

# CORROSION TESTS AND STANDARDS

APPLICATION AND INTERPRETATION

2ND EDITION

ROBERT BABOIAN, EDITOR



# **Corrosion Tests and Standards: Application and Interpretation—Second Edition**

---

**Robert Baboian, Editor**

## **Section Editors**

**Robert Baboian  
Sheldon W. Dean, Jr.  
Harvey P. Hack  
Edward L. Hibner  
John R. Scully**

**ASTM Stock Number: MNL20—2nd**



ASTM International  
100 Barr Harbor Drive  
PO Box C700  
West Conshohocken, PA 19428-2959

Printed in the U.S.A

Library of Congress Cataloging-in-Publication Data

Corrosion tests and standards : application and interpretation /  
Robert Baboian, editor ; section editors, Robert Baboian ...  
[et al.].—2nd ed.

p. cm.—(ASTM manual series ; MNL 20)

ASTM Stock Number: MNL20—2nd

ISBN 0-8031-2098-2

I. Corrosion and anti-corrosives—Testing. I. Baboian, Robert.  
II. Series.

TA462.C666 2005

620.1'1223—dc22

2004025972

Copyright © 2005 ASTM International, West Conshohocken,  
PA. All rights reserved. This material may not be reproduced  
or copied, in whole or in part, in any printed, mechanical,  
electronic, film, or other distribution and storage media,  
without the written consent of the publisher.

**Photocopy Rights**

**Authorization to photocopy items for internal, personal,  
or educational classroom use, or the internal, personal, or  
educational classroom use of specific clients, is granted  
by ASTM International (ASTM) provided that the ap-  
propriate fee is paid to the Copyright Clearance Center,  
222 Rosewood Drive, Danvers, MA 01923; Tel: 978-750-  
8400; online: <http://www.copyright.com/>.**

**The Society is not responsible, as a body, for the  
statements and opinions expressed in this publication.**

Printed in Baltimore, MD  
January 2005

## THE EDITORS

### ROBERT BABOIAN,

#### Editor

Robert Baboian is a corrosion consultant with RB Corrosion Service. He received his B.S. degree in chemistry from Suffolk University in 1959 and his Ph.D. in physical chemistry from Rensselaer Polytechnic Institute in 1964. He did postdoctoral research at the University of Toronto in 1964 and subsequently received a faculty appointment to Senior Research Associate in 1965. He joined the Materials and Controls Group of Texas Instruments, Inc. in 1966, where he established the Electrochemical and Corrosion Laboratory. He retired from Texas Instruments in December 1996 as Principal Fellow and Head of the Electrochemical and Corrosion Laboratory. The Principal Fellow position at TI is the company's highest honor for scientific and technical achievement. He is an ASTM Honorary Member, a Fellow of ASTM, NACE, and SAE, and was a Ford Foundation Postdoctoral Fellow in 1964.

Dr. Baboian has been dedicated to the research and development of corrosion resistant materials and devices, environmental effects on materials, and the use of electrochemical techniques in corrosion testing for almost 40 years. He holds 15 U.S. patents, is the editor of 13 books, and has authored over 170 technical publications. He has served on a number of Government and Academic Committees and has lectured throughout the world, and his services were donated by TI to the National Park Service as a corrosion consultant on the Statue of Liberty restoration program. Recently, he has researched the sinking of the *Titanic* and has proposed theories on corrosion mechanisms causing the failure.

Recognized for his active involvement in the technical community, Dr. Baboian has received the Cavanaugh Award and the Award of Merit from ASTM, the ASTM Dudley Award for publications, the ASTM LaQue Award for outstanding contributions to corrosion testing and evaluation, the Speller Award for outstanding contributions in corrosion engineering, and the T. J. Hull Award for publications from NACE, the Science and Technology Award of the Suga Weathering Technology Foundation in Japan, the Vittorio de Nora Award from the Electrochemical Society, the Francis L. LaQue Award for contributions to marine corrosion and prevention from the LaQue Center Sea Horse Institute, and the National Materials Advancement Award from the Federation of Materials Societies. He has served on the Executive Committee and the Board of Directors of ASTM and NACE and was the Chairman of the ASTM Board of Directors in 1987. He also has chaired ASTM Committee G-1 on Corrosion of Metals, the SAE Automotive Corrosion and Protection Committee, and the NACE Research Committee.

## SECTION EDITORS

### SHELDON W. DEAN, JR.

is currently the President of Dean Corrosion Technology, Inc., a consulting firm in Allentown, Pennsylvania that provides expert advice on matters involving corrosion of metals. He is also Editor in Chief of the *Journal of ASTM International*. He received his A.B. from Middlebury College and his B.S. and Sc.D. from the Massachusetts Institute of Technology. He has received the ASTM Award of Merit, the Charles B. Dudley Award, the Sam Tour Award, the Francis L. LaQue Memorial Award, the ASTM Committee on Publications Award for Excellence, the ASTM Committee G-1 Certificate of Appreciation, the NACE Frank Newman Speller Award, the NACE Fellow Honor, and was named a Fellow of the American Institute of Chemical Engineers and the Materials Technology Institute. He has served as chairman of ASTM Committee G-1 for four years. He also served on and chaired the ASTM Committee on Publications and the ASTM Board of Directors, and chaired the Finance and Audit Committee. He has also served on and chaired the Board of Directors of the Materials Technology Institute. He has 12 U.S. patents, 96 publications, and has co-edited eight books.

### HARVEY P. HACK

Dr. Hack is an Advisory Engineer for Northrop Grumman Corporation, where he does materials selection and corrosion control for underwater vehicles and systems for the Department of Defense. He received his B.S. and M.S. from Carnegie-Mellon University, and his Ph.D. in Metallurgy from The Pennsylvania State University. He is the recipient of the ASTM International Award of Merit, and is past Chairman of the Board of Directors of ASTM International. Dr. Hack has received the Distinguished Service Award from NACE International, the Francis L. LaQue Memorial Award from ASTM Committee G-1 on Corrosion of Metals, and the Francis L. LaQue Award from the Sea Horse Institute. He is a NACE Corrosion Specialist, Cathodic Protection Specialist, and Coatings Inspector, a Fellow of NACE International, ASTM International, the Washington Academy of Sciences, and the Institute of Corrosion in the United Kingdom, and is a Registered Professional Engineer in Maryland. Dr. Hack is the Associate Editor for the Materials Performance and Characterization section of the *Journal of ASTM International (JAI)*, is on the Materials Advisory Board for the National Air and Space Museum of the Smithsonian Institution, and is a past President of the Council of Engineering and Scientific Specialty Boards. Dr. Hack has approximately 70 publications and is the author, editor, or major contributor to five books. He is the author of a regular column on corrosion in *Underwater Magazine*.

### EDWARD L. HIBNER

is a Senior Metallurgist and Code Manager at Special Metals Corporation, formerly Inco Alloys International, in Huntington, West Virginia. He received his B.S. in Chemistry from Marshall University and in Metallurgy from the University of Cincinnati. He is the recipient of the ASTM Award of Merit, the ASTM Committee G-1 Francis L. LaQue Memorial Award, the ASTM Committee G-1 Certificate of Appreciation, and the NACE Fellow Award, and is currently Vice-Chairman and the Editorial Review Chairman of ASTM Committee G-1 on Corrosion of Metals. He has served as Chairman and as Trustee of the West Virginia Section of NACE International and is currently serving on the NACE MR0175/ ISO 15156 Maintenance Panel. He has extensive experience in alloy development for chemical process, flue gas desulfurization, marine, and oil field applications. He has written widely on materials applications and corrosion topics in these fields and has four patents and 60 publications. In addition to ASTM International, he is a member of the International Desalination Association, the Society for Petroleum Engineers, ASME International, SAE International, NACE International, and the Naval Submarine League.

### JOHN R. SCULLY

received his B.S., M.S., and Ph.D. in Materials Science and Engineering from Johns Hopkins University. While pursuing his Ph.D., he worked at David Taylor Naval Ship R&D Center in Annapolis, Maryland in the Marine Corrosion Branch. He then joined Sandia National Laboratory after a term as a Visiting Scientist at AT&T Bell Laboratories. In 1990, he joined the faculty of the Department of Materials Science and Engineering at the University of Virginia and is a full professor and co-directs the Center for Electrochemical Science and Engineering. Professor Scully received the 1985 A. B. Campbell Young Author Award from NACE. He has also been selected as a National Science Foundation Young Investigator, and has received the H. H. Uhlig Award from NACE and the William Blum Award from the Electrochemical Society. Professor Scully has published over 100 technical papers and edited several books on corrosion.



# Reviewers

Dinesh Agarwal  
Vinod Agarwala  
Hira Ahluwalia  
Paul Aimone  
George Andersen  
Frank Ansuini  
Peter Ault  
Denise Aylor  
Robert Baboian  
Brian Baker  
Milan Bartos  
Neal Berke  
Thomas Britton  
C. Sean Brossia  
Rudolph G. Buchheit  
Kenneth Budinski  
James Bushman  
Paul Brewer  
Julie Brown  
Kirk Bundy  
Gustavo Cragnolino  
Lee Craig  
Sheldon Dean  
Terry DeBold  
Stephen Dexter  
George DiBari  
Jeffrey Didas  
Charles Dillon  
Marcia Domack  
George Downs  
Dave Duquette  
K. Daniel Efird  
Nathan Eisinger  
Peter Elliott  
David Enos  
Ed Escalante  
John Fitzgerald  
Anna Fraker  
Gerald Frankel

Jim Gossett  
Richard Granata  
Harvey Hack  
William Hartt  
Gardner Haynes  
George Hays  
Edward Hibner  
Stanley Hirozawa  
F. Galen Hodge  
Alfred Hopkins  
William Jarosinski  
James Jenkins  
Denny Jones  
Russell Jones  
Robert Kain  
Mike Katcher  
Robert Kelly  
Gerhardus Koch  
Simeon Krumbein  
Paul Labine  
Herbert Lawson  
Jason Lee  
Daoming Li  
Brenda Little  
Daryl Little  
Frank Lutze  
Florian Mansfeld  
Charles Marsh  
James Martin  
Peter Mayer  
Joseph Menke  
Jean-Marc Meyer  
Harold Michels  
Tom Mills  
James Moran  
Patrick Morris  
Max Moskal  
Jim Myers  
James Noel

Sankara Papavinasam  
Frederick Pettit  
Bopinder Phull  
Robert Puyear  
David Reiser  
Pierre Roberge  
Paul Rothman  
Ken St. John  
Alberto Sagues  
Stuart Saunders  
John Schemel  
George Schick  
John Scully  
K. Anthony Selby  
David Shifler  
Tetyana Shmyreva  
David Silverman  
J. Douglas Sinclair  
Raymund Singleton  
Joseph Slusser  
Gaylord Smith  
John Snodgrass  
Donald Snyder  
Narasi Sridhar  
Sridhar Srinivasan  
Anthony Stavros  
T. J. Summerson  
William Tillis  
Herbert Townsend  
Hector Videla  
Yash Virmani  
George Waid  
Robert Wei  
Paul Whitcraft  
Ian Wright  
George Young  
Walter Young

# Foreword

THE REVISED PUBLICATION, *Corrosion Tests and Standards: Application and Interpretation*, is sponsored by ASTM Committee G1 on Corrosion of Metals and edited by Robert Baboian, RB Corrosion Service. Section editors include Robert Baboian, Sheldon W. Dean, Dean Corrosion Technology, Harvey P. Hack, Northrup Grumman Corporation, Edward Hibner, Special Metals Corporation, and John R. Scully, University of Virginia. This is the second edition of Manual 20 in the ASTM Manual series.

# Preface

CORROSION CONTINUES to be a problem of worldwide importance. The second edition of this manual has been prepared and published to address this form of degradation. Corrosion is often neglected, but it seriously impacts our economy, jeopardizes human health and safety, and impedes technological progress. The most important factors in addressing corrosion and its control are: (1) recognizing and understanding the mechanisms, (2) developing solutions to the problems, and (3) implementing those solutions. Corrosion tests and standards are very significant in addressing each of these factors. Therefore, this manual includes guidelines for recognizing types of corrosion as well as fundamentals of testing and provides the tools required for making calculations, interpretations, and correlations. It serves as a source book of procedures, equipment, and standards used in testing.

The editor and section editors have coordinated the revision and update of this book so that most recent technologies are included in each section. In most cases, the original authors of chapters have made the revisions. In some cases, new authors needed to be chosen, or the editors performed that task. Users of the manual will find that it is an invaluable and instructive tool, as well as a source book on how to conduct corrosion tests, interpret results, and use standards.

The second edition of the manual is the result of a massive effort of planning, writing, reviewing, editing, production, and marketing. It would not have been possible without the outstanding efforts of the ASTM staff and the valuable and competent work of the editors and over 400 experts in the field that donated their time as authors and reviewers. They represent industrial, educational, and government organizations, and their contributions are greatly appreciated.

*Robert Baboian*  
Editor

# Contents

<b>Introduction</b>	<b>1</b>
---------------------	----------

## **I: GENERAL INFORMATION—*R. Baboian, Section Editor***

Unified Numbering System for Metals and Alloys	4
Examples of Common Names of Selected UNS Alloys	5
Standard Terminology Relating to Corrosion and Corrosion Testing	7
Glossary of Corrosion-Related Acronyms	12
Standard Abbreviations and Unit Symbols	14
International System of Units (SI)	17
General Conversion Factors	18
Condensed Metric Practice Guide for Corrosion	20
Multiplication Factors (SI Prefixes)	22
Corrosion Rate Conversion Factors	22
Corrosion Rate Calculation (from Mass Loss)	23
Corrosion Rate Conversion Factors	24
Densities/K Factors for Alloys	25
Overvoltage Values	26
Reference Potentials and Conversion Table	27
Equivalent Weight Values for Metals and Alloys	28
Constants Used in Faraday's Equation	30
Physical Properties of Gases and Liquids	31
Physical Properties of Elements	32
Densities of Metals and Alloys	33
Density of Materials	35
Thermal Expansion Coefficients for Alloys	36
Physical Properties of Water	37
Dew Point of Moist Air	38
Chemical Cleaning Procedures for Removal of Corrosion Products	43
Electrolytic Cleaning Procedures for Removal of Corrosion Products	46

## **II: TESTING AND EVALUATION—*R. Baboian, Section Editor***

<b>Chapter 1—Planning and Design of Tests</b>	<b>49</b>
<i>Stephen D. Cramer and Barnie P. Jones</i>	
<b>Chapter 2—Types of Data</b>	<b>59</b>
<i>David C. Silverman</i>	
<b>Chapter 3—Metallographic Analysis</b>	<b>66</b>
<i>Richard L. Colwell</i>	

viii CORROSION TESTS AND STANDARDS MANUAL

<b>Chapter 4—Surface Analysis</b> <i>Alfred G. Hopkins</i>	76
<b>Chapter 5—Statistical Treatment of Data, Data Interpretation, and Reliability</b> <i>Fred H. Haynie</i>	83
<b>Chapter 6—Computer Based Data Organization and Computer Applications</b> <i>Pierre R. Roberge</i>	89

III: TYPES OF TESTS—*H. P. Hack, Section Editor*

<b>Chapter 7—Electrochemical Tests</b> <i>John R. Scully</i>	107
<b>Chapter 8—Cabinet Tests</b> <i>Cynthia L. Meade</i>	131
<b>Chapter 9—Immersion Testing</b> <i>Richard A. Corbett</i>	139
<b>Chapter 10—High-Temperature and High-Pressure Corrosion Testing</b> <i>Russell D. Kane</i>	147
<b>Chapter 11—Atmospheric</b> <i>Sheldon W. Dean, Jr.</i>	159
<b>Chapter 12—Seawater</b> <i>James F. Jenkins</i>	170
<b>Chapter 13—Freshwater</b> <i>Walter T. Young and Philippa Fairer</i>	175
<b>Chapter 14—Soils</b> <i>Edward Escalante</i>	181
<b>Chapter 15—Industrial Applications</b> <i>Allan Perkins</i>	187
<b>Chapter 16—High-Temperature</b> <i>Gaylord D. Smith</i>	194

IV: TESTING FOR CORROSION TYPES—*J. R. Scully, Section Editor*

<b>Chapter 17—Uniform Corrosion</b> <i>James A. Ellor and John Repp</i>	205
<b>Chapter 18—Pitting</b> <i>Robert G. Kelly</i>	211
<b>Chapter 19—Crevice Corrosion</b> <i>Narasi Sridhar, Darrell S. Dunn, C. S. Brossia, Gustavo A. Cragnolino, and Jeffery R. Kearns</i>	221
<b>Chapter 20—Galvanic</b> <i>Harvey P. Hack</i>	233
<b>Chapter 21—Intergranular</b> <i>Michael A. Streicher</i>	244

<b>Chapter 22—Exfoliation</b>	266
<i>Donald O. Sprowls; revised by Kevin R. Cooper</i>	
<b>Chapter 23—Erosion, Cavitation, and Fretting</b>	273
<i>W. A. Glaeser</i>	
<b>Chapter 24—Dealloying</b>	278
<i>Ann Chidester Van Orden</i>	
<b>Chapter 25—Environmental Cracking—Stress Corrosion</b>	289
<i>W. Barry Lisagor</i>	
<b>Chapter 26—Environmental Cracking—Corrosion Fatigue</b>	302
<i>Richard P. Gangloff</i>	
<b>Chapter 27—Hydrogen Damage</b>	322
<i>C. G. Interrante and L. Raymond</i>	
 <b>V: TESTING IN ENVIRONMENTS—H. P. Hack, Section Editor</b>	
<b>Chapter 28—Outdoor Atmospheres</b>	343
<i>Herbert H. Lawson</i>	
<b>Chapter 29—Indoor Atmospheres</b>	349
<i>J. D. Sinclair</i>	
<b>Chapter 30—Seawater</b>	362
<i>David A. Shifler and Denise M. Aylor</i>	
<b>Chapter 31—Freshwater</b>	380
<i>Walter T. Young and Philippa Fairer</i>	
<b>Chapter 32—Soils</b>	387
<i>Lucien Veleva</i>	
<b>Chapter 33—Concrete</b>	405
<i>Neal S. Berke</i>	
<b>Chapter 34—Industrial Waters</b>	413
<i>A. S. Krisher</i>	
<b>Chapter 35—Industrial Chemicals</b>	418
<i>Robert B. Puyear</i>	
<b>Chapter 36—Petroleum</b>	425
<i>K. Daniel Efird</i>	
<b>Chapter 37—High-Temperature Gases</b>	434
<i>Gaylord D. Smith and Brian A. Baker</i>	
<b>Chapter 38—Organic Liquids</b>	448
<i>C. S. Brossia and D. A. Shifler</i>	
<b>Chapter 39—Molten Salts</b>	457
<i>F. S. Pettit</i>	
<b>Chapter 40—Liquid Metals</b>	465
<i>Chris Bagdall, Peter F. Tortorelli, Steven J. Pawel, Jack H. DeVan, and Steven L. Schrock</i>	

**x CORROSION TESTS AND STANDARDS MANUAL**

<b>Chapter 41—Corrosion Inhibitors</b> <i>Rudolf H. Hausler</i>	480
<b>Chapter 42—Corrosion Testing in <i>In Vivo</i> Environments</b> <i>K. J. Bundy</i>	500
<b>Chapter 43—Microbiological Effects</b> <i>Stephen C. Dexter</i>	509
<b>VI: MATERIALS TESTING—E. L. Hibner, Section Editor</b>	
<b>Chapter 44—Zinc</b> <i>Frank E. Goodwin and Safaa J. Alhassan</i>	525
<b>Chapter 45—Lead (and Alloys)</b> <i>Safaa J. Alhassan and Frank E. Goodwin</i>	531
<b>Chapter 46—Magnesium (and Alloys)</b> <i>James E. Hillis</i>	537
<b>Chapter 47—Aluminum (and Alloys)</b> <i>Bernard W. Lifka</i>	547
<b>Chapter 48—Steels</b> <i>M. E. Komp, D. L. Jordan, and R. Baboian</i>	558
<b>Chapter 49—Copper (and Alloys)</b> <i>Arthur Cohen</i>	565
<b>Chapter 50—Nickel (and Alloys)</b> <i>Edward L. Hibner</i>	580
<b>Chapter 51—Stainless Steels</b> <i>James W. Martin</i>	585
<b>Chapter 52—Cobalt-Base Alloys</b> <i>P. Crook</i>	591
<b>Chapter 53—Titanium</b> <i>Ronald W. Schutz</i>	598
<b>Chapter 54—Zirconium and Hafnium</b> <i>Te-Lin Yau</i>	613
<b>Chapter 55—Tantalum and Niobium Alloys</b> <i>E. B. Hinshaw and K. D. Moser</i>	617
<b>Chapter 56—Metallic Coatings on Steel</b> <i>T. C. Simpson and H. E. Townsend</i>	620
<b>Chapter 57—Nonmetallic Coatings</b> <i>Richard D. Granata</i>	632
<b>Chapter 58—Metal-Matrix Composites</b> <i>L. H. Hihara</i>	637
<b>Chapter 59—Electrodeposits</b> <i>T. P. Moffat</i>	656

<b>Chapter 60—Powder Metallurgy (P/M) Materials</b> <i>Erhard Klar and Prasan K. Samal</i>	664
<b>VII: TESTING IN INDUSTRIES—S. W. Dean, Jr., Section Editor</b>	
<b>Chapter 61—Automotive</b> <i>Robert Baboian</i>	673
<b>Chapter 62—Commercial Aircraft</b> <i>A. A. Adjorlolo and J. A. Marceau</i>	687
<b>Chapter 63—Military Aircraft and Associated Equipment</b> <i>Earl C. Groshart</i>	693
<b>Chapter 64—Pipeline</b> <i>Paul S. Rothman and Walter T. Young</i>	696
<b>Chapter 65—Highways, Tunnels, and Bridges</b> <i>James B. Bushman and Victor Chaker</i>	706
<b>Chapter 66—Marine—Piers and Docks</b> <i>James F. Jenkins</i>	716
<b>Chapter 67—Electric Power</b> <i>P. Mayer and A. D. Pellgrini</i>	722
<b>Chapter 68—Nuclear Power</b> <i>George J. Licina</i>	727
<b>Chapter 69—Steam Generation</b> <i>Otakar Jonas</i>	738
<b>Chapter 70—Flue Gas Desulfurization</b> <i>Harvey S. Rosenberg and Eldon R. Dille</i>	746
<b>Chapter 71—Electronics</b> <i>Robert Baboian</i>	754
<b>Chapter 72—Telecommunications</b> <i>George Schick</i>	762
<b>Chapter 73—Metals Processing</b> <i>Terry A. DeBold</i>	769
<b>Chapter 74—Chemical Processing</b> <i>Bert Moniz and Shi Hua Zhang</i>	779
<b>Chapter 75—Pulp and Paper</b> <i>Angela Wensley</i>	795
<b>Chapter 76—Petroleum Production and Refining</b> <i>R. N. Tuttle</i>	812
<b>Chapter 77—Food and Beverage</b> <i>W. E. Clayton and B. Tholke</i>	822
<b>Chapter 78—Water Handling Systems</b> <i>Bennett P. Boffardi</i>	826



**xii** *CORROSION TESTS AND STANDARDS MANUAL*

**Chapter 79—Medical and Dental** 834  
*Anna C. Fraker*

**Chapter 80—Pharmaceutical** 846  
*David F. Jensen*

**VIII: CORROSION-RELATED STANDARDS—*H.P. Hack and R. Baboian, Section Editors***

**LIST OF CORROSION-RELATED STANDARDS** 851

**Author Index** 865

**Subject Index** 867

# Introduction

ASTM'S AWARD-WINNING Manual 20 has been revised and updated to include current and state-of-the-art technologies in corrosion testing and standardization. The editors of this manual have many years of experience in this field and are well qualified in leading the task to provide state-of-the-art information on this subject for corrosion scientists and technologists throughout the world. The work of 80 highly qualified chapter authors and numerous reviewers has resulted in a revised, expanded, and updated Manual 20 on Corrosion Tests and Standards, Application and Interpretation.

Corrosion is the chemical or electrochemical reaction between a material, usually a metal, and its environment that produces a deterioration of the material and its properties. The direct cost of corrosion in countries throughout the world is estimated to be between 3 % and 4 % of the gross domestic product of each country. For example, that cost in the United States was estimated to be \$276 billion annually, for recent years. It was determined that a significant portion of these costs could be avoided through the more effective use of existing technologies and the use of sound corrosion management techniques. This manual is a key resource in addressing both of these subjects.

Corrosion testing is one of the most important aspects of corrosion control because it is used to advance technology and to determine the most effective and economical means to achieve acceptable performance. A large number of factors affect corrosion behavior so that there is no universal corrosion test. ASTM and other organizations such as NACE, ISO, and others have standardized many tests and practices. However, industry, government, and academic laboratories sometimes utilize in-house tests. Thus, this Manual provides a valuable resource describing and listing a large number of tests ranging from highly accelerated laboratory tests to field service trials.

Since standards are universally recognized as an important tool in effective corrosion control management, this Manual not only provides information required to find and use proper standards in specific applications, it also includes a CD with almost 200 of the most widely used ASTM and NACE corrosion standards. All of the chapter authors have included important standards specific to their topic and the Manual includes lists of standards according to subject, of which the most important are included in the CD.

The revised Manual is organized into eight sections.

Section I on **General Information** (R. Baboian, Section Editor) provides tools necessary for the corrosionist to define,

interpret, and evaluate the technology. This section is greatly expanded and includes a unified numbering system for metals and alloys and their common names, standards terminology, a glossary of terms and acronyms, abbreviations and units symbols, International System of Units and matrix guide, general conversion tables, corrosion rate calculations and all necessary conversion factors, chemical and physical properties of materials, properties of water and moist air, chemical and electrolytic cleaning procedures for corrosion products, physical properties of gases, liquids and elements, and densities of metals and alloys.

Section II on **Testing and Evaluation** (R. Baboian, Section Editor) is designed to provide important information on planning and design of tests and interpretation of results. This topic provides a foundation for corrosion testing and the use of corrosion standards. It includes chapters on planning and design of tests, types of corrosion data, metallographic and surface analysis, statistical treatment of data and data computerization and computer applications.

Section III covers **Types of Tests** (H. Hack, Section Editor) including laboratory-accelerated tests, field tests, and service tests. The chapters in this section provide basic principles, describe test techniques and specific considerations such as specimen preparation, test duration and acceleration factors, and cite pertinent standards. Chapters included under laboratory tests are electrochemical, cabinet, immersion, high temperature, and high pressure. Field Tests chapters include atmospheric exposure, seawater, fresh water, and soil. Under service tests are industrial applications and high temperature environments.

Section IV on **Testing for Corrosion Types** (J. Scully, Section Editor) describes the major forms of corrosion, how to recognize them and factors of influence. Each chapter includes an overview of basic principles and also descriptions of test techniques, methods of evaluation of test results, and standards used for testing. Subjects included are uniform, pitting, crevice, galvanic, intergranular, exfoliation, erosion, cavitation, fretting, dealloying, stress corrosion, corrosion fatigue and hydrogen damage.

Section V on **Testing in Environments** (H. Hack, Section Editor) includes chapters on outdoor and indoor atmospheres, seawater, fresh water, soils, concrete, industrial waters, industrial chemical, petroleum, high-temperature gases, organic liquids, molten salts, liquid metals, corrosion inhibitors, in-vivo, and microbiological effects. Each chapter provides a descriptive overview of the environment and factors and variables affecting corrosion rates and mechanisms,

## 2 CORROSION TESTS AND STANDARDS MANUAL

unique characteristics of testing, descriptions of appropriate laboratory and field tests and lists of standards used for corrosion testing in these environments.

Section VI is on **Materials Testing** (E. Hibner, Section Editor). This section provides overviews of important tests used in evaluating the corrosion behavior of metals and alloys. In addition, this testing information provides the means for the development of new and improved corrosion resistant materials. Each chapter includes a discussion of the nature of the material, such as the effect of composition, alloying, metallurgical treatments, microstructure, surface effects and natural films on the corrosion behavior. The chapter also includes descriptions of tests used for specific types of corrosion for the metals and alloys, methods of evaluation of corrosion damage and standards used for corrosion testing of the various materials. The chapters are zinc, lead (and alloys), aluminum (and alloys), steels, copper (and alloys), nickel (and alloys), stainless steels, cobalt-base alloys, titanium, zirconium and hafnium, tantalum and niobium alloys, metallic coatings on steel, nonmetallic coatings, metal matrix composites, electrodeposits, and powder metallurgy materials.

Section VII on **Testing in Industries** (S. Dean, Section Editor) provides an overview of corrosion testing unique to each industry and how these tests are used to address corrosion problems. Included are descriptions of environments encountered and materials used in specific industries. Test methods for corrosion control and evaluation are described along with appropriate standards. Chapters in this section include automotive, commercial aircraft, military aircraft

and equipment, pipeline, highways, tunnels and bridges, marine piers and docks, electric power, nuclear power, steam generation, flue gas desulfurization, electronics, telecommunications, metal processing, chemical processing, pulp and paper, petroleum production and refining, food and beverage, water handling systems, medical and dental, and pharmaceutical.

Section VIII on **Corrosion-Related Standards** (H. Hack and R. Baboian, Section Editors) is a comprehensive list of standards developed by various organizations including the American Petroleum Institute, American Waterworks Association, ASME International, ASTM International, International Electrotechnical Commission, ISO, NACE International, SAE International, and the Steel Structures Painting Council. The standards are listed and grouped according to subject within each organization. The accompanying CD includes many of the ASTM and NACE corrosion standards.

The revised Manual 20 on Corrosion Tests and Standards is certain to serve as a valuable resource for those in industry, government, and academia. Acknowledgment is given to the many authors who wrote the chapters providing the important information in this revision. Also acknowledged are the reviewers who work anonymously to help maintain a high level of quality throughout the book. The work of the editors can only be completed through the dedication and competence of these persons.

*Robert Baboian*  
Editor

# Section I: General Information

*R. Baboian, Editor*

## Contents

Unified Numbering System for Metals and Alloys  
 Examples of Common Names of Selected UNS Alloys  
 Standard Terminology Relating to Corrosion and Corrosion Testing  
 Glossary of Corrosion-Related Acronyms  
 Standard Abbreviations and Unit Symbols  
 International System of Units (SI)  
 General Conversion Factors  
 Condensed Metric Practice Guide for Corrosion  
 Multiplication Factors (SI Prefixes)  
 Corrosion Rate Conversion Factors  
 Corrosion Rate Calculation (from Mass Loss)  
 Corrosion Rate Conversion Factors  
 Densities/K Factors for Alloys  
 Overvoltage Values  
 Reference Potentials and Conversion Table  
 Equivalent Weight Values for Metals and Alloys  
 Constants Used in Faraday's Equation  
 Physical Properties of Gases and Liquids  
 Physical Properties of Elements  
 Densities of Metals and Alloys  
 Density of Materials  
 Thermal Expansion Coefficients for Alloys  
 Physical Properties of Water  
 Dew Point of Moist Air  
 Chemical Cleaning Procedures for Removal of Corrosion Products  
 Electrolytic Cleaning Procedures for Removal of Corrosion Products

Reference  
 NACE  
 NACE  
 ASTM G 15  
 NACE  
 ASTM  
 ASTM E 380  
 ASTM E 380  
 ASTM  
 ASTM E 380  
 Wranglén  
 ASTM G 1  
 NACE  
 NACE  
 Various  
 ASTM G 3  
 ASTM G 102  
 ASTM G 102  
 ASTM  
 ASTM  
 ASTM G 1  
 ASM  
 NACE  
 Various  
 NACE  
 ASTM G 1  
 ASTM G 1

# Unified Numbering System for Metals and Alloys<sup>1</sup>

## UNS SERIES

### Nonferrous Metals and Alloys

A00001-A99999  
C00001-C99999  
E00001-E99999  
L00001-L99999  
M00001-M99999  
N00001-N99999  
P00001-P00999  
P01001-P01999  
P02001-P02999  
P03001-P03999  
P04001-P04999  
P05001-P05999  
P06001-P06999  
P07001-P07999  
R01011-R01999  
R02001-R02999  
R03001-R03999  
R04001-R04999  
R05001-R05999  
R06001-R06999  
R07001-R07999  
R08001-R08999  
R10001-R19999  
R20001-R29999  
R30001-R39999  
R40001-R49999  
R50001-R59999  
R60001-R69999  
Z00001-Z99999

### Ferrous Metals and Alloys

D00001-D99999  
F00001-F99999  
G00001-G99999  
H00001-H99999  
J00001-J99999  
K00001-K99999  
S00001-S99999  
T00001-T99999

### Welding Filler Metals, Classified by Weld Deposit Composition

W00001-W09999  
W10000-W19999  
W20000-W29999  
W30000-W39999  
W40000-W49999  
W50000-W59999  
W60000-W69999  
W70000-W79999  
W80000-W89999

## Metal

Aluminum and aluminum alloys  
Copper and copper alloys  
Rare earth and rare earth-like metals and alloys  
Low melting metals and alloys  
Miscellaneous nonferrous metals and alloys  
Nickel and nickel alloys  
Gold  
Iridium  
Osmium  
Palladium  
Platinum  
Rhodium  
Ruthenium  
Silver  
Boron  
Hafnium  
Molybdenum  
Niobium (Columbium)  
Tantalum  
Thorium  
Tungsten  
Vanadium  
Beryllium  
Chromium  
Cobalt  
Rhenium  
Titanium  
Zirconium  
Zinc and zinc alloys  
  
Specified mechanical properties steels  
Cast irons  
AISI and SAE carbon and alloys steels (except tool steels)  
AISI H-steels  
Cast steels (except tool steels)  
Miscellaneous steels and ferrous alloys  
Heat- and corrosion-resistant (stainless) steels  
Tool steels  
  
Carbon steel with no significant alloying elements  
Manganese-molybdenum low-alloy steels  
Nickel low-alloy steels  
Austenitic stainless steels  
Ferritic stainless steels  
Chromium low-alloy steels  
Copper-base alloys  
Surfacing alloys  
Nickel-base alloys

<sup>1</sup>See *NACE Corrosion Engineers Reference Book, Third Edition*,  
R. Baboian, Ed., NACE International, 2002, p. 233.

# Examples of Common Names of Selected UNS Alloys<sup>1</sup>

Nonferrous		
A02420 Al 242.0	A02950 Al 295.0	A03560 Al 356.0
A05140 Al 514.0	A05200 Al 520.0	A24430 Al B443.0
A91060 Al 1060	A91100 Al 1100	A92014 Al 2014
A92024 Al 2024	A93003 Al 3003	A95052 Al 5052
A95083 Al 5083	A95086 Al 5086	A95154 Al 5154
A96061 Al 6061	A96063 Al 6063	A97075 Al 7075
C10200 OF Copper	C11000 ETP Copper	C12200 DHP Copper
C14200 DPA Copper	C22000 Commercial Bronze	C23000 Red Brass
C26000 Cartridge Brass	C27000 Yellow Brass	C28000 Muntz Metal
C44300 Admiralty Brass, As	C44400 Admiralty Brass, Sb	C44500 Admiralty Brass, P
C46500 Naval Brass, As	C51000 Phosphor Bronze A	C52400 Phosphor Bronze D
C60600 Aluminum Bronze, 6 %	C61300 Aluminum Bronze, 7 %	C61400 Aluminum Bronze D
C63000 Nickel Aluminum Bronze	C65500 High-Silicon Bronze	C67500 Manganese Bronze A
C68700 Aluminium Brass, As	C70600 90-10 Copper-Nickel	C71500 70-30 Copper-Nickel
C75200 Nickel Silver	C83600 Ounce Metal	C86500 Manganese Bronze
C90500 Gun Metal	C92200 M Bronze	C95700 Cast Mn-Ni-Al Bronze
95800 Cast Ni-Al Bronze	C96400 Cast 70-30 Cu-Ni	
L50045 Common Lead	L51120 Chemical Lead	L55030 50/50 Solder
M11311 Mg AZ31B	M11914 Mg AZ91C	M12330 Mg EZ33A
M13310 Mg HK31A		
N02200 Nickel 200	N02201 Nickel 201	N02230 Nickel 230
N04400 400 Alloy	N04405 R-405 Alloy	N05500 K-500 Alloy
N05502 502 Alloy	N06002 X Alloy	N06007 G Alloy
N06022 C-22 Alloy	N06030 G-30 Alloy	N06110 Allcor
N06333 RA333 Alloy	N06455 C-4 Alloy	N06600 600 Alloy
N06601 601 Alloy	N06617 617 Alloy	N06625 625 Alloy
N06690 690 Alloy	N06975 2550 Alloy	N06965 G-3 Alloy
N07001 Waspaloy	N07031 31 Alloy	N07041 Rene 41
N07090 90 Alloy	N07716 625 Plus	N07718 718 Alloy
N07750 X-750 Alloy	N08020 20Cb-3	N08024 20Mo-4
N08026 20Mo-6	N08028 Sanicro 28	N08320 20 Mod
N08330 RA-330	N08366 AL-6X	N08367 AL-6XN
N08700 JS700	N08800 800 Alloy	N08801 801 Alloy
N08810 800H Alloy	N08811 800HT Alloy	N08825 825 Alloy
N08904 904L Alloy	N08925 25-6Mo	N09706 706 Alloy
N09925 925 Alloy	N10001 B Alloy	N10002 C Alloy
N10003 N Alloy	N10004 W Alloy	N10276 C-276 Alloy
N10685 B-2 Alloy		
R03600 Molybdenum	R03630 Molybdenum Alloy	R03650 Molybdenum, low C
R04210 Niobium (Columbium)	R05200 Tantalum	R07005 Tungsten
R30003 Elgiloy	R30004 Havar	R30006 Stellite 6
R30031 Stellite 31	R30035 MP35N	R30155 N-155

<sup>1</sup> See *NACE Corrosion Engineers Reference Book, Third Edition*,  
R. Baboian, Ed., NACE International, 2002, pp. 234-235.

## 6 CORROSION TESTS AND STANDARDS MANUAL

Nonferrous		
R30188 HS-188 Alloy	R30260 Duratherm 2602	R30556 HS-556
R30605 L-605 Alloy	R50250 Titanium, Gr 1	R50400 Titanium, Gr 2
R50550 Titanium, Gr 3	R50700 Titanium, Gr 4	R52250 Titanium, Gr 11
R52400 Titanium, Gr 7	R53400 Titanium, Gr 12	R54520 Titanium, Gr 6
R56260 Ti6Al6Mo2Sn4Zr	R56320 Titanium, Gr 9	R56400 Titanium, Gr 5
R58640 Beta-C	R60702 Zr 702	R60704 Zr 704
R60705 Zr 705		
Z13000 Zinc Anode Type II	Z32120 Zinc Anode Type I	Z32121 Zinc Anode Type III
Ferrous		
F10006 Gray Cast Iron	F20000 Malleable Cast Iron	F32800 Ductile Iron 60-40-18
F41000 Ni-Resist Type 1	F41002 Ni-Resist Type 2	F41006 Ni-Resist Type 5
F43000 Ductile Ni-Resist D2	F43006 Ductile Ni-Resist D5	F47003 Dunron
G10200 1020 Carbon Steel	G41300 4130 Steel	G43400 4340 Steel
J91150 CA-15	J91151 CA-15M	J91153 CA-40
J91540 CA-6NM	J91803 CB-30	J92500 CF-3
J92600 CF-8	J92602 CF-20	J92603 HF
J292605 HC	J92615 CC-50	J92701 CF-16F
J92710 CF-8C	J92800 CF-3M	J92900 CF-8M
J93000 CG-8M	J93001 CG-12	J93005 HD
J93370 CD-4MCu	J93402 CH-20	J93423 CE-30
J93503 HH	J94003 HI	J94202 CK-20
J94203 HK-30	J94204 HK-40	J94213 HN
J94224 HK	N08604 HL	N08002 HT
N08007 CN-7M	N08004 HU	N08705 HP
K01800 A516-55	K02100 A516-60	K02403 A516-65
K02700 A516-70	K02801 A285-C	K03005 A53-B
K03006 A106-B	K11510 0.2Cu Steel	K11522 C-0.5Mo
K11576 HSLA Steel	K11597 1.25Cr-0.5Mo	K21590 2.25Cr-1Mo
K41545 5Cr-0.5Mo	K81340 9Ni Steel	K90941 9Cr-1Mo
K94610 KOVAR		
S13800 PH 13-8 Mo	S15500 15-5 PH	S15700 PH 15-7 Mo
S17400 17-4 PH	S17600 Stainless W	S17700 17-7 PH
S20100 201 SS	S20200 202 SS	S20910 22-13-5
S21400 Tenelon	S21600 216 SS	S21800 Nitronic 60
S21900 21-6-9	S24000 18-3 Mn	S28200 18-18 Plus
S30200 302 SS	S30300 303 SS	S30400 304 SS
S30403 304L SS	S30409 304H SS	S30451 304N SS
S30453 304LN SS	S30500 305 SS	S30800 308 SS
S30815 253MA	S30900 309 SS	S30906 309S SS
S31000 310 SS	S31006 310S SS	S31200 44LN
S31254 254 SMO	S31260 DP-3	S31400 314 SS
S31500 3RE60	S31600 316 SS	S31603 316L SS
S31609 316H SS	S31635 316Ti SS	S31640 316Cb SS
S31651 316N SS	S31635 316LN SS	S31700 317 SS
S31703 317L SS	S31725 317LM SS	S31726 317L4 SS
S31803 2205 Alloy	S32100 321 SS	S32109 321H SS
S32304 SAF 2304	S32404 Uranus 50	S32550 Ferralium 255
S32900 329 SS	S32950 7-Mo Plus	S34700 347 SS
S34709 347H SS	S34800 348 SS	S35000 AM 350
S35500 AM 355	S36200 Almar 362	S38100 18-18-2
S40300 403 SS	S40500 405 SS	S40900 409 SS
S41000 410 SS	S41400 414 SS	S41600 416 SS
S41800 Greek Ascoloy	S42000 420 SS	S42200 422 SS
S42400 F6NM	S42900 429 SS	S43000 430 SS
S43100 431 SS	S43400 434 SS	S43500 436 SS
S44002 440A SS	S44003 440B SS	S44004 440C SS
S44200 442 SS	S44400 18-2	S44600 446 SS
S44625 26-1	S44626 26-1 Ti	S44627 26-1 Cb
S44635 26-4-4	S44660 SC-1	S44700 29-4
S44735 29-4C	S44800 29-4-2	S45000 Custom 450
S45500 Custom 455	S50100 5Cr-0.5Mo	S50200 5Cr-0.5Mo
S50300 7Cr-0.5Mo	S50400 9Cr-1Mo	S66286 A286



**Designation: G 15-04**

## Standard Terminology Relating to Corrosion and Corrosion Testing<sup>1</sup>

This standard is issued under the fixed designation G 15; the number immediately following the designation indicates the year of original adoption or, in the case of revision, the year of last revision. A number in parentheses indicates the year of last reapproval. A superscript epsilon (ε) indicates an editorial change since the last revision or reapproval.

*This standard has been approved for use by agencies of the Department of Defense.*

### 1. Scope

1.1 This terminology covers commonly used terms in the field of corrosion. Related terms may be found in Terminologies D 16, D 4538, G 40, or other ASTM terminology standards. All terms defined by ASTM committees may be found in the *ASTM Dictionary of Engineering & Technology*.

### 2. Referenced Documents

#### 2.1 ASTM Standards:<sup>2</sup>

D 16 Terminology for Paint, Related Coatings, Materials, and Applications

D 4538 Terminology Relating to Protective Coating and Lining Work for Power

G 40 Terminology Relating to Wear and Erosion

### 3. Terminology

**AC impedance**—See **electrochemical impedance**.

**active**—the negative direction of electrode potential. (Also used to describe corrosion and its associated potential range when an electrode potential is more negative than an adjacent depressed corrosion rate [passive] range.)

**anion**—a negatively charged ion.

**anode**—the electrode of an electrolytic cell at which oxidation is the principal reaction. (Electrons flow away from the anode in the external circuit. It is usually the electrode where corrosion occurs and metal ions enter solution.)

**anode corrosion efficiency**—the ratio of the actual corrosion (weight loss) of an anode to the theoretical corrosion (weight loss) calculated by Faraday's law from the quantity of electricity that has passed.

**anodic inhibitor**—a corrosion inhibitor whose primary action is to slow the kinetics of the anodic reaction, producing a positive shift in corrosion potential.

**anodic polarization**—the change of the electrode potential in the noble (positive) direction due to current flow. (See **polarization**.)

**anodic protection**—a technique to reduce the corrosion rate of a metal by polarizing it into its passive region where dissolution rates are low.

**anolyte**—the electrolyte adjacent to the anode of an electrolytic cell.

**auxiliary electrode**—See **counter electrode**.

**breakdown potential**—the least noble potential where pitting or crevice corrosion, or both, will initiate and propagate.

**cathode**—the electrode of an electrolytic cell at which reduction is the principal reaction. (Electrons flow toward the cathode in the external circuit.)

**cathodic corrosion**—corrosion of a metal when it is a cathode. (It usually happens to metals because of a rise in pH at the cathode or as a result of the formation of hydrides.)

**cathodic inhibitor**—a corrosion inhibitor whose primary action is to slow the kinetics of the cathodic reaction, producing a negative shift in corrosion potential.

**cathodic polarization**—the change of the electrode potential in the active (negative) direction due to current flow. (See **polarization**.)

**cathodic protection**—a technique to reduce the corrosion rate of a metal surface by making it the cathode of an electrochemical cell.

**catholyte**—the electrolyte adjacent to the cathode of an electrolytic cell.

**cation**—a positively charged ion.

**caustic cracking**—stress corrosion cracking of metals in caustic solutions. (See also **stress-corrosion cracking**.)

**caustic embrittlement**—See **caustic cracking**.

**cavitation**—the formation and rapid collapse within a liquid of cavities or bubbles that contain vapor or gas or both.

**cavitation corrosion**—the conjoint action of cavitation-erosion and corrosion.

**cavitation damage**—the degradation of a solid body resulting from its exposure to cavitation. (This may include loss of material, surface deformation, or changes in properties or appearance.)

**cavitation-erosion**—loss of material from a solid surface due to mechanical action of continuing exposure to cavitation.

**chemical conversion coating**—a protective or decorative nonmetallic coating produced *in situ* by chemical reaction of a metal with a chosen environment. (It is often used to prepare the surface prior to the application of an organic coating.)

<sup>1</sup> This terminology is under the jurisdiction of ASTM Committee G01 on Corrosion of Metals and are the direct responsibility of Subcommittee G01.02 on Terminology.

Current edition approved Jan. 1, 2004. Published January 2004. Originally approved in 1971. Last previous edition approved in 2003 as G 15-03a.

<sup>2</sup> For referenced ASTM standards, visit the ASTM website, [www.astm.org](http://www.astm.org), or contact ASTM Customer Service at [service@astm.org](mailto:service@astm.org). For *Annual Book of ASTM Standards* volume information, refer to the standard's Document Summary page on the ASTM website.

- concentration cell**—an electrolytic cell, the emf of which is caused by a difference in concentration of some component in the electrolyte. (This difference leads to the formation of discrete cathode and anode regions.)
- corrosion**—the chemical or electrochemical reaction between a material, usually a metal, and its environment that produces a deterioration of the material and its properties.
- corrosion fatigue**—the process in which a metal fractures prematurely under conditions of simultaneous corrosion and repeated cyclic loading at lower stress levels or fewer cycles than would be required in the absence of the corrosive environment.
- corrosion fatigue strength**—the maximum repeated stress that can be endured by a metal without failure under definite conditions of corrosion and fatigue and for a specific number of stress cycles and a specified period of time.
- corrosion inhibitor**—a chemical substance or combination of substances that, when present in the proper concentration and forms in the environment, prevents or reduces corrosion.
- corrosion potential**—the potential of a corroding surface in an electrolyte relative to a reference electrode measured under open-circuit conditions.
- corrosion rate**—the amount of corrosion occurring in unit time. (For example, mass change per unit area per unit time; penetration per unit time.)
- counter electrode**—the electrode in an electrochemical cell that is used to transfer current to or from a test electrode.
- crevice corrosion**—localized corrosion of a metal surface at, or immediately adjacent to, an area that is shielded from full exposure to the environment because of close proximity between the metal and the surface of another material.
- critical anodic current density**—the maximum anodic current density observed in the active region for a metal or alloy electrode that exhibits active-passive behavior in an environment.
- critical humidity**—the relative humidity above which the atmospheric corrosion rate of some metals increases sharply.
- critical pitting potential**—the least noble potential where pitting corrosion will initiate and propagate. (See breakdown potential.)
- current density**—the electric current to or from a unit area of an electrode surface.
- current efficiency**—the ratio of the electrochemical equivalent current density for a specific reaction to the total applied current density.
- deactivation**—the process of prior removal of the active corrosive constituents, usually oxygen, from a corrosive liquid by controlled corrosion of expendable metal or by other chemical means, thereby making the liquid less corrosive.
- dealloying**—See **parting**.
- depolarization**—not a preferred term. (See **polarization**.)
- deposit corrosion**—localized corrosion under or around a deposit or collection of material on a metal surface. (See also **crevice corrosion**.)
- dezincification**—See **parting**; specific to copper-zinc alloys.
- differential aeration cell (oxygen concentration cell)**—a concentration cell caused by differences in oxygen concentration along the surface of a metal in an electrolyte. (See **concentration cell**.)
- diffusion limited current density**—the current density, often referred to as limiting current density, that corresponds to the maximum transfer rate that a particular species can sustain due to the limitation of diffusion.
- electrochemical admittance**—the reciprocal of the electrochemical impedance,  $\Delta I/\Delta E$ .
- electrochemical cell**—an electrochemical system consisting of an anode and a cathode in metallic contact and immersed in an electrolyte. (The anode and cathode may be different metals or dissimilar areas on the same metal surface.)
- electrochemical impedance**—the frequency dependent, complex valued proportionality factor,  $\Delta E/\Delta I$ , between the applied potential (or current) and the response current (or potential) in an electrochemical cell. This factor becomes the impedance when the perturbation and response are related linearly (the factor value is independent of the perturbation magnitude) and the response is caused only by the perturbation. The value may be related to the corrosion rate when the measurement is made at the corrosion potential.
- electrochemical noise**—fluctuations of the current, or both, originating from uncontrolled variations in a corrosion process.
- electrochemical potential (electrochemical tension)**—the partial derivative of the total electrochemical free energy of the system with respect to the number of moles of the constituent in a solution when all other factors are constant. (Analogous to the chemical potential of the constituent except that it includes the electrical as well as the chemical contributions to the free energy.)
- electrode potential**—the potential of an electrode in an electrolyte as measured against a reference electrode. (The electrode potential does not include any resistance losses in potential in either the solution or external circuit. It represents the reversible work to move a unit charge from the electrode surface through the solution to the reference electrode.)
- electrolysis**—production of chemical changes of the electrolyte by the passage of current through an electrochemical cell.
- electrolytic cleaning**—a process of removing soil, scale or corrosion products from a metal surface by subjecting it as an electrode to an electric current in an electrolytic bath.
- Electromotive Force Series (EMF Series)**—a list of elements arranged according to their standard electrode potentials, with “noble” metals such as gold being positive and “active” metals such as zinc being negative.
- embrittlement**—the severe loss of ductility or toughness or both, of a material, usually a metal or alloy.
- environmentally-assisted cracking**—the initiation or acceleration of a cracking process due to the conjoint action of a chemical environment and tensile stress.
- equilibrium (reversible) potential**—the potential of an electrode in an electrolytic solution when the forward rate of a given reaction is exactly equal to the reverse rate. (The equilibrium potential can only be defined with respect to a specific electrochemical reaction.)
- erosion**—the progressive loss of material from a solid surface due to mechanical interaction between that surface and a fluid, a multi-component fluid, or solid particles carried with the fluid.

- erosion-corrosion**—a conjoint action involving corrosion and erosion in the presence of a moving corrosive fluid, leading to the accelerated loss of material.
- exchange current density**—the rate of charge transfer per unit area when an electrode reaches dynamic equilibrium (at its reversible potential) in a solution; that is, the rate of anodic charge transfer (oxidation) balances the rate of cathodic charge transfer (reduction).
- exfoliation**—corrosion that proceeds laterally from the sites of initiation along planes parallel to the surface, generally at grain boundaries, forming corrosion products that force metal away from the body of the material, giving rise to a layered appearance.
- external circuit**—the wires, connectors, measuring devices, current sources, and so forth, that are used to bring about or measure the desired electrical conditions within the test cell.
- filiform corrosion**—corrosion that occurs under some coatings in the form of randomly distributed threadlike filaments.
- fretting corrosion**—the deterioration at the interface between contacting surface as the result of corrosion and slight oscillatory slip between the two surfaces.
- galvanic corrosion**—accelerated corrosion of a metal because of an electrical contact with a more noble metal or nonmetallic contactor in a corrosive electrolyte.
- galvanic couple**—a pair of dissimilar conductors, commonly metals, in electrical contact (See **galvanic corrosion**.)
- galvanic current**—the electric current between metals or conductive nonmetals in a galvanic couple.
- galvanic series**—a list of metals and alloys arranged according to their relative corrosion potentials in a given environment.
- galvanodynamic**—refers to a technique wherein current, continuously varied at a selected rate, is applied to an electrode in an electrolyte.
- galvanostaircase**—refers to a galvanostep technique for polarizing an electrode in a series of constant current steps wherein the time duration and current increments or decrements are equal for each step.
- galvanostatic**—an experimental technique whereby an electrode is maintained at a constant current in an electrolyte.
- galvanostep**—refers to a technique in which an electrode is polarized in a series of current increments or decrements.
- grain dropping**—the dislodgement and loss of a grain or grains (crystals) from a metal surface as a result of intergranular corrosion.
- graphitic corrosion**—the deterioration of metallic constituents in gray cast iron, which leaves the graphic particles intact. (The term “graphitization” is commonly used to identify this form of corrosion but is not recommended because of its use in metallurgy for the decomposition of carbide to graphite.)
- hot corrosion**—an accelerated corrosion of metal surfaces that results from the combined effect of oxidation and reactions with sulfur compounds and other contaminants, such as chlorides, to form a molten salt on a metal surface which fluxes, destroys, or disrupts the normal protective oxide.
- hydrogen blistering**—the formation of blisters on or below a metal surface from excessive internal hydrogen pressure. (Hydrogen may be formed during cleaning, plating, corrosion, and so forth.)
- hydrogen embrittlement**—hydrogen-induced cracking or severe loss of ductility caused by the presence of hydrogen in the metal.
- immunity**—a state of resistance to corrosion or anodic dissolution of a metal caused by thermodynamic stability of the metal.
- impingement corrosion**—a form of erosion-corrosion generally associated with the local impingement of a high-velocity, flowing fluid against a solid surface.
- impressed current**—an electric current supplied by a device employing a power source that is external to the electrode system. (An example is dc current for cathodic protection.)
- intensistatic*—See **galvanostatic**.
- intercrystalline corrosion*—See **intergranular corrosion**.
- intergranular corrosion**—preferential corrosion at or adjacent to the grain boundaries of a metal or alloy.
- internal oxidation**—the formation of isolated particles of corrosion products beneath the metal surface. (This occurs as the result of preferential oxidation of certain alloy constituents by inward diffusion of oxygen, nitrogen, sulfur, and so forth.)
- knife-line attack**—intergranular corrosion of an alloy, usually stabilized stainless steel, along a line adjoining or in contact with a weld after heating into the sensitization temperature range.
- local action corrosion**—corrosion caused by local corrosion cells on a metal surface.
- local corrosion cell**—an electrochemical cell created on a metal surface because of a difference in potential between adjacent areas on that surface.
- localized corrosion**—corrosion at discrete sites, for example, pitting, crevice corrosion, and stress corrosion cracking.
- long-line current**—electric current through the earth from an anodic to a cathodic area of a continuous metallic structure. (Usually used only where the areas are separated by considerable distance and where the current result from concentration-cell action.)
- Luggin probe or Luggin-Haber capillary**—a device used in measuring the potential of an electrode with a significant current density imposed on its surface. (The probe minimizes the IR drop that would otherwise be included in the measurement and without significantly disturbing the current distribution on the specimen.)
- macrocell corrosion**—corrosion of a metal embedded in porous media (for example, concrete or soil) caused by concentration or galvanic cells which exist on a scale at least as large as the smallest major dimension of the corroding item (for example, the diameter of a bar pipe).
- metal dusting**—accelerated deterioration of metals in carbonaceous gases at elevated temperature to form a dust-like corrosion product.
- metallizing*—See **thermal spraying**.
- microbial corrosion**—corrosion that is affected by the action of microorganisms in the environment.
- microbiologically influenced corrosion (MIC)**—corrosion inhibited or accelerated by the presence or activity, or both, of microorganisms.
- mixed potential**—the potential of a specimen (or specimens in a galvanic couple) when two or more electrochemical reactions are occurring simultaneously.
- noble**—the positive (increasingly oxidizing) direction of electrode potential.

**noble metal**—a metal with a standard electrode potential that is more noble (positive) than that of hydrogen.

**occluded cell**—an electrochemical cell created at a localized site on a metal surface which has been partially obstructed from the bulk environment.

**open-circuit potential**—the potential of an electrode measured with respect to a reference electrode or another electrode when no current flows to or from it.

**overvoltage**—the change in potential of an electrode from its equilibrium or steady state value when current is applied.

**oxidation**—loss of electrons by a constituent of a chemical reaction. (Also refers to the corrosion of a metal that is exposed to an oxidizing gas at elevated temperatures.)

**parting**—the selective corrosion of one or more components of a solid solution alloy.

**parting limit**—the minimum concentration of a more noble component in an alloy, above which parting does not occur in a specific environment.

**passivation**—the process in metal corrosion by which metals become passive. (See **passive**.)

**passivator**—a type of inhibitor which appreciably changes the potential of a metal to a more noble (positive) value.

**passive**—the state of the metal surface characterized by low corrosion rates in a potential region that is strongly oxidizing for the metal.

**passive-active cell**—a corrosion cell in which the anode is a metal in the active state and the cathode is the same metal in the passive state.

**pitting**—corrosion of a metal surface, confined to a point or small area, that takes the form of cavities.

**pitting factor**—ratio of the depth of the deepest pit resulting from corrosion divided by the average penetration as calculated from weight loss.

**polarization**—the change from the open-circuit electrode potential as the result of the passage of current.

**polarization admittance**—the reciprocal of polarization resistance ( $di/dE$ ).

**polarization resistance**—the slope ( $dE/di$ ) at the corrosion potential of potential ( $E$ )—current density ( $i$ ) curve. (It is inversely proportional to the corrosion current density when the polarization resistance technique is applicable.)

**potentiodynamic**—refers to a technique wherein the potential of an electrode with respect to a reference electrode is varied at a selected rate by application of a current through the electrolyte.

**potentiostaircase**—refers to a potentiostep technique for polarizing an electrode in a series of constant potential steps wherein the time duration and potential increments or decrements are equal for each step.

**potentiostat**—an instrument for automatically maintaining an electrode in an electrolyte at a constant potential or controlled potentials with respect to a suitable reference electrode.

**potentiostatic**—the technique for maintaining a constant electrode.

**potentiostep**—refers to a technique in which an electrode is polarized in a series of potential increments or decrements.

*poultice corrosion*—See **deposit corrosion**.

**Pourbaix diagram (electrode potential-pH diagram)**—a graphic representation showing regions of thermodynamic stability of species in metal-water electrolyte systems.

**primary passive potential (passivation potential)**—the potential corresponding to the maximum active current

density (critical anodic current density) of an electrode that exhibits active-passive corrosion behavior.

**protection potential**—the most noble potential where pitting and crevice corrosion will not propagate.

**redox potential**—the potential of a reversible oxidation-reduction electrode measured with respect to a reference electrode, corrected to the hydrogen electrode, in a given electrolyte.

**reduction**—the gain of electrons by a constituent of a chemical reaction.

**reference electrode**—electrode having a stable and reproducible potential, which is used in the measurement of other electrode potentials.

*rest potential*—See **open-circuit potential**.

**rust**—a corrosion product consisting primarily of hydrated iron oxide. (A term properly applied only to ferrous alloys.)

**sample**—a portion of material taken from a larger quantity and representative of the whole, to be used for test purposes.

*season cracking*—See **stress-corrosion cracking**.

**sensitization**—a process resulting in a metallurgical condition which causes susceptibility of an alloy to intergranular corrosion or intergranular environmentally assisted cracking in a specific environment.

**specimen**—a prepared portion of a sample upon which a test is intended to be performed.

**stray current corrosion**—the corrosion caused by electric current from a source external to the intended electrical circuit, for example, extraneous current in the earth.

**stress-corrosion cracking**—a cracking process that requires the simultaneous action of a corrodent and sustained tensile stress. (This excludes corrosion-reduced sections which fail by fast fracture. It also excludes intercrystalline or transcrystalline corrosion which can disintegrate an alloy without either applied or residual stress.)

*subsurface corrosion*—See **internal oxidation**.

**sulfidation**—the reaction of a metal or alloy with a sulfur-containing species to produce a sulfur compound that forms on or beneath the surface of the metal or alloy.

**Tafel slope**—the slope of the straight line portion of a polarization curve, usually occurring at more than 50 mV from the open-circuit potential, when presented in a semi-logarithmic plot in terms of volts per logarithmic cycle of current density (commonly referred to as volts per decade).

**thermal spraying**—a group of processes wherein finely divided metallic or nonmetallic materials are deposited in a molten or semimolten condition to form a coating. (The coating material may be in the form of powder, ceramic rod, wire, or molten materials.)

**thermogalvanic corrosion**—the corrosive effect resulting from the galvanic cell caused by a thermal gradient across the metal surface.

**transpassive region**—the region of an anodic polarization curve, noble to and above the passive potential range, in which there is a significant increase in current density (increased metal dissolution) as the potential becomes more positive (noble).

**tuberculation**—the formation of localized corrosion products that appear on a surface as knoblike prominences (tubercles).

**uniform corrosion**—corrosion that proceeds at about the same rate over a metal surface.

**weld decay**—not a preferred term. Intergranular corrosion, usually of stainless steels or certain nickel-base alloys,

that occurs as the result of sensitization in the heat-affected zone during the welding operation.

**working electrode**—the test or specimen electrode in an electrochemical cell.

*This standard is subject to revision at any time by the responsible technical committee and must be reviewed every five years and if not revised, either reapproved or withdrawn. Your comments are invited either for revision of this standard or for additional standards and should be addressed to ASTM International Headquarters. Your comments will receive careful consideration at a meeting of the responsible technical committee, which you may attend. If you feel that your comments have not received a fair hearing you should make your views known to the ASTM Committee on Standards, at the address shown below.*

*This standard is copyrighted by ASTM International, 100 Barr Harbor Drive, PO Box C700, West Conshohocken, PA 19428-2959, United States. Individual reprints (single or multiple copies) of this standard may be obtained by contacting ASTM at the above address or at 610-832-9585 (phone), 610-832-9555 (fax), or [service@astm.org](mailto:service@astm.org) (e-mail); or through the ASTM website ([www.astm.org](http://www.astm.org)).*

# Glossary of Corrosion-Related Acronyms<sup>1</sup>

ABS	Acrylonitrile-butadiene-styrene plastics	FBC	Fluidized bed combustion
AC	Air-cooled	FBE	Fusion-bonded epoxy coating
AE	Acoustic emission	FC	Furnace cooled
AES	Auger electron spectroscopy	FCGR	Fatigue crack growth rate
ANN	Annealed	FEP	Fluorinated ethylene propylene polymer
AUSS	Austenitic stainless steel	FGD	Flue gas desulfurization
AVT	All volatile treatment for BFW	FPM	Fluorocarbon elastomers
BFW	Boiler feedwater	FRP	Fiber-reinforced plastic
BWR	Boiling water reactor	FSS	Ferritic stainless steel
CAB	Cellulose acetate-butyrate	GMAW	Gas metal arc welding
CCI	Crevice corrosion index	GTAW	Gas tungsten arc welding
CCT	Critical crevice corrosion temperature	HAZ	Heat-affected zone
CD	Current density	HB	Brinell hardness number
CDA	Corrosion data acquisition	HE	Hydrogen embrittlement
CF	Corrosion fatigue	HIC	Hydrogen induced cracking
CH	Cold work hardened	HK	Knoop hardness number
CHA	Cold work hardened, aged	HLLW	High level liquid waste (nuclear)
CN	Concentric neutral	HPW	High-purity water
CP	Cathodic protection	HR	Hot-rolled
CPP	Critical pitting potential	HRA	Hot-rolled, aged
CPT	Critical pitting temperature	HRB	Rockwell B hardness number
CPVC	Chlorinated poly(vinyl chloride)	HRC	Rockwell C hardness number
CR	Cold-rolled	HSC	Hydrogen stress cracking
CRA	Corrosion-resistant alloy	HSLA	High-strength low-alloy steel
CS	Carbon steel	HTR	Heat treatment
CSE	Copper/copper sulfate electrode	HVN	Vickers hardness number
CW	Cooling water	IGC	Intergranular corrosion
DCB	Double cantilever beam test	IGSCC	Intergranular stress corrosion cracking
DIMA	Direct imaging mass analyzer	IMMA	Ion microprobe mass analyzer
DSS	Duplex stainless steel	IOZ	Inorganic zinc coating
DTA	Differential thermal analysis	ISS	Ion scattering spectroscopy
DW	Distilled water	ISWS	Illinois State Water Survey tester
EC	Environmental cracking	KIC	Critical stress intensity
EDXA	Energy dispersive X-ray analysis	LAS	Low-alloy steel
EIS	Electrochemical impedance spectroscopy	LMC	Liquid metal cracking
ELN	Electrochemical noise technique	LSI	Langelier saturation index
EPMA	Electron beam microprobe analysis	MAS	Maraging steels
EPDM	Ethylene propylene elastomer	MCA	Multiple crevice assembly
EPR	Electrochemical potentiokinetic reactivation	MIC	Microbial induced corrosion
ER	Electrical resistance	MSS	Martensitic stainless steel
ESCA	Electron spectroscopy for chemical analysis	MT	Magnetic particle inspection
EW	Electric welded	NG	Nuclear grade
		NHE	Normal hydrogen electrode
		NMR	Nuclear magnetic resonance
		NPS	Nominal pipe size
		NT	Normalized and tempered

<sup>1</sup> See *NACE Corrosion Engineers Reference Book, Third Edition*, R. Baboian, Ed., NACE International, 2002, p. 33.

OCTG	Oil country tubular goods	SIMS	Secondary ion mass spectroscopy
OQ	Oil-quenched	SMAW	Shielded metal arc welding
OTEC	Ocean thermal energy conversion	SMLS	Seamless pipe or tubing
OZ	Organic zinc coating	SMYS	Specified minimum yield strength
PC	Polycarbonate	SRA	Stress relief anneal
PD	Pit depth	SRB	Sulfate-reducing bacteria
PE	Polyethylene	SRC	Solvent-refined coal
PFA	Perfluoro(alkoxy-alkane) copolymer	S/N	Fatigue test
PHSS	Precipitation hardenable stainless steel	SRE	Scanning reference electrode
PPC	Polymer modified portland cement	SS	Stainless steel
PP	Polypropylene	SSC	Sulfide stress cracking
PR	Polarization resistance	SSMS	Spark sources mass spectroscopy
PT	Dye penetrant survey	SSR	slow strain rate test
PTA	Polythionic acids	SSW	Substitute seawater
PTFE	Polytetrafluoromethylene	STA	Solution treated and aged
PU	Polyurethane	STEM	Scanning transmission electron microscopy
PVC	Poly(vinyl chloride)	STQ	Solution treated and quenched
PVDC	Poly(vinylidene chloride)	SW	Seawater
PVDF	Poly(vinylidene fluoride)	TEM	Transmission electron microscopy
PWHT	Post-weld heat treatment	TFE	Tetrafluoroethylene
PWR	Pressurized water reactor	TS	Tensile strength
QT	Quenched and tempered	TTS	Temperature, time, sensitization diagram
RH	Relative humidity	URD	Underground residential distribution systems
RSI	Ryzner saturation index	UT	Ultrasonic survey
RT	X-ray or gamma ray survey	UV	Ultraviolet spectroscopy
RTP	Reinforced thermoset plastics	VCI	Volatile corrosion inhibitor
RX	Recrystallized	WFMT	Wet fluorescent magnetic particle inspection
SAM	Scanning Auger microscopy	WQ	Water-quenched
SAW	Submerged arc welding	WOL	Wedge-opening load test
SBR	Styrene-butadiene rubber	XPS	X-ray photoelectron spectroscopy
SCC	Stress-corrosion cracking	XRD	X-ray diffraction
SCE	Saturated calomel electrode	YS	Yield strength
SEM	Scanning electron microscopy	ZRP	Zinc-rich paint



# ASTM Standard Abbreviations and Unit Symbols

absolute	abs	Department	Dept. <sup>b</sup>
academic degrees	use periods and run together (M.S., Ph.D., etc.)	diameter	dia (in figures and tables only)
		differential	d
alternating current, <i>n.</i>	AC	direct current, <i>n.</i>	DC
alternating current, <i>adj.</i>	A-C	direct current, <i>adj.</i>	D-C
American	Am. <sup>a</sup>	Division	Div. <sup>b</sup>
American wire gage	AWG	dollar	\$
ampere	A	effective horsepower	ehp
ampere hour	Ah	electromotive force	emf
angstrom	Å	electronvolt	eV
ante meridiem	a.m.	Engineers	Engrs. <sup>a</sup>
Association	Assn. <sup>b</sup>	equation(s)	Eq(s)
atmosphere	atm	farad	F
average	avg	figure(s)	Fig(s). <sup>d</sup>
barrel	bbl	foot	ft
becquerel	Bq	footcandle	fc
billion electronvolts	(use GeV, gigaelectronvolts)	foot pound-force	ft · lbf (use for work, energy) (see lbf · ft)
Birmingham wire gage	BWG		gal
brave horsepower	bhp	gallon	gal
brake-horsepower hour	bhp · h	gauss	G
Brinell hardness number	HB (see ASTM E 10)	gilbert	Gb
British thermal unit	Btu	grain	<i>spell out</i>
Brown and Sharpe (gage)	B&S	gram	g
bushel	bu	gravity (acceleration)	g
calorie	cal	gray	Gy
candela	cd	half hard	½ H
centimetre	cm	henry	H
centipoise	cP	hertz	Hz
centistokes	cSt	horsepower	hp
circular mil	cmil	horsepower hour	hp · h
coefficient	<i>spell out</i>	hour	h
Company	Co. <sup>b</sup>	Hurter and Driffield scale	H&D
Corporation	Corp. <sup>b</sup>	(film density)	
coulomb	C	hydrogen ion concentration,	pH
cubic	use exponential form <sup>c</sup>	negative logarithm of	
cubic centimetre	cm <sup>3</sup>	inch	in.
cubic decimetre	dm <sup>3</sup>	inch of mercury	in. Hg
curie	Ci	inch of water	in. H <sub>2</sub> O
cycles per minute	cpm	inch pound-force	in · lbf (use for work, energy) (see lbf · in.)
cycles per second	(use Hz. hertz)		incl (in figures and tables only)
day	<i>spell out</i>	inclusive	Inc. <sup>b</sup>
decibel	dB	Incorporated	ihp
degree (angle)	°	indicated horsepower	ID (in figures and tables only)
degree Celsius	°C	inside diameter	Inst. <sup>b</sup>
degree Fahrenheit	°F	Institute	nvt. n/cm <sup>2</sup>
degree Rankine	°R	integrated neutron flux	IPS
degrees of freedom	df	iron pipe size	

joule	J	millimetre	mm
K alpha radiation	K $\alpha$	millimetre of mercury	mm Hg
kelvin	K	million electronvolts	MeV
kilocalorie	kcal	milliroentgen	mR
kilocycle per second	(see note on cycles per second)	millisecond	ms
kilogram	kg	millivolt	mV
kilogram-calorie	kg · cal	milliwatt	mW
kilogram-force	kgf	minimum	min (in figures and tables only)
kilogram metre	kg · m	minute	min ( <i>spell out</i> when used with minimum)
kilometre	km		
kilovolt	kV	molal	<i>spell out</i>
kilovolt ampere	kVA	molar	M
kiloelectronvolt	keV	mole	mol
kilovolt peak	kVp	month (When followed by a date use Jan., Feb., March, April, May, June, July, Aug., Sept., Oct., Nov., Dec. When there is no date, <i>spell out</i> . Examples: Jan. 15, 1983; January 1983)	<i>spell out</i>
kilowatt	kW		
kilowatt hour	kWh	nanometre (formerly millimicron)	nm
kip (1000 lbf)	<i>spell out</i>	National	Nat. <sup>a</sup>
kip (1000 lbf) per square inch	ksi	newton	N
Knoop hardness number	HK (see ASTM E 384)	normal	N
lambert	L	number(s) (This abbreviation can often be omitted entirely. It is usually understood (as in STP 325, Specimen 8, Test 14, etc).)	No(s). <sup>d</sup>
linear	<i>spell out</i>	oersted	Oe
litre	L	ohm	$\Omega$
logarithm (common)	log	ortho	<i>o</i>
logarithm (natural)	ln	ounce	oz
lumen	lm	outside diameter	OD (in figures and tables only)
lux	lx	page	p.
magnetomotive force	mmf	pages	pp.
mass-to-charge ratio	<i>m/e</i>	para	<i>p</i>
maximum	max (in figures and tables only)	parts per billion	ppb
maxwell	Mx	parts per million	ppm
median effective concentration	EC <sub>50</sub>	pascal	Pa
median effective dose	ED <sub>50</sub>	per	use the diagonal line in expressions with unit symbols <sup>e</sup>
median lethal concentration	LC <sub>50</sub>	percent	%
median lethal dose	LD <sub>50</sub>	pico (prefix)	p
megacycles per second	(see note on cycles per second)	picofarad	pF
megawatt	MW	pint	pt
meta	<i>m</i>	poise	P
metre	m	Poisson's ratio	$\mu$ ( $\nu$ is preferred in applied mechanics)
microampere	$\mu$ A	post meridiem	p.m.
microcurie	$\mu$ Ci	pound	lb
microfarad	$\mu$ F	pound-force	lbf
microgram	$\mu$ g	pound-force foot	lbf · ft (use for torque) (see ft · lbf)
microhenry	$\mu$ H		
microinch	$\mu$ in.	pound-force inch	lbf · in. (use for torque) (see in · lbf)
microlitre	$\mu$ L		
micro-micro (prefix. use pico)	p	pound-force per square foot	lbf/ft <sup>2</sup>
micrometre (formerly micron)	$\mu$ m	pound-force per square inch	psi or lbf/in. <sup>2</sup>
microroentgen	$\mu$ R	pound-force per square inch absolute	psia
microsecond	$\mu$ s		
microvolt	$\mu$ V		
microwatt	$\mu$ W		
mil	<i>spell out</i>		
mile	<i>spell out</i>		
miles per hour	mph		
milliampere	mA		
milli-angstrom	mÅ		
millicurie	mCi		
milliequivalent	meq		
milligram	mg		
millihenry	mH		
millilitre	mL		

## 16 CORROSION TESTS AND STANDARDS MANUAL

pound-force per square inch	psig	standard taper (tables and drawings only)	§
gage quart		steradian	sr
quart	qt	stokes	St
rad (dose unit)	rd	tensile strength	<i>spell out</i>
radian	rad	tertiary	<i>tert</i>
radio frequency, <i>n.</i>	rf	tesla	T
radio frequency, <i>adj.</i>	r-f	thousand electronvolts	keV
radius	R (in figures and tables only)	thousand pounds	kip
Railway	Ry. <sup>b</sup>	thousand pounds-force per square inch	ksi
Railroad	R.R. <sup>b</sup>	ton	<i>spell out</i>
reference(s)	Ref(s)	torr	<i>spell out</i>
relative humidity	RH (in figures and tables only)	United States, <i>n.</i>	<i>spell out</i>
		United States, <i>adj.</i>	U.S.
revolution per minute	r/min	United States Pharmacopeia	USP
revolution per second	r/s	versus	<i>spell out</i>
Rockwell hardness, C scale	HRC (see ASTM E 18)	Vickers hardness number	HV (see ASTM E 92)
roentgen	R	volt	V
root mean square	rms	volume (of a publication)	Vol <sup>d</sup>
Saybolt Furol seconds	SFS	watt	W
Saybolt Universal seconds	SUS	watt hour	Wh
second	s	weber	Wb
secondary	<i>sec</i>	week	<i>spell out</i>
siemens	S	yard	yd
Society	Soc. <sup>b</sup>	year	<i>spell out</i>
socket joint (tables and drawings only)	§	Young's modulus	E
specific gravity	sp gr		
square	use exponential form (exception: psi, ksi) <sup>c</sup>		

<sup>a</sup>In footnotes and references only.

<sup>b</sup>At end of name only.

<sup>c</sup>With unit symbols only.

<sup>d</sup>Only when followed by a number.

<sup>e</sup>Exceptions: cpm, mph, psi.

# International System of Units (SI)<sup>1</sup>

Quantity	Unit	Formula
<b>Base Units</b>		
length	metre (m)	
mass	kilogram (kg)	
time	second (s)	
electric current	ampere (A)	
thermodynamic temperature	Kelvin (K)	
amount of substance	mole (mol)	
luminous intensity	candela (cd)	
<b>Supplementary Units</b>		
plane angle	radian (rad)	
solid angle	steradian (sr)	
<b>Derived Units</b>		
acceleration	metre per second squared	$\text{m/s}^2$
activity (of a radioactive source)	disintegration per second	(disintegration)/s
angular acceleration	radian per second squared	$\text{rad/s}^2$
angular velocity	radian per second	$\text{rad/s}$
area	square metre	$\text{m}^2$
density	kilogram per cubic metre	$\text{kg/m}^3$
electric capacitance	farad (F)	$\text{A} \cdot \text{s/V}$
electric conductance	siemens (S)	$\text{A/V}$
electric field strength	volt per metre	$\text{V/m}$
electric inductance	henry (H)	$\text{V} \cdot \text{s/A}$
electric potential difference	volt (V)	$\text{W/A}$
electric resistance	ohm ( $\Omega$ )	$\text{V/A}$
electromotive force	volt (V)	$\text{W/A}$
energy	joule (J)	$\text{N} \cdot \text{m}$
entropy	joule per kelvin	$\text{J/K}$
force	newton (N)	$\text{kg} \cdot \text{m/s}^2$
frequency	hertz (Hz)	(cycle)/s
illuminance	lux (lx)	$\text{lm/m}^2$
luminance	candela per square metre	$\text{cd/m}^2$
luminous flux	lumen (lm)	$\text{cd} \cdot \text{sr}$
magnetic field strength	ampere per metre	$\text{A/m}$
magnetic flux	weber (Wb)	$\text{V} \cdot \text{s}$
magnetic flux density	tesla (T)	$\text{Wb/m}^2$
magnetomotive force	ampere (A)	—
power	watt (W)	$\text{J/s}$
pressure	pascal (Pa)	$\text{N/m}^2$
quantity of electricity	coulomb (C)	$\text{A} \cdot \text{s}$
quantity of heat	joule (J)	$\text{N} \cdot \text{m}$
radiant intensity	watt per steradian	$\text{W/sr}$
specific heat	joule per kilogram-kelvin	$\text{J/kg} \cdot \text{K}$
stress	pascal (Pa)	$\text{N/m}^2$
thermal conductivity	watt per metre-kelvin	$\text{W/m} \cdot \text{K}$
velocity	metre per second	$\text{m/s}$
viscosity, dynamic	pascal-second	$\text{Pa} \cdot \text{s}$
viscosity, kinematic	square metre per second	$\text{m}^2/\text{s}$
voltage	volt (V)	$\text{W/A}$
volume	cubic metre	$\text{m}^3$
wavenumber	reciprocal metre	(wave) m
work	joule (J)	$\text{N} \cdot \text{m}$

<sup>1</sup> See ASTM E 380, Practice for Use of the International System of Units (SI) (The Modernized Metric System).

# General Conversion Factors<sup>1</sup>

Unit	Conversion to	Multiply by	Reciprocal
<b>Linear Measure</b>			
mil (0.001 inch)	micrometre	25.4	0.03937
mil (0.001 inch)	millimetre	0.0254	39.37
inch	millimetre	25.4	0.03937
foot	metre	0.3048	3.281
yard	metre	0.9144	1.0936
mile	kilometre	1.6093	0.6214
nautical mile	kilometre	1.8532	0.5396
<b>Square Measure</b>			
square inch	square millimetre	645.2	0.00155
square inch	square centimetre	6.452	0.155
square foot	square metre	0.0929	10.764
square yard	square metre	0.8361	1.196
acre	hectare	0.4047	2.471
acre	square metre	4047.	0.0002471
acre	square foot	43560.	0.00002296
square mile	acre	640.	0.001562
square mile	square kilometre	2.590	0.3863
<b>Volume</b>			
cubic inch	cubic centimetre	16.387	0.06102
cubic foot	cubic metre	0.02832	35.31
cubic foot	gallon (U.S.)	7.48	0.1337
cubic foot	litre	28.32	0.03531
cubic yard	cubic metre	0.7646	1.3079
ounce (U.S., liq.)	cubic centimetre	29.57	0.03382
quart (U.S., liq.)	litre	0.9464	1.0566
gallon (U.S.)	gallon (Imperial)	0.8327	1.2009
gallon (U.S.)	litre	3.785	0.2642
barrel (U.S. Petroleum)	gallon (U.S.)	42.	0.028
barrel (U.S. Petroleum)	litre	158.98	0.00629
<b>Mass</b>			
grain	milligram	64.8	0.01543
ounce (avoirdupois)	gram	28.35	0.03527
pound (avoirdupois)	kilogram	0.4536	2.205
short ton	metric ton	0.9072	1.1023
long ton	metric ton	1.0161	0.9842
<b>Pressure or Stress</b>			
atmosphere	mm Hg (@ 0°C)	760.	0.001316
atmosphere	pound force per inch <sup>2</sup>	14.696	0.06805
atmosphere	bar	1.013	0.9872
atmosphere	megapascal (MPa)	0.1013	9.872
torr (mm Hg)	pascal	133.32	0.007501
inch of water	pascal	248.8	0.004019

<sup>1</sup>See ASTM E 380, Practice for Use of the International System of Units (SI) (The Modernized Metric System).

Unit	Conversion to	Multiply by	Reciprocal
foot of water	pound force per inch <sup>2</sup>	0.4335	2.307
dyne per centimetre <sup>2</sup>	pascal	0.1000	10.00
pound force per inch <sup>2</sup> (psi)	kilopascal (kPa)	6.895	0.1450
kip per inch <sup>2</sup> (ksi)	megapascal (MPa)	6.895	0.1450
pound force per inch <sup>2</sup>	bar	0.06895	14.50
kip per inch <sup>2</sup>	kilogram per millimetre <sup>2</sup>	0.7031	1.4223
<b>Work, Heat, and Energy</b>			
British thermal unit (Btu)	joule	1055.	0.0009479
foot pound-force	joule	1.356	0.7375
calorie	joule	4.187	0.2389
Btu	foot pound-force	778.	0.001285
kilocalorie	Btu	3.968	0.252
Btu	kilogram metre	107.56	0.009297
Btu per hour	watt	0.2929	3.414
watthour	joule	3600.	0.0002778
horse power	kilowatt	0.7457	1.341
<b>Thermal Properties</b>			
(Btu per foot <sup>2</sup> , hour, °F) per inch	(kilocalorie per metre <sup>2</sup> , hour, °C) per metre	0.1240	8.064
(Btu per foot <sup>2</sup> , hour, °F) per inch	watt per metre, K	0.144	6.944
Btu per foot <sup>2</sup> , hour, °F	kilocalorie per metre <sup>2</sup> , hour, °C	4.882	0.2048
Btu per foot <sup>2</sup> , hour, °F	watt per metre <sup>2</sup> , K	5.674	0.1762
Btu per foot <sup>2</sup>	kilocalories per metre <sup>2</sup>	2.712	0.3687
Btu per foot <sup>2</sup>	joule per metre <sup>2</sup>	11360.	0.00008803
<b>Miscellaneous</b>			
pound per foot <sup>3</sup>	kilogram per metre <sup>3</sup>	16.02	0.06242
pound per gallon (U.S)	gram per litre	119.8	0.00835
grains per 100 foot <sup>3</sup>	milligram per metre <sup>3</sup>	22.88	0.0437
ounces per foot <sup>3</sup>	gram per metre <sup>2</sup>	305.2	0.003277
pound mole (gas)	cubic foot (STP)	359.	0.00279
gram mole (gas)	litre (STP)	22.4	0.0446
day	minute	1440.	0.000694
week	hour	168.	0.00595
year	hour	8766.	0.0001141
U.S. bag cement	kilogram	42.63	0.02346
gallon (U.S) per bag cement	litre per kilogram	0.0888	11.26
ksi (inch) <sup>1/2</sup>	megapascal (metre) <sup>1/2</sup>	1.0989	0.9100
cubic foot of water (60°F)	pound of water	62.37	0.01603
board foot	cubic metre	0.00236	423.7
milliampere per foot <sup>2</sup>	milliampere per metre <sup>2</sup>	10.76	0.0929
gallons (U.S.) per minute	metre <sup>3</sup> per day	5.451	0.1835
pound-force	newton	4.448	0.2248

# Condensed Metric Practice Guide for Corrosion<sup>1,2</sup>

Multiply	By	To Convert to SI Units:
<b>Area</b>		
inch <sup>2</sup>	645.2	millimetre <sup>2</sup> (mm <sup>2</sup> )
inch <sup>2</sup>	6.452	centimetre <sup>2</sup> (cm <sup>2</sup> )
foot <sup>2</sup>	0.092 90	metre <sup>2</sup> (m <sup>2</sup> )
foot <sup>2</sup>	929.0	centimetre <sup>2</sup> (cm <sup>2</sup> )
yard <sup>2</sup>	0.836 1	metre <sup>2</sup> (m <sup>2</sup> )
<b>Bending Moment (Torque)</b>		
dyne centimetre	0.000 000 1	newton metre (N·m)
pound-force inch	0.113 0	newton metre (N·m)
pound-force foot	1.356	newton metre (N·m)
<b>Corrosion Rate</b>		
mil per year (mpy)	0.025 40	millimetre per year (mm/y) <sup>a</sup>
mil per year	25.40	micrometre per year (mm/y)
inch per year (ipy)	25.40	millimetre per year (mm/y)
inch per month (ipm)	304.8	millimetre per year (mm/y)
milligram per decimetre <sup>2</sup> day (mdd)	0.100 0	gram per metre <sup>2</sup> day (g/m <sup>2</sup> ·d) <sup>a</sup>
milligram per decimetre <sup>2</sup> day	0.004 167	gram per metre <sup>2</sup> hour (g/m <sup>2</sup> ·h)
milligram per decimetre <sup>2</sup> day	100.0	milligram per metre <sup>2</sup> day (mg/m <sup>2</sup> ·d)
<b>Current Density</b>		
milliampere per millimetre <sup>2</sup>	1000.	ampere per metre <sup>2</sup> (A/m <sup>2</sup> )
milliampere per centimetre <sup>2</sup>	10.00	ampere per metre <sup>2</sup> (A/m <sup>2</sup> )
microampere per centimetre <sup>2</sup>	0.010 00	ampere per metre <sup>2</sup> (A/m <sup>2</sup> )
milliampere per metre <sup>2</sup>	0.001 000	ampere per metre <sup>2</sup> (A/m <sup>2</sup> )
microampere per millimetre <sup>2</sup>	1.000	ampere per metre <sup>2</sup> (A/m <sup>2</sup> )
microampere per foot <sup>2</sup>	10.76	milliampere per metre <sup>2</sup> (mA/m <sup>2</sup> )
ampere per inch <sup>2</sup>	1 550.	ampere per metre <sup>2</sup> (A/m <sup>2</sup> )
ampere per foot <sup>2</sup>	10.76	ampere per metre <sup>2</sup> (A/m <sup>2</sup> )
ampere per centimetre <sup>2</sup>	10 000.	ampere per metre <sup>2</sup> (A/m <sup>2</sup> )
ampere per decimetre <sup>2</sup>	100.0	ampere per metre <sup>2</sup> (A/m <sup>2</sup> )
<b>Energy</b>		
British thermal unit (Btu) (60°F)	1055.	joule (J)
calorie (mean)	4.190	joule (J)
foot-pound-force	1.356	joule (J)
kilocalorie (mean)	4190.	joule (J)
kilowatt hour	3.600	megajoule (MJ)
<b>Flow, Volume Per Unit Time</b>		
foot <sup>3</sup> per second	0.028 32	metre <sup>3</sup> per second (m <sup>3</sup> /s)
foot <sup>3</sup> per second	2445.	metre <sup>3</sup> per day (m <sup>3</sup> /d)
foot <sup>3</sup> per minute	40.78	metre <sup>3</sup> per day (m <sup>3</sup> /d)
gallon (U.S. liquid) per minute	5.451	metre <sup>3</sup> per day (m <sup>3</sup> /d)
gallon (U.S. liquid) per hour	0.090 85	metre <sup>3</sup> per day (m <sup>3</sup> /d)
gallon (U.S. liquid) per day	0.003 785	metre <sup>3</sup> per day (m <sup>3</sup> /d)
<b>Force</b>		
dyne	0.000 01	newton (N)
kilogram-force	9.807	newton (N)
ounce-force	0.278 0	newton (N)
pound-force	4.448	newton (N)
<b>Length</b>		
angstrom	1 x 10 <sup>-10</sup>	metre (m)
angstrom	0.100 0	nanometre (nm)
micron	0.001 0	millimetre (mm)
micron	1.000	micrometre (µm)
mil	0.025 40	millimetre (mm)
mil	25.40	micrometre (µm)



Multiply	By	To Convert to SI Units:
inch	2.540	centimetre (cm)
inch	25.40	millimetre (mm)
inch	25 400.	micrometre ( $\mu\text{m}$ )
foot	0.304 8	metre (m)
yard	0.914 4	metre (m)
mile	1.609	kilometre (km)
Mass		
grain	64.80	milligram (mg)
ounce	28.35	gram (g)
pound	0.453 6	kilogram (kg)
pound	453.6	gram (g)
ton (short, 2000 lb)	907.2	kilogram (kg)
Mass Per Unit Area		
ounce-mass per foot <sup>2</sup>	305.1	gram per metre <sup>2</sup> (g/m <sup>2</sup> )
pound-mass per foot <sup>2</sup>	4.882	kilogram per metre <sup>2</sup> (kg/m <sup>2</sup> )
pound-mass per foot <sup>2</sup>	4882.	gram per metre <sup>2</sup> (g/m <sup>2</sup> )
pound-mass per inch <sup>2</sup>	703.1	kilogram per metre <sup>2</sup> (kg/m <sup>2</sup> )
Mass Per Unit Volume (Density)		
gram per centimetre <sup>3</sup>	1000.	kilogram per metre <sup>3</sup> (kg/m <sup>3</sup> )
ounce (mass) per inch <sup>3</sup>	1730.	kilogram per metre <sup>3</sup> (kg/m <sup>3</sup> )
ounce (mass) per gallon (U.S. liquid)	7.489	kilogram per metre <sup>3</sup> (kg/m <sup>3</sup> )
ounce (mass) per gallon (U.S. liquid)	7.489	gram per litre (g/L)
pound (mass) per foot <sup>3</sup>	16.02	kilogram per metre <sup>3</sup> (kg/m <sup>3</sup> )
pound (mass) per gallon (U.S. liquid)	119.8	kilogram per metre <sup>3</sup> (kg/m <sup>3</sup> )
Power		
Btu (thermochemical) per second	1054.	watt (W)
horsepower (electric)	746.0	watt (W)
kilocalorie (thermochemical) per second	4184.	watt (W)
Pressure or Stress		
atmosphere (normal = 760 torr)	101 300.	pascal (Pa)
centimetre of mercury (0°C)	1 333.	pascal (Pa)
dyne per centimetre <sup>2</sup>	0.100 0	pascal (Pa)
inch of mercury (60°F)	3377.	pascal (Pa)
inch of water (60°F)	248.8	pascal (Pa)
kilogram-force per metre <sup>2</sup>	9.807	pascal (Pa)
kip per inch <sup>2</sup>	6.895	megapascal (MPa)
pound-force per inch <sup>2</sup>	6.895	kilopascal (kPa)
pound-force per foot <sup>2</sup>	47.88	pascal (Pa)
Stress Intensity		
(pound-force per inch <sup>2</sup> ) inch <sup>1/2</sup>	0.034 75	newton per millimetre <sup>3/2</sup> (N/mm <sup>3/2</sup> )
(kip per inch <sup>2</sup> ) inch <sup>1/2</sup>	34.75	newton per millimetre <sup>3/2</sup> (N/mm <sup>3/2</sup> )
(pound-force per inch <sup>2</sup> ) inch <sup>1/2</sup>	0.001 099	megapascal metre <sup>1/2</sup> (MPa · m <sup>1/2</sup> ) <sup>a</sup>
(kip per inch <sup>2</sup> ) inch <sup>1/2</sup>	1.099	megapascal metre <sup>1/2</sup> (MPa · m <sup>1/2</sup> ) <sup>a</sup>
Temperature		
degree Celsius	$T_K = T_C + 273.15$	kelvin (k)
degree Fahrenheit	$T_C = (T_F - 32)/1.8$	degree Celsius (°C)
Time		
hour (mean solar)	3600.	second (s)
day (mean solar)	86 400.	second (s)
month (calendar)	2.628	megasecond (Ms)
year (calendar)	31.54	megasecond (Ms)
Velocity (Speed)		
inch per second	25.40	millimetre per second (mm/s)
foot per second	0.304 8	metre per second (m/s)
Inch per minute	0.423 3	millimetre per second (mm/s)
mile per hour	1.609	kilometre per hour (km/h)
mile per hour	0.447 0	metre per second (m/s)
Volume		
inch <sup>1</sup>	16.39	centimetre <sup>3</sup> (cm <sup>3</sup> )
fluid ounce (U.S.)	29.57	centimetre <sup>3</sup> (cm <sup>3</sup> )
pint (U.S. liquid)	473.2	centimetre <sup>3</sup> (cm <sup>3</sup> )
quart (U.S. liquid)	946.4	centimetre <sup>3</sup> (cm <sup>3</sup> )
gallon (U.S. liquid)	0.003 785	metre <sup>3</sup> (m <sup>3</sup> )
gallon (U.S. liquid)	3.785	litre (L)

<sup>1</sup>This condensed guide is under the jurisdiction of ASTM Committee G-1 on Corrosion of Metals.<sup>2</sup>This guide is based on ASTM E 380.<sup>a</sup>Preferred units.

# Multiplication Factors<sup>1</sup>

Multiplication Factor	Prefix	Symbol
1 000 000 000 000 000 000 = $10^{18}$	exa	E
1 000 000 000 000 000 = $10^{15}$	peta	P
1 000 000 000 000 = $10^{12}$	tera	T
1 000 000 000 = $10^9$	giga	G
1 000 000 = $10^6$	mega	M
1 000 = $10^3$	kilo	k
1 00 = $10^2$	hecto <sup>a</sup>	h
1 0 = $10^1$	deka <sup>a</sup>	da
0.1 = $10^{-1}$	deci <sup>a</sup>	d
0.01 = $10^{-2}$	centi <sup>a</sup>	c
0.001 = $10^{-3}$	milli	m
0.000 001 = $10^{-6}$	micro	μ
0.000 000 001 = $10^{-9}$	nano	n
0.000 000 000 001 = $10^{-12}$	pico	p
0.000 000 000 000 001 = $10^{-15}$	femto	f
0.000 000 000 000 000 001 = $10^{-18}$	atto	a

<sup>a</sup>To be avoided where practical.

## Relationships among Some of the Units Commonly Used for Corrosion Rates<sup>2</sup>

Unit	Factor for Conversion to					
	mdd	g/m <sup>2</sup> /d	μm/yr	mm/yr	mils/yr	in./yr
Milligrams per square decimetre per day (mdd)	1	0.1	36.5/ <i>d</i>	0.365/ <i>d</i>	1.144/ <i>d</i>	0.00144/ <i>d</i>
Grams per square metre per day (g/m <sup>2</sup> /d)	10	1	365/ <i>d</i>	0.365/ <i>d</i>	14.4/ <i>d</i>	0.0144/ <i>d</i>
Micrometres per year (μm/yr)	0.0274 <i>d</i>	0.00274 <i>d</i>	1	0.001	0.0394	0.0000394
Millimetres per year (mm/yr)	27.4 <i>d</i>	2.74 <i>d</i>	1000	1	39.4	0.0394
Mils per year (mils/yr)	0.696 <i>d</i>	0.0696 <i>d</i>	25.4	0.0254	1	0.001
Inches per year (in./yr)	696 <i>d</i>	69.6 <i>d</i>	25400	25.4	1000	1

NOTE: *d* is metal density in grams per cubic centimetre (g/cm<sup>3</sup>).

<sup>1</sup> See ASTM E 380, Practice for Use of the International System of Units (SI) (The Modernized Metric System).

<sup>2</sup> Wranglén, G. An Introduction to Corrosion and Protection of Metals, Chapman and Hall, 1985, p. 233.

# Corrosion Rate Calculation (from Mass Loss)<sup>1</sup>

$$\text{Corrosion rate} = \frac{(K \times W)}{(A \times T \times D)}$$

where

$K$  = a constant (see below),

$T$  = time of exposure in hours to the nearest 0.01 h,

$A$  = area in  $\text{cm}^2$  to the nearest 0.01  $\text{cm}^2$ ,

$W$  = mass loss in g, to nearest 1 mg (corrected for any loss during cleaning (see 9.4)), and

$D$  = density in  $\text{g/cm}^3$ , (see Appendix X1 of ASTM G 1).

Many different units are used to express corrosion rates. Using the above units for  $T$ ,  $A$ ,  $W$ , and  $D$ , the corrosion rate can be calculated in a variety of units with the following appropriate value of  $K$ :

Corrosion Rate Units Desired	Constant ( $K$ ) in Corrosion Rate Equation
mils per year (mpy)	$3.45 \times 10^6$
inches per year (ipy)	$3.45 \times 10^3$
inches per month (ipm)	$2.87 \times 10^2$
millimetres per year (mm/y)	$8.76 \times 10^4$
micrometres per year ( $\mu\text{m/y}$ )	$8.76 \times 10^7$
picometres per second (pm/s)	$2.78 \times 10^6$
grams per square metre per hour ( $\text{g/m}^2 \cdot \text{h}$ )	$1.00 \times 10^4 \times D^a$
milligrams per square decimeter per day (mdd)	$2.40 \times 10^6 \times D^a$
micrograms per square metre per second ( $\mu\text{g/m}^2 \cdot \text{s}$ )	$2.78 \times 10^6 \times D^a$

<sup>a</sup>Density is not needed to calculate the corrosion rate in these units. The density in the constant  $K$  cancels out the density in the corrosion rate equation.

<sup>1</sup>See ASTM G 1, Practice for Preparing, Cleaning and Evaluating Corrosion Test Specimens.

# Corrosion Rate Conversion Factors

$$\text{Mils/year (mpy)} = C \times \frac{\text{weight loss}}{\text{area} \times \text{time}} \times K$$

$$\text{Millimetres/year (mm/y)} = 0.0254 \text{ mpy}$$

Weight Loss	Area	C Factors				
		Hour	Day	Week	Month	Year
mg	cm <sup>2</sup>	437	18.2	2.59	0.598	0.0498
	dm <sup>2</sup>	4.37	0.182	0.0259	$5.98 \times 10^{-3}$	$4.98 \times 10^{-4}$
	m <sup>2</sup>	0.0437	$1.82 \times 10^{-3}$	$2.59 \times 10^{-4}$	$5.98 \times 10^{-5}$	$4.98 \times 10^{-6}$
	in <sup>2</sup>	67.7	2.82	0.402	0.0927	$7.72 \times 10^{-3}$
	ft <sup>2</sup>	0.470	0.0196	$2.79 \times 10^{-3}$	$6.44 \times 10^{-4}$	$5.36 \times 10^{-5}$
g	cm <sup>2</sup>	$437 \times 10^3$	$182 \times 10^2$	2590	598	49.8
	dm <sup>2</sup>	4370	182	25.9	5.98	0.498
	m <sup>2</sup>	43.7	1.82	0.259	0.0598	$4.98 \times 10^{-3}$
	in <sup>2</sup>	$677 \times 10^2$	2820	402	92.7	7.72
	ft <sup>2</sup>	470	19.6	2.79	0.644	0.0536
lb	cm <sup>2</sup>	$198 \times 10^6$	$825 \times 10^4$	$118 \times 10^4$	$271 \times 10^3$	$226 \times 10^2$
	dm <sup>2</sup>	$198 \times 10^4$	$825 \times 10^2$	$118 \times 10^2$	2710	226
	m <sup>2</sup>	$198 \times 10^2$	825	118	27.1	2.26
	in <sup>2</sup>	$307 \times 10^5$	$128 \times 10^4$	$182 \times 10^3$	$420 \times 10^2$	3500
	ft <sup>2</sup>	$213 \times 10^3$	8880	1270	292	24.3

K is a density factor  
 K = 1.000 for carbon steel  
 K factors for other alloys  
 are given on the next page

EXAMPLE: A 5.0 square inch specimen of copper has a weight loss of 218 mg in 40 hour corrosion test.

$$\text{mpy} = 67.7 \times \frac{218}{5.0 \times 40} \times 0.88 = 65$$

$$\text{mm/yr} = 0.0254 \times 65 = 1.65$$

<sup>1</sup>See *NACE Corrosion Engineers Reference Book, Second Edition*, R. S. Treseder, R. Baboian, and C. G. Munger, Eds., NACE International, Houston, TX, 1991.

# Densities of Common Alloys<sup>1</sup>

(K = ratio of carbon steel density to that of alloy)

UNS	Common Name	Density g/cm <sup>3</sup>	K	UNS	Common Name	Density g/cm <sup>3</sup>	K
A91100	Al 1100	2.72	2.89	N06007	G Alloy	8.34	0.94
A93003	Al 3003	2.74	2.87	N06022	C-22 Alloy	8.69	0.90
A95052	Al 5052	2.68	2.93	N06030	G-30 Alloy	8.22	0.96
A96061	Al 6061	2.70	2.91	N06455	C-4 Alloy	8.64	0.91
A97075	Al 7075	2.80	2.81	N06600	600 Alloy	8.47	0.93
C11000	ETP Copper	8.94	0.88	N06601	601 Alloy	8.11	0.97
C22000	Commercial Bronze	8.89	0.88	N06625	625 Alloy	8.44	0.93
C23000	Red Brass	8.75	0.90	N06985	G-3 Alloy	8.30	0.95
C26000	Cartridge Brass	8.53	0.92	N07001	Waspalloy	8.19	0.96
C27000	Yellow Brass	8.39	0.94	N07041	Rene 41	8.25	0.95
C28000	Muntz Metal	8.39	0.94	N07718	718 Alloy	8.19	0.96
C44300	Admiralty brass. As	8.52	0.92	N07750	X-750 Alloy	8.28	0.95
C46500	Naval Brass. As	8.41	0.93	N08020	20Cb-3	8.08	0.97
C51000	Phosphor Bronze A	8.86	0.89	N08024	20Mo-4	8.11	0.97
C52400	Phosphor Bronze D	8.78	0.90	N08026	20M0-6	8.13	0.97
C61300	Aluminum Bronze 7 %	7.69	1.00	N08028	Sanicro 28	8.0	0.98
C61400	Aluminum Bronze D	7.78	1.01	N08366	AL-6X	8.0	0.98
C63000	Ni-Al Bronze	7.58	1.04	N08800	800 Alloy	7.94	0.99
C65500	High-Silicon Bronze	8.52	0.92	N08825	825 Alloy	8.14	0.97
C67500	Manganese Bronze A	8.36	0.94	N08904	904L Alloy	8.0	0.98
C68700	Aluminum Brass. As	8.33	0.94	N08925	25-6Mo	8.1	0.97
C70600	9-10 Copper-Nickel	8.94	0.88	N09925	925 Alloy	8.05	0.98
C71500	70-30 Copper-Nickel	8.94	0.88	N10003	N Alloy	8.79	0.89
C75200	Nickel Silver	8.73	0.90	N10004	W Alloy	9.03	0.87
C83600	Ounce Metal	8.80	0.89	N10276	C-276 Alloy	8.89	0.88
C86500	Manganese Bronze	8.3	0.96	N10665	B-2 Alloy	9.22	0.85
C90500	Gun Metal	8.72	0.90	R03600	Molybdenum	10.22	0.77
C92200	M Bronze	8.64	0.91	R04210	Niobium	8.57	0.92
C95700	Cast Mn-Ni-Al Bronze	7.53	1.04	R05200	Tantalum	16.60	0.47
C95800	Cast Ni-Al Bronze	7.64	1.03	R50250	Titanium, Gr 1	4.54	1.73
F10006	Gray Cast Iron	7.20	1.09	R50400	Titanium, Gr 2	4.54	1.73
F20000	Malleable Cast Iron	7.27	1.08	R53400	Titanium, Gr 12	4.52	1.74
F32800	Ductile Iron	7.1	1.11	R56400	Titanium, Gr 5	4.43	1.77
F41002	Ni-Resist Type 2	7.3	1.06	R60702	Zr 702	6.53	1.20
F43006	Ductile Ni-Resist, D5	7.68	1.02	S20100	201 SS	7.94	0.99
F47003	Duriron	7.0	1.12	S20200	202 SS	7.94	0.99
G10200	1020 Carbon Steel	7.86	1.00	S30400	304 SS	7.94	0.99
G41300	4130 Steel	7.86	1.00	S30403	304L SS	7.94	0.99
J91150	CA-15 Cast SS	7.61	1.03	S30900	309 SS	7.98	0.98
J91151	CA-15M Cast SS	7.61	1.03	S31000	310 SS	7.98	0.98
J91540	CA-6NM Cast SS	7.7	1.02	S31254	254 SMO	8.0	0.98
J92600	CF-8 Cast SS	7.75	1.01	S31500	3RE60	7.75	1.01
J92800	CF-3MN Cast SS	7.75	1.01	S31600	316 SS	7.98	0.98
J92900	CF-8M Cast SS	7.75	1.01	S31603	316L SS	7.98	0.98
J94204	HK-40 Cast SS	7.75	1.01	S31700	317 SS	7.98	0.98
J95150	CN-7M Cast SS	8.00	0.98	S32100	321 SS	7.94	0.99
K11597	1.25Cr-0.5Mo Steel	7.85	1.00	S32550	Ferralium 255	7.81	1.01
K81340	9Ni Steel	7.86	1.00	S32950	7 Mo Plus	7.75	1.01
L51120	Chemical Lead	11.3	0.70	S34700	347 SS	8.03	0.98
M11311	Mg AZ31B	1.77	4.44	S41000	410 SS	7.70	1.02
N02200	Nickel 200	8.89	0.88	S43000	430 SS	7.72	1.02
N04400	400 Alloy	8.80	0.89	S44600	446 SS	7.65	1.03
N05500	K-500 Alloy	8.44	0.93	S50100	5Cr-0.5Mo Steel	7.82	1.01
N06002	X Alloy	8.23	0.95	S50400	9Cr-1Mo Steel	7.67	1.02

<sup>1</sup>See NACE Corrosion Engineers Reference Book, Third Edition, R. Baboian, Ed., NACE International, 2002, p.105.

# Table 1—Overvoltage values

$$n = b \log i / i_0$$

## HYDROGEN OVERVOLTAGE

Material	Ovevoltage (Volts) at 1 ma/cm <sup>2</sup>
	25°C, 2 N H <sub>2</sub> SO <sub>4</sub>
Platinum (Platinized)	0.0005
Platinum (Smooth)	0.15
Palladium	0.05
Nickel	0.25
Iron	0.40
Tungsten	0.2
Molybdenum	0.15
Bismuth	0.70
Lead	1.2
Tin	0.65
Carbon	0.5
Aluminum	0.70
Mercury	1.15
Cadminum	0.9
Zinc	0.85
Gold	0.15
Silver	0.30
Copper	0.5

## OXYGEN OVERVOLTAGE

Material	Overvoltage (Volts) at 1 ma/cm <sup>2</sup>
	25°C, 1 N KOH
Platinum (Platinized)	0.52
Platinum (Smooth)	0.82
Nickel	0.53
Graphite	0.89
Gold	0.96
Silver	0.73
Copper	0.58

Data from: *The Encyclopedia of Electrochemistry*, Reinhold, NY, 1964. Glasstone's *Textbook of Physical Chemistry*, Van Nostrand, NY, 1958. Kochler's *Electrochemistry*, 2nd Edition, Wiley, NY, 1950. Uhlig's *Corrosion and Corrosion Control*, Wiley, NY, 1971.

# Standard Reference Potentials and Conversion Table<sup>1</sup>

## Reference Potentials and Conversion Factors

Electrode	Potential (V) at 25°C		Thermal Temperature Coefficient <sup>A</sup> (mV/°C)
	$E'^B$	$E''^C$	
(Pt)/H <sub>2</sub> ( $\alpha = 1$ )/H <sup>+</sup> ( $\alpha = 1$ )(SHE)	0.000	...	+0.87
Ag/AgCl/1M KCl	+0.235	...	+0.25
Ag/AgCl/0.6 M Cl <sup>-</sup> (seawater)	+0.25	...	...
Ag/AgCl/0.1 M Cl <sup>-</sup>	+0.288	...	+0.22
Hg/Hg <sub>2</sub> Cl <sub>2</sub> /sat KCl (SCE)	+0.241	+0.244	+0.22
Hg/Hg <sub>2</sub> Cl <sub>2</sub> /1M KCl	+0.280	0.283	+0.59
Hg/Hg <sub>2</sub> Cl <sub>2</sub> /0.1M KCl	+0.334	0.336	+0.79
Cu/CuSO <sub>4</sub> sat	+0.30	...	+0.90
Hg/Hg <sub>2</sub> SO <sub>4</sub> /H <sub>2</sub> SO <sub>4</sub> <sup>D</sup>	+0.616	...	...

<sup>A</sup> To convert from thermal to isothermal temperature coefficients, subtract 0.87 mV/°C. Thus the isothermal temperature coefficient for Ag-AgCl is - 0.62 mV/°C.

<sup>B</sup>  $E'$  is the standard potential for the half cell corrected for the concentration of the ions.

<sup>C</sup>  $E''$  also includes the liquid junction potentials for a saturated KCl salt bridge.

To convert from one scale to another, add the value indicated.

<sup>D</sup> Potential given is for a range of H<sub>2</sub>SO<sub>4</sub> molalities as discussed in Ref (10).

From (E')	To SHE Scale	To SCE Scale (E')
H <sub>2</sub> /H <sup>+</sup>	...	-0.241
Ag/AgCl/1 M KCl	+0.235	-0.006
Ag/AgCl/0.6 M Cl (seawater)	+0.25	+0.009
Ag/AgCl/0.1 M Cl	+0.288	+0.047
Hg/Hg <sub>2</sub> /Cl <sub>2</sub> /sat KCl (SCE)	+0.241	...
Hg/Hg <sub>2</sub> Cl <sub>2</sub> , 1 M	+0.280	+0.039
Hg/Hg <sub>2</sub> Cl <sub>2</sub> , 0.1 M	+0.334	0.093
Cu/CuSO <sub>4</sub> sat	+0.30	+0.06
Hg/Hg <sub>2</sub> SO <sub>4</sub> /H <sub>2</sub> SO <sub>4</sub>	+0.616	...

### Example:

An electrode potential of +1.000 V versus SCE would be (1.000 + 0.241) ± +1.241 V versus SHE.

An electrode potential of -1.000 V versus SCE would give (-1.000 + 0.241) = -0.759 V versus SHE.

<sup>1</sup>See ASTM G 3, Practice for Conversions Applicable to Electrochemical Measurements in Corrosion Testing.

# Equivalent Weight Values for Metals and Alloys<sup>1</sup>

Common Designation	UNS	Elements w/Constant Valence	Lowest		Second		Third		Fourth	
			Variable Valence	Equivalent Weight	Variable Valence	Equivalent Weight	Element/ Valence	Equivalent Weight	Element/ Valence	Equivalent Weight
Aluminum Alloys										
AA1100	A91100	Al/3		8.99						
AA2024	A92024	Al/3, Mg/2	Cu/1	9.38	Cu/2	9.32				
AA2219	A92219	Al/3	Cu/1	9.51	Cu/2	9.42				
AA3003	A93003	Al/3	Mn/2	9.07	Mn/4	9.03	Mn 7	8.98		
AA3004	A93004	Al/3, Mg/2	Mn/2	9.09	Mn/4	9.06	Mn 7	9.00		
AA5005	A95005	Al/3, Mg/2		9.01						
AA5050	A95050	Al/3, Mg/2		9.03						
AA5052	A95052	Al/3, Mg/2		9.05						
AA5083	A95083	Al/3, Mg/2		9.09						
AA5086	A95086	Al/3, Mg/2		9.09						
AA5154	A95154	Al/3, Mg/2		9.08						
AA5454	A95454	Al/3, Mg/2		9.06						
AA5456	A95456	Al/3, Mg/2		9.11						
AA6061	A96061	Al/3, Mg/2		9.01						
AA6070	A96070	Al/3, Mg/2, Si/4		8.98						
AA6101	A96161	Al/3		8.99						
AA7072	A97072	Al/3, Zn/2		9.06						
AA7075	A97075	Al/3, Zn/2, Mg/2	Cu/1	9.58	Cu/2	9.55				
AA7079	A97079	Al/3, Zn/2, Mg/2		9.37						
AA7178	A97178	Al/3, Zn/2, Mg/2	Cu/1	9.71	Cu/2	9.68				
Copper Alloys										
CDA110	C11000		Cu/1	63.55	Cu/2	31.77				
CDA220	C22000	Zn/2	Cu/1	58.07	Cu/2	31.86				
CDA230	C23000	Zn/2	Cu/1	55.65	Cu/2	31.91				
CDA260	C26000	Zn/2	Cu/1	49.51	Cu/2	32.04				
CDA280	C28000	Zn/2	Cu/1	46.44	Cu/2	32.11				
CDA444	C44300	Zn/2	Cu/1, Sn/2	50.42	Cu/1, Sn/4	50.00	Cu/2, Sn/4	32.00		
CDA687	C68700	Zn/2, Al/3	Cu/1	48.03	Cu/2	30.29				
CDA608	C60800	Al/3	Cu/1	47.114	Cu/2	27.76				
CDA510	C51000		Cu/1, Sn/2	63.32	Cu/1, Sn/4	60.11	Cu/2, Sn/4	31.66		
CDA524	C52400		Cu/1, Sn/2	63.10	Cu/1, Sn/4	57.04	Cu/2, Sn/4	31.55		
CDA655	C65500	Si/4	Cu/1	50.71	Cu/2	28.51				
CDA706	C70600	Ni/2	Cu/1	56.92	Cu/2	31.51				
CDA715	C71500	Ni/2	Cu/1	46.69	Cu/2	30.98				
CDA752	C75200	Ni/2, Zn/2	Cu/1	46.38	Cu/2	31.46				
Stainless Steels										
304	S30400	Ni/2	Fe/2, Cr/3	25.12	Fe/3, Cr/3	18.99	Fe/3, Cr/6	15.72		
321	S32100	Ni/2	Fe/2, Cr/3	25.13	Fe/3, Cr/3	19.08	Fe/3, Cr/6	15.78		
309	S30900	Ni/2	Fe/2, Cr/3	24.62	Fe/3, Cr/3	19.24	Fe/3, Cr/6	15.33		
310	S31000	Ni/2	Fe/2, Cr/3	24.44	Fe/3, Cr/3	19.73	Fe/3, Cr/6	15.36		
316	S31600	Ni/2	Fe/2, Cr/3, Mo/3	25.50	Fe/3, Cr/3, Mo/4	25.33	Fe/3, Cr/6, Mo/6	19.14	Fe/3, Cr/6, Mo/6	16.111
317	S31700	Ni/2	Fe/2, Cr/3, Mo/3	25.26	Fe/3, Cr/3, Mo/4	25.03	Fe/3, Cr/6, Mo/6	19.15	Fe/3, Cr/6, Mo/6	15.82
410	S41000		Fe/2, Cr/3	25.94	Fe/3, Cr/3	18.45	Fe/3, Cr/6	16.28		
430	S43000		Fe/2, Cr/3	25.30	Fe/3, Cr/3	18.38	Fe/3, Cr/6	15.58		
446	S44600		Fe/2, Cr/3	24.22	Fe/3, Cr/3	18.28	Fe/3, Cr/6	14.46		
20CD3 <sup>a</sup>	N08020	Ni/2	Fe/2, Cr/3, Mo/3 Cu/1	23.98	Fe/2, Cr/3, Mo/4, Cu/1	23.83	Fe/3, Cr/3, Mo/6, Cu/2	18.88	Fe/3, Cu/6, Mo/6, Cu/2	15.50

<sup>1</sup> See ASTM G 102, Practice for Calculation of Corrosion Rates and Related Information from Electrochemical Measurements.



Common Designation	UNS	Elements w/Constant Valence	Lowest		Second		Third		Fourth		
			Variable Valence	Equivalent Weight	Variable Valence	Equivalent Weight	Element/Valence	Equivalent Weight	Element/Valence	Equivalent Weight	
Nickel Alloys											
200	N02200		Ni/2	29.36	Ni/3	19.57					
400	N04400	Ni/2	Cu/1	35.82	Cu/2	30.12					
600	N06600	Ni/2	Fe/2, Cr/3	26.41	Fe/3, Cr/3	25.44	Fe/3, Cr/6	20.73			
800	N08800	Ni/2	Fe/2, Cr/3	25.10	Fe/3, Cr/3	20.76	Fe/3, Cr/6	16.59			
825	N08825	Ni/2	Fe/2, Cr/3, Mo/3, Cu/1	25.52	Fe/3, Cr/3, Mo/4, Cu/1	25.32	Fe/3, Cr/3, Mo/6, Cu/2	21.70	Fe/3, Cr/6, Mo/6, Cu/2	17.10	
B	N10001	Ni/2	Mo/3, Fe/2	30.05	Mo/4, Fe/2	27.50	Mo/6, Fe/2	23.52	Mo/6, Fe/3	23.23	
C-22 <sup>b</sup>	N06022	Ni/2	Fe/2, Cr/3, Mo/3, W/4	26.04	Fe/2, Cr/3, Mo/4, W/4	25.12	Fe/2, Cr/3, Mo/6, W/6	23.28	Fe/3, Cr/6, Mo/6, W/6	17.88	
C-276	N10276	Ni/2	Fe/2, Cr/3, Mo/3, W/4	27.09	Cr/3, Mo/4	25.90	Fe/2, Cr/3, Mo/6, W/6	23.63	Fe/3, Cr/6, Mo/6, W/6	19.14	
G	N06007	Ni/2	(1)	25.46	(2)	22.22	(3)	22.04	(4)	17.03	
(1) = Fe/2, Cr/3, Mo/3, Cu/1, Nb/4, Mn/2			(3) = Fe/3, Cr/3, Mo/6, Cu/2, Nb/5, Mn/2								
(2) = Fe/2, Cr/3, Mo/3, Cu/2, Nb/5, Mn/2			(4) = Fe/3, Cr/6, Mo/6, Cu/2, Nb/5, Mn/4								
Carbon Steel											
			Fe/2	27.92	Fe/3	18.62					
Other Metals											
Mg	M14142	Mg/2		12.15							
Mo	R03600		Mo/3	31.98	Mo/4	23.98	Mo/6	15.99			
Ag	P07016		Ag/1	107.87	Ag/2	53.93					
Ta	R05210	Ta/5		36.19							
Sn	L13002		Sn/2	59.34	Sn/4	29.67					
Ti	R50400		Ti/2	23.95	Ti/3	15.97	Ti/4	11.98			
Zn	Z19001	Zn/2		32.68							
Zr	R60701	Zn/4		22.80							
Pb	L50045		Pb/2	103.59	Pb/4	51.80					

<sup>a</sup>Registered trademark Carpenter Technology.<sup>b</sup>Registered trademark Haynes International.

NOTE 1—Alloying elements at concentrations below 1 % by mass were not included in the calculation, for example, they were considered part of the basis metal.

NOTE 2—Midrange values were assumed for concentrations of alloying elements.

NOTE 3—Only consistent valence groupings were used.

NOTE 4—Equation 4 in ASTM G 102 was used to make these calculations.

# Values of Constants for Use in Faraday's Equation<sup>1</sup>

*Calculation of Corrosion Rate*—Faraday's Law can be used to calculate the corrosion rate, either in terms of penetration rate (CR) or mass loss rate (MR)

$$CR = K_1 \frac{i_{\text{cor}}}{\rho} EW$$

$$MR = K_2 i_{\text{cor}} EW$$

where

CR is given in mm/yr,  $i_{\text{cor}}$  in  $\mu\text{A}/\text{cm}^2$ ,

$K_1 = 3.27 \times 10^{-3}$ , mm g/ $\mu\text{A cm yr}$ ,

$\rho$  = density in  $\text{g}/\text{cm}^3$ , (see ASTM G 1 for density values for many metals and alloys used in corrosion testing),

MR =  $\text{g}/\text{m}^2\text{d}$ , and

$K_2 = 8.954 \times 10^{-3}$ ,  $\text{g cm}^2/\mu\text{A m}^2 \text{ d}$ .

Other values for  $K_1$  and  $K_2$  for different unit systems are given in the following table.

Rate				
A				
Penetration Rate Unit (CR)	$I_{\text{cor}}$ Unit	$\rho$ Unit	$K_1$	Units of $K_1^a$
mpy	$\mu\text{A}/\text{cm}^2$	$\text{g}/\text{cm}^3$	0.1288	mpy g/ $\mu\text{A cm}$
mm/yr <sup>b</sup>	$\text{A}/\text{m}^{2b}$	$\text{kg}/\text{m}^{3b}$	327.2	mm kg/A m y
mm/yr <sup>b</sup>	$\mu\text{A}/\text{cm}^2$	$\text{g}/\text{cm}^3$	$3.27 \times 10^{-3}$	mm g/ $\mu\text{A cm y}$
B				
Mass Loss Rate Unit	$I_{\text{cor}}$ Unit	$K_2$	Units of $K_2^a$	
$\text{g}/\text{m}^2\text{d}^b$	$\text{A}/\text{m}^{2b}$	0.8953	g/Ad	
mg/dm <sup>2</sup> d (mdd)	$\mu\text{A}/\text{cm}^2$	0.0895	mg cm <sup>2</sup> / $\mu\text{A dm}^2 \text{ d}$	
mg/dm <sup>2</sup> d (mdd)	$\text{A}/\text{m}^{2b}$	$8.953 \times 10^{-3}$	mg m <sup>2</sup> /A dm <sup>2</sup> d	

<sup>a</sup>EW is assumed to be dimensionless.

<sup>b</sup>SI unit.

<sup>1</sup> See ASTM G 102, Practice for Calculation of Corrosion Rates and Related Information from Electrochemical Measurements.

# Physical Properties of Gases and Liquids

Name	Formula	Molecular Weight	Density, g/L	Melting Point, °C	Boiling Point, °C	Auto-Ignition Point °C	Explosive Limits Percent by Vol. in Air	
							Lower	Upper
Acetylene	C <sub>2</sub> H <sub>2</sub>	26.04	1.173	-81	-83.6 subl.	335	2.5	80.0
Air			1.2929					
Ammonia	NH <sub>3</sub>	17.03	0.7710	-77.7	-33.4	780	16.0	77.0
Argon	Ar	39.94	1.784	-189.2	-185.7			
Butane-n	C <sub>4</sub> H <sub>10</sub>	58.12	0.601	-138	0.6	430	1.6	8.5
Butylene-n	C <sub>4</sub> H <sub>8</sub>	56.10	0.595	-185	-6.3		1.7	9.0
Carbon dioxide	CO <sub>2</sub>	44.01	1.977	-57	-78.5 subl.			
Carbon monoxide	CO	28.01	1.250	-207	-191	650	12.5	74.2
Chlorine	Cl <sub>2</sub>	70.91	3.214	-101	-34			
Ethane	C <sub>2</sub> H <sub>6</sub>	30.07	0.572	-172	-88.6	510	3.1	15.0
Ethylene	C <sub>2</sub> H <sub>4</sub>	28.05	0.384	-169	-103.7	543	3.0	34.0
Helium	He	4.003	0.1785	-272	-268.9			
Heptane-n	C <sub>7</sub> H <sub>16</sub>	100.20	0.684 g/cm <sup>3</sup>	-90.6	98.4	233	1.0	6.0
Hexane-n	C <sub>6</sub> H <sub>14</sub>	86.17	0.6594 g/cm <sup>3</sup>	-95.3	68.7	248	1.2	6.9
Hydrogen	H <sub>2</sub>	2.016	0.0899	-259.2	-252.8	580	4.1	74.2
Hydrogen chloride	HCl	36.47	1.639	-112	-84			
Hydrogen fluoride	HF	20.01	0.921	-92.3	19.5			
Hydrogen sulfide	H <sub>2</sub> S	34.08	1.539	-84	-62		4.3	45.5
Methane	CH <sub>4</sub>	16.04	0.7168	-182.5	-161.5	538	5.3	13.9
Nitrogen	N <sub>2</sub>	28.016	1.2506	-209.9	-195.8			
Octane-n	C <sub>8</sub> H <sub>18</sub>	114.23	0.7025 g/cm <sup>3</sup>	-56.8	125.7	232	0.8	3.2
Oxygen	O <sub>2</sub>	32.00	1.4290	-218.4	-183.0			
Pentane-n	C <sub>5</sub> H <sub>12</sub>	72.15	0.626 g/cm <sup>3</sup>	-131	36.2	310	1.4	8.0
Propane	C <sub>3</sub> H <sub>8</sub>	44.09	0.501	-189	-44.5	465	2.4	9.5
Propylene	C <sub>3</sub> H <sub>6</sub>	42.05	0.519	-184	-48	458	2.0	11.1
Sulfur dioxide	SO <sub>2</sub>	64.06	2.926	-75.7	-10.0			

Density of gases in g/L at 0°C and 760 mm Hg.

Density of liquids in g/cm<sup>3</sup> at 20°/4°C.

# Physical Properties of Elements

	Symbol	Atomic Weight	Density g/cm <sup>3</sup> 20°C	Valencies	Melting Point, °C	Crystal Structure
Aluminium	Al	29.98	2.70	3	660	1
Antimony	Sb	121.75	6.68	3/5	630	5
Argon	Ar	39.948	1.784 <sup>a</sup>	0	-189.2	1
Arsenic	As	74.92	5.73	3/5	814	5
Barium	Ba	137.34	3.5	2	725	2
Beryllium	Be	9.01	1.85	2	1280	3
Bismuth	Bi	208.98	9.80	3/5	271	5
Boron	B	10.81	2.3	3	2300	—
Bromine	Br	79.91	3.12	1/3/5/7	-7.2	6
Cadmium	Cd	112.40	8.65	2	321	3
Calcium	Ca	40.08	1.55	2	842	1
Carbon	C	12.01	2.25	2/3/4	3550	4
Chlorine	Cl	35.45	1.56 <sup>b</sup>	1/3/5/7	-103	7
Chromium	Cr	52.00	7.2	2/3/6	1890	2
Cobalt	Co	58.93	8.9	2/3	1495	3
Copper	Cu	63.54	8.92	1/2	1083	1
Fluorine	F	19.00	1.69 <sup>a</sup>	1	223	—
Gold	Au	196.97	19.32	1/3	1063	1
Helium	He	4.003	0.177 <sup>a</sup>	0	-272.2	—
Hydrogen	H	1.008	0.090 <sup>b</sup>	1	-259.2	4
Iodine	I	126.90	4.93	1/3/5/7	113.5	6
Iron	Fe	55.85	7.87	2/3/6	1535	2
Lead	Pb	207.19	11.35	2/4	327.4	1
Lithium	Li	6.94	0.53	1	186	2
Magnesium	Mg	24.31	1.74	2	651	3
Manganese	Mn	54.94	7.2	2/3/4/6/7	1260	10
Mercury	Hg	200.59	13.55	1/2	-38.9	5
Molybdenum	Mo	95.94	10.2	2/3/4/5/6	2620	2
Nickel	Ni	58.71	8.90	2/3	1455	1
Niobium	Nb	92.91	8.55	3/5	2500	2
Nitrogen	N	14.007	1.25 <sup>a</sup>	3/5	-209.9	4
Oxygen	O	15.9994	1.429 <sup>a</sup>	2	-218.4	10
Phosphorus	P	30.98	1.82	3/5	44.1	10
Platinum	Pt	195.09	21.37	2/4	1773	1
Potassium	K	39.10	0.87	1	62.3	2
Rhodium	Rh	102.91	12.5	1/2/3/4	1966	1
Selenium	Se	78.96	4.8	2/4/6	220	4
Silicon	Si	28.09	2.42	4	1420	8
Silver	Ag	107.87	10.50	1	960.5	1
Sodium	Na	22.99	0.97	1	97.5	2
Sulfur	S	32.06	2.07	2/4/6	119	9
Tantalum	Ta	180.95	16.6	3/5	2996	2
Tin	Sn	118.69	7.31	2/4	231.9	7
Titanium	Ti	47.90	4.5	2/3/4	1800	3
Tungsten	W	183.85	19.3	2/4/5/6	3370	2
Vandium	V	50.94	5.96	2/3/4/5	1710	2
Zinc	Zn	65.73	7.14	2	419.5	3
Zirconium	Zr	91.22	6.4	4	1857	3

<sup>a</sup> g/L (0°C and 760 mm Hg)<sup>b</sup> Liquid at boiling point -37°C<sup>c</sup> Crystal structures:

- 1 Face-centered cubic
- 2 Body-centered cubic
- 3 Close packed hexagonal
- 4 Hexagonal

- 5 Rhombohedral
- 6 Orthorhombic
- 7 Tetragonal
- 8 Diamond cubic

- 9 Face-centered orthorhombic
- 10 Cubic (complex)

# Densities for a Variety of Metals and Alloys<sup>1</sup>

UNS Number	Alloy	Density, g/cm <sup>3</sup>
<b>Aluminum Alloys</b>		
A91100	1100	2.71
A91199	1199	2.70
A92024	2024	2.78
A92219	2219	2.84
A93003	3003	2.73
A93004	3004	2.72
A95005	5005	2.70
A95050	5050	2.69
A95052	5052	2.68
A95083	5083	2.66
A95086	5086	2.66
A95154	5154	2.66
A95357	5357	2.69
A95454	5454	2.69
A95456	5456	2.66
A96061	6061	2.70
*	6062	2.70
A96070	6070	2.71
A96101	6101	2.70
A97075	7075	2.81
A97079	7079	2.75
A97178	7178	2.83
<b>Stainless Steels</b>		
S20100	Type 201	7.94
S20200	Type 202	7.94
S20200	Type 302	7.94
S30400	Type 304	7.94
S30403	Type 304L	7.94
S30900	Type 309	7.94
S31000	Type 310	7.98
S31100	Type 311	7.98
S31600	Type 316	7.98
S31603	Type 316L	7.98
S31700	Type 317	7.98
S32100	Type 321	7.94
S32900	Type 329	7.98
N06330	Type 330	7.98
S34700	Type 347	8.03
S41000	Type 410	7.70
S43000	Type 430	7.72
S44600	Type 446	7.65
S50200	Type 502	7.82
<b>Other Ferrous Metals</b>		
FIXXXX	Gray cast iron	7.20
GXXXXX-KXXXXX	Carbon steel	7.86
*	Silicon iron	7.00
KXXXXX	Low alloy steels	7.85

<sup>1</sup> See ASTM G 1, Practice for Preparing, Cleaning, and Evaluating Corrosion Test Specimens.

UNS Number	Alloy	Density, g/cm <sup>3</sup>
<b>Copper Alloys</b>		
C38600	Copper	8.94
C23000	Red brass 230	8.75
C26000	Cartridge brass 260	8.52
C28000	Muntz metal 280	8.39
*	Admiralty 442	8.52
C44300	Admiralty 443	8.52
C44400	Admiralty 444	8.52
C44500	Admiralty 445	8.52
C68700	Aluminum brass 687	8.33
C22000	Commercial bronze 220	8.80
C60800	Aluminum bronze, 5 % 608	8.16
*	Aluminum bronze, 8 % 612	7.78
*	Composition M	8.45
*	Composition G	8.77
C51000	Phosphor bronze, 5 % 510	8.86
C52400	Phosphor bronze, 10 % 524	8.77
*	85-5-5-5	8.80
C65500	Silicon bronze 655	8.52
C70600	Copper nickel 706	8.94
C71000	Copper nickel 710	8.94
C71500	Copper nickel 715	8.94
C75200	Nickel silver 752	8.75
<b>Lead</b>		
L53305-53405	Antimonial	10.80
L5XXXX	Chemical	11.33
<b>Nickel Alloys</b>		
N02200	Nickel 200	8.89
N04400	Nickel copper 400	8.84
N06600	Nickel chromium iron alloy 600	8.51
N06625	Nickel chromium molybdenum alloy 625	8.14
N08825	Iron nickel chromium alloy 825	8.14
N08020	Iron nickel chromium alloy 20	8.08
	Cb-3	
*	Iron nickel chromium cast alloy 20	8.02
N10665	Nickel molybdenum alloy B2	9.2
N10276	Nickel chromium molybdenum alloy C-276	8.8
N06985	Nickel chromium molybdenum alloy G-3	8.3
<b>Other Metals</b>		
MIXXXX	Magnesium	1.74
R03600	Molybdenum	10.22
P04980	Platinum	21.45
P07016	Silver	10.49
R05200	Tantalum	16.60
L13002	Tin	7.30
R50250	Titanium	4.54
Z13001	Zinc	7.13
R60001	Zirconium	6.53

**NOTES**—All UNS numbers that include the letter X indicate a series of numbers under one category. An asterisk(\*) indicates that a UNS number not available.

# Density of Materials

Material	Density (g/cm <sup>3</sup> )	Density (lb/in. <sup>3</sup> )	Material	Density (g/cm <sup>3</sup> )	Density (lb/in. <sup>3</sup> )
Iridium	22.65	0.82	Nickel aluminide (NiAl)	6.05	0.22
Osmium	22.61	0.82	Gallium	5.91	0.21
Platinum	21.45	0.77	Zirconia (partially stabilized)	5.70	0.21
Rhenium	21.00	0.76	Germanium	5.32	0.19
Tungsten	19.40	0.70	Titanium nitride	5.29	0.19
Gold	19.30	0.70	Titanium carbide	4.94	0.18
Uranium	19.07	0.69	Titanium diboride	4.52	0.16
Tungsten carbide	17.20	0.62	Titanium	4.51	0.16
Tantalum	16.60	0.60	Ti-6Al-4V	4.50	0.16
Tantalum carbide (TaC)	14.53	0.52	Titanium dioxide	4.25	0.15
Hafnium	13.10	0.47	Aluminum oxide	3.98	0.14
Ruthenium	12.45	0.45	Spinel (MgO · Al <sub>2</sub> O <sub>3</sub> )	3.57	0.13
Rhodium	12.41	0.45	Aluminum nitride	3.26	0.12
Palladium	12.02	0.43	Sialon	3.20	0.12
Thallium	11.85	0.43	Silicon nitride	3.19	0.12
Thorium	11.50	0.42	Mullite(3Al <sub>2</sub> O <sub>3</sub> · 2SiO <sub>2</sub> )	3.16	0.11
Lead	11.34	0.41	Silicon carbide	3.10	0.11
Silver	10.49	0.38	Hydroxyapatite	3.10	0.00
Molybdenum	10.20	0.37	Aluminum carbide	2.99	0.11
Bismuth	9.80	0.35	Wollastonite	2.90	0.10
Thulium	9.31	0.34	Aluminum copper alloy	2.84	0.10
Cast high leaded tin bronze	9.29	0.34	Aluminum zinc alloy	2.78	0.10
Nickel-moly (Hastelloy B-2)	9.20	0.33	Aluminum	2.70	0.10
Copper	8.96	0.32	Cordierite	2.65	0.10
Nickel	8.90	0.32	E-glass fiber	2.62	0.10
Copper nickel (64Cu-14Ni-227n)	8.85	0.32	Pyrex glass	2.52	0.09
Cobalt	8.85	0.32	Boron carbide	2.52	0.09
Nickel silver	8.70	0.31	Boron	2.40	0.09
Brass (61.5Cu-3Pb-35.5Zn)	8.70	0.31	Silicon	2.33	0.08
Bronze (57Cu, 40Zn, 39Pb)	8.70	0.31	PTFE (polytetrafluoroethylene)	2.30	0.08
Cadmium	8.65	0.31	Graphite	2.26	0.08
Niobium (Columbium)	8.57	0.31	Boron nitride	2.25	0.08
Nickel chromium cobalt alloy	8.21	0.30	Sulfur	2.07	0.07
Nickel-chromium (Inconel 718)	8.20	0.30	Unsaturated polyester	2.00	0.07
Copper zinc alloy	8.19	0.30	Polyimide thermoset	2.00	0.07
Maraging steel	8.02	0.29	Phenolic resin	1.99	0.07
Austenitic stainless steel	8.00	0.29	Beryllium	1.85	0.07
Iron-nickel (Invar)	8.00	0.29	Phosphorus	1.83	0.07
Iron	7.87	0.28	Carbon fiber	1.74	0.06
Nickel iron superalloy	7.86	0.28	Magnesium	1.74	0.06
Chromium steel	7.83	0.28	PPS (polyphenylene sulfide)	1.67	0.06
Nonresulfurized carbon steel	7.83	0.28	Nylon 6	1.64	0.06
Stainless steel (17Cr-4Ni)	7.81	0.28	Acetal resin	1.57	0.06
Hot work tool steel	7.75	0.28	Epoxy resin	1.56	0.06
Aluminum bronze	7.64	0.28	Calcium	1.55	0.06
Babbitt	7.50	0.27	Rubidium	1.53	0.06
Samarium	7.49	0.27	Polycarbonate	1.53	0.06
Manganese	7.43	0.27	Aramid fiber	1.45	0.05
Indium	7.31	0.26	Aromatic polyamide	1.44	0.05
Niobium nitride	7.30	0.26	Bismaleimide resin	1.36	0.05
Tin	7.30	0.26	Silicone	1.35	0.05
Cerium dioxide	7.28	0.26	PEEK (polyetheretherketone)	1.32	0.05
Austempered ductile iron	7.20	0.26	Cellulose acetate	1.30	0.05
Pewter (Sn,Sb,Cu)	7.20	0.26	Human Bone	1.30	0.05
Chromium	7.19	0.26	Polyurethane	1.27	0.05
Zinc	7.13	0.26	ABS (acrylonitrile butadiene styrene)	1.26	0.05
Neodymium	7.00	0.25	Polysulfone	1.24	0.04
Praseodymium	6.77	0.24	Acrylic	1.19	0.04
Cerium	6.77	0.24	Polypropylene	1.05	0.04
Chromium carbide	6.70	0.24	Sodium	0.97	0.04
Antimony	6.65	0.24	PE (polyethylene)	0.95	0.03
Zirconium	6.49	0.23	UHMWPE		
Lanthanum	6.15	0.22	(ultrahigh molecular weight PE)	0.93	0.03
Vanadium	6.11	0.22	Potassium	0.86	0.03
			Lithium	0.53	0.19

Source: GEM 2001, p. 35, ASM 2000.

# Coefficients of Thermal Expansion of Common Alloys<sup>1</sup>

UNS	Common Name	in/in/°F x 10 <sup>-6</sup>	mm/mm/°C x 10 <sup>-6</sup>	Range, °C
A24430	Cast Al B443.0	12.3	22	20-100
A91100	Al 1100	13.1	24	20-100
A95052	Al 5052	13.2	24	20-100
C11000	ETP Copper	9.4	16.9	20-100
C23000	Red Brass	10.4	18.7	20-300
C28000	Muntz Metal	11.6	21	20-300
C44300	Admiralty Brass, As	11.2	20	20-300
C61400	Aluminum Bronze D	9.0	18.2	20-300
C70600	90-10 Copper-Nickel	9.5	17.1	20-300
C71500	70-30 Copper-Nickel	9.0	16.2	20-300
C83600	Ounce Metal	10.2	18.4	0-100
F10006	Gray Cast Iron	6.7	12.1	0-100
G10200	Carbon Steel	6.7	12.1	0-100
J94224	HK Cast SS	9.4	16.9	20-540
L13002	Tin	12.8	23	0-100
L51120	Chemical Lead	16.4	30	0-100
L55030	50/50 Solder	13.1	24	0-100
M11311	Mg AZ31B	14.5	26	20-100
M13310	Mg HK31A	14.5	26	20-100
N02200	Nickel 200	7.4	13.3	20-90
N04400	400 Alloy	7.7	13.9	20-90
N06600	600 Alloy	7.4	13.3	20-90
N10276	C-276 Alloy	6.3	11.3	20-90
N10665	B-2 Alloy	5.6	10.1	20-90
R03600	Molybdenum	2.7	4.9	20-100
R05200	Tantalum	3.6	6.5	20-100
R50250	Titanium, Gr 1	4.8	8.6	0-100
R56400	Titanium, Gr 5	4.9	8.8	0-100
R60702	Zr 702	2.9	5.2	0-100
S30400	304 SS	9.8	17.3	0-100
S31000	310 SS	8.0	14.4	0-100
S41000	410 SS	6.1	11.0	0-100
S44600	446 SS	5.8	10.4	0-100
S50200	5Cr-0.5Mo Steel	7.3	13.1	20-540
Z13001	Zinc	18	32	0-100

<sup>1</sup>See *NACE Corrosion Engineers Reference Book, Third Edition*, R. Baboian, Ed., NACE International, 2002, p. 291.



# Physical Properties of Water

Temperature, t	Density <sup>1</sup> , d	Specific Volume <sup>1</sup> , v	Vapor Pressure <sup>2</sup> , p	Viscosity <sup>3</sup> , $\eta$	Dielectric Constant <sup>4</sup> , $\epsilon$
°C	g/mL	mL/g	mm Hg*	Centipose	
0**	0.99987	1.00013	4.580	1.787	87.74
5	.99999	1.00001	6.538	1.517	85.76
10	.99973	1.00027	9.203	1.306	83.83
15	.99913	1.00087	12.782	1.138	81.95
18	.99862	1.00138	15.471	1.053	80.84
20	.99823	1.00177	17.529	1.002	80.10
25	.99707	1.00293	23.753	0.8903	78.30
30	.99567	1.00434	31.824	.7974	76.55
35	.99406	1.00598	42.180	.7194	74.83
38	.99299	1.00706	49.702	.6783	73.82
40	.99224	1.00782	55.338	.6531	73.15
45	.99025	1.00985	71.90	.5963	71.51
50	.98807	1.01207	92.56	.5471	69.91
55	.98573	1.01448	118.11	.5044	68.34
60	.98324	1.01705	149.47	.4669	66.81
65	.98059	1.01979	187.65	.4338	65.32
70	.97781	1.02270	233.81	.4044	63.86
75	.97489	1.02576	289.22	.3782	62.43
80	.97183	1.02899	355.31	.3547	61.03
85	.96865	1.03237	433.64	.3340	59.66
90	.96534	1.03590	525.92	.3149	58.32
95	.96192	1.03959	634.04	.2976	57.01
100***	.95838	1.04343	760.00	.2822	55.72

1 – M. Thiesen, *Wiss. Abh. der Physikalisch-Technischen Reichsanstalt* 4, No. 1, 1904; *International Critical Tables* 3, 25 (1928).

2 – F. G. Keyes, *J. Chem. Phys.*, 15, 602 (1947).

3 – J. F. Swindells, J. R. Coe, and T. B. Godfrey, *J. Research Nat. Bur. Standards*, 48, 1 (1952); R. C. Hardy and R. L. Cottingham, *ibid.*, 42, 573 (1949); J. R. Coe and T. B. Godfrey, *J. App. Phys.*, 15, 625 (1944).

4 – C. G. Malmberg and A. A. Maryott, *J. Research Nat. Bur. Standards*, 56, 1 (1956).

\* – 760 mm Hg = 1 atmosphere =  $1,013,250 \text{ dyn cm}^{-2}$  =  $101,325 \text{ newtons m}^{-2}$  on the *Système International d'Unites*, adopted in a resolution, 11th General Conference on Weights and Measures, Paris, October 1960, the international unit of pressure is the Newton per square meter.

\*\* – The freezing point is zero degrees Celsius, exactly; the triple point of water is 0.001°C or 273.16°K.

\*\*\* – The boiling point.

# Dew Point of Moist Air<sup>1</sup>

The temperature drop required for condensation to occur at a specified air temperature and relative humidity is given in the table below. The temperature drops are mean values for the indicated air temperature ranges.

RH %	Air Temperature °C		RH %	Air Temperature °F	
	0-20	20-35		32-68	68-95
55	9	10	55	16	18
60	7	9	60	13	15
65	6	7	65	11	13
70	5	6	70	9	11
75	4	5	75	8	9
80	3	4	80	6	7
85	2	3	85	4	5
90	1.6	1.8	90	3	3
92	1.2	1.4	92	2.2	2.5
95	0.8	0.9	95	1.4	1.6
98	0.3	0.3	98	0.5	0.5

Example: At 30°C (86°F) and 80 % RH, a temperature drop of 4°C (7°F) would result in condensation.

Dew point temperatures of moist air as a function of air temperature and relative humidity are tabulated on the following four pages.

<sup>1</sup> See *NACE Corrosion Engineers Reference Book, Third Edition*, R. Baboian, Ed., NACE International, 2002, pp. 69-73.

# Dew Point of Moist Air °C<sup>1</sup>

Air Temperature °C													
RH %	0	2	4	6	8	10	12	14	16	18	20	22	24
1	-50	-49	-47	-46	-45	-44	-42	-41	-40	-39	-38	-36	-35
3	-40	-39	-37	-36	-34	-33	-32	-30	-29	-28	-26	-25	-24
5	-35	-34	-32	-31	-29	-28	-26	-25	-24	-22	-21	-19	-24
7	-32	-30	-29	-27	-26	-24	-23	-21	-20	-18	-17	-15	-14
9	-29	-27	-26	-24	-23	-21	-20	-18	-17	-15	-14	-12	-11
11	-27	-25	-24	-22	-21	-19	-17	-16	-14	-13	-11	-10	-8
13	-25	-23	-22	-20	-19	-17	-15	-14	-12	-11	-9	-8	-6
15	-23	-22	-20	-19	-17	-15	-14	-12	-11	-9	-7	-6	-4
17	-22	-20	-19	-17	-15	-14	-12	-11	-9	-7	-6	-4	-2
19	-21	-19	-17	-16	-14	-12	-11	-9	-8	-6	-4	-3	-1
21	-20	-18	-16	-15	-13	-11	-10	-8	-6	-5	-3	-1	0
23	-19	-17	-15	-14	-12	-10	-8	-7	-5	-3	-2	0	2
25	-18	-16	-14	-13	-11	-9	-7	-6	-4	-2	-1	1	3
27	-17	-15	-13	-12	-10	-8	-6	-5	-3	-1	1	2	4
29	-16	-14	-12	-11	-9	-7	-5	-4	-2	0	2	3	5
31	-15	-13	-12	-10	-8	-6	-5	-3	-1	1	2	4	6
33	-14	-13	-11	-9	-7	-6	-4	-2	0	2	3	5	7
35	-14	-12	-10	-8	-7	-5	-3	-1	1	2	4	6	8
37	-13	-11	-9	-8	-6	-4	-2	0	1	3	5	7	9
39	-12	-10	-9	-7	-5	-3	-1	0	2	4	6	8	9
41	-12	-10	-8	-6	-4	-3	-1	1	3	5	6	8	10
43	-11	-9	-7	-6	-4	-2	0	2	4	5	7	9	11
45	-11	-9	-7	-5	-3	-1	1	2	4	6	8	10	11
47	-10	-8	-6	-5	-3	-1	1	3	5	7	8	10	12
49	-9	-8	-6	-4	-2	0	2	4	5	7	9	11	13
51	-9	-7	-5	-3	-1	0	2	4	6	8	10	12	13
53	-8	-7	-5	-3	-1	1	3	5	7	8	10	12	14
55	-8	-6	-4	-2	-1	1	3	5	7	9	11	13	14
57	-7	-6	-4	-2	0	2	4	6	8	9	11	13	15
59	-7	-5	-3	-1	1	2	4	6	8	10	12	14	16
61	-7	-5	-3	-1	1	3	5	7	9	11	12	14	16
63	-6	-4	-2	0	2	3	5	7	9	11	13	15	17
65	-6	-4	-2	0	2	4	6	8	10	11	13	15	17
67	-5	-3	-2	0	2	4	6	8	10	12	14	16	18
69	-5	-3	-1	1	3	5	7	8	10	12	14	16	18
71	-5	-3	-1	1	3	5	7	9	11	13	15	17	19
73	-4	-2	0	2	4	6	7	9	11	13	15	17	19
75	-4	-2	0	2	4	6	8	10	12	14	15	17	19
77	-4	-2	0	2	4	6	8	10	12	14	16	18	20
79	-3	-1	1	3	5	7	8	10	12	14	16	18	20
81	-3	-1	1	3	5	7	9	11	13	15	17	19	21
83	-3	-1	1	3	5	7	9	11	13	15	17	19	21
85	-2	0	2	4	6	8	10	12	14	16	18	19	21
87	-2	0	2	4	6	8	10	12	14	16	18	20	22
89	-2	0	2	4	6	8	10	12	14	16	18	20	22
91	-1	1	3	5	7	9	11	13	15	17	19	21	23
93	-1	1	3	5	7	9	11	13	15	17	19	21	23
95	-1	1	3	5	7	9	11	13	15	17	19	21	23
97	0	2	4	6	8	10	12	14	16	18	20	22	24
99	0	2	4	6	8	10	12	14	16	18	20	22	24

Continued on Next Page

<sup>1</sup> See NACE Corrosion Engineers Reference Book, Third Edition, R. Baboian, Ed., NACE International, 2002.

**Dew Point of Moist Air °C<sup>1</sup> (Cont.)**

RH %	Air Temperature °C												
	26	28	30	32	34	36	38	40	42	44	46	48	50
1	-34	-33	-32	-30	-29	-28	-27	-26	-25	-24	-22	-21	-20
3	-22	-21	-20	-18	-17	-16	-14	-13	-12	-11	-9	-8	-7
5	-16	-15	-14	-12	-11	-10	-8	-7	-5	-4	-3	-1	0
7	-12	-11	-9	-8	-7	-5	-4	-2	-1	1	2	4	5
9	-9	-8	-8	-5	-3	-2	0	1	3	4	6	7	9
11	-7	-5	-4	-2	-1	1	3	4	6	7	9	10	12
13	-4	-3	-1	0	2	3	5	6	8	10	11	13	14
15	-3	-1	1	2	4	5	7	9	10	12	13	15	16
17	-1	1	2	4	6	7	9	10	12	14	15	17	18
19	1	2	4	6	7	9	10	12	14	15	17	19	20
21	2	4	5	7	9	10	12	14	15	17	19	20	22
23	3	5	7	8	10	12	13	15	17	18	20	22	23
25	5	6	8	10	11	13	15	16	18	20	21	23	25
27	6	7	9	11	12	14	16	18	19	21	23	24	26
29	7	8	10	12	14	15	17	19	20	22	24	25	27
31	8	9	11	13	15	16	18	20	21	23	25	27	28
33	9	10	12	14	16	17	19	21	22	24	26	28	29
35	9	11	13	15	16	18	20	22	23	25	27	29	30
37	10	12	14	16	17	19	21	23	24	26	28	30	31
39	11	13	15	16	18	20	22	24	25	27	29	31	32
41	12	14	15	17	19	21	23	24	26	28	30	31	33
43	13	14	16	18	20	22	23	25	27	29	31	32	34
45	13	15	17	19	20	22	24	26	28	29	31	33	35
47	14	16	17	19	21	23	25	27	28	30	32	34	36
49	15	16	18	20	22	24	26	27	29	31	33	35	36
51	15	17	19	21	23	24	26	28	30	32	34	35	37
53	16	18	20	21	23	25	27	29	31	32	34	36	38
55	16	18	20	22	24	26	27	29	31	33	35	37	38
57	17	19	21	23	24	26	28	30	32	34	36	37	39
59	17	19	21	23	25	27	29	30	32	34	36	38	40
61	18	20	22	24	26	27	29	31	33	35	37	39	41
63	19	20	22	24	26	28	30	32	34	35	37	39	41
65	19	21	23	25	27	28	30	32	34	36	38	40	42
67	19	21	23	25	27	29	31	33	35	37	38	40	42
69	20	22	24	26	28	30	31	33	35	37	39	41	43
71	20	22	24	26	28	30	32	34	36	38	40	42	43
73	21	23	25	27	29	31	32	34	36	38	40	42	44
75	21	23	25	27	29	31	33	35	37	39	41	42	44
77	22	24	26	28	29	31	33	35	37	39	41	43	45
79	22	24	26	28	30	32	34	36	38	40	41	43	45
81	23	25	26	28	30	32	34	36	38	40	42	44	46
83	23	25	27	29	31	33	35	37	39	40	42	44	46
85	23	25	27	29	31	33	35	37	39	41	43	45	47
87	24	26	28	30	32	34	36	37	39	41	43	45	47
89	24	26	28	30	32	34	36	38	40	42	44	46	48
91	25	27	29	31	32	34	36	38	40	42	44	46	48
93	25	27	29	31	33	35	37	39	41	43	45	47	49
95	25	27	29	31	33	35	37	39	41	43	45	47	49
97	26	28	30	32	34	36	38	40	42	44	46	48	50
99	26	28	30	32	34	36	38	40	42	44	46	48	50

# Dew Point of Moist Air °F

## Air Temperature °F

RH %	32	35	38	41	44	47	50	53	56	59	62	65	68	71	74
1	-57	-56	-54	-52	-50	-48	-46	-45	-43	-41	-39	-37	-36	-34	-32
3	-40	-38	-36	-34	-32	-30	-28	-25	-23	-21	-19	-17	-15	-13	-11
5	-31	-29	-27	-25	-22	-20	-18	-16	-14	-12	-9	-7	-5	-3	-1
7	-25	-23	-20	-18	-16	-14	-11	-9	-7	-5	-2	0	2	4	6
9	-20	-18	-15	-13	-11	-9	-6	-4	-2	1	3	5	7	10	12
11	-16	-14	-12	-9	-7	-5	-2	0	2	5	7	9	12	14	16
13	-13	-11	-8	-6	-3	-1	1	4	6	8	11	13	16	18	20
15	-10	-8	-5	-3	0	2	4	7	9	12	14	16	19	21	24
17	-8	-5	-3	0	2	5	7	10	12	15	17	19	22	24	27
19	-5	-3	0	2	5	7	10	12	15	17	19	22	24	27	29
21	-3	-1	2	4	7	9	12	14	17	19	22	24	27	29	32
23	-1	1	4	6	9	11	14	16	19	21	24	26	29	31	34
25	0	3	5	8	11	13	16	18	21	23	26	28	31	33	36
27	2	5	7	10	12	15	17	20	23	25	28	30	33	35	38
29	4	6	9	11	14	17	19	22	24	27	29	32	35	37	40
31	5	8	10	13	16	18	21	23	26	29	31	34	36	39	42
33	6	9	12	14	17	20	22	25	27	30	33	35	38	41	43
35	8	10	13	16	18	21	24	26	29	31	34	37	39	42	45
37	9	12	14	17	20	22	25	28	30	33	36	38	41	44	46
39	10	13	15	18	21	23	26	29	32	34	37	40	42	45	48
41	11	14	17	19	22	25	27	30	33	35	38	41	44	46	49
43	12	15	18	20	23	26	29	31	34	37	39	42	45	48	50
45	13	16	19	21	24	27	29	32	35	38	40	43	46	49	51
47	14	17	20	22	25	28	31	33	36	39	42	44	47	50	52
49	15	18	21	24	26	29	32	35	37	40	43	46	48	51	54
51	16	19	22	24	27	30	33	36	38	41	44	47	49	52	55
53	17	20	23	25	28	31	34	37	39	42	45	48	50	53	56
55	18	21	23	26	29	32	35	37	40	43	46	48	51	54	57
57	19	21	24	27	30	33	35	38	41	44	47	50	52	55	58
59	19	22	25	28	31	33	36	39	42	45	48	50	53	56	59
61	20	23	26	29	32	34	37	40	43	46	49	51	54	57	60
63	21	24	27	29	32	35	38	41	44	47	49	52	55	58	61
65	22	25	27	30	33	36	39	42	44	47	50	53	56	59	62
67	22	25	28	31	34	37	40	42	45	48	51	54	57	60	62
69	23	26	29	32	35	37	40	43	46	49	52	55	58	60	63
71	24	27	30	32	35	38	41	44	47	50	53	55	58	61	64
73	24	27	30	33	36	39	42	45	48	51	53	56	59	62	65
75	25	28	31	34	37	39	42	45	48	51	54	57	60	63	66
77	26	29	32	34	37	40	43	46	49	52	55	58	61	64	66
79	26	29	32	35	38	41	44	47	50	52	55	58	61	64	67
81	27	30	33	36	39	42	44	47	50	53	56	59	62	65	68
83	27	30	33	36	39	42	45	48	51	54	57	60	63	66	68
85	28	31	34	37	40	43	46	49	52	55	58	60	64	66	69
87	29	32	34	37	40	43	46	49	52	55	58	61	64	67	70
89	29	32	35	38	41	44	47	50	53	56	59	62	65	68	71
91	30	33	36	39	42	45	48	51	54	56	60	62	65	68	71
93	30	33	36	39	42	45	48	51	54	57	60	63	66	69	72
95	31	34	37	40	43	46	49	52	55	58	61	64	67	70	73
97	31	34	37	40	43	46	49	52	55	58	61	64	67	70	73
99	32	35	38	41	44	47	50	53	56	59	62	65	68	71	74

Continued on Next Page

<sup>1</sup> See *NACE Corrosion Engineers Reference Book, Third Edition*, R. Baboian, Ed., NACE International, 2002.

**Dew Point of Moist Air °F (Cont.)**

		Air Temperature °F														
RH %	77	80	83	86	89	92	95	98	101	104	107	110	113	116	119	122
1	-30	-28	-27	-25	-23	-21	-20	-18	-16	-14	-13	-11	-9	-7	-6	-4
3	-9	-7	-5	-3	-1	1	2	4	6	8	10	12	14	16	18	20
5	1	3	5	8	10	12	14	16	16	20	22	24	26	28	30	32
7	8	11	13	15	17	19	22	24	26	28	30	32	35	37	39	41
9	14	16	19	21	23	25	28	30	32	34	36	39	41	43	45	47
11	19	21	23	26	28	30	32	35	37	39	41	44	46	48	50	53
13	23	25	27	30	32	34	37	39	41	44	46	48	51	53	55	57
15	26	28	31	33	35	38	40	43	45	47	50	52	54	57	59	61
17	29	31	34	36	39	41	44	46	48	51	53	55	58	60	63	65
19	32	34	37	39	42	44	46	49	51	54	56	59	61	63	66	68
21	34	37	39	42	44	47	49	52	54	56	59	61	64	66	69	71
23	37	39	42	44	47	49	51	54	56	59	61	64	66	69	71	74
25	38	41	44	46	49	51	54	56	59	61	64	66	69	71	74	76
27	41	43	46	48	51	53	56	58	61	64	66	68	71	74	76	79
29	42	45	48	50	53	55	58	60	63	65	68	71	73	76	78	81
31	44	47	49	52	55	57	60	62	65	67	70	73	75	78	80	83
33	46	48	51	54	56	59	61	64	67	69	72	74	77	80	82	85
35	47	50	53	55	58	60	63	66	68	71	74	76	79	81	84	87
37	49	52	54	57	60	62	65	67	70	73	75	78	81	83	86	89
39	50	53	56	58	61	64	66	69	72	74	77	80	82	85	87	90
41	52	54	57	60	62	65	68	70	73	76	78	81	84	86	89	92
43	53	56	58	61	64	68	69	72	75	77	80	83	85	88	91	93
45	54	57	60	62	65	68	70	73	76	78	81	84	87	89	92	95
47	55	58	61	63	66	69	72	74	77	80	82	85	88	91	93	96
49	56	59	62	65	68	70	73	76	78	81	84	87	89	92	95	98
51	58	60	63	66	69	71	74	77	80	82	85	88	91	93	96	99
53	59	62	64	67	70	73	75	78	81	84	86	89	92	95	97	100
55	60	62	65	68	71	73	76	79	82	85	87	90	93	96	98	101
57	61	64	66	69	72	75	78	80	83	86	89	91	94	97	100	103
59	62	64	67	70	73	76	78	81	84	87	90	92	95	98	101	104
61	63	66	68	71	74	77	80	82	85	88	91	94	96	99	102	105
63	64	66	69	72	75	78	81	83	86	89	92	95	98	100	103	106
65	64	67	70	73	76	79	82	84	87	90	93	96	98	101	104	107
67	65	68	71	74	77	80	82	85	88	91	94	97	100	102	105	108
69	66	69	72	75	78	80	83	86	89	92	95	98	100	103	106	109
71	67	70	73	76	79	81	84	87	90	93	96	99	101	104	107	110
73	68	71	74	76	79	82	85	88	91	94	97	100	102	105	108	111
75	69	71	74	77	80	83	86	89	92	94	97	100	103	106	109	112
77	69	72	75	78	81	84	87	90	93	96	98	101	104	107	110	113
79	70	73	76	79	82	84	87	90	93	96	99	102	105	108	111	114
81	71	74	77	80	82	85	88	91	94	97	100	103	106	109	112	115
83	71	74	77	80	83	86	89	92	95	98	101	104	107	109	112	115
85	72	75	78	81	84	87	90	93	96	99	102	105	108	110	113	116
87	73	76	79	82	85	88	91	94	96	99	102	105	108	111	114	117
89	73	76	79	82	85	88	91	94	97	100	103	106	109	112	115	118
91	74	77	80	83	86	89	92	95	98	101	104	107	110	113	116	119
93	75	78	81	84	87	90	93	96	99	102	105	108	111	114	117	120
95	76	79	82	85	87	90	93	96	99	102	105	108	111	114	117	120
97	76	79	82	85	88	91	94	97	100	103	106	109	112	115	118	121
99	77	80	83	86	89	92	95	98	101	104	107	110	113	116	119	122

# Chemical Cleaning Procedures for Removal of Corrosion Products<sup>1</sup>

Designation	Material	Solution	Time	Temperature	Remarks
C.1.1	Aluminum and Aluminum Alloys	50 mL phosphoric acid (H <sub>3</sub> PO <sub>4</sub> , sp gr 1.69) 20 g chromium trioxide (CrO <sub>3</sub> ) Reagent water to make 1000 mL	5 to 10 min	90°C to Boiling	If corrosion product films remain, rinse, then follow with nitric acid procedure (C.1.2).
C.1.2		Nitric acid (HNO <sub>3</sub> , sp gr 1.42)	1 to 5 min	20 to 25°C	Remove extraneous deposits and bulky corrosion products to avoid reactions that may result in excessive removal of base metal.
C.2.1	Copper and Copper Alloys	500 mL hydrochloric acid (HCl, sp gr 1.19) Reagent water to make 1000 mL	1 to 3 min	20 to 25°C	Deaeration of solution with purified nitrogen will minimize base metal removal.
C.2.2		4.9 g sodium cyanide (NaCN) Reagent water to make 1000 mL	1 to 3 min	20 to 25°C	Removes copper sulfide corrosion products that may not be removed by hydrochloric acid treatment (C.2.1).
C.2.3		100 mL sulfuric acid (H <sub>2</sub> SO <sub>4</sub> , sp gr 1.84) Reagent water to make 1000 mL	1 to 3 min	20 to 25°C	Remove bulky corrosion products before treatment to minimize copper redeposition on specimen surface.
C.2.4		120 mL sulfuric acid (H <sub>2</sub> SO <sub>4</sub> , sp gr 1.84) 30 g sodium dichromate (Na <sub>2</sub> Cr <sub>2</sub> O <sub>7</sub> · 2H <sub>2</sub> O) Reagent water to make 1000 mL	5 to 10 s	20 to 25°C	Removes redeposited copper resulting from sulfuric acid treatment.
C.2.5		54 mL sulfuric acid (H <sub>2</sub> SO <sub>4</sub> , sp gr 1.84) Reagent water to make 1000 mL	30 to 60 min	40 to 50°C	Deaerate solution with nitrogen. Brushing of test specimens to remove corrosion products followed by re-immersion for 3 to 4 s is recommended.
C.3.1	Iron and Steel	1000 mL hydrochloric acid (HCl, sp gr 1.19) 20 g antimony trioxide (Sb <sub>2</sub> O <sub>3</sub> ) 50 g stannous chloride (SnCl <sub>2</sub> )	1 to 25 min	20 to 25°C	Solution should be vigorously stirred or specimen should be brushed. Longer times may be required in certain instances.

<sup>1</sup> See ASTM G1, Standard Practice For Preparing, Cleaning, and Evaluating Corrosion Test Specimens.

#### 44 CORROSION TESTS AND STANDARDS MANUAL

Designation	Material	Solution	Time	Temperature	Remarks
C.3.2		50 g sodium hydroxide (NaOH) 200 g granulated zinc or zinc chips Reagent water to make 1000 mL	30 to 40 min	80 to 90°C	Caution should be exercised in the use of any zinc dust since spontaneous ignition upon exposure to air can occur.
C.3.3		200 g sodium hydroxide (NaOH) 20 g granulated zinc or zinc chips Reagent water to make 1000 mL	30 to 40 min	80 to 90°C	Caution should be exercised in the use of any zinc dust since spontaneous ignition upon exposure to air can occur.
C.3.4		200 g diammonium citrate ((NH <sub>4</sub> ) <sub>2</sub> HC <sub>6</sub> H <sub>5</sub> O <sub>7</sub> ) Reagent water to make 1000 mL	20 min	75 to 90°C	Depending upon the composition of the corrosion product, attack of base metal may occur.
C.3.5		500 mL hydrochloric acid (HCl, sp gr 1.19) 3.5 g hexamethylene tetramine Reagent water to make 1000 mL	10 min	20 to 25°C	Longer times may be required in certain instances.
C.3.6		Molten caustic soda (NaOH) with 1.5–2.0 % sodium hydride (NaH)	1 to 20 min	370°C	For details refer to Technical Information Bulletin SP29-370, "DuPont Sodium Hydride Descaling Process Operating Instructions."
C.4.1	Lead and Lead Alloys	10 mL acetic acid (CH <sub>3</sub> COOH) Reagent water to make 1000 mL	5 min	Boiling	...
C.4.2		50 g ammonium acetate (CH <sub>3</sub> COONH <sub>4</sub> ) Reagent water to make 1000 mL	10 min	60 to 70°C	...
C.4.3		250 g ammonium acetate (CH <sub>3</sub> COONH <sub>4</sub> ) Reagent water to make 1000 mL	5 min	60 to 70°C	...
C.5.1	Magnesium and Magnesium Alloys	150 g chromium trioxide (CrO <sub>3</sub> ) 10 g silver chromate (Ag <sub>2</sub> CrO <sub>4</sub> ) Reagent water to make 1000 mL	1 min	Boiling	The silver salt is present to precipitate chloride.
C.5.2		200 g chromium trioxide (CrO <sub>3</sub> ) 10 g silver nitrate (AgNO <sub>3</sub> ) 20 g barium nitrate (Ba(NO <sub>3</sub> ) <sub>2</sub> ) Reagent water to make 1000 mL	1 min	20 to 25°C	The barium salt is present to precipitate sulfate.
C.6.1	Nickel and Nickel Alloys	150 mL hydrochloric acid (HCl, sp gr 1.19) Reagent water to make 1000 mL	1 to 3 min	20 to 25°C	...
C.6.2		100 mL sulfuric acid (H <sub>2</sub> SO <sub>4</sub> , sp gr 1.84) Reagent water to make 1000 mL	1 to 3 min	20 to 25°C	...
C.7.1	Stainless Steels	100 mL nitric acid (HNO <sub>3</sub> , sp gr 1.42) Reagent water to make 1000 mL	20 min	60°C	...
C.7.2		150 g diammonium citrate ((NH <sub>4</sub> ) <sub>2</sub> HC <sub>6</sub> H <sub>5</sub> O <sub>7</sub> ) Reagent water to make 1000 mL	10 to 60 min	70°C	...
C.7.3		100 g citric acid (C <sub>6</sub> H <sub>8</sub> O <sub>7</sub> ) 50 mL sulfuric acid (H <sub>2</sub> SO <sub>4</sub> , sp gr 1.84) 2 g inhibitor (diorthotolyl thiourea or quinoline ethyiodide or betanaphthol quinoline) Reagent water to make 1000 mL	5 min	60°C	...



Designation	Material	Solution	Time	Temperature	Remarks
C.7.4		200 g sodium hydroxide (NaOH) 30 g potassium permanganate (KMnO <sub>4</sub> ) Reagent water to make 1000 mL <i>followed by</i> 100 g diammonium citrate ((NH <sub>4</sub> ) <sub>2</sub> HC <sub>6</sub> H <sub>5</sub> O <sub>7</sub> ) Reagent water to make 1000 mL	5 min	Boiling	...
C.7.5		100 mL nitric acid (HNO <sub>3</sub> , sp gr 1.42) 20 mL hydrofluoric acid (HF, sp gr 1.198–48 %) Reagent water to make 1000 mL	5 to 20 min	20 to 25°C	...
C.7.6		200 g sodium hydroxide (NaOH) 50 g zinc powder. Reagent water to make 1000 mL	20 min	Boiling	Caution should be exercised in the use of any zinc dust since spontaneous ignition upon exposure to air can occur.
C.8.1		150 g trisodium phosphate (Na <sub>3</sub> PO <sub>4</sub> · 12H <sub>2</sub> O) Reagent water to make 1000 mL	10 min	Boiling	...
C.8.2	Tin and Tin Alloys	50 mL hydrochloric acid (HCl, sp gr 1.19) Reagent water to make 1000 mL	10 min	20°C	...
C.9.1	Zinc and Zinc Alloys	150 mL ammonium hydroxide (NH <sub>4</sub> OH, sp gr 0.90) Reagent water to make 1000 mL <i>followed by</i> 50 g chromium trioxide (CrO <sub>3</sub> ) 10 g silver nitrate (AgNO <sub>3</sub> ) Reagent water to make 1000 mL	15 to 20 s	Boiling	The silver nitrate should be dissolved in water and added to the boiling chromic acid to prevent excessive crystallization of silver chromate. The chromic acid must be sulfate free to avoid attack of the zinc base metal.
C.9.2		100 g ammonium chloride (NH <sub>4</sub> Cl) Reagent water to make 1000 mL	2 to 5 min	70°C	...
C.9.3		200 g chromium trioxide (CrO <sub>3</sub> ) Reagent water to make 1000 mL	1 min	80°C	Chloride contamination of the chromic acid from corrosion products formed in salt environments should be avoided to prevent attack of the zinc base metal.
C.9.4		85 mL hydriodic acid (HI, sp gr 1.5) Reagent water to make 1000 mL	15s	20 to 25°C	Some zinc base metal may be removed. A control specimen (3.1.1) should be employed.
C.9.5		100 g ammonium persulfate (NH <sub>4</sub> ) <sub>2</sub> S <sub>2</sub> O <sub>8</sub> ) Reagent water to make 1000 mL	5 min	20 to 25°C	Particularly recommended for galvanized steel.
C.9.6		100 g ammonium acetate (CH <sub>3</sub> COONH <sub>4</sub> ) Reagent water to make 1000 mL	2 to 5 min	70°C	...

# Electrolytic Cleaning Procedures for Removal of Corrosion Products<sup>2</sup>

Designation	Material	Solution	Time	Temperature	Remarks
E.1.1	Iron, Cast Iron, Steel	75 g sodium hydroxide (NaOH) 25 g sodium sulfate (Na <sub>2</sub> SO <sub>4</sub> ) 75 g sodium carbonate (Na <sub>2</sub> CO <sub>3</sub> ) Reagent water to make 1000 mL	20 to 40 min	20 to 25°C	Cathodic treatment with 100 to 200 A/m <sup>2</sup> current density. Use carbon, platinum or stainless steel anode.
E.1.2		28 mL sulfuric acid (H <sub>2</sub> SO <sub>4</sub> , sp gr 1.84) 0.5 g inhibitor (diorthotolyl thiourea or quinoline ethyliodide or betanaphthol quinoline). Reagent water to make 1000 mL	3 min	75°C	Cathodic treatment with 2000 A/m <sup>2</sup> current density. Use carbon, platinum or lead anode.
E.1.3		100 g diammonium citrate ((NH <sub>4</sub> ) <sub>2</sub> HC <sub>6</sub> H <sub>5</sub> O <sub>7</sub> ) Reagent water to make 1000 mL	5 min	20 to 25°C	Cathodic treatment with 100 A/m <sup>2</sup> current density. Use carbon or platinum anode.
E.2.1	Lead and Lead Alloys	28 mL sulfuric acid (H <sub>2</sub> SO <sub>4</sub> , sp gr 1.84) 0.5 g inhibitor (diorthotolyl thiourea or quinoline ethyliodide or betanaphthol quinoline) Reagent water to make 1000 mL	3 min	75° C	Cathodic treatment with 2000 A/m <sup>2</sup> current density. Use carbon, platinum or lead anode.
E.3.1	Copper and Copper Alloys	7.5 g potassium chloride (KCl) Reagent water to make 1000 mL	1 to 3	20 to 25°C	Cathodic treatment with 100 A/m <sup>2</sup> current density. Use carbon or platinum anode.
E.4.1	Zinc and Cadmium	50 g dibasic sodium phosphate (Na <sub>2</sub> HPO <sub>4</sub> ) Reagent water to make 1000 mL	5 min	70°C	Cathodic treatment with 110 A/m <sup>2</sup> current density. Specimen must be energized prior to immersion. Use carbon, platinum or stainless steel anode.
E.4.2		100 g sodium hydroxide (NaOH) Reagent water to make 1000 mL	1 to 2 min	20 to 25°C	Cathodic treatment with 100 A/m <sup>2</sup> current density. Specimen must be energized prior to immersion. Use carbon, platinum or stainless steel anode.
E.5.1	General (excluding Aluminum, Magnesium and Tin Alloys)	20 g sodium hydroxide (NaOH) Reagent water to make 1000 mL	5 to 10 min	20 to 25°C	Cathodic treatment with 300 A/m <sup>2</sup> current density. A S31600 stainless steel anode may be used.

<sup>2</sup> See ASTM G1, Standard Practice for Preparing, Cleaning, and Evaluating Corrosion Test Specimens.

## **Section II: Testing and Evaluation**

*R. Baboian, Editor*

# Planning and Design of Tests

*Stephen D. Cramer<sup>1</sup> and Barnie P. Jones<sup>2</sup>*

CORROSION TESTS ARE an important tool for evaluating the performance of materials used in scientific, industrial, engineering, consumer, and aesthetic applications, where corrosion was estimated to cost the U.S. economy \$276 billion in direct costs annually in 1998, or 3.1 % of the U.S. Gross Domestic Product [1–3]. Corrosion tests are widely used to evaluate the durability of materials of construction in reactive environments. They have a profound impact on society by the influence they have on the choice of materials used, for example, in chemical plants, drilling and mining equipment, energy production facilities, communications equipment, buildings, bridges, spacecraft, monuments, computers, food processing equipment, medical implants, automobiles, and manufacturing facilities. Corrosion tests evaluate a range of material degradation processes that affect the final performance of these materials and directly influence the materials chosen for these applications. These processes involve chemical and electrochemical reactions, and include mechanically assisted corrosion processes and synergies between wear and corrosion. Corrosion tests are used to examine the performance of materials, evaluate alternate materials, develop strategies for protection of materials, and determine the corrosivity of specific environments.

Typical corrosion and materials engineering requirements are shown in Fig. 1 for three stages in the evolution of a manufacturing process for the chemical process industries (CPI) [4]. Thorough corrosion test planning and design is essential to achieve satisfactory materials performance for each of these stages. Corrosion tests lay the foundation for obtaining adequate information on materials performance in the process environments, for ensuring resources are efficiently used, and that materials choices are compatible with long-term economic goals for the plant. The corrosionist is challenged to influence materials decisions in each of these stages. This is particularly true of the first stage where trends in process simulation have greatly reduced the time between research and development and plant design.

Corrosion test planning and design has been discussed by others [5–9]. This chapter provides a general background for planning and design of corrosion tests and the basic statistical considerations affecting the design of these tests.

While corrosion testing of metallic materials is the focus here, planning and design of environmental performance tests for nonmetallic materials, such as paints, plastics, ceramics, and refractories is similar. Specific corrosion test methods have been developed by ASTM International [10–12], NACE International [13], and the International Organization for Standardization (ISO) [14].

Corrosion test planning and design typically involves the following five steps:

- Define goals and objectives
- Design corrosion test
- Develop test protocol
- Engineer test
- Modify test

These steps are affected by the nature of the corrosion process, the types of data acquired, the analytical resources available, the statistical treatments to be applied, and the outcomes sought. Preliminary or early data can help determine whether the fifth step, modification of the test design, will be needed.

As with other technical endeavors, adequate and ongoing documentation is a necessary element of planning, designing, and conducting corrosion tests [15]. It is the basis for effective communications between management and the corrosionist from the earliest planning stages, ensuring agreement on goals and objectives and the availability of necessary resources. It provides a way to assess, review, and modify the test plan with regard to data quality objectives, use of resources, and the outcomes achieved. It provides the continuity for other investigators to continue and complete tests and to evaluate the results when personnel changes occur, especially when tests are conducted over long time spans.

## DEFINE GOALS AND OBJECTIVES

Clearly defined goals and objectives are needed if corrosion tests are to produce results that affect materials selection, and methods of corrosion protection and corrosion control. Goals and objectives define test purpose and what is to be achieved. Economic considerations are always a factor in defining goals and objectives, along with other considerations (workforce, public safety, and environment). Figure 2 shows some of the quality criteria that affect plant economics in the CPI. The criteria have been grouped

<sup>1</sup>Materials Conservation Division, Albany Research Center, 1450 Queen Ave. SW, U.S. Department of Energy, Albany, OR 97321.

<sup>2</sup>Research Unit, Oregon Department of Transportation, 200 Hawthorne SE, Suite B-240, Salem, OR 97310.

Research and Development, Pilot Plant Materials Selection	Preliminary Plant Design, Detailed Engineering, Procurement, Fabrication and Construction Considerations	Plant Operation, Code Inspection, Maintenance Considerations
<ul style="list-style-type: none"> <li>• Corrosion resistance</li> <li>• Ductility</li> <li>• Weldability</li> <li>• Long time performance</li> <li>• Non-destructive testing (NDT)</li> <li>• Corrosion effects on product</li> <li>• Availability</li> </ul>	<ul style="list-style-type: none"> <li>• Operating conditions</li> <li>• Corrosion performance at operating conditions, start-up and shutdown conditions</li> <li>• Design demands on materials selection</li> <li>• NDT</li> <li>• Inspection</li> </ul>	<ul style="list-style-type: none"> <li>• Corrosion monitoring</li> <li>• NDT in maintenance strategy</li> <li>• Inspection program</li> <li>• Maintenance and repair</li> <li>• Failure analysis</li> </ul>

**FIG. 1—Corrosion and materials engineering requirements characteristic of research and development, plant design, and plant operation in the CPI [4]. © Copyright 1993 by NACE International. All rights reserved by NACE; reprinted by permission.**

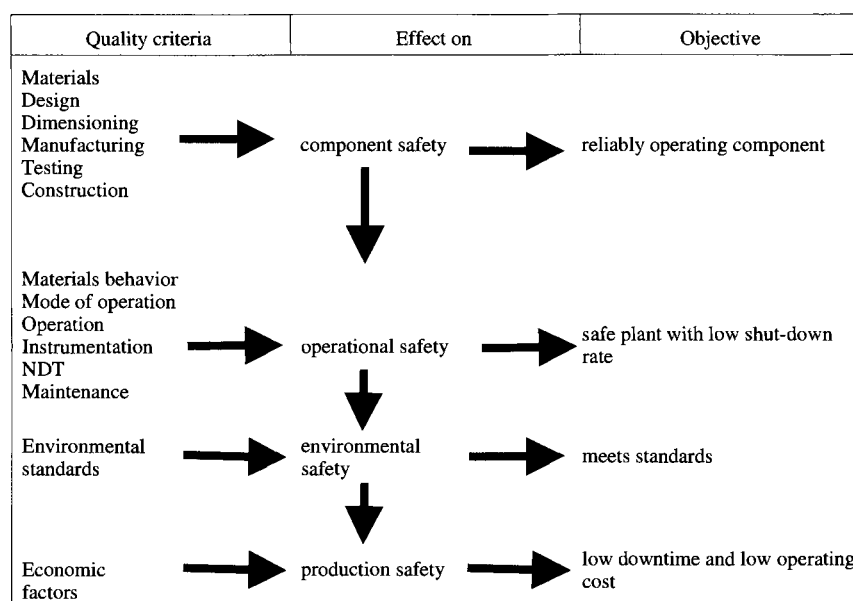


**FIG. 2—Component, operational, and production safety as criteria of plant economics [4]. © Copyright 1993 by NACE International. All rights reserved by NACE; reprinted by permission.**

according to their effect on a hierarchy of safety factors that determine the long-term economic success of the plant. These safety factors are component safety, operational safety, and production safety, and represent, in increasing order of importance, the economic risks associated with the plant. Corrosion tests establish some of the quality criteria for these safety factors. The corrosionist must ultimately help balance the costs of corrosion control against the benefits to be achieved in each of these areas.

In the CPI, maintenance is one of the quality criteria in operational safety and involves the impact of corrosion on the service life of components, on plant productivity, and on maintenance strategies. Figure 3 shows how component exploitation and risk factors are affected by three different maintenance strategies, and the maintenance actions that result from these strategies. To be able to influence maintenance costs, the goals and objectives must be guided by pragmatic considerations of plant operation.

Failure analysis is an important aspect of corrosion testing since failed components inform the corrosionist about the severity of actual steady-state and transient operating conditions, improperly identified or selected materials, and faulty equipment design. Figure 4 outlines typical steps in failure analysis that are applicable to the CPI and other industries. At the heart of this process is testing to determine chemical, corrosion, and mechanical contributions to the failure and to validate the results of the analysis. Failure analysis is an effective means to lower maintenance costs and a strategy to limit risk to operational safety.

In each of these examples, the crucial issue for the corrosionist is to identify what information is to be generated by the corrosion test, and the connection of that information to production safety. While asking the right technical questions is a necessary element of the planning and design process, in an increasingly important sense, the definition of goals and objectives can reach beyond the corrosionists expertise and require input from the public. Thus, in addition

Component Exploitation and Risk Factors; Maintenance Action	Maintenance Strategy		
	Waiting for Component Failure	Preventive Maintenance	State of Component Monitored in Real Time
Component exploitation	<ul style="list-style-type: none"> <li>• operate up to failure</li> <li>• exploiting component 100 pct</li> <li>• redundancy necessary</li> </ul>	<ul style="list-style-type: none"> <li>• repair after assigned time intervals</li> <li>• exploiting component 60–80 pct</li> <li>• life time assignment necessary</li> </ul>	<ul style="list-style-type: none"> <li>• repair according to test of state</li> <li>• exploiting component 60–80 pct</li> <li>• diagnostic method necessary</li> </ul>
Failure risk	<ul style="list-style-type: none"> <li>• no influence on plant availability</li> <li>• secondary plant components</li> <li>• no risk of consecutive failures</li> </ul>	<ul style="list-style-type: none"> <li>• influence on plant availability</li> <li>• important plant components</li> <li>• risking future failures</li> </ul>	<ul style="list-style-type: none"> <li>• influence on plant availability</li> <li>• important plant components</li> <li>• risking future failures</li> </ul>
Maintenance action	<ul style="list-style-type: none"> <li>• exchange of component</li> </ul>	<ul style="list-style-type: none"> <li>• setting repair schedule</li> </ul>	Early failure diagnosis by: <ul style="list-style-type: none"> <li>• plant supervision</li> <li>• recurrent testing</li> </ul>

FIG. 3—Maintenance strategies and their effects on component exploitation, failure risk, and plant availability [4]. © Copyright 1993 by NACE International. All rights reserved by NACE; reprinted by permission.

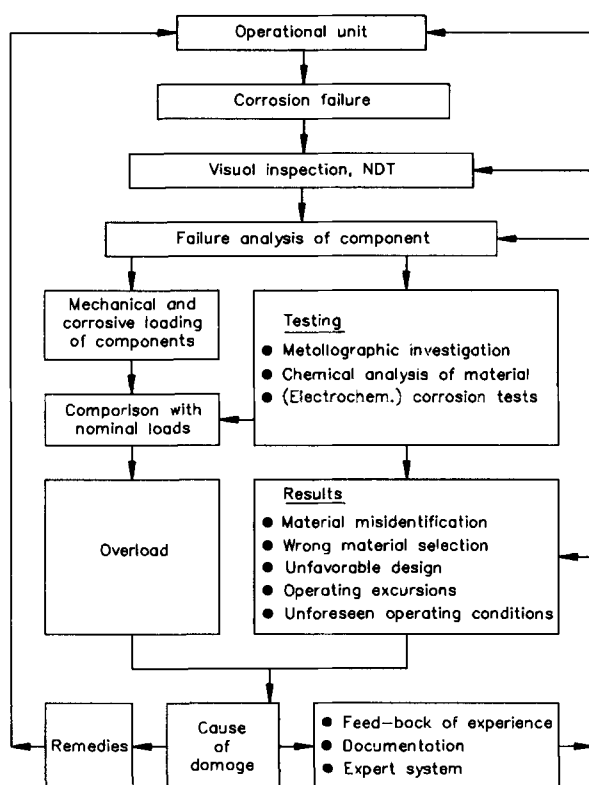


FIG. 4—Corrosion failure analysis in the CPI [4]. © Copyright 1993 by NACE International. All rights reserved by NACE; reprinted by permission.

to the expected economic and safety issues, corrosion testing can involve legal [15], regulatory, health, and environmental issues. In this context, the goals and objectives may include not only technical but nontechnical factors. Ultimately, the goals and objectives may include standards of quality, quantity, and timeliness on matters that are both technical and nontechnical.

## DESIGN CORROSION TEST


Corrosion data are developed from service experience, field tests, pilot plant tests, and laboratory tests. Confidence in the reliability of corrosion data increases the more closely results are based on performance in similar or identical process environments, Table 1 [16]. Understandably, the most reliable information on corrosion performance is developed from service experience in identical or nearly identical process environments. Laboratory tests offer the flexibility of a broad range of standard and fundamental corrosion measurements. Sound practice requires that laboratory tests be verified by pilot plant tests and/or field tests before materials specifications are adopted.

Standard corrosion tests such as those developed by ASTM, NACE, and ISO often will address the technical requirements established in the goals and objectives though, in some cases, they may need to be modified. The quality of data produced by standard tests has been well established by critical evaluation and review, and results can readily be compared to others obtained using the same test. Even the highly specialized techniques used in fundamental corrosion research, while not especially amendable to standardization, eventually achieve codification through continued publication and use [9,17–20].

As a practical matter, corrosion tests are integrated with other functions in plant development at the laboratory and pilot plant stage in the ongoing process of specifying materials of construction, Fig. 5. At each stage the corrosionist must evaluate and re-evaluate the material properties and performance necessary to achieve the production safety (Fig. 2) defined by plant management. This is done by considering the operating environment, extremes in the operating environment, and startup and shutdown conditions. Table 2 identifies reasons why the corrosionist may consider selecting more expensive materials than those judged to provide adequate performance at the laboratory or pilot plant stage. Critical or key components in a process may warrant the added expense of more corrosion resistant materials.

The service conditions upon which materials selection is based are most often the nominal process or environmental conditions. However, transients at startup and shutdown,

**TABLE 1**—Corrosion data reliability levels [16].

Corrosion data source	
<ul style="list-style-type: none"> <li>Plant performance data obtained in identical processes</li> <li>Coupon or equipment data obtained in similar processes</li> <li>Laboratory coupon (including electrochemical tests) data obtained in simulated service conditions</li> <li>Published data in recognized journals</li> <li>Advertising literature from industrial sources</li> </ul>	

and during operating excursions, can produce service conditions that require consideration when selecting a material. Less obvious factors such as trace reactant levels, stray currents, mechanical energy bursts, or combinations of these may also be important. Finally, stability of corrosion products, inhibitors, and coatings must be considered. Potential-pH diagrams [21–23] are a valuable resource for showing conditions that may lead to corrosion, immunity, or passivity of metals in many applications.

Corrosion tests must address many types of corrosion [24,25]. These include uniform corrosion, galvanic corrosion, and various forms of localized corrosion, such as intergranular, crevice, or pitting corrosion, that can rapidly cause materials failure without apparent uniform damage. Mechanically-assisted corrosion, such as stress-corrosion cracking (SCC) [26], corrosion fatigue, erosion corrosion, and wear/corrosion synergism, are complex and important corrosion processes, about which better understanding is being achieved through ongoing research.

Corrosion tests are intended to identify materials that provide adequate corrosion performance and service life at a low materials cost. To ensure this, as noted earlier, corrosionists evaluate the performance of materials, the effectiveness of protection strategies (coatings, inhibitors, cathodic protection), and the mechanism and kinetics of corrosion processes in specific environments in service tests, pilot plant tests, and laboratory tests. Increasingly, materials costs are being evaluated in the context of component or structure service life. In this way, factors such as maintenance, repairs, replacement, rehabilitation, process downtime, and interest rates are added into the cost of providing adequate corrosion performance over the service life of the component or structure. Finding or producing the necessary data from corrosion tests for such

**TABLE 2**—Reason for selecting more expensive materials [4].

Concern	Importance
Component/material cost ratio high	moderate
Risk of pitting	high
Risk of stress-corrosion cracking	high
Environmental consequences	high
Safety consequences	highest
Key component failure results in plant shutdown	highest

an evaluation is often daunting, particularly since most corrosion testing is conducted over relatively short time frames relative to the service life of the component or structure. Nevertheless, with necessary assumptions regarding long-term corrosion performance, lifetime cost estimates can provide an effective means for evaluating materials choices.

Cited here are some corrosion studies requiring differing levels of planning and statistical design. Materials selection and protection strategies for specific environments are widely determined in pilot plant tests and by performance in service environments [27–31]. Understanding the mechanism and kinetics of specific corrosion processes under one set of conditions provides a fundamental basis for transferring that knowledge to related corrosion processes under somewhat different conditions [32,33]. Corrosion testing in specific environments includes acceptance testing for materials and for environments [34,35], corrosivity mapping [36], and modeling the effects of environmental factors on materials performance [37–40].

### Basic Statistical Topics

Corrosion test design should reflect the statistical basis of the data analyses (see ASTM G 16, Guide for Applying Statistics to Analysis of Corrosion Data; and E 1488, Guide for Statistical Procedures to Use in Developing and Applying ASTM Test Methods; or for a general statistical reference see Snedecor and Cochran [41]). Whether done intuitively or deliberately, this is a necessary step towards achieving the goals and objectives of the test. However, corrosion test design is more encompassing than the application of statistical methods alone. The design must efficiently provide the needed information. In this regard, the design should employ both statistical and economic types of analyses and address the range of technical and nontechnical issues that are important. Fortunately, most statistical designs are both efficient and economical.

Five statistical topics are introduced here in increasing order of complexity. They are:

- Probability sampling and randomization
- Determining the required numbers of observations
- Curve fitting and simple statistical modeling
- Designing experiments
- Statistical tests for experiments

These represent only a fraction of the techniques and approaches that are available to the corrosionist. Chapter 5, “Statistical Treatment of Data, Data Interpretation, and

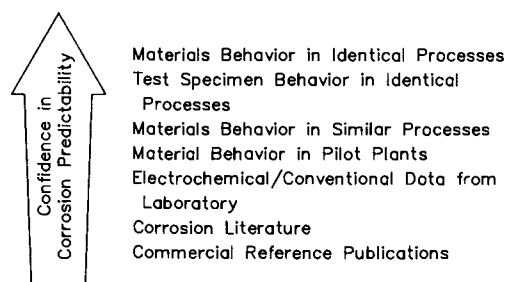


**FIG. 5—Materials selection in research and development for CPI plant facilities [4]. © Copyright 1993 by NACE International. All rights reserved by NACE; reprinted by permission.**

Reliability,” covers some of these topics in detail and summarizes the statistical terminology (see also ASTM E 456, Terminology Relating to Quality and Statistics; and E 1325, Terminology Relating to Design of Experiments).

### Probability Sampling and Randomization

There are two related but conceptually different uses of probability sampling, sampling from a larger population, and randomization. Sampling from a population is usually intended to establish *external* validity, or to obtain a sample that can be used to make an inference to the larger population. An example might be quality control sampling of coated steel from a production line, corrosion resistance measurements on a medical implant, or samples of reinforced concrete from bridges of a particular type.

Randomization is largely an identical process, except its focus is on *internal* validity. An example might be random assignment of 48 prepared material specimens to three groups. In this example, three “samples” of 16 observations (specimens) each are drawn from the “population” of 48 material specimens. The purpose is to create three test groups that are equivalent and statistically independent of one another. In both situations, chance alone determines assignment of *observations* (observations and cases are interchangeable terms) to a given *sample* (the aggregate of observations or cases).

### Determining the Required Number of Observations

There are three considerations in determining the number of observations to be included in the case of sampling from a larger population or in randomization. One consideration is the variance in the dependent variable. Other things being equal, the larger the variance, the larger the required number of observations. A second consideration is the number of factors that will be included in any statistical analysis. The larger the number of variables, the more observations that are needed.

Finally, the level of precision required to successfully complete the study affects the required number of observations. Again, the same considerations apply in randomization and in sampling from a larger population: other things being equal, a large number of observations is needed to detect a small change or to obtain a higher level of confidence in the result. For example, larger samples are needed to accurately predict whether there is a difference in corrosion performance between two alloys with similar compositions. Also, since statistical tests and estimates are conditioned by probabilities, larger samples reduce the risk of drawing the wrong inference from a sample (see the discussion of probability distributions and confidence limits in Part II Chapter 5.)

The effect of replicate samples for each variable on statistical error and confidence is illustrated in Fig. 6. The top curve is the statistical confidence as a function of the number of observations per test variable, with the number of observations and the corresponding statistical confidence (as a percent) also shown in parentheses. The bottom curve is the statistical error, which was generated for three magnitudes of variability in the data. For large numbers of

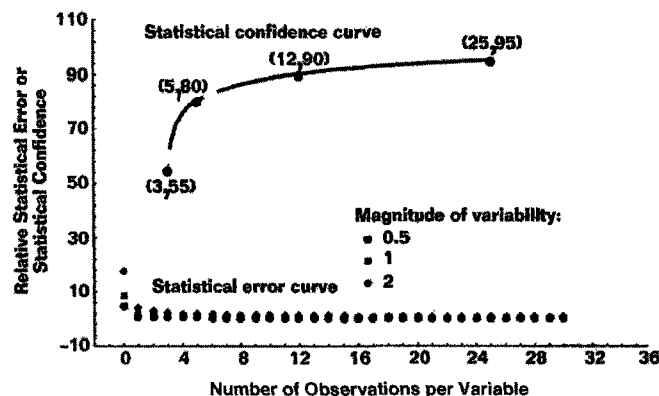


FIG. 6—Statistical confidence and statistical error curves as a function of the number of observations per test variable [42]. © Copyright 2001 by NACE International. All rights reserved by NACE; reprinted by permission.

observations per variable, confidence in the results is high and the error is small regardless of the variability. For small numbers of observations per variable, the confidence decreases substantially and is sensitive to the number of observations taken. With only three observations per variable, the level of confidence is only 55 %, corresponding to a risk level of 45 %, i.e., a 45 % risk that the wrong conclusion may have been reached about corrosion performance or service life. When resources permit, some statisticians recommend 12–18 observations per variable corresponding to 90–93 % confidence in the data, or a 10–7 % level of risk [42].

### Curve Fitting and Simple Statistical Modeling

Often a relationship is sought between corrosion performance and some controllable variable, such as exposure time. Random error can produce enough scatter in the data to make visual curve fitting imprecise. What is desired is the best data fit. One way used frequently to accomplish a good fit is to use regression analysis to minimize the sum of the square of the data deviations about the fitted curve. This is the “method of least squares.” Many physical relationships are not linear functions. For example,

$$\text{logarithmic} \quad y = a + b \ln X \quad (1)$$

$$\text{exponential} \quad y = be^{ax} \quad (2)$$

$$\text{power} \quad y = bX^a \quad (3)$$

However, they can be put in linear form by data transformation. Fitting these functions by least squares is not necessarily straightforward, but fortunately there are user-friendly curve fitting software utilities included with most major spreadsheets and statistical packages that will find the best fit for these and other functions.

Another method is to use a polynomial in the independent variable and then use multiple linear regression, considering each power of the independent variable in the polynomial as a separate linear variable. Powers of a single independent variable can be used to fit a complex curve in two dimensions (Eq 4). For example, many growth processes in



nature, when charted over time, will tend to follow a sinusoidal curve as they transition from one state of equilibrium to another. This can be approximated using a third-order polynomial regression with one independent variable. With two independent variables, a complex surface can be fit in three dimensions. A second order example with two independent variables is given in Eq 5 and the approach can be extended to third and higher order models.

$$y = a + b_1X + b_{11}X^2 + b_{111}X^3 + \dots + b_{111\dots1}X^k \quad (4)$$

$$y = a + b_1X_1 + b_2X_2 + b_{11}X_1^2 + b_{22}X_2^2 + b_{12}X_1X_2 \quad (5)$$

An estimate for a multiplicative model (Eq 6) can be obtained through simple log transformations as shown in Eq 7.

$$y = aX_1^{b_1}X_2^{b_2}X_3^{b_3} \quad (6)$$

$$\ln y = \ln a + b_1 \ln X_1 + b_2 \ln X_2 + b_3 \ln X_3 \quad (7)$$

Each of these approaches will yield a best fit based on the criterion of least squares. A standard measure to express this is the coefficient of determination,  $R^2$ .  $R^2$  has a range from 0 to 1 and can be expressed as the ratio:

$$R^2 = 1 - SSE/SST \quad (8)$$

where:

$SST$  = sum of squared deviations of  $y$  from the mean of  $y$ .

$SSE$  = sum of squared deviations of  $y$  from the fitted curve or trend line.

However, in interpreting  $R^2$  and especially in comparing  $R^2$  values, it is important to keep in mind that a perfect fit can always be obtained with a sufficiently complex curve. An alternative is the "adjusted  $R^2$ ," which is a more realistic measure of goodness of fit and expressed as:

$$\text{Adjusted } R^2 = 1 - (n-1/n-p)SSE/SST \quad (9)$$

where  $n$  is the number of observations and  $p$  represents the number of predictors in the regression equation. Note that if  $p$  is greater than 1, the "adjusted  $R^2$ " will always be smaller than  $R^2$ .

## Designing Experiments

In statistical terms, the primary goal of an experimental design is to introduce controls that eliminate or significantly reduce statistical dependence between the factor of interest and other factors that might influence the test outcome or dependent variable. To illustrate, consider three variables:  $X$ ,  $Y$ , and  $Z$ .  $X$  is an experimental factor,  $Y$  is a test outcome measure or dependent variable, and  $Z$  is an independent variable that is correlated with both  $Y$  and  $X$ . For example, in atmospheric corrosion, the corrosion rate ( $Y$ ) is influenced by both temperature ( $X$ ) and rainfall ( $Z$ ). However, a wet season will also tend to be a cool one in the natural environment, so temperature and rainfall will be correlated, or confounded.

Controlling  $Z$  makes it possible to assess the influence that  $X$  and only  $X$  has on  $Y$ .  $Z$  is effectively controlled

**FIG. 7—Cyclic polarization curves from six nominally identical samples of UNS C10920 copper exposed to a high viscosity, high pH solution [42]. © Copyright 2001 by NACE International. All rights reserved by NACE; reprinted by permission.**

whenever  $X$  and  $Z$  can be made *statistically independent*, and this can be accomplished in a variety of ways. Referring back to the previous example, atmospheric corrosion experiments can be conducted in chambers, where both temperature and moisture (rainfall) can be controlled completely and independently, or experiments can be conducted in a climate where moisture does not vary significantly compared to temperature.

An experiment in which all other relevant variables are held constant is an effective approach when it can be achieved. However, all relevant factors may not be known. Furthermore, circumstances often preclude the ability to hold some variables constant. For example, there may be unforeseen factors that affect the course of a corrosion experiment, as in the polarization curves in Fig. 7 for nominally identical samples of copper (UNS C10920). Most of the curves indicate the copper will actively corrode in the solution. However, one curve indicates the copper will passivate over a narrow range of potentials. Had a structure or device been built based on the passive curve it would have failed unexpectedly. Fortunately, enough replicate curves were measured to show that the passive curve was the exception [42].

**Completely Randomized Designs**—The concept of randomization was discussed above in relation to probability sampling, and also with regard to two sample tests. Given sufficient sample size, random assignment of observations to two or more groups will tend to result in statistical independence between the groups. The larger the groups, the better the approximation to perfect statistical independence.

As an example, reinforced concrete slabs are prepared for an experiment to compare effectiveness of arc-sprayed zinc and titanium anodes. All the slabs will be put under impressed current cathodic protection, and exposed to controlled applications of chloride to the concrete to promote corrosion of the reinforcing bar. Slabs are assigned randomly to be coated with either arc-sprayed zinc or titanium. In this case, randomization is a desirable precaution to control small inconsistencies due to mixing of the concrete, the chemical composition of the concrete, or the distribution of aggregate in the concrete.

An important advantage of randomization is that it will effectively control not only factors that are known, but also factors that are not known. Consequently, randomization is particularly useful in studies where no well-developed knowledge base exists. The primary disadvantage of a completely randomized design is that, other things being equal, it requires more cases than other designs. In determining the required number of test cases for a completely randomized design, the same considerations apply that were discussed earlier in this chapter under "Probability sampling and randomization."

**Factorial Designs**—Sometimes more than one treatment variable is of interest in an experiment. Whenever an experiment involves the manipulation of two treatments, it is referred to as a factorial design. For example one might wish to test the effects of a chemical wetting agent on the conductivity of concrete at varying levels of relative humidity. A full factorial design involves testing all combinations of two or more treatment factors. A fractional factorial study excludes some treatment combinations [43].

**Block Designs**—As noted already, the primary disadvantage of a randomized design is the number of observations that may be required to effectively control other factors. The number of required observations can often be reduced through blocking. Blocking can be applied to single factor or multi-factor studies. Variables may be incorporated as blocking factors or as additional treatment factors. A treatment factor is usually part of the primary focus of an experiment, while a blocking factor is more typically a "nuisance" factor to be controlled. More important, a treatment factor is manipulated directly by the corrosionist, while a blocking factor is controlled indirectly through selection and organization of observations.

Consider the simplest case for blocking in which one particular independent variable is known to have a strong statistical relationship (correlation) with the dependent variable in an experiment. Observations can be sorted on that independent variable and formed into homogeneous groups. Treatments are then conducted within each of these homogeneous groupings of the blocking variable. Blocking effectively holds the criterion variable constant within blocks, and therefore the treatments will be statistically independent of the blocking variable. Also, because the blocking variable is known to be correlated with the dependent variable, blocking will reduce the variance of the dependent variable within blocks. It is this latter consequence of blocking that improves efficiency over a fully randomized design.

More than one variable can be used as blocking criteria, but adding blocking criteria increases the number of blocks, and this compounds the number of times an experiment must be replicated. Consider an experiment in which a treatment is administered at six levels. Consider further that two blocking factors have been selected, and that each of these has six levels. The minimum required cases for a randomized block design is  $6 \times 6 \times 6 = 216$ .

To illustrate randomized block designs, consider the following example: an experiment is conducted to test the effectiveness of two humectants (wetting agents) on the operation of impressed current cathodic protection systems on reinforced concrete bridges. There are 120 reinforced

concrete test slabs left over from other experiments, and we will assume for the purpose of illustration that they are suitable for use in this new test. The test slabs have been coated with either a carbon, titanium, or zinc anode, and as a result of a previous experiment they have been electrochemically aged to simulate in-service lives ranging from 0–20 years.

Conceptually, the simplest design would involve using all 120 test slabs in the experiment, and randomly assigning the slabs to three groups, one for each humectant, and one to serve as a control group. This would constitute a simple randomized experiment. However, the efficiency of the experiment could be improved by using a randomized block design. This would involve, as a first step, specifying levels of each blocking factor to include in the experiment. In this instance there are the three "levels" of anode type. In addition, three age categories can be established representing: young (0–6 years), medium (7–13 years), and old (14–20 years) slab electrochemical age. The advantage introduced by blocking is that it assures that two variables known to be important (anode type and slab electrochemical age) are forced to be independent of the treatment. Also, by grouping the blocked factor, variance is reduced.

The next step would be to assign slabs to the blocks based on the three levels of treatment (and control). Assignment should be random within the nine blocks defined by anode electrochemical age and anode type. A random process would assign three slabs within each of the nine blocks to the three levels of treatment/control; remaining slabs would be dropped from the experiment. This process requires only  $3 (\text{anode type}) \times 3 (\text{anode age}) \times 3 (\text{treatment/control}) = 27$  slabs. Organization of the experiment is described in Table 3.

This is the minimum number of slabs required for the experimental design. In some cases it might be advisable to include replications within blocks. The purpose of replications would be to preclude unanticipated attrition (e.g., a test accident) or to control unidentified variables through randomization. If the experimenter is confident that no uncontrolled or unidentified variables are present, there is no need for replications within blocks.

By using a randomized block design the number of test specimens was reduced from 120 to 27. However, to do so required some assumptions. One assumption was that no unidentified or uncontrolled variables were present to confound the experiment; hence there was no benefit in including replications within blocks. The second was that the factors used in blocking were in fact correlated with the treatment; if not, nothing was gained through blocking.

To improve the efficiency of the experiment even further one could go to an incomplete block design. An incomplete block design does not run all treatments in all blocks. The most extreme case is the Latin square design. In a Latin

TABLE 3—A randomized block experiment.<sup>a</sup>

Electrochemical Age	Anode Type		
	Carbon	Titanium	Zinc
Young	A <sub>11</sub> , B <sub>11</sub> , C <sub>11</sub>	A <sub>21</sub> , B <sub>21</sub> , C <sub>21</sub>	A <sub>31</sub> , B <sub>31</sub> , C <sub>31</sub>
Medium	A <sub>12</sub> , B <sub>12</sub> , C <sub>12</sub>	A <sub>22</sub> , B <sub>22</sub> , C <sub>22</sub>	A <sub>32</sub> , B <sub>32</sub> , C <sub>32</sub>
Old	A <sub>13</sub> , B <sub>13</sub> , C <sub>13</sub>	A <sub>23</sub> , B <sub>23</sub> , C <sub>23</sub>	A <sub>33</sub> , B <sub>33</sub> , C <sub>33</sub>

<sup>a</sup>A, B, and C represent humectant treatments.

**TABLE 4**—A Latin square design.<sup>a</sup>

Electrochemical Age	Anode Type		
	Carbon	Zinc	Titanium
Young	B <sub>11</sub>	A <sub>21</sub>	C <sub>31</sub>
Medium	A <sub>12</sub>	C <sub>22</sub>	B <sub>32</sub>
Old	C <sub>13</sub>	B <sub>23</sub>	A <sub>33</sub>

<sup>a</sup>A, B, and C represent humectant treatments.

square design each level of each blocking factor receives each treatment just once, as in Table 4. However, note that each row and each column contains all three treatments. The primary advantage of a Latin square is that the experiment can be conducted with nine specimens. One important disadvantage is that a Latin square requires two blocking factors, and both blocking factors, along with the treatment factor must have the same number of levels. However, the main disadvantage of a Latin square, and to some extent all incomplete block designs, is that interactions are confounded. For instance, suppose that the different humectant treatments affect the anodes very differently. What is actually an interaction between anode type and the treatment, would be impossible to disentangle from the effects of anode age.

### Statistical Tests for Experiments

In a statistically designed corrosion experiment the goal is to infer a cause and effect relationship between a treatment variable and a dependent variable. By whatever means this is achieved, there is an implicit assumption that, except for the treatment itself, there is an equivalence between the sample of units that received a treatment and the sample (controls) that did not. In statistical analysis of results from experiments, all tests start with this assumption of equivalence between or among groups in all regards except for the factors being tested. Experimental designs are intended to assure, or at least approximate, conditions that make that assumption credible.

The simplest category of testing in an experimental design is the two-sample test. There are a number of nonparametric tests that are appropriate for comparisons of two groups. The most familiar is the two-sample Chi square ( $\chi^2$ ) test, but there is also Fisher's Exact Test, the median test, Mann and Whitney's U, and many others [44]. Nonparametric tests are usually applicable when the dependent variable is categorical, but whenever the dependent variable will support computation of a mean, the most typical test to be applied is the difference of means test. If two groups are created through random assignment from a common pool, differences can be expected to be attributable to either sampling error or some external influence occurring subsequent to assignment. By effectively ruling out chance on the basis of probability, one is left with the implication that some factor subsequent to assignment accounts for the difference. In a well-designed experiment, the only possible candidate should be the treatment factor.

This same basic approach can be extended to any of the experimental designs discussed above using analysis of variance (ANOVA). ANOVA was developed early in the 1920s by the British statistician, R. A. Fischer, to apply statistical methods to agricultural experiments. In fact, the

F ratio is named for R. A. Fischer [41]. The simplest extension involves comparisons of three or more groups. Another involves introduction of more than one factor. Also, it should be noted that whenever more than one factor is included in an experiment, it becomes possible to test for interaction effects. Interaction refers to a situation in which the effects of two variables are nonadditive, or that the effect of one variable depends on the level of a second variable.

Analysis of variance becomes more complicated with more complex designs. It is often the case with incomplete block and fractional factorial designs that some or all interactions cannot be tested. In the case of more complex designs, it is advisable to consult an experienced statistician for assistance, both in the design of the experiment and in setting up the analysis.

### DEVELOP TEST PROTOCOL

A test protocol transforms the corrosion test design into a set of reliable and reproducible measurements that achieve the goals and objectives of the test. The test protocol may simply be a guide or "road map" to the raw or uninterpreted measurements defining methods and standards. When measurements must meet legal, regulatory, or customer challenges, the test protocol may be codified into a quality assurance (QA) plan [45,46]. The test protocol typically specifies criteria for precision, accuracy, completeness, representativeness, and comparability of the corrosion and related measurements. It can address sampling and analytical procedures, calibration procedures and standards, data reduction and processing methods, data validation, data reporting, and data audits.

Many of the measurements involved in corrosion tests are defined in standards to establish precision, accuracy, representativeness, and comparability [10–14]. Analytical techniques and measurements used to characterize the environment and corrosion product chemistry, and to evaluate coatings properties and inhibitor performance, are largely covered by "good laboratory practices" standards [45]. In addition, the requirements for certain analytical and environmental measurements used in regulatory efforts have been established in the Code of Federal Regulations (CFR) [47]. The corrosionist should become familiar with and use these sources of information as they apply to the goals and objectives of the study. Table 5 lists some of the ASTM standards that are more widely used by corrosionists.

### ENGINEER TEST

Engineering the test assures that materials, equipment, instrumentation, personnel, and supporting services are available and used in a timely and effective manner. The test plan must be examined with a clear understanding of problems that may arise to thwart its successful completion. Critical supplies, equipment, and schedule steps must be identified; options developed; tasks simplified; resources allocated; and adequate time allotted. The cost and effort of this step is usually recouped in a more efficient, trouble-free corrosion test.

**TABLE 5**—Widely used ASTM corrosion and related standards [10–12].

Standard	Standard Title
G 1	Preparing, Cleaning, and Evaluating Corrosion Test Specimens
G 3	Conventions Applicable to Electrochemical Measurements in Corrosion Testing
G 4	Conducting Corrosion Coupon Tests in Plant Equipment
G 5	Making Potentiostatic and Potentiodynamic Anodic Polarization Measurements
G 15	Terminology Relating to Corrosion and Corrosion Testing
G 16	Applying Statistics to Analysis of Corrosion Data
G 31	Laboratory Immersion Corrosion Testing of Metals
G 38	Making and Using C-Ring Stress-Corrosion Test Specimens
G 40	Terminology Relating to Wear and Erosion
G 46	Examination and Evaluation of Pitting Corrosion
G 50	Conducting Atmospheric Corrosion Tests on Metals
G 57	Field Measurement of Soil Resistivity Using the Wenner Four-Electrode Method
G 59	Conducting Potentiodynamic Polarization Resistance Measurements
G 71	Conducting and Evaluating Galvanic Corrosion Tests in Electrolytes
G 82	Development and Use of a Galvanic Series for Predicting Galvanic Corrosion Performance
G 102	Calculation of Corrosion Rates and Related Information from Electrochemical Measurements
G 119	Determining Synergism Between Wear and Corrosion
C 876	Half Cell Potentials of Uncoated Reinforcing Steel in Concrete
E 380	Use of the International System (SI) of Units
E 527	Numbering Metals and Alloys

Pilot plant and service tests may be more vulnerable to unforeseen difficulties as a consequence of constraints and demands from external technical and nontechnical sources. Laboratory tests avoid some of these difficulties because there is usually more flexibility in the allocation of supplies and equipment and in the scheduling of personnel. Certain common sense practices can improve laboratory, pilot plant, and service tests. Use good quality water for the preparation of aqueous solutions (systems are available at reasonable cost that routinely supply Type 1 water) (see ASTM D 1193, Specification for Reagent Water, part 9). Provide regulated and filter power for operating critical electronic instruments and computers. Establish a well-defined ground system for test equipment.

Support personnel provide a valuable base of additional experience and often serve as assistants to the investigator. To use support personnel effectively, they must understand the goals and objectives of the test, have adequate training, and clearly understand their role and responsibilities.

## MODIFY TEST

Test plan execution is the point where the corrosionist must cope with changes that affect resource allocation, personnel schedules, and goals and objectives. These changes may alter the test design, the nature of the results, and the analysis and interpretation of results. Even when external factors cause no changes, the investigator should examine data early in the test, incomplete as they may be, to ensure that the results will meet the goals and objectives of the test while time and resources may exist to modify the plan.

Many changes can be anticipated and their impact on the test plan minimized. Changes arise in the planning and design stage through interactions with others who manage, operate, oversee, study, maintain, or fund related technical areas. Changes that cannot be anticipated have a more significant impact on the plan. These can range from loss of personnel, damaged equipment, vandalism, major changes

in the corrosive environment, lost or damaged corrosion samples, or loss or failure of monitoring capability.

Comparing test results with the goals and objectives of the test is the clearest measure of the success of the test. In this way, opportunities to improve the test by revising its design, exploiting scientific and technological advances, and considering new or additional information can be achieved.

## SUMMARY

Corrosion tests provide information about materials and their applications that have an important effect on the economic vitality and quality of life. An overview of the key steps in planning and designing corrosion tests includes identifying goals and objectives, developing a test design using statistical and economic analysis, establishing the protocol for reliable and reproducible measurements, efficiently engineering the corrosion test with limited resources, and coping with modifications to the test plan.

## REFERENCES

- [1] "Corrosion Costs and Preventive Strategies in the United States," in a supplement to *Materials Performance*, NACE International, Houston, TX, July 2002, 11 pp.
- [2] Virmani, Y. P., "Corrosion Costs and Preventive Strategies in the United States," Tech Brief, FHWA-RD-01-157, Federal Highway Administration, U.S. Department of Transportation, Washington, DC, March 2002.
- [3] Koch, G. H., Brongers, M. P. H., Thompson, N. G., Virmani, Y. P., and Payer, J. H., "Corrosion Cost and Preventive Strategies in the United States," FHWA-RD-156, Federal Highway Administration, U.S. Department of Transportation, Washington, DC, March 2002.
- [4] Spahn, H., "Corrosion Control for Low-Cost Reliability," *Proceedings of 12th International Corrosion Congress*, NACE International, September 1993, Plenary 4–19.
- [5] Ailor, W. H., *Handbook on Corrosion Testing and Evaluation*, John Wiley and Sons, New York, 1971, pp. 1–112.

- [6] Dean, S. W., Jr., *Atmospheric Corrosion*, W. H. Ailor, Ed., John Wiley and Sons, New York, 1982, pp. 195–216.
- [7] Sprowls, D. O., *Corrosion*, ASM Metals Handbook, Vol. 13, 9th ed., ASM International, Metals Park, OH, 1987, pp. 193–196 and pp. 316–317.
- [8] Fontana, M. G. and Greene, N. D., *Corrosion Engineering*, McGraw-Hill, NY, 1978.
- [9] Haynes, G. S. and Baboian, R., *Laboratory Corrosion Tests and Standards*, ASTM STP 866, ASTM International, West Conshohocken, PA, 1985.
- [10] "American Society for Testing and Materials, Wear and Erosion; Metal Corrosion," *Annual Book of ASTM Standards*, Vol. 03.02, ASTM International, West Conshohocken, PA, 1993.
- [11] "American Society for Testing and Materials, General Methods and Instrumentation," *Annual Book of ASTM Standards*, Vol. 14.02, ASTM International, West Conshohocken, PA, 1993.
- [12] ASTM International, 100 Barr Harbor Drive, West Conshohocken PA 19428-2959; see also <http://www.astm.org/>; make the following selections: ASTM Store; Search for individual standards; ASTM Designation only – Search for "corrosion."
- [13] NACE International, 1440 South Creek Drive, Houston TX 77084-4906; see also NACE Standards at <http://www.nace.org/nace/content/nacesecondstandards.cfm>.
- [14] International Organization for Standardization (International Standards Organization, ISO), 1, rue de Varembé, Case postale 56, CH-1211 Geneva 20, Switzerland; see also <http://www.iso.ch/iso/en/ISOOnline.opennerpage>. Make the following selections: International Standards; ICS field 77 (Metallurgy); 77.060 (Corrosion of Metals).
- [15] Rak, G. F., "The Corrosion Professional's Role in a Regulated and Litigious Environment," *Materials Performance*, Vol. 40, No. 5, 2001, pp. 18–21.
- [16] Verink, E. D., Koltz, J., Rumble, J., and Ugiansky, G. N., "Corrosion Data Program Workshop Summary," *Materials Performance*, Vol. 26, No. 4, 1987, pp. 55–60.
- [17] Mansfeld, F. and Bertocci, U., *Electrochemical Corrosion Testing*, ASTM STP 727, ASTM International, West Conshohocken, PA, 1981.
- [18] Geef, R., Peat, R., Peter, L. M., et al., *Instrumental Methods in Electrochemistry*, John Wiley and Sons, NY, 1985.
- [19] *Electrochemical Impedance: Analysis and Interpretation*, ASTM STP 1188, J. R. Scully, D. C. Silverman, and M. W. Kendig, Eds., ASTM International, West Conshohocken, PA, 1993.
- [20] Bard, A. J. and Faulkner, L. R., *Electrochemical Methods*, John Wiley and Sons, NY, 1980.
- [21] Pourbaix, M., *Atlas of Electrochemical Equilibria in Aqueous Solutions*, NACE International, Houston, TX, 1974.
- [22] Frankenthal, R. P. and Kruger, J., *Equilibrium Diagrams—Localized Corrosion*, Electrochemical Society, Pennington, NJ, 1984.
- [23] Chen, C. M., Aral, K., and Theus, G. J., *Computer-Calculated Potential pH Diagrams to 300 °C*, Vol. 2, EPRI NP-3137, Electric Power Research Institute, Palo Alto, CA, 1983.
- [24] Shreir, L. L., Jarman, R. A., and Burstein, G. T., Eds., *Corrosion: Metal/Environmental Reactions*, Vol. 1, 3rd ed., Butterworth/Heinemann, Oxford, U.K., 1994.
- [25] *Uhlig's Corrosion Handbook*, 2nd edition, R. W. Revie, Ed., Wiley, NY, 2000.
- [26] McElvily, A. J., Jr., *Atlas of Stress-Corrosion and Corrosion Fatigue Curves*, ASM International, Materials Park, OH, 1990.
- [27] Schlain, D., *Corrosion Properties of Titanium and Its Alloys*, Bulletin 619, U.S. Bureau of Mines, 1964.
- [28] *Corrosion in Sulfuric Acid*, Symposium Proceedings, CORROSION/85, NACE International, Houston, TX, 1985.
- [29] *Corrosion Rates of Steel in Concrete*, ASTM STP 1065, N. S. Berke, V. Chaker, and D. Whiting, Eds., ASTM International, West Conshohocken, PA, 1990.
- [30] *Effects of Soil Characteristics on Corrosion*, ASTM STP 1013, V. Chaker and J. D. Palmer, Eds., ASTM International, West Conshohocken, PA, 1989.
- [31] *Corrosion*, ASM Metals Handbook, Vol. 13, 9th ed., ASM International, Metals Park, OH, 1987, pp. 377–1367.
- [32] Mansfeld, F., *Corrosion Mechanisms*, Marcel Dekker, NY, 1987.
- [33] Szklarska-Smialowska, Z., *Pitting Corrosion of Metals*, NACE International, Houston, TX, 1986.
- [34] Baloun, C. H., *Corrosion*, Metals Handbook, Vol. 13, 9th ed., ASM International, Materials Park, OH, 1987, p. 207.
- [35] Corbett, R. A. and Saldanha, B. H., *Corrosion*, Metals Handbook, Vol. 13, 9th ed., ASM International, Materials Park, OH, 1987, pp. 239–240.
- [36] King, G. A., "Corrosivity Mapping—A Sensitive and Cost Effective Means of Characterizing a Region's Level of Atmospheric Corrosion," Paper 93638, CORROSION/93, NACE International, Houston, TX, 1993.
- [37] Spence, J. W., Haynie, F. H., Lipfert, F. W., et al., "Atmospheric Corrosion Model for Galvanized Steel Structures," *Corrosion*, Vol. 48, No. 12, 1992, pp. 1009–1019.
- [38] Graedel, T. E., Nassau, K., Franey, J. P., et al., "Copper Patina Formation," *Corrosion Science*, Vol. 27, No. 7, 1987, pp. 639–782.
- [39] Cramer, S. D., Matthes, S. A., Covino, B. S., Jr., Bullard, S. J., and Holcomb, G. R., "Environmental Factors Affecting the Atmospheric Corrosion of Copper," *Outdoor and Indoor Atmospheric Corrosion*, ASTM STP 1421, H. E. Townsend, Ed., ASTM International, West Conshohocken, PA, 2002, pp. 245–264.
- [40] Cramer, S. D., Matthes, S. A., Holcomb, G. R., Covino, B. S., Jr., and Bullard, S. J., "Precipitation Runoff and Atmospheric Corrosion," Paper No. 00452, CORROSION/2000, NACE International, Houston TX, 2000.
- [41] Snedecor, G. and Cochran, W., *Statistical Methods*, Eighth ed., Iowa State University Press, Ames, Iowa, 1989.
- [42] Tait, W. S., "Increase Your Confidence in Corrosion Test Data," *Materials Performance*, NACE International, Houston TX, Vol. 40, No. 3, 2001, pp. 58–61.
- [43] Neter, J., Kutner, M., Nachtsheim, C., and Wasserman, W., *Applied Linear Statistical Models*, 4th ed., McGraw-Hill, Boston, 1996, pp. 795–797.
- [44] Siegel, S., Chapters 5 and 6, *Nonparametric Statistics for the Behavioral Sciences*, McGraw-Hill Book Company, NY, 1956.
- [45] Garner, W. Y., Barge, M. S., and Ussary, J. P., *Good Laboratory Practice Standards*, American Chemical Society, Washington, DC, 1992.
- [46] Ratliff, T. A., Jr., *The Laboratory Quality Assurance System*, Van Nostrand Reinhold, NY, 1990.
- [47] *Code of Federal Regulations*, U.S. Government Printing Office, Office of the Federal Register, National Archives and Records Service, General Services Administration, Washington, DC, 1993.

# Types of Data

David C. Silverman<sup>1</sup>

CORROSION TESTS ARE performed to provide information on material degradation in specific environments, information that is not available from other sources. Corrosion testing can be divided into two broad categories, electrochemical and nonelectrochemical. Within these categories, test results are presented in a number of ways, ranging from numerical output to qualitative examination of the test specimen. Both types of data are represented in each category. A very complete listing of data formats for collection and compilation for computerized databases is presented in ASTM G 107, Guide for Formats for Collection and Compilation of Corrosion Data for Metals for Computerized Database Input. The information in that standard includes a significant portion of the type of test data that might be recorded during corrosion testing. Since required data are test-dependent, not every test would include all of the data listed, but the standard does provide a reasonable, first pass checklist and should be used to ensure that needed information is not overlooked.

The purpose of this chapter is to provide an overview of types of corrosion data for metals and alloys that might be obtained from or be relevant to different types of corrosion tests. The examples discussed are not meant to be all-inclusive. They are meant to provide a flavor of the types of data that might be recorded. The reader is strongly encouraged to refer to the references and cited standards for a more complete discussion of the types of data relevant to the test discussed.

## ELECTROCHEMICAL TEST DATA

The main variables that are measured in an electrochemical test are the voltage and the current. The goal is to translate this information into a corrosion rate or some other information that describes the corrosion process. ASTM G 3, Practice for Conventions Applicable to Electrochemical Measurements in Corrosion Testing, provides guidelines for conventions for reporting a myriad of electrochemical data for the more common tests.

### Potential

One very common electrochemical measurement is the corrosion potential. This potential is the voltage of the corroding

electrode measured at open circuit in an electrolyte. The voltage is measured relative to a reference electrode. For example, ASTM G 69, Practice for Measurement of Corrosion Potentials of Aluminum Alloys, describes how to measure the corrosion potential of aluminum alloys, and ASTM G 82, Guide for Development and Use of a Galvanic Series for Predicting Galvanic Corrosion Performance, describes the development and use of a practical galvanic series for predicting relative corrosion performance. Very often, the attempt is made to relate the measured potential to potentials calculated from thermodynamic data, e.g., as presented in Pourbaix Diagrams [1], in order to understand better the corrosion mechanism. One reason this approach requires caution is that the measured corrosion potential is at best a steady state potential in which reactions are not at equilibrium and the potential on the Pourbaix diagram is a thermodynamic or equilibrium potential.

Confusion sometimes exists with the sign convention when reporting voltage with respect to the reference electrode. The thermodynamic electrochemical potential of a reaction written as oxidizing ( $M \rightarrow M^{n+} + ne^-$ , where  $M$  is the metal and  $e^-$  is the electron) has the opposite sign as when the same reaction is written as reducing ( $M^{n+} + ne^- \rightarrow M$ ). The recommended approach is to use the Stockholm sign invariant convention. In this convention, the positive direction (increasing potential) implies increasingly oxidizing conditions at the electrode surface (noble). The negative direction (decreasing potential) implies increasingly reducing conditions at the electrode surface (active). For example, the potential of the gold couple with its ion would be more positive than the couple of zinc with its ion. Care must be taken when recording the potential of a specimen in an electrolyte relative to a reference electrode so that the recorded potentials are consistent with this convention. One can always make sure that the connection is correct, i.e., the leads are hooked up properly, by checking against a known couple (see ASTM G 3).

### Current or Current Density

Measurement of current or current density is the most common output of electrochemical corrosion tests. This quantity is usually related either to the corrosion rate or to some features of the corrosion process, such as surface redox reactions that can change the corrosion characteristics. The relationship between the measured current and the corrosion rate or mechanism depends to some degree on

<sup>1</sup>Principal Consultant, Argentum Solutions, Inc., 14314 Strawbridge Ct., Chesterfield, MO 63017, e-mail: dcsilverman@argentumsolutions.com, web site: www.argentumsolutions.com.

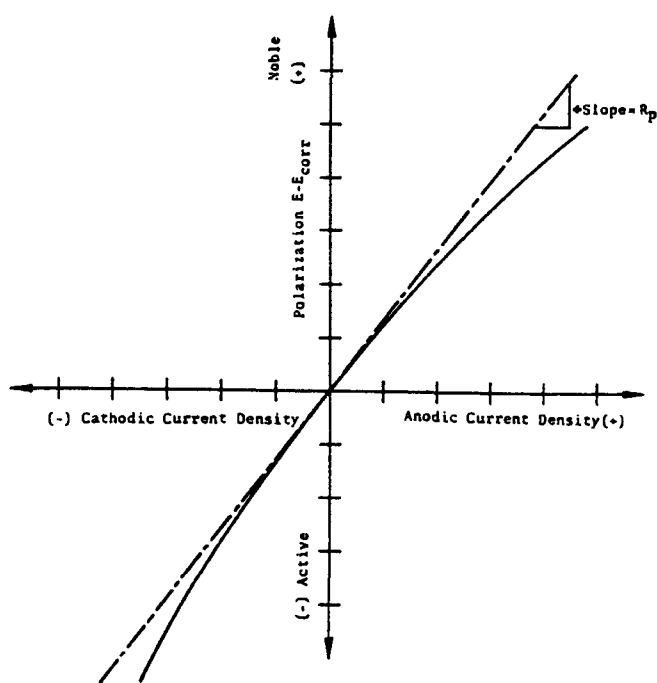


FIG. 1—Hypothetical polarization resistance or linear polarization plot (from ASTM G 3).

the technique used to obtain the current. The type of data obtained and the format by which the information is displayed depend on the test. Some tests display voltage versus current, others display voltage versus the logarithm of the current, others display information about the impedance (voltage divided by the current), and others examine fluctuations in the current around some average value. These different types of current data have different uses and may require additional types of data or analysis programs to translate the data into usable information.

Polarization resistance or linear polarization measurements are used to determine the polarization resistance, a quantity related to the corrosion rate. Current is measured as a function of voltage in the vicinity of the corrosion potential. The two values are plotted as voltage versus current. The polarization resistance is the slope of the curve at the corrosion potential. The importance of this quantity lies in the fact that it is (usually) inversely proportional to the corrosion current, the proportionality constant being related to the Tafel slopes. ASTM G 59, Practice for Conducting Potentiodynamic Polarization Resistance Measurements, describes a method by which these measurements are made and the polarization resistance is calculated. Figure 1 shows a hypothetical plot as a function of current. A very extensive discussion of the historical development, theory and assumptions, and pitfalls provides an excellent background to ASTM G 59 [2]. Additional experimental artifacts have also been discussed [3].

Data in addition to the slope as estimated from a curve, such as in Fig. 1, are required when calculating the corrosion rate from polarization resistance measurements. ASTM G 102, Practice for Calculation of Corrosion Rates and

Related Information from Electrochemical Measurements, provides the methodology and equations. The method is summarized as follows. The slope actually contains contributions from the polarization resistance (shown) and the uncompensated resistance. The latter term contains several contributions, two of which are the electrical resistance in the solution between the reference electrode sensing point and the working electrode and the electrical resistance of the leads and measuring circuit. This uncompensated solution resistance must be subtracted from the resistance calculated from the slope to obtain the actual polarization resistance. The corrosion current is estimated from this corrected value. The procedure is to divide the Stern Geary constant by the polarization resistance. ASTM G 102 and Refs 2 and 3 provide details on how the Stern Geary constant might be estimated. If the current measurement is in current, e.g., amp, and not current per unit area of working electrode, e.g., amp/cm<sup>2</sup>, the corrosion current density is estimated from the corrosion current by dividing it by the exposed specimen surface area. The specimen area must be measured. Finally, the corrosion rate as a mass loss is obtained from the corrosion current density. The corrosion current density is divided by the density of the alloy and is multiplied by the alloy equivalent weight and a constant to obtain the corrosion rate in the proper units. The alloy equivalent weight is the reciprocal of the sum taken over all of the elements in the alloy of the valence of the element times its mass fraction divided by its atomic weight. The reader is referred to ASTM G 102 for the details and justification of using the alloy equivalent weight. Thus, more information than that in Fig. 1 is needed for the corrosion rate to be estimated from polarization resistance measurements.

A second type of presentation of current is as the plot of voltage versus logarithm of the current density (current divided by the surface area). ASTM G 5, Standard Reference Test Method for Making Potentiostatic and Potentiodynamic Anodic Polarization Measurements, and ASTM G 61, Test Method for Conducting Cyclic Potentiodynamic Polarization

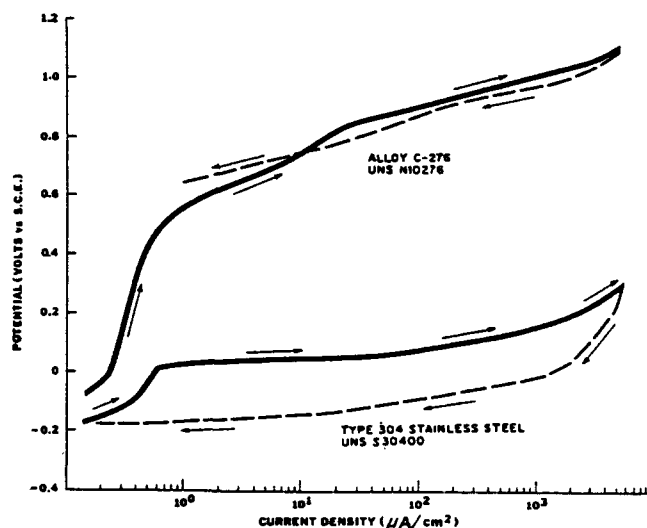


FIG. 2—Representative cyclic potentiodynamic polarization curves (from ASTM G 61).

Measurements for Localized Corrosion Susceptibility of Iron-, Nickel-, or Cobalt-based Alloys, show examples of these types of plots. They are generated by ramping the voltage at a preset rate in the anodic direction with respect to the corrosion potential. Sometimes, the voltage ramp is then reversed so that the potential is driven at a slow rate back to the corrosion potential. This procedure of using a forward and reverse ramp of voltage is called cyclic potentiodynamic polarization. Figure 2 shows an example of a cyclic potentiodynamic polarization scan. One of the purposes of performing this type of experiment and presenting the data in this manner is to estimate the susceptibility of an alloy to undergo localized corrosion in the form of crevice corrosion and pitting. Certain relationships among “characteristic” voltages, e.g., the difference between the “repassivation potential” and the corrosion potential and the difference between the “pitting potential” and the corrosion potential, as well as other features related to the current, can be used to make a judgment about corrosion [4]. Both quantitative and qualitative information constitute the data that are used to interpret the polarization scan.

The electrochemical reactivation technique provides a different way of presenting and using current (see ASTM G 108, Test Method for Electrochemical Reactivation (EPR) Test Method for Detecting Sensitization of AISI Type 304 and 304L Stainless Steels). This test, like the one above, involves a voltage ramp, but in this case, the voltage ramp is from the passive region of the alloy to the active region. The required test result is the integration of the current or the total charge passed. This charge is related to the degree of sensitization of the alloy. In this case, the charge is divided by both the surface area and often the average grain size so it, too, must be measured.

Coupling of dissimilar metals can create a current caused by the potential difference between the two alloys. Such galvanic currents are measured by a zero resistance ammeter placed in an external circuit that connects the two alloys immersed in an electrolyte (see ASTM G 71, Guide for Conducting and Evaluating Galvanic Corrosion Tests in Electrolytes). Sometimes, the current when divided by the surface area can be used to calculate the corrosion rate from Faraday's law. Often when using this type of test the coupled specimens have different surface areas so the surface area of each specimen is a type of data. If corrosion is localized on the alloy surfaces, however, conversion of current to a mass-loss based corrosion rate may not be meaningful.

## Impedance

Measurement of impedance of a corroding electrode has become important in corrosion prediction for such diverse applications as coatings and corrosion rate estimation in low conductivity media. As most commonly practiced, an electrode is subjected to a small amplitude (e.g., 5–10 mV) sinusoidal variation in the voltage of varying frequency, usually about the corrosion potential. The current is measured. The applied voltage is divided by this measured current. Since both the voltage and current have a sinusoidal component with respect to time and are usually out-of-phase, the division results in the impedance, which itself has real and imaginary contributions. Often, the current is

divided by the surface area, and the impedance has the units of ohm-cm<sup>2</sup>. Details are provided in ASTM G 106, Standard Practice for Verification of Algorithm and Equipment for Electrochemical Impedance Measurements. The impedance is usually plotted in one of two ways, as the inverse of the imaginary component versus the real component, as in Fig. 3a, or as a pair of plots in which the magnitude of the impedance and the inverse of the phase angle are plotted as function of the logarithm of the frequency, as in Figs. 3b and 3c (see ASTM G 106 and G 107).

A plethora of literature exists that discusses how to relate the structure of the impedance spectrum to the corrosion mechanism and corrosion rate. In the limit of zero frequency, the impedance becomes equal to the polarization resistance discussed above. Situations arise in which this value is not inversely related to the corrosion rate [5]. The reader is referred to two recent symposia on electrochemical impedance spectroscopy that provide excellent “snapshots” of the state of the art in determining corrosion rates and mechanisms from the impedance spectra and provide information on the additional types of data needed to make the connection [6,7]. In addition, Ref 3 provides an overview of practical applications of this technology, as well as those mentioned previously [3].

## Electrochemical Noise

The technique that has been labeled as electrochemical noise is the measurement and analysis of fluctuations in potential or current that arise from uncontrolled variations in a corrosion process. This technique has received much attention both for laboratory studies and on-line monitoring for localized corrosion (pitting, crevice corrosion, and stress corrosion cracking), coating degradation, and general corrosion [8]. Though no ASTM standard yet exists with respect to measurement procedure or analysis algorithm, a brief discussion of types of data associated with this technique is warranted because of the attention that this technique has received. The recorded data themselves are current and voltage recorded at constant time intervals. The method used to analyze the data points is as important as the data points themselves.

The methods used for expressing the data fall into two categories, time domain techniques and frequency domain techniques. The two methods are related because frequency and time are the reciprocals of each other. The analysis technique influences the data requirements. Reference 9 provides a brief overview of the various mathematical methods and a multitude of additional references. Specialized transforms (Fourier) can be used to transfer information between the two domains. Time domain measures include the normal statistical measures such as mean, variance, third moment, skewness, fourth moment, kurtosis, standard deviation, coefficient of variance, and root mean square as well as an additional parameter, the ratio of the standard deviation to the root mean square value of the current (when measuring current noise) used in place of the coefficient of variance because the mean could be zero. An additional time domain measure that can describe the degree of randomness is the autocorrelation function of the voltage or current signal. The main frequency domain



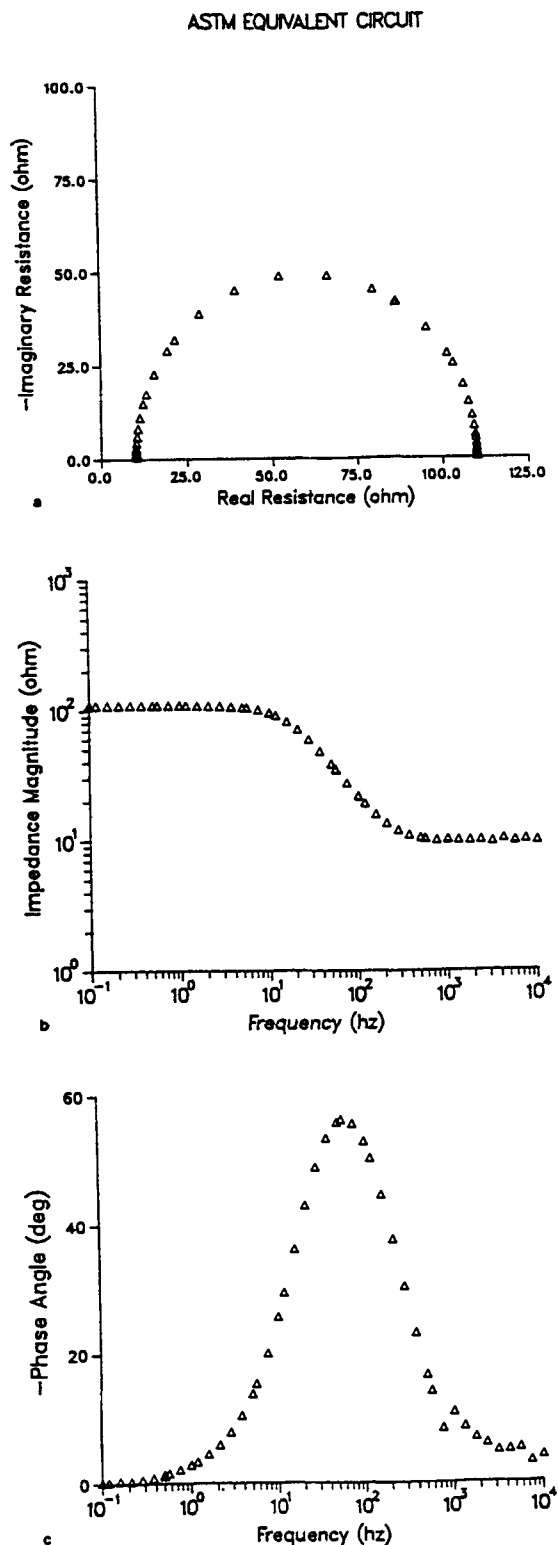


FIG. 3—Plot of electrochemical impedance spectrum in: (a) Nyquist format, inverse of the imaginary impedance versus real impedance; (b) Bode format, logarithm of the impedance magnitude versus logarithm of the frequency; (c) Bode format, inverse of the phase angle versus logarithm of the frequency (from ASTM G 106).

measure is the power spectral density of the corrosion potential noise or the current noise. The power spectrum is the Fourier Transform of the autocorrelation function and is the distribution of power of the signal in the frequency domain. The power spectral density is usually estimated by the Fast Fourier Transform algorithm or the maximum entropy algorithm. Another transform that is presently being investigated but has not found widespread use is the wavelet transform [10]. This transform has been proposed to overcome some of the shortcomings of the more traditional Fourier transform by using a family of basis functions that are localized in both the time and frequency domains. Debate remains as to which measures provide the most information, so all are found in the literature.

The types of data mentioned in the previous paragraph pertain to the results from analyzing fluctuations in either the voltage or current signal individually. One additional analysis is to divide the standard deviation of the voltage signal by the standard deviation of the current signal to obtain the noise resistance [11]. This parameter can be equivalent to the polarization resistance discussed in the previous section.

## NONELECTROCHEMICAL TEST DATA

Though a significant fraction of metallic corrosion involves electrochemical processes, much of corrosion testing involves techniques that do not have as the main goal the measurement of current or voltage. These techniques are used to examine a number of different forms of corrosion. Sometimes the data that result from the tests are quantitative. Sometimes the data are qualitative. Pictures of either the actual corroded sample or magnified portions of the corroded sample are often very useful and must be considered as types of data.

## Corrosion Rate from Mass Loss

The most common method for estimating the corrosion rate is from the mass loss of a metal specimen of known dimensions immersed in a fluid for a known amount of time. The weight of the specimen is obtained before and after the exposure. The corrosion rate is obtained by dividing by the exposed area, the time, and the density. The procedure is outlined in ASTM G 31, Practice for Laboratory Immersion Corrosion Testing of Metals. An example of a typical vessel for conducting such a test is shown in that standard. Different units exist for expressing the corrosion rate (mils/year for penetration rate or  $\text{mg}/\text{dm}^2/\text{day}$  for mass loss rate). Though a number of assumptions are made about the test and specimen when making this estimate, reasonably reliable values can be obtained when corrosion is not localized but extends reasonably uniformly across the specimen. Guidelines have been presented as to the error associated with measurements of weight, time, and surface area when these are the only sources of error [12].

In the case of rectangular panels or coupons, the area may be calculated from the exposed flat sides plus the four edges. Many investigators have chosen not to include the edge area, though its inclusion is fairly easily done. In the

case of a wire specimen, the exposed area decreases as corrosion proceeds. In order to take this effect into account, a somewhat different approach must be used to calculate the mass loss per unit area.

*Flat panel:*

$$A = 2lw + 2lt + 2wt \quad (1)$$

where

$l$  = length,  
 $w$  = width,  
 $t$  = thickness,  
 $A$  = exposed specimen area.

*Wire specimen radius loss:*

$$\Delta r = \frac{d_i}{2} \left[ 1 - \sqrt{\frac{m_f}{m_i}} \right] = \frac{d_i}{2} \left[ 1 - \sqrt{1 - \frac{\Delta m}{m_i}} \right] \quad (2)$$

$\Delta r$  = radius reduction from corrosion loss,  
 $d_i$  = initial diameter before exposure,  
 $m_i$  = initial mass,  
 $m_f$  = final mass after exposure,  
 $\Delta m$  = mass loss.

The specimen must be cleaned after exposure in order to obtain mass loss results. In many cases weighing the panel before cleaning is desirable so that an estimate of the corrosion product thickness or mass can be obtained. In some cases, removal of the corrosion products should be done nondestructively from at least a small area on some of the panels so that chemical analyses of the corrosion products may be carried out. Such removal may be done by scraping the surface or by using replicating tape. Replicating tape is not very effective in removing rust from steel specimens. ASTM G 1, Standard Practice for Preparing, Cleaning, and Evaluating Corrosion Test Specimens, provides additional information.

The laboratory immersion test in which a specimen is exposed for a period of time and then removed for examination assumes that the corrosion rate remains constant with time. This assumption is not completely valid, even if the environment remains static over the exposure time. The corrosion rate might decrease from a high rate during which passivation occurs or inhibitors adsorb, or the corrosion rate might increase as different kinetic processes establish themselves. When the amount of change is great, one might use a modified immersion test in which identical specimens are immersed for differing time periods in the same environment [13]. The mass loss, exposure time associated with that mass loss, and area are used to calculate the corrosion rate for each interval. By comparing the rates during the different time periods, one can judge if the corrosion rate is constant, increasing, or decreasing. Again, the types of data needed are time, mass, and dimensions, but the exposure intervals are shorter than the total time of the test.

## Localized Corrosion

Required data can sometimes be a mixture of qualitative observations and quantitative measurements that are combined to provide an overall picture of corrosion. As mentioned

above, certain features of the cyclic potentiodynamic polarization scan are used to estimate somewhat qualitatively the risk of localized corrosion in the form of pitting and crevice corrosion. Likewise, the results from coupon immersion tests used to estimate the risk of crevice corrosion and pitting also contain both types of information. In the case of crevice corrosion, a common procedure is to immerse a coupon upon which is mounted an artificial crevice former. ASTM G 78, Guide for Crevice Corrosion Testing of Iron-Base and Nickel-Base Stainless Alloys in Seawater and Other Chloride-Containing Aqueous Environments, describes a typical procedure. Typical observations include a recording of the general appearance of the specimen, its mass change, the maximum depth of corrosion in each crevice, the number of crevices that had attack under them, and the severity of that attack. A picture sometimes becomes part of the data. This information might be used to rank alloy performance in the environment either qualitatively or even semi-quantitatively.

Similar types of qualitative and quantitative data are also combined when examining pitting. When a specimen is exposed to an environment, the depths of pits are often measured. However, the relationship between such depth and a pitting growth rate is not straightforward because pits do not necessarily grow at a continuous rate. Sometimes a sample is sectioned near the pit to examine its structure. ASTM G 46, Guide for Examination and Evaluation of Pitting Corrosion, provides a standard rating chart for pits in which the density of pits on a surface is rated on a scale of 1–5 (1 being the fewest pits, shallowest attack), as well as diagrams of different types of pit shapes. Comparing actual appearance to that shown in the standard can provide important information about the resistance of the alloy, how it is being attacked, and possible ways to overcome the attack. The appearance of the specimen is a type of data. ASTM G 46 discusses a number of detection and analysis techniques that could be used for analyzing pitting and the types of data that each technique can supply. In addition, the standard provides a methodology by which a pitting probability might be estimated from an immersion test.

Pitting corrosion is a phenomenon that may or may not proceed at a constant rate. Pitting can initiate, propagate, stop, reinitiate, propagate, stop, etc., many times before the entire specimen is penetrated completely. The mere presence of pitting does not necessarily indicate failure. Only when the deepest pit has penetrated and a leak has occurred has the alloy actually failed. The time for such penetration to occur may be impossible to estimate. In the laboratory, test time and specimen surface area can be far different from the expected field exposure time and surface area of the equipment being used. One method that has been proposed to bridge the large differences in space and time is using the statistical theory of extreme values [14,15]. The test and actual environments are assumed to be the same. Pit depths are measured on the laboratory specimen. The values are fit to a probability distribution function. If the fit is good, then by introducing the concept of return period, which is the ratio of the surface area of the object to the surface area of the specimen, the maximum pit depth can, in principle, be estimated for the object. The technique still requires more validation to determine the extent of usefulness.

If valid, it could provide a quantitative methodology for relating measured pit depths to equipment life. In terms of required data, one needs to know the surface area of both the laboratory coupon and the object being examined by the coupon and the depths of the pits on the coupon.

Types of data recorded for detection of intergranular corrosion are both qualitative and quantitative. Qualitative data are visual. They are obtained by examining under magnification a mounted and polished specimen that is etched appropriately. The etched structure is usually compared to photographs of specimens suffering similar types of corrosion (see ASTM A 262, Practices for Detecting Susceptibility to Intergranular Attack in Austenitic Stainless Steels) to determine if intergranular corrosion is observed on the specimen under examination [16]. The observed surface structure becomes the data. Characteristic information that might be recorded are evidence of grains missing from the structure, pits in the grain ends, and ditches between the grains.

Quantitative data relating to intergranular corrosion are actually relative corrosion rates between different materials or the same material treated differently. For example, the alloy under examination is exposed to a strongly acidic solution (see ASTM G 28, Test Methods of Detecting Susceptibility to Intergranular Attack in Wrought, Nickel-Rich, Chromium Bearing Alloys) for a specified length of time [16]. The corrosion rate is calculated from the mass loss of the specimen, its area, and the time of exposure (see ASTM G 31). This rate is compared to that obtained for a properly annealed material. Large differences between the two corrosion rates can mean the presence of intergranular corrosion.

### Stress Corrosion Cracking

The most common form of evaluation is time to failure for stress corrosion specimens. Failure usually means observation of the first crack. In relatively brittle materials, small cracks propagate rapidly causing the material to break into pieces. For specimens with constant loads, the rate of crack propagation increases as cracking proceeds, and failure is usually manifested as breaking of the specimen. Most specimens, however, are stressed by means of a constant strain. In such cases, the rate of propagation decreases after the initial crack is formed and, consequently, the best measure of time to failure is the time to observation of the first crack.

A number of tests are available that are used to estimate the alloy most resistant to stress corrosion cracking in an environment or to estimate a relative ranking of resistance among alloys. These tests employ a number of different types of specimens including U-bends, C-bends, precracked (Fracture Mechanics) specimens, tuning fork specimens, tension specimens, etc. The type of data generated depends on the specimen and the test. The reader is encouraged to consult two reviews [17,18] and the considerable number of citations to which the articles refer. These references discuss the type of data obtainable in stress corrosion cracking tests in considerable detail, as well as the behavior of a number of alloys. One of the reviews also contains references to a number of the ASTM standards that discuss test methods for stress corrosion cracking [17].

### Velocity Sensitive Corrosion (Single Phase Flow)

Corrosion can be sensitive to fluid motion, and often, fluid motion is included when testing for corrosion susceptibility. When fluid motion becomes part of the experimental protocol, measurements not only have to be made under dynamic conditions, but the data recorded must characterize the fluid motion in addition to corrosion rate or other indications of corrosion. This brief discussion is provided only to point out the type of information that must be obtained and recorded to integrate fluid motion into the estimation of corrosion. Though ASTM standards for testing for velocity sensitive corrosion do not yet exist, a recent NACE International Report reviews several methods for making these measurements [19]. While the techniques described all have different geometries, certain types of data are common to all. Merely recording fluid velocity or agitation rate is not sufficient to characterize the relationship between fluid motion and corrosion. Fluid motion is often quantified in terms of the dimensionless group the Reynolds number ( $Re$ ). Quantities such as fluid shear stress at the wall and the friction factor used to characterize the relationships between fluid flow field and the geometry are functions of this dimensionless group. If mass transfer controls or influences corrosion, the Schmidt number ( $Sc$ ) and Sherwood number ( $Sh$ ) are included in the description. These dimensionless groups are:

$$Re = \frac{(\text{velocity})(\text{characteristic\_length})}{(\text{kinematic\_viscosity})} \quad (3)$$

$$Sc = \frac{(\text{kinematic\_viscosity})}{(\text{diffusivity})} \quad (4)$$

$$Sh = \frac{(\text{mass\_transfer\_coefficient})(\text{characteristic\_length})}{(\text{diffusivity})} \quad (5)$$

The dimensionless groups can usually be related by the following equation:

$$Sh = a Re^b Sc^c \quad (6)$$

where  $a$ ,  $b$ , and  $c$  are constants that depend on the geometry of the test apparatus.

Equation 6 is usually assumed to model the relationship among these dimensionless groups and the variables  $a$ ,  $b$ , and  $c$  are determined by curve-fitting to actual data for the geometry in question.

Finally, when the corrosion rate is under complete mass transfer control, the corrosion rate can be derived from an equation of the form:

$$\text{Corrosion Rate} = (\text{Mass Transfer Coefficient}) \times (\text{Concentration Gradient}) \quad (7)$$

In theory, one could estimate the mass transfer controlled corrosion rate from knowledge of velocity, the characteristic dimension, and certain physical properties. In practice, such a simplified approach would not be prudent though

differences between measured and calculated values might provide insight into the corrosion mechanism.

The background and methodology for using these parameters in real situations to relate the laboratory geometry to the field and estimate corrosion rates are presented in detail elsewhere [20,21]. The equations point to the information deficiency if only velocity is recorded. Such physical properties as the diffusivity, viscosity (kinematic viscosity = absolute viscosity/density), and density need to be included in the recorded data. The characteristic length is a parameter that scales the geometry to the flow field and is used as a scaling factor for distance from the wall. Examples are the diameter of a rotating cylinder or the diameter of a pipe. The concentration gradient between the corroding surface and the bulk fluid can often be approximated by the bulk concentration (e.g., oxygen diffusion controlling) or the saturation concentration (e.g., steel corroding in concentrated sulfuric acid). Either should be measurable. The reader should consult the references for more details.

## OTHER DATA

Though this brief discussion has focused on the various types of corrosion data that might be recorded during certain corrosion tests or upon the analysis of the data, there also are noncorrosion data that should be recorded. Temperature, alloy type, heat number, surface condition, and environment chemistry are a few examples. Many more exist and may be required to complete the analysis. ASTM G 107, and especially its Table 1, contains a reasonably comprehensive list of the type of data that might be recorded during a corrosion test. ASTM G 161, Standard Guide for Corrosion Related Failure and Analysis, and especially its Appendix X1, list the type of qualitative and quantitative data that should be considered when analyzing corrosion-related failures. Though not all of the data types listed are relevant to every test, the contents serve as a useful checklist. Experimenters are encouraged to consult these listings prior to setting up an experiment to help ensure that key data and observations are not omitted from the measurements or records during the testing. An important concept to keep in mind is that recording too much information is always better than not recording enough information.

## REFERENCES

- [1] Pourbaix, M., *Atlas of Electrochemical Equilibria in Aqueous Solutions*, National Association of Corrosion Engineers, Houston, TX, 1974.
- [2] Mansfeld, F., "The Polarization Resistance Technique for Measuring Corrosion Currents," in *Advances in Corrosion Science and Engineering*, M. G. Fontana and R. W. Staehle, Eds., Vol. 6, Plenum Press, NY, 1976, p. 163.
- [3] Silverman, D. C., "Practical Corrosion Prediction Using Electrochemical Techniques," Chap. 68 in *Uhlig's Corrosion Handbook*, 2nd ed., R. W. Revie, Ed., John Wiley and Sons, 2000, p. 1179.
- [4] Rosen, E. M. and Silverman, D. C., "Corrosion Prediction from Polarization Scans Using an Artificial Neural Network Integrated with an Expert System," *Corrosion*, Vol. 48, No. 9, 1992, p. 734.
- [5] Gabrielli, C., Keddam, M., and Takenouti, H., "The Use of AC Impedance Techniques in the Study of Corrosion and Passivity," in *Treatise in Materials Science Technology*, J. C. Scully, Ed., Vol. 23, Academic Press, San Diego, CA, 1993, p. 395.
- [6] *Electrochemical Impedance: Analysis and Interpretation*, ASTM STP 1188, J. R. Scully, D. C. Silverman, and M. W. Kendig, Eds., ASTM International, West Conshohocken, PA, 1993.
- [7] *Proceedings of the Second International Conference on Electrochemical Impedance Spectroscopy*, Santa Barbara, CA, 1992, D. D. Macdonald, Ed., in *Electrochimica Acta*, Vol. 38, 1993.
- [8] Eden, D. A., "Electrochemical Noise," Chap. 69 in *Uhlig's Corrosion Handbook*, 2nd ed., R. W. Revie, Ed., John Wiley and Sons, 2000, p. 1227.
- [9] Eden, D. A., "Electrochemical Noise - The First Two Octaves," Paper 386, presented at CORROSION/98, March, 1998, reprint available from NACE International, Conferences Division, P. O. Box 218340, Houston, TX 77218-8340.
- [10] Motard, R. L., Dai, X. D., Joseph, B., Silverman, D. C., "Improved Discrimination of Electrochemical Noise Signals Using Wavelet Analysis," *Corrosion*, Vol. 57, No. 5, 2001, p. 394.
- [11] Chen, J. F. and Bogaerts, W. F., "The Physical Meaning of Noise Resistance," *Corrosion Science*, Vol. 37, No. 11, 1995, p. 1839.
- [12] Freeman, R. A. and Silverman, D. C., "Error Propagation in Coupon Immersion Test," *Corrosion*, Vol. 48, No. 6, 1992, p. 463.
- [13] Fontana, M., *Corrosion Engineering*, McGraw-Hill Book Company, New York, 1986, p. 164.
- [14] Shibata, T., "Corrosion Probability and Statistical Evaluation of Corrosion," Chap. 22 in *Uhlig's Corrosion Handbook*, 2nd ed., R. W. Revie, Ed., John Wiley and Sons, New York, 2000, p. 367.
- [15] Ault, J. P. and Gehring, G. A., "Statistical Analysis of Pitting Corrosion in Condensor Tubes," in *Corrosion Testing in Natural Waters*, ASTM STP 1300, Vol. 2, ASTM International, West Conshohocken, PA, 1996.
- [16] "Failure Analysis and Prevention," *Metals Handbook*, Vol. 11, 9th ed., ASM International, Metals Park, OH, 1986.
- [17] Phull, B., "Evaluating Stress-Corrosion Cracking," *Corrosion: Fundamentals, Testing, and Protection*, ASM Handbook, Vol. 13A, Materials Park, OH, 2003, p. 575.
- [18] *Corrosion—Metal/Environmental Reactions*, L. L. Shreir, R. A. Jarman, and G. T. Burstein, Eds., Vol. 1, Chap. 8, Butterworth-Heinemann, Oxford, 1998.
- [19] "State-of-the-Art Report on Controlled-Flow Laboratory Corrosion Tests," NACE Publication 5A195, NACE International, Houston, TX, 1995.
- [20] Silverman, D. C., "Rotating Cylinder Electrode-Geometry Relationships for Prediction of Velocity-Sensitive Corrosion," *Corrosion*, Vol. 44, 1988, p. 42.
- [21] Efird, K. D., "Flow-Induced Corrosion," Chap. 14 in *Uhlig's Corrosion Handbook*, 2nd ed., R. W. Revie, Ed., John Wiley and Sons, 2000, p. 233.

# Metallographic Analysis

*Richard L. Colwell<sup>1</sup>*

A NEW DOOR opened into the study of materials in the late 19th century (1863) when a British geologist named Henry C. Sorby decided to polish a piece of steel, etch it with acid, and examine it under a microscope. Since that time, metallographic examinations have been performed on most every engineering material developed.

Metallographic examination is a valuable tool in providing an understanding of structure/property relationships in many engineering materials. The true value in these examinations cannot be obtained without an intimate knowledge of a materials thermodynamic phase equilibria, and the effects of environmental factors on that equilibria. While this knowledge can be gleaned from the numerous technical volumes available, first hand experience can be a far better teacher.

## SAMPLE SELECTION

The selection of samples can be very important to the outcome of metallographic analysis. If the component is very large, it may require sectioning to provide manageable metallographic samples. The location for removal of metallographic samples should be considered carefully. Samples should contain areas representative of the corroded or fractured component. Samples of unaffected areas can reveal contrasting structures, thus distinguishing damage. Sometimes multiple samples must be taken at different orientations to understand the true nature of failure mechanism.

When sectioning, care should be taken to keep the sample cool. Elevated temperatures can promote phase transformations and exfoliation of surface deposits and scales. Heat can also promote volatilization of chemical species on the surface. Keeping the sample cool may require slow cutting to avoid heat generation. If samples must be cut using a torch, make sure that large areas are removed, thus leaving enough unaffected area for later saw cuts. Recently, the plasma cutting torch has gained much acceptance for use in obtaining samples in steels. The plasma torch transfers very little heat to the steel, thus creating very small heat-affected areas.

Cutting may also require use of a coolant. One should be careful of liquid coolants, especially if chemical analysis of surface scales and deposits will be required. Introduction of cooling liquids can contaminate areas of interest. In addition,

chemical species responsible for damage may dissolve and be washed away.

## PROCEDURES FOR SAMPLE PREPARATION

### Fixturing and Mounting

Once a sample has been obtained, it can be prepared for metallographic examination. Preparation usually involves taking a representative sample of usable size and fixturing it for easy handling during grinding. The sample may be fixtured in a mechanical assembly by using a clamping load supplied by threaded fasteners. Most often the sample is sandwiched between two pieces of material of similar hardness. This sandwiching promotes good edge retention. One should be sure that the sandwich material is nonreactive with the sample, especially in the presence of water and other fluids. In order to prevent capillary draw of fluid into the crevices inherent to the clamping fixture, paraffin can be used to fill the voids and gaps.

Another fixturing technique involves the use of either thermoplastic, or thermosetting polymer granules and powders. These powders and granules have different values of wearability. Mounting resins with high wear resistance promote good edge retention, but slow the material removal rate. Mounting polymers can also be transparent and electrically conductive. Conductive mounts are required to keep the sample from charging when examination using a scanning electron microscope is required.

Mounting involves inserting a specimen, to-be-polished side down, into a heated cylindrical cavity of fixed diameter so that the area to be examined is flat against one end of the cylinder. The sample may require support, such as clip rings, to keep it in the desired position. Next, polymer granules or powder, or both, are carefully added to the cavity, care being taken to not disturb the sample. Once sufficient material has covered the sample, the other end of the cylinder is secured, and the cylinder is pressurized. Heat and pressure cause the polymer to liquify and then set, thus encapsulating the sample. Thermoplastic polymers should be allowed to cool to near room temperature before releasing pressure. At temperatures above their glass transition, flow will result, causing the polymer to pull away from the sample.

When encapsulating samples, it is advisable, if possible, to remove any sharp corners, sharp protrusions, and burrs

<sup>1</sup>Bechtel Corporation, Houston, TX.

from the sample edges. Their presence tends to concentrate stresses during polymer cool-down and can promote cracking. Once cool, the sample can be handled easily during grinding and polishing.

Another method of sample fixturing uses cold-set epoxy resins. This method is helpful when samples are large or when cutting affects the physical integrity of the sample. Samples can be mounted in mold release coated metal molds or bakelite preforms. Molds or preforms, or both, are then affixed (rubber cement, Seal-All™, etc.) to an aluminum foil or PTFE covered flat surface. The sample is then placed on the flat foil/PTFE surface, in the preform, side-to-side polished down. Mixed, bubble-free epoxy resin is then poured over the sample, filling the mold. When using epoxy resins, it is helpful to have access to a bell jar and vacuum pump. A few minutes under vacuum tends to draw any air and gas bubbles out of the sample. The best method using liquid resins involves introducing it to the sample while under vacuum. Upon venting to atmosphere, resin is actually forced into microcavities. The sample is then placed in the preform mold and resin is added to fill the mold.

For some resins, raising the temperature of reaction significantly reduces the time required for the resin to cure, but there are some drawbacks. If the temperature is too high, the resin can oxidize, causing discoloration, thus decreasing visibility of the sample. More important, the amount of shrinkage is significantly higher for resins cured at temperatures above room temperature. This shrinkage can lead to cracking of the epoxy glass. Curing at high temperatures can also cause the epoxy to pull away from the sample, which promotes staining during etching.

If metallographic examination of coatings, specifically oxide coatings, is required, the following special techniques are helpful in preserving the integrity of the coating. The basis of coating preservation involves minimizing shrinkage associated with the curing resin. Blank mounts are made by filling bubble-free liquid resin in 1.25 in. diameter bakelite preforms. After a 24 h cure, two parallel saw cuts are made (approximately 7/8 in. apart) through the sample, creating flats (Fig. 1). Next, a thin slot is cut normal to the flats, half-way through the mount thickness. The ends of the slot are dammed up using cellophane tape. The sample is vacuum impregnated and then placed in the slot. The sample is then shimmed up using thin stainless steel strips. "The strips minimize rounding and reduce the chance of separation at the specimen-resin interface by providing a preferential site for such separation, if any should occur" [1].

Other methods are available and the reader is advised to explore them. A good outline of additional mounting methods and materials is given in *Metallography Principles and Practice* by G. Vander Voort, Ref 2, section 2.4, and ASTM E 3, *Methods of Preparation of Metallographic Specimens*, sections 7 through 9.

## Grinding

Once the sample is fixtured properly, the surface should be ground smooth and flat. Grinding is traditionally performed using silicon carbide papers, but sometimes diamond impregnated grinding media are used. Grinding can be done manually with stationary abrasive papers, manually

FIG. 1—Mounting arrangement for preserving oxide scales.

using rotating abrasives, or automatically (usually encompassing rotating abrasives, a counterrotating sample platen, and downwards pressure of the sample onto the abrasive). The choice between these methods depends on the number of samples and economy.

Whatever method is used, the principle is still the same: material removal. Material is removed for two reasons. The first involves removal of gross scratches and deformities from the surface. The second, which is equally important, especially for softer materials, is to remove subsurface damage. During grinding, abrasive particles actually cut gouges in the sample surface. While cutting, the material just beneath the surface of the gouge is plastically deformed. This plastically deformed material has a higher dislocation density, and is therefore higher in internal strain energy than the material around it. During etching, these higher energy areas are preferentially attacked, thus leaving traces of scratches and etch pits. It is very important to not only remove the scratches you see, but remove subsurface damage you cannot see.

During grinding, the metallographer should keep in mind that increasing the pressure on the sample will result in greater material removal rates, but will not increase the amount of subsurface damage [3]. The maximum depth of subsurface damage is independent of pressure [4].

Traditionally, grinding starts at grits numbered 60 or 120, depending on the initial condition and flatness of the sample. Grinding should start with the finest grit capable of rendering a flat specimen and removing damage from sectioning. Coarse grinding should be minimized in order to limit subsurface deformation. Figure 2 shows the relationship between scratch

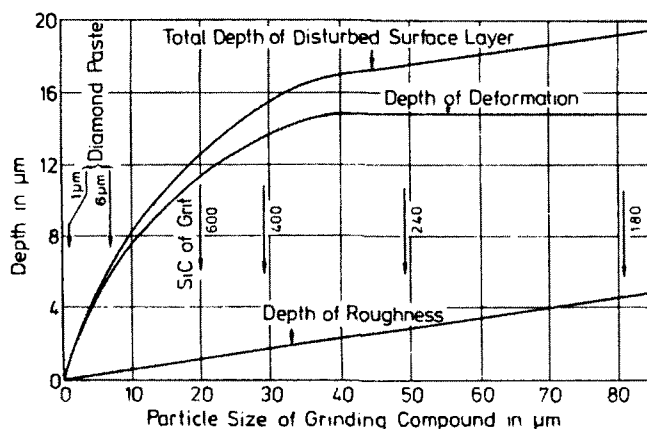


FIG. 2—Depth of scratches (roughness) and subsurface deformation in steels as a function of abrasive grit size.

depth (roughness) and depth of deformation in steels for various grit sizes [5]. Additional grinding is performed using successively finer abrasives, typically using 240, 400, and 600 grit abrasives sequentially.

During grinding, the sample surface should be kept cool. Cooling is usually provided by use of water, alcohol, or other organic compounds. Nonaqueous coolants are used to inhibit leaching of water soluble compounds from the sample or oxide scales.

Once grinding using 600 grit paper is completed, it is usually a good idea to chamfer the edges of the sample mount. This chamfer minimizes damage to the polishing cloth nap.

## Polishing

There are basically two types of polishing: electrolytic (electrochemical) and mechanical. Each will be discussed separately.

### Mechanical Polishing

Subsequent to grinding and prior to polishing, the metallographer's hands and the sample should be thoroughly washed. Washing keeps any residual grinding abrasives from contaminating the polishing cloth.

The polishing operation is very similar to grinding, but the size of the polishing abrasives is considerably smaller than the size of grinding abrasives. Again, the sample should be washed between each polishing step to inhibit abrasive carryover and contamination of the polishing cloths. Ultrasonic baths are highly recommended for cleaning during polishing. Ultrasonic waves promote superior cleaning by agitating small particles out of cracks and voids. However, metallographers beware: extended use can result in cavitation and pitting on the sample surfaces.

Typically, a sample will first be rough polished using 6  $\mu\text{m}$  or 3  $\mu\text{m}$  diamond compound, or similarly sized alumina slurries. Choice of polishing cloth is a function of sample material hardness, polishing rate, desired edge retention, and relief. A listing of various polishing cloths and their uses is presented in Table 1. It is a good idea to keep separate wheels for both soft and hard materials.

TABLE 1—Polishing cloth selection table.\*

Cloth	Recommended Uses
Canvas	Rough general polishing. Use with coarse grades of SiC and $\text{Al}_2\text{O}_3$ .
Billiard Cloth (Sheared Virgin Wool)	Rough general polishing of ferrous-based materials.
Red Felt (Plucked Virgin Wool Pile)	Rough or intermediate polishing.
Cotton-Medium Nap	Intermediate polishing. Commonly used with diamond, $\text{Al}_2\text{O}_3$ , and colloidal silica.
Cotton-Fine Nap	Rough diamond polishing of soft metals. Use with polishing grades of $\text{Al}_2\text{O}_3$ , $\text{Cr}_2\text{O}_3$ , and silica.
Nylon	Rough polishing with diamond. Helps maintain flatness.
Silk	Use with diamond in rough polishing of extremely friable materials and rough polishing of metals.
Woven Wool	Rough and intermediate polishing of hard materials.
Wool (Short Pile)	Use in all final polishing stages.
Rayon (Flock on Cotton Backing)	Final polishing with diamond, $\text{Al}_2\text{O}_3$ .
Rayon-Fine	Superior final polishing with diamond, $\text{Al}_2\text{O}_3$ , and colloidal silica.
Synthetic Velvet	Intermediate and final polishing. Minimizes relief and edge rounding.
Synthetic Velvet-Fine	Use in vibratory polisher, especially with soft materials.
Medium Napped Polyurethane Cloth on Polyester	Polishing oxide films. Use with cerium oxide.

\*Courtesy of South Bay Technology, Inc.

A diamond extender (i.e., fine cutting oil) is used during polishing. This oily compound allows diamond particles to adhere to the fibers of the polishing cloths, removes abraded material, and permits dissipation of heat during polishing.

For very soft materials, it is sometimes necessary to etch the sample and repeat the previous step before continuing. This repetition is required to remove subsurface damaged material.

Once the sample has been polished to 3  $\mu\text{m}$ , a final step (fine polishing) usually involving either an alumina slurry or colloidal silica slurry is used. The size of particles in these aqueous slurries can be as small as 0.02  $\mu\text{m}$ . Once finished with this step, the sample is ready for etching. If elemental analysis of the polished sample is to be performed using SEM/EDS or other X-ray techniques, extra care should be taken. Often times artifact silicon or aluminum peaks can be introduced by accumulation of polishing abrasives in cracks and pores, and sometimes, depending on the metal hardness, by intrusion into the sample surface.

### Vibratory Polishing

Vibratory polishing is another method commonly used. Mounted samples are weighted down and allowed to randomly circulate on a cloth covered vibrating platen. The platen holds an aggressive slurry of polishing abrasives and is usually covered to avoid evaporation and splashing. The downside of vibratory polishing is that it requires much more time than traditional mechanical or electrolytic polishing. Fortunately, this time is unattended. Vibratory polishing is very good at

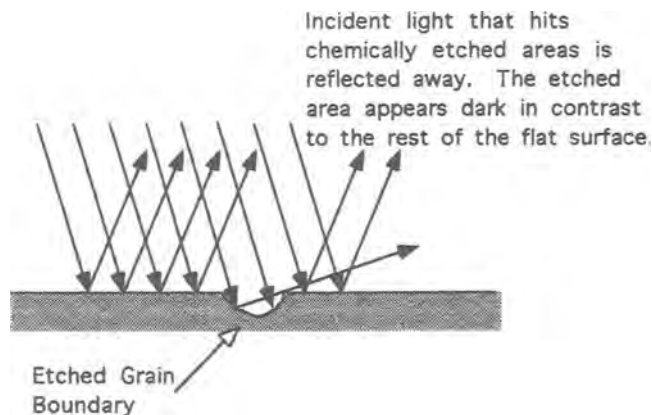


Fig. 4—Simplistic representation of the principle of chemical etching.

Fig. 3—Diagram of a simple electrolytic polishing cell.

producing scratch-free samples for soft metals. After polishing, samples should be washed, rinsed in alcohol, and blown dry to avoid staining.

### Electrolytic Polishing

Electrolytic polishing is a convenient way to polish metallic samples in the fine grinded (600 grit) or machined surface states. This method requires formation of an electrical circuit in which the sample is the anode (Fig. 3). A suitable electrolyte flows across the surface of the sample. The current density is adjusted for the type of material and size of the polished sample to facilitate suitable dissolution of metal ions from the to-be-polished surface. As the electrolyte washes over the sample, any perturbations in the surface (high energy sites) are selectively dissolved. The result is a flat surface with no mechanical damage.

Although this method is easy to use, storage and use of potentially dangerous electrolytes limit its use. For example, some solutions of perchloric ( $\text{HClO}_4$ ) can become explosive if allowed to evaporate to concentrated solutions.

### Etching

Etching is performed in order to observe microstructural constituents, including grain boundaries, twin planes, slip lines, and second phase particles. In addition, etching can sometimes, as will be discussed later, reveal a material's propensity towards certain corrosion mechanisms.

Safe laboratory work practices are very important. A metallographer is useless without his or her eyes. Use proper protective equipment (gloves, safety glasses, etc.) when using laboratory chemicals.

There are three basic types of etching mechanisms: chemical etching, staining, and optical etching. Chemical etching uses the anisotropy in a material. The reaction rates of the chemical etchant on a polished sample's surface are dependent on the energy state of materials microstructure. The higher the energy state of one region, the faster it will react, and more etching (localized material removal) occurs.

In other words, some microstructural constituents are anodic to others. Grain boundaries and twin boundaries are more energetic (anodic) than the material in the center of a grain. Likewise, regions under elastic tensile strain, or regions that have undergone plastic deformation will etch faster than nonstrained, nondeformed material. In a multiphase material, one phase may be more reactive than another.

Similarly, grain orientation on polished surfaces can affect the degree of etching. Close packed orientations can etch slightly faster than lesser packed planes.

Under reflected light, etched material will appear darker than the unetched material. Indentations created by etching act as holes, reflecting light away at different angles. The "off-reflected" light cannot be reflected back to the objective lens, and therefore appears as regions of darkness (Fig. 4).

Some materials etch more easily than others. Grain boundary delineation in aluminum alloys is perhaps one of the most difficult tasks for a metallographer. In aluminum alloys, it is sometimes necessary to experiment with many etchants in order to obtain the desired grain boundary resolution.

Table 2 contains a number of chemical etchants that have proved useful for a limited number of the more popular engineering alloys. Included are the microstructural characteristics highlighted by the etch.

After chemical etching, samples should be rinsed in water, followed by alcohol and blown dry to avoid staining. Samples should be stored in desiccators to inhibit corrosion on the highly polished surfaces. If a desiccator is not available, use of commercial clear coat paints is recommended.

Electrolytic etching is similar to chemical etching, but the electrochemical reaction is forced by means of an externally applied potential. If the sample is embedded in a polymeric mounting material, provisions for making electrical contact must be made (i.e., prepared mount, drilling through the mount, removal from mount, etc.).

A family of chemical etchants known as deposit etchants works slightly different than chemical etchants. Like electrolytic etchants, deposit etchants promote dissolution of metal on the polished surface. However, the dissolved metal ions react with agents in the etchant solution, promoting



TABLE 2—A brief list of etchants for revealing microstructure in popular engineering alloys.

Alloy	Etchant	Uses
Aluminum and Al Alloys	0.5–25 g NaOH	General purpose etch.
	1 g zinc chloride	Grain boundary delineation.
	100 mL water	Immerse up to 2 min.
	1 mL HF (48 %)	Outlines microconstituents.
	200 mL water	Immerse for 30–40 s.
	12.5 mL HNO <sub>3</sub> (conc.)	General purpose etch.
	2.5 mL HF (48 %)	Grain boundary delineation.
	85 mL water	Immerse up to 1 min.
	2 mL HF (48 %)	Modified Keller's Rgnt.
	3 mL HCl (conc.)	General purpose etch for Al & Al alloys. Immerse 10–60 s.
	20 mL HNO <sub>3</sub> (conc.)	Wash in warm water, blow dry.
	175 mL water	
	10 mL NH <sub>4</sub> OH	General purpose etch.
Copper and Copper Alloys	10 mL H <sub>2</sub> O <sub>2</sub> (3 %)	Grain boundary delineation.
	Can dilute up to 20 mL water	Use fresh, swab, or immerse up to 1 min.
	10 g (NH <sub>4</sub> ) <sub>2</sub> S <sub>2</sub> O <sub>8</sub>	General purpose etch.
	90 mL water	Grain boundary delineation.
		Immerse up to 1 min.
	10 g Cr <sub>2</sub> O <sub>3</sub>	Swab or immerse up to 30 s.
	4 drops HCl	
Nickel and Nickel Alloys	75–100 mL water	
	20 mL HNO <sub>3</sub>	AquaRegia
	60 mL HCL	Grain boundary, carbide, and $\sigma$ contrast. Use fresh and under hood. Discard after use.
		Swab or immerse up to 1 min.
	3 parts glycerol	Glyceregia.
	2–3 parts HCl	Popular etch. Use fresh and under hood. Discard after use.
	1 part HNO <sub>3</sub>	Swab or immerse up to 1 min.
	10 g CuSO <sub>4</sub>	Marble's Reagent.
	50 mL HCl	Grain boundary delineation
	50 mL water	Swab or immerse up to 1 min.
Iron and Iron Alloys		A few drops of H <sub>2</sub> SO <sub>4</sub> increase etch activity.
	2 mL HNO <sub>3</sub>	Nital.
	98 mL ethanol	Gives good pearlite-ferrite-grain boundary contrast in carbon and low alloy steels.
		Swab or immerse up to 1 min.
	4 g picric acid	Picral. Promotes good resolution of pearlite, bainite, martensite, and carbides.
	100 mL ethanol	Swab or immerse up to 1 min.
	4–5 drops of zephiran chloride (wetting agent)	
Stainless Steel	100 mL picric acid (sat.)	Reveals prior austenitic grain boundaries in martensitic steels.
	1 g tridecylbenzene	
	1 part HNO <sub>3</sub>	General purpose etch for stainless steels.
	1 part HCl	Promotes grain boundary contrast.
	1 part water	Immerse in a gently stirred solution.
	1 g picric acid	Viella's Reagent.
	5 mL HCl	Outlines carbides, $\sigma$ , and $\delta$ .
	100 mL ethanol	Immerse up to 1 min.
	1 part glycerol	Glyceregia for SS's.
	3 parts HCl	Reveals grain structure.
	1 part HNO <sub>3</sub>	Outlines $\sigma$ and carbides.
		Use fresh and under hood. Discard after use.
		Swab or immerse up to 1 min.
	10 g oxalic acid	Electrolytic etch (sample is anode). Use at 1–6 V @ 0.1–1.0 A/cm <sup>2</sup> .
	100 mL water	Resolves $\sigma$ in 5–10 s. Resolves carbides in 15–30 s. Resolves grain boundaries in 45–60 s.

precipitation of insoluble compounds on the sample surface. The relative thickness of the coating is dependent on the reaction rate, which again is variant depending on microstructure and chemical composition.

Heat tinting is another type of deposit etch. Exposing a polished sample (not in a plastic mount!) to elevated temperatures in air causes oxidation to occur. On the microscopic level, oxidation rates of microstructural constituents vary according to their reactivity in a given environment.

The second type of etching is more of a staining operation than etching. Staining has been more involved with the

identification and differentiation of oxide films than in outlining microstructural constituents.

Optical etching is a nondestructive method. The term optical etching is a misnomer. Optical methods do not involve etching, but are useful in showing microstructural features in certain alloys. In this method, microstructural contrast, specifically crystallographic contrast of polished samples, is produced by using the "Kohler" principle of illumination (Fig. 5). Modes of illumination including polarized light, differential interference contrast (Nomarski), and dark field illumination can produce vivid and sometimes colorful contrast.

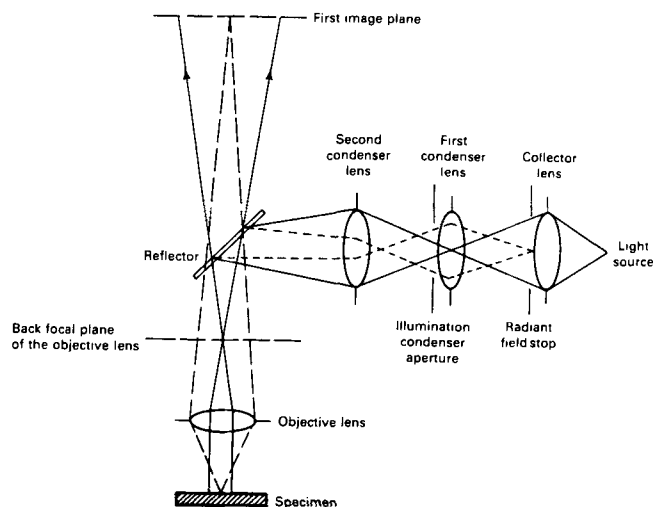


FIG. 5—The Kohler Principle of Illumination.

A comprehensive list of chemical etchants and etching procedures can be found in Refs 2, 6, and 7.

### Metallographic Interpretation

In the preparation of metallographic samples, not only are good hygiene and technique required, but also a good understanding of the sample material and its properties. Most metallographers have at least once been surprised by a structural anomaly that turned out to be an artifact. Experience and an inquisitive nature are necessary for good metallographic interpretation.

## METALLOGRAPHIC EXAMINATION AND EVALUATION OF CORROSION MECHANISMS

### Stress Corrosion Cracking (SCC)

The nature of stress corrosion cracking (SCC) can be directly observed by metallographic examination. The distinction between intergranular (IGSCC) and transgranular

cracking. TGSCC is best revealed by etching materials to reveal grain boundaries (Fig. 6). In addition, the magnitude of crack branching and crack initiation sites is best revealed by metallographic examination.

Susceptibility of SCC is highly dependent on the metals stress state. Tensile stresses, either applied or residual, above a threshold value (material dependent), are required for cracking to occur. Chemical etching of metals can sometimes provide clues into a material's thermomechanical history. Signs of plastic deformation (deformation twins, slip lines), and thus knowledge of exceeding of material yield strength, can be revealed through etching.

Some stainless steels can be made susceptible to IGSCC by exposure to elevated temperatures ( $823^{\circ}\text{K} < T < 1073^{\circ}\text{K}$ ). At these temperatures, carbon atoms migrate to grain boundaries where they combine with chromium atoms to produce chromium carbides. Since chromium atoms are tied up as carbides, they are not available for matrix corrosion resistance, and the near-grain boundary regions are locally depleted in chromium (Fig. 7). This depletion renders grain boundary regions susceptible to corrosion, and the alloy is then termed "sensitized." The degree of sensitization is a function of temperature and time at temperature. In many cases, a prediction of the susceptibility of austenitic stainless steels to IGSCC can be obtained by a simple electrolytic etch (ASTM A 262, Practices for Detecting Susceptibility to Intergranular Attack in Austenitic Stainless Steels, practice A).

### Pitting

Metallographic examination can be quite useful in determining severity of pitting, and can also be used to qualify materials for use in specific environments. A procedure for metallographic preparation of pitted samples is cited here, quoting ASTM G 46, Guide for Examination and Evaluation of Pitting Corrosion, section 5.1.5: "Select and cut out a representative portion of the metal surface containing pits and prepare a metallographic specimen in accordance to the recommended procedures in Methods E 3. Examine microscopically to determine whether there is a relation between pits and inclusions or microstructure, or whether

FIG. 6—Transgranular (left) and intergranular (right) stress corrosion cracking in type 304 stainless steel (magnification 200 $\times$ )

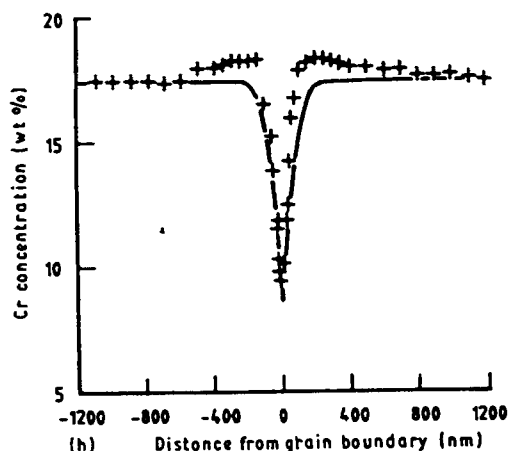


FIG. 7—Electron microprobe analysis showing depletion of chromium at and near grain boundaries of sensitized type 304 stainless steel [14].

the cavities are true pits or might have resulted from metal dropout caused by intergranular corrosion, dealloying, etc.”

Evaluation of the metallographic samples of pitted materials can be performed easily using charts A, B, and C in ASTM G 46, section 7.2.1. (Figs. 8 and 9). These charts characterize a sample's pit density, pit size, and pit depths. These data are convenient ways of relating and illustrating the severity of pitting to the lay person. It is sometimes helpful to reassess a sample after additional grinding and

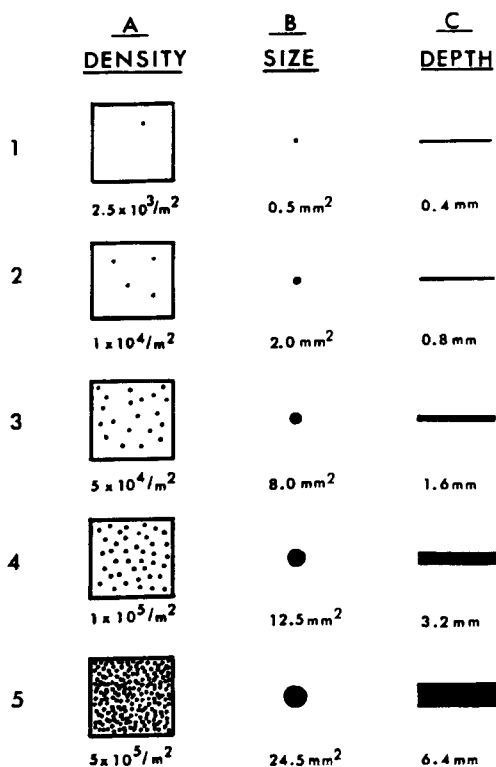


FIG. 8—ASTM pitting chart for density, size, and depth (see ASTM G 46).

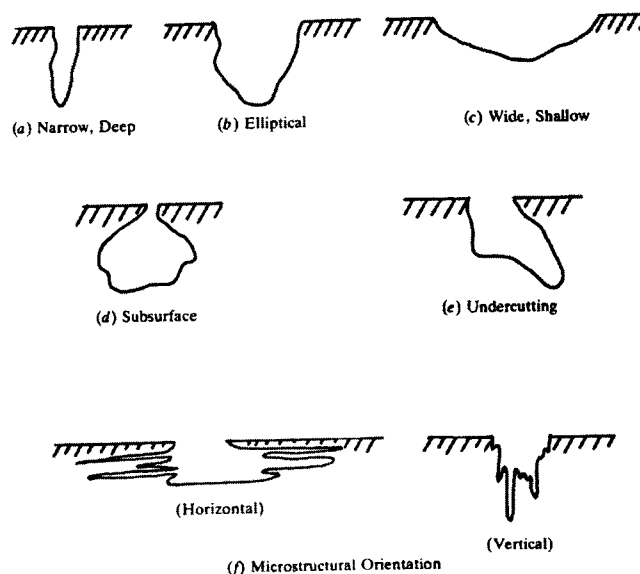


FIG. 9—ASTM pitting chart for pit shape (see ASTM G 46).

polishing. Material removal can eliminate overly conservative measurements caused by the three-dimensional (3-D) travel path of corrosion pits.

Another way to quantify the extent of pitting is to just examine the pitted surface of an unprepared sample under a laboratory microscope. By measuring the vertical difference, via micrometer measurements on focus knob, between the top of sample and bottom of pit, the pit depth can be measured. One should use this method with caution because pits are not always straight. Pits may travel a circuitous path, and measurement of the perceived pit bottom will result in an overly conservative depth.

## Dealloying

Dealloying is a corrosion mechanism where one element in a multielement system is selectively leached from the matrix by action of a fluid system. Two alloy systems that are widely known for dealloying are cast iron (graphitic corrosion) and copper zinc (Zn > 15 wt. %) brasses. In gray cast irons (in the presence of sulfate reducing bacteria, salt water, or weak acids), alpha iron is anodic to graphite and corrodes, leaving behind a porous mass of graphite and iron sulfates. In brasses, zinc is selectively leached from the matrix, leaving behind a porous mass of copper [8,9]. Dealloying severely reduces the mechanical properties of components made from them. Metallographic examination can confirm visual indications of dealloying (Fig. 10). Not only will the microstructure appear changed as one element is selectively leached from the matrix, but changes in microchemistry can also be observed. Dealloying can be observed optically or by analyzing the polished specimen in a scanning electron microscope (SEM). Back scatter electron images will show contrast in regions of varying atomic number. Another SEM method that graphically displays differences in microstructural elemental composition is the digital X-ray line scan or X-ray dot map. The line scan can

**FIG. 10—Photomicrograph showing selective dezincification of the continuous phase in an  $\alpha$ - $\beta$  brass (magnification 200  $\times$ ).**

show variations in elemental composition along a line (Fig. 11). The dot map shows compositional differences over the examined area. Depending on computer capabilities and software, some systems can map out the concentrations of up to 16 elements simultaneously.

### Corrosion Due to Phase Changes ( $\sigma$ Phase Formation in Cr-Ni-Fe and Fe-Cr Alloys)

Exposure of certain alloys to elevated temperatures can produce phase changes within the alloy. These phase changes can sometimes lead to corrosive attack of the alloy. Corrosion can occur if the phase change alters the formation of protective barriers on surface. Examples of this mechanism are sensitization of stainless steels (discussed earlier) and sigma phase ( $\sigma$ ) formation. Sigma phase formation occurs in nickel-chromium-iron and chromium-iron alloys containing a minimum of 16.5 %

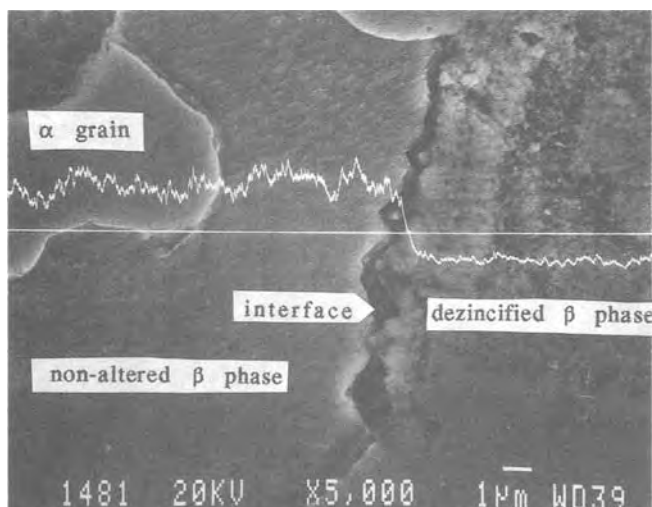


**FIG. 11—EDS line scan showing a reduction in zinc concentration across a dezincified interface in an  $\alpha$ - $\beta$  brass alloy.**

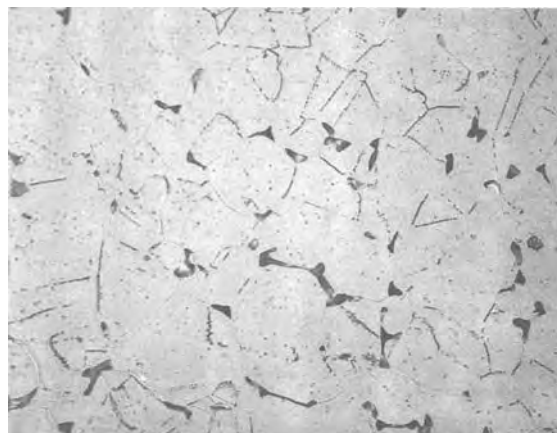


**FIG. 12—Photomicrograph showing  $\sigma$  phase precipitation along austenitic grain boundaries in a type 310 stainless steel (magnification 500  $\times$ ).**

Cr exposed to temperatures between 1100° and 1700°F (593.3° and 926.7°C) over long periods of time [10]. Sigma phase is an iron chromium rich phase that precipitates along austenitic grain boundaries and delta ferrite precipitates (Fig. 12). Test results have shown that sigma phase stainless steels undergo significant intergranular corrosion in boiling 65 %  $\text{HNO}_3$  and in hot concentrated sulfuric acid solutions. Sigma phase formation also results in loss of room temperature base metal ductility.

Sigma phase formation can be easily assessed by metallographic examination. One of the easiest ways of determining the presence of sigma phase is by using a 45 % aqueous KOH solution as an electrolytic etch. Sigma grains are revealed as distinct reddish-brown islands in the austenitic matrix.

### General Corrosion

In conditions where general corrosion occurs, metallographic samples can be used to verify the extent of metal loss through microscopic measurements of sample thickness. Reduction of thickness coupled with weight loss information provides a checks and balances program into the analysis and reveals any corrosion rate differences due to anisotropy.

### Liquid Metal Embrittlement

Liquid metal embrittlement (LME) is not a very common mechanism. Only a small number of liquid metals can cause LME in any given alloy system. LME is an inter- and intragranular cracking mechanism produced by a liquid metal on the surface of a sensitive solid metal in the presence of a tensile stress, either applied or residual. The mechanism occurs only above a threshold stress value and has an incubation period. Table 3 shows a few of the solid and liquid systems exhibiting LME. More alloys systems exhibiting LME are tabulated in the ASM Metals Handbook, 9th edition, Vol. 11, p. 238.

**TABLE 3**—Solid and liquid systems exhibiting LME.

Solid Metal	Liquid Metals Promoting Embrittlement
Aluminum Alloys	Mercury, Gallium, Sodium, Indium, Tin
Brass (70/30-Cu/Zn)	Mercury, Lithium Bismuth
Iron or Steel	Lithium
Nickel Copper Alloys	Mercury, Lead
Stainless Steels	Zinc, Cadmium
Ni-Cr-Fe Alloys	Lead

Metallographic examination can assist in identifying LME. Liquid metal penetration can be observed readily, usually without use of an etchant (Fig. 13). However, etching for grain boundaries can distinguish between inter- and intra-granular cracking. In addition, SEM/EDS (energy dispersive spectroscopy) analysis, as discussed in the section covering Dealloying, can positively identify the presence of foreign metals at grain boundaries within a matrix. Care should be taken when trying to identify mercury using SEM/EDS. High vacuum and electron beams promote evaporation of mercury. Low kV settings should be used over wide areas to inhibit burning off highly volatile mercury. In addition, mercury X-ray energy peaks (M) and sulfur (K $\alpha$ ) peaks are easily mistaken for each other. Wet chemical spectroscopy is perhaps the best method for absolute identification of liquid metal species.

Radiography can be used as a check for LME in large structures. By virtue of the large difference in liquid and solid metal system densities, cracks can be revealed easily on X-ray film, even when they are not visible on the surface.

### High Temperature Corrosion—Metal Dusting

Metal dusting of heat-resistant alloys (Ni-Cr-Fe) occurs in carbonaceous atmospheres at temperatures above 800°F (426.7°C), with very high activity in the temperature range of 1450°F to 1550°F (787.7° to 843.3°C) and above 1700°F (926.6°C). In metal dusting environments, a black “sooty” residue (graphite) usually covers the surface in most of the wasted areas. The residual metal is usually thinned and contains multiple rounded pits. The originally austenitic matrix

transforms to a brittle ferromagnetic material and can be checked with a simple magnet.

Metallographic examination reveals an inward diffusion layer of gross carburization and grain “pop out”.

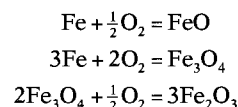
### Sulfidation

Metallographic examination of metals which have exhibited wastage due to sulfidation usually show a two-layer scale, the upper layer being red, the lower being black and shiny. A few drops of aqueous hydrochloric acid on the deposit can release a noticeable H<sub>2</sub>S odor and verify the presence of sulfides. In addition, creation of a “sulfur print” can verify sulfidation damage. A cross section sample of thinned metal with surface scale is sanded to a 120 grit finish. Next, wash a piece of black and white photographic paper in 2–3 % sulfuric acid. Wipe away excess acid with a clean sponge. The sample is placed on the photographic paper for a few seconds. The paper is then stopped and fixed as in normal circumstances. An image of the sulfide distribution on the tube will appear [11].

### Oxidation

Oxidation, perhaps the most visible of all corrosion mechanisms, is responsible for consuming a significant amount of maintenance dollars. Metallography of oxidized metals can provide information about the type of reaction. Types of oxidation reactions (general, internal, intergranular) can be differentiated by microexamination. Knowing the oxide scale thickness and composition can provide data on time-temperature exposure by knowing the oxidation rate laws of the material. In addition, knowledge of the mass ratio of oxide species in the scale can determine exposure temperature.

Metallographic examination of different phases within oxide scales has proven difficult, but some techniques are available. For example, in steels the scales formed at high temperature are generally composed of three layers: wüstite (FeO), hematite (Fe<sub>2</sub>O<sub>3</sub>), and magnetite (Fe<sub>3</sub>O<sub>4</sub>). The formation of these three oxides can be described by the following reactions:



The mineralogical names are used to emphasize their specific physical and chemical properties. Wüstite forms at high temperatures (>565°C) adjacent to the steel surface. Magnetite is an intermediate layer and hematite is the outer layer. Usually a layer of mixed hematite and magnetite is observed.

An etchant containing 0.5 % selenic acid (H<sub>2</sub>SeO<sub>4</sub>) and 4 % HCl in ethanol can produce a nice contrast between the oxide phases on polished samples after immersion at room temperature [12]. Selected dyes have also been used with various degrees of success. The reader is encouraged to read Ref 13 for further information on dying oxide scales.

**FIG. 13**—Unetched photomicrograph showing diffusion of Pb/Sb into steel (magnification 500 $\times$ ).

## REFERENCES

- [1] Hussey, R. J., Beaubien, P. E., and Caplan, D., "Metallography of Oxide Scales on Metals," *Metallography*, Vol. 6, 1973, pp. 27–36.
- [2] Vander Voort, G., *Metallography Principles and Practice*, McGraw-Hill, 1984.
- [3] Samuels, L. E., *Metallographic Polishing by Mechanical Methods*, ASM, Materials Park, OH, 1982, p. 57.
- [4] Samuels, L. E., *Metallographic Polishing by Mechanical Methods*, ASM, Materials Park, OH, 1982, p. 111.
- [5] Petzow, G., *Metallographic Etching*, ASMI, Materials Park, OH, 1978, pp. 10–11.
- [6] Petzow, G., *Metallographic Etching*, ASMI, Materials Park, OH, 1978, pp. 30–101.
- [7] *ASM Metals Handbook*, 9th ed., Vol. 9, ASMI, Materials Park, OH, 1985.
- [8] Uhlig, H. J., *Corrosion Handbook*, John Wiley and Sons, 1948, pp. 139–198.
- [9] *Corrosion*, Vol. 1, L. L. Shreir, Ed., Newnes-Butterworths, reprinted 1977, pp. 446–447.
- [10] Gaertner, D. J., "Characterization of Sigmatized Austenitic Stainless Steels," *Materials Performance*, January 1985, pp. 18–24.
- [11] Gaertner, D. J., "Characterization of Sigmatized Austenitic Stainless Steels," *Materials Performance*, January 1985, p. 15.
- [12] Chicco, B. and Heijkoop, T., "Metallographic Reagent for the Characterization of Oxide Scales on Iron and Steel," *Prakt. Metallographic*, Vol. 20, 1983, pp. 321–326.
- [13] Chicco, B., "Dye Adsorption—A New Technique for the Color Metallography of Oxide Scales on Steels," *Metallography*, Vol. 14, 1981, pp. 319–328.
- [14] Tekin, A., Martin, J., and Senior, B., *Journal of Materials Science*, Vol. 26, 1991, pp. 2458–2466.

# Surface Analysis

*Alfred G. Hopkins<sup>1</sup>*

BECAUSE CORROSION is fundamentally a surface phenomenon, those interested in the fundamental processes of corrosion have always been among the first to explore the utility of surface analysis techniques. These techniques have had, and will continue to have, great success in illuminating many facets of corrosion phenomena.

For those seeking a more detailed treatment of the application of surface analysis techniques to the study of corrosion than can be given here, there are a number of Symposium Proceedings from the Electrochemical Society and from ASTM that are of great utility [1–6]. For those interested in more depth on the subject of surface analysis in general or on particular surface techniques, the following are some useful references [7–13]. Systems that are particularly amenable to surface analysis include inhibitor films and protective coatings, stable oxide films, and corroded surfaces.

## LIMITATIONS

There are, however, a number of limitations that have prevented these techniques from being even more widely used. The first is that corrosion is inherently a dynamic process, while these techniques are essentially static in nature. They can only give a snapshot in time of the chemical state of the system. These techniques are obviously of more use in those systems that change slowly in time versus those that change rapidly.

The second limitation is that most of these techniques require that the sample be removed from the corrosive environment and placed into a high vacuum environment before analysis can be performed. This is a major problem for those systems that can change structure upon drying or loss of absorbed water.

The third major limitation is that the analysis process itself can change the composition of the surfaces to be analyzed. The two most common types of this problem are analysis beam-induced damage and inhomogeneities caused by the sputtering process, which is used often to probe past the topmost surface of the sample.

The final major limitation is cost/availability. Some of the techniques are not widely available, and even those that are easily available (XPS and Auger) are still quite expensive.

This limits the number of analysis points that can be obtained. All of the above limitations result in most studies being done on stable films on metals and making these techniques of lesser utility on unstable or rapidly changing systems.

## GENERAL PRINCIPLES

These techniques generally require the sample to be placed in an ultrahigh vacuum (on the order of  $10^{-7}$  Pa/  $10^{-9}$  torr) to prevent contamination from residual gases in the analysis chamber. A rule of thumb is that up to an atomic layer per second can be formed at pressures of  $10^{-4}$  Pa ( $10^{-6}$  torr) if each collision of a gas molecule results in its sticking to the surface. Fortunately, the sticking coefficients are often much less than unity, especially for oxidized samples such as often are of interest in corrosion studies. Some samples are especially prone to reacting with residual gases; this is often accelerated by electron beam-induced degradation at the sample surface with techniques such as Auger. In these cases, it may be necessary to bake the analysis system to reach vacuums in the low  $10^{-8}$  Pa range or better. With some techniques (such as Secondary Ion Mass Spectroscopy), the vacuum requirements can be relaxed since the surface that is actually being analyzed will only be exposed to the vacuum for a very short period of time.

Near surface techniques, in contrast to true surface techniques, do not require an ultrahigh vacuum. Secondary Electron Microscopy-Energy Dispersive X-ray Spectroscopy (SEM-EDS) is an example of a particularly useful near surface technique that will be discussed in a later section. Micro surface electrochemical techniques, such as the Scanning Kelvin probe, overcome these limitations and do give detailed electrochemical (rather than elemental) information about the system in question.

In classic surface analysis techniques, the surface is illuminated (interrogated) with high-energy electrons, photons, or ions. Depending on the illuminating species, any or all of these types of species will be generated from the ensuing collision. Elemental identification is then made based on characteristic energies or masses of the ejected species. One common way of characterizing surface analysis techniques is by tabulating the incoming and outgoing particles. Table 1 shows such a table, which was adapted from previously published ones [8–10]; this paper will concentrate on the most frequently used techniques. Because surface analysis

<sup>1</sup>Distinguished Member, Technical Staff, Texas Instruments Inc., Attleboro, MA 02703-0964.

**TABLE 1**—Comparison of surface analysis techniques.

Category Technique	Incident Particle	Analyzed Particle	Measured Quantity	Analysis Depth in Monolayers	Sample Damage	Sensitivity (Atomic Fraction)	Standardless Quantification
Auger	Electron	Auger Electron	Energy	2–10	No-Mod	$10^{-3}$	fair
XPS-ESCA	X-Ray	Photo-Electron	Energy	2–10	No-Min	$10^{-3}$	fair
Dynamic Sims	Ions	Sec Ions	Mass	10–20	Mod-Ext	$10^{-7}$	poor
Static Sims	Ions	Sec Ions	Mass	1–2	Mid-Mod	$10^{-8}$	poor
SNMS	Ions	Neutrals	Mass	5–10	Min-Ext	$10^{-7}$	fair
SALI	Ions	Neutrals	Mass	1–2	Min-Ext	$10^{-7}$	fair
RBS	Ions	Input Ions	Energy	many	Min-Mod	$10^{-3}$	good
ISS	Ions	Input Ions	Energy	1	No	$10^{-3}$	good

NOTES—NO: NONE; MOD: MODERATE; MED: MEDIUM, EXT: EXTENSIVE.

is an extremely specialized field, it has its own nomenclature; the reader is referred to ASTM E 673, Terminology Relating to Surface Analysis.

Surface analysis is mainly used in two separate modes. One is in surface science where the goal is to fundamentally understand the root causes and mechanisms that are occurring in a system. Usually a model system is picked to eliminate as many confounding variables as possible to get a system about which firm conclusions can be drawn. Often, many different techniques will be used on the same problem in order to illuminate as many facets of the problem as possible. The other mode is failure analysis. The goal here is to determine which of the failure modes (previously discovered by surface science) is the most important one for a particular failure. The samples are real, and hence, non-ideal. This analysis mode is often used to identify the elements present, their distribution pattern and their oxidation state.

The first and second most common of the true surface analysis techniques are Auger Electron Spectroscopy (AES) and X-ray Photoelectron Spectroscopy. They are electron spectroscopies that quantify the energy of electrons that are emitted by the surface during analysis. A good reference for those seeking more detail is "Uses of Auger Electron and Photoelectron Spectroscopes in Corrosion Science" by McIntyre and Chan in Practical Surface Analysis [12].

## AUGER ELECTRON SPECTROSCOPY (AES)

AES is the most commonly used surface technique on metal samples because of the following advantages:

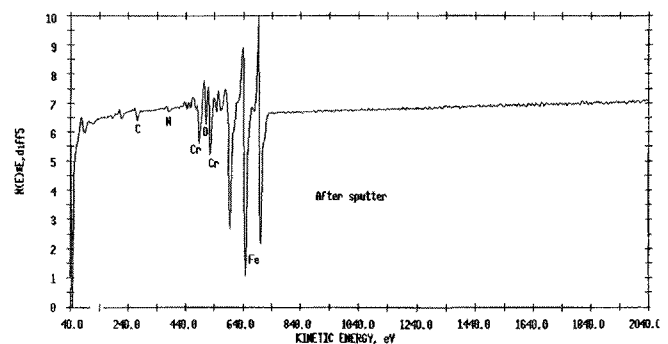
- High-surface sensitivity.
- Acceptable detectability for many corrosion problems.
- Simultaneous detection of all elements (except hydrogen and helium).
- Very good small area analysis (mapping).
- Ability to probe deeper into the surface by sputter profiling.
- Analysis time not excessively long.
- Readily available instrumentation.

With AES, the sample is subjected to a high-energy (typically 2–20 KeV) electron beam that can cause ejection of a core electron from an atom to form an atomic inner shell vacancy. An outer-level electron will then fill the inner-level vacancy, which will induce an excited state. One of the ways that the atom can then relax is by emitting another electron to form a doubly ionized species. This electron is the Auger electron (named for Pierre Auger, who recognized the effect

in a Wilson Cloud Chamber and first described it in 1923) [14]. Because the emission of an Auger electron is, in reality, a three-electron process, Auger transitions are named for the energy levels of the three-electron orbitals involved, such as KLL.

The Auger process releases electrons of characteristic energy for each element, which are determined by the differences in energy of the orbitals involved. In addition to the Auger electrons, there are also much more plentiful secondary electrons with a broad energy distribution that overlay the characteristic peaks. To highlight the characteristic peaks, differentiation is performed on a plot of the number of electrons emitted by the sample versus the energy of those electrons. This results in a spectrum that ignores the more plentiful background (secondary) electrons and emphasizes the characteristic electrons that are used to identify the elements present. In some cases, the exact peak shape and energy can be used to identify the oxidation state of the elements present. To more clearly discern the peaks, the spectra are derivatized; such a spectrum is shown in Fig. 1.

One of the attractions of Auger analysis is that it is quite surface-sensitive since an Auger spectrum typically represents information about the composition of the top (0.5–2 nm) of the surface depending on the sample analyzed and the analysis conditions. Although Auger electrons can be generated at depths of several micrometers into the sample, in order to be detected, the Auger electrons must be able to escape to the surface without undergoing an inelastic collision. The presence of overlaying material exponentially decreases the probability of the electron reaching the detector unscathed. The exponential constant is the inelastic mean-free path of the electron, which depends on the kinetic energy of the Auger electron and the material it must

**FIG. 1**—Auger spectra of stainless steel surface.



traverse in order to reach the detector. Empirical graphs of the relationship between the electron kinetic energy and its mean-free path are often of use in understanding detectability issues. The effective depth of analysis varies from element to element, even varying between lines of a particular element. This results in high-energy Auger electrons being detectable from deeper in the surface than low-energy ones. For example, a thin, adsorbed carbon (organic) film will preferentially mask the low-energy (68 eV) peak of aluminum as compared to the high energy one (1396 eV). These same types of considerations are applicable to all related electron spectroscopies such as XPS.

Auger spectroscopy also offers acceptable detectability for many situations encountered in corrosion science. This can be as low as 0.01 %, although this is seldom realized in common practice since low detectability conflicts with other desirable qualities such as resolution, analysis time, and the need to minimize beam current to minimize beam damage.

Almost all Auger spectrometers have a scannable incident electron beam such as is used in a Scanning Electron Microscope (SEM). Such an instrument can also be called a Scanning Auger Microscope (SAM). This can provide spatial resolution as low as 15 nm. The ability to scan allows elemental concentration maps of the surface to be generated. This qualitative analysis of small areas is AES's greatest strong point. Its ability to determine element identity and distribution via mapping provides insights into many corrosion problems. In particular, the breakdown of passivity and the initiation of pitting corrosion are often associated with the presence of heterogeneous elements, which include both internal inclusions and corrosive species. Auger maps

are shown in Fig. 2. Variations in signal intensity caused by geometric effects can often be eliminated by ratioing the intensity of the peak of interest to that of adjoining background areas. Elemental mapping is also an important tool in techniques such as SIMS, SEM-EDS, Scanning Kelvin Probe and others.

As in most surface analysis techniques, qualitative identification of the elements present is the easiest type of analysis. Most elements have more than one Auger peak due to having either multiple transitions or fine structure within a transition. It is fairly easy to identify from an Auger spectrum what elements are present on the surface of the sample based on the following: peak position, peak intensity ratios for a particular element, and peak shape. Compilations of elemental spectra and charts of atomic number versus electron energy are available to help assign peaks. Modern data processing (background subtraction, peak fitting to standard spectra) has made it possible to correctly resolve many peak identification problems caused by peak overlap. The analyst should be familiar with ASTM E 827, Standard Practice for Identifying Elements In Auger Electron Spectroscopy. There have been some variations in peak electron energy between different systems and handbooks, but this should be minimized in the future as a result of standardization efforts of ASTM.

Both peak energy and peak shape can vary depending upon the chemical state of the element. This is particularly true for the low-energy transitions of valence electrons. It can also be seen in core-level transitions in those cases where the electrons experience strong energy losses in escaping from metallic surfaces but not from the oxide; for

FIG. 2—Auger elemental distribution maps.

instance; aluminum, magnesium, and silicon. A more detailed description can be found in ASTM E 984, Guide for Identifying Chemical Effects and Matrix Effects in Auger Electron Spectroscopy.

Auger spectrometers are normally equipped with ion-beam sputter guns that can slowly remove the surface while the sample is being analyzed in the vacuum chamber. This results in a depth profile that plots the composition of the freshly generated surface as it varies with depth into the surface. The following three basic issues must be faced when sputter profiling is employed: difficulties in determining the sputter rate, variations in depth resolution, and changes in the sample that are induced by the ion beam.

Sputter rates vary greatly depending on such factors as the identity of the ions (argon is most typical), the accelerating voltage, the angle of incidence, the chemical nature of the sample, and sample surface structure. Although published sputtering yields can be helpful, they cannot replace running known thickness standards on an individual instrument. Two standards that are easiest to accurately fabricate, and therefore are the most common, are tantalum oxide on tantalum and silicon oxide on silicon. Further complications are added by the dependence of sputter yield on depth and on surface roughness.

Depth resolution can be considered to be equal to the observed broadening of an originally atomically sharp interface. It is not constant; it worsens as one sputters into the material. Inert gas ion sputtering is used in the great majority of surface analysis techniques, either as a method of seeing deeper into the sample (Auger, XPS) or as a way of generating particles to be analyzed (SIMS). A discussion of some of the effects of the sputtering process is given in the SIMS section of this chapter. An important publication on the subject is ASTM E 1127, Guide for Depth Profiling in Auger Electron Spectroscopy. A review of sputtering is given in "Depth Profiling in Corrosion Research" in Ref 15. For Auger spectroscopy, a simplistic method of generating a sputter profile by plotting net peak heights works well if there are no problems such as: peak overlap, peak shape change, and peak shift. Modern data manipulation techniques such as factor analysis minimize the effects of these problems. An Auger sputter profile is shown in Fig. 3.

Absolute quantification of surface composition by electron-energy spectral techniques such as Auger and ESCA is a very difficult goal. Current efforts are concentrated in abstracting

quantifiable peaks from the spectra and in minimizing inter-instrument and inter-laboratory variations. ASTM Committee E-41 on Laboratory Apparatus has a number of subcommittees dealing with these issues for a number of surface analysis techniques including Auger, ESCA, and SIMS. A relevant publication is ASTM E 995, Guide to Background Subtraction Techniques in Auger Electron Spectroscopy. Auger analysis is subject to a number of possible artifacts due to effects such as sample charging, electron beam desorption, electron beam decomposition, and variations induced by sputter profiling. These are treated in ASTM E 983, Standard Guide for Minimizing Unwanted Electron Beam Effects in Auger Electron Spectroscopy. To prevent the analyst from adding contamination to the sample, he should be aware of ASTM E 1078, Guide for Specimen Handling in Auger Electron Spectroscopy, X-Ray Photoelectron Spectroscopy, and Secondary Ion Mass Spectrometry.

## X-RAY PHOTOELECTRON SPECTROSCOPY (XPS)

Einstein received the Nobel Prize for his explanation of the photoelectric effect in which atoms can be ionized by an incoming photon [16]. Siegbahn's [17] realization that the energy of the ejected photoelectron could be used to determine the chemical state of an atom caused him to coin the name ESCA (Electron Spectroscopy for Chemical Analysis). Because X-ray photons are necessary to generate appropriate electrons, the technique is also called X-ray Photoelectron Spectroscopy (XPS).

XPS shares the Auger characteristics of good surface sensitivity since this is driven by the same need for the electrons to be able to reach the detector unscathed. It is possible to vary the depth of analysis in both techniques by varying the tilt angle with regard to the detector. This technique is used more extensively in XPS where it is often called angle resolved depth profiling.

XPS also has the very important advantage of being able to obtain chemical state information on most atoms. It becomes easy to observe the effect of differing chemical environments in both the photoelectron peaks and in the Auger peaks, which are also generated by XPS's X-ray excitation. Often, the chemical shifts in the Auger peaks of an XPS spectrum are larger than the shifts in the photoelectron peaks. Another aid to assigning the proper oxidation state to a peak is the presence of satellite shake-up lines due to a simultaneous promotion of a valence electron to a higher orbital as the photoelectron is being ejected. Proper interpretation of the implications of peak shifts requires the knowledge of sample charging on the spectra. A useful reference is ASTM E 1523, Guide to Charge Control and Charge Referencing Techniques in X-Ray Photoelectron Spectroscopy. Another advantage of XPS is that peak identification is more easily done than in Auger because of the narrow line width, as well as the presence of both Auger peaks and photoelectron peaks in the spectra as is shown in Fig. 4.

XPS is also preferable in that it is able to analyze non-conducting samples and has a lesser tendency towards sample degradation than other techniques. XPS is not as preferable

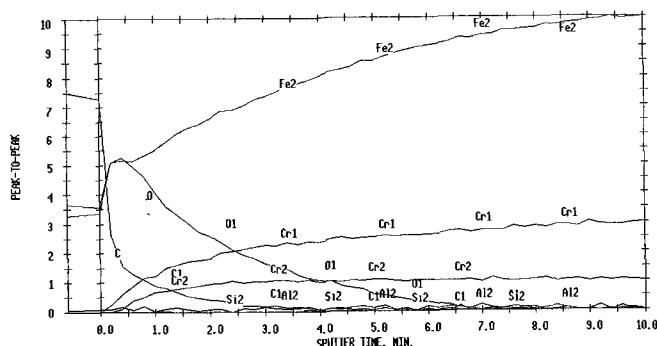


FIG. 3—Auger sputter profile.

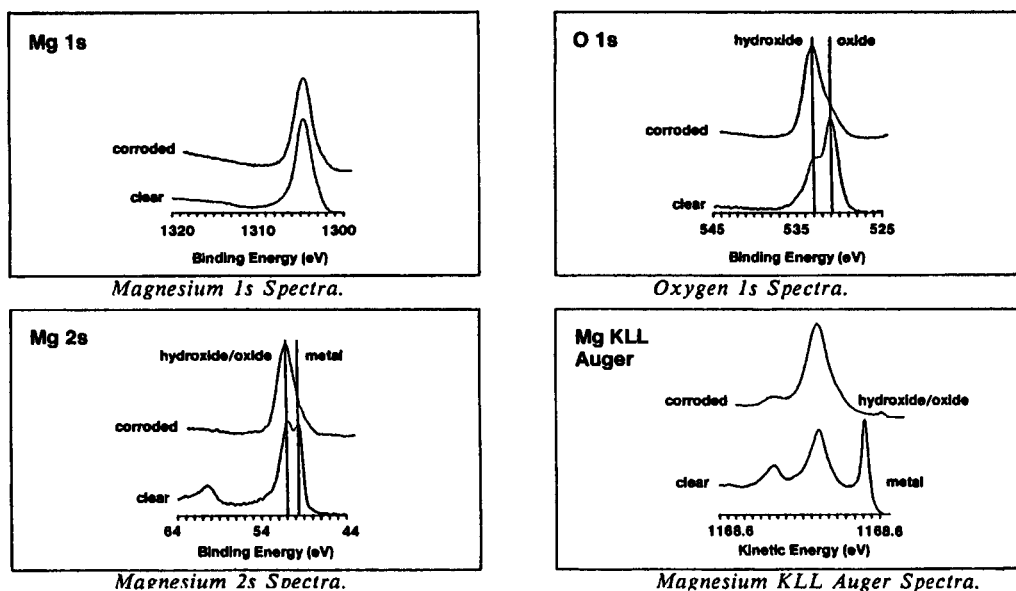


FIG. 4—Ultraviolet photon spectroscopy: uses of narrow scans for corrosion problem solving.

because it does not have Auger's very small spot size since it is much more difficult to focus X-ray beams than electron beams. Therefore, it is necessary to mask or abstract only a portion of the available analysis area which negatively impacts the signal to noise ratio. Relevant information is found in ASTM E 1217, Practice for Determination of Specimen Area Contributing to the Detected Signal in X-Ray Photoelectron Spectroscopy and Auger Electron Spectroscopy. However, 10–30  $\mu\text{m}$  size analysis is possible on a routine basis. The longer time necessary for an XPS spectrum often results in the analyst settling for a lower signal-to-noise ratio and, hence, poorer detectability than with Auger.

## SECONDARY ION MASS SPECTROSCOPY (SIMS)

Secondary Ion Mass Spectroscopy (SIMS) is the third of the three most common surface analysis techniques. A good reference to SIMS and other ion spectroscopies is Czanderna's and Hercules' "Ion Spectroscopies for Surface Analysis" in Ref 11. In SIMS, the sample is irradiated with a primary ion beam (normally argon), the impact of which sputters away the surface atoms, some as neutrals and others as ions. Those atoms that become ionized are then detected in a mass spectrometer where their masses are measured. The most common variant is Dynamic SIMS in which a high-energy ion beam is used that removes layers of the surface. The beam is so energetic that little chemical information is retained since the vast majority of any molecular species is fragmented. Although destroying the surface obviously prevents its re-examination, it is not a total disadvantage since it allows depth profiling to occur.

Some of the advantages of SIMS are that it has a very low detection limit (PPM to PPT) and it can detect all elements. These advantages make it able to address many problems that neither AES nor XPS are suitable for. Reasonably small (micrometer or smaller) spot sizes allow elemental mapping.

A major disadvantage of SIMS is that there is a very great range of ionization rates for different elements. Furthermore, the rates will vary depending on the other species present (matrix effects). Either a beam of positive or negative ions can be used as the exciting beam, although the response factors are much different between them. The biggest differences are found with the very electronegative halogens and the electropositive alkali metals. The variability in response factors makes quantification very difficult and closely matched standards critical. Of use is ASTM E 1505, Guide for Determining SIMS Relative Sensitivity Factors from Ion Implanted External Standards.

In SIMS, as in sputter profiling in Auger and XPS, there are other effects in addition to simply removing the surface atoms. For instance, there is implantation of the sputtering gas and a rearrangement or interfacial mixing of the surface layers. Also, compositional changes caused by preferential sputtering of one element versus another also occur. This is actually a bigger problem for Auger and XPS, which measure the surface, as compared to SIMS, which measures the elements ejected from the surface which soon reach an equilibrium with the actual composition.

Static SIMS uses a much less intense ion beam than Dynamic SIMS. This gives the advantage of not destroying all the molecular species on the surface, which results in one being able to obtain significant chemical information from the surface. It also maintains the integrity of the surface during analysis so that it is much more of a surface technique than Dynamic SIMS. Time of Flight (TOF) SIMS refers to the mode of analysis of the ionized particles rather than their generation process. It provides a very wide mass range plus very high sensitivity.

## OTHER SURFACE TECHNIQUES

The highly variable response factors that are the main limitation of SIMS are almost eliminated by Secondary Neutral

Mass Spectroscopies (SNMS), which provides relatively non-selective ionization of the sputtered species. Separating the sputtering and ionizing functions of SIMS not only eliminates matrix effects but also allows for much less aggressive sputtering conditions. The higher cost of the systems is an inevitable trade-off. There are three ways that the sputtered neutral species can be ionized. Surface Analysis by Laser Ionization (SALI) uses a high-power laser for photoionization, while Glow Discharge Mass Spectroscopy ionizes the neutrals in a glow discharge plasma. The third method is Electron Impact Ionization, and it is labeled by the name of the overall technique, SNMS. Both Electron Impact SNMS and SALI can give SIMS-type information on point defects without the quantification problems that SIMS is prone to. SALI is available with a time of flight (TOF) mass spectrometer which is desirable if higher mass range and resolution is needed than can be provided by standard mass spectrometers.

Rutherford Backscatter Spectroscopy (RBS) requires a monoenergetic beam of high-energy particles (helium ions) that is bounced off of the surface to be analyzed. By analyzing the energy of the backscattered particles, a standardless, nondestructive, quantitative depth profile of the top several micrometers of the surface can be obtained. A related technique is Ion Scattering Spectroscopy (ISS) in which a low-energy monoenergetic beam of ions is directed onto the surface and the energy of the scattered ions is measured. This technique is perhaps the most selective technique of all with regard to only analyzing the topmost layer of atoms. Its major limitations are that it is not able to detect elements at low concentration levels, and it has poor ability to discriminate between elements with similar atomic mass.

## NEAR SURFACE TECHNIQUES

Although not a true surface technique, SEM-EDS often provides useful information in regard to surface corrosion mechanism. The ubiquitous nature, low cost, and ease of use of this technique cause it to be used as a tool in many failure analyses involving corrosion. Because its analysis depth is much larger (approximately a micrometer) than the true surface techniques, it is not necessary to analyze samples that are high-vacuum compatible. This results in the necessity of almost no sample preparation for many different kinds of samples.

The sample is scanned with a high-energy (typically 5–30 KeV) electron beam in a raster pattern, which causes the ejection of a number of particles including secondary electrons, backscattered electrons, and X-rays. Secondary electrons (with energies less than 50 eV) are only detectable if they are generated in the top surface of a sample; this causes the secondary electron output to be responsive to topographical detail and therefore gives an image that is remarkably similar to that seen with an optical microscope. Added advantages are greater magnification and depth of field. The contrast in backscattered electron images is mainly dependent on atomic number, so these images provide rough elemental distribution information.

Element identification is provided by analysis of the characteristic X-rays that are emitted with an Energy Dispersive

Spectrometer (EDS). Quantification can be quite good if appropriate standards are used. The X-ray detector can be set to only detect and count X-rays that have energies within a narrow range. This output can then be used to generate elemental distribution maps, or line scans. Newer detectors with ultrathin windows can easily detect all elements with an atomic number of 5 (boron) or greater. Some applications of SEM-EDS analysis are given in the metallography chapter of this manual.

Particle Induced X-Ray Emission (PIXE) is similar to EDS analysis except that it uses high-energy particles instead of electrons to create the vacancies that lead to X-ray emission. It offers orders of magnitude better detection limits for trace elements than does EDS. Transmission Electron Microscopy (TEM) and Scanning Transmission Electron Microscopy (STEM) require extensive sample preparation. When coupled with another technique (EDS for example), they can be useful in determining the nature of surface films or in illuminating the microstructural causes of corrosion. Environmental Scanning Electron Microscopes (ESEM) that are equipped with EDS spectrometers allow SEM-EDS type data to be obtained from samples in the hydrated state.

Fourier Transform Infrared Spectroscopy (FTIR) and Laser Raman Spectroscopy (LRS) provide complementary views of chemical bonding in a sample by studying the vibrational energies of the bonds. Surface Enhanced Raman Spectroscopy (SERS) can give vibrational spectra of in situ films. A useful review of the application of these vibrational spectroscopies is available [19].

## IN SITU METHODS

Because of the changes that can occur in preparing and analyzing surfaces for high-vacuum techniques, there is great interest in techniques that can obtain information as to the chemical state of metal surfaces while they are in aqueous environments. Some of the most exciting research on the fundamentals of corrosion are using these new techniques. Scanning Tunneling Microscopy (STM) and especially Scanning Force Microscopy (SFM) were the first techniques to give an atomic scale and three-dimensional (3-D) image of a surface that would permit observation in aqueous environments. Since the first scanning probe microscope was invented in 1981 by Gerd Binnig and Heinrich Rohrer, a whole family of scanning probe microscopies have evolved. All of these Scanning Probe Microscopies operate by scanning a small probe tip over the surface to be imaged and creating distributional maps of the response. Two of the most useful for corrosion science are Scanning Kelvin Probe Atomic Force Microscopy (SKPAFM) and Scanning Electrochemical Microscopy (SECM). Two valuable resources on these and other techniques are the Electrochemical Society's *Proceedings on the Symposium on Localized In Situ Methods for Investigating Electrochemical Interfaces* [2] and *Scanning Electrochemical Microscopy*, which has been edited by Bair and Mirkin [20].

SECM is discussed elsewhere in this handbook. The Scanning Kelvin Probe is an updating and miniaturization of the classic method that was first postulated by Lord Kelvin in 1861. It is essentially a non-contact vibrating capacitor

formed between the sample and a vibrating electrode tip, which measures the work function of the sample. Since the work function is extremely dependent on surface condition, the SKP can be used to study such phenomena as oxide layer imperfections, surface and bulk contamination, surface charging, etc.

The availability of high intensity, synchronous X-ray sources at national synchrotron centers has allowed the development of a number of new tools that can study passive or corrosion films as they are forming in aqueous environments. Surface X-Ray Diffraction (SXRD) provides a direct determination of the crystal structure of the atoms of the surface. Surface Extended X-Ray Absorption Fine Structure (SEXAFS) can provide information on the geometric structure of atoms within a few angstroms around the absorbing atom.

These are truly exciting times for the application of surface analysis to corrosion problems.

## REFERENCES

- [1] Baer, D. R., Clayton, C. R., Halada, G. P., and Davis, G. D., "State-of-the-Art Application of Surface and Interface Analysis Methods to Environmental material Interactions," The Electrochemical Society, Inc., Pennington, NJ, 2001.
- [2] Hillier, A. C., Seo, M., and Taylor, S. R., *Proceedings of the Symposium on the Localized In Situ Methods for Investigating Electrochemical Interfaces*, The Electrochemical Society, Inc., Pennington, NJ, 1999.
- [3] Hebert, K. R., Lillard, R. S., and MacDougall, B. R., *Oxide Films*, The Electrochemical Society, Inc., Pennington, NJ, 2000.
- [4] Mansfeld, F., Huet, F., and Mattos, O., "New Trends in Electrochemical Impedance Spectroscopy and Electrochemical Noise Analysis," The Electrochemical Society, Inc., Pennington, NJ, 2000.
- [5] Hansen, D. C., Isaacs, H. S., Sieradzki, K., and Porter M. D., "Scanning Probe Microscopy for Electrode Characterization and Nanometer Scale Modification," The Electrochemical Society, Inc., Pennington, NJ, 2000.
- [6] *Application of Surface Analysis Methods to Environmental/ Material Interactions*, D. R. Baer, C. R. Clayton, and G. D. Davis, Eds., The Electrochemical Society, Inc., Pennington, NJ, 1991.
- [7] *Surface Analysis—The Principal Techniques*, J. C. Vickerman Ed., John Wiley & Sons, 1997.
- [8] *Encyclopedia of Materials Characterization: Surfaces, Interfaces, Thin Films*, C. R. Brundle, C. A. Evans, Jr., and S. Wilson, Eds., Butterworth-Heinemann, Boston, MA, 1992.
- [9] Powell, C. J., et al., "Methods of Surface Characterization," *Beam Effects, Surface Topography and Depth Profiling in Surface Analysis*, Vol. 5, Kluwer Academic Publishers, 1998.
- [10] *Surface Characterization: A User's Sourcebook*, D. Brune et al., Eds., John Wiley & Sons, 1997.
- [11] *Ion Spectroscopies for Surface Analysis*, A. W. Czanderna and D. Hercules, Eds., Plenum, New York, 1991.
- [12] McIntyre, N. S. and Chan, T. C., "Uses of Auger Electron and Photoelectron Spectroscopies in Corrosion Science," *Practical Surface Analysis*, 2nd ed., Vol. A, Auger and X-Ray Photoelectron Spectroscopy, John Wiley & Sons Ltd., Chichester, U.K., 1990.
- [13] Thompson, M., Baker, M. D., Christie, A., and Tyson, J. F., *Auger Electron Spectroscopy*, John Wiley & Sons, New York, 1985.
- [14] Auger, P. J., *J Phys Radium*, Vol. 6, 1925, pp. 205–208.
- [15] Hoffman, S., "Depth Profiling in Corrosion Research," *The Application of Surface Analysis Methods to Environmental/ Material Interactions*, The Electrochemical Society, Pennington, NJ, 1991.
- [16] Einstein, A., *Annals Physik*, Vol. 17, 1905, p. 132.
- [17] Siegbahn, K., et al., "Electron Spectroscopy for Chemical Analysis Atomic, Molecular and Solid State Structure Studies by Means of Electron Spectroscopy," *Nova Acta Geogiae Societate Upsaliensis*, Series IV, No. 20, 1967.
- [18] Czanderna, A. W., "Ion Spectroscopies for Surface Analysis," *The Application of Surface Analysis Methods to Environmental/ Material Interactions*, The Electrochemical Society, Pennington, NJ, 1991.
- [19] Czanderna, A. W. and Hercules, D. M., "Methods of Surface Characterization," *Surface Infrared and Raman Spectroscopy*, Vol. 3, Kluwer Academic Publishers, 1998.
- [20] Bard, A. J. and Mirkin, M., *Scanning Electrochemical Microscopy*, 2001, Marcel Dekker, New York.

# Statistical Treatment of Data, Data Interpretation, and Reliability

Fred H. Haynie<sup>1</sup>

MOST PHYSICAL AND CHEMICAL measurements, performed under nominally identical conditions, yield differing data. The results of corrosion tests are no exception. Sometimes the difference between values is less than the measurement accuracy and cannot be detected. At other times the difference approaches the magnitude of the values. Unfortunately, corrosion test data tend to be in the latter category more often than in the former.

Because of this variation in results it is necessary to apply some type of statistical treatment to the data (e.g., the arithmetic averaging of replicate values). When analyzing data, however, it helps to know some basics. Statistical techniques can be misused and give the researcher a false sense of security. One must be aware of limitations as well as advantages.

*Statistics in Research* by Bernard Ostle [1] is an excellent text that can be used as a handbook. In addition, Standard G 16 (Guide for Applying Statistics to Analysis of Corrosion Data) is a useful document. Statistical techniques are particularly useful in planning and designing experiments. This chapter describes some of the advantages and limitations of applying statistical techniques in corrosion research.

## BASICS

Three statistical methods that are often important in corrosion experiments are (1) probability distributions, (2) design of experiments, and (3) analysis of data. Most investigators use some kind of data analysis technique. Less attention is given to experimental design, and probability distribution is the most neglected of the three methods.

## Terminology

Certain words have specific meanings to the statisticians. These same words may have different meanings to those who are not familiar with statistics. In order to avoid confusion, a discussion of some of the basic terminology is presented.

### Error

Error is the amount by which a value is incorrect or inaccurate.

<sup>1</sup> Corrosion consultant, Cary, NC 27511, and updated and revised by S. W. Dean.

Unfortunately, all experiments have limitations and these limitations cause the existence of error. Whereas random error is acceptable, biased error is not. For example, if, when comparing the corrosion resistance of two alloys in a salt cabinet, the replicate samples of one alloy are placed at one end of the cabinet and the other alloy at the other end, it is possible that the results will be biased by the spray pattern. The within-sample error may be small, and the difference between samples may appear to be significant when the only true significance is a difference in spray pattern. The same type of biased error may be introduced when results obtained on a new alloy are compared to previously obtained results on an old alloy. Because such environmental conditions cannot be controlled exactly, it is necessary to compensate for them in the experimental designs by random exposure of sample replicates in both time and space. This procedure tends to counteract the effects of biased error but generally increases the within-sample error. Both effects reduce the probability of producing results from which erroneous conclusions are made.

### Population, Sample, and Replication

All units having a common set of conditions form a population described by those conditions. For example, if we wish to determine the corrosion behavior of an alloy in a particular type of chemical solution, the population consists of all heats of that alloy exposed to all solutions of the specified type. A much smaller population would be one particular heat of the alloy exposed to a single batch of the solution. It would be incorrect to assume that the smaller population is representative of the larger population.

A sample is some fraction, usually small, of the population. A good sample is representative of the population. Random selection of the proper number of units from a population should assure a good sample. In chapter 1 on *PLANNING AND DESIGN OF TESTS* both random selection and minimum sample size are discussed.

Replication is the repetition of a specified set of experimental conditions that describe the population. Repeated measurements on a single specimen constitute replication only if the population is the set of all such measurements on the specimen.

### Probability Distribution

If mass losses on a large number of replicate specimens are determined, it is often observed that there is one most frequently occurring value, and as other values deviate from

it, their frequencies of occurrence decrease. This peak is called the mode, and the shape of the curve produced by plotting frequency versus measured value is the probability distribution. Most such curves are symmetrical about the mode and have a bell-shaped normal distribution as shown in Fig. 1.

A normal distribution can be mathematically described with two terms: (a) the arithmetic mean ( $\bar{x}$ ) of all values in the population, and (b) the standard deviation ( $\sigma$ ). The mean, which is a measure of central tendency, is equal to the mode for a normal distribution. It is determined from the relationship

$$\bar{x} = \sum_{i=1}^n x_i / n \quad (1)$$

where  $n$  is the number of units in the population. The standard deviation ( $\sigma$ ) is the square root of the variance ( $\sigma^2$ ) and is a measure of the dispersion of values about the mean. The variance is the arithmetic average of all the squares of the deviations about the mean. Mathematically

$$\sigma^2 = \sum_{i=1}^n (x_i - \bar{x})^2 / n \quad (2)$$

Thus, 68.26 % of all the population will be contained within 1 standard deviation either side of the mean. Similarly, 95.46 % and 99.73 % will be contained within 2 and 3 standard deviations, respectively.

#### Best Estimate of Variance and Standard Deviation

The sample sizes in corrosion work are usually not large enough to establish either a true mean ( $\bar{x}$ ) or a true variance ( $\sigma^2$ ). Therefore, best estimates must be made. The number of bits of information that possibly can be obtained from a finite sample is restricted by the data collected. This restriction is known as the total degrees of freedom. As bits of information are obtained from the sample, the degrees of freedom are reduced. Thus, in order to estimate both a mean ( $\bar{x}$ ) and a variance ( $s^2$ ), which are two bits of information, we must have a minimum sample size of two. The best estimate of the mean ( $\bar{x}$ ) is calculated from the sample data using Eq 1. With any size sample ( $n$ ), 1 degree of freedom is said to be used in estimating the mean, thus leaving  $(\bar{n})$  1 degrees of freedom with which to calculate the best

estimate of variance ( $s^2$ ). Equation 2 is used to estimate variance by substituting  $(\bar{n})$  1 for  $n$ .

#### Confidence Limits for the Mean

In general the larger the sample size, the more closely the sample average ( $\bar{x}$ ) approaches the population mean since, if the entire population were measured, we could calculate the population mean. As the sample size decreases, however, the sample average probably deviates more from the population mean. We would like to know how the sample average deviates from the population mean in order to have confidence in the calculated average value.

Gossett [2] (who signed his article "Student") provided a relationship from which the confidence limits on the true mean can be estimated. The relationship is

$$\bar{x} - \bar{x} = \pm s_m \cdot t \quad (3)$$

where  $s_m$  is the square root of the best estimate of sample variance of the mean ( $s^2$ ) and  $t$  is the tabular value "Student's  $t$ " [which is a function of the degrees of freedom and probability ( $P$ )]. If, for example, a sample of five specimens is available and it is desired to establish 95 % confidence limits for the true mean ( $\bar{x}$ ) (i.e., it is desired to have some measure of assurance that 19 out of 20 times the true mean will lie within these limits), the table of " $t$ " values is consulted at 4 degrees of freedom ( $\bar{n}$ ) 1 and a probability  $P$  of 0.05, and a value of 2.776 for " $t$ " is found. If the best estimate of variance is 10,  $s_m$  is calculated to be  $\pm 1.414$ . Therefore, the 95 % confidence limits for the true mean  $\bar{x}$  are  $\bar{x} \pm 3.92$ .

## PROBABILITY DISTRIBUTION

Probability distribution was introduced in the section in this chapter on **Terminology**, and the components of a normal distribution and how to work with them were discussed. Some distributions are not normal because they are skewed to one side of the mode. Unless the values can be treated by some mathematical function to yield a new set of values that approximates a normal distribution, the use of normal statistical techniques could lead to erroneous conclusions. Sometimes the distribution is skewed in such a way that the logarithms of the values have a normal distribution. Fortunately, although the values are not amenable to standard statistical methods, their logarithms are. In contrast, maximum pit depths have an extreme value distribution and should be treated with extreme value statistics. We will discuss these three distributions.

#### Normal Distribution

The normal distribution has the familiar symmetrical bell shape as shown in Fig. 1 and is the basis for the most common statistical techniques of experimental design and data analysis. The characteristics of this distribution are described in the section on **Terminology**. Mass loss, mass gain, thickness loss, corrosion potential, corrosion rate, and pitting area may have a normal distribution. Although this may not be an established fact, in the past many researchers have assumed normal distributions for such data with apparent success.

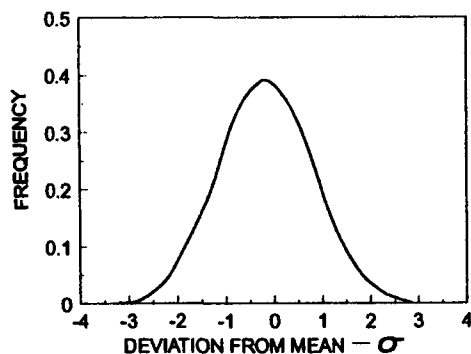


FIG. 1—Normal distribution.

### Log-Normal Distribution

In some cases better results can be produced by assuming a log-normal distribution. A log-normal distribution is simply data that have a normal distribution after they are converted to logarithms. The data then can be analyzed using normal statistical techniques.

Some indicators that generally indicate a log-normal distribution are: (a) data values that physically cannot be negative, (b) normal standard deviations that are proportional to arithmetic means, (c) arithmetic means that are consistently greater than median values, and (d) dependent parameters whose logarithms are proportional to the values of independent parameters. Some types of corrosion data that are likely to be log-normally distributed are: (a) mass loss, (b) thickness loss, (c) time to initial stress corrosion cracks, (d) time to stress-corrosion cracking failures, and (e) polarization currents in the Tafel slope range.

### Extreme Value Distribution

The depths of deepest pits on specimens, the times to first leaks in pipe lengths, times to initial stress-corrosion cracking failures, and the number of cycles to first corrosion-fatigue failures are, by definition, extreme values. The depth of the deepest pit on a specimen is the upper tail of the distribution of depths of all pits on that specimen.

The Weibull distribution [3] often is used in analyzing extreme value data. Expressed in a linear form [4]

$$\ln[-\ln[1 - F(x)]] = c \ln(x - a) - c \ln(1/b) \quad (4)$$

where  $F(x)$  is cumulative probability,  $x$  is a ranked measured value equal to or greater than  $a$ ,  $a$  is the minimum value of  $x$  and is equal to or greater than 0,  $b$  is a scaling parameter, and  $c$  is a shape factor. When working with finite samples, the cumulative probability or plotting position is estimated by [5]

$$F(x_m) = m/(n + 1) \quad (5)$$

where  $m$  is the ordered rank of the measured value (1,2,3, . . . ,  $n$ ) and  $n$  is the total number of the sample.

### Data Distribution Evaluation

Corrosion scientists seldom have enough replicate data to analyze distributions using such techniques as histograms and tests of fit. Sometimes, however, enough data are available to order and plot as a function of linearized forms of the different kinds of probability distributions. Also, nonlinear least squares curve fitting may be used. The best approach is to choose the type of distribution that clearly produces the best approximation to a straight line. If an extreme value distribution is only slightly better than a normal distribution, a normal distribution may be assumed because the statistical techniques are easier to use and more universally understood.

## DESIGN OF EXPERIMENTS

The philosophy incorporated into the design of corrosion experiments is more encompassing than the application of

statistical methods. The purpose of any experimental design should be to efficiently provide a maximum amount of relevant information. In this optimization process, statistical methods, economic analysis, as well as knowledge of corrosion processes is normally employed. Therefore, the use of statistical techniques in design of experiments, is covered in more detail in the chapter on *PLANNING AND DESIGN OF TESTS*. It is discussed here to show how it subsequently affects the analysis of data.

### Types of Experiments

Corrosion scientists work with two basic types of experiments, (1) controlled and (2) uncontrolled. In controlled experiments, levels of independent variables (factors such as temperature and chemical composition) are controlled and the dependent variables (corrosion rate, pitting potential, etc.) are measured. In uncontrolled experiments such as atmospheric exposures, uncontrolled independent variables such as temperature and relative humidity are measured along with the dependent corrosion results. Properly designed controlled experiments are much more amenable to statistical analysis of variance than are properly designed uncontrolled experiments. Many scientists prefer some form of factorial design for controlled experiments.

#### Factorial Experiments

Each controlled variable with more than one controlled level is considered a factor in an experiment. The main advantage of a factorial design experiment is that interaction as well as direct effects can be studied with less replication than several one-way analyses of variances. An example of an interaction effect is a change of slope of a corrosion rate versus relative humidity curve with a change in temperature.

Researchers use two-level factorial experiments to determine which variables or factors cause direct or interaction (synergistic) effects on the measured parameter. Each new factor introduced, however, doubles the number of test conditions. Thus, the need to include a large number of factors in a complete experimental design often results in an impractical number of test conditions. To circumvent this problem, statisticians can design fractional experiments that produce nearly all of the information that researchers need by confounding some possible effects such as higher order interactions. At this point, corrosion researchers have the knowledge and background to assess which physical and chemical relations may control the corrosion process. Some high-order interaction effects may be physically impossible or very unlikely, and statisticians may be able to confound these with direct or lower-order interaction effects that may be possible. Without such guidance, statisticians normally will assume that the higher-order interactions will have little effect, and therefore will design a fractional factorial experiment accordingly.

The Greco-Latin square is a fractional, four-level, four-factor factorial experiment composed of a total of 16 sets of conditions. The complete factorial experiment requires 256 test conditions. It is a very efficient experiment when the data are commensurate with a model containing no interaction terms. Unfortunately, in corrosion experiments it is a



rare situation when a study of four variables does not involve some interaction effects.

### *Uncontrolled Experiments*

In the real world, metals are seldom exposed to controlled environments. Thus, the development of materials for use in the real world normally requires exposure studies in uncontrolled environments.

A properly designed uncontrolled experiment is one that considers all the possible effects of uncontrolled variables. The corrosion researcher's knowledge of physical and chemical processes is most valuable in this respect. Changes in variables that are believed to cause effects along with the resulting effects should be measured. If an important variable is missed, all of the other data become less meaningful.

For proper subsequent analysis, uncontrolled experiments require the collection of considerable data. For example, it is possible to collect ten sets of data involving nine uncontrolled variables and the measured corrosion results. The total is 100 bits of information that can be subjected to multiple regression analysis. If all of the variables are included in the analysis, a perfect mathematical fit can be obtained that is both physically and statistically meaningless. The experimental design does not consider the possibility of nonlinearity effects, interaction effects, nor error effects. One approach to assure that enough data sets are collected is to count all of the physically and chemically (not mathematically) possible direct and interaction effects of the measured variables and multiply by 4 or 5 to account for possible nonlinearity and error.

## ANALYSIS OF DATA

With the use of desktop computers and work stations now common, it is possible for corrosion researchers to put in their data and come out with analysis of variance tables for factorial experiments and multiple linear regression analysis tables for uncontrolled experiments. Most such tables include a statistical test of significance for observed effects. That test (such as a F test) is a measure of the probability that an observed effect either exists or is caused by random error.

Handbooks usually tabulate F values for 0.05 and 0.01 probability levels. If a proper probability distribution has been assumed and an experiment has been designed and executed properly, calculated F values exceeding tabulated values at the 0.05 probability level indicate that the observed effect is likely to be caused by random error only one in 20 or more times. Those are rather good odds involving relatively little risk. Such odds establish a relatively high degree of confidence in the decisions that are based on the corresponding experimental results. When complex tradeoff decisions are to be made, it may be necessary to assume a higher degree of risk. More complete F tables are available that include other probability levels; nothing is magical about 95 or 99 % confidence levels. Researchers should be able to weigh the involved risks in decisions and act accordingly.

### **Analysis Techniques**

A lot of sophisticated statistical software can be used to analyze data. These comprehensive packages can be expensive.

Most of the popular spreadsheet programs can perform multiple regression analysis, and most of the information that is needed can be obtained from this process. Regression analysis as well as other techniques that deal with normal statistics are based on two basic assumptions that are seldom completely accurate; these are (1) independent variables upon which dependent variables are regressed are truly independent, or not associated with each other in any way, and (2) the values of the independent variables are fixed (that is, each one is not just a sample of a distribution of values and thus is not subject to error). In the real world of corrosion research, it is extremely difficult to design or conduct an experiment where these criteria are met. Thus, it is necessary to evaluate how these assumptions might affect the data analysis. The different statistical techniques discussed in the following paragraphs consider the effects of these assumptions.

### *Simple Linear Regression*

This technique fits a straight line to data as dependent values related to a single set of values of an independent parameter. The set of equations that are used minimizes the sum of the squares of differences between the dependent values and the line.

This technique may be illustrated by the analysis of a conceptually simple experiment, galvanic current as a function of dewpoint-temperature and ambient-temperature differences. Assume the experiment was conducted in an environmental chamber that can control conditions uniformly within the measurement accuracy of temperature and dewpoint. We have spaced replicate specimens randomly in the chamber and have measured currents from each very accurately. Three tests were performed at each of three levels of dewpoint (28, 26, and 24°C) holding temperature constant at 30°C. For each new test, at each level, old specimens were retained while new specimens were added and measurements made on both. If three specimens were added for each test replication, there would be 18 current measurements at each level for a total of 54 measurements. That may seem like a lot of measurements just to establish two points that define a straight line. This approach has taken into consideration that both time and space may have an unexpected effect on our current responses, and that our environmental measurements and their resulting controls on chamber conditions truly may not be fixed. For example, although continuous temperature measurements may be within a tenth of a degree, dewpoint measurements may be accurate only within a degree.

Spreadsheet programs consider independent variables as in the  $x$  range and the dependent variable as the  $y$  range. The resulting statistics are placed in an output range in the form of a table. The primary results of interest are the intercept ( $a$ ), the slope ( $b$ ), the estimated standard deviation of the slope ( $s_b$ ), the square of the correlation coefficient ( $R^2$ ), and the number of degrees of freedom for error. In simple linear regression, only one independent value or one column for  $x$  is considered. In multiple regression, several variables ( $x_i$ ) may be included in a like number of columns and the results include a coefficient ( $b_i$ ) and estimated standard deviation ( $s_{bi}$ ) for each.

TABLE 1—Fractional factorial design and results.

	Natural Logarithm of Current in Microamps								
	28°C			26°C			24°C		
	1st Time	2nd Time	3rd Time	1st Time	2nd Time	3rd Time	1st Time	2nd Time	3rd Time
First Exposure	2.0656	...	...	1.4563	...	...	0.2700	...	...
	2.0656	...	...	1.5195	...	...	0.3075	...	...
	2.1294	...	...	1.4231	...	...	0.4055	...	...
Second Exposure	2.2905	2.3224	...	1.3762	1.2119	...	-0.3011	-0.3011	...
	2.3523	2.4105	...	1.2641	1.3762	...	-0.1744	-0.4463	...
	2.3523	2.2905	...	1.2119	1.1410	...	-0.4463	-0.2107	...
Third Exposure	1.8625	1.8991	1.8625	1.2613	1.1086	1.1725	0.0862	0.2390	0.0862
	2.0980	2.1564	2.0360	1.1725	0.9670	1.1410	0.1484	-0.0513	0.0198
	1.8991	2.1282	1.9359	1.0750	1.2326	1.0403	0.0198	0.1222	0.1823

The results of a simple linear regression of our data are:  $-a = 44.01$ ,  $b = 1.859$ ,  $s_b = 0.094$ , and  $R^2 = 0.882$  (the fraction of the variability explained by the regression). However, it is known that current is an exponential function of dewpoint, and the current values are log-normally distributed. One reason to think so is that current cannot be negative when the dewpoint is zero as is indicated by the intercept value. Regressing the natural logarithms of the current with dewpoint yields  $-a = 12.68$ ,  $b = 0.532$ ,  $s_b = 0.018$ , and  $R^2 = 0.943$ . The exponential model produces a better fit than the linear model.

How does dewpoint not being fixed affect these coefficients? If dewpoint is regressed with log-current and the resulting equation transposed, the coefficients  $a$  and  $-b$  are 13.52 and 0.563, respectively. This result shows that the inability to precisely measure and control the dewpoint results in an underestimate of the slope and an overestimate of the intercept.

#### Multiple Regression Analysis and Analysis of Variance

The hypothetical experiment described previously was performed considering the possibility that time and space effects could bias our results. This possibility can be tested using multiple linear regression and analysis of variance. The experimental design has included two variables (other than dewpoint) we will call time and exposure. Values for exposure are 1, 2, and 3 for the first, second, and third exposures at a set dewpoint, respectively. Values for time are 1, 2, and 3 for specimens exposed only to the first exposure, to the first and second exposures, and to the first, second, and third exposures, respectively. With three variables, four interaction effects are possible: (1) dewpoint X time, (2) dewpoint X exposure, (3) time X exposure, and (4) dewpoint X time X exposure. The values for these interactions are the products of the differences between the values and their means. For example, a value for dewpoint X exposure is  $(28 - 26) \times (-12.33) = -2.67$ . By using formulas in a spreadsheet it is possible to create an  $x$  matrix of 7 columns with 54 rows that can be regressed against the measured current data  $y$ . The data in this fractional factorial experiment are presented in Table 1.

Multiple regression of the data for this three-factor, three-level factorial experiment can produce an analysis of variance. Calculated values for  $F$  are used to determine statistical significance of direct and synergistic effects.  $F$  may be determined using the following relationship

$$F = (b/s_b)^2 \quad (6)$$

Each coefficient uses one degree of freedom ( $DF$ ). In this experiment with an intercept and 7 slopes the remaining

error degrees of freedom are 46. The  $F$  tables are entered with 1  $DF$  for the greater mean square and 46  $DF$  for the lesser mean square. The  $F$  values associated with better than 0.95 and 0.99 probabilities of statistical significance for these  $DF$ s are 4.05 and 7.21, respectively.

The results of regression analysis and analysis of variance are given in Table 2. Only those effects containing dewpoint are statistically significant at greater than 0.95 or 0.99 probability. A regression including only those terms yields the results in Table 3. Only the intercept is slightly different from that in Table 2. The best estimate of the functional relationship between current and dewpoint at a constant temperature of 30°C is  $\text{Current} = \exp [0.581(DP - 24.2)]$ .

#### Covariance of "Independent" Variables

In many corrosion experiments, exposure conditions are uncontrolled and the independent variables of interest are measured and recorded. Multiple regression analysis is very useful in analyzing these data. The results of multiple regression analysis of uncontrolled experiments do not within themselves prove cause-effect relationships. Possible correlations between supposedly independent variables are a serious problem. When two "independent" variables are perfectly correlated, it is impossible to determine which variable actually correlates with the dependent variable results. Thus, when such strong correlations exist, although one variable may appear to be statistically more significant than the other, it may be mathematically serving as the other variable's proxy or stand-in a cause-effect relationship. Such might be the case when the error of measurements for the proxy variable is much less than the error of measurements for the variable actually causing the effect.

Significant proxy variables may be used within limits with some success as predictors and still not have any real physical significance. A good example is corrosion rates that correlate with distance from a seashore when the actual cause is the amount of salt spray deposited on the specimens.

Simple linear regressions between each of the independent variables can be used to produce a correlation matrix. The values of  $R$  in this matrix can be used to identify possible covariance problems. Once statistical significance of various factors is established, the corrosion researcher should consider the corrosion processes and first principles in reaction kinetics to evaluate the consistency of the statistical model with a physical model. Best fits of data to physical models can yield valuable information such as activation energies that can point toward diffusion controlled or activation controlled processes.

**TABLE 2**—Regression analysis and analysis of variance.

Intercept $a$ -13.81	$R^2$ 0.9643		DF 46
Effect	$b$	$s_b$	$F$
Dewpoint (DP)	0.5809	0.0196	876.70
Time (T)	-0.0457	0.0513	0.79
Exposure (E)	-0.0533	0.0513	1.08
DP $\times$ T	0.0836	0.0314	7.08
DP $\times$ E	-0.1087	0.0314	11.96
T $\times$ E	0.0778	0.0728	1.14
DP $\times$ T $\times$ E	-0.1811	0.0446	16.52

**TABLE 3**—Regression analysis of significant effects.

Intercept $a$ -13.99	$R^2$ 0.9572		DF 49
Effect	$b$	$s_b$	$F$
Dewpoint (DP)	0.5809	0.0208	778.21
DP $\times$ T	0.0836	0.0334	6.28
DP $\times$ E	-0.1087	0.0334	10.62
DP $\times$ T $\times$ E	-0.1811	0.0473	14.66

## SUMMARY

Corrosion researchers can gain a greater degree of confidence in their experimental results if they have a basic understanding and use statistical techniques of experimental design and data analysis. Statisticians cannot properly design

an experiment nor analyze the resulting data without the help of corrosion researchers. Statistical techniques have both advantages and limitations related to the types of data to be collected. Overall, corrosion researchers should have a better feel for the physical constraints that may limit statistical models than do statisticians. The statistician will have a better feel for how these constraints can be incorporated into the layout of the design which predetermines the style of statistical analysis to be used. Statistical techniques should not control the research to the point that it becomes the "tail that wags the dog." The research objectives must be kept in sight, and statistics is one of many tools that can be valuable to reach them.

## REFERENCES

- [1] Ostle, B., *Statistics in Research*, Second Edition, Iowa State College Press, Ames, IA, 1963, pp. 585.
- [2] Mickley, H. S., Sherwood, T. K., and Reed, C. E., *Applied Mathematics in Chemical Engineering*, Second Edition, McGraw-Hill, New York, 1957, pp. 46-99.
- [3] Weibull, W., "A Statistical Distribution of Wide Applicability," *Journal of Applied Mechanics*, Vol. 18, 1951, pp. 293-297.
- [4] Harshbarger, J. H., Kemppinen, A. I., and Strum, B. W., "Statistical Treatment of Nonnormally Distributed Stress-Corrosion Data," *Handbook on Corrosion Testing and Evaluation*, W. H. Ailor, Ed., John Wiley and Sons, New York, 1971, p. 90.
- [5] Pathak, B. R., "Testing in Fresh Waters," *Handbook on Corrosion Testing and Evaluation*, W. H. Ailor, Ed., John Wiley and Sons, New York, 1971, p. 568.

# Computer Based Data Organization and Computer Applications

Pierre R. Roberge<sup>1</sup>

## INTRODUCTION

COMPUTERS PLAY IMPORTANT roles in data acquisition in laboratory and field environments, data processing and analysis, data searching and data presentation in understandable and useful formats. The rapid development of accessible computing power since the 1980s has led to the use of computers and direct or indirect applications of machine intelligence in every sphere of science and engineering. As a modern science philosopher has written, "The emergence of machine intelligence during the second half of the twentieth century is the most important development in the evolution of this planet since the origin of life two to three thousand million years ago" [1]. Computers also assist engineers to transform data into usable and relevant information. The connectivity of computers to the outside world through the Internet and the Web has opened up tremendous channels of communication that never existed before.

## Compilation of Corrosion Data

Corrosion data for metals are measures of time dependent material/environment interactions that are manifested in many forms; for example, pitting, stress corrosion cracking, corrosion-fatigue, crevice corrosion, and fretting. If nonmetals are considered, swelling, property changes, and cracking are important manifestations. Data are available from many sources including standardized laboratory and field tests, industrial exposures, and the results of failure analyses, and are recorded in many formats that may or may not include sufficient information for independent understanding and reliability assessment. As with many other material property studies, the data often are developed for proprietary purposes by an individual or a small group of users who have a common understanding of unique terminology, algorithms, test methods, and data report formats and have no motivation to modify their data compilations for sharing with other potential users [2].

## Standardized Data Recording Formats

The need to develop standardized data recording formats was recognized by Committee G01 on Corrosion of Metals. The committee efforts addressed material identification and recording of test details along with guidelines for assessing data quality, data interchange formats, and consistent terminology

as it relates to computerization. ASTM G 107, Guide for Formats for Collection and Compilation of Corrosion Data for Metals for Computerized Database Input, serves as a master list with a total of 125 individual data entry fields, each defined with preferred units and category sets (acceptable entries) to assure consistency. Not all fields are required for any one data record, but an estimated 25–50 often are required to fully describe the material, environment, and test results for an individual test. Table 1 describes the eight basic data categories detailed in the standard as being considered essential for the complete documentation of corrosion data. Rarely is this detail provided in the published literature, a factor that compounds the difficulties in comparing published data from different sources [2].

**TABLE 1**—Corrosion database input categories for metals in ASTM G 107.

Type of Test	<ul style="list-style-type: none"> <li>• Standardized test</li> <li>• Laboratory or field test</li> <li>• Relation to specific process (e.g., pulp bleaching)</li> <li>• Relation to specific application (e.g., production tubing)</li> </ul>
Test Emphasis Environment	<ul style="list-style-type: none"> <li>• Type(s) of corrosion evaluated</li> <li>• Generic description</li> <li>• Concentration and state of principal components</li> <li>• Contaminants</li> <li>• Form (e.g., solid, liquid, aqueous solution)</li> </ul>
Exposure Conditions	<ul style="list-style-type: none"> <li>• Duration</li> <li>• Temperature</li> <li>• pH</li> <li>• Hydrodynamic conditions</li> <li>• Aeration</li> <li>• Agitation</li> </ul>
Material Identification	<ul style="list-style-type: none"> <li>• Class(e.g., metals)</li> <li>• Subclass</li> <li>• Family</li> <li>• Common name</li> <li>• Standard designation</li> <li>• Condition</li> <li>• Manufacturing process</li> <li>• Product form</li> </ul>
Specimen Identification	<ul style="list-style-type: none"> <li>• Specimen no.</li> <li>• Size</li> <li>• Surface condition</li> <li>• Composition</li> <li>• Properties</li> </ul>
Specimen Performance	<ul style="list-style-type: none"> <li>• Mass change</li> <li>• Property change</li> <li>• Type and severity of localized attack (e.g., pitting, crevice corrosion, stress corrosion cracking)</li> </ul>
Documentation	<ul style="list-style-type: none"> <li>• Reference or source</li> <li>• Published or unpublished data</li> </ul>

<sup>1</sup> Department of Chemistry and Chemical Engineering, Royal Military College of Canada, Kingston, Ontario K7K 7B4, Canada.

**FIG. 1—Time and environment dependency of databases and models.**

ASTM G 135, Guide for Computerized Exchange of Corrosion Data for Metals, defines the techniques used to encode corrosion of metals test results for exchange between computer systems. The guide establishes formalism for transferring corrosion test data between computer systems in different laboratories and defines a generic approach to structuring data files. The guide is designed for standards developers to help them specify the format of files containing test results and create programs that read and write these files.

### Data Quality

Physical and mechanical property data are normally generated using established standard test procedures that permit direct comparisons of test results. However, the transformation of corrosion testing results into usable real life functions for service applications can be a rather difficult task, often generating unreliable or questionable data as illustrated in Fig. 1 [3]. In the best cases, laboratory tests can provide a relative scale of merit in support of the selection of materials exposed to specific corrosive conditions and environments. Data can be classified by a variety of schemes that reflect the extent of the data generated and the level to which the data have been processed [2]:

- Raw (unanalyzed) individual test results.
  - Analyzed individual test results.
  - Mathematically reduced (average or statistically based) values representative of sets (multiple replicates) or results.
  - Validated data, meeting the validity requirements of the appropriate test standards.
  - Evaluated data, representing parametric analysis of data sets, including in some cases judgmental interpretation by one or more experts.
  - Certified values, representing approval by some referee on certification groups for some specific application (for example, design).
- Several distinct steps should be taken to assess the quality of any material property or performance data. While the data evaluation and validation steps reflect more on the quality of the data generated, data verification reflects on the data search and retrieval system used to ensure the retrieved data are consistent with the original source [2].
1. Evaluation: The process of establishing the accuracy and integrity of data. Evaluation may involve examination and appraisal of the data presented, assessment of experimental technique and associated errors, consistency checks for allowed values and units, comparison with other experimental or theoretical values, reanalysis and recalculation of derived quantities as required, selection of best values, and assignment of probable error or reliability.
  2. Validation: The process of substantiating that the data have been generated according to standard methods and practices or other indices of quality, reliability, and precision.
  3. Verification: The process of substantiating the accuracy of the data transcription and manipulation within the data system.
- A number of corrosion data evaluation studies have described the scope of the effort required [4]. Unfortunately,

the complexities of corrosion data tend to discourage attempts to undertake this type of rigorous data analysis. A more accepted approach is to develop expert consensus, often through peer review or technical committee activities, resulting in publication of summary documents addressing specific environments or applications with judgmental appraisals of the quality, reliability, and adequacy of available data for the intended purpose or application.

### Overcoming Knowledge Gaps

Humans are used to working with imprecise information. They naturally accept vague use of language, making continuous interpretations of the information they receive based upon context. Computers are much less forgiving. This section introduces a generic framework linking mechanistic principles leading to corrosion damage with the observable signs of a corrosion attack.

Six important corrosion factors have been identified in a review of scientific and engineering work on SCC damage [5], generally regarded as the most complex corrosion mode. According to Staehle's materials degradation model, all engineering materials are reactive and their strength is quantifiable, if all the variables involved in a given situation are properly diagnosed and their interactions understood. For characterizing the intensity of SCC the factors were material, environment, stress, geometry, temperature and time. These factors represent independent variables affecting the intensity of SCC. Furthermore, a number of subfactors have been identified by Staehle for each of the six main factors, as shown in Table 2.

The term "form" of corrosion is generally well known from Fontana's popular corrosion engineering textbook [6]. The different forms of corrosion represent corrosion phenomena categorized according to their visual appearance. Dillon [7] considered Fontana's eight basic forms of corrosion and divided them into three groups, based on their ease of identification:

- Group 1—readily identifiable by ordinary visual examination
  - Uniform corrosion
  - Pitting
  - Crevice corrosion
  - Galvanic corrosion
- Group 2—may require supplementary means of examination
  - Erosion
  - Cavitation
  - Fretting
  - Intergranular
- Group 3—verification by microscopy is usually required
  - Exfoliation
  - Dealloying
  - Stress corrosion cracking
  - Corrosion fatigue

An empirical correlation was established between the factors listed in Table 2 and these forms of corrosion. Fifteen recognized corrosion experts agreed to complete an opinion poll listing the main subfactors and the common forms of corrosion. The responses were then analyzed and represented in a graphical way, such as illustrated in Fig. 2, for

the most important factors leading to different forms of corrosion failures. An obvious application of the results shown in Fig. 2 would be to help optimize the number of fields required for the development of an efficient knowledge based system.

Context sensitivity is fundamental to failure analysis. For one, the criticality of a specific failure is very much system dependent. While the general description of the corrosion types presented in Table 2 is sufficient to explain the general appearance of most specific problems, it can lead to great confusion when one tries to quantify the attributes associated with them. Pitting corrosion, which, for example, is almost a common denominator in all types of localized corrosion attack, may assume different shapes. Pitting corrosion can produce pits with their mouth open (uncovered) or covered with a semipermeable membrane of corrosion products. Pits can be either hemispherical or cup-shaped. In some cases, they are flat-walled, revealing the crystal structure of the metal, or they may have a completely irregular shape [8]. The severity associated with pitting corrosion can also vary greatly and is directly dependent on the criticality of the systems subjected to this form of damage.

A more detailed analysis of these survey results reveals some interesting features that relate to the terminology used in corrosion science and engineering. The results of interviews were analyzed with Box-and-Whisker plots. These plots divide the data for each sample into four areas of equal frequency. A box encloses the middle 50 %, and the median is drawn as a vertical

**TABLE 2**—Factors and subfactors controlling the occurrence of a corrosion failure.

Factor	Subfactors and contributing elements
Material	Chemical composition of alloy Crystal structure Grain boundary (GB) composition Surface condition
Environment	
<i>chemical definition</i>	Type, chemistry, concentration, phase, conductivity
<i>circumstance</i>	Velocity, thin layer in equilibrium with relative humidity, wetting and drying, heat transfer boiling, wear and fretting, deposits
Temperature	At metal surface exposed to environment Change with time
Stress	
<i>stress definition</i>	Mean stress, maximum stress, minimum stress, constant load/constant strain, strain rate, plane stress/plane strain, modes I, II, III, biaxial, cyclic frequency, wave shape
<i>sources of stress</i>	Intentional, residual, produced by reacted products, thermal cycling
Geometry	Discontinuities as stress intensifiers Creation of galvanic potentials Chemical crevices Gravitational settling of solids Restricted geometry with heat transfer leading to concentration effects Orientation versus environment
Time	Change in GB chemistry Change in structure Change in surface deposits, chemistry, or heat transfer resistance Development of surface defects, pitting, or erosion Development of occluded geometry Relaxation of stress

	Uniform	Pitting	Crevice	Galvanic	Erosion	Cavitation	Fretting	Intergranular	De-Alloying	SCC	Fatigue	Scaling	Internal Attack
<b>Material</b>													
Composition	■	■		■		■	■	■	■	■	■	■	■
Crystal Structure								■					
GB Composition								■		■			
Surface Condition		■								■			
<b>Environmental</b>													
Nominal	■	■		■	■			■	■	■	■	■	
Circumstantial		■	■							■			
<b>Stress</b>													
Applied										■	■		
Residual										■			
Product Build-Up										■			
Cyclic											■		
<b>Geometry</b>													
Galvanic Potentials				■									
Restricted Geometries			■										
Settling of Solids		■											
<b>Temperature</b>													
Changing Temperature												■	
Temperature of Surface		■										■	■
<b>Time</b>													
Changes Over Time	■											■	■

Based on response where  $\bar{x} > 7$  and  $\sigma < 3$

**FIG. 2—Results of an expert opinion poll indicating the most important factors causing different types of corrosion failures.**

line inside the box. Horizontal lines or whiskers extend on each side of the box to represent the smallest data point within 1.5 interquartile for the lower quartile (left) and the highest data point within 1.5 interquartile for the upper quartile (right). Individual points drawn outside of these ranges signify the presence of data values within three interquartile ranges (suspect outliers) or even farther apart as outliers.

Figure 3 presents the Box-and-Whisker plots of the results obtained with pitting corrosion, and Table 3 summarizes two features of the plot by prioritizing the importance associated with each subfactor included in the framework (the median) and the sharpness of the responses (inverse of the breadth of the whiskers). When presented in this fashion, such results provide a useful spectrum of factor and subfactor confidence levels. While the important and sharp subfactors can be used reliably to predict the occurrence of pitting corrosion, the least focused results provide a good indication of the ambiguities related to this form of corrosion.

## MODELING AND LIFE PREDICTION

Models of materials degradation processes have been developed for a multitude of situations using a great variety of methodologies. For scientists and engineers working at developing materials, models have become an essential benchmarking element for the selection and life prediction associated with the introduction of new materials or processes. For systems

managers the corrosion performance or under-performance of materials has a very different meaning. In the context of life cycle management, corrosion is only one element of the whole picture, and the main difficulty with corrosion knowledge is in incorporating it at the system management level.

### Bottom Up Approach

Scientific models can take many shapes and forms, but they all seek to characterize response variables through relationship with appropriate factors. Traditional models can be divided into two main categories: mathematical or theoretical models and statistical or empirical models [9]. Mathematical models have the common trait that the response and predictor variables are assumed to be free of specification error and measurement uncertainty [10]. Statistical models, on the other hand, are derived from data that are subject to various types of specification, observation, experimental and/or measurement errors. In general terms, mathematical models can guide investigations while statistical models are used to represent the results of these investigations.

### Mathematical Models

Some specific situations lend themselves to the development of useful mechanistic models that can account for the principal features governing corrosion processes. These models are most naturally expressed in terms of differential

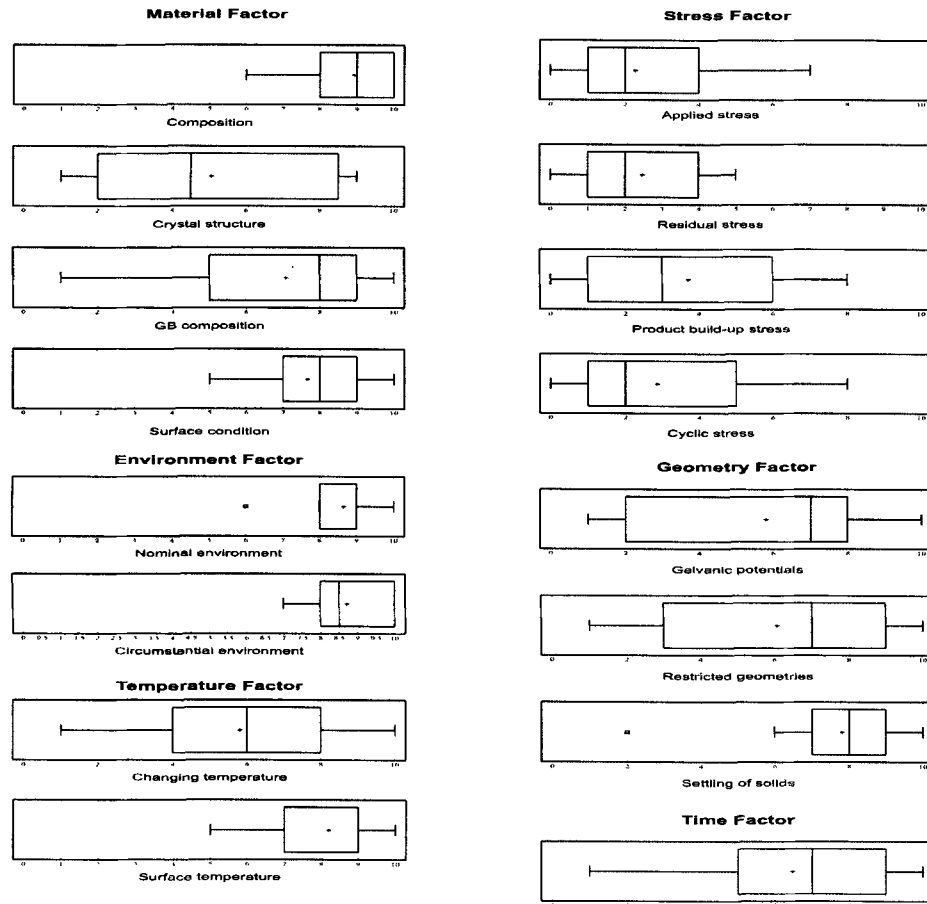


FIG. 3—Box-and-whisker plots of the survey results obtained for the factors and subfactors underlying the appearance of pitting corrosion.

equations or in another nonexplicit form of mathematics. However, modern developments in computing facilities and in mathematical theories of nonlinear and chaotic behaviors

TABLE 3—Ranking of the subfactors causing pitting corrosion in decreasing order of importance and distribution sharpness.

Order of importance*		Order of sharpness**	
Factor	Subfactor	Factor	Subfactor
Material	Composition	Environment***	Nominal
Temperature	Surface	Environment	Circumstantial
Environment	Nominal	Material	Composition
Environment	Circumstantial	Geometry***	Settling
Material	GB	Temperature	Surface
Material	Surface	Material	Surface
Geometry	Setting	Stress	Residual
Geometry	Galvanic	Stress	Applied
Geometry	Restricted	Material	Microstructure
Time		Stress	Product
Temperature	Changing	Stress	Cyclic
Material	Microstructure	Material	GB
Stress	Product	Geometry	Galvanic
Stress	Applied	Temperature	Changing
Stress	Residual	Geometry	Restricted
Stress	Cyclic	Time	

\*The median

\*\*The inverse of the breadth of the whiskers

\*\*\*Presence of one suspect outlier

have made it possible to cope with relatively complex problems. A mechanistic model has the following advantages [11]:

- It contributes to our understanding of the phenomenon under study;
- It usually provides a better basis for extrapolation;
- It tends to be parsimonious, i.e., frugal, in the use of parameters and to provide better estimates of the response.

The modern progress in understanding corrosion phenomena and controlling the impact of corrosion damage was greatly accelerated when the thermodynamic and kinetic behavior of metallic materials was made explicit in what became known as E-pH or Pourbaix diagrams (thermodynamics) and mixed potential or Evans diagrams (kinetics). These two models, both established in the 1950s, have become the basis for most of the mechanistic studies carried out since then. The multidisciplinary nature of corrosion science is reflected in the multitude of approaches that have been proposed to explain and model fundamental corrosion processes. The following list illustrates some scientific disciplines with examples of modeling efforts one can find in the literature:

- **Surface science:** atomistic model of passive films
- **Physical chemistry:** adsorption behavior of corrosion inhibitors



- **Quantum mechanics:** design tool for organic inhibitors
- **Solid state physics:** scaling properties associated with hot corrosion
- **Water chemistry:** control model of inhibitors and anti-scaling agents
- **Boundary element mathematics:** cathodic protection

### Statistical Models

Mechanisms underlying corrosion processes are frequently not understood sufficiently well or are simply too complicated to allow an exact model to be built from theory. In such cases empirical models may be useful. The degree of complexity that should be incorporated in an empirical model can seldom be assessed in the initial phase of designing such model. A most common approach is to first build a simple model based on a limited set of variables and increase its complexity with growing evidence and confidence.

Statistical assessment of time to failure is a basic topic in reliability engineering for which many mathematical tools have been developed. Evans, who also pioneered the mixed potential theory to explain basic corrosion kinetics, launched the concept of corrosion probability in relation to localized corrosion. According to Evans, an exact knowledge of corrosion rate was less important than the ascertainment of the statistical risk of its initiation [12]. The following examples illustrate the application of empirical modeling in two areas of high criticality.

### Extreme Value Statistics

A number of statistical transformations have been proposed to quantify the distributions in pitting variables. Gumbel is given the credit for the original development of extreme value statistics (EVS) for the characterization of pit depth distribution [13]. The EVS procedure is to measure maximum pit depths on several replicate specimens that have pitted, then arrange the pit depth values in order of increasing rank. The Gumbel distribution expressed in Eq 1, where  $\lambda$  and  $\alpha$  are the location and scale parameters, respectively, can then be used to characterize the dataset and estimate the extreme pit depth that possibly can affect the system from which the data was initially produced.

$$F(x) = \exp\left(-\exp\left[-\frac{x-\lambda}{\alpha}\right]\right) \quad (1)$$

In reality there are three types of extreme value distributions [14]:

- **Type 1:**  $\exp(-\exp[-x])$  or the Gumbel distribution
- **Type 2:**  $\exp(-x^{-k})$  Cauchy distribution
- **Type 3:**  $\exp(-[\omega - x]^k)$  Weibull distribution

where  $x$  is a random variable, and  $k$  and  $\omega$  are constants.

A goodness-of-fit test is required to verify which of these three distributions best fits a specific data set. The Chi square test or Kolmogorov-Smirnov test has often been used for this purpose. A simpler graphical procedure is also possible using a generalized extreme value distribution with a shape factor dependent on the type of distribution. There are two expressions for the generalized extreme value distribution, i.e., Eq 2 when  $kx \leq (\alpha + uk)$  and  $k \neq 0$ ,

$$F(x) = \exp\left(-1 - k \frac{x-u}{\alpha}\right)^{1/k} \quad (2)$$

and Eq 3 when  $x \geq u$  and  $k = 0$ .

$$F(x) = \exp\left(-\exp\left[-\frac{x-u}{\alpha}\right]\right) \quad (3)$$

EVS were put to work on real systems on several occasions in the oil and gas industries for two main reasons. The 1st reason was the critical nature of many operations associated with the transport of gas and other petroleum products, and the 2nd is the predictability of localized corrosion of steel, the main material used by the oil and gas industry. Meany has, for example, reported four detailed cases where extreme value distribution proved to be an adequate representation of corrosion problems in underground piping and power plant condenser tubing [15]. In another study, data from water injection pipeline systems and from the published literature were used to simulate the sample functions of pit growth on metal surfaces [16]. It was concluded that maximum pit depths were adequately characterized by extreme value distribution, that a Gaussian distribution could model corrosion rates for water injection systems, and that an exponential pipeline leak growth model was appropriate for all operation regimes.

## PROPAGATION OF PROBABILITY FUNCTIONS

The regulations pertaining to the geologic disposal of high-level nuclear waste, in the U.S. and Canada, require that the radionuclides remain substantially contained within the waste package for 300–1000 years after permanent closure of the repository. The current concept of a waste package involves the insertion of spent fuel bundles inside a container that is then placed in a deep borehole, either vertically or horizontally, with a small air-gap between the container and the borehole. For vitrified wastes, a pour canister inside the outer container acts as an additional barrier. Currently, no other barrier is being planned, making the successful performance of the container material crucial to fulfilling the containment requirements over long periods of time.

A model developed to predict the failure of Grade-2 titanium was published in which two major corrosion modes were included [17]: failure by crevice corrosion and failure by hydrogen induced cracking (HIC). A small number of containers were assumed to be defective and fail within 50 years of emplacement. The model was probabilistic in nature, and each modeling parameter was assigned a range of values resulting in a distribution of corrosion rates and failure times. The crevice corrosion rate was assumed to be only dependent on properties of the material and the temperature of the vault. Crevice corrosion was also assumed to initiate rapidly on all containers and subsequently propagate without repassivation. Failure by HIC was assumed to be inevitable once a container temperature fell below 30°C. However, the concentration of atomic hydrogen to render a container susceptible to HIC would occur only very slowly and might even be negligible if that container had never been subject to crevice corrosion.

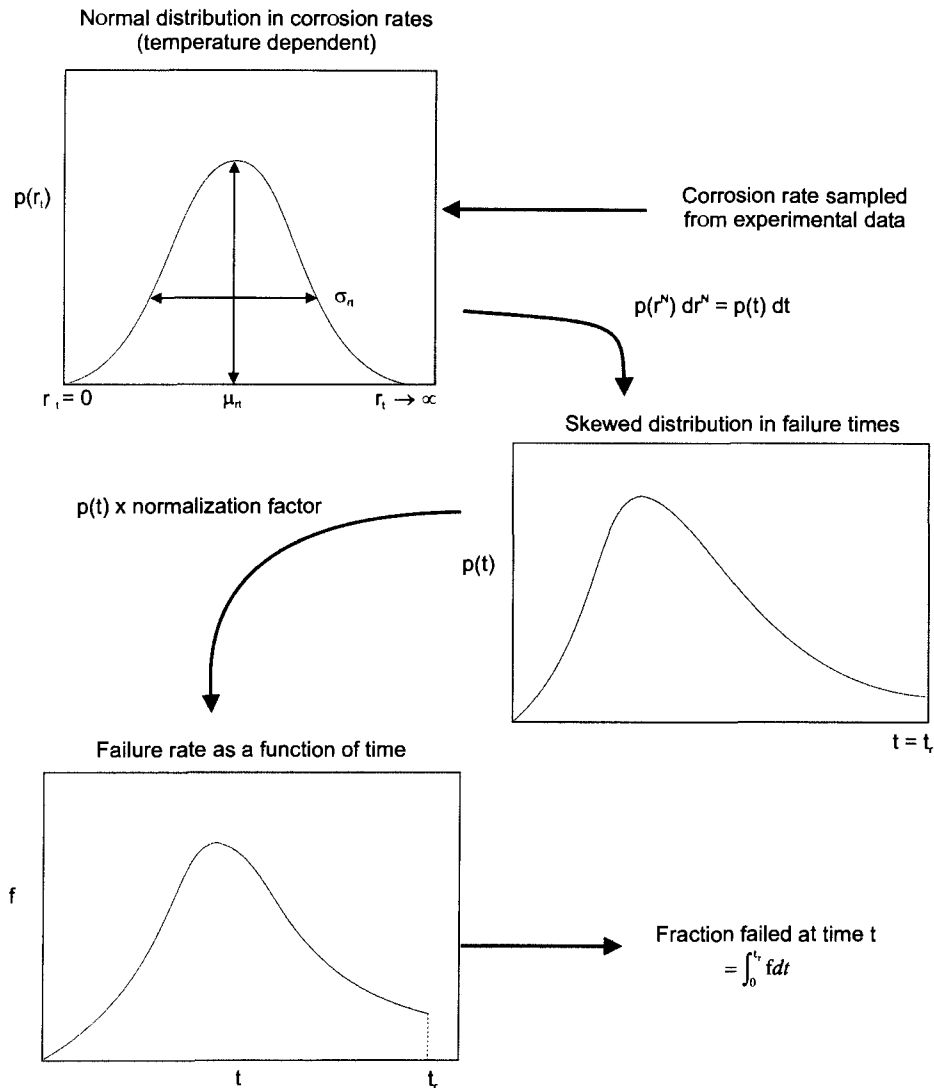


FIG. 4—Procedure used to determine the failure rate of hot containers as a function of time.

The mathematical procedure to combine various probability functions and arrive at a failure probability of a hot container due to crevice corrosion at a certain temperature is illustrated in Fig. 4. The failure rate due to HIC was arbitrarily assumed to have a triangular distribution in order to simplify the calculations, and knowing that HIC is only a predicted marginal failure mode in the considered burial conditions.

On the basis of these assumptions and the calculations described in the full paper, it was predicted that 96.7 % of all containers would fail by crevice corrosion and the remaining by HIC. However, only 0.137 % of the total number of containers were predicted to fail before 1000 years (0.1 % by crevice corrosion and 0.037 % by HIC) with the earliest failure after 300 years.

### Top Down Approach

Some of the issues involved in deciding on a cost-effective solution for combating corrosion are generic to sound system

management. Others are specifically related to the impact of corrosion damage on system integrity and operating costs. The following examples illustrate how these considerations are put into practice and integrated into efficient management systems.

### A Fault Tree for the Risk Assessment of Gas Pipeline

This first top-down model example briefly describes the fault tree analysis (FTA) methodology adopted by Nova Corporation for the risk assessment of its 18 000 km gas pipeline network [18]. FTA is a very efficient method for reviewing and analytically examining a system or equipment in its details to emphasize the lower level fault occurrences that directly or indirectly could contribute to a major fault or undesired event. By performing an FTA from lower-level failure mechanisms, a global overview of the system is achieved. Once completed, the fault tree allows the risk engineer to evaluate fully a system safety or reliability by altering the various lower-level attributes of the

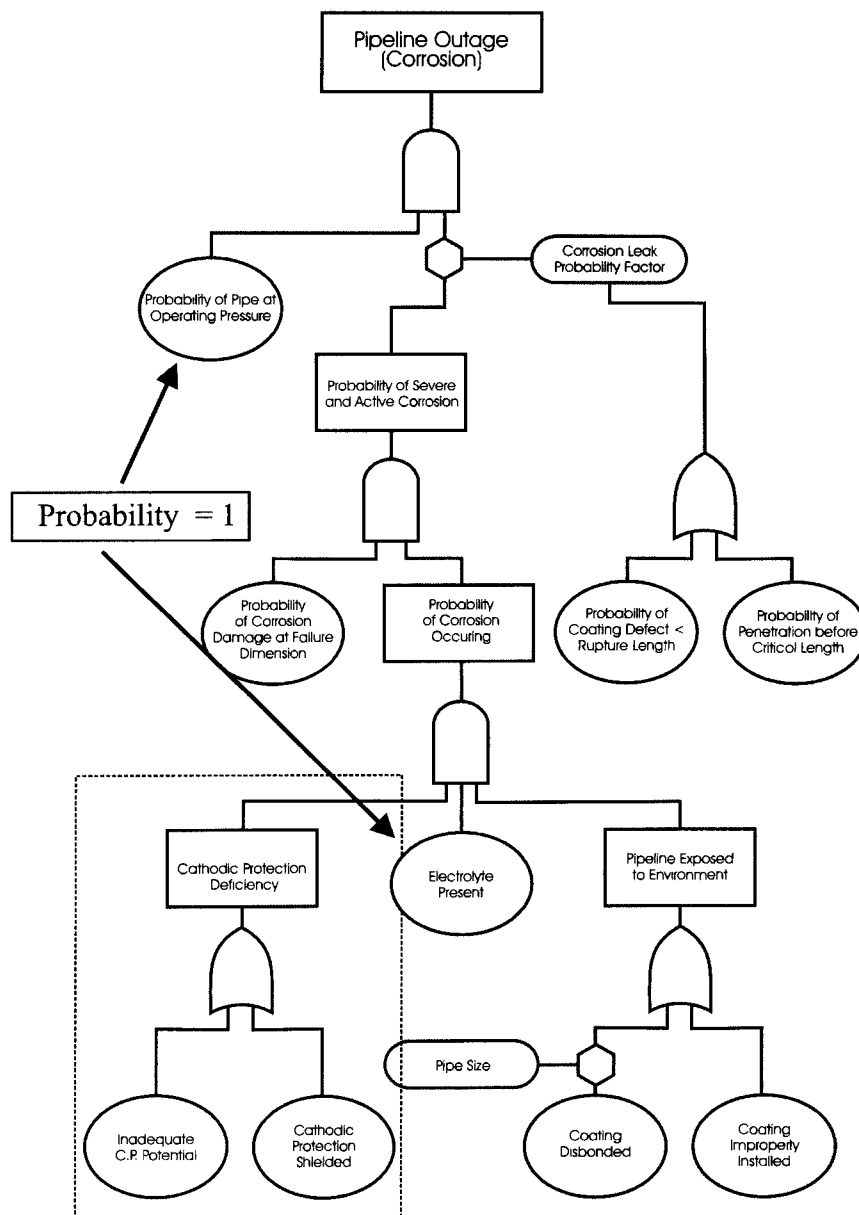


FIG. 5—Fault tree for natural gas pipeline outage due to general corrosion.

tree. Through this type of modeling, a number of variables may be visualized in a cost-effective manner.

The Nova rupture risk FTA is normally performed for the review and analytical examination of systems or equipment to emphasize the lower-level fault occurrences, and the results of the FTA calculations are regularly validated with inspection results. These results also serve to schedule maintenance operations, conduct surveys, and plan research and development efforts. Figure 5 presents the uniform corrosion branch pipeline outage FTA system. Each element of the branch in this figure contains numeric probability information related to technical and historical data for each segment of the 18 000 km pipeline. In some cases, it is simpler to assume some probability

values for an entire system. The probabilities of operating at maximum permitted pressure and the presence of electrolyte were both set at value unity in Fig. 5, therefore forcing the focus on worst case scenarios. Other more verifiable variables can be developed fully, as is shown in Fig 6 for the two basic events describing the probable impact of a cathodic protection deficiency on the pipeline network. As can be seen in this figure, the probability values used for fault-tree calculations are written directly in the database program.

#### Maintenance Steering Group (MSG) System

The aircraft industry and its controlling agencies have developed, over the past few decades, a top down system to

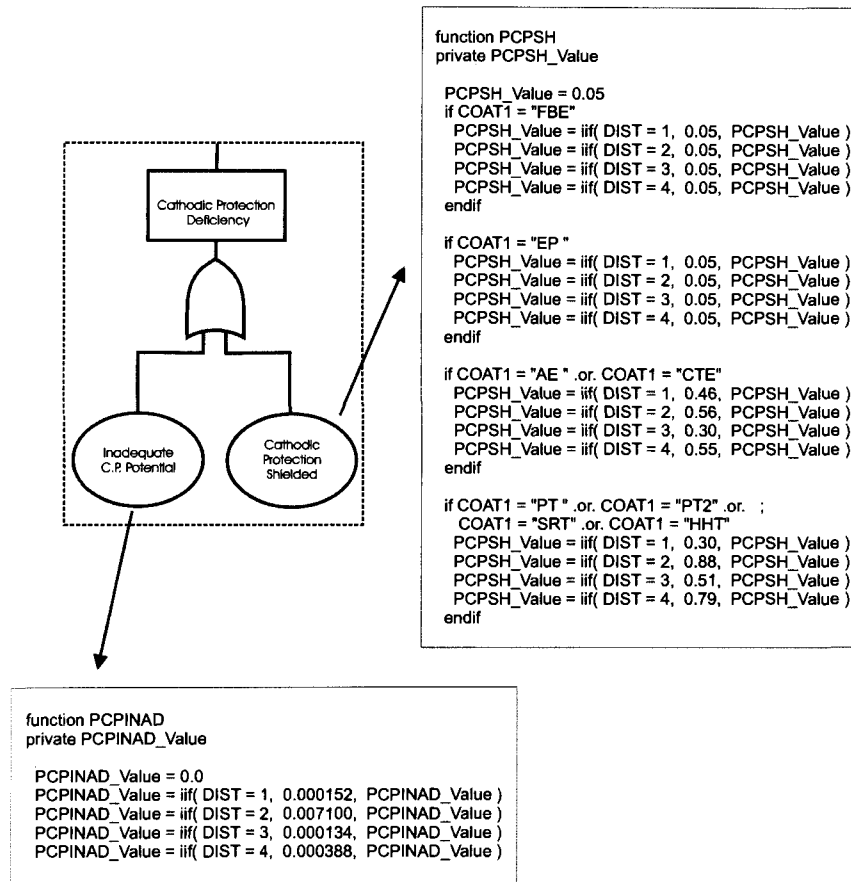


FIG. 6—Detailed code for the basic events leading to a cathodic protection deficiency.

represent potential failures of aircraft components, the Maintenance Steering Group (MSG). The first generation of formal air carrier maintenance programs was based on the belief that each part on an aircraft required periodic overhaul. As experience was gained, it became apparent that some components did not require as much attention as others and new methods of maintenance control were developed. Condition monitoring was, thus, introduced in the decision logic of the initial maintenance steering group document (MSG-1) and was applied to Boeing 747 aircraft.

The most recent major update to the system was initiated in 1980. The resultant MSG-3 system is based on the basic philosophies of MSG-1 and MSG-2, but prescribes a different approach in the assignment of maintenance requirements. In 1991, industry and regulatory authorities began working together to provide additional enhancements to MSG-3. As a result of these efforts, Revision 2 was submitted to the Federal Aviation Administration (FAA) in September 1993 and accepted a few weeks later. One particularly interesting addition in this revision is a procedure for incorporating corrosion damage in the MSG logic. The environmental deterioration analysis (EDA) involves the evaluation of the structure against probable exposure to adverse environments. The evaluation of deterioration is based on a series of steps supported by reference materials containing baseline data expressing the susceptibility of structural materials to various types of environmental damage.

The MSG-3 (Revision 2) structures analysis begins by developing a complete breakdown of the aircraft systems, down to the component level. All structural items are then either classified as Structure Significant Items (SSIs) or other structure. An item is classified as an SSI depending on consideration of consequences of failure and likelihood of failures as well as material, protection, and probable exposure to corrosive environments. All SSIs are then listed and categorized as damage tolerant or safe life items to which life limits are assigned [19]. Accidental damage, environmental deterioration corrosion prevention and control, and fatigue damage evaluation are then performed for these SSIs following the logic diagram illustrated in Fig. 7. Once the MSG-3 structure analysis is completed, each element of the structural analysis diagram (Fig. 7) can be expanded right to the individual components and associated inspection and maintenance tasks. The logic of the EDA, illustrated in Fig. 8, requires the input of a multitude of parameters such as component part number, location, material composition, and protective coating that can be actuated in practical templates.

#### *A Corrosion Index for Pipeline Risk Evaluation*

The third example of top down models is the pipeline risk assessment methodology that is described in much detail in the 2nd edition of a popular book on pipeline risk management [20]. Since this book was published, many systems

**FIG. 7—Overall MSG-3, Revision 2, structural analysis logic diagram.**

based on similar logic have been produced with much more data and complexity. Thus, the following description should serve more as an example than a state-of-the-art description of the technology.

The methodology proposed in that document is based on subjective risk assessment, a method particularly well adapted to situations where knowledge is incomplete and judgments are based on opinions, experience, and other nonquantifiable factors. The technique used for quantifying risk factors is described as a hybrid of several methods allowing the user to confide in scores obtained by combining statistical failure data with operator experience. The subjective scoring system

permits an assessment of the pipeline risk picture in two general parts:

**First Part:** In the first part, a detailed itemization and relative weighting of all reasonably foreseeable events that may lead to the failure of a pipeline are carried out. The itemization is further broken into the four indexes illustrated in Fig. 9, corresponding to typical categories of pipeline accident failures. By considering each item in each index, an expert evaluator arrives at a numerical value for that index. The four index values are then summed to obtain the total index value.

**Second Part:** The second part of the scoring system is a detailed analysis of potential consequences of each failure, considering product characteristics, pipeline operating conditions, and line location.

The risk of a pipeline failure caused by corrosion, directly or indirectly, is a common hazard associated with steel pipelines. The corrosion index was organized in three categories to reflect three types of environment to which pipelines are typically exposed, i.e., atmospheric corrosion, soil corrosion, and internal corrosion. Table 4 contains the elements contributing to each of the contributing type of environments and suggested weighting factors. Building the risk assessment tool is said to require the following four steps:

**1. Sectioning:** Dividing a system into smaller sections. The size of each section should reflect practical considerations

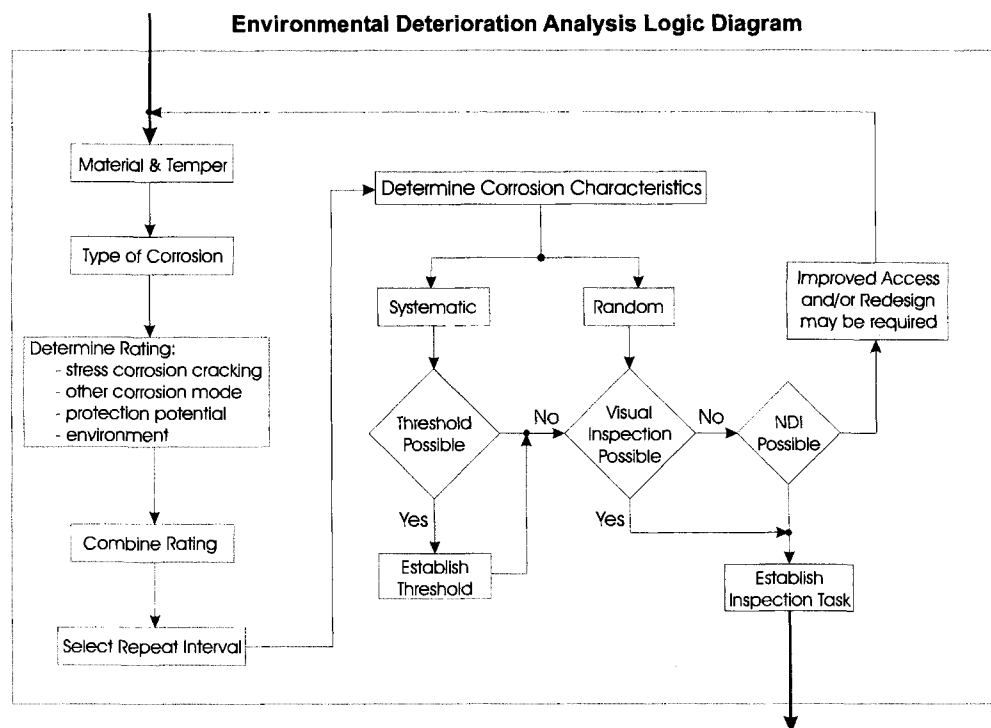


**FIG. 8—Environmental deterioration analysis logic diagram.**

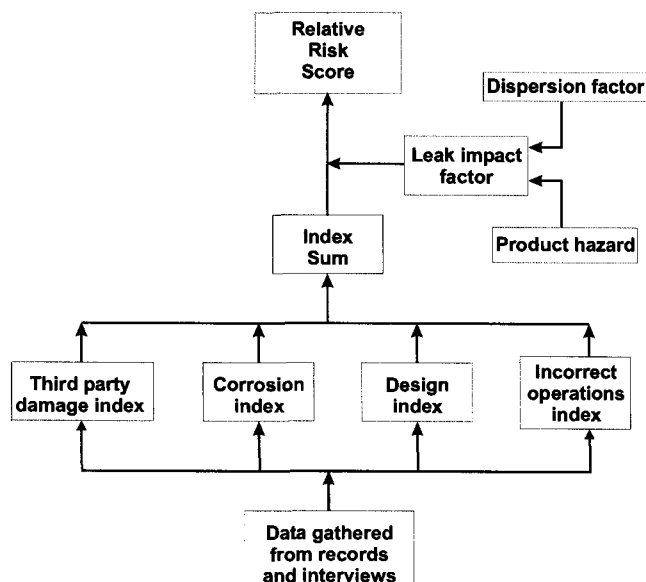


FIG. 9—Pipeline risk assessment model.

of operation, maintenance, and cost of data gathering versus the benefit of increased accuracy;

2. **Customizing:** Deciding on a list of risk contributors and risk reducers and their relative importance;
3. **Data Gathering:** Building the database by completing an expert evaluation for each section of the system;
4. **Maintenance:** Identifying when and how risk factors can change and updating these factors accordingly.

## APPLICATIONS OF ARTIFICIAL INTELLIGENCE

The modern world has produced an unprecedented level of technical information that merits being preserved and

managed. In an age of conservation and recycling, it is important to recognize the fact that the most valuable commodities are information as a vehicle and knowledge as the essence. It is surely sensible to preserve and reuse these most valuable commodities. The adequate transfer and reuse of information covering corrosion problems and solutions involve the development of information-processing strategies that can become very complex. Some of the artificial intelligence tools that have been developed recently in support of corrosion control and protection will be reviewed in the following sections.

### Expert Systems (ESs)

During the 1970s, research in Expert Systems (ES) was mostly a laboratory curiosity. The research focus then was really centered on developing ways of representing and reasoning about knowledge in a computer, and much less on designing actual systems [21]. In 1985 approximately 50 systems were deployed and reported, but the success of some of these captured the attention of many organizations and individuals. The corrosion community reacted with interest to the advent of these new information-processing technologies by establishing programs to foster and encourage the introduction of ES in the workplace. While some of these programs were relatively modest, others were quite ambitious and important both in scope and in funding. The advantages and limitations of using ES technology were analyzed in great detail in one of the first reported efforts on combating corrosion with ES [22]. The Stress Corrosion Cracking (SCC) ES (SCCES) had been created to calculate the risk of various factors involved in SCC, such as crack initiation, when the user supplied evidence. The main goal of this effort was to support the decision process of "general" materials engineers. The system would initially play the role of a consultant, but it was anticipated that SCCES had the potential to become:

- An intelligent checklist;
- A trainer;
- An expert sharpener;
- A communication medium;
- A demonstration vehicle.

The transfer of corrosion expertise into ES has been realized in a multitude of projects. The NACE Conference Proceedings, for example, regularly contain papers that illustrate the continuous interest in the application of knowledge engineering to corrosion. Unfortunately, many systems reported in the literature have never been commercialized. This has resulted in a lack of impartial and practical information concerning the performance and accuracy of these systems. It is, indeed, very difficult to believe everything that is said in a paper, or even more so when the information is some form of publicity. To remedy this situation, the European Federation of Corrosion (EFC) and Materials Technology Institute (MTI) have performed two surveys, between 1988 and 1990, requesting recognized developers of ES in corrosion-related areas to provide very specific information concerning the availability, scope, and performance of their systems [23]. A review of the information presented in these reports was summarized [24]

TABLE 4—Pipeline Corrosion Risk Subjective Assessment.

Corrosion problem	Risk weight
<i>Atmospheric corrosion</i>	
1. Facilities	0-5 pts
2. Atmospheric type	0-10 pts
3. Coating inspection	0-5 pts
total	0-20 pts
<i>Internal corrosion</i>	
1. Product corrosivity	0-10 pts
2. Internal protection	0-10 pts
total	0-20 pts
<i>Soil corrosion</i>	
1. Cathodic protection	0-8 pts
2. Coating condition	0-10 pts
3. Soil corrosivity	0-4 pts
4. Age of system	0-3 pts
5. Other metals	0-4 pts
6. a-c induced currents	0-4 pts
7. SCC and HIC	0-5 pts
8. Test leads	0-6 pts
9. Close internal surveys	0-8 pts
10. Inspection tool	0-8 pts
total	0-60 pts
Total	0-100 pts

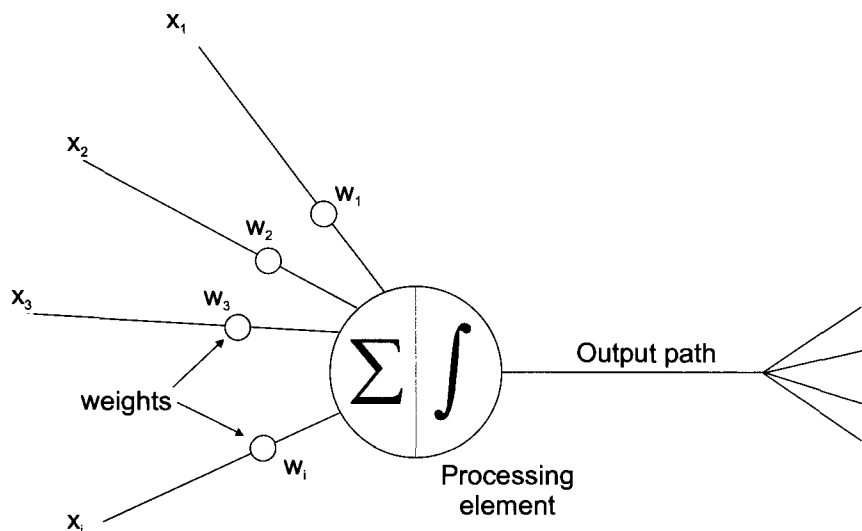


FIG. 10—Schematic of a single processor or neuron in an artificial neural network.

and other developments in expert systems for corrosion prevention and control reported subsequently [25].

### Neural Networks

An artificial neural network (ANN) is a network of many very simple processors or neurons (Fig. 10), each possibility having a small amount of local memory. The interaction of the neurons in the network is roughly based on the principles of neural science. Unidirectional channels that carry numeric data based on the weights of connections connect these neurons that operate only on their local data and on the inputs they receive via the connections. Most neural networks have some sort of training-rule. The training algorithm adjusts the weights on the basis of presented patterns. In other words, neural networks “learn” from examples. ANNs excel particularly at problems where pattern recognition is important and precise computational answers are not required. When ANNs inputs and/or outputs contain evolved parameters, their computational precision and extrapolation ability significantly increases and can even outperform more traditional modeling techniques. Only a few applications of ANN to solving corrosion problems have been reported so far. Some of these systems are briefly described here:

- **Predicting the SCC Risk of Stainless Steels:** The risk of encountering a stress corrosion cracking (SCC) situation was functionalized in terms of the main environment variables [26]. Case histories reflecting the influence of temperature, chloride concentration, and oxygen concentration have been analyzed by means of a back-propagation network. Three neural networks were developed. One was created to reveal the temperature and chloride concentration dependency (Fig. 11) and another to expose the combined effect of oxygen and chloride content in the environment. The third ANN was trained to explore the combined effect of all three parameters. ANNs were found to outperform, during this project, traditional mathematical regression

techniques where the functions have to be specified before performing the analysis.

- **Corrosion Prediction from Polarization Scans:** ANN was put to the task of recognizing certain relationships in potentiodynamic polarization scans in order to predict the occurrence of general or localized corrosion, such as pitting and crevice [27]. The initial data inputs were derived by carefully examining a number of polarization scans for a number of systems and recording those features that were used for the predictions. Table 5 lists the initial inputs used and how the features were digitized for computer input. The variables shown were chosen because they were thought to be the most significant in relation to the predictions (Table 5). The final ANN proved to be able to make appropriate predictions using scans outside the initial training set. The resulting ANN was imbedded in an ES to facilitate the input of data and the interpretation of the numerical output of the ANN.
- **Modeling CO<sub>2</sub> Corrosion:** A CO<sub>2</sub> corrosion “worst case” model based on an ANN approach was developed and the model validated against a large experimental database [28]. An experimental database was used to train and test the ANN. It consisted initially of six elemental descriptors (temperature, partial CO<sub>2</sub> pressure, ferrous and bicarbonate ion concentrations, pH, and flow velocity) and one output, i.e., the corrosion rate. The system demonstrated superior interpolation performance compared to two other well known semi-empirical models. The ANN model also demonstrated extrapolation capabilities comparable to a purely mechanistic electrochemical CO<sub>2</sub> corrosion model.
- **Predicting the Degradation of Nonmetallic Lining Materials:** An ANN was trained to recognize the pattern between results from a sequential immersion test for nonmetallic materials and behavior of the same material in field applications [29]. Eighty-nine cases were used for the supervised training of the network. Another 17 cases were held back for testing of the trained network. An effort was made to ensure that both sets had experimental data taken from the same test but using different samples. Appropriate

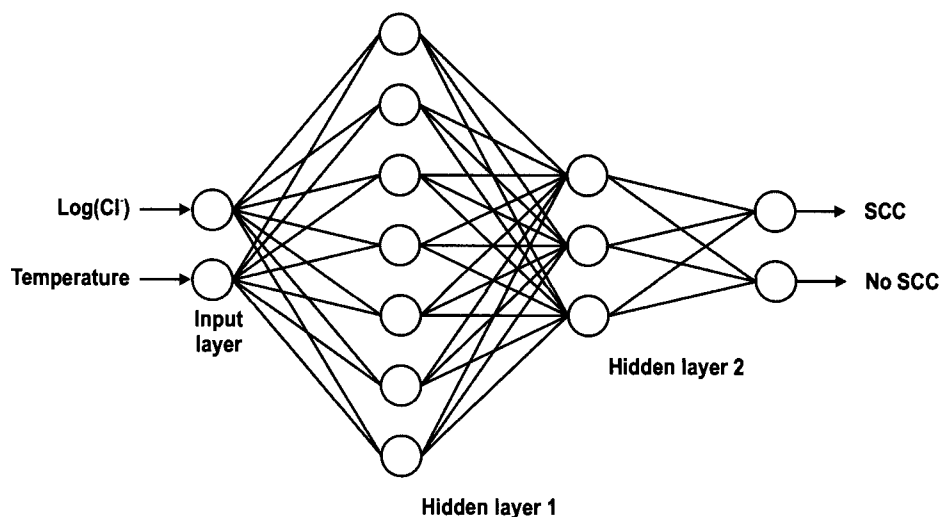


FIG. 11—Neural network architecture for the prediction of SCC risk of austenitic stainless steels in industrial processes.

choice of features enabled the ANN to mimic the expert with reasonable accuracy. The successful development of this ANN was another indication that ANNs could seriously aid in projecting laboratory results into field predictions.

- **Validation and Extrapolation of Electrochemical Impedance Data:** The ANN developed in this project had three independent input vectors, frequency, pH, and the applied potential [30]. The ANN was designed to learn from the invisible or hidden information at high and low frequencies and to predict in a lower frequency range than that used for training. Eight sets of impedance data acquired on nickel electrodes in phosphate solutions were used for this project. Five sets were used for training the ANN and three for its testing. ANN proved to be a powerful technique for generating diagnostics in these conditions.

### Case-Based Reasoning

Much of human reasoning is case-based rather than rule-based. When people solve problems, they frequently are

TABLE 5—Data inputs and outputs for predicting corrosion out of polarization scans with an Artificial Neural network.

Input parameter	Value of feature
Repassivation potential	$E_{\text{prot}} - E_{\text{corr}}$
Pitting potential	$E_{\text{pit}} - E_{\text{corr}}$
Hysteresis	+1 = Positive 0 = None -1 = Negative
Current density at scan reversal	$\mu\text{A cm}^{-2}$
Anodic nose	+1 = Yes 0 = No
Passive current density	$\mu\text{A cm}^{-2}$
Potential at anodic-cathodic transition	$E_{\text{A to C}} - E_{\text{corr}}$
Output parameter	Value of feature
Crevice corrosion predicted	+1 = Yes 0 = No
Pitting predicted	+1 = Yes 0 = No
Should general corrosion be considered	+1 = Yes 0 = No

reminded of previous problems they have faced. For many years, both law and business schools have used cases as the foundation for knowledge in their respective disciplines. Within AI, when one talks of learning, it usually means the learning of generalizations, either through inductive or through explanation-based methods. Case-Based Reasoning (CBR) is unique in making the learning little more than a byproduct of reasoning [31]. CBR has met with tangible success in such diverse human decision-making applications as banking, auto-clave loading, tactical decision-making, and foreign trade negotiations. The CBR approach is particularly valuable in cases containing ill-structured problems, uncertainty, ambiguity, and missing data. Dynamic environments can also be tackled, or when there are shifting, ill-defined, and competing objectives. Cases where there are action feedback loops, multiple human involvement, and multiple and potentially changing organizational goals and norms can also be tackled.

A critical issue for the successful development of such systems is the creation of a solid indexing system, since the success of a diagnosis depends heavily on the selection of the best stored case. Any misdirection can lead a query down a path of secondary symptoms and factors. Therefore, it is very important to establish an indexing system that will effectively indicate or counter-indicate the applicability of a stored case. Three issues are particularly important in deciding on the indices [32]:

- Indices must be truly relevant;
- Indices must be generalized, otherwise only an exact match will be the criterion for case applicability;
- But indices shall not be over-generalized.

Failure analysts and corrosion engineers also reason by analogy when faced with new situations or problems. Two CBR systems have been developed recently in support of corrosion engineering decisions. Both systems derived their reasoning from a combination of two industrial alloy performance databases. The general architecture of these two



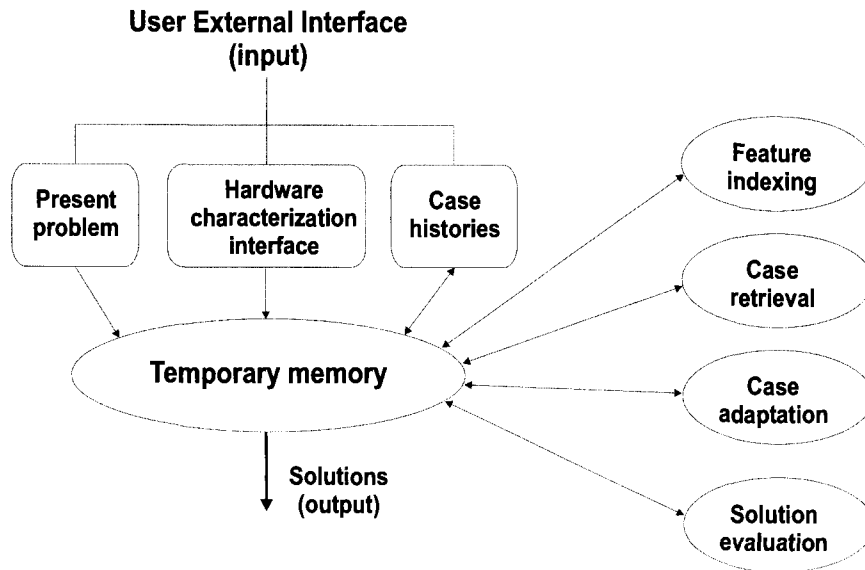


FIG. 12—Case-based reasoning architecture for the prediction of materials behavior.

FIG. 13—Compilation of the results to the questions, “What is the most dependable information source you depend upon to carry your work?” and “What is the least dependable information source you depend upon to carry your work?”

CBR systems is presented in Fig. 12. The first, “M-BASE,” facilitates the process of retrieving materials according to a given set of desired properties and/or specifications. The second, “C-BASE,” helps the materials engineer in the difficult task of selecting materials for corrosion resistance in complex chemical environments.

## INTERNET AND THE WEB

The Internet has revolutionized both the computer and communication worlds like nothing before. The invention of the telegraph, telephone, radio, and computer set the stage for this unprecedented integration of capabilities. The

Internet is at once a world-wide broadcasting capability, a mechanism for information dissemination, and a medium for collaboration and interaction between individuals and their computers without regard for geographic location.

Besides being extremely efficient tools for transferring documents and data of all types, the Internet and the Web are also gigantic repositories of information. However, there are some doubts concerning the quality of that information. The confidence professionals have in the information currently available on the Web was verified during a survey carried out directly from a Web site. That survey was conducted by inviting the active participants of two well-known Internet corrosion discussion groups [33,34], totaling approximately 1200 active members, to reach a specific page of the Corrosion Doctors site and answer a set of both short and specific questions. In the survey designed to reveal the importance of different information sources used by corrosion engineers, the participants were asked to select among a series of optional answers the one that best fitted a specific question:

- Books
- Journals
- Conferences and their associated activities and publications
- Software systems (databases, CDs, etc.)
- Own network of friends and contacts
- Internet discussion groups such as UMIST, NACE, and others
- Internet sources others than above, e.g., Web sites
- Other

The questions themselves were semirepetitive, asking of the 52 participants that registered to this particular survey to identify which of the proposed information sources was either the most dependable, the least dependable, or a gradation of these questions. Fig. 13 shows the breakdown of answers to the question, "What is the most dependable information source you depend upon to carry your work?" and to the question, "What is the least dependable information source you depend upon to carry your work?" The information explaining the survey and the survey results have been edited and processed into a page of the site for further consultation. The histograms presented in Fig. 13 indicate rather clearly that the confidence level people have on the information displayed on the Web in general or shared in discussion lists is presently rather low. This situation will probably change as the technology matures into a credible repository of useful information.

## SUMMARY

The difficulties associated with recording corrosion information are many, ranging from the basic lack of details in failure analyses to the inherent complexity of the variables involved. The complexities associated with corrosion damage information are compounded by a general lack of standard schemes to represent materials in their operational environments. Data gathered in controlled laboratory environments can usually be obtained with more precision and for such data standards have been developed to stream-

line the exchange of information between organizations. However, it is evident that the progress made in recent years with communication tools and protocols has been much greater than the progress in the quality of data that are generated and cumulated. Improvement in this area has to precede the development of generalized models of corrosion failures and the subsequent reuse of the information by applying methodologies related to artificial intelligence.

## REFERENCES

- [1] Stonier, T., *Beyond Information*, London, UK: Springer-Verlag, 1992.
- [2] Anderson, D. B., "Computerization of Data," *Corrosion Tests and Standards: Application and Interpretation*, R. Baboian, Ed., ASTM International, West Conshohocken, PA, 1995, pp. 68–72.
- [3] Tomiura, A., "Lessons for a Case Study of Property Databases in Materials Development," *Computerization/Networking of Materials Databases, ASTM STP 1311*, S. Nishijima, S. Iwata, C. H. Newton, Eds., West Conshohocken, PA, ASTM International, 1996, pp. 3–20.
- [4] Anderson, D. B., "Evaluation of Corrosion Data—A Review," *Computer Modeling in Corrosion*, R. S. Munn, Ed., ASTM International, West Conshohocken, PA, 1992, pp. 162–173.
- [5] *Understanding "Situation-Dependent Strength": a Fundamental Objective in Assessing the History of Stress Corrosion Cracking*, NACE International, Houston, TX, 1989.
- [6] Fontana, M. G., *Corrosion Engineering*, 3rd ed., McGraw Hill, New York, NY, 1986.
- [7] Dillon, C. P., *Forms of Corrosion: Recognition and Prevention*, NACE International, Houston, TX, 1982.
- [8] Szklarska-Smialowska, Z., *Pitting Corrosion*, NACE International, Houston, TX, 1986.
- [9] Box, G. E., Hunter, W. G., and Hunter, J. S., *Statistics for Experiments*, New York, NY, John Wiley and Sons, 1978.
- [10] Mason, R. L., Gunst, R. F., and Hess, J. L., *Statistical Design and Analysis of Experiments*, John Wiley and Sons, New York, NY, 1989.
- [11] Box, G. E. P. and Draper, N. R., *Empirical Model-Building and Response Surfaces*, John Wiley and Sons, New York, NY, 1987.
- [12] Evans, U. R., Mears, R. B., and Queneau, P. E., "Corrosion Probability and Corrosion Velocity," *Engineering*, 1933, Vol. 136, p. 689.
- [13] Gumbel, E. J., *Statistical Theory of Extreme Values and Some Practical Applications*, Vol. 33, 1954, Washington, D.C., National Bureau of Standards, Mathematics Series.
- [14] Shibata, T., "Statistical and Stochastic Approaches to Localized Corrosion," *Corrosion*, Vol. 52, No. 11, 1996, pp. 813–830.
- [15] Meany, J. J. and Ault, J. P., "Extreme Value Analysis of Pitting Corrosion," *Life Prediction of Corrodible Structures*, R. N. Parkins, Ed., Vol. 1, NACE International, Houston, TX, 1994, pp. 306–319.
- [16] Sheikh, A. K., Boah, J. K., and Hansen, D. A., "Statistical Modeling of Pitting Corrosion and Pipeline Reliability," *Corrosion*, Vol. 46, No. 3, 1990, pp. 190–197.
- [17] Shoesmith, D. W., Ikeda, B. M., and LeNeveu, D. M., "Modeling the Failure of Nuclear Waste Containers," *Corrosion*, Vol. 53, No. 10, 1997, pp. 820–829.
- [18] Roberge, P. R., "Eliciting Corrosion Knowledge through the Fault-Tree Eyeglass," *Modelling Aqueous Corrosion: From Individual Pits to Corrosion Management*, K. R. Trethewey and P. R. Roberge, Eds., Kluwer Academic Publishers, Dordrecht, The Netherlands, 1994, pp. 399–416.
- [19] *BBAD Maintenance Program: Policy and Procedures Handbook*, Montreal, Canada, Bombardier, 1994.

- [20] Muhlbauer, W. K., *Pipeline Risk Management Manual*, 2nd ed., Gulf Publishing Company, Houston, TX, 1996.
- [21] Durkin, J., *Expert Systems: Design and Development*, MacMillan Publishing Company, New York, NY, 1994.
- [22] Basden, A., "On the Applications of Expert Systems," *International Journal of Man Machine Studies*, Vol. 19, 1983, pp. 461-472.
- [23] MTI, *Report of Task Group 1 of the Working Party on Expert Systems in Materials Engineering*, Materials Technology Institute, Vol. 1-124, 1990, St. Louis, MO.
- [24] Roberge, P. R., "Bridging the Gap Between the World of Knowledge and the World that Knows," *Materials Performance*, Vol. 33, No. 3, 1994, pp. 52-56.
- [25] Roberge, P. R., "Expert Systems for Corrosion Prevention and Control," *Corrosion Reviews*, 1997, Vol. 15, No. 1-2, pp. 1-14.
- [26] Smets, H. M. G. and Bogaerts, W. F. L., "SCC Analysis of Austenitic Stainless Steels in Chloride-Bearing Water by Neutral Network Techniques," *Corrosion*, Vol. 48, No. 8, 1992, pp. 618-623.
- [27] Rosen, E. M. and Silverman, D. C., "Corrosion Prediction from Polarization Scans Using Artificial Neural Network Integrated with an Expert System," *Corrosion*, Vol. 48, No. 9, 1992, pp. 734-745.
- [28] Netic, S. and Vrhovac, M., "A Neural Network Model for CO<sub>2</sub> Corrosion of Carbon Steel," *Journal of Corrosion Science and Engineering*, Vol. 1, No. 6, 1998, pp. 1-11.
- [29] Silverman, D. C., "Artificial Neural Network Predictions of Degradation of Nonmetallic Lining Materials from Laboratory Tests," *Corrosion*, Vol. 50, No. 6, 1994, pp. 411-418.
- [30] Urquidi-Macdonald, M. and Egan, P. C., "Validation and Extrapolation of Electrochemical Impedance Spectroscopy Data," *Corrosion Reviews*, Vol. 15, Nos. 1-2, 1997, pp. 169-194.
- [31] Kolodner, J., *Case-Based Reasoning*, Morgan Kaufmann Publishers, San Mateo, CA, 1993.
- [32] *Explanation-Based Indexing of Cases*, MIT Press, Cambridge, MA, 1988.
- [34] CORROS-L: The corrosion discussion list, <http://www.cp.umist.ac.uk/>
- [35] NACE International List Servers, <http://www.nace.org/>

## **Section III: Types of Tests**

*H.P. Hack, Editor*

# Electrochemical Tests

John R. Scully<sup>1</sup>

SEVERAL TEXTBOOKS AND SYMPOSIA proceedings cover the application of electrochemical methods in corrosion testing [1–16]. This chapter highlights many of the commonly used laboratory methods after presenting a brief review of thermodynamics and kinetic aspects of electrochemical reactions that describe corrosion processes. Techniques discussed include Tafel extrapolation, polarization resistance, electrochemical impedance spectroscopy, electrochemical noise resistance, use of rotating disks, and cylinders to study aspects of corrosion affected by solution flow, polarization methods for assessing susceptibility to localized corrosion, scratch repassivation, potential-step repassivation, electrochemical noise applied to pitting, potentiodynamic repassivation techniques for assessing sensitization, the barnacle electrode and permeation methods for hydrogen concentration analysis, and methods for evaluating anodized layers and coatings on metals.

## ELECTRODE REACTION THERMODYNAMICS AND KINETICS IN CORROSION

Metallic corrosion is usually an electrochemical process. Electrochemical processes require anodes and cathodes in electrical contact, as well as an ionic conduction path through an electrolyte. The electron flow between the anodic and cathodic areas quantifies the rates of the oxidation and reduction reactions. When anodes are physically separated from cathodes, the current can be readily measured by replacing direct electrical contact with a zero resistance ammeter. The conversion of the reaction rate per unit area,  $J$ , from units of mol/cm<sup>2</sup>-s to electrical current density,  $i$  (A/cm<sup>2</sup>) is accomplished with Faraday's constant,  $F$ , and knowledge of the number of electrons transferred to complete the electrochemical reaction a single time,  $n$

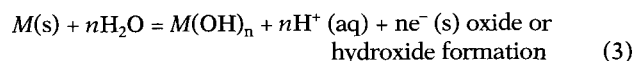
$$i = nFJ \quad (1)$$

where

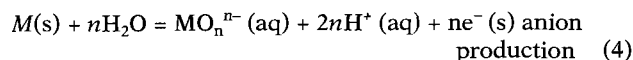
$n$  = number of electrons transferred, equivalents/mol, and  
 $F$  = Faraday's constant, 96,484.6 coulombs/equivalent.

<sup>1</sup>Professor of Materials Science and Engineering, Co-director, Center for Electrochemical Science and Engineering, Department of Materials Science and Engineering, University of Virginia, Charlottesville, VA 22903-2442.

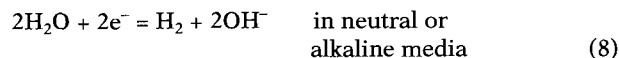
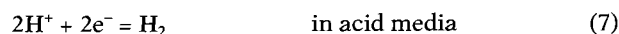
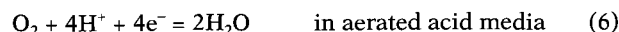
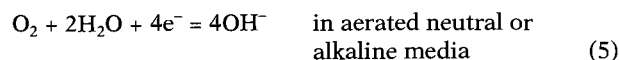
Monitoring this current provides the means of assessing the kinetics of the corrosion process, not just the thermodynamic tendencies for corrosion nor merely the mass of metal loss registered after the test. There are three typical half cell reactions by which a metal ( $M$ ) may be oxidized in water



or



In all cases, metal atoms in the solid ( $s$ ) metallic state (in the electronic conductor) are converted to an oxidized state. These species remain either on the metallic surface or are ejected into the aqueous ( $aq$ ) solution (the ionic conducting phase). Typical cathodic half-cell reactions in aqueous media involve the reduction of oxygen, protons, and water at the interface between the metallic and ionic conducting phases. This process involves consumption of electrons liberated during oxidation:



The Nernst equation describes the reversible electrode or equilibrium potential,  $E_{\text{redox}}$ , associated with the thermodynamic tendency for an electrochemical half-cell reaction to occur spontaneously. At potentials more positive than the equilibrium potential associated with a particular electrochemical half-cell reaction, oxidation proceeds spontaneously, while at potentials more negative, reduction occurs. The forms of the Nernst equation for the oxidation reactions given in Eqs 2 and 7 are, respectively,

$$E_{\text{redox}} = E_o + (2.303RT/nF) \log (M^{n+}) \quad (9)$$

and

$$E_{\text{redox}} = E_o - 2.303RTpH/F \quad (10)$$

where

$R$  = the ideal gas constant, cal/mol-K,  
 $T$  = temperature, K,

$n$  = the number of electrons to complete the half-cell reaction a single time, and

$E_0$  = the specific standard half-cell potential for the reaction cited at unity activity for dissolved species and 1 atmosphere fugacity for gaseous substances at 25°C. The standard half cell potential for the reaction  $2\text{H}^+ + 2\text{e}^- = \text{H}_2$  is defined as 0.0 V versus the normal hydrogen electrode (NHE) at 25°C.

Concerning corrosion in aqueous media, metal oxidation reactions (see Eqs 2-4) with Nernst or redox potentials more negative than the Nernst or redox potentials associated with typical cathodic reactions given by Eqs 5-8 will occur spontaneously [4-5].

The reaction rate for any single reduction-oxidation process is a function of overpotential  $E - E_{\text{redox}}$ , where  $E$  is the applied potential. For a single charge transfer controlled redox reaction,  $i_{\text{net}}$  is described by:

$$i_{\text{net}} = i_{\text{ex}} [\exp[\alpha_a F(E - E_{\text{redox}})/RT] - \exp[-\alpha_c F(E - E_{\text{redox}})/RT]] \quad (11)$$

where the exchange current density,  $i_{\text{ex}}$ , describes the non-zero rate at which the forward (oxidation) and reverse (reduction) reactions occur equally at  $E_{\text{redox}}$ . Since  $E_{\text{redox}}$  represents an equilibrium condition, the forward and reverse rates of the reaction must be equal.  $\alpha$  is known as the symmetry factor (such that  $\alpha_c = 1 - \alpha_a$ ) in the case of single step electron transfer processes representing a reduction oxidation process.  $\alpha$  represents a transfer coefficient for a multi-step reaction process (in this case,  $\alpha_c + \alpha_a \neq 1$ ). The factor  $2.303 RT/\alpha_a F$  is equal to the anodic Tafel slope,  $\beta_a$ . Similarly, the factor  $2.303 RT/\alpha_c F$  is equal to the cathodic Tafel slope,  $\beta_c$ . If  $E - E_{\text{redox}}$  is a large positive voltage (i.e., such that the term  $[\alpha_a F(E - E_{\text{redox}})/RT]$  is greater than about 2.303 or  $(E - E_{\text{redox}})/\beta_a > 1$ , then the following simplification known as the Tafel approximation applies for a charge transfer controlled process:

$$i_{\text{ox}} = i_{\text{ex}} \exp[\alpha_a F(E - E_{\text{redox}})/RT] \quad (12)$$

Similarly, when  $E - E_{\text{redox}}$  is a large negative number (i.e., such that  $(E - E_{\text{redox}})/\beta_c > 1$ ), another analogous simplification applies in the case of a single cathodic reaction:

$$i_{\text{red}} = i_{\text{ex}} \exp[-\alpha_c F(E - E_{\text{redox}})/RT] \quad (13)$$

Typical corrosion processes occurring under freely corroding conditions involve at least one cathodic and one anodic reaction. The thermodynamics discussed above dictate the circumstances where these reactions will proceed spontaneously. The current density measured during a polarization experiment,  $i_{\text{app}}$ , involving a single charge transfer controlled oxidation and single charge transfer controlled reduction reaction is

$$i_{\text{app}} = i_{\text{corr}} \left[ \exp\left(\frac{\alpha_a F(E - E_{\text{corr}})}{RT}\right) - \exp\left(\frac{\alpha_c F(E - E_{\text{corr}})}{RT}\right) \right] \quad (14)$$

The corrosion potential,  $E_{\text{corr}}$ , is a kinetically and thermodynamically determined "mixed" potential given by the interception of the lines describing the total anodic and cathodic reaction rates. At  $E_{\text{corr}}$ ,  $i_{\text{ox}} = i_{\text{red}}$  and  $i_{\text{corr}}$  is described by the magnitude of  $i_{\text{ox}}$  at  $E_{\text{corr}}$  as shown in Fig. 1. Either reaction

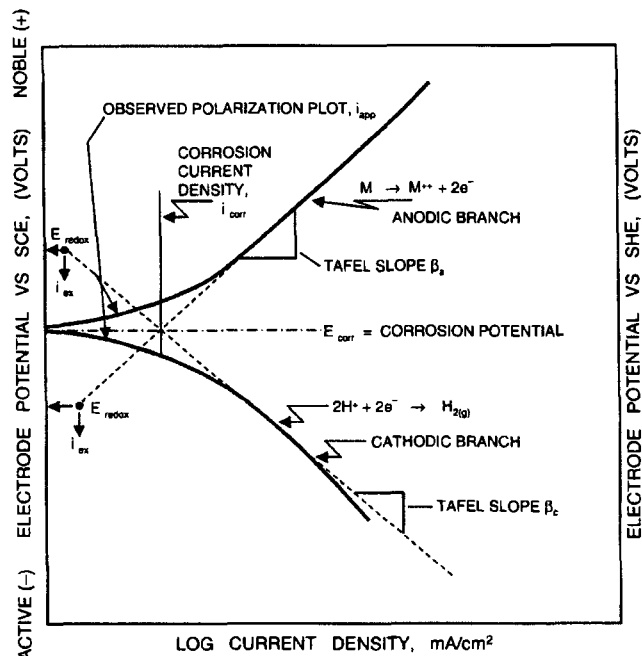


FIG. 1—Application of mixed potential theory showing the electrochemical potential-current relationship for a corroding system consisting of a single charge transfer controlled anodic reaction and single charge transfer controlled anodic electrochemical reaction.  $\beta_a$  and  $\beta_c$  are Tafel slopes.

rate may become mass transport limited under certain circumstances, in which case Eqs 12, 13, and 14 do not apply.

### Obtaining Corrosion Rates from Electrochemical Kinetic Data

According to mixed-potential theory, any overall electrochemical reaction can be algebraically divided into half-cell oxidation and reduction reactions, and there can be no net electrical charge accumulation [17]. For open-circuit corrosion in the absence of an applied potential, the oxidation of the metal and the reduction of some species in solution occur simultaneously at the metal/electrolyte interface, as described by Eq 14. Under these circumstances, the net measurable current density,  $i_{\text{app}}$ , is zero. However, a finite rate of corrosion defined by  $i_{\text{corr}}$  occurs at anodic sites on the metal surface, as indicated in Fig. 1. When the corrosion potential,  $E_{\text{corr}}$ , is located at a potential that is distinctly different from the reversible electrode potentials ( $E_{\text{redox}}$ ) of either the corroding metal or the species in solution that is cathodically reduced, the oxidation of cathodic reactants or the reduction of any metallic ions in solution becomes negligible. Because the magnitude of  $i_{\text{ox}}$  at  $E_{\text{corr}}$  is the quantity of interest in the corroding system, this parameter must be determined independently of the oxidation reaction rates of other adsorbed or dissolved reactants.

The information obtained in a polarization experiment is  $i_{\text{app}}$  as a function of the potential,  $E$ , as shown by the thick solid line in Fig. 1, where  $i_{\text{app}} = i_{\text{ox}} - i_{\text{red}}$ . To obtain  $i_{\text{app}}$  as a function of  $E$ , the applied potential between the reference electrode and working electrode is controlled and scanned

at constant rate (potentiodynamic), instantaneously increased a fixed amount (potentiostatic), or stepped at various times (potentiostaircase) [18].  $I_{app}$  is measured and normalized with respect to the surface area,  $A$  (i.e.,  $i_{app} = I_{app}/A$ ). Conversely,  $i_{app}$  can be supplied between the working and counter-electrodes under galvanostatic or galvanostaircase control, and the resulting potential between the working and reference electrodes is monitored. Several ASTM standards discuss methods for performing these experiments.<sup>2</sup> Several approaches are available to determine  $i_{corr}$  from such experimental information. These methods are discussed below.

### Conversion of Corrosion Rates to Mass Loss and Penetration Rate

Determination of  $I_{ox}$  at open circuit potential or other potential of interest, where  $I_{ox} = i_{ox} \times A$ , over a known period of time leads to direct determination of the mass loss

$$M = \frac{I_{ox}t(A.W.)}{nF} \quad (15)$$

where:

$M$  = the mass loss, g,

$I_{ox}t$  = the product of current and time, coulombs, and

$A.W.$  = the atomic weight of the electroactive species, g/mol.

This relation is known as Faraday's 1st Law. Rearrangement of Eq 15 leads to a straightforward determination of the penetration rate (applicable only when  $i_{ox}$  ( $\mu A/cm^2$ ) is uniformly distributed over the entire wetted surface area, or where the localized actively corroding area,  $A$ , is known), as follows

$$CR = \frac{K_1 i_{ox}(E.W.)}{\rho} \quad (16)$$

where

$CR$  = the corrosion rate, in mm/year,

$E.W.$  = the equivalent weight (considered dimensionless in this calculation), and

$\rho$  = the metal or alloy density, g/cm<sup>3</sup>.

The constant  $K_1 = 3.27 \times 10^{-3}$  when  $i_{ox}$  is expressed as  $\mu A/cm^2$ .  $K_1$  has units of mm-g/ $\mu A$ -cm-y when  $CR$  is desired in mm/yr. ASTM standard G 102<sup>3</sup> gives other values for this constant when  $CR$  is expressed in other units. Expressions are also available to calculate mass loss rate per unit area from knowledge of electrochemical corrosion rate. For instance,

$$MR = K_2 i_{ox}(E.W.) \quad (17)$$

where  $K_2 = 8.954 \times 10^{-3}$  g-cm<sup>2</sup>/ $\mu A$  m<sup>2</sup> d when  $MR$  is expressed as g/m<sup>2</sup> d. For alloys, the equivalent weight  $E.W.$  should be calculated as outlined in ASTM G 102<sup>3</sup>

$$E.W. = \frac{1}{\sum \left( \frac{n_i f_i}{A.W._i} \right)} \quad (18)$$

<sup>2</sup>ASTM G 5, Reference Test Method for Making Potentiostatic and Potentiodynamic Anodic Polarization Measurements; and ASTM G 59, Practice for Conducting Potentiodynamic Polarization Resistance Measurements.

<sup>3</sup>ASTM Standard G 102, Practice for Calculation of Corrosion Rates and Related Information from Electrochemical Measurements.

where

$f_i$  = the mass fraction of the  $i$ th component of the alloy (–),

$A.W._i$  = the atomic weight of the  $i$ th component element, g/mol

$n_i$  = the number of electrons transferred or lost when oxidizing the  $i$ th component element under the conditions of the corrosion process (equivalents/mol), and

$i$  = the number of component elements in the alloy.

$n$  is usually equal to the stable valence of the elements oxidized, or must be determined from either a Pourbaix (potential-pH) diagram or experimentally from an analysis of the ions in the corrosive solution. This expression assumes that all component elements oxidize when the alloy corrodes and that they are all oxidizing at essentially a uniform rate. In some situations, these assumptions are not valid and the calculated corrosion rate will be in error. For example, if an alloy is composed of two or more phases and one phase preferentially oxidizes, the calculation must take this into consideration.

### ELECTROCHEMICAL METHODS FOR THE STUDY OF UNIFORM CORROSION: POLARIZATION METHODS

One method for examining the corrosion behavior of a metal is to determine the  $E$ - $i_{app}$  relationship by conducting a polarization experiment. The following  $E$ - $i_{app}$  relationship is often experimentally observed between applied current and potential. The expression is applicable to charge transfer controlled corrosion processes, regardless of the exact number of charge transfer controlled reactions or reaction steps. It provides the basis for the electrochemical polarization technique [1,2,17,19].

$$i_{app} = i_{corr} \left[ \left( \exp \left\{ \frac{2.303(E - E_{corr})}{\beta_a} \right\} \right) - \exp \left\{ -\frac{2.303(E - E_{corr})}{\beta_c} \right\} \right] + C \frac{\partial E}{\partial t} \quad (19)$$

where

$C$  = the interfacial capacitance associated with the electrochemical doublelayer [1,2], and

$\beta_a$  and  $\beta_c$  = the anodic and cathodic Tafel slopes ( $\partial E / \partial \log i_{app}$ ) given by the slopes of the polarization curves in the anodic and cathodic Tafel regimes, respectively, and

$\partial E / \partial t$  = the time rate of change in applied potential, or voltage scan rate.

The second term of the expression ( $C \partial E / \partial t$ ) approaches 0 at low voltage scan rates  $dE/dt$ . Steady state is desirable, since the goal is to obtain  $i_{corr}$  at  $E_{corr}$ . Note that  $i_{app}$  becomes approximately equal to either  $i_{ox}$  or  $i_{red}$  at large  $\eta$ , where  $\eta = (E - E_{corr})$ . At very large anodic or cathodic overpotentials, Eq 19 can be rearranged in the form of the Tafel expression [1-3,5,7,18,19]

$$\begin{aligned} \eta_a &= \beta_a \log \left( \frac{i_{app}}{i_{corr}} \right) \\ \eta_c &= -\beta_c \log \left( \frac{i_{app}}{i_{corr}} \right) \end{aligned} \quad (20)$$

where:

$\eta_a$  and  $\eta_c$  = the anodic and cathodic overpotentials, respectively.

Equations 20 are only strictly valid for a single anodic or cathodic reaction, respectively, although approximately linear behavior can be observed despite several reactions. The linear portion of the solid line describing  $E-i_{app}$  in Fig. 1 above  $E_{corr}$  describes a single anodic reaction that can be described by Eq 20. Similarly, the linear portion of the solid line describing  $E-i_{app}$  in Fig. 1 below  $E_{corr}$  describes a single cathodic reaction that can be described by Eq 20.

### Tafel Extrapolation to Determine Corrosion Rate

In cases where Eq 20 is valid,  $\eta$  can be plotted versus  $\log(i_{app})$  over a sufficient range to obtain a linear relationship between the logarithm of current density and potential [1,5,7,19].  $i_{corr}$  can be determined from extrapolation of  $i_{app}$  from either the anodic or the cathodic Tafel region to the open-circuit potential (zero overpotential). Figure 1 illustrates this method. The method is potentially damaging to the corroding metal, since a large overpotential must be applied. This is particularly true in the case of anodic polarization, in which the surface is changing because of corrosion and or passivation of the metal. No ASTM standard currently exists for this method.

### Complications with the Polarization Method Involving Solution Resistance

Tafel extrapolation, as well as other polarization techniques, can be complicated by several factors. One such factor, ohmic resistance, arises from the resistivity of the solution, cell geometry, location of the reference electrode, and magnitude of applied current [2,6]. Ohmic resistance can contribute a voltage error to the measured potential. This error is summed algebraically with the true interfacial overpotential across the electrochemical interface (the potential usually sought in electrochemical measurements) measured with respect to a reference electrode. Placement of the reference electrode near the working electrode with a Luggin-Haber capillary is used to minimize the solution resistance error, which can be estimated from the product of the applied current density, the solution resistivity, and the perpendicular distance from the Luggin probe to the specimen surface in a planar electrode geometry. The error contributes to the measured overpotential  $\eta_{app}$ :

$$\eta_{app} = \eta_{true\ interfacial} + i_{app}R_s \quad (21)$$

$R_s$  ( $\Omega\text{-cm}^2$ ) is the uncompensated solution resistance between the working electrode and the position where the reference electrode senses the potential in solution (at the tip of the Luggin-Haber capillary). Thus,  $\eta_{app} > \eta_{true}$  at high anodic, current densities high  $R_s$  or high cathodic applied current density,  $E_{app} > E_{true}$  and the Tafel slope desired from a fit of Eq 19 or 20 to  $E$  versus  $i_{app}$  data cannot be obtained from  $E$ - $\log i$  data. When the dominant term in Eq 21 is the second term, a linear relationship between  $\eta$  ( $\eta = \eta_{app}$ ) and  $i_{app}$  is obtained instead of the semi-logarithmic relationship discussed above. The true scan rate in the potentiodynamic technique may also be altered, since the applied potential that contains the ohmic component

is controlled during the scan, not the true overpotential. Several excellent reviews are available on the subject of the voltage error introduced from solution resistance [20–23].

### Complications Involving Concentration Polarization Effects

The Tafel relationship established through Eqs 19 and 20 is valid for pure activation control, or charge transfer control. An additional consideration involves the concept of concentration polarization. In this case, the reaction rate is fast enough that the reacting specie is depleted (reduction reaction) or concentrated (oxidation) at the reacting surface. In order to maintain the reaction rate, diffusion through the electrolyte becomes the kinetic limitation. The reaction becomes completely diffusion controlled at the limiting current density,  $i_L$ . The deviation from activation control in the case of a cathodic reaction can result in an additional overpotential known as a mass transport overpotential,  $\eta_{conc}$ . This overpotential is described by [4,5]

$$\eta_{conc} = \left[ \frac{2.303RT}{nF} \right] \log \left[ 1 - \frac{i_{app}}{i_L} \right] \quad (22)$$

where

$i_L$  = the mass transfer limiting current density defined by Fick's first law at steady state.

As  $i_{app}$  approaches  $i_L$ , the concentration overpotential,  $\eta_{conc}$ , becomes very large. The cathodic reaction may be under mixed charged transfer-mass transport or mass transport control for many corrosion situations, particularly if the cathodic reaction is  $O_2$  reduction [5]. The cathodic polarization behavior associated with "mixed" charge transfer—mass transfer control can be described mathematically by the algebraic combination of Eqs 20 and 22. Tafel extrapolation of cathodic data becomes difficult under these conditions because the Tafel region may not be extensive.

For a completely mass transport limited corrosion process, the concentration of the cathodic reacting species  $C_b$  approaches zero at the electrode interface and  $i_{corr} = i_L$  (Fig. 2) [2]. The diffusional boundary layer thickness,  $\delta$ , is decreased by increasing solution stirring or rotation rate,  $\Omega$  (rad/s), in the case of a rotating cylinder or disk electrode [1]. The limiting current density  $i_L$  is a linear function of concentration gradient [15]. The concentration gradient ( $C_b/\delta$ ) increases as a function of  $\Omega^{0.5}$  or  $\Omega^{0.7}$  for the rotating disk and cylinder, respectively [2,15]. For a mass transport controlled cathodic reaction,  $i_{corr}$  is increased with flow as shown in Fig. 2. The governing equation for the rotating cylinder electrode is [15]

$$i_L = 0.079nFC_bD^{0.64}\nu^{-0.34}\Omega^{0.7}r^{0.4} \quad (23)$$

and for the rotating disk electrode is [2,15]

$$i_L = 0.621nFC_bD^{0.67}\nu^{-0.167}\Omega^{0.5} \quad (24)$$

where

$C_b$  = the reacting species concentration in the bulk solution, moles/cm<sup>3</sup>,

$D$  = the diffusion coefficient for the reacting specie, cm<sup>2</sup>/s,

$\nu$  = the kinematic viscosity of the solution, cm<sup>2</sup>/s, and

$r$  = cylinder or disk radius, cm.



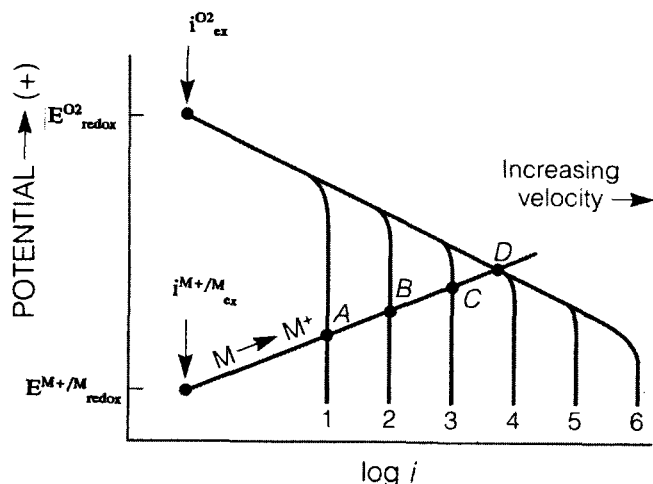


FIG. 2—Application of mixed potential theory showing the electrochemical potential-current relationship for a corroding system consisting of a mass transport controlled cathodic reaction and a charge transfer controlled anodic reaction. As the fluid velocity increases from 1 to 4, the corrosion rate increases from A to D.

Corrosion engineers often favor the rotating cylinder to simulate flow in turbulent piping systems, since this flow regime is readily obtained [15]. In contrast, the rotating disk electrode operates in the laminar flow regime, even at high rotation rates, and does not accurately represent many corrosion situations [15]. No ASTM methods currently exist to examine mass transport controlled corrosion.

### Polarization Resistance Methods

Stern and Geary simplified the kinetic expression describing charge transfer controlled reaction kinetics (Eq 19) for the case of small overpotentials with respect to  $E_{corr}$  [24,25]. Equation 19 can be linearized when  $\eta/\beta < 0.1$ . This simplified relationship has the following form if the second term describing the capacitive current,  $C(dE/dt)$ , is negligible

$$i_{corr} = \left( \frac{\Delta i_{app}}{2.3 \Delta E} \right) \left( \frac{\beta_a \beta_c}{(\beta_a + \beta_c)} \right) \quad (25)$$

rearranging

$$i_{corr} = \left( \frac{1}{2.3 R_p} \right) \left( \frac{\beta_a \beta_c}{(\beta_a + \beta_c)} \right) = \frac{B}{R_p} \quad (26)$$

where  $R_p$  is the polarization resistance ( $\Omega\text{-cm}^2$ ) given by  $\partial E / \partial i$  at  $t = \infty$ ,  $\Delta E = 0$ , and  $B$  is a constant given by the constant terms shown in Eq 26.

$i_{app}$  is often approximately linear with potential within  $\pm 5\text{--}10$  mV of  $E_{corr}$ , as shown for AISI 430 stainless steel in  $\text{H}_2\text{SO}_4$  (Fig. 3). The slope of this plot,  $\Delta E / \Delta i$ , when determined at  $E_{corr}$  as shown in Fig. 3 defines the polarization resistance, which is inversely proportional to corrosion rate [26,27]. The surface area of the working electrode must be known. Knowledge of  $R_p$ ,  $\beta_a$ , and  $\beta_c$  permits direct determination of the corrosion rate at any instant in time using Eq 26 [24,25,27,28].

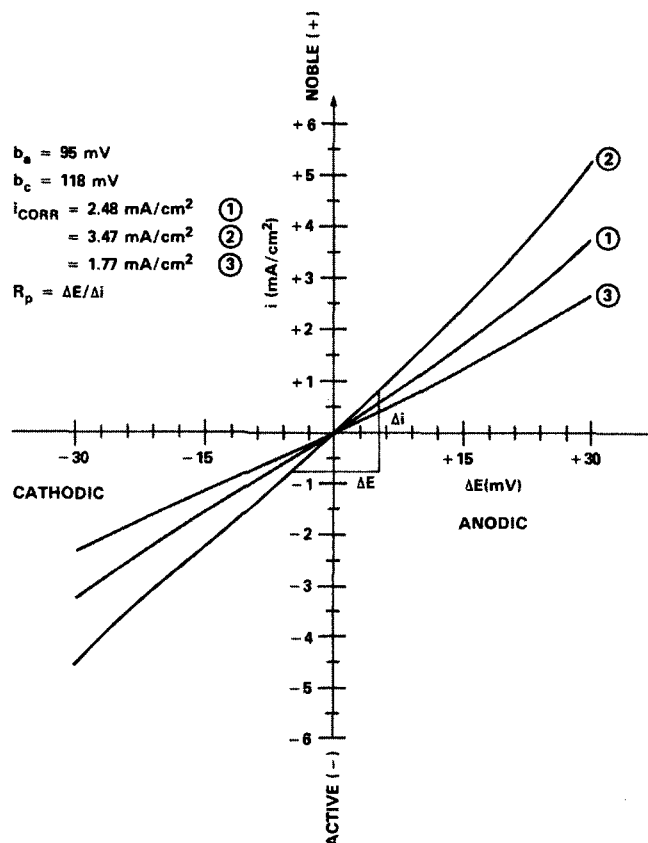


FIG. 3—ASTM G 59 polarization curves used for polarization resistance determinations based on the results from eight independent laboratories for AISI type 430 stainless steel in 1N  $\text{H}_2\text{SO}_4$ . Curve 1 is the mean result, with Curves 2 and 3 showing the 95 % confidence limits from the laboratory round robin.

ASTM standards G 59<sup>2</sup> and G 96<sup>4</sup> describe standard procedures for conducting polarization resistance measurements.<sup>a</sup>

Other techniques exploit nonlinearity at larger overpotentials that invalidates the approximation given by Eq 25 [29]. The Oldham-Mansfeld method calculates  $i_{corr}$  from nonlinear  $E$  versus  $i_{app}$  data obtained usually within  $\pm 30$  mV of  $E_{corr}$ , using tangent slopes and intercepts to calculate corrosion rate without high overpotential determination of  $\beta_a$  and  $\beta_c$  [30a]. Computerized curve fitting can exploit nonlinearity to calculate  $\beta_a$  and  $\beta_c$  from low overpotential data, avoiding the destructive nature of large overpotentials [30b]. The

<sup>4</sup>ASTM Standard G 96, Guide for On-line Monitoring of Corrosion in Plant Equipment (Electrical and Electrochemical Methods).

<sup>a</sup>This review focuses on corroding systems with different cathodic and anodic half-cell reactions. However, the concept of polarization resistance applies equally well to reduction-oxidation systems involving a single half-cell reaction. Here, the exchange current density,  $i_o$ , may be calculated from the polarization resistance, where  $R$  is the ideal gas constant,  $F$  is Faraday's constant,  $T$  is the temperature, and  $\alpha_a$  and  $\alpha_c$  are the anodic

$$R_n (\text{ohm-cm}^2) = \left[ \frac{\Delta E}{\Delta i} \right]_{(E-E_{corr}) \rightarrow 0} = \left( \frac{RT}{i_o F (\alpha_a + \alpha_c)} \right)$$

and cathodic multi-step electron transfer coefficients, respectively, for the reduction-oxidation process.

Mansfeld technique substitutes Eq 26 into Eq 19, eliminating  $i_{corr}$  [30b].  $\beta_a$  and  $\beta_c$  are determined from the best fit of the resulting expression containing  $\beta_a$  and  $\beta_c$  as unknowns to a nonlinear plot of  $\eta$  versus  $2.3i_{app}R_p$ .  $\eta$  versus  $i_{app}$  data are obtained within  $\pm 30$  mV of  $E_{corr}$ .  $R_p$  is determined from the linear slope of  $E$  versus  $i_{app}$  within  $\pm 5$  mV of  $E_{corr}$ .  $i_{corr}$  is subsequently determined from Eq 25 using  $R_p$ ,  $\beta_a$ , and  $\beta_c$ .

### Complications with Polarization Resistance Measurements

Complications related to the polarization resistance method and possible remedies are reported in the literature [29–34]. Three of the most common errors involve: (1) invalidation of the results through oxidation or reduction of some other electroactive species besides the corroding metal in question, (2) a change in the open-circuit or corrosion potential during the time taken to perform the measurement, and (3) use of a large  $\eta$ , invalidating the assumption of a linear relationship between  $i_{app}$  and  $E$  required by Eqs 25 and 26.

Another source of error involves cases in which both the anodic and cathodic reactions are not charge transfer controlled processes, as required for the derivation of Eq 25. Modifications to Eq 25 exist for cases in which pure activation control is not maintained, such as in the case of partial diffusion control or passivation [35]. Other researchers have attempted to calibrate the polarization resistance method with gravimetrically determined mass loss [36]. In fact, polarization resistance data for a number of alloy-electrolyte systems have been compared to the observed average corrosion currents determined from mass loss via Faraday's law [28]. A linear correspondence was obtained over six orders of magnitude in corrosion rates.

Two other frequently encountered complications are the need to correct polarization data for errors that arise from the contribution of solution resistance,  $R_s$ , and the addition of capacitive current,  $C dE/dt$ , which occurs with increasing scan rate [16]. Capacitive current gives rise to hysteresis in current-potential plots [37]. Solution resistance contributes to a voltage error as discussed above, as well as a scan rate error. Since the applied potential is increased by an ohmic voltage component, an apparent value of polarization resistance  $R_p'$  is obtained which overestimates  $R_p$  by an amount equal to  $R_s$ . Consequently, the corrosion rate is underestimated. Hysteresis in the current density-applied potential plot is brought about for combinations of high voltage scan rate and large interfacial capacitances, as well as large polarization resistances. Attempting to determine  $R_p$  at too fast of a scan rate underestimates its true value, leading to an overestimation of corrosion rate. This error can be minimized by determining the polarization resistance at a slow scan rate, or extrapolating the results at several slow scan rates to zero scan rate. Alternatively, one may take two or more current density measurements from potentiostatic data after long time periods near  $E_{corr}$  to minimize fast scan rate effects. These complications and others have been reviewed elsewhere [38].

Many treatments of this subject have used an electrical equivalent circuit model to simulate the corroding metal/electrolyte interface [1,38,39]. The simplest form of such a model is shown in Fig. 4. The three parameters discussed above

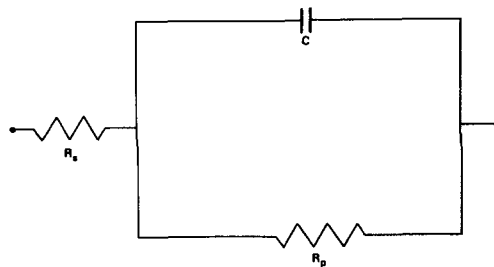


FIG. 4—Electrical equivalent circuit model simulating a simple corroding metal/electrolyte interface. See also Fig. 5.  $R_s$  is the solution resistance.  $R_p$  is the polarization resistance.  $C$  is the double layer capacitance.

( $R_p$ ,  $R_s$ , and  $C$ ) that approximate a corroding electrochemical interface are shown. The algebraic sum of  $R_s$  and  $R_p$  is measured when a d-c measurement is performed. The impedance associated with a capacitor approaches infinity as the voltage scan rate approaches zero, and parallel circuit elements are always dominated by the element with the smallest impedance. Therefore, the sum of  $R_s$  and  $R_p$  is measured and the true corrosion rate will be underestimated when  $R_s$  is appreciable. Conversely, any experiment conducted at a fast voltage scan rate causes the algebraic sum of the ohmic resistance and the resultant impedance of the parallel resistive-capacitive network to be measured. This value will be lower than the sum of  $R_p$  and  $R_s$  determined at an infinitely slow scan rate, as current leaks through the parallel capacitive element at higher scan rate due to its low impedance at high frequency. This will usually result in an overestimation of the true corrosion rate. These complications can be overcome by using the electrochemical impedance method.

### Electrochemical Impedance Methods

One approach for determining the polarization resistance of a metal involves the electrochemical impedance (sometimes known as a-c impedance) method [2,37–41]. ASTM Standard G 106,<sup>5</sup> Practice for Verification of Algorithm and Equipment for Electrochemical Impedance Measurements, contains an appendix reviewing the technique. In this technique, typically a small-amplitude sinusoidal potential perturbation is applied to the working electrode at a number of discrete frequencies,  $\omega$ . At each one of these frequencies, the resulting current waveform will exhibit a sinusoidal response that is out of phase with the applied potential signal by a certain amount ( $\Phi$ ) and has a current amplitude that is inversely proportional to the impedance of the interface. The electrochemical impedance,  $Z(\omega)$ , is the frequency-dependent proportionality factor that acts as a transfer function by establishing a relationship between the excitation voltage signal and the current response of the system

$$Z(\omega) = V(\omega)/i(\omega) \quad (27)$$

<sup>5</sup>ASTM G 106, Practice for Verification of Algorithm and Equipment for Electrochemical Impedance Measurements.

where

$V$  = the time varying voltage across the circuit,  $V = V_o \sin(\omega t)$ ,

$i$  = the time varying current density through the circuit,  $i = i_o \sin(\omega t + \Phi)$ ,

$Z(\omega)$  = the impedance,  $\Omega\text{-cm}^2$ , and

$t$  = time, s.

$Z(\omega)$  is a complex-valued vector quantity with real and imaginary components whose values are frequency-dependent

$$Z(\omega) = Z'(\omega) + jZ''(\omega) \quad (28)$$

where

$Z'(\omega)$  = the real component of impedance,  $Z'(\omega) = |Z(\omega)|\cos(\Phi)$ ,

$Z''(\omega)$  = the imaginary component of impedance,  $Z''(\omega) = |Z(\omega)|\sin(\Phi)$ ,

$j^2$  = the square of the imaginary number,  $-1$ ,

$|Z(\omega)|$  = the impedance magnitude, where  $|Z(\omega)| = (Z'(\omega)^2 + Z''(\omega)^2)^{1/2}$

The electrochemical impedance is a fundamental characteristic of the electrochemical system it describes. A knowledge of the frequency dependence of impedance for a corroding system enables a determination of an appropriate equivalent electrical circuit describing that system. Table 1 shows the transfer functions for resistors, capacitors, and inductors.

Figure 4 illustrates for a simple case the equivalent electrical circuit model for an actively corroding metal. The following expression describes the impedance for that system

$$Z(\omega) = R_s + R_p / (1 + \omega^2 R_p^2 C^2) - j\omega C R_p^2 / (1 + \omega^2 R_p^2 C^2) \quad (29)$$

where

$\omega$  = the frequency of the applied signal where  $\omega = 2\pi f$ , rad/s

$f$  = the frequency of the applied signal, Hz (cycles/sec),

$R_s$  = the solution resistance, and

$C$  = the interfacial capacitance,  $F/\text{cm}^2$ .

The Bode magnitude and phase information of Fig. 5 and Eq 29 show that at very low frequencies

$$Z\omega \rightarrow 0(\omega) = R_s + R_p \quad (30)$$

while at very high frequencies

$$Z\omega \rightarrow \infty(\omega) = R_s \quad (31)$$

Determination of  $R_p$  is attainable in media of high resistivity because  $R_p$  can be mathematically separated from  $R_s$  by taking the difference between  $Z(\omega)$  obtained at low and high  $\omega$  ( $R_p = Z(\omega \rightarrow 0) - Z(\omega \rightarrow \infty)$ ). Determination of the corrosion rate using Eq 25 also requires knowledge of  $\beta_a$ ,  $\beta_c$ , and electrode area,  $A$ , which are not obtained in the impedance experiment [42]. The minimum applied frequency required to obtain  $R_s + R_p$  can be approximated by

$$f_{min} < f_{bp} = \frac{1}{2\pi C(R_s + R_p)} \quad (32)$$

**TABLE 1**—Linear circuit elements commonly used in electrochemical impedance.

Circuit Element	Impedance
Resistor	$Z(\omega) = R$
Capacitor	$Z(\omega) = -j/\omega C$
Inductor	$Z(\omega) = j\omega L$

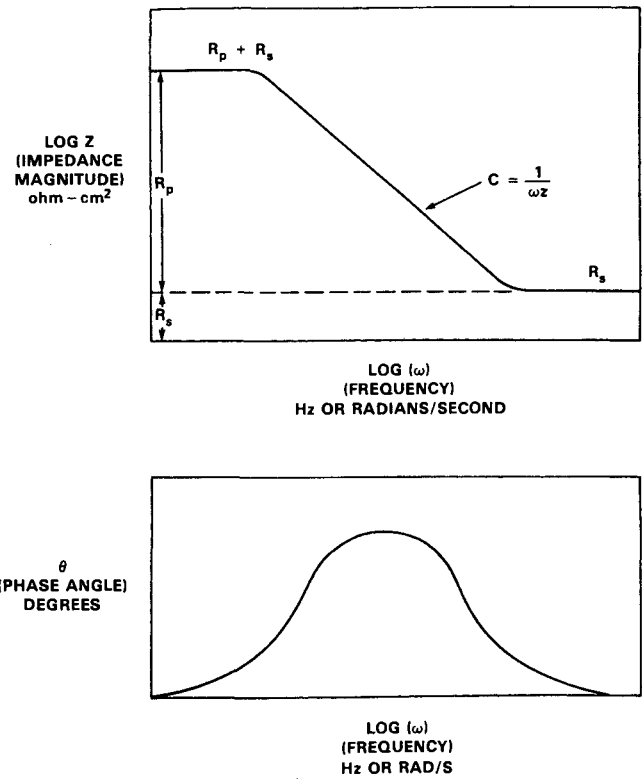


**FIG. 5**—Bode phase angle and magnitude plots demonstrating the frequency dependence of the electrochemical impedance for the circuit model shown in Fig. 4.

where

$f_{bp}$  = the lower breakpoint frequency approximated by the point on the  $\log |Z(\omega)|$  versus  $\log f$  plot where the low frequency plateau dominated by  $R_s + R_p$  and slope  $-1$  region dominated by capacitance produce equal values of  $Z(\omega)$ , Hz, and

$f_{min}$  = the minimum required test frequency required according to Eq 32, Hz.

Since the magnitudes of  $C$ ,  $R_s$ , and  $R_p$  are not known explicitly a priori, prudence dictates that  $f_{min}$  be selected as 0.1–0.5 of the estimated  $f_{bp}$ . Thus, large values of  $C$ ,  $R_s$ , or  $R_p$  dictate that a low  $f_{min}$  is required to accurately obtain  $R_p + R_s$  at  $Z(\omega) \rightarrow 0$ . One mHz is typically chosen as a reasonable initial choice of  $f_{min}$ , but it is obvious from Eq 32 that either a lower frequency may be required or a higher frequency permitted, depending on circumstances.

Either the anodic or cathodic half-cell reaction can become mass transport limited and restrict the rate of corrosion at  $E_{corr}$ . The presence of diffusion controlled corrosion processes does not invalid the EIS method, but does require extra precaution and a modification to the circuit model of Fig. 4. In this case, the finite diffusional impedance is added in series with the usual charge transfer parallel resistance shown in Fig. 4. The transfer function for the frequency dependent finite diffusional impedance,  $Z_D(\omega)$ , has been described [43]:

$$Z_D(\omega) = R_D \left[ \frac{\tanh \sqrt{(j\omega s)}}{\sqrt{(j\omega s)}} \right] \quad (33)$$

Here,  $s = l_{eff}^2/D$  where  $l_{eff}$  is the actual finite diffusion length and  $D$  is the diffusivity of the diffusing species that limits the interfacial reaction. The value of  $Z_D(\omega)$  approaches the real component of diffusional resistance,  $R_D$ , as  $\omega \rightarrow 0$ . The frequency required to obtain  $R_D$  depends on the value of  $s$ . The larger the value of  $s$ , such as when  $l_{eff}$  is large or  $D$  is small, the lower the frequency required.  $R_p$ , defined as  $[\partial E / \partial i_{app}]$  as  $\omega \rightarrow 0$ , is the sum of the charge transfer controlled,  $R_{ct}$  and diffusion controlled,  $R_D$ , contributions to the polarization resistance assuming that  $R_D + R_{ct} \gg R_s$ .

$$R_p = R_{ct} + R_D \quad (34)$$

A very low frequency or scan rate may be required to obtain  $R_p$  defined by Eq 34 under circumstances where reactions are mass transport limited, as indicated by Eq 32. Here, a  $l_{eff}$  of 0.1 cm and  $D = 10^{-5}$  cm<sup>2</sup>/sec requires that a frequency below 0.1 mHz be implemented to obtain  $R_p$  from  $|Z(\omega)|$  at the zero frequency limit. Hence, a common experimental problem in the case of diffusion controlled electrochemical reactions is that extremely low frequency (or scan rates) are required to complete the measurement of  $R_p$ . In the case where  $R_p$  is dominated by contributions from mass transport such that Eq 33 applies, the Stern approximation of Eqs 25 and 26 must be modified to account for a Tafel slope for either the anodic or cathodic reaction under diffusion controlled conditions (i.e.,  $\beta_a$  or  $\beta_c = \infty$ ). In fact, Eq 19 becomes invalid.

Similarly, a frequency above  $f_{max}$  must be applied to obtain  $R_s$ .

$$f > f_{max} = \frac{1}{2\pi C R_s} \quad (35)$$

where

$f_{max}$  = the frequency required such that  $Z(\omega)$  is dominated by  $R_s$ .

Typically,  $f_{app}$  must be in the kHz range to determine  $R_s$ . These issues equally plague time as well as frequency domain methods for obtaining  $R_p$ , since in the time domain measurement, the triangle waveform is simply the Fourier synthesis of a series of sinusoidal signal functions.

The capacitance is also determined from the impedance technique. In many corroding systems, an interfacial capacitance associated with the electrified double layer scales linearly with the true electrochemical surface area. An electrochemically based estimate of the surface area may be obtained if the area-specific capacitance is known or determined from the slope of a plot of  $C$  versus surface area [42].

A common issue in the use of impedance-derived capacitance concerns the use of constant phase elements (CPE). The impedance associated with a CPE has been given by the following expression [44]:

$$Z_{CPE}(\omega) = \left( \frac{1}{Y_o (j\omega)^n} \right) \quad (36)$$

$Y_o$  and  $n$  are usually assumed to be frequency independent parameters. The units for  $Y_o$  are s<sup>n</sup>/ohm, while those for capacitance ( $C$ ) are s/ohm. Hence, in the case of an ideal

capacitor or resistor,  $n = 1$  or 0, respectively, and either the magnitude of  $Y_o$  equals the magnitude of  $C$  with the dimensions s/ohms or  $1/Y_o = R$  (ohms). In the case of  $n = 0.5$ , an infinite diffusional impedance best describes the constant phase element. At issue is the task of extracting physically meaningful parameters conveyed by the capacitance in the case of impedance data that is best represented in an electrical circuit model by a constant phase element. Examples of such parameters extracted from ideal interfacial capacitance include electrode area in the case of a double layer capacitance, surface coverage in the case of an adsorption pseudo-capacitance, and dielectric constant or dielectric layer thickness in the case of a coating or oxide with dielectric properties. Other parameters may be extracted from capacitance associated with solid state impedance experiments, but these are beyond the scope of the present paper. In the case where  $n = 0.8-0.99$ , the CPE is often treated as a nonideal capacitance value, and attempts are made to extract physically meaningful parameters from the CPE data. One equation proposed to convert  $Y_o$  into  $C$  is [45]:

$$C = Y_o (\omega''_{max})^{n-1} \quad (37)$$

where  $\omega''_{max}$  is the frequency where the imaginary component of impedance,  $Z''$ , is maximized. This frequency is independent of  $n$ . In an earlier approach,  $C = Y_o (\omega)^{n-1} / \sin(n\pi/2)$  was suggested as a method for extracting capacitance,  $C$ , from  $Y_o$ , where  $\omega$  was taken as the frequency where the phase angle was maximized [46]. This method has the disadvantage that the exact value of  $\omega$  associated with the phase angle maximum changes with the value of  $n$ .

## Frequency Modulation Methods

Both harmonic and electrochemical frequency modulation (EFM) methods take advantage of nonlinearity in the E-I response of electrochemical interfaces to determine corrosion rate [47-50]. A special application of harmonic methods involves harmonic impedance spectroscopy [51]. The EFM method uses one or more a-c voltage perturbations in order to extract corrosion rate. The electrochemical frequency modulation method has been described in the literature [47-50] and has recently been reviewed [52]. In the most often used EFM method, a potential perturbation by two sine waves of different frequencies is applied across a corroding metal interface. The E-I behavior of corroding interfaces is typically nonlinear, so that such a potential perturbation in the form of a sine wave at one or more frequencies can result in a current response at the same and at other frequencies. The result of such a potential perturbation is various AC current responses at various frequencies such as zero, harmonic, and intermodulation. The magnitude of these current responses can be used to extract information on the corrosion rate of the electrochemical interface or conversely the reduction-oxidation rate of an interface dominated by redox reactions as well as the Tafel parameters. This is an advantage over LPR and EIS methods, which can provide the  $Z(\omega)$  and, at  $\omega = 0$ , the polarization resistance of the corroding interface, but do not uniquely determine Tafel parameters in the same set of data. Separate experiments must be used to define Tafel parameters. A special extension of the method involves

**TABLE 2**—Governing equations for extraction of  $i_{corr}$ , as well as  $b_a$  and  $b_c$ , from harmonic and intermodulation frequency data [52].

Reaction Type	Governing Equation	Determination of $i_{corr}$	Determination of Tafel Parameters
Charge transfer control Tafel behavior	Eq 19	$i_{corr} = \frac{i_{\omega_1\omega_2}^2}{2\sqrt{8i_{\omega_1\omega_2}i_{2\omega_2\pm\omega_1} - 3i_{\omega_2\pm\omega_1}^2}}$	$b_a = \frac{i_{\omega_1\omega_2}V_o}{i_{\omega_1\omega_2} + \sqrt{8i_{\omega_1\omega_2}i_{2\omega_2\pm\omega_1} - 3i_{\omega_2\pm\omega_1}^2}}$ similar expression for $b_c$
Passive or Anodic mass transport control	$i = i_{corr} \left[ 1 - \exp\left(\frac{-\eta}{b_c}\right) \right]$	$i_{corr} = \frac{i_{\omega_1\omega_2}^2}{2i_{\omega_2\pm\omega_1}}$	$b_c = \frac{i_{\omega_1\omega_2}}{2i_{\omega_2\pm\omega_1}} V_o$
Cathodic mass transport control	$i = i_{corr} \left[ \exp\left(\frac{\eta}{b_a}\right) - 1 \right]$	$i_{corr} = \frac{i_{\omega_1\omega_2}^2}{2i_{\omega_2\pm\omega_1}}$	$b_a = \frac{i_{\omega_1\omega_2}}{2i_{\omega_2\pm\omega_1}} V_o$

Note that  $b_a = \beta_a/\ln 10$ , and  $b_c = \beta_c/\ln 10$   
 $i_{2\omega_1\pm\omega_2}$  can be evaluated at  $i_{2\omega_1+\omega_2}$  or  $i_{2\omega_1-\omega_2}$   
 $i_{\omega_1\pm\omega_2}$  can be evaluated at  $i_{\omega_1+\omega_2}$  or  $i_{\omega_1-\omega_2}$   
 $i_{\omega_1\omega_2}$  can be evaluated at  $i_{\omega_1}$  or  $i_{\omega_2}$

harmonic impedance spectroscopy where the harmonic currents are converted to harmonic impedance values at various frequencies through knowledge of the magnitude of the a-c perturbation.

In the EFM method, an a-c voltage perturbation is applied at two frequencies,  $\omega_1$  and  $\omega_2$ . As an example, the voltage perturbation could be given as:

$$\eta = V_o [\sin(\omega_1 t) + \sin(\omega_2 t)] \quad (38)$$

where

$$\eta = E - E_{corr}$$

$V_o$  = the magnitude of the voltage amplitude applied.

Harmonic current responses occur at  $\omega_1$ ,  $2\omega_1$ ,  $3\omega_1$ , as well as at  $\omega_2$ ,  $2\omega_2$ , and  $3\omega_2$ , etc. Additionally, a current response can be seen at various intermodulation frequencies, such as  $2\omega_1\pm\omega_2$  and  $2\omega_2\pm\omega_1$ . Consider the application of this method to a charge transfer controlled corrosion process with an E-I response that behaves according to Eq 19. Under the assumption that  $\omega_2 > \omega_1$  and  $\beta_a < \beta_c$ , the corrosion current density,  $i_{corr}$ , and Tafel parameters,  $b_a$  (where  $b_a = \beta_a/\ln 10$ ) and  $b_c$ , can be determined from the equations summarized in Table 2. The current components at the angular frequency  $\omega_1$  or  $\omega_2$  can be measured at  $\omega_1$  or  $\omega_2$ . The intermodulation components  $\omega_1\pm\omega_2$  can be determined from the signal response at  $\omega_1+\omega_2$  or  $\omega_1-\omega_2$ , etc. The method is one of the few that enables extraction of corrosion rate and Tafel parameters directly from a single measurement (see Refs 29 and 30). Currently, there are no ASTM standards for this technique.

### Electrochemical Noise Resistance

Electrochemical noise analysis can provide a parameter called the electrochemical noise resistance,  $R_n$ , [53–59]. It is desirable to utilize this parameter in an analogous fashion as the polarization resistance. One electrode configuration that enables such a measurement involves connecting a zero resistance ammeter between two nominally identical corroding electrodes immersed in the same solution. A third, nominally identical electrode can be immersed in solution and connected to the first two using a high impedance voltmeter. This electrode serves as a “noisy” pseudoreference electrode. This approach is attractive in field applications due to the more rugged nature of the metallic electrode compared to laboratory electrodes, but complicates the analysis

because two uncorrelated potential sources (i.e., from the couple and the pseudoreference) are measured in the collection of potential noise,  $V_n$ . Since  $V_{n(meas)} = (V_{n(couple)} + V_{n(pseudo-ref)})^{1/2}$ ,  $V_{n(meas)}$  must be divided by 2 [60] to yield  $V_{n(couple)}$ . Another alternative is a four electrode arrangement where the first pair is coupled through a zero resistance ammeter to monitor current, and the second pair is connected with a high impedance voltmeter to sample an uncorrelated  $V_{n(couple)}$ . Alternatively, a less noisy, conventional reference electrode may be utilized in the three electrode arrangement. In this case  $V_{n(meas)}$  and  $I_{n(meas)}$  are correlated. The reference electrode noise can be separately defined as the electrochemical voltage noise between two nominally identical reference electrodes [61]. If the reference electrode noise is low, then the correction factor of 2 is not needed. In either case, the third electrode (reference electrode) is connected to the first two via a high impedance voltmeter. These arrangements enable simultaneous recording of the galvanic current with time and the galvanic couple potential versus time. The standard deviation of the voltage noise divided by the standard deviation of the current noise has been proposed to yield a statistical parameter called the noise resistance  $R_n$  [53–60,62]. Analysis of simulated noise data has led to the conclusion that the ratio of the standard deviations of the current and voltage noises measured between two identical electrodes can be normalized by surface area by multiplying by the square root of  $A_v A_i$  [59]:

$$R_n (\text{ohm-cm}^2) = \left[ \frac{\sigma_{V(meas)}}{\sigma_{I(meas)}} \right] \sqrt{A_v A_i} \quad (39)$$

where  $\sigma_{V(meas)}$  is the standard deviation of the voltage noise,  $\sigma_{I(meas)}$  is the standard deviation of the current noise, and  $A_v$  and  $A_i$  are the surface areas of the corroding electrodes used for voltage and current measurement, respectively. Correlations between this parameter and conventionally determined polarization resistance, as well as mass loss-based corrosion rates, have been obtained [54,60]. Unfortunately, experimental confirmation of the area normalization factor has not been extensively performed. Recall that in the case of a polarization resistance determined from  $E-i_{app}$  data or EIS data at the zero frequency limit, measured resistance can be multiplied by electrode area and will yield the same area-normalized polarization resistance over a broad range of electrode areas.

Moreover, the correlation has lacked a rigorous fundamental foundation for correlating  $R_n$  with corrosion rate, despite the intuitive connection between  $\sigma_V$  and  $\sigma_I$  given by the proportionality factor  $R_n$ . The surface of one freely corroding electrode could be divided into areas that experience fluctuations in interfacial resistance that produce changes in anodic and cathodic half-cell reaction rates in any one patch. The electrode potential must then change in each patch to drive the half-cell reactions, such that the sum of all the anodic half-cell currents from all patches equals the sum of all cathodic half-cell currents, regardless of whether the source of cathodic half-cell current is from capacitive discharge or electrochemical reaction [58]. Some global change in potential also occurs on the electrode. If the first electrode is now connected to a second electrode whose interfacial properties and global electrode potential don't change on their own at the same instant in time and by the same degree as on the first electrode, then a galvanic cell is momentarily created which induces a further difference in anodic and cathodic half-cell currents on the first electrode. Current now flows between the first and second electrode, such that the sum of anodic and cathodic half-cell currents over all patches on both electrodes is equal. When the interfacial resistances return to normal values over all patches, the potential difference between the two electrodes is eliminated and so is the measurable current between the two electrodes. Bertocci argued that the external current fluctuation measured between two identical electrodes is identical to the fluctuation in one electrode [58,59]. Others have argued using concepts of mixed potential theory that, at worst, the current sampled is only one half of the total for equal size electrodes.

Theoretical relationships establishing the connection between  $R_n$  and  $R_p$  have been sought by several researchers [59,63–66], but their validity has been questioned. A great concern has been that the largest current peaks would occur during the most rapid voltage fluctuations, since the electrode interface contains a capacitance through which current can be shorted [58,59]. Thus, when voltage fluctuations are rapid, the measured noise current will be shorted through the interfacial capacitance, assuming a simple electrical equivalent circuit model consisting of a two parallel resistor-capacitor network describing the interface for each electrode connected in series through  $R_s$ . This situation would lead to the lowest impedance between the two electrodes during the most rapid voltage fluctuations that, in turn, produce the greatest current fluctuations. The theoretical maximum measured current would be given by the voltage fluctuation divided by  $R_s$ . The outcome would be a statistical noise resistance parameter that is proportional to, or heavily influenced by, higher frequency data. Indeed,  $R_n$  was found to equal an absolute impedance at some frequency that depended on the frequency of the voltage fluctuations and the RC time constant of the electrode interface in one study of simulated noise [58]. Unfortunately, a  $R_n$  value obtained at high frequency would be smaller in magnitude than the  $R_p$  obtained at the zero frequency limit. Hence, it would not represent the desired zero frequency limit interfacial resistance,  $R_p$ . Indeed, such underestimations in the true value of  $R_p$  have been observed experimentally [60,62].

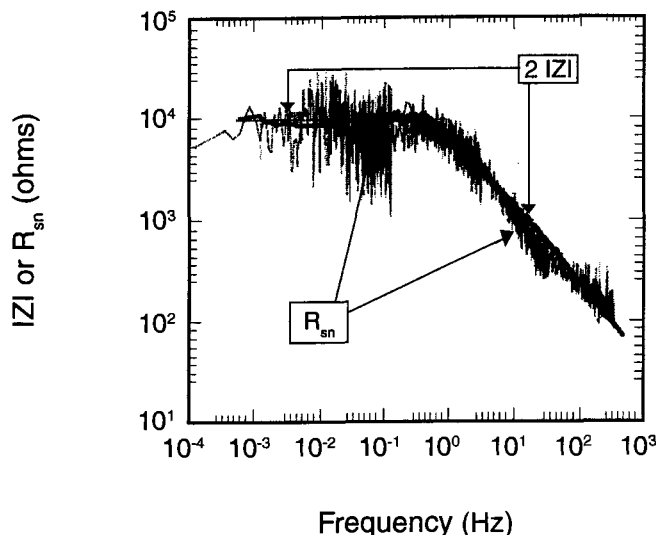


FIG. 6— $R_{sn}(\omega)$  versus frequency for iron in 1 M  $\text{Na}_2\text{SO}_4$  at pH 4 with a “noisy” iron reference electrode compared to two times the impedance  $|Z(\omega)|$  versus frequency using the EIS method. Impedance measurements were performed in a two electrode cell with two iron electrodes to produce  $2|Z(\omega)|$ . The value of  $R_{sn}(\omega)$  calculated is equal to  $\sqrt{3}|Z(\omega)|$  for the case of two iron electrodes coupled through a ZRA and a third iron electrode as reference electrode [71].

Recently, a more rigorous theoretical and experimental analysis has been made comparing the spectral noise resistance obtained at each frequency with both the polarization resistance obtained from the zero frequency limit of impedance data  $|Z(\omega=0)|$  as well as the frequency dependent impedance of two electrodes [67–71]. The spectral noise resistance  $R_{sn}(\omega)$  was determined by taking the square root of power spectral density of the voltage noise  $(V^2/\text{Hz})^{1/2}$  and dividing it by the square root of power spectral density of the current noise  $(A^2/\text{Hz})^{1/2}$  at each frequency using the same two-electrode arrangement as discussed above [70,71].

$$R_{sn}(\omega) = \frac{\sqrt{(V_{PSD})}}{\sqrt{(I_{PSD})}} \quad (40)$$

$R_{sn}(\omega)$  is proportional to the magnitude of the cell impedance,  $|Z(\omega)|$  in the two electrode arrangement [70,71]. The proportionality factor is unity in the case of identically-sized electrodes in a two electrode cell with identical impedances and a noise-less reference electrode [70,71]. Therefore, the spectral noise resistance at the zero frequency limit equals the interfacial impedance at the zero frequency limit  $|Z(\omega=0)|$  in the theoretical case of identical electrode impedances with negligible  $R_s$ . In this case  $R_{sn}(0) = R_p$ . Figure 6 illustrates data for identical Fe electrodes in 1 M  $\text{Na}_2\text{SO}_4$  with an iron reference electrode. Here  $R_{sn}(\omega) = \sqrt{3}|Z(\omega)|$  due to the noisy RE. Thus,  $2|Z(\omega)|$  and  $R_{sn}(\omega)$  appear to be similar. For a corroding system,  $|Z(\omega=0)|$  equals  $R_p$ . For a corroding system  $R_{sn}(0) = R_p$ . Even  $R_n$  may equal  $R_{sn}(\omega=0) = |Z(\omega=0)| = R_p$  if  $|Z(\omega)|$  equals  $R_p$  in the frequency regime dominating

the  $R_n$  value. The frequency range dominating the  $R_n$  value is determined by several factors, but this statement is more likely to be true if  $|Z(\omega)|$  and  $R_{sn}(\omega)$  both exhibit long low frequency plateaus over a broad frequency range that encompasses the  $f_{min}$  and  $f_s$  utilized in the  $R_n$  measurement. Here  $f_{min}$  is given by the total sampling time,  $T$ , where  $f_{min} = 1/T$  and  $f_s$  equals the data sampling rate.  $R_n$  typically varies with  $f_s$  and underestimates  $|Z(\omega = 0)|$ . Unfortunately,  $R_{sn}(\omega \rightarrow 0)$  does not equal  $R_p$  in the zero frequency limit under many other conditions, such as when  $\log(R_s/R_p) > 0$  or in the case of very noisy reference electrodes [70,71]. Moreover,  $R_{sn}(\omega)$  can be dominated by the properties of the high impedance electrode in the case of dissimilar electrode impedances that are equally noisy, but this is not always the case. For instance, the low impedance electrode in a two electrode cell with a third reference electrode can be sensed by  $R_{sn}(\omega)$  if the higher impedance electrode is much noisier than the low impedance electrode [70,71]. Recent attempts have been made to address circumstances where  $R_{sn}(\omega)$  lies in between  $|Z(\omega)|_1$  and  $|Z(\omega)|_2$  representing the high and low impedance electrodes. Methods have been suggested for sensing the current fluctuations on both electrodes [72]. The reader is referred to these articles for further information.

## ELECTROCHEMICAL METHODS FOR THE STUDY OF GALVANIC CORROSION

Galvanic corrosion is defined and described in Section IV of this manual on corrosion types.

### Methods Based on Mixed-Potential Theory

The thermodynamic tendency for galvanic corrosion may be determined from the electromotive series [5] or from the construction of a galvanic series as discussed in ASTM G 82,<sup>6</sup> Guide for Development and Use of a Galvanic Series for Predicting Galvanic Corrosion Performance. Galvanic corrosion rates can also be determined from mixed-potential theory as schematically illustrated in Fig. 7. In the case of bimetal or multimetal galvanic attack in which two or more metals are electrically in contact with one another, there is in theory a minimum of two cathodic and two anodic reactions. One of each of these reactions is occurring on each metal. In this case, the more noble of the two metals is cathodically polarized, and its anodic reaction rate will thus be suppressed. Conversely, the less noble or anodic material is anodically polarized and the anodic reaction rate is accelerated. The mixed potential (the galvanic couple potential,  $E_{couple}$ ) of the galvanic couple and the resulting galvanic current can be uniquely determined from the sums of all of the individual anodic and cathodic currents obtained for each material at each potential when the following condition is met

$$\sum i_a A_a = \sum i_c A_c \text{ at } E_{couple} \quad (41)$$

where

$i_a, i_c$  = the anodic and cathodic current densities,  $\mu A/cm^2$ , and  
 $A_a, A_c$  = the anodic and cathodic areas,  $cm^2$ .

<sup>6</sup>ASTM Standard G 82, Guide for Development and Use of a Galvanic Series for Predicting Galvanic Corrosion Performance.

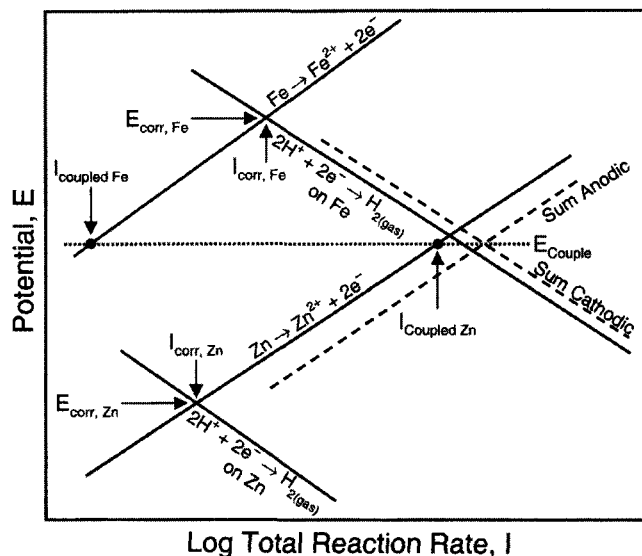


FIG. 7—Potential-current relationships for the case of a galvanic couple between two corroding metals. Steel is the more noble metal, zinc is the less noble metal [5]. The corrosion rate of zinc is increased significantly when coupled while the corrosion rate of steel is decreased.

The galvanic couple potential is defined by the potential where the sum of the anodic currents equals the sum of the cathodic currents for all reactions on all of the metals in the couple. The galvanic couple potential can be determined either by direct measurement with a reference electrode or from polarization data if:

1. Polarization data are available for each material in the galvanic couple,
2. The area of each metal is known, and
3. The current distribution is uniform.

Once  $E_{couple}$  is determined, the galvanic corrosion rate may be estimated for the metal of interest in the couple if a relationship such as given in Eq 19 is known for that metal. In simple bimetal cases, direct superposition of polarization data (corrected for wetted surface area) can yield  $E_{couple}$  and the galvanic corrosion rate [73]. However, because applied currents instead of true anodic or cathodic currents are measured in any polarization experiment, the E-log(I) superposition technique will introduce the least error when the cathodic reduction reaction rate on the anode is negligible and the anodic oxidation reaction rate on the cathode is negligible at the galvanic couple potential. Obviously, when the OCPs of the anode and cathode are similar, error is more likely. Fortunately, galvanic corrosion may be less significant in these cases. In addition, special care must be taken in the procedures used to develop the polarization data [73], especially if time effects are to be taken into consideration when evaluating long-term galvanic corrosion behavior.

### Direct Measurement of Galvanic-Corrosion Rates

A more straightforward procedure involves immersing the two dissimilar metals in an electrolyte and electrically

connecting the materials together using a zero-resistance ammeter to measure the additional galvanic current [9, 74,75]. In this method, the galvanic current is directly determined as a function of time. The galvanic corrosion rate so determined is the additional corrosion created with the couple and will not equal the true corrosion rate. This is given by the sum of the galvanic corrosion rate and the corrosion rate under freely corroding conditions, unless the latter is negligible. Recall that the corrosion rate of the uncoupled anode is undetermined by this method, since an equal cathodic reaction rate is occurring on the same surface. A reference electrode connected to the galvanic couple can be used to determine the galvanic couple potential. ASTM standards do not exist for direct measurement of galvanic corrosion or scanning potential probe methods.

### Potential Probe Methods

Potential probe methods may be used to determine and map the local ionic currents associated with galvanic corrosion cells between dissimilar metals or heterogeneities on complex alloy surfaces [76–79]. In the most straightforward application, the local potential is mapped over a planar electrode oriented in the x-y plane to give an indication of local current. The basic concept is that the ionic current density in three dimensions can be mapped by either scanning an array of reference electrodes or by vibrating a single electrode. The following equation expresses the orthogonal ionic current flow in terms of solution conductivity and the gradient in potential in the solution above the galvanic couple,

$$i = -\kappa(\nabla E) \quad (42)$$

where  $\kappa$  is the solution conductivity and  $\nabla E = \delta_1 dE/dx + \delta_2 dE/dy + \delta_3 dE/dz$ , where  $x, y, z$ , define axes in a coordinate system and  $\delta_i$  are unity vectors. The advantage of the vibrating technique is that minor differences between the reference potential of separate electrodes is eliminated by using a single vibrating reference electrode. The ionic current density so recorded is the component of current density flowing perpendicular to iso-potential lines in solution established due to the galvanic couple and the established potential gradient. Therefore, a map of local current can be constructed by scanning over a planar electrode in the x-y plane, where  $z$  is the vertical distance in the solution above the electrode. Locations of high local current imply significant galvanic interactions.

## ELECTROCHEMICAL METHODS FOR THE STUDY OF PASSIVITY AND LOCALIZED CORROSION

Pitting and crevice corrosion are associated with the breakdown of passivity [80]. Electrochemical tests for evaluating the susceptibility of a material to pitting and to crevice corrosion include potentiodynamic, potentiostatic, scratch potentiostatic, potentiostaircase, tribo-ellipsometric methods, pit-propagation rate curves, galvanostatic, and electrochemical noise measurements [80–82].

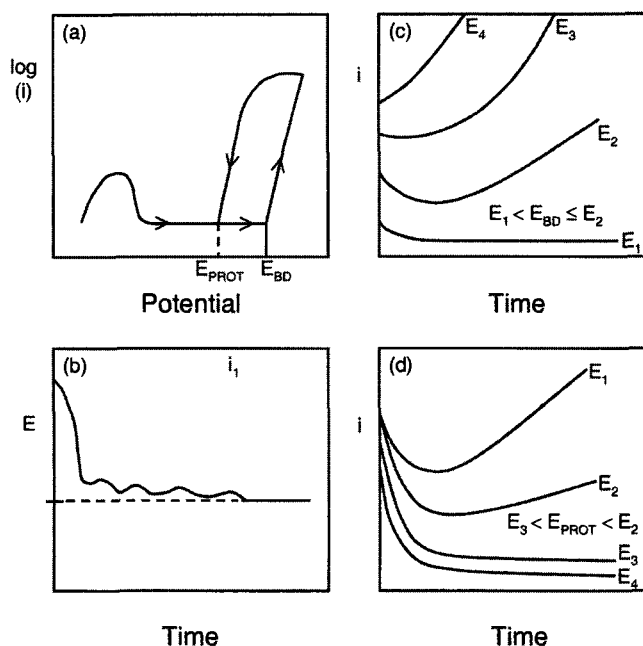


FIG. 8—Schematic representations of experimental data for (a) a cyclic potentiodynamic polarization curve; (b) galvanostatic potential-time curve for a material; (c) potentiostatic current-time curve for a previously passivated surface which pits at  $E_1 < E_{bd} < E_2$ ; and (d) potentiostatic current-time curve for active surface. The protection potential is found as  $E_3 < E_{prot} < E_2$  [80].

### Cyclic Potentiodynamic Polarization Methods to Determine $E_{bd}$ and $E_{prot}$

ASTM G 61<sup>7</sup> describes a procedure for conducting cyclic potentiodynamic polarization measurements to determine relative susceptibility to localized corrosion. The method is designed for use with iron- or nickel-based alloys in chloride environments. In this test, a cyclic anodic polarization scan is performed at a fixed voltage scan rate. Figure 8a shows a schematic of the cyclic potentiodynamic method. Particular attention is focused on two features of cyclic polarization behavior (Fig. 8a). The first is the potential at which the anodic current increases significantly with applied potential (the breakdown potential,  $E_{bd}$ ). In general, the more noble this potential, obtained at a fixed scan rate in this test, the less susceptible the alloy is to the initiation of localized attack. The second feature of great interest is the potential at which the hysteresis loop is completed during reverse polarization scan after localized corrosion propagation. This potential is often taken as the repassivation potential or protection potential,  $E_{prot}$ . In general, once initiated, localized corrosion sites can propagate only at some potential more positive than the potential at which the hysteresis loop is completed (when determined at a fixed scan

<sup>7</sup>ASTM Standard G 61, Test Method for Conducting Cyclic Potentiodynamic Polarization Measurements for Localized Corrosion Susceptibility of Iron-, Nickel-, or Cobalt-Based Alloys.



rate). In other words, repassivation will occur at more negative potentials, even after localized corrosion initiation. Therefore, the more positive the potential at which the hysteresis loop is completed, the less likely that localized corrosion will propagate. Additionally, the difference in potential between  $E_{corr}$  and  $E_{prot}$  ( $E_{prot} - E_{corr}$ ) is often taken to indicate relative resistance to local corrosion. ASTM G 61 illustrates cyclic polarization behavior for Hastelloy C-276 and 304 stainless steel in 3.5 % sodium chloride solution. Based on this criterion, it is evident that Hastelloy C-276 is more resistant to localized corrosion in this environment than AISI 304 stainless steel.

### Complications with Cyclic Potentiodynamic Polarization Methods

Although the cyclic method is a reasonable method for screening variations in alloy composition and environments, the cyclic potentiodynamic polarization method has been found to have a number of shortcomings [80–85]. One major problem concerns the effect of the potential scan rate. The values of both  $E_{bd}$  and  $E_{prot}$  are a strong function of the manner in which the tests are performed, particularly the potential scan rate employed. Experimental values of  $E_{bd}$  are linked to the induction time required for pitting. Another complication arises from allowing too much pitting propagation to occur before reversing the scan direction. This either alters the localized chemistry in pits, affects pit depth, or both. Pit depth alters the diffusion length associated with the dilution of pit chemistry necessary for repassivation. This factor affects the polarization behavior after the reversal in the direction of scanning and influences  $E_{prot}$ . From an engineering standpoint, metal surfaces held at potentials below the repassivation potential of the deepest pits should be safe against stable pit propagation. That is to say, stable pits should not propagate. It has been found that  $E_{bd}$  observed after potentiostatic holds or the slowest scan rates approaches the protection potential found after minimal pit growth when pits are small [85]. This suggests the existence of a single critical potential,  $E_c$ , for pit initiation and growth in the absence of crevices or other occluded sites [85]. If the potential can be maintained below  $E_c$ , pitting does not occur.

### Potentiostatic and Galvanostatic Methods for Localized Corrosion

The shortcomings of the cyclic potentiodynamic polarization method have become the basis for several other electrochemical techniques. Other methods are schematically illustrated in Fig. 8. In the galvanostatic or galvanostaircase technique (Fig. 8b), potential is measured versus time at various constant applied currents that are incrementally increased in steps, then reversed and decreased. In the case of passive materials, a potential rise during galvanostatic testing indicates passive film growth, while a decline indicates breakdown and growth of local corrosion sites. In the galvanostaircase technique, the current is step increased. Potential measurements are made until the time rate of change in potential approaches zero. These forward and reverse potential-current density data are extrapolated to the zero current density to obtain  $E_{bd}$  and  $E_{prot}$ . The technique

is described by ASTM G 100<sup>8</sup> (Method of Conducting Cyclic Galvanostaircase Polarization) as a test method for aluminum alloys. Potentiostatic methods can overcome the inherent problems involving scan rate. A more conservative estimate of  $E_{bd}$  can be obtained by polarizing individual samples for long periods of time at potentials above and below the values of  $E_{prot}$  and  $E_{bd}$  previously determined from the potentiodynamic method (Fig. 8c). Eventual initiation is indicated by a current increase. In another approach (Fig. 8d), initiation of pits is intentionally induced by applying a “stimulation” potential well above  $E_{bd}$  and then quickly shifting to a preselected potential below that value. If this second applied potential is above  $E_{prot}$ , propagation of the existing pits will continue and the current will increase. However, at potentials less than  $E_{prot}$  the pits will eventually repassivate and the current will subsequently decrease with time. The critical potential for pitting is defined as the most noble potential at which pits repassivate after the stimulation step. This approach is covered in ASTM F 746<sup>9</sup> (Test Method for Pitting or Crevice Corrosion of Metallic Surgical Implant Materials).

### Determination of $E_{prot}$ by Potential Step-down or Scan-down Methods

As stated above,  $E_{bd}$  and  $E_{prot}$  often depend strongly on the method by which they are determined and, therefore, do not uniquely define intrinsic material properties. The  $E_{prot}$  values determined from the scanning method can be complicated by scan rate, pit size or depth, vertex potential/current, polarization curve shape, and specimen geometry [86,87]. Investigators have found more consistent  $E_{prot}$  values after a critical charge has passed, while others report a single critical potential [85]. Often this potential is difficult to choose from E-I data and has been taken at various points on the reverse scan of a cyclic potentiodynamic polarization curve [89].

What is needed is a method for determination of  $E_{prot}$  that defines a conservative value of this potential that likely reflects a true pit or crevice repassivation potential. Tsujikawa has developed a method for determination of  $E_{prot}$  from previously grown pits and crevices [90,91]. This method and its variations have been successfully used by several research groups and associates the critical potential for repassivation  $E_{prot}$  with the need to grow local corrosion sites to a critical minimum size [92]. The method is an enhancement of the determination of  $E_{prot}$  from potentiodynamic E-I scans that involve scan reversal to the point where pits are repassivated. In the potential step-down method, the potential is first set at a high enough value to induce and grow stable pits to the specified size. The potential can then be stepped down or scanned downward, while the pit propagation current is recorded. Subsequently, the potential may be held after a pit has been initiated in order to determine the time until repassivation [93]. Moreover, long potential holds at selected applied potentials enable confirmation of a true

<sup>8</sup>G 100, Test Method for Conducting Cyclic Galvanostaircase Polarization.

<sup>9</sup>ASTM F 746, Test Method for Pitting or Crevice Corrosion of Metallic Surgical Implant Materials.

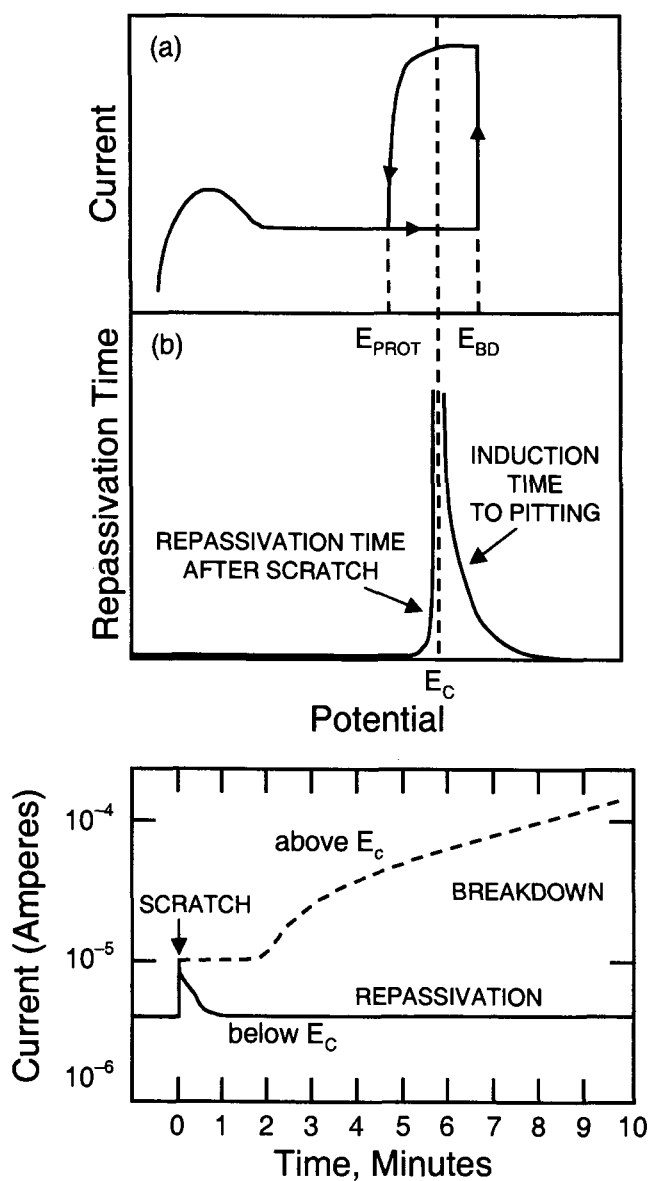


FIG. 9—(a)  $E$ -log( $i$ ) curve showing location of  $E_{bd}$  and  $E_{prot}$ . (b) Time versus applied potential plot from scratch test illustrating a possible location of the critical potential,  $E_c$ , as it relates to the induction time and the repassivation time [80]. (c) Current versus time plot for a scratched specimen when scratched above and below  $E_c$ .

repassivation potential, often indicated by an abrupt decrease in current density at the time when the chemical conditions favoring pit stability (often expressed as some fraction of the salt saturation concentration) are no longer maintained. Abrupt transitions in finite repassivation time towards infinity with increasing hold potential may indicate that conditions favorable to pit growth are sustained. Another benefit of determining  $E_{prot}$  from controlled growth of pits and crevices is that the repassivation potential can be determined from pits of preselected sizes that can be controlled by the duration of the potential holds. The method

has been successfully applied to nickel-base alloys, stainless steels, and Al-base alloys, and is being standardized by the committee for Japanese Industrial Standards. When a one-dimensional pit or pencil electrode is tested, the pit propagation kinetics can be recorded from a single pit [94]. Whether pit growth is ohmic, mass transport, or charge transfer controlled may also be determined. Moreover, the effects of various material and solution parameters (e.g., flow rate, conductivity, and solution composition) on pit propagation rates can be determined.

### The Scratch-Repassivation Method for Localized Corrosion

An additional potentiostatic technique to be mentioned in the area of localized corrosion involves the scratch method [95]. In this method, the alloy surface is scratched at a constant potential and the current is measured as a function of time. The potential dependencies of the induction time and the repassivation time are determined by monitoring the current change over a range of different potentials. This is illustrated in Fig. 9. From this information the critical pitting potential,  $E_c$ , thought to be more negative than  $E_{bd}$  determined by potentiodynamic scan, can be determined. Other methods of studying localized corrosion are also available [80]. An ASTM standard exists for the critical pitting temperature measurement method under the designation ASTM G 150.<sup>10</sup>

### Statistical Distributions in Critical Potentials

$E_{bd}$  is typically observed to be a significantly "statistically distributed" property compared to the repassivation potential. This is often observed when critical potentials are determined by potentiodynamic scanning, but also can be observed during potentiostatic tests where the pit incubation time and subsequent survival probabilities are also seen to be distributed.  $E_{prot}$  distributions are often attributed to distributions in pit size. However,  $E_{prot}$  is not distributed when pits are uniformly large [88] and may not depend on the depth of corrosion damage at all during crevice corrosion when a crevice former controls mass transport [96]. Statistical distributions in pitting potentials have been observed for AISI 304 [97], Fe-Cr-X (where  $x$ =Nb, Mo, or Ti) alloys [98], AISI 316 [99], Ti [100], high purity Al [101], AA 2024-T3 [102], and amorphous Al-base alloys [103]. These statistical distributions imply that significant variations exist when a number of specimens are tested under identical conditions. These distributions have been attributed to the stochastic nature of pitting [99], distributions in oxide film cation vacancy transport properties [104], the effects of potential on the nature of the eligible sites for the metastable pit nucleation process [97], and the population of fatal flaws or pit initiating defects on an electrode surface [105]. The possibility that oxide defects at densities exceeding millions of sites/cm<sup>3</sup> produces specimen-to-specimen variations appears unlikely for specimens with surface areas of the order of cm<sup>2</sup>. It appears to be more reasonable to expect that

<sup>10</sup>ASTM Standard G 150, Test Method for Electrochemical Critical Pitting Temperature Testing of Stainless Steels.

sample-to-sample variations are, instead, associated with distributions in the population of micrometer scale defects, such as sulfide inclusions in stainless steel [106] and constituent particles in Al alloys [105] that control the density of pit nucleation sites and produce micropit to micropit variations in growth rates and diffusive transport characteristics (e.g.,  $D_{eff}$ , pit shape) for a large population of metastable pits grown at a single potential. A statistical distribution of the product  $i_{pit} * r_{pit}$  (where  $i_{pit}$  is the pit current density and  $r$  is pit radius) was observed for a large population of pits at a fixed potential in high purity Al [101]. This product is linearly related to the acid pit chemistry. Although not rigorously proven, it is reasonable to argue that a slightly slower rate of pit transport or slightly larger  $i_{pit} * r_{pit}$  product for a given pit might lead to pit stabilization through achievement of the critical acid pit chemistry at different applied potentials on an electrode with a population of pits sites. Moreover, such behavior is likely controlled by micrometer scale defects spaced at tens of micrometer lateral separation distances across planar electrode surfaces. Investigators seeking information on critical potentials for engineering use should consider appropriate specimen sizes relative to critical defect densities and spacings. There are no ASTM standards that address these issues. However, the sizes of test specimens recommended in many ASTM standards are conservatively large so as to include many possible pit sites.

### Electrochemical Noise Methods

Electrochemical noise (EN) methods are used increasingly as a nondestructive tool for evaluating susceptibility to localized corrosion as well as stress-corrosion cracking (SCC), particularly in field or process plant applications [107–112]. EN is appealing because it may be conducted at open circuit without perturbing the corroding system. However, currently no consensus exists as to the most appropriate test procedure or analysis method, or how well results correlate with coupon exposures. The origins of EN current and potential signals are discussed in more detail in the chapter on Testing for Corrosion Types: Pitting. The transient development of bare metal at newly formed pit or cracking sites as a result of temporary propagation and repassivation can result in potential noise (open circuit EN), current noise (potentiostatic EN), or both. In the latter case, the current noise is measured with a zero resistance ammeter (ZRA) used to monitor a galvanic couple consisting of two identical electrodes, while the potential noise comes from the reference electrode (or, third metallic electrode) monitoring the couple potential. The noise signal, hereafter referred to as a potential or current time record, is caused by the galvanic couple formed between the very small anode sites corroding at current densities (c.d.) approaching 10 A/cm<sup>2</sup> in pitting corrosion and the much larger remaining cathode surface operating at lower cathodic current densities (c.d.) (e.g., 10 μA/cm<sup>2</sup>). Regarding pitting phenomena, a negative shift in measured potential is observed (OCP and galvanic couple EN), an increase in current is observed for potentiostatic EN, and current fluctuations of either polarity are observed for galvanic couple EN.

Several analysis methods exist, including electrochemical [113], statistical [111,112], spectral [107–110], and autocorrelation [109]. Some of the approaches for determination of spectral noise resistance during uniform corrosion are discussed above in the section on polarization resistance. Electrochemical analysis may also enable the determination of pit sizes from the charge associated with each pitting event [101], or from attempting to determine pit current densities. Statistical analyses include determining the root mean square (rms), variance, and standard deviations of the EN voltage or current time records, as well as a noise resistance,  $R_N$ , taken as the ratio of the rms or standard deviation of the potential and current time records acquired over various periods of time [111]. Spectral analysis consists of Fourier transformation of EN data acquired in the time domain to create a power spectral density plot [109, 110,112,114]. Qualitative assessment of the benefits of inhibitors, or the effects of process stream variations are made possible by comparing statistical or spectral results. Quantitative analysis and predictive capability still require further development.

### Use of Shot Noise Methods During Pitting

In the prepitting stage, multiple subcritical pitting events are often observed. The current time record shows exponential decaying or rising transients associated with discrete pitting events. In many systems these prepitting events occur at potentials far more negative than  $E_{bd}$  and sometimes  $E_{prot}$ . Numerous investigators have proposed that the ratio of peak pit current to pit radius during metastable pitting or product of pit current density times pit radius ( $I_{pit}/r_{pit}$  or  $i_{pit} * r_{pit}$ ) provides a insightful parameter that can be used to characterize the risk of stable pit propagation based on the critical acid pit chemistry theory of Galvele [115].

When anodic current is monitored near the pitting potential, multiple overlapping metastable pitting events are often detected as current spikes at potentials just below  $E_{bd}$ . EN analysis provides one method for extracting information on pitting from such complicated current time records. That is, the power spectrum for a population of spikes of similar amplitude and duration is the sum of the spectra for each spike and should have the same shape as an individual spike. The use of Shot noise analysis has been proposed to calculate the pit charge from power spectral density (PSD) analysis obtained from a current-time record [116–118]. According to this approach, pit charge,  $q_{pit}$ , and, through Faraday's Law the pit radius,  $r_{pit}$ , for the pit events that dominate the current-time record can be determined from the PSD of a pitting current noise spectrum. The following equation describes the theoretical power spectral density (PSD) of current fluctuations for the case of randomly occurring, exponentially decaying current spikes associated with metastable pitting events during the prepitting stage [115]:

$$\frac{I^2}{\Delta f} = \left[ \frac{2q_{pit}I_{mean}}{1 + (2\pi f\tau)^2} \right] \quad (43)$$

where  $f$  is the spectrum frequency,  $\Delta f$  is the frequency resolution given by the data acquisition frequency divided by the number of data points collected,  $q_{pit}$  is the pit charge,

$I_{mean}$  is the mean current from a  $I-t$  record containing multiple current fluctuations associated with pit events after subtraction of any background passive current,  $I$  is the amplitude of pit current fluctuations, and  $\tau$  is the time constant for individual exponentially decaying current transients that comprise the current fluctuations. Hence, the low frequency limit of a  $\log I^2/\Delta f$  versus  $\log f$  plot provides information on  $q_{pit}$  for known  $I_{mean}$ . The frequency of the intercept (or breakpoint frequency) of the sloping part of the high frequency PSD with the low frequency plateau,  $f_{bpt}$ , provides information on the time constant for exponentially decaying pitting events,  $\tau$ ;  $f_{bpt} = 1/2\pi\tau$ . Therefore,  $q_{pit}$  and  $\tau_{pit}$  may be extracted from current PSD plots constructed from current-time data containing many overlapping metastable pitting events. This analysis method has been successfully applied to Al alloys [119,120]. Unfortunately, the approach has its shortcomings. The parameters recovered are heavily biased towards smaller more numerous pitting events that dominate the current time record. The biggest and/or fastest growing pits that might readily form stable propagating pits may not be detected. However, the method does enable determination of pit sizes at various potentials and allows the comparison of one environment, temperature, or set of plant conditions to another. No ASTM standard currently exists on this topic.

## ENVIRONMENTALLY ASSISTED CRACKING

There are several electrochemical techniques for assessing susceptibility to environmental cracking. For alloys that are susceptible to SCC by a mechanism of slip induced passive film rupture and anodic dissolution, electrochemical measurement of dissolution rate has obvious practical advantages. In this case, the increment of crack growth is defined by the anodic charge associated with each film rupture event. The crack growth rate is defined by this repetitive process. In the case of hydrogen embrittlement (HE) phenomena, determination of the mobile hydrogen concentration in the metallic lattice is an important consideration. Such a determination is possible using an electrochemical approach. Several pertinent methods are discussed below.

### Scratch Repassivation

The scratch repassivation technique discussed above may be more useful for studying SCC than pitting [107]. This is because natural pitting is often initiated at defect sites in the passive film that are electronic or chemical in nature. Such sites are not necessarily probed by a mechanical scratch. Scratching can simulate SCC where mechanical film rupture processes are operative and anodic dissolution controls the SCC process. In general, once the passive film is mechanically disturbed at some potential, an electrochemical current can be measured that will decay back to a low level when repassivation has occurred. A measure of the crack growth rate,  $V$ , (cm/s) can be obtained from these data

$$V = \left( \frac{E.W.}{\rho F} \right) \left[ Q_f \frac{\epsilon_{ct}}{\epsilon_f} \right] \quad (44)$$

where  $E.W.$ ,  $\rho$ , and  $F$  have been defined previously, and

$$Q_f = \int i_{ox} dt$$

$Q_f$  = the anodic charge density (coulombs/cm<sup>2</sup>),

$\epsilon_f$  = the fracture strain of the film, and

$\epsilon_{ct}$  = the crack tip strain rate (s<sup>-1</sup>).

## Tribo-ellipsometric Methods

The tribo-ellipsometric method is an advancement of the scratch method and has been used to distinguish between cases where an alloy is susceptible to localized corrosion, such as pitting or SCC, as opposed to general dissolution. The total anodic current transient following film destabilization consists of the algebraic sum of the repassivation current and the current corresponding to dissolution of the exposed bare metal in lieu of film formation. The electrochemical current measurement is conducted in conjunction with the optical ellipsometric method to measure the rate of film growth and repassivation film thickness. This combination offers a method of separating the two currents (dissolution versus repassivation), assuming that the valence state and density of the oxide are known so that charge can be determined from its volume. Based on the ratio of the charge involved in dissolution and the charge associated with repassivation, a criterion for stress corrosion is established by the parameter  $R_{sc}$ :

$$R_{sc} = 1 + Q_d/Q_r \quad (45)$$

where

$Q_d$  = the charge involved in dissolution, and

$Q_r$  = the charge associated with repassivation.

For example, a low-carbon steel was not found to be susceptible to SCC in a solution in which  $R_{sc}$  was 2.8. In this case, repassivation occurred very rapidly. However, the steel was found to be susceptible when that ratio was 26, and it was not susceptible again in a solution in which  $R_{sc}$  was 75 [121]. In the latter case, widespread pitting occurred instead. Hence, a balance between repassivation and widespread dissolution is required for anodically controlled SCC. Only under intermediate conditions is SCC possible.

## Potentiodynamic Methods

Parkins has devised a slow and rapid potentiodynamic scanning method to determine both the relative susceptibility to slip-film rupture-repassivation SCC susceptibility, as well as possible ranges of potential where SCC might occur [60]. The method applies to metals and alloys whose oxide films can initially be cathodically reduced. The validity of the method relies on the notion that SCC only occurs when crack walls are readily passivated while the crack tip dissolves at a high rate due to continual destabilization of the passive film. In this method, the rapid scan anodic polarization curve provides a measure of the bare dissolution kinetics over a range of anodic potentials. A slow anodic potentiodynamic scan provides a measure of the passive crack flank dissolution kinetics over the same range of potential. Alloy-electrolyte combinations that produce potential

ranges where a difference in dissolution rate of 100–1000 is observed for the two scan rates are more SCC susceptible. Caution is warranted, however, over concern that the differences in current do not merely reflect capacitive current as indicated in Eq 19. All of the techniques mentioned in this section suffer from the need to perform testing in solutions that simulate the relevant crack tip chemistry and at the potentials actually experienced by the crack tip. No ASTM standard exists for these methods.

### The Barnacle Electrode Technique for Determination of Diffusible Hydrogen Concentration

The degradation of fracture toughness below levels obtained in dry air or vacuum is a strong function of the internal diffusible hydrogen concentration for alloys prone to HE. Therefore, it is often important to determine this concentration, hereafter referred to as  $C_H$ .  $C_H$  can be determined by measuring the anodic current density associated with the oxidation of mobile hydrogen, which has diffused to the surface. Of course, precaution must be taken to ensure that  $i_{ox}$  is associated only with the reactions given by Eqs 7 or 8 and does not include a contribution from other oxidation processes, such as metal oxidation. The source of the adsorbed hydrogen is internal hydrogen in a precharged specimen that diffuses to the surface across the concentration gradient created when the surface concentration is lowered to zero as a consequence of hydrogen oxidation and extraction. In the Barnacle Electrode method, a hydrogen-containing steel part with initial uniform diffusible hydrogen concentration,  $C_H$ , is galvanically coupled to a nickel/nickel oxide electrode in an alkaline electrolyte [123,124]. This couple polarizes the steel to a potential at which the hydrogen is oxidized as it diffuses out while metal oxidation is minimized.  $i_{ox}$  is related to mobile hydrogen concentration in the metal by the first term solution to Fick's second law [123]. The appropriate boundary conditions for this equation are:  $\partial C_H / \partial x = 0$ ,  $x = 0$ ,  $t \geq 0$ ;  $C_H = 0$ ,  $x = L$ ,  $t > 0$ ;  $C = C_H$ ,  $0 \leq x \leq L$ ,  $t \leq 0$ .

$$\frac{i_{ox}}{nF} = C_H \left( \frac{D_H}{\pi t} \right)^{1/2} \quad (46)$$

where

- $C_H$  = the mobile or diffusible hydrogen concentration (1 gram-mole  $H/cm^3$  Fe  $\equiv 1.3 \times 10^5$  wt. ppm),
- $D_H$  = the apparent diffusion coefficient for  $H$  ( $cm^2/s$ ),
- $t$  = time, s, and
- $L$  = one-half the sample thickness so that  $x = L$  at the extraction surface and  $x = 0$  is the center of the specimen, cm.
- $i_{ox}$  = the current density associated with hydrogen oxidation ( $A/cm^2$ ).

The first term solution given in Eq 46 is valid if  $L^2/Dt \geq 4$ . The slope of a plot of  $\log(i_{ox})$  versus  $\log(t)$  should be  $-0.5$ .  $C_H$  is determined from measured values of  $i_{ox}$  and  $t$  if  $D_H$  is known and the data fit Eq 46. If  $D_H$  is not known, then the product  $C_H D_H^{1/2}$  is obtained.

### The Permeation Method for Determination of Diffusible Hydrogen Concentration

In this method, an electrochemical technique is used to measure the diffusion coefficient,  $D$ , and the solubility,  $C_o$ , of

hydrogen in iron or other metallic foil, under a variety of experimental conditions [125,126]. The advantages of the electrochemical technique are twofold. First, as noted above, by adjusting the potential one can apply a wide range of equivalent hydrogen pressures to the charging side of the metal membrane without resorting to high-pressure or high-vacuum techniques. Secondly, the hydrogen forced through a thin metal foil can be transformed to  $H^+$  ions ( $H \rightarrow H^+ + e^-$ ) when it reaches the solution on the other side of the permeation foil, and thus, the permeation rate will be proportional to the oxidation current required on the exit side of the membrane. Very accurate and sensitive measurements of the permeation rate to be made, can be seen from the fact that a current density of  $1 \mu A/cm^2$  corresponds to a permeation rate of  $H_2$  of about  $10^{-7} mL/cm^2 sec^{-1}$  at STP in palladium.

The diffusion equation given by Fick's second law where  $C_H(x, t)$  is the position dependent diffusible hydrogen concentration,  $t$  is time,  $D$  is the diffusion coefficient, and  $x$  is distance through the foil has been solved for the initial conditions  $C_H(x, t = 0) = 0$  and for the boundary conditions  $C_H(0, t = \infty) = C_o$ ,  $C_H(L, t = \infty) = 0$ . In other words, the conditions are that before the experiment is started, the foil contains no hydrogen and, at any time after the start of the experiment, the concentration,  $C_H$ , on one side ( $x = 0$ ) is a constant,  $C_o$ , and on the other side ( $x = L$ ) it is equal to zero. The time  $t = 0$ , in this case, corresponds to the time at which the concentration is switched from 0 to  $C_o$ . The solution of Eq 47 with the above initial and boundary conditions yields a series, which, to a good approximation,\* can be given by its first term:

$$\frac{i(t)}{i(\infty)} = \left( \frac{2}{\pi} \right) \left( \frac{1}{\tau^{1/2}} \right) \exp \left( -\frac{1}{4} \right) \quad (47)$$

in which  $i(t)$  and  $i(\infty)$  are the measured currents (proportional to the permeation rate of hydrogen) at a time  $t$  and at steady state, respectively, and  $\tau$  is a dimensionless parameter given by  $\tau = Dt/L^2$  where  $L$  is the thickness of the membrane. Figure 10 depicts the relation between  $i(t)/i(\infty)$  and  $\tau$ . The values of  $\tau$  corresponding to some selected values of  $\gamma$  are given in Table 3.

The diffusion coefficient may be determined from the transient permeation current density at various times  $t\gamma$  for  $\tau\gamma$  and selected foil thickness,

$$D = \tau\gamma L^2/t\gamma \quad (48)$$

where  $t\gamma$  is the time required to reach a current  $i(t) = \gamma i(\infty)$  and  $\tau\gamma$  is the corresponding value of  $\tau$ . This forms the basis of the lag time and breakthrough time methods discussed in ASTM standard G 148.<sup>11</sup> A test of the validity of the assumptions leading to Eq 47 is to calculate  $D$  from Eq 48 for different values of  $\gamma$  and show that it is independent of  $\gamma$ . An alternative approach facilitates determination of  $D$  from a linear regression of many data points, instead of relying on a single data point on the rise transient. Here, the solution given by McBreen for the rise transient is used based on a rearrangement of Eq 47:

\* This approximation is valid for  $i(t)/i(\infty) < 0.96$ .

<sup>11</sup>ASTM Standard G 148, Practice for Evaluation of Hydrogen Uptake, Permeation, and Transport in Metals by an Electrochemical Technique.

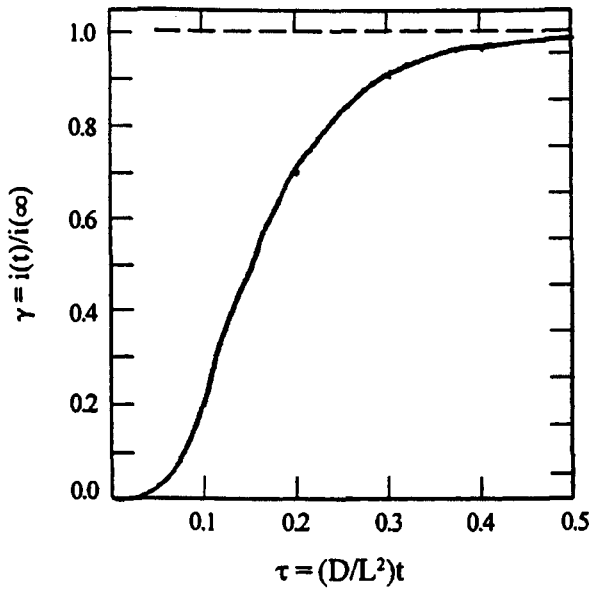


FIG. 10—Plot of permeation rise transient  $H$  oxidation current density expressed as the ratio of the transient current density to the steady state current density ( $\gamma = i(t)/i(\infty)$ ) versus  $\tau = (D/L^2)t$ . The constants associated from the breakthrough and lag time methods can be obtained from this plot. Selected values are given in Table 3.

TABLE 3—Selected values of  $\gamma$  and  $\tau$ .

$\gamma = i(t)/i(\infty)$	$\tau = Dt/L^2$
0.10	0.066
0.30	0.101
0.50	0.138
0.63	0.167
0.70	0.192
0.90	0.304

$$\text{Log}(i(t)\sqrt{t}) = \text{Log}\left(\frac{2FC_0\sqrt{D}}{\sqrt{\pi}}\right) - \frac{L^2\text{Log}(e)}{4D} \cdot \frac{1}{t} \quad (49)$$

such that a plot of  $\log(i(t)\sqrt{t})$  vs.  $1/t$  is linear and has a slope of:

$$\frac{-L^2\text{Log}(e)}{4D} \quad (50)$$

where  $t$  is time after start of charging in seconds,  $i(t)$  is the time dependent permeation flux in amps/cm<sup>2</sup>,  $L$  is foil thickness in cm, and  $D$  is the diffusion coefficient in cm<sup>2</sup>/sec. This solution assumes that the initial subsurface hydrogen concentration ( $C_0$ ) is zero. This solution is valid for  $0.02 < \tau < 0.9$ . This method has been used to determine the effective diffusion coefficient in high strength steels [127].

For steady-state conditions we have

$$i(\infty) = \frac{nFDC_0}{L} \quad (51)$$

and knowing the value of  $D$  from the transient, the concentration  $C_0 = C(0, t)$  at  $t = \infty$  can be calculated. This is the diffusible

hydrogen concentration under the conditions of interest. Hydrogen embrittlement severity is often proportional to this steady state diffusible hydrogen concentration when specimens are charged at the same hydrogen overpotential as used in the permeation experiment. ASTM Standard G 148, Standard Practice for Evaluation of Hydrogen Uptake, Permeation, and Transport in Metals by an Electrochemical Technique,<sup>11</sup> describes this method.

### Evaluation of Alloy Sensitization

Measurement of the coulombs generated during the electrochemical polarization of a material from the passive range to the active corrosion potential can be used to quantify the susceptibility to intergranular attack associated with the precipitation of chromium carbides and chromium nitrides at grain boundaries [128–130]. The method is described by ASTM G 108.<sup>12</sup> A modification of this procedure, called the double loop electrokinetic repassivation test [131, 132], involves a potentiodynamic polarization of the metal surface initially from the open-circuit potential in the active region to a potential in the passive range. This is immediately followed by reverse polarization in the opposite direction back to the open-circuit potential. The second method is less dependent on surface finish and precise knowledge of the grain size. Both variations of the method are illustrated in Fig. 11. In the latter method, the degree of sensitization is determined by the ratio, ( $I_r/I_a$ ), of the maximum current generated in the reactivation,  $I_r$ , or reverse scan compared to that generated in the initial anodic scan,  $I_a$ . The procedure is contingent on the presence of anodic current during the reactivation scan that results mainly from incomplete passivation of the zone adjacent to the grain boundaries that is depleted of chromium due to carbide precipitation at grain boundaries. For nonsensitized material, the passive film remains essentially intact during the reverse scan and the magnitude of the reactivation polarization peak remains small. For the same reasons, the charge,  $Q$ , obtained from integration of current versus potential for a known voltage scan rate in the single loop method is small for nonsensitized material. As a refinement to the method, the charge is normalized by the grain-boundary area (GBA) because this is the area from which most of the current arises in the single reactivation scan [130]

$$P = Q/GBA \quad (52)$$

$$GBA = A_s [5.09544 \times 10^{-3} \times \exp(0.34696 \times GS)] \quad (53)$$

where

$P$  = the reaction charge density associated with the sensitized area, coulombs/cm<sup>2</sup>,

$A_s$  = the wetted specimen surface area,

$GBA$  = grain boundary area, and

$GS$  = the ASTM grain size in accordance with ASTM E 112, Test Methods for Determining the Average Grain Size.

The same procedure can be used to normalize the ratio  $I_r/I_a$  [132]. The current peak,  $I_r$ , for the reactivation scan is normalized

<sup>12</sup>ASTM Standard G 108, Test Method for Electrochemical Reactivation (EPR) for Detecting Sensitization of AISI Type 304 and 304L Stainless Steels.

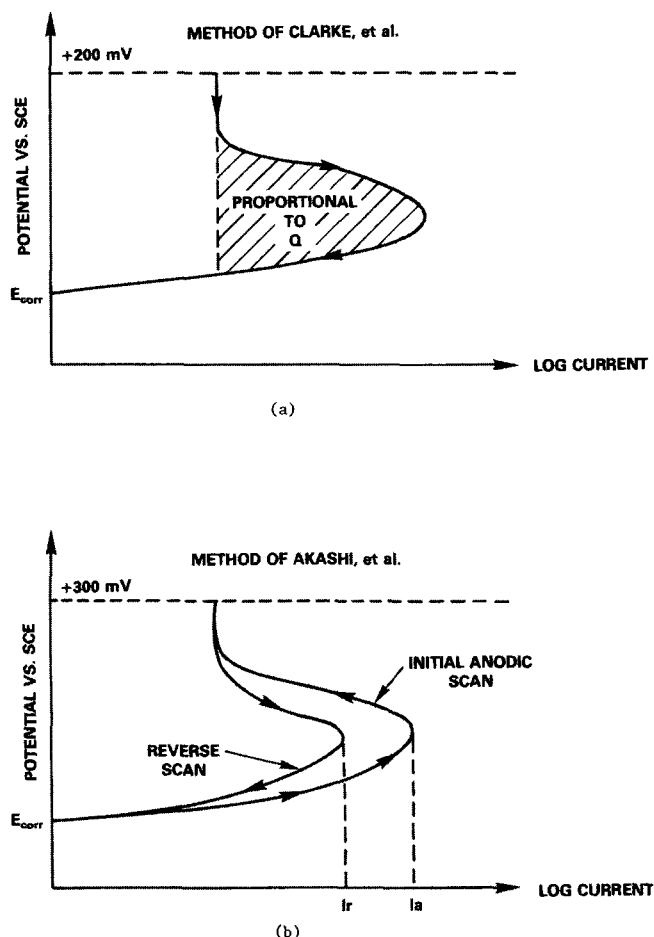


FIG. 11—Schematics of two procedures for anodic reactivation polarization testing. (a) The Clarke method involves a downward reactivation scan [129–130]; (b) The Akashi method involves an upward scan to the passive state followed by a reverse scan [131,132].

for the grain boundary area, while the initial anodic current peak remains normalized to  $A_s$ .

$$\frac{i_r}{i_a} = \left[ \frac{I_r}{I_a \times [5.09544 \times 10^{-3} \exp(0.34696 \times GS)]} \right] \quad (54)$$

$I_r/I_a$  ratios approaching 1 imply sensitization. A number of investigators have correlated this electrochemically derived ratio with optical metallographic evaluations of the degree of material sensitization, such as those outlined in ASTM A 262.<sup>13</sup> This has been accomplished for several different iron-nickel-chromium alloys [133–135]. The technique is nondestructive to the underlying metal and can be applied in the field.

## ELECTROCHEMICAL EVALUATION OF PROTECTIVE COATINGS AND FILMS

Numerous ac and dc electrochemical methods have been used to study the performance and the quality of protective

coatings, which include passive films on metallic substrates, and to evaluate the effectiveness of various surface pre-treatments. Several are discussed below.

### Anodized Aluminum Corrosion Test

The Ford anodized aluminum corrosion test (FACT) [136] involves the cathodic polarization of the anodized aluminum surface by using a small cylindrical glass clamp-on cell and a special 5 % NaCl solution containing cupric chloride ( $\text{CuCl}_2$ ) acidified with acetic acid. A large voltage is applied across the cell by using a platinum auxiliary electrode. The alkaline conditions created by the cathodic polarization promote dissolution at small defects in the anodized aluminum. As the coating resistance is decreased, more current begins to flow, and the voltage decreases. The cell voltage (auxiliary electrode to test specimen voltage) is monitored for 3 min and the cell voltage multiplied by time is recorded. The former standard ASTM B 538<sup>14</sup> described this method. This standard has been withdrawn because some aluminum alloys failed the test but still performed well in service. A similar test, known as the cathodic breakdown test, involves cathodic polarization to  $-1.6$  V versus saturated calomel electrode (SCE) for a period of 3 min in acidified NaCl [137]. Again, the test was designed for anodized aluminum alloys because the alkali created at the large applied currents will promote the formation of corrosion spots at defects in the anodized film. Today, impedance spectroscopy provides a more informative approach to examining anodized aluminum (see below).

### The Electrolytic Corrosion Test

This test was designed for electrodeposits of nickel and chromium on less noble metals, such as zinc or steel [138–140]. Special solutions are used, and the metal is polarized to  $+0.3$  V versus the standard calomel electrode. The metal is taken through cycles of 1 min anodically polarized and 2 min unpolarized. An indicator solution is then used to detect the presence of pits that penetrate to the substrate. Each exposure cycle attempts to simulate one year of exposure under atmospheric-corrosion conditions. The former standard ASTM B 627,<sup>15</sup> Test Method of Electrolytic Corrosion Testing (EC Test), described the method but has been withdrawn.

### The Paint Adhesion on a Scribed Surface Test

This involves the cathodic polarization of a small portion of painted metal. The area exposed contains a scribed line that exposes a line of underlying bare metal. The sample is cathodically polarized for 15 min in 5 % NaCl. At the end of this period, the amount of delaminated coating is determined from an adhesive tape pulling procedure.

<sup>14</sup>ASTM Standard B 538-70, Method of FACT (Ford Anodized Aluminum Corrosion Test) (Withdrawn 1987).

<sup>15</sup>ASTM Standard B 627, Test Method for Electrolytic Corrosion Testing (EC Test) (Withdrawn 1998).

<sup>13</sup>ASTM Standard A 262-01, Practices for Detecting Susceptibility to Intergranular Attack in Austenitic Stainless Steels.

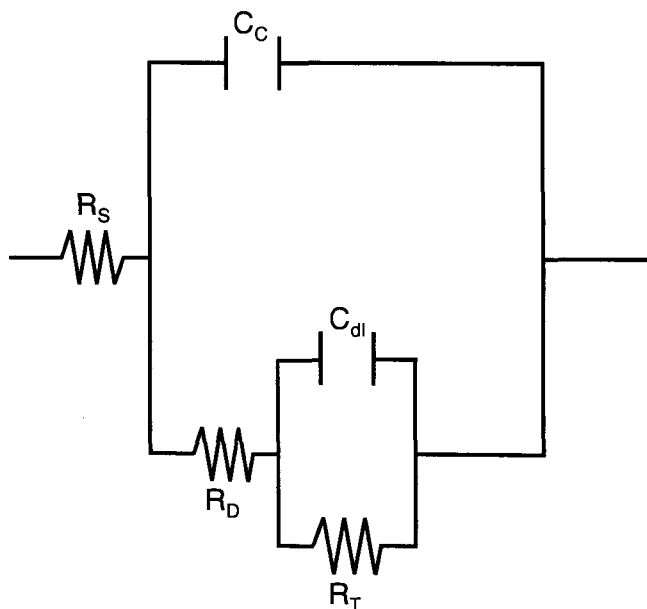


FIG. 12—Electrical equivalent circuit to simulate a coated steel panel with a defect [146,147,149].  $R_D$  is the coating defect resistance,  $R_T$  is a charge transfer resistance (similar to  $R_p$ ) at the metal interface where water has penetrated.  $C_c$  is the coating capacitance.

### The Single Frequency Impedance Test for Anodized Aluminum

The method described by ASTM B 457,<sup>16</sup> Test Method for Measurement of Impedance of Anodic Coatings on Aluminum, is used to study the seal performance of anodized aluminum [141,142]. This method uses a 1-V rms 1-kHz signal source from an impedance bridge to determine the sealed anodized aluminum impedance. The test area is again defined with a portable cell, and a platinum or stainless steel auxiliary electrode is typically used. The sample is immersed in 3.5 % NaCl (see ASTM B 457).

### Electrochemical Impedance Spectroscopy (EIS) Methods

The electrochemical impedance technique offers an advanced method of evaluating the performance of metallic-based coatings (passive film forming and/or conversion coatings) and the barrier properties of organic coatings and corrosion rates under paints [143–151]. The method does not accelerate the corrosion reaction and is non-destructive. The technique is quite sensitive to changes in the resistive-capacitive nature of coatings as well as the electrochemical interface. It is possible to monitor the polarization resistance of the corroding interface under the coating with this technique. In this respect, the electrochemical impedance technique offers several advantages over d-c electrochemical techniques in that resistances related to

the corrosion rate can be separated from the high d-c resistance of the dielectric coating. This is not possible with the d-c methods. Because a large frequency bandwidth is used for the applied signal (usually from the mHz range to the kHz range), the electrochemical impedance technique is “spectroscopic” and surpasses the capabilities of single-frequency impedance methods. The reason for this lies in the capability of the electrochemical impedance technique to discriminate between the resistive properties of the coating or passive film because of its ionic and/or electronic conductivity and the capacitive nature of the passive film or coating due to its dielectric constant, area, and thickness. Although impedance circuit models for coatings (Fig. 12) contain more elements than the model shown in Fig. 4 for bare metals, frequency regimes in which impedance information is primarily due to the coating capacitance or coating resistance can be separated from one another and analyzed independently by using a broad frequency bandwidth. If the coating or passive film capacitance can be determined by impedance analysis and if the dielectric constant is known, then the film thickness can be estimated for a given exposed area:

$$C = \frac{\epsilon \epsilon_0 A}{d} \quad (55)$$

where

$A$  = the surface area,  $\text{cm}^2$ ,

$d$  = the dielectric thickness,  $\text{cm}$ ,

$\epsilon_0$  = the electric permittivity of a vacuum ( $8.854 \times 10^{-12} \text{ F/m}$ ), and

$\epsilon$  = the dielectric constant for the passive film or coating.

In addition to this relationship between thickness and area of dielectric and capacitance, the uptake of water in an organic coating can be monitored because the dielectric constant for water is over an order of magnitude greater than the dielectric constant for the dry organic coating. The quantity of water absorbed in the organic coating can be estimated as follows [144,146]:

$$\text{vol.\%H}_2\text{O} = \left[ \frac{100 \log \left( \frac{C_t}{C_0} \right)}{\log(79)} \right] \quad (56)$$

where

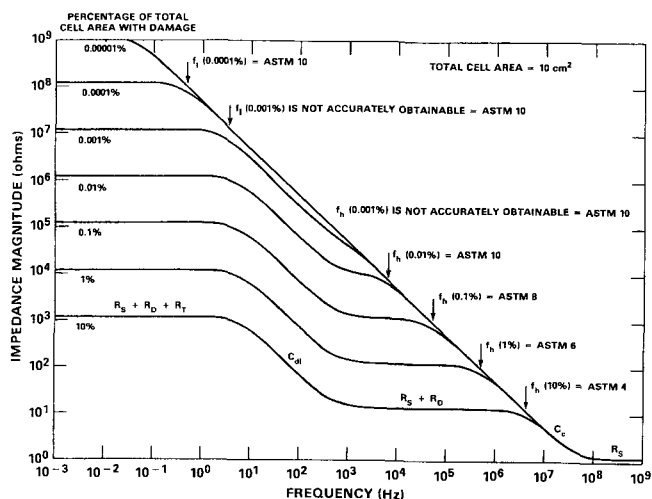
$C_t$  = the coating capacitance after some exposure time, and  
 $C_0$  = the initial coating capacitance at time zero when the exposure begins.

The coating resistance can also be monitored as a function of exposure time. Large decreases signify permeation of ionic species through the coating or the presence of defects in the coating [150,151]. The breakpoint frequency is a useful method for estimating the area fraction of physical defects in an organic coating [149–152]. The following expression describes the dependency between the high-frequency breakpoint frequency and defect area:

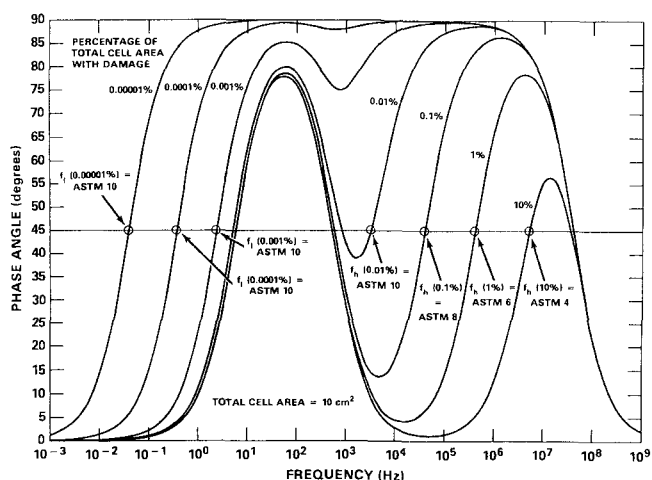
$$f_{bpt} = \left( \frac{1}{2\pi\epsilon\epsilon_0\rho} \right) \left( \frac{A_d}{A} \right) \quad (57)$$

<sup>16</sup>ASTM Standard B 457, Test Method for Measurement of Impedance of Anodic Coatings on Aluminum.





A 2) Effect of Defect Area Percentage on Impedance Magnitude Behavior of a Coated Steel Equivalent Circuit. Total Cell Area Assumed is 10 cm<sup>2</sup>.



B 3) Effect of Defect Area Percentage on Impedance Phase Behavior of a Coated Steel Equivalent Circuit. Total Cell Area Assumed is 10 cm<sup>2</sup>.

**FIG. 13—Theoretical Bode Magnitude and Phase Angle Plots for various known electrochemically active defect areas for a coating containing a cylindrical defect penetrating to the metal substrate and no delaminated regions. (a) Bode magnitude, (b) Bode Phase Angle. ASTM visual ratings with the % of area damaged as blisters or rust spots according to standards D 610 and D 714 are included for comparison [152].**

where

$A_d$  = the defect area where electrochemical reactions operate,  
 $A$  = the total painted surface area, and  
 $\rho$  = the resistivity of the coating at defects.

Thus,  $f_{bpt}$  can track with change in defect area provided that decreases in  $\rho$  over time and increase in  $\epsilon$  with electrolyte uptake do not dominate. Under such circumstances, the term preceding the ratio ( $A_d/A$ ) remains constant. In this case, increases in  $f_{bpt}$  occur mainly as a function of the increases in the defective area. However, circumstances may exist where small increases  $A_d$  in  $\epsilon$  and very large decreases in  $\rho$  occur so that  $f_{bpt}$  does not relate linearly to defect area.

Moreover, bare metal under delaminated coating regions may not be detected under all circumstances, especially if the coating resistivity over the delaminated area and dielectric constant are identical to those in regions where the coating is not delaminated. The hypothetical relationship between  $f_{bpt}$  and open defect area is shown in Fig. 13 [152]. No ASTM standard currently exists for conducting impedance measurements on coated metals.

### Electrochemical Noise Methods for Organic Coating Evaluation

Electrochemical noise (EN) methods have also been explored as a method to analyze the degradation of polymer coated metals [153–157]. A variety of methods have been used. A common method involves the use of a cell with two identical working electrodes connected through a zero resistance ammeter. The entire galvanic couple is coupled through a high impedance voltmeter to an ideally noiseless reference electrode. Two samples often experience drastically different behavior; for instance, if one electrode has a coating defect and the other does not, then asymmetrical electrode behavior results. The spectral noise impedance obtained is equivalent to the geometric mean of the moduli of individual electrode impedances. Instrument noise should be carefully considered when this approach is used to analyze high resistance coatings. No ASTM standard currently exists for conducting EN tests on coated metals.

### CHARACTERIZATION OF ANODIZED SURFACES AND CONVERSION COATINGS ON METALS

The impedance technique also provides a useful approach for characterizing anodization [158–160], conversion coatings, sealing of anodized layers, and passivity [161]. ASTM STP 1188, *Electrochemical Impedance: Analysis and Interpretation*, covers some of these applications [162]. EIS methods have also been applied to the study of conversion coatings [163–165]. In the case of conversion coatings, an impedance modulus of 1–2 megaohm-cm<sup>2</sup> at the DC limit is a threshold value required in order for the conversion coating to pass an ASTM B 117<sup>17</sup> salt spray test [166]. This value must be passed after a 24 h exposure to aerated 0.5 M NaCl solution [167]. EIS studies of synthesized bulk Cu-based intermetallic compounds have improved insight on the role of conversion coatings in affecting the electrochemical properties of intermetallic compounds [168]. Such phases are often responsible for microgalvanic corrosion of Al-base alloys.

### REFERENCES

- [1] Bockris, J. O'M. and Reddy, A. K. N., *Modern Electrochemistry-2*, Plenum Press, New York, 1970.
- [2] Gileadi, E., *Electrode Kinetics for Chemists, Chemical Engineers and Materials Scientists*, VCH Publishers, New York, 1993.

<sup>17</sup>ASTM Standard B 117, Practice for Operating Salt Spray (Fog) Apparatus.

- [3] Tomashov, N. D., *Theory of Corrosion and Protection of Metals*, Macmillan Publishing, New York, 1966.
- [4] Jones, D. A., *Principles and Prevention of Corrosion*, Macmillan Publishing, New York, 1992.
- [5] Fontana, M. G. and Greene, N. D., *Corrosion Engineering*, McGraw-Hill, New York, 1978.
- [6] Newman, J., *Electrochemical Systems*, Prentice-Hall, 1973.
- [7] Uhlig, H. H. and Revie, R. W., *Corrosion and Corrosion Control*, John Wiley & Sons, New York, 1985.
- [8] *Electrochemical Materials Science, Vol. 4, Comprehensive Treatise of Electrochemistry*, J. O'M. Bockris, B. E. Conway, E. Yeager, and R. E. White, Eds., Plenum Press, New York, 1981.
- [9] *Electrochemical Techniques for Corrosion*, R. Baboian, Ed., National Association of Corrosion Engineers, Houston, TX, 1977.
- [10] *Electrochemical Corrosion Testing, ASTM STP 727*, U. Bertocci and F. Mansfeld, Eds., ASTM International, West Conshohocken, PA, 1979.
- [11] *Laboratory Corrosion Tests and Standards, ASTM STP 866*, G. Haynes and R. Baboian, Eds., ASTM International, West Conshohocken, PA, 1985.
- [12] *Corrosion Monitoring in Industrial Plants Using Nondestructive Testing and Electrochemical Methods, ASTM STP 908*, G. C. Moran and P. Labine, Eds., ASTM International, West Conshohocken, PA, 1986.
- [13] *Electrochemical Techniques for Corrosion Engineers*, R. Baboian, Ed., National Association of Corrosion Engineers, Houston, TX, 1986.
- [14] *Galvanic and Pitting Corrosion-Field and Laboratory Studies, ASTM STP 576*, R. Baboian, W. D. France, Jr., L. C. Rowe, and J. F. Rynewicz, Eds., ASTM International, West Conshohocken, PA, 1974.
- [15] Poulson, B., *Corrosion Science*, Vol. 23, No. 4, 1983, pp. 391-430.
- [16] MacDonald, D. D., *Transient Techniques in Electrochemistry*, Plenum Press, New York, 1977.
- [17] Wagner, C. and Traud, W. Z., *Electrochem*, Vol. 44, 1938, p. 391.
- [18] France, W. D., Jr., "Controlled Potential Corrosion Tests. Their Application and Limitations," *Materials Research Standardization*, Vol. 9, No. 8, 1969, p. 21.
- [19] Tafel, Z., *Physical Chemistry*, Vol. 50, 1904, p. 641.
- [20] Britz, D., *Journal of Electroanalytical Chemistry*, Vol. 88, 1978, p. 309.
- [21] Hayes, M. and Kuhn, J., *Journal of Power Sources*, Vol. 2, 1977-1978, p. 121.
- [22] Mansfeld, F., *Corrosion*, Vol. 38, No. 10, 1982, p. 556.
- [23] *The Measurement and Correction of Electrolyte Resistance in Electrochemical Tests, ASTM STP 1056*, L. L. Scribner and S. R. Taylor, Eds., ASTM International, West Conshohocken, PA, 1990.
- [24] Stern, M. and Geary, A. L., *Journal of the Electrochemical Society*, Vol. 104, 1957, p. 56.
- [25] Evans, S. and Koehler, E. L., *Journal of the Electrochemical Society*, Vol. 108, 1961, p. 509.
- [26] Stern, M. and Roth, R. M., *Journal of the Electrochemical Society*, Vol. 104, 1957, p. 390.
- [27] Stern, M. and Geary, A. L., *Journal of the Electrochemical Society*, Vol. 105, 1958, p. 638.
- [28] Stern, M. and Weisert, E. D., "Experimental Observations on the Relation between Polarization Resistance and Corrosion Rate," *Proceedings of the American Society of Testing and Materials*, Vol. 59, ASTM International, West Conshohocken, PA, 1959, p. 1280.
- [29] S. Barnartt, *Electrochimica Acta*, Vol. 15, 1970, p. 1313.
- [30a] Oldham, K. B. and Mansfeld, F., *Corrosion Science*, Vol. 13, 1973, p. 813.
- [30b] Mansfeld, F., *Journal of the Electrochemical Society*, Vol. 120, 1973, p. 515.
- [31] Mansfeld, F. and Kendig, M., *Corrosion*, Vol. 37, No. 9, 1981, p. 556.
- [32] Bandy, R. and Jones, D. A., *Corrosion*, Vol. 32, 1976, p. 126.
- [33] Danielson, M. J., *Corrosion*, Vol. 36, No. 4, 1980, p. 174.
- [34] Reeve, J. C. and Bech-Nielsen, G., *Corrosion Science*, Vol. 13, 1973, p. 351.
- [35] Epelboin, I., Gabrielli, C., Keddam, M., and Takenouti, H., *Electrochemical Corrosion Testing, ASTM STP 727*, F. Mansfeld and U. Bertocci, Eds., ASTM International, West Conshohocken, PA, 1981, p. 150.
- [36] Makrides, A. C., *Corrosion*, Vol. 29, No. 9, 1973, p. 148.
- [37] MacDonald, D. D. and McKubre, M. C. H., *Electrochemical Corrosion Testing, ASTM STP 727*, F. Mansfeld and U. Bertocci, Eds., ASTM International, West Conshohocken, PA, 1981, p. 110.
- [38] Scully, J. R., *Corrosion*, Vol. 56, No. 2, 2000, pp. 199-218.
- [39] Bard, A. J. and Faulkner, L. R., *Electrochemical Methods: Fundamentals and Applications*, John Wiley & Sons, New York, 1980.
- [40] Mansfeld, F., *Corrosion*, Vol. 36, No. 5, 1981, p. 301.
- [41] Mansfeld, F., Kendig, M. W., and Tsai, S., *Corrosion*, Vol. 38, 1982, p. 570.
- [42] Murray, J. N., Moran, P. J., and Gileadi, E., *Corrosion*, Vol. 44, No. 8, 1988, p. 533.
- [43] Franceschetti, D. R. and Macdonald, J. R., *Journal of Electroanalytical Chemistry*, Vol. 101, 1979, p. 307.
- [44] Boukamp, B. A., *Solid State Ionics*, Vol. 20, 1986, pp. 31-44.
- [45] Hsu, C. H. and Mansfeld, F., *Corrosion*, Vol. 57, 2001, p. 747.
- [46] Mertens, S. F., Xhoffer, C., De Cooman, B. C., and Temmerman, E., *Corrosion*, Vol. 53, 1997, p. 381.
- [47] Devay, J. and Meszaros, L., *Acta Chimica Academy of Sciences Hungary*, Vol. 100, 1979, p. 183.
- [48] Gill, J. S., Callow, M., Scantlebury, J. D., *Corrosion*, Vol. 39, 1983, p. 61.
- [49] Rao, G. P. and Mishra, A. K., *Journal of Electroanalytical Chemistry*, Vol. 77, 1977, p. 121.
- [50] Meszaros, L. and Devay, J., *Acta Chimica Academy of Sciences Hungary*, Vol. 105, 1980, p. 1.
- [51] McKubre, M. C. H. and Syrett, B. C., *Corrosion Monitoring in Industrial Plants Using Nondestructive Methods, ASTM STP 908*, G. C. Moran, P. Labine, Eds., ASTM International, West Conshohocken, PA, 1986, p. 433.
- [52] Bosch, R. W., Hubrecht, J., Bogaerts, W. F., and Syrett, B. C., *Corrosion*, Vol. 57, 2001, pp. 60-70.
- [53] Eden, D. A., Rothwell, A. N., Dawson, J. L., *Paper 444 in Proceedings of the Corrosion Conference*, National Association of Corrosion Engineers, 1991.
- [54] Dawson, J. L., *Electrochemical Noise Measurement for Corrosion Applications, ASTM STP 1277*, J. Kearns, J. R. Scully, P. R. Roberge, D. L. Reichert, J. L. Dawson, Eds., ASTM International, West Conshohocken, PA, 1996, pp. 3-35.
- [55] Eden, D. A., Hladky, K., John, D. G., and Dawson, J. L., *Paper 276 in the Proceedings of the Corrosion Conference*, National Association of Corrosion Engineers, 1986.
- [56] Eden, D. A. and Rothwell, A. N., *Paper 292 in the Proceedings of the Corrosion Conference*, National Association of Corrosion Engineers, 1992.
- [57] Rothwell, A. N. and Eden, D. A., *Paper 223 in the Proceedings of the Corrosion Conference*, National Association of Corrosion Engineers, 1992.
- [58] Bertocci, U., *Electrochemical Noise Measurement for Corrosion Applications, ASTM STP 1277*, J. Kearns, J. R. Scully, P. R. Roberge, D. L. Reichert, J. L. Dawson, Eds., ASTM International, West Conshohocken, PA, 1996, pp. 39-58.
- [59] Bertocci, U. and Huet, F., *Corrosion*, Vol. 51, 1995, p. 131.
- [60] Reichert, D. L., *In Electrochemical Noise Measurement for Corrosion Applications, ASTM STP 1277*, J. Kearns, J. R. Scully, P. R. Roberge, D. L. Reichert, J. L. Dawson, Eds., ASTM International, West Conshohocken, PA, 1996, pp. 79-89.

- [61] Searson, P. C. and Dawson, J. L., *Journal of the Electrochemical Society*, Vol. 135, No. 8, 1988, p. 1908.
- [62] Mansfeld, F. and Xiao, H., In *Electrochemical Noise Measurement for Corrosion Applications*, ASTM STP 1277, J. Kearns, J. R. Scully, P. R. Roberge, D. L. Reichert, J. L. Dawson, Eds., ASTM International, West Conshohocken, PA, 1996, pp. 59–78.
- [63] Bierwagen, G. P., *Journal of the Electrochemical Society*, Vol. 141, 1994, L155.
- [64] Mansfeld, F. and Xiao, H., *Journal of the Electrochemical Society*, Vol. 141, 1994, p. 1403.
- [65] Huet, F., *Journal of the Electrochemical Society*, Vol. 142, 1995, p. 2861.
- [66] Chen, J. F. and Bogaerts, W. F., *Corrosion Science*, Vol. 37, 1995, p. 1839.
- [67] Xiao, H. and Mansfeld, F., *Journal of the Electrochemical Society*, Vol. 141, 1994, p. 2332.
- [68] Mansfeld, F. and Xiao, H., *Journal of the Electrochemical Society*, Vol. 140, 1993, p. 2205.
- [69] Mansfeld, F., Han, L. T., and Lee, C. C., *Journal of the Electrochemical Society*, Vol. 143, 1996, L286.
- [70] Bertocci, U., Gabrielli, C., Huet, F., and Keddam, M., *Journal of the Electrochemical Society*, Vol. 144, 1997, p. 31.
- [71] Bertocci, U., Gabrielli, C., Huet, F., and Keddam, M., *Journal of the Electrochemical Society*, Vol. 144, 1997, p. 37.
- [72] Bautista, A. and Huet, F., *Journal of the Electrochemical Society*, Vol. 146, 1999, p. 1730–1736.
- [73] Hack, H. and Scully, J. R., *Corrosion*, Vol. 42, No. 2, 1986, p. 79.
- [74] Baboian, R., *Galvanic and Pitting Corrosion-Field and Laboratory Studies*, ASTM STP 576, R. Baboian et al., Eds., ASTM International, West Conshohocken, PA, 1974, p. 5.
- [75] Mansfeld, F. and Kenkel, J. V., *Galvanic and Pitting Corrosion-Field and Laboratory Studies*, ASTM STP 576, R. Baboian et al., Eds., ASTM International, West Conshohocken, PA, 1974, p. 20.
- [76] Kasper, R. G. and Crowe, C. R., "Comparison of Localized Ionic Currents as Measured from 1-D and 3-D Vibrating Probes," *Galvanic Corrosion ASTM STP 978*, H. P. Hack, Ed., ASTM International, West Conshohocken, PA, 1988, p. 118.
- [77] Kasper, R. G. and Crowe, C. R., "Comparison of Localized Ionic Currents as Measured from 1-D and 3-D Vibrating Probes," *Journal of the Electrochemical Society*, Vol. 33, 1986, p. 879.
- [78] Isaacs, H. S., "The Measurement of Galvanic Corrosion of Soldered Copper Using the Scanning Vibrating Electrode Technique," *Corrosion Science*, Vol. 28, 1988, p. 547.
- [79] Voruganti, V. S., Huft, H. B., Degeer, D. and Bradford, S. A., "Scanning Reference Electrode Technique for the Investigation of Preferential Corrosion of Weldments in Offshore Applications" *Corrosion*, Vol. 47, 1991, p. 343.
- [80] Szklarska-Smialowska, Z., *Pitting Corrosion of Metals*, National Association of Corrosion Engineers, Houston, TX, 1986.
- [81] Wilde, B. E., *Corrosion*, Vol. 28, 1972, p. 283.
- [82] Syrett, B. C., *Corrosion*, Vol. 33, 1977, p. 221.
- [83] Pessall, N. and Liu, C., *Electrochimica Acta*, Vol. 16, 1971, p. 1987.
- [84] Wilde, B. E. and Williams, E., *Journal of the Electrochemical Society*, Vol. 118, 1971, p. 1057.
- [85] Thompson, N. G. and Syrett, B. C., *Corrosion*, Vol. 48, No. 8, 1992, p. 649.
- [86] Wilde, B. E. and Williams, E., *Electrochimica Acta*, Vol. 16, 1971, p. 1671.
- [87] Starr, K. K., Verink, E. D., Jr., and Pourbaix, M., *Corrosion*, Vol. 2, 1976, p. 47.
- [88] Sridhar, N. and Cragnolino, G.A., *Corrosion*, Vol. 49, 1993, p. 885.
- [89] Yasuda, M., Weinburg, F., and Tromans, D., *Journal of the Electrochemical Society*, Vol. 137, 1990, p. 3708.
- [90] Tsujikawa, S., Hasamatsu, T., and Boshoku, G., *Corrosion Engineering*, Vol. 29, 1980, p. 37.
- [91] Shinohara, T., Tsujikawa, S., and Boshoku, G., *Corrosion Engineering*, Vol. 39, 1990, p. 238.
- [92] Tsujikawa, S., Heng, Z., Hisamatsu, Y., and Boshoku, G., *Corrosion Engineering*, Vol. 32, 1983, p. 149.
- [93] Dunn, D. and Sridhar, N., In *Critical Factors in Localized Corrosion II*, P. M. Natishan, R. G. Kelly, G. S. Frankel, R. C. Newman, Eds., *Proceedings Volume of the Electrochemical Society* 95–15, 1996, p. 79–90.
- [94] Gaudet, G. T., Mo, W. T., Hatton, T. A., Tester, J. W., Tilly, J., Isaacs, H. S., and Newman, R. C., *American Institute of Chemical Engineers Journal*, 32 (60), p. 949 (1986).
- [95] Ambrose, J. R. and Kruger, J., *Journal of the Electrochemical Society*, Vol. 121, 1974, p. 599.
- [96] Kehler, B. A., Ilevbare, G. O., and Scully, J. R., *Corrosion*, Vol. 57, No. 12, 2001, pp. 1042–1065.
- [97] Pistorius, P. C. and Burstein, G. T., *Philosophical Transactions of the Royal Society of London*, Vol. 341, 1992, p. 531.
- [98] Shibata, T., *Transactions ISIJ*, Vol. 23, 1983, p. 785.
- [99] Shibata, T. and Takeyama, T., *Corrosion*, Vol. 33, 1977, p. 243.
- [100] Shibata, T. and Zhu, Y-C., *Corrosion Science*, Vol. 36, No. 1, 1994, pp. 153–163.
- [101] Pride, S. T., Scully, J. R., and Hudson, J. L., *Journal of the Electrochemical Society*, Vol. 141, 1994, p. 3028.
- [102] Ilevbare, G. O., Scully, J. R., Yuan, J., and Kelly, R. G., *Corrosion*, Vol. 56, No. 3, 2000, pp. 227–242.
- [103] Sweitzer, J. E., Shiflet, G. J., and Scully, J. R., *Electrochimica Acta*, Vol. 48, 2003, pp. 1223–1234.
- [104] Macdonald, D. D., In "Critical Factors in Localized Corrosion", G. S. Frankel and R. C. Newman, Eds., PV 92–9, p. 144, *The Electrochemical Society Proceedings Series*, Pennington, NJ (1992).
- [105] Suter, T. and Alkire, R. C., *Journal of the Electrochemical Society*, Vol. 148, No. 1, 2001, B36–B42.
- [106] Burstein, G. T. and Ilevbare, G. O., *Corrosion Science*, Vol. 38, 1996, pp. 2257–2265.
- [107] Hladky, K. and Dawson, J. L., *Corrosion Science*, Vol. 22, 1982, pp. 231–237.
- [108] Hladky, K. and Dawson, J. L., *Corrosion Science*, Vol. 21, 1982, pp. 317–322.
- [109] Bertocci, H. S., *Proceedings of the 2nd International Conference on Localized Corrosion*, NACE-9, Isaacs, Bertocci, Kruger, and Smialowska, Eds., National Association of Corrosion Engineers, Houston, TX, 1990.
- [110] Bertocci, H. S. and Kruger, J., *Surface Science*, Vol. 101, 1980, pp. 608–618.
- [111] Eden, D. A. and Rothwell, A. N., "Electrochemical Noise Data: Analysis and Interpretation," *Paper 92 in the Proceedings of the Corrosion Conference*, National Association of Corrosion Engineers, Houston, TX, 1992.
- [112] Searson, P. C. and Dawson, J. L., *Journal of the Electrochemical Society*, Vol. 135, 1988, pp. 1908–1915.
- [113] Williams, D. E., Stewart, J., and Balkwill, B. H., *Proceedings of the Symposium on Critical Factors in Localized Corrosion*, G. S. Frankel and R. C. Newman, Eds., Electrochemical Society, Vol. 92–9, 1992, p. 36.
- [114] Pride, S. T., Scully, J. R., and Hudson, J. L., *Electrochemical Noise Measurement for Corrosion Applications*, STP 1277, J. R. Kearns, J. R. Scully, et al., Eds., ASTM International, West Conshohocken, PA, 1996, p. 307.
- [115] Galvele, J. R., *Journal of the Electrochemical Society*, Vol. 123, 1976, p. 464.
- [116] Turgoose, S. and Cottis, R. A., "Corrosion Testing Made Easy: Electrochemical Impedance and Noise," NACE International, Houston, TX, 2000.

- [117] Cottis, R. A., *Corrosion*, Vol. 57, 2001, p. 265.
- [118] Gabrielli, C., Huet, F., Keddam, M., and Oltra, R., "Localized Corrosion as a Stochastic Process," *NACE -9 Advances in Localized Corrosion*, H. Isaacs, U. Bertocci, J. Kruger, and S. Smialowska, Eds., National Association of Corrosion Engineers, Houston, TX, 1990, pp. 93-108.
- [119] Scully, J. R., Pride, S. T., Scully, H. S., and Hudson, J. L., In *Critical Factors in Local Corrosion II*, R. G. Kelly et al., Eds., *Proceedings, Volume 95-15 of the Electrochemical Society*, 1996, p. 15.
- [120] Cottis, R. A. and Turgoose, S., *Materials Science Forum*, Vol. 2, 1995, pp. 192-194.
- [121] Ambrose, J. R. and Kruger, J., *Proceedings of the Fifth International Congress on Metallic Corrosion*, National Association of Corrosion Engineers, Houston, TX, 1974, p. 406.
- [122] Parkins, R. N., *Corrosion Science*, Vol. 20, 1990, pp. 147-166.
- [123] DeLuccia, J. J. and Berman, D. A., *Electrochemical Corrosion Testing*, ASTM STP 727, F. Mansfeld and U. Bertocci, Eds., ASTM International, West Conshohocken, PA, 1981, pp. 256-273.
- [124] Berman, D. A. and Agarwala, V. S., *Hydrogen Embrittlement: Prevention and Control*, ASTM STP 962, L. Raymond, Ed., ASTM International, West Conshohocken, PA, 1988, pp. 98-104.
- [125] Devanathan, M. A. V. and Stachurski, Z., *Proceedings of the Royal Society, A* 270, 1962, pp. 90-102.
- [126] McBreen, J., Nanis, J., and Beck, W., *Journal of the Electrochemical Society*, Vol. 113, 1966, pp. 1218-1222.
- [127] Scully, J. R. and Moran, P. J., "Influence of Strain on Hydrogen Entry and Transport in a High Strength Steel in Sodium Chloride Solution," *Journal of the Electrochemical Society*, Vol. 135, No. 6, 1988.
- [128] Novak, P., Stefec, R., and Franz, F., *Corrosion*, Vol. 31, No. 10, 1975, p. 344.
- [129] Clarke, W. L., Romero, V. M., and Danko, J. C., *Paper (preprint 180) in the Proceedings of the Corrosion Conference, 1977*, National Association of Corrosion Engineers, Houston, TX, 1977.
- [130] Clarke, W. L., Cowan, R. L., and Walker, W. L., *Intergranular Corrosion of Stainless Alloys*, ASTM STP 656, R. F. Steigerwald, Ed., ASTM International, West Conshohocken, PA, 1978, p. 99.
- [131] Akashi, M., Kawamoto, T., and Umemura, F., *Corrosion Engineering*, Vol. 29, 1980, p. 163.
- [132] Majidi, A. P. and Streicher, M. A., *Corrosion*, Vol. 40, No. 11, 1984, p. 584.
- [133] Lee, J. B., *Corrosion*, Vol. 42, No. 2, 1986, p. 67.
- [134] Roelandt, A. and Vereecken, J., *Corrosion*, Vol. 42, No. 5, 1986, p. 289.
- [135] Scully, J. R. and Kelly, R., *Corrosion*, Vol. 42, No. 9, 1986, p. 537.
- [136] Stone, J., Tuttle, H. A., and Bogart, H. N., *Plating*, Vol. 43, 1965, p. 877.
- [137] Michaelson, C. E., Dean, S. W., and Strousky, *CORROSION/69, Proceedings 25th Conference*, NACE, p. 648, 1969.
- [138] Saur, R. L. and Basco, R. P., *Plating*, Vol. 53, 1966, p. 33.
- [139] Saur, R. L. and Basco, R. P., *Plating*, Vol. 53, 1966, p. 981.
- [140] Saur, R. L. and Basco, R. P., *Plating*, Vol. 53, 1966, p. 320.
- [141] Englehart, E. T. and Sowinski, G., Jr., *Society of Automotive Engineers Journal*, Vol. 72, 1974, p. 51.
- [142] Englehart, E. T. and George, D. J., *Materials Protection*, Vol. 3, 1964, p. 25.
- [143] Scantlebury, J. D., Ho, K. N., and Eden, D. A., *Electrochemical Corrosion Testing*, ASTM STP 727, F. Mansfeld and U. Bertocci, Eds., ASTM International, West Conshohocken, PA, 1981, p. 187.
- [144] Narian, S., Bonanos, N., and Hocking, M. G., *Journal of Oil Colour Chemical Association*, Vol. 66, No. 2, 1983, p. 48.
- [145] Strivens, T. A. and Taylor, C. C., *Materials Chemistry*, Vol. 7, 1982, p. 199.
- [146] Mansfeld, F., Kendig, M. W., and Tsai, S., *Corrosion*, Vol. 38, No. 9, 1982, p. 478.
- [147] Kendig, M., Mansfeld, F., and Tsai, S., *Corrosion Science*, Vol. 23, No. 4, 1983, p. 317.
- [148] Touhsaent, R. and Leidheiser, H., *Corrosion*, Vol. 28, No. 12, 1982, p. 435.
- [149] Haruyama, S., Asari, M., and Tsuru, T., in *Corrosion Protection by Organic Coatings*, M. Kendig and H. Leidheiser, Jr., Eds., *The Electrochemical Society Proceedings Series*, Pennington, NJ, 1980, p. 197.
- [150] Scully, J. R., *Journal of the Electrochemical Society*, Vol. 136, No. 4, 1989, p. 979.
- [151] Kendig, M. W. and Scully, J. R., *Corrosion*, Vol. 46, No. 1, 1990, p. 22.
- [152] Hack, H. P. and Scully, J. R., *Journal of the Electrochemical Society*, Vol. 138, No. 1, 1991, pp. 33-40.
- [153] Mansfeld, F. and Lee, C. C., *Journal of the Electrochemical Society*, Vol. 144, 1997, pp. 2068-2071.
- [154] Mansfeld, F., Han, L. T., Lee, C. C., Chen, C., Zhang, G., and Xiao, H., *Corrosion Science*, Vol. 39, 1997, pp. 255-279.
- [155] Xia, H., Han, L. T., Lee, C. C., and Mansfeld, F., *Corrosion*, Vol. 53, 1997, pp. 412-422.
- [156] Tallman, D. E. and Bierwagen, G. P., *Paper No. 380 in the Proceedings of the Corrosion Conference*, Houston, TX, 1998.
- [157] Aballe, A., Bautista, A., Bertocci, U., and Huet, F., *Corrosion*, Vol. 57, 2001, p. 35.
- [158] Hoar, J. P. and Wood, G. C., *Electrochimica Acta*, Vol. 7, 1962, p. 333.
- [159] Hitzig, J., Juttner, K., Lorenz, W. J., and Paatsch, W., *Journal of the Electrochemical Society*, Vol. 133, 1986, p. 887.
- [160] Mansfeld, F. and Kendig, M., *Journal of the Electrochemical Society*, Vol. 135, 1988, p. 828.
- [161] Kolman, D. G. and Scully, J. R., *Journal of the Electrochemical Society*, Vol. 140, 1993, p. 2771.
- [162] *Electrochemical Impedance: Analysis and Interpretation*, ASTM STP 1188, J. R. Scully, D. Silverman, and M. W. Kendig, Eds., ASTM International, West Conshohocken, PA, 1993.
- [163] Mansfeld, F., Wang, V., and Shih, H., *Journal of the Electrochemical Society*, Vol. 138, 1991, L74.
- [164] Shih, H. and Mansfeld, F., *ASTM STP 1134*, ASTM International, West Conshohocken, PA, 1992, p. 180.
- [165] Mansfeld, F., Lin, S., and Shih, H., *Corrosion*, Vol. 45, 1989, p. 615.
- [166] Kendig, S., Jeanjaquet, M., and Cunningham, M., "Replacement for Chromate Conversion Coating and Anodization," *Final Report to Rockwell International Space Systems Division and the South Coast Air Quality Management District*, September 1993.
- [167] Buchheit, R. G., Cunningham, M., Jensen, H., Kendig, M. W., and Martinez, M. A., *Corrosion*, Vol. 54, 1998, p. 61.
- [168] Ilevbare, G. O. and Scully, J. R., "Mass Transport Limited Oxygen Reduction Reaction Rates on AA 2024-T3 and Selected Intermetallic Compounds in Chromate-Containing Solutions," *Corrosion*, Vol. 57, 2001, pp. 134-152.

# Cabinet Tests

Cynthia L. Meade<sup>1</sup>

CABINET CORROSION TESTS have been used since the early 1900s as a means of evaluating the performance of coatings as a quality control tool for monitoring processes, and in some cases, as a method for accelerating corrosive activity.

A cabinet corrosion test is one in which a test chamber (or cabinet) is used to produce an environment that will cause the occurrence of a corrosion product on a test sample. Some common corrosive environments produced in a test chamber are salt fog, humidity, hot and cold temperatures, ultraviolet exposure, and corrosive gases. These environments may be used individually or in combination with each other.

Corrosion test cabinets have evolved from homemade water-and-spray tanks that operated at fixed or ambient temperatures and humidity to computer-controlled, multi-environmental laboratory apparatus that are not only functional, but are also an attractive addition to the laboratory. Sizes range from small benchtop units to large walk-in and drive-in chambers capable of testing full vehicles or other large specimens. ISO requirements have led to the use of NIST traceable devices for measurement of temperature, humidity, and/or other critical conditions to enhance the accuracy and repeatability of the test conditions. A list of commonly used cabinet tests is shown in Table 1.

## SALT SPRAY (FOG) TEST

The most commonly used cabinet corrosion test is the Salt Spray (Fog) Test. Although originally adopted as a test method, ASTM B 117 is actually a practice—Standard Practice for Operating Salt Spray (Fog) Apparatus [1].

The salt spray test was adopted by ASTM in 1939 after considerable developmental work by the National Bureau of Standards [2]. It has widespread use in many industries, including automotive, aerospace, paints and coatings, etc. ASTM B 117 can be found as a reference in many material and performance standards as a stand-alone test or as part of other environmental conditions to which a specimen is subjected prior to acceptance.

While typically called a salt 'spray' test, it actually consists of a fog produced by air atomization of a 5 % sodium chloride solution. The cabinet temperature is maintained at 35°C. Variations of the test, using a 20 % salt solution or

higher temperatures, exist within specific industries. Historically, salt fog chambers were heated via a water jacket, which surrounded the sides and bottom. Newer designs utilize heated air jackets and alternative heater configurations. Figure 1 illustrates typical salt fog chamber designs as depicted in ASTM B 117 [1].

Salt fog testing is performed by placing samples in a test cabinet that has been designed and operated in accordance with Paragraph 4, Apparatus, of B 117. A 5 % salt solution, prepared by dissolving sodium chloride into water that meets the requirements of ASTM D 1193, Specification for Reagent Water, Type IV, is supplied to the chamber. At the time the samples are placed into test, the cabinet should be preconditioned to the operating temperature of 35°C and fogging a 5 % salt solution at the specified rate of 1–2 mL/h. The fog collection rate is determined by placing a minimum of two 80 cm<sup>2</sup> funnels inserted into two 100 mL graduated cylinders inside the chamber. One collection device is located nearest the nozzle, and one in the farthest corner.

Unless otherwise agreed upon, the samples are placed at a 15–30° angle from vertical. (Automotive components, however, are often tested in 'in-car' position.) This orientation allows the condensation to run down the specimens and minimize condensation pooling. Overcrowding should be avoided. An important aspect of the test is utilization of a free-falling mist, which uniformly settles on the test samples. Samples should be placed in the chamber so that condensation does not drip from one to another. Test durations are typically in 24-h increments and can range from 24–5000 h. (Where salt fog exposure is a part of a more complex test method, exposure time can be as little as 15 min.) Except for sample rotation and daily monitoring of collection rates, the cabinet should remain closed for the duration of the test.

In 1987, Appendix X.3 was added to B 117 to suggest the use of mass loss panels as a means for checking the corrosive conditions in a given salt spray chamber. The procedure calls for SAE 1008 commercial grade cold-rolled carbon steel panels, measuring 76 × 127 × 0.8 mm, to be cleaned, weighed, and placed in the chamber in the proximity of the collector funnels. After an exposure time of 48, 96, or 168 h, the panels are removed, cleaned, and reweighed. When conducted on a regular basis, the final mass loss number can be used as a tool for monitoring consistent corrosive conditions within the chamber. The frequency of conducting this test should be determined by the user, but common practice suggests the test be conducted monthly,

<sup>1</sup>National Exposure Testing, Sylvania, OH 43560, e-mail: cmeade@core.com

TABLE 1—Commonly-used cabinet tests.

Test Designation	Title
ASTM B117	Standard Practice for Operating Salt Spray (Fog) Apparatus
ASTM B827	Standard Practice for Conducting Mixed Flowing Gas (MFG) Environmental Tests
ASTM B368	Standard Method for Copper-Accelerated Acetic Acid-Salt Spray (Fog) Testing (CASS Test)
ASTM B380	Standard Method of Corrosion Testing of Decorative Electrodeposited Coatings by the Corrodkote Procedure
ASTM D870	Standard Practice for Testing Water Resistance of Coatings Using Water Immersion
ASTM D1735	Standard Practice for Testing Water Resistance of Coatings Using Water fog Apparatus
ASTM D1748	Standard Test Method for Rust Protection by Metal Preservatives in the Humidity Cabinet
ASTM D2247	Standard Practice for Testing Water Resistance of Coatings in 100% Relative Humidity
ASTM D2803	Standard Guide for Testing Filiform Corrosion Resistance of Organic Coatings on Metal
ASTM D5894	Standard Practice for Cyclic Salt Fog/UV Exposure of Painted Metal
ASTM G85	Standard Practice for Modified Salt Spray (Fog) Testing
ASTM G87	Standard Practice for Conducting Moist SO <sub>2</sub> Testing
BI 103-01 (Ford Motor)	Salt Spray Resistance Test for Painted Panels and Parts
BI 104-01	Water Immersion Test for Painted Parts and Panels
BI 104-02	Condensing Water Vapor Test
BQ 105-01	Copper-Accelerated Acetic Acid Salt Spray Testing (CASS Test)
BI-123-01	Painted Sheet Metal Corrosion Test
CCT	Various Cyclic Corrosion Tests
DIN 50017	Condensation Water Test Atmospheres
DIN 50018	Testing in Saturated Atmospheres in the Presence of Sulfur Dioxide
DIN 50021	Salt Spray Testing
GM4298P (General Motors)	Salt Spray Test
GM4465P	Water Fog Humidity Test
GM4476P	Copper-Accelerated Acetic Acid Salt Spray Test (Fog)
GM9505P	Automotive Environmental Cycles
GM9511P	SCAB Corrosion Creepback of Paint Systems on Metal Substrates
GM9540P	Accelerated Corrosion Test
GM9682P	Filiform Corrosion Test Procedure for Painted Aluminum Wheels and Painted Aluminum Wheel Trim
ISO 3231	Paints & Varnishes—Determination of Resistance to Humid Atmospheres Containing Sulfur Dioxide
ISO 4541	Metallic & Other Organic Coatings—Corrodkote
ISO 6270-1	Paints & Varnishes—Determination of Resistance to Humidity
ISO 7253	Paints & Varnishes—Resistance to Neutral Salt Spray
ISO 9227	Corrosion Tests in Artificial Atmospheres—Salt Spray Tests
ISO 10062	Corrosion Tests in Artificial Atmospheres at Very Low Concentrations of Polluting Gas(es)
ISO DIS 16701	Corrosion in Artificial Atmospheres
JASO M610	Cosmetic Corrosion Test Method for Automotive Parts
JIS Z2371	Methods of Neutral Salt Spray Testing
LP-463PB-10-01 (DC)	Salt Spray Test
LP-463PB-22-01	Cycle Testing of Painted Surfaces
LP-463PB-45-01	Water Immersion Test for Painted Parts
MIL-STD-810F	Environmental Engineering Considerations & Laboratory Tests
NES M0140 (Nissan)	Methods of Salt Spray Testing
NES M0158 (Nissan)	Methods of Compound Corrosion Test
SAE J2334	Cosmetic Corrosion Lab Test
SAE USCAR-1	Salt Spray Testing & Evaluation of Fastener Finishes
VDA 621-415	Cyclic Corrosion Test

Note: Thanks to Harold Hilton, Atlas Electric Devices, for his assistance in compiling this list.

or whenever any change occurs which might affect the cabinet—change of location, salt, water, operators, etc.

Whether due to the lack of an alternative test method or other reasons, the salt spray test has endured in spite of clear data that, in some cases, it is misapplied and misused, thereby providing erroneous information. As indicated in paragraph 3.2, 'Prediction of performance in natural environments has seldom been correlated with salt spray results when used as stand alone data.' Significance and Use, a modification made to ASTM B 117 in 1985, paragraph X2.2 specifically states, 'It should be noted that there is usually not a direct relation between salt (fog) resistance and resistance to corrosion in other media because the chemistry of the reactions, including the formation of films and their protective value, frequently varies greatly with the precise conditions encountered.'

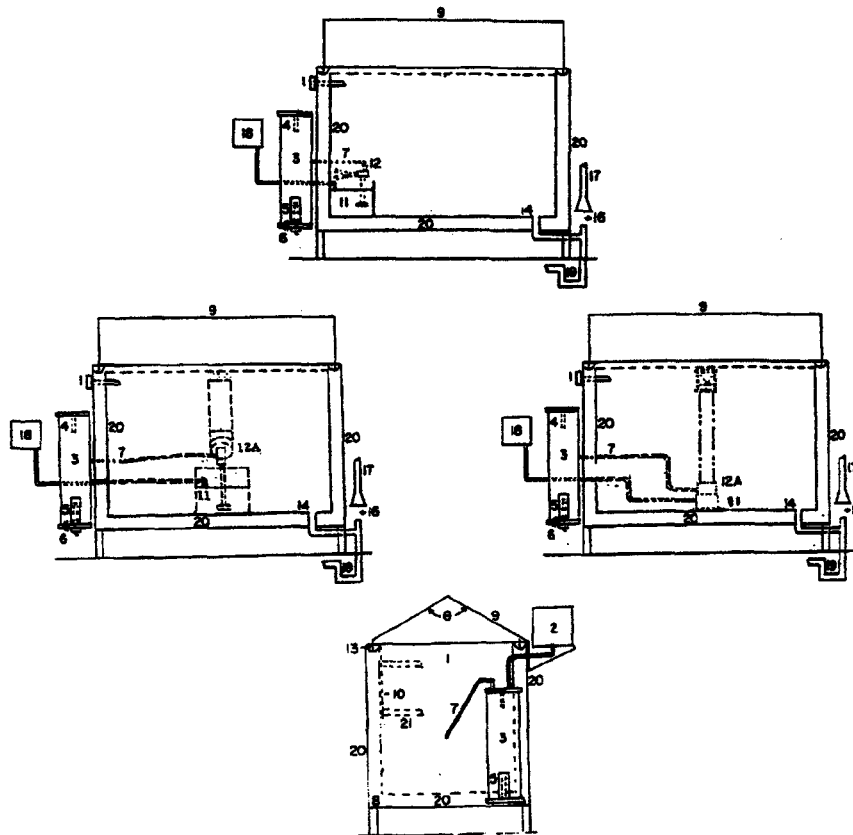
The salt spray test is a useful process control tool. For example, if a given product, when plated, coated, or painted

properly, passes X number of hours of salt spray exposure, any failure prior to that target number would be a good indication that the **process** is out of specification. As evidence of its continuing popularity, B 117 is one of the top ten best-selling standards published by ASTM [3].

## MODIFIED SALT FOG TESTS

### Acetic Acid Salt Spray (Fog) Tests

A compilation of modified salt fog tests, ASTM G 85, includes five annexes. The first, Acetic Acid Salt Spray (Fog) Testing, was originally published as ASTM B 287. In this annex, the salt solution is prepared in accordance with B 117, then adjusted to a pH in the 3.1–3.3 range with the acetic acid. The acetic acid salt spray test is used for decorative chromium plating on steel [4]. The test duration is typically 144–240 h.



NOTE 1— $\theta$ —Angle of lid, 90 to 125°

- 1—Thermometer and thermostat for controlling heater (Item No. 8) in base
- 2—Automatic water leveling device
- 3—Humidifying tower
- 4—Automatic temperature regulator for controlling heater (Item No. 5)
- 5—Immersion heater, nonrusting
- 6—Air inlet, multiple openings
- 7—Air tube to spray nozzle
- 8—Heater in base
- 9—Hinged top, hydraulically operated, or counterbalanced
- 10—Brackets for rods supporting specimens, or test table
- 11—Internal reservoir
- 12—Spray nozzle above reservoir, suitably designed, located, and baffled
- 12A—Spray nozzle housed in dispersion tower located preferably in center of cabinet (typical examples)
- 13—Water seal
- 14—Combination drain and exhaust. Exhaust at opposite side of test space from spray nozzle (Item 12), but preferably in combination with drain, waste trap, and forced draft waste pipe (Items 16, 17, and 19).
- 16—Complete separation between forced draft waste pipe (Item 17) and combination drain and exhaust (Items 14 and 19) to avoid undesirable suction or back pressure.
- 17—Forced draft waste pipe
- 18—Automatic leveling device for reservoir
- 19—Waste trap
- 20—Air space or water jacket
- 21—Test table or rack, well below roof area

NOTE 2—This figure shows the various components including alternate arrangements of the spray nozzles and solution reservoir.

FIG. 1—Typical Salt Spray Cabinet.

### Cyclic Acidified Salt Fog Test

The second annex, Cyclic Acidified Salt Fog Testing, originally ASTM G 43, was used for exfoliation testing on certain aluminum alloys [4]. It is often referred to as the

MASTMAASIS test and is used for exfoliation testing of aluminum. Annex 2 uses a 5 % sodium chloride solution that has been adjusted to a pH between 2.8 and 3.0 with acetic acid [4]. The test cycle is a 6-h cycle of  $\frac{3}{4}$ -h spray, 2-h dry air purge, and  $\frac{3}{4}$ -h soak at high humidity. The

chamber exposure temperature is held at a constant 49°C, and the humidifying tower is operated at 57°C. An important aspect of this test is that the specimens dry during the purge cycle, leaving a white corrosion product. Note: Both ASTM B 287 and G 43 were discontinued in 1988 and incorporated into G 85 [5].

### Acidified Synthetic Sea Water (Fog) Test

Annex 3, Acidified Synthetic Sea Water (Fog) Testing, is commonly referred to as the SWAAT test and is often used to test aluminum alloys. Rather than a 5 % salt solution, a synthetic seawater solution is used with the pH adjusted to 2.8–3.0. This annex includes recommendations regarding the chamber operating temperature for different substrates. The chamber must be equipped with a device to conduct the following cycle: 30-min seawater spray (fog), followed by a 90-min period at a relative humidity greater than 98 %. The high relative humidity is achieved by maintaining approximately 1 in. of water in the bottom of the chamber [4].

### Salt/SO<sub>2</sub> Spray (Fog) Test

Annex 4, Salt/SO<sub>2</sub> Spray (Fog) Testing, may be performed using either a 5 % salt solution or synthetic seawater solution. Like the salt spray test, it is conducted at 35°C. The fog may be continuous or intermittent. Depending upon the chosen cycle, the sulfur dioxide is injected into the chamber four times a day for 1 h or within a cycle of ½-h salt fog, ½-h SO<sub>2</sub> injection, and 2-h soak [4]. The test was developed by the Navy to simulate exfoliation corrosion on aircraft carriers [6].

### Dilute Electrolyte Cyclic Fog/Dry Test

The latest addition to G 85 is Annex 5, Dilute Electrolyte Cyclic Fog/Dry Test. This test, often referred to as the Prohesion test, was developed by F. D. Timmins with Mebon Paints in the 1970s [7]. This test utilizes a wet/dry cycling operation. The wet cycle is conducted at room temperature, while the dry cycle is at 35°C. This method causes the specimens to be visibly wet, then dry, thereby creating a concentrated corrosive agent on the specimens [7]. This annex has widespread use in the industrial protective coatings market. It has recently become a performance requirement by the United States Postal Service for curbside mailboxes as part of 39CFS Part 111 [8].

The equipment needed to conduct any of the above tests is typically a traditional salt spray chamber that meets the requirements of B 117, with additional electronic control packages for cycling air, solution, and/or corrosive gas flow, while monitoring time and temperature.

### Cyclic Salt Fog/UV Exposure

ASTM D 5894, Standard Practice for Cyclic Salt Fog/UV Exposure of Painted Metal, was adopted in 1996 and incorporates a UV exposure cycle following G 85 Annex 5 exposure [9]. The addition of the UV exposure cycle added a weathering effect to the test conditions and produced results that more closely resembled field exposure. Due to the alternating Salt Fog/UV exposure, two separate test chambers are required.

The Steel Structures Paint Council and the Cleveland Society of Coatings Technology Technical Committee have done extensive studies and published and presented numerous papers on the virtues of this procedure, as well as G 85 Annex 5 [10,11].

### CASS Test

The Copper-Accelerated Salt Spray Test, ASTM B 368, commonly known as the CASS test, is typically used for testing copper-nickel chrome products. It was developed by the American Electroplaters Society as AES Research Project 15 [12], along with the Corrodokote Test (ASTM B 380) and incorporated into ASTM in 1965.

The CASS test is conducted at an exposure zone temperature of 120°F. The electrolyte solution is a 5 % salt solution, with the addition of copper chloride and glacial acetic acid. The sodium chloride used *must be* reagent grade in order to produce the mass loss specified on the nickel panels. Similar to B 117, collection rates should be at 1–2 mL/h.

Nickel panels are used to calibrate and monitor CASS test chamber conditions. The panels must be 7.5 × 10 × 0.09 cm and made from higher grade carbon as described in ASTM B 162. The panels are weighed and placed in each of the four corners of the chamber. After a 22-h exposure period, the panels are removed, cleaned, and reweighed. ASTM B 368 identifies the target weight loss as 0.45–0.85 mg/cm<sup>2</sup> [13].

Although a salt spray (fog) chamber and CASS test chamber may be structurally identical, users are discouraged from using a chamber that has previously been used for CASS testing as a salt fog chamber.

## HUMIDITY TESTS

Humidity tests generally fall into two categories: controlled humidity that targets a specific relative humidity range such as 85 %, or high humidity conducted at humidity levels in excess of 95 %. A list of commonly used humidity tests is included in Table 1.

A number of tests exist within ASTM, SAE, ISO, and automotive standards that include a controlled humidity cycle as part of a total test procedure.

### Corrodokote Test

The Corrodokote test, ASTM B 380 [14], was developed by the American Electroplaters Society to improve the performance of decorative plating used on automobiles. The original test protocol used actual Detroit city road slush consisting of dirt, road salt, and water [12]. The Corrodokote test uses a slurry consisting of kaolin, cupric nitrate (Cu(NO<sub>3</sub>)<sub>2</sub> · 3H<sub>2</sub>O), ferric chloride (FeCl<sub>3</sub> · 6H<sub>2</sub>O), and ammonium chloride (NH<sub>4</sub>Cl) in deionized water [14]. The slurry is applied to the samples being tested. They are then placed in the humidity chamber maintained at 38 ± 2°C and a relative humidity between 80 and 90 %, with no condensation on the parts. Twenty hours is considered one cycle [20]. Upon completion of the test, the specimens shall be cleaned with a mild abrasive and fresh running water. Additional



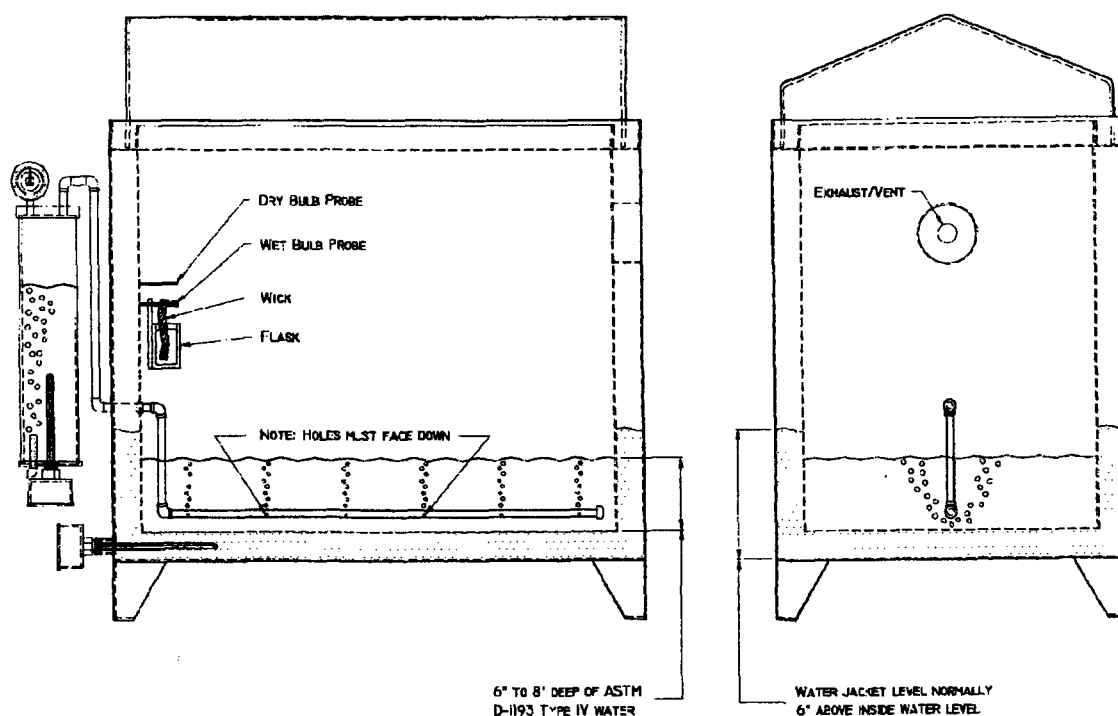


FIG. 2—Humidity Cabinet.

exposure to salt fog or humidity may be necessary after cleaning to provide evidence of corrosion products [14].

### Filiform Test

ASTM D 2803, Standard Guide for Testing Filiform Corrosion Resistance of Organic Coatings on Metal, was originally published in 1969 [15]. The test typically begins with a salt spray exposure according to ASTM B 117, followed by humidity exposure at 70–90 % relative humidity. Variations of the test exist that vary the length of the salt spray exposure and percent of relative humidity. General Motors Engineering Standard GM9682P, Filiform Corrosion Test Procedure for Painted Aluminum Wheels and Painted Aluminum Wheel Trim, incorporates a CASS Test exposure for 6 h, prior to the humidity cycle [16]. Care must be taken to maintain the proper humidity, as filiform corrosion only occurs at humidities between 70 and 95 %.

Filiform corrosion, identified by threadlike strands, is formed under finishes such as powder-clear-coated aluminum [17].

### High Humidity Tests

ASTM D 2247, Standard Practice for Testing Water Resistance of Coatings in 100% Relative Humidity, was originally published in 1966. As the title implies, it is primarily used to test the water resistance of coated specimens. The apparatus as depicted in D 2247 is shown in Fig. 2.

The chamber and humidifying tower temperatures are maintained at 38°C. As described in Annex A1.1, the apparatus may be a water tank with an immersion heater or test chamber with an air dispersion pipe assembly. The key design feature is that condensation is formed on the speci-

mens. A modified salt fog chamber as described in ASTM B 117 is commonly used for this type of test. (Note: The fogging apparatus must be removed and replaced with a water tank or air dispersion pipe assembly. The water level in the heated water jacket must be reduced to a level above the inside humidified water.)

### CORROSIVE GAS TESTS

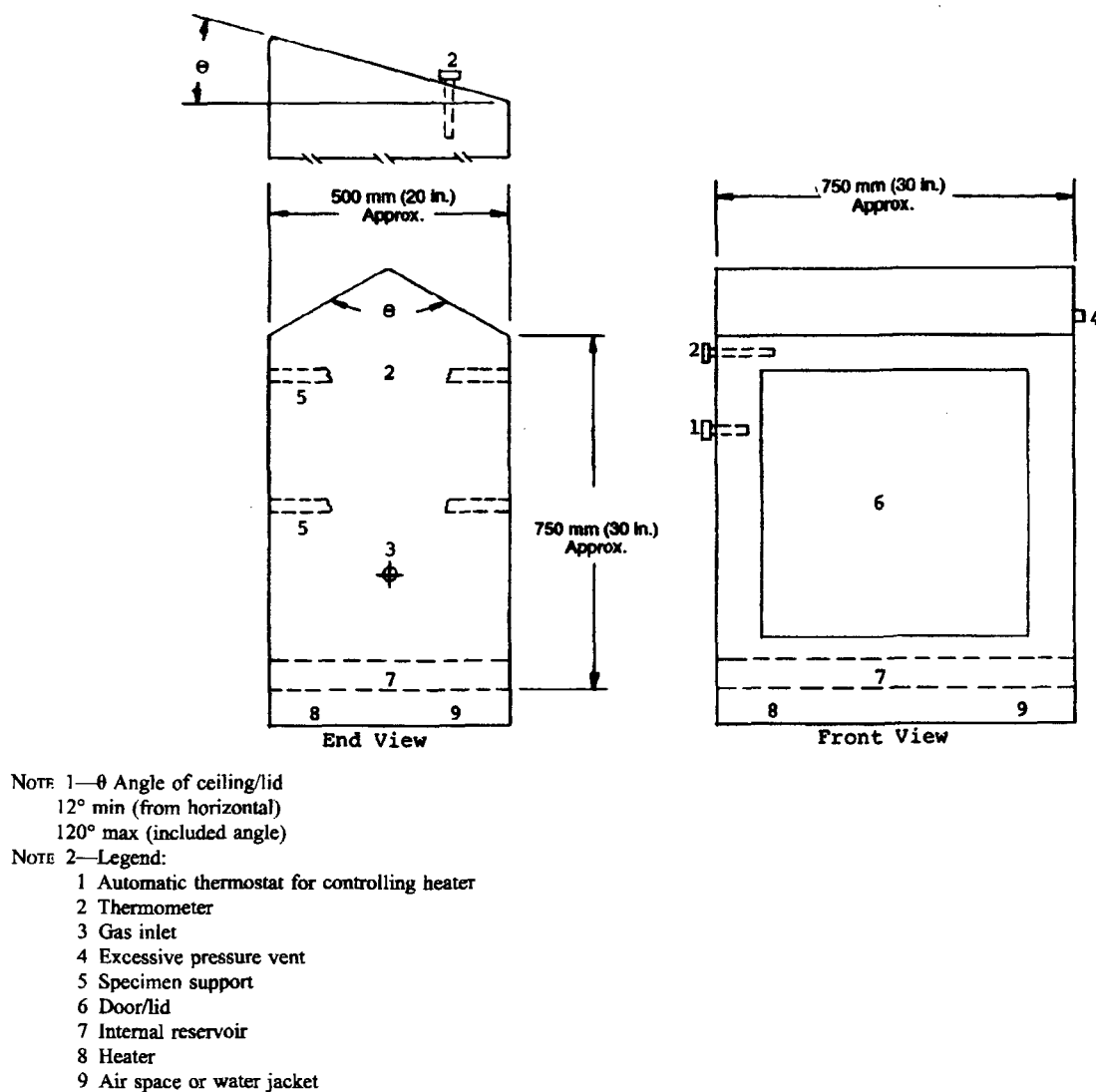
Corrosive gas tests are often a combination of a gas introduced into a high humidity atmosphere and typically used as a porosity test. A few examples of these tests are:

- ASTM G 87, Standard Practice for Moist SO<sub>2</sub> Testing
- ASTM B 827, Mixed Flowing Gas Test
- DIN 50018, Testing in Saturated Atmospheres in the Presence of Sulfur Dioxide
- ISO 3231, Determination of Resistance to Humid Atmospheres Containing Sulfur Dioxide

### ASTM G 87

ASTM G 87, Standard Practice for Conducting Moist SO<sub>2</sub> Tests, was modeled after the German standard DIN 50018, and is commonly referred to as the Kesternich test. The test incorporates low volumes of sulphur dioxide gas (usually 2 liters or less) into a 100 % humid atmosphere. The test is conducted at a temperature of 40°C. A typical chamber design is shown in Fig. 3a as depicted in G 87.

G 87 and DIN 50018 are used in the electronics industry, as well as on roofing materials and fasteners (ASTM D 6294) [18]. A recent ASTM Guide for Coil Coatings

FIG. 3a—Typical Moist SO<sub>2</sub> Test Chamber.

(D 3794) [19] references G 87 as a performance standard. Variations of the test exist that incorporate other gases, such as carbon dioxide.

### Mixed Flowing Gas

The Mixed Flowing Gas Test, ASTM B 827, is used extensively in the electronics industry. As the name implies, the test method uses a combination of various gases at controlled temperatures and humidities to produce the desired conditions. The MFG test requires equipment of a more complex nature than other corrosive gas tests. A schematic of a typical chamber is shown in Fig. 3b, as depicted in ASTM B 827.

## CYCLIC CORROSION TESTS

Typical cyclic corrosion tests include one or more steps of salt solution exposure, humidity, drying, and/or ambient conditions. A list of commonly used cyclic tests is included in Table 1.

### SAE J2334

The automotive industry has taken a lead role in the development of cyclic corrosion tests that can produce results that better correlate with field exposure. In 1984, a joint effort, Automotive Corrosion and Prevention Committee, began between the Corrosion Task Force of the American Iron and Steel Institute and the Society of Automotive Engineers. Nearly 20 years later, and after considering over 130 available laboratory, proving ground, and outdoor corrosion tests, SAE Surface Vehicle Standard, J2334, Cosmetic Corrosion Lab Test, was published in June 1998 [20].

The development of SAE J2334 was arduous, but thorough. Ten materials were used to provide a wide range of anticipated results. At least two substrates were chosen because of proven corrosion testing results, to assure the consistency of the test. Canadian on-vehicle tests were conducted at Montreal, Quebec, and St. John's, Newfoundland for five years. The panels were placed in horizontal and vertical orientations. The corrosion mechanisms of on-vehicle tests were

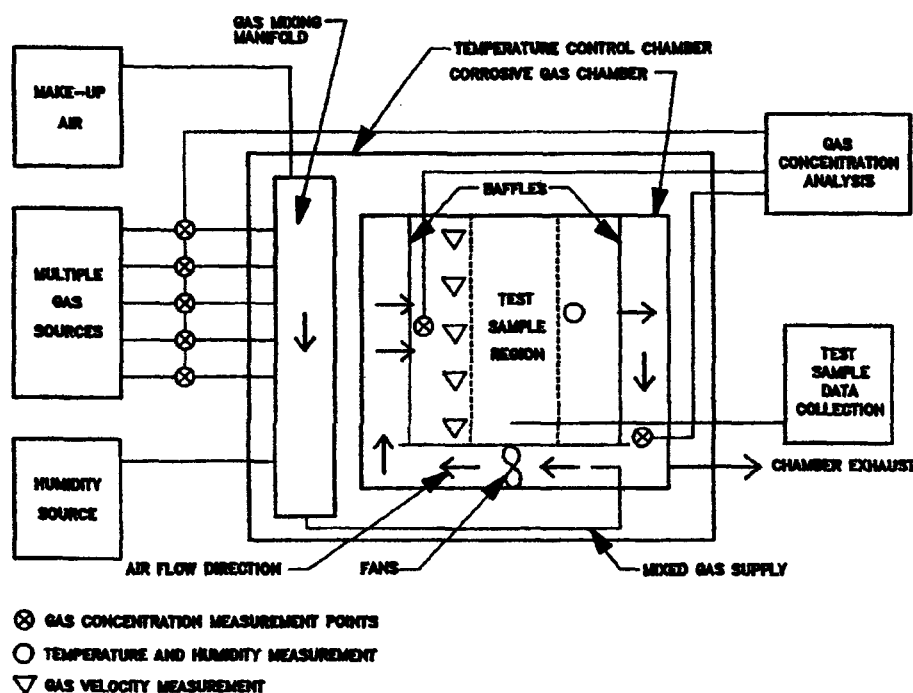


FIG. 3b—MFG Chamber.

studied by Lehigh University, where it was determined that similar corrosion products and modes were found when compared to those found after conducting J2334 [21].

The test procedure is:

1. Humid stage at 50°C and 100 % humidity for 6 h,
2. Salt application stage for 15 min at ambient conditions,
3. Dry stage at 60°C and 50 % humidity for 17 h and 45 min.

A typical test duration is 60 cycles, although longer cycles are commonly used for heavier coating systems.

The use of corrosion coupons is included in the test procedure as a means for monitoring corrosive activity within a given chamber. A minimum of six corrosion coupons, made of 25.4 × 50.8 mm AISI 1006-1010 steel, are used. The coupons are cleaned and weighed in accordance with the procedure described in J2334 and mounted in a nonmetallic rack. One coupon from each end of the rack is removed, cleaned, and reweighed every 20 cycles. At the present writing, no target mass loss numbers for each cycle or end-of-test mass loss have been published.

Efforts to improve the correlation and repeatability are underway as of this writing.

### General Motors GM9540P

Another commonly used cyclic corrosion laboratory test is GM9540P, Accelerated Corrosion Test [22]. The operating conditions are as follows:

Condition	Temperature	Humidity
Fog Humidity (GM4465P)	49 ± 2°C	100 %
Salt Solution Spray*	Ambient	Ambient
Dry Off	60 ± 2°C	< 30 %
Ambient	25 ± 2°C	40–50°C

\* The solution consists of 0.9 % sodium chloride, 0.1 % calcium chloride, and 0.25 % sodium bicarbonate mixed with ASTM D 1193 Type IV water.

The test cycle consists of four applications of salt solution every 90 min, 8 h of exposure in the humidity cabinet, and 8 h in the ambient environment.

The use of mild steel corrosion coupons is required and GM9540P provides end-of-test target mass loss numbers depending upon the number of cycles performed and coupon thickness.

### Typical Cyclic Corrosion Test Chamber

### Other Cyclic Tests

The number of available cyclic corrosion tests are too many to outline. ASTM Subcommittee D 01.27, Accelerated Test Methods, has formalized a document on laboratory corrosion tests that is published as ASTM D 6899.

### Evaluation of Cabinet Corrosion Test Results

Cabinet corrosion tests can be a useful tool in determining the production quality or suitability of given material.

**TABLE 2**—Commonly-used evaluation standards.

Standard Designation	Description
ASTM B537	Standard Practice for Rating of Electroplated Panels Subjected to Atmospheric Exposure
ASTM D610	Standard Test Method for Evaluating Degree of Rusting on Painted Steel Surfaces
ASTM D714	Standard Test Method for Evaluating Degree of Blistering on Paints
ASTM D1654	Standard Test Method for Evaluation of Painted or Coated Specimens Subjected to Corrosive Environments
ASTM G1	Preparing, Cleaning and Evaluating Corrosion Test Specimens
ASTM G46	Standard Guide for Examination and Evaluation of Pitting Corrosion
GM9102P	Corrosion Creepback Test Method

However, the results of cabinet tests should be considered in conjunction with field performance data.

Performance criteria are found in material and engineering standards. ASTM standards offer a scope, significance and use paragraphs, and precision and bias statements to assist the user of test methods and practices in defining the validity of the results. Common evaluation criteria include blistering, corrosion creepback, rust spots, etc.

A list of commonly used evaluation standards is shown in Table 2.

## REFERENCES

- [1] ASTM Standard B 117-97: Standard Practice for Operating Salt Spray (Fog) Apparatus, *Annual Book of ASTM Standards*, Vol. 03.02, ASTM International, West Conshohocken, PA, 2001.
- [2] Waldron, L., "Basic Requirements in the Standardization of the Salt Spray Corrosion Test," *ASTM Proceedings*, Vol. 44, 1944, pp. 654-662.
- [3] Coppa, C., "A Coating Test that Covers the Globe," *Finishers' Management*, March 1999.
- [4] ASTM Standard G 85-98: Standard Practice for Modified Salt Spray (Fog) Testing, *Annual Book of ASTM Standards*, Vol. 03.02, ASTM International, West Conshohocken, PA, 2001.
- [5] *Corrosion Tests and Standards: Application and Interpretation*, MNL 20, R. Baboian, Ed., ASTM International, West Conshohocken, PA, 1995.
- [6] Sprowls, D. O., "Exfoliation," Chap. 22 in *Corrosion Tests and Standards: Application and Interpretation*, MNL 20, R. Baboian, Ed., ASTM International, West Conshohocken, PA, 1995, p. 220.
- [7] Cremer, N. D., "Prohesion Compared to Salt Spray and Outdoors," Presented at *Federation of Societies for Coatings Technology 1989 Paint Industries Show*.
- [8] *Federal Register*, Vol. 66, No. 27, February 8, 2001, pp. 5909-5922.
- [9] ASTM Standard D 5894: Standard Practice for Cyclic Salt Fog/UV Exposure of Painted Metal, *Annual Book of ASTM Standards*, Vol. 6.01, ASTM International, West Conshohocken, PA, 2001.
- [10] Simpson, C., Ray, C., and Skerry, B., "Accelerated Corrosion Testing of Industrial Maintenance Paints Using a Cyclic Corrosion Weathering Method," *Journal of Protective Coatings and Linings*, Vol. 8, No. 5, May 1991, pp. 28-36.
- [11] Andrews, J., et al., "Correlation of Accelerated Exposure Testing and Exterior Exposure Sites," *Journal of Coatings Technology*, Vol. 66, No. 837, October 1994, pp. 49-67.
- [12] Pinner, W., "Accelerated Corrosion Tests for the Performance of Plated Coatings," AESF Research Project No. 15, Fourth Progress Report.
- [13] ASTM Standard B 368: Standard Method for Copper-Accelerated Acetic Acid-Salt Spray (fog) Testing (CASS Test), *Annual Book of ASTM Standards*, Vol. 03.02, ASTM International, West Conshohocken, PA, 2001.
- [14] ASTM Standard B 380: Standard Method of Corrosion Testing of Decorative Electrodeposited Coatings by the Corrodokote Procedure, *Annual Book of ASTM Standards*, Vol. 03.02, ASTM International, West Conshohocken, PA, 2001.
- [15] ASTM Standard D 2803: Standard Guide for Testing Filiform Corrosion Resistance of Organic Coatings on Metal, *Annual Book of ASTM Standards*, Vol. 6.01, ASTM International, West Conshohocken, PA, 2001.
- [16] GM9682 General Motors Engineering Standard, Filiform Corrosion Test Procedure for Painted Aluminum Wheels and Painted Aluminum Trim, June 1997.
- [17] Coyle, J., Fortier, M., and McKeon, J., "Studying Filiform Corrosion of Powder-Clearcoated Aluminum Wheels," *Powder Coating*, March 1997, pp. 22-35.
- [18] ASTM Standard D 6294: Standard Test Method for Corrosion Resistance of Ferrous Metal Fastener Assemblies Used in Roofing and Waterproofing, *Annual Book of ASTM Standards*, Vol. 01.08, ASTM International, West Conshohocken, PA, 2001.
- [19] ASTM Standard D 3794: Guide for Coil Coatings, *Annual Book of ASTM Standards*, Vol. 06.01, ASTM International, West Conshohocken, PA, 2001.
- [20] SAE J2334, Lab Cosmetic Corrosion Test, Society of Automotive Engineering Surface Vehicle Standard, June 1998.
- [21] Schafer, J. and Lutze, F., "The New SAE Cyclic Corrosion Standard, J2334—A Simulation in the Laboratory of Automotive Corrosive Environments," Presented at Eurocorr 2000.
- [22] GM9540P General Motors Engineering Standard, Accelerated Lab Corrosion Test, December 1997.

# Immersion Testing

*Richard A. Corbett<sup>1</sup>*

MOST CHEMICAL PLANT processes are complex. Materials of construction for process equipment and piping must be selected with care to assure corrosion-free operation of those plants. In a well designed plant, materials selection is based on a number of factors: prior service history, field in-plant corrosion tests, pilot plant corrosion tests and laboratory corrosion tests, in that relative order of usefulness. <sup>1</sup>Often, actual service history regarding materials performance is not available because plants kept poor records, plant personnel were not trained to evaluate corrosion failures, or, in the case of new processes, because there is no service history. The same can be said for field in-plant corrosion tests. Pilot plant testing is usually the best alternative in such cases, but such facilities are typically operated only for short runs and are not well suited for gathering long-term corrosion performance data.

For all of these reasons, laboratory corrosion tests are frequently the best available source of data for materials selection. If these tests are well planned, they can provide the information necessary for intelligent plant design and proper selection of materials of construction. Laboratory tests also offer unique advantages over in-plant tests: acceleration of results through variation of parameters or use of electrochemical methods, ability to vary process conditions at will to develop safe "windows" of operation for selected materials, plus the ability to look at a limitless number of candidate materials quickly and at relatively low cost. If poorly designed or improperly run and interpreted, all corrosion tests can give misleading information likely to lead to costly materials selection errors.

## BASIC PRINCIPLES

For any given chemical process it is not always possible to predict which forms of corrosion will occur, or even which chemical or parameter will dominate the corrosion scenario. Process flowcharts define certain chemicals and "normal" operating conditions, but frequently overlook trace elements (impurities), transient conditions, or chemical intermediates. Such factors can have a major effect on corrosion in that process. Subtle changes in pH, for example, can shift electrochemical potentials from, say, a passive range into a pitting range. Certain ionic species, while having little effect in the bulk environment, can act as accelerating charge carriers

when concentrated inside a pit or crevice. Such factors must be considered when designing a laboratory corrosion test.

Laboratory corrosion test parameters are usually separated into two groups: chemical and physical. Chemical parameters include not only the concentration of various compounds, but also such factors as dissociation, pH, phase equilibrium (especially vapor phase chemistry), dissolved gases, conductivity, and degradation reactions caused by the construction materials themselves. Relevant physical parameters include temperature (including temperature gradients and heat transfer), pressure, flow velocity, surface area effects (such as ratio of volume-to-surface area), and time (test duration). Also important are cyclical changes in these parameters. It is often impractical to study effects of all these variables, so educated decisions must be made as to which variables might be important in a particular process and how many variations of each shall be included in the corrosion test program.

Depending upon the expected mechanism of corrosion (i.e., general or localized pitting, crevice, cracking or galvanic attack), different tests can be designed to detect the susceptibility to attack. Table 1 summarizes some of the more common forms of corrosion and the appropriate laboratory tests used to evaluate the susceptibility of a material to a specific mode of attack [1]. Many of these tests are accelerated rather than simulated service (e.g., an accelerated test used to detect susceptibility to a form of corrosion), and are routinely performed to provide information for use in:

- fundamental corrosion evaluation
- failure analysis
- corrosion prevention or control
- acceptance of quality assurance
- environmental issues involving corrosion
- new alloy/nonmetallic or product process development

Custom and unique test set-ups to evaluate heat transfer, thermal shock, velocity, fatigue, or abrasion/wear effects are also used to determine the susceptibility of a material to a specific environment or process.

## Test Conditions

The selection of the conditions for a laboratory corrosion test should be determined by the expected results and the purpose of the test. If the test is to be a guide for the selection of a material for a particular application, then the limits of the controlling factors under service conditions must

<sup>1</sup>Corrosion and Materials Research Institute, 60 Blue Hen Drive, Suite 1000, Newark, DE 19713-3406

TABLE 1—Common forms of corrosion and laboratory evaluation tests.

Mode of Attack	Occurrence in Industry (Typical)	Evaluation Tests	ASTM Std. (Typical)
General Corrosion	28 %	Total Immersion Tests (Atmospheric & Autoclave)	G 31
		Multiphase (liquid, vapor, condensate, interface) Tests	G 31
		Hot Wall	
		Electrochemical Polarization	G 5
Stress Corrosion Cracking	24 %	Electrochemical Impedance	G 106
		Boiling Chloride U-Bend Tests	G 36
		Wick Test	C 692
		Polythionic Acid Cracking Test	G 35
		Caustic Solution Cracking Tests	
		Custom Process Solution Testing	
Pitting Corrosion	15 %	Ferric Chloride Immersion Test	G 48
		Cyclic Potentiodynamic Polarization (Hysteresis)	G 61
		Critical Pitting/Crevice Temperature Determination	G 48
		Seawater/Marine Exposure Testing	G 78
		Surgical Implant Test	F 2129
		Green Death Test	
		Critical Pitting Potential Test (Potentiostatic)	G 5
Crevice Corrosion	2 %	Critical Pitting/Crevice Temperature Determination	G 61
		Multi-Crevice Washer/Process Solutions	G 48
Intergranular	15 %	Electrolytic Oxalic Acid Screening Test	A 262[A]
		Ferric Sulfate-Sulfuric Acid (Streicher Test)	A 262[B]
		Nitric Acid (Huey Test)	A 262[C]
		Copper Sulfate-Sulfuric Acid Test	A 262[D]
		EPR Test (Electrochemical Potentiokinetic Reactivation)	G 108
Erosion Corrosion	7 %	Miller Test	G 75
		Rotating Disk Test	
De-alloying	2 %	Total Immersion Testing for De-alloying	G 31
		Galvanic Couple Test	G 71
		Electrochemical Tests	G 5
		Exfoliation of Aluminum Tests	G 34
Galvanic	1 %	Dissimilar Metal Couple Immersion Test	G 31
		Galvanic Couple Test	G 71
		Zero Resistance Ammeter Electrochemical Tests	G 3

be determined. Normally these factors include, but are not limited to, service temperature ranges, process fluid flow rates, atmosphere (i.e., air, nitrogen, argon, etc.), aqueous/organic phases, and other characteristics of the bulk solution (e.g., impurities or contaminants). There should be an effort to ensure duplication of the service conditions in the laboratory corrosion test, with conditions adequately controlled during the entire test duration to ensure reproducible results.

Experience shows that at least duplicate test specimens should be exposed in each test. Under laboratory tests, corrosion rates of duplicate specimens are usually within  $\pm 10\%$  of each other, when the attack is uniform. Occasional exceptions, in which a large difference is observed, can occur under conditions of borderline passivity of alloys that depend on a passive film for their resistance to corrosion. If the rate difference exceeds  $10\%$ , re-testing should be considered, unless it is observed that localized attack is predominant. Corrosion rates are calculated assuming a uniform loss of metal, and therefore when specimens are attacked non-uniformly, the calculated corrosion rates indicate only the relative severity of attack and should not be used to predict the performance of an alloy to the test solution. In such cases, weight loss per unit of surface area may be used to avoid implying a uniform penetration rate.

Ideally, laboratory tests should use actual solutions from plant processes, which is often impractical. Therefore, test

solutions are prepared from reagent chemicals and water. No matter what the source of the test solution, its composition should be controlled accurately and should be described in the test report as completely as possible. Minor constituents should not be overlooked because they often affect the corrosion rate. Chemical content should be reported as percentage by weight, molarity, or normality. If percentage is given, the solution density should also be provided so that molarity can be calculated. The composition of the test solution should be checked before and after testing by analysis to determine the extent of change in composition. Evaporation losses should be controlled by a constant level device, or by frequent additions of the evaporating solution, to maintain the original volume within  $\pm 1\%$ .

In some situations, the composition of the test solution may change as a result of the build-up of corrosion products in the solution, catalytic decomposition, or by reaction with the test specimens. If possible, these changes should be determined, and where required, the consumed constituents should be replenished or a fresh solution provided periodically.

Experience has shown that wherever possible, only one type of alloy or family of nonmetallics should be exposed in a given test apparatus. If several alloys or nonmetallics are exposed in the same apparatus the corrosion products from one material may affect the corrosion rate on another material. For example, copper corrosion products can inhibit corrosion of stainless steel but accelerate corrosion of aluminum.

If different alloys are coupled in a particular process, these couples must be reproduced in the laboratory test. For example, in ASTM Standards D 1384, D 2570, or D 2758, copper, brass and solder, found in the radiator and heaters in automobiles, are electrically connected and tested in the same laboratory apparatus.

## Physical Parameters

### *Temperature*

The temperature of the test solution should be controlled within  $\pm 1^\circ\text{C}$  and should be stated as such in the report of test results. If no specific temperature, such as boiling, is required or if a temperature range is selected, this should also be reported. For processes that are conducted under ambient conditions, the laboratory tests should be conducted at the highest temperature anticipated for stagnant storage during the summer months. This temperature may be as high as  $55^\circ\text{C}$ . Laboratory tests conducted at the temperature of a process solution may provide misleading results if heat transfer occurs as the metal heats the process stream.

### *Aeration/Deaeration*

Unless specified, the test solution should not be aerated or deaerated. Most laboratory tests used to replicate process equipment should be controlled with the natural atmosphere inherent under process conditions, such as the vapors of the boiling solution. If aeration or deaeration is used, the test specimens should not be located in the direct stream of the gas sparge tube. Undesirable effects can be encountered if the gas stream impinges on the test specimens.

### *Solution Velocity*

The effect of process solution velocity is not usually determined in normal laboratory tests, although specific tests have been designed for this purpose. Tests under boiling conditions should be conducted with minimal heat input, and inert material boiling chips should be used to avoid excessive turbulence and bubble impingement. For tests conducted below the boiling point, thermal convection generally is the only source of liquid velocity in the laboratory test. For test solutions with high viscosities or multiple phases, supplemental controlled stirring may be recommended.

### *Test Solution Volume*

The volume of the test solution should be large enough to avoid any appreciable change in its corrosiveness either through depletion of the corrodant or accumulations of corrosion products that may affect further corrosion. The preferred minimum solution volume-to-specimen surface area ratio is  $20 \text{ mL/cm}^2$ .

### *Methods of Supporting Test Specimens*

It is important that the supporting device and the test apparatus should not be affected by or cause contamination of the test solution. The method of supporting test specimens will vary with the apparatus used for conducting the test, but should be designed to insulate the specimen from

each other physically and electrically, and to insulate the specimens from any metallic container or supporting device used with the apparatus. The shape and form of the specimen support should assure free contact of the specimen with the test solution, the liquid/vapor interface or the vapor phase, whichever is applicable.

Common supports include glass or ceramic rods or hooks, glass cradles, fluorocarbon plastic thread or string, and various insulated or coated metallic supports.

## Test Duration

The duration of any laboratory test should be determined by the nature and purpose of the experiment. The amount of corrosion attack under any given test condition will be directly dependent on the duration of the test. Often it is assumed that corrosion is a linear function of time, and often this is incorrect. Yet this assumption is implied when a corrosion rate is stated.

Since corrosion may not be linear, it is important that tests be made with specimens exposed for an increasing increment of time, with some durations as long as possible to enable reliable extrapolation of performance. Under such test parameters, it is recommended to expose several identical specimens in the corrodant and remove them individually at different times over an extended duration. This technique is called the "Planned Interval Test" [2], and the procedure and evaluation of the results are presented in Table 2.

Materials that experience severe corrosion usually do not require long duration exposure to obtain accurate corrosion rates, and common testing periods are 24–240 h. Although this assumption is valid in many cases, there are situations where it is not valid. For example, aluminum exposed to solutions of sodium hydroxide corrodes at an extremely high rate, often in excess of an inch per year, while it is building a protective corrosion product film; then the rate decreases dramatically so that further corrosion is almost negligible, provided the film is not damaged. Likewise, stainless steels that form passive films may have that film broken down under prolonged exposure and subsequently experience rapid attack. Experience suggests that laboratory tests of long periods are considerably more realistic than those conducted for short duration. However, this must be qualified because corrosion should not proceed to where the original specimen size or the exposed area is drastically reduced or where the material is perforated or dissolved.

## TYPES OF TESTS

The type of laboratory immersion test to be used will be determined mostly by the environmental conditions that are to be simulated. For example, if the equipment is immersed in service, then the test specimens should be immersed in the laboratory test; if the exposure is alternating immersion and atmospheric exposure, then a cyclic exposure test to wet/dry conditions should be used. Another determining factor is the duration of exposure for arriving at the desired results, which is associated with the degree of acceleration that will be required of the test method.

TABLE 2—Planned interval test.

Specimen #	0	1	Time	t	t+1
1	←	→			
2	←	→			
3	←	→			
4				←	→
5				←	→

Calculated Specimen #3 - #2

The test specimens are placed in the same test vessel which contains the corrosive solution. The test conditions are kept constant during the duration of the test program. The parameter being measured is the penetration<sup>a</sup>, as defined below.

Interpretation	Criteria
Liquid Corrosiveness	—Unchanged if 1 = 4 —Decreases if 1 > 4 —Increases if 1 < 4
Metal Corrodibility	—Unchanged if 4 = 5 —Decreases if 4 > 5 —Increases if 4 < 5

Other Combinations of Interpretation:

Liquid Corrosiveness	Metal Corrodibility	Criteria
1. unchanged	unchanged	1 = 4 = 5
2. unchanged	decreases	1 = 4 > 5
3. unchanged	increases	1 = 4 < 5
4. decreases	unchanged	1 > 4 = 5
5. decreases	decreases	1 > 4 > 5
6. decreases	increases	1 > 4 < 5
7. increases	unchanged	1 < 4 = 5
8. increases	decreases	1 < 4 > 5
9. increases	increases	1 < 4 < 5

## Example of Planned Interval Corrosion Test Program

Exposure: Test specimens were of AISI Type 316L (UNS S31603) stainless steel (density 7.98 g/cm<sup>3</sup>), with dimensions of 25 × 50 × 3 mm (1 × 2 × 1/8 in.), immersed in 500 mL of 15 % methylsulfonic acid + 5 % sulfuric acid, balance water, at atmospheric pressure and 45°C.

Specimen Number	Duration Days	Mass Loss, mg	Penetration <sup>a</sup>		Apparent Corrosion Rate <sup>b</sup>	
			mm	mils	mm/y	mpy
1	0-1	1495	0.064	2.4	23	880
2	0-4	2240	0.095	3.6	8.7	330
3	0-5	2280	0.097	3.7	7.1	270
4	4-5	95	0.004	0.15	1.5	55
5	calc. 3-2	40	0.002	0.06	0.7	22

$$^a \text{Penetration} = \frac{(\text{mass loss in mg})(C\text{-factor})}{(\text{area in mm}^2 \text{ or in.}^2)(\text{density in g/cm}^3)}$$

where C = 1 for mm; or C = 0.061 for mils

$$^b \text{Apparent Corrosion Rate} = \frac{(\text{Penetration in mm or mils})365}{\text{time in days}}$$

From penetration information: Specimen 1 > 4 > 5

Based on the interpretation criteria, the liquid has decreased its corrosiveness during the test, and suggests the formation of a protective film owing to a decrease in metal corrodibility.

The principal reason for accelerated testing is the need to obtain results sooner than can be obtained under field conditions. Acceleration is achieved by lengthening the exposure to the critical conditions, or by intensifying the conditions so that the corrosion rate is increased. The former may be achieved by exposing a test specimen to a process condition an order of magnitude longer than actual practice. For example, if a vessel is to be batch processed with a chemical for 24 h, then a laboratory corrosion exposure of 240 h should be considered. Intensifying the test conditions may be achieved by increasing the solution acidity, salt concentration, temperature, or other parameters. In some cases, the physical parameters may be changed, such as the amount of stress or the degree of fatigue.

Once the service conditions of the test have been determined, and evaluation tests for all forms of corrosion that

might occur have been designed, then they should be repeated a sufficient number of times to determine whether it meets the desired reliability standard for reproducibility. Changes in the test procedure may be required if the reliability is not satisfactory.

If the test procedure is to be used by other laboratories, either to qualify on the basis of a specification or simply to compare results among laboratories, then it is important that reproducibility of results be determined. This is accomplished through round-robin tests that are conducted among interested laboratories to develop standard test procedures, such as those that are developed by ASTM International, Comité European Normalization (CEN), International Organization for Standardization (ISO), Japanese Standards Association (JSA), Materials Technology Institute (MTI) of the Chemical Process Industries, and NACE International.



TABLE 3—Standard corrosion test procedures.

**NACE STANDARD**

No.	Title
TM0169	Laboratory Corrosion Testing of Metals at Atmospheric Pressure
TM0171	Autoclave Testing of Metals in High Temperature Water
TM0174	Laboratory Methods for the Evaluation of Protective Coatings Used as Lining Materials for Immersion Service
TM0274	Dynamic Corrosion Testing of Metals in High Temperature Water
TM0374	Laboratory Screening Tests to Determine the Ability of Scale Inhibitors to Prevent the Precipitation of Calcium Sulfate and Calcium Carbonate from Solution
TM0177	Testing of Metals for Resistance to Sulfide Stress Cracking at Ambient Temperatures
TM0284	Test Method for Evaluation of Pipeline Steels for Resistance to Stepwise Cracking
TM0185	Evaluation of Internal Plastic Coatings for Corrosion Control of Tubular Goods by Autoclave Testing
TM0286	Cooling Water Test Units Incorporating Heat Transfer Surfaces

**ASTM STANDARDS**

No.	Title
A 262	Practices for Detecting Susceptibility to Intergranular Attack in Austenitic Stainless Steels
A 763	Practices for Detecting Susceptibility to Intergranular Attack in Ferritic Stainless Steels
C 692	Method for Evaluation of Insulation (used to measure susceptibility to stress corrosion cracking)
D 1384	Test Method for Corrosion Test for Engine Coolants in Glassware
D 2570	Test Method for Simulated Service Corrosion Testing of Engine Coolants
D 2758	Method of Testing Engine Coolants by Engine Dynamometer
F 2129	Standard Test Method for Conducting Cyclic Potentiodynamic Polarization Measurements to Determine the Corrosion Susceptibility of Small Implant Devices
G 1	Practice for Preparing, Cleaning, and Evaluating Corrosion Test Specimens
G 3	Practice for Conventions Applicable to Electrochemical Measurements in Corrosion Testing
G 4	Method for Conducting Corrosion Coupon Tests in Plant Equipment
G 5	Recommended Practice for Standard Reference Method for Making Potentiostatic and Potentiodynamic Measurements
G 28	Test Methods of Detecting Susceptibility to Intergranular Attack in Wrought Nickel-Rich, Chromium-Bearing Alloys
G 31	Practice for Laboratory Immersion Corrosion Testing of Metals
G 34	Test Method for Exfoliation Corrosion Susceptibility in 2XXX and 7XXX Series Aluminum Alloys
G 35	Practice for Determining the Susceptibility of Stainless Steels and Related Nickel-Chromium-Iron Alloys to Stress-Corrosion Cracking in Polythionic Acids
G 36	Practice for Performing Stress-Corrosion Cracking Tests in a Boiling Magnesium Chloride Solution
G 44	Recommended Practice for Alternate Immersion Stress Corrosion Testing in 3.5% Sodium Chloride Solution
G 46	Practice for Examination and Evaluation of Pitting Corrosion
G 48	Test Method for Pitting and Crevice Corrosion Resistance of Stainless Steels and Related Alloys by the Use of Ferric Chloride Solution
G 49	Recommended Practice for Preparation and Use of Direct Tension Stress Corrosion Test Specimens
G 50	Practice for Conducting Atmospheric Corrosion Tests on Metals
G 60	Test Method for Conducting Cyclic Humidity Tests
G 61	Practice for Conducting Cyclic Potentiodynamic Polarization Measurements for Localized Corrosion
G 71	Guide for Conducting and Evaluating Galvanic Corrosion Tests in Electrolytes
G 75	Test Method for Determination of Slurry Abrasivity (Miller Number) and Slurry Abrasion Response of Materials (SAR Number)
G 78	Guide for Crevice Corrosion Testing of Iron-Base and Nickel-Base Stainless Alloys in Seawater and Other Chloride-Containing Aqueous Environments
G 106	Practice for Verification of Algorithm and Equipment for Electrochemical Impedance Measurements
G 108	Test Method for Electrochemical Reactivation (EPR) for Detecting Sensitization of AISI Type 304 and 304L Stainless Steels

**MTI METHODS**

No.	Title
MTI 1	Laboratory Testing of Wrought Iron and Nickel Based Alloys for Relative Resistance to Corrosion in Selected Media
MTI 2	Laboratory Testing of Wrought Iron and Nickel Based Alloys for Relative Resistance to Crevice Corrosion in a Standard Ferric Chloride Solution
MTI 3	Laboratory Testing of Wrought Iron and Nickel Based Alloys for Relative Resistance to Stress Corrosion Cracking in a Boiling Magnesium Chloride Solution
MTI 4	Laboratory Testing of Wrought Iron and Nickel Based Alloys for Relative Resistance to Crevice Corrosion in Sodium Chloride Solutions
MTI 5	Laboratory Testing of Wrought Iron and Nickel Based Alloys for Relative Resistance to Stress Corrosion Cracking in a Sodium Chloride Drop Evaporation System

It is not unusual to use a laboratory test procedure for which there is no direct correlation with service or field results. Sometimes correlation cannot be obtained immediately because service results are either not available or are not practical to obtain in a reasonable time. For example,

suppose a company wishes to offer a lifetime warranty of a coating exposed to an industrial environment but needs data to back up their claim. Humidity chamber tests plus ultraviolet light exposure can give "best guess" results in a matter of weeks rather than years of actual exposure to the elements.

Because the laboratory test is designed around a synthesized or contrived environment, it is important that the results provide reliable information that can be used to make decisions on candidate materials of construction.

### Simple Immersion Tests

There are many variations in a laboratory immersion test. ASTM G 31 and NACE International Standard Test Method TM-01-69 are general guides on how these tests may be performed (see Table 3 for these and other standard corrosion test procedures). Basically, small pieces (i.e., 2.5-cm by 5-cm by 0.3-cm thickness) of the candidate material are exposed to the test medium, and the loss of weight of the material is measured for a given period of time. Immersion testing remains the best method for screening and eliminating from further consideration those materials that obviously should not be considered as useable materials. This technique is frequently the quickest and most economical means for providing a preliminary selection of the best candidate materials. Probably the most serious disadvantage of this method of corrosion study is the assumed average-time weight loss. The corrosion rate could be high initially and then decrease with time. In other cases, the rate of corrosion might increase very gradually with time, it could cycle, or it could be some combination of these things. Remember, "corrosion is not an exact science," and no written information can take the place of a corrosion consultant.

Besides the full immersion test, there are several variations that could be used to accentuate certain types of exposure conditions. For example, the test specimen can be partially immersed in an electrolyte (liquid or solid) to create an oxygen concentration cell at the vapor-liquid/solid interface (as opposed to an occluded cell).

### Alternate Immersion Testing

Another variation of the immersion test is the cyclic test procedure where a test specimen is immersed for a period of time in the test environment, then removed and dried (either air dry or use of heat lamps), then re-immersed to continue the cycle. Normally hundreds of these cycles are completed during the course of the test program. In ASTM G 60, test specimens are dipped in a test solution before being exposed to atmospheres varying in relative humidity. The intent of the test is to develop a layered corrosion product similar to that found on sheltered outdoor exposure test specimens. These tests can be either manually performed or conducted in apparatus equipped for automatic cycling.

### Simulation and Acceptance Testing

The laboratory test should try to simulate actual service conditions. Occasionally, this may be accomplished simply by building a scaled-down model of a particular operation. If the service operation is not too large, actual parts of the system can be modified to a laboratory bench-top to permit a better simulation of the actual process.

There are many examples where this approach has been applied. An excellent example is depicted in Fig. 1 of a circulating brine cooling/heating heat exchanger system. The effect

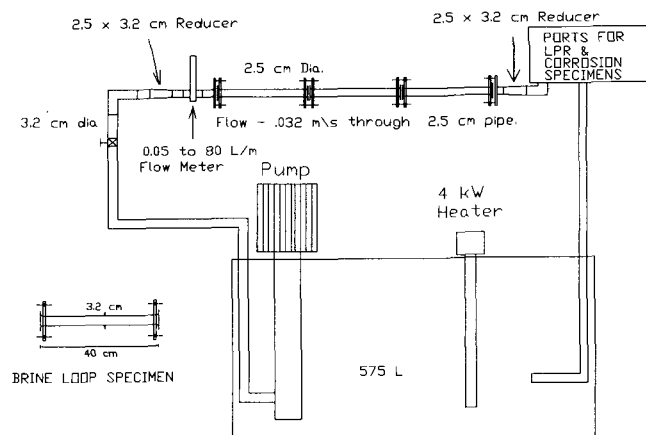


FIG. 1—Scaled-down model, circulating brine cooling/heating heat exchanger system.

of brine corrosion, and use of inhibitors, in the piping system is simulated by the use of full-sized pipe spool pieces of different alloy composition. The test model further incorporates the use of small test specimens and electrochemical monitoring probes.

Acceptance tests attempt to use actual service conditions and environments to control the quality of the material being supplied as material of construction. A classic example is the use of acceptance testing for susceptibility of alloys to intergranular corrosion under boiling nitric acid service using the ASTM A 262, Method C test procedure. Another example is to simulate down-hole sour gas or sour oil piping environments by use of the NACE International TM-01-77 procedure for hydrogen induced cracking susceptibility exposure to aqueous hydrogen sulfide.

## TEST SPECIMEN PREPARATION, CLEANING, AND EVALUATION

### Preparation

One of the most important parts of corrosion testing is the preparation of the specimen or part to be tested. Although it is desirable to use the same surface conditions for the tests as those found in service, this is not always possible because of the variability of the material's surface in service, but it should always be a desirable objective.

Test specimens should have many of the characteristics of the material that will be used for the service application, which typically includes composition (elemental chemistry), mechanical properties (strength, hardness, etc.), form (sheet, plate, bar, etc.), size and shape (surface area-to-corrodant volume ratio, flat-stock, end-grain exposure, etc.), metallurgical treatment (heat treatment, welding, hot or cold working, etc.), surface finish (dye-cut, sheared, saw-cut, mill scale, ground and polished, electropolished, etc.), identification procedures (stamped, engraved, etc.), and cleaning procedures (passivated, degreased, water washed, etc.).

Although the size and shape of the specimen will depend on the purpose of the test, rectangular specimens of the dimensions 2.5 cm by 5 cm by 0.3 cm thick are common. A typical variation is found when a corrosion test requires the specimen to be mechanically stressed as part of the evaluation procedure. It would be normal in this case to use a standard tensile test specimen for the corrosion test. Other examples are the use of disk-shaped specimens for rotational erosion tests, or special configurations for stress corrosion, exfoliation, or crevice tests.

A reproducible surface finish is desirable for repetitive testing. A common final surface finish for test specimens is No. 120 grit abrasive paper or cloth, or their equivalent. Whenever possible or known, the same metallurgical treatment should be used for the test specimen as used for the service part, because heat treatment or cold work can change the surface composition, grain size and structure, and residual stresses. Mechanical operations can affect the materials surface. Cutting, shearing, grinding, and polishing operations should be performed to avoid excessive work-hardening or stresses.

There are many ways to identify test specimens, such as marking with ink or paint, incise marking, or stamping numbers or letters with a tool that leaves an impression in the surface. Precautions should be observed with the use of any system to avoid excessive stresses, the creation of sites for pit initiation, or the use of materials that will be reactive with the metal. It is important that the identification endures the duration of the test, so some of these problems may have to be tolerated.

### Cleaning Specimens Before Testing

After the test specimen has been prepared for testing, it must be cleaned to remove oil, soil, and fingerprints. Either chemical or electrochemical means can be used for the final cleaning, but the effects of cleaning on surface topography must be considered. A recommended procedure involves scrubbing with a toothbrush and a bleach-free scouring powder, followed by thorough rinsing in water and a suitable solvent (such as acetone or methanol) and warm air-drying. For relatively soft metals (such as aluminum, magnesium and copper) scrubbing with abrasive powder is not always desirable as it can mar the surface of the specimen. Ultrasonic techniques may be used, as necessary.

If coatings are to be evaluated, it is important that the metal surface be cleaned and the coating applied in a similar manner to that used in the service application. This step may involve using regular production facilities.

After cleaning, the test specimens are weighed on an analytical balance to an accuracy of  $\pm 0.5$  mg, and dimensional measurements are made to  $\pm 0.001$  cm to permit accurate calculation of the exposed surface area.

### Cleaning Specimens After Testing

The effect that corrosion and the resulting corrosion products have on the test specimen should be determined in order to evaluate the severity of the attack. Locations of deposits or corrosion products are important in evaluating localized attack such as pitting, crevice attack or cracking.

Therefore before cleaning the exposed specimens should be observed and their appearance recorded. Although this method is qualitative it is helpful in assessing the nature and extent of corrosion.

Corrosion rates are based on weight loss (consumption of the base material) during the duration of exposure. Therefore cleaning the specimens of their corrosion products is a vital step in the corrosion test protocol. Generally, the cleaning procedure should remove all corrosion products from the specimen with a minimum removal of sound material. Set procedures for specimen cleaning vary depending on the type of the material being cleaned, and on the degree of adherence of corrosion products. Cleaning methods are divided into three general categories: mechanical, chemical, and electrolytic. Detailed procedures are described in ASTM G 1.

After cleaning, the specimens are re-weighed. The weight loss during the test duration is used as the principal measure of corrosion: the corrosion rate.

### Evaluation of Results

Even though each step of the corrosion test procedure is important, if not properly evaluated the results can be misused or can lead to erroneous conclusions. It is important to remember that the corrosion rate is based on the extrapolation of results from short-term tests. For example, corrosion rates may be reported in the terms of millimeters per year (mmpy) on the basis of results obtained from exposure of one month, one week, or one day. The degree of extrapolation ranges from a multiple of 12 to 365. Since corrosion is rarely linear, with initial rates being extremely high, it is important that the extent of extrapolation be considered in the evaluation phase of the test program.

After the specimens have been re-weighed, they should be carefully examined visually and under low-power magnification for the presence of localized attack. If there are pits or creviced areas, the extent of the depth of attack can be measured with a pit gauge or a calibrated microscope which is first focused on the bottom of the pit and then the specimen surface edge (see ASTM G 46 for details).

If the test material is suspected of being subject to dealloying (such as dezincification) or intergranular corrosion, a cross section of the specimen should be microscopically examined. If embrittlement is suspect, simply bending the specimen may determine this susceptibility.

### PRECAUTIONS AND VALIDITY OF RESULTS

Most metals and alloys are thermodynamically unstable and will therefore attempt to revert back to their native stable state (e.g., red rust or ferric oxide). The rate at which this reversion (corrosion) occurs varies with the particular alloy and the environment to which it is exposed. The purpose of the laboratory corrosion test is to best simulate these conditions, determine corrosion rates, and predict the various modes of attack. Although each data point is important, the results can be misinterpreted and lead to the wrong conclusion if they are not properly evaluated. Therefore, a laboratory corrosion test can be most useful only if the test results can be compared with actual plant or process service experience.

The precautions mentioned throughout this section focus on the planning and execution of the laboratory test and particularly in the interpretation of results. These cautions are not intended to provide a false impression that corrosion tests are unreliable. Rather, they are intended to emphasize that when corrosion test procedures are executed carefully and interpreted intelligently our knowledge of corrosion may be enhanced. That this is true is evident by the few number of cases of unexpected failures by corrosion or gross misapplication of corrosion resistant materials.

## STANDARDS

Reference is made throughout this section to standards and test methods issued regularly by technical societies such as

ASTM International and NACE International. Other organizations, which also issue standards for the many types of corrosion tests, are CEN, ISO, JSA, and MTI. These professional organizations have produced industry accepted recommended practices and test procedures (see Table 3), which allow comparison with others through direct interaction or published data.

## REFERENCES

- [1] Corbett, R. A., "Using Corrosion Tests Effectively," *Chemical Processing*, Vol. 50, No. 12, Oct. 1987, pp. 28–32.
- [2] Wachter, A. and Treseder, R. S., "Corrosion Testing Evaluation of Metals for Process Equipment," *Chemical Engineering Progress*, Vol. 43, June 1947, pp. 315–326.

# High-Temperature and High-Pressure Corrosion Testing

Russell D. Kane<sup>1</sup>

AUTOCLAVE CORROSION TESTS are a convenient means for laboratory simulation of many service environments for the purpose of evaluating the corrosion resistance of materials and for determining the effects of metallurgical, processing, and environmental variables on corrosion processes. The reason for such tests is to more closely recreate the high temperatures and pressures commonly occurring in commercial or industrial processes.

In many of these cases, the factors affecting corrosion behavior are intimately linked to the conditions of total system pressure, partial pressures of various soluble gaseous constituents and temperature. Table 1 provides a listing of several HT/HP environments of commercial interest. Therefore, corrosion tests conducted at room temperature or ambient pressure, or both, simply cannot produce conditions which allow simple glassware experiments to be totally adequate for the purpose of determining corrosion behavior. In these situations, greater effort must be taken to carefully reproduce conditions of high temperature and pressure in laboratory test vessels in which corrosion coupon, electrochemical, or environmentally assisted cracking (EAC) experiments can be conducted.

## BASIC PRINCIPLES

HT/HP corrosion tests by their nature have special requirements not common to conventional corrosion experiments

conducted in laboratory glassware. There are basic considerations that are necessary when these conditions are used for laboratory corrosion tests. There are several standards documents that have been developed for specific purposes which describe equipment and experimental methods for HT/HP corrosion testing. However, in many situations, the procedures used by laboratory personnel for conducting such tests are not always found in accepted standards documents, but have been developed through years of experience. In general, the degree of difficulty and amount of expense required for HT/HP corrosion tests increases with increasing test pressure and temperature.

## Pressurized Corrosion Tests

### Equipment

The simplest type of HT/HP corrosion test is that which is conducted in a sealed, static, pressurized test vessel as shown schematically in Fig. 1. The test vessel contains a solution and a vapor space above the solution. The liquid and gas phases will be determined by the amount and vapor pressures of the constituents in the test vessel as well as by the test temperature. Corrosion coupons can be placed in the aqueous phase, vapor space, or at phase interfaces depending on the specific interest involved. Additionally, it is also possible to conduct electrochemical tests (i.e., linear polarization resistance (LPR), polarization curve generation

TABLE 1—Typical high temperature/high pressure test conditions.

No.	Application	Environment	Temp, C	Pressure, MPa (bar)
1	Nuclear Power	high-purity water/steam/H <sub>2</sub>	280 to 500	≤ 7 (170)
2	Fluidized Bed Combustion	air, gas, coal	600 to 750	1 (10)
3	Deep Sea	seawater, Cl <sup>-</sup>	0 to 70*	<5 (50)
4	Oil and Gas Production	brine, H <sub>2</sub> S, CO <sub>2</sub> , S <sup>o</sup> , Cl <sup>-</sup>	20 to 250	≤130 (1300)
5	Aerospace Propulsion	hydrogen	-200 to 900	0.1 to 67 (1 to 670)
		oxygen	-200 to 480	≤8 (80)
6	Petroleum Refining	H <sub>2</sub> , H <sub>2</sub> S, hydrocarbons, CO	350 to 650	≤10 (100)
7	Compressed Natural Gas Storage	methane w/trace H <sub>2</sub> S	0 to 100	≤8 (80)
8	Ammonia Storage	NH <sub>3</sub> , H <sub>2</sub> O	0 to 70	≤4 (40)
9	Thermodynamic Power Generation	NH <sub>3</sub> , H <sub>2</sub> O	100 to 650	1.5 to 11 (15 to 110)
10	Exhaust Gas Processing	H <sub>2</sub> , N <sub>2</sub> , CO, CO <sub>2</sub>	≤70	≤35 (350)
11	Natural Gas Pipeline	CH <sub>4</sub> , w/trace H <sub>2</sub> S/CO <sub>2</sub> /O <sub>2</sub>	≤60	≤13 (130)
12	Geothermal Power	brine, steam, H <sub>2</sub> S	≤370	≤17 (170)
13	Steam Boiler	water/steam	≤300	≤9 (90)

\*Pipeline surface temperature.

<sup>1</sup>InterCorr International, Inc., 14503 Bammel North Houston Road, Suite 300, Houston, TX 77014; rkane@intercorr.com.

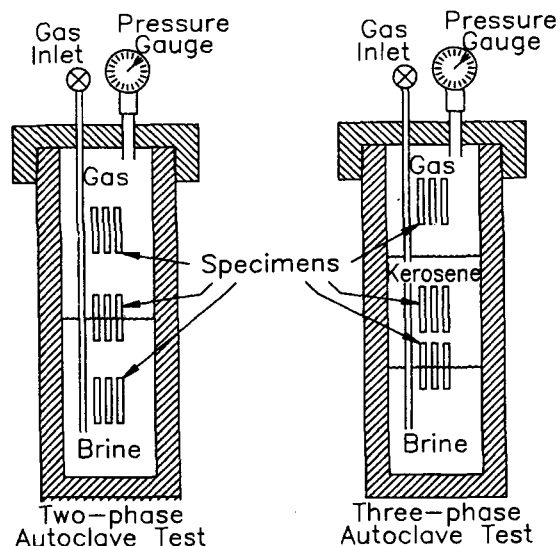


FIG. 1—Simple static HT/HP test vessel configuration.

and cyclic polarization, electrochemical noise (ECN), harmonic distortion analysis (HDA). In these cases, it is often necessary to modify the simple static test vessels with additional electrical feed-throughs to accommodate the electrodes required for electrochemical testing while maintaining a pressure containment.

### Static Tests

In the simplest case of HT/HP corrosion tests conducted under static conditions, it is common to use a single liquid medium. However, in some cases, exposure to a single gaseous phase is required as found in studies of the compatibility of materials to environments containing high-pressure hydrogen gas, oxygen, or other chemical environments. In most situations involving aqueous corrosion, this involves a water-based solution containing various dissolved salts such as chlorides, carbonates, bicarbonates, alkali salts, acids, and various mixtures of these and other constituents. In many cases, the aim is to simulate a particular service environment rather than a simple test environment commonly found in many standardized test methods.

HT/HP corrosion tests can use many of the same test procedures and similar specimens commonly found in conventional aqueous corrosion testing as per ASTM G 31, Practice for Laboratory Immersion Corrosion Testing of Metals. However, in general, somewhat smaller corrosion coupons and stressed EAC specimens are used for HT/HP testing than those used in glassware experiments. The reason for this is that vessels for HP/HT experiments often are of limited internal volume. Volume generally decreases with increasing pressure rating of the equipment due to the increasing wall thickness required to contain the pressure and the high costs associated with particularly larger test vessels. Most laboratory test vessels have an internal volume of between 500 mL and 5 L. In some special cases, however, this type of equipment may have an internal volume in excess of 120 L. To minimize the wall thickness and associated equipment costs, most large test vessels tend to be long

so that volume can be maximized while minimizing the vessel diameter. In most cases, the equipment is designed to specification given in the ASME Boiler and Pressure Vessel Code.

### Agitated Tests

In static corrosion tests, the only form of agitation of the test environment is convection produced by heating of the solution. However, if multiple liquid phases are present (e.g., aqueous along with liquid hydrocarbon phases) it is often necessary to stir or agitate the media or test vessel to produce mixing and conditions whereby the corrosion test specimens are contacted by all of the phases present. Special magnetic and mechanical stirrers and flow loops are available that can be used (see Fig. 2a–c) to produce movement of the fluid to produce a mixing of the phases. In some cases where contact of the specimens with both liquid and gaseous phases is important in the corrosion process, it may be necessary to slowly rotate, rock or shake the test vessel to produce the intended results.

Magnetic or mechanical stirring equipment can also be employed to spin the specimens in the test environment as commonly used in spinning disk or spinning cylinder tests. To study the effects of velocity, it is usually more practical to spin the specimens while minimizing fluid movement by placing baffles in the test vessel. In some applications, turbulent or high-velocity flow is a critical factor in materials performance and must be simulated under temperature and pressure. Test systems can use jet impingement techniques to simulate such conditions using a pressurized flow system up to 350°C. In these tests, it is necessary to not simulate service conditions based on linear flow velocity. A more important and relevant parameter used when assessing field, plant and laboratory test environments is the wall shear stress, which is a measure of the mechanical action (and frictional force) produced at the interface between the flowing media and the metal surface.

### Refreshed and Recirculating Tests

The limited volume of corrosive environment in HT/HP tests makes issues such as solution volume to specimen surface area ratio a critical factor. In most cases, it is advantageous to limit this ratio to no less than 30 mL/cm<sup>2</sup>.

$$\text{Solution volume to surface area ratio} = V / (N \times A_s)$$

where:

$A_s$  = Exposed surface area of an individual test specimen  
(area calculation depends on size and shape)

$N$  = Number of test specimens in experiment

$V$  = Volume of corrosive solution used in test vessel

In any event, care should be taken to prevent depletion of critical corrosive species or contamination of the test solution with unacceptably high levels of metal ions produced by corrosion. Such conditions may require periodic changes in the test constituents after a certain period of testing time (e.g., 3 days, 7 days, 1 month, etc.) depending on their rate of consumption or contamination by corroding specimens.

In particularly critical situations, it is possible to minimize such concerns by using constant or periodic replenishment of either the gaseous or liquid phases in the autoclave

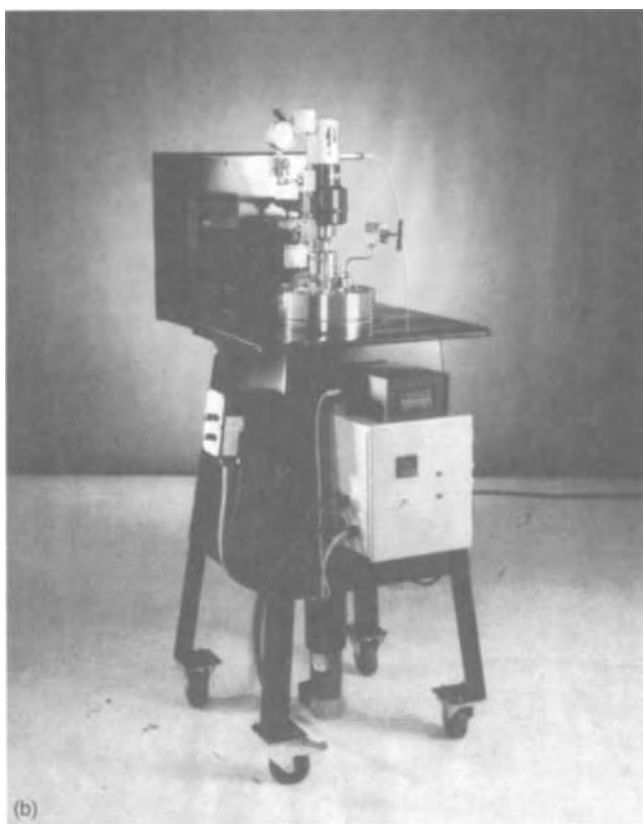
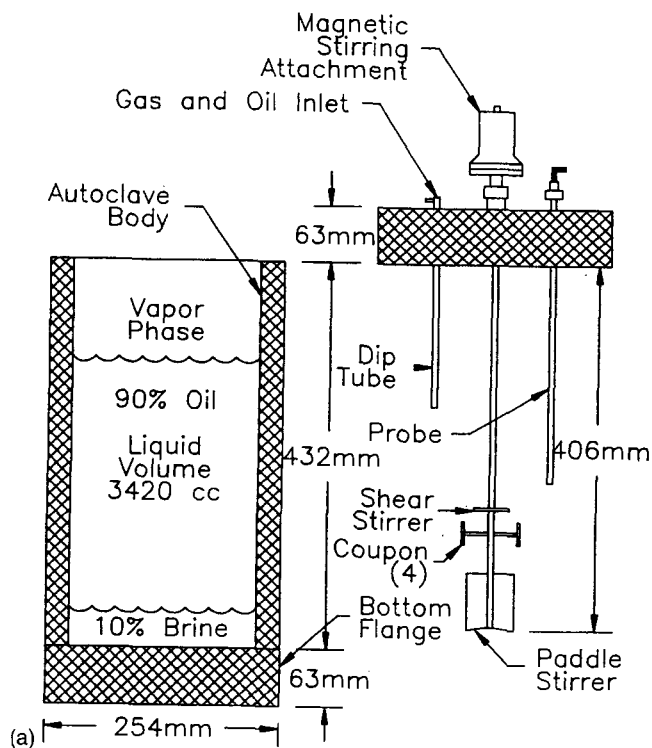


**FIG. 2—HT/HP test vessel with stirring attachment; (a) vessel schematic, (b) High pressure test vessel, (c) High pressure flow loop.**

while under pressurized conditions. An example of a pressurized liquid phase replenishment system used in HT/HP corrosion testing is shown in Fig. 3. These include systems that can refresh the liquid or gas phases with continuous or periodic additions by simply flowing through the test cell while at pressure. In other cases it may be possible to recirculate the solution after it has been recharged with particular corrosive species or been regenerated to attain certain compositional requirements.

### Factors Affecting HT/HP Test Environments

For simple HT/HP exposure tests involving either aqueous or nonaqueous phases with a gas cap over the solution, the total pressure is usually determined by the sum of the partial pressures of the constituents of the test environment, which will vary with temperature. Where liquid constituents are being used for the test environment, the partial pressure is usually taken to be the vapor pressure of the liquid at the intended test temperature (see Table 2 for steam pressure versus temperature). Vapor pressures for several other volatile compounds used in HT/HP corrosion testing can usually

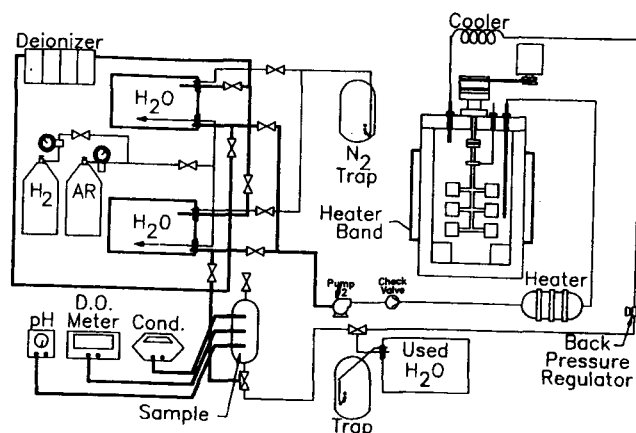


FIG. 3—HT/HP test vessel with recirculation loop and environmental monitoring.

be found in the chemistry literature. In some cases, higher test pressures can be obtained by pumping additional gas (either inert or corrosive) into the test vessel using a special gas pump depending on the situation being simulated. Alternately, hydrostatic pressurization may be employed to increase test pressure whereby there is no gas phase in the test vessel and the pressure is increased by pumping additional liquid into the test vessel in a controlled manner. However, this requires very careful techniques as the hydrostatic pressure increases very rapidly due to the incompressibility of the most liquids.

For mixed gases, the partial pressure of the constituents are usually represented as the product of their respective mol fractions (in the gas phase) times the total pressure (see below):

$$P_g = P_t \times X_g$$

where:

$P_g$  = partial pressure of gaseous constituent

$P_t$  = total system pressure, and

$X_g$  = is the mole fraction of the constituent in the test gas

For example, if a sealed, 2-L test vessel containing 75 % water was heated to 200°C, then the total pressure would be expected to be approximately 1.5 MPa. This is based on the vapor pressure of water as given in steam tables (Table 2). However, if a 10:90 mixture of carbon dioxide and nitrogen was added to the vessel to increase its pressure by 1.5 MPa to 3.0 MPa, then after saturation of the solution, the partial

pressure of the constituents would be estimated to be as follows: (1)  $PCO_2 = 0.15$  MPa; (2)  $PN_2 = 1.35$  MPa;  $PH_2O = 1.5$  MPa. Other liquid and gaseous constituents usually act similarly to the cases given. However, in cases where the gas phase is extremely soluble in the liquid gas more complicated ionic models can be used to predict the total and partial pressures of the constituents in the test vessel and their solubility in the liquid phases. Prior to initiating HT/HP corrosion tests, it is usually prudent to consult various sources of solubility and vapor pressure for the specific test constituents. This will usually prevent unintentional over-pressurization of the test cell.

The importance of partial pressure in HT/HP corrosion testing is that the solubility of the gaseous constituents in the liquid phase is usually determined by its partial pressure. For a particular mol fraction of gas in the vapor phase, its concentration in the liquid will usually increase with increasing total pressure. This is why the effects of low-level (ppm) corrosive impurities such as oxygen, hydrogen,  $H_2S$ , and many other species on corrosion and cracking are often found to be magnified at high pressure and exhibit corrosive effects not commonly found in conventional low-pressure corrosion tests.

### Special HT/HP Corrosion Test Conditions

HT/HP testing has been used to simulate corrosive environments commonly found in many industrial and commercial processes. Those which have been highly studied and which highlight some of the important effects and considerations of HT/HP corrosion testing are discussed briefly in this section.

#### Oxygen

In many cases, the effects of oxygen (or aeration) in solution are important due to its effect on the corrosion potential of materials, particularly alloys, which exhibit active/passive corrosion behavior. One example of the effects of oxygen on corrosion behavior is the combined effect of oxygen and chloride concentrations on the stress corrosion cracking (SCC) of stainless steel in HT/HP water systems [1]. Such conditions represent a wide range of aqueous applications. In general, the severity of SCC in stainless steel increases with both dissolved oxygen and chloride concentrations in an aqueous solution at elevated temperature. Additionally, if the oxygen concentration can be reduced to very low levels (0.1 ppm) through extensive deaeration procedures, this material can be used in systems with a reduced tendency for SCC compared to systems where the dissolved oxygen level is high.

Figure 4 shows a laboratory test vessel specially designed to examine the effects of oxygen on engineering materials. In such systems, it is very important to design the test equipment to (1) contain minimum volume of reactive constituents, and (2) to resist rapid oxidation or even burning of materials of construction. ASTM G 88, Guide for Designing Systems for Oxygen Service, gives guidelines that can be used for the design of such systems. The particular system shown includes the use of copper or copper/nickel alloys for test cells. In this case, alloy N04400 was used as the material of construction for the vessel. However, in some cases stainless or nickel-base alloys will provide sufficient oxidation

TABLE 2—Pressure of dry saturated steam versus temperature.\*

Temperature, °C	Absolute Pressure, MPa (bar)
100	0.1 (1.0)
150	0.5 (5.0)
200	1.5 (15.0)
250	4.0 (40.0)
300	8.5 (85.0)
350	16.5 (165.0)

\*In closed container with liquid phase present.



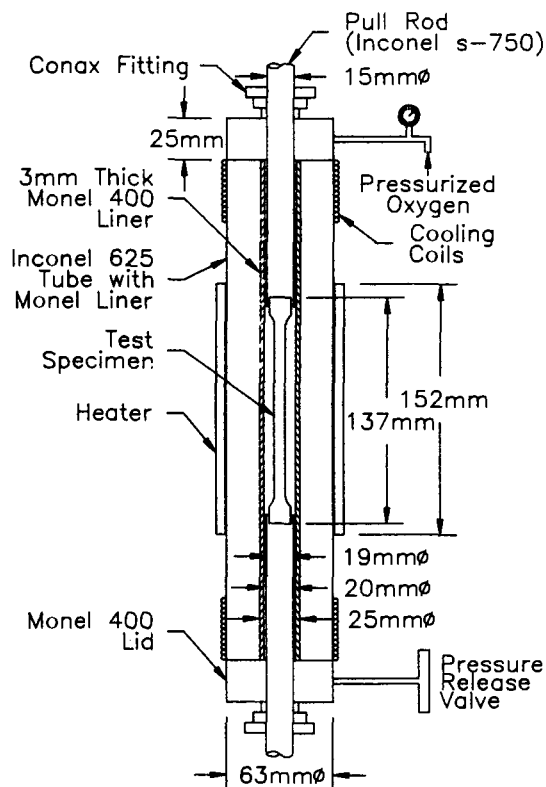


FIG. 4—Schematic of HT/HP oxygen test cell.

resistance in less severe environments. It is also important to carefully select all polymeric materials used in the system to resist deterioration and combustion in oxygen environments. This requires attention to both the partial pressure of oxygen in mixed gas environments as well as the maximum operating temperature of the system when selecting materials for the test vessel and ancillary equipment.

### Hydrogen

Another chemical species whose chemical behavior impacts corrosion resistance and materials performance is hydrogen. It has been known for decades that atomic hydrogen can produce embrittlement in many metallic materials to varying degrees, particularly under conditions of high-pressure hydrogen. Under high hydrogen environment pressure or electrochemical reaction, or both, hydrogen atoms can enter the material where it can react by one of the following mechanisms:

1. Recombination to form pressurized molecular hydrogen blisters at internal sites in the metal.
2. Chemical reaction with metal atoms to form brittle metallic hydrides.
3. Solid state interaction with metal atoms to produce a loss of ductility and cracks.

There has been much interest in conducting hydrogen embrittlement cracking (HEC) tests in aqueous media which can produce atomic hydrogen on the surface of materials as a result of corrosion or cathodic charging. In most cases, these tests can be conducted at ambient pressure and at

temperatures from ambient to elevated depending on the application. When aqueous hydrogen charging is involved, pressure is usually not a major factor. However, as in the case of steels exposed to aqueous hydrogen sulfide containing environments, the atomic hydrogen is produced as a result of sulfide corrosion. The severity of the mass-loss corrosion and hydrogen charging is directly dependent on the amount of hydrogen sulfide dissolved in the aqueous solution. In applications involving petroleum production and refining, compressed natural gas storage, chemical, processing and heavy water production such effects are compounded by exposure to HT and/or HP conditions. Additionally, variations in pH which control the type and amount of dissolved sulfide species and the severity of corrosion and hydrogen charging can be affected by hydrogen sulfide pressure.

The hydrogen flux produced by exposure to aqueous hydrogen sulfide containing environments can be categorized based on the hydrogen sulfide partial pressure. The effect of solution pH produced by the combined effect of certain soluble corrosive gases (i.e., hydrogen sulfide and carbon dioxide) is also important.

Service environments that contain a high partial pressure of gaseous hydrogen as found in hydrogen-fueled aerospace or transportation vehicles can only be simulated using HT/HP test methods. The environments involved in hydrogen storage, active cooling systems, and hydrogen combustion can vary in hydrogen partial pressure from less than 0.1 MPa to over 70 MPa (10 000 psi) and temperatures that range from cryogenic to over 925°C. In these situations, the concerns for absorption of atomic hydrogen lead to the need for laboratory HT/HP testing of engineering materials which include high-strength steels as well as advanced materials such as nickel-base and titanium alloys, intermetallic compounds and composites, high-conductivity microcomposites, and nonmetallic structural materials and composites [2].

### Other Dissolved Gas Systems

In other systems, similar effects of dissolved gaseous species can be important and may require the use of HT/HP corrosion test procedures to give accurate simulation of service environments. Examples of such conditions are those that contain carbon dioxide, sulfur dioxide, and  $\text{NO}_x$ , which can determine the pH of the aqueous phase and affect the severity of corrosion reactions.

To simulate dissolved gas conditions in the laboratory it is important to simulate their partial pressures in the gas phase over the test solution since this, in turn, will determine the amount of dissolved species present. If low (generally <1 %) levels of these constituents or high reaction rates are present, then some form of continuous or periodic replenishment of these species during testing may be necessary. For very low (ppm) levels of these constituents in pressurized systems, such procedures are usually always required to provide for valid test conditions to be maintained.

### Test Variations

The HT/HP corrosion test methods described previously require many specialized procedures, evaluation techniques and test equipment. In this section, four variations of common

HT/HP test methods that have been found to be useful in materials evaluation involving corrosion phenomena will be briefly described. These include:

1. Windowed test vessels.
2. Electrochemical measurements.
3. Hydrogen permeation measurements.
4. Mechanical property testing.

Typically, the major differences between these types of tests conducted at high pressure and in conventional low-pressure glassware are the special requirements and limitations imposed by the test vessel, vessel feed-throughs, and the high-pressure environment. However, these types of evaluations can be accomplished through careful planning and test vessel design.

#### Windowed Test Vessels

It may be necessary to make visual measurements or observations within the confines of the test vessel. Additionally, it may be necessary to introduce radiation into the test vessel to produce reactions on metal surfaces as in the case of photo-assisted chemical or electrochemical reactions or for conducting analytical techniques such as Raman Spectroscopy.

To accomplish direct visual contact with specimens in laboratory test vessels, it is common to use special transparent windows and fixtures which can withstand the pressures, temperatures, and corrosive environments commonly used in these experiments. An example of such a test cell is shown in Fig. 5. In this case, it is necessary to provide energy from an external light source to provide stimulation of a corroding metal surface. The transparent port is provided by a special connection in the end of the test vessel containing a sealed sapphire window which allows transmission of the light to the specimen surface. The specimen is also being monitored using electrochemical methods for its potential/current response under varying conditions of light stimulus [3].

Other types of specimen monitoring that can be performed by this technique are (1) visual observation of the development of localized corrosion phenomena with time, (2) monitoring of environmental crack initiation, and (3) crack growth rate measurements. In these cases, it is important to be able to provide for incoming light and for reflection of light from the specimen in order to visually observe the test specimen. Therefore, such measurements often require somewhat larger transparent ports and are usually limited to lower pressure systems.

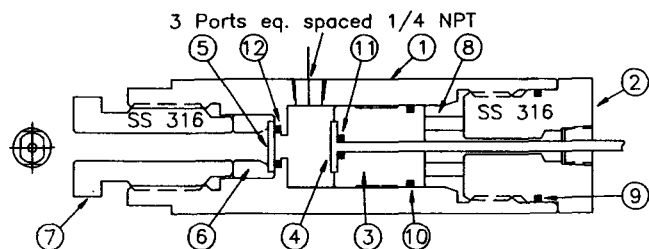


FIG. 5—Schematic of HT/HP optical test vessel.

FIG. 6—HT/HP electrochemical test cell with electrical feed-throughs for working electrodes.

It is also possible to use fiber optics to provide an optical conduit into pressurized systems. In either case, it is possible to use photographic or video techniques to magnify, supplement, and record the direct visual monitoring and examination of corrosion processes first-hand. The main concern for such systems is that they be constructed of materials that are compatible with the test environment and have adequate pressure ratings. This is possible in lower pressure and less aggressive systems, but may prevent the use of such methods in some highly corrosive or ultrahigh-pressure applications.

#### Electrochemical Measurements

Electrochemical corrosion measurements can be conducted in HT/HP environments with modification of conventional test vessels and by using few special techniques. In general, most all of the conventional electrochemical techniques performed in glassware have also been conducted inside of HP test equipment. Figure 6 shows a test system that uses cylindrical electrodes where only the lower portion of the electrode is exposed to the liquid phase of the test environment and where the electrical connections are made externally to the test vessel.

In general, the most critical portion of any electrochemical system is the reference electrode. The design and construction of the reference electrode for HT/HP corrosion testing is particularly important as it must provide a stable

reference potential (relatable to other common reference electrodes) to which the working electrode (i.e., test specimen) can be compared. It must also give a reasonable service life to remain functional throughout the intended test period.

In many applications, a test vessel modified with an external reference electrode cell has become the most common system to minimize effects of temperature, pressure, or contamination, or a combination thereof, from the corrosive environment. This approach helps to prolong the usable life of the reference electrode. One of the most common reference electrode systems used in HT/HP corrosion testing is Ag/AgCl [4]. However, other reference systems have been developed and are used for application in specific environments [5]. The external reference electrode is usually contained in a separate pressurized compartment. The reference electrode is then connected to the test vessel using a bridge or conductive solution conduit.

To minimize penetrations into the test vessel for HT/HP electrochemical tests, it is possible to use the test vessel directly as the counter-electrode. This requires special selection of materials of test vessel construction so that it will be effectively inert to the test environment.

In systems that contain impurities which will contaminate common reference electrode systems and degrade their performance, it is possible to pressure balance the electrode [6] and to even provide a reverse flow into the test vessel to minimize ingress of the contaminant species into the reference electrode.

Another type of reference system that can be employed effectively in HT/HP systems where conventional stable reference electrodes are not usable is the use of an inert (i.e., graphite or platinum) or a corroding metal to produce a stable potential [7]. Such electrodes are considered “pseudo-reference” systems since they may tend to exhibit a drift in potential with time. However, in environments where no other convenient reference electrodes are available, they can provide at least a measurement of relative potential between materials in the environment even if their reference potentials cannot be considered truly constant.

### *Hydrogen Permeation Measurement*

In some environments that produce hydrogen charging in metals, it is necessary to measure hydrogen permeation rates and diffusion constants in order to predict hydrogen attack rates or time-to-failure by HEC. It may also be important to determine the effects of additions of inhibitors into the environment and surface barriers which may act to reduce the level of hydrogen flux. At ambient temperatures and pressures, such measurements are easily obtained through the use of various forms of the standard glass permeation cell reported in the literature [8,9]. Such procedures and equipment are generally limited to ambient pressure and to the atmospheric boiling point of the aqueous solutions in the permeation cell. For higher temperatures and pressures, further modifications must be made which involve adaptation of this system along with incorporation of a high pressure test vessel [10].

As shown in Fig. 7a and b, HT/HP systems have been used for both laboratory and field measurements of hydrogen flux commonly called a “patch probe” or “barnacle cell” [11]. They have typically been used for the monitoring of

**FIG. 7—Hydrogen permeation cell for conducting tests on HT/HP system with external electrochemical hydrogen patch probe.**

hydrogen permeation in steel refinery plant vessels and piping or pipelines exposed to corrosive wet H<sub>2</sub>S environments. For hydrogen permeation measurements in higher temperature systems, it is necessary to use solid state methods since systems involving liquids in the measurement compartment will be subject to evaporation or breakdown with increasing temperature. These systems depend on monitoring of either the pumping rate of a vacuum pump or the pressure

buildup rate in an evacuated compartment to determine the hydrogen flux through a membrane in contact with the hydrogen environment.

#### *Mechanical Property Testing in HT/HP Corrosive Environments*

In cases where susceptibility to HEC, SCC, liquid metal embrittlement (LME), or other EAC mechanism may be suspected, it is common to evaluate the actual mechanical behavior of the alloys under consideration in the corrosive environment of interest. For decades, these techniques were developed and conducted in low-pressure aqueous environments and are referred to as slow strain rate (SSR) testing or constant extension rate testing (CERT) [12]. The important aspect of such techniques is the requirement for these tests to be conducted in a range of strain rate or cross-head extension rate in which the material under evaluation is going to experience cracking if it is susceptible.

In general, it is necessary to conduct such tests slow enough so that the environment has adequate time to affect the material and produce cracking. These strain rates are typically in the range of  $10^{-4}$  to  $10^{-7}$  s $^{-1}$  for SCC in many common metals/environment systems. For HEC, the critical strain rate is somewhat higher (i.e.,  $10^{-2}$  to  $10^{-4}$  s $^{-1}$ ) in most susceptible iron, nickel, and titanium alloys. SSR tests are particularly adapted to HT/HP in simulated environments. Since the test is accelerated mechanically by the application of the dynamic straining, it is possible to use simulated test environments rather than the overly aggressive chemical environments commonly used in conventional standardized tests.

Figure 8a and b shows a vessel used to conduct SSR tests at HT/HP conditions. In aqueous environments, the heating is accomplished from the outside of the vessel to uniformly heat the entire test solution surrounding the specimen. For high-temperature gaseous environments it may be possible to heat the specimen within the pressurized test vessel. If not, the configuration of the test cell should be changed to reduce the radial distance between the internal diameter (I.D.) of the vessel and the specimen to minimize gas volume required and to reduce heat transfer problems. In either case, it is important to monitor the temperature of the gage section of the test specimen to obtain accurate measurement of test temperature.

In some cases, it may be possible to use the similarly designed HT/HP test vessels to conduct fracture or fatigue loading, or both. For such tests, accommodations must be made to be able to handle the generally larger specimen configuration of fracture mechanics specimens. Additionally, there is the need to closely monitor crack opening displacement or crack growth, or both, directly using various methods including (1) pressure and environmentally compatible clip gages, (2) mechanical fixtures which exit the pressure vessel, or (3) potential drop across the specimen. In the case of potential drop techniques, as the specimen cross section is reduced due to crack growth, the electrical resistance measured across the cracked region increases and can be monitored as a measure of crack growth. Alternately, in some cases, direct measurements of crack opening displacement can be conducted using special mechanical feed-throughs in the test vessel. This technique, while

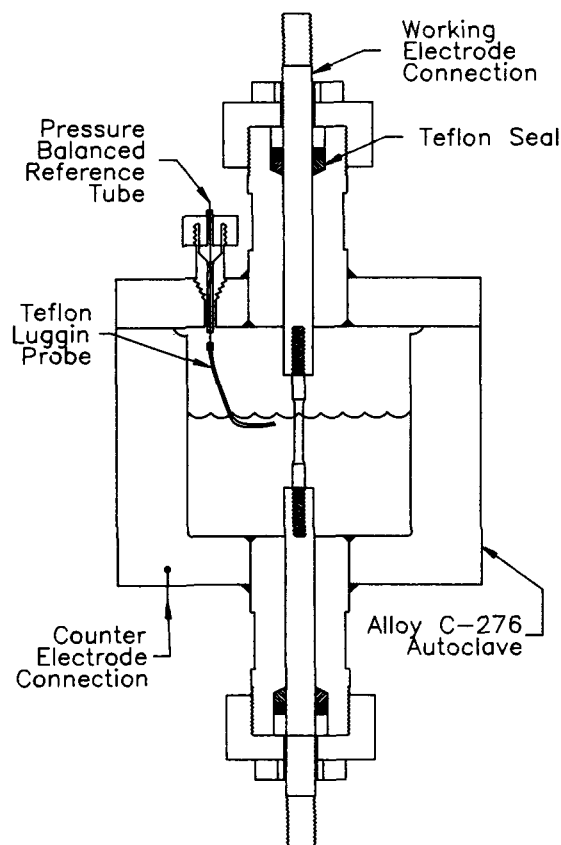


**FIG. 8—HT/HP test vessel for slow strain rate tension testing.**

cumbersome, is preferred where the test environment is particularly corrosive and may attack clip gages and interfere with electrical feed-throughs for use with potential drop techniques.

#### **Safety**

HT/HP corrosion tests require attention to safety on many levels since this type of testing involves handling high pressures, high temperatures, and exposure to corrosive and potentially hazardous and/or toxic chemical test constituents. Special care should be taken to obtain properly designed and constructed test equipment and facilities, and to develop safe test procedures. Additionally, safety planning should be carried out well in advance of the initiation of testing and it should include training of technical personnel in the aspects of safely handling chemical environments at HT and HP as well as the development of contingency and emergency procedures in the event of problems.

#### *Pressure*

To safely handle high pressure environments, it is critical that all equipment including test vessels, piping, fittings, gages, and other ancillary components be properly designed and constructed to withstand the intended test pressure.

It is common to design test vessels and piping per methods given in Section VIII of the ASME Boiler Code even though in many cases compliance with this specification may not be mandatory [13]. Additionally, all test equipment and pressure vessels should be fabricated from materials that are highly resistant to the corrosive environments that they are going to contain. This is needed both from the standpoint of safety and to prevent depletion of reactive constituents from the test environment. Consideration should also be given to the full range of chemical environments that the test equipment will be exposed to during its useful service life. Major emphasis should be placed on selecting material(s) that are resistant to not just mass-loss corrosion but to localized corrosion and EAC. It is recommended that many sources of information be consulted in the process of materials selection along with any relevant service experience which can be obtained from field/plant operations and from manufacturers experienced in providing pressurized test equipment.

It is common for most corrosion test vessels to be designed to be periodically hydrostatically tested at pressures from 1.25 to 1.5 times their maximum working pressure depending on the nature of the service. It is also a good practice to limit the test conditions in the test vessel to less than the maximum working pressure limits. This will prolong the service life of fittings and seals. Also, prior to each use, a leak check of all fittings and seals with an inert gas will minimize problems later when the vessel contains corrosive and potentially hazardous test environments. Vessels can also be used with liners which are made from corrosion resistant metallic materials or nonmetallic materials such as TFE or glass depending on the nature of the test environment. This technique can prolong the useful life of a test vessel; however, it is important not to totally rely on liners to protect the test vessel. Situations can occur that result in breakage or leakage from the liner, thus exposing the test vessel to direct contact with the corrosive environment.

In some cases, chemical reactions in the test environment or interactions between the test environment and the specimens can produce unexpected increases in pressure or temperature, or both. Conditions that can result in large or rapid pressure increase inside of the test vessel should be carefully studied prior to testing and eliminated unless adequate safety precautions and/or pressure relief methods can be provided.

### *Temperature*

For tests conducted at high temperature, there are several concerns regarding safety that should be taken into account. The first is that HT corrosion tests may involve test conditions that are above the atmospheric boiling point of the aqueous solution or even above the flash point of various combustible constituents in the test environment. Therefore, all precautions to prevent leakage from the test vessel should be taken prior to the initiation of testing. This usually includes a pressure test of all fittings and seals with an inert gas prior to introduction of the corrosive environment.

In some cases, bolted closure vessels that are being used to conduct tests which involve very high temperatures (>250°C) may experience thermal expansion of the bolts in the closure. This situation can result in a relaxation of the

sealing force and can produce leakage from the test vessel at high temperature even though the vessel was leak-tight at low temperature. Similarly, when using test vessels that have elastomeric seals, it is important to limit the test temperature to conditions that will not produce either mechanical or chemical deterioration or thermal decomposition of the elastomeric seals. This situation can also result in leakage from the test vessel when it is hot.

Second, in most HT/HP corrosion tests, heating of the test environment is used to produce at least a portion of the total test pressure. Therefore, overheating as a result of loss of temperature control can lead to overpressurization of the test vessel and associated equipment. Unexpected pressure increases can be obtained during heating through volume expansion of test fluids. It is normal to take into account such conditions when determining the amounts of constituents to be added to the test vessel. Adequate precautions need to be taken to prevent temperature excursions through failure of temperature control equipment with the use of overtemperature controllers or thermostats. The exact needs in any particular test should be carefully considered.

### **Simulation of Service Environments**

In many situations, actual service environment samples are retrieved and brought to the laboratory to provide the most representative media in which to conduct such tests. In these cases, sampling techniques play a major role in determining the successful usage of simulated environment corrosion tests.

In some cases, the actual service environment may not be readily available or accessible for laboratory evaluation. Such cases include situations where the effects of changes in environment composition on corrosion behavior are being examined. Additionally, simulated service environment tests are used to select materials that are resistant to new processes that are not yet commercial. This necessitates the formulation of a simulated service environment from reagent grade chemicals. Judgments must be made concerning the effects of impurities found in process equipment which are not commonly found in reagent grade chemicals. In some cases, these impurities may act as inhibitors and in others they may act to promote corrosion or SCC. These judgments require a basic knowledge of alloy sensitivities to environment species and test parameters obtained through both service and testing experience and through review of the published literature and available corrosion databases.

### *Temperature Effects*

The service temperature is normally duplicated exactly in laboratory simulations. Unlike glassware experiments, HT/HP corrosion tests can be conducted at temperatures above the atmospheric boiling point of the test environment. This is an important benefit of HT/HP testing which normally results in better simulation of actual service conditions. However, problems may arise when the corroding system is not isothermal as in the case under heat transfer conditions commonly found in many types of industrial process equipment such as heat exchangers and dynamic process vessels. Temperature can also be used to accelerate reactions in the laboratory. This can have its drawbacks which

**FIG. 9—Test assembly for prototype component test with internal HT/HP hydrogen gas exposure.**

mainly arise when elevating the test temperature over the service temperature changes the operating corrosion mechanisms. Therefore, care must be taken to choose the test temperature that best typifies the service condition including normal operation and upset conditions.

#### *Pressure Effects*

Pressure stresses can be duplicated allowing simulation of actual components exposed to corrosive environments [14]. In the actual vessel tests, the environment is often pressurized hydrostatically. This testing arrangement allows for nondestructive inspection using techniques such as ultrasonics and acoustic emission to be used from the outside while the test is being conducted. It also provides for evaluation of complex situations involving fabrication, welding, stress relief, etc. It should be mentioned that, under such test configurations, careful test control and containment must be used. The consequences of failure can be minimized through the use of fully hydrostatic pressure conditions. Another example is shown in Fig. 9, which represents the evaluation of an actual component prototype pressurized with high-pressure hydrogen. Each chamber was monitored for internal hydrogen pressure versus exposure time so that time-to-failure from hydrogen attack could be determined [15].

In other cases, total system pressure may be of less importance in laboratory simulations. Usually, simulation of partial pressure of soluble gaseous constituents is the important parameter which affects the corrosion test results.

However, total pressure can be a major effect under conditions where total pressure affects phase behavior or flow conditions or where it may be a driving force in a particular chemical reaction or in diffusion of a particular species in the test environment. In these cases (e.g., where volatile inhibitors or polymeric coatings or seals are being evaluated), it is important to simulate the total pressure so that the proper relationships between liquid and gaseous phases or permeation of corrosive media can be obtained. An example of the effect of total pressure is the performance of sacrificial anodes under simulated conditions of varying depths of water.

### **STANDARDS: SCOPE, SIGNIFICANCE, AND USE**

The number of standards involving HT/HP corrosion testing is somewhat limited. In general, the procedures used for HT/HP corrosion tests have been highly specialized to the particular nature of the corrosion test and the test environment. Those that have been identified are described in this section.

#### **NACE Standards**

NACE has developed several standards involving HT/HP corrosion testing. These have involved the laboratory simulation of two types of corrosive environments: (1) Aqueous oilfield production environments containing corrosive acid gases (i.e., hydrogen sulfide and carbon dioxide) and water, and (2) nuclear reactor high-purity water environments.

#### *Oilfield Corrosion Test Environments*

NACE Standard Test Method TM0185 (Evaluation of Internal Plastic Coatings for Corrosion Control of Tubular Goods by Autoclave Testing) was developed to provide manufacturers, applicators, and users of internal pipe coatings with a method of comparing the performance of these coatings for corrosion control. The test method establishes a laboratory method for evaluation of plastic coatings for downhole tubulars in specific HT/HP environments for the purpose of corrosion control. The intent was to standardize existing laboratory methods used by various laboratories.

NACE TM0185 was not developed to provide results that correlate directly with any particular set of field conditions, but solely for the purpose of comparing materials under uniform laboratory test procedures. Controls are given for specimen size, test environment, test duration, and depressurization rate. It allows for post-test evaluation of the coating performance based on visual examination and various physical and mechanical evaluations.

NACE has standardized test methods (TM0177 and TM0198) for the evaluation of environmentally assisted cracking—EAC—(sulfide stress cracking of steels and SCC of stainless and nickel-base alloys exposed to simulated aqueous environments containing hydrogen sulfide. TM0177 involves exposure of tensile, bent beam, C-ring, and fracture mechanics specimens and TM0198 involves smooth and notched tensile and pre-cracked specimens using the slow strain rate testing technique. The purpose of these

specimens and test methods are to provide a basis to screen materials for EAC in environments containing both sulfide and chloride species in an aqueous environment. These tests are not meant to simulate service behavior directly, but to provide a reproducible method of comparing alloy performance, thus aiding the determination of the effects of various metallurgical and environment parameters. Suggested environmental conditions for testing are provided in these standards and may include HP/HT exposures in some cases. The standards provide meaningful information relative to specimen preparation and various methods that can be used to attain HT/HP test environments containing various partial pressures of hydrogen sulfide.

### *Corrosion Tests in High-Purity Water*

NACE has standardized two test methods that deal specifically with conducting corrosion tests in high-purity water for nuclear applications. These are NACE Standards TM0171 (Autoclave Corrosion Testing of Metals in High Temperature Water) and TM0274 (Dynamic Corrosion Testing of Metals in High Temperature Water). The two test methods discuss corrosion testing in high-purity water under dynamically replenished and recirculated conditions, respectively.

NACE TM0171 establishes suggested laboratory procedures for determining the extent and the rate of uniform corrosion of metals in high-temperature water or aqueous solutions at temperatures in the range 100°C to 360°C. This is to aid in the standardization of laboratory procedures and in the evaluation of corrosion test specimens exposed to HT/HP aqueous conditions. The standard is not applicable to the testing of cladding fissionable materials or neutron absorbing materials, which are the subject of ASTM G 2 (see next subsection). It is not intended that the data be used to determine the release rate of metallic elements to the test medium or to determine the effects of velocity on corrosion.

This method provides for the descriptions of test apparatus for the purification, storage, heating, pumping, and replenishment of a high-purity water environment and the exposure of test specimens in this environment. Techniques are provided for cleaning the test equipment and specimens, fixturing, solution purity levels, flow rates and testing procedures. Procedures are also given for the evaluation of the corrosion specimens and the corrosion films produced on them and for determination of corrosion rate. A critical part of the test method is the maintenance of the test environment within specific environmental limits.

NACE TM0274 appears to be an outgrowth of the previously mentioned TM0171 test method. It is similar in many aspects. The major difference is the use of a dynamic recirculation loop which accommodates both a high temperature test station and a low temperature test station in which corrosion coupons can be placed. This method can be used for (1) the quantitative measurement of the general corrosion rates of metallic materials for consideration for use in high-purity water, (2) the determination of the effects of flow velocity, and (3) the estimation of the release rate of metallic elements to the aqueous medium. No provisions

are made for simulation of heat transfer conditions or steam/water environments.

### **ASTM Standards**

There are also several ASTM standards that describe testing techniques for the evaluation of corrosion and materials compatibility which involve HT/HP conditions. These are:

- G 2M Test Method for Corrosion Testing of Products of Zirconium, Hafnium, and Their Alloys in Water at 633K or in Steam at 673K
- G 4 Method for Conducting Corrosion Coupon Tests in Plant Equipment
- G 72 Standard Test Method for Autogenous Ignition Temperature of Liquids and Solids in a High-Pressure Oxygen-Enriched Environment
- G 86 Test Method for Determining the Ignition Sensitivity of Materials to Mechanical Impact in Pressurized Oxygen Environments
- G 94 Guide for Evaluating Metals for Oxygen Service
- G 111 Standard Guide for Corrosion Tests in High Temperature or High Pressure Environment, or Both
- G 124 Standard Test Method for Determining the Combustion Behavior of Metallic Materials in Oxygen-Enriched Atmospheres
- G 129 Standard Practice for Slow Strain Rate Testing to Evaluate the Susceptibility of Metallic Materials to Environmentally Assisted Cracking
- G 142 Standard Test Method for Determination of Susceptibility of Metals to Embrittlement in Hydrogen Containing Environments at High Pressure, High Temperature, or Both
- G 146 Standard Practice for Evaluation of Disbonding of Bimetallic Stainless Alloy/Steel Plate for Use in High-Pressure, High-Temperature Refinery Hydrogen Service
- G 170 Standard Guide for Evaluating and Qualifying Oil-field and Refinery Corrosion Inhibitors in the Laboratory

Example of other ASTM standards which high pressure methods for evaluation of materials and corrosion apply include:

- D 572 Standard Test Method for Rubber-Deterioration by Heat and Oxygen
- D 3632 Standard Test Method for Accelerated Aging of Adhesive Joints by the Oxygen-Pressure Method
- D 6396 Standard Test Method for Testing of Pipe Thread Sealants on Pipe Tees
- E 712 Standard Practice for Laboratory Screening of Metallic Containment Materials for Use With Liquids in Solar Heating and Cooling Systems

These standards involve a variety of test conditions and environmental parameters. The ASTM standards listed provide specialized information on specific combinations of environments and materials and give guidelines for test procedures, equipment, and evaluation techniques required to measure or monitor corrosion resistance and material compatibility. ASTM G 111 is a standard guide that is directed at providing general guidelines for a broad range of tests that can be conducted under HT/HP conditions involving corrosion, environmentally assisted cracking, and electrochemical measurements.

## REFERENCES

- [1] *Metals Handbook, Volume 13—Corrosion*, 9th Edition, ASM International, Metals Park, OH, 1987, p. 274.
- [2] Kane, R. D. and Chakachery, E. A., "Behavior of Titanium Aluminide and Carbon-Carbon Composite Materials for Hydrogen Gas Service," *Proceedings of ADVMAT/91*, NACE, Houston, TX, p. 20-1.
- [3] Wilhelm, S. M., "Photoelectrolysis of Liquid Hydrogen Sulfide by Cadmium Sulfide," *Journal of the Electrochemical Society*, to be published.
- [4] Wilde, B. E., "Some Considerations in the Design of Electrodes for Electrochemical Studies at High Temperature and Pressure," *High Temperature, High Pressure Electrochemistry in Aqueous Solutions*, NACE, Houston, TX, 1976, pp. 277-287.
- [5] Case, B. and Bignold, G. J., "The Mercury/Mercuric Oxide Electrode in High Temperature Alkaline Solutions," *High Temperature, High Pressure Electrochemistry in Aqueous Solutions*, NACE, Houston, TX, 1976, pp. 334-340.
- [6] Danielson, M. J., "A Long-Lived External Reference Electrode for Use in High Temperature/Pressure Environments," Batelle Pacific Northwest Laboratories, Report No. PNL-SA-10424, U.S. D.O.E. Contract DE-AC0G-76RLO-1830.
- [7] McKie, A. S., "The Development and Functional Testing of an External Reference Electrode for Use with Autoclaves," *High Temperature, High Pressure Electrochemistry in Aqueous Solutions*, NACE, Houston, TX, 1976, pp. 325-333.
- [8] Devanathan, M. A. V. and Stackwaski, Z., *Proceedings of the Royal Society A270*, 1962, p. 90.
- [9] Devanathan, M. A. V. and Stackwaski, Z., *Journal of the Electrochemical Society*, Vol. 110, 1963, p. 866.
- [10] Hay, M. G., "Correlation of Laboratory Hydrogen Induced Cracking Test Environments with Field Sour Gas Environments Using Hydrogen Permeation Measurements," *Corrosion/92*, Paper 13, NACE, Houston, TX.
- [11] French, E. C. and Hurst, L. R., "Hydrogen Monitoring by the Hydrogen Patch Probe," *Corrosion/80*, Paper 47, NACE, Houston, TX.
- [12] *Slow Strain Rate Testing for the Evaluation of Environmentally Induced Cracking: Research and Engineering Applications*, ASTM STP 1210, R. D. Kane, Ed., ASTM International, West Conshohocken, PA, 1993.
- [13] American Society of Mechanical Engineers, ASME Boiler and Pressure Vessel Code, Section VIII, ASME, New York.
- [14] Cayard, M. S. and Kane, R. D., Status Report: API/MPC Full Scale HIC Program, American Petroleum Institute Refining Committee Meeting, September 1992.
- [15] Cayard, M. S., Internal Report, InterCorr International, Inc., Houston, TX, 1992.



# Atmospheric

*Sheldon W. Dean, Jr.*<sup>1</sup>

EXTENSIVE EXPERIENCE, TOGETHER with many exposure programs, has shown that atmospheric corrosion is a phenomenon that varies greatly from location to location [1]. Studies throughout the world have revealed that the rate of atmospheric corrosion is a function of the metal being tested, the location, the climate, the proximity to pollutants, and a variety of other factors. Most people understand that atmospheric corrosion can occur in outdoor exposures, but more recent experience has shown that corrosion can occur from indoor atmospheres under certain circumstances [2].

Outdoor atmospheric exposure tests have been carried out for a variety of purposes [3]. Alloy producers have used this type of testing to evaluate the performance of new alloys in a variety of atmospheric conditions. Atmospheric corrosion testing has also been used to test both metallic and nonmetallic coatings to demonstrate their performance in atmospheric conditions [4]. Manufacturers of items designed to be used in outdoor conditions sometimes expose components to various atmospheres to demonstrate their performance and develop data on the service life that may be expected from such components. In some cases, atmospheric exposure programs are run to evaluate the corrosivity of specific atmospheres. This type of information can be helpful in selecting coatings or other corrosion protection systems to be used at specific sites.

## BASIC PRINCIPLES

### Types of Exposures

Probably the most common type of atmospheric exposure is conducted in a static location; that is, racks or holding devices are fixed in a location and specimens are exposed for a test period at that site. This type of exposure can be carried out in sheltered sites or boldly exposed sites. A wide variety of different types of specimens may be employed in long-term tests.

Another type of test is the dynamic or mobile test where panels are mounted on vehicles to simulate the service conditions of cars or trucks. Vehicles are exposed to significant amounts of spray and splash from the road surface and, as a consequence, this environment is significantly different from that normally seen in the static exposures. In some

cases, panels have been mounted on the sides of trucks to allow a larger number of panels to be mounted in approximately the same type of environment [5]. Panels mounted on automobiles are generally mounted in locations where they are not visible, although in some cases bumper-mounted panels have been used [6]. Variability in dynamic tests is substantial because no two vehicles see exactly the same environment. A similar situation exists for ocean-going vessels. The atmospheric corrosion that occurs on aircraft carriers, for example, is unique because it incorporates both marine spray from the ocean and flue gases from the engines.

Because of the rather substantial variability in dynamic tests, coupled with the problem of having very limited numbers of panels on each vehicle, some investigators have employed an approach of spraying static panels with simulated road splash solutions, for example, mixtures of sodium and calcium chloride. This is, of course, a much more severe environment than normal static atmospheric exposure. However, it does have the advantage of being more reproducible than a vehicular exposure while allowing many panels to be exposed at the same time under the same conditions. Such an approach also allows for the natural wetting and drying that is normally seen in atmospheric exposures. These conditions are difficult to simulate in cabinet-type tests.

### Monitoring Atmospheric Variables

A conventional weather station approach has often been used to monitor atmospheric variables regarding atmospheric corrosion [7]. Temperature and relative humidity may be recorded continuously, and these data are used to produce average temperatures for periods of time such as days, weeks, or months. Electrical monitoring sensors have been developed to measure when wetness exists on the surface by means of detecting a potential difference between dissimilar metals [8]. A standard device is shown in ASTM G 84, Practice for Measurement of Time of Wetness on Surfaces Exposed to Wetting Conditions as in Atmospheric Corrosion Testing. The information on time of wetness is usually reduced to a percentage or fraction of time a surface is wet in a month or in a year.

Atmospheric sulfur, usually in the form of sulfur dioxide, is measured by means of a volumetric sampling approach in which samples of the air are passed through a detector that directly measures the sulfur dioxide concentration. Another

<sup>1</sup>President, Dean Corrosion Technology, Inc., 1316 Highland Ct., Allentown, PA 18103.

approach is to use a sulfation plate or sulfation candle [9] (Fig. 1). These devices rely on lead dioxide to react with the sulfur compounds in the atmosphere to form lead sulfate. At the conclusion of a fixed exposure period, usually 30 days, the sulfation plate or candle is removed from exposure and analyzed for the presence of lead sulfate. ASTM G 91, Practice for Monitoring Atmospheric  $\text{SO}_2$  Using the Sulfation Plate Technique, describes the sulfation plate method. Sulfation plates are exposed in a horizontal downward-facing position so that the lead dioxide reagent is not exposed to rainwater. ASTM D 2010, Test Methods for Evaluation of Total Sulfation Activity in the Atmosphere by the Lead Dioxide Technique, describes the sulfation candle, which is a similar type of collector except that it employs a vertical cylinder rather than a flat disk. Again, the sulfation candle must be protected from exposure to rain or snow. Neither the sulfation plate nor the sulfation candle is specific for sulfur dioxide. They will respond to reduced sulfur species such as hydrogen sulfide and carbonyl sulfide. However, the presence of these gases is relatively rare, and usually a source of such reduced species would be very apparent to investigators at the site. These gases dramatically enhance the corrosion of some alloys but are not equivalent to sulfur dioxide.

It should be noted that the volumetric measurement and the deposition rate measurement measure different phenomena. The transfer from the gas phase to the solid surface requires both convective diffusion and surface adsorption steps [10]. Air movement assists the convection process while the adsorption step is accelerated by the presence of

condensed moisture. As a result, correlations between volumetric concentration and deposition rate are approximate and may not necessarily apply from site to site. For corrosion correlation purposes, the deposition rate is a more relevant phenomenon. However, as a practical matter, the mass transfer rate that occurs on a sulfation plate or candle is probably not equivalent to what would occur on a flat surface or a wire. Therefore, the results obtained from devices such as sulfation plates provide a reasonable measure of the concentration of sulfur in the atmosphere but not an accurate measure of what deposits are on test samples or structures. The volumetric concentration monitoring instruments are clearly the preferred technique because they require less labor to expose and retrieve samples and can provide much more detailed information on how the sulfur dioxide concentration varies with time.

Sulfur dioxide deposition and chloride deposition have been designated dry depositions in studies concerned with the effects of acid precipitation in spite of the fact that these processes do occur when the specimen is physically wet with dew or rain. The term *wet deposition* refers to acidity delivered to the specimen during periods of rain or snow [11]. The reason for this distinction is that the source of acidity in precipitation is probably different from the source of either atmospheric sulfur dioxide or chloride. In order to monitor wet deposition, it is necessary to collect and analyze precipitation samples. In general, the damage to metals from acid precipitation is relatively small as compared to damage caused by significant levels of sulfur dioxide or chloride on most engineering metals.

Several techniques have been used to monitor chloride in the atmosphere. The wet candle method, ASTM G 140, Method for Determining Atmospheric Chloride Deposition Rate by Wet Candle Method, has been used in marine sites and consists of a fabric-wrapped tube in which the fabric is kept wet with water [12] (Fig. 2). The wet fabric acts as a collector for chloride particulates or droplets. Exposure periods of one week or up to one month have been used. The longer time periods can be a problem because the water source must not be allowed to dry. It is important to protect the wet candle from rain exposure so that wet candle assemblies are usually mounted with a cover over them. With the

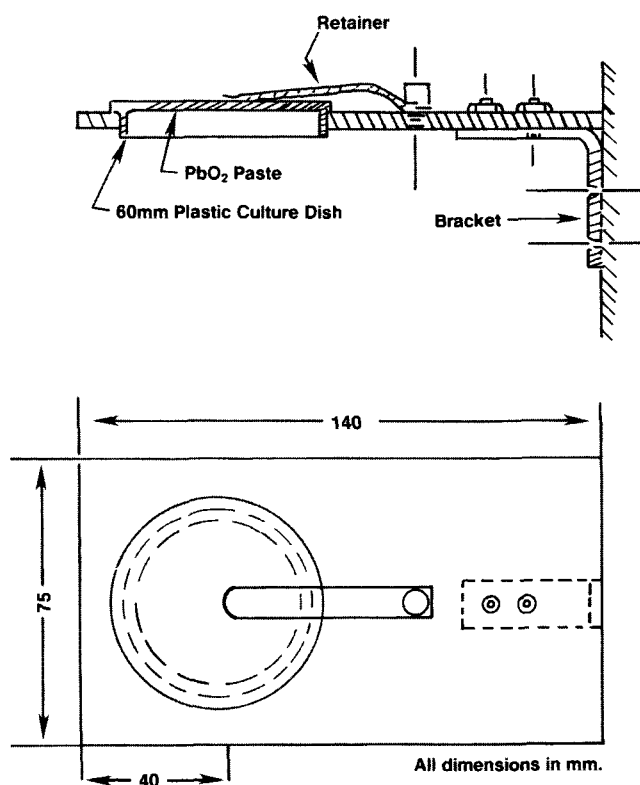


FIG. 1—Sulfation plate in holder (see ASTM G 91).

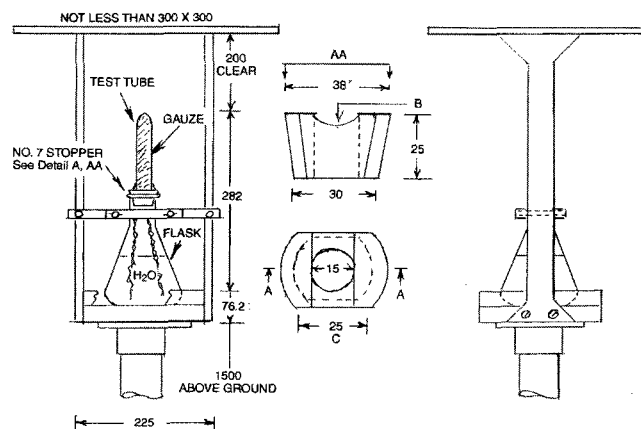


FIG. 2—Wet candle apparatus with holder (see ISO 9225).

**FIG. 3—Comparison of wet candle and dry plate results for atmospheric deposition at two sites. Reference ISO/TC156/WG4/N236.**

wet candle method it is necessary to employ an antifreeze solution in cold climates when freezing can occur. Glycerine has been used for this purpose, but if glycerine is used, it is necessary to add an inhibitor to prevent biological growth in the solution. Another technique that has been used is the dry plate method. In this case, a vertical assembly is used with fabric stretched over a frame. Chloride-containing particles adhere to the dry fabric and are extracted from the fabric and analyzed at the end of the exposure period. Figure 3 shows the relationship between chloride deposition rates measured by both methods at two sites.

Atmospheric chlorides generally originate from marine sources. Surf is a major contributor to atmospheric chlorides. The spray from surf is entrained in the air and carried inland by the wind. As a result, spray droplets tend to settle out and dry out as they move inland, becoming smaller and more concentrated in an almost exponential decay as they move. Chloride particles are very water soluble so that areas washed by rain tend to retain much less chloride than protected areas. Large smooth surfaces are much poorer collectors of salt particles than small diameter wires. As a result, devices such as the chloride candle or dry plate collector give only rough approximations of actual chloride depositions on test samples or structures exposed to the atmosphere.

Chlorine and hydrogen chloride are sometimes found in industrial atmospheres. These compounds can cause serious corrosion, but are not covered by the ISO standards.

### Classification of the Atmosphere—ISO Approach

The International Organization for Standardization Technical Committee on Corrosion of Metals and Alloys, ISO/TC156, has developed a systematic approach to classification of atmospheric corrosivity [13]. This approach is based on two different methods. The first method involves exposure of standard coupons of steel, zinc, copper, or aluminum to the atmosphere at the site where the classification is to be made. The selection of which metal is to be used will depend on the purpose of the test. Panels are

exposed for a one-year period, at which time they are retrieved and a mass loss per unit area obtained. This mass loss value can then be used to determine the corrosivity of the atmosphere at that location. Table 1 shows the corrosivity classes based on mass loss results.

The second method involves measurement of the temperature, time of wetness, amount of sulfur in the atmosphere, and the amount of chloride in the atmosphere. Temperature and humidity information can be used to estimate the time of wetness. This estimation is based on the percentage of time that the temperature is above freezing, 0°C, and the relative humidity is at the same time above 80 %. Once the time of wetness is known, it is then possible to determine a time of wetness class (Table 2). Sulfur dioxide content of the atmosphere can be estimated either by measurement of the concentration in the atmosphere over some period of time or by means of the sulfation plate or candle. This information is then used to develop a sulfur dioxide class or P class (Table 3). The chloride dry plate or wet candle method is used to obtain the chloride deposition rate of the atmosphere that is then converted to a chloride class or S class (Table 3). The corrosion class or C class can be obtained for the time of wetness, chloride, and sulfur dioxide classes (Table 4). Once the corrosion class is known, it is possible to estimate the corrosion damage that will occur in either short-term or long-term exposures for the five metals, steel, weathering steel, aluminum, copper, and zinc (Table 5). The detailed information on this method is discussed in Tables 2–5.

**TABLE 1—ISO corrosion classes for metals based on one-year exposure results—mass losses.**

Steel g/m <sup>2</sup>	Copper g/m <sup>2</sup>	Aluminum g/m <sup>2</sup>	Zinc g/m <sup>2</sup>	Corrosion Category
<10	<0.9	~0	<0.7	C1
10–200	0.9–5	<0.6	0.7–5	C2
201–400	5.01–12	0.6–2	5.01–15	C3
401–650	12.01–25	2.01–5	15.01–30	C4
651–1500	25.01–50	5.01–10	30.01–60	C5

Based on ISO 9223.

**TABLE 2—ISO wetness class based on time of wetness.**

Wetness Class	Time Wet. %	Hrs. Wet Per Yr.	Examples of Occurrence
T1	<0.1	<10	Indoor
T2	0.1–3	10–250	Indoor—Unheated
T3	3–30	250–2500	Shed Storage—Cold Climate
T4	30–60	2500–5500	Outdoor Temperate Climate
T5	60	5500	Tropical Outdoor or Surf

Based on ISO 9223.

**TABLE 3—Sulfur dioxide and chloride classes.**

SO <sub>2</sub> Class	SO <sub>2</sub>		Chloride	
	Deposit Rate, mg/m <sup>2</sup> Day	Concentration, mg/m <sup>3</sup>	Cl Class	Deposit Rate, mg/m <sup>2</sup> Day
P0	<10	<12	S0	<3
P1	10–35	12–40	S1	3–60
P2	36–80	41–90	S2	61–300
P3	81–200	91–250	S3	301–1500

Based on ISO 9223.

**TABLE 4—Corrosion classes for environmental classes.**

	T2			T3			T4			T5		
	S0-S1	S2	S3	S0-S1	S2	S3	S0-S1	S2	S3	S0-S1	S2	S3
Unalloyed Steels												
P0-P1	1	2	3-4	2-3	3-4	4	3	4	5	3-4	5	5
P2	1-2	2-3	3-4	3-4	3-4	4-5	4	4	5	4-5	5	5
P3	2	3	4	4	4-5	5	5	5	5	5	5	5
Zinc and Copper												
P0-P1	1	1-2	3	3	3	3-4	3	4	5	3-4	5	5
P2	1-2	2	3	3	3-4	4	3-4	4	5	4-5	5	5
P3	2	3	3-4	3	3-4	4	4-5	5	5	5	5	5
Aluminum												
P0-P1	1	2-3	4	3	3-4	4	3	3-4	5	4	5	5
P2	1-2	3-4	4	3	4	4-5	3-4	4	5	4-5	5	5
P3	3-4	4	4	3-4	4-5	5	4-5	5	5	5	5	5

Note: T = wetness class; P = SO<sub>2</sub> class; S = chloride class.  
Based on ISO 9223.

**TABLE 5—Atmospheric corrosion rates for corrosion class, µm/year.**

Corrosion Class	Steel		Copper		Zinc		Aluminum		Weathering Steel	
	ST	LT	ST	LT	ST	LT	ST	LT	ST	LT
1	<0.5	<0.1	<0.01	<0.01	<0.1	<0.05	<0.01	<0.01	<0.1	<0.1
2	0.5-5	0.1-1.5	0.01-0.1	0.01-0.1	0.1-0.5	0.05-0.5	0.01-0.025	0.01-0.02	0.1-2	0.1-1
3	5-12	1.5-6	0.1-1.5	0.1-1.0	0.5-2	0.5-2	0.025-0.2	0.02-0.2	2-8	1-5
4	12-30	6-20	1.5-3	1.0-3	2-4	2-4			8-15	5-10
5	30-400	20-90	3-5	3-5	4-10	4-10			15-80	10-80

Note: ST = average corrosion rate during the first ten years of exposure.  
LT = steady state corrosion rate for long-term exposures.  
Based on ISO 9224.

**TABLE 6—Gaseous and solid materials affecting indoor atmospheric corrosion.**

Substance	Concentration µg/m <sup>3</sup>	Comments
SO <sub>2</sub>	1-100	30-50% lower than outdoors
NO <sub>2</sub>	2-150	Similar to outdoors
H <sub>2</sub> S	1-3	Higher in some situations
Cl <sub>2</sub>	<0.1	
HCl	0.1-20	Usually very low
NH <sub>3</sub>	20	
Soot	5	Higher when fires are used
O <sub>3</sub>	2-25	Usually lower than outdoors

This system of atmospheric classification is now being revised to create a new approach based on dose-response functions for steel, copper, and zinc. Because the corrosion of aluminum occurs by a pitting or localized mechanism, the traditional approach of using mass loss to determine severity of attack is often misleading. Atmospheric corrosion problems with aluminum alloys are most frequently a result of metallurgical conditions rather than environmental conditions, and the behavior of aluminum may be excluded in the upcoming revision of the ISO 9223-6 documents.

### Indoor Atmospheres

Although the ISO approach to classification of the atmosphere was envisioned to cover both indoor and outdoor atmospheres, the classification range on indoor atmospheres was too broad to be useful for many applications. The corrosion concerns for indoor atmospheres covered three different categories. One major area of concern was storage of metallic parts and components in warehouses. The concern

here is that the storage conditions do not stain or damage the parts. The second area of concern is the use of metallic materials in indoor atmospheres where corrosive conditions can occur, for example, plumbing fixtures in humid environments such as kitchens and bathrooms. A third area of concern is for electronic components [14]. There have been serious problems with failures of measuring devices, computers, and related equipment in control rooms, and even in offices, that have been attributed to corrosion. The ISO system is adequate to deal with the concerns of warehouse storage but has not been adequate to deal with the concerns of electronic materials degradation. The reason for this is that the mechanism of corrosion that causes problems in electronic circuitry is quite different from that encountered by engineering materials in atmospheric outdoor exposure. The problems that occur in electronics are development of resistive films that interfere with switch operation and the migration of corrosion products causing short circuits or related problems. Two specific problems have been noted. One is the development of pore corrosion. This phenomenon has been observed on gold surfaces in the form of black spots distributed over the gold surface. The second problem is film creep that refers to a rapid diffusion of corrosion products across the gold surface. Other problems have also been noted.

In the case of corrosion in storage areas and the protection of materials in humid indoor atmospheres, conventional techniques that apply to outdoor corrosion are suitable. The primary mechanism seems to be the development of moisture films on the metallic surfaces that then promote corrosion. In the case of electronic components corrosion, the critical moisture contents are at substantially

lower values than are normally seen in outdoor corrosion. In addition, the critical pollutants seem to be reduced sulfur species such as  $\text{H}_2\text{S}$ , and also acid chloride species such as hydrogen chloride. These species are present in indoor atmosphere at very low levels, typically 0.1–10 ppb (Table 6).

## ATMOSPHERIC TESTING

### Program Development

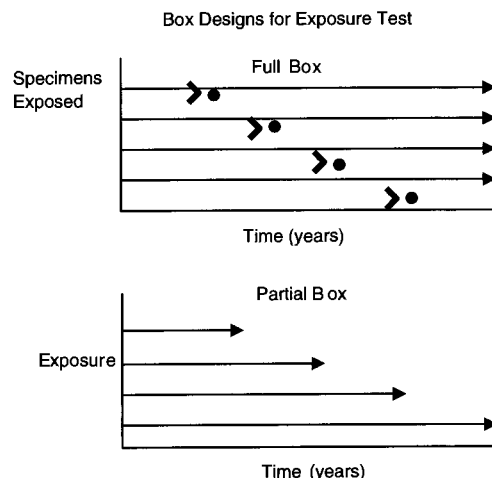
The first step in an atmospheric testing program is to develop a program that will provide answers to the question: What is the purpose of this program [15]? If the purpose of the program is to characterize the atmospheric performance of a new material, it is important to determine what time interval is relevant and what reference materials should be included so that a definite comparison can be made. It is also important to determine what type of exposure will be used and what the specimens should look like. Further, it is important to determine at this time how the results of the program will be evaluated. Understanding these issues at the beginning of the process is very helpful in determining later how many specimens are needed and what types of materials are required and, ultimately, what the cost of the exposure program will be. Table 7 supplies a list of the key issues that need to be decided at the beginning of any atmospheric testing program.

### Exposure Program

The simplest type of exposure program is a fixed material program in which a set of specimens is exposed for a fixed time period. At the conclusion of this period, the specimens are retrieved and evaluated. A variation on this approach is to inspect the specimens at the exposure site at intervals during the exposure period and report results.

A somewhat different approach is to expose a group of specimens initially and then retrieve portions of the group at intervals, e.g., 1 year, 3 years, 5 years, 10 years, and 20 years. This approach allows the investigator to estimate the kinetics of the process if an assumption can be made about the constancy of the environment. A variation of this approach is to replace each specimen removed with an unexposed specimen to be retrieved at the conclusion of the test. This approach allows variations in the environment to be averaged out or at least acknowledged (Fig. 4).

An important issue in exposure tests is the question of replication. It is desirable to use at least duplicate specimens in corrosion tests. However, in atmospheric tests it is good



Specimens exposed at dots and retrieved for evaluation at arrow head  
Full box allows atmospheric corrosivity change estimate as well as specimen corrodibility estimate Partial box estimates only specimen changes

**FIG. 4—Example of exposure program designs [15]. (Reprinted from Materials Performance. © Copyright 1988 by NACE International. All Rights Reserved by NACE; reprinted with permission.)**

practice to use a larger degree of replication, preferably five specimens for statistical analysis. Three specimens are generally considered the minimum acceptable in most cases to avoid problems from damage, loss, and unexpected events.

In general, indoor exposures are usually made for relatively short periods. In most cases, 30 days and 90 days are typical, although occasionally a 1-year exposure is used. Because the purpose of these exposures is generally to evaluate the environment, it is usually necessary to obtain results rapidly to determine what protective measures are necessary.

### Specimen Types

Once the purpose of the program is decided, the next question is: What type of specimen should be used? Some typical specimen types are listed in Table 8. Probably the most widely used specimen in atmospheric exposure programs is a 100 by 150 mm panel. This type of panel is very suitable for mass loss measurements. It is also used for evaluating coatings and is convenient to handle. For nonferrous metals, investigators have preferred to use larger panels, for example, 100 by 200 mm [16]. Larger sizes do lose some convenience and ability to fit on some balances.

Wire helix specimens have been used to monitor atmospheric corrosivity [17]. It should be noted that this type of specimen tends to show higher corrosion rates than flat panels of the same material. For this reason, it is likely that helix specimens will be dropped for the purpose of site monitoring. The reason that wire samples show higher corrosion rates seems to be related to the increased collection efficiency of small diameter cylinders in gathering other gaseous or solid particles and these materials tend to stimulate the corrosion process [18].

**TABLE 7—Program development issues.**

- Purpose of the program?
- Exposure time to achieve purpose?
- Reference materials?
- Results evaluation?
- Replication needed?
- Coating for the ground facing surface of panel?
- Edge preparation or masking?

TABLE 8—Types of specimen.

Type	Standards
Flat Panel	ASTM G 50
100 × 150 mm	
100 × 200 mm	
100 × 300 mm	
Helix Wire	
Stress Corrosion	
Bent Beam	ASTM G 39
C Ring	ASTM G 38
U Bend	ASTM G 30
Direct Tension	ASTM G 49
Welded	ASTM G 58
Galvanic	
Plate on Plate	ISO 7441
Disk on Disk	ASTM G 149
Wire on Bolt	ASTM G 116
Coated Specimen	ASTM D 1654
Fabricated Items	

Atmospheric stress corrosion tests are frequently run with U-bend specimens or two-point loaded specimens. U-bend specimens are used when the stress level is not a variable, but it is desired to determine if an alloy is susceptible to cracking (Fig. 5). Two-point loaded specimens have the advantage of being held at points of low stress and at locations where a crevice will do the least damage. It is relatively simple to construct racks to hold two-point loaded specimens. A two-point loaded specimen can be designed to cover a wide range of maximum stresses [19]. Other types of standard stress specimens may also be used, for example, direct tension specimens, C-ring specimens, and other bent beam configurations (Fig. 6). Table 8 has a list of standard stressed specimens that may be used in atmospheric corrosion.

It is occasionally desirable to evaluate galvanic corrosion effects from atmospheric exposures (see ASTM G 116, Conducting Wire-on-Bolt Test for Atmospheric Galvanic Corrosion and ASTM G 149, Conducting the Washer Test for Atmospheric Galvanic Corrosion). Several different types of specimens have been used for this purpose. One approach is

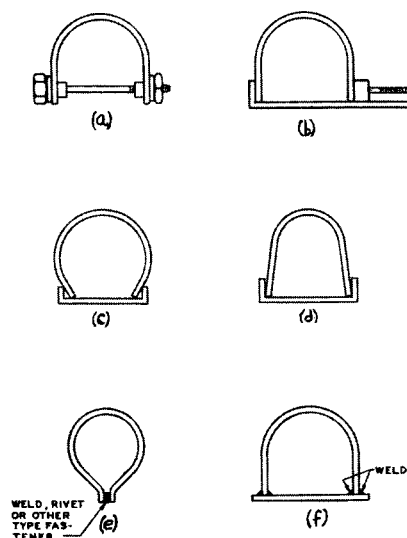


FIG. 5—U-bend specimen designs (see ASTM G 30).

to use washers bolted together as shown in Fig. 7 [20]. At the end of the test, it is possible to measure the depth of corrosive attack associated with the region of galvanic corrosion by means of mass loss measurements. Other types of galvanic exposure specimens that have been used have included plates of different metals bolted together. The third type that has been used is the helix wire on bolt type of specimen [21] (see ASTM G 116), and in this case the test specimen is usually a wire that is wrapped around a bolt of a different material to evaluate the galvanic corrosion that may occur from this couple. Mass loss measurements are usually used to evaluate the loss of metal from the wire specimen.

Atmospheric exposure programs are often run to evaluate coating performance. This is true for both organic coatings and for inorganic coatings including metallic coatings such as electroplated coatings [22], flame-sprayed coatings [23], and hot-dipped coatings [24]. The key issue in the case of organic coatings is the adhesion of the coating and particularly the ability of the coating to maintain adhesion and protection even in the face of mechanical damage. Consequently, it is often desirable to scribe an x-shaped mark on the surface of the panel after the coating process. The scribe should penetrate to the basis metal. At various times during the exposure, the panel is evaluated by noting how far the corrosion of the basis metal has proceeded under the

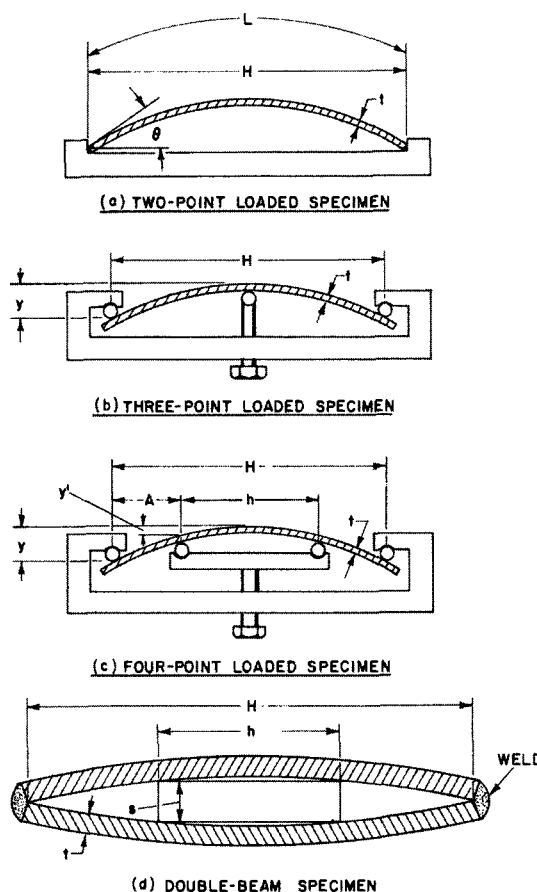


FIG. 6—Bent beam specimen designs (see ASTM G 39).

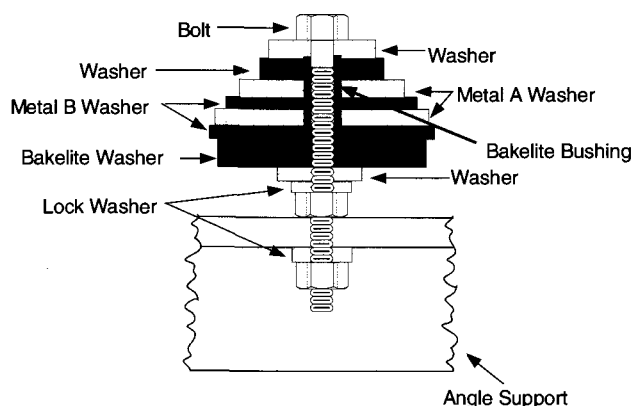


FIG. 7—Cross section of washer bimetal assembly (ASTM G 149).

paint or coating. In the case of metallic coatings, visual examinations are usually conducted during the life of the exposure to look for penetration of rust through the coating, spalling, or other degradation of the coating itself.

It is often desirable to expose fabricated items such as roofing panels, automotive trim parts, wire ropes, wire specimens, and a host of other hardware items. This type of program allows the performance of a finished product to be evaluated in a controlled exposure program. It is especially good for evaluating differences in finishes to determine if the difference in the finishing process has caused a change in the coating performance.

### Specimen Preparation

The type of preparation that a specimen will require depends very much on purposes of the exposure program [3]. In cases where bare metals are to be exposed to the atmosphere, a somewhat arbitrary decision must be made on what type of surface finish will be tested. Typical steps in an atmospheric exposure program are given in Table 9.

Characteristically for ferrous metals, it is generally desirable to employ a mechanical finishing technique that removes the mill scale. Surface grinding with 120-grit abrasive is a typical finish. Such finishes are rather active, and consequently panels must be wrapped with an inhibiting paper or protected by other means so that the surface rust does not develop during shipment. In this case, it is necessary

TABLE 9—Specimen preparation steps.

- Mechanical Preparation
  - Cut to size
  - Finish edges
  - Finish faces
- Identification and Cleaning
- Initial Measurement
  - Mass
  - Size
  - Optical
  - Photographic
- Shipment
- Final Cleaning and Edge Protection if Necessary
- Exposure

to remove any traces of inhibitor that might have transferred to the metal surface. A solvent cleaning step immediately before exposure is frequently used.

It is also necessary to place an identifying mark on the panels before exposure (Table 10). In the case of ferrous metals where heavy corrosion occurs, it is necessary to use techniques such as drilling holes in the panels in specific locations or milling notches in the side of the panel so that it will be possible to identify the panel even after extensive corrosion has occurred [16]. In the case of materials that do not suffer such extensive corrosion in atmospheric exposures, techniques such as stencil stamping may be used. It is desirable to use clean, sharp stencils and to avoid transferring foreign metals from the stencil stamps to the metal surface. In the case of coated samples, stencil stamping may not be acceptable. Other approaches may be used such as writing the panel identification on the back of the panel with a weather-resistant paint or attaching a tag to the panel with the panel identification stamped on it.

The panels should be carefully weighed and measured before exposure. This should be the last step before the panel leaves the laboratory. In the case of coated samples, an important issue is the edge protection. In some cases, specimens are sheared from larger sheets and, consequently, the edges are left uncoated. In this case, it is essential that measures be applied to edges to prevent edge damage from confusing the results. For short-term exposures, vinyl tape is sometimes used to protect the edges. It may also be necessary to carry out preliminary evaluations of the surface of coated samples, including reflectivity measurements, color measurements, or related optical measurements before placing them on exposure.

For indoor exposures, the metals used are usually copper, silver, or steel. Typical exposure panels are 10 by 50 mm by 0.5 mm thick. These panels are usually abraded with a fine silicon carbide abrasive paper; 1200 grit for copper and silver and 500 for steel. After polishing, the specimens should be cleaned in ethanol in an ultrasonic bath before exposure. Occasionally, nickel or zinc specimens may be used in special circumstances where these metals are to be used.

### Outdoor Exposure

Most outdoor exposures are carried out in static situations with the specimens mounted on racks. A standard system has been developed whereby racks are mounted on stands with the panels exposed, in the United States at an angle of 30° to the horizontal [16]. In Europe the exposure angle is generally 45° to the horizontal [25] (Fig. 8). Exposure racks have been designed so that panels can be placed in the rack without disturbing adjacent panels. It is general

TABLE 10—Specimen identifying systems.

Type of Panel	Appropriate System
Steel	Drilled holes according to matrix Mill or saw edge notches
Nonferrous and Stainless Steel Alloys	Stencil stamping
Metallic coated	Stencil stamping Plastic or nonferrous tags Paint on back side

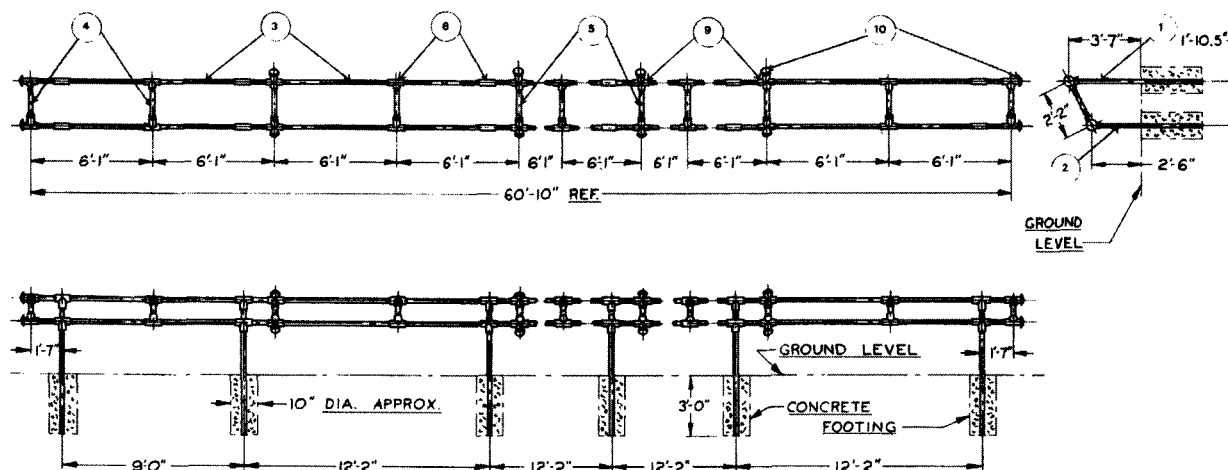


FIG. 8—Atmospheric exposure test rack support design (see ASTM G 50).

practice to have the panel racks facing south in the northern hemisphere. In the case of panels with organic coatings, the top surface will receive the greatest sun exposure if the panel is mounted at an angle to the horizontal equal to the latitude of the site. When panels are mounted in locations where sources of atmospheric-borne corrodants are present, generally it is desirable to have the racks face the source of the corrodant species. For example, at seacoast locations panels should face the surf. In cases where there are adjacent industrial sites, it may be desirable to orient the panels so that they face the source of the pollutants from the industrial source [3].

At the time panels are exposed, the weather should be recorded. It is also important to record the location of each panel on the rack and the rack identification and location at the site. Plans should also be made at this time for retrieving the panels or specimens. For short-term exposures this may not be a problem. However, for programs that go for many years, maintenance of the site can be a problem.

In the case of exposure programs where visual examination of the specimens is to be made at intervals during the program at the exposure site, it is important to set up an evaluation form so that the information desired is recorded along with the specimen identification (see ASTM G 33, Practice for Recording Data from Atmospheric Corrosion Tests of Metallic-Coated Steel Specimens). In the case of tests on stress corrosion specimens, it is desirable to remove specimens at regular intervals during the exposure period so that they may be examined for cracking. This is especially true for specimens that develop thick corrosion product films on their surface because such films often obscure the cracks. It is also desirable to retrieve broken specimens in stress corrosion programs so that the specimen may be evaluated for mode of cracking and presence of secondary cracks. For two-point loaded specimens, it is desirable to wire both ends to the holder in case the specimen fails by total fracture.

### Indoor Exposure

Indoor exposure sites generally employ vertical panels hung from hooks or wires through a hole near the top of the

specimen. In some cases, a plastic enclosure is used to protect the specimens from direct exposure to air currents and to shield the specimens from falling dust. In general, it is desirable to avoid locating the panels near walls and corners where unusual air currents may circulate. It is important that the site location be chosen to be representative of the conditions in question, but more importantly, that they not be damaged or disturbed by the activities in the area.

Indoor specimens may be evaluated by several techniques including mass gain, mass loss, electrochemical reduction, (coulometric measurement), and electrical resistance increase. Microbalance measurements on mass gain after removal of particulates is probably the most popular method because it requires the least specimen handling. However, it will detect dust and particulates on the surface that adhere strongly and may overestimate the corrosion damage in cases where this condition occurs.

Another approach to the microbalance concept is to deposit a thin layer of the metal in question on a quartz crystal and monitor the mass change due to oxidation by means of the change in resonance frequency of the crystal. Applying an AC potential across the thickness of the crystal and detecting the resonance frequency in the shear direction can activate the quartz crystal. By selecting a crystal orientation that has minimal temperature dependence on the resonance frequency, it is possible to obtain a device that can monitor mass changes on a continuous basis [26]. This technique can detect mass changes as low as  $10^{-6}$  g/cm<sup>2</sup>. The metal chosen for the test is typically deposited by vacuum evaporation onto the quartz surface.

### Site Monitoring/Evaluation of Environment

One of the distinguishing characteristics of atmospheric exposure programs is that the environment is not under the investigator's control. Sites may be selected to have specific properties or characteristics; however, unpredictable variations occur in weather patterns in both short- and long-term exposures. Furthermore, the presence of corrosive materials in the environment is often the function of activities that go on at some distance from the exposure site and, as such, are



entirely outside the control of the investigator. Consequently, it has long been a desire of investigators to develop techniques for evaluating the corrosivity of sites where exposure programs are taking place. One approach to measuring site corrosivity is to expose a set of standard panels of a known material that can be used as a control. Steel panels have been widely used for this purpose (see ASTM G 92, Practice for Characterization of Atmospheric Test Sites); however, zinc, copper, and aluminum have also been used [17]. The test material performance can be compared to the standard panel material performance and conclusions drawn from that. This is a very important approach and should be practiced as much as possible because we may never be able to measure all the variables that affect atmospheric corrosion.

The standard panel approach, however, does not provide information as to what caused corrosivity of the environment. In order to understand the factors that contribute to corrosivity, it is desirable to obtain data on the temperature, relative humidity, time of wetness, time during which precipitation occurred, and wind velocities [16]. It is also desirable to obtain samples of precipitation at various times during the exposure period and have it evaluated for acidity and the presence of ionic species. Another factor is the presence of sulfur species in the air, especially sulfur dioxide. The sulfation plate or actual volumetric sampling may be used. In addition, in marine locations it is desirable to have some estimate of the airborne salinity, either through a chloride candle or dry plate method [27]. Another variable that is very important, but seldom measured, is the temperature during the period which panels are wet. Corrosion occurs mainly during periods of wetness, so that the temperature during this period is most important in terms of determining the corrosion kinetics. Table 11 contains a list of atmospheric variables that are often monitored.

In the case of indoor corrosion, there are several parameters that can be measured to determine the corrosivity of the atmosphere. Unfortunately, there are no standards currently available that relate the corrosivity of the atmosphere to the concentrations of corrosive components, but the measurement of such components may be helpful in determining

what is causing problems with an indoor environment. For gaseous components, there are two types of measurements that can be used: active sampling and passive sampling. Active sampling requires a pump to draw a specific quantity of air into a measurement chamber. The gaseous components are measured by a specific method, e.g., IR absorption, and recorded. Passive samplers use either a diffusion cell or a direct deposition method. The diffusion cell employs a stagnant tube through which the components must diffuse and then be absorbed and measured. The deposition method eliminates the stagnant tube and relies solely on natural convection to transport the species in question to the reactive surface. The following gases have been monitored using diffusion cells: SO<sub>2</sub>, NO<sub>2</sub>, H<sub>2</sub>S, NH<sub>3</sub>, and O<sub>3</sub>. Particulates are more difficult to monitor and require different methods. Again, active sampling requires a pump to draw a specific volume of air through a filter or onto impingement plates that is then analyzed. Collection plates may also be used together with microscopic methods of analysis and evaluation. Temperature and humidity measurements are also important to measure for evaluation of the environment.

The corrosivity of indoor atmospheres must be determined by standard panel exposures. Currently ISO/TC 156 is developing standards on indoor corrosivity classification. These standards have not yet been adopted.

## ATMOSPHERIC EXPOSURE STANDARDS

ASTM Committee G01 has written a number of atmospheric exposure standards, which are listed in Table 12. ASTM G 50 provides a recommended practice for atmospheric corrosion test programs. ASTM G 33 covers visual

**TABLE 11**—Atmospheric variables for exposure program.

Variable	Measurement Frequency	Report	Typical Units
Temperature	Hourly	30 day A&R	°C
Temperature when wet	Hourly	30 day A	°C
Relative humidity	Hourly	30 day A	%
Time of wetness	Hourly	30 day T	h or %
Dewpoint temperature	Hourly	30 day A	°C
Insolation time	Hourly	30 day A	h
Insolation	Hourly	30 day A	J/m <sup>2</sup> h
Precipitation time	Hourly	30 day T	h
Precipitation	Hourly	30 day T	mm
Precipitation pH	Daily	30 day A&R	
SO <sub>2</sub> Concentration	Hourly	30 day A	ppb(vol)
SO <sub>2</sub> Deposition	30 day	30 day T	mgSO <sub>2</sub> /m <sup>2</sup> day
Chloride Deposition	30 day	30 day T	mgCl <sup>-</sup> /m <sup>2</sup> day

A = average

R = range (high and low value)

T = total

Insolation Time = time during sun exposure

Insolation = solar heating

**TABLE 12**—ASTM committee G01 atmospheric exposure standards.

Designation	Title
G 30	Practice for Making and Using U-Bend Stress—Corrosion Test Specimens
G 33	Practice for Recording Data from Atmospheric Corrosion Tests of Metallic Coated Steel Specimens
G 38	Practice for Making and Using C-Ring Stress—Corrosion Test Specimens
G 39	Practice for Preparation and Use of Bent Beam Stress—Corrosion Test Specimens
G 49	Practice for Preparation and Use of Direct Tension Stress—Corrosion Test Specimens
G 50	Practice for Conducting Atmospheric Corrosion Test on Metals
G 58	Practice for Preparation of Stress Corrosion Specimens for Weldments
G 84	Practice for Measurement of Time of Wetness on Surfaces Exposed to Wetting Condition as in Atmospheric Corrosion Testing
G 91	Practice for Monitoring Atmospheric SO <sub>2</sub> Using the Sulfation Plate Technique
G 92	Practice for Characterizing Atmospheric Test Sites
G 101	Guide for Estimating the Atmospheric Corrosion Resistance of Low Alloy Steels
G 116	Practice for Conducting Wire on Bolt Test for Atmospheric Galvanic Corrosion
G 149	Practice for Conducting the Washer Test for Atmospheric Galvanic Corrosion

**TABLE 13**—ISO standards relating to atmospheric corrosion.

Designation	Title
ISO 4540	Metallic Coating—Coatings Cathodic to the Substrate—Rating of Electroplated Test Specimen Subjected to Corrosion Tests
ISO 4542	Metallic and Other Non-organic Coatings—General Rules for Stationary Outdoor Exposure Corrosion Tests
*ISO 7441	Corrosion of Metals and Alloys—Determination of Bimetallic Corrosion in Outdoor Exposure Corrosion Tests
*ISO 8565	Corrosion of Metals and Alloys—Atmospheric Corrosion Testing—General Requirements
ISO 8994	Anodized Aluminum and Aluminum Alloys—Rating System for Evaluation of Pitting Corrosion Grid Method
*ISO 9223	Corrosion of Metals and Alloys Classification of the Corrosivity of Atmospheres
*ISO 9224	Corrosion of Metals and Alloys Guiding Values for the Corrosivity Categories of Atmospheres
*ISO 9225	Corrosion of Metals and Alloys—Aggressivity of Atmosphere-Methods of Measurement of Pollution Data
*ISO 9226	Corrosion of Metals and Alloys—Corrosivity of Atmospheres—Methods of Determination of Corrosion Rate of Standard Specimens for the Evaluation of Corrosivity
ISO 11303	Specification of Protection Methods on the Basis of Atmospheric Corrosivity Classification

\* Standards developed by ISO Technical Committee TC156 on corrosion of metals and alloys.

**TABLE 14**—NACE International Standards relating to atmospheric exposure tests.

Designation	Title
RP0172-72	Surface Preparation of Steel and Other Hard Materials by Water Blasting Prior to Coating or Recoating—Item #53008-P
RP0176-83	Corrosion Control of Steel, Fixed Offshore Platforms Associated with Petroleum Production—Item #53031-P
RP0281-86	Method for Conducting Coating (Paint) Panel Evaluation Testing in Atmospheric Exposure—Item #21026-P
RP0591-91	Coating for Concrete Surfaces in Non-immersion and Atmospheric Service—Item #21052-P
RP0692-92	Application of a Coating System to Exterior Surfaces of Steel Rail Cars—Item #21058-P
TM0170-70	Visual Standard for Surfaces of New Steel Air-blast Cleaned with Sand—Item #21201-P
TM0175-75	Visual Standard for Surfaces of New Steel Centrifugally Blast Cleaned with Steel Grit and Shot—Item #21209-P

examination of panels with metallic coatings such as galvanized or aluminized panels. There are several standards written by Committee G01 on stress corrosion specimens shown in this table. In addition, there are descriptions of galvanic specimen design, sulfation plate, time of wetness, and characterization of atmospheric test sites. ASTM Committee B08 has a standard on evaluating electroplated samples and atmospheric exposures. This standard, ASTM B 537, Practice for Rating of Electroplated Panels Subjected to Atmospheric Pressure, includes charts showing pit densities.

The International Organization for Standardization, ISO Technical Committee 156, has written six standards that

apply to atmospheric exposures, which are shown in Table 13. One standard covers galvanic corrosion specimens, one is a general procedure for atmospheric exposures, and four cover the subject of classification of atmospheres for corrosivity. ISO/TC156 is now considering the question of indoor atmospheric corrosivity classification and will be preparing standards in this area.

The National Association of Corrosion Engineers International (NACE) has several standards related to atmospheric corrosion, which are shown in Table 14. These standards apply mainly to coating systems to protect from corrosion.

The Instrument Society of America (ISA) has established a classification system for indoor corrosivity [28] that applies mainly to electronic devices.

## Acknowledgment

The author is grateful to Air Products and Chemicals, Inc. for permission to publish this paper.

## REFERENCES

- [1] Guttman, H. and Sereda, P. J., "Measurement of Atmospheric Factors Affecting the Corrosion of Metals," *Metal Corrosion in the Atmospheres*, ASTM STP 435, ASTM International, West Conshohocken, PA, 1968, pp. 326–359.
- [2] Knotková-Cermáková, D. and Barton, K., "Corrosion Aggressivity of Atmospheres (Derivation and Classification)," *Atmospheric Corrosion of Metals*, ASTM STP 767, S. W. Dean, Jr. and E. C. Rhea, Eds., ASTM International, West Conshohocken, PA, 1982, pp. 225–249.
- [3] Dean, S. W., Jr., "Planning Instrumentation and Evaluation of Atmospheric Corrosion Tests and A Review of ASTM Testing," *Atmospheric Corrosion*, W. H. Ailor, Ed., John Wiley and Sons, NY, 1982, pp. 195–216.
- [4] Dean, S. W., "Corrosion Testing of Materials with Metallic and Inorganic Coatings," *Testing of Metallic and Inorganic Coatings*, ASTM STP 947, W. B. Harding and G. A. DiBari, Eds., ASTM International, West Conshohocken, PA, 1987, pp. 177–192.
- [5] Black, H. L. and Lherbier, L. W., "A Statistical Evaluation of Atmospheric, In-Service, and Accelerated Corrosion of Stainless Steel Automotive Trim Material," *Metal Corrosion in the Atmosphere*, ASTM STP 433, ASTM International, West Conshohocken, PA, 1968, pp. 3–32.
- [6] Palmer, J. D., "Atmospheric Corrosion and the Automobile," *Atmospheric Corrosion*, W. H. Ailor, Ed., John Wiley and Sons, NY, 1982, pp. 705–710.
- [7] Dean, S. W., Jr., "Planning Instrumentation and Evaluation of Atmospheric Corrosion Tests (Part 3)," *Materials Performance*, Vol. 27, No. 12, December 1988, pp. 35–37.
- [8] Sereda, P. J., "Weather Factors Affecting Corrosion of Metals," *Corrosion in Natural Environments*, ASTM STP 558, ASTM International, West Conshohocken, PA, 1974, pp. 7–22.
- [9] Levadie, B., "Sampling and Analysis of Sulfur Dioxide with the Lead Dioxide Plate (Huey Plate)," *Journal of Testing and Evaluation*, Vol. 7, No. 2, March 1979, pp. 61–67.
- [10] Spence, J. W. and Haynie, F. H., "Derivation of a Damage Function for Galvanized Steel Structures: Corrosion Kinetics and Thermodynamic Considerations," *Corrosion Testing and Evaluation: Silver Anniversary Volume*, ASTM STP 1000, R. Baboian and S. W. Dean, Eds., ASTM International, West Conshohocken, PA, 1990, pp. 208–224.

- [11] Haynie, F. H., "Environmental Factors Affecting the Corrosion of Galvanized Steel," *The Degradation of Metals in the Atmosphere*, ASTM STP 965, S. W. Dean and T. S. Lee, Eds., ASTM International, West Conshohocken, PA, 1988, pp. 282–289.
- [12] Foran, M. R., Gibbons, E. V., and Wellington, J. R., "The Measurement of Atmospheric Sulfur Dioxide and Chlorides," *Chemistry in Canada*, Vol. 10, No. 5, May 1958, pp. 33–41.
- [13] Dean, S. W., "Corrosion Testing of Metals Under Natural Atmospheric Conditions," *Corrosion Testing and Evaluation: Silver Anniversary Volume*, ASTM STP 1000, R. Baboian and S. W. Dean, Eds., ASTM International, West Conshohocken, PA, 1990, pp. 163–176.
- [14] Abbott, W. H., "Field vs. Laboratory Experience in the Evaluation of Electronic Components and Materials," *Materials Performance*, Vol. 24, No. 8, August 1985, pp. 46–50.
- [15] Dean, S. W., Jr., "Planning Instrumentation and Evaluation of Atmospheric Corrosion Tests (Part 1)," *Materials Performance*, Vol. 27, No. 10, October 1988, pp. 56–59.
- [16] Money, K. L., "Corrosion Testing in the Atmosphere," *Metals Handbook Ninth Edition*, Vol. 13, Corrosion, ASM International, Materials Park, OH, 1987, pp. 204–206.
- [17] Dean, S. W., "ISO CORRAG Collaborative Atmospheric Exposure Program: A Preliminary Report," *Degradation of Metals in the Atmosphere*, ASTM STP 965, S. W. Dean and T. S. Lee, Eds., ASTM International, West Conshohocken, PA, 1988, pp. 385–431.
- [18] Dean, S. W. and Reiser, D. B., "Comparison of the Atmospheric Corrosion Rates of Wires and Flat Panels," *Corrosion 2000*, Paper 00455, NACE, Houston, March 2000.
- [19] Dean, S. W. and Copson, H. R., "Stress Corrosion Behavior of Maraging Nickel Steels in Natural Environments," *Corrosion*, Vol. 21, No. 3, March 1965, pp. 95–103.
- [20] Baboian, R., "Final Report on the ASTM Study: Atmospheric Galvanic Corrosion of Magnesium Coupled to Other Metals," *Atmospheric Factors Affecting the Corrosion of Engineering Metals*, ASTM STP 646, S. K. Coburn, Ed., ASTM International, West Conshohocken, PA, 1978, pp. 17–29.
- [21] Doyle, D. P. and Godard, H. P., *Proceedings*, 3rd International Congress on Metallic Corrosion, Moscow 1966, Vol. 4, 1969, pp. 429–437.
- [22] DiBari, G. A., Hawk, G., and Baker, E. A., "Corrosion Performance of Decorative Electrodeposited Nickel and Nickel Iron Alloy Coating," *Atmospheric Corrosion of Metals*, ASTM STP 767, S. W. Dean, Jr. and E. C. Rhea, Eds., ASTM International, West Conshohocken, PA, 1982, pp. 186–213.
- [23] Altorfer, K. J., "Service Evaluation of Zinc Thermal Spraying Systems," *Atmospheric Corrosion*, W. H. Ailor, Ed., John Wiley and Sons, NY, 1982, pp. 645–650.
- [24] German, G., "Behavior of Zinc-Coated Steel in Highway Environments," *Atmospheric Factors Affecting the Corrosion of Engineering Metals*, ASTM STP 646, S. K. Coburn, Ed., ASTM International, West Conshohocken, PA, 1978, pp. 74–82.
- [25] Kucera, V. H., Haagenrud, S., Atteraas, L., and Gullman, J., "Corrosion of Steel and Zinc in Scandinavia with Respect to Classification of the Corrosivity of Atmospheres," *Degradation of Metals in the Atmosphere*, ASTM STP 965, S. W. Dean and T. S. Lee, Eds., ASTM International, West Conshohocken, PA, 1988, pp. 264–281.
- [26] Seo, M., "Application of Quartz Crystal Microbalance to Corrosion Research," *Corrosion Engineering*, Vol. 48, 1999, pp. 809–828.
- [27] Phul, B. S. and Kirk, W. W., "Monitoring the Corrosivities of Atmospheric Exposure Sites," *Journal of Protective Coatings and Linings*, Vol. 8, No. 10, October 1991, pp. 152–162.
- [28] Instrument Society of America Standard ISA-S 71-04-1985: Environmental Conditions for Process Measurement and Control Systems: Airborne Contaminants, Instrument Society of America, Durham, NC, 1985.

# Seawater

James F. Jenkins<sup>1</sup>

## BASICS

AS IN OTHER NATURAL environments, corrosion testing in seawater is dependent upon the actual environmental conditions experienced by the exposed materials during the entire duration of exposure. These environmental conditions can vary widely in any specific location. Normal seasonal variations as well as variations from year to year and temporary natural or manmade conditions can dramatically affect the conditions of exposure that control overall corrosion behavior of materials. Seasonal variations include changes in temperature, dissolved oxygen content, and the type and extent of biological fouling. Significant year-to-year variations such as those caused by the aperiodic general ocean surface water warming in the eastern Pacific Ocean, called El Niño, also affect the seawater environment over a wide area. Temporary natural conditions may include natural proliferation of microorganisms such as the "red tide" blooms of algae that can significantly reduce dissolved oxygen availability. Temporary manmade conditions such as spills of oil, chemicals, and sewage can also have a dramatic effect on the local environment that can affect corrosion.

A further complication is that these variations may not affect the deterioration of materials in a simple manner. In many cases, metal corrosion is dependent upon surface films that form upon exposure to seawater. Variations of initial exposure conditions can affect the protective nature of these films, which can affect the further corrosion behavior of the material. Thus, a sample first exposed under conditions conducive to the formation of a protective film may perform very differently than the same material exposed for an identical period, but was first exposed to conditions that resulted in the formation of a film that was less protective. In other cases, short-term variations in environment may be sufficient to initiate attack that would not occur during typical conditions and that, once initiated, can continue over extended exposures.

The interaction between biological activity and material performance is very significant in seawater. Macrofouling such as barnacles and mussels can be either protective or can result in accelerated corrosion depending on the material exposed and the extent of the accumulation of fouling. Anaerobic conditions are frequently found at the base of extensive fouling accumulation and this can dramatically affect corrosion of many materials. Seasonal variations and

temporary upsets can also result in the death and sloughing off of specific types of fouling organisms, which can cause temporary upsets of conditions at the surface of the material.

Because of the highly variable nature of the seawater environment, the results of corrosion testing in seawater are subject to significant variability. Reference 1 describes several test programs that demonstrate this variability. Considerable variability in the corrosion behavior of steel, aluminum and copper-nickel was also demonstrated in a worldwide seawater corrosivity test program described in Ref 3. To properly interpret the results of such tests, it is important to include control samples in the testing program. These control samples should include materials whose corrosion performance in the environment is well established. One control should be a material such as mild steel, which corrodes significantly in the environment so that corrosion rates for the control can be established. Another control should be a material that has marginal resistance to the environment so that upset conditions that may cause unusual initiation of corrosion can be detected. Additional control materials with compositions and characteristics similar to those being tested should also be included. For example, if performance of a newly developed stainless steel is being evaluated, samples of previously tested stainless steels should be included as controls.

## SPECIMEN CONFIGURATION

There are no specific standards for the configuration of samples for seawater testing. A few general guidelines should be considered when determining the appropriate specimen configuration and size. As metallurgical condition is an important variable in the performance of many metals, specimens with metallurgical condition similar to that of the material of interest should be included in the test. For example, if plate material is of primary interest, plate material should be selected for testing. If the metallurgical condition of interest is not defined, or several conditions are of interest, specimens of the material with different metallurgical conditions should be exposed.

ASTM G 52 (see section on standards at the end of this chapter) recommends a nominal sample size of 100 by 300 mm. In general, larger specimens are preferred over smaller specimens. First, larger specimens will expose a greater amount of surface area which will increase the probability of initiation of localized attack such as pitting.

<sup>1</sup>329 Drake Street, Cambria, CA 93428.

Second, where measurement of corrosion rate by mass loss is important, mass losses for larger specimens will be greater, thus requiring lower precision in weighing for equivalent precision in mass loss per unit area. Third, for many sheet and plate materials, exposed edges may corrode differently than exposed faces. Corrosion potential differences resulting from these differences may accelerate the corrosion of either the edges or faces. This effect is minimized in larger samples because the ratio of face area to edge area is minimized. Increasing the sample size beyond approximately 300 by 300 mm, however, has little further effect in minimizing the influence of the edges on face behavior of most materials. Unlike laboratory tests where the volume of solution must be adjusted for sample size, this is not a factor in natural seawater exposures.

### Duration of Exposure

Because long-term durability is required for most marine applications, corrosion test exposures for periods of less than six months usually are not sufficient for engineering purposes. Exposures of 0.5, 1, 2, 5, 10, and 20 years are recommended in ASTM G 52. For control specimens, information on environmental variability can be obtained by exposing specimens for periods of one-fourth of a year where the specimens are initially exposed one-fourth of a year, a half-year, and three-quarters of a year after the start of the test. Year-to-year variability can be evaluated by exposing a series of specimens that are initially exposed at one-year intervals after the start of the test and removed after one year of exposure.

Testing for shorter periods may be appropriate when the test sample configuration intentionally provides more severe conditions than anticipated in service. Crevice corrosion tests using severe artificial crevice geometries may only require 30–90 days of exposure to establish relative crevice corrosion resistance.

### Number of Test Specimens

The number of replicate test specimens depends upon the desired reliability of the results of the test. ASTM G 16 gives guidance for establishing the required number of replicate specimens. In general, as recommended in ASTM G 52, triplicate specimens for each exposure period are sufficient for many seawater corrosion tests.

## TESTS FOR SPECIFIC TYPES OF CORROSION

If susceptibility to specific types of corrosion is of interest, specialized sample configurations can be used. If the corrosion performance of the material in seawater is completely unknown, at a minimum it should be evaluated for general corrosion and pitting, galvanic corrosion, crevice corrosion, and stress corrosion.

### General Corrosion and Pitting

Evaluation of general corrosion and pitting does not require any special specimen configuration. Mass loss and pit depths

can be measured on specimens of nearly any configuration. Specimen size, however, may dictate the type of instrumentation that is utilized in these measurements.

### Galvanic Corrosion

Galvanic corrosion tendencies can be evaluated by developing a galvanic series for the materials of interest as described in ASTM G 82. Galvanic corrosion rates can be established by exposure of galvanic couples as described in ASTM G 71.

### Crevice Corrosion

For many alloys such as stainless steels that rely on passivity for corrosion resistance, crevice corrosion can be a limiting factor in their seawater corrosion resistance. For a specific alloy, resistance to crevice corrosion in seawater is predominantly dependent upon the tightness and depth of the crevice formed and on the ratio of exposed surface inside and outside the crevice. Many crevice corrosion tests have been developed that attempt to control these three primary factors in crevice corrosion. ASTM G 78 describes a variety of crevice-forming assemblies and other test considerations. Both flat and cylindrical specimens are described in the latest version of ASTM G 78. It should, however, be remembered that even simple immersion tests include crevice testing because natural crevices form where the specimens are held in the test racks and may also be present at such features as sheared edges and drilled holes as well as under fouling organisms such as barnacles. Therefore, when specimens specifically configured for crevice corrosion evaluation are not included in a test program, special attention should be given to inspection of the specimens at these inherent crevice sites for indications of susceptibility to crevice attack. When artificial crevice formers are used, other crevices can be avoided by using the crevice former fastener to hold the specimen.

### Stress Corrosion

While many laboratory tests for resistance of metals to stress corrosion cracking have been developed, only a few tests are amenable to actual in-situ testing in seawater. These primarily consist of the exposure of statically stressed type test specimens such as described in ASTM G 30, G 38, G 39, and ISO 7539-2, ISO 7539-3, and ISO 7539-5. In addition, welded specimens such as described in ASTM G 58 are excellent for evaluation of the stress corrosion resistance of weldments in simple immersion tests. Evaluation of corrosion fatigue is usually limited to laboratory testing.

## SPECIMEN PREPARATION

Because multiple samples will normally be exposed in a seawater test program, specimens should be labeled in a manner whereby the sample can be easily identified during sample preparation and evaluation. ASTM G 52 recommends several methods of such specimen labeling including the use of coded drilled holes, edge notches, corrosion-resistant tags, and stamped numerals. In some cases, the use of stamped

numerals may introduce significant local residual stress in the sample which may cause cracking in susceptible materials. In addition, location of the specimens on the exposure racks should be recorded as a backup identification method.

To develop quantitative and reproducible corrosion performance data in any corrosion test program it is important to properly prepare the specimens for exposure. ASTM G 1, Practice for Preparing, Cleaning, and Evaluating Corrosion Test Specimens, gives guidelines for specimen preparation for exposure. This standard includes guidelines for cleaning, measuring, and weighing the samples prior to exposure. In many marine corrosion studies, multiple samples will be placed on racks before exposure and a considerable period of time may elapse between specimen cleaning and exposure. In these cases, it may be necessary to store the specimens and racks in a low-humidity environment prior to exposure. In addition, care must be taken in handling the specimens to prevent contamination of the specimens with oils, salts, or other contaminants on people's hands.

## SPECIMEN EXPOSURE AND RETRIEVAL

An obvious but not trivial consideration in seawater corrosion testing is that the samples must not become lost prior to the end of the exposure period. The test racks and suspension systems must be resistant to corrosion failures during the exposure period. In-surface exposures, storms, mechanical damage by floating debris, vandalism, and many others may result in specimen loss. Frequent inspection of the exposure site is necessary to identify potential problems before specimen loss occurs. In deep ocean exposures, storm damage is less of a problem, but methods for locating and handling the racks requires considerable planning and ocean engineering experience in order to expose and retrieve the specimens without loss or damage.

### Static Testing in Surface Environments

Several test rack designs are described in Ref 3. For surface exposures where fouling accumulations are likely to be extensive, test racks that boldly expose the specimen surfaces such as shown in Fig. 3-3 and 3-6 of Ref 3 are preferred over basket-type racks such as shown in Fig. 3-7, where the spaces between the faces of the specimens can become completely clogged with fouling organisms and potentially affect the test results. As described in ASTM G 52, test racks should be fabricated from materials that are reasonably corrosion resistant. Wooden racks are usually limited to a one-year life. Aluminum alloy 5086 test racks may be suitable for exposures of up to five years. Welded nickel-copper alloy 400 racks have essentially indefinite life in surface seawater, but are expensive and heavy. Nickel-copper alloy 400 is subject to crevice attack in seawater and this may be significant on fasteners. Reinforced plastic structural shapes, fastened with corrosion-resistant fasteners such as titanium, are relatively inexpensive, lightweight, and durable for long exposure periods.

In designing test racks and exposure facilities, consideration must be given to handling of the test racks. In many cases, material handling equipment will not be provided and the racks will be handled by hand. The total weight of the rack plus

specimens should be limited to about 50 kg for manual handling by two persons. Allowance should also be made for the fouling that will accumulate on the test specimens and racks.

To identify problems such as frayed suspension ropes and rack entanglement, inspection of the exposure site at weekly intervals as a minimum with additional inspections during stormy periods is recommended. In most cases, specimens that become detached can be replaced in the test racks without serious effect on the test results if the samples are retrieved and replaced in the racks within a few days.

### Velocity Testing

Testing of materials for resistance to seawater under velocity conditions such as testing for resistance to erosion-corrosion, cavitation, and direct impingement can be performed in the ocean but are more commonly performed in water pumped into tanks and troughs. Velocity can be achieved by moving the specimen through the water, but is more commonly accomplished by moving the seawater past fixed specimens. Flow troughs can be designed to give flow velocities up to 2 m/s. Tests at higher velocities are essentially laboratory tests performed in continuously or intermittently refreshed seawater. There are several testing procedures that have been developed to perform these tests under standardized conditions. ASTM G 32 and G 73 are standard methods for vibratory cavitation erosion and liquid impingement erosion testing, respectively, and can be performed using refreshed seawater. Jet impingement testing usually requires filtration of the incoming seawater to avoid clogging of the jet orifices. Tests using spinning disk samples are described in Ref 3. Other tests at very high velocities have been developed as described in Ref 5. For testing at extreme velocities, such as those encountered by hydrofoils, special test apparatus using spinning circular water troughs have been developed.

Other nonstandard velocity tests can be performed using subscale or even full-scale systems. An example of such tests is the evaluation of condenser tubing using pumped seawater. While these tests provide results useful for the development of specific systems, the results may not be readily applicable to systems of different design or using different materials. Where water is pumped, such as in testing of condenser tubes and pipes, particular attention must be paid to the effects of turbulence and surface shear stress. The hydrodynamics at the test sample surface must be similar to the hydrodynamics anticipated in service.

### Deep Ocean Testing

Deep ocean testing is performed to determine the effect of depth-related environmental variables on material performance. To determine the relative effects of variation in environment, tests sites with significant variation in environment should be selected. For example, where oxygen content is the major variable of interest, sites with high, minimum, and intermediate oxygen content should be used. To compare deep ocean test results with results from surface seawater, testing of replicate specimens in the deep ocean and in surface seawater is often performed.

The emplacement and retrieval of deep ocean test samples is expensive and involves the coordinated efforts of

various ocean engineering disciplines such as navigation, ship handling, rigging, oceanography, and marine geotechnology. As in all ocean operations, considerable planning is required for successful emplacement and retrieval of deep ocean corrosion test samples. Sample configuration and preparation for deep ocean testing is similar to that for surface seawater exposures. For deep ocean exposures it is common to emplace and retrieve large assemblies of multiple racks containing individual samples. The test samples should be protected from atmospheric and salt spray corrosion during transit to the test site. This can be accomplished by transporting the racks below deck for small racks or by covering larger racks with plastic sheeting.

The test rack assembly design is dependent on the deployment and retrieval method selected. One test rack assembly design and the method for emplacement and retrieval of the test rack is described in Ref 6. In deep ocean testing, the accumulation of fouling organisms is much less than in near surface waters and basket-type racks can be used as the spaces between the sample faces will not become clogged with fouling organisms. Contamination of samples by corrosion products from other test samples can be minimized by grouping samples of similar types in separate racks. Particular attention should be given to vertical location of test samples. For example, aluminum samples should be located above copper alloys as copper corrosion products falling onto the aluminum alloys can cause contamination of the aluminum alloys, whereas the aluminum corrosion products have little effect on the copper alloys. Painted carbon steel, 5083 and 5086 aluminum alloys, and reinforced plastic test racks and rack assemblies have all been successfully used for deep ocean testing.

To provide different removal times, replicate rack assemblies can be emplaced and retrieved separately. As an alternative to removal of replicate racks, it is possible to design a rack assembly such that individual racks or even individual samples can be removed by remote operated vehicles or manned submersibles. Although not proven, autonomous systems that release racks or individual specimens at intervals for surface retrieval are within the capability of modern ocean engineering technology. Once these racks reached the surface they could report their location through satellite systems for location and recovery by a surface vessel.

## SPECIMEN EVALUATION

The evaluation of the specimens in any corrosion test must be appropriate for the type of corrosion that actually occurs on the samples. In many cases, the actual sample evaluation requirements will not be known until the samples are retrieved and examined visually. This can complicate the administration of the testing program as the cost of specimen evaluation and the time to perform the evaluation cannot be planned in advance. For example, if general corrosion is the only form of corrosion experienced, the cost of sample evaluation by mass loss measurement is relatively inexpensive, whereas a form of corrosion such as stress corrosion cracking may require a high cost evaluation.

Upon removal from exposure, the specimens should be examined visually as soon as possible after retrieval. If more than a few hours will elapse between the removal of the specimens

and this initial examination, the samples should be rinsed with fresh water after removal. For deep ocean tests, this will usually be performed at sea and sufficient fresh water for this purpose must be provided. Whenever possible, the samples should be photographed to record their appearance upon retrieval.

After initial visual examination, the specimens should be cleaned. ASTM G 52 gives guidelines for evaluation of specimens after exposure to surface seawater. In surface seawater exposures, the accumulation of fouling organisms may be removed using wooden or plastic scrapers and bristle brushes prior to chemical cleaning. In deep ocean and velocity tests, the accumulation of fouling organisms is usually very limited and scraping is usually not required. It may be appropriate to visually re-examine the samples and rephotograph them at this stage of the evaluation.

The specimens should be cleaned in accordance with the methods recommended in ASTM G 1 or ISO 8407. The samples should then be remeasured to determine geometric changes and reweighed to determine mass loss. Nonuniform attack must be evaluated using methods appropriate for the type of attack experienced.

Pitting corrosion should be evaluated using the methods described in ASTM G 46. Pitting evaluation of aluminum alloys can also be performed using the practices recommended in ISO 8993 and 8994. As crevice corrosion often results in pitting attack, crevice attack is frequently evaluated using techniques outlined in ASTM G 46. Due to the effect of material and surface condition on pitting, statistical analysis methods described in ASTM G 16 should be applied to estimating the confidence interval of the pitting. In addition, the statistical analysis methods described in ASTM G 16 can be applied to crevice corrosion data where not only the material and surface condition, but also the inevitable variability in crevice tightness may influence susceptibility.

Other forms of attack such as exfoliation of aluminum alloys and dezincification of brasses require specialized evaluation and interpretation. Methods and standards for evaluation of exfoliation of aluminum alloys which are given in ASTM G 34 and G 66 are for materials exposed to artificial environments but may be used for evaluation of materials exposed to natural environments such as seawater. Many forms of attack can be best evaluated by microscopic or mechanical tests. ASTM E 3 gives standard methods for preparation of metallographic specimens, but does not provide specific guidelines for use of metallographic analysis in evaluation of corrosion. There are many standards for mechanical testing, such as ASTM A 370 for mechanical testing of steel products, that can be used in evaluating corrosion damage.

## STANDARDS

Standards applicable to field testing in natural seawater are given below:

### ASTM

- E 3 Methods of Preparation of Metallographic Specimens
- G 1 Practice for Preparing, Cleaning, and Evaluating Corrosion Test Specimens

- G 15 Terminology Relating to Corrosion and Corrosion Testing
- G 16 Guide for Applying Statistics to Analysis of Corrosion Data
- G 30 Practice for Making and Using U-Bend Stress-Corrosion Test Specimens
- G 32 Test Method for Cavitation Erosion Using of Vibratory Apparatus
- G 34 Test Method for Exfoliation Corrosion Susceptibility in 2XXX and 7XXX Series Aluminum Alloys (EXCO Test)
- G 38 Practices for Making and Using C-Ring Stress-Corrosion Test Specimens
- G 39 Practice for Preparation and Use of Bent-Beam Stress-Corrosion Test Specimens
- G 46 Practice for Examination and Evaluation of Pitting Corrosion
- G 52 Practice for Exposing and Evaluating Metals and Alloys in Surface Seawater
- G 58 Practice for the Preparation of Stress-Corrosion Test Specimens for Weldments
- G 66 Method for Visual Assessment of Exfoliation Corrosion Susceptibility of 5XXX Series Aluminum Alloys (Asset Test)
- G 71 Guide for Conducting and Evaluating Galvanic Corrosion Tests in Electrolytes
- G 73 Practice for Liquid Impingement Erosion Testing
- G 78 Guide for Crevice Corrosion Testing of Iron-Base and Nickel-Base Stainless Alloys in Seawater and Other Chloride-Containing Aqueous Environments
- G 82 Guide for Development of a Galvanic Series for Predicting Galvanic Corrosion Performance

### International Standards Organization (ISO)

- 7539-1 Corrosion of Metals and Alloys-Stress Corrosion Testing-Part 1: General Guidance on Testing Procedures

- 7539-2 Corrosion of Metals and Alloys-Stress Corrosion Testing-Part 1: Preparation and Use of Bent-Beam Specimens
- 7539-3 Corrosion of Metals and Alloys-Stress Corrosion Testing-Part 3: Preparation and Use of U-Bend Specimens
- 7539-5 Corrosion of Metals and Alloys-Stress Corrosion Testing-Part 5: Preparation and Use of C-Ring Specimens
- 8407 Metals and Alloys-Procedures for Removal of Corrosion Products from Corrosion Test Specimens
- 8993 Anodized Aluminum and Aluminum Alloys-Rating System for the Evaluation of Pitting Corrosion-Chart Method
- 8994 Anodized Aluminum and Aluminum Alloys-Rating System for the Evaluation of Pitting Corrosion-Grid Method

### REFERENCES

- [1] *Corrosion in Natural Waters*, ASTM STP 1086, C. H. Baloun, Ed., ASTM International, West Conshohocken, PA, 1990.
- [2] *Corrosion in Natural Waters—2nd Volume*, ASTM STP 1300, R. N. Kain & W. T. Young, Eds., ASTM International, West Conshohocken, PA, 1997.
- [3] La Que, F. L., *Marine Corrosion Causes and Prevention*, John Wiley & Sons, New York, 1975, pp. 45–52.
- [4] La Que, F. L., *Marine Corrosion Causes and Prevention*, John Wiley & Sons, New York, 1975, pp. 56–57.
- [5] La Que, F. L., *Marine Corrosion Causes and Prevention*, John Wiley & Sons, New York, 1975, pp. 62–63.
- [6] Reinhart, F. M., Technical Report R-834: Naval Civil Engineering Laboratory, Corrosion of Metals and Alloys in the Deep Ocean, February 1976.



# Freshwater

Walter T. Young<sup>1</sup> and Philippa Fairer<sup>1</sup>

THIS CHAPTER PROVIDES an overview of standard corrosion testing procedures for freshwater systems. Additional information is provided in Chapter 31—Freshwater. Freshwater can be defined simply as water that is not salty; brackish water as defined by the dictionary is water having a somewhat salty taste. A more quantitative definition of brackish water is water with a salinity between 0.5 and 17 parts per thousand [1]. Then freshwater can be further defined as water with a salinity of less than 0.5 parts per thousand. For the purposes of this chapter, freshwater systems include potable water, heating/cooling, steam, condensate, rivers, streams, lakes, and wastewater.

Corrosion studies are beneficial for both ensuring a safe operating system and containing costs associated with maintenance, downtime, and replacement parts. Testing aids in selecting a material, designing the physical and operating parameters of a system, selecting a water treatment program to mitigate corrosion, and monitoring the effectiveness of water treatment. These studies are especially useful when a system is in the design stage; however, existing systems also benefit from corrosion testing.

## FACTORS AFFECTING CORROSION

The environment must be considered when designing any testing program. Environmental factors that affect the corrosion rates of materials in freshwater systems can be divided into two categories. The first category, water chemistry, includes: pH, electrical resistivity, scaling ability, concentration of corrosives, suspended matter, and water treatment additives. Factors such as temperature, pressure, metallurgy, redox potential, biological effects, velocity, and galvanic effects comprise the second category. These factors must be identified for freshwater systems so that corrosive conditions may be simulated during testing. A full description of these factors is beyond the scope of this paper. The reader is referred to texts on corrosion [2–7].

### Water Chemistry

Factors that influence water corrosivity include pH, electrical resistivity, scaling ability, concentration of corrosive

species, and water treatment additives. Corrosive species include chlorides, sulfates, suspended matter, and dissolved gases.

In general, if the pH only is altered between pH 4 and 10, the corrosion rate of steel, copper, or stainless steel is not altered significantly. However, most common materials of construction for freshwater systems are adversely affected by waters with a pH less than 4. Zinc and aluminum will freely corrode in waters with a pH lower than 6 and higher than 9.

The electrical resistivity of water is a function of the concentration of electrically conductive ions it contains. Low resistivity waters are more corrosive generally because of the availability of ionic species to transport charge between anodic and cathodic sites. However, the magnitude of the resistivity is not the only determining factor for a water's corrosivity; waters with high resistivity may be corrosive due to the presence of corrosion-causing bacteria.

Some flowing waters have the ability to form protective scales (primarily calcium carbonates) on the surface of metals. This tendency is a function of the pH, temperature, alkalinity, and amount of total dissolved solids. Excessive amounts (above 100-ppm total) of ions such as chlorides or sulfates may inhibit the formation of protective scales. The Langelier and Ryznar Indices quantify the tendency of water to form a scale [1,8].

Chlorides and sulfates are common ions known to be aggressive towards metals. In general, environments with excessive amounts of chlorides or sulfates are considered to be aggressive towards most common materials of construction for freshwater systems.

The concentrations of dissolved gases in a freshwater system should also be determined to simulate corrosive conditions in a test. Of concern are oxygen, carbon dioxide, hydrogen sulfide, chlorine, and ammonia. Freshwater systems with at least 2 ppm of dissolved oxygen are considered to be corrosive. Oxygen is a necessary component for most corrosion reactions. However, oxygen is necessary for some metals, such as stainless steels and aluminum, to form a protective oxide film. This oxide is responsible for the corrosion resistance of these metals to many environments. Carbon dioxide and hydrogen sulfide in sufficient quantities may cause the pH of a freshwater system to decrease. Hydrogen sulfide is aggressive to copper, ferrous, and galvanized steel [9,10]. Chlorine and water form hypochlorous acid (HOCl) and the hypochlorite ion (OCl<sup>-</sup>). These are oxidizing agents and reduce pH and alkalinity, which can

<sup>1</sup>Principal Engineer and Former Engineer, respectively, Corropro Companies, Inc., 610 Brandywine Parkway, West Chester, PA 19380.

increase corrosion [2,11]. Ammonia causes corrosion of copper and copper alloys [4,11].

### Other

The second category of factors that affect corrosion includes: temperature, pressure, metallurgy, redox potential, biological effects, velocity, and galvanic effects [4,5]. In general, corrosion rates increase with increasing temperature or pressure. Both temperature and pressure affect reaction rates and gas solubility. Temperature will also affect the formation of protective scales.

Higher flow rates may have a beneficial or an adverse effect in freshwater systems. In many cases, the corrosion rate will increase with increased flow rates. This is mostly due to the removal of oxides or protective films that may form on the metal surface and the increased availability of oxygen to the surface. Erosion corrosion may occur on some alloys if critical velocities are exceeded. Critical velocities may be lowered by the presence of entrained solids or gases, which have the tendency to scour metal surfaces. One benefit of a higher velocity is the cleaning action, which makes it more difficult for biological organisms to attach to the walls of a system and form colonies. In addition, stainless steels benefit from higher flow rates because of the tendency to clean debris from surfaces and mitigate crevice corrosion and the increased oxygen availability to maintain the passive film.

The metallurgy of a system may have an impact on the type or magnitude of corrosion. In particular, the presence of inclusions or voids may lead to premature corrosion induced failures. In addition, grain boundaries that are formed during the manufacturing process may be different in composition from the rest of the material. This difference in composition may cause a form of galvanic corrosion commonly referred to as intergranular corrosion. Elements in an alloy may selectively corrode under certain conditions. This process, dealloying, is common in brass alloys containing more than 15 % zinc in certain waters. In addition, cast irons may preferentially corrode and an embrittled graphitic matrix will remain. The mechanical properties of the structure or piping will change, although the dimensions of the cast iron will be the same. Stainless steels and various copper alloys when subjected to (a minimum of 10 % yield strength) tensile stress, may fail prematurely due to stress corrosion cracking in water. Stainless steel may fail depending on the chlorine content. Avoiding manganese bronzes, leaded red brass and austenitic stainless steels that are not solution heat-treated may eliminate these problems.

Several types of bacteria are known to be corrosive to metals. Acid producing, sulfate reducing, thiobacillus, slime forming, and gallowella are among the most common forms of these bacteria. Acid producing bacteria (APB) may produce acids by their metabolic process. These acids will attack the base metal in very localized areas, usually beneath their colonies. Other organisms, not directly involved with redox reactions, may benefit from the corrosion process. Although some forms of bacteria thrive in deaerated systems, they may also be found in aerated systems underneath deposits of corrosion products or colonies of aerobic bacteria. For more information regarding

microbiologically influenced corrosion, the reader is referred to Refs 12 and 13.

Galvanic corrosion occurs when two dissimilar metals in the same environment are electrically connected. This type of corrosion may also exist in localized areas on the same metal. For example, a galvanic corrosion cell is formed if an area of piping is at a higher temperature than adjacent piping. In this case, the metal in the hotter zone is more active and will corrode. As another example, galvanic corrosion may occur if a new section of piping is welded into a system that contains older piping containing deposits. The new section (with its clean surface) will be more active than the older section of piping. Crevice corrosion occurs due to the formation of a differential oxygen cell that leads to galvanic corrosion. The crevice area is at a more active potential than the surrounding metal that has better access to oxygen. This form of corrosion is typically expected with materials (such as stainless steels or aluminum) that depend on a naturally occurring oxide film for their corrosion protection. However, crevice corrosion may also occur on steel and copper.

### Corrosion Considerations

The system's layout, operating conditions, maintenance procedures, and materials of construction should be defined so that corrosion tests can be designed to simulate conditions that exist or will exist in the system. For piping systems, the presence of elbows, tees, valves, placement of pumps, and presence of insulating joints should be known. For cooling water systems, the degree of cycling or concentrating before blowdown should be known.

## BASIC CORROSION TESTING TECHNIQUES

### Methods of Exposure

Corrosion testing may be conducted in the laboratory, pilot plant, or field. Systems that are either in the design phase or operating, benefit from laboratory and pilot plant testing. In-situ testing is useful for pilot plant testing and for providing information for systems that are currently operating [7].

Laboratory tests should simulate the water chemistry and operating conditions of the freshwater system. A sample of water from the system may be used if it is available. Immersion testing and electrochemical testing are commonly used for laboratory tests. Laboratory tests are often used to simulate a process in order to confirm a failure mode.

In-situ testing is commonly conducted in pilot plants. This testing is useful in evaluating or monitoring a water treatment system or the effects of varying operating parameters, such as flow rate and temperature. In addition, the performance of different alloys in a system may be studied by in-situ testing. In-situ testing provides information on uniform corrosion rate, types of corrosion, and pitting tendencies. In the case of utilities or others testing water treatment procedures to comply with the maximum permissible lead-copper concentrations in potable water, pilot testing is performed using corrosion specimens arranged in

loops with the various metals used in the system included in the loop. Copper/lead concentrations in the recirculating water are tested under various treatment protocols [14].

In-situ testing is also performed in the field to determine the effectiveness of a water treatment system, the performance of difference alloys, and the effects of varying operating parameters such as flow rate and temperature. Uniform corrosion rates, types of corrosion, and pitting tendencies are identified with in-situ testing.

## Design

The expected forms of corrosion can be anticipated once the water chemistry, operating conditions, materials of construction, and system layout are defined. A corrosion test matrix can be designed by determining the expected forms of corrosion. Some of the common forms of corrosion found in freshwater systems are described in the chapter on Freshwater Testing in Section V of this manual. A list of test methods is presented in this chapter. The following section describes the applicability and significance of these standardized tests.

## Uniform Corrosion

Uniform corrosion rates may be determined by weight loss or electrochemical methods. Both methods average a specimen's corrosion rate over its surface area. Corrosion rates calculated from weight loss data also average the loss over the exposure period. Electrochemical methods may yield instantaneous or time averaged corrosion rates. Weight loss testing is performed by immersing a coupon in a test solution either in the laboratory or in-situ.

The following standardized test methods are relevant for determining a uniform corrosion rate of a material in a specific test environment:

*ASTM G 31, Practice for Laboratory Immersion Corrosion Testing of Metals*—This method describes typical test vessels, metal specimens (coupons), process controls, aeration techniques, coupon placement and supports, exposure times, and corrosion rate calculations.

*ASTM G 1, Practice for Preparing, Cleaning, and Evaluating Corrosion Test Specimens*—Methods for preparing, cleaning, and evaluating corrosion test specimens are discussed in this standard. Coupon preparation procedures include surface finish, specimen identification, degreasing, weighing, and dimensional measurement. After testing, several cleaning procedures are recommended that will remove common corrosion products for each type of alloy without causing significant additional corrosion to the specimen. The formula for calculating corrosion rates by weight loss testing is also presented in this standard.

*ASTM G 3, Practice for Conventions Applicable to Electrochemical Measurements in Corrosion Testing*—Conventions used for electrochemical corrosion testing are presented in this standard. Sign conventions for electrode potential, electrode potential temperature coefficients, and current and current density are discussed.

*ASTM D 2688, Test Method for Corrosivity of Water in the Absence of Heat Transfer (Weight Loss Methods)*—This standard contains two methods for performing corrosion rate

testing. The first method (Method A) uses flat, rectangular-shaped metal coupons that are mounted on pipe plugs and exposed to water flowing in metal piping such as in municipal, building, or industrial water systems. The corrosive and scaling tendencies of cooling waters can be evaluated by subjecting the coupons to the water in a bypass piping arrangement. Coupons are evaluated by measuring weight loss or gain (ASTM G 1), determining the characteristics of foreign matter on the coupon, measuring the depth and distribution of pits, and examining the coupon for other forms of localized corrosion. The second method (Method B) determines the weight loss or gain of metal pipe inserts that are installed in a plastic bypass assembly tailored to provide the same surface and flow conditions as in the normal metal piping system. Dimensions are selected so that water flow (distorted or no distortion) is the same as in the metal piping system. In both methods, meaningful data might require months or years to obtain depending on the corrosiveness of the water. Less corrosive waters require more exposure time. It should also be noted that several coupons might be needed in order to evaluate pitting since pits might not develop on a small coupon.

*ASTM G 4, Method for Conducting Corrosion Coupon Tests in Plant Equipment*—This standard outlines the procedures for performing immersion testing in an operating system. Typical mounting apparatus are described and illustrated. This standard discusses test specimen size, shape, preparation before testing, identification procedures, installation, exposure time, retrieval, cleaning, weighing, and examination.

*ASTM G 59, Practice for Conducting Potentiodynamic Polarization Resistance Measurements*—The technique of polarization resistance testing is described. This standard conducts electrochemical testing in 1.0 N H<sub>2</sub>SO<sub>4</sub>. The apparatus, specimen preparation, and test environment are described. In addition, the equipment, electrochemical test procedure, and standard reference plots are presented.

*ASTM G 96, Practice for On-Line Monitoring of Corrosion in Plant Equipment (Electrical and Electrochemical Methods)*—This standard outlines procedures for online corrosion monitoring in operating systems. The test methods described in this standard are used to determine the cumulative metal loss (electrical resistance method) or instantaneous corrosion rates (electrochemical method). Reference 15 provides a summary of electrical resistance and polarization resistance theory.

*ASTM G 102, Practice for Calculation of Corrosion Rates and Related Information from Electrochemical Measurements*—Corrosion rate equations and sample calculations are included. In this standard, corrosion rates are calculated from galvanic cell currents, polarization corrosion data (including Tafel extrapolations), and polarization resistance data.

*NACE TM0171, Autoclave Corrosion Testing of Metals in High Temperature Water*—A material's resistance to systems operating at high temperatures and high pressures may be evaluated by this method. In general, tests performed by this standard are conducted between 212°F and 680°F (100°C and 360°C). Weight loss and metallographic examinations are performed after test specimens are exposed in the test solution at the high temperature and pressure for a selected period of time. This test method contains

a description of the test apparatus, test specimens, test solution, test duration, and methods of specimens evaluation and reporting results.

*NACE TM0274, Dynamic Corrosion Testing of Metals in High Temperature Water*—This standard presents a method for evaluating a material's behavior with respect to corrosion in high temperature, high pressure, recirculating aqueous environments. Since this method is conducted in the pilot plant, it may be used to determine the effects of water velocity unlike NACE TM0171. This method is used to determine the uniform corrosion rate and is not designed to evaluate localized corrosion. In general, test specimens are placed in a test loop and exposed to the environment at select operating conditions. After exposure, the specimens are evaluated by visual, weight loss, and metallographic inspection. This method suggests test apparatus, test specimens, operating conditions, test duration, methods of evaluation, and reporting results.

*NACE TM0169, Laboratory Corrosion Testing of Metals for the Process Industries*—A method for laboratory immersion testing is presented. This method involves immersing test specimens in an environment and performing weight loss analysis after exposure. Specimen preparation, test equipment, test conditions and solution, methods of supporting specimens, test duration, cleaning methods, and evaluation of results are covered in this standard.

*NACE RP-0775-87, Preparation and Installation of Corrosion Coupons and Interpretation of Test Data in Oilfield Operations*—This practice is typically used for determining corrosion rates of materials in oil field operations; however, NACE RP0775 may be adapted for fresh water systems. This standard describes the preparation, handling, cleaning and weighing of corrosion coupons that will be installed in the environment of interest. In addition, methods for installation and calculating corrosion and pitting rate are presented in this guideline.

## Pitting and Crevice Corrosion

Pitting and crevice corrosion tendencies of a material in a select environment may be determined by immersion testing or by electrochemical techniques. Immersion testing generally involves visual examination and dimensional analysis after exposure of a test specimen to a select environment. Electrochemical methods usually involve exposure of a test specimen to a select environment and graphical interpretation of data.

The following standardized test methods describe relevant test procedures or practices for evaluating the pitting and crevice corrosion tendency of a material in a select environment:

*ASTM G 4, Method for Conducting Corrosion Coupon Tests in Plant Equipment*—This test method is described under uniform corrosion.

*ASTM G 16, Guide for Applying Statistics to Analysis of Corrosion Data*—Statistical analysis methods are presented. The methods discussed in this standard allow investigators to determine the significance of their results with the inherent variation observed in corrosion testing. This method includes error analysis, variability measures, standard statistical tests, curve fitting methods, and sample calculations.

*ASTM G 46, Practice for Examination and Evaluation of Pitting Corrosion*—This standard is used for evaluating and quantifying pitting corrosion. It presents guidelines for visual examination, nondestructive inspection (including radiographic, electromagnetic, sonics, and dye penetrants), and quantifying the extent of pitting. Methods for measuring pit depth, pit density, and pit size are included in this practice. A chart is provided for rating pit data. In addition, ASTM G 46 presents a procedure for determining the metal penetration rates.

*ASTM G 61, Test Method for Conducting Cyclic Potentiodynamic Polarization Measurements for Localized Corrosion Susceptibility of Iron-, Nickel-, or Cobalt-Based Alloys*—This standard presents a procedure for performing cyclic potentiodynamic polarization testing to determine the relative susceptibility of iron-, nickel-, and cobalt-based alloys to localized corrosion (pitting or crevice corrosion). It illustrates and presents test apparatus, reagents, and materials, test procedures, and interpretation of results.

*ASTM F 746, Test Method for Pitting or Crevice Corrosion of Metallic Surgical Implant Materials*—The susceptibility of an alloy to localized corrosion (pitting or crevice corrosion) may be determined using this standard. This procedure may be used to test alloys that have susceptibility to crevice corrosion in electrolytes of relatively low salt concentration although its intended purpose is to evaluate surgical implant alloys. In this standard, a specimen is allowed to stabilize in a test solution for approximately 1 h. After this time the potential is shifted to stimulate localized corrosion. The current is recorded with respect to time. A graphical analysis is then performed. ASTM F 746 describes test apparatus, reagents, preparation of specimens, test procedures, and report techniques typically used.

*ASTM G 78, Guide for Crevice Corrosion Testing of Iron-Base and Nickel-Base Stainless Alloys in Seawater and Other Chloride-Containing Aqueous Environments*—The tendency of an alloy to undergo crevice corrosion in chloride containing environments may be evaluated by using this standard. Specimens are prepared and intentional crevices are formed on the surface. These specimens are then immersed in a test environment and evaluated by visual means and depth of crevice areas. This guide lists suggestions for specimens dimensions, specimen preparation, crevice formers, specimen supports, test apparatus, test duration, and evaluation methods.

## Galvanic Corrosion

Galvanic corrosion is an electrochemical reaction that occurs between two different metals. This phenomenon may be studied by electrically connecting dissimilar metals in the same environment. Electrochemical analysis is typically used to evaluate the performance of two dissimilar metals when electrically connected in a select environment. The following standards and practices present methods for evaluating galvanic corrosion:

*ASTM G 82, Guide for Development and Use of a Galvanic Series for Predicting Galvanic Corrosion Performance*—This standard contains a method for predicting the galvanic effect when two metals are electrically connected in a given electrolyte. It outlines the procedures for creating a galvanic

series for materials in a select environment. This standard covers the precautions in the use of a galvanic series, test condition considerations in developing a galvanic series, and the theory of galvanic corrosion.

*ASTM G 71, Practice for Conducting and Evaluating Galvanic Corrosion Tests in Electrolytes*—The galvanic effects of materials in a select environment may be predicted by using this practice. Its method may be used in laboratory or field-testing. Two dissimilar metal specimens are electrically connected and immersed in an electrolyte. Galvanic current and potential measurements are recorded. The specimens are visually examined after exposure. This method covers test specimens dimensions, identification, the test environment, test procedures, evaluation of test specimens, and methods of reporting the results.

### Electrolyte Flow Effects

Movement of the electrolyte over a metal surface can cause erosion corrosion, impingement, or cavitation. The corrosiveness of the environment will accelerate the degree of corrosion. Standardized methods for evaluating erosion corrosion and cavitation involve immersion testing in the laboratory or operating system. Analysis is typically performed by visual examination and weight loss data. The following standards are commonly used to evaluate susceptibility to erosion corrosion and cavitation:

*ASTM G 40, Terminology Relating to Wear and Erosion*—This contains terms and their definitions relating erosion corrosion and cavitation of materials.

*ASTM G 73, Practice for Liquid Impingement Erosion Testing*—The behavior of solid specimens that are exposed to discrete impacts of liquid may be evaluated by conducting studies according to this standard. Specimens are subjected to liquid sprays or jets and the weight loss (or other metal loss data) is recorded with exposure time. This method presents test apparatus, test specimens, test procedures, and calculations and analysis of erosion resistance.

*ASTM G 32, Method for Vibratory Cavitation Erosion Test*—This standard presents a test method for determining the susceptibility of an alloy in an electrolyte to cavitation damage using high-frequency vibration. In general, the rate of erosion is determined by weight loss of the specimen. The method contains terminology definitions, a description of the apparatus, test specimen dimensions and preparation, test conditions, test procedures, interpretation of results, and report considerations.

### Stress-Corrosion Cracking

Stress-corrosion cracking (SCC) occurs on certain materials when exposed in select corrosive environments. Standards applicable for measuring the tendency of a material to undergo SCC involve immersion testing of stressed specimens and tension and slow strain rate testing. The following standards are applicable for evaluating a material's tendency for SCC in a select environment:

*ASTM G 30, Practice for Making and Using U-Bend Stress-Corrosion Test Specimens*—This describes methods for constructing specimens for evaluating SCC of metals. This standard includes specimen orientation, dimensions,

surface finish, and procedures for stressing. These coupons may be used for field or laboratory testing and evaluated by visual and microscopic methods.

*ASTM G 38, Practices for Making and Using C-Ring Stress-Corrosion Test Specimens*—This standard presents the design, machining, and procedures for stressing, exposing, and inspecting C-ring type stress-corrosion specimens. These coupons may be used for field or laboratory exposure and evaluated by microscopic methods.

*ASTM G 39, Practice for Preparation and Use of Bent-Beam Stress-Corrosion Test Specimens*—This describes methods for design, preparation, and use of bent-beam stress-corrosion specimens. This standard covers apparatus for supporting specimens, basic design of a specimen, stress calculations, test conditions, exposure, and inspection techniques.

*ASTM G 47, Test Method for Determining Susceptibility to Stress-Corrosion Cracking of High-Strength Aluminum Alloy Products*—Generalized procedures for characterizing the resistance to SCC of high-strength aluminum alloy wrought products are discussed. Test specimens are alternately exposed to wet and dry cycles in prepared solutions for ten to forty days. The specimens are then examined by microscopic and metallographic procedures. The major sections of this standard describe test specimen, test environment, loading procedure, examination, interpretation of results, and report considerations.

*ASTM G 49, Recommended Practice for Preparation and Use of Direct Tension Stress-Corrosion Test Specimens*—This presents the design, preparation, and use of ASTM standard tension test specimens for investigating susceptibility to SCC. Specimens are generally tested in a selected environment under axial load conditions until fracture occurs. This standard describes the apparatus for providing the load to the stressed specimens along with exposure considerations and inspection methods.

*ASTM G 58, Practice for Preparation of Stress Corrosion Test Specimens for Weldments*—This covers the manufacture and application of welded test specimens in stress corrosion testing. This practice is used to evaluate a total weldment, weld metal, or presence of notches and stress risers in weldments with respect to SCC in an environment. In addition, ASTM G 58 contains a method for evaluating the critical stress levels that will produce SCC in a weldment. The specimens are evaluated after exposure to an environment by microscopic methods. This standard includes typical specimens (stressed and tension), welding considerations, test specimen preparation, and inspection after exposure.

*ASTM E 3, Methods of Preparation of Metallographic Specimens*—This standard presents guidelines for proper selection and preparation of metallographic specimens. Recommendations for specimen size, cutting procedures, cleaning methods, various mounting techniques, and grinding and polishing practices are included.

*ASTM E 807, Practice for Metallographic Laboratory Evaluation*—This provides recommended practices for evaluating agencies that perform metallographic analysis. This guideline includes definitions of related terms, and recommended responsibilities, capabilities, and duties of the agency. In addition, ASTM E 807 recommends that an agency disclose a description of its staff, organization,

facilities, resources, and information relating to its procedural systems that directly affects the quality of services offered.

### Intergranular Corrosion

Intergranular corrosion is the preferential corrosion of a material at or along the grain boundaries. The standards commonly used for measuring a material's tendency to intergranular corrosion involve immersion testing followed by a visual and microscopic examination. The following standards predict a material's susceptibility to intergranular corrosion:

*ASTM G 108, Test Method for Electrochemical Reactivation (EPR) for Detecting Sensitization of AISI Type 304 and 304L Stainless Steels*—This method presents techniques for evaluating the susceptibility of 304 stainless steel, 304L stainless steel, other stainless steels and nickel alloys to intergranular corrosion and intergranular stress corrosion cracking caused by heat sensitization. Test specimens are subjected to anodic potentiodynamic testing from the passive to active regions of electrochemical potentials (from  $E_{corr}$  to  $E_{corr} + 200$  mV, back to  $E_{corr} - 50$  mV.) The test specimens are then metallurgically analyzed and the test data graphically analyzed. This method discusses apparatus, test specimens, test procedures, test solutions, metallographic inspection, graphical analysis, and calculations. This will provide meaningful results since as little as 10 ppm chlorides, which is present in most water, can make sensitized 304 and 316 stainless steels subject to SCC.

*ASTM G 1, E 3, and E 807*—ASTM G 1 is presented in the Uniform Corrosion section of this chapter; ASTM E 3 and E 807 are discussed in the Stress-Corrosion Cracking section.

### REFERENCES

- [1] *ASM Materials Engineering Dictionary*, J. R. Davis, Ed., ASM International, Materials Park, OH, 1992.
- [2] *Internal Corrosion of Water Distribution Systems*, 2nd Ed., AWWA, Denver, CO, 1996.
- [3] *Betz Dearborn Handbook of Industrial Water Conditioning*, Betz Dearborn, Trevose, PA, 1991.
- [4] Fontana, M., *Corrosion Engineering*, 3rd ed., McGraw-Hill, NY, 1986.
- [5] Uhlig, H. H. and Revie, R. W., *Corrosion and Corrosion Control*, 3rd ed., John Wiley & Sons, NY, 1985.
- [6] *Uhlig's Corrosion Handbook*, R. Winston Revie, 2nd ed., John Wiley & Sons, NY, 2000.
- [7] *Corrosion Handbook*, Vol. 13, Corrosion, ASM International, Metals Park, OH, 1987.
- [8] *Corrosion Control by Deposition of  $\text{CaCO}_3$  Films*, AWWA, Denver, CO, 1978.
- [9] *NALCO Guide to Cooling Water System Failure Analysis*, H. H. Herro and R. D. Port, McGraw-Hill, NY, 1993.
- [10] Jacobs, S., Reiber, S., and Edwards, M., "Sulfide Induced Copper Corrosion," *Journal AWWA*, Vol. 90, No. 7, July 1998, pp. 62–73.
- [11] *Economics of Internal Corrosion Control*, AWWA Research Foundation, Denver, CO, October 1989.
- [12] Borestein, S. E., *Microbiologically Influenced Corrosion Handbook*, Industrial Press, NACE International, Houston, TX, 1994.
- [13] *A Practical Manual on Microbiologically Influenced Corrosion*, G. Corbin, NACE International, 1993.
- [14] *Development of a Pipe Loop Protocol for Lead Control*, AWWA Research Foundation, Denver, CO, 1994.
- [15] *Electrochemical Techniques for Corrosion Engineers*, R. Baboian, Ed., NACE International, 1986.

# Soils

*Edward Escalante<sup>1</sup>*

## INTRODUCTION

MUCH OF THE underground infrastructure in the United States was constructed after World War II in the 1950s and '60s, and many of these structures, such as pipelines, utilities, and storage tanks, are approaching the end of their useful life. Thus, there is an increased need for data on the underground corrosion performance of materials used in these structures. The ideal measurement would nondestructively provide information on how much a structure has deteriorated and how rapidly this deterioration is occurring. With this information, engineers can predict the expected lifetime of a structure. With present day techniques, we can measure the rate of corrosion of an underground structure, but we lack a nonintrusive method that provides information on the extent of accumulated damage. Controlled tests are one way that data on accumulated damage can be obtained, and it is for this reason that this type of test is useful. This section on field measurements will concentrate on the types of underground corrosion measurements that can be made in controlled and uncontrolled conditions, with an emphasis on controlled site testing.

At a controlled exposure site, metal samples are intentionally exposed so that control of variables such as specimen surface area and size, depth of burial, minimum electrical and mechanical interference, and site accessibility are maximized. The design of this type of site allows retrieval of specimens from the ground without interrupting services as may be the case with a real structure. In an uncontrolled exposure site, the above variables may be in question, and this situation usually applies to any real underground structure. For example, the surface area of an underground pipeline is difficult to determine because from the standpoint of electrochemical polarization measurements, the pipeline is of infinite length. In addition, electrical isolation from other structures or services may not be possible with an underground system in use. In general, techniques for measuring corrosion are the same for controlled and uncontrolled sites, but some precautions and limitations must be kept in mind when these techniques are applied to real structures, and these will be discussed where appropriate. Assessing the corrosion of buried steel tanks is complicated by the presence of internal corrosion as well as external wall deterioration. This special case is addressed in ASTM G 158 [1].

<sup>1</sup>Corrosion Consultant, formerly with Corrosion Group, National Institute of Standards and Technology, Gaithersburg, MD.

## SPECIMEN AND SITE ACCOUNT

### Maintaining Records

Determining corrosion performance of metals in underground environments generally requires long-term testing, sometimes exposures of several years. Such long-term studies make it imperative that information be maintained in a readable, accessible, permanent system. Experience has shown that a bound notebook with numbered pages is one format that has proven successful for keeping these records. Today, computerized media such as CD ROMs provide other useful storage options. These data must include the exact location of the test site and its configuration. Identifying the location of the site with reference to survey markers or other reliable, long-term features may be warranted, and becomes more important as the length of exposure is increased. Using global positioning satellite (GPS) technology, a point on the surface of the earth can be identified with an error of less than  $\pm 1$  m, making it a very attractive means of identifying the location of buried specimens. One test site out of the direct control of this author was paved over for parking motorized equipment, and survey information allowed successful retrieval of the specimens. Specimen surface treatment, heat treatment, and identification marks must be carefully described in these records. Photographic records during all phases of preparation and burial are useful for future site and specimen evaluation. Finally, computer files on hard or floppy disks are invaluable for organizing and examining data, but they are a poor format for long-term storage of data. Changes in computer equipment or damage to magnetic disks may make it difficult or impossible to access old data files. CD ROMs, however, are not affected by magnetic fields, making them a good alternative storage media for data. The importance of maintaining good records cannot be overemphasized.

### Specimen Design

The design of specimens is determined by several factors, such as the form of corrosion expected (uniform corrosion, pitting, etc.), the type of structure in question (pipe, tank, etc.), and the measurements necessary for obtaining the data. Measurement requirements for determining the loss in cross section of a structural H-pile are different from measurements designed to examine pitting of a pipeline material. In general, the larger the sample exposed, the better the data,

but there may be a size limitation imposed by the measurements. Weight loss data requires weighing a specimen before and after exposure, and for this type of data, the size and weight of a sample is limited by the capabilities of the weighing equipment. Surface preparation of a sample must be considered. If the sample is a simulation of a real structure, then care should be taken to ensure that the specimen surface is representative of that structure. Thus, chemical cleaning, abrading, and polishing of the specimen surface may be undesirable if the real structure is not subjected to the same surface treatment.

For evaluation of pipeline materials, a segment of the pipe with endcaps to protect the interior may be the most suitable design for a test specimen. It is also common practice to use sheet material for specimens, where sheet metal is used for producing containers such as holding tanks. Where welds are encountered, it is valuable to include specimens with welded sections in the burial test. Coated panels and coated panels with intentional breaks in the coating may be desirable. Galvanic coupling of specimens is also a consideration, where two unlike metals are expected to be in contact. Stressed U-bend or C-ring type specimens are used for studies of stress corrosion failures. Specimen identification marks stamped or scribed must be easy to read, and in the case of large specimens, such as H-piles, identification marks can be applied with a welding torch. Thus, the design of the specimen is tailored to meet the needs of the study.

### Considerations for Physical Measurements

Weight loss, pit depth, or wall thickness determinations are physical measurements used as a reference to non-destructive electrochemical techniques. Physical measurements are considered destructive because, generally, the specimen must be removed from the site and cleaned. The process of extraction and preparation for examination changes the surface condition of the specimen, effectively destroying the possibility of continuing the exposure test with that particular specimen. Nevertheless, to rely solely on electrochemical measurements can result in misleading information, and it is strongly recommended that the test design include some form of physical verification of non-destructive measurements. To obtain corrosion data from physical measurements during long-term exposures, it is common practice to place enough samples in the ground to allow removals at intervals of time. The most meaningful data are obtained when duplicate samples are used for each removal, allowing averaging of data and providing a better representation of material performance.

### Burial Site

Choosing the correct burial site is important, since the environment will have a direct effect on the performance of buried materials. This choice must take into account more than just characteristics of a soil, and must include consideration of local conditions of temperature, rainfall, and location. For example, a soil located in a valley near a stream provides a different environment to the same soil on a nearby hill. In general, the best test site is near the structure

in question. Such a site has the added advantage that measurements can be made on the real structure, which can then be compared to data obtained from controlled specimens nearby. Where a variety of soils are encountered, several soil sites may be needed. If only one site is chosen, then the site with the "worst case" conditions will provide the most conservative data. Where anaerobic bacterial corrosion is of concern, redox potential measurements of the soil can identify the sites where these bacteria are most likely to be present [2]. Soil characterization is discussed in another section of this manual, but it is worth mentioning that the ASTM G01 committee on Corrosion of Metals has published useful techniques for measuring soil resistivity and soil pH [3,4].

### Specimen Emplacement

The manner in which a sample is buried is influenced by the configuration of the specimens. For example, steel piling specimens are driven into the ground with pile drivers, while small specimens will most likely be buried in trenches dug with a back hoe. A typical steel pile test site involves the placement of five pilings in a 2 m radius circle around a sixth centrally located pile, as illustrated in Fig. 1 [5]. The central pile was used as a counter electrode during electrochemical polarization measurements of the other piles as will be explained later. The top of each pile was 0.6 m below ground level, and to the top of each pile was welded a steel rod that extended to just below the surface of the ground. A removable concrete marker, extending above ground, was placed over the rod to help locate the steel rod. Since the study included examining the effect of disturbed soil, a seventh pile was buried horizontally in a nearby trench.

Small specimens can be buried in a long, narrow excavation made by a backhoe. Such a trench is typically 1 m deep, 0.6 m wide, and as long as necessary to accommodate all specimens, which are generally placed about 30 cm apart along the length of the trench. Where electrical wires from specimens extend above ground, wood posts are commonly used to serve as markers and hold the wires. Untreated wood is recommended, because leaching of chemicals from treated wood will modify the surrounding soil and possibly affect the results of the corrosion test. It is especially important to avoid placing wood treated with copper salts near aluminum specimens, since it is known that copper ions

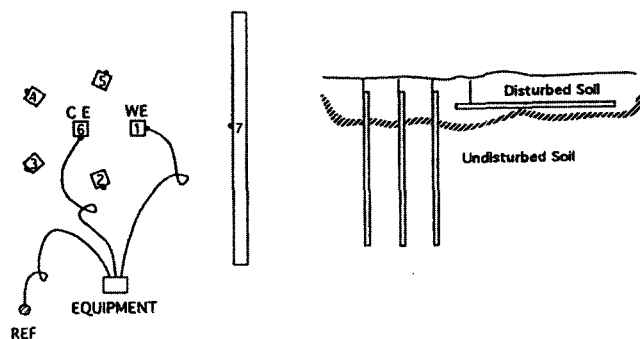


FIG. 1—Typical view of steel pile placement at an underground test site.



accelerate the corrosion of aluminum. Retrieval of specimens is simplified by tying specimens together with a small diameter plastic cord and attaching the cord to wood posts. In this way, finding the cord or one specimen allows retrieval of all other specimens in a group. Where several retrievals are to be made over a period of time, specimens for a given removal can be grouped together in one section of the trench, so that when a group is retrieved, those remaining are not disturbed during digging. Wooden posts can be used as trench markers to delineate groups of specimens, or metal markers located just below the ground surface will serve the same purpose and can later be found using a metal detector.

More than one system of specimen identification must be incorporated in the test. For example, stamping identification characters on the specimen and on an attached plastic label reduces problems of identification in the future. In addition, specimens can be buried in a known sequence for further verification of identity.

### Specimen Retrieval

Immediately after excavation, a rapid superficial cleaning of specimens with a scrubbing brush and water allows easy removal of oxides and soil/oxide conglomerates that harden as they dry, making later cleaning difficult. An immediate cursory examination of specimens on initial removal, coupled with photographic documentation, has several advantages. This examination can become important in those unfortunate cases where specimens are lost or damaged in transit. Furthermore, although identification of a specimen may be obvious on removal, later it may be difficult where tags are separated or lost, and documentation with photographs or notes becomes crucial for identification. Where specimens have corroded to the point of separation, it is important to tag the parts for later identification, and this may include placing specimens in envelopes or bags. In some cases metal specimens undergo surface changes after retrieval, especially if there is a long period of time between removal and final examination, and photographs help identify those instances where this happens, allowing the examiner to differentiate between burial damage and damage from subsequent handling. This can be especially important in cases where coatings are involved in the test. Thus, the employment of some precautions and documentation on initial removal of specimens will save time and effort in subsequent examination procedures.

Some information can be obtained from the soil at the time of sample extraction. For example, soil conditions may vary along the length of a trench, resulting in a variation in the corrosion performance of similar samples, and these soil differences should be noted. In some cases, where warranted, local measurements of soil pH or soil resistivity at the depth of the specimens, can provide insight to material performance. The use of pH paper is an excellent method of obtaining a rapid reading on a soil. Unusual conditions of pH found with pH paper can be verified with more traditional pH electrodes. The resistivity of small samples of soil can be measured using a soil cup or soil box. The use of these techniques is an excellent way of getting information on localized soil conditions in the vicinity of the specimens.

Always be aware that local, small soil sample readings can change dramatically from place to place in the same trench, and these readings must not be assumed as representative of the soil as a whole. Other techniques for measuring large soil samples must be used and are described in the ASTM Annual Book of Standards [4].

### Cleaning and Examination of Specimens

Examination of specimens at the time of excavation is a critical step in the process of obtaining information from underground exposure studies. As has already been suggested, it is instructive to examine and characterize the condition of specimens before the final cleaning process. The presence or absence of an oxide on a corroded surface, the color of an oxide, and its location on the metal surface provide clues to the mechanism of attack. This initial examination is followed by removal of all corrosion products from the specimen. Fortunately, information on this difficult process, removal of oxide layers with minimum substrate attack, has been published by the ASTM G01 Committee on Corrosion of Metals [6]. This publication describes reagents and detailed chemical and electrochemical methods for cleaning ferrous and nonferrous metallic specimens.

## PHYSICAL MEASUREMENTS

### Weight Loss

Determining weight loss resulting from exposure to soil is a common technique used to measure corrosion rate. This type of data is most meaningful when corrosion is uniform over the surface of the specimen, since normally the entire exposed surface area of the specimen is used for calculating corrosion rate. If corrosion attack is localized and the total exposed surface area is used for the corrosion rate calculation, then the result will underestimate penetration. One possible way around this problem is to measure the area where the localized attack has occurred and use this corrected area in the calculation of corrosion rate. Possible sources of error in weight loss determinations are a) excessive removal of metal during cleaning, b) inadequate cleaning of specimen, and c) using the total surface area for calculating corrosion rate when the attack is localized.

A typical approach that has been used to determine weight loss of specimens through physical measurements is as follows. Small steel coupons, weighing approximately 200 g, were exposed to a soil environment. The samples were weighed before and after exposure. Prior to the "after exposure" weighing, the samples were cleaned using the ASTM solution designation C.3.1, which is an inhibited hydrochloric acid solution described in detail in the ASTM G 1 Standard Practice [6]. To determine the immersion time necessary for removal of the oxide, the specimens were cleaned and weighed repeatedly, until weight loss stabilized, indicating that the cleaning reaction had gone to completion. Figure 2 is an example of these data. Note that specimen 9 required immersion of only 30 s to remove the oxide, while specimen 7 took approximately 2.5 min to clean. This cleaning and weighing procedure allows monitoring of the chemical cleaning

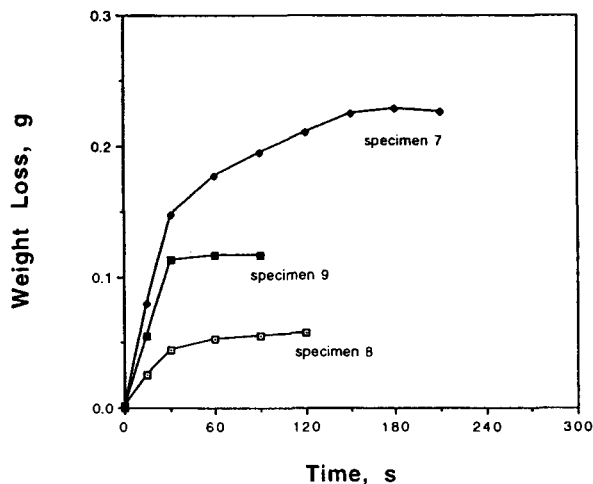


FIG. 2—A plot of weight loss versus time for three steel coupons in inhibited hydrochloric acid, showing the initial rapid oxide removal and the slower dissolution of metal as a function of time.

process, and reduces the likelihood of error from removing too much base metal. The ASTM publication also provides information on the mathematical procedure for calculating corrosion rate from weight loss in terms of a variety of units, both English and Metric.

### Pit Depth

Obtaining information of the degree of pitting involves some form of visual inspection, so that the shape, depth, and density of pitting can be determined. Large shallow pits are relatively easy to evaluate, compared to small, narrow, deep pits. The degree of pit penetration of wide pits can be measured with a pit depth micrometer or by the use of a microscope that allows measuring the change in movement of the stage when focusing between the bottom of the pit and the surface of the metal. Determining the shape and depth of a narrow, deep pit is more challenging and may involve a metallographic cross-sectional examination of the pitted area. This same metallographic technique may be the most effective way of examining pits that get wider with depth. A crude but effective way of measuring the depth of relatively straight line pits is to insert a small diameter wire into the pit and measuring the length of penetration by the wire. In some cases, the rate of wall penetration is critical, as for pipeline material, and identifying and measuring the deepest pit is important, along with information on the average penetration of the ten deepest pits. Density of pitting can be obtained by counting pits in a known area or by comparing the pitted surface to standard charts as described in the ASTM G 46 Standard Practice for Examination and Evaluation of Pitting Corrosion [7].

### Stress Induced Failure

Determining susceptibility of a material to stress corrosion cracking or hydrogen embrittlement in a soil environment has been studied using buried U-bend specimens [8].

This approach provides information on whether or not a specimen failed, but will not reveal when, during the exposure period, the failure occurred. One novel method for application of stress allows monitoring the condition of the specimen from the surface, using a steel ring located above ground level to apply the stress to a tubular tensile specimen in the soil via a steel rod [9]. By monitoring the load on the steel ring, the failure of the tensile specimen is detected. Another technique that provides a remote indication of failure is the above ground monitoring of gas pressure used to apply a hoop stress to small containers buried in the ground. The ASTM committee on the corrosion of metals has developed and published standard methods for the use of U-bend and C-ring specimens for the application of stress [10,11].

## ELECTROCHEMICAL MEASUREMENTS

### Polarization

The technique of electrochemical polarization is a useful tool for obtaining corrosion rate data nondestructively during exposure, with a minimum of disruption to the test. The polarization resistance measurement is especially attractive because its use is well documented, and it requires a minimal amount of equipment, some of which is commercially available. The measurement involves applying current to a specimen from a second electrode, changing the potential of the specimen by approximately 10 mV versus a reference electrode, and noting the amount of current needed to make that change. The slope of the change in potential versus the applied current is inversely related to the corrosion current of the specimen [12]. With information on the Tafel slope of the material in that environment, the corrosion current can be determined. This approach uses: 1) a specimen as the working electrode (WE), 2) a reference potential electrode (REF), and a counter electrode (CE) used to apply the polarizing current. Additional information is available in ASTM Standard Practice G 59 [13].

Corrosion current density, and corrosion rate, can be calculated when the entire specimen is polarized and its surface area is known. This is the case for finite area specimens, as illustrated in Fig. 1 for steel piling. The reference electrode is located at the soil surface approximately 30 m from the WE. For these measurements, each of the seven piles was polarized using the centrally located pile as the CE with the REF at a fixed location. In this way, measurements could be duplicated from year to year and the results compared [5]. From this corrosion current measured over a period of time, in this case 14 years, an estimate of weight loss can be calculated.

There are situations where the polarized area of the specimen is not known, as is the case where the WE is a long structure such as a pipeline or electric power utility. In this situation, the WE is essentially infinitely long and the CE can only supply current to a portion of the structure. An estimate of how much of the structure is polarized when current is applied can be made by measuring the potential of the structure in the vicinity of the CE, as illustrated in Fig. 3 [14]. In this example, polarization region extends from the 4 m mark to the 18 m mark. From this information, the approximate polarized area can be calculated.

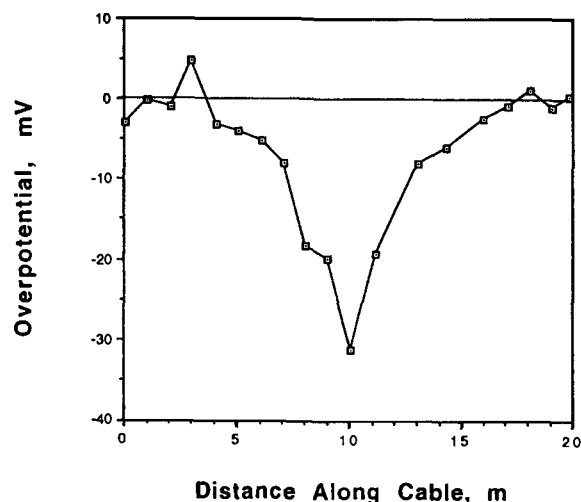


FIG. 3—A plot of overpotential versus distance, illustrating the distribution of current on an underground cable when 1.5 mA is applied from a rod placed 1 m to the side of the cable.

Special probes with associated measuring equipment that provide a means of determining the corrosion rate of a material in soil are commercially available. Generally, the probe and a specimen, built into the probe, are bought as a unit. An attractive feature of this equipment is that the data reads out directly in terms of corrosion rate. The biggest concern is that the specimen in the probe may not be representative of the structure of interest because of the small size of the probe specimen or its isolation from the structure. One type of probe system uses the change in electrical resistance of the coupon in the probe as an indicator of reduction in cross section due to corrosion attack. This reading is then converted to corrosion rate. Other types of probes use electrochemical polarization techniques and two or three electrodes to measure the corrosion rate of the WE in the probe [15,16]. Details on calculating corrosion rate from electrochemical data are discussed in ASTM G 102 [17].

In the laboratory, the technique of ac impedance is superseding polarization resistance, because it provides additional information on mechanisms of the processes involved. Guidance on performing corrosion tests in the laboratory in liquids or in soils is provided in ASTM G 31 and ASTM G 162 [18,19]. Ac impedance systems are now commercially available, but these units are limited to low polarization currents of 1 A or less, making them unsuitable for most field applications where larger current capabilities (>1 A) are needed.

### Galvanic Corrosion

The galvanic coupling of unlike metals in soil is an all too common occurrence, and the need to obtain information on the consequences of this condition is recognized. Copper ground rods and copper mesh ground beds are typically connected to steel piling supported structures and underground telephone, water, and fuel utilities to the detriment

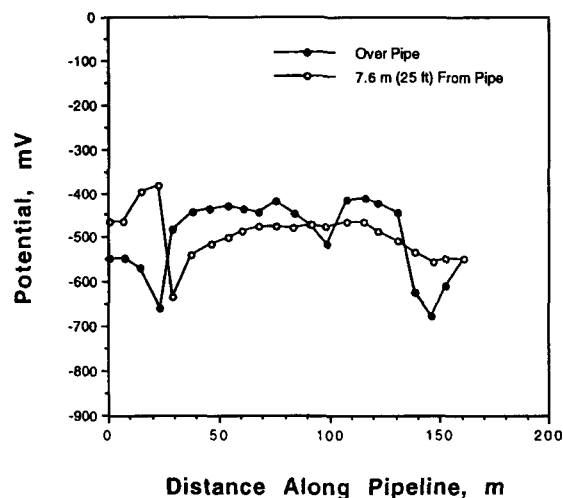


FIG. 4—A plot of potential over a pipeline and to the side of the pipeline versus distance, illustrating the presence of cathodic regions where "over the pipe" potentials are more positive than "beside the pipe" potentials.

of the less noble steel. Burial of galvanically coupled metals in soil provides information on the degree of corrosion and the possibility of hydrogen embrittlement. The effect of relative surface area of the coupled metals and the spacing between them are important [20].

Measuring the galvanic current of the coupled metals during the exposure period allows monitoring of changes in the magnitude of the current and direction of current flow. This can be accomplished by attaching insulated wire conductors that extend above the surface of the soil where they are connected together. Periodically, an ammeter is inserted in the circuit and the current is measured. To reduce the possibility of affecting the current during the measurement, which may involve currents in the milliamp range or less, the use of a zero-resistance ammeter is recommended [8].

### Potential Mapping

Measured potentials at the soil surface above a utility, such as a pipeline, are often used to evaluate the effectiveness of cathodic protection systems and coatings.

One technique that has been applied for many years uses two sets of measurements where one of the electrodes is positioned over the pipeline and the second electrode is placed several meters to the side. The data from this approach provide a comparison of the local potential to the more distant potential made to the side of the pipeline, as illustrated in Fig. 4. Regions where the "Over Pipe" potential are more positive than the "25 ft From Pipe" potential are cathodic to other sections of the pipe line. Potential effects of stray currents, galvanic currents, and cathodic protection interference are identified from this information [21].

A more recent technique relies on a set of potential measurements between the pipeline and a reference electrode, where the electrode is positioned directly over the pipeline, and measurements are made along its length at intervals. Computerized data logging permits a detailed analysis of

discontinuities in potentials that reveal areas of active corrosion [22]. Recent improvements in programming and equipment permit elimination of iR error from cathodic protection potential measurements and also incorporate use of "over the pipe" and "beside the pipe" potential data [23].

## SUMMARY

Underground corrosion is particularly insidious in that, generally, we are not aware of its progress until a failure occurs. However, there are physical and electrochemical techniques available that will provide information on corrosion processes. Physical measurements furnish cumulative corrosion information obtained at the final removal stage, while electrochemical measurements supply data during the period of exposure to soil.

## REFERENCES

- [1] ASTM G 158: Standard Guide for Three Methods of Assessing Buried Steel Tanks, *Annual Book of Standards*, Vol. 03.02, ASTM International, West Conshohocken, PA, 1998.
- [2] Booth, G. H., Cooper, A. W., and Cooper, P. M., "Criteria of Soil Aggressiveness Towards Buried Metals, I. Experimental Methods," *British Corrosion Journal*, Vol. 2, 1967, pp. 104-108.
- [3] ASTM G 51: Standard Test Method for pH of Soil For Use In Corrosion Testing, *Annual Book of Standards*, Vol. 03.02, ASTM International, West Conshohocken, PA, 1993.
- [4] ASTM G 57: Standard Method for Field Measurement of Soil Resistivity Using the Wenner Four-Electrode Method, *Annual Book of ASTM Standards*, Vol. 03.02, ASTM International, West Conshohocken, PA, 1993.
- [5] Escalante, E., "Measuring the Underground Corrosion of Steel Piling at Turcot Yard, Montreal, Canada - A 14 Year Study," *Corrosion Forms and Control for Infrastructure*, ASTM STP 1137, V. Chaker, Ed., ASTM International, West Conshohocken, PA, 1992, pp. 339-355.
- [6] ASTM G 1: Standard Practice for Preparing, Cleaning, and Evaluating Corrosion Test Specimens, *Annual Book of ASTM Standards*, Vol. 03.02, ASTM International, West Conshohocken, PA, 1990.
- [7] ASTM G 46: Standard Practice for Examination and Evaluation of Pitting Corrosion, *Annual Book of Standards*, Vol. 03.02, ASTM International, West Conshohocken, PA, 1993.
- [8] Escalante, E. and Gerhold, W. F., "Galvanic Coupling of Some Stressed Stainless Steels to Dissimilar Metals Underground," *Galvanic and Pitting Corrosion - Field and Laboratory Studies*, R. Baboian, et al., Ed., ASTM International, West Conshohocken, PA, 1976, pp. 81-93.
- [9] Escalante, E., "Corrosion Testing In Soil," *Corrosion*, J. R. Davis, Ed., ASM International: Materials Park, OH, 1987, pp. 208-211.
- [10] ASTM G 38: Standard Practice for Making and Using C-Ring Stress-Corrosion Test Specimens, *Annual Book of Standards*, Vol. 03.02, ASTM International, West Conshohocken, PA, 1993.
- [11] ASTM G 30: Standard Practice for Making and Using U-Bend Stress-Corrosion Test Specimens, *Annual Book of Standards*, Vol. 03.02, ASTM International, West Conshohocken, PA, 1993.
- [12] Mansfeld, F., "The Polarization Resistance Technique For Measuring Corrosion Currents," *Advances in Corrosion Science and Technology*, M. G. Fontana and R. W. Staehle, Ed., Plenum Press, NY, 1976, pp. 163-262.
- [13] ASTM G 59: Standard Practice for Conducting Potentiodynamic Polarization Resistance Measurements, *Annual Book of Standards*, Vol. 03.02, ASTM International, West Conshohocken, PA, 1993.
- [14] Escalante, E., "Measuring the Corrosion of Metals in Soil," *Corrosion Testing and Evaluation*, R. Baboian and S. W. Dean, Ed., ASTM International, West Conshohocken, PA, 1990.
- [15] Kilpatrick, J. M., "Measuring Corrosion Rate—Now," *Oil & Gas Journal*, March 1964, pp. 155-157.
- [16] Marsh, G. A., "The Measurement of Instantaneous Corrosion Rates," *2nd International Congress on Metallic Corrosion*, NACE, Houston, TX, 1963, pp. 936-941.
- [17] ASTM G 102: Standard Practice for Conducting Potentiodynamic Polarization Resistance Measurements, *Annual Book of Standards*, Vol. 03.02, ASTM International, West Conshohocken, PA, 1993.
- [18] ASTM G 31: Standard Practice for Laboratory Immersion Corrosion Testing of Metals, *Annual Book of Standards*, Vol. 03.02, ASTM International, West Conshohocken, PA, 1993.
- [19] ASTM G 162: Standard Practice for Conducting and Evaluating Laboratory Corrosion Tests in Soils, *Annual Book of Standards*, Vol. 03.02, ASTM International, West Conshohocken, PA, 1999.
- [20] Fontana, M. G. and Greene, N. D., *Corrosion Engineering*, McGraw-Hill, NY, 1978, p. 35.
- [21] Husock, B., "Use of Pipe-to-Soil Potential In Analyzing Underground Corrosion Problems," *Corrosion*, Vol. 17, No. 8, 1961, pp. 97-101.
- [22] Kroon, D. and Nicholas, K. W., "Computerized Potential Logging: Results On Transmission Pipelines" *NACE Corrosion/82*, NACE, Houston, TX, 1982.
- [23] Kroon, D., Private Communication, 1993.

# Industrial Applications

Allan Perkins<sup>1</sup>

## PURPOSE AND IMPORTANCE OF IN-PLANT TESTING

THERE ARE A CONSIDERABLE number of sources of material testing data that have been accumulated over the years and are available to process plant designers to assess the most suitable materials selection for a particular plant and operating conditions. However, many of the factors involved in the selection of an optimum choice are subject to variability, and this makes the selection process more complex.

The ranking of the most valuable corrosion data for plant designers is generally understood to be as follows:

1. Operating experience on full-scale equipment under the actual process environment.
2. Operating experience on a pilot plant with similar feed-stock and operating conditions.
3. Sample tests in the field, corrosion test specimens, electrical resistance (ER) probes, or stressed samples exposed to the process environment.
4. Laboratory evaluations in "actual" plant fluids, or simulated environments.
5. Materials and Corrosion Database.

It should also be recognized that the economics of the various material selection choices is not constant. A decision that makes economic sense at the design time, or at the materials selection time, may not make sense by the time the plant is actually built or operating. In addition, the economics of plant shutdowns due to failure can depend on the market for the product being generated by the plant, although these costs are generally ever upward.

The choice must be made between the use of more expensive corrosion-resistant alloys, and the use of a less expensive, less corrosion-resistant alloys protected by chemical treatment. Changes in the raw material costs of chromium, nickel, and other constituents in corrosion-resistant alloys affect the initial construction costs. A less expensive material, that would otherwise be unacceptable due to low corrosion resistance, can still be the best choice when used with chemical corrosion inhibitors, or other protection methods such as anodic or cathodic protection.

In some process applications, the material selection may have been the optimum choice for the specified operating conditions.

However, unintended minor changes in the operating conditions may have a major influence on corrosion rates.

For these reasons, periodic and continuous in-plant corrosion monitoring is frequently used for materials evaluation. The main uses for corrosion monitoring are summarized in Table 1.

A range of material evaluation tools is available for in-plant use. Some of these may be classified as inspection methods, and some of them as on-line continuous corrosion monitoring methods. The difference between the two is the sensitivity and, consequently, the frequency with which measurements are taken. The lower-sensitivity measurement methods may be useful for long-term life prediction. Short-term continuous online methods may be used more for corrosion prevention, by allowing changes to the inhibitor injection rates or operating conditions before significant damage occurs.

## MEASUREMENT TECHNOLOGIES

There is a considerable number of technologies available for assessment of material degradation, each with its own benefits and limitations. Corrosion is rarely uniform throughout a plant, or even in a localized area, and it is preferable to use more than one method of assessment. An alternate measurement technology will improve confidence levels in the results obtained and avoid unrepresentative results.

The various types of measurement technologies for assessment of corrosion may be summarized as shown in Tables 2 to 5. These techniques cover both laboratory and field use. However, many of the direct methods, particularly the electrochemical methods of potentiodynamic polarization and electrochemical impedance spectroscopy (EIS) are generally more suited to laboratory evaluation. In the laboratory, test conditions are clean and more controlled. Consequently, more sophisticated measurement electrode systems can be used that take advantage of their more sophisticated measurements technologies. In the field, practicalities of changing process conditions, high flow rates, debris, electrical noise, and electrical safety limit their use.

**TABLE 1**—Main objectives of in-plant monitoring.

- Predict behavior of materials in full scale plant from a pilot plant.
- Assess choices of materials for plant replacement in an operating plant.
- Assess the corrosion penalty of uprating the maximum process capacity, or otherwise increase operating parameters.
- Assess the effectiveness and to optimize the costs of various corrosion inhibitors, or modified operating conditions.

<sup>1</sup>Rohrback Cosasco Systems, Sante Fe Springs, CA 90670.

**TABLE 2**—Direct intrusive measurement methods.

Physical Methods	<ul style="list-style-type: none"> <li>• Corrosion test specimens</li> <li>• Electrical resistance</li> </ul>
Electrochemical Methods	<ul style="list-style-type: none"> <li>• Linear polarization resistance</li> <li>• Potentiodynamic polarization</li> <li>• Galvanic (Zero Resistance Ammetry)</li> <li>• Electrochemical impedance spectroscopy (EIS)</li> <li>• Electrochemical noise</li> </ul>

**TABLE 3**—Direct nonintrusive measurement methods.

Physical Methods for Metal Loss	<ul style="list-style-type: none"> <li>• Ultrasonic thickness measurement</li> <li>• Radiography</li> <li>• Surface activation and gamma radiometry</li> <li>• Direct electrical resistance</li> </ul>
---------------------------------	--

**TABLE 4**—Indirect intrusive measurement methods.

Corrosion By-products	• Hydrogen probes
Electrochemical Methods	• Corrosion potential
Water Chemistry	• pH, conductivity, dissolved oxygen, redox potential (ORP)
Fluid Dynamics	• Flow regime, flow velocity
Process Parameters	• Pressure, temperature
Dewpoint	
Deposition Monitoring	• Fouling
Failure Analysis	

**TABLE 5**—Indirect nonintrusive measurement methods.

<ul style="list-style-type: none"> <li>• Alkalinity</li> <li>• Metal Ion Analysis</li> <li>• Concentration of Dissolved Solids</li> <li>• Gas Analysis</li> <li>• Residual Oxidant</li> <li>• Microbiological Analysis</li> <li>• Residual Inhibitor</li> <li>• Chemical Analysis</li> </ul>
--

In general, the most widely used field technologies for inspection are ultrasonic thickness measurement, while for online methods they are corrosion test specimens, electrical resistance, and linear polarization probes. Both of the inspection methods and the first two online methods measure metal loss. The last method measures corrosion rate, but only in a sufficiently conductive process environment, normally water.

Measurement sensitivity divides the metal loss methods. Ultrasonics and radiography are usually considered as inspection methods. Typically, ultrasonics has a measurement resolution of around 50  $\mu\text{m}$  (0.002 in.), and radiography 250  $\mu\text{m}$  (0.010 in.). Consequently, these types of measurements are typically made annually. Corrosion test specimens (coupons) assess metal loss typically over a one to three month interval. Electrical resistance probes, as an "automatic coupon," assess metal loss typically over a few hours to a few weeks.

It should also be noted that there is a difference between measurements made directly on the plant material compared to measurements made on a test specimen. The methods for the former are generally less sensitive than the latter. Hence, to be effective, overall inspection methods on the plant material should be as comprehensive as possible to

ensure location of severely corroded areas. Correspondingly, measurements on a test specimen to determine the corrosiveness of the process should be taken at representative locations, namely at the points of most severe corrosion.

## INSTALLATION OF MONITORING DEVICES

Ultrasonic and radiographic inspection techniques are used for long-term evaluations because of their lower sensitivity. The advantages of these techniques are that they are nonintrusive and do not normally require special mounting equipment or access to the process. The common intrusive techniques of corrosion test specimens, electrical resistance, and linear polarization probes require exposure to the process.

Corrosion test specimens in particular, and electrical resistance or linear polarization probes to a lesser extent, need to be removed and replaced, or inspected at intervals. These intervals most probably will not coincide with plant shutdowns.

Probes and corrosion test specimens that are mounted rigidly in the process by some form of fixed mounting do not allow removal online. This may suit some applications but may be inconvenient where shutdowns are not made except for emergencies or major planned overhauls at one, two, or even five year intervals. For these applications, removal of probes and corrosion test specimens under operating conditions may be achieved by various insertion and retrieval systems.

Evaluation of alternate materials of construction is often undertaken in operating plants with multiple corrosion test specimen holders of various types, typically over months or years. This type of test is useful for assessing alternate alloys that may be used for replacement of those already used. The tests may comprise simple unstressed immersion tests of various alloys, or specially strained or notched specimens to evaluate stress corrosion cracking (SCC) properties. Since a relatively large number of specimens are frequently used, with multiple specimens of each alloy that permit successive removal of the corrosion test specimens, these racks and fixtures can be quite bulky. Consequently, these racks are most commonly installed within vessels or sometimes in large pipe sections. Care must be taken in the latter case to avoid excessive restriction due to the bulk of the corrosion test specimen rack or assembly. Because of the size of the test rack, these assemblies are generally only removable at plant shutdown. The key features of corrosion test specimens support structures are strength and durability of the corrosion test specimen support structure and electrical isolation of the corrosion test specimens from the rack and each other.

Positioning of the rack is also critical to make the corrosion test specimens a good representation of the required test conditions. This should consider the phases that are present, the separation of phases, the velocity of the phase or phases in multiphase flow, and the velocity changes due to the test rack itself. Even greater care is required with mounting and construction of stressed specimens to ensure that the applied stresses are held constant by the stressing mechanism. The other more common aspect of material evaluation is to monitor the ongoing performance of the existing plant alloys, or a few alternate materials, through changes in feedstock, operating conditions, various inhibitors, and inhibitor feed rates.

Retractable corrosion test specimen holders allow removal under process operating conditions without process shut-down. The requirement for assessing only one or possibly two alloys permits a more compact construction. This assists the design of the retractable mechanism and permits more flexibility in positioning the corrosion test specimen correctly, to pick up the corrosive water phase in the bottom of an oil/water pipeline, for example.

Electrical resistance and linear polarization probes generally monitor a single alloy at a time, but permit much more rapid responses to dynamic corrosion rate changes that occur. Most commonly the probes are retrievable to allow replacement at required intervals or for inspection of probe elements.

## SPECIMENS

Any specimen used in a plant evaluation, whether it is a test specimen or a probe, has certain limitations that must be recognized:

1. It is a small sample compared to the plant equipment.
2. The sample may differ from the actual plant material in composition, preparation, orientation to the process, previous history, and exposure to the process.

Where corrosion test specimens are used, care is required in the preparation, identification, cleaning, and evaluation to ensure reasonable reliability and accuracy of the data. These requirements are well detailed in ASTM G 4, Guide for Conducting Corrosion Tests in Field Applications.

Corrosion test specimens are used to evaluate average corrosion rate over the exposure period and are also useful for assessment of crevice corrosion, pitting, and end grain attack, and may be used for metallographic examination of the corrosion test specimen or analysis of any deposits. Special corrosion test specimens may be prepared with welds to assess corrosion problems particular to weld material or heat affected zones. SCC may be monitored with specially mounted and loaded corrosion test specimens.

Identification of the corrosion test specimens is achieved by using low-stress stamping of an identification number directly on the corrosion test specimen surface. Signs of preferential attack on the stamped area can indicate susceptibility to corrosion when cold worked, and it may also be possible to detect stress corrosion cracking. However, tests for such problems of corrosion on cold worked areas and stress corrosion cracking should be made on specimens designed specifically for this purpose. On electrical resistance probe elements and linear polarization probe electrodes, the element alloy is identified on the probe body, thereby avoiding any stressing or damaging of the element material.

## TESTING APPROACHES

### Corrosion Test Specimens (Coupons)

Corrosion test specimens are convenient for determining average corrosion rates over periods of typically one to three months. They are also a relatively economical way of comparing various alloys for extended periods. Corrosion test

specimens are not suitable for determining the timing or magnitude of corrosion upsets within the exposure period.

### Electrical Resistance Probes

Electrical resistance probes are essentially "automatic" coupons, since they may be measured without removal from the system. The physical loss of material is measured by the increase in electrical resistance that is created in the test specimen as it corrodes. The resistance of the test specimen is compared to a reference specimen of the same material that does not corrode, since it is protected from the corrosive environment. This method of measurement compensates to a first order for resistance changes due to temperature. This technique is the most widely used system for automatic monitoring on a continuous basis. It is the only method of this type capable of use in virtually all environments—gases, liquids, or solids—whether conductive or nonconductive. It is not dependent on the variability of factors that apply to electrochemical methods. Changing the thickness of the element varies the sensitivity of the measurement. Probe span is typically half of the measurement element thickness. Measurement resolution of electrical resistance systems is typically 1 part in 1000 of the probe element span when using conventional electronic systems. With more recently developed high-resolution probes and electronic systems, this resolution has been increased to as much as 1 part in 262,144 (18 bit). Corrosion rate changes are detected by changes in the slope of the graph of metal loss against time [see Fig. 1, taken from ASTM G 96, Guide for On-Line Monitoring of Corrosion in Plant Equipment (Electrical and Electrochemical Methods)]. Changes in corrosion rate are detected typically in a period of a few hours to a few days with conventional electrical resistance systems, and in minutes to an hour or two for high-resolution systems. The response time to detect corrosion rate changes is inversely proportional to the probe element thickness. Temperature transients can cause second order noise on the measurement that can increase the time required to detect a corrosion upset. The sensitivity of electrical resistance systems is well-suited to detect quickly the loss of corrosion inhibitor, changes in corrosion caused by changes in operating conditions, or for adjustment of inhibitor treatment frequency.

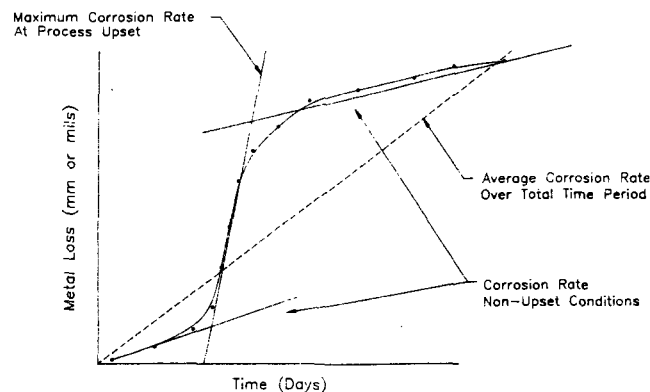


FIG. 1—Typical plot of metal loss versus time (reprinted from ASTM G 96).

In the same way as mass loss on corrosion test specimens, resistance measurements on electrical resistance probes indicate metal loss by general corrosion. Pitting is generally not noticeable until near the end of probe life, where the effect of pitting becomes "runaway" on the resistance measurement.

The measured resistance of these elements is very low so that noise interference can be significant from thermal effects, and electrical noise if the probes are not well designed. Some deposits such as iron sulfide are sufficiently conductive to provide some apparent reduction in the corrosion rate, and a few molten ionic salts may have sufficient bulk conductivity to prevent the use of these probes.

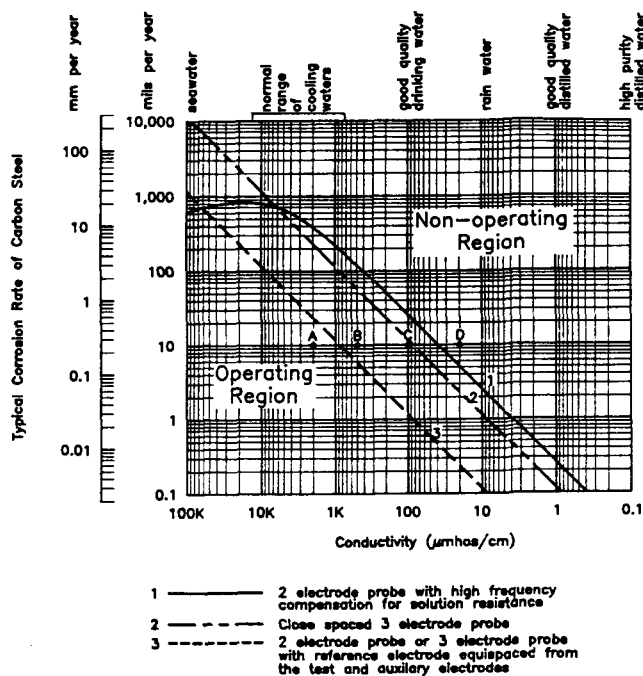
## Electrochemical Probes

Any electrochemical method of corrosion measurement has the advantage of determining corrosion rates generally over a few minutes. For field methods, the primary electrochemical method is linear polarization resistance (LPR). Electrochemical methods can only be used in sufficiently conductive media. This essentially means sufficiently conductive

water systems. They cannot be applied to gases and solids unless the water phase completely covers and connects the measurement electrodes. For a practical guide on the operating range of such probes see Fig. 2, taken from ASTM G 96.

In addition, electrochemical measurements require a critical conversion factor between the measured electrical current and the corrosion rate of the alloy. These conversion factors are variable. The factor depends on the valency of the corrosion reaction, on how each element that makes up an alloy corrodes individually in the environment, and on the empirically determined Tafel slope for the corrosion mechanism (see ASTM G 102, Practice for Calculation of Corrosion Rates and Related Information from Electrochemical Measurements).

For a given situation, such as a controlled laboratory environment, these factors may be more constant and more easily measured. In the laboratory, electrical noise can be minimized and a higher sensitivity achieved with short leads, special reference electrodes, and clean solutions. In the real world of operating plant conditions, damage of electrodes, screening of the electrodes by oil or other nonconductive



NOTE 1—See Appendix X1 for derivation of curves and Table X1.1 for description of points A, B, C and D.

NOTE 2—Operating limits are based on 20 % error in measurement of polarization resistance equivalent circuit (see Fig. 1).

NOTE 3—In the Stern-Geary equations, an empirical value of  $B = 27.5$  mV has been used on the ordinate axis of the graph for "typical corrosion rate of carbon steel".

NOTE 4—Conductivity  $\frac{\mu\text{mhos}}{\text{cm}} = \frac{1}{\text{Resistivity (ohm} \cdot \text{cm)}}$

NOTE 5—Effects of solution resistance are based on a probe geometry with cylindrical test and auxiliary electrodes of 4.75 mm (0.187 in.) diameter, 31.7 mm (1.25 ft) long with their axes spaced 9.53 mm (0.375 in.) apart. Empirical data shows that solution resistance (ohms  $\cdot$  cm<sup>2</sup>) for this geometry = 0.55  $\times$  resistivity (ohms  $\cdot$  cm<sup>2</sup>).

NOTE 6—A two-electrode probe, or three-electrode probe with the reference electrode equidistant from the test and auxiliary electrode, includes 50 % of solution resistance between working and auxiliary electrodes in its measurement of  $R_p$ .

NOTE 7—A close-space reference electrode on a three electrode probe is assumed to be one that measures 5 % of solution resistance.

NOTE 8—In the method for Curve 1, basic polarization resistance measurement determines  $2R_p + R_s$  (see Fig. 1). High frequency measurement short circuits  $C_{dl}$  to measure  $R_s$ . By subtraction polarization resistance,  $R_p$  is determined. The curve is based on high frequency measurement at 834 Hz with  $C_{dl}$  of 40  $\mu\text{F}/\text{cm}^2$  on above electrodes and  $\pm 1.5$  % accuracy of each of the two measurements.

NOTE 9—Curve 1 is limited at high conductivity to approximately 700 mpy by error due to impedance of  $C_{dl}$  at frequency 834 Hz. At low conductivity it is limited by the error in subtraction of two measurements where difference is small and the measurements large.

NOTE 10—Errors increase rapidly beyond the 20 % error line (see Appendix X1, Table X1.1).

FIG. 2—Guidelines on operating range for polarization resistance (reprinted from ASTM G 96).



deposits, physical bridging, and dynamic conditions are much more of a practical problem. Careful design of probes, cabling, and electronic equipment manages some of the inevitable compromises, and provides very effective dynamic corrosion monitoring so that the electrochemical methods have become the standard for the cooling water treatment industry.

For field use, linear polarization is the most commonly used technique for water-based process streams. For conductive waters, above about 2500 microsiemens the LPR technique may be used in its simplest form with an error of less than 20 % (see Fig 2). For a wider range of operation, the error due to solution resistance may be reduced with a close-space reference electrode, or with high-frequency measurements, which are modifications or components of the EIS laboratory technique.

Galvanic probes to monitor the effects of galvanic corrosion are much less common. Special care must be taken to consider the effect of relative areas of the different alloys in the plant as compared to those on the probe elements.

The other techniques of potentiodynamic scanning, EIS, harmonic impedance spectroscopy (HIS), and pure electrochemical current and potential noise are primarily laboratory methods that are used only in a limited way in field investigations. This is because of their relative expense, requirement for a low noise measurement environment, and clean and stable process conditions. However, simple qualitative electrochemical noise or pitting indications are used in a simple way in field applications to look at uniform versus nonuniform corrosion. Greater fluctuations and instability in the noise measurements are generally indicative of conditions leading to nonuniform or pitting corrosion.

## Other Corrosion Measurements

### *Hydrogen Probes*

Hydrogen probes may be used to assess susceptibility to hydrogen induced damage. Nascent (or atomic) hydrogen is generated from the cathodic part of the corrosion reaction in acid to neutral solution. This nascent hydrogen can permeate the steel and cause hydrogen embrittlement, hydrogen-induced cracking, and hydrogen blistering. Various types of hydrogen probes are available for detection of the hydrogen from simple pressure types to electrochemical types. While the cause of the hydrogen is the corrosion process, the method is not necessarily a good measure of corrosion rate, since hydrogen is not evolved from the cathode in alkaline environments. In addition, the proportion of evolved hydrogen that passes into the process and into the steel varies depending on contaminants in the process such as hydrogen sulfide, cyanide, or arsenic. Hydrogen measurements must generally be used in a rather qualitative empirical form since even the same grades of steel can behave differently to the same hydrogen flow rates. Separate laboratory tests on the actual plant material are best used to measure susceptibility to hydrogen damage.

### *Crevice Corrosion*

Crevice corrosion sites may be inherent with specimen mounting and may also be intentionally created at specimen or probe element locations. For example, a corrosion test

specimen mounting insulation normally provides a suitable crevice against the corrosion test specimen, and crevices may be measured at the time of removal. Some corrosion test specimens are specifically designed for crevice corrosion by having insulators with a variety of crevice gaps. On electrical resistance probes, multiple crevice-forming beads or insulations may be added to create multiple crevice corrosion sites and increase the total metal loss from crevice corrosion so that it can be detected by this "average metal loss" measurement method.

Some linear polarization probes incorporate a zero resistance ammeter to compare identical electrodes. O-rings may be added to one electrode to form crevices. Localized attack from crevice corrosion shows as an increase in the current measured between the electrodes in a zero resistance ammeter mode.

### *Galvanic Corrosion*

Galvanic corrosion may be monitored in-situ by placing a zero resistance ammeter in the electrical circuit between the electrodes of the galvanic couple under test. This may be useful as a qualitative measurement to monitor comparative corrosion inhibition treatments against galvanic corrosion. It is difficult to estimate representative plant galvanic corrosion rates. The relative areas of the two alloys in the plant, their geometry, the conductivity of the solution, and the connection path all affect the galvanic current and its consequential metal loss. Metal loss from galvanic corrosion depends on the magnitude of the galvanic current density. Consequently, the metal loss due to the galvanic current on a large area produces a much smaller metal loss per unit area than if the same galvanic current is concentrated in a small area.

### *Stress Corrosion Cracking*

This is a difficult phenomenon to monitor online. Mostly investigations are carried out over relatively long-term exposure of stressed corrosion test specimens. Slow strain rate tests that are carried out in laboratory evaluations are difficult to reproduce in the field environment. Techniques such as acoustic emission have been used on-line to detect process conditions that produce SCC, but the data analysis is still relatively lengthy, complex, and in the developmental stage.

## Online Monitoring

Online monitoring is most commonly employed to provide feedback for the control and regulation of corrosion within acceptable limits in the dynamic environment of real plant conditions. The use of inhibitors and modification of operating conditions can then be used to achieve control of corrosion. In many batch process systems, online monitoring is used to identify the part of the process causing corrosion problems. This narrows down the field of investigation for laboratory testing or simulations. In some instances, automatic samples are triggered by the measurement of high corrosion rates, for subsequent chemical analysis of the process corresponding to these excessive corrosion rates.

To be effective the specimens under test must be representative of the worst or most severe operating conditions from a corrosion viewpoint. This means positioning of the probe element or corrosion test specimen in the correct location

where the corrosion is occurring. This may be more difficult where no previous experience exists. If process simulators or side-streams are used, care must be taken to simulate accurately the process conditions that give rise to the corrosion. This can involve producing the appropriate phase (such as in condensation areas) correct temperatures and pressures, correct flow velocities, and so on.

## TESTING PRECAUTIONS

Corrosion by its very nature is rarely uniform, even over one area of a plant or even the area of a single test piece, corrosion test specimen, or probe. Considerable care needs to be exercised to ensure that monitoring is carried out effectively in order to measure the most severe conditions. The most effective or appropriate location to monitor the most severe corrosion conditions with probes or corrosion test specimens may not be the most convenient or accessible. However, priority should be given to monitoring at the correct location.

"Where should we monitor?" is probably the often most commonly asked question. This is where previous plant experience of corrosion problems is extremely important. On an existing plant this can usually be ascertained from experienced maintenance staff. On a new plant, previous experience on a similar plant is usually most helpful. Since the monitoring is being done on a test specimen rather than the actual plant, the probe or corrosion test specimen must be in a "representative" location. General location of probes and corrosion test specimens are listed in Table 6.

The combined effects of corrosion and erosion can be particularly severe and special care is required to capture its effect. In processes such as oil production, where sand may be present, erosion along the outside of bends and high velocity areas can be very high, necessitating careful probe or corrosion test specimen location to capture these most critical areas. When corrosion-resistant alloys and their durable passive films are present, this aggravates the difficulty of making accurate measurements. Erosion or cavitation may remove the protective film and then expose the base metal which corrodes at a comparatively high rate as it reforms its protective film. In such situations, small changes in the velocity can produce a very rapid change in metal loss due to this double effect.

In these cases, flow around the probe or corrosion test specimen should be carefully considered to ensure a representative measurement. Frequently in such situations, a flush mounting probe or corrosion test specimen will be most effective.

Thermal effects may also be a factor in the method of monitoring and the location of monitoring. Higher temperatures can produce a marked increase in corrosion rates. Location of a probe or corrosion test specimen in the highest temperature area with everything else being equal will generally show the higher corrosion rates. For example, on a cooling water system it is normal to measure corrosion rates at the high temperature outlet return to the cooling tower. However, it should be recognized that since the probe or corrosion test specimen is rarely heated to the surface temperature of the heat exchanger, the probe or corrosion test

TABLE 6—Probe locations.

Single Phase Flows	<ul style="list-style-type: none"> <li>• High flow rate (erosion or cavitation) areas</li> <li>• High temperature/low alloy areas</li> </ul>
Multiphase Flows	<ul style="list-style-type: none"> <li>• Usually monitor the water phase (bottom of line)</li> <li>• Points of condensation</li> <li>• Where acid gases pass into solution or organic acids are present</li> </ul>
Vessels	<ul style="list-style-type: none"> <li>• At the liquid vapor interface</li> <li>• Where concentration of contaminants occur</li> <li>• Where noncondensable gases cannot escape</li> </ul>
Heat Exchangers	<ul style="list-style-type: none"> <li>• On low pressure side of exchanger to detect corrosion leaks</li> <li>• At high temperatures, where the product is naturally corrosive</li> </ul>

specimen may not corrode at the same rate as the heat exchanger surfaces. Also, since scale will tend to occur at the hot end of the cooling water side of the heat exchanger, this may provide more corrosion protection that may not exist at lower temperatures where scale is not occurring.

The most suitable type of corrosion monitoring is dependent on the type of corrosion occurring. For general or localized corrosion, the choices are relatively easy. For cracking, online methods are currently very difficult and experimental.

## SUMMARY

Making measurements of corrosion rates and corrosion mechanisms in plant equipment is more complex than is often appreciated. There are many aspects to designing an effective in-plant monitoring program, which we have briefly covered here. A badly designed program, or even one compromised for practical difficulties, such as the correct monitoring location, can render measurements totally unrepresentative and thereby useless. However, dealing with the inherent variability of corrosion in real world application makes the use of in-plant measurements a vital requirement. A well designed corrosion monitoring program operated by skilled personnel can make an exceptionally good return on investment, when integrated into a complete process analysis. Although it sometimes seems difficult to obtain all of the corrosion management data we would like, the existing technologies are well able to make a major contribution to the reduction of the enormous annual worldwide costs of corrosion, when correctly applied. It is regrettable that in many situations, there is a lack of knowledge, or even the existence, of some of these corrosion measurement techniques by management. Automated monitoring systems using these existing techniques can make a major contribution to better asset and risk management with a relatively small investment of time and money.

## STANDARDS

### ASTM Standards

- G 1, Practice for Preparing, Cleaning, and Evaluating Corrosion Test Specimens
- G 4, Guide for Conducting Corrosion Tests in Field Applications

- G 16, Guide for Applying Statistics to Analysis of Corrosion Data
- G 30, Practice for Making and Using U-Bend Stress-Corrosion Test Specimens
- G 38, Practice for Making and Using C-Ring Stress-Corrosion Test Specimens
- G 39, Practice for Preparation and Use of Bent-Beam Stress-Corrosion Test Specimens
- G 46, Practice for Examination and Evaluation of Pitting Corrosion
- G 61, Test Method for Conducting Cyclic Potentiodynamic Polarization Measurements for Localized Corrosion Susceptibility of Iron-, Nickel-, or Cobalt-Based Alloys
- G 78, Guide for Crevice Corrosion Testing of Iron-Base and Nickel-Base Stainless Steel Alloys in Seawater and Other Chloride-Containing Aqueous Environments
- G 96, Guide for On-Line Monitoring of Corrosion in Plant Equipment (Electrical and Electrochemical Methods)
- G 102, Practice for Calculation of Corrosion Rates and Related Information from Electrochemical Measurements

### NACE Standards

- Test Method TM0169, Laboratory Corrosion Testing of Metals for the Process Industries
- Recommended Practice RP0775, Preparation and Installation of Corrosion Coupons and Interpretation of Test Data in Oil Production Practice
- Recommended Practice RP0189, On-Line Monitoring of Cooling Waters
- Standard Material Requirement MR0175, Sulfide Stress Cracking Resistant Metallic Materials for Oil Field Equipment
- Publication 3D170, "Electrical and Electrochemical Methods for Determining Corrosion Rates" (1984 Revision)

### Other References

*Perry's Chemical Engineers' Handbook*, 6th ed., McGraw-Hill Book Co., NY, 1984.

*Corrosion Monitoring Primer*, Rohrback Cosasco Systems, Santa Fe Springs, CA, 1989.

# High-Temperature

Gaylord D. Smith<sup>1</sup>

SERVICE TESTS CHARACTERIZE the performance of materials in specific applications and should mimic the environment of the actual application as much as possible. This includes simulating the chemical composition of the atmosphere, the temperature and thermal cycle profiles, stress states, fatigue conditions, and design. These tests may be accomplished by exposing test racks to actual service conditions or through the use of prototype apparatus designed and constructed to duplicate the end-use application. Additionally, laboratory service tests designed to evaluate the effect of one or more critical aspects of the exposure conditions may be employed. Service test data enable one to determine failure mechanisms, component or material life, or to screen materials for an application.

Focus here is on service tests that evaluate materials in applications that involve both high-temperature and corrosive conditions. Basic chemical, thermodynamic, and physical principles are discussed. Specimen preparation, environment synthesis and evaluation are briefly reviewed and, where appropriate, reference is made to more detailed information and studies available in the technical literature.

## CORROSION BASICS

Kinetics, chemical, thermodynamic, and physical principles will all be operating in high-temperature service test environments, requiring each investigator to have an adequate familiarity of basic mechanisms and corrosion phenomena. A brief introduction to these aspects of service testing is presented here.

### Kinetics of High-Temperature Corrosion

Reaction kinetics is the study of the speed of chemical reactions. The factors driving these reactions are a complex interaction between the test material and the environment of the service test. Environmental issues include:

- temperature
- time/thermal cycle conditions
- corrosive species and their concentration
- chemisorption and dissociation characteristics
- stress states and cyclic strains

An incomplete list of material characteristics affecting high-temperature corrosion are:

- scale integrity
- the free energy of formation of oxides of the alloying elements
- alloy composition
- alloy substructure
- alloy interdiffusion coefficients in the material and in the scale
- coefficient of expansion differences in the scale and substrate
- specimen size and shape
- solubility of gaseous components of the atmosphere in the scale and substrate
- scale adhesion
- oxide formation during different stages of the service test

Materials frequently undergo changes in corrosion mechanisms that confound elucidation of reaction kinetics. For example, the corrosion of an alloy may initially follow parabolic kinetics (see below for a description of kinetic behavior) during scale formation, then enter a stage of linear behavior as another rate-limiting mechanism controls scale growth and, finally, upon depletion of scale-forming elements, catastrophic corrosion conditions occur and the rate of corrosion changes dramatically.

Reactions depicting high-temperature corrosion can be most commonly classified as one of three types: linear, parabolic, or logarithmic [1].

### Linear Reaction Kinetics

Linear rate kinetics are most often associated with materials that do not form protective scales or whose scales are highly porous, crack-prone, or poorly adherent, thus experiencing a relatively constant surface area to the corrosive environment.

Integrated, the rate equation that describes linear reaction kinetics (Fig. 1) is

$$x = k_1 t \quad (1)$$

where  $x$  is the scale thickness or mass gain per unit area and  $k_1$  is the linear rate constant. The units of  $k_1$  depend upon the manner in which the equation is used. Where oxide scale thickness is measured, then  $k_1$  has the units  $\text{cm s}^{-1}$ ; if mass gain measurements are used, then the rate constant has the units  $\text{g cm}^{-2} \text{s}^{-1}$ .

<sup>1</sup>Technical Manager, Product Development, Special Metals Corporation, Huntington, WV 25705.

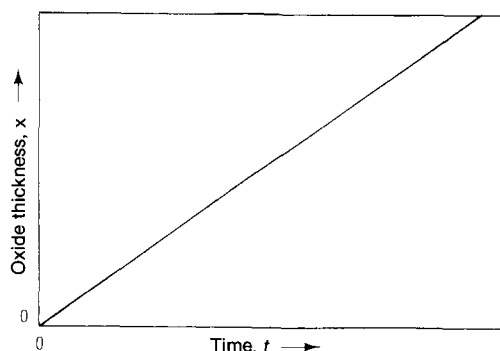


FIG. 1—Linear reaction kinetics [6].

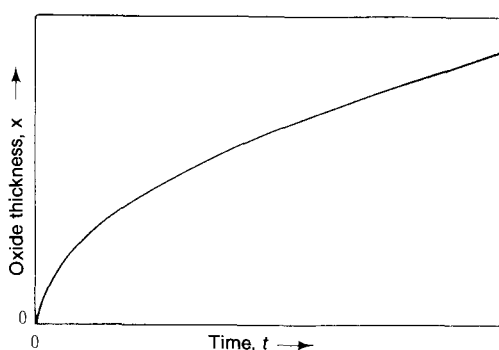


FIG. 2—Parabolic reaction kinetics [6].

### Parabolic Reaction Kinetics

Parabolic reaction kinetics describe high-temperature corrosion where the rate determining step is diffusion. This is often associated with protective scales and with internal penetration by such corrosive species as oxygen, carbon, or sulfur in certain materials.

Integrated, the rate equation describing parabolic reaction kinetics (Fig. 2) is

$$x^2 = k_2 t \quad (2)$$

where  $x$  is the scale thickness or mass gain per unit area,  $k_2$  is the parabolic rate constant with the units  $\text{cm}^2 \text{s}^{-1}$  for scale thickness measurements and the units  $\text{g}^2 \text{cm}^{-4} \text{s}^{-1}$  for mass gain measurements. The high-temperature corrosion resistance of most chromia ( $\text{Cr}_2\text{O}_3$ ) and alumina ( $\text{Al}_2\text{O}_3$ ) scale-forming materials follow parabolic reaction kinetics.

Internal penetration or attack can also be defined by parabolic rate equation. This term describes the formation of precipitates (both inter- and intragranular) by the interaction of one or more constituents of the atmosphere with the substrate. The reactive species of the atmosphere dissolves in the substrate if the gas pressure is below the dissociation pressure of the compounds formed by the reactive species with components of the substrate. The reactive species of the atmosphere diffuse into the substrate and form the most stable precipitate possible. Internal penetration

occurs only if the reactive component of the substrate diffuses outwardly more slowly than the gaseous species diffuses inwardly. Wagner developed a simplified equation to approximate internal attack [2].

$$X = \left[ \frac{2N^s D t}{v N_B^i} \right]^{1/2} \quad (3)$$

where

$X$  = depth of internal penetration at time  $t$ ,

$N^s$  = mole fraction of reactive gaseous species in the substrate at the surface,

$D$  = diffusion coefficient of the reactive species in the substrate,

$t$  = time,

$v$  = ratio of reactive gaseous species atoms to substrate reactive component atoms in the precipitate, and

$N_B^i$  = mole fraction of reactive component initially in the substrate.

### Logarithmic Reaction Kinetics

Logarithmic reaction kinetics are most often associated with low-temperature service tests, the initial stages of oxidation of certain materials, and with thick scale behavior where internal scale cavities or precipitates interfere with diffusion mechanisms [3]. The rate equation describing logarithmic reaction kinetics (Fig. 3) is

$$x = k_{\log}(t + t_0) + A \text{ (direct log law)} \quad (4)$$

$$1/x = B - k_{il} \log t \text{ (inverse log law)} \quad (5)$$

where  $A$ ,  $B$ ,  $t_0$ ,  $k_{\log}$ , and  $k_{il}$  are constants at constant temperature.

Logarithmic rate behavior can occur when the diffusion paths for ions or vacancies are reduced as a function of time. For example, this can occur when vacancies collect at the metal/scale interface and result in cavity formation or partial scale detachment, which, in turn, inhibits pre-existing scale growth mechanisms. It can also occur in alloys when particles of a very stable but slow growing precipitate form within the scale or at the metal/scale interface and restrict the growth of a much faster growing scale component. Growth stresses within the scale may also result in logarithmic rate kinetics if they cause the scale to develop short cracks parallel to the substrate interface. Inverse logarithmic rates have been associated with copper, aluminum, and iron at temperatures near room temperature.

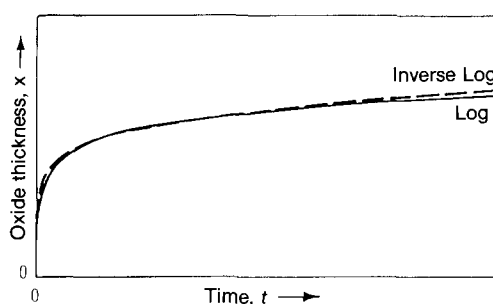


FIG. 3—Logarithmic reaction kinetics [6].

Two not uncommon forms of high-temperature corrosion that do not lend themselves to mathematical modeling are (1) breakaway corrosion and (2) catastrophic corrosion.

#### Breakaway Corrosion

Breakaway corrosion (Fig. 4) commonly occurs if numerous cracks continuously form and extend rapidly through the scale. It can also occur for alloys that have had one component (principally the most stable scale former) either effectively depleted from the alloy through repeated scale formation and spallation or through selective internal compound formation. Breakaway corrosion leaves bare substrate continuously exposed. Mass change measurements are meaningless during breakaway corrosion as scales rapidly form and break away from the substrate. Efforts to predict the onset of breakaway corrosion have been attempted for iron-base oxide dispersion alloys [4].

#### Catastrophic Corrosion

Catastrophic corrosion refers to the unique situation where a liquid phase is formed as a consequence of the corrosion process. This can occur either when the metal is exposed to the vapors of a low melting point compound or during corrosion of a substrate having a component that

forms a low melting point compound with one or more of the corrosive species of the service test atmosphere. Table 1 lists a few common oxides, sulfides, and chlorides known to initiate catastrophic corrosion.

While the exact mechanism of catastrophic corrosion is debated, it is clear that a liquid phase is essential and that it initiates at the scale/atmosphere interface and penetrates the scale along grain boundaries and pores to reach the substrate. Once at the scale/substrate interface, the liquid phase spreads out by capillary action destroying scale adhesion. Predictable corrosion rates under conditions of catastrophic corrosion are unlikely as different areas of the substrate undergo ever changing corrosive attack. Catastrophic corrosion can be unpredictably temperature-dependent as observed in waste incinerator simulation testing [5]. Iron-base heat-resistant alloys are subject to chlorine attack that forms  $\text{FeCl}_2$  at 676°C and above. For example, this attack is initially quite high upon formation of the liquid  $\text{FeCl}_2$  phase, then decreases somewhat as the sublimation rate increases only to begin increasing mass loss rates once again as a result of further increasing temperature.

#### Determining Kinetic Effects

Each investigator is encouraged to graphically plot the test results (mass change, scale thickness, etc.) as a function of time at constant temperature and pressure and as a function of temperature at constant time and pressure or if pressure is of prime importance as a function of pressure at constant time and temperature. These plots will permit the investigator to gain an insight into the form of the kinetics operating in the service test. Caution is offered not to extrapolate short time data into life predictions or to necessarily assume a smooth change in corrosion rates over a wide range of temperatures.

### CHEMICAL, THERMODYNAMIC, AND PHYSICAL PRINCIPLES OF HIGH-TEMPERATURE CORROSION

Chemical, thermodynamic, and physical principles underpin the corrosion mechanisms and their rates, which occur in any given service test. Each investigator must address the relevant principles operating in the test environment to fully understand the factors influencing performance.

Due to extensive data on crystal structures (both scales and substrates) and their properties, including melting points, boiling or sublimation temperatures, vapor and dissociation pressures, coefficients of expansion, molar volumes, free energy of reaction, and phase stability, it is left to each investigator to consult with the appropriate sources for the necessary data. One excellent source describing the fundamentals of high-temperature corrosion with accompanying tables of data is found in Ref 6.

Of particular importance to high-temperature corrosion investigators are isothermal phase stability diagrams. These diagrams fix temperature and plot the other variables of gas pressures or alloy composition against each other. These diagrams show the species that will be most stable for a given set of conditions. Stability diagrams for selected metal-carbon-oxygen, metal-chlorine-oxygen, and

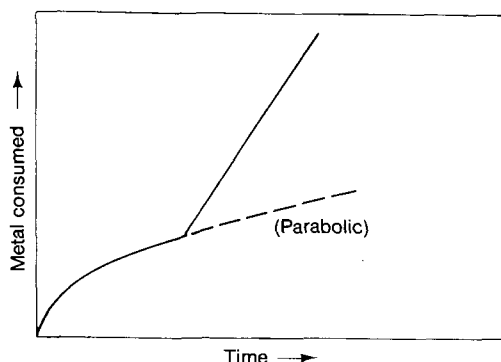


FIG. 4—Breakaway corrosion kinetics [6].

TABLE 1—Example of Low Melting Compounds and Eutectics that Could Lead to Catastrophic Corrosion.

	Melting Point °C
Oxides	
$\text{V}_2\text{O}_5$	674
$\text{MoO}_3$	795
$\text{Bi}_2\text{O}_3$	817
$\text{PbO}$	885
$\text{WO}_3$	1470
Chlorides	
$\text{MoCl}_5$	194
$\text{WCl}_5$	240
$\text{MnCl}_2$	652
$\text{FeCl}_2$	676
$\text{CoCl}_2$	740
$\text{NiCl}_2$	1030
Metal-Sulfide Eutectics	
$\text{Ni-Ni}_3\text{S}_2$	645
$\text{Co-Co}_3\text{S}_3$	877
$\text{Fe-FeS}$	988
$\text{Cu-Cu}_2\text{S}$	1067

metal-sulfur-oxygen systems are found in Ref 7, and for coal gasification/combustion atmospheres in Ref 8. An example of a stability diagram for the Fe-Cr-Ni-S-O<sub>2</sub> system is given in Fig. 5 [9].

Investigators can derive their own stability phase diagrams from standard free energy diagrams. The relative stability of the compounds of gas-metal reactions is usually shown on a Gibbs energy-temperature diagram. Gibbs energy-temperature diagrams for numerous elements and bromine, chlorine, fluorine, iodine, nitrogen, and sulfur are available [10]. The standard Gibbs energies of formation of selected oxides as a function of temperature are shown in Fig. 6 [11]. For an explanation of how to interpret a Gibbs energy-temperature diagram, the reader is referred to Ref 6.

Knowledge of the diffusion coefficients in the scale and substrate are important in relating performance to fundamentals. The diffusion coefficient  $D$  increases exponentially with temperature according to the Arrhenius equation:

$$D = D_0 \exp - Q/RT \quad (6)$$

$D_0$  = constant that is a function of the diffusing species and the medium,

$Q$  = activation energy for diffusion,

$R$  = gas constant, and

$T$  = absolute temperature.

The activation energy  $Q$  is a measure of the temperature dependence of a diffusion process. The higher the value of  $Q$ , the more rapid is the diffusion at high temperature and the slower it is at low temperatures. Activation energies for interstitial diffusion are much lower than for vacancy diffusion.

Epitaphial effects of a scale can influence diffusivity as does any defect such as porosity, grain boundaries, cracks, dislocation substructures, etc. Impurity cations can have a great effect on diffusivity in the oxide depending on the valence of the impurity ion and the semiconducting properties of the scale. Common scales formed from oxides, sulfides, and nitrides can be classified as  $p$ -type,  $n$ -type, or amphoteric semiconductors. The  $p$ -type, metal-deficit scales are nonstoichiometric with cation vacancies present. Impurity ions with valencies greater than the  $p$ -type semiconductor will tend to increase the concentration of cation vacancies and, hence, diffusivity. Lower vacancy ions will have the opposite effect. Impurity ions with the same valence should have little effect on diffusion. The  $n$ -type semiconductors

have negatively charged free electrons as the major charge carriers;  $n$ -type semiconductors have either excess cations or deficient anions. The effect of impurities on diffusivity is the opposite of that which occurs in  $p$ -type semiconductors.

Physical factors can play a major role in service, and each investigator should be alert to the significance of these factors. Included here are such factors as the volume of scale to the volume of substrate from which it is produced, the so-called Pilling-Bedworth ratio [12], the coefficient of expansion differences between the scale and substrate, the effect of the relative scale thicknesses, scale transformation stresses, thermal stresses, imposed stresses, plasticity of the scale, and the physical condition of the scale (porosity, presence and nature of any cracking, decohesion, and number of layers). Specimen size and shape can influence test results. Edges and corners behave differently than planar surfaces.

## BASIC MODES OF HIGH-TEMPERATURE CORROSION

The principal forms of high temperature corrosion can be classified as:

- oxidation
- carburization
- metal dusting
- nitridation
- halogen corrosion
- sulfidation
- ash/salt deposit corrosion
- molten salt corrosion
- molten metal corrosion

The first six modes of corrosion are the result of interaction between reactive gaseous species and the material of the substrate. Testing in gaseous environments is discussed in detail in the chapter on **Testing in Environments**. Ash/salt deposit corrosion is generally associated with gas turbines, fossil fuel power generation, coal gasification, waste incineration, and certain molten metal corrosion with metallurgical processing. Special service tests can be found in the literature that mimic molten metal, salt, and glass industry environments. Especially helpful is the text by Lai, *High Temperature Corrosion of Engineering Alloys* (1990).

## TESTING IN ENVIRONMENTS

Oxidation is the most commonly encountered high-temperature corrosion reaction. It is likely found as one of the constituents in most mixed oxidant environments and serves to either aggravate or ameliorate sulfidation, carburization, halogen corrosion, nitridation, and ash/salt deposit corrosion. Oxidation environments may be classified on the basis of their oxygen activity being either "oxidizing" (excess free oxygen) or "reducing" (no free oxygen) at equilibrium for the gas mixture. Mixed oxidant environments with low oxygen activities are generally more corrosive.

As with oxygen, sulfur-containing environments are quantified on the basis of their sulfur activity. Solid sulfide scales

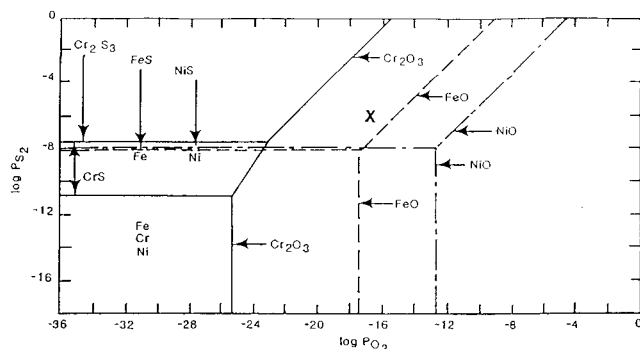


FIG. 5—M-S-O stability diagram for the Fe-Cr-Ni system at 870°C [9].

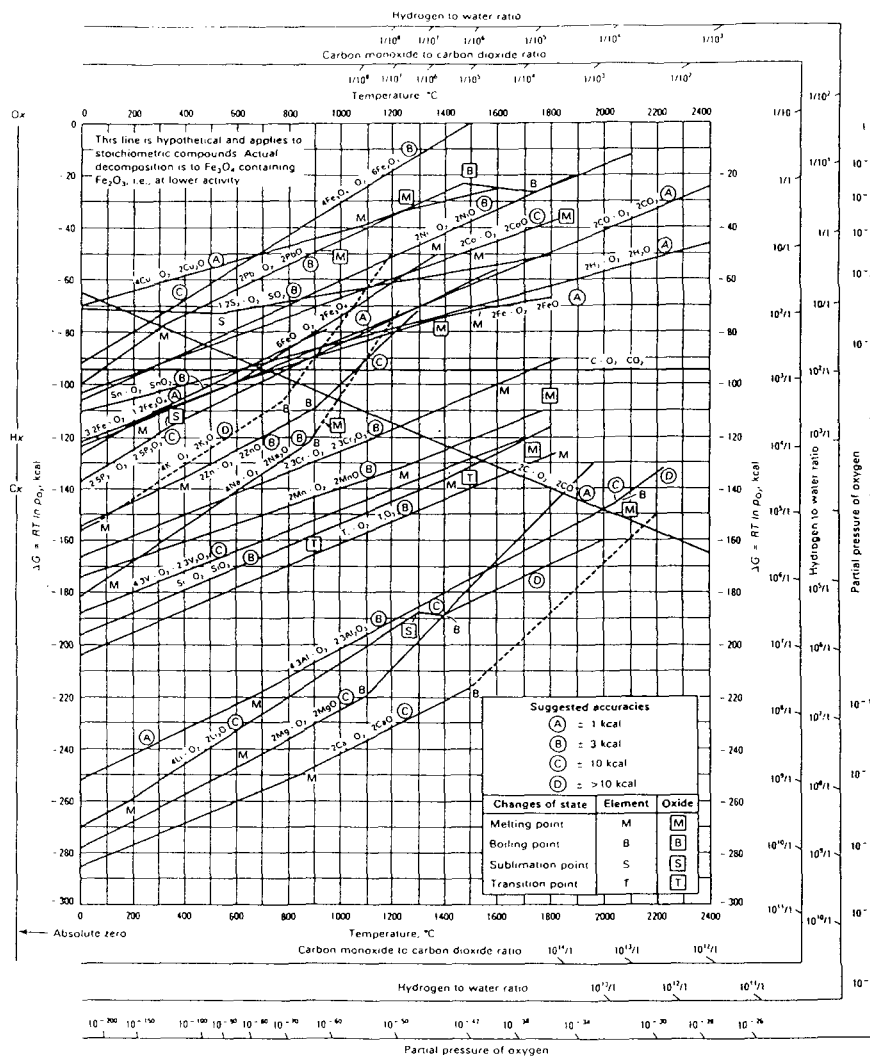


FIG. 6—Standard Gibbs energies of formation of selected oxides as a function of temperature [17].

generally grow at faster rates than their corresponding oxides. Liquid sulfide phases are especially damaging and can be troublesome for alloys containing more than 20 % nickel as the nickel-sulfide eutectic melts at about 645°C. Ash and slag from combustion products may aggravate sulfidation by shielding the substrate from oxygen or fluxing protective scales.

Carburization is typically controlled by both carbon and oxygen activities. Generally, the lower the oxygen activity, the greater the tendency for carburization to occur. While carbide scales do form, it is more frequently observed that inward diffusion of carbon has occurred. This inward diffusion can create a number of material problems, notably embrittlement, distortion, and reduction in oxidation resistance.

Nitridation characteristics are similar in behavior to that of carburization, although not as industrially common in occurrence. It is frequently observed in materials exposed in air at relatively high homologous substrate temperatures, in ammonia production, and in nitrogen-based atmospheres. As with carburization atmospheres, increasing oxidation activity decreases nitridation at a given temperature.

Service testing to simulate ash/salt deposit corrosion is of importance to a number of industries. The fossil-fired power generation industry must deal with what is called "fuel ash corrosion" from sulfur- and vanadium-containing fuels and alkali, chlorine, and sulfur in coal. The gas turbine industry must deal with "hot corrosion" problems arising from sulfur in fuel and sodium salts from ingested air. Waste incineration environments can become even more complex with refuse containing sulfur, chlorine, phosphorus, and numerous metallic elements.

## SERVICE TESTING

### Specimen Preparation

The subject of specimen selection and preparation is given thorough treatment in ASTM G 1, Practice for Preparing, Cleaning, and Evaluating Corrosion Test Specimens and each investigator is encouraged to review this information. Attention to detail is critical to successful service testing



and it begins with a complete metallurgical profile on the material to be tested. Included here is the chemical composition, fabrication history, and a knowledge of the microstructure. Positive identification of all specimens is essential. Stamping numbers on all specimens is frequently used for identification purposes. Brittle materials can be notched. Setting up a pedigree reference material to be used over and over again in order to "calibrate" each run of the service test is strongly recommended. Duplicate samples will aid in assuring a certain accuracy of the data.

If the ultimate purpose of the service test is to evaluate wrought materials for a particular application, then the majority of the materials tested should reflect the selection of appropriate wrought materials. Similarly, cast components should have a bias toward cast substitutes. This is because costs, physical properties, and available forms lend themselves to either wrought or cast alloy construction. If welded construction is involved in the end-use, welded specimens should be part of the service test series. Again, the investigator must know the welding products and welding conditions used. Size and shape of service test specimens can vary widely but must be large enough to obtain meaningful quantitative data. In testing where internal penetration occurs, such as in carburization, it is important to have a specimen large enough to not become saturated prior to completion of the test. Edges and corners do not behave the same as planar surfaces. The investigator should consider which to emphasize through test specimen geometry. For wrought specimens, large surface to edge area is desirable to more accurately reflect typical equipment. If the effects of service conditions on mechanical properties are sought, machined test specimens should be exposed.

Although clean, uniform, and defect-free surfaces are rarely found in plant equipment, it is important to strive for a clean, uniform surface condition in order to assure meaningful and reproducible results. A common surface finish is produced by dry polishing with nominally #120 abrasive cloth or paper. The sample is polished until the surface is of uniform condition. Machining may be necessary to remove scale or other defects prior to polishing. Carburized or decarburized layers should be removed. Sheared metal may have a cold-worked layer that requires removal although this could be less important in high-temperature test environments. Certain materials may require special handling or safety procedures that can be obtained from the manufacturer.

After surface preparation, the sample must be carefully measured to permit an accurate calculation of surface area. The sample is then thoroughly cleaned in a solvent, dried, and weighed as precisely as possible. Typically, small specimens should be weighed to within 0.1 mg. Changes in mass and dimensions will occur during service testing and the precision of the results will be no better than those of the "before and after" mass and dimensions. Once weighed, the samples should be inserted into the test environment or stored in a desiccator.

### Service Test Atmospheres

Simulating the environment of an industrial process or application is a compromise in most situations. Most

atmospheres consist of mixed oxidants of varying partial pressures (activities), temperature gradient profiles, and, in some cases, velocity and erosion parameters as well. Key application variables should be identified and care should be taken to see that these variables are suitably simulated in the service test. Characterization of gas composition is as essential as the control of temperature and gas flow rate. This will assure that the system is at equilibrium and is free of extraneous components. If accurate and dependable atmospheres are to be maintained, care must be paid to flow stability and to maintaining calibrations. Atmosphere synthesis may require a stream of apparatus consisting of such units as an inlet saturator, exhaust condensers, gas preheater beds, catalyst beds, heat shields, bubblers, mass flow meters, and analytical instrumentation. It is helpful to fix flow meter inlet pressure at a constant, uniform level and meter the gaseous components with electronic mass flow controllers of the proper capacity range. Simple flow meter-needle valve controls should be limited to single component gases or for purge streams. Mass flow controllers will maintain uniform flow rates until a back pressure of 36 kPa is reached. Any service test environment that could cause system blockage through condensation, sulfate formation, coking, or line corrosion should be constantly monitored and relief valving provided. Corrosive gases such as sulfur trioxide will require corrosion-resistant materials of construction. Polyethylene is a convenient tubing material and does not appear to affect gas dewpoints as low as  $-73^{\circ}\text{C}$  (approximately 2 ppm). If the system is to be monitored using a gas chromatograph, septums must be appropriately located in the gas stream, preferably both immediately before and after the specimen reaction chamber. For more information on atmosphere simulation and analysis, the reader is referred to Refs 13 and 14. References to methods for purifying elemental gas streams are described in Ref 1.

### Service Testing Techniques

Data collection depends on the purpose of the service test. Measuring techniques include mass and dimensional changes, volumetric measurement of reactive gas consumption, changes in mechanical and physical properties, metallography, and radiographic analysis. These techniques are described in detail throughout this text, and it is the intent here to only caution a new investigator of several common mistakes that can occur in high-temperature corrosion testing. Any determination method that measures film formation during the initial period of scale growth can be highly misleading (and usually is) when it comes to extrapolating the results to long-term service. Only in the few instances where linear oxidation kinetics prevail over time would gravimetric data be valid for predicating service life. Care must be taken to assure that corrosion behavior has been measured over the entire range of temperature and pressure expected in actual service. For example, liquid phase formation is a function of temperature and can quite suddenly alter corrosion behavior in sulfur-containing atmospheres. Dependence on mass change data can be deceptive. Use of metallography to measure loss of metal and depth of internal penetration by the reactive gaseous species is essential to assess potential material degradation not

necessarily apparent by mass change data. For example, a net zero mass change effect for chromia-forming alloys can be observed at elevated temperatures in mixed oxidant environments where simultaneous mass loss of chromium by evaporation (as  $\text{CrO}_3$ ) occurs while internal attack by one or more of the oxidants (mass gain) is occurring.

## SERVICE TEST EXAMPLES

Service tests are meant to bridge the gap between fundamental data and end-use applications. These tests are used to evaluate existing materials or to screen candidate compositions for their suitability for a given application. In selected industries, service testing has become "semi-standard." Design of any given service test is a practical compromise of the critical aspects of the service conditions and a means of obtaining engineering data that in some way have their origins in fundamental data. It is assumed that at least some readers intend to design and construct a service test for their particular application and wish to assess the typical degree of test complexity found in established service tests.

It is not uncommon to find test methods in the literature used by companies or individuals to investigate specific service applications. Readers should be cautioned about using these types of tests. While they may be valid service tests, most have not been through any formal "standardization process," including peer review and interlaboratory testing. Thus no data are available to assess precision issues of the procedure such as "repeatability" (precision issues of the procedure) and "reproducibility" (precision between different laboratories). When possible, each investigator is encouraged to follow ASTM, ASME, or NACE standards in their service testing.

Examples of specific service tests for selected applications are cited below that have achieved a high degree of acceptability. Additional discussion on high temperature corrosion testing in specific laboratory and field environments can be found in the chapter on **Testing in Environments**.

### Electric Heater Wire Tests

Two service tests have been reported in the literature for life testing electric heater wire. The first test is described by ASTM B 76, Method for Accelerated Life Test of Nickel-Chromium and Nickel-Chromium Iron Alloys for Electrical Heating. The useful life of a material is determined by electrically heating a section of wire in air to a given temperature where it is held for 2 min, followed by 2 min of cooling. This cycling is repeated until a 10 % increase in electrical resistance is noted and reported as the useful life of the material. This testing can take about one week.

A faster technique has been proposed [15]. Based on analysis of the mechanisms of electrical heater wire failure, these authors derived a test incorporating a 2 % plastic strain in the wire after a preset degree of oxidation. A microbalance was used to obtain the parabolic rate constants before and after straining. A reduced parabolic rate constant after prestraining correlated well with the ASTM B 76

Life Test results. This service test could be accomplished in a few hours.

### Residual Fuel Oil Corrosion Tests

Because residual fuel oils contain sulfur, vanadium, and sodium, these fuels for power generation can be highly corrosive as a result of combustion. Consequently, a number of investigators have described test methods for evaluating residual fuel oil corrosivity, its inhibition, and the resistance of materials to it [16–21]. In these tests, specimens are partially or completely immersed in actual or synthetic ash and heated in air, followed by mass change measurement and metallographic evaluation of internal depth of penetration. Crucible tests gain increased credibility where their results can be correlated with test rack data obtained from an operating boiler using the same fuel. Viswanathan and Spengler have devised a laboratory test method for exposing specimens to synthetic or real combustion gases [22].

### Sulfur Corrosion Tests

Sulfur-bearing gases are found in many processes in numerous industries. The petroleum and petrochemical industries are particularly plagued by sulfur-bearing, elevated temperature process streams and, consequently, have been active in test method development and material evaluation [23–25]. A pilot plant size test reactor is described in Ref 23. In sulfur-bearing environments, metal loss and total depth of penetration are the principal measurement techniques. Numerous investigators have compared their service test data with actual operating conditions. A synthetic gas environment test was formulated to evaluate the effect of heating during the manufacture of heat-resistant alloys using sulfur-bearing fuels [26]. When sodium, usually from sea salt, reacts with any residual sulfur in a combustion gas stream, sodium sulfate ( $\text{Na}_2\text{SO}_4$ ) is formed, which is a particularly aggressive corrosion accelerator of nickel- and cobalt-base superalloys. This form of attack is called "hot corrosion." Seybolt has compared sodium sulfate crucible testing to  $\text{H}_2\text{S}/\text{H}_2$  gas mixture testing at 1000°C [27]. Sulfur dioxide ( $\text{SO}_2$ ) plus air mixtures have been used [28] and saturated solutions of sodium sulfate have been sprayed on alloys at 120°C and subsequently exposed to oxygen in a heated furnace and evaluated using a thermobalance [29]. More common and also much more elaborate and expensive is "hot corrosion" testing in a burner rig apparatus. A schematic of a G. E. Lynn burner rig is shown in Fig. 7. The typical burner rig meters fuel (usually JP-4 or JP-5 aviation fuel) to the fuel nozzle where it is atomized and combusted with an excess of air, usually at an air-to-fuel ratio ranging from 15:1 to 60:1. Sea salt and any other soluble component, such as additional sulfur, can also be injected through additional nozzles. The combustion tube is usually made from ceramic and electrically heated to assure a uniform, constant temperature in the specimen test zone of the rig. The sample holder is rotated at speeds to 200 r/min and the cycle between time in the combustion zone and time in a blast of room temperature air is programmable. A typical cycle is 58 min in the combustion zone and 2 min in the air blast.

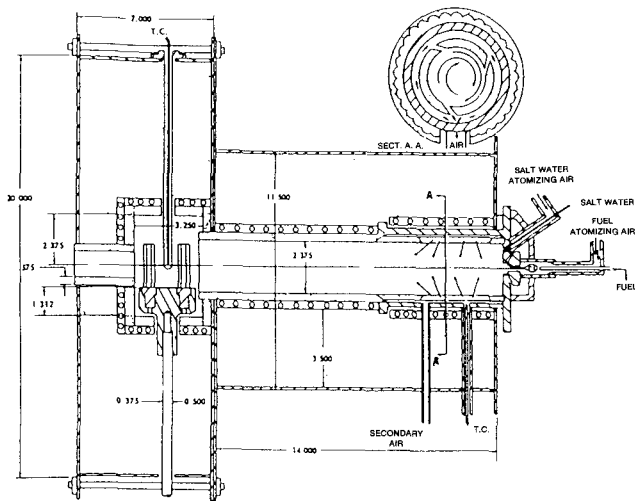


FIG. 7—Schematic cross-sectional view of a hot corrosion rig.

The test specimens are evaluated for dimensional and mass change effects, the types of scale formed, and metallographically, for metal loss and depth of attack. Evaluation methods are further described in the section of this text on **Testing in High Temperature Gases**. Just, et al. have developed a test in which a synthetic ash, similar in composition to that found on blades of gas turbines used in industrial processes, covers the test specimens and a gas atmosphere containing sulfur dioxide is passed over the sample and ash [30].

### Molten Salt Corrosion Tests

Molten salt technology is employed in a number of industries including metal heat-treating, nuclear and solar energy systems, reactive metal extraction, high-temperature batteries, and fuel cells. Because molten salts tend to flux the inherent scales that form on heat-resistant alloys, the intrinsic resistance of the metal or alloy to the molten salt is of paramount importance. Oxygen and water vapor tend to accelerate molten salt corrosion that can either be uniform thinning, pitting, or internal or intergranular attack. Testing is often done in quartz crucibles either in air or in a controlled atmosphere. Molten salts can cause significant mass transport due to thermal gradients within the system. This form of corrosion involves dissolution of an alloying element in the higher temperature regions and subsequent deposition of the element in the cooler parts of the system. This can result in system fouling as shown in studies by Adamson in thermal convection loop [31] and by Misra and Whittenberger for a heat-storage medium in an advanced solar space power system [32]. A high temperature test to evaluate candidate automotive exhaust system materials for resistance to road salts has been developed by Crum, et al. [33].

### Carburization Corrosion Tests

Carburization atmospheres are extensively found in the metal fabrication and heat-treating industries where furnaces

are heated and the atmospheres maintained by hydrocarbon fuels. The petrochemical industry operates a great number of high-temperature hydrocarbon processes where carburization is the major degradation mechanism. Mason, et al. describe a pack carburization test method that is common for evaluating the resistance of materials to carburizing environments in the heat-treating industry [34]. More common are gaseous carburization test methods that use gaseous environments with varying carbon activity and various oxygen potentials [35]. Lai has a similar technique and controls the partial pressure of oxygen to dictate the type of protective scale that forms [36]. ASTM G 79, Practice for Evaluation of Metals Exposed to Carburization Environments, describes various methods of measuring the degree of carburization of a material. One test method to evaluate the resistance of alloys to metal dusting has been described by Baker et al. [37].

## SERVICE TEST STANDARDS

High-temperature service test standards are available from ASTM. No other technical organization has yet published any standards pertaining to high-temperature corrosion service.

### ASTM G 54, Practice for Simple Static Oxidation Testing

This service test practice covers determination of preliminary information on the relative growth, scaling, and microstructural characteristics of an oxide on the surface of a pure metal or alloy under isothermal conditions in still air.

### ASTM B 76, Method for Accelerated Life Test of Nickel-Chromium and Nickel-Chromium-Iron Alloys for Electrical Heating

This service test method covers the determination of the resistance to oxidation of nickel-chromium-iron electrical heating alloys at elevated temperatures under intermittent heating using a constant temperature cycle test. This test is used for internal comparative purposes only.

### ASTM B 78, Method for Accelerated Life Test of Iron-Chromium-Aluminum Alloys for Electrical Heating

This practice covers the determination of the resistance to oxidation of iron-chromium-aluminum alloys for electrical heating alloys at elevated temperatures under intermittent heating using a constant temperature cycle test. This test is used for internal comparative purposes only.

### ASTM G 79, Practice for Evaluation of Metals Exposed to Carburization Environments

This practice covers procedures for the identification and measurement of the extent of carburization in a metal sample and for the interpretation and evaluation of the effects of carburization. It applies mainly to iron- and nickel-based alloys for high temperature applications.

Four methods are described:

- Method A: Total Mass Gain
- Method B: Metallographic Evaluation
- Method C: Carbon Diffusion Profile
- Method D: Change in Mechanical Properties

These methods are intended, within the limitations as noted for each, to evaluate either laboratory or commercial product samples that have been exposed in carburizing environments.

## REFERENCES

- [1] Scharfstein, L. R. and Henthorne, M., "Testing at High Temperatures," *Handbook on Corrosion Testing and Evaluation*, W. H. Ailor, Ed., John Wiley and Sons, Inc., NY, 1971, pp. 291-366.
- [2] Wagner, C., "Types of Reaction in the Oxidation of Alloys," *Zeitschrift für Elektrochemie*, Vol. 63, 1959, pp. 772-782.
- [3] Evans, U. R., *The Corrosion and Oxidation of Metals*, Edward Arnold, London, England, 1960, pp. 836-837.
- [4] Smith, G. D. and deBarbadillo, J. J., "Exploring the Temperature and Environmental Limits for MA ODS Alloys Based on High Temperature Corrosion Performance," *Proceedings of the International Conference on PM Aerospace Materials*, 4-6 November 1991, Lausanne, Switzerland.
- [5] Smith, G. D. and Ganesan, P., "Performance and Scale Formation of Selected High Temperature Alloys in Simulated Waste Incineration Environments Containing Gaseous Bromides and Chlorides," presented at *Corrosion 87*, 9-13 March 1987, San Francisco, CA, National Association of Corrosion Engineers, Houston, TX.
- [6] Bradford, S. A., "Fundamentals of Corrosion in Gases," *Metals Handbook, Ninth Edition, Vol. 13, Corrosion*, ASM International, Metals Park, OH, 1987, pp. 61-76.
- [7] Lai, G. Y., "Carburization and Metal Dusting," "Corrosion by Halogens," and "Sulfidation," *High Temperature Corrosion of Engineering Alloys*, ASM International, Metals Park, OH, 1990, pp. 47-72, pp. 85-115, and pp. 117-144.
- [8] Hemmings, P. L. and Perkins, R. A., "Thermodynamic Phase Stability Diagrams for the Analysis of Corrosion Reactions in Coal Gasification/Combustion Atmospheres," EPRI FP-539, Project 716-1, Electric Power Research Institute, Palo Alto, CA, 1977.
- [9] Lai, G. Y., "Sulfidation," *High Temperature Corrosion of Engineering Alloys*, ASM International, Metals Park, OH, 1990, p. 123.
- [10] Lai, G. Y., "Corrosion by Halogens," *High Temperature Corrosion of Engineering Metals*, ASM International, Metals Park, OH, 1990, pp. 85-115.
- [11] Birks, N. and Meier, G. H., *Introduction to High Temperature of Metals*, Edward Arnold, London, England, 1983.
- [12] Pilling, N. B. and Bedworth, R. E., "The Oxidation of Metals at High Temperature," *Journal of the Institute of Metals*, Vol. 29, 1923, pp. 529-582.
- [13] Kane, R. H. and Goodell, P. D., "Gas Analysis Techniques for High Temperature Corrosion Testing," *Journal of Testing and Evaluation*, Vol. 10, No. 6, November 1982, pp. 286-291.
- [14] Makavos, E. B. and Liu, C. C., "A Method for Creating Predictable Conditions in High Temperature Reactive Gases," *High Temperature Materials and Processes*, Vol. 10, No. 2, 1992, pp. 127-136.
- [15] Gulbransen, E. A. and Andrew, K. F., "Effect of Strain on the Oxidation of Nickel-Chromium Heater Alloy," *Symposium on Basic Effects of Environment on Strength, Scaling, and Embrittlement of Metals at High Temperatures*, ASTM STP 171, ASTM International, West Conshohocken, PA, 1955, p. 35.
- [16] Buckland, B. O., Gardiner, C. M., and Sanders, D. G., ASME Paper No. 52-A-161, 1952.
- [17] Oliver, D. A. and Harris, G. T., "Some Proven Gas Turbine Steels and Related Developments," *Special Report 43*, The Iron and Steel Institute, Vol. 51, 1952.
- [18] Fitzer, E. and Schwab, J., "Attack of Scaling-Resistant Materials by Vanadium Pentoxide and Effect of Various Alloying Elements Thereon," *Corrosion*, Vol. 12, 1956, p. 459.
- [19] Harris, G. T., Child, H. C., and Kerr, J. A., "Effect of the Composition of Gas-Turbine Alloys on Resistance to Scaling and to V<sub>2</sub>O<sub>5</sub> Attack," *Journal of the Iron Steel Institute*, Vol. 179, 1955, p. 241.
- [20] Witmeter, J. R., Naval Boiler and Turbine Lab, Test Report AD-143765, 26 June 1957.
- [21] Witmeter, J. R., Naval Boiler and Turbine Lab, Test Report AD-147471, 27 July 1957.
- [22] Viswanathan, R. and Spengler, C. J., "Corrosion of 85 Ni-15 Cr Alloy at 1600°F in Controlled Atmospheres Containing O<sub>2</sub>, SO<sub>3</sub>, H<sub>2</sub>S and N<sub>2</sub>," *Corrosion*, Vol. 26, 1970, p. 29.
- [23] Backensto, E. B., Drew, R. D., and Stapleford, C. C., "High Temperature Hydrogen Sulfide Corrosion," *Corrosion*, Vol. 12, 1956, p. 6.
- [24] NACE Technical Committee Report, 56-7, "Collection and Correlation of High Temperature Hydrogen Sulfide Corrosion Data," *Corrosion*, Vol. 12, 1956, p. 213.
- [25] NACE Technical Committee Report, 56-8, "High Temperature Hydrogen Sulfide Corrosion in Thermofar Catalytic Reformers," *Corrosion*, Vol. 12, 1956, p. 235.
- [26] Kane, R. H., "Corrosion of Commercial High Temperature Alloys in Simulated Coal Gasification Environments," *Materials Performance*, October 1984, pp. 9-19.
- [27] Seybolt, B. V., "Contribution to the Study of Hot Corrosion," *Transactions, Metallurgical Society, AIME*, Vol. 242, 1968, p. 1955.
- [28] Llewellyn, G., "Protection of Nickel-Base Alloys Against Sulfur Corrosion by Pack Aluminizing," *Hot Corrosion Problems Associated with Gas Turbines*, ASTM STP 421, ASTM International, West Conshohocken, PA, 1967, p. 3.
- [29] Final Report, H91063-4, Investigation of Sulfidation, United Aircraft Research Labs, USNSRDL Contact N00600-68-0639, April 1969.
- [30] Just, C. H., Huber, P., and Bauer, R., *Proceedings, 13th International Congress on Combustion Engines*, Council International des Machines a Combustion (CIMAC), Paris, France, 1979, Paper GT 34.
- [31] Adamson, G. M., Crouse, R. Se., and Manly, W. D., *Interim Report on Corrosion by Alkali-Metal Fluorides*, ORNL-2337, Oak Ridge National Laboratory, Oak Ridge, TN, 5 June 1959.
- [32] Misra, A. K. and Whittenberger, J. D., "Fluoride Salts and Container Materials for Thermal Energy Storage Applications in the Temperature Range 973 to 1400K," *NASA Technical Memorandum 89913*, NASA Lewis Research Center, Cleveland, OH, 1987.
- [33] Crum, J. R., Smith, G. D., Flower, H. L., "Resistance of Automobile Exhaust Flexible Coupling Alloys to Hot Salt Attack, Stress Corrosion Cracking and High Temperature Embrittlement," *SAE 1999-01-0372*, SAE International, Warrendale, PA, 1999.
- [34] Mason, J. F., Moran, J. J., and Skinner, E. N., *Corrosion*, Vol. 16, 1960, p. 593.
- [35] Kane, R. H. and Hosier, J. C., "Carburization Resistance of Some Wrought Nickel-Containing Alloys in Simulated Industrial Environments," *Inco Alloys International Technical Report*, 1985.
- [36] Lai, G. Y., in *High Temperature Corrosion in Energy Systems, Proceedings of the TMS-AIME Symposium*, M. F. Rothman, Ed., The Metallurgical Society of AIME, Warrendale, PA, 1985, p. 551.
- [37] Baker, B. A. and Smith, G. D., "Metal Dusting Behavior of High-Temperature Alloys," *Paper No. 54, Corrosion99*, NACE International, Houston, TX, 1999.

# **Section IV: Testing for Corrosion Types**

*J. R. Scully, Editor*

# Uniform Corrosion

James A. Ellor<sup>1</sup> and John Repp<sup>2</sup>

TESTING FOR UNIFORM corrosion is one of the most common corrosion tests employed to determine material suitability in a wide variety of applications. The following is intended to be an introduction into the subject of testing for uniform corrosion, its applications, basic methodology, and limitations. The reader is referred to applicable standards fully detailing the procedures.

ASTM G 15, Terminology Relating to Corrosion and Corrosion Testing, defines uniform corrosion as: "corrosion that proceeds at about the same rate over a metal surface." The standard does not define the term "about." This discussion defines uniform corrosion as equivalent material loss across the continuous surface of a material. This very rarely occurs in practice. The degree to which the loss is indeed identical across a surface, as opposed to localized at some material feature, is a direct indication of compliance with this definition of uniform corrosion. The analyses described are not applicable to test specimens that show significant localized corrosion—for example, if only 20 % of the surface area appears attacked, or if certain sections have areas of metal loss ten times that of other areas. Should the corrosion pattern show such characteristics of nonuniformity, the researchers will need to consider these factors in their final analysis. Often, this might be addressed by running and reporting on both uniform and nonuniform corrosion tests.

## BACKGROUND AND THEORY

An appreciation of the basic principles guiding uniform corrosion aids in discussion of test methods. In general, corrosion is the net result of chemical or electrochemical reactions occurring at the surface of a metal. An example is red-rust occurring on iron exposed to the atmosphere. In most atmospheres, bright iron or steel surfaces are not favored by nature—nature instead favors iron oxide or "rust."

Most simply, uniform corrosion results when no single region or area of a metallic surface is favored over another. Over an exposure period, the active corrosion areas are evenly distributed over a surface. In localized corrosion, some feature of the material, a local crevice, defect, or surface metallurgy, acts to promote one particular site as the most active region of corrosion.

Two aspects of corrosion should be introduced: one is the tendency for a corrosion reaction and the second is the rate at which the reaction will occur. Often, one of these principles is considered without regard for the other, leading to improper conclusions.

In uniform corrosion on a metallic surface, the tendency for a corrosion reaction results from the magnitude of the electromotive force of the corrosion cells comprising the corrosion process [1]. In some materials, the corrosion cell may arise from the heterogeneous nature of the surface, the often discussed "local cell." Conceptually the local cell is similar to a battery, often used to discuss corrosion reactions, where oxidation occurs at an anode and reduction at a cathode. Yet unlike a battery, which is comprised of different materials immersed in a common electrolyte, a local cell on an otherwise uniform piece of material can be related to, among other factors, surface impurities, alloy phases, or nonuniform stress distributions. On a pure, homogeneous surface, corrosion may still occur. Practically, the corrosion rate of a pure material is often lower than a nonhomogeneous material. Corrosion is believed to occur through simultaneous oxidation and reduction reactions taking place at a common point [2]. In either case, the tendency for the reaction can be determined by inspection of the thermodynamic equilibrium potentials of the anodic and cathodic reactions.

Consider the corrosion of iron in an acidic environment. The anodic reaction is  $\text{Fe} = \text{Fe}^{+2} + 2\text{e}^-$ . The cathodic reaction is  $2\text{H}^+ + 2\text{e}^- + \frac{1}{2}\text{O}_2 = \text{H}_2\text{O}$ . The standard thermodynamic equilibrium potential at unity  $\text{Fe}^{+2}$  concentration for the anodic reaction is  $-0.44\text{V}$  versus the normal hydrogen electrode (NHE). The thermodynamic equilibrium potential for the cathodic reaction at unit activity for  $\text{H}^+$  is  $1.229\text{V}$  versus NHE [3]. The overall cell electromotive force (EMF) is  $1.669\text{V}$ . If  $V > 0$ , then the reaction has a tendency to proceed as written. In this case, iron would go into solution and oxygen would be reduced. Similar calculations can be made for different metals in solutions with varying cathodic reactions to determine the tendency for corrosion. For instance, iron would still corrode in an oxygen-free acid. Here  $2\text{H}^+ + 2\text{e}^- = \text{H}_2$  at  $0.0\text{V}$  (NHE) and  $\text{Fe} = \text{Fe}^{+2} + 2\text{e}^-$  at  $-0.44\text{V}$  (NHE) results in a cell potential of  $0.44\text{V}$ . Fontana and Greene, among many others, provide a good description of this type of analysis [4].

While such calculations can be made to investigate the tendency for corrosion, they do not indicate the rate of corrosion. Greater cell EMF values do not necessarily indicate

<sup>1</sup>P.E., Vice President, Corpro, Ocean City, NJ 08226.

<sup>2</sup>Manager, Corpro/Ocean City Research Corporation, Ocean City, NJ 08226.

higher corrosion rates. The corrosion rate is the parameter of concern in most practical problems. The corrosion reaction itself is complex, consisting of numerous steps. The overall reaction rate, and thus, the corrosion rate, can be no faster than the slowest of these steps (the rate determining step). Each portion of the reaction sequence imparts a resistance to the corrosion reaction, i.e., limits the corrosion current resulting from the thermodynamically favored anodic and cathodic reactions.

The key rate-controlling steps are commonly referred to as concentration control and activation control [4]. Concentration control implies that the rate determining step is the rate at which reactants or products move to or from the corroding surface. Concentration control is also referred to as mass transfer or diffusion control. Common illustrations of concentration control include the ability of a reactant, e.g., dissolved oxygen, to diffuse to a steel surface in an aqueous electrolyte or the ability of a reaction product, e.g., hydroxide, to diffuse from a steel surface. High supply rates of reactants favor a higher corrosion rate; low diffusion rates of products from a surface hinder corrosion rate.

Activation control refers to the rate of oxidation and reduction that takes place at a metallic surface. Activation control is also referred to as charge transfer control. For zinc in an acid environment, one reaction product is typically hydrogen gas. Given that the solution is sufficiently acidic, there is a large abundance of hydrogen ions in the solution; thus, mass transfer of hydrogen ions to the zinc surface is not usually the rate-controlling step. The rate-controlling step can be the transfer of electrons from the zinc to the hydrogen ions to form adsorbed atomic hydrogen on the zinc surface. Charge transfer rates can vary as material properties in different chemical environments (e.g., catalytic properties).

Other factors may influence uniform corrosion rates, such as the development of oxide layers on a metallic surface. In reality, such layers limit the corrosion rate by affecting diffusion and imparting concentration control.

## UNIFORM CORROSION TESTS

The uniform corrosion test methodologies outlined below are intended to provide the user with an overview to the process. They are centered on tests in aqueous applications, but can also be adopted to monitor uniform corrosion concerns in an atmospheric exposure. Uniform corrosion tests are only useful if the test results demonstrate that the corrosion was indeed uniform. The tests described below discuss the general procedures and areas of concern. The test results will be valid to the extent that the test simulates the potential material in-service application.

Factors that affect the in-service corrosion rate by influencing the controlling thermodynamic and/or kinetic parameters that are not accounted for by the experimental design limit the usefulness of the test. Typical operational parameters of concern include, but are not limited to, exact material composition and forming techniques, service temperature, electrolyte chemistry, electrolyte velocity, time-of-wetness (wet/dry cycles), exposure duration, and mechanical forces (e.g., abrasion or stress). Often, neglect of the key

operational parameters for testing convenience provides for erroneous results. Any testing method should attempt to determine which of these parameters is key and to simulate that parameter as closely as possible during the test.

It should be noted that there is often a desire to accelerate corrosion tests by increasing the corrosive stress factors, e.g., temperature or chemical concentrations. Before accepting the results from such tests, it is wise to confirm their validity, especially in light of the importance discussed above of matching the key operational conditions. In accelerated tests, it is suggested that one confirm (1) the acceleration factor and (2) that novel or unnatural corrosion processes do not result. Running a series of tests where the stress factors are incrementally increased and the resultant corrosion rate determined can assess acceleration factors. Severe discontinuities in this relationship or the formation of novel corrosion products or corrosion morphologies can be indications that novel or unnatural corrosion processes are occurring. In such cases, the acceleration factors should be decreased.

## MASS LOSS TESTS

The simplest uniform corrosion tests are those based on coupon immersion and mass loss tests. The tests provide data on the uniform metallic corrosion rate most often expressed in English units as mils per year (mpy) or in metric units as millimeters per year (mm/y). While there are various standards for such tests, the predominant methods are those prescribed by ASTM G 1, "Practice for Preparing, Cleaning, and Evaluating Corrosion Test Specimens." This standard contains a comprehensive reference list of other ASTM standards that also apply, depending on the type of tests of interest to the investigator.

These mass loss tests consist of preparing metallic coupons, cleaning them before testing, weighing them before exposure, exposing them to the corrosive media, post-test removal of visible corrosion products, and reweighing. The corrosion rate is calculated from the mass loss measured, converted to a volume of metal loss by the material density, and finally to a corrosion rate by dividing this volume by the material surface area and the test time.

The reader is directed to ASTM G 1 for the procedure details. The following comments apply to these standard procedures and should be considered. The test coupon size selected should be large enough to minimize the ratio of edges to general surface area. On some sensitive materials, corrosion often preferentially takes place at an edge, thereby limiting the measurement of "uniform" corrosion. There are no advantages to using small coupon sizes other than the size of the test equipment. Specimens should be as large as practically possible considering the size of the test chamber, material cost, and capacity of an analytical balance for coupon mass measurements. This author has used samples as small as 2.5-cm by 5-cm by 0.3-cm, and as large as 15-cm by 10-cm by 0.6-cm.

The volume of the test media should be sufficient to ensure that the corrosion products formed or dissolved within the media do not significantly affect its properties. One may make an estimate of the required volume by estimating the

total volume of material possibly dissolved into the media based on an approximate corrosion rate and the size of the test coupon. ASTM G 31, "Practice for Laboratory Immersion Corrosion Testing of Metals" also addresses this same issue.

The exposure test(s) should be designed such that the expected mass loss of coupons is within detection limits of the measurement instrumentation. Variations to coupon dimensions and/or test duration can accomplish this. Coupons should always be large enough so that the mass loss expected over the test duration is resolvable above minimum, but does not exceed maximum detection limits. With low corrosion rates, larger coupons are necessary. Alternatively, the duration of exposure may also be changed to obtain detectable mass loss. However, this method is typically not favored, since significantly increased test durations may result.

Coupons must be identifiable before and after testing. Most simply, the coupons can be identified by a mark made directly onto the sample. However, with some notch-sensitive materials such as stainless steels that may have a tendency to favor localized corrosion over uniform corrosion, such a mark can modify the sample corrosion behavior. For the most sensitive materials, even a tag attached to the sample can affect the corrosion. In these cases, the materials should be identified by location within a test environment. Of course, the larger the test sample, the less of an influence some small mark will have on the overall results.

The material surface should be representative of the finish expected in-service. If the exact service finish is not known, the test surface finish should be noted. For stainless steel or aluminum alloys, where corrosion phenomena can attack specific elements of the metallic structure preferentially, the coupon forming process should also be noted (e.g., annealed, heat-treated, cold-rolled, cast, etc.).

ASTM G 1 provides specific details on the accuracy of the coupon weighing procedures before and after testing. Data to the fifth significant digit are suggested. While this is good practice, the practitioner should also consider the expected corrosion rate. Often in situations where the corrosion rate is expected to be quite high, data are not required to the fifth significant digit. This can be a significant time-saver if many coupons are to be tested and must be weighed on an analytical balance. The precision of electronic digital scales often makes this an unnecessary consideration.

Removal of visible corrosion products, after testing, is accomplished by cleaning of the coupon surface. Cleaning is accomplished by chemical stripping, mechanical removal (i.e., abrasive blasting or brushing), and electrolytic methods to remove corrosion products. This author's experience suggests that the best methods are abrasive blasting and chemical stripping. These techniques are more likely to remove all of the visible corrosion products without harming the metallic surface.

With respect to the chemical procedures described by ASTM G 1, the immersion time suggested for coupons in the alternative chemical baths should be used as a guideline only. There are many times when tenacious corrosion products can take significantly longer to remove than that expressed by the standard. All corrosion products must be removed without resulting in additional corrosion of the metallic substrate for an accurate mass loss measurement.

Furthermore, the standard does not describe a correction procedure for mass loss of the base metal. The standard suggests that the mass loss be plotted as a function of the number of cleaning cycles. The breakpoint in this curve is regarded as the corrosion mass loss; further mass losses are suggested to be the mass loss of base material. The standard urges that a cleaning procedure be selected such that the slope of this latter curve is "zero," i.e., the cleaning procedure is having no effect on the base metal. This is not always possible.

It is suggested that the cleaning cycle time be standardized and the number of cleaning cycles recorded. After cleaning, a clean coupon of the same base material should be subject to the same cleaning procedure and cleaning cycle. The mass loss of this material should be recorded as a function of cleaning cycles. For each cleaning cycle of the corroded specimens, an adjustment should be made for the mass loss of the base metal as a result of the cleaning procedure.

Some may argue that the base material mass loss per cleaning cycle is not the same for an already clean sample and a sample covered with corrosion products. This is a valid point; yet, if the base material is significantly affected by the cleaning solution, a correction should be attempted and the procedure described is appropriate. If the base material is not significantly affected, application of this correction factor will have no effect on the test results.

Abrasive grit blast methods for removal of corrosion products have increased in popularity in recent years. Some test specifications specifically list this as the preferred cleaning method [5]. Fine abrasive grit (the author has used 120 grit glass bead) is used in an air-powered blast cabinet. The surface of the coupon is blasted until removal of all visible corrosion products is observed. Mass loss and corrosion rates are then determined by standard methods.

The use of abrasive grit blasting has several advantages over chemical stripping. This cleaning method eliminates the use and disposal of hazardous chemicals during the cleaning processes. Eliminating hazardous chemicals also reduces the need for personal protective equipment (PPE) and reduces potential worker health and safety issues. This method also reduces the amount of time necessary to remove all corrosion products both during the cleaning and disposal operations.

The author has used this method to clean carbon steel coupons following exposure tests. Similar results were obtained from samples using this and the chemical stripping cleaning methods. Use of this method on uncorroded test samples resulted in negligible mass loss of sound base metal. Before using this method on other materials, similar comparisons between cleaning methods and removal of base metal are suggested.

The duration of the test can have a significant effect on the test data. Most materials will corrode most rapidly in the early stages of exposure to an environment—before oxide films are developed that may inhibit the corrosion rate by limiting the diffusion rate of reacting species to and from the metallic surface. Thus, tests of 24-h duration extrapolated to 30-day or 1-year behavior may be extremely conservative. Where time allows, multiple test durations may be evaluated to determine the actual effect of exposure time on uniform corrosion.



One last factor that should be considered in the design of mass loss tests is metallic plated specimens, e.g., galvanized steel. It is often difficult to distinguish between the corrosion of the zinc-galvanizing and the base steel and difficult to clean the zinc corrosion products without damaging the steel. For this example, it is suggested that the test design include both bare steel and solid zinc coupons as additional materials. Coupons of the base metal and plating materials should be evaluated for other samples, e.g., aluminum and nickel for nickel-plated aluminum samples. The corrosion rates of the homogeneous materials can aid in distinguishing the corrosion of the base metal and plating materials.

After completion of the test, the corrosion rate may be calculated from the mass loss as follows:

$$\text{Corrosion Rate} = (K \times W) / (A \times T \times D)$$

where

$K$  = constant,  
 $T$  = time of exposure, h,  
 $A$  = area,  $\text{cm}^2$ ,  
 $W$  = mass loss, g, and  
 $D$  = density,  $\text{g/cm}^3$ .

$K = 3.45 \times 10^6$  for a corrosion rate in mpy. Other constants include  $K = 8.76 \times 10^4$  for a corrosion rate in mm/y. Refer to ASTM G 1 for a complete listing of constants. Common material densities include about  $7.9 \text{ g/cm}^3$  for most steels and many stainless steels,  $8.9 \text{ g/cm}^3$  for copper alloys, and  $2.7 \text{ g/cm}^3$  for aluminum. Refer to ASTM G 1 for a detailed listing of material densities.

It should be realized that the utility of the tests is limited if the corrosion is not uniform. If there is extensive localized corrosion, the mass loss data will greatly underestimate the maximum corrosion rate, as it will distribute the corrosion over the entire surface of the coupon. Where localized corrosion may be a concern, the investigator may use a micrometer or other type of sensitive instrument to measure the coupon thickness before and after test. Multiple measurements should be made to ensure that the coupon surface is well-characterized. The thickness loss in mils divided by the test duration in years should be compared to the corrosion rates calculated by the above formula. The degree to which the two results agree indicates the degree to which the coupon did indeed undergo uniform corrosion.

## ELECTROCHEMICAL TESTS

Electrochemical tests are often preferred to mass loss studies as a method of measuring uniform corrosion. Such tests are preferred because in theory they: (1) provide a real-time measurement of the metallic corrosion rate, (2) can provide time-corrosion rate data on a single coupon, and (3) are rapid to perform. Disadvantages of the electrochemical tests include the requirements for comparatively expensive equipment (versus mass loss tests) and higher levels of technical expertise for data analysis. Furthermore, the data reduction requires the use of conversion-“constants,” factors applied to the results of the electrical measurements to convert the data to a corrosion rate. These “constants”

are usually developed from theoretical behavior of metals in an environment and are checked through actual mass-loss data for materials in the test environment. However, when evaluating a material in a new environment or novel operating condition, the assumption that similar conversion-“constants” apply can be misleading and result in erroneous conclusions. In such cases, a limited number of mass loss tests (or other physical tests) should be run in parallel to the electrochemical tests to confirm the validity of the conversion-“constants.” Often, if the test is only intended to develop the relative order of magnitude of corrosion, as opposed to an exacting value, this is not necessary and historical “constants” may be used.

With the advent of advanced electronics and computerization, electrochemical techniques have evolved rapidly. The most common technologies today are the polarization resistance technique, electrochemical impedance, and Tafel extrapolation. Regardless of the technique used, each relies on the same basic principles: in each test, a metallic coupon in an electrolyte is subject to an electrical perturbation. This perturbation is the application of a current from an external source (power supply). This current stimulates the surface corrosion reactions. The voltage (potential) response of the coupon is measured and correlated with the current applied—a galvanodynamic test. Conversely, the coupon potential is controlled and correlated with the requisite current—a potentiodynamic test. In either case, the resultant current is representative of the rate determining mass transfer or charge transfer rate. This may be related to the corrosion rate.

Standard test procedures are defined within ASTM standards: ASTM G 59, “Practice for Conducting Potentiodynamic Polarization Resistance Measurements”; G 5, “Standard Reference Test Method for Making Potentiostatic and Potentiodynamic Anodic Polarization Measurements”; G 106, “Practice for Verification of Algorithm and Equipment for Electrochemical Impedance Measurements”; and G 102, “Practice for Calculation of Corrosion Rates and Related Information from Electrochemical Measurements.” Each of these methods describes a standard procedure or practice for the test method. A complete discussion of the technologies is beyond the scope of the current text. For the current text, the focus is on the application of the most simple and most widely used of these techniques, the polarization resistance measurement, ASTM G 59. The parameters discussed are, however, applicable concerns for all electrochemical tests.

The ASTM G 59 standard experiment described determines the uniform corrosion rate of 430 stainless steel in  $1.0 \text{ N H}_2\text{SO}_4$  solution, purged with oxygen-free hydrogen. The procedure described is adequate for learning the basic polarization resistance techniques, equipment calibration, and operator training. However, as acknowledged by the standard, the techniques are not applicable to all material and environment combinations. The reader should consider the following modifications to the standard procedure when dealing with materials other than the calibration standards.

Consider a metal in a flowing natural water. The standard procedure suggests establishing a coupon in a standard “polarization cell.” This exposure is valid to the extent that the in-service application of the material is similar to a

polarization cell. If the electrolyte is expected to flow past the metallic surface, this will influence the local mass transfer rate, and data from a polarization cell will be of little utility if either the anodic or cathodic reaction is affected by mass transport. Agitation in the polarization cell by a stirring mechanism is perhaps better than testing under completely quiescent conditions, yet is no guarantee that the data will be representative of the actual field conditions. Experience and correlation of the test data with field results provide the best confirmation of the test setup. The test setup concerns are not limited to electrolyte flow but include electrolyte chemistry, temperature, material preparation, etc. As with mass loss tests, the closer one comes to duplicating the in-service conditions, the more confidence can be placed in the resultant data. For a more complete discussion of uniform corrosion testing under mass transport controlled conditions, the reader is referred to the chapter on electrochemical testing in this manual.

The standard procedure suggests that sample potential be monitored through 55 min of exposure before initiating the scan. This is not always an adequate time for coupon stabilization. The coupon potential versus time should be monitored for a sufficient time (even greater than 24 h if necessary) to ensure stability before beginning the scan. Stability is a relative term. However, consider that the testing will polarize (perturb) the material only a few millivolts (10–20) around its corrosion potential in a period of a few minutes. This suggests that stability is a variation of  $\pm 1$ –2 mV (less than 10 %) per the anticipated polarization resistance test period. While some may argue that the requirement for a long stabilization period eliminates the ability to get rapid data early in the exposure, it should be recalled that the procedure relies on measuring the coupon response from an external perturbation. If the natural perturbations are of the same magnitude as those imposed on the sample (external), the test data are difficult to interpret. In some cases, if the natural perturbation can be documented to be a consistent factor, this input can be subtracted from the effects of the external perturbation, and polarization resistance tests can be run before complete stabilization. Such data interpretation is beyond the current discussion.

The standard procedure suggests that the polarization scan be initiated by polarizing the material 30 mV active. The scan is then run through the corrosion potential (previously measured stabilized potential) to 30 mV noble to this value. This range may be appropriate for the standard test, but can be significantly too much for many materials in a natural environment. In many natural environments, the actual external perturbation should be limited to  $\pm 10$  mV about the corrosion potential.

It is also interesting to note that the standard procedure suggests that the scan be initiated by shifting the coupon potential 30 mV active and then scanning in a noble direction at 0.6 V/h. The standard prescribes the scan rate from the cathodic to the anodic side of the corrosion potential but not a time for polarizing the material 30 mV active. This appears contradictory. Scan rate is very important in these experiments. If the sample is “immediately” driven to a potential 30 mV active with a potentiostatic input, the sample surface can be strongly influenced. In many “real-life” experiments the procedures described are not adequate. It is

suggested that the scan be started from the corrosion potential at a standard scan rate in the active direction until the sample is polarized 10 mV active (versus 30 mV). At this point, the scan should be reversed in polarity, and the material polarized until it is 10 mV noble to the initial corrosion potential. At all times the scan rate is kept the same. The polarization resistance value is obtained as described by ASTM G 59.

With respect to the actual value of scan rate, the ASTM standard suggests a value of 0.6 V/h. Again, this is adequate for the standard test but may not be for a wider variety of materials. The primary objective of the scan rate is to perturb the sample yet minimize any “capacitive” effects at each point along the scan. If a potentiodynamic scan is run too fast, the amount of current required to “hold” the indicated potential is too high. Thus, the calculated polarization resistance value is too low.

One simple way of determining an appropriate scan rate is to use a scan rate slow enough so that if the scan is stopped (and the applied potential or current is maintained constant), the current does not decrease with time under a potential controlled scan, nor does the potential continue to shift under a current controlled scan. A little trial and error will determine the optimal scan rate. Often times it can be much faster than 0.6 V/h, especially in well-aerated, flowing solutions. Under quiescent conditions with oxidized materials, the necessary scan rate is much slower than 0.6 V/h. A detailed discussion on effects of scan rate, ohmic voltage error, choice of over-potential, and other factors appears in the chapter on electrochemical test methods in this manual.

Under any conditions, the choices of scan rate and magnitude of the potential scans about the corrosion potential dictate the individual test duration. With multiple samples and frequent testing, a significant amount of labor and time can be consumed in the testing. The test designer must balance the alternatives of the test matrix with the available testing time and budget.

Following acquisition of the polarization resistance value, a corrosion rate can be calculated by ASTM G 102. Briefly,

$$\text{Corrosion rate} = (K \times i_{\text{corr}} \times EW)/(D)$$

where

Corrosion rate = mm/y,

$i_{\text{corr}}$  = corrosion current density,  $\mu\text{A}/\text{cm}^2$ ,

$K = 3.27 \times 10^{-3}$ , mm g/ $\mu\text{A cm yr}$ ,

$EW$  = equivalent weight = atomic weight of the primary alloy element/number of electrons involved in the oxidation process,

$D$  = material density, g/cm<sup>3</sup>,

$i_{\text{corr}} = B/R_p$  where  $B$  = Stern-Geary constant, mV, and  $R_p$  = polarization resistance,  $\Omega\text{-cm}^2$ .

The derivation of the value for the term  $B$  is a central focus of ASTM G 102 and need not be repeated within the current text. As an approximate value for quick calculation only,  $B$  often is about 20 mV.  $EW$  values include 9 for aluminum alloys, 50 for copper alloys, and 27 for carbon steel.

Refer to ASTM G 102 for more precise values and determination methods for multi-element alloys. Yet these data can be used to estimate the corrosion rate predicted by the  $R_p$  value obtained.

It is also noted that Scully provides an excellent summary of electrochemical tests in Section III: Type of Tests in this text.

## OTHER TECHNIQUES

There are many other techniques for measuring corrosion. Some of these may rely on chemical solution analysis or physical measurement of metal loss. One widely used additional technique is provided by ASTM G 96, Practice for On-Line Monitoring of Corrosion in Plant Equipment (Electrical and Electrochemical Methods). This guide covers two basic procedures. In one, a sample of the material, usually in the form of a continuous wire, is immersed into the environment of interest (liquid, air, solid, or multiphase). The electrical resistance through the wire is determined. As corrosion consumes the cross section of the wire, the resistance increases proportionately. The second procedure uses the polarization resistance technique described in ASTM G 59 to determine the corrosion rate in the environment.

Both of these techniques have their utility and drawbacks. The resistance probe is limited because it is difficult to determine if the electrical resistance increases being monitored are the result of localized or uniform corrosion without visual inspection of the probe. However, the resistance probe is of great use in that it may be used in multiphase environments, whereas the polarization resistance probe is mostly limited to use in conductive aqueous

environments. The primary advantage of the polarization resistance probes is that they can provide a rapid indication of the corrosion rate on a real-time basis. As with any polarization resistance technique, the procedure assumes that the predominant corrosion mode is uniform attack and not pitting. Polarization resistance-type probes are not suited for monitoring where pitting corrosion is of concern. On both types of probes, one additional concern has to be the presentation of the probes to the environment being monitored. In typical installations, the probes are used as through wall fittings in process piping. The flow characteristics imparted on the probes is not the same as that observed on the pipe walls, and therefore, the corrosion rates may not be similar. This is less of a problem in process vessels, yet is always a concern. ASTM G 96 describes additional precautions in the use of the probes.

## REFERENCES

- [1] Uhlig, H. H. and Revie, R. W., "Corrosion Tendency and Electrode Potentials," *Corrosion and Corrosion Control, An Introduction to Corrosion Science and Engineering*, 3rd ed., John Wiley and Sons, New York, 1985.
- [2] Bockris, J. O'M. and Reddy, A. K. N., *Modern Electrochemistry*, Plenum Press, New York.
- [3] *Handbook of Chemistry and Physics*, 68th ed., R. C. Weast, Ed., CRC Press, Boca Raton, FL, 1987.
- [4] Fontana and Greene, *Corrosion Engineering*, McGraw-Hill Book Company, New York, 1987.
- [5] General Motors Corporation, "GM 9540P, Accelerated Corrosion Testing," September 1997.

# Pitting

Robert G. Kelly<sup>1</sup>

## INTRODUCTION

PITTING CORROSION occurs when discrete areas of a material undergo rapid attack, although the vast majority of the surface remains virtually unaffected. This morphology is in sharp contrast to uniform corrosion in which all parts of the exposed surface recede at approximately the same rate. Essentially, all metals and alloys undergo pitting corrosion under some set of experimental conditions, although the relative susceptibility varies widely. The basic requirement for pitting is the existence of a passive state for the material in the environment of interest. Pitting occurs when portions of the metal surface lose their passivity and dissolve rapidly. This loss of passivity often occurs at heterogeneities in the surface (either physical or chemical). Pitting of a given material depends strongly on the presence of an aggressive species in the environment and a sufficiently oxidizing potential (e.g.,  $\text{Cl}^-$  ion in neutral, aerated aqueous solution for Type 304 stainless steel). There are many metal/environment combinations that can lead to pitting, as extensively reviewed by Szlarska-Smialowska [1] and more recently by Frankel [2]. In many situations, pitting can severely limit the performance of the material.

Testing for localized corrosion resistance usually aims at meeting one (or more) of four general goals: (a) alloy ranking for selection or development; (b) failure analysis; (c) determination of the effects of changes in process parameters; and (d) prediction of penetration rates. Of the four, the last is by far the most difficult to accomplish, but also the most important in many cases. This chapter discusses the different types of tests that have been developed for pitting corrosion. The physical and chemical basis for each test is described, as are some of the practical applications and limitations. The first section describes coupon exposure testing, while the second describes electrochemical testing.

## COUPON TESTING

The exposure of test coupons to the corrosive solutions to evaluate localized corrosion resistance has a long and successful history. The materials of interest are typically machined into coupon form before being measured, cleaned, weighed, and exposed to the corrosive medium. After a set

period of time, the coupons are removed; the surfaces are carefully cleaned and evaluated for attack. General requirements and information on coupon testing can be found elsewhere in this manual as well as in other sources [3,4]. ASTM G 1, Practice for Preparing, Cleaning, and Evaluating Corrosion Test Specimens, describes the details of the preparation of test coupons. ASTM G 4, Method for Conducting Corrosion Coupon Tests in Plant Equipment, details related information on the performance of such tests in plant equipment under operating conditions. The advantages of properly conducted coupon testing include the fact that actual process streams can be used, a large number of coupons can be exposed simultaneously, and various forms of corrosion can be detected. Disadvantages include the inability to monitor the time dependence of the corrosion process and the long exposure times usually required to characterize both the initiation period and the propagation rate.

## Coupon Preparation and Analyses

Because detailed information on coupon testing is available elsewhere, this section will focus on the aspects of such testing that are specific to the evaluation of pitting corrosion. When performing coupon exposures, it is important to include alloys whose corrosion behavior in the environment of interest is well characterized and reproducible to serve as an internal standard. This protocol is of particular importance when localized corrosion is studied. Because pitting has a stochastic nature, the use of these "controls" increases the confidence with which final material selection choices are made. If the control materials behave as expected, it is probable that the results for the other materials reflect typical behavior for the environment of interest.

Whereas mass loss characterizes the rate of uniform corrosion well, such measurements can be extremely misleading for pitting corrosion. Badly pitted specimens can exhibit negligible weight loss if the attack is extremely localized. In fact, the more a given amount of attack is localized, the more severe the pitting problem. ASTM G 46, Practice for the Examination and Evaluation of Pitting Corrosion, describes different methodologies for evaluating pitting corrosion attack. Visual attack of both cross sections and plan views of pitted specimens can be ranked as shown in the standard. Whereas pit density (number/cm<sup>2</sup>) is important, pit depth measurement is often the most directly applicable measurement. Values for both average pit size and for the deepest pit observed are useful. To quantitatively evaluate the depth of attack, a variety

<sup>1</sup>Associate Professor, Department of Materials Science and Engineering, University of Virginia, P.O. Box 400745, 116 Engineer's Way, Charlottesville, VA 22904.

of measurement methods can be used including depth gages, metallographic examination of cross sections, or change in the focus plane on a metallurgical microscope, depending on the size of the pits. Direct measurement of pit depth using confocal laser scanning microscopy is attractive in that pit depths and distributions can be obtained rapidly. All line-of-sight methods are unable to detect and characterize undercutting pits (i.e., those with “ink-bottle” shapes or those with lacy covers [6]). The pitting factor (PF) is the ratio of the average of the ten deepest observed pits to the average metal penetration by uniform dissolution, with higher values indicating a greater susceptibility to pitting. Statistical methods have also been applied to the evaluation of pitting corrosion (see ASTM G 16, Guide for Applying Statistics to Analyses of Corrosion Data, and Refs 7 and 8). In terms of predictive capability, the use of extreme value statistics is attractive [8]. Plotting the measured maximum pit depths for a large number of small samples has been used to estimate the probability that a pit of a specific depth will occur under the same conditions for a larger area [8].

### Exposure Environments

There are two general types of environments used in coupon testing for pitting corrosion: those that simulate service conditions and those that seek to accelerate the pitting process. Tests in simulated (or actual) service solutions are extremely valuable due to their direct applicability. However, because time is often of the essence, the long exposure times required usually limit the use of such tests to (a) confirmation of decisions made on the basis of accelerated laboratory tests, and (b) corrosion monitoring. The aim of testing in accelerating environments is usually alloy ranking or screening. Thus, little information is gained on the expected rate of attack in the actual application. However, the relative susceptibility of different alloy compositions or the effects of heat treatments, welding, or other processing can be assessed rapidly and quantitatively.

There is a variety of accelerated exposure tests that have been developed to aid engineers in material selection for corrosion resistance. This section will review some of those that are useful for localized corrosion resistance. Besides a brief description of the test, the scientific reasoning behind it is presented, along with comments concerning the limits of its applicability, and alterations one can make to improve the utility of the test for a specific application. An experimenter should not feel bound by the strictures of the ASTM standards if he or she can justify that by changing the procedure, more relevant information can be gained. However, it should be noted that these ASTM tests are probably the most widely used tests for localized corrosion resistance. Thus, an understanding of them can be of great importance in analyzing the results of testing performed in other labs or by manufacturers.

#### *ASTM G 48, Test Method for Pitting and Crevice Corrosion Resistance of Stainless Steels and Related Alloys by the Use of Ferric Chloride Solution*

This test involves exposure of the material to a highly oxidizing, highly acidic, concentrated metal chloride solution. In essence, it is an attempt to simulate very roughly the composition of the environment within a localized corrosion

site in a stainless steel. Briefly, a material is exposed to a 10 wt%  $\text{FeCl}_3$  solution for a relatively short time (24–72 h) at either ambient or elevated (usually 50°C) temperature. At the end of the test, the sample is examined for weight loss and localized attack (see ASTM G 46 for a recommended practice for evaluating the extent of pitting corrosion). If pitting and crevice corrosion are of concern, artificial crevices can be applied by the use of Teflon® blocks held tightly to the sample surface by rubber bands (see ASTM G 48).

The basic concept behind this test is the application of a high potential using a chemical potentiostat in an acidic, concentrated chloride solution. The ferric salt forms a  $\text{Fe}^{3+}/\text{Fe}^{2+}$  redox couple with a potential of approximately +0.45 V(SCE). The high concentration of ferric ion allows the couple to provide a large current without an appreciable change in potential (approaching an ideally nonpolarizable electrode). The cathodic reaction (reduction of ferric to ferrous ion) occurs on the boldly exposed passive surface of the material under test. Thus the redox couple serves the role of the *chemical* potentiostat. The high potential in turn nearly guarantees that the pitting potential will be exceeded, especially in such a concentrated  $\text{Cl}^-$  solution (and even more so if the test temperature is raised to 50°C). The low pH of the solution (typically about 1.3) inhibits repassivation and lowers the stability of the passive film. Thus, the ferric chloride test is a test of the resistance of an alloy to propagation of localized corrosion for most alloys, because their pitting potentials are well below +0.45 V(SCE). However, more highly alloyed materials can resist initiation in this solution, and thus the time of the test can be extended to a period of many days or the temperature increased.

This very popular test does have a number of limitations. Very few industries operate in 10 wt%  $\text{FeCl}_3$ . Thus, the relation of the results of this test to material performance in real service environments that are profoundly different is questionable, and in fact, reversals in alloy ranking can occur. For nickel-base materials, the use of a ferric ion solution is also of questionable value. Despite these limitations, the  $\text{FeCl}_3$  test will continue to be an important tool in alloy development and screening for historical, if for no other reasons.

The ferric chloride test details can be modified and still fall within the spirit of the requirements of the published method. The exposure time and temperature can be altered, as can the surface finish. As mentioned above, surface finish can have important impact on the localized corrosion behavior. For example, it can affect the geometry of occluded sites and, in some cases, it can alter the surface area for cathodic reactions. Thus, it is important that the surface finish be chosen with care to simulate the expected conditions of the application.

#### *B 117 Standard Practice for Operating Salt Spray (Fog) Apparatus and G 85 Standard Practice for Modified Salt Spray (Fog) Testing*

Probably the most widely used test for pitting resistance is salt spray. B 117 describes the experimental arrangements to be used and mandates the use of 5 wt.% NaCl at slightly elevated temperature (35°C). The test chamber allows the solution to be sprayed within its confines, creating a salt fog environment around the coupons. Such a constantly moist, salty environment is quite aggressive.

G 85 describes modifications to B 117 involving a variety of solution chemistries and exposure regimens that can be used, including acetic acid-NaCl solution, acidified synthetic sea water, NaCl solution with SO<sub>2</sub> gas added and a 0.05 % NaCl +0.35 % (NH<sub>4</sub>)<sub>2</sub>SO<sub>4</sub> solution. In addition, a variety of cycles (wet/dry) are described that have been found to be more aggressive than the constant moisture of B 117. In general, a spraying period is followed by a longer time at high relative humidity during which the sample can partially dry.

This cyclic type of exposure represents a more aggressive condition for most alloys than does constant, full immersion. Although still the subject of some debate, the generally accepted explanation involves the increased kinetics for oxygen reduction within the thin electrolyte layer that is present. Due to its limited solubility in water, oxygen reduction is usually under mixed or fully diffusion control for most alloys, particularly those undergoing stable pitting. The thin electrolyte layer present during wet/dry cycling increases the rate of delivery of oxygen to the surface by reducing the diffusion boundary layer thickness from ca. 0.05 cm characteristic of stagnant solution to the thickness of the solution layer (often between 25 and 100 microns [9]). In addition, the concentration of aggressive ionic species increases dramatically during drying periods to the point of saturation.

Although reams of salt spray data exist, their use must be approached with care. As with ferric chloride, few industries actually operate in continuous salt spray (coastal regions and ships being notable exceptions). A number of industries have found that the standard salt spray testing not only does not reproduce the damage observed in service, but also is not particularly accelerating. Thus, the auto industry has developed a more complicated cyclic test known as GM 9540 [10]. The reasons for the discrepancies between service experience and these laboratory tests are not clear, and users of the test should bear them in mind.

#### *G 69 Standard Test Method for Measurement of Corrosion Potentials of Aluminum Alloys*

Aluminum alloys are highly susceptible to localized corrosion, including pitting. For many years, G 69 has been used to determine the so-called "solution potential" of Al alloys. The test solution described in G 69 is a strongly oxidizing, near-neutral pH chloride solution. The oxidizing power originates in the 3 g/L (0.09 M) hydrogen peroxide that is added. In the 1 M NaCl, virtually all precipitation-hardened Al alloys will undergo stable pitting. The solution potential measurement is made over a period of 1 h. It represents a mixed potential between the passive portions of the surface on which peroxide reduction is occurring and the pitting sites. Thus, the potential depends on (a) the cathodic kinetics of peroxide reduction, (b) the pit dissolution kinetics, and (c) the number and size of the pits. As these characteristics vary from alloy to alloy as well as with time, quantitative interpretation of the solution potential is challenging. Mixed potential theory can be used to demonstrate that the solution potential cannot be used to rank the resistance of Al alloys to stable pitting. Nonetheless, it has been used as a type of quality control test to probe batch-to-batch variations within a given alloy. This solution is also specified in G 110, a standard practice for evaluating intergranular corrosion of heat treatable aluminum alloys.

### **Alteration of Test Methods**

When considering how to accelerate a test, the two most commonly applied methods are to increase the temperature and/or increase the concentration of aggressive species (e.g., Cl<sup>-</sup> or H<sup>+</sup>). Either can be effective, and some of the electrochemical tests described below use the strong temperature dependence of pit stabilization as a parameter to quantify pitting resistance. That said, such changes must be introduced with care to ensure that the mechanism of attack in the accelerated test is the same as that in the actual service environment. Decreased time required for the testing should be balanced against the decreasing relevance of the results, and the consequential increase in the uncertainty in their interpretation. In addition, results from accelerated tests are useful for material selection, but not life prediction, as there is no means currently to connect the rates of pitting corrosion observed in these tests to other environments. This situation can be contrasted with crack growth testing where the similitude of the stress intensity factor, *K*, has been repeatedly demonstrated. This similitude allows results from laboratory scale test samples to be applied to service structures if the stress and flaw size and shape are known.

### **ELECTROCHEMICAL TESTS**

The main advantage of electrochemical testing is the opportunity to investigate corrosion phenomena in the solution of interest rather than in a (possibly) more aggressive and (probably) less relevant environment. In addition, a great deal of information can be gained about the dependence of the phenomena on external variables in a short time. Finally, the determination of critical potentials for initiation and propagation of localized corrosion can be useful in design decisions. For example, the use of mixed potential theory can allow prediction of the protection (either anodic or cathodic) criteria, as well as information on the galvanic couples to avoid.

#### **Specimen Mounting**

Probably the main problem associated with electrochemical testing for localized corrosion resistance is sample mounting. It can be extremely difficult to mount a sample with an insulated electrical contact and a controlled exposed surface area without introducing a crevice at the sample/mount interface. Because crevice corrosion will occur at lower potentials than pitting, the sample invariably begins to be attacked at the crevice, leading to an underestimation of the resistance of the sample to pitting. Some may argue that for the same reason, this type of testing is not overly conservative, as in service, one wants to know the potential at which any localized corrosion can occur, not just pitting. The flaw in this argument is that most crevices formed during sample preparation are not reproducible either in position or geometry, making comparisons extremely difficult. In addition, there may be applications where crevice corrosion is not the failure mode of concern, but pitting is. Such testing with crevices present would lead one to choose a more resistant (and therefore more expensive) alloy than one would actually need.

**FIG. 1—Stern-Makrides electrode assembly. (A) glass tube that protects threaded steel rod from solution, (B) PTFE gasket, (C) specimen. For more details, see ASTM G 5.**

A number of suggested solutions have been made for sample mounting, including the use of “knife-edge” Teflon washers [11], various mounting compounds and procedures [12], the use of wire loops [13], and flag geometries [14]. One experimental design even includes a crevice area that is continually washed with deionized water [15]. All of these have their limitations, and one must choose the most appropriate for the particular alloy/environment combination. The knife-edge PTFE washer, in combination with what has been known as the Stern-Makrides assembly (Fig. 1), has been used successfully in a number of applications in which a tight seal can be formed, which (a) prevents ingress of any electrolyte, and/or (b) causes the IR drop into the crevice to be so high as to prevent any polarization of the creviced surface away from  $E_{\text{corr}}$ . Because the latter of these is unlikely to occur, the prevention of ingress is critical. This prevention of solution ingress is closely related to the quality of the surface finish both in terms of its fineness (i.e., final polishing step particle size) and its uniformity. One large scratch can allow capillary action to draw electrolyte into an otherwise impervious crevice and start the crevice corrosion initiation process. This is the prime reason for the failings of this type of approach. In addition, due to the cost of the PTFE washers, many experimenters tend to try to reuse them. However, after the knife edge is deformed once, it will not form a watertight seal again, thus allowing crevice corrosion to occur.

The cell designed by Quarfort [15,16] uses a slow flow (4 mL/min) of deionized water into the creviced area to prevent the accumulation of dissolution products inside the occluded area, the hydrolysis of which leads to crevice corrosion. The design has been successfully applied to the study

of the pitting of a wide variety of stainless steels at both ambient and elevated temperature [15,16]. However, this cell can only be used for flat samples. In addition, one must be careful to ensure that the deionized water flow is uniform throughout the crevice. If a dead spot were to develop, crevice corrosion will very likely be initiated. Details of the cell can be found in Annex X2 of G 150.

One example of the effect of crevices is shown in Fig. 2 for a 18Cr-8Ni stainless steel in a solution in which propagating crevice corrosion will not occur (1 N  $\text{H}_2\text{SO}_4$ ) [12]. In this case, the higher passive current densities are observed for the insulating materials that perform poorly. In a  $\text{Cl}^-$ -containing solution, this would translate into a lower  $E_{\text{bd}}$ . As can be seen from Fig. 2, some mounting materials perform well in this solution, though it should be pointed out that these results cannot be extrapolated to other solutions. For example, the alkyd varnish is used in electroplating to mask off areas that should not be plated. Although it works well in acid solutions, it performs very poorly in neutral or basic solutions, especially on materials with passive films such as stainless steel.

If mounting cannot be accomplished, three other approaches can be used. The first is the use of a wire loop electrode, as shown in Fig. 3a. Stockert et al. [13] have used this approach to study pitting without the complications of crevice corrosion. This approach works extremely well if one can get the material in wire form, though there is always the concern of metallurgical differences between material in wire form and that in plate or tube form, which are more likely to be used in engineering applications. A related approach is the use of a flag electrode configuration, as shown in Fig. 3b. This works well with plate material by minimizing the shaft size and thereby minimizing any effects of the waterline. If localized corrosion at the waterline continues to be a problem, deaeration of the solution and the air space above it can be of help as well. When deaerating, a baffle should be placed between the sample and the bubbler in

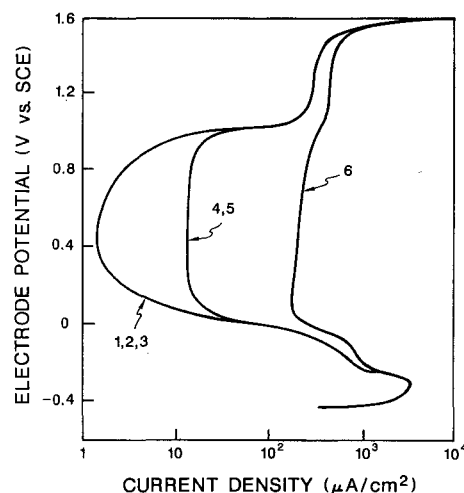


**FIG. 2—Polarization curves of stainless steel in 1 N sulfuric acid using different specimen mounting methods: (1) Stern-Makrides compression gasket, (2) heat-cured epoxy, (3) alkyd-varnish, (4) phenol-formaldehyde, (5) polymethyl methacrylate, (6) cold-cured epoxy [12].**

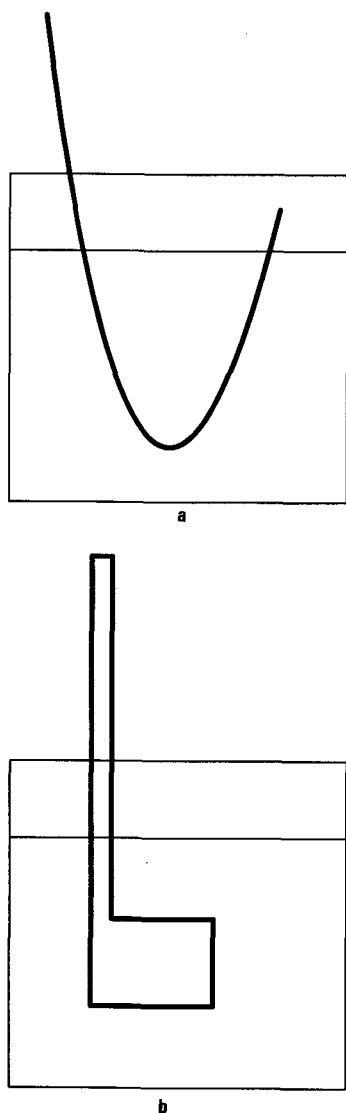


FIG. 3—(a) Wire loop configuration for electrochemical testing, (b) flag electrode configuration for electrochemical testing.

order to prevent oscillations of the waterline. It should be noted that flag electrodes can suffer edge attack that is not indicative of the behavior of the flat surface. Thus, post-test inspection of the location of the attack and careful interpretation of the results are important, as is the case for all electrochemical testing.

Suter [17] developed a third approach to delineation of the surface area of interest. By using a microcapillary attached to a conventional optical microscope, Suter was able to define small areas of stainless steel surfaces and generate polarization curves. The area probed is defined by the diameter of the capillary with results demonstrated for capillaries between 2 and 1000 microns [18]. The cell is of particular use when the behavior a particular microstructural feature is of interest [19–21], as the design allows the matrix contribution to be minimized.

### Cyclic Polarization

By far the most common electrochemical test for localized corrosion resistance is cyclic polarization. ASTM G 61, Test Method for Conducting Cyclic Potentiodynamic Polarization Measurements for Localized Corrosion Susceptibility of Iron-, Nickel-, or Cobalt-based Alloys, has been developed to allow experimenters to test their equipment and procedures on systems that are well characterized. The potential is scanned from  $E_{\text{corr}}$  (or slightly below it) in the anodic direction until localized corrosion initiates as indicated by a large increase in the applied current. At this point, the direction of the scan is reversed, and the current decreases until it changes polarity (i.e., becomes cathodic). Representative scans are shown in Fig. 4 for Type 304 SS and Hastelloy C-276. Conventional wisdom states that  $E_{\text{bd}}$  (the breakdown potential) is the potential above which pits are initiated, while  $E_{\text{rp}}$  (the repassivation potential) is the potential below which pits repassivate. The breakdown potential is usually defined as the potential at which there is a large increase in the applied current, whereas the repassivation potential is the potential on the reverse scan at which the applied anodic current becomes zero (i.e., the current changes polarity). Thus, the higher the value of  $E_{\text{bd}}$ , the more resistant is the alloy to the initiation of localized attack. The higher  $E_{\text{rp}}$ , the more easily the alloy can repassivate. At potentials between  $E_{\text{bd}}$  and  $E_{\text{rp}}$ , sites that have initiated can propagate. Based upon this argument, one would favor an alloy that had both a high  $E_{\text{bd}}$  and a high  $E_{\text{rp}}$ .

Examples of the range of data that can be expected are shown in the standard. The scatter in the data is apparent, especially in the forward scan. This scatter points out the statistical nature of the nucleation of pitting. The average  $E_{\text{bd}}$  of Type 304SS was found to be approximately +0.15 V(SCE), while the average  $E_{\text{rp}}$  was found to be approximately -0.21 V(SCE). The reverse scans are much more reproducible, because the local chemistry controls the repassivation. Another

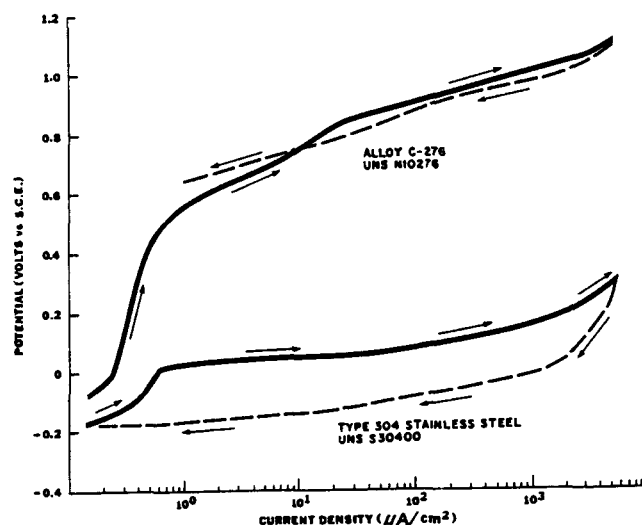


FIG. 4—Representative cyclic potentiodynamic polarization curves (ASTM G 61). The average  $E_{\text{bd}}$  for Type 304SS was approximately +0.15 V(SCE), while the average  $E_{\text{rp}}$  was approximately -0.21 V(SCE).



example of the inherent scatter in  $E_{bd}$  is shown in Fig. 5 [22] for three variants of Type 304SS in 1000 ppm NaCl. The large variation in  $E_{bd}$  arises despite the fact that all of the samples of each type were from the same heat of material and were tested under identical conditions.

There have been numerous attempts to use the amount of hysteresis in the cyclic scan as a measure of localized corrosion susceptibility, with varying degrees of success. In this approach, the larger the hysteresis, the more likely a localized corrosion site will propagate once initiated. In the presence of a well-defined crevice, a good correlation has been found and the relative crevice corrosion susceptibility of alloys can be obtained. Wilde [23] demonstrated this for Hastelloy C, Incoloy 825 and Carpenter 20Cb3 in seawater where the amount of hysteresis correlated well with the amount of weight loss (due to crevice corrosion) in a two-year exposure to seawater. There is not a linear correlation, however, so local penetration rates cannot be predicted, but the test has been used successfully for alloy selection. However, in studies that have attempted to study the relative pitting susceptibility of alloys, it has been found that comparisons are valid only if no crevices are present on any of the specimens tested. An example of the differences that one can observe is shown in Fig. 6. In the absence of crevices, the Fe-30Cr-3Mo alloy performs well in 1 M NaCl, with a high  $E_{bd}$  and a small hysteresis. Microscopic examination showed the attack occurred only at the grain boundaries. However, when a crevice was intentionally applied, the alloy performed poorly. The possible problems in comparing one specimen that had a crevice with another that did not are obvious; incorrect conclusions concerning the relative resistance of two materials could easily be reached. Independent of the mounting method used, one should always examine the specimen for localized attack after the test is completed. At a minimum, microscopic examination of likely creviced areas should be performed. Some samples should be broken out of their mounts for more thorough examination.

While the interpretation of breakdown and repassivation potentials remains controversial, progress towards a consensus

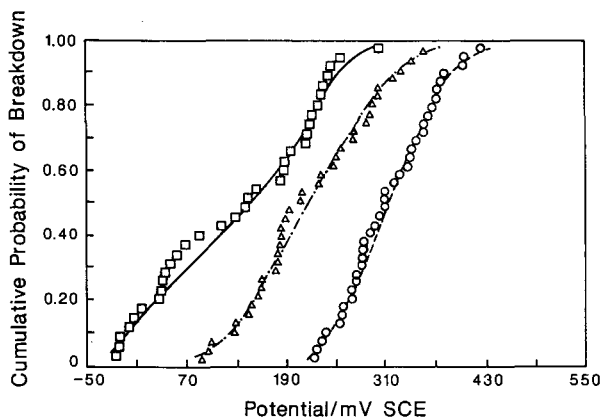


FIG. 5—Cumulative probability distributions of pitting breakdown potentials for three Type 304 stainless steels in 1000 ppm NaCl with different sulfur contents: high sulfur (□), commercial purity (△), and high purity (○) [22].

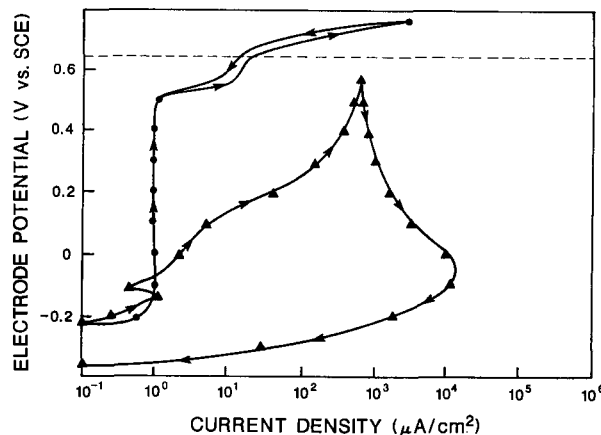


FIG. 6—Cyclic polarization curve for Fe-30Cr-3Mo alloy in deaerated 1 M NaCl for specimens (a) without a crevice (●) and (b) with a crevice (▲) [23].

is being made. The large scatter in the breakdown potential is thought to be due to the sensitivity of pit initiation to the initial conditions. Its dependence on scan rate is most likely the result of the time dependence of the localized corrosion site chemistry development. In addition, it is now generally accepted that corrosion-resistant designs should not use  $E_{bd}$  as the important parameter, but the appropriate value of  $E_{rp}$ , because this is the potential below which pits should repassivate. Under these circumstances, the determination of the proper value of  $E_{rp}$  becomes the focus.

Thompson and Syrett [24] attempted to address the problem of the proper pitting potential by performing a variety of electrochemical tests on Type 317L and Alloy 825 in simulated flue gas desulfurization environments to determine  $E_{bd}$  and  $E_{rp}$  as a function of the extent of pitting damage, characterized in terms of the time during which localized attack was allowed to occur. In terms of cyclic polarization, this time would be inversely proportional to the sweep rate on the reverse portion of the scan, with lower sweep rates leading to greater attack. As shown in Fig. 7 for Type 317L, their results indicate the convergence of  $E_{bd}$  and  $E_{rp}$  at a single potential of +0.2 V(SCE). This "unique potential" can be interpreted as the potential below which the smallest pit will neither initiate nor grow. Quantifying the size of the "smallest" pit remains an important task. However, the work is important support for the hope of eventually developing quantitative, engineering-relevant criteria for material selection against pitting.

One of the historical controversies with regard to  $E_{rp}$  as a "material property" are the results of Wilde [23] in which the repassivation potential was shown to depend to some extent on the amount of localized dissolution that has been allowed to occur, and therefore depends on both the scan rate and the current at which the scan is reversed. The more attack that has been allowed to occur, the more negative is the  $E_{rp}$ . However, there are other data on stainless steels that show a limiting value for large pits (0.05–0.5 mm deep) [25,26], complementing the work of Thompson and Syrett [24], where a limiting value is also found for small pits.

**FIG. 7—Critical potentials ( $E_{bd}$  and  $E_{rp}$ ) for Type 317L stainless steel exposed to a simulated flue gas desulfurization environment as a function of the time during which localized corrosion was allowed to propagate before repassivation occurred. Symbols denote different methods used to determine values: cyclic polarization (filled and open squares and triangles); constant potential tests (filled and open circles and diamonds) [24].**

Despite the problems, polarization testing is useful for comparing alloys with respect to propagation of localized corrosion, though its use gives little information on the initiation time that is necessary for accurate lifetime prediction. One alloy may have superior resistance to propagation, but have much inferior resistance to initiation, and thus result in a shorter application lifetime.

### Galvanostatic Measurements

Controlled current tests for pitting are seeing increased popularity. Galvanostatic measurements involve the application of a series of small, step changes in the applied current. The potential is followed as the current is increased as described in ASTM G 100, Method for Conducting Cyclic Galvanostaircase Polarization. In some cases, more reproducible values for  $E_{rp}$  can be obtained galvanostatically in some systems, notably aluminum in inhibited water [27]. However, potential oscillations at constant current can sometimes occur, which, while of scientific interest, can make interpretation of the results difficult, as the choice of potential becomes almost arbitrary.

### Potentiostatic Measurements

By far the most common electrochemical tests used is cyclic polarization. Nonetheless, potentiostatic measurements can be powerful tools in evaluating pitting behavior. Ideally, potentiostatic tests would be conducted over long time periods to avoid being fooled by long initiation times. Potentiostaircase tests can be performed in lieu of potentiodynamic tests, though, at equivalent potential scan rates, the results should be identical. Unfortunately, long-term potentiostatic testing is extremely time-consuming and expensive.

In addition, the time frames involved are usually still very short compared to the projected life. Thus, a number of approaches have been developed for accelerating the process of initiation.

Mechanical scratching is favored by some as a means by which a bare surface can be created. In this technique, one is ascribing no importance to initiation time. The surface is held at a constant potential and then a portion of it is scratched, usually with a diamond-tipped stylus. The current is monitored with time. For potentials below  $E_{rp}$ , the surface will repassivate rather rapidly, as shown in Fig. 8. Just above  $E_{rp}$ , the surface will try to repassivate, but will fail, and the current will eventually increase. The closer the potential to  $E_{rp}$ , the longer is the time before the current increases. Thus, in most cases, the  $E_{rp}$  measured by this method is not conservative, as usually no more than 10 min is spent at any one potential. If one had waited long enough at the potential used just before the measured  $E_{rp}$ , localized corrosion might have occurred. However, this does not denigrate its utility as a screening test. One problem with scratching tests of this type is the dependence on the weight of the scratch. For scratching by hand, the  $E_{rp}$  decreases with increasing damage. A mechanical system improves the reproducibility. A more difficult problem concerns the site of pitting. In many cases, pitting occurs at inclusions or second-phase particles of one type or another. Such inclusions are usually present at small volume fractions, so the probability of scratching across one (or more) with a fine diamond tip is extremely small. This paucity of sites can lead to erroneously high values of  $E_{rp}$ , which reflect the pitting susceptibility of the matrix material, but ignore the susceptibility of the weakest link, the inclusions.

There are also purely electrochemical methods that can be used to produce a bared surface. In one technique, the entire exposed surface is activated by a large positive voltage excursion, which is followed by a voltage step back to (or towards)  $E_{corr}$ . In this way, any potential pitting sites are initiated, and the test measures the ability of the material to resist propagation and to repassivate. One version of this test (Fig. 9) involves a step to +2 V for 3 s followed by a step back to  $E_{corr}$ , during which time the current is monitored. The potential is held there for 5 min before it is again

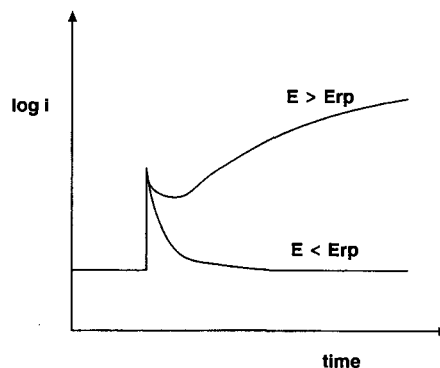


**FIG. 8—Scratch test current-time curves for a specimen held potentiostatically above the repassivation potential ( $E_{rp}$ ) and below  $E_{bd}$ .**

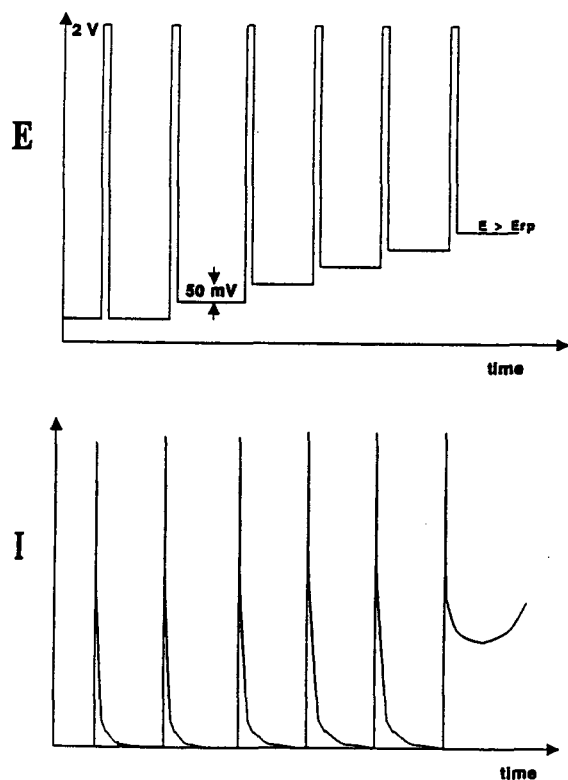


FIG. 9—Schematic  $E(t)$  and  $I(t)$  for electrochemical scratch method for determining the repassivation potential.

stepped to +2 V for 3 s to reinitiate localized corrosion. At this point, the potential is stepped back to a potential 50 mV above  $E_{\text{corr}}$  and the current is monitored for 5 min. The process is repeated until the current does not decay upon the step in the negative direction. In this way, an estimate of  $E_{\text{rp}}$  can be made, with better estimates resulting from the use of smaller increments in the test potential (e.g., 25 mV instead of 50 mV). This method is essentially using the potentiostat to “electrochemically scratch” the specimen surface. A related method is described in ASTM F 746, Test Method for Pitting or Crevice Corrosion of Metallic Surgical Implant Materials, for determining the pitting and crevice corrosion susceptibility of materials used in medical implants.

In another electrochemical test that focuses on pit propagation, the potential is scanned at 10 mV/s to a potential  $E_1$  between  $E_{\text{bd}}$  and  $E_{\text{rp}}$  where it is held to determine the background passive current density. After 10 min, the potential is scanned anodically past  $E_{\text{bd}}$  until the current density is 10 mA/cm<sup>2</sup>, at which time the potential is stepped back to  $E_1$ . The current is then monitored for 10 min, after which the potential is held at  $E_{\text{corr}}$  for 5 min to repassivate the pits. Finally, the potential is stepped back to  $E_1$  and the current is monitored to ensure that the background current has not changed appreciably. The amount of charge passed during the propagation stage is compared to the pitted area (determined by optical microscopy) to determine an average pit penetration rate. This test is known as the Pit Propagation Rate (PPR) Test [28].

Frankel [29,30] has developed a means of testing pit propagation using thin foils. The geometry of the foil restricts the dissolution to two spatial dimensions, allowing optical measurements of changes in diameter to be related to the measured current, thereby establishing an accurate rate of pit propagation as well as conditions under which such pits repassivate. The method has been applied to sputtered Al thin films [30] as well as Al alloys [29]. The primary experimental challenge is the creation of foils that are sufficiently thin to produce a stable, two-dimensional pit. While sputter deposition is an excellent method, the production of thin foils of engineering alloys provides more of a challenge, although not always an insurmountable one.

### Critical Temperature Tests

Although ASTM tests use temperature to accelerate attack during exposures, temperature can also be used in combination with electrochemical techniques. One example of this is the determination of critical pitting temperatures (CPT) [16,31,32] for alloy development or selection, or both. An anodic potential is applied to an electrode at low temperature (room or below) in the solution of interest and the temperature slowly increases in order to determine the temperature at which initiation of localized corrosion occurs, as signified by an increase in the current above some criterion. Such a method allows a quantitative ranking of materials in terms of resistance to pitting.

ASTM G 150 (Standard Test Method for Electrochemical Critical Pitting Temperature Testing of Stainless Steels) describes in detail how to perform such experiments. The solution prescribed is 1 M NaCl, the suggested applied potential is +700 mV(SCE) and the starting temperature is deemed to be 0°C, with the temperature being increased at 1°C/min. The CPT is defined as the temperature at which the current exceeds 100  $\mu\text{A}/\text{cm}^2$  and remains so for greater than 1 min. The test method clearly states that alternative potentials can be used if they are within the range for which the CPT is potential independent.

Salinas-Bravo and Newman [33] developed variation on the critical pitting temperature test for welded stainless steels in which a large, unwelded specimen was coupled to a welded sample via a zero resistance ammeter (ZRA). The unwelded specimen polarizes the welded sample to a positive potential. As the temperature is raised, the galvanic current between the two remains low until the CPT is reached. At that point, the welded sample undergoes stable pitting and a large current is observed. The attractiveness of this test is that it probes the inherent galvanic couple that is the essence of localized corrosion: the large, passive cathode, and the small, active pit.

### Electrochemical Noise

Recently, electrochemical noise has seen increased interest as a tool for both corrosion science and corrosion engineering. By monitoring the galvanic current between two nominally identical electrodes or the corrosion potential of a single electrode carefully, metastable pitting can be detected. The localization of the dissolution inherent in localized corrosion implies a separation of the anodic and cathodic reactions that

constitute the corrosion couple. This physical separation of reactions distinguishes localized corrosion from uniform corrosion in which it is traditionally thought that the anodic and cathodic sites are in very close proximity to one another. The majority of the anodic (oxidative dissolution) reaction occurs inside the localized corrosion site, while the majority of the cathodic (reduction) reaction occurs on the boldly exposed surface. Thus, a galvanic couple is created. The spatial separation of the processes necessitates the passage of current between the two sites. This passage of current leads to the various electrochemical noise signals measured.

Under open circuit conditions, bursts of dissolution at localized corrosion sites require the generation of bursts of cathodic current from the surrounding boldly exposed surface. This increased demand typically causes a decrease in the measured open circuit potential. Localized corrosion sites are typically very small ( $<100\text{ }\mu\text{m}$  diameter). However, the current densities inside these cavities during transient bursts can be on the order of  $1\text{ A/cm}^2$ . These rates are possible because of the extremely aggressive environments that develop inside localized corrosion sites. Thus, even though the sites are geometrically small, they can influence the electrochemical potential of the much larger boldly exposed surface on which the electrode kinetics are far slower. This difference in relative current densities on separated anodes and cathodes is what accounts for the ability to detect the electrochemical noise associated with localized corrosion. When the potential of the surface is controlled with an external device, the same burst of dissolution requires the device to supply a burst of current, which can be recorded. Usually, these bursts are transient, with temporary repassivation of the localized corrosion site occurring and allowing the system to return to the previous steady-state condition. On a metal surface of appreciable size ( $>1\text{ cm}^2$ ), there can be many localized corrosion sites. They will usually propagate independently, so that a series of current (or potential) fluctuations is observed due to the summation of the signals from the individual sites. These fluctuations are referred to as "electrochemical noise." Because electrochemical noise can be observed often under open circuit conditions, it has been hailed as the only truly noninvasive electrochemical method.

Changes in the noise signal are often taken as an indication that conditions are favorable for pit initiation to occur. Thus, if one is monitoring a process stream, corrective action can be taken. The disadvantage of noise monitoring is that it does not give sufficient information about what level of this metastable pitting is acceptable. For example, there may be literally millions of metastable pits forming and repassivating in a vessel wall, but only one needs to penetrate completely for a leak to develop. It may not be possible to differentiate between conditions that will allow that and those in which the extent of pitting is negligible. Experience and correlations with coupon exposures are critical factors in the use of noise for localized corrosion monitoring. No ASTM standard currently exists for noise measurements.

## PREDICTIVE CAPABILITIES

With the caveats mentioned previously in mind, the study of metastable pitting can be used to assist in lifetime prediction studies. If pitting is truly a stochastic phenomenon, then one

can apply statistics to allow prediction of the likelihood of pit propagation, given sufficient information. The information needed is (a) the probability that a pit will nucleate under a given set of conditions, and (b) the probability that once a pit nucleates, it will survive (i.e., become stable). Such information could be used to estimate component lifetimes, which could then be used to make design decisions based on the consequences of a failure. For example, a 3 % chance of perforation may be acceptable for an easily shutdown and repaired vessel if it allows a cheaper alloy to be used, but such a probability would not be acceptable for a critical component in an inaccessible submersible.

Analyses of these current and potential transients due to metastable pits can provide information regarding the controlling factors and their dependence on environmental, metallurgical, and applied potential conditions. For example, Pride et al. [34] characterized the metastable pitting behavior of high-purity Al and aged Al-2%Cu. They found that the frequency of pitting events was proportional to both the applied potential and the chloride concentration. The rate of pitting was also found to decrease with increasing exposure time. These kinds of analyses can serve as the basis for the pitting prediction methodologies described below.

Shibata et al. [7] and Williams et al. [35] have applied such statistical arguments to pitting of stainless steel. To develop these models, a large amount of data that can be treated as an ensemble must be gathered. In other words, variations in results from test to test are expected, even for nominally identical tests. This variation is used to develop the cumulative probability curve for pitting under a certain set of conditions. Both groups used multiple specimen testing apparatus to gather up to 12 data points for critical potentials and metastable pit nucleation rates simultaneously. The results for one set of 30 tests are shown in Fig. 5 [22]. This shows that the breakdown potential  $E_{bd}$  follows a distribution. Thus, there is a 20 % chance that the breakdown potential of commercial 304 SS will be below +160 mV(SCE) in 1000 ppm NaCl. The argument is that there was nothing "wrong" with those tests whose  $E_{bd}$  was less than +160 mV(SCE), but that the variation reflects the stochastic nature of the pitting process. Qualitatively similar data have been developed for Al alloys and their constituent second phase particles [36].

The development of commercially available multipotentiostats has made measurements of pitting conditions and the underlying factors more tractable. Lunt et al. [37] used an array of nominally identical electrodes to characterize the strengths and extent of the types of interactions that occur among active pits. In addition, such instrumentation makes the determination of the statistical distribution of pitting potentials via the testing of a large number of specimens much less time intensive, as multiple electrodes (up to 100) [38] can be independently tested simultaneously.

## CONCLUDING REMARKS

The goals of this chapter were to give a brief overview of the exposure tests used to determine localized corrosion susceptibility, and to introduce a variety of electrochemical techniques that can provide important information concerning localized corrosion susceptibility. Although none of the

methods is perfect or a panacea, when used judiciously and in combination, a better picture of the localized corrosion process can be gained, even in complicated solutions. This allows for more informed decisions on alloy selection, process alteration, or failure analysis. While prediction of localized penetration rate remains a goal of electrochemical testing, applications of statistics to the process appear promising.

## REFERENCES

- [1] Szlarska-Smialowska, Z., *Pitting Corrosion of Metals*, NACE, 1986.
- [2] Frankel, G. S., "Pitting Corrosion of Metals. A Review of the Critical Factors," *Journal of the Electrochemical Society*, Vol. 145, 1998, p. 2186.
- [3] *Corrosion Tests and Standards: Application and Interpretation, Manual 20* (Sec. III, Types of Tests), ASTM International, West Conshohocken, PA, 1995 (this publication).
- [4] *Handbook on Corrosion Testing and Evaluation*, W. H. Ailor, Ed., John Wiley, New York, 1971.
- [5] Streicher, M. A., "Pitting Corrosion of 18Cr-8Ni Stainless Steel," *Journal of the Electrochemical Society*, Vol. 103, 1956, p. 375.
- [6] Ernst, P., Laycock, N. J., Moayed, M. H., and Newman, R. C., "The Mechanism of Lacy Cover Formation in Pitting," *Corrosion Science*, Vol. 39, 1997, p. 1133.
- [7] Shibata, T. and Takeyama, T., "Stochastic Theory of Pitting Corrosion," *Corrosion*, Vol. 33, 1977, p. 243.
- [8] Aziz, P. M. and Godard, H. P., "Influence of Specimen Area on the Pitting Probability of Aluminum," *Journal of the Electrochemical Society*, Vol. 102, 1955, pp. 577-579.
- [9] Leygraf, C. and Graedel, T. E., *Atmospheric Corrosion*, Wiley-Interscience, 2000, p. 11.
- [10] Singleton, R., *Corrosion: Fundamentals, Testing and Protection, ASM Handbook*, Vol. 13A, ASM International, Materials Park, OH, 2003, p. 470.
- [11] Stern, M. and Makrides, A. C., "Electrode Assembly for Electrochemical Measurements," *Journal of the Electrochemical Society*, Vol. 107, 1960, p. 782.
- [12] Greene, N. D., France, W. D., and Wilde, B. E., "Electrode Mounting for Potentiostatic Anode Polarization Studies," *Corrosion*, Vol. 21, 1965, p. 275.
- [13] Stockert, L., Hunkeler, F., and Bohni, H., "A Crevice-Free Measurement Technique to Determine Reproducible Pitting Potentials," *Corrosion*, Vol. 41, 1985, p. 676.
- [14] Shaw, B., Ph.D. dissertation, Johns Hopkins University, 1988.
- [15] Quarfort, R., "New Electrochemical Cell for Pitting Corrosion Testing," *Corrosion Science*, Vol. 28, 1988, p. 135.
- [16] Quarfort, R., "Critical Pitting Temperature Measurements of Stainless Steels with an Improved Electrochemical Method," *Corrosion Science*, Vol. 29, 1989, p. 987.
- [17] Suter, T. and Bohni, H., "Microelectrodes for Corrosion Studies in Microsystems," *Electrochimica Acta*, Vol. 47, Nos. 1-2, 2001, p. 191.
- [18] Park, J. O., Suter, T., and Bohni, H., "Role of Manganese Sulfide Inclusions on Pit Initiation of Super Austenitic Stainless Steels," *Corrosion*, Vol. 59, 2003, p. 59.
- [19] Staemmler, L., Suter, T., and Bohni, H., "Glass Capillaris as a Tool in Nanoelectrochemical Deposition," *Electrochemical and Solid-State Letters*, Vol. 5, 2002, p. C61.
- [20] Suter, T. and Alkire, R. C., *Journal of the Electrochemical Society*, Vol. 148, 2001, p. B36.
- [21] Leard, R. R. and Buchheit, R. G., "Electrochemical Characterization of Copper-Bearing Intermetallic Compounds and Localized Corrosion of Al-Cu-Mg-Mn Alloy 2024," *Materials Science Forum*, Vol. 396-402 (Pt. 3, Aluminium Alloys 2002), 2002, p. 1491.
- [22] Stewart, J., Ph.D. dissertation, University of Southampton, U.K., 1990.
- [23] Wilde, B. E., *Localized Corrosion*, R. W. Staehle, B. F. Brown, J. Kruger, and A. Agarwal, Eds., NACE, Houston, TX, 1974, p. 342.
- [24] Thompson, N. G. and Syrett, B. C., "Relationship Between Conventional Pitting and Protection Potentials and a New, Unique Pitting Potential," *Corrosion*, Vol. 48, 1992, p. 649.
- [25] Sridhar, N. and Cragolino, G. A., "Applicability of Repassivation Potential for Long-Term Prediction of Localized Corrosion of Alloy 825 and Type 316L Stainless Steel," *Corrosion*, Vol. 49, 1993, p. 885.
- [26] Hakkareinen, T., *Passivity of Metals and Semiconductors*, M. Froment, Ed., Elsevier Science Publishers B.V., Amsterdam, The Netherlands, 1983, p. 367.
- [27] Hirozawa, S. T., *Laboratory Corrosion Tests and Standards, ASTM STP 866*, G. S. Haynes and R. Baboian, Eds., ASTM International, West Conshohocken, PA, 1985, p. 108.
- [28] Syrett, B. C., "PPR Curves—a New Method of Assessing Pitting Corrosion Resistance," *Corrosion*, Vol. 33, 1977, p. 221.
- [29] Sehgal, A., Frankel, G. S., Zoofan, B., and Rokhlin, S., "Pit Growth Study in Al Alloys by the Foil Penetration Technique," *Journal of the Electrochemical Society*, Vol. 147, No. 1, 2000, pp. 140-148.
- [30] Frankel, G. S., Newman, R. C., Jahnes, C. V., and Russak, M. A., "On the Pitting Resistance of Sputter-Deposited Aluminum Alloys," *Journal of the Electrochemical Society*, Vol. 140, No. 8, 1993, pp. 2192-2197.
- [31] Brigham, R. J. and Tozer, E. W., "Temperature as a Pitting Criterion," *Corrosion*, Vol. 29, No. 1, 1973, pp. 33-36.
- [32] Lau, P. and Bernhardsson, S., *Electrochemical Techniques in Corrosion Engineering*, R. Baboian, Ed., NACE, Houston, TX, 1986, p. 281.
- [33] Salinas-Bravo, V. M. and Newman, R. C., "An Alternative Method to Determine Critical Pitting Temperature of Stainless Steels in Ferric Chloride Solution," *Corrosion Science*, Vol. 36, No. 1, 1994, pp. 67-77.
- [34] Pride, S. T., Scully, J. R., and Hudson, J. L., "Metastable Pitting of Aluminum and Criteria for the Transition to Stable Pit Growth," *Journal of the Electrochemical Society*, 1994, Vol. 141, No. 11, pp. 3028-3040.
- [35] Williams, D. E., Westcott, C., and Fleischman, M., "Stochastic Models of Pitting Corrosion of Stainless Steels. II. Measurement and Interpretation of Data at Constant Potential," *Journal of the Electrochemical Society*, Vol. 132, No. 8, 1985, pp. 1804-11.
- [36] Ilevbare, G. O., Scully, J. R., Yuan, J., and Kelly, R. G., "Inhibition of Pitting Corrosion on Aluminum Alloy 2024-T3: Effect of Soluble Chromate Additions Versus Chromate Conversion Coating," *Corrosion*, Vol. 56, 2000, p. 227.
- [37] Lunt, T. T., Scully, J. R., Brusamarello, V., Mikhailov, A. S., and Hudson, J. L., "Spatial Interactions Among Localized Corrosion Sites Experiments and Modeling," *Journal of the Electrochemical Society*, 2002, Vol. 149, No. 5, pp. B163-B173.
- [38] Budiansky, N. D., Hudson, J. L., and Scully, J. R., "Origins of Persistent Interaction Among Localized Corrosion Sites on Stainless Steel," *Journal of the Electrochemical Society*, Vol. 151, No. 4, 2004, pp. B233-B243.

# Crevice Corrosion

Narasi Sridhar,<sup>1</sup> Darrell S. Dunn,<sup>1</sup> C. S. Brossia,<sup>1</sup>  
Gustavo A. Cragnolino,<sup>1</sup> and Jeffery R. Kearns<sup>2</sup>

CREVICE CORROSION OCCURS IN regions of a metal that are not directly exposed to an environment such as flanged joints, lap joints, and under corrosion deposits. The metals that undergo crevice corrosion are otherwise protected by a surface film. Alloys that are not protected by a surface film tend to corrode outside the crevice region where there is greater access to cathodic reduction reactions. In this regard, there are many similarities between pitting and crevice corrosion. Indeed, for some classes of materials, a case can be made that the same mechanism operates both phenomena. It must be emphasized that the crevice corrosion tendency is not the property of a particular alloy class; rather it is a function of the alloy's response to a given environmental condition. For example, carbon steels do not suffer crevice corrosion in acidic solutions because of the absence of a passive film, but do suffer crevice corrosion in alkaline solutions when there is a passive film. Similarly, some alloys suffer crevice corrosion in the presence of a corrosion inhibitor, whereas corrosion occurs outside the crevice in the absence of the inhibitor.

Several tests have been developed over the years to determine the crevice corrosion resistance of alloys. The objectives of these tests include comparison of alloys, qualification of alloys for a given service, evaluation of the effects of fabrication processes on crevice corrosion resistance, quality control, and life prediction. This chapter will briefly describe the types of tests, and their applicability and limitations, with a focus on tests that have been or are now being considered by ASTM Committee G-1 on Corrosion of Metals. While these test principles are applicable to a wide variety of alloys, the information presented is focused on stainless and nickel-base alloys.

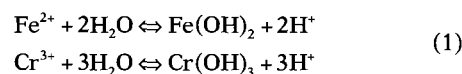
## THE MECHANISMS OF CREVICE CORROSION

It was realized early on that crevice corrosion occurs because the protective film on the metal is somehow removed or made less protective. Mears and Evans [1] and Uhlig [2] suggested that oxygen depletion inside the crevice was responsible for the destabilization of the protective passive film.

However, Rosenfeld and Marshakov [3] in the late 1950s conducted a detailed examination of processes occurring in the crevice that was a precursor to many experimental studies that are being conducted even today. They suggested that crevice corrosion occurs through a combination of reduction in oxygen or a corrosion inhibitor in the crevice, a reduction in pH, and shift in the potential within the crevice to a more negative value such that the potential is in the active regime. Since these early ideas, many conceptual models of crevice corrosion have been developed [4–39] that have elaborated one or more aspects of this model. Quantitative modeling of crevice corrosion was first performed by Crolet and Defraux [11], who considered only the effect of passive dissolution rate on pH reduction within the crevice and ignored the effect of transport of species in and out of the crevice. This was further improved by Galvele [12] and Oldfield and Sutton [14,15], who considered transport of species in and out of the crevice. These early models have since been improved considerably both in terms of the conceptual models and the numerical solutions [13,16–21].

The crevice corrosion process can be described in four stages: (1) deoxygenation, (2) increase of the salt and acid concentrations, (3) depassivation, and (4) propagation, as illustrated in Fig. 1. Crevice corrosion begins when discrete areas on a passive surface are physically isolated or occluded. Convection between the solution entrapped within an occluded area on a passive surface and the bulk environment is slow, so the dissolved oxygen in a crevice solution is rapidly depleted (Fig. 1, stage [a]). A localized galvanic cell is established due to the difference in the oxygen concentrations of the solutions within a crevice (anode) and the surrounding surface (cathode). The depletion of oxygen in the crevice solution shifts the corrosion potential for a passive surface in the active direction. Although “differential aeration” [1] is sufficient to induce crevice corrosion of certain metals and alloys, it only provides the initial driving force for the crevice corrosion of stainless alloys.

As metallic dissolution continues within a crevice, the metal cations (e.g., Fe<sup>2+</sup>, Cr<sup>3+</sup>, Al<sup>3+</sup>, etc.) are concentrated in the stagnant solution within a crevice. They also react with water (called hydrolysis reaction) to generate acidity.



Mobile anionic species (e.g., Cl<sup>−</sup>) are attracted to the crevice and charge neutrality is maintained. The crevice solution

<sup>1</sup>Southwest Research Institute, 6220 Culebra Road, San Antonio, TX 78238-5166.

<sup>2</sup>Previous Author of the chapter, Alcoa Technical Center, Alcoa Center, PA 15069-0001.

**FIG. 1—Processes leading to crevice corrosion.**

becomes concentrated in metallic chlorides even when only small quantities of chloride anions are present in the bulk environment (Fig. 1, stage [b]). Active metallic dissolution occurs when the pH of the crevice solution is sufficiently low and the concentration of chlorides is high enough to break down the passive film. The development of a critical crevice solution is controlled by alloy composition, crevice geometry, and bulk solution chemistry [35,36]. The length of time (or incubation period) required to develop a critical crevice solution with a particular crevice geometry determines the effective crevice corrosion resistance of a stainless alloy. The critical crevice solution criterion has proven to be useful for ranking alloy performance [15,35,36].

Following Karlberg and Wranglen [8], many investigators [22–29] have shown that a small potential gradient in the crevice can result in the shift of the electrochemical behavior from passive to active (Fig. 1, stage [c]) and thus result in high corrosion at an intermediate distance into the crevice. Once corrosion has been initiated, the reaction can proceed rapidly due to the unfavorable area ratio of the small, anodic crevice to the large, cathodic surrounding surface. For corrosion resistant alloys that do not exhibit a large active-passive slope at near-neutral pH, stages [b] and [c] are both required because an active-passive peak is not observed unless low pH values are attained [22,23,29].

Pits in crevices were reported early on by Karlberg and Wranglen [8]. An alternative mechanism was originally proposed by Stockert and Bohni [30] and later enhanced by Laycock et al. [37]. This suggests that pit nucleation occurs

in the crevice even at small applied potentials leading to current noise (Fig. 1, stage [d]), but above a critical potential, the dissolution rate increases steadily as pit stabilization occurs. The pit stabilization, in turn, is linked to formation of metal-chloride salt films [38,39].

## REVIEW OF TEST METHODS FOR CREVICE CORROSION RESISTANCE

The tests can be classified into three general categories: (i) non-electrochemical tests, (ii) electrochemical tests under open-circuit conditions, and (iii) electrochemical tests under controlled potential or current conditions. Brief descriptions of the more established methods for evaluating crevice corrosion appear in Table 1 along with comments concerning limits of applicability. Details of each method can be found in the literature cited. The reader is also advised to consider one or more of the excellent reviews on test techniques for crevice corrosion [40–45,76,114].

## NON-ELECTROCHEMICAL TESTS

In these tests, specimens fitted with crevice-forming devices (artificial crevices) are exposed for varying lengths of time to environments containing an anionic species that promotes crevice corrosion (e.g., chloride) and an oxidizing agent to accelerate initiation of crevice corrosion (e.g., ferric ions). The crevice corrosion resistance is then measured by mass-loss and visual methods. ASTM G 48<sup>3</sup> (2000 version) involves four test methods. Methods A and C apply to pitting corrosion. Method B measures the crevice corrosion resistance at two fixed temperatures, whereas Method D measures the crevice corrosion resistance in terms of a critical crevice temperature. These two methods will be described in greater detail below, but the standards provide a comprehensive description of the methods.

### ASTM G-48, Method B

Method B employs a 6 weight percent  $\text{FeCl}_3$  solution (equivalent to 10 %  $\text{FeCl}_3 \cdot 6\text{H}_2\text{O}$ ), with an exposure period of 72 h at either  $22 \pm 2$  or  $50 \pm 2^\circ\text{C}$ , or both. It involves the use of crevice formers (i.e., cylindrical TFE-fluorocarbon blocks) that are held tightly against the sample surface by two rubber bands. These methods produce localized corrosion of type 304L stainless steel at ambient temperature and can be used to rank other materials with respect to this stainless steel and to a lesser extent with respect to each other. The limited ability of Method B to rank a wide range of alloys stems from the limited temperatures used and the fact that the extent of localized corrosion at a given temperature, even if it can be measured accurately, is not often as important in materials selection as the initiation of localized corrosion. Method B employs two tetrafluoro ethylene (TFE)

<sup>3</sup>Standard Test Methods for Pitting and Crevice Corrosion Resistance of Stainless Steels and Related Alloys by Use of Ferric Chloride Solution.

**TABLE 1**—Comparison of tests for resistance to crevice corrosion.

Test	Summary
(a) Non-Electrochemical Test	
FeCl <sub>3</sub> Test, ASTM G 48, Method B [78,79]	Maximum corrosion depth perpendicular to the crevice plane and/or mass-loss are measured after exposure of creviced specimens to 22°C, 50°C, or both. Crevice device is a TFE block without serrations. The test can provide qualitative ranking of an alloy's resistance with respect to type 304L SS, but is not adequate in ranking a number of corrosion resistant alloys. The rubber band holding the crevice blocks provide additional, uncontrolled crevice sites.
FeCl <sub>3</sub> + HCl Test, ASTM G 48, Method D [47,48,72,77]	A serrated TFE crevice block is used and critical crevice temperature is determined through a series of tests at 5°C increments. The test can be used to rank alloys. Test is limited to 85°C because of instability of FeCl <sub>3</sub> . The pitting resistance equivalents used to determine starting temperature can be misleading because they do not consider synergism between alloying elements. Critical crevice temperature is dependent on specimen preparation, test time, and solution composition.
Other solutions	A procedure similar to ASTM G 48 or ASTM G 78 should be followed.
(b) Electrochemical Open-Circuit Potential Tests	
Remote Crevice Assembly Test [87–89] ASTM G 71 can be used for guidance	A sample with crevice block is electrically coupled to a larger open sample through a zero-resistance ammeter. The current flowing in the external circuit is an indicator of crevice activation and growth. It provides a more sensitive and continuous record of crevice initiation and growth processes. It simulates a real crevice condition. At present, there is no standard test procedure for this. Test time, area ratio of open to creviced sample are important factors.
(c) Electrochemical Applied Potential/Current Tests	
Critical Temperature Tests [48,50,64,73–75,79,90–93]	The temperature is varied in steps or continuously while the potential is held at a constant value. The temperature at which a sustained increase in current is observed is noted as the critical temperature. While phenomenologically equivalent to ASTM G 48D, it provides greater freedom in choice of potential and sensitivity in current measurements.
Critical Potential Tests (ASTM G 61 and variants)	The potential can be scanned continuously or varied in a stepwise manner. The potential at which current increases during the upward scan or stepping of potential is called the initiation potential, $E_{\text{crev}}$ or $E_p$ . The potential at which current decreases to a low value during downward scan or stepping of potential is called repassivation potential, $E_{\text{rcrev}}$ or $E_{\text{tp}}$ . The value of $E_{\text{rcrev}}$ is independent of prior growth of crevice corrosion provided a sufficient extent of growth is maintained. For corrosion resistant alloys, too high an initial potential at which crevice corrosion is initiated can result in erroneous measurement of $E_{\text{rcrev}}$ .

fluoropolymer blocks and either rubber band or o-rings to fasten the blocks to a flat specimen and create crevices (Fig. 2, top). The rubber-band crevice assembly is inexpensive, easy, and fast to assemble, and produces useful results in a reasonably short period of time. However, the rubber band crevice assembly has certain drawbacks:

1. The test is invalid if either rubber band breaks.
2. The compressive pressure associated with the rubber band is not uniform.
3. The ratio of the creviced area to the bold exposed area ratio cannot be accurately measured [66].
4. The surface finish of the TFE-block is not specified.
5. Crevice attack often initiates on the edges of the specimen in contact with rubber bands rather than under the TFE blocks. The edge attack may be related to a combination of crevice geometry as well as metallurgical condition (e.g., inclusion stringers). This may lead to uncertainties about correlating the test results to service conditions where edges of plates/sheets may not be exposed. At the end of the test, the sample is evaluated visually for signs of attack. ASTM G 46,<sup>4</sup> Practice for Examination and Evaluation of Pitting Corrosion, can provide guidelines for evaluating the extent of crevice corrosion after the sample has been removed from the test solution. A mass loss measurement is also recommended, but no acceptance criteria or test data for visual or gravimetric evaluations are presented in the standard. Criteria such

as a maximum of 0.038 mm depth of penetration and maximum of 0.2 mg/cm<sup>2</sup> mass loss have been commercially accepted by certain metals producers and users. As previously stated, many important aspects of the test that influence the result, such as the method of examination and evaluation criteria, must be agreed to by the vendor and user of the product to be tested.

### ASTM G 48, Method D

To overcome these limitations, Method D measures the critical crevice corrosion temperature, using a multiple crevice assembly (MCA). The test solution is 6 wt. percent FeCl<sub>3</sub> acidified with 1 wt. percent HCl. This test method is also referenced in ASTM G 157<sup>5</sup> for evaluating the corrosion properties of wrought iron- and nickel-based corrosion resistant alloys for the chemical process industries.

The multiple crevice assembly (MCA) consists of two “serrated” washers made of TFE-fluorocarbon bolted together through a hole drilled in the specimen, as illustrated in Fig. 2(b). The bolts, made of a highly corrosion resistant alloy, are electrically isolated from the specimen. The MCA eliminates the crevices created where the rubber band contacts the specimen and facilitates the measurement of the crevice area to boldly exposed area ratio. The advantage of the MCA is that the crevice geometry can be made very severe by

<sup>5</sup>Standard Guide for Evaluating the Corrosion Properties of Wrought Iron- and Nickel-Based Corrosion Resistant Alloys for the Chemical Process Industries.

<sup>4</sup>Standard Guide for Examination and Evaluation of Pitting Corrosion.



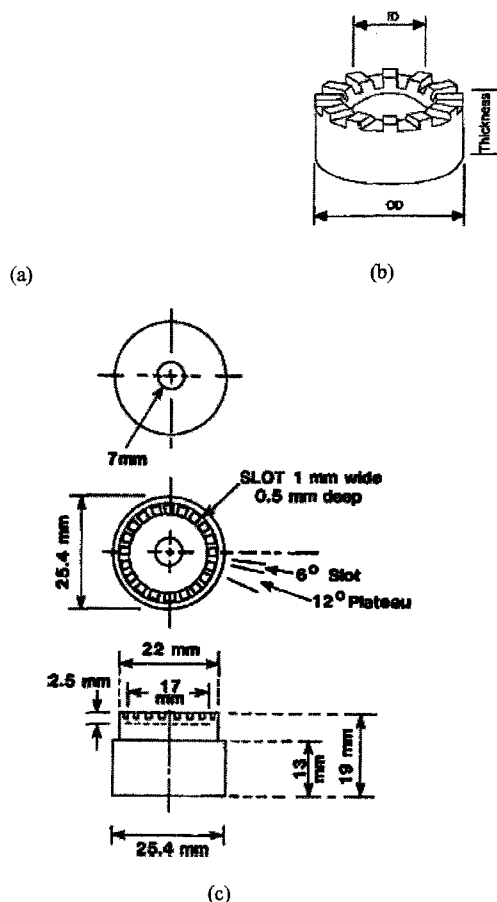


FIG. 2—Standardized crevice corrosion test specimen assemblies described in ASTM G 48 B (top) [25,44] and ASTM G 78 (bottom) [78,79], commonly referred to as the rubber band assembly and multiple crevice assembly (MCA), respectively.

applying greater torque to the bolt and the multiple small contact points. A torque of 0.28 Nm is recommended by ASTM G 48, based on interlaboratory testing. Higher torque may be used, but creep of the crevice washer is an important concern. The depth and number of crevice sites attacked under the washer are reported and can be statistically analyzed if desired, although statistical analysis is not required by ASTM G 48, Method D. Also shown in Fig. 2(c) is the multiple crevice assembly specified in ASTM G-78<sup>6</sup>. Although the design and material of the crevice device are different, the underlying principle is the same in these crevice designs.

The test consists of exposing the MCA in the  $\text{FeCl}_3$  solutions at different temperatures to determine the temperature at which crevice corrosion can be observed when examined at a magnification of 20X. As a guidance to estimating the starting temperature, two multiple regression equations are suggested by ASTM G 48:

For Ni-base alloys:

$$\text{CCT} (^{\circ}\text{C}) = (1.5 \times \% \text{Cr}) + (1.9 \times \% \text{Mo}) + (4.9 \times \% \text{Nb}) + (8.6 \times \% \text{W}) - 36.2 \quad (\text{Eq. 1})$$

For Iron-base alloys:

$$\text{CCT} (^{\circ}\text{C}) = (3.2 \times \% \text{Cr}) + (7.6 \times \% \text{Mo}) + (10.5 \times \% \text{N}) - 81.0 \quad (\text{Eq. 2})$$

ASTM G 48 recommends that tests shall be started within 5°C of the critical temperature estimated by the above equation. The minimum and maximum test temperatures are recommended to be 0°C and 85°C, respectively. Separate samples are to be used for each temperature and a test duration of 72 h is recommended. The main limitation of Eqs 1 and 2 is that they do not recognize the interactive effects of some alloying elements and are regression estimates based on a limited number of commercial alloys. For example, according to Eq 1, alloy C-276 (Ni-15.5%Cr-16%Mo-4%W) would have a CCT of 52°C, whereas alloy C-22 (Ni-22%Cr-13%Mo-3%W) would have a CCT of 47°C. However, the observed CCT of alloy C-276 is significantly lower than that of alloy C-22.

Critical temperature test values determined by various methods have been used for ranking and comparing the localized corrosion resistance of a large number of commercial alloys and to develop new alloys [41,43,46–69]. Critical crevice temperature has been used as a convenient and quantitative measure of the relative ranking of various alloys. However, it must be used with caution in predicting the performance of an alloy in a given service. This is because the localized corrosion dependence on temperature is a function of the test technique, corrosion potential of the alloy in a given environment, and the concentration of chloride or other anionic species. For example, higher corrosion potentials, longer exposure time, and higher chloride concentrations have a tendency to lower the critical crevice temperature. However, the presence of inhibitive species such as nitrate can increase the critical crevice temperature.

The Immersion Critical Pitting Temperature (ICPT) and Immersion Critical Crevice-Corrosion Temperature (ICCT) tests produce results that follow similar trends relative to alloy composition, as demonstrated by the well-known work of Garner (Fig. 3). Garner found that the ICPT values were approximately 20°C higher than the ICCT values for a broad range of alloy compositions [47,70,71]. Crevice corrosion typically occurs at lower temperatures and in less time than pitting [71,73]. Consequently, a pitting test will typically take longer than a crevice test in the same test environment. However, since the problems associated with the geometry of the gap created by the crevice former are avoided, ICPT tests are more sensitive to differences in alloy composition [50,74,75] and are more reproducible (+2.5°C for ICPT versus ±10°C for ICCT) than are ICCT values [50,57]. The scatter in ICCT can be reduced by extending the test exposure period (e.g., from 24 to 72 h [76]) or testing more samples.

### Precision in Critical Temperature Tests

The variability of critical crevice temperature measurement was originally addressed by Brigham [63]. The round

<sup>6</sup>Standard Guide for Crevice Corrosion Testing of Iron-Base and Nickel-Base Stainless Alloys in Seawater and Other Chloride-Containing Aqueous Environments.

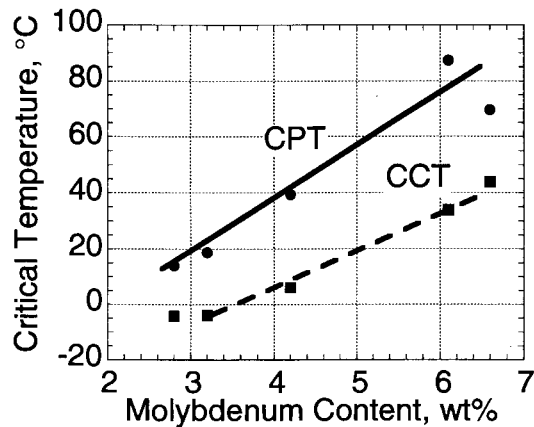


FIG. 3—Immersion Critical Pitting Temperature (CPT) and Immersion Critical Crevice Corrosion Temperature (CCT) curves for molybdenum-bearing austenitic alloys. The dots represent, from left to right: UNS S31600, S31700, N08904, S31254, and N08366. Data are replotted from Refs 45,47,70.

robin test program using G 48, Method D is given in Table 2. The interlaboratory test program found that the pooled repeatability standard deviation and the 95 % confidence limit for Method D were 2°C and 6°C, respectively. The pooled reproducibility standard deviation and 95 % confidence interval for Method D were 6°C and 16°C, respectively. Previous studies [48,70,71] have established  $\pm 10^\circ\text{C}$  as the variation for immersion ICPT values above 40°C.

One significant difference in the results of ICPT and ICCT tests that use acidified ferric chloride (Table 2) versus straight ferric chloride is that the values obtained are significantly lower in the acidified solution. For example, the AL-6XN<sup>®4</sup> alloy (UNS N08367) has an ICCT of 43°C when tested in conventional ferric chloride but, as shown in Table 2, it has a value of 30°C in acidified ferric chloride. Although it is an apparently insignificant part of ASTM G 48, the preparation of 2.5 by 5 cm (1 by 2 in.) corrosion specimens from sheet, strip, and, particularly, plate is a time-consuming and costly part of product testing. Many corrosion-resistant alloys are nonmagnetic, very tough, and, therefore expensive to machine into corrosion specimens. Even properly machined/polished coupon edges are subject to preferential attack because either (a) the rubber bands holding the crevice-former on the sample surface form a very tight crevice on the sample edges, or (b) a subsurface microstructural constituent is exposed and

TABLE 3—Results of crevice corrosion tests in natural seawater from the LaQue Center for Corrosion Technology, circa 1993 [77].

UNS No.	PRE <sup>a</sup>	Percentage of 32 Sites Resistant <sup>b</sup>
N06059	73	100
S32654	56	100
N08367	45	100
N10276	69	97
N08031	51	97
N08926	45	94
S31254	43	94
S32550	37	87
S31600	24	25

<sup>a</sup>Pitting Resistance Equivalent =  $\text{Cr} + 3.3\text{Mo} + 16\text{N}$ .

<sup>b</sup>Eight different combinations of alloys and crevice-formers were tested.

suffers preferential attack. The bias of test results by edge attack is unacceptable because, in general, product corrosion performance is determined by the surface, not the through-thickness microstructure.

### Applications of ASTM G 48 Tests

As noted in Table 3 [77], the results of multiple alloy tests in seawater are correlated to the Pitting Resistance Equivalence (PRE) number [47,48,72,77], which also correlates to alloy performance in  $\text{FeCl}_3$ . Anderson [78] and Streicher [79] used MCA in seawater tests to compare alloy performance. More recently, a simple, flat, plastic (specifically, polymethylmethacrylate, which is often referred to as “perspex”) washer has been successfully used to evaluate a series of alloys in seawater [77]. One application of the ASTM G 48 test has been in simulating leaking tube-to-tube sheet joints in seawater heat exchangers and condensers [81]. When certain highly corrosion-resistant alloys were paired in a dissimilar metal crevice (DMC) with alloys that would be expected to suffer crevice corrosion in the particular test solution, the more corrosion-resistant alloy was found to corrode due to the accelerating effects of the corrosion products from the less resistant alloy. The results of DMC tests in ferric chloride were confirmed by long-term DMC exposures in seawater [82].

TABLE 2—Results of interlaboratory test program

NOTE 1—Minimum temperature (°C) to produce attack at least 0.025-mm (0.001-in.) deep on bold surface of specimen. Edge attack ignored.

Alloy/Laboratory	Method C—CPT Critical Pitting Corrosion Temperature (C)				Method D—CCT Critical Crevice Corrosion Temperature (C)			
	UNS S31603	UNS N08367	UNS S44735	UNS N06022	UNS S31603	UNS N08367	UNS S44735	UNS N06022
1	20/20/20	75/^-/^	85/85/85	>85/>85/>85	<0/<0/<0	30/30/30	42/35/42	50/^-/50
2	20/20/20	70/70/70	80/80/80	>85/>85/>85	<0/<0/<0	25/25/25	35/35/^-	50/55/55
3	20/20/20	85/85/85	75/85/85	>85/>85/>85	<0/<0/<0	25/30/30	35/40/40	55/60/60
4	19/19	75/80	81/81	>85/>85	<0/<0	34/34	40/40	67/67
5	20/20/20	75/75/75	70/70/75	>85/>85/>85	<0/<0/<0	20/20/20	45/45/45	
6	20/20	75/80	75/85	>85/>85	<0/<0	30/30	40/40	55/55

<sup>^</sup>Test run but no attack observed.

### ASTM G 78 Test

ASTM G 78 describes crevice corrosion testing using a number of specimen geometries. While the standard is primarily devoted to seawater testing, it can be adopted for other applications. In addition to variations of multiple crevice assembly, ASTM G 78 describes other geometries, including cylindrical pipe geometries with flexible polymeric sheaths as a crevice-forming device. The test method involves exposing the specimens to the applicable environment and evaluating the crevice corrosion susceptibility through mass-loss, measurement of the area of corrosion, and depth of penetration.

### Other Non-Electrochemical Tests

Immersion tests have also been conducted in other environments, notably seawater. The test procedures for preparing the crevice samples can be similar to that in G 48, Method D. The results from seawater tests are shown in Table 3 [79]. It must be emphasized that natural seawater behaves quite differently than synthetic seawater in that the corrosion potential is often much higher in natural seawater [83]. The  $\text{FeCl}_3$  solution is not stable above about 85°C, necessitating use of more aggressive environments for highly corrosion resistant alloys. On the other hand, the  $\text{FeCl}_3$  solution can be too aggressive for some alloys, making it difficult to differentiate between alloys. Crevice corrosion tests in other oxidizing, chloride solutions have been reported in the literature [84]. Caution should be exercised in ranking alloys for their localized corrosion resistance in one oxidizing chloride solution based on their ranking in another chloride environment. For example, the ranking of alloys in  $\text{FeCl}_3$  solution has been found to be in variance with that in chlorine dioxide-containing solutions [85,86]. The localized corrosion resistance in chloride containing solutions may also not be an accurate indicator of their resistance to non-chloride environments.

### ELECTROCHEMICAL TESTS UNDER OPEN-CIRCUIT CONDITIONS

Electrochemical tests are the most rapid way of detecting localized corrosion and measuring corrosion rates. With proper calibration and control, corrosion can be detected and quantified online and in real-time. Electrochemical tests can be conducted at open-circuit potential conditions by galvanically coupling a creviced specimen to an open (non-creviced) specimen and measuring the current flow using a zero-resistance ammeter [87–90]. Such an arrangement is called the remote crevice assembly. The area ratio between the creviced and non-creviced specimens can be varied depending upon the specific application. The advantage of this technique is the sensitivity with which early stages of crevice corrosion and later growth and repassivation can be measured, without perturbing the system away from its open-circuit potential. Care should be taken to minimize exposed (non-crevice) area in the anodic member of the remote crevice assembly. The test specimen geometry can be designed to reproduce anticipated macroscopic crevice geometries in many applications.

The crevice can be formed in the same manner as for G 48, Method D. Care must be taken in exposing only the crevice with controlled gap. The crevice where electrical contact is made with the specimen is uncontrolled. This crevice area can be designed to be above the solution level. The choice of area ratio between cathode (non-creviced specimen) and anode (creviced specimen) depends upon the application. For example, in a low conductivity solution or an environment where a condensed water film controls corrosion, the cathode to anode area ratio is expected to be relatively small (less than 2:1). In flowing seawater systems, this ratio can be quite large. For example a ratio of 300:1 has been used [90]. Visual examination at the end of the test is essential in correlating the observed galvanic currents with degree of crevice corrosion. The open-circuit potential can be changed as in the non-electrochemical tests by changing the redox species or concentration. At present, there is no specific ASTM standard for his test. However, ASTM G 71<sup>7</sup> can be used as guidance.

### ELECTROCHEMICAL TESTS UNDER APPLIED POTENTIAL/CURRENT

These techniques for evaluating crevice corrosion resistance involve holding (static) or incrementally changing (step or scan) the potential or current. Some of the more frequently used techniques for evaluating crevice corrosion resistance are listed below, following the definitions given in ASTM G 15:

1. Potentiostatic technique—Changes in current density are monitored for a sample maintained at a constant potential. The potential can be varied from sample to sample.
2. Galvanostatic technique—changes in potential are monitored for a sample maintained at a constant current in a test solution.
3. Potentiostep or potentiostaircase technique—Changes in current density are monitored for a sample that is polarized in a series of potential increments or decrements. Typically, the time duration or potential steps in a crevice corrosion tests are not equal.
4. Potentiodynamic technique—The potential is changed scanned continuously at a predetermined rate (ASTM G 5).
5. Cyclic potentiodynamic technique—The potential is scanned forward from some low value to a high value and scanned backward to a predetermined potential or current value (ASTM G 61).
6. Galvanostep or galvanostaircase technique—Changes in potential are monitored for a sample that is polarized in a series of current increments or decrements. (For more information the reader is referred to a related standard, ASTM G 100, Method for Conducting Cyclic Galvanostaircase Polarization.)

<sup>7</sup>Standard Guide for Conducting and Evaluating Galvanic Corrosion Tests in Electrolytes. The work of Qvarfort [51] represents a different approach to critical temperature testing that is intended to study pitting rather than crevice corrosion. See the previous chapter, Pitting, for a discussion of this approach.

These four basic techniques are used alone, combined, or in combination with other corrosion-accelerating factors such as increased temperature or chloride concentration. For example, ASTM F 746, Test Method for Pitting or Crevice Corrosion of Metallic Surgical Implant Materials, test involves alternatively controlling the potential until a specified current density is achieved and then following the current until a specified potential is achieved. One way of determining the critical crevice corrosion temperature is with a series of potentiostatic tests conducted at uniform increments of increasing temperature until a limit in current density is exceeded. In the electrochemical tests, it should be noted that some of the measured parameters are sensitive to crevice geometry.

### Measurement of Critical Temperature

Electrochemical critical temperature (ECT) testing has been evolving for more than two decades [48,50,64,73–75,79,91–94,101].<sup>7</sup> The programmed changes in applied potential and temperature that constitute the ECT method are schematically illustrated in Fig. 4. (Note that the corresponding changes in current density are not illustrated in Fig. 4.)

The periodic decreases in the applied potential and current density shown in Fig. 4 are due to the fact that the potential is not applied during the rise in temperature. Several workers have found that the continuous application of potential while temperature is increased continuously at a constant rate to be a more efficient and less complex method of testing [102]. The primary reason for preferring the intermittent or step method (the latter is illustrated in Fig. 4) over the continuous method of ECT testing is that the step method better simulates the conditions of the conventional immersion-type test, in which samples are removed from the test solution after exposure at each temperature and inspected, then reimmersed.

Under some combination of elevated temperature and applied potential, localized corrosion will initiate and result

in a rapid increase in current density. Eventually, the change in current density is sustained at a level two or more orders of magnitude higher than the passive current level. The temperature at which this occurs is taken to be the electrochemical critical crevice corrosion temperature (ECCT) or electrochemical critical pitting temperature (ECPT), depending on whether a crevice-former was used. The transient surges of current density that occur below the ECT are usually ignored since such changes represent the initiation and rapid repassivation of pits.

The results achieved by using the ECT technique have very good correlation with long-term exposure tests in brine as well as the same ranking as found in cyclic polarization work [55]. ECT test methods have been found to be very effective in detecting rather subtle differences in the composition and microstructure of stainless steels [95,96,103].

The most important aspect of ECT testing is that a wide range of alloys can be ranked by a single parameter. Another advantage of ECT testing over immersion testing is that different degrees of polarization can be used to simulate the corrosion potentials that are characteristic of various environments. If the corrosion potential ( $E_{\text{corr}}$ ) of an alloy in a service environment is known, a specimen of that alloy can be polarized to that potential in a simulated solution or to a value typically 200–600 mV more anodic than  $E_{\text{corr}}$  in order to accelerate pitting or crevice corrosion.

An extension of the ECT method described above that has been used to evaluate alloys for service on North Sea oil platforms [97,98] has been referred to as cyclic thermammetry [99]. The technique involves exposing a coupon fitted with an MCA to a test solution under an applied potential that simulates a process environment. The current density of the crevice specimen is monitored as the temperature of the test solution is slowly changed (e.g., 4°C/24 h) in a cyclic manner up to a critical value and then back toward room temperature. The test results are in the form of a curve (Fig. 5) that looks very much like a conventional anodic polarization curve [97] with the exception that temperature rather than applied potential is the independent variable. Values for a critical crevice corrosion

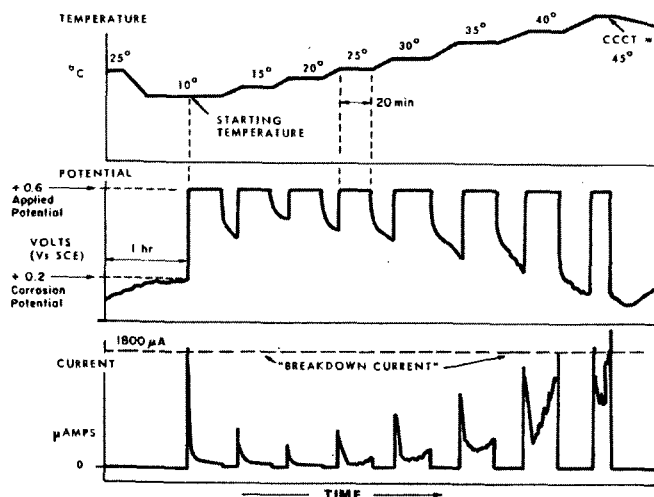


FIG. 4—Schematic illustration of changes in test variables in the course of an intermittent type of ECT test [93].

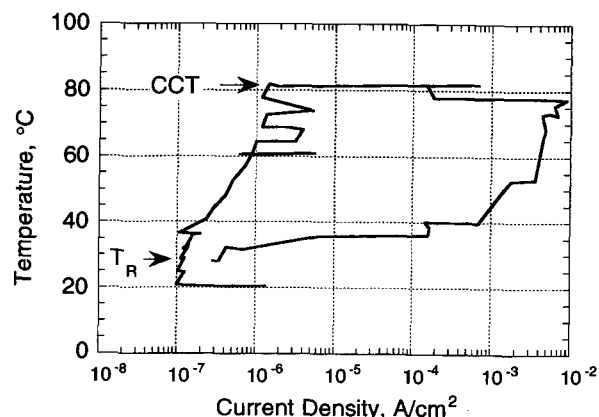


FIG. 5—Cyclic thermammetry plot for N08367 alloy exposed in a crevice assembly to aerated 3 wt% NaCl under an applied potential of 600 mV (SCE). The temperature was changed by 4°C/24 h; data from Ref 97.

temperature (CCT) and a repassivation temperature ( $T_R$ ) can be determined from a cyclic thermammety curve, as indicated in Fig. 5 [98].

### Bias in ECT Tests

The current limit for the ECT, like mass loss or crevice depth, is crucial in establishing a value for the ECT. No criteria for ECT have yet been established by any internationally recognized standards writing organization. A limited survey of the literature yielded test parameter values ranging from 0.01–1.8 mA/cm<sup>2</sup>, depending on test environment and sample configuration. One method for establishing the current limit for an ECT test that has been used by several workers involves conducting a series of cyclic potentiodynamic polarization tests (after ASTM G 61<sup>5</sup>) at various temperatures to determine the current density associated with the pitting potential. The influence of the rate of temperature increase in an ECT is analogous to that of potential scan rate in cyclic potentiodynamic polarization test. Figure 6 shows that lower rates of temperature increase result in lower ECCT values.

With regard to intermittent versus continuous ECT test, intermittent tests generally produce higher ECT values than do continuous tests. The reason is that metastable pits are more likely to stabilize and propagate in a continuous test; intermittent tests pits or crevices can repassivate during the intervals when the specimen is allowed to return to open circuit potential.

### Measurement of Critical Potentials

Critical potentials are important in determining the resistance of a metal to localized corrosion because they have a mechanistic underpinning and they are rapid measurements. Two potentials have been used as a measure of the crevice corrosion resistance—crevice/pit initiation potential ( $E_{crev}$  or  $E_p$ ) and crevice/pit repassivation potential ( $E_{rcrev}$  or  $E_{rp}$ ). The  $E_{crev}$  or  $E_p$  is the potential at which the current

increases significantly when the potential is raised from a lower value either in a stepwise or continuous fashion. The  $E_{rcrev}$  or  $E_{rp}$  is the potential at which the current decreases to a low value when the potential is decreased (Fig. 7).

However, there has been considerable debate about the validity of these parameters for determining the long-term performance of a given alloy and their dependence on measurement techniques [39,103–107]. It is well known that the  $E_p$  and  $E_{rcrev}$ , the potential at which the current increases from a low passive value to a high active value, depends on the scan rate [104], among other factors. Another reason cited against the use of critical potential as a measure of the localized corrosion resistance is the observation made by Wilde and Wilde and Williams [106,107] that the  $E_{rp}$  decreased with the extent of prior pit growth. Since then, a number of studies [39,108–110] have shown that the  $E_{rcrev}$  and  $E_{rp}$  attain a lower bound value beyond a certain pit or crevice corrosion depth (Fig. 8). Longer-term, potentiostatic tests have also shown that the  $E_{rp}$  measured for deep pits is a reasonable parameter to predict long-term localized corrosion occurrence [39,108].

The techniques for measuring the repassivation potential have not been standardized, although existing methods can be adapted. For alloys that exhibit low to moderate resistance to localized corrosion, the ASTM G 61 method is adequate in defining the repassivation potential, provided sufficient growth in crevice corrosion is assured. For highly corrosion resistant alloys, the use of cyclic, potentiodynamic polarization method (ASTM G 61) can lead to misleading results. For example, hysteresis between the forward and backward scans has traditionally been used as an indicator of localized corrosion. In highly corrosion resistant alloys, such a hysteresis can be observed without any visual appearance of crevice corrosion (Fig. 9a and b). This is because the initiation of crevice corrosion in the forward scan is monitored by the magnitude of current density. In highly corrosion resistant alloys high currents can be attained during continuous scanning by polarizing to high potentials (above 1 V SCE) where transpassive dissolution takes place. The fact that this is not crevice corrosion is

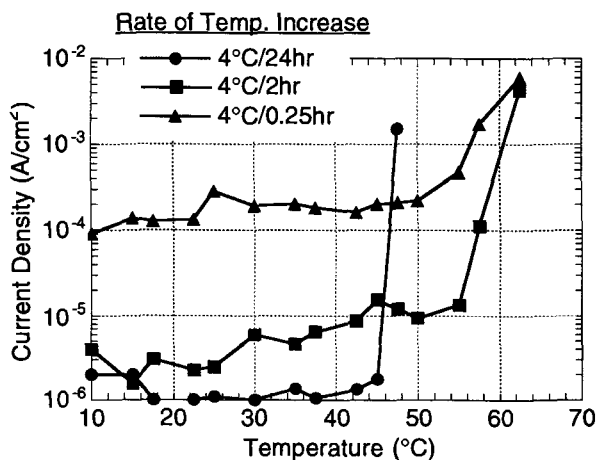


FIG. 6—Effect of the rate of temperature increase on the anodic current density for welded S31254 in natural seawater at an applied potential of +400 mV (SCE). The solution temperature was increased continuously at the cited rates. Data from Ref 99.

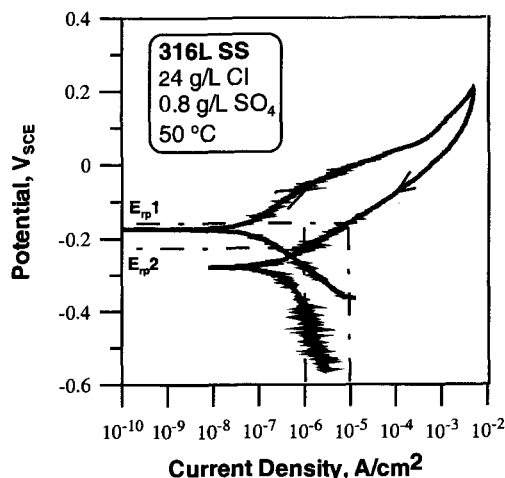


FIG. 7—Cyclic potentiodynamic polarization curve for type 316L SS showing hysteresis and crevice corrosion.

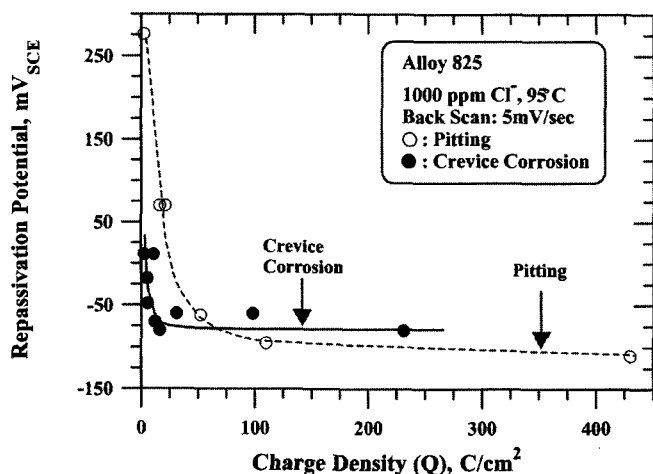


FIG. 8—The repassivation potential as a function of prior crevice corrosion and pit depth showing a bounding value less sensitive to penetration depth [39].

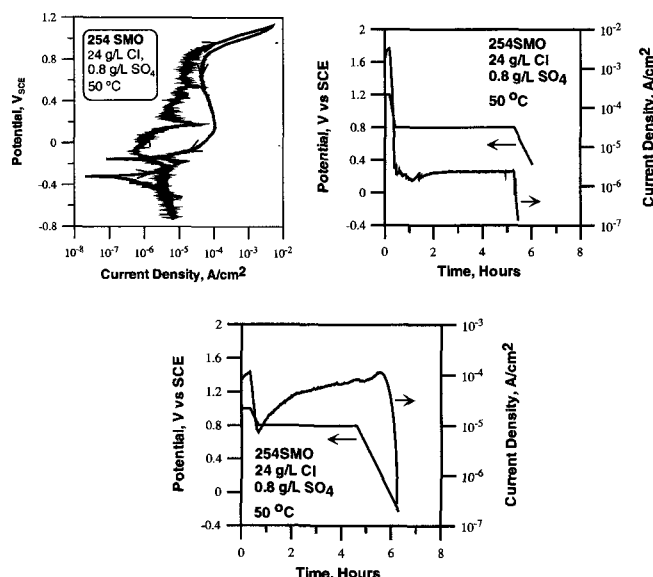


FIG. 9—Cyclic potentiodynamic polarization curve for alloy 254 SMO showing a large hysteresis, but no crevice corrosion (a). If potentiostep tests were performed with the initial potential value at 1.2 V SCE, no crevice corrosion is initiated upon subsequent growth at 0.8 V SCE, as noted by lack of current increase (b). If the initial potential was held at 1.0 V SCE, then crevice corrosion growth occurred at 0.8 V SCE subsequently as noted by the current increase (c).

seen in Fig. 9b, where the potential is held at 0.8 V SCE after initiating corrosion at 1.2 V SCE. The current in this case does not increase even after relatively long time periods. In such a case, backward scanning will indicate a misleading value for repassivation potential. On the other hand, if the corrosion is initiated at a lower potential, the current increases and crevice corrosion is observed visually. Therefore, a combination of cyclic polarization test to determine

the overall characteristics of the polarization curve, followed by potentiostep technique is recommended for highly corrosion resistant alloys.

### Precision in Measuring Critical Potentials

ASTM G 61 shows the precision in these measurements. The scatter in the  $E_p$  and  $E_{crev}$  is much larger than the scatter in  $E_{tp}$  or  $E_{tcrev}$  [39,108–110]. Limited experimental data [108] indicate a scatter in the  $E_{tcrev}$  values of about 100 mV.

### Measurement of Depassivation pH

Following a number of crevice corrosion modeling approaches [11,12,14], another measure of the crevice corrosion resistance of an alloy was established in terms of the depassivation pH,  $pH_d$ . This is the pH below which an alloy does not exhibit any passivity and thus represents the conditions at an active crevice corrosion site. It must be noted that in some of the experimental investigations criteria are adopted that may not always result in complete depassivation. For example, Oldfield and Sutton [14] assume a certain current density under potentiostatic conditions as the criterion for depassivation. The  $pH_d$  values have been measured for a number of alloys [36,113]. The  $pH_d$  can be measured either by generating polarization curves in various simulated crevice solutions with decreasing pH using ASTM G 5 or G 61 method or by monitoring the potential of a specimen under galvanostatic conditions while simultaneously decreasing the pH by the addition of HCl. There is no standard procedure established for this measurement.

## REFERENCES

- [1] Mears, R. B. and Evans, U. R., "Corrosion at Contact with Glass," *Transactions of the Faraday Society*, Vol. 30, 1934, pp. 417–423.
- [2] Uhlig, H. H., "Pitting of Stainless Steels," *Transactions of AIME*, Vol. 140, 1940, pp. 387–432.
- [3] Rosenfeld, I. L. and Marshakov, I. K., "Mechanism of Crevice Corrosion," *Corrosion*, Vol. 20, No. 4, 1964, pp. 115t–125t.
- [4] Schafer, G. J. and Foster, P. K., "The Role of the Metal-Ion Concentration Cell in Crevice Corrosion," *Journal of the Electrochemical Society*, Vol. 106, No. 5, 1959, p. 468.
- [5] Schafer, G. J., Gabriel, J. R., and Foster, P. K., "On the Role of the Oxygen Concentration Cell in Crevice Corrosion and Pitting," *Journal of the Electrochemical Society*, Vol. 107, No. 12, 1960, pp. 1–1.
- [6] Bombara, G., "Stress-Corrosion Cracking and Crevice Corrosion in Passivable Alloys," *Corrosion Science*, Vol. 9, No. 7, 1969, pp. 519–533.
- [7] Brown, B. F., "Technical Note: Concept of the Occluded Corrosion Cell," *Corrosion*, Vol. 26, No. 8, 1970, pp. 249–250.
- [8] Karlberg, G. and Wranglen, G., "On the Mechanism of Crevice Corrosion of Stainless Cr Steel," *Corrosion Science*, Vol. 11, 1971, pp. 499–510.
- [9] Pickering, H. W. and Frankenthal, R. P., "On the Mechanism of Localized Corrosion of Iron and Stainless Steel I. Electrochemical Studies," *Journal of the Electrochemical Society*, Vol. 119, No. 10, 1972, pp. 1297–1304.
- [10] Pickering, H. W. and Frankenthal, R. P., "On the Mechanism of Localized Corrosion of Iron and Stainless Steel II. Morphological Studies," *Journal of the Electrochemical Society*, Vol. 119, No. 10, 1972, pp. 1304–1310.

- [11] Crolet, J. L. and Defranoux, J. M., "Calculation of Incubation Times in Crevice Corrosion of Stainless Steels," *Corrosion Science*, Vol. 13, No. 7, 1973, pp. 575-585.
- [12] Galvele, J. R., "Transport Process and the Mechanism of Pitting of Metals," *Journal of the Electrochemical Society*, Vol. 123, No. 4, 1976, pp. 464-474.
- [13] Gravano, S. M. and Galvele, J. R., "Transport Processes in Passivity Breakdown - III. Full Hydrolysis Plus Ion Migration Plus Buffers," *Corrosion Science*, Vol. 24, No. 6, 1984, pp. 517-534.
- [14] Oldfield, J. W. and Sutton, W. H., "Crevice Corrosion of Stainless Steels—I. A Mathematical Mode," *British Corrosion Journal*, Vol. 13, No. 1, 1978, pp. 13-22.
- [15] Turnbull, A., "Chemistry Within Localized Corrosion Cavities," in *Advances in Localized Corrosion*, H. S. Isaacs, U. Bertocci, J. Kruger, and S. Smialowska, Eds., National Association of Corrosion Engineers, 1990, Vol. NACE-9, pp. 359-373.
- [16] Alkire, R. C. and D. Siitari, "Initiation of Crevice Corrosion - II, Mathematical Model for Aluminum in Sodium Chloride Solutions," *Journal of the Electrochemical Society*, Vol. 129, No. 3, 1982, pp. 488-496.
- [17] Sharland, S. M., "A Mathematical Model of the Initiation of Crevice Corrosion in Metals," *Corrosion Science*, Vol. 33, No. 2, 1992, pp. 183-201.
- [18] Watson, M. K. and Postlethwaite, J., "Numerical Simulation of Crevice Corrosion," *Corrosion*, Vol. 46, No. 8, 1990, pp. 522-530.
- [19] Gartland, P. O., "Modeling Crevice Corrosion of Fe-Ni-Cr-Mo Alloys in Chloride Solutions," 12th International Corrosion Congress, NACE International, 1993, Vol. 3B, pp. 1901-1914.
- [20] Walton, J. C., "Mathematical Modeling of Mass Transport and Chemical Reaction in Crevice and Pitting Corrosion," *Corrosion Science*, Vol. 30, No. 8/9, 1990, pp. 915-928.
- [21] Walton, J. C., Cragnolino, G. A., and Kalandros, S. K., "A Numerical Model of Crevice Corrosion for Passive and Active Metals," *Corrosion Science*, Vol. 38, No. 1, 1996, pp. 1-18.
- [22] Lillard, R. S. and Scully, J. R., "Modeling of the Factors Contributing to the Initiation and Propagation of the Crevice Corrosion of Alloy 625," *Journal of the Electrochemical Society*, Vol. 141, No. 11, 1994, pp. 3006-3015.
- [23] Lillard, R. S., Jurinski, M. P., and Scully, J. R., "Crevice Corrosion of Alloy 625 in Chlorinated ASTM Artificial Oceanwater," *Corrosion*, Vol. 50, No. 4, 1993, pp. 251-265.
- [24] Nisancioglu, K. and Holtan, H., "Correlation of the Protection Potential and the Ohmic Potential Drop," *Electrochimica Acta*, Vol. 23, No. 3, 1978, pp. 251-253.
- [25] Pickering, H. W., "The Limiting IR Voltage within Electrolyte in Cavities During Localized Corrosion and Hydrogen Charging of Metals," *Corrosion and Corrosion Protection*, R. P. Frankenthal and F. Mansfeld, Eds., The Electrochemical Soc., Inc., Pennington, NJ, 1981, p. 85.
- [26] Pickering, H. W., "The Significance of the Local Electrode Potential within Pits Crevices and Cracks," *Corrosion Science*, Vol. 29, No. 2/3, 1989, pp. 325-341.
- [27] Xu, Y. and Pickering, H. W., "A Model of the Potential and Current Distribution within Crevices and Its Application to the Iron-Ammoniacal System," *Critical Factors in Localized Corrosion*, G. S. Frankel and R. C. Newman, Eds., The Electrochemical Society, Pennington, NJ, 1992, pp. 389-406.
- [28] Shaw, B. A. and Moran, P. J., "The Role of Ohmic Potential Drop in the Initiation of Crevice Corrosion on Alloy 625 in Seawater," *Corrosion Science*, Vol. 32, No. 7, 1991, pp. 707-719.
- [29] Kehler, B. A., Ilevbare, G. O., and Scully, J. R., "Crevice Corrosion Behavior of Ni-Cr-Mo Alloys: Comparison of Alloys 625 and 22," *Research Topical Symposium on Localized Corrosion*, G. S. Frankel and J. R. Scully, Eds., Houston, TX, NACE International, 2001, pp. 30-64.
- [30] Stockert, L. and Boehni, H., "Metastable Pitting Processes and Crevice Corrosion on Stainless Steels," *Advances in Localized Corrosion*, H. S. Isaacs, U. Bertocci, J. Kruger, and S. Smialowska, Eds., National Association of Corrosion Engineers, Orlando, FL, 1-5 June 1987, 1990, Vol. NACE-9, pp. 467-473.
- [31] Sridhar, N. and Dunn, D. S., "Effect of Applied Potential on Changes in Solution Chemistry Inside Crevices on Type 304. Stainless Steel and Alloy 825," Paper 347, NACE CORROSION/94, NACE International, Baltimore, MD, 1994.
- [32] Ogawa, H., Denpo, K., and Miyasaka, A., "Criteria for Passivity Breakdown of High Alloy Materials in Relation to Crevice Corrosion Nucleation," *Corrosion Science*, Vol. 31, No. 1, 1990, pp. 459-464.
- [33] Sato, N., "Some Concepts of Corrosion Fundamentals," *Corrosion Science*, Vol. 27, No. 5, 1987, pp. 421-433.
- [34] Sato, N., "Toward a More Fundamental Understanding of Corrosion Processes," *Corrosion*, Vol. 45, No. 5, 1989, pp. 354-368.
- [35] Crolet, J. L., Defranoux, J. M., Seraphin, L., and Tricot, R., "Electrochemical Characterization of the Crevice Corrosion Resistance of Stainless Steels," *Memoires Scientifiques Revue Metallurgie*, Vol. 71, No. 12, 1974, pp. 797-805.
- [36] Crolet, J. L., Seraphin, L., and Tricot, R., "Influence of Chloride Content on the Depassivation pH of Stainless Steels," *Memoires Scientifiques Revue Metallurgie*, Vol. 73, No. 1, 1976, pp. 1-8.
- [37] Laycock, N. J., Stewart, J., and Newman, R. C., "The Initiation of Crevice Corrosion in Stainless Steels," *Corrosion Science*, Vol. 39, No. 10-11, 1997, pp. 1791-1809.
- [38] Isaacs, H. S., "The Behavior of Resistance Layers in the Localized Corrosion of Stainless Steel," *Journal of the Electrochemical Society*, Vol. 120, No. 11, 1973, pp. 1456-1462.
- [39] Sridhar, N., Dunn, D. S., Brossia, C. S., and Cragnolino, G. A., "Stabilization and Repassivation of Localized Corrosion," Research Topical Symposium on Localized Corrosion, G. S. Frankel and J. R. Scully, Ed., Houston, TX, NACE International, 2001, pp. 1-29.
- [40] Oldfield, J. W. and Sutton, W. H., "Crevice Corrosion of Stainless Steels—II. Experimental Studies," *British Corrosion Journal*, Vol. 13, No. 3, 1978, pp. 104-111.
- [41] Isseling, F. P., "Electrochemical Methods in Crevice Corrosion Testing: Report Prepared for the European Federation of Corrosion Working Party 'Physico-Chemical Testing Methods of Corrosion,'" *British Corrosion Journal*, Vol. 15, No. 2, 1980, pp. 51-69.
- [42] Kruger, J. and Rhyne, K., "Current Understanding of Pitting and Crevice Corrosion and Its Application to Test Methods for Determining the Corrosion Susceptibility of Nuclear Waste Metallic Containers," *Nuclear and Chemical Waste Management*, Vol. 3, No. 4, 1982, pp. 205-227.
- [43] Postlethwaite, J., "Electrochemical Tests for Pitting and Crevice Corrosion Susceptibility," *Canadian Metallurgical Quarterly*, Vol. 22, No. 1, 1983, pp. 133-141.
- [44] Oldfield, J. W., "Test Techniques for Pitting and Crevice Corrosion Resistance of Stainless Steels and Nickel Base Alloys in Chloride Containing Environments," *International Materials Reviews*, Vol. 32, No. 3, 1987, pp. 153-170.
- [45] Kain, R. M., "Evaluation of Crevice Corrosion," *Corrosion*, Vol. 13, L. J. Korb and D. L. Olson, Eds., ASM, Materials Park, OH, 1988, p. 405.
- [46] Streicher, M. A., "Development of Pitting Resistant Fe-Cr-Mo Alloys," *Corrosion*, Vol. 30, No. 3, 1974, pp. 77-91.
- [47] Garner, A., "Crevice Corrosion of Stainless Steels in Seawater: Correlation of Field Data with Laboratory Ferric Chloride Tests," *Corrosion*, Vol. 37, No. 3, 1981, pp. 178-184.
- [48] Nagaswami, N. S. and Streicher, M. A., "Accelerated Laboratory Tests for Crevice Corrosion of Stainless Alloys," Paper 71, NACE CORROSION/83 Conference, NACE, Anaheim, CA, 1983.
- [49] Hibner, E. L., "Modification of Critical Crevice Temperature Test Procedures for Nickel Alloys in a Ferric Chloride Environment," *Materials Performance*, Vol. 26, No. 3, 1987, pp. 37-40.

- [50] Brigham, R. J., "Temperature as a Crevice Corrosion Criterion," *Corrosion*, Vol. 30, No. 11, 1974, pp. 396–398.
- [51] Qvarfort, R., "New Electrochemical Cell for Pitting Corrosion Testing," *Corrosion Science*, Vol. 28, No. 2, 1988, pp. 135–140.
- [52] Qvarfort, R., "Critical Pitting Temperature Measurements for Stainless Steels with an Improved Electrochemical Method," *Corrosion Science*, Vol. 29, No. 8, 1989, pp. 987–993.
- [53] Dean, S. W., "Electrochemical Methods for Corrosion Testing in the Process Industries," *Electrochemical Corrosion Testing with Special Consideration of Practical Applications: Papers and Discussions of an International Workshop*, J. C. Rowlands and F. Mansfeld, Eds., VCH, Deerfield Beach, FL, Ferrara, Italy, 1985, pp. 1–15.
- [54] Schofield, M. J. and Kane, R. D., "Critical Review of Corrosion Test Methods for Duplex Stainless Steels," Paper 90572, CORROSION/90, NACE International, Las Vegas, NV, 23–27 April 1990.
- [55] Bardal, E., Drugli, J. M., and Gartland, P. O., "Behavior of Corrosion-Resistant Stainless Steels in Seawater: A Review," *Corrosion Science*, Vol. 35, No. 1–4, 1993, pp. 257–267.
- [56] Streicher, M. A., "Pitting Corrosion of 18Cr-8Ni Stainless Steel," *Journal of the Electrochemical Society*, Vol. 103, No. 7, 1956, pp. 375–389.
- [57] Renner, M., Heubner, U., Rockel, M. B., and Wallis, E., "Temperature as a Pitting and Crevice Corrosion Criterion in the  $\text{FeCl}_3$ ," *Werkstoffe und Korrosion*, Vol. 37, No. 4, 1986, pp. 183–190.
- [58] Lizlovs, E. A., "Crevice Corrosion of Some High Purity Ferritic Stainless Steels," *Localized Corrosion—Cause of Metal Failure*, ASTM STP 516, ASTM International, West Conshohocken, PA, 1972, pp. 201–209.
- [59] Bond, A. P. and Dundas, H. J., "Resistance of Stainless Steels to Crevice Corrosion in Seawater," *Materials Performance*, Vol. 23, No. 7, 1984, pp. 39–43.
- [60] Bond, D. P., Dundas, H. J., Ekerot, S., and Semchyshen, M., "Stainless Steels for Seawater Service," *Stainless Steel '77*, Climax Molybdenum Co., Ann Arbor, MI, 1977, p. 197.
- [61] Tsujikawa, S., Kudo, K., Ogawa, H., et al., "A New Test for Predicting Pitting Corrosion Resistance of CRA's in Sour Environments," Paper 65, NACE CORROSION/88 Conference, NACE International, St. Louis, MO, 1988.
- [62] Wallen, B., Bergqvist, A., and Olsson, J., "Testing of Three Highly Alloyed Stainless Steels According to the MTI Corrosion Tests," E., Risbergs, Ed., 11th Scandinavian Corrosion Congress, Swedish Corrosion Institute, Stockholm, Sweden, Stavanger, Norway, 1989, pp. 1–9.
- [63] Brigham, R. J., "On the Variability of Crevice Corrosion Initiation in Ferric Chloride Exposure Tests," *Corrosion*, Vol. 37, No. 10, 1981, pp. 608–609.
- [64] Brigham, R. J. and Tozer, E. W., "Localized Corrosion Resistance of Mn-Substituted Austenitic Stainless Steels: Effect of Molybdenum and Chromium," *Corrosion*, Vol. 32, No. 7, 1976, pp. 274–276.
- [65] Christie, D. W., "Effect of Post-Weld Cleaning on Corrosion Resistance of Austenitic and Duplex Stainless Steel Weldments in Bleach Plant Service," NACE Western Canadian Region Conference, NACE, Edmonton, Canada, 1992, pp. 1–14.
- [66] Degerbeck, J., "On Accelerated Pitting and Crevice Corrosion Tests," *Journal of the Electrochemical Society*, Vol. 120, No. 2, 1973, pp. 175–182.
- [67] Kolts, J. and Sridhar, N., "Temperature Effects in Localized Corrosion," *Corrosion of Nickel-Base Alloys*, R. C. Scarberry, Ed., ASM International, Metals Park, OH, 1985, pp. 191–198.
- [68] Lagerberg, S., Bernhardsson, S., and Lau, P., "Electrochemical Testing Methods for the Study of Localized Corrosion," 10th Scandinavian Corrosion Congress, Swedish-Corrosion Institute, Stockholm, Sweden, 1986, pp. 271–277.
- [69] Lau, P. and Bernhardsson, S., "Electrochemical Techniques for the Study of Pitting and Crevice Corrosion Resistance of Stainless Steels," *Electrochemical Techniques for Corrosion Engineering*, R. Baboian, Ed., NACE International, Houston, TX, 1977, pp. 281–286.
- [70] Garner, A., "The Effect of Autogenous Welding on Chloride Pitting Corrosion in Austenitic Stainless Steels," *Corrosion*, Vol. 35, No. 3, 1979, pp. 108–113.
- [71] Garner, A., "Materials Selection for Bleached Pulp Washers," *Pulp & Paper Canada*, Vol. 82, No. 12, 1981, pp. 109–120.
- [72] Strandmyr, O. and Hagerup, O., "Field Experience with Stainless Steel Materials in Seawater Systems," *Corrosion/98*, Paper 707, Houston, TX: NACE International, 1998.
- [73] Brigham, R. J., "Pitting and Crevice Corrosion Resistance of 18% Cr Stainless Steel," *Materials Performance*, Vol. 13, No. 11, 1974, pp. 29–31.
- [74] Brigham, R. J. and Tozer, E. W., "Effect of Alloying Addition on the Pitting Resistance of 18%Cr Austenitic Stainless Steel," *Corrosion*, Vol. 30, No. 5, 1974, pp. 161–166.
- [75] Brigham, R. J. and Tozer, E. W., "Temperature as a Pitting Criterion," *Corrosion*, Vol. 29, No. 1, 1973, pp. 33–36.
- [76] Rockel, M. B. and Renner, M., "Critical Review of Laboratory Methods Testing the Resistance of High Alloyed Stainless Steels and Nickel Alloys Against Localized Corrosion in Chloride Solutions," 8th European Congress of Corrosion, Vol. 1, Centre Francais de la Corrosion, Societe de Chimie Industrielle, F75007 Paris, France, Nice, France, 19–21 November 1986.
- [77] Kain, R. M., "Seawater Testing to Assess the Crevice Corrosion Resistance of Stainless Steel and Related Alloys," 12th International Corrosion Congress, NACE International, Vol. 3B, 1993, pp. 1889–1900.
- [78] Anderson, D. B., "Statistical Aspects of Crevice Corrosion in Seawater," *Galvanic and Pitting Corrosion—Field and Laboratory Studies*, ASTM STP 576, ASTM International, West Conshohocken, PA, 1976, pp. 231–242.
- [79] Streicher, M. A., "Analysis of Crevice Corrosion Data from Two Sea Water Exposure Tests in Stainless Alloys," *Materials Performance*, Vol. 22, No. 5, 1983, pp. 37–50.
- [80] Kain, R. M., "Crevice Corrosion Testing in Natural Seawater Significance and Use of Multiple Crevice Assemblies," *Journal of Testing and Evaluation*, Vol. 18, No. 5, 1990, pp. 309–318.
- [81] Kearns, J. R., Johnson, M. J., and Grubb, J. F., "Accelerated Corrosion in Dissimilar Metal Crevices," Paper 228, NACE CORROSION/86 Conference, NACE, Houston, TX, 1986.
- [82] Maurer J. R., "Long-Term Exposure of Dissimilar Metal Crevice in Filtered Seawater," *Materials Performance*, Vol. 33, No. 4, 1994, pp. 51–54.
- [83] Gallagher, P., Malpas, R. E., and Shone, E. B., "Corrosion of Stainless Steels in Natural, Transported, and Artificial Seawater," *British Corrosion Journal*, Vol. 23, No. 4, 1988, pp. 229–233.
- [84] Manning, P. E., "Comparison of Several Accelerated Laboratory Tests for the Determination of Localized Corrosion Resistance of High-Performance Alloys," *Corrosion/82*, Paper No. 176, Houston, TX: NACE International, 1982.
- [85] Wensley, D. A., Reid, R. C., and Dykstra, H., "Corrosion of Nickel-Based Alloys in Chlorine Dioxide Washer Service," *Corrosion/90*, Paper 537, Houston, TX: NACE International, 1990.
- [86] Nadezhdin, A. and Wensley, D. A., "Composition Factors Affecting Resistance of Ni-Cr-Mo-N Alloys to Crevice Corrosion," *Materials Performance*, Vol. 31, No. 11, 1991, pp. 57–59.
- [87] Lee, T. S., "A Method for Quantifying the Initiation and Propagation Stages of Crevice Corrosion," *Electrochemical Corrosion Testing*, ASTM STP 727, F. Mansfield and U. Bertocci, Eds., ASTM International, West Conshohocken, PA, 1981, pp. 43–68.



- [88] Kain, R. M. and Lee, T. S., "Recent Developments in Test Methods for Investigating Crevice Corrosion," *Laboratory Corrosion Tests and Standards*, ASTM STP 866, G. S. Haynes and R. Baboian, Eds., ASTM International, West Conshohocken, PA, 1985, pp. 299–323.
- [89] Kain, R. M., "Electrochemical Measurement of the Crevice Corrosion Propagation Resistance of Stainless Steels: Effect of Environmental Variables and Alloy Content," *Materials Performance*, Vol. 23, No. 2, 1984, pp. 24–30.
- [90] Steinsmo, U., Rogne, T., and Drugli, J., "Aspects of Testing and Selecting Stainless Steels for Seawater Applications," *Corrosion*, Vol. 53, No. 12, 1997, pp. 955–964.
- [91] Brigham, R. J., "The Initiation of Crevice Corrosion on Stainless Steels," *Materials Performance*, Vol. 24, No. 12, 1985, pp. 44–48.
- [92] Bernhardtsson, S., Mellström, R., and Brox, B., "Limiting Chloride Contents and Temperatures with Regard to Pitting of Stainless Steels," Paper 85, NACE CORROSION/80 Conference, Anaheim, CA, 1980.
- [93] Bernhardtsson, S. and Mellström, R., "Performance of a Highly Alloyed Stainless Steel in Marine Environments," *Anti-Corrosion*, 1985, p. 7.
- [94] Davis, G. O. and Streicher, M. A., "Initiation of Chloride Crevice Corrosion of Stainless Alloys," Paper 205, NACE CORROSION/85 Conference, Boston, 1985.
- [95] Davison, R. M., "Characterization of Stainless Steel Plates for Paper Machine Headbox Applications," Paper 90542, CORROSION/90, NACE International, Las Vegas, NV, 23–27 April 1990.
- [96] Alfonsson, E. and Qvarfort, R., "Investigation of the Applicability of Some PRE Expressions for Austenitic Stainless," Materials Science Forum: Electrochemical Methods in Corrosion Research (EMCR) 4, Vol. 111–112, 1992, pp. 483–491.
- [97] Steinsmo, U., Rogne, T., Drugli, J. A., and Gartland P. O., "High Alloyed Stainless Steels for Chlorinated Seawater Applications—Critical Crevice Temperatures," *Engineering Solutions to Industrial Corrosion Problems*, NACE International, Sandefjord, Norway, 1993.
- [98] Gartland, P. O., Steinsmo, U., Drugli, J. M., and Solheim, P., "High, Alloyed Stainless Steels for Chlorinated Seawater Applications: A Summary of Test Results for Eleven Austenitic and Duplex Materials," Paper 646 NACE CORROSION/93, NACE Nashville, TN, 1993.
- [99] Martinchek, G. A. and Yaffe, M. R., CMS 110 Critical Pitting Test System Operator's Manual, GAMRY Instruments, Inc., Langhorne, PA, 1992.
- [100] Drugli, J. M. and Johnsen, R., "Corrosion Testing of Stainless Steel Weldments in Seawater, NaCl- and FeCl<sub>3</sub> Solutions," Paper 410, NACE CORROSION/88, St. Louis, MO, 1988.
- [101] Arvig, P. O. and Davison, R. M., "Measuring Corrosion Resistance of Stainless Steels Using the 'Avesta Cell'—Experiences and New Applications," 12th International Corrosion Congress, NACE International, Vol. 3A, 1993, pp. 1477–1490.
- [102] Kane, R. D., Wilhelm, S. M., and McIntyre, D. R., "Application of the Critical Pitting Temperature Test to the Evaluation of Duplex Stainless Steel," *Corrosion Testing and Evaluation: Silver Anniversary Volume*, ASTM STP 1000, R. Baboian and S. W. Dean, Eds., ASTM International, West Conshohocken, PA, 1990, pp. 289–302.
- [103] Thompson, N. G. and Syrett, B. C., "Relationship between Conventional Pitting and Protection Potential and a New, Unique Pitting Potential," *Corrosion*, Vol. 48, No. 8, 1992, pp. 649–659.
- [104] Szklarska-Smialowska, Z., "Pitting Corrosion of Metals," Houston, TX: NACE International, 1986.
- [105] Rogne, T., Drugli, J. M., and Johnsen, R., "Testing for Initiation of the Crevice Corrosion of Welded Stainless Steel in Natural Seawater," *Materials Performance*, Vol. 26, No. 9, 1987, pp. 29–34.
- [106] Wilde, B. E., "A Critical Appraisal of Some Popular Laboratory Electrochemical Test for Predicting the Localized Corrosion Resistance of Stainless Alloys in Seawater," *Corrosion*, Vol. 28, No. 8, 1972, pp. 283–291.
- [107] Wilde, B. E. and Williams E., "The Use of Current/Voltage Curves for the Study of Localized Corrosion and Passivity Breakdown on Stainless Steels in Chloride Media," *Electrochimica Acta*, Vol. 16, No. 11, 1971, pp. 1971–1985.
- [108] Dunn, D. S., Cragolino, G. A., and Sridhar, N., "An Electrochemical Approach to Predicting Long-Term Localized Corrosion of Corrosion-Resistant High-Level Waste Container Materials," *Corrosion*, Vol. 56, No. 1, 2000, pp. 90–104.
- [109] Tsujikawa, S. and Okayama, S., "Repassivation Method to Determine Critical Conditions in Terms of Electrode Potential, Temperature and NaCl Concentration to Predict Crevice Corrosion Resistance of Stainless Steels," *Corrosion Science*, Vol. 31, No. 1, 1990, pp. 441–446.
- [110] Tsujikawa, S., "Critical Depth for Initiation of Growing Crevice Corrosion," *Critical Factors in Localized Corrosion*, G. S. Frankel and R. C. Newmans, Eds., The Electrochemical Society, Pennington, NJ, 1992, pp. 378–388.
- [111] Syrett, B. C., "Technical Note: PPR Curves—A New Method of Assessing Pitting Corrosion Resistance," *Corrosion*, Vol. 33, No. 6, 1977, pp. 221–224.
- [112] Imai, H., Fukumoto, I., and Masuko, N., "Repassivation Potential for Crevice Corrosion of Austenitic SUS304 Stainless Steel with Teflon Ball Crevice," *Corrosion Engineering*, Vol. 36, 1987, pp. 461–466.
- [113] Okayama, S., Tsujikawa, S., and Kikuchi, K., "Effects of Alloying Elements on Stainless Steel Depassivation pH," *Corrosion Engineering*, Vol. 36, 1987, p. 631.
- [114] Betts, A. J. and Boulton, L. H., "Crevice Corrosion: Review of Mechanisms, Modeling, and Mitigation," *British Corrosion Journal*, Vol. 28, No. 4, 1993, pp. 279–295.

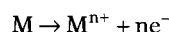
# Galvanic

Harvey P. Hack<sup>1</sup>

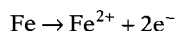
## BASIC PRINCIPLES

### Electrochemical Reactions

IN ORDER TO BE able to properly design and interpret the results from galvanic corrosion tests, it is necessary to have some appreciation of the electrochemical theory behind galvanic corrosion. Metal corrosion consists of at least two reactions. The first is the metal going into solution in the electrolyte

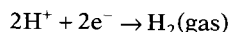


For iron in steel corroding in water at room temperature, this reaction would be

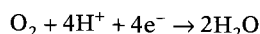


Since the metal is transformed from an atom with no net charge to an ion in solution with a net positive charge, this type of reaction is called an oxidation reaction, and generates electrons. Oxygen need not be involved in an oxidation reaction, only a net increase in charge of the metal. The oxidation reaction involved in the corrosion process is also called the anodic reaction.

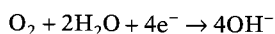
Since electrons are generated by the oxidation reaction, and since there can be no net accumulation of charge in these reactions, there must be another reaction occurring that uses up these electrons. This is the cathodic or reduction reaction, and it will always result in some species reducing its charge as it gains electrons. The three common reduction reactions in water are hydrogen reduction, occurring primarily in acids



oxygen reduction occurring primarily in acids



and oxygen reduction occurring primarily in bases or neutral water



The first of these cathodic reactions generates hydrogen gas and is readily observed when zinc or iron are placed in certain strong acids. The last two cathodic reactions use

oxygen molecules that are dissolved in the water. Other reduction reactions not illustrated include metal ion reduction and plating.

All of these reactions generate or use up electrons and, therefore, involve the flow of a current. For this reason, they are called electrochemical reactions, and their rates are influenced by externally applied currents and potentials. For example, if electrons are forcibly removed from the anodic corrosion reaction, the reaction will occur more rapidly. Removing electrons also causes the potential of the corroding metal, as measured relative to a device with a very stable potential called a reference electrode, to become more positive. This is plotted in Fig. 1. The relationship is illustrated as a straight line where potential is plotted against the log of the reaction rate. This straight-line relationship was first noted by Tafel [1], and the slope of the line honors him by being called the Tafel slope. Anodic reactions usually have a positive Tafel slope. Ideal reactions frequently yield these straight lines, but in practice it is common to see curved lines. The process of changing potential by applying a current is called polarization.

The cathodic reactions can also be plotted on the same type of graph. Adding electrons to the hydrogen reduction reaction (or to any cathodic reaction) will speed up that reaction and shift the potential more negative. This is shown in Fig. 1 as another straight line with a negative Tafel slope. Electrochemical reactions generate or use up electrons, and therefore, the rate of a reaction is equivalent to the electron current generated or used up by that reaction.

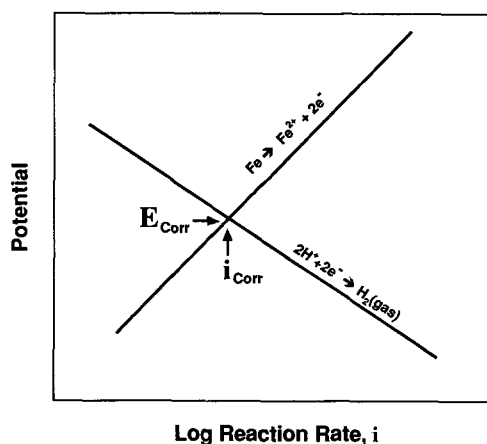


FIG. 1—Evans diagram for iron in an acid.

<sup>1</sup>Northrop Grumman Corporation, Oceanic Systems, Annapolis, MD 21404.

## Galvanic Series

Since no charge can accumulate on any metal surface, the electrons generated by the anodic reaction must all be used up by the cathodic reaction. This can only occur in Fig. 1 where the anodic and cathodic reaction lines cross. At this point, the rate of the anodic reaction, the corrosion rate, equals the rate of the cathodic reaction—in this case, hydrogen generation. This rate is called the open-circuit corrosion rate, abbreviated  $i_{\text{corr}}$ . The potential at which the lines cross is called the open-circuit corrosion potential, abbreviated  $E_{\text{corr}}$ . This type of plot is called an Evans Diagram, after U. R. Evans, a pioneer in corrosion electrochemistry. Any corroding metal should, under open-circuit conditions, exist at  $E_{\text{corr}}$  corroding at a rate  $i_{\text{corr}}$ , which can be predicted from the Evans Diagram. The value of  $E_{\text{corr}}$  will depend on the position of the curves. The anodic curve is a function of the type of metal and the charge it receives when it goes into solution. The cathodic curve is a function of the type of cathodic reaction, the type of surface on which that reaction takes place, the concentration of reacting species, and other factors, most of which are dependent on the environment in which the metal sits.

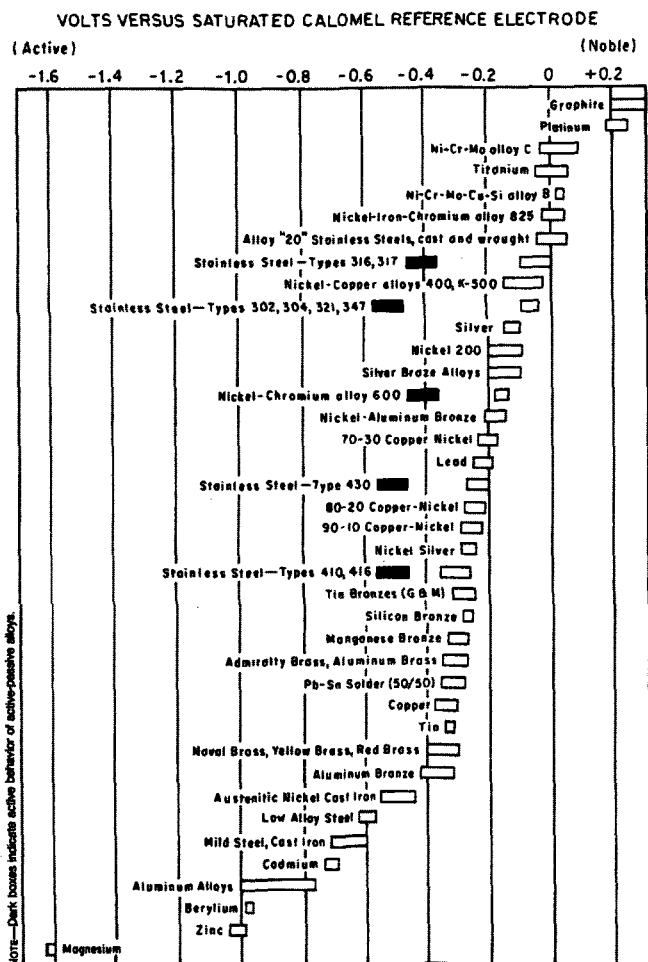


FIG. 2—Galvanic series of various metals in flowing seawater at 2.4–4.0 m/s for 5–15 days at 5–30°C (redrawn from original in Ref 21; taken from ASTM G 82).

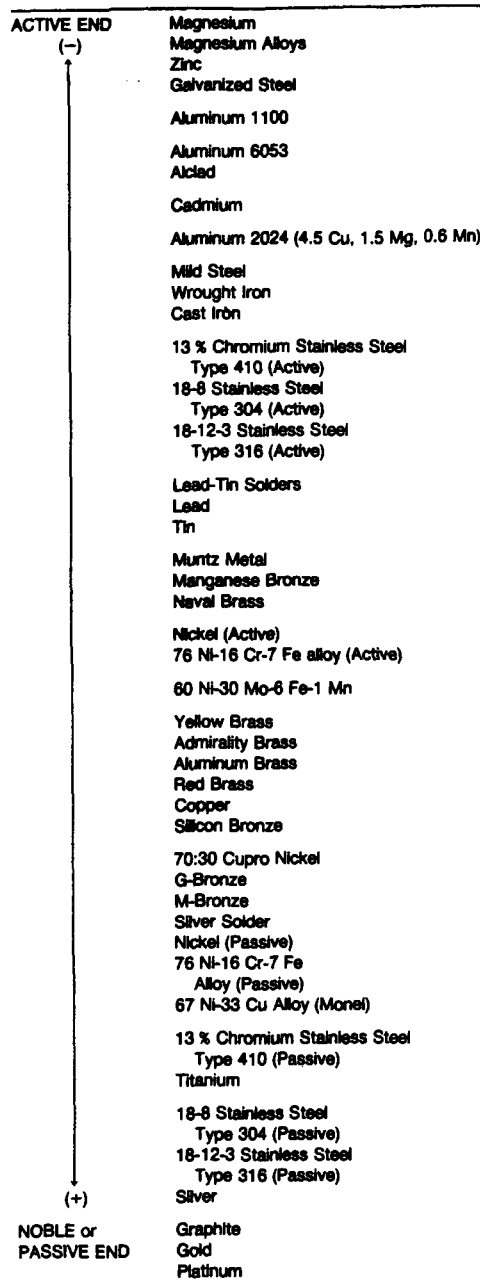


FIG. 3—Galvanic series of various metals exposed to seawater (taken from ASTM G 82).

Each metal/environment combination, therefore, exists at a unique potential. For a given environment, the potentials of various materials can be listed in a form called a galvanic series. Galvanic series can be expressed either as a graph giving the numerical values of the potentials of the materials in the given environment, as in Fig. 2, or as a list in order of increasing or decreasing potential without the specific values, as in Fig. 3. The galvanic series is important because it helps to predict what happens when two metals are placed in electrical contact in that environment. The metal that is more negative in the galvanic series will have

a driving force to lose electrons to a metal in electrical contact that is more positive in the series. This will cause the corrosion rate of the more negative metal to increase when the electrical connection is made. It is this increase in corrosion of the more negative metal upon contact with a more positive metal that is called galvanic corrosion. The galvanic series allows prediction of which of the metals in contact, the galvanic couple, will suffer increased corrosion.

### Mixed Potential Theory

It is tempting to say that the farther apart two metals are in the galvanic series, the more corrosion will occur on the more negative material, or anode. Unfortunately, this is not the case. In order to predict the rate of galvanic corrosion, an Evans Diagram of both metals involved must be considered. This approach is called Mixed Potential Theory.

In Fig. 4, Evans Diagrams are shown for two materials of equal surface area that have different potentials on the galvanic series in an acid: iron and zinc. The anodic material, zinc with the more negative  $E_{\text{corr,Zn}}$ , corrodes uncoupled at a rate of  $I_{\text{corr,Zn}}$ . The cathodic material, iron with the more positive  $E_{\text{corr,Fe}}$ , corrodes uncoupled at a rate of  $I_{\text{corr,Fe}}$ . When these metals are electrically connected, electrons can flow between them, upsetting their individual balances. Since there are four reactions to consider, and since electrons can now flow freely between all four reactions, the charge balance must be handled differently than for the individual metals. All of the electrons generated by the anodic reactions must still be consumed by the cathodic reactions. Therefore, the sum of the anodic reactions is plotted as a dashed line with a positive Tafel slope, and the sum of the cathodic reactions is plotted as a dashed line with a negative Tafel slope. The intersection of these two sum lines is where all charges balance, and the potential so defined is called the mixed potential of the galvanic couple, or coupled potential,  $E_{\text{couple}}$ . The mixed potential of the couple is shown as a dotted line in Fig. 4. The points where the individual reaction lines cross the mixed potential define the rates of

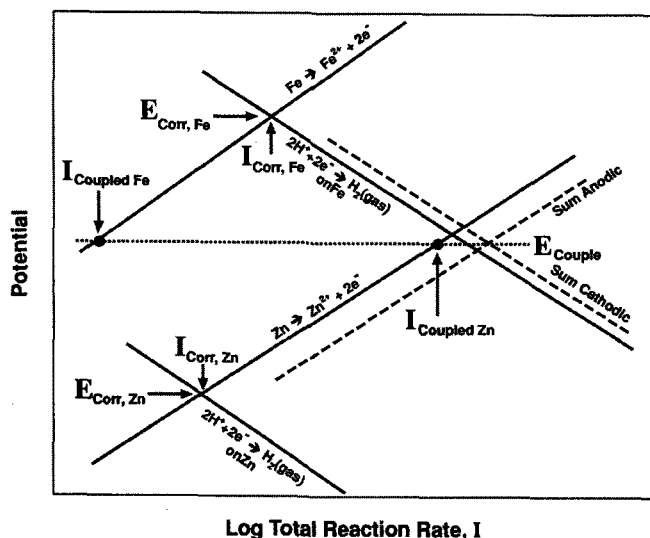


FIG. 4—Evans diagram for iron and zinc in acid.

those reactions. The zinc corrosion rate has increased from  $I_{\text{corr,Zn}}$  to  $I_{\text{coupled,Zn}}$ . This increase is the galvanic corrosion rate. The iron corrosion rate has decreased from  $I_{\text{corr,Fe}}$  to  $I_{\text{coupled,Fe}}$ . This decrease is called cathodic protection.

### Effects of Anode/Cathode Area Ratio

There was a shift in axis labeling between Figs. 4 and 1. Figure 1 expressed reaction rate as lower case  $i$ , the reaction current per unit area, which is appropriate for considering single metals. Figure 4 was forced to switch to total reaction current  $I$ , because it is the total current from each metal that must be considered in the summation. The effect of changing the relative areas of the anode and cathode is illustrated in Fig. 5. If the cathode is small, the original Evans diagram for the cathodic material must have the current densities multiplied by a small area to obtain total currents. This makes the lines appear far to the left in Fig. 5, and results in only a small increase in anodic corrosion rate,  $I_{\text{coupled,anode,small cathode}}$  over  $I_{\text{corr,anode}}$ . If the cathode is large, the original Evans diagram for the cathodic material must have the current densities multiplied by a large area to obtain total currents. This makes the lines appear far to the right in Fig. 5, and results in a large increase in anodic corrosion rate,  $I_{\text{coupled,anode,large cathode}}$  over  $I_{\text{corr,anode}}$ . This illustrates the area ratio effect in galvanic corrosion. A small anode and large cathode result in a large anodic corrosion rate, whereas a large anode and small cathode are far more desirable.

### Flow Rate

Changing the electrolyte flow rate can have significant effects on the curves in the Evans diagram, and therefore, can dramatically influence galvanic corrosion rate. The direction of the effect can only be predicted using Evans diagrams, however.

If the cathodic reaction is oxygen reduction rather than hydrogen reduction, oxygen must be supplied to the metal surface by diffusion in order to react. Diffusion can be a slow process relative to the electron exchange, and this can make the cathodic line in the Evans diagram deviate from

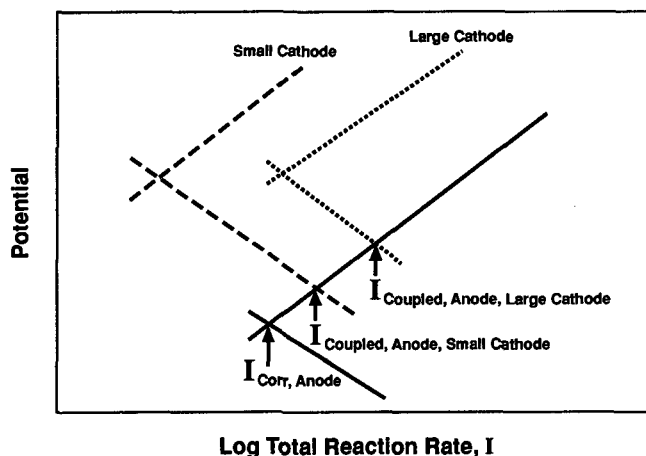


FIG. 5—Effect of cathodic area on couple current.

a straight line. Oxygen diffusion occurs through a relatively stationary boundary layer, which becomes thinner as flow increases. Diffusion rate therefore increases with flow, and the maximum rate of the oxygen reduction reaction,  $i_L$ , increases with flow. This is shown in Fig. 6. When the diffusion-limited cathodic curve is present in a galvanic couple, the total cathodic current will increase with increasing flow, causing corrosion rate of the anode to increase with increasing flow.

Flow can also have an effect on the anodic reaction. Many materials exhibit passivity, which causes the anodic reaction to deviate dramatically from a straight line. This is caused by the corrosion products formed during the anodic reaction becoming firmly attached to the metal surface, blocking the reaction from proceeding further. The anodic line in the Evans diagram will be straight until the corrosion product forms, after which the current will rapidly drop even though potential is still increasing. The low current will persist until the potential becomes sufficiently positive to break down the corrosion product or to produce oxygen directly from water by electrolysis. In either event,

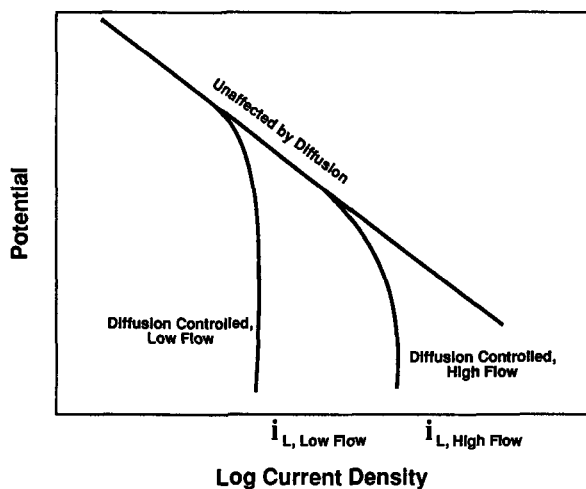


FIG. 6—Effect of flow on diffusion-limited current density.

the current will then rise sharply. This is shown in Fig. 7. Some of the most protective passivating corrosion products are on stainless steels. These films form more readily in the presence of oxygen, and so are enhanced by flow. This leads to the situation shown in Fig. 8 where increasing flow increases oxygen delivery, which increases the amount of protective corrosion products, lowering the anodic currents. This can cause corrosion rates in a galvanic couple to decrease with increasing flow, opposite to the oxygen effect on the cathodic reaction discussed above.

### Measured Currents

Much of the current that flows between reactions in a galvanic couple will flow between the anodic and cathodic metals, but some also flows within these metals. Internal current is not directly measurable, although it can be inferred from other test methods that use external current that can be measured. Measurable external currents can be predicted from the Evans diagrams as follows. When a metal is corroding by itself, as in Fig. 9, the corrosion current is  $i_{corr}$ , which flows entirely between anodic and cathodic sites in the metal and cannot be measured. All

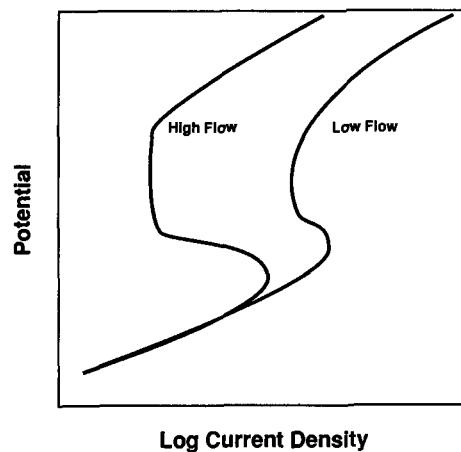


FIG. 8—Effect of flow on passivity.

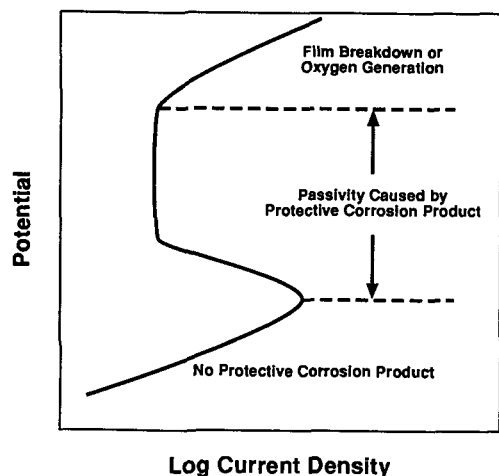


FIG. 7—Effect of passivity on anodic polarization curve.

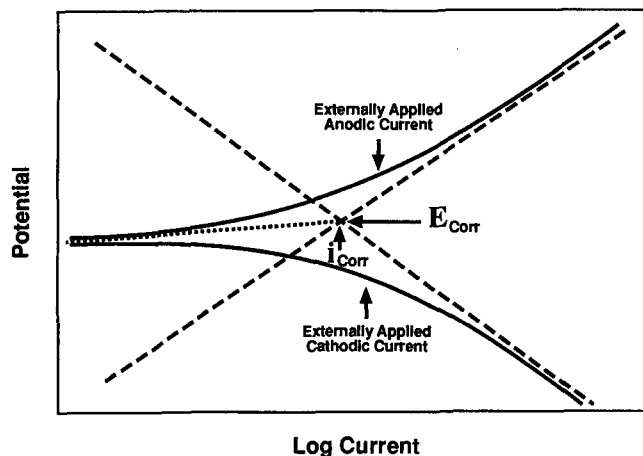


FIG. 9—Creating polarization curves from Evans diagrams.

electrons produced by the anodic reaction are consumed by the cathodic reaction. If an external source, such as a power supply or another metal electrically connected to the first, removes electrons, the anodic reaction will increase to supply more electrons and the cathodic reaction will decrease to use up less electrons. The externally applied anodic current will be the difference between the anodic and cathodic reaction currents. At very positive potentials, the cathodic current will be negligible, and the applied current will roughly equal the anodic corrosion rate. At very negative potentials, the anodic current will be negligible, and the applied current will roughly equal the cathodic current. At  $E_{\text{corr}}$  the external current will be zero. The externally applied current will follow a shape called a polarization curve, shown in Fig. 9.

Galvanic corrosion rate can be roughly predicted by superimposing the polarization curves of the anodic and cathodic materials. This is shown in Fig. 10. When the open-circuit potentials of the anode and cathode are relatively far apart, more than roughly 120 mV depending on the slopes of the curves, this prediction is fairly accurate. The polarization curves for the anodic and cathodic materials are multiplied by their respective wetted surface areas and placed on the diagram. The intersection of the anodic curve for the anodic material with the cathodic curve for the cathodic material provides an indication of the galvanic corrosion rate,  $I_{\text{galvanic}}$ , and the exact coupled potential,  $E_{\text{couple}}$ .

### Current and Potential Distributions

For galvanic corrosion to occur, there must exist at least two metals with different corrosion potentials, a metal path for electrons to flow between them, and an ionic path through the electrolyte to complete the electronic circuit. The latter is sometimes not considered, but contributes to nonuniformity of galvanic current and potential on large structures.

Figure 11 shows two metals electrically connected in an electrolyte that has a significant resistivity, such as tap water. Current  $I_1$  must travel through some small electrolyte resistance  $R_1$  to go the short distance from the anode to the cathode, and undergoes a voltage drop according to Ohm's

law of  $I_1 R_1$ . Current  $I_2$  must travel farther, through an increased resistance  $R_2$ , and will therefore be smaller than  $I_1$ . The voltage drop here is  $I_2 R_2$ . The largest distance is traversed by current  $I_4$ , through the largest resistance  $R_4$ , and will therefore be the smallest current and undergo a voltage drop of  $I_4 R_4$ . The falloff of current (and corrosion rate) as distance from the second metal increases is a common method for recognizing galvanic corrosion. Although current decreases with distance, the product of current times resistance will increase with distance. The largest voltage drop in this example would be  $I_4 R_4$  and the smallest would be  $I_1 R_1$ . The voltage drops are shown in Fig. 11. The presence of an IR drop not only decreases the current on the anodic and cathodic materials, but also allows the anode to be at a different potential than the cathode. The potentials will be closest to  $E_{\text{couple}}$  where the anode and cathode are closest, and will shift towards  $E_{\text{corr}}$  for each material as separation distance increases. This creates a potential distribution over the structure that can be measured.

### Factors Controlling Galvanic Corrosion

Any factor that controls corrosion of a single metal may control galvanic corrosion by its effect on one or more of the reaction lines on the Evans diagram. Besides flow and pH, these factors include temperature, electrolyte composition, surface condition of the metals, thermomechanical and potential history of the surfaces, and many more too numerous to mention. Factors unique to galvanic corrosion include anode/cathode area ratio, electrolyte resistivity, and geometry. Sometimes it is important to know which reactions control or limit galvanic corrosion rates. The polarization curves in Fig. 12a illustrate how a diffusion-limited cathodic reaction will control the rate of galvanic corrosion. Changing the shape of the anodic polarization curve, for example, by the use of an anodic inhibitor, has no effect on galvanic corrosion rate determined by the curve intersection, whereas changes in the cathodic diffusion-limited current result in equivalent changes in galvanic corrosion rate. Similarly, galvanic corrosion of passive materials, as

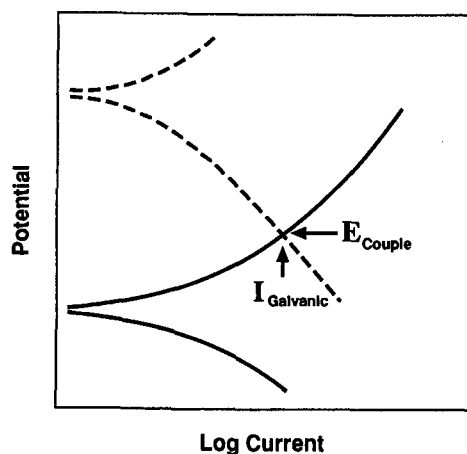


FIG. 10—Rough prediction of galvanic current from overlapping polarization curves.



FIG. 11—Effect of distance on IR drop and current density.

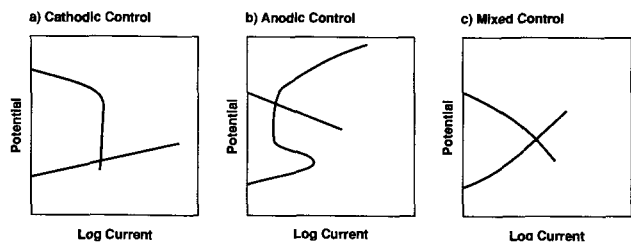


FIG. 12—Type of control of galvanic corrosion reactions: (a) cathodic control; (b) anodic control; (c) mixed control.

shown in Fig. 12b, is frequently under anodic control, with the shape of the cathodic polarization curve making little difference. Mixed control as in Fig. 12c is also possible.

## TESTING TECHNIQUES

### Exposure of Galvanic Couples

The most obvious method of testing for galvanic corrosion is to construct a couple between the materials of interest and place it in the environment of interest. Material condition, environment, and geometry should simulate the application as closely as possible. Care should be taken during assembly to ensure adequate electrical connection, and this connection should be checked before, after, and occasionally during the exposure using an appropriate ohmmeter. In some cases, it may be possible to electrically isolate the individual metals from each other and connect them through an external wire, which can be used to measure galvanic current during exposure. For small specimens it is permissible to use a 1- $\Omega$  resistor in the line to measure voltage drop and calculate current. Where currents are larger or where corrosion potentials are close for the materials involved, use of a zero-resistance ammeter may be more appropriate for current measurement. The potential of the couple can also usually be monitored during the exposure using a suitable reference electrode. More detail on galvanic corrosion testing in electrolytes can be found in ASTM G 71, Guide for Conducting and Evaluating Galvanic Corrosion Tests in Electrolytes.

Important material factors to consider when simulating a galvanic corrosion situation include chemical composition, thermal history, and surface condition. Changes in these parameters may change the corrosion behavior of a material when it is not in a galvanic couple without affecting its galvanic corrosion behavior, or may affect its galvanic corrosion behavior without a significant effect on its corrosion properties when it is used alone.

Any environmental factor that can influence corrosion can also affect galvanic corrosion. Environmental factors to consider when designing a test include major chemical components, dissolved gases, minor constituents, organic materials, biological organisms and activity, temperature, flow, and electrical conductivity. In atmospheric galvanic couples, atmospheric factors such as time-of-wetness, orientation relative to prevailing winds, sunlight exposure, height above ground, and other unique atmospheric conditions should also be considered. Some important atmospheric

factors affecting corrosion are discussed in ASTM G 33, G 50, G 84, and G 92.<sup>2</sup>

The relative geometry of the parts of interest in the galvanic couple can also influence corrosion behavior. In low conductivity environments, the distance of separation of the dissimilar metals will affect galvanic corrosion rate. Even in high conductivity environments, it is difficult for galvanic current to travel into long narrow crevices or down the insides of tubes. The relative wetted surface areas of the dissimilar metals will dramatically influence galvanic corrosion rate. In atmospheric exposures, geometry can control water trapping and drainage, and thermal mass, which controls dew retention.

Ensuring adequate electrical contact between the dissimilar metals in a galvanic couple can be difficult. Pressure contact, such as between two plates bolted together, is subject to corrosion products forming between the plates and wedging them apart. Attachment of wires by soldering or brazing will work with some materials, but the use of drilled and tapped holes for screw attachment or through holes for bolting may be required for others. In some cases, spot welding can be used for electrical attachment. Finally, a wire may be inserted into a drilled hole and the hole peened closed around the wire, although this method is not reliable over long exposure periods. Whatever connection method is used, the connection area and wire are subject to corrosion, which can affect both the electrical contact and the performance of the galvanic couple being tested. For this reason, coatings are frequently used on the connection area. When electrical contact is maintained by physical contact of the dissimilar metals, periodic measurement is desirable to ensure that electrical continuity is maintained. If continuity is checked frequently relative to the length of the exposure, it will be possible to adjust the materials to regain this continuity without significantly affecting the results. This should be done without disassembly or gross movement, such as by tightening tensioning bolts.

Mounting of galvanic couples for testing should be done carefully using insulator materials to avoid the possibility of establishing electrical continuity with the mounting device or test chamber. Mounting techniques include gasketed seals, rod mounting, epoxy mounting, press-fit, partial immersion, full immersion, and others. The mounting technique chosen is related to the type of corrosion expected, the electrical connection method, the type of exposure desired, presence or absence of water-line effects, and the materials chosen.

Duration of exposure is extremely important in galvanic corrosion testing. In many galvanic couples, the amount of corrosion is highly variable with time. Initial high corrosion rates may fall dramatically, initial low rates may suddenly increase, and the relationship between anodic and cathodic materials can even reverse with time. For these reasons, the duration of the test exposure should be of sufficient length to ensure that the corrosion processes have reached steady

<sup>2</sup>ASTM G 33, Practice for Recording Data from Atmospheric Corrosion Tests of Metallic-Coated Steel Specimens; G 50, Practice for Conducting Atmospheric Corrosion Tests on Metals; G 84, Practice for Measurement of Time-of-Wetness on Surfaces Exposed to Wetting Conditions as in Atmospheric Corrosion Testing; G 92, Practice for Characterization of Atmospheric Test Sites.

state if long-term performance is being evaluated. Test duration should be similar to service duration for short-term service. In atmospheric testing, the season of the year when exposure is initiated may influence the test. Multiple exposures of different time periods may be used to give corrosion rate information as a function of time.

Exposures can be conducted on full-scale components or on scaled down or simplified geometries. Full-scale components have a number of advantages, including not needing to consider details of geometry and ease of relating the results to service performance. However, full-scale component testing may be impractical or too expensive, in which case scale modeled components may have to be used. If scale modeling is used, details of scaling laws must be understood before designing the test. For example, when galvanic corrosion current distribution is important, the conductivity of the electrolyte may need to be scaled by the same factor as the physical size. This procedure, called Dimension and Conductivity Scaling (DACS), would involve the use of an electrolyte of one-tenth conductivity for a one-tenth-scale model. DACS scales only primary current distribution, which is controlled by IR drop in the electrolyte. Secondary and tertiary current distribution are influenced by polarization behavior of the material involved, and are best approximated by the use of full-conductivity electrolytes. Both types of current distributions cannot be modeled simultaneously, so a decision must be made as to which is most important. Small structures in highly conductive electrolytes should generally be tested in full-conductivity electrolytes, whereas DACS should be used primarily for large structures in low-conductivity electrolytes. To date, DACS has been used primarily for ship cathodic protection system design. More information on scaling can be found in Refs 2 through 5.

## Electrochemical Tests

Accelerated testing to get a result in a shorter time period than would be possible naturally should be avoided whenever possible, because the mechanism of galvanic corrosion can change if the rate is altered significantly. For this reason, electrochemical tests are frequently chosen to evaluate galvanic corrosion performance. The sensitivity of these tests allows for obtaining results fairly quickly without accelerating the corrosion process.

Electrochemical galvanic corrosion tests can be placed into three categories: sensitive galvanic current measurement, galvanic series determination, and polarization curve measurement. Sensitive current measurement involves an ordinary galvanic couple exposure, but with current between the dissimilar metals forced to flow through an external wire where it can be measured with a zero-resistance ammeter or by voltage drop across a 1- $\Omega$  shunt resistor. This type of testing is described in ASTM G 71.

Determination of a galvanic series involves placing the materials of interest from the galvanic couple individually in the environment of interest and monitoring their electrochemical potential over time. The material with the more electronegative potential will become the anode and suffer accelerated corrosion when placed in a galvanic couple. Galvanic series are extremely useful during the materials

selection process to make sure that the anodic areas are large compared to the cathodic areas in complex structures. The galvanic series is influenced by all of the environmental variables described earlier, so the series should only be used if it is developed in the environment in which the galvanic couple will see service. One disadvantage of the galvanic series is that it is frequently misapplied. A series developed in one environment is used to predict performance in another environment. A second disadvantage of the galvanic series is that it does not predict rate. Separation in potential between dissimilar materials does not relate to the rate of corrosion in a couple. More details of the development and use of galvanic series are given in ASTM G 82, Guide for Development and Use of a Galvanic Series for Predicting Galvanic Corrosion Performance.

Galvanic corrosion can be predicted by overlaying polarization curves, as described earlier. The determination of polarization curves is, therefore, an important method for galvanic corrosion testing. These curves can be obtained galvanostatically, potentiostatically, or potentiodynamically. Galvanostatic testing is typically used for determining the efficiency of sacrificial anodic materials, such as is done in ASTM G 97, Test Method for Laboratory Evaluation of Magnesium Sacrificial Anode Test Specimens for Underground Applications, or NACE Standard RP0387, Metallurgical and Inspection Requirements for Cast Sacrificial Anodes for Offshore Applications.

The most common method of obtaining polarization curves is potentiodynamically. Potentiodynamic testing is described in an earlier section of this manual. For galvanic corrosion, the scan rate for these tests should be as slow as possible, since long-term polarization behavior is usually what is sought in predicting long-term galvanic corrosion behavior.

Potentiostatic polarization curve generation is advantageous for situations where polarization is time-dependent and prediction of long-term galvanic corrosion performance is desired. This involves exposing a series of individual specimens of each material at a variety of different potentials for a duration sufficient to ensure steady-state behavior. The steady-state current at each potential is obtained, and polarization curves constructed from the potential/current data pairs.

Using electrochemical tests to predict galvanic corrosion performance has the same caveats as in any other type of predictive testing. Conditions must be as close as possible to those being modeled. This includes not only solution chemistry and flow, but also the surface condition of the samples. Polished samples can behave quite differently from samples with more representative surface conditions and corrosion products developed by pre-exposure.

More detail on using electrochemical tests for galvanic corrosion can be found in Refs 6 and 7.

## Computer Modeling

Although not a laboratory testing technique, computer modeling is still an important tool in understanding and predicting galvanic corrosion performance. As mentioned above, exposure of scaled components of a galvanic couple leads to scaling problems in that the primary current



distribution cannot be scaled at the same time as the secondary and tertiary current distributions. Computer modeling is usually best for making accurate predictions of the distribution of galvanic corrosion over a structure in which both solution IR drop and polarization behavior both control current distribution. Computer models require the geometry of the structure to be input. Additional inputs include the electrolyte conductivity and the polarization behavior of the surfaces of all materials, usually obtained from laboratory testing. Although finite element analysis and finite difference analysis have both been used to predict distribution of galvanic currents on structures, the boundary element technique is becoming the computer tool of choice. This technique requires only that the surfaces of the structure be defined, whereas the other methods require that the volume of the electrolyte be divided into a three-dimensional grid, a time-consuming and difficult process for complex structures. The disadvantage of the boundary element method is that at present the commercially available software for performing this analysis is not very user-friendly.

### Atmospheric Tests

Unlike galvanic corrosion testing in electrolytes, galvanic corrosion testing in the atmosphere can be standardized because special circumstances exist that limit the number of test variables.

Three factors that are different in atmospheric testing from most other galvanic corrosion testing are the presence of a limited amount of electrolyte, the need for a very long duration of exposure, and the importance of specimen

orientation. Since rainwater and dew are fairly poor electrical conductors, and since they are usually present only as thin layers on the surfaces of materials exposed to the atmosphere, there is a large IR drop between the anode and the cathode in any atmospheric corrosion exposure. This limits the effective distance over which galvanic interactions take place to about 0.5 cm, which in turn means that the effective area ratio of anode to cathode in an atmospheric exposure is almost always about 1:1. The limited electrolyte also makes electrochemical measurements impractical.

Atmospheric corrosion typically occurs only during a small percentage of the total exposure time, typically when the surfaces are wet from precipitation, dew, fog, or when hygroscopic compounds on the surface absorb moisture during periods of high humidity. For this reason, atmospheric corrosion occurs slowly, and long exposure durations are usually necessary. Most tests typically involve minimum durations of 1 to 3 years, with 20 years maximum exposure not unusual. Tests of shorter duration than one year not only have so little corrosion as to make evaluation of mass loss difficult, but also suffer from the effects of seasonal variation of corrosion rate.

Finally, the time that a specimen is wet depends on sunlight heating, prevailing winds, and specimen geometry. Specimen orientation is, therefore, much more critical in atmospheric galvanic corrosion testing. Standard orientations are specified in ASTM G 50 as 30° to the horizontal facing south or the nearest source of corrodent (the sea).

Three standardized atmospheric galvanic corrosion tests are the plate test, the wire-on-bolt test, and the disk test. The plate test, described in ISO Standard ISO7441, Determination

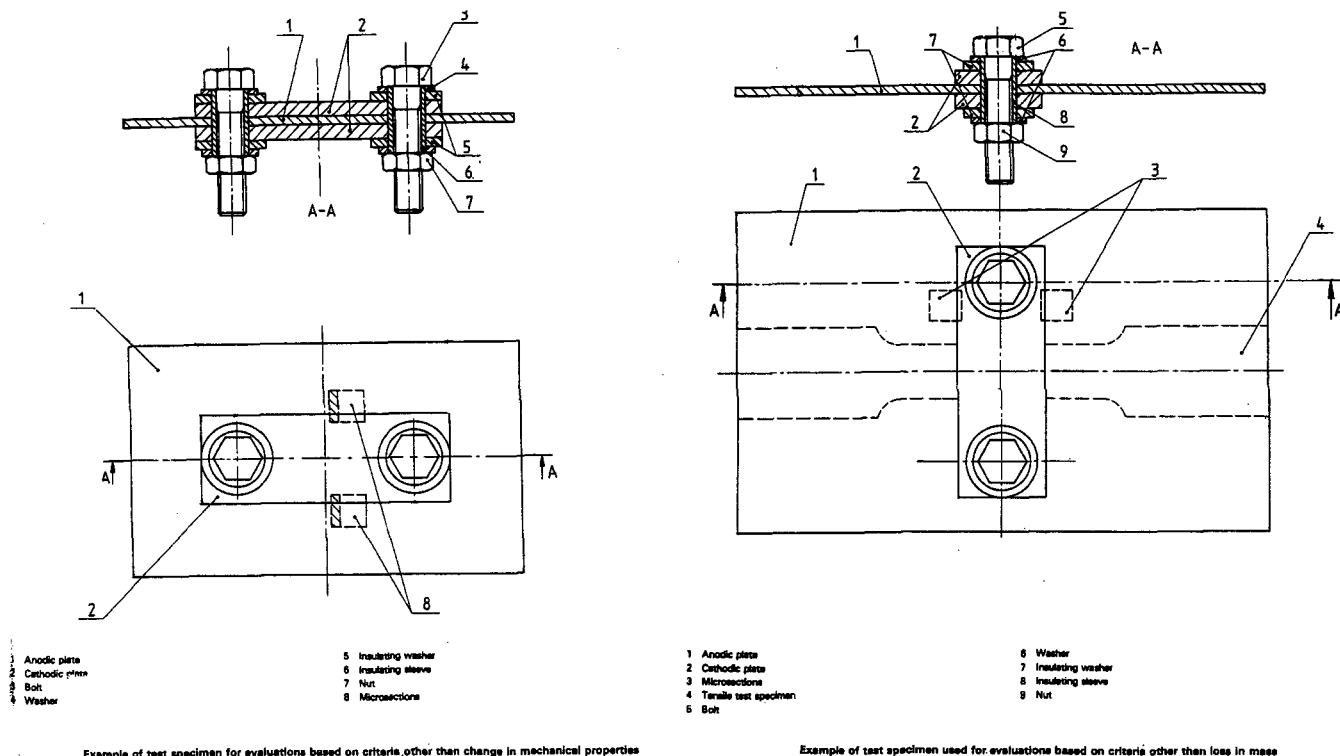


FIG. 13—Plate test assembly for galvanic corrosion testing (redrawn and simplified from ISO 7441).

of Bimetallic Corrosion in Outdoor Exposure Corrosion Tests, consists of a large plate of the anodic material sandwiched between two small plates of the cathodic material and held together with nonmetallic or insulated bolts. Sometimes the crevice area between the plates is coated with an organic material. The two possible configurations are shown in Fig. 13. Typical exposure durations are 1 to 20 years. At the end of this time, the anodic plate may be evaluated metallographically, visually, by mass loss, or by material property loss (typically using tension testing). The advantages of this test are that materials are usually available in plate form, and a wide range of analyses can be used on the exposed panels. The disadvantages include the need to know which material is the anodic beforehand, the long exposure duration, the difficulty of maintaining electrical continuity between panels, and the possibility of confusing crevice effects with galvanic effects. At one time, ASTM also had a standard for this test method, but dropped this standard due to these disadvantages and lack of use.

The wire-on-bolt test, described in ASTM G 116 (Practice for Conducting the Wire-on-Bolt Test for Atmospheric Galvanic Corrosion), has been used with standard materials as an atmospheric corrosivity test under the names of the CLIMAT and ATCORR tests. This test consists of wrapping a 1.0-m length of wire of the anodic material around a threaded bolt or rod of the cathodic material. Post-test evaluation is typically done by mass loss only. Since the wire diameter is much smaller than the 0.5-cm galvanic interaction distance in the atmosphere, the effective anode-to-cathode area ratio is well below 1:1, making this a fast test. A typical exposure duration is 90 days. The short duration is

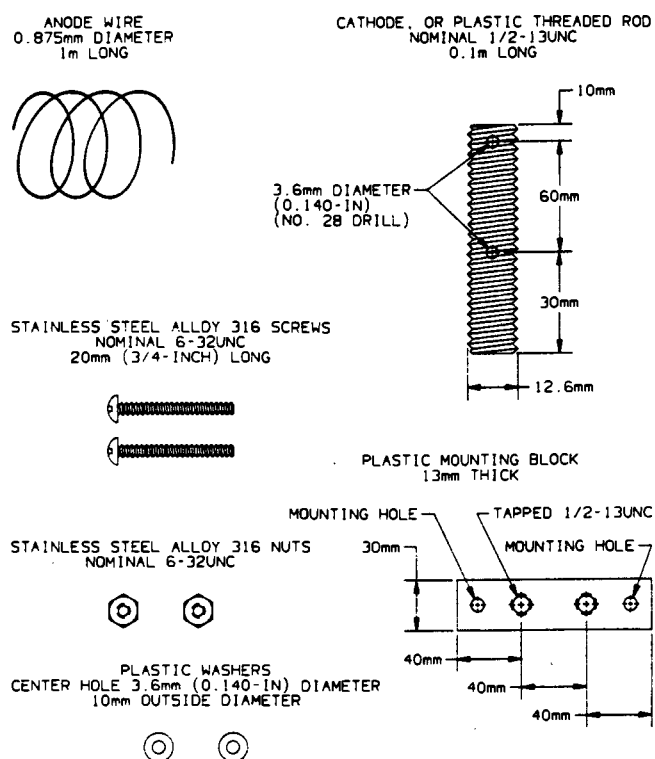


FIG. 14—Components for making wire-on-bolt atmospheric exposure assemblies (taken from ASTM G 116).

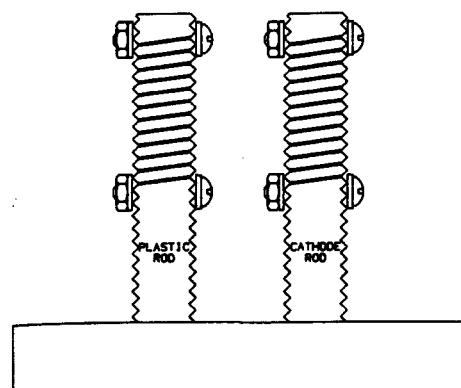


FIG. 15—Schematic of completed wire-on-bolt assemblies mounted for exposure (taken from ASTM G 116).

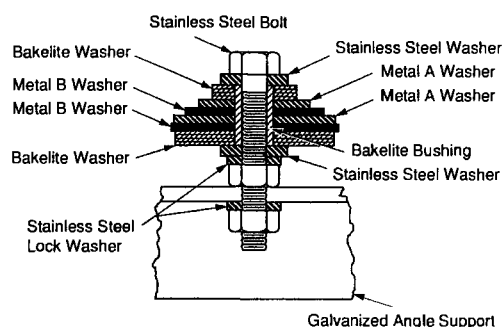


FIG. 16—Cross section of disk test assembly for atmospheric galvanic corrosion.

a significant advantage to this test. The disadvantages include materials needing to be in wire and threaded rod form, the beforehand knowledge of which material is the anode, and the seasonal variations in exposures of such short duration. A diagram of the sizes and forms of the components needed to construct an assembly is given as Fig. 14, and a completed assembly is shown as Fig. 15.

The disk test, described in Refs 8 and 9 and in ASTM G 149, Practice for Conducting the Washer Test for Atmospheric Galvanic Corrosion, consists of a set of four washers of alternating anodic and cathodic materials of graduated sizes bolted together with an insulated bolt. Only the center two washers are used for the analysis. A cross-sectional assembly view is shown in Fig. 16. The duration of this test is usually 1 to 20 years. Post-test evaluation usually consists only of mass loss. Advantages to this test are that material is usually easy to find, the anodic material need not be known beforehand, and it is easy to set up and evaluate. The disadvantages include the long test duration and the lack of information on corrosion morphology or mechanical property degradation.

## EVALUATION OF TEST RESULTS

### Exposure of Galvanic Couples

If the different materials can be disassembled after testing, mass loss measurements can be performed. In some

cases, loss of strength may also be of interest. If disassembly is not possible, the specimens may still be examined for pitting, cracking, color and extent of corrosion products, and, in some geometries, thickness loss. Mass loss of an assembly may still be useful if corrosion of the cathode was minimal. After exposure, destructive techniques such as metallographic examination may also provide information about the extent and morphology of corrosion. Useful standards for cleaning samples after immersion and evaluating mass loss, pitting, and degradation in properties are ASTM G 1, G 46,<sup>3</sup> and G 71. Applying the results of a set of measurements designed to generate a galvanic series is described in ASTM G 82.

### Electrochemical Tests

When the potentials of two materials in a galvanic couple are widely separated, Faraday's Law can be used to calculate the galvanic corrosion rate from the galvanic current measured between them. This calculation can be done by the procedures in ASTM G 102.

Overlaying of polarization curves of the different materials in a galvanic couple must be done by first converting the current densities into total currents by multiplying the polarization curves by the exposed wetted surface area for each material. The curves then may be overlaid, and if IR drop is not important, the couple current and potential may be predicted. If the coupled potential deviates by 50–100 mV from the open-circuit potential of the anode, then the current may be converted by Faraday's Law into a corrosion rate. If the coupled potential deviates by less than 50–100 mV from the open-circuit potential of the anode, then it is conservative to add the open-circuit corrosion rate of the anode to the corrosion rate calculated from Faraday's Law to get the total anodic corrosion rate. Neither of these methods is exactly accurate, but both will give a reasonable approximation to the true corrosion rate of the anode in the couple.

If the polarization curve for the anode is known, the coupled potential may be measured to predict corrosion performance. The couple current is the current on the anodic material polarization curve at the measured coupled potential. Corrosion rate may be calculated from the couple current determined in the same way as in the previous paragraph.

### Computer Modeling

Interpretation of results from computer models is straightforward, since the results are usually potential maps that can be related back to current density maps by using the polarization curves of the appropriate materials, or the current density maps, themselves. Faraday's Law can be applied to the current densities to determine the corrosion rates over the various surfaces. The results of this type of analysis always look good intuitively, with the potential

profiles deviating in the right places in the right directions. This does not mean that the answer is correct, however. Discontinuities in potentials between adjacent areas could be caused by discretization error, resulting from the selection of boundary elements that are too big. The analysis should always be checked to ensure that the total anodic and cathodic currents are equal. Inequality could mean a lack of mathematical convergence of the model. The most important check on the results of a computer model occurs before the model is ever run. The input polarization curves must be accurate in order for the model predictions to be meaningful. Model results should be spot-checked against the real structure whenever possible.

### Atmospheric Tests

Only mass loss information is obtained from the standard atmospheric galvanic corrosion tests, with the exception of the plate test. The plate test specimens can also be evaluated by metallography, visual examination, probe-type attack depth gages, or mechanical tests such as tensile strength.

## STANDARDS

Laboratory testing for galvanic corrosion involves so many variables that it is difficult to write a single standardized test. For this reason, there are no standardized laboratory testing procedures specifically for galvanic corrosion. If another form of corrosion is being studied, then a slight modification to a standardized test for that corrosion form may be used. For example, to study galvanically accelerated stress corrosion testing, ASTM G 30, Practice for Making and Using U-Bend Stress-Corrosion Test Specimens, may be used, adding only a wire between the specimen and a second material to create the galvanic couple. To study the breaking strength of a piece of metal, a standard mechanical pull test such as that found in ASTM E 8, Test Methods for Tension Testing of Metallic Materials, may be used. To study the effect of galvanic corrosion on breaking strength, the same test may be used on pieces of metal after exposure to the environment of interest, both with and without galvanic coupling to a second material. Subtracting the strength of the metal with galvanic coupling from that without it will give the effect due to galvanic corrosion. There are two guidelines for galvanic corrosion testing published by ASTM: ASTM G 71 and G 82. Specific test standards for atmospheric galvanic corrosion can be found in ASTM G 116 and G 149, and ISO 7441, as described above.

## ADDITIONAL INFORMATION

Additional information and details of galvanic corrosion testing are available in the standards referred to above and in Refs 10 and 11. Additional information on the theory of galvanic corrosion is available in Refs 12 to 22. A good series of articles summarizing galvanic corrosion theory and application in various industries is available in Ref 23. Galvanic corrosion testing descriptions are written at the level of a corrosion technician in Ref 11.

<sup>3</sup>ASTM G 1, Practice for Preparing, Cleaning, and Evaluating Corrosion Test Specimens; G 46, Practice for Examination and Evaluation of Pitting Corrosion.

## REFERENCES

- [1] Tafel, J., *Zeitschrift für Elektrochemie und Angewandte Physikalische Chemie*, Vol. 50, 1905, p. 641.
- [2] Hack, H. P., "Scale Modeling for Corrosion Studies," *Corrosion*, Vol. 45, No. 7, July 1989, pp. 601–606.
- [3] Tighe-Ford, D. J., McGrath, J. N., and Hodgkiss, L., "Design Improvements for a Ship's Cathodic Protection System Using Dimension and Conductivity Scaling (DACS)," *Corrosion Prevention and Control*, Vol. 32, No. 5, October 1985, pp. 89–91.
- [4] DeCarlo, E., "Computer Techniques for Offshore Corrosion Protection," *Sea Technology*, September 1981.
- [5] Clerbois, L., Heintz, E., IJsseling, F., et al., "Principles for Scaling of Corrosion Tests," *British Corrosion Journal*, Vol. 20, No. 3, 1985, pp. 107–116.
- [6] Scully, J. R., "Electrochemical Methods of Corrosion Testing," *Metals Handbook*, Vol. 13, *Corrosion*, ASM, Metals Park, OH, 1987, pp. 212–216.
- [7] Baboian, R., "Prediction of Galvanic Corrosion Using Electrochemical Techniques," *Electrochemical Techniques for Corrosion Engineering*, R. Baboian, Ed., NACE, Houston, TX, 1986, pp. 253–258.
- [8] Baboian, R., "Final Report on the ASTM Study: Atmospheric Galvanic Corrosion of Magnesium Coupled to Other Metals," *Atmospheric Factors Affecting the Corrosion of Engineering Metals*, ASTM STP 646, S. Coburn, Ed., 1978, ASTM International, West Conshohocken, PA, pp. 17–29.
- [9] Blum, W., *Symposium on Properties, Tests and Performance of Electrodeposited Metallic Coatings*, ASTM STP 197, 1956, ASTM International, West Conshohocken, PA, p. 49.
- [10] Hack, H. P., "Evaluation of Galvanic Corrosion," *Metals Handbook*, Vol. 13, *Corrosion*, ASM, Metals Park, OH, 1987, pp. 234–238.
- [11] Hack, H. P., "Corrosion Testing Made Easy," *Galvanic Corrosion*, NACE International, Houston, TX, 1993.
- [12] Rowe, L. C. and Chance, R. L., "Fundamentals of Corrosion Testing," *Automotive Corrosion by Deicing Salts*, R. Baboian, Ed., pp. 142–146.
- [13] Uhlig, H. H., *Corrosion and Corrosion Control*, John Wiley and Sons, New York, 1985.
- [14] Fontana, M. G., *Corrosion Engineering*, McGraw-Hill, New York, 1986, Chapters 9–10.
- [15] Shoesmith, D. W., "Kinetics of Aqueous Corrosion," *Metals Handbook*, Vol. 13, *Corrosion*, ASM, Metals Park, OH, 1987, pp. 29–36.
- [16] Baboian, R., "Electrochemical Techniques for Predicting Galvanic Corrosion," *Galvanic and Pitting Corrosion—Field and Laboratory Studies*, ASTM STP 576, R. Baboian, W. France, Jr., L. Rowe, and J. Rynewicz, Eds., ASTM International, West Conshohocken, PA, 1976, pp. 5–19.
- [17] Baboian, R., "New Methods for Controlling Galvanic Corrosion," *Machine Design*, Vol. 11, October 1979, pp. 2–9.
- [18] Tomashov, N. D., *Theory of Corrosion and Protection of Metals*, MacMillan Company, New York, 1966.
- [19] Baboian, R., "Investigations of Galvanically Induced Localized Corrosion," *Localized Corrosion—Cause of Metal Failure*, ASTM STP 516, ASTM International, West Conshohocken, PA, 1972, pp. 145–163.
- [20] Compton, K. G., "Current Density Distribution on Composite Structures under Cathodic Protection in Seawater," *Galvanic and Pitting Corrosion—Field and Laboratory Studies*, ASTM STP 576, R. Baboian, W. France, Jr., L. Rowe, and J. Rynewicz, Eds., ASTM International, West Conshohocken, PA, 1976, pp. 48–55.
- [21] Hack, H. P., Moran, P. J., and Scully, J. R., "Influence of Electrolyte Resistance on Electrochemical Measurements and Procedures to Minimize or Compensate for Resistance Errors," *The Measurement and Correction of Electrolyte Resistance in Electrochemical Tests*, ASTM STP 1056, L. L. Scribner and S. R. Taylor, Eds., ASTM International, West Conshohocken, PA, pp. 1–16.
- [22] LaQue, F. L., *Marine Corrosion, Causes and Prevention*, John Wiley and Sons, New York, 1975.
- [23] *Galvanic Corrosion*, ASTM STP 978, H. P. Hack, Ed., ASTM International, West Conshohocken, PA, 1988.

# Intergranular

Michael A. Streicher<sup>1</sup>

THERMAL EXPOSURES, such as during welding, fabrication, and faulty heat treatment, can change the composition of grain boundaries of metals and alloys by equilibrium segregation of impurities and/or alloying elements and, most frequently, by the formation of precipitates, such as chromium carbides in stainless steels. These changes can make the grain boundaries susceptible to rapid, preferential attack (sensitization) in many, mostly acid, environments in which the materials are otherwise considered to have an acceptable degree of corrosion resistance for industrial purposes. The materials of construction most widely used for severely corrosive applications and which may also be subject to sensitization are the numerous iron-base austenitic and ferritic stainless steels and certain nickel-rich alloys with chromium or chromium and molybdenum.

Since 1926, a large variety of tests has been developed to detect susceptibility to intergranular attack in these materials and thereby to investigate this phenomenon, monitor production procedures, screen for plant use as acceptance tests, analyze plant failures, and develop improved and new alloy compositions. The first of these tests to be incorporated in the ASTM Book of Standards for detecting and quantitatively measuring susceptibility to intergranular attack in some austenitic and ferritic stainless steels was the boiling, 65 % nitric acid test, ASTM A 262<sup>2</sup>, in 1943. Five other standard practices have since then been added to ASTM A 262, and one of them has been removed. Thus, there are now five tests deployed for testing 19 wrought and cast austenitic stainless steel compositions. In 1971, the boiling 50 % sulfuric acid-ferric sulfate test, which was one of the five tests added to ASTM A 262, was also specified for application to 13 Ni-Cr and Ni-Cr-Mo alloys in a new standard, ASTM G 28<sup>3</sup>, along with a second test for three of these alloys. In 1979, a separate standard with four test methods was devised for a group of twelve old and new ferritic stainless steels, ASTM A 763<sup>4</sup>. Most recently, a standard

for an electrochemical method for detecting quantitatively mild degrees of sensitization in Types 304 and 304L has been developed, ASTM G 108<sup>5</sup>.

The following discussion on testing for detecting susceptibility to intergranular attack is limited to the tests included in the above four ASTM standards for stainless alloys. The only other ASTM standards on intergranular corrosion testing, ASTM G 67<sup>6</sup> and G 110<sup>7</sup>, are for certain aluminum alloys. These two tests are discussed in the chapter by Lifka in this manual.

## BASIC PRINCIPLES [1]<sup>8</sup>

Metals and alloys generally consist of agglomerations of variously oriented, individual crystals or grains. At the boundaries between these crystals, lattices of different orientations meet and zones of less perfect structure are formed whose properties depend, in part, on the relative orientations of the adjacent grains. Two properties of these boundary zones are of particular importance in corrosion. Small amounts of impurities in solid solution in metals and alloys may segregate at grain boundaries while remaining in solid solution, defined as equilibrium segregation [2]. In addition, precipitates, which form during heat treatments in some alloys, frequently nucleate more readily at or within the boundaries. Thus, as a result of structural imperfections, the chemical composition and, consequently, the electrochemical properties and the corrosion resistance of grain boundaries may be appreciably different from those of the interior of grains. It is apparent that the surfaces of metals consist of a two-dimensional network of such grain-boundary zones which surrounds cross sections through variously oriented grain interiors of greater structural perfection.

<sup>1</sup>Consultant, Wilmington, DE 19803; formerly with E. I. Du Pont de Nemours and Co., Inc. Engineering Research Laboratory, Wilmington, DE and University of Delaware, Newark, DE.

<sup>2</sup>Practice for Detecting Susceptibility to Intergranular Attack in Austenitic Stainless Steels. (Ferritic Stainless Steels are now in ASTM A 763.)

<sup>3</sup>Test Methods for Detecting Susceptibility to Intergranular Attack in Wrought Nickel-Rich, Chromium-Bearing Alloys.

<sup>4</sup>Practice for Detecting Susceptibility to Intergranular Attack in Ferritic Stainless Steels.

<sup>5</sup>Test Method for Electrochemical Reactivation (EPR) Test Method for Detecting Sensitization of AISI Type 304 and 304L Stainless Steels.

<sup>6</sup>Test Method for Determining the Susceptibility of Intergranular Corrosion of 5XXX Series Aluminum Alloys by Mass Loss after Exposure to Nitric Acid (NAMLT Test).

<sup>7</sup>Practice for Evaluating Intergranular Corrosion Resistance of Heat Treatable Aluminum Alloys by Immersion in Sodium Chloride + Hydrogen Peroxide Solution.

<sup>8</sup>Text by the author within this section is reprinted with permission from Van Nostrand Reinhold, New York, NY.

Intergranular attack on these surfaces may range from light etching of grain boundaries, which merely outlines the granular structure, to rapid penetration, which may lead to loss of mechanical strength or even a residue of completely separated grains, "sugaring." Whether corrosion is predominantly by intergranular or by general attack depends on the difference between the rate of corrosion of the grain-boundary zones and that of the grain faces. This difference in rates is determined not only by the metallurgical structure and composition of the boundary but also by the characteristics of the corroding solution.

Surprisingly, even in cases of pronounced intergranular attack, the rate of grain-face corrosion plays an important role. The grain-boundary zone along which there is rapid intergranular penetration is usually very narrow. As a result, even though grain boundaries have all been dissolved, the grains tend to remain linked together and do not drop out of the surface of the metal. However, if there is also some appreciable grain-face corrosion, the narrow groove formed by intergranular penetration is gradually widened by corrosion of the grain faces making up the walls of the grooves and grains drop out readily. In addition, the size of the grains determines how much time is required to undermine and dislodge a grain. Small (and in the first layer, sectioned) grains drop out sooner than large grains. Because of these factors—the ratio of intergranular to grain-face corrosion and the grain size—the results of quantitative measurements of intergranular corrosion depend not only on the type of solution that causes intergranular attack, but also on the method used for the measurement.

Measurements of changes in electrical resistance clearly show the reduction in effective cross section of the corroding metal, even when the undermined grains remain in place. In contrast, weight-loss determinations depend on undermining and dropping-out of grains. Therefore, the two methods provide identical results only on metals corroding in solutions in which there is sufficient grain-face corrosion to lead to ready removal of undermined grains. Specific examples of various types of intergranular corrosion and of different techniques of measurement are described below.

The effect of grain-boundary imperfections on intergranular attack is illustrated by the attack of hydrochloric acid on high-purity (99.998 %) aluminum (Fig. 1). Corrosion varies with the curvature of the boundary. Corrosion may be intensified by equilibrium segregation of traces of iron and/or copper impurity in zones at the boundary with high concentrations of imperfections. For example, corrosion of aluminum in hydrochloric acid is increased by a factor of 1000 in the presence of 0.03 % iron [3].

Intergranular corrosion associated with precipitates is clearly observed on 18Cr-8Ni stainless steels. Upon heating in the range of 1000–1700°F (538–927°C), a precipitate of chromium carbide forms preferentially at grain boundaries in steels containing about 0.02 %, or more, carbon (sensitization). Its presence can be readily detected by metallographic examination. Because of the industrial importance of these steels, their susceptibility to intergranular corrosion has been investigated extensively, and a number of rapid methods for detecting susceptibility to intergranular attack has been developed [4–6].

**FIG. 1—Intergranular attack on pure aluminum (250×). Attack of 20 % solution of hydrochloric acid on 99.9998 % aluminum specimen at 25°C.**

A solution of boiling 50 % sulfuric acid containing ferric sulfate as a passivating inhibitor is used for one of these evaluation tests. Typical weight-loss data obtained on two specimens of the same 18Cr-8Ni steel are plotted in Fig. 2. One of these specimens is free of chromium carbides and has a low, constant rate of corrosion. In contrast, the corrosion rate (slope of the curve) of the other specimen, which had been previously heated to produce profuse precipitation of chromium carbides at grain boundaries, increases rapidly because of intensive dropping of grains. An early phase of this intergranular attack is shown in Fig. 3.

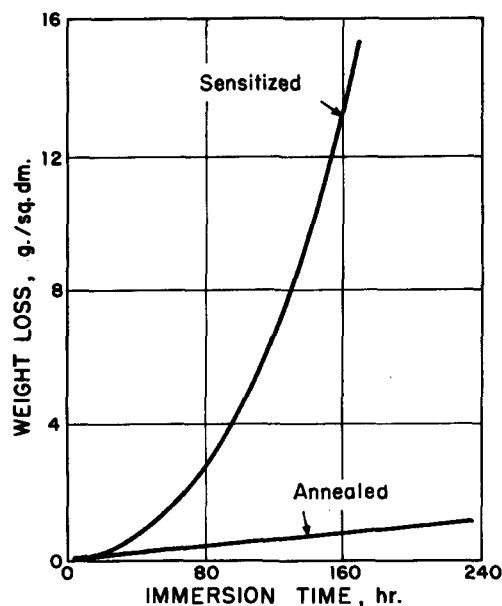


**FIG. 2—Corrosion of stainless steel in ferric sulfate-sulfuric acid solution. Effect of carbide precipitation in 18Cr-8Ni steel on corrosion in boiling 50 % sulfuric acid containing ferric sulfate inhibitor. Sensitized: chromium carbide precipitate at grain boundaries. Annealed: no intergranular precipitate, all carbides dissolved in solid solution.**

FIG. 3—Intergranular attack on stainless steel (500 $\times$ ). Initial stages of corrosion in boiling 50 % sulfuric acid containing ferric sulfate. Steel was sensitized and shows some grain face corrosion and rapid intergranular attack which has undermined and dislodged several grains.

Differences in the type of intergranular corrosion produced on identical, sensitized specimens of 18Cr-8Ni steel in various acid solutions are shown in Fig. 4. Measurements of weight loss and of the corresponding increase in electrical resistance are plotted for intergranular corrosion in three boiling solutions: (1) sulfuric acid containing ferric sulfate inhibitor, (2) sulfuric acid containing copper sulfate inhibitor, and (3) nitric acid. The dotted line shows the relationship of weight loss and change of resistance on a specimen corroding uniformly (no intergranular attack). For a given change in resistance (i.e., penetration of intergranular attack) the weight loss is lowest in the copper sulfate-sulfuric

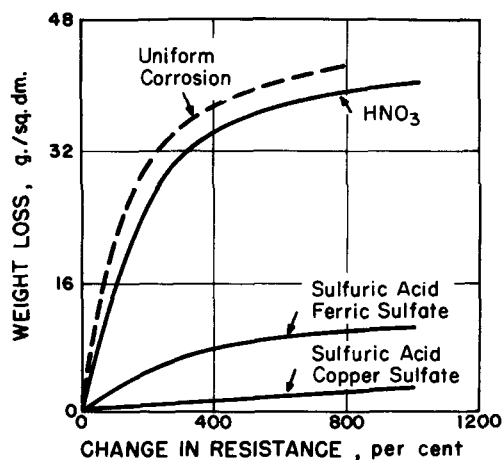


FIG. 4—Comparison of intergranular corrosion in various acid solutions. Measurement of weight-loss and change in electrical resistance on sensitized stainless steel corroding in boiling 65 % nitric acid, and boiling sulfuric acid solutions containing cupric or ferric sulfate. Specimen: 0.15 by 0.60 cm in cross section.

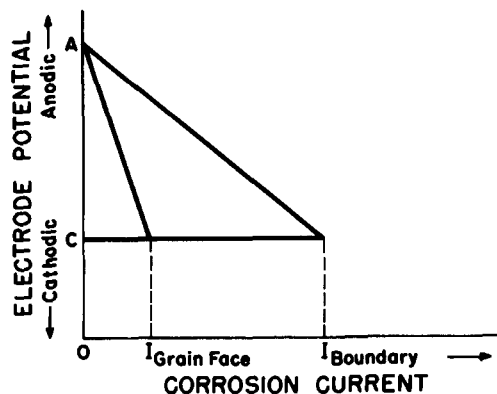


FIG. 5—Local cell polarization on grain faces and boundaries of corroding stainless steel. In ferric sulfate-sulfuric acid solutions grain faces and grain boundaries are both polarized to the oxidation-reduction potential of the solution. The corrosion current at corroding boundaries is greater than that on grain faces.

acid solution and highest in the nitric acid solution. As expected, in all cases the weight loss is lower than on a uniformly corroding metal because some of the grains adhere even though they have been undermined. The reason for these differences is that the ratio of intergranular penetration to grain-face corrosion is different for each solution. It is highest for the copper sulfate-sulfuric acid solution because of the very low rate of grain-face corrosion and lowest in the nitric acid because of the high rate of grain-face corrosion.

Electrochemical measurements [6] show that in nitric acid and in sulfuric acid solutions inhibited with cupric or ferric salts the grain faces and the grain boundaries containing chromium carbide precipitate are both passive. This passive state is a dynamic condition in which there is continual dissolution (breakdown) and re-formation (repair) of a protective, passive film by a reaction between the dissolving metal and the corroding solution. The weight loss of stainless steel actually dissolved in sulfuric acid-ferric sulfate solutions is electrochemically equivalent to the weight of ferric ions reduced. There is no evolution of hydrogen gas, even on rapidly corroding grain boundaries. However, at these boundaries the corrosion current (metal dissolution) required to keep the film in repair, and, thereby, to polarize the boundaries to the same passive potential as the grain faces, is much greater (Fig. 5). The reason for this is that precipitation of chromium carbides (Cr<sub>23</sub>C<sub>6</sub>) at boundaries greatly depletes adjacent metal in chromium.

Variations in the composition of grain boundaries of 18Cr-8Ni stainless steel containing 2-3 % molybdenum may also be caused by precipitation of sigma phase, a chromium- and molybdenum-rich constituent. This precipitate forms during heating in the range of 1000-1600°F (538-871°C). In some cases there may merely be a form of "equilibrium segregation," which is not visible in the microstructure when examined by light or electron microscopy [7]. Nevertheless, such steels are rapidly attacked at grain boundaries by nitric acid, even in the absence of any

TABLE 1—Compositions of stainless steels (ASTM A 262) and related alloys (ASTM G 28).

Composition, Percent by Weight							
UNS	Type <sup>a</sup>	Iron	Chromium	Nickel	Molybdenum	Carbon Max	Other
S30400	304	~69	18.0 to 20.0	8.0 to 10.5	...	0.08	Mn—2.0 max; Si—1.0 max
S30403	304L	~68	18.0 to 20.0	8.0 to 12.0	...	0.03	Mn—2.0 max; Si—1.0 max
S31000	310	~53	24.0 to 26.0	19.0 to 22.0	...	0.25	Si—1.50 max
S31600	316	~66	16.0 to 18.0	10.0 to 14.0	2.00 to 3.00	0.08	Mn—2.0 max; Si—1.0 max
S31603	316L	~66	16.0 to 18.0	10.0 to 14.0	2.00 to 3.00	0.03	Mn—2.0 max; Si—1.0 max
S31703	317L	~63	18.0 to 20.0	11.0 to 15.0	3.0 to 4.0	0.03	Mn—2.0 max; Si—1.0 max
S32100	321	~70	17.0 to 19.0	9.0 to 12.0	...	0.08	%Ti = 5 × %C min
S34700	347	~69	17.0 to 19.0	9.0 to 13.0	...	0.08	Cb = 10 × %C min
N08020	Alloy 20 Cb-3	~40	19.0 to 21.0	32.5 to 35.0	2.00 to 3.00	0.06	%Cb + Ta = 8 × %C; Cu—3.00 to 4.00
N10002	Alloy C	~5	14.5 to 16.5	~54	15.0 to 17.0	0.08	W—4; Co—2.5
N10276	Alloy C-276	~5	14.5 to 16.5	~54	15.0 to 17.0	0.02	W—4; Co—2.5 max; Si—0.05 max
N06985	Alloy G-3	~19	21.0 to 23.5	~49	6.0 to 8.0	0.015	Cu—1.5–2.5; W—1
N06007	Alloy G	~19	18.0 to 21.0	~47	5.5 to 7.5	0.05	Cu—2; Nb—2
N06030	Alloy G-30	~15	28.0 to 31.5	~52	4.0 to 6.0	0.03	Cu—2; Cb + Ta = 0.3–1.5
N06600	Alloy 600	~8	14.0 to 17.0	72 min	...	0.15	Fe—8; Cu—0.5
N06625	Alloy 625	~4	20.0 to 23.0	~62	8.0 to 10.0	0.10	Cb—3.6; Fe—5 max
N08800	Alloy 800	~45	19.0 to 23.0	30.0 to 35.0	...	0.10	Ti—0.5; Cu—0.75
N08825	Alloy 825	~33	19.5 to 23.5	38.0 to 46.0	2.5 to 3.5	0.05	Ti—0.9; Cu—2.2
N06455	Hastelloy Alloy C-4 <sup>b</sup>	~3	14.0 to 18.0	60 to 67	14.0 to 17.0	0.015	Mn—1 max; Co—2
N06022	Hastelloy Alloy C-22 <sup>b</sup>	~4	20.0 to 22.5	57 to 61	12.5 to 14.5	0.015	Mn—0.5 mas; Co—2.5
N06686	Inconel Alloy 686 <sup>c</sup>	~5	19.0 to 23.0	52 to 58	15.0 to 17.0	0.01	Mn—0.75 max; W—3.5
N06059	VDM Alloy 59 <sup>d</sup>	~1	22.0 to 24.0	59	15.0 to 16.5	0.010	Mn—0.5 max
N08367	AL-6XN <sup>e</sup>	~49	20.0 to 22.0	23.5 to 25.5	6.00 to 7.00	0.03 max	N—0.22; Cu—0.1

<sup>a</sup>The tests in ASTM A 262 are also applicable to a number of other alloys, e.g., AISI, 201, 202, 301, 304H, 316H and cast equivalents of some alloys.

<sup>b</sup>Trademark Haynes International, Kokomo, IN.

<sup>c</sup>Trademark Special Metals Corp., Huntington, WV.

<sup>d</sup>Trademark Houston, TX Thyssen Krupp, VDM.

<sup>e</sup>Trademark Allegheny Ludlum Corp., Brackenridge, PA.

chromium carbides. Because sigma phase may not be visible in the microstructure, exposure to nitric acid solution provides a simple method whereby this change in metallurgical structure may be detected.

## DETECTING SUSCEPTIBILITY TO INTERGRANULAR ATTACK IN STAINLESS ALLOYS<sup>9</sup>

A large group of these iron-base alloys (Tables 1 and 2) has been found to be susceptible to rapid intergranular attack in a wide range of plant environments when the compositions at the grain boundaries have been changed by equilibrium segregation of alloying elements and especially by the precipitation of chromium carbides and nitrides, the formation of separate intermetallic phases (e.g., sigma or mu-phase), and molybdenum carbides. These changes are a result of exposures of the alloys during production of mill forms (rods, plates, sheet, tubes) to temperatures at which solid state reactions occur preferentially at grain boundaries. Because welding operations are used in the production of tubes from sheet and during shop fabrication and field

erection, there are further opportunities for the exposure of alloys in the range of temperatures which may result in the formation of deleterious phases at grain boundaries.

An example of weld effects is shown in Fig. 6. Four different 18Cr-8Ni stainless steel panels were joined by welding and were then immersed in a solution of nitric-hydrofluoric acids. This solution produces rapid attack on grain boundaries containing chromium-rich carbide precipitates, which are surrounded by chromium-depleted zones. The attack is similar to that shown in Fig. 3. Dislodgement of grains in the weld-decay zones leads to the formation of grooves on both sides of the panel of Type 304 (about 0.06 % C) steel that are parallel, but not adjacent to the weld bead. If immersion had been continued, the panel would have dropped off from the assembly.

The absence of intergranular attack on the rest of the Type 304 panel shows that the original sheet had been properly annealed (1066°C, 1950°F) at the mill and had been rapidly cooled (quenched) from the annealing temperature through the range of 871–427°C (1600–800°F). This is the range of temperatures in which chromium carbides might form most readily. During welding, the temperatures of the metal in the zone adjacent to the molten zones were raised well above the chromium carbide precipitation range and were cooled rapidly enough to prevent carbide precipitation. But in the weld-decay zone, the base-metal was exposed long enough in the precipitation range, with a maximum rate of precipitation near 677°C (1250°F), so that there was profuse formation of carbides which made this zone susceptible to rapid intergranular attack.

<sup>9</sup>The term *stainless alloys* includes the austenitic and ferritic stainless steels with 12 % or more chromium and certain austenitic nickel-rich chromium-bearing alloys. From this section through the discussion on the oxalic acid etch test, the text is an update and condensation of material in Ref 9. All figures are from this publication except where other references are shown. The latter are reprinted with permission, copyright NACE International. All rights reserved by NACE.



**TABLE 2—Nominal compositions of ferritic stainless steels from ASTM A 763.**

UNS Designation	Alloy	Weight % Maximum Unless Otherwise Specified											Practice(s)
		C	Mn	P	S	Si	Cr	Ni	Mo	Cu	N	Ti	Other
S43000	430 <sup>a</sup>	0.12	1.00	0.040	0.030	0.75	16.0–18.0	0.5	...	...	...	...	...
S43400	434 <sup>a</sup>	0.12	1.00	0.040	0.030	1.00	16.0–18.0	...	0.75–1.25	...	...	...	...
S43600	436 <sup>a</sup>	0.12	1.00	0.040	0.030	1.00	16.0–18.0	...	0.75–1.25	...	...	...	...
S43035	XM8	0.07	1.00	0.040	0.030	0.75	17.0–19.0	0.5	...	...	0.04	0.2 + 4(C + N) min, 1.10 max	0.15 Al
S44400	18Cr-2Mo	0.025	1.00	0.040	0.030	1.00	17.5–19.5	1.00	1.75–2.50	...	0.025	Ti + Cb = 0.2 + 4(C + N) min, 0.80 max	...
S44600	446 <sup>a</sup>	0.20	1.50	0.040	0.030	0.75	23.0–27.0	0.50	...	...	0.10 0.25	...	...
S44626	XM33	0.06	0.75	0.040	0.020	0.75	25.0–27.0	0.50	0.75–1.50	0.20	0.040	0.2–1.0, 7(C + N) min	...
S44627	XM27	0.01	0.4	0.02	0.02	0.40	25.0–27.5	0.5 <sup>b</sup>	0.75–1.50	0.2	0.015	...	...
S44660	26-3-3	0.030	1.00	0.040	0.030	1.00	25.0–28.0	1.0–3.5	3.0–3.5	...	0.040	(Ti + Nb) = 0.20 to 1.00 and 6(C + N) min	0.05–0.2 ...
S44700	29Cr-4Mo	0.010	0.3	0.025	0.02	0.2	28.0–30.0	0.15	3.5–4.2	0.15	0.020 <sup>c</sup>	...	...
S44735	29-4C	0.030	1.0	0.040	0.030	1.00	28.0–30.0	1.0	3.6–4.2	...	0.045	Ti + Cb = 0.2–1.0, 6(C + N) min	...
S44800	29Cr-4Mo- 2Ni	0.010	0.3	0.025	0.02	0.2	28.0–30.0	2.0–2.5	3.5–4.2	0.15	0.020 <sup>c</sup>	...	...

<sup>a</sup>Types 430, 434, 436, and 446 are nonstabilized grades that are generally not used in the as-welded or sensitized condition in other than mildly corrosive environments. In the annealed condition, they are not subject to intergranular corrosion. For any studies of IGA on Types 430, 434, 436, or 446, the indicated test methods are suggested.

<sup>b</sup>Nickel plus copper.

<sup>c</sup>Carbon plus nitrogen = 0.025 max.

**FIG. 6—Weld decay and methods for its prevention. The four different panels were joined by welding and then exposed to a hot solution of nitric-hydrofluoric acids. The weld decay, such as shown in Type 304 steel, is prevented by reduction of the carbon content (Type 304L) or stabilization of carbon with titanium (Type 304L) or niobium (Type 347).**

Weld-decay zones can be prevented by reducing the carbon content to less than 0.03 % (Type 304L)<sup>10</sup> or by addition of “stabilizing” elements, titanium or niobium. By heating such stabilized alloys near 900°C (1650°F), most of the carbon reacts to form “harmless” titanium and niobium carbides, and, as a result, the formation of chromium carbides is prevented during exposure in the range of 871–427°C (1600–800°F).

In ferritic stainless steels, such as Types 430 and 446 (Table 2), diffusion rates of carbon and chromium are much higher than in the nickel-bearing, austenitic alloys, e.g., Type 304. As a result, the precipitation of chromium carbides is so rapid that it cannot be prevented even during water-quenching of small specimens in water from annealing temperatures. Such specimens have extensive amounts of precipitates at grain boundaries and are, therefore, sensitized. However, because of the high rate of diffusion of chromium, a heat treatment at 1500°F (816°C) will diffuse chromium into the depleted zones around the chromium-rich carbide precipitates and will thereby eliminate sensitization, i.e., make the material resistant to intergranular attack even though the grain boundaries still contain chromium carbides. (Because of the much lower rate of diffusion in the austenitic alloys, and, consequently, the long heat treatments required, elimination of sensitization by rediffusion of chromium into depleted zones is not practical.)

<sup>10</sup>By argon-oxygen decarburization (AOD) the carbon content of commercial heats of 304L can now be reduced consistently to 0.01 %. AOD and vacuum induction melting are used to produce the new high-purity Fe-Cr-Mo ferritic stainless steels in Table 2.

All of the alloys listed in Tables 1 and 2 may become sensitized; that is, form various precipitates at grain boundaries when exposed to certain temperatures and thereby become subject to intergranular attack. Chromium-rich carbides are the most common precipitates in the alloys of Tables 1 and 2, except in the Ni-Cr-Mo alloys in which molybdenum carbide is formed. All of the evaluation tests discussed below detect susceptibility to intergranular attack associated with chromium and molybdenum carbide precipitates.

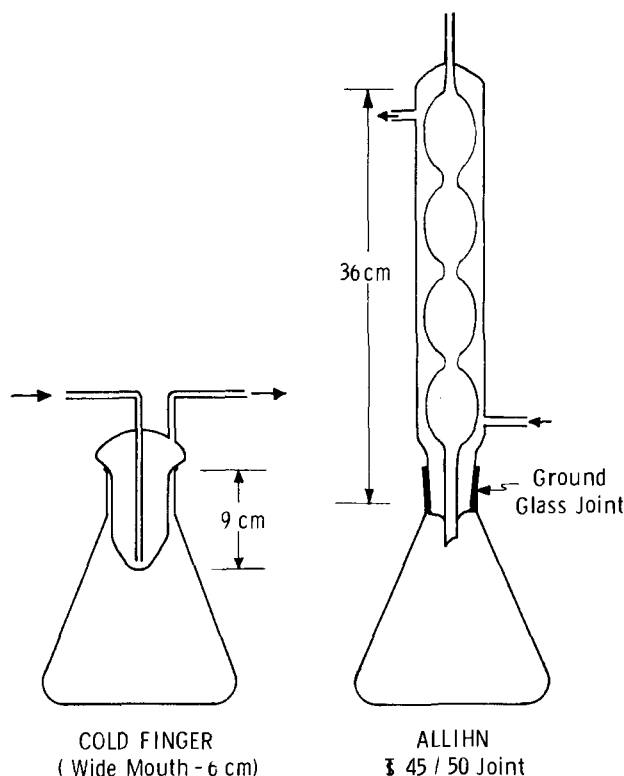
The stainless steels in Table 1 containing molybdenum (Types 316, 317, 316L, and 317L) may also contain molybdenum-rich sigma phase. Furthermore, the nickel-rich alloys with molybdenum in Table 1 may form an intermetallic, molybdenum-rich compound, mu-phase. When these phases are present at grain boundaries, even in some cases as a preprecipitation form (i.e., not visible in the microstructure, see above in the previous section), they may also lead to intergranular attack, but only in certain oxidizing solutions, for example, boiling 65 % nitric acid in which the redox potential (the potential of a platinized platinum electrode) is about +1.0 V versus SCE. In the 50 % sulfuric acid test with ferric sulfate (redox potential +0.6 V versus SCE) only mu-phase, which may be present in Ni-Cr-Mo alloys (C, C-276, and C-4) causes susceptibility to intergranular attack, but not sigma-phase in Types 316, 316L, 317, and 317L stainless steels. Alloys 625 and 825 also contain molybdenum that can in some cases lead to phases that increase corrosion rates in oxidizing (especially nitric acid) solutions.

Precipitates at grain boundaries may make the costly alloys of Tables 1 and 2 subject to intergranular corrosion in a very wide range of mostly acid plant environments in the chemical process industries, as well as pulp and paper, food processing, and petroleum refining plants. A number of solutions that have resulted in intergranular attack on sensitized austenitic stainless steels is given in Table 3. These solutions range from highly reducing (−0.6 V versus SCE) redox potentials, e.g., in sulfuric acid, to highly oxidizing (+1.0 V versus SCE) in nitric acid. Under severe conditions, i.e., higher concentrations and temperatures, many of these solutions may also produce intergranular attack in the nickel-rich, chromium-bearing alloys of Table 1, e.g., sulfuric, hydrochloric, chromic, and nitric acids.

Chromium and molybdenum carbide precipitates have also been found to result in susceptibility to other forms of corrosion. Some examples are stress accelerated intergranular attack on Type 304 and alloy 600 in polythionic acid and stress corrosion cracking (SCC) of ferritic stainless steels, such as Type 446 in boiling sodium chloride with 50 ppm Cl<sup>−</sup>. Molybdenum carbide precipitates make alloys C and C-276 subject to stress corrosion in boiling 45 % magnesium chloride solution, and to crevice attack in ferric chloride. Finally, sensitization of Type 304 stainless steel during circumferential welding to join pipe segments has made the heat affected zones, which run parallel to these welds, subject to intergranular stress corrosion cracking (IGSCC) on boiling water nuclear plants. The pipes contain water at 289°C and crack when the concentration of oxygen is in the range of 0.2–8 ppm. Cracks have been found in pipes from 4 to over 30 in. (10.2 to over 76.2 cm) diameter on many plants, which has necessitated costly replacement operations [9].

**TABLE 3**—Corrosives that induce intergranular corrosion in austenitic stainless steels [8].

Acetic acid	Oxalic acid
Acetic acid + salicylic acid	Phenol + naphthenic acid
Ammonium nitrate	Phosphoric acid
Ammonium sulfate	Polythionic acid
Ammonium sulfate + sulfuric acid	Salt spray
Beet juice	Seawater
Calcium nitrate	Silver nitrate + acetic acid
Chromic acid	Sodium bisulfate
Chromium chloride	Sodium hydroxide + sodium sulfide
Citric acid	Sodium hypochlorite
Copper sulfate	Sulfamic acid
Crude oil	Sulfite cooking liquor
Fatty acids	Sulfite digester acid
Ferric chloride	(calcium bisulfite + sulfur dioxide)
Ferric sulfate	Sulfite solution
Formic acid	Sulfur dioxide (wet)
Hydrocyanic acid	Sulfuric acid
Hydrocyanic acid + sulfur dioxide	Sulfuric acid + acetic acid
Hydrofluoric acid + ferric sulfate	Sulfuric acid + copper sulfate
Hydroxyacetic acid	Sulfuric acid + ferric sulfate
Lactic acid	Sulfuric acid + methanol
Lactic acid + nitric acid	Sulfuric acid + nitric acid
Maleic acid	Sulfurous acid
Nitric acid	Water + starch + sulfur dioxide
Nitric acid + hydrochloric acid	Water + aluminum sulfate
Nitric acid + hydrofluoric acid	



ONE LITER ERLLENMEYER FLASKS

**FIG. 7—Types of condensers.**

## ORIGIN OF EVALUATION TESTS

The first laboratory tests for detecting susceptibility to intergranular attack were simulated service tests. In 1926, Hatfield [10] observed intergranular attack on an austenitic stainless steel used for a pickling tank containing sulfuric acid and some copper sulfate. To prevent the selection of material that might be susceptible to intergranular corrosion for this service, he used an 8 % sulfuric acid solution containing copper sulfate to evaluate steels before use. By 1930, Hatfield's test solution was being used to investigate intergranular corrosion and to develop methods for overcoming this problem. Strauss et al. [11] and Aborn and Bain [12] established that the cause of intergranular attack is the precipitation of chromium carbides,  $(\text{Cr,Fe})_{23}\text{C}_6$ , at grain boundaries. Because these chromium-rich precipitates are surrounded by metal that is depleted in chromium, there is more rapid attack at these zones than on undepleted metal surfaces.

## 65 % NITRIC ACID TEST

In 1930, Huey [4] described another simulated service test used at the Du Pont Co. since 1927 to quantitatively detect variations in the performance of iron-12 to 18 % chromium alloys intended for service in nitric acid plants. For rapid results, he selected a concentrated solution of 65 % nitric acid, which is near the constant boiling concentration of 68.5 %. Five 48-h periods, each with fresh acid solution, were proposed. Fresh solutions are needed to minimize the effect of corrosion products as described below. The weight

loss was converted to a corrosion rate. A glass flask fitted with a reflux condenser via a ground glass joint was specified. Later, the less costly cold finger condenser (Fig. 7) was used at many laboratories, apparently without recognition that this change in condensers lowers corrosion rates, by keeping the concentration of hexavalent corrosion products at relatively low levels [13,14].

Hexavalent chromium greatly increases both general and intergranular corrosion. It is formed when stainless steel dissolves in hot, concentrated nitric acid as divalent chromium ions (blue), which are then oxidized by nitrate ions to the trivalent (green) and then the hexavalent (orange) state. Concurrently, nitric oxide gas (NO) is formed. When this is absorbed in the cold condensate on the surfaces of the condensers and thereby recirculated into the boiling nitric acid solution it reduces the hexavalent ions to the tri- and divalent states. The cold finger condenser provides a more efficient method for recirculating nitric oxide than the Allihn or drip-tip condenser. (Contact of nitric oxide gas (colorless) with air (oxygen) results in nitrogen dioxide ( $\text{NO}_2$ , brown.) The latter also reduces hexavalent chromium ions) [14].

It was soon found that among the variables affecting corrosion rates were certain heat treatments that made not only the ferritic stainless steels subject to intergranular attack, but also the austenitic, 18Cr-8Ni alloys. From this simulated service test in boiling 65 % nitric acid, there evolved Practice C of ASTM A 262. Its large-scale use by one

of the first and largest purchasers of stainless steels, the Du Pont Co., made it the leading method for acceptance testing of stainless steels for many years in the United States.

## COPPER SULFATE-SULFURIC ACID TESTS

In England and Germany, the copper sulfate test with sulfuric acid has been the most frequently used. Evaluation in this test is qualitative by examination for fissures (cracks) on the test specimen, which is bent after exposure to the test solution. In the United States, this test was not standardized by ASTM until 1955. ASTM A 393, which later became A 708, Practice for Detection of Susceptibility to Intergranular Corrosion in Severely Sensitized Austenitic Stainless Steel, specified a solution of 6 % anhydrous copper sulfate and 16 % sulfuric acid, by weight. Evaluation of results after only 72 h of testing was also done by bending the tested specimen over a mandrel and examining the outer surface for fissures. In this short form, the test was useful only for detecting very severe cases of sensitization. This limitation, along with the qualitative nature of evaluation, greatly limited the usefulness of this form of the copper sulfate-sulfuric acid test. It eventually resulted in the removal of ASTM A 708 from the ASTM Book of Standards because several other tests can detect severe cases of sensitization as well as mild and medium conditions of sensitization.

In Germany, the rate of intergranular attack in this solution has been greatly increased by Rocha [15] since 1950. He added zinc dust to precipitate metallic copper and later simply embedded the stainless steel specimens in metallic copper chips or shot. This has the effect of changing the corrosion potential of the test specimen in the less noble direction to that of the metallic copper and thereby reducing the testing time from 200 to less than 48 h.

Quantitative measurements of the effect of metallic copper in the copper sulfate-sulfuric acid solution on intergranular attack were reported in 1959 [6]. Three types of tests were made in flasks with cold finger or pine cone condensers (Fig. 7): (a) without metallic copper, (b) with a specimen of copper not in contact with the stainless steel specimen, and (c) with copper (turnings) in contact with the stainless steel specimen. Results are shown in Fig. 8. Simultaneous immersion of a copper specimen increased the rate of corrosion on a sensitized Type 316 specimen by a factor of 8 in a 200-h test period. Contact of the stainless steel with the copper increased this factor to 34.

The three electrode potentials plotted in Fig. 9 provide data on the changes taking place in the cupric sulfate-sulfuric acid solutions during these tests in a flask with a finger condenser. As in the case of ferric ions, cupric ions make stainless steels passive in sulfuric acid. Measurements on the platinized platinum electrode give the oxidation-reduction potential of the solution. The potentials on the stainless steel and the copper specimens are the corrosion potentials of these materials. In the presence of the stainless steel specimen whose corrosion potential is constant, there is a gradual decrease (change in the active direction) in the redox potential of the solution resulting from the formation of cuprous ions on the surface of the specimen.

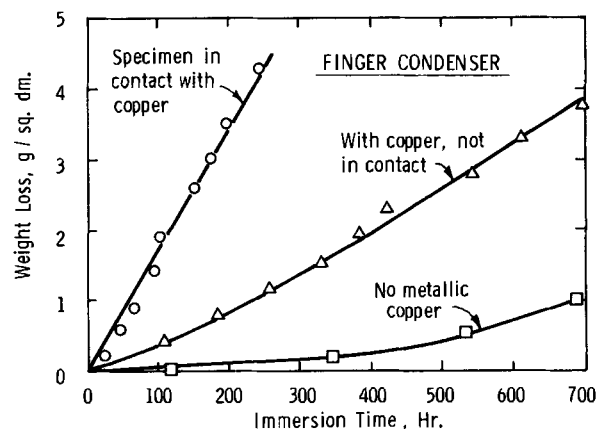


FIG. 8—Corrosion of sensitized Type 316 steel in boiling copper sulfate-sulfuric acid solution. Specimen: 17.4 Cr; 12.7 Ni; 1.89 Mo; 0.053 C. Heated 1 h at 677°C. Solution: 15.7 % sulfuric acid with 5.7 % anhydrous copper sulfate.



This produces a change in the relative concentrations of cupric and cuprous ions. The rate of this change is greatly increased by the addition of metallic copper (40 cm<sup>2</sup> surface area in 600 mL) whose dissolution is governed by the rate of the cathodic reaction:



Within an hour in boiling solutions, the potentials of the stainless steel and of the platinized platinum electrode become constant at +0.13 V versus SCE; that is, the stainless steel assumes the redox potential which remains constant at a relatively low potential. However, the corrosion potential of the copper specimen is even lower, and when contact is made between the stainless steel specimen and the copper, the steel assumes the potential of the copper. The redox

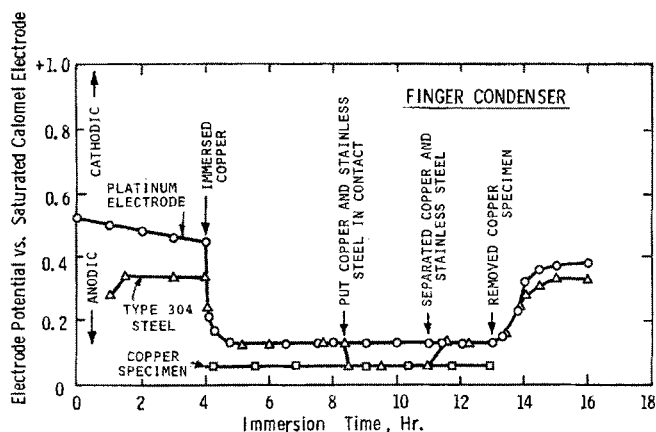


FIG. 9—Electrode potential measurements in boiling copper sulfate-sulfuric acid solution. Solution: 15.7 % sulfuric acid with 5.7 % anhydrous copper sulfate.

**TABLE 4—Boiling copper sulfate tests in ASTM A 262 and A 763.**

ASTM Designation	Solution		Metallic Copper		Testing			Alloys
	CuSO <sub>4</sub>	H <sub>2</sub> SO <sub>4</sub> (By Weight %)	Type	Contact	Apparatus	Evaluation	Time (h)	
A 262-E	6%	16	shot or turnings <sup>a</sup>	yes	Allihn condenser, 1-L flask	bend test	24	austenitic stainless steels
A 262-F	72g CuSO <sub>4</sub> •5H <sub>2</sub> O in 600 mil	50	specimen or shot	no	Allihn condenser 1-L flask	weight loss	120	Cast 316 Cast 316L
A 763 Practice Y	72g CuSO <sub>4</sub> •5H <sub>2</sub> O in 600 mil	50	specimen	no	Allihn condenser 1-L flask	weight loss, bend test, no grain dropping	120	Fe-Cr with more than 25% Cr, Type 446(96 h) Fe-26Cr-1Mo Fe26Cr-1Mo-Ti 29Cr-4Mo 29Cr-4Mo-2Ni
Practice Z	6%	16	shot or turnings <sup>a</sup>	yes	Allihn condenser 1-L flask	bend test	24	Fe-Cr with 16 to 20% Cr 430 (17Cr) 434 (17Cr-1Mo) 436 (17Cr-1Mo-Nb) 18 Cr-Ti 18 Cr-2Mo-Ti

<sup>a</sup>Amount not specified; enough to cover the specimen.**TABLE 5—ASTM standard practices in A 262 for detecting susceptibility to intergranular corrosion in austenitic stainless steels.**

Designation	Test	Temperature	Testing Time	Applicability	Evaluation Method
Practice A	Oxalic Acid Etch Screening Test	ambient	1.5 min	Chromium carbide sensitization only	Microscopic Examination; Classification of etch structure
B	Ferric Sulfate-50% Sulfuric Acid	boiling	120 h	Chromium carbide	Weight-loss/corrosion rate
C	65% Nitric Acid	boiling	240 h	Chromium carbide and sigma phase	Weight-loss/corrosion rate
D	10% Nitric-3% Hydrofluoric Acids (This test is being removed from A 262)	70°C	4 h	Chromium carbide in 316, 316L, 317, 317L	Ratio of corrosion; Rates of "unknown" over that of a solution annealed specimen
E	6% Copper Sulfate 16% Sulfuric Acid with metallic copper	boiling	24 h	Chromium carbide	Examination for fissures after bending
F	Copper Sulfate 50% Sulfuric Acid with metallic copper	boiling	120 h	Chromium carbide in cast 316 and 316L	Weight-loss/corrosion rate

**TABLE 6—ASTM standard practices in A 763 for detecting susceptibility to intergranular attack in ferritic stainless steels.**

Designation	Test	Temperature	Testing Time	Applicability	Evaluation Method
Practice W	Oxalic Acid Etch	ambient	1.5 min	stabilized (Ti, Cb) grades only	Classification of etch structures
X	Ferric Sulfate-50% Sulfuric Acid	boiling	24 to 120 h	17 to 29% Cr	Weight-loss 17 to 26% Cr, microscopic examination, 29% Cr
Y	Copper Sulfate 50% Sulfuric Acid with metallic copper	boiling	96 to 120 h	25–29% Cr	Weight-loss 26% Cr, microscopic examination, 29% Cr
Z	Copper Sulfate 16% Sulfuric Acid with metallic copper	boiling	24 h	17–18% Cr	Check for fissures in bend test

potential (platinum electrode) remains unchanged. Reversing these steps, that is, breaking contact and removing the metallic copper, reverses the potential changes. The potentials of the platinized platinum and the stainless steel move in the noble direction. Thus, in tests with finger condensers there must be contact between the copper and the stainless steel test specimen to obtain reproducible and maximum corrosion rates.

In contrast, when a flask with an Allihn condenser (Fig. 7) is used, it is unnecessary to have physical (electrical) contact

between the copper and the stainless steel specimen. The corrosion rate is the same for the "no contact" and the "contact" tests [9]. This difference in the performance of the two condenser systems is caused by the greater concentration of oxygen from air in the condensate from the cold finger condenser as compared with that coming from the Allihn condenser [9].

Two versions of the copper sulfate test are now included in the ASTM standards (Tables 4–6). For both versions, Allihn condensers and the addition of metallic copper are

specified. In ASTM A 262, Practice E, the 6 % copper sulfate–16 % sulfuric acid test is specified for austenitic stainless steels. The specimen is to be embedded in copper shot or turnings. (However, as mentioned above, with the Allihn condenser it is not really necessary to make contact between the stainless steel specimen and the copper metal.) Evaluation of results after 24 h is by examination for fissures on a bent specimen. The same test method is also specified for certain ferritic stainless steels in ASTM A 763 as Practice Z. (This method is favored by the petroleum industry where the concern is IGSCC in polythionic acid.)

ASTM A 763 also includes a copper sulfate 50 % sulfuric acid test with metallic copper and an Allihn condenser, Practice Y. In place of copper shot or turnings, a copper specimen (2.5 by 2.5 cm) is immersed in a second glass cradle. Thus, there is no contact between it and the specimen. The use of 50 % sulfuric acid for the 120-h test on higher chromium (25–29 %) ferritic stainless steels increases the rate on sensitized specimens so that weight-loss can be used as a quantitative method of evaluation in addition to bending for fissures and microscopic examination for evidence of dropped grains (Table 4). The use of 50 % sulfuric acid was taken over from the boiling 50 % sulfuric acid ferric sulfate test [16].

## FERRIC SULFATE-50 % SULFURIC ACID TEST

This test solution was introduced in 1958 [17] to reduce the 240-h testing time of the boiling 65 % nitric acid test to 120 h and to limit intergranular attack to grain boundaries containing chromium carbides. As mentioned above, the nitric acid test also causes intergranular attack on austenitic, molybdenum-bearing stainless steels containing sigma-phase in Types 316, 316L, 317, and 317L. The ferric sulfate test was the first test that was not derived from a plant service problem. The oxalic acid etch test (described below), which is used as a screening test, had already established the concept (1953) that all of the evaluation tests were simply a means for determining the presence and degree of sensitization, i.e., whether or not a given stainless alloy had been made susceptible to intergranular attack in certain chemical solutions by faulty heat treatments or welding. They do not predict service life in the way that the results of a simulated service test might be used. Although the nitric acid and the copper sulfate tests were originally derived from simulated service tests, they became tools for providing information on the presence and extent of damaging precipitates at grain boundaries [13].

Allihn condensers are specified for the ferric sulfate test (Figs. 7 and 10). However, this is not an essential requirement. Other condensers can be used. Also, because corrosion products do not affect the rate of corrosion, there is no need to change the solution during the 120-h test period and several specimens may be tested in the same flask. The only requirement is that the ferric sulfate inhibitor, which is consumed during the inhibition process, must be replenished in proportion to the total amount of metal dissolved from the test specimen. This is in contrast to the 240-h 65 % nitric acid test in flasks for which the solution must be changed

FIG. 10—Apparatus for ferric sulfate-sulfuric acid test.

every 48 h to avoid the buildup of chromium ion corrosion product for reasons described above. The ferric sulfate-50 % sulfuric acid test has been standardized for use on austenitic (Table 5) and ferritic (Table 6) stainless steels, as well as Ni-base alloys (Table 7).

Table 8 provides a summary of the redox potentials of various tests for austenitic and ferritic stainless steels. Because both carbides and molybdenum-rich sigma-phase may result in intergranular attack in highly oxidizing solutions, the nitric acid test should be specified for materials to be used in nitric acid or other highly oxidizing environments.

## OXALIC ACID ETCH TEST

The gradual introduction of various new stainless steels, as well as a variety of evaluation tests, has resulted in a relatively large numbers of ASTM test methods, and, consequently, a rather involved set of choices to be made for a specific evaluation procedure. Sometimes a short testing time is a prime requirement. The original 65 % nitric acid

**TABLE 7**—ASTM standard test methods in G 28 for detecting susceptibility to intergranular attack in wrought, nickel-rich, chromium-bearing alloys.

Designation	Test	Temperature	Testing Time	Applicability	Evaluation Method
Method A	Ferric Sulfate 50% Sulfuric Acid	boiling	24 to 120 h	Carbides and intermetallic phases <sup>a</sup>	Weight-loss/corrosion rate and/or microscopic examination
B	23% Sulfuric 1.2% Hydrochloric 1% Ferric Chloride 1% Cupric Chloride	boiling	24 h	Carbides and intermetallic phases Alloys C-276, C-22, 59	Weight-loss/corrosion rate and/or microscopic examination

<sup>a</sup>Alloys C-4, C-276, 20 Cb-3, 600, 625, 800, 825, C-22, 59, G, G-3, G-30, and 6XN Compositions in Table 1; alloy C has been removed and alloy 686 has not yet been included.

**TABLE 8**—Corrosion potentials of wrought stainless steels in acid solutions.

			Precipitates and Phases Detected							
			Solutions <sup>a</sup>	Austenitic Steels		Ferritic Steels				
				Cr-Carbide	Sigma	Cr-Carbide and Nitride		Intermetallics (Fe-Cr-Mo(Ti))		
						Fe-Cr	Fe-Cr-Mo			
Electrode Potential (V) versus Saturated Calomel Electrode (SCE)	<div>Passive (Noble)</div> <div>Active</div>		+1.0	←nitric acid, 65% (0.75 to 1.0 V during test)	yes	316, 321 316L, 317, 317L	yes	yes	yes	
			+0.6	←ferric sulfate-sulfuric acid	yes	no <sup>b</sup>	yes	yes	yes <sup>c</sup>	
			+0.35	←copper sulfate-sulfuric acid	yes	no	yes	yes	no	
			+0.1 0.0	←copper sulfate-sulfuric acid with metallic copper	yes	no	yes	yes	no	
			-0.1	←10% nitric-3% hydrofluoric acid (oscillates between +0.3 and -0.1 V)	yes	no	yes	yes	no	
			-0.6	←5% sulfuric acid	yes	no	no	yes <sup>c</sup>	no	

<sup>a</sup>The potential of the specimen in the oxalic acid etch test while being anodically etched at 1A/cm<sup>2</sup> is 1.7 V vs calomel scale. In austenitic stainless steels only chromium carbides are detected and sigma phase when present as a second phase; also in stabilized ferritic stainless steels.

<sup>b</sup>There is some effect of sigma phase in Type 321 steel.

<sup>c</sup>In unstabilized Fe-Cr-Mo alloys (29Cr-4Mo and 29Cr-4Mo-2Ni) sigma- and chi-phases do not cause intergranular attack.

test took 240 h of actual testing time, plus the preparation of fresh solutions for each of the five 48 h test periods. In addition, specimen preparation, shipping, and calculations resulted in a total delay of as much as three weeks for test results. This provided the motivation for the introduction and acceptance of the oxalic acid etch test for screening specimens by classifying microstructures [18]. These are obtained simply by making a polished surface anodic in 10 % oxalic acid solution for 1.5 min with a current density of 1.0 amp/cm<sup>2</sup>. This results in an "over etch" which facilitates interpretation. On specimens that are free of chromium carbides at grain boundaries the different rates of dissolution of variously oriented metal grains results in steps between grain (Fig. 11, Step Structure). When the boundaries contain enough carbides to surround completely at least one grain there can be expected to be undermining of grains in the boiling acid tests and an increase in the corrosion rate with testing time (Fig. 12, Ditch Structure). When the ditching does not surround grains completely the classification is Dual Structure (Fig. 13).

Specimens with step and dual structures do not drop grains in boiling acid tests, and therefore have acceptable or "passing" corrosion rates in weight-loss tests. Materials represented by such specimens can therefore be accepted for plant use on the basis of the 1.5 min oxalic acid etch test. Only those materials that have a ditch structure must be submitted for testing in the hot acid tests to determine whether or not their corrosion rates fall below or above the acceptance rate for the given alloy.

Type 304 and especially Type 304L are now by far the steels produced in the largest quantity. During the last 15 years all producers have switched to argon-oxygen refining. This makes it possible to keep the carbon content of Type 304L in the range of 0.01–0.02 %. Low carbon grades are used specifically for materials that will be welded (tubes, shop and field fabrication). To anticipate welding effects, specimens of Types 304L and 316L are heated for 1 h at 677°C (1250°F) before corrosion testing. Before the introduction of argon-oxygen refining, low-carbon alloys had carbon contents between 0.02 and 0.03 %, and in these the

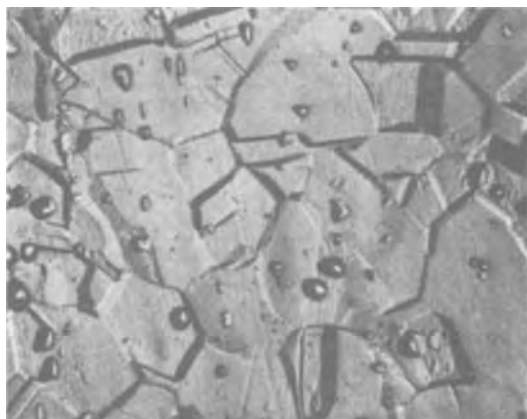


FIG. 11—Oxalic acid etch (500 $\times$ ). Step structure. Etched 1 A/cm<sup>2</sup> for 1.5 min.

FIG. 12—Oxalic acid etch (500 $\times$ ). Ditch structure. Etched 1 A/cm<sup>2</sup> for 1.5 min.

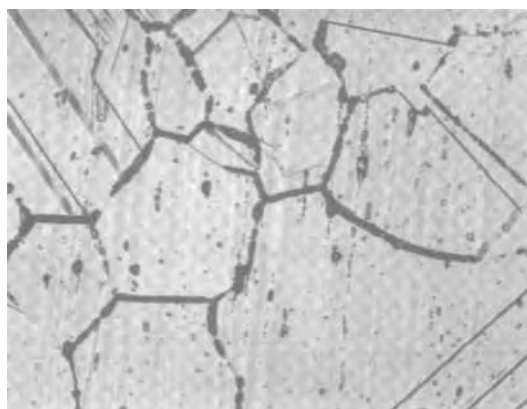


FIG. 13—Oxalic acid etch (250 $\times$ ). Dual structure. Etched 1 A/cm<sup>2</sup> for 1.5 min.

heat treatment at 677°C resulted in more carbides than the newer heats with 0.01 to 0.02 % carbon. The result is that an ever larger proportion of low-carbon heats can now be

screened by the oxalic acid etch test from the hot acid tests after the heat treatment of 1 h at 677°C (1250°F).

The oxalic acid etch test has been incorporated as Practice A in ASTM A 262 for screening a large number of wrought and cast austenitic stainless steels. It has also been included in ASTM A 763 for screening of stabilized ferritic stainless steels, Practice W (Table 6).

## NITRIC-HYDROFLUORIC ACID TEST

The 10 % nitric-3 % hydrofluoric acid test at 70°C (Practice D in ASTM A 262) was developed into a quantitative, 4 h method specifically for Types 316 and 316L material to detect sensitization associated only with chromium carbide precipitates, and not with that caused by sigma phase (Table 5) [19]. Because hydrofluoric acid attacks glassware, special apparatus is required made of polyvinyl chloride. For this reason and because of the unique hazards involved in handling hydrofluoric acid, this test has never been used widely. It was found recently that it was not being used at all and was, therefore, removed from ASTM A 262 in 1993. There are several other tests that accomplish the same objectives: the ferric and the cooper sulfate tests with the oxalic acid etch test as a screening method. A large percentage of Types 316 and 316L can be "accepted" without further testing in boiling acid tests, even after heating Type 316L specimens for 1 h at 677°C (1250°F) in the case of material to be welded. This percentage is even higher for 316L than for 304L because the 2.5 % molybdenum in Type 316L retards formation of chromium carbides.

## EPR TESTS

### Single Loop (SL)

The failures by SCC of welded Type 304 piping exposed to water at 289°C with 0.2–8 ppm of oxygen on boiling water nuclear power plants created a demand for a nondestructive method for detecting quantitatively the degrees of sensitization in these pipes. A nondestructive method was needed so that measurements could be made directly on the heat-affected zones of pipes on the plants. For this purpose, Clarke et al. [20] selected and applied the electrochemical potentiokinetic reactivation (EPR) technique. A cell was designed that could be attached to pipes.

This EPR method has now been incorporated in the ASTM Book of Standards as a laboratory test, ASTM G 1085. A mounted and highly polished specimen of Type 304 or 304L material is polarized in a special cell from its corrosion potential of about -400 mV versus SCE to a passive potential of +200 mV versus SCE and then reactivated to the corrosion potential at rates of 6 V per h (Fig. 14). During this sweep the total charge (area under the curve) passing through the cell (coulombs) is measured. The counter-electrode is a graphite rod and the solution consists of 0.5M sulfuric acid with 0.01M potassium thiocyanide. The temperature must be controlled at  $30 \pm 1^\circ\text{C}$  and the solution must be freshly prepared. Automatic scanning, data recording, and plotting are carried out with computerized instrumentation. The



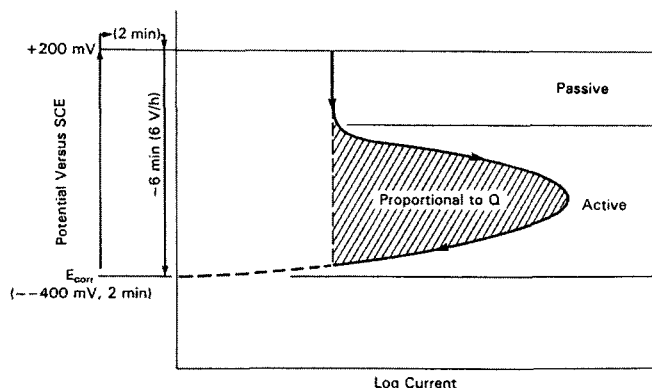


FIG. 14—Schematic diagram of electrochemical potentiokinetic reactivation, (SL-EPR), method for AISI 304 and 304L stainless steels [27]. ©NACE International. All Rights Reserved by NACE; reprinted with permission.)

results,  $P_a$ , are calculated as coulombs,  $Q$ , per  $\text{cm}^2$  of grain boundary area, GBA

$$P_a = \frac{Q}{\text{GBA}}$$

$\text{GBA} = A_s [5.09544 \times 10^{-3} \exp(0.34696 X)]$  where  $A_s$  = the specimen area and  $X$  = the ASTM grain size in accordance with ASTM E 112, Test Methods for Determining Average Grain Size.

The assumption in this procedure is that dissolution takes place uniformly at all grain boundaries and that there is no increment of current coming from other areas in the surface, such as pits. However,  $P_a$  values should not be pictured too literally because there are many specimens for which this is not the case, because only segments of the boundaries are attacked (dual structures) and there are pits at nonmetallic inclusions [21].

For comparisons, data from the EPR, ferric sulfate, and oxalic acid etch tests have been plotted on log-log scales in Fig. 15, along with information on pitting in the EPR structures. It has been observed that  $P_a$  values on nonsensitized (step structure) AISI 304 or 304L material exceeding 0.10 coulomb/ $\text{cm}^2$  are evidence of significant amounts of pitting in the EPR etch structures.

The line at 2.0 coulomb/ $\text{cm}^2$  has been drawn because Clarke et al. [20] selected it as the upper limit for acceptance testing of incoming stainless steel to ensure a "lack of discernible intergranular carbide precipitation." This is in agreement with our findings as shown in Fig. 15, i.e., the limit of 2.0 coulomb/ $\text{cm}^2$  essentially covers the range of step structures in the oxalic acid etch test. However, any  $P_a$  value in excess of 0.10 coulomb/ $\text{cm}^2$  denotes the presence of some random pitting in the microstructure.

Figure 15 also shows that for certain values of  $P_a$  there is an overlap of step and dual structures in the oxalic acid etch. Dual structures extend down to  $P_a$  values of about 0.4 coulomb/ $\text{cm}^2$ . Thus, in the case of  $P_a$  values in the range of 0.4 to 2.0 coulomb/ $\text{cm}^2$ , it is essential to look at the microstructure produced by the EPR test to establish whether it is a result of pitting in a step structure or of a mild case of sensitization (dual structure). The cause for the second overlap between dual and ditch structures is also pitting.

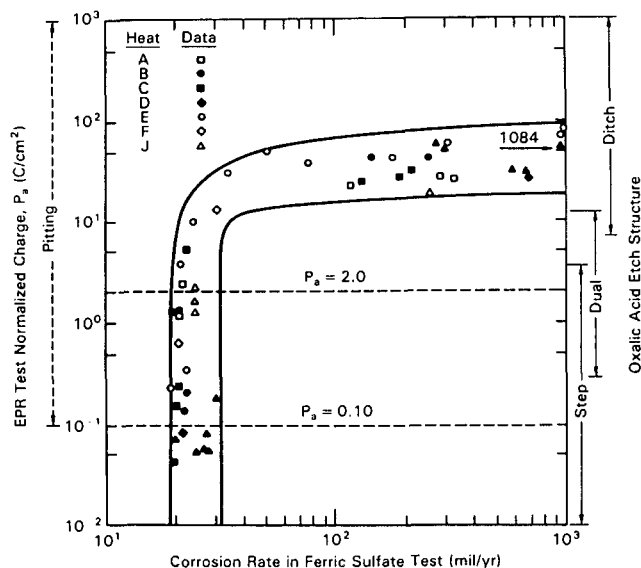


FIG. 15—Correlation of SL-EPR, oxalic acid etch, and ferric sulfate tests for AISI 304 and 304L stainless steels [27]. ©NACE International. All Rights Reserved by NACE; reprinted with permission.)

The curves in Fig. 15 can be divided into three ranges [21]:

1. In the range of  $P_a$  values from 0.01–5.0 coulomb/ $\text{cm}^2$ , there is essentially no effect on the rate in the ferric sulfate test. The EPR test can provide a sensitive measure of sensitization in this range in which the weight-loss, boiling acid tests are insensitive because there are no grain droppings. This is the range of step and dual structures in the oxalic acid etch test.
2. From a  $P_a$  of 5.0–20 coulomb/ $\text{cm}^2$ , there is a transition region in which there is an increase in corrosion in the ferric sulfate test as  $P_a$  values increase. (The small overlap between dual and ditch structures falls in this range.)
3. Above about 20 coulomb/ $\text{cm}^2$ , the EPR test almost saturates; i.e., even though corrosion rates in the ferric sulfate test increase, there is essentially no increase in  $P_a$  values.

In terms of the data in Fig. 15, the requirement as mentioned above for freedom of sensitization corresponds to a requirement for a step structure in the oxalic acid etch test. Even though the oxalic acid etch is not a quantitative test, the step microstructure can be readily identified and has been used for laboratory acceptance testing in industry for more than 40 years to identify and screen acceptable material which needs no further testing in one of the boiling tests that provide quantitative data. The much simpler oxalic acid etch test also has been used as a nondestructive test on equipment in chemical plants.

### Double Loop (DL)

It has been found [22] that the problem of pitting mentioned above for the single loop EPR test can be eliminated by the use of a double loop test. This test was proposed by Akashi et al. [23] to reduce the amount of polishing

required in the field on the surface to be tested from a 1  $\mu\text{m}$  surface for the SL test to 100 grit (140  $\mu\text{m}$ ) finish for the DL test. Otherwise, the requirements for the DL test are the same as those for the SL test except for the polarization procedure and the criteria for evaluation of the results. The polarization sequence is shown in Fig. 16. The specimen is polarized anodically from the corrosion potential of about  $-400$  mV versus SCE to a potential of  $+300$  mV versus SCE at a rate of  $6$  V/h. As soon as this potential is reached, the scanning direction is reversed and the potential is decreased at the same rate to the corrosion potential. The maximum current for each loop is measured:  $I_a$  for the large anodic loop, which was generated first, and  $I_r$  for the smaller loop generated during reactivation. The measure of sensitization is the ratio of  $I_r/I_a$ .

DL data have been plotted in Fig. 17 as a function of corrosion rates in the ASTM standard ferric sulfate test and the classifications obtained in the oxalic acid etch test. They show that the current ratio is very sensitive for detecting the absence of sensitization and for differentiating mild degrees of sensitization for which the oxalic acid test shows step or dual structures. Current ratios are in the range of  $0.0001$ – $0.001$  for step structures and between  $0.001$ – $0.05$  for dual structures. Corrosion rates in the ferric sulfate test do not differentiate between these small levels of sensitization. However, for severely sensitized materials with ditch structures, current ratios become less effective in making distinctions between medium and severe levels of sensitization, while the corrosion rates vary over a wide range. These specimens have DL ratios in a wide band extending from  $0.05$ – $0.3$ .

Note that there are no overlaps in oxalic acid etch structures for any values of current ratios (Fig. 17). In contrast, two overlaps were found for the SL test (Fig. 15). The absence of an overlap in Fig. 17 indicates that nonmetallic inclusions do not affect values of current ratios in the DL test and that it is, therefore, unnecessary to examine the microstructure after the DL test. (The same specimens were used for the data in Figs. 15 and 17.)

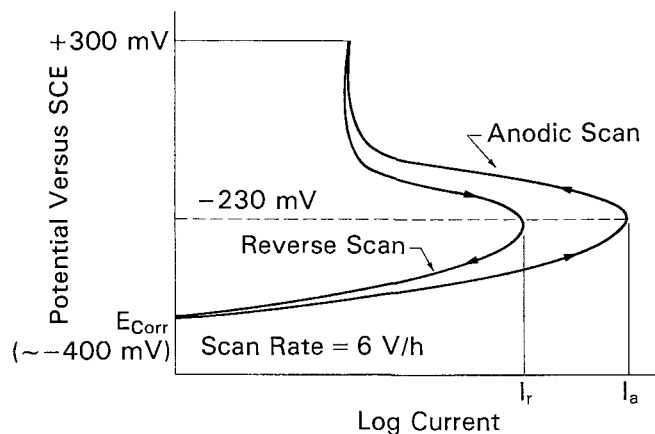


FIG. 16—Schematic diagram of the double loop EPR test. Evaluation is by the ratio  $I_r/I_a$  [22]. (©NACE International. All Rights Reserved by NACE; reprinted with permission.)

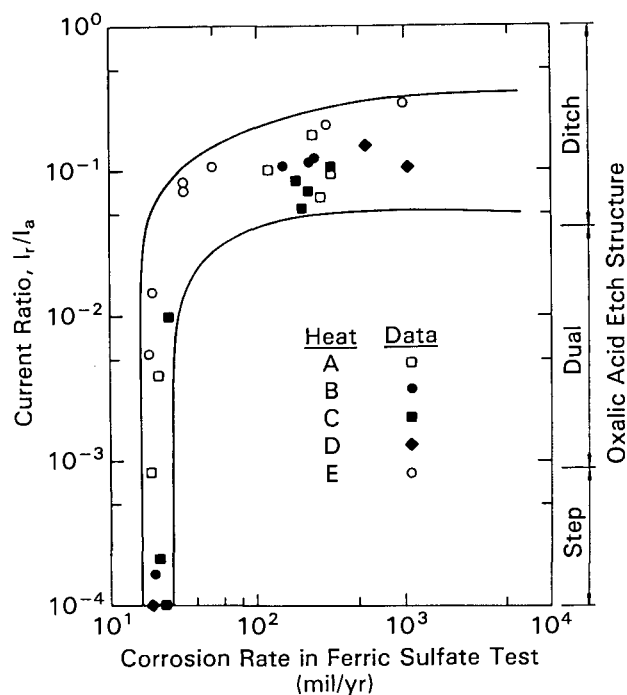


FIG. 17—Correlation of the DL test with the ferric sulfate and oxalic acid etch tests on AISI 304 stainless steels [22]. (©NACE International. All Rights Reserved by NACE; reprinted with permission.)

The advantages [22] of the DL over the SL EPR test are its relative independence not only of the surface finish, but also of the presence of nonmetallic inclusions that cause pitting in the SL test. It is more reproducible than the SL test and less sensitive to variations in scan rate and solution composition. It provides a quantitative, nondestructive method for detecting relatively mild degrees of sensitization which match the metallographic classifications obtained in the oxalic acid etch test.

Test procedures for the DL test are being considered for inclusion in ASTM G 108 as Method B, along with those for the SL test, Method A (Table 9).

## NICKEL-RICH, CHROMIUM-BEARING ALLOYS

It was known that alloy C (Table 1) could also become susceptible to intergranular attack as a result of exposure to a range of elevated temperatures. However, there was no reliable quantitative method available for detecting this condition until the publication in 1963 [24] of the results shown in Fig. 18. To demonstrate the applicability of the ferric sulfate-50 % sulfuric acid test, specimens were heat-treated for 1 h at temperatures between  $900$  and  $2450^{\circ}\text{F}$  ( $482$ – $1343^{\circ}\text{C}$ ), and tested for 24 h. (This is much shorter than the 120-h period used for Type 304 because of the 2 % lower chromium content and the 16 % molybdenum in alloy C.) It was found in the ferric sulfate test that there are two maxima in corrosion rates: one at  $1300^{\circ}\text{F}$  ( $704^{\circ}\text{C}$ ), which is

**TABLE 9**—Test methods for electrochemical reactivation (EPR) for detecting sensitization of AISI 304 and 304L stainless steels.

Designation	Test	Temperature	Testing Time	Applicability	Evaluation Method
Method A G 108	EPR-SL (Single Loop)	$30^{\circ} \pm 1^{\circ}\text{C}$	10 min	Chromium carbides in 304 and 304L	Coulombs per $\text{cm}^2$ of grain boundary area, $P_p$ . $P_p$ values $>2.0$ coulombs per $\text{cm}^2$ denote onset of sensitization. (Equivalent to Dual Structure in Oxalic Acid Etch.)
"Method B" (proposed)	EPR-DL (Double Loop)	$30^{\circ} \pm 1^{\circ}\text{C}$	15 min	Chromium carbides in 304 and 304L	Ratio of currents; $I_p/I_a$ . Values $>0.001$ denote onset of sensitization. (Equivalent to Dual Structure in Oxalic Acid Etch.)

associated with the formation of a molybdenum-rich carbide at grain boundaries, and another at 1900°F (1038°C), which is associated with a molybdenum-rich intermetallic compound, mu-phase. It is apparent from Fig. 18 that reducing acids, such as hydrochloric acid, result in high rates near 1300°F, and highly oxidizing acids, such as chromic acid, near 1900°F.

These results on the effect of heat treatments on corrosion resistance of the original (Hastelloy) alloy C are discussed here because they show clearly the different effects of molybdenum-rich carbides and molybdenum-rich mu-phase on corrosion in reducing and oxidizing acids. This alloy has been replaced during the past 30 years by a series of compositions that were designed to minimize the formation of second phases and to enhance

the general corrosion resistance in oxidizing acids, as well as the resistance to intergranular stress corrosion in chloride solutions.

The first improvements by Haynes International resulted from a reduction of the carbon (0.02 % max) and silicon (0.05 % max) contents in alloy C-276. These improvements in properties were facilitated by the application of the ferric sulfate test [25]. Reductions of the carbon and silicon contents greatly reduced the formation of both types of precipitates (Fig. 19) [26,27]. Further improvements are represented by Hastelloy alloys C-4 [25] and C-22 [28], Inconel Alloy 686 [29] and VDM Alloy 59 [30] (Table 1). At present, all but alloy 686 of this class of alloys are included in ASTM G 28 (Table 7), as well as alloys G-3, G-30, and A.L.6XN.

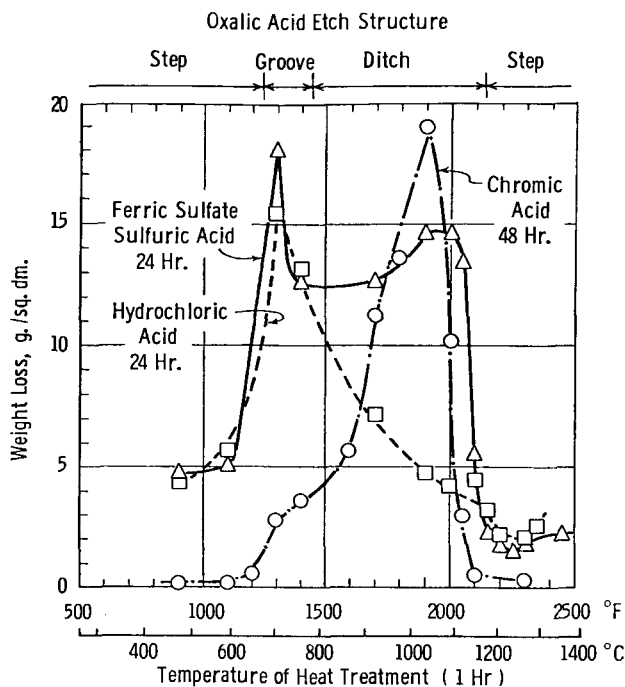


**FIG. 18**—Effect of heat treatment on corrosion and etch structures of Hastelloy alloy C. Solutions: boiling 50 % sulfuric acid with 42 g/L ferric sulfate; boiling 10 % hydrochloric acid; boiling 10 % chromic ( $\text{CrO}_3$ ) acid; specimens: 0.06 % carbon [24]. (©NACE International. All Rights Reserved by NACE; reprinted with permission.)

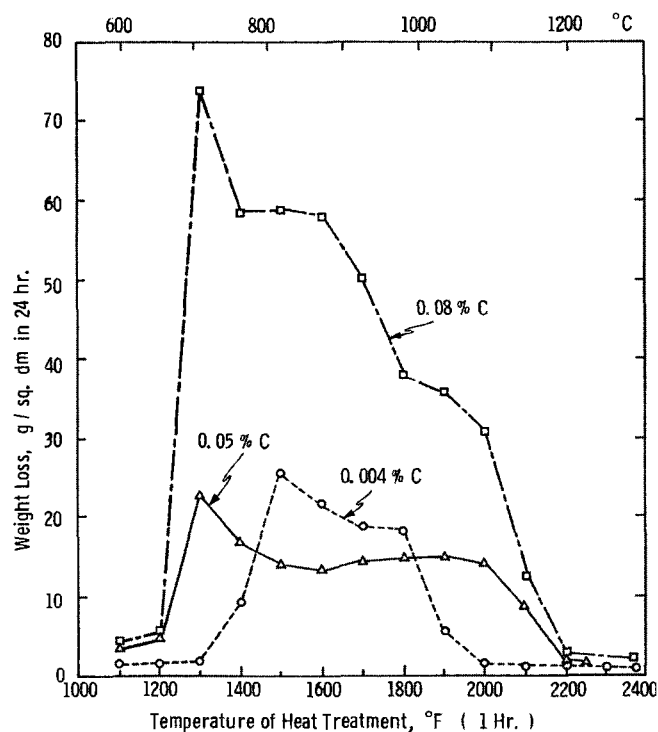


**FIG. 19**—Effect of carbon content in Ni-Cr-Mo alloys on corrosion in the ferric sulfate-50 % sulfuric acid test [25]. (©NACE International. All Rights Reserved by NACE; reprinted with permission.)

Generally, evaluation in the 50 % sulfuric acid ferric sulfate test is by weight-loss. However, on alloys C and C-276 the relatively low chromium content of about 15 % (i.e., 3 % less than in Type 304 steel) results in a somewhat high rate of general corrosion that tends to mask low rates of intergranular attack. Therefore, to establish evidence of intergranular attack, microscopic examination is recommended in ASTM G 28 to supplement the corrosion rate (weight-loss) data. The newer C-type alloys (Table 1) have 20 to 23 % chromium, and therefore do not pose this problem.

In 1974, the ferric sulfate test was applied by Brown [31] to other nickel-rich, chromium-bearing alloys and found to be applicable for detecting susceptibility to intergranular attack in alloys G, 20 Cb-3, 600, 625, 800, and 825 (Table 1). All of these alloys have been incorporated in ASTM G 28, Practice A (Table 7).

In 1985, Manning [32] proposed the use of a boiling solution of 23 % sulfuric acid, 1.2 % hydrochloric acid, 1 % cupric chloride, and 1 % ferric chloride for a 24-h test in order to provide a more sensitive measure of the presence of molybdenum-rich precipitates at grain boundaries of alloy C-276. When such precipitates are present there is severe pitting attack at grain boundaries that results in a large increase in corrosion rates. This test, which was first applicable only to wrought alloy C-276, has been incorporated in ASTM G 28 as Method B and is now also being applied to C-22 and 59 alloys. Weldments can be tested only when the welds have been annealed after welding. The test is not applicable to as-welded specimens because weld metal is severely attacked by this solution probably because of segregation of alloying elements in the dendritic structure of weld metal.

Because there are many successful applications of alloy C-276 for which weldments cannot be annealed after welding, e.g., in shop fabrication and field erection, it seems that this test may be too severe in detecting mild forms of sensitization. This is also suggested by the results with 14 different solution compositions [32]. Only two of the 14 resulted in a large increase in rates on mildly sensitized alloy C-276. The two were the Method B solution and a second version of this solution with 2.4 % hydrochloric acid in place of the 1.2 % specified for Method B. This is now used on sheets of alloy C-276 for sulfuric acid coolers to monitor the success of final annealing heat treatments. These solution-annealing treatments require heating of large objects to a relatively high temperature [2050°F (1121°C)] to dissolve precipitates and rapid enough cooling to prevent their reformation during cooling through the range of 2000° to 1000°F (1093 to 538°C).

For recent results and discussion on alloys C-276, C-22, and 682 weld metals, see item 7 in Future Developments section.

## WHEN TO EVALUATE FOR SUSCEPTIBILITY TO INTERGRANULAR ATTACK

All the stainless steels and nickel-rich alloys to which the various evaluation tests are applied (Tables 1 and 2) are relatively costly. However, for critical applications in the process and power industries, the replacement cost of alloys may be only a relatively small part of the total cost of corrosion

failures. The loss in production due to plant shutdowns can greatly exceed the costs of new equipment. For such critical applications, it is essential that the alloys be in their optimum metallurgical condition for resisting intergranular attack and other forms of corrosion associated with precipitates at grain boundaries. The laboratory equipment and apparatus required for the boiling acid tests and the oxalic acid etch test are generally available in metallurgical laboratories. Only the EPR tests require relatively costly computerized electronic equipment.

Sensitized alloys, i.e., materials containing potentially damaging precipitates at grain boundaries, may come into use on plants inadvertently when:

- (a) regular carbon Types 304 or 316 are used unknowingly in place of Types 304L and 316L for fabrication involving welding;
- (b) the final mill annealing heat treatments and quenching operations are not effective, e.g., on regular carbon grades of Type 304 and alloy 600, in dissolving chromium carbides and nitrides and intermetallic phases and keeping them in solution during cooling;
- (c) there is incomplete stabilization of titanium- or niobium-bearing alloys (Types 321, 347, alloys 625, 825, 18Cr-2Mo-Ti, and 26Cr-1Mo-Ti) either because of inadequate amounts of these elements or because of ineffective stabilizing heat treatments;
- (d) heat is applied for unscheduled forming operations during fabrication or installation of equipment;
- (e) there is interior carburization of tubes resulting from decomposition during annealing heat treatments of incompletely removed drawing lubricants;
- (f) the carbon and/or nitrogen contents of any of the extra low-carbon austenitic stainless steels, of the new high-purity ferritic iron-chromium-molybdenum alloys or of alloys C-276, C-22, 59, 686, 6XN, and G-30 exceeds the specified limits; and
- (g) in a very few certain cases, sensitized material is accepted knowingly to reduce costs or even is specified to minimize failures by stress corrosion in certain caustic environments. When it is known that there will be no intergranular attack on sensitized material by the process stream during the life of the equipment, such material may be used. It can reduce costs in three ways: (1) the regular carbon grades cost less than the extra low-carbon grades; (2) they have somewhat higher yield strengths which permit the design of smaller sections; and (3) solution-annealing treatments can be omitted.

## Testing Strategy

1. When available plant experience shows clearly that there will be intergranular or other localized attack on sensitized material, the alloy intended for such service must obviously be free of damaging grain-boundary precipitates and should, therefore, be resistant to intergranular attack in an appropriate evaluation test.
2. Only when available data from plant service or long-time plant tests show definitely that a certain plant environment does not cause intergranular attack on sensitized alloys and when it is known that the process conditions

**TABLE 10**—Corrosion rates indicating susceptibility to intergranular attack. Corrosion rates higher than those listed indicate grain dropping in unwelded specimens.

Alloy (AISI Type)	Condition	Test Practice	Time, h	Corrosion Rate	
				mil/year	mm/year
304	as-received	Nitric Acid Practice C ASTM A 262	240	12 (18) <sup>a</sup>	0.30 (0.46)
304L	20 min, 677°C		240	12 <sup>a</sup>	0.30
304L	60 min, 677°C		240	12 (24) <sup>a</sup>	0.30 (0.61)
316	as-received		240	12 (18) <sup>a</sup>	0.30 (0.46)
316L	20 min, 677°C		240	12	0.30
316L	60 min, 677°C		240	12 (24)	0.30 (0.61)
321	60 min, 677°C		240	24 <sup>a</sup>	0.61
347	60 min, 677°C		240	24 <sup>a</sup>	0.61
825	60 min, 677°C		240	36 <sup>a</sup>	0.91
304	as-received	Ferric Sulfate, Practice B, ASTM A 262	120	48 <sup>a</sup>	1.20
304L	20 min, 677°C		120	48 <sup>a</sup>	1.22
304L	60 min, 677°C		120	48 <sup>a</sup>	1.22
316	as-received		120	48 <sup>a</sup>	1.22
316L	20 min, 677°C		120	48 <sup>a</sup>	1.22
316L	60 min, 677°C		120	48 <sup>a</sup>	1.22
317L	20 min, 677°C		120	48 <sup>a</sup>	1.22
321	60 min, 677°C		120	36	0.91
430	as-received		24	540 <sup>a</sup>	13.71
446	as-received		72	120 <sup>a</sup>	3.05
Alloy C	as-received	Ferric Sulfate, ASTM G 28, Method A	24	480	12.00
Alloy C-276	as-received		24	360 (480)	9.14 (12.18)
Alloy G	as-received		120	20	0.51
Alloy 20Cb-3	as-received		120	24 <sup>a</sup>	0.61
Alloy 600	as-received		24	24	0.61
Alloy 625	as-received		120	18 (36)	0.46 (0.90)
Alloy 800	as-received		120	18	0.46
Alloy 825	as-received		120	18	0.46

<sup>a</sup>Used as acceptance rates by the du Pont de Nemours Co. When two rates are listed, the rate in parentheses is the acceptance rate.

will not change, there is no need to specify an evaluation test, or even to specify costly low-carbon grades.

But, because service life may range from ten to 40 years, the degree of sensitization that can be tolerated can be decisive. Therefore, the knowledge that sensitized material has been found to be free of intergranular attack for five to ten years in plant service can be used as a guide for future action only when there is information on the severity and type, carbide or sigma, of sensitization involved and on the effect of time on the rate of intergranular attack over the length of the expected service life.

Another example is a process in which stainless steels are used to prevent product contamination by corrosion products. In such cases, even carbon steel may have the necessary corrosion resistance from an engineering standpoint, but the corrosion products formed by the small amount of corrosion of carbon steel are not acceptable, and for this reason a stainless steel is used, e.g., to prevent discoloration of polymers on certain textile fiber plants. Finally, sensitization may not be a problem when stainless steel is used for appearance or ease of maintenance.

3. This leaves new environments for which there are no actual or even comparable data on their effects on sensitized alloys. Even when such a new environment is thought to be harmless, evaluation tests should, nevertheless, be applied to assure optimum metallurgical conditions. There have been a number of costly corrosion failures on material sensitized by welding when exposed

to previously unknown factors, such as oxygen in water at elevated temperatures. Also, when the original environment is known not to cause intergranular attack on sensitized alloys, there may be changes later in process conditions which may cause such attack.

Information on "acceptable" and "nonacceptable" corrosion test results has been given for the two EPR tests in the section above on these tests. Acceptable etch structures (step, and in some cases, dual) are also identified for the oxalic acid etch test. The absence of fissures in bends after certain copper sulfate tests is considered an indication of acceptable results. However, in the case of weight-loss tests (nitric acid, ferric sulfate, and certain copper sulfate tests) the standard ASTM test methods merely show how corrosion rates are calculated without identification of rates which are evidence of the onset of susceptibility to intergranular attack.

Data on corrosion rates in the nitric acid and the ferric sulfate-sulfuric acid tests that are indicative of the onset of enough intergranular attack to dislodge grains from the surface (sugaring) during the specified testing times are given in Table 10 for a group of alloys. Most of these rates are being used as a cut-off for acceptance of material for use on plant equipment. However, for some of these alloys these rates have proven to be unnecessarily low. In these cases it has been found that considerably higher rates can safely be used for industrial applications. These rates are also shown in Table 10.

The following references provide some examples of major applications of evaluation tests and of problems associated with sensitization. The uses of evaluation tests for the study of the effects of complex microstructures on corrosion have been illustrated in a detailed investigation of titanium stabilized, Type 321 stainless steel [33]. Industrial experience at Du Pont with the application of evaluation tests to more than 10 000 specimens of Type 300 series steels has been reported by Brown [34]. On the subject of IGSCC at weldments of Type 304 stainless steel piping on boiling water nuclear plants, a detailed report is available from the U.S. Nuclear Regulatory Commission [35], which provides information on the origin and extent of the problem, remedial procedures, and the selection of replacement alloys.

## FUTURE DEVELOPMENTS

The numerous tests in ASTM A 262, A 763, and G 28 are the results of the introduction of a great number of commercial stainless alloys over a period of about 80 years and the development of a great variety of methods for determining susceptibility to intergranular attack in these alloys. (The accidental discovery of both the ferritic and austenitic stainless steels in 1912 and the subsequent evolution of various stainless alloy compositions have been described in Ref 36.) The result has been considerable overlap in tests; e.g., Types 304 and 304L stainless steels, which are produced in the largest tonnage of all of the alloys listed in Tables 1 and 2, can be evaluated in the nitric acid, oxalic acid, ferric sulfate-sulfuric acid, and copper sulfate tests, and even the EPR tests. Simplifications in the test programs could be made by removing alloys that are no longer of commercial importance from the lists and by removing tests that are rarely or no longer used. Also, changes in production of alloys, such as the introduction of argon-oxygen refining for reducing the carbon contents to the range of 0.01 to 0.02 %, can and have resulted in greater "resistance to sensitization" in Type 304L and other alloys. As a result, a greater proportion of test specimens are found acceptable in the simple and rapid oxalic acid etch test, and therefore do not have to be tested in the boiling acid or EPR tests.

The following are some initial steps that would further simplify the test program:

1. Remove the Nitric Acid Test from ASTM A 262 and establish it as a separate ASTM Test: At present, the boiling 65 % nitric acid test (Practice C) is specified for materials to be used in nitric acid service. Only this test is sensitive to sigma-phase in molybdenum-bearing austenitic stainless steels. Also, problems such as end-grain corrosion associated with hexavalent chromium derived from corrosion products are unique to this solution. While this test also detects susceptibility to intergranular attack associated with chromium carbide precipitates, there are other tests that perform this function in less time and with greater simplicity.

Thus, the nitric acid test should be used primarily as a kind of simulated service test for alloys to be used in nitric acid environments. This is a return to its original function as defined by Huey [4]. When used in this way, it will be

essential to specify the test apparatus, including the condenser, the ratio of surface area of test specimens to solution volume, and the number of changes of solution to provide a close simulation of the severity of the hexavalent chromium problem which the material being tested is to encounter in plant service. In ASTM A 262, Practice C, a wide-mouth Erlenmeyer Flask with a cold finger condenser (Fig. 7) is recommended for the nitric acid test.

It has been shown [14] that this condenser results in lower corrosion rates than the Allihn condenser. The lowest rates are obtained with (glass) apparatus in which there is continuous flushing of (chromium) corrosion products [6,14]. A design for such conditions has also been provided by Corbett [38]. In this apparatus, up to 100 specimens can be tested simultaneously with corrosion products kept so low that the test simulates a "once through" industrial application.

2. Drop the Single Loop EPR Test: If and when the double loop version of the EPR test is approved for inclusion in ASTM G 108, the single loop version can be dropped due to the greater clarity of the results and simpler test procedures for the double loop as compared to the single loop (see section, EPR Tests).
3. Apply EPR Tests to Castings in ASTM G 108: Because of the relatively large grains in castings, it takes longer to undermine grains (and register corrosion as weight-loss) on sensitized castings than on the small-grained, wrought stainless steels. Therefore, much longer testing times are needed for castings in the ferric sulfate-50 % sulfuric acid test, perhaps two or three times 120 h; or two or three times the 240 h used for the 65 % nitric acid test [9].

To reduce greatly the time required for testing of castings, consider the inclusion in ASTM G 108 of the double loop practice to cast alloy CF-8 as described by Reichert and Stoner [39] and Sydow et al. [40]. By applying the double loop EPR test to cast alloys such as CF-8 and CF-3 (the cast equivalents of Types 304 and 316), quantitative data on sensitization may be obtained in less than an hour.

The application of an EPR test to castings to provide rapid, quantitative data on sensitization may prove to be the main use of the EPR technique.

4. Consider the Use of a Simplified EPR Test: Such a test has been proposed in Ref 41. It is based on the maximum current measured for the reactivation loop (Fig. 14) which is proportional to the area within the loop, and therefore to  $Q$ , the total charge.

Attempts to assess sensitization in Type 304 alloy by means of 5–15 min potentiostatic electrochemical tests in solutions that simulated exactly the plant conditions have been shown to be invalid [42]. This testing period is much too short for testing in simulated service conditions, i.e., the electrode potential applied to the specimen in the laboratory test, the solution compositions, and temperature were the same as those to be used in plant service. Thus, there was no accelerating factor in the laboratory test and it would have had to be just as long as a plant test, perhaps 3–12 months, to determine whether or not the material would be subject to intergranular attack in plant service.

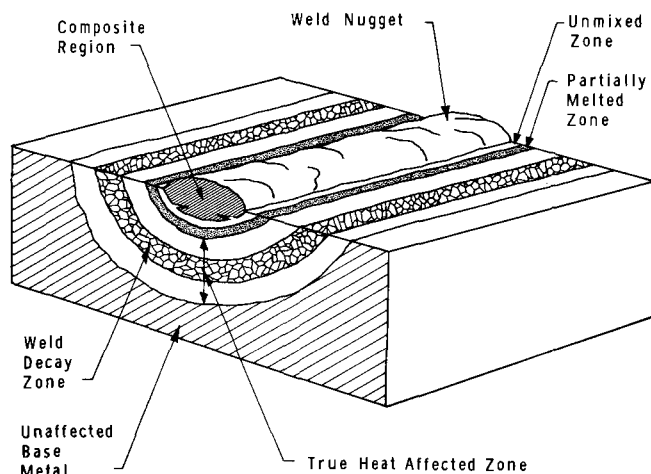


**FIG. 20—Schematic diagram of components of weldments in austenitic stainless steels. Diagram based on findings of W. F. Savage [43].**

5. Eliminate the Two Copper Sulfate Tests with 6 % Sulfuric Acid, Practice E in A 262 and Practice Z in ASTM A 763 (Tables 5 and 6): Similar results can be obtained with the 50 % sulfuric acid-copper sulfate tests, Practice F in ASTM A 262 and Practice Y in ASTM A 763.

At present, the copper sulfate test with 50 % acid is specified in ASTM A 763 only for ferritic alloys with 25 % or more chromium. Tests on Type 430 (14–18 % chromium) [37] and on Type 321 (17–19 % chromium) steels [33] show that the 50 % acid test is also applicable to these alloys. Thus, Practices Z in ASTM A 763 and E in ASTM A 263 could be eliminated. All remaining copper sulfate tests (Practices F and Y) would then be in 50 % acid solution.

6. Establish criteria for evaluation of weldments. The various components of weldments are shown in Fig. 20, which is based on the classification scheme of W. F. Savage [43]. The weld nugget or the composite region contains the bulk of filler metal which is somewhat diluted with material melted from surrounding base metal. Adjacent to the nugget is a zone of base metal that melted and solidified during welding without experiencing mechanical mixing with the filler metal, the unmixed zone. In these two regions, there is complete melting, resulting in a cast structure. Beyond this weld interface, there is a partially melted zone within which the proportion melted ranges from 100–0 %. The heat-affected zone is that portion of the base metal within which all microstructural changes produced by welding occur in the solid state. The maximum temperature reached in the heat-affected zone is highest near the molten zone and decreases with distance from this interface.

As shown in Fig. 6, the weld decay zone which contains chromium carbide precipitate is not adjacent to the cast metal, but at some distance from it, in austenitic stainless steels. The reason for this is that the temperature of the metal in the zone adjacent to the molten zones has been

raised above the chromium carbide precipitation range. During cooling, the precipitation range is traversed from above. It has been shown [25] that carbide precipitation is much slower when the sensitizing range is entered from above. Thus, both because of this factor and because the total time in the precipitation range is relatively short, there is no carbide precipitate in the zone adjacent to the partially melted zone. In the weld decay zone, the metal is heated into the carbide precipitation range, and the time in this range is longer than that of the zone adjacent to the partially melted zone [44]. Beyond the weld decay zone, the temperature remains below the sensitizing range during the welding operation.

In effectively stabilized austenitic stainless steels (Types 321 and 347), there is no weld decay zone (Fig. 6). However, immediately adjacent to the partially melted zone, the temperature is so high that the titanium or niobium carbides are dissolved in the solid solution before rapid cooling through the sensitizing range. As in the case of unstabilized steels, cooling from above the sensitizing range is rapid enough to keep the carbon in solid solution and is too rapid to form titanium or columbium carbides. However, when weldments in stabilized steels are later heated into the sensitizing range, for example, during a stress-relieving treatment or another weld pass, chromium carbides form, and this zone becomes sensitized. Exposure to certain acid solutions results in intergranular attack in a narrow zone next to the partially melted zone, knife-line corrosion [45]. It can be prevented by heating the weldment at 900°C to react the stabilizing element with carbon to form niobium or titanium carbides. As a result, there is no carbon available to form chromium carbides during subsequent exposure in the carbide precipitation range, 430–870°C.

Figure 21 illustrates intergranular attack on an autogenous weldment (made with tungsten electrode without filler metal) in a ferritic, 29Cr-4Mo, alloy with a nitrogen content that greatly exceeds the maximum permissible concentration of 200 ppm. Intergranular attack takes place in the melted metal and in a narrow zone immediately adjacent to it. Apparently, the high temperatures in these zones resulted in the slowest rates of cooling through the sensitizing range (Fig. 22) and the precipitation of chromium nitrides at grain boundaries.

When weldments are made to simulate fabrication welds or when they are part of the tube producing process, they then contain the very components that will be exposed in service, the same compositions, structures, and thermal cycles. Any evidence of intergranular attack in any of the components of the weldments will, therefore, be an indication of susceptibility during long time exposure in those service environments that are known to cause such attack on sensitized material. Because of this, assessment of weldments after exposure in laboratory evaluation tests must be based on very strict criteria for the onset of intergranular attack. Such criteria include the appearance of fissures on specimens bent after testing and evidence of dropped grains. Weight loss measurements are generally too insensitive to detect intergranular attack confined to narrow zones of a weldment. To implement this method of assessing corrosion on weldments, tests are needed in nitric, ferric sulfate, and cupric sulfate solutions on weldments prepared



**FIG. 21—Intergranular attack on weldment in ferritic stainless steel caused by high nitrogen content (5 $\times$ ). Autogenous weld in 28.5 %Cr-4.2 %Mo alloy with 22 ppm carbon and 388 ppm nitrogen after exposure in ferric sulfate-50 % sulfuric acid test.**

by the various methods applicable to each alloy for which the new assessment criteria are to be established. In addition, where applicable, the results should be compared with the oxalic acid etch structure of the weldment on cross sections perpendicular to the weld bead.

In some cases, there is preferential attack on weld filler metal in austenitic stainless steels related to its ferrite content.

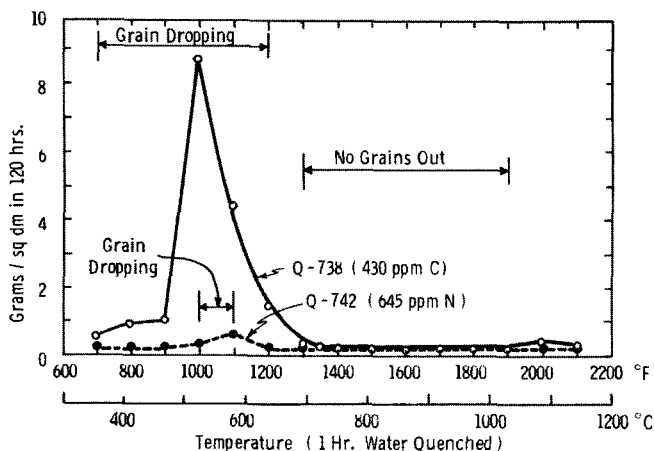


**FIG. 22—Effect of heat treatment on intergranular corrosion of Fe-29 %Cr-4 %Mo alloy. Specimens: heat treatment 1 h as shown, water-quenched. 2.5 by 2.5 by 0.2 cm. Q-738: 40 ppm nitrogen; Q-742: 120 ppm carbon. Solution: boiling ferric sulfate-50 % sulfuric acid.**

R. W. Gurry et al. [46] have found that chloride-containing acids, strong organic acids, and sulfuric acid preferentially attack weld metal containing more than about 5 % ferrite, whereas the oxidizing acids, nitric and ferric sulfate-sulfuric acid, used in evaluation tests do not cause preferential attack on ferrite-bearing weldments. Removal of the ferrite by cold-working and annealing eliminates this form of preferential attack. Thus it may be possible to screen weldments for service in reducing acids by microscopic (oxalic acid etch) testing for the presence of ferrite. To establish a series of standard etch structures for evaluation, comparisons are needed between etch structures containing various amounts of ferrite and the corrosion in reducing acids of these same weldments.

7. Testing Weld Metal of Alloys C-276, C-22, and 686: In the previous section, Nickel-Rich, Chromium-Bearing Alloys, tests with Practice B in ASTM G 28 are discussed. Twenty-four hour tests in a boiling mixture of sulfuric and hydrochloric acids with cupric and ferric chloride are used as a very sensitive method for detecting the presence of molybdenum-rich precipitates in wrought alloys C-276, C-22, and 686. Practice B is considered too severe for as-welded material because it fails by pitting in the dendritically segregated, cast structure of the weld deposit. High-temperature annealing treatments (2050°F, 1121°C) eliminate this problem [32].

In a recent investigation of the corrosion resistance of as-welded C-276, C-22, and alloy 686 specimens, Saldanha [47] has shown that such weld metal is also susceptible to rapid and severe pitting in a simulated plant solution, boiling 80 % acetic acid with 1000–5000 ppm ferric chloride. There was severe pitting on all three alloy weldments; see Fig. 23 for pitting in C-276 weld metal in only five days of testing. There was no attack in the heat-affected zones or in the base-plate. Thus, there are plant environments in which

**FIG. 23—Alloy C-276 plate with C-276 weld metal (7 $\times$ ). Pitting attack in weld deposit after exposure of five days in boiling 80 % acetic acid with 1000 ppm ferric chloride. No attack in heat-affected zones or on base plate [47].**



as-welded C-276, C-22, and alloy 686 may be susceptible to rapid localized attack in service. For such applications welded equipment must be annealed. Practice B tests on weldments provide a needed tool for acceptance testing in addition to the process control application on wrought sheet as described in the above-mentioned section.

Additional investigations are needed to establish the limits of use of as-welded C-276, C-22, and alloy 686 and the extent to which Practice B should be specified as a requirement for acceptance testing of weldments. Practice B may also serve as a tool for the development of new weld-rod compositions which result in welds that can be used without post-weld annealing treatments for use in environments that are known to cause pitting of alloys C-276, C-22, and 686 weld-deposits. Such new compositions are needed especially for field welding of equipment that cannot be annealed.

## Acknowledgments

The author would like to thank F. Galen Hodge and Stephen Corey, Haynes International, Inc., Kokomo, Indiana; Robert F. Steigerwald, Bechtel, San Francisco, California; and John R. Scully, University of Virginia, Charlottesville, Virginia, for information on current developments. He also expresses his appreciation and thanks to Brian J. Saldanha, E. I. DuPont Co., Wilmington, Delaware, for making the results of his recent tests on alloys C-276, C-22, and 686 weldments available for inclusion in this chapter.

## REFERENCES

- [1] Streicher, M. A., "Intergranular Corrosion," *Encyclopedia of Electrochemistry*, C. A. Hampel, Ed., Reinhold Publishing Corp., NY, 1964, pp. 720-723 (published with permission).
- [2] McLean, D., *Grain Boundaries in Metals*, The Clarendon Press, Oxford, 1957.
- [3] Roald, B. and Streicher, M. A., *Journal of the Electrochemical Society*, Vol. 97, 1950, pp. 283-289.
- [4] Huey, W. R., *Transactions of the American Society of Steel Treating*, Vol. 18, 1930, p. 1126.
- [5] Monypenny, J. H. G., *Stainless Iron and Steel*, Vol. 1, Chapman and Hall, Ltd., London, 1951, p. 99.
- [6] Streicher, M. A., *Journal of the Electrochemical Society*, Vol. 106, 1959, pp. 161-180.
- [7] Binder, W. O. and Brown, C. M., "Influence of Carbon and Molybdenum on the Intergranular Corrosion Resistance of Austenitic Chromium-Nickel Steels With and Without Columbium," *Symposium on Evaluation Tests for Stainless Steels*, ASTM STP 93, ASTM International, West Conshohocken, PA, 1949, pp. 146-182.
- [8] Fontana, M. G., *Corrosion Engineering*, 3rd ed., McGraw-Hill Book Co., New York, 1986, p. 82.
- [9] Streicher, M. A., "Theory and Application of Evaluation Tests for Detecting Susceptibility to Intergranular Attack in Stainless Steels and Related Alloys—Problems and Opportunities," *Intergranular Corrosion of Stainless Alloys*, ASTM STP 656, R. F. Steigerwald, Ed., ASTM International, West Conshohocken, PA, 1978, pp. 3-84.
- [10] Hatfield, W. H., *Journal of the Iron and Steel Institute*, Vol. 127, 1933, pp. 380-383.
- [11] Strauss, B., Schottky, H., and HinnÜber, J., *Zeitschrift für Anorganische Allgemeine Chemie*, Vol. 188, 1930, pp. 309-324.
- [12] Aborn, R. H. and Bain, E. C., *American Society for Steel Treating*, Vol. 18, 1930, pp. 837-893.
- [13] DeLong, W. B., "Testing Multiple Specimens of Stainless Steels in a Modified Boiling Nitric Acid Test Apparatus," *Symposium for Evaluation Tests for Stainless Steels*, ASTM STP 93, ASTM International, West Conshohocken, PA, 1949, pp. 211-216.
- [14] Streicher, M. A., "The Effect of Condenser Design on the Corrosion of Stainless Steels in Nitric Acid," Paper 87, Corrosion/1980, NACE, Chicago, March 1980.
- [15] Rocha, H. J., *Stahl und Eisen*, Vol. 75, 1955, p. 579; and Vol. 70, 1950, pp. 608, 609.
- [16] Streicher, M. A., *Corrosion*, Vol. 29, 1973, pp. 337-362.
- [17] Streicher, M. A., ASTM Bulletin No. 229, ASTM International, West Conshohocken, PA, 1959, pp. 77-86.
- [18] Streicher, M. A., ASTM Bulletin No. 188, ASTM International, West Conshohocken, PA, February 1953, pp. 35-38.
- [19] Warren, D., ASTM Bulletin No. 230, ASTM International, West Conshohocken, PA, May 1958, pp. 45-56.
- [20] Clarke, W. L., Cowan, R. L., and Walker, W. L., "Comparative Methods for Measuring Degree of Sensitization in Stainless Steels," *Intergranular Corrosion of Stainless Alloys*, ASTM STP 656, R. F. Steigerwald, Ed., ASTM International, West Conshohocken, PA, 1978, p. 99.
- [21] Majidi, A. P. and Streicher, M. A., *Corrosion*, Vol. 40, 1984, pp. 393-408.
- [22] Majidi, A. P. and Streicher, M. A., *Corrosion*, Vol. 40, 1984, pp. 584-592.
- [23] Akashi, M., Kawamoto, T., and Umemura, F., *Corrosion Engineering (Japan)*, Vol. 29, 1980, p. 163.
- [24] Streicher, M. A., *Corrosion*, Vol. 19, 1963, pp. 272t-284t.
- [25] Streicher, M. A., *Corrosion*, Vol. 32, 1976, pp. 79-93.
- [26] Hodge, F. G., *Corrosion*, Vol. 29, 1973, p. 375.
- [27] Hodge, F. G. and Kirchner, R. W., *Corrosion*, Vol. 32, 1976, p. 332.
- [28] Manning, P. E. and Schoebel, J. D., *Werkstoffe und Korrosion*, Vol. 37, 1986, p. 137.
- [29] Crum, J. R. and Schoemaker, L. E., "Advances in Molybdenum-Bearing, Corrosion Resistant Alloys for FGD Service," Paper 423, Corrosion/93, New Orleans.
- [30] Agarwal, D. C., Heubner, U., and Herda, W., "Corrosion Characteristics and Applications of Newer High and Low Nickel Containing Ni-Cr-Mo Alloys," Paper 179, Corrosion/91, Cincinnati, OH, 1991.
- [31] Brown, M. H., *Corrosion*, Vol. 25, 1969, pp. 438-443.
- [32] Manning, P. E., "An Improved Intergranular Corrosion Test for Hastelloy Alloy C-276," *Laboratory Corrosion Tests and Standards*, ASTM STP 866, G. S. Haynes and R. Baboian, Eds., ASTM International, West Conshohocken, PA, 1985, pp. 437-454.
- [33] Streicher, M. A., *Corrosion*, Vol. 20, 1964, pp. 57t-72t.
- [34] Brown, M. H., *Corrosion*, Vol. 30, 1974, pp. 1-12.
- [35] Bush, S. H., "Investigation and Evaluation of Stress Corrosion Cracking in Piping of Boiling Water Reactor Plants," NUREG-1061, Vol. 1, U.S. Nuclear Regulatory Commission, Washington, DC 20555, August 1984.
- [36] Streicher, M. A., "Stainless Steels: Past, Present and Future," *Stainless Steels '77*, Climax Molybdenum Co., August 1978, pp. 1-34; *The Metallurgical Evolution of Stainless Steels*, F. B. Pickering, Ed., The American Society for Metals, 1979, pp. 442-475; *Corrosion*, Vol. 30, 1974, pp. 77-91, 115-124.
- [37] Streicher, M. A., *Corrosion*, Vol. 29, 1973, pp. 337-360.
- [38] Corbett, R. A., "Using Multisample Test Apparatus for the ASTM A 262, Practice C Nitric Acid Corrosion Testing of Types 304 and 304L Stainless Steels," *Corrosion Testing and Evaluation, Silver Anniversary Volume*, ASTM STP 1000, R. Baboian and S. W. Dean, Eds., ASTM International, West Conshohocken, PA, 1990, pp. 335-347.
- [39] Reichert, D. L. and Stoner, G. E., *Journal of Electrochemical Society*, Vol. 137, 1990, pp. 411-413.

- [40] Sydow, J. P., Reichert, D. L., and Stoner, G. E., *Materials Performance*, January 1991, pp. 68–70.
- [41] Majidi, A. P. and Streicher, M. A., *Nuclear Technology*, Vol. 75, 1986, pp. 356–369.
- [42] Streicher, M. A., *Corrosion Science*, London, Vol. 9, 1969, pp. 53–56; and Vol. 11, 1971, pp. 275–276.
- [43] Savage, W. F., “New Insight into Weld Cracking and a New Way of Looking at Welds,” *Welding Design and Engineering*, December 1969.
- [44] Henthorne, M., *Corrosion*, Vol. 30, 1974, pp. 39–46.
- [45] Fontana, M. G., *Industrial and Engineering Chemistry*, Vol. 44, 1952, pp. 87A–90A.
- [46] Gurry, R. W., Jacob, E. M., and Allen, S. H., *Industrial and Engineering Chemistry, Product Research and Development*, Vol. 10, 1971, pp. 112–119.
- [47] Saldanha, B. J., DuPont Experimental Station, Wilmington, DE, Private communication with author, February 1995.

# Exfoliation

Donald O. Sprowls;<sup>1</sup> revised by Kevin R. Cooper<sup>2</sup>

## EVALUATION OF EXFOLIATION CORROSION

HISTORICALLY, exfoliation corrosion problems have been associated principally with high-strength aluminum alloys used in aircraft construction and by the U.S. Department of Defense. This chapter, therefore, will deal mainly with test procedures developed for alloys of aluminum.

### Basic Principles

Exfoliation is defined in ASTM G 15, Terminology Relating to Corrosion and Corrosion Testing, as a form of “corrosion that proceeds laterally from the sites of initiation along planes parallel to the surface, generally at grain boundaries, forming corrosion products that force metal away from the body of the material, giving rise to a layered appearance.” An example is shown in Fig. 1.

For a metal to exfoliate, a highly directional grain structure is necessary along with electrochemically active corrosion paths parallel to the metal surface. The severity of exfoliation in susceptible materials is influenced to a marked degree by environmental conditions [1]. Figure 2 shows the broad range of behavior of a particular material in different types of atmospheres [2]. Taking an example from service, it is recognized that forged motor truck wheels made of an aluminum copper alloy (AA2024-T4) give corrosion-free performance for many years in the warm dry climates of the southern and western United States, but they exfoliate severely in only one or two years in the northern states where deicing salts are used on the highways during the winter months [3].

### Susceptible Metal Alloy Systems

#### Aluminum

Exfoliation corrosion of aluminum is an industrial problem chiefly with the higher strength AA2XXX, AA5XXX, and AA7XXX alloy wrought products in which the grains of metal are elongated during manufacture. The alloy typically is in a temper that is susceptible to dominant intergranular corrosion. The severity of the exfoliation will depend not

**FIG. 1—Three degrees of resistance to exfoliation produced by variations in heat treatment of a AA2024 alloy extruded 13-mm thick bar. T/10 and T/2 are designations for the interior machined test surfaces (refer to the subsection, Test Specimens, in this chapter). The stepped specimens were exposed for 55–61 months in an industrial environment at Brookfield, IL [3]. (Reprinted with permission from EMAS, Ltd., U.K.)**

only on the extent to which the grains have been elongated, but also to the continuity of the anodically active paths and to the environmental conditions. These materials also have a low resistance to environment-assisted cracking when stressed in the short transverse direction, and the two phenomena may be mutually accelerating when short transverse tension stresses are involved [3,4]. A more detailed discussion of the importance of the macrostructure of the exfoliation test specimens is given in Refs 3–4 and in the ASTM G 112, Standard Guide for Conducting Exfoliation Corrosion Tests in Aluminum Alloys.

Exfoliation also can occur in the directional fragmented grain structure of severely cold-rolled products of certain lower strength strain-hardening alloys of the AA3XXX and

<sup>1</sup>Consultant; retired, Alcoa Technical Center, Alcoa Center, PA 15069.

<sup>2</sup>Research Scientist, Luna Innovations, Inc., 705-A Dale Ave, Charlottesville, VA 22903.

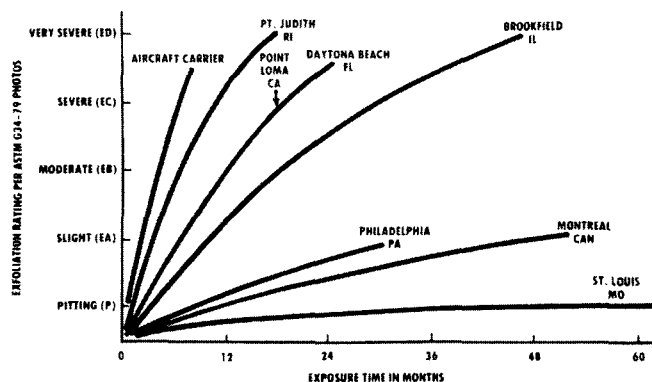


FIG. 2—Influence of environmental conditions on the exfoliation corrosion of a material with a low resistance to exfoliation. AA2124-T351 rolled 51-mm thick plate rated ED in the standard EXCO test, ASTM G 34 [2].

AA5XXX families. The anodic corrosion path in these materials is not in the grain boundaries, but rather it is in deformation bands of aluminum or Al-Mg solid solutions interspersed between relatively cathodic strata of Al-Mn and/or Al-Cr phases depending on the composition of the alloy and the thermal history during processing. Although this form of intragranular exfoliation corrosion rarely presents industrial problems, it is possible, however, as a result of inappropriate ingot homogenizing thermal treatments, to encounter exfoliation susceptibility of severely cold-rolled products in aggressive environments [3].

Severe exfoliation has been reported with graphite/aluminum metal matrix composites in marine environments [5]. Localized corrosion along wire-wire and wire-foil diffusion bonds resulted in disbondment of the precursor wires and aluminum foils. See also the discussion by Hihara on corrosion of metal-matrix composites in Section VI of this manual.

### Other Metals

Although exfoliation corrosion has been reported in a few other metal systems, incidents of this form of corrosion are few and presumably not of practical importance. Therefore, no attempts have been made to develop and standardize specific tests for detecting susceptibility to exfoliation for these other metals. The following notes from published literature may be of interest to some readers.

"A peculiar form of attack (exfoliation) has been reported with 80/20 or 70/30 cupro-nickel tubes in high-pressure feed-water heaters. A severe form of general corrosion on the steam side consists of an exfoliating scale mainly of a mixture of metal oxides in the same proportions as the metals present in the alloy. The attack has only been observed on tubes heated intermittently and the mechanism is obscure . . . materials which are immune are copper or 90/10 cupro-nickel" [6].

Wrought iron, produced by piling several plates on top of one another, subjected to heat, and passed through a rolling mill, develops zones that behave differently from one another when subjected to corrosive conditions. Evans considers this zonal corrosion of wrought iron to have much in common with the layer corrosion (exfoliation) of light alloys [7].

An experimental magnesium-base alloy sheet containing 14 % lithium and 2 % aluminum was reported to have experienced intergranular layer attack similar to the exfoliation of aluminum-copper alloys [8].

## Test Procedures for Aluminum Alloys

### Relation to Service Conditions

Laboratory corrosion tests for exfoliation corrosion susceptibility are a necessary tool for research and quality control engineers; however, the validity of such accelerated tests depends on their relationship to realistic service conditions and their sensitivity to various degrees of susceptibility. The tests must be discriminating and yet not so severe as to be unrealistic. For the majority of engineered structures, exposure to outdoor atmospheres provides a baseline that is representative of many service conditions, except for structures that are subjected to unusual chemical environments. Experience has shown that seacoast conditions are more corrosive to aluminum alloys than inland urban and industrial conditions (see Fig. 2), and seacoast atmospheric exposure tests have been particularly useful for the validation of accelerated exfoliation tests [9].

Accelerated tests do not precisely predict long-term corrosion behavior; however, answers are needed quickly in the development of new materials. For this reason, accelerated tests are used to screen candidate alloys before conducting atmospheric exposures or other field tests. They also are used for production control of exfoliation-resistant heat treatments for the AA2XXX, AA5XXX, and AA7XXX aluminum alloys. ASTM has standardized several laboratory tests for susceptibility to exfoliation corrosion in recent years.

### Selection of Appropriate Test Procedures

Selection of the most appropriate test procedure(s) depends on the type of alloy to be tested, the anticipated service environment, and the purpose of the test.

When testing an experimental alloy or product form, one would normally select a procedure known to be applicable to a similar commercial alloy. The investigator is cautioned, however, that even a small difference in alloy chemistry or changes in processing method can markedly affect the resistance to exfoliation of the new material and the appropriateness of a specific test method. Therefore, when investigating a new type of material, it is advisable to initially use more than one laboratory test procedure and compare the test results. If they do not agree, determine which procedure is the most applicable by conducting a seacoast atmospheric exposure. It is unrealistic to expect a single laboratory test to be applicable to all materials and purposes [2]. The known applicability of each of the standardized test procedures is discussed below.

These several tests, developed by the producers of aluminum alloys and U.S. Government laboratories, have been used mainly for research and alloy development. Certain test procedures are also used for production control of exfoliation-resistant materials. If they are considered for quality assurance purposes, however, limits of acceptable performance should be the subject of an agreement between concerned parties.

**Salt Spray (Fog) Tests**—Three different cyclic acidified salt spray tests have been widely used for exfoliation testing in the aluminum and aircraft industries. These are described in Annexes A2, A3, and A4 in ASTM G 85, Practice for Modified Salt Spray (Fog) Testing. The three practices are not equivalent, and the user should determine which one is best suited for the alloy and application under investigation. The following notes were taken from the ASTM G 112, which contains additional details regarding their usage:

- Annex A2 describes a cyclic salt spray test (MAST-MAASIS) that uses a 5 % sodium chloride solution acidified to pH 3 with acetic acid in a spray chamber at a temperature of 49°C (120°F). This test is applicable for exfoliation testing of AA2XXX (dry-bottom operation) and AA7XXX (wet-bottom operation, that is, with approximately 25 mm (1 in.) of solution present in the bottom of the test chamber) aluminum alloys with test duration of 1–2 weeks. Results with AA7075 and AA7178 alloys in various metallurgical conditions have been shown to correlate well with results obtained in a seacoast atmosphere (four-year exposure at Point Judith, RI) [9]. The exfoliation behavior of lithium-containing aluminum alloys AA2090-T8, AA2091-T3 and T8 and AA8090-T8 obtained with dry bottom MASTMAASIS agree with marine environments [10–12]. There is no record of this test being unrealistically aggressive, that is, causing exfoliation of a material that did not exfoliate at the seacoast.
- Annex A3 describes a cyclic salt spray test (SWAAT) that uses a different exposure cycle and a 5 % synthetic sea salt solution acidified to pH 3 with acetic acid in a spray chamber at a temperature of 49°C (120°F). This test is applicable to the production control of exfoliation-resistant tempers of the AA2XXX, AA5XXX, and AA7XXX aluminum alloys. Wet-bottom operating conditions are recommended with test durations of 1–2 weeks [13,14].
- Annex A4 describes a salt-sulfur dioxide (SO<sub>2</sub>) spray test that uses either 5 % sodium chloride or 5 % synthetic sea salt solution in a spray chamber at a temperature of 35°C (95°F). The spray may be either cyclic or continuous, which, along with the type of salt solution and test duration, is subject to agreement between the purchaser and the seller. This test, which was developed to simulate the hostile environment on the deck of an aircraft carrier, reproduces in two weeks the exfoliation attack on susceptible AA2XXX and AA7XXX aluminum alloys that occurs on a carrier in about eight months [2]. However, the sulfur dioxide salt spray does not well reproduce the exfoliation behavior of aluminum lithium alloys AA2020, AA2090 and AA8090 observed when exposed to the environment encountered on aircraft carriers [15,16].

**Immersion Tests**—Continuous total immersion tests were developed more recently to provide simpler, rapid, and more reproducible test methods than the salt spray tests. Although plain sodium chloride solutions do not cause exfoliation during the desirable short periods of immersion, formulations of chloride-nitrate solutions were found that produced severe exfoliation of highly susceptible alloys of various types in only one to four days. Optimum test conditions differed for separate alloy families [1].

ASTM G 66, Method for Visual Assessment of Exfoliation Corrosion Susceptibility of AA5XXX Series Aluminum Alloys (ASSET Test), describes a procedure for the continuous immersion exfoliation testing of AA5XXX alloys containing 2.0 % or more magnesium. Specimens are immersed for 24 h at 65°C (150°F) in a solution containing 1.0 M ammonium chloride, 0.25 M ammonium nitrate, 0.01 M ammonium tartrate, and 0.09 M hydrogen peroxide. This method provides a reliable prediction of the exfoliation corrosion behavior of AA5XXX alloys in marine environments including seawater [17,18]. This test is useful for alloy development studies and quality control of mill products such as sheet and plate.

ASTM G 34, Method for Exfoliation Corrosion Susceptibility in 2XXX and 7XXX Series Aluminum Alloys (EXCO Test), provides an accelerated test for AA2XXX and AA7XXX aluminum alloys by continuous immersion of test materials in an aqueous solution containing 4 M sodium chloride, 0.5 M potassium nitrate, and 0.1 M nitric acid at 25°C (77°F) (with a starting pH of 0.4 rising to 3.2 during the first 7–20 h of exposure) for periods of 24–48 h. “This test method is primarily used for research and development and should not be construed as a method for quality acceptance.” Seacoast atmospheric exposures of six to twelve years have proven the EXCO test to be a reliable indicator of service performance for the following alloys used in an interlaboratory testing program: AA2024 and AA2124 in T351 and T851 tempers; AA7075 in T651, T7351, and T7651 tempers; and AA7178 in T651 and T7651 tempers [14,15,19].

The EXCO test has been reported as being too aggressive and not representative of outdoor atmospheres for more recently developed alloys, such as AA2219, AA2419, and AA2519 in the T851 tempers [20], for aluminum-lithium alloys AA2020, AA2090, AA2091, and AA8090 in both as-quenched and artificially aged tempers [10,11,15,21] and for AA7050 and AA7150 in the T7XX type tempers [21]. The problem is that EXCO test specimens of these materials quickly become covered with corrosion products from general attack making it difficult to visually distinguish the general attack from genuine exfoliation. The result is that test specimens frequently have been rated as being overly susceptible to exfoliation (EA or EB) whereas little or no exfoliation occurred in extended seacoast exposures. Metallographic examination is often required to establish a true rating for these relatively resistant materials. Similar problems related to the severity of the EXCO test have also been experienced with copper-free AA7XXX alloys and wrought products of powder metallurgy AA7XXX alloys. This sort of difficulty contributes to variability in the assessment of the exfoliation.

Modified EXCO test solutions not yet standardized that cause less general corrosion have been investigated with promising results in that the reduced general attack favored positive identification of the exfoliation and more accurate estimation of the intensity of it without the necessity of metallographic examination. One approach was to reduce the acidity to pH 3.2 and to add a small amount of aluminum ion while keeping the molarities of chloride and nitrate the same. A 96 h exposure to this modified EXCO solution appears more capable of reliably predicting exfoliation performance in seacoast environments and of distinguishing

between various commercial tempers of AA7075, AA7050, and AA7150 alloys. With a 48 h exposure at a slightly elevated temperature of 52°C (125°F) this modified solution also reflected accurately the performance in a seacoast atmosphere of alloys AA2024 and aluminum-lithium AA2090, in both the T3 and T8 type tempers [21].

Another approach involved the addition of a corrosion inhibitor. Sinyavsky et al. [4], using an addition of 10 g/L potassium dichromate to the standard EXCO solution, reported that the exfoliation trends were the same as in the standard solution for all of the alloys examined (AA2124-T3, T8; AA2618-T6; and AA7175-T6, T76, T73), and because of less general corrosion the exfoliation was easier to identify and to assess in the inhibited solution.

Additional testing of these and other possible modifications, including interlaboratory comparisons, is needed to verify the promising results noted. An ideal modification would hopefully work well with a variety of alloys and be shown to have good reproducibility before it is proposed as a new standard test method.

Historically, various investigators in Europe have used hydrochloric acid-potassium dichromate solutions for testing the exfoliation susceptibility of all types of aluminum alloys. An example is the Russian Standard GOST 9.904-82, Aluminum Alloys: Methods of Accelerated Exfoliation Corrosion Testing [22]. It should be noted, however, that hexavalent chromium ( $\text{Cr}^{6+}$ ) solutions are considered undesirable for health and environmental considerations and have been prohibited in some countries.

*Electrochemical and Conductivity Tests*—These are useful techniques that indicate expected exfoliation corrosion performance but do not actually produce corrosion. Both the electrochemical corrosion potentials and the electrical conductivity are secondary characteristics that relate to the metallurgical condition of the metal and must be correlated to actual exfoliation corrosion tests.

Several researchers experimented with electrochemically driven techniques. Budd and Booth used a potentiostatic approach [23]. Others have tried impressed current tests. Although both appeared promising, these procedures did not lend themselves to the multiple testing required for production control of heat treatment. Neither type of test has been standardized to date.

A useful measure of the degree of improvement in exfoliation resistance of the overaged T7X tempers for AA7075 and similar copper-containing AA7XXX alloys is available from a correlation of the decrease in yield strength combined with the increase in electrical conductivity as the alloy is overaged [3]. Such lot acceptance criteria are included in certain specifications for the T7X temper products of these alloys.

### Test Specimens

Specimens may be of any practical size or shape. However, it is advisable not to use too small a specimen since visual examination is the key evaluation method. It is recommended that flat specimens at least 50 mm by 75 mm in size and full section thickness be used with the specimen length oriented in the direction of principal deformation of the mill product. Larger sized panel specimens are desirable for salt spray testing or outdoor exposures.

The test surface is either the as-fabricated surface or some other specified plane(s). Interior planes typically used are: (a) T/10 = 10 % of the thickness removed (this is representative of a minimal cut to obtain a flat surface free of traffic marks), (b) T/4 = quarter plane, 25 % of the thickness removed, or (c) T/2 = midplane, 50 % of the thickness removed. These interior planes are representative of many of the exposed surfaces of parts machined for aircraft components and they also may expose regions in the grain structure with the highest likelihood of exfoliation susceptibility. When removing test specimens from extrusions and die forgings, locations where the grain structure is variable, such as underneath flanges and ribs, should be avoided. The roughness parameter of machined test surfaces,  $R_a$ , should not exceed 2.5  $\mu\text{m}$ , unless it is required to simulate an as-manufactured surface condition.

Edges of the test specimens should preferably be sawed or machined. If specimens are obtained by shearing, the plastically deformed edges should be dressed by machining, sanding, or filing to a depth equal to the specimen thickness to remove residual short transverse tensile stresses. With very susceptible materials stress-corrosion cracks parallel to the surface may initiate in the edges.

### Test Duration

The length of time to develop exfoliation in a susceptible material can vary appreciably depending on the degree of directionality of the grain structure and the heat treatment of the test specimen. Therefore, it can be helpful when the purpose is to compare various items in a series to examine and assign exfoliation ratings after increasing periods of exposure during the test.

*Accelerated Tests*—Standard tests generally are conducted for the recommended exposure period. However, if no appreciable exfoliation is observed on a new alloy or temper, the period may be doubled. If this still does not produce significant exfoliation it generally can be concluded that the material is not susceptible to exfoliation in that test medium.

*Outdoor Tests*—Past experience has shown that materials that are very prone to exfoliation in service conditions will show marked exfoliation within four years of exposure at severe outdoor sites, such as seacoast and certain highly industrialized urban areas. If test space is limited, specimens surviving this length of exposure at outdoor sites known to cause exfoliation can be terminated and considered “not highly susceptible.” However, some investigators now have programs of 20 or more years duration showing that exposures exceeding four years still may discriminate between materials with the “better and best” resistance.

### Evaluation of Test Results

One of the problems with evaluating exfoliation corrosion is the lack of a generally accepted numerical measure of the corrosion damage. Mass loss is a poor indicator of exfoliation behavior because the degree of attack can be spatially nonuniform. Delaminated layers that are not completely detached from the specimen also complicate accurate mass loss determination. Cross-sectional metallographic examination can add valuable information on the degree and mode of attack, but is time consuming and no relative ranking system has been devised.

Therefore, the usual practice is to inspect the specimens and to assign visual ratings with reference to standard photographs illustrating four degrees of severity as in ASTM G 34 and G 66. To choose a rating, the inspector must make a judgment, and herein lies the main source of variability in the test results from the relatively uncomplicated immersion tests. It is often desired for the record to make photographs of the exposed test specimens as well as to rate them using the standard photographs.

*Classification of Exfoliation*—The following classifications (Table 1) are recommended when reporting the visual ratings of corroded test specimens by comparison with standard photographs in Figs. 3–8 (after ASTM G 34, G 66, and G 112):

TABLE 1—Classifications for corroded test specimens.	
Classification	Rating
No appreciable attack	N
Pitting	P
General	G
Exfoliation	EA, EB, EC, ED

(a) N—No appreciable attack: surface may be discolored or superficially etched.

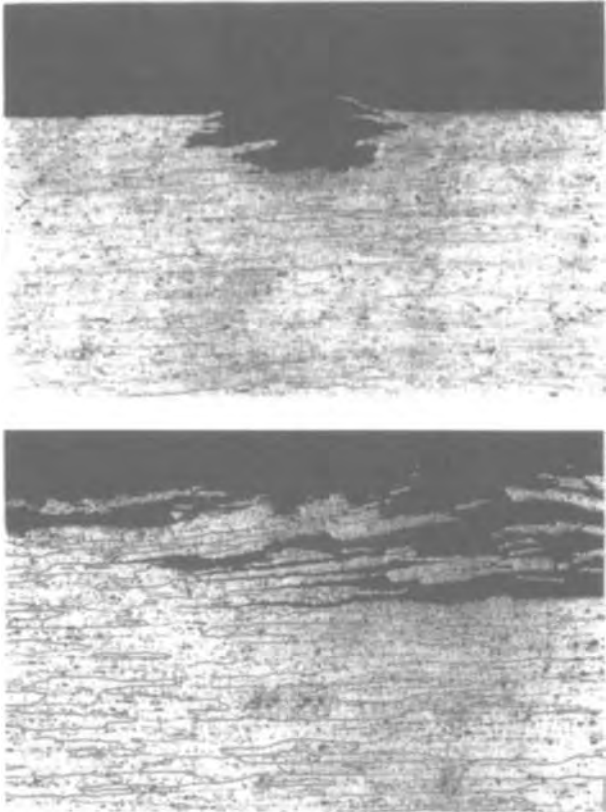


**FIG. 3—Metallographic sections illustrating two different types of attack (reprinted from ASTM G 34): (a) undermining pitting that may from the surface give the appearance of the beginning of exfoliation (Keller's Etch: 100×); (b) exfoliation resulting from rapid lateral attack of selective grain boundaries or strata forming wedges of corrosion product that force layers of metal upward giving rise to a layered appearance (Keller's Etch: 100×).**

**FIG. 4—Examples of exfoliation rating EA (superficial): tiny blisters, thin slivers, flakes, or powder, with only slight penetration into the metal (reprinted from ASTM G 34).**

- (b) P—Pitting: discrete pits, sometimes with a tendency for undercutting and slight lifting of metal at the pit edges (Fig. 3a).
- (c) G—General: fairly uniform corrosion with accumulation of powdery corrosion products; the basic type of attack may be either pitting or intergranular.
- (d) EA to ED—Exfoliation: visible separation of the metal into layers manifested in various forms such as blisters, slivers, flakes, fairly continuous sheets, and sometimes granular particles resulting from disintegration of thin layers of metal; attack may be wide-spread or localized. Various degrees of exfoliation with increasing area, penetration, and loss of metal are shown in Figs. 4–8.

*Inspection of Specimens*—After discontinuation of the exposure, performance should be rated while the specimens are still moist, taking into account all corrosion products adhering to the metal surface or lying on the bottom of the test container. Photographs may be advisable at this stage. If in some cases it is impossible to positively distinguish mild forms of exfoliation from general corrosion it may be helpful to chemically clean the specimens by soaking them in concentrated nitric acid (70 % HNO<sub>3</sub>, specific gravity 1.19) at room temperature for only a few minutes, just long enough to dissolve corrosion products without dislodging layers or flakes of true exfoliation, followed by gently rinsing again with tap water. When the presence of exfoliation is still questionable because of remaining powdery deposits or if real exfoliation actually was removed, metallographic examination of a cross section of the corrosion will be required to determine the correct rating (Fig. 3). The purpose is to avoid giving a specimen an unrealistic visual rating of EA or EB when there is no microscopic evidence of actual delamination or conversely giving an erroneous visual rating of P or G when the evidence of real exfoliation was destroyed. Experience has shown that material that is roughened and exhibiting a loosely adherent powdery deposit in the standard EXCO test does not exfoliate during exposure of five years in the seacoast atmosphere at Point Judith, RI [24].

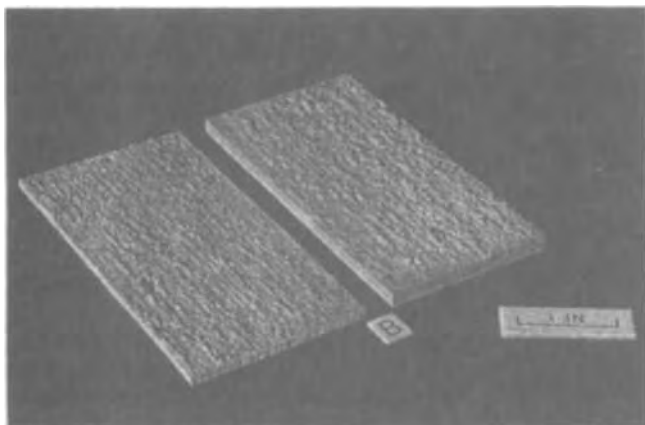


FIG. 5—Examples of exfoliation rating EB (moderate): notable layering and penetration into the metal (reprinted from ASTM G 34).

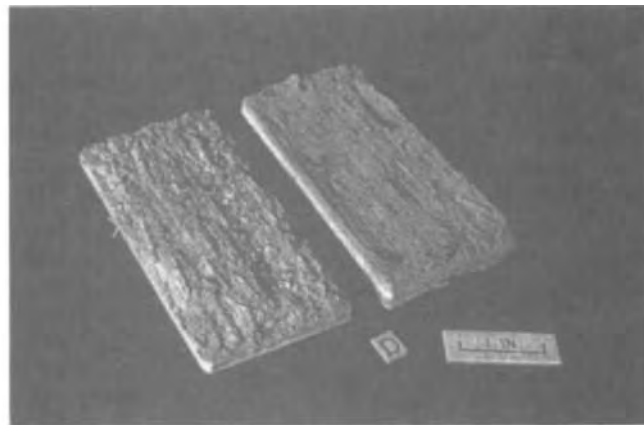


FIG. 7—Examples of exfoliation rating ED (very severe): similar to EC except for much greater penetration and loss of metal (reprinted from ASTM G 34).

FIG. 6—Examples of exfoliation rating EC (severe): penetration to a considerable depth into the metal (reprinted from ASTM G 34).

When a test specimen appears to be borderline, choose the rating indicating higher susceptibility. And when exfoliation occurs at isolated sites, rate the worse condition observed.

Care must be taken not to over interpret the inherently subjective ratings. As an example, the difference in the amount of attack between samples rated on the severe end of the EA range and mild end of the EB range is small such that samples receiving those designations may not in fact have different exfoliation susceptibilities. In addition, material with exfoliation resistance between highly susceptible and highly resistant can be difficult to rate visually, as highlighted in an interlaboratory test program that used two non-commercial heat treatments of AA7075 with different levels of resistance (see ASTM G 34-01 section 14). Results from this round-robin test program indicate that the visual rating system gives consistent classification designation for highly susceptible samples but may produce a large amount of variation for moderately resistant tempers. Experience also suggests that the visual rating system produces more consistent results for highly resistant material than it does for aging conditions of moderate to low resistance.

FIG. 8—Examples of four degrees of exfoliation corrosion, EA-ED of several AA5XXX alloys (reprinted from ASTM G 66).

Another approach based on visual examination has been used in the former Soviet Union [4,22]. Three rating criteria are used to express the degree of damage on a scale of 1–10:

- (a) Percent area of swelling and exfoliation of test surface,
- (b) Maximum diameter in mm of swellings (blisters) on test surface, and
- (c) Percent length of cracking in specimen perimeter (edges).

The material is evaluated by calculating the arithmetic mean of these three criteria. Although a numerical result is generated, it is calculated from subjective visual estimates and is more complicated.

A classification system for exfoliation attack based on an objective and quantitative rating method and criteria would be a beneficial alternative to the existing subjective visual rating method.

#### *Test Procedures for Other Metals*

Exploratory investigations of the possible susceptibility to exfoliation corrosion of alloys of other metals would be advisable if wrought mill products have highly directional grain structures and if it is known that they may be susceptible to intergranular



or lamellar corrosion. It is recommended that, if practicable, exposure tests be conducted under environmental conditions of anticipated service applications. Otherwise, consider a severe seacoast atmosphere, one of the cyclic salt spray tests described in ASTM G 85, or one of the immersion type tests.

### Test Controls

It is always advisable to include control specimens from known materials representing both high and low resistance to exfoliation. This is recommended for both accelerated and outdoor tests. Such controls verify the validity of a particular test environment and permit the investigator to make some assessment of the normalcy of a particular test run. For example, one cannot conclude that a new material is resistant to exfoliation if the susceptible control specimen did not exfoliate to the usual degree. In outdoor tests, the condition of the susceptible control serves as an indicator of when a meaningful length of exposure has been reached. Control specimens are especially advisable in outdoor environments that encounter variable conditions of temperature, precipitation, airborne pollutants, and the like.

### REFERENCES

- [1] Sprowls, D. O., Walsh, J. D., and Shumaker, M. B., "Simplified Exfoliation Testing of Aluminum Alloys," *Localized Corrosion—Cause of Metal Failure, ASTM STP 516*, ASTM International, West Conshohocken, PA, 1972, pp. 38–65.
- [2] Ketcham, S. J. and Jankowsky, E. J., "Developing an Accelerated Test: Problems and Pitfalls," *Laboratory Corrosion Tests and Standards, ASTM STP 866*, G. S. Haynes and R. Baboian, Eds., ASTM International, West Conshohocken, PA, 1985, pp. 14–23.
- [3] Summerson, T. J. and Sprowls, D. O., "Corrosion Behavior of Aluminum Alloys," *Conference Proceedings Volume III, Aluminum Alloys: Their Physical and Mechanical Properties*, E. A. Starke, Jr. and T. H. Sanders, Jr., Eds., Engineering Materials Advisory Services Ltd., West Midlands, U.K., 1986, pp. 1576–1662.
- [4] Sinyavski, V. S., Kalinin, V. D., and Dorokhina, V. E., "Study of Correlations Between Structural, Electrochemical and Physical Characteristics and Resistance to Exfoliation Corrosion of Aluminum Alloys," *Proceedings of the Second International Conference on Aluminum Alloys—Their Physical and Mechanical Properties*, International Academic Publishers, A Pergamon-CNPIEC Joint Venture, 1990, pp. 692–697.
- [5] Aylor, D. M., "Corrosion of Metal Matrix Composites," *Metals Handbook*, 9th ed., Vol. 13 Corrosion, ASM International, Metals Park, OH, 1987, pp. 859–863.
- [6] Butler, G. and Ison, H. C. K., "Corrosion and Its Prevention in Waters," Reinhold Publishing Corp., New York, NY, 1966, p. 48.
- [7] Evans, U. R., *The Corrosion and Oxidation of Metals*, Edward Arnold Ltd., London, U.K., 1961.
- [8] Loose, W. S., "Magnesium and Magnesium Alloys," *The Corrosion Handbook*, 1st ed., John Wiley and Sons, Ltd., New York, NY, 1976, pp. 218–252.
- [9] Lifka, B. W. and Sprowls, D. O., "Relationship of Accelerated Test Methods for Exfoliation Resistance in 7XXX Series Aluminum Alloys with Exposure to a Seacoast Atmosphere," *Corrosion in Natural Environments, ASTM STP 558*, ASTM International, West Conshohocken, PA, 1974, pp. 306–333.
- [10] Colvin, E. L. and Lifka, B. W., "Accelerated and Atmospheric Exfoliation Corrosion Performance of Al–Li Alloys," *Advances in Localized Corrosion: Proceedings of the Second International Conference on Localized Corrosion, NACE-10*, H. S. Isaacs, U. Bertocci, J. Kruger, and S. Smialowska, Eds., National Association of Corrosion Engineers, Houston, TX, 1989, pp. 215–220.
- [11] Colvin, E. L. and Murtha, S. J., "Exfoliation Corrosion Testing of Al–Li Alloys 2090 and 2091," *Proceedings of the Fifth International Aluminum–Lithium Conference*, T. H. Sanders Jr. and E. A. Starke Jr., Eds., Materials and Component Engineering Publications Ltd., Birmingham, U.K., 1989, pp. 1251–1260.
- [12] Braun, R., "Exfoliation Corrosion Testing of Aluminium Alloys," *British Corrosion Journal*, Vol. 30, No. 3, 1995, pp. 203–208.
- [13] Romans, H. B., "An Accelerated Laboratory Test to Determine the Exfoliation Corrosion Resistance of Aluminum Alloys," *Materials Research Standards*, Vol. 9, No. 11, 1969, pp. 31–34.
- [14] Ketcham, S. J. and Jeffrey, P. W., "Exfoliation Corrosion Testing of 7178 and 7075 Aluminum Alloys," *Localized Corrosion—Cause of Metal Failure, ASTM STP 516*, ASTM International, West Conshohocken, PA, 1972, pp. 273–302.
- [15] Thompson, J. J., "Exfoliation Corrosion Testing of Aluminum–Lithium Alloys," *New Methods for Corrosion Testing of Aluminum Alloys, ASTM STP 1134*, V. S. Agarwala and G. M. Ugiansky, Eds., ASTM International, West Conshohocken, PA, 1992, pp. 70–81.
- [16] Tankins, E., Kozol, J., and Lee, E. W., "The Shipboard Exposure Testing of Aircraft Materials," *Journal of Metals*, Vol. 47, No. 9, 1995, pp. 40–44.
- [17] "Technical Report: Exfoliation Corrosion Testimony of Aluminum Alloys 5086 and 5456," The Aluminum Association.
- [18] Summerson, T. J., "Interim Report, Aluminum Association Task Group on Exfoliation and Stress-Corrosion Cracking of Aluminum Alloys for Boat Stock," *Proceedings of the Tri-Service Corrosion Military Equipment Conference, Technical Report AFML-TR-75-42, Vol. II*, Air Force Materials Laboratory, 1975, pp. 193–221.
- [19] Sprowls, D. O., Summerson, T. J., and Loftin, F. E., "Exfoliation Corrosion Testing of 7075 and 7178 Aluminum Alloys—Interim Report on Atmospheric Exposure Tests," *Corrosion in Natural Environments, ASTM STP 558*, ASTM International, West Conshohocken, PA, 1974, pp. 99–113.
- [20] Lifka, B. W. and Lee, S., "Exfoliation Test Results on 2519–T87 Plate: Disparity of Results in EXCO Versus Other Environments," *Presentation of ASTM Subcommittee G01.05 Workshop on Exfoliation Corrosion*, 1988.
- [21] Lee, S. and Lifka, B. W., "Modification of the EXCO Test Method for Exfoliation Corrosion Susceptibility in 7XXX, 2XXX and Aluminum–Lithium Alloys," *New Methods for Corrosion Testing of Aluminum Alloys, ASTM STP 1134*, V. S. Agarwala and G. M. Ugiansky, Eds., ASTM International, West Conshohocken, PA, 1992, pp. 1–19.
- [22] Formin, G. S., "Corrosion and Corrosion Protection," *Encyclopedia of International Standards*, Moscow Standards Publishing House, 1994, pp. 193–194.
- [23] Budd, M. K. and Booth, F. F., "An Accelerated Test For Indicating Susceptibility Of Aluminum Alloys To Layer Corrosion," *Corrosion*, Vol. 18, 1962, pp. 197–203t.
- [24] Lifka, B. W., "Corrosion Resistance of Aluminum Alloy Plate in Rural, Industrial, and Seacoast Atmospheres—Paper #420," *Corrosion/87*, National Association of Corrosion Engineers, Houston, TX, 1987.

# Erosion, Cavitation, and Fretting

W. A. Glaeser<sup>1</sup>

## BASIC PRINCIPLES

### Review of Mechanisms

#### Erosion

SOLID PARTICLE and liquid drop erosion are surface removal processes caused by impingement of solid particles or droplets carried in a moving gas or liquid stream against a surface. Erosion can also occur when the surface is the moving body impacting suspended particles or drops, as happens on a helicopter blade moving through rain.

The mechanism of erosion differs for various materials. For ductile materials, impacting particles produce craters that have material extruded from the surface, as shown in Fig. 1.

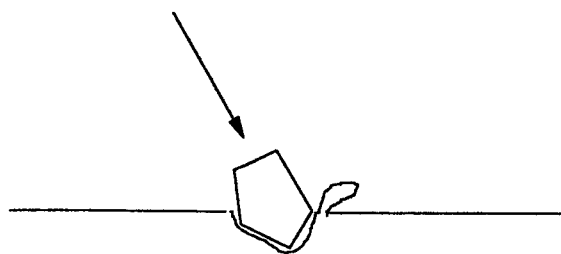


FIG. 1—Crater formed in the surface of a ductile material by an impacting particle.

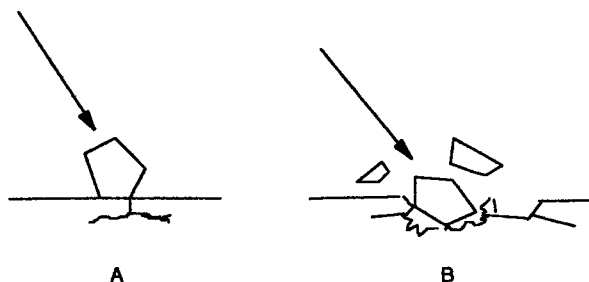


FIG. 2—Particle erosion of brittle material: (A) subsurface crack formed by impacting particle; (B) the result of multiple impacts causing fracture linkage and chipping out of material.

The arrow in Fig. 1 shows the direction of travel by the impacting particle. The crater formed is shaped by the particle and by the angle of impact. A lip of material has been thrown up on one side of the crater. Population density of craters increases with time until the entire surface is covered. The time to develop this condition is called the induction period. During the induction period, surface removal is small. After the induction period, erosion rate increases as the crater lips are broken off by impacting particles.

For brittle materials such as glass, the surface removal mechanism is different. Impact by particles causes micro fractures in the surface and as fractures increase in numbers they grow together and produce chips, as shown in Fig. 2.

### Factors Controlling Particle Erosion

- **Impingement angle:** Ductile materials show the highest erosion rate at low impingement angles. Brittle materials show highest erosion rates at impingement angles around 90° to the surface. These effects are shown in Fig. 3. The dashed line shows ductile material erosion characteristics while the solid line represents ceramics. The dashed line is shown to vary with the impingement angle  $\alpha$  by theory. However, in practice, erosion of metals departs from the dashed line at about 40° as shown. It can be seen that for ductile materials a maximum volume of removal occurs at an impingement angle of about 28°. For brittle materials, minimum removal occurs at low impingement angles, while the maximum removal occurs from 70 to 90°. Concentration of particles in the gas or liquid stream can influence the erosion. When concentration becomes heavy, erosion rate decreases owing to the interference among particles.
- **Velocity:** Particle velocity has a significant effect on erosion rate. Erosion is generally given as mass loss per unit mass of particles impinging.

For a given impingement angle, the erosion rate can be expressed as follows:

$$E = kv^n$$

where:

$E$  = erosion rate

$v$  = velocity

$n$  = exponent that ranges between 2 and 2.5 for metals and 2.5 and 3 for ceramics.

<sup>1</sup>Research Leader, Battelle Laboratories, 505 King Ave., Columbus, OH 43201.

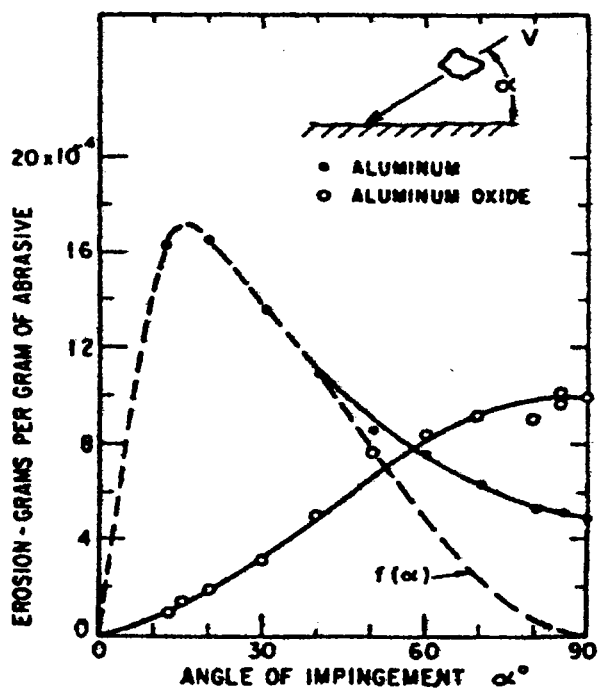


FIG. 3—Chart showing the effect of impingement angle on erosion weight loss for metals and ceramics. Aluminum characteristics (typical for ductile metals) are shown in the dashed line. Aluminum oxide (ceramics) is represented by the solid line. The dashed line follows theory while the solid line deviation at about 40° represents practical experience (from Ref 1).

- Particle size: Erosion rates for metals decrease significantly when particle size drops below 100  $\mu\text{m}$ . For ceramics, erosion rate increases to the two-thirds power of particle diameter.
- Material hardness: For steels, hardening by working or by heat-treating has little effect on erosion resistance. For pure face centered cubic metals, erosion resistance increases with hardness. Thus, tantalum has twice the erosion resistance of aluminum. (Hardness for pure aluminum is 37 DPH, for tantalum the hardness is 70 DPH.)

Liquid drop erosion is a different process from solid particle impingement. When a droplet impacts a solid surface, the contact stress distribution is maximum at the edges of the drop and minimum at the center of the contact. This is the opposite of a Hertzian concentrated contact for a solid point pressed against a flat surface. The droplet rapidly spreads radially at very high velocity and causes a roughening of the periphery of the circular contact. Thus, the deformation left by the impacting drop is a ring indentation with a little depression in the center of the circle. The circular indentation is roughly the diameter of the impinging drop. As the surface roughens with accumulation of drop impacts, the indentations deepen and fill with liquid. The presence of liquid in the pits tends to cushion the drop impacts and reduces the rate of erosion.

The appearance of the eroded surface impacted by liquid drops is different from solid particle erosion. Liquid drop

impacts leave roughly circular pits while solid particle impacts leave irregular pits with shapes that show the angle of impingement.

- Droplet velocity influences erosion rate. Heyman [1] suggests that maximum erosion rate varies as the fourth or fifth power of impact velocity.
- Impact angle also influences erosion rate. Rate is maximum around 90°.
- Erosion rate increases with droplet size increase.

## EROSION-CORROSION

Titanium alloys are being used in increasing quantities in the aerospace industry because of their high corrosion resistance. The reduction in the passivating films caused by particle erosion as observed in stainless steel has been investigated for titanium and titanium alloys [2].

Solid particle erosion in salt water was found to increase anodic passivation in titanium. The rate of erosion for pure titanium was compared with the same for titanium alloys. It was found that titanium alloys like Ti-6Al-4V showed significant increased resistance to erosion-corrosion. The addition of 0.1 % Ru to Ti-6Al-4V further increased the erosion-corrosion resistance of the alloy.

## Cavitation

The most familiar is cavitation of ship propellers. At the periphery of the rotating propeller, the moving velocity is highest. Fluid dynamic effects cause the formation and collapse of gas bubbles near the tips. The collapse of the gas bubbles is so rapid that it causes violent pressure impulses that are audible. These pressure pulses shock the solid surfaces and cause localized pitting. The origin of the bubbles can be trapped air bubbles, dissolved air coming out of solution or water vapor.

Cavitation in a liquid medium requires a rapidly changing pressure distribution. This can happen in oil-lubricated journal bearings around a discontinuity like an oil inlet hole. The shear rates in the thin oil film supporting the bearing load are very high. Thus, when the moving oil encounters a hole or slot, flow rate and local pressures change abruptly. Bubbles in the vicinity collapse. The bubble collapse is much like a violent implosion and the shock wave will deform and pit the bearing material. Cavitation in oil can be more damaging than in water [2].

## Fretting

One definition of fretting is "Wear phenomena occurring between two contacting surfaces having oscillatory relative motion of small amplitude." **Note:** *Fretting* is a term frequently used to include fretting corrosion. This usage is not recommended.

Another is the "Small amplitude oscillatory motion, usually tangential, between two solid surfaces in contact." **Note:** Here the term fretting refers only to the nature of the motion without reference to wear, corrosion or other damage that may follow. The term *fretting* is often used to denote fretting corrosion and other forms of fretting wear.

Usage in this sense is discouraged due to the ambiguity that may arise.

### Fretting Corrosion

"A form of fretting in which chemical or electrochemical reaction predominates. Note: Fretting corrosion is often characterized by the removal of particles and subsequent formation of oxides, which are often abrasive and so increase the wear. Fretting corrosion can involve other chemical reaction products that may not be abrasive."

The above quote is from the Tribology Volume of the Metals Handbook [3] and serves to point out the confusion that can exist in defining fretting.

The term *fretting* means removal of material from between two contacting surfaces when one oscillates against the other at a very small amplitude (sometimes from vibration). Godfrey [4] showed that for iron and steel, metal particles are removed and pushed to the edge of the contact where they oxidize. He demonstrated that oxidation did not start within the contact region. He also showed that inert metals like platinum and gold will produce fretting debris under the same conditions.

### Factors Controlling Fretting [5]

- Number of cycles: Volume removed is about proportional to number of fretting cycles.
- Load: Damage increases linearly with increasing normal load.
- Amplitude: Fretting wear volume increases with amplitude. Above about 100  $\mu\text{m}$  the rate increases owing to a change in the wear mode. Wear rate can go to zero at very low amplitudes if motion is purely elastic.
- Frequency: Fretting wear per cycle increases at low frequency in oxidizing environment or corrosive conditions. Frequency has little effect when inert environment exists.
- Temperature: The nature of oxide chemistry influenced by temperature will affect fretting. Some oxides become quite refractory at elevated temperatures and inhibit fretting.

R. C. Bill [6], discussing high-temperature fretting, suggests three conditions: (1) adhesive asperity contact and removal of metal in the absence of an oxide film, (2) removal of oxide film as it grows, and (3) oxidative attack of fretting pit walls causing weakening and removal of wall surfaces.

### Fretting Fatigue

Fretting of clamped joints will reduce the fatigue strength of the joint significantly. In fact just fretting a joint reduces its inherent fatigue strength. Figure 4 shows a fatigue S-N curve for both classic fatigue and for fretting fatigue (where S is stress and N is number of fatigue cycles).

Waterhouse [7], using Mindlin's state of stress for fretting contacts, found that the action of fretting was to increase the areas of real contact and to increase the coefficient of friction until a sufficient volume of material is subjected to sufficiently high stress field to enable a crack (or cracks) to

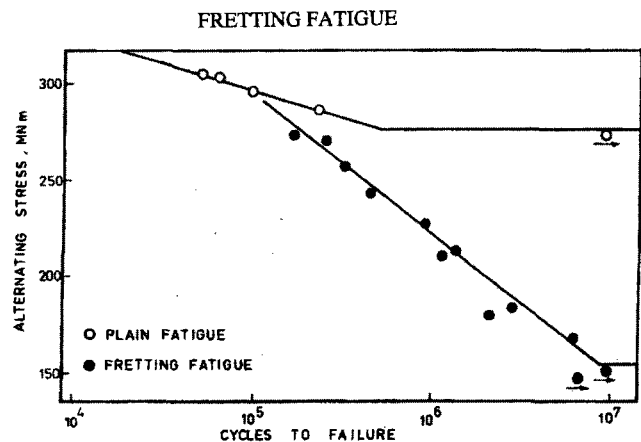


FIG. 4—S-N curve showing the reduction in fatigue strength caused by fretting.

be generated. Coefficient of friction can reach values of 0.8 during fretting.

Hills and Nowell [8] propose that the contact stress state (assuming a ball-on-flat configuration) involves a maximum shear stress oriented at 45° to the surface which produces slip and eventual persistent slip bands. Cracks are then generated in these bands.

More recent experimental work in fretting fatigue [9] has shown that fretting alone can develop cracks. These cracks are oriented at approximately 45° to the surface and are likely shear induced. An example is shown in Fig. 5. This is a photomicrograph of a right section through a titanium alloy test bar showing several fretting generated cracks that did not propagate to failure.

## TESTING TECHNIQUES

ASTM International has a number of standard test methods for erosion, cavitation, and fretting wear.

### Particle Erosion

The ASTM standard for conducting erosion tests by solid particle impingement is ASTM G 76-95 (2000) [10]. ASTM scope: "This practice covers the determination of material loss by gas-entrained solid particle impingement erosion with a jet - nozzle type erosion equipment. This practice may be used in the laboratory to measure the solid particle erosion of different materials and has been used as a screening test for ranking solid particle erosion rates of materials in simulated service environments. Actual erosion service involves particle size, velocities, attack angles, environments, etc., that will vary over a wide range. Hence, any single laboratory test may not be sufficient to evaluate expected service for solid particle impingement erosion measurement for which interlaboratory test results are available."

Since particle velocity has a strong influence on erosion rate, accurate results require knowledge of this parameter.

**FIG. 5—Photomicrograph showing fretting caused surface cracks in a metallographic section through a Ti-6Al-4V fretting fatigue specimen.**

The particles in a pressurized gas jet do not necessarily move at the gas velocity. Measurement of gas entrained particle velocities is difficult. Therefore, another test method, involving moving the specimen through a suspended column of particles can also be used. The specimen or specimens are mounted on a rotating arm or wheel with set approach angles and rotated through a stream of particles dropped in their path or suspended in a fluidized bed. There is no ASTM standard for this; however, recommended practice does exist for liquid particle impingement (see below).

### Liquid Impingement Erosion

The same methods used in particle erosion tests can be used in liquid impingement tests. Liquid gun devices in which a small quantity of liquid is ejected through a nozzle are used in the study of drop impact effects on materials [11]. The rotating arm method, carrying specimens through suspended drops, is often used for testing aircraft leading edges and helicopter rotor blades erosion characteristics in rain fields. ASTM G73-98, Practice for Liquid Impingement Erosion Testing, gives recommendations for setting up a liquid drop impingement test [12].

### Cavitation Erosion

ASTM G 32-98, Test Method for Cavitation Erosion Using Vibratory Apparatus [13], describes a standard method for performing cavitation tests. Its scope is listed as follows: "This test method produces cavitation damage on the face of a specimen vibrated at high frequency while immersed in a liquid. The vibration induces the formation and collapse of cavities in the liquid, and the collapsing cavities produce the damage to and erosion (material loss) of the specimen."

"Although the mechanism for generating fluid cavitation in this method differs from that occurring in flowing systems and hydraulic machines, the nature of the material damage mechanism is believed to be basically similar. The method therefore offers a small-scale, relatively simple and

controllable test that can be used to compare the cavitation erosion resistance of different materials, to study in detail the nature and progress of damage in a given material, or by varying some of the test conditions to study the effect of test variables on the damage produced."

### Fretting Wear

A number of test methods are used to evaluate the fretting resistance of various materials and lubricants. The object of the tests is to bring two surfaces into contact under a known load and contact geometry and to move one surface relative to the other under an oscillating motion with a very small amplitude.

Conventional wear test configurations can be adapted to fretting. Ball-on-flat, block-on-ring, and crossed cylinders can be modified so that the sliding motion can be made oscillatory and the amplitude small (less than 100  $\mu\text{m}$ ).

Fretting fatigue configurations are generally adaptations of standard bending fatigue machines. By clamping metal pads to the fatigue bar in the maximum bending strain region, the relative motion developed between the pads and the bar surface as it flexes produces fretting in the bending fatigue zone. This will cause acceleration of the fatigue process.

ASTM Method D 4170, Test Method for Fretting Wear Protection by Lubricating Greases [14], evaluates the fretting wear protection to rolling contact bearings afforded by various greases. This test was developed in response to a fretting problem found in long distance transportation of automobiles. Fretting of the wheel bearings (sometimes called "false brinelling") is caused by small oscillations cause by swaying movements of the transporters (barges and automobile truck transports). This test can be used for ball bearings under small amplitude oscillatory movement.

The above test methods do not exactly simulate the actual fretting conditions. The surface damage produced by the test should be compared to the damage on parts damaged in service. If there is significant difference between scar morphologies, the wear mode may not be correctly simulated in the test. Corrections can be made in contact geometry, contact stress, and amplitude and velocities of movement.

### Fretting Fatigue

Currently, there is no recognized standardized test for fretting fatigue. A number of tests have been developed. Most involve either bearing balls or cylindrical bars clamped on either side of a fatigue "dog bone" specimen. The dog bone is either subjected to push pull tensile loading or reversed bending. Both cause elastic deformation in the bar contact zone on the order of 10 to 100  $\mu\text{m}$  providing relative motion between the contacting surfaces. Some tests involve fretting alone and then subjecting the fretted specimen to classic fatigue conditions. A variety of contact geometries have been tried for fretting fatigue testing including "bridges," or flat specimens with a channel cut in the contact surface or the flat end of chamfered rectangular coupon. Descriptions of these various test configurations can be found in Ref 8, Chapter 7.

## REFERENCES

- [1] Heymann, F. J., "Liquid Impingement Erosion," *ASM Handbook, Vol. 18, Friction, Wear and Lubrication Technology*, American Society of Metals, Materials Park, OH, 1992, pp. 222–232.
- [2] Neville, A. and McDougall, B. A. B., "Erosion – and Cavitation – Corrosion of Titanium and its Alloys," *Wear*, 250, 2001, pp. 726–735.
- [2] Rao, B. C. S. and Buckley, D. H., "Cavitation Pitting and Erosion of Aluminum 6061-T6 in Mineral Oil and Water," NASA-TP-2146, 1983.
- [3] "Tribology, Glossary of Terms," *ASM Metals Handbook, Vol. 18, Friction, Wear and Lubrication Technology*, Materials Park, OH, 1992, p. 9.
- [4] Godfrey, D., NACA Report 1009, NASA Center for AeroSpace Information, Hanover, MD, 1951.
- [5] Waterhouse, R. B., *Fretting Corrosion*, Pergamon Press, NY, 1972.
- [6] Bill, R. C., "The Role of Oxidation in the Fretting Wear Process," *Proceedings Wear of Materials 1981 Conference*, ASME, NY, pp. 238–250.
- [7] Waterhouse, R. B., *Fretting Fatigue*, Applied Science Publishers, Ltd., London, 1981.
- [8] Hills, D. A. and Nowell, D., "Mechanics of Fretting Fatigue," Kluwer Academic Publishers, NY, 1994.
- [9] Glaeser, W. A. and Lawless, B., "Behavior of Alloy Ti-6Al-4V under Prefretting and Subsequent Fatigue Conditions," *Wear*, 250, 2001, pp. 621–630.
- [10] ASTM Test Method G 76-95: Standard Method for Conducting Erosion Tests by Solid Particle Impingement, *Annual Book of ASTM Standards*, Vol 03.02, ASTM International, West Conshohocken, PA.
- [11] Brunton, J. H., "Deformation of Solids by Impact of Liquids at High Speeds," *Symposium on Erosion and Cavitation, ASTM STP 307*, ASTM International, West Conshohocken, PA, 1961, pp. 83–98.
- [12] ASTM G 73-98: Standard Practice for Liquid Impingement Erosion Testing, *Annual Book of ASTM Standards*, Vol 03.02, ASTM International, West Conshohocken, PA.
- [13] ASTM G 32-98: Standard Test Method for Cavitation Erosion Using Vibratory Apparatus, *Annual Book of ASTM Standards*, Vol. 03-02, ASTM International, West Conshohocken, PA.
- [14] ASTM D 4170-97: Standard Test Method for Fretting Wear Protection by Lubricating Greases, *Annual Book of ASTM Standards*, Vol. 05.02, ASTM International, West Conshohocken, PA.

# Dealloying

*Ann Chidester Van Orden*<sup>1</sup>

DEALLOYING HAS BEEN KNOWN for many years, in many alloy systems, under many different conditions. A number of mechanisms have been proposed and examined over time. Six specific mechanisms are reviewed here with information regarding systems wherein they have been observed, temperature regime, solutions, microstructural features, and the evidence that was cited for their origination. The literature regarding these mechanistic models is outlined along with possible problems not addressed by each model. Methods used for examination of dealloying are mentioned along with evaluation methods for considering the results of the examination. Although few standards exist dealing with dealloying, the lack of standards is discussed along with the few standards in existence. Test methods such as those used in examining stress corrosion cracking (SCC), which may be influenced by dealloying, are outlined and the effect of dealloying on these test methods is discussed.

## FUNDAMENTALS

ASTM International defines dealloying, or parting, as “the selective corrosion of one or more of the components of a solid solution alloy” [1]. This preferential removal or parting has been known for as long as alloys have been exposed to corrosive environments. An early study by Calvert and Johnson [2] discussed the action of acids on metals and alloys, specifically 50Cu-50Zn submerged in concentrated HCl for several days. The authors stated that, over the duration of the experiment, the zinc was totally removed from the alloy, rendering the specimen copper-colored and quite soft. This explanation of the preferential removal of the zinc is one of the earliest discussions of a mechanism for dealloying.

Dealloying is known to occur in many alloy systems at ambient and high temperatures, in aqueous and vapor environments, and in mild-to-severe acids or bases [3–10]. Examples of systems that show dealloying include removal of zinc from copper-zinc [10–13], nickel from copper-nickel and Cu or Ni from monels [7,14–16], aluminum from aluminum-bronzes [5,14,15], manganese from copper-manganese [17], tin from copper-tin [18], copper from copper-gold [19–24], and from Al-Cu-Li [25,26]. Nickel can be dissolved preferentially from steels [27]. At high temperatures, chromium will dissolve preferentially from steels [28] as well. Cobalt

is known to dissolve from Co-Ni-Cr [29,30], chromium and iron can be removed from Fe-Ni-Cr [31,32], and iron will dissolve preferentially from gray cast iron [33]; carbon (graphite) can also be preferentially removed from cast iron [34] and from steels [35,36]. In high-temperature hydrogen environments and certain oxidizing atmospheres as early as 1917, the preferential removal of iron from Fe-Cu alloys was reported [37]. In addition to the much studied removal of copper from Cu-Au [32–38], gold can be removed from Pt-Au [38–40], silver from Ag-Pd [41] and from Ag-Au [42–51], and lead from Pt-Pb [52]. Several authors have surveyed the literature on dealloying and summarized the information up to the time of their published work [8,35,51,53].

Dealloying is characterized by the formation of a porous microstructure, much like that of a microscopic sponge. The pores are interconnected and open to the environment. Selective dissolution and preferential leaching are other terms for dealloying. Dezincification is the specific term given to preferential removal of zinc from brasses. Other words have developed that are similar to dezincification (such as denickelification) and refer to dealloying in specific cases. The term “dealloying” is universally acceptable and is preferred by ASTM [54]. Alloys in which a specific phase is susceptible to dealloying include some of the systems mentioned earlier, such as gray cast iron, stainless steels, and copper-zinc alloys [55].

In alloys that form solid solutions, the microstructure formed by dealloying is characterized by islands of the more noble material, with open channels between the islands. This unique microstructure is one of the characteristic features of dealloying. Figure 1 shows an example of this microstructure in a 90Ag-10Au alloy, dealloyed electrochemically in perchloric acid. Although the dimensions of the microstructure may vary with alloy composition [19], and dealloying conditions such as solution, temperature, and time [49], the dimensions of the islands and channels are approximately equal and are characteristic of the specific set of dealloying conditions applied. In some cases, the microstructure can be viewed without magnification or with low-power light microscopy [3]; under other circumstances, the microstructure is of small enough dimensions that it can only be viewed with transmission electron microscopy (TEM) [51] or high resolution scanning electron microscopy (HRSEM) [56].

Many of the alloys that undergo selective dissolution (or dealloying) are also prone to stress corrosion cracking (SCC).

<sup>1</sup>Formerly, Mechanical Engineering Department, Old Dominion University, Norfolk, VA 23529. Now deceased.

**FIG. 1—The microstructure of silver-gold anodically polarized in perchloric acid. The microstructure consists of islands of the more noble material (the dark areas) and empty channels (the light areas), which are of equal dimensions. The islands and channels are interconnected and cover the entire specimen following the electrochemical polarization treatment to produce dealloying. (160 000  $\times$ .)**

From the ASTM definition, stress corrosion cracking is “the simultaneous action of a corrosive environment and a sustained tensile stress promoting rupture” [54]. Both SCC and dealloying often occur in the same environment. By the 1940s, dealloying was considered to be involved in the initiation of SCC [57].

Examining the relationship of dealloying to initiation of SCC involves, first, exposing susceptible alloys to environments that promote dealloying. A mechanically weak, porous layer forms, either on the surface or at pre-existing crack tips, and with addition of stress, ductile fracture occurs in this corroded material and may propagate into the surrounding uncorroded region leading to failure. The study of the initiation of SCC by dealloying is of continuing technological importance [58–60]. Recent studies have focused attention on crack initiation in dealloyed material [22,61–64].

Biological activity has been found to cause the dealloying of Cu-Ni alloys under some conditions [65]. Dealloying may also be a problem in copper-gold and silver-gold alloys used for connections on printed circuit boards [66–68]. Since the vapor-deposited layers of silver-gold on printed circuit boards are very thin, even mild environments may cause enough dealloying to be of serious consequence and result in failure. A new class of aerospace alloys based on the aluminum-lithium system may also be affected by dealloying [25,26]. The removal of zinc from brasses (dezincification) has been of concern for many years [69], especially since it

occurs under ambient conditions in seawater and does not require application of a potential to initiate the dealloying.

In some cases, dealloying may have beneficial applications; for example, in the Raney process, patented in 1925 [70,71], dealloying produces a high-surface-area of nickel for applications such as catalysis, by the preferential removal of aluminum from Al-Ni alloys, leaving “active” nickel behind. This is a beneficial use for the porous metal resulting from dealloying. Another example of a beneficial use of dealloying is a recent one. Novel work by Verink and coworkers showed that the inner surfaces of faucets can be dealloyed to preferentially remove the lead from the surfaces and eliminate lead contamination to the drinking water coming into contact with the interiors of the faucets [72]. These examples show that dealloying continues to be of commercial interest and benefits of the microstructure and composition of dealloying can be found.

## MECHANISTIC MODELS AND MECHANISMS OF DEALLOYING

In order to exercise control over the process, the mechanism by which an alloy is parted (or dealloyed) needs to be understood. Mechanisms of dealloying have been discussed as long as the phenomenon has been known [2,69]. The specific example of dealloying in silver-gold alloys will be used to help explain and demonstrate features of the models outlined here. Six separate mechanistic models have developed for describing how dealloying takes place. The mechanistic models may be designated: Volume diffusion, vacancy diffusion, surface diffusion, oxide formation, percolation, and dissolution and reprecipitation. With these six models and the amount of experimental work that has gone into their creation, varying opinions on the results of experimental work exist and can be used to reinforce more than one of the models.

Preceding the discussion of the six proposed models for dealloying is Table 1, which summarizes the basic features of each model, along with information such as the temperature regime and the alloy systems to which each has been applied.

### Volume Diffusion Model

As the less noble component is removed by ionization and diffusion away from the metal surface, a constant supply of the less noble metal must be maintained by its diffusion toward the corroding interface from the bulk or diffusion of the more noble components away from the interface, or both (interdiffusion). At high temperatures, diffusion may be fast enough in some alloys to account for the constant supply of ionizable metal [73–75]. It was in this high-temperature regime where this model was first proposed by Wagner [73]. Since diffusion measurements are most often made at high temperatures, extrapolations of diffusivities to lower temperatures are often used in dealloying studies performed at room temperature. These extrapolations show that diffusion is too slow under steady state conditions to account for the extent of dealloying. Diffusion at ambient temperatures may be faster than extrapolations show, due to effects of grain boundaries, dislocations, or enhanced numbers of vacancies.



**TABLE 1**—Representation of the six mechanistic models for dealloying with information on temperature regimes, microstructural features, and evidence for the existence of the specific models.

Mechanism	Temp.	Features	Evidence	Alloys
Volume Diffusion	HT	Bulk diffusion accounts for all atoms ionized at interface	Intermediate composition phases found by X-ray diffraction	Au-Ag, Au-Cu, Cu-Ni, Co-Pt,
Vacancy Diffusion	RT	di- and trivacancies create pipeline diffusion	Mathematical model and X-ray diffraction data	Au-Cu, Co-Pt, others
Surface Diffusion	RT	High Energy Sites (Kinks and Jogs) allow dissolution of less noble metal	Mathematical simulation	Au-Cu, Au-Ag, Cu-Zn, others
Oxide Formation	RT	Noble metal oxide is metastable phase oxide rearranges to noble metal islands	Electron diffraction pattern shows extra spots	Au-Ag only
Percolation	RT	Inner-connectedness of lattice allows less noble metal to be removed	Mathematical simulation of structure	Au-Ag, Fe-Cr, Ni-Co, others
Dissolution and Reprecipitation	RT	Dissolution of both components, reprecipitation of more noble component, as islands	Solution chemistry crystals of pure metals electron diffraction shows rings	Au-Ag, Cu-Zn, Fe-Ni, others

A mathematical explanation for the severity of the room temperature diffusion problem, exemplified by silver-gold, can be summarized as follows: Data [76,77] demonstrate that interdiffusion at room temperature is too slow to account for dealloying. Diffusion coefficients previously used were extrapolated from values taken above 600°C. Data taken nearer room temperature cast doubt on earlier extrapolations and allow much more reliable values for diffusion coefficients to be obtained. These values could not account for diffusion of the silver to the solution interface, which would require diffusion of many orders of magnitude faster for removal of all of the silver from the alloy. Since, in some alloy compositions at room temperature, all of the silver can be ionized and removed from the alloy within a few minutes, bulk diffusion cannot be the means for moving the silver to the surface for ionization. There must be a much faster method by which the less noble metal can reach the solution metal interface, because volume diffusion can only account for a fraction of the movement required to ionize all of the less noble metal at the alloy-solution interface.

### Enhanced Diffusion Models

Mechanisms seeking to explain dealloying by enhanced diffusion have been considered by many authors. Vacancy Diffusion, where atoms associated with vacancies are transported rapidly through the lattice, is known to be faster than equilibrium bulk diffusion. This atomic diffusion coupled to vacancy diffusion is at the center of a model proposed by Pickering [78]. The model involves the formation of a large number of di- and trivacancies on the surface as a result of the dealloying process. Monovacancies have been shown to be too slow to account for the diffusion and so are not considered in Pickering's model [78]. In a later article, Pickering showed that with a divacancy concentration of approximately 10<sup>-2</sup>, his model can account for the diffusion of the less noble metal to the surface [79]. This is several orders of magnitude higher than the equilibrium vacancy content in well-annealed samples [77], and di- and trivacancies are generally at concentrations lower than the equilibrium monovacancy concentrations. This suggests that any model that relies on large numbers of vacancies to enhance diffusion must account for the energy required to form these vacancies in the dealloyed material, and this energy of formation is not included in Pickering's model.

Recent work by Jones et al. [80] has shown an enhancement of diffusion due to vacancies formed by anodic polarization. He has once again suggested that vacancies formed at room temperature by anodic dissolution are implicated in dealloying, embrittlement, and stress corrosion cracking. Specifically, divacancies are the species that migrate to the dissolving interface and enhance diffusion at that site. Other authors [81] have also recently returned to the vacancy enhanced mechanism for dealloying and SCC.

### Surface Diffusion

This is a critical feature of most models. Surface diffusion is faster than interdiffusion, discussed heretofore. Tischer and Gerisher [42] first proposed that surface diffusion could account for replenishment of the less noble metal to the corroding interface; Vermilyea [82] followed the initial lead, while theoretical advancements were made by Forty [43,45,83] and Galvele [84]. In Forty's model, the dissolution is thought to occur from kink sites on the surface, with the more noble metal diffusing to form islands. Forty suggests the dissolution of the less noble metal forms large numbers of surface vacancies that migrate inward and assist in the rearrangement. Vacancies initially create a disordered region that decomposes into noble metal islands that grow by surface diffusion, allowing removal of the less noble metal. However, even at the surface there is an energy barrier in vacancy formation, and data from Cook and Hilliard [77] found vacancies did not affect the overall diffusion rate significantly. Recently, surface diffusion has been the mechanism of most interest and several new groups have added their research to the growing body favoring surface diffusion as the mechanism that best explains the dealloying phenomenon [85-87].

Work has been conducted by Moffat et al. [88] involving scanning tunneling microscopy on copper-gold alloys. Several methods, including scanning tunneling microscopy, have been used by other authors [84-87] focusing on more rapid surface diffusion as the means for dealloying in various alloys. In all cases, the surface diffusion rates that are needed for complete dealloying are many orders of magnitude faster than the bulk diffusion rates. In some of the studies [85,87] new values quoted for the surface diffusion rates at room temperature are much faster than the rates previously accepted for surface diffusion.

Similar to surface diffusion is grain boundary diffusion, which is also much faster than bulk lattice diffusion. Pryor

and Lin [88] suggest both grain boundaries and pipe diffusion are active during dealloying with applied strain in copper-based alloys. Diffusion along grain boundaries has been considered as a possible means of allowing the less noble metal to rapidly diffuse to the surface and contribute to the rate at which dealloying occurs [82]. Grain boundaries were found to move during dealloying or under the influence of diffusion. This phenomenon, diffusion-induced grain-boundary migration (DIGM) [89–93], has been detected in single crystals and thin-film polycrystals. It may be worth consideration in dealloying studies, since direct movement of grain boundaries can occur in both alloying [92] and in dealloying [93], with solute diffusion leading to the formation of new grains (diffusion-induced recrystallization) [94].

Another form of the surface diffusion model relies on atomic rearrangement to create noble metal-rich islands and was proposed in a study of Ag-Au alloys by Forty [45]. Galvele makes use of rearrangement in his model [84,87], as does Young [95]. It is a way of managing the need for creating more surface without expending a great deal of energy. Young suggests that the remaining material will rearrange to accommodate the loss of the less noble material at the reaction front. He also cites surface diffusion along the interface between the dealloyed region and that which has not undergone dealloying as the mechanism of segregation of the less noble material. Forty, on the other hand, uses rearrangement to explain how the less noble material reaches the surface to be ionized. The more noble material rearranges, thus opening up pathways for the ionization to occur. In Galvele's model [87], rearrangement is an intermediate step on the way to formation of the porous microstructure.

### Oxide Formation Model

In the oxide formation model, oxidation of the more noble metal (gold, in the example of Forty [45] and Durkin and Forty [43]) occurs as a result of the change of chemical environment brought about by the selective dissolution of the less noble silver. The gold oxide is thought to be a metastable phase, which accounts for the rapid rearrangement of the gold into the islands noted in the microstructure. Surface diffusion is the mechanism by which this rearrangement occurs. Evidence cited for oxide formation involves electron diffraction patterns and dark field electron microscopy, but these interpretations are not without problems. One concern with this model is that stable oxides are not known to form in several of the alloy/environment systems where dealloying takes place [96,97]. Generally, this model can be considered as a subset of the surface diffusion model, since the formation of the oxide is merely an intermediate step.

### Percolation Model

Diffusion plays a minor role in a mechanistic model described recently by Sieradzki et al. [98] and Halley [99], which relies on the interconnected nature of the lattice material. As the less noble component goes into solution, percolation allows the solution to move into the bulk and ionize the less noble component because each atom of noble

metal is less interconnected to another less noble metal atom. This model relies on the new science of chaos theory to explain the complex behavior of the systems undergoing dealloying [99]. Mathematical modeling involving Monte Carlo simulation for diffusion, using percolation theory, with simple rules for dissolution of the less noble component was combined with known morphological features of the phenomenon. But in the initial simulation, these rules lead to cessation of the dealloying process if surface diffusion was not employed. When simulations of dealloying take place, involving the same rules of dissolution but with surface diffusion added, the results for the 2D square and the 3D simple cubic lattices produce many of the features usually associated with dealloying, such as a porous island/channel structure and coarsening of the porous structure on annealing, but on an atomic rather than molecular scale. Although the dimensions do not match the microstructure found experimentally, the mathematical model is interesting in its ability to produce an island/channel structure. A percolation model for dealloying was originally proposed by Keir and Pryor [17] and the contribution of Sieradzki et al. [98] is primarily in the computer-generated modeling of the lattice and the mathematical description of the model. Recent work on coarsening of dealloyed microstructures with annealing has shown microstructural features similar to those seen in the mathematical modeling [49,63,85,98–100].

There are some concerns about using percolation theory itself, which limits removal to 30 % of the original composition of the more noble component [101]. In work by Halley, mention is made that at high surface potentials, percolation will not occur since the surface will not be fractal, and an additional feature is needed to explain dealloying beyond the limits of percolation theory [99]. Sieradzki et al. [98] overcomes this limitation by allowing a small amount of surface diffusion to occur, which will initiate further fractal formation at the surface.

### Dissolution and Reprecipitation Model

One model that involves essentially no diffusion in the bulk or on the surface could be characterized as dissolution and reprecipitation. Dissolution of the entire alloy surface under anodic conditions is followed by reprecipitation of the more noble component. Early in this century, many authors postulated this as the most likely mechanism for dealloying [3,37,102]. Much of the early work was done on brasses and involved chemical analysis of the solutions during dealloying. This analysis showed the presence of both copper and zinc, under most conditions.

Holloman and Wulf [103] and Fink and Evans [104] suggested that electrochemical inhomogeneities could contribute to the redeposition, at copper-rich cathodic sites, of the copper that had been dissolved from anodic sites along with the zinc. More recently, Heidersbach [105,106] and Heidersbach and Verink [55] have shown, definitively, that under certain conditions, dissolution and reprecipitation occur in brasses. Swann [107] also showed that particles of pure gold were formed on the insides of tunnels formed by dealloying of copper gold alloys in nitric acid. The study of linear instability was the major thrust of the work by Halley [99], who

considered both the dissolution and deposition cases. Hamilton [108], who also considered only deposition, showed that the surface instability leads to the formation of particles rather than a smooth surface. Young [95] describes dealloying of copper-aluminum alloys and cites dissolution and reprecipitation of the copper as the mechanism by which the porous microstructure coarsens. Mathematical modeling by Newman et al. [109] has shown that for Fe-Cr alloys, particles of chromium can form on the surface under conditions of incomplete passivation.

The dissolution and reprecipitation model fell out of favor for certain alloy systems like copper-gold when no gold could be detected by chemical analysis of the solution sampled during dealloying [110]. Electrochemical techniques such as measurement with a ring disk electrode also showed that no gold was plated onto the surface of the ring, while the disk of copper-gold was under dealloying conditions, suggesting that no dissolution of gold occurred from copper-gold alloys.

Other possible difficulties with this model include the appearance of intermediate compositions between those of the noble metal and the original alloy, when precipitation of only the noble metal is predicted by this model. Dealloying is also known to occur at potentials far from the known dissolution potential for the more noble metal, leading to questions as to whether any of the more noble metal would dissolve under these conditions.

In summary, regarding the mechanistic models proposed for dealloying, none has been shown to be without problems. The volume diffusion model is much too slow at room temperature to allow dealloying to go to completion. Enhanced diffusion mechanisms have sought to remedy this problem by applying faster means of diffusion. The vacancy diffusion model encounters difficulty in explaining the energy required to form large numbers of di- or trivacancies, which are necessary for this model's success. Surface diffusion has been shown to be fast enough to account for the diffusion required for complete dealloying, if all the diffusion occurred by this means. The difficulty here is that much more surface would need to be created for surface diffusion to be the only means of diffusion needed. The percolation model, as it is presently discussed, involves a certain amount of surface diffusion. This model can account for the removal of the less noble alloy, but it cannot provide a means for formation of new surfaces such as the crystallites seen in some studies [51]. Currently, the only model able to explain formation of crystallites is the dissolution and reprecipitation model, which encounters problems explaining dealloying far from the dissolution potential of the more noble alloy.

### Discussion of "Parting Limits"

In some alloy systems, studies of dealloying appear to show a "parting limit." ASTM defines parting limit as:

"The minimum concentration of the more noble component in an alloy, above which parting (or preferential dissolution) does not occur" [1].

Parting limits have been suggested in many alloy systems, particularly binary alloys. A thorough review of parting limits up to the time of its publication is Pickering's 1983 article [8]. In order to explain the development of a parting limit,

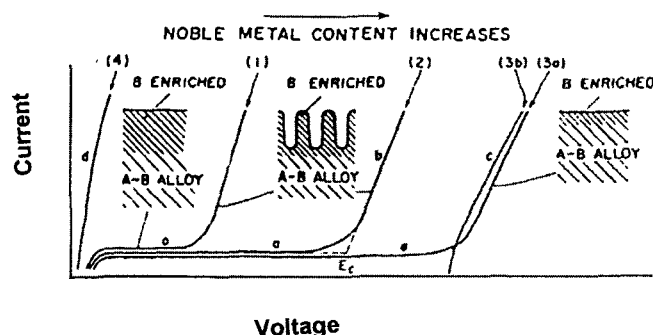


FIG. 2—After a figure by Pickering in Ref. 8, outlining the polarization behavior of alloys that undergo dealloying. The value of potential, shown as  $E_c$ , is the value of the critical potential above which Type II dealloying behavior is expected.

the silver-gold system is considered as an example. In silver-gold alloys, a parting limit was first reported in the extraction of gold from native silver-gold alloys by beneficiation involving dissolution [111]. It is quite likely that the existence of certain compositions of gold-rich silver-gold alloys, which were virtually impossible to "part" by static dissolution processes, had been known since ancient times, and this knowledge was instrumental in determining the composition of alloys that were made from native ores [38,112]. Native gold is almost always alloyed with some silver. One gold-silver alloy that was well known in ancient times is called electrum and is approximately 20 % silver. Development of the concept of a parting limit in other binary alloys followed much the same path, from origins in the mining industry or from phenomenological studies that were usually chemical rather than electrochemical in nature, or from case studies in aqueous solutions [102–104,113]. Few electrochemical studies have questioned the existence of parting limits in a number of binary systems [22]. Most of the work on binary alloys has concentrated on the initiation of dealloying rather than its completion [24,105–109].

Parting of gold from silver was usually done with acids such as nitric or sulfuric acid. In order to separate fully the silver from the gold-rich alloys, additional silver was added before the acid dissolution process took place. Textbooks mention complete parting of gold from a silver-gold alloy; the amount of silver must be at least 2.5 times the amount of gold. Compositions of 20–25 % gold are suggested as best compositions for parting in mining textbooks. Even in textbooks that describe parting limits, the removal of gold from alloys containing various amounts of gold greater than 50 % is mentioned, but is deemed not "efficient" [111]. Reports of dealloying of other binary alloys in compositions beyond the parting limits have occasionally been seen, but have been considered controversial [55,114].

In approaching the issue of parting quite broadly, Pickering, in 1983, provided a widely used schematic representation of the anodic polarization behavior of any binary alloy (A-B), such as copper-gold, silver-gold, most brasses, and many others, which are known to undergo dealloying [8]. He covers the electrochemical behavior of binary alloys, as well as the parting limit. A figure of the same type as that by Pickering is shown here as Fig. 2; the markings follow

those of the original. Pickering designated three regions of dissolution behavior. In the first region (Region 1), which is characterized by very low current values over a wide range of potentials, the alloy is undergoing dissolution of the less noble component (A) and a buildup of the more noble component (B) on the surface. No porosity is expected in Region 1, only uniform dissolution of A. Region 2 begins with the initiation of a higher dissolution rate of A, and a marked increase in current with only a small increase in potential. Dissolution of the less noble component, A, preferentially occurs in this region. Dealloying occurs in this region over a range of potentials and for a range of alloy compositions, with the formation of a porous layer as the less noble component is dissolved. Pickering's explanation for the transition from this region of typical dealloying behavior to the next region is not absolutely clear, but is thought to go no further than the potential at which the more noble component, B, begins to dissolve. Above the dissolution potential for B, Region 3 behavior occurs. He describes this region as being characterized by nonselective dissolution with no porosity formed. The behavior in Region 2 is referred to by Pickering as Type I and Region 3 is said to exhibit Type II behavior. The transition from Type I to Type II behavior is dependent on potential and alloy composition. This transition from Type I behavior, with preferential dissolution and porous microstructure formed, to Type II behavior, with no porous microstructure and uniform dissolution, has been used by a number of authors to define the parting limit for several alloy systems. For example, in silver-gold alloys, the value cited for the transition from Type I to Type II dissolution (the parting limit) is a mole fraction of gold of 35–45 % for perchloric acid solutions, and references the work by Tischer and Gerisher. In their study, Tischer and Gerisher report that these alloys [42] show no microstructural evidence of the formation of porosity above 50 % gold when they were exposed to large anodic potentials.

Other systems such as brasses, copper-gold, platinum-copper, and several others are described by Pickering as having a mole fraction of the more noble metal above which Type I behavior is not found [7]. However, in copper-base alloys, other authors have shown dealloying occurring in all of the phases, even those assumed to be resistant to dealloying [20,55,114].

In the case of silver-gold, the value for the parting limit for silver-gold alloys has been reported in the literature from just below 50 % Au [111] to above 55 % Au [42]. In 1931, Tamman and Brauns [113] found that alloys containing more than 50 % Au were not attacked by immersion in hot sulfuric acid. More recent work connects the value for a parting limit to the mechanism outlined for dealloying. Duffo and Galvele, for example, defended a mechanism for dealloying related to surface diffusion and formation of a low melting point intermediate compound, a value for the parting limit of 20 % Ag [87] in Ag-Au alloys, 10 % Pd in Ag-Pd alloys, and 30 % Ag in Ag-Cd alloys. When the percolation model for dealloying is considered for silver-gold alloys in perchloric acid, a limit of 30 % Ag is cited [98,112], since this is the value at which an interconnected path of silver atoms can be found. In recent work involving scanning tunneling microscopy [44,85], alloys with Au content

as high as 96 % Au were shown to exhibit preferential silver dissolution and formed a porous surface. The example of silver-gold alloys shows that the concept of a parting limit, while widely accepted, has questions remaining behind it, which are beginning to be addressed. This is also true of other binary alloys where a parting limit has been found, and in some cases re-evaluation has taken place [24,55,114].

## TESTING TECHNIQUES USED IN STUDYING DEALLOYING

Since the existence of dealloying was first noted visually [2], much of the early work on dealloying involved discovery of the systems that were susceptible [3–10], and, to some extent, the environment and temperature where dealloying was found. Earliest work involved aqueous systems [2,69], but a short time later, work at high temperatures detected the existence of dealloying under those conditions as well [53,73]. When dealloying was linked with SCC [5,64], the testing of materials for dealloying became intertwined with testing alloys for SCC, with the initiation thought to involve dealloying at the crack-tip surface [7,12,22,29–31,48–51,64,85–87].

Dealloying has been found to initiate in small areas or patches and spread over the entire surface in stages [4,11,29]. Much of the work done on the mechanism of dealloying and on the initiation and the fundamental aspects of dealloying has been done electrochemically [8,11,14,29–32,60]. Electrochemical methods involve application of constant potential, constant current, or cyclic potential. Methods used for examining dealloying involve standard ASTM methods for making electrochemical measurements [1,54]. Examination of dealloyed microstructure may require SEM, TEM, or HRSEM. Recent work has made use of scanning tunneling microscopy [24,44,49].

## Immersion and Observation

The first method for examining susceptibility of alloys to dealloying was reported by Calvert and Johnson in 1866, who reported the complete removal of zinc when brass was immersed in sulfuric acid for several days [2]. The effects of dealloying had certainly been noted as long as brasses had been used in seawater. The ability to part silver from alloys of silver-gold had been noted much earlier, since it was used by pre-Columbian civilizations in production of gold-surfaced objects centuries before Columbus [112]. Systematic studies of dealloying seem to have begun in 1866. It could be speculated that the original reason for testing copper-zinc alloys in sulfuric acid was a result of the knowledge of the behavior of certain compositions in seawater (those which show dealloying behavior). The method of immersion of an alloy in certain acids, bases, or other solutions can also be cited as the beginning of the study of corrosion of metals.

Observing the effects of solutions on the alloys was done visually and with light microscopy. The examination of brasses by light microscopy is somewhat fortuitous, since the porous microstructure can be noted in most of these

alloys with only a light microscope. Had an alloy such as silver-gold been examined initially, the brittleness would have been noted but the microstructure would have been invisible, since it is on the order of a few hundred angstroms in size (dimensions of both the islands and the channels). When the porous microstructure of Cu-Zn was first noted, as Calvert and Johnson had done, most early authors suggested that one element had been dissolved, leaving the matrix of the other element [2,23].

Dealloying occurs over a wide temperature range from aqueous to gaseous environments [3-6,28,73,74], and in a large number of solutions [3-10,16-36]. Therefore, when one considers immersion, the term must be expanded to include gaseous environments as well as aqueous ones. Some of the most widely referenced studies of dealloying, such as that of Wagner [73,74], were done at high temperatures. The mechanistic information that was derived from such studies has been extended to room temperature and aqueous environments and forms the basis for much of the understanding of the mechanisms of dealloying still accepted presently [9,22].

One recent development in the static immersion testing from Newman et al. [116] originated with Bengough and May [115]. Recent experimentation [116] involved exposing samples of alpha-brass in NaCl solutions with additions to simulate the local environment in crevices or otherwise inhibited transport. Under these severe conditions, dealloying can be shown to occur without an applied potential and may be reduced or eliminated by addition of arsenic to the alloy. The authors suggest that these results support the percolation mechanism with surface diffusion for dealloying rather than mechanisms that rely on formation of metastable phases or disproportionation of the less noble element.

### Electrochemical Methods

In some cases, initiation of dealloying may require polarization of specimens to a potential where the less noble element in the alloy will begin to be dissolved. In addition to the applied potential, a specific combination of solution and alloy is required for dealloying to occur. Silver-gold in perchloric acid is an example of the combination of alloy and solution, which will not initiate dealloying without polarization. By contrast, however, silver-gold alloys in nitric acid will begin to dealloy immediately upon immersion. For combinations of alloy and solution where potential application is necessary to initiate dealloying, there is a value of potential below which bulk dealloying does not occur. This value is usually referred to as the critical potential. Investigation of the specific values of the critical potential for alloy systems has been an important part of the study of dealloying by electrochemical methods [8,10,19-26].

The nature of the critical potential has been debated as part of the mechanistic studies of dealloying. Authors such as Forty [45], who subscribe to a rearrangement model for dealloying, suggest that the critical potential is the potential at which dissolution from kinks and jogs on the surface is activated, while authors who argue for a diffusion-related mechanism suggest that the critical potential relates to the unblocking of pathways for the transport of the less noble metal to the surface [48-50,98-100]. Probably the most comprehensive discussion

of the critical potential is included in Pickering's graphical representation of dealloying and the parting limit [8]. Above the critical potential, dissolution of the less noble component, A, preferentially occurs over a range of potentials and for a range of alloy compositions. The formation of a porous layer as the less noble component is dissolved is the visible sign that dealloying has occurred.

Alloys that have a wide range of potentials where dealloying occurs, such as silver-gold alloys, provide an opportunity to examine closely the initiation and growth of dealloying as a function of applied potential. Under some carefully controlled conditions, one sample may be exposed to several different electrochemical conditions and examined following each exposure [51]. This minimizes sample-to-sample variation and allows examination of a specific region in the sample while the conditions are varied. In most cases, however, samples are exposed to only one potential and then examined [46]. Scanning tunneling microscopy has allowed even closer observation of the surfaces of alloys with applied potentials. Movement of the atoms on the surfaces as the potential is changed has been noted [24,44,49]. This and other in situ techniques may provide the electrochemical evidence needed to discern which mechanism of dealloying is operating under specific circumstances.

When electrochemical methods are used to ionize the less noble metal, current flow can be quantitatively measured. The number of moles of metal ionized can be calculated and compared with the mass lost from the sample. Detection of the relative amount of current can be used as a basis for deciphering the initiation or completion of dealloying. When current at constant potential drops to zero or nearly zero, dealloying will have stopped. Monitoring of the current can be used as an electrochemical indicator of the type of attack as well [117].

### Microstructural Examination

Transmission electron microscopy (TEM) has been used for examining dealloying for almost 30 years. The difficulty in preparing thin samples of uniform composition and also of dealloying very thin samples has made this type of study quite involved [19,42,46,47,62]. When the microstructure formed by dealloying was examined, several interesting issues were raised. Variations in the dimensions of the island/channel microstructure have been noted by several authors [42,44,46,118]. It has been shown that the dimensions of the microstructure vary with annealing [43], while other effects on the island/channel microstructure of potential are not quite so clear, but investigation on this segment of dealloying is continuing [44,49]. Use of scanning tunneling microscopy may lead to interesting information related to the island/channel dimensions.

## EVALUATION OF TEST RESULTS

### Service Performance versus Test Results

Samples that are dealloyed have a microstructure that is recognizable, depending on the magnification used and the extent of dealloying, since dealloying initiates in patches and

grows to cover the entire sample, with time in solution or at constant potential. The existence of the island/channel microstructure is often used to identify dealloying. Chemical examination of the solution is also used to detect the presence of the less noble metal when it is being dissolved in the dealloying process.

Examination of the surface to detect the presence of the porous microstructure can be used as a qualifying test for the presence of dealloying. Under laboratory conditions, dealloying is usually detected visually, using some type of microscopy. In service conditions, this may be far too late to prevent the dealloying from leading to catastrophic failure due to the lack of structural strength provided by the porous material or due to SCC following the dealloying [58]. Detection of the less noble metal in solution may be made at very low levels depending on the chemical test method used. This method could be done under conditions such as may be found in the electronics industry where dealloying of printed circuits may be a problem. Test methods have been developed to detect susceptibility to SCC [119–122], and these methods could be applied to dealloying since the two phenomena are linked, in many cases. Tests that are electrochemical, mechanical, or both have been used to investigate SCC for some time [119–122]. Electrochemical test methods exist for examination of dealloying and could be combined with chemical methods to provide instantaneous evidence of initiation of dealloying.

Other methods with possible application to dealloying include electrochemical noise measurements, which some authors have used to detect SCC [117]. Electrochemical impedance measurements have been used to evaluate dealloying, but not specifically to predict its existence [49]. Verink and Parish have shown that making use of overlaid Pourbaix diagrams for alloys, in the way that Pourbaix himself suggested [114,122], can yield information on the potential for dealloying in aqueous solutions. No specific electrochemical method exists for determination of susceptibility to dealloying, such as the polarization test showing a hysteresis suggestive of pitting; however, use of electrochemical techniques can provide data that can be used to support conclusions of dealloying sensitivity, and the development of sensitive monitoring methods, such as electrochemical noise, may lead to such specific tests.

## STANDARDS

### ISO Standards

The relationship between dealloying and initiation of SCC is the area of greatest technological interest and emphasis. The International Standards Organization (ISO) has developed a standard related to initiation of SCC by dealloying [124]. As the porous and mechanically weak surface layer develops on the surface or at the tip of a pre-existing crack by dealloying, additional stress will cause a brittle fracture to propagate in this otherwise ductile material. The level of stress may be such that the crack may even extend into the uncorroded material beyond the dealloyed region. It is the initiation and propagation of these brittle cracks in otherwise ductile material that leads to failure.

Consideration is given to the susceptibility of the alloy in the specific environment of interest in the ISO document. However, extension of the limits of the known ranges, compositions, and temperatures leading to dealloying is not addressed in the ISO draft standard. Predictability beyond accepted limits is often an issue with application of standards, and the study of dealloying is not unique in this area. Dealloying specifically is mentioned in the ISO draft standard, and reference to initiation of SCC is also mentioned.

### ASTM and NACE Standards

Although ASTM has a definition for dealloying [1], there are no ASTM active or draft standards that involve testing or examination of alloys for dealloying. In standards that deal with SCC, dealloying is not mentioned explicitly, although inferences are made to initiation by means of SCC [54].

By contrast, NACE has not published any standards that mention dealloying. NACE does have several standards and reference publications that deal with SCC [118–121], but dealloying is not mentioned in any of these.

### Use of Standards in Industry

Industries, such as the power industry, where dealloying continues to be a significant problem, use combinations of solutions and alloy composition in specifying materials for redesign. This is due, in part, to knowledge of some conditions where dealloying causes condensers to fail. The elimination of combinations of solutions and alloy compositions where dealloying may contribute to premature condenser failure [12] appears as an *ipso facto* industrial standard. In the mining industry, where the ability to part alloy compositions is related to dealloying, a series of procedures rather than actual standards is used to separate alloys of specific compositions. The efficient removal of the less noble metal is the primary goal, along with the minimization of the amount of energy used to accomplish this goal.

Recycling of precious metal alloys from diverse sources, such as electronics, jewelry, and medical or dental supplies, may require development of procedures for separation and removal of the less noble metal and concentration of the more noble metal. Dealloying and the effect of the composition of the starting material on the amount of energy needed to fully separate the more noble metal may be of importance with continued growth of the recycling industry and increased pressure on pricing of precious metals and alloys. Work is continuing on use of alloys containing lower content of noble metal for environments where corrosion continues to be a problem (such as dentistry) [125]. Increased usage by the aerospace or aircraft industry of age-hardenable high-strength aluminum alloys, such as the low-density aluminum-copper-lithium alloys, may further the discussion of dealloying in these alloys in order to lower the risk of corrosion (dealloying) related failure [25,26].

## SUMMARY AND CONCLUSIONS

Historically, dealloying has been known and studied for more than 150 years. The mechanism for dealloying has

been speculated upon for nearly that long. Many alloys are known to be susceptible to dealloying, which has been implicated in the initiation of stress corrosion cracking for a number of different alloys. Currently, dealloying is still of interest to scientists, but not as an industrial problem, although several industries such as the electronics industry were mentioned where the possibility of dealloying seems significant.

Six different mechanisms for dealloying were outlined with data on the features noted and the evidence cited for each mechanistic model. Alloys where each model has been studied were also noted. Detailed descriptions of the models were presented and information given regarding how well the models can explain what has been seen about dealloying. Most current research is focused on surface diffusion as the mechanism for dealloying, although vacancy formation and dissolution and reprecipitation have been suggested as well. In addition, recent results have led to questions regarding the parting limit in some alloys.

The initiation and growth of dealloying has been well documented and can be detected visually, using microscopy (including HRSEM and TEM) or chemically by analysis of the less noble metal ions in solution. Electrochemically, no specific test exists to detect dealloying, but passage of significant anodic current in susceptible alloys in well-known solutions can give evidence for dealloying. Some methods such as electrochemical noise seem to have promise for detection of dealloying by electrochemical means.

## REFERENCES

- [1] ASTM Standard G 31-72: Practice for Laboratory Immersion Corrosion Testing of Metals, *Annual Book of ASTM Standards*, Vol. 3.02, ASTM International, West Conshohocken, PA, 1992.
- [2] Calvert, C. and Johnson, R., "Action of Acids Upon Metals and Alloys," *Philosophical Magazine*, 1866, pp. 434-455.
- [3] Bird, D. B. and Moore, K. L., "Dezincification of Brasses in Seawater," *Materials Protection*, Vol. 1, 1962, pp. 70-74.
- [4] Stewart, W. C. and LaQue, F. L., "Removal of Nickel from Copper Alloys," *Corrosion*, Vol. 8, 1940, pp. 259-266.
- [5] Britton, S. C., "Dealloying in Aluminum Bronzes," *Journal of the Institute of Metals*, Vol. 67, 1941, pp. 119-123.
- [6] Trautzel, P. and Treadwell, W. D., "Corrosion of Bronzes," *Helvetica Chimica Acta*, Vol. 34, 1951, pp. 1723-1744.
- [7] Fontana, M. G., "Stress Corrosion Cracking in Nickel Alloys," *Industrial Chemical Engineering*, Vol. 39, No. 5, 1947, pp. 87a-89a.
- [8] Pickering, H. W., "Characteristic Features of Alloy Polarization Curves," *Corrosion Science*, Vol. 23, No. 10, 1983, pp. 1107-1120.
- [9] Hiller, K., Kaiser, H., Kaesche, H., et al., "Dealloying for Silver-Palladium in Chloride Systems," *Werkstoffe und Korrosion*, Vol. 33, 1982, pp. 83-95.
- [10] Marshkov, I. K., Bolychev, V. S., and Potapova, D. P., "Review of Dealloying in Copper-Zinc Alloys" (approximate translation of title), *Z. Metallv.*, Vol. 9, 1973, pp. 3-15.
- [11] Pickering, H. W. and Byrne, P. J., "Partial Currents During Anodic Dissolution of Cu-Zn Alloys at Constant Potential," *Journal of the Electrochemical Society*, Vol. 116, No. 11, 1969, pp. 1492-1496.
- [12] Cohen, A., *Process Industries Corrosion*, W. I. Pollock and B. J. Monez, Eds., NACE, Houston, TX, 1986, p. 500.
- [13] Marshkov, I. K., Bolychev, V. S., and Potapova, D. P., "Prevention of Dezincification," *Prot. Metals*, Vol. 9, 1973, pp. 1-14.
- [14] Schussler, M. and Napolitan, D. S., "Selective Dissolution from Copper-Based Alloys," *Corrosion*, Vol. 12, 1956, p. 107t.
- [15] Serre, J. and Lawreys, J., "Selective Dissolution from Copper-Based Alloys," *Corrosion Science*, Vol. 2, 1965, p. 135.
- [16] Copson, H. and Cheng, C., "Stress Corrosion Cracking of Monel in Hydrofluoric Acid," *Corrosion*, December 1956, p. 71.
- [17] Keir, D. S. and Pryor, M. J., "The Dealloying of Copper-Manganese Alloys," *Journal of the Electrochemical Society*, Vol. 127, No. 10, 1980, pp. 2138-2144.
- [18] Ammar, I. A., Darwish, S., Khalil, M. W., and El-Taher, S., "Anodic Oxide Film Formation on Tin," *Corrosion*, March 1990, p. 197.
- [19] Pickering, H. W., "Metallurgical Aspects of Electrolytic Dissolution of Alloys," in *Proceedings of the Darken Conference*, 1976, pp. 1-21.
- [20] Pickering, H. W. and Byrne, P. J., "Stress Corrosion of  $\alpha$ -Brass in an Acid Sulfate Solution," *Corrosion*, August 1973, p. 325.
- [21] Lichter, B. D. and Wagner, C., "The Attack of Copper-Gold, Silver-Gold, Nickel-Copper and Silver-Copper Alloys by Sulfur at Elevated Temperatures," *Journal of the Electrochemical Society*, Vol. 107, No. 3, 1960, pp. 168-180.
- [22] Cassagne, T. B., Flanagan, W. F., and Lichter, B. D., "Stress-Corrosion Cracking of Copper-24 Gold Single Crystals in Aqueous Chloride Media," in *Chemistry and Physics of Fracture*, D. H. Jones and R. M. Lattinison, Eds., NATO, Brussels, 1988, pp. 659-669.
- [23] Gerischer, V. H. and Rickert, H., "Über das Electrochemische Verhalten von Kupfer-Gold-Legierungen und den Mechanismus der Spannungskorrosion," *Z. Metallkde.*, Vol. 46, No. 9, 1955, pp. 681-689.
- [24] Moffat, T. P., Fan, F. R. F., and Bard, A. J., "Electrochemical and Scanning Tunneling Microscopic Study of Dealloying of  $\text{Cu}_3\text{Au}$ ," *Journal of the Electrochemical Society*, Vol. 138, No. 11, 1991, pp. 3224-3235.
- [25] Bavarian, B., Becker, J., Parikh, S. N., and Zamanzadeh, H., "Localized Corrosion of 2090 and 2091 Al-Li Alloys, Aluminum-Lithium Alloys," *Proceedings of the 5th International Aluminum-Lithium Conference*, T. H. Sanders, Jr. and E. A. Starke, Jr., Eds., 1989, pp. 1227-1236.
- [26] Buchheit, R. G. and Stoner, G. E., "The Corrosion Behavior of the  $\text{T}_1$   $\text{Al}_2\text{Cu-Li}$  Intermetallic Compound in Aqueous Environments, Aluminum-Lithium Alloys," *Proceedings of the 5th International Aluminum-Lithium Conference*, T. H. Sanders, Jr. and E. A. Starke, Jr., Eds., 1989, pp. 1347-1356.
- [27] Dvorak, A., (no title translation available), *Strojeirentsvi*, Vol. 12, No. 1, 1962, pp. 39-46.
- [28] Trax, R. V. and Holzwarth, J. C., "High Temperature Oxidation of Stainless Steels," *Corrosion*, Vol. 16, 1960, pp. 105-108.
- [29] Fontana, M. G., "Selective Dissolution from Stellite," *Industrial and Engineering Chemistry*, Vol. 39, No. 5, 1947, p. 87A.
- [30] Clark, W. D., "Selective Dissolution from Stellite," *Journal of the Institute of Metals*, Vol. 73, 1947, pp. 263-273.
- [31] Clarke, W. L. and Gordon, G. M., "Investigation of Stress Corrosion Cracking Susceptibility of Fe-Ni-Cr Alloys in Nuclear Reactor Water Environments," *Corrosion*, January 1973, p. 1.
- [32] Bakish, R. and Kern, F., "Preferential Dissolution of Chromium and Iron from Inconel," *Corrosion*, Vol. 16, 1960, pp. 89-90.
- [33] Larson, T. and Skold, R., "Laboratory Studies Relating Mineral Quality of Water to Corrosion of Steel and Cast Iron," *Corrosion*, June 1958, p. 43.
- [34] Bloom, P. R. and Tuovinen, O. H., "Characterization of Graphitic Corrosion Residue of Cast Iron in a Water Distribution System," *Materials Performance*, February 1984, p. 21.
- [35] Heidersbach, R., "Regarding the Mechanism of Dealloying in Cu-Zn," *Corrosion*, Vol. 24, 1968, p. 38-X.
- [36] Steigerwald, R. F., "The Effects of Metallic Second Phases in Stainless Steels," *Corrosion*, September 1977, p. 338.
- [37] Storey, H. T., "Corrosion of Metallic Brasses," *Met. Chem. Eng.*, Vol. 17, 1917, pp. 650-654.



- [38] Scott, D. A., *Pre-Hispanic Colombian Metallurgy: Studies of Some Gold and Platinum Alloys*, University of London, Institute of Archeology, 1982, pp. 46–134.
- [39] Armstrong, G., Himsworth, F. R., and Butler, J. A. V., "The Kinetics of Electrode Processes—Part III. The Behavior of Platinum and Gold Electrodes in Sulphuric Acid and Alkaline Solutions Containing Oxygen," *Proceedings of the Royal Society A*, Vol. 138, 1933, pp. 89–103.
- [40] Handwerker, C. A., Lechtman, H. N., Marinenko, R. B., and Bright, D. S., "Fabrication of Platinum-Gold Alloys in Pre-Hispanic South America: Issues of Temperature and Microstructure Control," *Materials Research Society Proceedings*, Vol. 185, Materials Research Society, 1991, pp. 649–664.
- [41] Hiller, K., Kaiser, H., Kaesche, H., et al., *Werkstoffe und Korrosion*, Vol. 33, No. 83, 1982.
- [42] Tischer, V. R. P. and Gerischer, H., "Elektrolytische Auflösung von Gold-Silber-Legierungen und die Fränge der Reistengrenzen," *Z. für Elektrochem.*, Vol. 62, No. 5, 1958, pp. 50–64.
- [43] Forty, A. J. and Durkin, P., "A Micromorphological Study of the Dissolution of Silver-Gold Alloys in Nitric Acid," *Philosophical Magazine A*, Vol. 42, No. 3, 1989, pp. 295–318.
- [44] Oppenheim, I. C., Trevor, D., Chidsey, C. E. D., et al., "In Situ Scanning Tunneling Microscopy of Corrosion of Silver-Gold Alloys," *Science*, Vol. 254, No. 1, November 1991, pp. 687–689.
- [45] Forty, A. J., "Micromorphological Studies of the Corrosion of Gold Alloys," *Gold Bull.*, Vol. 14, No. 1, 1981, pp. 25–35.
- [46] Carter, D., *Electrochemical and Electron-Microscopical Studies of Anodically Corroded Silver-Gold Alloys*, University of Warwick, Department of Physics, 1985, pp. 1–145.
- [47] Van Orden, A. C., "Dealloying of Ag-Au an Interface Morphology Problem," Paper 156, *Corrosion/88*, NACE, 1988, pp. 156–1–156–8.
- [48] Li, R. and Sieradzki, K., "Mechanical Properties of Dealloyed Microstructure and Coarsening," *Phys. Rev. Lett.*, Vol. 45, No. 6, 1993, pp. 634–642.
- [49] Kelly, R. G., Young, A. J., and Newman, R. C., "The Coarsening of Dealloyed Layers by EIS and Its Correlation with Stress-Corrosion Cracking," in *Electrochemical Impedance: Analysis and Interpretation*, ASTM STP 1188, J. R. Scully, D. C. Silverman, and M. W. Kendig, Eds., ASTM International, West Conshohocken, PA, 1993, pp. 94–112.
- [50] Newman, R. C., Kim, J. S., and Sieradzki, K., "Dealloying and Growth of Cracks in Ductile Materials," in *Modelling Environmental Effects on Crack Growth Processes*, D. H. Jones and S. Gerbrick, Eds., TMS-AIME, 1986, pp. 127–140.
- [51] Van Orden, A. C., "Dealloying of Silver-Gold in Perchloric Acid," Dissertation, University of Maryland, College Park, MD, 1994, pp. 1–186.
- [52] Shreir, L. L., "Anodic Polarization of Lead-Platinum Bielectrodes in Chloride Solutions," *Corrosion*, March 1961, p. 90.
- [53] Graf, L., "Zur Spannungskorrosion Heterogener Legierungen," *Z. Metall.*, Vol. 46, 1949, p. 275.
- [54] *Annual Book of ASTM Standards*, Vol. 3, ASTM International, West Conshohocken, PA, 1992, p. 77.
- [55] Heidersbach, R. H., Jr. and Verink, E. D., Jr., "The Dezincification of Alpha and Beta Brasses," *Corrosion*, Vol. 28, No. 11, 1972, pp. 397–418.
- [56] Sieradzki, K., Dienes, G. J., Paskin, A., and Massoumzadeh, B., "Atomistics of Crack Propagation," *Acta Metallurgica*, Vol. 36, No. 3, 1988, pp. 651–663.
- [57] Bakish, R. and Robertson, W. D., "Structure-Dependent Chemical Reaction and Nucleation of Fracture in Cu<sub>3</sub>Au Single Crystals," *Acta Metallurgica*, Vol. 4, July 1956, pp. 342–351.
- [58] Copson, H. R. and Cheng, C. F., "Some Case Histories of Stress Corrosion Cracking of Austenitic Stainless Steels Associated with Chlorides," *Corrosion*, June 1957, p. 55.
- [59] Rooyen, D. V., "Qualitative Mechanism of Stress Corrosion Cracking of Austenitic Stainless Steels," *Corrosion*, September 1960, p. 93.
- [60] Williams, W. L., "Stress Corrosion Cracking: A Review of Current Status (An Educational Lecture)," *Corrosion*, July 1961, p. 92.
- [61] Sieradzki, K. and Newman, R. C., "Brittle Behaviour of Ductile Metals during Stress-Corrosion Cracking," *Philosophical Magazine A*, Vol. 51, No. 1, 1985, pp. 95–132.
- [62] Pickering, H. W. and Swann, P. R., "Electron Metallography of Chemical Attack Upon Some Alloys Susceptible to Stress Corrosion Cracking," *Corrosion*, Vol. 19, September 1963, pp. 373–389.
- [63] Sieradzki, K., Dienes, G. J., Paskin, A., and Massoumzadeh, B., "Atomistics of Crack Propagation," *Acta Metallurgica*, Vol. 36, No. 3, 1988, pp. 651–663.
- [64] Cassagne, T. B., Flanagan, W. F., and Lichter, B. D., "On the Failure Mechanism of Chemically Embrittled Cu<sub>3</sub>Au Single Crystals," *Metallurgical Transactions A*, Vol. 17A, 1986, pp. 703–710.
- [65] Little, B. J. and McNeil, M., "Technical Note: Mackinawite Formation During Microbial Corrosion," *Corrosion*, July 1990, p. 599.
- [66] Oesch, U. and Janata, J., "Electrochemical Study of Gold Electrodes with Anodic Oxide Films—I. Formation and Reduction Behaviour of Anodic Oxides on Gold," *Electrochimica Acta*, Vol. 28, No. 9, 1983, pp. 1237–1246.
- [67] Handwerker, C. A., *Diffusion Phenomena in Thin Films and Microelectronic Materials*, Vol. 1, Chap. 5, Noyes Publications, 1990, pp. 245–322.
- [68] Duncan, B. S. and Frankenthal, R. P., "Effect of pH on the Rate of Corrosion of Gold in Acid Sulfate Solutions," *Journal of the Electrochemical Society*, Vol. 126, 1979, pp. 95–104.
- [69] Tilden, R. C., "Report on the Study of Brasses in Seawater," *Journal of Soc. Chem. Ind.*, Vol. 5, 1886, pp. 80–93.
- [70] Patent: Raney, M., U.S. 1,563,587, (1925).
- [71] Raney, M., "Increased Surface Area Catalysts," *Ind. Eng. Chem.*, Vol. 32, 1940, pp. 1199–1203.
- [72] Verink, E. D., Jr., unpublished results.
- [73] Wagner, C., "Theoretical Analysis of the Diffusion Processes Determining the Oxidation Rate of Alloys," *Journal of the Electrochemical Society*, Vol. 99, No. 10, 1952, pp. 369–380.
- [74] Wagner, C., "Oxidation of Alloys Involving Noble Metals," *Journal of the Electrochemical Society*, Vol. 103, No. 10, 1956, pp. 571–580.
- [75] Harrison, J. D. and Wagner, C., "The Attack of Solid Alloys by Liquid Metals and Salt Melts," *Acta Metallurgica*, Vol. 7, November 1959, pp. 722–735.
- [76] Cook, H. E. and Hilliard, J. E., "Interdiffusion in Au-Ag Alloys at Low Temperatures," *Journal of Applied Physics Letters*, Vol. 8, No. 1, 1966, pp. 24–26.
- [77] Cook, H. E. and Hilliard, H. E., "Interdiffusion in Gold Silver," *Journal of Applied Physics*, Vol. 40, 1969, pp. 2191–2193.
- [78] Pickering, H. W., "Formation of New Phases during Anodic Dissolution of Zn-Rich Cu-Zn Alloys," *Journal of the Electrochemical Society*, Vol. 117, No. 1, January 1970, pp. 8–15.
- [79] Pickering, H. W. and Wagner, C., "Electrolytic Dissolution of Binary Alloys Containing a Noble Metal," *Journal of the Electrochemical Society*, Vol. 114, No. 7, 1967, pp. 698–706.
- [80] Jones, D. A. and Jankowski, A. F., "Anodically Enhanced Diffusion in Cu/Ag Thin Film Couple," *Scripta Metallurgica*, Vol. 29, 1993, pp. 701–706.
- [81] Melitis, E. S., Liam, K., and Huang, W., "Embrittlement and Stress Corrosion Cracking," *Proceedings of the Conference on Corrosion-Deformation Interactions*, 1992, pp. 21–32.
- [82] Vermilyea, D. A., "Dissolution of MgO and Mg(OH)<sub>2</sub> in Aqueous Solution," *Journal of the Electrochemical Society*, Vol. 116, No. 11, 1969, pp. 1487–1492.
- [83] Forty, A. J. and Rowlands, G., "A Possible Model for Corrosion Pitting and Tunnelling in Noble-Metal Alloys," *Philosophical Magazine A*, Vol. 43, No. 1, 1981, pp. 171–188.
- [84] Galvele, J. R., "A Stress Corrosion Cracking Mechanism Based on Surface Mobility," *Corrosion Science*, Vol. 27, 1987, pp. 1–33.



- [85] Oppenheim, I. C., Chidsey, C. E. D., Trevor, D. J., and Sieradzki, K., "Surface Morphology Alterations Occurring During Selective Dissolution of Ag-Au Alloys," *Research in Progress Symposium*, T. M. Devine and A. J. Sedricks, Eds., NACE, Houston, TX, 1990, pp. 3-4.
- [86] Pryor, M. J. and Lin, L., "The Mechanism of Stress Corrosion Cracking of Cu-Base Alloys," *Corrosion Science*, Vol. 30, No. 2/3, 1990, pp. 267-280.
- [87] Duffo, G. S. and Galvele, J. R., "Experimental Confirmation of the Surface Mobility-Stress Corrosion Cracking Mechanism: Ag-15Pd, Ag-15Au, and Ag-30Cd Alloys in Hallide and Sulphate Containing Solutions," *Corrosion Science*, Vol. 30, No. 2/3, 1990, pp. 249-265.
- [88] Pryor, M. J. and Lin, L., "Part II: The Mechanism of Stress Corrosion Cracking of Cu-Base Alloys," *Corrosion Science*, Vol. 30, No. 2/3, 1990, pp. 280-291.
- [89] Balluffi, R. W. and Alexander, B. H., "Development of Porosity During Diffusion in Substitutional Solid Solutions," *Journal of Applied Physics*, Vol. 23, No. 11, 1952.
- [90] Hillert, M. and Purdy, G. R., "Chemically Induced Grain Boundary Migrations," *Acta Metallurgica*, Vol. 26, 1978, pp. 333-340.
- [91] den Broder, F. J. A., "Interface Reaction and a Special Form of Grain Boundary Diffusion in the Cr-W System," *Acta Metallurgica*, Vol. 20, 1972, pp. 319-332.
- [92] Balluffi, R. W. and Cahn, J. W., "Mechanism for Diffusion Induced Grain Boundary Migration," *Acta Metallurgica*, Vol. 29, 1981, pp. 493-500.
- [93] Handwerker, C. A., Cahn, J. W., Yoon, D. N., and Blendell, J. E., *Diffusion in Solids: Recent Developments*, TMS/AIME Publishers, Warrendale, PA, 1985, pp. 127-148.
- [94] Kirsch, R. G., Poate, J. M., and Eibschutz, M., "Interdiffusion Mechanisms in Ag-Au Thin-film Couples," *Applied Physics Letters*, Vol. 29, No. 12, 1976, pp. 772-774.
- [95] Young, D. J., "Dealloying Reactions as Cellular Phase Transformations," in *Advances in Phase Transformations*, Pergamon Press, 1988, pp. 116-130.
- [96] "Reduction du Film D'Oxyde Forme Anodiquement par la Method de Chronoamperometrie a Variation Lineaire de Potentiel," *Journal of Electroanalytical Chemistry*, Vol. 70, 1976, pp. 291-315.
- [97] Sotto, M., "Oxydation Anodique de L'or, Partie II, Etude de la Reduction du Film D'Oxyde par la Methode de Chronoamperometrie a Variation Lineaire de Potentiel," *Journal of the Electroanalytical Chemistry*, Vol. 2, 1976, pp. 287-306.
- [98] Sieradzki, K., Corderman, R. R., and Shukla, K., "Computer Simulations of Corrosion: Selective Dissolution of Binary Alloys," *Philosophical Magazine A*, Vol. 59, 1989, pp. 713-746.
- [99] Halley, J. W., "Superlattices and Microstructures," in *Topics in the Physics of Electrochemistry*, Vol. 2, Academic Press, 1986, pp. 165-172.
- [100] Li, R., "Studies of the Mechanical Properties of Solids with Random Porosity," dissertation, City University of New York, Queens, New York, 1990, pp. 1-220.
- [101] Witten, A. and Sander, L., "Diffusion-Limited Aggregation," *Physical Review B*, Vol. 27, 1983, pp. 5686-5697.
- [102] Bengough, G. D., Jones, G., and Pirret, R., "Diagnosis of Brass Condenser Tube Corrosion," *Journal of the Institute of Metals*, Vol. 23, 1920, pp. 65-137.
- [103] Holloman, J. H. and Wulf, J., "Dezincification of Alpha and Beta Brasses," *Transactions AIME*, Vol. 147, 1942, p. 297.
- [104] Fink, F. W. and Evans, U. R., "Dezincification of Alpha-Brass with Special Reference to Arsenic," *Journal of the Electrochemical Society*, Vol. 75, 1939, pp. 441-448.
- [105] Heidersbach, R. H., Jr., "The Dezincification of Alpha and Beta Brasses," dissertation, University of Florida, College of Engineering, Gainesville, FL, 1971, pp. 1-145.
- [106] Heidersbach, R. H., Jr., "Clarification of the Mechanism of the Dealloying Phenomenon," *Corrosion*, Vol. 24, No. 2, 1968, pp. 38-44.
- [107] Swann, P. R., "Morphological Aspects of Stress Corrosion Failure," in *Theory of Stress Corrosion Cracking in Alloys*, R. M. Latanision, Ed., NATO, Brussels, Belgium, 1971, pp. 113-126.
- [108] Hamilton, D. R., "A Theory of Dendritic Growth in Electrolytes," *Electrochimica Acta*, Vol. 8, 1963, pp. 731-740.
- [109] Newman, R. C., Meng, F. T., and Sieradzki, K., "Validation of a Percolation Model for Passivation of Fe-Cr Alloys: Current Efficiency in the Incompletely Passivated State," *Corrosion Science*, Vol. 28, No. 5, 1988, pp. 523-527.
- [110] Pickering, H. W. and Kim, Y. S., "Dealloying at Elevated Temperatures and at 298 K—Similarities and Differences," *Corrosion Science*, Vol. 22, No. 7, 1982, pp. 621-635.
- [111] Laist, J., *Comprehensive Inorganic Chemistry, Copper, Silver and Gold*, Vols. 2 and 3, Van Nostrand Company, 1954, pp. 184-238.
- [112] Forty, A. J., "Selective Dissolution in Depletion Gilding, Nature," Vol. 282, 1979, pp. 597-598.
- [113] Tammans, Z. and Brauns, E., "Gold-Silber-Legierungen Elektrolytische Auflösung und der Reistenzgrenzen," *Anorg. Chem.*, Vol. 200, 1931, pp. 209-234.
- [114] Verink, E. D. Jr. and Parrish, P. A., "Use of Pourbaix Diagrams in Predicting the Susceptibility to De-Alloying Phenomena," *Corrosion*, Vol. 26, No. 5, 1970, pp. 214-217.
- [115] Gibbs, W. E., Smith, R. H., and Bengough, G. D., "Third Report to the Corrosion Committee of the Institute of Metals," *Journal of the Institute of Metals*, Vol. 15, 1916, pp. 41-157.
- [116] Newman, R. C., Shahrabi, T., and Sieradzki, K., "Direct Electrochemical Measurement of Dezincification Including the Effect of Alloyed Arsenic," *Corrosion Science*, Vol. 28, No. 9, 1988, pp. 873-886.
- [117] Eden, D. A., Rothwell, A. N., and Dawson, J. L., "Electrochemical Noise for Detection of Stress Corrosion Cracking," Paper 444, *CORROSION/89*, NACE, Houston, TX, 1989.
- [118] Dull, D. L. and Raymond, L., "A Test Procedure to Evaluate the Relative Susceptibility of Materials to Stress Corrosion Cracking," *Corrosion*, May 1973, p. 205.
- [119] Langenegger, E. E. and Robinson, F. P. A., "Effect of the Polarization Technique on Dezincification Rates and the Physical Structure of Dezincified Zones," *Corrosion*, December 1968, p. 411.
- [120] Schmidt, H. W., Gegner, P. J., Heinemann, G., et al., "Stress Corrosion Cracking in Alkaline Solutions-TP-5C—Sub-Surface Corrosion by Alkaline Solutions, A Technical Practices Committee Report," *Corrosion*, Pub. 51-3; September 1951, p. 295.
- [121] NACE, Report by Technical Unit Committee 1-G on Sulfide Stress Corrosion Cracking: Sulfide Corrosion Cracking of Production Equipment, Publication 54-5, November 1954, p. 413.
- [122] Pourbaix, M., *Atlas of Electrochemical Equilibria in Aqueous Solutions*, Pergamon Press, New York, 1966, pp. 1-305.
- [123] Green, J. A. S. and Haney, E. G., "Relationships Between Electrochemical Measurements and Stress Corrosion Cracking of Maraging Steel," *Corrosion*, January 1967, p. 5.
- [124] International Standards Organization, Corrosion of Metals and Alloys—Determination of Dezincification Resistance of Brass, International Standard Number 6509:1981, 2001.
- [125] Bidez, M. W., Lemons, J. E., and Isenberg, B. P., "A Corrosion Study of Gold and Nickel-Based Dental Systems Using Distal Abutment Dental Implants," World Congress in Biomaterials, Paper 60, Society for Biomaterials, Washington, DC, 1984.

# Environmental Cracking— Stress Corrosion

*W. Barry Lisagor<sup>1</sup>*

WITH THE PUBLICATION of the first edition of *Corrosion Tests and Standards—Interpretation and Application* (Manual 20), this chapter concluded with the prediction that future work in the study and characterization of stress corrosion cracking (SCC) of engineering alloys would be directed to more quantitative information based on improved test control, procedures, and techniques to better serve the engineering community, and improved modeling and life prediction techniques. This same theme has been reiterated in the most recent ASTM sponsored conference [1] by Wei, who stated that the community should take a role in development of quantitative methodologies for assurance of reliability and continued safety of engineered systems [2]. In that same conference, Staehle [3] elaborated on a technique for predicting SCC using a corrosion-based design approach (CBDA), and a location for analysis matrix (LAM). More quantitative methodologies and SCC prediction are still recognized as desired entities. The initial publication of this chapter compiled a historical perspective of the SCC phenomenon as well as discussion of testing standards and techniques, and evaluation and interpretation of test results. To that end, the narrative included in the first edition is essentially preserved in the current chapter with additions included based on research and development since the first publication.

The first edition of *Corrosion Engineering* [4] identified stress corrosion cracking (SCC) as the eighth of the famous eight forms of corrosion. This phenomenon has been the basis for countless studies and engineering service problems over a wide spectrum of applications. It has been experienced in the process chemical, energy, and utility exploration and delivery, and aerospace industries, as well as in consumer products. Although SCC has certainly not been the most widely experienced form of corrosion, it has certain characteristics that are particularly troublesome from an applications' standpoint. Notable among these include the frequent lack of early warning or detection by evidence of corrosion products and the fact that catastrophic structural failure can be the first sign of an unfortunate material/environment combination, placed in service by design. Although Uhlig [5] and Fontana and Greene [4] cite riveted steam boilers as early examples of service failures attributed to SCC, the earliest examples frequently cited as the "season cracking" of brass cartridge cases were identified by Fontana, and more

recently by Jones [6], noting a 1906 reference in *Brass World* [7] in his preface. Historically, the period of most vigorous activity addressing SCC from both a research and technological understanding, and an applications standpoint, would likely be the period from the mid- to late 1960s to the mid-1970s, although it still remains an important corrosion topic as new high-strength alloys are considered for service to improve performance. During that period, a great deal of activity occurred relative to standards development and information interchange, through the sponsorship of ASTM Committee G.01 on Corrosion of Metals. Through Subcommittee G.01.06 on Stress Corrosion Cracking and Corrosion Fatigue, numerous test standardization activities were initiated, and many conferences and symposia were organized and held. The current chapter will highlight both the developments of the various activities during that time, as well as activities and standards development since the first edition, and provide an update on standards development regarding SCC testing. Test standardization procedures being pursued by other organizations including the International Standards Organization (ISO) and the National Association of Corrosion Engineers (NACE) were cited in the original edition, and remain essentially unchanged.

## BASIC PRINCIPLES

General theories regarding stress corrosion mechanisms initially supported one of two fundamental considerations: anodic dissolution or hydrogen-related phenomena. Much effort was expended in attempts to show which was the obvious predominant controlling mechanism. Studies over the last 30 years have shown that the factors controlling the SCC process are much more complex, and likely unique to alloy composition, metallurgical condition, chemical environment, electrochemical state, and state of mechanical stress. Considerable detail on mechanisms has been elaborated on in notable monographs published in the early 1970s [8] and later in 1992 [6]. Emphasis has shifted from attempts to relate all SCC phenomena to a single or near single mechanism to a better understanding of all factors contributing to its occurrence and control. Typically, alloy/environment systems susceptible to SCC do not suffer a more general form of corrosion, and the phenomenon is considered one of activation/passivation interaction. Frequently, the alloy system produces a protective film, making it more resistant to general corrosion in natural environments as in the case of aluminum and titanium alloys.

<sup>1</sup>Senior Scientist, Analytical Services and Materials, Inc., Hampton, VA 23666.

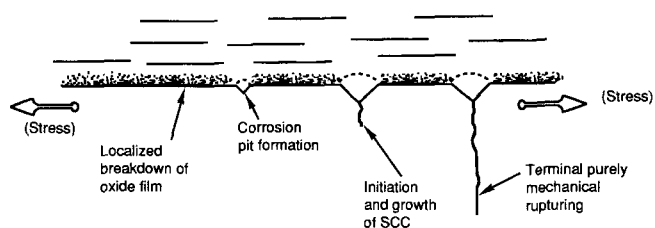


**FIG. 1—Sequence of events (left to right) in a stress corrosion test on an initially smooth specimen. For low-alloy steels in seawater, the rate of growth of SCC is faster than it is for pitting by a factor of about 106, and fast fracture propagates at about 1010 times faster than SCC [8].**

Originally it was considered a process of nucleation and propagation where breakdown of the protective film or establishment of localized electrochemical conditions were necessary for the cracking process to reach a propagation condition. This sequence is reflected in Fig. 1 [8], where an SCC crack results from localized breakdown of a protective film and initial formation of a corrosion pit. Traditional testing for SCC susceptibility was accomplished through time-to-failure tests of specimens exposed in the test environment under various levels of applied tensile stress. Although this approach has resulted in tremendous contributions to the understanding of behavior, and ranking of alloy and environmental combinations, it can also produce some misleading results, as evidenced by the sequence of conditions reflected in Fig. 2 [8]. Figure 2 reflects four conditions of failure phenomena, which, based solely on time to failure tests, could result in misinterpretation of SCC susceptibility by erroneously combining effects of pitting, SCC, and fracture toughness in the results. Young et al. [9] have reported on interaction of electrode potential and temper in aluminum alloy 7050, which describes that SCC susceptibility versus applied potential cannot be used to prove anodic dissolution or hydrogen embrittlement.

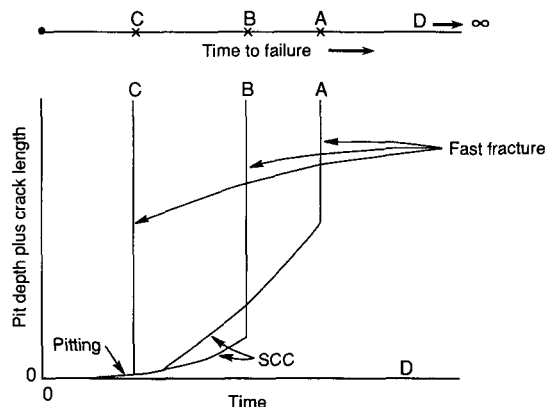


**FIG. 2—Kinetics for pitting (or, in D, nonpitting), SCC (A and B only), and fast fracture (lower plot). Line at top shows how time-to-failure combines the three phenomena to produce misleading results [8].**

The introduction of precracked specimens as a means of studying and characterizing SCC behavior led to the acceptance of another factor in the overall SCC process—that of incubation. Initially, it was thought that the initiation period was principally related to establishment of conditions producing a crack-like flaw for propagation. An early ASTM sponsored interlaboratory test program [10] exploring the use of precracked specimens for SCC testing showed that substantial periods of time were necessary for incubation, before a pre-existing crack would begin to propagate via SCC. In this study, specimens were tested under certain conditions of applied stress intensity that were known to be above the threshold level for SCC propagation of this high-strength steel in the chloride-containing aqueous test environment. In some instances, thousands of hours of exposure were necessary before onset of SCC propagation occurred in modified compact wedge loaded specimens. In this test program the pre-existing crack was introduced by fatigue, at stress intensity levels considerably below that which the SCC tests were performed. The specimens were then loaded in the test media to stress intensity levels which should have created local crack tip conditions expected in more traditional tests, and yet significant exposure times were necessary before propagation occurred. This gave rise to the recognition of the incubation period, a time period necessary perhaps to establish local crack tip chemistry and electrochemical conditions necessary for propagation. Based on the author's participation in interlaboratory test programs on high-strength steels and aluminum alloys, incubation times will be dependent on the combination of alloy and environment and the local stress state based on starting test conditions, and can vary from near zero to extended periods of time. Examples include thousands of hours for high-strength steels initially loaded to stress intensities only marginally above threshold levels, to hundreds of hours for aluminum alloys, to minutes or even seconds for titanium alloys under certain test conditions.

## FACTORS INFLUENCING SCC

Factors that influence SCC response will generally affect one of four basic variables in the process: the material or alloy system, the chemical service environment, the electrochemical state of the system relative to surroundings, and the state of mechanical stress. Nearly all structural alloy systems can be found susceptible to SCC under certain alloy chemistry, metallurgical condition, and service environmental conditions. SCC behavior relative to alloy system was detailed in an American Society for Metals (ASM) publication [6], for a broad range of structural alloys, and has also been covered extensively for aluminum, titanium, and high-strength steels [8].

### Alloying Additions

Alloying additions can have considerable effect on SCC behavior, impacting the formation of protective films on the alloy systems and impacting metallurgical condition, and subsequently impacting the electrochemical and chemical environmental states. These factors are evidenced by the

references cited throughout the chapter. Most notable among these is probably metallurgical condition, which in turn affects the local galvanic or electrochemical state. Precipitation processes and segregation resulting from casting and processing practices can produce inhomogeneous microstructural conditions and second phases that are more resistant or susceptible to crack propagation and produce a profound effect on response. Examples of these include the high-strength aluminum alloys that produce precipitate free zones adjacent to grain boundaries, which in turn are considered to greatly affect anodic dissolution behavior, and alpha/beta titanium alloys, where discontinuous beta significantly retards aqueous crack propagation depending on volume fraction and morphology of the discontinuous phase. Further treatment of effect of alloy composition can be found in the cited references.

### Metallurgical Factors

In addition to metallurgical factors related to alloy composition that result in complex microstructures, both yield strength and grain size effects can affect SCC behavior depending on alloy type and environment. In systems where crack propagation proceeds along intergranular paths, grain size can significantly affect response. In the case of low-alloy steels, yield strength effects can overshadow composition and metallurgical effects and are treated in some detail for both low and high yield strength conditions [6]. For other alloy systems, similar heat treatment and associated temper effects can be seen, although they cannot be generalized without considering composition. For instance, in high-strength aluminum alloys it is generally known that 7XXX series alloys have the highest SCC susceptibility in the peak-aged condition, whereas 2XXX series alloys have more SCC resistance in the peak-aged condition than the naturally aged condition. Connolly and Scully [11] have reported SCC in aluminum-lithium alloys, which show more susceptibility in underaged and overaged conditions, but more resistance in intermediate tempers.

### Environmental Factors

Chemical environmental factors play a major role as one of the four major variables in the SCC process. Chemical environments associated with SCC of the major structural alloy systems range from the naturally occurring environments such as marine and industrial atmospheric conditions to complex chemical environments like anhydrous nitrogen tetroxide ( $N_2O_4$ ). Minor contaminants or concentration level changes, or even minor process changes, can have massive effects on SCC susceptibility. One example of a minor process change that resulted in a near catastrophic result occurred in the aerospace application of titanium alloy Ti-6Al-4V, the workhorse aerospace alloy. Severe SCC was reported in oxidizer tanks undergoing exposure tests associated with the Gemini program [12]. The SCC susceptibility was ultimately determined to be the result of a modest process change in the production of  $N_2O_4$  to ensure lower oxides of nitrogen were not present in the oxidizer. Extensive SCC characterization was conducted and correlation between laboratory specimen tests and stored tank

tests was demonstrated [13]. Similarly, subtle changes in low-level chloride ion concentration and water of hydration have rendered Ti-6Al-4V susceptible in methanol, used as a test medium to simulate propellant fuel [14,15]. More familiar effects of oxygen, chlorides, sulfides, and sulfates, and their effects on SCC response of low-alloy steels and corrosion-resistant alloys for oil, gas, and energy industry applications are reported extensively [16–18]. In these applications, changes in exposure or service temperature may have a substantial effect on SCC response of a material; however, temperature does not always produce rate change effects but should always be considered in characterization or in alloy selection.

### Electrochemical Factors

Electrochemical factors are known to contribute to overall SCC response, dependent on the given material/environment system. For a low-alloy steel, such as 4340 heat-treated to various yield strength levels, applied potential has been shown to have little effect on threshold stress intensity ( $K_{ISCC}$ ) levels (Fig. 3), but significant effect on crack growth rates at stress intensity levels above the threshold value as shown in Fig. 4 [8]. For maraging steels, however, impressed electrochemical potentials had a significant effect on  $K_{ISCC}$  [19]. These effects can further be exacerbated by crack tip chemistries, which can be substantially different from that of the bulk chemistry [20–25]. This can produce changes in a number of variables affecting SCC behavior, including mass transport to the crack tip, protective film attack, adsorption and diffusion, and reaction with the material. Extensive work has been conducted and reported on electrochemical factors contributing to environment assisted cracking (EAC) response of AA 7XXX high strength aluminum alloys [26–30]. This work has included techniques to measure localized chemistry of the environment within the crack wall using capillary electrophoresis [26,27], studies addressing crack chemistry as well as effects of applied and localized measurements of electrode potential [28,29], and crack potential

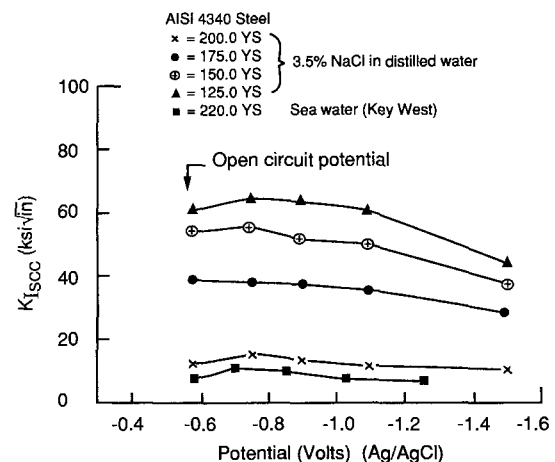


FIG. 3—Effect of (impressed) potential on cracking threshold stress intensity of AISI 4340 steel [8].

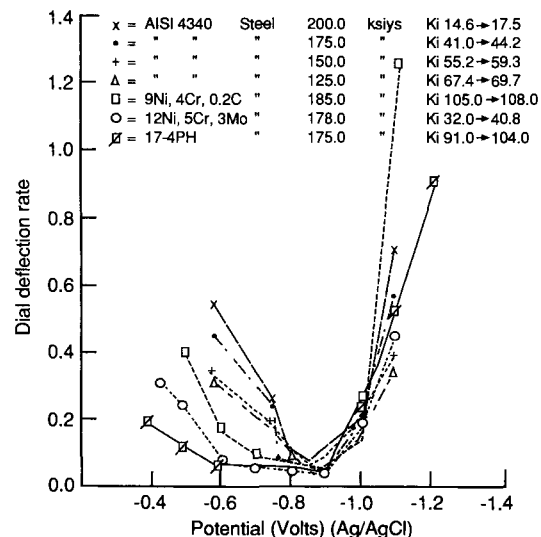


FIG. 4—Effect of (impressed) potential on cracking rates [8].

and modeling of the EAC process [30]. Discussion of mechanisms in this material/environment system [28,30] is elucidating but still leaves room for speculation on the relative significance of hydrogen environment embrittlement (HEE) and anodic dissolution (AD) as principal mechanistic contributors in the cracking process.

### Mechanical Stress Conditions

The mechanical stress conditions are the remaining major consideration necessary for the SCC process to occur and its importance is obvious, considering that most structural engineering applications result in applied loads and resulting stresses that increase the local stress state at the tip of an advancing crack. This means that sudden structural failure is likely if the crack initiation and growth process is allowed to continue in service. Failure will often be manifested by another consideration, such as fatigue, embrittling phenomena, or their interaction, which can reduce resistance to fracture. The mechanical stress condition can also be very complex, considering complex geometry of structural alloy designs as well as complex loading conditions including tensile and shear stress modes, plane stress and plane strain conditions, and biaxial loading modes. All of these factors ultimately affect the local strain and stress conditions in the vicinity of an initiation site or zone beyond an advancing crack front. These factors can also contribute to complex stresses even in relatively simple test specimens. Two factors are considered primary in consideration of the stress distribution and include the tensile or opening mode element of the stress condition, and the degree of constraint beyond the advancing crack front. Other factors may contribute to SCC response but may be secondary in nature. It is reported generally that SCC produces a three-stage initiation, growth, and failure or fast fracture process, often exhibiting a lengthy period of

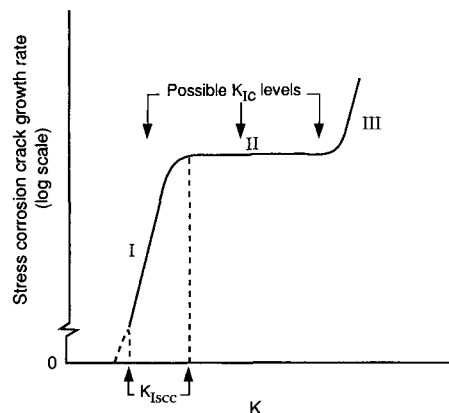


FIG. 5—Generalized SCC kinetics. Fast fracture at one of the points marked  $K_{Ic}$  may preclude development of Region III or of Regions II and III. There may be a true threshold  $K_{Isc}$  or the kinetics may simply decrease continuously to ever smaller but finite values as  $K$  is decreased, denoted by broken line prolongation of Region I [37].

Stage II growth period where crack growth rate is independent of observed stress intensity or associated local stresses. This “plateau velocity” is observed in numerous material/environment systems, schematically represented in Fig. 5 [31]. The relative degree or observance of the three distinct stages depends on a number of factors including the inherent fracture toughness of the material, as well as the specimen geometry and the initial or continuous loading condition during test or exposure. The figure shows how variations in threshold stress intensity for onset or arrest of environmental cracking, and inherent fracture toughness (represented by possible  $K_{Ic}$  levels) may impact whether or not a classical three-stage behavior is observed. The observation of a well-defined “plateau velocity” in many systems suggests that a combination of known variables achieve a resultant steady state condition, and that such a condition will subsist as long as the interaction of those variables to create such a steady state are maintained. The four major variables (material, environment, electrochemical state, and stress) will also be affected secondarily by specimen geometry (affecting compliance and stress and strain rate behavior at the crack tip). Each in itself is complex, and this certainly gives rise to the degree of variability generally encountered in development of SCC data.

The interaction of these important variables to the process is often the most overlooked factor and should be carefully considered in future work regarding SCC. The greatest deficiency currently existing relative to this important form of corrosion is in behavior modeling to develop improved life-prediction capabilities and development of more quantitative data to be input into future developed models.

### TESTING TECHNIQUES

Test technique development has been related closely to purpose and application, and in some cases has been targeted to either specific alloy system and product form, or

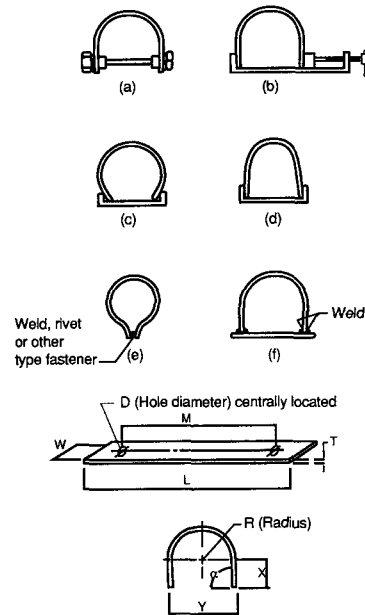
specific test environment. Early work relative to ASTM technical committee standards development and technology interchange (with heaviest activity beginning in the mid-1960s) focused on smooth specimen configurations and specific test environments of interest to materials producers, and users in the aerospace, process chemical, and oil, gas, and other energy related applications. General categories for test technique development were initially focused in three areas: test specimens and loading equipment, test environments, and corrosion fatigue. As standards development continued, additional areas of focus were included. Precracked specimens were added as interests in this configuration of specimens were accelerated by both corrosion and fracture toughness specialists. Dynamic testing was also added as a result of increased activities associated with slow strain rate testing. SCC of aluminum alloys was the most recent organizational addition, a result of the extensive continuing activity with characterization and understanding of the SCC behavior of the high-strength alloys.

### Test Specimens and Loading Equipment

Smooth test specimens developed in various standards included the U-bend, C-ring, bent beam, and direct tension specimens, and a special compilation of specimens directed toward testing of weldments. The specimens considered for standards development were chosen based on widespread use, or by decision of the SCC specialists participating in ASTM technical committee activities.

The U-bend specimen was the first of the SCC specimen types to be included in the *Annual Book of ASTM Standards*, first published in 1972. Many standards activities were underway during that time, with the U-bend standard practice being the initial one reaching completion. The current standard practice (ASTM G 30, Practice for Making and Using U-Bend Stress-Corrosion Test Specimens) includes many details on specimen stressing, surface considerations, and combinations of specimen dimensions (Fig. 6) suitable for achieving a successfully formed specimen for material of adequate engineering ductility. This specimen achieved widespread use in early studies where SCC susceptibility for a given material environment system was desired. It continues to be extensively used by producers of specialty and corrosion-resistant alloys used in the process chemical and energy related applications. The standard now includes reference relative to use of the split tube U-bend (STUB) specimen [32], extensively used in the nuclear power industry, and use of the U-bend specimen for testing in pressurized water [33]. All standards included in the *Annual Book of ASTM Standards* are required to be reviewed for correctness and updating at least every five years, and standards may undergo major technical revision, minor editorial revision, or reapproval without change. Infrequently, standards are balloted for withdrawal, if they are judged to be no longer viable or needed.

The C-ring specimen has also received widespread use in development of SCC data on many alloy systems, but was probably pioneered by SCC specialists with the aluminum producers. Many of those specialists worked on the development of the standard practice, and provided research data to demonstrate its performance. The specimen lends itself



Examples of typical dimensions (SI Units)

Example	L, mm	M, mm	W, mm	T, mm	D, mm	X, mm	Y, mm	R, mm	$\alpha$ , mm
a	80	50	20	2.5	10	32	14	5	1.57
b	100	90	9	3.0	7	25	38	16	1.57
c	120	90	20	1.5	8	35	35	16	1.57
d	130	100	15	3.0	6	45	32	13	1.57
e	150	140	15	0.8	3	61	20	9	1.57
f	310	250	25	13.0	13	105	90	32	1.57
g	510	460	25	6.5	13	136	165	76	1.57

FIG. 6—Typical U-bend specimen dimensions (examples only; not for specification) [32].

particularly to thinner gage plate and tubing product based on its configuration. It can be used in a constant deflection or constant load configuration with the use of springs to obtain the necessary spring constant response for eliminating load drop-off with crack extension. The specimen is almost always used in constant deflection, however. The standard practice includes details of stress considerations, stressing methods, and formulas and tables used for determining stress as a function of measured deflection. Figure 7 shows several C-ring configurations and how the methods of stressing can be accomplished, whereas Fig. 8 shows the correlation of deflection with applied stress based on experimentally measured

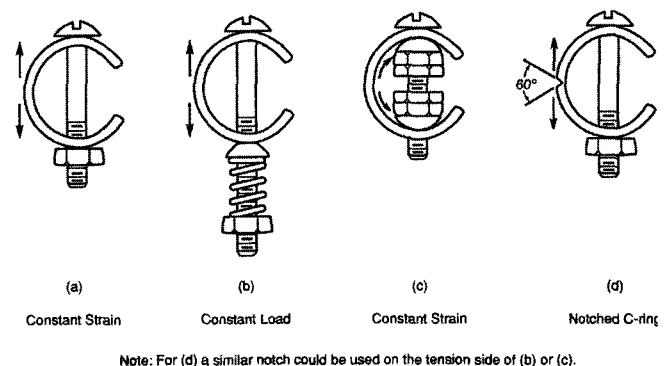


FIG. 7—Methods of stressing C-rings (see ASTM G 38).

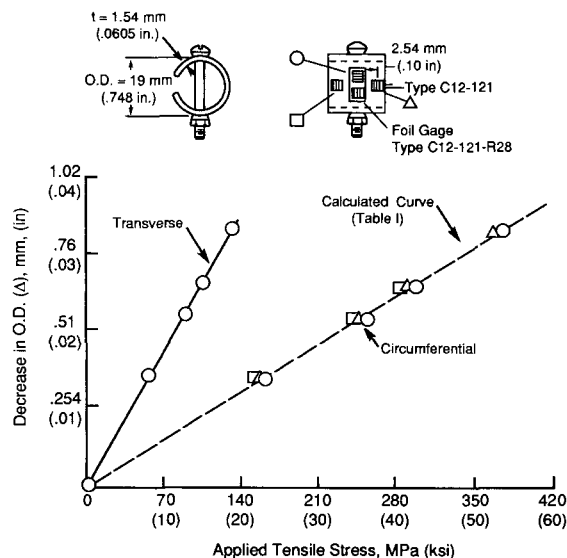


FIG. 8—Stresses in 7075-T6 aluminum alloy C-ring stress-corrosion specimen (see ASTM G 38).

strains for 7075-T6 aluminum alloy from the current standard practice (ASTM G 38, Practices for Making and Using C-Ring Stress Corrosion Test Specimens).

Materials producers and users for its simplicity in stress application, particularly in the two-point loaded configuration, used the bent beam specimen extensively in atmospheric exposure studies. For a given specimen length and thickness, fixturing is relatively easy once the proper calculations to provide the correct shortening for the desired stress has been determined. The standard practice was initially published in the 1973 Book of Standards. The current version (ASTM G 39, Practice for Preparation and Use of Bent-Beam Stress-Corrosion Test Specimens) includes stress calculations for two-, three-, and four-point loaded configurations, and for a double beam configuration essentially achieving four-point loading. Figure 9 shows the four configurations described, while Fig. 10 shows an array of two-point loaded specimens on an outdoor atmospheric exposure rack. There are other configurations of bent beam specimens, one of which is used in a double beam configuration, but which achieves a uniform stress throughout the gage section as a result of the unique specimen geometry [34].

The direct tension specimen is also widely used in developing SCC data and conducting fundamental studies of a broad range of alloy/environment systems. The specimen is usually tested by axially loading along the test section, which is usually of a round or rectangular cross section. Specimen geometry is typical of that used for mechanical testing to obtain tensile properties. It is used in both constant deflection and constant load configurations, although most constant deflection stressing frames used are sufficiently compliant to result in some elevation of stress, as exposure and cracking or reduction in area of the net section of the specimen proceeds during test. ASTM G 49, Practice for Preparation and Use of Direct Tension Stress Corrosion Specimens, describes stress considerations in using this

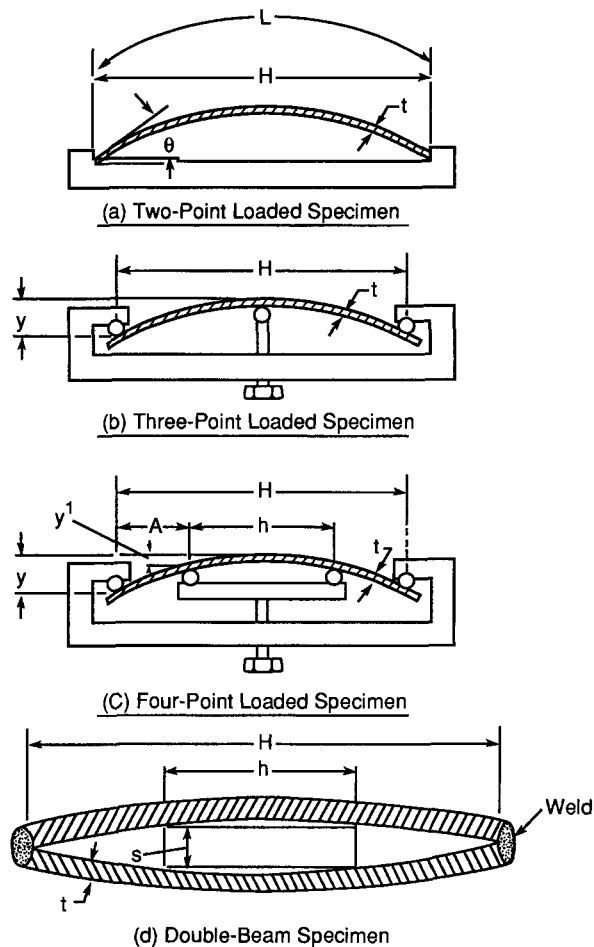
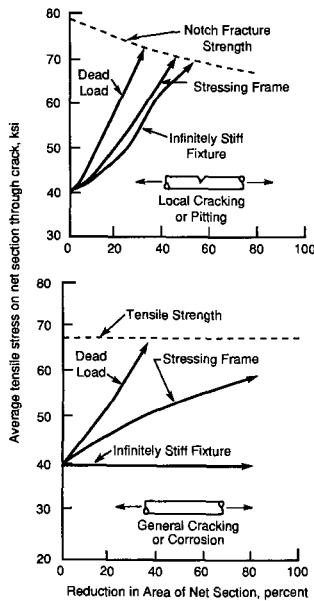


FIG. 9—Schematic specimen and holder configurations (see ASTM G 39).

FIG. 10—Bent-beam specimens on atmospheric exposure rack (reprinted from ASTM G 39).

specimen configuration, as well as methods of loading. Figure 11 shows the effect of reduction of area on the net section of a test specimen on the resultant stress level for three conditions of compliance. This can affect the observed response, particularly if time-to-cracking or time-to-failure criteria are being used to evaluate test results. The direct tension specimen is widely used in dynamic testing, where applied stress is intentionally being varied. This includes



Note: The behavior shown is generally representative, but the curves will vary with specific alloys and tempers.

FIG. 11—Effect of loading method and extent of cracking or corrosion pattern on average net section stress (see ASTM G 49).

slow strain rate and breaking load testing, to be described subsequently.

ASTM G 58, Practice for the Preparation of Stress Corrosion Test Specimens for Weldments, describes use of all of the before-mentioned smooth test specimen configurations. It also includes some configurations unique to welding practices, and references citing use of specimens and procedures unique to SCC testing of weldments.

### Test Environments

Laboratory testing methods associated with specific test environments have been developed for two general purposes: producing accelerated SCC response for a given alloy system, or developing a test medium that more closely simulates SCC response with service for alloy systems known to be susceptible under given conditions. Test environments for specific alloy systems include polythionic acid for stainless steels and other nickel-chromium-iron systems<sup>2</sup>, boiling magnesium chloride for stainless steels and related alloys<sup>3</sup>, Mattsson's solution for copper-zinc alloys<sup>4</sup>, hot hydrated salt for high-strength alloys<sup>5</sup>, and the alternate immersion

3.5 % sodium chloride<sup>6</sup>, and boiling 6 % sodium chloride<sup>7</sup> tests primarily used for aluminum alloys. The alternate immersion test was developed primarily for aluminum alloys, but is also used for ferrous alloys. The boiling 6 % sodium chloride solution test is used primarily for low copper-containing Al-Zn-Mg alloys and has been shown to correlate better with atmospheric exposure tests than other accelerated tests [35]. ASTM G 123 (Test Method for Evaluating Stress-Corrosion Cracking of Stainless Alloys with Different Nickel Content in a Boiling Acidified Sodium Chloride Solution) is a standard test method for producing better correlation of accelerated test and service performance for stainless alloys with varying nickel content.

### Precracked Specimens

Precracked specimens and linear elastic fracture mechanics analysis methods have also been widely used in SCC testing. As was noted earlier, this type of specimen and technique was originally anticipated to result in revolutionary improvements in SCC understanding and development of quantitative information for use in selection and design.

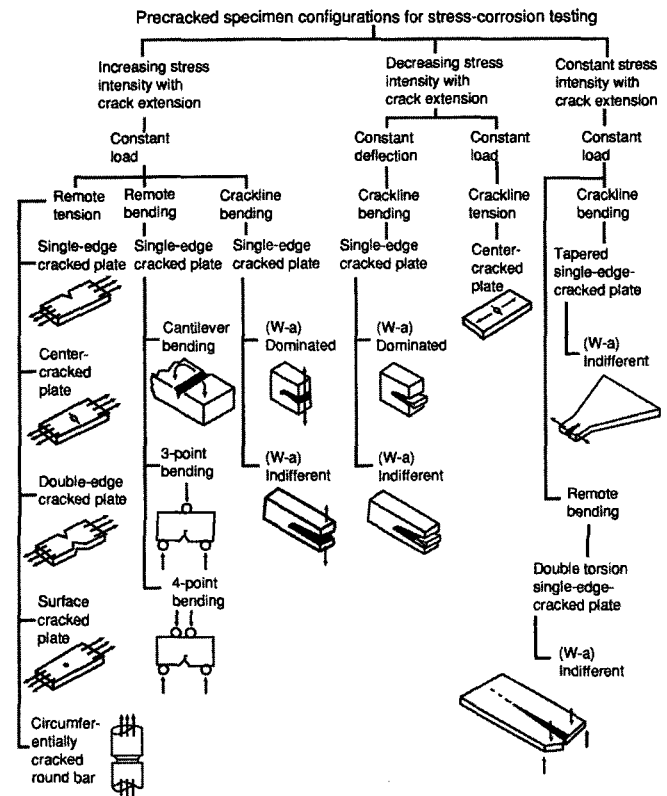


FIG. 12—Classification of precracked specimens for stress corrosion testing [8].

<sup>2</sup> See ASTM G 35, Practice for Determining the Susceptibility of Stainless Steels and Related Nickel-Chromium-Iron Alloys to Stress Corrosion Cracking in Polythionic Acids.

<sup>3</sup> See ASTM G 36, Practice for Performing Stress-Corrosion Cracking Tests in a Boiling Magnesium Chloride Solution.

<sup>4</sup> See ASTM G 37, Practice for Use of Mattsson's Solution of pH 7.2 to Evaluate the Stress-Corrosion Cracking Susceptibility of Copper-Zinc Alloys.

<sup>5</sup> See ASTM G 41, Practice for Determining Cracking Susceptibility of Metals Exposed under Stress to a Hot Salt Environment.

<sup>6</sup> See ASTM G44, Practice for Evaluating Stress Corrosion Cracking Resistance of Metals and Alloys by Alternate Immersion in 3.5 % Sodium Chloride Solution.

<sup>7</sup> See ASTM G 103, Test Method for Performing a Stress-Corrosion Cracking Test of Low Copper Containing Al-Zn-Mg Alloys in Boiling 6 % Sodium Chloride Solution.



Although precracked specimens have proven to be an invaluable tool for SCC studies, SCC information developed using precracked specimens has not been well standardized. Effective use of precracked specimens resulting in reproducible results has, in fact, proven to be very difficult to standardize with respect to appropriate test control and in analysis and reporting of results, including their significance. Notable unanswered questions that continue to perplex researchers and corrosion and fracture specialists include whether or not  $K_{Isc}$  can be considered a material property, whether the same threshold value will be measured from both increasing and decreasing stress intensity test techniques, and whether the same values will be measured from both constant deflection and constant load techniques. There is also considerable controversy over the relative accuracy with which crack growth rates or velocities can be measured. Figure 12 shows a broad classification of precracked specimen configurations for stress corrosion testing [8]. They represent configurations used for both increasing and decreasing stress intensity with crack extension, as well as two configurations that result in a constant value of stress intensity with increasing crack extension under constant load. Although all of these configurations likely have been used in experimental programs, relatively few have been included in interlaboratory test programs to address inter- and intralaboratory variability and to assess

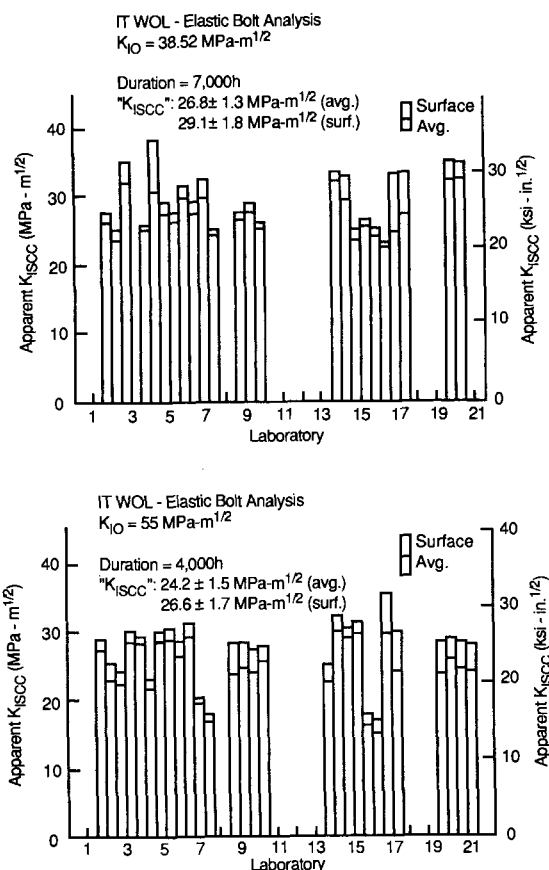


FIG. 13— $K_{Isc}$  results for modified compact specimens from ASTM Interlaboratory Program [10].

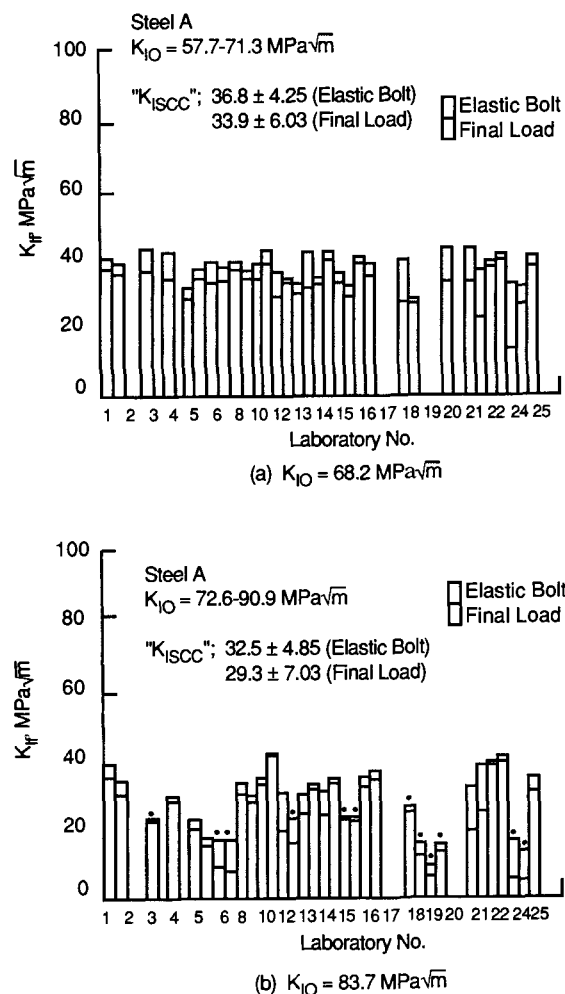


FIG. 14— $K_{Isc}$  results for modified compact specimens from the Japan Society for the Promotion of Science [38].

validity of concepts and techniques. Three studies have been reported in ASTM publications [10, 36–38], two of which were cosponsored by ASTM technical subcommittees on stress corrosion cracking and corrosion fatigue, and subcritical crack growth [10,36,37]. The first of these on low-alloy steel dates back to 1974 and has been reported summarily [36], and in some detail [10]. The second on high-strength aluminum alloy was initiated in 1981 and summarily reported [37]. The third study, conducted in Japan, was essentially similar to the ASTM sponsored study on low-alloy steel [38]. In the test programs, variables included specimen configuration (modified compact bolt loaded specimens, cantilever bend specimens, and double beam bolt loaded specimens), increasing and decreasing stress intensity with increasing crack growth, and alloy composition (AISI 4340 steel, heat-treated to 1240 MPa yield strength, JIS SNCM 439 steel heat-treated to 1170 and 1240 MPa, and 7075 aluminum alloy in the T6 temper). For the aluminum program, method of precracking was also varied. Figures 13 and 14 show representative data from the ASTM sponsored and the Japanese

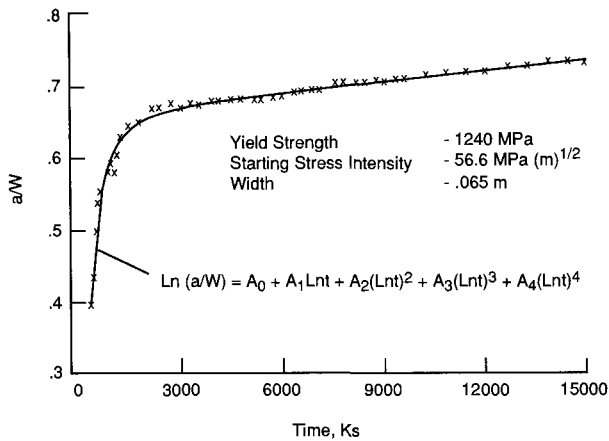


FIG. 15—Crack growth behavior for AISI 4340 steel in 3.5 % NaCl solution [40].

studies. As can be seen from the figures, similar inter- and intralaboratory variability was observed in each of the studies, although for a given starting stress intensity, the ASTM sponsored study indicated slightly less scatter. It is also apparent that initial starting stress intensity had a significant effect on the reported  $K_{Isc}$  value. The total range of reported data would suggest that variations in test environment (3.5 % sodium chloride) over these long duration tests may have influenced the total scatter band. Lack of monitoring of the electrode potential in these tests is of concern, as well as solution chemistry changes, and control of these important parameters may be necessary for test reproducibility and comparison between laboratories to be meaningful [39]. The two studies did not reach the same conclusion regarding specimen configuration. Although the Japanese study reported good agreement between the two specimen configurations, the ASTM study chose to report preference to the modified compact configuration for a number of reasons. Results reported from one of the laboratories participating in the ASTM sponsored program raised the issue of a change in mechanism near the final stages of crack growth for the modified compact configuration [40]. Figure 15 shows a typical crack length versus time curve for a modified compact specimen, which shows the rapid transition from relatively high crack growth rate to significantly low rate. This seemed to occur at or very near the reported  $K_{Isc}$  value for the study. There was also examination of stress intensity solution equations and compliance calibrations in at least one of the participating laboratories individually reported [40]. Tables 1–3 show comparisons of stress intensity solution equations and crack mouth and load line displacement calibrations for the modified compact wedge loaded and cantilever bend specimens. These data suggest that different stress intensity solutions vary slightly, but do not appear to contribute significantly to the variability observed in reported  $K_{Isc}$ . Compliance calibration values, however, can be significantly different, and care must be taken to evaluate response in the crack length regime most insensitive to variation by different analysis techniques. General conclusions based on the ASTM sponsored programs suggest that  $K_{Isc}$  be considered a distributed quantity [10],

TABLE 1—Stress intensity calibrations for modified compact bolt-loaded specimen [30].

$a/W$	$KBW/P(a)^{1/2}$		
	Wilson	Newman (1978)	Newman (Current Study)
0.30	12.06	11.97	12.20
0.25	12.39	12.35	12.47
0.40	12.93	12.87	12.91
0.45	13.64	13.58	13.59
0.50	14.59	14.60	14.59
0.55	15.96	16.06	16.05
0.60	18.05	18.17	18.17
0.65	21.28	21.27	21.31
0.70	26.17	25.96	26.04
0.75	33.36	33.38	33.48
0.80	43.60	45.99	46.02

TABLE 2—Calculated crack mouth opening and load-line compliance calibrations for modified compact bolt-loaded specimen [30].

$a/W$	Novak	Newman (1978)	Newman (Current Study)
$EB(2V_0)/P$			
0.30	29.2	30.4	27.0
0.40	42.6	45.3	42.2
0.50	65.0	67.8	64.8
0.60	101.0	105.8	102.5
0.70	173.3	185.3	182.7
0.80	399.7	404.9	414.5
$EB(2V_{LL})/P$			
0.30	15.8	17.7	19.3
0.40	26.0	28.6	30.4
0.50	43.1	45.3	47.2
0.60	70.9	74.3	76.0
0.70	127.0	135.8	138.1
0.80	303.1	322.6	319.0

TABLE 3—Stress intensity calibrations for single-edge-cracked bend specimens [30].

$a/W$	$KBW^2/6M(a)^{1/2}$			
	Tada	Gross	Kies	Experimental (Current Study)
0.30	1.946	1.988	2.011	1.643
0.35	2.048	2.090	2.130	1.338
0.40	2.188	2.226	2.281	1.475
0.45	2.373	2.408	2.475	1.838
0.50	2.614	2.649	2.725	2.283
0.55	2.935	2.968	3.054	2.780
0.60	3.365	3.386	3.496	3.344
0.65	3.959		4.110	4.004
0.70	4.815		4.992	4.799
0.75	6.120		6.343	5.762
0.80	8.285		8.853	6.915

and identify a number of sources for variance including measurement of crack length, starting stress intensity, and test duration.

As a result of these interlaboratory test programs, standardized test technique development has proceeded even slower than ever anticipated, realizing the difficulties encountered in defining acceptable levels of reproducibility and control of test variables. Since publication of the first edition of Manual 20, ASTM Standard G 168, Standard Practice for Making and Using Pre-cracked Double Beam Stress Corrosion Specimens has been developed, a result of the interlaboratory program conducted on aluminum alloy 7075 [32].

## Dynamic Testing

The term dynamic testing is used here to mean intentional variation in applied load while accomplishing the actual stress corrosion test. It includes a wide variety of applied loading techniques including step loading of both smooth and precracked specimens for rapid estimates of threshold stress and stress intensity for SCC, ripple loading approaches to accelerate response of film passivating materials, and the slow strain rate test technique, used initially for mechanism studies but now also a tool for lot acceptance and material quality control. It is not intended to include interaction of corrosion and fatigue, which is extensively discussed as a separate area in itself. Both step and ripple loading techniques have been used in fundamental studies, and each has been proposed to have sufficient merit and use to be candidates for standardization. However, neither has yet been the subject of interlaboratory evaluation by sponsoring technical societies. The slow strain rate test has received more widespread use, both for fundamental studies of material classes and for a wide variety of test environments. It has been included as a principal topic in several technical symposia (see, for example, Ref 41), and has been the highlighted subject in a symposium dedicated to the technique [42]. The technique has been reported in studies on aluminum-base materials [43,44], as well as steels and nickel-base alloys [45,46]. An overview summary of the use and status of the technique was reported [47] and describes the efforts of both ASTM and NACE to develop appropriate standards for desired test control and general use of the slow strain rate test.

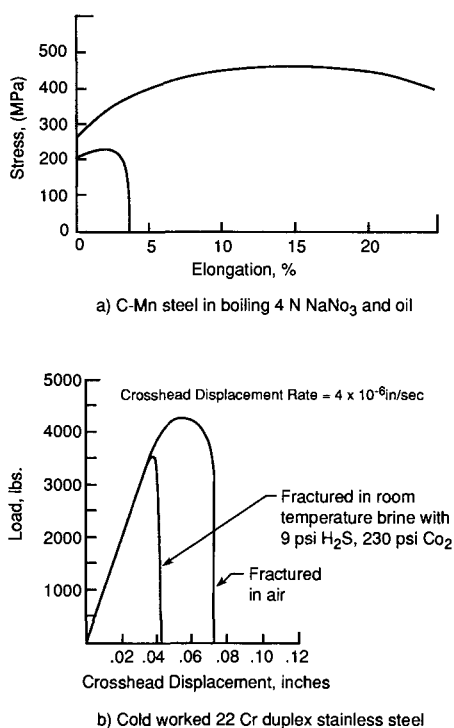


**FIG. 16—Load deflection curves for ferritic and duplex stainless steels using slow strain rate test techniques [47].**

As a result of the interest and activity using slow strain rate testing, ASTM Standard G 129, Standard Practice for Slow Strain Rate Testing to Evaluate the Susceptibility of Metallic Materials to Environmentally Assisted Cracking was developed. Additional papers by Kolman [48] and Little [49] describe issues to be addressed when using slow strain rate testing on beta titanium and aluminum-copper-magnesium-silver alloys, respectively. ISO has adopted a standard on the test that will be described subsequently. Figure 16 shows examples of load deflection response of ferritic and duplex stainless steels for selected aggressive environments along with inert environment response.

## EVALUATION OF TEST RESULTS

Stress corrosion test results have been traditionally evaluated and reported as time-to-failure data for a given set of test conditions related to test environment, electrochemical condition, and magnitude of stress or stress intensity. This has resulted in compiled data in the formal literature that is relatively unsystematic and is difficult for designers and material selectors to use. The results are usually targeted to report or define a threshold stress or stress intensity below which SCC is not expected to occur for a given set of environmental conditions. Lack of reproducibility, range of data scatter, and inability to adequately define anticipated service conditions have typically resulted in efforts by designers to use alloys and metallurgical conditions thought to be immune to SCC susceptibility.

### Correlation of Test Results with Service Performance

Numbers of service failures began to increase in the 1960s as higher strength alloys were used in a broad range of service applications where high structural performance was desired. Many of the standardized test environments were developed to produce accelerated results that would also rank materials in anticipated service (see footnotes 2–7). The development of new environments and techniques often has been the objective of better correlation with service performance. The most recent of these has been the adoption of ASTM G 123, which has been shown to correlate better with service performance of specialty stainless alloys in process chemical application than ASTM G 36, previously widely used. The new standard was developed on completion of an interlaboratory test program [50] that showed better correlation with service performance for the alloys tested.

An honorable goal of the SCC research community is that of predicting service life. It is also a very difficult endeavor at best and must be approached with caution considering the complexity of defining service conditions and lack of adequate models [51]. On the other hand, Staehle [3] maintains that SCC occurrence has nothing to do with the lack of good models for prediction, but with limitations of useable strength in a given environment. SCC data scatter, variables affecting material response, and uncertainties associated with correlation of test and service experience all contribute to relative scarcity of life prediction models.

## STATISTICAL TREATMENT OF SCC DATA

SCC test data are at best considered to be relatively imprecise. Variability in test results can be the result of inadequate control of factors contributing to the process, discussed previously in some detail. In the development of standardized test techniques, some effort has been aimed at identifying the level of data scatter to be expected. In ASTM standards, test methods are required to define expected precision and bias and be supported by results from an interlaboratory test program, while practices, guides, and other publications are not. Traditional pass/fail tests have typically resulted in data scatter sufficiently broad to prevent differentiation of performance of alloys in different heat-treat tempers. Figure 17 shows typical test results from an interlaboratory test program using traditional pass/fail evaluation (see ASTM G 47, Test Method for Determining Susceptibility to Stress-Corrosion Cracking of High-Strength Aluminum Alloy Products). A test technique based on measuring residual strength after exposure was developed to provide more quantitative data using fewer test specimens and to differentiate differences in SCC response of tempers, which could not be done with pass/fail tests [52–57]. The technique originally used extreme value statistics [52–54] and later Box-Cox transformations [55,56] to evaluate SCC response of 7075 aluminum alloy in tempers with little difference in susceptibility. Figure 18 [56] illustrates the concept of defining a statistical threshold stress determined from 99 % survival stress. This was accomplished with far fewer specimens and shorter exposure times than would be required for pass/fail results. These efforts resulted in the development of ASTM G 139 Standard Test Method for Determining Stress-Corrosion Cracking Resistance of Heat Treatable Aluminum Alloy Products Using the Braking Load Method.

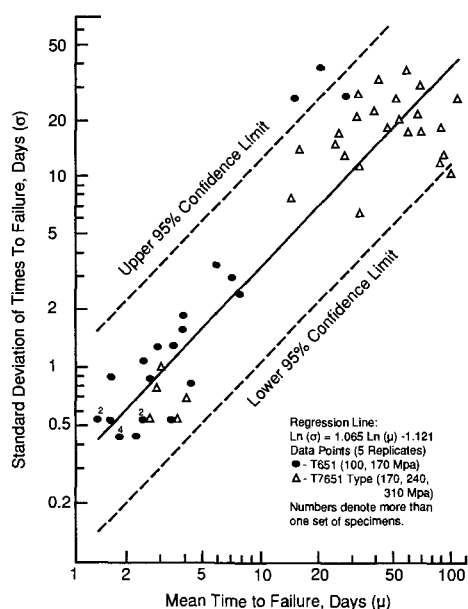


FIG. 17—Aluminum alloy 7075 short transverse tension specimens at various levels and exposed in quintuplicate to 3.5% NaCl solution by alternate immersion per ASTM G 44.

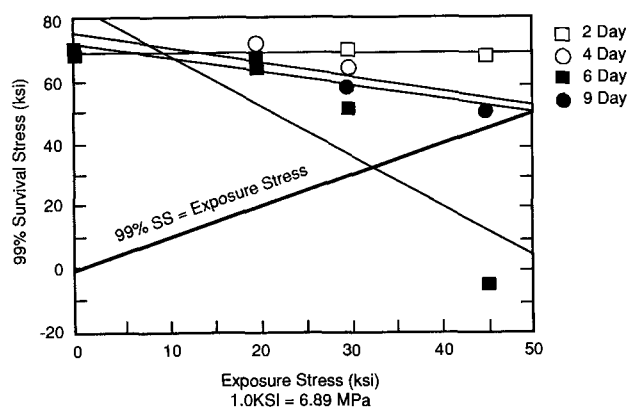


FIG. 18—Plot of breaking load test results demonstrating the concept of statistical threshold stress [57].

## STANDARDS: SCOPE, SIGNIFICANCE, AND USE

The development and use of appropriate standards for SCC response in both research and characterization for application is extremely important if continued improvements in the literature database are to be realized. ASTM has put forth the most extensive effort in this endeavor, dating to the early 1960s, with the first standard published in 1972 (ASTM G 30). Since that time, 17 standards have been published on specimens, environments, alloys, and classifications, but only three have been added since the first edition of Manual 20. The development of such standards dealing with stress corrosion has been the responsibility of ASTM Subcommittee G01.06 on Stress Corrosion Cracking and Corrosion Fatigue, under ASTM Committee G01 on Corrosion of Metals. An additional important contribution to the standards development process is the sponsorship of technical symposia, which provide an effective technical forum for specialists to present current work in progress. The subcommittee has sponsored nine such symposia [1,41,58–64], which have served as catalysts for many developed standards.

NACE is also involved extensively in standards development pertinent to SCC. Two Specific Technology Groups, SG32 and SG62 on oil and gas and testing have oversight on the task group STG 85, which has jurisdiction over a multipart standard [65] that addresses specimens also incorporated in the ASTM standards. ISO, through work of its Technical Committee 156 Working Group 2, has adopted a multipart standard [66] related to SCC published in separate parts primarily based on test specimen design or technique [67–72]. These documents include standardization of precracked specimens as well as a slow strain rate test technique. The procedures described in the ISO standard relative to precracked specimens and slow strain rate would be better described as guides, rather than methods or practices. They do not include sufficient detail related to test control, or important test variables to provide users with adequate information to conduct well controlled tests that would result in reproducible interlaboratory results. This lack of agreement in test control has been, in fact, a major drawback in achieving approved standards through ASTM and NACE. Although

some progress has been made since the first edition of Manual 20, there has been little major breakthrough in SCC technology, and perhaps a diminished effort on research and development of the phenomenon, definitely on the part of industry. It is perhaps timely to quote Staehle [3] in conclusion, that in general, SCC continues to occur because designers do not have a useful conception on how environments affect the mechanical properties of materials nor of the circumstances when SCC occurs.

## REFERENCES

- [1] *Environmentally Assisted Cracking: Predictive Methods for Risk Assessment and Evaluation of Materials, Equipment and Structures*, ASTM STP 1401, R. D. Kane, Ed., ASTM International, West Conshohocken, PA, 2000.
- [2] Wei, R. P., "Material Aging and Reliability of Engineered Systems," *ASTM STP 1401*, ASTM International, West Conshohocken, PA, 2000, pp. 3–19.
- [3] Staehle, R. W., "Framework for Predicting Stress Corrosion Cracking," *ASTM STP 1401*, ASTM International, West Conshohocken, PA, 2000, pp. 131–165.
- [4] Fontana, M. G. and Greene, N. D., *Corrosion Engineering*, McGraw-Hill, New York, 1967.
- [5] Uhlig, H. H., *Corrosion and Corrosion Control: An Introduction to Corrosion Science and Engineering*, 2nd ed., John Wiley & Sons, Inc., New York, 1971.
- [6] *Stress-Corrosion Cracking: Materials Performance and Evaluation*, R. H. Jones, Ed., ASM International, Metals Park, OH, 1992.
- [7] Sperry, E. S., *Brass World*, Vol. 2, 1906, p. 39.
- [8] *Stress-Corrosion Cracking in High Strength Steels and in Titanium and Aluminum Alloys*, B. F. Brown, Ed., Naval Research Laboratory, Washington, DC, 1972.
- [9] Young, L. M., et al., "The Effects of Electrode Potential and Temper on Environment Assisted Cracking in AA 7050," *Light Weight Alloys for Aerospace Applications IV*, The Minerals, Metals and Materials Society, 1997, pp. 3–18.
- [10] Wei, R. P. and Novak, S. R., "Interlaboratory Evaluation of  $K_{Isc}$  and  $da/dt$  Determination Procedures for High-Strength Steels," *Journal of Testing and Evaluation*, Vol. 15, No. 1, 1987, pp. 38–75.
- [11] Connolly, B. J. and Scully, J. R., "Corrosion Cracking Susceptibility in Al-Li-Cu Alloys 2090 and 2096 As a Function of Isothermal Aging Time," *Scripta Materialia*, Vol. 42, 2000, pp. 1039–1045.
- [12] King, E. J., Kappelt, G. F., and Field, C., "Titanium Stress Corrosion Crackings in  $N_2O_4$ ," Presented at NACE Conference and 1966 Corrosion Show, Miami Beach, FL, April 1966.
- [13] Lisagor, W. B., Manning, C. R., Jr., and Bales, T. T., "Stress-Corrosion Cracking of Ti-6Al-4V Titanium Alloy in Nitrogen Tetroxide," NASA TN D-4289, January 1968.
- [14] Johnston, R. L., Johnson, R. E., Ecord, G. M., and Castner, W. L., "Stress-Corrosion Cracking of Ti-6Al-4V Alloy in Methanol," NASA TN D-3868, 1967.
- [15] Lisagor, W. B., "Some Factors Affecting the Stress-Corrosion Cracking of Ti-6Al-4V Titanium Alloy in Methanol," NASA TN D-5557, December 1969.
- [16] Chaung, H. E., Watkins, M., and Vaughn, G. A., "Stress Corrosion Cracking Resistance of Stainless Alloys in Sour Environments," CORROSION/85, Paper 227, NACE, Houston, TX, 1985.
- [17] Miyasa, A., Denpo, K., and Ogawa, H., "Environmental Aspects of SCC of High Alloys in Sour Environments," CORROSION/88, Paper 70, NACE, Houston, TX, 1988.
- [18] Craig, B. D., Collins, J. C., Patrick, R. L., and Gilbert, T., "Testing and Evaluation of Corrosion-Resistant Alloys," *Materials Selection and Design*, December 1991, pp. 51–55.
- [19] Dautovich, D. P. and Floreen, S., "The Stress Corrosion and Hydrogen Embrittlement Behavior of Maraging Steels," *Stress Corrosion Cracking and Hydrogen Embrittlement of Iron Base Alloys*, NACE-5, R. W. Staehle, et al., Eds., NACE, Houston, TX, 1971, pp. 798–815.
- [20] Brown, B. F., Fujii, C. T., and Dahlberg, E. P., *Journal of the Electrochemical Society*, Vol. 116, No. 2, 1969, p. 218.
- [21] Suzuki, T., Yamabe, M., and Kitamura, Y., *Corrosion*, Vol. 29, No. 18, 1973.
- [22] Mankowski, J. and Szlarska-Smialowska, Z., *Corrosion Science*, Vol. 15, 1975, p. 493.
- [23] Turnbull, A., *Embrittlement by the Localized Crack Environment*, R. P. Gangloff, Ed., TMS-AIME, Warrendale, PA, 1973, p. 3.
- [24] Holroyd, N. J. H., Scamans, G. M., and Hermann, R., *Corrosion Chemistry Within Pits, Crvices and Cracks*, A. Turnbull, Ed., HMSO, London, Butterworth, 1987, p. 495.
- [25] Nash, B. K. and Kelley, R. G., "The Use of Ion Chromatography for the Study of Localized Corrosion," *Journal of the Electrochemical Society*, Vol. 139, 1992, L48.
- [26] Cooper, K. R., Kelly, R. G., and Colvin, E. L., "The Correlation between Crack Chemistry and Crack Growth Behavior of 7XXX Series Aluminum Alloys: A Comparison of Field and Laboratory Tests," NACE Corrosion 1999, paper No. 153, San Antonio, TX.
- [27] Cooper, K. R. and Kelly, R. G., "Using Capillary Electrophoresis to Study the Chemical Conditions within Cracks in Aluminum Alloys," *Journal of Chromatography*, Vol. A. 850, 1999, pp. 381–389.
- [28] Cooper, K. R., Young, L. M., Gangloff, R. P., and Kelly, R. G., "The Electrode Potential Dependence of Environment-Assisted Cracking of AA 7050," *Materials Science Forum*, Vols. 331–337, 2000, pp. 1625–1634.
- [29] Cooper, K. R. and Kelly, R. G., "Crack Tip Chemistry and Electrochemistry of Environmental Cracks in AA 7050," *Advances in the Metallurgy of Aluminum Alloys, Proceedings of the James T. Staley Honorary Symposium on Aluminum Alloys*, Indianapolis, IN, November 2001, pp. 73–82.
- [30] Cooper, K. R. and Kelly, R. G., "Measurement and Modeling of Crack Conditions During the Environment-Assisted Cracking of an Al-Zn-Mg-Cu Alloy," *Chemistry and Electrochemistry of Stress Corrosion Cracking: A Symposium Honoring the Contributions of R. W. Staehle*, R. H. Jones, Ed., TMS (The Minerals, Metals & Materials Society), 2001, pp. 523–542.
- [31] Dahlberg, E. P., "ARPA Coupling Program on Stress Corrosion Cracking: (Seventh Quarterly Report)," NRL Memorandum Report 1941, Naval Research Laboratory, Washington, DC, November 1968, p. 49.
- [32] Copson, H. R. and Dean, S. W., "Effect of Contaminants on Resistance to Stress Corrosion Cracking of Ni-Cr Alloy 600 in Pressurized Water," *Corrosion*, Vol. 21, No. 1, January 1965, pp. 1–8.
- [33] Totsuka, N., Lunarska, E., Cragnolino, G., and Szlarska-Smialowska, Z., "Effect of Hydrogen on the Intergranular Stress Corrosion Cracking of Alloy 600 in High Temperature Aqueous Environments," *Corrosion*, Vol. 43, No. 8, August 1987, pp. 505–514.
- [34] Heimerl, G. J. and Braski, D. N., "A Stress Corrosion Test for Structural Sheet Materials," *Materials Research & Standards*, Vol. 5, No. 1, January 1965, pp. 18–22.
- [35] Craig, H. L. Jr., Sprowls, D. O., and Piper, D. E., *Handbook on Corrosion Testing and Evaluation*, Ch. 10, W. H. Ailor, Ed., John Wiley and Sons, Inc., New York, 1971, pp. 275–277.
- [36] Wei, R. P. and Novak, S. R., "Interlaboratory Evaluation of KISCC Measurement Procedures for Steels: A Summary," *Environment-Sensitive Fracture: Evaluation and Comparison of Test Methods*, ASTM STP 821, S. W. Dean, E. N. Pugh, and G. M. Ugiansky, Eds., ASTM International, West Conshohocken, PA, 1984, pp. 75–79.
- [37] Domack, M. S., "Evaluation of  $K_{Isc}$  and  $da/dt$  Measurements for Aluminum Alloys Using Pre-cracked Specimens," *Environmentally*

- Assisted Cracking: Science and Engineering*, ASTM STP 1049, W. B. Lisagor, T. W. Crooker, and B. N. Leis, Eds., ASTM International, West Conshohocken, PA, 1990, pp. 391–409.
- [38] Yokobori, T., Watanabe, J., Aoki, T., and Iwadate, T., "Evaluation of the  $K_{Isc}$  Testing Procedure by Round Robin Tests on Steel," *Fracture Mechanics (Eighteenth Symposium)*, ASTM STP 945, D. T. Read and R. P. Reed, Eds., ASTM International, West Conshohocken, PA, 1988, pp. 843–866.
- [39] Turnbull, A., "Test Methods for Environment Assisted Cracking," *British Corrosion Journal*, 1992, Vol. 27, No. 4, pp. 271–289.
- [40] Lisagor, W. B., "Influence of Precracked Specimen Configuration and Starting Stress Intensity on the Stress Corrosion Cracking of 4340 Steel," *Environment Sensitive Fracture: Evaluation and Comparison of Test Methods*, ASTM STP 821, S. W. Dean, E. N. Pugh, and G. M. Ugiansky, Eds., ASTM International, West Conshohocken, PA, 1984, pp. 80–97.
- [41] *Stress Corrosion Cracking: The Slow Strain Rate Technique*, ASTM STP 665, G. M. Ugiansky and J. H. Payer, Eds., ASTM International, West Conshohocken, PA, 1979.
- [42] Indig, M. E., "SSRT for Hydrogen Water Chemistry Verification in Boiling Water Reactors," *Slow Strain Rate Testing for the Evaluation of Environmentally Induced Cracking: Research and Engineering Applications*, ASTM STP 1210, R. D. Kane, Ed., ASTM International, West Conshohocken, PA, 1993.
- [43] Khobaib, M. and Lynch, C. T., "Slow-Strain-Rate Testing of Al 7075-T6 in Controlled Atmospheres," *Environment-Sensitive Fracture: Evaluation and Comparison of Test Methods*, ASTM STP 821, ASTM International, West Conshohocken, PA, pp. 242–255.
- [44] Holroyd, N. J. and Scamans, G. M., "Slow-Strain-Rate Stress Corrosion Testing of Aluminum Alloys," *Environment-Sensitive Fracture: Evaluation and Comparison of Test Methods*, ASTM STP 821, ASTM International, West Conshohocken, PA, 1984, pp. 202–240.
- [45] Wilhelm, S. M. and Kane, R. D., "Effect of Heat Treatment and Microstructure on the Corrosion and SCC of Duplex Stainless Steels in H<sub>2</sub>S/Cl Environments," Paper 154, CORROSION/83, NACE, Houston, TX, April 1983.
- [46] Kane, R. D., Greer, J. B., Hanson, J. R., et al., "Stress Corrosion Cracking of Nickel Base Alloys in Chloride Containing Environment," Paper 174, CORROSION/79, NACE, Atlanta, GA, April 1979.
- [47] Kane, R. D., "The Acceptance of Slow Strain Rate Testing Techniques for Environmentally Assisted Cracking," *ASTM Standardization News*, May 1993, pp. 34–39.
- [48] Kolman, D. G. and Scully, J. R., "On the Requirement for a Sharp Notch or Precrack to Cause Environmentally Assisted Crack Initiation In Beta Titanium Alloys Exposed to Aqueous Chloride Environments," *ASTM STP 1298*, ASTM International, West Conshohocken, PA, pp. 61–73.
- [49] Little, D. A. and Scully, J. R., "An Electrochemical Framework to Explain Intergranular Stress Corrosion Cracking in an Al-5.4% Cu-0.5%Mg-0.5%Ag Alloy," *Chemistry and Electrochemistry of Stress Corrosion Cracking: A Symposium Honoring the Contributions of R. W. Staehle*, R. H. Jones, Ed., The Minerals, Metals and Materials Society, 2002, pp. 555–571.
- [50] "Interlaboratory Test Data for G 123, Test for Evaluating Stress-Corrosion Cracking of Stainless Alloys with Different Nickel Content in a Boiling Acidified Sodium Chloride Solution," *ASTM Research Report*, G01-1013, April 1994.
- [51] Sprowls, D. O., "Evaluation of Stress-Corrosion Cracking," *Stress-Corrosion Cracking: Materials Performance and Evaluation*, ASM International, 1992, pp. 363–415.
- [52] Sprowls, D. O., "A Study of Environmental Characterization of Conventional and Advanced Aluminum Alloys for Selection and Design," Phase 1: Literature Review, NASA CR 172387, August 1984.
- [53] Sprowls, D. O., Bucci, R. J., Ponchel, B. M., et al., "A Study of Environmental Characterization of Conventional and Advanced Aluminum Alloys for Selection and Design," Phase 2: The Breaking Load Test Method, NASA CR 172387, August 1984.
- [54] Bucci, R. J., Brazill, R. L., and Brockenbrough, J. R., "Assessing Growth of Small Flaws from Residual Strength Data," *Small Fatigue Cracks: Proceedings of the Second International Conference/Workshop*, Santa Barbara, CA, 5–10 January 1986, (A87- 34651 14-26), Metallurgical Society, Inc., Warrington, PA, 1986, pp. 541–556.
- [55] Domack, M. S., "Stress Corrosion Evaluation of Powder Metallurgy Aluminum Alloy 7091 with the Breaking Load Test Method," Presented at the Tri-Service Corrosion Conference, Colorado Springs, CO, 5–7 May 1987, p. 21.
- [56] Lukasak, D. A., Bucci, R. J., Colvin, E. L., and Lifka, B. W., "Damage-based Assessment of Stress Corrosion Performances Among Aluminum Alloys," *New Methods for Corrosion Testing of Aluminum Alloys*, ASTM STP 1134, ASTM International, West Conshohocken, PA, 1992, pp. 101–116.
- [57] Colvin, E. L. and Emptage, M. R., "The Breaking Load Method: Results and Statistical Modification from the ASTM Interlaboratory Test Program," *New Methods for Corrosion Testing of Aluminum Alloys*, ASTM STP 1134, ASTM International, West Conshohocken, PA, 1992, pp. 82–100.
- [58] *Stress Corrosion Testing*, ASTM STP 425, ASTM International, West Conshohocken, PA, West Conshohocken, PA, 1967.
- [59] *Stress Corrosion Cracking of Metals—A State of the Art*, ASTM STP 518, ASTM International, West Conshohocken, PA, 1971.
- [60] *Stress Corrosion—New Approaches*, ASTM STP 610, H. L. Craig, Ed., ASTM International, West Conshohocken, PA, 1975.
- [61] *Corrosion-Fatigue Technology*, ASTM STP 642, H. L. Craig, T. W. Crooker, and D. W. Hoepfner, Eds., ASTM International, West Conshohocken, PA, 1976.
- [62] *Environment-Sensitive Fracture: Evaluation and Comparison of Test Methods*, ASTM STP 821, S. W. Dean, E. N. Pugh, and G. M. Ugiansky, Eds., ASTM International, West Conshohocken, PA, 1982.
- [63] *Environmentally Assisted Cracking: Science and Engineering*, ASTM STP 1049, W. B. Lisagor, T. W. Crooker, and B. N. Leis, Eds., ASTM International, West Conshohocken, PA, 1987.
- [64] *Slow Strain Rate Testing for the Evaluation of Environmentally Induced Cracking: Research and Engineering Applications*, ASTM STP 1210, R. D. Kane, Ed., ASTM International, West Conshohocken, PA, 1993.
- [65] Standard Test Method—Laboratory Testing of Metals for Resistance to Sulfide Stress Cracking in H<sub>2</sub>S Environments, TM0177-90, NACE, Houston, TX.
- [66] Corrosion of Metals and Alloys—Stress Corrosion Testing—Part 1: General Guidance on Testing Procedures, ISO 7539-1, 1st ed., ISO, Geneva, Switzerland, 1987.
- [67] Corrosion of Metals and Alloys—Stress Corrosion Testing—Part 2: Preparation and Use of Bent Beam Specimens, ISO 7539-2, 1989.
- [68] Corrosion of Metals and Alloys—Stress Corrosion Testing—Part 3: Preparation and Use of U Bend Specimens, ISO 7539-3, 1989.
- [69] Corrosion of Metals and Alloys—Stress Corrosion Testing—Part 4: Preparation and Use of Uniaxially Loaded Tension Specimens, ISO 7539-4, 1989.
- [70] Corrosion of Metals and Alloys—Stress Corrosion Testing—Part 5: Preparation and Use of C-Ring Specimens, ISO 7539-5, 1989.
- [71] Corrosion of Metals and Alloys—Stress Corrosion Testing—Part 6: Preparation and Use of Pre-cracked Specimens, ISO 7539-6, 1989.
- [72] Corrosion of Metals and Alloys—Stress Corrosion Testing—Part 7: Slow Strain Rate Testing, ISO 7539-7, 1989.

# Environmental Cracking— Corrosion Fatigue

Richard P. Gangloff<sup>1</sup>

CORROSION FATIGUE (CF) is an important but complex mode of failure for high-performance structural metals operating in deleterious environments. This view is based on the likelihood of cyclically varying loads and chemical environments in service, the need for predictable long-life component performance and life extension, the universal susceptibility of pure metals and alloys to CF damage, and the time-dependent multivariable character of corrosion fatigue. For example, stress corrosion cracking (SCC) immune alloys are susceptible to CF. Corrosion fatigue has affected nuclear power systems, steam and gas turbines, aircraft, marine structures, pipelines, and bridges; CF issues are central to the behavior of many aging systems [1–3].

The objective of this chapter is to highlight modern laboratory methods for characterizing the corrosion fatigue behavior of metals in aqueous electrolytes. The principles and mechanisms of CF are summarized in the first section of this chapter, followed by discussions of experimental methods in the second section. Specimen design and loading, environment control, strain and crack size measurement, and computer automation are discussed. The emphasis throughout is on exemplary experimental methods and results, as well as on CF data analysis and interpretation. The third section of this chapter cites applications of CF data to service, the advantages and limitations of the experimental methods, and directions for research on CF experimentation. Symbols and terms are defined in the Nomenclature. This chapter, with extensive references, extends previous reviews of corrosion fatigue test techniques [4,5]. This chapter was published originally in 1995, the following literature in the Bibliography reflects new developments in Corrosion Fatigue.

## Nomenclature

$\Delta\sigma$	applied engineering true stress range in a fatigue load cycle, $\sigma_{\max} - \sigma_{\min}$ , where $\sigma$ is load/initial cross-sectional area
$\Delta\epsilon_p$	true plastic axial strain range in a fatigue load cycle, $\epsilon_{p\max} - \epsilon_{p\min}$
$\Delta\epsilon_T$	true total axial strain range in a fatigue load cycle, $\epsilon_{T\max} - \epsilon_{T\min}$
$\epsilon$	true axial strain, $\ln(l/l_0)$
$\epsilon_d$	true diametral strain, $\ln(d/d_0)$

$l, d$	gage length and specimen diameter, respectively
$\sigma'_f, b$	Basquin relationship material property parameters
$\epsilon'_f, c$	Coffin-Manson relationship material property parameters
$N_f$	number of load cycles for specimen failure by fatigue
$N_i$	number of load cycles for fatigue crack initiation
$N_T$	transition fatigue life, or number of load cycles where the magnitudes of the elastic and plastic axial strain ranges are equal
$da/dN$	macroscopically averaged fatigue crack growth rate
$a$	fatigue crack length
$N$	fatigue load cycle count
$\Delta K$	applied stress intensity factor range, $K_{\max} - K_{\min}$
$A, m$	Paris Law material property constants
$\Delta K_{TH}$	threshold stress intensity range
$R$	stress ratio, $K_{\min}/K_{\max}$
$\rho$	notch tip radius
$f$	loading frequency in cycles per s or Hz
$1/\alpha_f$	time-portion of the load cycle where CF damage occurs
$K_{ISCC}$	threshold stress intensity for monotonic load SCC
$da/dt$	velocity of monotonic load SCC
$E_C$	free corrosion potential
$E$	modulus of elasticity
$\Delta K_{eff}$	effective stress intensity range, $K_{\max} - K_{cl}$
$K_{cl}$	stress intensity value in a fatigue load cycle where crack-surface closure contact is experimentally resolved and operationally defined
$\Delta K_o$	stress intensity range at a fixed crack length, $a_o$
$C$	constant in the $\Delta K$ -control equation with units of $\text{mm}^{-1}$
$da/dt_f$	time-based crack growth rate in fatigue, often approximated by $(da/dN)(f)$
CF	corrosion fatigue
SCC	stress corrosion cracking
HCF	high-cycle fatigue
LCF	low-cycle fatigue
FCP	fatigue crack propagation
HEE	hydrogen environment embrittlement
H	atomic hydrogen
HCP	hexagonal-closed-packed
LEFM	linear elastic fracture mechanics
SN	stress range versus life
CP	cathodic polarization
cpm	cycles per minute
Mode I	applied load perpendicular to the crack plane and growth direction [6–8]
Mode II	applied load parallel to the crack plane and the crack growth direction

<sup>1</sup>Professor and Chair, Department of Materials Science and Engineering, University of Virginia, Charlottesville, VA 22903.

Mode III	applied load parallel to the crack plane and perpendicular to the growth direction
$\nu_e$	Poisson's ratio for isotropic elastic deformation, often taken as 0.33
LVDT	Linear Variable Differential Transformer
EPD	electrical potential difference

## BASIC PRINCIPLES

### Fundamentals of Corrosion Fatigue

#### Definition

Corrosion fatigue is defined as the sequential stages of metal damage that evolve with accumulated load cycling, in an aggressive environment compared to inert or benign surroundings, and resulting from the interaction of irreversible cyclic plastic deformation with localized chemical or electrochemical reactions. Environment-enhanced fatigue is a modern term; however, corrosion fatigue is traditionally used when emphasizing electrochemical environments. Mechanical fatigue experiments and analyses, detailed in recent textbooks [6–8], provide the basis for understanding CF.

#### Stages of Corrosion Fatigue

CF damage accumulates with increasing load cycle count ( $N$ ) and in four stages: (1) cyclic plastic deformation, (2) microcrack initiation, (3) small crack growth to linkup and coalescence, and (4) macrocrack propagation. A cardinal principle is to design a CF experiment to isolate and quantitatively characterize one of these four stages. The methods in this chapter are organized as follows: (1) smooth specimen life for high cycle fatigue (HCF) described by  $\Delta\sigma$  versus  $N_f$  data, (2) smooth uniaxial or notched specimen life for low cycle fatigue (LCF) described by  $\Delta\epsilon_p$  versus  $N_f$  or  $\Delta K/\sqrt{p}$  versus  $N_f$ , respectively, and (3) fatigue crack propagation (FCP) kinetics described by  $da/dN$  versus the fracture mechanics  $\Delta K$ .

#### Mechanisms

It is important to understand damage mechanisms in order to correctly interpret and extrapolate laboratory CF data. Similar to SCC, the mechanism for CF may involve hydrogen embrittlement, film rupture, dissolution and repassivation, enhanced localized plasticity, interactions of dislocations with surface dissolution, films or adsorbed atoms, and complex combinations of these processes [9–16]. The contribution of each mechanism is controversial and depends on metallurgical and environment (thermal and chemical) variables. While providing significant insight, existing mechanism-based models are generally not capable of accurately predicting CF behavior beyond the range of laboratory data.

Hydrogen environment embrittlement (HEE) is an important mechanism for CF crack propagation in ferritic and martensitic steels, as well as aluminum, titanium, and nickel-based alloys exposed to gases and electrolytes within order of 100°C of ambient temperature [15–21]. This hypothesis is supported by extensive but circumstantial evidence, and is most readily accepted for high-strength alloys in strong hydrogen-producing environments. In HEE atomic hydrogen

chemically adsorbs on strained-clean initiation sites or crack surfaces as the result of electrochemical reduction of hydrogen ions or water. (Adsorbed hydrogen is also produced by the reactions of  $H_2$ ,  $H_2O$ ,  $C_2H_2$ , or  $H_2S$  molecules with metal surfaces.) Hydrogen production follows mass transport within the occluded crack (pit or crevice) solution, crack tip dissolution, and hydrolysis of cations for local acidification; and precedes hydrogen diffusion by lattice, interface, or dislocation processes in the initiation-volume or crack tip plastic zone. Fatigue damage is promoted by hydrogen-affected lattice bond decohesion, grain or dislocation cell boundary decohesion, enhanced localized plasticity, or metal hydride formation (in materials such as HCP titanium-based alloys). Hydrogen-enhanced CF cracking is either intergranular or transgranular, with the latter involving dislocation substructure, low index crystallographic planes, or interfaces.

A second mechanism for CF is based on damage by passive film rupture and transient anodic dissolution at a surface initiation site or crack tip. This model was developed with several necessary empirical elements to predict CF propagation in carbon and stainless steels in high-temperature pure water [22,23], and is sometimes applied to titanium and aluminum alloys in aqueous chloride solutions. Localized plastic straining, described by continuum mechanics or dislocation plasticity, ruptures the protective film. Crack advance occurs by transient anodic dissolution of metal at the breached film, and at a decreasing rate while the surface repassivates pending repetition of this sequence. The increment of CF growth depends Faradaically on the anodic charge (transient current-time integral) passed per load cycle. Charge is governed by clean-repassivating surface reaction kinetics for the CF-sensitive alloy microstructure in occluded crack solution, and by the time between ruptures given by local strain rate and film ductility. As with the hydrogen mechanism, film rupture modeling is complex and controversial; confirming data exist [22,23], but other research shows the model to be untenable for specific alloy/environment systems [24].

Several CF mechanisms were proposed based on interactions between dislocations and environment-based processes at initiation sites or crack tip surfaces. For example, in-situ transmission electron microscopy and dislocation modeling show that adsorbed hydrogen localizes plastic deformation in several pure metals and alloys [25]. Second, reaction-product films are not capable of extensive plastic deformation relative to the underlying metal, and may cause CF damage by one or more processes, viz: (1) interference with the reversibility of slip, (2) localization of persistent slip bands, (3) reduction of near-surface plasticity leading to reduced or enhanced CF depending on the cracking mechanism, (4) localization of near-surface dislocation structure and voids, or (5) film-induced cleavage [14,15,26–28]. Adsorbed cations could similarly affect fatigue [29]. Finally, anodic dissolution may eliminate near-surface work hardening and hence stimulate fatigue damage [30]. These mechanisms have not been developed and tested quantitatively.

### Factors Controlling Corrosion Fatigue

Two considerations are central to understanding the effects of mechanical, metallurgical, and chemical variables



on CF. The influences of electrolyte composition, conductivity, pH, electrode potential, temperature, viscosity, and biological activity are governed by the mass transport and electrochemical reaction conditions within occluded pits, crevices, or cracks, including the role of strain in creating reactive clean surfaces [31,32]. Second, CF can be time-dependent. Crack growth is often rate-limited by one or more of the slow steps in the mass transport and crack surface reaction sequence; slow loading rates enhance CF damage [17]. Increased crack tip strain rate is deleterious when the extent of per-cycle electrochemical reaction is promoted [22–24].<sup>2</sup>

Variables that affect CF were reviewed elsewhere [15–17]. Important factors are cited here to illustrate important CF test methods and to guide data interpretation.

### Mechanical Variables

An important issue is the influence of an electrochemical environment on the cyclic deformation behavior of metals [14,33–35]. As illustrated by the data in Fig. 1 for a carbon-manganese steel in high-temperature water, environment does not typically affect the relationship between stresses and strains derived from the maximum tensile (or compressive) points of steady-state (saturation) hysteresis loops [36]. Such loops should relate to elastic and plastic deformation prior to substantial CF microcracking. CF data of the sort shown in Fig. 1 are produced by either stress or total strain controlled uniaxial fatigue experiments, identical to the methods

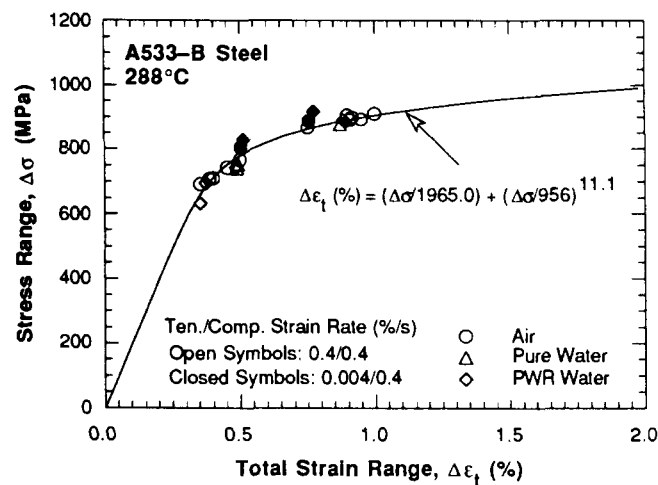


FIG. 1—The nil effect of environment on the cyclic stress-strain response of a C-Mn steel in moist air and pressurized water at 288°C [36]. Data are represented as true stress—true total strain range.

<sup>2</sup>Considering HEE, it is important to consider the primary hydrogen source when designing CF experiments and interpreting results. In addition to occluded crack tip hydrogen production, hydrogen can diffuse over long distances from production sites at mildly strained bulk-solution-exposed specimen surfaces to the propagating CF crack tip. Bulk-surface hydrogen production is important for ferrous alloys at long exposure times in acidic or H<sub>2</sub>S-bearing solutions, and with cathodic polarization [21]. This hydrogen source is less important for aluminum and titanium alloys in electrolytes that form passive surface films capable of blocking hydrogen uptake.

developed for measuring purely mechanical cyclic stress-strain data [8,37]. While macroscopic constitutive properties may not be environment sensitive, slip localization can be affected by electrochemical reactions [14,33].

### Mechanical Driving Forces

Considering smooth specimens, the ranges of applied stress or plastic strain control the fatigue or CF responses of metals for HCF and LCF conditions, respectively. For HCF, smooth specimen CF life increases with decreasing elastic stress range, at cycles in excess of the transition fatigue life,  $N_T$ , according to the Basquin equation

$$\Delta\sigma = \sigma'_f (N_f)^{-b} \quad (1)$$

and due to decreasing globally plastic strain at cycles less than  $N_T$ , according to the Coffin-Manson equation for LCF

$$\Delta\epsilon_p = \epsilon'_f (N_f)^{-c} \quad (2)$$

Alternatively, Eq 1, divided by  $E$  to relate  $N_f$  to elastic strain range ( $\Delta\sigma/E$ ), is added to Eq 2 in order to relate  $N_f$  to total applied strain range, the sum of the elastic and plastic strain ranges.

The material property parameters for HCF and LCF ( $b$ ,  $c$ ,  $\sigma'_f$ , and  $\epsilon'_f$ ) depend on metallurgical, environmental, and time variables. Data in Fig. 2 show that the HCF life of AISI 4140 steel is degraded by aerated neutral NaCl solution, compared to similar fatigue lives for dry and moist air as well as deaerated chloride [38,39]. The data in Fig. 3 show that distilled water and aqueous 3 % NaCl similarly degrade the LCF resistance of an unrecrystallized precipitation-hardened aluminum alloy [35]. The Basquin and Coffin-Manson relationships are generally obeyed for fatigue in electrochemical environments; however, multiple power law segments may occur. Critically, the HCF endurance limit or threshold stress range can be

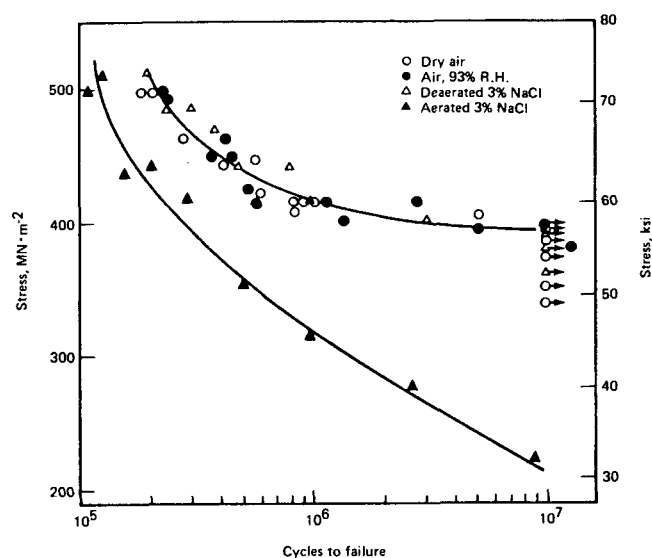


FIG. 2—The deleterious effect of aerated aqueous chloride solution on the HCF life of smooth specimens of tempered martensitic AISI 4140 steel. Symbols with horizontal arrows indicate that CF failure has not occurred after 10<sup>7</sup> load cycles [38].

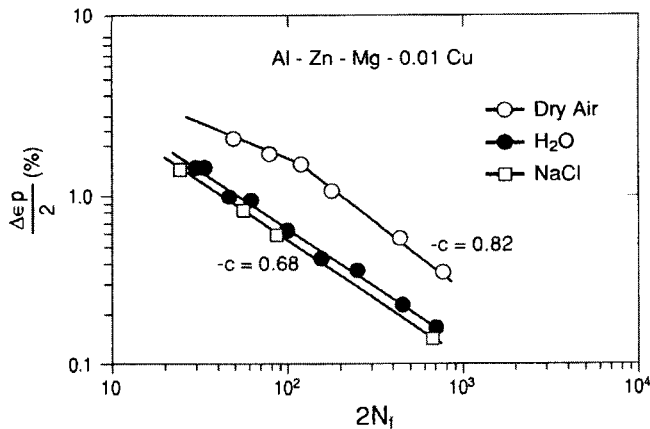


FIG. 3—The deleterious effect of aqueous chloride solution on the LCF life of a precipitation hardened aluminum alloy [35].

eliminated by the action of the electrolyte, as illustrated in Fig. 2. A common explanation for this effect is pitting-based CF crack initiation.

Rates of CF crack propagation are uniquely defined by the linear elastic fracture mechanics stress intensity factor range that combines the effects of applied load, crack size, and geometry [17,40]. The similitude principle states that fatigue and CF cracks grow at equal rates when subjected to equal values of  $\Delta K$  [6–8]. The  $da/dN$  versus  $\Delta K$  relationship may be complex; however, an effective approach is based on a power (or Paris) relationship of the form [41]

$$da/dN = A \Delta K^m \quad (3)$$

$\Delta K$  is limited to stress intensity changes above zero because compressive loads do not cause appreciable crack tip plastic strain and damage. The material properties ( $A$  and  $m$ ) depend on environmental and time variables. For metals in vacuum and moist air, FCP is described by a single power law and an apparent threshold stress intensity range below which  $da/dN$  tends to zero [42]. More complex cracking behavior is observed for CF, as illustrated for aqueous chloride solution-enhanced FCP in titanium (Fig. 4) and advanced aluminum-lithium-copper alloys (Fig. 5) [43,44]. Note the complex  $\Delta K$ -dependence of  $da/dN$  for FCP in chloride solution, but not vacuum or moist air. Environmental effects on Paris regime FCP have been characterized broadly; however, data on near-threshold CF ( $da/dN < 10^{-6}$  mm/cycle) are scarce [16,42].

Crack closure can strongly affect fatigue and CF [45]. This phenomenon is based on crack surface contact during unloading, critically at stress intensity levels above zero and applied-positive  $K_{min}$  values. Crack wake contact is caused by corrosion debris, plasticity, crack path roughness, or phase transformation products; each mechanism may be sensitive to aqueous environmental reactions [6]. To account for closure,  $da/dN$  is correlated with an effective stress intensity range that is defined operationally as the difference between applied  $K_{max}$  and the  $K_{cl}$  level where surface contact is resolved (see Data Analysis and Evaluation in this chapter).

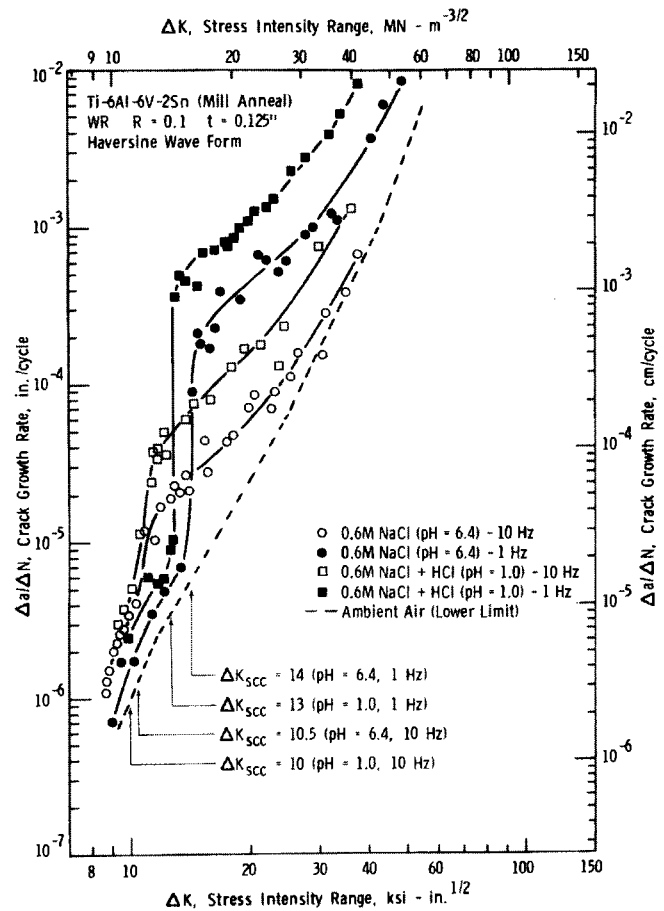


FIG. 4—The effect of solution pH and loading frequency on CF crack propagation in an  $\alpha/\beta$  titanium alloy exposed to aqueous chloride [43].

CF crack formation in notched specimens is most effectively characterized by the notch-root plastic strain range calculated by Neuber's method, elastic-plastic finite elements, or fracture mechanics approximation [7,8]. The latter approach is illustrated in Fig. 6, showing the results of over 100 experiments with C-Mn and alloy steels in aqueous chloride solution compared to moist air [8,46–48]. The load cycles to produce 1 mm of fatigue crack extension, measured optically, increase with decreasing  $\Delta K/\sqrt{\rho}$ , an estimate of notch root  $\Delta \epsilon_p$ , for air and chloride solution.<sup>3</sup> At fixed  $\Delta K/\sqrt{\rho}$ ,  $N_i$  is reduced by chloride exposure at free corrosion, relative to fatigue in moist air. An endurance limit is observed for moist air, but not this CF case. Cathodic polarization (CP) restores a portion of the moist air fatigue initiation/early growth life, as discussed in an ensuing section.

**Loading Frequency**—Slow frequency CF experiments may be necessary because of mass transport and electrochemical reaction rate limitations on damage, but are challenging

<sup>3</sup> $\Delta K$  is calculated assuming a sharp crack of length and geometry equivalent to the notch. This method is a reasonable alternative to a finite element or Neuber analysis of notch strain, but only for crack-like notches of the sort shown by the insert in Fig. 6 [7].

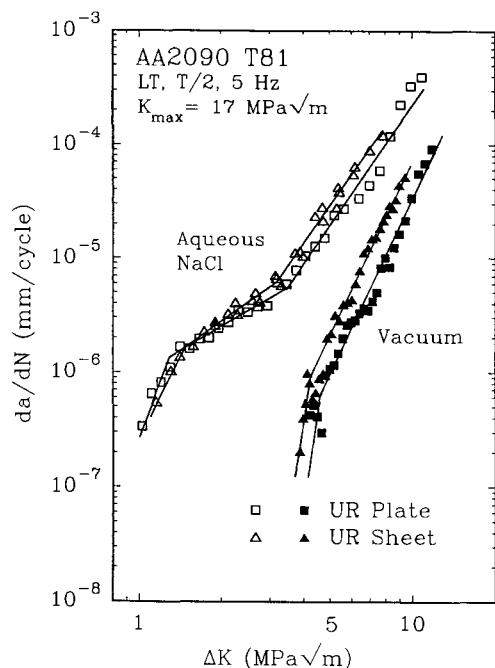


FIG. 5—The effect of aqueous NaCl on the CF crack propagation response of unrecrystallized sheet and plate of an advanced Al-Li-Cu-Zr alloy [44].

because of prolonged test time. The generally deleterious effect of decreasing  $f$  on smooth specimen CF life is illustrated in Fig. 7 for an LCF case involving a C-Mn pressure vessel steel, corroding freely in high-temperature water with varying dissolved oxygen levels between 0.01 and 8 ppm. (The free corrosion potential for these steel CF specimens increases as the dissolved oxygen concentration increases.) For fixed  $\Delta\epsilon_p$ , the ratio of  $N_f$  for fatigue in water to that for air, each at 270°C, declines with decreasing average total strain rate (proportional to frequency) [36]. LCF lives are rate-independent for fatigue in laboratory air at low to moderate temperatures where creep is minimal.

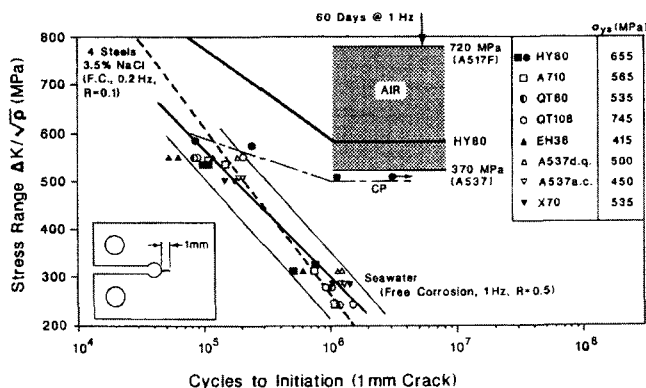


FIG. 6—The effect of chloride on the CF crack formation and early (<1 mm) growth resistance of notched steel specimens; solid line for four steels in NaCl, data points for seawater, and dashed line for four steels in NaCl [46–48].

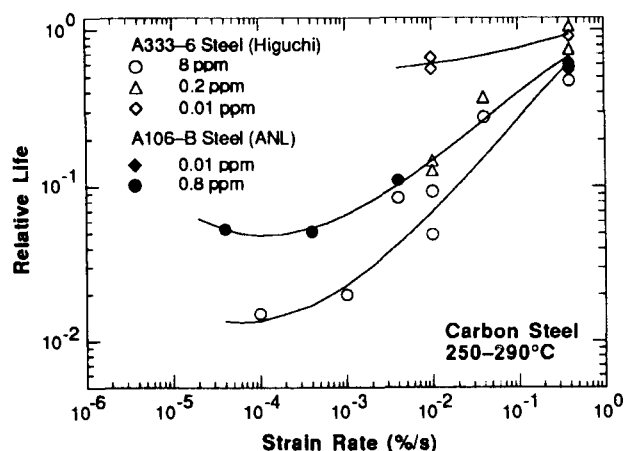


FIG. 7—The effect of strain rate on low cycle CF in the C-Mn steel/high-temperature water system. The dissolved oxygen content of the pure water environment was varied, as indicated by the weight-parts-per-million values in the legend [36].

Frequency effects on CF crack propagation have been characterized broadly and modeled based on the HEE and film rupture mechanisms [16–18,22–24]. FCP rates are  $f$ -independent for alloys in moist air, inert gases such as  $N_2$  or  $Ar$ , or vacuum at low to moderate temperatures. For CF, there are three possible frequency responses: (1) purely time-dependent, where  $da/dN$  increases with decreasing frequency proportional to  $(1/\alpha f)$ , (2) cycle-time-dependent, where  $da/dN$  increases with decreasing frequency proportional to  $(1/\alpha f)^\beta$  with  $\beta$  on the order of 0.5, and (3) cycle-dependent, where  $da/dN$  is environmentally enhanced but frequency-independent. The parameter  $\alpha$  gives the proportion of the load-cycle time that produces CF damage, and is often taken as 2 for a symmetrical cycle, since environmental cracking may not occur during unloading [16]. An alternative model of the frequency effect considers that electrochemical reactions occur

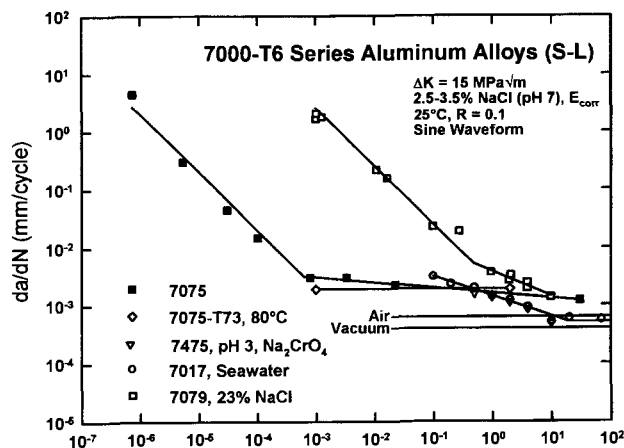


FIG. 8—The varied effects of loading frequency on CF crack propagation rate in peak aged AA7075, 7017, 7475, and 7079 exposed to aqueous chloride solution (free corrosion) at constant  $\Delta K$  and  $R$ . The fatigue crack is parallel to the plate rolling plane in the SCC sensitive S-L orientation [50].

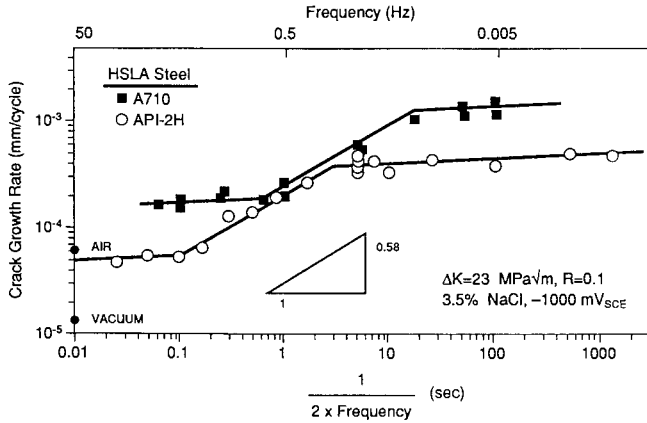


FIG. 9—The effect of loading frequency on CF propagation in API-2H and A710 steels, at the 625 to 750 MPa yield strength level, exposed to aqueous NaCl solution with CP to  $-1000$  mV<sub>SCE</sub> at constant  $\Delta K$  and  $R$  [51].

throughout the entire load-cycle [17]. A single alloy/environment system can exhibit each  $da/dN$ - $f$  relationship, depending on  $\Delta K$ ,  $f$ , and alloy composition, as illustrated for aged 7000 series aluminum alloys (AA) (Fig. 8) and steels (Fig. 9) [18,49–51]. These plots illustrate the two usual ways of presenting frequency-dependent CF  $da/dN$  data, with the abscissa as either  $\log(f)$  or  $\log(1/f)$ . The  $f$  range where  $da/dN$  is most cycle-time dependent varies with mass transport and reaction kinetics that are material-environment sensitive.

Time-dependent cracking is observed for high-strength SCC-prone alloys when  $K_{max}$  in the fatigue cycle is above  $K_{ISCC}$  and  $da/dt$  is rapid. This case, illustrated in Fig. 8 for AA7079 at  $f < 1$  Hz and for AA7075 at  $f < 0.001$  Hz, is modeled by linear superposition of SCC  $da/dt$  and inert environment  $da/dN$  data [49,52,53]. Cycle-time-dependent CF (or cyclic stress corrosion cracking) involves substantial CF at  $\Delta K$  levels that are below  $K_{ISCC}$  or where  $da/dt$  is slow. This

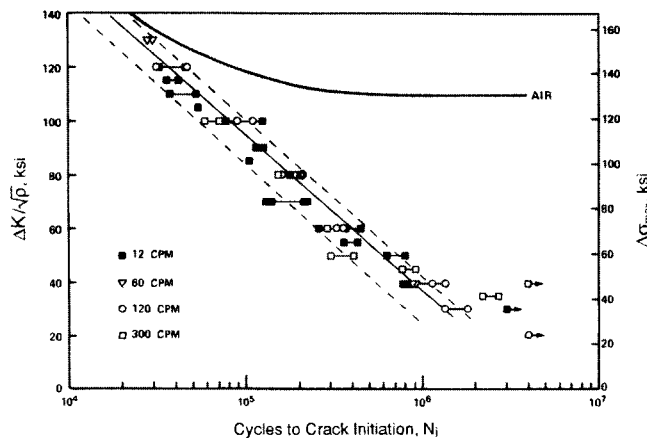


FIG. 10—The frequency independence of CF life for blunt notch specimens of A517 steel, freely corroding in aqueous 3.5 % NaCl as a function of notch root strain range [46]. (Initiation here is in fact crack formation plus early growth to a 1-mm depth.)

response is illustrated for AA7017 and AA7475 (Fig. 8) in seawater and acidified NaCl, respectively, and for two steels in neutral NaCl with cathodic polarization (Fig. 9), each at fixed  $\Delta K$  and  $R$  [18,50,51]. In both systems,  $\beta$  is 0.3 to 0.6. Note (Fig. 9) that cycle-time-dependent  $da/dN$  achieves a plateau or saturation level at slow frequencies below a critical value that depends on steel composition. The third case,  $f$ -independent CF, is illustrated for AA7075 in 80°C chloride solution (Fig. 8) and for the two steels at high frequencies in NaCl at 25°C (Fig. 9) [49,51]. This response (true corrosion fatigue) is often observed at low  $\Delta K$ , at high loading frequencies, or for alloys that resist environmental cracking. In some cases CF  $da/dN$  increases with increasing  $f$ . This behavior is illustrated in Fig. 4 for a titanium alloy at low  $\Delta K$ ; in addition, note a crossover to time-dependent CF above 20 MPa $\sqrt{m}$  and time-cycle-dependent CF at intermediate  $\Delta K$  [43].

Figure 10 illustrates the minimal effect of loading frequency on CF crack formation and early growth for blunt notched steel specimens in aqueous chloride solution at free corrosion [46]. These data are notable for the rare combination of low  $f$  and high cyclic lives (175 days were required to obtain  $3 \times 10^6$  cycles at 12 cpm), and for the lack of a frequency effect on the cycles required to produce 1 mm of CF cracking. This result indicates that one or more of the early

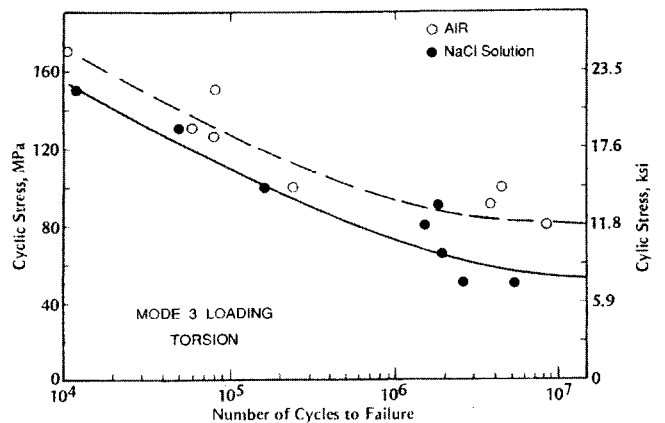
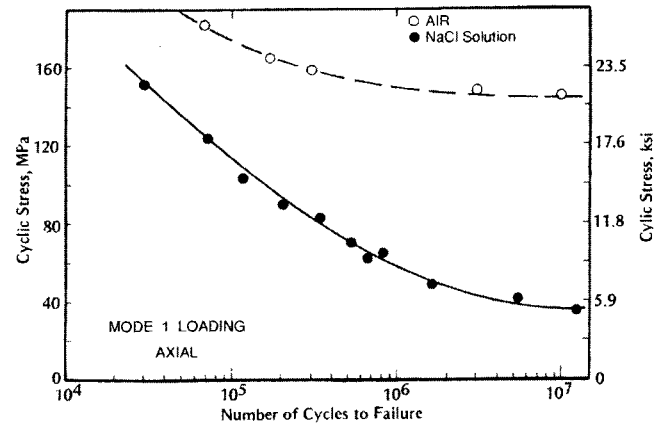


FIG. 11—The effect of environment on tensile and torsional high-cycle corrosion fatigue in the 7075/NaCl solution system [57].

stages of CF (cyclic plastic deformation, pitting, crack nucleation, and small crack growth) are frequency-insensitive, consistent with the  $f$ -independence of long crack CF at low  $\Delta K$  for many alloys including steels in NaCl [16,51]. Results of the sort shown in Fig. 10 are limited and this behavior has not been modeled.

### Other Mechanical Factors

Applied load or strain waveform, stress ratio, load spectrum, and overloads can affect CF [16,22,23,54–56]. This chapter emphasizes uniaxial tensile loading of CF specimens because environmental effects on fatigue under torsional or multiaxial loading have not been studied. An exception is illustrated in Fig. 11, showing fatigue life data for smooth specimens of AA7075 in moist air and aqueous NaCl [57]. Note the strong environmental degradation of  $N_f$  for uniaxial loading represented by normal stress range ( $\Delta\sigma$ ), but a reduced effect for torsion at a given applied shear stress range. Such results can be explained based on the deleterious role of triaxial tensile stresses, and the associated high hydrostatic (mean) tension, in CF propagation by HEE; this stress state is present for uniaxially loaded Mode I cracks, but not for torsional loading and Mode II or III cracks. Fatigue initiation may be similarly environment-enhanced for uniaxial tensile and torsional loading, explaining the modest reduction in  $N_f$  for torsion (Fig. 11).

## Electrochemical Variables

### Electrode Potential

Both anodic and cathodic polarization can affect CF, with different trends observed for crack initiation compared to propagation, and for steels compared to either aluminum or titanium alloys. For ferritic and martensitic steels in aqueous chloride solution, high-cycle CF occurs at electrode potentials near free corrosion for aerated solution ( $E_c \approx -650$  mV<sub>SCE</sub>), but is often reduced in severity or eliminated by cathodic polarization to near  $-1000$  mV<sub>SCE</sub> [58]. This behavior is illustrated in Figs. 6 and 12 for notched and smooth-uniaxial

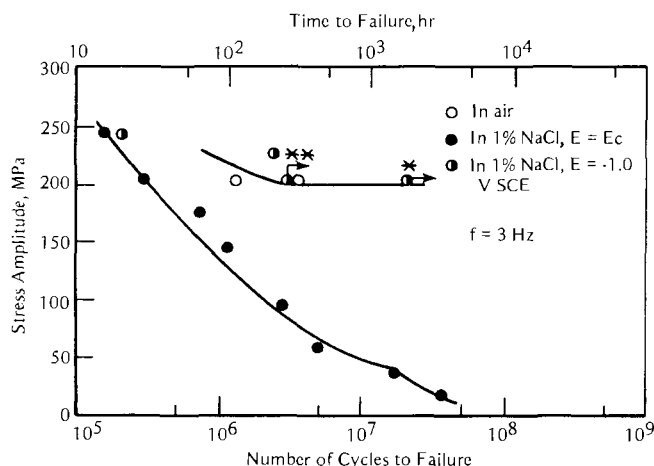


FIG. 12—The beneficial effect of cathodic polarization on high-cycle CF crack initiation in a C-Mn steel in 1 % NaCl solution [59].

fatigue specimens, respectively [47,59]. CF of polished specimens of 1020 and 4140 steels, exposed to NaCl during high-frequency rotating bending, occurred only if a critical anodic current was exceeded [38,39]. In this study, CF was essentially eliminated by solution deaeration which reduced the steel corrosion rate current and free corrosion potential (Fig. 2). Applied cathodic polarization similarly reduced CF of polished specimens.

Understanding the effect of applied polarization on CF propagation requires a description of crack tip electrochemistry, particularly local pH and potential, as affecting the kinetics of passive film formation, dissolution, hydrogen production, and hydrogen entry. Occluded crack processes are complex, as are the observed dependencies of CF  $da/dN$  on electrode potential. For example, CF crack growth rates for steels in chloride increase with increasing cathodic polarization, with a modest minimum in  $da/dN$  at about 200 mV active to the free corrosion potential [16,20]. Figure 13 illustrates that the environmental enhancement of  $da/dN$  increases with the total rate of H production at the crack tip, raised to the  $-1/4$  power, for C-Mn steel in NaCl ( $E_c = -675$  mV<sub>SCE</sub>), polarized between  $-750$  and  $-1325$  mV<sub>SCE</sub> [16]. Hydrogen production was calculated from a crack chemistry model [60]. For this system, solution deaeration does not affect CF  $da/dN$  when electrode potential is fixed potentiostatically [61]. The opposite effects of polarization on smooth specimen CF life and crack propagation in steel can be reconciled. Dissolution and pitting probably govern environment-enhanced fatigue crack initiation [14,38,39]; hydrogen plays a secondary role for the fast loading frequencies, near-threshold stress intensities, and uniaxial stress states typical of smooth specimen studies. Slow loading frequencies and crack tip hydrostatic tension promote crack growth by HEE. Here, important contributions to crack tip hydrogen production are from crack acidification near free corrosion and water reduction at cathodic potentials [16,60].

Cathodic polarization of aluminum and titanium alloys in chloride provides an interesting contrast to steels. Duquette

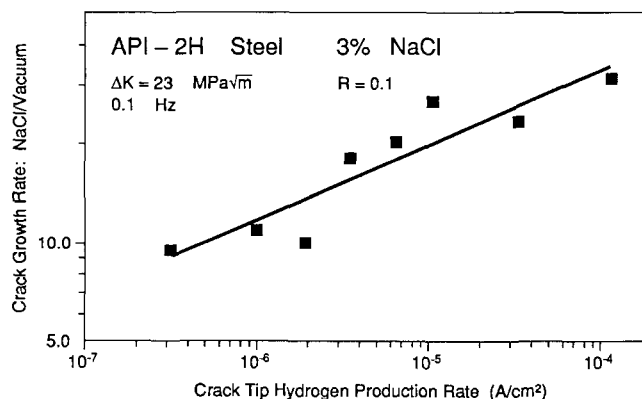


FIG. 13—The effect of electrode potential on relative CF crack propagation rate in the C-Mn steel/chloride system, as portrayed by the crack tip hydrogen production current calculated from a crack chemistry model. The equation of the line from regression analysis is:  $y = 2.39 + 0.22 x$ , where  $y$  is the normalized (dimensionless) crack growth rate and  $x$  is crack tip hydrogen production rate in A/cm<sup>2</sup> [16].

and others reported that the fatigue lives of smooth specimens of AA7075 and Al-Mg-Li in NaCl solution were maximum at potentials mildly active of free corrosion; both anodic and highly cathodic polarization degraded corrosion fatigue life [15,57,58]. CF propagation occurs at the free corrosion potential, is exacerbated by either anodic polarization or extreme cathodic polarization, and is arrested by modest cathodic polarization. This trend was demonstrated for AA7079, AA7075 and AA2090 in NaCl and explained based on HEE [19,62,63]. At negative potentials from cathodic polarization, crack tip hydrogen production may be reduced by the effect of alkaline occluded-crack solution on the overpotential and exchange current density for hydrogen production on strain-bared surfaces, and hydrogen uptake may be blocked by crack surface films.

### Sulfur Ion Content

Sulfur ions in electrolytes exacerbate CF crack propagation in many alloys. Various forms of sulfur are important in sour oil or gas well and geothermal brine environments, and are also produced in unlikely ways. For example, the  $da/dN$  versus  $\Delta K$  data in Fig. 14 show the CF behavior of martensitic HY130 steel in sterile 3.5 % NaCl solution with CP, an environment that enhances cracking by two- to eight-fold relative to moist air and more compared to FCP

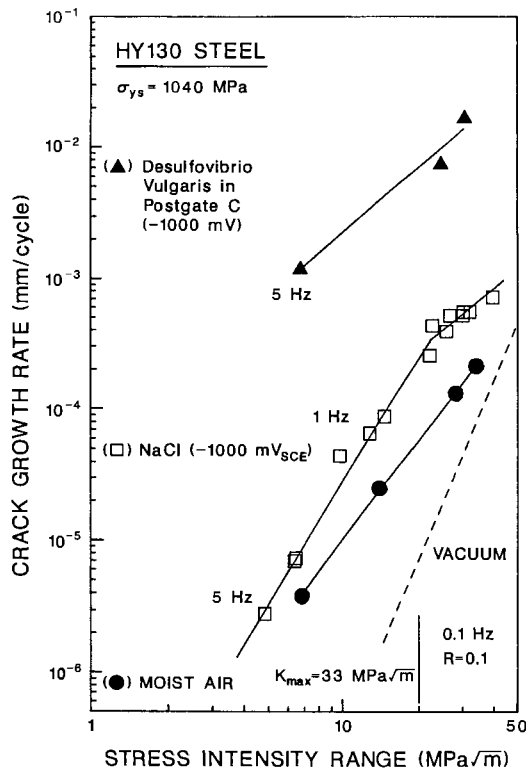


FIG. 14—CF crack propagation in HY130 steel in aqueous (sterile) chloride and active sulfate-reducing bacteria environments, both with CP to  $-1000 \text{ mV}_{\text{SCE}}$ .  $\Delta K$  values above  $20 \text{ MPa}\sqrt{\text{m}}$  were applied at  $R$  of 0.1 and  $f$  of 0.1 Hz, while  $\Delta K < 20 \text{ MPa}\sqrt{\text{m}}$  was applied at constant  $K_{\text{max}}$  of  $33 \text{ MPa}\sqrt{\text{m}}$  and  $f$  of 1 or 5 Hz. The dashed line represents literature data for FCP in the steel/vacuum system [64].

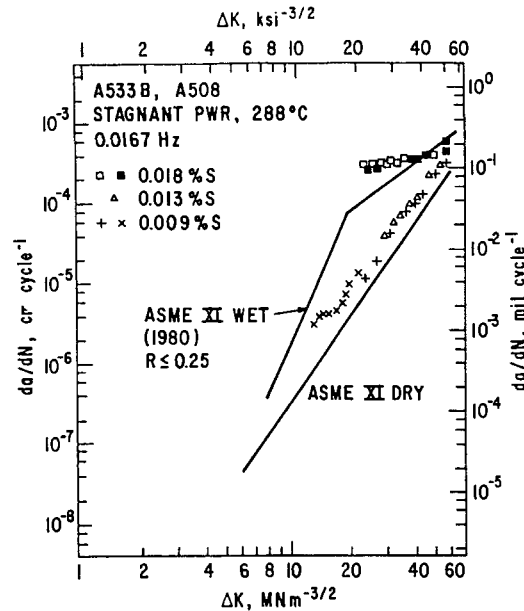


FIG. 15—The effect of alloy impurity-sulfur content on CF crack propagation in the C-Mn steel/high-temperature pure water system [22].

in vacuum. Note the strong environmental effect caused by a sulfate reducing bacteria (SRB; *desulfovibrio vulgaris*) cultured in Postgate C food-medium and with cathodic polarization [64]. These, and similar data for both biologically active and abiotic gaseous  $\text{H}_2\text{S}$  saturated sterile chloride solutions, are interpreted based on sulfide-stimulated HEE [64,65]. Bacteria metabolize the food-source and consume hydrogen to produce sulfide ions and other sulfur species. These anions poison recombinant hydrogen desorption to reduce  $\text{H}_2$  production and increase hydrogen entry into the metal at the crack tip, similar to the deleterious effect of dissolved  $\text{H}_2\text{S}$ .

In a second example, CF is promoted by increased impurity-sulfur in ferritic steels subjected to low-frequency loading in pressurized pure water at  $288^\circ\text{C}$  (Fig. 15) [22,23]. MnS inclusions, which intersect crack flank surfaces, dissolve to enrich the occluded crack solution in sulfide. These anions promote crack advance by increasing the anodic charge that is passed per film rupture event, or perhaps by the HEE mechanism. This effect of steel sulfur content is severe for a stagnant environment within the autoclave, and is eliminated by turbulent solution flow which reduces sulfide buildup within the crack [66].

### Other Chemical Factors

Solution pH, ionic composition, conductivity, and temperature can affect CF [14–17,22, 23,43,58].

### Metallurgical Variables

Metallurgical factors can influence CF crack initiation and growth. Prominent in this regard are sensitization of grain boundaries in austenitic stainless steels [22,23], locally intense slip in aluminum alloys from dislocation interactions

with shearable precipitates [67], and metalloid impurities segregated to grain boundaries in steels [68]. CF crack initiation often occurs at surface intersecting inclusions that concentrate strain and may dissolve to produce a locally aggressive environment [69]. CF crack propagation in the ferritic steel/aqueous chloride system is apparently not affected by substantial changes in steel composition, microstructure, and yield strength [51]. In another case, aluminum alloy processing route, and the resulting degree of recrystallization and grain size, did not substantially affect aqueous environmental LCF life and FCP kinetics [35,44,70]. Increasing copper content in precipitation-hardened Al-Zn-Mg alloys reduced the environmental enhancement of  $da/dN$ , with the importance of the effect depending on aging condition [67].

### Relationship between CF and SCC

Corrosion fatigue is related to, but uniquely distinct from, SCC [71]. Purely time-dependent CF crack propagation in SCC-prone alloys is governed by the integrated amount of time-based crack extension per fatigue load cycle. In such cases CF and SCC occur by the same mechanism and are affected by the same variables, as modeled by simple linear superposition [49,52,53]. SCC is discussed elsewhere in this manual.

Time-cycle and cycle-dependent CF are more complex, involve unique mechanisms, and occur at stress intensities where SCC is insignificant. In these cases, the CF damage mechanism is unique for reasons traceable to cyclic loading, and including: (a) increased crack tip strain rate [22–24], (b) resharpening of the blunted crack geometry during unloading, particularly at high  $\Delta K$ , (c) altered crack chemistry by convective mixing [72], (d) evolution of persistent slip band, slip step, and dislocation cell structures into embryonic damage, often at low  $\Delta\epsilon_p$  or low  $\Delta K$  [73,74], and (e) mobile dislocation transport of hydrogen in the crack tip process zone [18,50]. These additional factors must be considered when interpreting and modeling CF data [16].

### Literature Sources for CF Data and Mechanisms

In addition to the examples presented in Figs. 1 through 15, extensive CF data have been published in several volumes [1,2,9–12,58,75–78].

## TESTING TECHNIQUES

### Common Elements of a Corrosion Fatigue Experiment

An experiment to characterize the CF properties of a metal involves cyclic straining of a precisely machined specimen in an electrolyte. (Precorrosion effects on fatigue are not considered.) Environment containment about the specimen must guarantee constant solution purity and composition. Specimen potential should be monitored, often controlled potentiostatically, and not affected by galvanic coupling to the grips or test machine. The mechanical parameters that must be measured depend on the experiment, be it HCF, LCF, LEFM-crack propagation or notched, and are progressively more difficult to monitor from the HCF to notched cases. CF

experiments follow directly from procedures for mechanical tests with benign environments; the latter are well-developed and standardized, while CF experiments are not. For example, ASTM Committee G-1 has published 14 standards or practices for SCC experiments (see Volume 03.02, Section 3 of the Annual Book of ASTM Standards), but none for corrosion fatigue.

CF experiments are hindered by several common factors. Aggressive environments are difficult to contain at a constant condition, and hinder precise measurements of specimen displacement, load, and crack size. CF is influenced by many interactive mechanical, chemical, and microstructural variables that must be factored into experimental design. It is often necessary to investigate slow-rate deformation and cracking phenomena in a realistic time; experiments must be conducted for one day to one year or more. CF damage is localized at surface slip structure and near the crack tip; high resolution observations are not generally available and behavior must be interpreted from indirect measurements.

### Smooth Specimen $\Delta\sigma$ -Life Method for High Cycle CF

#### Governing Standards

Experiments to characterize high cycle CF life according to the Basquin Law (Eq 1) follow from ASTM standards for metals in moist air (see ASTM E 466, Practice for Conducting Constant Amplitude Fatigue Tests of Metallic Materials; and E 468, Practice for Presentation of Constant Amplitude Fatigue Test Results for Metallic Materials). Such methods were detailed for steels and aluminum alloys in aqueous chloride solutions [38,39,57–59,69,79,80]. Typical data are presented in Figs. 2, 11, and 12.

#### Specimens and Loading

High-cycle CF specimens focus failure in a carefully prepared reduced-uniform or mild-blend-radius gage section, often of circular cross section and with ends for gripping in the fatigue machine. Typical specimen designs are shown elsewhere, including methods for low-damage gage machining and polishing (see ASTM E 466 and Ref 81). HCF specimens are loaded in uniaxial tension or bending (three-point, four-point, or cantilevered) with electromechanical, servohydraulic, or rotating wheel/mass machines, and grips of various designs (see ASTM E 466 and Ref 81). Elastic straining is load or displacement controlled; involves either negative, zero, or positive mean stress; and varies with time symmetrically in a sinusoidal or linear-ramp waveform. Since CF is dominated by electrochemical surface damage,  $N_f$  could decrease and variability may increase with increasing surface area that is stressed.

High-cycle corrosion fatigue experiments are conducted for  $10^5$  to  $10^9$  cycles to failure, at a relatively high frequency of 25 to 100 Hz to conserve time. ( $N_f$  of  $10^6$  cycles requires 5.5 h, while  $10^9$  cycles require 230 days of continuous loading at 50 Hz.) Multiple, reliable, and inexpensive rotating-bend machines are often dedicated to these experiments. Caution is required when extrapolating the results of relatively rapid frequency experiments, to lower  $f$  and/or the very long life regime in excess of  $10^9$  cycles.

### Environmental Cell Design

The design of the environmental cell depends on electrolyte and temperature. A typical cell is illustrated in Fig. 16 for containing aqueous chloride solution at ambient temperature [79]. Glass, Plexiglas®, Teflon®, or other plastics are adequate cell materials. The specimen is gripped outside of the test solution to preclude galvanic effects, and the cell is sealed to the round or square/rectangular specimen with O-rings away from the high-stress gage section. Solution can be circulated from a large storage volume and at a constant flow rate. The cell should include reference and counter electrodes to enable specimen (working electrode) polarization with standard potentiostatic (or galvanostatic) procedures [38,39,59,79]. When fixing potential or current, care should be taken to correctly ground or isolate the test specimen, to uniformly polarize the gage surface, to account for IR effects when necessary, and to isolate counter-electrode reaction products. Provided that potential is controlled, there is probably no reason to control the oxygen content of the solution. Temperature is maintained between subzero and boiling levels with a heater or cooling coil, a specimen thermocouple, control electronics, and a condensation apparatus. Cells for more complex environments are detailed in ensuing subsections on Environmental Cell Design.

### Parameter Measurement, Control, and Computer Automation

The maximum and minimum applied loads (or, alternately, displacements) are measured with a load cell (or remotely attached extensometer/LVDT) and controlled during a HCF experiment.  $\Delta\sigma$  is calculated from standard elastic solutions for bars under uniaxial tension, or beams subjected to bending. Elastic strain range is calculated from  $\Delta\sigma/E$  and gage displacement is not typically measured.

### Crack Detection

Total load cycles to failure are measured, but crack initiation and growth are not monitored during an HCF experiment. Information on these stages of HCF is critical, but difficult to obtain. Methods for CF crack detection are discussed in the subsection on Small Crack CF Methods.

### Data Analysis and Evaluation

High-cycle CF data are presented in a logarithmic plot of stress range versus cycles to failure according to the Basquin Law (Eq 1). Data are also plotted as stress amplitude ( $\Delta\sigma/2$ ) versus reversals to failure ( $2N_f$  for simple waveforms). The Basquin Law is based on the initial applied elastic stress range and does not consider the complicating effect of a growing crack on  $\Delta\sigma$ . Material property constants  $\sigma'_f$ ,  $b$ , and the endurance limit (or fatigue strength at a given number of cycles) are environment-sensitive. The mechanical information that should be reported with HCF data is standardized (see ASTM E 468), and electrochemical factors should be cited as discussed in this manual.

Design and alloy development studies require mean as well as minimum (lower bound) Basquin relationships and statistics on the distribution of  $\Delta\sigma$  versus  $N_f$  data. This distribution depends on the fatigue damage mechanism. Most

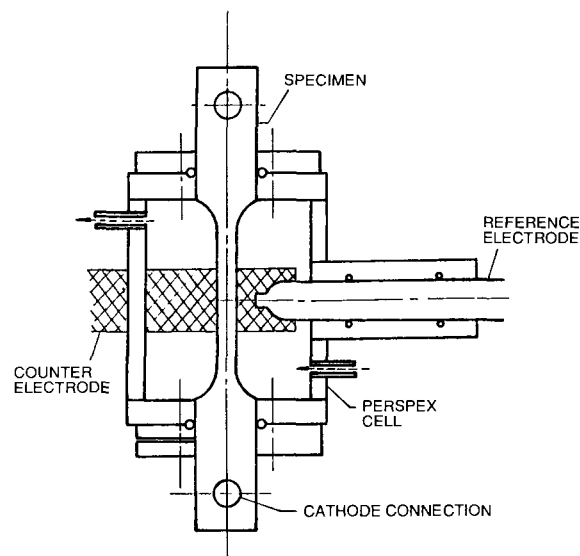


FIG. 16—Uniaxially loaded smooth-gage specimen and environmental chamber for high-cycle CF experimentation with aqueous chloride solutions at near ambient temperatures [79].

CF studies have not provided such information, often because of time-intensive slow frequency experiments and the many important variables. A sense of the variability in CF data is portrayed by the extensive HCF results collected for C-Mn and alloy steels in marine environments [58]. The distribution of HCF lives at a given stress range was analyzed based on Weibull statistics applied to a database of 30 000 points for steels in benign environments [82]. While instructive, these statistical results are not necessarily relevant to high-cycle CF where electrochemical reactions introduce additional variability.

Future work must address two areas to provide the foundation for statistically based analyses of high-cycle CF (as well as environmental LCF and FCP). For simple laboratory conditions, the Weibull analysis of mechanical HCF failure probability [82] must be extended to include CF. Second, variable load, temperature, and environment chemistry histories are likely to be complex in applications and significantly affect CF life. Such history effects have not been studied. The scaling of Basquin relationship data to predict the life of a structure is qualitative and uncertain. Either the local strain approach to CF crack formation/early growth life or the fracture mechanics analysis of CF propagation provide a better foundation for life prediction and failure analysis.

### Smooth Specimen $\Delta\epsilon_p(N)$ Method for Low-Cycle CF

#### Governing Standards

Experiments to characterize low-cycle CF life according to the Coffin-Manson relationship (Eq 2) follow from an ASTM standard for LCF of metals in air, and a classic ASTM manual on laboratory methods (see Ref 37 and ASTM E 606, Practice for Strain-Controlled Fatigue Testing). Low-cycle CF



experiments are detailed elsewhere [33–36, 74,83], and typical data are presented in Figs. 3 and 7.

### Specimens and Loading

Uniform-gage or mild-radius (hourglass) round specimens are subjected to uniaxial tensile loading with rigid gripping and a test machine that provides for either tension-compression or tension-tension strain cycling. Square or rectangular specimens have also been successfully employed. Specimen alignment is critical for this rigid gripping system [81]. Total axial displacement is generally controlled, with regard to maximum and minimum limits as well as time-dependence, while load is measured, often with a computer-automated servoelectric or servohydraulic closed-loop test machine. Such machines provide a variety of strain-time profiles. Loading frequencies are typically less than those employed for HCF experiments because failure occurs in less than 10<sup>4</sup> cycles. Low-cycle CF experiments differ from the HCF case in that gage displacement must be measured with sufficient resolution to apply  $\Delta\epsilon_p$  between 10<sup>-4</sup> and 10<sup>-1</sup>.

### Environmental Cell Design

Cells for environment containment and control are identical for LCF and HCF (see previous subsection with this title). LCF cells are, however, more complicated because of the requirement to measure specimen gage displacement, as illustrated in Fig. 17 [33,36]. For simple aqueous environments, diametral or axial displacement is measured by a contacting (but galvanically insulated) extensometer, perhaps employing pointed glass or ceramic arms extending from a body located outside of the solution. A hermetically sealed extensometer or LVDT can be submerged in many electrolytes over a range of temperatures and pressures. Alternately, the specimen can be gripped in a horizontally mounted test machine, and half-submerged in the electrolyte, with the extensometer contacting the dry side of the gage (Fig. 17a) [33]. For both simple and aggressive environments, grip displacement can be measured external to the cell-contained solution, as shown in Fig. 17b for high-temperature water in a pressurized autoclave [34,36]. It is necessary to conduct LCF experiments in air (at temperature), with an extensometer mounted directly on the specimen gage, to relate grip displacement and specimen strain.

### Parameter Measurement, Control, and Computer Automation

Applied load and gage displacement are measured throughout an LCF experiment. From these data, it is possible to calculate true  $\Delta\sigma$ ,  $\Delta\epsilon_T$ , and  $\Delta\epsilon_p$ , where axial plastic strain range equals  $(\Delta\epsilon_T - \Delta\sigma/E)$ . For the hourglass specimen, true total diametral strain can be measured at any time, and converted to axial strain according to [37]

$$\epsilon = (\sigma/E)(1 - 2\nu_e) - 2\epsilon_d \quad (4)$$

If  $\Delta\epsilon_T$  or  $\Delta\epsilon_d$  is maintained constant by the test machine, then  $\Delta\sigma$  increases and  $\Delta\epsilon_p$  decreases until the hysteresis loop stabilizes at a constant form for a cyclically hardening material, and vice-versa for a softening alloy [7,37]. The stabilized-loop value of axial  $\Delta\epsilon_p$  is used in the Coffin-Manson Law to correlate  $N_f$ . When substantial crack growth occurs, these

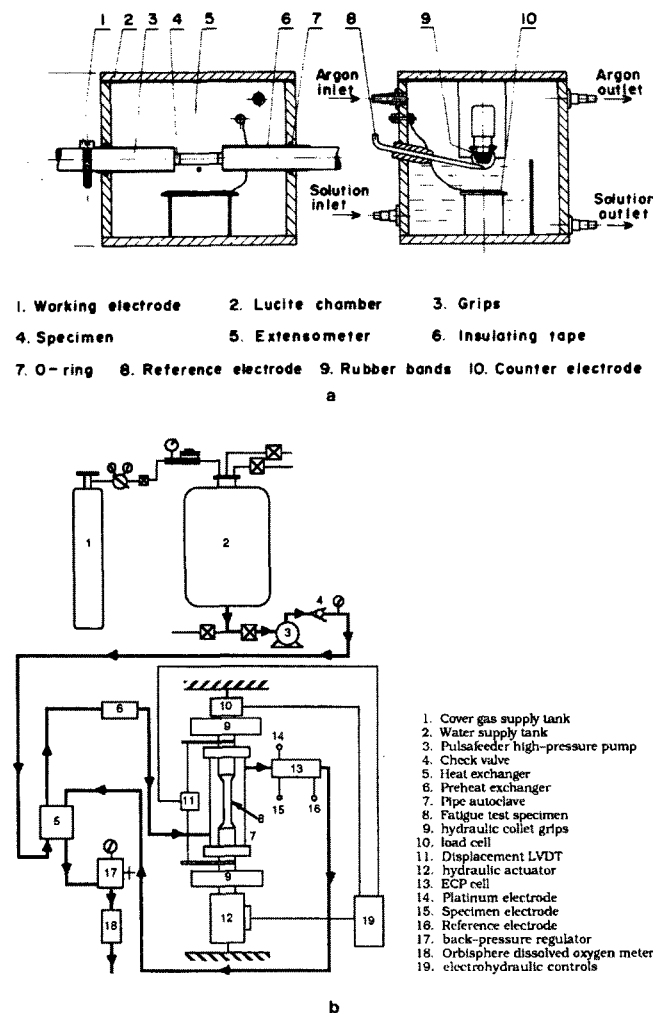


FIG. 17—Environmental chambers for low-cycle CF in: (a) an electrolyte at ambient temperature [33], and (b) high-temperature water [36].

stress and strain range calculations are not accurate. Experiments are often terminated and failure is defined for a percent decline in  $\Delta\sigma$ . Total strain rate, average plastic strain rate, or the frequency of displacement cycling should be maintained constant during the low-cycle corrosion fatigue experiment.

Personal computer programs are available to control the closed-loop test machine during an LCF experiment and to analyze load-displacement-time data.

### Crack Detection, Data Analysis, and Evaluation

These procedures are identical for LCF and HCF, as discussed in the previous subsections, Crack Detection and Data Analysis and Evaluation.

### Fracture Mechanics Methods for Corrosion Fatigue Crack Propagation

#### Governing Standards

Experiments to characterize CF crack propagation kinetics, in terms of LEFM Paris relationships (Eq 3) and near- $\Delta K_{TH}$

data, are guided by an ASTM standard for metals in air (ASTM E 647, Test Method for Measurement of Fatigue Crack Growth Rates), a compilation of laboratory experience with this standard [84], and a review of inert environment FCP testing [85]. The ASTM standard contains an appendix specific to CF crack growth in marine environments (ASTM E 647 and Ref 86). Procedures for CF in other environments are not standardized; however, methods have evolved for specific technologies [2,4]. CF  $da/dN$  data are presented in Figs. 4, 5, 8, 9, and 13 to 15.

### Specimens and Loading

CF crack propagation data are obtained with a variety of notched and precracked specimen geometries that are well-characterized in terms of stress intensity and compliance functions [85,87]. The Mode I compact tension, single-edge crack, three- or four-point bend, and center-cracked tension specimens are used commonly, and are prepared based on standardized procedures (ASTM E 647). Specimen in-plane dimensions are selected to guarantee elastic deformation with limited small-scale crack tip plasticity. Specimen thickness, and the plane stress or plane strain deformation state, is a variable. Closed-loop servohydraulic test machines are most effective for CF propagation experiments, with the control parameter being load. (Load-line displacement or crack mouth opening displacement control are sometimes used.) Such machines provide a range of load or displacement waveforms (sinusoidally time-dependent is typical) and frequencies ( $10^{-4}$  to 100 Hz are typical values).

### Environmental Cell Design

Cells for CF crack propagation experiments are designed to control solution composition and specimen electrochemistry analogous to HCF and LCF (see previous subsections with this title), while allowing for measurements of applied load, crack opening displacement, and crack length. A variety of approaches is reviewed elsewhere, including electrochemical details for several environments [4]. Two cells for ambient temperature electrolytes are shown in Fig. 18. If the test machine and loading axis are mounted in a horizontal plane ( $90^\circ$  to the normal orientation), then the compact tension crack tip can be dipped into solution which is exposed to air without complex sealing (Fig. 18a). The alternate approach in Fig. 18b employs a vertical loading axis with a segmented Plexiglas or Teflon cell, sealed to the faces of the compact tension specimen with O-rings and including a short segment in the notch mouth. Solution flow is through the notch, parallel to the crack front. Small cells clamped to specimen surfaces (Fig. 18b) are equally effective for center-through-cracked plate specimens. Specimens with surface cracks or single-edge cracks are effectively contained in environmental cells that are large and sealed to the round or flat ends inboard from the gripping points [88]. Compact tension and surface crack specimens have been contained in pressurized metal autoclaves with electrolytes or steam at elevated temperature (Fig. 19) [89]. In this particular study, a yoke was employed to simultaneously test two specimens in one autoclave and load frame.

Reference and counter electrodes are readily employed in the various cells (e.g., Fig. 18b), perhaps with salt bridges to

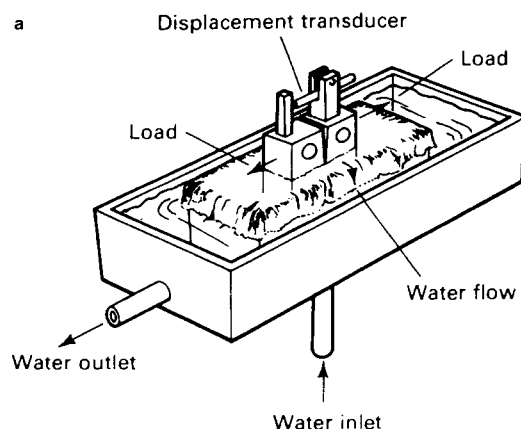


**FIG. 18—Environmental chambers for CF in electrolytes where: (a) the CT specimen is loaded horizontally and dipped into solution [4], and (b) the CT crack is enclosed by a clamped cell and polarized potentiostatically. In part b load (P)-displacement ( $\Delta$ ) data are recorded by computer and autographically for compliance measurement of crack length and  $K_{ci}$ .**

remote containers and including high pressure and temperature compensation capabilities. Procedures to eliminate galvanic couples and to maintain solution purity and composition are identical to those employed in HCF and LCF experiments. Crack opening displacement is measured with a remote or immersed extensometer or LVDT. The cell must not interfere with specimen loading or displacement. For example, in Fig. 18b, the shaded midportion is a flexible membrane designed so that cell clamping forces do not alter specimen compliance. This is important for accurate measurements of crack closure.

Typically, metal-bellows/gasket sealed high vacuum chambers are utilized for environmental fatigue experiments in inert or deleterious gaseous environments [4]. Such an apparatus is outside the scope of this review.

**FIG. 19—Two compact tension specimens mounted in a high pressure-temperature stainless steel autoclave capable of containing water, steam, or acidified H<sub>2</sub>S bearing brine environments [4,89].**

### Crack Length Measurement

CF propagation experiments are unique in the need to monitor crack length, often over a long time. Much has been written on two widely employed methods, direct or alternating current electrical potential difference and compliance (see ASTM E 647, and Refs 84,90,91), as well as on less-tried methods such as eddy current, acoustic wave, optical, or crack surface marking [92]. Compliance and EPD are broadly calibrated and well-suited for precision ( $\pm 25 \mu\text{m}$  or better), long-term-stable monitoring of crack length in many common fracture mechanics specimens and aggressive CF environments. These methods can be computer-automated for test machine and stress intensity control (see following subsection). The principles and instrumentation for each method are detailed elsewhere (ASTM E 647 and Ref 84).

Several points are pertinent to CF. First, compliance allows monitoring of both crack length and crack closure [93]. The advantage of the EPD method is simplicity; it is not necessary to immerse a displacement gage in the electrolyte. (The compliance scheme illustrated in Fig. 18b avoids this complication.) The EPD method is best-suited for monitoring the growth of surface fatigue cracks. Second, there is no evidence that the 1 to 50 A direct or alternating current used in the potential difference method affects CF kinetics. Presumably, the resistance to current flow through the metal is orders of magnitude lower compared to that of the most conductive solutions in an occluded crack. Voltage differences along a crack surface, and

due to this current distribution in the metal, are small (less than 1 mV) and probably unimportant. Nonetheless, prudence dictates that the influence of applied current be tested by employing an independent monitor of crack length in limited qualification and calibration experiments. Third, the electrical potential signal often increases with increasing load in the fatigue cycle because electrically conductive crack surfaces are increasingly parted. Accordingly, potential should be measured at maximum load, and errors in crack length due to residual "crack surface-shorting contact" should be corrected based on post-test crack length measurements [94]. Finally, solution flow or temperature changes can upset the stability of the electrical potential signal due to thermally-induced voltages and material resistance changes.

Ground-loops between potentiostat and electrical potential crack monitoring electronics degrade the quality of polarization as well as CF crack length and growth rate measurements. A successful approach to this problem is based on a specimen (working electrode) that is grounded commonly with the test machine, constant-current power supply and EPD amplifier, coupled with a potentiostat that uses a grounded working electrode. In this case the specimen should not be grounded virtually through an operational amplifier. With this procedure, and the several-ohm (or larger) alternate current path through the typical loading system and test machine, it is not necessary to electrically isolate the CF specimen from the grips. As a test of ground-loop integrity in CF, guarantee that specimen electrochemical current does not change, at fixed electrode potential, upon reversing the polarity of the crack monitoring current.

Given the success of the direct-EPD method, with current applied through the bulk of the CF specimen, there is generally no need to employ an indirect method based on a foil gage bonded to the specimen surface and solely carrying the applied current. This latter method eliminates the effect of applied current on crack electrochemistry (if such an effect exists); however, long-term crevice and galvanic corrosion associated with the attached foil may be important. CF crack growth in the midregion of a specimen is reasonably indicated by compliance or direct EPD, but not by the surface-mounted foil gage method.

### Parameter Measurement, Control, and Computer Automation

Applied load and crack length from electrical potential or compliance are measured as a function of load cycles during a CF experiment. Apart from simple constant load range (increasing  $\Delta K$ ) loading, modern FCP and CF experiments are computer-automated to control the  $\Delta K$ -history, with the mode selection based on the goal of the work, be it mechanism- or application-based. Load is computer-varied, in real time and at frequencies between  $10^{-4}$  and 50 Hz, to maintain the crack length dependence of stress intensity range according to (ASTM E 647)

$$\Delta K = \Delta K_0 \exp[C(a - a_0)] \quad (5)$$

R-value is typically maintained constant as  $\Delta K$  changes. A programmed  $C$  of 0 yields a constant  $\Delta K$  experiment,

which is useful for establishing transient and steady state CF growth rates for mechanistic research. Negative  $C$ -values provide for a  $\Delta K$ -decreasing experiment for measuring near- $\Delta K_{TH}$  CF. Positive  $C$  gives a  $\Delta K$ -increasing experiment that yields data in a reasonable time and confirms stress intensity governed cracking when used in conjunction with a negative  $C$  experiment. Guidance on those values of  $C$  that minimize the effect of prior load history is standardized (see ASTM E 647).<sup>4</sup>

### Data Analysis and Evaluation

Applied stress intensity range and CF crack growth rate are calculated at regular crack length intervals, based on standardized analytical procedures (ASTM E 647). For continuously increasing or decreasing  $\Delta K$  experiments,  $da/dN$  is calculated by either a point-to-point difference (secant) or incremental polynomial method. For constant  $\Delta K$ ,  $da/dN$  is determined by linear regression of cyclic crack length data. The simple secant calculation amplifies  $da/dN$  variability, while polynomial methods average the growth kinetics over seven (typically)  $a$  versus  $N$  points. Growth rate variations depend on the size of the crack growth interval. It is particularly challenging to establish physically meaningful variations from an average growth rate law.

FCP variability was considered in conjunction with an interlaboratory test program that measured  $da/dN$  versus  $\Delta K$  for a well-behaved high-strength steel in moist air [95]. For this best case and 14 laboratories,  $da/dN$  variability from replicate standardized experiments within a single laboratory equaled between  $\pm 13\%$  and  $\pm 50\%$  ( $\pm$  two residual standard deviations about the mean regression curve) at fixed  $\Delta K$ . Variability in CF experiments has not been addressed quantitatively; however, the results from the moist air FCP program provide a lower bound. The increased complexity and prolonged test times typical of CF experiments, as well as the FCP behavior of more complex alloys, should lead to increased variability and uncertainty.

Two complications are notable for CF experimentation. CF  $da/dN$  versus applied  $\Delta K$  data may be affected by a crack closure mechanism that depends on aqueous environment exposure (see subsection, Mechanical Variables) [6,45]; such CF growth kinetics are defined as an extrinsic property that may be test method-specific. As a diagnostic, if CF  $da/dN$  depends strongly on  $R$ , if the environmental  $\Delta K_{TH}$  value is high and increases with decreasing loading frequency, or if crack arrest occurs during CF propagation at constant applied  $\Delta K$ , then environment-sensitive crack closure should be suspected. A bilinear specimen compliance trace (of applied load versus crack mouth or load line displacement) confirms the presence of crack closure.

Closure is characterized and eliminated approximately for a given  $da/dN$  by reducing the applied  $\Delta K$  to  $\Delta K_{eff}$ , the difference between  $K_{max}$  and  $K_{cl}$  rather than  $K_{max}$  and  $K_{min}$ .  $K_{cl}$  is determined by a global compliance method that is nearing

standardization [96]. CF  $da/dN$  versus  $\Delta K_{eff}$  data, as well as results obtained at high constant  $R$  (above about 0.7) or high constant  $K_{max}$  (see Fig. 5 and subsection, Programmed Stress Intensity Experimentation), are reasonably closure-free and are an intrinsic property for a given material-environment system [62]. Closure-free CF data are necessary for basic studies of crack tip process zone damage mechanisms, while crack closure phenomena may be important to applications. As an example, corrosion fatigue cracks in steels exposed to seawater at low  $R$  are arrested by cathodic polarization, because calcareous corrosion products precipitate within the growing crack and cause crack surface closure contact at  $K$  levels well above zero [20,97].  $\Delta K_{eff}$  is substantially less than both the applied  $\Delta K$  and the intrinsic  $\Delta K_{TH}$ . Rough intergranular CF crack surfaces, coupled with local Mode II displacements, may also promote crack closure. Closure benefits may, however, be limited to simply loaded laboratory specimens. For example, compression elements of a complex load history can crush corrosion debris and crack surface roughness asperities, and can thus reduce crack closure.

As a second complication, crack tip stress, strain, and strain rate within the process zone are more fundamental than  $\Delta K$  or  $\Delta K_{eff}$ , and govern CF crack growth kinetics. It is not presently possible to unambiguously calculate the stress intensity dependence of these more fundamental parameters [16,22–24]. Shoji and coworkers argue that the time-based rate of mechanical FCP ( $da/dt_f$ ) in an inert environment is proportional to the rate of dislocation emission from the crack tip, or equivalently, to the crack tip strain rate [98]. The value of  $da/dt_f$  for FCP in vacuum, or more typically moist air, is therefore an indirect crack tip driving force parameter for correlating CF  $da/dN$  data which are also often stated with respect to a time-rate. In this approach,  $da/dt_f$  is the product of  $da/dN$  and  $f$ . An example of this correlation is shown in Fig. 20 which represents the CF enhancement in  $da/dN$  relative to the air

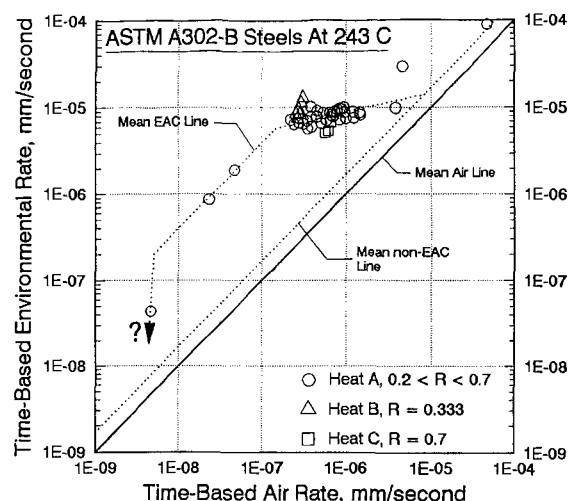


FIG. 20—Time-based CF propagation rate for several heats of A302-B steel in high-temperature water versus mechanical  $da/dt$  for the same alloy in moist air and at several  $R$  values [99].

<sup>4</sup>During fatigue and CF crack propagation, a sudden large decrease or increase in the maximum stress intensity level of the load cycle produces a strong reduction in subsequent growth rates, or so-called delay retardation. These growth rates are important, but are not steady-state and not simply governed according to Eq 3 [6–8]. Most CF experiments are designed and conducted to avoid such overload effects.

case for three high-sulfur-content heats of a C-Mn steel in elevated-temperature water [99]. The speculation is that this relationship between the benign and CF time-based rates of cracking is followed independent of  $\Delta K$ ,  $R$ ,  $f$ , and loading waveform, as demonstrated for several material-environment systems [98]. In Fig. 20 these parameters are varied widely; for example,  $f$  between 10–4 Hz and 10–1 Hz, and  $R$  between 0.2 and 0.7, but a single CF crack growth law is observed. Based on the film rupture (and perhaps HEE) mechanism, environmental  $da/dt$  should increase with increasing crack tip strain rate [22–24], and hence with the mechanical  $da/dt_f$ , as suggested in Fig. 20.

### Specialized Corrosion Fatigue Experiments

Several new CF experimental methods have evolved over the past decade.

#### Programmed Stress Intensity Experimentation

Real-time computer-control of stress intensity during a CF experiment provides important benefits. For example, CF experiments can be designed with a large negative  $C$ -value (Eq 5) to produce continuously decreasing  $\Delta K$  at constant applied  $K_{\max}$  and increasing  $R$  [62,100]. This approach minimizes the complicating effect of crack closure and provides near- $\Delta K_{TH}$  data, albeit at high  $R$ . The CF results presented in Fig. 5 were obtained based on this method [44]. Since both  $\Delta K$  and  $R$  change during this type of experiment, the effects of these two mechanical parameters must be characterized and understood when using the constant  $K_{\max}$  method in CF [16]. Second, variables such as electrode potential, solution composition, or frequency are easily changed as the crack grows at constant  $\Delta K$  to probe subtle growth rate changes for basic research [61,64]. A constant  $\Delta K$  segment can be conducted over an interval of CF crack extension, then  $\Delta K$  can be step-increased or decreased at constant  $K_{\max}$  [51,62,64]. The data presented in Figs. 9, 13, and 14 were obtained with this method.

#### Cyclic Strain-Induced Dissolution

The cyclic-mechanical depassivation method involves measurement of transient electrochemical current during cyclic plastic straining of a smooth specimen in an electrolyte at fixed potential [34,101]. A three-electrode cell, coupled with a fast-response potentiostat and the mechanical LCF procedures described in the subsection on the Smooth Specimen Method, are employed in this regard. Data include time-dependent applied plastic strain, stress, and anodic current density. The phase difference between the mechanical and electrochemical parameters, the strain dependence of the current density during repeated repassivation repair of ruptured surface films, the anodic charge passed per fatigue cycle, and the charge accumulation with increasing cycles and time are interpreted to probe CF damage mechanisms. For example, peak anodic current density and the cycle-cumulative charge increased with increasing strain rate for LCF of a ferritic stainless steel in NaCl, consistent with the film rupture model [34]. (This current reflects metal oxidation to produce cations in solution and in formation of the passive film, or, collectively, metal removal.) Additionally, the time dependence of repassivation and the magnitude of current

transients depended on the sign of the plastic strain, and the repassivation characteristics for this system varied with cycle count, demonstrating the complexity of CF. This method was employed to rank the susceptibility of alloys to CF, based on the stability of surface passive films [101].

#### Small Crack CF Methods

An important goal of CF experimentation and modeling is to quantitatively couple smooth specimen and fracture mechanics approaches to understand the total life of components with microscopic defects. Studies of the so-called “small crack problem” have contributed in this regard [6]. Small crack size can be a particularly important variable that affects CF propagation rates [102,103]. For example, CF cracks sized between 100 and 1000  $\mu\text{m}$  grew up to 1000-fold faster than predicted compared to long crack compact tension specimen  $da/dN$  data at fixed  $\Delta K$ , for the case of a high-strength martensitic steel in NaCl [104]. Such crack geometry effects are traced to differences in crack solution mass transport and crack surface electrochemical reactions that govern HEE and film rupture processes [16,102,103].

Both electrical potential and high magnification optical methods have been developed to monitor the formation and growth of CF cracks smaller than 500  $\mu\text{m}$  [105,106]. Each method is capable of micron-level resolution. The electrical potential approach monitors average short crack growth into the specimen bulk, while microscopic methods focus on surface crack interactions with specific microstructural features including inclusions and corrosion pits. The data presented in Fig. 21 were obtained from in situ monitoring of AA2024 in aqueous chloride solution with a long focal length (15 to 40 cm) and high magnification (500 $\times$  with 1  $\mu\text{m}$  resolution) optical microscope interfaced with a servohydraulic test machine and video system [106]. Microstructurally small CF cracks initiated at constituent particles and grew at rates that were equal to values obtained with the standard LEFM method discussed in the subsection on Fracture Mechanics Methods. While the chemically small crack

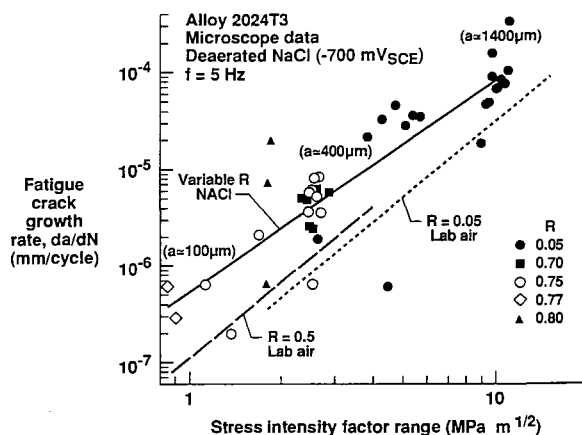


FIG. 21—CF propagation rate versus  $\Delta K$  for microstructurally small cracks in AA2024 exposed to deaerated aqueous chloride at fixed potential. Crack growth was monitored by in situ optical microscopy [106].

effect is not observed for the system in Fig. 21 [106], data of this type are important and lacking for a range of materials and environments [102–105].

The use of short crack specimens provides an important benefit for corrosion fatigue experimentation. Since high-resolution crack monitoring is employed, crack growth rates are quantitatively defined with small crack extensions and the associated reduced  $N$ . It is possible to obtain accurate low growth rate CF data at low loading frequencies. For example, a short crack specimen was employed to measure a  $da/dN$  value of  $0.5 \mu\text{m}/\text{cycle}$  at constant  $\Delta K$  and  $f$  of  $0.0 \text{ Hz}$  during a CF test time of 10 days [16,105]. A 10- to 20-fold longer test time is required to obtain this measurement with a standard long crack method.

#### Measurement of CF Crack Solution pH and Potential

It is important to measure occluded crack pH, potential, and solution composition because these factors govern CF by either HEE or film rupture mechanisms. Several experimental approaches have succeeded in this regard for simple ambient temperature and complex high-temperature pressurized water electrolytes [107,108]. Reference and pH electrodes were located in small holes drilled in the compact tension specimen to intersect the CF crack plane growing from the notch, as shown in Fig. 22 [108]. This method provides information on the crack size and position dependence of local pH and potential, as well as on the effects of  $\Delta K$ ,  $R$ , and  $f$ . Additionally, crack solution can be sampled from crack-intersecting holes for composition analysis by ion chromatography and capillary electrophoresis [109]. Important data were obtained to test models of crack chemistry [72,108] and to understand solution-dissolved oxygen and metal sulfide effects on CF [22,23,109]. Given the very small volume of a typical CF crack, solution extraction methods are likely to upset crack electrochemistry and alter  $da/dN$ .

## APPLICATIONS OF CORROSION FATIGUE TEST RESULTS

### Modern Approach to CF Life Prediction

A cardinal principle is to design the CF experiment to isolate and characterize quantitatively any one of the four stages of fatigue damage defined in the Definition subsection of this chapter. The choice of stage depends on the problem, be it pitting-based crack nucleation in a polished and rigorously inspected medical implant or steam turbine blade, or macrocrack propagation from a weld defect in a large offshore marine structure. If a CF experiment measures total life, without quantifying the four damage stages, then basic understanding and component life prediction are compromised. This is the situation for standardized high- and low-cycle fatigue experiments that measure total  $N_f$  of a small laboratory specimen. The CF material properties embodied in the Basquin and Coffin-Manson relationships Eqs 1 and 2) are not directly scalable to predict the lives of components of alternate geometries and perhaps containing preexisting flaws. These data cannot be used to test models of CF because  $N_f$  embodies cyclic deformation, microcrack

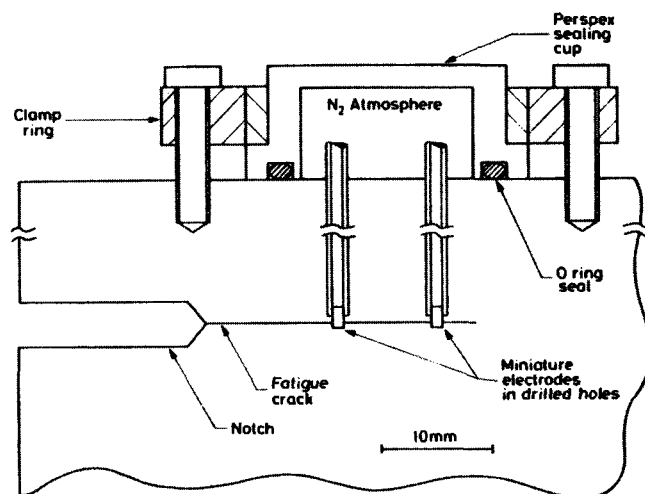


FIG. 22—Compact tension specimen and electrode arrangement for in situ measurement of crack electrode potential, pH, and solution composition during CF growth [108]. ©NACE International. All rights reserved by NACE; reprinted with permission.

nucleation and coalescence, small/short crack growth, and long crack propagation.

Implementing the correct method for CF life prediction and CF-resistant alloy development is often controversial, as existing approaches (often based on smooth specimen HCF data) are challenged by more modern approaches. A consensus is perhaps developing; an effective method couples the local strain approach to CF crack formation and early growth to a given detection threshold with the LEFM approach to propagation in order to calculate the summed total component life. The recommendation is that the Coffin-Manson approach be employed, but that the number of cycles to form a (reasonably) resolvable crack size (perhaps 0.1 to 1 mm) be measured in place of total cycles to failure. Equation 2 then describes the CF crack formation resistance of a given alloy-environment system, with the size of the initiated crack defined operationally. These material-environment property data are coupled with Neuber's method or finite element calculations of local plastic strain range in a component to define service initiation life [7].

The fracture mechanics approach should be employed to characterize CF crack propagation kinetics, with emphasis on both the microstructurally small, physically short, and conventional long crack regimes [6,8]. The Paris relationship (Eq 3), or more complex formulations, are employed with stress intensity similitude and an analysis of the stress and stress intensity conditions of the component to predict CF propagation life, integrated from the size of the crack formed in the initiation stage [41]. A variety of desktop computer programs have been developed for the LEFM portion of the fatigue life prediction problem [110]. If non-destructive testing so indicates, then the LCF initiation portion of the problem can be equated to zero, and the fracture mechanics integration started at the appropriate existing flaw size.

The output of an integrated CF prediction method is plots of total cyclic life as a function of applied stress range, or

crack length versus load cycles at constant applied  $\Delta\sigma$ , for specific material, time, and environment chemistry variables. Coffin-Manson and Paris Law data depend on the variables cited in the section, Factors Controlling Corrosion Fatigue. Since a legion of variables is important, and since prolonged CF test times are often required, mechanistic modeling of the nucleation and crack propagation processes is a critical tool to develop algorithms for extrapolating the results of limited laboratory experiments [111].

### Examples of Component Service Life Prediction with Laboratory CF Data

Corrosion fatigue problems have been attacked aggressively in several technologies over the past decade. The coupled local strain-formation and LEFM-propagation approach has not, however, been broadly employed. Early codified design predictions, using elastic smooth-specimen fatigue data (HCF-SN) adjusted empirically for deleterious time-dependent environmental effects, are being replaced by LEFM predictions of crack propagation from an inspection-based or estimated initial crack size [111]. Examples of this procedure were reported for CF in welded offshore structures in the marine environment [1,3,58,111–113], in-core and out-of-core components in commercial light water nuclear reactors [2,22,111,113], oil and gas pipelines [114], and aircraft [115,116]. Emphases focused on the conflicting effect of cathodic polarization on CF crack formation and growth (marine structures), the unifying role of crack tip strain rate (nuclear reactors), the deleterious effect of sulfur contaminants (nuclear reactor systems and pipelines), and the CF kinetics of small multiple fatigue cracks (aircraft). Tens of man-years are typically required to address a complex CF problem, and large databases for SCC and CF resulted from these efforts [58,117].

### Future Research Needs in CF Experimentation

Environmental effects have not been rigorously incorporated in fatigue life prediction procedures [110]. The time dependence of CF, the many important interacting variables, and several uncertainties confound the problem. From the experimental perspective, LCF and LEFM-based laboratory CF methods must be improved to address the following uncertainties:

1. Methods must be further developed to probe the growth of single small CF cracks sized below 500  $\mu\text{m}$ , and the interaction and coalescence of multiple small cracks must be characterized. Both LCF and LEFM approaches must be modified in this regard.
2. Near-threshold CF crack formation and propagation, and environment-dependent crack closure, must be characterized including the important effect of low loading frequency [118].
3. Load- and environment-spectrum history effects on CF crack formation and propagation must be characterized.
4. The statistical distribution of CF initiation/early growth and crack propagation properties must be defined.

5. High-resolution probes must be developed to measure occluded crack chemistry, transient crack surface electrochemical reactions, crack tip process zone damage processes, and microcrack advance.
6. Fractographic analyses of CF must be improved, including quantitative measurement of crack surface crystallography [119], and computerized image analysis methods to characterize and reconstruct the CF process [120].
7. For mechanistic modeling, CF results must be coupled with transient electrochemical reaction kinetics, hydrogen permeation, and hydrogen trapping analyses described elsewhere in this manual.

### Acknowledgments

This chapter was written based on the support of the Office of Naval Research (Grant N00014-91-J-4164, with Dr. A. John Sedriks as the Scientific Officer), the NASA Langley Research Center (Grant NAG-1-745, with Mr. D. L. Dicus as Grant Monitor), and the Virginia Center for Innovative Technology (Technology Development Center for Electrochemical Science and Engineering, with Professor G. E. Stoner as Director).

### BIBLIOGRAPHY

- Gangloff, R. P., "Environment Sensitive Fatigue Crack Tip Processes and Propagation in Aerospace Aluminum Alloys," in *Fatigue '02*, Anders Blom, Ed., Engineering Materials Advisory Services, West Midlands, UK, 2002, pp. 3401–3433.
- Gasem, Z. and Gangloff, R. P., "Rate-Limiting Processes in Environmental Fatigue Crack Propagation in 7000-Series Aluminum Alloys," in *Chemistry and Electrochemistry of Corrosion and Stress Corrosion Cracking: A Symposium Honoring the Contributions of R.W. Staehle*, R. H. Jones, Ed., TMS, Warrendale, PA, 2001, pp. 501–521.
- In addition, the emerging body of literature on the effect of precorrosion on fatigue life, particularly of aerospace alloys, is important. These include the following:
- Barter, S. A., Sharp, P. K., Holden, G., and Clark, G., "Initiation and Early Growth of Fatigue Cracks in an Aerospace Aluminum Alloy," *Fatigue and Fracture of Engineering Materials and Structures*, Vol. 25, 2002, pp. 111–125.
- DuQuesnay, D. L., Underhill, P. R., and Britt, H. J., "Fatigue Crack Growth from Corrosion Damage in 7075-T65511 Aluminum Alloy Under Aircraft Loading," *International Journal of Fatigue*, Vol. 25, 2003, pp. 371–377.
- Fawaz, F. A., "Equivalent Initial Flaw Size Testing and Analysis of Transport Aircraft Skin Splices," *Fatigue and Fracture of Engineering Materials and Structures*, Vol. 26, 2003, pp. 279–290.
- Spence, S. H., Williams, N. M., Stonham, A. J., Bache, M. R., Ward, A. R., Evans, W. J., Hay, D., Urbani, C., Crawford, B. R., Loader, C., and Clark, G., "Fatigue in the Presence of Corrosion Pitting in an Aerospace Aluminum Alloy," in *Fatigue '02*, Anders Blom, Ed., Engineering Materials Advisory Services, West Midlands, UK, 2002, pp. 701–708.
- Sharp, P. K., Mills, T., Russo, S., Clark, G., and Liu, Q., "Effect of Exfoliation Corrosion on the Fatigue Life of Two High-Strength Aluminum Alloys," *Aging 2000*, DOD/FAA/NASA, 2000.
- Gruenberg, K. M., Craig, B. A., Hillberry, B. M., Bucci, R. J., and Hinkle, A. J., "Predicting Fatigue Life of Pre-Corroded 2024-T3

- Aluminum from Breaking Load Tests," *International Journal of Fatigue*, Vol. 26, 2004, pp. 615–627.
- Gruenberg, K. M., Craig, B. A., Hillberry, B. M., Bucci, R. J., and Hinkle, A. J., "Predicting Fatigue Life of Pre-Corroded 2024-T3 Aluminum," *International Journal of Fatigue*, Vol. 26, 2004, pp. 629–640.
- ## REFERENCES
- [1] *Proceedings Institute of Mechanical Engineers Conference on Fatigue and Crack Growth in Offshore Structures*, Institute of Mechanical Engineers, London, England, 1986.
  - [2] *Proceedings of the Second International Atomic Energy Agency Specialists Meeting on Subcritical Crack Growth*, Vols. I and II, U.S. Nuclear Regulatory Commission Document, NUREG CP-0067, Washington, DC, 1986.
  - [3] Hudak, S. J., Burnside, O. H., and Chan, K. S., *Journal of Energy Resources Technology*, ASME Transactions, Vol. 107, 1985, pp. 212–219.
  - [4] Gangloff, R. P., in *Metals Handbook: Mechanical Testing*, 9th edition, Vol. 8, ASM International, Metals Park, OH, 1985, pp. 403–410.
  - [5] Turnbull, A., Test Methods for Environment-Assisted Cracking, National Physical Laboratory Report DMM(A)66, Teddington, U.K., 1992.
  - [6] Suresh, S., *Fatigue of Materials*, Cambridge University Press, Cambridge, U.K., 1991.
  - [7] Dowling, N. E., *Mechanical Behavior of Materials*, Prentice Hall Inc., Englewood Cliffs, NJ, 1993.
  - [8] *Fatigue and Fracture Control in Structures*, 2nd ed., J. M. Barsom and S. T. Rolfe, Eds., Prentice-Hall, Inc., Englewood Cliffs, NJ, 1987.
  - [9] *Environment Induced Cracking of Metals*, R. P. Gangloff and M. B. Ives, Eds., NACE, Houston, TX, 1990.
  - [10] *Corrosion Fatigue, Chemistry, Mechanics and Microstructure*, O. Devereux, A. J. McEvily, and R. W. Staehle, Eds., NACE, Houston, TX, 1972.
  - [11] *Stress Corrosion Cracking and Hydrogen Embrittlement of Iron Based Alloys*, J. Hochmann, J. Slater, R. D. McCright, and R. W. Staehle, Eds., NACE, Houston, TX, 1977.
  - [12] *Hydrogen Effects on Material Behavior*, N. R. Moody and A. W. Thompson, Eds., TMS-AIME, Warrendale, PA, 1990.
  - [13] *Chemistry and Physics of Fracture*, R. M. Latanision and R. H. Jones, Eds., Martinus Nijhoff Publishers BV, Netherlands, 1987.
  - [14] Duquette, D. J., in *Environment Induced Cracking of Metals*, R. P. Gangloff and M. B. Ives, Eds., NACE, Houston, TX, 1990, pp. 45–53.
  - [15] Duquette, D. J., Mechanisms of Corrosion Fatigue of Aluminum Alloys, AGARD Report No. AGARD-CP-316, 1981.
  - [16] Gangloff, R. P., in *Environment Induced Cracking of Metals*, R. P. Gangloff and M. B. Ives, Eds., NACE, Houston, TX, 1990, pp. 55–109.
  - [17] Wei, R. P. and Gangloff, R. P., in *Fracture Mechanics: Perspectives and Directions (Twentieth Symposium)*, ASTM STP 1020, R. P. Wei and R. P. Gangloff, Eds., ASTM International, West Conshohocken, PA, 1989, pp. 233–264.
  - [18] Holroyd, N. J. H. and Hardie, D., *Corrosion Science*, Vol. 23, 1983, pp. 527–546.
  - [19] Speidel, M. O., Blackburn, M. J., Beck, T. R., and Feeney, J. A., in *Corrosion Fatigue, Chemistry, Mechanics and Microstructure*, O. Devereux, A. J. McEvily, and R. W. Staehle, Eds., NACE, Houston, TX, 1972, pp. 324–345.
  - [20] Scott, P. M., Thorpe, T. W., and Silvester, D. R. V., *Corrosion Science*, Vol. 23, 1983, pp. 559–575.
  - [21] Griffiths, A. J., Hutchings, R., and Turnbull, A., *Scripta Metallurgica*, Vol. 29, 1993, pp. 623–626.
  - [22] Ford, F. P., *Journal of Pressure Vessel Technology, Transactions of ASME*, Vol. 110, 1988, pp. 113–128.
  - [23] Ford, F. P., in *Environment Induced Cracking of Metals*, R. P. Gangloff and M. B. Ives, Eds., NACE, Houston, TX, 1990, pp. 139–166.
  - [24] Hudak, S. J., "Corrosion Fatigue Crack Growth: The Role of Crack-Tip Deformation and Film Formation Kinetics," Ph.D. dissertation, Lehigh University, Bethlehem, PA, 1988.
  - [25] Birnbaum, H. K., in *Environment Induced Cracking of Metals*, R. P. Gangloff and M. B. Ives, Eds., NACE, Houston, TX, 1990, pp. 21–29.
  - [26] Sudarshan, T. S. and Louthan, M. R. Jr., *International Metallurgical Review*, Vol. 32, 1987, pp. 21–151.
  - [27] Grinberg, N. M., *International Journal of Fatigue*, April 1982, pp. 83–95.
  - [28] Sieradzki, K., in *Environment Induced Cracking of Metals*, R. P. Gangloff and M. B. Ives, Eds., NACE, Houston, TX, 1990, pp. 125–137.
  - [29] Duquette, D. J., in *Environment Sensitive Fracture of Engineering Materials*, Z. A. Foroulis, Ed., TMS-AIME, Warrendale, PA, 1979, pp. 521–537.
  - [30] Jones, D. A., in *Environment Induced Cracking of Metals*, R. P. Gangloff and M. B. Ives, Eds., NACE, Houston, TX, 1990, pp. 265–270.
  - [31] *Embrittlement by the Localized Crack Environment*, R. P. Gangloff, Ed., TMS-AIME, Warrendale, PA, 1984.
  - [32] *Corrosion Chemistry Within Pits, Crevices and Cracks*, A. Turnbull, Ed., National Physical Laboratory, Teddington, U.K., 1987.
  - [33] Yan, B., Farrington, G. C., and Laird, C., *Acta Metallurgica*, Vol. 33, 1985, pp. 1533–1545.
  - [34] Magnin, T. and Coudreuse, L., *Materials Science and Engineering*, Vol. 72, 1985, pp. 125–134.
  - [35] Lin, F. S. and Starke, E. A. Jr., *Materials Science and Engineering*, Vol. 39, 1979, pp. 27–41.
  - [36] Chung, H. M., Chopra, O. K., Ruther, W. E., et al., Environmentally Assisted Cracking in Light Water Reactors, U.S. Nuclear Regulatory Commission Report NUREG/CR-4667, Vol. 16, ANL-93/27, 1993.
  - [37] *Manual on Low-Cycle Fatigue Testing*, ASTM STP 465, ASTM International, West Conshohocken, PA, 1969.
  - [38] Lee, H. H. and Uhlig, H. H., *Metallurgical Transactions*, Vol. 3, 1972, pp. 2949–2957.
  - [39] Duquette, D. J. and Uhlig, H. H., *Transactions of ASM*, Vol. 61, 1968, pp. 449–456.
  - [40] Feeney, J. A., McMillan, J. C., and Wei, R. P., *Metallurgical Transactions*, Vol. 1, 1970, pp. 1741–1757.
  - [41] Paris, P. C., Gomez, M. P., and Anderson, W. E., *The Trend in Engineering*, University of Washington, Seattle, Vol. 13, 1961, pp. 9–14.
  - [42] Taylor, D., *Fatigue Thresholds*, EMAS, Ltd., Warley Heath, U.K., 1982.
  - [43] Dawson, D. B. and Pelloux, R. M., *Metallurgical Transactions A*, Vol. 5A, 1974, pp. 723–731.
  - [44] Slavik, D. C., "Environmental Fatigue Crack Growth and Microscopic Damage Mechanisms in AA2090," Ph.D. dissertation, University of Virginia, Charlottesville, VA, 1993.
  - [45] *Mechanics of Fatigue Crack Closure*, ASTM STP 982, J. C. Newman and W. Elber, Eds., ASTM International, West Conshohocken, PA, 1988.
  - [46] Taylor, M. E. and Barsom, J. M., in *Fracture Mechanics (Thirteenth Conference)*, ASTM STP 743, R. Roberts, Ed., ASTM International, West Conshohocken, PA, 1981, pp. 599–622.
  - [47] Rajpathak, S. S. and Hartt, W. H., in *Environmentally Assisted Cracking: Science and Engineering*, ASTM STP 1049, W. B.



- Lisagor, T. W. Crooker, and B. N. Leis, Eds., ASTM International, West Conshohocken, PA, 1990, pp. 425-446.
- [48] Novak, S. R., in *Corrosion-Fatigue Technology*, ASTM STP 642, H. L. Craig, Jr., T. W. Crooker, and D. W. Hoepfner, Eds., ASTM International, West Conshohocken, PA, 1978, pp. 26-63.
- [49] Speidel, M. O., in *Stress Corrosion Research*, H. Arup and R. N. Parkins, Eds., Sijthoff & Noordhoff, Alphen aan den Rijn, Netherlands, 1979, pp. 117-183.
- [50] Mason, M. E. and Gangloff, R. P., "Modeling Time-Dependent Corrosion Fatigue Crack Propagation in 7000 Series Aluminum Alloys," in *Proceedings, FAA/NASA International Symposium on Advanced Structural Integrity Methods for Airframe Durability and Damage Tolerance*, C. E. Harris, Ed., NASA Conference Publication 3724, Part 1, NASA-Langley Research Center, Hampton, VA, 1994, pp. 441-462.
- [51] Krishnamurthy, R., "Microstructure and Yield Strength Effects on Hydrogen Environment Fatigue of Steels," Ph.D. dissertation, University of Virginia, Charlottesville, VA, 1991.
- [52] Wei, R. P. and Landes, J. D., *Materials Research and Standards*, Vol. 9, 1969, pp. 25-28.
- [53] Bucci, R. J., "Environment Enhanced Fatigue and Stress Corrosion Cracking of a Titanium Alloy Plus a Simple Model for the Assessment of Environmental Influence on Fatigue Behavior," Ph.D. dissertation, Lehigh University, Bethlehem, PA, 1970.
- [54] Selines, R. J. and Pelloux, R. M., *Metallurgical Transactions*, Vol. 3, 1972, pp. 2525-2531.
- [55] Vosikovsky, O., *Journal of Testing and Evaluation*, Vol. 8, 1980, pp. 68-73.
- [56] Barsom, J. M., in *Corrosion Fatigue, Chemistry, Mechanics and Microstructure*, O. Devereux, A. J. McEvily, and R. W. Staehle, Eds., NACE, Houston, TX, 1972, pp. 424-436.
- [57] Duquette, D. J., in *Environment Sensitive Fracture of Metals*, R. P. Wei, D. J. Duquette, T. W. Crooker, and A. J. Sedriks, Eds., Office of Naval Research, Arlington, VA, 1987, pp. 1-16.
- [58] *Corrosion Fatigue of Metals in Marine Environments*, C. E. Jaske, J. H. Payer, and V. S. Balint, Eds., Metals and Ceramics Information Center, MCIC-81-42, 1981.
- [59] Endo, K., Komai, K., and Kinoshita, S., in *Proceedings of the 22nd Japan Congress on Materials Research*, Kyoto, Japan, 1978, pp. 193-198.
- [60] Turnbull, A. and Saenz de Santa Maria, M., *Metallurgical Transactions A*, Vol. 19A, 1988, pp. 1795-1806.
- [61] Gangloff, R. P., in *Embrittlement by the Localized Crack Environment*, R. P. Gangloff, Ed., TMS-AIME, Warrendale, PA, 1984, pp. 265-290.
- [62] Piascik, R. S. and Gangloff, R. P., *Metallurgical Transactions A*, Vol. 22A, 1991, pp. 2415-2428.
- [63] Stoltz, R. E. and Pelloux, R. M., *Metallurgical Transactions*, Vol. 3, 1972, pp. 2433-2441.
- [64] Gangloff, R. P. and Kelly, R. G., *Corrosion*, Vol. 50, 1994, pp. 345-354.
- [65] Thomas, C. J., Edyvean, R. G. J., and Brook, R., *Biofouling*, Vol. 1, 1988, pp. 65-77.
- [66] Scott, P. M., Truswell, A. E., and Druce, S. G., *Corrosion*, Vol. 40, 1984, pp. 350-357.
- [67] Lin, F. S. and Starke, E. A. Jr., *Materials Science and Engineering*, Vol. 45, 1980, pp. 153-165.
- [68] Hipsley, C. A., "Hydrogen and Temper Embrittlement Interactions in Fatigue of 2 1/4Cr-1Mo Steel," Harwell Laboratory Report AERE R 12322, Oxon, U.K., 1986.
- [69] Cottis, R. A., Markfield, A., Boukerrou, A., and Haritopoulos, P., in *Environment Induced Cracking of Metals*, R. P. Gangloff and M. B. Ives, Eds., NACE, Houston, TX, 1990, pp. 223-227.
- [70] Lin, F. S. and Starke, E. A. Jr., *Materials Science and Engineering*, Vol. 43, 1980, pp. 65-76.
- [71] Wei, R. P. and Gao, M., *Scripta Metallurgica*, Vol. 17, 1983, pp. 959-962.
- [72] Turnbull, A. and Ferriss, D. H., *Corrosion Science*, Vol. 27, 1987, pp. 1323-1350.
- [73] Magnin, T. and Coudreuse, L., *Materials Science and Engineering*, Vol. 72, 1985, pp. 125-134.
- [74] Yan, B., Farrington, G. C., and Laird, C., *Fatigue and Fracture of Engineering Materials and Structures*, Vol. 8, 1985, pp. 259-273.
- [75] *Atlas of Stress-Corrosion and Corrosion Fatigue Curves*, A. J. McEvily, Ed., ASM International, Metals Park, OH, 1990.
- [76] *Corrosion Fatigue Technology*, ASTM STP 642, H. L. Craig, Jr., T. W. Crooker, and D. W. Hoepfner, Eds., ASTM International, West Conshohocken, PA, 1978.
- [77] *Corrosion Fatigue: Mechanics, Metallurgy, Electrochemistry and Engineering*, ASTM STP 801, T. W. Crooker and B. N. Leis, Eds., ASTM International, West Conshohocken, PA, 1984.
- [78] "Proceedings of the Conference on Low Frequency Cyclic Loading Effects in Environment Sensitive Fracture," *Corrosion Science*, Vol. 23, No. 6, Pergamon Press, Oxford, U.K., 1983.
- [79] Derrick Jones, W. J. and Blackie, A. P., in *Environmentally Assisted Cracking: Science and Engineering*, ASTM STP 1049, W. B. Lisagor, T. W. Crooker, and B. N. Leis, Eds., ASTM International, West Conshohocken, PA, 1990, pp. 447-462.
- [80] Lee, E. U., in *Corrosion Cracking*, V. S. Goel, Ed., ASM International, Metals Park, OH, 1986, pp. 123-128.
- [81] Czyryca, E. J., in *Metals Handbook: Mechanical Testing*, 9th edition, Vol. 8, ASM International, Metals Park, OH, 1985, pp. 366-375.
- [82] Tanaka, T., Sakai, T., and Iwaya, T., in *Fatigue Lives and Fatigue Strengths of Ferrous Metals*, 1986, pp. 125-157.
- [83] Bernstein, H. and Loeby, C., in *Offshore and Arctic Operations*, I. Konuk, Ed., PD-Vol. 10, ASME, New York, 1987, pp. 253-259.
- [84] *Fatigue Crack Growth Measurement and Data Analysis*, ASTM STP 738, S. J. Hudak and R. J. Bucci, Eds., ASTM International, West Conshohocken, PA, 1981.
- [85] Utah, D. A., Cullen, W. H., Majno, L. C., et al., in *Metals Handbook: Mechanical Testing*, 9th edition, Vol. 8, ASM International, Metals Park, OH, 1985, pp. 376-402.
- [86] Crooker, T. W., Bogar, F. D., and Yoder, G. R., "Standard Method of Test for Constant-Load-Amplitude Fatigue Crack Growth Rates in Marine Environments," Naval Research Laboratory Report 4594, Washington, DC, 1981.
- [87] Smith, H. R. and Piper, D. E., in *Stress Corrosion Cracking in High Strength Steels and in Titanium and Aluminum Alloys*, B. F. Brown, Ed., Naval Research Laboratory, Washington, DC, 1972, pp. 17-78.
- [88] Young, L. M., "Environment-Assisted Cracking in Beta Titanium Alloys," M.S. thesis, University of Virginia, Charlottesville, VA, 1993.
- [89] Ceschini, L. J., Liaw, P. K., Rudd, G. E., and Logsdon, W. A., in *Environmental-Sensitive Fracture: Evaluation and Comparison of Test Methods*, ASTM STP 821, S. W. Dean, E. N. Pugh, and G. M. Ugiansky, Eds., ASTM International, West Conshohocken, PA, 1984, pp. 426-442.
- [90] *Advances in Crack Length Measurement*, C. J. Beevers, Ed., EMAS, Cradley Heath, Warley, West Midlands, U.K., 1982.
- [91] *Fatigue Crack Measurement: Techniques and Applications*, K. J. Marsh, R. A. Smith, and R. O. Ritchie, Eds., EMAS, Cradley Heath, Warley, West Midlands, U.K., 1991.
- [92] *Small-Crack Test Methods*, ASTM STP 1149, J. M. Larsen and J. E. Allison, Eds., ASTM International, West Conshohocken, PA, 1992, pp. 116-168.
- [93] James, L. A. and Ceschini, L. J., *Journal of Testing and Evaluation*, Vol. 13, 1985, pp. 409-415.
- [94] Donald, J. K. and Ruschau, J., in *Fatigue Crack Measurement: Techniques and Applications*, K. J. Marsh, et al., Eds., EMAS, West Midlands, U.K., 1991, pp. 11-37.
- [95] Clark, W. G. Jr. and Hudak, S. J. Jr., *Journal of Testing and Evaluation*, Vol. 3, 1975, pp. 454-476.

- [96] Phillips, E. P., "Results of the Second Round Robin on Opening-Load Measurement," NASA TM 109032, Langley Research Center, Hampton, VA, 1993.
- [97] Van der Velden, R., Ewalds, H. L., Schultze, W. A., and Punter, A., in *Corrosion Fatigue: Mechanics, Metallurgy, Electrochemistry, and Engineering*, ASTM STP 801, T. W. Crooker and B. N. Leis, Eds., ASTM International, West Conshohocken, PA, 1984, pp. 64–80.
- [98] Shoji, T., Takahashi, H., Suzuki, M., and Kondo, T., *Journal of Engineering Materials Technology, Transactions of ASME*, Vol. 103, 1981, pp. 298–304.
- [99] James, L. A., "Effect of Temperature and Cyclic Frequency Upon Fatigue Crack Growth Behavior of Several Steels in an Elevated Temperature Aqueous Environment," *Journal of Pressure Vessel Technology*, Vol. 116, ASME, May 1994.
- [100] Herman, W. A., Hertzberg, R. W., and Jaccard, R., *Journal of Fatigue and Fracture of Engineering Materials and Structures*, Vol. 11, 1988, pp. 303–320.
- [101] Amzallag, C., Mayonobe, B., and Rabbe, P., in *Electrochemical Corrosion Testing*, ASTM STP 727, F. Mansfeld and U. Bertocci, Eds., ASTM International, West Conshohocken, PA, 1981, pp. 69–83.
- [102] Gangloff, R. P. and Wei, R. P., in *Small Fatigue Cracks*, R. O. Ritchie and J. Lankford, Eds., TMS-AIME, Warrendale, PA, 1986, pp. 239–264.
- [103] Hudak, S. J. and Ford, F. P., in *Small Fatigue Cracks*, R. O. Ritchie and J. Lankford, Eds., TMS-AIME, Warrendale, PA, 1986, pp. 289–310.
- [104] Gangloff, R. P., *Metallurgical Transactions A*, Vol. 16A, 1985, pp. 953–969.
- [105] Gangloff, R. P., Slavik, D. C., Piascik, R. S., and Van Stone, R. H., in *Small-Crack Test Methods*, ASTM STP 1149, J. M. Larsen and J. E. Allison, Eds., ASTM International, West Conshohocken, PA, 1992, pp. 116–168.
- [106] Piascik, R. S. and Willard, S. A., *Fatigue and Fracture of Engineering Materials and Structures*, Vol. 17, 1994, pp. 1247–1259.
- [107] Gabetta, G. and Rizzi, R., *Corrosion Science*, Vol. 23, 1983, pp. 613–620.
- [108] Turnbull, A., Dolphin, A. S., and Rackley, F. A., *Corrosion*, Vol. 44, 1988, pp. 55–61.
- [109] Andresen, P. L. and Young, L. M., "Crack Tip Chemistry and Growth Rate Measurements in Low Alloy Steel in High Temperature Water," *Corrosion*, March 1995.
- [110] Forman, R. G., Shivakumar, V., Newman, J. C. Jr., et al., in *Fracture Mechanics (Eighteenth Symposium)*, ASTM STP 945, ASTM International, West Conshohocken, PA, 1988, pp. 781–803.
- [111] Andresen, P. L., Gangloff, R. P., Coffin, L. F., and Ford, F. P., in *Fatigue 87*, Vol. III-A, R. O. Ritchie and E. A. Starke, Jr., Eds., EMAS, West Midlands, U.K., 1987, pp. 1723–1751.
- [112] Scott, P. M., *Memoires et Etudes Scientifiques Revue de Metallurgie*, November 1983, pp. 651–660.
- [113] Dover, W. D., *International Journal of Fatigue*, Vol. 3, 1981, pp. 52–60.
- [114] Vosikovskiy, O. and Cooke, R. J., *International Journal of Pressure Vessels & Piping*, Vol. 6, 1978, pp. 113–129.
- [115] Gangloff, R. P., Piascik, R. S., Dicus, D. L., and Newman, J. C., *Journal of Aircraft*, Vol. 31, 1994, pp. 720–729.
- [116] *Durability of Metal Aircraft Structures*, S. N. Ataluri, C. E. Harris, A. Hoggard, et al., Eds., Atlanta Technology Publishers, Atlanta, GA, 1992.
- [117] EPRI Database for Environmentally Assisted Cracking, Project RP2006-2, J. Gilman, Manager, Electric Power Research Institute, Palo Alto, CA.
- [118] "Threshold Corrosion Fatigue of Welded Shipbuilding Steels," Ship Structures Committee Report SSC-366, Washington, DC, 1992.
- [119] Slavik, D. C., Wert, J. A., and Gangloff, R. P., *Journal of Materials Research*, Vol. 8, 1993, pp. 2482–2491.
- [120] Kobayashi, T. and Shockey, D. A., "Computational Reconstruction of Environmentally Accelerated Cyclic Crack Growth in Reactor Steels," Paper 563, Corrosion 89, NACE, Houston, TX, 1989.

# Hydrogen Damage

C. G. Interrante<sup>1</sup> and L. Raymond<sup>2</sup>

## ENVIRONMENTAL CRACKING— HYDROGEN DAMAGE

THIS CHAPTER BEGINS with a brief review of the fundamental behavior of hydrogen in steels. It is presented as a primer that should aid in the understanding of (1) behaviors of hydrogen in materials, (2) the damage caused by hydrogen in various materials, and (3) the selection of appropriate test methods for a particular hydrogen problem.

## UNDERSTANDING THE BEHAVIORS OF HYDROGEN IN MATERIALS

### Basic Principles

Basic aspects of the problem of hydrogen in steels involve its limited solubility in the lattice, its high propensity for adsorption on internal and external surfaces, its absorption into the lattice and the transport by diffusion and by the motion of dislocations and the localization of hydrogen at internal sites in the bulk metal. This localization behavior is called trapping. A trap is a void, interface, or other physical site but may include a region of high stress.

Although it is not highly soluble in steels, hydrogen interacts readily with its host material in many ways that involve precipitates, inclusions, grain boundaries, and other imperfections in the lattice, and it may react with selected elements to form hydrides. These interactions and reactions frequently require transport of hydrogen within the bulk metal and the high mobility of the hydrogen contributes to the damaging character that it has in steels and other alloys.

Hydrogen molecules are relatively large and only the smaller atomic form of hydrogen can diffuse effectively. In gaseous hydrogen only a small fraction of  $H^+$  (hydrogen ions) are present, whereas they are abundant in aqueous solutions. Thus, aqueous solutions can be potent sources for "charging" steels with hydrogen. The uptake of hydrogen involves surface adsorption, followed by absorption into the lattice where it can be driven to diffuse through the bulk of the material. The driving force for diffusion is a gradient in the chemical potential which results from a gradient in one

of the following: the lattice hydrogen concentration, the hydrostatic component of an elastic stress field [1,2], an electric field, and temperature. Hydrogen diffuses away from a region of high chemical potential and towards lower chemical potential. For example, when a concentration gradient exists in the lattice of an unstressed body of uniform temperature without an electric gradient present, hydrogen atoms will diffuse from a region of higher interstitial concentration and towards a region of lower concentration.

In addition to its effects on decreasing the ductility of materials, the localization of hydrogen at regions of high levels of triaxial stress is well-known to be a very important factor in the characteristic delayed-failure behavior of steels containing hydrogen. The driving forces provided by gradients (in concentration, stress, etc.) act independently. Thus, the concentration gradient may be opposed or augmented by a gradient in stress. Hydrogen will diffuse towards an elastic stress field that is tensile in character. For example, this may occur from stress gradients nearby to notches, sharp defects (inclusions or microcracks), bending moments, and the stress field of a dislocation. Each can lead to hydrogen motion, with a hydrogen buildup occurring in the tensile regions, near the defects, and with the flux of hydrogen being proportional to the gradient in the triaxial component of stress.

### Diffusivity, Solubility, and Fugacity

#### Diffusivity

The lattice diffusivity and solubility both can be expressed by an Arrhenius-type equation. The diffusivity can be given by

$$D = D_0 \exp(-Q/RT) \quad (1)$$

where  $D_0$  is a pre-exponential term related to the vibrational frequency of hydrogen and the crystal structure of the metal,  $Q$  is an activation energy or heat of solution,  $R$  is the universal gas constant, and  $T$  is the absolute temperature.

Figure 1 gives results of diffusivity measurements on alpha iron [3,4], a ferritic steel [5], gamma iron [3], and stainless steel [3] by various investigators. These plots are shown to point out some general trends. Apart from the scatter in  $D$  for alpha iron and ferritic steels, the plots show that the lattice diffusivity of hydrogen in gamma iron is much lower than in alpha iron. The values for stainless steel are lower than those for gamma iron, presumably reflecting an influence of the alloy content. See Caskey [55] for a summary of "Hydrogen Effects in Stainless Steels."

<sup>1</sup>U.S. Nuclear Regulatory Commission, Senior Materials Engineer, Rockville, MD, 20852.

<sup>2</sup>L. Raymond & Associates, A Professional Consulting Engineering Corporation, a.k.a. LRA., www.louraymond.com, Director of Technical Operations, Newport Beach, CA 92660.

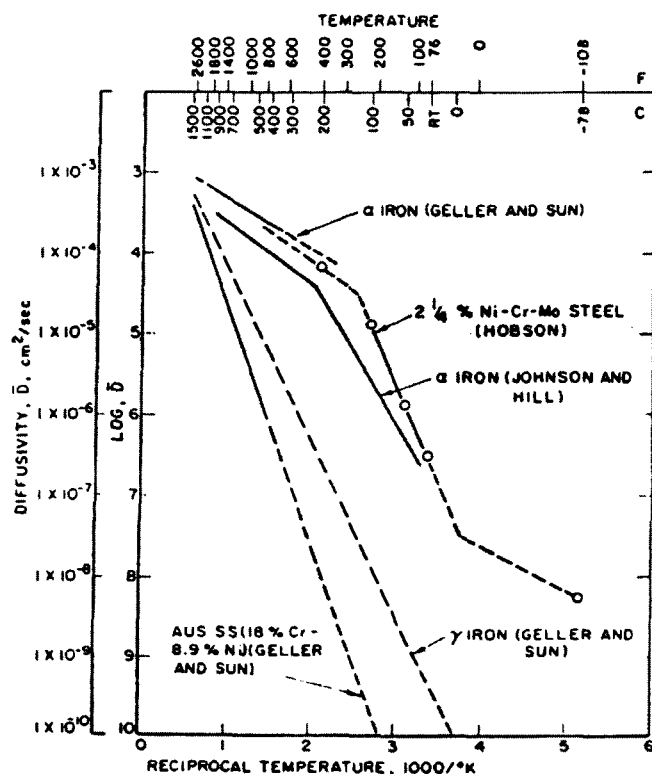


FIG. 1—Diffusivity of hydrogen in iron and steel, after Geller and Sun [3] and Johnson and Hill [4], and in steels after Hobson [5] and Geller and Sun [3].

### Solubility

The solubility embodies Sieverts' law,  $C_H = k \times P^{1/2}$ , as the pre-exponential term, so as to account for the effects of pressure of hydrogen ( $P$ ) on the soluble concentration of hydrogen in metallic solution ( $C_H$ )

$$S = (k \times P^{1/2}) \exp(-Q'/RT) \quad (2)$$

Some materials are endothermic absorbers, while others are exothermic absorbers of hydrogen. For exothermic absorbers solubility decreases with increasing temperature for palladium, titanium, etc., and for endothermic absorbers like copper, iron, nickel, zirconium, etc., it increases with temperature, as illustrated below for iron.

Equation 2 for the solubility ( $S$ ) contains three constants— $k$ ,  $R$ , and  $Q'$ —and it demonstrates the dependence of the lattice concentration of hydrogen,  $C_H$ , on the square root of pressure. This dependence of  $C_H$  on the partial pressure of hydrogen in the environment is illustrated in Fig. 2, which gives hydrogen contents for iron for a range of values of partial pressure of hydrogen ranging from 0.01 atmospheres to 100 atmospheres [6].

Figure 2 also illustrates the effect of crystal structure, by the higher values over the range of temperatures (910°C to 1400°C) at which the FCC gamma phase exists. Solubility in the delta phase is an extrapolation of the alpha values indicating similar behavior for these BCC phases. In the liquid, solubility is much higher than in the solid. This plot is based upon measurements taken above 400°C (750°F).

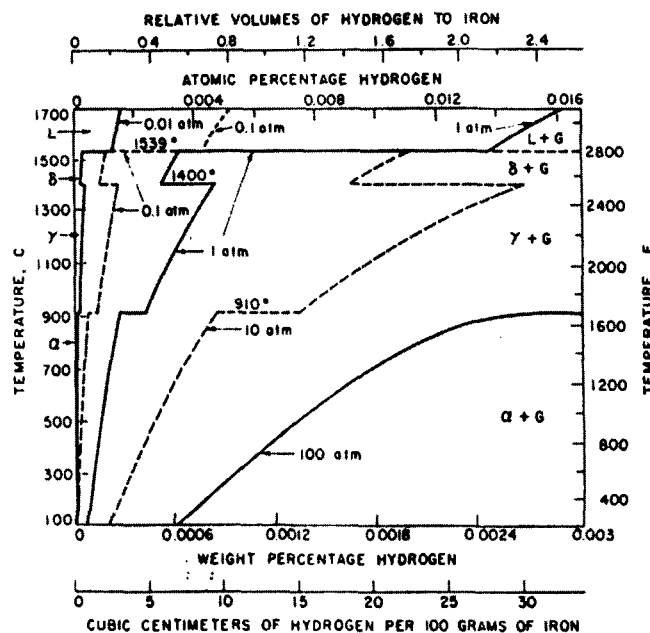


FIG. 2—Equilibrium diagram, iron-hydrogen system, by Zapf [6].

When the solubility of hydrogen in iron is measured at temperatures below about 400°C (750°F), the observed values are generally much higher than those extrapolated from high temperature measurements, and this is taken as evidence of "traps." The subject of hydrogen traps is briefly introduced later in this chapter.

### Fugacity

Fugacity ( $f$ ) is a measure of the escaping tendency from liquid or solid solution to the surrounding environment or into the lattice or a void within a metal. In an ideal gas, the fugacity is equal to the vapor pressure, but hydrogen is not an ideal gas and the proportionality expressed by Sieverts' law is not exact. To account for this deviation in thermodynamic behavior, the fugacity of hydrogen furnishes a correction [51]. For hydrogen, and other diatomic gases like nitrogen and oxygen, when the partial molar Gibbs free energy ( $G$ ), which is synonymous with the chemical potential, is computed, the gas behaves like an ideal gas with a (equivalent) pressure ( $P$ ) equal to the fugacity ( $f$ ). When  $f$  is used in place of  $P$ , in Eq 2, the calculated lattice concentration is exact.

From data given by Baranowski [7], Fig. 3 is given to show the pressure for values of fugacity that extend over a very large range. At higher values of hydrogen pressure, the increases in fugacity, and hence in the concentration of hydrogen in the lattice, are comparatively much greater. Further, it is seen that as  $f$  increases, the difference between  $f$  and  $p$  increases, so that the values of  $f$  become increasingly greater than the corresponding values of  $P$ , which correspond to the internal pressure that can be exerted from within internal voids in the steel. In general, the pressure, e.g., that at internal sites, will not exceed that which corresponds with the fugacity of hydrogen at the exposed input

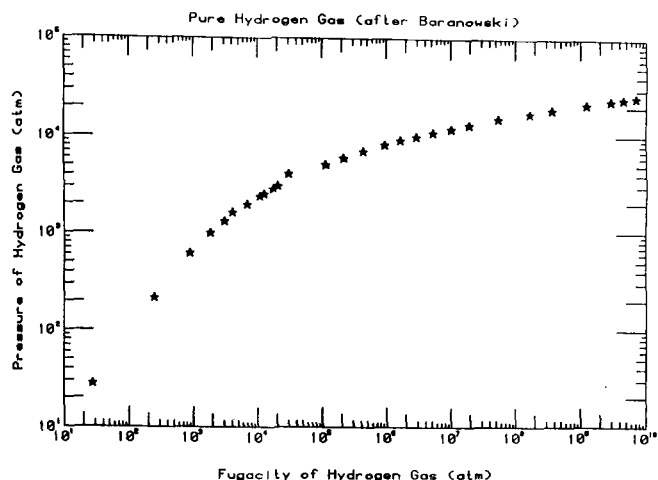


FIG. 3—Plot of the relationship between pressure and fugacity of hydrogen derived from data of Baranowski [7].

surface (where hydrogen enters the material) or that within the lattice. Figure 3 indicates that a pressure limit of under 20,000 atm (<300 ksi) can be imposed by hydrogen and that the hydrogen behavior is that of an ideal gas up to at least 200 atm.

In an analogous way, the non-ideality of solutions (liquid or solid) is accounted for when the chemical potential is computed for real solutions. The thermodynamic activity ( $a$ ) is used in place of the concentration ( $C$ ) in the Nernst equation; the equation is exact even if the concentration is high and the behavior is non-ideal. The activity is the driving force for the reaction of hydrogen within the lattice and is related to the concentration by a proportionality factor  $\gamma$ :  $a_i = \gamma_i C_i$ . Use of the activity is more important at higher concentrations, as the difference ( $C - a$ ) increases with concentration. Thus, the activity ( $a$ ) can be used to correct for the nonideality of the solution.

### Trapping Behavior

Hydrogen in excess of the solubility (interstitial) limit is believed to be contained not at interstitial lattice sites but at other sites referred to as "traps." In general, these trapping sites apparently do not affect solubility at elevated temperatures, as indicated for several ferrous materials in Fig. 1. At room temperature their ability to trap hydrogen is so great that only a small fraction of total hydrogen content is dissolved in the lattice for steel. The trapping behavior is affected greatly by cold work and the presence of nonmetallic inclusions. Other factors such as chemical composition of the matrix have a minor role. A "trapping state" defines a unique trap, i.e. dislocations, MnS inclusions, grain boundaries, etc. For every trapping state, there may be multiple "trapping sites."

The tendency for hydrogen to be trapped, the jump probabilities for the hydrogen atoms [8], is governed by the energy of motion  $G_m$  of the hydrogen atom, as well as by both the energy and the nature of the traps [9]. Attractive traps are regions of the lattice at which atoms are subject to a drawing force, for example, a region of local strain that

pulls the hydrogen to the center of the local region. Physical traps are modifications of the ideal crystal lattice, such as may result from high-angle grain boundaries, incoherent particle-matrix interfaces, and voids [52,57].

At lower temperatures, e.g., room temperature, at which a significant fraction of the hydrogen resides in traps, the trap acts like reservoirs whose behavior is governed by the fugacity of hydrogen in the adjacent lattice. Under equilibrium conditions, a net uptake of hydrogen by the trap occurs while the adjacent lattice hydrogen fugacity is higher, in relation to that inside the trap, whereas traps in a low-fugacity lattice region can lose hydrogen to the lattice. The kinetics of the uptake and loss during steady-state permeation are governed by behaviors at input and exit surfaces, the local fugacity through the lattice, the binding energy (reversibility) of the traps as well as the number of traps.

Traps are of two principal types, physical and attractive [52,53,57]. When a purely physical trap is compared with a purely attractive trap of the same depth, it is easier for hydrogen to escape the attractive trap, as smaller jump increments will lead to escape from it. Thus, attractive traps are regarded as being more reversible than physical traps, i.e., hydrogen that enters can leave more readily. Thus, the amount of trapped hydrogen is governed by both the nature of the defects and the fugacity of hydrogen in the lattice.

In general, it is observed that the very high values of the fugacity that can be achieved electrochemically (from aqueous solutions) are much greater than the fugacities that occur under hydrogen gas storage and industrial applications. Whereas from aqueous solutions, the fugacity can obtain values of hundreds of thousands of atmospheres, values of about 1000 atmospheres is about the limit for industrial gas; e.g., in hydrogen storage, chemisorption of hydrogen atoms at the charging surface is frequently less from the gas phase than that from aqueous solutions—fewer hydrogen atoms are made available for adsorption from the gas phase. This means that the gas-charged metal has a lower fugacity, a decreased tendency to escape or diffuse. Therefore, except for the cases of thermal charging and charging under the ionized atmosphere created by a welding arc, which are not dealt with in this chapter, gaseous environments have diminished effects in relation to those of some severe aqueous environments. The gaseous behavior further can often be greatly ameliorated by the presence of surface contaminants, e.g., oxygen gas, that block surface entry sites into the bulk lattice [10,11]. In many instances, this has proven to be an effective remedy to the deleterious effects of gaseous hydrogen. Very low levels of oxygen ( $10^{-3}$  atm) can have significant effects and the behavior can be abated completely using 1 to 10 % oxygen in hydrogen gas. The behavior observed under hydrogen gas strongly indicates that surface behavior governs the properties of steel in gaseous hydrogen environments.

## DAMAGE CAUSED BY HYDROGEN IN VARIOUS MATERIALS

### Effects of Hydrogen

There are few if any favorable effects of hydrogen in materials, while numerous types of mechanical damage may

result. While incomplete understanding exists on the details associated with the mechanisms by which hydrogen damage arises, the various mechanistic descriptions [12–18,54] that have been developed are adequate for problem solving by scientists and engineers. The most prominent and complex effects of hydrogen are those in steels. Hydrogen embrittlement is reported to occur in stainless steels [55], but austenitic materials including the stainless steels are much more tolerant of hydrogen when compared with ferritic steels. The damaging effects in austenite are generally most pronounced under high fugacities and where epsilon and alpha-prime martensite are present. Hence, this review focuses mainly on hydrogen damage in ferritic materials, as from a practical view these steels are most significantly affected by hydrogen damage. Hydrogen damage takes as many forms as there are mechanistic explanations for the effects of hydrogen:

1. At temperatures near room temperature, hydrogen in steel may cause a decrease in ductility, blistering, step-wise cracking or delayed cracking, which is crack extension that occurs at levels of stress intensity much below those required for crack growth in the absence of hydrogen.
2. At temperatures that are usually above room temperature, hydrogen gas at high pressure that diffuses into the steel can decrease the strength level of the steel by reacting with carbon, forming methane that can form internal bubbles that coalesce, usually at grain boundaries, and exert significant pressure that expands voids and causes decarburization. These are part of the problem called hydrogen attack, as described by Nelson [33].
3. In niobium, tantalum, titanium, and zirconium, brittle hydride phases can form and this may lead to loss of ductility and crack extension at decreased levels of stress intensity. The damage due to these hydride phases is governed not only by their quantity but by their orientations in relation to stress states in the nearby matrix.

### Internal Hydrogen Embrittlement (IHE)

Internal hydrogen embrittlement (IHE) is caused by hydrogen, contained (pre-existing) in the material, that acts in combination with extant stress, residual and applied. When a steel part fractures while sitting in air on a shelf, with no externally applied stress, this process of time-delayed fracture is caused by residual stress in a process that is classically termed internal hydrogen embrittlement (IHE). This behavior is usually associated with steels of relatively high strength levels, such as those used in bolts or landing gears. It is caused by the presence of residual hydrogen and residual stresses from processing. These “causes” initiate microcracking that proceeds eventually to rupture. Applied tensile stresses in combination with residual stresses from processing can also produce time-delayed fracture or IHE, as in electrochemically plated tensile bolts. Commercially, IHE is treated differently than environmental hydrogen embrittlement (EHE), which includes any gaseous or aqueous environment that promotes hydrogen charging of the material. In both processes, the cracking is associated with diffusion and localization of hydrogen near defects and microcracks.

### Environmental Hydrogen Embrittlement (EHE) and Stress Corrosion Cracking (SCC)

When cracking occurs in an aqueous solution, a distinction is made between two forms Environmentally Assisted Cracking (EAC): stress corrosion cracking (SCC), and Environmental Hydrogen Embrittlement (EHE). An impressed cathodic current may often provide protection against SCC, but steel that is “protected” against corrosion by this means may be subject to EHE by cathodic hydrogen absorption/adsorption. For an impressed anodic current, the converse is true. Although this is a simplistic view of SCC, it is sometimes useful. Nevertheless, it would be remiss to fail to note that under anodic polarization, hydrogen production might still result at a crack tip where its presence can be most harmful. Bulk anodic polarization does not ensure that the crack tip is polarized.

Differences and similarities between SCC and EHE are further described by Latanision [19], who also discusses hydrogen-induced phase transformations in the solid, the observation of hydrogen evolution from the tip of a propagating crack, fractography, crystal structure, and the influence of solid-state impurities.

Thompson, Bernstein and Pressouyre [20,52] discuss the significance of a number of metallurgical variables (including chemical composition), microstructural components (precipitates, grain size and shape, crystallographic texture), heat treatment and its effects on these variables, and processing, especially thermomechanical treatments for enhancement/optimization of properties.

Treseder [21] indicates ranges of electrode potentials for SCC in various environments and indicates that EHE may be a factor in complex environments of sulfides, cyanides, carbonates, and ammonia, and he notes that the term SCC is attributed to various literature references where EHE is the appropriate environmental influence.

### Effects on Ductility

Hydrogen contained in steel that is tested in air can lead to a decrease in ductility and the true stress at fracture. This effect is manifested in tension tests with smooth specimens as a decrease in reduction of area and elongation, but in notched specimens as a degradation in strength (in notched tension tests as a decrease in notch tensile strength) and in notched bend tests as a decrease in bend ductility. The magnitude of the decrease in ductility increases with decreasing strain rate, and for an SAE 1020 steel [31] this effect on ductility was observed to occur within the range of temperatures from about -250F to 130F after cathodic pre-charging with hydrogen.

Figure 4 illustrates the effects of hydrogen on ductility in a smooth bar tensile test. Steels containing residual hydrogen can be characterized by fracture after the onset of necking but at lower than normal strain values, as illustrated by data from Hobson and Sykes [22] for smooth bars. The table corresponding to this figure shows that the bars had hydrogen contents of from 0.1 ppm to 4.8 ppm, as the hydrogen content was decreased by baking. The plot shows that the true stress at fracture decreases as the hydrogen concentration in the steel increases, but fracture occurs only

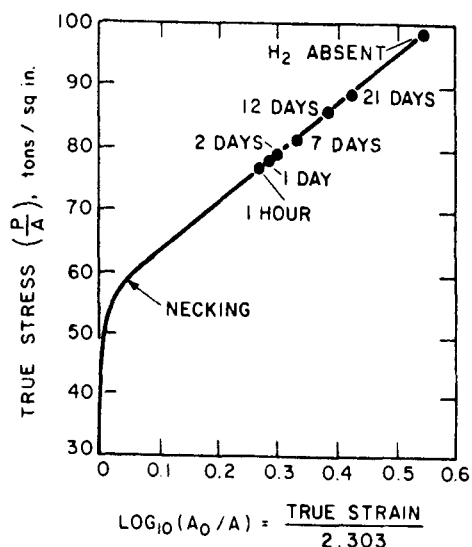


FIG. 4—True stress-true strain curves for a hydrogen-impregnated 3Cr-Mo steel after standing in air for varying periods [22].

after the apparent maximum stress has been reached and necking is already in progress. Thus, in this study, the presence of hydrogen led to fracture after the apparent maximum stress has been reached, and necking is already in progress, so that the flow or yield behavior does not appear to have been affected, but fracture occurs at levels of true strain and true stress that decrease progressively as the hydrogen content is increased. In steels of higher strength level, which are more greatly affected by hydrogen effects, the presence of hydrogen may have substantial effects on both the tensile strength as well as on measures of ductility.

These effects of hydrogen are often reversible if no microcracking has occurred. Whenever specimens that have contained hydrogen have been outgassed of hydrogen but still exhibit decreased ductility, the observed effects are generally attributable to microcrack damage that occurred prior to outgassing and during the period of hydrogen containment.

It was shown that in IHE the plastic flow behavior after the point of maximum load is the dominant effect in smooth-bar testing, which is to say that ductility and toughness are decreased. As has been suggested by Beachem [17], hydrogen facilitates dimpled rupture and/or crack propagation. Hence, it is expected that the fracture toughness at the onset of crack propagation will not be as greatly influenced by hydrogen at conventional ASTM E 8 loading rates, when compared with propagation behavior. In J-integral and R-curve tests Nagumo's Figs. 22, 21, and 15 illustrate [59] significant effects for the "region of crack propagation" [<http://www.msm.cam.ac.uk/phase-trans/2003/nagumo/IMG/22.gif>]. Hirth discusses plastic instability in the presence of hydrogen [58]. Nagumo [59] attributes the role of hydrogen in decreasing the resistance to ductile crack-growth (Nagumo Figs. 18–20) as an increase in the density of vacancies and their agglomeration, a mechanism that he supports with recent findings of amorphization associated with crack growth (s.a. Nagumo Figs. 23–25). The classification

	Aging Period	Hydrogen Concentration ml/100g	Hydrogen Concentration ppm
H <sub>2</sub> gas	ABSENT	0.1	0.1
	21 days	1.4	1.3
	12 days	2.8	2.5
	7 days	3.7	3.3
	2 days	4.6	4.1
	1 day	4.4	4.0
	1 hour	5.3	4.8

of models in his Fig. 25 was adapted from his ISIJ International (2001) article [60].

### Effect of Notches

The decreased tensile ductility and true fracture stress/strength of steels containing hydrogen are particularly significant in respect to behavior at notches and other stress concentrators, as the local plastic strain that precedes fracture at these local sites is affected as described above, except that the result is a decrease in notched tensile or fracture strength. Because notched tensile strength (NTS) or notched fracture strength (NFS) is affected by ductility of the steel, those factors that govern the effects of hydrogen on the ductility of steels containing hydrogen, such as hydrogen content, strain rate, and temperature, are expected to similarly affect the behavior of the NFS. Thus, the effects on strength of notched specimens are qualitatively similar to the effects on ductility of smooth specimens.

### Delayed Failure

When subject to a sustained load, a steel containing residual hydrogen may exhibit a considerable degradation in strength. Thus, after an incubation period, hydrogen in steel can decrease the fracture strength, and for very-high-strength steels this behavior may occur at very low levels of hydrogen. This behavior is variously termed delayed failure, hydrogen-stress failure, and delayed, low-stress brittle failure, static fatigue, cold (or delayed) cracking, and internal hydrogen embrittlement (IHE). It represents a manifestation of the decreased fracture strength (or strain at fracture) in the presence of hydrogen, as exemplified by the results of the notch tension tests just described. These delayed fractures initiate in regions of highly localized stress in which hydrogen is concentrated as a result of locally augmented solubility,

which promotes diffusion of hydrogen into triaxially stressed sites near flaws, notches, and discontinuities. The term "brittle" sometimes used for this effect of hydrogen is an embrittlement observed to occur with a change from higher- to lower-energy fracture, with corresponding changes in the modes of failure. Thus, the fractographic features change from dimpled rupture to some combination of modes from quasi-cleavage to intergranular and cleavage.

The discovery and early exploitation of the understanding of this behavior was by Troiano and coworkers [13], who showed that in precharged samples, fracture occurs as a series of events: incubation, crack initiation, crack propagation, and finally failure. In the schematic drawing shown as Fig. 5 this behavior is represented by two stress-time curves, one for crack initiation and one for failure. Each curve is bounded by two stress levels, an upper-critical stress (UCS) and lower-critical stress (LCS), which are the highest and lowest applied-stress levels leading to delayed failure. Above the UCS, failure occurs without a time delay, and at stresses below the LCS (or threshold stress), hydrogen is not damaging and time-delayed failure will not occur. At intermediate stress levels, failure is inevitable and occurs as a series of events involving initiation and propagation of a crack.

After the specimen is loaded in tension at intermediate stress levels, an incubation period is required to initiate a crack. During this time, lattice-contained or weakly-trapped hydrogen diffuses ahead of the notches and local stress raisers, so as to equilibrate under the influence of any triaxial stress created there—this equilibration involves hydrogen redistribution associated with the equilibration of its chemical potential, under the combined influences of all factors that affect it. The first cracks will be initiated in this region after a critical hydrogen concentration has accumulated. The kinetics of the crack-initiation process are therefore dependent on the temperature and the stress gradient as they relate to the diffusion and concentration of hydrogen at the site of maximum triaxial stress in the steel.

The delayed-failure behavior of precharged steels may be affected by various factors, principal among which are the

hydrogen concentration and the strength level or hardness, but composition and processing may also affect the susceptibility of the steel. Other important factors are notch acuity and temperature, both of which strongly influence the observed behavior. An increase in either the hydrogen concentration or the strength level normally leads to a decrease in both the upper and the lower critical stresses, and to shorter delay times for failure.

## THE SELECTION OF APPROPRIATE TEST METHODS FOR A PARTICULAR HYDROGEN PROBLEM

### Interpretation of Test Results

Due to the complex nature of hydrogen embrittlement, the selection of a test method requires much thought to insure that the results truly predict the in-service behavior of a structural component. Test results may be influenced by a large number of variables: (1) those that affect the local concentration of hydrogen and state of stress; i.e., test specimen geometry (notched tension or bend specimens, cantilever, beam specimen, wedge-opening specimen), and specimen preparation (machining, grinding, fatigue precracking), (2) the susceptibility of the material that depends on the specific material, hardness and melting procedure i.e., air, vacuum, electroslag or vacuum arc remelting, etc., and (3) the environmental conditions i.e., potential, pH, oxygenation level, temperature, environment. As a result, test methods to assess hydrogen damage on a quantitative scale, are very difficult to design and control, and therefore, the test method should address a very specific set of conditions, so that the interpretation is facilitated and the results may be applied to solve a specific problem.

### Testing Techniques to Measure Hydrogen Concentration

Many test methods have been developed over the years [23–25] and new techniques to monitor the various aspects of hydrogen embrittlement are constantly being incorporated into ASTM Standards<sup>3</sup>. What many consider to be the most direct approach is to measure the concentration of diffusible hydrogen in the material. ASTM Committee E 3 focuses on these methods. No suitable fusion method has been developed to reproducibly measure hydrogen content at the precision of a part per million (or less) that may sometimes cause embrittlement in high-strength steels. For this reason, indirect mechanical test methods of measurement such as the amount of degradation in strength are being used.

### ASTM Test Methods Related to Hydrogen Uptake of Plated Materials

These ASTM standards are based on three types of controls: (1) monitoring indirectly the concentration of diffusible

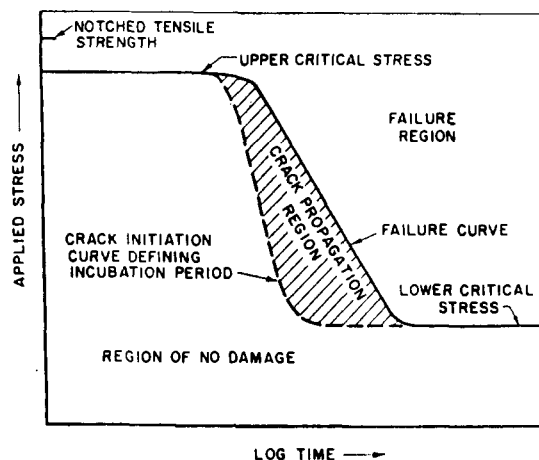


FIG. 5—Schematic drawing of characteristic failure behavior of notched tension specimens containing hydrogen.

<sup>3</sup> *Annual Book of Standards*, American Society for Testing and Materials, West Conshohocken, PA.



hydrogen in the material (ASTM F 1113<sup>4</sup>), (2) minimizing the amount of hydrogen introduced into the steel by keeping the hydrogen in a plating bath at acceptably low levels (ASTM F 326<sup>5</sup>) and (3) using mechanical tests to ensure that the amount of residual hydrogen after baking is below acceptable levels (ASTM F 519<sup>6</sup>).

### ASTM F 1113: Barnacle Electrode

A nondestructive electrochemical method for measurement of diffusible hydrogen in steels has been devised and standardized. The purpose of this test method is to evaluate the potential for hydrogen embrittlement based on the amount of diffusible hydrogen in steel. The method is limited to room temperature testing of flat carbon or alloy steels, excluding austenitic stainless steel specimens. The specimens must be bare or re-plated after the plating has been removed. One of the significant findings in the development of this technique is that 100-h baking time at 400°F (204.4°C) was shown to be required for a sufficient removal of all the hydrogen from a cadmium plated quenched-and-tempered 4340 steel specimen at 53 HRC.

### ASTM F 326: Lawrence Gage

This standard method electronically detects hydrogen in the plating bath and is related to hydrogen absorbed by the steel parts during plating and to the hydrogen permeability of the plating during post-plate baking. A specific application of this method involves controlling cadmium-plating processes in which the plate porosity relative to hydrogen is critical, such as with cadmium plating of high-strength steel.

This method uses a metal-shelled vacuum probe as an ion gage. A section of the probe shell is cadmium-plated at the lowest current density encountered during the electroplating process. During the subsequent baking, the probe ion current, which is proportional to hydrogen pressure, is recorded as a function of time. The slope of this curve has an empirical relationship to failure data, as discussed in ASTM STP 543 [26].

## MECHANICAL TESTING

An indirect, less expensive, and often more precise method for determining the amount of residual hydrogen due to processing is to quantitatively measure the change in a mechanical property that is sensitive to small variations in the hydrogen concentration [27–29]. This works best in higher strength steels in which comparatively small amounts of hydrogen lead to large changes in properties; in steels of lower strength levels, greater hydrogen contents are required to obtain significant effects. Measured tensile properties are affected by the temperature and strain rate of the test, the stress concentration of the specimen, the strength level of the steel, and the

amount of prior cold work. In fatigue-tests, the effects of hydrogen can be masked because hydrogen may not have sufficient time for diffusion to the crack-tip process zone for any significant effects of hydrogen to be observable. Nevertheless, in hydrogen “charging” environments significant effects of hydrogen may be observed.

Standard mechanical testing procedures are commonly used to measure the effects of hydrogen. Test results expressed as differences or ratios of the hydrogen-affected and nonaffected specimens are compared as a measure of the hydrogen effect.

Hydrogen embrittlement can also be revealed by a change in ductility of smooth-bar specimens and of strength level of notched-bar specimens. Likewise, the results of various other qualitative tests that are commonly used in corrosive environments, e.g., U-bend, C-ring, three- and four-point bend specimens, as well as stress-rupture constant load, constant-extension or slow strain rate tension and step-modified slow strain rate bend test specimens are used to detect embrittlement due to hydrogen. In addition, hydrogen attack, caused by high-pressure hydrogen at elevated temperatures, can result in decreases in absorbed energy in impact tests as well as decreases in other mechanical properties [30,32,33].

### Temperature and Strain Rate

Temperature and strain rate strongly affect the magnitude of the effect that hydrogen has on the ductility of (nonaustenitic) steels [33]. Hydrogen influences ductility over the range of temperatures from about –160°C (about –250°F) to above 200°C (400°F). The effect on ductility is a function of factors that influence the overall behavior, but the greatest effects occur near room temperature. The magnitude of the decrease in ductility increases with decreasing strain rate [31]. For the austenitic steels (in which effects are much less pronounced) the greatest effects are generally at and just below room temperature [55].

### Potential

Galvanic coupling from the use of dissimilar metals or the actual implementation of cathodic protection systems introduce hydrogen into the test environment in varying amounts. The amount of absorbed hydrogen is, of course, governed by the potential, and steel that is very resistant to EHE under open circuit potential may fail under galvanic action. Once exposed to a cathodic potential, the threshold stress required for subcritical crack growth can decrease significantly. Therefore potential is an extremely important test variable in evaluating a materials resistance to EHE.

### Process Control

Two standard test methods are used for hydrogen embrittlement prevention and control during processing of steel products. ASTM F 519 is directed at the plating process and maintenance chemicals used in aircraft such as landing gear (high-hardness steels, 45–52 HRC) and ASTM F 1940 is primarily directed at plating processes for fasteners (lower-hardness steels, 33–44 HRC).

<sup>4</sup> Ibid., Vol. 15.03, F1113, “Test Method for Electrochemical Measurement of Diffusible Hydrogen in Steels (Barnacle Electrode).”

<sup>5</sup> Ibid., Vol. 15.03, F326, “Method for Electronic Hydrogen Embrittlement Test for Cadmium Electroplating Processes.”

<sup>6</sup> Ibid., Vol. 15.03, F519, “Method for Mechanical Hydrogen Embrittlement Testing of Plating Processes and Aircraft.”

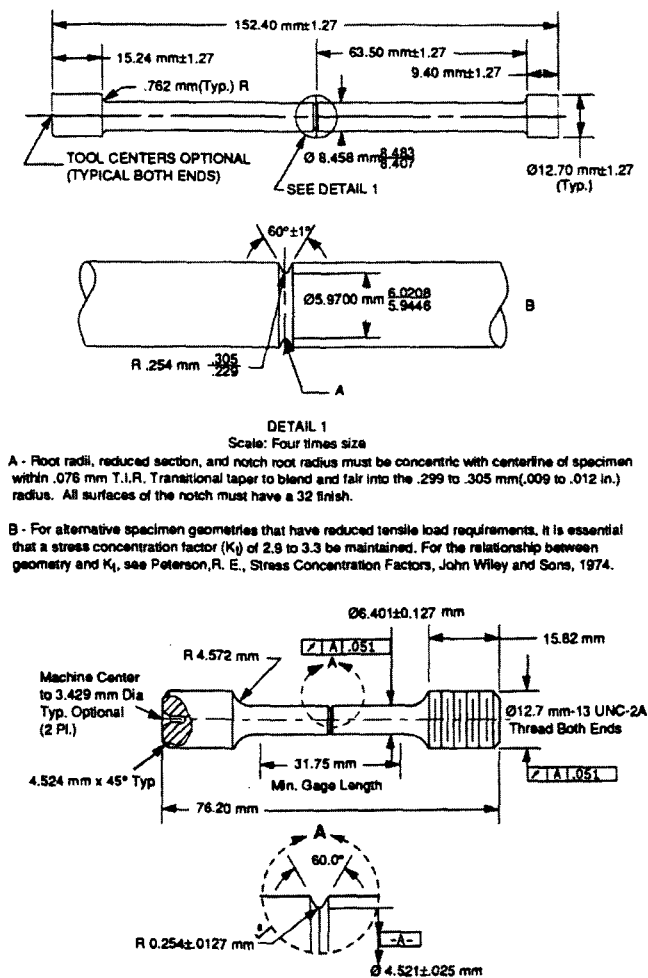


FIG. 6—Dimensional requirements for Type 1a specimens (reprinted from ASTM F 519, Type 1a).

Over 30 other military (MIL) and Federal (FED) specifications include hydrogen embrittlement relief treatments. Structural elements, such as springs or fasteners, are tested directly under constant load, constant displacement or decreasing extension rates (slow-strain-rate testing) for evaluation of the effectiveness of treatments directed at amelioration of hydrogen embrittlement.

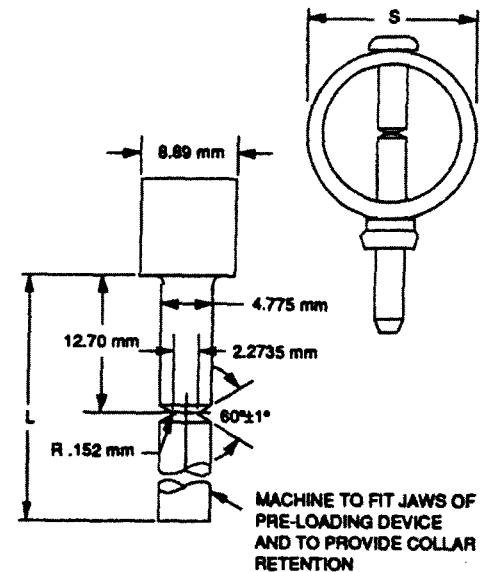
### ASTM F 519: Aerospace & Aircraft

The ASTM F 519 method covers the evaluation of hydrogen introduced by electroplating processes and aircraft maintenance chemicals. The standard was originally written just for cadmium plated aircraft components, and specifically for high-hardness landing gear. Now the standard is being modified to evaluate other platings, some as replacements to cadmium and chromium because of their carcinogenic nature.

Test specimens are installed into the plating bath during the plating of hardware to monitor indirectly the amount of hydrogen in the plating bath. The acceptable level of hydrogen has been historically determined in a pass/fail test with

### Assembly of Type 1b Specimens with Type 1b Stress Ring with Locking Collar.

A flexible Plastic Collar is inserted over loaded specimen for protection.



Note 1—"L" to be 38.1 mm (1.5 in.) or greater.  
Note 2-Tolerance (unless otherwise specified):

XXX ±1.27 mm (.05 in.)  
XXOX ±.025 mm (.001 in.)  
XXXX ±.0051 mm (.0002 in.)

Note 3-Specimens and loading device that have been found to meet the standard are available from Stapleton Co., 1350 W 12th St., Long Beach, Calif. 90813.

FIG. 7—Dimensional requirements of Type 1b tension specimen (reprinted from ASTM F 519, Type 1b).

the fail being failure in less than 200 h under a sustained load with the specimen being stressed to 75 % of its notched tensile strength. With accelerated production schedules of 4- to 6-weeks, the 200 h (> 8 days) test period is creating an unacceptable and unnecessary time burden on production leading to the need and development of an accelerated, ≤ 24 h test method.

The procedures and requirements for ASTM F 519 are specified for the following six types of AISI 4340 steel test specimens grouped into three different loading methods are shown in Fig. 6 through Fig. 11:

#### • Constant Load

Type 1a: notched round bars, stressed in tension, under constant load (Fig. 6).

#### • Constant Displacement

Type 1b: notched round bars loaded in tension with loading rings (Fig. 7).

Type 1c: notched round bars loaded in bending with loading bars (Fig. 8).

Type 1d: notched C-rings loaded in bending with loading bolt (Fig. 9).

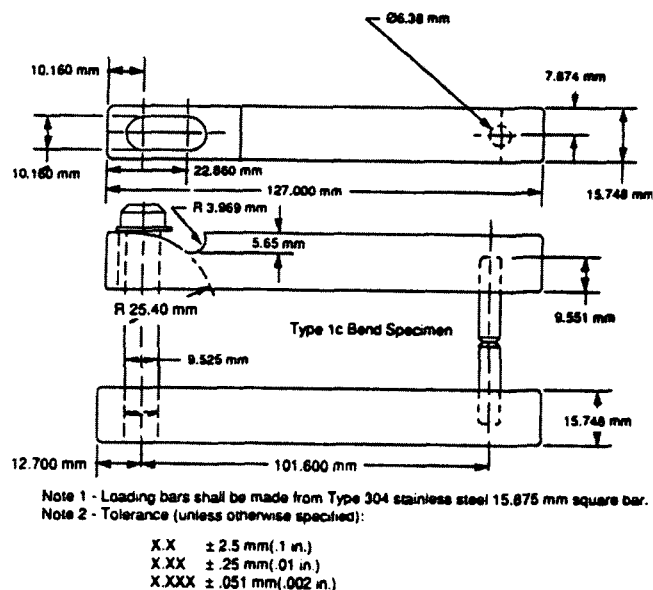


FIG. 8—Dimensional requirements of Type 1c loading bending bars (reprinted from ASTM F 519, Type 1c).

Type 2a: unnotched ring specimens loaded in bending with displacement bars (Fig. 10).

#### • Displacement Control

Type 1e: notched square bar loaded in bending (Fig. 11).

The Type 1e specimen is designed to incorporate the best attributes of all of the other specimens. The Type 1e has the same a notch acuity or stress concentration factor as the Type 1d specimen, which is the highest of all of the other specimens ( $k_t = 4.1 \text{ v } 3.1$ ), and therefore is considered to be

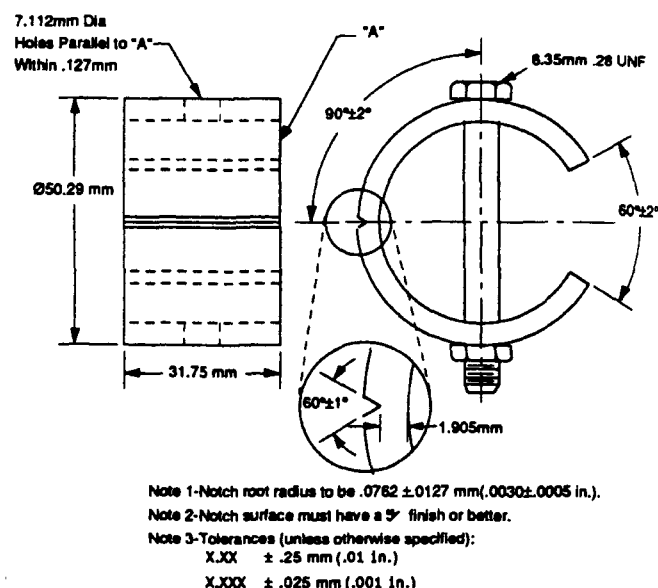


FIG. 9—Dimensional requirements of Type 1d ring bend specimens with loading bolt (reprinted from ASTM F 519, Type 1d).

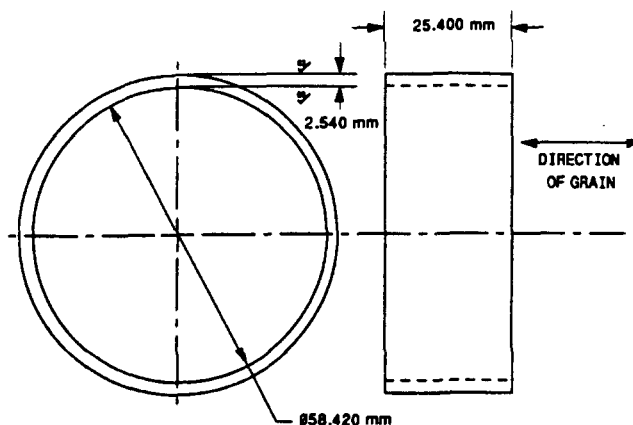


FIG. 10—Dimensional requirements of Type 2a smooth ring specimens (reprinted from ASTM F 519, Type 2a).

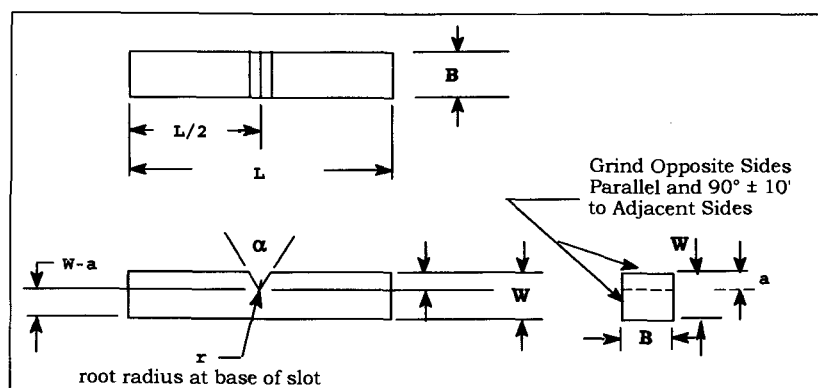
FIG. 10—Dimensional requirements of Type 2a smooth ring specimens (reprinted from ASTM F 519, Type 2a).

the most sensitive. The Type 1e specimen can have the same orientation relative to grain direction as all of the other specimens, which is the opposite of that in the Type 1d specimen. The Type 1e specimen is loaded in bending as with the Type 1c specimen, eliminating the need to establish axial tensile loads with great precision and minimizing the load requirements in addition to maximizing attainable stress levels. The Type 1e specimen is under displacement control as with the Type 1b, Type 1c, and Type 1d specimens. The Type 1e specimen has more size constraint than even the large diameter Type 1a specimen that is so designed to increase sensitivity. The Type 1e specimen has a larger notch angle for making deposition of a plating or coating more accessible. Finally, the Type 1e specimen is relatively inexpensive to manufacture, having the overall dimensions of a blank for a Charpy specimen.

The load is applied as a rising step load or step-modified slow strain rate testing protocol under displacement control that measures the threshold load for the onset of hydrogen assisted stress cracking by a drop in load that can be used as a quantitative, accelerated ( $\leq 24$  h) test method. Equivalence between the displacement control test method is assumed to occur when the threshold load in the accelerated test is  $\geq 75\%$  of the notched fracture strength of the square bar in bending.

For platings, no stress is applied until the parts have been baked, and baking must be initiated within one hour after plating. For maintenance chemicals and cleaners, stress is applied before the test specimens are exposed to the environment.

ASTM F 519 is based on the assumption that air-melted AISI 4340 at a hardness level of  $52 \pm 1$  HRC is a 'worst-case' condition. It is assumed that if no fracture occurs in the specimen after 200 h at 75 % or at a threshold of 75 % of the



All dimensions are in millimeters except for  $\alpha$ , which is in degrees.

$K_t$	$W = B$	$W - a$	$R$	$\alpha$	$L$ min	$L/2$ min
$4.1 \pm 0.2$	10.0	6.50	$0.28 \pm 0.03$	$90^\circ \pm 1^\circ$	50	25
$3.1 \pm 0.2$	10.0	6.50	$0.52 \pm 0.03$	$90^\circ \pm 1^\circ$	50	25

FIG. 11— Dimensional requirements of Type 1e Notched Square Bar Bend specimens (reprinted from ASTM F 519, Type 1e).

notched strength, then other 4340 steels processed by alternate melting processes (even steels with higher hardness levels that are vacuum-melted) will not have residual levels of atomic hydrogen that are high enough to produce sustained load (delayed) failure in the environment of concern. This test method is not intended to be a relative susceptibility test. The specimens are not to be fabricated from any material other than AISI 4340 according to MIL S-5000E.

### ASTM F 1940<sup>7</sup>: Automotive/Fasteners

This test method parallels the use of F 519, specimen Type 1e in specimen design and concept. The steel specimen has been modified to have a lower hardness of  $51 \pm 1$  HRC, and the notch root radius is 20-mil instead of 9-mil in order to reduce the stress concentration. The modifications were made with the intent of making the specimen less sensitive because the application was lower hardness fasteners (33-44 HRC) for automotive applications as compared to the higher hardness (45-52 HRC) steel used in aerospace applications.

The concept focuses on an accelerated  $\leq 24$  h test using a rising step load-modified, slow strain rate testing protocol to measure the threshold. An equivalence was established between the  $\geq 75$  % threshold acceptance level for the specimens and the  $\geq 90$  % threshold for product at 45 HRC.

As with F 519, the specimen is plated with the parts. A 'worst case' condition is again assumed since the hardness of the specimen is greater than the parts. A threshold of 75 % of the notched fracture strength of a bare specimen tested at ASTM E 8<sup>8</sup> loading rates is used as the acceptance

criterion. As a referee test, actual fasteners that have a lower hardness can be tested, but the threshold must be  $\geq 90$  % of the notched fracture strength of the fastener tested in bending.

It should be emphasized that this test method is not intended to be a relative susceptibility test, nor are the steel specimens to be fabricated with any material other than AISI 4340 steel.

### RELATIVE SUSCEPTIBILITY OF MATERIALS

#### ASTM F 1459<sup>9</sup>: Disk Pressure Test

The disk-pressure testing method is intended to measure the susceptibility to hydrogen embrittlement of metallic materials using a high-pressure gaseous environment [34]. The relative susceptibility to hydrogen embrittlement is based on the ratio of the burst pressure using hydrogen gas as compared to the burst pressure using helium. The test can be used for the selection and quality control of materials, and to evaluate the influence of protective coatings, surface finishes, and other processing variables.

In this test, a thin disk of the metallic material is placed as a membrane in a test cell and subjected to helium pressure until it bursts. Because helium is inert, the fracture is caused by mechanical overload; no secondary physical or chemical action is involved. An identical disk is placed in the same test cell and subjected to hydrogen pressure until it bursts. Metallic materials that are susceptible to gaseous hydrogen embrittlement will fracture at a pressure that is lower than the helium burst pressure; materials that are not susceptible will fracture at the same pressure for both hydrogen and helium.

<sup>7</sup> Ibid., Vol. 01.08, F1940, "Standard Test Method for Process Control Verification to Prevent Hydrogen Embrittlement in Plated and Coated Fasteners."

<sup>8</sup> Ibid., Vol. 03.01, E 8, "Standard Test Methods for Tension Testing of Metallic Materials."

<sup>9</sup> Ibid., Vol. 15.03, F 1459, "Standard Test Method for the Determination of the Susceptibility of Metallic Materials to Hydrogen Gaseous Embrittlement."

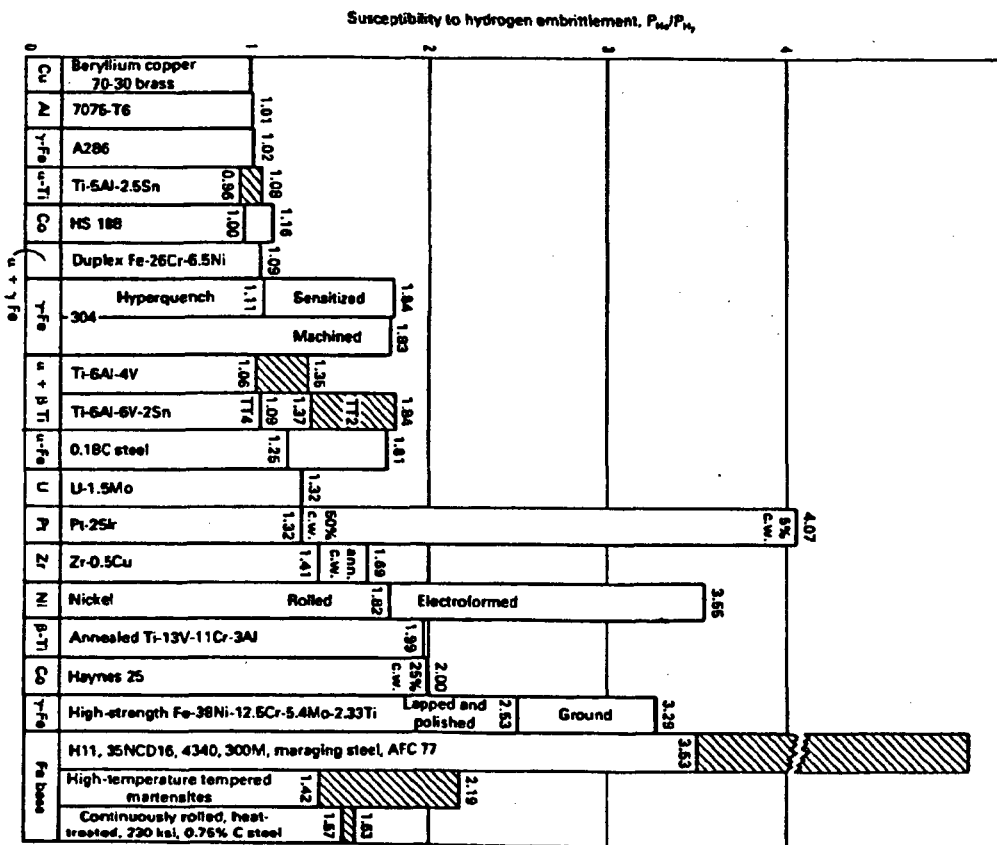


FIG. 12—Relative hydrogen susceptibility of various metals and alloys tested at a rate of 65 bars/min (6.5 MPa/min) at room temperature: c.w. is cold-worked; ann. is annealed [34].

The ratio between the helium burst pressure,  $P_{He}$ , and the hydrogen burst pressure,  $P_{H_2}$ , is a measure of the susceptibility of the material to gaseous hydrogen embrittlement or  $P_{He}/P_{H_2}$ .

If  $P_{He}/P_{H_2} \leq 1$ , the material is not susceptible to gaseous hydrogen embrittlement. When  $P_{He}/P_{H_2} > 2$ , the material is considered to be highly susceptible. At values between 1 and 2, the material is moderately susceptible, with failure expected after long exposure to hydrogen, and the material must be protected against exposure.

Alloys having little or no sensitivity are claimed to be 7075-T6 aluminum; Haynes 188 (cobalt-base); beryllium copper (copper-base); Types 304, 316, and 310 austenitic stainless steels; Type 430 high-hardness ferritic steel; and age-hardened austenitic A286 steel. Titanium-base alloy Ti-6Al-4V exhibits moderate sensitivity. Alloys with high sensitivity are Haynes 25 (cobalt-base) and iron-base alloys, including medium- and high-strength steels.

Specific test results are shown in Fig. 12. As noted, the test results can be significantly influenced by processing variables such as cold work that primarily affect the hardness.

## FRACTURE MECHANICS TESTING

In recent years, fracture mechanics methods have received increased usage in studies of the effects of hydrogen

and have been adapted to many of the testing protocols developed for notched specimens. Fatigue precracked specimens are used instead of notched specimens to eliminate the crack nucleation step, providing a quantitative design parameter in terms of stress intensity that can provide analysis not only in terms of fracture but also in terms of life based on measurement of crack growth rates. For hydrogen assisted cracking, design is generally based on 'infinite life' or designing to operate below the threshold stress intensity.

Hydrogen can cause a degradation in strength with time. It can cause subcritical crack growth or accelerate subcritical crack growth rates or rates of slow crack extension and lower the threshold stress-intensity for subcritical crack extension. The effect of hydrogen on materials can be monitored and characterized by plots of crack velocity ( $da/dt$ ) as a function of applied stress intensity  $K_{Ia}$ , as shown in Fig. 13. At high levels of  $K_I$ , Stage III, the critical value at which rapid failure would occur is designated as the plane-strain fracture toughness,  $K_{Ic}$ . The effect of hydrogen is to cause subcritical (below  $K_{Ic}$ ) extension of cracks. This behavior in Stage II yields crack-extension rates that increase with the hydrogen content. The effects are more pronounced for materials of higher strength. The Stage I effect of hydrogen is a decrease in the threshold value  $K_{Ith}$  ( $K_{Ith/IHE}$  or  $K_{Ith/EHE}$ ), which may be only a small fraction of  $K_{Ic}$ . In general, this subcritical behavior is affected by the parameters of strength level, hydrogen concentration, microstructure, etc.

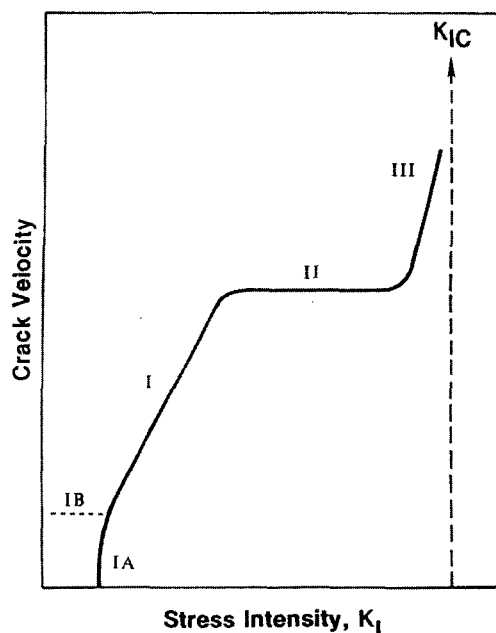


FIG. 13—Schematic of crack velocity versus  $K_I$  curve showing three stages of subcritical crack-extension behavior.

The crack extension in Stage II occurs over a broad range of stress-intensity values at which failure can occur in times of only minutes to days. The behavior is generally governed by bulk diffusion, but may also be controlled by the kinetics of adsorption and absorption on external surfaces [35], and in high-strength steels by dislocation sweeping [36].

In the absence of a hydrogen or other environments, under plane-strain conditions, the material would fail only at the critical value of stress-intensity,  $K_{IC}$ , the plane-strain fracture toughness<sup>10</sup>. Elastic-plastic methods of calculating the fracture toughness are given in ASTM E 1290<sup>11</sup> by a crack tip opening displacement method and in ASTM E 1820<sup>12</sup> by a J-integral method. The threshold values are of great practical significance, as they represent the limiting values above which crack extension may be so rapid as to greatly curtail service life. The threshold stress intensity delineates the region of finite life from infinite life.

Conventional fracture mechanics testing specimens, such as the compact, cantilever beam, modified bolt-load compact previously referred to as wedge-opening load (WOL), and contoured double-cantilever beam specimens, have been adapted for testing in both aqueous environments and in a high-pressure gaseous hydrogen environment.

These various specimens are shown in Fig. 14. While, in tests of IHE, precharged specimens (IHE) or specimens in the hydrogen charging environments (EHE) can be tested in servohydraulic or equivalent motorized test machines, or

in self-loading frames as preloaded compact, double-beam specimens or three- or four-point bend specimens.

### Ripple Loads

Caution must be taken in designing against sustained load stress cracking in a hydrogen environment when low-amplitude fatigue or "ripple" loads are also encountered in service [37]. The ripple load can have significant effect on the threshold stress-intensity parameter  $K_{Isc}$  or  $K_{Ith}$  (Fig. 12). The benefits of using a softer steel, tempered back to a lower hardness to increase the threshold stress intensity for sustained load hydrogen stress cracking can be completely neutralized.

It has been shown [38] that under cathodic protection, AISI Type 4340 steel at 43 HRC (1400 MPa) with  $K_{Ith}$  equal to 50  $\text{MPa}\sqrt{\text{m}}$  and at 55 HRC (2070 MPa) with  $K_{Ith}$  equal to 25  $\text{MPa}\sqrt{\text{m}}$ , exhibited thresholds that decreased and converged to the same value of about 17  $\text{MPa}\sqrt{\text{m}}$  as the amplitude of the ripple load increased from 3  $\text{MPa}\sqrt{\text{m}}$  to 6  $\text{MPa}\sqrt{\text{m}}$ . Below 3  $\text{MPa}\sqrt{\text{m}}$ , there was no effect on  $K_{Isc}$ .

The test program was conducted on four-point bend specimens with a root radius of 0.25 mm under a rising step load-displacement controlled test method with the amplitude of the ripple load maintained constant and superimposed at each step load level. The hydrogen charging potential applied during ripple load testing was  $-1.2$  V versus SCE in a 3.5 % salt water environment.

### ASTM E 1681<sup>13</sup>: Threshold Stress Intensity for EAC

This test method can be used to measure the relative susceptibility of materials by "Determining the Threshold Stress Intensity Factor for Environment-Assisted Cracking EAC of Metallic Materials." Constant load specimens, both the fatigue precracked single edge beam SE(B) and precracked compact specimens are tested in bending. The SE(B) was originally referred to as the Cantilever Beam Test.

The specimen is inserted along a portion of the beam and enclosed by an environmental chamber (Fig. 15). A crack is initiated and extended by fatigue before testing. The specimen thickness requirement can often be excessive for high-toughness steels, requiring large size specimens if plain strain test conditions are to be maintained up to the critical stress intensity value or fracture toughness of the material. The specimen is subjected to a constant load over a predetermined run-out period of time. As the crack grows, the stress intensity increases. Time-to-failure is plotted versus applied stress intensity. The lower limit on this plot is a threshold stress intensity for hydrogen embrittlement,  $K_{EHE}$ , as shown in Fig. 16. Below the threshold stress intensity, no failures should occur.

The  $K_{EHE}$  results of a cantilever beam test can depend on how much time elapses before the test is terminated. Recommended test times for establishing the true threshold

<sup>10</sup> Ibid., Vol. 03.01, E 399, "Standard Test Method for Plane-Strain Fracture Toughness of Metallic Materials."

<sup>11</sup> Ibid., Vol. 03.01, E 1290, "Standard Test Method for Crack-Tip Opening Displacement (CTOD) Fracture Toughness Measurement."

<sup>12</sup> Ibid., Vol. 03.01, E 1820, "Standard Test Method for Measurement of Fracture Toughness."

<sup>13</sup> Ibid., Vol. 10.05, E 1681, "Standard Test Method for Determining a Threshold Stress Intensity Factor for Environmentally Assisted Cracking of Metallic Materials."

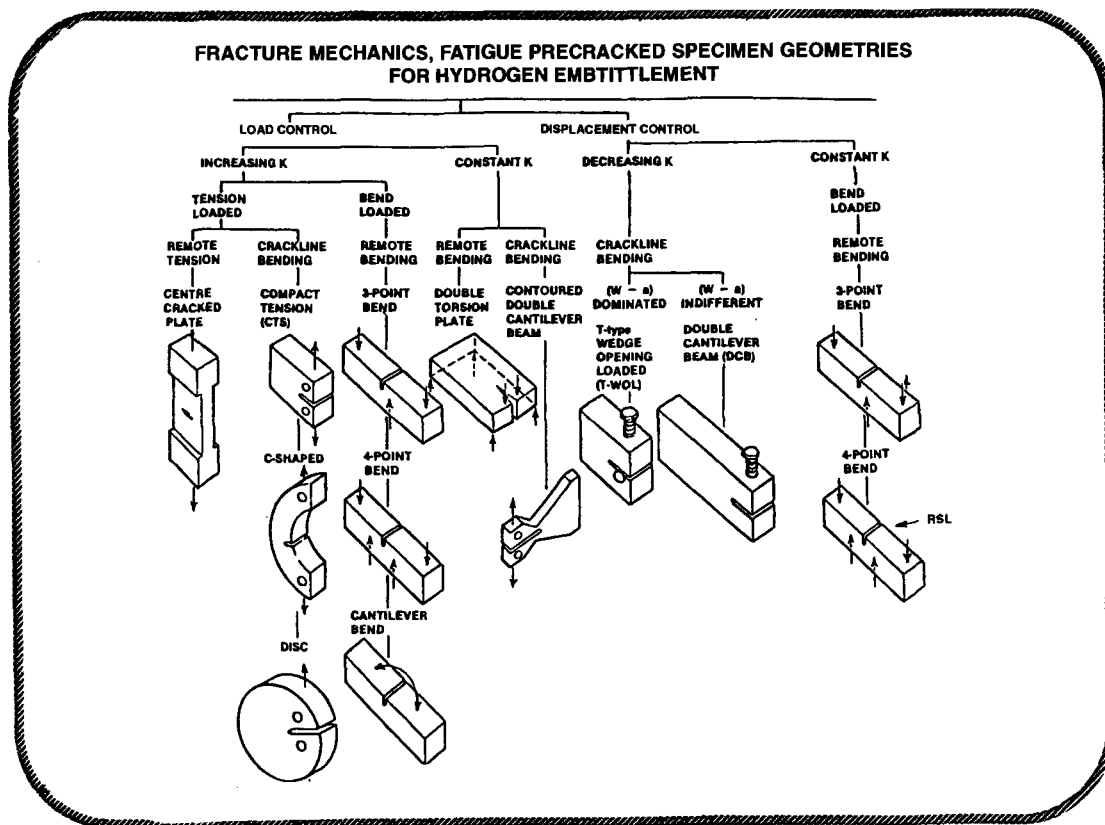
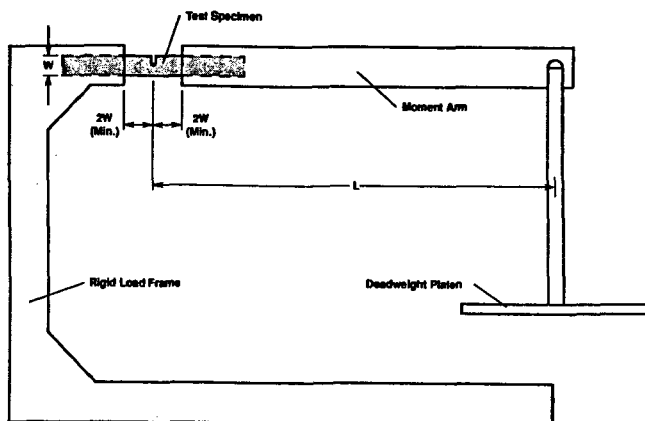


FIG. 14—Fracture mechanics, fatigue precracked specimen geometries for hydrogen embrittlement testing. (Courtesy of Naval Research Laboratory, Washington, DC and LRA Labs, Newport Beach, CA.)

stress intensity, range from 5 000 h to 10 000 h. A limitation of this test method is that it can be expensive in terms of materials, machining and test time. As many as 12 specimens placed under different loads in separate test machines are needed for each test in order to obtain valid  $K_{EHE}$  values. The Navy uses as much as 4–5 years for run-out times to establish the true threshold for HY 130 steels at 33–35 HRC [39].

The modified bolt-load compact specimen, originally referred to as the Wedge Opening Load (WOL) specimen under constant displacement (Fig.17) is best used for quality control rather than performing research studies. In concept it can be used to measure the threshold stress intensity but the result are extremely sensitive to the various material environment combinations with retardation and crack blunting playing a major role in the final test results, such that



Note: The length of the moment arm (L) should be equal to or greater than 8W

FIG. 15—Typical configuration of a Dead-Weight Beam loading fixture. (Source: ASTM E 1681.)

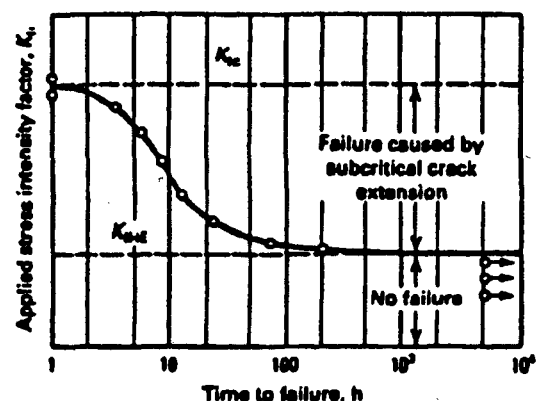


FIG. 16—Procedure to obtain  $K_{EAC}$  for internal (IHE) or environmental (EHE) embrittlement with pre-cracked cantilever beam test specimen [23].

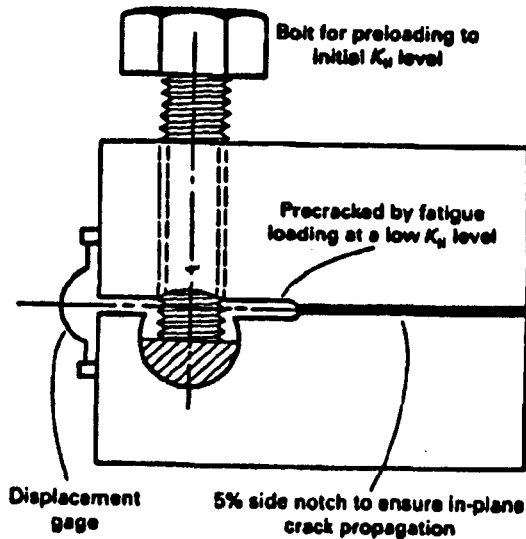


FIG. 17—Schematic showing basic principle of Modified Bolt-Load Compact specimen (Source: ASTM E 1681).

from a practical point of view, the test method is very limited. It is best applied systems where the material sensitivity to test variable and threshold stress intensity are already well established.

A constant value of the wedge- or crack-opening displacement is used to generate the initial load for this type of specimen. As the crack extends, the stress intensity decreases until crack arrest occurs. The initial load is assumed to be slightly above  $K_{EHE}$ . The specimen is maintained under these conditions for about 5000 h to establish the threshold. The crack extends to a point after which further extension is not measured ( $K_{EHE}$ ). However, it is difficult to determine precisely when the "no-growth" criterion is met.

As subcritical crack extension occurs, stress intensity increases in the cantilever beam test and decreases in the WOL test (Fig. 18). Generally, the threshold stress intensity measured with the WOL test is lower than that measured with

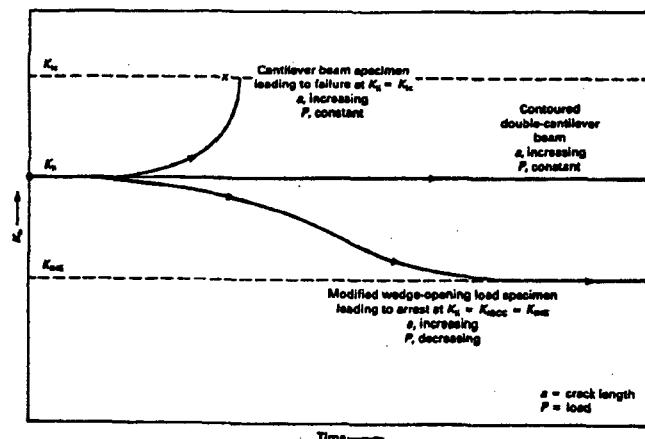


FIG. 18—Change of stress-intensity with time of constant load cantilever beam compared to a contoured double-cantilever beam test specimen and a constant displacement bolt-load compact specimen [28].

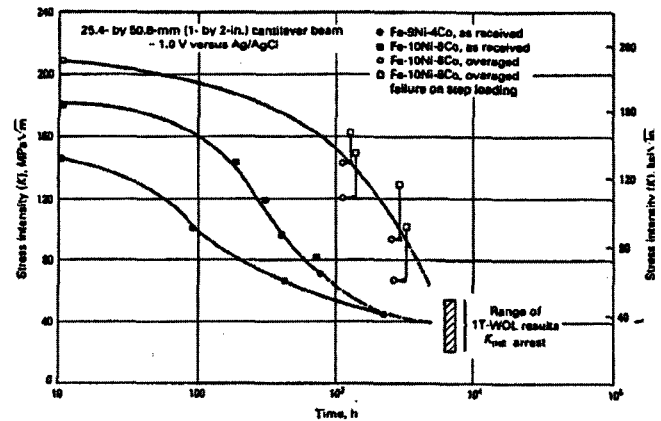


FIG. 19—Comparison of single-edge-notched bend cantilever beam and wedge-opening load test results for hydrogen embrittlement threshold of iron-nickel-cobalt steels [28].

the cantilever beam test [40]. The advantage of the WOL test is that only one specimen is required to measure  $K_{EHE}$ .

In long-term tests, it is essential to ensure that the concentration and the composition of the environmental solution do not change over time, in ways that do not reflect service behavior. In addition, evaporation may cause the solution level to drop below the crack line of the specimen; this would render the test invalid.

The results of WOL and cantilever beam tests conducted on 25.4 mm (1 in.) thick iron-nickel-cobalt alloy steel specimens are presented as Fig. 19. The data imply that the WOL  $K_{Ith}$  threshold is the lower limit for the cantilever beam threshold.

The open circles in Fig. 19 represent "no fracture" at various exposure times for an overaged Fe-10Ni-8Co alloy in a cantilever beam test. The open squares indicate failure at increased stress intensities, following step-loading from the lower stress-intensity values of the open circles. This test was conducted at various exposure times. The results suggest that increasing the load leads to a shorter induction, indicating a more aggressive hydrogen embrittlement condition than at the lower value of the constant load. The change in behavior may be due to the breakdown of repassivation, i.e., cracking of the oxide film on the surface. When the load is increased, the oxide film is broken, exposing fresh metal, and more hydrogen is adsorbed and absorbed at the crack tip. For this reason, tests that use a rising load can be more aggressive than the constant-load cantilever beam test, which does not provide worst-case (fresh metal exposed) loading conditions.

The data also suggest that the cantilever beam test can generate an artificially high  $K_{EHE}$  threshold when the time under load is too short. If the test is terminated at 200 h rather than at 5000 h, the reported  $K_{EHE}$  values from the cantilever beam test (Fig. 19) are four times higher than those measured after the longer time period. Similarly, if insufficient time is allowed in the WOL test, the incubation period may not be exceeded, and no crack extension will be observed.

The cantilever bend test method is costly and time-consuming. However, it does furnish a quantitative fracture



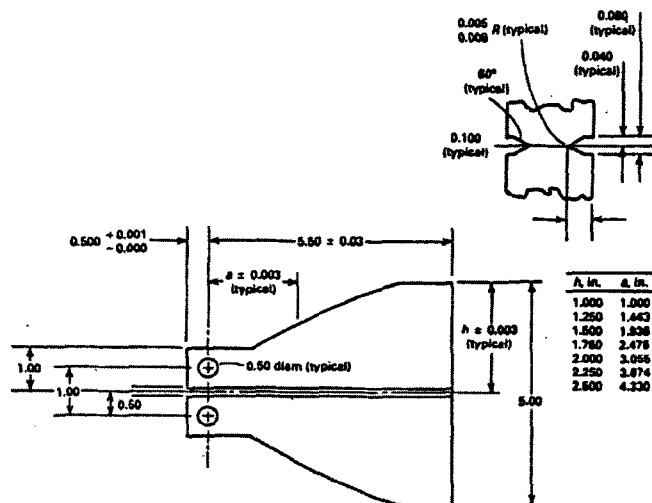


FIG. 20—Dimensions and configurations for double-cantilever beam test specimen. Specimen contoured to  $3a^2/h^3 + 1/h + C$ , where  $C$  is a constant [28]. All values given in inches. (Note: 1 in. = 25.4 mm.)

mechanics threshold stress intensity parameter that can be used for designing against effects due to hydrogen. The WOL specimen, on the other hand, is more useful as a quality control test because the initial preload can significantly affect the results by the magnitude of the large plastic zone introduced at the onset of the test, which could retard crack extension.

### G 168<sup>14</sup>: Double-Cantilever Beam

Although this specimen can be used to measure the threshold stress intensity, the double-cantilever beam specimen was developed primarily for measuring crack growth rate. That is the reason for the extended gage length section for subcritical crack growth to occur. The specimen can be stressed by either constant displacement or constant load. ASTM G 168 provides the standard practice for "Making and Using Double Beam Stress Corrosion Specimens," formerly designated double cantilever beam (DCB) specimens.

The *contoured* double-cantilever beam test specimen is a modification that is used to measure crack growth rate at a constant applied stress intensity. This test simplifies the calculation of stress intensity by using a contoured specimen, as its stress intensity is proportional to the applied load and independent of the crack length. Under a constant load, the stress intensity for this specimen remains constant with crack extension. For the test geometry shown in Fig. 20, the magnitude of the stress-intensity factor  $K$  is observed to equal 20 times the load.

When relatively thin specimens must be used, data on hydrogen embrittlement can sometimes be obtained by using side grooves on subthickness specimens, even at values in excess of the ASTM requirement of  $K_{max}^2 \leq 0.4 B/YS^2$  (where  $B$  is the thickness and  $YS$  is the yield strength of the

material). The enhanced triaxial stress that is introduced by side grooves enables plane-strain conditions in a thinner specimen.

The contoured double-cantilever beam test can be particularly useful in studies of the effects of a single fracture mechanics or environmental parameter. For example, in Fig. 21, the incubation time, for the onset of hydrogen-stress cracking is shown to be dependent on the type of steel [41]. A decrease in the stress intensity factor ( $\Delta K$ ), from 44 to 22 MPa $\sqrt{m}$  or  $\Delta K/K_f = 1$ , may change the incubation time from less than one hour for AISI 4340 steel to about one year for Type D6Ac steel, which means that crack extension would initiate at the lower stress intensity in about one hour for the AISI 4340 steel, but would take over one year to initiate in the D6Ac steel. This method has been extensively used to study the effect of heat treatment (hardness) and environment on the hydrogen stress cracking of AISI 4340 steels.

The fact that the incubation times can vary by as much as three orders of magnitude for steels that are compositionally very similar provides the technical basis for exercising caution in using the WOL displacement controlled test specimen on new alloys to measure the threshold stress intensity. A rapid drop in load would produce an artificially high threshold stress.

### Three-Point and Four-Point Bend Tests

The contoured double-cantilever beam test, as described above, uses a contoured geometry to maintain a constant stress-intensity factor as the crack extends under constant load. Similar advantages can be produced by using a three- or four-point bend test under constant displacement. These tests use a ASTM E 1290 single-edge-notched bend SE(B) specimen that has the overall dimensions of a standard Charpy specimen. Because crack-opening displacement is constant as the crack extends, the load decreases; therefore, the stress intensity is approximately constant until the ratio of crack depth to specimen width exceeds 0.5. Typically, the stress intensity is

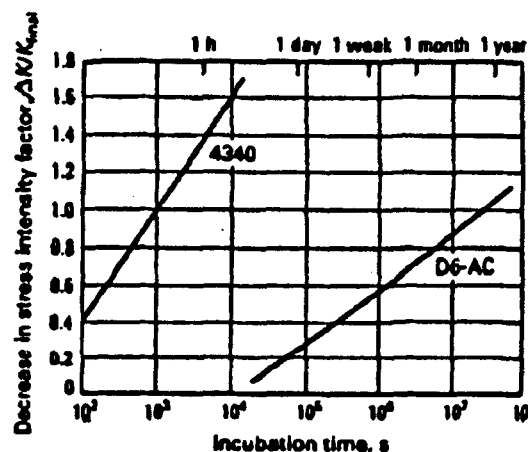


FIG. 21—Incubation time for crack extension as a function of decrease in stress intensity in AISI Type 4340 and Type D6Ac steels using contoured double-cantilever beam test specimen [28].

<sup>14</sup> Ibid., Vol. 03.02, G168, "Standard Practice for Making and Using Double Beam Stress Corrosion Specimens."

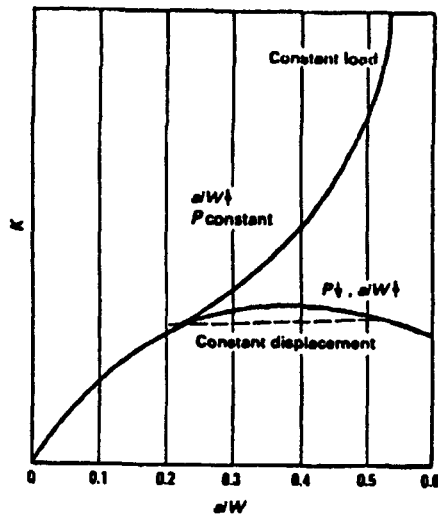


FIG. 22—Change in stress intensity factor with crack extension for a three-point bend specimen under load control compared to displacement control [28].

regarded to be constant within a small range of 0.25 to 0.5. In Fig. 22, the change in stress-intensity factor as a function of crack extension is shown for both the load control and the displacement control conditions, using a three-point bend specimen.

#### ASTM G 129<sup>15</sup>: Slow-Strain-Rate Tension Tests

This test method was developed and is most often used to measure the relative susceptibility of materials to hydrogen stress cracking (HSC) or hydrogen sulfide stress cracking (HSSC) in the petroleum industry using *smooth* tensile bars. The concept was also utilized and developed to measure the degree of embrittlement due to plating, the relief from baking and as a process control test in the aerospace industry using high-hardness, *notched* round tensile bars.

This test method can be useful in screening many product forms, including plate, rod, wire, sheet, and tubing, as well as welded parts. Smooth, notched, or precracked specimens can be used. The principal advantage of this test is that the relative susceptibility in a hydrogen-producing environment (for a particular metal-environment combination) can be rapidly assessed. ASTM G 129 is the standard practice for "Slow Strain Rate Testing to Evaluate the Susceptibility of Metallic Materials to Environmentally Assisted Cracking."

The test method was initially developed as the Slow Strain Rate (SSR) smooth bar Tensile Test (SSRTT), but more recently, it has incorporated the use of notched and precracked or fracture mechanic types of specimens. The SSR is conducted in tension at a constant displacement rate in the strain range of  $10^{-4}$  to  $10^{-7}$  s<sup>-1</sup> and always produces fracture of the test specimen. The degree of susceptibility is measured as a SSR-ratio in terms of the rupture properties, being more susceptible as the value of the SSR-ratio decreases from unity until it reaches a threshold (Fig. 23).

<sup>15</sup> Ibid., Vol. 03.02, G 129, "Standard Practice for Slow Strain Rate Testing to Evaluate the Susceptibility of Metallic Materials to Environmentally Assisted Cracking."

A variety of specimen shapes and sizes can be used; but the most common is a smooth-bar tensile coupon, as described in ASTM E 8, "Test Method for Tension Testing of Metallic Materials." In smooth-bar tests, the changes are measured in terms of time to failure, ductility (elongation or reduction-in-area), maximum load achieved, and area bounded by a nominal stress-elongation curve or a true stress/true strain curve, which are often supported by fractographic examination. The specimen is exposed to the environment while it is stressed under a constant displacement rate.

Some of the original studies with the use of smooth bar specimens found "It lacks correlation with service conditions. Interpretation of results is difficult. It often indicates stress corrosion cracking in alloy-environment combinations that do not cause failures in service. It does not address notch sensitivity" [42].

Pollack [43] addressed notch sensitivity when he initiated the SSR work on notched round bar tensile coupons of high hardness Type 4340 steel at 52 HRC for the aerospace industry. He demonstrated their usefulness as a screening test in evaluating different platings, coatings, and cleaners relative to hydrogen embrittlement per ASTM F 519. He found the measurement of the notched tensile strength to be a more discriminating and analytically definitive parameter. More recent work has been performed on fatigue precracked fracture mechanics type specimens, but use of the stress intensity data in design is not recommended unless long term tests per ASTM E 1681 are performed with identical material in an identical environment.

#### ASTM F 1624<sup>16</sup>: Step-modified SSR Test

The bridge between the long-term E 1681 and the accelerated or short-term G 129 testing protocols is ASTM F 1624,

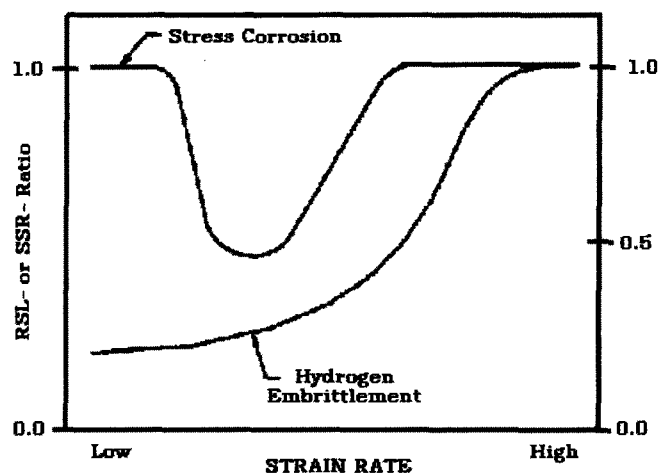


FIG. 23—A comparison of the load-time curves of SSR-T and RSL-T tests under displacement control. The RSL-T test is used to detect crack initiation or threshold the onset of subcritical crack growth, while the SSR-T records the entire tensile curve to rupture [49].

<sup>16</sup> Ibid., Vol. 15.03, F 1624, "Standard Test Method for Measurement of Hydrogen Embrittlement Threshold in Steel by the Incremental Step Load Technique."

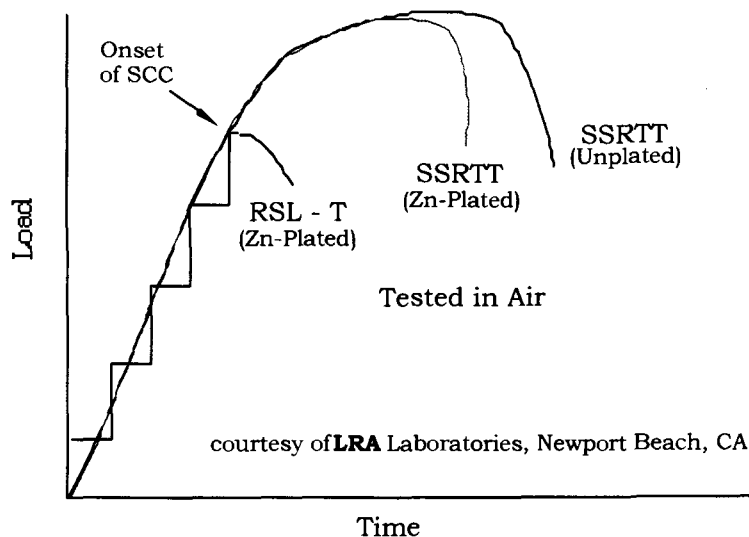


FIG. 24—A schematic of the effect of the strain rate range on the apparent threshold for EAC/SCC and HSC testing. The threshold stress intensity for hydrogen stress cracking is the minimum at the slowest rate (after Fig. 2, G 129).

the (Accelerated) Standard Test Method for Measurement of the Hydrogen Embrittlement Threshold in Steel by the Incremental Step Loading Technique.

A step-modified slow-strain-rate test is used to provide a threshold stress intensity that does correlate with long-term tests in the same environment [44]. Figure 24 is a graphical comparison between the two methods. By progressing in incremental steps, the onset of hydrogen assisted stress cracking can be accurately detected in a rigid testing system by a drop in load under displacement control. As with the slow strain rate test, the rate is progressively decreased from  $10^{-4} \text{ s}^{-1}$  to  $10^{-8} \text{ s}^{-1}$  until the measured value of the apparent threshold stress intensity becomes an invariant, which is the true threshold,  $K_{\text{IHSC}}$  that can be used as a comparison of the relative susceptibility of different materials and is considered to be the material property that can be incorporated into design.

The slow strain-rate test method ( $10^{-4} \text{ s}^{-1}$  to  $10^{-8} \text{ s}^{-1}$ ) is an accelerated test method when compared with a sustained-load test method. The “slow” strain-rate test provides an “accelerated” test for measuring the threshold when compared with the 5000 hours required by ASTM E 1681, for steels at a hardness of 50-52 HRC.

The step-modified slow strain-rate or Rising Step-Load™ (RSL™) test produces an increasing stress intensity that is different at each step-load but remains constant with crack extension for a Charpy-sized SE(B) four-point bend specimen while each load level is maintained constant for a period of time. The rising step-load test was developed as an accelerated low-cost test for measuring the resistance of steels and weldments to IHE or EHE [45,46]. The load is constantly increased under displacement control, but incrementally in steps with each step being sustained for a period of time so that the onset of subcritical crack extension can be detected, which is the threshold for the onset of IHE or EHE. The RSL test differs from the SSRTT, which measures the differences in ductility parameters over the

entire loading range to ultimate fracture and only provides relative parameters to index hydrogen embrittlement. When used with notched or fatigue precracked specimens, it has been found that the threshold is overestimated with the SSRTT. By comparison, the RSL is tested over the same range of strain rates but it detects the onset of subcritical cracking by a load drop (Fig. 24) and thus is considered to be quantitative and accelerated relative to a SSRTT.

The RSL is an economical test, as only one specimen may be required to obtain a measure of the threshold value, as compared to the dozen or so normally required to conduct sustained load run-out tests as with the cantilever beam type (ASTM E 1681). The test method takes advantage of using small specimens to measure the fracture toughness [47] and utilizes potentiostatic test methods to simulate conditions of galvanic coupling on the specimen [48].

The test can be conducted in tension or in the bending, which has lower load requirements than tension and thus may be helpful in testing larger diameter fasteners. The use as a bend test also has several advantages relative to alignment and increased sensitivity, since the limit load in bending is greater than the limit load in tension. This test can be conducted using either precracked specimens (that can be used to measure threshold stress intensities within the framework of fracture mechanics) or actual fasteners (to obtain an ‘effective’ threshold stress). The results from either test can be incorporated into design and the calculation of maximum installation torques to prevent in-service failures of fasteners [49,50].

### Choosing the Appropriate Method

Whatever test method is selected, whether it is for quality control, process control, or material susceptibility, it is imperative that the results be related to service conditions. The proper selection of torque or stress for a hydrogen embrittlement test should exceed the stress in service. If the stress

levels in the quality control test are less than the stress levels of service, the test is meaningless. The state of stress must also be accurately represented. For example, as was mentioned previously, the superposition of a low-amplitude cyclic or ripple load can totally negate the effects of the measured threshold stress-intensity parameter under sustained loading conditions.

It is also important to ensure that the actual types of environmental service conditions are adequately represented in a hydrogen-stress cracking test, including the pressure (fugacity) of hydrogen from the environment before the results can be used in design. Choosing a test method should always be critically reviewed before the results are related to service performance, especially in conducting long-term life analysis that takes into account the possibility of hydrogen embrittlement.

## REFERENCES

- [1] Oriani, R. A., "Hydrogen in Metals," *Proceedings of Conference on Fundamental Aspects of Stress Corrosion Cracking*, Staehle, Forty, and van Roogen, Eds., NACE, Houston, TX, 1967, pp. 32–50.
- [2] Oriani, R. A., "Hydrogen Embrittlement of Steels," *Ann. Rev. Mater. Sci.*, 1978, pp. 327–357.
- [3] Geller, W. and Sun, T., "Influence of Alloy Additions on Hydrogen Diffusion in Iron and Contributions to the System Iron-Hydrogen," *Arch. Eisenhüttenw.*, Vol. 21, 1950, pp. 423–430.
- [4] Johnson, E. W. and Hill, M. L., "The Diffusivity of Hydrogen in Alpha Iron," *Transactions, AIME*, Vol. 218, 1960, pp. 1104–1112.
- [5] Hobson, J. D., "The Diffusion of Hydrogen in Steel at Temperatures of  $-78^{\circ}\text{C}$  to  $200^{\circ}\text{C}$ ," *JISI*, Vol. 189, 1958, pp. 315–321.
- [6] *Metals Handbook*, ASM International, Metals Park, OH, 1948, p. 1208.
- [7] Baranowski, B., "Thermodynamics of Metal/Hydrogen Systems of High Pressure," *Ber. Bunsenges Phys. Chem.*, 1972, pp. 714–724.
- [8] Manning, J. R., *Theory of Diffusion*, ASM, Metals Park, OH, 1973, pp. 1–24.
- [9] Pressouyre, G. M., "A Classification of Hydrogen Traps in Steel," *Metallurgical Transactions*, Vol. 10A, October 1979, pp. 1571–1579.
- [10] Hofmann, W. and Rauls, W., "Ductility of Steel Under the Influence of External High Pressure Hydrogen," *Welding Journal*, Vol. 44, No. 5, May 1965, pp. 225s–320s.
- [11] Hancock, G. G. and Johnson, H. H., "Hydrogen, Oxygen, and Subcritical Crack Growth in a High-Strength Steel," *Transactions, AIME*, Vol. 236, April 1966, pp. 513–516.
- [12] Zapffe, C. A. and Sims, C. E., "Hydrogen Embrittlement, Internal Stress, and Defects in Steel," *Transactions, AIME*, Vol. 145, 1941, pp. 225–259.
- [13] Troiano, A. R., "The Role of Hydrogen and Other Interstitials in the Mechanical Behavior of Metals," *Transactions, ASM*, Vol. 12, No. 52, 1960, pp. 54–80.
- [14] Oriani, R. A., "A Mechanistic Theory of Hydrogen Embrittlement of Steels," *Ber. Bunsenges. Phys. Chem.*, Vol. 76, 1972, pp. 848–857.
- [15] Petch, N. J. and Stables, P., "Delayed Fracture of Metals under Static Load," *Nature*, Vol. 169, 1952, pp. 842–843.
- [16] Petch, N. J., "Lowering of the Fracture Stress Due to Surface Adsorption," *Philosophy Magazine*, Vol. 1, 1956, pp. 331–335.
- [17] Beachem, C. D., "A New Model for Hydrogen Assisted Cracking (Hydrogen 'Embrittlement')," *Metallurgical Transactions*, Vol. 3, No. 2, February 1972, pp. 437–451.
- [18] Westlake, D. G., "A Generalized Model for Hydrogen Embrittlement," *Transactions, ASM*, Vol. 62, 1969, pp. 1000–1006.
- [19] Latanision, R. M., Gastine, O. G., and Compeau, C. R., "Stress Corrosion Cracking and Hydrogen Embrittlement: Differences and Similarities," *Environment-Sensitive Fracture of Engineering Materials*, 1977, pp. 48–70.
- [20] Thompson, A. W. and Bernstein, I. M., "Metallurgical Variables in Hydrogen-Assisted Environmental Fracture," *Advances in Corrosion Science and Technology*, Vol. 7, 1980, pp. 53–175.
- [21] Treseder, R. S., "Influence of Yield Strength on Anodic Stress Corrosion Cracking Resistance of Weldable Carbon and Low Alloy Steels with Yield Strengths Below 100 ksi," *WRC Bulletin*, Vol. 243, November 1978, pp. 27–33.
- [22] Hobson, J. D. and Sykes, C., "Effect of Hydrogen on the Properties of Low-Alloy Steels," *JISI*, Vol. 169, October 1951, pp. 209–220.
- [23] Raymond, L., "Hydrogen Embrittlement Control," *ASTM Standardization News*, Vol. 13, No. 12, December 1985, p. 46.
- [24] Raymond, L., "The Many Faces of Hydrogen Embrittlement," *ASTM Standardization News*, Vol. 24, No. 10, October 1996, p. 40.
- [25] Raymond, L., "The Enemy Within: Hydrogen Embrittlement," *ASTM Standardization News*, Vol. 27, No. 3, March 1999, p. 28.
- [26] *Hydrogen Embrittlement Testing*, ASTM STP 543, L. Raymond, Ed., ASTM International, West Conshohocken, PA, 1972, p. 83.
- [27] Raymond, L., "Tests for Hydrogen Embrittlement," *ASM Metals Handbook*, Vol. 8, 9th ed., American Society for Metals, 1985, pp. 537–543.
- [28] Raymond, L., "Evaluation of Hydrogen Embrittlement," *ASM Metals Handbook*, Vol. 13, 9th ed., Corrosion, American Society for Metals, 1987, pp. 283–290.
- [29] *Hydrogen Embrittlement: Prevention and Control*, ASTM STP 962, L. Raymond, Ed., ASTM International, West Conshohocken, PA, 1988.
- [30] Cialone, H. J. and Holbrook, J. H., "Sensitivity of Steels to Degradation in Gaseous Hydrogen," Symposium on Hydrogen Embrittlement—Prevention and Control, May 1985, Los Angeles, ASTM International, West Conshohocken, PA.
- [31] Toh, T. and Baldwin, W. M., "Ductility of Steel with Varying Concentrations of Hydrogen," *Stress Corrosion Cracking and Embrittlement*, W. D. Robertson, Ed., John Wiley and Sons, New York, 1956, pp. 176–186.
- [32] Shewman, P. G., "Hydrogen Attack of Carbon Steel," *Metallurgical Transactions*, Vol. A7A, 1976, pp. 279–286.
- [33] Interrante, C. G., Nelson, G. A., and Hudgens, C. M., "Interpretive Report on Effect of Hydrogen in Pressure Vessel Steels," *WRC Bulletin*, Vol. 145, October 1969, pp. 33–42.
- [34] Fidelle, J. P., Bernardi, R., Broudeur, R., et al., "Disk Pressure Testing of Hydrogen Environment Embrittlement," in *Hydrogen Embrittlement Testing*, ASTM STP 543, ASTM International, West Conshohocken, PA, 1974, pp. 221–253.
- [35] Wei, R. P., Klier, K., Simmons, G. W., and Chou, Y. T., "Fracture Mechanics and Surface Chemistry Investigations of Environmental-Assisted Crack Growth," A.R. Troiano Festschrift on Hydrogen Embrittlement and Stress Corrosion Cracking, Case Western Reserve University, 2–3 June 1980.
- [36] Tien, J. K., Nair, S. V., and Jensen, R. R., "Dislocation Sweeping of Hydrogen and Hydrogen Embrittlement," *Hydrogen Effects in Metals*, Bernstein and Thompson, Eds., The Metallurgical Society of AIME, Warrendale, PA, 1980, pp. 36–56.
- [37] Pao, P. S., Bayles, R. A., and Yoder, G. R., "Effect of Ripple Load on Stress Corrosion Cracking in Structural Steels," *Journal of Engineering Materials and Technology*, Vol. 113, Jan. 1991, pp. 125–129.
- [38] Krams, W. E., "Effect of Cyclic Loading on the Resistance of 4340 Steel to Stress Corrosion Cracking," M.S. thesis, California State University, Long Beach, CA, December 1985.

- [39] Kaznoff, A. I., Department of the Navy, NAVSEA, Director, Materials Engineering Office, Private communication with author, 1993.
- [40] Zanis, C. A., "Subcritical Cracking in High Strength Steel Weldments—A Materials Approach," *SAMPE Quarterly*, January 1978, pp 8–12.
- [41] Dull, D. L. and Raymond, L., "Stress History Effect on Incubation Time for Stress Corrosion Crack Growth in AISI 4340 Steel," *Metallurgical Transactions*, Vol. 3, November 1972, pp. 2943–2947.
- [42] Wolfe, L. H., Burnette, C. C., and Joosten, M. W., "Hydrogen Embrittlement of Cathodically Protected Subsea Bolting Alloys" *Metal Progress*, July 1993.
- [43] Pollack, W. J., "Assessment of the Degree of Hydrogen Embrittlement Produced in High-Strength 4340 Steel by Plating and Baking Process Using Slow Strain Rate Testing," pp. 698–80, and "Assessment of the Degree of Hydrogen Embrittlement Produced in Plated High-Strength 4340 Steel by Paint Strippers Using Slow Strain Rate Testing," pp. 372–386, *Hydrogen Embrittlement: Prevention and Control*, ASTM STP 962, L. Raymond, Ed., ASTM International, West Conshohocken, PA, 1988.
- [44] Raymond, L., "Accelerated Stress Corrosion Cracking Screening Test Method for HY-130 Steel", under SBIR Phase I and Phase II NAVSEA contract No. N00024-89-C-3833, LRA Labs, Final Report No. NAVSEA 80058, Dec. 1989 and Dec. 1993, respectively.
- [45] Fast, P. J., Susskind, C. S., and Raymond, L., "Charpy V-Notched Specimens for Indexing Stress Corrosion Cracking in HY Ship Steels and Weld Metals," Final report under contract F04701-78-C-0079, The Aerospace Corporation, August 1979.
- [46] Interrante, C. G. and Pressouyre, G. M., Current Solutions to Hydrogen Problems in Steels: Proceedings of the First International Conference, Washington, DC, ASM, Metals Park, OH, November 1982, Raymond, L. and Crumly, W. R., "Accelerated, Low-cost Test Method for Measuring the Susceptibility of HY-steels to Hydrogen Embrittlement," p. 477.
- [47] "Rapid Inexpensive Tests for Determining Fracture Toughness," NMAB-328, National Academy for Sciences, 1976.
- [48] Dull, D. L. and Raymond, L., "Electrochemical Techniques," in *Hydrogen Embrittlement and Testing*, ASTM STP 543, ASTM International, West Conshohocken, PA, 1974, pp. 20–33.
- [49] Raymond, L., "Test Methods for Hydrogen Embrittlement of Fasteners: Meaning and Use," *American Fastener Journal*, May/June 1994.
- [50] Raymond, L., "The Susceptibility of Fasteners to Hydrogen Embrittlement and Stress Corrosion Cracking," Chapter 39, Bickford, J. H. and Nassar, S., Eds., Marcel Dekker, Inc., New York, N.Y., 1998.
- [51] Oriani, R. A., Hirth, J. P., and Smialowski, M., Hydrogen Degradation of Ferrous Alloys, Noyes Publications, Park Ridge, New Jersey, U.S.A., I: Equilibria Properties, Ch. 2, p. 16, van Leeuwen, Henri P., "Fugacity of Gaseous Hydrogen."
- [52] Ibid 51: p. 641, IV: Cracking and Failure Mechanisms, Ch. 26, Bernstein, Melvin I. and Pressouyre, G. M., "The Role of Traps in the Microstructural Control of Hydrogen Embrittlement of Steels."
- [53] Ibid 46: p. 23.
- [54] Ibid 51: pp. 454–509, IV: Cracking and Failure Mechanisms, Ch. 19, Thompson, Robb, "Fundamentals of Fracture."
- [55] Ibid 51: p. 822, V: Hydrogen Effects in Classes of Steels, Ch. 31, Caskey, George R. Jr., "Hydrogen Effects in Stainless Steels."
- [56] Ibid 51: p. 763, V: Hydrogen Effects in Classes of Steels, Ch. 29, McIntyre, Paul, "Hydrogen Effects in High Strength Steels."
- [57] Ibid 46: p. 18.
- [58] Hirth, J. P., *Hydrogen Effects in Materials*, edited by A. W. Thompson and Moody, N. R., 1996, ASTM, pp. 507–522.
- [59] Nagumo, M., An overview paper along the lines of the Cambridge paper has been submitted to *Materials Sci. Tech.*, in which characterization of the fracture process in terms of R-Curve is described. [<http://www.msm.cam.ac.uk/phase-trans/2003/nagumo/IMG/22.gif>].
- [60] Nagumo, M., *ISIJ International*, (The Iron and Steel Institute of Japan), Vol. 41, 2001, pp. 590–598.

# **Section V: Testing in Environments**

*H. P. Hack, Editor*

# Outdoor Atmospheres

Herbert H. Lawson<sup>1</sup>

IT IS ESTIMATED THAT half the total cost of corrosion in the United States is spent on the protection of materials in the atmosphere [1]. Therefore, atmospheric testing has assumed a great degree of importance throughout the world, especially because of the emphasis on conserving natural resources.

## CLASSIFICATION OF ATMOSPHERES

On the basis of worldwide testing, atmospheres have been broadly classified into three qualitative categories: rural, marine, and industrial [2]. In rural atmospheres, there is minimal presence of ionic species to cause a strongly conductive electrolyte. Hence, the rural classification implies little, or at most moderate, corrosion. The corrosion depends primarily on temperature, humidity, and moisture retention. In industrial environments, the severity of corrosive attack also depends on these factors, but is significantly affected by the presence of industrial pollutants such as solid or gaseous sulfur compounds, and other emissions that increase the corrosion by strengthening the electrolyte, frequently by lowering the pH. Marine atmospheres are usually the most consistently severe environments, their corrosiveness being affected by the chloride ion, and influenced significantly by humidity, temperature, time-of-wetness (TOW), wind direction, and distance from the breaking surf [3,4].

Considering the above, test sites should be selected to provide general corrosion performance in one or more of these atmospheric classifications. ASTM Committee G01.04 on Atmospheric Corrosion operates sites that include all three, and testing can be done in these providing the data accumulated become part of the public record. In addition, there are several private, government, and commercial testing facilities already established where exposure space can be rented.

Exposure in the classified environments consists of testing in a "macroclimate," i.e., there are usually no significant point sources of industrial pollutants to unduly affect the corrosivity. There are instances, however, when testing is desirable to evaluate a "microclimate." This can generally be accomplished by less expensive means than full-scale testing in a formal test site. These means will be covered later in this section.

<sup>1</sup>Lawson Consultants, Inc., 4821 Manchester Rd., Middletown, OH 45042.

## SITE SELECTION AND PREPARATION

When planning a new test facility, possible point sources of contamination should be avoided, i.e., the atmosphere should represent the area rather than a specific corrosive source. This can be illustrated by the data in Table 1. Comparison of the two exposures in Halifax, N. S. shows significant differences, although the sites are relatively close together. The more severe corrosion at the Federal Building is the result of the presence of a coal-fired boiler stack at the site. Also, the effects of distance from a corrosive source as well as height above the ground are shown by the Kure Beach and Cape Kennedy [*sic*] data.

Test yards should be planned so that the test rack orientation for proper exposures can be maintained. In most instances, test yards in the northern hemisphere are situated so that the exposures will face south. The opposite orientation would be the case in the southern hemisphere (to achieve near maximum exposure to the sun). Quite frequently, marine exposure sites are oriented so that the racks face the surf; it is usually the case, however, that these are accompanied by the normal north or south facing racks, somewhat removed from the possibility of direct spray, but still within the macroclimate under study. In all cases, at least 100 ft (30.5 m) of clear space should be maintained

**TABLE 1**—Relative corrosivity of zinc and steel exposed for one year at various locations (State College, PA = 1.00).<sup>a</sup>

Site	Steel	Zinc
Phoenix, AZ	0.26	0.32
Detroit, MI	0.93	1.03
State College, PA	1.00	1.00
Halifax, NS (York Redoubt)	1.27	1.43
Middletown, OH	1.44	1.01
Pittsburgh, PA	1.60	1.90
Columbus, OH	1.65	1.54
London, UK	2.25	1.55
Newark, NJ	2.90	2.80
East Chicago, IN	4.43	2.38
Cape Kennedy, FL (0.5 mile from surf)	1.65	1.21
Cape Kennedy, FL (60 yds/60 ft elevation)	2.46	2.53
Cape Kennedy, FL (60 yds/30 ft elevation)	2.84	2.89
Kure Beach, NC (250 m)	3.41	2.09
Halifax, NS (Federal Bldg.)	5.50	6.56
Cape Kennedy, FL (60 yds/ground level)	7.66	3.16
Kure Beach, NC (25 m)	28.50	5.44
Cape Kennedy, FL (beach)	42.50	—

<sup>a</sup>From "Corrosiveness of Various Atmospheric Test Sites as Measured by Specimens of Iron and Zinc," A Report of Subcommittee G01.04, *Metal Corrosion in the Atmosphere*, STP 435, ASTM International, West Conshohocken, PA, 1968, pp. 360–391.

between the sample rack and the property line to avoid shading or disturbance of the existing wind patterns. Additional detail on test yards and much of the following information on hardware and testing appears in ASTM G 50, Recommended Practice for Conducting Atmospheric Corrosion Tests on Metals.

## HARDWARE AND TERMINOLOGY

For the sake of consistency, a terminology has developed within the atmospheric corrosion testing community with respect to testing. The test facility itself is commonly referred to as a corrosion yard. Racks, commonly fabricated from pipe or wood, are installed to hold the fixtures for the individual test specimens. The latter are referred to as "frames," and can be fabricated from wood or metal (nickel-copper alloy, stainless steel, aluminum, etc.). These frames are usually designed to hold approximately 75 specimens, isolated from each other and the test frame by porcelain, plastic, or rubber "insulators." Thus, a corrosion yard



FIG. 1—Typical atmospheric corrosion test yard at Middletown, Ohio, showing exposure racks and instrumentation. Reprinted with permission of Armco, Inc. [sic]

contains racks upon which frames are mounted to hold specimens isolated from metal-to-metal contact by insulators. Details for construction and use of these are contained in ASTM G 50. Figure 1 shows a typical corrosion yard, illustrating the appearance and use of racks, frames, and insulators. Figure 2 shows an overall view of the LaQue Center for Corrosion Technology [sic] test yard at Kure Beach, NC. Any fasteners employed to assemble racks, frames, and insulators should have corrosion resistance commensurate with the anticipated life of the installation. Common fastener materials include stainless steel, nickel-copper alloy, aluminum, or bronze. The exposure angle is usually 30 or 45° from the horizontal (the higher angle usually recommended for testing paints and other organic systems; see ASTM G 07, Recommended Practice for Atmospheric Environmental Exposure Testing of Nonmetallic Materials). The lower edge of the exposure frames should not be less than 760 mm (30 in.) from the ground. Although the foregoing specifies details of hardware, these should not be construed as limits to exposure requirements that might be necessary to measure corrosion at other angles or heights for specific purposes.

## CORROSION YARD INSTRUMENTATION

Most corrosion yards around the world have little or no weather instrumentation within their confines. As mentioned earlier, the temperature-relative humidity interaction is one of the foremost combinations of weather factors in affecting corrosion of metals. The installation of a thermograph and hygrograph is valuable as a means to determine TOW. Knowing the temperature is important for several reasons. Below freezing corrosion normally does not occur, as ice is a poor electrolyte. At elevated temperatures, adsorbed or phase water cannot exist. Therefore, most corrosion typically occurs between 0 and 25°C. Higher temperatures also contribute to more rapid drying after specimens become wet with rain, dew, or adsorbed water. At high values of relative humidity, relatively small drops in specimen temperature can exceed the dewpoint, resulting in condensation of water on the specimen surface. It has been observed, however, that wet conditions (dew) can exist in tropical environments up to 35°C.

Other standard weather instrumentation that has been used includes wind direction and velocity equipment and rain gages.

There are several other aspects of atmospheric characterization which, if measured, can provide pertinent information related to the performance of materials. Probably the most important and universal is the determination of the TOW, described earlier. ASTM G 84, Practice for Measurement of Time-of-Wetness on Surfaces Exposed to Wetting Conditions as in Atmospheric Corrosion Testing, describes instrumentation and techniques for measuring TOW. This parameter can most easily (and adequately) be estimated from weather bureau records. It is generally accepted that metal atmospheric test specimens are wet when the temperature is above freezing and the relative humidity is above 80 %. There are indications that corrosion can occur under arctic conditions down to 0°F if

FIG. 2—Marine atmosphere testing site at Kure Beach, NC. Reprinted with permission of LaQue Center for Corrosion Technology, Inc.



salt deposits are present. This will be discussed further when describing contributions to the science of atmospheric testing that have been made by investigators in Eastern Europe.

It is advantageous to measure the levels of other atmospheric corrosives; e.g., chlorides at marine sites and gaseous and particulate sulfur compounds at known industrial sites, or at sites where long-range sulfur contamination may be suspected. There are techniques available for adequately measuring both of these corrosives.

With respect to chlorides ( $\text{Cl}^-$ ), the most widely used procedure is the "chloride candle," a gauze wick in a flask of reagent water. The candles are exposed for a fixed period of time, usually 30 days, then removed. After leaching the exposed gauze into the flask water, the total chlorides are determined analytically, and reported as chloride deposition per unit of exposed area per unit of time ( $\text{mg}/\text{m}^2/\text{day}$ ). This method is described in ASTM G 140, Test Method for Determining Atmospheric Chloride Deposition Rate by Wet Candle Method. The other method more recently introduced uses a dry fabric panel, which is also exposed for a predetermined length of time, usually 30 days. Then the chlorides are washed out of the fabric and analyzed. Both procedures are currently described in ISO Standard 9225; however, the dry plate method has been found to produce inconsistent results, and probably will be dropped from the ISO document at its next revision.

There are two accepted methods for determining the sulfur dioxide ( $\text{SO}_2$ ) concentration in the atmosphere of interest. Both employ the affinity of lead oxide for sulfur dioxide. The most common technique uses sulfation plates. This procedure is covered in detail in ASTM G 91, Test Method for Monitoring Atmospheric  $\text{SO}_2$  Using the Sulfation Plate Technique. These devices are no longer available for purchase, but must be prepared in the laboratory. The second method is the peroxide candle, similar in its function to the chloride candle. The procedure suggests a 30-day exposure, followed by a standard sulfate analysis. This procedure is covered by ASTM D 2010, Test Methods for Evaluation of Total Sulfation Activity in the Atmosphere by the Lead Dioxide Technique. In both cases, the results are calculated as the capture rate of  $\text{SO}_2$  per unit area, normally per  $\text{m}^2$ .

If electric power is available, both  $\text{Cl}^-$  and  $\text{SO}_2$  levels in the atmosphere can be obtained by taking volumetric samples of the air into reagent water, and analyzing to obtain the actual concentration. Representative and frequent sampling should be carried out to obtain a realistic appraisal of the range and average of the contamination over a period of time. Chloride candles and sulfation plates measure deposition per area per time rather than instantaneous atmospheric content per unit volume. Therefore, the results of one can provide an indication of the other, but are not directly comparable.

## SITE CALIBRATION

Most atmospheric corrosion yards are monitored for consistency or to quickly identify any sudden changes in corrosivity. This is most often accomplished through

periodic exposure of standard materials, usually pure zinc (99.95 % Zn), and a copper-bearing steel (0.20 % Cu, min). The details of site characterization can be found in ASTM G 92, Practice for Characterization of Atmospheric Test Sites. Other materials are used sometimes, e.g., aluminum and copper, but in many environments their corrosion rates are too low to be definitive. As these are intended to be standards, it is advisable to purchase a quantity sufficient to provide many years of continuing calibration. As it is valuable to measure both short- and long-term corrosion rates, a statistically significant number of specimens should be exposed each year. The short-term exposures will alert the investigator to sudden changes in his environment, while the extended exposures will provide a continuing record of the corrosivity of the site.

## TEST SPECIMENS AND IDENTIFICATION

Accepted terminology for atmospheric testing includes sample, the material to be tested; specimens (or panels), the individual pieces of the sample that are actually exposed; and lot, a group of specimens, usually three to five, intended for a specific exposure time. Thus, a typical exposure plan might involve 40 specimens of a given sample divided into eight lots composed of five specimens each for removal at eight different times. The most frequently used specimen size is 4 in. by 6 in. (100 mm by 150 mm). This does not imply, however, that other sizes cannot be used. It is common that larger or smaller, thick or thin, specimens can be tested, as well as various shapes such as bolts, nuts, fasteners, angles, channels, pipes, and fabricated assemblies. It may also be desirable to evaluate galvanic corrosion in the atmosphere. The method for this is described in ASTM G 116, Practice for Conducting the Wire-on-Bolt Test for Atmospheric Galvanic Corrosion. This latter procedure has also been used to calibrate and monitor test sites by employing aluminum wire on nylon, steel, and copper bolt material. This calibration procedure will be discussed later.

There are almost as many means of marking specimens for identification as there are investigators engaged in atmospheric corrosion testing. The primary consideration is to select a system that will maintain the identification for the intended test period. The most common method is stenciling (metal stamping), which is easy, and adequate for short-term testing or for more corrosion-resistant materials. Another common means depends on drilling an identification code into the specimens. A typical template for accomplishing this is shown in ASTM G 92. Other investigators notch the edges, while still others put the identification on a corrosion resistant tag and attach it to the specimen by means of insulated wire through a drilled hole. The drilling technique has a distinct advantage in that several specimens can be identified at a time. However, it also has the disadvantage that edge corrosion may make decoding difficult.

After shearing and identification, the specimens should be properly cleaned prior to either additional processing or exposure. Cleaning procedures can be found in ASTM G 1, Practice for Preparing, Cleaning, and Evaluating Corrosion Test Specimens. Information specific to stainless steel alloys can also be found in ASTM A 380, Practice for Cleaning and

Descaling Stainless Steel Parts, Equipment, and Systems. After cleaning, extreme care should be taken when handling the specimens to avoid contamination and fingerprinting. As mass loss is involved in evaluation of the samples in most cases, the individual specimens are then weighed. Analytical balances are used, and the precision of the weighing depends on the anticipated corrosion resistance of the material. It is common to weigh to the nearest milligram.

In addition to mass loss, some materials are further evaluated by determining changes in their mechanical properties. This is most frequently the case with materials that demonstrate good corrosion resistance, but may suffer pitting in the atmosphere. Nonmetals and organic finishes also suffer deterioration of properties due to ultraviolet (UV) effects. The possibility of this type of damage occurring points up the need to keep a supply of untested control samples.

Record keeping and tracking of exposure and materials can be as simple or as sophisticated as the laboratory needs. A simple card file or notebook system is adequate. By simply numbering the frames and using the row numbers, the location of every specimen exposed can be defined. A card file arranged by month and year can keep track of removals.

The site should be visited periodically to make certain everything is as it should be, i.e., panels are still properly exposed, and the site and facilities maintenance is satisfactory. Special attention should be paid to fences, gates, and locks. (Corrosion affects facilities as well as specimens.)

## CLEANING AND EVALUATION

After removal at the specified exposure period, the specimens are evaluated. Visual examination of the specimens upon removal is usually performed, and a photographic record of appearance is valuable. ASTM G 33, Practice for Recording Data from Atmospheric Corrosion Tests of Metallic-Coated Steel Specimens, can provide guidance for evaluation procedures. Before determination of mass loss, or for most other evaluation techniques, the specimens must be cleaned. Again, cleaning procedures are described in ASTM G 1 and A 380 for most materials of interest. ASTM G 1 also includes a procedure for determining when the corrosion products have been removed. After cleaning, specimens should be placed in a desiccator with fresh dessicant until ready for further evaluation.

The specimens are reweighed to the same precision as prior to exposure and the mass loss determined. Mass losses can then be used to calculate corrosion rates as follows:

$$\text{Corrosion Rate} = \frac{(K \times W)}{(A \times T \times D)}$$

where

- $K$  = a constant based on the rate units desired (see ASTM G 1),
- $T$  = time of exposure in h,
- $A$  = area in  $\text{cm}^2$ , and
- $D$  = density in  $\text{g/cm}^3$ .

Other means of evaluation can be used. Pit depth and pit density measurements are frequently employed. ASTM G 46, Guide for Examination and Evaluation of Pitting Corrosion, provides information on this means of evaluation. Once all the pertinent nondestructive tests have been completed, various destructive tests can be employed to further define the nature and extent of the corrosion. The measurement of changes in mechanical properties has already been mentioned. Metallographic examination will provide information on the nature of the corrosion that has occurred (parting, exfoliation, cracking, intergranular corrosion, pitting, etc.).

In the case of plastics or organic coatings, other factors must be considered. These include but are not limited to the size and density of blistering, delamination, loss of gloss, loss of adhesion, fading, chalking, crazing, cracking, and creep. In tropical and subtropical environments, algal and fungal growth can also be problems. Much more use is made of the loss of properties in the evaluation of organic materials than in the case of metals.

With the proper statistical design of exposure tests, including proper replication and multiple exposures, atmospheric corrosion data are readily amenable to statistical analysis. An excellent review of an applicable statistical procedure can be found in ASTM G 16, Guide for Applying Statistics to Analysis of Corrosion Data.

## SPECIAL TESTING PROCEDURES

To this point, the discussion has centered on standard conditions of exposure and evaluation of materials. Earlier it was mentioned that the details described in the various ASTM standards cited would allow investigators to develop data that are directly comparable to that determined by other investigators at other sites using the same procedures. However, sometimes there is a need to develop information related to some specific commercial need. Therefore, the standard conditions of exposure are frequently varied to develop the requisite data. All testing described, for instance, infers specimens boldly exposed at  $30^\circ$  from the horizontal facing the equator. This is the matter of obtaining consistency between tests and investigators. It has been demonstrated, however, that corrosion varies considerably if the specimens are exposed to face the poles rather than the equator, or if the specimens are sheltered from the direct effects of the elements. As recommended in ASTM G 50, the specimens receive almost the maximal solar effects, particularly in the middle latitudes. North or south facing racks (depending on hemisphere) receive no direct sun at all. This results in slower drying, and therefore longer times of wetness. Sheltered specimens can accumulate airborne contaminants but do not receive the washing action of rain. Therefore, the corrosive contaminants remain on the surface for a longer period of time, and the surfaces remain wet for longer periods. Vertical exposures corrode less than samples exposed at the recommended angle, because of better drainage, a poorer view of the sky that can slow dew formation, and less accumulation of deposits. However, these conditions exist in many atmospheric applications of materials, so testing under these conditions is certainly justified in some cases.

**FIG. 3—Wire-on-bolt assembly for measuring atmospheric corrosivity and/or galvanic corrosion.**

**TABLE 2—Evaluation of various atmospheres using the CLIMAT sample.**

Location	Season	Corrosivity Values <sup>a</sup>		
		ACI <sup>b</sup>	MCI <sup>b</sup>	ICI <sup>b</sup>
Middletown, OH	Summer	N	N	N
	Winter	N	N	N
	Spring	N	N	N
Kure Beach, NC 250 m lot	Summer	N	M	
	Spring	N	M	
	Fall	M	S	
Kure Beach, NC 25 m lot	Summer		S	
	Fall		VS	
Voerde, Ger.	Summer	N		M
	Winter	M		VS
	Spring	N		M
Hamburg, Ger.	Winter	M	MS	VS
	Spring	N	N	MS
Antwerp, Bel.	Winter	M		VS
	Spring	N		M
Liege, Bel.	Winter	N		VS
	Spring	N		MS
Dunkerque, Fr.	Winter	N	MS	
	Spring	N		S
Goteborg, Sw.	Winter	N	MS	M
	Spring	M	VS	
Jiddah, S. Arabia	Winter	N	N	N
	Spring	N		MS
Teheran, Iran	Winter	N		N
	Spring	M		VS
Leeds, U.K.	Winter	N		VS
	Spring	N	M	
London, U.K.	Winter	N	N	N
	Spring	N	N	N

<sup>a</sup>N = negligible; M = moderate; MS = moderately severe; S = severe; VS = very severe.

<sup>b</sup>ACI = Atmospheric Corrosion Index; MCI = Marine Corrosion Index; ICI = Industrial Corrosion Index.

It has been established that corrosive conditions vary considerably with distance from a corrosive source, as well as height above the ground. Therefore, there can be a need for such evaluations to be made for determining such differences. One relatively easy way to accomplish this has been developed by the Alcan Research Laboratories from previous work done by ASTM Committee B-3 [5–7]. This technique is the basis for the wire-on-bolt practice

described in ASTM G 116. This means of rapidly developing data on the comparative corrosivity of a site or several sites has become very well accepted and has been widely used by various investigators. The procedure is identified as the CLIMAT test (from Classification of Industrial and Marine Atmospheres). Originally designed to measure galvanic effects between aluminum strands and the steel reinforcement in aluminum overhead conductors [8], particularly in marine environments, the test has been extended to provide information on the general corrosivity of atmospheres. It has proven valuable in assessing storage areas, microclimates, indoor corrosion, and in providing quantitative evaluations of the corrosivity of various atmospheres.

The assembly used for the corrosivity measurements consists of preweighed 1100 aluminum wire fastened to and tightly wound on threaded lengths of steel, copper, and nylon. Figure 3 shows a completed assembly. The details of preparation are given in ASTM G 116. The data derived from the individual wire-bolt combinations are used to develop "corrosion indices"; the aluminum-nylon results reflect the general atmospheric corrosion (ACI), the aluminum-steel the marine index (MCI), and the aluminum-copper the industrial index (ICI).

The rod assemblies are usually exposed to the environment in question for 90 days, after which the wires are removed, cleaned, and reweighed. The percentage mass loss of the aluminum is the corrosion index for that time period. The data obtained can then be used to describe the severity of the atmosphere by comparing the values obtained to those empirically determined by experience or by relevant testing. Environmental corrosivity is classified from "negligible" to "very severe" on this basis. Some typical atmosphere assessments made using this procedure are shown in Table 2. It has been found that a series of exposures must be made to fully characterize an environment, as the corrosion varies with the season of the year and the exposure is only for three months.

## ISO CORROSION CLASSIFICATION SYSTEM

The rural, industrial, and marine atmospheres described earlier are very broad classifications, and do not adequately define specific exposure conditions. Other categories have been proposed, such as desert, tropical, urban, semi-industrial, and industrial-marine, but even these are not satisfactory for predictive purposes [9]. In the mid-1970s, Technical Committee 156 on Corrosion of Metals and Alloys of the International Organization for Standardization (ISO) identified atmospheric corrosion as a priority area for study. From that, a classification system was developed, and described by four standards (Table 3). The system is based on quantitative values for TOW, SO<sub>2</sub>, and Cl<sup>-</sup> deposition rates, and/or mass loss of steel, aluminum, zinc, and copper samples exposed for at least one year. The TOW can be determined from meteorological data or measured by devices such as described in ASTM G 84, the ionic species deposition rates by ASTM G 92 and either of the Cl<sup>-</sup> methods described earlier, and the mass losses determined by the procedures discussed earlier in this section. The levels of ionic species, TOW, and mass losses are placed in categories as to

**TABLE 3**—ISO standards concerned with classification of atmospheric corrosivity [10].

ISO 9223,	Corrosion of metals and alloys—Classification of the corrosivity of atmospheres
ISO 9224,	Corrosion of metals and alloys—Guiding values for the corrosivity categories of atmospheres
ISO 9225,	Corrosion of metals and alloys—Aggressivity of atmospheres—Methods of measurement of pollution data
ISO 9226,	Corrosion of metals and alloys—Corrosivity of atmospheres—Methods of determination of corrosion rate of standard specimens for the evaluation of corrosivity

severity, and from these corrosivity categories can be derived [10]. The system is currently being evaluated on a worldwide basis by means of the ISO CORRAG program [11].

## LABORATORY SIMULATION TESTS

It has long been the desire of investigators studying atmospheric corrosion to have a laboratory test that would duplicate and accelerate the behavior of materials in the atmosphere. Many years ago, the salt spray test was developed to evaluate defects in metallic coatings, but later extended as a means to simulate marine environments [12]. Similarly, the humidity cabinet has been used in an attempt to accelerate corrosion that might occur in less severe atmospheres. These test procedures are covered by ASTM B 117, Test Method of Salt Spray (Fog) Testing, and ASTM G 60, Method for Conducting Cyclic Humidity Tests. The ultimate aim of accelerated testing is to obtain realistic data in an abbreviated time period (atmospheric testing may take years to effect a failure of a material). As in the case of many other accelerated test procedures, laboratory tests frequently are misused or misinterpreted, often giving a quick answer in lieu of the right one. In addition to the above, there are several other tests used to evaluate materials intended for atmospheric usage. These include other variations of the humidity cabinet, ASTM G 87, Practice for Conducting Moist SO<sub>2</sub> Tests, and a variety of other cabinet tests which may include cyclic wetting and drying, exposure to salt spray, temperature cycles, the use of UV radiation, and the introduction of small concentrations of various corrosive gases into a single test regime. There has been considerable interest in these last described cyclic test systems on the part of the automotive industry worldwide, and several tests are being used.

In the development of any accelerated tests, several significant factors have been identified as contributing to corrosion [13]. These include the following:

- (a) Precipitation—a liquid film present, containing dissolved pollutants and salts
- (b) Evaporation—a liquid film present, salts and pollutants concentrating
- (c) Dry—liquid film absent, solid salts on surface
- (d) Re-wetting—liquid film present, salts diluting, or possibly removed under rain conditions

Step b in the above is very important, because it points out that the corrodents may concentrate on the surface

under drying conditions, providing a more corrosive condition should the material be wetted by condensation rather than being cleaned by the washing action of rain.

Therefore, a meaningful accelerated test must include each of the above to be realistic, i.e., it must include cycling the surface of the test material through both wet and dry conditions. Concentrations of the corrosives (other than water) must be realistic—not so concentrated that they dominate the reaction, nor so acid that they alter the corrosion products that would develop in normal environments. Care must be taken to avoid distorting the naturally occurring reactions. Perhaps the only effective acceleration can be in the frequency of wetting and drying, and the use of heat to facilitate the latter. Additional discussion of laboratory testing can be found in Section VIII of this manual.

## REFERENCES

- [1] Munger, C. G., *Corrosion Prevention by Protective Coatings*, NACE International, Houston, TX, 1984, pp. 37–38.
- [2] Dean, S. W., "Corrosion Testing of Metals under Natural Atmospheric Conditions," *Corrosion Testing and Evaluation: Silver Anniversary Volume*, ASTM STP 1000, R. Baboian and S. W. Dean, Eds., ASTM International, West Conshohocken, PA, 1990, pp. 163–176.
- [3] Kucera, V. and Mattsson, E., "Atmospheric Corrosion," *Corrosion Mechanisms*, Marcel Dekker, NY, 1987, pp. 211–284.
- [4] Ambler, H. R. and Bain, A. A. J., "Corrosion of Metals in the Tropics," *Journal of Applied Chemistry*, Vol. 5, London, 1955, pp. 437–467.
- [5] "Report of Committee B3 on Corrosion of Non-Ferrous Metals and Alloys," *Proceedings, American Society for Testing and Materials*, Philadelphia, 1954, pp. 147–159.
- [6] Compton, K. G. and Mendizza, A., "Galvanic Couple Corrosion Studies by Means of the Threaded Bolt and Wire Test," *Symposium on Atmospheric Corrosion of Non-Ferrous Metals*, ASTM STP 175, ASTM International, West Conshohocken, PA, 1955, pp. 116–125.
- [7] Doyle, D. P. and Godard, H. P., "Rapid Determination of Corrosivity of an Atmosphere to Aluminum," *Proceedings of 3rd International Congress on Metallic Corrosion*, Moscow, 1966.
- [8] Doyle, D. P. and Wright, T. E., "A Rapid Method for Predicting Adequate Service Lives for Overhead Conductors in Marine Atmospheres," presented at the IEEE Power Meeting, New York, 1971.
- [9] Dean, S. W., "Atmospheric Corrosion after 80 Years of Study," *Materials Performance*, Vol. 26, No. 7, NACE International, Houston, TX, 1987, pp. 9–11.
- [10] Dean, S. W., "Classifying Atmospheric Corrosivity: A Challenge for ISO," *ISO Bulletin*, Vol. 23, No. 12, December 1992.
- [11] Dean, S. W., "ISO CORRAG Collaborative Atmospheric Exposure Program: A Preliminary Report," *Degradation of Materials in the Atmosphere*, ASTM STP 965, ASTM International, West Conshohocken, PA, 1988, pp. 365–431.
- [12] Capp, J. A., "A Rational Test for Metallic Protective Coatings," *Proceedings, American Society for Testing and Materials*, Vol. XIV, Part II, Philadelphia, 1914, p. 474.
- [13] Lyon, S. B., Cox, W. M., and Dawson, J. L., "Atmospheric Degradation and Testing of Materials," *Standardization News*, July 1987, ASTM International, West Conshohocken, PA, 1987, pp. 52–56.

# Indoor Atmospheres

*J. D. Sinclair*<sup>1</sup>

## DESCRIPTION OF THE ENVIRONMENT

CORROSION in indoor environments is an exceedingly complex process. Few environments have as many components that participate in the corrosion of materials as the indoor environments in which we live and work. While the indoor environment is less harsh than many other environments, e.g., chemical reactors and jet engines, its effects are particularly difficult to mimic through accelerated life testing because of the many possible chemical and physical interactions that can take place between environmental components and materials.

It can be argued that indoor environments are even more difficult to simulate than outdoor environments because they contain all the components present in outdoor environments, e.g., gases derived from fossil fuel combustion (sulfur dioxide (SO<sub>2</sub>) and nitrogen oxides (NO<sub>x</sub>)), particulate matter, and microbes, as well as components derived from indoor sources, e.g., outgassed vapors from carpets, paints, plastic furnishings, cooking, manufacturing activities, office equipment, appliances, cleaning solutions, waxes, and wax strippers. Also, items designed for indoor use may well be more sensitive to environmental effects. The optimum design is frequently one using materials that are no more resistant to the environment than is necessary to satisfy specified reliability criteria. Examples of common household or office items that are not designed for outdoor use include many computers, photocopiers and similar office machines, some plastics, silver-plated utensils and serving dishes, brass fixtures, and kitchen appliances.

In this chapter, the applicable environmental factors include temperature, vapor phase and condensed moisture, corrosive inorganic gases, organic vapors, particles, electric fields, and air velocity. While vibration, mechanical stress, thermal shock, and solar radiation can occasionally contribute to materials degradation in indoor environments, these subjects are covered in other chapters and MIL-STD-810E.

The relevant material components in indoor environments can be conveniently segregated into six categories. Corrosive gases include SO<sub>2</sub> and NO<sub>x</sub> (primarily NO and NO<sub>2</sub>), as well as organic acids such as formic and acetic

acids, hydrochloric acid (HCl), hydrogen sulfide (H<sub>2</sub>S), carbonyl sulfide (COS), mercaptans (RSH, where R is an alkyl group), and organic sulfides including dimethylsulfide ((CH<sub>3</sub>)<sub>2</sub>S) and dimethyl disulfide ((CH<sub>3</sub>)<sub>2</sub>S<sub>2</sub>). The concentrations of SO<sub>2</sub> and NO<sub>x</sub> are usually reduced by a factor of 2 to 10 from their outdoor concentrations in air-conditioned office buildings, while the concentrations of organic acids, hydrochloric acid, and other sulfur-containing substances can be less than, similar to, or even greater than the outdoor concentrations, depending on the existence of indoor sources. In parts of the world where air conditioning is less prevalent, exchange of outdoor air for indoor air can be quite rapid, making the indoor environment more like the outdoor environment than an air-conditioned environment. Air conditioning designs also vary significantly in different parts of the world. For example, in North America and Europe, the common practice is to positively pressurize buildings relative to outdoors by continuously pumping conditioned outside air into the building. With this approach, the quality of the filtration and the rate of air exchange are the largest determinants of indoor concentrations for all components except those that have substantial indoor sources. On the other hand, for many Asian countries, the common practice, especially for equipment rooms, is to eliminate air exchange pathways as much as possible and continuously re-circulate the indoor air through heat exchangers and air filters. No outside air is intentionally drawn into the building. In this case, corrosive gas concentrations are frequently much less than outdoor concentrations because the balance between the ingress rate (through leakage) and the consumption rate on surfaces is dominated by the consumption rate. At the same time, species with substantial indoor sources, such as outgassed substances from building and housekeeping materials, can reach much higher concentrations than commonly found in North America and Europe.

Typical indoor and outdoor concentrations of gases that equipment should be able to tolerate without exhibiting significant degradation are shown in Table 1. The values listed in Table 1 are based on U.S. Environmental Protection Agency (EPA) reports, published air quality studies, and proposed standards currently under consideration by such organizations as ASTM International, the International Electrotechnical Committee (IEC), and the European Telecommunications Standards Institute (ETSI). They are intended to represent average annual concentrations at roughly the 95th percentile, i.e., only 5 % of all locations are

<sup>1</sup>Currently Vice President of Engineering, Nova Crystals, San Jose, CA 95135. Formerly, Director, Materials Reliability and Electrochemistry Research Department, Bell Laboratories, Murray Hill, NJ 07974.

**TABLE 1**—Design guidelines for atmospheric gaseous pollutants.<sup>a</sup>

Species	North America and Europe		Southern and Eastern Asia	
	Outdoor	Indoor	Outdoor	Indoor
SO <sub>2</sub>	50	25	100	50
H <sub>2</sub> S	2	2	6	4
NH <sub>3</sub>	50	0.5	50	2
NO <sub>x</sub>	60	40	50	35
HNO <sub>3</sub>	4	2	2	1
O <sub>3</sub>	50	30	50	30
Reactive Chlorine <sup>b</sup>	4	2	6	3
Volatile Organics <sup>c</sup>	1200	1500	1200	5000

<sup>a</sup>Parts per billion of air by volume.<sup>b</sup>Mostly HCl, but includes Cl<sub>2</sub> and HOCl.<sup>c</sup>Methane is excluded. Concentrations are expressed in ppbv of carbon.

likely to exhibit higher average annual concentrations than those indicated. Some judgment was exercised in setting these values, as the available data are frequently insufficient to be quantitative. It is also now generally accepted that environments in parts of Southern and Eastern Asia tend to be much more polluted than many other parts of the world but reliable data is very limited. Thus, the reader should exercise caution in using these values for materials and equipment intended for use in Southern and Eastern Asia.

A variety of techniques is used for determining the concentrations of pollutant gases. Where possible, instruments certified by government agencies such as the U.S. EPA are recommended. These are available for SO<sub>2</sub>, NO<sub>x</sub>, and ozone (O<sub>3</sub>). For the other gases, the techniques are more difficult and require specialized expertise and extensive standardization. In many cases these are proprietary or inadequately documented to be referenced. The reactivity of these gases for materials is very material specific. Atmospheric moisture is a critical ingredient for many of these degradation processes. Most corrosion processes depend strongly on relative humidity (RH). A couple of examples illustrate the complexity of RH effects. Silver is very reactive to H<sub>2</sub>S, with a strong RH dependence. However, silver shows no RH dependence in its reactivity with vapors of elemental sulfur. Iron, on the other hand, is rapidly corroded by SO<sub>2</sub> at RH about 75 % or greater but reacts much more slowly below this RH. Vernon [1] first described this critical relative humidity (CRH) concept in the 1930s. Outdoor RH spans a wider range than indoor RH in most climates. RH > 75 % is rare for most office buildings or homes, but typical outdoor conditions may be present in many manufacturing environments, storage sheds, and equipment huts used by utility companies.

Organic gases are usually not directly corrosive but can play an important mitigating role in the aging of surfaces. These gases may be derived from natural or anthropogenic (manmade) sources. The typical total abundance of all organic gases, shown in Table 1, is much higher than the total of all inorganic pollutant gases combined. Many of these organic species have much higher concentrations indoors than outdoors, especially those derived from outgassing of indoor materials. Some typical arrays of organic vapors found indoors and their likely sources have been described elsewhere [2]. These gases competitively adsorb on surfaces with the corrosive gases and atmospheric moisture. The presence of an organic film on a surface can alter

its wettability. The effects of these adsorbed films on corrosion rate have generally not been quantified and have rarely been considered in accelerated testing. The test engineer should, however, be aware of their existence.

The other major material component of indoor environments is particles. Most of the mass of particulate matter in the atmosphere exists in the size range 0.1–15 µm. Within this range, the mass exhibits a bimodal distribution. Particles 2.5–15 µm are largely derived from natural materials and are usually called coarse particles, while particles 0.1–2.5 µm are called fine particles. Coarse particles are largely mineralogical in composition and form predominantly as a result of human activity (mechanical processes) or by the action of wind or other abrasion processes on soils. Design guidelines for particulate mass are given in Table 2. Indoor and outdoor concentrations of water soluble ions in fine and coarse particles for a typical North American telecommunications office building and an electronics assembly environment [3,4] are shown in Table 3. All particle concentrations shown in Table 3 were determined using a dichotomous sampler, which provides particle collection on Teflon® filters. Mass concentrations are determined from the volume of air passed through each filter and gravimetric measurement of the mass of collected material. An important distinction between fine and coarse particles is their corrosivity. The higher the fraction of water soluble ions, the higher the corrosivity. The concentrations shown in Table 3 are determined by ion chromatography after the particles have been collected on the Teflon filters and then water extracted. Coarse particles tend to have a much lower fraction of water soluble ionic components (5–20 %) than fine particles (25–50 %), excluding

**TABLE 2**—Design guidelines for atmospheric particulate matter.<sup>a</sup>

Species	North America and Europe			Southern and Eastern Asia	
	Indoor Filtered	Indoor Nonfiltered	Outdoor	Indoor Filtered	Outdoor Nonfiltered
Coarse Particles	7	15	50	50	350
Fine Particles	7	25	25	40	50

<sup>a</sup>Micrograms per cubic metre.**TABLE 3**—Average airborne concentrations (ng m<sup>-3</sup>).

	Newark, NJ, USA Telecommunications Center		Andover, MA, USA Manufacturing Plant	
	Indoor	Outdoor	Indoor	Outdoor
Fine Particles				
Chloride	4	66	15	37
Sulfate	721	5214	2840	4339
Sodium	14	103	39	69
Ammonium	168	1631	846	1573
Potassium	19	53	36	52
Magnesium	2	14	4	8
Calcium	10	25	17	31
Coarse Particles				
Chloride	4	502	43	300
Sulfate	25	725	104	376
Sodium	3	446	35	269
Ammonium	0	1	13	26
Potassium	2	30	24	28
Magnesium	1	90	5	29
Calcium	20	297	101	245

**TABLE 4**—Total Suspended Particulate (TSP) and airborne concentrations in Eastern Asia (micrograms/m<sup>3</sup>).

City	Location	TSP	Chloride	Sulfate	Nitrate	Ammonium	Potassium	Calcium
Qingdao	Indoor	7.4	0.01	1.4	0.03	0.55	0.16	0.02
	Outdoor	199	0.42	14	2.8	4.3	1.4	1.1
Jinan	Indoor	34	0.03	7.6	1.1	1.8	2.1	0.51
	Outdoor	165	1.4	21	6.9	2	5.3	11
Beijing	Indoor	26	0.04	4.7	0.44	1.3	1.2	0.27
	Outdoor	269	2.2	19	7.9	3.5	4.9	13
Wuhan	Indoor	11	0.01	2.8	0.07	0.92	0.78	0.09
	Outdoor	141	0.3	16	3.7	2.5	4.1	6.6
Guangzhou	Indoor	18	0.02	3.7	0.18	0.82	2.8	0.29
	Outdoor	182	0.82	22	5.4	1.1	14	12
Zigui	Indoor	46	0.05	5.8	1.1	2.9	1.3	1.5
	Outdoor	175	0.7	25	14	6.5	5.6	11
Wenzhou	Indoor	32.9	0.06	4.8	0.27	1.3	1.1	0.2
	Outdoor	146	0.65	13	2.5	1.7	2.6	3.9
Chengdu	Indoor	46	0.12	7.9	0.57	2.4	2.9	0.9
	Outdoor	231	3.8	32	9.9	7.8	10	7.9

hydrogen ion (H<sup>+</sup>), hydroxyl ion (OH<sup>-</sup>), and carbonate (CO<sup>3-</sup>) [4]. As a result, coarse particles are less corrosive than fine particles. Recent work by the author and colleagues for telecommunications facilities in Eastern Asia, as shown in Table 4, found concentrations of particles to be typically 3–10 times higher than those found in North American facilities. The particles also tend to have a higher concentration of corrosive anions. In this work, fine and coarse particles were collected on the same Teflon filter (referred to as total suspended particulate).

Fine particles are largely of anthropogenic origin, though volcanic activity can sometimes be a significant source. The predominant source in developed parts of the world is fossil fuel combustion. These particles are formed by a complex ensemble of chemical and photochemical processes in which SO<sub>2</sub> and NO<sub>x</sub> formed by fossil fuel combustion are further oxidized over a period of days to sulfuric acid (H<sub>2</sub>SO<sub>4</sub>) and nitric acid (HNO<sub>3</sub>). These acids are neutralized to varying extents, depending on the environment, by ambient ammonia (NH<sub>3</sub>) derived from fertilization of farms, feedlot activity, and humans. The particles that initially form are smaller than 0.1 µm but rapidly grow, through condensation, on seed nuclei of carbonaceous material (also from fossil fuel combustion) to the stable size range of fine particles. The stability of this size range is attributable to the decreasing diffusivity and hence collision rate of particles, as their size increases. The mass abundance of fine particles outdoors is typically of the same order of magnitude as that of coarse particles, while their number density (typically 10<sup>7</sup> to 10<sup>8</sup> particles/ft<sup>3</sup>) is three or four orders of magnitude greater.

The concentrations of coarse particles within air conditioned office buildings, regardless of location in the world, are usually much lower than their outdoor concentrations, as shown in Tables 2 and 4, due to the effectiveness of even modest filtration systems in capturing particles in this size range. Within homes with open windows or doors, and within sheds and utility huts, the concentrations will be appreciably higher than for office buildings. If homes are well-sealed, the indoor concentrations are likely to be comparable to office buildings, except when items such as wood stoves, space heaters, and cooking appliances are operating. Mechanical processes in manufacturing environments, such

as cutting, grinding, welding, and polishing, can also generate locally high concentrations of coarse particles with the composition reflecting the source.

The indoor concentrations of fine particles in office buildings commonly range from 20–50 % of the outdoor concentrations, depending on: (1) the efficiency of the air filtration system, (2) the rate at which outdoor air is brought into the building or enclosure, and (3) indoor sources such as smoking or vigorous human activity. Concentrations within homes, sheds, and utility huts can range from 20–75 % of the outdoor concentration due to: (1) the penetrability of these particles through air-leakage pathways or open doors or windows; (2) the low efficiency of any air filtration; and (3) indoor sources like those mentioned above for coarse particles. Manufacturing environments typically have abundant sources of fine particles and their compositions may reflect the processing activity as much as ingress of outdoor particles.

An important distinction between coarse and fine particles is their predominant mode of transport through the air, which is determined by the combined effects of gravity, air velocity, temperature, electric fields, and surface configuration. Air velocity and flow direction are critical to the migration of fine particles but have little effect on coarse particles at normal indoor air velocities. Since coarse particles are sufficiently large to deposit by gravitational settling, they are found almost exclusively on topside horizontal surfaces, unless air velocities are very high and surfaces are tacky. Their residence time suspended in the air of an ordinary room is a maximum of a few minutes.

Many of the transport properties of fine particles are comparable to those of gas phase species. They migrate by convective diffusion and can remain in the air of a room for hours and even days, depending on the air exchange rate of the room. In the absence of thermophoretic forces or electric fields, they deposit with roughly equal propensity on all surface configurations and are more able to penetrate narrow spaces than coarse particles. The ratio of the surface accumulation rate (units of mass per unit area per unit time) to the airborne concentration (units of mass per unit volume) is a useful physical parameter that is commonly referred to as the deposition velocity (units of distance divided by time). The deposition velocity is the transfer

coefficient for transport across the concentration boundary layer that exists next to all surfaces.

With respect to corrosion processes, more important than the transport rate of particles or gases through air is their arrival rate and sticking probability on surfaces. These are determined by: (1) the air velocity across the surface and the resulting concentration boundary layer at the surface that controls transport to the surface; (2) the temperature of the surface relative to ambient; (3) the electrical charge on the surface and on nearby particles (electric field is not important for gases); and (4) bond strength between the surface and a freshly deposited particle or molecule. Typical deposition velocities for fine and coarse particles in various environments (in the absence of significant thermophoretic forces or electric fields) are shown in Table 5. Air velocity is well-established to have a dramatic effect on the arrival rate of gases and fine particles at surfaces. For example, the deposition velocity of fine sulfate containing particles was measured to be 0.005 cm/s in electronic equipment rooms where the linear air flow velocity is typically a few meters per minute [4]. However, for electronic equipment cabinets within these rooms, rapid airflow may be required to dissipate the high heat loads. In these situations, the air velocity is comparable to the typical outdoor wind velocity across the surfaces of vegetation (100 to 600 m/min). Deposition velocities to these surfaces has been found to range from 0.1–1.0 cm/s. From these data, the predicted arrival rate of particles on surfaces within forced-air-cooled electronic equipment cabinets is 20–200 times that for a normal office building environment at the same airborne concentration. The need to use forced-air cooling requires that the designer take steps to ensure that equipment has been adequately tested and hardened to the increased risk from environmental effects.

Particle transport through boundary layers in the presence of thermophoretic and electric forces is complex but predictable [5]. For coarse particles, thermophoretic and electric forces can usually be ignored. For fine particles, they can be very important. If the material to be tested is expected to exist in the field at  $>10^{\circ}\text{C}$  cooler or warmer than the ambient, or if the surface is expected to be  $>100\text{ V}$  above or below ground potential, these effects need to be considered. Cool surfaces increase the particle deposition rate while warm surfaces decrease it (analogous to condensation but for different reasons). Experience has shown that surfaces biased at a few hundred volts can collect fine particles at  $>5$  times the rate of grounded surfaces.

Detailed discussion of the modulating chemical and physical processes associated with continuing accumulation of fine and coarse particles over many years is beyond the scope of this chapter but can be found elsewhere [4]. Both

fine and coarse particles are expected to have sticking probabilities close to 1. Thus, in the absence of cleaning, accumulation will be continuous and linearly related to airborne concentration for all species that are chemically stable.

Bond strength of particles to the surface depends on many factors. Coarse particles do not normally adhere to vertical or bottom side surfaces unless the surface is very rough or tacky to human touch. The relationship between relative humidity and surface moisture can affect the degree of tackiness. For fine particles, chemical bonding and physical forces (van der Waals) are sufficiently strong to permanently hold all particles on surfaces, regardless of configuration, unless substantial mechanical forces, such as wiping or high-pressure air jets, are used to clean the surfaces. It is usually appropriate to assume that the sticking probability is 1 for both coarse and fine particles, recognizing that coarse particles only collect on top side horizontal surfaces. This behavior contrasts sharply with that of gas phase species, where sticking probabilities range from 0 to 1, depending on the surface, gas, and exposure time.

In electronic equipment, coarse particles sometimes cause malfunctions by interrupting electrical contact between mating pairs of contacts on connectors or relays. In manufacturing environments where air velocities may be high, these particles may erode passive surface films or coatings, resulting in accelerated corrosion. The CRH at which coarse particles begin to adsorb ambient moisture is substantially higher than that for fine particles, typically well over 80 %. In contrast, the CRHs of some of the major ionic components found in fine particles in most urban environments, given in Table 6 [6,7], are below 60 %. The electrolyte films that form upon moisture acquisition on surfaces contaminated with fine particles are responsible for their high corrosivity to many metals and can lead to electrolytic corrosion in electronics. Hygroscopic dust is a frequent cause of malfunction in electronics.

Another possible cause of materials degradation in indoor environment is microbes. A few research groups are investigating the effects of specific microbes on materials exposed to much harsher environments than are generally encountered indoors. Microbial corrosion has been largely ignored by the indoor design community. The test engineer concerned about indoor environments should be aware of microbial corrosion but will need to rely on engineering intuition to decide if microbial corrosion could be an issue. Since most corrosion engineers, including the author, have limited knowledge of how microbes interact with materials, the best approach seems to be to solicit the advice of a good microbiologist when devising a test method.

Finding a single accelerated test to evaluate materials against all these possible environmental hazards is unrealistic at this time. Each material needs to be evaluated by a series of tests to elucidate the possible degradation mechanisms.

**TABLE 5**—Deposition velocities of airborne particles (cm/s).

Conditions (Air Velocity)	Fine (0.1–2.5 $\mu\text{m}$ )	Coarse (1–15 $\mu\text{m}$ )
Outdoor (250–1000 cm/s)	0.6	0.6
Office Bldg (2–4 cm/s)	0.006	0.6
Cleanroom (50 cm/s)	0.009–0.09	0.6

**TABLE 6**—Critical relative humidity for saturated salt solutions,  $75^{\circ}\text{F}$  ( $23.9^{\circ}\text{C}$ ).

Salt	RH, %
$\text{NH}_4\text{HSO}_4$	40
$\text{NH}_4\text{NO}_3$	65
$\text{NaCl}$	75
$(\text{NH}_4)_2\text{SO}_4$	81



Experience has shown that our ability to predict what test to use when field failure data are not available falls well short of needs. In reality, the corrosion engineer must rely on past experience to make an educated judgment about potential failure scenarios and which accelerated-life-tests to run.

## UNIQUE ASPECTS OF TESTING

As has already been briefly discussed, the unique challenge facing the test engineer responsible for evaluating the effects of indoor atmospheres is the complexity of these environments. Each material or combination of materials and each product have unique considerations. The first step in deciding on a test protocol is to conduct a literature search on the atmospheric corrosion of each material. Consultations with experts in the corrosion of each material are also suggested. After establishing, as best possible, what the known corrosion tendencies are, the appropriate test(s) should be selected from among those described or referenced below.

At this time, the knowledge base and experience in conducting temperature/humidity testing (or temperature/humidity/bias for electronics) and corrosive gas testing is more developed than that for coarse and fine particles, organic vapors, and microbes. The test engineer should have little difficulty in finding a well-seasoned test procedure for accelerating the effects of temperature, humidity, and bias [8]. Unfortunately, for corrosive gas testing, there is still some disagreement among the various standards organizations about what combinations of corrosive gases are appropriate for each type of environment. A few of these tests, as will be outlined below, are in sufficiently widespread use to serve as acceptable evidence in most forums that a product will perform reliably in the intended use environments. Some national and regional standards organizations may insist that their test is the only acceptable test. Test engineers for companies with broad international sales may be required to perform several different tests.

Testing for the effects of particles is much less advanced than corrosive gas testing, but further along than organic vapors or microbial testing. A few proprietary, one-of-a-kind chambers have been developed for testing the effects of coarse particles. The typical dusts used in these tests include red china clay, fine sand, Arizona Road Dust, talc, silica, quartz, feldspar, fire extinguisher powder (usually sodium or potassium bicarbonate with additives to keep it free flowing), or some combination of ground materials that may include silica, calcite, iron oxide, alumina, gypsum, paper fibers, cotton fibers, polyester fibers, carbon black, and human hair. In a few cases, complex mixtures of ionic and water insoluble materials have been blended to produce a composition that resembles that of fine and coarse atmospheric particles combined. MIL-STD-810E, EIA Standard RS-364-50, proposed IEC Test L: Dust and Sand, and the published literature provide relevant background information.

With fine particles, work to develop test methods is just beginning. While experimental work in recent years has shown that these highly ionic particles can have severe

corrosion effects, especially for electronic equipment and devices [9], only in the past few years have test procedures and chambers been developed for evaluating effects [10,11]. These methods will be discussed below. Since only a few standards organizations have even recognized the need for fine particle testing, the test engineer has free reign in selecting a test. Often the most demanding customers only expect a good faith effort in demonstrating immunity to fine particle effects. Recent research may stimulate standards activity in the next few years. It should be noted that salt spray tests are usually too harsh for simulating fine particle effects in indoor environments, especially for electronics.

A valuable test, in conjunction with standard laboratory testing, is to deploy a prototype of the product in the harshest environment that can be found and to monitor and evaluate the performance of the materials for any early signs of unexpected behavior. High airflow velocity and elevated humidity will frequently provide even further acceleration. If unacceptable degradation is found that is representative of what would occur in a less severe environment, the originally selected laboratory tests should be re-evaluated to determine if they appropriately accelerate the observed condition.

Experience has shown that our best efforts to predict potential problem areas frequently miss the fatal flaws. For this reason it is advisable to perform at least one broad, severe corrosive gas test and one similarly harsh particle test, even if no obvious failure scenario can be envisioned that would be expected to be manifested through these tests. It is also helpful to stress the material or product sufficiently to produce significant corrosion or malfunction, even if this requires unrealistically harsh conditions. Such a test helps ensure that the designer understands the materials limitations and may indicate that the product is over-designed. Less resistant, less expensive materials may be sufficient for the intended use.

A danger in using extreme conditions is that unrealistic failures may occur. Several examples illustrate this hazard:

1. When testing the permeability of plastics or coatings to moisture and the possibility of corrosion of underlying materials, extreme humidity conditions, such as those present in steam bombs, can lead to unrealistic failures. An RH extreme that produces condensed water may result in degradation that would never occur in a field situation.
2. Many degradation processes are thermally activated. Use of extreme temperatures can give very high but unrealistic acceleration factors if there is a change in failure mechanism at the extreme condition. Further, if phase changes, e.g., recrystallization or plastic deformation, are induced that would not occur at the maximum conceivable operating temperature, the test may not give an accurate indication of material performance.
3. Breakdown of protective oxide films on many metals, e.g., aluminum, requires that environmental stresses exceed some threshold condition. Aluminum is likely to rapidly pit when exposed to high chloride concentrations at humidity levels sufficiently high to adsorb several monolayers of moisture. Most home and office environments do not cause these conditions.

4. In electronics, a common metallization used for connectors on printed wiring boards is copper with an overplate of nickel and then gold. Under most environmental conditions, the gold prevents oxidation of the underlying copper. However, if the conditions are harsh enough, very small pores that are always present even in the best quality commercial gold electroplates allow sufficient access to the underlying copper for it to oxidize. In time, the copper corrosion products creep over the surface of the gold, producing an insulating film and breaking the electrical integrity of the connection. Except for unfiltered air near pulp mills, oil fields, and similar extreme environments, gold-plated connectors have been used indoors for decades without experiencing harmful corrosion.

Testing of electronic equipment is particularly challenging because the degree of complexity is even higher than for most other indoor materials. The number of different materials typically ranges from dozens to hundreds and all the environmental influences discussed above are important. A detailed discussion is beyond the scope of this chapter. A recent review on testing of electronic components and assemblies covers this subject [10].

In fortunate cases, sufficient field and laboratory data are available and the failure mechanism is sufficiently well-understood to accurately determine acceleration factors. The corrosion rate of some metals, e.g., copper, silver, and nickel, can be accurately predicted for environments in which the major corrodents are  $\text{SO}_2$ ,  $\text{NO}_x$ ,  $\text{H}_2\text{S}$ , and  $\text{Cl}_2$ . (Note:  $\text{Cl}_2$  is too reactive to be a significant corrodent in field environments but is used in corrosive gas testing to simulate the effects of HCl and other corrosive chlorine-containing gases). The aging behavior (cracking, discoloration) of many plastics as a function of temperature, oxidant concentration, e.g., ozone, and sunlight can also be predicted with fair accuracy. In electronics, temperature/humidity/bias testing has reached a useful level of sophistication with respect to component testing and evaluation of plastic and hermetic packages for devices. Such testing is typically required by the customer as part of the data that go into evaluating the temperature/humidity performance of an entire assembly of electronic components.

In less fortunate cases, for example particle-related degradation, the best that can be done at this time is to compute acceleration factors for particle loading. How the rate of materials degradation brought on by gradual particle loading in field environments compares with the rate brought on by rapid loading in a test chamber is only beginning to be investigated. RH effects are widely agreed to be important in degradation induced by fine particles, but are not quantifiable at this time. The time-of-wetness (TOW) concept [12,13] can predict the corrosion rate of some metals in outdoor environments, but it is not applicable to most indoor environments where the RH is usually lower than that required for condensation to occur. A model that explains the dependence of surface conductance and electrical leakage of printed wiring boards as function of temperature and humidity exists [14], but it is not yet useful for predictions because the conductance also depends on the composition and amount of contamination on the surface in ways that are not fully understood.

Useful work on acceleration factors for degradation induced by organic vapors or microbes in indoor environments does not exist.

## IMPORTANT VARIABLES

The number of variables important to corrosion in indoor atmospheres is very large. The most important of these are: (1) the range and periodicity of temperature variations; (2) the range and periodicity of humidity variations; (3) the average and spread in concentration of corrosive gases such as  $\text{SO}_2$ ,  $\text{H}_2\text{S}$ ,  $\text{NO}$ ,  $\text{NO}_2$ ,  $\text{HNO}_3$ ,  $\text{HCl}$ , and organic acids; (4) the number concentration of coarse particles in air and their composition; (5) the number concentration, composition, ionic content, and CRH of fine particles; (6) microbial activity; (7) the concentration of organic vapors in air, their rate of condensation on surfaces, and their effects on surface wettability over time; (8) airflow velocity and turbulence; and (9) electric fields. Complicating all of these factors is the sequence of events that age the surface during the exposure. Some species may quickly reach a saturation concentration on the surface, while others will continuously accumulate over time (in the absence of cleaning). Many organic vapors are expected to saturate. Some corrosive gases initially reach an apparent saturation level but are then gradually consumed and replenished while residing on the surface. Other corrosive gases react with some materials as rapidly as they arrive at the surface until the material is consumed. All particles continuously accumulate on surfaces in the absence of mechanical effects or cleaning, though some components of the particles may react with the surface or some surface contaminants to form new products. Microbes may come and go depending on the nutrients available on the surface, relative humidity, and oxygen accessibility. The continuous accumulation of contaminants on indoor surfaces is an important difference from what occurs outdoors, where rain periodically removes components through solubilization or mechanical action.

Air velocity effects are frequently ignored in conducting life tests and in determining acceleration factors. This is unfortunate because, as discussed, the rate of arrival of gases and fine particles at surfaces depends on their rate of transport across the viscous boundary layer. The rate of transport increases rapidly as velocity increases and the boundary layer thickness decreases. Deposition velocities have been measured for enough different species and air velocities to reasonably estimate the deposition velocity for most situations of concern to the test engineer. The values given in Table 5 have been used by the author and colleagues [10] for approximate work, and are suggested as a guideline.

The two important points to recognize from this discussion of deposition velocity are: (1) the critical concentration parameter in accelerated life testing is not the airborne concentration but rather the surface arrival rate; (2) if airborne concentration is known, the surface arrival rate can be calculated from the equation: surface arrival rate = (airborne concentration)/(deposition velocity). Few workers in this field have evaluated the surface arrival rate of the corrodents in their test chambers. As long as airflow conditions

are constant and the corrosion rates of materials have been accurately standardized for the chamber, it is acceptable to base acceleration factors on airborne concentration. However, the test engineer needs to recognize that airflow velocities and turbulence can change dramatically with minor changes in the configuration of the exposure apparatus. Insistence on using airborne concentration instead of surface arrival rate also means that results from different chambers are not comparable. Much of the disagreement among test groups when round robin tests have been run can possibly be attributed to this factor.

## LABORATORY TESTING

### Testing for Thermal, Humidity, and Bias Effects

Thermal, humidity, and bias testing can be done individually or in any combination. Simple thermal testing without humidity or bias is usually done in conjunction with a mechanical stress or as a temperature cycling experiment. Both of these are intended to evaluate the effects of mechanical stress on materials degradation. These kinds of tests are covered in other chapters of this book. Occasionally, materials may be exposed to elevated temperature for extended periods to uncover instabilities like phase segregation, recrystallization, or oxidation under ambient conditions. Ambient in this case means room air with whatever contaminants may be present. The assumption is that oxygen or moisture in the air dominates any oxidation process and that the contaminating components have negligible effect. These tests are straightforward, usually follow Arrhenius behavior, and will not be discussed further.

Humidity testing is nearly always carried out at temperatures ranging from 351–100°C with relative humidity from nearly zero to 100 %. Occasionally, steam bombs are used so tests can be run above 100°C. In the last ten years, highly accelerated stress tests have been developed to enable materials to be tested at temperatures above 100°C, but at a non-condensing relative humidity, typically 85 %. The most common applications for these tests are in evaluating coatings, paper, adhesives, adhesion between mechanically or chemically bonded materials, and, in electronics, for evaluating the effectiveness of device encapsulation.

Bias is frequently added for testing of electronic devices, printed wiring boards, and assemblies of electronic equipment. The 85°C, 85 % RH, bias test has been the predominant one in electronics for many years [8]. While it sometimes misses failure mechanisms that later occur in the field, it also finds many weak points in new products. It is especially useful for quality control of seasoned devices for which long-term reliability is known to be high if the product passes this test. There are many commercial suppliers of temperature/humidity/bias test chambers and software is widely available to automate the operation, data collection, and data interpretation. Attention to data management is mandatory when hundreds of devices are tested simultaneously. This is frequently required in electronics to obtain sufficient data to make statistically valid predictions of lifetime and failure rate under use conditions.

### Corrosive Gas Testing

Corrosive gas testing became commonplace in the mid-1970s as a result of the need of the electronics industry to reduce the cost of materials used as electrical contacts on connectors and as conducting pathways on various kinds of insulating substrates. Studies at IBM [15–18] and Battelle [19] played a key role in the development of this technology. Studies at both institutions compared laboratory data to field data and achieved results in the laboratory that accurately reproduced field results. Field exposures of 20 years can be simulated in 5–30 days in the laboratory. Based on metal coupon exposures and simultaneous air pollutant measurements from over a hundred locations around the world, a four-level environmental classification scheme for environmental severity, which is now in common use around the world, was developed by the industry-sponsored Battelle group.

Differences of opinion have existed for decades with respect to the mixture of corrosive gases that should be used in test chambers. For air-conditioned electronic equipment rooms in urban environments that are well removed from industrial pollution (Class II Battelle environment, G1 IBM environment, and IEC Class II environment), the appropriate Battelle accelerated life test calls for use of 200 ppb NO<sub>2</sub>, 10 ppb H<sub>2</sub>S, and 10 ppb Cl<sub>2</sub> at an RH of 70 %. This test does an excellent job of simulating corrosion films on silver, copper, tin, and some gold-plated metals, but has been criticized in recent years because the films it produces on nickel are unrealistic.

Several groups, including Siemens and Bellcore, now prescribe a four-gas test that does a better job of simulating nickel corrosion. Their test gas contains 200 ppb NO<sub>2</sub>, 10 ppb H<sub>2</sub>S, 10 ppb Cl<sub>2</sub>, and 200 ppb SO<sub>2</sub>. Bellcore calls for a RH of 70 %, while Siemens stipulates 75 %. Standard setting organizations have not agreed on a standard test for electronic equipment, but the engineer can use the Battelle test with a high degree of confidence for silver, copper, and tin, and the Siemens or Bellcore test for nickel.

The greatest difficulty in using corrosive gas tests comes in deciding how to test entire assemblies of equipment, rather than just the metallization schemes used for connectors, and in evaluating equipment for those indoor environments where the RH may reach close to 100 %. The Battelle, Bellcore, and Siemens test conditions are intended for simulations of metals that will be used in office buildings, homes, and other air-conditioned environments. Enclosed environments such as sheds, utility huts, and non-air-conditioned manufacturing environments are more like outdoor than indoor environments with respect to RH. Standardized test conditions are not available. At this time, the test engineer has little alternative but to use the conditions that work for metals in indoor environments to cover all “enclosed” environments.

Suggested test conditions that cover both “indoor” and “outdoor” environments are given in Table 7. It can reasonably be argued both for and against using the same humidity for indoor and outdoor testing. Since most chambers have been set up to operate stably at 70 or 75 % RH, one possible approach is to do all corrosive gas exposure testing at this RH but, for outdoor simulations, to follow the

**TABLE 7**—Corrosive gas test conditions.

Location	Atmosphere	Test Duration, days
Indoors (Environmentally Controlled)	25°C, 75 % RH, 10 ppb Cl <sub>2</sub> , 10 ppb H <sub>2</sub> S, 200 ppb NO <sub>2</sub> , 200 ppb SO <sub>2</sub> , balance air	10
Outdoors <sup>a</sup> (Uncontrolled)	25°C, 75 % RH, 10 ppb Cl <sub>2</sub> , 10 ppb H <sub>2</sub> S, 200 ppb NO <sub>2</sub> , 200 ppb SO <sub>2</sub> , balance air	20

<sup>a</sup>Subsequent to the corrosive gas exposure, equipment intended for outdoor use should be exposed to cyclic high/low humidity (95/20 % RH) with the equipment powered. An appropriate exposure sequence is 12 h high, 12 h low for 20 days.

corrosive gas exposure with a cyclic RH exposure that covers the full range of expected outdoor conditions. Some would also argue that a factor of 2 difference in exposure time to the environments indicated in Table 7 for indoor and outdoor testing is insufficient. For the harshest environments, the test engineer needs to make a best judgment estimation of the proper test duration. With mechanical and electronic equipment and assemblies, it is also essential to undertake a complete series of functional tests following the testing prescribed in Table 7. Typically, the functional testing should be undertaken in a chamber in which RH is cycled during the testing over ranges representative of the expected use environment. It may also be desirable to undertake the testing at elevated temperature. For electronics, 85°C is frequently used.

Helpful guidance for conducting corrosive gas tests is provided in ASTM B 827, Practice for Conducting Mixed Flowing Gas (MFG) Environmental Tests. Proper technique for use of metal coupons for calibrating chambers is described in ASTM B 810, A: Test Method for Calibration of Atmospheric Corrosion Test Chambers by Change in Mass of Copper Coupons and other references [20–23]. A guide to commonly used gas mixtures and their historical significance is given in ASTM B 845, B: Guide for Mixed Flowing Gas (MFG) Tests for Electrical Contacts.

Occasionally failure mechanisms in the field are encountered that suggest the use of simpler one component gas tests. For example, design engineers for electronic equipment like to use fired silver paste to produce low-cost conductor patterns on insulating substrates. Silver is susceptible to silver migration under conditions of elevated humidity and bias. The presence of a reduced sulfur gas greatly accelerates the formation of metal dendrites between oppositely biased conductors. This condition eventually leads to short circuits. The susceptibility of these devices to silver migration can be easily evaluated using a simple bell jar with a feedthrough for supplying bias to the circuit pattern, a salt solution for achieving humidity control (described below), and elemental sulfur as the source of reduced sulfur. The test is typically run at 50°C. Elemental sulfur is much easier and safer to work with than hydrogen sulfide.

Exposure to organic vapors, when needed to simulate degradation of a plastic or perhaps change the wettability of a surface, can also be conducted in a simple bell jar. In this case it may be desirable also to collect material on a

quartz crystal microbalance to monitor absorption rate and possible saturation.

Whether these corrosive gas tests are realistic for materials other than those used for connectors or for operating electronic equipment is not clear. The test should be carried out, but the observation of no failures should not be taken to mean there will be no field failures in typical urban environments. Similarly, any failures that are observed should be carefully evaluated to ensure that the same mechanism would be operative in field situations. Connectors are a somewhat unique part of an electronic assembly in that the active part is frequently a noble metal and the sensitivity of the mated surfaces to failure may be lower than many other parts of electronic assemblies. Most failures in electronic assemblies attributable to the environment are due to ionic particle contamination in conjunction with atmospheric moisture. In 20 years of evaluating field failures in the United States, the author has never seen a failure that could be attributed to the effects of SO<sub>2</sub>, has seen a few caused by H<sub>2</sub>S or HCl, has heard of a few caused by NO<sub>x</sub>, and has seen several hundred that were caused by ionic contamination. Clearly, valid accelerated testing of electronic components, circuit boards, and assemblies must include ionic contamination. Emerging methods are discussed in the Fine Particle Testing section in this chapter.

### Coarse Particle Testing

Occasionally, some materials have been subjected to coarse particle dust tests in which the test dust is frequently a “real world” standard material such as Arizona Road Dust, talc, silica, or other mineralogically-derived substances, as discussed above. MIL-STD-810E, EIA Standard RS-364-50, proposed IEC Test L: Dust and Sand and the published literature provide relevant background information. Typically, the test dust is dispersed by mechanical means into a rapidly moving air stream that is directed at the test specimen. Internationally recognized standards for indoor coarse particle testing are not likely to be available for many years. Most of the existing or emerging tests use particle sizes much larger than would likely be encountered in indoor environments, except perhaps for some manufacturing processes. While typical indoor dust particles are within the size range 2.5–15 µm, many of the suggested tests use particles that span the size range 1–150 µm. Some standards prescribe that 100 % of the dust pass through a minimum screen size of 100 mesh (149 µm). MIL-STD-810E, Method 510.2, Sand and Dust considers sand particles in the size range 140–850 µm. The transport characteristics of these very large particles in an air stream, and their penetrability into narrow spaces, are very unrealistic of real indoor coarse particles.

In a typical test apparatus, coarse particles are mechanically injected into a rapidly moving air stream that is projected at the equipment undergoing the test. Deposition is largely by gravitational settling with some inertial impaction. A commonly encountered problem with this kind of test is that the dust tends to collect at certain points in the chamber, depending on how and where the dust is dispersed and how the test piece disturbs the airflow. Typically, the dust collects in thick deposits on some parts of the

test piece but hardly deposits on other parts. Recent failures of mechanical assemblies in wind-swept deserts, despite best efforts to harden the equipment against the effects of coarse dust through experiments in coarse particle test chambers, have had tragic consequences. These methods are fraught with difficulty that test engineers need to take into account when deciding on the confidence level of the result.

In electronics, these kinds of tests have been used to evaluate the effects of coarse particles on the insulation resistance of connectors. When the tests are done with the connectors mated, the connectors are sometimes vibrated in an attempt to drive particles into the interface. In other cases the connectors are exposed unmated. After exposure they are mated and the resistance is measured. Sometimes these tests are carried out iteratively, or multiple insertion cycles are undertaken to evaluate the ability of the contact metal (typically a gold or other noble metal finish) to withstand the abrasion from coarse particles. Acceleration factors either are not determined or, if they are, the confidence level is low because they are based on tests as simple as the weight gain of metal coupons. Under fortunate circumstances, these tests may point out opportunities for design changes that extend life, at least in a qualitative way.

Following coarse particle deposition on the surfaces of test specimens or equipment, a full series of surface characterizations and functional tests should be carried out. Ideally, testing of mechanical or electrical performance is carried out in-situ during particle deposition but frequently this is not practical. Since coarse particles usually have low chemical reactivity, post-deposition testing usually produces realistic results. In some cases it may be advantageous to carry out an iterative series of particle depositions followed by functional tests (mechanical and electrical).

In the absence of a widely accepted test suitable for indoor environments, the test engineer will have to use best judgment in deciding how to carry out coarse particle testing. Fortunately, the effects of coarse particles indoors are usually small.

### Fine Particle Testing

Physical designers are just now becoming aware of the need to harden materials and products against the effects of submicron particle contamination. Bellcore [24] recently suggested a test for simulating the electrical leakage effects on circuit boards of ionic contamination derived from particles. The test is intended to simulate the effects of fine particle deposition, though it uses an atomized spray of an aqueous solution to deposit the contamination.

Development of a suitable test chamber for evaluating the effects of submicron particles on indoor surfaces, including electronic equipment and devices, requires: (1) the capability to produce suspended ionic particles that accurately simulate the composition and size distribution of airborne particles responsible for the observed effects; (2) designing a chamber that combines continuous air-recirculation, filters out all background and once-through particles, and provides parallel airflow with uniform particle concentration over the flow cross section of the test area; (3) fabrication and evaluation of suitable test samples or devices; and

(4) for electronics, understanding what environmental factors cause electrical leakage and arcing. Over the last 20 years, the author and colleagues have been gradually and somewhat serendipitously acquiring this expertise [9].

In the mid-1980s, experiences with field failures in electronic equipment made it clear that existing accelerated test methods were inadequate for discovering failure processes caused by fine particle deposition. A method was needed to apply a realistic layer of particles on circuit boards or test substrates to answer questions such as: (1) Are the line separations and circuit voltages in a particular design safe with respect to electrical leakage or arcs that may occur on particle-contaminated surfaces? (2) Are pore defects in cover coats on substrates of sufficiently high density to present a significant risk of component damage due to electrical leakage or arcs between leads on components and metal lines running under the covercoat? (3) Will electric fields near components substantially accelerate deposition of fine particles? (4) What level of atmospheric moisture (RH) produces a sufficiently thick electrolyte film on particle-contaminated surfaces to observe soft electrical defects, e.g., cross talk, or, in the worst case, component failure?

Over the last several years, a series of methods for depositing particles on surfaces that are representative of submicron atmospheric particles has been developed. The first uses a synthetic dust produced by grinding. The finely ground dust is then mechanically dispersed on the test substrate. This test is useful for solving field problems because it is quick. The limitations in using this dust are: (1) the particle size is too large, so that gravitational settling dominates the deposition process; and (2) deposition on partially shielded surfaces, especially vertical and top-side horizontal surfaces, is inadequate. To overcome this problem, a recirculating chamber with a continuous feed stream of submicron atmospheric-like particles was developed. The details of these two methods are described in the following sections.

### Ground Synthetic Dust Mixture

Hand-grinding of a mixture of ammonium sulfate, ammonium bisulfate, sodium chloride, potassium bicarbonate, and talc in dry nitrogen produces a dust that can readily be dispersed onto test substrates. The resulting particles are typically 1–5  $\mu\text{m}$  in diameter. A typical composition is shown in Table 8. The composition of the dust can be adjusted to match the electrical leakage properties on circuit boards of fine particle dust found in telecommunications switching equipment centers [9]. Two methods of dispersion were found to be effective: (1) blasting a high-pressure stream of dry nitrogen into a dust-filled container with circular perforations in the top; and (2) applying the dust from a salt shaker or sieve. Subsequent exposure of an

**TABLE 8**—Composition of synthetic dust.

Component	Weight, g
Talc	66
$\text{NaHCO}_3$	1
KCl	1
$\text{NH}_4\text{HSO}_4$	3
$(\text{NH}_4)_2\text{SO}_4$	29

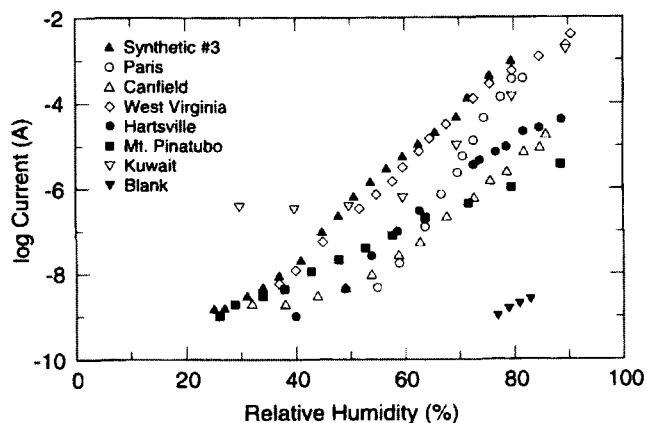


FIG. 1—Leakage current as a function of RH, showing exponential dependence. The Blank is a clean circuit. Synthetic No. 3 is a finely ground mixture of the dust, as described in Table 7. Paris, Canfield, West Virginia, and Hartsville are U.S. sites. Mt. Pinatubo is volcanic ash collected at the time of the 1991 eruption. Its low dependence on RH is explained by its lower fraction of water-soluble ionic material. Kuwait dust was collected at the height of the oil fires in 1991. Its high conductivity at low RH is caused by its high graphitic carbon content.

interdigitated test substrate to an air environment in which the RH was gradually increased from 20–85 % produced a slow increase in the electrical leakage current until the CRH of ammonium sulfate (81 %) was reached, at which point the leakage current increased rapidly. This behavior was similar to the exponential dependence of surface conductance on RH seen for many different samples of atmospheric dust from locations all over the United States, as seen in Fig. 1. With the synthetic dust, it is possible to vary the effective CRH over the range of 40–81 %, depending on the relative amounts of ammonium sulfate (CRH of 81 %) and ammonium bisulfate (CRH of 40 %).

### Test Chamber for Fine Particles

A new, more realistic approach for fine particle dust testing is to disperse water-soluble, hygroscopic salts representative of those found in fine environmental particles into a chamber that is designed to provide uniform airflow of otherwise particle-free air across a rack of circuit boards [11]. Generation of submicron particles is achieved by atomizing an aqueous solution of the appropriate salt, followed by thorough drying of the resulting aerosol laden air stream. A picture of the dust generator and the dust chamber is shown in Fig. 2.

The specifications for the chamber are: particle size, 0.01–1  $\mu\text{m}$ ; particle concentration,  $1 \times 10^{10}/\text{m}^3$ ; flow velocity, 35 m/min; parallel airflow; and uniform dust concentration. The air velocity is similar to that found in forced-air-cooled telecommunications equipment cabinets. Air is re-circulated upwards through the chamber. Particles are introduced into the chamber at a point above a HEPA filter that removes the particles with 99.9995 % efficiency at

FIG. 2—Photograph of the fine particle exposure chamber with the HEPA filter and controls underneath and particle generation equipment at the right. The funnels are part of the distribution system. The two racks in the upper part of the chamber can hold up to 48 circuit boards.

0.12  $\mu\text{m}$  after they have made one pass through the chamber. With a 60 by 60 cm cross section and a height of 110 cm, the chamber is sufficiently large to hold a rack that supports up to 48 circuit boards. The HEPA filter, which is situated immediately below the chamber, and a screen just above the filter ensure that the airflow in the chamber is parallel to the vertical walls. The air velocity can be controlled at speeds up to 36 m/min.

Submicron (0.01–1  $\mu\text{m}$ ) ionic particles, such as ammonium sulfate, are generated from an aqueous solution of the salt by compressed high-purity, filtered air in an atomizer. The aerosol droplets are dried by a stream of preheated air. Residual moisture is removed from the particles by passing them through a diffusion dryer. Since the particles are highly charged when they exit the atomizer, they are neutralized with a Kr-85 source, which brings them to a Boltzmann equilibrium. The average size of the particles varies as the cube root of the solution concentration.

The particles are introduced into the exposure chamber through a 16-nozzle distribution system that was designed to give a uniform concentration of particles throughout the chamber. This was achieved by having all particles travel the identical distance and encounter the same type of obstructions and turns. The distribution system is made

from type 316 stainless steel the interior of which has been electropolished to minimize particle deposition and shedding. Steady-state conditions in the chamber are achieved by recirculating the air while constantly introducing new particles immediately downstream from the HEPA filter.

The air velocity distribution, measured at 49 points over the cross section of the chamber at a height corresponding to the middle of the rack that holds the specimens, exhibited an average speed of 38.2 m/min with a standard deviation of 10.6 m/min. The concentration of  $(\text{NH}_4)_2\text{SO}_4$  particles generated from a 0.01 M solution of the salt was found to be quite uniform over the cross section of the chamber (see Fig. 3). Variation of the deposition rate to surfaces being tested is accomplished by regulating the airflow velocity.

From the compositional data for Eastern Asia (Table 4), we know that airborne concentrations and surface deposition rates are substantially higher than those in the U.S. One approach to simulating the worst-case environment for Eastern Asia is to reduce the ammonium to sulfate ratio of the ground dust mixture. However, hand grinding salt mixtures is a tedious process that must be carried out in a dry box. A more appropriate approach for high volume testing is to use the fine particle test chamber. In this approach the proportions of ionic substances used for the Test Dust #3 are dissolved in water at a concentration that appropriately simulates a worst-case hazard for the environment under study based on comparing the surface conductance versus RH behavior of test dusts with the behavior of samples from the field. The amount of salt to be deposited is determined from knowledge of the worst-case environmental conditions and the expected lifetime of the component. Typically, airborne sulfate concentrations are used to estimate the expected deposition over the product life. The sulfate deposition rate in the field is estimated by multiplying the worst-case airborne sulfate concentration by the deposition velocity appropriate for the airflow rate across the component. For example, the highest sulfate concentration in this work was  $8.0 \mu\text{g}/\text{m}^3$ . Presuming the component is cooled by forced-air with a linear velocity of 250 cm/s, the appropriate deposition velocity is 0.6 cm/s.

For a lifetime of 20 years, the sulfate accumulation is expected to reach  $3000 \mu\text{g}/\text{cm}^2$ . (It should be noted that electric fields can increase this deposition rate by as much as 100 but this effect is ignored here.)

Following particle deposition, the test specimens should be evaluated in a temperature/humidity environmental chamber. With electronic equipment, bias should be applied to the specimen as well, and the device or equipment assembly should undergo a full series of functional tests.

While this method of testing is new and still being refined, it has been demonstrated to accurately simulate the deposition and electrical effects of fine particle dust as are found in a forced-air-cooled equipment frame. The resulting electrical effects on circuit boards and equipment assemblies are comparable to those found in field environments. This approach was found quite effective for testing the sensitivity of circuit boards intended for use in Eastern Asia to electrical leakage, and to evaluate the effectiveness of covercoats in preventing leakage. At the very least, use of this test demonstrates a state-of-the-art goodwill effort to show that equipment will operate reliably in the presence of fine, hygroscopic dust. The acceleration factor for fine particle deposition is about 200, depending on the surface area and configuration of the equipment undergoing test.

## FIELD TESTING

### Temperature, Humidity, and Dewpoint Monitoring

Since relative humidity plays such a key role in the corrosiveness of many environments, it is always desirable to monitor the interrelated humidity factors: temperature, humidity, and dewpoint temperature. Since reliable commercial equipment is widely available, it will not be discussed further. Closely related to dewpoint is time-of-wetness (TOW), which is measured by monitoring the resistance between oppositely biased electrical conductors as a function of relative humidity. Bias can be applied through an external power source [12]. Alternatively, adjacent metal conductors can be selected to have substantially different corrosion potentials [13]. Above a critical level of relative humidity, the test specimen will adsorb a sufficient amount of moisture to produce a sharply lower resistance between conductors. The fraction of time of lowered resistance is commonly referred to as the time-of-wetness. It is one useful measure of the corrosivity of an environment. Such measurements were popular in the 1960s and 1970s. More recently, the preferred measurement, due to ease of use, is fraction of time the dewpoint is reached. A procedure for measuring time-of-wetness is contained in ASTM G 84, Standard Practice for Measurement of Time-of-Wetness on Surfaces Exposed to Wetting Conditions as in Atmospheric Corrosion Testing.

### Metal Coupon Exposures

Relating laboratory exposures to field results is commonly accomplished through metal coupon tests. Three extensive studies of this type are described in Refs 16, 17,

**FIG. 3—Particle concentration distribution profile across the exposure chamber at the middle height of the test rack for particles within the approximate size range 0.018–0.032  $\mu\text{m}$ .**

19, and 25. While the results are only appropriate for validating the corrosion testing of the metals undergoing test, they are frequently used as an indication of test validity for all types of materials and functional assemblies. This leap of faith is usually necessitated by resource limitations. Environmental classifications that have been developed, e.g., the Battelle Class I-IV [19] or the IBM G1-G3 [18] environments, are a way of categorizing the severity of corrosion and the composition of corrosion products that are expected for the full range of environments found in the world, and for selecting appropriate test conditions to simulate these environments in the laboratory. The standard coupons used to classify environments using the Battelle scheme are: (1) a plated metallization consisting of porous gold over nickel over copper, and (2) unprotected copper. The Battelle Classifications, in order of increasing corrosion rate, are as follows:

Class I—No significant corrosion observed.

Class II—Mild pore corrosion of Au/Ni/Cu with chloride, oxide, and smaller amounts of sulfide in the corrosion product; corrosion product on unprotected copper contains oxide and chloride.

Class III—Pore and creep corrosion of Au/Ni/Cu with major amounts of sulfide, chloride, and oxide in the corrosion product; corrosion product on unprotected copper is rich in sulfide and oxide.

Class IV—Severe creep corrosion of Au/Ni/Cu with major amounts of sulfide, oxide, and chloride in the corrosion product; corrosion product on copper is primarily a sulfide film with some oxide.

### Measurements of Corrosive Gas Concentrations

The most commonly used method to measure the concentrations of corrosive gases in field environments is to adsorb the gases on chemically treated filter paper, sometimes followed by a water extraction or chemical treatment, and then to determine the composition and quantity spectroscopically. IBM [15] developed a stacked canister sampler that was adapted for use in the Battelle studies [19]. Each element in the canister stack collects a specific pollutant. The canisters are easily deployed anywhere in the world, the only inconvenience being that an air pump is required to draw a well-controlled air volume. The reliability of these pumps, based on the author's experience, is less than desirable but adequate. A similar technique, developed largely under the sponsorship of the U.S. EPA, is the "denuder" tube. This method is also based on species-specific absorption of pollutants on a chemically treated surface, but in this case a permanent honeycomb substrate is mounted inside a tube. For field sampling, the tubes are stacked, the number depending on the number of species to be analyzed. Airflow pumps are also required in this approach. While this method is more cumbersome than the IBM/Battelle canisters, all the equipment and follow-up chemical analysis can be obtained commercially.

The advantage of these adsorption methods is that the expensive analytical equipment remains in the laboratory. With all these methods, however, the sample integration period is typically days to weeks. The resulting average

concentration provides no information on variations or daily maxima, which may be important for some degradation phenomena, particularly where thresholds are important. If such measurements are required, equipment is commercially available for determining low ppb concentrations of common pollutants like SO<sub>2</sub>, NO<sub>x</sub>, O<sub>3</sub>, and H<sub>2</sub>S, though at a much higher cost than for the absorption methods. Unfortunately, no practical instruments are available for real-time measurements of corrosive chlorine-containing gases at the low ppb level.

### Measurements of Fine and Coarse Particle Concentrations

Because of the health implications of airborne particles, a large number of techniques has been developed in recent years for sampling fine and coarse particles. The most sophisticated, a high-volume cascade impactor, can separate particles into five or more size classifications between about 0.1 and 15 µm. These instruments are labor-intensive and usually provide much finer detail than is needed for evaluating environmental severity with respect to particles.

Two other sampling methods are preferred by the author. The least expensive and simplest to use is a plastic cassette containing filter paper that is connected to a low-volume sampling pump. A convenient filter and cassette size is 37 mm. Both are commercially available. The typical air sampling rate is 1–3 L/min. Particle mass concentration is determined gravimetrically, while composition can be determined by X-ray fluorescence, ion chromatography (preceded by water extraction), or other common laboratory techniques. Commercial analytical laboratories can also perform these techniques. This method provides the volumetric concentration (mass and individual components) of total suspended particulates (usually referred to as TSP). TSP is often sufficient for the experienced evaluator to gage relative corrosivity of all particulates. The disadvantage of this method is that no distinction can be made between fine and coarse particles. As has been discussed, fine particles tend to be the most corrosive, while coarse particles tend to be insulating and abrasive. Knowing the fraction of each and the chemical components of each fraction provides a more accurate assessment of the degradation hazard.

The equipment most commonly used for separating fine and coarse particles is a dichotomous sampler. Again, particles are collected on filter papers and the analysis is accomplished in the same way. The typical sampler operates at high airflow velocity (about 17 L/min, depending on the design) so that sufficient sample can be collected in hours to days, compared to days or weeks for the TSP sampler. The drawback of this method is that the sampling equipment is too large to conveniently ship as an ordinary parcel and requires a trained operator to set it up properly.

## STANDARDS

MIL-STD-810E-14 July 1993-Environmental Test Methods and Engineering Guidelines—Pressure, temperature, temperature shock, solar radiation, rain, humidity, fungus, salt fog, sand and dust, explosive atmospheres, acceleration,



vibration, acoustic noise, shock, temperature/humidity/vibration/altitude.

Electronic Industries Association Standard RS-364-50, Test Procedure No. 50 Sand and Dust Test Procedure for Electrical Connectors, Electrical Industries Association, Washington, DC, 7 October 1983.

European Telecommunications Standards Institute, Environmental Conditions and Environmental Tests for Telecommunications Equipment: Part I-Introduction and Terminology, Document prETS 300 019-2; Part II-Classification of Environmental Conditions, Document prETS 300 019-2; Part III-Specifications of Environmental Tests, Document prETS 300 019-3. ETSI Secretariat, Valbonne, France.

International Electrotechnical Commission, Environmental Testing, Part 2: Test Ke: Corrosion Tests in Artificial Atmosphere at Very Low Concentration of Polluting Gas(es), Document 68-2-60 TTD, Bureau Central de la Commission Electrotechnique Internationale, Geneva, 1990.

ASTM B 810, Test Method for Calibration of Atmospheric Corrosion Test Chambers by Change in Mass of Copper Coupons.

ASTM B 827, Practice for Conducting Mixed Flowing Gas (MFG) Environmental Tests.

ASTM B 845, Guide for Mixed Flowing Gas (MFG) Tests for Electrical Contacts.

## REFERENCES

- [1] Vernon, W. H. J., *Transactions of the Faraday Society*, Vol. 31, 1935, p. 1668.
- [2] Shields, H. C. and Weschler, C. J., "Volatile Organic Compounds Measured at a Telephone Switching Center From 5/30/85-12/6/88: A Detailed Case Study," *Journal of Air Waste Management Association*, Vol. 42, 1992, pp. 792-804.
- [3] Sinclair, J. D., Psota-Kelty, L. A., Peins, G. A., and Ibidunni, A. O., "Indoor/Outdoor Relationships of Airborne Ionic Substances: Comparison of Electronic Equipment Room and Factory Environments," *Atmospheric Environment*, Vol. 26A, 1992, p. 871.
- [4] Sinclair, J. D., Psota-Kelty, L. A., Weschler, C. J., and Shields, H. C., *Atmospheric Environment*, Vol. 24A, 1990, p. 627.
- [5] Donovan, R. P., Locke, B. R., Osburn, C. M., and Caviness, A. L., *Journal of the Electrochemical Society*, Vol. 132, 1985, p. 2731.
- [6] Nelson, G. O., *Controlled Test Atmospheres*, Ann Arbor Science Publishers, Inc., Ann Arbor, MI, 1972.
- [7] Lide, D. R., *Handbook of Chemistry and Physics*, 71st ed., CTC Press, Inc., Cleveland, OH.
- [8] *Microelectronics Packaging Handbook*, R. R. Tummala and E. J. Rymaszewski, Eds., Van Nostrand Reinhold, NY, 1989, pp. 629-649.
- [9] Comizzoli, R. B. and Sinclair, J. D., "Electronic Components and Assemblies: Reliability and Testing," *Encyclopedia of Applied Physics*, Vol. 6, VCH Publishers, Inc., 1993.
- [10] Comizzoli, R. B., Frankenthal, R. P., Lobnig, R. E., et al., "Corrosion of Electronic Materials and Devices by Submicron Atmospheric Particles," *The Electrochemical Society Interface*, Vol. 2, No. 3, 1993, pp. 26-33.
- [11] Frankenthal, R. P., Siconolfi, D. J., and Sinclair, J. D., "Accelerated Life Testing of Electronic Devices by Atmospheric Particles: Why and How," *Journal of the Electrochemical Society*, Vol. 140, 1993, pp. 2134-3129.
- [12] Sereda, P. J., ASTM Bulletin No. 246, 1960, p. 47; *Corrosion in Natural Environments*, ASTM STP 558, ASTM International, West Conshohocken, PA, 1974, p. 7.
- [13] Mansfeld, F. and Kenkel, J. V., "Electrochemical Measurements of Time-of-Wetness and Atmospheric Corrosion Rates," *Corrosion-NACE*, Vol. 33, 1977, pp. 13-16.
- [14] Comizzoli, R. B., "Surface Conductance on Insulators in the Presence of Water Vapor," *Materials Developments in Micro-electronic Packaging Conference Proceedings*, Montreal, Quebec, Canada, 19-22 August 1991, pp. 311-316.
- [15] Rice, D. W., Cappell, R. J., Kinsolving, W., and Laskowski, J. J., "Indoor Corrosion of Metals," *Journal of the Electrochemical Society*, Vol. 127, 1980, pp. 892-901.
- [16] Rice, D. W., Phipps, B. P. B., and Tremoureux, R., "Atmospheric Corrosion of Cobalt," *Journal of the Electrochemical Society*, Vol. 129, 1979, pp. 1459-1466.
- [17] Rice, D. W., Phipps, B. P. B., and Tremoureux, R., "Atmospheric Corrosion of Nickel," *Journal of the Electrochemical Society*, Vol. 127, 1980, pp. 563-568.
- [18] Gore, R. R., Witska, R. W., Kirby, J. R., and Chao, J. L., "Corrosive Gas Environmental Testing for Electrical Contacts," *IEEE Transactions on Components, Hybrids, and Manufacturing Technology*, Vol. 13, 1990, pp. 27-32.
- [19] Abbott, W. H., "The Development and Performance Characteristics of Mixed Flow Gas Test Environment," *IEEE Transactions on Components, Hybrids, and Manufacturing Technology*, Vol. 11, 1988, pp. 22-35.
- [20] Schubert, R., "A Second Generation Accelerated Atmospheric Corrosion Chamber," *Degradation of Metals in the Atmosphere*, ASTM STP 965, ASTM International, West Conshohocken, PA, 1988, pp. 374-384.
- [21] Schubert, R. and Neuberger, G. G., "Rapid Determination of Corrosion Chamber Uniformity," *Journal of the Electrochemical Society*, Vol. 137, 1990, p. 1048.
- [22] White, L., *Proceedings of the 33rd IEEE Holm Conference*, Electrical Contacts, 1982, p. 87.
- [23] Denure, D. G. and Sproles, E. S. Jr., *IEEE Transactions on Components, Hybrids, and Manufacturing Technology*, Vol. 14, 1991, p. 802.
- [24] Sandroff, F. S. and Burnett, W. H., "Reliability Qualification Test for Circuit Boards Exposed to Airborne Hygroscopic Dust," *Proceedings of the Electronic Components and Technology Conference*, San Diego, CA, May 1992, pp. 1-6.
- [25] Kucera, V., Coote, A. T., Henriksen, J., et al., *Proceedings*, 11th International Corrosion Congress, Florence, Vol. 2, 1990, p. 433.

# Seawater

David A. Shifler<sup>1</sup> and Denise M. Aylor<sup>1</sup>

## INTRODUCTION

SEAWATER IS AN AGGRESSIVE, complex fluid that affects nearly all common structural materials to some extent [1]. There are two competing processes that operate simultaneously in seawater environments: (1) the chloride ion activity, which tends to destroy the passive film, and (2) dissolved oxygen, which acts to promote and repair the passive film on metallic materials of construction [2]. Metals and alloys that develop protective films by the formation of thin metal oxides can have the formation of passive films delayed or have films destroyed by chloride ions in seawater [3].

The type of corrosion testing required depends on the extent and type of information desired and the environmental conditions expected in service for an alloy component. Seawater corrosion is dependent on a number of factors including, but not limited to, alloy composition, water chemistry, pH, biofouling, microbiological organisms, pollution and contamination, alloy surface films, geometry and surface roughness, galvanic interactions, fluid velocity characteristics and mode, oxygen content, heat transfer rate, temperature, and the environmental zone to which the material is exposed. Understanding how these factors may affect experimental results can help the design of seawater corrosion testing to minimize experimental variations and to best simulate service conditions.

## DESCRIPTION OF THE SEAWATER ENVIRONMENT

### Composition

Seawater, the Earth's most abundant resource, covers 71 % of the Earth's surface. This electrolyte approximates a 3.5 weight percent sodium chloride solution but it is much more complex, containing almost all naturally occurring elements [4,5]. The major chemical constituents of seawater, listed in Table 1, are consistent throughout the world [1]. The minor constituents, including dissolved trace elements and gases, can vary substantially due to seasonal changes, storms, or tidal cycles. Biological organisms, which, combined with the minor constituents, often control

**TABLE 1**—Major seawater constituents at (35 parts per thousand (‰) salinity) and 25°C [1].

Ion or Molecule	Concentration	
	mmol/kg	g/kg
Na <sup>+</sup>	468.5	10.77
K <sup>+</sup>	10.21	0.399
Mg <sup>+2</sup>	53.08	1.290
Ca <sup>+2</sup>	10.28	0.4121
Sr <sup>+2</sup>	0.090	0.0079
Cl <sup>-</sup>	545.9	19.354
Br <sup>-</sup>	0.842	0.0673
F <sup>-</sup>	0.068	0.0013
HCO <sub>3</sub> <sup>-</sup>	2.30	0.140
SO <sub>4</sub> <sup>-2</sup>	28.23	2.712
B(OH) <sub>3</sub>	0.416	0.0257

the rate of the corrosion reactions occurring on metals in seawater [1,5,6]. In addition, the concentration of seawater can vary from full strength ocean water to coastal seawater or brackish conditions. The type of corrosion and the corrosion rate occurring on metals and alloys in seawater are highly dependent on the specific seawater composition, its salinity, and the environmental zone to which the material is exposed.

Seawater is a unique environment that cannot be duplicated in the laboratory. Throughout the world, seawater can vary widely in terms of its specific chemical composition, oxygen content, temperature, salinity, pH, and biological activity. At a given location, seawater is also prone to variations from seasonal influences. All of these variables, combined with the long-term time dependence of many metal reactions, will affect the corrosion occurring on metals and alloys in seawater. In addition, the composition of corrosion products and of calcareous deposits formed under cathodic polarization conditions will influence metal corrosion.

Seawater pH ranges from 7.8–8.3. This narrow pH range is due to reactions that cause the interchange of carbon dioxide in the air with seawater and photosynthesis. Changes in the pH of seawater are buffered by the carbonate system and the presence of undissociated boric acid [7]. The buffering capacity and the constancy of natural waters such as seawater are discussed in Ref 8.

### Environmental Zones

Environmental zones involving seawater include marine atmosphere, splash/spray, tidal, submerged/shallow ocean, deep ocean, and mud. Figure 1 illustrates the relative

<sup>1</sup>Carderock Division, Code 613, Naval Surface Warfare Center, 9500 MacArthur Boulevard, West Bethesda, MD 20817-5700.

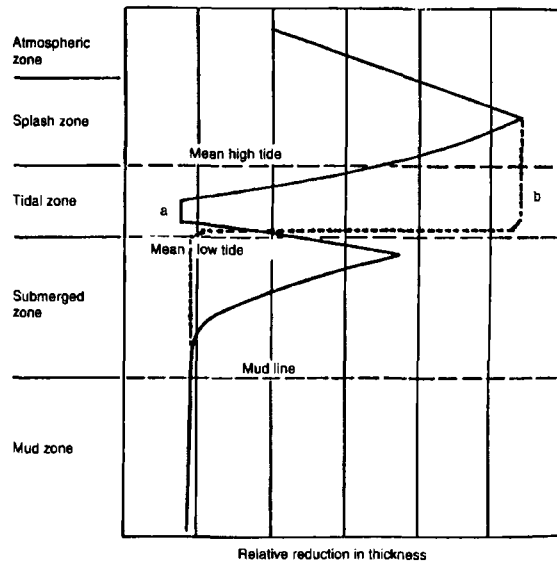


FIG. 1—Corrosion profile of steel piling in seawater. Curve (a) represent behavior of uncoated piling; curve (b) represent steel piling corrosion at coating defect coated with organic, insulating substance [15].

corrosion rates of steel pilings in the different environmental zones [9]. The marine environment is generally considered a highly aggressive environment.

**Atmospheric**—Atmospheric corrosion is responsible for a large fraction of the total corrosion in the world. Factors that affect the atmospheric corrosion of materials in a marine environment are the time of wetness, temperature, material, atmospheric contaminants and pollutants, solar radiation, composition of the corrosion products, wind velocity, and biological species [10]. Atmospheric corrosion of a passive alloy tends to be localized. For electrochemical processes related to corrosion to occur, an electrolyte must be present to allow current to pass via diffusion and electrochemical migration of cations and anions. Seawater is a very conductive electrolyte. The severity of corrosion in an atmospheric environment is related to the time of wetness during which electrochemical processes and corrosion take place. There is also a direct relationship between atmospheric salt content and measured corrosion rates [10].

Atmospheric corrosion rates will tend to increase with winds directly from the ocean to the site, the lower the elevation, and the closer the ocean is to the specimen as shown in Table 2. The direction and velocity of the wind can affect the accumulation of entrained seawater-related particles on specimen surfaces. Generally, the closer the site to the ocean in the face of a prevailing wind the greater the corrosion rate of metals and alloys. Magnesium and calcium chlorides are hygroscopic and tend to keep surfaces wet or moist. Sulfur dioxide lowers the critical humidity required to activate corrosion [10] and increases the aggressiveness of the marine atmospheric environment such as found in an industrial marine environment versus a rural marine environment (Table 2). The dew-point temperature and the component/specimen temperature will influence the rate of corrosion.

TABLE 2—Corrosion rates of uncoupled steel panels after two years at different atmospheric test sites.

Location	Distance from Ocean (m)	Steel Corrosion Rate 2-yr. test	
		Mpy	mm/y
Cape Canaveral ground level	55	17.37	0.44
Cape Canaveral 9 m elevation	55	6.48	0.165
Cape Canaveral 18 m elevation	55	5.17	0.131
Cape Canaveral	800	3.39	0.086
Point Reyes, CA	400	19.71	0.50
Kure Beach, NC	25	21.00	0.53
Kure Beach, NC	250	5.73	0.145
Dungeness, England	Industrial Marine	19.22	0.49
Pilsey Island, England	Industrial Marine	4.04	0.013
Durban, Salisbury I., S. Africa	10	2.20	0.056
Esquimalt, B.C.	Rural Marine	0.53	0.013

(Data compiled from Table 13 [6])

Solar radiation tends to degrade the performance of organic coatings and plastics, and stimulates biological formation and photosensitive electrochemical/corrosion reactions on copper or iron. Ultraviolet radiation can embrittle polymers unless UV stabilizers are added [10].

**Splash/Spray**—The splash/spray zone can be characterized as an aerated seawater environment where exposed metals are almost continually wet and biofouling organisms do not attach [11,12]. In an excessively windy seawater environment, the corrosion of metals can be increased as a result of seawater impinging on their surfaces. The aerated condition of the splash/spray environment is detrimental to many metals such as steel, where its corrosion rate is higher than in any of the other marine environments. This is because dissolved oxygen is easily accessible for electrochemical reactions and chlorides can concentrate during drying of moist films created by spray and condensation [13]. As illustrated by curve (a) in Fig. 1, the most severe corrosion occurs in the splash/spray zone for uncoated steel pilings. The splash/spray environment is also destructive to protective coatings such as organic coatings. Passive film-forming alloys such as stainless steels and titanium have good resistance in this well-aerated environment [12].

**Tidal**—The tidal zone is an environment where metals are alternately submerged in seawater and exposed to the splash/spray zone as the tide fluctuates. In the submerged condition, metals are exposed to well-aerated seawater and biofouling does occur [11,12]. A continuous cover of biofouling organisms protects some metal surfaces such as steel, while the presence of biofouling on stainless steel surfaces can accelerate localized corrosion. Steel is influenced by tidal flow, where increased movement due to tidal action causes an increased steel corrosion rate [12]. Curve (b) in Fig. 1 shows that steel corrosion at exposed coating defect sites is as severe in the tidal zone as it is in the splash/spray zone.

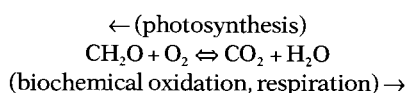
**Submerged/Shallow Ocean**—The submerged/shallow ocean environmental zone usually is characterized by well aerated water combined with marine biofouling organisms of both the plant and animal variety. As in the tidal zone, the

biofouling can either protect the metal surface from attack or can accelerate localized corrosion at the site of the attachment [11,12]. The temperature of the seawater in this environmental zone is dependent on seasonal and specific geographical location but, other than in the polar regions, it is substantially warmer than in the deep ocean environment. The corrosion rate of metals in the shallow ocean varies. Titanium exhibits excellent corrosion resistance in this environment while the corrosion resistance of steel is largely dependent on the availability of oxygen to be transported to cathodic sites on the surfaces [12].

**Deep Ocean**—The deep ocean environment is very different from the ocean at the surface. At sites in the North Atlantic and North Pacific Oceans, oxygen, temperature, and salinity vary with depth. At the ocean surface, the oxygen concentration in the North Pacific is 1.4 times the oxygen content in the North Atlantic. In addition, both the surface temperature and surface salinity are lower in the North Pacific than in the North Atlantic. Below about 1500 m, however, temperature and salinity levels are approximately the same at these two ocean sites [1,6].

The oxygen concentration also varies with seawater depth, as shown in Fig. 2. This figure compares the concentration level with depth at sites in both the North Atlantic and North Pacific Oceans. As the depth is increased to an intermediate level, the oxygen concentration decreases at both sites; however, the reduction in oxygen is much greater in the Pacific Ocean than in the Atlantic. As the depth is then increased even further, the concentration of oxygen increases once again at both ocean sites [6].

As a general rule, the pH varies with the change in dissolved oxygen content. Both variables decrease with depth and reach a minimum value before increasing again (as shown in Fig. 2 for oxygen content). The dissolved oxygen and carbon dioxide concentrations are related to pH in the ocean according to the following reaction [14]:



As organic matter decomposes, the dissolved oxygen content decreases and carbon dioxide is produced. The

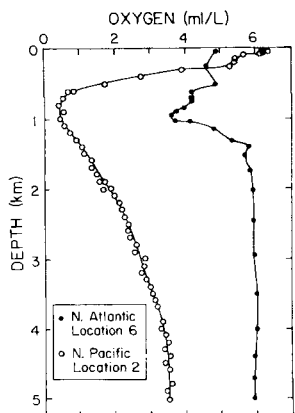


FIG. 2—Variation in oxygen concentration with depth at sites in the northwest Atlantic (36°44' N, 64°28' W) and northeast Pacific (38°21' N, 133°38' W) [3].

production of carbon dioxide, a weak acid, results in a pH reduction in seawater. With photosynthesis, the above reaction is reversed [1,6].

Beyond a depth of 18–30 m, plant biofouling ceases due to the lack of solar radiation and any biofouling present is entirely due to animal life sources. In general, the degree of fouling decreases substantially as the depth is increased, an effect which is independent of the distance from the shoreline [12]. On the other hand, at a given depth, as one moves away from the shoreline where breeding of macroorganisms takes place, significantly less fouling on metal surfaces is observed.

**Mud**—The bottom sediments of the ocean comprise the mud zone. Anaerobic sediments contain bacteria that develop gases such as  $\text{NH}_3$ ,  $\text{H}_2\text{S}$ , and  $\text{CH}_4$ . Sulfides present in the mud zone can attack metals such as steels and copper alloys. The corrosion rate of low-carbon steel (as shown in Fig. 1) in this environment is, however, usually lower than that in the other seawater environmental zones described above, predominantly due to the reduced supply of oxygen [12].

## Uniqueness

Seawater is a unique environment. A recent worldwide test program was recently completed by ASTM Task Group G1.09.02.03 to evaluate the corrosivity of seawater at a number of sites [15]. Though these results indicated the uniqueness of natural seawater, corrosivity was site-specific and influenced by numerous factors. Seawater can vary widely in terms of chemical composition, dissolved oxygen content, temperature, salinity, pH, carbonate levels, flow, degree of fouling, biological activity, and pollution [16].

## ENVIRONMENTAL VARIABLES AFFECTING CORROSION RATES IN SEAWATER

### Temperature

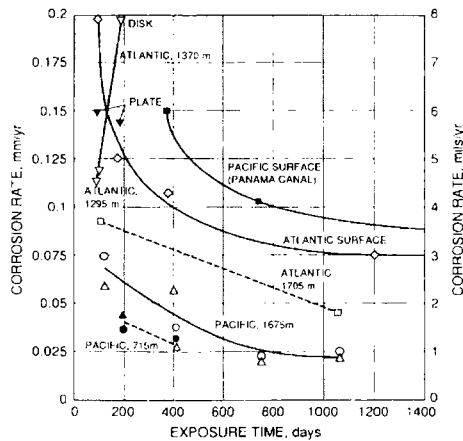
As a general rule, the corrosion reaction rate in seawater increases as the temperature is increased. This applies only when the effect of temperature alone is a factor. Other variables such as oxygen concentration, diffusion rates, salinity, calcareous deposit formation, and biological activity vary as a function of temperature and must also be considered as to how it affects the overall corrosion rate of a material, component, or system.

Surface water temperatures vary mainly by latitude, with the temperature ranging from approximately  $-2^\circ\text{C}$  in the Arctic to about  $35^\circ\text{C}$  in the tropics [16]. Table 3 shows the variation of surface temperatures in selected oceans as a function of latitude in the northern and southern hemispheres [6]. The data suggest that for a given latitude, corrosion test results may vary slightly depending on the ocean location chosen. Also, metal corrosion rates are usually higher at the surface where temperatures are warmer than in the deep ocean where the temperatures are colder [6,12]. The effect of temperature as a function of ocean depth for low-carbon steel alloys is presented in Fig. 3.

**TABLE 3**—Average surface temperature (°C) of the oceans as a function of latitude.

North Latitude	Atlantic Ocean	Indian Ocean	Pacific Ocean	South Latitude	Atlantic Ocean	Indian Ocean	Pacific Ocean
70°–60°	5.60	—	—	70°–60°	–1.30	–1.50	–1.30
60°–50°	8.66	—	5.74	60°–50°	1.76	1.63	5.00
50°–40°	13.16	—	9.99	50°–40°	8.68	8.67	11.16
40°–30°	20.40	—	18.62	40°–30°	16.90	17.00	16.98
30°–20°	24.16	26.12	23.38	30°–20°	21.20	22.53	21.53
20°–10°	25.81	27.23	26.42	20°–10°	23.16	25.85	25.11
10°–0°	26.66	27.88	27.20	10°–0°	25.18	27.41	26.01

NOTE: Data compiled from Ref 6 (original data courtesy of Prentice-Hall Inc. USA).

**FIG. 3**—Corrosion rate of low carbon steels at varying ocean depths [12].

Metal corrosion rates are similar at different locations throughout the world due to a number of controlling factors that compensate for one another [17]. Increasing seawater temperatures increases diffusion rates, but decreases oxygen solubility. Though increasing temperatures do tend to increase corrosion rates, rising temperatures also promote the formation of calcareous deposits [6,12] and microbiological colonization, which form barrier layers that often throttle corrosion attack [17]. Bacteria may participate in anaerobic corrosion reactions that replace the cathodic, oxygen reduction reaction.

Temperature variations due to seasonal changes may also affect corrosion rates in seawater. For many copper and iron alloys, the corrosion rates increase during the warmer months of the year. The start of the corrosion test, therefore, may be affected by the time that a corrosion test is initiated, and there is a tendency for corrosion rates to slow down with increased times of exposure to the natural seawater environment, depending on the actual environmental zone.

However, some of the highest corrosion rates in the world are found in cold weather climates. Corrosion rates in Alaska are reported to be twice as high as those in the North Sea and six times greater than the rates reported in the Gulf of Mexico. The high corrosion rates are caused by the high dissolved oxygen levels, abrasion from glacial silts, tidal changes of over 30 ft (9.1 m), and the action of ice floes in winter [18]. Corrosion rates on steel in the splash zones on docks in the Aleutians are estimated to be as high as 30–35 mpy (761–889  $\mu\text{m/y}$ ) [19].

## Dissolved Oxygen

Dissolved oxygen in seawater has a major influence on corrosivity since oxygen is the principal reactant involved in the cathodic reaction and is involved in the passivation reactions that occur for most metals and alloys in seawater. The solubility of oxygen decreases as the temperature is increased. The oxygen content in surface seawater can be as high as 11–12 ppm in the Arctic as compared to 6 ppm in the tropics. Oxygen solubility in surface seawater can become supersaturated by as much as 200 % of its equilibrium concentration due to photosynthesis by marine plants and by wave action [16]. Conversely, the dissolved oxygen concentration can decrease and become undersaturated due to oxygen consumption created by the decomposition of organic matter.

The combined influence of these natural cycles on the dissolved oxygen content can vary as a function of seasonal changes and the ocean depth at any given location [12]. Oxygen solubility in seawater goes through a minimum at intermediate ocean depths: the depth of minimum oxygen solubility ranges from 400 m in the equatorial Eastern Pacific to 2400 m in the Central Pacific Ocean. The minimum oxygen concentration at these ocean depths ranges from 0.16–6.4 ppm [6].

Seawater temperature and salinity also affect the dissolved oxygen content, with temperature having the larger influence on the oxygen solubility. The general rule is that as either the temperature or the salinity is decreased, the dissolved oxygen content increases [1,6]. The equilibrium concentration of dissolved oxygen in seawater as a function of salinity and temperature is shown in Table 4 [6].

The effect of the dissolved oxygen level on corrosion is dependent on the metal. For metals that form passive films like stainless steel and aluminum, a high oxygen content is favorable in that it helps to delay the initiation of pitting on

**TABLE 4**—Equilibrium concentration of oxygen in seawater as a function of temperature and salinity.<sup>a</sup>

Temperature (°C)	Salinity (ppt)					
	0	8	16	24	31	36
Oxygen Solubility (ppm) at Specific Salinity Levels						
0	14.6	13.9	13.1	12.4	11.8	11.4
5	12.5	11.9	11.3	10.7	10.2	9.9
10	10.9	10.4	9.8	9.4	8.9	8.7
15	9.5	9.1	8.7	8.2	7.9	7.7
20	8.5	8.1	77.7	7.3	7.0	6.8
25	7.6	7.2	6.9	6.6	6.3	6.2
30	6.8	6.5	6.2	6.0	5.7	5.6

<sup>a</sup> Calculated based on data from Ref 6.

the metal surface. However, once pitting is initiated, the propagation rate is increased with high oxygen content in the seawater. For common steels and copper alloys, the effect of dissolved oxygen is dependent on the seawater flow velocity. The oxygen concentration has a negligible effect on copper alloy corrosion rates in quiescent seawater while at a seawater flow rate of 1.8 m/sec, an increasing oxygen content accelerates the copper corrosion rate. For metals such as iron and steel, the corrosion rate increases linearly with a rising oxygen concentration at a constant temperature [12,20].

Oxygen concentration cells can be created from deposits on a metal's surface or may be due to improper component design, which introduces crevices. Differences in oxygen content due to discrete films or deposits randomly scattered along a metal surface can cause pitting and/or crevice corrosion at these localized sites. In contrast, complete coverage of a surface by a film or a deposit can provide an effective barrier and reduce corrosion of the metal [6,21].

### Salinity

Salinity is defined as the total weight of solids dissolved in 1000 g of water. For example, 35 parts per thousand (‰) salinity is equivalent to 35 g of solids dissolved in 1000 grams of water or a dissolved matter content of 35 000 ppm [12]. Salinity usually is determined by measuring chlorinity and then deriving the salinity from the following relation:

$$S = 1.80655 Cl$$

where *S* (salinity) and *Cl* (chlorinity) are measured in parts per thousand [1,6].

The salinity of open ocean water at the surface typically varies from 32–37.5 ‰. Generally, this degree of variation does not alter metal corrosion rates. Some of the more isolated seas, such as those shown in Table 5, can have large variations in salinity, which may influence metal corrosion rates. Salinity variations can affect a metal's uniform corrosion rate. For example, in areas where there are high evaporation rates, the salinity can be very high. Conversely, at the mouth of a river, the salinity is more dilute than in the open ocean.

Variations in salinity can also alter the localized corrosion resistance of metals in seawater. As the salinity is increased, the chloride ion activity increases and can result in increased pit and crevice corrosion initiation and propagation [6].

### pH and Carbonates

The pH of open ocean water varies from approximately 7.5–8.3 and is buffered by a complex carbonate system. This

variation in pH does not affect the corrosion of most metals, except for aluminum. As the pH decreases from 8.2 at the surface to 7.5–7.7 in deep water, the initiation of pitting and crevice corrosion in aluminum alloys is accelerated [1,6].

Depending on various conditions, calcareous deposits form when the solubility of calcium and magnesium ions is exceeded. Calcareous deposits form at pH levels between 8 and 10 and consist mainly of  $\text{CaCO}_3$ ,  $\text{MgCO}_3$ , and  $\text{Mg}(\text{OH})_2$  [12]. Although changes in pH do not directly alter the corrosion behavior of most metals, pH variations can influence the formation of protective calcareous scales that subsequently can affect the corrosion rate of the substrate alloy. Spontaneous calcareous deposits are more likely to occur at higher pH values, but the function of these deposits is limited due to the presence of organic matter and seawater salinity [16].

At the surface, the ocean waters throughout most of the world are 200–500 % supersaturated in calcium carbonates and precipitation of these carbonate scales will influence the corrosion reaction occurring at the metal surface [6]. The buildup of protective calcareous deposits by cathodic protection can lower the subsequent current demand in natural seawater [22–24].

Dilute seawater is undersaturated in carbonates, which reduces the likelihood of forming protective calcareous films on a metal surface. In deep ocean waters, the calcareous deposits are not spontaneously formed in an ambient environment and are often not precipitated under cathodic protection conditions [6]. In the cold waters of the deep ocean environmental zones, the precipitation and/or dissolution of the calcareous deposits is mainly controlled by the calcium carbonate saturation level,  $\Omega$  [25].

$$\Omega = \frac{[\text{Ca}^{+2}][\text{CO}_3^{-2}]}{K'_{\text{sp}}}$$

where  $[\text{Ca}^{+2}]$ ,  $[\text{CO}_3^{-2}]$  = calcium, carbonate measure concentrations, respectively,  $K'_{\text{sp}}$  = apparent solubility product, and  $\Omega$  is the calcium carbonate saturation value. The calcareous deposits formed by cathodic protection will be stable when the degree of saturation is  $\Omega > 0.6$  as in most ocean areas down to depths of 3000 m [25]. However, at depths greater than 3000 m, the calcium carbonate formation may be unstable. At  $\Omega = 0.6$ , the dissolution rate of calcium carbonate may be at around 1  $\mu\text{m}/\text{y}$ .

### Biological Organisms

Seawater is a living medium sustaining a wide variety of organisms [26]. Marine biological organisms consist of either micro (bacterial) or macro (algae, barnacles) speciation. These organisms can affect the corrosion behavior of metals and alloys in a number of ways including: (a) influencing either or both the prevailing anodic and cathodic reactions, (b) influencing the formation and/or maintenance of protective films, (c) producing deposits on metal surfaces, and (d) creating a corrosive environment. The factors listed above can act singly or combine with one or more sources to alter a metal's corrosion behavior [21].

One of the keys to alternating conditions at the metallic surface, and the subsequent delay or acceleration of corrosion, is the formation of a biofilm. The exact sequence of

**TABLE 5**—Total solids in different seawater locations.

Body of Water	Total Dissolved Solids, ppm
Baltic Sea	8000
Caspian Sea	13 000
Black Sea	22 000
Irish Sea	32 500
Atlantic Ocean	37 000
Mediterranean Sea	41 000
Arabian Sea	39 000–47 000
(Doha, Kuwait)	
Dead Sea	260 000

events leading to biofilm formation depends on the environment and the organisms present [26]. Biological organisms attach and multiply on any solid surface in seawater. Within two hours of immersion, a non-living organic conditioning film develops on a solid surface. Within the first 1–2 days, a bacterial slime film develops over the conditioning film. The slime film creates a partial barrier to diffusion between the liquid/metal interface and the bulk seawater environment. These slime films are usually not continuous and can create oxygen or chemical concentration cells on the metal surface, which can result in accelerated localized corrosion.

Biofilms are structured, but complex assemblages of microorganisms embedded in exopolymers (extracellular material produced by microorganisms that define their shape, their ability to adhere to solid surfaces, and their ability to trap particulate nutrients) [26]. Biofilms include communities of colonies, consortia, newly created cells, dying cells, extracellular products, polymers, and trapped inorganic material. Biofilms and individual organisms that are contained within the biofilm interact with external influences originating from the substratum and the bulk medium to cause oxygen or chemical concentration gradients and other localized effects related to mitigating or accelerating corrosion [26,27].

Ammonia and sulfides can also be produced from the decay of organic matter within the slime film, resulting in increased corrosion of some alloys [28]. Sulfur-oxidizing organisms produce sulfuric acid from sulfur or other reduced sulfur species [28]. The presence of ammonia is known to cause stress corrosion cracking of copper alloys, while sulfides may lead to accelerated attack on copper alloys and steel. The presence of the slime film on the metal surface can locally change the local environment at the liquid/metal interface such that the corrosion behavior of a metal can be considerably altered from one that normally displays low corrosion rates in seawater to conditions where corrosion is accelerated [6].

The reduction or complete elimination of marine organisms in dilute seawater reduces the probability of forming protective biofilms and could result in increased metal corrosion [12].

Macrofouling films begin to develop over the conditioning and slime films within 2–3 days after immersion in seawater [6]. If the macrofouling is continuous along the solid surface, the film can decrease the amount of dissolved oxygen present at the surface and thus decrease the overall metal corrosion rate. If, however, the macrofouling is discontinuous, the film acts in the same manner as discontinuous slime films where oxygen or chemical concentration cells can be formed and result in localized corrosion of the metal [6].

The macrofouling organisms attach in embryonic form to the slimed solid surfaces. Once attached, they metamorphose and mature. The most common sessile fouling organisms in seawater include: (a) organisms with hard shells, annelids, barnacles, encrusting bryzoa, mollusks, and corals, and (b) organisms without hard shells: marine algae, filamentous bryzoa, coelenterates or hydroids, tunicates, and calcareous and siliceous sponges [12]. The accumulation of these biological organisms is dependent on specific environmental conditions. Conditions which are most conducive

to their development are: (a) relatively shallow water such as in a harbor, (b) warm temperatures, (c) low seawater flow, and (d) smooth, hard surfaces [21].

Both macro and microfouling can have a major impact on the performance of marine components [6,12,21]. Macro and microfouling organisms can break down protective paint films on a component surface. On ship hulls, these organisms increase drag and power requirements. In heat exchangers, fouling limits the heat transfer and seawater flow, and severe fouling can result in complete blockage [21]. Fouling also shields the component surface from any oxygen supply thereby creating the possibilities that differential aeration cells can develop. Fouling can cause catalytic effects [7]. Fouling, in addition to causing drag or blockage, can cause localized turbulence. Plant decay or secretion products from animal life can accelerate corrosion processes [7].

### Velocity of Seawater

Fluid velocity can significantly affect metal corrosion rates in seawater. Flow-assisted corrosion is dependent on variables such as water chemistry, pH, component geometry, surface roughness, biofouling, microbiologically influenced corrosion, pitting and crevice corrosion, water pollution and contamination, alloy composition and surface films, galvanic interaction, fluid velocity and mode, oxygen content, heat transfer rate, and temperature [29].

Corrosion rates and the type of corrosion are often dependent on environmental factors such as fluid flow and the availability of appropriate species required to drive electrochemical reactions [30]. A change in the motion of a corroding metal or alloy relative to its environment by fluid flow can increase corrosion rates by removing protective films or by increasing the diffusion or migration of deleterious species. However, an increase in fluid flow can decrease corrosion rates by eliminating aggressive ion concentration or enhancing passivation or inhibition by transporting the protective species to the fluid/metal interface [21].

Under high flow conditions, corrosion may take the form of impingement, erosion corrosion, or cavitation [12]. In any given velocity domain, different local velocities may exist over diverse areas of the component due to factors such as geometry or mode of fabrication [2]. The effect of seawater velocity on a metal's corrosion rate varies with the particular alloy. Alloys such as 304 and 316 stainless steel or nickel-chromium-molybdenum alloys exhibit deep pitting in low flow conditions, yet at high seawater velocities their corrosion rate decreases to less than 25  $\mu\text{m}$  per year. Contrary to this, iron and copper show significantly lower corrosion rates at low flow velocities than under high seawater flow conditions [31]. The corrosion rates for various metals as a function of seawater velocity are included in Fig. 4.

Seawater velocity for immersed samples may decrease to a lower magnitude as the seawater depth is increased; this decrease typically begins at depths of 18–30 m. Lack of flow can exacerbate crevice corrosion, which takes place with passive oxide film formers such as stainless steels where occluded, stagnant areas become oxygen-deficient anodic sites as compared to outer cathodic, oxygenated regions [21,32].

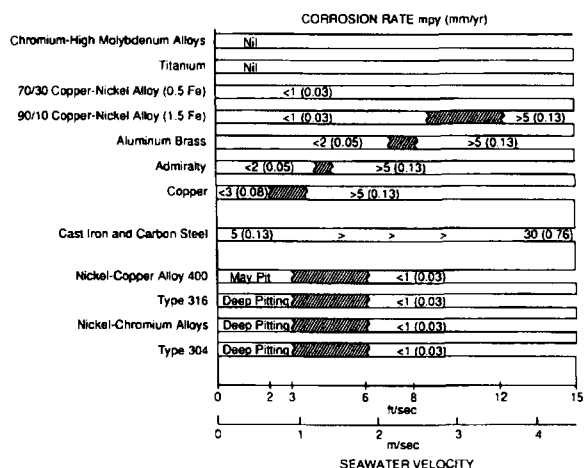


FIG. 4—Corrosion rate of metals and alloys in seawater as a function of flow velocity (Source: LaQue Center for Corrosion Technology). denotes critical range.

Removal of the corrosion product or oxide layer by excessive flow velocities leads to increased corrosion rates of the metallic material. Corrosion rates are often dependent on fluid flow and the availability of appropriate species required to drive electrochemical reactions. Surface shear stress is a measure of the force applied by fluid flow to the corrosion product film. For seawater, this takes into account changes in seawater density and kinematic viscosity with temperature and salinity [33]. Accelerated corrosion of copper-based alloys under velocity conditions occurs when the shear surface stress exceeds the binding force of the corrosion product film. Alloying elements such as chromium improve the adherence of the corrosion product film on copper alloys in seawater based on measurements of the surface shear stress. The critical shear stress for C72200 ( $297 \text{ N/m}^2$ ,  $6.2 \text{ lb}_f/\text{ft}^2$ ) far exceeds the critical shear stresses of both C70600 ( $43 \text{ N/m}^2$ ,  $0.9 \text{ lb}_f/\text{ft}^2$ ) and C71500 ( $48 \text{ N/m}^2$ ,  $1.0 \text{ lb}_f/\text{ft}^2$ ) copper-nickel alloys [33].

Alloys such as 304 and 316 stainless steel or nickel-chromium alloys exhibit deep pitting in low flow conditions, yet at high seawater velocities their corrosion rate decreases to less than  $25 \mu\text{m}$  per year. Contrary to this, iron and copper show significantly lower corrosion rates at low flow velocities than under high seawater flow conditions [31].

Seawater turbulence can substantially alter the flow rates and subsequent corrosion rate of metals. Consider, for example, a seawater piping system that operates at a  $1.8 \text{ m/sec}$  velocity. Increases of pipe diameter will increase the thickness of the velocity boundary layer and the diffusion boundary layer. The thicker velocity boundary layer leads to a decreased velocity gradient and reduced shear stresses at the piping wall. For design purposes, a single velocity value marking the initiation of erosion corrosion can provide misleading service life prediction [29]. Factors that affect erosion in pipe bends include the degree of internal ellipticity and asymmetry, sudden changes in cross section, and a reduction in cross-sectional area [34]. As the radii of directional change are reduced, the erosion corrosion rates are expected to increase. Ledges, crevices, deposits, and other obstructions disturb laminar flow and result in turbulence

at sometimes significant velocities [21]. In a turbulent area such as downstream of a valve, velocities far exceeding the  $1.8 \text{ m/sec}$  nominal velocity may occur and cause accelerated corrosion of the metal. In testing piping systems, turbulent areas should be accounted for and mitigated by choosing appropriate erosion and cavitation-resistant materials [31] and by implementing a proper design [35].

## Sulfides

Sulfides, sulfur, and other sulfur compounds can produce pitting, crevice corrosion, dealloying, stress corrosion cracking, and stress-assisted hydrogen induced cracking of susceptible metals and alloys [28]. Polluted waters, like those found in coastal harbors and estuaries, contain hydrogen sulfide and sulfur-containing compounds. Sulfides can be generated in several ways: (1) bacterial reduction of naturally occurring sulfates in seawater; (2) rotting vegetation; and (3) industrial waste discharge [29]. Hydrogen sulfides are known to adversely affect the corrosion rate of various metals and alloys. Sulfates themselves are not usually harmful; however, sulfates can be reduced to harmful sulfides by sulfate-reducing bacteria. These sulfide pollutants can contribute to the corrosion of steels, stainless steels, copper, and aluminum alloys [6].

Sulfide corrosion has been found to occur on a number of different copper-base alloys. Wrought 90/10 copper-nickel can exhibit sulfide-induced attack in the form of accelerated pitting with as little as  $0.01 \text{ ppm}$  sulfide concentration while 70/30 copper-nickel is susceptible at sulfide concentrations of  $0.05 \text{ ppm}$  or greater [36]. The presence of sulfide-modified films interferes with the formation of normal passivating films of copper nickel alloys found in unpolluted waters [37,38]. Sulfide-modified films generally are more loosely adherent than the normal cuprous oxide films; turbulence tends to selectively remove the sulfide-modified films. The accelerated corrosion rates of copper-nickel alloys in aerated sulfide-containing seawater remain high since the sulfides prevent protective corrosion product layers from forming [39].

A number of variables contributing to sulfide-influenced corrosion include duration of sulfide exposure, system operating velocity, and degree of turbulence must be assessed in conjunction with the sulfide concentration in order to accurately predict the sulfide susceptibility of copper-nickel alloys. Other research [12] on copper-base alloys has found that  $3\text{-ppm}$  hydrogen sulfide significantly increases the corrosion rates of several copper alloys as indicated in Table 5.

## Heavy Metals

Concentrations of copper in seawater can cause accelerated corrosion of metallic components. In unpolluted seawater, the copper concentration is  $0.2 \text{ ppb}$ , which is typically not high enough to influence a metal's corrosion behavior. If, however, the copper concentration is increased above approximately  $30 \text{ ppb}$ , corrosion of aluminum alloys can occur. The copper concentration may be increased due to a number of factors including copper leaching from anti-fouling paints, pollutants containing copper, or nearby copper alloy corrosion. If the copper deposits onto aluminum



**TABLE 6**—Corrosion of copper-base alloys in clean and polluted seawater [12].

Seawater Velocity, 7.5 fps (2.3 m/sec), Test Duration, 64 Days			
		Corrosion Rate, mpy (mm/yr)	
Alloy	CDA No.	Clean Seawater	Seawater (3 ppm H <sub>2</sub> S)
90/10 Cu-Ni	706	3 (0.08)	34 (0.86)
70/30 Cu-Ni	715	5 (0.13)	26 (0.66)
2% Al Brass	687	3 (0.08)	22 (0.56)
6% Al Brass	608	5 (0.13)	21 (0.53)
As-inhibited Admiralty Brass	443	13 (0.33)	35 (0.89)
Phosphor Copper	122	14 (0.36)	105 (2.67)

alloy surfaces, a galvanic couple is formed, resulting in localized pitting of the aluminum [6].

The corrosion products generated from iron and steel have also been known to cause corrosion of aluminum alloys in desalination plants. However, the iron contamination effects are less and are not as consistent as for copper [6].

## CORROSION MECHANISMS

Seawater is an aggressive, complex aqueous medium that has unique properties that affect most common structural materials somewhat differently than in most other natural media. As stated earlier, two competing processes operate simultaneously in seawater environments: (1) the chlorinity in seawater tends to destroy alloy passive films, while (2) dissolved oxygen acts to promote and repair passive films on metallic materials [2]. Though oxygen is the reactant involved in the major cathodic (oxygen reduction) reaction that occurs in seawater, species such as hydrogen (involved with cathodic protection applications), sulfates, nitrates, or ammonium compounds (related to with reactions via bacteria or other microorganisms in polluted waters) can be involved in other cathodic reactions in seawater. Seawater is also a very conductive medium due to its inherent electrolyte content leading to reactions detrimental to alloy performance.

Corrosion can occur by numerous pathways. Fontana [40] lists eight forms of corrosion: (1) uniform corrosion, (2) pitting, (3) crevice corrosion, (4) galvanic corrosion, (5) intergranular corrosion, (6) selective leaching or dealloying, (7) erosion corrosion, and (8) stress corrosion. Some of these "classic" forms of corrosion are somewhat simplistic and are discussed in more detail [41]. Some additional background information on these corrosion mechanisms is discussed in Section IV: Testing for Corrosion Types.

Uniform corrosion is characterized by an electrochemical/corrosion reaction that proceeds over an entire surface area. This form of corrosion can be measured easily and is conducive to prediction of component failure.

Pitting is a mode of localized dissolution leading to the formation of cavities within a passivated surface that is boldly exposed [41]. Pitting is a probabilistic or stochastic corrosion mechanism that is dependent on electrochemical

potential, alloy chemical composition and microstructure, electrolyte composition, and temperature [41]. Natural seawater, with a relatively high concentration of chlorides, contributes to the development of pitting of passive alloys such as stainless steels.

Pitting corrosion usually initiates at surface inhomogeneities such as intermetallic phases, nonmetallic inclusions, grain boundaries, dislocations, defects, or mechanically damaged sites [41]. At low potentials, pitting is followed by repassivation; this is termed metastable pitting. Above a certain potential or potential range, a transition from metastable pitting to stable pitting formation occurs. If the environmental conditions do not change in the anodic pit site(s), the pit continues to grow due to, in part, the large cathode (where oxygen reduction occurs) to anode ratio over the specimen or component surface.

Crevice corrosion is localized corrosion that occurs within crevices or at shielded surfaces where a stagnant solution exists. To develop as a corrosion site, a crevice must be wide enough to permit entry of a corrodent, but sufficiently narrow to cause and maintain a stagnation environment. Crevices can be formed at metal-metal or nonmetal-metal junctions or at holidays that form in coatings on metals or alloys. The parameters leading to crevice geometries that will cause crevice corrosion of an alloy are difficult to quantify [40]. Like pitting, crevice corrosion involves both initiation and propagation processes. During the initiation stage, discrete areas develop within the crevice [42,43]. In a creviced site exposed to a seawater environment, the crevice becomes oxygen-deficient. The increasing concentration of metal cations causes an associated migration and build-up of chloride ions within the crevice in order to maintain electroneutrality. Metal chlorides are then hydrolyzed by water to form an insoluble metal hydroxide and free acid (in the case of chloride environments, HCl) thus creating overall acidification of the crevice site. The loss of oxygen, chloride ion buildup, acidification, and a large IR drop between the boldly exposed cathodic sites outside of the crevice and the anodic crevice propagate crevice corrosion [44].

Under-deposit attack or "poultice" corrosion may occur when a metal is locally covered by foreign, absorbent (organic or inorganic) materials [40,45]. In this case, attack can proceed even when the bulk of the system is dry due to retention of moisture in the poultice. The corrosion mechanism is similar to crevice corrosion in that the deposits act to limit the migration of oxygen to the covered area. This leads to acidic shifts in pH, concentration of Cl<sup>-</sup> ions in the shielded area, and a shift to a more active corrosion potential under the deposit. Local corrosion rates can be very high due to the large cathode-to-anode area ratio.

The coupling of dissimilar alloys in conductive, corrosive solutions such as seawater is called galvanic corrosion and can lead to accelerated corrosion of the more anodic, electronegative alloy and protection of the more cathodic, electropositive alloy. The extent of galvanic corrosion depends on factors such as: (1) the effective area ratio between the anodic and cathodic members of the couple; (2) solution conductivity; (3) flow characteristics of the solution; (4) temperature; (5) system geometry; (6) the potential difference of the dissimilar alloys; (7) solution composition and

environment; and (8) the cathodic efficiency of the more noble metal or alloy [46–48]. Galvanic corrosion and erosion corrosion can synergistically attack the passive films of susceptible alloys. Galvanic action between dissimilar metals can destroy the passive film of the more anodic member exposing the bared substrate to possible erosion corrosion. The removal of the protective films on copper-nickel alloys by flow may promote dissolution of the bare, exposed areas by galvanic interaction with the surrounding surfaces covered by corrosion product scales.

Under certain conditions, grain boundary interfaces are very reactive, causing intergranular corrosion. Intergranular corrosion can be caused by impurities at the grain boundaries, or enrichment or depletion of one of the alloying elements in the grain boundary region [40]. Iron segregation at the grain boundaries of aluminum alloys can initiate intergranular corrosion. Depletion of chromium in sensitized, unstabilized, austenitic stainless steels are susceptible to intergranular corrosion [40]. A form of intergranular corrosion called knife-line attack may occur on welded, stabilized austenitic stainless steels if proper post-weld heat treatment is not implemented [40].

Selective leaching or dealloying is the selective removal of one element from an alloy by corrosion processes. The most common example is the selective removal (dezincification) of zinc in brass alloys. Dezincification may either be plug-type or uniform. In other alloy systems, aluminum, iron, cobalt, nickel, chromium, and other elements may be selectively removed [49]. Little work has been done in differentiating susceptibility of selective leaching of alloys in synthetic and natural seawater [6].

A change in the motion of a corroding metal or alloy relative to its environment by fluid flow can increase corrosion rates by removing protective films or by increasing the diffusion or migration of deleterious species. An increase in fluid flow can also decrease corrosion rates by eliminating aggressive ion concentration or enhancing passivation or inhibition by transporting the protective species to the fluid/metal interface. Accelerated corrosion due to flow has been termed flow-assisted, flow-influenced, flow-induced, or flow-accelerated corrosion. There are several mechanisms described by the conjoint action of flow and corrosion that result in flow-influenced corrosion: (1) mass transport-controlled corrosion; (2) phase transport-controlled corrosion; (3) erosion corrosion; and (4) cavitation [50].

Mass transport-controlled corrosion implies that the rate of corrosion is dependent on the convective mass transfer processes at the metal/fluid interface. Mass transfer can have a significant effect on corrosion rates of metals and alloys depending on factors such as bulk solution chemistry, temperature, flow conditions, surface roughness, and geometry.

Phase transport-controlled corrosion suggests that the wetting of the metal surface by a corrosive phase is flow-dependent. This may occur because one liquid phase separates from another or because a second phase forms from a liquid. The distribution and morphology of the corrosive attack will be related to the distribution of the corrosive phase; the corroded sites will frequently display rough, irregular surfaces and be coated with or contain thick, porous corrosion deposits [29].

Erosion corrosion is associated with a flow-induced mechanical removal of the protective surface film that results in subsequent corrosion rate increases via either electrochemical or chemical processes. It is often accepted that a critical fluid velocity must be exceeded for a given material. The mechanical damage by the impacting fluid imposes disruptive shear stresses or pressure variations on the material surface and/or the protective surface film. Erosion corrosion may be enhanced by particles (solids or gas bubbles) and impacted by multi-phase flows [29]. Increased flow stream velocities and increases of particle size, sharpness, density, and concentration increase the erosion corrosion rate. Increases in fluid viscosity, density, target material hardness, and/or pipe diameter tend to decrease the corrosion rate. The morphology of surfaces affected by erosion corrosion may be in the form of shallow pits or horseshoes or other local phenomena related to the flow direction.

Factors that affect erosion in pipe bends include the degree of internal ellipticity and asymmetry discussed earlier, sudden changes in cross section, and reduction in cross-sectional area [51]. As the radii of directional change are reduced, the erosion corrosion rate is expected to increase. Ledges, crevices, deposits, and other obstructions disturb laminar flow and result in turbulence at significant velocities [40]. Short distances less than 10 diameters after directional changes or obstructions do not allow turbulence to dissipate [52].

Cavitation sometimes is considered a special case of erosion corrosion and is caused by the formation [53] and collapse of vapor bubbles in a liquid near a metal surface. Cavitation is a process by which a liquid is ruptured by decreasing the pressure at roughly constant liquid temperature. Cavitation removes protective surface scales by the implosion of gas bubbles in a fluid; calculations have shown that the implosions produce shock waves with pressures approaching 60 ksi [40]. Cavitation damage often appears as a collection of closely-spaced, sharp-edged pits or craters on the surface. It has been suggested [54] that the corrosion rate by cavitation can be influenced by surface roughness that permits a large number of nuclei for bubble formation. Under this condition, the concentration of deleterious ions in solution next to the metal surface will be greater, and the observed corrosion damage indicates that the steam bubbles may provide crevices or enhanced possibilities for dissolution at the solution/metal/steam interface.

Environmental cracking can take several forms: (1) stress corrosion cracking, (2) corrosion fatigue, and (3) hydrogen embrittlement. Stress corrosion cracking is caused by the presence of a tensile stress and a specific corrosion medium to a susceptible alloy. Failures from corrosion fatigue of alloys occur with time after the application of repeated cyclic stresses below the yield stress in a corrosive environment. It is generally considered that steels stressed below a fatigue limiting stress will endure an infinite number of cycles without fracture in non-corrosive environments [40]. Corrosion fatigue is influenced by the corrosive medium, pH, temperature, oxygen content, and the presence of any contaminants. In seawater, aluminum bronzes and austenitic stainless steels retain about 70 and 80 % of the normal fatigue resistance while high-chromium alloys retain only 30–40 % of normal fatigue resistance [40].

Hydrogen embrittlement lowers the yield stress and the ultimate tensile stress of a metal or alloy due to the diffusion of atomic hydrogen into susceptible alloys. This may occur in seawater for high-strength steels subjected to overprotection from cathodic protection systems. The term hydrogen embrittlement is used to characterize the near room temperature effects of hydrogen on materials. Among these effects are loss of ductility, loss of load carrying capability, delayed cracking, and loss of true stress at fracture. Although there is an incomplete understanding of the mechanisms of hydrogen related failures, the evidence indicates there is no single dominant mechanism operative over a broad range of materials. This may be mitigated if calcareous deposits have formed on alloy surfaces that can act as barriers to hydrogen permeation.

More recently, attention has been directed to the "ninth" form of corrosion, biologically influenced corrosion, which includes studies on an area referred to as "ennoblement." The presence of biofilms on metals and alloys immersed in natural seawater produces a complex, heterogeneous chemistry along the metallic surface. It has usually been observed that passive alloys such as aluminum, stainless steels, nickel-base alloys, or titanium show an increase to more noble (electropositive) potentials or ennoblement of several hundred millivolts with exposure time in natural seawater, thus magnifying the potential differences that may exist between dissimilar alloys [26,55–64]. Ennoblement is likely caused by the formation of microbiological films, which increase the kinetics of the cathodic reaction [55–63].

The ennoblement of these passive alloys by biofilms has been attributed to increasing the kinetics of the oxygen reduction reaction, or by the introduction of alternative redox reactions such as peroxide production or heavy metal (Mn or Fe) reduction [60]. The ennoblement caused by the influence of cathodic reactions occurring on these passive alloys results in increasing the initiation and propagation of crevice corrosion [26,61], pitting [61], and galvanic corrosion [63,64].

Figure 5 illustrates that the ennoblement of Alloy 625 occurred between 37 and 51 days of exposure to flowing natural seawater [64]. This ennoblement of Alloy 625 increased the driving force for increased galvanic corrosion of the

70/30 copper-nickel pipe [64]. Continued buildup of the microbiological film thickness gradually decreased the potential difference between the Alloy 625 and the copper-nickel alloy [64].

## CORROSION TESTING

Corrosion testing is important in evaluating materials in seawater and related marine environments. Tests can ascertain the performance of different materials, measure the degradation processes, and evaluate alternative materials and designs that optimize service life for given marine environments. Marine environments may include high temperature oxidizing or reducing conditions found in marine gas turbines or waste incinerators; testing may also be done in the marine environmental zones discussed earlier. Although most details are discussed in the chapter on High Temperature Gases, high temperature testing for marine applications must consider the presence of seawater salts contained in the air intake of the turbines or waste incinerators since such electrolytes enhance the high temperature corrosion processes of hot corrosion, sulfidation, and carburization.

Testing should be properly planned as discussed in Planning and Design of Tests. Tests should be relevant and correlate with actual field use. Accelerated tests often provide useful information, but degradation processes in such tests may not reflect the actual corrosion mechanisms by which the materials naturally deteriorate. Testing may require laboratory, field, simulated service evaluations, or a combination of the tests. Specific test methods are discussed in the following sections.

Before testing components in most practical applications, one should be knowledgeable of the corrosion properties of possible candidate materials, have an idea of the type and complexity of testing desired, and have a sufficient level of experience to comprehend possible materials interactions that a component may have with other material components and be able to interpret and translate the test results into the requirements of the service application [6].

The objective for performing a corrosion test should be identified during the initial phase of designing the testing procedure. The test conditions including specimen size, test environment vs. service environment, geometry, sample preparation, temperature, flow velocity, potential, and type of corrosion test (general, crevice, pitting resistance, galvanic, stress-related, dealloying, etc.) should be considered.

## Laboratory Evaluation

The corrosion behavior of metals or coatings is often evaluated in the laboratory rather than in an actual service environment due to time and/or budget limitations. Laboratory evaluation is generally of relatively short duration and is often used to study environmental effects on a metal's corrosion behavior because the specific environmental conditions can be controlled. The major disadvantage of testing in the laboratory is that the actual service environment and conditions may not be evaluated. Service conditions are being simulated, which involves accepting certain

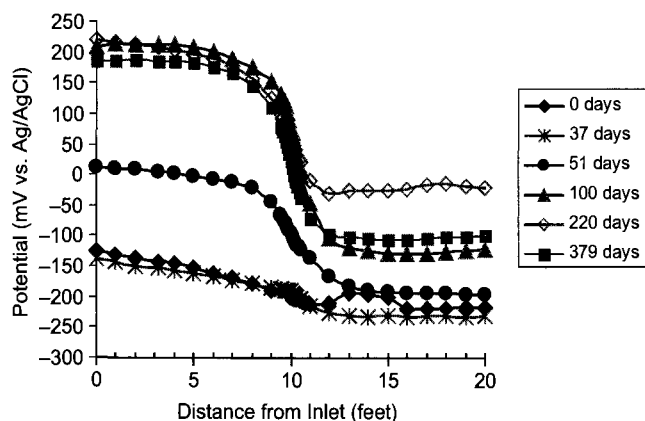


FIG. 5—Alloy 625/70:30 Copper-Nickel Piping Couple. Potential profile shown as a function of time and location along the pipe (junction between the dissimilar alloys is located 10 ft (3 m) from inlet).

assumptions. It is important when testing in the laboratory to correlate field data with laboratory data so that the validity of the laboratory information can be assessed [65].

Natural seawater is the preferred environment for laboratory testing, but synthetic seawater solutions are often utilized. The term natural seawater refers to fresh seawater that is pumped directly into the laboratory, rather than seawater that has been stored and possibly shipped to an onshore location for the testing. Once seawater is removed from its natural environment, its composition changes and this can have a large impact on the resultant metal corrosion rate. Synthetic seawater solutions that are typically used include 3.5-weight percent sodium chloride (NaCl) and substitute ocean water per ASTM D1141 [66]. The substitute ocean water can be used either with or without heavy metals added according to the ASTM D1141 specification [66]. Both 3.5 % NaCl and substitute ocean water solutions do not contain the same organic and biological components as natural seawater. Substituting ocean water with heavy metals most nearly approximates the actual composition of natural seawater. The disadvantage in using any of the synthetic solutions is that, like the stored natural seawater, the composition varies from that of fresh, natural seawater and thus the corrosion behavior of the metals evaluated can be considerably affected. However, one advantage of using 3.5 % NaCl is that calcareous deposits will not form under cathodic polarization conditions in this solution. This is extremely useful in fracture surface evaluation of metal specimens, where the presence of calcareous deposits often prohibits examination of the surfaces unless the deposits are dissolved or mechanically removed, which could alter the original fracture surface.

### Immersion Testing

Immersion testing is usually performed on panel specimens or small component parts such as fasteners. Specimens are exposed to the seawater environment in fully immersed, partially immersed, or alternately wetted and dried in a cyclic pattern. Sample weight loss, physical surface changes, visually assessed modifications, as well as surface compositional changes can be documented. For example, long-term uniform corrosion testing is usually performed in test racks or in test loops. Immersion testing is useful to examine different variables such as environmental compositions, alloying elements, coating type, surface condition, controlled defects, etc. Immersion testing may be done in either natural or synthetic seawater. Natural seawater for laboratory immersion testing is often filtered to prevent macrofouling on the specimen surfaces. The filtering can be accomplished by passing seawater through a sequence of coarse to fine filters, with final filtering through 5–10  $\mu\text{m}$  pore size filter cartridges. Stagnant natural seawater solutions are not recommended for testing due to decay of the marine biological organisms, which will alter the seawater composition and can affect the resultant corrosion behavior [67].

### Salt Spray/Salt Fog Testing

Salt spray (fog) testing is an accelerated laboratory method for assessing the corrosion behavior of coated and

uncoated metals. The generally accepted methods in the United States for salt spray testing are discussed in ASTM B117 (Method of Salt Spray (Fog) Testing), ASTM G85 (Practice for Modified Salt Spray (Fog) Testing) and GM9540P [68]. These tests have been successfully used to screen both coated and uncoated metals and to evaluate coating performance, particularly in terms of thickness uniformity and porosity. Cyclically acidified salt spray tests have also been used to determine the exfoliation corrosion resistance of aluminum alloys [69].

Outdoor corrosion is influenced by a number of factors, including corrosive atmospheres, UV light, wet/dry cycling, and temperature cycling that can occur to varying degrees in environmental zones discussed earlier. ASTM D5894 (Cyclic Salt Fog/UV Exposure of Painted Metals) alternatively exposes samples to UV light with ASTM G85 salt fog exposures. Although salt spray testing is commonly used as a screening test, this method is not reliable for accurately predicting the corrosion rate of a metal in its service environment [6].

### Electrochemical Testing

*Direct Current Methods*—Laboratory test methods include a number of direct current measurement techniques that are commonly used in electrochemical testing. Specific methods include potentiodynamic polarization, potentiostatic polarization, galvanostatic polarization, Tafel extrapolation, and polarization resistance determinations. In seawater, passive film forming alloys like aluminum or stainless steel require an induction time for pitting to occur, and thus the scan rate in a potentiodynamic test can significantly influence the results obtained. Also, the dynamic nature of these test methods may preclude the natural formation of films on a metal or alloy surface, which can cause the distorted results. Potentiostatic and galvanostatic polarization methods are often applied in studying localized corrosion. Electrochemical methods to measure the susceptibility of alloys to pitting corrosion are reviewed elsewhere [70,71]. The disadvantages associated with selecting the proper scan rate in the potentiodynamic method do not apply to the potentiostatic and galvanostatic methods [69].

The Tafel extrapolation test is capable of determining very low metal corrosion rates in a short period of time. When conditions are ideal, its accuracy is equivalent to or better than weight loss measurements. However, to maintain accuracy, the Tafel regions must encompass at least one order of magnitude of current. Also, this method can only be applied to systems that have one reduction process or the Tafel region may be distorted and corrosion rate determinations will be inaccurate. Finally, the Tafel method only yields an average, uniform corrosion rate and is not sensitive to localized corrosion. Therefore, use of this technique in seawater is considered to be limited primarily to obtaining an indication of the corrosion rate within an order of magnitude [16,72].

*Nondestructive Electrochemical Methods*—Many of the disadvantages discussed above for the Tafel extrapolation method can be eliminated by using the polarization resistance technique. This nondestructive method can be used on systems that are under either activation or diffusion

control. Very low corrosion rates can be determined accurately, quickly, and monitored as a function of time. Polarization resistance can also be used to measure the corrosion rate of a component such as a seawater tank or piping system, where inspections and weight loss tests are difficult if not prohibitive [16]. The major disadvantage with this technique is that, like the Tafel extrapolation method, the calculated corrosion rate represents a uniform corrosion value and does not measure localized corrosion [73].

Electrochemical impedance spectroscopy (EIS) uses a small amplitude, sinusoidal potential perturbation to the test material for examining the corrosion behavior of nonconductive coated metals [72–79]. This method is essentially nondestructive and does not cause any acceleration of the corrosion reaction. The EIS technique can be used to monitor corrosion of a system or coating resistance as a function of time. Decreases in the measured coating resistance suggest that the electrolyte has permeated through the coating or that there are defects in the coating [69]. Reducing the distance between the working and counter electrodes to approximately 50  $\mu\text{m}$  allows local EIS measurements to be done over uncoated and coated metal and alloy surfaces to discern surface inhomogeneities that may lead to corrosion initiation before corrosion is visually observed [80].

Electrochemical noise involves the nondestructive measurement of electrochemical transients or noise generated during corrosion processes without disturbing the system. Measurements are made by (1) monitoring potential noise through measurement of potential difference between two identical electrodes, or (2) monitoring the current noise by assessing the current fluctuations between two short identical electrodes through a zero resistance ammeter, or (3) monitoring both potential and current perturbations. Electrochemical noise has been used to evaluate localized corrosion, stress corrosion cracking or uniform corrosion in laboratory or field applications [79,81–86]. Electrochemical voltage or current noise can determine the onset of pitting or crevice attack [87–89].

### High Velocity Flow Testing

A variety of high velocity tests have been designed to evaluate cavitation and erosion properties in seawater environments. Specific tests are as follows: (a) high velocity flow tests which include venturi tubes, rotating disks, and ducts with specimens positioned in the throat sections, (b) high frequency vibration tests that utilize magnetostriction or piezoelectric devices (described in ASTM G32 (Cavitation Erosion Using Vibratory Apparatus)), and (c) impinging jet tests where rotating or stationary specimens are exposed to a high-velocity jet or droplet impact (described in ASTM G73 (Liquid Impingement Erosion Testing)) [90]. A test loop using flowing artificial seawater and 1 weight % sand was able to evaluate the relative erosion resistance of materials under consideration for valves in a piping system [91].

There are a number of disadvantages in high velocity flow laboratory testing. First of all, the results from these tests can vary widely due to differences in test technique, specimen size and shape, and environmental conditions like salinity, pH, temperature, and oxygen content. Secondly,

these tests are designed to expose small specimens to high intensity flow conditions; however, the edges of the small specimens utilized can alter turbulent flow conditions in such a manner that the results do not simulate the actual service environment. The flow dynamics and conditions produced by the different high velocity techniques vary significantly. Although these high velocity laboratory tests may not accurately simulate the desired service condition, they are still useful in ranking different metals according to their resistance to velocity effects. For reproducibility among test laboratories, it is important to run a standard control material along with the candidate test materials so that the data can be normalized with respect to the control standard [69,90].

### Environmental Cracking Test Methods

A wide variety of stress corrosion cracking, corrosion fatigue, and hydrogen embrittlement tests to study environmental cracking phenomena have been developed. These tests, which employ either a static or a dynamic load, can vary widely in terms of specimen configuration, cost, test duration, etc. A detailed summary can be found in the chapters on Environmental Cracking and Hydrogen Damage in Section IV—Testing for Corrosion Types. These tests, which employ either a static or a dynamic load, can vary widely in terms of specimen configuration, cost, test duration, etc. These tests may include the effects of cathodic protection on the susceptibility of materials to environmental cracking. In general, they fall into three major categories:

1. Constant displacement techniques include bent-beam, U-bend, wedge-open loading, and proving ring tests. In these tests, specimens are loaded to some fixed displacement and then exposed to the corrosive environment. Initiation of cracking causes the stress to be relieved, thus causing crack arrest. These tests tend to be plagued by a high degree of data scatter and in many cases do not result in providing useful design parameters.
2. Rising load techniques include the slow strain rate (SSR) test [92]. In this technique, axially-loaded tension test specimens or fatigue precracked (fracture mechanics) specimens are subjected to a rising stress, typically applied by a screw-driven testing machine. SSR tests produce a result in a reasonably short time, usually within 1–2 days. The dynamic straining reduces incubation time to the onset of cracking in susceptible materials and sustains the cracking process. The SSR method allows for evaluation of the effects of metallurgical variables such as alloy composition, heat treatment, and processing and or environmental parameters in shorter times than is usually possible with constant load or stress specimens [93]. SSR evaluation of materials via environmentally assisted cracking is generally obtained through the comparison of test results conducted in a corrosive environment versus corresponding SSR results obtained in an inert environment [93].

SSR tests tend to produce conservative results (i.e., materials that show susceptibility in these tests may not show susceptibility in service) in a relatively short period of time. This conservatism may result from the fact that engineering structures are rarely loaded in this fashion.

As such, these tests are typically used only to relatively rank susceptibility of materials to different environments [94].

3. Load controlled techniques comprise methods such as the cantilever beam test. In these tests, specimens are dead-weight loaded to produce the desired stress. Any cracks that initiate grow into an increasing stress field, resulting in failure of the specimen. Unfortunately, these tests are time-consuming and costly. However, a critical linear elastic stress intensity factor can be obtained from these tests and this parameter can subsequently be used in design or to determine the flaw tolerance of an engineering structure.

ASTM E1681 [95] provides a standard method for determining a threshold stress intensity factor for environmentally-assisted cracking of metallic materials under constant load using a cantilever beam. The cantilever beam technique utilizes long term static load testing of fatigue pre-cracked, single-edge notched beam specimens (SEN-B) manufactured to guidelines designed to produce plane-strain SCC data [96]. Test durations range from several hours to over 10 000 hours. The 10 000-hour runout time is preferred to ensure sufficient time for crack incubation (hydrogen entry and transport to the crack tip region in the case of hydrogen embrittlement) without being excessively long. The threshold stress intensity ( $K_{Isc}$ ) obtained from these tests can subsequently be used in design or to determine the flaw tolerance of an engineering structure.

## FIELD EVALUATION

### In-Service Testing

In-service testing provides the advantage of examining the corrosion behavior of a metal in the actual service environment. The advantages and disadvantages of some of these tests are briefly described below. More detail can be found in the article titled "In-Service Monitoring" in Ref 69. Section III—Types of Tests—Seawater, describes further details on seawater testing.

*Small Specimen Testing*—Small specimen testing allows a large number of variables to be evaluated at minimal cost. Small specimens can be designed to determine specific types of corrosion; for example, creviced specimens can be exposed to assess localized corrosion [69]. ASTM G16 provides guidance for establishing the number of replicate samples required for the desired reliability of the test results.

Although small specimen testing allows examination in the actual service environment, the corrosion rate determined on a small specimen is usually not consistent with the corrosion rate of a large-scale piece of equipment predominantly because it is difficult to duplicate all of the metallurgical conditions of the large equipment on a small specimen. In addition, it is difficult to simulate erosion-corrosion by small specimen testing, since small specimens can shield each other from turbulence, thus providing inaccurate results [69]. The use of spool pieces for piping/tubing may provide useful test information related to in-service performance for similar components.

*Electrical Resistance Probes*—Electrical resistance probes are small in size and can be easily installed in the service environment; however, the walls of the test equipment must be penetrated for the probes to be installed and consequently, care must be taken to avert leakage in the system. The usefulness of the probes is limited in that they provide a measurement of uniform corrosion and can be continuously monitored, but provide no information on localized corrosion such as pitting or crevice corrosion. In addition, errors can result in the probe data if the temperature is varied during the time of the measurement [69].

*Ultrasonic Measurements*—The ultrasonic thickness measurement method is quite popular for in-service corrosion testing. The major advantage of this method is that the equipment is portable and very easy to use. The major disadvantage is that a bare metal surface is required for accurate measurements. The presence of coatings and/or corrosion products can introduce errors into the thickness measurements [69]. Curved surfaces such as piping bends and small tubing diameters require special attention.

### Simulated Service Testing

Like in-service testing, simulated service testing provides the advantage of exposure to the actual environment. Fluctuations in the weather, the influence of geographical location, and bacteriological influences are part of the simulated service test environment and are factors that cannot be simulated in the laboratory [69]. Simulated service testing in seawater typically consists of panel specimens exposed on test racks suspended from a pier or a float [11]. Testing in this environment is discussed in ASTM G52 (Exposing and Evaluating Metals and Alloys in Surface Seawater). Specimens may be exposed in full immersion, splash/spray, or tidal conditions. The disadvantage of exposing panel specimens in the full seawater immersion environment is the occurrence of extensive macrofouling on the panel surfaces. The presence of these organisms prohibits inspection of the test panels during the exposure period and can result in the difficult task of removing the macrofouling after testing to obtain accurate weight loss measurements. For coated specimens, removal of the macrofouling after testing could cause partial removal of the coating as well, making an accurate corrosion assessment impossible. For this reason, simulated service testing in the full immersion testing is often conducted using filtered natural seawater to eliminate microorganisms.

## STANDARDS FOR SEAWATER TESTING

The standard listed below is specific to testing in seawater.

- ASTM G52—Standard Practice for Exposing and Evaluating Metals and Alloys in Surface Seawater

The following standards apply only to artificial seawater environments.

- ASTM D1141—Specification for Substitute Ocean Water
- ASTM D5894—Practice for Cyclic Fog/UV Exposure of Painted Metal, (Alternating Exposures in a Fog/Dry Cabinet and a UV/Condensation Cabinet)

- ASTM E1524—Standard Test Method for Saltwater Immersion and Corrosion Testing of Photovoltaic Modules for Marine Environments
- ASTM G44—Practice for Evaluating Stress Corrosion Cracking Resistance of Metals and Alloys by Alternate Immersion in 3.5 % Sodium Chloride Solution
- ISO 4623—Paints and Varnishes—Filiform Corrosion Test on Steel
- ISO 7384—Corrosion Tests in Artificial Atmosphere—General Requirements

The standards listed below describe corrosion testing and data evaluation in natural seawater or artificial seawater environments.

- ASTM E606—Recommended Practice for Constant Amplitude Low-Cycle Fatigue Testing
- ASTM E647—Test Method for Measurement of Fatigue Crack Growth Rates
- ASTM E1681-99e1—Standard Test Method for Determining a Threshold Stress Intensity Factor for Environment-Assisted Cracking of Metallic Materials
- ASTM E739—Standard Practice for Statistical Analysis of Linear or Linearized Stress-Life (S-N) and Strain-Life (e-N) Fatigue Data
- ASTM E1049—Standard Practices for Cycle Counting in Fatigue Analysis
- ASTM G1—Practice for Preparing, Cleaning, and Evaluating Corrosion Test Specimens
- ASTM G5—Reference Test Method for Making Potentiostatic and Potentiodynamic Anodic Polarization Measurements
- ASTM G15—Terminology Relating to Corrosion and Corrosion Testing
- ASTM G16—Practice for Applying Statistics to Analysis of Corrosion Data
- ASTM G30—Practice for Making and Using U-Bend Stress-Corrosion Test Specimens
- ASTM G31—Practice for Laboratory Immersion Corrosion Testing of Metals
- ASTM G32—Test Method for Cavitation Erosion Using Vibratory Apparatus
- ASTM G38—Practice for Making and Using C-Ring Stress-Corrosion Test Specimens
- ASTM G39—Practice for Preparation and Use of Bent-Beam Stress-Corrosion Test Specimens
- ASTM G46—Practice for Examination and Evaluation of Pitting Corrosion
- ASTM G47—Test Method for Determining Susceptibility to Stress-Corrosion Cracking of High-Strength Aluminum Alloy Products
- ASTM G49—Practice for Preparation and Use of Direct Tension Stress-Corrosion Test Specimens
- ASTM G59—Practice for Conducting Potentiodynamic Polarization Resistance Measurements
- ASTM G61—Test Method for Conducting Cyclic Potentiodynamic Polarization Measurements for Localized Corrosion Susceptibility of Iron-, Nickel-, or Cobalt-Based Alloys
- ASTM G71—Guide for Conducting and Evaluating Galvanic Corrosion Tests in Electrolytes
- ASTM G73—Practice for Liquid Impingement Erosion Testing
- ASTM G78—Guide for Crevice Corrosion Testing of Iron-Base and Nickel-Base Stainless Alloys in Seawater and Other Chloride-Containing Aqueous Environments
- ASTM G82—Guide for Development and Use of a Galvanic Series for Predicting Galvanic Corrosion Performance
- ASTM G100—Test Method for Conducting Cyclic Galvanostaircase Polarization
- ASTM G102—Practice for Calculation of Corrosion Rates and Related Information from Electrochemical Measurements
- ASTM G129—Standard Practice for Slow Strain Rate Testing to Evaluate the Susceptibility of Metallic Materials to Environmentally Assisted Cracking
- ASTM G139—Determining Stress Corrosion Cracking Resistance of Heat Treatable Aluminum Alloy Products Using Breaking Load Method
- GM9540P—Accelerated Corrosion Test ©.
- ISO 1462—Metallic Coatings—Coatings Other than Those Anodic to the Basis Metal—Accelerated Corrosion Tests—Method for the Evaluation of the Results
- ISO 4540—Metallic Coatings—Coatings Cathodic to the Substrate—Rating of Electroplated Test Specimens Subjected to Corrosion Tests
- ISO 7539—Corrosion of Metals and Alloys—Stress Corrosion Testing—Parts 1–7
- ISO 8993—Anodized Aluminum and Aluminum Alloys—Rating System for the Evaluation of Pitting Corrosion—Chart Method
- ISO 8994—Anodized Aluminum and Aluminum Alloys—Rating System for the Evaluation of Pitting Corrosion—Grid Method
- ISO 9591—Corrosion of Aluminum Alloys—Determination of Resistance to Stress Corrosion Cracking
- ISO 11306—Corrosion of Metals and Alloys—Guidelines for Exposing and Evaluating Metals and Alloys in Surface Sea Water
- ISO 11463—Corrosion of Metals and Alloys—Evaluation of Pitting Corrosion
- ISO 11782-1—Corrosion of Metals and Alloys—Corrosion Fatigue Testing—Part 1: Cycles to Failure Testing
- ISO 11782-2—Corrosion of Metals and Alloys—Corrosion Fatigue Testing—Part 2: Crack Propagation Testing Using Precracked Specimens
- ISO 11845—Corrosion of Metals and Alloys—General Principles for Corrosion Testing
- NACE RP0173-73—Collection and Identification of Corrosion Products

## CORROSION PERFORMANCE OF SPECIFIC MATERIALS

Metals and alloys commonly used in the seawater environment include carbon steels, stainless steels, nickel alloys, copper alloys, titanium alloys, and aluminum alloys. All of these alloys exhibit differing degrees of corrosion resistance in seawater, and in general, coatings or cathodic protection are often applied to increase the corrosion resistance of these metals. The corrosion resistance within a class of alloys may also be dependent on metallurgical differences caused by fabrication and processing or heat treatments. Joining processes such as welding, brazing, and soldering,



use of adhesives or coatings, surface roughness, and proximity to dissimilar metals or alloys also will cause changes in the corrosion resistance of materials.

Carbon steels corrode in aerated seawater conditions. Their corrosion rate decreases with time as protective barrier films are formed on the carbon steel surfaces. These protective films may be a rust layer, calcareous deposits, or biofouling. The corrosion rate of carbon steels increases in high velocity seawater because the protective barrier layer is either not allowed to form or is stripped away under the flow conditions. Also, the available oxygen at the metal surface is increased in flowing seawater, which promotes a higher carbon steel corrosion rate.

Stainless steels are susceptible to localized corrosion in quiet seawater but maintain good corrosion resistance in seawater flow conditions due to the increased oxygen supply, which promotes passivity of these alloys. Biofouling is also minimized in high velocity conditions, and this in turn minimizes the number of sites for crevice or poulitice attack [12]. Type 304 and 316 stainless steels are not recommended in flow conditions less than approximately 1.5 m/s due to deep pitting of these alloys from crevices created by biofouling [19].

Nickel-copper and nickel-chromium-molybdenum alloys are the nickel-base alloys that are typically used in seawater. The nickel-copper alloys have good corrosion resistance in high velocity seawater, but do exhibit localized corrosion in quiescent seawater [19]. Alloy 625, a nickel-chromium-molybdenum alloy, is susceptible to crevice corrosion in both quiescent and flow conditions [97–100]. Other nickel-chromium-molybdenum alloys, such as Alloys C-276, C-22, 59 and 686 have increased seawater crevice corrosion resistance as compared to Alloy 625 [97,98].

A variety of copper alloys are used in seawater applications. Their generally good resistance is due to the formation of a protective film of cuprous oxide on the metal surface. Additional deposits such as copper-containing compounds and calcareous materials often form on top of this film, which can further increase the corrosion resistance [12]. Cu-30Ni (C71500) and Cu-10Ni (C70600) have excellent general and pitting corrosion resistance in seawater [12,19].

Copper and some copper alloys do exhibit corrosion under advanced velocity conditions. Their corrosion resistance is dependent on the growth and maintenance of the protective layers formed on the metal surface. The maximum velocity recommended for copper in seawater is 0.9 m/sec. Alloying with nickel or aluminum increases the resistance of copper alloys to impingement attack [12,19].

Copper-zinc alloys (brasses) with more than 15 % zinc are susceptible to a type of dealloying called dezincification. Some aluminum bronze (Cu-Al) alloys, especially those containing more than 8 % aluminum, are also susceptible to dealloying. The dealloying in Cu-Al alloys can be prevented by adding more than 3.5 % nickel or by heat treating to obtain an  $\alpha + \beta$  microstructure [19].

Aluminum alloys are susceptible to localized corrosion in seawater under both low and high velocity conditions. However, these alloys, particularly 5XXX series and 6061 aluminum, are commonly used in marine applications [12,19].

Titanium alloys have the best corrosion resistance of the metals and alloys typically used in seawater. Titanium is a passive film-forming alloy and retains excellent resistance in both low and high velocity seawater. Some titanium alloys, specifically the all alpha and near-alpha alloys, do exhibit a susceptibility to stress corrosion cracking [12].

In addition to metals, organic composites such as graphite-reinforced epoxy are gaining increasing use in the marine environment. The advantage of these composites over conventional materials is in their high strength-to-weight and stiffness-to-weight ratios. These composites also offer excellent marine corrosion resistance [101,102], but may be susceptible to attack from the alkaline environment produced by cathodic protection techniques.

## REFERENCES

- [1] Dexter, S. C. and Culberson, C., "Global Variability of Natural Sea Water," *Materials Performance*, Vol. 19, No. 9, 1980, p. 16.
- [2] Danek, G. J., "The Effect of Sea-Water Velocity on the Corrosion Behavior of Metals," *Journal of Naval Engineers*, Vol. 78, 1966, pp. 763–769.
- [3] Hoar, T. P., *Journal of Applied Chemistry*, Vol. 11, April 1961, p. 121.
- [4] Horne, R. A., *Marine Chemistry*, Wiley-Interscience, NY, 1969, pp. 2–7.
- [5] Rowlands, J. C., "Seawater," *Corrosion: Metal/Environment Reactions*, 3rd ed, L. L. Sheir, L. L. Jarman, and G. T. Burnstein, Eds., Butterworths-Heinemann, Oxford, 1994, pp. 2:60–2:71.
- [6] Dexter, S. C., Griffin, R. B., Montemarano, J. A., Smart III, J. A., and Heidersbach, R. H., "Corrosion in Specific Industries and Environments: Marine Corrosion," *Metals Handbook: Corrosion*, 9th ed, Vol. 13, ASM International, Materials Park, OH, 1987, pp. 893–926.
- [7] Ijsseling, F. P., "General Guidelines for Corrosion Testing of Materials for Marine Applications," *British Corrosion Journal*, Vol. 24, 1989, p. 55.
- [8] Stumm, W. and Morgan, J., *Aquatic Chemistry: An Introduction Emphasizing Chemical Equilibria in Natural Waters*, 2nd ed., John Wiley & Sons, NY, 1981, pp. 556–580.
- [9] Humble, H. A., *Corrosion*, Vol. 5, 1949, p. 292.
- [10] Griffin, R. B., "Marine Atmosphere," *Metals Handbook: Corrosion*, 9th ed., Vol. 13, ASM International, Materials Park, OH, 1987, pp. 902–906.
- [11] Compton, K. G., "Seawater Tests," *Handbook on Corrosion Testing and Evaluation*, W. H. Ailor, Ed., John Wiley and Sons, NY, 1971, pp. 507–514.
- [12] Boyd, W. K. and Fink, F. W., *Corrosion of Metals in Marine Environments*, Metals and Ceramics Information Center, Columbus, OH, 1978, pp. 1–6, 13–16, 23–25, 35–39, 42–44, 48–51, 53–62.
- [13] Jones, D. A., *Principles and Prevention of Corrosion*, 2nd Ed., Prentice Hall, Upper Saddle River, NJ, 1996, p. 366.
- [14] Horne, R. A., *Marine Chemistry*, Wiley-Interscience, NY, 1969, pp. 253–259.
- [15] Phull, B. S., Pikul, S. J., and Kain, R. M., "Seawater Corrosivity Around the World: Results from Five Years of Testing," *Corrosion Testing in Natural Waters: Second Volume, ASTM STP 1300*, R. M. Kain and W. T. Young, Eds., ASTM International, West Conshohocken, PA, 1997, pp. 34–73.
- [16] Matsushima, I., "Carbon Steel—Corrosion by Seawater," *Uhlig's Corrosion Handbook*, 2nd ed., R. W. Revie, Ed., John Wiley & Sons, New York, 2000, pp. 545–553.



- [17] Laque, F. L., *Corrosion Handbook*, H. H. Uhlig, Ed., Wiley, NY, 1948, p. 383.
- [18] Perrigo, L. D., "An Overview of Corrosion in Cold Climates," Paper 306, CORROSION/2001, NACE International, Houston, TX, 2001.
- [19] Talkington, J. P. and Perrigo, L. D., "Special Aspects of Corrosion Control in the Arctic and Subarctic," *Proceedings of the International Conference of Offshore Mechanics and Arctic Engineering*, American Society of Mechanical Engineers, NY, 1994, pp. 337–344.
- [20] "Corrosion of Specific Alloy Systems," *Metals Handbook: Corrosion*, 9th ed., Vol. 13, J. R. Davis, Ed., ASM International, Materials Park, OH, 1987, pp. 556, 583–598, 612–616, 622–625, 653–654.
- [21] Fontana, M. G., *Corrosion Engineering*, 3rd ed., McGraw-Hill, NY, 1986, pp. 51–59, 100–102, 373–378, 392–398, 499–503.
- [22] Fischer, K. P. and Finnegan, J. E., "Cathodic Protection Behavior of Steel in Sea Water and the Protective Properties of the Calcareous Deposits," Paper 582, CORROSION/89, NACE International, Houston, 1989.
- [23] Luo, J. S., Lee, R. U., Chen, T. Y., Hartt, W. H., and Smith, S. W., *Corrosion*, Vol. 47, 1991, p. 189.
- [24] Mantel, K. E., Hartt, W. H., and Chen, T. Y., "Substrate, Surface Finish, and Flow Rate Influences on Calcareous Deposits," *Corrosion*, Vol. 48, 1992, pp. 489–500.
- [25] Fischer, K. P., Espelid, B., and Schei, B., "A Review of CP Demand and Anode Performance for Deep Water," Paper 13, CORROSION/2001, NACE International, Houston, 2001.
- [26] Videla, H. A., *Manual of Biocorrosion*, CRC Press, NY, 1996, pp. 13–46, 47–72, 121–136, 259–262.
- [27] Dexter, S. C., "Role of Biofilms in Determining the Rate of Localized Marine Corrosion," *Critical Factors in Localized Corrosion III*, PV 98-17, R. G. Kelly, G. S. Frankel, P. M. Natishan, R. C. Newman, Eds., The Electrochemical Society, Pennington NJ, 1999, pp. 339–352.
- [28] Little, B. J., Ray, R. I., and Pope, R. K., "The Relationship between Corrosion and the Biological Sulfur Cycle," Paper 00394, CORROSION/2000, NACE International, Houston, 2000.
- [29] Shifler, D. A., "Environmental Effects in Flow-Assisted Corrosion of Naval Systems," Paper 99619, CORROSION/99, NACE International, Houston, 1999.
- [30] Poulson, B., *Corrosion Science*, Vol. 23, 1983, p. 391.
- [31] Tuthill, A. H. and Schillmoller, C. M., *Guidelines for Selection of Marine Materials*, International Nickel Co., NY, 1971, pp. 11–13.
- [32] Shreir, L. L., "Localized Corrosion" *Corrosion: Metal/Environment Reactions*, Vol. 1, 3rd ed., L. L. Shreir, R. A. Jarman, G. T. Burnstein, Eds., Butterworths-Heinemann, Oxford, 1994, pp. 1:151–1:212.
- [33] Efird, K. D., "Effect of Fluid Dynamics on the Corrosion of Copper-Based Alloys in Seawater," *Corrosion*, Vol. 33, No. 1, 1977, p. 3.
- [34] Poulson, B. and Robinson, R., *International Journal of Heat & Fluid Flow*, Vol. 31, 1988, p. 1289.
- [35] Chexal, B., Horowitz, J., Jones, R., Dooley, B., Wood, C., Bouchacourt, M., et al., *Flow-Accelerated Corrosion in Power Plants*, EPRI and Electricite' de France, Palo Alto CA, 1996, pp. 4–11.
- [36] Gudas, J. P. and Hack, H. P., "Sulfide Induced Corrosion of Copper Nickel Alloys," Paper 93, CORROSION/77, NACE International, Houston, TX, 1977.
- [37] MacDonald, D. D., Syrett, B. C., and Wing, S. S., "The Corrosion of Cu-Ni Alloys 706 and 715 in Flowing Seawater. II," *Corrosion*, Vol. 35, 1979, p. 367.
- [38] Syrett, B. C., "The Mechanism of Accelerated Corrosion of Copper-Nickel Alloys in Sulfide-Polluted Seawater," *Corrosion Science*, Vol. 21, 1981, p. 187.
- [39] Eiselstein, L. E., Syrett, B. C., Wing, S. S., and Caligiuri, R. D., "The Mechanism of Accelerated Corrosion of Cu-Ni Alloys in Sulfide-Polluted Seawater: Mechanism No. 2," *Corrosion Science*, Vol. 23, 1983, p. 223.
- [40] Fontana, M. G. and Greene, N. D., *Corrosion Engineering*, 2nd ed., McGraw-Hill, NY, 1978, pp. 28–115.
- [41] *Uhlig's Corrosion Handbook*, 2nd ed., R. W. Revie, Ed., John Wiley & Sons, NY, 2000.
- [42] Oldfield, J. W. and Sutton, W. H., *British Corrosion Journal*, Vol. 13, 1978, p. 104.
- [43] Eklund, G. S., *Journal of the Electrochemical Society*, Vol. 123, 1976, p. 170.
- [44] Sedriks, A. J., *Corrosion of Stainless Steels*, 2nd ed., John Wiley & Sons, NY, 1996, pp. 176–184.
- [45] Hare, C. H., *Journal of Protective Coatings and Linings*, Vol. 15, No. 1, 1998, p. 67.
- [46] Oldfield, J. W., "Electrochemical Theory of Galvanic Corrosion," *Galvanic Corrosion*, STP 978, H. P. Hack, Ed., ASTM International, West Conshohocken, PA, 1988, p. 5.
- [47] Francis, R., *British Corrosion Journal*, Vol. 29, 1994, p. 53.
- [48] Hack, H. P., "Galvanic Corrosion of Piping and Fitting Alloys in Sulfide-Modified Seawater," DTNSRDC/SME-79-31, May, 1979.
- [49] Steigerwald, R., "Metallurgically Influenced Corrosion," *Metals Handbook: Corrosion*, 9th ed., Vol. 13, ASM Handbook, ASM International, Materials Park, OH, 1987, p. 131.
- [50] Eiselstein, L. E., Syrett, B. C., Wing, S. S., and Caligiuri, R. D., *Corrosion Science*, Vol. 23, 1983, p. 223.
- [51] Poulson, B. and Robinson, R., *International Journal of Heat & Fluid Flow*, Vol. 31, 1988, p. 1289.
- [52] Hirota, N. S., "Erosion-Corrosion in Wet Steam Flow," *Metals Handbook: Corrosion*, 9th ed., Vol. 13, ASM International, Materials Park, OH, 1987, p. 967.
- [53] Kuiper, G., *Cavitation and Multiphase Flow Forum*, J. W. Hoyt and O. Furuya, Eds., Vol. 23, ASME, New York, 1985, p. 1.
- [54] Butler, G. and Ison, H. C. K., *Proceedings of 1st International Congress on Metallic Corrosion*, Butterworths, London, 1961.
- [55] Scotto, V., Cintio, R. D., and Marcenaro, G., "The Influence of Marine Aerobic Microbial Film on Stainless Steel Corrosion Behaviour," *Corrosion Science*, Vol. 25, 1985, pp. 185–194.
- [56] Dexter, S. C. and Gao, G. Y., "Effects of Seawater Biofilms on Corrosion Potential and Oxygen Reduction of Stainless Steel," *Corrosion*, Vol. 44, 1988, p. 717.
- [57] Mansfield, F. and Little, B. J., "The Application of Electrochemical Techniques for the Study of MIC: A Critical Review," Paper 108, CORROSION/90, NACE International, Houston, 1990.
- [58] Mansfield, F., Tsai, R., Shih, H., Little, B. J., Ray, R., and Wagner, P., "Results of Exposure of Stainless Steel and Titanium to Natural Seawater," Paper 109, CORROSION/90, NACE International, Houston, TX, 1990.
- [59] Zhang, H. J. and Dexter, S. C., "Effect of Biofilms on Crevice Corrosion of Stainless Steels in Coastal Seawater," *Corrosion*, Vol. 51, 1995, pp. 56–66.
- [60] Dexter, S. C., "Effects of Biofilms on Marine Corrosion of Passive Alloys," *Bioextraction and Biodeterioration of Metals*, C. C. Gaylarde and H. A. Videla, Eds., Cambridge University Press, Cambridge, 1995, p. 129.
- [61] Zhang, H. J. and Dexter, S. C., "Effect of Biofilms on Critical Pitting Potentials for Stainless Steels S30400 and S31600 in Seawater," *International Conference on Microbiologically Influenced Corrosion*, P. Angell, Ed., NACE International, Houston, TX, 1995, pp. 70–71.
- [62] Scotto, V. and Lai, M. E., "The Ennoblement of Stainless Steels in Seawater: A Likely Explanation Coming from the Field," *Corrosion Science*, Vol. 40, 1998, pp. 1007–1018.
- [63] Dexter, S. C. and LaFontaine, J. P., "Effect of Natural Marine Biofilms on Galvanic Corrosion," *Corrosion*, Vol. 54, No. 11, 1998, p. 851.

- [64] Shifler, D. A., "Advanced Measures to Control Galvanic Corrosion in Piping Systems," CARDIVNSWC-TR-61-99-18, September 1999.
- [65] Treseder, R. S., "An Engineering View of Laboratory Corrosion Tests," *Laboratory Corrosion Tests and Standards*, ASTM STP 866, G. S. Haynes and R. Baboian, Eds., ASTM International, West Conshohocken, PA, 1985, pp. 5-13.
- [66] ASTM D1141-98e1: Standard Practice for Substitute Ocean Water, *Annual Book of ASTM Standards*, ASTM International, West Conshohocken, PA, 2001.
- [67] Compton, K. G., "Seawater Tests," *Handbook on Corrosion Testing and Evaluation*, W. H. Ailor, Ed., John Wiley and Sons, NY, 1971, pp. 507-514.
- [68] GM 9540P: Accelerated Corrosion Test, General Motors Engineering Standards: Materials and Processes-Procedures, General Motors Corporation, Detroit, MI, December 1997.
- [69] "Corrosion Testing and Evaluation," *Metals Handbook: Corrosion*, Vol. 13, J. R. Davis, Ed., ASM International, Materials Park, OH, 1987, pp. 197-204, 212-220, 225-226, 311-313.
- [70] Szlarska-Smialowska, Z., *Pitting Corrosion of Metals*, NACE International, Houston, TX, 1986.
- [71] Sedriks, A. J., *Corrosion of Stainless Steels*, 2nd ed., John Wiley & Sons, NY, 1996, p. 104.
- [72] Siebert, O. W., "Laboratory Electrochemical Test Methods," *Laboratory Corrosion Tests and Standards*, ASTM STP 866, G. S. Haynes and R. Baboian, Eds., ASTM International, West Conshohocken, PA, 1985, pp. 65-90.
- [73] Mansfeld, F., et al., "Evaluation of Corrosion Behavior of Coated Metals with AC Impedance Measurements," *Corrosion*, Vol. 38, No. 9, 1982, pp. 478-485.
- [74] Scantlebury, J. D., et al., "Impedance Measurements on Organic Coatings on Mild Steel in Sodium Chloride Solutions," *Electrochemical Corrosion Testing*, ASTM STP 727, F. Mansfeld and U. Bertocci, Eds., ASTM International, West Conshohocken, PA, 1981, pp. 187-197.
- [75] Murray, J. N. and Hack, H. P., "Testing Organic Architectural Coatings in ASTM Synthetic Seawater Immersion Conditions Using EIS," *Corrosion*, Vol. 48, No. 8, 1992, pp. 671-685.
- [76] Scully, J. R., "Electrochemical Impedance of Organic Coated Steel: Correlation of Impedance Parameters with Long Term Coating Deterioration," DTRC/SME-86/108, David Taylor Research Center, Annapolis, April 1988.
- [77] MacDonald, D. D. and McKubre, M. C. H., "Electrochemical Impedance Techniques in Corrosion Science," *Electrochemical Corrosion Testing*, ASTM STP 727, F. Mansfeld and U. Bertocci, Eds., ASTM International, West Conshohocken, PA, 1981, pp. 110-149.
- [78] *Electrochemical Impedance: Analysis and Interpretation*, ASTM STP 1188, J. R. Scully, D. C. Silverman, and M. W. Kendig, Eds., ASTM International, West Conshohocken, PA, 1993.
- [79] Mansfeld, F., Han, L. T., and Lee, C. C., "Analysis of Electrochemical Impedance and Noise Data for Polymer Coated Metals," *Corrosion Science*, Vol. 39, 1997, pp. 255-279.
- [80] Lillard, R. S., Kruger, J., and Tait, W. S., "Using Local Impedance Spectroscopy for Monitoring Coating Performance in Condensing Environments," *Corrosion*, Vol. 51, 1995, pp. 251-259.
- [81] Bertocci, U., "Electrochemical Noise and Its Analysis to Corrosion," Paper 24, CORROSION/89, NACE International, Houston, TX, 1989.
- [82] Bertocci, U., "Statistics of Localized Breakdown Noise," *Proceedings of the 2nd International Conference on Localized Corrosion*, NACE-9, H. Isaacs, U. Bertocci, J. Kruger, and S. Smialowska, Eds., NACE International, Houston, TX, 1990, pp. 127-136.
- [83] Eden, D. A., Rothwell, A. N., and Dawson, J. L., "Electrochemical Noise for Detection of Susceptibility to Stress Corrosion Cracking," Paper 444, CORROSION/91, NACE International, Houston, TX, 1991.
- [84] Syrett, B. C. and Cox, W. M., *Proceedings of the First Intl. Symposium on Electrochemical Noise Measurements for Corrosion Applications*, ASTM STP 1277, J. R. Kearns, J. R. Scully, P. R. Roberge, D. L. Reichert, and J. L. Dawson, Eds., ASTM International, West Conshohocken, PA, 1996, p. 173.
- [85] Mansfeld, F., Sun, Z., Speckert, E., and Hsu, C. H., "Electrochemical Noise Analysis (ENA) for Active and Passive Systems," Paper 418, CORROSION/2000, NACE International, Houston, TX, 2000.
- [86] Edgemon, G. L. and Barr, E. E., "Applications of Electrochemical Noise: Real Time Plant and Field Challenges," Paper 283, CORROSION/2001, NACE International, Houston, TX, 2001.
- [87] Mansfeld, F., Sun, Z., Hsu, C. H., and Nagiub, A., "Electrochemical Impedance (EIS) and Electrochemical Noise Analysis (ENA) for Active and Passive Systems in Chloride Media," *New Trends in Electrochemical Impedance (EIS) and Electrochemical Noise Analysis*, PV2000-24, F. Mansfeld, E. Huet, and O. R. Mattos, Eds., The Electrochemical Society, Pennington, NJ, 2001.
- [88] Cottis, R. A., Bagley, G., Alawadhi, A. A., Al-Mazeedi, H., and Laycock, P. J., "Electrochemical Parameter for the Identification of Localized Corrosion," *New Trends in Electrochemical Impedance (EIS) and Electrochemical Noise Analysis*, PV2000-24, F. Mansfeld, E. Huet, and O. R. Mattos, Eds., The Electrochemical Society, Pennington, NJ, 2001.
- [89] Berthome, G. and Baroux, B., "Crevice Corrosion of Stainless Steel: Electrochemical Noise Analysis at Rest Potential," *New Trends in Electrochemical Impedance (EIS) and Electrochemical Noise Analysis*, PV2000-24, F. Mansfeld, E. Huet, and O. R. Mattos, Eds., The Electrochemical Society, Pennington, NJ, 2001.
- [90] Lichtman, J. Z., Kallas, D. H., and Rufolo, A., "Evaluating Erosion (Cavitation) Damage," *Handbook on Corrosion Testing and Evaluation*, W. H. Ailor, Ed., John Wiley and Sons, NY, 1971, pp. 453-472.
- [91] Ruedisueli, R. L. and Aylor, D. M., "Erosion Resistance Testing for Candidate Seawater Valve Materials," Paper 468, CORROSION/2001, NACE International, Houston, TX, 2001.
- [92] Parkins, R. N., "Slow Strain Rate Testing—25 Years Experience," *Slow Strain Rate Testing for the Evaluation of Environmentally Induced Cracking, Research and Engineering Applications*, ASTM STP 1210, R. D. Kane, Ed., ASTM International, West Conshohocken, PA, 1993.
- [93] Kane, R. D., "Testing for Environmentally Assisted Cracking," *Uhlig's Corrosion Handbook*, 2nd ed., R. W. Revie, Ed., John Wiley & Sons, Inc., NY, 2000, p. 1117.
- [94] ASTM G139-00: Slow Strain Rate Testing to Evaluate the Susceptibility of Metallic Materials to Environmentally Assisted Cracking, *Annual Book of ASTM Standards*, ASTM International, West Conshohocken, PA, 2000.
- [95] ASTM E1681-99e1: Standard Test Method for Determining a Threshold Stress Intensity Factor for Environmentally Assisted Cracking of Metallic Materials, *Annual Book of ASTM Standards*, ASTM International, West Conshohocken, PA, 1999.
- [96] Novak, S. R. and Rolfe, S. T., "Comparison of Fracture Mechanics and Nominal Stress Analyses in Stress Corrosion Cracking," *Corrosion*, Vol. 26, No. 4, April 1970.
- [97] Klein, P. A., Ferrara, R. J., and Kain, R. M., "Crevice Corrosion of Nickel-Chromium-Molybdenum Alloys in Natural and Chlorinated Seawater," Paper 112, CORROSION/89, NACE International, Houston, TX, 1989.
- [98] Aylor, D. M., et al., "Crevice Corrosion Performance of Candidate Naval Ship Seawater Valve Materials in Quiescent and Flowing Natural Seawater," Paper 329, CORROSION/99, NACE International, Houston TX, 1999.

- [99] Kain, R. M. and Klein, P. A., "Crevice Corrosion Propagation Studies for Alloy N06625: Remote Crevice Assembly Testing in Flowing Natural and Chlorinated Seawater," Paper 158, CORROSION/90, NACE International, Houston TX, 1990.
- [100] Jurinski, M. P. and Scully, J. R., "Crevice Corrosion of Alloy 625 in Chlorinated ASTM Seawater," *Proceedings of the 46th Meeting of the Mechanical Failures Prevention Group*, Virginia Beach, VA, April 1992, pp. 87–102.
- [101] Brown, S. R. and Deluccia, J. J., "Corrosion Characteristics of Naval Aircraft Metals and Alloys in Contact with Graphite-Epoxy Composites," *Proceedings of the Environmental Materials Conference*, Blacksburg, VA, October 1977, pp. 277–288.
- [102] *Handbook of Composites*, G. L. Lubin, Ed., Van Nostrand Reinhold Company, NY, 1982, pp. 699–702.

# Freshwater

Walter T. Young<sup>1</sup> and Philippa Fairer<sup>1</sup>

CORROSION TESTING in freshwater environments is performed to determine the corrosion characteristics of water, evaluate the behavior of various materials when exposed to water, and evaluate various corrosion mitigation methods. For example, waters in cooling systems are often analyzed to determine how much and what forms of corrosion might occur on a given metal. Screening tests are used to select the most appropriate metal for use as piping material. Various water treatment alternatives can be tested in the laboratory or in a pilot plant. Tests are used to monitor the selected treatment scheme. Laboratory screening tests, detailed simulations, pilot plant studies, and system monitoring are typical corrosion testing methods. In any event, the selection of the appropriate test method will depend on the objectives of the test, details of the system, and the process parameters (e.g., flow, temperature, and chemistry). Test design and analysis are covered elsewhere in this book as well as in the referenced documents. This chapter discusses the causes and types of corrosion common in freshwater systems and the standardized tests used for evaluation. Freshwater can be defined simply as water that is not salty and brackish water is defined by the dictionary as water having a somewhat salty taste. A more quantitative definition of brackish water is water with a salinity between 0.5 and 17 parts per thousand [1] (Ref *ASM Materials Engineering Dictionary*, J. R. Davis Ed., ASM International, Materials Park, OH, 1992). Then freshwater can be further defined as water with a salinity less than 0.5 parts per thousand. For the purposes of this chapter, freshwater systems include potable water, heating/cooling, condensate, rivers, streams, and lakes.

## THE FRESHWATER ENVIRONMENT

In designing an effective laboratory test program, it is important to consider factors that influence corrosion in a freshwater environment. The following discussion summarizes these factors, but the complexity of the topic does not permit a detailed discussion in this chapter. Details on corrosion processes affecting metals in freshwaters are found in the references provided at the end of this chapter [1–5].

<sup>1</sup>Principal Engineer and Former Engineer, respectively, Corpro Companies, 610 Brandywine Parkway, West Chester, PA 19380.

## Water Chemistry

Although water has a definite molecular structure, freshwater is not a pure substance and may contain numerous ions, dissolved minerals, and gases. Examples of dissolved solids include calcium, magnesium, manganese, nitrates, iron, copper, lead, chlorides, sulfates, carbonates, and bicarbonates. Chemistry is one of the most important factors affecting the corrosion of metals in water. Dissolved salts, such as chlorides and sulfates, cannot only increase the aggressiveness of the water, but also affect the ability of the water to form protective deposits. Generally, waters with higher dissolved salt contents are more corrosive. Dissolved gases also affect the corrosivity of water. Oxygen and carbon dioxide concentrations can increase corrosivity, as does hydrogen sulfide. Not all metals are affected the same in a given water composition.

Acidity and alkalinity affect the corrosion rate. Generally, alkaline conditions favor lower corrosion rates; however, some metals, such as aluminum and zinc, are amphoteric and show increased corrosion at pH values above 9. For iron alloys, the corrosion rate is relatively steady between a pH of 4 and 10 at ambient temperature and where oxygen reduction is the primary cathodic corrosion reaction; however, the corrosion rate increases rapidly below pH 4 [4]. Iron passivates and the corrosion rate decreases rapidly above a pH of 10, except at very high pH levels where the corrosion rate again can increase.

The solubility of elements in freshwater is limited and the solubility of calcium and magnesium carbonates are of particular importance in freshwaters. The solubility of carbonates is inversely proportional to the temperature of the water. In other words, as the water temperature increases, calcium and magnesium carbonates become less soluble. If the solubility decreases sufficiently, carbonates will precipitate and form a scale on the surfaces of the system. This scale can provide a protective barrier to prevent corrosion of the metallic elements in a system. Excessive scale deposits can interfere with water flow and heat transfer. The quality of the scale is dependent on the quantity of calcium that can precipitate as well as water flow and the chloride and sulfate content of the water. The tendency of water to precipitate a carbonate scale is estimated from corrosion indices such as the Langelier Saturation Index (LSI) and Caldwell-Lawrence calculations [6–8] which use calcium, alkalinity, total dissolved solids, temperature and pH properties of the water. Other indices, such as the Ryznar Index

purport to indicate corrosivity directly using the same elements as the LSI [6]. Manganese in excess of 0.50 mg/L can cause pitting of copper in hot water systems [1]. Copper in excess of 0.1 mg/L causes pitting of galvanized steel and aluminum if the zinc and aluminum are downstream of the copper [1]. The reversal of the potential between zinc galvanizing and steel can occur in some water resulting in the steel becoming the anode in a bimetallic couple. This normally occurs in hot water with relatively high carbonates, bicarbonates, phosphates, and silicates relative to sulfate and chlorides.

### Process Conditions

Water velocity and turbulence can damage protective films and deposits on metal surfaces causing increased corrosion. Soft metals, such as copper, are particularly susceptible to erosion corrosion, but steel and other metals are also susceptible if the water velocity is sufficiently high. The critical velocity for erosion-corrosion of copper in freshwater is about 5 fps (1.52 m/s), but this velocity can drop sharply as the chemical corrosivity of the water increases. Suspended solids in the water can increase the erosion characteristics of the water [1]. Deposits can result in accelerated corrosion from the formation of oxygen differential concentration corrosion cells.

Generally, higher temperatures cause an increase in corrosion activity and a corresponding increase in metal loss, particularly in a closed (pressurized) system. If the system is open, increasing the temperature beyond 91°C causes a decrease in corrosion since oxygen is removed from the water. Higher temperatures can also cause the solids in a system (where evaporation occurs) to concentrate, which can lead to increased corrosion rates. Increased temperature can cause an increase in the scaling tendency of the water resulting in lower corrosion rates.

The use of water treatment can increase or decrease corrosion rate. Excessive amounts of chlorine (used as a biocide) can increase corrosion. Water softening can also lead to increased corrosion rates. On the other hand, additions of caustic, soda ash, or corrosion inhibitors are used to decrease corrosion rates. Aeration can decrease corrosion rates when used to remove carbon dioxide. Deaeration is also used to decrease corrosion rates in some systems.

### Biological Factors

Biological corrosion is not a separate corrosion type, but biological activity can increase corrosion rate either by increasing the occurrence of concentration cell corrosion beneath the biomass or by producing corrosives from metabolic processes. Corrosion occurs as one of the common forms discussed below. Bacteria can survive under most conditions found in water systems and are either aerobic or anaerobic. *Desulfovibrio desulficans* is an anaerobic sulfate reducing bacterium that can be found in cooling towers and potable water piping. *Thiobacillus thiooxidans* (an acid producer) is another anaerobic bacterium known to influence corrosion. An example of aerobic bacteria is iron bacteria (*Gallionella*), which are found in some water wells. Slimes also influence corrosion by promoting concentration cell corrosion [2]. Metal reducing

bacteria cause pitting of stainless steel. Manganese in the presence of anaerobic manganese fixing bacteria (e.g., *Gallionella*, *Sphaerotilus*) and chloride, can cause pitting corrosion of stainless steel in fresh water.

### Metallurgy

In gray cast iron, the iron can be selectively removed leaving the graphite matrix—a process called graphitization. High-zinc brasses and aluminum-bronzes might be subject to selective leaching of specific elements in the alloy. In brass, the zinc selectively corrodes, leaving behind a weak, spongy, porous, copper-rich matrix. The process, dezincification, generally occurs in relatively corrosive, soft, and acidic waters. Aluminum bronzes can undergo selective leaching of aluminum (dealuminification) under conditions similar to dezincification. Stainless steels can undergo intergranular corrosion at welds and elsewhere caused by the effective removal of chromium from the metal matrix by combination with carbides under high temperature exposure. Denickelification is the selective removal of nickel from copper-nickel alloys, which has been found in fresh waters under conditions of high heat flux and low water velocity [16]. Brass is also subject to stress corrosion cracking in water where tensile stress and a corrosion species, such as nitrate or ammonia, are present in the water.

### Other Factors

Poor workmanship and defective materials can increase corrosion. Water turbulence effects can be increased by poor workmanship, such as the failure to ream burrs from cut ends of copper pipe. This increases the turbulence at the joints and results in erosion of the copper. Excessive and corrosive flux used in soldered coppers joints results in pitting corrosion along the flux runs. Incomplete longitudinal welds in electric resistance welded (ERW) steel pipe result in concentration cell corrosion and rapid corrosion.

Contamination of the water system can increase the corrosion rate. In cooling tower systems, water corrosivity is increased by the absorption of sulfur gases from the atmosphere. Airborne salts can contaminate open water systems. Process water systems can be contaminated with process debris, such as fibers and chemicals that can increase the corrosion rate.

## TEST METHODS

Table 1 shows the most common forms of corrosion that affect metals in the freshwater environment. These corrosion forms are described in ASTM G 15, Terminology Relating to Corrosion and Corrosion Testing.

The following section provides information about the use and applicability of various corrosion tests. Details of performing the tests are provided in the cited references and in the chapter on Types of Tests. Tables 2 through 10 list the test methods applicable to the various tests.

### Electrolyte Chemistry

In designing a test program, it is important to know the chemistry of the system water in order to accurately simulate

**TABLE 1**—Corrosion forms affecting common engineering metals in freshwater.

Metal	Corrosion Form
Steel	Uniform
	Pitting
	MIC
	Erosion
	Galvanic
	Fretting
Galvanized steel	Concentration cell
	Uniform
	Pitting
	Galvanic
	MIC
Cast and ductile iron	Concentration cell
	Uniform
	Pitting
	MIC
Copper	Concentration cell
	Uniform
	Pitting
	Crevice
	Erosion corrosion
	Cavitation
	Galvanic
Bronze	Concentration cell
	Pitting
	De-alloying
	Cavitation
Brass	Concentration cell
	Pitting
	Cavitation
	De-alloying
	Stress corrosion cracking
Aluminum	Concentration cell
	Pitting
	Galvanic
	Bacterial
Stainless Steel	Concentration cell
	Pitting
	MIC
	Stress corrosion cracking
	Crevice
	Intergranular corrosion
	Concentration cell

MIC = Microbiologically Influenced Corrosion

the environment of interest. Knowledge of the water chemistry will not provide quantitative corrosion data, but will provide insight into the corrosivity of the water. The chemical constituents of importance in corrosion are: pH, conductivity (or resistivity), total dissolved solids, chlorides, sulfates, suspended solids, alkalinity, carbonates, bicarbonates, hardness, carbon dioxide, oxygen, sulfur dioxide, nitrates, manganese and heavy metals. Also, the scaling tendency of the water should be determined by either the LSI or Caldwell-Lawrence diagrams [7,8]. A computer program for calculating the scale-forming tendencies is available from the American Water Works Association, Denver, Colorado.

Applicable test methods can be found in the following publications:

1. ASTM Annual Book of Standards, Volume 11.01
2. Standard Methods for the Examination of Water and Wastewater, 20th Ed., American Public Health Association, Washington, D.C., 1998
3. NACE TM0374, Laboratory Screening Tests to Determine the Ability of Scale Inhibitors to Prevent the Precipitation

of Calcium Sulfate and Calcium Carbonate from Solution, NACE International, Houston, Texas

## Uniform Corrosion

Uniform corrosion is readily measured with standard test procedures. Weight loss testing, polarization resistance, Tafel extrapolation, resistance change measurements, and AC impedance all measure the average corrosion rate of a sample surface. Each test is conducted by immersing the sample in the environment and averaging the corrosion losses, current flows, or volume changes over the entire surface area. However, nonuniform corrosion will provide inaccurate corrosion rates since the results are averaged over the surface area. Specimens must be visually examined for signs of pitting, crevice corrosion, stress-corrosion cracking (SCC), or other localized corrosion. When using electrochemical or resistance tests, parallel immersion testing should be conducted to determine if localized corrosion will occur.

Weight loss is the easiest and least expensive method since that method requires only test specimens, the solution, a container, and the appropriate environmental parameters. Weight loss tests can be conducted in low and low conductivity solutions, even in the atmosphere. An analytical balance is required for both before and after weight measurements. Multiple specimens must be used when evaluating the change in corrosion rate over time. Specimens cannot be reused for corrosion rate versus time measurements after first exposed and cleaned because high initial corrosion rates will occur each time the specimen is used. This will lead to artificially high corrosion rate data.

Weight loss testing is widely used both in the laboratory and for in-plant testing. For in-plant tests, racks of corrosion samples or single coupons are inserted at locations where corrosion rates are desired. Test specimens can be inserted in pipes or other structures using "hot-tap" devices and in bypass loops. Weight loss testing is slow (especially in systems with low corrosion rates) and does not allow instantaneous measurement. Extreme care must be exercised in designing weight loss tests since velocity, crevice, stagnation, and heat transfer conditions will influence the results.

DC polarization measurements, both polarization resistance and Tafel extrapolation, provide the ability to measure instantaneous corrosion rates and corrosion rate variation over time [9,10]. Standard polarization techniques assume a uniform corrosion rate, although special techniques can be used to evaluate localized corrosion. The solution must have sufficient conductivity to perform this test. Solutions with low conductivity require correction factors or special techniques to account for the effect of voltage drops on the measured specimen potential caused by current flow through the solution (IR drop). Tafel extrapolation requires relatively large changes to the electrochemical potential that can damage the specimen. In addition, relatively long test times are required. Corrosion reactions that are not under activation control will obscure the Tafel slope. On the other hand, significant information on the corrosion process is obtained from full anodic and cathodic polarization curves. Polarization resistance requires only small changes in specimen electrochemical potential; therefore, this method is fast and does less damage to the specimen compared to

**TABLE 2**—Test methods for evaluating uniform corrosion.

Test Method	Test Title	Application
ASTM D 2688	Test Method for Corrosivity of Water in the Absence of Heat Transfer (Weight Loss Methods)	Provides weight loss methods to evaluate corrosion directly in piping systems.
ASTM G 1	Standard Practice for Preparing, Cleaning, and Evaluating Corrosion Test Specimens	Provides methods for cleaning and evaluating weight loss coupons.
ASTM G 3	Standard Practice for Conventions Applicable to Electrochemical Measurements in Corrosion Testing	Information on reporting and displaying polarization measuring techniques, including both DC and AC methods.
ASTM G 4	Standard Method for Conducting Corrosion Coupon Tests in Plant Equipment	Provides guidelines for in-plant testing—weight loss coupons, specimen racks, reporting.
ASTM G 31	Standard Practice for Laboratory Immersion Corrosion Testing of Metals	Describes procedures for conducting laboratory weight loss tests Provides information on reporting and factors to be aware of.
ASTM G 59	Standard Practice for Conducting Potentiodynamic Polarization Resistance Measurements	Provides details on how to conduct DC polarization resistance tests.
ASTM G 96	Standard Guide for On-Line Monitoring of Corrosion in Plant Equipment (Electrical and Electrochemical Methods)	Provides details on conducting polarization resistance and electrical resistance tests.
ASTM G 102	Standard Practice for Calculation of Corrosion Rates and Related Information from Electrochemical Measurements	Describes practice for converting corrosion current data from electrochemical polarization measurements to corrosion rate.
NACE TM-01-71 <sup>a</sup>	Autoclave Testing of Metals in High Temperature Water	Methods for testing water at temperatures greater than 100°C but less than 360°C Test is weight loss method, but could be modified for electrochemical techniques.
NACE TM-02-74	Dynamic Corrosion Testing of Metals in High Temperature Water	Similar to TM-01-71, but uses circulating loop and heat exchangers Weight loss method.
NACE TM-01-69	Laboratory Corrosion Testing of Metals for the Process Industries	Discusses factors of concern for laboratory testing. Discusses planning tests and evaluation Emphasizes weight loss methods.
NACE RP-0775-87 <sup>b</sup>	Preparation and Installation of Corrosion Coupons and Interpretation of Test Data in Oilfield Operations	Discusses the use of weight loss coupons, interpretation of data, and analysis Principals are applicable to freshwater systems.

<sup>a</sup>Test method.<sup>b</sup>Recommended practice.

Tafel extrapolation. Polarization can be applied to field testing and monitoring. Computerized equipment is available for both types of tests. Instruments based on the polarization resistance technique are widely used for process monitoring.

Resistance probes are used for in-plant corrosion testing. As a metal corrodes, its volume decreases with a corresponding increase in resistance. Resistance probe instruments are commercially available on the market. Probes can be made from many different metals and alloys. The probes are inserted into the environment and the loss of cross-sectional area of the probe element is detected by its increase in electrical resistance with time. The data obtained by plotting resistance against time of exposure provide a graphic history of corrosion rate. Resistance probes can be used in low-conductivity solutions. Visual inspection is necessary to differentiate between pitting and general metal loss. Pitting can result in the appearance of low corrosion rate followed by rapid increases in corrosion. The method is not very sensitive either to very low or to rapid changes in corrosion rate. The positions of the probe in the environment, the fluid velocity, and heat transfer have a pronounced effect on the results. ASTM Test Method G 96 provides the details about conducting this test.

Electrochemical impedance spectroscopy (EIS) provides detailed information on the corrosion reaction by determining the equivalent electrical circuit of a corroding system.

The method requires low potential changes in the system and can be used in low-conductivity solutions. Complex equipment is needed to conduct the tests and specialized knowledge is needed to interpret the data [11,12]. Table 2 provides information on standard test methods for evaluating uniform corrosion.

### Pitting Corrosion

Pitting corrosion is difficult to evaluate because it can initiate at random locations on a metal surface. Large areas of a surface can be corrosion-free with pits only at a few locations. Small corrosion coupons might not show pitting or might not provide enough pit depth data for a reliable analysis. On the other hand, the surface can have a large number of pits over a given area. Immersion testing using specimens of sufficient size and number should be used to measure corrosion rate accurately. The depth of pitting follows the normal probability distribution. Extreme value statistical analysis provides a useful tool to evaluate pitting [13,14]. Pit depths can be measured using calipers, micrometer, or metallurgical microscope with a calibrated focus. Cyclic anodic polarization curves are used to provide relative susceptibility to pitting corrosion. This method does not provide specific corrosion rate data. Table 3 provides the standard test methods for evaluating pitting corrosion.

**TABLE 3**—Test methods for evaluating pitting corrosion.

Test Method	Test Title	Application
ASTM F 746	Standard Test Method for Pitting or Crevice Corrosion of Metallic Surgical Implant Materials	Measurement of pitting or crevice tendency by measuring repassivation tendency after polarization at noble potential. Applicable only to passive alloys.
ASTM G 16	Standard Guide to Analysis of Corrosion Data	Discusses statistical analysis methods of corrosion data.
ASTM G 46	Standard Practice for Examination and Evaluation of Pitting Corrosion	Provides information needed for collecting and interpreting pitting data.
ASTM G 61	Standard Test Method for Conducting Potentiodynamic Polarization Measurements for Localized Corrosion Susceptibility of Iron-, Nickel-, or Cobalt-Based Alloys	Provides information on conducting cyclic anodic polarization tests. Useful procedure for evaluating pitting and crevice corrosion susceptibility. Can be modified for other alloys that exhibit passive behavior.

### Crevice and Concentration Cell Corrosion

Crevice corrosion, and concentration cell corrosion, susceptibility can be measured directly, by exposing test specimens to the environment. ASTM F 746, G 48, and G 78 can be used for evaluating these forms of corrosion. These methods were designed to measure crevice corrosion in severe electrolytes such as salt solutions, but can be modified for freshwaters.

Electrochemical polarization can also be used by conducting cyclic anodic polarization scans. This technique, described in ASTM G 61, provides a qualitative approach to evaluating crevice corrosion. Polarization can be used to provide a more quantitative analysis by applying a graphical technique. This approach uses the same general method as described under galvanic corrosion in ASTM G 82. Its use requires knowledge of the solution chemistries inside and outside of the crevice and the ability to simulate these environments for the anodic and cathodic tests. Table 4 provides information on standard test procedures for evaluating crevice corrosion.

### Galvanic (Bimetallic) Corrosion

The galvanic series might be used to predict the possibility of galvanic corrosion, but it cannot be used to predict the quantity of corrosion that can occur. Most published

galvanic series apply only to the seawater environment and some metals behave differently in different environments. For example, stainless steels can behave either in the active state or in the passive state depending on the environment and the metals they are connected to. Sometimes the behavior of a galvanic couple in a particular environment can be the reverse of that shown in most published galvanic series. Also, metals polarize (change potentials as a result of current flow) when connected to each other in an electrolyte. This will affect the corrosion behavior and cannot be predicted from the galvanic series. The area ratio of the two metals has a marked influence on the corrosion rate of the bimetallic couple. The solution operating conditions (e.g., aeration, movement) also can have significant effect(s).

Two test methods can be employed to determine the susceptibility of two metals to galvanic corrosion in an electrolyte. In the first method, the two metals are immersed in the electrolyte and the current flow between them is measured using a zero resistance ammeter. The corrosion current is calculated according to the following relationship:  $I_{cl} = I_g + I_{la}$ , where  $I_{cl}$  is the total current,  $I_g$  is the measured galvanic corrosion current, and  $I_{la}$  is the local action corrosion current measured by another technique. The galvanic corrosion rate is calculated using Faraday's Law. ASTM G 71 describes the method.

The galvanic corrosion behavior can be predicted using polarization behavior. Electrochemical potential measurements

**TABLE 4**—Test methods for evaluating crevice corrosion.

Test Method	Test Title	Application
ASTM F 746	Standard Test Method for Pitting or Crevice Corrosion of Metallic Surgical Implant Materials	Measurement of pitting or crevice tendency by measuring repassivation tendency after polarization at noble potential. Applicable only to passive alloys.
ASTM G 48	Standard Test Methods for Pitting and Crevice Corrosion Resistance of Stainless Steels and Related Alloys by the Use of Ferric Chloride Solution	Method for characterizing crevice and pitting resistance of metals. Specific to chloride containing environment, but useful for any environment where ion concentration or oxygen differential corrosion can occur.
ASTM G 61	Standard Test Method for Conducting Potentiodynamic Polarization Measurements for Localized Corrosion Susceptibility of Iron-, Nickel-, or Cobalt-Based Alloys	Provides information on conducting cyclic anodic polarization tests. Useful procedure for evaluating pitting and crevice corrosion susceptibility. Can be modified for other alloys that exhibit passive behavior.
ASTM G 78	Standard Guide for Crevice Corrosion Testing of Iron-Base and Nickel-Base Stainless Alloys in Seawater and Other Chloride Containing Aqueous Environments	Useful for evaluating crevice corrosion susceptibility in any environment where ion or oxygen concentration cells can occur.



**TABLE 5**—Test methods for evaluating galvanic (bimetallic) corrosion.

Test Method	Test Title	Application
ASTM G 71	Standard Guide for Conducting and Evaluating Galvanic Corrosion Tests in Electrolytes	Evaluation of galvanic corrosion using two dissimilar metals in an electrolyte connected through a zero resistance ammeter.
ASTM G 82	Standard Guide for Development and Use of a Galvanic Series for Predicting Galvanic Corrosion Performance	Procedure for development of a galvanic series in an electrolyte.

**TABLE 6**—Test methods for evaluating erosion corrosion.

Test Method	Test Title	Application
ASTM G 40	Standard Terminology Relating to Wear and Erosion	Definition of terms for erosion and wear.
ASTM G 73	Standard Practice for Liquid Impingement Erosion Testing	Resistance to erosion from impacts of liquid drops or jets.

**TABLE 7**—Test method for evaluating cavitation corrosion.

Test Method	Test Title	Application
ASTM G 32	Standard Test Method for Cavitation Erosion Using Vibratory Apparatus	Test for comparing cavitation resistance of different alloys.

**TABLE 8**—Test methods for evaluating stress corrosion cracking.

Test Method	Test Title	Application
ASTM E 3	Methods for Preparing Metallographic Specimens	Techniques for preparing metal samples for metallographic examination.
ASTM E 807	Practice for Metallographic Laboratory Evaluation	Techniques for preparing metal samples for metallographic examination.
ASTM G 30	Standard Practice for Making and Using U-bend Stress Corrosion Test Specimens	Procedures for preparing and testing strip specimens for stress corrosion testing.
ASTM G 38	Standard Practice for Making and Using C-Ring Stress Corrosion Test Specimens	Procedures for preparing and testing tube samples or ring samples from thick solid material for stress corrosion cracking immersion testing. For testing above the elastic limit of the alloy.
ASTM G 39	Standard Practice for Preparation and Use of Bent-Beam Stress Corrosion Test Specimens	Testing strip specimens from sheet or plate for stress corrosion cracking immersion tests. For testing below the elastic limit of the alloy.
ASTM G 47	Standard Test Method for Determining Susceptibility to Stress Corrosion Cracking of High Strength Aluminum Alloy Products	Procedure for using ring or strip samples for testing 2xxx and 7xxx series aluminum alloys.
ASTM G 49	Standard Practice for Preparation and Use of Direct Tension Stress Corrosion Test Specimens	Procedures for testing axially loaded specimens. Specimens may be straight, or joined (welded, riveted or other means).
ASTM G 58	Standard Practice for Preparation of Stress Corrosion Test Specimens for Weldments	Procedures for producing welded test specimens for use in other stress corrosion tests.
ASTM G 64	Classification of Resistance to Stress-Corrosion Cracking of Heat Treatable Aluminum Alloys	

**TABLE 9**—Test methods for evaluating intergranular corrosion.

Test Method	Test Title	Application
ASTM G 61	Standard Test Method for Conducting Potentiodynamic Polarization Measurements for Localized Corrosion Susceptibility of Iron-, Nickel-, or Cobalt-Based Alloys	Provides information on conducting cyclic anodic polarization tests. Useful procedure for evaluating pitting and crevice corrosion susceptibility. Can be modified for other alloys that exhibit passive behavior.
ASTM G 108	Standard Test Method for Electrochemical Re-activation (EPR) for Detecting Sensitization of AISI Type 304 and 304L Stainless Steels	Describes cyclic polarization technique for evaluation of sensitivity to intergranular corrosion. Specific to 300 series stainless steel, but might be adaptable to other passive alloys with laboratory evaluation.

**TABLE 10**—Test method for evaluating fretting corrosion.

Test Method	Test Title	Application
ASTM F 897	Practice for Fretting Corrosion of Osteosynthesis Plates/Screws	

are used to predict which metal is the anode and which is the cathode. Anodic and cathodic polarization curves are produced for the anticipated environments then superimposed on each other at the known initial potential difference. The corrosion current is graphically determined. ASTM G 82 describes the method as does Ref 15. Table 5 provides information on standard test methods for evaluating galvanic corrosion.

### Erosion-Corrosion

Erosion corrosion resistance is measured by immersion testing and impinging an electrolyte flow onto the metal of interest. ASTM G 73 provides standardized methods for performing erosion tests. See Ref 14 for a detailed discussion about various erosion tests. Table 6 provides standard tests for evaluating erosion corrosion.

### Cavitation

ASTM G 32 provides a standardized method of conducting a cavitation test. Another nonstandard method is to construct a flow channel and mount the specimens in such a manner as to produce cavitation on the downstream side of the specimen. See Ref 16 for a detailed discussion about various cavitation tests. Table 7 provides information on G 32.

### Stress-Corrosion Cracking (SCC)

Stress corrosion cracking susceptibility is directly evaluated by immersing stressed specimens in water, then evaluating the specimens for cracks using high-magnification metallographic or low-magnification macrographic examination. ASTM G 30, G 38, G 39, G 47, G 49, G 58, and G 64 provide methods of preparing specimens and conducting immersion tests. ASTM E 3 and E 807 provide methods of metallurgical examination.

SCC susceptibility is more readily detected using slow strain rate techniques than normal tension testing. This is because the slow straining procedure allows the corrosion effects to occur [17]. Table 8 provides information on standard test methods for evaluating SCC.

### Dealloying

Dealloying is a localized phenomenon that can be evaluated through the use of immersion testing and metallographic techniques (ASTM E 3 and E 80). Energy dispersive X-ray spectroscopy (EDS) and wavelength dispersive X-ray spectroscopy (WDS) are used to detect small amounts of dealloying. Using EDS and WDS, the surface chemistry of the sample is examined to detect losses in the active element(s) and enrichment in the noble alloying element(s).

### Intergranular Corrosion

Since intergranular corrosion is limited to corrosion at or immediately adjacent to grain boundaries and is detectable at the microstructural level, simple corrosion rate calculations using weight loss measurements provide no information. Standard ASTM tests, such as the oxalic acid etch test

(ASTM A 262) provide relative susceptibility only for austenitic stainless steels. These tests have little usefulness in freshwater environments. A metallographic analysis performed after test samples are exposed provides the most useful information about susceptibility to intergranular corrosion (ASTM E 3 and E 80).

Cyclic polarization measurements provide relative information about susceptibility as described in ASTM G 61. ASTM G 108 provides a test method applicable to type 304 stainless steel. Table 9 provides information on standard test methods.

### Fretting Corrosion

Fretting corrosion can occur between two metal parts having an electrolyte and slight vibratory movement. Although ASTM F 897 is intended specifically for surgical implants, it can be modified for use in other environments. Table 10 provides information on ASTM F 897.

## REFERENCES

- [1] *Internal Corrosion of Water Distribution Systems*, 2nd ed., AWWA, Denver, CO, 1996.
- [2] Herro, H. M. and Port, R. D., *Cooling Water Systems Failures*, McGraw-Hill, New York, 1993.
- [3] Fontana, M. and Greene, N., *Corrosion Engineering*, McGraw-Hill, New York, 1967.
- [4] Uhlig, H. H., *Corrosion and Corrosion Control*, John Wiley & Sons, New York, 1967.
- [5] Lane, R. W., *Control of Scale and Corrosion in Building Water Systems*, McGraw-Hill, New York, 1993.
- [6] *Prevention & Control of Water Caused Problems in Building Potable Water Systems*, 2nd ed., NACE TPC Publ 7, 1995, NACE International, Houston, TX.
- [7] Powell, S. T., *Water Conditioning for Industry*, McGraw-Hill, New York, 1954.
- [8] *Corrosion Control by Deposition of CaCO<sub>3</sub> Films*, AWWA, Denver, CO, 1978.
- [9] Stern, M. and Geary, A. L., "Electrochemical Polarization," *Journal of the Electrochemical Society*, Vol. 104, 1957, p. 56.
- [10] Stern, M., "A Method for Determining Corrosion Rates from Linear Polarization Data," *Corrosion*, September 1958, p. 440t.
- [11] Mansfeld, F., "Recording and Analysis of AC Impedance Data for Corrosion Studies, Part I. Background and Analysis," *Materials Performance*, Vol. 36, No. 5, May 1981, p. 301.
- [12] Mansfeld, F., Kendig, M., and Tsai, M. W., "Recording and Analysis of AC Impedance Data for Corrosion Studies, Part II. Experimental Approach and Results," *Materials Performance*, Vol. 38, No. 11, November 1982, p. 510.
- [13] Aziz, P. M., "Application of Statistical Theory of Extreme Values to the Analysis of Maximum Pit Depth Data for Aluminum," *Corrosion*, Vol. 12, 1956, pp. 495-506t.
- [14] Rowe, L. C., "Measurement and Evaluation of Pitting Corrosion," *Galvanic and Pitting Corrosion—Field and Laboratory Studies*, ASTM STP 576, ASTM International, West Conshohocken, PA, 1976, p. 203.
- [15] Jones, D. A., "Polarization Studies of Brass-Steel Galvanic Couples," *Corrosion*, Vol. 40, No. 4, April 1984, p. 181.
- [16] *Corrosion Handbook*, Vol. 13, *Corrosion*, ASM International, Metals Park, OH, 1987, p. 311.
- [17] "Stress Corrosion Cracking—The Slow Strain Rate Technique," *ASTM STP 665*, G. M. Ugiansky and J. H. Payer, Eds., ASTM International, West Conshohocken, PA, 1979.

# Soils

Lucien Veleva<sup>1</sup>

## DESCRIPTION OF SOILS

### Definition and Classification [1-4,6,8]

SOIL AS A CORROSIVE ENVIRONMENT is probably of greater complexity than any other environment. The corrosion process of buried metal structures is extremely variable and can range from rapid to negligible. In fact, pipes in soil can be perforated within one year, presenting very localized or uniform corrosion attack (Figs. 1-2). With background knowledge of the principal soil specifics and their influence on metal corrosion, the most serious corrosion problems can be prevented.

In discussion of the soil as an environment for corrosion, no strict definitions exist. However, soil itself has been defined in the Soil Survey Manual of the United States Department of Agriculture as "a collection of natural bodies occupying portions of the earth's surface that support plants and that have properties due to the integrated effects of climate and living matter, acting upon parent material as conditioned by relief over periods of time." The term "soil" has also been defined as "the first few feet of finely divided, modified rock material covering the level and moderately inclined portion of the earth." The origin of soil is in the earth's crust and four main classes of soil have been proposed:

1. Soils formed in situ from soft rocks, such as chalk and volcanic ash;
2. Soils formed in situ from hard rocks such as granite, limestone, and marble;
3. Soils transported from their place of origin before weathering to form soils; they include those moved by water, such as marine and beach sediments, and also those moved by wind, such as sands and those moved by glacial drift;
4. Soils formed in situ from organic material, such as peat.

Soils are commonly named and classified according to the size range of their particulate matter. For example, **sand**, **silt**, and **clay** derive their name from the predominant size range of their inorganic constituents. Particles between 0.02 and about 2 mm are classed as fine (0.02–0.2 mm) and coarse (0.20–2.00 mm) sands. Silt particle size is from 0.002 to 0.02 mm and clay particles have a mean

diameter <0.002 mm down to colloidal matter. Table 1 presents the terminology for different soils according to ASTM Practice for Description and Identification of Soils (Visual-Manual Procedure) (D 2488). The United States and over 50 other countries now use a more detailed classification of their soils, which includes 11 major orders and 47 suborders.

Variation of the proportion of soil size groups determines many of the properties of the soil. Terms commonly used for soil classification include sandy clay, clay loam, silt loam, loamy sand, silty clay loam, sandy loam, gravel, etc. The clays are very plastic mixtures with a high moisture content and are considered to be the most important inorganic constituents of the soil. Often the clays are grouped depending upon the weathering conditions (for example, montmorillonite, illite, kaolinite). Soils of fine texture, due to high clay content, present more packed particles and have less pore capacity for moisture and gases (oxygen) diffusion than an open-type soil such as sand. The clay mineralogy and properties are closely related to the corrosion aggressiveness of soil, and this fact needs attention.

Soil has a specific gravity from 1.1 to 1.7, which is measured as described in ASTM Test Method for Density of Soil in Place by the Drive-Cylinder Method (D 2937).

The main chemical constituent of soils, such as loam, clay, and silt is  $\text{SiO}_2$ , usually along with  $\text{Al}_2\text{O}_3$ . Commonly dissolved species in wet soils are  $\text{H}^+$ ,  $\text{Cl}^-$ ,  $\text{SO}_4^{2-}$ ,  $\text{HCO}_3^-$  ions. The soil mineralogy and chemistry determine the corrosion aggressiveness of soil and need attention. Soils with the poorest drainage, like clay, silt, and loam, are the most corrosive, while soils with excellent and good drainage (gravel and sand, respectively) are the least corrosive.

Because of the complex content of the soil (including organic matter and organisms, gases, mineral particles, moisture), the relative size range does not represent the whole nature of the soil. In fact, most soils consist of aggregates of particles, which gives the possibility for moisture penetration, less erosion by water and wind, and generally great aeration and biological activity. The destruction of this structure by mechanical action or chemical alteration (such as excess alkali accumulation) can alter the physical nature of the soil. To understand the corrosion behavior of buried metal, it is also important to have information about the soil profile (section through the soil showing the various layers).

Complex physical, chemical and biological nature, corrosion aggressiveness, and dynamic interactions with the environment

<sup>1</sup>Research Professor (Corrosion Engineer and Ph.D. in Electrochemistry) at Applied Physics Department, CINVESTAV-IPN, Unidad Merida, Yucatan, C.P. 97310, Mexico

FIG. 1—Buried pipe with detected corrosion failure.

distinguish the soil. Climatic changes of sun irradiation, air temperature and relative humidity, rainfall, winds, mechanical action of natural forces, various physical, chemical and biological factors, and man's manipulation can alter the soil properties, which directly affect the corrosion rate of metals buried in the soil. The amounts of moisture and rainfall are considered of primary importance in soil evolution. They affect the type of soil that forms, the weathering process, and all changes taking place within the soil. Plant and animal life with their soil-building action, acid or base reactions in the parent material, dissolution of soluble components, the leaching out of alkaline minerals of the weathering rock, and other phenomena are strictly influenced by the changes of all the above factors.

The metal corrosion in soils is *aqueous* (in an electrolyte) and its mechanism is *electrochemical*. Three elements are necessary for the operation of the corrosion cell:

1. Galvanic **corrosion cells** operating on the metal surface formed by **anode** and **cathode** sites. Usually the metal is a good conductor for electron flow. The corrosion reaction is done on the anode areas.
2. **Electrolyte** (moisture) on the metal surface. The moisture containing dissolved ionic substances is a good ionic conductor.
3. **Oxidizing agent** (such as oxygen in air).

The conditions in soils can range from atmospheric to completely immersed metal, depending on the soil compactness

(existence of capillaries and pores) and moisture content. The corrosiveness of a soil depends upon an interaction between climate and soil reactions. The variation in soil composition and structure can create distinct corrosive environments, which results in different metal activities and oxygen concentrations (differential aeration) at the metal/soil interface.

### Characteristics of Soils Related to Corrosion [1-6,9,10]

The metal corrosion in soils is determined primarily by such factors as moisture content and its level of electrical (ionic) conductivity, aeration and oxygen content, relative acidity or alkalinity, and amount of dissolved salts. The two conditions necessary to initiate metal corrosion in soil are water (moisture) and oxygen. After these factors, a number of variables can affect the corrosion process.

#### Soil Moisture

Principally three types of water provide the soil moisture: free ground water, gravitational water, and capillary water. They have significant influence on the metal/environmental characteristics and determination of the corrosion rate. The amount of moisture in a soil can be determined by the method described in ASTM Test Method for Laboratory Determination of Water (Moisture) Content of Soil and Rock by Mass (D 2216).

FIG. 2—Corrosion produced in soil on buried metal structure.

TABLE 1—ASTM terminology for soils (Standard D 2488).

Term	Description
Clay	<0.75 $\mu\text{m}$ (passes No. 200 sieve)
Gravel	<75 mm and >4.75 mm (No. 4 sieve)
Organic clay	Clay except that its liquid limit values after oven drying are <75 % of its liquid limit value before oven drying.
Organic silt	Silt except that its liquid limit values after oven drying are <75 % of its liquid limit value before oven drying.
Peat	Soil, primarily vegetable tissue, in various stages of decomposition, usually with organic odor, dark brown or black, spongy consistency, with fibrous to amorphous texture.
Sand	Rock particles passing No. 4 sieve (4.75 mm) and retained on a No. 200 (75 $\mu\text{m}$ ).
Silt	Soil passing No. 200 sieve; nonplastic or very slightly plastic, and exhibiting little or no strength when air-dried.

The **free ground water** is present in the soil at some depth (a few meters to hundreds of meters) below the surface and usually only river crossing pipelines are surrounded by ground water. In such a situation metal corrosion occurs in an aqueous environment, e.g., on a fully-immersed metal structure.

The principal sources of the **gravitational water** are rainfall, snow, flood, and irrigation. This water enters and flows through the soil, governed by its physical structure,

including pore and capillary spaces at various zones in the soil profile, and usually percolates to the level of permanent ground water. A measure of the compactness of mineral soils is the **apparent specific gravity index**. The amount of organic matter influences this value markedly. Some impervious soils, such as clay and water resistant materials, act as effective barriers to the passage of gravitational water and cause zones of water accumulation and saturation. The tendency of the soil to crack on drying and swell when wetted is defined by the term **volume shrinkage** and it is an indicator of the colloidal nature of the clay and loam particles in a soil. In drying, the soil forms cracks that allow oxygen to flow freely to buried metals.

The **capillary water** represents an important reservoir of water in soil. A considerable amount is held in the capillary spaces of silt and clay particles. The term **moisture equivalent of soil** is a measure of the retentiveness or water holding capacity of the soil. The water retained by a soil is a consequence of equilibrium between capillary and gravitational forces. The permeability and moisture retention of granular soils can be measured by the method described in ASTM Test Method for Permeability of Granular Soils (Constant Head) (D 2434). For the water-holding capacity of peat, one can use ASTM Test Method for Volume Weights, Water-Holding Capacity, and Air Capacity of Water-Saturated Peat Materials (D 2980). The existence of moisture in good conductivity soil indicates high ion content and a possibility for very strong corrosion attack.

### Aeration and Oxygen Content

The percentage of the volume of the soil occupied by air at a certain moisture content is defined by *air-pore space* and is used for permeability characterization of the soil. High values of air-pore space could provide a dry soil environment, which does not permit the electrochemical development of corrosion. The aeration and oxygen content in soil moisture are very important for the corrosion process, because the oxygen is the principal oxidizing agent in the cathodic (electron consumption) corrosion reaction. It is generally assumed that the gases of the upper layers of soil are similar in composition to the atmosphere above the soil, except for a higher carbon dioxide content. By the fact that the plant roots require oxygen to penetrate a soil, it may be assumed that soil gases at depths of 6 m or more contain a significant amount of oxygen. For soils with coarse texture, such as sand and gravel, the circulation of air is relatively free and the corrosion rate may reach that in the atmosphere.

From a corrosion perspective, the solubility of oxygen in soil moisture (electrolyte) is one of the most significant effects. The dissolved oxygen concentration increases until the saturation limit is reached. The solubility of oxygen in water is a function of temperature and the oxygen solubility decreases as soil temperature increases. However, the temperature also increases the corrosion kinetics, even at lower levels of oxygen concentration. Some specific climates, such as warm and tropical humid (and their daily temperature variations), may cause expansion and contraction of the surface-soil gases. The oxygen content also depends on the biological activity within the soil and the consumed oxygen can be replaced with gases from metabolic activity, such as carbon dioxide.

### Relative Acidity (pH) of Soil

The soil moisture (electrolyte) can be described as acidic ( $\text{pH} < 7$ ), neutral ( $\text{pH} = 7$ ), or alkaline ( $\text{pH} > 7$ ), based on the relative ratio of hydrogen ions ( $\text{H}^+$ ) to hydroxyl ions ( $\text{OH}^-$ ). When  $\text{H}^+$  ions predominate over  $\text{OH}^-$  ions, the soil is acidic and vice versa. In a neutral solution both ions are in balance. (The value of pH indicates only the hydrogen ion concentration.) Fresh water and seawater typically have a near neutral pH. The concrete environment has a strongly alkaline  $\text{pH} \approx 13$ . The corrosion effect of soil moisture acidity or alkalinity depends very much on the specific metal of interest.

Acidity in soils is the result of natural processes of weathering under humid conditions, such as mineral leaching, decomposition of acidic plants, industrial wastes, acid rain, and certain forms of microbiological activity. Most soils range from pH 4.5 to pH 8. In this range, pH is generally not considered to be a problem for buried steel pipelines and tanks. More acid soils (pH lower than 4.5) can cause rapid metal corrosion and serious risk to common construction materials, including some stainless steel grades. In areas with moderate rainfall, soluble salts accumulate only where the water concentrates in depressions. In areas with considerable rainfall, soluble salts and bases are removed, resulting in increased acidity.

### Dissolved Salts and Corrosion Agents

The soil water is a good solvent for salts of the soil, which dissociate to form cations and anions and render the soil

conductive. In moderate rainfall areas the soil solution is relatively dilute (80 to 1500 ppm total dissolved salts). Lower salt concentrations characterize regions with extensive rainfall as a result of leaching action. Soils in arid regions are usually quite high in salts, due to surface evaporation.

The most common *cations* in the soil electrolyte are potassium and sodium in alkaline soils, magnesium and calcium in basic (calcareous) soils. Salts containing the four cations,  $\text{K}^+$ ,  $\text{Na}^+$ ,  $\text{Mg}^+$ , and  $\text{Ca}^{2+}$ , can accelerate metal corrosion. However, in non-acid soils, calcium and magnesium tend to form insoluble metal oxides or carbonates, which act as an effective barrier against corrosion. The corrosion rate in these soils may diminish significantly.

The *anions* also play a very important role in the corrosion process. If they react with metal ions, produced during the anodic corrosion reaction, and form an insoluble salt precipitate on the metal surface, this layer could act as an effective barrier against corrosion. This is the case of corrosion of lead sheathing for power and communications cables in a soil solution that contains sulfate ions ( $\text{SO}_4^{2-}$ ). The most corrosive anion for metals is the chloride ion ( $\text{Cl}^-$ ), which is usually naturally present in soils and sands of the marine-coastal regions, or it may be present as a result of external sources such as de-icing salts applied to roadways. Its attack is localized and more dangerous than the uniform corrosion, because the formed pits could perforate the metal surface. The chloride ion concentration in corrosive soil electrolytes (moisture) varies as soil conditions alternate between wet and dry.

Compared to the corrosion aggressivity of chloride ions, sulfate ions are generally considered to be less aggressive. However, they can be converted to highly corrosive sulfide ions by anaerobic sulfate reducing bacteria (SRB).

The *salt* content of soil may be altered by several human activities, such as fertilizer use in heavy doses, industrial wastes, deicing salts on road and walk ways, salt brines from petroleum production, and many others.

Another important relationship between the salt in the soil and corrosion has to do with *biological activity*. Since the growth of plants and microorganisms depend on the proper inorganic mineral nutrients, the action of these forms of life varies with the salt content of the soil.

### Microbiological Activity

The role of microbes or bacteria in the corrosion of metals is due to the chemical activities associated with their metabolism, growth, and reproduction. For example, the *microbiologically induced corrosion* (MIC) of metals by sulfate-reducing bacteria (SRB) is a recognized problem in pipelines. These bacteria are anaerobic and live in poorly drained wet soils, with a pH from 6 to 8, that contain sulfate ions, organic compounds, and minerals in the absence of oxygen and temperature from 20 to 30°C. In well-aerated soils the anaerobic bacteria cause no problem. During metabolism of the bacteria, oxygen is extracted from the sulfate ions and this reaction converts the soluble sulfates to sulfides, which attack the metal surface, forming, for example, iron sulfide ( $\text{FeS}$ ). Numerous studies established the relationship of sulfides and sulfates to bacterial activity in microbiologically induced metal corrosion [11–17].

FIG. 3—Localized corrosion attack on buried pipe accelerated by the presence of sulfate-reducing bacteria.

The corrosive microbial effect on metals can be attributed to removal of electrons from the metal and formation of corrosion products principally by:

- a) Direct chemical action of metabolic products, such as sulfuric acid, inorganic or organic sulfides and chelating agents, such as organic acids;
- b) Changes in oxygen content, salt concentration, and pH that increase the possibilities for differential diffusion and concentration gradients, etc., which establish local electrochemical corrosion cells.

Anaerobic bacteria have been reported to accelerate the normal corrosion process and convert noncorrosive soil to a very aggressive environment (Fig. 3). The environmental conditions under which the microorganisms normally operate are: temperature from 20 to 30°C, pH from 6 to 8, and soil resistivity from 500 to 20 000 ohm-cm. Rate and extent of corrosion are related directly to bacterial growth in contact with the metallic surface. Bacteria have been found that are capable of growing on many kinds of coating materials, including hydrocarbons.

#### *Disturbance of Natural Soils*

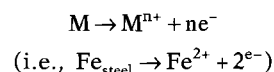
Experience shows that the pipeline ditch markedly disturbs natural soil. The operation of ditching and back-filling create several zones around the metal structure. The soil in the ditch is less compact and sometimes the disturbed soil is a mixture of surface and sub-surface soils. This new

heterogeneous soil environment may have higher moisture content, increased aeration, and microbial population. Contact with organic matter in coatings applied over the pipeline and the above factors create conditions for accelerated localized corrosion attack.

### CORROSION IN SOILS [1-6,9,10]

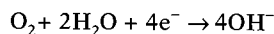
The electrochemical corrosion of metals buried in wet soils is based on the creation of multiple **corrosion cells**, formed by coupled *anodes* and *cathodes*. The *cathodes* are characterized by metal areas with a higher level of potential energy (Gibbs Free Energy) and the *anodes* have a lower potential energy. This energy difference between anodes and cathodes sites is usually due to the heterogeneity of composition of the metal structure. The soil in which the metal resides could also contribute to corrosion cell formation.

The metal corrosion is an *oxidation process* and it occurs at the **anode** areas where the metal goes into soil moisture as metal cation (ion), leaving electrons. The principal **anodic reaction** is:

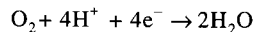


The generated free electrons flow through the metal to the **cathode** areas, where they are accepted by oxidizing

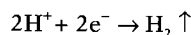
agents, such as air oxygen dissolved in the moisture. The oxidizing agents undergo a *reduction process* in the **cathodic reaction**:



In weak acid soils the cathodic reaction involves the participation of oxygen molecules and hydrogen ions ( $\text{H}^+$ ):



In strong acid soil the principal oxidizing agent is the hydrogen cation:



Different oxygen contents in the soil moisture at the metal surface can create local **oxygen concentration cells**. Wet soil with lower oxygen usually gives rise to anodic areas, while well-aerated soils form cathodic areas on the metal surface (Fig. 4). In most cases when the metal structure is exposed to different temperatures, the areas at higher temperatures become anodes and those at lower temperatures become cathodes. Since soils usually are a mixture of different kinds of soils, they often provide no uniform environment for the metal structure. This heterogeneous environment creates different and local aeration zones on the metal surface, and as a consequence can cause serious localized corrosion attack (Figs. 5–6).

Sometimes pipes are buried with mill scale ( $\text{FeO}$  and  $\text{Fe}_3\text{O}_4$  gray oxide layer) that is formed on their surface as a product of high temperature chemical corrosion during hot-rolling production and thermal treatments. This layer is an efficient protective coating for the metal, since it is resistant

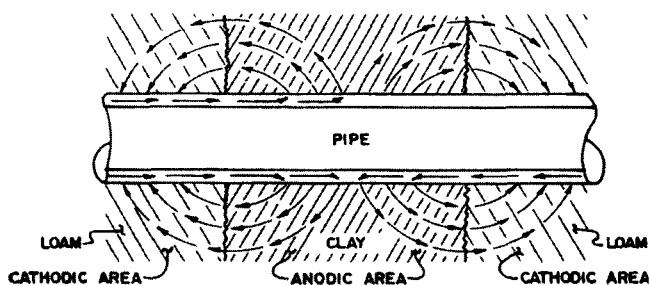


FIG. 4—A metallic pipe is anodic in wet soil with lower oxygen content and cathodic in better oxygenated soil.

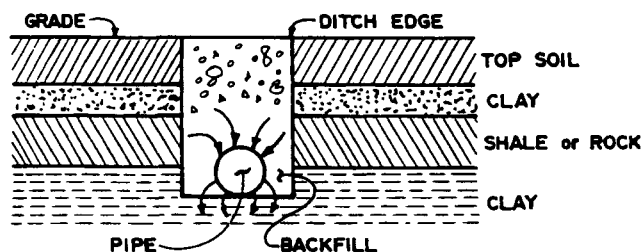


FIG. 5—Oxygen concentration corrosion cells caused by a mixture of different soils.

to corrosion and quite adherent. However, it is brittle and its structure presents a lot of heterogeneity and cracks that contribute to creation of local corrosion cells at the interface metal/scale. The *scale oxides* are electronic semiconductors, and they can serve as *cathodes*. Areas covered with scale are more cathodic than those where the metal is not covered and open to the environment. Such bare area can be a perfect *anode* for a corrosion cell (Fig. 7).

If the buried metal structure involves contact between different metals (such as mild steel, copper, bronze, brass, aluminum, zinc, lead, stainless steel, cast iron, etc.), it is possible that local **galvanic cells** can form in the contact areas (Figs. 8–9). Each metal has its own tendency to corrode. An alternative way to express the metal reactivity is to look at the excess of its free energy (standard electrochemical metal potential) and predict the *electromotive force (emf)* between metals in contact, as a general indication for the corrosion process (Table 2). The metal that has a more positive potential is nobler in the galvanic cell, and it is a cathode. The metal with a more negative potential is more active and acts as an anode in the corrosion cell, e.g., it suffers corrosion.

As corrosion proceeds, the steel changes its surface physical-chemical properties because of the formed corrosion layer. Insoluble corrosion products partially act as a physical barrier against the corrosion process. In this case, when a new repaired part of steel is connected to old steel, which has been in the soil for a relatively long time, the new section suffers corrosion because it is anodic with respect to old steel, even when the steel composition is identical.

*Stray currents*, picked up by a buried structure, could also cause metal corrosion. They are usually direct electric currents (dc) deflected from their principal service. Sources of stray currents could be direct current equipment and systems, such as electric railway systems, grounded d-c power supplies, electric welders, cathodic protection systems for underground natural gas pipelines, and electroplating plants, that are not well insulated from the earth. The metal structure suffers severe **stray current corrosion** at the area where the stray current discharges and leaves the metal, as it seeks for a new low resistance path. As shown in Fig. 10, when tracks are laid at ground level and not insulated well from the earth, some part of the load current enters the ground where the tracks are most positive (at the load) and follows an earth path back to the substation. The stray current corrosion looks like pitting on an otherwise smooth surface, and only a light rust and black carbon dust cover the spots where the stray current is discharged. Stray current prevention measures are corrective drainage and good insulation. Lead pipelines and lead cable sheathing also can suffer severe stray current corrosion caused by minor earth currents.

In certain specific soil chemistries the metal corrosion may be nonuniform, concentrated in relatively small areas that form sharply defined local holes called *pits* (Figs. 11–12), that grow deep into the metal and can cause failure by perforation. The pits are usually small in diameter, isolated from each other, and occur in more anodic metal areas with respect to the rest of the surface. The **pitting corrosion** is a very dangerous form of localized metal attack and sometimes cannot be detected by simple visual examination.



FIG. 6—General view of corrosion attack in soil at local aeration zones.

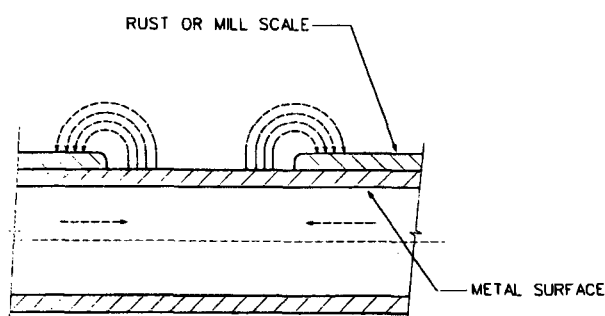


FIG. 7—Corrosion cell created on metal surface due to the presence of heterogeneity in the formed corrosion layer.

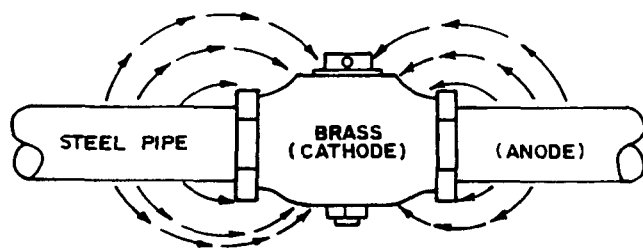


FIG. 8—Galvanic corrosion caused by contact of dissimilar metals. Steel is the anode, which suffers corrosion, and brass is the cathode. Electrons leave the steel and flow to brass.

For example, when pitting corrosion occurs together with slight or moderate general corrosion, the corrosion products often mask the pits. Soils in marine-coastal environments, containing relatively high concentrations of chloride ions (active anions), cause chloride-induced pitting corrosion on the metal structure. Once a pit initiates, an active corrosion cell is set up as shown in Fig. 13. The rapid dissolution of metal in the pit produces an excess of positive metal ions, which hydrolyze in the water solution, causing a high concentration of hydrogen ions. The cause of pitting could be associated with local inhomogeneity on the metal surface, mechanical or chemical defects (holidays) in a protective organic or oxide coating (Fig. 14), galvanic corrosion, or the presence of biological organisms. Pitting corrosion occurs in most commonly used buried metals and alloys.

Some specific corrosion environments, in the presence of applied tensile stress on the metal surface (above some threshold value), can cause **stress-corrosion cracking (SCC)**. The source of stresses can be external, but residual stresses can also cause SCC failures. Specific corrosive pollutants, which may contribute to the SCC of carbon steels, are for example, the carbonates in water. **Sulfide stress cracking (SSC)** commonly occurs on the outside of a pipe where sulfate-reducing bacteria are present at a soil pH of 3–7. Because of the produced iron sulfide (FeS), which adsorbs readily on the steel surface, hydrogen atoms generated

FIG. 9—Galvanic corrosion attack produced on the surface of buried pipe.

during the cathodic corrosion reaction cannot combine to form molecular hydrogen, and therefore, enter into the iron crystal, causing hydrogen embrittlement and initiating microcracks.

#### General Methods for Corrosion Protection

The electrochemical corrosion of metals occurs at the metal/corrosive electrolyte (metal/soil moisture) interface. Consequently, the first group of methods for corrosion protection aims to *create an efficient separation* of the metal from the aggressive environment, using metallic, organic, and inorganic coatings.

The second method includes *chemical treatment of the corrosive environment*, for decreasing its aggressiveness, by changing its pH, salt and moisture content, existing microbes, and existing bacteria, when it is economically and technically feasible.

The third method is *decreasing the metal activity*, by alloying with metals, like chromium, nickel, molybdenum, cobalt, titanium, copper, etc., that usually form passive oxide layers, that are resistant in a given environment.

From the thermodynamic point of view, some metals can be *polarized* in a range of potentials where the metal enters into an *immune* (no corrosion) or *passive state* (creation of resistant oxides). These states could be achieved, respectively, by *cathodic* and *anodic electrochemical methods of protection*, applying external polarization (potential) using direct current. *Pourbaix diagrams* provide useful

thermodynamic information on the possible metal states using metal *potential-pH* of water solution coordinates.

#### Steels, Lead, and Copper in Soils

The most frequently used materials for buried metal structures are the *carbon steels*. For prevention of their corrosion the most recommended, economical, and effective method is *cathodic protection* (CP). The use of CP is now standard procedure for long-term corrosion protection of underground pipelines, oil and gasoline tanks, and other structures. With a shift of the metal potential to more of a negative value of  $-0.85$  V versus a  $\text{Cu}/\text{CuSO}_4$  reference electrode, it is possible to make the metal surface a *cathode*, which ensures an immune (no corrosion) state of the carbon steel. Cathodic polarization is achieved by direct current, which can be supplied either by *sacrificial anodes* in galvanic contact with the steel structure, or by *impressed current* from a rectifier.

Some *organic coatings* like polymers, plastics and rubbers, other than paint, are used to advantage along with cathodic protection of steels. Coatings of coal tar, coal tar/epoxy, or fusion-bonded epoxy powders are used to ensure a passive metal protection, isolating the metal from the soil environment, and also to decrease the current required for CP. *Painting and chemical treatment* of the metal surface are seldom used. *Metal coatings* such as electroplating or thermal spraying are not recommended. Making *alloying additions* to steel buried in soils is considered not to be an

TABLE 2—Electromotive series of metals.

Metal	Metal / Formed Ion	Potential* (V)
Lithium	Li / Li +	-2.96
Rubidium	Rb / Rb +	-2.93
Potassium	K / K +	-2.92
Strontium	Sr / Sr ++	-2.92
Barium	Ba / Ba ++	-2.90
Calcium	Ca / Ca ++	-2.87
Sodium	Na / Na +	-2.71
Aluminum	Al / Al +++	-1.70
Beryllium	Be / Be ++	-1.69
Manganese	Mn / Mn ++	-1.10
Zinc	Zn / Zn ++	-0.76
Chromium	Cr / Cr ++	-0.56
Iron (Ferrous)	Fe / Fe ++	-0.44
Cadmium	Cd / Cd ++	-0.40
Indium	In / In +++	-0.34
Thallium	Tl / Tl +	-0.33
Cobalt	Co / Co ++	-0.28
Nickel	Ni / Ni ++	-0.23
Tin	Sn / Sn ++	-0.14
Lead	Pb / Pb ++	-0.12
Iron (ferric)	Fe / Fe +++	-0.04
Hydrogen	H <sub>2</sub> / H +	0.00
Antimony	Sb / Sb +++	+0.10
Bismuth	Bi / Bi +++	+0.23
Arsenic	As / As +++	+0.30
Copper (cupric)	Cu / Cu ++	+0.34
Copper (cuprous)	Cu / Cu +	+0.47
Tellurium	Te / Te ++++	+0.56
Silver	Ag / Ag +	+0.80
Mercury	Hg / Hg ++	+0.80
Platinum	Pt / Pt ++++	+0.82
Palladium	Pd / Pd ++++	+0.86
Gold (auric)	Au / Au +++	+1.36
Gold (auras)	Au / Au +	+1.50

\*The metal that has a more positive potential is more noble in a galvanic cell between two metals, and it is the *cathode*. A more negative potential corresponds to the more active (*anodic*) metal.

The state of oxidation of the metal ion (cation) is equal to the number of electrons liberated by the metal during the anodic corrosion process. For example,  $\text{Ni} \rightarrow \text{Ni}^{2+} + 2\text{e}^-$ .

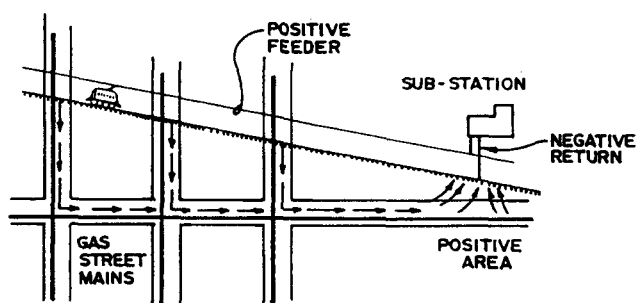


FIG. 10—Stray current in street railways. The area near the substation, where a current flowing in a pipeline leaves its surface to return to the negative bus bar, can suffer very severe corrosive attack.

effective method for prevention of *galvanic corrosion*. Elimination of galvanic contact between steel and more noble metals, selection of more compatible dissimilar metals in a junction, introduction of insulators, and protective coatings are recommended.

Stainless steel (SS) is also used as a material for buried metal structures. In principle, the SS should be in the passive

state in soils, due to the naturally formed very resistive oxide layer on its surface, composed of oxides of different alloying elements (nickel, chromium, molybdenum, copper, etc.) and iron. However, the presence of chloride in the soil can cause stainless steels to pit or corrode in crevices, so this material should be avoided in chloride containing soils. It is also known that SS can be attacked by certain species of microbes, contributing to their microbial corrosion (MIC).

Another metal with a successful service record in soils is *lead*. Thousands of kilometers of lead-sheathed power and communication cables and lead pipes have shown good performance underground. They are directly buried in the ground or installed in ducts or conduits. Lead corrodes less on the average than does steel. Most of the initially formed corrosion products of lead are relatively insoluble salts, such as carbonates, silicates, or sulfates. They are deposited on the lead surface and ensure very compact and dense protective layers for the metal. The formation of such a layer is responsible for the high resistance of lead to corrosion. Due to its less negative potential (Table 2), the lead is *cathodic* when connected to steel (except for strongly alkaline environments), aluminum, zinc, or cadmium, and thus will accelerate the corrosion process of these metals. Only in galvanic contact with copper, stainless steel, and titanium, will lead be an *anode* in the formed corrosion cell and suffer corrosion attack. In poorly aerated soils or soils high in organic acids, the corrosion rate may be four to six times higher than the average. Other factors that may accelerate the corrosion of lead are stray currents, microorganisms (like sulfate-reducing bacteria), a high concentration of hydroxides (up to 1000 ppm, for example, in a wet concrete tunnel), and contact with acetic acid (in a wooden duct).

*Copper* is also a metal used for underground cables and usually has very good corrosion resistance. Copper on the average corrodes at about one sixth the rate of iron, but in tidal marsh the rate is higher than in most other soils, about half that of iron. When connected to buried steel or iron, the copper will be a cathode of the galvanic cell and will not suffer any corrosion.

An increase in chromium content of steel decreases the observed weight loss in a variety of soils, but above 6 % chromium, the depth of pitting increases.

## TESTING IN SOILS [8,18-26]

### Direct and Indirect Measurements and Techniques for Use

The corrosion behavior of a buried metal structure needs to be indirectly controlled or monitored to determine the time for direct examination when repairs will be necessary. Looking at the corroded surface is usually expensive and is acceptable only for a special corrosion situation. However, direct external surface assessment is sometimes imperative, for example, to verify some indirect measurements or for visual examination of the coating for damage. Several *NACE Recommended Practices* are useful in this situation:

**RP0502**—Pipeline External Corrosion Direct Assessment Methodology;

**RP0169**—Control of External Corrosion on Underground or Submerged Metallic Piping Systems;



FIG. 11—General view of localized pitting corrosion on underground pipe surface.

- RP0285**—Corrosion Control of Underground Storage Tank Systems by Cathodic Protection;
- RP0274**—High-Voltage Electrical Inspection of Pipeline Coatings;
- RP0286**—Electrical Isolation of Cathodically Protected Pipelines;
- RP0375**—Wax Coating Systems for Underground Piping Systems;
- RP0487**—Considerations in the Selection and Evaluation of Rust Preventives and Vapor Corrosion Inhibitors for Interim (Temporary) Corrosion Protection;
- RP0174**—Corrosion Control of Underground Residential Distribution Systems;
- RP0177**—Mitigation of Alternating Current and Lightning Effects on Metallic Structures and Corrosion Control Systems.

Direct assessment gives a possibility for *direct mechanical* or *ultrasonic measurement* of pit depth and wall thickness change due to the corrosion. *X-ray radiography* is used to inspect welds immediately after they are made. This technique can also show stress corrosion cracks and corrosion pits in the weld area, where the coating has failed to seal the metal structure. A promising method of mapping corrosion on the metal surface is the use of *laser scanning equipment*.

Direct measurement of metal corrosion rate can be achieved using preweighed *metal coupons*. They are buried

in the pipeline trench, unconnected or connected to the structure at a controlled test post. Periodically, they can be removed and processed for their weight loss due to corrosion. A simple calculation can give the corrosion rate value, expressed, for example, in  $\text{g/m}^2$  year. This method is time-consuming, especially when a large number of samples are needed for removal at consistent intervals.

The buried coupons have no standard size or shape and are made of the same metal as the structure. Comparing the mass loss of connected and unconnected coupons may provide information about the effectiveness of cathodic protection. Connected coupons have not been fully accepted as a cathodic protection monitoring test, because the coupon may not always polarize to the same potential value as the metal structure.

An *electrical resistance (ER) probe* is designed to measure corrosion in soil, without the necessity to be dug up for examination. This is an advantage over the coupons. The ER of the probe, made of the same metal as the structure, will change its value because of loss of metal, due to conversion to corrosion products on the metal surface. The ER probe also gives indirect information about the soil corrosivity and its changes with time.

#### *Field and Laboratory Tests*

Several field and laboratory tests are used to correlate soil corrosion aggressivity to its physical and chemical properties. Sampling errors are the most common errors encountered

FIG. 12—General view of pit formed on buried corroded pipe surface.

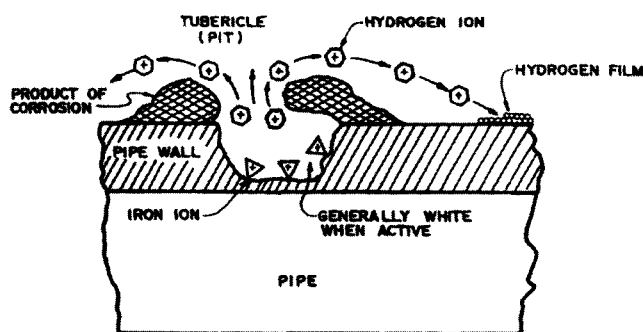


FIG. 13—Pit action and active pitting cell.

in soil analysis, due to the extreme heterogeneity of the material. In the laboratory, grinding and mixing can minimize such errors, but the largest sampling error occurs in field measurements.

#### Potential Measurement *in Situ*

This measurement establishes the corrosion potential of buried metal in a given soil. Its value is an indication of the degree and extent of corrosion attack and the efficiency of applied cathodic protection. The metal potential usually shifts with time to less negative values, if the corrosion products form an inert and compact layer on the metal surface. Due to this fact, it is possible to observe more positive potential values on an old structure than those measured on

a new metal surface. A new, coated steel pipe may have a potential of  $-0.7$  V versus a  $\text{Cu}/\text{CuSO}_4$  reference electrode, while an old pipe surface is more positive ( $-0.1$  to  $-0.3$  V). The surface areas where the potential is less negative will be more cathodic, and as a consequence they will suffer less corrosion. Stray currents or interference from foreign cathodic protection systems may cause potential fluctuations and have to be taken into account.

The *in situ* cathodic protection test criteria for full protection of steel is that all measured points are close to  $-0.85$  V versus a  $\text{Cu}/\text{CuSO}_4$  reference electrode. For long pipelines, passing through different types of soil, the potential is usually measured every 30 m or less (often at 1.5 m).

Experience indicates that the corrosion potential value of buried copper cable correlates with its corrosion behavior (Table 3). A potential value of  $-0.50$  V or more negative, versus a  $\text{Cu}/\text{CuSO}_4$  reference electrode, indicates full cathodic protection of this metal, typically provided by a connection to a steel structure.

An indicator of soil corrosivity is the value of *soil oxidation-reduction* (ORP) or *redox potential*. It is calculated from the potential difference measured with a probe that contains an inert platinum (Pt) electrode and a saturated calomel electrode ( $\text{Hg}/\text{Hg}_2\text{Cl}_2/\text{KCl}$ ,  $+0.241$  V versus SHE) as a reference electrode. The value of this soil redox potential depends on the dissolved oxygen content in the pore water and provides some information on the conditions under which sulfate-reducing bacteria could grow. The use of redox potentials to predict soil corrosivity is presented in Table 4.

FIG. 14—Localized corrosion on buried metal structure, concentrated on holidays (defects) of the coated surface.

TABLE 3—Copper potential and corrosion behavior.

Potential vs. Cu/CuSO <sub>4</sub>	Corrosion Behavior
Positive to -0.1 V	Probably corroding
-0.1 to -0.25 V	Possibly corroding
-0.25 to -0.50 V	Probably not corroding
-0.50 V or more negative	Full protection

TABLE 4—Soil redox potentials as an indicator for soil corrosivity.

Redox Potential (vs. SHE*)	Aeration	Soil Corrosivity Category
Negative	Not aerated	Extremely severe
0–100 mV	None to weak	Severe
100–200 mV	Weakly aerated	Moderate
200–400 mV	Aerated	Slight
Above 400 mV	Strongly aerated	Noncorrosive

\* Standard Hydrogen Electrode (SHE), conventionally accepted to be 0.00 V.

Potential measurements of metal in soil require the use of some assistance tools, such as insulated wire, reels, alligator clips, terminal connectors, hand tools, a reference electrode (RE), and specialized equipment like voltmeters and ammeters.

The *saturated copper/copper sulfate reference electrode* (Cu/CuSO<sub>4</sub>) is the most used in soils (+ 0.316 V versus SHE

standard potential). This RE has poor reproducibility and needs to be frequently checked and renewed. In high chloride environments the most appropriate electrode is a *silver/silver chloride RE* (Ag/AgCl/KCl (0.1N) +0.288 V versus SHE standard potential). Usually it provides reproducible and reliable values. The *lead sulfate RE* (Pb/PbO<sub>2</sub>/PbSO<sub>4</sub>/H<sub>2</sub>SO<sub>4</sub> (0.1M), + 1.565 V versus SHE standard potential) is connected to lead-sheathed cables for measurement of their potential. Very dry soils may be wetted or a shallow hole dug to establish good electrical contact between the electrode and the soil moisture. The RE should be placed near the metal structure, augering a hole down to near the pipeline surface, to minimize ohmic potential drop (IR) due to the soil and coating resistance. The tester must avoid any damage to the coating or protective scale on the metal. The potentials over well-coated pipelines do not vary much over distance.

Factors affecting the potential measurements are broken test leads, corroded contact points, and defective insulation of test leads. An improperly calibrated RE can also be an important source of errors. The existence of vegetation or of other metals may introduce errors of over 100 mV.

The metal potential can be measured using *voltmeters* with more than 10 MΩ internal resistance. *Ammeters* are used to measure electric current passing through the structure protected by CP and are relatively low-resistance instruments.

### Soil Resistivity

The soil resistance ( $R$ ) to passage of electrical current is the most used parameter as an indicator of corrosion aggressivity of soils. It is related to three terms in the equation

$$R = \rho \cdot l / A$$

where  $\rho$  is *specific resistivity* of the particular soil,  $l$  is a length of the electrical path, and  $A$  is the cross-sectional area of the electrodes.

The resistivity indicates the probable corrosivity of the soil. Its value depends on the soil water content on the layers and on types of soils underneath (sand, rock, gravel, clay, mud, etc.). Vertically homogeneous soils are virtually nonexistent. Thus, it is convenient to consider a nonuniform soil to consist of different layers or strata [7]. Electron flow will deflect downward in the case of a high resistivity strata over a low resistivity one, and vice versa, as shown in Figs. 15 and 16. The electrical resistivity of the surface strata has greater influence on test results than does that of deeper strata. Also, the soil resistivity decreases with increasing water content and with increasing water salinity because of high contents of ions. Thus, nonporous soils exhibit relatively high values of resistance, since the water content is small. These include nearly all of the igneous and metamorphic rocks such as granite, plus many sedimentary rocks such as dense limestone or sandstone. The resistivity of bedrock can vary considerably depending upon the type of bedrock and the extent of weathering and fracturing.

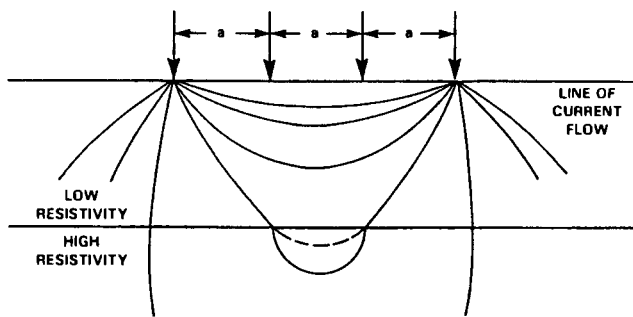


FIG. 15—Low resistivity layer over high resistivity layer.

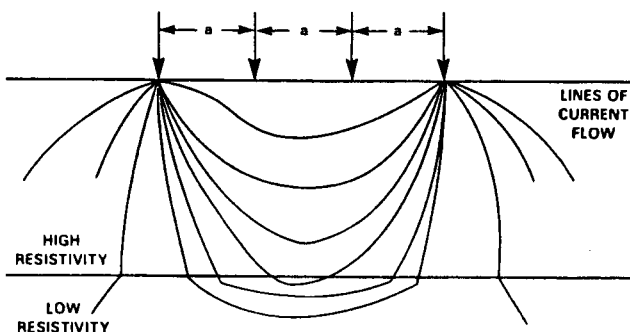


FIG. 16—High resistivity layer over low resistivity layer.

The resistivity of sand and gravel deposits is generally high and uniform, while many bedrock formations have high but erratic resistivity. Table 5 gives typical resistivity values of various minerals and soils.

Along the length of the pipe, variations in soil resistivity may stimulate localized metal corrosion and can cause long line currents; in the area of *lower resistivity* soil the buried metal surface is usually *anodic*, with a more negative potential, compared to that in the soil of higher resistivity.

Soil resistivity measurements are carried out by the *Wenner technique*, *four-pin method*, with or without Barnes Procedure, according to procedures of ASTM Standard Test Method for Field Measurement of Soil Resistivity Using the Wenner Four-Electrode Method (G 57) using commercially available instruments. Four steel electrodes, each spaced an equal distance from the next, are driven into the ground. An alternating current (ac) or direct current (dc) is passed between the outer two pins, and the corresponding potential drop (voltage  $\Delta V$ ) is measured between the inner pins, as shown in Fig. 17. The resistance  $R = \Delta V / I$ , where  $I$  is the applied current. This procedure is usually used to measure the average resistivity of the soil where a cathodically protected structure is to be installed.

The average resistivity value depends on how many measurements are taken in the area and when they were taken. Measurements should be made at various times and weather conditions (dry or rainy seasons, summer or winter, etc.). It is, therefore, impossible to give any precise assessment as to the rate at which corrosion will occur

TABLE 5—Electrical resistivity of various minerals and soils.

Minerals and Soils	Resistivity, $\Omega$ -cm
<b>Minerals</b>	
Pyrite	0.1
Magnetite	0.6–1.0
Graphite	0.03
Rock Salt (impure)	3000–500 000
Serpentine	20 000
Siderite	7000
<b>Igneous Rock</b>	
Granite	500 000–100 000
Diorite	1 000 000
Gabbro	10 000 000–1 400 000 000
Diabase	310 000
<b>Metamorphic Rocks</b>	
Garnet gneiss	20 000 000
Mica chist	130 000
Biotite gneiss	100 000 000–600 000 000
Slate	64 000–6 500 000
<b>Sedimentary Rock</b>	
Chattanooga shale	2000–130 000
Michigan shale	200 000
Calumet and hecla conglomerates	200 000–1 300 000
Muschelkalk sandstone	7000
Ferruginous sandstone	18 000
Muschelkalk limestone	18 000
Marl	7000
Glacial till	50 000
<b>Type of Soil</b>	
Sand	10 000–500 000
Oil sand	400–22 000
Gravel	20 000–400 000
Loam	3000–20 000
Clay	500–2000
Silt	1000–2000

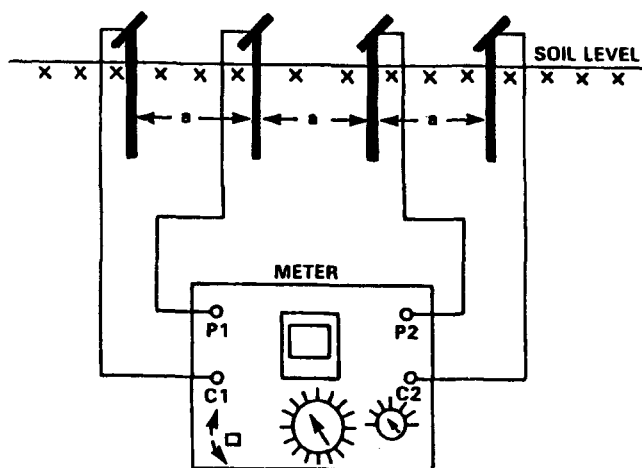


FIG. 17—Four-electrode method for the electrical soil resistance measurement.

under any particular conditions, and the results of any survey must be taken as giving only a general indication of the probability of corrosion. Chemical and other forms of industrial contamination of the soil can significantly influence soil resistivity and corrosivity. In real life, the soil is not homogeneous and layers are not always horizontal. In fact, as the spacing between Wenner pins changes, soil resistivity readings may also change.

There are several *commercial meters* that allow measurement of soil resistivity. A commonly used resistance meter is shown in Fig. 18. One reliable and widely used instrument uses an alternating current 97 Hz square wave. It has several advantages such as eliminating the effect of polarization that can affect the measurements when using dc, and eliminating interference by 60 Hz sinusoidal currents.

Soil resistivity can be measured under either field or laboratory conditions. In the laboratory, the soil sample is placed and compacted to the same amount as the soil at the site in a *soil box*, with typical internal dimensions of  $4.0 \times 3.1 \times 21$  cm. The resistivity is measured between the two pins inserted in the sides of the box, applying low voltage dc or ac. Errors could result from polarization when using a d-c or a-c current of too low a frequency. The soil box measurement (representing a specific soil sample) is a point measurement, not an average soil resistivity as is the Wenner method. Another alternative way to measure soil resistivity is to combine the Wenner four-pins with the soil-box (Fig. 19) and follow the standard test method of ASTM G 57. In laboratory tests the soil resistivity can also be measured at 100 % water saturation using distilled water, which gives a value that could correspond to that of rainy climatic periods, when a lot of salts may be dissolved and cause a decrease of the soil resistivity. The temperature changes have only a slight effect on the soil resistivity value until total freezing of soil moisture occurs. However, the ice resistance increases sharply as temperature drops. Table 6 shows an approximate relationship between soil resistivity values and soil corrosivity categories for buried mild steel structures.

The soil box could be used also in laboratory tests to determine the corrosion rate (weight loss) of metal samples buried in a given soil for some period of time. This test can be conducted using ASTM Standard Practice for Preparing, Cleaning, and Evaluating Corrosion Test Specimens (G 1). The soil in the box may be maintained in a saturated state with distilled water to keep all salts dissolved (dissociated as ions). Visual examination of the metal samples will give information on the corrosion appearance, especially useful when the corrosion is localized, such as pitting. Pitting can be evaluated in accordance with ASTM Standard Guide for Examination and Evaluation of Pitting Corrosion (G 46). Corrosion products could be analyzed for their composition. Figure 20 shows general views of mild steel samples corroded in different types of soils.

#### *Field and Laboratory Measurement of Relative Acidity (pH) of Soil*

Soil acidity, or its pH, is the most important measured parameter. Details for conducting field measurements of pH in soils for use in corrosion testing are covered in ASTM Test Method for Measuring pH of Soil for Use in Corrosion Testing (G 51). Two electrodes, glass and calomel, of a standard pH meter are pressed on undisturbed soil at a given site, and the value of their potential difference is linearly related to pH. Salts such as fertilizers in the soil can affect the correct value.

A sample of soil can be collected and taken back to the laboratory for pH analysis. There, the soil can be mixed with distilled water (1:1 by volume), shaken well, and then the pH measured in a sample of the filtered extract solution. In the case of soils rich in sulfide, the pH value could be more acidic because of the oxidation of sulfides to sulfates as the soil dries out. The treatment of the soil prior to pH measurement is still an open issue. Drying of soil samples and addition of distilled water are two of the treatments used. However, the soil resistivity value is not sufficient to unambiguously indicate the soil corrosivity. For example, a neutral soil (pH 6.6–7.3) could be very corrosive due to the presence of chloride ions. Table 7 presents an approximate relationship between pH of soil water extract and soil corrosivity.

In some cases a determination of the *total acidity* is desirable. Additional measurement requires a soil treatment by mixing the soil with a solution of neutral salts like KCl,  $\text{CaCl}_2$ , etc., to determine the *exchange* or *total acidity* of the soil, which includes the hydrogen ions loosely bonded to soil minerals. This extraction method is practically unaffected by fertilizers or other salts that may be present in the soil.

#### *Laboratory Measurement for Presence of Ions*

From a corrosion point of view, the important ions that can be found in soil and in soil moisture are:

1. *anions*: chloride ( $\text{Cl}^-$ ), sulfate ( $\text{SO}_4^{2-}$ ), nitrate ( $\text{NO}_3^-$ ), phosphate ( $\text{PO}_4^{3-}$ ), carbonate ( $\text{CO}_3^{2-}$ ), bicarbonate ( $\text{HCO}_3^-$ ), and
2. *cations*: calcium ( $\text{Ca}^{2+}$ ), potassium ( $\text{K}^+$ ), ammonium ( $\text{NH}_4^+$ ), magnesium ( $\text{Mg}^{2+}$ ), sodium ( $\text{Na}^+$ ), and ferrous ( $\text{Fe}^{2+}$ ) and ferric ( $\text{Fe}^{3+}$ ) ions.

Their concentration determines the ionic conductivity and resistivity of the soil moisture, and also the tendency



FIG. 18—General view of four-pin soil resistance meter

for formation of a precipitated layer on the metal, which may protect its surface from future corrosion attack. The most dangerous ion is chloride, which may accelerate the metal corrosion, causing deep pitting. In some cases, the presence of sulfides such as hydrogen sulfide ( $\text{H}_2\text{S}$ ) should be determined also. The ion concentration is measured in a water soil extract using various analytical techniques. Slightly alkaline ground water usually contains  $\text{Na}^+$ ,  $\text{Ca}^{2+}$ ,  $\text{Mg}^{2+}$ ,  $\text{SO}_4^{2-}$ , and  $\text{HCO}_3^-$  ions, as part of the dissolved salts (<1000 mg/L or in a higher range of 1000–10,000 mg/L). In slightly acidic water the principal ions are  $\text{Na}^+$ ,  $\text{Ca}^{2+}$ ,  $\text{Mg}^{2+}$ , and  $\text{HCO}_3^-$ , with a lower concentration of total dissolved solids of <100 mg/L.

#### *Biological Activity Test*

Tests for sulfate-reducing bacteria include counts of total viable sulfate reducers. Other tests include measurement of the hydrogen uptake of a soil, and the time for a soil sample to blacken a medium used to grow sulfate reducers. Chemical analysis of the water source and the soil is helpful in determining the critical nutrients necessary to support microbiological activity. These tests should be conducted under the direction of a microbiologist who has experience in microbiologically influenced corrosion. Field test kits are currently available that employ an antibody tagging technique to identify and facilitate the determination of the population of microbes [27,28]. Microbiologically influenced corrosion (MIC) can be studied using field survey and other techniques, such as electrochemical polarization curves, polarization resistance, electrochemical impedance spectroscopy (EIS), thin-film electrical resistance (ER) probe, galvanic current measurement, SEM and EDS surface analysis, etc. [17].

#### *Electrochemical Laboratory Tests [29–32]*

Several electrochemical tests have been used successfully over the years to estimate the corrosion behavior of a given metal in soil or to determine the soil corrosivity. These tests can be carried out in water extract of soil and/or in water saturated soil, when all dissolved salts (ions) are present. The electrochemical test methods and practices are described in several *ASTM Tests Methods and Practice*:

- Standard Practice for Conventions Applicable to Electrochemical Measurements in Corrosion Testing (G 3);
- Standard Reference Test Method for Making Potentiostatic and Potentiodynamic Anodic Polarization Measurements (G 5);
- Standard Test Method for Conducting Potentiodynamic Polarization Resistance Measurements (G 59);
- Standard Test Method for Conducting Cyclic Potentiodynamic Polarization Measurements for Localized Corrosion Susceptibility of Iron-, Nickel-, or Cobalt-Based Alloys (G 61);
- Standard Guide for Conducting and Evaluating Galvanic Corrosion Tests in Electrolytes (G 71);
- Standard Practice for Calculation of Corrosion Rates and Related Information from Electrochemical Measurements (G 102);
- Standard Practice for Verification of Algorithm and Equipment for Electrochemical Impedance Measurements (G 106);
- Standard Practice for Evaluation of Hydrogen Uptake, Permeation and Transport in Metals by an Electrochemical Technique (G 148);

FIG. 19—Soil box in use, with inserted Wenner four-pin electrodes.

**TABLE 6**—Corrosivity categories of soils for buried mild steel based on soil resistivity ( $\rho$ ) values

Corrosivity of soil	Soil resistivity ( $\rho$ ) $\Omega$ -cm
Very severe	< 500
Severe	500–2000
High	2000–5000
Moderate	5000–10 000
Medium	10 000–25 000
Light	25 000–50 000
Low	>50 000

These standard methods and practices provide the necessary information for electrochemical potentiostatic and potentiodynamic anodic measurements, calculation of corrosion rate from electrochemical measurements, and conducting potentiodynamic polarization resistance measurements. Recently, *Electrochemical Impedance Spectroscopy* (EIS) has been introduced for corrosion measurements of steel structures corroding in soils. These tests can be

performed using a *commercial potentiostat*, appropriate computer software for analysis of the results, a standard electrochemical cell, a platinum or carbon counter electrode, a reference electrode, and a sample of the metal as a working electrode. Figure 21 presents a general view of equipment in use for electrochemical measurements. Recently, an Electrochemical Impedance Spectroscopy (EIS) technique has been introduced for measurements of steel structure corroding in soil.

*External Corrosion Direct Assessment (ECDA) of Buried Pipelines [33,34]*

As a result of regulatory changes in the U.S., the pipeline industry needed an alternative method to pressure testing on in-line tool inspection to assess buried pipelines [33]. *EDCA is a four-step process* consisting of:

- *Preassessment*: pipe data, construction data, soil/environmental conditions, corrosion protection data, and operating parameters/history;

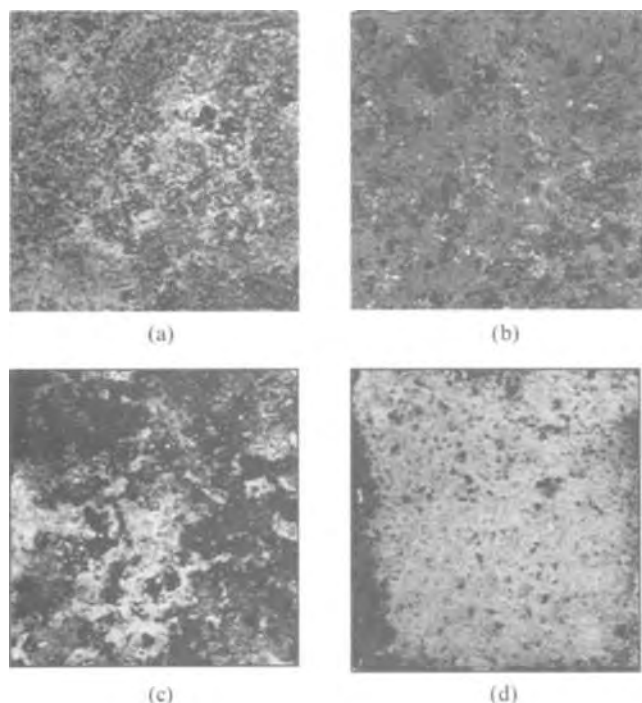


FIG. 20—General view of mild steel samples corroded in different soil samples (a) clay, (b) sand, (c) and (d) calcareous sandy soil. These soils are part of Southeastern Mexico in the Mexican Caribbean Gulf.

TABLE 7—Corrosivity categories of soils for buried steel based on pH of water soil extract.

Corrosivity of soil	Relative acidity (pH) of soil extract
Low	>12
Moderate	7.5–12
High	4–7.5
Very high	< 4

- *Indirect inspection*: the purpose is to identify the locations of coating faults, insufficient cathodic protection, and electrical shorts (close-interval, on/off potential surveys, electromagnetic current attenuation surveys, alternating current voltage gradient surveys, etc.), interference, geological current surveys, and other anomalies along the pipeline.
- *Direct examination*, excavating the pipe and performing physical inspections and tests on the pipe surface and the surrounding soil/water electrolytes, to assess the degree of corrosion;
- *Post-assessment* gives one an opportunity to assess the overall effectiveness of direct assessment and to define re-assessment intervals based on remaining-life calculations.

The EDCA process incorporates standard techniques for compiling historical information, pipeline and soil surveys, external pipeline inspections, and data analysis. The procedure includes no new measurement techniques, but it does allow for the future addition of such techniques. Some rules and information about EDCA are present in NACE **RP0502**—Pipeline External Corrosion Direct Assessment Methodology.

New advances in satellite technology may soon help pipeline operators and utilities observe encroachments and

FIG. 21—General view of equipment for electrochemical measurements.

ground movements near their assets with unprecedented details [34].

## REFERENCES

- [1] *Corrosion, Volume 1: Metal/Environment Reactions*, L. L. Shreir, R. A. Jarman, and G. T. Burstein, Eds., Butterworth Heinemann, 1994.
- [2] Romanoff, M., "Underground Corrosion," NACE International, Houston, TX, 1989.
- [3] Ulig, H. H., "Corrosion and Corrosion Control," John Wiley & Sons, New York, 1985.
- [4] "Corrosion, Understanding the Basics," J. R. Davis, Ed., ASM International, Ohio, 2000.
- [5] Stansbury, E. E. and Buchanan, R. A., "Fundamentals of Electrochemical Corrosion," ASM International, Ohio, 2000.
- [6] Parker, M. E., "Corrosion by Soils," *NACE Basic Corrosion Course*, NACE International, Houston, TX, 1975.
- [7] "Earth Resistivity Manual," Soiltest Inc., Evanston, IL, 1968.
- [8] Bradford, S. A., "Practical Handbook of Corrosion Control in Soils," CASTI Publishing, Canada, and ASTM International, West Conshohocken, PA, 2000.
- [9] Escalante, E., "Concepts of Underground Corrosion," *Effects of Soil Characteristics on Corrosion, ASTM STP 1013*, V. Chaker and J. D. Palmer, Eds., ASTM International, West Conshohocken, PA, 1989, pp. 81–94.
- [10] Fitzgerald, J. H., III, "The Future as a Reflection of the Past," *Effect of Soil Characteristics on Corrosion, ASTM STP 1013*, V. Chaker and J. D. Palmer, Eds., ASTM International, West Conshohocken, PA, 1989, pp. 1–4.
- [11] Pont, E. G., "Association of Sulfate Reduction in the Soil with Anaerobic Iron Corrosion," *Journal of Australian Inst. Agr. Science*, Vol. 5, No. 5, 1939, pp. 170–171.
- [12] Seelmeyer, G., "Biological Corrosion of Iron and Steel," *Werkstoffe und Korrosion*, Vol. 4, 1953, pp. 241–247.
- [13] Senez, J. C., "Investigation in Biological Corrosion in Anaerobic Soils by Sulfate-Reducing Bacteria," *Corrosion and Anti-Corrosion*, Vol. 1, 1953, pp. 131–132.
- [14] Harris, J. O., "Bacterial Activity at the Bottom of Back-Filled Pipe-Line Ditches," *Corrosion*, Vol. 16, 1960, pp. 149–154.
- [15] Iverson, W. P., "Biological Corrosion," *Advanced Corrosion Science and Technology*, Vol. 2, 1972, pp. 1–42.
- [16] Prakash, N., Srivastava, K., and Gupta, S., "Corrosion of Mild Steel by Soil Containing Sulfate-Reducing Bacteria," *Microbiological Biotechnology*, Vol. 3, No. 2, 1988, pp. 79–84.
- [17] Li, S. Y., Kim, Y. G., Jeon, K. S., Kho, Y. T., and Kang, T., "Microbiological Influenced Corrosion of Carbon Steel Exposed to Anaerobic Soil," *Corrosion*, Vol. 57, No. 9, 2001, pp. 815–828.
- [18] Chaker, V., "Corrosion Testing in Soils—Past, Present, and Future," *Corrosion Testing and Evaluation: Silver Anniversary Volume, ASTM STP 1000*, R. Baboian and S. W. Dean, Eds., ASTM International, West Conshohocken, PA, 1990, pp. 95–111.
- [19] Bushman, J. B. and Mehalick, T. E., "Statistical Analysis of Soil Characterization to Predict Mean Time to Corrosion Failure of Underground Metallic Structures," *Effects of Soil Characteristics on Corrosion, ASTM STP 1013*, V. Chaker and J. D. Palmer, Eds., ASTM International, West Conshohocken, PA, 1989, pp. 107–118.
- [20] Dillon, C. P., "Corrosion Control in the Process Industries," McGraw-Hill, New York, 1986.
- [21] Chaker, V., "Simplified Method for Electrical Soil Resistivity Measurement," *Underground Corrosion, ASTM STP 741*, E. Escalante, Ed., ASTM International, West Conshohocken, PA, 1981, pp. 61–91.
- [22] Escalante, E., "The Effect of Soil Resistivity and Soil Temperature on the Corrosion of Galvanically Coupled Metals in Soil," *Galvanic Corrosion, ASTM STP 978*, H. P. Hack, Ed., ASTM International, West Conshohocken, PA, 1988, pp. 193–202.
- [23] Iverson, W. P., "An Overview of the Anaerobic Corrosion of Underground Metallic Structures, Evidence for a New Mechanism," *Underground Corrosion, ASTM STP 741*, ASTM International, West Conshohocken, PA, 1981.
- [24] Escalante, E., "Measuring the Corrosion of Metals in Soils," *Corrosion Testing and Evaluation: Silver Anniversary Volume, ASTM STP 1000*, R. Baboian and S. W. Dean, Eds., ASTM International, West Conshohocken, PA, 1990, pp. 112–124.
- [25] Palmer, J. D., "Environmental Characteristics Controlling the Soil Corrosion of Ferrous Piping," *Effects of Soil Characteristics on Corrosion, ASTM STP 1013*, V. Chaker and J. D. Palmer, Eds., ASTM International, West Conshohocken, PA, 1989, pp. 5–17.
- [26] Palmer, J. D., "Field Soil Corrosivity Testing—Engineering Considerations," *Corrosion Testing and Evaluation: Silver Anniversary Volume, ASTM STP 1000*, R. Baboian and S. W. Dean, Eds., ASTM International, West Conshohocken, PA, 1990, pp. 125–138.
- [27] Pope, D. H., "Discussion of Methods for the Detection of Microorganisms Involved in Microbiologically Influenced Corrosion," *Biologically Induced Corrosion—Proceedings of the International Conference*, NACE International, 1986, p. 275.
- [28] Stoecker, J. G., "Guide for the Investigation of Microbiological Induced Corrosion," *Materials Performance*, Vol. 20, No. 9, p. 32.
- [29] Scully, J. R. and Bundy, K. J., "The Use of Electrochemical Techniques for Measurement of Pipe Steel Corrosion Rates in Soil Environments," *Corrosion* 83, NACE International, Houston, TX, 1983, Paper 253.
- [30] Levlin, E., "Aeration Cell Corrosion of Carbon Steel in Soil: In Situ Monitoring Cell Current and Potential," *Corrosion Science*, Vol. 38, No. 12, 1996, pp. 2083–2090.
- [31] Kasahara, K. and Kajiyama, F., "Application of AC Impedance Measurements to Underground Monitoring," *Corrosion*, Vol. 39, June 1983, pp. 296–302.
- [32] Murphy, J. C., Hartong, G., Cohn, R. F., et al., "Magnetic Field Measurement of Corrosion Processes," *Electrochemical Science and Technology*, Vol. 135, No. 2, February 1988, pp. 310–313.
- [33] Kroon, D. H., "External Corrosion Direct Assessment of Buried Pipelines: The Process," *Materials Performance*, Vol. 42, June 2003, pp. 28–32.
- [34] Veazey, M. V. and Writer, S., "The Next Big Thing in Pipeline Monitoring," *Materials Performance*, Vol. 42, June 2003, pp. 16–21.

# Concrete

Neal S. Berke<sup>1</sup>

## DESCRIPTION

### The Concrete Environment

CONCRETE IS ONE OF THE most widely used construction materials due to its good durability and relatively low cost. When reinforced with steel and other materials it has very good structural properties allowing for its use in numerous structures such as bridge decks, parking structures, marine piles and piers, and large buildings. The embedded steel does not corrode due to the high alkalinity of concrete which results from the portland cement used in its manufacture.

The pH of concrete is typically  $\geq 12.5$  with some measurements on squeezed pore water suggesting even higher values [1]. Thus in the absence of a depassivating ion such as chloride, or carbonation of the concrete to a lower pH value, steel will remain passive. Note that steel in concrete subjected to high stray voltages could corrode under environmental conditions that would normally be benign.

In addition to providing a high pH environment, concrete also has a high resistivity compared to most aqueous environments. Resistivities in water saturated concrete range from 2000 to over 300 000  $\Omega\cdot\text{cm}$  and are even higher in dry concrete [2,3]. Correction for high resistance is needed in making electrochemical corrosion rate measurements.

The high resistivity of concrete is related to a reduced permeability of concrete to the ingress of water and chloride [4–6]. Thus, it can take several years to decades for corrosion activity to initiate on steel embedded in concrete, even when the exposure to chloride is severe.

### Simulated Concrete Environments

The concrete environment is often simulated by a concentrated calcium hydroxide solution [7,8]. Addition of additional sodium or potassium hydroxide, or both, to increase the pH has no effect on changing the corrosion mechanisms, but increases the chloride threshold level [9]. Typically the effects of chlorides and corrosion inhibitors on the susceptibility of steel to pitting can be determined in these environments [7–9].

More realistic simulated environments are mortar or cement paste mixtures. The chemistry is much closer to that occurring in concrete. The drawback of these mixtures is that they

do not necessarily reproduce true concrete behavior due to the effects of coarse aggregates in concrete. For example, porosity and calcium hydroxide plate precipitation is highest at the coarse aggregate paste boundaries, and this plays an important role in the corrosion processes [10].

## ASPECTS THAT MAKE TESTING UNIQUE

### High Resistivity

The high resistivity of concrete requires the use of techniques to correct for the voltage drop through the electrolyte (IR drop). This is especially the case for concrete produced with pozzolans, such as silica fume, or latex modified concretes in which the resistivities of the wet concrete can be in excess of 300 000  $\Omega\cdot\text{cm}$ . It has been shown that IR interruption and electrochemical impedance spectroscopy are effective in properly correcting for the IR drop in laboratory specimens [3].

In addition to the high resistivity due to the concrete, the IR drop can be significant depending upon the placement of the reference electrode. This is due to the fact that concrete surrounds the embedded working electrode, and often the distance between the two electrodes is over 20 mm.

### Complexities Associated with Corrosion Evaluation

Determination of the area polarized in a concrete specimen is not clearly defined in most field applications. Typically bars are meters in length and spaced on the order of 25–30 cm in multiple mats. When a counter-electrode is at the surface of the concrete along with the reference electrode it is not a trivial matter to determine the area of bars being polarized. Furthermore, the area polarized is affected by whether or not the steel is passive [11].

Another hurdle involves making electrical connections to the steel. In laboratory specimens this can be performed by bringing the bar out of the concrete or by pre-attaching a wire and insulating the area at the connection point. The connection point must be electrically isolated and remain dry to prevent galvanic corrosion.

In the field one must locate the bar and drill or core to make an electrical connection. If there is good continuity between the bars, one connection can allow for testing at multiple sites. However, in the case of poor continuity, e.g., epoxy-coated rebars, multiple connections will be needed.

<sup>1</sup>Research and Development Fellow, Grace Construction Products, W. R. Grace & Co.-Conn., Cambridge, MA 02140.

It is not possible to perform a visual examination of the bars nondestructively. This requires concrete removal and replacement if necessary. In field structures this could be a site of future corrosion activity if the patch area is more permeable than the original concrete, or excessively cracks due to shrinkage or other causes. Laboratory specimens are typically removed from testing if the bars are to be examined. It is possible to make visual examinations of the concrete surface for staining or cracking, or both, and delamination determinations can be performed non-destructively.

Mass loss tests are a common means of testing many metals in atmospheric and submerged exposure. For steel in concrete they are destructive to the concrete and difficult to perform. Laboratory specimens typically have a portion of the embedded bar coated or taped to define a specific test area. These materials are often hard to remove and could gain or lose mass. Furthermore, at the initial stages of corrosion most of the damage is in pits which have relatively low mass loss relative to that lost in the formation of the passive film [12], and thus mass loss is not necessarily a good indicator of corrosion activity.

### Outdoor Exposures

Concrete in the field undergoes large changes in temperature and moisture content. Often these occur in the course of only a few hours. Thus, even on the same day corrosion rates can change at the same location, and over the course of the year corrosion rates can vary by orders of magnitudes.

Corrosion rates are typically under 25  $\mu\text{m}$  per year, thus requiring electrochemical corrosion rate measurements with longer scan times than those adequate for highly corroding specimens [13]. This can present difficulties due to problems with traffic control, assessability, and weather since long polarizations might see a change in the specimen due to a moisture or temperature change.

## IMPORTANT VARIABLES

### Chloride Ingress

In North America corrosion of rebars in concrete is primarily due to chloride induced pitting. The chloride ingress comes from exposures in marine environments, most notably the splash-tidal zone, and from deicing salts. The onset of corrosion is generally associated with chloride values above 0.9  $\text{kg/m}^3$  (1.5  $\text{lb/yd}^3$ ), even though there are several chloride threshold values that have been reported in the literature with values ranging from 0.17–2.5 % by mass of cement (approximately 0.5–7.5  $\text{kg/m}^3$ ) [14–20]. Therefore, one indirect method of assessing corrosion is to determine the chloride content of the concrete at the reinforcing bar level. If it is below 0.9  $\text{kg/m}^3$  corrosion rate measurements are frequently not performed.

### Admixed Chemicals

Numerous chemical additives are added to concrete to improve its plastic or hardened properties. The vast majority of

these chemical admixtures is noncorrosive. However, some admixtures such as calcium chloride, which is added to decrease setting time and increase early strength, could be corrosive. The presence of these admixtures at high dosage rates could initiate rebar corrosion even in a normally benign exposure. To prevent this, calcium chloride is usually not allowed in steel-reinforced concrete. Ionic salts could also affect the measurement of concrete resistivity [21].

### Carbonation

Though not considered a major problem in North America, carbonation of concrete is a major cause of steel corrosion in the world. Calcium hydroxide in the concrete can react with carbon dioxide or carbon monoxide to produce calcium carbonate. The calcium carbonate is not detrimental to the mechanical properties, but in the process the pH of the concrete drops below 10. At that point the corrosion rate of embedded steel can significantly increase. This phenomenon is mostly found in concretes with low cement contents, high permeability, and low concrete cover over the rebars.

## LABORATORY TESTING

### Solution Tests in Concrete-Like Solutions

As mentioned in the subsection on Simulated Concrete Environments, saturated calcium hydroxide solutions with various combinations of sodium or potassium hydroxide are often used to simulate concrete. Chloride salts are added to these solutions to represent the effects of chloride ingress into the concrete to the rebar level. Rebars or other metal specimens can be examined for corrosion when added to these solutions.

The simplest tests are mass loss and nonquantitative visual examination. Bars are weighed before and after immersion and are examined for surface rusting and pitting. Since pitting is the failure mechanism in alkaline solutions, there is little difference in the mass loss measurements until there is a substantial degree of corrosion, and these tests might have to run for several months or years. Furthermore, since oxygen availability and conductivities are much higher in solutions, corrosion rates will not be directly comparable to those expected in concrete. More quantitative approaches are to actually measure pitting depths. The qualitative effects of inhibitors can be noticed. Useful ASTM methods that can be used in this type of testing are ASTM G 1, Practice for Preparing, Cleaning, and Evaluating Corrosion Test Specimens; G 16, Guide for Applying Statistics to Analysis of Corrosion Data; G 33, Practice for Recording Data from Atmospheric Corrosion Tests of Metallic-Coated Steel Specimens; and G 46, Practice for Examination and Evaluation of Pitting Corrosion.

Another more informative solution test is to perform cyclic polarization in the saturated calcium hydroxide solutions mentioned above. This quickly demonstrates whether the corrosion mechanism is one of pitting and determines the primary mechanisms of corrosion inhibitors [7–9]. A modified version of ASTM G 61, Test Method for Conducting

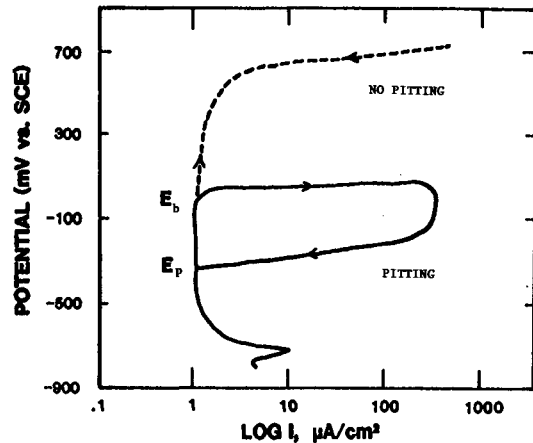


FIG. 1—Idealized cyclic polarization curve for steel in alkaline environments.

Cyclic Potentiodynamic Polarization Measurements for Localized Corrosion Susceptibility of Iron-, Nickel-, or Cobalt-Based Alloys, is quite effective [8,9,22]. A sample curve showing the effects of a corrosion inhibitor is in Fig. 1. An increase in the pitting ( $E_p$ ), and breakdown ( $E_b$ ) potentials is indicative of a good anodic inhibitor.

### Testing in Laboratory Concrete Specimens

The best environment in which to test rebars is concrete, and several test methods are available. A new ASTM test method, G 109, Test Method for Determining the Effects of Chemical Admixtures on the Corrosion of Embedded Steel Reinforcement in Concrete Exposed to Chloride Environments, was issued in 1992. This method uses relatively high water-to-cement (w/c) ratio concrete at a low concrete cover. Because these conditions are not representative of recommended field applications [23], this is a screening test method.

ASTM G 109 involves the measurement of a galvanic current between a single upper layer bar and two bars at a lower level, for concrete that is cyclically ponded with 3 % sodium chloride. When chloride permeates through the concrete the upper bar begins to corrode, with the bottom bars acting as cathodes. A schematic of the specimen is shown in Fig. 2. Visual observations of the bars at the completion of the test is required as is determination of the chloride content at the reinforcing bar depth.

Effective corrosion inhibitors will increase the time to initiation of severe corrosion currents and detrimental concrete admixtures will reduce the time to initiation of severe corrosion. A composite curve from the ASTM round robin is given in Fig. 3. The integrated macrocell current (Coulombs) is a measurement of the total corrosion due to the macrocell. The test is not designed to evaluate materials such as silica fume that increase the resistance between the steel bars and significantly decrease chloride ingress.

Since chloride ingress is relatively quick compared to that observed in field specimens, the difference in time to corrosion initiation between the control and a specimen with corrosion inhibitor is not directly proportional to the

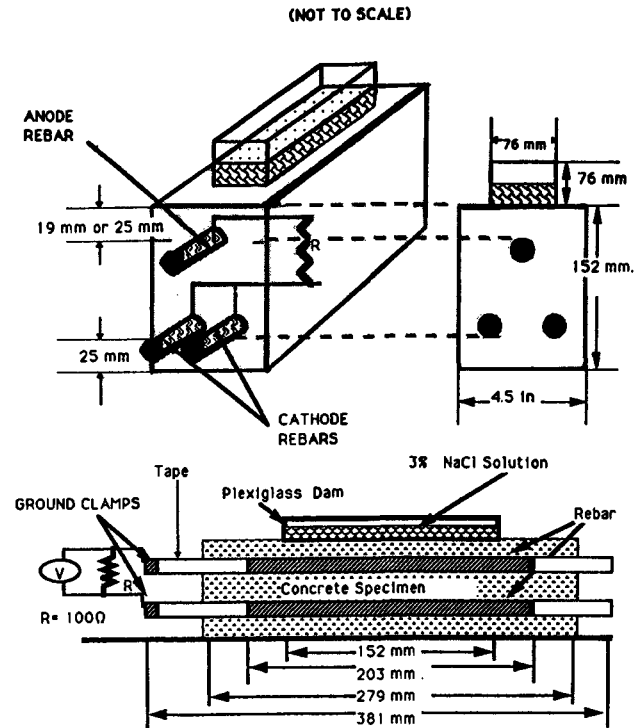


FIG. 2—Diagram of a concrete minibeam (see ASTM G 109).

difference expected in better quality concrete with increased cover, and actually underestimates the improved performance of inhibitors that protect to a given chloride level [24].

The preferred concrete for laboratory studies is one that is representative of field concrete. The concrete mixture would follow the code and recommendations of the American Concrete Institute. For severe chloride exposures this would require a w/c ratio at or below 0.4 and minimum concrete covers of 38 mm (1.5 in.). Testing of these kinds of specimens will take two to five years even under accelerated laboratory test conditions. Though this is a disadvantage for specification writers, it provides a much better representation of expected field performance.

One method of testing would be to use a modified version of ASTM G 109. This would use the same specimen configuration

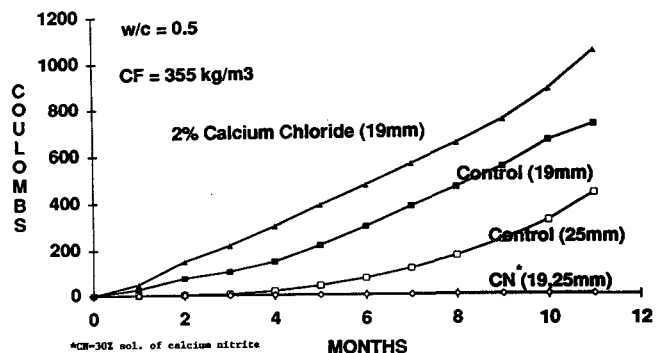


FIG. 3—Macrocell corrosion versus time for concrete mini-beams.

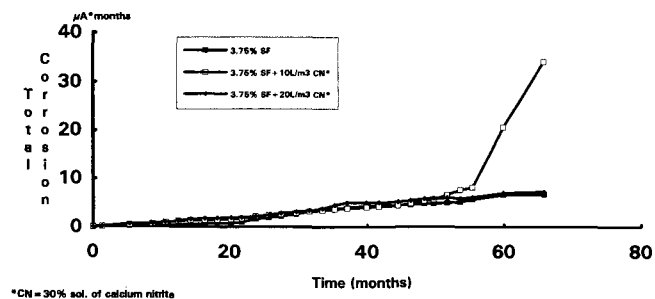


FIG. 4—Total corrosion of minibeam with  $w/c = 0.38$  and concrete cover = 35 mm.

with increased concrete cover and a better quality concrete mixture design. The test procedures would be the same as in ASTM G 109, except for the above changes. Figure 4 gives an example of longer-term testing using a modified version of ASTM G 109. In this figure, the integrated macrocell current over time is represented versus time.

The Southern Exposure Test Method is macrocell test similar in nature to G 109 with some major differences [25,26]. This method uses larger specimens, but the main difference is that one cycle involves four days of ponding with chloride solution followed by three days of accelerated drying at low RH at 40°C. Marine environments will not have the low relative humidity achieved in this method, which could lead to misleading results due to the drying of the concrete. Even in non-marine exposures, weather histories show that the relative humidity, where deicing salts are used, remains above 80 % in the summer, especially on the few days when the temperatures approach 40°C or higher [weather]. Thus, while this test method accelerates chloride ingress, it might change the performance of characteristics corrosion prevention systems that have enhanced performance under accelerated drying conditions.

In addition to the simple macrocell current measurement as described in ASTM G 109, polarization resistance and electrochemical impedance spectroscopy (EIS) can be performed. A modified version of ASTM G 59 (Practice for Conducting Potentiodynamic Polarization Resistance Measurements) using IR drop correction is recommended for the polarization resistance measurements [3,9]. EIS is conducted using equipment as described in ASTM G 106, Practice for Verification of Algorithm and Equipment for Electrochemical Impedance Measurements. The experimental data are commonly displayed using Nyquist or Bode plots. By applying an alternating current over a range of frequencies, which in concrete is generally between 0.4 mHz to 20 000 Hz [9], more mechanistic information of the corrosion process can be obtained than when a direct current method is used. This is because the electrochemical processes respond similarly as a network of capacitances and resistances which can be identified by measurements at various frequencies.

Another geometry for laboratory specimens is a concrete cylinder with an embedded reinforcing bar known as a lollipop specimen. These specimens can be used to simulate marine piles, and frequently are partially immersed to represent the splash tidal zone area [9]. Concrete mixtures

representing those used in the field are often tested with the only acceleration being a reduced concrete cover of approximately 35 mm, constant exposure to 3 % sodium chloride, and a laboratory temperature that is 22°C.

Corrosion tests that are performed on lollipops are corrosion potential readings as described in ASTM C 876 (Test Method for Half-Cell Potentials of Uncoated Reinforcing Steel in Concrete), polarization resistance as described in ASTM G 59, using IR correction [3,9], and EIS [9]. Specimens are broken open to visually examine the bars for confirmation of the electrochemical results, and chloride analyses are performed. The chloride analysis correlates the chloride content to the corrosion activity.

Testing in cracked concrete specimens can provide an indication of performance in less than ideal circumstances. These tests should be conducted in concrete meeting the minimum requirements of codes and recommended practices since mechanisms might be significantly affected by improper specimen design [27,28].

Testing procedures for cracked concrete are essentially the same as used for other laboratory specimens exposed to chloride solutions continuously or cyclically. Methods that can be used include polarization resistance, electrochemical impedance, and macrocell corrosion which were discussed above. Procedures for conducting these tests are described in Refs 27 and 28.

Large-scale laboratory specimens are typically about 2 m<sup>2</sup> in surface area or larger. They have depths exceeding 100 mm that are typical of field concretes that are actually used. The decks are reinforced with one to two mats of steel as would be found in actual use. For acceleration purposes the spacing of the steel can be less than used in the field.

One method of conducting these tests is to have two mats of reinforcing bars with or without admixed chlorides in the top mat and to pond with chloride. The macrocell current between the top and bottom mats as well as the corrosion potentials are measured according to ASTM C 876. This procedure is described in Ref 29.

Testing with one layer of reinforcing bars using a fine grid can also give good results [30]. The 51 mm (2-in.) grid gave very good potential contours that can be used to estimate the corrosion activity. The use of polarization resistance as described by Clear [31], Escalante [32], Andrade et al. [11], and the Strategic Highway Program [33] could also be employed on these kinds of slabs.

## FIELD TESTING

### Specimens in the Field

One method of field testing is to place laboratory size specimens in the field. These specimens could then be tested using the same techniques used in the laboratory. One advantage of this is the ability to have well-defined specimen dimensions and control of exposed steel areas.

### Field Structures

Test methods for field structures almost always include corrosion potential mapping as described in ASTM C 876.



Note that it is essential that the deck be moist without puddles on the surface. This method only gives an idea of the corrosion activity and does not provide corrosion rate data. A recent Transportation Research Board (TRB) paper on work in Virginia indicated that a 0.61 m (2 ft) spacing for the potential grid was much better than the typical 1.2 m (4 ft) spacings in relating corrosion damage to corrosion potential contours [34].

Polarization resistance methods can be used to measure the corrosion rates of steel embedded in concrete. This can be performed on embedded probes of known area or by having the counter-electrode and reference electrode at the surface. The high resistivity of the concrete requires some form of IR correction. The Strategic Highway Research Program Project (SHRP) C101 looked at several devices to measure corrosion rates [35]. These devices included the three electrode linear polarization (3LP) device [31] and the guard ring device [11] and a two frequency electrochemical impedance device [33]. A single galvanic current with current interruption as described by Escalante has also been used [32], as has traditional polarization resistance [36].

Though the absolute values for the corrosion rate do not agree for the various instruments described above, the devices show the same trends in the rates; that is, if one device shows a higher corrosion rate at one location, the others will also show a higher rate. More work is needed in this area.

EIS can be used in the field, but long test periods at low frequencies are impractical. This is because there are large temperature and moisture changes which affect the corrosion activity. One possible means to get an idea of the corrosion rate is to examine the inflection point of the Bode curve. If it occurs at a frequency above 1 mHz there is a good possibility that severe corrosion is occurring [37,38].

Several nonelectrochemical techniques for field corrosion assessment are the measurement of spalled and delaminated concrete from visual and chain drag operations. A measurement of the chloride contents at the reinforcing level also gives some idea as to the potential corrosion activity with chloride contents of 0.9 kg/m<sup>3</sup> (1.5 lb/yd<sup>3</sup>) typically being considered to be the threshold value for corrosion initiation.

## STANDARDS

ASTM C 876: Describes a technique to measure the corrosion potential of steel in concrete. In the past researchers have used absolute corrosion potential values to give probabilities of the existence of corrosion and to estimate corrosion rates. This is no longer the case and current thoughts are that the contours are an indication of corrosion activity for larger structures, but absolute corrosion rates must be determined by some other method.

ASTM G 109: This method is used as a screening test to determine if chemical admixtures inhibit or accelerate the corrosion of steel in concrete subjected to chloride ponding. The technique is useful for chemical admixtures, but due to the low concrete cover and relatively high w/c ratio does not provide quantitative results as to expected long-term performance in concrete meeting the minimum recommendations of the American Concrete Institute (ACI) [23]. As mentioned above, variations of this test method with better

quality concrete can be used to predict field performance more accurately.

## European Standards

The European organization for standards (Comite European de Normalisation-CEN) is considering a harmlessness test method based on polarizing steel embedded in a mortar, made with a cement with less than 5 % C<sub>3</sub>A, to +260 mV versus a saturated calomel electrode [39]. Admixtures would be tested to see if they gave detrimental effects (high currents, and corrosion damage on the bar) relative to a mortar without admixture. This method is still in committee at this time.

Work in Germany has resulted in a new admixture specification for Passivating Corrosion Inhibitors [40]. Schiessl et al. describe several of the test methods used by the specification [41].

## MATERIALS

A brief description of materials used to improve the corrosion resistance of steel in reinforced concrete is given in this section. The reader is encouraged to go to other sources for a more detailed description, since this article is emphasizing test methods.

### Concrete Admixtures

ASTM C 494 (Specification for Chemical Admixtures for Concrete) classifies several types of concrete admixtures. Of particular use for steel in concrete are the high range water reducers that are classified as type F or G admixtures. These chemicals significantly improve concrete workability at low w/c ratios, which is needed to produce low permeability concrete.

Corrosion inhibitors are also used to provide corrosion protection for steel in concrete. A TRB document describes the several corrosion inhibitors used in concrete [42] as do ACI 212 [43] and ACI 222 [44]. The corrosion inhibitor that is most used at this time is calcium nitrite [45]. Additional inhibitors and methods of predicting life-cycle costs are now addressed in the literature [46–51].

Damp-proofing admixtures or water repellents can also be added to concrete. However, several researchers indicate that they offer little benefit to corrosion protection in good quality concrete [52,53]. Succinate type admixtures have been tested at the Universities of Connecticut and Massachusetts [54,55]. Good dampproofing and corrosion resistance properties were shown; however, due to the extreme drying conditions and artificial cracks, it is not known if these materials raise the chloride threshold level at the reinforcing steel for corrosion initiation.

Mineral admixtures can be used to reduce concrete permeability. These are typically fly ash, microsilica, or blast furnace slag and are also addressed by TRB [42], and by ASTM Committee C09 on Concrete.

### Reinforcing Bar Coatings

The most popular coating for reinforcing bars is fusion bonded epoxy. Epoxy-coated steel is addressed in ASTM A 775M,

Specification for Epoxy-Coated Reinforcing Steel Bars; and ASTM D 3963M, Specification for Fabrication and Jobsite Handling of Epoxy-Coated Reinforcing Steel, and epoxy-coated wire and wire fabric in ASTM A 884, Specification for Epoxy-Coated Steel Wire and Welded Wire Fabric for Reinforcement. A TRB symposium [56] and circular [57] discusses the pros and cons of this approach. The general consensus was that much more attention to minimizing defects and damage to the coatings is needed from the manufacturing point up to the placement of the bars in the field.

Galvanized steel was found to be of marginal effectiveness in earlier Federal Highway Administration (FHWA) studies [58]. More recent work indicates that galvanized steel can offer increased protection and can be especially beneficial in carbonated concrete [59,60]. The ASTM standard for galvanized steel bars is A 767.

Other inorganic and metallic coatings have been applied to steel rebars, but their use is not widespread.

### Concrete Sealers

Concrete sealers have been used to reduce chloride and moisture ingress into concrete. Work in the Strategic Highway Research Program (SHRP) C 103 project indicated that they have a finite lifetime and need to be reapplied in bridge applications [61].

### Membranes

Membranes are widely used in Europe and Canada as well as some areas in the United States to limit the ingress of chloride into concrete. They provide good protection as long as the membrane remains leak-free and the riding surface does not deteriorate exposing the membrane. The lifetime of membranes in bridge applications was also addressed by SHRP C 103 [61].

### Cathodic Protection

Cathodic protection is typically used as a rehabilitation technique, but is also used in new construction. The steel in the concrete is made into a cathode and thus its corrosion rate is kept low. Broomfield reviewed the current state of cathodic protection systems in the United States [62]. Further information can be obtained from a SHRP report on cathodic protection of concrete structures [63]. NACE International holds symposiums on cathodic protection of steel in concrete on a biannual basis [64].

### New Steels

Stainless steel bars and cladding are now available [65] and ASTM is working on a standard. Results are significantly improved over standard reinforcing bars in testing, but dependent upon which alloys are used [65,66]. Though corrosion is reduced, it is not necessarily prevented [66].

Steel processed to have untransformed nano-sheets of austenite sandwiching dislocated martensite laths is available. There are no carbon containing phases present, so cathodic reaction rates are claimed to be low on this steel. The version with the most promise contains over 8 % chromium [67].

### Additional Information

More information relating concrete properties, corrosion, and corrosion protection systems is available in reference books. A few of these are included in the references [17,68,69].

### REFERENCES

- [1] Hansson, C. M. and Berke, N. S., "Chloride in Concrete," *MRS Symposium Proceedings*, Pore Structure and Permeability of Cementitious Materials, L. R. Roberts and J. P. Skalny, Eds., Vol. 137, No. 99, November 1988, pp. 253-270.
- [2] Dawson, J. L., Callow, L. M., Hladky, K., and Richardson, J. A., "Use of Electrochemical Impedance Measurements Applied to the Corrosion of Reinforcing Steel in Concrete," *Corrosion/78*, Paper 125, NACE, Houston, TX, 1978.
- [3] Berke, N. S., Shen, D. F., and Sundberg, K. M., "Comparison of the Polarization Resistance Technique to Macrocell Corrosion Technique," *Corrosion Rates of Steel in Concrete*, ASTM STP 1065, Berke, Chaker, and Whiting Eds., ASTM International, West Conshohocken, PA, 1990.
- [4] Andrade, C., Sanjuan, M. A., and Alonso, C., "Measurements of Chloride Diffusion Coefficient from Migration Tests," *Corrosion/93*, Paper 319, NACE, New Orleans, March 1993.
- [5] Arup, H., Sorensen, B., Frederiksen, J., and Thaulow, N., "The Rapid Chloride Permeation Test—An Assessment," *Corrosion/93*, Paper 334, NACE, New Orleans, March 1993.
- [6] Berke, N. S. and Hicks, M. C., "Predicting Chloride Profiles in Concrete," *Corrosion/93*, Paper 341, NACE, New Orleans, March 1993.
- [7] Page, C. L. and Treadaway, K. W. J., "Aspects of the Electrochemistry of Steel in Concrete," *Nature*, Vol. 297, 13 May 1982, pp. 109-115.
- [8] Berke, N. S., "The Use of Anodic Polarization to Determine the Effectiveness of Calcium Nitrite as an Anodic Inhibitor," *Corrosion of Rebars in Concrete*, ASTM STP 906, ASTM International, West Conshohocken, PA, 1986, pp. 78-91.
- [9] Berke, N. S. and Hicks, M. C., "Electrochemical Methods of Determining the Corrosivity of Steel in Concrete," *Corrosion Testing and Evaluation, Silver Anniversary Volume*, ASTM STP 1000, R. Baboian and S. Dean, Eds., ASTM International, West Conshohocken, PA, 1990, pp. 425-440.
- [10] Berke, N. S., Scali, M. J., Regan, J. C., and Shen, D. F., "Long-Term Corrosion Resistance of Steel in Silica Fume and/or Fly Ash Containing Concrete," *Second International Conference on Concrete Durability*, Montreal, Canada, 1991, ACI, SP-126, pp. 393-422.
- [11] Andrade, C., Maribona, I. R., Feliu, S., et al., "The Effect of Macrocells between Active and Passive Areas of Steel Reinforcements," *Corrosion Science*, Vol. 23, No. 2, 1992, pp. 237-249.
- [12] Berke, N. S., Dallaire, M. P., and Hicks, M. C., "Effect of Calcium Nitrite on the Corrosion Fatigue of Steel Reinforcing in Cracked Concrete," *Corrosion/91*, Paper 550, NACE, Houston, TX, 1991.
- [13] Mansfeld, F. and Kendig, M., "Concerning the Choice of Scan Rate in Polarization Measurements," *Corrosion*, Vol. 37, No. 9, September 1981, pp. 545-546.
- [14] Rasheduzzafar, M., Al-Sandoun, S. S., Al Gahtani, A. S., and Dakhil, F. H., "Effects of Tricalcium Aluminate Content of Cement on Corrosion of Reinforcing Steel in Concrete," *Cement and Concrete Research*, Vol. 20, 1990, p. 723.
- [15] Slater, J. E., *Corrosion of Metals in Association with Concrete*, ASTM STP 818, ASTM International, West Conshohocken, PA, 1983.

- [16] Kayyali, O. A. and Haque, M. N., "The Ratio of Cl-/OH- in Chloride Contaminated Concrete: A Most Important Criterion," *Mag. Concrete Res.*, Vol. 47, 1995, pp. 235-242.
- [17] Tuutti, K., *Corrosion of Steel in Concrete—CBI Research Report 4:82*, Swedish Cement and Concrete Research Institute, Stockholm, 1982.
- [18] Hansson, C. M. and Sorensen, B., "Threshold Concentration of Chloride in Concrete for Initiation of Reinforcement Corrosion," *Corrosion Rates of Steel in Concrete*, ASTM STP 1065, N. S. Berke, V. Chaker, and D. Whiting, Eds., ASTM International, West Conshohocken, PA, 1988, pp. 3-16.
- [19] Bamforth, P. B. and Chapman-Andrews, J. F., "Long Term Performance of Reinforced Concrete Elements Under UK Coastal Conditions," *Corrosion and Corrosion Protection of Steel in Concrete—I*, R. N. Swamy, Ed., Sheffield Academic Press, Sheffield (1994), pp. 139-156.
- [20] Lukas, W., "Relationship Between Chloride Content in Concrete and Corrosion in Untensioned Reinforcement in Austrian Bridges and Concrete Road Surfacing," *Betonwerk Fertigeil-Tech* 51, 1985, p. 730.
- [21] Berke, N. S. and Hicks, M. C., "Estimating the Life Cycle of Reinforced Concrete Decks and Marine Piles Using Laboratory Diffusion and Corrosion Data," *Corrosion Forms and Control for Infrastructure*, ASTM STP 1137, V. Chaker, Ed., ASTM International, West Conshohocken, PA, 1992, pp. 207-231.
- [22] Tourney, P. and Berke, N. S., "Put to the Test," *Civil Engineering*, December 1992, pp. 62-63.
- [23] ACI 318, "Building Code Requirements for Reinforced Concrete," American Concrete Institute, Detroit, 2002.
- [24] Berke, N. S., Pfeifer, D. E., and Weil, T. G., "Protection Against Chloride Induced Corrosion—A Review of Data and Economics on Microsilica and Calcium Nitrite," *Concrete International*, Vol. 10, No. 12, December 1988, pp. 45-55.
- [25] Clear, K. C. and Harrigan, E. T., "Sampling and Testing for Chloride Ion in Concrete," Report No. FHWA/RD-77-85, Federal Highway Administration, August 1977.
- [26] Pfeifer, D. W., Landgren, J. R., and Zoob, A., "Protective Systems for New Prestressed and Substructure Concrete," Report No. FHWA/RP-86/193, Federal Highway Administration, Washington, DC, April 1987, 113 pp.
- [27] Berke, N. S., Dallaire, M. P., Hicks, M. C., and Hoopes, R. J., "Corrosion of Steel in Cracked Concrete," *Corrosion/93*, Paper 322, NACE, Houston, TX, March 1993.
- [28] Hansson, C. M. and Okulaja, S. A., "Corrosion of Reinforcing Steel in Cracked High Performance Concrete," *Advances in Cement and Concrete Proceedings of Copper Mountain, CO Conference*, August 10-14, 2003, Engineering Conferences International, D. A. Lange, K. L. Scrivener, and J. Marchand, Eds., University of Illinois, Urbana, 2003, pp. 223-232.
- [29] Virmani, Y. P., Clear, K. C., and Pasko, T. J., "Time-to-Corrosion of Reinforcing Steel in Concrete Slabs, Vol. 5—Calcium Nitrite Admixture and Epoxy-Coated Reinforcing Bars as Corrosion Protection Systems," Report FHWA-RD-83-012, Federal Highway Administration, Washington, DC, September 1983, p. 71.
- [30] Rosenberg, A. H. and Gaidis, J. M., "The Mechanism of Nitrite Inhibition of Chloride Attack on Reinforcing Steel in Alkaline Aqueous Environments," *Materials Performance*, Vol. 18, No. 11, 1979, pp. 45-48.
- [31] Clear, K., "Measuring Rate of Corrosion of Steel in Field Concrete Structures," Transportation Research Record 1211, Transportation Research Board, Washington, DC, 1989, pp. 28-37.
- [32] Escalante, E., "Measuring the Underground Corrosion of Steel Piling at Turcot Yard, Montreal, Canada—A 14 Year Study," *Corrosion Forms and Control for Infrastructure*, ASTM STP 1137, V. Chaker, Ed., ASTM International, West Conshohocken, PA, 1992, pp. 339-355.
- [33] Strategic Highway Research Program, "Condition Evaluation of Concrete Bridges Relative to Reinforcement Corrosion, Volume 2: Method for Measuring the Corrosion Rate of Reinforcing Steel," SHRP-S/FR-92-104, National Research Council, Washington, DC, September 1992.
- [34] Clemena, G., Jackson, D., and Crawford, G., "Inclusion of Rebar Corrosion Rate Measurements in Condition Surveys of Concrete Bridge Decks," Transportation Research Board, Paper 920344, Washington, DC, January 1992.
- [35] Flis, J., Sehgal, A., Li, D., et al., "Condition Evaluation of Concrete Bridges Relative to Reinforcement Corrosion—Vol 2: Method for Measuring Corrosion Rate of Reinforcing Steel," Strategic Highway Research Program, National Research Council, Final Report C-101, SHRP-S/FR-92-104, Washington, DC, 1992.
- [36] Berke, N. S., Dallaire, M. P., Weyers, R. E., et al., "Impregnation of Concrete with Corrosion Inhibitors," *Corrosion Forms and Control for Infrastructure*, ASTM STP 1137, V. Chaker, Ed., ASTM International, West Conshohocken, PA, 1992, pp. 328-338.
- [37] Berke, N. S., "Corrosion Rates of Steel in Concrete," *ASTM Standardization News*, March 1986.
- [38] Berke, N. S., "Electrochemical Tests to Determine Corrosion Rates of Rebar in Field Concrete," ASTM Workshop G01.14.06, Oral Presentation, Miami, FL, November 1992.
- [39] Comité Européen de Normalisation, CEN/TC104, Zurich, Switzerland.
- [40] General Building Inspection Approval No. Z-3.212-1737: Concrete Additive Passivator "DCI S," German Institute for Building Technology, Berlin, Germany, February 2002.
- [41] Schiessl, P. and Dauberschmidt, C., "Evaluation of Calcium Nitrite as a Corrosion Inhibitor," Sixth CANMET/ACI International Conference on Superplasticizers and Other Chemical Admixtures in Concrete, Supplementary Papers, M. Malhotra, Ed., American Concrete Institute, Detroit, 2000, pp. 105-119.
- [42] Transportation Research Board, "Admixture and Ground Slag for Concrete," Circular 365, National Research Council, Washington, DC, December 1990.
- [43] ACI 212, "Chemical Admixtures in Concrete," *Manual of Concrete Practice, Part I—Materials and General Properties of Concrete*, American Concrete Institute, Detroit, 2000.
- [44] ACI 222, "Corrosion of Metals in Concrete," *Manual of Concrete Practice, Part I—Materials and General Properties of Concrete*, American Concrete Institute, Detroit, 2003.
- [45] Berke, N. S., "Corrosion Inhibitors in Concrete," *Concrete International*, Vol. 13, No. 7, July 1991, pp. 24-27.
- [46] Johnson, D. A., Miltenberger, M. A., and Almy, S. L., "Determining Chloride Diffusion Coefficients for Concrete Using Accelerated Test Methods," Third CANMET/ACI International Conference on Concrete in Marine Environment, St. Andrews by-the-Sea, New Brunswick, Canada, August 4-9, 1996, Supplementary Papers, pp. 95-114.
- [47] Vogelsang, J. and Meyer, G., "Electrochemical Properties of Concrete Admixtures," *Fourth International Symposium on Corrosion of Reinforcement in Concrete Construction*, Cambridge, UK, July 1-4, 1996, Page, C. L., Bamforth, P. and Figg, J. W., Eds., pp. 579-588.
- [48] Berke, N. S., Aldykiewicz, Jr., A. J., Hicks, M. C., and MacDonald, A., "Life-Cycle Cost Modeling for Steel Reinforced Concrete Structures," *Ion and Mass Transport in Cement-Based Materials*, R. D. Hooton, M. D. A. Thomas, J. Marchand, and J. J. Beaudoin, Eds., The American Ceramic Society, Westerville, OH, 2001, pp. 341-366.
- [49] Elsener, B., "Corrosion Inhibitors for Steel in Concrete," *European Federation of Corrosion Publications*, No. 35, W. S. Manney and Son, Ltd., 2001.
- [50] Thomas, M. D. A. and Bentz, E. C., "Life 365," Computer Program for Predicting Service Life and Life-Cycle Costs of

- Reinforced Concrete Exposed to Chlorides, University of Toronto, August 2000.
- [51] Berke, N. S., Aldykiewicz, A. J., Jr., and Li, L., "What's New in Corrosion Inhibitors, *Structure*, July/August 2003, pp. 10–12.
  - [52] Rixom, M. R. and Mailvaganam, N. P., *Chemical Admixtures for Concrete, Second Edition*, E & FN Spon Publishers, New York, 1986, p. 140.
  - [53] *Concrete Admixtures Handbook*, V. S. Ramachandran, Ed., Noyes Publications, Park Ridge, NJ, 1984, p. 518.
  - [54] Allyn, M., Frantz, G. C., and Stephens, J. E., "Protection of Reinforcement with Corrosion Inhibitors, Phase 1," Final Report JHR 98-266 Project 96-2, Connecticut Department of Transportation, November 1998.
  - [55] Civjan, S. A., LaFave, J. M., Lovett, D., Sund, D. J., and Trybalski, "Performance Evaluation and Economic Analysis of Combinations of Durability Enhancing Admixtures (Mineral and Chemical) in Structural Concrete for the Northeast U.S.A.," NETCR36 Project No. 97-2, The New England Transportation Consortium, February 2003.
  - [56] Transportation Research Board Annual Meeting, 1993, Taped Oral Session on Epoxy-Coated Steel Reinforcement, Washington, DC, January 1993, available from Transportation Research Board, National Research Council, Washington, DC.
  - [57] Transportation Research Circular, "Epoxy-Coated Reinforcement in Highway Structures," No. 403, March 1993, Transportation Research Board, National Research Council, Washington, DC.
  - [58] Clear, K. C., "Time-to-Corrosion of Reinforced Steel in Concrete Slabs," Vol. 4—Galvanized Reinforcing Steel, Interim Report, December 1981, Federal Highway Administration Report No. FHWA/RD-82/028, FHA, U.S. Department of Transportation, Washington, DC.
  - [59] Yeomans, S. R., "Aspects of the Characteristics and Use of Coated Steel Reinforcement in Concrete," *Corrosion/93*, Paper 329, NACE, New Orleans, March 1993.
  - [60] Gonzalez, J. A. and Andrade, C., "Effect of Carbonation, Chlorides and Relative Ambient Humidity on the Corrosion of Galvanized Rebars Embedded in Concrete," *British Corrosion Journal*, Vol. 17, No. 1, 1993, pp. 21–28.
  - [61] Whiting, D., Borge, O., Nagi, M., and Cady, P., "Condition Evaluation of Concrete Bridges Relative to Reinforcement Corrosion—Vol. 5: Methods for Evaluating the Effectiveness of Penetrating Sealers," Strategic Highway Research Program, National Research Council, Final Report C-101, SHRP-S/FR-92-107, Washington, DC, 1992.
  - [62] Broomfield, J., "Field Survey of Cathodic Protection on North American Bridges," *Materials Performance*, Vol. 31, No. 9, September 1992, pp. 28–33.
  - [63] "Cathodic Protection of Reinforced Concrete Elements—State of the Art Report," SHRP S337, Strategic Highway Research Program, National Research Council, Washington, DC, 1993.
  - [64] NACE International, Houston, TX.
  - [65] McDonald, D. B., Sherman, M. R., Pfeifer, D. W., and Virmani, Y. P., "Stainless Steel Reinforcing as Corrosion Protection," *Concrete International*, May 1995, pp. 65–70.
  - [66] Flint, G. N. and Cox, R. N., "The Resistance of Stainless Steel Partly Embedded in Concrete to Corrosion by Seawater," *Magazine of Concrete Research*, Vol. 40, No. 142, 1988, pp. 13–27.
  - [67] Darwin, D., Browning, J., Nguyen, T. V., and Locke, C., Jr., "Mechanical and Corrosion Properties of a High-Strength, High Chromium Reinforcing Steel for Concrete," SM Report No. 66, South Dakota DOT Office of Research, Pierre, SD, (March 31, 2002).
  - [68] Bentur, A., Diamond, S., and Berke, N. S., *Steel Corrosion in Concrete—Fundamental and Civil Engineering Practice*, E & FN Spon, London, 1998.
  - [69] Broomfield, J., *Corrosion of Steel in Concrete: Understanding, Investigation and Repair*, Routledge and E & FN Spon, October 1997.



## CONSIDERATIONS AFFECTING TEST PROGRAMS

The corrosivity of water to mild steel is related to certain chemical aspects of the water. The more important variables are dissolved oxygen, alkalinity,<sup>2</sup> pH, chloride, sulfate, hydrogen sulfide, carbon dioxide, and ammonia.

The most important single variable affecting corrosivity is pH. The relationship, with regard to carbon steel, is shown in Fig. 2 [1]. At a pH below about 4, corrosion increases rapidly with decrease in pH. In the pH range 4 to 9, changes in pH have a relatively minor effect on corrosivity to steel. Above pH 9, corrosivity decreases as pH increases.

Within the pH range of primary interest (the 5 to 9 range) dissolved oxygen is the dominant corrosive agent to carbon steel. The corrosion mechanism involves dissolution of metallic ions in an anodic area combined with consumption of the released electrons at a cathodic area. In the pH range of 5 to 9, the dominant cathodic reaction is reduction of dissolved oxygen. At a low pH (pH <4) the dominant cathodic reaction is generation of hydrogen.

At a given level of pH and dissolved oxygen content, the next most important determinants of corrosivity are the concentration of aggressive ions (primarily chloride and sulfate) and the buffering capacity of the water, which is roughly proportional to alkalinity. A number of attempts have been made to derive a reliable corrosion index. None have been fully successful. One approach to a usable "corrosivity index" is calculated by dividing chloride plus sulfate by alkalinity, all expressed in terms of equivalents per liter. This value, developed by Larson and Skold [2], is sometimes called the Larson-Skold Index. One reference [3] suggests that a value of this index <0.8 indicates that "chlorides and sulfates probably will not interfere with natural film formation"; while a value >1.2 "suggests that high local corrosion rates may be encountered." While useful, this index is only a crude guideline.

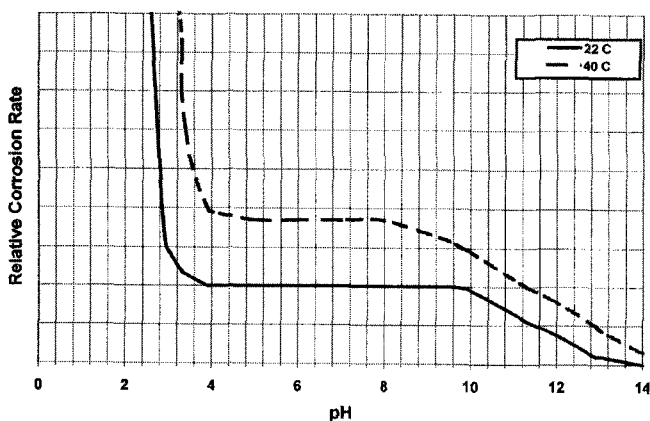


FIG. 2—Effect of pH on corrosion of steel in water in the absence of an inhibitor.

<sup>2</sup>Alkalinity, as used in water treating, is defined as the ability of a water to neutralize acid. It is measured by titration and the results are usually expressed "as  $\text{CaCO}_3$ ."

The rate of corrosion is controlled by the rate of dissolved oxygen reaction on the surface, which is controlled by the rate of transport of dissolved oxygen to the surface. Similar mass transfer mechanisms control the rate of transfer of fouling ions to the surface. In a system containing a corrosion inhibitor, the transfer of inhibitor to the surface is also controlled by the same factors. Once the reactants are at the surface, reaction rates are affected by temperature. Temperature also affects the properties of the fluid film in contact with the surface. For example, viscosity typically decreases in the film on the surface of a hot wall, facilitating reactant transfer. It is difficult to generalize about the affect of temperature on corrosion rates in a system treated with corrosion inhibitor. Increased temperature is likely to accelerate the corrosion inhibition reactions as well as the corrosion reaction. The net change in corrosion rate could be either an increase or a decrease, depending upon the effectiveness of the corrosion inhibition treatment.

In the near neutral pH range, corrosion rate is nonlinear with respect to time. Almost any clean carbon steel surface in contact with aerated water will corrode at a rapid rate for the first few hours. The rate decreases with time, eventually reaching a steady state. This steady state corrosion rate is the rate of practical interest in water systems.

The critical consideration in most industrial cooling operations is the situation on heat transfer surfaces exposed to flowing water. In order to simulate these conditions, the hydrodynamics must be properly modeled. The important variable is not velocity but turbulence, which is qualitatively proportional to the Reynolds Number. The second critical variable is temperature, particularly the temperature in the relatively slow-moving, laminar film flowing next to the heated wall.

In the following sections, test methods will be discussed in terms of how effectively each test method models these variables.

## LABORATORY TESTING

Laboratory corrosion tests in industrial water are used to help understand corrosion and inhibition mechanisms and to develop treatment systems. They are helpful in selecting treatments for a given system, but usually fail to model accurately the critical aspects of a field system.

The most common test method is the coupon immersion test, usually conducted under static or near-static conditions. Other methods, used to a lesser degree, include rotating electrodes, of which the best arrangement for water is probably the rotating cylinder, and small recirculating systems. Electrochemical tests and polarization studies are used primarily to elucidate the corrosion mechanism. Surface analysis is also used, primarily for mechanistic studies.

## PLANT TESTING

NOTE: Biological monitoring or testing is not discussed in this section. However, one should recognize that biological control is the first requirement in a cooling water system. If biological growth is not properly controlled, serious corrosion or fouling, or both, are almost certain to occur.

Virtually all definitive test work is done in a pilot plant or plant. The final test is performance of actual operating equipment. A systematic, quantitative inspection program is the final measure of success of a corrosion control program. All other methods are evaluated in terms of how closely they approximate this method. Other methods used are listed and described briefly below.

### Coupon Tests

Coupon tests are by far the most commonly used test method. The usual method is to mount coupons in the middle of a stream, frequently in a serpentine bypass loop as shown in Fig. 3. Detailed procedures for coupon tests are described in ASTM D 2688, Test Method for Corrosivity of Water in the Absence of Heat Transfer (Weight Loss Methods) (Method A). Tests with very low water flow (suspended coupons in the cooling tower basin, for example) are not recommended unless the objective is to measure corrosion under near stagnant conditions.

Coupon tests give reliable comparative numbers indicative of changes in average water corrosivity during the exposure period, provided tests are run for a long enough period (30 days or more) and only data from tests of comparable exposure time and velocity are compared. For interpretive purposes, some reasonably reliable rules-of-thumb have been developed. For systems using modern non-metallic based inhibitors, a coupon corrosion rate on steel for a 30-day test of  $<50 \mu\text{m/yr}$  (2 mpy) is indicative of excellent control of water corrosiveness. A rate of  $50\text{--}75 \mu\text{m/yr}$  (2–3 mpy) or less on a 30-day test is indicative of satisfactory results. A rate of  $75\text{--}125 \mu\text{m/yr}$  (3–5 mpy) are considered fair, possibly acceptable in some cases. Rates of  $>125 \mu\text{m/yr}$  (5 mpy) are usually considered excessively high. Note that these rules-of-thumb assume reasonably general corrosion. Severe localized attack on the coupon is a clear indication that the corrosion prevention treatment is not achieving acceptable results.

A basic limitation of coupon testing is that it fails to model properly either the hydrodynamic or thermal conditions on plant equipment. The coupon is exposed in the

most highly turbulent area and the coupon causes additional turbulence by its presence. As previously discussed, high turbulence facilitates inhibitor transfer to the surface; thus, the coupon has a better chance of being adequately protected than the wall of a tube or pipe. While not common, there have been cases where the treatment system protected the coupons but not the plant equipment.

The use of tubular (pipe or tube) samples with internal flow should be more reliable than conventional coupon tests because of the closer approach to proper hydrodynamic conditions. Such tests are seldom used in industrial water systems, despite the fact that ASTM standards, i.e., ASTM D 2688 (Method B), cover the use of tubular samples.

### Electrical and Electrochemical Methods

There are two commonly used tests. One is called “linear polarization (LP)” using either two element or three element probes. If a very low DC voltage (10 mV or so) is imposed between two identical metallic electrodes in an electrolyte, the observed current flow is approximately proportional to the corrosion rate of the probes. This was first demonstrated in the 1950s [5–7]. Stern and Geary [8,9] later developed a quantitative equation that allows estimation of the corrosion rate. Although this technique, when used with commercially available probes, does not replicate the hydrodynamic or heat transfer conditions, it is widely used because of its simplicity. It provides an instantaneous indication of corrosion rate. By arranging the instrumentation so that the DC potential is applied with one polarity, then reversed, two readings are obtained. The difference between the two readings is believed by some to be an indication of the tendency toward localized corrosion. There is a lack of consensus about the utility and reliability of this measurement.

The second method, called “electrical resistance” (ER), exposes a sample of the metal of interest, mounted on a probe inserted into the system. As the sample corrodes, the cross-sectional area decreases, increasing the electrical resistance of the sample. This increase, measured through suitable instrumentation, provides a continuous record of metal loss. This method does not give proper quantitative results in systems characterized by localized attack, a common situation in water systems.

While these methods have been used with success, they have deficiencies for water systems. As with coupons, the hydrodynamic and thermal conditions of critical plant surfaces are not properly modeled.

Both LP and ER methods are covered by ASTM G 96, Practice for On-line Monitoring of Corrosion in Plant Equipment (Electrical and Electrochemical Methods).

### Test Exchangers

A better method of replicating the hydrodynamics and thermal conditions of critical operating equipment is a test heat exchanger, using a small side stream of water from the cooling tower water circuit. This technique is more complex and expensive; as a result, it has been used less extensively than the techniques described previously. In a test heat exchanger, water flow and heat flux can be controlled. If

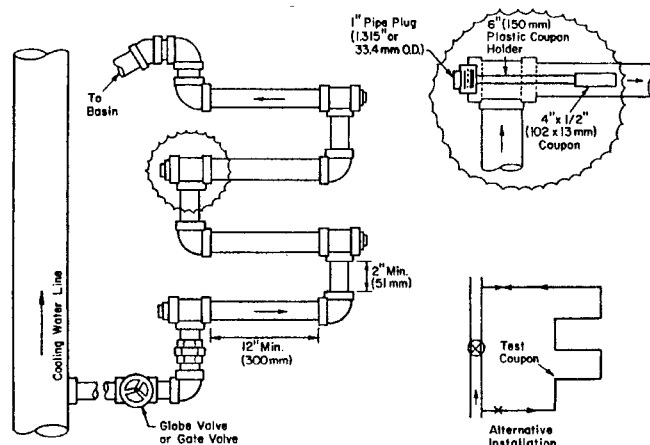


FIG. 3—Serpentine bypass loop used for coupon test in plant (see ASTM D 2688, Method A).

the test exchanger contains multiple tubes, tubes can be removed at different time periods and depth of attack measured quantitatively. Plotting these depths against time of exposure allows an estimate of the rate at which corrosion is penetrating the wall. In addition, thermal measurements allow calculation of heat transfer coefficients and fouling factors, providing a quantitative measure of fouling.

Test exchangers require both operating attention and maintenance work, making their use relatively expensive and troublesome. The method has the distinct advantage that it correlates reliably with equipment performance. While used less extensively than the methods described previously, a number of examples of use have been documented [10–13].

The type of test exchanger preferred by the author [14–18] is one that has multiple easily removable tubes, allowing data to be collected as a function of time. This method is covered by NACE Standard TM 286 [10].

Most water-treating suppliers supply single tube, electrical resistance heated fouling measurement units. These units consist of a heat exchanger tube with an internal electrical resistance heater. The water flow is in the annular space between the tube and an outer tube, which is frequently transparent to allow direct observation. These units are excellent for monitoring fouling. They are amenable to automated data acquisition. Heat transfer coefficients and fouling factors can be easily calculated. The fouling factor, a direct measure of resistance to heat transfer, is the preferred measure.

In addition to the direct thermal measurements, the weight of deposit formed per unit time is sometimes used as a measure of fouling. While this gives a measure of the quantity of fouling material precipitated, it does not tell how that deposit affects heat transfer efficiency.

## INNOVATIVE NEW TECHNIQUES

The techniques described above are well established. They are the primary tools used for most practical day-to-day monitoring. There are a number of newer techniques that show promise of giving better data, usually more quickly and sometimes more easily automated. These are discussed briefly below.

### Miniature Heat Exchanger with Combined Corrosion and Fouling Evaluation

This technique [19], developed by Capsis-March Ltd. for Amoco (now part of BP), is probably the most advanced attempt at an on-line continuous instrumental monitor of both fouling and corrosion of a heat exchanger tube. The test assembly consists of several short lengths of exchanger tube, electrically isolated by non-conductive gasketing. The assembly is carefully assembled to assure that the tube segments are precisely aligned and the gasketing does not introduce additional turbulence. Electrical heating elements are mounted outside each discrete tube section, with temperature sensors mounted to allow calculation of the heat flux and heat transfer coefficients.

Corrosion is monitored continuously by means of Electro Chemical Noise (ECN). Using this technique involves measuring the variance of both potential and current flow between adjacent, electrically isolated tube segments. The degree of variance (noise) provides an indication of corrosion activity on the tube segments. While there remains some debate concerning interpretation of such data, there is substantial evidence that increased noise is a reliable indicator of increased corrosion activity.

This approach shows promise of providing a real-time indication of both corrosion and fouling on a heat exchanger surface. The Winters et al. [19] paper shows instances where ECN changes indications correlated with changes in corrosion and fouling.

### Thin Layer Activation (TLA)

TLA was developed in the United Kingdom [20,21]. The surface of a sample (which can be a coupon or a section or tube or pipe) is irradiated to make it slightly radioactive. Two samples are irradiated. One sample is protected from corrosion; the second is exposed to the corrosive fluid, in this case the water system. The radioactivity of each of two samples is monitored as a function of time. There will be a radioactive decay curve characteristic of the protected sample and a second decay curve for the exposed sample. The difference between the two curves indicates metal loss, which can be converted to corrosion rate. This technique has not been broadly used, but some field use has been reported [21,22]. It shows promise of being an “automated coupon” which provides a continuous record of corrosion. Figure 4 shows a pipe specimen with an activated area, and Fig. 5 shows data generated in an inhibited cooling tower system.

### Synthetic Crevice Devices

Some work [23–25] has been done in which an occluded cell condition is set up, with electrically isolated anode and cathode connected through a zero resistance ammeter. The current flow between the electrodes is proportional to the corrosion occurring on the anode. This technique provides a measure of the rate of corrosion penetration in occluded areas. With this technique, it is possible to allow the corrosion reaction to start (forming oxide deposits) and then determine the ability of different inhibitors to control the corrosion in the presence of the deposits.

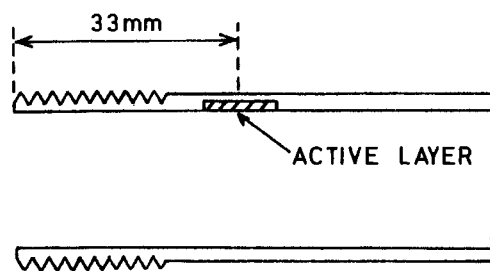


FIG. 4—Diagram of the test pipe section showing the position of the active layer.



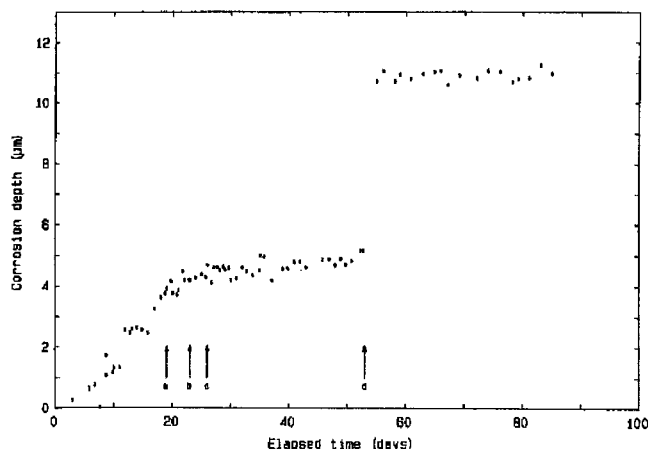


FIG. 5—Plot of metal loss versus exposure time for a carbon steel pipe, as determined by TLA. The depth of corrosion is deduced from the activity loss of the test component. The correct inhibitor conditions were established between points a and c. At d, the component was removed for inspection and cleaned. After replacement, the apparent corrosion rate was very low, indicating the effectiveness of the inhibitor.

### Differential Flow Cell Technique

This recently reported [26] technique is similar to the Synthetic Crevice approach. In this method, two parallel flow channels are operated at different water flow rates. The low flow channel becomes an active anode, which is connected through a zero resistance ammeter to the high flow channel, which acts as a cathode. The current flow then indicates the corrosion rate of the anodic surface. This technique shows promise as a continuous on-line instrumental monitor that will show changes in corrosion rate under deposits.

## DISCUSSION

This presentation has focused on corrosion test methods in open recirculated cooling tower systems. This area is the most challenging, difficult, and important area of corrosion testing in industrial water. For economic and environmental reasons, water and inhibitor lost through blowdown must be minimized. Cooling tower systems are the systems that are most subject to operational upsets and operational variables.

The corrosion testing techniques described can also be used in closed cooling systems, once-through cooling systems, boiler feed water systems, etc.

## REFERENCES

- [1] Whitman, W. G., Russell, R. P., and Altieri, V. J., *Industrial Engineering Chemistry*, Vol. 16, 1924, pp. 665–670.
- [2] Larson, T. E. and Skold, R. V., *Corrosion*, Vol. 14, 1958.

- [3] Anon., Technical Manual for WaterCycle software, Version 1.1, page 1-6, French Creek Software, Inc., Valley Forge, PA.
- [4] Strauss, S. and Puckorius, P., "Cooling-Water Treatment for Control of Scaling, Fouling, Corrosion," Special Report in Power, June 1984.
- [5] Schwerdtfeger, W. J. and McDorman, O. N., *Journal of the Electrochemical Society*, Vol. 99, 1952, p. 407.
- [6] Simmons, E. J., *Corrosion*, Vol. 11, No. 6, 1955, p. 255t.
- [7] Skold, R. V. and Larson, T. E., *Corrosion*, Vol. 13, No. 2, 1957, p. 139t.
- [8] Stern, M. and Geary, A. L., *Journal of the Electrochemical Society*, Vol. 104, No. 1, 1975, p. 56.
- [9] Stern, M., *Corrosion*, Vol. 14, No. 9, 1958, p. 40t.
- [10] Anon., "Standard Heat Exchanger for Cooling Water Tests," *Materials Performance*, August 1965.
- [11] Silva, J. O., "Corrosive Water—A Brazilian Reality," Paper No. TP-87-14 presented at CTI 1987 Annual Meeting, New Orleans, LA, 25–27 February 1987.
- [12] Kanuth, J. G. and Binks, K., "Cooling Water Treatment Transition—Zinc-Chromate to All Organic," Paper No. TP-85-3, CTI 1985 Annual Meeting, New Orleans, LA, 21–25 January 1985.
- [13] Degnan, T. F. and Fynsk, A. W., "Improved Techniques for Cooling Water Corrosion Control," presented at Cooling Water Symposium, 21st NACE Conference, St. Louis, MO, 15–19 March 1965.
- [14] Krisher, A. S., "NACE Standard Heat Exchanger Monitors Cooling Tower Water Corrosion," *Materials Performance*, August 1965.
- [15] Krisher, A. S., "Test Exchangers Permit Better Evaluation of Cooling Water Treatment," *Materials Protection*, April 1963.
- [16] Krisher, A. S., "Evaluation of Nonmetallic Cooling Water Inhibitors," *Materials Performance*, January 1979.
- [17] Krisher, A. S., "Evaluation of Nonmetallic Cooling Water Inhibitors—Phase 2," *Materials Performance*, May 1982.
- [18] Krisher, A. S. and Sanders, B. J., "Evaluation of Nonmetallic Cooling Water Inhibitors—Phase 3," presented at AIChE St. Louis One-day Technical Seminar, Spring 1985.
- [19] Winters, M., Stokes, P., Zuniga, P., and Schlottenhler, D., "Developments in On-Line Corrosion and Fouling Monitoring in Cooling Water Systems," Paper No. 392, Corrosion/93, NACE International.
- [20] Asher, J., Webb, J. W., Wilkins, N. J. W., and Lawrence, P. F., Report published by AERE Harwell AERE-R-10391, December 1981.
- [21] Asher, J., Conlon, T. W., Tofield, B. C., and Wilkins, N. J. M., Report published by AERE Harwell AERE-R-10871, March 1983.
- [22] Marshall, A., Paper No. 248, Corrosion/88, NACE, Houston, TX, 1988.
- [23] Krisher, A. S., Paper No. 153, Corrosion/81, NACE, Houston, TX, 1981.
- [24] Shim, S. and Johnson, D. A., Paper No. 86, Corrosion/91, NACE, Houston, TX, 1991.
- [25] Pathok, B. R., Ch. 20, *Handbook of Corrosion Testing and Evaluation*, W. H. Ailor, Ed., 1971.
- [26] Yang, B., "Real-Time Localized Corrosion Monitoring in Industrial Cooling Water Systems," *Corrosion*, Vol. 56, No. 7, July 2000, pp. 743–756.

# Industrial Chemicals

*Robert B. Puyear<sup>1</sup>*

## DESCRIPTION

THIS SECTION INCLUDES TESTS for determining the materials of construction requirements for equipment used for manufacturing chemicals. This includes both bulk chemicals, which are typically manufactured in dedicated equipment in large quantities, and specialty chemicals, which are most often made in smaller quantities and often in equipment used for more than one process. Tests for both organic and inorganic chemicals are included. Because some tests require the presence of an electrolyte, they are not suitable for many pure organic processes. Equipment intended for use in the pharmaceutical, petrochemical, or high-temperature gas phase or molten salt processes have special requirements that are not included in this section.

## ASPECTS THAT MAKE TESTING FOR INDUSTRIAL CHEMICAL EQUIPMENT UNIQUE

Unlike refineries and many petrochemical plants where each company has similar equipment, many industrial chemical units are one-of-a-kind. This characteristic means there may not be any history of similar equipment to use for making materials selections. Also, it may be only a few years before technology advances make the process obsolete. A third consideration is that the equipment may be called on to make more than one product. Sometimes this multiproduct use is part of the original design and sometimes it is the result of changing conditions or technology, or both. These factors create a tension between selecting materials that will give long, reliable life and materials of lesser reliability, but also of lower cost. There is no correct answer as to what strategy to use. However, whatever strategy is chosen it is always important that the tests conducted provide reliable results so that materials selection choices are made on the basis of accurate and meaningful data.

### Batch and Continuous Processes

Industrial chemical processes include both batch and continuous operations and some can include a combination

of the two. Each operation mode presents its own set of requirements on the tests that are to be used to characterize materials requirements.

In many cases continuous processes are easier to characterize because when the process is operating under control the environment in any part of the process is fairly constant. This permits the development of laboratory tests that can simulate the process conditions with some accuracy. Care must be taken to assure that the effects of process startups, shutdowns, and upsets are considered since the most corrosive conditions may occur during these times.

Process understanding is required to select the proper environments for corrosion tests in a continuous process. In some equipment such as distillation towers there is a continuous change in process conditions through the unit. It is not practical to conduct tests at all of these conditions, yet the raw material or product streams may not represent the most severe conditions. The use of a good process simulation model with good physical property data can go a long way in helping to identify the range of conditions present and therefore help select the best test conditions.

Another characteristic of continuous processes is that each unit supplies the raw materials to the following unit. Thus, if any piece of equipment fails, the entire plant is shut down until it is repaired. This adds a premium to the reliability of continuous process equipment and to our ability to predict the remaining life of equipment components.

In batch processes the equipment sees a continuing change in process conditions throughout the batch cycle. This requires the materials of construction to resist the entire range of environments encountered. On the other hand, it means that there may be a surface condition created in one step of the process that provides protection in a subsequent step where the material would otherwise corrode.

One approach to testing materials for a batch process is to expose samples of the candidate materials of construction in a number of batch cycles in a plant, pilot plant, or research laboratory. However, when this option is not available the problem of creating meaningful test environments is difficult and the results are subject to considerable error. A good understanding of the process chemistry and the behavior of candidate materials in various chemical environments is very helpful in improving the validity of these tests.

<sup>1</sup>Principal, Robert B. Puyear, P.E., 226 River Valley Dr., Chesterfield, MO 63017-2629.

## IMPORTANT VARIABLES

Any variable that can influence a reaction between the material of construction and its environment is important. Some of these variables are:

- temperature,
- pressure,
- pH,
- velocity (fluid motion),
- temperature and heat transfer,
- presence of chlorides and other halides, and
- presence of small quantities of contaminating chemicals.

### Temperature

Plastics, coatings, linings, and the like have rather severe temperature limits and can be used only within these limits. Table 1 lists the maximum operating temperatures for a number of plastics and coatings used by industrial chemical firms. A word of caution is in order about the temperatures listed in this table. These temperatures are for noncorrosive applications. The maximum temperature for a specific application may be much different. For example, the maximum temperature for vinyl ester reinforced thermosetting resin construction for air immersion is 177°C and for steam it is 104°C. For deionized water the maximum recommended temperature is 82°C and for dichloroethane it is only 27°C. To be safe the person selecting a plastic for chemical service must obtain data on the behavior of that material in the specific environment. In addition to chemical degradation, plastics, coatings and linings are subject to permeation of process fluids through these organic materials. Permeation is a temperature-sensitive behavior. A recent Materials Technology Institute Publication [14] provides a comprehensive discussion of this issue. Even with materials of construction that do not have narrow inherent temperature limits such as alloys and ceramics, we are faced with the fact that temperature influences the rate of chemical reactions, and hence the corrosion rate.

Some forms of corrosion such as stress corrosion cracking and pitting are especially sensitive to temperature. This was borne out by the results of a study sponsored by the Materials Technology Institute [15] which showed a strong correlation between temperature and stress corrosion cracking of stainless steels in cooling water with low chloride concentrations (Fig. 1). This work showed that there was no true threshold temperature for the onset of stress corrosion cracking as failures were reported down to cryogenic temperatures in certain circumstances involving concentrated brines, low pH, microbial attack, or sulfur compounds. The data shown are for near neutral waters where there is an apparent threshold of about 60°C.

### Pressure

In most cases pressure does not have a large influence on corrosion behavior. However, it can affect the composition of the corrodent fluid and thereby have an influence. A classic example is the difference in corrosion behavior of carbon steel in water in an open and closed vessel [16–18] (Fig. 2). Dissolved oxygen is a major source of corrosion of steel by

**TABLE 1**—Maximum operating temperature of plastics and coatings.

Materials		Maximum Operating Temperature, Deg C <sup>a</sup>	Ref
<b>Thermoplastics</b>			
Perfluoroalkoxy (PFA)		260	1
Polytetrafluoroethylene (PTFE)		260	1
Fluorinated Ethylene Propylene (FEP)		200	1
Ethylene Tetrafluoroethylene (ETFE)		180	1
Ethylene Chlorotrifluoroethylene (ECTFE)		165	1
Polyvinylidene Fluoride (PVDF)		150	1
Nylon 6/6, heat stabilized		130	2
Polypropylene (PP)		120	3
Polyvinylidene Chloride (PVDC)		120	4
Polyvinyl Fluoride (PVF)		110	1
Polyvinyl Chloride (PVC)		105	5
Polybutylene		100	6
Polyethylene, high density (HDPE)		90	7
<b>Reinforced Thermosetting Resin Construction</b>			
Vinyl Ester		230	8
Polyester		177	9
Epoxy		150	10
<b>Coatings and Linings</b>			
Vinyl Ester		180	11
Epoxy		120	11

Materials	ASTM Desig	Maximum Operating Temperature, Deg C	Ref
<b>Elastomers</b>			
Perfluoroelastomer	FFKM	260	12
Silicone	VMQ	232	13
Fluoroelastomer	FPM	204	13
Ethylene Propylene	EPM, EPDM	204	13
Polyacrylate	ACM, ANM	177	13
Fluorosilicone	FVMQ	177	13
Neoprene	CR	149	13
Epichlorohydrin	CO, ECO	135	13
Nitrile (high temperature type)	NBR	121	13
Chlorosulfonated Polyethylene	CM	121	13
Polysulfide	PTR	107	13
Nitrile (low temperature type)	NBR	107	13
Butyl	BR	107	13

<sup>a</sup>These temperatures are typical of the maximum operating temperature for these materials in noncorrosive environments. The maximum temperature for specific applications depends on the environment and may be very much lower than indicated here. Contact the manufacturer or its agent before selecting these materials for high-temperature or corrosive applications.

water. As the temperature increases, the corrosion rate increases until about 80°C. In this region the water vapor pressure increases rapidly, thereby reducing the oxygen partial pressure. This results in essentially zero oxygen in the open system at the boiling point. However, if the system is closed the oxygen cannot escape and the corrosion rate continues to increase as the temperature rises. This is why it is so important to remove dissolved oxygen from boiler feed water.

### pH

Dillon [19] provides a good discussion of the role pH and total acidity (or alkalinity) have on materials selection

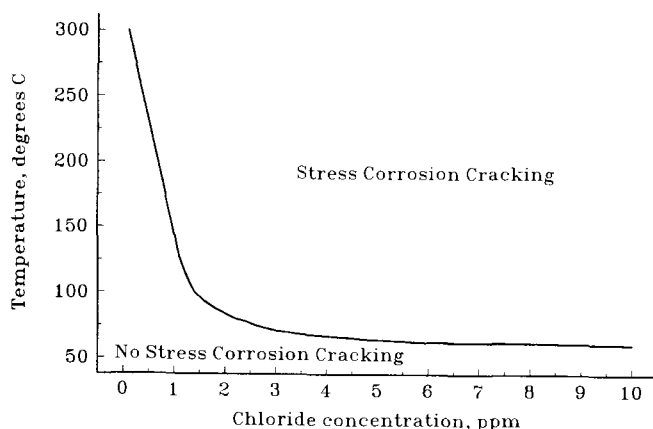


FIG. 1—Chloride stress corrosion cracking of types 304 and 316 stainless steel as a function of chloride concentration and temperature [15].

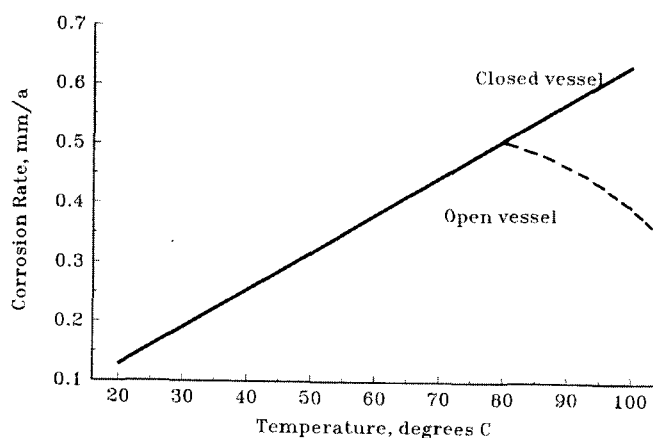


FIG. 2—Retaining dissolved oxygen in a closed vessel boosts corrosion. (Based on curves in Refs 16–18.)

requirements. The following is a synopsis of this discussion. pH is defined as the negative of the base ten logarithms of the hydrogen ion activity. In strong acids and bases it is a valid measure of the total acidity or alkalinity because of the total ionization of the electrolyte. For weaker acids and alkalis, which are less completely ionized, total acidity (or alkalinity) is a better indication of corrosivity than is pH. With these acids (or alkalis) the unionized material serves as a reservoir of potential protons available for potential corrosion. Corrosion data are a more reliable indication than either pH or total acidity (or alkalinity) in complex process mixtures. Nevertheless, pH and total acidity (or alkalinity) are useful indicators of potential corrosion behavior and should be identified whenever possible.

Aluminum is a classic example of a metal where the corrosion resistance has strong pH dependency. Aluminum is a very active metal and its corrosion resistance depends on a barrier oxide film. This film contains two layers, an inner compact amorphous barrier layer and a thicker,

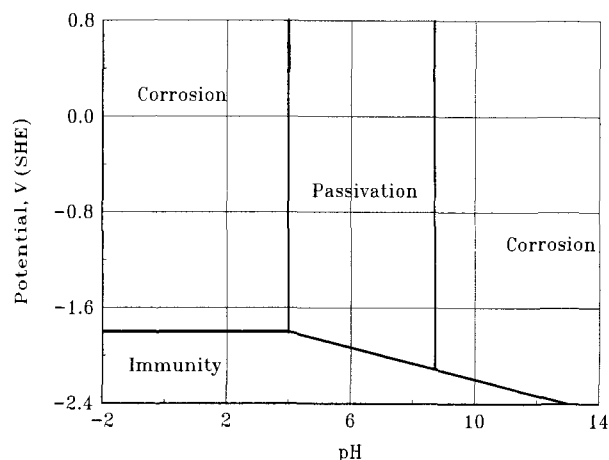


FIG. 3—EMF-pH (Pourbaix) diagram for aluminum in water at 25°C [20].

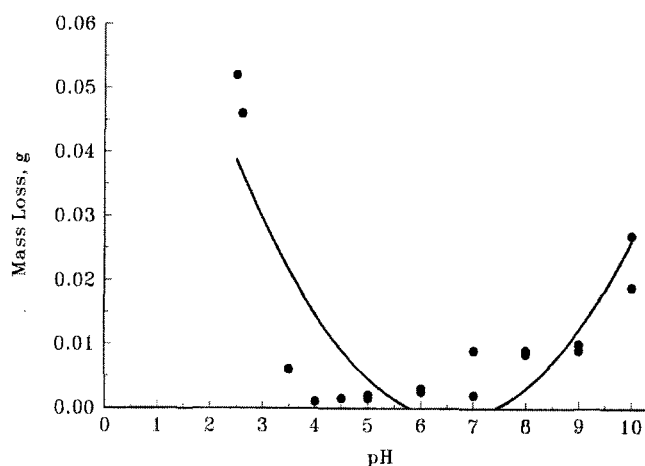


FIG. 4—Weight loss of aluminum alloy 3-H14 exposed one week in solutions of various pH values. pH values were adjusted with HCl and NaOH [20].

more permeable outer layer [20]. Potential-pH (Pourbaix) diagrams are used to map where the barrier layer would be expected to be effective (Fig. 3). These diagrams are based largely on the solubility of the solid species. In Pourbaix's terminology, passivity is achieved when the solubility of the solid species is less than  $10^{-6}$  moles/L. In this case aluminum would be expected to have good corrosion resistance between pH 4 and 8.5, but the corrosion rate might be well above zero. This correlates well with experimental data (Fig. 4).

In a similar manner carbon steel is sensitive to pH. In the pH 4.5–9 range the corrosion rate is governed by dissolved oxygen. (See the following discussion on velocity effects.) Below pH 4.5 the corrosion rate is controlled by hydrogen evolution and above about pH 9, the rate is suppressed by an insoluble film of ferric hydroxide (Fig. 5) [18]. At very high pH levels, especially at elevated temperatures, steel is susceptible to stress corrosion cracking [21].

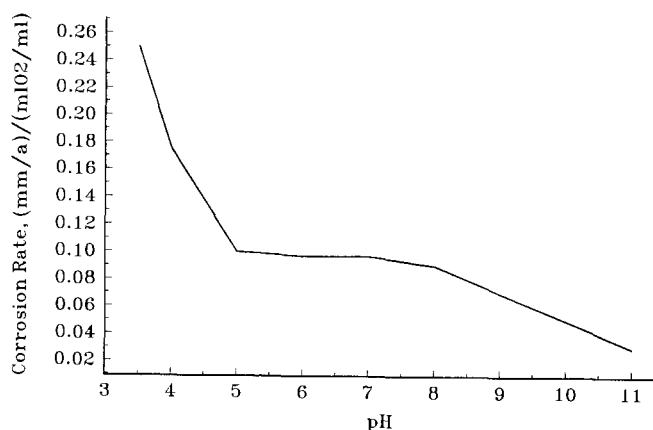


FIG. 5—Corrosion of carbon steel versus pH in water at 25°C [18].

### Velocity (Fluid Motion)

The influence of fluid flow rate on corrosion is dependent on the alloy, fluid constituents, fluid physical properties, geometry, and corrosion mechanism. In some cases the dependence is fairly direct. For example, the corrosion of carbon steel and UNS S44626 (26Cr1Mo) in concentrated  $H_2SO_4$  is governed by the rate of mass transfer of  $FeSO_4$  from a saturated layer on the surface [21–23]. Carbon steel corrosion in water in the near-neutral pH range is governed by the rate of mass transfer of dissolved oxygen from the bulk fluid to the surface [21].

The presence of fluid flow can sometimes be beneficial in preventing or decreasing localized attack such as pitting and crevice corrosion. For example, alloys such as types 304 and 316 stainless steel and nickel chromium alloys will pit in quiescent seawater more readily than in flowing seawater. When the water is quiet, the mass transfer rate of oxygen is insufficient to maintain a completely passive surface and pitting can result [24]. Low flow rates in seawater also contribute to the formation of marine growth such as mollusks and barnacles and sedimentation, both of which create deposits that promote crevice corrosion attack.

Under other circumstances fluid flow can cause erosion of the surface through the mechanical force of the fluid itself. When solids are present in the liquid they can cause wear or solid particle erosion. In either case, the rate of attack can be accelerated by the combined effects of erosion and corrosion. Erosion corrosion results when the passive films that form on alloys are removed and the underlying metal is attacked [25]. The rate can be very rapid.

### Temperature and Heat Transfer

As a general rule corrosion rate increases with temperature. One notable exception is the corrosion of carbon steel by water in an open container (Fig. 2) that was discussed earlier. Temperature also influences the onset of localized corrosion such as pitting and crevice corrosion of passive alloys.

Fluid temperature changes can affect the polarity of galvanic couples. An example is the iron-zinc couple in some domestic waters where the iron may become anodic to the zinc at temperatures over 82°C [26].

The effects of heat transfer on corrosion rates depend on the system. If corrosion is under activation control the presence of heat transfer might not have much effect. On the other hand, if corrosion is controlled by diffusion of a species, such as oxygen, to the surface, then heat transfer may greatly change the corrosion rate. There are three possible causes. First, a temperature difference between the wall and bulk solution may affect the solubility and diffusion coefficient of the diffusing species. Second, boiling at the surface can increase turbulence or increase diffusion. Third, heat transfer in the absence of fluid flow, as in a stagnant tank, can cause natural convection currents that enhance mass transfer [19].

### Presence of Chlorides and Other Halides

Chloride ion accelerates the corrosion of iron in acidic solutions. The role of other halides is less clear and iodides and perhaps bromides may even serve as corrosion inhibitors. At near neutral pH values chloride has less effect than dissolved oxygen [21].

The most notable effects of the chloride ion are pitting and crevice corrosion of passive alloys and stress corrosion cracking of stainless steels and related alloys. Most pitting and crevice corrosion is associated with chlorides, bromides, and hypochlorites. Fluorides and iodides have comparatively little pitting tendencies [27].

Crevice corrosion may occur under deposits, under gaskets, or any other place where the opening is wide enough to permit liquid entry but narrow enough to create a stagnant zone. While halides are not necessary for crevice corrosion to occur, their presence promotes the formation of more acidic conditions in the crevice and much more rapid corrosion [28].

Oxidizing metal ions with chlorides are aggressive pitting agents. Even the most corrosion resistant alloys can be pitted by cupric chloride and ferric chloride. By comparison, chlorides of non-oxidizing metal ions such as sodium chloride and calcium chloride cause pitting to a much lesser degree.

Chloride stress corrosion cracking is a constant concern when stainless steels are used at elevated temperatures. There is no true threshold of chloride concentration or temperature below which stress corrosion will not occur, but experience has provided some guidelines where stainless steel can be used with confidence. An example of chlorides in cooling water was discussed earlier (Fig. 1). Equipment designed to reduce opportunities for chlorides to concentrate is helpful. The presence of deposits also provides an opportunity for chloride concentration.

### Presence of Small Quantities of Contaminating Chemicals

One variable frequently overlooked in designing tests for selecting materials for industrial chemical applications is the presence of small quantities of chemicals present as contaminants; that is, chemicals that are there unintentionally. Often these chemicals have no effect on corrosion behavior and can be safely ignored. However, all too often this is not the case. Consider, for example, the effect of a few

drops of water in an otherwise all-organic environment [29]. This water may have no effect on the process, but it completely changes the corrosion picture. Whereas carbon steel might have been satisfactory without the water, stainless steel may be required to avoid contaminating the process with iron corrosion products. If the organic chemicals include a halogenated compound, higher alloys or glass lining may be required to avoid pitting or stress corrosion cracking, or both.

A small quantity of a contaminating compound resulted in equipment failure at a gulf coast chemical plant that had a fiber reinforced plastic (FRP) tank for a process stream that was essentially dilute hydrochloric acid (HCl), a service where the FRP tank would be completely satisfactory. However, this stream contained a small quantity of benzene. Over time the benzene dissolved in the plastic resin, softening it to the point that the tank suddenly failed, sending a wave of HCl into a nearby control room. Fortunately no one was hurt, but the process was down until the tank was replaced.

In another case leaks developed in type 316 stainless steel (UNS S31600) piping in a new chemical plant during startup. None of the chemicals in the process were known cracking agents. Investigation determined that a chlorinated hydrocarbon had been used for "water batching" since ambient temperature was below freezing. This compound was not completely removed and it reacted with the process chemicals to form a very aggressive cracking environment [30].

## CORROSION TESTING

Refer to Sections II and III for information on designing tests and for detailed descriptions of common laboratory tests. Considerable skill is required to develop a corrosion test program that adequately defines materials requirements. First, we must identify those conditions that will limit the materials selections. This includes the conditions that will be encountered under nonstandard conditions such as startup, shutdown, and process upsets. In many cases we also need to consider the conditions encountered when the unit is in standby status; that is, when the unit is not operating but is being maintained so that it can be put back into operation when it is needed. The best materials selections are made when the full range of these conditions is identified and considered before the test program is started.

### Testing Methods

Corrosion test methods can be divided into electrochemical and non-electrochemical methods. Among the electrochemical techniques that have been used successfully for corrosion prediction are potentiodynamic polarization scans, electrochemical impedance, corrosion current monitoring, controlled potential tests for cathodic and anodic protection, and the rotating cylinder electrode for studies of velocity effects [31,32]. Though not literally a test, potential-pH (Pourbaix) diagrams have been used as road maps to help understand the results of other tests.

The non-electrochemical techniques include direct immersion of materials samples in the test fluid in either the laboratory or plant. These samples sometimes have an artificial crevice generated with a serrated washer. They may be welded to determine the effects of welds and weld heat affected zones. Real-time information can be obtained using electrical resistance probes. Heat transfer effects can be evaluated by having a test sample that is exposed to the corrodent on one side and the other side heated or cooled. Stressed samples are used to evaluate stress corrosion cracking tendencies [33].

The need for more rapid evaluation of plastics and elastomers prompted the development of a sequential absorption test to provide useful information on the durability of these materials in a few weeks [34]. A refinement to this test was developed more recently [35,36].

### Test Design

The selected test program must adequately simulate the limiting conditions. However, not all tests must be under process conditions. One strategy is to start the test program by sorting the promising and less promising materials with simple tests such as immersion corrosion tests in environments that crudely simulate the process conditions. There is a danger that this approach will exclude a material that would in fact be satisfactory in the process because the test environment did not properly simulate the process conditions. However, unless you already have a pretty good idea of the type of materials that are candidates, some sort of sorting process is necessary before detailed testing is conducted. Otherwise, the test program will be too cumbersome to manage.

Once the list of candidate materials has been reduced to a manageable number we can begin a program to understand how each behaves under the range of process conditions. Details of the test methods used for laboratory corrosion testing are included in Section III and special tests for corrosion types are included in Section IV. The specific program for a process must be based on the requirements of that process and each will be different. A typical program might include immersion and electrochemical tests in process fluids (simulated or from operating units). It might also include tests for velocity sensitivity, crevice corrosion, pitting, and stress corrosion cracking. If plastics or coatings are being considered it will be necessary to conduct the tests long enough for degradation to be measured. We would like to have six months or longer for these tests but often must settle for six weeks or less.

### For Existing Processes

There is a place for both plant and laboratory tests for exploring materials for a new unit of an existing process. Plant tests can be used to explore the behavior of new materials under current operating conditions far better than can laboratory tests. These tests do not require the simulation of plant conditions, which is always imperfect. Also, in most situations these tests can be conducted with more materials at a far lower cost than is possible with laboratory tests. One drawback to in plant testing is that it may be

necessary to time the start and end of the test with scheduled equipment outages, which may postpone the data collection. An advantage of laboratory tests is that they permit exploring the effects of process changes on corrosion behavior without putting plant equipment at risk.

Some of the more sophisticated corrosion tests are suitable for use in a laboratory setting only. These tests can give more information about a material's tendencies toward localized corrosion, velocity-influenced corrosion, and the like than can the conventional plant tests. Where these are of concern, a combination of plant and laboratory tests is probably the best choice. The following is an example of how complementary use of laboratory and plant tests was used to solve a complex chemical plant corrosion problem [36]. The problem was to determine how to treat a waste stream from an entire chemical plant so it could be handled in carbon steel equipment. One characteristic of waste streams is that their compositions vary widely over time. Therefore, a grab sample from the stream might not be representative of the most corrosive conditions to be experienced. The fluid for laboratory testing was prepared from "typical" compositions of the various plant streams that are combined to create the waste product. This fluid was used in the laboratory to evaluate the effects of a proprietary sulfite-containing inhibitor, pH, and fluid velocity using a combination of electrochemical impedance and rotating cylinder electrode techniques. Plant tests included corrosion coupons and electrical resistance probes. The laboratory tests indicated that the combination of inhibitor and pH control at pH 9 provided adequate protection to carbon steel. It also suggested that pH control was critical with the corrosion rate increasing by an order of magnitude at pH 7. The plant test results supported the laboratory data but showed that extended exposure to pH 9 fluid resulted in a steel surface that withstood short excursions to pH 7 without rapid corrosion.

### For New Processes

With a new process there is no history of materials performance and no existing operating unit available for plant testing. Therefore, laboratory testing is required to determine the relative performance of materials under the expected operating conditions. The exact conditions each unit will be exposed to may not be known. However, with modern process simulation models we can have a pretty good idea of what the operating conditions will be. Simulating these conditions in the laboratory may be quite another thing. From a practical standpoint we are usually restricted to testing in raw materials, reaction products and various cuts from distillation processes. In some cases we can test in intermediate reaction products, but often these compounds are not stable. For more information on designing a test program for a new chemical process see Ref 37. This reference includes a list of corrosion testing standards by ASTM and other organizations.

### REFERENCES

- [1] Fifoot, R. E., "Fluoroplastics," *Modern Plastics Encyclopedia*, R. Juran, Ed., McGraw-Hill, NY, 1988, pp. 24–26.

- [2] Kohan, M. I. and Ward, R. L., "Nylon," *Modern Plastics Encyclopedia*, R. Juran, Ed., McGraw-Hill, NY, 1988, pp. 30–31.
- [3] Amoco Chemicals Co., "Introduction to Polypropylene," *Modern Plastics Encyclopedia*, R. Juran, Ed., McGraw-Hill, NY, 1988, p. 86.
- [4] Clark, D. L., "Vinylidene Chloride," *Modern Plastics Encyclopedia*, R. Juran, Ed., McGraw-Hill, NY, 1988, p. 127.
- [5] Martello, G. A., "Chlorinated PVC," *Modern Plastics Encyclopedia*, R. Juran, Ed., McGraw-Hill, NY, 1988, pp. 118–125.
- [6] Schard, M. P., "Polybutylene," *Modern Plastics Encyclopedia*, R. Juran, Ed., McGraw-Hill, NY, 1988, pp. 36–38.
- [7] Bussone, D. D., "High Density Polyethylene," *Modern Plastics Encyclopedia*, R. Juran, Ed., McGraw-Hill, NY, 1988, pp. 66–67.
- [8] Derakane Vinyl Esters from Dow, *Chemical Resistance Guide*, Dow Chemical, Midland, MI, July 1985.
- [9] *A Guide to Corrosion Control with ATLAC Polyester Resin*, ICI Americas, Inc., Wilmington, DE, September 1982.
- [10] *Chemical Resistance of Fibercast Piping Systems*, Fibercast Company, Sand Springs, OK.
- [11] Plasite Technical Bulletins for Vinyl Ester and Epoxy Coatings, Wisconsin Protective Coatings Corp., Green Bay, WI, 1985.
- [12] Chemical and Fluid Resistance of DuPont Kalrez Perfluoroelastomer Parts, E. I. DuPont de Nemours and Company, Inc., Wilmington, DE, March 1984.
- [13] *Parker Seals O-Ring Handbook*, Parker Hannifin Corporation, Lexington, KY, 1977.
- [14] Campion, R. P., *Permeation Through Polymers for Process Industry Applications*, MTI Publication No. 53, St. Louis, MO, 2000.
- [15] McIntyre, D. R., "Experience Survey Stress Corrosion Cracking of Austenitic Stainless Steels in Water," MTI Publication 27, Materials Technology Institute of the Chemical Process Institute, Inc., St. Louis, MO, February 1977.
- [16] Kemmer, F. N., *The NALCO Water Handbook*, 2nd ed., McGraw-Hill, NY, 1988, p. 20.8.
- [17] Ashbaugh, W. G., "Corrosion of Steel and Stainless Steel under Thermal Insulation," *Process Industries Corrosion—The Theory and Practice*, B. J. Moniz and W. I. Pollock, Eds., National Association of Corrosion Engineers, 1986, pp. 759–768.
- [18] Dillon, C. P., *Corrosion Control in the Chemical Process Industries*, McGraw-Hill, NY, 1986, p. 145.
- [19] Dillon, C. P., *Materials Selection for the Chemical Process Industries*, McGraw-Hill, NY, 1992, pp. 315–317.
- [20] Hollingsworth, E. H. and Hunsicker, H. Y., "Corrosion of Aluminum and Aluminum Alloys," *Metals Handbook, Ninth Edition*, Vol. 13, Corrosion, J. R. Davis, Sr., Ed., ASM International, Materials Park, OH, 1987, pp. 583–609.
- [21] Silverman, D. C. and Puyear, R. B., "Effect of Environmental Variables on Aqueous Corrosion," *Metals Handbook, Ninth Edition*, Vol. 13, Corrosion, J. R. Davis, Sr., Ed., ASM International, Metals Park, OH, 1987, pp. 37–44.
- [22] Ellison, B. T. and Schmeal, W. R., "Corrosion of Steel in Concentrated Sulfuric Acid," *Journal of the Electrochemical Society*, Vol. 125, No. 4, 1978, p. 524.
- [23] Silverman, D. C. and Zerr, M. E., "Application of Rotating Cylinder Electrode-E-Brite 26-1/Concentrated Sulfuric Acid," *Corrosion*, Vol. 42, No. 11, 1986, p. 633.
- [24] Fontana, M. G., *Corrosion Engineering*, 3rd ed., McGraw-Hill, NY, 1986, p. 376.
- [25] Fontana, M. G., *Corrosion Engineering*, 3rd ed., McGraw-Hill, NY, 1986, p. 91.
- [26] Fontana, M. G., *Corrosion Engineering*, 3rd ed., McGraw-Hill, NY, 1986, p. 45.
- [27] Fontana, M. G., *Corrosion Engineering*, 3rd ed., McGraw-Hill, NY, 1986, p. 69.
- [28] Fontana, M. G., *Corrosion Engineering*, 3rd ed., McGraw-Hill, NY, 1986, pp. 51–59.

- [29] Turner, M. E. D., "Corrosion Tests for Materials Selection: Standard or Plant Simulation?" *Materials Performance*, Vol. 28, No. 3, March 1989, pp. 77–80.
- [30] Puyear, R. B., "A Little of This and That Can Cause Big SCC Problems," *Materials Performance*, Vol. 31, No. 4, April 1992, p. 74.
- [31] Silverman, D. C., "Electrochemical Techniques—Simple Tests for Complex Predictions in the Chemical Process Industries," *Corrosion Reviews*, Vol. 10, Nos. 1 and 2, 1992, pp. 31–77.
- [32] Liening, E. L., *Electrochemical Corrosion Testing Techniques, Process Industries Corrosion—The Theory and Practice*, B. J. Moniz and W. I. Pollock, Eds., National Association of Corrosion Engineers, 1986, pp. 85–122.
- [33] Moniz, B. J., "Field Coupon Corrosion Testing," *Process Industries Corrosion—The Theory and Practice*, B. J. Moniz and W. I. Pollock, Eds., National Association of Corrosion Engineers, 1986, pp. 67–83.
- [34] Carpenter, C. N. and Fisher, A. O., "Sequential Absorption Techniques for Evaluating Elastomers," *Materials Performance*, Vol. 20, No. 1, 1981, pp. 40–45.
- [35] Rosen, E. M. and Silverman, D. C., "Sorption/Diffusion Prediction in Nonmetallics Using Fick's Law," *Corrosion*, Vol. 46, No. 11, 1990, p. 945.
- [36] NACE Standard tm0169-96, Standard Test Method, Chemical Resistance of Polymeric Materials by Periodic Evaluation, NACE International, Houston, TX, 1996.
- [37] McGuire, R. E. and Silverman, D. C., "Complementary Use of Laboratory and Plant Tests to Solve Complex Chemical Plant Corrosion Problems," *Corrosion*, Vol. 47, No. 11, November 1991, pp. 894–902.
- [38] Puyear, R. B., "Pick the Right Material for Process Hardware," *Chemical Engineering*, Vol. 99, No. 10, October 1992, pp. 90–94.



# Petroleum

*K. Daniel Efird<sup>1</sup>*

THE PETROLEUM PRODUCTION environment provides a unique challenge for corrosion testing in that it is not a controlled chemistry, as a chemical process environment, but is an environment provided by nature, with all the potential variability in phase distribution and chemical composition this implies. Petroleum environments are always complex, and often change during production from a formation, or may change due to production from formations that were not included or anticipated in the original planning for field exploitation. The corrosion test program for petroleum environments must, therefore, account for the environment nature has created with very little ability to alter or control it. In a very real sense the petroleum chemistry environment is a case of "what you see is what you get." The primary concern with corrosion testing in petroleum environments is to ensure that what you "see" is, in fact, what is really in the actual production environment.

The effect of petroleum chemistry on corrosion lies primarily in its influence on the formation, chemical composition, and characteristics of a liquid water phase, since liquid water in contact with the containing material is a necessary condition for corrosion to occur for the operating temperatures and pressures encountered in petroleum production. This fact dictates the direction of the discussion on the influence of petroleum chemistry in corrosion testing. This chapter deals solely with the effects of naturally occurring petroleum chemistry on corrosion testing and methods to deal with the effects of petroleum chemistry in corrosion testing. There is no elaboration on the actual test techniques except as they are affected by the petroleum chemistry considerations, and there is no consideration of refinery operations or alterations to the petroleum chemistry used to control corrosion.

## CHEMICAL AND PHYSICAL CHARACTERIZATION OF PETROLEUM ENVIRONMENTS

Petroleum production is generally classified on the basis of existing phases in the production stream, the relative proportions of these phases, and the presence or absence of hydrogen sulfide. Carbon dioxide, hydrogen sulfide, hydrocarbons, and organic compounds (gas and liquid), water,

and dissolved salts are the primary constituents of the petroleum environment, and provide the basis for additional characterization. The acid gases, CO<sub>2</sub> and H<sub>2</sub>S, have the primary effect on corrosion, and hence provide a primary basis of classification.

The term "sweet" is commonly applied to petroleum production environments containing carbon dioxide (CO<sub>2</sub>) and no hydrogen sulfide. These environments are generally defined for corrosion purposes on the basis of the partial pressure of carbon dioxide in the gas phase. This grossly defines the level of dissolved CO<sub>2</sub> in the water phase and, according to many sources, roughly defines the relative aggressiveness of the water phase.

The term "sour" is applied to petroleum production environments containing hydrogen sulfide. Sour environments generally contain carbon dioxide as well as hydrogen sulfide. The concentration of H<sub>2</sub>S required to consider an environment "sour" is not well defined. The most widely used definition is found in NACE Specification MR0175 [1], which defines sour as greater than 0.003 bar (0.05 psia) partial pressure H<sub>2</sub>S in the gas phase. This definition is based on safety considerations and the susceptibility of materials to sulfide stress corrosion cracking and is not related to general or localized corrosion. The term sour could be more broadly defined as an environment containing sufficient H<sub>2</sub>S to produce primarily iron sulfides as a corrosion product on steel. The H<sub>2</sub>S concentration in the water phase required for this to occur is not well defined; however, a concentration of >50 ppm H<sub>2</sub>S in the water phase is sometimes used as a criterion for a sour environment.

The physical phases in a petroleum environment [gas, liquid hydrocarbon (gas condensate and/or crude oil), and liquid water phases] may occur singly or in combination in a wide range of phase ratios, and these phase ratios and compositions may change during production. Producing fields and individual wells are broadly classified as gas or oil fields and/or wells depending on the primary phase produced. Other types of wells or systems for which corrosion testing may be considered are used for subsurface injection, e.g., CO<sub>2</sub>, water or gas injection wells, and produced water disposal wells. A "gas" well is defined as one whose production consists primarily of a gas phase with possibly some gas condensate, condensed water and/or produced water, but no crude oil. An "oil" well is defined as one whose production consists of crude oil with varying amounts of gas, and produced water. The relative proportion of gas and crude oil in the well production is expressed as the gas to oil

<sup>1</sup>Efird Corrosion International, Inc., The Woodlands, TX.

ratio (GOR) in units of volume of gas at standard conditions per volume of crude oil at 20°C (68°F).

### Temperatures and Pressures Encountered

The temperatures and pressures encountered in oil and gas production can vary widely. In general, high pressures and high temperatures go together for gas wells, but this is not necessarily the case for crude oil wells. The total bottom hole pressure in gas wells can range from a low of 40–60 bar to a high of over 1500 bar. Bottom hole temperatures can range from 50°C to well over 150°C. The temperatures and pressures normally encountered in surface production facilities are generally significantly lower.

Changes in temperature and pressure occur along the length of a tubing string during well production. The temperature and pressure variations for a typical well are shown in Fig. 1 [2]. The significance of the change in temperature and pressure is that the phase behavior of the fluids present in the formation can change in the tubing string during production and in surface facilities. This can result in the formation of liquid water and gas condensate that were not present in the original produced fluid, which can dramatically affect corrosion. A valid corrosion test procedure must account for this effect.

### Gas Phase and Gas Condensate Phase

The gas phase is composed of various combinations and ratios of methane, heavier hydrocarbons (ethane, propane, etc.), acid gases ( $\text{CO}_2$  and  $\text{H}_2\text{S}$ ),  $\text{H}_2\text{O}$ ,  $\text{N}_2$ , and helium. The primary gas is usually methane. A typical gas analysis for a producing well is given in Table 1. The gases of greatest importance to corrosion are the acid gases  $\text{CO}_2$  and  $\text{H}_2\text{S}$ . The other gases in the well stream are important to corrosion primarily because of their influence on the concentration of the acid gases dissolved in a liquid water phase.

The gas condensate phase is composed of C3 and heavier alkanes and alkenes, present in the gas phase at reservoir conditions, that condense due to the temperature and pressure drop in the well string during production or in flowlines and production facilities. The gas condensate phase can occur in gas wells, flowlines, and in crude oil well gas processing facilities after separation of gas from the crude

TABLE 1—Typical gas analysis for a producing well.

Compound	Mole %
Methane ( $\text{CH}_4$ )	81.5
Ethane ( $\text{C}_2\text{H}_6$ )	3.6
Propane ( $\text{C}_3\text{H}_8$ )	2.0
Butane ( $\text{C}_4\text{H}_{10}$ )	0.4
Pentane ( $\text{C}_5\text{H}_{12}$ )	0.2
> $\text{C}_5$	1.0
$\text{CO}_2$	4.6
$\text{H}_2\text{S}$	1.4
$\text{N}_2$	5.2
He	0.04

oil. The primary effect of gas condensate on corrosion is the displacement of liquid water from the metal surface by the gas condensate, which prevents corrosion of the metal by the water phase. This relative condensation of liquid hydrocarbon and liquid water is very difficult to simulate in laboratory tests, but the effect on corrosion must be accounted for in assessing the corrosivity of production from a well. At this time there is no simple answer to the problem. Calculations of relative condensation from well data are about the only recourse.

### Liquid Water Phase

The liquid water phase in petroleum production can consist of produced water, injected water, and/or condensed water, and combinations of these in varying proportions. Produced water is present in the reservoir as a liquid water phase, and is produced along with the gas, gas condensate, and/or crude oil. Condensed water is liquid water condensed directly from gaseous  $\text{H}_2\text{O}$  in the gas phase as a result of changes in temperature and pressure along the length of a tubing string during production and in flowlines and surface facilities. The condensed water contains dissolved acid gases ( $\text{CO}_2$  and  $\text{H}_2\text{S}$ ) and low levels of dissolved corrosion product from the well tubing. Condensed water is the fluid studied by de Waard and Milliams in their landmark work on the effects of  $\text{CO}_2$  on steel corrosion in gas transmission lines, and the equations developed apply to condensed water [3]. The equation has since been modified to account for additional variables [4].

A special case of corrosion by condensed water occurs in the vapor phase of pipelines and vessels. This condensed water can be very corrosive, and must be accounted for in designing a corrosion test program, if the phenomenon is anticipated in the specific production system being studied. Extensive discussion of vapor phase corrosion by water condensation and possible remedies are given by Dugstad, Lunde, and Olsen [5], Olsen and Dugstad [6], and Nyborg, Dugstad, and Lunde [7].

Produced water is an extremely complex chemical solution, comprised of liquid water, minerals dissolved from formation rocks, and water soluble organics from the hydrocarbon phase. The most important inorganic compounds with corrosion implications are chlorides and buffering compounds (bicarbonate, borate, silicate, etc.). The presence of buffering compounds reduces corrosion by raising the solution pH, compensating for the effect of dissolved acid gases. An accurate, detailed analysis of the

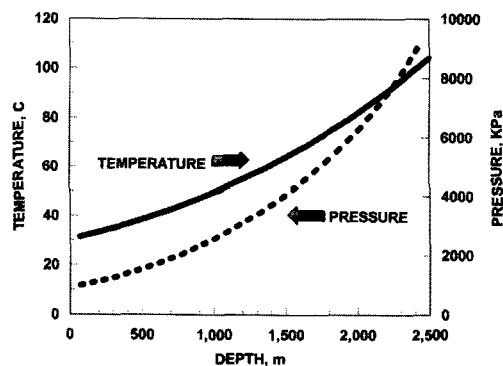


FIG. 1—Subsurface variation in temperature and pressure in a well as a function of depth from downhole surveys [2].

**TABLE 2**—Recommended analysis for produced waters.

Anions	Cations	Additional
Na	Cl	pH <sup>a</sup>
K	SO <sub>4</sub>	TDS
Ca	HCO <sub>3</sub>	CO <sub>2</sub> <sup>a</sup>
Mg	CO <sub>3</sub>	H <sub>2</sub> S <sup>a,b</sup>
Ba	F	O <sub>2</sub> <sup>a,b</sup>
Sr	NO <sub>3</sub>	
Fe	CH <sub>3</sub> COO	

<sup>a</sup> Analysis at the time of taking the sample is preferred.<sup>b</sup> Sampling technique must prevent iron contamination.

produced water is essential so it can be accurately reproduced for corrosion testing, and accurate simulation of the produced water is essential for realistic laboratory corrosion test results. The basic analytical detail needed for produced water is given in Table 2. This degree of detail is necessary to allow the required simulation of the produced water for the laboratory corrosion experiments. Research into the effects of produced water chemistry have been reported by Crolet and Bonis [8,9], Schmidt [10], Murata [11], and Videm [12].

The original produced water chemistry can be altered during production by dilution with condensed water in the tubing string and in production facilities. The effect of this dilution is to reduce the concentration of buffering compounds in the produced water, resulting in potentially lower pH and increased corrosion.

### Crude Oil Phase

The crude oil phase is the most chemically complex phase in the petroleum environment. Crude oil contains aliphatic and aromatic hydrocarbons, heterocyclic and metal organic compounds, high molecular weight organic compounds, and a broad assortment of nitrogen, sulfur, and oxygen containing organic compounds.

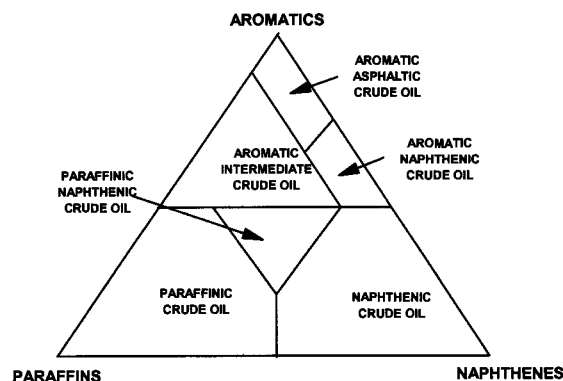
## CHEMICAL AND PHYSICAL CHARACTERIZATION OF CRUDE OIL

Crude oils are generally classified according to API gravity (inversely proportional to the crude oil density), sweet or sour, and asphaltenic or paraffinic (hydrocarbon characteristics). A so-called "heavy" crude oil has a low API gravity (<20), a "medium" crude oil has an intermediate density (20 to 34), while a "light" crude oil has a high API gravity (>34). These ranges are not absolutely defined, but serve as a general reference. All crude oils are composed of some or all of eight basic classes of organic compounds, as given in Table 3. Another way of classifying crude oils is based on the nature of the organic compounds that make up the crude oil, specifically the proportions of paraffins, aromatic compounds, and naphthenic compounds, as shown in Fig. 2 [13].

The recommended physical and chemical analyses for determination of the general characteristics of a crude oil are given in Tables 4 and 5. Results of these analyses provide a solid basis for comparison of crude oils from different formations and fields. The crude oil components that have the greatest potential effect on corrosion are the polar organic

**TABLE 3**—Basic organic compound groups for crude oils.

1. n-alkanes
2. iso-alkanes
3. mono- and poly-nuclear naphthenes
4. mono- and poly-nuclear aromatics
5. mono- and poly-nuclear naphthenoaromatics
6. hetero-compounds
7. asphaltenes
8. carbenes

**FIG. 2**—Classification of crude oils based on petroleum fractions [8].**TABLE 4**—Recommended analysis for crude oils.

1. Gravity, API @ 15°C	
2. Pour Point, °C (°F)	
3. Flash Point, Pensky-Martens	
4. Base Sediment & Water, Vol%	
5. Carbon Residue, Conradson	
6. Salt Content, ptb	
7. Ash Content, wt%	
8. Wax Content, wt%	
9. Neutralization Number, mg/g	
10. N-heptane Insoluble, wt%	
11. Toluene Insoluble, wt%	
12. Colloid Content (ethyl acetate pptn), wt%	
13. Bubble Point Pressure	
14. Element Analysis: Sulfur, wt%	Nitrogen (total), wt%
Copper, ppm	Iron, ppm
Nickel, ppm	Vanadium, ppm
Calcium, ppm	Magnesium, ppm
Sodium, ppm	

**TABLE 5**—TBP crude oil distillation.

1. Light Ends [to 32°C (90°F)], vol%
2. Light Naphtha [32 to 171°C (90 to 340°F)], vol%
3. Kerosene [171 to 260°C (340 to 500°F)], vol%
4. Diesel [260 to 353°C (500 to 700°F)], vol%
5. Light Distillate [353 to 409°C (700 to 800°F)], vol%
6. Medium Distillate [409 to 464°C (800 to 900°F)], vol%
7. Heavy Distillate [464 to 520°C (900 to 1000°F)], vol%
8. Residue [520°C + (1000°F +)], vol%

compounds, since the polar organic compounds are the most water-soluble components in the crude oil and are surface active. A flow chart diagram for the extraction of the polar components of a crude oil published by Donaldson is shown in Fig. 3 [14].

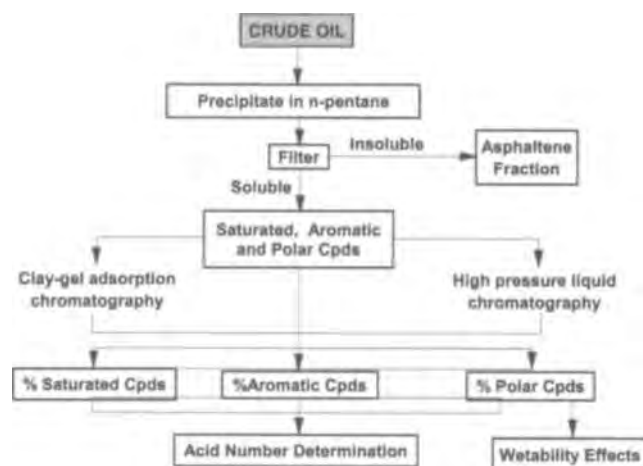


FIG. 3—Schematic diagram of chromatographic separation procedures for extraction of polar compounds from crude oil [9].

### Chemical Constituents of Crude Oil that Affect Corrosion

As stated earlier, the effect of petroleum chemistry on corrosion lies primarily in its influence on the formation, composition, and characteristics of a liquid water phase. This discussion deals with the chemical constituents in crude oil that affect the chemical composition of the liquid water phase. The water-soluble constituents in crude oil are primarily the heterocyclic and metal organic compounds, and the nitrogen, sulfur, and oxygen containing organic compounds. These include pyridines, indoles, benzofurans, phenols, amines, organic acids, thiols, ketones, and aldehydes. All are organic compounds, which are water-soluble and surface active to varying degrees [14–16].

The effect of these organic compounds on the corrosivity of the water phase is not well understood, but probably results from either direct chemical interaction with the metal surface in the manner of a chemical corrosion inhibitor, and/or their effect on wettability. An example of the effect of the crude oil acid number on crude oil wettability is given in Fig. 4 [14]. The relative wettability of the crude oil and water phases determines whether the metal surface will be oil wet or water wet, with significant effects on corrosion [17]. There is a great deal of scatter in these data, allowing determination of only a general trend.

There are also data correlating the corrosion rate of steel in crude oil/brine mixtures with the total nitrogen and sulfur content of the crude oil as shown in Fig. 5 [18]. For this set of crude oils, there is a definite decrease in the carbon steel corrosion rate with increased nitrogen and sulfur. This result is not surprising, since organic nitrogen and organic sulfur compounds are common active ingredients in formulated corrosion inhibitor packages.

### Variability of Crude Oil

The problem with corrosion testing for crude oil environments is the wide variability in the composition of the crude oils and the resulting variability in their effect on

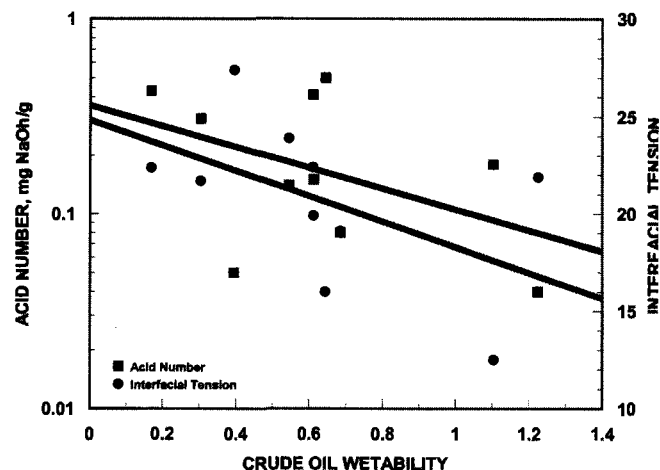


FIG. 4—Effect of acid number and interfacial tension of the crude oil water interface on crude oil wettability [9].

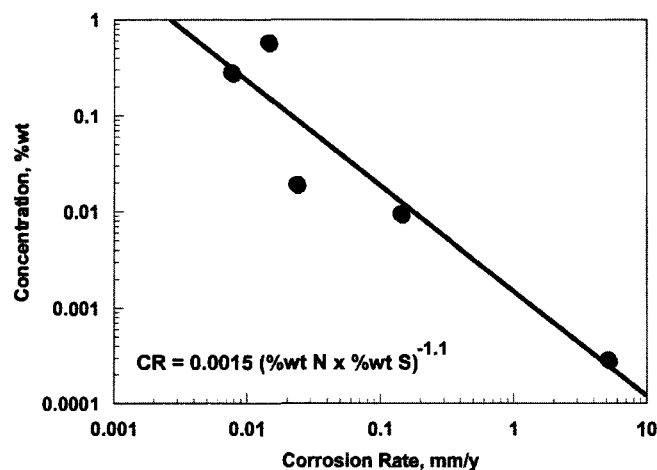


FIG. 5—The relationship of the organic nitrogen and organic sulfur content of crude oil on carbon steel corrosion rate in crude oil/brine mixtures [13]. (4% NaCl brine at 5.2 mPa CO<sub>2</sub> pressure and 85°C.)

FIG. 6—Chromatographic analysis of ten crude oils for aromatic and polar organic compounds, with the balance saturated organic compounds [9].

FIG. 7—Acid number for the ten crude oils in Fig. 6. The acid number is defined as mg NaOH/g of sample.

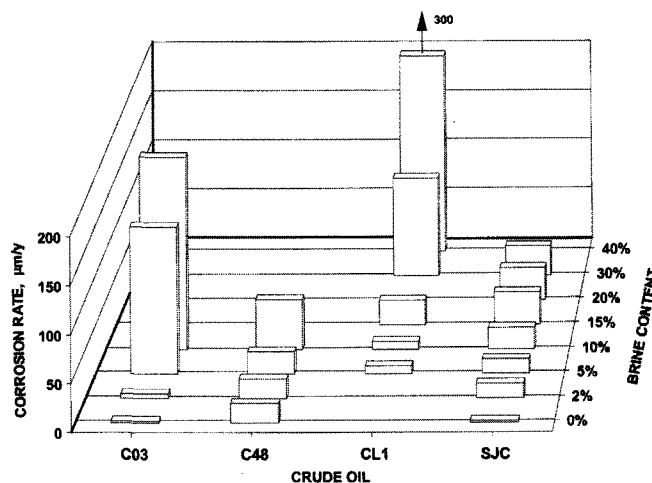


FIG. 8—Carbon steel corrosion rate on a logarithmic scale for crude oil/brine mixtures using different crude oils with the same brine composition (4 % NaCl solution) [13].

corrosion. An example of the variability in composition is shown for ten crude oils in Figs. 6 and 7 [14]. Differences in aromatic and polar organic content for the ten crude oils is given in Fig. 6, while differences in the acid numbers for these same crude oils are given in Fig. 7. The crude oil components shown in these figures are some of the components that can affect carbon steel corrosion.

These differences in composition result in wide variability in the influence of the various crude oils on corrosion of carbon and alloy steels. The effect of specific crude oils on the corrosion rate of carbon steel as a function of the produced water content with a constant produced water composition is shown in Figs. 8 and 9 [18].

This compositional variation also results in differences in the way the amount of brine in a crude oil stream affects carbon steel corrosion, as shown in Fig. 10 [19]. The three curves in Fig. 10 demonstrate the three main characteristics observed for a number of crude oils. Crude oil A demonstrates a crude

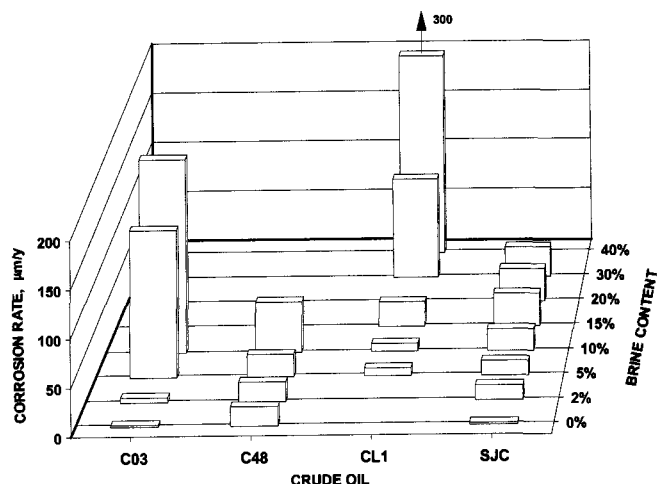


FIG. 9—Carbon steel corrosion rate on a linear scale for crude oil/brine mixtures using different crude oils with the same brine composition (4 % NaCl solution), showing different effects of increasing brine content [13].

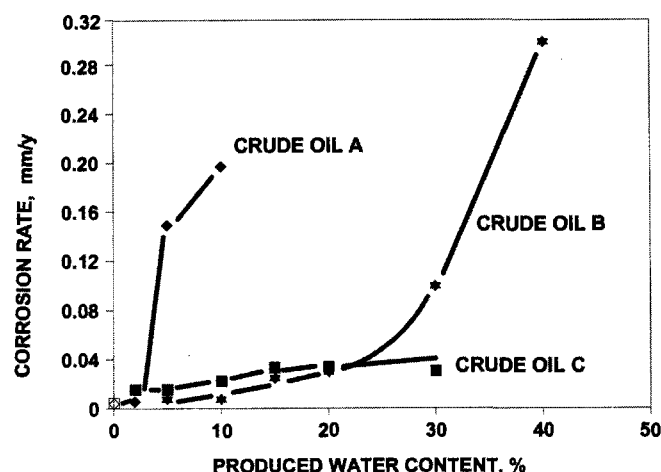


FIG. 10—The change in carbon steel corrosion rate of steel in crude oil/produced water mixtures with increasing produced water content showing the three general types of behavior observed.

oil that provides very little protection for carbon steel, even at water concentrations that would be expected to result in an oil wet, and thus essentially corrosion free, surface. Crude oil B provides corrosion inhibition to a high water concentration, with a subsequent rapid increase in corrosion rate. Crude oil C maintains significant corrosion inhibition at the full range of water concentrations tested.

## LABORATORY CORROSION TESTING

The unique characteristics of petroleum chemistry have a major effect on corrosion test methodology, experimental techniques, and considerations. The most important step preliminary to conducting corrosion tests is to ensure that the actual petroleum chemistry that occurs in the production system is the one investigated. This requires accurate field

data and rigorous sampling techniques. No corrosion test in the petroleum environment can be more precise than the accuracy of the production temperature and pressure data, the gas composition data, and the fluid sample analyses. The well fluids composition, particularly the gas, crude oil, and produced water analysis, must be correct.

Six basic test principles should be followed to preserve the petroleum chemistry for corrosion testing and allow valid laboratory corrosion tests in petroleum environments:

1. A representative production environment for the area of interest, or the most potentially corrosive or highest risk area in a production system, should be duplicated as nearly as possible for all corrosion testing, and its composition should not be altered, except for the purpose of investigating specific field or composition variable, e.g., changes in produced water level, CO<sub>2</sub> partial pressure, change in H<sub>2</sub>S partial pressure (field souring).
2. The composition of corrosive gases in the test solution should be calculated on the basis of gas fugacity not partial pressure for correlation with the production environment. The higher the total pressure of the production environment, the more important this becomes.
3. For crude oil corrosion tests, the actual production crude oil should be used for all corrosion testing, and oxygen must not be allowed to contact the crude oil at any time before corrosion testing.
4. Artificial produced water may be used, however, if crude oil is produced in service, the artificial produced water must be intimately contacted with the crude oil before testing to ensure that the soluble organics from the crude oil are present in the test solution.
5. Great care must be taken to prevent oxygen contamination during corrosion testing, unless oxygen is one of the test variables.
6. Each individual corrosion test must be completed before the chemistry of the water phase in the test environment is changed significantly by the corrosion process, or a flow through system must be used to maintain the solution chemistry.

### Corrosion Testing for Hydrocarbon Gas Systems

The following discussion applies to corrosion testing of hydrocarbon gas systems, and to the gas phase used for produced/condensed water and crude oil system corrosion testing.

Accurately reproducing the composition of the concurrently produced water phase is the primary concern with corrosion testing for hydrocarbon gas systems. The concentration of corrosive gases in the water phase must be accurately simulated, and simple equalizing of the partial pressure with the production environment is not sufficient. As stated previously, gas production wells are generally at high pressure. It is the high pressure that causes the error with the use of partial pressure as the determinant of acid gas concentration in the liquid water phase. This error is not as great for surface facilities operating at much lower pressures.

Using equality of gas fugacity rather than partial pressure to reproduce the production environment in the corrosion

test accounts for the effect of nonideality in the solubility of the gas in the water phase at increasing total pressure. For example, a test conducted at 1.5 bar total pressure of pure CO<sub>2</sub> will not result in the same CO<sub>2</sub> concentration in the water phase as 1.5 bar CO<sub>2</sub> partial pressure in a well with a total pressure of 350 bar with CH<sub>4</sub> as the other gas. There is significantly less CO<sub>2</sub> dissolved in the water phase at the high pressure well than in the low pressure test, even though the partial pressures are the same. This can have a major effect on the application of corrosion test results to the operating system, since the concentration of acid gas dissolved in the water phase strongly affects its corrosivity.

Care is required to ensure that unwanted oxygen is removed from the gas phase to prevent it from being introduced into the water phase. Oxygen contamination, even at a level in the water phase of 100 ppb, can result in significant errors in the test results. Anaerobic gases should be used wherever possible. Initial oxygen removal is obtained by passing the gas through commercial oxygen removal cartridges. Final oxygen removal is accomplished by passing the prescrubbed gas through an NiCl<sub>2</sub> catalyzed 10 000 ppm solution of hydrazine chloride.

Where hydrogen sulfide gas or gas mixtures containing hydrogen sulfide are used, there is rarely any oxygen in the supplied gas. However, these situations do require removal of oxygen from the test solution and the test cell gas space before introduction of the hydrogen sulfide containing test gas. Oxygen remaining in the test cell can react with the hydrogen sulfide to form oxy-sulfide compounds, which can greatly affect corrosion.

### Corrosion Testing for Produced Water Systems

The following discussion applies to corrosion testing in produced/condensed water systems and to the liquid water phase used for hydrocarbon gas and crude oil system corrosion testing.

Produced water is an extremely complex chemical solution, comprised of liquid water, minerals dissolved from formation rocks, and water soluble organics from the hydrocarbon phase, and simulated produced water used in corrosion testing must reproduce this complexity. Good initial analysis of the produced water to be tested is essential for success of the test program.

Removal of oxygen from the solution before testing is vital, since oxygen contamination can result in significant errors in the test results. The test solution is best deaerated by purging with a low oxygen test gas. Hydrogen absorption cells and/or heated copper turnings (300°C) can be employed to remove the final traces of oxygen in the test gas. Purging times must be sufficient to lower the oxygen concentration to <20 ppb. The actual purge time required will vary with the solution concentration and temperature. A hydrazine salt solution can be added to the test solution prior to its use to remove residual oxygen and maintain the solution in a reducing condition for the duration of the test period, if this is required. Hydrazine can interfere with some corrosion inhibitors, which must be considered when using hydrazine.

The test gas must be in equilibrium with the test solution before corrosion testing begins. Since chemical equilibrium

between the gas phase and the water phase, particularly for carbon dioxide, can require four to eight hours, purging overnight before testing begins is often necessary. If the gas and water phases are not at equilibrium, errors in the corrosion test results are possible. However, caution must be exercised if there are volatile components in the test solution that could be stripped out by the purge gas. The primary goal is to generate a test solution that accurately simulates the production environment.

### Corrosion Testing for Crude Oil Systems

The actual production crude oil must be used for all testing to evaluate corrosion in crude oil, and oxygen should not be allowed to contact the crude oil at any time if at all possible. The crude oil samples used in corrosion tests must be obtained in a manner designed to prevent contact of the crude oil with air. The sample container must be purged with inert gas before filling with crude oil, and the crude oil must be shipped under positive inert gas pressure. The sample container construction must be Type 316 stainless steel or a material of greater corrosion resistance, or the container must be lined with an inert material. The crude oil sample must be stored under an inert gas blanket. The crude oil must be transferred from its shipping container into the test cell using inert gas pressure or vacuum.

The extreme measures used to ensure the complete exclusion of oxygen are taken because oxygen can react with some crude oils to form organic acids that were not present in the original crude oil, and could alter the test results. Figure 11 shows the effect air exposure (oxygen) can have on the concentration of acid compounds in a crude oil. Acids in the crude oil sample were extracted with 0.06 M NaOH, which was then titrated with 0.01 M HCl. The crude oil sample not exposed to air shows a titration curve that implies carbonate/bicarbonate as the titrated species, probably originating from the carbon dioxide in the crude oil reacting with the NaOH. The crude oil sample that was

exposed to air contains 1.5 milliequivalents per liter of acidic compounds that are not present in the unexposed sample. This phenomenon does not occur for all crude oils, but it is not possible at this time to know which crude oils will be affected.

### Preventing Changes in Solution Chemistry

Contamination of the test solution with corrosion products is a very real problem, particularly for corrosion testing with carbon and alloy steel. In designing the corrosion test program, calculations using an estimated corrosion rate should be made to estimate the solution volume and maximum exposure time for the test. During the test, and at test termination, solution samples should be taken and analyzed to ensure that no significant changes in solution chemistry occurred that could affect the results. The formation of one mole of ferrous ion will generate two moles of bicarbonate in a sweet environment. For many produced water compositions, this is not necessarily a problem. For condensed water, however, the bicarbonate can result in a significant increase in solution pH. As a general guide iron concentrations should not be allowed to exceed 10 ppm during a test.

However, the above discussion assumes that there is no dissolved iron in the produced water. If dissolved iron is present in the produced water, this iron level should be duplicated in the tests. In this case the requirement becomes to not allow significant changes in the iron concentration during the test period. Many produced waters do contain dissolved iron, but care must be exercised to make sure that the iron concentration analyzed is actually contained in the produced water and not an extraneous artifact resulting from tubular corrosion.

Maintaining the dissolved acid gas concentration in the solution during the test period can be a problem, particularly when testing carbon and alloy steel for periods of over 30 days. This is generally overcome for corrosion tests in glassware by rapid stirring and sparging gas below the liquid surface. Autoclave testing is a particularly difficult problem in that the liquid volumes are small, and stirring efficiency for long time periods is difficult to assess. The most effective method for maintaining the solution dissolved acid gas concentration in autoclaves is to recirculate the test solution and allow it to fall through the gas phase on re-entering the autoclave.

### APPLICATION OF CORROSION TESTING TO NEW PRODUCTION

An approach using corrosion testing for application to new production is given in the logic diagram of Fig. 12 [20]. Carbon and low alloy steels, including corrosion testing of steels, are appraised before any consideration is given to corrosion resistant alloys. This is done because the very heavy cost penalty for alloys dictates that steels should generally be used if technically feasible.

The first step is to obtain valid field production data and samples. As discussed previously, no corrosion test is any more accurate than the accuracy of the temperature, pressure and composition data, and the sampling methodology.

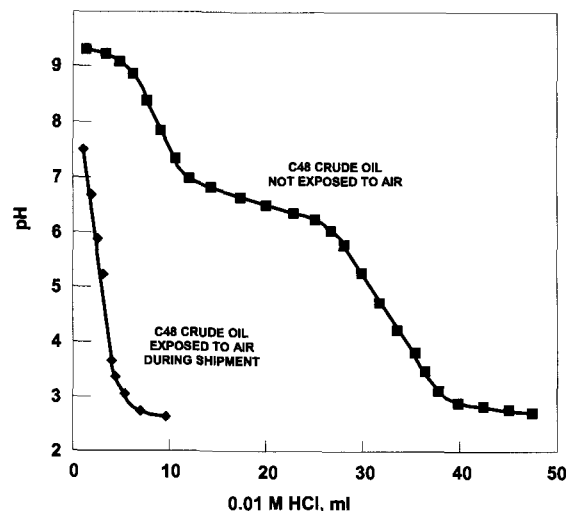


FIG. 11—The effect of exposure to air on the titration curve for acidic compounds extracted from 200 mL of a crude oil with 10 mL of 0.06 M NaOH using 0.01 M HCl as the titrant.

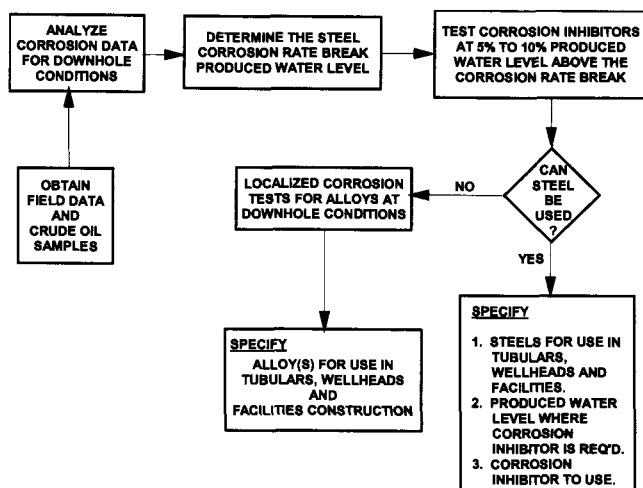


FIG. 12—The logic diagram for new field corrosion testing to determine the Corrosion Rate Break produced water level for carbon or low alloy steel corrosion, corrosion inhibitor application, and corrosion resistant alloy selection.

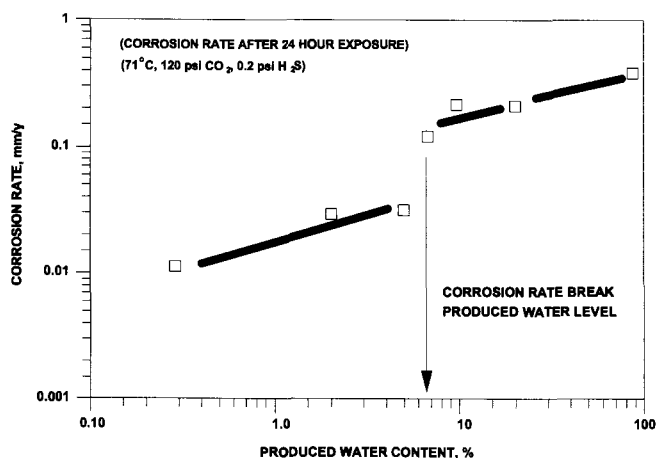


FIG. 13—Change in the corrosion rate of carbon steel in crude oil/produced water mixtures with increasing produced water content, showing a corrosion rate break at approximately 7 % produced water.

The well fluids composition, particularly the gas analysis and produced water analysis, must be reasonably accurate. The crude oil samples used in the corrosion tests must be obtained as described previously. The field data are evaluated as they relate to known corrosion information and corrosion prevention practices.

The corrosion tests are conducted to determine the Corrosion Rate Break produced water level for carbon or low alloy steel. The corrosion rate break is defined as a sudden increase in the corrosion rate between two produced water levels when testing in a series of produced water levels [20]. Generally, only one or two of the carbon or low alloy steels will need to be tested, since there is no significant difference in the Corrosion Rate Break produced water level measured for the various carbon and low-alloy steels commonly used

in crude oil service. The Corrosion Rate Break produced water level is determined from corrosion tests conducted at 10 % by volume produced water increments starting with 100 % crude oil until a high corrosion rate is obtained, the expected produced water limit for the field is reached, or to 90 % produced water level. If a Corrosion Rate Break is observed, additional corrosion tests are conducted at 2 % produced water increments between the two produced water levels that form the break [20]. An example of the results form this type of test sequence is shown in Fig. 13 [20].

The corrosion test methods may be any method that can provide corrosion data in the low water environments. This is generally coupon testing, but may include electrochemical tests that are applicable to the high resistivity crude oil continuous environments at low water levels, e.g., electrochemical impedance spectroscopy and electrochemical noise.

The Corrosion Rate Break tests are followed by tests for corrosion inhibitor effectiveness at a produced water content above the Corrosion Rate Break level. At this point the decision is made on whether or not carbon or low alloy steel can be used, based on the corrosion rate data and corrosion inhibitor effectiveness coupled with estimates of future produced water levels during the life of the field.

If carbon or low alloy steel can be used, the Corrosion Rate Break data are employed to specify:

1. The carbon or low alloy steels to use for tubulars, wellheads, and facilities,
2. The produced water level where the injection of corrosion inhibitor is required, and
3. The corrosion inhibitor to use when the corrosive produced water level is reached.

If carbon or low alloy steel cannot be safely used, corrosion resistant alloys must be evaluated. The production environment must be duplicated in alloy corrosion tests in the same manner as for carbon or low alloy steels. Standard corrosion tests modified to use the production environment are conducted for the corrosion resistant alloys with due consideration given the probable failure modes, e.g., crevice and pitting corrosion for stainless steels. On completion of this test sequence, the corrosion resistant alloy or alloys to use for tubulars, wellheads, and facilities construction are specified.

The possibility of sulfide stress corrosion cracking, including consideration of the possibility for future H<sub>2</sub>S occurrence even though it is not presently contained in the produced fluids is not addressed in this procedure. If sulfide stress corrosion cracking is a concern only resistant carbon or low alloy steels are included in the corrosion testing. The consideration of sulfide stress corrosion cracking must be made for the corrosion resistant alloys in the same manner as for carbon or low alloy steels.

## SUMMARY

Petroleum chemistry is very complex and very sensitive to error when translated to the laboratory. Great care must be taken when designing and conducting corrosion tests for the petroleum environment to ensure that the corrosion



measurements made are relatable to the intended service environment. These six basic principles will aid immensely in obtaining successful results.

1. Duplicate the production environment as nearly as possible including specific field or composition variables.
2. Use fugacity to calculate the composition of corrosive gases in the test solution.
3. Use the actual production crude oil excluding any contact with oxygen.
4. Artificial produced water must be intimately contacted with the crude oil before testing.
5. Prevent oxygen contamination during corrosion testing.
6. Complete each individual corrosion test before the chemistry of the water phase significantly changes.

The preventive corrosion engineering technique for determination of the Corrosion Rate Break produced water level for steel, corrosion inhibitor treatment requirements, and alloy selection can be used to minimize the cost of corrosion protection, while at the same time maximizing its effectiveness.

## REFERENCES

- [1] NACE MR0175, "Sulfide Stress Cracking Resistant Metallic Materials for Oilfield Equipment," National Association of Corrosion Engineers, Houston, TX, 1992.
- [2] Shock, D. A. and Sudbury, J. D., "Prediction of Corrosion in Oil and Gas Wells," Carbon Dioxide Corrosion in Oil and Gas Production, L. E. Newton, et al., Eds., National Association of Corrosion Engineers, Houston, TX, 1984, pp. 394-401.
- [3] de Waard, C. and Milliams, D. E., "Carbonic Acid Corrosion of Steel," *Corrosion*, Vol. 31, No. 5, 1975, pp. 177-181.
- [4] de Waard, C., Lotz, U., and Milliams, D. E., "Predictive Model for CO<sub>2</sub> Corrosion Engineering in Wet Natural Gas Pipelines," Paper 577, CORROSION/91, NACE, Houston, TX, 1991.
- [5] Dugstad, A., Lunde, L., and Olsen, S., "Dewing Corrosion—A Possible Problem Area for Pipelines Transporting Unprocessed Gas over Long Distances," 5th International Conference on Multiphase Production, British Hydrodynamics Research Group, Cranfield, U.K., 1991.
- [6] Olsen, S. and Dugstad, A., "Corrosion under Dewing Conditions," Paper 472, CORROSION/91, NACE, Houston, TX, 1991.
- [7] Hyborg, R., Dugstad, A., and Lunde, L., "Top-of-the-Line Corrosion and Distribution of Glycol in a Large Wet Gas Pipeline," Paper 77, CORROSION/93, NACE, Houston, TX, 1993.
- [8] Crolet, J.-L. and Bonis, M. R., "A Tentative Method for Predicting the Corrosivity of Wells in New CO<sub>2</sub> Fields," *Advances in CO<sub>2</sub> Corrosion*, Vol. 2, National Association of Corrosion Engineers, Houston, TX, 1985, pp. 23-38.
- [9] Crolet, J.-L. and Bonis, M. R., "pH Measurements in Aqueous CO<sub>2</sub> Solutions under High Temperature and Pressure," *Carbon Dioxide Corrosion in Oil and Gas Production*, L. E. Newton et al., Eds., National Association of Corrosion Engineers, Houston, TX, 1984, pp. 178-184.
- [10] Schmitt, G. and Engels, D., "SEM/EDX Analysis of Corrosion Products for Investigation of Metallurgy and Solution Effects in CO<sub>2</sub> Corrosion," Paper 149, CORROSION/88, National Association of Corrosion Engineers, Houston, TX, 1988.
- [11] Murata, T., Sato, E., and Matsuhashi, R., "Factors Controlling Corrosion of Steels in CO<sub>2</sub>-Saturated Environments," *Advances in CO<sub>2</sub> Corrosion*, Vol. 1, National Association of Corrosion Engineers, Houston, TX, 1985, pp. 64-71.
- [12] Videm, K. and Koren, A. M., "Corrosion, Passivity, and Pitting of Carbon Steel in Aqueous Solutions of HCO<sub>3</sub><sup>-</sup>, CO<sub>2</sub>, and Cl<sup>-</sup>," *Corrosion*, Vol. 49, No. 9, September 1993, pp. 746-754.
- [13] Neumann, H.-J., Paczynska-Lahme, B., and Severin, D., *Geology of Petroleum, Volume 5—Composition and Properties of Petroleum*, Halsted Press, NY, 1985, p. 125.
- [14] Donaldson, E. C., "Characterization of the Crude Oil Polar Compound Extract," U.S. Department of Energy Publication DOE/BETC/RI-80/5, October 1980.
- [15] Snyder, L. R., "Petroleum Nitrogen Compounds and Oxygen Compounds," *Accounts of Chemical Research*, Vol. 3, No. 9, September 1970, pp. 290-299.
- [16] Hasiba, H. H. and Jessen, F. W., "Film Forming Compounds from Crude Oils, Interfacial Films and Paraffin Deposition," *Journal of Canadian Petroleum Technology*, Vol. 7, No. 1, January-March 1968, pp. 1-12.
- [17] Smart, J. S., "Wetability—A Major Factor in Oil and Gas System Corrosion," Paper 70, NACE CORROSION/93, New Orleans, March 1993.
- [18] Efird, K. D. and Jasinski, R. J., "Effect of the Crude Oil on Corrosion of Steel in Crude Oil/Brine Production," *Corrosion*, Vol. 45, No. 2, February 1989, pp. 165-171.
- [19] Efird, K. D., "Predicting Corrosion of Steel in Crude Oil Production," *Materials Performance*, Vol. 30, No. 3, March 1991, pp. 63-66.
- [20] Efird, K. D., "Preventive Corrosion Engineering in Crude Oil Production," OTC Paper 6599, Offshore Technology Conference, Houston, TX, 1991.

# High-Temperature Gases

*Gaylord D. Smith<sup>1</sup> and Brian A. Baker<sup>1</sup>*

## IMPORTANCE AND USES OF LABORATORY AND FIELD TESTING

LABORATORY AND FIELD TESTING is aimed at characterizing material performance for specific applications, or at evaluating the effect of variations in test conditions on candidate materials. The test environment should mimic, as faithfully as possible, the environment of the actual application. This includes simulating the chemical composition of the atmosphere, temperature and thermal cycle profiles, stress states, fatigue conditions, and design. Test racks placed in actual use are frequently employed. In other cases, prototype or scaled-down apparatus are designed and constructed to duplicate the end-use application. Laboratory service tests are commonly engineered specifically to evaluate the effect of one or more critical aspects of the exposure conditions. The data on material performance are then used to determine failure of mechanisms, components, or material life, or to screen materials for the application. This chapter will focus on high-temperature gaseous environment testing used to evaluate materials where the applications simultaneously involve high temperature and corrosive conditions. Common basic principles will be described that an investigator must consider in conducting and evaluating these tests. Generalized testing methods associated with specimen preparation, environment synthesis, and evaluation are briefly reviewed. Where applicable, reference is made to more detailed information and studies that are found in the technical literature.

## SAMPLE PREPARATION

Attention to detail in sample preparation begins with obtaining a complete metallurgical profile on the material to be tested. Included here are the chemical composition, fabrication history, and a knowledge of the microstructure. In general, if wrought materials are used in the end-use, the majority of materials tested should be wrought, while cast components should be modeled in test by cast materials. This is because cost, physical properties, and available forms are dependent on whether the alloys are of wrought or cast construction. If welded construction is involved in

the end-use, welded specimens should be part of the laboratory or field test series. The investigator must know the welding products and welding conditions used.

## Size and Shape

Size and shape of laboratory and field test specimens can vary widely but specimens must be large enough to obtain meaningful quantitative data. In testing where internal penetration occurs, such as in carburization, specimens must be large enough to not become saturated prior to completion of the test. Edges and corners do not behave the same as planar surfaces. The investigator should consider which to emphasize through test specimen geometry. For wrought specimens, large surface to edge area is desirable to more accurately reflect typical equipment. If the effect of environmental conditions on mechanical properties is sought, machined test specimens should be exposed.

## Identification

Positive identification of all specimens is essential. Stenciling of samples is frequently used, and brittle materials can be notched. Identification marks should be located to minimize the likelihood of being obscured by corrosion effects or corrosion products. If stress is a critical component of service performance, stamped numbers should not be permitted to be a stress raiser or serve as a notch.

## Replication

Because variations in test parameters cannot be guaranteed over time or place within the test apparatus, replication is essential. Duplicate samples will generally suffice, although a larger number of samples may be necessary for highly variable materials or test conditions. Consistency of test materials and parameters will reduce test result scatter and, hence, the need for multiple samples.

## Surface Preparation

Although clean, uniform, and defect-free surfaces are rarely found in plant equipment, it is important to strive for a clean, uniform surface condition in order to ensure meaningful and reproducible results. A common surface finish is produced by polishing with nominally #120 abrasive cloth or paper until the surface is uniform. Machining

<sup>1</sup>Technical Manager–New Products, and Metallurgist–Advanced, respectively, Special Metals Corporation, 3200 Riverside Drive, Huntington, WV 25705.

may be necessary to remove scale or other defects prior to polishing. Carburized or decarburized layers should be removed. Sheared metal may have a cold-worked layer that requires removal, although this could be less important in high-temperature test environments. Certain materials may require special handling or safety procedures that can be obtained from the manufacturer. After surface preparation, the sample must be carefully measured to permit an accurate calculation of surface area. The sample is then thoroughly cleaned in a solvent such as acetone, dried, and precisely weighed. Typically, small specimens should be weighed to within 0.1 mg. Changes in mass and dimensions will occur during service testing. Once weighed, the samples should be inserted into the test environment or stored in a desiccator. Direct handling of the specimens at any time is to be avoided.

### Controls (Reference Materials)

Setting up a pedigree material to be used repeatedly in order to "calibrate" each laboratory or field test is strongly recommended. This will ensure reproducibility of the test procedure. This material should be thoroughly characterized as to its chemical composition, process history, and microstructure. The size and shape of the reference material should reflect that of the candidate product forms being screened.

## LABORATORY AND FIELD TESTING CONTROLS

Simulating the environment of an industrial process or application can be as rudimentary or complex as the investigator chooses. Most industrial atmospheres consist of mixed oxidants of varying partial pressures (activities), temperature gradient profiles, and, in some cases, velocity and erosion parameters as well. Key application variables should be identified and suitably simulated in the laboratory or field test. Characterization of gas composition is as essential as the control of temperature and gas flow rate. The system should be at equilibrium and free of extraneous components. Care must be paid to flow stability and to maintaining calibration of equipment. Atmosphere synthesis may require multiple units, such as inlet saturators, exhaust condensers, gas preheater beds, catalyst beds, heat shields, bubblers, mass flow controllers, and analytical instrumentation. Flowmeter inlet pressure should be fixed while the gaseous components are metered with electronic mass flow controllers of the proper capacity range. Simple flowmeter-needle valve controls should be limited to single component gases or for purge streams. Mass flow controllers will maintain uniform flow rates until a back pressure of 36 kPa is reached. Any test environment that could cause system blockage through condensation, sulfate formation, coking, or line corrosion should be constantly monitored and relief valving provided. Corrosive gases, such as sulfur trioxide, will require corrosion-resistant materials of construction. Polyethylene is a convenient tubing material and does not appear to affect gas dew points as low as  $-73^{\circ}\text{C}$  (approximately 2 ppm). If the system is to be monitored using a gas chromatograph, septums must be appropriately

located in the gas stream, preferably both immediately before and after the specimen reaction chamber. For more information on atmosphere simulation and analysis, the reader is referred to Refs 1 and 2. Methods for purifying elemental gases are described in Ref 3.

Too infrequent data collection can lead to misleading conclusions, and perhaps complete failure of the test. It is common to space out field test observations to match plant shutdowns only to find complete disintegration of one or more specimens. Conversely, too frequent data collection could be unnecessarily time-consuming and expensive. Data collection can take on numerous forms depending on the purpose of the service test, including mass and dimensional changes, volumetric measurement of reactive gas consumption, changes in mechanical and physical properties, metallography, and radiographic analysis. These techniques are described in detail throughout this text. Common mistakes that can occur in high-temperature corrosion testing are described below. Gravimetric analysis that measures film formation during the initial period of scale growth usually is misleading when the results are extrapolated to long-term service. Only in the few instances where linear oxidation kinetics prevail over time would gravimetric data be valid for predicting service life. Care must be taken to assure that corrosion behavior has been measured over the entire range of temperature and pressure expected in actual service. For example, liquid phase formation is a function of temperature and can quite suddenly alter corrosion behavior in sulfur and chlorine containing atmospheres. Dependence on mass change data can be deceptive. Use of metallography to measure loss of metal and depth of internal penetration by the reactive gaseous species is essential to assess potential material degradation not necessarily apparent by mass change data only. For example, a net zero mass change effect for chromia ( $\text{Cr}_2\text{O}_3$ ) forming alloys can be observed at elevated temperatures in mixed oxidant environments where simultaneous mass loss of chromium by evaporation (as  $\text{CrO}_3$ ) and possibly scale spallation occurs, in addition to mass gain via internal attack by one or more oxidants.

## SPECIFIC ENVIRONMENTS

The principal high-temperature gaseous atmospheres to be discussed are:

- oxidation
- carburization
- sulfidation
- halogenization

Testing in each of these types of atmospheres will be discussed separately, but many industrial gas streams are best described as "mixed oxidant" atmospheres containing a combination of reactive gases. The interaction of these atmospheres with materials can be complex and vary dramatically with changing conditions of reactive gas species, temperature, pressure, and time. Another form of gaseous attack that can occur at high temperatures for a given substrate is nitridation. It shows characteristics of both oxidation and carburization. The reader is referred to the text by Lai for an overview of nitridation [4].

## Oxidation

An understanding of oxidation enhances the understanding of other types of high-temperature gaseous mechanisms [5-7]. Oxidation is often responsible for part, or all, of an engineering alloy's resistance to attack from these other gaseous environments.

### Oxide Formation

An understanding of protective oxidation of metal is enhanced by knowledge of the mechanisms of solid-state diffusion. For a particular metal, the reaction mechanism will in general be a function of pretreatment and surface preparation, temperature, gas composition and pressure, and elapsed time of reaction. When the large variations in properties of different metals and alloys and their oxides are also considered, it is not surprising that a large theoretical base is needed to describe the oxidation behavior of metals. Thermodynamics and kinetics are two basic factors associated with the formation and subsequent protection by these oxide layers at high temperatures.

### Thermodynamics

The overall driving force of metal-oxygen reactions is the free energy change associated with the formation of the oxide from the reactants. Thermodynamically, the oxide will be formed only if the ambient oxygen pressure is higher than the dissociation pressure of the oxide in equilibrium with its metal. See Fig. 1. Free energy of formation of metal oxides as a function of temperature is included in many reference books [7]. The fact that the activity of the oxide-forming metal will be less than unity should be considered as well. This information allows the determination of whether or not a particular oxide will form under a given set of operating conditions.

### Kinetics

Once it has been determined that the thermodynamic conditions are met for the formation of a particular oxide, the kinetics need to be considered [8]. A number of methods can be used to study the oxidation mechanism quantitatively. One of the simplest is to plot mass change per unit surface area of a metallic specimen versus time of exposure and examine the applicable oxidation rate laws. Using the maximum depth of attack, or penetration, is another excellent means of gaging an alloy's resistance to oxidation. It requires additional time and the internal examination of the sample. An ideal way of using both of these methods is to periodically weigh the sample and finally conduct a metallographic examination after the desired total exposure time has been reached.

An oxide layer that forms on an engineering alloy can generally be classified as a "good" (protective) oxide or as a "poor" (non-protective) oxide. The performance of this oxide, good or poor, determines whether a satisfactory alloy has been selected for the particular application.

## Oxidation Rate Laws

The most commonly encountered reaction equations are rate laws [9,10]; by determining which reaction rate law or

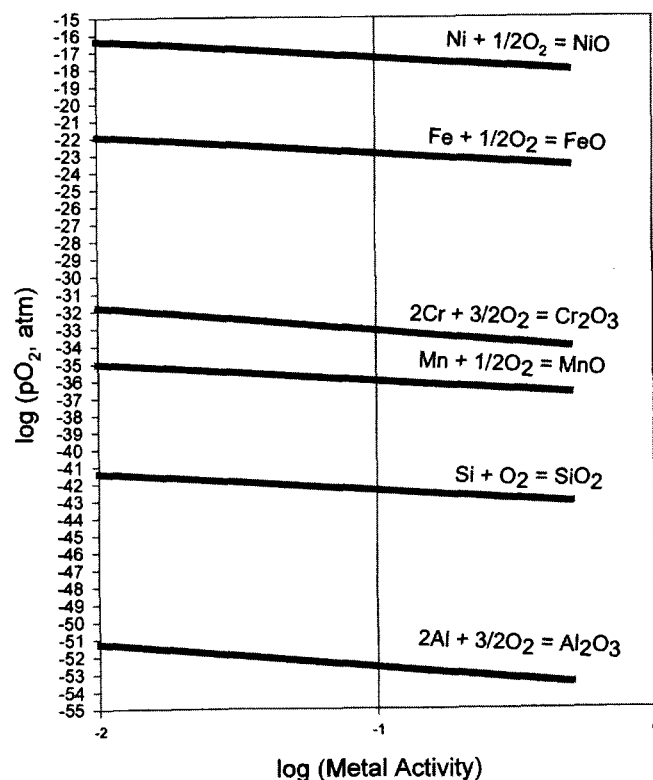


FIG. 1—Equilibria between the dissociation pressure of the certain elemental oxides and their metal activity (Ellingham Diagram [23,24].

laws apply, the corrosion resistance of an alloy can be categorized for a particular set of conditions and time.

### Linear Rate Law

The linear rate suggests the rate-controlling step is simply the reaction of metal with oxygen. Any corrosion product or scale formed is generally assumed to be non-protective, due to its porous, non-adherent, powdery, or volatile structure. In some cases, the corrosion product may even be a liquid. Overall reaction rates may be very fast up to and including ignition. Magnesium, cerium, and lanthanum are typical examples of pure metals that exhibit linear oxidation rates over a wide variety of conditions.

### Parabolic Rate Law

The parabolic rate law is applicable when the controlling step is by diffusion of the oxide-forming metal through a barrier such as an oxide or passive film. The oxidation rate is inversely proportional to time and approaches a slow constant rate after finite time. This is the most common type of high-temperature oxidation found on engineering materials.

### Paralinear Rate Law

In most practical oxidation processes, any particular rate law lasts for only a limited time. At the end of that time, the reaction rate is immediately describable by another law, or passes through a transition period before another rate law

is established. This change may be associated with failure of the protective scale. The slower process step may become more rapid and another may take over as rate controlling. If the mechanism of oxidation changes, oxide morphology may also change, giving another clue to the mechanism.

Many commercial alloys exhibit what is called a parabolic rate law. Initial scale buildup is parabolic, followed after some time by scale breakaway [11]. A linear weight loss then develops. This linear rate may be related to the initial parabolic rate, as in the case of scale breakaway and reformation. It may also be independent of the parabolic rate if the reformed oxide is non-protective in nature. The changing of rate laws, over time, is one of the reasons for the desirability of long-term test exposures.

## Testing

ASTM G 54, Practice for Simple Static Oxidation Testing, describes standard procedures for this test. This service test practice covers determination of preliminary information on the relative growth, scaling, and microstructural characteristics of an oxide on the surface of a pure metal or alloy under isothermal conditions in still air. The advantages of laboratory testing include being able to use small amounts of material, having a controlled environment where the parameters can be closely monitored and adjusted as desired, and being able to test with alternate materials for comparison [3]. The main disadvantage is that laboratory tests seldom, if ever, completely duplicate actual service conditions. While laboratory test data can be beneficial in assisting in selecting materials for construction, the overall test conditions, especially time duration of testing, should be closely examined. Some laboratory testing is conducted for short periods of time, i.e., less than 100 h. This type of testing can be beneficial in studying initial scale formation or oxidation theories, but is often of little benefit to actual service conditions. Laboratory oxidation tests of 500–1000 h and longer should generally be used to select materials.

Field testing can be conducted using test coupons in actual service environments or by using service equipment. The coupons offer the advantage of being able to test small samples and compare materials by testing several materials at the same time. They still, however, may not provide conditions that are identical to actual service.

Field testing of real equipment may be conducted on small, or pilot plants, or full-scale installations. The main disadvantage of this type of testing is the expense and time required. The advantage is that the data and information more accurately reflects actual operating conditions than that obtained in the laboratory. In these pilot plant environments, materials may be evaluated to determine the type of oxides formed and the degree of protection provided. This in turn provides information to permit selection of the material that will provide the required service life.

## CARBURIZATION AND METAL DUSTING

Metals and alloys are susceptible to carburization when exposed at elevated temperatures to atmospheres containing carbon-based species, such as CO or CH<sub>4</sub>. Carburization,

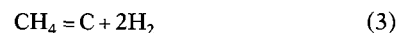
a form of internal attack resulting in carbide formation, can be highly embrittling. A unique mode of carburization is metal dusting in which a metal or alloy experiences significant pitting or thinning, or both, due to disintegration of a carbide-saturated surface layer. The distinguishing characteristic of metal dusting is that it requires that the calculated carbon activity be greater than unity; carburization can occur when the carbon activity is less than unity. Metal dusting environments, which commonly contain H<sub>2</sub>, CO, and various hydrocarbons, are relatively stagnant and usually between 430 and 900°C (806 and 1652°F) [12,13].

Carburization is common in heat treatment equipment, especially where endothermic gas is used for creating a protective atmosphere [14]. A typical endothermic atmosphere consists of about 40 % N<sub>2</sub>, 20 % CO, 39 % H<sub>2</sub> with less than 1 % CH<sub>4</sub>, and a dew point of –20 to –4°C (–5 to +25°F). An endothermic atmosphere, enriched in CH<sub>4</sub> or C<sub>3</sub>H<sub>8</sub>, etc., is used for gas carburizing steels (case-hardening). Carburization is also found in equipment for carbon and carbon fiber production. In the petrochemical industry, ethylene and olefins are produced in pyrolysis furnaces where petroleum feed stocks, such as ethane and naphtha, are cracked at temperatures up to 1150°C (2102°F) [15]. Of more recent origin are the carbonaceous problems associated with emerging energy conversion systems. Problems with carburization of high-temperature alloys have been identified in both liquid metal and gas-cooled nuclear reactors and in equipment for gasification and coal combustion.

## Carburization Variables

Carburization is a function of both the carbon activity of the environment and of the metal or alloy. Thermodynamically, one can determine the carbon activity of the atmosphere as follows:

When the environment contains CH<sub>4</sub>, CO or H<sub>2</sub>, the reactions are:



Then the carbon activity in the environment of Eq 1 can be calculated as follows:

$$\Delta G^\circ = -RT \ln \left( \frac{a_c \cdot P_{\text{H}_2\text{O}}}{P_{\text{CO}} \cdot P_{\text{H}_2}} \right) \quad (4)$$

Rearranging

$$a_c = e^{-\Delta G/RT} \left( \frac{P_{\text{CO}} \cdot P_{\text{H}_2}}{P_{\text{H}_2\text{O}}} \right) \quad (5)$$

Similarly, the carbon activity in the environment (2) can be calculated as follows:

$$\Delta G^\circ = -RT \ln \left( \frac{a_c \cdot P_{\text{CO}_2}}{P_{\text{CO}}^2} \right) \quad (6)$$

Rearranging

$$a_c = e^{-\Delta G/RT} \left( \frac{P_{CO}^2}{P_{CO_2}} \right) \quad (7)$$

For Eq 3, the carbon activity in the environment can be calculated as follows:

$$\Delta G^\circ = -RT \ln \left( \frac{a_c \cdot P_{H_2}^2}{P_{CH_4}} \right) \quad (8)$$

Rearranging

$$a_c = e^{-\Delta G/RT} \left( \frac{P_{CH_4}}{P_{H_2}^2} \right) \quad (9)$$

Computer programs to determine the carbon activity, as well as other constituents of the gas are available, including SOLGAS-MIX-PV developed by Besmann [16] and CORGA, developed by Bresselers et al. [17]. More recently, computer programs have become available including Thermo-Calc® developed by Sundman [18], ChemSage® by Eriksson and Hack [19], F\*A\*C\*T\*® by Thompson et al. [20], and MTDATA by Davies et al. [21].

An excellent description of the use of the Brinkley method for characterization of high-temperature gaseous environment is given in Ref 22. The Brinkley method is an iterative one, based on solving two sets of equations alternately until a consistent set of values is obtained for the mole number of each species and the total number of moles. The first step is to select the major components, i.e., those expected to constitute the bulk of the equilibrated mixture. Chemical reactions are then written for the formation of each expected minor constituent in terms of only the major ones selected, and a set of equations (Series I) is formed by the equilibrium relations for these reactions. The magnitude of each major component is then estimated, and the equations are solved to obtain trial values of the minor species.

New values for the major components are derived from a second set of equations constructed from a mass balance (Series II). The first series of equations is solved again, using the new values of the major components or weighted averages of new and old ones and the process repeated until values calculated on successive iterations converge to a consistent set of mole numbers. Partial pressures or activities can then be computed.

Reactions (1) and (2) will show decreasing carbon activity with increasing temperature while reaction (3) exhibits the reverse. Thus, at high temperatures, the carburizing tendencies of atmospheres containing  $CH_4$ ,  $CO$ , and  $CO_2$  will be dominated by reaction (3). See Fig. 2. Carbonaceous atmospheres tend to be slow in reaching equilibrium. Consequently, preheating furnaces containing an appropriate catalyst may be necessary in laboratory testing to properly simulate actual process conditions.

The carbon activity of a metal or alloy in equilibrium with its environment can be determined using similar thermodynamic principles. The relative stabilities of selected binary carbides are depicted in Fig. 3 for various partial pressures of the constituents in equations in Refs 2 and 3 versus  $a_c$ . Stability diagrams (modified Ellingham

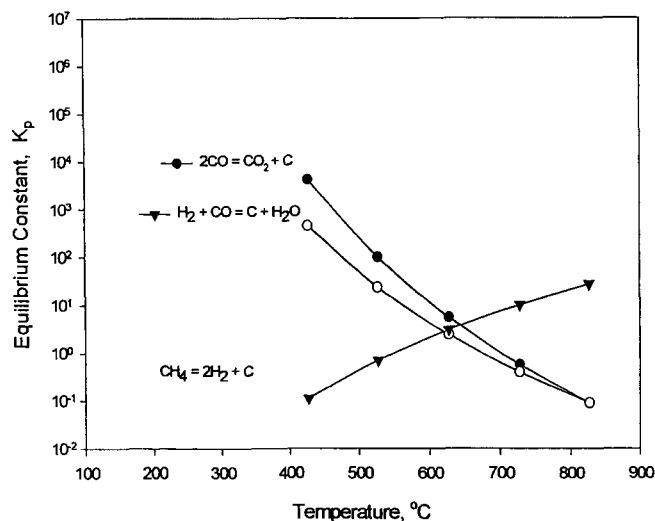


FIG. 2—Equilibrium constant,  $K_p$ , versus temperature for various reactions producing carbon.

diagrams) of selected metals in equilibrium with both carbon and oxygen are available in various publications [23,24]. These diagrams are generated by computer programs similar to those developed by Besmann and the others [16–22]. Figure 4 is an example of one such diagram for Cr-C-O at 620°C (1150°F). These diagrams may not represent the actual events of any given alloy since the activity of the scale-forming elements will vary with their concentration in the alloy. Also, the characteristics of the scale that forms will influence carbon activity in the substrate by controlling carbon diffusion through the scale.

## Carburization Effects

Carburization usually results in the formation of internal carbides, which initially strengthen and harden a metal or alloy and then in excess begin to degrade the mechanical properties, ultimately resulting in embrittlement and potential brittle fracture at low temperatures and creep failure at elevated temperatures. Carburization is a diffusion-controlled reaction that results in a carbon gradient with its maximum at the reaction surface. Grain boundary diffusion of carbon tends to be significantly faster than intragranular diffusion, usually producing a carbide network around grains. Carbon will react with the alloy constituents that are energetically favored at any given temperature, pressure, and carbon activity. It is not uncommon to see a variation in carbide type from the surface to the interior, as dictated by the carbon activity within the alloy matrix such as  $Cr_3C_2$  to  $Cr_7C_3$  to  $Cr_{23}C_6$  to carbon in solid solution in a high-nickel austenitic alloy. Carbide formation resulting from carburization can lead to loss of both aqueous and high-temperature corrosion resistance. This is due principally to the loss of chromium from solid solution, although other elements can be involved as well. Initial carbide formation in some structural alloys can cause slight shrinkage, but gross carburization is more likely to cause expansion.

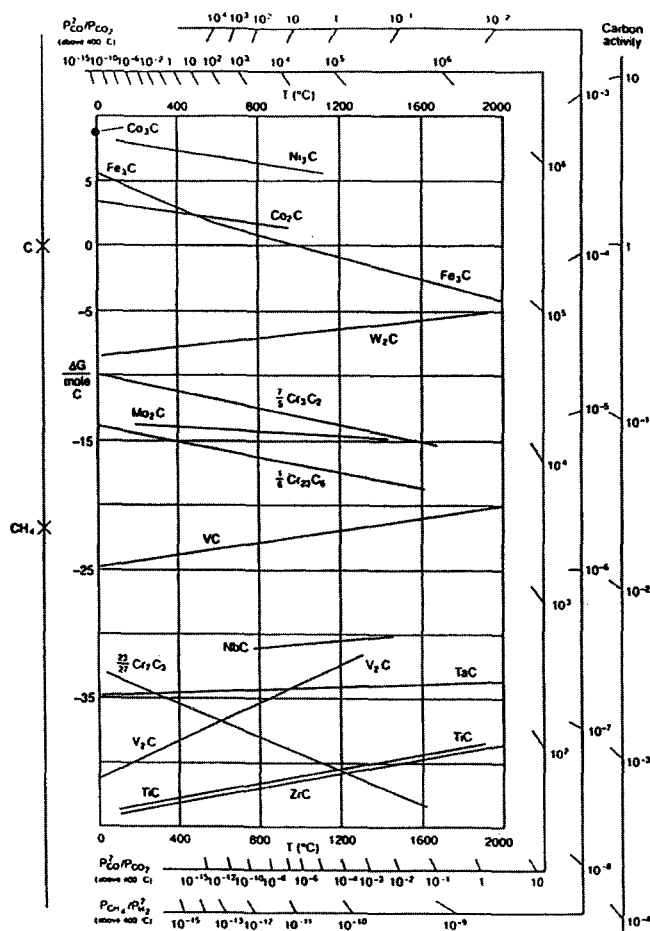


FIG. 3—Standard free energies of formation for carbides [22].

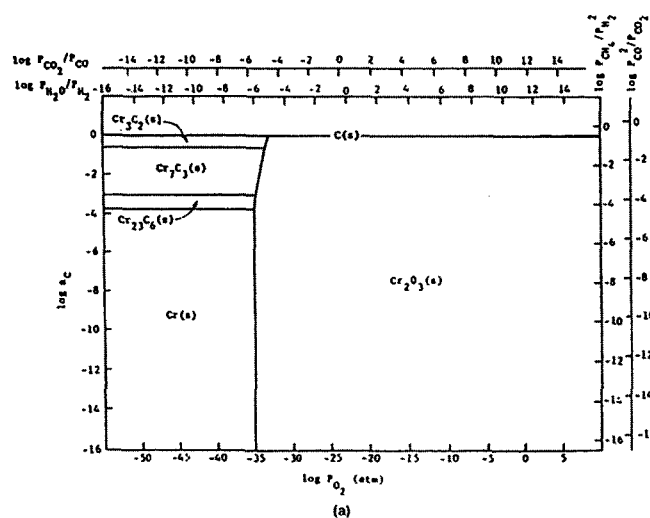


FIG. 4—Stability diagrams of Cr-C-O system at 620°C (1150°F) [22].

Mixed oxidant environments such as those that contain both carbon and O<sub>2</sub> or both carbon and sulfur can result in simultaneous internal carburization and breakaway oxidation (rapid and unpredictable metal loss) or, in other cases,

internal carburization and accelerated carbide scaling reactions [25,26]. Cycling conditions may cause a phenomenon called “green rot” in nickel-chromium alloys, whereby chromium carbides are precipitated along grain boundaries during a reducing (carburizing) cycle and subsequently oxidized during an oxidizing cycle [27].

### Testing

High-temperature carburization studies have become quite complex in the past few years resulting in much better simulations of industrial environments. Laboratory testing can now duplicate the atmospheres of coal gasification and liquefaction atmospheres, combustion gases, petrochemical process streams, and gas-cooled reactor environments. Much of this progress has been enabled by the availability of electronic flow meters to synthesize the atmosphere, and gas analysis equipment such as the gas chromatograph, mass spectrometer and individual analyzers including the electrolytic cell for oxygen, the dew point hygrometer, the chemiluminescence detector for nitrogen oxides, and the infrared absorption cell for carbon monoxide. For a detailed guide to practical usage of this equipment, the reader is referred to Ref 3.

### Laboratory Testing

Pack carburization testing as described by Mason et al. is perhaps the oldest method for characterizing the carburization resistance of alloys [28]. In such a test, the samples are packed in a heat-resistant alloy retort containing usually a 20 % mixture of alkali or other metal carbonates bound to a hardwood charcoal by oil, tar, or molasses. Approximately 20 % of coke is added to act as a diluent and to enhance heat transfer. While variations on the pack carburization test are still currently being used for screening purposes, although now typically with carbon granules, the current popularity of gas carburization technology has nearly led to its replacement.

Gaseous environmental testing, usually in multiple component atmospheres, is much more versatile and accurate and one such test configuration is depicted in Fig. 5. The dry inlet gases pass through pressure regulators and filters and are then metered through flow meters and electronic flow controllers at the desired total flow rate. The gas streams then pass through a mixing manifold and optional equipment to add water vapor or alcohol, or both. The addition of water vapor requires a water saturator and a constant temperature bath. Due to the sluggish tendency of carbonaceous atmospheres to equilibrate, it is recommended that the gas stream pass through a preheater containing a suitable catalyst, such as 0.3 % platinum on alumina. Electrically heated ceramic tube furnaces with end caps make ideal retorts for carburization testing. Specimens can be readily positioned on EX-20 cordierite [Mg<sub>2</sub>Al<sub>3</sub>(AlSi<sub>5</sub>)O<sub>18</sub>] boats drilled to accept the test specimens. Cordierite boats avoid the use of reactive metallic specimen holders in the hot zone. Cordierite is readily available in corrugated monolithic form, extremely resistant to both corrosion and thermal shock, and is easily machined. Alumina (Al<sub>2</sub>O<sub>3</sub>) is preferred for test temperatures above 1000°C (1832°F) due to the volatilization of silicon

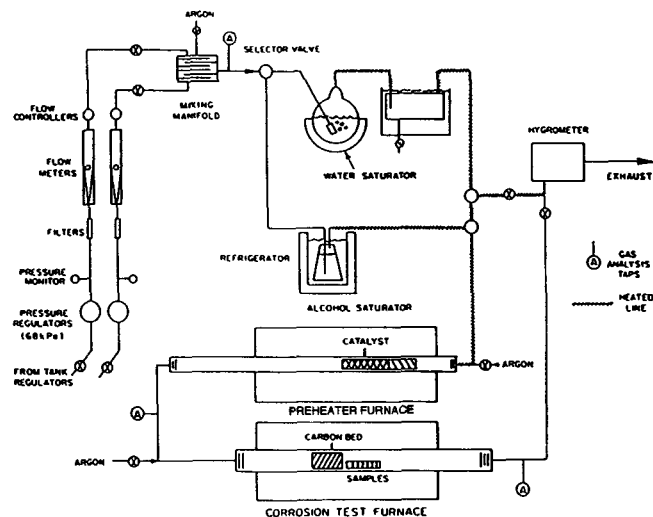


FIG. 5—Schematic representation of carburization-oxidation test apparatus.

oxide from silicon-containing ceramics. Inlet and outlet piping may be constructed with polyethylene or stainless steel tubing. Furnace end caps may be gasketed with castable silicone rubber. A plunger, which passes through an O-ring cell in the end cap, inserts and extracts the boat from the hot zone. This prevents atmospheric exposure from oxidizing reactive surfaces during thermal cycling (to weigh the samples). In the case of metal dusting testing, typically done in mixtures of  $H_2$ ,  $CO$ , and water vapor, attention to the iron content of refractory specimen holders is warranted to avoid catalytic carbon deposition on non-metallic surfaces.

The composition of the inlet mixtures and the test gases can be monitored by gas chromatography, dew point hydrometry, and individual gas component analyzers. This procedure is essential in maintaining consistency of test results, to assure equilibrium, and to check for leaks. Properly placed rubber septums in the transfer lines make monitoring relatively easy. Placing the septums in a T-type compression tube fitting using a rubber septum squeezed between a back ferrule and the fitting nut works well. The systems are usually good for dozens of injections before replacement is necessary. If properly done, less than 0.15 % air is entrained in the gas specimen.

Furnace purging for up to 1 h prior to inserting specimens into the hot zone is recommended to assure that all air trapped in the furnace during loading is expelled. Similarly, upon removal of the specimens from the hot zone, the furnace should be flushed with argon while the specimens cool to room temperature in the end of the furnace tube. This procedure negates any explosion hazard and protects the specimens from oxidation.

Mass change data can be collected from each cycle of the specimens (cycle time is entirely arbitrary and can vary from daily to weekly or longer depending on the aim of the investigation). Upon completion of the testing, the specimen can be sectioned for metallographic evaluation, hardness profile measurements or serially machined for

carbon profile analysis as described in ASTM G 79, Practice for Evaluation of Metals Exposed to Carburization Environments.

### Field Testing

Carburization testing in the field usually requires dedicating all or a portion of a particular piece of equipment for evaluating alloys' performance or for evaluating the effect of process variables on the materials of construction. Such testing is performed to confirm laboratory data because of a lack of access to laboratory equipment or professional material expertise, or because of difficulty in duplicating certain carburization conditions in the laboratory. Atmospheres of low oxygen potential have proven difficult to duplicate in the laboratory. Direct simulation of ethylene furnaces is difficult in the laboratory because of the simultaneous interaction of long-term creep and high-temperature corrosion by carbonaceous atmospheres on the inner diameter and oxidizing combustion gases on the outer diameter of the furnace tubes.

Carburization testing in the laboratory offers the convenience of access to the necessary equipment for precise control of conditions along with the ability to control measurement schedules. However, the laboratory test may not mimic all environmental and mechanical conditions such as stress, design effects (corners, crevices, dead zones, etc.), thermal fluctuations in service abrasive damage, flow stream effects, and metal-to-metal contact reactions. The investigator may not be able to reproduce the complete atmosphere that is being simulated in the laboratory and thereby runs the risk of missing a key element in determining the rate of carburization degradation. This concern prompts many investigators to seek confirming field test data.

### Materials

Because of the multiplicity of carbeneous environments in industry and the broad spectrum of mechanical property, product form, and cost requirements, a large number of heat-resistant, carburization-resistant, cast, and wrought alloys are currently available. Nickel-containing austenitic alloys are widely used in the thermal processing and petrochemical industries to resist carburization. The typical workhorse of the pyrolysis furnace tube market in ethylene cracking is now an HP-type cast (35 %Ni-25 %Cr) iron-base alloy. Many modifications, both cast and wrought, compete for this market [29,30]. High-nickel alloys find application in carburizing environments, particularly where high stress, thermal fatigue, and exceptional carburization resistance is required [31]. Alumina ( $Al_2O_3$ ) scales are deemed more protective than chromia ( $Cr_2O_3$ ) scales in conveying carburization resistance to an alloy, making alloys such as Haynes® alloy 214 UNS N07214 or INCOLOY® alloy MA 956 (UNS S67956) likely candidates for extremely carburizing environments. Silicon additions, which form silica ( $SiO_2$ ) subscales beneath chromia, offer enhanced carburization resistance; INCOLOY® alloys DS and 890 plus alloy 330 (UNS 08330) are three examples of silicon-containing, carburization-resistant alloys.



## SULFIDATION

At high temperature, sulfur is very damaging to materials of construction as many of the metallic elements that compose an alloy form low melting eutectic sulfides. The extent of corrosion depends on the partial pressure of sulfur relative to oxygen at a given temperature and the relative stability of the oxides and sulfides at the same temperature. High-temperature sulfidic corrosion of metals and alloys occurs in petroleum refining and processing. Sulfur-induced hot corrosion also occurs in gas turbine components during combustion of fuels that contain sulfur as an impurity. Similarly, sulfide corrosion is possible in environments associated with coal combustion and conversion systems.

In petroleum processing, sulfur compounds originate with crude oils and include polysulfides, hydrogen sulfide, mercaptans, aliphatic sulfides, disulfides, and thiophenes [32]. Corrosion by these sulfur compounds occurs between 260°C (500°F) and 538°C (1000°F). The corrosion rate increases with temperature to 454°C (850°F) and then decreases. Corrosion rate curves as a function of temperature for various steels with different chromium levels for a specific amount of sulfur in the processing streams are called McConomy curves [33] or modified McConomy curves [32]. If the sulfur content in the system is different, a corrosion multiplier is then applied for varying sulfur amounts. In addition, Copper-Gormen curves have been developed for various alloys that predict corrosion rate with respect to temperature for a range of H<sub>2</sub>S composition [34].

## Laboratory Testing

In the laboratory, corrosion from sulfur-containing gases can be assessed by exposing samples to the environment simulating the process. Most of the chemical processes involving sulfur would most likely have a significant partial pressure of oxygen as well. Although there is no standard sulfidation test, a typical oxidizing environment can be represented by H<sub>2</sub>-45 %CO<sub>2</sub>-1 %H<sub>2</sub>S mixture and a H<sub>2</sub>-1 %H<sub>2</sub>S mixture for reducing conditions (simulation of a coal gasification environment). The volume of gas used in the test should be sufficient so as not to influence the specimens placed in front as compared to specimens located in the back of the chamber. A flow rate of about 500 cm<sup>3</sup> per min [at standard temperature and pressure (STP)] should be more than adequate for the size of the furnace tube and the sample size mentioned below. Bottled gas premixed to the required composition can be used. Gases can also be mixed in-situ using electronic flow meters and a mixing chamber.

The sulfidation test is normally done in an electrically heated mullite tube 100 mm in diameter. The gases are mixed and passed into the mullite tube furnace. Typical specimens are in the form of pins 7.6 mm (0.3 in.) diameter by 19 mm (0.75 in.) length. Specimens are placed in a cor-dierite boat that can hold about 10 to 20 specimens at a time. To avoid any oxidation during cooling to room temperature for weighing, the samples are pulled by means of pusher rod to the cold end of the furnace and cooled in argon. After weighing, the samples are pushed into the hot zone under argon and switched to the sulfidizing environment as soon as the test temperature is attained. The test

data are plotted in the form of mass change versus exposure time. Mass change is reported as mg/cm<sup>2</sup> obtained from the measured mass change, and dimensions of the samples measured at the beginning of the experiment. The data are used to compare all the alloys tested.

The mass change in sulfidation tests is usually negative. One has to be careful in using sulfidation testing to measure weight gain using thermogravimetric equipment. Some alloys may form, at certain temperatures, low melting eutectics resulting in molten droplets dripping off the coupons under investigation. Such testing should be limited to lower temperatures or preoxidized specimens that do not form eutectics on the surface.

Another laboratory test that has been successfully used in screening candidate gas turbine alloys uses a mixture of 96 % O<sub>2</sub> and 4 % SO<sub>2</sub> [35]. When using O<sub>2</sub>-SO<sub>2</sub> gas mixtures a platinum catalyst should be used to aid establishment of equilibrium. In this oxidation/sulfidation environment, sub-surface sulfides normally get oxidized, releasing sulfur for further ingress into the metal. The extent of corrosion in this case should be assessed by cross section metallographic examination of the test specimens at the conclusion of the test, in addition to the measurement of mass change.

Another oxidation/sulfidation test to assess the performance of gas turbine alloys is the burner rig test. A schematic of the burner rig is shown in Fig. 6. Here a jet fuel is burned in a combustion chamber with an air-fuel ratio of 30:1. The flame passes down a tube at the end of which are the samples to be evaluated, mounted in a rotating platen. The samples are in the form of pins. The jet fuel normally contains a certain amount of sulfur. There are provisions to add additional sulfur in the form of volatile sulfur compounds. In addition, seawater can be added into the gas stream to simulate a marine environment. The samples are typically exposed to the flame temperature for 58 min and cooling air for 2 min in a 1-h cycle. The test is typically conducted for about 500 h.

In a standard burner rig test, mass change data are not usually acquired during testing. The metal loss and depth of maximum attack can be obtained after completion of the test by mounting transverse sections cut from the

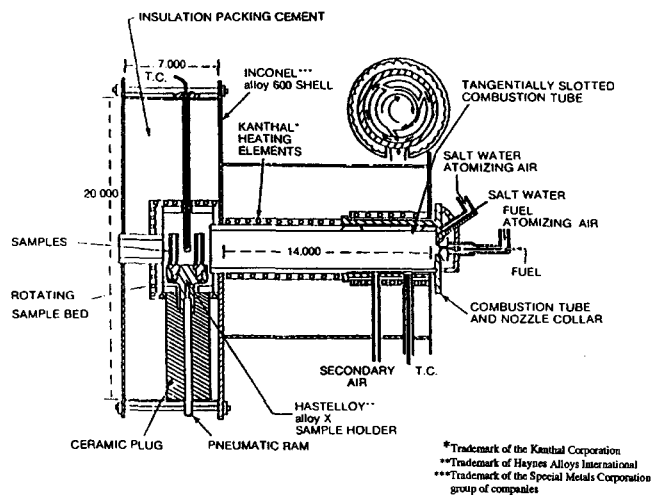


FIG. 6—Schematic of the G. E. Lynn burner-rig test setup.

specimens and polishing using standard metallographic procedures. Samples can then be evaluated using the criteria described below under Metallographic Analysis.

In addition to burner rig tests, additional laboratory tests such as the Dean test and modified Dean tests have been developed to study the hot-corrosion resistance of gas turbine alloys [36]. These differ from the burner rig in the way salt is carried to the specimens at a specific temperature.

Considerable work has been done on the performance of conventional engineering alloys and advanced nickel- and cobalt-based alloys in environments simulating low oxygen partial pressures and moderate to high sulfur partial pressures that are typical of coal gasification and substoichiometric combustion systems [37]. Figure 7 shows the schematic of a laboratory setup used for evaluation of materials. The setup is used to internally air-cool the specimens to simulate heat exchanger tubes exposed in a coal gasification type environment. Thermocouples are welded on the inside and outside surfaces of the metal tube. The gas temperature is measured by another thermocouple in the thermowell. The fireside temperature of the metal is controlled by adjusting the coolant flow rate. Flow rates of the mixed gases such as  $\text{CO-CO}_2\text{-CH}_4$  and  $\text{H}_2\text{-H}_2\text{S}$  are adjusted

through a gas flow system to achieve the desired oxygen and sulfur partial pressures in the reaction mixture.

### Field Testing

Coal ash corrosion is a widespread problem for superheater and reheater tubes in coal fired power plants that burn high-sulfur coals. The accelerated corrosion is caused by liquid sulfates on the surface of the metal beneath an overlying ash deposit. Coal ash corrosion is very severe between 540 and 740°C (1000°F and 1364°F) because of the formation of molten alkali iron-trisulfate. Considerable work has been done to predict corrosion rates based on the nature of the coal (its sulfur and ash content). This was accomplished by the exposure of various alloys to synthetic ash mixtures and synthetic flue gases. The corrosion rates of various alloys were reported in the form of iso-corrosion curves for various sulfur dioxide, alkali sulfate, and temperature combinations. An equation was developed to predict corrosion rates for selected alloys from details of the nature of ash by analyzing deposits removed from steam generator tubes and from test probes installed in a boiler [38]. Then laboratory tests were conducted using coupons of various alloys coated with synthetic coal ash that was exposed to simulated combustion gas atmospheres.

The U.S. Department of Energy sponsored various materials testing projects in operating coal gasification pilot plants. The results for several coal gasification pilot plants are summarized in Ref 39.

Atmospheric and Pressurized Fluidized Bed Combustion (AFBC and PFBC) of coal using calcium oxide as a sulfur absorbent is an emerging technology that burns coal efficiently and eliminates the need for expensive flue gas desulfurization systems, as sulfur in this case, is removed in solid form. However, solid-state oxygen sensors have shown that the average oxygen concentration is not a valid indication of the in-bed combustion chemistry [40]. The oxygen sensors identified localized areas within the fluidized bed that have very low (as low as  $10^{-25}$  atmospheres) or oscillating oxygen partial pressures. Low oxygen partial pressures result in relatively high sulfur activity (as high as  $10^{-5}$  atmospheres). Several corrosion studies of coupons and tubular specimens exposed in various pilot plants have shown that heat exchanger alloys can undergo very severe sulfidation attack within the bed environment [41].

### Materials for Test Equipment and Reference Samples

The most effective way to combat sulfidation is to develop a protective oxide layer using adequate amounts of chromium and/or aluminum. High-temperature alloys should contain at least 20 % chromium to form a continuous chromium oxide scale to prevent sulfur from getting into the metal. High nickel-containing alloys are often not suitable for use in reducing sulfur-containing environments. Depending upon the relative partial pressures of sulfur and oxygen, nickel-containing alloys can be used in oxidizing environments containing small amounts of sulfur. INCONCLAD® alloy 800H/671 has been used in coal ash corrosion involving coals containing appreciable amounts

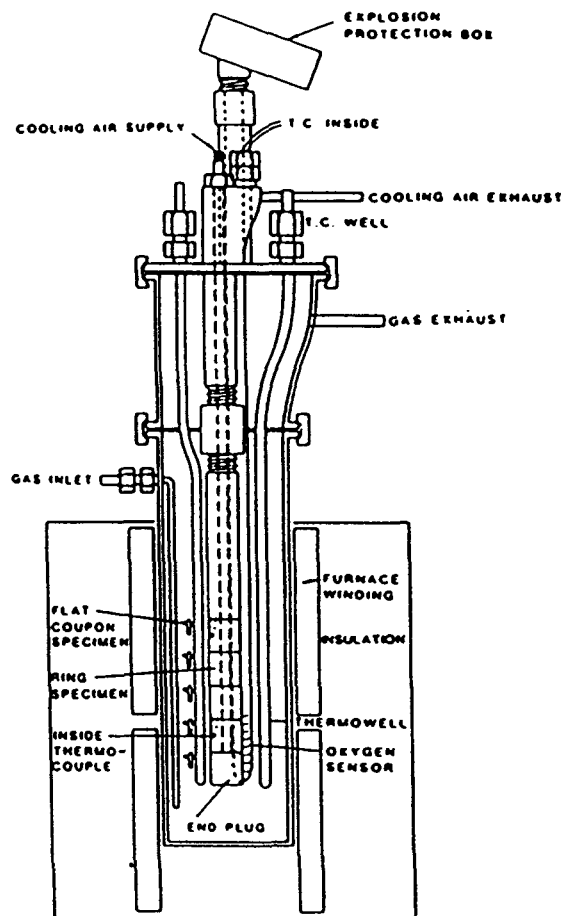


FIG. 7—A schematic of the corrosion setup developed by Argonne National Lab to study the corrosion rates of alloys in cooled and uncooled condition at selected partial pressures of oxygen and sulfur.

of sulfur. Alloy 309 SS (UNS S30900), alloy 310 SS (S31000) and INCOLOY® alloy MA 956 (S67956) can be effectively used in reducing environments containing sulfur.

## HALOGENIZATION

High-temperature, halogen-containing environments are potentially extremely aggressive. The reaction products of halogen gases can be liquid or can possess a high vapor pressure, depending on the reactions and temperature. In either case, degradation of most metals and alloys can be rapid. Table 1 lists 14 metal chlorides, their melting and boiling points, and the temperature for  $10^{-4}$  atmosphere vapor pressure [42].

### Laboratory Testing

Laboratory testing environments are divided into two groups, those halogen environments possessing no measurable oxygen and those environments containing both halogens and oxygen. In the oxygen-free environments, liquid phases and volatile reaction products may lead to erratic corrosion attack. Halogen plus oxygen environments exhibit parabolic behavior as oxide scale and volatile halide reactions occur simultaneously.

Halogen testing is properly conducted in electrically heated furnaces using ceramic tubes with end caps containing pusher rods to manipulate the corrosion specimens under atmosphere. The end caps should be protected with a corrosion-resistant sealing gasket. Gas compositions may be either purchased or synthesized from the components using halogen-resistant electronic flow controllers and mixers. Polyethylene is recommended for the tubing and cordierite is ideally suited for the specimen holder. The specimens are in the form of pins with dimensions similar to those mentioned for sulfidation tests. Gas flow streams of a total flow rate of  $500 \text{ cm}^3/\text{min}$  ( $30.5 \text{ in.}^3/\text{min}$ ) are considered adequate to assure a consistent environment for all specimens. The effluent stream should be reacted with a caustic solution before venting to remove the reacted and unreacted halogens. At the completion of testing, the specimens should be examined metallographically for evidence of voiding or liquid phase corrosion. Scale identification by X-ray

diffraction or SEM-EDX can be helpful in clarifying reaction mechanisms.

Two representative laboratory test programs are those depicted by Brown et al. who conducted short-term studies in chlorine on various temperatures [43,44]. Tyreman and Elliott have described a laboratory procedure for testing in fluorine as has Jackson [45,46].

Laboratory screening of alloys and weld overlay compositions has become increasingly important as efforts to utilize waste incinerators for disposal of waste gains momentum. One such procedure is described in a paper by Baker et al. [47]. Testing was performed in a sealed electrically heated muffle furnace having a 100 mm (3.94 in.) diameter mullite tube. To form the test gas mixtures,  $\text{O}_2$  and  $\text{N}_2$  were passed through a constant temperature water bath before the addition of  $\text{CO}_2$ . The  $\text{SO}_2$  and  $\text{HCl}$  test gases, pre-mixed with  $\text{N}_2$ , were then added to the gas stream. All flow rates were measured using electronic mass flow controllers. The flow of the gas mixtures was  $250 \text{ cc/min}$  ( $15.3 \text{ in.}^3/\text{min}$ ). The test gases flowed through a nickel oxide catalyst before reaching the samples to ensure gas equilibrium. The resultant gas mixture was composed of  $\text{N}_2$ -10 %  $\text{O}_2$ -20 %  $\text{H}_2\text{O}$ -1500ppm  $\text{HCl}$ -300ppm  $\text{SO}_2$ .

Samples were exposed in the flowing gas with and without the application of one of two chloride slurries. The slurries were prepared by first grinding the chloride salts into a fine powder in a mortar and pestle and then mixed with acetone and applied to the specimens with a soft bristle brush. Mass gain resulting from application of the coating averaged  $40 \text{ mg/cm}^2$ . Samples painted with the slurry were cycled at one-week intervals during which loose scale was lightly removed mechanically and the slurry re-applied. The composition of the two salt mixtures were (a) 20 %  $\text{ZnCl}_2$ -40.9 %  $\text{PbCl}_2$ -21.9 %  $\text{KCl}$ -17.2 %  $\text{NaCl}$  by weight and (b) 4.7 %  $\text{ZnCl}_2$ -0.7 %  $\text{PbCl}_2$ -2.0 %  $\text{KCl}$ -2.60 %  $\text{NaCl}$ -6.1 %  $\text{K}_2\text{SO}_4$ -4.9 %  $\text{Na}_2\text{SO}_4$  (equimolar amounts of each salt) -70 %  $\text{Al}_2\text{O}_3$  by weight. Testing was conducted at  $650^\circ\text{C}$  ( $1202^\circ\text{F}$ ) for 336 h with and without the application of the first salt mixture and at  $550^\circ\text{C}$  ( $1022^\circ\text{F}$ ) for 336 h with the application of each salt mixture. Corrosion performance of each candidate alloy was sectioned and evaluated metallographically after each test. Additionally, mass change results were obtained when salt mixture (a) was not used during one of the test cycles.

Spiegel and Warnecke employed a crucible test using a salt mixture of 46 %  $\text{KCl}$ -46 %  $\text{ZnCl}_2$ -8 %  $\text{PbCl}_2$  which was molten at  $350^\circ\text{C}$  ( $662^\circ\text{F}$ ) to test their thermal spray coated specimens [48]. The furnace atmosphere was controlled by a gas metering system in which  $\text{N}_2$ -5 %  $\text{O}_2$  was added as a pre-mix and  $\text{HCl}$  added by passing a portion of the gas flow through a saturator of azeotropic  $\text{HCl}$  solution placed in a thermostat.  $\text{SO}_2$  was added from a pre-mix of  $\text{N}_2$ -5 %  $\text{O}_2$ -1 %  $\text{SO}_2$ . This gas was dried by passing through columns filled with  $\text{Pb}_2\text{O}_5$  and mixed before entering the furnace. Each test was conducted for 360 h.

### Field Testing

An excellent example of field testing in conjunction with laboratory testing to solve a heat exchanger corrosion problem in an industrial chlorinated solvent incinerator is described in Ref 49. A corrosion rack containing three

TABLE 1—High-temperature properties of 14 chlorides.

Chlorides	Melting Point	Temperature $^\circ\text{C}$ at $10^{-4}$ atm	Boiling Point
$\text{FeCl}_2$	676	536	1026
$\text{FeCl}_3$	303	167	319
$\text{NiCl}_2$	1030	607	987
$\text{CoCl}_2$	740	587	1025
$\text{CrCl}_2$	820	741	1300
$\text{CrCl}_3$	1150	611	945
$\text{CrO}_2\text{Cl}_2$	-95	—	117
$\text{MoCl}_3$	195	58	268
$\text{WCl}_5$	240	72	—
$\text{WCl}_6$	280	11	337
$\text{TiCl}_2$	1025	921	—
$\text{TiCl}_3$	730	454	750
$\text{TiCl}_4$	-23	-38	137
$\text{AlCl}_3$	193	76	—

stainless steels, two high-nickel austenitic alloys and three nickel-base alloys was placed within the hot gas stream of a heat exchanger containing HCl and chlorine. The in-situ test results were correlated with laboratory tests of the same alloys for this application.

Waste incinerator effluent streams contain halogen compounds arising principally from the burning of plastics and organic matter. A ten-year study of candidate alloy boiler tubes in several field test sites is described in Ref 50. Again, these field results were confirmed by simulated laboratory tests. Metallography and scanning electron microscopy (SEM) were used to define the corrosion modes of this mixed oxidant environment. Ultrasonic thickness measuring equipment was used to follow tube corrosion/erosion rates at the field sites. Tubes were periodically removed from service for laboratory evaluation. Use of test racks to evaluate the performance of candidate materials for municipal incinerator hardware is discussed in Ref 51. Test racks have proven to be a valuable source of performance information for waste incinerator environments [52].

### Materials

Nickel and nickel-base alloys have consistently been proven to be the most resistant materials to halogen- and halide compound-containing environments. An extensive summary of alloy performance data in these environments is presented in Refs 53 and 54.

## CORROSION SAMPLE ANALYSIS

### Analysis of Corrosion Products

Corrosion products should be examined for both composition and morphology. Compositional analysis can be wet chemical analysis, X-ray diffraction, high and low energy electron diffraction, X-ray fluorescence, electron probe microanalysis, or mass spectrometry. Morphology can be determined using light microscopy, hardness measurements, transmission electron microscopy, SEM, field ion microscopy, plus other techniques. For details on these methods, the reader may refer to basic texts and pertinent review articles, such as Ref 3.

SEM is excellent for observing scale features providing photographs and permitting simultaneous chemical analysis of surface features. Along with scale composition, the phases present in the scale should be determined by X-ray diffraction or other methods. Care should be taken to assure the sample is taken from a representative area. Care must also be taken during metallographic preparation to avoid spalling of the scale during cutting, mounting, or polishing. Mounting in liquid epoxy resin or nickel or copper plating the surface aids significantly in preserving original structure. For subsequent metallographic analysis, it is important to ensure that the sample is mounted perpendicular to the cut surface. Due to the friable nature of oxide scales, it is recommended that more time than normal is spent on each successive abrasive paper in order to remove any damage to the scale caused by each grade of abrasive paper. If chemical analysis is to be done by SEM or other methods

and the scale is water soluble (as in halogen corrosion), it is best to avoid water during cutting and polishing. In such cases, use of non-aqueous lubricants, such as kerosene is recommended for polishing. The mount should be examined in the unetched condition to properly assess the true depth of penetration. Etching can result in voiding due to galvanic pitting of the substrate near the surface where alloy depletion has occurred. Care must also be taken to remove any etchant absorbed by porous scale since the etchant may subsequently ooze from the scale and stain the substrate. Techniques for analysis of the metallographic sample are described below.

### Metallographic Analysis

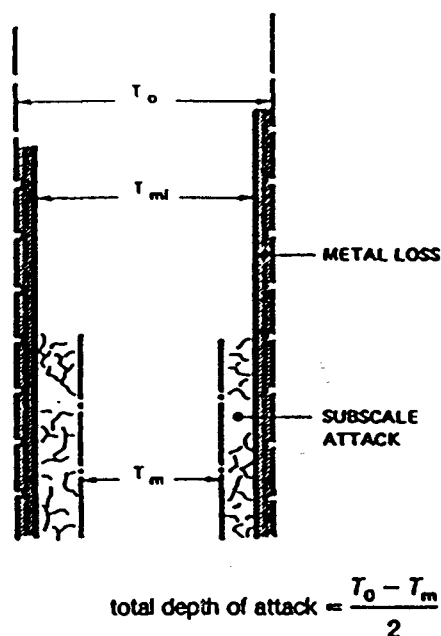
Metal loss is defined as one half the difference between the original thickness and the remaining thickness after exposure. This thickness extends to just beneath the scale/substrate surface and excludes the thickness of internal attack. This is schematically shown in Fig. 8, as depicted in ASTM G 54, Practice for Simple Static Oxidation Testing. Thus metal loss is defined as:

$$\text{Metal Loss} = \frac{T_o - T_{mi}}{2} \quad (10)$$

where:

$T_o$  = original thickness or diameter, mm

$T_{mi}$  = as-exposed sample thickness or diameter, mm.



where:

$T_o$  = original coupon thickness,

$T_{mi}$  = as-exposed coupon thickness, and

$T_m$  = remaining good metal.

FIG. 8—Schematic showing thickness measurements.

Metal loss may be assumed to be that position of the substrate lost to scale formation and no longer capable of fully participating in bearing a load over time.

Depth of attack describes the formation of voids or internal precipitates. This is sometimes referred to as depth of penetration or in the case of oxidation as internal oxidation. This attack can occur when an alloy constituent is lost to the scale or to the high-temperature gaseous environment. Voids are generally associated with grain boundaries as they are the path of fast diffusion of the alloying element being lost. Alloying elements of high vapor pressure or which form volatile species with the gaseous environment are especially prone to cause voids. Conversely, internal precipitates form if the gas pressure is below the dissociation pressure of the precipitate. When a gaseous species diffuses into a substrate it will form the most stable compounds possible. These are usually the precipitates of the most reactive components of the alloy. Internal precipitates can form only if the reactive element diffuses outward more slowly than the gaseous component diffuses inward; otherwise, only surface scale will form. From Fig. 8, depth of attack is described as:

$$\text{Depth of Attack} = \frac{T_o - T_m}{2} \quad (11)$$

where:

$T_m$  = remaining round metal, mm.

It may be necessary to quantify the extent of attack (voids or precipitation) as a function of depth beneath the surface. It is likely that the extent of voids will decrease with depth. Generally, the extent of precipitation is relatively uniform to a given depth and then tapers off rapidly. In making metal loss and depth of attack measurements, it is recommended that at least three measurements across the thickness of the metallographic section be averaged. Measurements should be made to the nearest 0.0025 mm (0.0001 in.).

### Structural Changes

Structural changes in the substrate can result due to alloy depletion and thermal effects on the stability of the alloy. An example of a typical alloy depletion effect is the dissolution and thermal effects on the stability of the alloy. An example of a typical alloy depletion effect is the dissolution of carbides near the substrate surface due to the loss of carbon and carbide-forming elements resulting from high temperature exposure. A common thermal effect is the precipitation of topologically close packed phases such as Mu, Sigma, etc., over time within certain high-temperature ranges. SEM X-ray diffraction of extracts and other methods can be used to confirm these structural changes.

### Mass Change Analysis

Mass change measurements are made by calculating the weight change per unit area, usually as a function of time, temperature, and pressure. Mass change is typically calculated as follows:

$$\text{Mass Change} = \frac{W_f - W_o}{A} \quad (12)$$

where:

$W_f$  = final weight, g,

$W_o$  = original weight, g,

$A$  = original area, cm<sup>2</sup>.

A plus or a minus sign indicates a net gain or loss, respectively. Report whether the sample has been descaled or not descaled. If mass change data are collected as a function of time, it is customary to not descale the sample until the exposure is complete, although the loose scale may be gently dislodged by tapping the sample against a clean solid surface. Descaling can be difficult for a tightly adhering scale or a deep oxide substructure. If descaling is felt to be necessary, ASTM G 1, Practice for Preparing, Cleaning, and Evaluating Corrosion Test Specimens should be consulted for typical electrolytic and chemical techniques. Gentle grit blasting is another alternative for removing adherent scale. Specimen weighing should be to the nearest 0.1 mg.

Carburizing atmospheres result in considerable internal attack and ASTM G 79, Practice for Evaluation of Metals Exposed to Carburization Environments describes the four methods of evaluating samples exposed to these environments. Besides total mass gain and metallographic evaluation, ASTM G 79 describes techniques for measuring carbon diffusion profiles and changes in mechanical properties. Additionally, ASTM E 10, Test Method for Brinell Hardness of Metallic Materials, is applicable for measuring hardness profiles due to carbon absorption.

As a final precaution, whatever the test atmosphere, single data points and single analytical measurements can be potentially highly misleading. Corrosion rates and modes vary with time. Data as a function of extended time are vital to define true performance in engineering applications. Because of the multiplicity of corrosion modes that can occur simultaneously in many environments, it is important to use as many analytical techniques as practical to fully understand all factors affecting performance.

### SERVICE TEST STANDARDS

High-temperature service test standards have been prepared by ASTM. No other technical organization has as yet published any standards pertaining to high-temperature corrosion service.

#### ASTM G 54, Practice for Simple Static Oxidation Testing

This service test practice covers determination of preliminary information on the relative growth, scaling, and microstructural characteristics of an oxide on the surface of a pure metal or alloy under isothermal conditions in still air.

#### ASTM B 76, Method for Accelerated Life Test of Nickel-Chromium and Nickel-Chromium-Iron Alloys for Electrical Heating

This service test method covers the determination of the resistance to oxidation of nickel-chromium-iron electrical

heating alloys at elevated temperatures under intermittent heating. Procedures for a constant temperature test are provided. The test method is used for comparative purposes only.

### ASTM B 78, Method for Accelerated Life Test of Iron-Chromium-Aluminum Alloys for Electrical Heating

This service test method covers the determination of the resistance to oxidation of iron-chromium-aluminum alloys for electrical heating alloys at elevated temperatures under intermittent heating using a constant temperature cycle test. This test is used for comparative purposes only.

### ASTM G 79, Practice for Evaluation of Metals Exposed to Carburization Environments

This service test method covers procedures for the identification and measurement of the extent of carburization in a metal sample and for the interpretation and evaluation of the effects of carburization. It applies mainly to iron- and nickel-based alloys for high-temperature applications. Four methods are described:

- Method A, Total Mass Gain.
- Method B, Metallographic Evaluation.
- Method C, Carbon Diffusion Profile.
- Method D, Change in Mechanical Properties.

These methods are intended, within the limitations as noted, to evaluate either laboratory or field samples that have been exposed in carburizing environments.

## REFERENCES

- [1] Kane, R. H. and Goodell, P. D., "Gas Analysis Techniques for High Temperature Corrosion Testing," *Journal of Testing and Evaluation*, November 1982, pp. 286-291.
- [2] Makavos, E. B. and Liu, C. C., "A Method for Creating Predictable Conditions in High Temperature Reactive Gases," *High Temperature Materials and Processes*, Vol. 10, No. 2, 1992, pp. 127-136.
- [3] Sdcharfstein, L. R. and Henthorne, M., "Testing at High Temperatures," *Handbook on Corrosion Testing and Evaluation*, W. H. Ailor, Ed., John Wiley and Sons, Inc., NY, 1971, pp. 291-366.
- [4] Lai, G. Y., "Nitridation," *High Temperature Corrosion of Engineering Alloys*, ASM International, Materials Park, OH, 1990, pp. 73-84.
- [5] Evans, U. R., *The Corrosion and Oxidation of Metals*, Edward Arnold, London, England, 1960.
- [6] Lai, G. Y., *High Temperature Corrosion of Engineering Alloys*, ASM International, Materials Park, OH, 1990.
- [7] Birks, N. and Meir, G. H., *Introduction to High Temperature Oxidation of Metals*, Edward Arnold, London, England, 1983.
- [8] Pilling, N. B. and Bedworth, R. E., "The Oxidation of Metals at High Temperature," *Journal of the Institute of Metals*, Vol. 29, 1923, pp. 529-582.
- [9] Wagner, C., "Types of Reaction in the Oxidation of Alloys," *Zeitschrift für Elektrochemie*, Vol. 63, 1959, pp. 772-782.
- [10] Bradford, S. A., "Fundamentals of Corrosion in Gases," *Metals Handbook, Ninth Ed.*, Vol. 13, Corrosion, ASM International, Metals Park, OH, 1987, pp. 61-76.
- [11] Haycock, E. W., "Transitions from Parabolic to Linear Kinetics in Scaling of Metals," *Journal of the Electrochemical Society*, Vol. 106, 1959, pp. 771-775.
- [12] Perkins, R. A., Coons, W. C., and Radd, F. J., *Properties of High Temperature Alloys*, Proceedings of the 1976 Fall Meeting of the Electrochemical Society, The Electrochemical Society, Pennington, NJ.
- [13] Prange, F. A., *Corrosion*, Vol. 15, No. 12, December 1959, p. 619.
- [14] *Metals Handbook*, 8th ed., Vol. 2, Heat Treating, Cleaning and Finishing, ASM International, Metals Park, OH, 1964, p. 93.
- [15] Moeller, G. E. and Warren, C. W., "Survey of Tube Experience in Ethylene and Olefins Pyrolysis Furnaces," Paper 237, presented at Corrosion/81, National Association of Corrosion Engineers, Houston, TX.
- [16] Besmann, T. M., "SOLGASMIX-PV, A Computer Program to Calculate Equilibrium Relationships in Complex Chemical Systems," ORNL/TM-5775, Oak Ridge National Laboratory, Oak Ridge, TN, April 1977.
- [17] Bresselers, C., Gavision, R., Harrison, J., et al., Report EUR 6203EN, Joint Research Center, Petten Establishment, The Netherlands, 1978.
- [18] Sundman, B., *User Aspects of Phase Diagrams*, F. M. Hayes, Ed., Institute of Metals, London, 1991, p. 130.
- [19] Eriksson, G. and Hack, K., *Metallurgical Transactions B*, Vol. 21B, 1990, p. 1013.
- [20] Thompson, W. T., Eriksson, G., Pelton, A. D., and Bale, C. W., *Proceedings of the Metallurgical Society*, Vol. 11, 1987, p. 87.
- [21] Barry, T. I., Dinsdale, A. T., Davies, R. H., Gisby, J., Pugh, N. J., Hodson, S. M., et al., *MTDATA Handbook: Documentation for the NPL Metallurgical and Thermochemical Databank*, National Physics Laboratory, Teddington, U.K., 1987.
- [22] Brinkley, S. R., Jr., *Journal Chemistry and Physics*, Vol. 14, No. 9, 1946, p. 563.
- [23] Kane, R. H., "Characterization of High Temperature Gaseous Environments," *Corrosion*, Vol. 36, No. 3, March 1980, pp. 112-118.
- [24] Hemmings, P. L. and Perkins, R. A., "Thermodynamic Phase Stability Diagrams for the Analysis of Corrosion Reactions in Coal Gasification/Combustion Atmospheres," EPRI FP-539, Project 716-1, Electric Power Research Institute, Palo Alto, CA, 1977.
- [25] Lai, G. Y., "Sulfidation," *High Temperature Corrosion of Engineering Alloys*, ASM International, Materials Park, OH, 1990, pp. 117-144.
- [26] Gibbs, G. B., *Oxidation of Metals*, Vol. 3, 1973, pp. 173-184.
- [27] Lai, G. Y., "Carburization and Metal Dusting," *High Temperature Corrosion of Engineering Alloys*, ASM International, Materials Park, OH, 1990, pp. 47-72.
- [28] Mason, J. F., Moran, J. J., and Skinner, E. N., *Corrosion*, Vol. 16, 1960, p. 593.
- [29] Steel, C. and Engel, W., *AFS International Cast Metals Journal*, September 1981, p. 28.
- [30] Norton, J. F. and Barnes, J., *Corrosion in Fossil Fuel Systems*, I. G. Wright, Ed., The Electrochemical Society, Pennington, NJ, 1983, p. 277.
- [31] Kane, R. H. and Hosier, J. C., "Carburization Resistance of Some Wrought Nickel-Containing Alloys in Simulated Industrial Environments," Inco Alloys International Technical Report, 1985.
- [32] Gutzeit, J., "High Temperature Sulfidic Corrosion of Steels," *Process Industries Corrosion*, pp. 367-372.
- [33] McConomy, H. F., "High Temperature Sulfidic Corrosion in Hydrogen-Free Environment," *Proceedings API*, Vol. 43 (III), 1963, pp. 78-96.
- [34] Cooper, A. S. and Gormen, J. W., "Computer Correlations to Estimate High Temperature H<sub>2</sub>S Corrosion in Refinery Streams," *Materials Protection and Performance*, Vol. 10, No. 1, 1971, pp. 31-37.

- [35] Ganesan, P. and Smith, G. D., *Journal of Materials Engineering*, Vol. 9, No. 4, 1988, pp. 337–343.
- [36] Steinments, P., Duret, C., and Morbioli, R., *Materials Science and Technology*, Vol. 2, 1986, pp. 262–271.
- [37] Natesan, K., “Corrosion and Mechanical Behavior of Materials for Coal Gasification Applications,” Argonne National Laboratory, Report ANL-80-5, May 1980.
- [38] Shigeta, J., Hamao, Y., Aoki, H., and Kajigaya, I., *Journal of Engineering Materials Technology*, Vol. 109, October 1987, pp. 299–305.
- [39] Judkins, R. R. and Bradley, R. A., presented at ASM Materials Week ‘87, 15 October 1987.
- [40] Minchener, A. J., Lloyd, D. M., and Sutcliffe, P. T., EPRI Report CS-1853, May 1981.
- [41] Rocazella, M. A., Wright, I. G., and Holt, C. F., “The Corrosive Environment in the Fluidized-Bed Heat Exchanger for CCGT Service,” ASME Paper 83-GT-249, ASME International, NY, 1983.
- [42] Lai, G. Y., “High-Temperature Corrosion: Issues in Alloy Selection,” *Journal of Metals*, November 1991, pp. 54–60.
- [43] Brown, M. H., DeLong, W. B., and Auld, J. R., *Industrial and Engineering Chemistry*, Vol. 39, No. 7, 1947, p. 839.
- [44] Downey, B. J., Bermel, J. C., and Zimmer, P. J., *Corrosion*, Vol. 25, No. 12, 1969, p. 502.
- [45] Tyreman, C. J. and Elliott, P., Paper No. 135, Corrosion ‘88, NACE, Houston, TX.
- [46] Jackson, R. B., “Corrosion of Metals and Alloys by Fluorine,” NP-8845, Allied Chemical Corp, Morristown, NJ, 1960.
- [47] Baker, B. A., Smith, G. D., and Shoemaker, L. E., “Performance of Commercial Alloys in Simulated Waste Incineration Environments,” Paper No. 01183, CORROSION2001, NACE, Houston, TX.
- [48] Spiegel, M. and Warnecke, R., “Performance of Thermal Spray Coatings Under Waste Incineration Conditions,” Paper No. 01182, CORROSION2001, NACE, Houston, TX.
- [49] Baker, B. A., “Heat Exchanger Corrosion in a Chlorinated Solvent Incinerator,” *Handbook of Case Histories in Failure Analysis*, ASM International, Materials Park, OH, 1992, pp. 118–123.
- [50] Harris, J. A., Lipscomb, W. G., and Smith, G. D., “Field Experience of High Nickel Containing Alloys in Waste Incinerators,” Paper No. 402, Corrosion ‘87, NACE, Houston, TX.
- [51] Smith, G. D. and Tassen, C. S., “Performance of Alloys 825 and 625 in Waste Incinerator Environments,” *Materials Performance*, Vol. 28, No. 12, December 1989, pp. 41–43.
- [52] Materials Performance in Waste Incineration Systems, G. Y. Lai and G. Sorrell, Eds., NACE, Houston, TX, 1992.
- [53] Lai, G. Y., “Corrosion by Halogen,” *High Temperature Corrosion of Engineering Alloys*, ASM International, Metals Park, OH, 1990, pp. 85–115.
- [54] Agarwal, D. C. and Grossmann, G. K., “Case Histories on the Use of Nickel Alloys in Municipal and Hazardous Waste Fueled Facilities,” Paper No. 01177, CORROSION2001, NACE Houston, TX.

# Organic Liquids

*C. S. Brossia<sup>1</sup> and D. A. Shifler<sup>2</sup>*

## DESCRIPTION OF ENVIRONMENT

### Overview

ORGANIC LIQUIDS ARE USED in a wide variety of industrial applications. They can be characterized as liquids that consist of one or more carbon atoms joined to other atoms via covalent bonds. Common atoms included in organic molecules are hydrogen, oxygen, nitrogen, sulfur, and halogens. Both the rate and yield of certain reactions have been found to greatly increase when performed in organic liquids. Thus, they are widely used in the chemical process industry for synthesis. With the increase in the use of organic liquids, increases in observed corrosion problems associated with the exposure of materials to them have also occurred. In some cases, failures involve an unacceptably large loss of metal or degradation of material properties. However, in many other cases, the major issue is discoloration or degradation of the organic solution resulting from corrosion of the processing vessel, as the solution is the product of commercial interest. For example, many pharmaceuticals are synthesized in organic solutions in large vessels. For these applications, the corrosion resistance requirements for materials used are stringent. The introduction of metals into a product can lead to rapid degradation of the product, as well as health and safety concerns.

While corrosion in pure organic liquids can occur, many corrosion problems in organic liquids involve solutions with multiple components. For example, a solution containing ethanol, water, oxygen, and hydrogen chloride (HCl) contains four components. Some of the components may be present at small concentrations, but have dramatic effects. This is often the case with water due to its low molecular mass compared to many organic liquids. Small mass percentages of water can represent significant concentrations in moles/L. For example, 100 ppm water in acetonitrile results in a water concentration of over 4 mM.

Organic liquids are classified in a variety of ways. A common classification scheme is based on the nature of the bonding between molecules during solvation. Three general categories exist: protic liquids, nonpolar aprotic liquids, and dipolar aprotic liquids. Protic liquids (e.g., alcohols, carboxylic acids, amines, amides) are those that can provide protons to

other molecules. Solvation in protic organic solvents occurs through dipole-dipole interaction, ion-dipole interaction, and hydrogen bonding. These are generally miscible with water (another protic liquid) and can solvate both organic and inorganic acids. Nonpolar, aprotic liquid molecules (e.g., aromatic and aliphatic hydrocarbons) interact through weak van der Waals bonds and have little solvating ability. The protons in these liquids do not dissociate to any measurable extent. Dipolar, aprotic liquid molecules (e.g., acetonitrile, aldehydes, esters, ethers, dimethyl sulfoxide, tetrahydrofuran, dimethylformamide) interact via ion-dipole and dipole-dipole forces and usually strongly solvate cations and tend to be poor acceptors of electrons and poorly solvate anions in solution.

Organic solvents may also have functional groups that are either hydrophobic, which repel water molecules, or hydrophilic, where the functional groups readily react with water. It has been shown that the predominant interaction of a metal with an organic adsorbate is through its functional groups [1].

The wide variety of organic liquids leads to complexity in the analysis of corrosion problems. In addition, the large number of different liquids leads to difficulties due to the limited physical and chemical data on specific liquids. This has ramifications both for the recording of corrosion data, and for the development of a broad-based understanding of the important corrosion processes. The lack of physical and chemical information is a limiting factor in any broad description of behavior, such as found in this chapter. Also, while many testing considerations can be generalized for organic liquids, the corrosion behavior of materials in nonaqueous solvents is not nearly as well understood as in aqueous solutions.

### Types of Corrosion

The types of corrosion (i.e., the morphology of attack and the oxidation process) that can be encountered in organic liquids are the same as those observed in aqueous solutions. The solution chemistry and solution electrochemistry may be different, but the types of fundamental corrosion processes that occur remain the same. An excellent review of examples of corrosion in various organic solutions can be found in the work of Heitz [2]. In addition to a review of the fundamental principles involved, Heitz critically evaluates the literature published before 1973 and describes a number of industrial case histories of component failures due to

<sup>1</sup>Manager, Environmental Performance of Materials Section, Southwest Research Institute, San Antonio, TX 78238.

<sup>2</sup>Materials engineer, Marine Corrosion Branch, Naval Surface Warfare Center, West Bethesda, MD 20817.





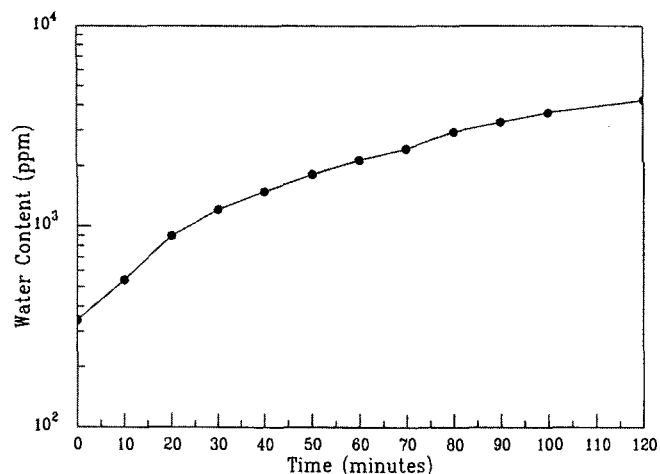


FIG. 2—Increase in water content in methanol due to absorption from ambient atmosphere [7].

pure, dramatic differences in corrosion rate due to small water additions are observed. This can also be true for other impurities that are often present in organic liquids. Thus, the measurement and control of water levels can be a key aspect to corrosion testing in organic liquids.

A popular technique to measure water content is the Karl Fischer Titration method [6]. This method can reliably analyze water contents as low as 100 ppm (0.01 mass %). Aliquots of solution can be taken before, during, and after an experiment to follow any changes in water content. Such changes can occur due to the tendency of some organics to absorb water from the ambient atmosphere. For example, it has been found that the water content of a 100 mL sample of methanol, exposed to laboratory air at 25°C with a relative humidity of approximately 55 %, increased from 0.035 mass % to 0.42 mass % in 2 h, as shown in Fig. 2 [7]. This illustrates the need for incorporating a sealed experimental cell or a dry glove box when working at low water levels. By using one or both of these, water absorption can be minimized and water levels of 100 ppm and below can be realized in the pure liquid. Care must be taken when adding other components to the anhydrous liquid, as most salts as well as electrodes can add appreciable amounts of water to the solution, which is then very difficult to remove. Also, extremely dry solutions can sometimes pose a safety hazard if suddenly exposed to air or water.

Organic liquids encompass an extremely wide variety of compounds. However, they can be classified into two main categories: aprotic (which are generally water insoluble) and protic (which are generally water soluble). Many solution properties, such as solvating power, depend on the primary functional groups of the organic liquid. Thus, the protic nature of a given organic liquid will determine the solubility of various impurities and corrosion products. Even within a type of organic liquid, important differences emerge among individual liquids. For example, the corrosion rate of iron decreases in monocarboxylic acids as the chain length increases (Fig. 3) [2]. These differences among similar organic liquids add another layer of complexity to the corrosion phenomena as compared to aqueous solution.

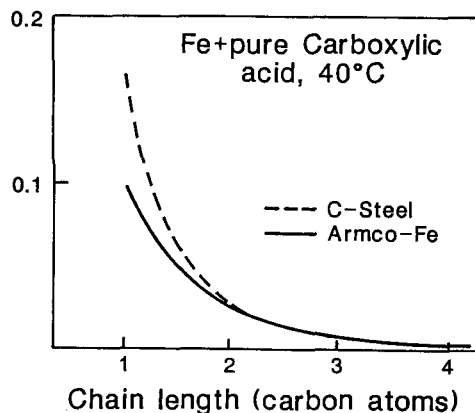


FIG. 3—Corrosion rate (mm/yr) of iron in mono-carboxylic acids of different chain lengths (formic acid, acetic acid, propionic acid, butyric acid) [2].

Related to liquid composition effects are cosolvent interactions. In many applications, a mixture of liquids (organic/organic, organic/inorganic) is of interest. Several aspects need to be considered when testing in such organic liquid mixtures, which are not considered in aqueous solutions. First, there exists the possibility that when two or more liquids are combined they are either immiscible or have limited miscibility. This results in the formation of multiple liquid phases (phase separation) where the properties of each phase could be significantly different from others. The net result is that testing in mixtures can be difficult. The difficulty arises in trying to determine which phase or composition is detrimental to material behavior and may also involve partitioning of dissolved species between the various phases present. The possibility also exists that it is not an individual phase, but rather the interface between two phases in solution that is deleterious. Multiphase solutions cause special problems, such as concentration of aggressive species into one phase (e.g., HCl into the aqueous phase of a HCl/water/dioxane mixture) [2], specific adsorption of one phase at the metal surface, and preferential attack at the phase boundary (akin to water line attack). Additional discussion of multiphase attack is outside the scope of this chapter, but can be found in Heitz's review [2].

One important manifestation of the large variety of organic liquids is the paucity of thermodynamic data. Thus, no equivalent to Pourbaix diagrams [8], used widely in aqueous solution, has been developed for any organic liquid. In fact, pH in organic liquids is not relevant in aprotic organic solvents, since there is no readily available hydrogen. However, in nonaqueous solutions, it is possible to generate more powerful proton donors than the hydronium ion found in aqueous solutions. The strength of extremely strong acids in nonaqueous solution is measured by the Hammett acidity function, which is defined for the reaction  $B + H^+ \rightleftharpoons BH^+$  [9]:

$$H_o = pK_{BH^+} - \log ([BH^+]/[B])$$

where B is the nonaqueous solvent. No standard metal/solution potential difference has been defined for all liquids. Some of the behavior in organic liquids can be explained by using the concept of Lewis acids and bases employed in

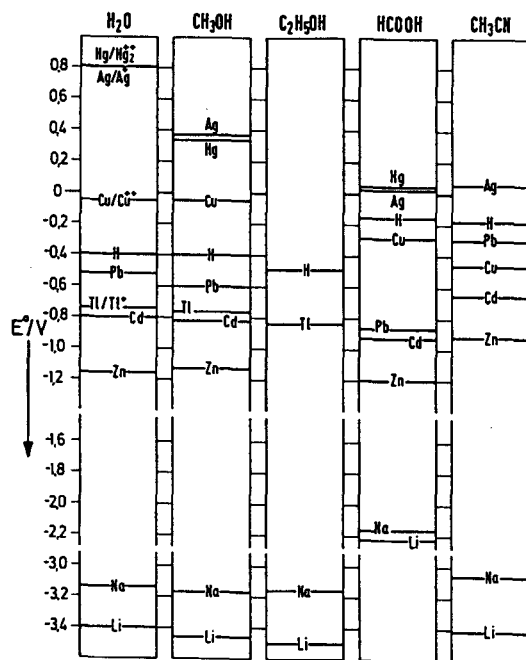
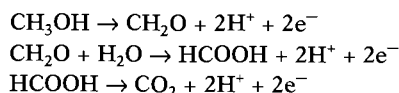


FIG. 4—Normal electrode potentials of metals in different liquids on the ferrocene/ferricinium<sup>+</sup> scale at 25°C [2].

the aqueous chemistry. A Lewis acid is an electron pair acceptor, while Lewis base is an electron pair donor. All the usual ligands can be considered Lewis bases and metal ions as Lewis acids.

In general, thermodynamic data in the literature pertaining to specific material/aqueous solution systems (e.g., Pourbaix diagrams) may not necessarily be valid for the same material in organic liquids. Some efforts have been made to develop electromotive series in different liquids, as shown in Fig. 4. The reference point is given by the ferrocene/ferricinium<sup>+</sup> couple. The selection of a reference electrode is discussed in a later section in this chapter. In general, the order of reversible potentials is maintained from aqueous solution, though the numerical values can change appreciably.

Finally, as is the case for water, organic liquids have a limited range of electrochemical stability. The products of these reactions are often also electroactive and can become involved in electrochemical or chemical reactions of interest. While solution oxidation or reduction can also occur in aqueous solutions, the products are simple bases or acids (i.e., H<sup>+</sup> and OH<sup>-</sup>). However, the products resulting from electroactive liquids are usually a mixture of complex organic acids. These complex organic acids can combine with other ions in solution and form other chemicals that could be even more aggressive than the acid from which they were derived. This has been shown to be an issue in methanol by Smialowska [10], who found that galvanostatic polarization of stainless steel in pure methanol resulted in the formation of formic acid as follows:



The observed oxidation current was a mixture of metal dissolution and methanol oxidation, complicating comparisons

of material loss and charge passed based upon Faraday's Second Law.

## IMPORTANT ENVIRONMENTAL VARIABLES

The environmental variables that influence corrosion testing in organic liquids include metal, alloy or nonmetallic material in contact with the organic solution, solution conductivity, solution acidity, water content of the solution, presence and stability of oxide or other pre-existing films, type and concentration of surface contaminants or inclusions, functional group and concentration of organic solvent, solvent oxidation or reduction products, type and concentration of supporting electrolyte, applied potential, possible mechanistic paths for passivation, and temperature. As in all corrosion testing, matching the test environment to the actual service environment is critical for obtaining useful information. In addition, by studying the effects of these variables on the corrosion processes, better insights into the controlling mechanisms, as well as the sensitivity of the corrosion processes to changes in the service environment, can be gained.

As mentioned above, the high resistances often associated with organic solutions can distort electrochemical measurements. To minimize these ohmic losses, supporting electrolytes are often used. Ideally, supporting electrolytes dissociate and increase the solution conductivity without altering the corrosion process under study. A commonly used electrolyte is lithium perchlorate (LiClO<sub>4</sub>) in concentrations ranging from 10<sup>-2</sup> to 5 × 10<sup>-1</sup> mol/L. The perchlorate anion is thought to be inert in most solutions, and very weakly adsorbing to surfaces. Thus, LiClO<sub>4</sub> is not expected to affect the electrochemical reactions considered in most organic liquids. The addition of 0.1 M lithium perchlorate as a supporting electrolyte to methanol can increase the conductivity from 10<sup>-6</sup> S/cm [4] to 6 × 10<sup>-3</sup> S/cm, thereby reducing the ohmic resistance by a factor of 200. This reduction allows the experimenter to more easily compensate for the ohmic drop. For fundamental studies of corrosion in organic liquids, the addition of a well-chosen supporting electrolyte is a reasonable approach to allow electrochemical information to be gathered. For more applied measurements, the addition should be carefully considered and comparison tests (e.g., coupon exposures) should be performed to verify the absence of an effect of the supporting electrolyte on the corrosion process. If a supporting electrolyte is not added, caution must be used in the gathering and interpretation of electrochemical data. In some cases, where a supporting electrolyte cannot be added and the solution resistance is very high, the performance of meaningful electrochemical measurements is extremely difficult.

Acids have often been used as supporting electrolytes [4]. Strong acids (e.g., H<sub>2</sub>SO<sub>4</sub>, HCl, HNO<sub>3</sub>) generally enhance the conductivity of organic solutions greatly. However, some organics are susceptible to degradation in acids. When water is present, acid hydrolysis becomes an additional degradation pathway [11]. Also, the acidity of the solution can have a controlling effect on the corrosion behavior of metals in organic solutions. For example, a recent review [3] of the

literature on the corrosion of metals in aprotic liquids has shown that corrosion behavior, and more specifically, the mechanisms of passivity, are affected by the acidity of the solution. The mechanisms of passivation were classified into four types: (1) air-formed film, (2) salt film, (3) chemisorption of the liquid, and (4) oxide/oxyhydroxide formation. Acidity is deleterious to all four passivation mechanisms in organic solutions. Hence, control of acidity is important. In addition to  $H^+$ , acidity also implies the presence of a corresponding anion. Its presence can alter material behavior by adsorbing to the surface in addition to increasing the solution conductivity. Thus, acids should not be considered as supporting electrolytes, since they influence the behavior observed, unless the service environment contains acids, in which case they should be included in the test solution. An additional passivation mechanism has been proposed by Shifler et al. involving the formation of a passive electropolymerized film (polymer films in which the polymerization process is electrochemically activated) on bare steel surfaces in dimethoxyethane(DME)/LiAsF<sub>6</sub> solutions at potentials above the oxidation potential of DME [12]. The complex electropolymerization mechanism for carbon steel in dimethoxyethane/propylene carbonate mixtures with LiAsF<sub>6</sub> as the supporting electrolyte is dependent on: (1) DME concentration, (2) cationic intermediate adsorbed concentration and degree of coverage, (3) LiAsF<sub>6</sub> concentration, (4) applied potential, (5) rate of iron cation dissolution, and (6) water concentration. Decreases in any of these factors will either decrease the rate of electropolymerization or may prevent electropolymerization entirely [13]. Numerous other investigators have also examined the role of electropolymerized films as a means of metal passivation in dioxolane [14,15], ether [16–19], pyrrole [20,21], and carbazoles/dicarbazoles with polyether chain substitution [22], and phenol [23]. For clarification purposes, Table 2 contains the physical data for many solvents commonly encountered. Table 2 is not intended to be a complete list, but rather to provide the reader with a sense of the range of physical properties of organic solvents.

The supporting electrolyte may also play an integral role in passivation processes. In supporting electrolytes, increasing the size of the counter-ions may lead to a decreased film mobility and polyvalent ions, acting as stronger acids, may enhance the formation of cross-links between chains and electrolyzed films [24]. It has also been observed that AsF<sub>6</sub><sup>-</sup>, added as a supporting electrolyte, can be an integral component of the polymerization process on iron [19] and carbon steel [12] in DME; the use of either tetrabutylammonium

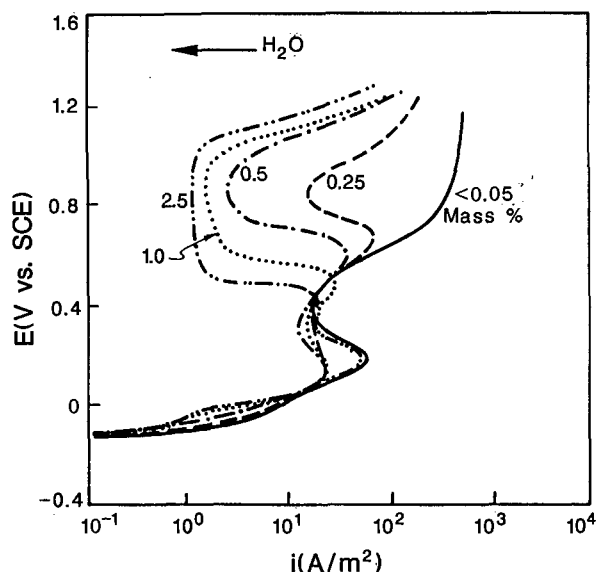


FIG. 5—The effect of water content on the anodic polarization behavior of nickel in methanol containing 1 M H<sub>2</sub>SO<sub>4</sub> [29].

perchlorate (TBAP) or lithium perchlorate as supporting electrolytes leads to alloy breakdown around the solvent oxidation potential [25]. The oxidation of aluminum was found to be influenced by the nature of the passivation mechanisms in nonaqueous solutions, which depended on the kind of electrolyte salt [26].

The water concentration in the experimental testing solution should duplicate as accurately as possible the water concentration found in the actual service solution. This is because the concentration of water present in the testing environment affects material behavior and the solvating ability of the solution. The presence of water in minimal concentrations (0.1–0.5 mass %) in acidified protic organic liquid solutions leads to the passivation of several materials. For example, iron, stainless steel, and nickel exhibit this behavior in methanol [27–29], as shown in Fig. 5. Water concentrations outside this range generally lead to increased corrosion rates [28,29]. In neutral aprotic organic solutions, water in any concentration, except in high concentrations (i.e., 80 + mass %), tends to be deleterious. For example, iron and nickel in neutral dimethylsulfoxide were passive only when the water content was low (0.02 mass % for iron and 0.01 mass % for nickel) [30,31]. Iron in neutral propylene carbonate solutions exhibits similar behavior

TABLE 2—Some typical physical properties of selected solvents at 25°C.

Solvent	M.W. g/mole	Density g/cm <sup>3</sup>	Dielectric constant - $\epsilon$	Viscosity cP	Dipole moment (Debye)	Formula
Waters	18.0152	0.997044	78.30	0.8904	1.87	H <sub>2</sub> O
Methanol	32.042	0.7864	32.66	0.5513	2.87	CH <sub>3</sub> O
Propylene Carbonate	102.090	1.1951	64.92	2.53	4.94	C <sub>3</sub> H <sub>6</sub> O <sub>3</sub>
Dimethoxyethane	76.95	0.859	7.20	0.455	1.07	C <sub>4</sub> H <sub>10</sub> O <sub>2</sub>
Tetrahydrofuran	72.12	0.880	7.58	0.46	1.71	C <sub>4</sub> H <sub>8</sub> O
Dioxolane (1,3-D)	74.079	1.0640 (20°C)	7.13	0.589	1.47	C <sub>3</sub> H <sub>6</sub> O <sub>2</sub>
Acetonitrile	41.052	0.88649	35.95	0.341	3.53	C <sub>2</sub> H <sub>3</sub> N
Dimethylsulfoxide	78.129	1.09537	46.45	1.991	4.06	C <sub>2</sub> H <sub>6</sub> OS
Dimethylformamide	73.094	0.94873	36.71	0.802	3.24	C <sub>3</sub> H <sub>7</sub> ON
Pyrrole	67.09	0.9691 (20°C)	7.5 @ 17°C			C <sub>4</sub> H <sub>5</sub> N
Phenol	94.11	1.07	4.3 @ 10°C			C <sub>6</sub> H <sub>5</sub> OH

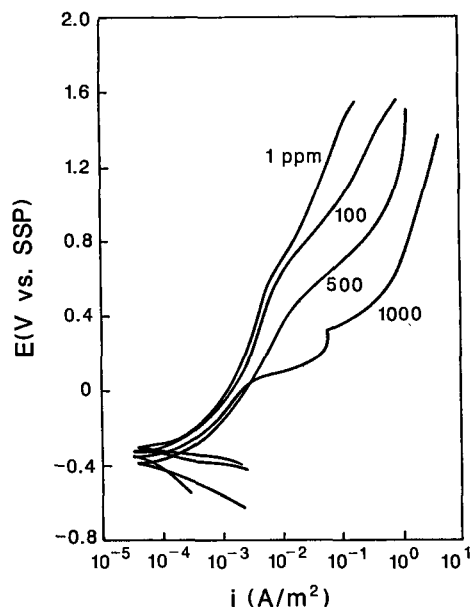


FIG. 6—The effect of water content on the anodic polarization of iron in propylene carbonate at 25°C [33].

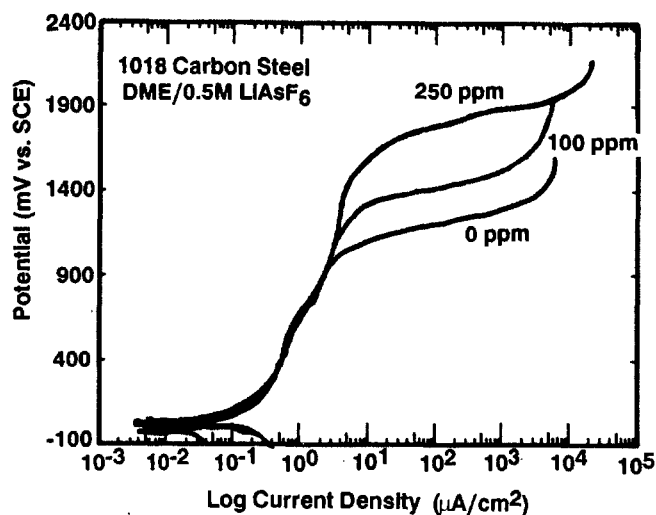


FIG. 7—The effect of water content on the anodic polarization of carbon steel in dimethoxyethane at 25°C [12].

[32,33], as shown in Fig. 6. For other materials and liquids, for example, molybdenum and chromium in methanol and dimethylformamide, and iron in acidified dimethylformamide, no clear dependence upon water content is observed [29,34]. Additionally, water can decrease the solvation ability of organic liquids, thus inhibiting the solvation of impurities and corrosion products. On the other hand, anhydrous ethers cannot form hydrogen bonds, but the small additions of water allow hydrogen bonds to form between the water hydrogen and the ether oxygen. Water added to dimethoxyethane (DME) increases the passive range of steel, as shown in Fig. 7, by several hundred millivolts [12] and of iron by contributing to hydrogen bonding or as a Lewis acid [35]. Thus, as stated above, water content needs to be closely monitored and controlled.

The pre-existence of a surface film can affect testing in organic solutions in several ways. In the absence of aggressive species, an air-formed film can be protective even under anodic polarization. Examples of this include iron in propylene carbonate [32,33] and ferritic stainless steel (Fe-18 %Cr) in methanol [36]. The presence of competing mechanisms may also contribute to breakdown of metals and alloys in multicomponent organic mixtures as observed for steel in PC/DME mixtures [37]. Propylene carbonate interferes with DME electropolymerization by solvating organic cations or cationic radical, or by contaminating the polymer to form pores that allow charge and ionic species to pass through. Adding water to PC-DME mixtures allows the possibility of aqueous passivating mechanisms that further complicate solvent interactions and competition [13]. However, even if aggressive species are present in the solution, the air-formed film may be protective until sufficient anodic polarization is achieved. This creates the need for a testing technique that permits removal of the film, enabling examination of the base metal. This can be accomplished by using a stylus to scratch the surface, thereby removing any pre-existing protective film to expose new metal. By monitoring the current over time, the corrosion behavior of the material in the absence of any pre-existing film can be observed. The long-term stability of air-formed oxides in organic solutions is not known, and thus, the corrosion processes that occur on bared surfaces may be the most relevant to the service conditions. In aqueous solution, cathodic polarization is often used to remove air-formed films. Extensive work in the literature on iron and ferrous alloys [38], as well as other materials [39], support the idea that this approach leads to an oxide-free surface. Such information does not exist for oxide reduction in organic liquids. However, many workers cathodically polarize their samples before performing electrochemical measurements [28,40-43].

Since the composition and purity of the organic liquid can strongly affect the corrosion process, a key feature to testing is the choice of an appropriate experimental testing solution. This solution should be as close in composition and impurity concentrations to the service solution as possible, unless accelerated testing is desired. The composition of organic liquids can influence the corrosion rate. For example, the corrosion rate of iron in monocarboxylic acids of different chain lengths was studied and showed that as the chain length increased, the corrosion rate decreased [2]. Often, organic liquids contain impurities such as water, acids, and metal ions. While these impurities generally have low concentrations in commercially purchased organic liquids, these concentrations could still be significant. For example, nickel in dimethylsulfoxide was only passive when the water concentration was below 100 ppm. Therefore, the testing solution may need to be purified such that the experimental testing solution closely matches the service solution. On the other hand, some corrosion problems develop due to the presence of impurities, so that an initially pure liquid may need to have impurities added to mimic the attack observed. Additionally, if accelerated testing is desired, care should be taken to ensure that the corrosion mechanisms and the location of the corrosion attack (e.g., vapor phase, immersed phase, etc.) accurately mimic in-service observations.

In most organic solutions, the nature of the cathodic process is unclear. In aqueous solutions, water reduction is the most common cathodic reaction, with the reduction of dissolved oxygen also being very important. However, the electrochemical reduction of many organics is very sluggish, and usually poorly characterized. Often, the reduction of residual water is assumed to be the predominant cathodic reaction. The role of molecular oxygen on the corrosion process in organic solutions has not been characterized. However, its solubility is nearly ten times higher in methanol than in water [2,44], making it a potentially much more influential oxidant. Additionally, aliphatic ethers are slowly converted to unstable peroxides when in contact with oxygen or air, leading to an unsafe condition that could induce a violent explosion during distillations [11]. Deaeration by the passage of an inert gas through the solution must be performed with care to avoid the selective evaporation of the liquid. For low boiling point liquids such as methanol, this is of particular importance. For high boiling point liquids such as propylene carbonate, the passage of ultrahigh-purity nitrogen through the solution for extended times can be used to selectively evaporate the water, leading to higher purity solutions, even after the addition of electrolytic salts [33]. The study of solution electrochemistry on platinum can often give insight into the nature of the cathodic as well as anodic reactions.

Temperature affects corrosion testing in organic liquids in that the reaction rates, charge transport diffusional coefficient, and rate of liquid evaporation are increased and the potential for ignition or explosion is greater. The effect of temperature on reaction kinetics, in general, follows the same principles that hold true for other heterogeneous chemical reactions [2]. Corrosion rates of iron in monocarboxylic acids increase by a factor of 8 to 20 by increasing the temperature from 25 to 80°C. While this behavior is not unique to organic liquids, it is important to realize that deviations in testing temperature compared to service temperature could lead to erroneous conclusions. Elevated temperatures may also lead to alternative reaction pathways, leading to other organic intermediate species. Temperature may result in hysteresis in macroscopic polymer properties such as swelling, elasticity, and turbidity [24]. If testing at elevated temperatures is called for, caution and appropriate safety preparations are needed.

## LABORATORY TESTING

Laboratory testing can be of two types: coupon testing and electrochemical testing. This section discusses the special considerations for each type of testing when organic liquids are involved.

### Coupon Testing

Exposure of coupons to the solution of interest with post-test evaluation according to accepted standards, such as ASTM G 31, Practice for Laboratory Immersion Corrosion Testing of Metals, is the most directly applicable method of testing in organic liquids. Because of the general lack of data on corrosion in organic liquids, coupon testing often

takes on additional importance. While standard test practices have been developed mostly for aqueous solutions, the protocols are essentially independent of the chemical nature of the environment, with minor exceptions. More detailed information on laboratory coupon testing can be found in the relevant chapter of this manual, as well as in ASTM G 31. One of the most important caveats for such testing in organic solutions is the need to check that the materials that make up the test apparatus are not affected by the liquid. Many nonmetallics are degraded by or preferentially absorb organic liquids, leading to dimensional and mechanical property changes. If such materials are used as spacers in a coupon exposure rack, unexpected experimental variability can result. For example, the nonmetallics may act as getters for aggressive species, produce aggressive species that would not normally be present, or produce inhibiting agents that bias the results. Compounds that have been used as mounting materials successfully in aqueous solution often do not perform well in either completely organic solutions or in mixed organic/aqueous solutions. Thus, a first step in coupon testing is careful selection of the exposure rack and spacer materials. Often, information of this sort is available from the material manufacturer. For example, many nonmetallics have been tested for weight loss/gain and mechanical properties after exposure to a range of different types of organics (e.g., alcohols, aliphatics, aromatics, etc.) at ambient and elevated temperature. While these data can provide general guidance, accelerated tests in the environment of interest may often be warranted.

A second important aspect of laboratory coupon testing in organics is the possibility of an evolution of the solution composition during the test. These changes can be severe, especially at elevated temperatures used to accelerate the corrosion process. Elevated temperature will also accelerate many organic liquid degradation processes, including oxidation by ultraviolet (UV) light. This can be severe in some instances. Thus, it is important to run solution blanks simultaneously. In these tests, no coupon is added to the solution under test, so its composition can be checked both before and after the testing to see if any significant changes in composition have occurred. Degradation reactions for many organics are well studied and available in the organic chemistry literature. This allows an identification of the by-products expected. Analysis of solutions after the exposure will allow a quantitative measurement of the degradation rate of the liquid in the absence of any interaction with the corroding materials. Comparison of the results with analyses of the liquid exposed to metal coupons may also give insight into the nature of the cathodic reaction that occurs.

Water ingress during coupon testing must also be monitored if it is suspected that water concentrations are important in the system under study. During testing, seals can develop minute leaks, allowing water levels to increase. Constant purging with an inert gas is an option if the boiling point of the solution is high. For many organics, this is the case. For example, the boiling point of propylene carbonate is over 200°C. However, for low boiling point liquids, such as methanol (b.p. = 64.9°C), constant purging will drive off liquid, increasing the concentration of the dissolved, nonvolatile species with time [45].

## Electrochemical Testing

For the most part, electrochemical testing in organic solutions is no different than such testing in aqueous solutions. The same experimental arrangements are used, and the appropriate standards, such as ASTM G 5, G 59, and G 61, are still applicable (see section titled Relevant ASTM Standards in this chapter). The chapter in this manual that describes electrochemical testing [4] should be consulted for other information on that subject. This section will focus on the special considerations in electrochemical testing in organic solutions.

The most central difficulty in electrochemical testing of materials in organics is the choice of a suitable reference electrode. Aqueous reference electrodes, such as saturated calomel (SCE), have been widely used in such studies, [28,34,36,40,43,45,46], but can suffer from three types of problems. Since these reference electrodes are in contact with the test solution, water can diffuse from the reference electrode into the test solution, thereby changing the concentration of water during the test. The organic liquid will also diffuse into the reference electrode, and may foul the interface, leading to irreversible changes in its potential. Such a change cannot be detected easily, as it would be superimposed on any change in the potential of the working electrode. A second difficulty with using aqueous reference electrodes is the development of a liquid junction potential. This potential develops at the interface of the aqueous solution and the nonaqueous solution due to the large difference in composition. Such potentials are extremely difficult to measure or calculate and vary with time due to the interdiffusion of the two solutions. The third possible difficulty that may be encountered is reference electrode plugging. This is particularly troublesome when potassium chloride-based reference electrodes are used in perchlorate solutions. As the potassium diffuses out of the reference electrode, precipitation of  $\text{KClO}_4$  may occur.

Some literature exists on organic liquid-based reference electrodes that have been successfully used in electrochemical studies [47–49]. These include the  $\text{Ag}/\text{AgClO}_4$  (propylene carbonate) [47],  $\text{Ag}/\text{AgCl}$  (methanol) [48], and numerous others, as detailed in Ref 49. The  $\text{Ag}/\text{AgClO}_4$  (propylene carbonate) reference electrode developed by Kirowa-Eisner and Gileadi [47] is easy to prepare, stable over time, highly reproducible, and easily stored. This electrode has been used successfully in conducting electrochemical experiments in propylene carbonate solutions. Similarly, the  $\text{Ag}/\text{AgCl}$  (methanol) reference electrode developed by Brossia and Kelly [48] has similar characteristics and has been successfully employed in electrochemical experiments conducted in methanolic solutions. Using a reference electrode where the electrolyte is based upon the testing solution will minimize contamination of the testing solution, and fouling of the reference electrode and the liquid junction potential.

Another aspect of electrochemical testing in organic solutions is the isolation of the counter-electrode from the working electrode. In aqueous solutions this is often ignored, since the predominant reactions at the counter-electrode are either oxygen evolution (producing  $\text{H}^+$ ) or hydrogen evolution (producing  $\text{OH}^-$ ) during cathodic and anodic polarization of the working electrode, respectively.

Especially in a buffered solution, these reaction products have little effect. However, in an organic solution, the products of the reactions at the counter-electrode are often more complex, and usually unknown. Thus, it is usually good practice to isolate the counter-electrode from the working electrode with porous frits. This will minimize, though not eliminate, any effects of those reaction products.

## Relevant ASTM Standards

- E 203 Test Method for Water Using Volumetric Karl Fischer Titration
- E 1064 Test Method for Water in Organic Liquids by Coulometric Karl Fischer Titration
- G 1 Practice for Preparing, Cleaning, and Evaluating Corrosion Test Specimens
- G 5 Standard Reference Test Method for Making Potentiostatic and Potentiodynamic Anodic Polarization Measurements
- G 31 Practice for Laboratory Immersion Corrosion Testing of Metals
- G 59 Practice for Conducting Potentiodynamic Polarization Resistance Measurements
- G 61 Test Method for Conducting Cyclic Potentiodynamic Polarization Measurements for Localized Corrosion Susceptibility of Iron, Nickel, or Cobalt-based Alloys

## FIELD TESTING

The approach to field studies of corrosion in organic liquids is no different than that used for aqueous corrosion. The choice of coupon size, rack design, test length, and other variables is more strongly influenced by the goals of the testing than by the testing medium. Safety concerns must also be addressed. Different organic liquids have different properties and safety issues, and appropriate references and experts should be consulted. More guidance on the general topic of field testing can be found in the relevant chapter in this manual and in ASTM G 4, Standard Guide for Conducting Corrosion Tests in Field Applications. However, the concerns expressed in the section above on laboratory coupon testing with regard to the effects of the organic liquid on the nonmetallic components of the mounting hardware should be considered.

Since the corrosion behavior of materials in organic liquids can be influenced by low levels of water, minimizing the introduction of water from the ambient atmosphere during the introduction of samples or probes should be carefully considered. For long-term testing at sites where there is a constant turnover of solution, these effects may be small for a one-time insertion of coupons. However, if, for example, a retractable electrochemical probe is used, the solution with which it comes into contact should be flushed in order to allow it to sample the most relevant environment.

In all field testing, the effects of variability in the composition of the stream being studied on the corrosion processes must be considered. Since small changes in the composition in organic solutions can have dramatic effects on the corrosion rate as well as the stability of passive films,

large transients in corrosion rate may be experienced. Thus, it is important to complement the corrosion measurements with solution composition measurements in order to develop an understanding of the role of stream composition on the corrosion behavior. Besides ionic composition, water concentrations and the level of liquid by-products should be monitored.

## SUMMARY

Corrosion testing in organic liquids has taken on greater importance in recent years due to the increase in the use of nonaqueous and mixed liquids in material and chemical synthesis as well as energy production. While the basic types of corrosion processes are similar in both aqueous and organic liquid environments, special attention must be given to the direct application of testing tools to organic testing due to the complexity of organic systems. The wide variety of organic liquids and mixtures increases the number of experimental variables that need to be considered and controlled.

## REFERENCES

- [1] Trasatti, S., *Electrochimica Acta*, Vol. 32, 1987, p. 843.
- [2] Heitz, E., "Corrosion of Metals in Organic Solvents," in *Advances in Corrosion Science and Technology*, Vol. 4, M. G. Fontana and R. W. Staehle, Eds., Plenum Publishing, New York, 1974.
- [3] Kelly, R. G. and Moran, P. J., *Corrosion Science*, Vol. 30, 1990, p. 495.
- [4] Hronsky, P., *Corrosion*, Vol. 137, 1981, p. 161.
- [5] Scully, J. R., Chapter on Electrochemical Tests, in *Corrosion Tests and Standards: Application and Interpretation*, Manual 20, 2nd ed., R. Baboian et al., Eds., ASTM International, West Conshohocken, PA, 2004 (this publication).
- [6] *Methods of Quantitative Micro-Analysis*, 2nd ed., R. F. Milton and W. A. Waters, Eds., Edward Arnold Publishers, 1955.
- [7] Brossia, C. S., "Iron Corrosion in Methanol Solutions," M.S. Thesis, University of Virginia, 1994.
- [8] Pourbaix, M., *Atlas of Electrochemical Equilibria in Aqueous Solutions*, NACE International, Houston, 1974.
- [9] Rochester, C. H., "Acidity Functions" in *Organic Chemistry*, a series of monographs, Vol. 17, Academic Press, New York, 1970.
- [10] Szklarska-Smialowska, Z. and Mankowski, J., *Corrosion Science*, Vol. 22, 1982, p. 1105.
- [11] Morrison, R. T. and Boyd, R. N., *Organic Chemistry*, Allyn and Bacon, Boston, 1973.
- [12] Shifler, D. A., Moran, P. J., and Kruger, J., *Electrochimica Acta*, Vol. 38, 1993, p. 881.
- [13] Shifler, D. A., Moran, P. J., and Kruger, J., in *Proceedings of the Symposium on Passivity and Its Breakdown*, PV 97-26, Natishan et al., Eds., The Electrochemical Society, Pennington, NJ, 1998, p. 432.
- [14] Glugla, P. G., in *Power Sources for Biomedical Implantable Applications and Ambient Temperature Lithium Batteries*, B. B. Owens and N. Margalit, Eds., The Electrochemical Society, Pennington, NJ, 1980.
- [15] Foos, J. S. and Erker, S. M., *Journal of the Electrochemical Society*, Vol. 134, 1987, p. 1724.
- [16] Koch, V. R., *Journal of the Electrochemical Society*, Vol. 126, 1979, p. 181.
- [17] Abraham, K. M., Goldman, J. L., and Natwig, D. L., *Journal of the Electrochemical Society*, Vol. 129, 1982, p. 2404.
- [18] Odziemkowski, M., Krell, M., and Irish, D. E., *Journal of the Electrochemical Society*, Vol. 139, 1992, p. 3052.
- [19] Scanlon, J. F., Moran, P. J., and Kruger, J., in *Critical Factors in Localized Corrosion*, PV92-9, G. S. Frankel and R. C. Newman, Eds., The Electrochemical Society, Pennington, NJ, 1992, p. 525.
- [20] Prejza, J., Lundstrom, I., and Skotheim, T., *Journal of the Electrochemical Society*, Vol. 129, 1982, p. 1685.
- [21] Beck, F., Oberst, M., and Jansen, R., *Electrochimica Acta*, Vol. 35, 1990, p. 1841.
- [22] Marrec, P., Dano, C., Gueguen-Simonet, N., and Simonet, J., *Synthetic Metals*, Vol. 89, 1997, p. 171.
- [23] Mengoli, G. and Musiani, M. M., *Journal of the Electrochemical Society*, Vol. 134, 1987, p. 643C.
- [24] Inzelt, G., *Electrochimica Acta*, Vol. 34, 1989, p. 83.
- [25] Brossia, C. S. and Kelly, R. G., *Corrosion Science*, Vol. 37, 1995, p. 1455.
- [26] Kanamura, K., *Journal of Power Sources*, Vol. 81-82, 1999, p. 123.
- [27] Schmidt, W., *Zashchita Metallov*, Vol. 5, 1970, p. 529.
- [28] Capobianco, G., Venti, P., and Bellucci, F., *British Corrosion Journal*, Vol. 25, 1990, p. 133.
- [29] Banas, J., in *Passivity of Metals and Semiconductors*, M. Froment, Ed., Elsevier Science Publishers, 1983.
- [30] Agladze, T. R., Kolotykin, Y. M., Malysheva, T. G., and Denisova, O. O., *Zashchita Metallov*, Vol. 22, 1986, p. 509.
- [31] Safonov, V. A., Komissarov, L. Y., and Petril, O. A., *Protection of Metals*, Vol. 22, 1978, p. 178.
- [32] Kelly, R. G., Moran, P. J., Gileadi, E., and Kruger, J., *Electrochimica Acta*, Vol. 34, 1989, p. 823.
- [33] Kelly, R. G., Moran, P. J., and Kruger, J., *Journal of the Electrochemical Society*, Vol. 136, 1989, p. 3262.
- [34] Farina, C. A., Faita, G., and Olivani, F., *Corrosion Science*, Vol. 18, 1977, p. 465.
- [35] Scanlon, J. F., Moran, P. J., and Kruger, J., *Journal of Power Sources*, Vol. 54, 1995, p. 85.
- [36] Bellucci, F., Faita, G., Farina, C. A., and Olivani, F., *Journal of Applied Electrochemistry*, Vol. 11, 1981, p. 781.
- [37] Shifler, D. A., Kruger, J., and Moran, P. J., *Journal of the Electrochemical Society*, Vol. 145, 1998, pp. 23-96.
- [38] Bardwell, J. A., Sproule, G. I., and Graham, M. J., *Journal of the Electrochemical Society*, Vol. 140, 1993, p. 50.
- [39] Speckmann, H. D., Haupt, S., and Strehblow, H.-H., *Surface and Interface Analysis*, Vol. 11, 1988, p. 148.
- [40] Mazza, F., Torchio, S., and Ghislandi, N., *International Congress on Metallic Corrosion*, Vol. 1, 1984, p. 102.
- [41] Capobianco, G. and Faita, G., *International Congress on Metallic Corrosion*, Vol. 3, 1984, p. 532.
- [42] Bellucci, F., Capobianco, G., Faita, G., et al., *Corrosion Science*, Vol. 28, 1988, p. 371.
- [43] Bellucci, F., Nicodemo, L., and Licciardi, B., *Corrosion Science*, Vol. 27, 1987, p. 1313.
- [44] Lewis, R. J., *Hazardous Chemicals Desk Reference*, 2nd ed., Van Nostrand Reinhold, 1991.
- [45] Singh, V. K. and Singh, V. B., *Journal of Applied Electrochemistry*, Vol. 19, 1989, p. 317.
- [46] Banas, J., *Corrosion Science*, Vol. 22, 1982, p. 1.
- [47] Kirowa-Eisner, E. and Gileadi, E., *Electroanalytical Chemistry and Interfacial Electrochemistry*, Vol. 25, 1970, p. 481.
- [48] Brossia, C. S. and Kelly, R. G., *Electrochimica Acta*, Vol. 41, 1996, pp. 25-79.
- [49] *Reference Electrodes, Theory and Practice*, D. J. G. Ives and G. J. Janz, Eds., Academic Press, 1961.



# Molten Salts

*F. S. Pettit<sup>1</sup>*

MOLTEN SALT INDUCED CORROSION may be encountered whenever molten salts contact metallic or ceramic surfaces at elevated temperatures. There are numerous industrial processes in which such conditions can develop. For example, during combustion, deposits such as  $\text{Na}_2\text{SO}_4$  can accumulate on hardware and cause corrosion. The combustion may occur, for example, in gas turbines, incinerators, or in diesel engines. The conditions are such that the deposits form as a thin ( $\sim 1 \mu\text{m}$ ) liquid layer separating the alloy from the gas phase. There are also other industrial processes, such as molten carbonate fuel cells, where molten salts are held in metallic or ceramic containers at elevated temperatures. The molten salts can corrode the container materials, but the conditions differ from the combustion environments because the amount of salt is very large with much larger diffusion distances between the gas phase and the container material. Because of the complexity of the environments, no tests have been developed that find general acceptance. In this section, testing in molten salts present as thin layers and as deep melts will be discussed, using illustrative examples to show some of the tests that have been developed.

## SELECTION OF TEST CONDITIONS

Test conditions should be the same as the application under consideration. Unfortunately, the application conditions are often not precisely known, and even when known, can be extremely difficult to establish as a controlled test. Moreover, true simulation testing is usually impractical because we want the material to perform for much longer times than we are willing and able to test. The answer to this problem is accelerated, simulation testing.

Accelerated, simulation testing requires knowledge of microstructure and morphological changes of the exposed material. All materials used in engineering applications exhibit a microstructural evolution, beginning during fabrication and ending upon termination of their useful lives. In an accelerated test, we must select test conditions that cause the microstructures to develop that are representative of the application, but in a much shorter time period. In order to use this approach some knowledge of the degradation process is necessary.

In selecting the conditions for molten salt corrosion testing, the application must be considered, but it is also useful to have some knowledge of the degradation process, especially the microstructural and morphological changes that occur. When metallic alloys or ceramics are exposed to molten salts at elevated temperatures, the reactions that occur depend upon a number of factors that include: the composition of the molten salt; the amount of molten salt, especially its thickness or depth; alloy or ceramic composition; gas composition over the molten salt; and temperature including thermal cycles. Some examples of molten salt corrosion are useful to illustrate factors relevant to accelerated, simulation testing. In some cases of molten salt corrosion, the alloy or ceramic would react with components in the gas phase had the molten salt not been present, and it is necessary to consider how the molten salt affects such reactions. If the molten salt is very thin and the corrosion products are insoluble in the molten deposit, the reactants from the gas can diffuse through the deposit to react with the alloy or ceramic. For example, in the case of  $\text{Na}_2\text{SO}_4$  on a Ni-30Cr-6Al (wt%) alloy [1] in oxygen at  $1000^\circ\text{C}$ , a continuous layer of alumina is formed on the alloy separating it from the molten deposit during isothermal oxidation. However, during cyclic oxidation, the alumina scale cracks and spalls, and eventually sulfides are formed in the alloy, which cause much more rapid oxidation. The gas phase usually does not play as important a role if the molten deposit is so thick that diffusion of reactants from the gas is negligible. When pure nickel is immersed in a crucible containing  $\text{Na}_2\text{SO}_4$  at  $1000^\circ\text{C}$  in air, the reaction involves sulfur and some oxygen from the  $\text{Na}_2\text{SO}_4$  with the nickel [2]. There is little influence from the gas environment. In all cases, the important point is how the molten salt affects the protectiveness of the corrosion products.

## SOME ILLUSTRATIVE TESTS

The European Federation of Corrosion has begun to attempt to develop standards for high temperature corrosion testing [3], including the case of molten salt deposits [4]. Some progress has been made but they have concluded more work is necessary. For the case of deposit-induced corrosion, Saunders [4] has shown that there are a number of key parameters that control the corrosion rate. Some of these factors have been mentioned previously in the present paper, but will be presented again, along with some of Saunders' remarks.

<sup>1</sup>Materials Science and Engineering Department, University of Pittsburgh, Pittsburgh, PA 15261.

**Deposit Composition:** The deposit should be present as a solid or liquid phase because direct reaction between this deposit and the material being tested plays an important role in the corrosion process.

**Deposit Structure:** Solid deposits can contain porosity that may affect the corrosion process, and consequently, good simulation of the pore structure may be necessary.

**Deposition Rate:** In most processes deposition takes place more or less continuously. The deposition rate plays a critical role in determining the corrosion rate and should be simulated.

**Aerodynamics/Gas Velocity:** Deposition is affected by gas flow over the component. At high velocities, depending upon the size of the deposit, erosion may occur. Deposition will also be affected by the shape of the component.

**Gas Atmosphere Control:** The gas atmosphere can affect the nature of the deposit. In some equipment the gas atmosphere can be cyclic with fluctuations in the oxidizing potential. Such fluctuations must be incorporated into the test.

**Gas and Metal Temperatures:** Generally these are different, and consequently, temperature gradients can exist across the deposits.

**Catalytic Effects:** Deposition is affected by the condition of the surface and the time that deposit particles are in contact with one another on the component surface. Whether the component surface provides catalytic activity may be questioned, but relevant surface preparation procedures must be used.

**Time:** The corrosion process may go through different stages with time, and it is important to account for such conditions in the design of the experiment.

**Thermal Cycles:** Most hardware is subjected to thermal cycles in use, and such cycling can exert profound effects on protectiveness of the corrosion products. The test must simulate thermal cycles.

In discussing molten salt corrosion tests, the task is to develop guidelines that may be used to develop tests for various situations. Since no standardized tests for molten salt-induced corrosion are available, the tests to be described are presented by way of example. Tests for other situations could, in principle, be devised by following procedures used in these examples. It is also important to emphasize that this chapter is not concerned with the various mechanisms for molten salt corrosion, but only the conditions that cause attack.

## Metals and Alloys

In discussing molten salt tests, it is useful to consider first thin deposits where diffusion through the deposit of reactants from the gas plays a significant role in the corrosion process, and thick deposits where such diffusion is less important and sometimes negligible.

### Thin Molten Salt Deposits

Thin molten deposits of  $\text{Na}_2\text{SO}_4$  are formed on alloys used in gas turbines. Depending upon conditions, different types of hot corrosion attack can occur. High-temperature hot corrosion is observed during operation of gas turbines when deposits of  $\text{Na}_2\text{SO}_4$  accumulate on alloys at temperatures above

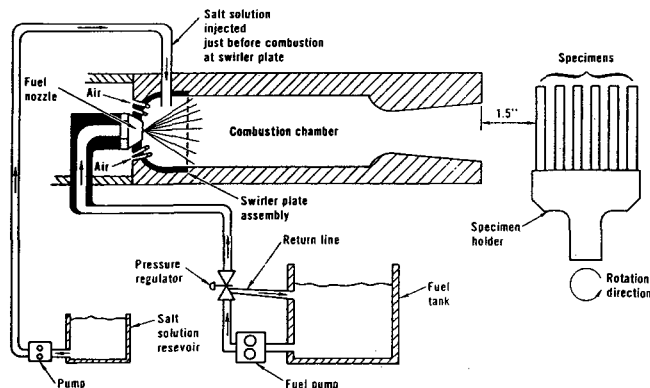


FIG. 1—Diagram of burner rig used to test alloys for high-temperature hot corrosion.

about  $800^\circ\text{C}$ . Nonprotective reaction products are developed because sulfides are formed in the alloys and also because some oxides dissolve in the molten deposit via basic fluxing reactions [2,5–8]. Low-temperature hot corrosion occurs at temperatures below about  $800^\circ\text{C}$ , where the accelerated attack involves dissolution of oxides in the molten deposits via acidic fluxing reactions [2,5–8]. Still another form of hot corrosion occurs when elements from the alloys enter the molten deposit and cause self-sustaining hot corrosion [1]. Each of these types of hot corrosion have distinctive microstructural features. Three types of tests have been used to examine alloys for resistance to these types of hot corrosion attack.

**Simulation Burner Rigs**—In the gas turbine industry, burner rigs have been developed to rank materials. The designs may

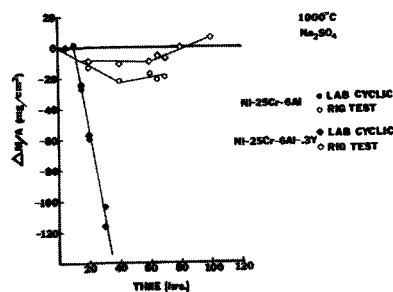


FIG. 2—Weight change data and degradation microstructures for alloys tested in a burner rig and a laboratory cyclic hot corrosion test. The microstructures after 70 h in the burner rig (left) are similar to those of the laboratory test after 12 h exposure (right).

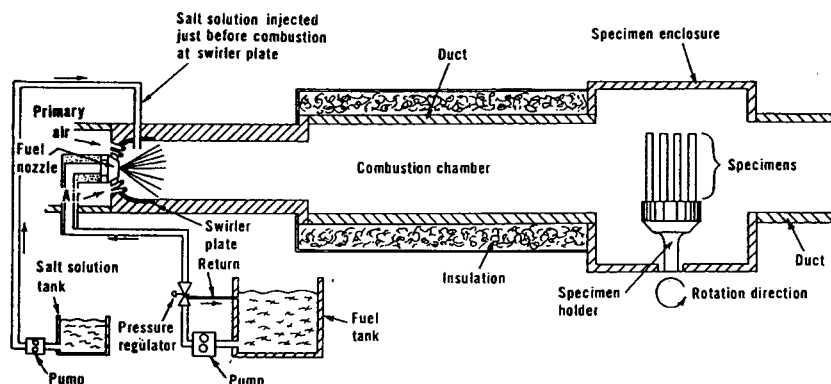


FIG. 3—Diagram of ducted burner rig used in low-temperature hot corrosion tests.

vary [9–13], but as shown in Fig. 1 the essential features are a combustion chamber, a means to ingest the salt, and a specimen holder that is rotated and often periodically removed from the hot gas stream to induce thermal stresses. The specimens are usually bars about 10–11 cm in length and about 1 cm in diameter. In the burner rig tests the specimens are periodically removed from the test to measure weight changes, or thicknesses, and to be examined visually. Upon conclusion of the tests the specimens are sectioned, metallographically prepared, and examined using optical metallography and scanning electron microscopy. Some typical weight changes and degradation microstructures are presented in Fig. 2 for the high-temperature hot corrosion of a Ni-25Cr-6Al alloy. The degradation microstructure contains a sulfide phase accompanied by oxidation, which is typical of high-temperature hot corrosion attack.

Burner rigs were initially developed to rank alloys for hot corrosion resistance in aircraft gas turbines. The various types of rigs and the important operating parameters are described in detail in Refs 14 and 15. When gas turbines began to be used on ships, hot corrosion with different microstructural features was observed. In order to duplicate such degradational microstructures, the burner rigs had to be ducted and operated at lower temperatures to establish the  $\text{SO}_3$  pressures in the gas necessary to produce low-temperature hot corrosion [16]. A schematic of a ducted burner rig is presented in Fig. 3, and the microstructural features typical of low-temperature hot corrosion are presented in Fig. 4.

The important feature of the burner rig approach to testing is simulation; for example, high gas velocities and hot gases with continuous deposition of molten salts as occurs in gas turbines. Very often, the exact conditions in the simulation test are not known. For example, some of the conditions established by the burner rigs were not known for 20 to 30 years after their inception [17]. The conditions are always more severe than in the application of interest, because the purpose is to accelerate failure. These types of tests are effective in ranking alloys for use in the application for which the simulation test was designed. It is also important to note that testing in burner rigs is expensive. Furthermore, the construction and operation of burner rigs requires experienced designers and operators.

*Controlled Laboratory Testing*—Hot corrosion testing has also been performed using conditions much different than those typical of gas turbine engines. For example, tube furnaces have been used with controlled compositions of flowing gases where the salt is deposited intermittently at specified times. In this type of testing the conditions are well defined and precisely controlled, but they are far removed from the environment of the gas turbine. The testing conditions must be varied until degradation microstructures are obtained representative of those observed in service. A laboratory test used for high-temperature hot corrosion testing consists of cyclic oxidation using periodic applications of  $\text{Na}_2\text{SO}_4$ . The alloy specimens can be small coupons (1 cm by 1 cm by 0.1 cm). The  $\text{Na}_2\text{SO}_4$  is applied at predetermined intervals (e.g., every 20 h or 100 h). The specimens are cycled from the test temperature to room temperature every hour. The gas can be air, oxygen, or oxygen with about 1 wt %  $\text{SO}_2$ . The specimens are weighed and visually examined at selected times. Based upon weight changes and visual examination, the specimens are removed from the test when degradation has

FIG. 4—Scanning micrographs showing low-temperature hot corrosion degradation microstructure after 4800 h of gas turbine marine service (upper micrographs) and after 17 h at 700°C in a laboratory low-temperature hot corrosion test (lower micrographs).

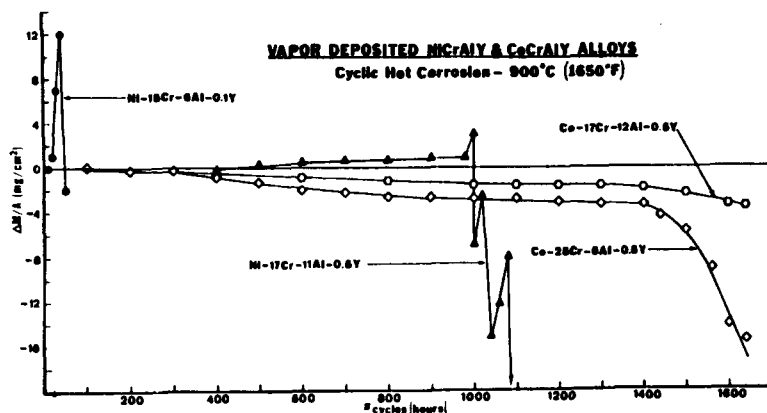


FIG. 5—Weight change versus time data obtained for high-temperature hot corrosion testing of specimens in a laboratory cyclic apparatus. Large weight increases or weight losses indicate failure.

progressed to failure limits. Typical results are presented in Fig. 2. The weight changes are different from the burner rigs, but the microstructures are virtually identical. In the laboratory cyclic test, the weight changes must be correlated with the amount of hot corrosion attack. In the case of the Ni-25Cr-6Al alloy for which the data are presented in Fig. 2, a protective  $\text{Al}_2\text{O}_3$  scale is developed initially, and the weight changes are small. As the testing is continued, the  $\text{Al}_2\text{O}_3$  cracks and spalls and eventually sulfides are formed that result in more rapid oxidation. This phase of the attack corresponds to the large weight losses evident in Fig. 2. Cyclic hot corrosion test results are presented for a number of alloys in Fig. 5. Abrupt changes in weight indicate a change in the corrosion mechanism and indicate failure is imminent. Usually this type of test results in large weight losses as the products spall from the surfaces of the specimens, but if spalling does not occur, large weight gains can be observed. The results presented in Fig. 5 show that the CoCrAl alloys have better high-temperature hot corrosion resistance than the NiCrAl alloys, which is consistent with burner rig test results. Various versions of these type of tests have been used by numerous investigators [1,2,5,8].

For low-temperature hot corrosion, the conditions must be altered to produce the appropriate microstructures [8,16]. The temperature must be lowered to 650–750°C, and most importantly an oxygen- $\text{SO}_2$  gas must be used. This gas must be passed over a platinum catalyst to ensure equilibrium conditions whereby  $\text{SO}_3$  pressures between  $10^{-3}$  to  $10^{-5}$  atm (101.3–1.013 Pa) are established. Deposits of  $\text{Na}_2\text{SO}_4$  are applied periodically. The tests may be isothermal or cyclic. For such conditions, degradation microstructures shown in Fig. 4 are developed that are very similar to degradation observed in service.

Most superalloys contain some refractory elements such as molybdenum and tungsten. When the oxides of these elements accumulate in molten deposits, very severe hot corrosion attack can occur. The degradation is characterized by an incubation period during which the attack is not severe, followed by much more rapid attack as the refractory metal oxide in the molten deposit reaches a level to produce catastrophic degradation. Microstructures typical

of this type of attack can be produced in both burner rigs and in a laboratory cyclic oxidation test with  $\text{Na}_2\text{SO}_4$  deposits [1]. It is important to emphasize that the incubation time prior to the onset of catastrophic attack is much longer in a burner rig than in the laboratory cyclic oxidation test. This occurs because some of the refractory metal oxides are removed from the molten deposits by the high gas velocities in the burner rig, and longer times are required for the refractory metal oxides to reach the critical level required for hot corrosion attack. In Fig. 6, data are presented to show that the incubation period prior to the onset of hot corrosion attack is increased in a flowing gas compared to static conditions.

**Immersion Test**—Immersion tests involve placing coupons in deep melts. This type of test is usually used for deep melts. Some investigators have attempted to use electrochemical techniques to measure corrosion kinetics. These techniques will be discussed in the following section on deep melts. The results from immersion tests must be used

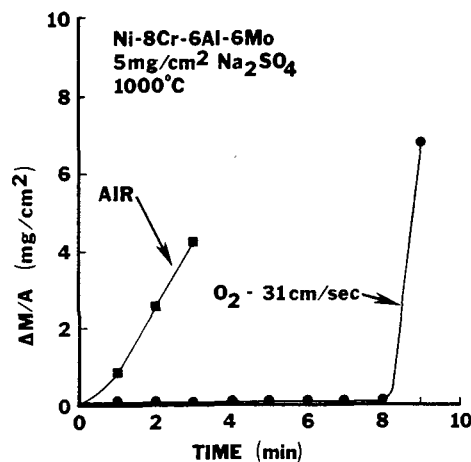


FIG. 6—Weight change versus time measurements for the isothermal hot corrosion of a Ni-8Cr-6Al-6Mo alloy in static air and in oxygen having a linear flow rate of 31 cm/s.

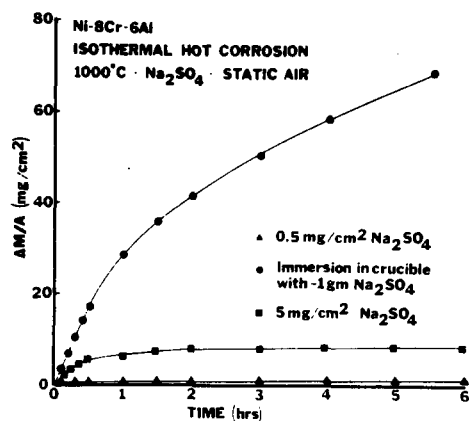


FIG. 7—Weight changes versus time data for the hot corrosion attack of Ni-8Cr-6Al specimens with different amounts of  $\text{Na}_2\text{SO}_4$ . The amount of degradation increases as the amount of deposit is increased.

FIG. 8—Surface and microstructural features developed for Ni-8Cr-6Al-6Mo specimens after exposure at 1000°C in air to (a) thin ( $\sim 5 \mu\text{m}$ , 7 min exposure) and (b) thick (1 cm, 4 min exposure) melts of  $\text{Na}_2\text{SO}_4$ . Attack with the thin deposit was evident visually after less than 1 min and usually spread laterally over the surface from the point of initiation. The specimen in the thick melt showed no attack after 4 min.

with great care when applied to cases where the molten salts are present as thin layers in practice. For example, as shown in Fig. 7, the hot corrosion attack of a Ni-8Cr-6Al alloy becomes more severe in an immersion test, but the hot corrosion of a Ni-8Cr-6Al-6Mo is less (Fig. 8). In the case of the latter alloy, the attack is more severe with the thin layer of molten salt, because the degradation process involves the

accumulation of  $\text{MoO}_3$  in the molten salt, and a critical level is reached sooner with a smaller amount of deposit.

### Thick Molten Salt Deposits

Tests for corrosion of alloys in deep melts should involve primarily immersion tests. The procedures to be followed in using immersion or crucible tests are similar to those used for thin deposits; namely, exposure of specimens with weight change versus time measurements and metallographic examination of the exposed specimens.

Electrochemical techniques have been used by a number of investigators to determine the corrosion resistance of alloys [18–24] and also to investigate the properties of salt mixtures [25–28]. When attempting to measure the corrosion resistance of alloys, the molten salt is used as the electrolyte with the alloy as the working electrode of the cell. A typical cell used by Kim and Devereux [23] to investigate the corrosion of alloys in molten  $\text{Na}_2\text{CO}_3$  is described schematically in Fig. 9. By using a reference electrode and auxiliary electrodes, electrochemical voltages and currents are measured and the results are interpreted by using principles and concepts applicable to aqueous corrosion [29]. Rahmel and coworkers [19,20,24] have used electrochemical cells to investigate the hot corrosion of superalloys in sulfate melts at temperatures of 800 and 900°C. They observed a strong dependence of corrosion behavior on the cell potential and showed that positive potentials established acidic conditions in the sulfate melts, whereas basic conditions were developed with negative potentials. In Fig. 10, data are presented for some superalloys exposed to a  $(\text{NaK})_2\text{SO}_4$  melt at 900°C where the depths of attack, measured metallographically after 100 h of exposure, are presented as a function of electrode potential. The potential range over which negligible attack occurred was used to compare the resistance of alloys to attack by this molten salt. Hence, the hot corrosion resistance was concluded to increase in the order IN-738 < IN-657 < IN-939, IN-597. These investigators also used current versus time measurements to detect the breakdown of protective scales on some of the alloys studied. Shores [18] has used electrochemical techniques to determine corrosion currents for a number of nickel- and cobalt-base alloys exposed to fused  $\text{Na}_2\text{SO}_4$  and showed that the corrosion currents could be related to the depths of attack of these alloys in a burner rig.

Electrochemical cells can also be used to attempt to obtain data on the mechanisms of the salt-induced corrosion processes. Cyclic voltammetry has been used [18–22] to obtain information on the oxidation and reduction reactions that may occur during molten salt corrosion. Chronopotentiometric investigations with platinum as the working electrode in cells can also be used to determine and control the compositions of molten salts, as well as to measure the solubilities of various oxidation products in melts [25–28,30].

Electrochemical techniques are difficult to use for thin deposits. Otsuka and Rapp [31], however, have constructed a cell that uses thin deposits of  $\text{Na}_2\text{SO}_4$  and have obtained results consistent with the  $\text{Na}_2\text{SO}_4$ -induced hot corrosion of nickel [2].

### Ceramics

The testing of ceramics in molten salts is similar to that for metals and metallic alloys. This is especially the case for

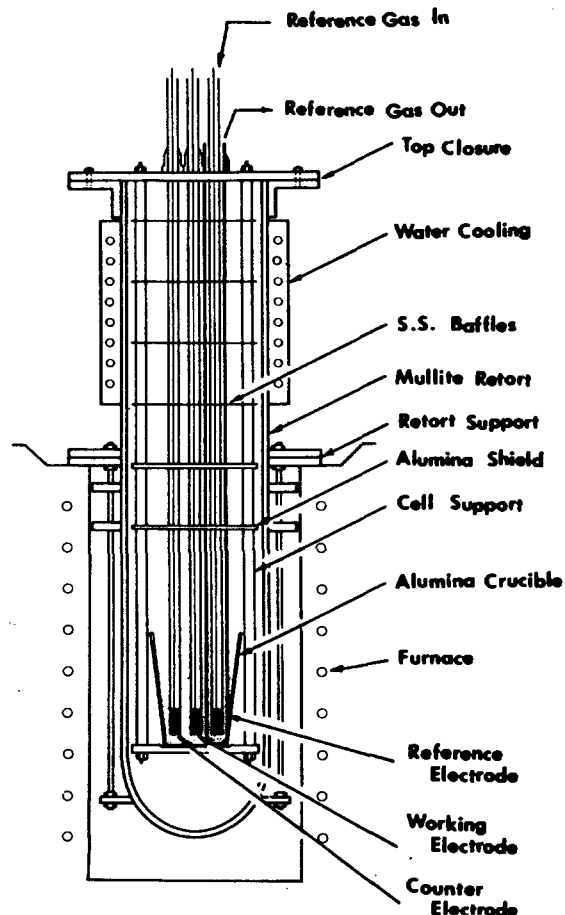


FIG. 9—Schematic diagram of a polarization cell used to investigate the corrosion of materials in molten salts.

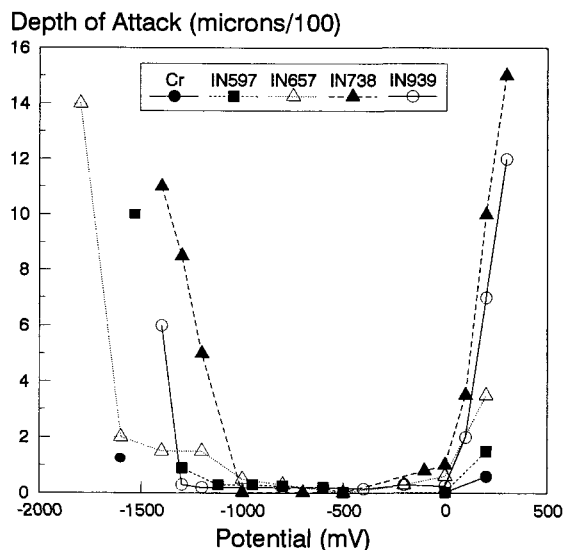


FIG. 10—Results obtained in an electrochemical test at 900°C to compare the hot corrosion of some superalloys.

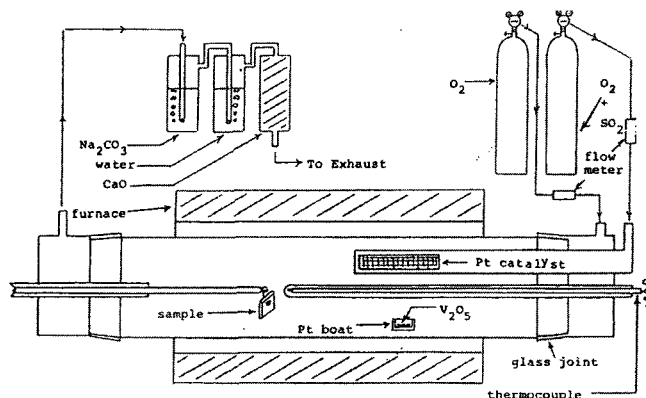


FIG. 11—Schematic diagram showing an apparatus to test coupons in gases containing SO<sub>3</sub> and vanadium oxides.

monoxide ceramics such as SiC and Si<sub>3</sub>N<sub>4</sub>, where resistance to degradation derives from the formation of silica scales. In the case of oxide ceramics, the testing techniques used for metallic alloys have been used with good results, but testing using immersion in deep melts has also been used to good advantage. Since ceramics are often not good electronic conductors, testing with electrochemical cells has been confined to investigations concerned with the solubilities of oxides in melts.

In Fig. 11, a laboratory apparatus to test coupons of metallic alloys and ceramics is presented. The coupons are coated periodically with thin deposits of Na<sub>2</sub>SO<sub>4</sub> or a Na<sub>2</sub>SO<sub>4</sub>-NaVO<sub>3</sub> mixture, and the gas composition is controlled to maintain the stability of the deposit [32]. The specimens are removed at selected time intervals to examine the corrosion. Typical results obtained for Al<sub>2</sub>O<sub>3</sub> [32,33] are presented in Figs. 12 and 13, showing a porous zone that developed in accordance with a parabolic rate.

FIG. 12—Photomicrograph showing porous zone that developed in alumina specimen after 46 h at 700°C with a deposit of Na<sub>2</sub>SO<sub>4</sub> containing 20 mol % NaVO<sub>3</sub>.

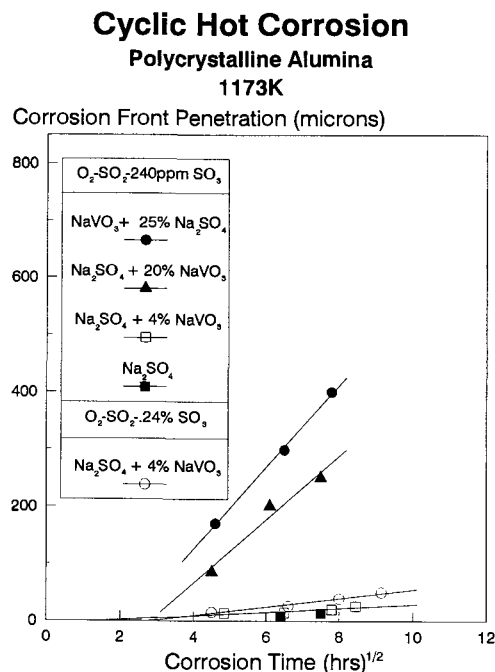


FIG. 13—Depths of corrosion front penetration for alumina exposed to various deposits in gases containing oxygen, SO<sub>2</sub> and SO<sub>3</sub>.

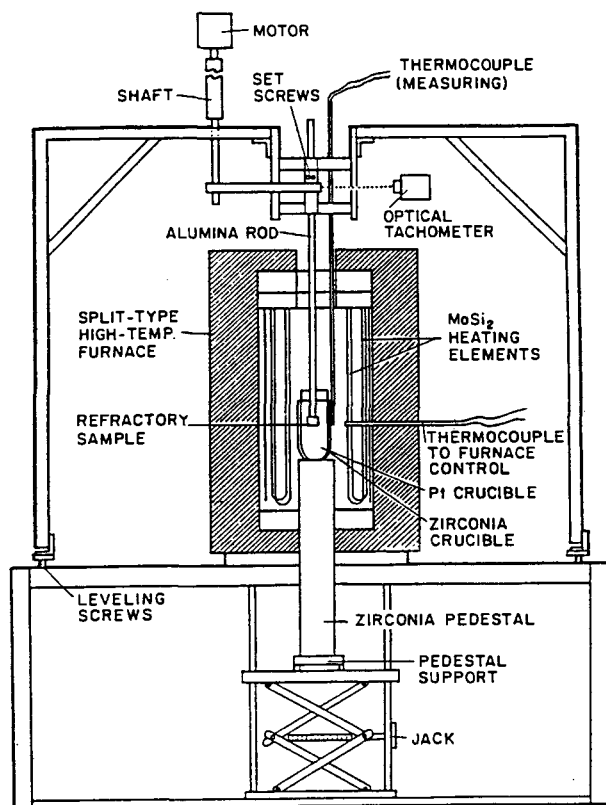


FIG. 14—Schematic of apparatus used to test ceramics in deep melts of molten salts.

The effects of deep melts on the dissolution of solid oxides have been studied by numerous investigators [34,35]. Dissolution studies of oxides are often performed using a rotating disk apparatus shown in Fig. 14 [35]. This apparatus can be used to measure the rates of corrosion under well-defined fluid dynamic conditions. After exposure, the specimens are examined by using optical metallography and scanning electron microscopy (SEM). The rates of corrosion can be determined by thickness measurements and by weight change measurements.

## CONCLUDING REMARKS

Standardized tests using molten salts are not available. In order to develop tests for the molten salt corrosion of materials, hardware should be obtained after service in the application of interest. The microstructures and surface morphologies of this hardware should be characterized in detail using optical metallography, X-ray diffraction (XRD), SEM, and other surface analytical techniques as required. The test must then be designed to duplicate the degradation microstructures documented in the service hardware. A wide range of tests is possible and extends from simulation of the presumed exposure conditions to conditions far removed from the actual exposure conditions.

## REFERENCES

- [1] Goebel, J. A., Pettit, F. S., and Goward, G. W., *Metallurgical Transactions*, Vol. 4, 1973, p. 261.
- [2] Goebel, J. A. and Pettit, F. S., *Metallurgical Transactions*, Vol. 1, 1970, p. 1943.
- [3] Grabke, H. J. and Meadowcraft, D. B., *Guidelines for Methods of Testing and Research in High Temperature Corrosion*, Chapters 1-9, The Institute of Materials, London, 1995.
- [4] Saunders, S. R. J., "Corrosion in the Presence of Melts and Solids," Chapter 6 in *Guidelines for Methods of Testing and Research in High Temperature Corrosion*, H. J. Grabkes and D. B. Meadowcraft, Eds., The Institute of Materials, London, 1995.
- [5] Bornstein, N. S. and De Crescente, M. A., *Transactions AIME*, Vol. 245, 1969, p. 1947.
- [6] Rapp, R. A., *Corrosion*, Vol. 42, 1986, p. 568.
- [7] Pettit, F. S. and Giggins, C. S., "Hot Corrosion," *Superalloys II*, C. T. Sims, N. S. Stoloff, and W. C. Hagel, Eds., John Wiley and Sons, New York, 1986, pp. 327-358.
- [8] Luthra, K. L., *Metallurgical Transactions*, Vol. 13A, 1982, p. 1843.
- [9] Doering, H. and Bergman, P., *Materials Research Standards*, Vol. 9, 1969, p. 35.
- [10] Lowell, C. E. and Deadmore, D. L., *Corrosion Science*, Vol. 18, 1973, p. 747.
- [11] Saunders, S. R. J., Hossain, M. K., and Ferguson, J. M., in *High Temperature Alloys for Gas Turbines*, R. Brunetaud, et al., Eds., D. Reidel Publishing Company, Dordrecht, 1982, p. 177.
- [12] Hancock, P., *Corrosion Science*, Vol. 22, 1982, p. 51.
- [13] Nicholls, J. R. and Saunders, S. R. J., *High Temperature Technology*, Vol. 7, 1989, p. 193.
- [14] Booth, G. C. and Clarke, R. L., *Materials Science and Technology*, Vol. 2, 1986, p. 2729.
- [15] Shifler, D. A., "High Temperature Gaseous Corrosion Testing," *ASM Handbook*, Vol. 13A, in press.
- [16] Aprigliano, L. F., "Burner Rig Simulation of Low Temperature Hot Corrosion," *Proceedings of the 1978 Tri-Service Conference on Corrosion*, October 1978.
- [17] Dils, R. R. and Follansbee, P., *Corrosion*, Vol. 33, 1977, p. 385.

- [18] Shores, D., *Corrosion*, Vol. 31, 1975, p. 435.
- [19] Rahmel, A., Schmidt, M., and Schorr, M., *Oxidation of Metals*, Vol. 19, 1983, p. 201.
- [20] Wu, W. T., Rahmel, A., and Schorr, N., *Oxidation of Metals*, Vol. 19, 1983, p. 201.
- [21] Gribaudo, L. M. and Rameau, J. J., *Corrosion Science*, Vol. 24, 1984, p. 291.
- [22] Azzi, M. and Rameau, J. J., *Corrosion Science*, Vol. 24, 1984, p. 935.
- [23] Kim, K. Y. and Devereux, O. F., "Electrode Polarization Studies Under CO/CO<sub>2</sub> and CO/CO<sub>2</sub>/H<sub>2</sub>/H<sub>2</sub>O/H<sub>2</sub>S in Molten Na<sub>2</sub>CO<sub>3</sub>," *High Temperature Corrosion*, R. A. Rapp, Ed., NACE-6, Houston, TX, 1983, pp. 539-549.
- [24] Rahmel, A., *Werkstoffe und Korrosion*, Vol. 28, 1977, p. 299.
- [25] Zhang, Y. S. and Rapp, R. A., *Journal of the Electrochemical Society*, Vol. 132, 1985, p. 2498.
- [26] Zhang, Y. S. and Rapp, R. A., *Journal of the Electrochemical Society*, Vol. 133, p. 655.
- [27] Gupta, D. K. and Rapp, R. A., *Journal of the Electrochemical Society*, Vol. 127, 1980, p. 2194.
- [28] Liang, W. W. and Elliot, J. F., *Properties of High Temperature Alloys*, Z. A. Foroulis and F. S. Pettit, Eds., The Electrochemical Society, Princeton, NJ, 1976, p. 557.
- [29] Fontana, M. G. and Greene, N. D., *Corrosion Engineering*, McGraw-Hill, New York, 1978, Chapters 9 and 10.
- [30] Rapp, R. A., "Hot Corrosion of Materials," *Selected Topics in High Temperature Chemistry*, O. Johannesen and A. Andersen, Eds., Elsevier, New York, 1989, p. 291.
- [31] Otsuka, N. and Rapp, R. A., *Journal of the Electrochemical Society*, Vol. 137, 1990, p. 46.
- [32] Warnes, B. M., "The Influence of Vanadium on the Sodium Sulfate Induced Hot Corrosion of Thermal Barrier Coating Materials," Ph.D. dissertation, University of Pittsburgh, Pittsburgh, PA, 1990.
- [33] Warnes, B. M., Hwang, S. Y., Caola, J. R., et al., "Hot Corrosion of Metallic and Ceramic Coatings in Heat Engines," *Proceedings of the 1990 Coatings for Advanced Heat Engines Workshop*, J. Fairbanks, Ed., U.S. Department of Energy, ONF-9008151, 1991, pp. IV-1-IV-38.
- [34] Cooper, A. R., Jr. and Kingery, W. D., *Journal of the American Ceramic Society*, Vol. 47, 1964, p. 37.
- [35] Sandage, K. H. and Yurek, G. J., *Journal of the American Ceramic Society*, Vol. 71, 1988, p. 478.



# Liquid Metals

Chris Bagnall,<sup>1</sup> Peter F. Tortorelli,<sup>2</sup> Steven J. Pawel,<sup>2</sup>  
Jack H. DeVan,<sup>3</sup> and Steven L. Schrock<sup>4</sup>

## DESCRIPTION OF ENVIRONMENT

THIS SECTION ADDRESSES the design, control, and interpretation of corrosion tests conducted in liquid metals. The emphasis in this chapter is placed on techniques that should be employed for determining the suitability of metals and alloys for liquid metal containment. Because one of the most important applications of liquid metal is for heat transfer, or thermal management within an engineered system, a focus will be placed on methods for study and measurement of corrosion in a circulating system in which there is a temperature gradient. Metals and alloys with relatively low melting points and high thermal conductivities are commonly used for these applications. A range of heat capacities and boiling points then permits specific selection for a variety of applications; for example, a lead system for applications below 500°C, sodium for operation up to 700°C, and lithium up to about 1300°C. The properties of potassium make it suitable for use as a working fluid in a two-phase Rankine cycle. In each case, however, the combination of liquid metal and candidate containment material requires careful evaluation before a final selection is made.

The environmental boundaries of a liquid metal system are set by the containment material. This material may experience other types of corrosion on the exterior surface (of pipe or tubing for example), but it isolates the liquid metal from interaction with any external atmosphere. This specification of "contained and isolated" sets the limits for the liquid metal corrosion system. Other more general areas of liquid metal/metal interaction, such as that produced when, for example, liquid steel or aluminum come into contact with materials employed in their production, are excluded by this definition. Liquid metal embrittlement will not be addressed. Information on this topic can be found elsewhere [1–3].

## UNIQUE ASPECTS

The approach to testing in liquid metals involves design of the test system, design and placement of samples, the control and monitoring of test conditions, the assurance of

wetting, and the measurement and evaluation of corrosion damage. One unique aspect is that liquid metals are excellent conductors, and hence electrochemical techniques cannot be employed to determine rates. Another important issue is that the containment material has its own effect on test results in systems in which dissimilar metals or alloys are involved. The chemical balance between dissolution and deposition is strongly influenced by all materials (i.e., containment and test coupons) exposed to the circulating liquid metal. Relative surface areas of different metals and alloys and surface:liquid metal volume ratios are important points to consider when designing small-scale tests for corrosion trends in a large multicomponent heat transport system. In general, materials with large compositional differences should not be exposed together to determine relative corrosion behavior.

The chemical activities of individual species in the system and the "corrosion potential" of the liquid metal are important factors in understanding the corrosion process. Reactions are complex; they involve the following phenomena:

- Dissolution—in its simplest form, or through compound or complex formation with one or more impurity elements in the liquid metal.
- Diffusion in the solid and liquid states—supply of dissolving or dissolved species to the liquid/solid interface.
- Influence of activity and temperature gradients.
- Mass transport by the liquid metal, even when elemental concentration gradients are at the lowest levels of detection.
- Influence of impurities in the liquid metal and the containment material.
- Influence of operating parameters, system geometry, and thermomechanical condition of the exposed materials.

The simplest corrosion reaction that can occur in a liquid metal environment is direct dissolution: the release of atoms from the containment (or test coupons) into the liquid metal, driven solely by solubility relationships, and independent of impurity elements. The solution reaction is governed by the rate controlling step in the dissolution reaction. The net rate,  $J$ , at which an elemental species can enter solution may be described by the expression

$$J = k(C - c) \quad (1)$$

where  $k$  is the solution rate constant for the rate controlling step,  $C$  is the solubility of the particular element in the liquid metal, and  $c$  is the actual instantaneous concentration of

<sup>1</sup> MCS Associates Inc., Greensburg, PA 15601.

<sup>2</sup> Oak Ridge National Laboratory, Oak Ridge, TN 37831.

<sup>3</sup> Oak Ridge National Laboratory, deceased.

<sup>4</sup> Oak Ridge National Laboratory, retired.

the element in the liquid metal. Under isothermal conditions, the rate of dissolution would decrease with time as  $c$  increases. After a period of time, the actual elemental concentration becomes equal to the solubility, and the dissolution rate is then zero. Therefore, in view of Eq 1, corrosion by the direct dissolution process can be minimized by selecting a containment material whose elements have low solubilities in the liquid metal of interest and/or by saturating the liquid metal before actual exposure. Measurements of weight changes as a function of time for a fixed  $C - c$  (see discussion below) yield the kinetic information necessary for determination of the rate-controlling mechanism.

Corrosion resulting from dissolution in a nonisothermal liquid-metal system is more complicated than the isothermal case. Although Eq 1 can be used to describe the net rate at any particular temperature, the movement of liquid—for example, due to thermal gradient or forced circulation—tends to make  $c$  the same around the liquid-metal system. Therefore, at temperatures where  $C > c$ , dissolution of an element into the liquid metal will occur. But at lower temperatures in the circuit, where  $C < c$ , a fraction of the particular element, dependent on nucleation kinetics and system variables, will tend to come out of solution and be deposited on the containment material in systems where wetting occurs. A schematic of such a mass transfer process is shown in Fig. 1. If net dissolution or deposition is measured by weight changes, a mass transfer profile such as the one shown in Fig. 2 can be established. There are exceptions to such behavior, however. For example, the movement of carbon in a  $\Delta T$  stainless steel/sodium system is found to be counter to the activity gradient (i.e., cold-to-hot) due to the overriding effect of liquid metal transport, even though concentration differences (in the liquid metal) are in the ppb–ppm range. Or, maximum corrosion in a two-phase potassium system is not found in the region of boiling (liquid-to-vapor), but in the area of condensation where the (liquid) metal is in its purest state and its corrosion potential is greatest. Liquid metal corrosion studies have led to

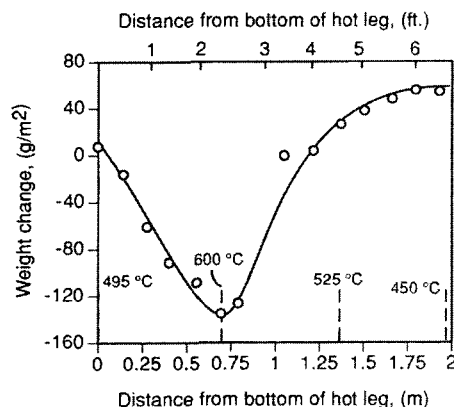


FIG. 2—Mass transfer as characterized by the weight changes of type 316 stainless steel coupons exposed around a nonisothermal liquid lithium type 316 stainless steel circuit for 9000 h [93]. (Reprinted with permission from Elsevier Science, New York, NY.)

considerable understanding of the mechanisms involved and the reader is referred to the selected bibliography for additional insight into specific systems [4–16]. Careful design of corrosion experiments and experimental apparatus is essential to eliminate unwanted, unexpected, or unpredictable results.

Liquid metal corrosion is also unique in the degree of selectivity with which certain constituents of a metal sample may be attacked. In aqueous or atmospheric corrosion, it is not uncommon for one phase or metal constituent in an alloy to be preferentially attacked. However, in liquid metals, the ability to remove interstitial elements from depths more than an order of magnitude greater than the surface damage can impart major degradation to mechanical strength, and may, under severe conditions, result in a breach of the containment. Furthermore, the design of most heat transfer systems involves narrow pathways for liquid metal flow, so that the useful life of a system may be as dependent on deposition phenomena as on corrosion. Corrosion deposits may increase pressure drops through an increase in surface roughness as well as restriction of the flow channel(s), and therefore place greater demand on pumping power and reduce heat transfer efficiencies. Understanding the process of deposition may be as vital as monitoring corrosion rate.

The goal of any scientist or engineer is to conduct tests that will allow predictions to be made for long-term behavior. For the liquid metal experimenter, the task is formidable since, in many cases, large size factors must be taken into consideration (a commercial nuclear reactor versus a laboratory test loop, for example), activity conditions of the complete system must be simulated, and the high chemical reactivity of the test medium (especially alkali metals) causes a major concern for safety of operation. In addition, the difficulties of sample handling, cleaning, and evaluating are challenging. An example is the removal of solidified lead or sodium from a test coupon without damaging the coupon surface or destroying a layer of deposit. However, perfect predictions are neither sought nor required; rather, a methodology for testing backed by a depth of understanding

FIG. 1—Schematic of thermal gradient mass transfer in a liquid-metal circuit [92].

for the physical and chemical changes occurring within the system is needed. This will permit design of liquid metal containment systems to meet basic operational criteria within acceptable limits of safety.

## IMPORTANT VARIABLES

There are at least 15 factors of major importance that require special attention in the consideration of corrosion by liquid metals:

1. Thermophysical condition of the material and base composition
2. Physical and chemical condition of the containment surface
3. Exposure temperature
4. Reactive impurity content in the liquid metal
5. Liquid metal velocity
6. Location (test coupons or containment), in relation to heat input/removal zones
7. Type of liquid metal circulation
8. Axial heating rate
9. Mechanical stress of material
10. Loop temperature differential,  $\Delta T$
11. Test specimen configuration
12. Exposure time
13. Monometallic or multi-metal/alloy containment system
14. Deposition of corrosion products
15. Effect of external environment

In liquid metal corrosion testing, all of these variables should be recognized and addressed. It is not possible in this chapter to provide a full account of the ramifications of each of them. Instead, one or two of the more important ones have been selected for illustrative purposes; in some cases, these illustrations are presented as specific examples of behavior in liquid sodium or liquid lithium. Numerous references are cited from the literature for information on the variables not described in detail.

### Thermophysical Condition of the Material and Base Composition

The thermophysical state of a material may be defined as the end result of prior thermal treatment and its interaction with mechanical deformation introduced in the final fabrication process. All of these conditions can have an effect on corrosion and must be characterized for definitive analysis. Surface condition of a specimen may also have an important influence on corrosion rate. The thermophysical condition of a material under test may be affected by the exposure environment. For example, if the intended application for a given metal or alloy is as a component in a nuclear reactor, then care should be exercised to ensure that high neutron fluxes do not significantly alter predicted corrosion behavior. Radiation can enhance nucleation reactions, and this may result in precipitation at lower than normal temperatures, or precipitation of normally unstable phases. In addition, radiation can dramatically affect the defect structure of a material and, therefore, significantly

influence solid state mass transport. These radiation effects may have an impact on corrosion rate or corrosion behavior.

A surface layer partially transformed to, or approaching the composition of, ferrite has been found to form on all austenitic materials exposed in a corrosion zone of nonisothermal systems based on sodium, lithium, lead, mercury, and other liquid metals, principally due to the preferential loss of nickel (or other soluble austenite stabilizing elements such as manganese and carbon) according to the mechanism described by Eq 1 [4,7,9-11,16-19]. The effect varies in degree and depth, depending on the operating parameters of the system, the liquid metal, and the time/temperature/location data of a given specimen. The plot in Fig. 3 illustrates this phenomenon in a more general sense. The figure shows the depth variation of a depleted zone as a function of corrosion rate in sodium. This depleted zone is formed as a result of two processes, either one of which may be rate-controlling; the diffusion of alloy species (including iron) down the activity gradient to the steel/sodium interface, and the removal of each element from the interface with subsequent transport by the liquid metal. The removal step may be either by direct dissolution (e.g., nickel, manganese) or by formation of a sodium-oxygen-metal complex (e.g., iron, chromium). The result is the eventual establishment of an equilibrium condition where the growth of the depleted zone is balanced by the receding corrosion surface [4,20]. Example A (Fig. 3) shows that an austenitic steel corroding in liquid sodium at  $5 \mu\text{m/y}$  will require 1000 h at  $700^\circ\text{C}$  to establish a steady-state depleted zone depth of  $10 \mu\text{m}$ . Example B indicates that corrosion at a rate of  $0.5 \mu\text{m/y}$  results in a  $100 \mu\text{m}$  depleted zone depth, but that about 60 000 h would be required to reach this condition at  $700^\circ\text{C}$ . However, at  $650^\circ\text{C}$  about the same depth of depletion ( $10 \mu\text{m}$ ) would be reached as in Example A after 10 000 h of exposure. Finally, since the corrosion rate in sodium is proportional to oxygen concentration [21], either parameter could be used as the variable on the abscissa axis in Fig. 3.

The amount of nickel present in an alloy exposed to liquid sodium, lithium, mercury, lead, and others has a direct impact not only on the overall weight loss, but also on the

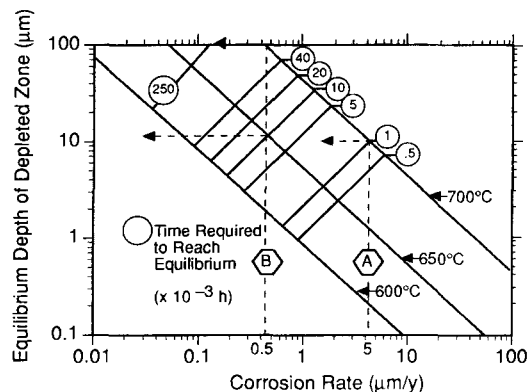


FIG. 3—Elemental depleted zone depth as a function of corrosion rate: type 316 stainless steel exposed to flowing sodium [69] (copyright 1980 by the American Nuclear Society, La Grange Park, IL).

morphology of the corroded surface. Features may range from relatively planar, where wall thinning is equivalent to weight loss, to a situation in which there is negligible wall thinning and corrosion produces a labyrinthine structure below the original liquid metal interface. In contrast to the behavior of nickel, molybdenum (as an alloy addition or as the primary metal) is very resistant to corrosion by many liquid metals. For example, if the molybdenum content is in excess of about 2 %, nodes of Laves phase,  $\text{Fe}_2\text{Mo}$ , form in the ferrite layer at the corroding surface and produce highly dissolution-resistant particles. With increasing molybdenum content, the surface structure can develop into coral-like features [22]. This has led to the development of corrosion-resistant coatings [23].

The ferrite regions on the austenitic steels often exhibit a porous-like structure that may be related to surface destabilization due to selective leaching [7,11,16,17], dissolution-triggered phase separation [18], or a localized corrosion product [19]. In contrast, the ferritic/martensitic steels tend to dissolve more slowly and maintain planar surfaces in contact with the liquid metal (although such surfaces are not smooth on a microscopic basis).

Solubility-driven reactions are not the only significant degradation mechanism for steels. Nitrogen in lithium has deleterious effects [24–28]. For stainless steel surfaces exposed to molten lithium [25,26], a specific nitrogen-related corrosion product was identified ( $\text{Li}_3\text{CrN}_3$ ). This key finding has formed the basis for a much better understanding of the various corrosion processes in lithium/steel systems. Furthermore, there is also definite evidence that carbides can play an important role in the corrosion of steels by lithium [25,29–33].

Refractory metals and alloys are generally dissolution-resistant in liquid metals and corrosion is often controlled by reactions with impurity/interstitial elements [13,14,27]. In the case of refractory metal alloys based on niobium or tantalum, the concentration of oxygen in the alloy is an important parameter with respect to corrosion in alkali metals, particularly lithium [34–38]. As little as 300 wppm of oxygen in niobium will induce catastrophic penetration of the niobium by lithium. Interstitial oxygen will also cause penetration of niobium and tantalum by sodium or potassium, but the threshold of oxygen concentration is higher.

In liquid metals other than the alkali series, such as lead, bismuth, and lead-lithium, solubility considerations tend to dominate and corrosion rates are usually higher than they are in many of the alkali metals. In general, increasing the nickel and/or manganese content of containment alloys results in significant increases in corrosion rates [9,16,39–46]. However, impurities, particularly oxygen and nitrogen, and additives to the liquid metals can play important roles in forming surface layers that, in some cases, can inhibit the dissolution process [9,47–50].

### Physical and Chemical Condition of the Containment Surface

Important considerations include the topography that results from the final preparation treatment given to the containment or corrosion test coupons and the chemical

condition of the surfaces to be exposed to the liquid metal. Several factors are clearly important in this regard:

- Smoothness—A corrosion test coupon should start its period of exposure with a relatively smooth and readily reproducible surface condition.
- Characterization—The surface morphology and microstructure should be thoroughly characterized and documented.
- Chemical condition—The starting chemical condition of the specimen surfaces is important, not as much as for the transient effect on the corrosion reactions of interest, but because contaminants can inhibit wetting, particularly for the heavier liquid metals like lead and mercury. Specimens should be free of finger oils, films from cleaning agents, and surface oxides or other products that form during materials processing. Otherwise, corrosion can be inadvertently delayed due to lack of wetting or atypical reactions and results will not be reproducible. Apparent incubation times can be quite long in some cases, even using specimen surfaces that were carefully cleaned prior to exposure—see, for example, the work of Pawel et al. with a mercury/stainless steel system [16].

### Exposure Temperature

Under dissolution-controlled conditions, corrosion by liquid metals should increase with increasing temperature. For example, assuming all other factors affecting corrosion are fixed, the corrosion rate-temperature relationship can be expected to follow the classical Arrhenius expression,  $\log k \propto \exp(-Q/RT)$ , where  $k$  is corrosion rate,  $Q$  is the activation energy,  $R$  is the gas constant, and  $T$  is the absolute temperature. This is shown graphically in Fig. 4 for type 316 stainless steel in sodium. In this case, the corrosion rate can be related directly to mass loss, which can be expressed in terms of wall thinning.

Mass transport of elemental or alloy constituents from the hot to cold regions around nonisothermal systems can be

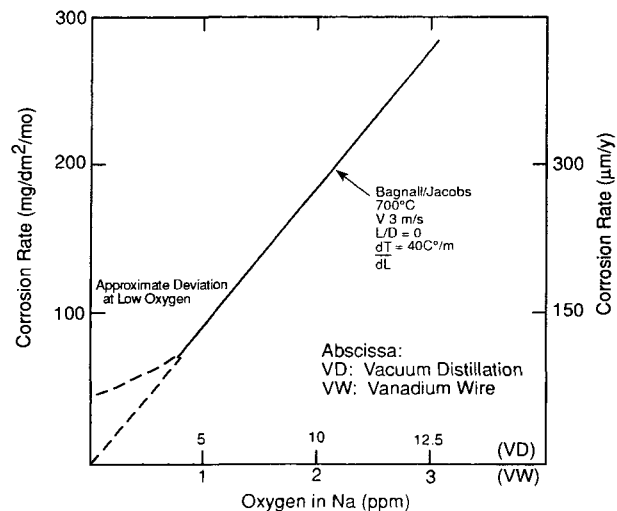


FIG. 4—Corrosion rate versus oxygen in sodium (type 316 stainless steel) [69] (copyright 1980 by the American Nuclear Society, La Grange Park, IL).

obscured or substantially altered by effects of reactions involving impurities. For example, in molten lithium-steel systems, nitrogen and carbon can lead to irregular mass transfer profiles, particularly at lower temperatures (400–500°C) [7,19,25,26,32,33,51–53]. Therefore, nature of the corrosion of steels by lithium can be very sensitive to the temperature range of interest and the magnitude of corrosion losses does not necessarily scale with the maximum temperature of the system. Depending on the temperature range, corrosion can be dominated by formation of  $\text{Li}_3\text{CrN}_5$  and/or carbides, carbon transport around the lithium system, and, at sufficiently high temperatures, solubility-driven reactions. At higher temperatures, for steels containing substantial amounts of soluble elements such as nickel and manganese, reactions involving nitrogen and carbon can often be minimal compared to mass transport by solubility-driven dissolution and deposition. In theory, such competing reactions can occur in most all liquid metal systems, particularly when solubilities are limited and care must be taken in evaluating corrosion as a function of temperature.

Another complicating factor in correlating corrosion rate data for certain systems stems from surface area-to-volume and temperature gradient effects. For example, for lithium, stainless steel corrosion rates determined for a given temperature condition are very reproducible among test systems (test loops) of the same geometry [54]. However, altering the dimensions of the system significantly changes the corrosion rate and also mass transfer profiles, even for the same maximum and minimum temperature conditions [54–56]. Similarly, the inclusion of a bypass, continuous flow cold trap system can affect mass transfer by extending the effective cold leg surface area of the loop.

### Reactive Impurity Content in the Liquid Metal

While reactive impurities are of concern for most liquid metals, most studies related to such have been with alkali metals, lead, and bismuth. As examples, some of these findings are described immediately below.

Oxygen in sodium is a key factor influencing the corrosion rate in sodium. Methods of measurement have included on-line and off-line vacuum distillation, mercury amalgamation, the use of a plugging meter or a cold trap temperature, vanadium wire equilibration, and several electrochemical metering devices. All methods suffer from some inherent fault or are open to reasonable doubt in regard to absolute interpretation of oxygen in ppm. For detailed information related to the various types of determination of oxygen in sodium, the reader is referred to several conference proceedings in which individual sessions devoted to this topic can be found [57–62].

Nitrogen is the main impurity element in lithium with respect to the rate of corrosive attack. Off-line monitoring techniques based on the Kjeldahl method are routinely used to determine nitrogen concentration.

While metering devices for on-line monitoring of oxygen in sodium and for hydrogen in both sodium and lithium have been successfully developed [63], only small-scale experiments have been attempted for direct measurement of nitrogen in lithium. The method is based on resistivity measurements in which it is assumed that total resistivity

increase, measured from a base value for “pure Li,” is due to the sum of resistivity contributions from hydrogen and nitrogen activities. Nitrogen concentration is hence determined by difference, using the base value for pure lithium and a value for the hydrogen resistivity contribution, determined from hydrogen activity measurements using an on-line hydrogen meter [64]. The reader is referred to a book by Addison [65] for additional information regarding the chemistry of liquid alkali metals.

In liquid metal systems that are oxidizing with respect to the solids they contact, corrosion inhibition is dependent on formation of protective surface films. For example, in lead or lead-bismuth, [47–49] equilibria controlling film formation are governed by the following: the uniform distribution of calcium, (or magnesium), to reduce the activity level of oxygen impurity in the lead (one common “alloy” often selected is Pb-225 ppm Mg) and the constant presence of active zirconium at the containment surface, where it reacts with nitrogen (or carbon, or both) diffusing from the containment bulk, to form a protective layer. (NOTE: The solubility of zirconium in pure lead is nil, and is only about 100–300 ppm in Pb-Mg or Pb-Bi alloys.)

### Liquid Metal Velocity

Much work on liquid metal velocity has been done with sodium and serves to illustrate its influence on corrosion. Bagnall and Jacobs [21] have attempted to unify the available data in the literature and correlate corrosion rate with temperature. Sodium velocity and oxygen were the two major variables taken into consideration. With oxygen interpreted on the vanadium wire equilibration scale, it was shown statistically that corrosion rate,  $R$ , was independent of velocity above about 3 m/s and directly proportional to oxygen concentration. An example of this correlation is shown in Fig. 4 where the variation of  $R$  with oxygen is plotted for type 316 stainless steel at 700°C. Data obtained at very low oxygen levels (<0.5 ppm by vanadium wire) deviate from the predictive curve. At these low concentrations, mass loss appears to approach the model developed by Weeks and Isaacs [4]. Such behavior is not unreasonable since it is clear that mass loss will, in any event, not drop to zero at zero oxygen. Also, an approximate correlation between the vanadium wire scale and vacuum distillation values is shown on the abscissa. Note that the latter scale is not linear and that the vacuum distillation analytical method becomes insensitive below about 5 ppm.

Another example of the influence of velocity on corrosion rate is from work with lead-lithium. Corrosion kinetics observed in the hot zones of austenitic steel loops containing Pb-17at.%Li show good agreement and appear to be linear after a nominal incubation period [49] in which differing initial surface conditions (e.g., oxidation, mechanical working) are eliminated (see above). The following corrosion expression, including an allowance for velocity effects, was derived by Flament et al. [9] for data collected in the temperature range 400–550°C:

$$v = 8 \times 10^9 e^{-25,600/1.98T} V^{0.875} d^{-0.125} \quad (2)$$

where  $v$  is metal loss rate in  $\mu\text{m/y}$ ,  $T$  is absolute temperature,  $V$  is the liquid metal velocity in m/s, and  $d$  is the hydraulic diameter in  $m$ .

### Location (Test Coupons or Containment) in Relation to Heat Input/Removal Zones

In sodium, corrosion rates have been shown to decrease as soon as heat input ceases to cause a temperature rise [7]. This phenomenon is known as the downstream effect and is applicable only in reference to isothermal zones. This effect is related to the hydraulic length-to-diameter ratio in the isothermal zone, and can be expressed as  $L/D$ , where  $L$  is the linear distance from the end of the temperature rise zone and  $D$  is the hydraulic diameter, defined as

$$D = \frac{4 \times \text{cross area of flow}}{\text{wetted perimeter}} \quad (3)$$

The decrease in corrosion rate with downstream position can be approximated by the equation

$$\log R_c = \log R_0 - K(L/D) \quad (4)$$

where

$R_c$  is corrosion rate at any value of  $L/D$ ,

$R_0$  is corrosion rate at  $L/D = 0$ , and

$K$  is the linear downstream coefficient.

This relationship is shown graphically in Fig. 5 for a liquid sodium corrosion test. In order to compare corrosion data between different laboratories, the corrosion rate at zero  $L/D$ , ( $R_0$ ), must be established. As an example, this was accomplished for the data in Fig. 7 by fitting a line by the least squares method and projecting this line to  $L/D = 0$ . Caution must be observed, however, when the data cover a limited range of  $L/D$  values. Corrosion experiments should be designed to cover a substantial range of  $L/D$ s ( $>200$ ), with data acquired as near  $L/D = 0$  as practical. Austenitic alloy/lithium  $\Delta T$  systems, apart from some interesting topographical changes, show little or no change in either chemical composition or mass loss as a function of  $L/D$  in isothermal corrosion zones

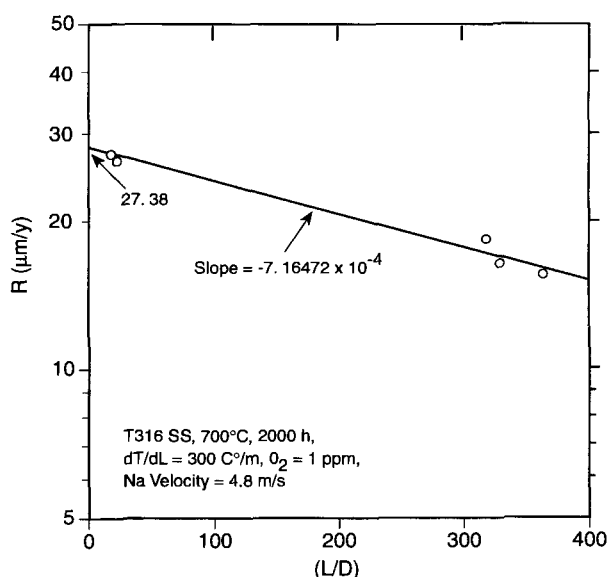


FIG. 5.—Typical downstream effect in a liquid sodium system [69] (copyright 1980 by the American Nuclear Society, La Grange Park, IL).

[66,67]. Downstream effects have not been observed for lithium and other liquid metals. However, the phenomenon has only been studied in detail for sodium.

### Type of Liquid Metal Circulation

Three basic types of liquid metal environment may be identified for engineering systems: forced circulation, thermal convection, or a stagnant isothermal containment system. These three types may be designed for single phase (liquid) or two-phase (liquid/vapor) operation. Laboratory testing, however, may involve numerous variations of the three types, and a description of the more important system configurations for data collection is given in the *Lab Testing* section of this chapter. In all liquid metal systems, the corrosion mechanisms will depend largely on the number of phases present, the concentration of active species available to participate in the process, and the characteristics of the various sources and sinks available to add or remove active elements. There are several considerations, however, that illustrate differences in behavior between the different liquid metals. Three examples are given:

In sodium, the corrosion rate generally increases in changing from static to thermal circulation to forced circulation systems.

In lithium, the same rules may not hold, because the solubility of nitrogen in lithium, even at its freezing point, is high (about 300 ppm). Hence, the best purification (“gettering”) techniques may not be good enough, and dissolution in a static system may remain high for a prolonged period.

In lead, or lead-bismuth systems, since the corrosion rate is highly dependent on the formation of surface films, the type of circulation has less effect on the corrosion rate than do those factors that affect film formation or spallation, (e.g., vibration or thermal/mechanical shocks).

### Axial Heating Rate

An increase in axial heating rate (i.e., increase in temperature divided by axial heat input distance), called  $dT/dL$ , has been related to an increase in corrosion rate in sodium [68]. Data were compared in experiments at three different laboratories. Results from two similar sodium loops, one with a  $dT/dL$  of  $\sim 40 \text{ C}^\circ/\text{m}$ , and the other with a  $dT/dL$  of  $300 \text{ C}^\circ/\text{m}$ , showed that consistently higher corrosion rates were obtained in the high  $dT/dL$  loop.

It is conceivable that the cause for the heating rate effect is closely linked to the mechanism controlling the downstream phenomenon. Sodium leaving the heater zone in the high  $dT/dL$  case has a greater “potential” for dissolution in the adjoining isothermal zone than in an otherwise identical low  $dT/dL$  case. The total change in solute concentration is extremely small in either case, but the change in terms of chemical activity may nevertheless be sufficient to affect the distribution of iron, nickel, and chromium atoms on active corrosion sites, a smaller number of “active” iron atoms existing in the lower  $dT/dL$  situation.

### Mechanical Stress of Material

There has been no detailed attempt to investigate the effects of stress on corrosion rate. It may be theorized that

an increase to some degree will result since diffusional processes, precipitation reactions, and dissolution kinetics at the solid/liquid interface will all be enhanced. However, the experimenter should bear in mind that the type of stress is important—whether it is tensile, compressive, cyclic, or residual. Residual stresses may be relieved at the test temperatures conventionally employed for liquid metal corrosion testing.

### Loop Temperature Differential, $\Delta T$

Temperature differences in a loop system provide the driving force for mass transport of corrosion products. Although no definitive experiments have been conducted, indications are that the magnitude of the  $\Delta T$  in sodium has no effect above a minimum value of about  $100^\circ\text{C}$  [69]. From a consideration of heat transfer properties, in any heat transfer system at a given flow velocity, different liquid metals would require different  $\Delta T$ s to deliver the same heat load. If the surface area and geometry are fixed by heat flux considerations, the  $\Delta T$  and/or flow velocity, and hence mass transfer fluxes, will change for liquid metals with different heat transfer characteristics.

### Test Specimen Configuration

Relative corrosion and mass transfer sources (dissolution) and sinks (deposition) are of vital importance in the analysis of corrosion experiments. It is important that the sink area is larger than the source area in order to determine the maximum corrosion effect at a given temperature. Cascading of test specimens in series or in parallel, as illustrated in Fig. 6, can lead to questionable conclusions about general corrosion results. Experiments in series, where different specimens are at different temperatures, can be particularly troublesome if some of the specimens act as both sources and sinks for corroding species, and careful post-exposure measurements of mass and surface composition changes are not made. Parallel experiments are more amenable to analysis providing all of the factors such as velocity,  $\Delta T$ , and  $L/D$  are known. The test geometry should always be given in detail when reporting corrosion results. The use of tubular (cylindrical) specimens allows a better hydrodynamic analysis of the flow conditions (e.g., Ref 32).

### Exposure Time

Experience has shown that accelerated corrosion takes place in the first few hours of exposure for certain alloys in liquid metals. After this initial period, which may vary for different materials, a steady-state corrosion rate is usually attained. Figure 7 graphically illustrates this phenomenon for sodium. Period  $t_1$  is generally on the order of 500–1000 h, but can extend appreciably beyond this duration. Period  $t_2$  indicates the steady-state corrosion rate that must be determined for long-term predictions. Historically,  $t_1$  and  $t_2$  have been combined when reporting corrosion data. This has little significance on long-term tests lasting thousands of hours, but becomes very important in short-term tests of a few hundred hours or less.

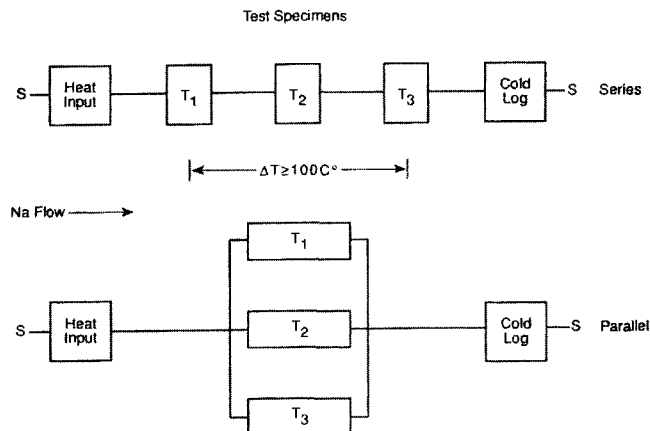


FIG. 6—Examples of series and parallel corrosion test circuits [69] (copyright 1980 by the American Nuclear Society, La Grange Park, IL).

### Monometallic or Multi-Metal/Alloy Containment System

The ideal corrosion experiment would contain only two materials: the liquid metal (or alloy), and the solid metal or alloy under test. This situation is rarely practical; every effort should therefore be made to prevent erroneous conclusions caused by masking. Masking can be described as the lowering of element loss from a downstream specimen because a specimen rich in this (these) element(s) is located upstream.

The removal of nickel from nickel-containing alloys is an important factor determining the corrosion rate of these materials in several liquid metals. If a high nickel source is placed upstream in an isothermal zone, the nickel removal rate from an alloy sample downstream could be reduced. If several alloys with different nickel contents are included in the same test it would seem appropriate to arrange them in

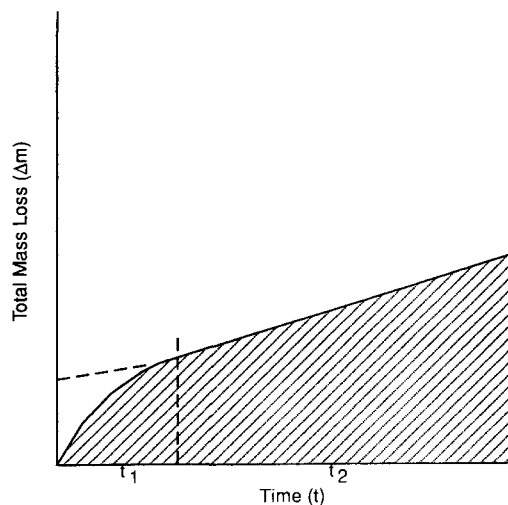


FIG. 7—Typical mass loss showing increased corrosion rate in first few hours of sodium exposure [69] (copyright 1980 by the American Nuclear Society, La Grange Park, IL).

order of increasing nickel concentration with respect to liquid metal flow direction. In the long term, this masking may become negligible in austenitic materials because all exposed surfaces move towards a ferritic composition with time.

Besides masking, elemental transfer can occur between two dissimilar materials in contact with the same liquid metal (even isothermally) due to an activity gradient. Again, experiments with only one solid material in contact with the liquid metal would avoid this complication. However, if this type of system cannot be used, careful surface analysis of as-exposed specimens should be used to try and understand mass transfer contributions from dissimilar material driving forces.

### Deposition of Corrosion Product

Deposition of corrosion products in a circulating  $\Delta T$  liquid metal system is important for three reasons. First, the degradation of heat transfer performance of heat exchangers must be predicted. Second, radiation exposure limits for maintenance in certain areas of nuclear reactor systems that transport and deposit radioactive species must be controlled. Third, the tendency for all deposits to become detached by thermal shock or flow perturbations must be known since there is concern that these types of debris could block critical coolant channels. It is therefore valuable, when possible, to monitor reactions involving deposition as well as dissolution.

The reader is referred to the literature for more information on deposits and deposition phenomena. Considerable work has been reported on characteristics of sodium, lithium, and lead-lithium systems [56,70–72].

### Effects of External Environment

Since the corrosion and mechanical properties of refractory metals and alloys based on niobium, vanadium, or tantalum are strongly affected by interstitial impurities (carbon, nitrogen, and oxygen), these metals must be maintained under ambient environments that do not contain sources of these impurities. In the case of lithium, the uptake of oxygen by niobium and Nb-1%Zr from the ambient atmosphere has induced localized penetration of the metal by lithium, with subsequent weeping or wicking to the outer surface of the containment [34]. In the case of liquid-vapor potassium or sodium systems, oxygen is depleted from the condenser regions and transferred to the evaporator [73]. Oxygen from the external atmosphere can thereby be transferred through the wall, and can increase the oxygen content of the liquid metal in the evaporator to levels where catastrophic corrosion will occur. Hydrogen embrittlement of refractory metals and alloys is also a potential problem during the removal of alkali metals after corrosion testing. The use of water- or alcohol-based solvents to remove the alkali metal residues can cause cracking as a result of the hydrogen generated from this reaction. Anhydrous ammonia is the preferred solvent for cleaning these metals.

### SUMMARY

Fifteen factors have been identified that can significantly affect the corrosion of materials in liquid metals. The collective

importance of all of these factors should be recognized and adequate information related to each of them should always be recorded. The more important of these factors are summarized below:

- Composition of the material being exposed and its thermophysical condition—The compositional variations and thermophysical condition of a material must be characterized prior to corrosion experiments in liquid metal.
- Exposure temperature—In general, corrosion rates increase with temperature. However, corrosion rate/temperature relationships can be strongly influenced by system geometry and impurity effects.
- Reactive impurities.
- Downstream effect.
- Axial heating rate.
- Liquid metal velocity.
- Loop  $\Delta T$ —There must be a difference in temperature in a forced circulation loop system to provide the driving force for solution-controlled mass transport.
- Exposure time—Accurate kinetic measurements must be made over an extended time period for useful comparisons and predictive analysis.
- Dissimilar materials—Care must be exercised to prevent dissimilar materials, whether in containment construction or in the sample inventory, from masking the true corrosion and mass transfer rates for individual materials.
- Deposition—Deposition can affect the efficient operation of a heat transfer system, and may lead to blockage of key flow channels. Characterization of deposition characteristics in a given system geometry is an important part of any liquid metal corrosion study.
- External environment—For tests involving reactive and refractory metals and alloys, care must be taken to preclude sources of carbon, nitrogen, and oxygen from the external environment, since their presence can adversely affect test data and the integrity of the liquid metal containment.

## LAB TESTING

### Test Procedures

Historically, testing routines have generally progressed from an evaluation of specimens encapsulated in static liquid metals through natural convection loops, forced convection loops, loops simulating reactor circuits, and large engineering experiments. As the tools have become more sophisticated, researchers have sought to identify the corrosion effects of system parameters such as temperature, geometry, flow velocity, turbulence, heat transfer rates, and system impurities.

In the case of the alkali metals, impurities such as oxygen, nitrogen, and carbon can have a significant effect on the corrosion of steels and refractory metals. For this reason, it is imperative that impurities initially present in the alkali metal and those entering during test be carefully monitored and controlled. In effect, any corrosion testing program must be designed around the sampling procedures and analytical techniques used to measure impurities in the alkali metals.



In the following sections, various test procedures are discussed and examples are given. The examples illustrate the principles involved in the test method. Each investigator's test design, although using these principles, may differ in detail. Alkali metals react vigorously with air. Consequently, although beyond the scope of this chapter, any operation on alkali metals (i.e., melting, loading, or welding the test system) must be performed in an inert gas or vacuum atmosphere. Additional details and references may be found in Ref 74. Some important safety aspects are reviewed in Ref 75, and devices for rapid leak detection are described in Ref 63.

### Specimen Examination

Correct interpretation of test results requires that the extent of wetting be confirmed for each test condition. In some liquid metal/containment combinations, many subtleties of surface condition may substantially influence wetting and thereby potential interactions (see above). In particular, wetting of metallic surfaces by Hg is very sensitive to precise temperature and extent of surface cleanliness/films [76,77]. As a result, wetting under test conditions can be easily disrupted and initial post-test examination of as-removed specimens must assure that complete wetting has taken place.

Mass loss alone is not a true indication of the total damage caused by corrosion in many materials. As indicated earlier, subsurface metal removal can be linked to the nickel content of the alloy, or any other element with high solubility; this is true for corrosion in sodium, lithium, mercury, and several other liquid metals. Subsurface attack can take the form of localized bulk removal producing a porous region in the depleted zone or a more general selective loss of alloy elements without microstructural damage. Either of these cases, or the presence of intergranular attack extending beneath the depleted zone into the base metal, causes damage greater than would be expected from wall thinning alone. In sodium studies, a total damage function was developed to express the corrosion process, as shown in Fig. 8. Here, total damage is shown as a combination of surface regression, a zone of degradation (with respect to mechanical properties) and intergranular attack. It should be noted, however, that this behavior is not limited to interaction with sodium, and this damage function can be used to describe corrosion damage produced by numerous liquid metals.

### Static Isothermal Capsules

Static capsules of the type shown in Fig. 9 are used to determine the extent of solid dissolution, interstitial transfer, or interalloying between the solid and liquid. The capsule can serve as the test specimen, or the test specimen can be incorporated as an insert in the capsule. In the latter case, it is a general requirement that the capsule and test specimen be of the same composition unless the test is intended specifically to study dissimilar-metal mass transfer effects. Incorporation of a test specimen simplifies the determination of any changes in weight, dimension, or mechanical properties due to liquid metal exposure.

Static capsules (Fig. 9) have also been used to determine the effect of oxygen on the compatibility of niobium and

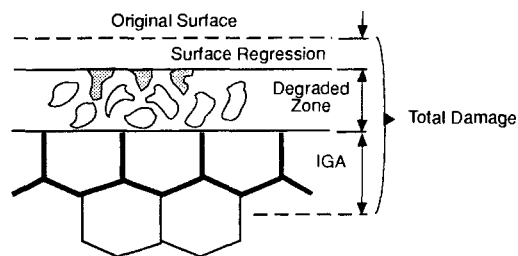


FIG. 8—Representative modes of surface damage in dynamic sodium or lithium systems [7].

tantalum with sodium and potassium [34–38]. The capsules were contained in the outer stainless steel container for protection against oxidation. By making weighed additions of  $K_2O$  to potassium, niobium dissolution was found to be strongly affected by the oxygen concentration of the potassium. Capsule tests with liquid metals have also been used to study carburization/decarburization behavior (see, for example, Refs 30 and 31) and nitrogen reactions (Ref 78).

Static isothermal capsules are also useful for studying dissimilar metal mass transfer. DiStefano [79] studied the interactions of type 316 stainless steel with niobium or Nb-1 % Zr in Na and NaK by exposing tension specimens of the niobium or Nb-1 % Zr to the liquid metal in a stainless steel container (Fig. 10). A transfer of carbon and nitrogen from the stainless steel to the niobium or Nb-1 % Zr was noted. The carbon and nitrogen transfer depended on temperature, time, and the surface area ratios of stainless steel to niobium (varied by changing the number of spacers shown in Fig. 10).

Static capsules or pots of special design are used to measure the solubility of solids in liquids. Eichelberger et al. [80] used bimetallic capsules made by welding two crucibles,

FIG. 9—Static capsule test system used to study the effect of oxygen on the corrosion of niobium by potassium (Note: 1.0 in. = 25.4 mm) [94].

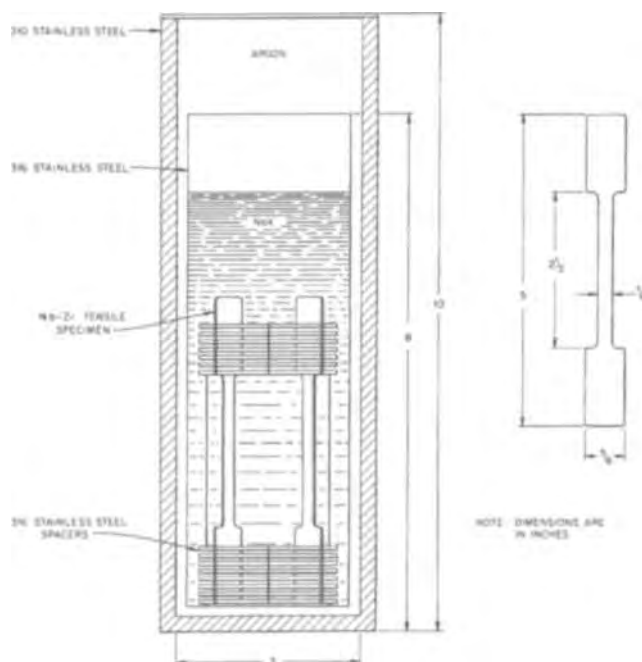


**FIG. 10—Dissimilar-metal test system (1.0 in. = 25.4 mm) [77].** (Reprinted with permission from the Oak Ridge National Laboratory, which is managed by Martin Marietta Energy Systems, Inc. for the U.S. Department of Energy.)

one of the test material (solute crucible) and one that contains none of this material (sampling crucible). The liquid was equilibrated in the solute crucible and inverted at temperature to allow the saturated liquid to drain into the sampling crucible. After cooling, the liquid was analyzed for the test material.

### Refluxing Capsules

In systems where a liquid metal is used as the working fluid (e.g., the Rankine-cycle), liquid is converted to vapor in one part of the system and vapor to liquid in another part. The distillation effects of the vaporization process result in extremely pure condensing vapor that may be able to dissolve and transport container material. As opposed to an all-liquid system, where the liquid is always partially saturated with container material constituents, dissolution in the condenser region can continue undiminished; the dissolution rate will depend on the condensation rate and temperature. In contrast, liquid in the evaporator section will ultimately become supersaturated with respect to container material constituents, so that the heated sections of a liquid metal boiling system will be subject to deposition rather than corrosion [81].

The effect of a boiling-condensing liquid metal on its container material is most easily studied in a refluxing capsule experiment. The capsule design illustrated in Fig. 11 was used for evaluating the effect of refluxing potassium on refractory metals. A 300 mm capsule containing machined insert specimens in the condenser section was half filled with potassium and heated. Liquid metal vaporizes, condenses in the water-cooled upper section of the capsule, and

**FIG. 11—Refluxing alkali metal test (1.0 in. = 25.4 mm) [79].** (Reprinted with permission from the Oak Ridge National Laboratory, which is managed by Martin Marietta Energy Systems, Inc. for the U.S. Department of Energy.)

flows back to the boiling pool. Under steady state conditions, the evaporation rate is determined by the vapor condensation rate, which in turn is determined by the amount of heat extracted from the vapor region. Knowing the water flow rate, the water temperature, and the latent heat of condensation of the liquid metal, the condensation rate can be calculated. After testing, the insert specimens are checked for changes in dimensions, weight, chemical composition, and microstructure.

DiStefano [82] has shown that the ratio of the diameter to length of a refluxing capsule is critical in achieving steady state boiling-condensing conditions. Also important in the case of refractory metals (e.g., niobium, tantalum) is the protective atmosphere maintained outside the capsule. Aside from limiting oxide film formation, the atmosphere must afford a sufficiently low-oxygen pressure to prevent oxygen infusion into the capsule. This is why such capsule (and loop) tests are often operated in vacuum systems.

### Seesaw (Tilting-Furnace) Capsules

The "seesaw capsule" provides the simplest technique for simultaneously introducing flow and a temperature gradient into a test. A capsule with specimens in both ends is partially filled with liquid metal and heated to maintain a temperature difference between the two ends. The capsule is then rocked slowly back and forth about a horizontal axis (perpendicular to the capsule axis) so that the liquid flows

from one end of the capsule to the other. After test, the extent of mass transfer is determined by examining test specimens from the alternate ends of the capsule. Although this device is useful for screening purposes, the dynamic nature of the heating and cooling cycles prevents a rigorous analysis of mass transfer in terms of time and temperature.

### Use of Capsules for Pre-Exposure

Capsule test facilities can also be used for pre-exposure of specimens for subsequent mechanical testing. Tortorelli and coworkers used this technique to study decarburization of ferritic steels in lithium under a variety of heat treatments. Weight change data, carbon analysis, and tension testing were collectively used in this evaluation [31].

### Rotating Cylinder (Disk) Technique

As noted above, the mass transfer kinetics of temperature gradient loops are usually described with reference to dissolution in the hot leg. It is possible to quantitatively study the dissolution step using the rotating cylinder technique. Unlike loop studies, this technique allows one to study dissolution in a system where the hydrodynamic conditions are fully defined. Experimentally, solid cylinders of the test material are rotated at various speeds in an isothermal liquid-metal bath. Changes in the concentration of solid in the liquid and changes in the cylinder radius are determined as a function of time. With these data it is possible to determine the mass transfer coefficient and the rate-controlling step for dissolution.

A rotating disk method has also been used to study effects of high-velocity corrosion, and the potential for damage from erosion mechanisms [83]. A rotating dissolution cell has also been used for measurements of corrosion in liquid mercury [84].

### Thermal-Convection Loops

The simplest nonisothermal flowing system where processes associated with dissolution and deposition occur is one in which flow is induced by thermal convection. This is accomplished by heating one leg of a closed loop and cooling another leg. The flow rate is dependent on the height of the heated and cooled sections, on the temperature gradient, and on the physical properties of the liquid. Both single-phase (all-liquid) and two-phase (liquid-vapor) loops have been tested. In some cases, thermal convection loops are destructively examined after operation [55,67]. In others, specimens are removed and replaced numerous times for cumulative periods of 10 000 h or more [22,54,68].

Figure 12 is a diagram of the loop used by DeVan and Sessions [85] to study the mass transfer of niobium-base alloys in flowing lithium. Each loop (254 by 610 mm) contained a continuous string of interlocking test specimens that gave a weight change profile around the loop along with information on changes in alloy composition and microstructure. These loops were heated by tantalum resistance furnaces placed concentrically about one vertical leg (hot leg). A water-cooled heat sink was located around the other vertical leg (cold leg), and the heat was rejected to this

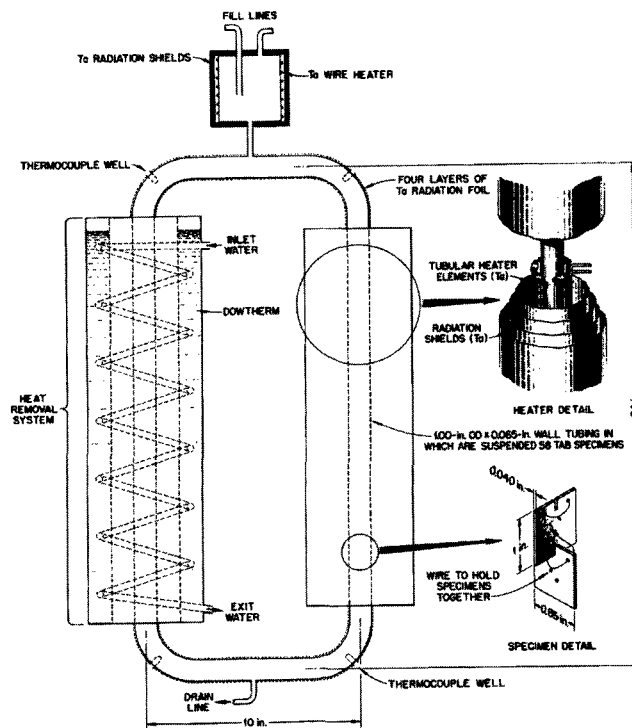


FIG. 12—Diagram of lithium thermal convection loop (1.0 in. = 25.4 mm) [83] (copyright 1967 by the American Nuclear Society, La Grange Park, IL).

sink together with the cold-leg entrance and exit temperatures was used to calculate the liquid flow rate. The remainder of the loop was insulated with tantalum foil to minimize heat losses. A temperature profile between the thermocouples on the loop corners was derived from a heat balance for each leg. During test, the loops were protected from oxidation by a bell-jar enclosure, which provided a vacuum of  $10^{-8}$  to  $10^{-9}$  Torr.

Similar loops, constructed of stainless steel and operated with radiant heating devices in air, have been used for liquid metal corrosion studies in laboratories around the world (e.g., Refs 16,54). In some cases, removable sample strings are situated in the hot and cold legs to facilitate removal of specimens without interruption to liquid metal flow [54].

The thermal convection loop is also useful for studying dissimilar-metal mass transfer. The bimetallic loop design shown in Fig. 13 was used by DeVan and Jansen [86] to determine the transport rates of nitrogen and carbon between vanadium alloys and stainless steels in a sodium circuit. Mass transfer rates and carbon and nitrogen effects on mechanical properties were monitored by means of insert specimens in the hot and cold legs. The effects of surface area ratios of the two materials were determined by adding or subtracting insert specimens.

Still another use [87] of thermal convection loops has been the study of corrosion effects in two-phase (vapor and liquid) potassium systems. In this case the lower half of the loop is filled with liquid and the upper half with vapor. The data derived from such a system are basically similar to

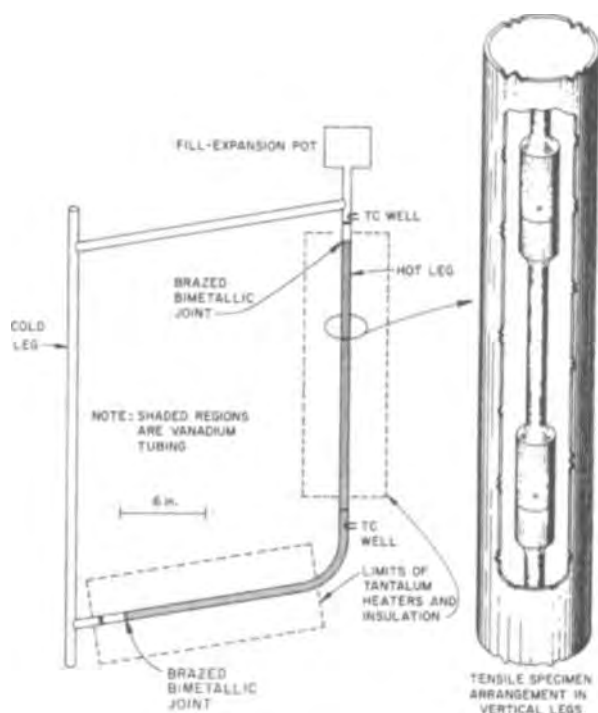


FIG. 13—Vanadium-stainless steel-sodium thermal convection loop (1.0 in. = 25.4 mm) [84]. (Reprinted with permission from the Oak Ridge National Laboratory, which is managed by Martin Marietta Energy Systems, Inc. for the U.S. Department of Energy.)

those obtained from refluxing capsule experiments discussed above. However, the use of a loop allows the boiler and condenser legs to be separated so that condensate flow parallels rather than opposes vapor flow.

### Forced-Convection Loops

The utility of thermal convection loops is limited by the low flow velocities (maximum of about 60 mm/s), making extrapolation to the higher velocities in operating systems doubtful. Higher flow velocities are obtained in forced convection loops where the liquid is moved through the loop with an electromagnetic or mechanical pump. Electromagnetic pumping is generally preferred for corrosion studies, since it alleviates the problem of pump seal leakage, but such pumps can act as traps for deposition of magnetic species. As with natural circulation systems, forced circulation loops have been developed to test both single-phase (all liquid) and two-phase (vapor and liquid) systems. The latter systems have been used to evaluate not only corrosion processes but also the effects of vapor impingement on turbine blade and nozzle simulators [88,89].

Figure 14 shows a schematic diagram of a simple "figure-of-eight" loop [90]. Basically, such loops consist of three parts: (a) the hot leg, where the liquid metal is heated to the maximum temperature, (b) an economizer or regenerative heat exchanger to minimize the energy transferred to and from the system, and (c) the cold leg, where the liquid is cooled to its minimum temperature. For the loop in Fig. 14,

FIG. 14—"Figure-of-eight" forced convection test loop: sodium-Inconel pumped loop (1.0 in. = 25.4 mm) [88].

the oxygen concentration of the alkali metal was controlled by bypassing a portion of the pump flow through a cold trap in parallel with the loop. The loop was completely closed except at the expansion tank, which was held under a positive pressure of purified helium to prevent pump cavitation. The material under test was used for constructing all parts of the loop, and the loop was destructively examined after a given test period.

Because forced-convection loops are costly to construct, it is now the usual practice to operate the loops as permanent testing facilities, with corrosion specimens cycled in and out of the facility. Test specimens of various materials are generally placed in the hot leg, and the effect of the flowing liquid on the specimens is determined from changes in weight, dimensions, composition, mechanical properties, and microstructure. Such an approach yields data on maximum corrosion rates as a function of temperature and liquid metal flow rate. Any attempt to elucidate corrosion mechanisms, however, is hampered by the inability to interrelate dissolution and deposition processes.

Forced convection systems have sometimes been used to screen test materials that differed widely in composition [91]. Corrosion data generated in such tests are useful to the extent that some information is gained about dissimilar-metal mass transfer among the materials, but it is normally not realistic to rate the thermal gradient mass transfer behavior of individual materials on the basis of such a test.

There are numerous accounts in the literature of liquid metal test facility design and operation, and it is not possible to list them all in this chapter. However, in addition to those already cited, the reader is referred to Refs 57 to 62 for a selection of reports addressing facility design for lithium, lithium-lead, lead, and sodium.

### Large Engineering Experiments

The final step in most testing programs is the design, construction, and testing of loops simulating the exact system for which data are needed. Here an attempt is made to duplicate all possible interactions involved in the operating system and to demonstrate system feasibility from an

**TABLE 1**—Range of applicability for various metals and alloys with liquid metals.

Material	Maximum Temperature of Operation for Nominal Corrosion(°C)			
	Na	Li	K	Pb,Pb-Bi
Stainless Steels	600	450	600	400
Cr-Mo Steels	600	500		425
Ti and Alloys		550		
Nb-1Zr	900	1300	750	

engineering standpoint. The reader is referred to numerous conference proceedings in which accounts of large facilities, including operating liquid metal-cooled nuclear reactors, are given [57–62].

## FIELD TESTING

Not applicable.

## STANDARDS

None.

## MATERIALS

As a general rule, assuming impurity and dissimilar metal effects are controlled and not overriding, the lower the nickel content of an alloy, the better is its corrosion resistance in liquid metals. The materials shown in Table 1 have proven to be corrosion-resistant to the specified liquid metals up to the temperature limit indicated. For additional information on materials compatibility, the reader is referred to the *Liquid Metals Handbook* [92,93].

## REFERENCES

- [1] *Embrittlement by Liquid and Solid Metals*, M. H. Kadmar, Ed., AIME, Warrendale, PA, 1984.
- [2] Lynch, S. P., "Metallographic Contributions to Understanding Mechanisms of Environmentally Induced Cracking," *Metallography*, Vol. 23, No. 2, September 1989, pp. 147–171.
- [3] Lynch, S. P., "Metal-Induced Embrittlement of Materials," *Materials Characterization*, Vol. 28, No. 4, June 1992, pp. 279–289.
- [4] Weeks, S. P. and Isaacs, H. S., "Corrosion and Deposition of Steels and Nickel-Base Alloys in Liquid Sodium," *Advances in Corrosion Science and Technology*, Vol. 3, Plenum Press, NY, 1973.
- [5] Epstein, L. F., "Static and Dynamic Corrosion and Mass Transfer in Liquid Metal Systems," *Liquid Metals Technology, Chemical Engineering Progress Symposium*, Ser. 20, No. 53, 1957, pp. 67–81.
- [6] Weeks, J. R. and Klamut, C. J., "Liquid Metal Corrosion Mechanisms," *Corrosion of Reactor Materials*, Vol. 1, International Atomic Energy Agency, pp. 106–132.
- [7] DeVan, J. H. and Bagnall, C., "A Perspective of the Corrosion Behavior of Lithium and Sodium," *Proceedings of the Third International Conference on Liquid Metal Engineering and Technology*, Vol. 3, The British Nuclear Energy Society, 1985, pp. 65–72.
- [8] Natesan, K., "Influence of Nonmetallic Elements on the Compatibility of Structural Materials with Liquid Alkali Metals," *Journal of Nuclear Materials*, Vol. 115, 1983, pp. 251–262.
- [9] Flament, T., Tortorelli, P. F., Coen, V., and Borgstedt, H. U., "Compatibility of Materials in Fusion First Wall and Blanket Structures Cooled by Liquid Metals," *Journal of Nuclear Materials*, 1992, Vol. 191–194, pp. 132–138.
- [10] Chopra, O. K. and Tortorelli, P. F., "Compatibility of Materials for Use in Liquid-Metal Blankets of Fusion Reactors," *Journal of Nuclear Materials*, 1984, Vol. 122, 123, pp. 1201–1212.
- [11] Tortorelli, P. F., "Fundamentals of High-Temperature Corrosion in Liquid Metals," *Metals Handbook, Ninth Edition, Volume 13*, ASM International, Metals Park, OH, 1987, pp. 56–60.
- [12] DeVan, J. H., DiStefano, J. R., and Hoffman, E. E., "Compatibility of Refractory Alloys with Space Reactor System Coolants and Working Fluids," *Proceedings of Symposium on Refractory Alloy Technology for Space Nuclear Power Applications*, U.S. Department of Energy Report CONF-8308130, January 1984, pp. 34–85.
- [13] Smith, D. L. and Natesan, K., "Influence of Nonmetallic Impurity Elements on the Compatibility of Liquid Lithium with Potential CTR Containment Materials," *Nuclear Technology*, Vol. 22, 1974, pp. 392–404.
- [14] Coen, V. and Fenici, P., "Compatibility of Structural Materials with Liquid Breeders—A Review of Recent Work Carried Out at JRC, Ispra," *Nuclear Engineering Design/Fusion*, Vol. 1, 1984, pp. 215–229.
- [15] DeVan, J. H., "Compatibility of Structural Materials with Boiling Potassium," *Proceedings of International Conference of Liquid Metal Technology in Energy Production*, CONF-760503-P1, U.S. Energy Research and Development Administration, 1976, pp. 418–426.
- [16] Pawel, S. J., DiStefano, J. R., and Manneschildt, E. T., "Thermal Gradient Mass Transfer of Type 316L Stainless Steel and Alloy 718 in Flowing Mercury," *Journal of Nuclear Materials*, Vol. 296, 2001, pp. 210–218.
- [17] Harrison, J. D. and Wagner, C., "The Attack of Solids by Liquid Metals and Salt Melts," *Acta Metallurgica*, Vol. 7, 1959, pp. 722–735.
- [18] Tas, H., De Schutter, F., LeMaitre, P., and DeKeyser, J., "Instability of Austenitic Stainless Steels in Contact with Liquid Metals," *Proceedings of Fourth International Conference on Liquid Metal Engineering and Technology*, Vol. 3, Societe Francaise d'Energie Nucleaire, 1988, pp. 523–1–523–12.
- [19] Barker, M. G., Sattler, P. F., and Schreinlechner, I. E., "Mechanism Determining the Corrosion Rate of Stainless Steels in Liquid Lithium," *Proceedings of Fourth International Conference on Liquid Metal Engineering and Technology*, Vol. 3, Societe Francaise d'Energie Nucleaire, 1988, pp. 34–85.
- [20] Brush, E. G., "Sodium Mass Transfer: XVI. The Selective Corrosion Component of Steel Exposed to Flowing Sodium," *Atomic Energy Commission Research & Development Program*, General Electric Corp. GEAP-4832, March 1965.
- [21] Bagnall, C. and Jacobs, D., "Relationships for Corrosion of Type 316 Stainless Steel in Liquid Sodium," Westinghouse Electric Corp. Topical Report, WARD-NA-3045-23, 1975.
- [22] Bagnall, C. and Witkowski, R. E., "Microstructure and Surface Characterization of Commercial Candidate LMFBR Fuel Cladding and Duct Alloys after Exposure to Flowing Sodium at 700°C," Westinghouse Electric Corp. Topical Report, WARD-NA3045-53, September 1978.
- [23] Witkowski, R. E., Arcella, F. G., Bagnall, C., and Shiels, S. A., "Molybdenum Coating Development for LMFBR Fuel Cladding," *Second International Conference on Liquid Metal Technology in Energy Production*, Richland Washington, 20–24 April 1980, pp. 7-62–7-71.
- [24] Hubberstey, P., "Dissolved Nitrogen in Liquid Lithium—A Problem in Fusion Reactor Chemistry," *Proceedings of the Third International Conference on Liquid Metal Engineering and Technology*, Vol. 2, The British Nuclear Energy Society, 1985, pp. 85–91.

- [25] Barker, M. G. and Frankham, S. A., "The Effects of Carbon and Nitrogen on the Corrosion Resistance of Type 316 Stainless Steel," *Journal of Nuclear Materials*, Vol. 107, 1982, pp. 218–221.
- [26] Barker, M. G., Hubberstey, P., Dadd, A. T., and Frankham, S. A., "The Interaction of Chromium with Nitrogen Dissolved in Liquid Lithium," *Journal of Nuclear Materials*, Vol. 114, 1983, pp. 143–149.
- [27] Hubberstey, P. and Roberts, P. G., "Corrosion Chemistry of Vanadium in Liquid Lithium Containing Dissolved Nitrogen," *Journal of Nuclear Materials*, Vol. 155-157B, 1988, pp. 694–697.
- [28] Hoffman, E. E., "Corrosion of Materials by Lithium at Elevated Temperatures," Oak Ridge National Laboratory Report, ORNL-2674, Oak Ridge National Laboratory, Oak Ridge, TN, March 1959.
- [29] Ruedl, E., Coen, V., Sasaki, T., and Kolbe, H., "Intergranular Lithium Penetration of Low-Ni, Cr-Mn Austenitic Stainless Steels," *Journal of Nuclear Materials*, Vol. 110, 1982, pp. 28–36.
- [30] Anderson, T. L. and Edwards, G. R., "The Corrosion Susceptibility of Ferritic Steels Lithium-17.6 Wt Pct Lead Liquid," *Journal of Materials for Energy Systems*, Vol. 2, 1981, pp. 16–25.
- [31] Tortorelli, P. F., DeVan, J. H., and Yonco, R. M., "Compatibility of Fe-Cr-Mo Alloys with Static Lithium," *Journal of Materials for Energy Systems*, Vol. 2, 1981, pp. 5–15.
- [32] Bell, G. E. and Abdou, M. A., "The Role of Carbides in the Corrosion of Fe-12Cr-1MoVW Steel in Liquid Lithium," *Fusion Technology*, Vol. 15, 1989, pp. 315–320.
- [33] Chopra, O. K. and Hull, A. B., "Influence of Carbon and Nitrogen Impurities on the Corrosion of Structural Materials in a Flowing-Lithium Environment," *Fusion Technology*, Vol. 15, 1989, pp. 309–314.
- [34] DiStefano, J. R., "Corrosion of Refractory Metals by Lithium," Oak Ridge National Laboratory Report, ORNL-3551, March 1964.
- [35] Klueh, R. L., "The Effect of Oxygen on the Corrosion of Niobium and Tantalum by Liquid Lithium," Oak Ridge National Laboratory Report, ORNL-TM-4069, March 1973.
- [36] Klueh, R. L., "The Effect of Oxygen in Sodium on the Compatibility of Sodium and Niobium," *Proceedings of the International Conference on Sodium Technology and Large Fast Reactor Design*, ANL 7520, Part 1, 7–9 November 1968, pp. 171–176.
- [37] Klueh, R. L., "The Effect of Oxygen on Tantalum-Sodium Compatibility," Oak Ridge National Laboratory Report, ORNL-TM-3590, December 1971.
- [38] Klueh, R. L., "The Effect of Oxygen on the Compatibility of Tantalum and Potassium," Oak Ridge National Laboratory Report, ORNL-4737, November 1971.
- [39] Romano, A. J., Klamut, C. J., and Gurinsky, D. H., "The Investigation of Container Materials for Bi and Pb Alloys, Part I. Thermal Convection Loops," Brookhaven National Laboratory Report, BNL-811, 1963.
- [40] James, J. A. and Trotman, J., "Corrosion of Steels in Liquid Bismuth and Lead," *Journal of the Iron & Steel Institute*, London, Vol. 194, 1960, pp. 319–323.
- [41] Cathcart, J. V. and Manly, W. D., "The Mass Transfer Properties of Various Metals and Alloys in Liquid Lead," *Corrosion*, 1955, pp. 43–47.
- [42] Asher, R. C., Davies, D., and Beetham, S. A., *Corrosion Science*, Vol. 17, 1977, pp. 545–557.
- [43] Sannier, J. and Santarini, G., "Etude de la Corrosion de Deux Aciers Ferritiques par le Plomb Liquide Circulant Dans un Thermosiphon; Recherche D'Un Modele," *Journal of Nuclear Materials*, Vol. 107, 1982, pp. 196–217.
- [44] Ali-Kahn, I., "Corrosion of Steels and Refractory Metals in Liquid Lead," *Material Behavior and Physical Chemistry in Liquid Metal Systems*, H. U. Borgstedt, Ed., Plenum Press, NY, 1982, pp. 85–91.
- [45] Broc, M., Flament, T., Fauvet, P., and Sannier, J., "Corrosion of Austenitic and Martensitic Stainless Steels in Flowing  $^{17}\text{Li}83\text{Pb}$ ," *Journal of Nuclear Materials*, Vol. 155-157B, 1988, pp. 710–714.
- [46] Tortorelli, P. F., "Corrosion and Mass Transfer of Ferrous Alloys in Pb-17 at.% Li," *Proceedings of Fourth International Conference on Liquid Metal Engineering and Technology*, Vol. 3, Societe Francaise d'Energie Nucleaire, 1988, pp. 528-1–528-10.
- [47] Weeks, J. R. and Klamut, C. J., "Reactions Between Steel Surfaces and Zirconium in Liquid Bismuth," *Nuclear Science and Engineering*, 1960, pp. 133–147.
- [48] Kammerer, O. F., Weeks, J. R., Sadofsky, J., et al., "Zirconium and Titanium Inhibit Corrosion and Mass Transfer of Steels by Liquid Heavy Metals," *Transactions of AIME*, Vol. 212, 1958, pp. 20–25.
- [49] Borgstedt, H. U. and Rohrig, H. D., "Recent Results on Corrosion Behavior of MANET Structural Steel in Flowing Pb-17Li Eutectic," *Journal of Nuclear Materials*, Vol. 179-181, 1991, pp. 596–598.
- [50] Barker, M. G., Lees, J. A., Sample, T., and Hubberstey, P., "Corrosion of Type 316L Stainless Steel in Pb-17Li," *Journal of Nuclear Materials*, Vol. 179-181, 1991, pp. 599–602.
- [51] Chopra, O. K. and Smith, D. L., "Influence of Temperature and Lithium Purity on Corrosion of Ferrous Alloys in a Flowing Lithium Environment," *Journal of Nuclear Materials*, Vol. 141-143, 1986, pp. 584–591.
- [52] Tortorelli, P. F. and DeVan, J. H., "Corrosion of an Fe-12 Cr-1 Mo VW Steel in Thermally-Convective Lithium," *Proceedings of Topical Conference on Ferritic Alloys for Use in Nuclear Energy Technologies*, AIME, 1984, pp. 215–221.
- [53] Tortorelli, P. F., "Corrosion of Ferritic Steels by Molten Lithium: Influence of Competing Thermal Gradient Mass Transfer and Surface Product Reactions," *Journal of Nuclear Materials*, Vol. 155-157, 1988, pp. 722–727.
- [54] Tortorelli, P. F. and DeVan, J. H., "Mass Transfer Kinetics in Lithium-Stainless Steel Systems," *Proceedings of Third International Conference on Liquid Metal Engineering and Technology*, 1984, The British Nuclear Energy Society, London, 1985.
- [55] Tortorelli, P. F., DeVan, J. H., and Selle, J. E., "Corrosion in Lithium-Stainless Steel Thermal Convection Systems," *Proceedings of the Second International Conference on Liquid Metal Technology in Energy Production*, CONF-801-P2, August 1980, pp. 13-44–13-54.
- [56] Tas, H., DeKeyser, J., Casteels, F., et al., "Mass Transfer in Pure Lithium and Lithium-Lead Dynamic Environments: Influence of System Parameters," *Journal of Nuclear Materials*, Vol. 141-143, 1986, pp. 571–578.
- [57] *Alkali Metal Coolants, Proceedings of a Symposium*, 28 November–2 December 1966, International Atomic Energy Agency, Vienna, 1967.
- [58] *International Conference on Liquid Metal Technology in Energy Production*, M. H. Cooper, Ed., CONF-760503-P1/P2, Champaign, PA, 3–6 May 1976.
- [59] *Second International Conference on Liquid Metal Technology in Energy Production*, J. M. Dahlke, Ed., CONF-801-P1/P2, Richland, WA, 20–24 April 1980.
- [60] *Third International Conference on Liquid Metal Engineering and Technology*, 1984, The British Nuclear Energy Society, London, 1985.
- [61] *Materials Behavior and Physical Chemistry in Liquid Metal Systems*, H. U. Borgstedt, Ed., Plenum Press, NY, 1982.
- [62] *Proceedings of the Fourth International Conference on Liquid Metal Engineering and Technology*, Societe Francaise d'Energie Nucleaire, Avignon, France, 17–21 October 1988.
- [63] Down, M. G. and Witkowski, R. E., "Instrumentation for Liquid Alkali Metals," *ISA Transactions*, Vol. 21 No. 4, 1982, pp. 49–55.

- [64] Adams, P. F., Down, M. G., Hubberstey, P., and Pulham, R. J., "Solutions of Lithium Salts in Liquid Lithium," *Journal of Chemical Society Faraday Transactions I*, Vol. 73, 1977, pp. 230–235; also, Calaway, W. F. et al., *Second International Conference on Liquid Metal Technology in Energy Production*, J. M. Dahlke, Ed., CONF-801-P1/P2, Richland, WA, 20–24 April 1980, pp. 20–24 to 20–32.
- [65] Addison, C. C., *The Chemistry of Liquid Alkali Metals*, John Wiley & Sons, New York, 1984.
- [66] Bauer, D. C., "Kinetics of the Degradation of Type 316 Stainless Steel by Liquid Lithium," Ph.D. thesis, University of Wisconsin-Madison, 1980.
- [67] Bagnall, C., "A Study of Type 304 Stainless Steel Containment Tubing From a Lithium Test Loop," *Journal of Nuclear Materials*, 1981, Vol. 103,104, pp. 639–644.
- [68] Shiels, S. A., Keeton, A. R., and Anantatmula, R. P., "The In-Sodium Corrosion Behavior of Candidate Commercial Fuel Cladding and Duct Alloys," Westinghouse Hanford Technical Report, HEDL TME-77-71 UC79b, February 1978.
- [69] Keeton, A. R. and Bagnall, C., "Factors that Affect Corrosion in Sodium," *Proceedings of the Second International Conference on Liquid Metal Technology in Energy Production*, Richland, WA, 20–24 April 1980, pp. 7-18–7-25.
- [70] Peric, Z., Drechsler, G., Frees, G., and Borgstedt, H. U., "The Corrosion of Steels in Liquid Pb-17Li Alloy," *Proceedings of Fourth International Conference on Liquid Metal Engineering and Technology*, Vol. 3, SocietÉ Francaise d'Energie Nucleaire, 1988, pp. 522-1–522-7.
- [71] Broc, M., Fauvet, P., Flament, T., et al., "Compatibility of 316L Stainless Steel with the Liquid Alloy Pb17Li," *Proceedings of Fourth International Conference on Liquid Metal Engineering and Technology*, Vol. 3, SocietÉ Francaise d'Energie Nucleaire, 1988, pp. 527-1–527-10.
- [72] Tortorelli, P. F., "Deposition Behavior of Ferrous Alloys in Molten Lead-Lithium," *Fusion Engineering and Design*, Vol. 14, 1991, pp. 335–345.
- [73] DiStefano, J. R. and DeVan, J. H., "Refluxing Capsule Experiment with Refractory Metals and Boiling Alkali Metals," *Nuclear Applications Technology*, Vol. 8, January 1970, pp. 29–44.
- [74] Klueh, R. L. and DeVan, J. H., "Liquid Metal Test Procedures," *Handbook on Corrosion Testing and Evaluation*, W. H. Ailor, Ed., John Wiley & Sons, NY, 1971.
- [75] Bagnall, C. and Brehm, W. F., "Corrosion in Liquid Metals," *Metals Handbook, Ninth Edition, Volume 13*, ASM International, Metals Park, OH, 1987, pp. 91–96.
- [76] Pawel, S. J., DiStefano, J. R., and Mannes Schmidt, E. T., "Corrosion of Type 316L Stainless Steel in a Mercury Thermal Convection Loop," Oak Ridge National Laboratory report, ORNL/TM-13754, April 1999.
- [77] Pawel, S. J., DiStefano, J. R., and Mannes Schmidt, E. T., "Effect of Surface Condition and Heat Treatment on Corrosion of Type 316L Stainless Steel in a Mercury Thermal Convection Loop," Oak Ridge National Laboratory report, ORNL/TM-2000/195, July 2000.
- [78] Tortorelli, P. F., DeVan, J. H., and Selle, J. E., *Effects of Nitrogen and Nitrogen Getters in Lithium on the Corrosion of Type 316 Stainless Steel*, National Association of Corrosion Engineers, No. 115, March 1979.
- [79] DiStefano, J. R., "Mass-Transfer Effects in Some Refractory Metal-Alkali Metal-Stainless Steel Systems," Oak Ridge National Laboratory Report, ORNL-4028, Oak Ridge National Laboratory, 1966.
- [80] Eichelberger, R. L., McKisson, R. L., and Johnson, B. G., "Solubility Studies of Refractory Metals and Alloys in Potassium and in Lithium," AI-68-110, Atomics International, 1969.
- [81] DeVan, J. H., "Compatibility of Structural Materials with Boiling Potassium," Oak Ridge National Laboratory Report, ORNL-TM-1361, April 1966.
- [82] DiStefano, J. R. and DeVan, J. H., *Nuclear Applications Technology*, Vol. 8, No. 29, 1970.
- [83] Down, M. G., Keeton, A. R., and Bagnall, C., "Erosive Effects in Liquid Lithium," *Journal of Materials for Energy Systems*, Vol. 4.2, 1982, pp. 69–77.
- [84] Bennett, J. A. R. and Lewis, J. B., "Dissolution Rates of Solids in Mercury and Aqueous Liquids: The Development of a New Type of Rotating Dissolution Cell," *A.I.Ch.E. Journal*, Vol. 4, 1958, pp. 69–77.
- [85] DeVan, J. H. and Sessions, C. E., *Nuclear Applications*, Vol. 3, 1967, p. 102.
- [86] DeVan, J. H. and Jansen, D. H., "Fuels and Materials Development Program Quarterly Progress Report," Oak Ridge National Laboratory Report, ORNL-4350, 30 September 1968, p. 91.
- [87] Jansen, D. H. and Hoffman, E. E., "Type 316 Stainless Steel, Inconel, and Haynes Alloy No. 25 Natural Circulation Boiling-Potassium Corrosion Test Loops," Oak Ridge National Laboratory Report, ORNL-3790, 1965.
- [88] Romano, A. J., Fleitman, A. H., and Klamut, C. J., *Proceedings of AEC-NASA Liquid Metals Information Meeting*, CONF-650411, 1965.
- [89] Fuller, C. J. and MacPherson, R. E., "Design and Operation of Stainless Steel Forced-Circulation Boiling-Potassium Corrosion-Testing Loops," Oak Ridge National Laboratory Report, ORNL-TM-2595, 1967.
- [90] DeVan, J. H., *Alkali Metal Coolants, Proceedings of a Symposium*, 28 November–2 December 1966, International Atomic Energy Agency, Vienna, 1967, p. 643.
- [91] Romano, A. J., Wachtel, S. J., and Klamut, C. J., *Proceedings of International Conference on Sodium Technology for Large Fast Reactor Design*, ANL-7520, Pt. I, Argonne National Laboratory, 1968, p. 151.
- [92] *Liquid-Metals Handbook, Second Edition (Revised)*, R. N. Lyon, Ed., NAVEXOS P-733(Rev), Atomic Energy Commission, Dept. of the Navy, Washington, DC, June 1952.
- [93] *Liquid-Metals Handbook, Sodium-NaK Supplement*, C. B. Jackson, Ed., TID 5277, Atomic Energy Commission, Dept. of the Navy, Washington, DC, 1 July 1955.

# Corrosion Inhibitors

Rudolf H. Hausler<sup>1</sup>

## SCOPE

THE PRESENT DISCUSSION IS neither intended as a review of the myriad products and formulations that have over the years been proposed for the inhibition of corrosion processes in a multitude of environments with various substrates, nor a dissertation of the many mechanistic concepts that have been proposed for corrosion inhibition. Rather, an effort shall be made to outline a methodology (or methodologies) narrowly focused on a specific objective: *the assessment of the reduction of the rates of corrosion (all manifestations thereof) caused by chemicals added to the environment for specific, well defined, purposes*. However, in pursuing a specific methodology neither the nature of the inhibitor, nor the underlying corrosion and corrosion mechanisms can be ignored, and all chemical, physical, and metallurgical realities, as well as their interactions and relationships, must be taken into consideration if the results shall have predictive value.

The most crucial aspect of the above definition of the objective, which must remain foremost in the technician's mind at all times, is "*the specific well-defined purpose*." Corrosion inhibition is no longer an academic endeavor. Rather, the focus must be on prolonging the useful life of a metallic structure in the realistic (or relevant) environment at an *acceptable cost advantage*. The design engineer in general has three options:

- Select the most economical metal for the environment and hope that the useful life of the structure will outlast the process for which the metal has been selected. (Example: The carbon steel tubing in an oil well may outlast the production capacity of the well. Similarly, it is often more economical to replace a carbon steel heat exchanger than build it out of an exotic material.)
- Select a high-grade material and save on maintenance, while avoiding the risk of catastrophic failure.
- Select a combination of low-grade material and corrosion inhibitor, and hope that the useful life of the structure is appropriately extended.

Experience has shown that the third option is viable, provided that inhibitor performance has been assessed predictably. Experience has also shown dramatic failures where these conditions had not been met. Selection of a corrosion inhibitor, therefore, boils down to *quantitative risk assessment and cost performance*, which can only be achieved on the basis of reliable/believable performance data.

<sup>1</sup>CORRO-CONSULTA, Kaufman, TX 75142, e-mail: rudyhau@msn.com

## INTRODUCTION

### Historical Perspective

Chemical corrosion inhibitors have been used for a long time, probably for as long as 150 years. Early applications involved the addition of inorganic chemicals to drinking and cooling water, and organic chemicals added to pickling acids. In the 1930s, and even more so after World War II, corrosion inhibition emerged as a separate science. The literature already in the 1950s has become vast, and reference needs be made to pertinent summaries. J. I. Bregman's book [1] published in 1963 has become a classic, but was soon out of print. NACE followed up with a second compilation in 1973, edited by C. C. Nathan, on the use of corrosion inhibitors across a broad spectrum of industries [2]. A further excellent update was generated by the European Federation of Corrosion in 1994 [3]. In 1983 the author brought together representatives from academia and industry in an attempt to discuss the interphase and its relevance to corrosion inhibition [4]. The interphase was defined as that three-dimensional region between metal and environment that is different in all its properties from either bulk phases.

All work on corrosion inhibition, indeed all work in the field of corrosion, is dependent on some sort of measurement or observation. In the early days weight loss, time to failure, or visual observation were the main tools. With the advent of electronic instrumentation, methods of measurement became more sophisticated. Electrochemistry and quantitative surface characterization became major tools. Unfortunately, emphasis was on the "electro-" part while the "-chemistry" often was sorely neglected. Mercer published a first overview of the various investigative techniques in 1985 [5], which was updated in 1994 [6].

The industry has always attempted to standardize materials and their applications. Despite great and protracted efforts to standardize test procedures, and there are many standard corrosion tests; there are no standard tests for corrosion inhibitor evaluation.<sup>2</sup> The reasons for this are complex as may become clear below. However, basically it had been thought that inhibitors, once evaluated under a specific set

<sup>2</sup>There are, however, currently efforts underway within ASTM Committee G-1 to develop a "Standard Guide for Evaluating and Qualifying Oilfield and Refinery Corrosion Inhibitors in the Laboratory." Such a guide, rather than specific standard test procedures, has become necessary for all the reasons spelled out in this chapter.



of circumstances, could be ranked according to efficiency, and that such ranking would carry through to other conditions as well. This proved to be erroneous for essentially all organic corrosion inhibitors and very likely for a good number of inorganic ones as well. Therefore, corrosion inhibitors have to be evaluated in an application specific manner; even the so-called screening procedures lead to faulty conclusions.

### The Importance of the System Analysis

The evaluation of corrosion inhibitor effectiveness is significantly different in many respects from corrosion testing for the purpose of evaluating material performance. The addition of a chemical to a corroding system requires compatibility, chemical and thermal stability, and in some cases physical stability as well. Transport properties become important where localized or gasphase corrosion (dew point) are an issue. Finally, no corrosion inhibitor, no matter how effective in preventing corrosion, can be considered successful if it causes process upsets. This latter aspect is usually summarized under secondary properties testing [7]<sup>3</sup> (cf. also Chapter 1 in this book).

- **Compatibility:** Corrosion inhibitors can undergo reactions with components of the environment. Amines react with H<sub>2</sub>S. Unsaturated fatty acids and derivatives thereof (imidazolines) are subject to vulcanization in the presence of elemental sulfur or oxygen in combination with H<sub>2</sub>S. Polyfunctional acids react with polyfunctional amines to form gels or solids. Such considerations are important, since production or process streams are often treated with more than one chemical (oil and gas production processing, transport and refining, cooling water circuits—the examples are endless).
- **Chemical Stability:** Since all inhibitors contain functional groups (carboxylic acids, amines, Schiff's bases, phosphates, phosphonates, sulfur derivatives, and many more), they are pH sensitive, and therefore, their activity varies over actually fairly narrow pH ranges. For example, it has been shown that certain amines in sour systems lose activity if the pH of the environment shifts from 4 to 7 [8], while in CO<sub>2</sub> systems the reverse has been observed [9].
- **Thermal Stability:** It is known that corrosion inhibitor effectiveness varies with temperature. This can be due to chemical degradation, decreased adsorption at higher temperature, or changes in surface properties (e.g., iron carbonate converts to magnetite at higher temperature).
- **Physical Stability:** Some corrosion inhibitors are polymeric in nature. As such, they become subject to degradation at high shear forces.
- **Transport Phenomena:** Many corrosion inhibitors are higher molecular compounds, and are usually present in small concentrations. If the objective is localized corrosion inhibition (crevice corrosion, under-deposit corrosion, etc.), the ability of the inhibitor to migrate where it is needed becomes a major concern that needs to be included in the design of the test methodology.

<sup>3</sup>Throughout this discussion predominantly examples from the oil field will be used. However, the principles discussed are universally valid.

Because of the above concerns, the first step in the development of any successful test methodology is the *systems analysis*, which must include the identification not only of the nominal levels of all prevailing physical, chemical, mechanical, and metallurgical parameters, but also their ranges and extreme values. For instance, the nominal temperature in a heat exchanger is that of the heated fluid exiting the tube bundle. The maximum temperature, however, is that of the tube surface. This becomes particularly important in direct fired boilers or reboilers. Other often overlooked parameters are flow rate (shear stress) and mechanical stresses (particularly alternating stresses), which tend to decrease inhibitor efficiency. Finally, a dark area of concern is the metallurgy. It is still not well understood why inhibitors are quite sensitive to small changes in the composition or physical properties of iron and/or carbon steels.

### Some Definitions

There are a myriad of tests that have been proposed, used, and will no doubt be developed in the future. The notion that a test per se can generate an understanding of the prevailing corrosion, or corrosion inhibition processes, and have some predictive value, even if performed under nominal conditions, is far from realistic. It may, therefore, be indicated to attempt to define the various concepts of testing, and apply certain critical measures to evaluate the validity of each. This shall lead to a set of broad quality criteria that, if applied consistently, will go a long way to improve overall the predictiveness of such testing.

### Quality Criteria

The objectives of corrosion testing and inhibitor evaluation may be varied and are often the preference of the technician, but they have to be clearly defined prior to selecting the test methodology. The simplest objective one can imagine may be to establish whether a substance added to a solution can retard the corrosion process. Uncomplicated immersion tests can easily fulfill such an objective. One may want to determine the mechanism by which such retardation occurs. This in itself can be a fascinating endeavor, but has little practical value, other than understanding the chemistry of interaction between a metal surface (in whatever state it may be) and the chemical added to the system. Many test procedures and methodologies have been proposed that can accomplish this, from the trivial to the most complicated [5,6]. Finally, however, corrosion inhibitors are being evaluated for the purpose of protecting metallic structures in some industrial process equipment, be it oil and gas production, refining and processing of crude oil, the pulp and paper industry, and many others. For this kind of testing, three *simultaneous* quality criteria have been defined [9]. The results have to be

- Unique,
- Relevant, and
- Predictive.

These terms are rigorously defined. Uniqueness, a mathematical term, refers to the fact that the end result, the

corrosion rate, must first of all be explainable by a unique set of corrosion kinetics. For example, the average weight loss corrosion rate can be explained by a decreasing, increasing, or steady state corrosion rate over the period of the test, and is, therefore, only for the steady state a unique value. It follows that almost all corrosion test results based on average weight loss violate the first quality criterion and have neither predictive nor mechanistic value.

Relevancy is obtained only if all operative parameters are controlled at constant levels during the test. The operative parameters are those that directly affect the corrosion mechanism. This definition creates a problem, in that the corrosion mechanism is itself based on results obtained from corrosion tests. Mechanistic understanding cannot possibly be complete if the relevancy condition has not been adhered to. Therefore, the study of corrosion and corrosion inhibition mechanisms is an ever-evolving field, as one can learn from history.<sup>4</sup> For example, inhibitor effectiveness is now known to be pH dependent. In CO<sub>2</sub> corrosion testing the pH increases continuously due to the formation in solution of bicarbonate (a buffering agent). It follows that unless the pH is maintained constant, the final result, even if at the end of the test a steady state corrosion has been measured, cannot be said to be relevant because the final pH is not defined. Similarly, if testing is performed in sour media, the build-up of (insoluble) iron sulfide results in a diminished inhibitor concentration due to generally unknown adsorption effects, and again, the results cannot be said to be relevant.

Predictiveness refers to the fact that during the corrosion test all operative parameters must be controlled at levels prevailing in the field. Even if relevancy has been adhered to under the above definition, the test results may not be predictive unless the test parameters mirror field conditions. In the past 20 years major problems arose because inhibitors tested in the laboratory under some flow conditions failed in the field at the predicted concentrations because the field flow conditions were not properly assessed and duplicated in the laboratory.

To illustrate the above, inhibitor evaluations by means of the so-called "Wheel Test" [10] fail all three quality criteria. This test has in the past been used extensively to evaluate corrosion inhibitors for use in oilfield applications. The results are always based on weight loss and are, therefore, not unique. They are not relevant, because as the test bottles turn on the wheel to which they are affixed, the flow regime or agitation is not defined. The results are also not predictive, because the controlling variables do in general not reflect field conditions.<sup>5</sup> Disregarding these most basic quality criteria has in the past been, and still is, a major reason for costly failures in the field of oil and gas production.

### Tests, Test Methods, and Test Methodology

The distinction between the three terminologies begins to approach a paradigm shift in the approach to corrosion

<sup>4</sup>A full discussion of this paradigm would exceed the framework of this article. However, one can readily understand that improved understanding of mechanisms can only come from discrepancies between new results and what might have been expected on the basis of mechanistic understanding. It therefore behooves the technician to be constantly on the lookout for such discrepancies.

<sup>5</sup>For a critical discussion of this test method see Ref 4.

testing. A **corrosion test**, many of which have been used to evaluate inhibitors, is nothing more than the hardware with which such evaluations are performed. A detailed compilation of all manner of corrosion tests has been presented by A. D. Mercer in 1985 [5] and updated recently in 1994 [6]. These compilations, however diligently brought together, merely describe and reference the various approaches to test apparatuses researchers have pursued over the years. It is interesting to note that Mercer characterized the state of the art of inhibitor testing as follows:

Since corrosion inhibitors are used in a wide range of applications, no universal test method is possible. Furthermore, even within one type of application, there will be a range of requirements and a diversity of opinion on the definition of effective inhibition [5].

In other words, the quest for a standardized corrosion inhibitor evaluation test is as elusive as it ever was and continues to be so.

More recently, particularly in discussions of various NACE or ASTM working groups, one encounters the terminology of **test method**. By this term one generally understands the combination of test (hardware) and the applications of it, which includes the preparation of the solutions, the metallurgy, the preparation of the test specimen, the monitoring of what happens during the test period, and the final evaluation of the results. Many of these steps have been standardized in various standards [11–21].

A third concept comprises the **test methodology**. Here one goes a step further and includes the system analysis (often complex and time consuming) of all the environments the test has to address and the objectives the results have to fulfill. What results from such analysis is not only a clear idea of the conditions to which a metal has to be resistant, or under which an inhibitor has to afford protection, but also an experimental test matrix that has to be executed before the application of the specific metallurgy in conjunction with an inhibitor can be reasonably recommended (see also Chapter 1).

## DISCUSSION OF SOME BASIC ASSUMPTIONS

### Protection and Inhibitor Adsorption

The conduct of corrosion or corrosion inhibition tests always aims at some objective, and therefore, is based on some implicit or explicit assumptions. For instance, the effectiveness of a corrosion inhibitor is preferentially expressed in terms of percent protection ( $P^*$ ) formulated by the well-known equation:

$$P^* = \left( \frac{cr^o - cr^i}{cr^o} \cdot 100 \right) \quad (1)$$

where:

$cr^o$  = uninhibited corrosion rate,

$cr^i$  = inhibited corrosion rate.

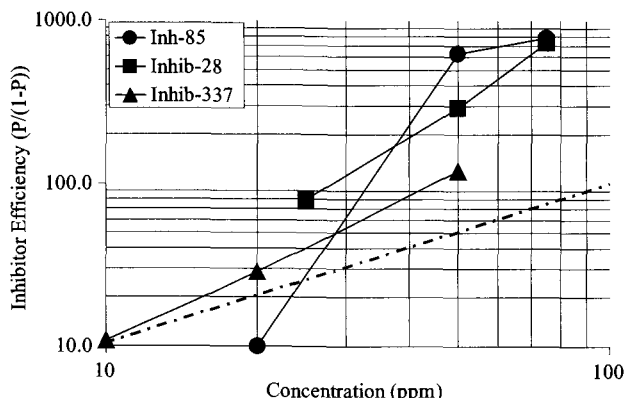


FIG. 1—Inhibitor performance in constant pH kettle test; note dashed line represents Langmuir behavior.

The assumption in Eq 1 is the notion that the blank (uninhibited) and inhibited corrosion rates are obtained under the same conditions. This is rarely the case and is certainly not true for the much studied  $\text{CO}_2$  corrosion. There are many other commonly held assumptions in corrosion inhibitor testing that are equally not true and will be discussed in greater detail below. Let's first look at some of the objectives that may be involved in corrosion inhibitor testing.

The degree of protection ( $P$ ), or percent protection ( $P^* = P \times 100$ ), has been used in the past extensively to assess inhibitor effectiveness and to compare the performance of different products. For this purpose,  $P^*$  is customarily plotted against inhibitor concentration. Because 100% protection is approached asymptotically as the concentration increases, differentiation between products is difficult. Alternatively, differentiation is accomplished numerically by comparing percent protection at a given concentration. This comparison neglects the different performance characteristics of inhibitors because, as will be shown below, one product may surpass another at one concentration while lagging behind at another concentration. For these reasons, and essentially totally practical purposes, another presentation of the results was proposed with some interesting conclusions.

Assume, as has been proposed in the past, that inhibition follows some basic law of adsorption of the inhibitor on the metal surface, or more realistically on a corrosion product covered surface, and that the degree of protection is somehow related to the degree of coverage. The simplest of adsorption isotherms is the Langmuir isotherm, which states that the degree of coverage is related to the concentration as follows:

$$\theta = \frac{K \cdot c}{1 + K \cdot c} \quad (2)$$

where:

$\theta$  equals the degree of coverage,  
 $K$  is the adsorption constant, and  
 $c$  is the (adsorbate) inhibitor concentration.

Assuming that degree of inhibition equals the degree of coverage,<sup>6</sup> one obtains an explicit relationship between the degree of inhibition and the concentration, which can be expressed as:

$$c = \frac{1}{K} \cdot \frac{P}{(1-P)} \quad (3)$$

Using Eq 3, presented graphically in double logarithmic fashion, as used below in Fig. 1, not only leads to better distinction between products, but also demonstrates some of the fundamentals that need to guide inhibitor testing and the interpretation of the results.

### Basic Test Procedures

There are two (perhaps three) basic corrosion tests that can be performed. The first, and certainly the most prevalent, is the so-called constant inventory test. Here, a metal specimen is exposed to a finite amount of test liquid (usually preconditioned) in a closed container. The test has a relatively short duration during which the corrosion rate asymptotically approaches a *pseudo* steady state. However, over this period of time all conditions keep changing, from the composition of the solution to the metallic surface conditions (real surface area, scale buildup, accumulation of iron carbide, and many more). Constant Inventory tests are characterized by the liquid volume to specimen surface area ratio. This ratio should always be maximized.

The second procedure is the flow through test. Here, a properly conditioned fluid is continuously flowed over the metal specimen [22]. While this does not eliminate initial effects, a more realistic steady state can be obtained if the test duration is long enough. The changes in the corrosive fluids are characterized by the flow rate and the total corrosion per unit time (corrosion rate  $\times$  surface area), and in some cases, the volume of the container holding the corrosion probe.

Third, a hybrid procedure is being used frequently where conditioned fluids are circulated over the test specimen from a reservoir [20]. If the reservoir is large enough, changes in fluid composition can be minimized. A particularly ingenious version of this hybrid test method has been developed in Norway [23], where the circulating fluids are continuously reconditioned by automatic pH maintenance and corrosion product removal. The distinction of these three approaches must always be kept in mind when discussing corrosion and inhibition tests.

The degree of protection afforded by an inhibitor ( $P$ ), or the percent of protection ( $P^* = P \cdot 100$ ) is based, as per Eq 1, on two measurements: the blank (uninhibited) and the inhibited corrosion rates. The measurements themselves will be discussed below. At this point we wish to point out that for  $P$  to have any real meaning, the measurements must be obtained under identical conditions. This means that not only the initial (nominal) conditions, but the final conditions as well must be identical. This requirement is hardly ever met in constant inventory tests, except perhaps in strong

<sup>6</sup>This assumption by no means implies a factual relationship, but is used as a working hypothesis to test whether corrosion inhibition might fulfill the assumptions underlying the Langmuir isotherm.

acid solutions, and can be most effectively approximated in flow through systems.<sup>7</sup> The reasons are obvious: during the test the composition of the solution, as well as the nature of the metal surface, keeps changing. These changes are more rapid and pronounced in the blank test. Therefore, it is impossible in constant inventory tests to obtain results that are strictly comparable, unless special provisions are taken.

### Effects of pH and Flow

Since the pH is probably the most important of the controlling test parameters, particularly in CO<sub>2</sub> corrosion, it can be held constant by continuous pH controlled acid injection as the corrosion process progresses [9]. This prevents the build-up of iron carbonate scale. Indeed, in the constant pH test, using a brine saturated with CO<sub>2</sub> at one bar, the blank corrosion rate was found to be constant (or slightly increasing) at about 220 mpy for at least 48 h, whereas in the simple constant inventory test without pH compensation the corrosion rate would decrease from an initial 220 mpy to 20 mpy after 24 h due to iron carbonate "passivation," with a concomitant pH increase of from 4 to about 6.

In order to keep conditions as constant as possible the constant pH "Kettle Test" was used to evaluate a large series of corrosion inhibitors of which a few results are shown in Fig. 1, represented according to Eq 3.<sup>8</sup> The inhibitors were intended for use in oil field systems and were, therefore, tested in fluids containing brine and a hydrocarbon phase saturated with 1 bar CO<sub>2</sub>. The results show the following:

- None of the inhibitors obeyed the Langmuir isotherm. In fact, all of them became more active than predicted with increasing concentration.<sup>9</sup>
- The slopes of the performance characteristics are not the same. As a consequence, comparison at an arbitrary concentration would be misleading.

When the same inhibitors were examined in the floating pH Kettle test,<sup>10</sup> under otherwise identical conditions (Fig. 2), it was observed that INHIB-28 performed slightly better in the cpHKT, while for INHIB-85 the slope of the performance changed leading to a crossover of the two curves. INHIB-337 performed better in the stdKT (higher pH) but exhibited saturation at already low concentrations. However, it needs to be noted that the degrees of protection derived from constant pH test results are real, because the blank corrosion rate was well identified. The blank rate in the floating pH test is not well defined. The continuously

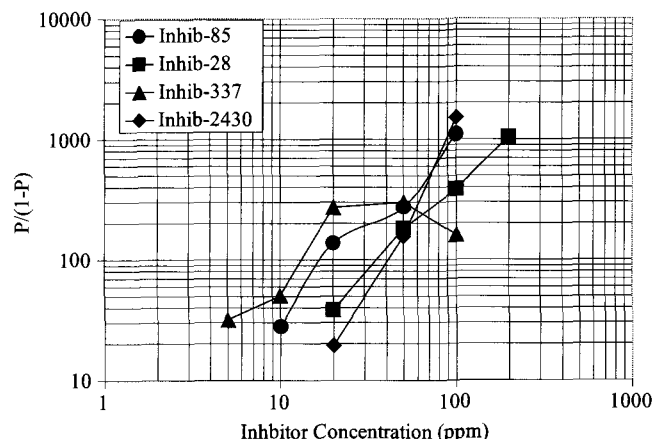


FIG. 2—Non-pH compensated std. kettle test (note that the blank corrosion rate was assumed to be 220 mpy, although in a floating pH test the blank rate is not defined).

increasing pH causes a continuous decrease of the blank rate. As a consequence, comparing the degrees of protection of inhibitors at different pH's is nearly impossible because of the nonsteady state blank corrosion rates.

These results show that practical corrosion inhibitors<sup>11</sup> are single-minded entities hard to squeeze into a mechanistic framework suitable for easy comparison. This means that ranking of inhibitor performance, by means of percent protection based on one test procedure and one concentration only, necessarily leads to erroneous, misleading, conclusions. Indeed, the work of Garber [24] had led to the same results. Garber tested some 50 oilfield corrosion inhibitors from different companies in six or seven different tests and found it impossible to arrive at a uniform performance ranking. Additional work by the author further substantiates these conclusions [25]. It is, therefore, nonsensical to argue that screening and ranking inhibitors are only for the sake of discarding the bad and then continuing to test only the good ones. It follows from the above that this is a totally arbitrary paradigm, which depends on the test procedure and the specific test conditions, and in general, bears no relationship to field application. In particular, the above demonstrates that the percent protection is not independent of pH.

The world, however, is not unidimensional, and there are many more parameters that affect inhibitor performance, including their interactions. One parameter that has caused workers in this field much concern and consternation is the flowrate under which the inhibitors are tested. Table 1 below summarizes some results obtained under controlled constant pH and various degrees of agitation in Kettle Test arrangements. Even though the experimental design was not complete, the data show that with the exception of Inhibitor D the other three are either pH or flow sensitive or both.

<sup>7</sup>Strictly speaking, the conditions of constancy of environment and true steady state can only be obtained with point measurements in flow-through systems.

<sup>8</sup>The degrees of protection were determined on the basis of the steady state corrosion rates obtained at the end of the test run determined from differential iron counts.

<sup>9</sup>From a mechanistic point of view this is not surprising because all inhibitors are either by nature, or due to formulation, surfactants. Therefore, as concentration increases the micelle concentration in the aqueous phase increases as well, and adsorption occurs by mechanisms other than envisaged by Langmuir.

<sup>10</sup>The blank corrosion rate here was assumed to be the same as in the cpH test, i.e., the initial corrosion rate.

<sup>11</sup>As opposed to single compounds with identical functional groups, and only distinguished by hydrocarbon chain length, as are often used in model studies.

**TABLE 1**—Average differential corrosion rates (in mpy) for the test period of 2 to 24 h, excluding initial corrosion transients.

pH	Inhibitor	Stirring Rate (rpm)	
		400	800
3.9	F		182
	C	0.15	21.6
	A		1.82
	D	0.5	0.57
4.9	F	0.3	3.6
	C	0.16	1.2
	A		0.2
	D	0.85	1

Note: Inhibitors F and C tested at 20 ppm; Inhibitors A and D at 50 ppm.

To summarize the above discussion of the status quo, it may have become clear that the degree of protection in general is a useless number because:

- It is defined only for one concentration, and
- Refers to only one test condition.

Furthermore, because the inhibitor performance characteristic (protection versus concentration)

- Is different for different inhibitors, and
- Varies from test condition to test condition,

ranking of inhibitors in so-called screening tests has no practical value within the quality criteria defined above.

## PURSuing A NEW PARADIGM

### The Steady State Corrosion Rate

Corrosion testing and corrosion inhibitor evaluation are done (apart from mechanistic studies) for the purpose of determining

- Whether corrosion preventive measures are necessary, and
- Whether the required life-time can be achieved with an inhibitor.

From a practical point of view it is only necessary to assess the level of the inhibited corrosion rate. The degree of inhibition is immaterial, once one has decided that inhibition is required. In order to answer these questions, it is necessary to establish a valid steady state corrosion rate that is predictive of field conditions. This is actually a rather demanding task because

- In the field the steady state is measured in years, while in the laboratory test, periods are generally of the order of 24 to a few hundred hours. Tests exceeding one week are usually only run in cases of extreme importance.
- In all laboratory tests the corrosion rates are subject to an initial transient characterized by a transition from high to low corrosion rates. During this transient the actual surface area adjusts to a steady state (constant roughness).<sup>12</sup>

<sup>12</sup>It has been observed that for polished probes the uninhibited corrosion rate increases, while for sandblasted coupons the initial corrosion rate shows a downward trend.

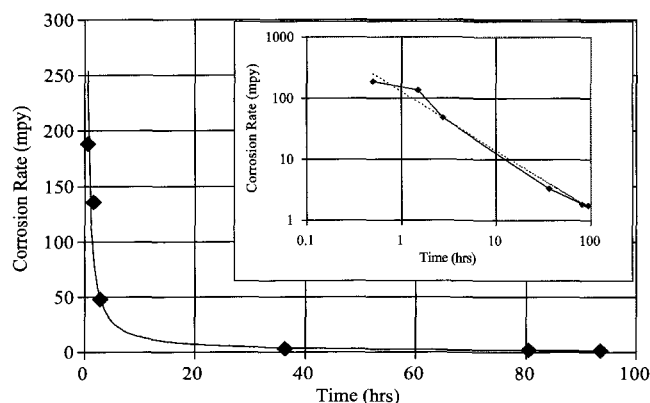


**FIG. 3**—Inhibited differential corrosion rates obtained in a HSACT experiment based on iron counts. The insert shows that the decrease of the corrosion rate follows a power law.

- Corrosion product scales can build up and inhibitors interact with these scales, or may actually become part of these scales (as, for instance, in the case of iron sulfide). Due to inhibitor adsorption the nature of the scales (crystal structure, porosity, and semiconducting properties) changes as well. While adsorption is usually considered fast (seconds or minutes), the structural relaxation of the metal surface composite is generally slow (hours to days).

The time dependent processes involved in inhibitor testing make it necessary to monitor the corrosion kinetics during the testing in order to estimate at what point a steady (or pseudo steady) state may have been achieved. A typical example is shown in Fig. 3. The data were obtained in the *High Speed Autoclave Test* [26] (HSACT, details see below) under 1000 psi CO<sub>2</sub> partial pressure and 1500 rpm of the cage holding the coupons. The inhibitor was added from the beginning. The individual points represent differential corrosion rates for subsequent time periods obtained by iron count measurements and confirmed by the overall weight loss.<sup>13</sup> The corrosion rates decrease in hyperbolic fashion, which actually translates to a near straight line decrease if plotted double logarithmically. The average corrosion rate for the entire test was 7 mpy, whereas the corrosion rate determined for the last 20 h was less than 2 mpy. Risk assessment of field conditions may indicate that 7 mpy is excessive, while 2 mpy is acceptable. This highlights the importance of the ultimate corrosion rate achievable under inhibited conditions. It must, however, be kept in mind that during the above constant inventory test, about 100 ppm of iron were introduced into the brine. This corresponds to about 210 ppm of bicarbonate, which in turn resulted in a calculable pH change. The closer these final conditions approach field conditions, the more predictive the results. Changes in the environment can be controlled by properly assessing the ratio of brine volume to surface area.

<sup>13</sup>The data are plotted in the center of the time period for which they were obtained, indicating the true average corrosion rate for that period.

### Alternate Performance Characteristics and Cost Effectiveness

If experiments of the above nature are carried out at different concentrations, an inhibitor performance characteristic can be obtained. A typical example is shown in Fig. 4. In most instances, one finds that double logarithmically again a straight line is obtained. Indeed, if Eqs 1 and 2 are combined, one obtains a relationship between the corrosion rate and the inhibitor concentration as expressed in Eq 4.

$$cr^i = cr^o \cdot \frac{1}{1 + K \cdot c} \quad (4)$$

If  $Kc \gg 1$  an inverse relationship between the concentration and the inhibited corrosion rate results where the position of the curve depends on  $cr^o/K$ , and the slope is 1 for the Langmuir assumptions. This is demonstrated in Fig. 4. However, the slope of the experimental line is much steeper than predicted, again demonstrating that these inhibitors adsorb much more strongly than the Langmuir assumption would predict. Another interesting effect, routinely observed, is the fact that with higher inhibitor concentration (better inhibition) the average and final corrosion rates are closer together. This is to be expected, since better inhibition also tends to minimize initial effects, which then become negligible over longer test periods.

From Fig. 4 one can now determine the effective inhibitor concentration, i.e., the concentration at which the desired steady state corrosion is obtained; and since the concentration translates directly to cost, Fig. 4 also lends itself to determine the cost-effectiveness of inhibition, which is defined as the cost to achieve a certain objective. Now, one has the means to compare different products objectively on a cost-effectiveness basis.

It is a general shortcoming of technicians in this field to assume that once such comparisons have been established for

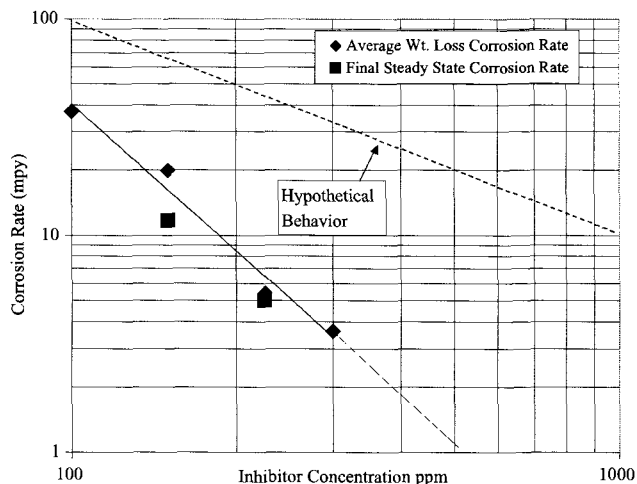


FIG. 4—Performance characteristic of an oilfield corrosion inhibitor in the HSACT at 1000 psi CO<sub>2</sub> partial pressure, 200°F and 1500 rpm. The hypothetical Langmuir behavior is shown to indicate the much stronger adsorption of the inhibitor.

one set of conditions, they can harmlessly be extrapolated to different conditions. This is far from reality. It has already been shown that different corrosion inhibitors behave differently under different conditions, while a single inhibitor can change its behavior unpredictably as conditions change. The example to be shown here in order to illustrate the point deals with the effects of pressure and velocity. Specifically, it was found that the CO<sub>2</sub> partial pressure and the speed of rotation of the cage in the HSACT affect the cost-effectiveness in a complex unpredictable fashion [27,28]. Figure 5 shows a contour plot of inhibited iso-corrosion rate lines from 5 to 30 mpy for 100 ppm inhibitor on a J-55 steel in a pressure-velocity grid. Clearly, the inhibited corrosion rates increase with both velocity and CO<sub>2</sub> partial pressure. However, there is a complex and unpredictable interaction between these two parameters, reflecting the nonlinearity of the effects.

Alternatively, one can focus in on the cost-effectiveness and present the data in terms of the necessary inhibitor concentration required to achieve a given corrosion rate (field performance). Figure 6 shows a contour plot for the inhibitor concentration necessary to achieve a steady state corrosion rate of 1 mpy in the velocity/pressure grid with the experimental data highlighted. The data are for a specific metal. Clearly, velocity (flow intensity, rpm) is a major parameter, but increased pressure also demands higher inhibitor concentrations, particularly at higher velocities. This reinforces the notion that there is an interaction between the two parameters and it is nonlinear. Additional parameters that affected this evaluation were the metallurgy and the brine to hydrocarbon ratio. Indeed, the inhibitor concentration required to inhibit L-80, an alternate oilfield carbon steel, was quite similar under the milder conditions but doubled under the most aggressive condition of 1500 rpm and 750 psi CO<sub>2</sub> partial pressure. Alternate inhibitors, which had been selected as promising in screening tests, performed worse in varying degrees.

The new paradigm discussed here recognizes that performance in a realistic parameter field is the predominant

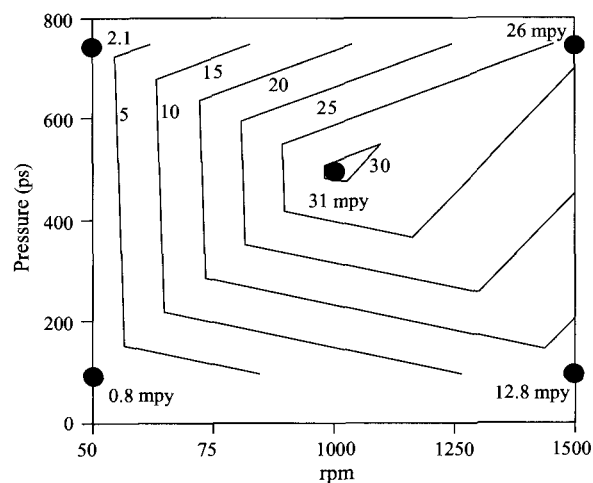


FIG. 5—Contour plot of iso-corrosion rate lines for J-55 at 100 ppm inhibitor evaluated in the HSACT. The points indicate the experimental matrix and results.

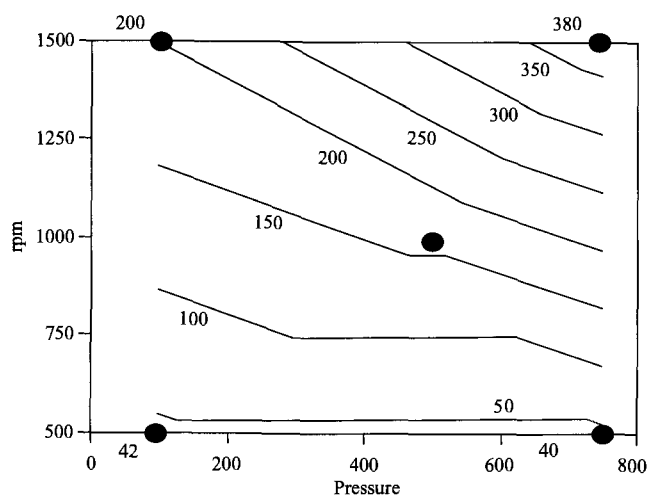


FIG. 6—Contour plot for J-55; inhibitor concentrations necessary to achieve 1 mpy; based on final corrosion rates from iron counts.

characteristic to be established for field application and, therefore, must focus on

- Steady state long-term performance of inhibitors within a realistic parameter field.
- The extent of the parameter field must be derived from a detailed system analysis.
- It can never be assumed that results from one set of conditions can be extrapolated to other conditions without penalty.

In order to follow such guidelines, one must also have a good grasp of the value of the results obtainable from certain experimental facilities, as well as the controlling parameters, such that they can be varied over the range of interest. Industry abounds with glaring examples where neglect of realistic evaluation of inhibitors resulted in catastrophic and expensive failures.

## CORROSION RATE MEASUREMENTS

Weight loss corrosion rates, which represent an average of corrosion over the test period, are useless from a predictive point of view, but are often used in conjunction with other measurements for quality assessments. Corrosion kinetics can be measured in different ways. Most favored are electrochemical techniques. They are, however, contrary to common belief, indirect techniques and must be properly calibrated and interpreted to be useful. If corrosion products are soluble in solution (as, for instance, iron carbonate), the buildup of such in solution can be used to monitor how corrosion progresses. Hydrogen, a byproduct of anaerobic corrosion, can also be used to monitor kinetics. Less common, but equally direct, are methods that use the removal of radioactivity from irradiated surfaces. Kinetic measurements have also been carried out with electrical resistance probes. As a general principle, no one method is in itself without some problems and should, therefore, always

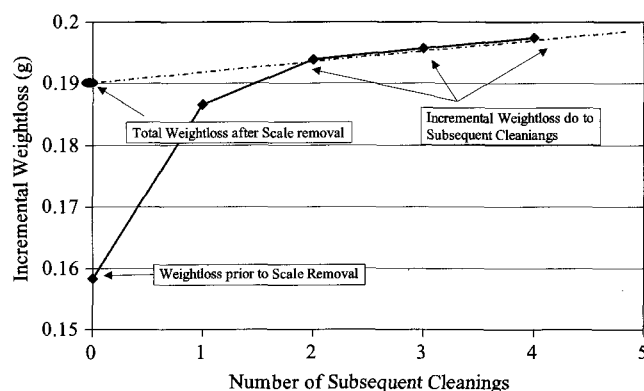


FIG. 7—Cleaning procedure of corrosion coupons for weight loss determination yields scale weight, total corrosion weight loss, and error due to cleaning procedure.

be interpreted on the basis of mechanistic understanding, and furthermore, be verified by multiple approaches.

## Weight Loss Corrosion Rate Measurements

While weight loss corrosion rate determinations by themselves are of little value because they are a priori not unique, they can and must often be used for verification of other data, or simply for quality control purposes. For example, iron count measurements for the purpose of determining corrosion kinetics can be misleading if, during the corrosion process, a corrosion product scale forms. In the above examples, the corrosion rates determined from iron counts were verified by establishing a mass balance between total weight loss, iron found in solution, and iron contained in the scale. Similarly, electrochemical measurements in inhibited solutions must at all times be verified by alternate measurements, weight loss being one of them.

In order to determine the weight loss on a corroded coupon, it is necessary in most instances to remove first adherent oil and inhibitor (which is usually done with acetone), and second, the corrosion product scale. In many instances, the scale weight is of interest as well, in which case the coupon is weighed before scale removal. There are many ways to remove the scale, some of which have been standardized [11]. For iron or steel samples, inhibited acid is used at an appropriate temperature. The important part of the cleaning procedure is an assessment of the metal loss during the cleaning procedure. This must be done by repeated timed immersions into the cleaning acid after the scale has been removed. Figure 7 illustrates the procedure. The additional weight loss due to the cleaning acid is extrapolated as shown. When the amount of metal removed in repeated cleanings is translated to a corrosion rate, one gains a measure of the possible error that can occur due to cleaning. In the above example, the total weight loss is 190.3 mg, corresponding to 24.4 mpy. When the weight loss due to cleaning is subtracted the corrosion rate is 23.5 mpy. The cumulative loss during four cleanings corresponds to about 1 mpy or 0.25 mpy per cleaning (about 2 mg). These numbers indicate more or less

the minimum corrosion rate that can be determined by weight loss in this example and highlight the importance of not only choosing the best conditions for cleaning, but controlling them, as well as an awareness of the possible errors introduced by cleaning. This is underlined by the fact that when inhibitors are used one often targets corrosion rates below 1 mpy in order to minimize and eliminate localized corrosion as well.

## CORROSION RATES FROM CORROSION PRODUCT ANALYSIS

### Iron Counts

The buildup of soluble corrosion products can be used to monitor corrosion kinetics. This method has been used extensively in oil field corrosion inhibitor testing, particularly in sweet ( $\text{CO}_2$ ) systems with only small amounts of  $\text{H}_2\text{S}$  present [29]. Iron analysis in the laboratory is most rapidly done on the bench with the Hach method (Phenanthridine) [30], although a host of other wet chemical methods are applicable. Instrumental methods include Atomic Absorption Spectroscopy (AAS) and Inductively Coupled Argon Plasma Spectroscopy (ICAP). While both these methods are well suited for high volume routine analysis, care must be taken that the samples are not contaminated by even traces of hydrocarbons. This includes soluble hydrocarbons such as methanol, chelating compounds such as EDTA, or scale inhibition products. Also used in the laboratory is Ion Chromatography (IC). This latter method is even more sensitive to sample composition and not recommended on a routine basis.

Iron counts are first used to confirm weight loss and scale weight. However, more interesting is the use of iron counts for kinetic studies, as shown in Fig. 4. The incremental increase of iron in solution between subsequent measurements is converted to a differential corrosion rate for the time period between measurements. Since the differential corrosion rate is an average for the specific time period, it should be plotted in the center of the period rather than at its end. Measurements of this kind are used for mechanistic studies in order to assess the rapidity of the onset of inhibition and related effects of inhibitor composition. However, it is also important, as has been pointed out above, to assess the steady state inhibited corrosion rate. A note of caution: Even if thermodynamically the corrosion products are soluble, they can still form on an actively corroding surface. For this reason the scale formation has to be monitored, and if important, the kinetics have to be corrected for scale formation. It has been observed, for instance, that iron carbonate formation in a corroding system is fast, but its dissolution rate is frustratingly slow.

## HYDROGEN MEASUREMENTS

### Direct Hydrogen Measurements

Molecular hydrogen is the other corrosion byproduct in aqueous anaerobic corroding system. In closed, oxygen free, constant inventory systems (by far the most prevalent test

systems), hydrogen builds up in the gas space at a rate reflecting the corrosion rate. By monitoring the hydrogen concentration versus time, and calculating the differential hydrogen evolution rates, corrosion kinetics can be determined. The method is old and predates in its application electrochemical measurements. In cases where electrochemical sensors made from the metal of interest are not available, or in systems where electrochemical measurements are virtually impossible, hydrogen evolution measurements have proved extremely valuable in recent times. The author has developed a methodology to study the behavior of corrosion inhibitors in high pressure, high temperature systems for oilfield steels under extreme flow intensities (HSACT) [31]. Using the rotating cage (see below) and oilfield tubular steel coupons (J-55, N-80, L-80, etc.), it would have been impossible to use electrochemical techniques, and iron counts were not applicable either when the brine was buffered into the pH range where solid iron carbonate could form. Small amounts of gas were continuously and automatically sampled from the gas space in the autoclave (mainly  $\text{CO}_2$ ) and analyzed by gas chromatography at a frequency of about 4 times per hour for the 100-h duration of the experiment. The sensitivity of this arrangement was 1 mpy in about 10 h, or sufficient to establish corrosion rates in the range of 0.2–0.5 mpy, which under the prevailing conditions corresponded to extremely efficient inhibition. The methodology was also used to establish inhibitor action on severely pre-corroded specimens, a feat that would have been literally impossible electrochemically (see below).

### Indirect Hydrogen Measurements

Hydrogen as a byproduct of corrosion can also diffuse into the metal. If corrosion occurs on one side of a metal wall, a hydrogen stream can be observed on the other side [32,33]. This phenomenon of hydrogen diffusion through metal has been routinely measured in the Devanathan-Stachurski cell and made use of in many different ways. In the field, it has been used to monitor inhibitor efficiency by means of various hydrogen probes [34]. Theories have been developed to assess the hydrogen concentration in the metal based on the diffusion rate and to establish correlations with the hydrogen cracking phenomenon. This area is complex and full of pitfalls, and for a detailed discussion the reader may be referred to some original literature. Suffice it to say here that in the presence of corrosion inhibitors, there is no general relationship between the corrosion rate on the corroding side of the metal and the hydrogen diffusion rate observed on the bare side of the metal. Corrosion inhibitors can either push hydrogen into the metal or prevent it from entering. Thus the reduction of the hydrogen diffusion rate observed upon the application of an inhibitor has no relationship to the degree of inhibition occurring on the corroding side. Similarly, the rate of hydrogen exiting the metal is controlled by the recombination reaction occurring on the exit side. If this rate is much faster than the diffusion rate, the hydrogen concentration on the exit side is zero and the hydrogen concentration in the metal can be estimated from the diffusion current on the basis of the first Fick's law. However, it is also known that the



recombination rate on the exit side depends on the surface condition and the nature of extraneously and fortuitously adsorbed chemicals. Thus, it has been observed that certain chemicals can retard the hydrogen exit reaction to a degree, such that the concentration in the metal is much greater than estimated from diffusion equations. Hydrogen diffusion measurements in the presence of inhibitors constitute waters difficult to navigate under the best of conditions. (For an in-depth discussion see also Ref 35.)

## ELECTRICAL RESISTANCE MEASUREMENTS

ER-measurements are based on the fact that as corrosion progresses the metal becomes thinner. Since the resistance of a metal strip (or wire) depends on its thickness, such probes lend themselves to direct corrosion rate measurements and the study of corrosion kinetics; hence, with respect to inhibitors, their effectiveness can in principle be studied with a minimum of basic assumptions.

The resistance for a metal strip can be expressed

$$R = \rho \cdot \frac{l}{A} = \rho \cdot \frac{l}{\Delta \cdot w} \quad (5)$$

where:

$R$  is the resistance in ohms,  
 $A$  is cross-sectional area in  $\text{cm}^2$ ,  
 $\rho$  is the specific resistance of the metal in  $\text{ohm} \cdot \text{cm}$ ,  
 $l$  is the length of the metal strip,  
 $w$  is the width of the strip.

A preferred probe for ER measurements is a wire. In this case, the resistance is inversely proportional to the square of the radius of the wire.

$$R = \rho \cdot \frac{l}{\pi \cdot r^2} \quad (6)$$

Practically, resistance measurements are made with a d-c or pulsed current Wheatstone bridge. There are many commercial instruments that incorporate this principle. The difficulty, of course, is the fact that resistance is inversely proportional to either the thickness or radius of the probe, and therefore, long-term results have to be interpreted carefully. Alternatively, such measurements can be made by measuring a d-c current at a constant potential (using, for example, a potentiostat).

$$I = V \cdot \frac{w}{\rho \cdot l} \cdot \Delta \quad (7)$$

Here, the current is directly proportional to the thickness of the probe via some probe constants.<sup>14</sup> Hence, the slope of the current/time curve is directly proportional to the corrosion rate, and changes in the slope represent the corrosion kinetics [36].

<sup>14</sup>The error introduced by the fact that the probe also corrodes from the side is generally minimal since the width is 10 to 20 times greater than the thickness.

It is well known that the specific resistance  $\rho$  is temperature dependent in a well-defined but metal specific way. In commercial instruments, this is accounted for by means of a noncorroding reference element built into the probe. However, commercial probes are, in general, still temperature sensitive because of the temperature gradient present when inside and outside temperatures differ significantly. If the measurements are accomplished according to Eq 7, temperature compensation can be accomplished by means of a thermocouple via microprocessors.

Whenever a current flows along a resistance element, a voltage (potential) drop establishes itself along the probe. This potential drop causes electrochemical reactions to proceed. The rate of these grows with the conductivity of the electrolyte. This phenomenon has actually been observed as an instantaneous current drop when inhibitors are added and is especially pronounced in concentrated hydrochloric acid. It is, however, an artifact and does not materially affect the  $I = f(\text{time})$  or the  $\Delta = f(\text{time})$  behavior. When corrosion product scales are present, however, the nature of this voltage drop along the probe can lead to artificially induced localized attack. This has also been observed in  $\text{H}_2\text{S}$  containing systems that were contaminated with oxygen.

## ELECTROCHEMICAL MEASUREMENTS

### Theoretical Principles

Electrochemical corrosion rate measurements have many advantages, in particular, because they are nearly instantaneous, they lend themselves to the study of corrosion kinetics, the assessment of the steady state, and, with regards to inhibitors, the inhibition transients. This is especially important in the laboratory where the exclusion of initial experimental effects is imperative for establishing predictive results.

The various electrochemical techniques employed for corrosion rate measurements have been discussed in detail by Scully in Chapter 7 and extensively referenced. This chapter also highlights the many pitfalls encountered with the interpretation of electrochemical polarization measurements. Some of these difficulties are generic to all polarization techniques, while others are more germane to inhibition. These latter ones will be discussed in greater detail.

At the core of all electrochemical techniques is the translocation of an external current flowing through a corroding electrode as a result of a potential perturbation. It does not matter whether this perturbation is the result of external d-c or a-c polarization, or manifests itself as electrochemical noise attributable to the inherent anisotropy of the metal. In all cases, one needs to come back to the fundamental relationships describing electron exchange at the metal surface. This relationship in its simplest form was established empirically by Tafel in 1904 [37] for general current/potential relationships, and later derived for corrosion currents by, among others, Stern and Geary [38] is:

$$\log i = \log i_{\text{corr}} + \frac{\eta}{\beta} \quad (8)$$

such that 
$$\frac{d(\eta)}{d(\log i)} = \beta \quad (9)$$

where

- $\log i$  is the external polarization current,
- $\eta$  is the polarization overpotential ( $E_{cor} - E_{applied}$ ),
- $\beta$  is the slope of the  $\log i$  versus potential curve, normally referred to as the Tafel slope.

The Tafel slope has a well-defined thermodynamic meaning: in essence, it represents the energy barrier for electron transfer across the metal/liquid interface. Anodic and cathodic Tafel slopes can easily be determined by polarization experiments. In order to fulfill the requirements of its definition, one should obtain a straight line of  $\log i$  versus  $\eta$  over two to three decades of current. In practice this is hardly ever the case, indicating that other controlling mechanisms are at play.

### Linear Polarization

In order to avoid some of the difficulties cited by Scully, Stern and Geary showed that for small potential perturbations Eq 8 can be linearized<sup>15</sup> such that

$$i_{cor} = \frac{i_{ext}}{\eta_{pol}} \cdot \frac{\beta_a \cdot \beta_c}{2.3 \cdot (\beta_a + \beta_c)} \quad (10)$$

where:

- $i_{ext}/\eta_{pol}$  = the polarization admittance, or  $1/R_p$ , the inverse of the polarization resistance, and the second term in Eq 10 is often referred to as the  $\beta$  factor.

Equation 10 is valid for small polarizations of about 10 mV. Ideally, anodic and cathodic Tafel slopes should be of the order of 60 and 120 mV, respectively. This would result in a  $\beta$ -factor of about 17 mV. However, in practice, Tafel slopes much larger than this are measured. Table 2 below shows  $\beta$ -factors for various anodic and cathodic "pseudo"-Tafel slopes.

These hypothetical calculations show that the assumption of ideal behavior can easily lead to underestimating the corrosion rate by a factor of 2.5. In practice, even higher Tafel slopes have been observed for a variety of reasons.

### The IR-Problem

The first problem encountered with electrochemical measurements (either potentiostatic or potentiodynamic) is the

**TABLE 2**— $\beta$ -Factors for various anodic and cathodic measured or pseudo Tafel slopes.

Cathodic Tafel Slopes	Anodic Tafel Slopes			
	60	100	150	200
60	13.04	16.30	18.63	20.07
120	17.39	23.72	28.99	32.61
150	18.63	26.09	32.61	37.27
200	20.07	28.99	37.27	43.48

fact that the applied overpotential ( $\eta$ ) not only reflects the charge transfer resistance, but also the resistance associated with current flow. One must, therefore, carefully think about this second component usually called the IR-drop. As discussed in Chapter 7, the most obvious cause for IR drop is the solution resistance. This can be minimized in the laboratory by properly positioning the reference electrode. However, in practice, where commercial three electrode arrangements of the same material are used, the reference electrode is hardly ever close enough to the working electrode to eliminate the IR drop. A typical example was shown in Ref 9, where the initial corrosion rate for CO<sub>2</sub> in a 300 ppm TDS brine measured by iron counts was 10 times higher than that measured by linear polarization. While this may be an extreme case, it reflects the magnitude of the effects one may encounter.

### Corrosion Product Layers

Resistance to current flow also occurs as a consequence of solid corrosion product buildup on the metal surface. This phenomenon is most pronounced in environments containing H<sub>2</sub>S. Iron sulfide is a semiconductor whose conducting properties depend on the nature of the environment. It had been observed [39] that the anodic and cathodic polarization curves on iron sulfide covered electrodes are linear rather than exponential. In this case, the current flow is entirely controlled by the charge transfer across the interphase (not interface) consisting of FeS. The polarization admittance ( $1/R_p$ ) becomes

$$\frac{i_{ext}}{\eta_{pol}} = \frac{a_c + a_a}{a_c \cdot a_a} \quad (11)$$

where  $a_a$  and  $a_c$  are the anodic and cathodic ohmic resistances (rather than Tafel slopes). The polarization admittance is no longer proportional to the corrosion current. Since most practical systems (oxides, carbonates, and many others [40,41]) exhibit mixed control, the  $\beta$ -factors can assume an almost infinite array of values.

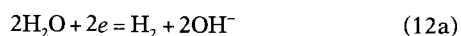
### The Interphase in the Presence of Corrosion Inhibitors

When corrosion inhibitors are present, the problems become infinitely more complex. First, inhibitors in most (perhaps all) practical systems adsorb on corrosion product layers. This notion has now been quite well accepted [39].<sup>16</sup> Second, most inhibitors that are effective enough to be used in practical systems are organic in nature and more or less hydrophobic. A schematic representation of the *Interphase* forming in most practical systems is shown in Fig. 8. In order to visualize the effects of a potential perturbation and current flow across this interphase, a number of phenomena need to be considered. In the steady state of a corroding surface, many different transfer reactions must occur. From the basic corrosion reactions

<sup>15</sup>For detailed derivation see also H. H. Uhlig, *Corrosion and Corrosion Control, An Introduction to Corrosion Science and Engineering*, John Wiley and Sons, New York, 1962, pg. 341.

<sup>16</sup>For many years it was believed that inhibitors adsorb on the metal surface, and test methods were developed to examine the "filming behavior" of inhibitors. It had been shown early that such filming inhibitors need an iron sulfide film to be effective. Later the same was shown for iron carbonate systems.

**FIG. 8—Schematic representation of corroding and inhibited metal surface.**



it is clear that the positive and negative ions generated have to come together in order to maintain electro-neutrality. From this simplified model a variety of interesting possibilities emerge. While Reaction 12 always occurs at the metal surface, Reaction 12a can occur either at the metal surface or at the scale-inhibitor interface, provided that in the first case the scale is porous and permeable to the corrodent, or is a semiconductor in the second case. If the scale is a semiconductor, it must be permeable to positive charges (electron holes of metal ions) or negative charges (electrons or anions). In either case, mass transfer occurs across the scale layer, and in the case of the semiconductor, charge transfer. Any of these transfer processes can be rate determining and then fall outside the Stern-Geary assumptions. This has been discussed in detail by Heitz and Schwenk [40] and by Ijsseling [41] among others. These authors have concluded that the polarization resistance methods are not applicable in cases where protective corrosion product layers are formed.

A problem, which is rarely discussed, presents itself by the fact that because of the ongoing surface reactions during corrosion, the surface pH is not equal to the solution pH. The steady state surface pH is also disturbed during polarization. This, in essence, manifests itself by a potential shift, which is superimposed to the external polarization [42].

Since essentially all corrosion product layers have some ion exchange properties, and since these result in an osmotic pressure gradient across the interphase, one can expect a structural relaxation following a potential perturbation. It has been shown that iron sulfide scale, for instance, has a different permeability for corrosion reactions depending on solution pH [39]. This structural relaxation due to surface pH changes is slow (much slower than interfacial capacitance charging) and makes it practically impossible to measure a representative polarization curve.<sup>17</sup>

<sup>17</sup>The effect is also noticeable at the low frequencies of EIS.

When an inhibitor is applied to a corroding specimen (or when the interphase forms in a corrosion test system containing an inhibitor), the situation becomes again much more complex, and one has to consider thermodynamic as well as transport effects. The presence of the inhibitor, in essence, represents a nonaqueous phase. (It does not matter whether one deals with a typical oilfield situation, HCl inhibitors, or in fact cooling water inhibitors. In all cases, a new phase will be formed on top of the metal-scale composite.) This new phase, first of all, changes all conditions that previously prevailed at the scale-brine interface. The water concentration is greatly reduced, and with it, occur changes in the ionic strength, the pH, and the osmotic pressure. More importantly, however, the corrosion reactions and associated transport processes must occur through this additional layer, which of course represents an additional resistance; otherwise, the chemical would not be an inhibitor. It is reasonable to postulate now that the rate determining steps are no longer the electron transfer reactions (basis for Stern-Geary theory), but transport processes. This, in essence, has been confirmed by Roy et al. [43] who indicated that in the absence of truly linear Tafel regions on polarization curves obtained in inhibited conditions, physically meaningful Tafel parameters cannot be obtained from polarization curves.

Now, it is known that uncharged molecules ( $\text{H}_2\text{O}$ ,  $\text{CO}_2$ ,  $\text{H}_2\text{S}$ , and under certain circumstances even  $\text{HCl}$ ) can diffuse through organic films. It is then perfectly possible and has again been observed with certain compounds, that corrosion can occur underneath such films without any exchange of charges with the environment.<sup>18</sup> Considering the nature of corrosion inhibitors, which are rarely single compounds, coupled with the fact that they need to be formulated to be "soluble," "dispersible," or "partitioning" into the corrosive environment, the proposition of measuring their effectiveness by electrochemical means alone becomes highly questionable.

## Practical Applications

Nevertheless, electrochemical measurements, particularly linear polarization, coupled with other qualifying measurements are a valuable tool to monitor corrosion kinetics — i.e., does inhibition occur and at what point in time does one observe a steady state inhibited corrosion rate? Under no circumstances, however, can results obtained from either linear polarization or potentiostatic polarization measurements be taken as realistic within the quality parameters outlined above.

Table 3 represents an example of a comparative study of weight loss and LPR corrosion rates in inhibited hydrochloric acid at 200°F [44]. The corrosion rate was continuously monitored and plotted as a function of time. Subsequently, the area under the curve was integrated, converted to weight loss, and compared with the actual weight loss. In this manner a ratio,  $R$ , of actual weight loss versus LPR

<sup>18</sup>This is not a case for chemical corrosion; it is a case for corrosion that cannot be measured electrochemically. It has been said that this can be overcome by electrochemical impedance spectroscopy measurements. However, the models are so complex that they have little practical value at this time.

**TABLE 3**—Corrosion inhibition measurements in 17 % HCl at 200°F on various steels with three different inhibitors.  $R$  = weight loss corrosion rate over integrated LPR measurement.  $R^2$  = same for first two hours of exposure,  $R^{22}$  same for 2 to 24 h,  $R$  = same for average of total exposure time. Average 24-h corrosion rates in mpy, P indicates coupon pitted or PP pitted severely.

Inhibitor Formulation	$R^1$	$R^{22}$	$R$	AISI 1020 mpy	N-80 mpy		
					1	2	3
1	5	5.2	5.7	75	117	89	320 P
2	2.8	6.8	3.6	49	52	68 P	1130 PP
3	2.3	15.5	8.2	61.4		85 P	1820 PP

weight loss was determined. Ideally, this ratio should be one if the  $\beta$ -factor (Eq 10) were 17 mV as corresponds to anodic and cathodic Tafel slopes of 60 and 120 mV, respectively. In fact, as can be concluded from the  $R$  ratios in Table 3,  $\beta$ -Factors from 3 to 15 times larger were observed. It is worth noting that the  $R$  ratios (and hence also the  $\beta$ -factors) increase with time (except for Inhibitor 1). The degree of inhibition in all these cases was very large and the inhibitors were such that a visible hydrophobic, protective layer formed with time. It would seem understandable, if not intuitive, that under such circumstances the electron transfer reactions are no longer rate determining and that, therefore, Tafel slopes have lost their traditional meaning. From a practical point of view it is clear that without calibration of the LPR response for each inhibitor, the electrochemical measurements would underestimate the real corrosion rates by a wide margin.

Similar results were presented in [9]. In uninhibited  $\text{CO}_2$  environments it was observed that in general the  $\beta$ -factors were of the order of 15–20 mV for pH-statted test procedures. However, as soon as a corrosion product layer formed, the factors increased. It is for this reason that the original PAIR<sup>19</sup>-meter by Petrolite pre-programmed a  $\beta$ -factor of 37 mV based on extensive laboratory and field calibrations [45].<sup>20</sup> Newer commercial instruments allow the user to dial in a value for the  $\beta$ -factor. However, this presupposes that the Tafel slopes are known, and since these cannot be reliably determined as indicated above, the user is still left to guess, unless calibration procedures are in place, such as weight loss determinations or iron counts.

In general,  $\beta$ -factors increase with the presence of corrosion product layers, the density and thickness of these layers, the presence of inhibitors, and the degree of inhibition. These effects, however, are unfortunately both metal and inhibitor specific and do not lend themselves to modeling, to the point where a model could be used uniformly, or electrochemical methods could be standardized to the point where the results were meaningful without qualifications.

<sup>19</sup>PAIR stands for Polarization Admittance Instantaneous (Corrosion) Rate and is Petrolite trade mark. PAIR is the inverse of polarization resistance, and was considered a more practical terminology since the corrosion current is directly proportional to  $I/V$ , the admittance.

<sup>20</sup>This had the effect of overestimating the blank corrosion rate and underestimating the inhibited rates, thus leading to higher degrees of inhibition, because of the compounded error.

## Other Approaches

Many other techniques and methodologies have been used to monitor effectiveness in inhibitor testing and the evaluation of inhibitors. Some of these are EIS (electrochemical impedance spectroscopy), EN (electrochemical noise measurements), galvanic testing, and many variations of these methods. The theoretical bases for these techniques have been discussed by Scully in Chapter 7 of this book, and specific applications are extensively referenced there.

## Electrochemical Impedance Spectroscopy

EIS basically determines the polarization and ohmic resistances, capacitance, and inductive impedances of electrochemical systems. While these electrical terms are straightforward and can be determined relatively easily with today's frequency spectrum analyzers, their chemical meaning is considerably more complex. In simple systems consisting of a metal surface and an electrolyte polarization resistance, capacitance and ohmic resistance simply represent the electron exchange, the solution resistance, and the Helmholtz double layer capacitance, and they can be determined independently in various ways. However, when the interphase is as complex as shown for instance in Fig. 8, the chemical meaning of these electrical terms is anything but straightforward. Without expanding this discussion into a lengthy mechanistic discourse of EIS and the underlying chemical realities, let's just look at three major difficulties.

Both the corrosion product layer and the inhibitor layer constitute resistances both to the transport of charged and uncharged species. The transport of water, carbon dioxide, oxygen, etc., through this interphase cannot be measured electrochemically and manifest themselves as diffusion resistance, also called a Warburg resistance. In the EI spectrum the Warburg resistance is observed only at very low frequencies, at which the corroding system is not in steady state any longer. An attempt to separate the polarization resistance from the Warburg resistance does not make any sense, because the system is under partial or full diffusion control to begin with.

The next difficulty has to do with the inherently anisotropic corrosion under the inhibitor film. It has been observed that on inhibited carbon steels corrosion often occurs along grain boundaries, while the grain faces can be well inhibited. This is particularly prevalent in the  $\text{CO}_2$  corrosion of carbon steels where often corrosion burrows into the steel, sometime to great depths, without affecting the surface to a great extent. The corroding surface, therefore, is much smaller than the apparent surface. Hence, translating the EIS polarization resistance to a corrosion rate would result in uncharacteristically low values. (This problem, of course, is inherent in all electrochemical measurements.)

Finally, corrosion inhibitors often lead to so-called inductive loops, the chemical meaning of which is totally unclear.

Nevertheless, EIS has its place in mechanistic studies. For instance, organic inhibitor films constitute imperfect dielectric barriers. The capacitance of the interphase is no doubt affected by the inhibitor film. Therefore, if the system were to lend itself to the measurement of the incremental capacitance due to the presence of the inhibitor film, such change

could be related to the chemical nature of the inhibitor. Such speculations, however, are way off in the future.

If the system under study is in a transitional state, or inherently unsteady because of local corrosion, EIS measurements will be unstable and noisy as well. Systems that exhibit this kind of behavior consist of passive metals in an environment that has a destructive effect on the passive layer (stainless steels and valve metals (such as aluminum)). Inhibitors (both inorganic and organic) have been observed to “tame” this noisy behavior. However, in such cases, electrochemical noise measurements may be more indicated.

In summary, EIS may have its place in mechanistic studies of corrosion inhibitors and should be used to elucidate some of the mysteries of corrosion inhibition from a chemical point of view. For routine evaluations of inhibited systems EIS has no specific advantages over LPR and is afflicted with the same uncertainties discussed above.

### Electrochemical Noise Measurements

Electrochemical noise of a corroding system manifests itself as potential fluctuations (measured against reference electrode), current fluctuations (measured at constant potential via a zero resistance ammeter), or both current and potential fluctuations (when measured between two identical electrodes in the same medium). Measurements of electrochemical noise have also been discussed by Scully in Chapter 7. Inhibitors have an attenuating effect on the noise and have often been associated with the inhibition of localized corrosion. Noise measurements are passive and inherently the ideal methodology for corrosion measurements, because the electrode is not polarized in an external circuit, and hence, the steady state of all interfacial constituents and processes is not disturbed. However, in order to translate the noise signals to a corrosion rate, both the potential and the current spectra have to be reduced to a single value each, which can then be processed according to the Stern-Geary equation. What's missing in this process, however, is the assessment of the corroding surface.

Again, EN is a very useful technique for the study of inhibition of localized corrosion, and tremendous progress has been made in the evaluation of the data using mostly proprietary computer algorithms [60]. It is a methodology that certainly lends itself for monitoring purposes. However, the results are strictly qualitative.

### Galvanic Measurements

An early method for the assessment and monitoring of corrosion inhibitor effectiveness in the oilfield, for instance, consisted of the coupling of a steel electrode with a copper electrode via a zero resistance ammeter. It can readily be understood that the inhibitor can or might reduce the rate of the electrochemical reactions on both electrodes and not necessarily to the same degree. The measured galvanic current in the inhibited situation indicates that inhibition occurred, but it might be the copper electrode that was inhibited rather than the steel electrode. The latter might continue to corrode. While this may be the extreme case, anything from inhibition of the steel to inhibition of the copper to inhibition of both may occur. The residual

galvanic current after inhibition is, therefore, no direct indication of the inhibited corrosion rate of the steel.

Additionally, there are situations where the system that needs to be inhibited contains several metals, which are already galvanically coupled. Such a system was encountered in nuclear steam generators where the shell is high strength carbon steel and the tubes are Inconel metal. Under normal operating conditions this is not a problem; however, when the generator needed to be cleaned (removal of iron oxides), the most effective cleaning solution also turned out to be most aggressive to carbon steel and needed to be chemically inhibited. The work was described in detail in Ref 63. It was found that the large Inconel surface in the generator accelerated the steel corrosion dramatically. Inhibitor dosage had to take into consideration this acceleration, and needed to be much higher than in the uncoupled condition. When an attempt was made to assess the degree of inhibition on couples with varying steel to Inconel surface area ratios, it was found that the galvanic current was always smaller than the actual corrosion rate of the carbon steel. The technician has to be very much aware of this problem. The galvanic current is only a measure for the galvanic acceleration of corrosion. The total corrosion consists of both the self-corrosion of the steel plus the galvanic acceleration. If the potential differences between the two electrodes is relatively small, the self-corrosion of the steel may not be suppressed to a large degree by the galvanic couple, and may therefore still be substantial, as was the case in the steam generator. The decrease of the galvanic current due to the inhibitor, therefore, has to be calibrated against the weight loss of the corroding electrode before zero resistance ammeter currents can be used as an indication of corrosion rate.

In summary, all electrochemical methods used and proposed for corrosion monitoring and evaluation of corrosion inhibitors serve useful purposes and certainly have their place in the industry. However, careful interpretation of the results is always called for. In this context, it must be emphasized that all commercial instruments employing one or the other technique are sold with exaggerated claims of accuracy, reliability, or usefulness.

## TEST PROCEDURES AND PRIMARY VARIABLES

### Atmospheric Testing

Corrosion inhibitor testing was in the past mostly performed under atmospheric pressure. Typical test procedures were the Wheel Test [10], the Bubble Test [46], the Kettle Test [47], and many variations thereof. While the Wheel Test is pretty much antiquated, the others are still used routinely by many technicians. A serious consideration in this type of testing is the exclusion of oxygen. Many procedures, even standardized ones, advise “bubbling” nitrogen through the solution at a given rate (100 mL/min) for a length of time (one hour) [48]. It has been the author's experience that bubbling nitrogen, even for longer periods of time, do not lead to full removal of oxygen. The solution needs to be heavily agitated to cause dispersion of the bubbles and increase

their residence time in the solution. Often overlooked is the fact that Tygon tubing, much used for connecting the source of the nitrogen to the test vessel, has a finite permeability to oxygen. The residual contamination of oxygen caused by this effect can easily be calculated from the oxygen diffusion coefficient, the length of the tubing, the tubing wall thickness, and the nitrogen gas flow.

Agitation can be achieved with magnetic stirrers, e.g., bubble test [46], or motor driven paddle or turbine driven stirrers [9,47]. The effective velocity for magnetic stirrers depends on the size of the magnet, the rpm, and the size of the vessel, and is in general ill defined. The effective velocity of the turbine stirrers also depends on the same parameters, but is in general higher because of the higher rpm that can be achieved. However, because of the drag on the vessel walls the actual velocity is again ill defined.

External stirrers, such as motor driven turbines or paddle stirrers, require some kind of a Teflon gland or bearing for pass through of the stirrer shaft. While it has been said that maintenance of a positive pressure in the vessel (a few centimeters of water) will prevent air entry into the vessel, such is not the case when the shaft is rotated at high speeds. If high velocities are a requirement for testing, the best solution is an airtight cover over the test vessel and a magnetically coupled stirrer such as are being used in autoclaves routinely. It is the only practical way to keep air from entering the test solution.

The pH of the test solution is, as has been pointed out above, a critical factor. Not only does the pH affect the effectiveness of the inhibitor, it also controls its partitioning behavior and other secondary properties of the chemicals such as foaming, and to a lesser extent chemical stability. The pH should be kept constant during the test. Compensation for the buildup of buffering components (e.g., bicarbonate) can be achieved inexpensively with a pH controlled acid injection pump [9]. Strong acids<sup>21</sup> that are not involved in the corrosion process, such as sulfuric or perchloric acids, have been used successfully. When high degrees of inhibition are achieved from the beginning of the test, pH maintenance may be less important, since the composition of the aqueous phase will not change much. However, when the concentration/performance characteristic of the product is to be established, it is important that all tests at different concentrations be carried out at the same pH all through each individual test.

In order to expand the usefulness of the constant inventory systems, flowloops were built such that brine and/or a combination of brine and hydrocarbon could be circulated from a large reservoir over relatively small corrosion coupons or probes. One of the first such systems [31] employed a reservoir constructed such that a mixture of brine and hydrocarbon could be pumped with a single pump at variable velocity and controlled by variable brine/hydrocarbon mixture ratio. The problem with flowloops used for inhibitor testing is cleaning; nevertheless, many laboratories built

such systems for a variety of purposes. High-pressure systems will be discussed below.

### High Pressure Testing: Autoclaves, Flowloops, and Flow-Through Systems

Many corrosive industrial systems operate under high pressure, either because of high temperature (above boiling point of water or brine), or because of a high pressure environment consisting of acid and inert gases. Autoclaves are constant inventory devices, and because of the severe corrosive conditions, the environment changes rapidly in the uninhibited situation. The results obtained from such tests have no other value than to demonstrate qualitatively the severity of corrosion and the corrosion morphology [26]. When inhibitors are used, it often takes a long time to reach a steady state corrosion rate [49]. The reason for this is the time necessary to build up a protective layer. It is, therefore, considered necessary to monitor the corrosion kinetics in autoclave tests. While this can be done electrochemically [50], it is an absolute must to verify the steady state corrosion rate through chemical analysis of the medium and weight loss measurements. Chemical analysis will also give the technician an idea of the composition of the brine after the test and will give him an opportunity to calculate the pH associated with the steady state.

Again, in order to extend the volume/surface area ratio of the test system, high pressure flowloops [51,52] were built and later high pressure flow-through systems [22,53<sup>22</sup>]. Both flowloops and flow-through systems were ideally suited to generate the type of shear stresses needed to study the effectiveness of inhibitors under extreme situations occurring in the field. These systems were not limited to the oil field but were also used to study corrosion in cooling water circuits, steam generation, and other technologies. More recently, the focus shifted to the interrelationships between pressure and flow intensity.

### The Effects of Flow and Pressure on Corrosion Inhibition

The effects of flow rate (flow intensity, turbulence, shear stress) on corrosion have been known for a long time and have been variously called erosion corrosion or flow induced localized corrosion (FILC), which latter term is preferred because it denotes a purely aqueous (liquid) phenomenon, while erosion generally includes the presence of a solid phase. An attempt was made in 1990 to summarize the state of the art of FILC in a symposium [54]. The following is a brief synopsis of the developments in this area, with emphasis on corrosion inhibitor testing.

Schmitt was one of the first to recognize that fundamental studies in this area were necessary [55]. This author developed the rotating cage to generate high flow intensities in autoclaves and demonstrated that corrosion phenomena

<sup>21</sup>The use of weak acids, such as acetic acid, would defeat the purpose for two reasons: first, such acids contribute to the buffering system (just like carbonic acid) and, second, organic acids in general are complexing moieties and become involved in the corrosion process.

<sup>22</sup>Mobil Oil company built a large flow-through installation wherein a mixture of brine, hydrocarbon, and acid gases was passed through an autoclave containing high shear devices. Inhibitors could be injected separately. The system resembled a large pilot plant and could operate at pressures up to 5000 psi with both CO<sub>2</sub> and H<sub>2</sub>S or mixtures thereof.

observed in the field could be duplicated in the laboratory and effectively inhibited. The rotating cage is a device where corrosion coupons are mounted between two discs, which in turn are fixed onto a rotating shaft. The assembly can be rotated in the autoclave using a magnetically coupled stirring motor. Schmitt then formulated a fundamental relationship between inhibition and flow intensity [47]: For every inhibitor at a given concentration there exists a critical flow intensity beyond which inhibition begins to be lost; and for every inhibitor concentration (for a given inhibitor) there exists a critical flow intensity beyond which inhibition begins to be lost. In addition, it was recognized that acid gas partial pressure can also play an important role.

The rotating cage, which subsequently was used by others [26,31,49,54], served its purpose in demonstrating that severe corrosion phenomena observed in the field could be qualitatively duplicated in the laboratory and inhibited. However, because it was necessary to quantify the flow intensity by some measurable parameter, e.g., shear stress, other methods were developed as well. Among these were the rotating disc and rotating cylinder electrodes, and the jet impingement technology. A detailed comparison of these methods and quantitative assessment of shear stress is given in [56]. At this stage, further development of both the jet impingement [57] and rotating cage occurred in parallel [58].

The drawback of the jet impingement method is the fact that the corrosion rates have to be monitored electrochemically and cannot easily be verified by alternate methods. While tests with the rotating cylinder electrode are also monitored electrochemically, the corrosion rate can be verified by weight loss. However, the rotating cylinder suffers in general from a limitation in the magnitude of the shear stress that can be achieved. Hence, it was desirable to attempt to quantify the shear stresses to which various parts of the coupons mounted in the rotating cage are subjected. Papavinasam et al. [58] attempted this in model experiments, but could not really derive a shear stress for the leading or trailing edges of the coupons.

That it would be necessary to obtain a quantitative assessment of shear stress on flow upsets in tubing had already earlier been demonstrated by Schmitt et al. [59]. The authors demonstrated by finite element analysis and experiments that peak shear stresses on the leading edge of a groove cut into 2-in. tubing and subject to full bore liquid flow velocities of up to 20 m/s were from 4 to 7 times higher than the nominal shear stress calculated for such flow. Thus, flow intensifier numbers were defined for flow upsets of different geometries. Since it was well known by this time that inhibitor concentrations had to be optimized for the maximum shear stress encountered in a practical system, it was understood that it would be desirable to quantify shear stresses in test systems as well. Schmitt developed microsensors with the help of which exact shear stress measurements could be achieved on the jet impingement electrodes [60] by means of limiting current measurements.

The next step, currently in progress [61], is the use of microsensors built into coupons used in the rotating cage for the determination of localized shear stresses in various locations of the coupons. By defining the exact geometry of the cage and the test vessels, as well as the fluids, the shear stresses will be mapped as a function of the speed of rotation

of the cage. This work, when completed, can lead to the first truly standardized test method for flow induced corrosion and the evaluation of inhibitors under FILC conditions.

## OTHER IMPORTANT VARIABLES

### Surface Preparation

The surface preparation of coupons or electrodes used in inhibitor testing has become so much of a routine that the problems involved with the state of the surface prior to testing are rarely given any thought. Mercer [6] put it as follows: "... The desirability of approximating the surface state of a test specimen to that encountered in service is opposed to by the need to generate a surface condition most conducive to producing reproducible results." The emphasis has almost exclusively been on reproducibility. Specimens are degreased with various solvents; at times, complex procedures are used (e.g., soxhlet type apparatus). Scale layers (including mill scale) are removed by sandblasting, acid etch, polishing with Emery paper, etc. (see also Ref 62). While all these procedures have improved the reproducibility, the question of relevance and predictiveness remains unanswered today. That inhibitors work in the field is unquestioned, but whether the cost-effectiveness has been reliably assessed does remain an open question.

Any specimen preparation procedure leaves the surface in some state of roughness. It has been observed that the corrosion on polished specimens tends to increase in the first stages of a test, while on rough surfaces the rate decreases. Eventually, both specimens will reach a similar steady state. However, a large real surface area requires more inhibitor for inhibition than a polished one. Thus, surface preparation will affect the determination of the effective inhibitor concentration, particularly in constant inventory tests with a small liquid volume to surface area ratio.

Corrosion specimens are usually cut from sheet metal or machined from rod material. Often, specimens are both machined and cut from tubing and piping material. Changes in the metallurgy due to these processes will alter the metallurgy and, thereby, the corrosivity and response to inhibitors. Anisotropic corrosion, particularly in presence of corrosion inhibitors, is a little known phenomenon, which should be paid more attention to (see below).

### Selection of Metallurgy

It is absolutely imperative that all corrosion inhibitor evaluations be made on metal specimens encountered in the field. It had been pointed out above that [27,28] the effective inhibitor concentration on two different oilfield steels (J-55 and L-80) was vastly different under severe conditions. Examples of this abound in the industry. Weldments of carbon steel piping containing a small amount of copper were more difficult to inhibit under relatively mild conditions.

A large study on the inhibition of carbon steel in 15 % hot hydrochloric acid showed that mild steel coupons could be extremely well inhibited [44] with degrees of protection in excess of 99.99 %, while at the same time coupons from oil field tubulars corroded from 4 to 30 times faster. While the

oilfield tubulars were designated as N-80 material, there were again big differences observed on N-80 material of different origin (see Table 3). The most perplexing observation during these investigations was the occurrence of anisotropic corrosion. Round electrodes, for instance, cut from AISI 1018 mild steel rod stock tended to be well inhibited on the sides, while the ends, the so-called cross-grain surfaces, corroded 10 to 20 times faster and exhibited pronounced intergranular corrosion. On the N-80 materials, it was observed that cross-grain surfaces were covered with a thin layer of ferritic steel (formed during cutting due to the heat generated), while the bulk of the material was martensitic. As it turned out, the ferritic material was well inhibited, while the martensite underneath corroded at a much increased rate.

Similarly, the development of an inhibitor for an EDTA based chemical cleaning solvent to be used in nuclear steam generator cleaning showed differences of the degree of inhibition for various structural carbon steels used in steam generators [63]. It was during this work that it was shown for the first time that corrosion inhibitor effectiveness may be dependent on the strength of the material. In these cases, it was also observed that surfaces parallel to the rolling direction were well inhibited while the cross-grain surfaces corroded much faster. All this points to the need to carefully select and prepare the test specimens.

### Conditioning of Environment

Under this heading, one needs to discuss the elimination or addition of gases to the test environment. Deoxygenation was discussed in some detail above. The diffusion of a dissolved gas from the liquid into an inert gas phase is a slow process, limited by the gas/liquid interface area and the contact time. It is, therefore, necessary to increase this area by finely dispersing the inert gas, and by extending the contact time. This can be achieved by vigorous agitation. Bubbling nitrogen through an electrolyte without agitation is never enough to fully deaerate a solution. The reverse process is equally slow. Saturating a solution with  $\text{CO}_2$  or  $\text{H}_2\text{S}$  must occur under vigorous agitation, particularly in high pressure testing.

While small amounts of residual oxygen (10 to 20 ppb) are not critical when inhibitors are evaluated in a  $\text{CO}_2$  atmosphere, except under high shear stress, the situation is different in the presence of  $\text{H}_2\text{S}$ . It has been shown that as little as 200 ppm of oxygen in the purge gas can dramatically alter the corrosion kinetics of iron in the presence of  $\text{H}_2\text{S}$  [36]. This corresponds to as little as 10 ppb oxygen in solution. It is, therefore, also important that the purge gases are analyzed for impurities. The  $\text{CO}_2$  purchased from a certain supplier was found at times to contain as much as 1000 ppm oxygen. This did not per se affect the inhibitor performance, but a residual corrosion due to the oxygen remained present, such that the steady state inhibited corrosion current was much larger than it would have been in the absence of oxygen. When inhibited corrosion rates of the order of 1 to 2 mpy or smaller are to be achieved, traces of oxygen can easily prevent this goal to be attained even with the best of products.

Another source of error often occurs when one must work with mixed gases, such as  $\text{CO}_2$  containing small amounts of

$\text{H}_2\text{S}$ . When a solution must be saturated with a mixed gas under atmospheric pressure by means of purging, the gas mixture may be equivalent to the partial pressure ratio to be achieved in the test. When, however, autoclaves are to be pressured with mixed gases, the gas composition must be carefully predetermined such that the correct partial pressure ratio in the autoclave will be achieved. The reason for this is that the gases have different solubilities. This problem was discussed in some detail by the author [64]. An in-depth analysis of test procedures carried out with mixed gases at high pressures reached the conclusion that most such tests carried out in the past were not done at the nominal partial pressure ratio. In some cases the discrepancies were rather large.

### Inhibition of Precorroded Surfaces

It had been demonstrated [39] early on that in hydrogen sulfide corrosion the inhibitor has to be in contact with a sulfided (precorroded) surface in order to show inhibition. This observation rendered useless all those test procedures in which the inhibitor is applied to a clean metal surface in so-called film persistency tests. While it is well established that certain chemicals, such as high molecular weight fatty acids, have an affinity for metal surfaces and can form a water repellent film, they are readily replaced by other compounds that have a stronger affinity, for instance  $\text{H}_2\text{S}$ . Fatty amines, on the other hand, adsorb strongly on iron sulfide, and their desorption from sulfided surfaces takes much longer than the desorption of fatty acids from bare metal surfaces in the presence of  $\text{H}_2\text{S}$ .

Table 1 shows that some inhibitors are active in  $\text{CO}_2$  corrosion at pH 4 where it is believed that no iron carbonate scale builds up, while others are only effective at the higher pH where a certain amount of passivation occurs due to iron carbonate buildup. Indeed, the inhibitors of the first kind are also the most effective ones against flow induced localized corrosion (also called "Mesa corrosion"), where due to high turbulences the protective iron carbonate is washed away. However, some interesting observations were made when carbon steel was precorroded in a  $\text{CO}_2$  environment [65]. Figure 9 shows that, at a constant inhibitor

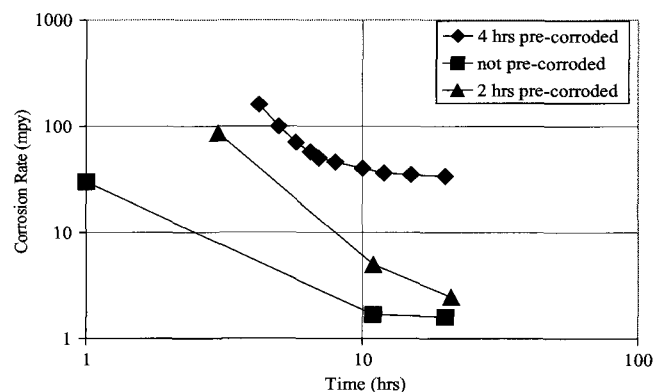


FIG. 9—Effect of precorrosion on inhibitor performance. Constant pH kettle test, 55°C, 1 bar  $\text{CO}_2$ , 100 ppm inhibitor. Corrosion rates monitored by Fe-counts or weight loss corrected LPR measurements.



concentration in the constant pH Kettle test at pH 4, inhibition is much less effective when the specimens are precorroded for 4 h. On the other hand, when the same tests were performed without maintaining the pH constant, such that a carbonate layer could in fact build up during the test procedure, precorrosion had very little effect, if any.

The relationship between a corrosion product layer and inhibitors has also been discussed, among others, by Lorenz [66], and Lorenz and Mansfeld [67]. These authors point out that in many practical systems, for instance aerated water and carbon steel, an interaction occurs between, in this case, iron oxide and the inhibitor to the point where the inhibitor is not only adsorbed on the oxide surface, but actually incorporated into the three-dimensional oxide layer. Clearly, three-dimensional or interphase inhibition cannot be achieved in short tests or by filming procedures. Furthermore, measuring techniques have to take into consideration the altered chemical and electrochemical conditions across such bulk interphase layers. It is unfortunate that this aspect of corrosion and corrosion inhibition has not received more attention, and it is suggested that this lack of attention has seriously held back all aspects of corrosion inhibitor applications and monitoring of effectiveness.

## SUMMARY

Corrosion inhibitor testing has over the years progressed from the trivial (immersion tests) to the most complex (high flow rates under verifiable shear stress). The presence of inhibitors in a corroding system adds a new dimension to corrosion testing and measuring in general. The presence of an inhibitor in the interphase between the metal and the liquid environment negates and invalidates in all but perhaps a few cases the electrochemical assumptions underlying electrochemical measuring techniques so prevalent in the industry today.

Within the framework of carefully defined quality criteria, it has become necessary to reinterpret the all too prevalent weight loss measurements and the methodology of constant inventory test systems. Since all corrosion inhibitor tests experience a corrosion rate transient in the early stages of the test for a multitude of reasons, the corrosion rates during the test must be monitored as a function of time in order to assess attainment of the steady state. Furthermore, the environment changes with time in most constant inventory test vessels. Therefore, there has been a tendency to either counteract these changes (continuous fluid conditioning) or minimize such changes by optimizing the liquid volume to surface area ratio.

The effectiveness of inhibitors is affected by a number of environmental, physical, and metallurgical parameters. These variables interact with each other in unpredictable nonlinear fashion, and moreover, such interactions are inhibitor specific. This state of affairs negates the validity of screening or standardized testing. Relevant and predictable inhibitor evaluation must be carried out under conditions simulating as closely as possible those of ultimate usage.

The ultimate objective of using corrosion inhibitors is failure inhibition. Failures always occur under the most aggressive conditions, be it due to flow intensity, pH, metallurgy,

or the combination of high pressure and temperature. Failure inhibition requires the largest inhibitor concentration and is the most costly option. Therefore, the technician must begin to model corrosion inhibition within the parameter field of the operating facilities in order to optimize overall inhibitor cost. One such model, empirical as it may have been, has recently been developed for the first time [27,28].

## REFERENCES

- [1] Bregman, J. I., *Corrosion Inhibitors*, McMillan, New York, 1963.
- [2] Nathan, C. C., *Corrosion Inhibitors*, NACE Official Publication, 1973.
- [3] European Federation of Corrosion (EFC), Publication No. 11, 1994.
- [4] NACE, *Corrosion Inhibition, Proceedings of the International Conference on Corrosion Inhibition*, R. H. Hausler, Ed., Dallas, 1983.
- [5] Mercer, A. D., "Test Methods for Corrosion Inhibitors," *British Corrosion Journal*, Vol. 20, No. 2, 1985 (updated in 1994), p. 61.
- [6] Mercer, A. D., "Test Methods for Corrosion Inhibitors," in EFC Publication No. 11, pp. 145–163.
- [7] Kapusta, S. D., "Corrosion Inhibitor Testing and Selection for E&P: A User's Perspective," *CORROSION/99 NACE*, Paper No. 16, 1999.
- [8] Hausler, R. H., *Corrosion Inhibition, Corrosion Chemistry*, ACS Symposium Series, Vol. 89, 1979, G. R. Brubaker and P. B. P. Phipps, Eds., p. 316.
- [9] Hausler, R. H., Stegmann, D. W., and Stevens, R. F., "The Methodology of Corrosion Inhibitor Development for CO<sub>2</sub> Systems," *Corrosion*, Vol. 45, No. 10, 1989, p. 857.
- [10] NACE Technical Committee Report, "Wheel Test Method Used for Evaluation of Film Persistent Inhibitors for Oilfield Applications," NACE Technical Publication 1D 182, *Materials Performance*, December 1982, p. 45.
- [11] ASTM Standard G 1-90 (Reapproved 1999): Practice for Preparing, Cleaning, and Evaluating Corrosion Test Specimens, *Annual Book of ASTM Standards*, Vol. 3, ASTM International, West Conshohocken, PA.
- [12] ASTM Standard G 16-95 (Reapproved 1999): Guide for Applying Statistics to Analysis of Corrosion Data, *Annual Book of ASTM Standards*, Vol. 3, ASTM International, West Conshohocken, PA.
- [13] ASTM Standard G 46-94 (Reapproved 1999): Guide for Examination and Evaluation of Pitting Corrosion, *Annual Book of ASTM Standards*, Vol. 3, ASTM International, West Conshohocken, PA.
- [14] ASTM G 5-87: Standard Reference Test Method for Making Potentiostatic and Potentiodynamic Anodic Polarization Measurements, *Annual Book of ASTM Standards*, ASTM International, West Conshohocken, PA, March 27, 1987.
- [15] ASTM Standard G 3-89 (Reapproved in 1999): Practice for Conventions Applicable to Electrochemical Measurements in Corrosion Testing, *Annual Book of ASTM Standards*, Vol. 3, ASTM International, West Conshohocken, PA.
- [16] ASTM Standard G 96-90: Guide for On-line Monitoring of Corrosion in Plant Equipment (Electrical and Electrochemical Methods), *Annual Book of ASTM Standards*, Vol. 3, ASTM International, West Conshohocken, PA.
- [17] ASTM Standard G 102-89: Practice for Calculation of Corrosion Rates and Related Information from Electrochemical Measurements, *Annual Book of ASTM Standards*, Vol. 3, ASTM International, West Conshohocken, PA.
- [18] ASTM Standard G 61-86: Test Method for Conducting Cyclic Potentiodynamic Polarization Measurements for Localized Corrosion Susceptibility of Iron-, Nickel-, or Cobalt-Based

- Alloys, *Annual Book of ASTM Standards*, Vol. 3, ASTM International, West Conshohocken, PA.
- [19] NACE TM 0169-95, Laboratory Corrosion Testing of Metals (item #21200).
- [20] NACE TM 0171-95, Autoclave Corrosion Testing of Metals in High-Temperature Water (item # 21203).
- [21] NACE TM 0172-93, Determining Corrosive Properties of Cargoes in Petroleum Product Pipelines (item # 212040).
- [22] Kapusta, S. D., Rhodes, P. R., and Silverman, S. A., "Inhibitor Testing Procedures for CO<sub>2</sub> Environments," *CORROSION 91, NACE Annual Conference 1991*, Paper No. 471.
- [23] Dugstad, A., Lunde, L., and Videm, K., "Influence of Alloying Elements upon the CO<sub>2</sub> Corrosion Rate of Low Alloyed Carbon Steels," *CORROSION/91, NACE Annual Conference 1991*, Paper No. 473.
- [24] Garber, J. D. (Unpublished data from a Joint Industry Project performed at the University of Southern Louisiana at Lafayette. Selected results were published by Garber, J. D.), "Comparison of Various Test Methods in the Evaluation of CO<sub>2</sub> Corrosion Inhibitors for Downhole and Pipeline Use," *CORROSION/94, NACE Annual Conference*, Paper No. 42, 1994.
- [25] Hausler, R. H. and Stegmann, D. W., "Studies Relating to the Predictiveness of Corrosion Inhibitor Evaluations in Laboratory and Field Environments," *SPE Production Engineering*, August 1990, p. 286.
- [26] Stegmann, D. W., Hausler, R. H., Cruz, C. I., and Sutanto, H., "Laboratory Studies on Flow Induced Localized Corrosion in CO<sub>2</sub>/H<sub>2</sub>S Environments, I. Development of Test Methodology," *CORROSION/90, NACE Annual Corrosion Conference*, Paper No. 5, 1990.
- [27] Hausler, R. H., Martin, T. G., Stegman, D. W., and Ward, M. B., "Development of a Corrosion Inhibitor Model I: Laboratory Studies," *CORROSION/99, NACE Annual Conference 1999*, Paper No. 2.
- [28] Martin, T. G., Cox, M. T., Hausler, R. H., Dartez, R. J., Pratt, P., and Roberts, J. C., "Development of a Corrosion Inhibitor Model II: Verification of Model by Continuous Corrosion Rate Measurements Under Flowing Conditions with a Novel Downhole Tool," *CORROSION/99, NACE Annual Conference 1999*, Paper No. 3.
- [29] NACE Recommended Practice RP 0192-92, Monitoring Corrosion in Oil and Gas Production with Iron Counts (item #21053).
- [30] *Hach Water Analysis Handbook*, Hach Company, Loveland, CO, 1989.
- [31] Hausler, R. H. and Stegmann, D. W., "Laboratory Studies on Flow Induced Localized Corrosion in CO<sub>2</sub>/H<sub>2</sub>S Environments, IV: Assessment of the Kinetics of Corrosion Inhibition by Hydrogen Evolution Measurements," *CORROSION/91, NACE Annual Corrosion Conference 1991*, Paper No. 474.
- [32] Devanathan, M. A. V. and Stachurski, Z., "The Adsorption and Diffusion of Electrolytic Hydrogen in Palladium," *Proceedings*, Royal Society, London, A 270, 1962, p. 90.
- [33] Devanathan, M. A. V., Stachurski, Z., and Beck, W., "A Technique for the Evaluation of Hydrogen Embrittlement Characteristics of Electroplating Baths," *Journal of the Electrochemical Society*, Vol. 110, 1963, p. 886.
- [34] Schmitt, G., "Wasserstoff Permeations Messungen (Hydrogen Permeation Measurements)," in *Wasserstoff und Korrosion (Hydrogen and Corrosion)*, D. Kuron, Ed., 2nd ed., 2000, Irene Kuron, Bonn, Germany, p. 407.
- [35] Schmitt, G., Sadlowski, B., Noga, J., and Siegmund, G., "Inhibition of Hydrogen Effusion from Steel—An Overlooked and Underestimated Phenomenon," *CORROSION/2000, NACE Annual Conference*, 2000, Paper No. 466.
- [36] Hausler, R. H., Stanski, C., and Nevins, A., "Process Corrosion and Corrosion Inhibitors in the Petroleum Industry," *Materials Performance*, Vol. 13, No. 9, 1974.
- [37] Tafel, J., *Z. Physikal. Chem.*, Vol. 50, 1904, p. 641.
- [38] Stern, M. and Geary, A., *Journal of the Electrochemical Society*, Vol. 104, No. 56, 1957 (see also Stern, M., *Corrosion*, Vol. 14, 440t (1958)).
- [39] Hausler, R. H., Goeller, L. A., and Rosenwald, R. H., "Contribution to the Mechanism of Hydrogen Sulfide Corrosion Inhibition," *Proceedings of the 3rd European Symposium on Corrosion Inhibitors*, Ferrara, Italy, 14–17 September 1970, p. 399.
- [40] Heitz, E. and Schwenk, W., "Bases Théoriques de la Détermination des Densités de Courant de Corrosion Partir des Résistances de Polarisation; Métaux," *Corrosion - Industrie*, No. 644, April 1979.
- [41] Ijsseling, F. P., "Application of Electrochemical Methods of Corrosion Rate Determination to Systems Involving Corrosion Product Layers," *Br. Corros. J.*, Vol. 21, No. 2, 1986, p. 95.
- [42] Kuhn, A. T. and Chan, C. Y., "pH Changes at Near-Electrode Surfaces," *J. Appl. Electrochem.*, Vol. 13, 1983, pp. 189–207.
- [43] Roy, S. C., Roy, S. K., and Sircar, S. C., "Critique of Inhibitor Evaluation by Polarization Measurements," *Br. Corros. J.*, Vol. 23, No. 2, 1988, p. 102.
- [44] Hausler, R. H., "On the Use of Linear Polarization Measurements for the Evaluation of Corrosion Inhibitors in Concentrated Hydrochloric Acid at 200°F," *Corrosion*, Vol. 42, No. 12, 1986, p. 729.
- [45] Petrolite internal documents, no longer retrievable.
- [46] Dawson, J. L., Miller, R. G., John, D. G., and King, R. A., "Inhibitor Evaluation Methodology for Oilfield Application," *CORROSION/88, NACE Annual Conference*, Paper No. 361, 1988.
- [47] Stegmann, D. W. and Asperger, R. G., "New Test for Oil Soluble/Water Dispersible Gas Pipeline Corrosion Inhibitors," *CORROSION/87, NACE Annual Conference*, Paper No. 35, 1987.
- [48] NACE Standard TM0177-90; Standard Test Method: Laboratory Testing of Metals for Resistance to Sulfide Cracking in H<sub>2</sub>S Environments (NACE Item 53040 1990).
- [49] Hausler, R. H., Stegmann, D. W., Cruz, C. I., and Tjandros, D., "Laboratory Studies on Flow Induced Localized Corrosion in CO<sub>2</sub>/H<sub>2</sub>S Environments, III. Chemical Corrosion Inhibition," *CORROSION/90, NACE National Conference*, 1990, Paper No. 7.
- [50] Dougherty, J. A. and French, E. C., "Selection of Inhibitors and Treating Methods for Deep Hot Gas Wells," *Materials Performance*, Vol. 25, No. 19, 1986, pp. 44–50.
- [51] Schmitt, G., Simon, T., and Hausler, R. H., "CO<sub>2</sub> Corrosion and its Inhibition under Extreme Shear Stress I. Development of Methodology," *CORROSION/90, NACE Annual Conference 1990*, Paper 22.
- [52] Schmitt, G., Simon, T., and Hausler, R. H., "CO<sub>2</sub> Corrosion and its Inhibition under Extreme Shear Stress II. Performance of Inhibitors," *CORROSION/93, NACE Annual Conference*, Paper No. 86, 1993.
- [53] Mobil Oil Company, internal documents
- [54] NACE, *Flow Induced Corrosion: Fundamental Studies and Industry Experience*, K. J. Kennelly, R. H. Hausler, and D. C. Silverman, Eds., An Official NACE Publication, 1991.
- [55] Schmitt, G., Steinmetz, D., Engels, D., and Bruckhoff, W., "Investigations on Localized Corrosion of Low Alloy Steels in Sweet Gas Production," SPE Paper 13553, Society of Petroleum Engineers, 1985.
- [56] NACE Technical Committee Report: State of the Art Report on Conducting Controlled-Flow Laboratory Corrosion Tests, December 1995, Item 24187.
- [57] Eifird, K. D., "Jet Impingement Testing for Flow Accelerated Corrosion," *CORROSION/2000, NACE Annual Corrosion Conference*, 2000, Paper No. 2000.
- [58] Papavinasam, S., Revie, R. W., Attard, M., Demoz, A., Sun, H., Donini, J. C., and Michaelian, K., "Inhibitor Selection for Internal Corrosion Control of Pipelines 1. Laboratory Methodologies," *CORROSION/99, NACE Annual Conference 1999*, Paper No. 1.

- [59] Schmitt, G., Bücken, W., and Fanebust, R., "Modelling Microturbulences at Surface Imperfections as Related to Flow Induced Localized Corrosion and its Prevention," *CORROSION/91, NACE Annual Conference 1991*, Paper No. 465.
- [60] Schmitt, G., Werner, C., and Schöning, M. J., "Microelectrochemical Efficiency Evaluation of Inhibitors for CO<sub>2</sub> Corrosion of Carbon Steel under High Shear Stress Gradients," *CORROSION/2002, NACE Annual Conference, 2002*, Paper No. 280.
- [61] Schmitt, G., private communication of work in progress
- [62] Uhlig, H. H., *Corrosion Handbook*, John Wiley and Sons, New York, 1948 (section on corrosion testing).
- [63] Hausler, R. H., *Nonproprietary Corrosion Inhibitors for Nuclear Steam Generators*, EPRI Final Report NP-3030, The Electric Power Research Institute, Palo Alto, CA, June 1983 (300+ pages).
- [64] Hausler, R. H., "Methodology for Charging Autoclaves at High Temperatures and Pressures with Acid Gases," *Corrosion*, Vol. 54, No. 8, 1998, p. 641.
- [65] Hausler, R. H., unpublished results
- [66] Morsi, M. A., Elewady, Y. A., Lorbeer, P., and Lorenz, W. J., "The Inhibition of Iron Corrosion in Aqueous Solutions Containing Oxygen," *Werstoffe und Korrosion*, Vol. 31, 1980, pp. 108–114.
- [67] Lorenz, W. J. and Mansfeld, F., "Interface and Interphase Inhibition," *Corrosion Inhibition*, NACE Official Publication No. 7, R. H. Hausler, Ed.

# Corrosion Testing in *In Vivo* Environments

K. J. Bundy<sup>1</sup>

## DESCRIPTION OF THE ENVIRONMENT

THE *in vivo* corrosion environment is complex, characterized by dynamic, constantly changing chemical and physiological processes, mechanical loading patterns, and bioelectric potentials. There is, in fact, more than one *in vivo* environment. Subenvironments, each presenting rather discrete corrosion conditions, exist, e.g., the oral cavity, the cardiovascular system, the environment surrounding orthopaedic implants, etc. Implant materials are vulnerable to various forms of corrosion attack. For some materials under certain conditions, uniform attack, pitting, crevice corrosion, galvanic corrosion, and various forms of interaction between applied loads and corrosion (fretting, corrosive wear, corrosion fatigue, and stress-corrosion cracking) have been reported.

One aspect of this environment that is different from the situation usually encountered in other environments is that the interaction between the metal surface and the electrolyte is modulated by an adsorbed protein conditioning film layer. Another atypical aspect is that, in some situations, the influence of the corrosion products on the environment (in terms of biocompatibility problems) may be of primary importance, while the damage to the material by the environment may be a secondary consideration.

In this chapter the variables affecting *in vivo* corrosion, the tests used to assess it, the materials used for implants (and the standards governing them), and various aspects that make the *in vivo* corrosion environment unique are discussed. Much useful information related to these subjects is found in the Medical and Dental chapter in the "Testing in Industries" section.

## ASPECTS THAT MAKE TESTING UNIQUE

The corrosion response within the human body is of most interest in this field. However, direct electrochemical testing in humans ranges from difficult (in the mouth) [1], to virtually impossible (for orthopaedic devices for example) because of ethical, safety, legal, and regulatory considerations. Consequently, much effort has been devoted to identifying alternative environments which, to a greater (or lesser) degree, simulate the corrosion conditions *in vivo* in humans.

Animal experimentation and testing in cell cultures represent alternative possibilities in this regard. When testing in animals, one important consideration, not always accounted for in earlier work in this area, is that significant IR drops occur *in vivo* (and require compensation) because of limited conductivities of certain tissues and anatomical difficulties that preclude optimal electrode placement. Another possibility for obtaining insight into *in vivo* corrosion is simulation of the conditions in the laboratory. Tests in such environments are more controlled, but in some ways less realistic, than tests with animals or cells. The determination of variables needed in a given case to adequately simulate the environment is difficult because of the many parameters that affect the relevant electrochemical processes.

## IMPORTANT VARIABLES AFFECTING *IN VIVO* CORROSION

Temperature is an important factor influencing *in vivo* electrochemical behavior. Internal body temperature is homeostatically regulated at 37°C, so it is important to test at this value in the laboratory. For dental materials exposed to the oral cavity, the temperature fluctuates due to food and drink intake and can range from about 0–70°C. Dissolved salts, particularly chlorides, are probably the most influential components for implant corrosion *in vivo* [2], although by no means the only ones. The internal body electrolyte has the equivalent of 0.9 % NaCl in solution.

The gases dissolved in body fluids also can play an important role in implant alloy corrosion. The most important of these is oxygen, whose partial pressure within the body is widely variable from about  $2.67 \times 10^2$  to  $1.33 \times 10^4$  Pa [3]. Sometimes implant surfaces can be in contact with areas of widely different  $pO_2$ , creating the possibility for differential aeration cells to develop. Carbon dioxide is another gas that can be important for *in vivo* corrosion, because of its influence on pH.

The pH of the *in vivo* electrolyte(s) has an important effect on corrosion of implant materials. pH usually is homeostatically regulated to a value of 7.4, but in certain circumstances the value may be quite different from the normal 7.4. Gastric juice [3], for example, has pH = 1.0. Saliva pH is variable and has been reported in the 5.5 to 8 range, although 6 to 7 is most common [4]. At sites of inflammation, there is a so-called transient "acid tide" in which the pH may fall to as low as 4.5 for a period of hours, or longer if a hematoma is present [5].

<sup>1</sup>Professor, Biomedical Engineering Department, Tulane University, New Orleans, LA 70118.

The role played by proteins regarding corrosion *in vivo* is one of the most important aspects of the unique environment within the body and can cause differences between corrosion behavior in laboratory chloride environments and *in vivo*. There are many thousands of proteins *in vivo*, and the influence of each individual species on corrosion processes is usually far from clear. Virtually from the time an implant is inserted into the body, it will become covered with a layer of adsorbed protein [6]. The characteristics of this layer can change with time, because both thermodynamic and kinetic factors are involved in the adsorption [7] and because cells in the vicinity are actively involved in protein synthesis [8]. The effects of proteins on corrosion are complex, and generally the influence of each protein is different. For example, a specific protein may sharply increase the corrosion rate of one alloy while not influencing the rate of another, or may even reduce the rate [9]. The fundamental effect is how the protein influences the passive layer, i.e., whether it disrupts it, or, conversely, whether it acts as a sort of "passive film," protecting the underlying surface from the electrolyte. Characteristics of the surface itself, such as charge, also influence adsorption of specific proteins.

Metallic biomaterials are generally stronger than other classes of biomaterials. Thus, they are customarily used in situations where they are subjected to significant static and dynamic forces, e.g., the loads in dentistry associated with mastication and, in orthopaedic applications, the forces applied to the skeletal system in standing, walking, stair climbing, etc. These loads may be of sufficient magnitude to cause corrosion fatigue [10], or on very rare occasions, stress-corrosion cracking (SCC) [11]. Many cases of fretting corrosion have also been reported [12]. Additionally, these loads may increase corrosion rate, while the mechanical integrity of the biomaterial is maintained. Such stress-enhanced ion release may occur for both static and dynamic loads [13] and has been observed at stress magnitudes below those that cause gross macroscopic plastic deformation.

An additional unique feature of the *in vivo* corrosion environment is the existence of bioelectric effects. These are potentials and ionic currents of physiological origin resulting from nerve and muscle activity, heart and brain function, stresses applied to skeletal tissues, etc. Since their magnitudes are small, usually they cannot be expected to have much influence on *in vivo* corrosion processes. In cases of border-line passivity, however, it is possible that these potentials could polarize portions of implant surfaces sufficiently to exacerbate pitting processes [14].

Implant design can alter the corrosion performance of alloys *in vivo*. A case in point of a device whose complex design has spurred much interest in its corrosion behavior is that of the cardiovascular stent [15,16]. To consider another example, many prosthetic devices and fracture fixation implants are by nature multicomponent or modular. This means they have various pieces that mate together, e.g., screws and screw holes in plates. These locations may be foci of localized corrosion processes such as crevice corrosion or (in the case of relative motion) fretting corrosion or both. Careful design of such components can minimize *in vivo* corrosion problems.

Galvanic contact between dissimilar metals is another aspect of the *in vivo* environment, which is important under

certain conditions. For example, in dentistry, two opposing teeth may have different alloys, e.g., an amalgam restoration and a gold-based crown, that come into contact during chewing [17]. Modular total hip replacements are often made from titanium- and cobalt-based alloys in contact. Although it was once thought that such devices would not suffer excessive corrosion because of the markedly passive behavior of both alloys, retrieval studies have shown otherwise [18]. The degree to which this form of attack is related to fretting, crevice corrosion, and galvanic contact has been controversial and the subject of intensive research [19–22].

The presence of inflammatory processes [5] or microorganisms [23], or both, at implant sites *in vivo* may affect corrosion behavior due to effects such as changes in pH. Conversely, the release of ions and other aspects of corrosion processes may affect these physiological events, leading, in the worst case, to a type of destructive feedback loop, in which cells release agents that exacerbate corrosion processes (which in turn provoke a more severe tissue response).

## LABORATORY TESTING

Because of the manifold complexities associated with the *in vivo* corrosion process, much attention has been devoted to control of the environment in the corrosion cell used for testing. The basic environment is a physiological saline solution usually kept at 37°C and pH 7.4, but there is no consensus regarding the exact composition that is appropriate. Ringer's solution, Hanks's solution, and 0.9 % NaCl are commonly used test environments for orthopaedic alloys. For environments simulating the oral cavity, termed artificial salivas, there is a similar lack of consensus, and a number of variations exist on a basic environment that has the equivalent of 0.1 % NaCl [24,25]. The chemical compositions of various solutions that are used for *in vitro* testing of orthopaedic and dental materials are given in the Medical and Dental chapter. There has also been a wide range of aeration used in testing. Aerated and deaerated solutions have been used as well as ones exposed to ambient conditions. When solutions containing protein are required for testing orthopaedic implants, it is most common to use albumin, an ubiquitous plasma protein. For dental materials, mucin, an important salivary protein, is widely used.

Testing in the laboratory allows the many complex variables discussed in the previous section to be investigated individually and in combination with each other. The *in vivo* corrosion environment is one that is sufficiently aggressive to cause a variety of corrosion phenomena. Therefore, a number of different types of tests have been developed and should be used to assess the *in vivo* resistance to corrosion of newly developed materials.

Considerable attention has been devoted to the interaction between mechanical loading and corrosion phenomena. Corrosion fatigue has been investigated with sinusoidal loading [26] and with force patterns more representative of actual *in vivo* stresses [27]. Both specimens of simple geometry [28] and actual prosthetic devices [29] have been tested. SCC has been studied using U-bend [30], stress ring [31], bent beam [31], and fracture mechanics [32] type

specimens (to obtain crack growth rate versus stress intensity curves). The fracture mechanics approach has also been employed in corrosion fatigue research [33]. Special corrosion cells have been developed for study of fretting corrosion [34–36] and corrosive wear [37]. Stress-enhanced ion release is also investigated with specialized specimen geometries, sample holders, corrosion cells, and a variety of loading patterns.

A number of additional corrosion phenomena have been the focus of laboratory testing. Crevice corrosion has been investigated using a variety of specimen designs with artificial crevices [38,39]. Galvanic corrosion has been investigated mainly via polarization curves and mixed potential theory [40]. Uniform corrosion and pitting also are examined by polarization curve measurement. Passive film stability may be investigated using methods that combine polarization and controlled surface scratch testing [41–43].

Most electrochemical testing conducted to date has used various DC approaches. The most common methods involve linear polarization (to determine the polarization resistance for calculation of corrosion current via the Stern-Geary equation) [44] and potentiodynamic polarization (to determine breakdown and repassivation potentials). Other tests are also conducted, however. For example, long-term open circuit potential versus time measurements, potentiostatic chronoamperometry, and galvanostatic measurements are occasionally conducted for specialized purposes.

In the past decade or so, there has been increasing interest in the use of electrochemical impedance spectroscopy (EIS) to study *in vivo* corrosion of implant materials [45,46]. An equivalent circuit modeling approach has been used to measure circuit parameters in order to gain insight into corrosion rates, surface areas of irregular surfaces (such as porous-coated implant alloys), and *in vivo* IR drop; to study corrosion mechanisms (e.g., charge transfer versus diffusion control); and to identify cracking processes and crevice corrosion, to name just some of the applications. Because protein adsorption is so important to implant corrosion processes, EIS has been used to measure capacitance versus applied bias potential [47]. Surface charge can be determined from these data. Since proteins themselves are charged, electrostatic interactions with charged surfaces play an important role in their adsorption.

A variety of surface observational tools have been used to assess various aspects of implant corrosion. For example, scanning electron microscopy (SEM) is often employed to study surface damage [48]. Scanning electrochemical microscopy (SECM) can be used to image localized corrosion currents with a high degree of spatial resolution [49]. The identification of released corrosion products has been another important focus of laboratory corrosion testing of implants. Electron microprobe analysis, Auger electron spectroscopy, and X-ray photoelectron spectroscopy of implant alloy surfaces (before and after corrosion has taken place) have been used to monitor surface changes and damage due to electrochemical action [50,51].

Atomic absorption spectrophotometry has often been used to analyze total amounts of released trace metals in the electrolyte [52]. In some circumstances, it is desirable to know the actual valence states of released corrosion products. Chromium, for example, as shown by Pourbaix

diagrams [53], may exist in either trivalent or hexavalent form for potential/pH ranges expected *in vivo*. The hexavalent form poses potentially much greater toxicity hazards. Polarographic methods have been used to differentiate between these two states [54–56]. Additionally, this electrochemical technique can perform trace element analysis in the part per billion range and has been employed for chemical analysis of the electrolyte. Ion exchange resins have also been used for chromium speciation [57]. Another analytical method that can be used for valence state determination is ion chromatography [58], which is capable of simultaneous measurement of multiple ions. A biologically-based technique that uses an assay of monoclonal antibody inhibition has recently been described [59] to measure the concentration of free ions in solution.

To simulate loading for fretting experiments, devices known as joint simulators are often used. Such apparatus attempts to duplicate the loading and motion patterns in actual prosthetic joints [60–63]. Other equipment (based upon universal testing machines) uses specimens of simple geometry, with more or less realistic loading patterns, to investigate interaction of stress and corrosive environments. Corrosion fatigue and some aspects of stress-enhanced ion release are investigated in this manner [26,27,64].

Because many corrosion phenomena *in vivo*, and therefore in laboratory environments, have long incubation times associated with them, the question of accelerated corrosion testing has arisen. Increasing the temperature can, via the Arrhenius equation, substantially increase corrosion rate [65], but there are pitfalls associated with this technique to be considered. It works best when the main component affecting corrosion is the chloride ion. Since proteins denature at relatively low temperatures, elevated temperature testing is less suitable for proteinaceous environments.

Testing in a chemical environment related to *in vivo* conditions, but more severe than that associated with the body, for example, the testing of dental materials in Ringer's solution [66] rather than artificial saliva, is another accelerated testing approach. The limitation of accelerated methods is that one cannot straightforwardly extrapolate the data to determine what the corrosion rate would be under *in vivo* conditions. Regardless of the medium used, *in vitro* testing will only serve as a comparative screening technique for materials, since it is not a direct determinant of *in vivo* rates.

Specimen geometry is also a concern for corrosion testing to simulate *in vivo* conditions. When studies involve material behavior alone, then usually simple shapes are used, but when functional behavior (such as fretting due to applied loads), or implant design (presence of crevices of given geometry), is at issue, then actual implant devices are usually tested.

Since there is such uncertainty regarding corrosion of implant materials, there are few standards that govern this field. Those that do exist, as well as future needs in this area, are discussed later.

## FIELD TESTING

Because of the many previously mentioned difficulties associated with electrochemical testing in humans, most of the information about corrosion resistance *in vivo* has come

from other methods. Foremost among these is retrieval analysis [67–70]. Here implants that have been removed, either routinely or for cause, along with adjacent tissue, are examined. Visual, low-power light microscopy, and SEM examinations are usually performed. Often a metallurgical examination is conducted, as well, to determine hardness, grain size, nonmetallic inclusion content, and other parameters [71].

Many large-scale retrieval studies have been conducted involving hundreds of implants. Although corrosion of the devices is only one of many topics that are the subjects of retrieval analyses, this type of investigation has yielded the majority of the knowledge that has been amassed regarding corrosion *in vivo*. ASTM F 561, Practice for Retrieval and Analysis of Implanted Medical Devices, and Associated Tissues, governs the performance of implant retrieval analyses.

Another “field testing” methodology for *in vivo* corrosion involves measuring corrosion product concentrations in blood and other physiological fluids, usually via atomic absorption spectrophotometry [72]. Such studies may be of a clinical nature, involving human patients. Elevated concentrations of various elements have been reported [73,74]. In other studies, controlled injections of implant corrosion products in animals are made to assess kinetics and modes of their excretion and storage in various body tissue compartments [75]. An alternative strategy has been to implant materials with large surface areas (e.g., powders) to simulate large degrees of corrosion product release, with storage and clearance monitored as before [76].

*In vivo* electrochemical testing is possible in humans (in the oral cavity) under restricted conditions [77,78]. Open circuit potentials and galvanic currents between dissimilar metals have been measured. Linear polarization and AC impedance tests have been conducted. The paramount concern for these measurements is obtaining accurate data under conditions that present no hazard to the human subjects.

A more wide-ranging set of experimental methods can be employed for testing in animals. Potential versus time data have been obtained over periods of 60 days [79]. Linear polarization tests have been conducted to determine corrosion rates via the Stern-Geary equation [80]. Potentiodynamic polarization tests (which are effectively impossible to conduct in humans because of safety concerns) have also been conducted in animals [81,82]. A diverse group of animal species including goats, rabbits, rats, and primates has been used for corrosion testing *in vivo*.

As previously pointed out, one difficulty with these tests is that, due to geometrical problems regarding electrode placement and somewhat limited ionic conductivities of certain tissues, significant IR drops are created that need compensation [83]. Electrochemical impedance spectroscopy would provide an excellent means for measurement of the ohmic resistance, but so far, this method has been very infrequently employed in *in vivo* animal testing. Nonelectrochemical approaches have been used to investigate the corrosion of implant materials *in vivo*. U-bends and stressed rings have been placed in rabbits to investigate the stress corrosion cracking behavior of implant alloys [30,31]. Dynamic loads have also been applied *in vivo* to investigate the corrosion fatigue process [84].

An additional field-testing approach that has increasingly been employed in the past decade to assess corrosion *in vivo* involves the use of cell culture techniques. Although systemic effects such as circulation that could impact corrosion processes are not modeled with this method [3], the basic biological environment at the metal/electrolyte interface, the protein conditioning layer, is simulated with some degree of realism, as are active cellular processes. The response of biomaterials in a cell culture environment can be gaged either through use of electrochemical techniques [47] or from chemical analysis of corrosion products in solution [85,86]. An advantage of the cell culture approach is that various assays related to cell viability, proliferation, histochemical status, function, gene expression, etc. can be performed in addition to corrosion measurements, thus providing insight into the material's biocompatibility [87,88] as well as its electrochemical behavior. A variety of cell types has been used in such studies including fibroblasts, osteoblasts, macrophages, as well as carcinoma, neuroblastoma, and bacterial cells. This approach appears to offer considerable promise of yielding further valuable information on corrosion and biocompatibility in the future.

## STANDARDS

Only four ASTM standards are explicitly concerned with corrosion of surgical implant materials. ASTM F 746, Test Method for Pitting or Crevice Corrosion of Metallic Surgical Implant Materials, is a test in which a specimen has an inert sleeve simulating a crevice. Anodic polarization is used to raise the potential and initiate pitting, as determined by a large and rising current. The potential is then potentiostatically controlled to various values, and the current is monitored to establish the highest potential not resulting in repassivation.

ASTM F 897, Test Method for Measuring Fretting Corrosion of Osteosynthesis Plates and Screws, is concerned with the fretting behavior of orthopaedic fracture fixation plates. A plate is attached to a rod with bone screws, and the assembly is loaded with a fretting apparatus described in the standard. The degree of fretting is gaged with gravimetric methods, atomic absorption spectrophotometry of the solution, and observation of surface appearance. There is another standard that deals specifically with fretting of the modular total hip replacement devices mentioned previously, F1875, Practice for Fretting Corrosion Testing of Modular Implant Interfaces: Hip Femoral Head-Bore and Cone Taper Interface. F1801, Practice for Corrosion Fatigue Testing of Metallic Implant Materials, is another test for monitoring the interaction between applied loads and corrosion processes.

Besides the standards mentioned above, there are several additional ones that have some bearing on the corrosion behavior of implant materials *in vivo*. A number of standards govern the chemical composition and metallurgical conditions of metallic implant materials.

The following ASTM standards govern the use of stainless steels:

- F 138, Specification for Wrought 18 Chromium-14 Nickel-2.5 Molybdenum Stainless Steel Bar and Wire for Surgical Implants (UNS S31673)

- F 139, Specification for Wrought 18 Chromium-14 Nickel-2.5 Molybdenum Stainless Steel Sheet and Strip for Surgical Implants (UNS S31673)
- F 621, Specification for Stainless Steel Forgings for Surgical Implants
- F 745, Specification for 18 Chromium-12.5 Nickel-2.5 Molybdenum Stainless Steel for Cast and Solution-Annealed Surgical Implant Applications
- F 1314, Specification for Wrought Nitrogen Strengthened- 22 Chromium-12.5 Nickel-5 Manganese-2.5 Molybdenum Stainless Steel Bar and Wire for Surgical Implants
- F 1350, Specification for Wrought 18 Chromium-14 Nickel-2.5 Molybdenum Stainless Steel Surgical Fixation Wire (UNS S31673)
- F 1586, Specification for Wrought Nitrogen Strengthened- 21 Chromium-10 Nickel-3 Manganese-2.5 Molybdenum Stainless Steel Bar for Surgical Implants

The following ASTM standards are concerned with titanium-based material:

- F 67, Specification for Unalloyed Titanium for Surgical Implant Applications (UNS R50250, UNS R50400, UNS 50550, UNS 50700)
- F 136, Specification for Wrought Titanium-6 Aluminum-4 Vanadium ELI (Extra Low Interstitial) Alloy (UNS R56401) for Surgical Implants Applications
- F 620, Specification for Alpha Plus Beta Titanium Alloy Forgings for Surgical Implants
- F 1108, Specification for Ti6Al4V Alloy Castings for Surgical Implants
- F 1295, Specification for Wrought Titanium-6 Aluminum-7 Niobium Alloy for Surgical Implant Applications (UNS R56700)
- F 1341, Specification for Unalloyed Titanium Wire (UNS R50250, UNS R50400, UNS R50550, UNS R50700) for Surgical Implant Applications
- F 1472, Specification for Wrought Titanium-6 Aluminum-4 Vanadium Alloy (UNS R56400) for Surgical Implant Applications
- F 1580, Specification for Titanium and Titanium-6% Aluminum-4% Vanadium Alloy Powders for Coatings of Surgical Implants
- F 1713, Specification for Wrought Titanium-13 Niobium-13 Zirconium Alloy for Surgical Implant Applications
- F 1813, Specification for Wrought Titanium-12 Molybdenum-6 Zirconium-2 Iron Alloy For Surgical Implant Applications
- F 2066, Specification for Wrought Titanium-15 Molybdenum Alloy for Surgical Implant Applications (UNS R58150)

The following standards apply to the nickel-titanium shape memory alloy:

- F 2004, Test Method for Transformation Temperature of Nickel-Titanium Alloys by Thermal Analysis
- F 2005, Terminology for Nickel-Titanium Shape Memory Alloys
- F 2063, Specification for Wrought Nickel-Titanium Shape Memory Alloys for Medical Devices and Surgical Implants

- F 2082, Test Method for Determination of Transformation Temperature of Nickel-Titanium Shape Memory Alloys by Bend and Free Recovery

Cobalt-chromium alloy systems are covered by the following ASTM standards:

- F 75, Specification for Cobalt-28 Chromium-6 Molybdenum Casting Alloy and Cast Products for Surgical Implants (UNS R30075)
- F 90, Specification for Wrought Cobalt-20 Chromium-15 Tungsten-10 Nickel Alloy for Surgical Implant Applications (UNS R30605)
- F 562, Specification for Wrought Cobalt-35 Nickel-20 Chromium-10 Molybdenum Alloy for Surgical Implant Applications
- F 563, Specification for Wrought Cobalt-20 Nickel-20 Chromium-10 Molybdenum Alloy for Surgical Implant Applications
- F 688, Specification for Wrought Cobalt-35 Nickel-20 Chromium-10 Molybdenum Alloy Plate, Sheet, and Foil for Surgical Implants (UNS R30035)
- F 799, Specification for Cobalt-28 Chromium-6 Molybdenum Alloy Forgings for Surgical Implants (UNS R31537, R31538, R31539)
- F 961, Specification for Cobalt-35 Nickel-20 Chromium-10 Molybdenum Alloy Forgings for Surgical Implants (UNS R30035)
- F 1058, Specification for Wrought Cobalt-Chromium-Nickel-Molybdenum-Iron Alloy for Surgical Implant Applications
- F 1091, Specification for Wrought Cobalt-20 Chromium-15 Tungsten-10 Nickel Alloy Surgical Fixation Wire (UNS R30605)
- F 1377, Specification for Cobalt-28 Chromium-6 Molybdenum Powder for Coating of Orthopedic Implants (UNS-R30075)
- F 1537, Specification for Wrought Cobalt-28-Chromium-6-Molybdenum Alloy for Surgical Implants (UNS R31537, UNS R31538, and UNS R31539)

Tantalum is governed by ASTM F 560, Specification for Unalloyed Tantalum for Surgical Implant Applications.

ASTM standards that have additional relevance to *in vivo* corrosion behavior are F 86, Practice for Surface Preparation and Marking of Metallic Surgical Implants, and those that deal with biocompatibility. The efficacy of the passivation procedures described in F 86 has recently become controversial [89]. Examples of standards related to biocompatibility include F 763, Practice for Short-Term Screening of Implant Materials, and F 981, Practice for Assessment of Compatibility of Biomaterials for Surgical Implants with Respect to Effect of Materials on Muscle and Bone. The latter two standards describe how to detect untoward tissue reactions due to released corrosion products. F 748, Practice for Selecting Generic Biological Test Methods for Materials and Devices, provides general guidelines as to what biocompatibility tests are appropriate in given situations.

Some standards cover corrosion testing for devices used in specific medical applications. Examples in this area



include F 1089, Standard Test Method for Corrosion of Surgical Instruments, and F 2068, Specification for Femoral Prostheses-Metallic Implants.

In addition to the ASTM Committee F 4 standards mentioned above, some of the standards from Committee G 1 are useful for testing alloys that see *in vivo* service. The following are examples of ASTM standards that are useful for studying specific corrosion mechanisms of implant materials:

- A 262, Practices for Detecting Susceptibility to Intergranular Attack in Austenitic Stainless Steels
- G 30, Practice for Making and Using U-Bend Stress-Corrosion Test Specimens
- G 36, Practice for Evaluating Stress-Corrosion-Cracking Resistance of Metals and Alloys in a Boiling Magnesium Chloride Solution
- G 38, Practices for Making and Using C-Ring Stress-Corrosion Test Specimens
- G 39, Practice for Preparation and Use of Bent-Beam Stress-Corrosion Test Specimens
- G 46, Guide for Examination and Evaluation of Pitting Corrosion
- G 49, Practice for Preparation and Use of Direct Tension Stress Corrosion Test Specimens
- G 71, Guide for Conducting and Evaluating Galvanic Corrosion Tests in Electrolytes

Standards governing testing methodology such as:

- G 5, Test Method for Making Potentiostatic and Potentiodynamic Anodic Polarization Measurements
- G 59, Practice for Conducting Potentiodynamic Polarization Resistance Measurements
- G 61, Test Method for Conducting Cyclic Potentiodynamic Polarization Measurements for Localized Corrosion Susceptibility of Iron-, Nickel-, or Cobalt-Based Alloys are also useful for testing implant materials. Besides ASTM standards, international organizations such as the ISO and various national groups (such as in Britain and Germany) have standards that relate to corrosion of metals that are used *in vivo*. For example, ISO 5832 Implants for Surgery-Metallic Materials, is a twelve part standard governing various biomedical stainless steel, titanium-based, and cobalt-based alloys.

So far, except for specifications for use of 0.9 % NaCl and other "physiologic" solutions (including "protein" solutions) at 37°C (see ASTM F 746 and F 897), standards are lacking that provide guidelines as to environmental conditions that could simulate various aspects of *in vivo* behavior. Load levels and waveforms, bioelectric effects, and the details of environmental chemical composition so far have not been addressed in standards governing testing. Efforts in the future to fill these gaps would be helpful.

## MATERIALS

Because materials that are used *in vivo* face demanding requirements with respect to corrosion resistance, other engineering aspects (such as mechanical behavior), and biocompatibility, only a handful of metallic materials have been judged over the years to be suitable for *in vivo* service.

The majority of orthopaedic devices are fabricated from 316L stainless steel. Cobalt-chromium and titanium-based alloys are used for the remaining share. These latter materials tend to be more durable in *in vivo* fluids than 316L [90]. Thus, their use tends to be more prevalent in permanent applications such as total joints. 316L, on the other hand, is often used in temporary situations such as fracture fixation.

A wider spectrum of materials are useful in dental applications, perhaps because of the much lower chloride content in saliva [4] as compared to blood and extracellular fluids [3]. Besides resistance to chloride attack, the oral environment is one where resistance to tarnishing due to sulfur in foodstuffs is important [4]. Precious metal and base metal alloys are used for casting of various dental restorations. The former consists of compositions based on gold, platinum, silver, and palladium alloy systems. Base metals consist of nickel, chromium, and copper systems and have become more common in recent times as alternatives to high priced precious metals. The most commonly used metallic dental material is amalgam. This is a silver-tin alloy powder mixed with mercury. In the past decade the use of mercury in amalgam has become a controversial topic. Stainless steel is used in certain orthodontic applications. Wrought materials, particularly ones that are titanium based, are often used to fabricate dental implants. The most corrosion-resistant materials are the precious metal and titanium systems. The amalgams and copper-based materials are most prone to corrosion in the oral cavity, with some of the base metal casting systems having intermediate corrosion resistance. Compositions of common alloys used in dentistry are provided in the Medical and Dental chapter.

## CONCLUSION

The corrosion of materials *in vivo* is an extremely complex process. This area has been intensively investigated in the past, resulting in the accumulation of a great deal of knowledge on the subject. Much remains to be done, however, before optimal means for corrosion testing in *in vivo* environments can be fully developed. The most advanced methodology from the corrosion testing field as a whole should be brought to bear on this topic as rapidly as it becomes available. In addition, approaches that are biologically based have already yielded considerable insights into corrosion behavior and biocompatibility of biomedical alloys. These techniques should be exploited even more intensively in the future.

## REFERENCES

- [1] Bundy, K. J., Gettleman, L., Flores, A., et al., "In Vivo and In Vitro Electrochemical Response of Dental Materials," *Transactions of the 19th Annual Meeting of the Society for Biomaterials*, 1993, p. 263.
- [2] Kruger, J., "Fundamental Aspects of the Corrosion of Metallic Implants," *Corrosion and Degradation of Implant Materials*, ASTM STP 684, B. C. Syrett and A. Acharya, Eds., ASTM International, West Conshohocken, PA, 1979, pp. 107-127.
- [3] Black, J., *Biological Performance of Materials—Fundamentals of Biocompatibility*, 3rd ed., Dekker, NY, 1999.

- [4] Mueller, H. J., "Tarnish and Corrosion of Dental Alloys," *Corrosion*, Vol. 13, Metals Handbook, 9th ed., ASM, Materials Park, OH, 1987, pp. 1336-1366.
- [5] Laing, P. G., "Tissue Reaction to Biomaterials," *NBS Special Publication 472*, Gaithersburg, MD, 1977, pp. 31-39.
- [6] Rudee, M. L. and Price, T. M., "The Initial Stages of Adsorption of Plasma Derived Proteins on Artificial Surfaces in a Controlled Flow Environment," *Journal of Biomedical Materials Research*, Vol. 19, 1985, pp. 57-66.
- [7] Neumann, A. W., Hum, O. S., Francis, D. W., et al., "Kinetic and Thermodynamic Aspects of Platelet Adhesion from Suspension to Various Substrates," *Journal of Biomedical Materials Research*, Vol. 14, 1980, pp. 499-509.
- [8] Gristina, A. G., "Biomaterial-Centered Infection: Microbial Adhesion Versus Tissue Integration," *Science*, Vol. 237, 1987, pp. 1588-1595.
- [9] Clark, G. C. F. and Williams, D. F., "The Effects of Proteins on Metallic Corrosion," *Journal of Biomedical Materials Research*, Vol. 16, 1982, pp. 125-134.
- [10] Fraker, A. C., "Corrosion of Metallic Implants and Prosthetic Devices," *Corrosion*, Vol. 13, Metals Handbook, 9th ed., ASM, Materials Park, OH, 1987, pp. 1324-1335.
- [11] Sandborn, P. M., Cook, S. D., Kester, M. A., and Haddad, R. J., "Fatigue Failure of the Femoral Component of a Unicompartamental Knee," *Clinical Orthopaedics and Related Research*, Vol. 22, 1987, pp. 249-254.
- [12] Weinstein, A., Amstutz, H., Pavon, G., and Franchesini, V., "Orthopaedic Implants—A Clinical and Metallurgical Analysis," *Journal of Biomat. Res. Symposium*, Vol. 4, 1973, pp. 297-325.
- [13] Bundy, K. J., "Modification of Surgical Implant Alloy Corrosion Rates by Static and Dynamic Loading," *Extended Abstracts NACE Corrosion Research Symposium*, 1989, pp. 61-64.
- [14] Bundy, K. J. and Dillard, J., "Accelerated Corrosion of Implant Materials Induced by Physiological Bioelectric Potentials," *Transactions of the 19th International Biomaterials Symposium*, 1987, p. 232.
- [15] Venugopalan, R., "Corrosion Testing of Stents: A Novel Fixture to Hold Entire Device in Deployed Form and Finish," *Journal of Biomedical Materials Research (Applied Biomaterials)*, Vol. 48, 1999, pp. 829-832.
- [16] Shih, C.-C., Lin, S.-J., Chung, K.-H., et al., "Increased Corrosion Resistance of Stent Materials by Converting Current Surface Film of Polycrystalline Oxide Into Amorphous Oxide," *Journal of Biomedical Materials Research*, Vol. 52, 2000, pp. 323-332.
- [17] Moberg, L. E., "Long-Term Corrosion Studies In Vitro of Amalgams and Casting Alloys in Contact," *Acta Odontologica Scandinavica*, Vol. 43, 1985, pp. 163-177.
- [18] Collier, J. P., Surprenant, V. A., Jensen, R. E., and Mayor, M. B., "Corrosion at the Interface of Cobalt-Alloy Heads on Titanium-Alloy Stems," *Clinical Orthopaedics*, Vol. 271, 1991, pp. 305-312.
- [19] Brown, S. A., Fleming, C. A. C., Kawalec, J. S., et al., "Fretting Accelerates Crevice Corrosion of Modular Hip Tapers," *Journal of Applied Biomaterials*, Vol. 6, 1995, pp. 19-26.
- [20] Gilbert, J. L., Buckley, C. A., and Jacobs, J. J., "In Vivo Corrosion of Modular Hip Prosthesis Components in Mixed and Similar Metal Combinations. The Effect of Crevice, Stress, Motion, and Alloy Coupling," *Journal of Biomedical Materials Research*, Vol. 27, 1993, pp. 1533-1544.
- [21] Bundy, K. J. and Collier, J. P., "Mechanistic Studies of Corrosion of Galvanically Coupled Alloys Used in Modular Total Hip Replacement Devices," *Transactions of the Implant Retrieval Symposium*, 1992, Pheasant Run, IL, p. 55.
- [22] Kawalec, J. S., Brown, S. A., Payer, J. H., et al., "Mixed-Metal Fretting Corrosion of Ti6Al4V and Wrought Cobalt Alloy," *Journal of Biomedical Materials Research*, Vol. 29, 1995, pp. 867-873.
- [23] Williams, D. F., "Physiological and Microbiological Corrosion," *CRC Critical Reviews Biocompatibility*, Vol. 1, 1985, pp. 1-24.
- [24] Tani, G. and Zucchi, F., "Electrochemical Evaluation of the Corrosion Resistance of Commonly Used Metals in Dental Prostheses," *Minerva Stomatologica*, Vol. 16, 1967, pp. 710-713.
- [25] Marek, M. and Topfl, E., "Electrolytes for Corrosion Testing of Dental Alloys," *Journal of Dental Research*, Vol. 65:301, No. 1192, 1986.
- [26] Hahn, H., Lare, P. J., Rowe, R. H., et al., "Mechanical Properties and Structure of Ti-6Al-4V with Graded-Porosity Coatings Applied by Spraying for Use in Orthopaedic Implants," *Corrosion and Degradation of Implants Second Symposium*, ASTM STP 859, A. Fraker and C. Griffin, Eds, ASTM International, West Conshohocken, PA, 1985, pp. 179-191.
- [27] Wheeler, K. R. and James, L. A., "Fatigue Behavior of Type 316 Stainless Steel under Simulated Body Conditions," *Journal of Biomedical Materials Research*, Vol. 5, 1971, pp. 267-281.
- [28] Cahoon, J. R. and Holte, R. N., "Corrosion Fatigue of Surgical Stainless Steel in Synthetic Physiological Solution," *Journal of Biomedical Materials Research*, Vol. 15, 1981, pp. 137-145.
- [29] Wright, K. W. J., Bathgate, R. G., and Scales, J. T., "A Method for Studying the Corrosion Fatigue Properties of Femoral Components," *Evaluation of Biomaterials*, 1980, pp. 72-87.
- [30] Galante, J. and Rostoker, W., "Corrosion-Related Failures in Metallic Implants," *Clinical Orthopaedics and Related Research*, Vol. 86, 1972, pp. 237-244.
- [31] Bundy, K. J., Marek, M., and Hochman, R. F., "In Vivo and In Vitro Studies of the Stress-Corrosion Cracking Behavior of Surgical Implant Alloys," *Journal of Biomedical Materials Research*, Vol. 17, 1983, pp. 467-487.
- [32] Bundy, K. J. and Desai, V. H., "Studies of Stress-Corrosion Cracking Behavior of Surgical Implant Materials Using a Fracture Mechanics Approach," *Corrosion and Degradation of Implant Materials, 2nd Symposium*, ASTM STP 859, A. Fraker and C. Griffin, Eds, ASTM International, West Conshohocken, PA, 1985, pp. 73-90.
- [33] Bolten, J. D., Hayden, J., and Humphreys, M., "A Study of Corrosion Fatigue in Cast Cobalt-Chrome-Molybdenum Alloys," *Engineering in Medicine*, Vol. 11, 1982, pp. 59-68.
- [34] Brown, S. A., Hughes, P. J., and Merritt, K., "In Vitro Studies of Fretting Corrosion of Orthopaedic Materials," *Journal of Orthopaedic Research*, Vol. 6, 1988, pp. 572-579.
- [35] Xulin, S., Ito, A., Tateishi, T., et al., "Fretting Corrosion Resistance and Fretting Corrosion Product Cytocompatibility of Ferritic Stainless Steel," *Journal of Biomedical Materials Research*, Vol. 34, 1997, pp. 9-14.
- [36] Hendry, J. A. and Pilliar, R. M., "The Fretting Corrosion Resistance of PVD Surface-Modified Orthopedic Implant Alloys," *Journal of Biomedical Materials Research (Applied Biomaterials)*, Vol. 58, 2001, pp. 156-166.
- [37] Buchanan, R. A., Rigney, E. D., and Williams, J. M., "Wear-Accelerated Corrosion of Ti-6Al-4V and Nitrogen-Ion-Implanted Ti-6Al-4V: Mechanisms and Influence of Fixed-Stress Magnitude," *Journal of Biomedical Materials Research*, Vol. 21, 1987, pp. 367-377.
- [38] Syrett, B. C. and Davis, E. E., "Crevice Corrosion of Implant Alloys—a Comparison of In Vitro and In Vivo Studies," *Corrosion and Degradation of Implant Materials*, ASTM STP 684, B. C. Syrett and A. Acharya, Eds, ASTM International, West Conshohocken, PA, 1979, pp. 229-244.
- [39] Sutow, E. J. and Jones, D. W., "A Crevice Corrosion Cell Configuration," *Journal of Dental Research*, Vol. 58, 1979, pp. 1358-1363.
- [40] Lucas, L. C., Buchanan, R. A., and Lemons, J. E., "Investigations on the Galvanic Corrosion of Multialloy Total Hip

- Prostheses," *Journal of Biomedical Materials Research*, Vol. 15, 1981, pp. 731–747.
- [41] Goldberg, J. R. and Gilbert, J. L., "Electrochemical Response of CoCrMo to High-Speed Fracture of Its Metal Oxide Using an Electrochemical Scratch Test Method," *Journal of Biomedical Materials Research*, Vol. 37, 1997, pp. 421–431.
- [42] Rondelli, G. and Vicentini, B., "Evaluation by Electrochemical Tests of the Passive Film Stability of Equiatomic Ni-Ti Alloy Also in the Presence of Stress-Induced Martensite," *Journal of Biomedical Materials Research*, Vol. 51, 2000, pp. 47–54.
- [43] Goldberg, S. R. and Gilbert, J. L., "Transient Electric Fields Induced by Mechanically Assisted Corrosion of Ti-6Al-4V," *Journal of Biomedical Materials Research*, Vol. 56, 2001, pp. 184–194.
- [44] Stern, M. and Geary, A., *Journal of the Electrochemical Society*, Vol. 105, 1958, pp. 638ff.
- [45] Bundy, K. J., Dillard, J., and Luedemann, R., "Use of AC Impedance Methods to Study the Corrosion Behavior of Implant Alloys," *Biomaterials*, Vol. 14, 1993, pp. 529–536.
- [46] Gilbert, J. L., "Step-Polarization Impedance Spectroscopy of Implant Alloys in Physiologic Solutions," *Journal of Biomedical Materials Research*, Vol. 40, 1998, pp. 233–243.
- [47] Hallab, N., Bundy, K., O'Connor, K., et al., "Cell Adhesion to Biomaterials: Correlations Between Surface Charge, Surface Roughness, Adsorbed Protein, and Cell Morphology," *Journal of Long-Term Effects of Medical Implants*, Vol. 5, 1995, pp. 209–231.
- [48] Mueller, H. J., Lenke, J. W., and Bapna, M. S., "Surface Analysis of Tarnished Dental Alloys," *Scanning Microscopy*, Vol. 2, 1988, pp. 777–787.
- [49] Gilbert, J. L., Smith, S. M., and Lautenschlager, E. P., "Scanning Electrochemical Microscopy of Metallic Biomaterials: Reaction Rate and Ion Release Imaging Modes," *Journal of Biomedical Materials Research*, Vol. 27, 1993, pp. 1357–1366.
- [50] Sundgren, J. E., Bodo, P., Lunstrom, I., et al., "Auger Electron Spectroscopic Studies of Stainless-Steel Implants," *Journal of Biomedical Materials Research*, Vol. 19, 1985, pp. 663–671.
- [51] Ducheyne, P. and Healy, K., "Titanium: Immersion-Induced Surface Chemistry Changes and the Relationship to Passive Dissolution and Bioactivity," *The Bone-Biomaterial Interface*, J. E. Davies, Ed., University of Toronto Press, 1991, pp. 62–67.
- [52] Marek, M. and Treharne, R. W., "An In Vitro Study of the Release of Nickel from Two Surgical Implant Alloys," *Clinical Orthopaedics and Related Research*, Vol. 167, 1982, pp. 291–295.
- [53] Pourbaix, M., *Lectures on Electrochemical Corrosion*, Plenum Press, NY, 1973.
- [54] Bundy, K. J. and Arney, M. M., "Polarographic Determination of Released Ion Valence States and Implant Alloy Corrosion Rate Accuracy," *Transactions of the 15th Annual Meeting of the Society for Biomaterials*, 1989, p. 53.
- [55] Bundy, K. J. and Gettleman, L., "'Orphan' Problems in Biomaterials — Solution via Electrochemical Testing," *Proceedings of the Symposium on Compatibility of Biomedical Implants*, P. Kovacs and N. S. Istephanous, Eds., Proceedings, Vol. 94-15, Electrochemical Society, 1994, pp. 381–390.
- [56] Shetlemore, M. G. and Bundy, K. J., "Examination of In Vivo Influences on Bioluminescent Microbial Assessment of Corrosion Product Toxicity," *Biomaterials*, Vol. 22, 2001, pp. 2215–2228.
- [57] Merritt, K. and Brown, S. A., "Release of Hexavalent Chromium from Corrosion of Stainless Steel and Cobalt-Chromium Alloys," *Journal of Biomedical Materials Research*, Vol. 29, 1995, pp. 627–633.
- [58] Buldini, P. L., Mevoli, A., and Sharma, J. L., "Ion Chromatographic Determination of Metals in Biocompatibility Testing," *Journal of Biomedical Materials Research*, Vol. 50, 2000, pp. 131–137.
- [59] Yang, J. and Merritt, K., "Production of Monoclonal Antibodies to Study Corrosion Products of Co-Cr Biomaterials," *Journal of Biomedical Materials Research*, Vol. 31, 1996, pp. 71–80.
- [60] McKellop, H. and Clarke, I., "Evolution and Evaluation of Materials-Screening Machines and Joint Simulators in Predicting In Vivo Wear Phenomena," *Functional Behavior of Orthopaedic Biomaterials*, P. Ducheyne and G. Hastings, Eds., CRC Press, Boca Raton, FL, 1984.
- [61] Weightman, B., Paul, I. L., Rose, R. M., et al., "A Comparative Study of Total Hip Replacement Prostheses," *Journal of Biomechanics*, Vol. 6, 1973, p. 299.
- [62] Gold, B. L. and Walker, P. S., "Variables Affecting the Friction and Wear of Metal-on-Plastic Total Hip Joints," *Clinical Orthopaedics and Related Research*, Vol. 100, 1974, p. 270.
- [63] Freeman, M. A. R., Swanson, S. A. V., and Heath, J. C., *Annals of Rheumatic Disease*, (Suppl.) Vol. 28, 1969, p. 29.
- [64] Luedemann, R. E. and Bundy, K. J., "The Effect of Dynamic Stress on the Corrosion Characteristics of Surgical Implant Alloys," *Transactions of the 15th Annual Meeting of the Society for Biomaterials*, 1989, p. 56.
- [65] Gileadi, E., Kirowa-Eisner, E., and Penciner, J., *Interfacial Electrochemistry—An Experimental Approach*, Addison Wesley, Reading, MA, 1975.
- [66] Lucas, L. C., "Biodegradation of Restorative Metallic Systems," *Effects and Side Effects of Dental Restorative Materials*, NIH Technology Assessment Conference, 26–28 August 1991, pp. 40–44.
- [67] Weinstein, A. M., Spires, W. P., Klawitter, J. J., et al., "Orthopaedic Implant Retrieval and Analysis Study," *Corrosion and Degradation of Implant Materials*, ASTM STP 684, B. Syrett and A. Archarya, Eds., ASTM International, West Conshohocken, PA, 1979, pp. 212–228.
- [68] Harding, A. F., Cook, S. D., and Thomas, K. A., "Orthopaedic Implant Retrieval: Clinical Performance, Metallurgical Characteristics and Tissue Reaction in 250 Internal Fixation Devices," *Proceedings of the 5th Southern Biomedical Engineering Conference*, Pergamon Press, NY, 1985, pp. 282–288.
- [69] Baswell, I. L., Sander, T., Allen, B., and Bechtol, C. O., "Fracture Analysis of Retrieved Orthopaedic Wires," *Journal of Biomedical Materials Research*, Vol. 20, 1986, pp. 887–894.
- [70] Wright, T. M., Burstein, A. H., and Bartel, D. L., "Retrieval Analysis of Total Joint Replacement Components: A Six-Year Experience," *Corrosion and Degradation of Implant Materials: 2nd Symposium*, ASTM STP 859, A. C. Fraker and C. D. Griffin, Eds., ASTM International, West Conshohocken, PA, 1985, pp. 415–428.
- [71] Cook, S. D., Renz, E. A., Barrack, R. L., et al., "Clinical and Metallurgical Analysis of Retrieved Internal Fixation Devices," *Clinical Orthopaedics and Related Research*, Vol. 194, 1984, pp. 236–247.
- [72] Bartolozzi, A. and Black, J., "Chromium Concentrations in Serum, Blood Clot and Urine from Patients Following Total Hip Arthroplasty," *Biomaterials*, Vol. 6, 1985, pp. 2–8.
- [73] Coleman, R. F., Herrington, J., and Scales, J. T., "Concentration of Wear Products in Hair, Blood, and Urine after Total Hip Replacement," *British Medical Journal*, Vol. 1, 1973, pp. 527–529.
- [74] Hildebrand, H. F., Ostapczuk, P., Mercier, J. F., et al., "Orthopaedic Implants and Corrosion Products Ultrastructural and Analytical Studies of 65 Patients," *Biocompatibility of Co-Cr-Ni Alloys*, H. F. Hildebrand and M. Champy, Eds., Plenum Press, NY, 1988, pp. 133–153.
- [75] Merritt, K., Crowe, T. D., and Brown, S. A., "Elimination of Nickel, Cobalt, and Chromium Following Repeated Injections of High Dose Metal Salts," *Journal of Biomedical Materials Research*, Vol. 23, 1989, pp. 845–862.
- [76] Black, J., Oppenheimer, P., Morris, D. M., et al., "Release of Corrosion Products by F-75 Cobalt Base Alloy in the Rat. III:

- Effects of a Carbon Surface Coating," *Journal of Biomedical Materials Research*, Vol. 21, 1987, pp. 1213-1230.
- [77] Nilner, K., Glantz, P. O., and Zoeger, B., "On Intraoral Potential and Polarization-Measurements of Metallic Restorations. A Methodological and Time Dependent Clinical Study," *Acta Odontologica Scandinavica*, Vol. 40, 1982, pp. 275-281.
- [78] Bundy, K. J., Gettleman, L., and Fitzpatrick, P. C., "Electrochemical Corrosion Tests of Dental Alloys in Human Subjects," *Transactions of the 4th World Biomaterials Congress*, 1992, p. 121.
- [79] Escudero, M. L., Ruiz, J., Gonzalez, J. A., and Ruiz, J., "In Vivo Measurement of Electrical Parameters with Alumina-Covered Stainless Steel Electrodes," *Biomaterials*, Vol. 7, 1986, pp. 197-200.
- [80] Gettleman, L., Cocks, F. H., Darmiento, L. A., et al., "Measurement of In Vivo Corrosion Rates in Babboons, and Correlation with In Vitro Tests," *Journal of Dental Research*, Vol. 59, 1980, pp. 689-707.
- [81] Nakayama, Y., Yamamuro, T., Kotoura, Y., and Oka, M., "In Vivo Measurement of Anodic Polarization of Orthopaedic Implant Alloys: Comparative Study of In Vivo and In Vitro Experiments," *Biomaterials*, Vol. 10, 1989, pp. 420-424.
- [82] Lucas, L. C., Dale, P., Buchanan, R., et al., "In Vitro Versus In Vivo Corrosion Analyses of Two Alloys," *Journal of Investigative Surgery*, Vol. 4, No. 1, 1991, pp. 13-21.
- [83] Bundy, K. J. and Luedemann, R. E., "Factors which Influence the Accuracy of Corrosion Rate Determination of Implant Materials," *Annals of Biomedical Engineering*, Vol. 17, 1989, pp. 159-175.
- [84] Morita, M., Sasada, T., Hayashi, H., and Tsukamoto, Y., "The Corrosion Fatigue Properties of Surgical Implants in a Living Body," *Journal of Biomedical Materials Research*, Vol. 22, 1988, pp. 529-540.
- [85] Ryh nen, J., Niemi, E., Serlo, W., et al., "Biocompatibility of Nickel-Titanium Shape Memory Metal and Its Corrosion Behavior in Human Cell Cultures," *Journal of Biomedical Materials Research*, Vol. 35, 1997, pp. 451-457.
- [86] Bumgardner, J. D. and Johansson, B. I., "Effects of Titanium-Dental Restorative Alloy Galvanic Couples on Cultured Cells," *Journal of Biomedical Materials Research (Applied Biomaterials)*, Vol. 43, 1998, pp. 184-191.
- [87] Yamamoto, A., Honma, R., Tanaka, A., et al., "Generic Tendency of Metal Salt Toxicity for Six Cell Lines," *Journal of Biomedical Materials Research*, Vol. 47, 1999, pp. 396-403.
- [88] Locci, P., Marinucci, L., Lilli, C., et al., "Biocompatibility of Alloys Used in Orthodontics Evaluated by Cell Culture Tests," *Journal of Biomedical Materials Research*, Vol. 51, 2000, pp. 561-568.
- [89] Callen, B. W., Lowenberg, B. F., Lugowski, S., et al., "Nitric Acid Passivation of Ti6Al4V Reduces Thickness of Surface Oxide Layer and Increases Trace Element Release," *Journal of Biomedical Materials Research*, Vol. 29, 1995, pp. 279-290.
- [90] Williams, D. F., "Electrochemical Aspects of Corrosion in the Physiological Environment," *Fundamental Aspects of Biocompatibility*, Vol. 1, CRC Press, Boca Raton, FL, 1981, pp. 11-42.

# Microbiological Effects

Stephen C. Dexter<sup>1</sup>

## DESCRIPTION AND UNIQUENESS

THERE IS NO SINGLE, unique microbiological environment. Rather, the microscopic organisms present in all natural aqueous (and many artificial) environments should be regarded as having a potential influence on any corrosion reaction that takes place in that environment. Theoretically, that influence can range, as shown in Fig. 1, anywhere from the organisms being the sole causative agent for corrosion, to innocent bystanders having no influence on corrosion, to corrosion inhibitors. In practice, when the influence of the organisms is a significant factor in determining the overall rate and extent of corrosion, that influence will usually make the corrosion more localized, and the penetration rate higher, than it would be in a sterile environment with the same chemistry. In such cases the corrosion is often referred to as "microbiologically influenced corrosion," or MIC. As of late 2001, a significant influence of microorganisms has been reported on uniform corrosion of a variety of materials in both aerated (aerobic) and deaerated (anaerobic) environments [1,2], pitting and crevice corrosion [3-8], corrosion fatigue [9], galvanic corrosion [10,11] and cathodic protection [12,13]. Effects have also been reported on cracking and embrittlement related to hydrogen evolution [14]. For additional general information on various types of microbiologically influenced corrosion the reader is referred to the books by Borenstein [15], Gaylarde and Videla [16], Kobrin [17], Stoecker [18] and Videla [19] as well as a conference proceedings edited by Angel, et al. [20].

The critical issue for both corrosion testing and corrosion mechanisms is how microscopic organisms exert their influence on corrosion. Generally, they do so by changing the chemistry of the electrolytic solution in a thin layer at the metal surface [8]. In liquid environments they do this by colonizing the metal surface, forming a thin film, or biofilm (usually with thickness in the 10-500  $\mu\text{m}$  range). In buried soil environments, a film may form, but it is not necessary because the moist soil itself is able to localize organisms near the surface. In this latter case, all that is needed is a sufficient density of organisms to change the chemistry of the pore water in the soil at local sites adjacent to the metal surface. In either case, once corrosion initiates, it is common to find intense microbiological activity in the corrosion products at and immediately adjacent to the corrosion site.

The mass of corrosion products, microbes, and their polymeric byproducts often take the form of a tubercle. At the same time, there may or may not be a distributed film of microorganisms on the general metal surface. The organisms associated with a tubercle usually influence the chemistry under which the anodic dissolution reaction takes place, while the organisms in the distributed film influence the chemistry of the cathodic reduction reaction. In a given situation either the anode or cathode reaction may be rate limiting, and it is not always easy (or even possible) to determine which set of organisms has the greater influence.

The process of biofilm formation begins immediately upon immersion of the metal in the liquid environment. The first step is the adsorption of a nonliving macromolecular organic film. This "conditioning film" is nearly complete within the first 2 h of immersion in natural waters at 25°C, but the process may take longer at lower temperatures. The initially colonizing bacteria also begin to attach in substantial numbers within the first 2-4 h of immersion in natural fresh, brackish, and sea waters. The biofilm then goes on to develop a highly complex and spatially heterogeneous structure of microbial colonies and their extracellular polymers. In some cases this structure can be substantially developed

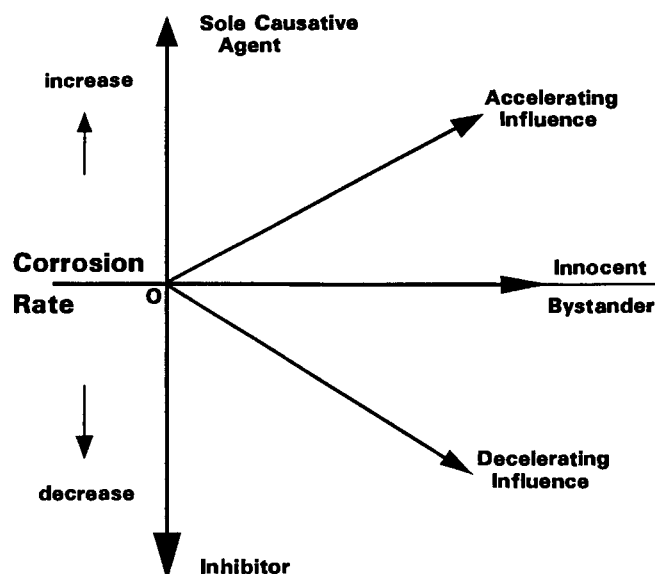


FIG. 1—Schematic diagram showing the range of influence microorganisms may have on corrosion.

<sup>1</sup>700 Pilottown Rd., College of Marine Studies, University of Delaware, Lewes, DE 19958.

within the first 48 h of immersion. In other cases the structure develops over a period of two weeks to a year depending on the temperature. The literature on biofilm formation is extensive, and the reader is referred to the proceedings volumes edited by Berkeley et al. [21], Costlow and Tipper [22] and Keevil et al. [23], and the books by Marshall [24] and Characklis and Marshall [25], Bryers [26], and An and Friedman [27] for further information.

Once formed, a microbial biofilm changes the chemistry at the metal-liquid interface in a number of ways that have an important bearing on corrosion [8]. As the biofilm grows, the bacteria in the film produce a number of metabolic byproducts. Among these are organic acids, hydrogen sulfide, and protein-rich polymeric materials commonly called exopolymers or "slime." The first effect of the composite film of microorganisms and their associated exopolymers is to create a highly heterogeneous micro-environment between the metal surface and the bulk electrolyte [28,29]. Since the biofilm itself is mostly water, it does not truly isolate the interface from the bulk environment, but it does support larger chemical concentration gradients both perpendicular to and parallel to the metal surface than would the laminar sub-boundary of liquid alone. Thus, the water chemistry at the interface may be quite different from that of the bulk solution, although the two chemistries will be coupled through diffusive and convective processes.

Two chemical species, oxygen and hydrogen, that are often implicated (or even rate controlling) in corrosion, are also important in the metabolism of microorganisms. A given biofilm can be a source or a sink for either oxygen or hydrogen. Moreover, biofilms are rarely homogeneous. Sometimes they provide only spotty coverage of the metal surface. Even when they provide nominally complete coverage, their thickness and composition may vary from point to point along the surface. Thus, they are capable of inducing oxygen (or other chemical) concentration cells. Even when the dissolved oxygen in the water is at air saturation, the oxygen tension at the metal surface under a microbial film can be zero [30–32]. In bringing this about, the biofilm acts both as a physical oxygen diffusion barrier and as an active oxygen sink in which the living organisms consume oxygen during respiration [8]. Alternatively, photosynthetic organisms consume carbon dioxide and produce oxygen.

Large changes in pH are also possible under biofilms. Values as low as 5 can be expected under general aerobic films containing acid producing bacteria [33]. Even more acid pH in the range of 1–2 can be expected under discrete biodeposits [34], and a pH of 3 is thought to be required for some of the effects produced by marine biofilms on passive alloys in seawater [35]. Recently, pH values in the 2–5 range have been directly measured at discrete locations within marine biofilms using micro-electrode techniques [36]. Some microbes are capable of directly producing acids such as formic, succinic, acetic, and sulfuric, while others are involved in metabolizing nitrogen compounds [37]. Some can reduce nitrates (used as corrosion inhibitors) to nitrite or nitrogen. Others can convert between nitrate and ammonia compounds, which cause stress corrosion cracking of copper alloys. Still other species of bacteria are involved in the sulfur cycle [38]. Some can oxidize sulfur or sulfides to

sulfate, and ultimately to sulfuric acid. Others, particularly the anaerobic sulfate reducing bacteria (SRB), can reduce sulfates to sulfides, often producing corrosive hydrogen sulfide ( $H_2S$ ) as an end product [39–41]. Many of these organisms have both fresh and salt water strains.

Organisms with a fermentative metabolism can be net producers or consumers for the dissolved gases carbon dioxide and hydrogen [37]. Finally, certain types of bacteria are directly involved in the oxidation of metal ions. Particularly damaging are those fresh water bacteria that oxidize ferrous and manganous ions to ferric and manganic [37,40]. Redox cycling of manganese dioxide within the biofilm matrix is currently thought to have a major effect on corrosion in both fresh [42–46] and seawater [32,47,48] environments. Dissolved manganese has been directly measured in seawater biofilms using microelectrodes [32], and it has been associated in those seawater biofilms with microorganisms of the correct morphological type to be manganese oxidizers [47]. Manganese dioxide has also recently been shown to have the current capacity to account for the observed increase in crevice and galvanic corrosion rates in the presence of marine biofilms [48].

In all these examples, the biofilm is able to substantially change the chemistry of the electrolyte at the metal-water interface. Thus, the corrosion rate may depend more on the details of the electrolyte chemistry at the interface under the biofilm than it does on the bulk environment chemistry. The fact that biofilms tend to be spatially heterogeneous allows them to support sharp chemical gradients both parallel and perpendicular to the metal surface. This is one of the reasons why corrosion tends to become more localized in the presence of microorganisms. On top of this is the tendency for films of microbes to develop and change with time. This can produce corrosion rates, which also vary with time and are thus hard to predict.

## IMPORTANT VARIABLES

It is difficult to specify just what the important variables are when corrosion is being influenced by microorganisms. In addition to their effects on corrosion itself, variables such as dissolved oxygen, pH, temperature, hydrodynamics of flow, and nutrient concentrations also affect the life cycle of the microorganisms. The difficulty is that in most cases, the organisms that affect corrosion are in a thin film or under a deposit on the metal surface. These structures support chemical gradients both parallel to and perpendicular to the metal surface. They can also shield the organisms from adverse chemical and physical situations. Thus, bulk electrolyte properties may have little relevance to the corrosion as influenced by organisms in a film on the metal surface.

The organisms present within the corroding system are also an important factor. A list of most of the types of organisms known to be directly implicated in corrosion, along with the environmental conditions that favor their growth, is shown in Table 1 [41]. This list should not be regarded as complete because new organisms are still being identified as having an influence on corrosion. In addition to these organisms, all microbes found in biofilms that form on metal surfaces have a potential effect on corrosion of that surface.

**TABLE 1**—Microorganisms most commonly implicated in microbiologically influenced corrosion. (Reprinted with permission from Ref 41.)

Genus or Species	pH Range	Temperature Range, °C	Oxygen Requirement	Metals Affected	Action
<b>Bacteria</b>					
<i>Desulfovibrio</i>					
Best known: <i>D. desulfuricans</i>	4–8	10–40	Anaerobic	Iron and steel, stainless steels, aluminum, zinc, copper alloys	Utilize hydrogen in reducing $\text{SO}_4^{2-}$ to $\text{S}^{2-}$ and $\text{H}_2\text{S}$ ; promote formation of sulfide films
<i>Desulfotomaculum</i>					
Best known: <i>D. nigrificans</i> (also known as <i>Clostridium</i> )	6–8	10–40 (some 45–75)	Anaerobic	Iron and steel, stainless steels	Reduce $\text{SO}_4^{2-}$ to $\text{S}^{2-}$ and $\text{H}_2\text{S}$ , (spore formers)
<i>Desulfomonas</i>	...	10–40	Anaerobic	Iron and steel	Reduce $\text{SO}_4^{2-}$ to $\text{S}^{2-}$ and $\text{H}_2\text{S}$
<i>Thiobacillus thiooxidans</i>	0.5–8	10–40	Aerobic	Iron and steel, copper alloys, concrete	Oxidizes sulfur and sulfides to form $\text{H}_2\text{SO}_4$ ; damages protective coatings
<i>Thiobacillus ferrooxidans</i>	1–7	10–40	Aerobic	Iron and steel	Oxidizes ferrous ( $\text{Fe}^{2+}$ ) to ferric ( $\text{Fe}^{3+}$ )
<i>Gallionella</i>	7–10	20–40	Aerobic	Iron and steel, stainless steels	Oxidizes ferrous (and manganous) to ferric (and manganic); promotes tubercule formation
<i>Sphaerotilus</i>	7–10	20–40	Aerobic	Iron and steel, stainless steels	Oxidizes ferrous (and manganous) to ferric (and manganic); promotes tubercule formation
<i>S. natans</i>	...	...	...	Aluminum alloys	
<i>Pseudomonas</i>	4–9	20–40	Aerobic	Iron and steel, stainless steels	Some strains can reduce $\text{Fe}^{3+}$ to $\text{Fe}^{2+}$
<i>P. aeruginosa</i>	4–8	20–40	Aerobic	Aluminum alloys	
<b>Fungi</b>					
<i>Horcomonis resiniae</i>	3–7	10–45 (best at 30–35)	...	Aluminum alloys	Produces organic acids in metabolizing certain fuel constituents

Just as bulk electrolyte chemistry does not necessarily define the conditions at the metal surface under a film of microorganisms, direct counts of organisms present in the bulk aqueous environment have also been found to indicate little of relevance to predicting their influence on corrosion. This is because it is the organisms right at the metal surface that influence corrosion, and those organisms multiply so rapidly on the surface that a low density of organisms in the bulk quickly becomes irrelevant.

In some cases where corrosion is being triggered by a single known microorganism, a change in temperature or pH of the environment outside the range of tolerance of that organism can alleviate the effect. It should not always be assumed, however, that such a tactic would work because there are organisms that can thrive, or at least survive, under extreme conditions including boiling water and space travel. In fact, some types of high-temperature corrosion are influenced by organisms that are only active at temperatures above 60°C (the so-called obligate thermophilic bacteria) [49].

## LABORATORY TESTS AND STANDARDS

Virtually all electrochemical tests used for corrosion in the laboratory are also applicable to corrosion as influenced by microorganisms. The reader is referred to the literature

on this subject for more detail than can be given here [50–52]. In general, the standards listed elsewhere in this publication for various types of corrosion will still be useful when that corrosion is being influenced by microorganisms. No standards have been written specifically for microbiologically influenced corrosion. However, a monograph on Microbiologically Influenced Corrosion [53] has recently been added to the “Corrosion Testing Made Easy” series. That monograph contains chapters on many types of testing that can be employed for looking at corrosion in cases where a microbial influence is suspected. These types of testing include: metallurgical, microbiological and biochemical, chemical and electrochemical, as well as procedures for specimen identification and collection. The reader is referred to this monograph for many additional references [53].

## Importance of Proper Sampling Techniques

Prior to discussing various testing techniques applicable to MIC, one must consider the proper sampling and specimen handling techniques to preserve the evidence. When evaluating a corrosion site in the field at which MIC is suspected, the evidence must be examined, recorded, and sampled and often transported from the site to a laboratory for further analysis. A suspected influence of microorganisms mandates that special procedures are followed to

preserve the microbiological evidence in addition to the procedures used for the chemical and physical evidence.

The sheer complexity of the corrosion process in the presence of microorganisms and microbial biofilms makes data interpretation difficult. Thus, whenever possible, multiple techniques should be used for assessing any microbial corrosion situation before conclusions are drawn. An outline of the laboratory techniques used most successfully in the past, along with any cautions for applying those techniques when the corrosion is influenced by microorganisms will be given below.

### Open Circuit Corrosion Potential

Due to its simplicity, open circuit corrosion potential measurements (see Chapter 20 of this manual) have been used in MIC studies for many years. Corrosion potential measurements as a function of time have been used to obtain information on MIC of steel, aluminum alloys, stainless steels, and other passive alloys. By itself, the corrosion potential of plain carbon and low alloy steels indicates very little because these steels can corrode at a wide range of potentials. Rapid changes in the corrosion potential, however, can be used to indicate cathodic depolarization, or an enhancement of the anodic reaction, or to the formation of a semi-protective film.

Changes in the corrosion potential with time have also been used to study the behavior of aluminum aircraft alloys in the presence of aggressive metabolites produced by *Horcomonis resiniae* during the degradation of jet fuel [54]. In this work it was possible to detect the onset of localized pitting due to microbial action by the change from a steady corrosion potential to one with strong oscillations.

There have been numerous reports in the literature in which variations in the corrosion potential of stainless steels and other passive alloys have been used to follow the effects of biofilms on localized corrosion in natural aqueous environments [3–8,55,56]. These data showed that the corrosion potentials of a variety of alloys were often, but not always [57,58], ennobled (shifted in the electropositive direction) to values above +400 mV SCE in the presence of a biofilm. Alloys with high resistance to chloride induced localized corrosion, such as the 4 % molybdenum ferritic and 6 % molybdenum austenitic stainless steels, the high-temperature superalloys and titanium, could sustain those high potentials indefinitely. Alloys with lesser corrosion resistance, such as the ordinary 300 series stainless steels, however, suffered corrosion initiation usually in the form of either pitting or crevice corrosion, with a sudden negative shift in the corrosion potential [5,59]. Similar data taken with the metal immersed in waters from which the film-forming microbes had been removed showed potentials remaining steady at values below +150 mV with greatly reduced corrosion initiation [59]. Several techniques for removing the film-forming organisms from natural waters without altering the inorganic chemistry of the water have been given in the literature [7,59,60]. These techniques, as discussed below in the section on Techniques for Crevice Corrosion, usually involve various combinations of filtering and low-temperature pasteurization.

### Redox Potential

Another potential that has been used to predict whether or not a given metal will suffer an increase in corrosion due to microorganisms is the reduction-oxidation (or redox) potential of the environment (see Chapter 7 of this manual). The redox potential in general is a measure of the oxidizing power of the environment. In a moist aerated soil, it is dominated by the pseudo-equilibrium potential of the oxygen reaction as measured on a platinum electrode immersed in the soil. At a given temperature and pH, the redox potential of most natural aqueous environments becomes more negative (or active) with decreasing dissolved oxygen concentration.

Redox potential measurements have been used frequently in microbiology to assess the suitability of a given environment for growth of the anaerobic SRB. Since these organisms grow only in the absence of oxygen, they require an environment with an active redox potential, generally less than –400 mV SHE. The redox potential has been used to estimate the aggressiveness of soils toward buried metals, and it has been considered by some authors to be the most significant factor in assessing the aggressiveness due to SRB [61]. Other authors, however, consider the combined use of several parameters such as electrical resistivity and water content of the soil in addition to redox potential to give a more reliable indication [62]. It is important to note that the redox potential is a function of soil pH as well as oxygen content. Therefore, when the purpose of measuring the redox potential is to learn something about the oxygen concentration or to detect when the oxygen content changes, it is necessary to concurrently measure and record the pH. It is also important when making such measurements to keep the immersion time of the platinum electrode short enough that it is not colonized by the microorganisms. Otherwise, the measured value will correspond to the chemistry at the platinum surface under the film of microorganisms, rather than to that of the bulk environment.

Redox potentials have also been used in conjunction with Pourbaix diagrams to predict the probable behavior of aluminum, nickel, and zinc alloys in aerated environments [63]. Unlike the negative redox potentials that signal corrosive conditions for steel in anaerobic environments, a positive redox potential usually indicates conditions favorable for corrosion under aerobic conditions. For example, positive redox potential values, along with positive corrosion potentials and negative pitting potentials, can explain the aggressiveness of *H. resiniae* toward aluminum [64]. In fuel/water systems where different species of bacteria and fungi often grow together, the redox potential can be useful in studying the role played by each species in modification of the environment. For active/passive metals like aluminum and its alloys, the use of redox potentials together with the corrosion potential and the pitting potential can be helpful in assessing when the oxidizing conditions of the environment reach the values needed to initiate localized corrosion [64]. It should be cautioned, however, that this can only be done reliably under conditions in which the organisms change the chemistry of the bulk environment, and that chemistry, along with the behavior of the metal, are easily simulated and measured. In contrast, as will be



discussed in a later section of this article, such measurements are much more difficult to both make and interpret when the organisms form a thin film on the metal surface and change the local chemistry within the film, rather than in the bulk solution.

### Direct Current Polarization Techniques

In this section the utility and limitations of various direct current electrochemical polarization techniques for investigating corrosion in the presence of microorganisms will be discussed. The reader is referred to other sections of this manual for a description of the techniques themselves.

### Polarization Resistance

The polarization resistance technique (described in Chapter 7 of this manual, and recently reviewed by Scully [65]) has been applied frequently to the measurement of corrosion rates as influenced by microorganisms. This technique is most useful for systems undergoing uniform corrosion controlled by a single set of anode and cathode reactions. An exact calculation of the corrosion rate by this technique requires the simultaneous determination of the polarization resistance itself and the anode and cathode Tafel slopes [66]. A simplified version of the technique, called linear polarization resistance (LPR), is based on the two assumptions [67] that (1) the corroding interface behaves as a simple resistor whose magnitude is inversely proportional to the corrosion current, and (2) there is a linear relationship between changes in an applied potential and the resultant current density when the applied potentials are within about 10 mV of the corrosion potential. Such small applied potentials are favorable for the study of MIC [50–52] because the minute changes they cause in chemistry at the interface are not likely to interfere with the metabolic processes of the microorganisms present. This allows the polarization resistance technique to be used repeatedly during an experiment to determine evolution of the biological influence with time.

In practical situations, electrochemical systems are often more complex than the simple model assumed by the polarization resistance method. The presence of biofilms on the metal surface may introduce a capacitance as well as resistance to the interface. Moreover, the biofilm may introduce additional electrochemical reactions and adsorptive processes, which can lead to nonlinear polarization behavior. Even so, a polarization resistance value can be found as long as a sufficiently slow polarization scan rate (determined by the rate of the slowest reaction present) is used to maintain steady state conditions and a correction can be made for solution and biofilm resistances.

Patchy biofilms and localized colonization give rise to localized corrosion reactions and to anodes and cathodes that are fixed in space and stable in time [68] as opposed to the randomly spaced and mobile oxidation and reduction reactions required by uniform corrosion. Under these conditions, the calculated polarization resistance value is correct but the anode and cathode areas are unknown, so that one does not know how to determine the current density (i.e., the penetration rate). Adding to the level of

uncertainty in the localized corrosion rate as measured by the polarization resistance technique is the observation that the data often show large fluctuations with time [51]. Even with these limitations, the polarization resistance method has been used successfully by many authors [69–76] to assess under what conditions microbes accelerate (or decelerate) corrosion rates.

### Tafel Polarization

Methods for making these measurements are given in the literature and in Chapter 7 of this manual. Polarization studies have been used for several decades in the study of anaerobic corrosion of iron by SRB. Anodic and cathodic polarization curves of mild steel in the presence of different strains of SRB were used to ascertain the effect of the enzyme hydrogenase on cathodic depolarization of the metal and to identify the basic mechanisms of anaerobic corrosion induced by SRB [77]. Others measured cathodic polarization curves for mild steel in sterile media containing suspensions of iron sulfide [78] or dissolved hydrogen sulfide [79] to demonstrate that cathodic depolarization can be enhanced in the presence of those chemical species. Polarization experiments have also been used to assess variations in the depolarizing effect of several species of microorganisms on steel under different experimental conditions [80,81] and to investigate the effects of natural biofilms on the cathodic kinetics of stainless steels [3–8,10,11,82,83].

Although these methods have been used with considerable success, several limitations should be kept in mind when applying them to situations in which the action of microorganisms may be important. First, the rather large polarizations required may change the electrochemical conditions (particularly the pH) in such a way as to be deleterious to microorganisms in the biofilm [84]. Thus, Tafel polarization measurements should not be made periodically during a microbial corrosion experiment. They may, however, give useful information for research purposes if done once at the end of an experiment. For purposes of following changes in the corrosion rate with time under the influence of microorganisms, the polarization resistance technique, which employs very small polarizations, should be used rather than Tafel polarization.

A second set of cautions about use of Tafel polarization in microbial corrosion experiments involves the tendency of films of microorganisms to (1) introduce new electrochemical reactions and diffusion barrier films [35], or (2) cause the corrosion potential to drift or fluctuate with time [5]. All of these effects make the linear region of the curve less distinct, and thus the extrapolated corrosion rates less reliable. Even so, data from the technique can still be useful for research purposes in that changes in shape of the curves from one experiment to the next can reveal that the organisms are changing conditions at the metal surface. If the changes are taking place slowly compared to the time for making a polarization run, the data can give valuable information on short-term effects, even though they will not be useful for measuring long-term corrosion rates. Finally, Tafel polarization measurements alone give no information on either the distribution of corrosion on the metal surface

(MIC is usually localized) or on the relative contribution to corrosion of the microorganisms as compared to other factors. This means that careful work and well-designed control experiments are required if the results are to be useful, or even interpretable.

### Potentiodynamic Sweep Techniques

The potentiodynamic sweep techniques are most useful for characterizing, and sometimes predicting, the corrosion behavior for metal-electrolyte systems in which the metal passivates by formation of a protective (or passive) film, as described in Chapter 20 of this manual. One of the main experimental variables that can be manipulated is the sweep rate. Relatively high scan rates (60 V/h) are used to indicate regions where intense anodic activity is likely. Slower scan rates (1 V/h) are used to identify regions in which relative inactivity is likely. High scan rates are used to minimize film formation so that the currents observed relate to thin film or nearly film free conditions, while slower scan rates allow time for film formation to occur. Slow scan rates provide for maximum stability of the metal surface conditions, but increase the chance of changes in the environment or in biofilms, particularly at the potentials furthest from the corrosion potential. High scan rates disturb the steady state reaction conditions at the metal surface, but better maintain stability of the environment.

At any scan rate, the large applied potentials often used in potentiodynamic experiments may disturb the organisms in the biofilm, as was the case for the Tafel polarization technique discussed above. Thus, the same caution against doing polarizations during the middle of a long-term experiment applies here as well [50]. MIC involves the action of relatively fragile organic and biological films that are affected by pH and the concentrations of oxygen and hydrogen at the metal-film interface. Thus, the scan rates and ranges discussed above, which can affect these variables, are very important when applying potentiodynamic techniques to MIC systems. Rapid scan rates can be used to develop a database for possible expected corrosion regimes for the film-free metal in a given environment. Intermediate scan rates may be selected to correspond to a particular biofilm formation rate, while very slow scan rates may be selected for measurements of the relatively steady state conditions in the presence of a mature biofilm. The combination of slow scan rate with a large scan range, however, maximizes the probability of adversely affecting organisms on the metal surface, so this type of experiment should only be done at the end of an experiment [e.g., 11]. Thus, no single scan rate is appropriate for use in all MIC investigations [50].

### Determination of Pitting Potentials

Pitting potentials in the presence of microorganisms are of interest because microbes often bring about localized corrosion. There is a wide variety of techniques for measuring pitting potentials as discussed in Chapter 18 of this manual. In general, the validity of these techniques is not changed by the microorganisms. The degree to which the

data can be interpreted, however, may be affected [85]. This is particularly true if the microorganisms that affect corrosion are present in the form of a thin biofilm on the metal surface. The chemistry within the film is often very complex and difficult to characterize. Thus, a measurement showing that the pitting or breakdown potential has decreased upon exposure to microorganisms will indicate correctly that conditions at the metal surface have become more conducive to localized corrosion, but it may not be possible to say anything about the mechanism without additional measurements [85]. Zhang and Dexter [86] used these techniques to show that the critical pitting and breakdown potentials of S30400 and S31600 stainless steels immersed in seawater changed upon natural biofilm formation.

### Alternating Current Methods

Direct current techniques assess the overall corrosion process occurring at a metal surface, but treat the metal-solution interface as if it were a pure resistor. Electrochemical impedance spectroscopy (EIS) using small alternating currents has been developed in part to eliminate this restriction. For a full description of the EIS technique itself, the reader is referred to the literature [87] as well as to Chapter 7 of this manual. EIS has been particularly useful in the presence of nonconducting and semiconducting surface films.

EIS data are most helpful and easiest to interpret for metal-electrolyte systems involving continuous thin films and low solution conductivity. Some caution, therefore, should be exercised in data interpretation from MIC systems because the adsorbed organic and biological films tend to provide spotty, rather than continuous, coverage, and these films can vary widely in thickness. Nevertheless, EIS can provide many useful types of information on biofilm covered electrodes [50–52].

Two examples of the successful use of EIS in determining the influence of microorganisms involve the deterioration of coatings and the localized corrosion of aluminum alloys. Mansfeld and co-workers have used EIS, along with electrochemical noise analysis (ENA), to monitor the impact of microorganisms on degradation of protective polymeric coatings on steel immersed in natural seawater for up to three years [88]. EIS spectra for most coatings showed a gradual decrease in the impedance modulus  $|Z|$  with immersion time, and they could be fit to suitable equivalent circuits. Using EIS data together with visual observation of the coatings surface the investigators also were able to follow the increase in percentage of damaged area of the sample (damage function) with time.

EIS has also been used to monitor the effect of microorganisms on localized corrosion of aluminum alloys [89,90]. In this effort [90] the EIS spectra were fitted to the pitting model of Mansfeld et al. [91], and a special software package [92] was used for data analysis. Tests on aluminum alloy 2024 were performed in sterile growth media as well as in the presence of three different bacterial strains, two of which were genetically engineered to produce a known metabolic product. Large differences in pit growth rates were observed, including some significant reductions in active pit growth rates.

Several difficulties with the use of the EIS technique for MIC research [50] recently have been alleviated through the development of improved instrumentation and software. First, the combination of microbial film and corrosion products often encountered in MIC causes the impedance to become very high at low frequencies. The large extrapolations needed in such cases with older equipment have been greatly reduced through the introduction of new instrumentation with increased frequency and impedance ranges. Second, the difficult task of developing equivalent electrical circuits required for quantitative EIS data interpretation can now be done automatically through commercially available software programs. A third difficulty stems from the nature of biofilms themselves. Microbial films are not static like paint or metal oxide films. Rather, microbial films are dynamic entities, within which changes are continually occurring under the influence of the organism's metabolism. Such changes can cause fluctuations in electrochemistry at the metal-film interface that are of shorter duration than the length of the EIS measurement. This can mean that the highest and lowest frequencies within the overall EIS signal may not be responding to the same interface conditions [93]. Once this difficulty is recognized, it can be addressed through proper experimental design.

### Scanning Vibrating Probe Techniques

The scanning vibrating probe is a technique in which the electrochemical potential field, or localized anodic and cathodic currents, above a corroding metal electrode, is mapped in a raster pattern. The generic apparatus developed by Isaacs [94,95] requires a flat horizontal specimen, with some means of vibrating, positioning, and scanning a fine-tipped platinum wire electrode, or alternatively a micro-reference electrode [96], above the metal surface. The scanning vibrating probe technique is ideally suited for mapping localized anodic and cathodic areas on a smooth metal surface. Franklin et al. [97–100] have used such a probe to study anodic areas associated with bacterial films. By coupling the scanning vibrating probe with autoradiography of bacterial cells labeled with  $^{14}\text{C}$  acetate, Franklin et al. were able to correlate sites of anodic activity with sites of bacterial activity [100].

### Microelectrode Techniques

Various microelectrode techniques can be powerful tools for evaluating effects of microbial activities on corrosion behavior at metal surfaces. Membrane type microelectrodes have been developed for measuring microprofiles of dissolved  $\text{O}_2$ ,  $\text{N}_2\text{O}$ ,  $\text{H}_2\text{S}$ , and pH across the thickness of microbial mats and biofilms [101–106]. These have been used successfully to determine oxygen diffusion fluxes [101,102], microbial photosynthetic and respiration rates [103], nitrogen cycling [104], and to locate the oxic/anoxic boundary [105,106].

Solid state voltammetric microelectrodes with tip diameters in the range of 10–50 microns are especially useful for measuring chemical profiles within thin biofilms on corroding metal surfaces. Lewandowski and coworkers have used iridium-iridium oxide microelectrodes for measuring

profiles of oxygen, peroxide, and pH perpendicular to the metal surface in natural and cultured fresh water biofilms [28,29,31,107–109]. Dexter and Chandrasekaran [36] also used the iridium-iridium oxide electrodes for measuring pH profiles within natural marine biofilms. Brendel and Luther developed Au-Hg amalgam voltammetric microelectrodes for measuring profiles of dissolved oxygen/peroxide,  $\text{Fe}^{+2}$ ,  $\text{Fe}^{+3}$ ,  $\text{Mn}^{+2}$ ,  $\text{Mn}^{+4}$  and various sulfur species in marine sediments [110]. Their original electrodes with tip diameters of 100 microns were too large for measuring chemical profiles across thin biofilms. Xu, Dexter, and Luther [32] further developed this technique to make the Au-Hg electrodes with tip diameters of 25 microns. These were used to directly measure  $\text{O}_2$ ,  $\text{H}_2\text{O}_2$ , Fe, Mn and sulfur species in natural marine biofilms using square wave voltammetry. These electrodes can also be used to measure pH values below 4 in the absence of iron [32]. When dissolved iron is present, the proton and  $\text{Fe}^{+2}$  peaks are so close together that the pH value is difficult to determine. All of the above measurements with solid state voltammetric microelectrodes showed that there are steep chemical gradients both perpendicular and parallel to the substratum surface, even in biofilms less than 50 microns in thickness. This was true for both fresh and seawater biofilms, and it is believed to be one of the major reasons why MIC tends to be localized.

Ideally, microelectrodes for use in thin biofilms grown on metal surfaces should have small tip diameters with small sensor surfaces to minimize distortion of the local environment and give optimal spatial resolution [111]. They should also produce a stable signal with low noise levels and high selectivity, and they should be robust enough to survive gentle contact with the solid surface [111] so that they can be reused. Tip diameters of 10–35 microns are necessary to achieve the spatial resolution needed to characterize the degree of heterogeneity in natural biofilms. However, the smaller the tip diameter, the more difficult the electrodes are to make and the more easily they are damaged.

Errors in the signal produced by microelectrodes can come from both chemical and physical sources. Contamination of the sensor element by reaction with the environment should be avoided. Investigators doing this type of work are careful to calibrate the electrode ahead of time for the species to be measured and then make sure the electrode will recalibrate after the measurement. One should consult the literature cited for specific procedures and cautions for using each type of electrode. Physical errors come from electrodes that are inappropriately sized for the variability of the environment. Problems may also come from vibration of the electrode tip or flow of bulk water along the outer sheath of the electrode into the measurement volume [31,36].

When coupled with observation of the surface by various techniques, the chemical data from microelectrodes can be correlated with the positions of microbial colonies and corrosion sites on the metal surface. Franklin et al. [97] have used confocal laser scanning microscopy (CLSM) to image microbes preferentially attached to corroding particles of zinc and iron. Xu [47] has used both CLSM and epifluorescence microscopy to image colonies of microorganisms associated with various combinations of oxygen, peroxide, and manganese revealed by the Au-Hg microelectrodes on passive metal surfaces.

### Dual Cell Techniques

The dual cell technique used for many years in galvanic couple studies and as biological fuel cells [112] can also be applied to the assessment of microbial activity in corrosion processes [113]. This type of cell consists of two similar compartments filled with the same electrolyte and each containing an identical metal electrode. For work on MIC, one of these cells is maintained under sterile conditions, while the other is inoculated with the microorganisms under study. The external circuit is completed through a zero-resistance microammeter, and the contact between the solutions in the two chambers is made across a semipermeable membrane. In this way, the current obtained under short-circuit conditions is considered as a measure of the biological effect on the inoculated electrode. Under ideal conditions this enables one to experimentally separate areas of sterile, bare metal surface from those of the same metal in the presence of microorganisms [113]. The corrosion currents flowing between these separated areas can then be measured. The method, however, does not separate the anodes and cathodes of local action microcells, but only measures the effect of coupling. Thus, it is not a simple matter to relate the data obtained from this method to MIC on real structures covered with spotty biofilms or discrete biodeposits. This type of device has been used successfully to study the effects of: a marine pseudomonad on corrosion of copper [114], an obligate thermophilic filamentous bacterium on the corrosion of nickel [115], an iron-oxidizing stalked bacterium on the corrosion of mild steel [113], and an aerobic acetic acid producing bacterium on the cathodic depolarization of stainless steel [116].

Inherent in this method is the assumption [50] that the two electrodes can be made identical, and that there would be no current flow as long as both cells were maintained in the sterile condition. This may be a reasonable assumption in the case of steady state uniform corrosion, or for stable passivity where neither electrode undergoes potential fluctuations in the absence of microorganisms. It may not be valid for systems, such as the 300 series stainless steels in seawater, where the electrode potentials are sufficiently variable that currents can flow in either direction whether or not microorganisms are present. In such systems, interpretation of the data will not be straightforward [50].

### Electrochemical Noise

In electrochemical noise (EN) measurements fluctuations in potential or current are measured as a function of time. The measurements can be done (see Chapter 7) either without or with an externally applied signal. In the first case one monitors the open circuit corrosion potential of the test metal versus a suitable reference electrode or versus a second electrode of the same material exposed under identical conditions. The advantage of this technique for use in MIC research is that there is no external signal to disturb the biological community on the metal surface. Alternatively, one can measure fluctuations in potential ( $E$ ) at an applied current ( $I$ ), or the reverse, fluctuations in  $I$  at an applied  $E$ . It has also been suggested that one could couple the metal of interest to a platinum electrode and measure the noise

across a resistor between the two electrodes [117]. As pointed out by Mansfeld and Little [51] this second technique applies an unknown polarization through the galvanic coupling to platinum. This has the dual disadvantage that the noise recorded could be due to that polarization and the applied signal may have an effect on processes within the biofilm.

Within the past decade there have been major developments in methods for analyzing and interpreting EN data [118–123]. Improved methods for collection of EN data also have been reviewed recently [124]. In spite of these developments, many of which have been summarized in the “Corrosion Testing Made Easy” series [87], there have been few applications of EN techniques to MIC. EN techniques have been applied to the study of anaerobic corrosion of iron by SRB [125]. Potential fluctuations accompanying the breakdown of an SRB produced iron sulfide film on iron have been recorded in the laboratory. Such fluctuations have also been recorded from steel pipelines in the field [126], and it may be possible to correlate these data with areas of anaerobic corrosion of the pipeline. In another study, EN techniques were used in combination with EIS to study the effects of SRB in the corrosion of reinforced concrete structures [127]. Little et al. used EN techniques together with EIS to examine the relationship between marine bacteria and the defect structure of polymer coatings on steel [128]. Very few bacteria became associated with the coating defects on cathodically protected samples, while many bacteria became associated with the corrosion products at the coating defects on unprotected samples.

Using EN techniques, it has been claimed that it is possible to detect the onset of corrosion, determine whether it is uniform or localized, and even distinguish between pitting and crevice corrosion [129]. There is evidence, however, that this claim should be taken with some caution [122]. At its present state of development the most common use for the EN technique has been in corrosion monitoring [124]. Although EN shows great promise for use in monitoring of MIC, there have been few applications to date.

### Electrical Resistance Probes

The electrical resistance method (see Chapter 15) is widely used as an industrial corrosion monitoring technique [130]. The electrical resistance method is excellent for indicating a change in the general corrosion rate, but the results are harder to interpret in the presence of localized forms of corrosion, such as pitting, crevice corrosion, stress corrosion cracking, and corrosion fatigue, which take place with very little mass loss. Workers have attempted to correlate characteristic jumps in resistance with localized forms of corrosion, but with only limited success. An electrical resistance probe will indicate very little corrosion if the corrosion products have an electrical conductivity approaching that of the metal, or if an electrically conducting film forms on the metal surface. MIC usually produces localized forms of corrosion, and it is sometimes associated with conductive corrosion product films. Therefore, in cases of known or suspected MIC, the electrical resistance method should be used only with caution, and in conjunction with other methods.

## RESEARCH TECHNIQUES FOR STUDYING CREVICE AND GALVANIC CORROSION IN THE PRESENCE OF BIOFILMS

### Multiple Crevice Assembly

The multiple crevice assembly technique (see Chapter 19) using a serrated washer to create many crevice sites on each side of a test panel, has become commonplace in the investigation of crevice corrosion. The multiple crevice assembly device, or the earlier version of it having a solid washer with only one crevice site per side, has been used to study biofilm effects on both initiation and propagation of crevice corrosion in natural waters by several authors [6,7,131]. Initiation can be inferred by observation of visible corrosion products or by a change in corrosion potential of the device. Propagation of corrosion is determined by measuring the weight loss and the number of sites (or percentage of area under the washer) attacked at the end of the experiment. The success of this technique for measuring the extent to which the microorganisms present affect either initiation or propagation depends on the ability to run a parallel experiment without any influence from microbes.

### Remote Crevice Assembly

The remote crevice assembly technique (see Chapter 19) is a research tool that allows one to separate the anode and cathode areas of a crevice corrosion test sample so that the current flowing between them can be measured with a zero-resistance ammeter. This technique is similar to the dual cell method, and it lends itself well to studies of microbial effects on crevice corrosion [7]. It allows direct measurement of microbial effects on both the initiation time and propagation rate for crevice attack, provided again that a suitable control experiment without the microbial influence can be done concurrently. The same technique of separating the anode and cathode can be used to study the influence of microbes in biofilms on galvanic corrosion [11].

### Performing the Test Without the Influence of Microbes

The most difficult problem to solve when using the two techniques above to demonstrate an effect (or lack thereof) of microorganisms on crevice and galvanic corrosion has been to devise an effective method for making the measurements with the same geometry and chemistry but without the organisms [132]. In a research context, this is called "running the control experiment." The word "control" as used in this section refers to running the same corrosion experiment without the microbes present. This should not be confused with a practical program designed to control, or mitigate, biocorrosion.

Ideally, one should have a sterile "control experiment" running concurrently, and under the same chemical and geometrical conditions as the one in the natural, or laboratory culture, environment. However, it is quite difficult to maintain truly sterile conditions in such corrosion experiments. The problem is compounded as the required duration of the experiment becomes longer and the volume of

water involved larger. For the long durations (several months) and large volumes of water required for most crevice corrosion experiments, it becomes impractical (some would say impossible) to maintain truly sterile conditions with no change in chemistry of the water. Given these difficulties, the objective of the control experiment changes from that of having no organisms present to that of delaying the onset of microbial effects long enough to do a meaningful experiment. If it is impossible for practical purposes to have an absolutely sterile control experiment, then some way must be found to have a control condition that is demonstrably effective in order for the data generated to be interpretable.

Several techniques, none of which is perfect, have been developed for creating such an effective, rather than an absolute, control condition. These techniques all involve one, or a combination of, three approaches: (1) use an artificial chemical water, (2) treat the natural water, or (3) treat the specimen surface. If the natural electrolyte is seawater, the first inclination will be to use a 3.5 % NaCl solution as the control water. This approach will not sterilize the water, but the organisms will be different from those in the marine environment. Thus, whatever biofilm does form will behave differently than a natural marine biofilm. This simple solution provides an electrolyte that is chemically stable over long periods of time, but it does not reproduce either the inorganic or organic chemistry of seawater very well [133]. A chemical improvement is to use an artificial seawater, such as the ASTM D 1141, Specification for Substitute Ocean Water. Other artificial seawaters that more accurately reproduce the chemistry of open ocean water than ASTM seawater have also been developed [134]. In general, however, the more chemically accurate the artificial formulation is, the more difficult it is to make, and the less stable it is over time. Moreover, no artificial seawater can reproduce the organic chemistry of natural seawater. It is important to realize that biofilms do eventually form in all the above artificial waters, and the investigator must be able to demonstrate that the level of biofilm control actually achieved is sufficient for the purposes of a given experiment.

The next approach to making an effective control is usually to modify the natural water itself in such a way as to eliminate the microorganisms, or at least to delay their tendency for biofilm formation over the desired length of the experiment. Many methods have been tried, but no one has yet devised an easy way to maintain sterile control conditions without also changing the water chemistry. Biofilm formation can be prevented by continuous photooxidation or addition of biocides to kill or inhibit the organisms, but these techniques also change the chemistry of the water. Perhaps the most successful technique has been to sterilize the water by combination of mechanical filtration at the 0.2 (or even 0.1) micrometer level with a low temperature (75–80°C) pasteurization [60]. This does not guarantee continued sterility of the water but it does delay the formation of a biofilm for four to eight weeks. This combination of filtration and pasteurization is usually the method of choice for short-term (<1 month) laboratory experiments. The disadvantage is that this control water has to be changed every two or three days to keep it fresh. Since filtration at the 0.2  $\mu\text{m}$  level is a slow process, this means that new water

must be continuously under preparation, and the experimental logistics become difficult if the volume of water required for a given experiment is more than about 5 L.

The final approach to creating an effective "control" experiment involves periodic removal of the biofilm by physical or chemical treatment of the metal surface. Techniques such as periodic wiping or scraping with or without chemical cleaning and even autoclaving the metal samples have been tried with varying degrees of success [135]. These techniques are all temporary, and they must be repeated frequently in order to be effective. Recently, Zhang and Dexter [7] found that the control condition for long-term crevice corrosion experiments requiring large volumes of water could be maintained by simple treatments of both the surface and the water. In their experiments the remote crevice assembly technique was used to measure the effect of biofilms on the cathode member of the assembly. They were able to maintain acceptable control conditions (i.e., no measurable biological effect) by pasteurizing the control water and recycling the cathodes. Two identical cathode panels were prepared for each experiment. These cathode panels were exchanged approximately every three days. The panel that was removed was immediately immersed in fresh water at 60°C for 1 h, then air-dried and kept in a desiccator until it was time for the next exchange. At that time the treated panel was connected into the circuit before disconnecting the old panel in order to avoid an open circuit condition on the anode. This simple method was found to be nearly as effective, and much less labor intensive than filtering the water. The disadvantage was that the current and potential record for the assembly showed large (although short-term) fluctuations each time the cathodes were changed, and each anode was momentarily connected to twice the normal area of cathode. It was not known exactly how these fluctuations affected the long-term corrosion of the anode. Nevertheless, the anodes connected continuously to cathodes with biofilms usually showed much higher weight losses at the end of the experiment and currents during the experiment one to three orders of magnitude higher than those of the control anodes [7].

None of the control methods described above is ideal, and the one chosen for a given experiment will depend on the intended purpose and duration of the experiment. The utility of these control methods is not limited to studies of crevice corrosion. In general, they can also be used for the study of any type of corrosion in which the effect of a natural or cultured biofilm is being measured.

## FIELD TESTS AND STANDARDS

As was the case in the laboratory, no standards have been written for field tests involving microbiologically influenced corrosion. Many of the electrochemical techniques evaluated above for use in the laboratory can also be taken into the field. The limitations on using these techniques on large structures in the field are described in other chapters of this manual. The same cautions outlined above for using them in laboratory MIC work should generally be carried into the field as well.

When attempting to analyze whether or not a particular type of corrosion on a real structure has been influenced by microorganisms, one should first observe proper procedures for dealing with the metallurgical and electrochemical aspects of the evaluation for that type of corrosion. Beyond those procedures, there are also some unique procedures for dealing with MIC. For the most part, these procedures, as outlined below, relate to the biological (i.e., living) nature of the evidence. For further information, the reader is referred to the review by Pope et al. [136], any of a number of books on microbiological laboratory methods [e.g., 137,138], the books by Borenstein [15], Videla [19], Kearns and Little, Eds., [139], Kobrin, Ed., [17] and Stoecker, Ed., [18], and the Corrosion Testing Made Easy volume on MIC [53].

When dealing with a suspected case of MIC in the field, it is of vital importance to remember that much of the evidence is living or is directly produced by living organisms. That evidence changes, or even disappears, very quickly when the specimen or structure is allowed to dry out or to sit under conditions different from those under which corrosion took place. Therefore, if MIC is to be either identified or eliminated, the proper type of sampling needs to be done quickly. In most cases, the evidence also needs to be transported to the analytical laboratory quickly. For nearly all metallic systems, there are several careful observations that need to be made while the corroding site is still fresh and wet. These include:

1. The form and distribution of corrosion (e.g., uniform or localized, tuberculation or not);
2. The color of the wet fouling and corrosion products;
3. The appearance and colors of the metal both within and immediately adjacent to the corrosion site (bright, shiny areas under corrosion products indicate active corrosion); and
4. The presence or absence of H<sub>2</sub>S odor as revealed by adding a drop or two of HCl to the corrosion products or the general environment adjacent to the corrosion site.

It is also important to gather information on the general state of the bulk water chemistry, including oxygen and sulfide concentrations, pH, salinity (or chloride ion concentration), and temperature (or temperature range) during the time of corrosion. These water chemistry measurements, however, need not be taken while the corrosion products are still wet, provided the bulk water chemistry does not change with time.

If it is suspected that a certain type of organism, such as the sulfate-reducing bacteria (SRB), sulfur oxidizing bacteria, any one of a number of acid producing bacteria or metal oxidizing bacteria is involved, then it is important to sample for and try to culture those bacteria. Generally, samples of the environment or corrosion products containing biological materials should be taken in duplicate, one preserved for microscopic and chemical analyses, and the other kept live for microbiological analysis. All such samples should be taken as soon as possible after the "normally corroding" material or structure is disturbed. It is vital that the live samples be handled properly, transported to the laboratory immediately and analyzed within 12–24 h. Procedures for

taking these samples are outside the scope of this manual, but the reader is referred to the review by Pope et al. [136] and the Corrosion Testing Made Easy volume on MIC [53] as a guide to the literature on the subject.

## REFERENCES

- [1] Tiller, A. K., "A Review of the European Research Effort on Microbial Corrosion between 1950 and 1984," *Proceedings, Biologically Induced Corrosion*, S. C. Dexter, Ed., NACE-8, National Association of Corrosion Engineers, Houston, TX, 1986, p. 8.
- [2] Videla, H. A., *Manual of Biocorrosion*, CRC Press, Inc (Lewis Publishers), Boca Raton, FL, 1996, p. 179.
- [3] Johnsen, R. and Bardal, E., "Cathodic Properties of Different Stainless Steels in Natural Seawater," *Corrosion*, Vol. 41, No. 5, 1985, p. 296.
- [4] Scotto, V., DeCintio, R., and Marcenaro, G., "The Influence of Marine Aerobic Microbial Film on Stainless Steel Corrosion Behavior," *Corrosion Science*, Vol. 25, No. 3, 1985, p. 185.
- [5] Dexter, S. C. and Gao, G. Y., "Effect of Seawater Biofilms on Corrosion Potential and Oxygen Reduction of Stainless Steel," *Corrosion*, Vol. 44, No. 10, 1988, p. 717.
- [6] Gallagher, P., Malpus, R. E., and Shone, E. B., "Corrosion of Stainless Steels in Natural, Transported and Artificial Seawater," *British Corrosion Journal*, Vol. 23, No. 4, 1988, p. 229.
- [7] Zhang, H. J. and Dexter, S. C., "Effect of Biofilms on Crevice Corrosion of Stainless Alloys in Coastal Seawater," *Corrosion*, Vol. 51, pp. 56–66.
- [8] Dexter, S. C., "Role of Microfouling Organisms in Marine Corrosion," *Biofouling*, Vol. 7, 1993, p. 97.
- [9] Edyvean, R. G. J., Thomas, C. J., Brook, R., and Austen, I. M., "The Use of Biologically Active Environments for Testing Corrosion Fatigue Properties of Offshore Structural Steels," *Proceedings, Biologically Induced Corrosion*, S. C. Dexter, Ed., NACE-8, National Association of Corrosion Engineers, Houston, TX, 1986, p. 254.
- [10] Mollica, A., Ventura, G., Traverso, E., and Scotto, V., "Cathodic Behavior of Nickel and Titanium in Natural Seawater," *International Biodeterioration*, Vol. 24, 1988, pp. 221–230.
- [11] Dexter, S. C. and LaFontaine, J. P., "Effect of Natural Marine Biofilms on Galvanic Corrosion," *Corrosion*, Vol. 54, No. 11, 1998, p. 851.
- [12] Dexter, S. C. and Lin, S. H., "Effect of Marine Biofilms on Cathodic Protection," *International Biodeterioration and Biodegradation*, Vol. 29, 1992, p. 231.
- [13] Edyvean, R. G. J., Maines, A. D., Hutchinson, C. J., Silk, et al., "Interactions Between Cathodic Protection and Bacterial Settlement on Steel in Seawater," *International Biodeterioration and Biodegradation*, Vol. 29, 1992, p. 251.
- [14] Ford, T. and Mitchell, R., "Microbiological Involvement in Environmental Cracking of High Strength Steels," *Proceedings, International Congress on Microbially Influenced Corrosion and Biodeterioration*, N. J. Dowling, M. W. Mittleman, and J. C. Danko, Eds., The University of Tennessee, Knoxville, TN, 1990, pp. 3–94.
- [15] Borenstein, S. W., *Microbiologically Influenced Corrosion Handbook*, Industrial Press, Inc., NY, 1994.
- [16] *Bioextraction and Biodeterioration of Metals*, C. Gaylarde and H. Videla, Eds., Cambridge University Press, Cambridge, UK, 1995.
- [17] *A Practical Manual on Microbiologically Influenced Corrosion*, G. Kobrin, Ed., NACE, International, Houston, TX, 1994.
- [18] *A Practical Manual on Microbiologically Influenced Corrosion, Volume 2*, J. Stoecker, II, Ed., NACE, International, Houston, TX, 2001.
- [19] Videla, H. A., *Manual of Biocorrosion*, CRC Press, Inc. (Lewis Publishers), Boca Raton, FL, 1996.
- [20] *Proceedings, 1995 International Conference on Microbiologically Influenced Corrosion*, P. Angel, et al., Eds., NACE International, Houston, TX, 1995.
- [21] *Microbial Adhesion to Surfaces*, R. Berkeley, J. Lynch, J. Melling, et al., Eds., Ellis Horwood, LTD., Chichester, U.K., 1980.
- [22] *Marine Biodeterioration*, J. D. Costlow and R. C. Tipper, Eds., Naval Institute Press, Annapolis, MD, 1984.
- [23] *Biofilms in the Aquatic Environment*, C. W. Keevil, A. Godfree, D. Holt, and C. Dow, Eds., The Royal Society of Chemistry, Cambridge, UK, 1999.
- [24] Marshall, K. C., *Interfaces in Microbial Ecology*, Harvard University Press, Cambridge, MA, 1976.
- [25] Characklis, W. G. and Marshall, K. C., *Biofilms*, John Wiley & Sons, Inc., NY, 1990.
- [26] Bryers, J. D., Ed., "Biofilms II: Processes Analysis and Applications," John Wiley & Sons, Inc., NY, 2000.
- [27] *Handbook of Bacterial Adhesion Principles, Methods and Applications*, Y. H. An and R. J. Friedman, Eds., Humana Press, Totowa, N.J., 2000.
- [28] DeBeer, D. P., Stoodley, P., Roe, F., and Lewandowski, Z., "Effects of Biofilm Structures on Oxygen Distribution and Mass Transport," *Biotechnology and Bioengineering*, Vol. 43, 1994, pp. 1131–1138.
- [29] Lewandowski, Z., Stoodley, P., and Roe F., "Internal Mass Transport in Heterogeneous Biofilms: Recent Advances," *Corrosion/95 Paper No. 222*, NACE, International, Houston, TX, 1995.
- [30] Hamilton, W. A. and Maxwell, S., "Biological and Corrosion Activities of Sulphate-Reducing Bacteria Within Natural Biofilms," *Proceedings, Biologically Induced Corrosion*, S. C. Dexter, Ed., NACE-8, National Association of Corrosion Engineers, Houston, TX, 1986, p. 131.
- [31] Lewandowski, Z., Roe, F., Funk, T., and Chen, D., "Chemistry Near Microbially Colonized Metal Surfaces," *Proceedings, Biocorrosion and Biofouling*, H. Videla, Z. Lewandowski, and R. Lutey, Eds., Buckman Laboratories Int., Memphis, TN, 1993, p. 52.
- [32] Xu, K., Dexter, S. C., and Luther, III, G. W., "Voltammetric Microelectrodes for Biocorrosion Studies," *Corrosion*, Vol. 54, No. 10, 1998, p. 814.
- [33] Pope, D. H., Zintel, T. P., Kuruvilla, A. K., and Siebert, O. W., "Organic Acid Corrosion of Carbon Steel," Paper 79, presented at Corrosion/88, NACE International, Houston, TX, 1988.
- [34] Pope, D. H., and Zintel, T. P., "Methods for Investigation of Underdeposit Microbiologically Influenced Corrosion," Paper 249, presented at Corrosion/88, NACE International, Houston, TX, 1988.
- [35] Chandrasekaran, P. and Dexter, S. C., "Factors Contributing to Ennoblement of Passive Metals Due to Biofilms in Seawater," *Proceedings, 12th International Corrosion Congress*, NACE International, Houston, TX, Vol. 5B, September 1993, p. 3696.
- [36] Dexter, S. C. and Chandrasekaran, P., "Direct Measurement of pH Within Marine Biofilms on Passive Metals," *Biofouling*, Vol. 15, No. 4, 2000, pp. 313–325.
- [37] Gaudy, A. and Gaudy, E., *Microbiology for Environmental Scientists and Engineers*, McGraw-Hill Book Co., NY, 1980, pp. 1–13.
- [38] Miller, J. D. A., *Microbial Aspects of Metallurgy*, American Elsevier, NY, 1970.
- [39] Hamilton, W. A., "The Sulphate-Reducing Bacteria: Their Physiology and Consequent Ecology," *Proceedings, Microbial Corrosion*, The Metals Society, London, U.K., 1983, p. 1.
- [40] Sharpley, J. M., "Microbiological Corrosion in Waterfloods," *Corrosion*, Vol. 17, 1961, p. 386t.



- [41] Dexter, S. C., "Localized Biological Corrosion," *Metals Handbook: Corrosion, Ninth Edition*, Vol. 13, American Society for Metals, Metals Park, OH, 1987, p. 118.
- [42] Dickinson, W. H. and Lewandowski, Z., "Manganese Biofouling and the Corrosion Behavior of Stainless Steel," *Biofouling*, Vol. 10, 1996, pp. 79-93.
- [43] Dickinson, W. H., Caccavo, F., and Lewandowski, Z., "The Ennoblement of Stainless Steel by Manganese Oxide Biofouling," *Corrosion Science*, Vol. 38, No. 8, 1996, pp. 1407-1422.
- [44] Linhardt, P., "Failure of Chromium-Nickel Steel in a Hydroelectric Power Plant by Manganese-Oxidizing Bacteria," Microbially Influenced Corrosion of Materials, Heitz, et al., Eds., Springer-Verlag, Berlin, 1996.
- [45] Olesen, B. H., Avci, R., and Lewandowski, Z., "Ennoblement of Stainless Steel Studied by X-ray Photoelectron Spectroscopy," *Corrosion/98 Paper No. 275*, NACE International, Houston, TX.
- [46] Renner, M. H. W., *Dechema Monogr.*, Vol. 133, 1996, p. 59.
- [47] Dexter, S. C., Xu, K., and Luther, III, G. W., "Mn Cycling in Marine Biofilms: Effect on Rate of Localized Corrosion," *Biofouling*, 2003, Vol. 19 (Supplement), pp. 139-149.
- [48] Ruppel, D. T., Dexter, S. C., and Luther, G. W., "Role of Manganese Dioxide in Corrosion in the Presence of Natural Biofilms," *Corrosion*, Vol. 57, No. 10, 2001, pp. 863-873.
- [49] Stoecker, J. G. and Pope, D. H., "Study of Biological Corrosion in High Temperature Demineralized Water," *Materials Performance*, Vol. 25, No. 6, 1986, p. 51.
- [50] Dexter, S. C., Duquette, D. J., Siebert, O. W., and Videla, H. A., "Use and Limitations of Electrochemical Techniques for Investigating Microbiological Corrosion," *Corrosion*, Vol. 47, No. 4, 1991, p. 308.
- [51] Mansfeld, F. and Little, B., "A Technical Review of Electrochemical Techniques Applied to Microbiologically Influenced Corrosion," *Corrosion Science*, Vol. 32, No. 3, 1991, p. 247.
- [52] Little, B. J. and Wagner, P. A., "Application of Electrochemical Techniques to the Study of MIC," Chapter 5, *Modern Aspects of Electrochemistry*, No. 34, J. O. Bockris, et al., Eds., Kluwer Academic/Plenum Publishers, NY, 2001.
- [53] Little, B. J., Wagner, P. A., and Mansfeld, F., "Microbiologically Influenced Corrosion," *Corrosion Testing Made Easy*, B. C. Syrett, Series Ed., Vol. 5, NACE International, Houston TX, 1997.
- [54] Salvarezza, R. C., de Mele, M. F. L., and Videla, H. A., "Mechanisms of the Microbial Corrosion of Aluminum Alloys," *Corrosion*, Vol. 39, No. 1, 1983, p. 26.
- [55] Eashwar, M. and Maruthamuthu, S., *Biofouling*, Vol. 8, 1995, pp. 203-213.
- [56] Dexter, S. C. and Maruthamuthu, S., "Response of Passive Alloys with N- and P-Type Passive Films to Manganese in Biofilms," *Corrosion/2001 Paper No. 01256*, NACE International, Houston, TX, 2001.
- [57] Little, B., Ray, R., and Wagner, P., et al., "Impact of Biofouling on the Electrochemical Behavior of 304 Stainless Steel in Natural Seawater," *Biofouling*, Vol. 3, 1991, p. 45.
- [58] Mansfeld, F., Tsai, R., Shih, H., et al., "Results of Exposure of Stainless Steel and Titanium to Natural Seawater," *Corrosion Science*, Vol. 33, No. 3, 1992, p. 445.
- [59] Dexter, S. C. and Zhang, H. J., "Effect of Biofilms on Corrosion Potential of Stainless Alloys in Estuarine Waters," *Proceedings, 11th International Corrosion Congress*, Florence, Italy, April 1990, p. 4.333.
- [60] Little, B., Gerchakov, S. M., and Udey, L. R., "A Method for Sterilization of Natural Seawater," *Journal of Microbiological Methods*, Vol. 7, 1987, pp. 193-200.
- [61] Starkey, R. L. and Wright, K. M., *Anaerobic Corrosion of Iron in Soil*, American Gas Association, NY, 1945.
- [62] Booth, G. H., *Microbiological Corrosion*, Mills and Boon, London, U.K., 1971.
- [63] Guillaume, I., Croissant, M., Grimadeau, J., et al., "Conditions d'immunité et de Corrosion de l'aluminium dans un Milieu Bactérien Doux et Marin (Conditions of Immunity and Corrosion of Aluminum in Fresh and Marine Bacterial Media)," *Corrosion Science*, Vol. 14, 1974, pp. 321-329.
- [64] Videla, H. A., "Mechanisms of MIC," *Proceedings, Argentina-USA Workshop on Biodeterioration*, H. A. Videla, Ed., Aquatec Química, A. A., São Paulo, Brazil, 1985, p. 43.
- [65] Scully, J. R., *Corrosion*, Vol. 56, 2000, pp. 199-218.
- [66] Shih, H. and Mansfeld, F., "Software for Quantitative Analysis of Polarization Curves," *Computer Modeling in Corrosion, ASTM STP 1154*, ASTM International, West Conshohocken, PA, 1992, pp. 174-185.
- [67] Stern, M. and Geary, A. L., "Electrochemical Polarization," *Journal of the Electrochemical Society*, Vol. 104, No. 1, 1957, pp. 56-63.
- [68] Little, B. J., Wagner, P., Characklis, J. W., and Lee, W., "Microbial Corrosion," *Biofilms*, J. W. Characklis and K. C. Marshall, Eds., John Wiley, NY, 1988, p. 635.
- [69] Obuekwe, C. O., Westlake, D. W. S., Flambeck, J. A., and Cook, F. D., "Corrosion of Mild Steel in Cultures of Ferric Iron Reducing Bacterium Isolated from Crude Oil, II. Mechanism of Anodic Depolarization," *Corrosion*, Vol. 37, No. 11, 1981, p. 632.
- [70] Castle, J. E., Parvizi, M. S., and Chamberlain, A. H. L., "Interaction of Marine Biofouling and Corrosion on Copper Based Alloys," *Proceedings Microbial Corrosion*, The Metals Society, London, U.K., 1983, p. 36.
- [71] Dowling, N., Guezennec, J., and White, D. C., "Methods for Insight into Mechanisms of Microbial Facilitation of Metal Corrosion," *Biodeterioration 7*, Elsevier Applied Science, Barking, Essex, U.K., 1988, pp. 404-410.
- [72] Kasahara, K. and Kajiyama, F., "Role of Sulfate Reducing Bacteria in the Localized Corrosion of Buried Pipes," *Proceedings, Biologically Induced Corrosion*, S. C. Dexter, Ed., NACE-8, National Association of Corrosion Engineers, Houston, TX, 1986, p. 171.
- [73] King, R. A., Skerry, B. S., Moore, D. C. A., et al., "Corrosion Behavior of Ductile and Grey Iron Pipes in Environments Containing Sulphate-Reducing Bacteria," *Proceedings, Biologically Induced Corrosion*, S. C. Dexter, Ed., NACE-8, National Association of Corrosion Engineers, Houston, TX, 1986, p. 83.
- [74] Nivens, D. E., Nichols, P. D., Henson, J. M., et al., "Reversible Acceleration of the Corrosion of AISI 304 Stainless Steel Exposed to Seawater Induced by Growth and Secretions of the Marine Bacterium *Vibrio Natriegens*," *Corrosion*, Vol. 42, No. 4, 1986, p. 204.
- [75] Mansfeld, F., Shih, H., Postyn, A., Deviny, J., Islander, R., and Chen, C., "Corrosion Monitoring and Control for Concrete Sewer Pipes," *Corrosion*, Vol. 47, 1991, pp. 369-376.
- [76] Keresztes, Z., Telegdi, J., Beczner, J., and Kalman, E., *Electrochim. Acta*, Vol. 43, 1998, pp. 77-85.
- [77] Booth, G. H. and Tiller, A. K., "Polarization Studies of Mild Steel in Cultures of Sulphate-Reducing Bacteria," *Transactions of the Faraday Society*, Vol. 56, 1960, pp. 1689-1696.
- [78] Booth, G. H., Elford, L., and Wakerley, D. S., "Corrosion of Mild Steel by Sulphate-Reducing Bacteria: An Alternative Mechanism," *British Corrosion Journal*, Vol. 3, 1968, pp. 242-245.
- [79] Costello, J. A., "Cathodic Depolarization by Sulfate Reducing Bacteria," *South African Journal of Science*, Vol. 70, No. 7, 1974, pp. 202-204.
- [80] Edyvean, R. G. J. and Terry, L. A., "Polarization Studies of 50D Steel in Cultures of Marine Algae," *International Biodeterioration Bulletin*, Vol. 19, No. 1, 1983, p. 1.
- [81] Westlake, D. W. S., Semple, K. M., and Obuekwe, C. O., "Corrosion by Ferric Iron Reducing Bacteria Isolated from Oil Production Systems," *Proceedings, Biologically Induced Corrosion*,



- S. C. Dexter, Ed., NACE-8, National Association of Corrosion Engineers, Houston, TX, 1986, p. 195.
- [82] Buchanan, R. A., Li, P., Zhang, X., et al., "Electrochemical Field Studies of Freshwater Microbiologically Influenced Corrosion," A Progress Report to the Electric Power Research Institute, Palo Alto, CA, December 1989.
- [83] Matoda, S., Suzuki, Y., Shinohara, T., and Tsujikawa, S., "The Effect of Marine Fouling on the Ennoblement of Electrode Potential for Stainless Steels," *Corrosion Science*, Vol. 31, 1990, pp. 515–520.
- [84] Bockris, J. O'M., Dahr, H. P., and Langham, L. R., "An Electrochemical Approach to the Prevention of Biofouling Phenomena," Final Report 14-34-0001-0446 to the U.S. Dept. of Interior, Bureau of Reclamation, Office of Water Research, 1983.
- [85] Dexter, S. C., Chandrasekaran, P., Zhang, H. J., and Wood, S., "Microbial Corrosion in Marine Environments: Effect of Microfouling Organisms on Corrosion of Passive Metals," *Proc., Biocorrosion and Biofouling*, H. Videla, Z. Lewandowski, R. Lutey, Eds., Buckman Laboratories, Int., Memphis, TN 1993, p. 171.
- [86] Zhang, H. J. and Dexter, S. C. "The Effect of Biofilms on Critical Pitting Potentials for Stainless Steels S30400 and S31600 in Seawater," *Proceedings, 1995 International Conference on Microbially Influenced Corrosion*, P. Angel, et al., Eds., NACE International, Houston, TX, 1995, p. 70/1.
- [87] Cottis, R. and Turgoose, S., "Electrochemical Impedance and Noise," *Corrosion Testing Made Easy*, B. C. Syrett, Series Ed., NACE International, Houston TX, 1997.
- [88] Mansfeld, F., Han, L. T., Lee, C. C., and Zhang, G., *Electrochim. Acta*, Vol. 43, 1998, pp. 2933–2945.
- [89] Mansfeld, F. and Shih, H., "Detection of Pitting with Electrochemical Impedance Spectroscopy," *Journal of the Electrochemical Society*, Vol. 135, No. 5, 1988, p. 1171.
- [90] Mansfeld, F., Hsu, C. H., Oernek, D., Wood, T. K., and Syrett, B. C., "Corrosion Control Using Regenerative Biofilms on Aluminum 2024 and Brass in Different Media," *Proceedings of New Trends in Electrochemical Impedance Spectroscopy and Electrochemical Noise Analysis*, F. Mansfeld, F. Huet, and O. Mattos, Eds., 2001, The Electrochemical Society, Proceedings, Vol. 2000-24, pp. 99–118.
- [91] Mansfeld, F., Lin, S., Kim, S., and Shih, H., *Materials Science Forum*, Vols. 44 & 45, 1989, pp. 83–95.
- [92] Mansfeld, F., Tsai, C. H., and Shih, H., "Software for Simulation and Analysis of Electrochemical Impedance Spectroscopy (EIS) Data," *Computer Modeling in Corrosion, ASTM STP 1154*, ASTM International, West Conshohocken, PA, 1992, pp. 186–196.
- [93] Lee, W., "AC Impedance and Microbial Corrosion," IPA Industrial Associates Report, Montana State University, Bozeman, MT, 1986, p. 2.
- [94] Isaacs, H. S., "Applications and Limitations of in situ Current Density Mapping," Paper 28, presented at Corrosion/89, National Association of Corrosion Engineers, Houston, TX, 1989.
- [95] Isaacs, H. S. and Ishikawa, Y., "Application of the Vibrating Probe to Localized Current Measurements," *Electrochemical Techniques for Corrosion Engineering*, R. Baboian, Ed., National Association of Corrosion Engineers, Houston, TX, 1986, p. 17.
- [96] Isaacs, H. S. and Vyas, B. "Scanning Reference Electrode Techniques in Localized Corrosion," *ASTM STP 727*, F. Mansfeld and U. Bertocci, Eds., ASTM International, West Conshohocken, PA, 1981, pp. 3–33.
- [97] Franklin, M. J., Isaacs, H. S., and White, D. C., "The Use of Current Density Mapping in the Study of Microbial Influenced Corrosion," NACE International, Houston, TX, 1990, p. 104.
- [98] Franklin, M. J., Guckert, J. B., White, D. C., and Isaacs, H. S., "Spatial and Temporal Relationships between Localized Microbial Metabolic Activity and Electrochemical Activity of Steel," Paper 115, presented at Corrosion/91, National Association of Corrosion Engineers, Houston, TX, 1991.
- [99] Franklin, M. J., Isaacs, H. S., and White, D. C., "Pitting Corrosion by Bacteria on Carbon Steel Determined by the Scanning Vibrating Electrode Technique," *Corrosion Science*, Vol. 9, pp. 945–952.
- [100] Franklin, M. J., White, D. C., Little, B. J., Ray, R. I., and Pope, R. K., *Biofouling*, Vol. 15, Nos. 1–3, 1999, pp. 13–23.
- [101] Rasmussen, H. and Jorgensen, B. B., *Marine Ecology Progress Series*, 81, 1992, pp. 289–303.
- [102] Revsbech, N., Sorensen, P. J., Blackburn, H. T., and Lomhoholt, J. P., *Limnol. Oceanogr.* 25, 1980, pp. 403–411.
- [103] Revsbech, N. P., Nielsen, L. P., Christensen, P. B., and Sorensen, J., *Applied Environmental Microbiology*, 54, 1988, pp. 2245–2249.
- [104] Revsbech, N. P., Christensen, P. B., and Nielsen, L. P., "Microelectrode Analysis of Photosynthetic and Respiratory Processes in Microbial Mats," *Microbial Mats*, Y. Cohen and E. Rosenberg, Eds., American Society for Microbiology, Washington, D.C., 1989.
- [105] Jorgensen, B. B., Cohen, Y., and Revsbech, N. P., *Applied Environmental Microbiology*, 51, 1986, pp. 408–417.
- [106] Alldredge, A. L. and Cohen, Y., *Science*, 235, 1987, pp. 689–691.
- [107] Lewandowski, Z., Lee, W. C., Characklis, W. G., and Little, B., *Corrosion/88* Paper No. 93, 1988, NACE International, Houston, TX.
- [108] Lewandowski, Z., *Corrosion/2000*, Paper No. 400, 2000, NACE International, Houston, TX.
- [109] Dickinson, W. H., Lewandowski, Z., and Geer, R. D., *Corrosion*, Vol. 52, 1996, pp. 910–920.
- [110] Brendel, P. J. and Luther, III, G. W., *Environ. Sci. Technol.*, Vol. 29, 1995, pp. 751–761.
- [111] Lee, W. and de Beer, D., *Biofouling*, Vol. 8, 1995, pp. 273–280.
- [112] Gray-Young, T., Hadjipetrou, L., and Lilly, M. D., "The Theoretical Aspects of Biological Fuel Cells," *Biotechnology and Bioengineering*, Vol. 8, 1966, pp. 581–593.
- [113] Little, B. J. and Wagner, P., "An Electrochemical Evaluation of Microbiologically Induced Corrosion by Two Iron-Oxidizing Bacteria," Paper 122, presented at Corrosion/86, National Association of Corrosion Engineers, Houston, TX, 1986.
- [114] Gerchakov, S. M., Little, B. J., and Wagner, P., "Probing Microbiologically Induced Corrosion," *Corrosion*, Vol. 42, No. 11, 1986, p. 689.
- [115] Little, B. J., Wagner, P., and Gerchakov, S. M., et al., "The Involvement of a Thermophilic Bacterium in Corrosion Processes," *Corrosion*, Vol. 42, No. 9, 1986, p. 533.
- [116] Little, B. J., Wagner, P., and Duquette, D., "Microbiologically Induced Cathodic Depolarization," Paper 370, presented at Corrosion/87, National Association of Corrosion Engineers, Houston, TX, 1987.
- [117] Iverson, W. P., "Transient Voltage Changes Produced in Corroding Metals and Alloys," *Journal of the Electrochemical Society*, Vol. 115, No. 6, 1968, p. 617.
- [118] Bertocci, U., Gabrielli, C., Huet, F., and Keddam, M., *Journal of the Electrochemical Society*, Vol. 144, 1997, pp. 31–37.
- [119] Bertocci, U., Gabrielli, C., Huet, F., Keddam, M., and Rousseau, P., *Journal of the Electrochemical Society*, Vol. 144, 1997, pp. 37–43.
- [120] Mansfeld, F., Lee, C. C., Chen, C., and Xiao, H., *Corrosion Science*, Vol. 38, 1996, pp. 497–513.
- [121] Mansfeld, F., Han, L. T., Lee, C. C., Chen, C., Zhang, G., and Xiao, H., *Corrosion Science*, Vol. 39, 1997, pp. 255–279.
- [122] Mansfeld, F., Sun, Z., Speckert, E., and Hsu, C. H., "Electrochemical Noise Analysis (ENA) for Active and Passive Systems," *Corrosion/2000*, Paper No. 418, NACE International, Houston, TX.

- [123] Mansfeld, F., Sun, Z., Hsu, C. H., and Naguib, A., *Corrosion Science*, Vol. 43, 2001, pp. 341–352.
- [124] Eden, D. A., "Electrochemical Noise—The First Two Octaves," *Corrosion/98*, Paper No. 386, NACE International, Houston, TX, 1998.
- [125] Iverson, W. P., Olson, O. J., and Heverly, L. F., "The Role of Phosphorous and Hydrogen Sulphide in the Anaerobic Corrosion of Iron and the Possible Detection of this Corrosion by an Electrochemical Noise Technique," *Proceedings, Biologically Induced Corrosion*, S. C. Dexter, Ed., NACE-8, National Association of Corrosion Engineers, Houston, TX, 1986, p. 154.
- [126] Iverson, W. P. and Heverly, L. F., "Electrochemical Noise as an Indicator of Anaerobic Corrosion," *Proceedings, Symposium on Nondestructive Testing and Electrochemical Methods of Monitoring Corrosion in Industrial Plants*, ASTM STP 908, ASTM International, West Conshohocken, PA, 1984, pp. 459–471.
- [127] Moosavi, A. N., Dawson, J. L., Houghton, C. J., and King, R. A., "Effect of Sulphate-Reducing Bacteria on Corrosion of Reinforced Concrete," *Proceedings, Biologically Induced Corrosion*, S. C. Dexter, Ed., NACE-8, National Association of Corrosion Engineers, Houston, TX, 1986, p. 291.
- [128] Little, B. J., Ray, R. L., Wagner, P. A., Jones-Meehan, J., Lee, C. C., and Mansfeld, F., *Biofouling*, Vol. 13, 1999, pp. 301–321.
- [129] Dawson, J. L., Hladky, K., and Eden, D. A., "Electrochemical Noise: Some New Developments in Corrosion Monitoring," U.K. National Corrosion Conference, Birmingham, U.K., 1983.
- [130] Cooper, G. L., "Proper Electrical Resistance Probe Span," *Electrochemical Techniques for Corrosion Engineering*, R. Baboian, Ed., National Association of Corrosion Engineers, Houston, TX, 1986, p. 327.
- [131] Streicher, M. A., "Analysis of Crevice Corrosion Data from Two Sea Water Exposure Tests on Stainless Alloys," *Materials Performance*, Vol. 22, No. 5, 1983, p. 37.
- [132] Dexter, S. C., "Effect of Biofilms on Crevice Corrosion," *Proceedings, Corrosion/96 Research Topical Symposium, Part II Crevice Corrosion*, J. W. Oldfield, and M. B. Ives, Eds., NACE International, Houston, TX, 1996, pp. 367–384.
- [133] Dexter, S. C., "Laboratory Solutions for Studying Corrosion of Aluminum Alloys in Seawater," *The Use of Synthetic Environments for Corrosion Testing*, ASTM STP 970, P. E. Francis and T. S. Lee, Eds., ASTM International, West Conshohocken, PA, 1988, p. 217.
- [134] Kester, D. R., Duedall, I. W., Connors, D. N., and Pytkowicz, R. M., "Preparation of Artificial Seawater," *Limnology and Oceanography*, Vol. 12, No. 1, 1967, p. 176.
- [135] Stevens, P., Genens, L., Thomas, A., et al., "OTEC Biofouling and Corrosion Study at the National Energy Laboratory of Hawaii, 1983–1987," ANL/ESD-10, Argonne National Laboratory, Argonne, IL, 1990.
- [136] Pope, D. H., Duquette, D., Wayner, P. C., and Johannes, A. H., "Microbiologically Influenced Corrosion: A State-Of-The-Art Review," MTI Publication No. 13, Materials Technology Institute of the Chemical Process Industries, Inc., Columbus, OH, June 1984.
- [137] *Manual of Methods for General Bacteriology*, P. Gerhardt, Ed., American Society for Microbiology, Washington, D.C., 1981.
- [138] Kemp, P. F., Sherr, B. F., Sherr, E. B., and Cole, J. J., *Handbook of Methods in Aquatic Microbial Ecology*, Lewis Publishers, Boca Raton, FL, 1993.
- [139] *Microbiologically Influenced Corrosion Testing*, ASTM STP 1232, J. R. Kearns and B. J. Little, Eds., ASTM International, West Conshohocken, PA, 1994.

# **Section VI: Materials Testing**

*E. L. Hibner, Editor*

# Zinc

*Frank E. Goodwin<sup>1</sup> and Safaa J. Alhassan<sup>1</sup>*

THE LARGEST USE OF zinc is as a protective coating for steel, and therefore corrosion tests and data [1,2], have been developed and widely used to describe its performance in specific situations or determine its usefulness for new applications. The corrosion resistance of zinc in cast or wrought form is less often a criterion for selection for a given application, although substantial published corrosion data on these product forms exist [2]. Another class of product, zinc anodes, is used to provide corrosion protection to iron and steel structures that are buried or immersed by simply making an electrical connection between the ferrous material and the anode. By this means, it is not necessary to provide a protective coating to the ferrous object. The use of a coating, however, reduces the current demand and extends anode life. Corrosion data for this application are also widely published [1].

Zinc-coated steel and monolithic zinc objects corrode similarly; a useful reference on the mechanism of corrosion of a galvanized coating is that of Daesen [3]. In dry air, a film of zinc oxide initially forms; however, the presence of moisture and carbon dioxide changes the corrosion product to a basic zinc carbonate film. Similarly, a dilute presence of sulfur compounds can result in a production of a basic sulfate film. Zinc oxide, basic zinc carbonate, and basic zinc sulfate are stable protective layers if left undisturbed; however, the pH of the environment can interfere with these layers, resulting in the formation of more soluble products. Because zinc forms an amphoteric oxide, both strong alkaline and acid conditions interfere with the formation of these protective layers. Attack is most severe at pH values below 6 and above 12.5. Within this range, corrosion is relatively slow.

Unalloyed zinc corrodes uniformly unless in contact with more cathodic materials, in which case a more localized galvanic corrosion can occur at the interface. In other cases, nonuniform corrosion is generally not encountered. Zinc alloys, particularly those with aluminum, can suffer from pitting and intergranular attack. This tends to be influenced by the fineness of the alloy microstructure.

The addition of aluminum to zinc is beneficial in improving its corrosion resistance and has resulted in development of coatings with aluminum contents between 5 and 55 %, like Galfan and Galvalume for hot dip and Zn-15 % Al alloy for thermal spray applications. In these coatings, the initial

surface layer formed is an aluminum oxide. Under humid conditions, additional corrosion products of aluminum and zinc hydroxides are formed as protective films. The addition of iron can improve the corrosion resistance of zinc in mildly acidic conditions, while copper additions up to 2 % can improve atmospheric corrosion by up to 20 % [1]. Lead was traditionally added to galvanized coatings to increase fluidity and produce a characteristic "spangle" solidification pattern. Segregation of lead to zinc grain boundaries, however, lowers corrosion resistance in comparison with pure zinc, especially in humid environments.

## GALVANIC PROTECTION

When zinc and steel are connected in the presence of an electrolyte, current flows from the zinc to the steel through the electrolyte so that the zinc becomes an anodic electron-producing area, while the steel is cathodic and electron-consuming. The zinc therefore corrodes in preference to the steel and in doing so protects the steel surface. This protection occurs with zinc anodes or with zinc coatings on steel surfaces subjected to cuts or scratches that expose the steel. Zinc's cathodic protection for steel depends upon the dimensions of the exposed steel and the coating thickness of the pure zinc layer. Scratches up to 5 mm wide and cut edges on galvanized parts up to 10 mm thick can be effectively protected by the surrounding zinc layer [1]. Under special situations in water immersion, zinc can become cathodic to steel; examples include immersion in fresh water between 60 and 90°C and 0.01M NaHCO<sub>3</sub> saturated with oxygen containing 1 % CO<sub>2</sub> at 65°C. In general, however, zinc is anodic to steel and is widely used for this property. There are a number of standard specifications for zinc-coated steels, while sacrificial anodes are covered by ASTM B 418, Specification for Cast and Wrought Galvanic Zinc Anodes. Application of zinc anodes is covered by BSI Code of Practice 7361, Part 1 (1991).

Zinc coatings are applied to steel by hot-dipping, electroplating, mechanical coating (i.e., tumbling in zinc dust at room temperature), sherardizing (i.e., tumbling in zinc dust just below the melting point of zinc), thermal spraying, and zinc-rich paints. The overwhelming tonnage of coatings is produced by hot-dip or electrogalvanizing processes. These coatings initially provide barrier protection, and then start to corrode sacrificially, therefore protecting the steel underneath.

<sup>1</sup>International Lead Zinc Research Organization, Inc., P. O. Box 12036, Research Triangle Park, NC 27709-2036.

Rolled zinc is produced as sheet, strip, plate, rod, and wire in numerous compositions and alloys. Sheet zinc for building uses contains copper and titanium and is covered by ASTM B 69, Specification for Rolled Zinc. Rolled zinc is also used for dry cell battery cans; however, composition and corrosion requirements for these are largely proprietary. Cast zinc is almost always in the form of zinc-aluminum-copper-magnesium alloys containing between 4 and 27 % aluminum. These alloys are covered by ASTM B 240 (Specification for Zinc Alloys in Ingot Form for Die Castings) and B 669 (Specification for Zinc Alloys in Ingot Form for Foundry and Die Castings).

The corrosion resistance of zinc can be improved by subsequent application of either conversion coatings or synergistic systems. In the former category are included processes such as zinc anodizing, using either phosphate-chromate-fluoride or silicate electrolytes to MIL-A-81801 (1971), and chromate conversion coatings. In the latter, the zinc surface is reacted to form a complex surface layer of chromium hydroxide, zinc hydroxychromate, and zinc chromate. Application of the chromate conversion coating is covered by ASTM B 201, Practice for Testing Chromate Coatings on Zinc and Cadmium Surfaces. Alternatives to chromating include phosphate, molybdate, silicate, and several organic coatings. Chromating is frequently found effective as an inhibitor against white rust. However, safety questions on chromate treatment tanks that contain sodium dichromate particularly with regard to spent solution disposal have been increasingly raised. Bans are already operating in some areas of Europe and North America. The issue of "white rust" is an important issue to galvanizers because it limits their market. White rust forms when freshly galvanized steel is exposed to water in the atmosphere in closely packed spaces. Zinc surfaces in this environment produce voluminous, bulky, and white deposits of zinc hydroxide/zinc oxide with thickness of the white rust layer of the order of 1000 Å. Zinc surfaces that already have a normal protective layer of corrosion products are seldom attacked. The protective layer on zinc consists of complex carbonate oxide films. Despite a considerable effort, researchers have yet to produce a direct replacement for sodium dichromate solution. The requirements for a chromate-free treatment are that it be nontoxic, water soluble, and environmentally safe, and that it maintain the original appearance, low cost, be easily painted over, and have an easy control and maintenance procedure.

Synergistic coatings include a variety of organic coatings applied by either coil coating or powder coating. If properly applied, the overall useful life of the organic coating-galvanized steel system will be longer than the sum of the lives of the individual components.

## SENSITIVITY TO PARTICULAR ENVIRONMENTAL FACTORS

In solutions with pH levels lower than 4.5, zinc reacts with hydrogen ions to produce zinc ions plus hydrogen gas. At pH values higher than 4.5, there is an insufficient supply of hydrogen ions to make this reaction significant and the rate of corrosion is controlled by the availability of oxygen diffusing

to the metal surface. Curves describing the effect of pH level have been published by Rotheli [4] for immersion corrosion and by Goodwin [5] for atmospheric corrosion.

In aqueous corrosion, the oxygen content of water is a controlling factor. Of other anions, chloride is the most corrosive to zinc in aqueous corrosion. The effectiveness of chloride becomes stronger as water softness increases and carbonate levels decrease; thus, a chloride content of 80 mg/L in soft water causes quite severe corrosion while in hard water no corrosion occurs, even with 700 mg/L chloride levels. Sulfate is less active than chlorides towards zinc. Nitrates are also fairly benign at normal levels. Hydrogen sulfide and other sulfides are sometimes produced by anaerobic decomposition of sulfur-containing organic matter in the water. Zinc is less sensitive to such waters than are copper and iron. Salts of metals more noble than zinc can sometimes be found in industrial waste streams. In these cases, the more noble metal will normally deposit onto the zinc, while an equivalent amount of zinc goes into solution. Small amounts of dissolved salts, such as copper, can set up local cells producing pits, while other salts can inhibit attack by sequestering corrosive species. Substances that form complexes with zinc but do not form protective films, such as salts of ammonia, may promote corrosion in water. Oxidizing salts may also stimulate attack under special conditions.

In aqueous corrosion, raising the temperature increases the dissolution of zinc in water. A marked increase occurs up to around 60°C followed, by a decrease at higher temperatures due to the decrease in oxygen supply and the formation of more compact and adherent scale. Intergranular corrosion of zinc casting alloys is a risk above 70°C in wet or humid conditions, such as in steam, when no protective layer can form and selective dissolution of the structure occurs. In hot hard waters, scale forms at water temperatures above 55°C. This scale has a coarse grain structure and does not adhere well to the zinc surface. Corrosion of the zinc occurs locally because of the discontinuities in the scale or local electrochemical action. Above 60°C, zinc usually becomes cathodic to steel; therefore, the steel will corrode to protect the zinc coating.

In air, sulfur dioxide is the most important contaminant to be considered. At relative humidities of 70 % or above, it usually controls the corrosion rate of zinc. Observed corrosion rates on atmospheric panels are much less than those calculated using available sulfur deposition levels from the atmosphere. This is related to washing of the panels by rain and an incomplete dissociation of hydrogen and zinc on the surface. Chlorides have far less effect on the atmospheric corrosion of zinc than sulfur. Results of tests in Nigeria indicated that an approximate linear relationship between corrosion rate and salinity. Appreciable corrosion, however, occurred only at sites very close to the sea [1]. Chloride corrosion in atmospheric exposures is usually accelerated because of the presence of sulfur gases, as occurs on the coast in highly industrial areas [1]. A similar situation exists for ammonia, which is usually found in high quantities near agricultural land and petrochemical plants. By itself, ammonia does not accelerate zinc corrosion, but it does react with atmospheric sulfur oxides to produce ammonium sulfate, which accelerates paint film degradation and zinc

corrosion. Ammonium can also react with NOX compounds to form ammonium nitrite and nitrate. Both compounds accelerate zinc corrosion, but to a much lesser extent than oxides of sulfur. Nitrogen oxides by themselves also increase the corrosion rate of zinc, but to a lesser extent than sulfur oxides. Atmospheric corrosion of zinc is roughly proportional to the time of wetness in a particular location, providing that the nature and quantity of environmental pollution does not change. Increasing temperature usually reduces the time of wetness, lowering the corrosion rate. Decreasing temperature can increase the time spent below the dew point of the surrounding atmosphere, increasing the time of wetness. Rain also increases time of wetness, but it can have an indirect beneficial effect by removing corrosive materials. Time of wetness is often in practice considered as the time when relative humidity exceeds 80 % and the temperature is above 0°C.

## SPECIFIC CORROSION PRACTICES

General approaches to a zinc corrosion testing program are described in the remainder of this chapter. A summary of tests and practices is provided in Table 1.

### Methods of Evaluation of Corrosion Damage

Under many situations, zinc corrosion is uniform in nature, while in other cases nonuniform or localized corrosion can occur. Overall determinations of corrosion mass loss in a galvanized coating can be made by “weigh-strip-weigh” methods such as described in ASTM G 1 (see Table 1) for zinc. This procedure dissolves some uncorroded zinc along with the corrosion products; correction procedures are given in the specification. It is also possible to electrolytically remove corrosion products using the procedure given in the same specification; however, electrolytic removal of corrosion products from zinc usually causes some of the zinc coating to be removed, especially in the case of zinc-aluminum coating alloys. Results from the “weigh-strip-weigh” method are reported as mass lost per unit area of coating. The results of this procedure can be validated, and further insights into the nature of corrosion obtained by metallographic cross sectioning of the corroded coating. Suitable etchants for preparing galvanized coatings are found in references such as Kehl [6].

Nondestructive determination of coating thicknesses can also be made by magnetic interference (like ASTM B 499 and ASTM E 376) or X-ray spectrometry (like ASTM B 568), provided that the measured surface is first cleaned to remove corrosion products that would otherwise result in measurement inaccuracies.

Impurities such as lead, tin, and cadmium are cathodic to zinc-aluminum alloys and can cause relatively rapid intergranular corrosion under humid conditions. The effects of these impurities are checked by humidity tests such as exposing test samples to saturated steam at 95°C for a period of ten days [1].

Nonuniform corrosion can be assessed using ASTM G 46. Cleaning procedures for examining specifications under this

procedure are covered by ASTM G 1. Pit density can be determined by the grid counting method noted in ASTM G 46. Metallographic examination allows for determination of pit depth and can allow determination of which coating constituents have actually been attacked.

## Tests for Specific Corrosion Types

### *Atmospheric Corrosion—Accelerated Tests*

The most widely used test to provide a rough determination of corrosion performance is the standard salt spray test, ASTM B 117. This is despite the fact that ASTM Committee B08, as early as 1943, confirmed that salt spray testing was a poor means of estimating coating performance and was especially unsuitable for coatings of a sacrificial nature. Despite this, the procedure continues to be widely used for manufacturing control purposes because of its simplicity and the availability of many results from this test for comparison. A better test for determining the behavior of galvanized coatings in a chloride-containing environment, such as for automotive applications where deicing salts are used or in marine environments, is a cyclic test such as that described by SAE J 2334 and Swedish Standard SS117211, Corrosion Tests in Artificial Atmosphere—Accelerated Outdoor Tests (1992). This test allows for simulation of a twelve-month outdoor test in a period of twelve weeks and is accomplished by artificial salting and other acceleration techniques along with outdoor exposure.

Accelerated simulation of industrial exposure environments can be carried out using the moist SO<sub>2</sub> test described in ASTM G 87. The concentration of sulfur dioxide gas used in this test will determine the degree of acceleration obtained relative to actual service. If past results using actual exposure sites are available to compare with accelerated test results, then some extrapolation is possible, provided that other variables do not change. Of these, the most important is likely the rate of sulfur oxide deposition on the exposure site that can be measured using ASTM G 91. One use of the sulfur dioxide ASTM G 87 test is to determine the location of any thin portions of the coating or pores. Such areas are the first to fail in this test. A more rapid test of such weaknesses or discontinuities, termed the Preece test, is covered by ASTM A 239. This test involves immersion of zinc-coated steel samples in a copper sulfate solution; however, continuous galvanized sheet products and all wire products are excluded from the ASTM A 239 test because of the additional forming undergone after coating. This test should only be used for materials that are coated after final forming operations; for other materials the sulfur dioxide ASTM G 87 test should be used. The endpoint of the Preece test is either the specified number of dips or the appearance of a bright adherent copper deposit where the zinc coating has been dissolved in its thinnest locations.

Accelerated tests such as ASTM B 201 are very useful in evaluating the quality of chromate films on zinc or zinc-coated surfaces. The test proceeds until white corrosion products have formed and should not be allowed to continue until red rust forms. Only the time to formation of “white rust” is relevant. The effects of impurities on the corrosion rate of zinc can be determined by humidity testing.

**TABLE 1**—Summary of standard tests and practices for evaluating zinc corrosion.

Standard Number	Description	Usage
ASTM G 1	Recommended Practice for Preparing, Cleaning and Evaluating Corrosion Test Specimens	Determines amount of corrosion loss on test samples by removing corrosion products.
ASTM B 499	Test Method for Measurement of Coating Thicknesses by the Magnetic Method: Nonmagnetic Coatings on Magnetic Basis Metals	Nondestructive measurement of coating thickness remaining after testing.
ASTM B 568	Test Method for Measurement of Coating Thickness by X-Ray Spectroscopy	Same as ASTM B 499.
ASTM G 46	Practice for Examination and Evaluation of Pitting Corrosion	Determines presence and density of pitting corrosion.
ASTM B 117	Test Method of Salt Spray (Fog) Testing	Most widely used accelerated test to determine general corrosion resistance of zinc coatings, particularly in marine and other salt-laden environments.
SS117211 (1992)	Corrosion Tests in Artificial Atmosphere-Accelerated Outdoor Tests	Twelve-month outdoor exposure test with artificial salting to determine general corrosion resistance.
ASTM G 87	Practice for Conducting Moist SO <sub>2</sub> Tests	Widely used accelerated test to determine corrosion resistance to industrial atmospheres.
ASTM G 91	Practice for Monitoring Atmospheric SO <sub>2</sub> Using the Sulfation Plate Technique	Determines rate of SO <sub>2</sub> deposition at corrosion site.
ASTM A 239	Test Method for Locating the Thinnest Spot in a Zinc (Galvanized) Coating on Iron or Steel Articles by the Preece Test (Copper Sulfate Dip)	Determines presence of discontinuities in zinc coatings.
ASTM B 201	Practice for Testing Chromate Coatings on Zinc and Cadmium Surfaces	Determines quality of chromate coatings by determining white rust resistance.
ASTM B 380	Methods of Corrosion Testing of Decorative Electrodeposited Coatings by the Corrodokote Procedure	Determines resistance to corrosion by chlorides.
ASTM G 92	Practice for Characterization of Atmospheric Test Sites	Gives information for comparison of results from one exposure site with others.
ASTM G 50	Practice for Conducting Atmospheric Corrosion Tests on Metals	Recommendations for locating test sites, constructing racks.
ASTM G 33	Practice for Recording Data from Atmospheric Corrosion Tests of Metallic-Coated Steel Specimens	Recommendations for recordkeeping practice for exposure programs.
ASTM G 31	Practice for Laboratory Immersion Corrosion Testing of Metals	Addresses issues relating to general immersion testing and its interpretation.
ASTM D 2688	Test Method for Corrosivity of Water in the Absence of Heat Transfer (Weight Loss Methods)	Determines water corrosivity by corrosion weight loss.
ASTM D 2776	Test Methods for Corrosivity of Water in the Absence of Heat Transfer (Electrical Methods)	Determines water corrosivity by solution conductivity.
ASTM G 61	Test Method for Conducting Cyclic Potentiodynamic Polarization Measurements for Localized Corrosion Susceptibility of Iron-, Nickel-, or Cobalt-Based Alloys	Determines susceptibility of named alloys to localized corrosion in immersion.
ASTM G 57	Method for Field Measurement of Soil Resistivity Using the Wenner Four-Electrode Method	Allows soil corrosion results to be compared with results of similar experiments.

The most effective test is termed "steam testing" and carried out at a temperature of 95°C. Samples are weighed and then placed in a cabinet for intervals up to several hundred hours. Samples are observed to undergo a mass gain in many cases after steam testing, which is usually related to the quantity of impurity elements in the zinc. This mass gain is caused by intergranular corrosion, with the formation of corrosion products occurring along zinc grain boundaries where impurities usually segregate.

Although originally intended for evaluation of nickel-containing decorative electroplated coatings, the Corrodokote test, ASTM B 380, has been used to qualify the performance of galvanized products for automotive applications. Apparently, the chloride ions introduced in this process provide a useful indication of automotive underbody performance for products such as tubing for containment of automotive fluids and other small components. The Corrodokote test applies a corrosive slurry to the

component to be tested, after which it is allowed to dry. Samples are then exposed to high humidity for a specific period of time.

#### *Atmospheric Corrosion—Extended Tests*

To determine suitability for service in atmospheric conditions, atmospheric exposure tests provide the most valid results, although testing time may be unacceptably long. Shorter test times are usually appropriate to detect defects in the coatings that usually appear quickly. Before beginning an atmospheric exposure program, sites should be characterized using the procedures described in ASTM G 92. The relevance of these characteristics to the intended service of the product should be carefully considered by suggesting sites with different characteristics to gain information for range of possible conditions. ASTM G 50 should also be referenced in locating test sites and specifying or constructing exposure racks for samples. As this specification notes, most published data on atmospheric corrosion of metals are based on an exposure angle of 30° from the horizontal facing south. ASTM G 33 describes recordkeeping methods that should be used for such long-term exposure tests.

#### *Immersion Corrosion—Accelerated Tests*

To simulate service of components that will be immersed in fluids, ASTM G 31 should be followed. This standard includes many precautions relating to how laboratory testing environments may differ from actual service. Issues such as immersion solution composition, temperature, aeration, velocity, and volume must be addressed thoroughly before the design of the test can be considered complete. For tests involving corrosion in water, two ASTM D 2688 and ASTM D 2776 should be referenced, which determine corrosivity by weight loss and electrical methods, respectively.

Many immersion tests based upon electrochemical principles can also be used to evaluate corrosion resistance. Most of these have been developed for automotive applications. For example, Dattilo [7] has developed a practice for measuring corrosion rates by Tafel line extrapolation and the polarization resistance technique. Value of the Tafel slopes and the corrosion currents can be compared for different coated products. The effects of the immersion medium employed can thus be determined. Electrochemical impedance measurements (e.g., ASTM G 106, Practice for Verification of Algorithm and Equipment for Electrochemical Impedance Measurements) are useful for determination of the rate of inhibition of corrosion. The frequency sweep with AC impedance measurements can passivate the electrode with an increasing product formation at intermediate reaction speeds. A key assumption is that observations at high frequency are also valid at low frequencies because of the high rate of zinc dissolution in acid environments [8]. ASTM G 61 describes a procedure for conducting cyclic potentiodynamic polarization on iron-, nickel-, and cobalt-based alloys. This test is also useful for determining susceptibility to localized corrosion such as pitting or crevice corrosion in zinc-coated steels, although all scratches or other cut surfaces exposing iron or steel to the solution

must be sealed so that only the zinc is exposed to the solution. ASTM G 61 could also be used to detect coating defects and holidays. For example, linear polarization techniques (like ASTM G 3) have been used to investigate the behavior of Zn and Zn + Al thermal spray coatings on steel.

#### *Soil Corrosion*

Corrosion in soil is largely influenced by soil chemistry. A summary of the characteristics and properties of soils is given in the National Bureau of Standards circular on underground corrosion [9]. There are over 200 soil types in the United States, categorized according to texture, color, and natural drainage. Physical properties of importance in corrosion are those of determining the permeability of the soil to air and water. Many chemicals are present in soils but those relevant to corrosion studies are those that are soluble in water. Analyses are usually made for base-forming elements such as sodium, potassium, calcium, and magnesium and for acid-formers such as carbonate, bicarbonate, chloride, nitrate, and sulfate. Electrical resistivity of the soil is determined by the nature and concentration of the ions formed by the chemical salts dissolved in the soil moisture. ASTM G 57 gives a method for measurement of soil resistivity. The U.S. Department of Agriculture Soil Conservation Service has developed a useful classification of soils that allows comparison between sites. Many galvanized samples buried in soil are also exposed to concrete, mortar, or plaster. Each of these substances attacks zinc, but the attack ceases after the materials have dried. However, the attack is sufficient to give a good bond [10–13]. Zinc is resistant to mildly alkaline conditions, unlike steel and aluminum, and thus is preferred for encasing of steel in concrete.

#### **Comparison of Corrosion Behavior among Zinc Coatings**

As noted before, the ASTM B 117 salt spray test is the most widely used accelerated test for determining coating performance even with its shortcomings, for manufacturing control purposes. The hours to a fixed fraction of red rust are widely accepted as a figure of merit, allowing comparison of different zinc coatings. Similarly the hours or cycles in accelerated sulfur dioxide tests such as ASTM G 87 are widely used to give accelerated information on the relative performance of zinc coatings in simulated industrial environments. These tests, and cyclic tests evolved from them, are the most widely used in providing comparative rankings of zinc coatings. Electrochemical tests are also used as screening techniques. A useful survey on applications of these techniques is given by Berke and Friel [14]. More detail is also provided in Chapter 7 of this manual.

#### **REFERENCES**

- [1] Porter, F. C., *Corrosion Resistance of Zinc and Zinc Alloys*, Marcel Dekker, NY, 1994.
- [2] Dale, C. and Nevison, H., "Corrosion of Zinc," *Metals Handbook*, Ninth Edition, Vol. 13, ASM International, Materials Park, OH, 1987, pp. 755–769.
- [3] Daesen, J. R., "Corrosion Resistance of Galvanized Coatings," *Second International Congress on Metallic Corrosion*, NACE, Houston, TX, 1965, pp. 686–705.



- [4] Rotheli, B. E., Cox, G. L., and Littreal, W. B., "Effects of pH on the Corrosion Products and Corrosion Rate of Zinc in Oxygenated Aqueous Solutions," *Metal Alloys*, Vol. 3, 1932, pp. 73–76.
- [5] Goodwin, F. E., "The Effect of Environmental Acidification on Atmospheric Corrosion of Zinc," *16th International Galvanizing Conference*, European General Galvanizers Association, London, 1991, pp. GH1/1–12.
- [6] Kehl, G. L., *Principles of Metallographic Laboratory Practice*, McGraw Hill, NY, 1949.
- [7] Dattilo, M., "Polarization and Corrosion of Electrogalvanized Steel—Evaluation of Zinc Coatings Obtained from Waste-Derived Zinc Electrolytes," *Journal of the Electrochemical Society*, Vol. 132, No. 11, 1985, pp. 2557–2561.
- [8] Troquet, M. and Pagetti, J., "Inhibition of Metallic Corrosion in an Acid Medium by Means of Phosphonium Salts: Zinc and Iron," (in German) *Werkstoffe und Korrosion*, Vol. 34, No. 11, November 1983, pp. 557–562.
- [9] Romanoff, M., *Underground Corrosion*, U.S. Government Printing Office for National Bureau of Standards, Washington, DC, Circular 579, 1957, 227 pp. (407 references).
- [10] A number of papers in *Corrosion and Corrosion Protection of Steel in Concrete*, *Proceedings of the International Conference on Corrosion and Corrosion Protection of Steel in Concrete*, R. N. Swamy, Ed., Sheffield Academic Press, Sheffield, 1994.
- [11] Fratesi, R., Moriconi, G., and Coppola, L., "The Influence of Steel Galvanization on Rebars Behaviour in Concrete," *Corrosion of Reinforcement of Concrete Construction*, C. L. Page, P. B. Bamforth, and J. W. Figg, Eds., SCI, London, 1996.
- [12] *Steel Corrosion in Concrete: Fundamental and Civil Engineering Practice*, A. Bentur, S. Diamond, and N. S. Berke, Eds., E & FN SPON, 1997, pp. 131–136.
- [13] Andrade, C., Arteaga, A., Lopez-Hombrados, C., and Vazquez, A., "Tests on Bond of Galvanized Rebar and Concrete Cured in Seawater," *Journal of Materials in Civil Engineering*, Vol. 13, No. 5, 2001, p. 319.
- [14] Berke, N. S. and Friel, J. J., "Applications of Electrochemical Techniques in Screening Metallic-Coated Steels for Atmospheric Use," *ASTM STP 866, Laboratory Corrosion Tests and Standards*, G. S. Haynes and R. Baboian, Eds., ASTM International, West Conshohocken, PA, 1985, pp. 143–158.

# Lead (and Alloys)

Safaa J. Alhassan<sup>1</sup> and Frank E. Goodwin<sup>1</sup>

## INTRODUCTION

LEAD IS A MEMBER OF Group IVB of the periodic table with two oxidation states ( $\text{Pb}^{2+}$  and  $\text{Pb}^{4+}$ ), but the chemistry of the element is dominated by  $\text{Pb}^{2+}$  ion. Lead has four isotopes with three of them being the ultimate decay products of uranium ( $^{238}\text{U}$  and  $^{235}\text{U}$ ) and, therefore, widely used in geological dating. The crystal structure of lead in solid form is face-centered cubic (FCC) with a lattice parameter of 4.95 Å at 20°C. Lead is a blue-gray metal with density (11.3 g/cm<sup>3</sup>) 50 % more than that of steel and four times that of aluminum. However, lead is malleable, soft, and melts at only 327°C, and therefore, readily cut and shaped into pipes and sheets since ancient times.

The total world consumption of refined lead in 2000 was 6 449 000 tonnes closely matching the total world production of refined lead in 2000, which was 6 630 000 tonnes. The total world production of primary lead in 2000 was 2 936 000 tonnes, meaning the balance of consumption was from recycled sources. The 3-month price for lead ranged between \$515.00 and \$419.00 per tonne [1]. The main ore deposit is galena,  $\text{PbS}$ , which contains an amount of silver and that adds economic value to ore deposits. Other lead deposits are in the form of sulfate and carbonate. Lead ranks fifth in tonnage consumed after iron, copper, aluminum, and zinc, but is rare in earth's crust where it ranks 34th among other elements.

The primary market for lead at the present time is in energy storage batteries, followed by the chemical, joining, and cable sheathing applications. About 95 % of the lead in spent batteries is recycled and used in new products. Lead can be used as cast, pipe, sheet, or as a thin protective coating for steel. A growing use of lead is in the manufacturing of seismic isolator (or earthquake dampers) for buildings. Several types of isolators are used, one of which is a lead rubber design combining bearing (support) and isolation (damping) functions. The isolator core is made of pure lead. Since the Hanshin (Kobe) earthquake of 1995, lead-containing seismic isolators have been used in Japan at an increasing rate with recent emphasis on residences and banks. In the USA, particularly California, bridge deck seismic isolation has also been increasingly used.

Inorganic lead compounds were used in paints and organic compounds in fuel to increase octane number, until concerns about lead's toxic properties arose. Lead is relatively opaque to ionizing radiation and is a valuable shielding material in X-ray applications and nuclear facilities. Another market for lead is in alloys that are used as solders in applications ranging from circuit boards to heat exchangers. Lead is also used in acoustic barrier panel, glassware and ceramic, and fiber optic cables.

## NATURAL PROTECTIVE FILMS

In a normal atmospheric exposure, a fresh lead surface will slowly be oxidized into a thin, protective lead oxide, which halts further oxidation of the metal. The rate of formation of lead oxide is determined by the absorption of oxygen and water vapor into the lead. Such factors as industrial and marine pollution, humidity, temperature, and rainfall profoundly affect the aggressiveness of the atmosphere, and most metals suffer accordingly. However, the protective films formed of lead are so effective that corrosion is insignificant in most natural atmospheres. The extent of this protection is demonstrated by the survival of lead roofing and auxiliary products after hundreds of years of atmospheric exposure that may continue for a much longer time if these films are not damaged [2].

The greatest value of lead is often in its very long service life and low maintenance costs, which when taken as part of an overall systems approach, often swings the materials selection choice balance in lead's favor, especially as labor costs continue to rise. Lead has an excellent record of service in three major types of environments: chemical, atmosphere, and underground. Resistance of lead to corrosion in contact with sulfuric acid has been critical in many chemical industries, like paper, plastics, petroleum, and photographic materials. Of particular importance in recent years has been the use of lead in the protection of devices for the removal of sulfur from industrial waste gases. Several industries, like ore roasting or burning of fossil fuels for power generation, produce large volumes of waste from which sulfur-containing species must be removed.

The current environmental regulations do not permit the use of lead in the drinking-water supply system, despite the excellent corrosion performance of lead and lead alloys in specific environments. This corrosion resistance is attributed to the formation of a strong, adherent, and impermeable

<sup>1</sup>International Lead Zinc Research Organization, P. O. Box 12036, Research Triangle Park, NC 27709-2036.

protective film that is stable or insoluble in these environments. Lead or lead-lined components continue to be used in the handling of alum used in industrial-water-treatment systems. Lead-sheathed cables have shown reliable long-term performance worldwide because of the extraordinary corrosion resistance of lead alloys to a variety of soils. Using lead-covered copper for grounding systems or in roofing has provided a superior performance in a variety of atmospheres around the world [3]. Lead with a small addition of bismuth is used in cable sheathing, while lead-calcium alloys are used in wire, pipe, anodes, and storage battery grid applications. Lead-copper alloys are of interest in cable sheathing and preferred by the chemical industry for its structural stability in handling sulfuric acid. Antimony additions increase hardness, tensile strength, and fatigue resistance, and such alloys are used in storage battery components. Lead-tin alloys are used in cable sheathing and as solders. A listing of lead alloys and their applications is reported in Ref 3.

## EFFECTS OF ALLOYING

There are four common grades of lead: pure lead, common lead, chemical lead, and acid-copper lead. These grades are covered by ASTM B 29-92, Standard Specification for Refined Lead. Pure lead and chemical lead contain 99.94 % minimum lead, while the latter two contain 99.9 % minimum. Typical impurities include Bi, Cu, Ag, Fe, Zn, Ni, Sn, and Sb [4]. Higher purity is also available in commercial quantities, like low bismuth low silver pure lead with 99.995 % minimum lead. However, because lead does not possess the level of required mechanical strength for material of construction, and in many cases, it is unable to support its own weight, alloys have been developed to improve its physical and mechanical properties, especially mechanical rigidity.

### Lead-Antimony

Lead alloy with 6 % antimony is frequently used in sheet and pipe forms for its superior strength and hardness over soft lead. Lead-antimony alloy is used to make battery plates. Antimony additions increase hardness, tensile strength, and fatigue resistance, and form alloys used in storage battery components.

### Lead-Tin

Lead-tin with lead-antimony alloys occupies the status of the most important alloy groups of lead. Pb-Sn alloys are used in cable sheathing, solders, or to wet steels [3]. Solders can contain between 50 and 95 % Sn and can be used for joining sheet metals for roofs, gutters, and downspouts. Pb-Sn solder has been used in joining copper radiators in the automotive industry and in the construction of other heat exchangers carrying fresh water with no significant galvanic corrosion. However, if a solder in the range of 10 to 25 % Sn has been used in radiator joints, movement during solidification should be avoided to prevent hot tearing in solders due to a wide freezing range [5]. Solders with 40–50 % Sn are widely used for general joining purposes. Furthermore,

solders with 60–63 % Sn are used most extensively in the electronic industries and sometimes with additions of silver to reduce dissolution of silver-based coatings. However, solders cannot be used in joining corrosion-resistant chemical equipment like tanks for photographic developers [2]. Pb-Sn coating used on steel is called "Terne" and contains 3–15 % Sn and is used to wet the steel, and therefore, allowing metallurgical bond formation between lead and steel. Painting of Terne further raises its resistance to corrosion in outdoor environments and makes it attractive to automotive industry for fuel tanks and small diameter tubing [5]. Other applications for lead-tin alloys are storage battery connectors, roofing, and type and bearing metal [4].

### Lead-Calcium

The addition of a small amount of calcium produces alloys of interest for wire, pipe, anodes, and storage battery grid applications. The addition of calcium to Pb-Sn alloys, and with proper processing, produces alloys with improved breaking strengths up to 75.8 MPa from 58.6 for the Pb-Sn binary alloy, due to a fine grain structure [4]. The corrosion resistance for Pb-Ca-Sn alloys is also higher than that of Pb-Sn in many applications.

### Lead-Copper

Lead-copper-tellurium alloys, up to commercial content of 0.08 % Cu and 0.04 % Te, are of interest in cable sheathing, and also in the chemical industry in handling sulfuric acid. Alloys containing copper have a superior mechanical strength due to grain growth inhibition and higher corrosion resistance than pure lead. Copper additions in the above range do not increase the corrosion rate of lead [4].

### Lead-Silver

Lead alloyed with silver shows excellent resistance to sulfuric acid. The addition of 1 % Ag produces alloy bars, extruded or cast, that are the excellent insoluble anodes with very good corrosion resistance over a wide range of current densities. Alloys with 1.5 % Ag and 1 % Sn are used as solders with high melting point [3].

## EFFECTS OF MICROSTRUCTURE

Since lead has a low melting point, lead based alloys can recover and recrystallize at room temperature, while high purity lead (99.99 %) may be subjected to grain growth at 25°C. The addition of elements, like Cu, Te, and Ca, to lead alloys is designed to inhibit grain growth. Grain growth can play an important role in intergranular corrosion, which can cause significant loss in strength [4].

## VARIOUS MILL PRODUCTS

As mentioned before, there are four common grades covered by ASTM B 29-92: pure lead, common lead, chemical lead, and acid-copper lead. Pure lead and common lead

contain 99.94 % minimum lead, while the latter two contain 99.9 % minimum, with Bi, Cu, Ag, Fe, Zn, Ni, Sn, and Sb being main impurities. Alloys with higher purity than 99.99 % are also available in commercial quantities. Corroding lead refers to a process that was formerly used, rather than to corrosion characteristic, and is another name for pure lead. This product is free of unwanted impurities and, therefore, is the most widely used grade of pure lead. Chemical lead is used in the chemical industry and contains small amounts of silver and copper, which increase the corrosion resistance and the mechanical strength of the grade. Common lead contains higher amounts of silver and bismuth than corroding lead and is used in battery oxide and general alloying. Acid-copper lead provides higher corrosion resistance than that of chemical lead in most applications that require corrosion resistance. Acid-copper is used in several types of fabricated lead products [4].

## GENERAL CORROSION OF LEAD

A fresh lead surface slowly oxidizes into a thin, protective lead oxide (PbO) that stops further oxidation of the metal. Lead gives satisfactory resistance to corrosion in rural, marine, and industrial environments. The corrosion rate data for lead is shown as 0.5–0.7  $\mu\text{m/y}$  in industrial (New York, NY), 1.2–2.2  $\mu\text{m/y}$  in marine (Kure Beach, NC), and 1.05–1.85  $\mu\text{m/y}$  in rural (State College, PA) [6]. Lead corrosion products in such environments, in addition to lead oxide, are sulfate, chloride, and carbonate, with lead chloride being the most soluble of all four products (see Table 1). However, lead in outdoor exposures was found to produce sulfate ( $\text{PbSO}_4$ ) and/or carbonate ( $\text{PbCO}_3$ ), and indoor exposures lead carboxylates. The primary atmospheric agents responsible for degradation of lead are  $\text{SO}_2$ ,  $\text{CO}_2$ , and carboxylic acid [7]. The corrosion rate of chemical lead in Key West, Florida, and La Jolla, California is 0.58 and 0.53  $\mu\text{m/y}$  (0.023 and 0.021 mpy), respectively [2].

Because of the toxicity of lead salts, lead should not be used to handle drinking water. The corrosion rate of lead is generally quite low in a wide variety of water environments, with major exceptions found in some pure waters containing oxygen and in soft natural water where contamination is an issue. Natural waters with hardness greater than 125 ppm calcium carbonate form protective films, and therefore, attack on lead is negligible. Certain salts, like silicate salts, enhance the resistance of lead to corrosion by water

because of its effect on water hardness and film formation [2]. In contrast, nitrate and chloride ions interfere with film formation and, thus, increase corrosion rates. The corrosion rate of lead is high in underground waters if they contain organic acids or carbonic acid. Furthermore, lead usually has low corrosion rates in seawater with influencing factors like flow, wave action, sand or silt content, temperature, and marine growth.

Lead has high corrosion resistance to chromic, sulfurous, sulfuric, and phosphoric acids and is widely used in their manufacture and handling, e.g., lining material for acid precipitators. Lead is not suitable for very dilute strengths of sulfuric acid [2] because lead does not develop protective film under these conditions.

Lead is a relatively active metal and is oxidized at the anode, and either enters the solution at the anodic sites as metallic cations or forms solid insoluble compound films. The reaction at the anode could be represented by:



The standard oxidation potential ( $E^\circ$ ) makes lead cathodic to most common metals like iron, aluminum, zinc, magnesium, and cadmium, but anodic to copper and silver. As a cathode, lead accelerates corrosion of steel, aluminum, and zinc. The cathodic reaction accompanying the lead dissolution is either the reduction of oxygen in neutral solutions or reduction of hydrogen ions in acid solutions. In the case of lead and its alloys, the physical characteristic of the film formed at the anode is the rate-determining step; therefore, the corrosion rate of lead is under anodic control. Furthermore, impurities in lead, especially Fe and Zn, which are anodic to Pb, can precipitate and segregate at the grain boundary. Therefore, it is important to keep Fe and Zn content to a minimum to avoid dissolution of their precipitates and subsequent strength loss due to grain boundary weakening. In contact with titanium and passivated stainless steels, lead itself would suffer accelerated corrosion. The formation of a protective film extends over a wide range of pH in aqueous solutions, except at very high and very low pH levels, which include both very weak and very strong sulfuric and phosphoric acids. The extent of protection depends on the compactness, adherence, and solubility of these films. The solubility of various lead compounds in water at room temperature, as shown in Table 1, is an indicator of the behavior of lead in solutions that promote the formations of these compounds. A comprehensive list of corrosion rates of lead in a variety of chemical environments

TABLE 1—Solubility of lead compounds [1].

Lead Compound	Formula	Temperature, °C	Solubility, g/100 mL $\text{H}_2\text{O}$
Acetate	$\text{Pb}(\text{C}_2\text{H}_3\text{O}_2)_2$	20	44.3
Carbonate	$\text{PbCO}_3$	20	0.00011
Chlorate	$\text{Pb}(\text{ClO}_3)_2 \cdot \text{H}_2\text{O}$	18	151.3
Chloride	$\text{PbCl}_2$	20	0.99
Chromate	$\text{PbCrO}_4$	25	0.0000058
Fluoride	$\text{PbF}_2$	18	0.064
Hydroxide	$\text{Pb}(\text{OH})_2$	18	0.0155
Nitrate	$\text{Pb}(\text{NO}_3)_2$	18	56.8
Oxalate	$\text{PbC}_2\text{O}_4$	18	0.00016
Oxide	$\text{PbO}$	18	0.0017
Sulfate	$\text{PbSO}_4$	25	0.00425
Sulfide	$\text{PbS}$	18	0.01244
Sulfite	$\text{PbSO}_3$	—	Insoluble

is given in Ref 2, and reported in Ref 4 as well, in which the corrosion data is divided into four categories. Categories A and B are environments where the corrosion rate is less than 0.05 and 0.5 mm/y (2 and 20 mpy), respectively, and in both cases lead is considered resistant and, therefore, recommended for use. Category C is for environments where corrosion rate is between 0.5 and 1.25 mm/y (20–50 mpy) and lead can be used if the effect of corroded lead can be tolerated. Category D is for environments where corrosion rate is more 1.25 mm/y (50 mpy) and lead is not recommended.

## SENSITIVITY TO PARTICULAR ENVIRONMENTAL FACTORS

The corrosion rate of lead in soils rich in sulfates or silicates is low, but in soils containing organic acids the rate might be higher than that of steel. Furthermore, lead-sheathed cable installed in continuous concrete ducts in concrete tunnels under waterways was found to be severely corroded [5]. That was because the seepage water was found to contain 1000 ppm of hydroxide ion (mainly from incompletely cured concrete), and the ducts were designed without the removal of seepage water. The use of completely cured, impervious concrete in ducts with proper drainage is the suggested remedy.

### Acidity/Alkalinity

Being amphoteric, lead can be susceptible to attack by both acids and alkalis under certain conditions. However, the formation of protective film extends over a wide range of pH in aqueous solutions, except at a very high and very low pH level, which includes very weak and very concentrated sulfuric and phosphoric acids. Lead is used commercially in equipment to handle sulfuric, sulfurous, chromic, and phosphoric acids in commercially used concentrations. However, lead is less resistant in hydrochloric and hydrofluoric acids. For example, lead is suitable to handle concentrated  $\text{H}_2\text{SO}_4$  up to less than 95 % strength at room temperature. Lead use in sulfuric acid depends on the protectiveness of its sulfate film with velocity limit up to 1 m/s. The protectiveness of a lead compound is directly related to its solubility in that specific environment. Lead sulfate is more soluble in water than in sulfuric acid. Even in the latter, the solubility of  $\text{PbSO}_4$  changes with acid concentration and temperature and reaches a minimum at  $\text{H}_2\text{SO}_4$  concentrations of 30–60 % at medium temperatures (25–50°C), resulting in a negligible corrosion. Furthermore, adding sulfuric acid to acids corrosive to lead will often lower the corrosion rate. Nitric acid of less than 50 % strength is quite corrosive to lead, while in presence of 54 % sulfuric acid, the corrosion rate for 1 and 5 % nitric acid is quite low, even at 118°C [2]. Lead has fair corrosion resistance to dilute hydrochloric acid up to 15 % at room temperature, with corrosion rate increasing as temperature and acid concentration increase. However, field experience has not been good, because of soluble corrosion products that can easily wash away. The presence of 5 % ferric chloride accelerates the acid attack

and doubles the corrosion rate. Lead has also a good corrosion resistance in dilute hydrofluoric acid (up to 10 %) at low temperature, given that the acid is air-free. Addition of sulfuric acid to hydrofluoric acid reduces the corrosion rate of lead as well.

In caustic solutions the use of lead is generally limited to concentrations of no more than 10 % up to 90°C. Little attack is seen in cold, strong amines, while dilute aqueous solutions will result in attack of lead. Lead can be attacked by calcium hydroxide solutions at room temperature, including solutions that have been in contact with fresh cement. The attack by caustic solutions also depends on several variables like temperature, concentrations, and aeration [4]. The influence of increasing additions of nitrate on the anodic features of lead in alkaline solutions was investigated [8]. The addition of 0.1–1.5 M sodium nitrate was found to enhance the anodic dissolution of lead in 0.1–1.5 M NaOH solutions and that the critical potential decreased linearly with logarithmic concentration of nitrate and temperature. Increasing the alkaline concentration increased the pitting potential. Originally, in nitrate-free alkaline solution,  $\text{PbO}$  was formed and the current density decreased, and there was no evidence of pitting.

### Soil

Soils vary widely in physical and chemical characteristics and, consequently, in their corrosive effect. More than 200 varieties of soil in the United States have been classified according to texture, color, and natural drainage. The physical properties of soils that are of most interest in corrosion are those that influence the permeability of soil to air and water. Lead can corrode less than steel and more than copper. Lead has been used in sheathing of underground cable for its resistance in soil. The corrosion resistance of Pb and Pb-Sb sheathing alloys depends upon the presence of silicate, carbonate, and to a lesser extent sulfates, which contribute to passive film formation. There is evidence that silicate and carbonate ions exert a marked inhibitive influence on corrosion of lead in soil. However, lead alloys might suffer from stray current effects due to street railways and can corrode rapidly in soils that contain some organic acids. Organic acid vapors, like acetic acid from wooden ducts for lead-sheathed cables or wood under lead roofing, have been the cause of corrosion in lead. Douglas fir and oak are known to give such vapors, while hemlock and cedar are not. However, and in general, test results indicate that corrosion in soil decreases with increasing particle size, and the average corrosion rate of lead in most soils is low and ranging from 2.5 to 10  $\mu\text{m}$  (0.1 to 0.4 mil) per year [2]. However, the depth of pitting is often a more important measure of corrosion in soil than the rate of general corrosion, as in the case of applications like cable sheathing.

### Salts and Gases

If lead is resistant to an acid, then it generally can resist the corresponding salt as well. Nitrates, for example, are corrosive and, therefore, cannot be handled with lead. Hydrochloric acid is corrosive to lead and so are most chlorides. Lead can be used with chlorine up to 100°C, wet or dry.

Gases of sulfur oxides can be handled in lead pipes. Hydrogen sulfide, on the other hand, can cause erosion to lead at high velocities. Furthermore, hydrogen fluoride is corrosive and, therefore, lead cannot be used with it.

## METHODS OF EVALUATION OF CORROSION DAMAGE

The procedures in ASTM G 1, Preparing, Cleaning, and Evaluating Corrosion Test Specimens, can be used in preparing bare, solid metal specimens for tests, for removing corrosion products after the test has been completed, and for evaluating the corrosion damage that has occurred. The chemical cleaning of lead and lead alloys for corrosion product removal suggests the use of either 10 mL of acetic acid in 990 mL of water for 5 min at boiling temperature, or 50 g of ammonium acetate in 1 L of water for 10 min at 60–70°C. A concentrated solution of 250 g of ammonium acetate in 1 L of water for 5 min can also be used at 60–70°C.

To simulate service of components that will be immersed in fluids, ASTM G 31, Practice for Laboratory Immersion Corrosion Testing of Metals, should be followed. This standard includes many precautions relating to how laboratory testing environments may differ from actual service. Issues such as immersion solution composition, temperature, aeration, velocity, and volume must be addressed thoroughly before the design of the test can be considered complete. For tests involving corrosion in water, two ASTM specifications relating to determination of water corrosivity should be referenced, D 2688, Test Method for Corrosivity of Water in Absence of Heat Transfer (Weight Loss Methods), and D 2776, Test Methods for Corrosivity of Water in Absence of Heat Transfer (Electrical Methods), which determine corrosivity by weight loss and electrical methods, respectively. The corrosion rate of lead and lead alloys by electrochemical method can be evaluated by using ASTM Standard G 102, Calculating of Corrosion Rates and Related Information from Electrochemical Measurements. This standard is intended to provide guidance in calculating mass loss and penetration rates for alloys. However, since the standard involves the conversion of electrical currents into mass loss rates or penetration rates, the calculations can be complicated for alloys and metals with elements having multiple valence values.

### Galvanic

Lead is cathodic to most elements but anodic to highly alloyed materials, and that could lead to galvanic corrosion. The effect of galvanic corrosion on lead or by lead on other metals immersed in an electrolyte can be evaluated by using ASTM Standard G 71, Conducting and Evaluating Galvanic Corrosion Tests in Electrolytes, and G 82, Development and Use of a Galvanic Series for Predicting Galvanic Corrosion Performance. In the latter standard, a list can be developed that arranges materials according to observed corrosion potentials in environment of interest. The metal that suffers increased corrosion in a galvanic couple can then be predicted from the relative position of the two metals in the

series. Precaution should be taken in the use of the galvanic series because environmental changes can reverse the galvanic positions of the two metals. For example, when lead is galvanically connected to a copper or a copper alloy in  $\text{H}_2\text{SO}_4$ ,  $\text{H}_2\text{CrO}_4$ , or  $\text{H}_3\text{PO}_4$  solution, lead is protected by a firm film, even though lead is considered the anode in the galvanic cell. However, corrosion of Monel (e.g., UNS N04400) will be accelerated if coupled with lead in 6 %  $\text{H}_2\text{SO}_4$  solution [5].

### Salt Spray

In seawater, lead may form oxide, chloride, carbonate, and chloride hydroxide as corrosion products. Only carbonate can protect lead from further corrosion. Furthermore, waters with hardness less than 125 ppm as calcium carbonate can cause significant corrosion. Therefore, the combination of soft water and sodium chloride can lead to significant corrosion to lead coatings. ASTM B 117, Salt Spray (Fog) Testing, can be used to evaluate the suitability of lead coatings in atmospheres containing salt spray or splash. This is an accelerated test in which time is reduced by exposing the specimens continuously to conditions which in service would arise only intermittently. It has been widely observed, however, that rankings of different alloys or coating systems do not fall in the same order as atmospheric tests in marine or road splash environments.

### Soil

As mentioned before, soil is a physically, chemically, and biologically complex system. Factors that affect corrosion in soil, in addition to specific ions, are resistivity of soil, oxygen content, and acidity. Field measurements of soil resistivity are covered in ASTM G 57, Method for Field Measurement of Soil Resistivity Using the Wenner Four-Electrode Method, which is the most widely used test, and using the proper meter produces accurate and reproducible results. Conducting field measurements of soil pH is covered in ASTM G 51, Test Method for pH of Soil for Use in Corrosion Testing. The corrosion resistance of lead and its alloys depends mainly upon the presence of silicate, carbonate, and to a lesser extent sulfates, in contributing to the passive film formation.

## LEAD IN ENERGY STORAGE BATTERIES

The main use of lead, with more than 70 % of the lead produced, is in the manufacturing of lead-acid batteries. It is hard to imagine a transportation industry today without lead-acid batteries. The total capacity of electrical energy storage of these batteries far exceeds any other competing devices. Lead-acid batteries are currently used in the electric vehicle (EV) to reduce air pollution. The relatively low cost and availability of raw materials, room-temperature operation, ease of manufacturing, long cycle life, versatility, and excellent reversibility of the electrochemical system make lead-acid batteries very attractive compared with other systems. Lead-acid cells have extensive use both as portable power sources for automobile service and traction and in

stationary applications ranging from small emergency supplies to load-leveling systems. Based on the application, there are three main types of batteries, namely SLI (starting, lighting, and ignition), industrial (traction and stationary), and small sealed portable batteries [3], with capacities ranging from 2 Wh to 40 MWh. The lead-acid battery system consists of negative electrodes of porous lead and positive electrodes of lead dioxide ( $\text{PbO}_2$ ) in a solution of sulfuric acid. Both electrodes form lead sulfate ( $\text{PbSO}_4$ ) on discharge, with a free-energy change of  $-372.6 \text{ kJ/mol}$  and standard potential of 1.93 V. Corrosion phenomena in a lead-acid battery occur during cyclic discharging and recharging. It is important to design grid so that corrosion on the positive grid is uniform. Very fine grain sizes promote a uniform corrosion morphology. Various alloys are used to make grids, including pure lead, Pb-Sn (0.5–6 % Sn), and Pb-Ca alloys. Pb-Sn alloys are widely used because of their higher strength compared with pure lead. However, antimony decreases hydrogen overvoltage. Grids made of lead-calcium alloys are widely used in batteries in the automotive industry in what is known as maintenance-free batteries over a normal service life. These batteries have smaller amounts of antimony; therefore, the amount of hydrogen and oxygen evolution is reduced. Lead-acid batteries are now completely recyclable.

## LEAD IN THE ENVIRONMENT

Health hazards posed by lead are a concern, and lead and its compounds should be handled with recommended precautions. Information on occupational protection in the workplace and publications on lead in architectural applications, in solders, and in batteries are available from the lead industry.\* Lead has been eliminated from applications like paint, gasoline, and water pipeline joints, in which lead recovery and recycling is difficult or human contact cannot be avoided. The toxic properties of lead have been known since the Roman period. When lead is released into the environment, it has a long residence time compared with most other pollutants. As a result, lead and its compounds tend to accumulate in surface soils and sediments where, due to their solubility and relative freedom from microbial degradation, they will remain accessible to the food chain and human consumption far into the future. Lead can reach the human body through the digestive system by entering the food chain (plant roots and leaves, canned food, cooking utensils), or through contaminated drinking water. Lead can also be inhaled (car exhausts, paint dust).

Lead runoff from outdoor surfaces was investigated, and it was found that lead corrosion products at unpolluted marine (in Albany) and unpolluted rural sites (in Newport) are composed of lead carbonate and lead hydroxy carbonate [9]. The average Pb concentration in the runoff, once the corrosion film was developed, was 2.1 mg Pb/L for both

sites. The steady-state Pb runoff rates were  $0.26 \mu\text{m Pb/y}$  for unpolluted marine and  $0.36 \mu\text{m Pb/y}$  for unpolluted rural site.

In most of the applications in which the use of lead is increasing and in which lead is expected to be used, the lead and its alloys have minimal contact with the user. The lead in these applications is expected to be recycled. However, the users must be aware of the health effects of lead absorption in the body [3]. Lead in the environment is regulated in different parts of the world, and there has been a significant increase in the public awareness on the health effects associated with lead exposure, particularly concerning young children. The current environmental regulations do not permit the use of lead in the drinking-water supply system. The World Health Organization stated that it intends to revise its guideline value for lead in water from 50 to  $10 \mu\text{g/L}$ , while the U.S. Environmental Protection Agency (EPA) proposed a lower level of  $5 \mu\text{g/L}$ . The EPA's air quality standards call for  $1.5 \mu\text{g/m}^3$  for lead averaged over 90 days. The U.S. Centers for Disease Control (CDC) guideline indicates that average blood lead in preschool children of  $10 \mu\text{g}$  of lead per dL (dL equal to 100 mL) of blood ( $10 \mu\text{g/dL}$ ) is a level of concern. However, the CDC does not recommend specific action, unless and until a blood lead value of 15–19  $\mu\text{g/dL}$  is reached [3]. The average blood-lead level among children has dropped in the U.S. from a national average of over  $30 \mu\text{g/dL}$  in the 1930s to an average level in 1994 of about  $2.7 \mu\text{g/dL}$ , according to the CDC.

## REFERENCES

- [1] International Lead and Zinc Study Group, *Lead and Zinc Statistics*, International Lead and Zinc Study Group, London, Vol. 41, No. 2, March 2001.
- [2] Lead Industries Association, *Lead for Corrosion Resistance Application-A Guide*, Lead Industries Association, New York, 1974.
- [3] Guruswamy, S., *Engineering Properties and Applications of Lead Alloys*, Marcel Dekker, New York, 2000.
- [4] Goodwin, F. E., "Lead and Lead Alloys," *Uhlig's Corrosion Handbook*, 2nd ed., New York, NY, 2000.
- [5] Smith, J. F., "Corrosion of Lead and Lead Alloys," *ASM Handbook, Corrosion*, Vol. 13, 6th ed., ASM International, 1998.
- [6] Cook, A. R. and Smith, R., "Atmospheric Corrosion of Lead and Its Alloys," in *Atmospheric Corrosion*, W. H. Ailer, Ed., Wiley, NY, 1982, p. 393.
- [7] Graedel, T. E., "Chemical Mechanisms for the Atmospheric Corrosion of Lead," *Journal of the Electrochemical Society*, Vol. 141, No. 4, pp. 922–927, April 1994, with excerpts in *Atmospheric Corrosion*, C. Leygraf and T. E. Graedel, Eds., Wiley, NY, 2000, pp. 295–304.
- [8] Abd El Rehim, S. S. and Mohamed, N. F., "Passivity Breakdown of Lead Oxide in Alkaline Nitrate Solutions," *Corrosion Science*, Vol. 40, No. 11, 1998, pp. 1883–1896.
- [9] Matthes, S. A., Cramer, S. D., Covino, B. S. Jr., Bullard, S. J., and Holcomb, G. R., "Precipitation Runoff from Lead," *Outdoor Atmospheric Corrosion, ASTM STP 1421*, Townsend, H. E., Ed., ASTM International, West Conshohocken, PA, 2002, p. 265.

\*Lead Industries Association, 13 Main Street, Sparta, NJ 07871; web site address, [www.leadinfo.com](http://www.leadinfo.com).

# Magnesium (and Alloys)

James E. Hillis<sup>1</sup>

## THE CORROSION CHARACTERISTICS OF MAGNESIUM AND MAGNESIUM ALLOYS

### Overview

THE USE OF MAGNESIUM METAL has grown significantly in recent years, averaging 7 % annually for the past six years. Its major applications include use in the production of aluminum alloys; for magnesium die cast alloys; in iron desulfurization for the production of high strength steels; in graphite nodularization for production of ductile iron; in the metal reduction industry—primarily for zirconium and titanium production; in chemical applications for the production of pharmaceuticals, organometallics, and silicone compounds; in electro-chemical applications—primarily as anodes for cathodic protection of ferrous metal structures; for magnesium wrought products, and for magnesium gravity cast parts. The three largest applications—aluminum alloying, die cast magnesium alloys, and iron desulfurization—accounted for almost 90 % of the total world-wide market of 367,000 metric tons in 2000 [1,2].

The discussion that follows deals with magnesium and its alloys in cast and wrought forms, but it may be noted that the discussion often focuses on the die cast alloy. This is mainly due to the fact that in 2000 die cast alloy accounted for roughly 90 % of all alloys produced and 30 % of the overall world-wide market for magnesium. The die cast market has experienced double-digit annual growth rates in North America and Europe over the past decade, a result of increasing use in automotive applications for weight reduction and enhanced performance. This growth is projected to continue well into the coming decade [2,3].

### Nature of Protective Films

With few exceptions, magnesium exhibits good resistance to corrosion at normal ambient temperatures, unless there is significant water content in the environment in combination with certain contaminants. The reaction, which typically occurs, is described by the equation



In neutral and alkaline environments the magnesium hydroxide product can form a surface film that offers considerable

protection to the pure metal or its common alloys. Electron diffraction studies of the film formed in humid air indicate that it is amorphous, with the oxidation rate reported to be less than 0.01  $\mu\text{m}/\text{yr}$  (0.0004 mpy). If the humidity level is sufficiently high, so that condensation occurs on the surface of the sample, the amorphous film is found to contain at least some crystalline magnesium hydroxide (brucite). On immersion in deionized water, weight loss studies indicate that the crystalline hydroxide formed is also protective at room temperature and that aeration of the water has little or no measurable effect. However, as the water temperature is increased to 100°C the protective capacity of the film begins to erode, particularly in the presence of certain contaminants in either the metal or the water [4,5].

In extended atmospheric exposures of magnesium and magnesium alloys, the reaction of the magnesium hydroxide with acid gases ( $\text{CO}_2$  and  $\text{SO}_2$ ) has been reported to play an important role in the stability and composition of the film present. X-ray diffraction analysis of the oxidation products present on unalloyed magnesium ingot revealed it consists of a mixture of crystalline hydroxycarbonates of magnesium: hydromagnesite [ $\text{MgCO}_3 \cdot \text{Mg}(\text{OH})_2 \cdot 9\text{H}_2\text{O}$ ], nesquehonite [ $\text{MgCO}_3 \cdot 3\text{H}_2\text{O}$ ], and lansfordite [ $\text{MgCO}_3 \cdot 5\text{H}_2\text{O}$ ]. In the case of a common commercial wrought alloy, AZ31B (magnesium, 3 % aluminum, 1 % zinc, 0.2 % manganese), analysis of the adherent corrosion product by X-ray diffraction revealed only two crystalline phases—hydromagnesite and hydrotalcite [ $\text{Mg}_6\text{Al}_2(\text{OH})_{16}\text{CO}_3 \cdot 4\text{H}_2\text{O}$ ]. In an industrial atmosphere with high  $\text{SO}_2$  content, traces of  $\text{MgSO}_4 \cdot 6\text{H}_2\text{O}$  and  $\text{MgSO}_3 \cdot 6\text{H}_2\text{O}$  were detected, in addition to the hydroxycarbonate products for unalloyed ingot. It was suggested that  $\text{SO}_2$  exposures accelerate the corrosion of magnesium through the conversion of the protective hydroxide and carbonate compounds to the highly soluble sulfate and sulfite, which are then eroded [4,6].

### Alloys and Compositional Effects

Table 1 lists some of the common commercial alloys of magnesium, plus two developmental alloys, AE42 and AJ52, along with their nominal compositions. The alloys, described in accordance with ASTM B 275, Practice for Codification of Certain Nonferrous Metals and Alloys, Cast and Wrought, can be generally classified as belonging to either the aluminum or zirconium families. These two elements play the critical role of nucleating the formation of magnesium grains during solidification such that reasonably fine

<sup>1</sup>Magnesium Technical Specialist, NORANDA MAGNESIUM, INC., Franklin, TN 37067.



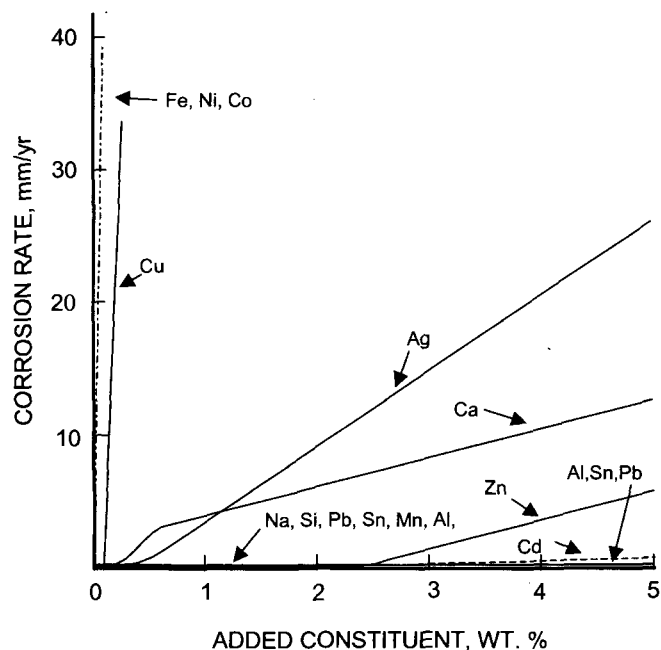
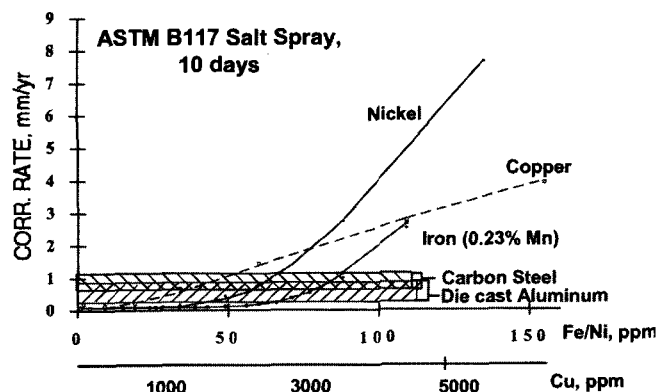
**TABLE 1**—Magnesium alloys and their nominal compositions.

Alloy Designation	Alloyed Elements, Nominal %								Product Form <sup>c</sup>
	Al	Zn	Mn	Ag	Zr	RE <sup>b</sup>	Y	Sr	
AE42X <sup>d</sup>	4	...	0.2	...	...	2	...	...	C
AJ52X <sup>d</sup>	5	...	0.4	...	...	...	...	2	C
AJ62X <sup>d</sup>	6	...	0.4	...	...	...	...	2	C
AM50A	5	...	0.4	...	...	...	...	...	C
AM60A, B	6	...	0.2	...	...	...	...	...	C
AZ31B, C, D	3	1	0.2	...	...	...	...	...	W, A
AZ61A	6	1	0.2	...	...	...	...	...	W
AZ63 A, B, C, D	6	3	0.2	...	...	...	...	...	C, A
AZ80A	8	0.5	0.2	...	...	...	...	...	C, W
AZ91B, C, D, E	9	1	0.2	...	...	...	...	...	C, W
EZ33A	...	2.5	...	...	0.5	2.5	...	...	C
M1C	...	...	1	...	...	...	...	...	W, A
QE22A	...	...	...	2.5	...	2	...	...	C
ZE41A	...	4.5	...	...	0.5	1.5	...	...	C
ZE63A	...	5.5	...	...	0.5	2.5	...	...	C
ZK40A	...	4	...	...	0.5	...	...	...	C, W
ZK60A	...	6	...	...	0.5	...	...	...	C, W
WE43A	...	...	...	...	0.5	3	4	...	C
WE54A	...	...	...	...	0.5	4	5	...	C

<sup>a</sup> For complete details see ASTM-B 80, B 90, B 93, B 94, B 107, or B 843.<sup>b</sup> Total Rare Earth content.<sup>c</sup> C-casting, W-wrought products, A-anodes for cathodic protection.<sup>d</sup> A developmental alloy; see Reference 11 or 14.

grain structures are produced, providing good mechanical properties, while simultaneously imparting no deleterious effects on the corrosion properties of the alloys. The aluminum content employed varies from 3 to 10 %, depending upon the product form and the properties desired. The zirconium alloys consistently employ about 0.5 % zirconium, which is near the solubility limit at normal metal processing temperatures.

Magnesium alloys have a reputation for poor corrosion performance, particularly in saltwater exposures. In large part, this is due to a lack of control, historically, of the

**FIG. 1**—Corrosion rates of magnesium binary alloys determined in alternate immersion testing in 3 % sodium chloride [7].**FIG. 2**—Effect of iron, nickel, and copper contaminant levels on ASTM B 117 salt spray corrosion rates in AZ91 alloy versus cold-rolled steel and 380 die cast aluminum [10, 19].

contaminant content. The importance of metal composition in determining the susceptibility to saltwater attack has been recognized for more than 50 years; however, the first complete definition of the compositional limits needed for common commercial alloys was only first accomplished in the mid 80s [8,9]. In 1942, Hanawalt et al. published a summary of the effects of 14 separate elements on the saltwater corrosion performance of magnesium (Fig. 1) [7]. Six elements (aluminum, manganese, sodium, silicon, tin, and lead) were identified as having a negligible effect at concentrations exceeding their solid solubility or up to 5 %. (In addition to these elements, thorium, zirconium, beryllium, cerium, praseodymium, and yttrium have also been found to have little or no effect [4].) Four elements (silver, calcium, zinc, and cadmium) had moderate effects, and four elements (iron, nickel, copper, and cobalt) were found to have severely degrading effects.

Of the four elements with degrading effects, three are common contaminants of standard commercial alloys: iron, nickel, and copper. It is these elements that, in large part, led to magnesium's poor reputation for saltwater corrosion durability. When these elements are controlled at levels lower than established limits (referred to as "tolerance limits") for a specific alloy composition, the saltwater corrosion rates may be reduced by more than 100-fold based on accelerated corrosion testing per ASTM B 117, Test Method for Salt Spray (Fog) Testing. Figure 2 illustrates the effect of reduced levels of iron, nickel, and copper on the corrosion rates of high pressure die cast AZ91 alloy, versus cold-rolled carbon steel and 380 die cast aluminum alloy [8,9].

Table 2 summarizes the known contaminant tolerance limits for the common commercially die cast alloys of magnesium plus the recently published tolerance limits for the developmental alloy AE42 [11]. As may be noted in Table 2, while the tolerance limits for nickel and copper are essentially independent of the alloy composition, within its normal

**TABLE 2**—Contaminant tolerance limits for cast alloys.

Element	AZ91 [9]	AM50 [10]	AM60 [55]	AS41 [58]	AE42 [11]
Iron (@ 0.2 % Mn)	64	32	42	20	40
Nickel	50	35	30	40	200
Copper	400	170	100	200	1000

limits the iron tolerance is directly dependent upon the specific level of manganese present in the alloy [9,10]. This is thought to be due to the formation of an electrochemically compatible, ternary intermetallic of iron, aluminum, and manganese on solidification  $[\text{Al}_5(\text{Fe-Mn})_2]$ , as opposed to the formation of the binary intermetallic,  $\text{Al}_3\text{Fe}$ , known to be an active cathodic phase relative to the magnesium matrix. While the manganese was recognized by Hanawalt et al. [7] to have a passivating effect on the nickel and copper contaminants, its passivating effect on iron in aluminum alloys was only recently recognized [9,12]. It was previously assumed that the manganese alloying addition was effective only through the precipitation of the iron contaminant from alloy melts prior to casting [13]. In addition to the beneficial effects of manganese, Hanawalt et al. [7] also published data indicating that zinc additions to magnesium or magnesium-aluminum alloys were beneficial in controlling the detrimental effects of nickel, copper, and iron contamination through increasing the alloy's tolerance limit for the contaminants.

In generating the tolerance limit data for the developmental alloy AE42, it was recognized that rare earth elements, in this case misch metal (the naturally occurring mixture of approximately 50 % cerium, 25 % lanthanum, 18 % neodymium, and 7 % praseodymium), also enhance the alloy's tolerance for each of the critical contaminants but most notably for nickel and copper [11]. Despite the good corrosion performance and elevated temperature properties of the AE42, the alloy has not seen commercial application since its introduction in 1990. Several new alloy compositions based on Al-Sr-Mn (e.g., AJ52), or a combination of Al-Ca-Mn-Sr, have recently been proposed for elevated temperature applications. While these alloys have been demonstrated to possess corrosion resistance equivalent to existing commercial high purity alloys, the effect of strontium and calcium on tolerance limits for the critical contaminants has yet to be reported [14–16].

In principle, the aluminum-containing alloys of magnesium should all be capable of providing corrosion performance competitive with that established for high-purity alloys AZ91D and AZ91E in die cast and sand cast applications (i.e., <0.25 mm/yr (10 mpy) in ASTM B 117 salt spray), if the critical contaminants are controlled at appropriate levels [9,17].

While the zirconium alloys should also be capable of providing competitive performance, many of these alloys possess zinc or silver contents at levels above that identified as detrimental to the alloys performance (Fig. 1); therefore, one should expect somewhat reduced corrosion resistance from these alloys, although the performance is typically better than that associated with the magnesium-aluminum alloys of the past with high contaminant levels. Of those zirconium alloys listed in Table 1, the WE43 alloy (as well as its forerunner WE54), with only yttrium and rare earth elements in addition to the zirconium, provides the best corrosion durability [17]. One advantage of the zirconium alloys is that the zirconium content strongly limits the solubility of the iron contaminant in the melt phase prior to casting, so that the purity of the alloys with respect to this detrimental element is naturally enhanced [18].

In addition to the cast and wrought alloys of magnesium used for structural applications, several alloys are used for cathodic protection of ferrous metal structures primarily in

underground applications, but also as in internal anodes for the protection of glass-lined water heaters. The alloys used are identified in Table 1 by the "A" designation. ASTM B 843 covers the specifications for these alloys, and ASTM G 97 describes the test method used in determination of anode performance, which is dependant on both the trace contaminant content and metallurgical factors.

## Effects of Metallurgical Treatments

The effects of grain refining and heat treatment, or temper, on standard purity AZ91C and high-purity AZ91E sand cast alloy were evaluated using salt spray testing [9]. Sand cast aluminum alloys of magnesium are commonly employed in one of four tempers: F—as cast, T4—solution-treated (condition of maximum ductility), T6—solution-treated and artificially aged (condition of maximum strength), or T5—artificially aged (condition of improved strength and dimensional stability); see ASTM B 661, Practice for Heat Treatment of Magnesium Alloys. Table 3 compares the ASTM B 117 salt spray performance of the alloys versus temper and grain size. The only significant difference in contaminant levels between the AZ91C and AZ91E alloys was the iron content, and this was the dominant factor in determining the corrosion performance obtained, although the best high-purity performance was obtained with samples in the aged T5 or T6 tempers, as may be noted. The critical iron, nickel, and copper contaminant tolerance limits have also been defined as a function of temper and reported in Refs 12 and 46.

The accelerated corrosion associated with cathodic contaminants occurs typically in the form of severe pitting, uniformly distributed over the exposed part surfaces, both cast and machined. It has been suggested that this attack is due to the segregation or precipitation of the contaminant phase within the alloy matrix. However, attempts to correlate the corrosion severity associated with the samples used in establishing the tolerance limits for AZ91 with the precipitate phases found within the microstructure using electron microscopy were not successful [8,9]. This may indicate that the "segregation" that occurs is a partitioning of the contaminant between the  $\alpha$ -magnesium phase and the aluminum-rich eutectic phase, as opposed to the precipitation of a discrete phase. This would appear to be consistent with the fact that microscopy studies of corroded magnesium samples reveal the attack occurs on the  $\alpha$ -phase within the individual grains, while the aluminum-rich grain boundary phase remains unaltered in the early stages of attack [12,21].

Highly localized pitting attack can be catalyzed by the presence of discrete phases within the microstructure; however, these are not introduced through the segregation of

**TABLE 3**—ASTM B 117 Corrosion performance of AZ91 versus temper, grain size, and iron-manganese content [9,10].

Alloy	Grain Size, $\mu\text{m}$	Mn %	Ratio Fe:Mn	Temper/Corrosion Rate, mm/yr			
				F	T4	T6	T5
AZ91C	187	0.18	0.087	18	15	15	...
AZ91C	66	0.16	0.099	17	18	15	...
AZ91E	146	0.23	0.008	0.64	4	0.15	0.12
AZ91E	78	0.26	0.008	2.2	1.7	0.12	0.12
AZ91E	160	0.33	0.004	0.35	3	0.22	0.12
AZ91E	73	0.35	0.004	0.72	0.82	0.1	0.1

the contaminants on solidification, but rather through the suspension of contaminants in molten metal processing and casting operations. Such contaminants are often associated with flux-oxide inclusions, which serve as suspension agents in the molten metal processing and casting operations, and later in the cast objects serve as a source of electrolyte when exposed to humid air. Such inclusions produce active localized corrosion cells on the magnesium surface. This may occur with both cast and wrought alloys; however, it is most commonly encountered on machined surfaces of sand cast alloys and often involves the iron-manganese-aluminum or the zirconium-iron intermetallic precipitates, which tend to associate with the suspended flux-oxide phase. The introduction of SF<sub>6</sub>-air-CO<sub>2</sub> gas mixtures for the control of magnesium oxidation in casting operations, however, has served to reduce the frequency of such failures [22,23]. The high global warming potential of SF<sub>6</sub> (23 900 times that of CO<sub>2</sub>), however, has recently brought pressure on magnesium producers and processors to find a new alternative for the control of melt oxidation. An industry-sponsored project has recently produced several promising alternatives, these include SO<sub>2</sub>, HFC-134a, and other fluorocarbons with low environmental impact [24,25].

### Magnesium Mill Products

As with magnesium cast alloys, the dominant type of general corrosive attack is of a pitting character. This can be catalyzed by the presence of the same critical contaminants already discussed—iron, nickel, and copper at the parts per million level within the alloy matrix—or by the presence of cathodic contaminants on the material surface. The surface contaminants could be imbedded contaminants from a blast operation, such as sand or steel shot blasting, or due to charred lubricants used in rolling, forging, or impact extruding the component. The surface contaminants can be readily removed by common surface cleaning methods such as sanding, abrading, or acid pickling. Typically, mill products are acid pickled and oiled prior to shipping or storage to protect against the surface contaminant effects.

Intergranular attack of magnesium mill products has not been a common mode of corrosive attack for the commercial alloys. An exception noted by Loose [5] was magnesium, 14 % lithium, 2 % aluminum alloy sheet, which suffered an intergranular layer attack similar to the exfoliation attack of aluminum-copper alloys. The 14 % lithium alloy adopts the body-centered cubic lattice structure of lithium over that of the magnesium and, consequently, possessed very high ductility. Unfortunately, the difficulty of handling the highly reactive alloy in the molten state, combined with a loss of ductility with aging, led to its demise as a commercial alloy some years ago.

### Stress-Corrosion Cracking and Corrosion Fatigue

Pure magnesium can be considered immune to stress-corrosion cracking (SCC) in both atmospheric and aqueous environments, with no reported failures occurring when loaded to its yield strength [5,26].

Aluminum containing alloys of magnesium are generally considered the most susceptible to SCC, with the tendency

increasing with the aluminum content. Thus the alloys AZ61, AZ80, and AZ91 with 6, 8, and 9 % aluminum, respectively, can show high susceptibility to SCC in laboratory and atmospheric exposures, while AZ31, a 3 % aluminum alloy used in wrought product applications, is considered to show good resistance [19,27,28].

Magnesium-zinc alloys such as ZK60 and ZE41 that are alloyed with zirconium, or zirconium and rare earth elements are typically considered only mildly susceptible, while magnesium alloys containing no aluminum or zinc are the most SCC-resistant. Thus, M1 alloy, a 1 % manganese alloy, like unalloyed magnesium itself, shows no evidence of SCC when placed under tensile stresses as high as its yield strength [5,8].

In controlled laboratory exposures it has been shown that SCC occurs only when the relative humidity exceeds 85–98 % with O<sub>2</sub> or CO<sub>2</sub> additions slightly accelerating the rate [29,30]. In atmospheric exposures rainfall, dew, and high humidity have been reported to accelerate SCC of magnesium alloys, with failures often occurring during the drying period following a rain [28,30]; yet a comparison of identical materials in rural, industrial, and seacoast exposures has produced nearly identical results, suggesting that SCC severity is not necessarily associated with the corrosivity of the environment [5,31]. To date, standard and preferred procedures for the evaluation of SCC in magnesium alloys have not been established.

In aqueous exposures, only strong alkalis, concentrated hydrofluoric acid, and chromic acid are considered not to induce SCC in magnesium alloys [5]. In other exposures from deionized water to a wide variety of aqueous salt solutions SCC failures have been observed in full, partial, or alternate immersion [32]. The most severe acceleration of failures has been found to occur with NaCl + K<sub>2</sub>CrO<sub>4</sub> solutions, which have been used in many laboratory studies of magnesium SCC; however, the results have been found to correlate poorly with service experience [28,31,33].

Both transgranular and intergranular crack propagation have been reported for magnesium alloys; however, transgranular failures with significant secondary cracking, or branching, are the most common mode of failure. Of the many mechanisms proposed over the years, hydrogen embrittlement is best supported by experimental evidence such as:

- Crack initiation and propagation are accompanied by hydrogen evolution;
- Immersion in a cracking solution before the stress is applied produces a fracture similar to a SCC fracture;
- The effect of pre-immersion in a cracking solution is reversed by vacuum annealing or exposure to room temperature air;
- Testing in gaseous hydrogen results in the same crack characteristics produced in aqueous solution test [34,40].

As with other metals, the control of magnesium SCC failures has involved the control of the three factors required for SCC to occur: the long-term tensile stress above a critical level, a susceptible alloy, and a SCC inducing environment. In practice, this has been interpreted as designing to continuous loads of 30–50 % of the yield stress and employing finishes that serve as effective corrosion barriers, combined with the selection of less susceptible alloys where feasible. Design precautions should also include limiting the stresses imparted in bolting and riveting

components together, and the use of heat treatments to relieve the stresses induced by welding [32,41].

The recent review by W. K. Miller, cited in Ref 22, provides an excellent summary of the published SCC literature on magnesium and magnesium alloys and provided the basis for the preceding summary.

Magnesium alloys in die cast and wrought forms, unlike some nonferrous alloys, show marked fatigue limits in dry air. In corrosive environments such as water or saltwater exposures the results have been less clear. For example, in a recent study the bending fatigue limit for AM50 die cast alloy (bending yield 142 MPa) was found to be 105 MPa in both air and seawater, but when tested in tap water or deionized water no endurance limit was found at stresses as low as 70 MPa. In contrast, testing on AZ91 die cast material (bending yield 164 MPa) in the same laboratory produced a fatigue limit of 110–115 MPa in air, but when tested in seawater the fatigue limit was significantly degraded, with failures still occurring at a stress of 70 MPa. Tests conducted with tap water, 3.5 % NaCl, and deionized water all produced very similar results to those generated in seawater [42]. In a separate study of die cast and wrought alloys roller burnishing was found to consistently produce superior results in both air and 3.5 % NaCl exposures, but the fatigue limits established for both AZ91 and AM50 in air in the roller burnished condition were still well below those established in the preceding study [43]. In a third recent study roller burnishing was again found beneficial to the fatigue performance of AZ31 and AZ80 alloys, but interestingly the burnished AZ31 alloy demonstrated very similar behavior in both air and 3.5 % NaCl with the data suggesting a fatigue limit of 110–120 MPa in both exposures [44].

In earlier studies Loose [5] summarized data for AZ61A and AZ31A sheet subjected to plate bending at 1500 cycles/min in both a dry air exposure and in a 0.01 % sodium chloride spray. At  $10^7$  cycles the observed fatigue strength was 103 MPa and 117 MPa (15 and 17 ksi), respectively, in air versus 34 MPa and 40 MPa (5.0 and 5.8 ksi), respectively, in the salt spray. In a summary by Bothwell [4] it was related that AZ31 subjected to an axial load cycled at  $10^5$  cycles/h in air, and then subjected to increasing levels of humidity showed a slow decrease in the fatigue strength once the humidity exceeded 50 %. At 93 % relative humidity, the measured fatigue strength had declined to about 75 % of that in dry air, or about 124 MPa (18 ksi), while in condensing humidity the strength was 89 MPa (13 ksi). Interestingly, in total immersion in deionized water or deionized water saturated with magnesium hydroxide the fatigue strength was reported to be 124 MPa (18 ksi). This improvement in the fatigue strength was suggested as due to the reduced exposure to atmospheric carbon dioxide in the total immersion environment.

As with SCC the effects of the environment on corrosion fatigue have been found to be mitigated by painting the components with a suitable organic coating [4,19,42].

## SENSITIVITY TO ENVIRONMENTAL FACTORS

### Acidity/Alkalinity

The chemical resistance of magnesium and magnesium alloys is typically considered opposite to that of aluminum and

its alloys. Magnesium resists attack by alkaline substances, but is attacked by acids, while aluminum is attacked by alkalis but has reasonable resistance to attack by mild acids. There are two notable exceptions to magnesium's lack of resistance to acids, and these are chromic ( $\text{H}_2\text{CrO}_4$ ) and hydrofluoric (HF) acids. In both cases the resistance is the result of the formation of insoluble protective films. Consequently, both acids are employed in formulations for pretreatments for painting and surface anodize treatments [19,42]. While pure chromic acid has a very limited affinity for metallic magnesium, it will readily dissolve magnesium hydroxide corrosion products. Consequently, a boiling solution of 20 % chromic acid is commonly used for the removal of magnesium corrosion products for refinishing parts as well as for establishing weight loss corrosion rates in the laboratory.

The strong alkalinity of the natural hydroxide film on magnesium means there is little tendency for the compound to give up a proton to strong alkalis; consequently, the film provides excellent protection even in strong hot alkali solutions that would readily attack aluminum or zinc alloys. Hot 10 % caustic or caustic plus alkali metal phosphate solutions maintained at a pH of 11–13 or more are the preferred cleaning solutions for magnesium castings and extrusions [19,42]. The protective capacity of the magnesium hydroxide film at high pH apparently overwhelms the effects of impurities in both the metal and aqueous media. Loose [5] points out that the measured corrosion rate for magnesium in 4 % aqueous NaCl solution is 0.31–0.62 mm/yr (12–50 mpy) at 35°C, while in 48 % caustic solution with the same 4 % NaCl content the corrosion is only 0.02–0.04 mm/yr (0.8–1.2 mpy). Magnesium's resistance to alkali attack combined with the metal's light weight has made it the preferred material for cement finishing tools for many years.

### Specific Ions/Salts

Salt solutions vary in their corrosivity to magnesium. Alkali metal or alkaline-earth metal (chromates, fluorides, phosphates, silicates, vanadates, or nitrates) cause little or no corrosion. Chromates, fluorides, phosphates, and silicates in particular are frequently used in the chemical treatment and anodizes for magnesium surfaces, due to their ability to form somewhat protective films [19,42–44]. Alkali or alkaline-earth metal (chlorides, bromides, iodides, and sulfates) will normally accelerate the corrosion of magnesium in aqueous solutions. Ammonium salts usually show greater activity than the alkali metal salts, apparently due to the somewhat high acidity of these salts. Practically all heavy metal salts are likely to cause corrosion, since magnesium will normally displace heavy metals from solution due to its high chemical activity. Such displaced metals may tend to plate on the magnesium surface and provide cathodic sites for galvanic corrosion [5,19]. There is at least one notable exception to this anticipated activity of heavy metal salts and that is iron phosphate solutions. Iron phosphates react to form surfaces suitable for paint application. Even parts treated or baked at elevated temperatures (300–400°F) show no evidence of active heavy metal deposits, even on high purity alloys [42,43]. This is consistent, however, with the ability of phosphate systems to sequester or strongly complex metal ions at moderate to high pHs.

## Elevated Temperature

Magnesium's corrosion performance in pure water is strongly dependent on temperature. In distilled water the corrosion rate of AZ61 alloy is reported to increase from less than 1 mm/yr to 20 mm/yr (<1 mpy to 20 mpy) at the boiling point. This trend is typical of the commercial magnesium-aluminum and magnesium-aluminum-zinc alloys, and these are reported to be among the best alloys for their resistance to aqueous corrosion environments [4,5,19]. Pure magnesium in distilled water is reported to corrode at 16 mm/yr (640 mpy) at the boiling point. Fluoride ion has been reported to be an effective inhibitor for the corrosion of magnesium in water, while sodium carbonate, sodium silicate, and sodium phosphate are not. Thus, A3A alloy (magnesium-3 % aluminum-0.2 % manganese) when boiled for 31 days in a 0.025 N  $\text{NH}_4\text{F}$  solution showed no discernible attack, while the corrosion rate in pure distilled water was reported to be 1.0 mm/yr (38 mpy) [4].

Magnesium corrosion resistance is typically considered to be good in dry air to about 400°C and to about 350°C in moist air. Magnesium with small alloy additions of zirconium or beryllium has been used in gas cooled nuclear reactors in England and France where operating temperatures exceed 350°C. These alloys are reported to have adequate corrosion resistance in wet  $\text{CO}_2$  and wet air at temperatures to 500°C [4,45].

## Organic Compounds

Organic compounds, with a few exceptions, have little effect on magnesium and its alloys. Reference 46 contains a large tabular summary of specific organic and inorganic substances with their compatibility, or incompatibility, appropriately noted. Magnesium is usable in contact with aromatic and aliphatic hydrocarbons, ketones, esters, ethers, glycols, phenols, amines, aldehydes, oils, and higher alcohols. Ethanol causes slight attack, but anhydrous methanol causes severe attack unless significant water content is introduced. Gasoline-methanol fuel blends in which the water content equals or exceeds about 0.25 % of the methanol content were found not to attack magnesium [46]. At room temperature ethylene glycol solutions produce negligible corrosion of magnesium alone or in galvanic couple with steel. At elevated temperatures such as 115°C (240°F), however, the rate raises and, unless an effective inhibitor level is maintained, significant corrosion will develop.

Most dry chlorinated hydrocarbons cause little attack on magnesium up to their boiling points. Chlorinated solvents have been used for years to degrease magnesium components without incident. (Parts that have been so cleaned, however, should be thoroughly baked to ensure that entrapped solvent is driven off, since it may cause degradation of subsequently applied coatings.) In the presence of water, particularly at high temperatures, chlorinated hydrocarbons may hydrolyze to form hydrochloric acid, causing corrosive attack of the magnesium [4,19].

Magnesium forms a highly stable fluoride film and, consequently, has good resistance to hot fluorine gas, HF solutions, and fluorinated hydrocarbons, such as refrigerants. Hydrofluorocarbons have recently been found to not only be noncorrosive at room and elevated temperatures, but very

effective oxidation inhibitors at a few tenths percent in air over molten metal at temperatures up to 700°C, and above [4,20,25,47].

In acidic foodstuffs, such as fruit juices and carbonated beverages, attack of magnesium is slow but measurable. Milk causes attack, particularly when souring. Continuous poultices of wet organic matter have also been noted to cause corrosive attack, as has continuous contact of wet wood products. In both cases the presence of organic acids produced by the decay process has been assumed to be the cause of the attack.

## Galvanic Corrosion

The severe corrosive attack suffered by magnesium components in salt water environments can generally be attributed to two basic causes: (1) poor alloy quality due to the lack of control of heavy metal contamination, and (2) poor design and assembly practices that can lead to severe galvanic corrosion attack on the magnesium components. The introduction of high-purity alloys in the 1980s (e.g., AZ91D, AM60B, AS41B, WE43A, and AE42) has done much to address the first basic cause of saltwater corrosion failures; however, these alloys offer no defense against the threat of galvanic corrosion. Because magnesium is anodic to all other engineering metals, the need for protective measures has long been recognized and measures to minimize such attack have been defined [4,19,48,49]. If the improved performance of high purity alloys is to be realized in completed assemblies, it is critical that these measures are understood and carefully applied. Recent evaluations of material selection and assembly practices in galvanic couples with magnesium have been based on weight loss and depth of penetration measurements following ASTM B 117 exposures [48,49].

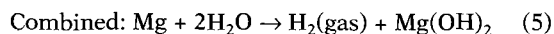
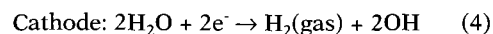
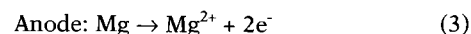
Galvanic corrosion is an electrochemical process with four fundamental requirements:

1. An anode (with magnesium assemblies this is the magnesium),
2. A cathode (e.g., a steel, brass, or graphite component),
3. Direct anode to cathode electrical contact, and
4. An electrolyte bridge at the anode and cathode interface (e.g., salt water bridging the adjacent surfaces of steel and magnesium components).

If any one of these is lacking, the process will not occur. The severity of the attack is determined by the galvanic current, which flows in the completed circuit. This can be expressed as

$$I_{\text{galv}} = (E_{\text{pc}} - E_{\text{pa}})/(R_{\text{m}} + R_{\text{e}}) \quad (2)$$

where  $E_{\text{pc}}$  and  $E_{\text{pa}}$  are the polarized potentials of the cathode and anode, respectively, and  $R_{\text{m}}$  and  $R_{\text{e}}$  are the resistance of the metal-metal contact and the electrolyte, respectively. The chemical process associated with the attack is normally summarized as follows:



The combined equation is the equivalent of that for general corrosion, described in Eq 1; however, due to the

**TABLE 4**—Compatibility of metals in galvanic couple with magnesium alloys AZ31B and AZ61A at Kure Beach, NC [6].

(Most Compatible)				(Least Compatible)
Group 1	Group 2	Group 3	Group 4	Group 5
Aluminum 5052	Aluminum 6063	AlClad 2024	Zinc Plated Steel	Carbon Steel
Aluminum 5056	AlClad 7075	Aluminum 2017	Cad. Plated Steel	Stainless Steel
Aluminum 6061	Aluminum 3003	Aluminum 2024	...	Monel
...	Aluminum 7075	Zinc	...	Titanium
...	...	...	...	Lead
...	...	...	...	Copper
...	...	...	...	Brass

electrochemical driving force involved, the product here is not protective and does not limit the process. Instead, the process continues indefinitely at a high rate typically causing severe pitting attack on the magnesium component at its interface with the cathodic component [4,19].

The most common means of controlling galvanic attack on magnesium is through minimizing the potential difference between the magnesium and the dissimilar metal,  $E_{pc} - E_{pa}$ . Because magnesium shows little, if any, tendency toward anodic polarization, the cathodic materials coupled with magnesium must be selected for their compatibility in the saltwater environment. In one evaluation of various metals with magnesium, the dissimilar metals were coupled to magnesium AZ31 and AZ61 alloy sheet and exposed to the marine environment of Kure Beach, NC. Based on the damage produced during the exposure, the metals were divided into five groups as summarized in Table 4 [4,19].

On steel fasteners, tin, cadmium, and zinc electroplates have long been recognized for their ability to reduce the galvanic attack induced by the fastener when compared to bare steel. The relative effectiveness of these electroplates has generally been accepted to be in descending order as listed. This is consistent with salt spray data presented by Hawke and summarized in Fig. 3. The data are based on the relative weight loss induced by similar fasteners coated with each of these electroplates and a number of alternative

fastener coatings. In addition to the correlation with past evaluations of electroplates, the data highlight two additional points of interest:

1. Certain proprietary zinc and aluminum filled polymers and some ion vapor deposited aluminum coatings, applied to steel fasteners may actually produce more damage than the untreated steel fastener itself. This was attributed to two possible causes: either the high surface area involved with each of the particulate coatings or the contamination of the particulate surface with active cathodic contaminants such as iron, nickel, or graphite;
2. A simple inorganic chromate treatment applied to a cadmium electroplate to preserve its brightness was as effective in further retarding the galvanic attack on magnesium, as was a coating of epoxy resin. (This is consistent with the known inhibitive effects of chromate on the cathodic reduction process and has been observed with other fastener coatings as well) [48,49].

As suggested by Eq 2 an alternate approach to controlling the galvanic corrosion activity in magnesium assemblies is to maximize the circuit resistance  $R_m + R_e$ , thus minimizing the current. There are several practical methods that may be employed depending on the demands of the application.

1. Electrically isolate the magnesium component from the cathodic material. In many applications, however, this is not a practical alternative due to the mechanical, electrical, or cost requirements.
2. Paint the cathodic material. This provides a barrier against electrolyte contact with the cathode; however, this is not simply accomplished in many cases due to the permeability of coatings by moisture combined with the generation of hydrogen and hydroxyl ion on the cathode surface. The combined effect is to strip all but the most alkali-resistant coatings.
3. Design to prevent pooling of the electrolyte in critical areas of fasteners and interfaces with other cathodic components. This is an effective method of control, since it limits both the electrolyte resistance and the period of its presence at the interface, since thin films of an electrolyte have reduced conductivity and higher rates of drying when compared to pools.
4. Use compatible shims or washers in association with fayed joints and fasteners. This control technique works well where exposure to the electrolyte is again intermittent and surfaces are well-drained. By using a shim or washer that extends 3–6 mm (1/8–1/4 in.) beyond the interface of the cathodic material with the magnesium surface, the electrolyte path is extended to a range where the resistance of typical aqueous saltwater electrolytes is

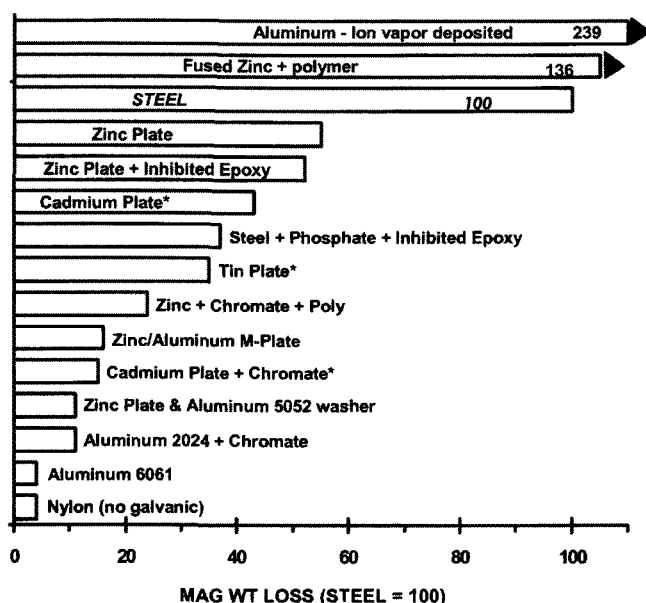


**FIG. 3**—Relative weight loss associated with dissimilar metal fasteners in AZ91 alloy exposed to ASTM salt spray [51,52].

sufficiently high to retard significantly the electrochemical activity. This compatible material may be a nonconductive ceramic, a polymeric material, or a compatible metal, such as an aluminum 5052 or 6061 alloy (Table 4). The use of an aluminum washer beneath the head of a steel fastener that extends 3–6 mm beyond the radius of the bolt head is a simple, effective method of control of the galvanic attack associated with fasteners in magnesium.

## METHODS OF EVALUATION OF CORROSION DAMAGE

Structural magnesium components may experience environmental exposures ranging from the clean, dry indoor atmospheres of computer disk drives and electronic components to the intermittent salt splash associated with automotive applications. Allowable corrosion in these applications may range from submicron attack in disk drives, to substantial attack of several millimeters for some automotive castings, which are judged on their functional performance over a defined period of time. High-purity magnesium alloys have demonstrated their ability to withstand the demands of these environments when components are properly designed, produced, and assembled.

Because magnesium corrosion studies have been limited and spread over several decades, there are few standard practices specific to the material. Perhaps the most commonly used accelerated corrosion test is the salt spray exposure defined in ASTM B 117. This, combined with automotive proving ground tests, has been instrumental in defining the metal quality and galvanic assembly practices required for the recent growth in automotive applications both in North America and Europe over the past decade [3,8,9,11,43,48]. Salt spray has also found a place in the qualification tests for aerospace applications of magnesium castings [50].

Unlike ferrous and aluminum alloys, electrochemical studies of magnesium corrosion have been very limited and as yet are not widely used in the predictive evaluation of its corrosion performance [20].

### Gravimetric Corrosion Rates

In ASTM B 117, salt spray testing exposure periods of seven or ten days are commonly used to evaluate the effects of trace contaminants within the alloy microstructure, as well as on surfaces of untreated and uncoated parts. The cleaning method used for the removal of corrosion products in determining weight loss corrosion rates consists of immersion in a hot (95–100°C) chromic acid solution (20 %  $\text{CrO}_3$  in water) for 1–2 min (or for 15 min at 25°C). The addition of approximately 1 %  $\text{AgCr}_2\text{O}_7$  prevents the accumulation of chlorides, which can lead to magnesium attack (see ASTM G 1, Practice for Preparing, Cleaning, and Evaluating Corrosion Test Specimens).

Two frequent alternatives to ASTM B 117 testing used in the evaluation of general and galvanic corrosion performance have been (1) alternate immersion testing (30 s immersion in 3 % NaCl followed by 2 min in air [4,5,7], or (2) continuous immersion in 3 or 5 % NaCl for a period of three

to seven days or more. In recent years, continuous immersion testing has been employed most often in Europe. A limited comparison of the test using 3 % NaCl as defined in ASTM G 31, Practice for Laboratory Immersion Corrosion Testing of Metals, suggests a reasonable correlation with salt spray performance; however, the measured weight loss corrosion rates typically run two or three times those measured in ASTM B 117 salt spray for the high-purity alloys.

The correlation of accelerated salt spray test results with real world atmospheric results have been very limited to date. Figure 4 represents one of the few direct comparisons published. The two-year marine atmospheric exposure was conducted at the ASTM Brazos River Test Site on the Texas Gulf Coast southwest of Galveston [19,51,52]. Duplicate panels of controlled-purity magnesium alloy AZ91 were employed in the atmospheric tests and in ASTM B117 salt spray. Although the salt spray corrosion scale is approximately 200 times higher than the atmospheric scale, some interesting correlations remain.

1. The break points, or tolerance limits, are the same in both exposures for the nickel and copper contaminants (about 50 and 500 ppm, respectively).
2. The corrosion rates, with respect to increasing iron content, remain low in both exposures throughout the range covered, confirming that the critical iron/manganese ratio was not significantly exceeded.

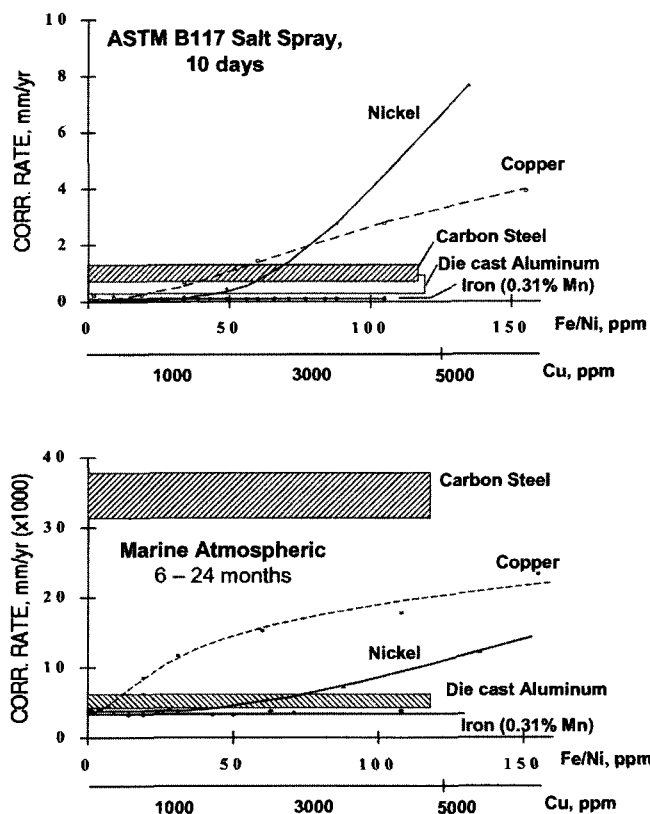


FIG. 4—AZ91 die cast alloy performance versus contaminant level: salt spray (ASTM B 117) versus two-year marine atmosphere (ASTM G 50) performance [19,55].

3. High-purity AZ91 clearly possesses lower overall corrosion rates than either cold rolled carbon steel or 380 die cast aluminum. But also noticeable are some significant contrasts: the relative effects of the nickel and copper contaminants in the atmospheric versus salt spray exposure are reversed, and the effect of both contaminants is mild in the atmospheric exposure when compared to their effects on the salt spray performance of AZ91 versus the carbon steel panels common to both tests.

### Painted Corrosion Performance

The evaluation of coatings and pretreatments for relative coating adhesion has been successfully evaluated in salt spray testing using ASTM D 1654, Test Method for Evaluation of Painted or Coated Specimens Subjected to Corrosive Environments, which employs the ASTM B 117 exposure for the acceleration of corrosive disbonding of the organic coating from the metal substrate. While the test is very effective in establishing the relative effectiveness of metal pretreatments and coatings, the correlation with real-world exposures suggests a test period of 28 days is significantly more severe than a five-year atmospheric exposure [43,53].

### Humidity Tests

Humidity testing is a common alternative to saltwater immersion and salt spray testing for evaluation of indoor corrosion performance and for the evaluation of potential flux contamination. Magnesium melts have traditionally been processed using molten eutectic salt mixtures, consisting principally of KCl and  $MgCl_2$ , as a protective barrier against excessive oxidation or burning during casting operations. Entrapment of these salts in association with unsettled oxides has been a common contributing factor to the poor corrosion performance of cast and extruded products. The introduction of protective gas mixtures ( $SF_6$ , HFC 134a,  $SO_2$ , or Novec™ 612—in a dilute blend with air, or air/ $CO_2$ ) [24,25,59,60] has dramatically reduced the frequency with which these problems are encountered; however, some foundries continue to use the traditional salt fluxes in casting operations today [22,23]. The exposure of a freshly machined surface to an atmosphere of 60–80 % relative humidity at 20–30°C will reveal the presence of flux inclusions within 24–48 h. E. F. Emley's *Principles of Magnesium Technology* describes a simple test chamber employing a saturated solution of sodium thiosulfate as a controlled source of 70 % relative humidity. Alternately, the corrosion product, suspected to be the result of flux inclusions, can be tested by dissolving a sample of the corrosion product in dilute nitric acid and then adding a small amount of a silver nitrate solution to verify the presence of chloride contamination via the readily visible precipitation of silver chloride. This procedure is again summarized by Emley [54].

### REFERENCES

- [1] VanFleteren, R. J., "Supply and Demand," *Proceedings of the International Magnesium Association*, Vancouver, BC, May, 2000.
- [2] The International Magnesium Association, news release—March 2001.
- [3] Esdaile, R. J., "Magnesium Casting Applications in the Automotive Industry," Paper 2001-01-0415, Society of Automotive Engineers, Detroit, MI, 2001.
- [4] Bothwell, M. R., *The Corrosion of Light Metals*, H. Godard, W. B. Jepson, M. R. Bothwell, R. L. Kane, Eds., John Wiley and Sons, New York, 1967, pp. 259–311.
- [5] Loose, W. S., *The Corrosion Handbook*, H. H. Uhlig, Ed., John Wiley and Sons, New York, 1948, pp. 218–252.
- [6] Bengough, G. D. and Whitby, L., *Transactions of the Institute of Chemical Engineers*, Vol. 11, 1933, pp. 176–189.
- [7] Hanawalt, J. D., Nelson, C. E., and Peloubet, J. A., "Corrosion Studies of Magnesium and Its Alloys," *Transactions AIME*, Vol. 147, 1942, pp. 273–299.
- [8] Hillis, J. E., "The Effects of Heavy Metal Contamination on Magnesium Corrosion Performance," Paper 830523, Society of Automotive Engineers, Detroit, MI, 1983.
- [9] Reichel, K. N., Clark, K. J., and Hillis, J. E., "Controlling the Salt Water Corrosion Performance of Magnesium AZ91 Alloy," Paper 850417, Society of Automotive Engineers, Detroit, MI, 1985.
- [10] Hillis, J. E., Murray, R. W., and Mercer, W. E., II, "Compositional Requirements for Quality Performance with High Purity Magnesium Alloys," *Proceedings of the International Magnesium Association*, San Diego, 1998, pp. 74–81.
- [11] Mercer, W. E. and Hillis, J. E., "The Critical Contaminant Limits and Salt Water Corrosion Performance of Magnesium AE42 Alloy," Paper 920073, Society of Automotive Engineers, Detroit, MI, 1992.
- [12] Lunder, O., Nisancioglu, K., and Hansen, R. S., "Corrosion of Die Cast Magnesium-Aluminum Alloys," Paper 930755, Society of Automotive Engineers, Detroit, MI, 1993.
- [13] Emley, E. F., *Principles of Magnesium Technology*, Pergamon Press, New York, 1966, pp. 181–183.
- [14] Pekguleryuz, M. and Baril, E., "Development of Creep Resistant Mg-Al-Sr Alloys," *Magnesium Technology 2001*, J. N. Hryn, Ed., The Minerals, Metals and Materials Society, Warrendale, PA, 2001, pp. 119–125.
- [15] Luo, A. A. and Powell, B. R., "Tensile and Compressive Creep of Magnesium-Aluminum-Calcium Based Alloys," *Magnesium Technology 2001*, J. N. Hryn, Ed., The Minerals, Metals and Materials Society, Warrendale, PA, 2001, pp. 137–144.
- [16] Bronfin, B., Aghion, E., von Buch, F., Schumann, S., and Katsir, M., "Die Casting Magnesium Alloys for Elevated Temperatures Applications," *Magnesium Technology 2001*, J. N. Hryn, Ed., The Minerals, Metals and Materials Society, Warrendale, PA, 2001, pp. 127–130.
- [17] Clark, K. J., "AZ91E Magnesium Sand Casting Alloy, The Standard for Excellent Corrosion Performance," *Proceedings of the International Magnesium Association*, Los Angeles, 1986.
- [18] Emley, E. F., *Principles of Magnesium Technology*, Pergamon Press, New York, 1966, pp. 183–185.
- [19] *Metals Handbook, Corrosion*, 9th ed., Vol. 13, ASM International, Metals Park, OH, 1987, pp. 740–754.
- [20] Hawke, D. L., Hillis, J. E., Pekguleryuz, M., and Nakatsugawa, I., "Corrosion Behavior," in *Magnesium and Magnesium Alloys*, A. Avedesian and H. Baker, Eds., ASM International, Materials Park, OH, 1999, pp. 194–210.
- [21] Nisancioglu, K., Lunder, O., and Aune, T. K., "Corrosion Mechanism of AZ91 Magnesium Alloy," *Proceedings of the International Magnesium Association*, Cannes, France, 1990.
- [22] Couling, S. L., "Use of Air/ $CO_2$ / $SF_6$  Mixtures for Improved Protection of Molten Magnesium," *Proceedings of the International Magnesium Association*, Oslo, Norway, 1979, pp. 54–57.
- [23] Busk, R. S., "Use of  $SF_6$  in the Magnesium Industry," *Proceedings of the International Magnesium Association*, Salt Lake City, UT, 1980, pp. 1–4.
- [24] Tranelle, G. and Pettersen, G., "Alternatives to  $SF_6$  in Magnesium Melt Protection," *Proceedings of the International Magnesium Association*, Brussels, May, 2001.



- [25] Milbrath, D. S. and Owens, J. G., "New Fluorochemical Cover Gases for Protection of Molten Magnesium," *Proceedings of the International Magnesium Association*, Brussels, May, 2001.
- [26] Beck, A., *The Technology of Magnesium Alloys*, 2nd ed., F. A. Hughes and Co., London, 1940, pp. 294–297.
- [27] Emley, E. F., *Principles of Magnesium Technology*, Pergamon Press, New York, 1966, pp. 720–721.
- [28] Logan, H. L. and Hessing, H., "Stress Corrosion of Wrought Magnesium Base Alloys," *Journal of Research of the National Bureau of Standards*, Vol. 44, 1950, pp. 233–243.
- [29] Kiszka, J. C., "Stress Corrosion Tests of Some Wrought Magnesium-Lithium Base Alloys," *Materials Protection*, Vol. 47, 1965, pp. 28–29.
- [30] Pelensky, M. A. and Gallaccio, A., "Stress Corrosion of Magnesium Alloys—Environmental Factors," in *Stress Corrosion Testing*, ASTM STP 425, ASTM International, West Conshohocken, PA, 1967, pp. 107–115.
- [31] Loose, W. S. and Barbian, H. A., "Stress-Corrosion Testing of Magnesium Alloys," in *Symposium on Stress Corrosion Cracking of Metals*, ASTM International, West Conshohocken, PA, 1945, pp. 273–292.
- [32] Miller, W. K., "Stress Corrosion Cracking of Magnesium Alloys," in *Stress-Corrosion Cracking: Material Performance and Evaluation*, ASM International, Metals Park, OH, 1992, pp. 251–263.
- [33] Sager, G. F., Brown, R. H., and Mears, R. B., "Tests for Determining Susceptibility to Stress-Corrosion Cracking," in *Symposium on Stress-Corrosion Cracking of Metals*, ASTM International, West Conshohocken, PA, 1945, pp. 15–36.
- [34] Liu, H. W., "Stress-Corrosion Cracking and the Interaction Between Crack-Tip Stress Field and Solute Atoms," *Transaction of the ASME, Journal of Basic Engineering*, Vol. 92, 1970, pp. 633–638.
- [35] Chakrapani, D. G. and Pugh, E. N., "The Transgranular SCC of a Mg-Al Alloy: Crystallographic, Fractographic and Acoustic Emission Studies," *Metallurgical Transactions*, Vol. 6A, 1975, pp. 1155–1163.
- [36] Bursie, A. J. and Pugh, E. N., "On the Mechanism of Transgranular Stress-Corrosion Cracking," in *Mechanisms of Environment Sensitive Cracking of Materials*, P. R. Swann, F. P. Ford, and A. R. C. Westwood, Eds., Materials Society, London, 1977, pp. 471–481.
- [37] Chakrapani, D. G. and Pugh, E. E., "Hydrogen Embrittlement of a Mg-Al Alloy," *Metallurgical Transactions*, Vol. 7A, 1976, pp. 173–178.
- [38] Makar, G. L., Kruger, J., and Sieadzki, K., "Environment-Assisted Cracking of Rapidly Solidified Mg-Al Alloys," *Proceedings of the International Magnesium Association*, 1990, pp. 37–42.
- [39] Stampella, R. S., Procter, R., and Ashworth, V., "Environmentally-Induced Cracking of Magnesium," *Corrosion Science*, Vol. 24, 1984, pp. 325–341.
- [40] Ebtehaj, K., Hardie, D., and Parkins, R. N., "The Influence of Chloride-Chromate Solution Composition on the Stress-Corrosion Cracking of Mg-Al Alloy," *Corrosion Science*, Vol. 9, 1988, pp. 849–851.
- [41] Ogarevic, V. V. and Stephens, R. I., "Fatigue of Magnesium Alloys," *Annual Review of Materials Science*, Vol. 20, 1990, pp. 141–177.
- [42] Ferguson, W. G., Liu, W., Ross, P. and MacCulloch, J., "Corrosion Fatigue of High Pressure Die Cast Magnesium Alloys," *Magnesium Technology 2001*, J. Hryn, Ed., TMS, New Orleans, LA, February, 2001, pp. 269–274.
- [43] Wendt, J., Hilpert, M., Kiese, J., and Wagner, L., "Surface and Environmental Effects on the Fatigue Behavior of Wrought and Cast Magnesium Alloys," *Magnesium Technology 2001*, J. Hryn, Ed., TMS, New Orleans, LA, February, 2001, pp. 281–285.
- [44] Hilpert, M. and Wagner, L., "Effect of Mechanical Surface Treatment and Environment on Fatigue of Wrought Magnesium Alloys," *Magnesium Alloys and their Applications*, K. U. Kainer, Ed., Wiley-VCH Verlag, Weinheim, Germany, 2000, pp. 463–468.
- [45] Murray, R. W. and Hillis, J. E., "Magnesium Finishing: Chemical Treatment and Coating Practices," Paper 900791, Society of Automotive Engineers, Detroit, MI, 1990.
- [46] Hillis, J. E. and Murray, R. W., "Finishing Alternatives for High Purity Magnesium Alloys," Paper G-T87, *Society of Die Casting Engineers 14th International Congress and Exposition*, Toronto, 1987.
- [47] Bartak, D. E., Schleisman, T. D., and Woolsey, E. R., "Electrodeposition and Characteristics of a Silicon-Oxide Coating for Magnesium Alloys," *Proceedings of the International Magnesium Association*, Quebec City, 1991, pp. 55–60.
- [48] Emley, E. F., *Principles of Magnesium Technology*, Pergamon Press, New York, 1966, pp. 858–898.
- [49] Hawke, D. L., "Compatibility of Magnesium Alloys with Methanol Fuels," Paper 86025, Society of Automotive Engineers, Detroit, MI, 1986.
- [50] Cashion, S. P., Ricketts, N. J., Frost, M. T., and Korn, C., "The Protection of Molten Magnesium and Its Alloys During Die-casting," *International Magnesium Association Automotive Seminar*, Aalen, Germany, 15 June 2000.
- [51] Hawke, D. L., "Galvanic Corrosion of Magnesium," Paper G-T87, *Society of Die Casting Engineers 14th International Die Casting Congress and Exposition*, Toronto, 1987.
- [52] Hawke, D. L., Hillis, J. E., and Unsworth, W., "Preventive Practice for Controlling the Galvanic Corrosion of Magnesium Alloys," Technical Brochure of the International Magnesium Association, McLean, VA, 1988.
- [53] SAE/AMS 4446, Magnesium Alloy Castings, Sand 8.7 Al-0.72 Zn-0.26 Mn (AZ91E-T6), Solution and Precipitation Heat Treated, Society of Automotive Engineers, Warrendale, PA, 1986.
- [54] Coburn, S. K., "Corrosiveness of Various Atmospheric Test Sites as Measured by Specimens of Steel and Zinc," *Symposium on Atmospheric Corrosion*, ASTM International, Boston, MA, 1967.
- [55] Hillis, J. E. and Reichek, R. N., "High Purity Magnesium AM60 Alloy: The Critical Contaminant Limits and the Salt Water Corrosion Performance," Paper 860288, *International Congress and Exposition of the Society of Automotive Engineers*, Detroit, MI, 1986.
- [56] Hawkins, J. H., "Assessment of Protective Finishing Systems for Magnesium," *Proceedings of the International Magnesium Association*, Washington, DC, 1993, pp. 46–58.
- [57] Emley, E. F., *Principles of Magnesium Technology*, Pergamon Press, New York, 1966, p. 909.
- [58] Shook, S. O. and Hillis, J. E., "Composition and Performance of an Improved Magnesium AS41 Alloy," Paper 890205, *International Congress and Exposition of the Society of Automotive Engineers*, Detroit, MI, 1989.
- [59] King, John F., "Environmental Challenges Facing the Magnesium Industry – SF<sub>6</sub> Replacement," *Proceedings of the IMA*, Stuttgart, Germany, May, 2003.
- [60] Milbrath, D. S., "3M™ Novec™ 612 Magnesium Protection Fluid—Its Development and Use in Full Scale Molten Magnesium Processes," *Proceedings of the IMA*, Stuttgart, Germany, May, 2003.

# Aluminum (and Alloys)

*Bernard W. Lifka*<sup>1</sup>

## OVERVIEW OF DOMINANT FACTORS

FOUR FACTORS SHOULD be considered in selecting corrosion tests for aluminum and aluminum alloys. These are: (1) the expected service environment, (2) the type of corrosion expected in service, (3) the primary material requirements of the application which should not be excessively degraded by corrosion, and (4) whether the material requires surface protection for use in the intended environment. Some form of surface protection is almost always necessary for the high-strength 2xxx and 7xxx series alloys.

Accelerated tests should produce the types of corrosion, pitting, or intergranular corrosion (IGC) that occur in service, and contain at least the major contaminants and environmental variables expected. Engineering requirements generally dictate the type of corrosion of most concern and the most significant method of evaluation. For example, for liquid containers the primary concern may simply be to avoid perforation and leaking. Depth of corrosion is the major concern. However, if the liquid is under pressure, the type of corrosion can be of importance as this can affect burst strength.

Tests of the bare, unprotected metal are useful to establish a minimum basis of performance and comparative ranking. However, the applicability to the end use and prediction of service life require evaluation of the protective coatings and maintenance procedures to be used in service.

## NATURE OF THE METAL

### Natural Protective Films

Aluminum is a highly reactive metal that has a high resistance to corrosion in many environments because of the presence of a thin, highly adherent film of aluminum oxide. When a fresh surface of aluminum is exposed to air or water, a surface film of aluminum oxide immediately begins to form and grow rapidly. The stable film thickness in air is about 5 nm (50 Å). The film is thickened when grown in the presence of water and oxygen at elevated temperatures. Pourbaix diagrams show aluminum oxide film is stable in the pH range of 4.0 to 9.0 [1]. In this pH range aluminum and its alloys normally undergo localized corrosion rather

than uniform corrosion. Outside this pH range, the aluminum oxide film dissolves rapidly in strong acids and bases, and the aluminum is then attacked uniformly. Notable exceptions are stability of the film in concentrated nitric acid and glacial acetic acid at pH 1 and lower; and in concentrated ammonium hydroxide and sodium disilicate at pH 11 to 13.

### Effect of Alloying (Composition)

Very high-purity aluminum, 99.99 % or purer, is highly resistant to pitting. Any alloying addition will reduce resistance to pitting corrosion. The 5xxx Al-Mg alloys and the 3xxx Al-Mn alloys resist pitting corrosion almost as well. The pure metal and the 3xxx, 5xxx, and 6xxx series alloys are resistant to the more damaging forms of localized corrosion, exfoliation, and stress-corrosion cracking (SCC). However, cold-worked 5xxx alloys containing magnesium in excess of the solid solubility limit (above 3 % magnesium) can become susceptible to exfoliation and SCC when heated for long times at temperatures of about 80–175°C [2,3].

Higher strength alloys are produced by the addition of magnesium and silicon (6xxx series); and by the addition of copper plus silicon, or copper plus magnesium and silicon (2xxx series). The highest strength alloys are produced by the addition of zinc plus magnesium, or magnesium and copper. The additions of these elements change the electrochemical potential of the alloy, which affects corrosion resistance even when the elements are in solid solution. Zinc and magnesium tend to shift the potential markedly in the anodic direction, while silicon has a minor anodic effect. Copper additions cause marked cathodic shifts. This results in local anodic and cathodic sites in the metal that affect the type and rate of corrosion.

### Effect of Metallurgical and Mechanical Treatments

Metallurgical and mechanical treatments often are interactive with regard to producing chemical-microstructural features in aluminum alloys, such as dislocations, precipitates, and the microstructural morphology (grain size and shape). For simplicity these two effects are discussed separately.

### Effect of Metallurgical Treatments

Variations in thermal treatments such as solution heat treatment, quenching, and precipitation heat treatment (aging)

<sup>1</sup>Former Technical Consultant, Alcoa Technical Center, Alloy Technology Division, Alcoa Center, PA 15069-0001; retired 3/1/93, contact at 724-337-8130.

can have marked effects on the local chemistry and hence the local corrosion resistance of high-strength, heat-treatable aluminum alloys [3]. Ideally, all the alloying elements should be fully dissolved and the quench cooling rate should be rapid enough to keep them in solid solution. The first objective usually is achieved, except when alloying elements exceed the solid solubility limit, e.g., alloy 2219; but a sufficiently rapid quench often is not obtained, either because of the physical cooling limitations, or the need for slower quenching to reduce residual stresses and distortion. Generally, practices that result in a nonuniform microstructure will lower corrosion resistance, especially if the microstructural effect is localized.

Precipitation treatment (aging) is conducted primarily to increase strength. Some precipitation treatments go beyond the maximum strength condition (T6 temper) to markedly improve resistance to IGC, exfoliation, and SCC through the formation of randomly distributed, incoherent precipitates (T7 tempers). This diminishes the adverse effect of highly localized precipitation at grain boundaries resulting from slow-quenching, underaging, or aging to peak strengths.

### Effect of Mechanical Treatments

Mechanical working influences the grain morphology and the distribution of alloy constituent particles. Both of these factors can affect the type and rate of localized corrosion.

Cast aluminum products normally have an equi-axed grain structure. Special processing routes can be taken to produce fine, equi-axed grains in thin rolled sheet and certain extruded shapes, but most wrought products (rolled, forged, drawn, or extruded products) normally have a highly directional, anisotropic grain structure. Rectangular products have a three-dimensional (3-D) grain structure. Figure 1 shows the three-directional Longitudinal (principal working direction), Long-Transverse, and Short-Transverse grain structure typically present in rolled plate and the two-directional grain structure of rolled rod. These directional structures markedly affect resistance to SCC and to exfoliation of high-strength alloy products (see ASTM G 34, Test Method for Exfoliation Corrosion Susceptibility in 2xxx and 7xxx Series Aluminum Alloys (EXCO Test)).

Most die forgings and many extrusions with irregular, complex cross sections have a metal flow that varies with the product contour. An example is shown in Fig. 2. Evaluation of such products requires knowledge of the metal flow pattern through either prior experience or macroetching. The grain structure and resultant corrosion behavior also vary from surface to center in products with appreciable thickness. This factor begins to be important at a thickness of about 12 mm. Almost all forms of corrosion, even pitting, are affected to some degree by this grain directionality. However, highly localized forms of corrosion, such as exfoliation and SCC, which proceed along grain boundaries, are highly affected by grain structure. Long, wide, and very thin pancake-shaped grains are virtually a prerequisite for a high degree of susceptibility to exfoliation. The photomicrograph shown in Fig. 2 of ASTM G 34 is an example of a highly laminated grain structure and the severe exfoliation corrosion that can occur.

Since SCC in aluminum alloys characteristically is intergranular, susceptible alloys and tempers are most prone to

SCC when the tensile stress acts in the short-transverse, or thickness direction, so that the crack propagates along the aligned grain structure. The same material, e.g., 7075-T651 plate, will show a much higher resistance to stress acting in the longitudinal direction, parallel to the principal grain flow. In this case the intergranular crack must follow a very meandering path and usually does not propagate to any major extent. Special agings to various, highly resistant T7 tempers have been developed to counteract this adverse effect of directional grain structure. Figure 3 [4] shows a

FIG. 1—(a) Three-dimensional grain structure of rolled plate, and (b) two-dimensional grain structure of rolled rod. Original magnification was 100 diameters. (Photographs courtesy of J. J. Liput, Alcoa Technical Center.)

FIG. 2—Transverse slice showing the variable grain structure in a die forging. (Photograph courtesy of J. J. Liput, Alcoa Technical Center.)

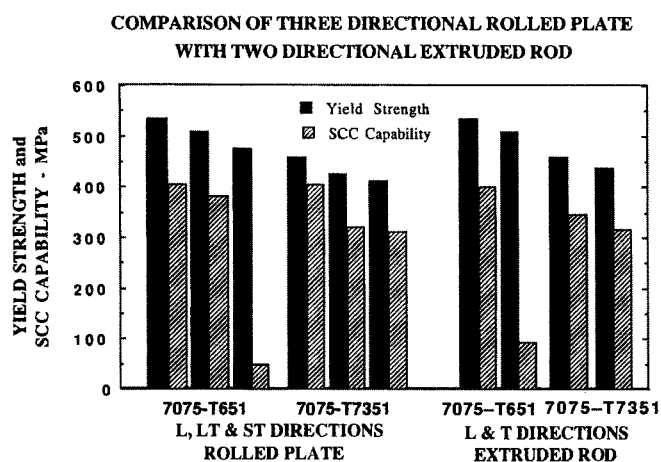


FIG. 3—Bar graph comparing tensile yield strength and the highest surviving SCC test stress for 7075-T6 and T73 in the L, LT, ST directions of plate and the Land T directions of rod. The SCC results are representative of tests in ASTM G 44 and in seacoast atmosphere at Point Judith, RI.

comparison of strength and SCC resistance for the principal grain directions in 7075 plate and rod in both the T651 and T7351 tempers. Various artificially aged tempers are available for both 2xxx and 7xxx alloys that provide a range of compromise choices between maximum strength and maximum resistance to exfoliation and SCC [5].

### Mill and Foundry Products

Cast aluminum products are produced by sand cast, die cast, and permanent mold casting methods. The alloys and tempers used are unique to castings, and their performance differs significantly from wrought products.

The most basic form of cast aluminum product is large ingot produced for subsequent fabrication into a wrought

product. Commercial ingots are cast by continual processes as rounds or rectangles, hence they can be of various lengths and as thick as 915 mm diameter or 619 mm thick. Corrosion tests are rarely made for products still in the ingot stage, but the homogenization (preheating) and hot- and cold-working processes given to ingot will affect the metallurgical structure and corrosion resistance of the final product. One has to establish, therefore, whether changes in ingot casting or processing affect the corrosion performance of the finished product.

Wrought aluminum products are produced by all of the standard hot- and cold-working processes. In general, the commercial alloys and tempers cross product lines. As such the main effect of various products on corrosion is that attributable to variations in grain structure, as discussed in the previous section.

### Role of Hydrogen

Hydrogen will dissolve in aluminum alloys in the molten state and during thermal treatments at temperatures close to the melting point in atmospheres containing water vapor or hydrocarbons. Upon solidification, this causes porosity and surface blistering.

Recent literature surveys [6,7] show there still is considerable dispute as to how much, if at all, high-strength aluminum alloys are embrittled by hydrogen. There is evidence that hydrogen evolving from anodic dissolution at a crack tip can dissolve into the metal at the grain boundary ahead of the crack tip, and thus be a factor in SCC of some 7xxx and possibly 2xxx alloys. Hydrogen embrittlement, however, has not restricted the commercialization of high-strength aluminum alloys.

### Protective Coatings

As mentioned earlier, pure aluminum, the 3xxx, 5xxx, and most 6xxx series alloys, are sufficiently resistant to be used in industrial atmospheres and waters without any protective coatings. Examples of this are cookware, boats, and building products. Generally, coatings are used to enhance an alloy's resistance and protection is considered necessary for the higher strength 6xxx alloys, such as alloy 6013, and for all 2xxx and 7xxx alloys.

One of the principal methods of protection is to enhance the thickness and quality of the natural oxide by prefilming in hot water, which can thicken the surface oxide by about a factor of 10. The film can be thickened even more (to 1000 or more times the natural thickness) by anodizing in special acid (e.g., sulfuric or chromic) electrolytes. Chemical conversion treatments also provide protection, but to a much lesser degree and are primarily used as a substrate for the subsequent application of organic films. A discussion of the effective use of organic coatings is beyond the scope of this chapter.

A protective measure unique to aluminum is the use of alclad, in which a thin layer of high-purity aluminum, or a special alloy designed to be sufficiently anodic, is metallurgically bonded to a less resistant alloy having more desirable engineering properties such as strength, toughness, or fatigue endurance. The cladding thickness is on the order of

2.5–5 % of the total product. Alclad sheet for the aerospace industry is the primary example, and almost all commercial airplanes currently use Alclad 2024-T3 sheet in the fuselage. A major advantage of alclad over other protective measures is that it provides both a protective barrier and electrochemical (cathodic) protection since the cladding alloy, by design, is anodic to the core alloy. This enables the cladding to continue to provide protection, even in the event of an intentional or inadvertent breach in the cladding, such as drilled holes and cut edges or accidental scratches or dings. The mechanism of alclad protection is analogous to that of the familiar galvanized steel, except the thin protective aluminum surface layer is applied by a fabrication process (generally hot-rolling or extrusion), whereas the zinc surface on steel is applied by a hot dip or plating process.

## SENSITIVITY TO PARTICULAR ENVIRONMENTAL FACTORS

### Acidity/Alkalinity

The aluminum oxide film generally is stable in the pH range of 4 to 9, but is readily dissolved in strong acids and alkalis, with some notable exceptions as mentioned in the section on Natural Protective Films. The rate of corrosion cannot be predicted solely by the pH, but depends on the specific ions present, their concentration, and the temperature. For example, the dissolution rate of aluminum in sulfuric acid becomes appreciable between 50–100 % concentration, with the maximum rate occurring at 70–90 % concentration. Furthermore, the corrosion rate at 50°C can be as much as four times more rapid than at 25°C [8–10].

A saturated solution of aluminum chloride ( $\text{AlCl}_3$ ) has a pH of 3.0–3.5 just into the range where the natural oxide is unstable. A saturated concentration can occur when aluminum corrodes in a chloride-containing solution under conditions where the electrolyte cannot be readily replenished, such as crevices, deep pits, and cracks. It also occurs in cyclic wet-dry environments, where the solution gradually evaporates and becomes concentrated. This tends to keep corrosion active at such a site, as opposed to the usual self-limiting effect.

Currently there is appreciable public concern over the effect of acidic precipitation (“acid rain”) on all materials of construction. Typically the pH ranges from 4–5.5 and rarely is less than 3.5. As such acidic precipitation does not cause severe damage to aluminum and its alloys from the standpoint of structural integrity. However, acid rain can cause cosmetic problems, such as dark brown to black stains.

### Specific Ions

Corrosion of aluminum requires the presence of moisture and oxygen. Aeration and oxygenating conditions will accelerate corrosion. Conversely, deaeration will retard corrosion. The amount of water may be minuscule, and present as isolated droplets or a continuous film. Soft waters tend to be less corrosive than hard waters. At ambient temperatures aluminum initially reacts with high-purity water, but this ceases after a few days as a result of the development of

a more protective oxide film [3]. A small amount of water can drastically affect resistance to certain anhydrous organic solutions, particularly halogenated hydrocarbons. Water vapor in the air is sufficient to cause staining upon condensation, and to support SCC.

Unlike steel, aluminum is resistant to steam, and steam or boiling water treatments can actually increase the protective oxide.

Halides, particularly the chloride ion, are corrosive to aluminum. Various mechanisms have been proposed, the most probable being localized breakdown and penetration of the oxide film. The corrosiveness of the chloride ion is a major concern because the ion is ubiquitous. Potable water and well water often are used to make up processing solutions and these normally contain small amounts of chlorides.

Small concentrations of heavy metals in solution (particularly copper, iron, lead, and even trace amounts of mercury) can plate out on the aluminum surface and can cause rapid localized pitting. Interactive effects can also occur, for example, the rate of pitting as a function of chloride content is highly accelerated by the addition of a few ppm of copper ions [3]. Consequently, the composition of etchants and other process solutions should be monitored and renewed on a regular basis. The depth of pitting occurring in such operations may be shallow, but can be adverse for cosmetic reasons, or as a site for subsequent corrosion.

Some ions are inhibitors and will reduce either the anodic or cathodic reactions that occur during the corrosion of aluminum. Examples are chromates (an anodic inhibitor) and phosphates (a cathodic inhibitor). Inhibition of circulating water systems is complex and professional consultation is recommended for the design of water treatment systems.

Corrosion rates tend to decrease as the electrolyte becomes spent and saturated with aluminum ions. Consequently, a greater amount of corrosion can be expected for conditions that prevent this, such as high flow rates, and a low ratio of area of metal surface to volume of solution. Contamination of a pure solution can increase, or decrease, the corrosion rate. Therefore, predictions of the corrosion performance should be obtained from Refs 8–10 or by experimentation.

### Elevated Temperature

In general, corrosion rates increase with increasing temperatures. In some cases this effect can be very marked, as noted previously for sulfuric acid.

In contrast to ambient temperature, high-purity water at high temperatures of 200 to 300°C can cause rapid disintegration of pure aluminum. Aluminum-nickel-iron alloys have been developed for use at such temperatures [11].

In atmospheric corrosion, slightly elevated temperatures can be beneficial by reducing the time of wetness. An example is electrical conductors that operate slightly above ambient temperatures and which usually incur little corrosion because the elevated operating temperature keeps them dry.

In addition to affecting the corrosion reactions, elevated temperatures can cause additional precipitation and changes in the metallurgical structure of the metal. The

2xxx and 7xxx alloys are affected beginning at temperatures of about 120°C. This effect initially is adverse, but with continued heating past peak strength conditions, a reversal and improved resistance can occur. The 5xxx series alloys containing more than 3 % magnesium are sensitized by exposure to temperatures on the order of 80 to 175°C. Exposure of these 5xxx alloys to even higher temperatures results in a coarsening of the precipitate, producing discontinuous grain boundary precipitation which reduces, or eliminates, the sensitization effect [12].

### Liquid Metals

Mercury is the primary liquid metal that degrades aluminum. Liquid mercury does not wet an aluminum oxide surface, but if the natural oxide film is penetrated aluminum dissolves in the mercury to form an amalgam starting a very rapid reaction. The dissolved aluminum oxidizes immediately in the presence of moisture and more aluminum dissolves. This reaction is assisted by the presence of halides. The mercury penetration tends to proceed along grain boundaries, and if tensile stresses are present in the metal, drastic splitting and the exposure of further film free metal occurs. Mercury can plate out of aqueous solutions to produce this effect. A mercury content of greater than 0.01 ppm is cause for concern. Detection of even lesser amounts of mercury may indicate a problem, since mercury tends to evaporate and low levels are difficult to analyze. Common sources of mercury are broken thermometers and mercury vapor bulbs, or mercury manometers that have been over-pressurized.

### Chemicals

Aluminum is suited for containment and production of many chemicals and foods. References 8–10 should be consulted to determine compatibility with specific chemicals. Caution is advised concerning compatibility with a specific chemical that has become contaminated. For liquid chemicals, especially with the use of closed aluminum containers, the resistance of the aluminum container can differ in the liquid and vapor phases and at the liquid-vapor interface. If the corrosion performance is unknown, all three conditions should be investigated.

### Galvanic Couples

Galvanic corrosion and the factors affecting it have been discussed in Chapter 20. However, a few precautionary comments are in order for aluminum, since it is anodic to most common materials of construction, with the exception of magnesium and zinc. In the presence of a good electrolyte, as little as 15 mV difference in corrosion potential of the two metals can have an effect, and if the difference is 30 mV or greater the anodic material will definitely corrode sacrificially to protect the contacting cathodic metal. A recently revised report on galvanic corrosion, with emphasis on automotive applications is available [13].

It is generally recognized that protection must be provided if aluminum and aluminum alloys contact copper, copper alloys, iron, or steel. Aluminum alloys are quite

anodic to these metals and an alloy change will have little effect. An exception is 2xxx series aluminum alloys containing 2 % or more copper in the solution heat-treated T3 or T4 tempers. These alloys can approach the corrosion potential of mild steel.

Designers often want to use aluminum in contact with stainless steel and titanium. Both these materials are quite cathodic to aluminum, but the effect of the couple depends to a large extent on whether or not the stainless steel or titanium passivates or stays active. If these metals passivate, such a couple often is tolerable, but one cannot assume passivity. The designer really needs to determine the expected environmental conditions and establish the performance of stainless steel and titanium. Conditions such as crevices, acidity, and oxygen availability are important.

Many users do not recognize that aluminum alloys themselves span a range of about 400 mV in their respective corrosion potentials. In aerated sodium chloride solutions, pure aluminum, 3xxx alloys, and many other alloys have a potential of about –740 mV when measured with a saturated calomel reference electrode (SCE). Aluminum alloys with high magnesium or zinc contents will be more anodic by as much as 260 mV, while high copper content alloys will be more cathodic up to about 140 mV. Care must be taken therefore, that all alloys and tempers are compatible, even in an all aluminum structure.

### Crevice

If an electrolyte can enter the crevice formed by the faying surfaces of two aluminum surfaces an oxygen concentration, and subsequently chemical concentration, cell can form and cause accelerated localized attack. As such, corrosion protection often is required in joints, even when not needed on the freely exposed aluminum. The severity of crevice corrosion depends on the electrolyte and how readily it is replenished. It also is influenced by the geometric shape of the crevice, and the ratio of active crevice cathode area to the adjacent external cathode area. The best protective measures are to design so that crevices will drain, and to effectively seal crevices to prevent ingress of the electrolyte.

## METHODS OF EVALUATION OF CORROSION DAMAGE

The various types of corrosion that occur in metals were covered in Section IV of this manual, Testing for Corrosion Types. Additional information also can be found in Refs 2, 3, and 14–16. This paragraph covers considerations more or less unique to aluminum. A brief summary of analytical methods used with aluminum is given in Table 1, listing the forms of corrosion in the order most prevalent in aluminum alloys.

Regardless of the type of corrosion, the initial, basic evaluation should be a visual inspection in the “as-corroded” condition, assisted by low-power (3 to 10×) magnification. A written description should be kept, preferably documented with photographs. If the sample is disassembled or cleaned, the visual/photographic inspection should be repeated. Cleaning in concentrated nitric acid, method

**TABLE 1**—Methods of evaluation of corrosion damage.

Type of Corrosion	Methods of Evaluation
Pitting Corrosion	Visual examination including low magnification, photographs, measurement of depth, assessment of size and number of pits, ASTM G 46. Determination of effect on mechanical properties.
Intergranular Corrosion	Metallographic determination of extent and depth of attack, ASTM G 110. Determination of effect on mechanical properties.
Exfoliation Corrosion	Visual and metallographic examination, photographs, photomicrographs, ASTM G 34 and G 66.
Stress-Corrosion Cracking	Determination of minimum stress level required for failure, number of failures, time to failure (log normal distribution), probability of percent survival (or failure) versus time, crack propagation rate and threshold stress intensity. Refer to Chapter 25.
Filiform Corrosion	Visual and metallographic examination. Photographs.
Staining	Visual examination and photographs. Measurement of reflectivity or image clarity.
Uniform Etching Corrosion	Rarely occurs, except in certain highly acidic or alkaline corrodents. Gravimetric methods in ASTM G 1.

C.1.2 in ASTM G 1, Practice for Preparing, Cleaning, and Evaluating Corrosion Test Specimens, is the procedure normally used for aluminum because it is simple and effectively removes most corrosion products.

Likewise, metallographic examination is performed in all but the most elementary evaluations. Typically this begins with optical microscopy at magnifications of 50–500 diameters to determine the type, depth, and extent of corrosion. Both pitting and intergranular corrosion of aluminum tend to be localized and nonuniform over the surface. Visual examination usually can define areas of most severe corrosion and metallographic examination generally is limited to such regions. Both forms of corrosion tend to develop in hemispherical shaped sites, and several (typically three) random metallographic sections of about 20 mm in length are examined to ensure a better chance of the plane of polish being at the deepest portion of the hemisphere. Repetitive polishing and measurement of the metallographic sections provide another means of assuring the maximum depth of penetration has been measured. The average depth of corrosion often provides a more repeatable assessment of the “overall” corrosion damage, which is useful for statistical evaluations. However, maximum depth is of prime importance in applications where service failure results from the penetration of the wall of a tube or vessel, or when corrosion sites act as initiation sites for other forms of metal damage, such as fatigue cracks.

Examination by scanning electron microscopy (SEM) permits examination of the actual corroded surface, with excellent resolution at high magnifications. Investigators often employ a mechanical test (tension or fatigue test) of a

corroded specimen, which inherently fractures at the deepest corrosion site. The fractured surface then is examined to measure the depth of corrosion at the fracture initiation site. Jones et al. [17] showed that, for more than half of their samples, the depth of corrosion measured by SEM examination of pre-corroded fatigue specimens was greater than that determined by optical microscopy.

Techniques involving probe instruments, sometimes used for ferrous alloys, are not reliable for measuring of the depth of narrow pits or IGC in aluminum.

### Pitting Corrosion

Pitting corrosion is normally encountered on all aluminum alloys and in all environments, i.e., laboratory tests, field tests, and service applications. It occurs randomly, but not necessarily uniformly, over the entire surface. The depth and frequency of pitting depend on the alloy and environment. Pitting can be locally accelerated by crevices and contact with dissimilar metals. Pitting in aluminum tends to be self-stopping, following a polynomial [14], or power function [16] depending on the environment. Because pitting tends to be nonuniform, the “Pitting Factor” (ratio of maximum to average penetration) discussed in paragraph 7.3.2. of ASTM G 46, Practice for Examination and Evaluation of Pitting Corrosion is not useful for aluminum.

### Intergranular Corrosion (IGC)

Intergranular (intercrystalline) corrosion also occurs randomly, over the entire surface, but corrosion is limited to the immediate grain boundary region and often is not apparent visually. This localization results from compositional differences between precipitates on the boundaries, the solute depleted grain margins, and the higher (normal) solute grain interior. IGC penetrates more quickly than does pitting corrosion, but it too reaches a self-limiting depth. This is due to limiting transport of oxygen and the corrodent down the narrow corrosion path. When the limiting depth has been reached, intergranular attack spreads laterally. If IGC results in splitting or exfoliation, the corrosion will not be self-limiting [18]. IGC has much sharper tips than pitting corrosion, hence it is a more drastic stress riser and has a more damaging contribution to corrosion fatigue.

### Exfoliation Corrosion

Exfoliation corrosion occurs in products having highly directional grain structure, such as that shown for plate in Fig. 1. The corrosion begins as lateral intergranular corrosion on subsurface grain boundaries parallel to the metal surface, but entrapped corrosion products produce internal stresses that tend to lift off the overlying metal. This spalling off of the metal creates fresh metal surfaces for continued corrosion. Consequently exfoliation corrosion does not become self limiting. Photographs of exfoliation can be found in Figs. 2–6 of ASTM G 34, and Figs. 1 and 2 of ASTM G 66, Method for Visual Assessment of Exfoliation Corrosion Susceptibility of 5xxx Series Aluminum Alloys (ASSET Test). These figures can also be found in Chapter 22 of this manual.

Highly cold-worked tempers of certain 3xxx and 5xxx alloys can incur a less aggressive form of exfoliation that proceeds in a transgranular mode, following selective precipitation along slip bands [16].

## STRESS CORROSION CRACKING (SCC)

Resistance to SCC is of prime importance in structural, load bearing applications. Considerable testing is performed to ensure adequate resistance because failure by this corrosion mode could be catastrophic, and because of the uncertainty of the time to initiate a failure.

SCC in aluminum alloys is typically intergranular, although transgranular SCC has been observed for a few alloys under highly specific environmental conditions [16,19] and may be part of the propagation mechanism in some 7xxx alloys. SCC requires the interaction of a metallurgically susceptible material, a corrosive environment (water vapor may be sufficient) and sustained (but not necessarily continuous) tensile stress.

Generally there is a threshold stress that must be exceeded in order for SCC to initiate, but this is dependent on the environment, the test specimen or part configuration, and the method of loading, (bending, direct extension, constant load, etc.). The initiation period increases as the applied stress is decreased and can vary from a few hours to many years. Once cracking has begun, the crack grows linearly at a constant velocity independent of the applied stress. This continues until either unstable crack growth occurs, leading to rapid failure, or the applied stress falls below the threshold required for crack propagation. Precracked, fracture toughness type specimens have been developed that can measure the crack growth rate, plateau velocity, and the threshold level of stress-intensity.

The use of precracked SCC specimens is necessary for some metals in which an SCC flaw will not initiate, but in which other types of flaws such as weld cracks can propagate by SCC. This is not necessary for aluminum alloys, which will initiate a SCC flaw on an unflawed, smooth specimen. Most SCC testing of aluminum has been done using smooth specimens because these specimens and test methods are faster and less expensive. Although the data from the two types of testing are not interchangeable, both methods tend to rank aluminum alloys in the same relative order of increasing resistance to SCC [20].

The most significant type of SCC data is determination of the safe stress level below which failure will not occur. Other data forms are time to failure, number of failures, and percent failure (or survival). SCC failure times are not normally distributed, but the logarithm of failure times tend to have a normal distribution. This permits probability plots of cumulative percent failure (or survival) versus exposure time. Refer to Chapter 25.

## FILIFORM CORROSION

Filiform corrosion is selective worm-track pitting corrosion of the surface of the metal beneath a pliable film. An example is shown in Fig. 4. This type of corrosion usually

**FIG. 4—Photograph of filiform corrosion that occurred on a medicinal “Uni-dose” cup during compatibility tests with various pharmaceuticals. The cup was formed from 0.15 mm aluminum foil coated with a clear lacquer. Corrosion did not perforate the cup but resulted in contamination of the liquid. (Photograph courtesy of F. S. Bovard, Alcoa Technical Center.)**

penetrates only a few hundredths of a millimeter; hence the concern generally is aesthetic appearance, except in the case of thin foils where perforation can occur, or where the packaged contents can be contaminated.

Resistance to filiform corrosion depends more on factors such as the environment, the type and thickness of coating, metal surface preparation, and coating application procedures than on the metal itself. However, there is evidence that higher copper content aluminum alloys are more susceptible. Primary environmental factors are the presence of moisture and chloride ions. An acidic electrolyte has an accelerating effect.

## UNIFORM CORROSION

Uniform corrosion of aluminum is rare, except in special, highly acidic, or alkaline corrodents, e.g., the preparation of specimens for exposure per paragraph 12.1 of ASTM G 66 by etching for 1 min in 5 % by weight sodium hydroxide at 80°C.

Under controlled conditions, the rate of dissolution is quite uniform and linear, depending primarily on the chemical concentration and temperature of the electrolyte. Several industrial processes use this principle to electrochemically machine or size parts. Thickness measuring devices, or gravimetric procedures, can be used in such cases.

## STAINING CORROSION

Bright aluminum surfaces incur staining in certain aqueous solutions. Frequently stains result from a roughening and thickening of the aluminum oxide, which causes a change in the refraction of incident light. This is important



in applications such as bright trim and reflector sheet. Assessment of damage is by visual inspection, photographs, and measurement of reflectivity or image clarity.

## TESTS FOR SPECIFIC TYPES OF CORROSION

The purpose of this section is to introduce standard test methods, practices and guides for evaluation of the various type of corrosion that occur in aluminum. Refer also to Section IV for additional information.

### General Pitting Corrosion

Pitting corrosion will occur in most environments, particularly those containing the chloride ion. Pitting can be evaluated on virtually any specimen, but flat panels usually are used when this is the principal purpose of the test. ASTM G 1 describes surface preparation of specimens for pitting tests, while ASTM G 46 covers specimen evaluation after test.

Specific tests frequently used are: (a) neutral 5 % Sodium Chloride salt spray (ASTM B 117, Test Method of Salt Spray (Fog) Testing), (b) 3.5 % Sodium Chloride by alternate immersion (ASTM G 44, Practice for Evaluating Stress Corrosion Cracking Resistance of Metals in 3.5 % Sodium Chloride Solution), and (c) exposure to various outdoor atmospheres. Guidelines for outdoor exposure are contained in ASTM G 50, Practice for Conducting Atmospheric Corrosion Tests on Metals. Generic types of atmospheres used are seacoast, industrial, urban, and rural. Sometimes specific geographical locations or local chemical conditions are important because they can produce unique results [21].

### Intergranular (Intercrystalline) Corrosion

Susceptibility to intergranular corrosion depends primarily on the type of alloy and fabrication process and can occur in most environments. The six-hour ASTM G 110 test (Practice for Evaluating Intergranular Corrosion Resistance of Heat Treatable Aluminum Alloys by Immersion in Sodium Chloride + Hydrogen Peroxide Solution) is most often used to determine inherent susceptibility to this form of corrosion. However, users are cautioned that the degree of susceptibility in this accelerated test may not be representative of performance in outdoor atmospheres [22].

A rather unique mass loss test method, ASTM G 67 (Test Method for Determining the Susceptibility of Intergranular Corrosion of 5xxx Series Aluminum Alloys by Mass Loss After Exposure to Nitric Acid [NAML Test]) has been developed to provide a quantitative measure of the intergranular susceptibility of 5xxx series Al-Mg and Al-Mg-Mn alloys. The technique is useful to determine whether material has become sensitized by exposure to elevated temperature. Development of the test is reported in Ref 23.

### Exfoliation

Exfoliation corrosion occurs only for certain tempers and alloys, but resistance to this form of corrosion should be

known, because the resultant damage can be quite severe. Also, protective coatings do little to prevent this type of corrosion.

ASTM standards have been prepared for several short time laboratory tests that range from one day to two weeks of exposure; namely, ASTM G 34 for 2xxx and 7xxx alloys, ASTM G 66 for 5xxx alloys, and three methods of Salt Spray (Fog) Testing, ASTM G 85 (Practice for Modified Salt Spray [Fog] Testing), Annexes A2, A3, and A4. The background of the development of these and other tests are contained in Refs 24–28. In addition ASTM G 112, Guide for Conducting Exfoliation Corrosion Tests in Aluminum Alloys, provides guidelines regarding specimen preparation, significant exposure periods, and inspection and evaluation techniques. The degree of susceptibility to exfoliation of some materials will vary in the different accelerated tests. Performance in seacoast atmosphere is generally regarded as the baseline against which the appropriateness of any accelerated test should be judged. Two years of exposure at the seacoast is considered the minimum exposure period for this purpose, and longer seacoast experience of four or more years is desirable [27,28] (see also Chapter 22).

### Stress Corrosion Cracking (SCC)

SCC tests differ from others corrosion tests in that specific types of specimens and loading methods are required to stress the specimens. Care must be taken to electrically insulate the specimen from any metallic loading fixtures.

### Smooth Specimens

Smooth specimens can be stressed by a constant load, by constant strain rate, or by constant deflection, which is the usual procedure. Typical specimens are (a) direct tension specimens, (b) C-ring specimens, (c) U-bend specimens, (d) bent beam specimens, and special techniques for weldments (see ASTM G 49, Practice for Preparation and Use of Direct Tension Stress-Corrosion Test Specimens; ASTM G 38, Practices for Making and Using C-Ring Stress-Corrosion Test Specimen; ASTM G 30, Practice for Making and Using U-Bend Stress-Corrosion Test Specimens; ASTM G 39, Practice for Preparation and Use of Bent-Beam Stress-Corrosion Test Specimens; and ASTM G 58, Practice for the Preparation of Stress-Corrosion Test Specimens for Weldments, respectively).

The most frequently used accelerated test is the 3.5 % NaCl alternate immersion test ASTM G 44 following procedures given in ASTM G 47, Test Method for Determining Susceptibility to Stress-Corrosion Cracking of High-Strength Aluminum Alloy Products. For 7xxx series alloys containing less than 0.25 % copper ASTM G 103, Test Method for Performing a Stress-Corrosion Test for Low Copper Containing Al-Zn-Mg Alloys in Boiling 6 % Sodium Chloride Solution is used.

Successful completion of any of these tests only assures a specific level of resistance and does not imply immunity to SCC. Field tests in outdoor atmospheres, especially seacoast and industrial atmospheres, are the primary baseline for determination of long-term service performance.

SCC tests involving constant strain rate loading are rarely used in the United States; however, a procedure for this type

of test is contained in the International Standards document ISO 7539-7 and in ASTM G 129, Practice for Slow Strain Rate Testing to Evaluate the Susceptibility of Metallic Materials to Environmentally Assisted Cracking (EAC).

A new technique for use with constant deflection specimens is the determination of the residual "breaking strength" (load carrying ability) after short exposures to an environment such as ASTM G 44, rather than use of pass/fail data. Both unstressed and stressed specimens are exposed, providing a measure of the effect of applied stress on corrosion and on resistance to SCC. An adequate number of replicate specimens (typically five), two or more stress levels (one being no stress), and three or more exposure periods (one being no exposure) are required. Such a method is in use for high-strength aluminum alloys [29] and the results of an ASTM round robin are contained in Ref 30. An expanded report version of Ref 30 containing all the tabular data is on file with ASTM. The advantages of the method are considerably shorter exposure periods and statistical analysis of results.

### Precracked Specimens

Tests involving precracked specimens are rarely used for aluminum alloys (except for mechanistic studies) because they require longer exposure and more expensive specimens. Specimens are loaded to a percentage of the fracture toughness and the loading method can result in a constant, an increasing, or a decreasing level of stress-intensity as the crack progresses. The last method is the usual one, using the double-cantilever notched, precracked specimens of the type shown in Ref 20. The data measured are crack lengths, from which crack velocity and the limiting stress-intensity

for crack growth can be calculated. The international standard ISO 7539-6 exists on this subject.

### Galvanic Corrosion

Electrochemical methods, such as anodic polarization curves electrochemical impedance spectroscopy (EIS), and measurement of the corrosion potential (open circuit or rest potential) are primarily laboratory tests. They require experience in interpretation of the results, but have the advantage of very short test times. As such, they are important in mechanistic studies, but certain commercial uses also exist.

ASTM electrochemical standards include ASTM G 3, Practice for Conventions Applicable to Electrochemical Measurements in Corrosion Testing; ASTM G 5, Standard Reference Test Method for Making Potentiostatic and Potentiodynamic Anodic Polarization Measurements; ASTM G 69, Practice for Measurement of Corrosion Potentials of Aluminum Alloys; and ASTM G 82, Guide for Development and Use of a Galvanic Series for Predicting Galvanic Corrosion Performance. The corrosion potential (ASTM G 69) often is used for metallurgical purposes, i.e., determination of the amount of material in solid solution, heat-affected areas from welding, and the validity of thermal treatments.

### Filiform Corrosion

To date there is no standardized filiform corrosion test, but it appears that chloride ions and high humidity are required for initiation and propagation. Laboratory tests that have been used are the 3.5 % NaCl alternate immersion test, ASTM G 44, or exposure to hydrochloric acid vapors

TABLE 2—Relative general corrosion and SCC ratings.

Ratings:<sup>a</sup>

- (1) *General Corrosion*: Relative ratings from A through D are in decreasing order of merit. Material rated A or B can be used in some applications without protection.
- (2) *SCC*: Ratings apply to the short transverse direction of products with a critical directional grain structure. Relative ratings from 1 through 5 are in decreasing order of merit. Material rating 1 is not susceptible to SCC, rating 2 is resistant at stresses up to 75% Y.S., rating 3 is resistant at stresses up to 50% Y.S., rating 4 is resistant at low stresses, 105 to 170 MPa, while rating 5 has incurred some failures even at the lowest stress level tested, 48 MPa.

Wrought, Strain-Hardened Alloys					
Type of Alloy	Commercial Examples	General Corrosion		Stress-Corrosion Cracking	
		Temper	Rating (1)	Temper	Rating (2)
Unalloyed Al	1100, 1230	All	A	All	1
Al-Mn	3003, 3004	All	A	All	1
Al-Mg	5052, 5454	All	A	All	1
Al-Mg-Mn	5083, 5456	All	A <sup>b</sup>	All	1 <sup>b</sup>
Wrought, Heat-Treated Alloys					
Al-Mg-Si	6061, 6013	T6	B	T6	2
Al-Cu	2024, 2324	T3, T39	C or D <sup>c</sup>	T3, T39	5
Al-Cu	2024, 2219	T8	C	T8	2
Al-Zn-Mg	7005	T6	B	T6	5
Al-Zn-Mg-Cu	7075	T6	C or D <sup>c</sup>	T6	5
Al-Zn-Mg-Cu	7075	T73	C	T73	2
Al-Zn-Mg-Cu	7050	T74	C	T74	3
Al-Zn-Mg-Cu	7075, 7150	T76	C	T76	4
Al-Zn-Mg-Cu	7150, 7055	T77	C	T77	4

<sup>a</sup>See Refs 34, 35, and ASTM G 64 for more detailed comparison, including other alloys.

<sup>b</sup>Ratings will be lower if material in a non-stabilized temper is heated at 80 to 175°C.

<sup>c</sup>The D rating applies to thick products susceptible to intergranular corrosion and exfoliation.

for 24 h followed by prolonged exposure to high humidity at slightly elevated temperatures of about 50–65°C [31].

Publications on filiform test methodology are anticipated in the near future due to the current interest in aluminum for auto body sheet, together with the need to maintain an aesthetically pleasing painted surface. This form of corrosion can occur during exposure to seacoast atmosphere, and it has been developed at inland atmospheric exposure sites by spraying the specimens periodically (about three times per week) with a 3–5 % solution of sodium chloride.

### Protective Coatings

Evaluation of the protective ability of coatings generally is made in salt spray cabinets, such as those covered in ASTM B 117 and G 85 or in the 3.5 % NaCl alternate immersion test (G 44).

Recent investigations, primarily on steel, have established the desirability of including ultraviolet (UV) light as part of the exposure cycle since UV light has a degrading effect on paints and other organic coatings. The significance of such tests on coated aluminum has not yet been fully established.

Furthermore, there is considerable interest in potentiodynamic polarization techniques to rapidly assess the durability of coated aluminum surfaces that have been painted or given various polymeric or anodic surface treatments [32,33]. Refer also to Chapter 56 in this section of the manual.

### RELATIVE COMPARISON OF CORROSION BEHAVIOR

A brief relative comparison of wrought, strain-hardened, and heat-treated alloys is given in Table 2. More detailed comparisons can be found in the following three references: Comparison of the general and the stress-corrosion resistance of registered alloys [34], Classification of SCC resistance of high-strength alloys (see ASTM G 64), and Comparison of the general corrosion resistance of weldments [35].

### REFERENCES

- [1] Pourbaix, M., *Atlas of Electrochemical Equilibria in Aqueous Solutions*, Pergamon Press, Oxford, 1966, p 169.
- [2] Ch. 7, *Aluminum—Properties, Physical Metallurgy and Phase Diagrams*, American Society for Metals, K. R. Van Horn, Ed., 1967.
- [3] Chs. 5–7, *Aluminum—Properties and Physical Metallurgy*, American Society for Metals, J. E. Hatch, Ed., 1984.
- [4] Sprowls, D. O. and Brown, R. H., "What Every Good Engineer Should Know About Stress Corrosion of Aluminum," *Metals Progress*, April 1962, pp. 79–85 and May 1962, pp. 77–83.
- [5] "TEMPERS for Aluminum and Aluminum Alloy Products Registered with The Aluminum Association," *The Aluminum Association*, 1 Sept. 1984.
- [6] Holroyd, N. J. H., "Environmental-Induced Cracking of High-Strength Aluminum Alloys," *Proceedings of the First International Conference on Environment-Induced Cracking of Metals*, October 1988, pp. 311–345.
- [7] Burleigh, T. D., "The Postulated Mechanisms for Stress Corrosion Cracking of Aluminum Alloys—A Review of the Literature 1980–1989," *Corrosion*, Vol. 47, No. 2, February 1991, pp. 89–98.
- [8] *The Corrosion Handbook*, H. H. Uhlig, Ed., John Wiley & Sons, Inc., NY, 1948.
- [9] Juniere, P. and Sigwaldt, M., *Aluminum—Its Application in the Chemical and Food Industries*, translated from French by W. C. Barnes, First American Edition, Chemical Publishing Co. Inc., NY, 1964.
- [10] "Guidelines for the Use of Aluminum with Food and Chemicals," *The Aluminum Association Handbook*, Fifth Edition, 1984.
- [11] Brown, M. H., Brown, R. H., and Binger, W. W., "Aluminum Alloys for Handling High Temperature Water," *Alcoa Green Letter*, March 1960.
- [12] Dix, E. H., Anderson, W. A., and Shumaker, M. B., "Development of Wrought Aluminum-Magnesium Alloys," Technical Paper 14, Aluminum Company of America, 1958.
- [13] Moran, J. P. and Byrne, S. C., "Galvanic Corrosion, Its Principles and Guidelines for Prevention," 15 July 1993, available on request from Information Department, Alcoa Technical Center, PA, 15069-0001.
- [14] Godard, H., *Corrosion of Light Metals*, John Wiley and Sons, NY, 1967.
- [15] Hollingsworth, E. H. and Hunsicker, H. Y., "Corrosion Resistance of Aluminum Alloys," *Metals Handbook*, 9th Edition, Vol. 2, Properties and Selections of Nonferrous Alloys, ASM, Materials Park, OH, 1979, pp. 204–236.
- [16] Summerson, T. J. and Sprowls, D. O., "Corrosion Behavior of Aluminum Alloys," International Conference of the Hall-Heroult Process, University of Virginia, 15–20 June 1986, Vol. III of Conference Proceedings, Engineering Materials Advisory Services Ltd., Warley, West Midlands, U.K., pp. 1576–1662.
- [17] Jones, S. A., Colvin, E. L., and Magnusen, P. E., "Synergistic Effects of Corrosion and Fatigue on Aluminum Fuselage Alloys," Presented at ASM AeroMet '92 Conference, Anaheim, CA, May 1992.
- [18] Lifka, B. W., "Corrosion Resistance of Aluminum Alloy Plate in Rural, Industrial and Seacoast Atmospheres," *Aluminum*, Vol. 63, No. 12, 1987, pp. 1256–1261.
- [19] Burleigh, T. D., Gillespie, E. H., and Biondich, S. C., "Blowout of Aluminum Alloy 5182 Can Ends Caused by Transgranular Stress Corrosion Cracking," Preprint from TMS Meeting, 15 November 1992.
- [20] Sprowls, D. O., Shumaker, M. B., Coursen, J. W., and Walsh, J. D., Final Report of NASA, Huntsville Contract NAS 8-21487, Part I, "Evaluation of SCC Susceptibility Using Fracture Mechanic Techniques: Aluminum, Titanium and pH Steels," 31 May 1973.
- [21] Lifka, B. W., "SCC Resistant Aluminum Alloy in Various Environments," *Aluminum*, Vol. 53, No. 12, 1977, pp. 750–752.
- [22] Lifka, B. W. and Sprowls, D. O., "Significance of IGC of High Strength Aluminum Alloy Products," *Localized Corrosion—Cause of Metal Failure, ASTM STP 516*, ASTM International, West Conshohocken, PA, 1972.
- [23] Craig, H. L., Jr., "Nitric Acid Mass Loss Test for the H116 and H117 Tempers of 5086 and 5456 Aluminum Alloys," *Localized Corrosion—Cause of Metal Failure, ASTM STP 516*, ASTM International, West Conshohocken, PA, 1972, pp. 17–37.
- [24] Sprowls, D. O., Walsh, J. D., and Shumaker, M. B., "Simplified Exfoliation Testing of Aluminum Alloys," *Localized Corrosion—Cause of Metal Failure, ASTM STP 516*, ASTM International, West Conshohocken, PA, 1972.
- [25] Sprowls, D. O., Summerson, T. J., et al., "Tentative Exfoliation Test for Al-Mg Alloys for Boat and Ship Hull Construction," *Aluminum Association*, 1970.
- [26] Lee, S. and Lifka, B. W., "Modification of the EXCO Test Method for Exfoliation Corrosion Susceptibility in 7xxx, 2xxx and Al-Li Aluminum Alloys," *New Methods for Corrosion Testing of Aluminum Alloys, ASTM STP 1134*, ASTM International, West Conshohocken, PA, 1992.

- [27] Lifka, B. W. and Sprowls, D. O., "Relationship of Accelerated Test Methods for Exfoliation Resistance in 7xxx Series Alloys with Exposure to a Seacoast Atmosphere," *Corrosion in Natural Environments*, ASTM STP 558, ASTM International, West Conshohocken, PA, 1974.
- [28] Ketcham, S. J. and Jankowsky, E. J., "Developing an Accelerated Test: Problems and Pitfalls," *Laboratory Corrosion Tests and Standards*, ASTM STP 866, ASTM International, West Conshohocken, PA, 1985.
- [29] Sprowls, D. O., Bucci, R. J., Ponchel, B. M., et al., "Phase II—The Breaking Load Test Method," NASA Contract Report 172387, 31 August 1984.
- [30] Colvin, E. L. and Emptage, M. R., "The Breaking Load Method: Results and Statistical Modification from the ASTM Interlaboratory Test Program," *New Methods for Corrosion Testing of Aluminum Alloys*, ASTM STP 1134, ASTM International, West Conshohocken, PA, 1992, pp. 82–100.
- [31] Ford Motor Company Specification for Filiform Corrosion Test, Number FLTMBI 124-1.
- [32] Mansfeld, F. and Kendig, M. W., "Evaluation of Anodized Aluminum Surfaces with Electrochemical Impedance Spectroscopy," *Journal of Electrochemical Society*, Vol. 135, Part 4, April 1988, pp. 828–833.
- [33] Nisancioglu, K., Lunden, O., and Holtan, H., "Improving the Corrosion Resistance of Aluminum Alloys by Cathodic Polarization in Aqueous Media," *Corrosion*, Vol. 41, No. 5, May 1985, pp. 247–255.
- [34] "Aluminum Standards and Data, Table 3.3, Comparative Characteristics and Applications," *The Aluminum Association, Tenth Edition*, 1990, pp. 51–53.
- [35] *ALUMINUM—Properties and Physical Metallurgy—Table 4a, b, and c, Aluminum Filler Alloy Chart (column C)*, American Society for Metals, J. E. Hatch, Ed., 1984, pp. 286–291.

# Steels

*M. E. Komp<sup>1</sup>, D. L. Jordan,<sup>2</sup> and R. Baboian<sup>3</sup>*

IN MOST INSTANCES, corrosion test methods for plain carbon steels, high-strength low-alloy steels, and alloy steels do not differ greatly. Therefore, these steels are grouped together for the purposes of this chapter. (Alloy steels here refers to heat treatable constructional and automotive steels, and does not include the stainless steels or other high alloys.) There are some differences in the corrosion test methods used for different mill products of this group of steels, and these will be discussed. The steels covered in this chapter are defined below.

Carbon steels are basically alloys of iron and carbon, with only small amounts of other elements present. For most of the steels discussed here, the carbon content ranges up to 1 %. However, there are some specialty steels in which carbon content may range up to 2 %. Carbon steels always contain some manganese, silicon, phosphorus, and sulfur; minor amounts of other elements may also be present. The American Iron and Steel Institute (AISI) specifies that carbon steel may contain up to 1.65 % manganese, 0.6 % silicon, and 0.6 % copper [1].

High-strength low-alloy (HSLA) steels contain additional alloying elements (up to a total of 3–4 %), which increase strength and, in some grades, improve atmospheric corrosion resistance. Usually they are supplied in the as-rolled or normalized condition, although some can be supplied in the quench-and-tempered condition. Alloying elements commonly present in HSLA steels include nickel, chromium, copper, silicon, phosphorus, columbium, vanadium, and titanium. Typical HSLA steels are described in the following specifications:

- ASTM A 242, Specification for High-Strength Low-Alloy Structural Steel
- ASTM A 572, Specification for High-Strength Low-Alloy Columbium-Vanadium Steels of Structural Quality
- ASTM A 588, Specification for High-Strength Low-Alloy Structural Steel with 50 ksi (345 MPa) Minimum Yield Point to 4 in. (100 mm) Thick
- ASTM A 606, Specification for Steel, Sheet and Strip, High-Strength, Low-Alloy, Hot-Rolled and Cold-Rolled, with Improved Atmospheric Corrosion Resistance

<sup>1</sup>Deceased, formerly with USS, a Division of USX Corporation, Monroeville, PA 15146.

<sup>2</sup>Formerly Staff Engineer, Inland Steel Flat Products Company, a Subsidiary of Inland Steel Industries, East Chicago, IN 46312.

<sup>3</sup>RB Corrosion Service, Greenville, RI 02828.

- ASTM A 852, Specification for Quenched and Tempered Low-Alloy Structural Steel Plate with 70 ksi (485 MPa) Minimum Yield Strength to 4 in. (100 mm) Thick

Minimum yield strengths for HSLA steels range from 40 000 to 70 000 psi (275–485 MPa.)

Alloy steels include the constructional alloy steels, which are normally supplied in the quenched-and-tempered condition with yield strengths of 100 000 psi (690 MPa) or higher, as described in the following specifications:

- ASTM A 514, Specification for High-Yield-Strength, Quenched and Tempered Alloy Steel Plate, Suitable for Welding
- ASTM A 517, Specification for Pressure Vessel Plates, Alloy Steel, High-Strength, Quenched and Tempered

Also included are the heat treatable constructional alloy steels identified in the Unified Numbering System (UNS) as designations between G13XXX and G94XXX, inclusive. These latter steels are also referred to as SAE-AISI alloy steels. The alloy steels generally contain somewhat higher carbon and alloy content than the HSLA steels (up to a total of about 5 %.) Stainless steels and other high alloys are not included in this category; they are covered in other chapters in this section. Mill products available in carbon, HSLA, and alloy steels include bar, plates, structural shapes, sheet, strip, tubular products, and wire.

## METALLURGICAL EFFECTS ON CORROSION

### Composition

Small amounts of alloying elements in steel can have a significant beneficial effect on corrosion in the atmosphere. Copper-bearing steels (0.2 % copper, minimum) have long been used for this purpose. In the HSLA weathering steels, small additions of elements such as chromium, silicon, copper, nickel, and phosphorus are used to achieve even greater resistance to atmospheric corrosion.

Under immersed conditions in natural waters, in neutral or alkaline solutions, or when buried in soil, the chemical composition of carbon, HSLA, and alloy steels has little effect on corrosion rates. In acid solutions, however, the composition can have a pronounced effect on corrosion. Rates of corrosion in acid increase with increasing carbon and nitrogen content of the steel. Sulfur and phosphorus

also increase the rate of attack, whereas copper additions counteract this effect.

### Microstructure

The microstructure of these steels has little effect on corrosion in the atmosphere or in neutral or alkaline solutions. In acids, however, microstructure can have a significant effect because the carbide morphology affects the hydrogen discharge reaction. Untempered martensitic and pearlitic structures generally show the lowest rates of attack in acids, whereas tempered martensite and spheroidized structures show much higher rates [2].

## ENVIRONMENTAL EFFECTS ON CORROSION

### Atmospheric

The main environmental factors that govern the corrosion rate of steel in the atmosphere are temperature, time-of-wetness, and type and amount of chemical contamination. Time-of-wetness includes not only time when the steel is wet from precipitation or dew, but also time above a certain "critical humidity," which can vary from about 50–70 % relative humidity, depending upon the contaminants present in the air [3]. For most inland sites, the most important chemical contaminant affecting atmospheric corrosion of steel is sulfur dioxide. At coastal sites, and locations where de-icing salts are used, chloride content is most important.

### Aqueous

In natural waters and other aqueous environments, corrosion of steel is controlled by the concentration of dissolved oxygen, temperature, acidity (pH), dissolved salts, and flow velocity. Corrosion rate is relatively constant between pH 4 and pH 10. At pH < 4, acid attack with hydrogen evolution generally occurs. In some acidic environments, particularly those containing sulfides or cyanides, or both, the hydrogen generated can diffuse into the steel and can result in blistering of low-strength steels and cracking of high-strength steels. Above pH 10, corrosion rate decreases. Dissolved salts generally increase corrosion rates because they increase the conductivity of the solution. However, in natural waters some calcium and magnesium salts (present in "hard" water) can be beneficial because they form insoluble protective films on the steel.

### Soils

Corrosion of steel buried in soil is largely controlled by moisture content, conductivity (dissolved salts), degree of aeration, and acidity (pH) of the soil. The effects of these factors are much the same as for immersed conditions in water. Corrosion caused by bacteria also may be important in soils. For example, under anaerobic (oxygen-free) conditions, sulfate-reducing bacteria in soil can form hydrogen sulfide, which attacks steel. Aerobic organisms can also cause corrosion. This entire subject is referred to as MIC (microbiologically influenced corrosion) [4].

### High Temperatures

The high temperature oxidation rate of carbon steels in air, steam, and other oxidizing gases is generally considered to be negligible below about 1000°F (540°C). For HSLA and alloy steels, the maximum temperature can be somewhat higher, depending primarily on the chromium, silicon, and aluminum contents of the steel. In reducing gases, the presence of sulfur and halogen compounds can create a much more aggressive environment and may preclude the use of these steels at elevated temperatures.

High-temperature hydrogen environments can cause severe damage to carbon steel at temperatures above about 425°F (220°C). Hydrogen diffuses into the steel and reacts with iron carbides to form methane. The resulting high internal pressures in the steel can result in cracking failures. Hydrogen damage in steel is effectively inhibited by alloying with strong carbide formers such as chromium, molybdenum, titanium, and vanadium. Diagrams showing the safe operating limits for carbon and alloy steels in high temperature hydrogen environments are available in the literature [5,6].

Some liquid metals can severely corrode carbon and low-alloy steels, usually by intergranular attack, and can also result in embrittlement and cracking failures. Molten lead-tin solder, brass, bronze, copper, and zinc are among the metals that reportedly can cause these problems under certain conditions [7].

## GENERAL CORROSION TESTING CONSIDERATIONS

In selecting a corrosion test method for steels, a number of issues must be considered and resolved. The purpose of the test must be carefully stated. Corrosion tests meant to predict long-term durability differ from those used to rank material performance in an idealized environment, which, in turn, differ from tests geared toward understanding why materials behave the way they do. The tests noted in this chapter are outlined in detail in standards published by ASTM, NACE International (formerly National Association of Corrosion Engineers), Society of Automotive Engineers (SAE), International Organization for Standardization (ISO), and German Standards Institution (DIN), and focus on long-term performance and ranking. Specialized tests for mechanism studies will not be addressed, since such tests are often developed specifically for a particular, sometimes unique, situation. Specialized tests are under constant refinement and are reported regularly in technical and scholarly journals. Corrosion testing of steels with metallic and organic coatings is covered in another chapter in this section. Details concerning mechanisms associated with the various corrosion types are discussed in another section of this manual.

The performance characteristic to be determined, e.g., mass loss, thickness loss, or strength loss, must be specified before selecting and performing the corrosion test. The environment must be specified, and a decision on whether or not to test in that specific environment (i.e., an in-plant or in-service test) or in a simulated environment (i.e., in a laboratory test) must be made. Any deviations from the actual

in-service conditions may make the testing simpler to accomplish, but will invariably introduce uncertainties into the data and resulting conclusions.

Before embarking on any corrosion testing program, the recommendations of the following documents should be read and understood:

- ASTM G 1, Practice for Preparing, Cleaning, and Evaluating Corrosion Test Specimens
- ASTM G 15, Definitions of Terms Relating to Corrosion and Corrosion Testing
- ASTM G 16, Practice for Applying Statistics to Analysis of Corrosion Data
- NACE Recommended Practice-Collection and Identification of Corrosion Products (RP0173)

Chemical cleaning of corroded iron and steel often involves hazardous chemicals, so recognition of the safety considerations listed in ASTM G 1 is mandatory.

Of particular interest to users of iron and steel is the presence of the passive film. The passive film and its breakdown are major controllers of iron and steel corrosion, so factors that influence the film (e.g., chloride ion, atmospheric oxygen, abrasion) must be carefully considered during test selection, sample preparation, and test execution.

## CORROSION TEST METHODS APPLICABLE TO ALL MILL PRODUCTS

### Uniform Corrosion

Uniform corrosion is responsible for the largest amount of corrosion damage, on a tonnage basis, of any type of corrosion. It is characterized by attack that occurs uniformly over the metal, with no concentrations in localized areas. Fortunately, methods are available to predict the corrosion rate, the extent of subsequent metal thinning, and the probable failure time, based on accurate knowledge of the metal and environment. This chapter will briefly describe the use of standard tests for uniform corrosion and will indicate possible testing pitfalls specifically associated with iron and steel.

In-service or in-plant tests are particularly useful in estimating the service life of steel, since the exposure conditions are considered to be realistic. The following documents clearly outline procedures to obtain meaningful corrosion rates for steels in their respective applications and environments:

- ASTM G 4, Guide for Conducting Corrosion Coupon Tests in Field Applications
- NACE Recommended Practice-Preparation and Installation of Corrosion Coupons and Interpretation of Test Data in Oil Production Practice (RP0775)
- SAE Recommended Practice for Undervehicle Coupon Corrosion Tests (J1293)
- ASTM G 52, Practice for Exposing and Evaluating Metals and Alloys in Surface Seawater

Care should be taken to prepare test materials with precisely the same processing history as those expected to be in service, since surface and bulk characteristics of the steel can dramatically influence the corrosion rate. Chemical

**TABLE 1**—Relative corrosivity of atmospheric corrosion test sites.<sup>a,b</sup>

Site	No. of Years			
	1	2	4	8
State College, PA (rural)	1.0	1.0	1.0	1.0
South Bend, PA (semi-rural)	1.5	1.5	1.6	1.7
Kure Beach, NC (marine)	2.0	2.5	3.5	5.8
Kearney, NJ (industrial)	3.3	2.7	2.5	2.6

<sup>a</sup>State College, PA as unity.

<sup>b</sup>From Ref 8.

cleaning, temper rolling, shot peening, or specialized heat treatments must be considered in that regard.

ASTM G 50, Practice for Conducting Atmospheric Corrosion Tests on Metals, is widely used, but care must be taken to interpret the results as being applicable only to the selected test site. Atmospheric corrosion testing involves exposing specimens of the test material to given environments for fixed periods of time. The typical measured response is mass loss, which can be converted to depth of penetration per unit time. Such a conversion assumes that the corrosion proceeds uniformly over the metal surface; localized corrosion is not considered in the treatment. It is common to test sheet or plate materials, due to their easily controllable geometry and placement in the corrosion environment. Shapes such as bolts, formed sheet, and fabricated parts, while often useful for product evaluation, complicate corrosion evaluation procedures. Different locations on irregular samples experience different exposure conditions; partially sheltered portions, skyward surfaces, groundward surfaces, and various angles from horizontal cannot be expected to experience the same corrosion rates. Table 1 shows that the measured corrosion rate for mild steel in one geographic location may differ significantly from that in another location [8]. Likewise, rankings of related materials may be different for different exposure locations. Clearly, selection of an atmospheric test location that adequately simulates the expected service environment is of utmost importance. Useful methods to determine and classify the corrosivities of different atmospheres are given in the following standards:

- ASTM G 92, Practice for Characterization of Atmospheric Test Sites
- ISO Standard-Corrosion of Metals and Alloys-Corrosivity of Atmospheres-Classification (9223)
- ISO Standard-Corrosion of Metals and Alloys-Corrosivity of Atmospheres-Guiding Values for the Corrosivity Categories (9224)

When it is impractical to test in service, laboratory simulations of the corrosive exposures may be necessary. Immersion tests, cabinet tests, and electrochemical measurements are in widespread use, but do not necessarily provide results that correlate with service exposures. However, relative rankings of selected materials under controlled testing conditions can be useful in materials development.

Guidelines for determining mass loss of a metal exposed in an apparatus that contains a solution of interest are provided in the following standards:

- ASTM G 31, Standard Practice for Laboratory Immersion Testing of Metals
- NACE Standard Test Method-Laboratory Corrosion Testing of Metals for the Process Industries (TM0169)

The apparatus may control temperature, aeration, agitation, or other parameters, depending on the service conditions that are to be simulated.

Guidelines for specialized cases of immersion testing of metals, including steels, are provided in the following standards:

- NACE Standard Test Method-Method of Conducting Controlled Velocity Laboratory Corrosion Tests (TM0270)
- NACE Standard Test Method-Autoclave Corrosion Testing of Metals in High Temperature Water (TM0171)
- NACE Standard Test Method-Dynamic Corrosion Testing of Metals in High Temperature Water (TM0274)
- ASTM G 129, Practice for Slow Strain Rate Testing to Evaluate the Susceptibility of Metallic Materials to Environmentally Assisted Cracking (EAC)

Many so-called cabinet tests are used to detect lot-to-lot variation of materials. Cabinet tests involve exposure of a material to an aqueous fog that may contain a variety of corrosive species (e.g., chlorides, sulfates), either singly or in combination. The exposure conditions (e.g., temperature, solution pH, solution specific gravity, fog delivery rate, position of specimens) are carefully specified and controlled. However, extensive efforts to correlate cabinet test results with those of service performance tests for many materials, including steel, have failed. The inability of the cabinet to reproduce the exposure conditions experienced in service is the primary contributor to that limitation. The unique interplay of the environment with the relatively fragile passive film on steel makes proper selection of exposure conditions mandatory. Standardized cabinet tests that could be adapted for quality control of uncoated steel are described in the following standards:

- ASTM B 117, Method of Salt Spray (Fog) Testing
- ASTM G 60, Test Method for Conducting Cyclic Humidity Tests
- ASTM G 85, Practice for Modified Salt Spray (Fog) Testing
- ASTM G 87, Practice for Conducting Moist SO<sub>2</sub> Tests

The electrochemical nature of corrosion may be studied effectively by a wide variety of electrochemical tests. Many of the tests require sophisticated instrumentation and expert interpretation and, therefore, have not been standardized. However, general guidelines for testing are described in the following standards:

- ASTM G 5, Reference Test Method for Making Potentiostatic and Potentiodynamic Anodic Polarization Measurements
- ASTM G 59, Practice for Conducting Potentiodynamic Polarization Resistance Measurements

It should be noted that many electrochemical measurements cause forced dissolution of the test material, and the actual corrosion rates of the material in service may have little or no correlation with the electrochemical results.

### Pitting Corrosion

Pitting is a type of localized corrosion where the corrosion rate differs at adjacent sites on the metal. Pits are frequently encountered during standard corrosion tests, expected to result in uniform corrosion. In those cases, only the interpretation of the results differs.

Testing for pitting corrosion is difficult, due to the probabilistic nature of its occurrence and the frequent difficulty of detecting the attack. Catastrophic perforation of the metal is often the first detectable manifestation of pitting.

The highly localized nature of pitting makes mass loss and mechanical property measurements meaningless. Pitting is usually characterized by measuring the maximum pit depth in a given area; measurements of average pit depth will not give an accurate indication of impending perforation.

ASTM G 46, Practice for Examination and Evaluation of Pitting Corrosion, recommends that pitting corrosion be quantified by destructive methods (metallographic or by machining) or by nondestructive methods (micrometer or microscopical measurements). A standard rating chart for pits is included in ASTM G 46.

ASTM G 61, Test Method for Conducting Cyclic Potentiodynamic Polarization Measurements for Localized Corrosion Susceptibility of Iron-, Nickel-, and Cobalt-Based Alloys, outlines an electrochemical procedure to screen and rank the pitting susceptibility of various metals. However, the electrochemical measurement does not necessarily correlate with pitting rates actually encountered in service.

### Crevice Corrosion

Crevice corrosion is associated with small amounts of stagnant electrolyte and frequently appears in lap joints, under bolt heads, or in other areas shielded from the surrounding environment. Many of the techniques used to characterize pitting corrosion are applicable to crevice corrosion.

### Galvanic Corrosion

Galvanic corrosion of a metal occurs as a result of electrical contact with a more noble conductor in a corrosive electrolyte. It is often called "dissimilar metal" corrosion. Galvanic corrosion can often be avoided by disconnecting the point of electrical contact. In cases where electrical isolation is not possible, proper material selection can help minimize the effect.

The primary detrimental effect of galvanic corrosion is electrochemical dissolution of the less noble member of the couple and is manifested in increased mass loss of that member. Therefore, techniques specified in ASTM G 1, ASTM G 15, and ASTM G 16 are applicable. In some instances, the more noble member of the couple can be adversely affected by cathodic reaction products OH<sup>-</sup>, H<sub>2</sub>, or H<sub>2</sub>.

ASTM G 71, Guide for Conducting and Evaluating Galvanic Corrosion Tests in Electrolytes, outlines recommended procedures and possible pitfalls in performing galvanic corrosion tests. Specimen geometry is the primary difference between galvanic corrosion testing and testing for uniform corrosion, due in part to its effect on current flow. Several useful sample geometries include wire-on-bolt, stacked washers, and stacked plates [9]. ASTM G 116, Practice for Conducting Wire-on-Bolt Test for Atmospheric Galvanic Corrosion, provides practical details for testing anodic metals.

### Stress Corrosion Cracking

SCC occurs in susceptible alloys and products under the simultaneous application of tensile stress and corrosive



environment. Methods of applying the test environment for SCC susceptibility screening tests for all mill products are described in the following standards:

- ASTM G 41, Test Method for Determining Cracking Susceptibility of Metals Exposed Under Stress to a Hot Salt Environment
- ASTM G 44, Practice for Evaluating Stress Corrosion Cracking Resistance of Metals and Alloys by Alternate Immersion in 3.5 % Sodium Chloride Solution

The atmospheric exposure outlined in ASTM G 50 may also be useful for SCC testing. Recommended exposure conditions, including solution composition, temperature, and drying cycles are listed. The time to first appearance of cracking is recorded. The stress state to be tested depends in large part on the geometry of the actual part, and methods to apply particular stress states to test specimens will be described in later paragraphs.

Slow strain-rate tests, in which standard tension test specimens are subjected to a constant extension rate of 10–4 to 10–6 m/s while being exposed to a corrosive environment, provide a relatively quick method for SCC screening of metals. Such methods are described in the following standards:

- ISO Standard-Corrosion of Metals and Alloys-Stress-Corrosion Testing-Part 7: Slow Strain-Rate Testing (7539-7)
- Proposed NACE Standard Test Method-Slow Strain Rate Test Method for Screening Corrosion Resistant Alloys (CRAs) for Stress Corrosion Cracking in Sour Oilfield Service (Task Group T-1F-9)

The methods are also discussed in detail in Ref 10.

The above methods for SCC testing are not widely used for carbon and low-alloy steels.

## CORROSION TEST METHODS APPLICABLE TO SPECIFIC MILL PRODUCTS

### Sheet and Strip

Nearly all of the standard test methods mentioned previously are applicable to sheet and strip. An important test that is best run on flat specimens is ASTM F 1113, Test Method for Electrochemical Measurement of Diffusible Hydrogen in Steels (Barnacle Electrode). This test measures the amount of diffusible (atomic) hydrogen in a steel sample by electrochemically oxidizing the atomic H to H<sup>+</sup>, which then combines with hydroxyl ions (OH<sup>-</sup>) in the electrolyte to form water. The atomic H can cause hydrogen embrittlement, a condition that reduces the ductility of a metal and results in cracking. Much of the testing for hydrogen embrittlement is associated with electroplated steels and is covered elsewhere in this section.

Procedures for making flat SCC specimens with specific stress states are outlined in the following standards:

- ASTM G 30, Practice for Making and Using U-Bend Stress-Corrosion Test Specimens
- ASTM G 39, Practice for Preparation and Use of Bent-Beam Stress-Corrosion Test Specimens
- ASTM G 49, Practice for Preparation and Use of Direct Tension Stress Corrosion Test Specimens

The specimens may then be tested by methods outlined in ASTM G 36, ASTM G 41, ASTM G 44, or ASTM G 50. A constant strain condition is maintained in the U-bend geometry specified in ASTM G 30; varying the bend radius controls the strain level. ASTM G 39 describes the bent beam SCC test specimen, which is similar in concept to the U-bend specimen, but is subject only to elastic strain. Axial loaded SCC test specimens are covered in ASTM G 49 and can be tested under constant strain, constant load, or varying strain rates. All of the SCC specimen preparation procedures for sheet and strip require careful sampling, due to the anisotropy introduced by rolling; specification of rolling direction on each specimen is mandatory.

### Bar, Plate, and Structural Shapes

Many applications for bar, plate, and structural steel require use of painting or other protective measures; therefore, there is not a great need for corrosion testing of the bare metal. An important exception to this, however, is the use of weathering steels, such as those specified in ASTM A 242, ASTM A 588, and ASTM A 852 in atmospheric exposure. The corrosion resistance of these steels is such that they can be used in the unpainted condition for many applications, depending on the environmental conditions. For these applications, there is a need for atmospheric corrosion testing to determine the suitability of bare weathering steels in specific locations.

The general recommendations given in ASTM G 50 can be followed for testing of weathering steels. Corrosion penetration calculated from mass loss after removal of corrosion products (per ASTM G 1) is the main criterion used, although pit depth and appearance are also used. However, it should be recognized that the corrosion rate of relatively small test panels of steel in the atmosphere may be substantially different than that of a massive structure, such as a bridge or large building. A large structure acts as a greater heat sink and has fewer temperature fluctuations, as compared to that of a small test panel; thus, time-of-wetness can be appreciably different. As indicated earlier, time-of-wetness is a significant factor in determining atmospheric corrosion rates.

For specific applications of bare weathering steel, it is desirable to test a mock-up containing the type of bolted and/or welded joints that will be used in the intended structure, and also the orientation conditions that the bare steel will encounter in the structure (e.g., horizontal, vertical facing north, 30° to the horizontal facing south, etc.). In addition to giving information on appearance and general corrosion rates in the specific environment, the mock-up can provide information on certain design details that should be avoided to prevent excessive localized corrosion.

ASTM G 101, Guide for Estimating the Atmospheric Corrosion Resistance of Low-Alloy Steels, presents two methods for use in estimating the performance of weathering steels in the atmosphere. The first method utilizes linear extrapolation of logarithmic plots of short-term atmospheric corrosion data to predict long-term performance. Examples of such predictions, taken from ASTM G 101, for ASTM A 242 and ASTM A 588 steels in industrial environments, are shown in Fig. 1.

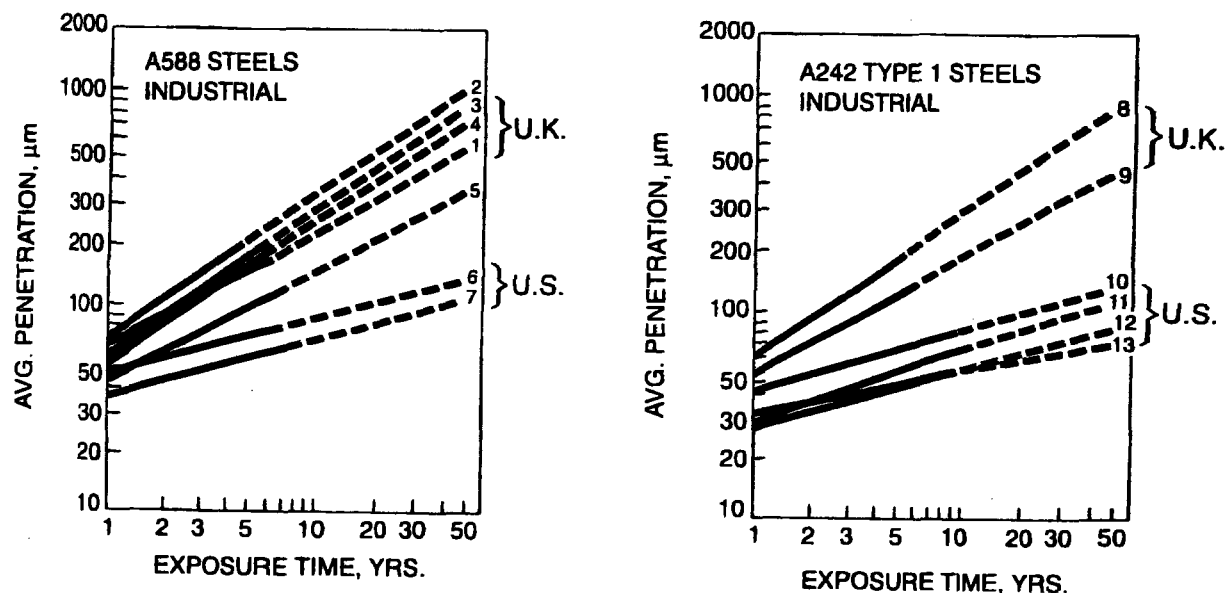


FIG. 1—Projected corrosion penetration of ASTM A 588 and ASTM A 242 Type 1 steels in industrial environments in the U.K. and the U.S. (see Table 2 for identification of lines). From ASTM G 101.

The specific locations from which these data were obtained are given in Table 2 (ASTM G 101).

The second method of ASTM G 101 uses a predictive equation, based on the chemical composition of the steel, to calculate a corrosion resistance index. If the index for a specific steel composition falls within the range normally expected for weathering steel, the indication is that the steel in question contains sufficient alloying elements (in the proper proportion) such that it should perform as a weathering steel. Averages and ranges of corrosion resistance indices, taken from ASTM G 101, for ASTM A 242 and ASTM A 588 steels, are shown in Table 3.

Additional tests that are used for bar and plate steels include those for sulfide stress cracking (SSC) and hydrogen-induced cracking (HIC), for applications involving exposure to oilfield environments containing hydrogen sulfide ( $H_2S$ ), and for applications in the petroleum refining industry. These tests are described in the subsection Tubular Products, which follows.

TABLE 2—Identification of penetration lines for industrial exposures, shown in Fig. 1.<sup>a</sup>

Line No.	Type of Steel	Exposure Site
1	A588 Grade A	Tinsley, U.K.
2	A588 Grade A	Teeside, U.K.
3	A588 Grade A	Battersea, U.K.
4	A588 Grade A	Middlesbrough, U.K.
5	A588 Grade A	Portishead, U.K.
6	A588 Grade B	Bethlehem, PA
7	A588 Grade B	Newark, NJ
8	A242 Type 1	Teeside, U.K.
9	A242 Type 1	Battersea, U.K.
10	A242 Type 1	Pittsburgh, PA
11	A242 Type 1	Pittsburgh, PA
12	A242 Type 1	Bethlehem, PA
13	A242 Type 1	Newark, NJ

<sup>a</sup>From ASTM G 101.

Because of the extensive use of steel reinforcing bars in concrete, corrosion tests of steel embedded in concrete are of interest. Procedures in the following standards are useful in this regard:

- ASTM C 876, Test Method for Half-Cell Potentials of Uncoated Reinforcing Steel in Concrete
- ASTM G 109, Test Method for Determining the Effects of Chemical Admixtures on the Corrosion of Embedded Steel Reinforcement in Concrete Exposed to Chloride Environments

Also, NACE Standard Recommended Practice-Design Considerations for Corrosion Control of Reinforcing Steel in Concrete (RP0187) contains recommendations for corrosion monitoring systems for steel in concrete.

### Tubular Products

Corrosion tests specifically applicable to tubular products involve primarily oil country goods exposed to sour ( $H_2S$ -containing) oil and brines. These test methods were developed and are published by NACE International.

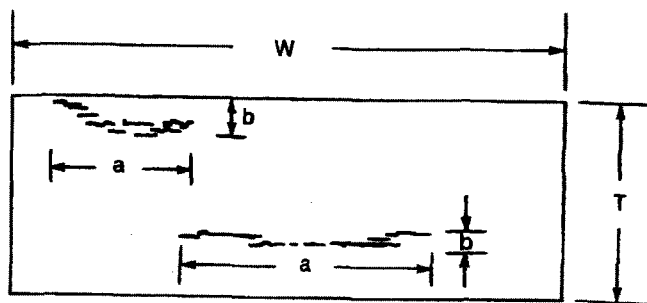
NACE Standard Test Method for Testing of Metals for Resistance to Sulfide Stress Cracking in  $H_2S$  Environments (TM0177) describes four test methods in which specimens stressed in tension are exposed to acidified brine saturated with  $H_2S$ . In Method A of this test, standard tension test specimens are used and the tensile stress is applied by either

TABLE 3—Atmospheric corrosion indices calculated from a modified Legault-Leckie equation for an industrial atmosphere<sup>a</sup> (36 heats of each steel).

Steel	Atmospheric Corrosion Index (1) <sup>b</sup>	
	Avg.	Range
A242 Type 1	8.5	7.9–9.1
A588 Grade A	6.8	6.4–7.0

<sup>a</sup>From ASTM G 101.

<sup>b</sup>The higher the index, the greater the corrosion resistance.



$$\text{Crack Sensivity Ratio, CSR} = \frac{\sum(a \times b)}{W \times T} \times 100\%$$

$$\text{Crack Length Ratio, CLR} = \frac{\sum a}{W} \times 100\%$$

$$\text{Crack Thickness Ratio, CTR} = \frac{\sum b}{T} \times 100\%$$

Where: a = crack length  
 b = crack thickness  
 W = section width  
 T = specimen thickness

FIG. 2—Schematic illustrating method of determination of CSR, CLR, and CTR in NACE TM0284. (© Copyright 1987 by NACE International. All Rights Reserved by NACE; reprinted by permission.)

a constant-load or a sustained-load device, per ASTM G 49. Method B uses bent-beam specimens stressed with a constant-deflection device employing three-point bending of the specimen. Method C uses C-ring specimens in accordance with ASTM G 38, Practice for Making and Using C-Ring Stress-Corrosion Test Specimens, and is intended primarily for transverse tests of pipe or tubing. Method D uses a double cantilever beam (DCB) specimen, in accordance with ISO Standard-Corrosion of Metals and Alloys-Stress Corrosion Testing-Part 6: Preparation and Use of Pre-Cracked Specimens (7539-6). This method is a crack arrest type of fracture mechanics test, and measures resistance of the steel to crack propagation by SSC in terms of critical stress intensity  $K_{Isc}$ .

NACE Test Method for Evaluation of Pipeline Steels for Resistance to Stepwise Cracking (TM0284) consists of exposing unstressed specimens to synthetic seawater saturated with  $H_2S$ , and subsequently examining polished cross sections of the specimens at magnifications up to 100× to determine the extent of internal cracking. This method is commonly referred to as the HIC (hydrogen-induced cracking) test. It is intended primarily to evaluate the resistance of pipeline steels to stepwise cracking caused by hydrogen absorption. "Stepwise" cracking refers to linking up of cracks on adjacent planes through the wall of the pipe, which can reduce the effective wall thickness and lead to overstressing and rupture. Three criteria are used to evaluate cracking in the steels: Crack Sensivity Ratio (CSR), which

is the summation of the crack areas divided by the area of the examined section; Crack Length Ratio (CLR), which is the summation of the crack lengths divided by the section width; and Crack Thickness Ratio (CTR), which is the summation of crack thicknesses divided by the specimen thickness. The determination of these ratios is shown schematically in Fig. 2, taken from NACE TM0284. The ratios are all multiplied by 100 to convert them to percent. The NACE test standard does not include acceptable values for these ratios; this is a matter of negotiation between the buyer and the producer.

For evaluation of the effect of flow velocity on corrosion in pipelines, NACE Standard Test Method of Conducting Controlled Velocity Laboratory Corrosion Tests (TM0270) can be used to evaluate several steel samples at one time, at velocities up to 8 ft/s (244 cm/s).

## Wire

In addition to the standard tests noted previously for uniform corrosion in the atmosphere and in aqueous electrolytes, two SCC tests specifically developed for wire must be noted. DNA Standard-Testing the Resistance of Aluminum Wrought Alloy Against Stress Corrosion (DIN 50908) outlines the Fry test, which consists of applying a bending load to a wire immersed in an appropriate test electrolyte and noting the time to fracture. Recognizing that bending loads are not always experienced by wire in service (e.g., concrete reinforcement) de Bondt developed a similar test that employs an axial load [11].

## REFERENCES

- [1] *The Making, Shaping and Treating of Steel*, 10th ed., W. T. Lankford et al., Eds., Association of Iron and Steel Engineers, Pittsburgh, PA, 1985, p. 1277.
- [2] Uhlig, H. H., *Corrosion and Corrosion Control*, 2nd ed., John Wiley & Sons, New York, 1971, pp. 119-126.
- [3] Uhlig, H. H., *Corrosion and Corrosion Control*, 2nd ed., John Wiley & Sons, New York, 1971, pp. 171-172.
- [4] *Biologically Induced Corrosion*, S. C. Dexter, Ed., International Corrosion Conference Series, Vol. NACE-8, National Association of Corrosion Engineers, Houston, 1986.
- [5] *Corrosion Data Survey: Metals Section*, 6th ed., National Association of Corrosion Engineers, Houston, 1985, p. 174.
- [6] Prescott, G. R., "Materials Problems in the Hydrogen-Carbon Processing Industries," *Alloys in the Eighties*, Climax Molybdenum Company, pp. 303-315.
- [7] Rostoker, W., McCaughey, J., and Markus, H., *Embrittlement by Liquid Metals*, Reinhold Publishing Corporation, New York, 1960.
- [8] Leckie, H. P., "Corrosion Standards and Control in the Steel Industry," *Manual of Industrial Corrosion Standards and Control*, ASTM STP 534, F. H. Cocks, Ed., ASTM International, West Conshohocken, PA, 1973, pp. 209-235.
- [9] Hack, H. P., "Evaluation of Galvanic Corrosion," *Metals Handbook*, 9th ed., Vol. 13, ASM International, Metals Park, OH, 1987, pp. 234-238.
- [10] *Stress Corrosion Cracking—The Slow Strain Rate Technique*, ASTM STP 665, G. M. Ugiansky and J. H. Payer, Eds., ASTM International, West Conshohocken, PA, 1979.
- [11] de Bondt, M., *Corrosion*, Vol. 30, No. 8, 1974, pp. 267-273.

# Copper (and Alloys)

Arthur Cohen<sup>1</sup>

COPPER AND COPPER ALLOYS are produced in various mill-product forms such as bar, pipe, rod, tube, plate, sheet, wire and as castings. They are used widely because of their excellent corrosion resistance particularly when combined with their other properties, including outstanding electrical and thermal conductivities and ease of fabrication and joining. The copper alloys also possess superior resistance to biofouling.

## NATURE OF PROTECTIVE FILM

Copper and its alloys are unique in that their superior performance is associated with two factors. The first is that in accordance with the electromotive force (or galvanic) series, they display noble potentials. Second, they form a cuprous oxide ( $\text{Cu}_2\text{O}$ ) product film that is responsible for their protection. This  $\text{Cu}_2\text{O}$  film is tenaciously adherent.

For any corrosion reaction to proceed, copper ions and electrons must migrate through the  $\text{Cu}_2\text{O}$  film. Reducing the ionic or electronic conductivity of this film by doping the alloy with divalent or trivalent cations further improves corrosion resistance. In practice, alloying additions of aluminum, zinc, tin, iron, beryllium, and nickel are used to dope the corrosion product films, which lead to significant corrosion rate reduction.

## EFFECT OF ALLOY COMPOSITIONS

The various wrought and cast copper and copper alloy families are listed in Table 1 [1]. The corrosion performance of these alloy families has been widely reported [1–4].

### Copper and High Copper Alloys

These alloys possess similar corrosion resistance. They have excellent resistance to seawater corrosion and biofouling but are susceptible to erosion-corrosion at high water velocities. The high-copper alloys are used primarily in applications that require enhanced mechanical performance, often at slightly elevated temperature, with good thermal or electrical conductivity. Processing for increased strength in the high-copper alloys generally improves their resistance to erosion-corrosion.

<sup>1</sup>Formerly, Arthur Cohen & Associates, Albuquerque, New Mexico. Now deceased.

TABLE 1—Generic classification of copper alloys.

Generic Name	UNS Numbers	Composition
<b>Wrought Alloys</b>		
Coppers	C10100-C15760	>99% Cu
High-copper alloys	C16200-C19600	>96% Cu
Copper Beryllium	C17000-C17600	Cu-Be-Co-Ni
Brasses	C20500-C28580	Cu-Zn
Leaded brasses	C31200-C38590	Cu-Zn-Pb
Tin brasses	C40400-C49080	Cu-Zn-Sn-Pb
Phosphor bronzes	C50100-C52400	Cu-Sn-P
Leaded phosphor bronzes	C53200-C54800	Cu-Sn-Pb-P
Copper-phosphorus and copper-silver-phosphorus alloys	C55180-C55284	Cu-P-Ag
Aluminum bronzes	C60600-C64400	Cu-Al-Ni-Fe-Si-Sn
Silicon bronzes	C64700-C66100	Cu-Si-Sn
Other copper-zinc alloys	C66400-C69900	—
Copper nickels	C70000-C79900	Cu-Ni-Fe
Nickel silvers	C73200-C79900	Cu-Ni-Zn
<b>Cast Alloys</b>		
Coppers	C80100-C81100	>99% Cu
High-copper alloys	C81300-C82800	>94% Cu
Red and leaded red brasses	C83300-C85800	Cu-Zn-Sn-Pb (75–89% Cu)
Yellow and leaded yellow brasses	C85200-C85800	Cu-Zn-Sn-Pb (57–74% Cu)
Manganese and leaded manganese bronzes	C86100-C86800	Cu-Zn-Mn-Fe-Pb
Silicon bronzes, silicon brasses	C87300-C87900	Cu-Zn-Si
Copper-bismuth and copper-bismuth-selenium	C88000-C89999	(Cu-Zn-Sn-Bi) (64–91% Cu)
Tin bronzes and leaded tin bronzes	C90200-C94500	Cu-Sn-Zn-Pb
Nickel-tin bronze	C94700-C94900	Cu-Ni-Sn-Zn-Pb
Aluminum bronzes	C95200-C95810	Cu-Al-Fe-Ni
Copper-nickels	C96200-C96800	Cu-Ni-Fe
Nickel silvers	C97300-C97800	Cu-Ni-Zn-Pb-Sn
Leaded coppers	C98200-C98800	Cu-Pb
Miscellaneous alloys	C99300-C99750	—

### Brasses

The most widely used group of copper alloys is the brasses, which are basically copper-zinc alloys. The resistance of brasses to corrosion by aqueous solutions does not change markedly as long as the zinc content does not exceed about 15 %; above 15 % zinc, dezincification (or dealloying) may occur. Selective removal of zinc leaves a relatively porous and weak layer of copper.

Dezincification may be either plug-type (Fig. 1) or layer-type (Fig. 2) as exhibited.

FIG. 1—Plug-type dezincification (cross section) in a yellow brass (alloy C26000) tube (magnification 15 $\times$ ).

By contrast, the resistance to pitting is almost total when the zinc content exceeds 15 %. But the brasses that resist pitting are severely degraded by dezincification, which causes them to lose much of their strength [2] as illustrated in Fig. 3.

Quiescent or slowly moving saline solutions, brackish waters and mildly acidic solutions are environments that often lead to the dezincification of unmodified brasses.

Brasses containing the highest amounts of zinc have the best resistance where exposure to sulfur compounds is involved. Susceptibility to stress corrosion cracking (SCC) is affected significantly by the zinc content; alloys containing more zinc are more susceptible with resistance to SCC increasing substantially as zinc content decreases from 15 % to zero.

Elements such as lead or tellurium have no effect on the corrosion-resistant properties of copper or the binary copper-zinc alloys as they are added only to enhance the property of machinability.

### Tin Brasses

Tin additions significantly increase the corrosion resistance of some brasses, especially dezincification. Uninhibited Admiralty metal is a variation of Cartridge brass (alloy C26000), which is produced by the addition of 1 % tin to

FIG. 2—Layer-type dezincification (cross section) in a yellow brass (alloy C26000) threaded fastener (magnification 15 $\times$ ).

the basic 70Cu-30Zn composition. Its use as a heat exchanger tube has been replaced completely by the inhibited Admiralty alloys C44300-C44500. Uninhibited Naval brass is the alloy resulting from the addition of 0.75 % tin to the basic 60Cu-40Zn composition of Muntz metal (alloy C28000), which is widely used in tube sheet applications.

Cast brasses for marine use also are modified by the addition of tin, lead and sometimes nickel. The cast marine brasses are used for plumbing goods in moderate-performance seawater piping systems or in deck hardware for which they subsequently are chrome plated.

### Aluminum Brass

Aluminum oxide ( $\text{Al}_2\text{O}_3$ ) is an important constituent of the corrosion product film on this brass. Its presence markedly increases resistance to impingement attack in turbulent high velocity saline water. Arsenical aluminum brass (alloy C68700) tube used to be widely specified for marine condensers and heat exchangers in which impingement attack was likely to pose a serious problem. This alloy is susceptible to dezincification unless it is inhibited with a small amount of arsenic.

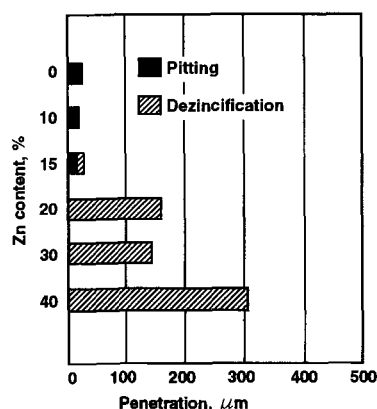
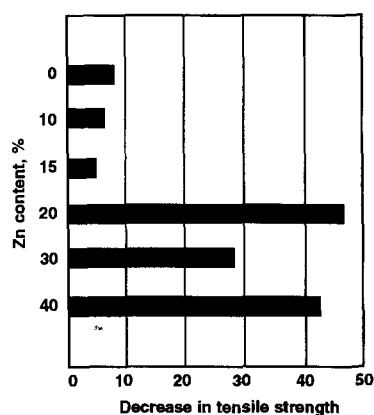


FIG. 3—Effect of zinc content on corrosion of brasses. Brass strip, 0.8 mm (0.032 in.) thick, was immersed for 60 days in 0.01M  $\text{NH}_4\text{Cl}$  solution at 45°C (113°F).

### Inhibited Alloys

The addition of arsenic, antimony, or phosphorus (typically 0.05 %) to Admiralty metal, Naval brass or aluminum brass produces high resistance to dezincification and SCC.

### Phosphor Bronzes

Additions of tin and phosphorus to copper produce alloys having good resistance to flowing seawater and to most non-oxidizing acids except hydrochloric. Alloys containing 8 to 10 % tin have high resistance to impingement attack. Phosphor bronzes are much less susceptible to SCC than bronzes and are similar to copper in their resistance to sulfur attack.

Tin bronzes tend to be used primarily in the cast form in which they are modified by further alloy additions of lead, zinc, and nickel. Contemporary uses include pumps, valves, gears, and bushings. This group of alloys has fair resistance to impingement and good resistance to biofouling.

### Copper Nickels

Alloy C71500 (70Cu-30Ni) has the best general resistance to aqueous corrosion of all the commercially important copper alloys, but C70600 (90Cu-10Ni) often is selected because it offers good resistance at lower cost. These alloys are used widely as condenser and heat exchanger tubes in recirculating steam systems in the chemical industry and are superior to copper and other copper alloys in resisting acid solutions and are highly resistant to impingement and SCC. They tend to be less resistant to pitting and crevice corrosion than the high copper alloys under certain conditions.

### Nickel Silvers

Alloy C75200 (nickel silver, 65-18) and C77000 (nickel silver 55-18), the two most common alloys in this family, have superior resistance to dezincification in both fresh and salt water over bronzes of similar copper content, chiefly because of their relatively high nickel contents.

### Copper-Silicon Alloys

These alloys generally have the same corrosion resistance as copper, but higher mechanical properties and superior weldability. They are somewhat better than the common bronzes in their resistance to SCC. However, evidence of their susceptibility to embrittlement by high-pressure steam makes them unsatisfactory in this application.

### Copper-Beryllium Alloys

As with other copper alloys used in electronics, beryllium copper can be supplied with solderability shelf life of 18 months or more. The alloys are essentially immune to cracking in sodium, potassium, magnesium, and mixed chloride salt solutions. They show no loss of ductility or strength under severe hydrogen charging conditions. Superior corrosion resistance and high hardness has led to their long successful service as undersea components, mold materials for plastic component manufacture, and instrument housings for oil and gas well drilling.

### Aluminum Bronzes

These alloys containing 5 to 12 % aluminum have excellent resistance to impingement corrosion and high-temperature oxidation. The corrosion characteristics of aluminum bronzes are related primarily to aluminum content. Alloys with up to 8 % aluminum have face-centered cubic alpha structures and good resistance to corrosion attack.

When the aluminum content exceeds 8 %, the alpha-beta duplex structures appear. The beta phase is a high-temperature phase retained at room temperature on fast cooling from 565°C (1050°F) or above. Slow cooling or long exposure at temperatures from 320 to 565°C (610 to 1050°F) tends to decompose the beta phase into a brittle alpha + gamma-2 eutectoid having either a lamellar or modular structure. The beta phase is less resistant to corrosion than the alpha phase, and eutectoid structures are even more susceptible to attack.

A corrosion mechanism similar to brass dezincification, known as dealuminification, can occur to the beta phase or eutectoid structure depending on environmental conditions. Proper quench and temper treatments produce a tempered beta structure with reprecipitated acicular alpha crystals, a combination often superior in corrosion resistance to the normal annealed structure. The nickel component in the more complex nickel aluminum bronzes alters the corrosion characteristics of the beta phase because of the nickel additive and gives greater resistance to dealloying and cavitation-erosion in most liquids.

### Cast Copper-Bismuth and Copper-Bismuth-Selenium

These cast alloys utilize bismuth and bismuth-selenium as a substitute for lead to facilitate machinability and pressure tightness in fluid carrying applications. Lead is not added intentionally to these alloys to minimize the amount that may leach in potable water systems and in other applications such as dairy product processing.

## SELECTION OF COPPER AND COPPER ALLOYS FOR SPECIFIC ENVIRONMENTS

In the following broad classifications, copper and copper alloys have demonstrated superior corrosion performance:

- Atmospheric exposure such as roofing and other architectural applications.
- Plumbing systems with superior corrosion resistance to both potable waters and soils.
- Marine applications involving supply lines, heat exchangers, and hardware where resistance to seawater and bio-fouling are mandatory.
- Industrial and chemical plant process equipment involving exposure to a wide variety of organic and inorganic chemicals.

While much corrosion performance data have been compiled by organizations such as the Copper Development Association (CDA) and the National Association of Corrosion Engineers (NACE), experience and field or laboratory

tests still remain the best criteria and are the most reliable guides for alloy selection for specific environments.

### Atmospheric Exposure

Copper and copper alloys perform well in industrial, marine, and rural atmospheres except in atmospheres containing ammonia which have been observed to cause SCC in brasses containing over 20 % zinc. Alloy C11000 (ETP copper) is the most widely used, particularly for roofing, flashing, gutters, and downspouts with alloys C22000 (commercial bronze), C23000 (red brass), C38500 (architectural bronze), and C75200 (65-12 nickel silver) accounting for much of the remainder.

### Water and Soils

The largest single application of copper tube is for hot and cold water distribution lines in building construction, with smaller amounts for heating and drainage lines and fire safety systems. Copper protects itself by forming a protective film, the degree of protection depending on mineral, oxygen, and carbon dioxide contents.

The brasses also perform well in unpolluted freshwaters but may experience dezincification in stagnant or slowly moving brackish or slightly acidic waters. The copper-nickels, silicon and aluminum bronzes display excellent resistance to corrosion.

Copper exhibits high resistance to corrosion in most soil types found throughout the United States. On the rare occasion where local soil conditions are unusually corrosive, some means of protection such as cathodic protection, neutralizing backfill (e.g., limestone), protective coatings, or wrappings may be helpful.

Studies on samples exposed underground have shown that tough pitch coppers, deoxidized coppers, silicon bronzes, and low-zinc brasses behave essentially alike. Soils containing cinders with high concentrations of sulfides, chlorides, or hydrogen ions corrode these materials. In this type of contaminated soil, alloys containing more than 22 % zinc experience dezincification. In soils that contain only sulfides, corrosion rates of the brasses decrease with increasing zinc content and no dezincification occurs.

For underground copper electric cables, the highest corrosion rate observed was in soils of lowest resistivity.

Due to the formation of a somewhat protective film, the corrosion rate of copper in quiescent ground waters tends to decrease with time, the rate depending on the amount of dissolved oxygen present.

### Steam

Copper and copper alloys resist attack by pure steam, but if carbon dioxide, oxygen, or ammonia is present, the condensate is corrosive.

### Steam Condensate

When the boiler feedwater is treated chemically to make the steam condensate relatively free of noncondensable gases, copper and copper alloys essentially are unattacked. The

presence of dissolved carbon dioxide, oxygen or both significantly increases the rate of attack.

Modern power utility boiler feedwater treatments commonly include the addition of organic amines to inhibit the corrosion of iron components of the system by scavenging oxygen and increasing the pH of the feedwater. These chemicals such as morpholine and hydrazine decompose in service to yield ammonia, which can be corrosive to some copper alloys. However, elevated oxygen levels are generally more deleterious than elevated ammonia levels.

### Salt Water

The superior performance of the inhibited admiralties, aluminum brass, aluminum bronzes, and copper-nickels over copper results from the combination of their corrosion product insolubility in seawater, erosion, and biofouling resistance.

Both alloys C70600 and C71500 display excellent resistance to pitting in seawater. The corrosion resistance of copper alloys in flowing seawater depends on the growth and maintenance of a protective film or corrosion product layers. The more adherent and protective the film on a particular alloy, the higher the velocity at which there is a transition from low- to high-corrosion rate and the greater its resistance to impingement attack or erosion-corrosion.

In general, the copper-base alloys are galvanically compatible with one another in seawater. While the copper-nickel alloys are slightly cathodic (noble) to the nickel-free copper base alloys, the small differences in corrosion potential generally do not lead to serious galvanic effects unless unusually adverse anodic/cathodic area ratios are involved.

### Polluted Cooling Waters

The primary causes of accelerated attack of copper alloys by polluted seawater are: (1) the action of sulfate-reducing bacteria under anaerobic conditions (bottom muds and sediments) on the natural sulfates in seawater in coastal harbors and estuaries, and (2) the putrefaction of organic sulfur compounds from decaying plant and animal matter within seawater systems during periods of extended shutdown.

### Biofouling

The copper alloys long have been recognized for their inherent resistance to marine fouling. Fouling resistance is a result of corrosion of the alloy. If galvanic effects or impressed cathodic protection suppresses the corrosion, the antifouling character will not be promoted.

### Acids

In general, copper alloys are used successfully with non-oxidizing acids as long as the concentration of oxidizing agents, such as dissolved oxygen (air), and ferric ( $\text{Fe}^{+3}$ ) or dichromate ( $\text{Cr}_2\text{O}_7$ )<sup>-2</sup> ions is low.

Acids that are oxidizing agents in themselves, such as nitric, cannot be handled in equipment made of copper or its alloys. Successful applications of copper and its alloys are in phosphoric, acetic, tartaric, formic, oxalic, malic, and other organic acids that react in a manner similar to sulfuric acid.

## Alkalies and Ammonia

Copper and its alloys resist alkaline solutions, except those containing ammonium hydroxide, or compounds that hydrolyze to ammonium hydroxide or cyanides. Ammonium hydroxide reacts with copper to form the soluble complex copper-ammonium compound  $\text{Cu}(\text{NH}_3)_4^{+2}$ .

Ammonium hydroxide solutions also attack copper-zinc alloys. Alloys containing more than 15 % zinc are susceptible to SCC when stressed and exposed to ammonium hydroxide, although it also is experienced by the copper-beryllium alloys which are zinc-free. The stress may be due to applied tensile service loads or to unrelieved residual tensile stresses.

## Salts

Copper metals are used widely in equipment for handling various kinds of salt solutions including the nitrates, sulfates, and chlorides of sodium and potassium. Chlorides usually are more corrosive than the other salts especially in strongly agitated aerated solutions.

Neutral salt solutions can be handled successfully by copper alloys. Hence, these alloys are selected for heat exchanger and condenser equipment exposed to seawater.

While alkaline sodium salts such as silicate, phosphate, and carbonate attack copper alloys at low rates, alkaline cyanide is aggressive and attacks copper alloys fairly rapidly because of the formation of the soluble complex copper cyanide anion  $\text{Cu}(\text{CN})_2^{-2}$ .

## Oxidizing Salts

Copper metals should not be used with oxidizing saline solutions except those that are very dilute. Temperature and acidity adversely affect the rate of attack.

## Liquid Metal Embrittlement

Intergranular cracking may be caused by liquid metal embrittlement if the alloy is under tensile stress, either residual or applied. While mercury embrittles copper, the severity increases when alloyed with aluminum or zinc. This embrittlement occurs in both tension and fatigue and varies with grain size and strain rate. Other alloying elements such as lithium, sodium, bismuth, gallium, and indium also affect embrittlement.

## Organic Compounds

Copper and many of its alloys resist corrosive attack by most organic compounds such as amines, alkanolamines, esters, glycols, ethers, ketones, alcohols, aldehydes, naphtha, gasoline, and most organic solvents.

Corrosion rates of copper and copper alloys in alkanolamines and amines, while low, can be increased significantly if these compounds are contaminated with water, acids, alkalies, salts or combinations of these impurities, particularly at high temperatures.

## CORROSION TESTS

### Mercurous Nitrate Test

The mercurous nitrate test (ASTM B 154, Method for Mercurous Nitrate Test for Copper and Copper Alloys) probably has been the most important and widely used accelerated test for detecting the presence of residual (internal) stresses in tension, which might result in failure of individual parts in storage or in service due to SCC.

The test method is not intended for assemblies under applied stress. If used for that purpose, it shall be for information only and not a cause for rejection of the assembly, its component parts, or the original mill product.

Basically, the procedure involves degreasing the test specimen in a suitable alkaline degreasing solution or organic solvent. If necessary, the specimen shall be immersed totally in an aqueous solution of sulfuric acid (15 vol %) or nitric acid (40 vol %) until all oxides are removed completely from its surface or pickle in such solutions as may be prescribed in the specification for the material being tested. Remove the specimen from the pickling solution and rinse it immediately in running water. Drain the specimen free of excess water and totally immerse it at room temperature into the mercurous nitrate solution for 30 min and rinse again in running water. Visual examination for cracks then takes place.

Test specimens are mercury-contaminated and may not be recycled for remelting or machined into product.

Because of mercury's health hazard and problems associated with the disposal of the test specimens and the mercurous nitrate test solutions, a substitute test based on an ISO ammonia test (see following) was adopted after modification to ASTM format.

### Ammonia Test

In response to the request from the U.S. Coast Guard and ASME's Boiler and Pressure Vessel Code for a replacement test for ASTM B154, ASTM B05 Committee undertook the effort. ASTM B858 (Method for Determination of Susceptibility to Stress Corrosion Cracking in Copper Alloys Using an Ammonia Vapor Test) was created in 1995. This test method is a conversion of ISO 6957 [5], Ammonia Test for Stress Corrosion Resistance with additional input from DIN 50916 [6] Stress Corrosion Cracking Test Using Ammonia, Research work performed by Mattson et al. [7] validates the technical integrity of the test method.

The test method uses an ammonia atmosphere to simulate service conditions under which stress corrosion cracking may occur. This test method is suitable only for products fabricated from copper alloys that are known to be susceptible to stress corrosion cracking in ammonia vapor atmospheres. It is intended to create an environmental condition of reproducible severity, but it is well known that the critical step in the cracking mechanism is the development of an environment in the condensate film that occurs on the test specimen, which is rich in complex copper ions.

This test method is an accelerated test to determine if a copper alloy product in a specific stress condition will be susceptible to stress corrosion cracking when exposed to a particular atmosphere condition during service with the appropriate risk



**TABLE 2**—Guidance for choice of the pH-value of the test solution [7,8].

Corrosiveness of Atmosphere	pH-value Safety Requirement	
	Low	High
<b>Low</b>		
Indoor atmosphere under dry conditions	9.3	9.5
<b>Moderate</b>		
Indoor atmosphere with risk of formation of condensation	9.5	10.0
Outdoor atmosphere, temperate climate	9.5	10.0
<b>High</b>		
Atmosphere with ammoniacal pollution, for example in stables	10.0	10.5

level (Table 2). Changing the pH value of the solution producing the ammoniacal atmosphere can regulate severity.

This test method generally is intended to determine if a copper alloy product will crack because of internal stresses when subjected to the test, and is not intended for testing assemblies under applied stress. If used for this purpose, it shall be for information only and not a cause for rejection of the assembly, its component parts, or the original mill product.

Detailed solution composition, test media, and procedure are illustrated in ASTM B 858. The major deficiency of this test method is that the exposure time is 24 h versus 30 min in the mercurous nitrate solution.

Also, the question arises as to how a crack is defined. Cracks can be very short, and the rim of the base, particularly at high magnification (10× or more) is not absolutely smooth. Distinguishing between an irregularity or a mark from the drawing die and the beginnings of a true crack becomes very difficult. The decision reached by IEC [9] was that if the "defect," however small, had characteristics that suggested a crack, it was called a crack.

Because a crack can become filled or covered with corrosion products, an acid dip or buffing frequently is necessary to clean the surface in order to verify that a crack exists beneath.

### Stress Corrosion Cracking Testing in Mattsson's Solution

ASTM G 37 (Practice for Use of Mattsson's Solution of pH 7.2 to Evaluate the Stress Corrosion Cracking Susceptibility of Copper-Zinc Alloys) is an accelerated stress corrosion cracking test environment for brasses (copper-zinc alloys). The use of this test environment is not recommended for other copper alloys since the results may be erroneous, providing completely misleading rankings. This is particularly true of alloys containing aluminum or nickel as deliberate alloying additions.

This practice is intended primarily where the test objective is to determine the relative stress corrosion cracking susceptibility of different brasses under the same or different stress conditions or to determine the absolute degree of stress corrosion susceptibility, if any, of a particular brass or brass component under one or more specific stress conditions. The tensile stresses may be known or unknown, applied or residual.

The practice may be applied to wrought brass products or components, brass castings, brass weldments, and to all brasses. Strict environmental conditions are mandatory.

There are no restrictions as to surface preparation or finish nor are particular stress corrosion test specimen configurations or methods of applying the stress recommended.

The practice consists of completely and continuously immersing a stressed test specimen in an aqueous solution containing 0.05 g-atom/L of  $\text{Cu}^{++}$  and 1 g-mol/L of  $\text{NH}_4^+$  and of pH 7.2. The copper is added as  $\text{CuSO}_4 \cdot 5\text{H}_2\text{O}$  and the  $\text{NH}_4^+$  as mixture of  $\text{NH}_4\text{OH}$  and  $(\text{NH}_4)_2\text{SO}_4$ . The ratio of these latter two compounds is adjusted to give the desired pH. Exposure time, criterion of failure are variable and are not specifically recommended.

The test environment correlates the service ranking for different brasses in environments that cause SCC, which are due to the combined presence of traces of moisture and ammonia vapor.

Linkage of the SCC of brasses to environments containing corroders other than ammonia is unknown. These alternate environments include marine atmosphere (chloride), severe industrial atmosphere (predominantly sulfur dioxide), or superheated ammonia-free steam.

Metallographic examination is necessary to distinguish between true SCC and mechanically induced cracking. The most widely used SCC agent for copper and copper alloys is ammonia ( $\text{NH}_3$ ). The  $\text{NH}_4^+$  ion does not appear to cause cracking in a stable salt such as ammonium sulfate whereas cracking will occur in a salt that disassociates (such as ammonium carbonate) to form ammonia.

For SCC of copper alloys to occur, however, the presence of air, oxygen, or an oxidizing agent along with the presence of moisture are essential, because cracking may appear to be caused by the presence of a condensed moisture film.

Detailed solution composition, test media, and procedure are illustrated in ASTM G 37.

### Salt Spray Test

Metal coatings are intended in most cases as corrosion protection barriers. In accelerated tests, the time required for corrosion should be reduced preferably by exposing the specimens continuously to conditions, which in service would arise only intermittently. At the same time, the conditions used should cause no damage of types other than that which would arise under conditions of natural exposure.

Early salt spray tests intended to reflect the rapid testing of metal coatings in an atmosphere comparable to that encountered at seacoasts were unsatisfactory because of the multiple variables involved [10].

The current salt spray test, in which the plated specimen is exposed to a spray or fog of sodium chloride solution, is the most widely used accelerated corrosion test for coatings, and various procedures have acceptance tests in standard specifications in numerous countries. Over the years, the procedure has employed sodium chloride solutions of concentrations between 3 and 20 %, sometimes with the addition of hydrochloric acid or hydrogen peroxide. The salt spray test [ASTM B 117, Test Method of Salt Spray (Fog) Testing] has largely fallen into disrepute because of the recognition that its reproducibility and correlation with outdoor exposure were often poor. Cyclic salt spray testing as well as alternate electrolytes such as the "prohesion" test solution have been found to produce more realistic results.

Detailed apparatus, test specimens, position of specimens during exposure, salt solution, air supply, conditions in the salt spray chamber, continuity and period of exposure and cleaning of tested specimens are illustrated in ASTM B 117.

The procedures of ASTM B 117 and a modified version of ASTM G 44 were employed to study the behavior of solid brass fittings with that of coated and zinc-plated steel fittings. While G 44 was developed originally as an accelerated test for determining the chloride stress corrosion cracking resistance of aluminum and ferrous alloys, the concept of the alternate wet and dry cycling was considered relevant.

G 44 can be used for both stressed and unstressed specimens. Historically, it has been used for stress corrosion cracking testing, but often is used for other forms of corrosion, such as uniform, pitting, intergranular, and galvanic. It uses a 1-h cycle that includes a 10-min period in a aqueous solution of 3.5 % sodium chloride (NaCl) followed by a 50-min period out of the solution, during which the specimens are allowed to dry. This 1-h cycle is continued 24 h/day for the total number of days for the particular alloy being tested.

### Modified Salt Spray (Fog) Testing

The addition of acetic acid to the salt solution used in the salt spray tests was introduced first in 1945 and is currently Annex A1 of ASTM G 85 [Practice for Modified Salt Spray (Fog) Testing]. The acidified test is much more corrosive than the normal salt spray test and is capable of producing a pattern of attack similar to that developed in outdoor service for decorative chromium plate on steel or zinc. It is much slower than the copper-accelerated acetic acid-salt spray (CASS) test in ASTM B 368 [Method for Copper-Accelerated Acetic Acid-Salt Spray (Fog) Testing (CASS Test)], [11] which resembles it in effect.

An improved salt spray test employed a mixture of sodium chloride and acetic acid. A solution containing 50 g/L of sodium chloride in distilled water is adjusted to a pH value between 3.2 and 3.4 (electrometric) with glacial acetic acid. The solution is sprayed through a small aperture atomizing nozzle and mixed with a compressed air stream. The solution usually is heated to 95 to 100°F (35 to 38°C). Failure under this test is assessed visually, and results generally are obtained within 48 to 72 h, depending on the coating system.

Additional information on salt spray testing can be found in Section III of this manual. Detailed information on apparatus, test solution, air supply, test specimens, procedure, and evaluation of results are illustrated in ASTM B 368.

### CASS [13,14] and Corrodokote Tests

[ASTM B 380 (Method of Corrosion Testing of Decorative Electrodeposited Coatings by the Corrodokote Procedure)].

The CASS test and Corrodokote procedure are employed primarily for testing decorative chromium systems, with the CASS test also being useful for testing anodized aluminum. These tests were developed to give a more rapid indication of corrosion resistance and a better correlation with service performance. They have come into prominence as the most widely used modifications of the salt spray test because of their greater speed. Both tests employ cupric ion in the corrodant

**TABLE 3**—Compositions of CASS and Corrodokote electrolytes.

CASS			Corrodokote		
	g/L	Moles/L		g/L	Moles/L
NaCl	50.0	0.86	NH <sub>4</sub> Cl	20.0	0.4
CuCl <sub>2</sub> ·2H <sub>2</sub> O	0.26	0.0015	FeCl <sub>3</sub> ·6H <sub>2</sub> O	3.3	0.012
			Cu(NO <sub>3</sub> ) <sub>2</sub> ·3H <sub>2</sub> O	0.7	0.005
	pH 3.1 (Acetic Acid)			pH 2.4	
	Temperature 124°F (51.1°C)			Temperature 100°F (37.8°C)	

solution. In the CASS test, a solution containing copper chloride, sodium chloride, and acetic acid is sprayed into a chamber like that employed in the neutral salt spray.

Specimens are cleaned by rubbing with a paste of magnesium oxide and water so that they become free from water breaks after rinsing. Articles then are exposed to the salt fog for 16 to 18 h, then washed in warm running water to remove salt deposits before being dried and inspected. Compositions of these electrolytes are given in Table 3.

The tests fairly accurately reproduce the corrosion pattern produced in outdoor exposure, although there is sometimes excessive spreading of corrosion product.

One important ingredient of the Corrodokote slurry is the application of a paste-containing copper nitrate and ferric and ammonium chlorides in a clay-water matrix to the specimen surface, followed by exposure in a high-humidity non-condensing atmosphere.

It had been established previously that the Annex A1 of ASTM G 85, applied to copper-nickel-chromium plated zinc castings, would produce the type of failure experienced on such articles in service. However, the 16 to 20 h required to produce such failure were considered by many to be undesirably long.

Detailed information on apparatus, procedure, and valuation of results is illustrated in ASTM B 380.

### The Salt Droplet Test

In the normal salt spray test, direct spraying is avoided and a fine mist envelops the specimens. The salt droplet test by contrast involves spraying the salt solution directly onto the test specimens.

The specimens are sprayed manually with a spray bottle once daily five times a week with an artificial seawater, the droplet size and distribution being required in the specification along with exposure time.

This test has the advantage over the salt spray test in that it excludes the effect of specimen shape and suspension method. In addition, it is possible to directly determine and control the droplet size. Moreover, effects due to the size and shape of the test chamber are excluded.

### Hydrochloric Acid Spray Test

It was reported that the early salt spray tests (ASTM B 117) did not yield useful results when applied to chromium-plated brass specimens, while the results of a hydrochloric acid spray test were claimed to be in good agreement with the behavior of this material during weathering [10].

A solution of 1.7 to 2.0 % hydrochloric acid is sprayed for 5 h at room temperature with the test specimens left in the test chamber for an additional 10 h without spraying.

Corrosion defects developed are similar to those observed on weathering (blisters, pits, cracks, flaking).

### Testing in Potable Water [12]

The corrosion of metals and alloys in potable water varies greatly depending on the water's composition. Among the factors that are most influential are: oxygen content, pH, temporary hardness, chloride, sulfate, total dissolved solids (TDS), and conductivity. Temporary hardness is sometimes referred to as carbonate hardness and is removed easily by boiling.

Testing frequently must take place in a combination of field and laboratory tests, possibly using electrochemical methods.

### Testing in Seawater [13,14]

Reverse osmosis (RO) desalination technology has become established over a number of years for producing potable water from various natural waters, including seawater. While some RO systems utilize nonmetallic construction materials for the pressure vessels to contain the membrane cartridges, metallic materials are desired where higher pressures and/or enhanced fire resistance are required.

Corrosion resistance is essential to the operation of RO systems constructed of metallic materials. This is because localized corrosion cannot be tolerated at the critical pressure seals which separate feedwater, brine, and the product water (permeate). Secondly, there is little tolerance for the generation of corrosion products, which can affect RO membrane performance.

Because of the extensive use of copper-nickel in shipboard piping, the potential corrosivity of RO ultrapure water on these systems is considered important, ASTM G 4 (Standard Guide for Conducting Corrosion Coupon Tests in Field Application) covers in-plant testing of metals and alloys without regard to alloy type, family, or class and generates test results by exposure of the materials to filtered seawater (RO feed stock), an intermediate-pass brine by-product, and ultrapure product water.

ASTM G 78 is employed specifically for crevice corrosion testing of iron and nickel-base type alloys. If susceptible, these materials exhibit attack within the crevice area. Other "nonstainless-type" alloys such as copper-nickels often tend to suffer localized corrosion just outside the crevice rather than within it. Traditional crevice corrosion test are performed routinely on Cu-Ni alloys.

Overall, the two ASTM Standard Guides (G 04 and G 78) provide valuable information applicable to the design and interpretation of these natural water corrosion tests.

While seawater is a ubiquitous environment and quite similar in terms of chloride content and pH, the corrosivity is site-specific, and likely to be influenced by a myriad of other factors such as temperature, dissolved oxygen concentration, flow, degree of fouling, bacterial activity, and pollution. All of these factors often are interrelated. The test program followed the guidelines provided in ASTM G 52 (Standard Practice for Conducting Surface Seawater Exposure Tests on Metals and Alloys).

Enhanced corrosion in seawater has been shown to be associated with sulfide contamination. Copper-nickel alloys

also have been shown to be susceptible to impingement attack in unpolluted but more so in polluted seawater. The corrosion behavior of copper-nickel alloys C70600 and C71500, respectively, under aerated static, aerated stirred, and under impingement attack in sulfide polluted seawater has been studied by Cyclic Current Reversal Chronopotentiometry (CRC) [15].

The application of this technique for evaluating the long-term corrosion behavior of copper-nickel alloys in sulfide-polluted and unpolluted seawaters employed an intentional abrupt change of current between anodic and cathodic values to determine the feasibility of using the CRC method.

Electrochemical corrosion measurements were conducted in a modified corrosion testing cell where a combination of a circulating pump and a jet nozzle simulated jet-impingement attack as shown in Figure 4.

The principle of the CRC technique is illustrated in Figure 5.

### Statistical Analysis of Pitting Corrosion in Condenser Tubes [16]

Corrosion performance is often the key to proper selection of tube alloy for steam surface condensers, particularly for those cooled by seawater and brackish water. Contamination of the working fluid will lower the steam quality, thus decreasing overall power generation efficiency.

One or more types of corrosion can cause condenser tube failures in seawater service. These corrosion types include turbulence/velocity stimulated corrosion at inlet ends or at partial tube blockages, galvanic-induced corrosion caused by a mismatch between tube and tubesheet/waterbox alloys, and selective corrosion attack caused by microstructural differences resulting from improper welding or fabrication techniques.

Pitting-type corrosion frequently causes condenser tube failures. Prediction of a particular alloy's propensity for pitting corrosion can involve some special problems. Sometimes, pitting corrosion becomes a problem in real-life service conditions even when laboratory studies indicate pitting immunity.

A statistical technique known as extreme value analysis for assessing pitting corrosion in condenser tubing is broadly

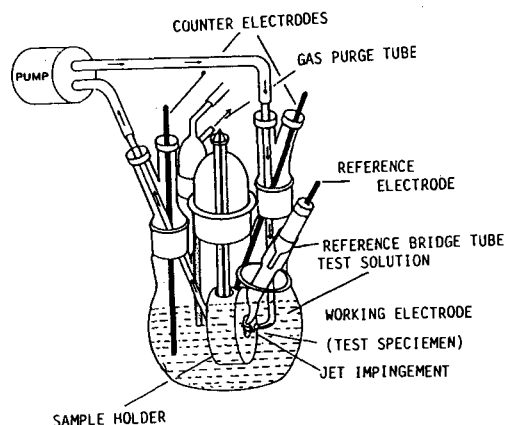


FIG. 4—The electrochemical cell used to simulate impingement attack.

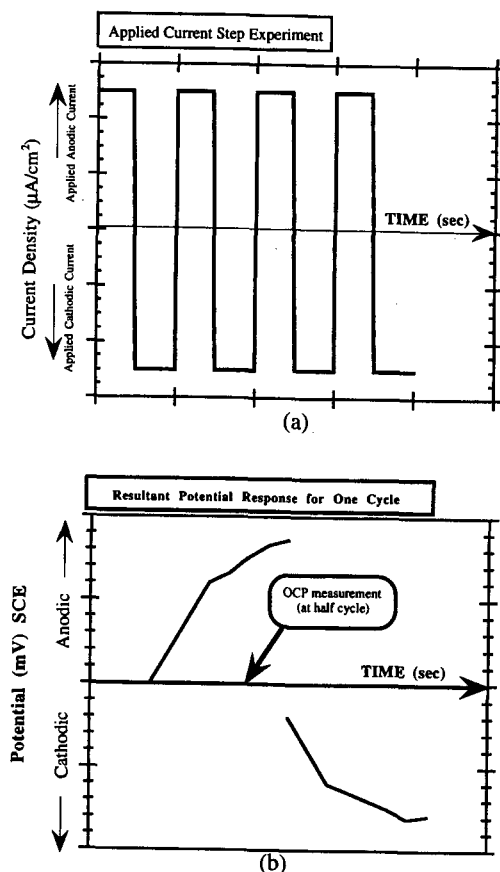


FIG. 5—A schematic diagram showing (a) the input applied current steps, and (b) the resultant potential response from a single current cycle for the cyclic current reversal chronopotentiometric experiment.

applicable to condition assessment, design problems, and applied research.

The normal probability relationship and its familiar bell-shaped curve represent a totality of data, all of the scores on a test, average soil resistivities, or all pit depths form the basis for the curve. Application of the cumulative probability function for an exponential extreme value distribution of a standard variate to practical situations requires statistically valid collection of data. A practical and consistent sample size must be selected and enough samples must be taken to attain reliable results.

The most important pit in piping systems where leakage is a concern is the deepest pit. This pit causes the first tubing wall penetration and the first leak. The time between the first tube failure and subsequent failures depends upon the statistical distribution of these pits and the rate at which corrosion continues.

### BNF Jet Test (Copper and Copper Alloy Deposits)

The apparatus consists of a separating funnel that is filled with the reagent solution to be used for attacking and gradually penetrating the plated coating. A rubber tube connects

the top of the funnel with a jet constructed to specified dimensions. A thermometer is immersed in the solution through a rubber plug at the top of the funnel.

The part to be tested is cleaned by wiping with magnesium oxide, rinsed, and wiped dry. It then is clamped in such a way that the surface is at an angle of  $45^\circ$  to the horizontal and  $1/4$  in. (6.35 mm) below the nozzle. When the tap is opened, a stopwatch is started simultaneously and the solution is permitted to flow until the coating is penetrated. The solution for testing copper or bronze deposits and multiple coatings of copper with nickel contains:

Ferric Chloride	300 g/L	(48 oz/gal)
Copper Sulfate	100 g/L	(16 oz/gal)

Calibration charts provided with the instrument give the relationship between penetrating time and plating thickness for various coatings.

The endpoint for copper on zinc-base or aluminum alloys is marked by the appearance of a black spot, and on nickel by a white spot. When testing copper on steel, the endpoint is detected as a black spot by placing with a pipette two drops of a 1 % antimony oxide solution in 50 % concentrated hydrochloric acid on the test area at intervals during the test. It is not required for bronze on steel.

When copper under nickel coatings are tested, the first endpoint (a copper spot) gives the thickness of nickel, after which the test is continued to the endpoint for copper as described previously.

### Cavitation Tests [17]

Cavitation is the dynamic phenomenon of repeated growth and collapse of bubbles in a liquid. It produces shock-like stresses in any solid in its vicinity. These stresses are not applied uniformly as the stress in a conventional test. Hence, no simple correlation exists between the cavitation erosion resistance of metals and alloys and any of their bulk mechanical properties.

Instead, the local modes of deformation in the metal play a major role in determining (1) the ability of the metal to absorb the impact energy, and (2) the mechanisms of subsequent material removal.

In one such test, the alloys studied were subjected to cavitation produced ultrasonically in distilled water by the piezoelectric device shown in Fig. 6. The damage produced then is evaluated metallographically and by microhardness measurements.

### Electrical Resistance Tests [18]

In a description of the methods summarizing soldering flux corrosivity, it was concluded that a quantitative method to replace the qualitative visual assessments was needed.

This short duration test method allows the corrosivity of liquid flux residues after wave soldering to be assessed and employed as a screening test prior to employment of the more time-consuming procedures.

The procedure to assess the corrosivity of flux residues towards a copper cable under controlled conditions of time, temperature, and humidity at an applied potential of 250 V

FIG. 6—Schematic representation of the vibratory cavitation probe.

DC involves measuring the changes in the strength of the copper cable.

The cable test piece consists of ten untwisted strands of bare copper wire mounted on a glass fiber-filled epoxy substrate with holes to allow flux residues to pass from the underside of the board to contaminate the cables on the topside during wave soldering. A DC power supply polarizes the test pieces anodically with respect to the copper conductor track on the laminate.

The environmental test chamber is maintained at 21°C with a relative humidity of 95 to 100 % using a reservoir of distilled or deionized water.

The strength is expressed in terms of all ten wires, even if some are broken, before the tensile strength of the cable is determined.

The increasing availability and reliability of digital equipment [19], both for performing analog-to-digital data conversion and for data reduction, analysis and digital filtering has become more widely used. The Fast Fourier Transform (FFT) techniques in performing digital faradaic impedance measurements (DFIM) on copper corrosion in acidic environments offers some advantages that make it appropriate for corrosion applications.

The measurement system consists of a calculator with a memory that controls data acquisition, data averaging, data storage, and data transmission to a large scale computer. These multifrequency impedance measurements are rapid and provide a rather complete description of the corrosion behavior in a very short time.

### Erosion-Corrosion Tests [20]

The repeated impact of liquid against a solid surface using an intermittent jet at sufficiently high speeds leads to a form of erosion. At impact, a liquid drop produces a very high compressive stress in the vicinity of the area of contact, and this is followed by outward, radial flow of liquid at very high speed which shears and erodes the surface. Erosion-corrosion in alpha-brass comprises two parts. The initial progressive plastic indentation is followed by the formation of an annulus where pits gradually form.

With the fastest jet of 218 m/s, an impression is made during the first impact. It consists of a flat circular region, approximately two thirds of the projected diameter of the jet, tapering at the outside up to the original surface of the specimen as indicated in Fig. 7.

Thereafter it remains constant throughout the remainder of the erosion process. The grains in the crater are marked clearly with many sliplines or extrusions, and during its deepening, the inner diameter of the depression does not change and the outer diameter alters only marginally. A central conical hole forms that is approximately twice the depth of the depression and this deepens with the number of impacts. However, the conical hole continues after the outer compressed region has reached its maximum depth; in fact,

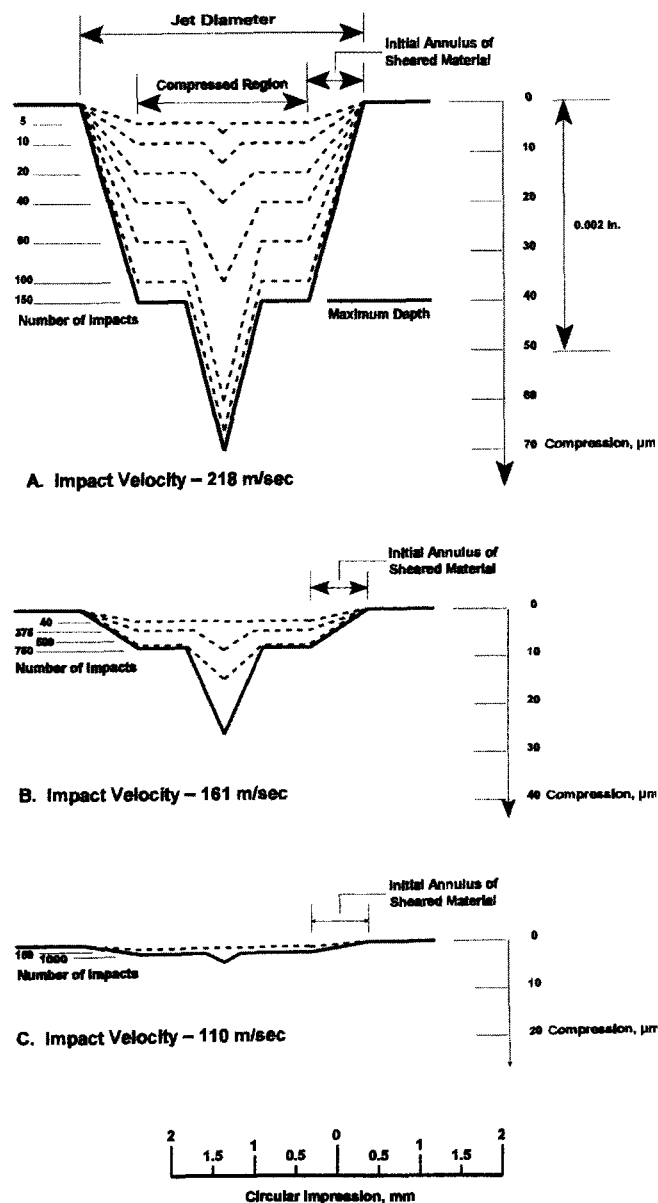


FIG. 7—Development of impact impression in alpha brass during the no-mass-loss stage of erosion.

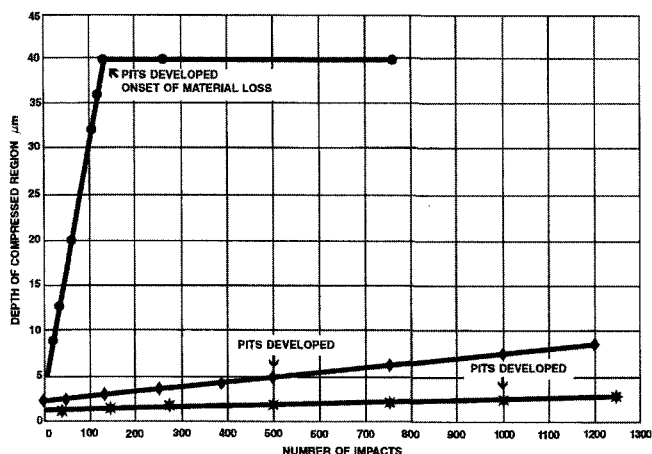


FIG. 8—Increase in depth of impression with number of impacts in alpha-brass. Water jet velocities (m/s): • is 218; ◇ is 161; \* is 110.

it deepens rapidly to about 20× the final depth of the compressed region. The central hole develops as the deepest part of the erosion crater.

In general, fluid velocity has two effects on corrosion: the mass transfer effect and the surface shear stress effect.

At low velocities, the rate of corrosion is completely or partially controlled by the rate of mass transfer. The effect of increasing velocity is to increase the surface concentration of the corrodent or to decrease the surface concentration of the corrosion product. Therefore, the rate of corrosion increases with increasing velocity. At higher velocities, the rate of mass transfer is much faster than the rate of charge transfer reaction at the metal surface. As a result, activation control of the overall corrosion process is observed. In this region, the corrosion rate is independent of fluid velocity and, in principle, also of the geometry involved. At still higher velocities, erosion-corrosion may occur if the surface shear stress is high enough to strip the protective film from the surface.

### Galvanic Corrosion Tests [21,22]

Components suffer most in areas where crevice-type conditions prevail. Thus, dealloyed nuts and bolts are common, with the influence of stagnant versus flowing fluid conditions playing a major role.

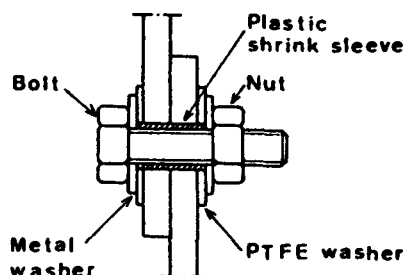


FIG. 9—Cross section of the metal-metal connection in a galvanic couple.

Dissimilar metal or galvanic couplings are created by firmly pressing the components together by means of an insulated bolt. Details of the arrangement are shown in Fig. 9.

In the specimens with the larger surface area, a hole is drilled. The galvanic couples and the uncoupled reference specimens are mounted in duplicate on wooden planks by means of an insulated bolt passing through the hole. PTFE washers insulate the test specimens from the plank and the bolt head.

Immediately before and after the exposure, the contact resistance between the metals in each galvanic couple is checked with an ohmmeter. Following exposure, initial cleaning of marine growth is done with a plastic scraper and nylon brush, then transferred to the laboratory for final cleaning.

Copper alloys are cleaned by immersion (15-s cycles) in 10 % sulfuric acid containing 4 % hydrogen peroxide at ambient temperature followed by scraping and brushing under flowing water several times until clean. After weighing, the specimens were studied under a stereomicroscope at 20×. For metallographic examination, etching was done in a 10 % solution of peroxodisulfate for 30 s at 20°C.

Additional information on galvanic corrosion tests may be found in Section IV of this manual.

The general effect of coupling dissimilar metals in a corrosive environment is that one metal will corrode more and the other less than would be expected from a consideration of the individual corrosion rates.

A popular practice has been to use a galvanic series in which the metals are arranged according to their potentials measured in a particular environment.

Several factors such as the formation of films on the surface, potential variation with time, and variation of polarizability of metals with environment can lead to drawbacks in the use of potential measurements and the galvanic series.

Connection of the multiple couples with the ammeter and voltmeter was made through a high-speed scanner with the galvanic cell and recirculating flow system as shown in Fig. 10.

Corrosion rates of uncoupled brass and bronze were determined both by potentiodynamic polarization and by weight loss and dezincification weight loss depth measurements.

### Oxidation Test [23]

Candidate container materials for high level nuclear wastes were evaluated as bare metal specimens exposed to an air atmosphere containing 12 % moisture in chambers maintained at temperatures of 150°C, 200°C, 250°C, and 300°C. Air was pumped through evaporators maintained at 50°C and then through the test chambers.

In the short-term testing with packing material, specimens were placed in the chambers in aluminum capsules packed with basalt-bentonite packing materials.

All specimens were polished through 600-grit abrasive before testing. Synthetic ground water used in these tests was prepared according to GR-4 specifications. The packing material used consisted of 75 % fine basalt and 25 % bentonite [24].

Penetration results were derived by calculating the weight loss per unit area from the weight change and dimensional measurements, then dividing by the density of the material.

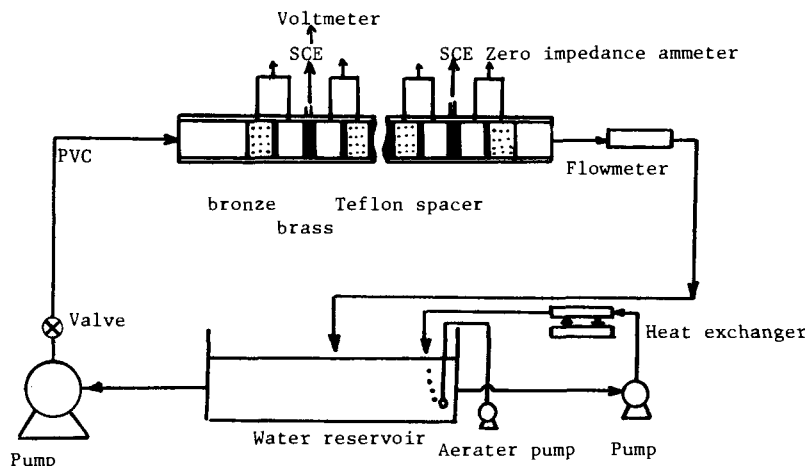


FIG. 10—Flow loop and galvanic cells.

### Potentiostatic Tests

Extensive cold water pitting corrosion was encountered in copper plumbing systems in the late 1940s and into the 1950s in the United Kingdom during the reconstruction of war-damaged housing [25]. The cause was circumstantially associated with carbon film residues resulting from the breakdown of drawing lubricants during bright annealing in the manufacturing process.

The BNF or the VTR tests for visual carbon have been recognized as being unsatisfactory because these simulated service tests are not reproducible between laboratories and take far too long. Also, they do not differentiate between acceptable and unacceptable tube in borderline cases.

This potentiostatic test method involves the monitoring and analysis of electrochemical current noise signals emitted by copper tubes immersed in a water that is linked to cold water pitting corrosion. It is claimed that the method provides a rapid and reliable means to distinguish between satisfactory and unsatisfactory tubes, especially in the borderline region.

Tubes with artificially controlled and produced levels of carbon films were produced by exposure to butane passing through the copper tubes when the traveling furnace heated them. Rates of flow of the gases and the temperature were varied to lay down different quantities of carbon film.

The synthetic pitting solution simulates a potable water composition known to cause cold water pitting [26]. It was prepared by bubbling carbon dioxide through a rapidly stirred suspension of calcium carbonate in distilled water to produce a solution of calcium hydrogen carbonate. Sodium sulfate (133 mg/L) and sodium chloride (49 mg/L) were dissolved in the solution and air then was bubbled through to adjust the pH to within the range of 7.0 to 7.5.

A pair of identical specimens was immersed in a container of synthetic pitting water, which was recirculated slowly and continuously throughout the test, generally 50 to 60 h, although some were extended to several hundred hours. This cell then was placed inside a grounded metallic drum, which acted as a Faraday cage. A zero resistance ammeter, programmable switch box, and high-resolution voltmeter were used to measure the current noise between these apparently identical specimens.

The current data were collected as a series of discrete time "windows" throughout the test. Typically, current-time windows were recorded once per hour during the early part of a test and at increasing intervals as the total test duration increased.

### Measuring the Corrosion of Metals in Soil [27,28]

Advances in technology have allowed measurements to be extended to field situations. Improved performance of electronic components, miniaturization of equipment, and development of portable computers and high impedance digital voltmeters are an important result of these advances.

Corrosion rate and galvanic current are the two measurement categories. Polarization measurements have shown that induced alternating current increases the corrosion rate of copper concentric neutrals compared to copper neutrals without alternating current. Galvanic current measurements provide valuable information on the behavior of galvanically coupled materials enabling the comparison of the corrosivity of soil environments.

The corrosiveness of a soil depends on a number of factors including resistivity, pH, aeration, moisture, and chemical contents. It is highly location-dependent and is influenced further by the presence of alternating current as well as galvanic couples with other buried metals.

Corrosion of copper shielding conforms to the mechanism of uniform corrosion. It is inherently resistant to differential aeration and only uniform corrosion of exposed areas occurs.

Copper is a relatively noble metal and is usually cathodic to other metals.

Losses in weight and maximum pit depths of copper and copper alloys are slight with the following exceptions: (1) in cinders; (2) in soils having high concentrations of sulfides; (3) in acid soils; and (4) in soils containing chlorides.

### Accelerated Corrosion Testing of Automotive Radiators

Automotive radiators have been made of copper and brass since the first water-cooled engines were produced. They

consist of an assembly of fluid-carrying tubes, which are joined either by heat conducting fins or by plates common to all tubes or groups of tubes or by corrugated conduction fins inserted between adjacent lines of tubes.

Radiators are composed of copper fins, tubes which until recently were soldered with a lead-tin solder. Currently, soldering with zinc and brazing are being studied.

Corrosion testing of radiators involves exposure of test pieces to a corrosive environment and determination of the corrosion effect arising during the exposure [29]. While field tests expose test pieces to the type of corrosive environment, where the material will be used, accelerated corrosion tests permits the corrosion rate to be increased through moderate changes such as temperature, the time of wetness or the contents of corrosion species. The changes, however, must not be so great that the corrosion mechanism or the corrosion products become significantly different from those in the service case. This increase of the corrosion rate can be expressed in terms of an acceleration factor.

Laboratory tests have many advantages over field and service tests as the exposure conditions can be controlled and the exposure time may be shortened.

The airside of the radiator, including the fins and the outside of the tubes, is exposed to the road climate. The atmospheric corrosion of radiators is influenced by the following parameters [28]: the time of wetness as corrosion of practical importance generally will take place only when the metal surface is covered with a moisture film; the types and contents of air pollutants from urban and industrial sources; splashing from the road.

Applicable test methods include [28]: Continuous Salt Spray Tests (ASTM B 117), Neutral Salt Spray Test (ASTM B 117), Acetic Acid Salt Spray Test, Copper-Accelerated Salt Spray Test (CASS) (ASTM B 368), Cyclic Salt Spray Tests, the Copper Development Association (CDA) Test, the Hitachi Salt Spray Test, Climate Tests, The Humidity Test, The International Electrotechnical Commission/International Organization for Standardization (IEC/ISO) Test and Mud Test.

Evaluation of corrosive effects arising during the exposure can be evaluated by visual inspection, metallographic examination of cross section under microscope with respect to pits, cracks, intergranular attack, and dezincification (of brass); and determination of loss in heat transmission capacity, a method which has direct relation to the function of automotive radiators.

An intensive study conducted for the Copper Development Association and reported by Beal [30] reported on two new soldered cup specimens that had been developed to evaluate blooming corrosion effects of solder and soldering parameters using ASTM D 1384 (Corrosion Tests for Engine Coolants in Glassware). Critical examination of the original test revealed wide variations in results in appearance and weight loss so that differences in solder alloy corrosion were difficult to interpret.

A new stressed solder specimen was shown to be sensitive to coolant conditions with experimental work confirming the validity of the new specimens by identifying the influences of the chosen test variables. In descending order of importance, antifreeze formula, flux, solder composition, and processing parameters were found to affect blooming corrosion.

## Microbiologically Influenced Corrosion Testing

Microbiologically influenced corrosion (MIC) is used to designate corrosion resulting from the presence and activities of microorganisms within biofilms on a material surface. Such microorganisms can accelerate and control corrosion reactions by several mechanisms: formation of differential or concentration cells, formation of metabolites, such as sulfides and organic and inorganic acids; metal oxidation and reduction, and deactivation of corrosion inhibitors.

Iron-oxidizing, sulfur-oxidizing, iron-reducing, sulfate-reducing, acid-producing, slime-producing, ammonia producing, and hydrogen-producing bacteria have been implicated in the corrosion of metals and alloys. Sulfate-reducing bacteria (SRB) are found commonly to be responsible for MIC in anaerobic environments through the production of  $H_2S$ . Metal-depositing bacteria, especially iron-oxidizing genera, form dense deposits of cells and metal ions, creating oxygen concentration cells and under-deposit corrosion. Acidic bacterial exopolymers can bind metal ions from the aqueous phase, increasing corrosion rates by providing an additional cathodic reaction [30].

While microorganisms attach to all engineering materials in contact with natural waters and colonize films to produce biofilms, these films are varied in composition, but usually include bacteria, algae, and fungi, in addition to exopolymeric material that provides attachment and structural integrity. A large fraction of the biofilm is adsorbed and entraps materials such as solutes, heavy metals, and inorganic particulates in addition to cellular constituents. Cells with biofilms grow, reproduce, and form colonies that are physical anomalies on a metal surface; local anodes and cathodes and differential aeration cells result as illustrated in Fig. 11.

Under aerobic conditions, areas under respiring colonies can become anodic and surrounding areas cathodic. A thick biofilm can prevent diffusion of oxygen to cathodic sites and diffusion of aggressive anions, such as chlorides to anodic sites. Outward diffusion of metabolites and corrosion products also is impeded. If areas within the biofilm become anaerobic, the cathodic mechanism can change to reduction of water or microbiologically produced  $H_2S$ .

Examination of a corrosion system experiencing MIC should include (1) metal composition; (2) macroscopic examination, (a) visible fouling, (b) localized corrosion, (1) forms, (2) location, (3) material within pits, and (c) corrosion products. Factors of interest in evaluating the environment of a corroding system include the following: (1) presence, absence, cycles of light, (2) aqueous medium, (a) temperature,

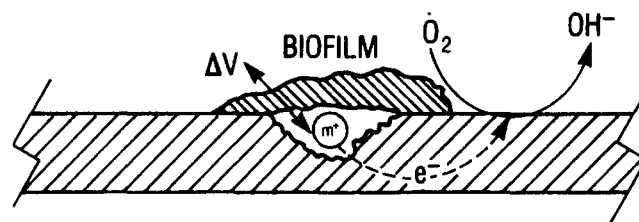


FIG. 11—Differential aeration cell resulting from microbial colony on metal surface.



(b) salinity, (c) dissolved oxygen, (d) water chemistries, (e) water microbiology, (f) direction, and velocity of flow, (3) system relationship to upstream industry, and (4) operating history of corroding system.

Additional laboratory and field procedures for evaluating microbiologically influenced corrosion resulting particularly from the sulfiding action of consortia are reported in Ref 31–34.

### Refractories in Copper Smelting [35]

Because of the high temperature corrosion resistance and thermal stability exhibited by magnesium-chromium oxide refractories in copper smelting, converting and fire refining furnaces, little research has been conducted on other refractory families. However, the concern for hexavalent chromium ( $\text{Cr}^{+6}$ ) as a potentially hazardous waste in spent refractories from copper production furnaces has prompted the recognition that a more environmentally acceptable material is needed for the copper industry.

Various chrome-free refractory materials have been studied by dip testing of these refractories in ferrous silicate and calcium ferrite slags typical of those used in copper production furnaces. More recently, a rotating sample test procedure has been employed.

A refractory sample exposed to a temperature of  $1300^{\circ}\text{C}$  was mounted on a stainless steel shaft with a section of stainless steel tubing placed around the shaft which in turn served as a high temperature “sacrificial anode.” Corrosion tests were conducted at rotation speeds of 60 and 120 rpm, along with a few under-static conditions.

The slag used for testing was a fayalite-based slag (70 %  $\text{FeO}$ ), produced using precipitated silica, reagent-grade hematite, and iron powders. The test durations were two and four hours.

However, the relatively mediocre corrosion resistance of the magnesia-based refractories suggests that its high temperature bonding strength is not sufficient, and that application of this material to copper smelting systems would be effective only under relatively static conditions, such as the bottom of stationary anode furnaces.

### REFERENCES

- [1] *Metals Handbook, Ninth Edition, Volume 13, Corrosion*, ASM International, Metals Park, OH, 1987, p. 611.
- [2] *Metals Handbook Desk Edition*, ASM, Metals Park, OH, 1985, pp. 7–39.
- [3] “Copper and Copper Base Alloys,” *Process Industries Corrosion*, National Association of Corrosion Engineers, Houston, TX, 1986, pp. 479–501.
- [4] Corrosion Data Survey—Metals Section, National Association of Corrosion Engineers, Houston, TX, 1967.
- [5] ISO 6957, Copper Alloys—Ammonia Test for Stress Corrosion Resistance, Geneva, Switzerland, 1988.
- [6] DIN 50916, Stress Corrosion Cracking Test Using Ammonia, Cologne, Germany, September 1985.
- [7] Mattsson, E., Holm, R., and Hassel, L., “Ammonia Test for Stress Corrosion Resistance of Copper Alloys,” *The Use of Synthetic Environments for Corrosion Testing*, ASTM STP 970, ASTM International, West Conshohocken, PA, 1988.
- [8] Landgren, W. and Mattsson, E., “Stress Corrosion of Brass: Field Test in Different Types of Atmosphere,” *British Corrosion Journal*, Vol. 11, No. 2, 1976, pp. 80–85.
- [9] International Electrotechnical Commission, Amendments to IEC Publication 238 by Working Group EPCI, Technical Committee No. 34, Subcommittee 34B Ammonia Vapor Test for Stress Corrosion, December 1987.
- [10] Kutzelnigg, A., “Corrosion Resistance,” in *Testing Metallic Coatings, Report No. 4*, Chap. 7, Robert Draper, Teddington, England, 1963, pp. 105–139.
- [11] Dibari, G. A., Hospardaruk, V., and Petrocelli, J. V., *Plating*, Vol. 49, January 1962, pp. 50–59.
- [12] Nielsen, K., “Corrosion Testing in Potable Water,” *International Symposium on Laboratory Corrosion and Standards*, Bal Harbour, November 1983, pp. 1–16.
- [13] Kain, R. M., Adamson, W. L., and Weber, B., “Corrosion Coupon in Natural Waters: A Case History Dealing with Reverse Osmosis Desalination of Seawater,” *Corrosion Testing in Natural Waters: Second Volume, ASTM STP 1300*, 1997, pp. 122–142.
- [14] Pikul, S. J. and Kain, R. M., “Seawater Corrosivity Around the World: Results from Five Years of Testing,” *Corrosion Testing in Natural Waters: Second Volume, ASTM STP 1300*, 1997, pp. 34–73.
- [15] Reda, M. R., and Alhajji, J. N., “Comparison of Current Reversal Chronopotentiometry (CRC) and Small Amplitude Cyclic Voltammetry (SACV) Method to Determine the Long-Term Corrosion Tendency of Copper-Nickel Alloys in Polluted and Unpolluted Seawater Under Jet-Impingement Conditions,” *Corrosion Testing in Natural Waters: Second Volume, ASTM STP 1300*, 1997, pp. 143–158.
- [16] Ault, J. P., and Gehring, G. A., “Statistical Analysis of Pitting Corrosion in Condenser Tubes,” *Corrosion Testing in Natural Waters: Second Volume, ASTM STP 1300*, 1997, pp. 109–121.
- [17] Preece, C. M., Dakshinamoorthy, S., Prasad, S., and Vyas, B., “The Influence of Microstructure on the Cavitation of Face Centered Cubic Metals and Alloys,” *Fourth International Conference on the Strength of Metals and Alloys*, Vol. 3, ENSIM, Nancy, France, 1976, pp. 1397–1403.
- [18] Bono, D., “The Assessment of the Corrosivity of Soldering Flux Residues Using Printed Copper Circuit Board Tracks,” *Solder Surface Mount Technology*, No. 2, June 1989, pp. 22–29.
- [19] Smyrl, W. H., “Digital Faradaic Impedance Measurements on Corroding Copper in Acid Solutions,” *Electrochemical Corrosion Testing*, ASTM STP 727, 1981, pp. 198–214.
- [20] Vickers, G. W. and Johnson, W., “The Development of an Impression and the Threshold Velocity for Erosion Damage in Alpha-Brass and Perspex Due to Repeated Water Jet Impact,” *Journal Institute of Mechanical Science*, Vol. 14, No. 11, November 1972, pp. 765–777.
- [21] Wallen, B. and Andersson, T., “Galvanic Corrosion of Copper Alloys in Contact with a Highly Alloyed Stainless Steel in Seawater,” *Proceedings of the 10th Scandinavian Corrosion Congress*, Stockholm, Sweden, June 1986, pp. 149–154.
- [22] Ishikawa, Y., Hosaka, N., and Hioki, S., “Galvanic Corrosion of Copper Alloys,” *Electrochemical Corrosion Testing*, ASTM STP 727, 1981, pp. 327–338.
- [23] Lutton, J. M., Dewees, D. A., Robinson, C. G., et al., Corrosion of Candidate Container Materials in Air-Steam Mixtures, Battelle, USA DE-AC06-76RLO 1830, U.S. Dept. of Energy, November 1987.
- [24] Lutton, J. M., Brehm, W. F., Maffei, H. P., et al., *General Corrosion Studies of Candidate Container Materials for the Basalt Waste Isolation Project in High Level Nuclear Waste Disposal*, II. C. Burkholder, Ed., Battelle Press, Columbus, OH, 1986, pp. 564–565.
- [25] Cohen, A., Discussion on paper by F. J. Cornwell, G. Wildsmith, and P. T. Gilbert, in *Pitting Corrosion in Copper Tubes in Cold Water Service*, ASTM STP 576, 1976, pp. 155–179.

- [26] Goodman, P. D., Lucey, V. F., and Maselkowski, C. R., in *The Use of Synthetic Environments for Corrosion Testing*, ASTM STP 970, 1988, p. 165.
- [27] Escalante, E., "Measuring the Corrosion of Metals in Soil," *Corrosion Testing and Evaluation: Silver Anniversary Volume*, ASTM STP 1000, 1990, pp. 112–124.
- [28] Haynes, G. and Baboian, R., "Field Corrosion Testing and Performance of Cable Shielding Materials in Soils," *MP*, September 1989, pp. 68–74.
- [29] Mattson, E., "Accelerated Corrosion Testing of Automotive Radiators of Copper Materials A Critical Survey," *SAE Technical Paper Series 920181*, Detroit, 1992, pp. 1–9.
- [30] Beal, R. E., "Testing of Solder for Corrosion by Engine Coolants," *Engine Coolant Testing; State of the Art*, ASTM STP 705, 1980, pp. 327–355.
- [31] McNeil, M. B. and Odom, A. L., "Thermodynamic Prediction of Microbiologically Influenced Corrosion (MIC) by Sulfate-Reducing Bacteria (SRB)," *Microbiologically Influenced Corrosion Testing*, ASTM STP 1232, 1994, pp. 173–179.
- [32] Little, B. J., Wagner, P., and Jones-Mehan, J., "Sulfur Isotope Fractionation in Sulfide Corrosion Products as an Indicator for Microbiologically Influenced Corrosion (MIC)," *Microbiologically Influenced Corrosion Testing*, ASTM STP 1232, 1994, pp. 180–187.
- [33] Wagner, D. H. J., Fischer, W. R., and Paradies, H. H., "Correlation of Field and Laboratory Microbiologically Influenced Corrosion (MIC) Data for a Copper Potable Water Installation," *Microbiologically Influenced Corrosion Testing*, ASTM 1232, 1994, pp. 253–265.
- [34] Fischer, W. R., Wagner, D. H. J., and Paradies, H. H., "An Evaluation of Countermeasures to Microbiologically Influenced Corrosion (MIC) in Copper Potable Water Supplies," *Microbiologically Influenced Corrosion Testing*, ASTM STP 1232, 1994, pp. 275–282.
- [35] Crites, M. D. and Schlesinger, M. E., "Corrosion Testing of Chrome-Free Refractories for Copper Production Furnaces," *Proceedings of Copper 99-Cobre 99 International Conference*, Volume VI-Smelting, Technology Department, Process Modeling and Fundamentals, The Minerals, Metals and Materials Society, 1999, pp. 187–194.

# Nickel (and Alloys)

*Edward L. Hibner<sup>1</sup>*

THIS CHAPTER HIGHLIGHTS the corrosion resistance of nickel and its alloys and identifies relevant ASTM standards associated with their evaluation. The test technique selected ultimately will depend upon the specific alloy involved, the type of corrosion in question, or the end application, or a combination thereof. The following discussions will deal primarily with aqueous corrosion and the nickel-base (greater than about 30 % nickel) alloys designed for aqueous corrosion resistance. High-temperature gaseous corrosion will be addressed in other sections.

For assistance in understanding corrosion terminology, please refer to ASTM G 15, Terminology Relating to Corrosion and Corrosion Testing.

## INHERENT CORROSION RESISTANCE OF NICKEL AND NICKEL ALLOYS

Nickel and its alloys spontaneously form passive oxide films upon exposure to the atmosphere at ambient temperature. This film helps to provide very useful corrosion resistance in a variety of environments. The protective nature of this film can be enhanced by specific alloying additions.

### Effects of Alloying (Composition) and Metallurgical Factors

Commercially pure nickel, e.g., alloy 200 (UNS N02200), is resistant to general corrosion and stress-corrosion cracking (SCC) in strong caustic solutions and in many mildly reducing environments. Nickel can be alloyed with high percentages of many elements for enhanced corrosion resistance while maintaining a stable austenitic structure.

The first practical alloying of nickel for enhanced corrosion resistance was the addition of copper to make the 70Ni-30Cu alloy commonly known as alloy 400 (UNS N04400). This provided improved general corrosion resistance in reducing environments. The addition of chromium to improve corrosion resistance in oxidizing environments such as nitric acid is demonstrated by the development of many Ni-Fe-Cr or Ni-Cr-Fe alloys. The presence of iron in these alloys is usually for economy, not necessarily corrosion resistance. Molybdenum improves corrosion resistance to strongly reducing environments such as hot concentrated hydrochloric acid, e.g. alloy B-2 (UNS N10665).

Molybdenum, and sometimes tungsten, are also added to Ni-Cr-Fe alloys for improved localized corrosion (pitting and crevice corrosion) resistance. An example is alloy C-276 (UNS N10276), which contains about 57Ni-15.5Cr-15.5Mo-4W-5Fe and is one of the most pit-resistant nickel-base alloys available.

Though these alloying additions are quite effective in improving resistance to a particular environment, the resulting alloy can be susceptible to other forms of corrosion such as intergranular attack (IGA). Heat treatment in the 650°C to 870°C (1200° to 1600°F) range, such as in the heat affected zone of a weld joint, can cause intergranular sensitization. This sensitization, resulting from grain boundary chromium depletion, makes the grain boundary area susceptible to IGA by highly oxidizing solutions. Additions of titanium or niobium are used for stabilization against the intergranular sensitization. A stabilizing anneal at about 940°C (1724°F) is used for these stabilized alloys. Unstabilized materials like alloy 600 (UNS N06600) are annealed at various temperatures required to achieve desired properties, but specific use of the 940°C (1724°F) temperature is ineffective without the required titanium or niobium additions.

Certain nickel alloys are age-hardened by additions of aluminum, titanium, and/or niobium in amounts greater than that used for stabilization against IGA (see above). The aging mechanism can adversely affect the SCC resistance of these alloys, making them more susceptible to chloride and caustic cracking than their nonagehardenable counterparts. Nevertheless, materials like the age-hardened alloy K-500 (UNS N05500) have performed successfully in many seawater applications even though it is susceptible to SCC in the very severe boiling magnesium chloride test, ASTM G 36 (Recommended Practice for Performing Stress-Corrosion Cracking Tests in Boiling Magnesium Chloride Solution).

### Microstructural Effects

The most common microstructural effect on the corrosion resistance of nickel alloys is intergranular sensitization, as previously mentioned. This is the result of chromium carbide precipitation in many Ni-Fe-Cr alloys but can result from intermetallic Mu-phase precipitation in low-carbon highly alloyed materials such as alloy C-276 (UNS N10276). Several standard IGA tests (discussed in the Intergranular Corrosion section) are available for determining (1) if stabilized alloys have been properly annealed to prevent subsequent sensitization, and (2) if nonstabilized alloys are free from significant sensitization as produced.

<sup>1</sup>Senior Metallurgist, Code Manager, and Specification Coordinator for Special Metals Corporation, Inc., Huntington, WV 25705.

Nickel-base alloys with at least about 30 % nickel are very resistant to SCC in chloride and caustic solutions. Increasing nickel content usually provides increasing SCC resistance. Many different specimen designs are used to provide the stress necessary for evaluating the SCC resistance of a material (see SCC section).

Grain orientation has little effect on corrosion resistance in nickel-base alloys, though preferential end grain or edge attack can occur due to attack of nonmetallic inclusions, which are elongated in the rolling direction. In general, there is little difference in the corrosion resistance of the various available mill product forms when in the same final condition. Heavily cold-worked or age-hardened material, with high yield strength, will be less resistant to SCC than annealed material. Standard tests will apply to all products such as sheet, plate, tubing, and rod.

## SENSITIVITY TO PARTICULAR ENVIRONMENTAL FACTORS

### Aqueous Solution Variables

Minor changes in acidity or alkalinity can have a significant effect on pitting and crevice corrosion resistance. High chloride concentrations may be tolerated at a neutral pH but cause severe pitting as the solution becomes more acidic. Acid-chloride solutions are the most common cause of localized corrosion (pitting and crevice corrosion) failures of nickel alloys. Though nickel-base alloys with greater than about 30 % nickel normally resist chloride SCC, exposure to concentrated caustic at elevated temperatures, 260° to 350°C (500° to 662°F), can result in intergranular SCC. Ni-Cr-Fe alloys 600 (UNS N06600) and age-hardened alloys X-750 (UNS N07750) and 718 (UNS N07718) have also failed by SCC in high-purity water at these temperatures. Alloy 690 (UNS N06690), with a higher chromium content, is resistant to this failure mechanism.

### Liquid Metals and Hydrogen

Ni-Cu alloy 400 (UNS N04400) is susceptible to intergranular cracking in mercury at ambient temperature or in molten bismuth. Other than this, nickel alloys are normally resistant to liquid metals at temperatures up to about 540°C (1000°F). Nickel alloys are susceptible to hydrogen embrittlement but are much more resistant than steels or titanium alloys. Of the nickel alloys, the age-hardened materials are the most susceptible. Hydrogen can diffuse into nickel alloys from low-temperature gaseous environments or in aqueous solutions under cathodic charging. The degree of damage is determined by measurement of mechanical properties or alloy hydrogen content, or both [1].

## METHODS OF EVALUATION OF CORROSION DAMAGE

### Gravimetric

The most common method of evaluating uniform corrosion damage is by measurement of mass loss per unit area and

time. These parameters, along with material density, are used to calculate a uniform rate of corrosion penetration in mm/y or other similar units. This procedure is described in detail in ASTM G 31, Recommended Practice for Laboratory Immersion Corrosion Testing of Metals. In addition to uniform corrosion, many intergranular corrosion tests rely upon mass loss measurements to calculate a corrosion rate. Though an overall rate is used, most of the mass loss occurs at grain boundaries. This is especially true for sensitized specimens that exhibit a high corrosion rate. Thus, an accurate measure of grain boundary attack is obtained from the overall mass loss measurement. In extreme cases, accelerated mass loss can be the result of actual grain removal (grain dropping) due to intergranular attack.

While mass loss may be used to quantify the overall corrosion damage due to pitting, corrosion rates based on mass loss should not be used to predict the rate of pitting.

### Depth of Attack

Depth of attack measurements are most often used to quantify the extent of localized corrosion due to pitting or crevice attack. ASTM G 46, Recommended Practice for Examination and Evaluation of Pitting Corrosion, describes various techniques for pit depth measurement and pit characterization. Pit depths are most often measured with a pointed needle depth gage or micrometer or by use of a focusing microscope with a calibrated eyepiece. In commercially pure nickel, alloy 200 (UNS N02200), and nickel alloys without chromium, such as alloy 400 (UNS N04400), pits are usually broad and shallow. In some aggressive high-chloride, low-pH media, nickel alloys containing chromium, such as alloy 800 (UNS N08800), may exhibit deep undercut pits with relatively small openings at the surface. Pit depth, which causes component perforation, is the most important measurement, but pit density is also measured. ASTM G 46 provides detailed procedures for pit depth and density measurement. In some cases, where pit density is high, a change in mechanical properties may result.

Depth of attack measurements are often used to characterize the severity of SCC. Sectioning of the sample is usually necessary to obtain an accurate measurement. Also, in some IGA tests the presence of cracking after an exposed specimen is bent indicates susceptibility to IGA.

## TESTS FOR SPECIFIC CORROSION TYPES

### Uniform Corrosion Testing

As with many other materials, nickel and nickel alloys can be evaluated for uniform corrosion resistance according to guidelines in ASTM G 31. Due to the active/passive nature of many nickel alloys, the length of the test exposure can affect test results and reproducibility. In a short test lasting only a few hours, duplicate specimens can provide very different corrosion rates in some environments, like sulfuric acid. It is not unusual for one sample to show active behavior and another passive behavior over short time periods. Thus, extended test periods of about 100–200 h often provide more accurate results than shorter tests. The following

**TABLE 1**—General corrosion rates for alloy 725 (UNS N07725), 0.125 in. (0.32 cm) sheet testing in acid environments for varied exposure times as specified in Ref 2.

Environment	Temp., °C	Corrosion Rate, mm/y		
		0–96 h	96–192 h	0–192 h
0.2 % HCl	Boiling	<0.01	<0.01	<0.01
1.0 % HCl	Boiling	0.12	0.05	0.26
1.0 % HCl	90	0.64	0.05	0.05
5.0 % HCl	70	4.92	5.16	4.31
5.0 % HCl	50	1.34	1.33	1.14
5.0 % HCl	30	0.24	0.17	0.18
10.0 % H <sub>2</sub> SO <sub>4</sub>	Boiling	0.25	0.55	0.12
60.0 % H <sub>2</sub> SO <sub>4</sub>	70	0.65	0.65	0.41
60.0 % H <sub>2</sub> SO <sub>4</sub>	50	0.59	0.02	0.74
60.0 % H <sub>2</sub> SO <sub>4</sub>	30	0.04	0.03	0.18
95.0 % H <sub>2</sub> SO <sub>4</sub>	70	1.68	1.71	1.07
95.0 % H <sub>2</sub> SO <sub>4</sub>	50	1.84	1.27	0.58
95.0 % H <sub>2</sub> SO <sub>4</sub>	30	0.28	0.34	0.33
85.0 % H <sub>3</sub> PO <sub>4</sub>	Boiling	0.78	0.79	1.47
85.0 % H <sub>3</sub> PO <sub>4</sub>	90	0.01	0.01	0.01

NOTES: Unpublished data developed by Inco Alloys International, Inc., by the test method specified in Ref 2.

equation gives a suggested test duration when expected corrosion rates are low to moderate (see ASTM G 31):

$$\text{Hours} = \frac{2000}{(\text{anticipated corrosion rate in mpy})}$$

(This method of estimating test duration is useful only as an aid in deciding, after a test has been made, whether or not it is desirable to repeat the test for a longer period. The most common testing periods are 48–168 h.)

The test exposure intervals specified in the Materials Technology Institute Manual No. 3 [2], for instance, are 96 and 192 h for immersion testing. Examples of corrosion rates determined for these time intervals are shown in Table 1. Even with these relatively long test periods, some variation in test results can be seen, especially in sulfuric acid.

Because variations in corrosion rates can result from different surface finishes, greater reproducibility can often be obtained if a common surface is used on all specimens. A common surface produced by wet grinding with 120 grit abrasive, e.g., SiC, or pickling will provide a better estimate of the inherent corrosion resistance of a material, though it is sometimes desired to evaluate a particular commercial surface.

### Intergranular Corrosion

Intergranular precipitation can occur in nickel alloys when exposed to temperatures in the range of 649–871°C (1200–1600°F) during some fabrication and welding operations. The resulting depletion of chromium or segregation of other elements can cause the material to become susceptible to IGA in highly oxidizing environments, SCC under certain conditions, and possibly accelerated localized corrosion.

Thus standard accelerated intergranular corrosion tests have been developed as a quality control test. They are designed to:

1. Determine if a stabilized alloy, such as alloy 825 (UNS N08825), has received a proper stabilizing anneal. In this case a 677°C (1250°F)/1 h sensitization heat treatment

will be applied to the mill annealed material prior to testing to determine if the material is resistant to intergranular sensitization caused by precipitation of chromium carbide at 677°C (1250°F).

2. Determine if an unstabilized material, such as alloy C-276 (UNS N10276), has received an adequate solution anneal that has effectively removed all Mu or other intergranular phases that may have been precipitated during earlier processing. A sensitization heat treatment is not applied in this case because the material is not stable after prolonged exposures at intermediate temperatures (though short exposures during welding can be tolerated). ASTM G 28 (Method for Detecting Susceptibility to Intergranular Attack in Wrought Nickel-Rich, Chromium-Bearing Alloys, Practice A) is an example of a test that can be used for either of the above alloys, though ASTM A 262 (Practices for Detecting Susceptibility to Intergranular Attack in Austenitic Stainless Steels, Practice C) is usually specified for alloy 825 (UNS N08825).

The most common intergranular corrosion tests are outlined in ASTM A 262 and G 28. Most of these test solutions are strong oxidizing acids or acids with added oxidizers that maintain the specimen at a stable electrochemical potential where accelerated intergranular corrosion will occur in a susceptible material. The test duration is typically 24–120 h, depending on the alloy. Recommended exposure periods for various nickel-base alloys are listed in ASTM G 28 but not in ASTM A 262. Though only austenitic stainless steels are listed in ASTM A 262, some of the test methods are used for nickel-base alloys. It is important to note that ASTM A 262, Practice A, the oxalic acid etch test, is recommended for stainless steels. It is not normally used for nickel-base alloys.

The corrosion rates determined in the various tests will vary greatly depending on the alloy being evaluated. Acceptance corrosion rates are not specified in the ASTM test procedures. They must be agreed upon by the supplier and user. Examples of typical acceptable corrosion rates determined for various alloys in ASTM G 28, Practice A are listed in Table 2 [3]. Due to test and material variations, the maximum acceptable rate will be somewhat higher than this nominal number.

In this oxidizing environment the corrosion rate of unsensitized, properly annealed material is determined primarily by the chromium content. Thus, the base rate for alloy C-276 (UNS N10276) with lower chromium content, for example, is higher than the other alloys. The relative suitability of an alloy for a particular application is sometimes mistakenly related to the annealed base corrosion rate in the IGA test. This concept is an error. The test is designed to flag out improperly produced material exhibiting a rate above the normal base corrosion rate (Table 2), not a rate higher than some other alloy.

**TABLE 2**—Typical corrosion rates for annealed nickel alloys in ASTM G 28, Practice A.

Alloy	Corrosion Rate, mm/y
C-276 (UNS N10276)	6.35
622 (UNS N06022)	1.02
C-22 (UNS N06022)	0.89
316 (UNS S31600)	0.51
625 (UNS N06625)	0.36

### Localized Corrosion (Pitting and Crevice Corrosion)

Factors affecting localized corrosion of nickel-base alloys are chloride concentration, pH, temperature, crevice geometry (depth and tightness), and crevice former material (non-metallic or similar or dissimilar metal, metal surface condition, area ratio of exposed to shielded metal). A wide range of results can be obtained as these factors are varied.

ASTM G 48, Test Method for Pitting and Crevice Corrosion Resistance of Stainless Steels and Related Alloys by the Use of Ferric Chloride Solution, covers procedures for determination of the resistance of stainless steels and related alloys to pitting and crevice corrosion when exposed to an oxidizing chloride environment (6 % FeCl<sub>3</sub>). Four procedures are identified as Methods A, B, C, and D.

- Method A—Ferric chloride pitting test.
- Method B—Ferric chloride crevice test.
- Method C—Critical pitting temperature test.
- Method D—Critical crevice temperature test.

Method A is designed to determine the relative pitting resistance of stainless steel and nickel-base, chromium bearing alloys, whereas Method B can be used for determining both the pitting and the crevice corrosion resistance of these alloys. Methods C and D allow for a ranking of alloys by minimum (critical) temperature to cause initiation of pitting and crevice corrosion, respectively, of stainless steels, nickel-alloy, chrome bearing alloys in a standard ferric chloride solution (acidified 6 % FeCl<sub>3</sub>). These tests may be used to determine the effect of alloying additives, heat treatment, and surface finishes on pitting and crevice corrosion resistance. Though the critical temperature cannot be extrapolated to other environments, the relative order of resistance of various materials to pitting or crevice corrosion in other acid chloride environments should be similar. These ferric chloride test procedures are not capable of producing pitting attack in nickel alloys containing more than about 13 % molybdenum, though crevice corrosion can usually be produced at elevated temperatures [up to about 85°C (185°F)].

ASTM G 78, Guide for Crevice Corrosion Testing of Iron Base and Nickel Base Stainless Alloys in Seawater and Other Chloride-Containing Aqueous Environment, describes the use of multiple crevice assemblies and other devices applicable to nickel alloy testing in chloride environments. These procedures can be used to identify conditions most likely to result in crevice corrosion and provide a basis for assessing the relative resistance of various alloys to crevice corrosion under certain specified conditions.

Localized corrosion propagation rates are highly variable and not normally measured unless the time to initiation of attack is determined visually or by electrochemical monitoring. Pits in nickel alloys such as alloy 400 (UNS N04400), which are usually of the broad and shallow variety, tend to propagate much more slowly than the narrow undercut types found in chromium-bearing nickel alloys. Electrochemical tests are useful to predict pit initiation, while immersion tests evaluate initiation and also provide some indication of the possibility of severe pit propagation.

Weld metal is usually attacked by localized corrosion to a greater extent than the base metal because of the dendritic

structure and segregation present in weld metal. All weld metal or combination weld metal/base metal samples can be evaluated in pitting or crevice corrosion tests. For some crevice corrosion tests, however, the weld must be machined flat prior to attaching the crevice assembly (designed for a flat surface). It should be recognized that significant weld metal removal may cause inaccurate results since final surface weld passes may exhibit different corrosion resistance than initial weld passes exposed by machining. Alternatively, a surface contouring type crevice-forming device or any applied coating such as epoxy (now described in ASTM G 78) may be employed.

### Stress Corrosion Cracking

SCC testing of nickel alloys is conducted using the same specimen designs and test solutions as for many other alloy systems. One of the most commonly used specimen designs is the simple U-bend specimen; see ASTM G 30, Practice for Making and Using U-Bend Stress Corrosion Test Specimens. This is a severe screening test used to determine if a material is susceptible to SCC in a specific environment. For determination of critical stress levels required to produce SCC, bent beam (ASTM G 39, Practice for Preparation and Use of Bent-Beam Stress-Corrosion Specimens) or C-ring (ASTM G 38, Practices for Making and Using C-Ring Stress Corrosion Cracking Test Specimen) specimen designs may be used.

One notable caution is in the use of precracked wedge open loaded (WOL) specimens. Nickel alloys are usually so ductile that a very thick specimen is required to obtain a plane strain stress state at the tip of the precrack. The minimum thickness required can be calculated from the following equation

$$B \geq 2.5(KIc/\sigma_{ys})^2$$

where B = thickness and  $\sigma_{ys}$  = yield strength of the material [4].

Nickel alloys also do not show a strong directional effect as in aluminum alloys. SCC resistance of most nickel alloys is nearly the same in the short transverse direction as in the longitudinal direction.

Because of their very good resistance to chloride SCC, nickel alloys are often tested in the severe boiling magnesium chloride test, ASTM G 36, rather than the alternate immersion sodium chloride test, ASTM G 44, Practice for Alternate Immersion Stress Corrosion Testing in 3.5 % Sodium Chloride Solution, or the recently developed ASTM G 123, Test Method for Evaluating Stress-Corrosion Cracking of Stainless Alloys with Different Nickel Content in a Boiling Acidified Sodium Chloride Solution acidified sodium chloride test. These sodium chloride tests, which cause cracking of stainless steels, usually do not cause failure of nickel alloys containing about 30 % or more nickel.

Though nickel alloys are more resistant to chloride and caustic SCC than stainless steels, they are equally susceptible to cracking in polythionic acid (PTA) when in the sensitized condition. See ASTM G 35, Practice for Determining the Susceptibility of Stainless Steels and Related Nickel-Chromium-Iron Alloys to Stress Corrosion Cracking in Polythionic Acids, for test details.

### Electrochemical Testing

Nickel-base alloys respond well to most electrochemical test techniques and show active-passive behavior in many environments. Due to their rapid repassivation, however, the results obtained with potentiodynamic techniques can sometimes be affected by scan rate and immersion time prior to starting the test [5,6]. Electrochemical techniques are useful for investigating localized corrosion resistance, ASTM G 61, Test Method for Conducting Cyclic Potentiodynamic Polarization Measurements for Localized Corrosion Susceptibility of Iron-, Nickel-, or Cobalt-Based Alloys, and general corrosion resistance, ASTM G 59, Practice for Conducting Potentiodynamic Polarization Resistance Measurements of nickel alloys. Electrochemical impedance measurement techniques have not been extensively applied to nickel alloys.

### COMPARISON OF CORROSION BEHAVIOR

The corrosion resistance of nickel alloys can be either very good or very poor depending on the alloy/environment combination. Each of the various alloys, by chance or design, has very good resistance to certain environments, while exposure to other environments may be highly detrimental (i.e., without failure). Alloying additions that increase resistance to one form of corrosion may decrease resistance to another form of corrosion. The design of alloys for various applications was discussed in the preceding section on Nature of Nickel and Nickel Alloys.

The limiting variable for usable corrosion resistance of nickel alloys, like many other alloys, is often temperature. Many nickel alloys, for instance, have good resistance to ambient temperature sulfuric or hydrochloric acid at all concentrations. As the temperature increases, the number of alloys withstanding severe attack diminishes rapidly. Other than certain limitations such as this, most aqueous

corrosion applications can be handled by nickel or some nickel alloy.

New nickel-base alloys such as alloy G-30 (N06030), alloy 59 (N06059), and alloy 686 (N06686) have been developed with higher levels of chromium or molybdenum, or both, for increased resistance to localized or general corrosion in severe environments. These materials are being included in test procedures such as ASTM G 28.

Cast equivalents are available for many nickel-base alloys. Some test procedures, such as ASTM G 28, do not apply to cast materials. In most cases, castings should be expected to have lower corrosion resistance than wrought materials of similar composition. Also, selective phase attack may be confused with other corrosion mechanisms such as pitting.

### REFERENCES

- [1] Harris, J. A., Scarberry, R. C., and Stephens, C. D., "Effects of Hydrogen on the Engineering Properties of MONEL Nickel-Copper Alloy K-500," *Corrosion*, Vol. 28, No. 2, February 1972, pp. 57-62.
- [2] *Materials Technology Institute*, Manual No. 3, The Materials Technology Institute of the Chemical Process Industries, Inc., Columbus, OH, May 1980.
- [3] Crum, J. R. and Shoemaker, L. E., "Advances in Molybdenum Bearing, Corrosion Resistant Alloys for FGD Service," CORROSION 93, NACE, Paper 423, New Orleans, LA, March 1993.
- [4] Proposed Method of Test for Plane Strain Fracture Toughness of Metallic Materials, ASTM Standards on Physical and Mechanical Testing of Metals; Nondestructive Test. Part 31, ASTM International, West Conshohocken, PA, May 1969, pp. 1099-1114.
- [5] Morris, P. E. and Scarberry, R. C., "Anodic Polarization Measurements of Active-Passive Nickel Alloys by Rapid-Scan Potentiostatic Techniques," *Corrosion*, Vol. 26, No. 7, July 1970, pp. 169-179.
- [6] Stoecker, J. G., Siebert, O. W., and Morris, P. E., "Practical Applications of Potentiodynamic Polarization Curves in Materials Selection," *Materials Performance*, November 1983, pp. 13-22.

# Stainless Steels

*James W. Martin<sup>1</sup>*

## NATURE OF STAINLESS STEELS

### Natural Protective Film

STAINLESS STEELS ARE iron-based alloys containing at least 10 % chromium [1]. Although iron may corrode in an ordinary rural environment, the chromium gives stainless steel its ability to form a protective or passive film that resists corrosion. It is this ability to resist the formation of rust that led to the name "stainless steel." Generally, it is thought that the passive film consists of hydrated chromium oxide. Other alloy elements such as iron, molybdenum, silicon, etc., have also been detected in the passive film. The passive film also tends to incorporate anions and cations that may be present in the environment in which the film forms. Stainless steels are aut passivating in the sense that the passive film is formed spontaneously upon exposure to air, moisture, or an oxidizing acid. When stainless steel is exposed to such an environment, its corrosion resistance approaches that of noble metals; however, when exposed to an environment that damages, reduces, or inhibits the formation of the passive film, corrosion resistance of the alloy is compromised.

The presence of exogenous surface contamination, including dirt, grease, or free iron from contact with steel tooling, may interfere with formation of a continuous passive film. The cleaning of these contaminants from stainless steel will facilitate spontaneous passivation by allowing uniform access of oxygen to the steel surface. The passive film may be augmented by chemical treatment that provides an oxidizing environment for the stainless steel surface.

Methods for cleaning and passivating stainless steels are presented in ASTM A 380, Practice for Cleaning, Descaling, and Passivation of Stainless Steel Parts, Equipment, and Systems and ASTM A 967, Specification for Chemical Passivation Treatments for Stainless Steel Parts.

### Effects of Alloying

Chromium is the main element that provides stainless steel with its corrosion resistance. However, several other

elements can be added to stainless steel to enhance corrosion resistance under various conditions.

### Aluminum

Additions of aluminum enhance high temperature oxidation resistance. Aside from corrosion performance, this element is added to some precipitation-hardening stainless steels to promote age hardening (e.g., S13800). In contrast, a small amount of aluminum is present in Type 405 stainless (S40500) to prevent hardening by stabilizing the ferrite phase.

### Niobium (Columbium)

Niobium is used to combine with carbon and nitrogen, thus reducing the formation of chromium carbonitrides. This reduces the possibility of intergranular corrosion when stainless is welded or heat-treated. Niobium also contributes to age hardening in some precipitation-hardening stainless grades.

### Copper

In austenitic stainless steels, copper can be added to provide corrosion resistance to sulfuric acid. Copper also is used as an age-hardening agent in precipitation-hardenable stainless steels, such as 15Cr-5Ni stainless (S15500). However, copper can be detrimental to stress-corrosion cracking resistance in some ferritic alloys.

### Nickel

Nickel is the primary element that stabilizes the austenite phase and provides stainless steels with resistance to corrosion in reducing environments.

### Nitrogen

Provides increased resistance to pitting and crevice corrosion, especially in the presence of molybdenum. Nitrogen is a strong austenite-stabilizing element.

### Manganese

Stabilizes austenite and can be used to replace nickel in some stainless steels. Manganese also increases nitrogen solubility.

<sup>1</sup>Specialist, Stainless Alloy R&D, Carpenter Specialty Alloys, Reading PA 19612. Original text authored by Mark J. Johnson—Research associate, Allegheny Ludlum Corp., Brackenridge, PA 15014.



## Molybdenum

Pitting and crevice corrosion resistance as well as resistance to reducing environments are enhanced by the addition of molybdenum.

## Silicon

In some alloys silicon is added for high temperature oxidation resistance. Silicon has also been shown to provide resistance to stress corrosion cracking, as well as resistance to corrosion by oxidizing acids.

## Titanium

Titanium can serve a similar purpose as niobium relative to carbonitride stabilization. Titanium is added to some precipitation-hardening stainless steels (e.g., S46500) as an age-hardening agent.

## Microstructure

There are more than 170 different basic compositions of stainless steel [2]. They may be divided into five families: (1) austenitic, (2) ferritic, (3) martensitic, (4) precipitation-hardening, and (5) duplex. Each family has some unique physical and mechanical properties; however, within each family there is a range of corrosion resistance that is achieved by varying the alloying elements. This allows for the substitution of an alloy from one family for that of another and thus takes advantage of these properties. UNS (Unified Numbering System) grade designations currently are assigned as a joint activity of SAE and ASTM. Heat and corrosion resistant (stainless) steels are assigned identities within the range of S00001 through S99999. Austenitic chromium-nickel-manganese steels typically are assigned as S2xxxx designations; austenitic chromium-nickel grades and duplex stainless steels typically are listed as S3xxxx. Ferritic and martensitic grades are normally categorized using S4xxxx designations. This system generally follows previous AISI-type grade designations. The precipitation-hardening stainless grades are unique in that they are grouped within the S1xxxx, S4xxxx or S6xxxx series.

## Austenitics

In this family, the alloys have a face centered cubic structure, are not hardenable by heat treatment, have excellent formability and weldability, and have a wide range of corrosion resistance. UNS S30400 (Type 304), or "18-8" as it was commonly known, is probably the most widely used stainless steel. Modifications of S30400 are the stabilized S32100 (Type 321—stabilized with titanium) and S34700 (Type 347—stabilized with niobium) grades. When improved corrosion resistance is needed, alloys with higher chromium, nickel or molybdenum content, or both, such as S31600, S31700, and the 4 and 6 % molybdenum alloys are used. For high temperature applications, the higher chromium S30900 and S31000 are used.

The 200 series alloys are also austenitic. In this group of alloys, the nickel content has been reduced and replaced

with manganese and nitrogen additions to stabilize the austenitic microstructure. Common alloys in this group are S20100 and S20430, which, in most environments, have corrosion resistance similar to S30400, and S20910, which compares favorably to S31600 in corrosion resistance.

The austenitic alloys are not hardenable by heat-treating, but they can be hardened by cold work. S20100 and S30100 are particularly amenable to such hardening. Various levels of strength and hardness can be produced by controlled cold reductions of strip or wire. Such processing can produce deformation-induced martensitic transformation in some of the lower alloy content (metastable) grades. Other austenitic grades are more stable and, thus, do not exhibit martensitic transformation after severe cold working. Such alloys are used when low magnetic permeability is critical to the intended application.

These alloys may be made sensitive to intergranular corrosion by some environments if they are improperly heat-treated or sensitized during welding. During heat-treating, if the alloy is held in the temperature range of about 550–850°C, chromium carbides will form at the grain boundaries, resulting in a chromium depleted envelope around individual grains. This envelope, having lower chromium content, will be less resistant to corrosion and may be attacked in certain environments. This type of corrosion is referred to as intergranular corrosion. The same sensitization can occur during welding. In this case, only a narrow band on either side of the weld is usually affected. This is where the temperature has remained between about 550 and 850°C for an extended period. Sensitization can be eliminated by annealing the alloy, or avoided by using the low carbon alloys (S30403, S31603, etc.) or the stabilized alloys (S32100, S34700). Sensitization does not significantly affect the mechanical properties of the stainless nor can it be readily observed visually. However, it may be detected by conducting corrosion tests, as outlined in ASTM A 262, Practices for Detecting Susceptibility to Inter-granular Attack in Austenitic Stainless Steels.

Some of the higher-alloyed austenitic stainless steels (S31600 and alloys with more chromium or molybdenum, or both, as well as the stabilized alloys) may form sigma or chi precipitates at temperatures between about 900 and 990°C. These precipitates are enriched with chromium and molybdenum and leave an envelope surrounding the grains depleted in these elements. ASTM A 262 describes testing methods to determine if an alloy has been subjected to precipitation of these phases.

The austenitic alloys are particularly susceptible to stress corrosion cracking (SCC) in hot chloride environments. This form of corrosion can be minimized by increasing the amount of nickel in the alloy.

## Ferritics

The ferritic alloys have a body centered cubic structure, are mildly hardenable by cold work, have good formability (particularly drawability), and have a range of corrosion resistance. The ferritic alloys are particularly noted for their SCC resistance. A widely used alloy in this group is S43000 (Type 430), which contains 16 % chromium. The S409xx series are 11 % chromium alloys stabilized with titanium,

niobium, or a combination of titanium and niobium that are commonly used for automotive applications. For improved pitting and general corrosion resistance, alloys with higher chromium and molybdenum should be chosen. There are ferritic alloys, known as superferritics, with chromium as high as 30 %, and molybdenum as high as 4 %. Such alloys provide excellent resistance to pitting, crevice, and general corrosion, but are somewhat limited in terms of maximum product section size.

The ferritic alloys are also susceptible to sensitization. They are sensitized by heating to temperatures above about 900°C where the carbon and nitrogen are in solution. Upon cooling to about 400 to 700°C, the solubility of these elements is lowered and they precipitate as chromium carbides and nitrides, thus causing chromium depletion. This sensitization can be corrected by heating the ferritic stainless steel to 800°C. At this temperature, chromium will rediffuse back into the depleted areas. ASTM A 763, Practices for Detecting Susceptibility to Intergranular Attack in Ferritic Stainless Steels, may be used for testing for the sensitization of these stainless steels.

### Martensitic

The alloys in this family have a body centered tetragonal structure. The most common alloy in this group is S41000 (Type 410) with about 11.5 % chromium. These alloys are hardenable by heat treatment but have the least corrosion resistance of the five stainless steel families. They are used primarily for their high strength and hardness. Other common alloys in this group include S42000 (Type 420) and S440xx (Type 440 grades). The carbon and chromium contents in these alloys are higher, which help produce a hard, wear-resistant martensitic structure.

### Precipitation-hardening Alloys

These alloys are used for their combination of strength, hardness, and corrosion resistance. By controlling alloying elements and heat-treatment processes to manipulate the balance between austenite, ferrite, martensite, and second phase precipitation, a wide range of properties can be produced. The precipitation-hardenable alloys can be classified as martensitic, austenitic, or semi-austenitic. In the latter case, the alloys are predominately austenitic in the solution-annealed condition for ease of forming, but are subsequently transformed to a martensitic structure to produce higher strength capability. Semi-austenitic alloys may be magnetic if they are martensitic, or nonmagnetic if they are fully austenitic. Precipitation-hardenable alloys are characterized by their ability to be aged to high strength levels. They may also be cold worked before age hardening to achieve even greater strength levels. Alloys representative of the martensitic, austenitic and semi-austenitic precipitation-hardenable stainless steel classifications are S17400, S66286, and S35500, respectively.

The precipitation-hardenable alloys do not have the range of corrosion resistance offered by some of the austenitic or ferritic alloys; however, they provide substantially higher strength and are not restricted by product form.

### Duplex

Duplex stainless steels represent a comparatively small, but growing, family of alloys. As the name suggests, the compositions of duplex stainless steels are balanced to contain two phases, austenite and ferrite. The resultant duplex microstructure exhibits higher strength and improved stress-corrosion cracking resistance compared with many austenitic grades, yet provides greater toughness and ductility than ferritic stainless steels. However, toughness and corrosion resistance can be impaired significantly by the precipitation of intermetallic phases. ASTM A 923, Test Methods for Detecting Detrimental Intermetallic Phase in Wrought Duplex Austenitic/Ferritic Stainless Steels, was developed to allow detection of such phases in certain duplex grades.

Traditional alloys, such as S32900, contain about 15–20 % austenite in a ferritic matrix. Modern duplex stainless steels (e.g., S32950, S32550, S32205) are alloyed with nitrogen to increase the austenite volume fraction to about 30–50 %. Because of their ferrite content, duplex stainless steels are magnetic.

### Mill Products

Stainless steels are versatile materials. They are manufactured into a wide variety of product forms including bar, wire, strip, sheet, plate, tubing, pipe, and castings. Stainless steels may be drawn, formed, spun, extruded, welded, and electropolished. Section sizes may range from fine surgical needle wire to large structural forgings.

Many finishes can be applied to stainless steels. They range from dull, to satin, to mirror. Pattern and other textured finishes may also be applied. Because of this diversity, stainless steels are frequently used for decorative purposes on automobiles, buildings and storefronts, and even for statues. The cleanability and corrosion resistance of stainless steels makes them ideal for use where stringent sanitary and health conditions are of utmost importance. The pharmaceutical, food processing, dairy, wine, brewing, and many other industries, as well as hospitals, restaurants, hotels, and the home, are some of the places where stainless steel equipment is found. Precipitation-hardening stainless steels are found in aerospace applications requiring a combination of good corrosion resistance with high strength and fracture toughness.

### Sensitivity to Particular Environments

#### Acids

The effect of pure acids on stainless steels depends on whether the acid is reducing or oxidizing. If the acid has low oxidizing strength, the stainless will corrode rapidly. If, however, the oxidizing strength of the acid is sufficiently high, the stainless steels will resist corrosion.

Hydrochloric acid is a good example of a reducing acid with very little oxidizing capacity. Stainless steels will readily corrode in this acid in all but the very low concentrations. The form of corrosion that will occur will be general corrosion. The stainless steels with higher nickel and molybdenum concentrations will perform better in reducing acids.

Nitric acid has a high oxidizing capacity and stainless steels will remain passive in nitric acid solutions. Although sulfuric acid is corrosive to stainless steels, it may be innocuous in low concentrations and in the presence of aeration. Similar performance can be expected in phosphoric acid and in many of the organic acids.

Stainless steels with higher chromium concentrations tend to have more corrosion resistance in oxidizing environments.

Metal salts, such as ferric and cupric sulfate, are oxidizing and will passivate stainless steel when added to sulfuric acid. The salt concentration may be controlled so that passivity will occur at a specific chromium concentration. Stainless steels or areas of a stainless surface (such as sensitized grain boundary areas) with lower chromium content will not be passivated. This is the basis for the intergranular corrosion tests for stainless steels.

### *Alkalies*

Generally, the stainless steels are not corroded by alkalies such as sodium and ammonium hydroxide at solution temperatures below 100°C. At higher temperatures the austenitics such as S30400 may corrode excessively and may also exhibit SCC. The higher chromium ferritics and duplex stainless steels (26 % chromium) resist corrosion by alkalies up to about 150°C.

### *Salts*

Stainless steels are resistant to corrosion by most salts. The exceptions are the halide salts that cause pitting, crevice corrosion, and SCC. Of these salts, those containing chlorides are the most corrosive, followed by fluoride, bromide, and iodide salts. Stainless steels with higher chromium, molybdenum, and nitrogen concentrations will resist pitting and crevice corrosion more effectively. Austenitic stainless steels with higher molybdenum and nickel, ferritic stainless steels with no nickel or copper, and duplex stainless steels will resist SCC.

### *Liquid Metals*

Low melting metal such as aluminum, cadmium, copper, magnesium, zinc, etc., will corrode stainless steels at or above their melting point. In mercury, the lower chromium ferritics are much more resistant than the higher alloyed stainless steels.

### *Outdoor Atmospheres*

The stainless steels have excellent corrosion resistance in outdoor environments. They will suffer some rust staining when exposed to chlorides (seacoast, deicing salts) and/or acid industrial fumes. The higher the alloy content of the stainless steel, particularly chromium, molybdenum, and nitrogen, the better the performance.

## **METHODS OF EVALUATION**

As with most metals, stainless steels are susceptible to most forms of corrosion. However, the most frequently encountered forms of corrosion are: general, intergranular, pitting, crevice, and SCC. Methods for evaluating stainless

steels for susceptibility to these forms of corrosion are described in the ASTM standards as outlined in this section.

## **Tests for Susceptibility to Forms of Corrosion**

In order to obtain accurate and consistent test results the specimens must be properly prepared before corrosion tests are conducted. Following ASTM G 1, Practice for Preparing, Cleaning and Evaluating Corrosion Test Specimens, will provide better reproducibility and will afford a commonality for comparing results compiled in the same laboratory at different times to results obtained at another laboratory.

### *General Corrosion*

General corrosion is the overall wastage of the material. This is a manageable form of corrosion in that the corrosion rate can be established, and an item may be built to last the length of time needed by selecting the correct thickness. The corrosion can be monitored and the life of the item can be estimated. Thus, no unexpected failures will occur. To test for susceptibility to this form of corrosion, samples may be exposed to the corrosive medium at the anticipated use temperature and a corrosion rate established. ASTM G 31, Practice for Laboratory Immersion Corrosion Testing of Metals, is an excellent guide for conducting such tests. Atmospheric corrosion tests may be conducted by following ASTM G 50, Practice for Conducting Atmospheric Corrosion Tests on Metals. The following electrochemical tests may also be used for establishing the relative corrosion resistance of stainless steels: ASTM G 3, Practice for Conventions Applicable to Electrochemical Measurements in Corrosion Testing; ASTM G 5, Standard Reference Test Method for Making Potentiostatic and Potentiodynamic Anodic Polarization Measurements; ASTM G 59, Test Method for Conducting Potentiodynamic Polarization Resistance Measurements; and ASTM G 102, Practice for Calculation of Corrosion Rates and Related Information from Electrochemical Measurements.

### *Intergranular Corrosion*

As described before, intergranular corrosion of stainless steels occurs when the material is sensitized. This condition produces a chromium-depleted envelope around each grain, which is less corrosion-resistant. This results in intergranular corrosion of the stainless steel in certain environments. The two ASTM standards that describe how to test stainless steels for susceptibility to this form of corrosion are ASTM A 262 and A 763. A third standard, G 28, is applicable to nickel-rich, chromium-bearing alloys.

### *Pitting Corrosion*

This is a localized type of corrosion. There could be only one or two pits on the surface of a tank containing a liquid and this very slight, highly localized corrosion could render that tank useless. Pitting of stainless steel usually starts as a small opening on the surface and then may spread like a balloon beneath it. Pitting can require an extended incubation period, and therefore short test periods may not provide useful data. A very high percentage of pitting of stainless steels is caused by chloride ions. The other halides

may also cause pitting, as will some sulfur species. Pitting susceptibility is usually established using chloride-containing solutions. Acid and oxidizing conditions tend to accelerate pitting. Alkaline conditions, on the other hand, tend to suppress pitting corrosion of the stainless steels. ASTM G 48, Test Methods for Pitting and Crevice Corrosion Resistance of Stainless Steels and Related Alloys by the Use of Ferric Chloride Solution, is used for testing pit susceptibility. ASTM G 46, Guide for Examination and Evaluation of Pitting Corrosion, may be used for evaluating the results of the tests. ASTM G 150, Test Method for Electrochemical Critical Pitting Temperature Testing of Stainless Steels, offers an electrochemical technique for evaluating relative susceptibility to pitting corrosion.

As previously mentioned, stainless steels with higher chromium, molybdenum, and nitrogen concentrations typically will resist pitting and crevice corrosion more effectively. Empirical formulas have been derived to express the relationship of chromium, molybdenum, and nitrogen concentrations to pitting and crevice corrosion resistance. For example, Eq 1 has been applied to austenitic stainless steels to define Pitting Resistance Equivalent or PRE number [3]. Elemental coefficients may differ depending upon the specific alloy family. For example, Eq 2 has been associated with duplex stainless steels. Results of such formulas are relative and should be used only as a guideline.

$$\text{PRE} = \% \text{Cr} + 3.3x\% \text{Mo} + 30x\% \text{N} \quad (1)$$

where elemental concentrations are expressed mass percent.

$$\text{PRE} = \% \text{Cr} + 3.3x\% \text{Mo} + 16x\% \text{N} \quad (2)$$

where elemental concentrations are expressed mass percent.

### Crevice Corrosion

This form of corrosion is very much like pitting corrosion. The only difference is that the attack occurs in a crevice such as lap joints, gaskets, bolts, rivets, dirt deposits, under disbonded paint, corrosion products, scale, etc. Everything stated above about pitting corrosion of stainless steel applies to crevice corrosion as well. There is an incubation period just like in pitting corrosion. The attack occurs, in this instance, on the surface of the stainless, immediately below the crevice former. As with pitting, metal dissolution can be very rapid once the passive film breaks down and attack has initiated. Corrosive ions, such as chlorides, tend to migrate to the crevice and concentrate, thus accelerating corrosion. The acidity of the solution in the crevice is also increased, which further accelerates corrosion. Given similar conditions, crevice corrosion will occur before pitting initiates.

ASTM G 48 is also used to evaluate stainless steels for crevice corrosion susceptibility. ASTM G 78, Guide for Crevice Corrosion Testing of Iron-Base and Nickel-Base Stainless Alloys in Seawater and Other Chloride-Containing Aqueous Environments, should be consulted prior to crevice corrosion testing.

### Stress Corrosion Cracking (SCC)

This form of corrosion is caused by the joint action of tensile stresses and corrosion. Almost all metals have some alloy systems that are susceptible to SCC. However, there are specific environments that cause cracking in each material.

A primary agent causing most stainless steel SCC failures is the chloride ion. The stainless steels that are most susceptible to this form of corrosion are the approximately 8–10 % nickel austenitic grades. However, as the nickel content of the austenitic steels increase beyond this level, the resistance to SCC increases. The ferritic stainless steels, with no nickel or copper, are resistant to this form of corrosion. However, ferritic grades are more prone to hydrogen-induced cracking or embrittlement.

Three factors are considered necessary to cause SCC in a susceptible austenitic stainless steel: (1) presence of chlorides, (2) elevated temperatures, and (3) tensile stresses. If any one of these is reduced or eliminated, the likelihood of SCC occurring is reduced.

SCC of the austenitic stainless steels has a characteristic morphology. The cracks are branching and transgranular in nature, unless the alloy is sensitized. In sensitized material the cracking will take an intergranular path. This form of corrosion also has an incubation period. Depending on the chloride ion concentration, the temperature, and the magnitude of tensile stresses, the failure can occur within hours or after many years.

The following ASTM standards may be used for testing susceptibility to SCC:

- G 30, Practice for Making and Using U-Bend Stress-Corrosion Test Specimens
- G 35, Practice for Determining the Susceptibility of Stainless Steels and Related Nickel-Chromium-Iron Alloys to Stress-Corrosion Cracking in Polythionic Acids
- G 36, Practice for Evaluating Stress-Corrosion Cracking Resistance of Metals and Alloys in a Boiling Magnesium Chloride Solution
- G 38, Practice for Making and Using C-Ring Stress-Corrosion Test Specimens
- G 39, Practice for Preparation and Use of Bent-Beam Stress-Corrosion Test Specimens
- G 41, Practice for Determining Cracking Susceptibility of Metals Exposed Under Stress to a Hot Salt Environment
- G 44, Practice for Exposure of Metals and Alloys by Alternate Immersion in Neutral in 3.5% Sodium Chloride Solution
- G 49, Practice for Preparation and Use of Direct Tension Stress-Corrosion Test Specimens
- G 58, Practice for Preparation of Stress-Corrosion Test Specimens for Weldments
- G 123, Test Method for Evaluating Stress-Corrosion Cracking of Stainless Alloys with Different Nickel Content in Boiling Acidified Sodium Chloride Solution
- G 129, Practice for Slow Strain Rate Testing to Evaluate the Susceptibility of Metallic Materials to Environmentally Assisted Cracking
- G 168, Practice for Making and Using Precracked Double Beam Stress Corrosion Specimens.

Refer to Chapter 25 for more information on testing for susceptibility to SCC.

## REFERENCES

- [1] "Properties and Selection: Stainless Steels, Tool Materials and Special-Purpose Metals," Vol. 3, *ASM Metals Handbook*, Ninth Edition, American Society for Metals, Metals Park, OH, 1980.

- [2] Sedriks, A. J., *Corrosion of Stainless Steels*, John Wiley & Sons, New York, 1979, p. 1.
- [3] Speidel, M. O., "High Nitrogen Stainless Steels: Austenitic, Duplex and Martensitic," *Stainless Steels '87*, The Institute of Metals, 1988.

### Bibliography

Ailor, W. H., *Handbook on Corrosion Testing and Evaluation*, John Wiley & Sons, Inc., NY, 1971.

*Liquid-Metals Handbook*, Oak Ridge National Laboratory, Second Edition, June 1952.

"Corrosion," Volume 13, *ASM Metals Handbook*, Ninth Edition, ASM International, Metals Park, OH, 1987.

Fontana, M. G., *Corrosion Engineering*, McGraw-Hill Book Co., NY, 1986.

NACE Standards, NACE, Houston, TX., [www.nace.org](http://www.nace.org).

Peckner, D. and Bernstein, I. M., *Handbook of Stainless Steels*, McGraw-Hill Publishing Co., NY, 1977.

# Cobalt-Base Alloys

P. Crook<sup>1</sup>

## THE NATURE OF COBALT AND ITS ALLOYS

COBALT OCCURS IN two atomic forms: a low temperature stable hexagonal close packed (hcp) form and a high temperature stable face centered cubic (fcc) form. The transformation temperature of pure cobalt is 417°C. Alloying elements such as nickel, iron, and carbon (within its soluble range) are known as fcc stabilizers, and suppress the transformation temperature. Chromium, molybdenum, and tungsten, on the other hand, are hcp stabilizers and have the opposite effect.

In reality, the transformation is extremely sluggish, and most cobalt-base alloys exhibit a (metastable) fcc structure at room temperature, even if their transformation temperatures are considerably higher. Partial transformation (from fcc to hcp) of most cobalt-based alloys is, however, easily induced at room temperature by plastic deformation (under the action of mechanical stress), the extent of the transformation being related to the composition (in particular the ratio of hcp stabilizers to fcc stabilizers). The transformation under stress is believed to progress by the creation of wide stacking faults (the fcc form of these alloys having very low stacking fault energies) and by subsequent coalescence. Extensive microtwinning is also observed in plastically-deformed, cobalt-based alloys.

By virtue of these crystallographic features, the cobalt-based alloys are inherently resistant to those forms of wear that involve a microfatigue constituent, namely sliding wear, fretting, cavitation erosion, and liquid droplet erosion [1].

From a corrosion standpoint, the roles of various alloying elements in the cobalt-base alloys parallel those seen in the nickel-base alloys. Chromium, molybdenum, and tungsten, for example, are highly soluble in both atomic forms of cobalt. Chromium is added to most of the commercially important alloys, and provides passivity over a wide range of potentials. Molybdenum and tungsten enhance resistance to corrosion within the active regime.

The cobalt-base alloys fall generally into two categories. Alloys in the first category contain low levels of carbon, and are intended for use in severely corrosive environments, at high temperatures, or where ductility is an important consideration. Alloys within the second category have high carbon contents; they exhibit high hardnesses and provide resistance to low stress abrasion (in addition to other forms of wear), but exhibit low ductilities and poorer corrosion resistance. Compositions from both categories are listed in Table 1.

Most of the low-carbon, cobalt-base alloys are available in the form of wrought products (plates, sheets, bars, etc.), from which industrial components can be fabricated. Some of these alloys are common in cast and weld overlay form also. The high-carbon alloys are not easily produced in wrought product form; they are therefore used mostly in cast or weld overlay form. From a microstructural standpoint, not only is there a large difference between the wrought and cast versions of certain cobalt-base alloys, but there is also an enormous microstructural difference

TABLE 1—Nominal compositions of selected cobalt-base alloys (wt%).

UNS Designation	Commercial Designation	Co	Cr	Ni	Fe	Mo	W	Si	Mn	C	Others
<b>Low-Carbon Alloys</b>											
R31233	ULTIMET	Bal	26	9	3	5	2	0.3	0.8	0.06	N-0.08
R30188	HAYNES 188	Bal	22	22	3*	—	14	0.4	1.25*	0.1	La-0.03
R30605	HAYNES 25/L-605	Bal	20	10	3*	—	15	0.4*	1.5	0.1	
R30021	STELLITE 21	Bal	28	2.5	2*	5.5	—	2*	1*	0.25	
—	STELLITE 306	Bal	25	5	—	—	2	—	—	0.4	Nb-6.0
<b>High-Carbon Alloys</b>											
R30006	HAYNES 6B/STELLITE 6	Bal	30	2.5	3*	1.5*	4	0.7	1.4	1	
R30012	STELLITE 12	Bal	30	3*	3*	1*	8.3	2*	1*	1.4	
R30002	STELLITE F	Bal	25	22	3*	1*	12.3	2*	1*	1.75	
R30001	STELLITE 1	Bal	31	3*	3*	1*	12.5	2*	1*	2.4	
—	STELLITE 3	Bal	31	3*	3*	1*	12.5	1*	1*	2.4	B-0.1
—	STELLITE 190	Bal	26	3*	3*	1*	14.5	2*	1*	3.3	

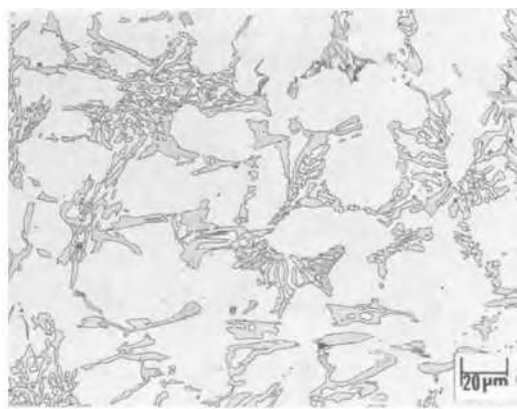
\*Maximum.

<sup>1</sup>Haynes International, Kokomo, IN 46901.

a. UNS R31233 Wrought Plate (Annealed)



c. UNS R30006 Multi-layer Oxy-Acetylene Weld Overlay (As-welded)



b. UNS R30006 Wrought Plate (Annealed)

d. UNS R30012 Multi-layer Oxy-Acetylene Weld Overlay (As-welded)

e. UNS R30001 Multi-layer Oxy-Acetylene Weld Overlay (As-welded)

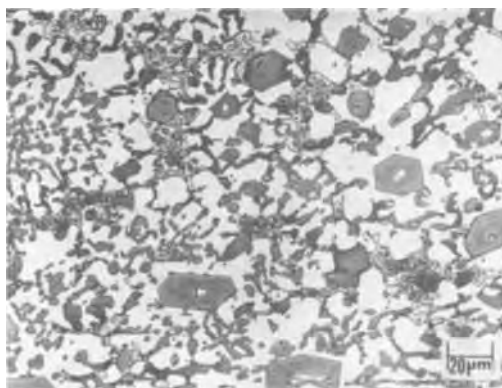


**FIG. 1—Microstructures of cobalt-base alloys. (a) UNS R31233 wrought plate; (b) UNS R30006 wrought plate; (c) UNS R30006 weld overlay; (d) UNS R30012 weld overlay; (e) UNS R30001 weld overlay.**

between the high- and low-carbon alloys [2]. During solidification, large quantities of carbide form in the microstructures of the high-carbon, cobalt-base alloys. At a carbon level of 2.4 wt% (STELLITE 3), for example, the carbides constitute about 30 wt% of the material [3]. These are of the  $M_7C_3$  (chromium-rich primary) and  $M_6C$  (tungsten-rich eutectic) types, where M represents the metal component (e.g.,  $M_7C_3$  corresponds to  $Cr_7C_3$ ). At 1 wt% carbon (UNS R30006), the carbides constitute about 13 wt% of the material, these being predominantly chromium-rich eutectic carbides of the  $M_7C_3$  type [3].

Carbides are much less abundant in the low-carbon alloys, and absent from the wrought, annealed microstructure of UNS R31233. In some of these low-carbon alloys, they play an important role. The  $M_6C$  precipitates in UNS R30605, for example, are important to its high-temperature, mechanical properties, partially because they restrict grain growth [4].

Microstructures of several cobalt-based alloys are presented in Fig. 1. From these, the influence of carbon content on the nature and volume fraction of carbide precipitates is evident.

With regard to corrosion resistance, carbide precipitates are very important in that they tie up critical alloying elements, and create, within the segregated cast microstructures at least, networks prone to preferential attack. Even in quenched, wrought microstructures, grain boundary sensitization due to carbide precipitation is common. In reviewing the high-carbon, cobalt-base alloy compositions, it should be appreciated that the (effective) solid solution chromium, molybdenum, and tungsten levels are relatively low, and that, in cast components and weld overlays, compositional inhomogeneity within the solid solution is to be expected.

## THE AQUEOUS CORROSION TESTING OF COBALT-BASE ALLOYS

Several tests are used to assess the suitability of the cobalt-base alloys for use in corrosive media. The most common is the immersion test, performed according to the procedures defined in ASTM G 31, Practice for Laboratory Immersion Corrosion Testing of Metals.

In special cases, such as UNS R31233, when general usage of the alloy in the chemical processing industries is anticipated, many immersion tests are performed in certain media, and isocorrosion curves generated. Comparative curves for UNS R31233 and UNS N06022 are shown in Fig. 2. These curves represent the concentrations and temperatures (in sulfuric, hydrochloric, nitric, and phosphoric acids) at which corrosion rates of 0.13 mm/y (5 mpy) and 0.51 mm/y (20 mpy) were encountered. At lower concentrations and temperatures, lower corrosion rates were measured. All of the immersion tests used to construct these curves were performed in duplicate, using samples of dimensions 25.4 by 12.7 by 3.2 mm and 1 L of solution per duplicate pair. The samples were each tested for four 24-h periods, with a new solution every period. Weights were measured after every test period.

Given the chromium and molybdenum levels that exist in UNS R31233, these curves suggest that the two elements are at least as effective in cobalt-base alloys as they are in the

iron- and nickel-based alloys, provided they remain in solution (i.e., do not partition to primary or secondary precipitates).

To evaluate the susceptibility of the cobalt-based alloys to localized attack, the procedures described in ASTM G 48, Test Method for Pitting and Crevice Corrosion Resistance of Stainless Steels and Related Alloys by the Use of Ferric Chloride Solution can be used. When tested in 6 % ferric chloride, for example, at a temperature of 65°C, the pit densities and depths for samples of UNS R31233 were less than those for UNS N10276.

The mode of degradation under which the nickel-base alloys are inherently superior to the cobalt-based materials is stress corrosion cracking. This is a result of their respective crystallographic characteristics. On the one hand, the nickel-base alloys possess stable fcc structures with high stacking fault energies, in which cross-slip is easily accomplished during plastic deformation. On the other hand, the cobalt-base alloys possess, in general, metastable fcc structures with low stacking fault energies, in which slip is predominantly planar. Such crystallographic characteristics are known to promote transgranular stress corrosion cracking [6].

Relative to the austenitic stainless steels, however, the low-carbon cobalt-base appear to exhibit reasonable resistance to stress corrosion cracking (equivalent to that of the high nickel grades). Although it has not been possible to differentiate between UNS R31233 and high-nickel stainless steels such as UNS N08020 by testing U-bend samples, prepared in accordance with ASTM G 30, Practice for Making and Using U-Bend Stress-Corrosion Test Specimens, in a boiling magnesium chloride solution (ASTM G 36, Practice for Performing Stress-Corrosion Cracking Tests in a Boiling Magnesium Chloride Solution), four-point bend tests at stresses within the elastic ranges of the materials have allowed the ranking of UNS R31233 relative to UNS N08020 and UNS S31603. The results of this test, which was performed in 30 % magnesium chloride at 118°C, are illustrated in Fig. 3.

Immersion testing according to the ASTM G 31 procedures can be used to evaluate the relative performance of the high- and low- carbon alloys. The data in Table 2 illustrate the difference in corrosion resistance between UNS R31233 (0.06 wt% carbon) and UNS R30006 (1 wt% carbon), when used in the cast form. All samples were prepared from investment castings. For comparison, data are presented also for investment castings of UNS R30605, CF-3M (the cast equivalent of UNS S31603 stainless steel), CW-12MW (equivalent to UNS N10276), and CX-2MW (equivalent to UNS N06022). The three cobalt-based alloys were tested in the as-cast condition (since castings of these alloys are not normally annealed); the stainless steel and nickel-base alloys were tested in the solution annealed condition.

These test media may be grouped into those that are oxidizing in nature (ASTM G 28A solution [Test Methods for Detecting Susceptibility to Intergranular Attack in Wrought Nickel-Rich, Chromium Bearing Alloys],  $P_2O_5$ , and  $HNO_3$ ), those that are non-oxidizing (HCl,  $H_2SO_4$ , and HF), and those that promote pitting (ASTM G 28B solution and  $FeCl_3$ ). For those in the oxidizing category, the chromium content of the alloy is critical in that it controls the



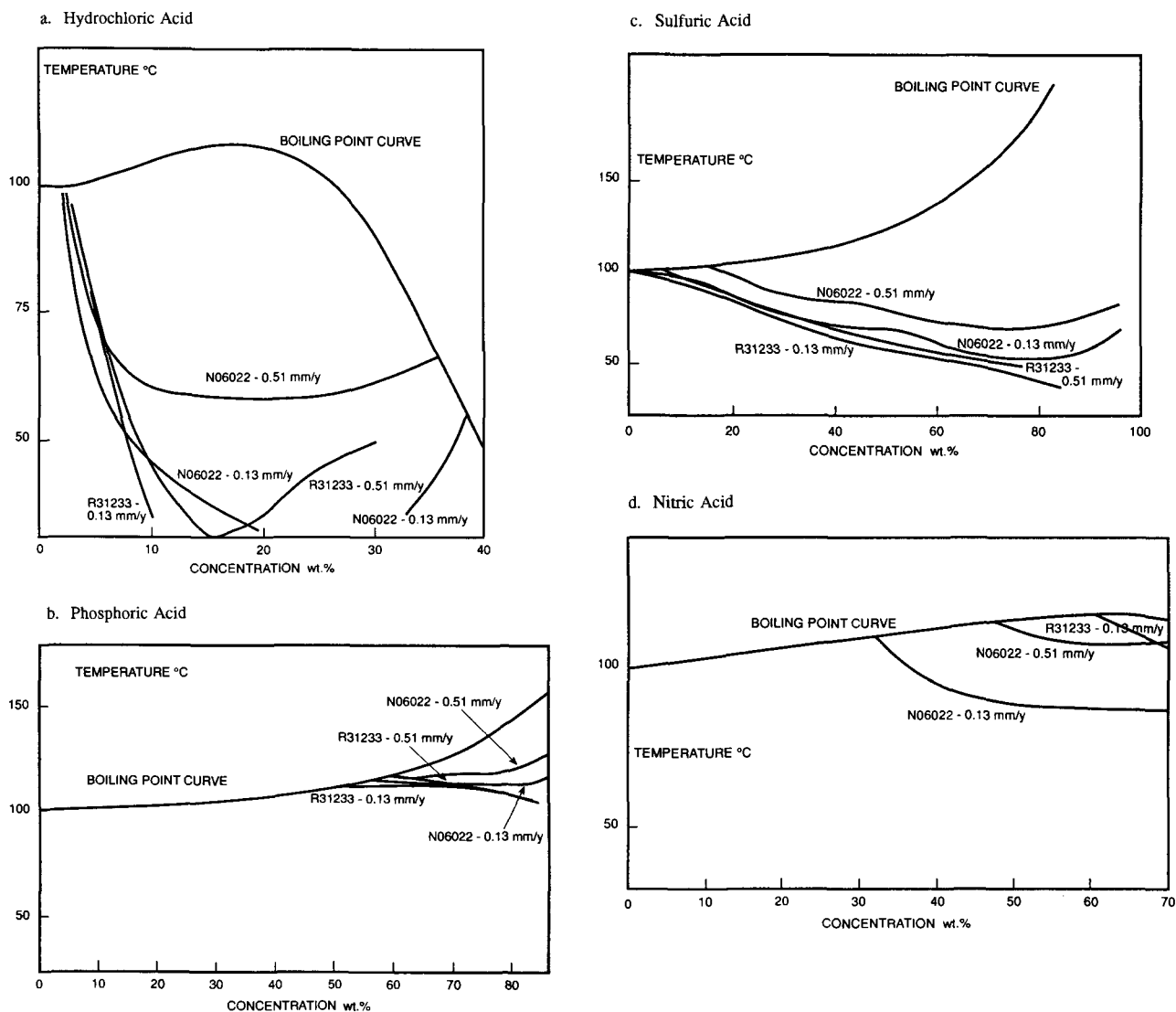


FIG. 2—Isocorrosion curves for UNS R31233.

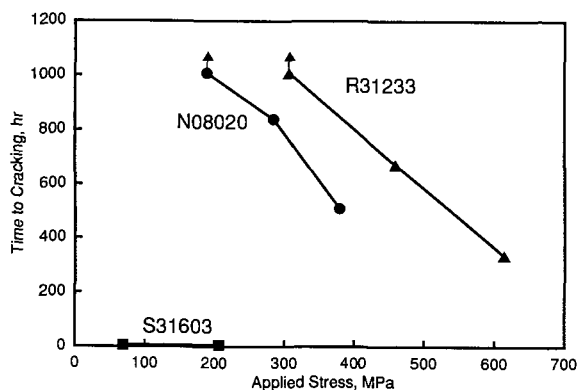


FIG. 3—Stress corrosion cracking data in 30 % magnesium chloride at 118°C.

active-passive behavior. In the case of multiphase alloys, it is important how the chromium partitions to the individual phases. In the case of castings, the distribution of chromium within each phase is critical also.

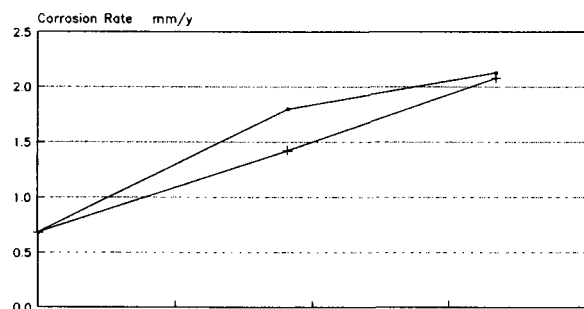
As discussed, a substantial proportion of the chromium in UNS R30006 partitions to the carbide phase. This explains the poor performance of UNS R30006 relative to UNS R31233 in the three oxidizing media.

For the non-oxidizing media, molybdenum and tungsten appear to be the most influential elements in cobalt-, nickel-, and iron-base alloys. Here the poorer performance of UNS R30006 can be explained by the atomic weight differences between molybdenum and tungsten (1 wt% of molybdenum being approximately equivalent to 2 wt% tungsten, in atomic terms), and the presence of the chemically-active carbides in the microstructure. Higher tungsten contents in the cobalt-base alloys are only effective when carbon

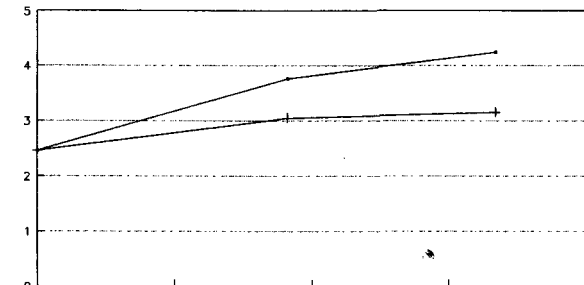
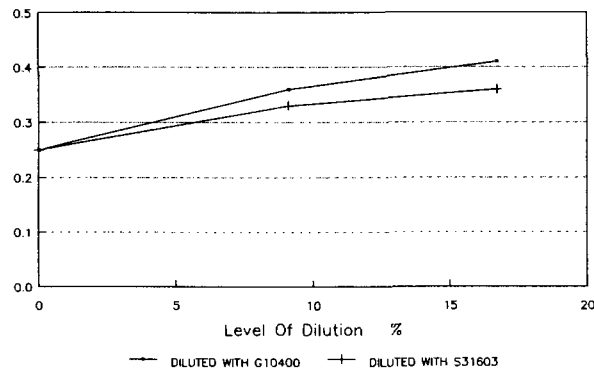
**TABLE 2**—Corrosion data for investment castings (corrosion rate, mm/y).

	ASTM G 28A Test	ASTM G 28B Test	3 % HCl 66°C	54 % P <sub>2</sub> O <sub>5</sub> 116°C	10 % H <sub>2</sub> SO <sub>4</sub> Boiling	65 % HNO <sub>3</sub> Boiling	2 % HF 70°C	10 % FeCl <sub>3</sub> Boiling
UNS R31233	0.3	1.0	0.0	0.2	2.1	0.2	0.5	0.0
UNS R30006	1.5	80.8	87.8	0.9	184.6	73.4	44.4	507.7
UNS R30605	0.7	40.9	15.6	0.2	3.6	1.3	5.1	335.7
CF-3M	0.7	90.3	10.2	0.7	16.1	0.4	14.8	531.5
CW-12MW	26.8	46.5	0.0	0.7	0.4	20.5	0.3	43.2
CX-2MW	1.8	0.7	0.0	0.3	0.7	3.0	0.3	4.0

a. 3% Hydrochloric Acid, 66°C



b. 10% Sulfuric Acid, Boiling

c. ASTM G28A Solution (50% H<sub>2</sub>SO<sub>4</sub> + 42 g/l Fe<sub>2</sub>(SO<sub>4</sub>)<sub>3</sub>, boiling)**FIG. 4—Corrosion rates versus dilution level for UNS R31233.**

contents are low, because of partitioning of the tungsten to the carbides.

For those media that promote localized attack (pitting and crevice corrosion), the combination of chromium and molybdenum appears to be important. Again, the distribution of these elements in the microstructure is believed to be important, as are second phases, which can act as initiation sites.

Since the cobalt-base alloys are widely used in weld overlay form, it is important to establish the effects of dilution (intermixing with the substrate material) by immersion testing, according to ASTM G 31 procedures. By means of such tests, it has been shown that intermixing of the cobalt-base alloys with either carbon steel or stainless steel is detrimental [7]. The extent to which dilution influences the corrosion resistance of UNS R31233, in selected oxidizing and non-oxidizing media, is illustrated in Fig. 4. These results may be attributed to the lower chromium and molybdenum levels in the diluted overlays; iron appears to degrade the corrosion resistance of the cobalt-base alloys also [7].

With regard to the use of corrosion tests for the quality control testing of cobalt-base alloys, only UNS R31233 appears to be subject to this. In this case, each wrought product (i.e., every thickness of plate, bar, and sheet from a given heat) is subjected to the ASTM G 28A (50 % H<sub>2</sub>SO<sub>4</sub> + 42 g/l Fe<sub>2</sub>(SO<sub>4</sub>)<sub>3</sub>, boiling) test prior to sale. A corrosion rate of less than 0.25 mm/y is necessary for release of the material. The test duration is 120 h.

## WEAR TESTING OF COBALT-BASE ALLOYS

The chief industrial attribute of the cobalt-base alloys is their resistance to wear. They hold a unique position in that they are also corrosion-resistant (when the carbon content is low), and maintain their strengths and wear resistance at high temperatures, by virtue of reasonable microstructural stability (relative to, say, the austenitic manganese steels, the tool steels, and the high-silicon stainless steels).

In evaluating the cobalt-base alloys in a wear sense, several ASTM standards, most involving room temperature tests, have been employed. Among these are:

- ASTM G 32, Test Method for Cavitation Erosion Using Vibratory Apparatus
- ASTM G 65, Test Method for Measuring Abrasion Using the Dry Sand/Rubber Wheel Apparatus
- ASTM G 98, Test Method for Galling Resistance of Materials

To illustrate the benefits of the cobalt-base alloys as compared to other alloys of moderate and high corrosion resistance, data generated using the ASTM G 32 and G 65 (Procedure B) tests are presented in Figs. 5 and 6. With regard to galling resistance, data are presented in Table 3.

The galling test used to generate the information in Table 3 was a modification of the ASTM G 98 procedure. It involved:

- (a) cyclic motion of the test pin through an arc of 120°,
- (b) application of the load by means of a Riehle Mechanical Tester (in the load holding mode), and

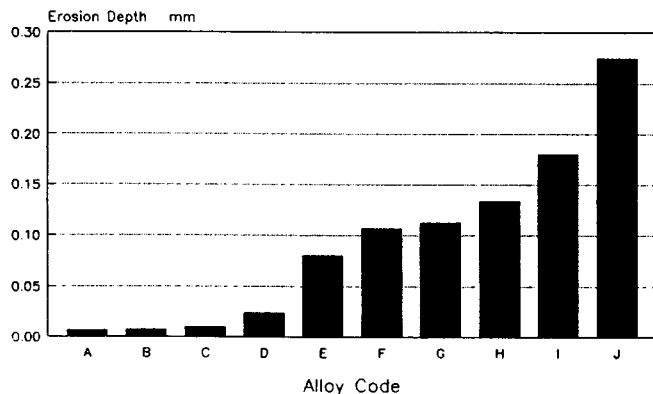
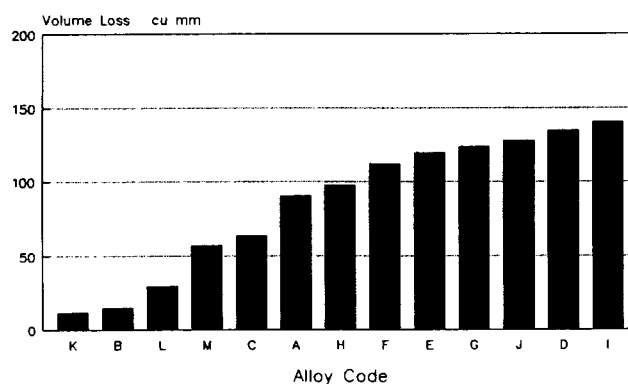


FIG. 5—Comparative cavitation erosion data (ASTM G 32 test).

(c) quantitative interpretation of the test scars by surface profilometry.

The cylindrical pins (of diameter 15.9 mm) and the counterface blocks (of dimensions 76.2 by 25.4 by 12.7 mm) were surface ground prior to test. During test, the pins were subjected to five rotational cycles (i.e., they were turned back and forth through ten arcs of 120°) by means of a wrench, at loads of 1361, 2722, and 4082 kg.

In visual terms, the cylindrical pins and the counterface blocks appeared to suffer the same degree of damage in each test. The blocks, therefore, were used in the quantitative determination of damage, since they were more amenable to profilometry, allowing travel of the stylus to and beyond the circumference of the scar. For accuracy, the stylus was passed twice over each scar (one pass along the diameter parallel to the sides of the block; the other along the diameter perpendicular to it). Measurement involved appreciable overlap of the adjacent unworn regions, to enable calculation of the initial peak-to-valley amplitude. By considering each radius as a distinct region of the scar, four values of final peak-to-valley amplitude were measured per scar. The



ALLOY CODES (FIGURES 5 AND 6)

CODE	ALLOY	CONDITION
A	R31233	Wrought-Annealed
B	R30006	Wrought-Annealed
C	R30006	2 Layer GTA Weld Overlay
D	R30605	Wrought-Annealed
E	N06625	Wrought-Annealed
F	S17400	Wrought-Hardened (H1025/4)
G	N10276	Wrought-Annealed
H	S32550	Wrought-Annealed
I	S31603	Wrought-Annealed
J	N08020	Wrought-Annealed
K	STELLITE 190	2 Layer GTA Weld Overlay
L	R30001	2 Layer GTA Weld Overlay
M	R30012	2 Layer GTA Weld Overlay

FIG. 6—Comparative low stress abrasion data (ASTM G 65 test).

average of these four values was used to determine the degree of damage incurred, by subtracting the average of four values of initial peak-to-valley amplitude.

With regard to the effects of dilution upon the wear properties of cobalt-base alloy weld overlays, tests have been performed on all-weld-metal samples made from admixtures of UNS R31233 and UNS G10400 (carbon steel) and of UNS R30006 and UNS G10400. The influence of dilution upon the resistance to cavitation erosion and galling of these two cobalt-base alloys was not strong, but both were affected markedly with regard to low stress abrasion, as measured using the ASTM G 65 procedure. The abrasion test results are presented graphically in Fig. 7.

TABLE 3—Comparative galling test data.

Test Couple		Degree of Damage (μm)		
Pin	Block	1361 kg	2722 kg	4082 kg
UNS R31233 (wrought-annealed)	UNS R31233 (wrought-annealed)	2.9	2.7	2.0
UNS R30006 (wrought-annealed)	UNS R30006 (wrought-annealed)	0.6	0.7	0.5
UNS R30605 (wrought-annealed)	UNS R30605 (wrought-annealed)	5.9	4.2	4.2
UNS N06625 (wrought-annealed)	UNS N06625 (wrought-annealed)	34.5	28.2	56.7
UNS N10276 (wrought-annealed)	UNS N10276 (wrought-annealed)	44.6	65.1	Not Tested
UNS S21800 (wrought-annealed)	UNS S21800 (wrought-annealed)	2.5	120.0	111.0
UNS S17400 (wrought-hardened)	UNS S17400 (wrought-hardened)	57.8	Seizure at 2722 kg	
UNS S32550 (wrought-annealed)	UNS S32550 (wrought-annealed)	—Seizure at 1361 kg—		
UNS S31603 (wrought-annealed)	UNS S31603 (wrought-annealed)	—Seizure at 1361 kg—		

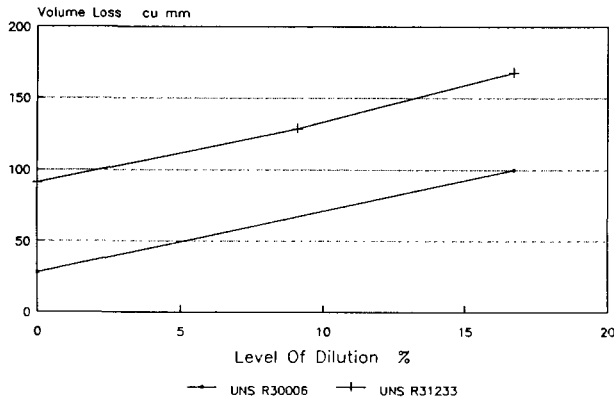


FIG. 7—Low stress abrasion resistance versus dilution (with UNS G10400) level for UNS R30006 and UNS R31233 (ASTM G 65 test).

## HOT CORROSION AND OXIDATION TESTING OF COBALT-BASE ALLOYS

As has been stated, the cobalt-base alloys are relatively strong and wear-resistant at elevated temperatures. Indeed, many applications of the alloys involve temperatures in the range of 500–1000°C. One of the important factors in their commercial success for high temperature applications is their excellent resistance to gaseous sulfidation. Data relating to this property are presented in Table 4. These data were generated by use of the test procedures described in Ref 8. Also of importance in high temperature applications is their good oxidation resistance. In particular, UNS R30188, which has an addition of the rare-earth lanthanum, is equal to the chromia-forming nickel-base superalloys from an oxidation standpoint, and is favored for many flying gas turbine parts because of its higher strength. With regard to other cobalt-based alloys, the wrought forms of UNS R30006 and UNS R31233 have been found to possess excellent resistance to oxidation under static conditions up to approximately 1000°C.

TABLE 4—Resistance to gaseous sulfidation. Environment: argon-5 % hydrogen-5 % carbon monoxide-1 % carbon dioxide-0.15 % hydrogen sulfide.

	Metal Loss, mm	Internal Attack	
		Average, mm	Maximum, mm
UNS R30006 (wrought)	less than 0.01	0.06	0.06
UNS R31233 (wrought)	less than 0.01	0.06	0.08
HAYNES HR-160 alloy (wrought)	less than 0.01	0.09	0.11
UNS R30556 (wrought)	0.11	0.29	0.36
UNS N08810 (wrought)	0.19	0.41	0.50
UNS N06625 (wrought)	Partially Consumed		

Time: 215 h.

Temperature: 871°C.

## SUMMARY

In summary, by corrosion and wear testing the cobalt-base alloys according to the procedures described in ASTM standards G 31, G 32, G 36, G 48, G 65, and G 98, it is possible to determine their suitability for many industrial situations. In general, the alloys are characterized by their carbon contents, the low-carbon alloys being generally much more corrosion-resistant and ductile than the high-carbon alloys.

## REFERENCES

- [1] Crook, P., "Practical Guide to Wear for Corrosion Engineers," *Materials Performance*, Vol. 30, No. 2, February 1991, pp. 64–66.
- [2] Crook, P., "Cobalt and Cobalt Alloys," *Metals Handbook*, Vol. 2, 10th ed., ASM International, 1990, pp. 446–454.
- [3] Silence, W. L., "Effect of Structure on Wear Resistance of Co-, Fe-, and Ni-Base," *Wear of Materials*, American Society of Mechanical Engineers, 1977, pp. 77–85.
- [4] Klarstrom, D. L., "Wrought Cobalt-base Superalloys," *Materials and Processes for Gas Turbine Engine Structures*, Canadian Institute of Metallurgists, August 1991.
- [5] ULTIMET Alloy, Haynes International Brochure H-2087, 1992.
- [6] Swann, P. R., "Dislocation Substructure vs Transgranular Stress Corrosion Susceptibility of Single Phase Alloys," *Corrosion*, Vol. 19, No. 3, National Association of Corrosion Engineers, March 1963, pp. 102–112.
- [7] Crook, P., "The Effects of Dilution upon the Corrosion and Wear Properties of Cobalt-Based Weld Overlays," *Corrosion Science*, Vol. 35, Pergamon Press, 1993, pp. 647–653.
- [8] Lai, G. Y., Rothman, M. F., and Fluck, D. E., "High Temperature Corrosion and Selection of Materials for Various Industrial Processing Equipment," *Industrial Heating*, August 1985.

# Titanium

Ronald W. Schutz<sup>1</sup>

APPLICATION OF TITANIUM and its alloys in aerospace, marine, energy chemical process, and other industrial sectors continues to expand. This has been motivated, in part, by trends in decreasing cost and increasing commercial availability of titanium mill products, improved designer and user knowledge and familiarity, and titanium's unique, attractive combination of engineering properties. These properties include, but are not limited to, relatively low density, low modulus, a wide range of strength, and exceptional corrosion resistance over a very wide span of environmental conditions [1,2].

Growing application of titanium and its alloys has stimulated increased laboratory and in-process (in situ) corrosion testing for the purpose of evaluation and service qualification. Although titanium alloys are evaluated via the same basic test methodologies used for other passive, film-forming CRAs (corrosion resistant alloys), its unique metallurgy, windows of susceptibility, and properties can require additional consideration toward or adjustments in certain testing details. This chapter overviews relevant corrosion test methods, and provides detailed guidelines to help ensure proper, meaningful evaluation of titanium alloy corrosion resistance and behavior.

## COMMERCIAL TITANIUM ALLOYS

The designations and nominal compositions of various commercial aerospace and industrial titanium alloys are listed in Table 1. The first eleven alloys listed are titanium alloys primarily used in chemical or industrial applications in which corrosion resistance is the main design consideration. These alloys consist of single alpha ( $\alpha$ ) phase (hexagonal close-packed crystal structure), or near-alpha alloys containing relatively small amounts of beta ( $\beta$ ) phase (body-centered cubic crystal structure) in an alpha phase matrix. The remaining alloys exhibit significantly higher strength and were developed for aerospace service, although several are rapidly finding applications in industrial service. Alloy strengthening is achieved via solid-solution alloying and stabilization of two-phase structures. These alpha-beta and beta alloys contain varying amounts of stabilized beta phase, and may be heat-treated (aged) to higher strength levels. Further

details on the metallurgy and mechanical/physical properties of titanium alloys can be found elsewhere [3–8].

## MECHANISM OF CORROSION RESISTANCE

The excellent corrosion resistance of titanium alloys results from the formation of very stable, continuous, highly adherent, and protective oxide films on the metal surfaces. Because titanium metal itself is highly reactive and has an extremely high affinity for oxygen, these beneficial surface oxide films form spontaneously and instantly when fresh metal surfaces are exposed to air or moisture, or both. In fact, a damaged oxide film can generally heal itself instantaneously if at least traces (that is, parts per million) of oxygen or water (moisture) are present in the environment. However, anhydrous conditions in the absence of a source of oxygen may result in titanium corrosion, because the protective film may not be regenerated if damaged.

The nature, composition, and thickness of the protective surface oxides that form on titanium alloys depend on environmental conditions. In most aqueous environments, the oxide is typically  $\text{TiO}_2$ , but may consist of mixtures of other titanium oxides, including  $\text{TiO}_2$ ,  $\text{Ti}_2\text{O}_3$ , and  $\text{TiO}$  [9]. High-temperature oxidation tends to promote the formation of the chemically resistant, highly crystalline form of  $\text{TiO}_2$ , known as rutile. Lower temperatures, oxidizing aqueous media, and anodizing favor generation of a less crystalline form of anatase  $\text{TiO}_2$ , or a mixture of rutile and anatase [9,10]. These naturally formed films are typically less than 10–30 nm thick and are invisible to the eye. The  $\text{TiO}_2$  oxide itself is highly chemical-resistant and is attacked by very few substances, including hot, concentrated  $\text{HCl}$ ,  $\text{H}_2\text{SO}_4$ ,  $\text{NaOH}$ , and (most notably)  $\text{HF}$ . This thin surface oxide is also a highly effective barrier to atomic and molecular hydrogen. With this hard, rehealable (ceramic-like) oxide film, titanium alloys exhibit elevated resistance to erosion, erosion-corrosion, and cavitation damage under high velocity, turbulent flow conditions [1].

The  $\text{TiO}_2$  film, being an n-type semiconductor, is electronically conductive. As a cathode, titanium permits electrochemical reduction of ions in an aqueous electrolyte. On the other hand, very high resistance to anodic current flow through the passive oxide film (i.e., significant anodic polarization) can be expected in most aqueous solutions. Elevated anodic pitting (breakdown and repassivation) potentials can also be expected with many titanium alloys.

<sup>1</sup>Corporate Specialist-Industrial Technology, RMI Titanium Company, Niles, OH 44446.

TABLE 1—Various commercial titanium alloys.

Common Alloy Designation	UNS Designation	Nominal Composition, wt %	ASTM Grade	Alloy Type
Grade 1	R50250	unalloyed titanium	1	$\alpha$
Grade 2	R50400	unalloyed titanium	2	$\alpha$
Grade 3	R50550	unalloyed titanium	3	$\alpha$
Grade 4	R50700	unalloyed titanium	4	$\alpha$
Ti-Pd	R52400/R52250	Ti-0.15Pd	7/11	$\alpha$
Ti-0.05-Pd	R52402/R52252	Ti-0.05Pd	16/17	$\alpha$
Ti-Ru	R52404/R52254	Ti-0.1Ru	26/27	$\alpha$
Grade 12	R53400	Ti-0.3Mo-0.8Ni	12	near $\alpha$
Ti-3-2.5	R56320	Ti-3Al-2.5V	9	near $\alpha$
Ti-3-2.5-Pd	R56322	Ti-3Al-2.5V-0.05Pd	18	near $\alpha$
Ti-3-2.5-Ru	R56323	Ti-3Al-2.5V-0.1Ru	28	near $\alpha$
Ti-6-4	R56400	Ti-6Al-4V	5	$\alpha$ - $\beta$
Ti-6-4-ELI	R56407	Ti-6Al-4V(0.13 % O max)	23	$\alpha$ - $\beta$
Ti-6-4-Ru	R56404	Ti-6Al-4V-0.1Ru (0.13 % O max)	29	$\alpha$ - $\beta$
Ti-5-2.5	R54520	Ti-5Al-2.5Sn	...	$\alpha$
Ti-8-1-1	...	Ti-8Al-1V-1Mo	...	near $\alpha$
Ti-6-2-4-2	...	Ti-6Al-2Sn-4Zr-2Mo	...	near $\alpha$
Ti-550	...	Ti-4Al-2Sn-4Mo-0.5Si	...	$\alpha$ - $\beta$
SP-700	...	Ti-4.5Al-3V-2Fe-2Mo	...	$\alpha$ - $\beta$
Ti-6-6-2	R56620	Ti-6Al-6V-2Sn-0.6Fe-0.6Cu	...	$\alpha$ - $\beta$
Ti-6-2-4-6	R56260	Ti-6Al-2Sn-4Zr-6Mo	...	$\alpha$ - $\beta$
Ti-6-22-22	...	Ti-6Al-2Sn-2Zr-2Cr-2Mo-0.15Si	...	$\alpha$ - $\beta$
Ti-10-2-3	...	Ti-10V-2Fe-3Al	...	near- $\beta$
Ti-15-3-3-3	...	Ti-15V-3Sn-3Cr-3Al	...	$\beta$
Beta-21S	R58210	Ti-15Mo-2.7Nb-3Al-0.2Si	21	$\beta$
Ti-3-8-6-4-4 (Ti Beta-C™)	R58640	Ti-3Al-8V-6Cr-4Zr-4Mo	19	$\beta$
Ti-13-11-3	...	Ti-3Al-13V-11Cr	...	$\beta$

Passivity and good corrosion resistance of titanium can be expected under conditions where these protective surface oxides are thermodynamically stable. Pourbaix (potential-pH) diagrams for the titanium-water system [1,11] reveal that oxide film stability occurs over a wide range of potentials, from highly oxidizing to mildly reducing conditions. As a result, titanium alloys can be expected to resist all natural waters (including seawater) and common salt solutions of halides (i.e., chlorides), sulfates, silicates, phosphates, nitrates, carbonates, etc., over the pH range of 3–12. However, oxide film breakdown and resultant corrosion of titanium occurs under moderate to strong reducing acid conditions. Thus, severe general corrosion is possible in strong uninhibited reducing acids such as HCl, HBr, H<sub>2</sub>SO<sub>4</sub>, or H<sub>3</sub>PO<sub>4</sub> solutions, particularly as acid concentration or temperature, or both, increases [1,2]. An especially severe attack of titanium occurs in acid fluoride (HF) solutions, even at relatively low concentrations (>10 to 15 ppm free fluorides) and temperatures. Titanium hydride formation is predicted under strongly reducing aqueous conditions (highly cathodic potentials) and is dependent on solution pH.

## FACTORS AFFECTING PASSIVITY IN AQUEOUS MEDIA

The passivation of titanium is favored and can be expanded in aqueous reducing acid media by any factor that shifts the alloy potential in the noble (positive) direction where oxide film stability is promoted. This beneficial ennobling influence may result from several factors including:

1. An increased surface oxide film thickness by anodizing or thermal oxidation;
2. Anodic polarization of the alloy by impressed anodic current, or galvanic coupling to a more noble metal (i.e., precious metals);
3. The presence of dissolved oxidizing species in the environment acting as cathodic depolarizers;
4. The presence of certain alloying elements in titanium that decreases the cathodic (hydrogen) overvoltage, thereby depolarizing the cathodic process.

The last two factors listed are most commonly encountered and can dramatically influence titanium alloy performance in reducing acid solutions. Dissolved reducible (oxidizing) species in solutions are common in many chemical process streams, whether intentionally added or present as minor background contaminants. Some common oxidizing inhibiting species in reducing acid solutions include Fe<sup>+3</sup>, Cu<sup>+2</sup>, Ni<sup>+2</sup>, Ti<sup>+4</sup>, Cr<sub>2</sub>O<sub>7</sub><sup>-2</sup>, O<sub>2</sub>, Cl<sub>2</sub>, and NO<sub>3</sub><sup>-2</sup>. For example, it is not uncommon for upstream steel corrosion to produce ferric corrosion products (i.e., Fe<sup>+3</sup> ions), which contaminate process streams. Several ppm concentrations or more of any of these species may partially or fully passivate titanium alloys in reducing aqueous media depending on acid concentration and temperature, and should be taken into account when evaluating alloy corrosion resistance.

These same oxidizing species can also stimulate and aggravate crevice corrosion of titanium in hot salt solutions. By depolarizing the cathodic process on open metal surfaces exposed to bulk solution, they effectively increase the potential difference between creviced and uncreviced metal surfaces, thereby driving the crevice cell [1,12,13]. This is why hot FeCl<sub>3</sub> solutions, Cl<sub>2</sub>-saturated solutions, or oxygenated brines are often selected as test media for accelerated test screening of alloy crevice corrosion resistance. Again, it is vital that these often minor background species

be accounted for in any crevice corrosion tests involving simulated laboratory environments.

The last factor listed addresses certain alloying element additions to titanium that may also enhance passivation in reducing acid solutions via cathodic depolarization (reduced hydrogen overvoltage on metal surfaces). This simultaneously enhances the alloy's resistance to crevice corrosion in hot salt solutions, since the solutions within an active crevice are essentially deaerated reducing acids. Alloying elements commonly added to commercial titanium alloys to achieve these improvements include the precious metals (i.e.,  $\geq 0.04$  wt % palladium or  $\geq 0.08$  wt % ruthenium), nickel ( $\geq 0.5$  wt %), and/or molybdenum ( $\geq 3.5$  wt %). Alloys incorporating these alloying additions for corrosion resistance enhancement in Table 1 include titanium Grades 7, 11, 12, 16, 17, 18, 19, 21, 26, 27, 28, and 29, and the Ti-6-2-4-6 alloy.

### Other Metallurgical Factors in Aqueous Media

The nature of the oxide film on titanium alloys basically remains unaltered in the presence of minor alloying constituents; thus, small additions ( $< 3$  %) of most commercially used alloying elements, or variations in trace alloy impurities (i.e., oxygen, nitrogen, carbon, and iron) generally have little effect on the general corrosion resistance of titanium in passivating environments. However, under active conditions (i.e., in strong reducing acids) in which titanium exhibits significant general corrosion, certain alloying elements such as iron or sulfur, or both, may accelerate corrosion. Thus, minor variations in alloy chemistry may only be of significance under conditions where the passivity of titanium is borderline or when the metal is fully active. Increasing aluminum content generally diminishes alloy corrosion resistance in strongly reducing or oxidizing acid media. Higher vanadium content can also result in higher corrosion rate in strong oxidizing acids, especially as temperature increases.

Weldments and castings of the first eleven titanium alloys listed in Table 1 generally exhibit corrosion resistance similar to that of their unwelded, wrought counterparts [1]. These titanium alloys contain so little alloy content and second phase that metallurgical instability and thermal effects are not significant. Protected by the same surface oxide film, titanium weldments and associated heat-affected zones will exhibit passive behavior (insignificant corrosion) for the same conditions under which the wrought base metal is passive. However, under marginal or active corrosion conditions (for corrosion rates  $\geq 0.10$  mm/yr, or 4 mils/yr), weldments may experience accelerated corrosion attack relative to the base metal, depending on alloy composition [14,15]. Microstructural and crystallographic texture, which often exists in many commercial titanium products, generally produces little or no effect on general or crevice corrosion test results. Thus, sample orientation and/or end-on (edge) grain texture effects are generally minor or insignificant in these two test modes. Unlike many metals, the introduction of severe cold work (plastic deformation/damage) has little impact on passivity and does not alter the basic corrosion resistance of titanium alloys.

Although little effect of heat treatment or annealing is observed with the leaner-alloy industrial titanium alloys (first eleven listed in Table 1), certain heat treatments (i.e., aging) may affect the corrosion resistance of higher strength  $\alpha$ - $\beta$  and  $\beta$  titanium alloys in reducing acid environments.

Evaluation of stress corrosion cracking (SCC) resistance of titanium alloys, on the other hand, does require attention to, and can be highly dependent on, alloy composition, heat treatment, microstructure, product processing, crystallographic texture, and orientation. Although the leaner industrial alloys (first eleven in Table 1) are generally SCC-resistant in aqueous environments, most higher strength titanium alloys generally exhibit SCC susceptibility in the form of  $K_{IC}$  or  $K_C$  reduction (i.e.,  $K_{ISCC}$  or  $K_{SCC}$ ) and/or increased environmental crack growth rates. With the exception of a few alloys in sensitized conditions (i.e., Ti-13-11-3 and Ti-8-1-1 alloys), most alloys will not exhibit SCC in stressed smooth or notched sample or component configurations when exposed to aqueous media. It is for this reason that aqueous SCC testing of titanium alloys is often conducted via precracked fracture mechanics or slow strain rate tests. Titanium alloying elements that decrease SCC susceptibility include molybdenum, vanadium, niobium, and tantalum, and precious metals (palladium and ruthenium) in high-temperature halide media. Detrimental effects may stem from increasing aluminum ( $\geq 5$  %), silicon, chromium, and manganese content in these alloys, as well as oxygen ( $\geq 0.2$  % in unalloyed Ti, or  $> 0.13$  % in higher strength alloys) and other interstitials. The influence of these metallurgical factors on titanium alloy SCC behavior is discussed in detail elsewhere [1,16-19].

It should be noted that titanium alloys are generally not susceptible to sulfide stress cracking (SSC) in  $H_2S$ -rich, sulfides, and/or sulfur containing environments (e.g., sour gas/oil well fluids). This inherent SSC resistance stems from the fact that formation of titanium sulfide corrosion products is not thermodynamically favored, such that stability of titanium's protective oxide surface film will prevail even at higher service temperatures. In these hot sour brine service environments, resistance to chloride-induced SCC is a more relevant issue for titanium alloys.

Due to the protective oxide film, titanium alloys generally exhibit anodic pitting (breakdown and repassivation) potential values that are elevated, and well above those of most corrosion engineering metals (i.e.,  $>> +1$  V). For example, pitting potentials in sulfate and phosphate solutions exceed  $+80$  V (versus SCE), and are typically in the  $+2$  to  $+10$  V range in chloride media depending on alloy composition, brine pH, and temperature. As a result, spontaneous pitting of titanium alloys in most aqueous environments does not occur and is usually not of engineering concern in the majority of applications. However, relatively low anodic pitting potential values near or just below  $+1.0$  V, which decrease with increasing temperature and acidity, may be observed in pure bromide or iodide salt solutions. Studies [20] have shown that increasing almost any alloying element reduces anodic repassivation potential values in titanium, whereas molybdenum, niobium, and zirconium generally have neutral and/or slightly beneficial influences. Unlike the intrinsic, conservative anodic repassivation potential value, the extrinsic anodic breakdown pitting potential is highly

dependent on metal surface condition. Roughened, mechanically damaged, ground, and sandblasted surfaces reduce values, whereas well-pickled, thermally-oxidized, and anodized surfaces elevate alloy anodic breakdown potentials [1].

## ROLE OF HYDROGEN

Titanium alloys are generally highly resistant to penetration by gaseous (diatomic) hydrogen and nascent (atomic) hydrogen due to the surface oxide barrier film. In hydrogen gas exposures, traces of moisture or oxygen are sufficient to maintain this protective film, whereas anhydrous gas can lead to hydrogen absorption, particularly as hydrogen gas pressures and temperature increase. Excessive cathodic charging of atomic hydrogen on titanium metal surfaces via galvanic coupling with active metals or impressed cathodic currents may induce excessive hydrogen uptake, depending on solution pH and temperature. Active corrosion of titanium in reducing acids, within active crevices, or exposure to high-temperature, strongly alkaline solutions, in which the oxide film is compromised, can also result in significant hydrogen pickup. Metallic iron embedded or galled into titanium metal surfaces can provide “windows” for enhanced penetration of hydrogen. On the other hand, surface treatments that increase oxide film thickness, such as anodizing and thermal oxidation, tend to thwart hydrogen absorption.

In  $\alpha$  and  $\alpha$ - $\beta$  alloys, excessive hydrogen uptake can induce the precipitation of titanium hydride phase in the  $\alpha$  phase. These acicular-appearing (needle-like) hydride platelets, shown in Fig. 1, are a relatively brittle phase. In most cases, small amounts of hydride precipitates are not detrimental from an engineering standpoint, but can cause severe reduction in alloy ductility and toughness when present in greater amounts. For example, hydride precipitates can be observed in Grade 2 titanium microstructures at hydrogen concentrations above approximately 40–100 ppm at 25°C, depending on the amount of  $\beta$  phase and interstitials

present. These precipitates do not result in gross embrittlement of Grade 2 titanium until hydrogen levels in excess of 500–600 ppm are reached. Since hydrogen solubility increases dramatically with temperature, hydride embrittlement may not be observed at higher temperatures. If significant absorption has occurred, embrittlement may manifest upon cooling as the hydride phase precipitates. Hydrogen solubility and tolerance generally increase with increasing volume% beta phase in  $\alpha$ - $\beta$  alloys. In Ti-6Al-4V, for example, hydride precipitates are not formed below hydrogen levels of 400–800 ppm, depending on product microstructure.

Although uniaxial tensile properties may experience little effect from increasing hydrogen levels, biaxial or triaxial stress properties, such as bend ductility, cold-drawing, and impact toughness in  $\alpha$  and near- $\alpha$  alloys may be very sensitive to hydrogen levels [21–24]. In  $\alpha$  and especially  $\alpha$ - $\beta$  alloys, hydrogen contents above critical levels (i.e., >80–120 ppm) can result in sustained-load cracking, which dramatically reduces useful maximum service loads in notched or cracked components under slow strain rate or constant tensile load situations [21–25].

Beta titanium alloys have a very high solubility for hydrogen. Therefore, embrittlement is generally not associated with hydride precipitation. Significant losses in ductility or formability do not occur below hydrogen levels of several thousand parts per million, although the tolerance to hydrogen decreases somewhat in the aged (high-strength) condition. In addition, hydrogen atom diffusivity (mobility) within the beta alloy is typically several orders of magnitude above that in alpha titanium.

## FORMS OF CORROSION AND RELEVANT TEST METHODS

It is important to know where titanium might exhibit susceptibility to corrosion attack in order to establish which corrosion test methods may be applicable or relevant to titanium alloys. Table 2 presents a list of specific environments where some form of corrosion susceptibility has been observed on titanium alloys in laboratory tests or service experience. The table indicates the relevant mode of corrosion degradation that can be expected, general scope of titanium alloys susceptible, and comments on critical factors that strongly influence each corrosion phenomenon.

Based on Table 2, the general forms of corrosion and corresponding test methods relevant to titanium alloys include: general corrosion, crevice corrosion, anodic pitting, SCC, hydrogen absorption/embrittlement, ignition/burning, and oxidation. The following sections will provide methods and guidelines for testing and evaluation of these seven basic forms of titanium alloy corrosion damage.

## TEST METHODS FOR EVALUATION OF CORROSION DAMAGE

### General Corrosion Testing

General corrosion rates for titanium alloys can be determined from weight loss data, dimensional changes, and

**FIG. 1—Photomicrograph of severely hydrided unalloyed titanium at 200 $\times$ . Note the acicular (needle-like) titanium hydride precipitate.**



TABLE 2—Environments where corrosion susceptibility of titanium alloys has been observed.

Environment	Corrosion Mode of Concern	Potentially Susceptible Ti Alloys	Comments
Strong Reducing Acids (HCl, HBr, HI, H <sub>2</sub> SO <sub>4</sub> , H <sub>3</sub> PO <sub>4</sub> , and especially HF)	general corrosion	all	Dependent on alloy composition, acid conc. and temp., and presence of inhibitive oxidizing species.
High-temp Halide and Sulfate Solutions	crevice corrosion	non-Pd or Ru alloys, or alloys with <3.5 % Mo or <0.6 % Ni	Dependent on alloy composition, brine pH and temp. Requires severe crevices.
Pure Bromide/Iodide Solutions	anodic pitting	all	Dependent on alloy composition and surface, and pH and temp.
High-temp Strongly Alkaline Solutions	hydrogen absorption	all	Occurs at pH >12 and >75°C.
High-temp Sour Brine (sulfide/H <sub>2</sub> S-rich)	galvanically induced hydrogen absorption	all	Requires galvanic couple to an active metal/alloy and >75°C.
Anhydrous Hydrogen Gas	hydrogen absorption	all	Occurs at higher temps. and gas pressures if water- or oxygen-free.
Anhydrous Methanol	stress corrosion cracking	all	Occurs when water content is below 2–3 wt %.
Red-fuming Nitric Acid or Nitrogen Tetroxide	stress corrosion cracking and/or pyrophoric reaction	all	Dependent on water and/or oxygen content.
Halide Salt Residues at High Temperatures (>230°C)	hot salt stress corrosion cracking	higher strength $\alpha/\beta$ and $\beta$ alloys	Dependent on alloy composition, stress load, temp., and exposure time.
Chlorinated Hydrocarbons	stress corrosion cracking	higher strength $\alpha/\beta$ and $\beta$ alloys	Dependent on alloy composition and condition.
Halide Salt Solutions	stress corrosion cracking	higher strength $\alpha/\beta$ and $\beta$ alloys	Dependent on alloy composition and condition, brine pH and temp., and test method.
Liquid Cadmium and Mercury, and Solid Silver (>230°C) and Cadmium	liquid or solid metal embrittlement	all	Requires direct, intimate contact with fresh unfilmed metal under high stress.
Dry Chlorine Gas	general corrosion and/or ignition/burning	all	Occurs when water content is below 0.5–1.0 wt % depending on temp.
Pure Oxygen Gas	ignition/burning	all	Dependent on alloy composition, component thermal mass, and gas pressure.
Warm Alkaline Peroxide Solutions	general corrosion	all	Dependent on peroxide solution composition, pH, and temp.
High-temp Air or Oxygen-containing Gas Exposures (>600°C)	metal oxidation, wastage, and/or embrittlement	all	Dependent on alloy composition, temp., and exposure time.

electrochemical methods. Electrochemical anodic and cathodic polarization testing is often used to supplement weight loss testing. Polarization testing can identify whether the alloy is truly fully passive or possibly metastable; this is often not discernible from weight loss tests alone. The immersion test procedures described in ASTM G 1 (Practice for Preparing, Cleaning, and Evaluating Corrosion Test Specimens) and G 31 (Practice for Laboratory Immersion Corrosion Testing of Metals) apply, provided several modifications are observed [1,26]. These modifications focus on test sample surface preparation and post-test sample-cleaning procedures. A typical laboratory test apparatus for weight-loss immersion testing in acid solutions at or below the boiling point is shown in Fig. 2.

The type of sample surface finish tested should resemble the one expected in service. For titanium alloys, this is frequently the pickled finish, although sandblasted, ground, or machined surfaces are also common. The initial degreasing of test samples should avoid chlorinated organic solvents (with higher-strength titanium alloys), anhydrous methanol, or hot alkaline cleaners. Acceptable cleaning solvents include methyl ethyl ketone (MEK), acetone, most alcohols, benzene, and most detergent solutions. The pickled finish

can be prepared by pickling the metal in a 35 vol % HNO<sub>3</sub>-5 vol % HF solution (based on 48 wt % HF and 70 wt % HNO<sub>3</sub> stock acid solutions, with the balance being water) at 20–55°C for 0.5–5 min or more. Typically, 0.005–0.05 mm (0.2–2 mils) of sample surface is removed in this process, depending on surface requirements. More dilute solutions, such as 12 vol % HNO<sub>3</sub>-1 vol % HF, can also be used if slower pickling rates are desired. In any case, a minimum 7:1 HNO<sub>3</sub>:HF stock acid vol % ratio should be maintained to avoid excessive uptake of hydrogen in titanium alloys during pickling. After pickling, a quick rinse in deionized water and air drying leaves a shiny gray specimen that is ready for weighing. The abraded surface finish can be obtained by wet grinding with fine grit SiC or Al<sub>2</sub>O<sub>3</sub> abrasive paper after the cleaning step. A final deionized water rinse and drying would prepare the specimens for weighing and testing. Prepared and weighed titanium samples may be stored in open air prior to exposure for several days without significantly affecting sample weight.

A mechanically abraded or polished coupon surface finish is highly recommended over pickled finishes when corrosion testing titanium alloys containing readily reducible (noble) alloying elements. These alloys include those containing

**FIG. 2—Typical Huey test apparatus with water-cooled condenser for conducting sample general corrosion (weight-loss) tests up to the solution boiling point. Samples are typically suspended in the solution by Teflon® string or glass rods.**

platinum group metals (Pd, Ru, Pt) and other metals (Ni, Cu), which may readily plate back in pure form onto titanium coupon surfaces during the pickling process. These plated metal residues can ennoble coupon test surfaces, and may not represent the most conservative test methodology.

Consideration should be given to the presence of certain test solution contaminants that may significantly affect the corrosion rate. More specifically, contamination of acid media with transition metal ions, such as ferric, nickel, cupric, and chromic ions, and other oxidizing species should be avoided because these ions act as cathodic depolarizers and inhibit corrosion in most acid media. In nitric acid testing, dissolved silicon,  $\text{Ti}^{+4}$ ,  $\text{Fe}^{+3}$ , and most precious metal ions are fairly effective inhibitors and will lower corrosion rates. In strong nitric acid media, it is best to avoid prolonged testing in glass, and the accumulation of dissolved  $\text{Ti}^{+4}$  corrosion product, which inhibits corrosion. This can be counteracted by frequent solution change or refreshment. In most reducing acids, such as HCl,  $\text{H}_2\text{SO}_4$ , or  $\text{H}_3\text{PO}_4$  (but not HF), testing in glass flasks is acceptable. The  $\text{Ti}^{+3}$  ion corrosion product normally formed and dissolved in a reducing acid medium does not appear to affect corrosion

significantly except at near-saturated concentrations, but mild oxidizing agents mentioned earlier, such as the transition metal ions (particularly those in higher oxidation states) may inhibit corrosion at concentrations above several ppm. It is recommended that the solution be constantly refreshed or changed at least every 24 h in corrosion tests where foreign ions are generated from corrosion processes in order to minimize their effects. It is also critical that the degree of aeration (dissolved  $\text{O}_2$  level) and other background chemistry variables in the test media that influence titanium passivity be taken into account to achieve valid and relevant test results.

The presence of surface corrosion products on titanium after testing depends on the environment to which the titanium was exposed. Removal of these products, when formed, is necessary for obtaining the proper weight loss data, and the correct corrosion rate. In media where the titanium has remained essentially passive, such as near-neutral brines, the original shiny metal luster will usually still exist, and the specimens need only be rinsed in distilled water before their final weighing. Most deposits from the medium that adhere to the specimen surface and are nontitanium corrosion products may be cleaned off in a warm ( $\leq 65^\circ\text{C}$ ) 25 vol %  $\text{HNO}_3$ -25 vol % HCl solution or a 50 vol %  $\text{HNO}_3$  solution. Other compatible post-test acid cleaning solutions include  $\leq 10$  wt % HCl or  $\text{H}_2\text{SO}_4$  inhibited with a minimum of 1000 ppm ferric ( $\text{Fe}^{+3}$ ), cupric ( $\text{Cu}^{+2}$ ), chromate ( $\text{Cr}^{+6}$ ), or molybdate ( $\text{Mo}^{+6}$ ) ions up to  $70^\circ\text{C}$ . Note that amine-type corrosion inhibitors are not effective for titanium. Siliceous scales may be removed in warm ( $< 65^\circ\text{C}$ ) solutions containing  $\leq 20$  % NaOH inhibited with 1 wt %  $\text{NaNO}_3$ , NaOCl,  $\text{NaCrO}_3$ , or  $\text{Na}_2\text{MoO}_4$ . The use of strong, uninhibited mineral acids such as HCl,  $\text{H}_2\text{SO}_4$ ,  $\text{H}_3\text{PO}_4$ , and especially HF are not recommended for cleaning, since they will corrode the metal samples; this also explains why the electrolytic cleaning method mentioned in ASTM G 1 is not used.

In media where the titanium does have a low but finite corrosion rate and where the dissolving titanium hydrolyzes back onto the surface of the specimen (such as dilute, hot reducing acids) or in very strongly oxidizing media (such as boiling concentrated  $\text{HNO}_3$ ), a titanium oxide-hydroxide corrosion product may build up slowly on the surface. This oxide film or deposit is not soluble in common mineral acids and cleaning solutions. The more desirable means of cleaning the specimen of titanium corrosion product or even stubborn nontitanium deposits is a fine grit- or glass bead-blasting procedure. Tests run in the laboratory suggest that the use of 120 or finer grit silica or alumina sand to lightly blast off titanium surfaces results in acceptably small weight losses in sample coupons. Weight losses in the  $10^{-4}$  g range may be incurred when light sandblasting ( $\leq 5$  s exposure) is used, and these can be corrected for by exposing an untested titanium specimen to the same blasting procedure and correcting for its weight loss. A final rinse in distilled water after sandblasting leaves the dried specimen ready for weighing. Titanium specimens that have been exposed to hot, strong reducing acids in which the corrosion rate is quite high generally exhibit chemically roughened matte-gray hydrided metal surfaces, which may not require surface cleaning.

Immersion testing will generate weight loss data, or corrosion current measurements can be obtained from standard electrochemical polarization tests (see ASTM G 5, Standard Reference Test Method for Making Potentiostatic and Potentiodynamic Anodic Polarization Measurements; see also Ref 27). Corrosion rates in millimeters per year (mpy) for titanium alloys can be calculated from sample weight loss data as follows:

$$\text{Corrosion rate (mm/y)} = \frac{(8.76 \times 10^4)(W)}{(d)(A)(t)}$$

where:

$d$  = alloy density in g/cm<sup>3</sup>,  
 $A$  = sample surface area in cm<sup>2</sup>,  
 $t$  = exposure time in h,  
 $W$  = weight change in g.

Corrosion rates in mpy (thousandths of an inch per year) can be derived using the formula:

$$\text{Corrosion rate (mpy)} = \frac{(534,700)(W)}{(d)(A)(t)}$$

where:

$W$  = weight change in g,  
 $d$  = alloy density in g/cm<sup>3</sup>,  
 $A$  = sample surface area in in.<sup>2</sup>,  
 $t$  = exposure time in h.

A list of density values for common commercial titanium alloys is given in Table 3.

Corrosion rates in mm/y can be calculated from electrochemical measurements by using the formula:

$$\text{Corrosion rate (mm/y)} = \frac{(3.3)(i_{\text{corr}})(EW)}{d}$$

where:

$i_{\text{corr}}$  = the measured corrosion current in mA per cm<sup>2</sup>,  
 $d$  = alloy density in g/cm<sup>3</sup>,  
 $EW$  = the equivalent weight (at. wt./valence state) for titanium.

**TABLE 3**—Room temperature density values for some commercial titanium alloys.

Alloy	Density, g/cm <sup>3</sup>
Ti Gr.1, 2, or 3	4.51
Ti Gr.7, 11, 16, 17, 26, or 27	4.51
Ti Gr.12	4.52
Ti Gr.9, 18, or 28	4.48
Ti Gr.5, 23, or 29	4.42
Ti-6-2-4-6	4.68
Ti-10-2-3	4.64
Ti-15-3-3-3	4.78
Ti-3-8-6-4-4 (Ti Gr.19)	4.82
Ti Gr.21	4.93

<sup>2</sup>ASTM Standard G 30, Practice for Making and Using U-Bend Stress-Corrosion Test Specimens; G 35, Practice for Determining the Susceptibility of Stainless Steels and Related Nickel-Chromium-Iron Alloys to Stress Corrosion Cracking in Polythionic Acids; G 36, Practice for Performing Stress-Corrosion Cracking Tests in a Boiling Magnesium Chloride Solution; G 47, Test Method for Determining Susceptibility to Stress-Corrosion Cracking of High-Strength Aluminum Alloy Products.

The equivalent weight for titanium is 16 g per equivalent under reducing acid conditions (Ti→Ti<sup>+3</sup>), and 12 g per equivalent under oxidizing conditions (Ti→Ti<sup>+4</sup>). The value of  $i_{\text{corr}}$  is typically determined from Tafel slope extrapolation or linear polarization methods [27–29].

## Crevice Corrosion Testing

Crevice corrosion is a form of localized attack of titanium alloys that may occur in higher temperature (>70°C) chloride, bromide, iodide, fluoride, and/or sulfate-containing solutions; its occurrence is highly dependent on alloy composition, solution pH, and temperature. Crevice attack on titanium requires the presence of large and very severe (tight) crevices, such as gasket-to-metal flange joints or seals, tube-to-tubesheet joints, metal-to-metal joints, or adherent process stream deposit/scale crevice formers found in service. Attack typically takes the form of irregularly shaped craters or pits, with voluminous, off-white, light gray, or sometimes black corrosion product caps as pictured in Fig. 3. Metal surfaces adjacent to active crevices may sometimes display vivid oxide film coloration from hydrolyzed acidic crevice solutions. The mechanism for titanium alloy crevice corrosion is generally similar to that for stainless steel and nickel alloys, in which oxygen-depleted reducing acid conditions develop within tight crevices as detailed elsewhere [1,30].

Crevice corrosion testing of titanium alloys generally aims at determining go/no-go performance information. The rate of crevice corrosion is of little practical interest, because crevice attack is generally insidious and very rapid. Thus, crevice corrosion cannot be tolerated in any form. Many crevice test assemblies have been used, including the multiple-crevice (serrated) washer (ASTM G 78, Guide for Crevice Corrosion Testing of Iron Base and Nickel Base Stainless Alloys in Seawater and Other Chloride-Containing Aqueous Environments), the Dutchman or spool rack (ASTM G 4, Method for Conducting Corrosion Coupon Tests on Plant Equipment) assembly, and the sheet sandwich-type assembly. The multiple-crevice (serrated) washer is generally not a conservative test and not recommended, since titanium is highly crevice-resistant and requires a relatively large creviced surface area for crevice corrosion initiation. The larger creviced surface area and depth of the sheet sandwich-type assembly, illustrated in Fig. 4, dramatically increases susceptibility to attack and is most commonly used. This method uses a test assembly in which thin gasket sheets (typically TFE, FEP, or other gasket material of interest) are interspersed between flat metal sheet or plate coupons to produce the desired number of metal-to-metal and/or metal-to-gasket crevices, or both. In some cases, even curable polymeric sealants (i.e., EPDM or polymethylacrylate) are applied to coupon surfaces prior to assembly. Coupons are typically 1 in. by 1 in. (25 mm by 25 mm) or larger to create large, deep creviced surfaces. Each test assembly is fastened together with a centerline titanium bolt and nut and tightened down to a torque of 25–90 in.·lb (2.8–10.1 m·N) to create tight, severe crevices. The titanium assembly bolts and nuts may be of the same titanium alloy being tested, or covered with an insulating, PTFE sleeve or tape wrap to avoid galvanic interferences.

It is important that coupon surfaces be flat and, especially, as smooth as possible (low RMS roughness) to minimize crevice gap and volume and, thereby, stimulate initiation. Highly roughened sandblasted or ground surfaces exhibit reduced crevice corrosion susceptibility. Although a 240 grit wet-ground coupon surface finish may be considered a minimum requirement, a 400 grit finish or finer is recommended for most conservative test results. Preparation of crevice test coupons follows the same procedures as that for general corrosion test coupons. Note that it is also vital that only the virgin grade of fluoropolymer gaskets (e.g., PTFE, FEP, or Viton) be used in these tests, since nonvirgin (reprocessed) grades may release fluorine compounds during test exposures that may falsely stimulate localized attack.

Laboratory crevice testing is usually conducted in glass flasks and vessels, titanium alloy autoclaves, or other resistant alloy autoclaves. The minor presence of background and/or contaminating metal ion species or other oxidizing species may aggravate crevice attack. Thus, it is also vital that suitable test vessels be selected and that the representative degree of aeration, pH, and other aspects of background solution chemistry be controlled and simulated. Although crevice corrosion can initiate within the first several hours of exposure, a minimum test duration of 30 days is recommended in order to develop a sufficient degree of attack for detection and measurement purposes.

Post-test evaluation of crevice test coupons may require removal of titanium oxide/hydroxide corrosion products (see Fig. 3) if crevice attack has occurred. Common mineral acids and reagents will not dissolve these tenacious deposits. A light ( $\leq 120$  grit and  $< 5$ – $8$  s) sandblasting or glass-bead blasting of coupon surfaces will readily remove these scales and facilitate visual examination of pitted surfaces (per ASTM G 46, Practice for Examination and Evaluation of Pitting Corrosion), and permit sample weighing after water rinsing. Creviced coupon surfaces are often highly colored after hot aqueous exposures, but reveal no visible pits after sandblasting. This is indicative of the very slight growth of a protective surface titanium oxide film, which is considered quite normal and acceptable from a performance standpoint. Slight coupon weight gain is often measured in this situation. In addition to visual examination and weight change measurements, monitoring of creviced specimen potential [31,32] and current [33] has been used to a limited extent to identify the initiation of crevice corrosion. Examination of polished and etched metallurgical sections through pitted areas of creviced coupons may also provide additional information concerning depth of attack and mechanisms of crevice initiation and propagation.

**FIG. 3—Typical example of crevice corrosion of titanium in hot chloride brines. (a) Irregularly-shaped crevice corrosion attack on Grade 2 titanium tubing. (b) Photomicrograph of cross section through crevice corrosion site in Grade 2 titanium showing the titanium oxide corrosion product cap and irregular attack profile (100 $\times$  magnification).**

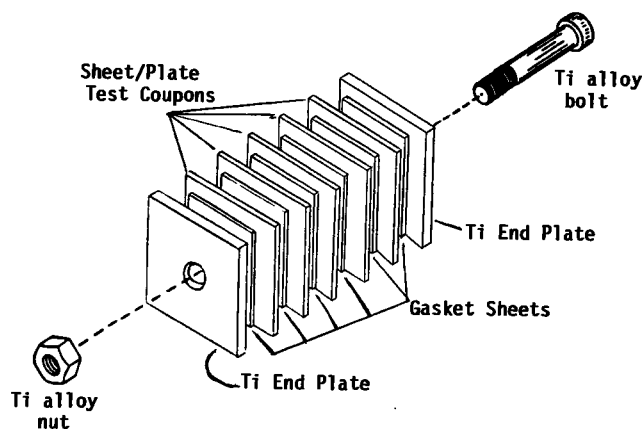


**FIG. 4—Typical crevice test assembly for crevice corrosion testing of titanium alloy sheet or plate coupons. Sequence of coupons and gasket sheets can be modified to form gasket-to-metal and/or metal-to-metal crevices.**

### Pitting Potential Testing

The susceptibility of an alloy to pitting on openly exposed surfaces (in the absence of crevices) in a given solution and fixed temperature is normally assessed by determination of anodic pitting potential values. The two pitting potentials of interest are (1) the extrinsic, surface-dependent anodic breakdown potential ( $E_b$ ), and (2) the conservative, intrinsic anodic repassivation potential (or protection potential ( $E_{prot}$ )) that defines the minimum potential at which pitting is possible in the test environment.

The anodic breakdown potential of titanium alloys is typically determined by the potentiodynamic (potential scan) technique (ASTM G 3, Practices for Conventions Applicable to Electrochemical Measurements in Corrosion Testing, and ASTM G 5) at slow scan rates ( $\leq 0.5$  mV/s). Since this value is sensitive to sample surface condition, it is vital that the representative metal surface anticipated in service be tested. Titanium alloy repassivation potential, on the other hand, may be measured by a galvanostatic method [34], the constant potential-surface scratch test [27,29,34], or reverse scan potentiodynamic method. The galvanostatic method is quick, easy, and generally preferred, and involves impressing a constant anodic current density of approximately  $+200$  mA/cm<sup>2</sup> on the specimen for at least several minutes before measuring the sample polarization potential relative to a reference electrode. This potential, once stabilized and corrected for electrolyte IR drop, represents the anodic repassivation potential. The constant potential-scratch method is more tedious and time-consuming, involving trial iterations for bracketing the critical potential. Potentiodynamic scan reversal (ASTM G 3 and G 5) after scanning anodically to induce breakdown pitting may produce ambiguous results with nonreproducible, scan rate dependent repassivation potential values.

The exceptionally high anodic pitting potentials of titanium alloys in most aqueous solutions means that: (1) oxidizing acid solutions such as FeCl<sub>3</sub> or Fe<sub>2</sub>(SO<sub>4</sub>)<sub>3</sub> solutions (ASTM G 28, Test Methods for Detecting Susceptibility to Intergranular Attack in Wrought Nickel-Rich Chromium-Bearing Alloys, and G 48, Test Method for Pitting and Crevice Corrosion Resistance of Stainless Steels and Related Alloys by the Use of Ferric Chloride Solution) cannot be used to identify critical pitting parameters, and (2) potential range and/or power requirements for potentiostats/galvanostats are greater than that for most other common metals and alloys. In chloride solutions, for example, a potentiostat or galvanostat with an impressed sample potential output range as high as  $+10$  to  $+12$  V may be required for pitting potential determinations. Practical counter-electrodes for these electrochemical techniques include glassy carbon and platinum.

### Stress Corrosion Cracking Testing

SCC test methods commonly used for metals [35] are all applicable to titanium alloys, as long as relevant mechanical and physical properties are accounted for. This means formulating applied stresses based on alloy strength and/or elastic modulus values for the appropriate sample orientation, which is corrected for test temperature when appropriate. The smaller spread between yield and ultimate strength and lower plastic strain limits exhibited by titanium alloys compared to most other CRAs also means limiting applied sample stresses values to  $\leq 105$  % yield strength in static- or deflection-loaded tests. Since many titanium alloy products can exhibit significant crystallographic texture depending on alloy type and processing history, it is advisable that SCC susceptibility be evaluated with regard to sample orientation as well. In  $\alpha$  and  $\alpha$ - $\beta$  alloy mill products, for example, greater susceptibility is often associated with the direction along hcp basal plane intensification (e.g., T-L direction in unidirectional processed products.)

Test methods for assessing the SCC resistance of titanium alloys can be grouped into three basic categories:

*Category 1* tests use smooth, statically loaded specimens, such as U-bend, C-ring, bent beam, and dead-loaded tension specimens (described in ASTM G 30, G 35, G 36, G 38, G 49, and G 472).

*Category 2* tests are fracture mechanics tests that use notched and precracked specimens that are statically or dynamically loaded, such as cantilever beam, compact tension, and double cantilever beam specimens, and are conducted per ASTM E 399, Test Method for Plane-Strain Fracture Toughness of Metallic Materials.

*Category 3* tests use smooth or notched tension specimens that are dynamically loaded at very low strain rates; the slow strain rate test (SSRT) is the primary example.

Selection of a suitable SCC test method for titanium alloys is primarily determined by the nature of the stress cracking data or design information desired and by the chemical nature of the test environment relative to titanium alloy passivation. For simple go/no-go assessment of SCC with no quantitative cracking parameters, the least costly Category 1 tests may be adequate if SCC initiation (incubation) periods are not too long. The data are typically considered in terms of sample stress versus time to failure, as shown in Fig. 5a. SSRT results are generally assessed as comparisons or ratios of test sample ductility and/or time-to-failure values to those from a reference (control) sample (tested in air or inert gas), providing some sense of relative SCC susceptibility. However, confirmation of SCC occurrence must also entail examination of SSRT sample fracture surfaces for indications of SCC (i.e., cleavage, intergranular cracking, and/or secondary cracking).

If fracture mechanics design information (i.e.,  $K_{ISCC}$  or Stage I or II crack growth parameters) is required, then the more sophisticated, costly Category 2 tests are the obvious choice (Figs. 5b and 5c).  $K_{ISCC}$  results for titanium alloys are stress- and time-dependent, such that  $K_{ISCC}$  values may be plotted as a function of time to failure to reveal true, conservative  $K_{ISCC}$  values. Sufficient test periods (typically 1–10 h) at each stress-intensity level tested should be allowed to ensure that the “plateau” shown in Fig. 5b has been reached.

Slow-strain-rate testing (SSR) is a highly sensitive, rapid, most discriminating, and conservative SCC test method for titanium alloys. In some cases, it is too conservative from a design/use standpoint because the surface-oxide film is continuously being broken during straining to failure. This method is particularly useful for rapid alloy screening and sorting, and provides a relative and/or semiquantitative sense of alloy SCC susceptibility. Discriminating strain rates for titanium alloys in aqueous and methanolic solutions lie within the  $10^{-5}$  to  $10^{-7}$  s<sup>-1</sup> window.

Selection of an appropriate SCC test method for titanium alloys may also be based on the particular type of environment to be tested. In environments where alloy repassivation (oxide film formation) is favored, and where Stage I subcritical cracking is generally not observed, Categories 2 and 3 tests are more severe and discriminating than Category 1 tests. This is the case for aqueous media, including salt water and brines, and chlorinated organic solvents in

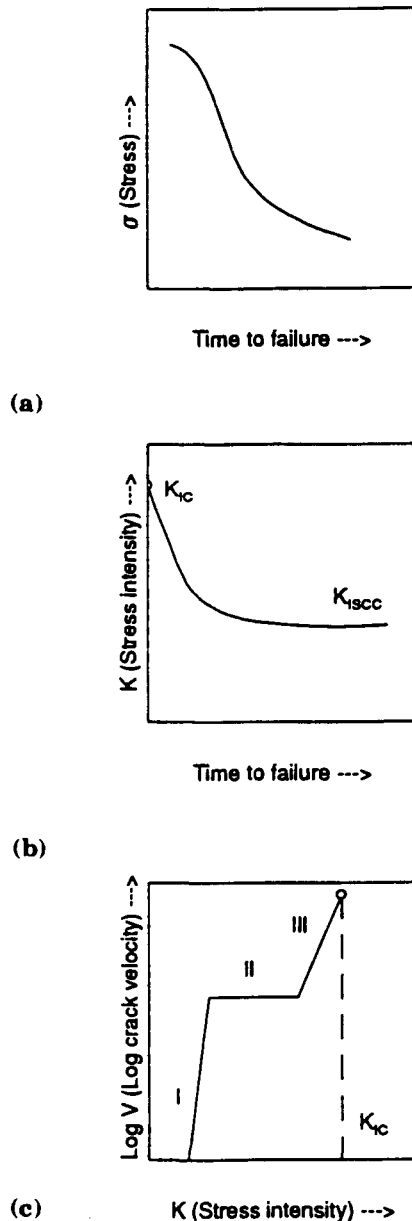


FIG. 5—Various types of SCC test data presentation: (a) typical for Category 1 tests, (b) and (c) typical for Category 2 tests.

which cracking failure of Category 1 specimens is generally not observed at near-ambient temperatures. One must provide initial or continued local oxide film breakdown, such as in Categories 2 and 3 tests, to expeditiously initiate and manifest potential SCC tendencies in these alloys. Exceptions to this rule are those very few titanium alloys that may exist in highly sensitized metallurgical conditions. For example, alloys susceptible to SCC in ambient neutral salt water in smooth or notched samples include step-cooled Ti-8Al-1Mo-1V and Ti-13V-11Cr-3Al alloys. Highly stressed Category 1 test specimens may also be applicable for testing in hot aqueous halides or chlorinated solvents, where higher temperatures may overcome SCC activation barriers in certain alloys after sufficient exposure periods.

For environments where Stage I subcritical cracking behavior occurs and repassivation is not favored, Category 1 tests are often preferred over Categories 2 and 3 tests for practical reasons. These environments include methanol, red-fuming nitric acid,  $N_2O_4$ , liquid/solid metals, molten salts, and hot salt. Note that Category 2 testing is not physically applicable to the evaluation of solid metal embrittlement and hot salt SCC in these alloys. Also, note that hot salt SCC testing of titanium follows the guidelines and procedures provided in ASTM G 41, Practice for Determining Cracking Susceptibility of Metals Exposed Under Stress to a Hot Salt Environment.

### Hydrogen Testing

Testing to determine the susceptibility of a titanium alloy to hydrogen uptake and embrittlement should simulate conditions expected in service. In hydrogen gas atmospheres, simple coupon exposures for as long as is deemed practical are recommended to ensure significant uptake, if it occurs. The gas atmosphere must duplicate exact gas chemistry, particularly with respect to water and oxygen content. Mere traces of moisture, for example, will effectively inhibit hydrogen absorption by titanium in dry hydrogen gas and possibly cause test interference.

Galvanic coupling tests or cathodic charging tests can also be conducted to evaluate susceptibility to hydrogen uptake. For a given environment and temperature, an active metal (iron, aluminum, etc.) sample is galvanically coupled to the titanium alloy sample, such that a specific anode-to-cathode surface area is tested. Impressed cathodic charging tests are performed in electrolytic cells containing a specific electrolyte. A power supply (potentiostat or galvanostat) impresses a constant potential or current on the cell, such that the titanium is cathodic relative to an inert counter-electrode such as graphite or platinum. A reference electrode can also be used to control or to measure the polarization potential of the test cathode. There are no standardized test methods or setups for cathodic charging studies; therefore, they are designed to best simulate conditions anticipated in service. Two examples of typical laboratory charging cell setups are depicted in Figs. 6a and 6b. Note the presence of a porous diaphragm in these cells to minimize unwanted intermixing of cathode/anode by-products and catholyte contamination. Catholyte refreshment should also be considered to maintain representative electrolyte composition and pH.

The surface condition of the test sample is a critical variable in all hydrogen uptake tests. Studies have shown that abraded or sandblasted surfaces absorb hydrogen more readily than as-pickled surfaces [7]. Thickening of the surface oxide film by anodizing or thermal oxidation further retards absorption. The actual surface finish anticipated in service should be evaluated.

After test exposure, sample evaluation for hydrogen may include tensile, notched tensile, bend, ductility (for example, drawn cup), and/or impact Charpy tests, hydrogen analysis, or cross-sectional microstructural examination, or a combination thereof. Uniaxial, smooth-specimen tension testing is generally of little value in diagnosing the subtle embrittling effects of hydrogen. Titanium alloys tend to

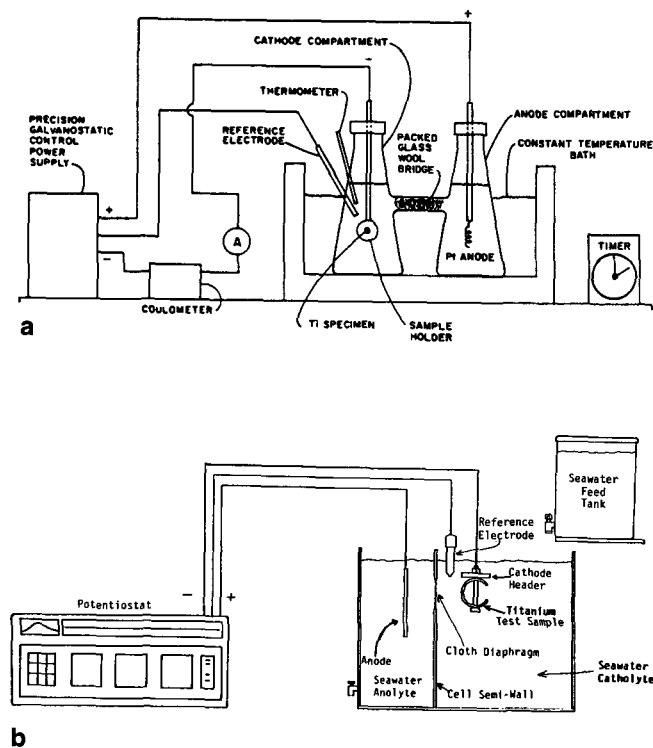


FIG. 6—Typical examples of laboratory cell setups for cathodic charging tests on titanium alloys. (a) Typical cell setup for short-term cathodic charging of titanium samples at constant current in hot acidic electrolytes. (b) Typical cell setup for longer-term cathodic charging of titanium samples at constant potential in seawater and brines.

exhibit susceptibility under biaxial or triaxial stress states; therefore, bend tests, cup tests, or notched tension tests are generally more sensitive to hydrogen effects. Impact toughness testing can be an especially sensitive indicator of hydrogen effects in  $\alpha$  alloys, whereas slow strain rate methods are very suitable for  $\alpha$ - $\beta$  alloys [21,22,25]. Because hydrogen content has relatively little effect on alloy hardness, hardness testing is generally of little use.

Some titanium alloys may be susceptible to sustained load cracking (SLC), also known as delayed cracking. This can occur on  $\alpha$ ,  $\alpha$ - $\beta$ , and aged  $\beta$  alloys that are highly stressed in tension for sustained periods. SLC susceptibility increases with increasing hydrogen content, alloy aluminum- or oxygen-equivalency, decreasing strain rate, and increasing stress intensity [23,36]. Highest susceptibility generally occurs at or somewhat below room temperature [23], and diminishes at higher temperatures.

SLC test severity increases (to the right) according to the following types of test specimens: smooth tensile << notched tensile << loaded pre-cracked specimen. Typical  $K_{ISLC}$  data dependence with test time (i.e., time-to-failure) is depicted in Fig. 7 with respect to  $K_{IC}$  (air) and  $K_{ISCC}$  (salt water). Approximate test time scale typically ranges anywhere from a few to 20 h [23,36]. Since alloy microstructure and, especially, product crystallographic texture strongly influence SLC susceptibility, it is important to consider the

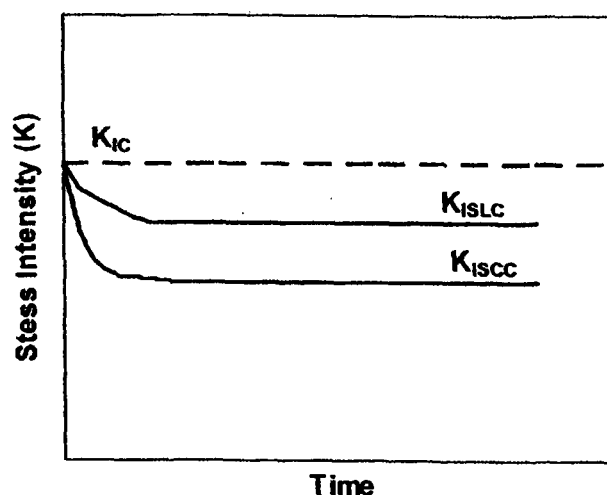


FIG. 7—Generalized test time dependence of  $K_{ISLC}$  values measured for high strength titanium alloys, as compared to their  $K_{IC}$  and  $K_{ISCC}$  values.

sample orientation of interest for testing. Examination of post-test specimen fracture surfaces should reveal low-energy facets of quasi-cleavage under high magnification SEM examination if SLC has occurred.

Hydrogen analysis of coupons is performed by the hot vacuum extraction method. In the hot vacuum extraction apparatus, a small sample is heated to between 1100 and 1400°C for several minutes within a chamber to reversibly release the absorbed hydrogen, which is subsequently measured. LECO Hydrogen Analyzers offer measurement resolution on the order of  $\pm 5$  ppm at sample hydrogen levels below 200 ppm. It is critical to note that the analyzed hydrogen content may be directly dependent on the test sample thickness tested if a nonhomogeneous distribution (i.e., hydrogen gradient or surface film) of absorbed hydrogen exists within the sample. If the hydrogen is uniformly distributed or diffused through the sample cross section (which is often not the case), no sample thickness dependence exists and the hydrogen content may be directly used to predict or correlate with metal behavior and properties.

Since hydrogen chemical analysis only provides the total hydrogen present in a given sample cross section, test samples are often metallurgically sectioned and examined for hydride phase to determine the hydrogen distribution. This technique, which is only useful in  $\alpha$ , near- $\alpha$ , and leaner  $\alpha$ - $\beta$  titanium alloys, involves wet-abrasive wheel- or saw-cutting through the sample cross section, wet-grinding down below any worked or heat-affected metal, and hand-polishing down through abrasive papers and slurry/cloth wheels down to 0.05  $\mu\text{m}$  alumina. Sample edge retention is vital in this hand-polishing technique. Final light etching with an HF/HNO<sub>3</sub> type etch (i.e., Kroll or Oxalic etches) should reveal the acicular hydride precipitates (Fig. 1), if present, which tend to etch out first. Intermediate electropolishing followed by etching may also be employed if sample edge (surface) retention is not critical or of interest. Basic guidelines and procedures for preparation of titanium alloy samples for metallographic examination can be found in Ref 37.

Microscopic examination of hydride phase precipitates is typically conducted at magnifications of 200 to 1000 $\times$ , depending on hydride size and quantity.

### Ignition Testing

Titanium alloys can be susceptible to ignition or burning, or both, in very few special gas environments, such as pure gaseous or liquid oxygen, oxygen-enriched gas mixtures, and dry chlorine gas [1]. These highly exothermic reactions generally increase with increasing gas pressure, concentration, flow rate, and temperature. Normally, the nonreactive, protective surface oxide film on titanium must be removed, damaged, or penetrated for ignition and reaction to occur. In the case of oxygen gas, burning is sustained only if the local metal surface temperature remains at or above the alloy's melting point, above which formation of the protective oxide film is not possible. Any factor that removes local heat generated, such as increased metal thermal conductivity and/or section thickness (i.e., increased thermal mass), will inhibit or diminish ignition and burning tendencies.

Although no standard metal ignition tests exist, testing has traditionally been aimed at identifying ignition and sustained burning thresholds of a metal as a function of gas pressure, concentration, and temperature. Ignition and burning tests may be categorized as either static or dynamic, depending on whether the reaction gas is nonflowing (static) or continuously flowing past the test sample through a test chamber. Since increased gas flow rate exacerbates metal ignition and burning, the dynamic tests tend to produce more conservative thresholds.

Ignition tests must incorporate a means of breaking or removing the surface oxide film and exposing fresh metal surface on the sample. This can be achieved by a variety of methods [38], including tensile straining to fracture, puncture, impact, severe surface abrasion or scratching, severe plastic straining, explosive shock, or high-energy beams (i.e., laser) [39] or electric sparks focused on the metal test sample. Tensile rupture of test samples within pressurized test vessels has been most commonly employed for testing in oxygen-rich gas mixtures [40–42] and dry chlorine gas [43]. A typical ignition test setup using tensile rupture is

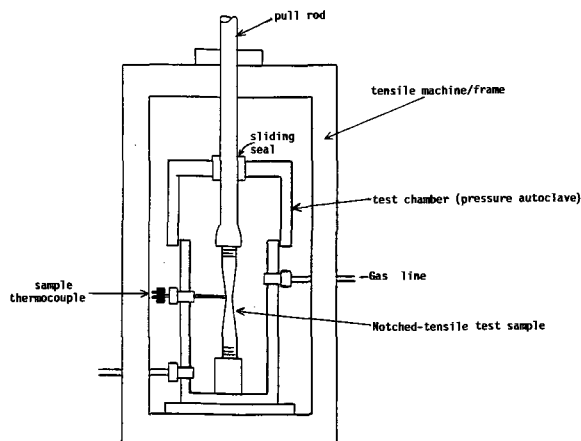


FIG. 8—Typical ignition test setup for titanium samples using tensile rupture.

depicted in Fig. 8. Continuous measurement of gas pressure and test sample temperature can provide an indirect means of assessing ignition occurrence. Go/no-go assessment of ignition is usually based on post-test visual examination of sample fracture surfaces for melting or oxide scaling, or both. More sophisticated burn testers may incorporate continuous video monitoring and pyrometers, or other heat sensors to track the ignition/burn event.

Burning or sustained combustion testing of titanium alloys typically involves intentional localized heating of a test sample at one end or location to a temperature above its melting point. This localized focused sample heating can be achieved by laser, electron beam, electric arc, electrical resistance, or plasma arc methods. Once sample ignition is induced, the ignition heating source is removed, and duration and extent of sustained sample burn is measured. One commonly used burn test uses a 4-in. (102-mm) long, 0.125-in. (3.18-mm) diameter test sample (rod) that is ignited on one end by electric arc. The rod length remaining after the test is measured and used to rate alloy burn susceptibility. Design details and setup of static and flow (dynamic) burn testers are presented in Figs. 9 and 10, and are discussed in more detail in Ref 44. Note that test sample size, geometry, and section thickness directly influence burn susceptibility, and must be standardized for comparative tests and specified in all cases.

FIG. 9—Static burn tester using promoted metal sample ignition [42].



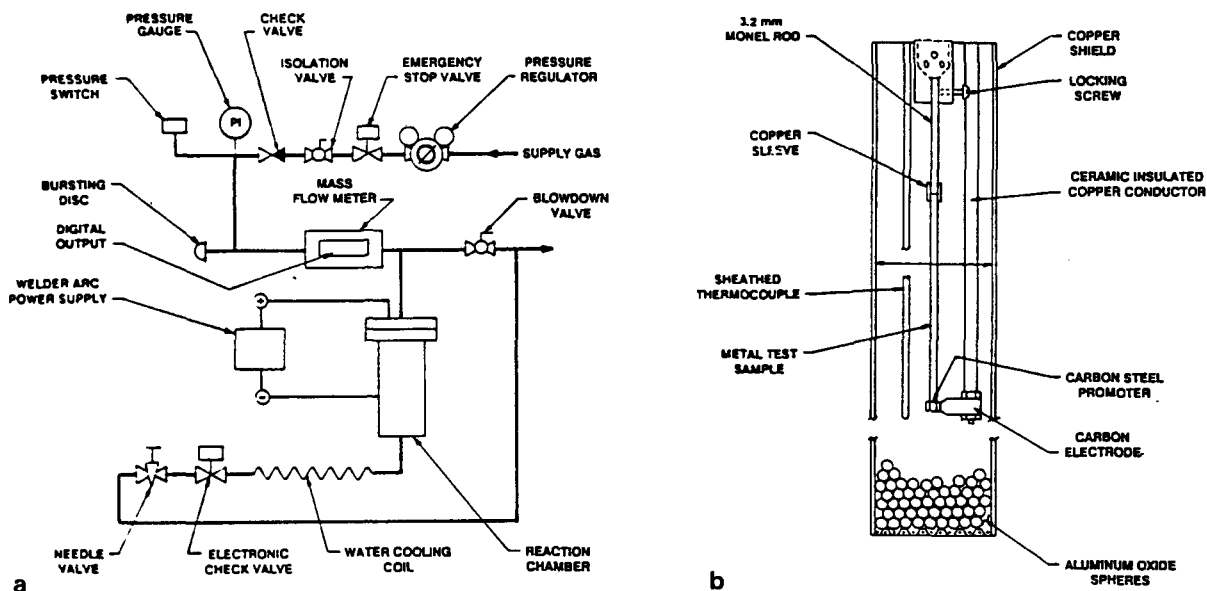


FIG. 10—Photomicrograph (400 $\times$ ) illustrating example of a hard oxygen-rich surface layer (alpha case) on  $\alpha/\beta$  and  $\beta$  titanium alloys after high-temperature air exposure.

### Oxidation Tests

Although titanium alloys are highly resistant to oxidation up to moderate temperatures, colored protective surface oxide films form in air at 370–595°C. Depending on exposure time at temperature and alloy composition, oxide film or scale growth may become excessive and unacceptable for engineering purposes above ~620°C. In terms of titanium alloy content, increasing vanadium, manganese, and zirconium concentrations are generally detrimental, whereas increasing molybdenum, niobium, silicon, and chromium concentrations tend to retard oxidation. Elevated aluminum content, as in the titanium aluminide intermetallics, markedly enhances oxidation resistance, elevating titanium alloy use windows by a few hundred degrees.

In addition to oxide film or scale formation at elevated temperatures, titanium alloys can also experience oxygen enrichment of metal surfaces beneath the oxide scale. These hard, brittle metal surface layers, known as “alpha case,” result from diffusion of oxygen or nitrogen interstitials, or both, into the metal. This time/temperature-dependent phenomenon becomes significant above ~540–590°C depending on alloy type, and severely reduces metal formability, ductility, and fatigue life, particularly as metal section thickness is reduced. Typical examples of an alpha case in  $\alpha/\beta$  and  $\beta$  titanium alloys are shown in Fig. 11.

Simple static oxidation testing of titanium alloys can be conducted per ASTM G 54, Practice for Simple Static Oxidation Testing, with a few unique considerations relative to post-test evaluation. Descaling of titanium samples after test exposure may employ mechanical scale removal or hot alkaline solution descaling. A light fine sand grit or glass-bead blast for several seconds are good mechanical descale methods if a procedure is prequalified to ensure insignificant substrate metal weight loss. Several high-temperature alkaline descale solutions based on concentrated KOH solutions

are available commercially for titanium alloys. Again, prequalification of the chemical descale procedure (i.e., exposure time and temperature) is recommended to avoid substrate metal corrosion. Conventional strong reducing acids will not dissolve heavy oxide films or scales on titanium and will attack the metal substrate and should, therefore, be avoided.

Metallographic examination offers valuable information once the sample is sectioned, mounted, hand-polished, and Kroll etched per recommended procedures outlined in Ref 37. The remaining metal sample thickness and the alpha-case layer thickness along the sample surface can be determined from the cross-sectioned mount. This alpha-stabilized layer is not visually discernable in  $\alpha$  alloys, but should be readily apparent when heavier than a few tenths of a mil in  $\alpha/\beta$  and  $\beta$  alloys (see Fig. 11). Subscale or

FIG. 11—Photomicrograph (400 $\times$ ) illustrating example of a hard oxygen-rich surface layer (alpha case) on  $\alpha/\beta$  and  $\beta$  titanium alloys after high-temperature air exposure.

internal oxidation attack is not typically observed with titanium alloys. Mechanical testing of samples after thermal exposure (i.e., tensile, bends, etc.) may also be of interest to assess extent of oxidation wastage and diffused interstitial embrittlement. Knoop or Vickers microhardness profiles of mounted and polished sample cross sections may also be useful in identifying heavy alpha case layers, since these oxygen-rich layers are substantially harder than the metal matrix.

## REFERENCES

- [1] Schutz, R. W. and Thomas, D. E., "Corrosion of Titanium and Titanium Alloys," in *ASM Metals Handbook*, 9th ed., Vol. 13, *Corrosion*, ASM International, Metals Park, OH, 1987, p. 669.
- [2] Schutz, R. W., "Titanium," in *Process Industries Corrosion—The Theory and Practice*, National Association of Corrosion Engineers (NACE), Houston, TX, 1986, p. 503.
- [3] *Titanium—A Technical Guide*, M. J. Donachie, Jr., Ed., ASM International, Metals Park, OH, 1988.
- [4] "Titanium and Its Alloys," Course 27, Lesson 3, Metals Engineering Institute, American Society for Metals (ASM), Metals Park, OH.
- [5] *Aerospace Structural Metals Handbook*, Mechanical Properties Data Center, U.S. Department of Defense, 1985.
- [6] Schwartzberg, F., Holden, F., Ogden, H., and Jaffee, R., "The Properties of Titanium Alloys at Elevated Temperatures," TML Report 82, Titanium Metallurgical Laboratory, Battelle Memorial Institute, September 1957.
- [7] Mote, M., Hooper, R., and Frost, P., "The Engineering Properties of Commercial Titanium Alloys," TML Report 92, Titanium Metallurgical Laboratory, Battelle Memorial Institute, June 1958.
- [8] *Titanium Alloys Handbook*, MCIC-HB-02, Metals and Ceramics Information Center, Department of Defense Information Analysis Center, December 1972.
- [9] Tomashov, N. D. and Altovskii, P. M., *Corrosion and Protection of Titanium*, Government Scientific-Technical Publication of Machine-Building Literature (Russian translation), 1963.
- [10] Andreeva, V. V., *Corrosion*, Vol. 20, 1964, p. 35.
- [11] Pourbaix, M., *Atlas of Electrochemical Equilibria in Aqueous Solutions*, National Association of Corrosion Engineers (NACE), Houston, TX, 1974, p. 217.
- [12] Griess, J. C., Jr., "Crevice Corrosion of Titanium in Aqueous Salt Solutions," *Corrosion*, Vol. 24, No. 4, April 1968, pp. 96–109.
- [13] Schutz, R. W., "Understanding and Preventing Crevice Corrosion of Titanium Alloys: Parts I and II," *Materials Performance*, October 1992, pp. 57–62, and November 1992, pp. 54–56.
- [14] Schutz, R. W., Grauman, J. S., and Hall, J. S., "Effect of Solid Solution Iron on the Corrosion Behavior of Titanium," in *Titanium—Science and Technology, Proceedings of the 5th International Conference on Titanium*, Deutsche Gesellschaft für Metallkunde E.V., 1985, pp. 2617–2624.
- [15] Covington, L. C. and Schutz, R. W., "Effects of Iron on the Corrosion Resistance of Titanium," in *Industrial Applications of Titanium and Zirconium*, ASTM STP 728, ASTM International, West Conshohocken, PA, 1981, pp. 163–180.
- [16] Schutz, R. W., "Stress Corrosion Cracking of Titanium Alloys," in *Stress-Corrosion Cracking—Materials Performance and Evaluation*, ASM International, Metals Park, OH, July 1992, pp. 265–297.
- [17] Wanhill, R. J. H., "Aqueous Stress Corrosion in Titanium Alloys," *British Corrosion Journal*, Vol. 10, No. 2, 1975, pp. 69–78.
- [18] Brown, B. F., *Stress Corrosion Cracking in High Strength Steels and in Titanium and Aluminum Alloys*, Naval Research Laboratory, Washington, DC, 1972.
- [19] Blackburn, M. J., Feeney, J. A., and Beck, T. R., *State-of-the-Art of Stress-Corrosion Cracking of Titanium Alloys*, Part 4 of Monograph Review, Boeing Company sponsored by the Advanced Research Projects Agency, ARPA Order No. 878 and NAS7-489, June 1970.
- [20] Schutz, R. W. and Grauman, J. S., "Compositional Effects on Titanium Alloy Repassivation Potential in Chloride Media," *Advances in Localized Corrosion, Proceedings of the 2nd International Conference on Localized Corrosion*, 1–5 June 1987, Orlando, FL, National Association of Corrosion Engineers (NACE), Houston, TX, 1990, pp. 335–337.
- [21] Paton, N. E. and Williams, J. C., "Effect of Hydrogen on Titanium and Its Alloys," in *Titanium and Titanium Alloys—Source Book*, ASM, Metals Park, OH, 1982, pp. 185–207.
- [22] Lenning, G. A., Spretnak, J. W., and Jaffe, R. I., "Effect of Hydrogen on Alpha Titanium Alloys," *Transactions of the Metallurgical Society of AIME*, October 1956, p. 1235.
- [23] Boyer, R. R. and Spurr, W. F., "Characteristics of Sustained-Load Cracking and Hydrogen Effects in Ti-6Al-4V," *Metallurgical Transactions*, Vol. 9A, January 1978, pp. 23–29.
- [24] Meyn, D. A., "Effect of Hydrogen on Fracture and Inert-Environment Sustained Load Cracking Resistance of  $\alpha$ - $\beta$  Titanium Alloys," *Metallurgical Transactions*, Vol. 5, November 1974, p. 2405.
- [25] Craighead, C. M., Lenning, G. A., and Jaffe, R. I., "Hydrogen Embrittlement of Beta-Stabilized Titanium Alloys," *Transactions of the Metallurgical Society of AIME*, August 1956, p. 923.
- [26] Schutz, R. W. and Covington, L. C., "Guidelines for Corrosion Testing of Titanium," in *Industrial Applications of Titanium and Zirconium*, ASTM STP 728, ASTM International, West Conshohocken, PA, 1981, pp. 59–70.
- [27] *ASM Metals Handbook*, 9th ed., Vol. 13, *Corrosion*, ASM International, Metals Park, OH, pp. 212–220.
- [28] Dean, S. W., Jr., "Electrochemical Methods of Corrosion Testing," in *Electrochemical Techniques for Corrosion*, National Association of Corrosion Engineers (NACE), Houston, TX, 1977, pp. 52–60.
- [29] Liening, E. L., "Electrochemical Corrosion Testing Techniques," in *Process Industries Corrosion*, National Association of Corrosion Engineers (NACE), Houston, TX, 1986, pp. 85–122.
- [30] Fontana, M. G. and Greene, N. D., *Corrosion Engineering*, McGraw-Hill, New York, 1967.
- [31] Bergman, D. D. and Grauman, J. S., "The Detection of Crevice Corrosion in Titanium and Its Alloys Through the Use of Potential Monitoring," *Titanium '92—Science and Technology*, The Minerals, Metals & Materials Society, 1993, pp. 2193–2200.
- [32] Kobayashi, M., Araya, Y., and Fujiyama, S., et al., "Study on Crevice Corrosion of Titanium," in *Titanium'80—Science and Technology*, Vol. 4, The Metallurgical Society, 1980, pp. 2613–2622.
- [33] Diegle, R. B., "Electrochemical Cell for Monitoring Crevice Corrosion in Chemical Plants," Paper 154, presented at Corrosion/81, Toronto, Canada, National Association of Corrosion Engineers (NACE), April 1980.
- [34] Szklarska-Smialowska, L. and Janik-Czachor, M., *Corrosion Science*, Vol. 11, 1971, pp. 901–914.
- [35] Sprowls, D. O., "Evaluation of Stress-Corrosion Cracking," *Metals Handbook*, 9th ed., Vol. 13, *Corrosion*, ASM International, Metals Park, OH, 1987, pp. 245–282.
- [36] Yoder, G. R., Griffis, C. A., and Crooker, T. W., "Sustained-Load Cracking of Titanium Alloys," NRL Report 7596, Naval Research Laboratory, Washington, D.C., August 1973.
- [37] *Metals Handbook*, 9th ed., Vol. 9, *Metallography and Microstructure*, ASM International, Metals Park, OH, 1985, pp. 458–475.

- [38] "Reactivity of Metals with Liquid and Gaseous Oxygen," DMIC Memorandum 163, Defense Metals Information Center, Battelle Memorial Institute, Columbus, OH, 15 January 1963.
- [39] Anderson, V. G. and Manty, B. A., "Titanium Alloy Ignition and Combustion," Report No. NADC 76083-30, United Technologies Corporation, Pratt & Whitney Aircraft Group, West Palm Beach, FL, 15 January 1978.
- [40] Littman, F. E., Church, F. M., and Kinderman, E. M., "A Study of Metal Ignitions—I. The Spontaneous Ignition of Titanium," *Journal of the Less-Common Metals*, Vol. 3, 1961, pp. 367–378.
- [41] Littman, F. E. and Church, F. M., "Reaction of Titanium with Water and Aqueous Solutions," Final Report—SRI Project No. SD-2116, Stanford Research Institute, 15 June 1958.
- [42] Krag, P. and Henson, R., "An Ignition Resistant Titanium Alloy for Acid Pressure Oxidation Applications," *Proceedings of the RANDOL Gold Forum*, Vancouver, B.C., 1992, p. 201.
- [43] Millaway, E. E. and Klineman, M. H., "Factors Affecting Water Content Needed to Passivate Titanium in Chlorine," *Corrosion*, Vol. 23, No. 4, 1972, p. 88.
- [44] McIlroy, K. and Zawierucha, R., "The Effects of Testing Methodology on the Promoted Ignition-Combustion Behavior of Carbon Steel and 316L Stainless Steel in Oxygen Gas Mixture," *Flammability and Sensitivity of Materials in Oxygen-Enriched Atmospheres, Fourth Volume, ASTM STP 1040*, ASTM International, West Conshohocken, PA, 1989, pp. 38–53.

# Zirconium and Hafnium

*Te-Lin Yau*<sup>1</sup>

## GENERAL CONSIDERATIONS

THE CHEMICAL PROCESS industry presents a complex set of materials selection challenges. Conducting corrosion testing of candidate materials under simulated or actual service conditions is widely used in the process of materials selection. ASTM G 4, Guide for Conducting Corrosion Tests in Field Applications and G 31, Practice for Laboratory Immersion Corrosion Testing of Metals, and NACE Standard TM-01-69, Laboratory Corrosion Testing of Metals are the general guides for conducting corrosion tests. While these standards can be very useful in making a preliminary list of the best candidate materials, they are designed primarily for the more common metals and alloys such as steel, aluminum alloys, and copper alloys. Certain portions of these procedures, e.g., cleaning methods, are not applicable to zirconium, hafnium, and their alloys. Although ASTM G 2 is designated specifically for zirconium, hafnium, and their alloys, it is a specific practice used in the nuclear industry. Therefore, a tailored practice for conducting corrosion specimen tests on zirconium, hafnium, and their alloys in chemical environments is needed. The use of test standards that have not been modified for zirconium or hafnium may lead to erroneous or invalid results.

For example, when field tests were conducted on zirconium and other materials in acetic acid environments, zirconium was the only metal tested to exhibit excellent corrosion resistance under most conditions [1]. However, severe general corrosion and pitting occurred in acetic acid when the acid contained both acetic anhydride and copper ions. The presence of copper ions was the result of the corrosion of copper specimens, which were tested at the same time. Zirconium resists attack by a wide range of acetic acid and anhydride environments when certain contaminants, such as copper ions, are avoided [2].

Standard practices must be modified for conducting laboratory or field tests on zirconium, hafnium, and their alloys. Emphasis must be placed on specimen quality and preparation, galvanic corrosion, test duration, contamination resulting from the corrosion of other metals, and handling of corroded specimens. The procedures recommended herein should be used in conjunction with the applicable ASTM and NACE standards previously mentioned. Additional information is available in Ref 3.

Zirconium and its alloys are susceptible to stress corrosion cracking (SCC) in such environments as  $\text{Fe}^{3+}$ - or  $\text{Cu}^{2+}$ -containing chloride solution,  $\text{CH}_3\text{OH}$  + halides, concentrated  $\text{HNO}_3$ , halogen vapors, and liquid mercury or cesium [4,5]. Common test methods, e.g., U-bend, C-ring, split ring, direct tension, double cantilever, and slow strain rate tension, have been used to determine zirconium's susceptibility to SCC.

## SPECIMEN IDENTITY

Zirconium ores generally contain a few percent of hafnium. Zirconium and hafnium are similar chemically and metallurgically but differ markedly in their nuclear properties. Zirconium is almost transparent to thermal neutrons and hafnium is highly opaque to thermal neutrons. As a result, there are nuclear and nonnuclear grades of zirconium, hafnium, and their alloys. The nuclear grades of zirconium materials are essentially hafnium-free, and the nonnuclear grades may contain up to 4.5 % hafnium. The alloy names Zircaloy, Zr-2.5Nb, and Zr1Nb apply to nuclear grade materials. Zircaloy is the general term for a series of zirconium-tin alloys containing minor amounts of iron, chromium, and nickel that were developed by the U.S. Navy Nuclear Propulsion Program. Only Zircaloy-2 and Zircaloy-4 are still in common usage. For commercial applications, ASTM specifications list three grades, namely, UNS R60702 (Grade 702), UNS R60704 (Grade 704), and UNS R60705 (Grade 705). Grade 702 is commercially pure zirconium, and Grades 704 and 705 are similar to Zircaloy-4 and Zr-2.5Nb, respectively.

For hafnium, Grade R1 materials, which are low in zirconium content, are for nuclear applications, and Grade R3 materials, which may contain a higher zirconium content, are intended for nonnuclear applications.

The first step in corrosion testing is to correctly identify corrosion specimens. When corrosion specimens need an identifying mark, a vibrating tool can be used.

## SPECIMEN QUALITY

Chemical composition and metallurgical condition are essential factors in determining corrosion properties. All specimens should be of known composition and metallurgical condition. Furthermore, each specimen should be examined

<sup>1</sup>Consultant, 1445 Belmont Avenue SW, Albany, OR 97321-3765.

**TABLE 1**—Results of EDX analyses of contaminated surface areas of untested specimens of Grade 702 zirconium from different sources.

Element	Composition, wt%									
	1	2	3	4	5	6	7	8	9	10
Zr	83.08	97.83	16.15	99.11	83.56	43.35	91.71	38.35	61.24	79.55
Ti	—	—	1.27	—	0.60	—	—	—	0.37	—
Fe	—	2.17	4.05	—	—	1.79	—	15.22	8.54	13.59
Cr	—	—	—	—	—	—	—	3.65	—	—
Cu	—	—	—	—	—	—	—	—	3.01	1.40
Cd	—	—	—	—	—	—	—	7.63	—	—
Al	—	—	1.59	0.89	—	7.70	—	—	—	1.21
Si	14.25	—	34.48	—	7.90	15.27	8.29	24.98	2.67	4.26
Na	—	—	—	—	—	7.60	—	—	7.01	—
Mg	—	—	13.50	—	—	—	—	—	—	—
Cl	—	—	5.14	—	4.87	9.56	—	7.79	0.62	—
S	—	—	8.98	—	—	—	—	—	—	—
K	—	—	1.53	—	3.07	4.75	—	1.47	—	—
Ca	2.67	—	12.46	—	—	6.37	—	0.91	0.16	—
Zn	—	—	—	—	—	3.61	—	—	16.37	—

visually for irregularities such as stains, scratches, foreign particles, etc. Unusual features should be recorded. Surface condition is very important in corrosion resistance.

Corrosion specimens may be unacceptable if they are not prepared properly. One of the major problems is cross contamination during specimen fabrication. Examples of contaminated surface areas of several Grade 702 zirconium specimens from different suppliers are given in Table 1. The specimen preparation can contaminate specimen surface as well when certain operations, such as bending and grinding, are employed. Tools should be clean in specimen-making processes. Surface condition plays an important role in corrosion and is particularly important to zirconium.

## PRECAUTIONS

Hazardous chemicals are frequently used in making and testing specimens of zirconium, hafnium, and their alloys. Detailed information on safe handling of involved chemicals should be obtained from competent sources.

## PREPARATION OF CORROSION SPECIMENS

### Corrosion Specimens

The size and shape of corrosion specimens are affected by several factors and cannot be rigidly defined. All convenient sizes are acceptable. Preferably, the edges of corrosion specimens should be machined in order to remove cold-worked metal. When the application demands, the specimens should include welds, cold-worked areas, and other features of the intended service.

### Cleaning

Usually corrosion specimens with as-manufactured surfaces are tested without further surface treatment other than cleaning. Corrosion specimens should be cleaned in a cleaner such as 5–10 % aqueous ammonia. An ultrasonic device can be used if available. Because of tightening regulation, organic solvents became undesirable cleaning agents recently. Use

a nylon brush or other nonmetallic brush if required. Rinse cleaned specimens in running cold water for five minutes. Then, specimens may be air-dried, wiped dry with a clean, lint-free cloth, or blown with clean, dry air. Handle cleaned specimens only with clean, lint-free gloves or forceps. When not being processed, enclose the specimens in a clean container or wrap in cloth, plastic, or clean heavy paper that will not affect weight or appearance.

### Pickling

Pickling is often applied to corrosion specimens to assure that the surfaces are free of surface contamination and uniform in nature. It is necessary if one of the following situations exists:

1. The surface of specimens is embedded with impurities.
2. The effects of pickling are being studied.
3. Specimens will be subsequently treated to form thick oxide films in air, water, steam, or molten salts.

Detailed procedures for pickling are given in ASTM G 2, Test Method for Corrosion Testing of Products of Zirconium, Hafnium, and Their Alloys in Water at 680°F or in Steam at 750°F.

### Dimensions, Weight, and Inspection

Measure and weigh each clean, dry specimen. Dimensions determined to the third significant figure and mass determined to an accuracy of 0.1 mg are suggested. Do not weigh specimens until they are thoroughly dry and at the same temperature as the balance. Examine each specimen for folds, cracks, blisters, foreign material, luster, brown acid stain, etc. Reject or reprepare any unacceptable specimen or record any significant observations prior to testing.

## CORROSION TESTING

### Specimen Mounting and Test Rack Installation

In laboratory testing, zirconium or hafnium specimens should not be placed in the same vessel with specimens of

other metals. The supporting device and vessel should also not cause contamination of the test solution.

In field testing, zirconium or hafnium specimens should be placed nearest the inlet of the process solution when other metals are also being tested. It is desirable to have the specimen or test rack securely fixed in place. Eliminate the possibility of galvanic effects resulting from metal-to-metal contact by using an insulating material.

A note should be made about the location and position of test specimens in the testing unit. Preferably, corrosion specimens should be placed so that any flow of liquid will be against the edges of the specimens. The same condition of agitation of the liquid should then be encountered by all specimens.

Tape, tube, and washers made of virgin fluorocarbon polymers can be used to prevent the galvanic coupling. Avoid insulated materials made of reprocessed fluorocarbon polymers, since free hydrofluoric acid may be formed from released fluoride ions. Properly oxidized zirconium or Zircaloy materials can also be used for this purpose. Zirconium oxide is an excellent insulating material.

### Test Solutions

Test solutions should be prepared accurately from chemicals conforming to the specifications of the committee on Analytical Reagents of the American Chemical Society and distilled water per ASTM D 1193 (Standard Specification for Reagent Water), unless they are naturally occurring solutions or plant solutions. The pH and specific gravity of fresh and tested solutions should be measured and recorded. Minor constituents should not be overlooked because they often affect corrosion rates. If there is any doubt, the composition of the test solutions should be checked by analysis. In corrosion testing, one should always expect the unexpected. For example, significant amounts of chloride and fluoride have been found in reagent grade nitric and sulfuric acids [6].

### Temperature of Solution

Temperature of the test solutions should be controlled within 2°C and the temperature must be reported with the test results.

### Aeration of Solution

Unless specified, the test solutions should not be aerated. Most tests related to process equipment should be run with the natural atmosphere inherent in the process, such as the vapors of the test solutions.

If aeration is required, test specimens should not be located in the direct oxygen or air stream from the sparger. Unrelated effects can be encountered if the gas stream impinges on the specimens.

If exclusion of dissolved oxygen is necessary, specific techniques are required, such as prior heating of the test solutions and sparging with an inert gas (usually nitrogen). A liquid atmospheric seal is required on the test vessel to prevent further contamination.

Tests at the boiling point should be conducted with the minimum possible heat input, and boiling chips should be

used to avoid excessive turbulence and bubble impingement. Cleaning may be needed to remove trace amounts of impurities in boiling chips before their usage. For example, amphoteric alundum granules, which may have some fluoride contamination, should be cleaned in boiling 20 % sulfuric acid for 24 h, rinsed in water, cleaned in boiling 40 % nitric acid for 24 h, rinsed in water, and dried.

### Duration of Test

Zirconium, hafnium, and their alloys can be either highly reactive or highly corrosion-resistant. In an incompatible environment, corrosion may occur within a short period of time, i.e., a few hours to a few days. On the other hand, in a compatible environment, there may be little change in mass (gain or loss) for years. Consequently, the commonly suggested test duration in hours, which is 50 divided by the corrosion rate in mm/y or 2000 divided by the corrosion rate in mpy, may be excessive and impractical. For example, if the corrosion rate determined from a short-term test is 0.0025 mm/y (0.01 mpy), the suggested test duration would be 20 000 h!

An often-used test schedule in testing zirconium or hafnium is the 2-4-2 day cycle. This schedule gives some indication about the time effect on the corrosivity of the test solution and the corrodibility of the test specimen.

Nevertheless, the duration of any test should be determined by the nature and purpose of the test. In studying the effects of a minor impurity, the duration of test can be 1 h or shorter, depending on the time required to measure an effect. In a confirmation test, the duration of the test can be 14 days to a year.

During the test, frequent checks should be made, if possible, at the test vessel for changes in solution color, temperature, pressure, bubbling, etc.

### Removal of Specimens from Test

The condition and appearance of the holder and specimens after removal from test should be noted and recorded. It is desirable to photograph the holder and specimens. Specimens should then be rinsed in water and dried. They can be cleaned with a nylon brush or other nonmetallic brush as required. In removing the specimens, care should be taken to keep them in proper order relative to each other so that any specimen may be identified from the original record of its position on the holder. This is important if corrosion has been so severe that identification marks have been removed. Tested specimens should be handled by forceps.

Specimens of zirconium and its alloys can be covered with a layer of pyrophoric film when they are tested under certain specific conditions, e.g., a stagnant solution of 77.5 % sulfuric acid and 200 ppm ferric ion at 80°C for ten days [7]. Treating in hot air or steam can eliminate this pyrophoric tendency. This takes 20 to 30 min at 250°C. It should be noted that most corroded specimens do not have a pyrophoric layer. The formation of pyrophoric films is possible, but not guaranteed when both the following conditions exist:

1. The test solution is stagnant or there are stagnant areas (e.g., under a gasket) on the test specimens.

2. The test solution can cause localized corrosion on a macroscale.

To clean exposed specimens, a nonmetallic brush or rubber stopper can be used if necessary. There is no applicable chemical or electrolytic cleaning method for zirconium, hafnium, and their alloys since their oxides and most of the other compounds are very inert.

### Interpretation and Calculation of Results

After exposed specimens have been cleaned, they should be reweighed with accuracy corresponding to that of the original weighing. The mass change during the test period can be the principal measure of corrosion. It should be noted that specimens of zirconium and hafnium may show weight gains after testing in certain oxidizing media, such as nitric acid, which result in the formation of insoluble oxide films.

The pH and specific gravity of spent solutions should be measured and recorded. Spent solutions should be saved for a reasonable period of time. They should be analyzed if test results are inexplicable.

Each tested specimen should be examined carefully for the presence of any pits or unusual marks. If there are any pits, the average and maximum depths of pits are determined with a pit gage or a calibrated microscope (refer to ASTM G 46, Practice for Examination and Evaluation of Pitting Corrosion).

If tested specimens are suspected of being subject to intergranular attack or hydrogen embrittlement, a cross section of the specimens should be metallographically examined for evidence of such attack.

Tested specimens may be subjected to simple bending tests to determine whether any embrittlement has occurred.

For corrosion-rate calculation, densities of Zr 702, Zr 704, Zr 705, and Hf are 6.50, 6.50, 6.53, and 13.1 g/cm<sup>3</sup>, respectively.

### REPORT

It is important to report all data as completely as possible. Expansion of the testing program in the future or correlating the results with other test results will be possible only if all pertinent information is properly recorded. The following checklist is a recommended guide for reporting all important information and data:

- Name of personnel and laboratory involved
- Date
- Identification of specimen material and number
- Form and metallurgical conditions of specimens
- Treatment used to prepare specimens
- Visual appearance remarks of each specimen before and after the corrosion testing
- Weights and dimensions of specimens before and after the corrosion testing
- Corrosive media and concentration (and any changes during test)
- Volume of test solution
- The color, pH and specific gravity of the test solution before and after the corrosion testing
- Temperature (maximum, minimum, and average)
- Aeration (describe conditions or technique)
- Agitation (describe conditions or technique)
- Type of apparatus used for test
- Duration of each test
- Number of specimens of each material tested, and whether specimens were tested separately or which specimens were tested in the same container
- Method used to clean specimens after exposure and the extent of any error expected by this treatment
- Evaluation of attack if other than general, such as crevice corrosion under support rod, pit depth and distribution, and results of microscopical examination or bend tests
- Corrosion rates for each specimen
- Minor occurrences or deviations from the proposed test program often can have significant effects and should be reported if known

### REFERENCES

- [1] Takaaki, S., Takamura, A., and Segawa, S., "Corrosion Behaviors of Various Metals and Alloys in Acetic Acid Environments," *Boshoku Gijutsu*, Vol. 15, No. 2, 1966, pp. 49–55.
- [2] Yau, T. L., "Performance of Zirconium and Zirconium Alloys in Organics," *Journal of Testing and Evaluation*, Vol. 24, No. 2, March 1996, pp. 110–118.
- [3] Yau, T. L., Andrews, J. A., Henson, H. R., and Holmes, D. R., "Practice for Conducting Corrosion Coupon Tests on Zirconium and Its Alloys," *Corrosion Testing and Evaluation: Silver Anniversary Volume, ASTM STP 1000*, ASTM International, West Conshohocken, PA, 1990, pp. 303–311.
- [4] Cox, B., "Stress Corrosion Cracking of Zirconium Alloys," *Langmuir*, Vol. 3, No. 6, 1987, pp. 867–873.
- [5] Yau, T. L., "Stress-Corrosion Cracking of Zirconium Alloys," *Stress-Corrosion Cracking*, R. H. Jones, Ed., ASM International, Metals Park, OH, 1992, pp. 299–311.
- [6] Yau, T. L., "Chemical Impurities Create New Challenges in Material Selection," *Outlook*, Vol. 9, No. 4, Teledyne Wah Chang Albany, Albany, OR, 1988, p. 4.
- [7] Yau, T. L., "Methods to Treat Pyrophoric Film on Zirconium," *Industrial Applications of Titanium and Zirconium (3rd Conference)*, ASTM STP 830, ASTM International, West Conshohocken, PA, 1984, pp. 124–129.

# Tantalum and Niobium Alloys

E. B. Hinshaw<sup>1</sup> and K. D. Moser<sup>2</sup>

## TANTALUM

### General

A MAJOR FACTOR IN determining the specific applications of tantalum for corrosion-resistant equipment is its price. The cost of tantalum metal is about 15 times that of nickel-copper, nickel, or titanium and about 50 to 100 times that of the stainless steels. Accordingly, the service requirements for tantalum components are to have practically no corrosion degradation over time periods of years—virtually indefinite life. This means that the use of tantalum is limited to a relatively small number of the most severe media and conditions in relatively thin cross sections or as lining compared to other materials of construction. Selection of tantalum for use is based on large, not moderate, improvements of performance over other materials. Therefore, testing data do not need to be highly quantified. If corrosion rates greater than 0.051 mm/yr. (2 mpy) are indicated the application very likely is not recommended [1].

### Nature of the Metal

#### Electrochemical Behavior

The corrosion resistance of tantalum is due to a naturally occurring oxide film. The film is dielectric and electronically rectifying. It is amorphous rather than crystalline. The integrity of the film can be breached at temperatures above 175 to 190°C (350–375°F) depending on the media composition. It is characteristic of tantalum that when the film loses effectiveness the very reactive metal is exposed and reaction can be vigorous. Accordingly, if tantalum is not highly resistant to media conditions it generally will be attacked rapidly and severely. In view of this behavior, and because only a slight amount of corrosive attack is tolerated in tantalum equipment, the practical evaluation of its corrosion characteristics can be relatively simple. In general, the preferred procedure is to do testing by exposure to the actual service conditions.

#### Alloys

Tantalum is similar in nature to the other passivating reactive-refractory metals (titanium, zirconium, and niobium)

but it is highly resistant to more species of chemicals and is susceptible to fewer types of attack. Alloys with these elements that have been evaluated have increased reactive tendencies in rough proportion to their compositional content as might be expected with solid solution alloys. Like all reactive metals tantalum and its alloys are susceptible to corrosion attack by fluoride ion or fluoride compound such as hydrogen fluoride at all temperatures. Caustic has a similar effect and readily attacks tantalum; however, tantalum is resistant to caustic corrosion at low concentrations <10 wt. % and temperatures <(38°C) 100°F, which is adequate for rinsing cycles in batch processing and continuous processing lines [2].

The only tantalum alloys of commercial importance are with tungsten. The Ta-2.5 % W alloy has corrosion resistance equivalent to that of the pure metal. The Ta-10 % W alloy has slightly less resistance in general but provides higher mechanical strengths.

### Sensitivity to Particular Environments

#### Hydrogen

Tantalum can be embrittled by exposure to hydrogen. It has a large solubility for hydrogen and embrittlement can occur without detectable formation of a hydride phase. Loss of ductility can range from moderate to extreme glass-like behavior. Embrittlement can be detected by a decrease in the normally high elongation or reduction of area values obtained in tension tests. When specimen size and shape selection are limited flex-bend tests and biaxial cup stretch tests are good indicators [3]. Successful NDE methods to determine hydrogen embrittlement could use *in-situ* hardness testing to detect increases in hardness of the material or determine the change in electrical conductivity by measuring the changes in the impedance [4]. In service tantalum normally assumes a cathodic potential when galvanically coupled and embrittlement can occur readily. Accordingly, evaluation for corrosive applications always should consider the possibility of embrittlement.

The use of platinum-plated spots on the chemical side of the tantalum surface at a surface ratio of 1/1000 to 1/10 000 can be effective in preventing hydrogen embrittlement in corrosive media [5].

#### Other Relevant Environments

Corrosive attack of tantalum is usually by uniform mass loss. No observations of stress-corrosion cracking (SCC) or of crevice corrosion have been reported in industrial service.

<sup>1</sup>CPI-Product Manager, H. C. Starck, Inc., 45 Industrial Place, Newton, MA 02161-1951.

<sup>2</sup>Senior Metallurgist, H. C. Starck, Inc., 45 Industrial Place, Newton, MA 02161-1951.



Pitting-type attack is rare and the mechanism is not understood. Extremely anhydrous or oxygen deficient conditions in association with halogen species have caused pitting [6].

Tantalum's major usage in corrosion resistant equipment is for the processing of primary chemicals, especially highly concentrated acids at elevated temperatures ( $>100^{\circ}\text{C}$ ). It can withstand moderately basic conditions, but caution is necessary for exposure in strong alkaline media. Two severe environments in which tantalum has been shown to be not susceptible to corrosion or cracking are:

1. NACE sulfide test [7,8] compositions at high temperature and pressure ( $250^{\circ}\text{C}$ –7 bar) ( $490^{\circ}\text{F}$ –100 psi).
2. Extended use in the production of 98 to 99 % fuming nitric acid [9].

No observations in industrial use have been reported wherein tantalum has been affected by increased anodic potential due to oxidizing ions (transpassive behavior). Neither microstructural-dependent attack nor interactive/selective attack involving welds and adjacent nonwelded metal has been observed.

Tantalum is unaffected by contact with most liquid metals at temperatures below  $600^{\circ}\text{C}$  ( $450^{\circ}\text{C}$  for zinc, tin) and up to  $1000^{\circ}\text{C}$  for some. Resistance to the alkali metals is dependent on maintaining very low levels of oxygen in the system [10].

No common organic compositions affect tantalum at temperatures below about  $200^{\circ}\text{C}$  except in compounds that have decomposition products of fluorine, sulfur trioxide, or strong alkalis. However, there is uncertainty about the effects of some complex species under highly anhydrous or oxygen-deficient conditions.

## NIOBIUM

### General

A major factor in determining the specific applications of niobium for corrosion-resistant equipment is its price. The cost of niobium metal is about 7 times that of nickel-copper, nickel, or titanium and about 25 to 50 times that of the stainless steels. Accordingly, the service requirements for niobium components are to have practically no corrosion degradation over time periods of years—virtually indefinite life. This means that the use of niobium is limited to a relatively small number of the most severe media and conditions in relatively thin cross sections or as lining compared to other materials of construction. Selection of niobium for use is based on large, not moderate, improvements of performance over other materials. Therefore, testing data do not need to be highly quantified. If corrosion rates greater than 2 mpy are indicated the application very likely is not recommended.

### Nature of the Metal

#### Electrochemical Behavior

The corrosion resistance of niobium is due to a naturally occurring oxide film. The film is dielectric and electronically rectifying. It is amorphous rather than crystalline.

The integrity of the film can be breached at temperatures above  $175$  to  $190^{\circ}\text{C}$  ( $350$ – $375^{\circ}\text{F}$ ) depending on the media composition. It is characteristic of niobium that when the film loses effectiveness the very reactive metal is exposed and reaction can be vigorous. Accordingly, if niobium is not highly resistant to media conditions it generally will be attacked rapidly and severely. In view of this behavior, and because only a slight amount of corrosive attack is tolerated in niobium equipment, the practical evaluation of its corrosion characteristics can be relatively simple. In general, the preferred procedure is to do testing by exposure to the actual service conditions.

### Alloys

Niobium is similar in nature to the other passivating reactive-refractory metals (titanium, zirconium, and tantalum) and has an inherent resistance to a wide range of chemicals. In general, compared to Zr and Ti, Nb has better corrosion properties in acids with small amounts of metal or organic contaminants. Niobium alloys with alloying elements such as Zr and Ti have been evaluated and have shown increased reactive tendencies in rough proportion to their compositional content as might be expected with solid solution alloys.

Commercially pure niobium (grade 1) is used commonly in nuclear reactors whereas niobium (grade 2) is used commonly for its corrosion resistance for lining of chemical equipment and as barrier shields in X-ray environments. The only niobium alloys of significant commercial importance are: the Nb with 1 % Zr for sodium vapor lamps, Nb with 55 % Ti for use in high purity oxygen injection parts/piping, Nb-Ti, Nb-Ti-Sn and Nb-Sn alloys for superconducting wires and magnets, and for extremely high temperature rocket nozzles which use the Nb-10 % Hf-1 % Ti alloy.

## Sensitivity to Particular Environments

### Hydrogen

Niobium can be embrittled by exposure to hydrogen. It has a large solubility for hydrogen and embrittlement can occur without detectable formation of a hydride phase. Loss of ductility can range from moderate to extreme glass-like behavior. Embrittlement can be detected by a decrease in the normally high elongation or reduction of area values obtained in tension tests. When specimen size and shape selection are limited, flex-bend tests and biaxial cup stretch tests are good indicators [3]. Successful NDE methods to determine hydrogen embrittlement could use *in-situ* hardness testing to detect increases in hardness of the material. In service niobium normally assumes a cathodic potential when galvanically coupled and embrittlement can occur readily. Accordingly, evaluation for corrosive applications always should consider the possibility of embrittlement.

### Other Relevant Environments

Corrosive attack of niobium is usually by uniform mass loss. No observations of stress-corrosion cracking (SCC) or of crevice corrosion have been reported in industrial service. Pitting type attack is rare and the mechanism is not understood. Extremely anhydrous or oxygen deficient conditions in association with halogen species have caused pitting [6].

Niobium's major usage in corrosion resistant equipment is for the processing of primary chemicals, especially in concentrating nitric acid at elevated temperatures  $>100^{\circ}\text{C}$  [11]. Niobium also has been used in chromic acid plating baths even with trace amounts of fluorine or fluoride-containing compounds; otherwise, niobium should not be considered in environments containing any amount of fluoride or fluoride compounds [12]. It can withstand moderately basic conditions, but caution is necessary for exposure in strong alkaline. Oxide scale formation and hydrogen absorption may occur in alkaline concentrations greater than about 10 % at ambient temperatures.

No observations in industrial use have been reported wherein niobium has been affected by increased anodic potential due to oxidizing ions (transpassive behavior). Neither microstructural dependent attack or interactive/selective attack involving welds and adjacent nonwelded metal have been observed.

Niobium has good resistance to most liquid metals but is not as resistant as tantalum.

Organic compositions do not affect niobium at temperatures at and below their boiling points except in compounds that have decomposition products of fluorine, sulfur trioxide, or strong alkalis.

However, there is uncertainty about the effects of some complex species under highly anhydrous or oxygen-deficient conditions.

## TANTALUM AND NIOBIUM

The most used chemical process industry equipment components made with tantalum and niobium are tanks/vessels, heat exchangers (tubing), immersion probes, and devices for instrumentation, valves, and glass lining repair assemblies [12].

### Recommended Corrosion Testing Procedures

The preferred procedure for corrosion testing tantalum and niobium materials, as stated previously, is to test by exposure to actual service conditions. However, in situations when this is not possible and it is necessary to obtain corrosion test data under simulated service conditions in the laboratory, guidance can be obtained from the following ASTM standards contained in the ASTM Annual Book of Standards Volume 03.02:

- G 4 Method for Conducting Corrosion Coupon Tests in Plant Equipment

- G 31 Practice for Laboratory Immersion Corrosion Testing of Metals
- G 1 Practice for Preparing, Cleaning, and Evaluating Corrosion Test Specimens
- G 46 Practice for Examination and Evaluation of Pitting Corrosion

Additional information on these standards can be obtained by referring to the index in this manual.

ASTM tantalum and niobium mill product specifications can be located in ASTM Annual Book of Standards, Section 2, Nonferrous Metal Products, and Volume 2.04 (ASTM Standards for Nb; B 898, B 391, B 391, B 394, B 393 and Ta Standards; B 898, B 364, B 365, B 521, B 708) and are also available through the ASTM website [www.astm.org](http://www.astm.org).

## REFERENCES

- [1] Hunkeler, F. J., *ASTM Manual on Corrosion Tests and Standards: Application and Interpretation, First Edition* Vol. 2, Chapt. 54.
- [2] Starck Inc., H. C., Moser, K., and Hinshaw, E., "Tantalum: Properties and Typical Uses," Reactive Metals Conference Proceedings, Sunriver OR, 1999.
- [3] *ASM Metals Handbook, Ninth Edition*, Vol. 13, ASM International, 1987, pp. 725–739.
- [4] Asahi Chemical Industry Co. Ltd., Seiichiro, T., and Nakahara, M., Nondestructive Evaluation of Hydrogen Absorption Embrittlement of Tantalum and Life Management in Chemical Plant, "Reactive Metals" Conference Proceedings, Sunriver OR, 1999.
- [5] Aimone, P. and Hinshaw, E. "Tantalum Materials in the CPI for the Next Millennium," NACE International Conference, Houston, TX, 2001.
- [6] Ribald, E., *Werkstoffe Korrosion*, Vol. 12, 1961, pp. 695–698.
- [7] NACE Standard MR-01-75.
- [8] NACE Standard Test Method 01-77.
- [9] Miles, Inc., New Martinsville, WV and Baytown, TX.
- [10] Sisco, F. T. and Epremian, E., *Cb and Ta*, John Wiley & Sons, Inc., New York, 1963, pp. 331–334.
- [11] Bayer Corp., Renner, M. "Niobium for Hot Concentrated Nitric Acid: Material Selection and Field Experiences with Nb Shell & Tube Heat Exchangers," Reactive Metals Conference Proceedings, Sunriver OR, 1999.
- [12] *Refractory Metals and Their Industrial Applications, ASTM STP 849*, R. E. Smallwood, Ed., ASTM International, West Conshohocken, PA, 1982.

# Metallic Coatings on Steel

*T. C. Simpson<sup>1</sup> and H. E. Townsend<sup>2</sup>*

## ENGINEERING PROPERTIES OF STEEL

EACH YEAR IN the United States, roughly 100 million tons ( $9.1 \times 10^{10}$  kg) of steel are consumed for a wide variety of applications. This enormous use results from a unique and favorable combination of characteristics that includes outstanding mechanical, physical, and magnetic properties, excellent manufacturability, low cost, availability, and ease of recycling. Because of its susceptibility to corrosion, steel is almost always used with a protective coating. The types of coatings and the kinds of corrosion test methods that are employed are as widely varied as the many end-uses [1–4].

## FUNCTIONS OF PROTECTIVE COATINGS

Protective metallic coatings are typically applied to metallic substrates for one of three reasons: to aid in corrosion resistance, to furnish high-temperature oxidation resistance, and/or to provide a base for painting. Although metallic coatings could also be applied for other user-specific reasons, such as appearance, to achieve the desired end-use product, the intent of this chapter is to focus on application of coatings to provide protection to the underlying substrate.

One very common reason for the application of metallic coatings to steel is to provide corrosion resistance. Metallic coatings can provide corrosion protection by one or more of several mechanisms including, barrier, sacrificial, or inhibitive protection. The details of these mechanisms of protection will be reviewed later in this chapter.

Metallic coatings can also be used to provide high-temperature oxidation resistance for specific applications. Aluminum and aluminum-zinc coatings are well suited for high-temperature applications (up to 675°C).

One additional attribute of metallic coatings, although not typically the only reason for their use, is their suitability to the application of paints. Metallic coatings, such as the iron-zinc coating galvalume, have a high degree of surface texture, which enhances paint adhesion compared to a relatively smooth steel surface.

This chapter will review the basic types of metallic coatings that are applied to steel substrates, the methods by which the coatings are applied, the mechanisms by which they protect the underlying substrate, and the common methods used to test metallic coatings on steel. In addition, a discussion of the important considerations in selecting/designing a corrosion test program for coatings on steel is included.

## COATING PROCESSES AND ALLOYS

The following two sections were designed to introduce the reader to the types of metallic coatings commonly applied to steel and the coating processes used to prepare them. The reader is also referred to a number of review articles that describe coating microstructure, preparation, and properties in further detail [2,26–30,57,58].

## COATING PROCESSES

### Hot Dip Coating

Hot dipping is the most widely used process to apply metallic coatings to steel. The hot dip process consists of immersion of clean steel into a molten bath of the material to be deposited. In the continuous hot dip process the material exits the bath and coating weight is controlled using a low pressure [typically, 50 psi (344.7 kPa) or less] gas wiping system prior to solidification. Hot dip coatings applied in the continuous process typically have coating thicknesses ranging from 6–20  $\mu\text{m}$ . Hot dip coatings can also be applied in a batch mode. Coating weight control for batch applications is controlled by letting the item drain, or bump, after application and/or by centrifugation. Hot dip coatings applied in a batch mode typically have coating thicknesses ranging from 50–130  $\mu\text{m}$ . Hot dip coatings are limited to use with metals having melting points  $\leq 732^\circ\text{C}$  (1350°F). The most common hot dip coatings are zinc, aluminum, and zinc-aluminum alloys [1,4,5,57].

### Electroplating

Another common method for coating application is electroplating. In electroplating, negatively charged steel sheet is immersed in a plating bath next to positively charged anodes.

<sup>1</sup>Research Supervisor, International Steel Group Inc., 116 Research Drive, Bethlehem, PA 18015.

<sup>2</sup>President, Townsend Corrosion Consultants, Inc., 3155 Balsam Road, Center Valley, PA 18034.

Metallic ions in an electrolyte bath are reduced and plated on the surface of the steel sheet forming the coating. Typical electroplated coating thicknesses range from 4–13  $\mu\text{m}$ . The bath composition, electrolyte velocity, current density, and temperature determine the chemistry and properties of the metallic/alloy coating. Typical electroplating baths are composed of aqueous salts of the ions to be deposited. Electroplating of highly electronegative metals such as aluminum, however, requires the use of molten salt or aprotic solvent plating baths, or both. Common coatings applied by electroplating are zinc, zinc-nickel, zinc-iron, tin, chromium, nickel, cadmium, and copper [6–8,58].

### Diffusion

Diffusion, also known as cementation, coatings are formed by heating the steel substrate in contact with the coating metal, usually in the form of powder at high temperature for sufficient time for interdiffusion to occur [9]. In Sheradizing, one of the oldest and most widely used cementation processes, zinc dust and steel parts are rotated in a drum at 370°C for several hours to form an iron-zinc alloy coating containing 8–10 % iron with thicknesses on the order of 50–100  $\mu\text{m}$ . Aluminum (calorized or Alonized) and chromium (chromized) coatings are also applied to steel as diffusion coatings for protection against high-temperature oxidation.

Diffusion coating is also done using a gaseous source of coating metal. For example, silicon diffusion coatings are applied by heating steel in the presence of hydrogen and silicon tetrachloride.

### Thermal Spray

In the most common type of thermal spray, also known as flame spray or metallizing, metal in the form of wire or powder is fed to an oxyacetylene flame [10]. Droplets of molten or semimolten metal are propelled toward the substrate by the flame where they splatter and form a coating. This method is most often used to coat large structures after they have been fabricated in the field. Zinc and aluminum are the most common coating metals applied by thermal spray and the coatings are usually applied in thicknesses on the order of 100  $\mu\text{m}$ . Because the coatings tend to be porous, they are generally used in conjunction with an organic topcoat.

Thermal spraying of small components is often done in an enclosed chamber with a reduced pressure or inert gas background. This technique facilitates safe containment of toxic or pyrophoric materials and minimizes oxidation.

Electric arc and plasma-arc thermal spraying are used when higher temperatures are required for improved bonding and coating density, or to liquefy higher melting point coating materials.

### Physical Vapor Deposition

In its simplest form, physical vapor deposition (PVD) is the evaporation of a coating metal source and condensation of the vapors on the substrate [11–13]. The process is carried out at low pressure, typically  $10^{-1}$  Pa, in order to avoid

oxidation of the metallic vapor. Virtually any coating metal can be applied by PVD and environmental concerns associated with liquid wastes can be avoided. Coatings up to about 10  $\mu\text{m}$  are deposited, and deposition rates are controlled by the rate of heat input used to vaporize the coating-metal source. Resistance and induction heating methods are often used, but the highest rates are obtained with electron beam heating.

Application of PVD coatings to coils of steel sheet in a continuous process was studied extensively in the United States during the 1970s, but the process was found to be more costly relative to other coating methods, such as electroplating and hot dipping. More recently, efforts are underway in Japan and Europe to further develop such a process.

Other types of PVD include ion-beam assisted deposition (IBAD), ion plating, and sputtering.

With the IBAD process, the coating surface is simultaneously bombarded with inert gas ions from an auxiliary source during coating deposition in order to improve adhesion and density of the PVD coating.

In ion plating, a negative bias, typically 3000–4000 V, is applied to the substrate, and the background pressure is increased with argon in order to create a glow discharge. Evaporated metal atoms are ionized and accelerated to the substrate with a resultant improvement in adhesion and density.

With sputtering, a target of coating metal is bombarded with argon ions in order to produce multiatomic fragments, which are then deposited on a substrate. Sputtering rates are generally less than that of ordinary PVD.

### Chemical Vapor Deposition

In chemical vapor deposition (CVD), a gas containing the coating metal is thermally decomposed on a heated substrate surface to form a deposit [14]. Typical coating thicknesses cover a very wide range (up to 100  $\mu\text{m}$ ) depending on the specific coating applied. Owing to the generally high temperatures required for thermal decomposition, CVD deposits usually have good adhesion and density. Gases used include halides, hydrides, carbonyls, and organometallics. Nickel, tungsten, and chromium are the most commonly applied CVD metal coatings. As an example, CVD tungsten coatings can be applied to steel by heating to 700–900°C in a mixture of tungsten hexachloride and hydrogen. Recent developments include the use of laser, microwave, or plasma energy in order to reduce the amount of substrate heating.

### Mechanical Coating

Mechanical coatings [15] are formed on steel surfaces by peening simultaneously with glass beads and metal powder, as described in ASTM B 695, Specification for Coatings of Zinc Mechanically Deposited on Iron and Steel, and ASTM B 696, Specification for Coatings of Cadmium Mechanically Deposited. A coating is built up by the cold-welding of successive layers of coating particles. The process is usually carried out by tumbling a barrel containing the substrate, coating metal powder, glass beads, and a proprietary

aqueous solution. It has been used primarily to coat fasteners and small hardware made of high-strength steel with zinc when it is desirable to avoid either the adverse effects of high temperatures in hot dipping on mechanical properties, or the possibility of hydrogen embrittlement in electroplating. Cadmium, tin, copper, lead, indium, and mixtures thereof have also been applied by mechanical coating. Coatings are typically in the range 5–25  $\mu\text{m}$  thick.

## COATING ALLOYS (COMPOSITIONS, APPLICATIONS, TYPICAL WEIGHTS, MICROSTRUCTURE)

### Zinc

Pure zinc coatings are usually applied to steel using the hot dip or electroplating methods. The hot dip process produces a predominately zinc coating containing an intermetallic layer at the zinc:steel interface. Hot dip zinc coatings are typically 6–20  $\mu\text{m}$  (40–140  $\text{g}/\text{m}^2$ ) thick. Electroplated zinc coatings consist of a single phase  $\alpha$  zinc coating. Electroplated zinc coatings applied at coating thicknesses of 4–13  $\mu\text{m}$  (20–90  $\text{g}/\text{m}^2$ ) are typically more uniform than hot dip zinc coatings. Hot dip coatings are typically less expensive than electroplated zinc coatings, particularly for heavier coatings and thinner steel sheet. Pure zinc coatings are used widely in the automotive and construction industries.

### Zinc Alloys (ZnAl, ZnNi, Zn-Fe)

Zinc alloy coatings are applied to steel by the hot dip or electroplating processes. Hot dip zinc-iron coatings are produced by heating zinc-coated strip just after it leaves the wiping dies. The extent of alloying is controlled by the time and temperature of the thermal process and by the addition of a small amount of aluminum to the zinc bath. Hot dip zinc-iron coatings, called galvaneal, typically contain 8–12 % iron and are 6–11  $\mu\text{m}$  (40–80  $\text{g}/\text{m}^2$ ). Hot dip zinc-iron coatings contain a microstructure consisting of several phases. A typical zinc-iron hot dip coating could have a zinc-rich zeta phase at the surface and progressively more iron-rich delta and gamma phases as one moves closer to the steel substrate. Electroplated zinc-iron coatings may contain 8–18 % iron and are applied at thicknesses up to 7  $\mu\text{m}$  per side. Similar to pure zinc coatings, zinc-iron hot dip coatings have the advantage of being less expensive and zinc-iron electroplated coatings have the advantage of being more uniform. Both coatings have the advantages of better weldability, and better paint adhesion (due to the microporous surface) than pure zinc coatings. Zinc-iron coatings are used primarily for automotive applications as body panels and other parts.

Zinc-nickel coatings contain 10–14 % nickel and are typically applied by electroplating at coating thicknesses ranging from 3–6  $\mu\text{m}$ . Zinc-nickel coatings are also commonly used by the automotive industry for exposed and unexposed panels because of their superior weldability (over pure zinc coatings) and good formability [16].

Zinc-aluminum coatings containing 5 % aluminum and small amounts of other elements are also commercially

available. One common 5 % aluminum coating also contains about 0.1 % mischmetal (cerium and lanthanum) to increase wettability of the bath and reduce the incidence of bare spots. Another contains 0.1 % magnesium to counteract the adverse effects of lead and tin impurities on intergranular corrosion and paint adhesion. These coatings can be used for enhanced corrosion properties over an equal thickness pure zinc coating in severe marine environments. In moderate marine, industrial, and rural environments, however, these coatings perform no better than pure zinc [17,18].

These 5 % aluminum coatings have no added lead and no spangle. As a result, they are free of spangle cracking and have better resistance to cracking during forming than ordinary spangled hot dip zinc coatings. The microstructure of a typical 5 % aluminum-zinc alloy coating is characterized by a matrix of 5 % aluminum eutectic and scattered regions of primary zinc. No intermetallic layer is visible on steel sheet coated with the eutectic alloy because the bath temperature is lower, and the aluminum content is higher, than with ordinary galvanized.

Enhancements of zinc alloy coatings are also commercially available. Zinc-nickel composite coatings are prepared by applying a chromium pretreatment followed by a thin (1–2  $\text{g}/\text{m}^2$ ) silicate containing organic topcoat to the zinc-nickel surface. The organic coating is typically applied to one side of the zinc-nickel, the side that will be the interior of the final panel. This provides additional protection to the areas where phosphating and priming may be inadequate after assembly. The other side of the steel sheet will typically contain zinc-nickel, but can be coated or uncoated. Perforation corrosion resistance is significantly enhanced in zinc-nickel composite coatings over conventional zinc-nickel coatings.

Plating of a thin iron-phosphorous (Fe-P) layer (2  $\text{g}/\text{m}^2$ ) or iron-zinc (3  $\text{g}/\text{m}^2$ ) layer on the surface of iron-zinc hot dip or electroplated coatings is also used for automotive applications. The thin electroplated layer is designed to improve formability and to reduce electrocoat cratering tendencies of the iron-zinc alloy coating.

### Aluminum and Aluminum Alloys

Aluminum coated steel sheet is produced in coil form by continuous hot dipping in a molten aluminum bath. The resultant coating consists of an iron-aluminum intermetallic layer and an aluminum overlay with a total thickness of 20–40  $\mu\text{m}$ . The product, referred to as Type 2 aluminum coated, is used mostly for light construction, e.g., metal buildings, silos, and highway culvert.

Another continuously coated steel sheet product, Type 1 aluminum-coated, is made by hot dipping in a molten bath of aluminum containing 5–11 % silicon [19]. Type 1 coatings are thinner, typically 10–20  $\mu\text{m}$ , and are more formable than Type 2 coatings. This product is widely used in high-temperature applications (up to 675°C), particularly for automobile tailpipes and mufflers.

Batch coating of steel hardware with aluminum to form aluminum-iron alloy coatings is also done by hot dipping or cementation. Pure aluminum coatings are applied on a batch basis by thermal spray, ion plating, and electroplating from nonaqueous solvents.

Aluminum-zinc alloy coatings are prepared by the hot dip process using a bath containing 55 % aluminum, 43.5 % zinc, and 1.5 % silicon. The coating consists of an aluminum/zinc matrix containing zinc-rich interdendritic areas. Coatings are typically 20–25  $\mu\text{m}$  (150 g/m<sup>2</sup>) thick. Aluminum-zinc coatings are most commonly used in the metal building industry. These coatings also provide high temperature resistance (up to 675°C) and are used by the automotive industry for heat shields, gas tank shields, mufflers, etc.<sup>3</sup>

### **Terne**

Terne is steel sheet that is hot dip coated with a lead-tin alloy [20]. Because lead does not readily wet steel, 2–25 % tin is added in order to ensure wetting and bonding of the coating to the substrate. Typical coating thicknesses are in the range of 5–15  $\mu\text{m}$ . The product has good weldability, solderability, and formability. Largest applications have been in the automobile industry, particularly for fuel tanks.

### **Tinplate**

Historically, tin was applied to individual cut lengths of steel sheet by fluxing and hot dipping [21]. Today, virtually all tin is electrolytically applied to steel sheet in continuous coil form for use in food containers. The tin serves as a base for protective organic coatings. Because of its favorably low frictional characteristic, tin also improves the formability of the steel substrate. Coating thicknesses are typically in the range of 0.4–1.6  $\mu\text{m}$ . As-deposited electrolytic tin coatings have a dull, matte appearance and normal practice is to brighten the deposit by melting it with in-line induction heating. This results in the formation of a thin iron-tin alloy layer at the coating-steel interface.

### **Chromium**

Chromium coatings [22–24] are batch-applied to steel components by diffusion, vacuum deposition, chemical vapor deposition, and most often by electrodeposition. Electroplated chromium coatings can be of two general types. Hard (also called industrial, functional, or engineering) coatings are applied in thicknesses of up to hundreds of  $\mu\text{m}$  in order to build up worn or improperly machined surfaces. Decorative chromium coatings, used for appearance purposes, are generally less than 2  $\mu\text{m}$  in thickness, and are applied as the outer layer of a multilayer system involving inner layers of electrodeposited nickel and copper. The chromium layer is often deliberately deposited in the crazed or microcracked condition in order to enhance corrosion resistance by minimizing adverse galvanic effects between the cathodic chromium and the anodic nickel. Automotive bumpers and trim are typical applications of decorative chromium coatings.

Although not truly metallic, a type of chromium coating is continuously applied to steel sheet in the production of “tin-free” steel (TFS). TFS was developed as an alternative to tinplate for the container industry. A mixture of chromium

oxide and metallic chromium is electrolytically applied in thickness on the order of 0.1  $\mu\text{m}$  or less. The TFS coating is an excellent base for coil-line applied organic coatings which, in turn, impart favorable forming and corrosion characteristics to the steel.

### **Cadmium**

Electrolytic cadmium coatings [25] have been widely used to protect fasteners, particularly for exposure in chloride environments. The lubricity of cadmium coatings aids in uniformly tightening threaded fasteners. However, use of cadmium is declining because of toxicity and environmental concerns.

## **CORROSION RESISTANCE**

### **Mechanisms**

Metallic coatings provide corrosion protection through one or more of the following mechanisms:

#### *Barrier*

In the barrier mechanism, the coating serves to isolate the underlying metal from the corrosive environment. The barrier mechanism is effective as long as the coating is continuous. Continuity is particularly important with noble coatings so that localized pitting due to galvanic attack is avoided. Barrier coatings should also corrode at a slower rate than the substrate.

#### *Galvanic*

In the galvanic mechanism, the coating is less noble than the underlying substrate, so that it corrodes preferentially and provides galvanic protection to any substrate that may be exposed at pores or cut edges.

#### *Inhibition*

In the inhibition mechanism, corrosion products from a sacrificial coating are deposited on the cathodic substrate where they act as a barrier to further corrosion.

In general, passive metals or noble metals provide only barrier protection to steel.

Studies of the corrosion mechanisms occurring in laboratory tests are often conducted in order to ensure that real-world conditions are being simulated, and to increase confidence in the test results [31]. Visual and microscopic examination is used to characterize the mode of attack, and a variety of analytical methods, including X-ray diffraction and fluorescence; and Raman, infrared, and Mossbauer spectroscopies are employed to identify corrosion products.

### **Specific Systems**

Tin coatings may be sacrificial or nonsacrificial, depending on the environment. In neutral, aerated solutions, tin acts cathodically to steel, resulting in pitting attack at coating pores. However, in deaerated, acid solutions, such as fruit juice within a closed container, tin behaves sacrificially and protects steel exposed at pores.

<sup>3</sup> In order to avoid embrittlement of the steel sheet during prolonged heating in the temperature range of 370–510°C, a phosphorus containing (>0.04 % P) steel substrate must be specified.

Aluminum coatings are passive in most environments where they provide only barrier protection. However, in chloride environments, aluminum may become active and provide sacrificial protection to steel.

Cadmium provides sacrificial protection to steel.

Zinc and zinc-alloy coatings can combine all three of the above protection mechanisms, a fact that forms the basis for their effectiveness and widespread use in protecting steel. As an example, consider electroplated zinc-alloy coatings containing approximately 13 % nickel. In order to explain why Zn-Ni alloy coatings perform remarkably well in salt-containing environments, such as the environment used for ASTM B 117, Test Method of Salt Spray (Fog) Testing, a detailed mechanistic study was conducted [32]. This work revealed how each of the three mechanisms comes into play during various stages during the lifetime of the coating (Fig. 1). As deposited, the Zn-12 % Ni alloy coating is composed of a uniform layer of gamma phase, a complex cubic structure  $\text{Ni}_5\text{Zn}_{21}$  intermetallic compound, which initially acts as a barrier. At this time, the coating corrodes at a potential that is anodic to steel, so that small areas of exposed substrate are galvanically protected. As the coating continues to corrode, zinc is preferentially dissolved, leaving behind a layer that becomes enriched in nickel and increasingly less sacrificial. At the same time, large tensile stresses are developed within the coating because of volume shrinkage associated with the loss of zinc. Eventually, cracks are formed as the shrinkage stresses exceed the tensile strength of the coating. Steel exposed at the base of the cracks at first is protected by the galvanic mechanism. Dissolved zinc cations are attracted to the cathodic sites where the steel is exposed and precipitate there because of the increased pH associated with the cathodic reactions. With further loss of zinc, the potential of the coating approaches that of the steel substrate, and sacrificial protection ceases. At that point, the coating consists of a cracked, nickel-rich layer with zinc corrosion products filling the cracks, and it acts only as an inert barrier. The superior performance of Zn-Ni alloy coatings compared to pure zinc coatings is attributed to the ability of the fine cracks to mechanically trap and retain zinc corrosion products.

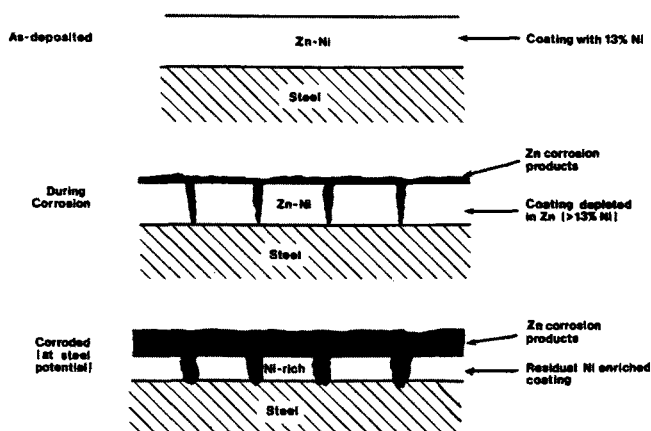


FIG. 1—Schematic of the corrosion mechanism of Zn-Ni alloy coatings [32].

## CORROSION TESTING

Testing of metallic coatings on steel will vary depending on the available resources and the desired degree of reliability. In the following list of test alternatives, the most reliable are at the top, but these are generally the most costly and time-consuming as well:

- Actual Field Service
- Simulated Field Service
- Static Atmospheric Testing
- Cabinet Testing
- Electrochemical Testing
- Service/Atmospheric Tests

Consider the cosmetic corrosion testing of coated steel sheet for autobody panels as an example [29]. The most reliable performance data are obtained by field surveys of vehicles in parking lots and junkyards after years of actual service. However, the time, effort, and sample-size requirements place practical limits on this approach.

The Society of Automotive Engineer's Automotive Corrosion and Prevention Committee (SAE/ACAP) has been publishing the results of parking lot surveys of five- to six-year-old vehicles randomly selected in parking lots [33,59,60]. Figure 2 shows survey results for cars manufactured from 1980 to 1993. The increases in automobile corrosion resistance that occurred during that time are believed to be the results of improvements in design, advances in pretreatment and paint technology, and increasing use of metallic-coated steel sheet.

Another approach to in-service testing is to monitor the behavior of the materials in a fleet of captive vehicles. This enables better control and recording of the exposure and driving conditions. The use of fleet vehicles also makes it possible to test coupons representing a wider range of materials. Coupons mounted on pickup trucks operated in Montreal, Quebec, and St. John's, Newfoundland for up to five years served as the real-world standard of performance in a laboratory test development by SAE/ACAP and The American Iron and Steel Institute's Corrosion Task Force. The materials being used in these tests are described in Table 1 and results after five years of testing at these sites are shown in Fig. 3 [64].

SAE Parking Lot Survey 5 to 6 Year Old Vehicles

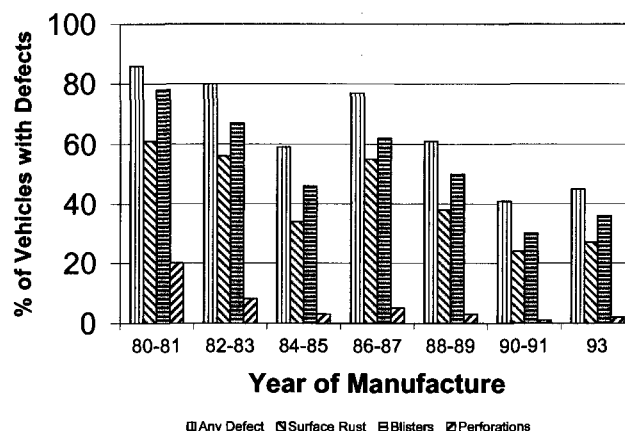
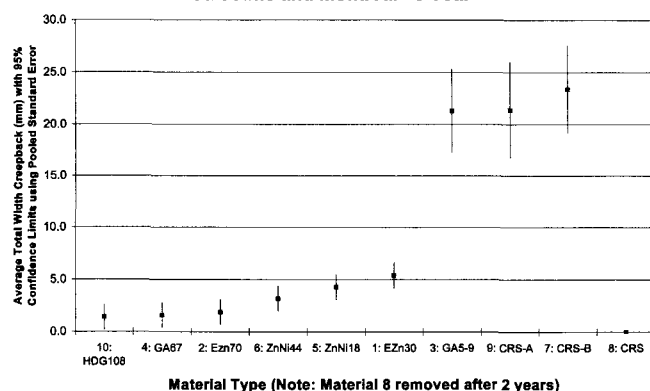


FIG. 2—Results of SAE's parking lot survey showing the increasing corrosion resistance of U.S. automobiles [59,60].

**TABLE 1**—Materials used in the AISI-SAE/ACAP cosmetic corrosion test study.

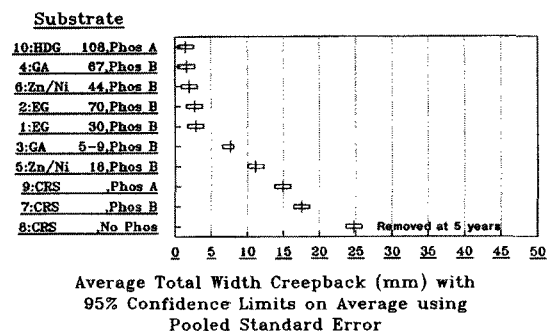
Identification No.	Material Description
1	Electroplated zinc (30 g/m <sup>2</sup> ), phosphate B
2	Electroplated zinc (70 g/m <sup>2</sup> ), phosphate B
3	Hot dip galvanized (5–9 g/m <sup>2</sup> ), phosphate B
4	Hot dip galvanized (67 g/m <sup>2</sup> ), phosphate B
5	Electroplated zinc/nickel (18 g/m <sup>2</sup> ), phosphate B
6	Electroplated zinc/nickel (44 g/m <sup>2</sup> ), phosphate B
7	Cold-rolled steel, phosphate B
8	Cold-rolled steel, no phosphate
9	Cold-rolled steel, phosphate A
10	Hot dip galvanized (108 g/m <sup>2</sup> ), phosphate A

**St. Johns and Montreal - 5 Year****FIG. 3**—Results of five-year on-vehicle tests of AISI materials at St. John's, Newfoundland and Montreal, Quebec, (see Table 1 for material identification codes) [67].

Automotive steel sheet coupons and components are usually tested in the painted condition. For evaluation of exterior cosmetic corrosion resistance, this includes application of phosphate, cathaphoretic primer, and one or more topcoats. Intentional damage to the paint system, usually in the form of a scribe that extends through the paint system and any metallic coating to the base steel, is an essential part of these tests. A number of practices for scribing are possible, using tungsten carbide engraving pencils, razors, and tungsten carbide lathe tools [34]. ASTM D 1654, Test Method for Evaluation of Painted or Coated Specimens Subjected to Corrosion Environments, and GM 9102P, Corrosion Creepback Test Method, describe a standardized scribing procedure. Other forms of intentional paint damage have been employed, including shot blasting, stone chipping, and diamond shot pecking. Results are generally reported in terms of the amount of underfilm delamination of the paint film (scribe creep), the degree of red rust at the scribe, and sometimes the extent of penetration of the steel substrate at the scribe.

### Simulated Service

Field service can be simulated at automotive proving grounds. Major automobile manufacturers operate proving ground test facilities that are intended to compress many years of service into a period of months. At these locations, production and prototype vehicles are repeatedly subjected to salt-water splash or spray, driven over rough roads, and

**GMPG Exposure - 10 Year Cosmetic****Total Width Creepback at Scribe (Ave. of 5 Measurements Per Panel)****FIG. 4**—Results of proving ground tests of AISI materials (see Table 1 for material identification codes) [35]. (Reprinted with permission, from SAE paper 912283, © 1991, Society of Automotive Engineers, Inc.).

parked in high humidity conditions. Small test coupons or individual components are also mounted on vehicles or trailers driven on the proving-ground circuit. Results of ten years of simulated road driving at an automotive proving ground are shown in Fig. 4 for the AISI/SAE test materials [35]. The data are plotted, similar to Fig. 3, as averages of total creepback from a scribe line with 95 % confidence limits shown. The main drawbacks to proving ground testing are that very few organizations have this type of resource, and there is a lack of uniform procedures practices. SAE J1950 is a guide to Proving Ground Vehicle Corrosion Testing.

Field service has also been simulated by mounting test coupons on a trailer that is towed over public roads and periodically sprayed with salt-water.

### Static Atmospheric Testing

Static atmospheric testing as described in ASTM G 50, Practice for Conducting Atmospheric Corrosion Tests on Metals, and ASTM G 1, Practice for Preparing, Cleaning, and Evaluating Corrosion Test Specimens, is used to test coated sheet steels intended for a variety of outdoor applications. In the case of automotive steel sheet, the practice has been modified to include a twice-weekly application of salt spray. Figure 5 shows the results of a 15-month exposure of the coated steel sheet products in the AISI/SAE test program [36]. The data are plotted as averages of total creepback from a scribe line and 95 % confidence intervals are shown in the figure.

In the case of metallic-coated steels intended for general outdoor applications such as metal buildings, normal testing practice is to expose multiple 100 by 150 mm coupons for determination of coating mass loss as a function of time. Several test locations should be employed in order to characterize performance in a range of representative environments, including marine, rural, and industrial atmospheres. Typical results for steel sheets coated with zinc, aluminum, and 55 % Al-Zn alloy are shown in Fig. 6, which gives the loss of coating thickness as calculated from mass loss during 13 years of testing at the marine site located 250 m from the ocean at the LaQue Corrosion Technology Center in Kure



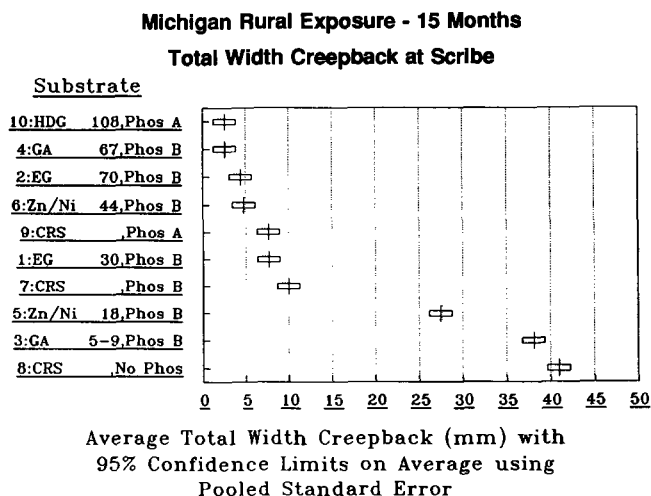


**FIG. 5—Results of modified atmospheric tests of AISI materials (see Table 1 for material identification codes) [36].**

Beach, NC [37]. The same data are plotted on a logarithmic scale in Fig. 6, where they fall on a straight line and can be easily fitted to an equation of the form

$$\log C = \log A + t \log B$$

where

$C$  is the corrosion loss,  $t$  is the exposure time, and  $A$  and  $B$  are constants.

This relationship facilitates extrapolation of the results in order to estimate coating life.

The above equation can also be written in exponential form,

$$C = A t^B$$

and differentiated with respect to time in order to conveniently calculate corrosion rate,  $dC/dt$ , as a function of time

$$dC/dt = A B t^{(B-1)}$$

as plotted in Fig. 6.

Another approach taken in atmospheric testing of metallic-coated steels is to monitor the appearance of test specimens during long-term exposure. Figure 7 shows how the life of zinc coatings on galvanized sheet increases with coating mass as determined by recording the percentage of rust on the surface of the test specimens in an industrial environment [38].

The visual approach is often used in the atmospheric testing of painted, metallic-coated sheet. Extent of paint blistering, paint undercutting, and appearance of corrosion products at edges, scribes, and formed areas are typically observed and recorded.

## Cabinet Tests

### Continuous Exposure Tests

Several tests are used to evaluate the performance of coated steel substrates that involve continuous exposure to

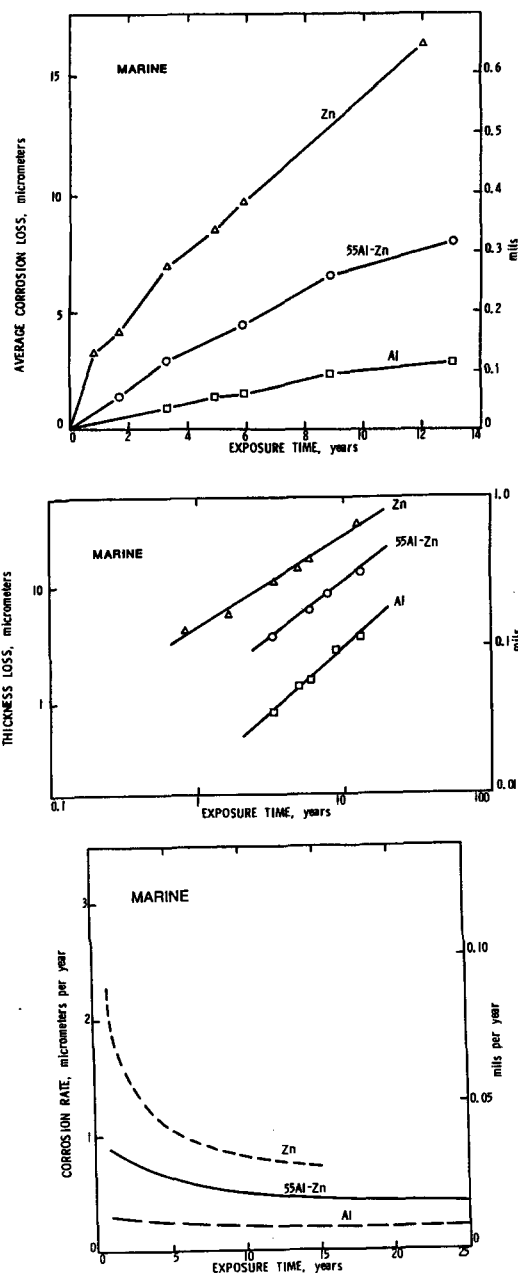


**FIG. 6—Quantitative test results for coated steel sheet in marine atmosphere (250-m lot at Kure Beach, NC) [39]; top: thickness loss versus time (linear scale); middle: thickness loss versus time (logarithmic scale); bottom: thickness loss rate versus time.**

one environment. ASTM B 117 (also GM 4298-P) involves continuous exposure to 5 % NaCl at elevated temperature (35°C). Some common continuous exposure tests include the Humidity Test, GM 4465P; the Cleveland condensation test (ASTM D 2247, Practice for Testing Water Resistance of Coatings in 100% Relative Humidity), the Kesternich/Moist SO<sub>2</sub> Test, (ASTM G 87, Practice for Conducting Moist SO<sub>2</sub> Tests), and the wet-storage stain test. The wet-storage stain test is commonly used for zinc and aluminum/zinc coated

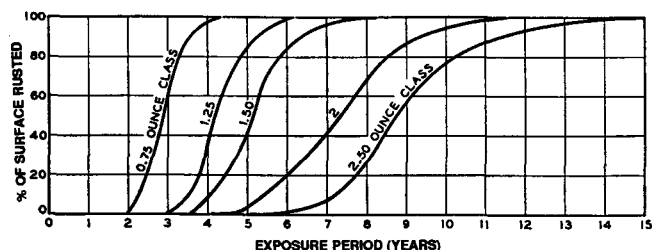


FIG. 7—Visual test results for zinc coatings of various masses in industrial atmosphere (Brunot Island, Pennsylvania) [9].

steel [39]. This test consists of stacking wet panels of the test material to simulate conditions that these materials may encounter during field storage. The test is often used to evaluate the quality of the passivation applied to the materials. Continuous exposure tests tend to be quite good at simulating a specific environment, but care must be taken in using them for the prediction of service life performance. For example, it has been clearly demonstrated that ASTM B 117 does not accurately predict the cosmetic corrosion performance of an automotive environment using the AISI/SAE materials [31].

### Cyclic Tests

Accelerated laboratory tests that have gained increasing support over the last several years typically combine several conditions into a cycle, and materials undergo repeated exposures to this cyclic environment. These tests are designed to take all potentially corrosive components of an exposure environment into consideration. The automotive industry has been using cyclic tests for a number of years as predictors of field performance and several other industries have recently begun investigating them as well. Some examples of cyclic tests are shown in Table 2. The first two tests shown in Table 2 are automotive tests that were developed by General Motors. The third test is a test used by investigators at the Sherwin Williams Company in recent years and combines aggressive exposure with accelerated weathering [40]. The Society of Automotive Engineers (SAE) has published an information report (SAE J1563) that provides guidelines including suggested control limits for test chambers, information about panel preparation, etc., to be used when running a cyclic test. In addition, the Automotive Applications Committee of the American Iron and Steel Institute (AISI) in cooperation with the Society of Automotive Engineers' Automotive Corrosion and Prevention (SAE/ACAP) Committee have developed a new cyclic cosmetic corrosion test. This test has is now designated as SAE J2334. Efforts are underway to develop a perforation corrosion test [62]. To date, the SAE J2334 also looks promising in predicting perforation corrosion behavior [65].

### Electrochemical Tests

Corrosion of metallic substances is an electrochemical process. An alternate approach to field or other accelerated tests in understanding and predicting metallic corrosion is the use of electrochemical parameters/tests. Electrochemical

TABLE 2

A. Test 1: GM 9511P-August 1989 SCAB Corrosion Creepback of Paint Systems on Metal Substrates	
Monday Only:	1 h 60C in air circulating oven 30 min cold cabinet (-25C) 15 min 5% NaCl immersion 21 h humidity cabinet (60C, 85% RH)
Tuesday Through Friday:	15 min 5% NaCl Immersion 1 h 15 min room temperature 22 h 30 min humidity cabinet (60C, 85% RH)
Saturday and Sunday:	humidity cabinet (60C, 85% RH)
Cycle is typically repeated to complete 20 cycles: One day of Monday through Friday exposure constitutes one cycle.	

B. Test 2: GM 9540P-May 1992 Accelerated Corrosion Test	
Monday Through Friday:	Salt mist applications in ambient environment (25C +/- 3C, 40-50% RH) every 1.5 hours (4 applications total for a total time of 4.5 hours)  Salt consists of: 0.9 % NaCl 0.1 % CaCl <sub>2</sub> 0.25 % NaHCO <sub>3</sub>  pH = 6-8  8 h humidity cabinet (49C, 95-100% RH) 8 h dry (60C +/- 2C, <30% RH) 8 h ambient (25C +/- 3C; 40-50% RH)
Saturday and Sunday:	ambient (25C +/- 3C; 40-50% RH)
Test is typically repeated for 40 cycles. One day of Monday through Friday exposure constitutes 1 cycle.	

C. Test 3: Combined Corrosion/Weathering Test	
Week 1	4 h UV light (UVA-340 bulbs), 60C 4 h H <sub>2</sub> O condensation, 50C
Week 2	1 h spray (0.35% (NH <sub>4</sub> ) <sub>2</sub> SO <sub>4</sub> + 0.05 wt% NaCl, ambient temperature) 1 h forced air dry, 35C
Test is repeated for 6 cycles. (One cycle consists of completion of week 1 and week 2 of exposure.)	

tests often complement other test methods by providing kinetic and mechanistic data that would be otherwise difficult to obtain. Electrochemical tests are typically grouped as DC or AC methods based on the type of perturbation signal that is applied in making the measurements. A number of investigators have used DC and AC electrochemical methods for the examination of metallic corrosion over the last several decades. This chapter will highlight a few sample applications of electrochemical methods to monitoring/examining metallic corrosion of coated sheet materials. These applications are provided for illustrative purposes only and the reader should not feel restricted to these applications. It is suggested that the reader consult the following review books/symposia proceedings and references contained within to see a much broader sampling of the ways electrochemical methods have been applied to study metallic corrosion, particularly corrosion of coated sheet products with or without organic coatings [41-46].

The simplest DC electrochemical method is the measurement of the electrochemical potential. Electrochemical potential measurements can be used to estimate the relative activity of a material in a particular environment and/or to compare materials in a particular environment. Tracking electrochemical potential as a function of time in a particular environment can provide information on how the corrosion process is proceeding. Investigators have used electrochemical potential/mixed potential measurements for numerous studies throughout the last several years. Efforts at Bethlehem Steel's Research Laboratories have used electrochemical potential monitoring to track the dissolution of active phases from zinc/aluminum alloy coatings on steel. Figure 8 is a representative plot of the potential change as a function of time in an aggressive environment for one of these alloy coatings. Regions of this curve have been labeled to indicate the dissolution expected to be taking place within each region. This monitoring method has been used to track the extent of dissolution of active phases from these coatings as a method of pre-exposure of these samples prior to field exposure. This method allows a significant decrease in the time involved in a field exposure to enable evaluation of effects of process/composition changes on performance of the material [47].

Other DC methods that are quite simple to use and provide important information to the corrosion scientist include polarization resistance (ASTM G 59, Practice for Conducting Potentiodynamic Polarization Resistance Measurements), potentiostatic and potentiodynamic polarization measurements (ASTM G 5, Standard Reference Test Method for Making Potentiostatic and Potentiodynamic Anodic Polarization Measurements), cyclic polarization measurements (ASTM G 61, Test Method for Conducting Cyclic Potentiodynamic Polarization Measurements for Localized Corrosion Susceptibility of Iron-, Nickel-, or Cobalt-based Alloys), and galvanic current monitoring. These DC techniques can be used to estimate the reactivity of a material in a particular environment, to determine the corrosion rate of a material in a particular environment, and/or to determine the susceptibility of a material to localized corrosion.

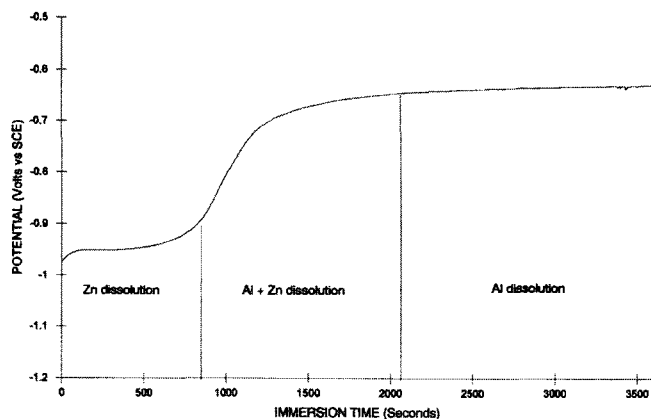


FIG. 8—Typical electrochemically monitored etching curve for zinc/aluminum alloy coatings on steel. Potential regions are labeled to indicate the dissolution occurring within each region [47].

Potentiodynamic polarization measurements are quite appropriate for determination of the pitting susceptibility of aluminum coatings, and/or the corrosion current density/corrosion rate of coated steel products in general. ASTM G 102, Practice for Calculation of Corrosion Rates and Related Information from Electrochemical Measurements, describes the calculation of corrosion rates and other information from electrochemical measurements. Another example of the use of DC electrochemical methods to examine the corrosion performance of coated sheet materials is a study by D. A. Jones et al. [48]. The study used polarization resistance measurements to examine the mechanism of steel and coated sheet degradation under conditions of alternate immersion. Jones compared the polarization resistance of samples of low-carbon steel, unpainted galvanized, aluminum-coated, and Zn-Ni alloy coated steel during continuous immersion and alternate immersion. Alternate immersion cyclic exposure produced a thick oxide that led to significant underfilm attack. Jones found that phosphate pretreatment tends to increase the resistance of these materials to underfilm attack. This study is an excellent example of the way electrochemical measurements can be used as a complement to other techniques to elucidate mechanistic information.

Additional electrochemical methods that involve some component of an AC signal include electrochemical impedance spectroscopy (ASTM G 106, Practice for Verification of Algorithm and Equipment for Electrochemical Impedance Measurements), galvanostatic staircase polarization (ASTM G 100, Method for Conducting Cyclic Galvanostaircase Polarization), and electrochemical noise monitoring. Efforts at the Research Laboratories of Bethlehem Steel have used electrochemical impedance spectroscopy (EIS) to evaluate phosphate coverage/stability on galvaneal [49]. Phosphate coatings are applied to coated steel products to enhance paint adhesion and alkaline stability of the painted system. A good correlation was observed between the near DC impedance value and the phosphate coating weight (determined gravimetrically) after exposure in a highly alkaline environment. A trend was also observed between the phosphate coating weight and near DC impedance value prior to any aggressive exposure. The value of using EIS in these types of studies is that EIS measurements can be nondestructive and gravimetric coating weight measurements are always destructive.

Another application of EIS to evaluation of metallic coatings on steel was reported by Ruiz and Davidson [50]. Samples of painted cold-rolled steel, electrogalvanized steel, and electrogalvanealed steel were evaluated by EIS, in a laboratory cyclic corrosion test (Chrysler Chipping Test) and in a cyclic corrosion test that is conducted outdoors (Volvo test). Prior to conducting EIS measurements, a gravelometer was used to intentionally damage the paint coatings. The laboratory cyclic corrosion test employed similar paint damage prior to test. EIS measurements were sensitive to the pretreatment type and substrate type. EIS data correlated well with the accelerated corrosion test conducted outdoors (Volvo test).

A relatively new application area for electrochemical techniques to corrosion studies that has gained considerable interest over the last several years is the use of electrochemical current and potential noise measurements. Skerry was one

of the early investigators to apply this technique to steel substrates [51,52]. Skerry found good relationships between the electrochemical noise parameters and performance data for a series of organic coatings on steel. Although these studies were not completed on coated steel substrates, the methods might be directly applicable to coated steel substrates.

## **SUMMARY: SELECTING CORROSION TESTS FOR COATED SHEET MATERIALS**

There are a number of factors to consider when selecting corrosion tests for coated sheet materials. The investigator must have a clear understanding of the materials to be tested, the exposure environments these materials are likely to encounter, and the levels/durations of these exposures. The most appropriate corrosion test(s) for a particular study can sometimes change based on the goal of the study. If the goal is to rank the corrosion performance of materials, or to select the best material for exposure in a specific environment, or both, field exposure data for those materials in that environment are the ideal. When time constraints prevent this type of data from being practical, accelerated test methods are often a reasonable alternative. Proving ground tests, laboratory cabinet tests, and/or other accelerated tests may be appropriate in these cases. One key in choosing an accelerated test to model performance is a good understanding of the exposure environment being simulated. Many investigators have been misled by accelerated tests because test conditions did not match the conditions of the exposure environment that the test was supposed to simulate. For example, it does not make sense to use a salt-spray test, for example, to simulate performance of materials in most natural environments, which involve alternating cycles of wetting and drying. By the same token, it may not make sense to use the Kesternich test to simulate performance of many of these materials either, since the conditions of this test may be too severe for an accurate simulation.

If the goal is a mechanistic/kinetic investigation of the corrosion process, again examination of samples after field exposure in the environment of interest may be the ideal. When this is not possible or practical, accelerated test methods should be used. If possible, these accelerated methods should have been previously verified to result in the same extent and mechanism of degradation as actual field exposure. Electrochemical methods can often provide important mechanistic/kinetic information about a corrosion process. Surface analytical, metallographic, or spectroscopic methods, or a combination thereof, can also be important components of any mechanistic study of metallic corrosion.

A second key to choosing an accelerated test is a good understanding of the material/materials being tested. In the subsection titled Specific Systems, a discussion of the way in which several coated sheet products provide corrosion protection was presented. Selection of a cyclic test that will yield good predictive information must take these factors into account. If the material of interest is known to provide barrier protection due to the formation of a passive film on the coating surface in the exposure environment of concern,

then it does not make sense to expose it in an accelerated test environment that results in rapid anodic dissolution of the coating. A viable approach to selection of a predictive accelerated test is to use the test or series of tests on materials of known field performance that are as similar as possible to the materials that require evaluation. If the accelerated test results in similar types (mechanisms) and extents of corrosion damage on known materials, then it is likely to be predictive on the test materials. The reader is referred to Refs 53 and 54 for additional information on test methods for coated sheet products.

Throughout the field of corrosion research, efforts have been ongoing to find better corrosion tests. For several years investigators have been aware of the current limitations in both continuous exposure and cyclic tests. Most laboratories have coped with these limitations by developing their own cyclic test, testing it on their own materials to determine performance correlations, and then using this test for further studies. Although this may work well in some instances, it leads to each laboratory having their own "preferred" test method and restricts interlaboratory- and/or industry-wide understanding of data, acceptance of results, etc. It also often leads to one laboratory having to test its material using many different cyclic tests to satisfy its customers. Not only does this result in added cost and time, but can often yield results that are not meaningful if the customer-preferred test is not appropriate for the material under study.

An approach to combating these problems is to unify the test methods used by different laboratories by finding/creating tests that are predictive of field performance and that are acceptable to a wide variety of users. Two industries, automotive and metal building, have taken the approach of trying to unify cyclic test methods for coated sheet products. In each case, committees have been formed with the charge of determining the most predictive cyclic tests for coated sheet products on steel. The formation of such committees is an important milestone in the testing of coated sheet products and for the field of corrosion research as well. These committees contain representatives from metal/coated sheet producers, paint and pretreatment companies, automotive companies, and other end-users. The impact of having such diverse representation of these committees is that committee consensus has the likelihood of changing the way testing is conducted throughout the entire industry rather than only at one company or in one supply group. Such groups have the added advantage of combining the expertise of personnel throughout each industry rather than being limited to one area of expertise. This should be a significant advantage in both designing the programs and in interpreting the results.

An excellent example of such a program was the one conducted by the automotive industry sponsored by the AISI's Corrosion Task Force in cooperation with SAE/ACAP that was described earlier in this chapter. In this study, ten materials (see Table 1) were placed on vehicles operated in the corrosive environments of Montreal, Quebec and St. John's, Newfoundland to determine a performance ranking for cosmetic (outside-in) corrosion resistance. These same materials were also exposed in a series of accelerated laboratory tests, at proving grounds, and at other exposure sites.

Correlation of the test methods to actual field performance is forming the basis of selection of the most predictive accelerated tests. This work led to the development of SAE J2334, a new standard accelerated laboratory cyclic corrosion test that accurately predicts the cosmetic corrosion performance of automotive coated steel sheet. The results of this study are described in a series of publications [31,35,36,55].

A similar program also conducted by the automotive industry is also a collaborative effort between AISI's Corrosion Task Force and SAE/ACAP led to the determination of appropriate test methods for predicting perforation (inside-out) corrosion on automotive coated sheet products. Development/determination of appropriate test methods for predicting perforation corrosion on coated sheet products [56,62,65].

A similar program began in the metal building industry through ASTM Subcommittee D01.27.31 on Corrosion Testing (Nonautomotive) and AISI CC-89 Task Force on Accelerated Test Methods for Coil Coated Steel for Construction. Materials were placed in field exposure at four sites for the AISI program during the summer of 1991. Details on the design of this program and the preliminary results were recently published [63]. Laboratory testing of these materials and evaluations are in progress. It is expected that once the work of these committees has been completed, significant improvements will occur in the cyclic tests that these industries use. Due to efforts like these, the next several years should yield important advances in the way that we test the corrosion behavior of coated steel products.

This chapter has attempted to give the reader some basic information about the types of coated steel products that are in common use, the methods by which they are prepared, the mechanisms by which they undergo corrosion, and the types of test methods that can be used to evaluate these corrosion processes. It is important for the investigator to use information obtained about the exposure environment, and the performance/corrosion properties or problems of the material in question to select an appropriate corrosion test. It is also important for the investigator to have a clear understanding of the goal of the test program. Only through careful evaluation of all of the information at the disposal of the investigator can the best test for a particular situation be selected.

## REFERENCES

- [1] Townsend, H. E., Allegra, L., Dutton, R. J., and Kriner, S. A., *Materials Performance*, August 1986, pp. 36-46.
- [2] Townsend, H. E., *Materials Performance*, October 1991, pp. 60-65.
- [3] *Steel Processing Flowlines*, American Iron and Steel Institute, Washington, DC, 1980.
- [4] *Metals Handbook*, Volume 5, Surface Cleaning, Finishing, and Coating, 9th ed., ASM International, Metals Park, OH, 1982, pp. 323-332.
- [5] Stavros, A. J. and Gambrell, J. W., *Metals Handbook*, Volume 13, Corrosion, 9th ed., ASM International, Metals Park, OH, 1987, pp. 432-445.
- [6] Bush, G. W., "Developments in the Continuous Galvanizing of Steel," *Journal of Metals*, August 1989, p. 34.
- [7] Austin, L. W. and Lindsay, J. H., *Continuous Steel Strip Electroplating*, American Electroplaters and Surface Finishers Society Press, Orlando, FL, 1989.
- [8] Mazia, J. and Lashmore, D., *Metals Handbook*, Volume 13, Corrosion, 9th ed., ASM International, Metals Park, OH, 1987, pp. 419-431.
- [9] Burns, R. M. and Bradley, W. W., *Protective Coatings for Metals*, 2nd ed., Reinhold Publishing Corp., NY, 1955, pp. 46-50.
- [10] Clare, J. H. and Crawmer, D. E., *Metals Handbook*, Volume 5, Surface Cleaning, Finishing, and Coating, 9th ed., ASM International, Metals Park, OH, 1982, pp. 361-374.
- [11] Rigney, D. V., *Metals Handbook*, Volume 5, Surface Cleaning, Finishing, and Coating, 9th ed., ASM International, Metals Park, OH, 1982, pp. 387-411.
- [12] Morita, A., Chohata, K., and Hirose, Y., *Proceedings: Second International Conference on Zinc Coated Steel Sheet*, Zinc Development Association, London, 1989, pp. SD1/1-5.
- [13] Lammermann, H. and Frommann, K., *Stahl u. Eisen*, Vol. 111, No. 11, 1991, pp. 76-84.
- [14] Blocher, J. M. Jr., *Metals Handbook*, Volume 5, Surface Cleaning, Finishing, and Coating, 9th ed., ASM International, Metals Park, OH, 1982, pp. 381-386.
- [15] O'Cone, A., "Mechanical Coating," *Metals Handbook*, Volume 5, Surface Cleaning, Finishing, and Coating, 9th ed., ASM International, Metals Park, OH, 1982, pp. 300-302.
- [16] Townsend, H. E., Paper 416, CORROSION'91, National Association of Corrosion Engineers, Houston, TX, 1991.
- [17] Friel, J. J. and Townsend, H. E., "Corrosion Resistance of Zinc and Zinc Aluminum Alloy Coatings," *Sheet Metal Industries*, Vol. 60, No. 9, 1983, pp. 506-507.
- [18] Townsend, H. E., *Materials Performance*, Vol. 32, No. 4, 1993, pp. 68-71.
- [19] Denner, S. G., Jones, R. D., and Thomas, R. J., *Iron and Steel International*, June 1975, pp. 241-252.
- [20] Gittings, D. O., *Metals Handbook*, Volume 5, Surface Cleaning, Finishing, and Coating, 9th ed., ASM International, Metals Park, OH, 1982, pp. 358-360.
- [21] Burns, R. M. and Bradley, W. W., *Protective Coatings for Metals*, 2nd ed., Reinhold Publishing Corp., NY, 1955, pp. 156-189.
- [22] Gannon, H. E., *The Making, Treating, and Shaping of Steel*, Herbeck and Held, Pittsburgh, PA, 1971, pp. 996-1021.
- [23] Chessin, H. and Fernald, E. H. Jr., *Metals Handbook*, Volume 5, Surface Cleaning, Finishing, and Coating, 9th ed., ASM International, Metals Park, OH, 1982, pp. 170-187.
- [24] Gianelos, L., *Metals Handbook*, Volume 5, Surface Cleaning, Finishing, and Coating, 9th ed., ASM International, Metals Park, OH, 1982, pp. 188-198.
- [25] Marce, R. E., *Metals Handbook*, Volume 5, Surface Cleaning, Finishing, and Coating, 9th ed., ASM International, Metals Park, OH, 1982, pp. 256-269.
- [26] Miyoshi, Y., "State of the Art in Precoated Steel Sheet for Automotive Body Materials in Japan," *ISIJ International*, Vol. 31, No. 1, 1991, p. 1.
- [27] Quantin, D., Deparis, D., and Charbonnier, J. C., "Coated Steel Sheets for the Automotive Industry," *Steel Technology International*, 1990/1991, p. 245.
- [28] Yamoto, K., Ichida, T., and Irie, T., "Progress in Precoated Steel Sheets for Automotive Use," *Kawasaki Steel Technical Report*, #22, May 1990, p. 57.
- [29] *Cracking Down on Corrosion*, American Iron and Steel Institute, Washington, DC, 1991.
- [30] Porter, F., *Zinc Handbook*, Marcel Dekker, Inc., New York, 1981.
- [31] Townsend, H. E., Granata, R. D., McCune, D. C., et al., *Proceedings of the 5th Automotive Corrosion and Prevention Conference*,

- P-250, Society of Automotive Engineers, Warrendale, PA, 1991, pp. 73–97.
- [32] Lambert, M. R., Hart, R. G., and Townsend, H. E., "Corrosion Mechanisms of Zn-Ni Alloy Coatings," *Proceedings of the Second Automotive Corrosion and Prevention Conference*, P-136, Society of Automotive Engineers, Warrendale, PA, 1983, pp. 81–87.
- [33] Bryant, A. W., Thompson, L. M., Oldenberg, W. C., et al., *Automotive Corrosion and Prevention Conference Proceedings*, P-228, Society of Automotive Engineers, Warrendale, PA, 1989, pp. 185–198.
- [34] Riffe, W. J., *Proceedings of the 5th Automotive Corrosion and Prevention Conference*, P-188, Society of Automotive Engineers, Warrendale, PA, 1986, pp. 209–212.
- [35] Petschel, M., *Proceedings of the 5th Automotive Corrosion and Prevention Conference*, P-250, Society of Automotive Engineers, Warrendale, PA, 1991, pp. 179–203.
- [36] Lutze, F. and Shaffer, R. J., *Proceedings of the 5th Automotive Corrosion and Prevention Conference*, P-250, Society of Automotive Engineers, Warrendale, PA, 1991, pp. 115–127.
- [37] Townsend H. E. and Zoccola, J. C., *Materials Performance*, Vol. 18, No. 10, 1979, pp. 13–20.
- [38] Reinhard, C. E., *ASTM Proceedings*, Vol. 44, 1944, p. 92.
- [39] Townsend H. E. and Zoccola, J. C., *Journal of the Electrochemical Society*, Vol. 125, No. 8, 1978, pp. 1290–1292.
- [40] Skerry, B. S. and Simpson, C. H., Paper #412, CORROSION'91, National Association of Corrosion Engineers, Houston, TX, 1991.
- [41] *Electrochemical Techniques for Corrosion Engineering*, R. Baboian, Ed., National Association of Corrosion Engineers, Houston, TX, 1986.
- [42] *Corrosion Testing and Evaluation: Silver Anniversary Volume*, ASTM STP 1000, R. Baboian and S. Dean, Eds., ASTM International, West Conshohocken, PA, 1990.
- [43] *Electrochemical Techniques for Corrosion*, R. Baboian, Ed., National Association of Corrosion Engineers, Houston, TX, 1977.
- [44] *Laboratory Corrosion Tests and Standards*, ASTM STP 866, G. Haynes and R. Baboian, Eds., ASTM International, West Conshohocken, PA, 1985.
- [45] *Corrosion Protection by Organic Coatings*, *Proceedings of the Electrochemical Society*, M. W. Kendig and H. Leidheiser, Jr., Eds., Vol. 87-2, The Electrochemical Society, Pennington, NJ, 1987.
- [46] *Electrochemical Impedance: Analysis and Interpretation*, ASTM STP 1188, J. Scully, D. Silverman, and M. Kendig, Eds., ASTM International, West Conshohocken, PA, 1992.
- [47] Simpson, T. C., "An Accelerated Corrosion Test Method for Galvalume and other Aluminum/Zinc Alloy Coatings," *Corrosion*, Vol. 49, No. 7, 1993, pp. 550–560.
- [48] Jones, D. A., Blitz, R. K., and Hodjati, I., *Corrosion*, Vol. 42, No. 5, 1986, pp. 255–262.
- [49] Simpson, T. C., Hoffman, J. D., and Unangst, W. C., Paper #912300, *Proceedings of the 5th Automotive Corrosion and Prevention Conference*, Society of Automotive Engineers, Warrendale, PA, 1991.
- [50] Ruiz, K. and Davidson, D., Paper #912299, *Proceedings of the 5th Automotive Corrosion and Prevention Conference*, Society of Automotive Engineers, Warrendale, PA, 1991.
- [51] Skerry, B. S. and Eden, D. A., *Progress in Organic Coatings*, Vol. 19, 1991, pp. 379–396.
- [52] Chen, C. T. and Skerry, B. S., Paper #413, CORROSION'91, National Association of Corrosion Engineers, Houston, TX, 1991.
- [53] LaQue, F. L., *46th Annual Technical Proceedings of the American Electroplaters Society*, 1959, pp. 443–445.
- [54] Lambert, M. R., Townsend, H. E., Hart, R. G., and Frydrych, D. J., *Industrial and Engineering Chemistry Product R & D*, Vol. 24, September 1985, pp. 378–384.
- [55] Roudabush, L. A., Townsend, H. E., and McCure, D. C., "Update on the Development of an Improved Cosmetic Corrosion Test by the Automotive and Steel Industries," *Automotive Corrosion and Prevention Conference Proceedings*, P-268, pp. 53–63.
- [56] Roudabush, L. A. and Dorsett, T. E., Paper #912285, *Proceedings of the 5th Automotive Corrosion and Prevention Conference*, P-250, Society of Automotive Engineers, Warrendale, PA, 1991, pp. 221–237.
- [57] Townsend, H. E., "Continuous Hot-Dip Coatings," *ASM Handbook*, Vol. 5, *Surface Engineering*, ASM International, Metals Park, OH, 1994, pp. 339–348.
- [58] Fountoulakis, S. G., "Continuous Electrodeposited Coatings for Steel Strip," *ASM Handbook*, Vol. 5, *Surface Engineering*, ASM International, Metals Park, OH, 1994, pp. 349–359.
- [59] Simpson, T. C., Bryant, A. W., Hook, G., et al., "U.S. Automotive Trends Over the Past Decade," SAE Congress '95, Paper 950375, SAE, Warrendale, PA, 1995.
- [60] Tiburcio, A. C. and Yergin, M. J., "U.S. Automotive Corrosion Trends: 1998 SAE (ACAP) Automotive Body Corrosion Survey Results," SAE International Corrosion Congress, Detroit, March 2001.
- [61] Ostermiller, M. R. and Townsend, H. E., "On-Vehicle Cosmetic Corrosion Evaluations of Coated and Cold Rolled Steel Sheet," Paper # 932335, *Proceedings of the 6th Automotive Corrosion and Prevention Conference*, P-268, 1993.
- [62] Townsend, H. E., Davidson, D. D., and Ostermiller, M. R., "Development of Laboratory Corrosion Tests by the Automotive and Steel Industries of North America," *Proceedings of the 4th International Conference on Zinc and Zinc Alloy Coated Steel Sheet (GALVATECH'98)*, Chiba, Japan, 1998.
- [63] Rommal, H. E. G., Lawson, K. M., Tiburcio, A. C., and Lawson, H. H., "Accelerated Test Development for Coil-Coated Steel Building Panels," Paper #356, CORROSION 98, NACE International, 1998.
- [64] Townsend, H. E., "Development of an Improved Laboratory Corrosion Test by the Automotive and Steel Industries," *Advanced Coatings Technology*, *Proceedings of the 4th Annual ESD Advanced Coatings Conference*, Dearborn, MI, November 1994, ESD, Ann Arbor, MI.
- [65] Davidson, D., Thompson, L., Lutze, F., Tiburcio, B., Smith, K., Meade, C., et al., "Perforation Corrosion Performance of Auto-body Steel Sheet in On-Vehicle and Accelerated Tests," *Advances in Coatings and Corrosion Prevention*, SP-1770, Society of Automotive Engineers, Warrendale, PA, 2003.

# Nonmetallic Coatings

*Richard D. Granata*<sup>1</sup>

## SCOPE

A LARGE NUMBER OF tests exist for establishing the reliability of nonmetallic protective coatings on metal substrates. Definitions, fundamentals, methodology, and practical examples are offered for a better understanding of tests for protective coatings and to demonstrate that well defined tests alone are not adequate without rational application and interpretation.

## Focus of Testing

Materials tests and standards of nonmetallic organic and inorganic coatings systems on corrodible substrates are described. Coatings systems may provide many properties in addition to corrosion resistance, e.g., appearance, insulation, and tack. Although test methods exist for a wide variety of coatings characteristics, the primary nonmetallic coatings tests addressed herein evaluate corrosion resistance, adhesion, and physical/chemical durability.

## Nonmetallic Coatings Materials

Two broad groups of nonmetallic coatings materials are considered:

1. Organic, including formulations containing dispersed inorganic or metallic materials. Examples: clear coatings, typical paints, metal flake coatings, organic-based galvanic (zinc-rich) coatings.
2. Inorganic, which may be modified by organic and metallic materials. Examples: phosphates, anodic coatings, oxides, carbides, nitrides, borides, silicides, inorganic-based galvanic (zinc-rich) coatings. Most of these inorganic coatings are applied. Some, such as anodic coatings, are formed by reaction on the surface.

Additional types of coatings exist, which are hybrids of these groups, and may be appropriately classified as metallic coatings or composite materials.

## Coatings and Coatings Systems

The term "coatings" implies that there is a supporting structure or substrate—an obvious point sometimes overlooked. The failure of otherwise acceptable coatings may be

due to the substrate. The machined, molded, or polished substrate may contain defects or trapped impurities that affect performance of the coatings system. A coatings test may assess the substrate properties. Likewise, the cleaning, surface preparation, and pretreatment methods influence the coatings system performance. Use of the term coatings system is intended to emphasize these interdependent properties. Most tests evaluate whole coatings systems, with emphasis on a particular component or processing step. (Conversely, the term film is appropriate when a coatings material can be evaluated independent of the substrate.)

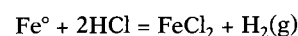
## FUNDAMENTALS

### Tests/Standards, Application/Selection and Specifications

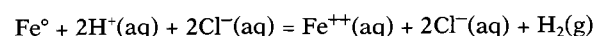
Tests and standards are intended to provide a means for determining the appropriateness of materials for the users' purposes. Example: The user requires excellent performance at low cost. The requirement must be translated to a set of tests and standards, collectively known as specifications, agreeable to supplier and user, often on a contractual basis. Achieving an agreement accrues benefits to both supplier and user; an efficient and effective agreement yields a competitive result. The major specification or objective in the context of corrosion testing is service life. Tests and standards must be selected and applied to satisfy user specifications (service and lifetime requirements). A difficulty is the often unsatisfactory relationship between long-term field service results to laboratory tests and standards results. Application and interpretation of tests for nonmetallic corrosion protective coatings is a dynamic, evolving process of satisfying specifications, including both short-term tests and long-term service performance. It is important to understand the limitations of tests and standards results.

### Electrochemical Mechanism of Corrosion

A typical corrosion process, the reaction of iron with hydrochloric acid (HCl) under anaerobic conditions, is represented by the equation

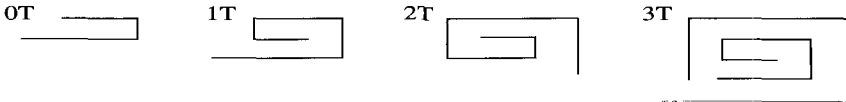


A more accurate representation is



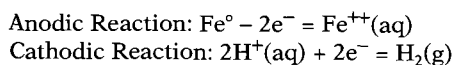
<sup>1</sup>Florida Atlantic University, Boca Raton, FL.

TABLE 1—Brief descriptions of selected tests.

Test	Description and Remarks
Salt Spray (ASTM B 117)	Most widely specified test. Atomized 5 % sodium chloride, neutral pH, 35°C*, follow details of ASTM B 117, Appendix X1. Emphasizes wet surfaces (nondrying), high oxygen availability, neutral pH, and warm conditions. Control or comparative specimens should be run simultaneously. Corrosivity consistency should be checked as described in ASTM B 117, Appendix X3. Notes: May be the most widely misused test. Requires correlation to service tests for useful results. Do not assume correlation exists.
100 % Relative Humidity (ASTM D 2247)	Widely used test. Condensing humidity, 100 % RH, 38°C. Emphasizes sensitivity to water exposure.
Acetic Acid-Salt Spray ASTM G 85, A 1 (formerly ASTM B 287)	Widely used test. Atomized 5 % sodium chloride, pH 3.2 using acetic acid, 35°C. More severe than ASTM B 117. The lower pH and the presence of acetate affect the solubility of corrosion products on and under the protective coatings.
Sulfur Dioxide-Salt Spray (ASTM G 85, A 4)	Atomized 5 % sodium chloride, collected solution pH = 2.5–3.2, 35°C, SO <sub>2</sub> metered (60 min × 35 cm <sup>3</sup> /min per m <sup>3</sup> cabinet volume) 4 times per day.
CASS(copper accelerated salt spray), (ASTM B 368)	Atomized 5 % sodium chloride, pH 3.2 with acetic acid, 0.025 % cupric chloride-dihydrate, 35°C. Galvanic coupling due to copper salt reduction to copper metal. More severe than ASTM B 117.
FACT(formely ASTM B 538)	Testing anodized aluminum specimens. Electrolyte as in salt-spray or CASS test. Specimen is made the cathode to generate high pH at defects.
Accelerated Weathering	Exposure of coated specimens to effects of UV radiation experienced in outdoor sunlight conditions which may be combined with other exposures such as moisture and erosion. Exposure cabinets use carbon arc (ASTM D 822), xenon lamp (ASTM G 26) or fluorescent lamp (ASTM G 53).
Lactic Acid	On substrates of brass and copper alloys, determines coatings porosity and resistance to handling (perspiration). Consists of immersion in 85 % lactic acid solution, drying and incubating above acetic acid vapors for 20 h to reveal discoloration spots at failure points or delaminations.
Acidified Synthetic Seawater Testing (SWAAT), ASTM G 85, A 3 (formerly ASTM G 43)	Atomized synthetic seawater (ASTM D 1141) with 10 mL glacial acetic acid per L of solution, pH 2.8 to 3.0, 35°C. More severe than ASTM B 117. The lower pH and the presence of acetate affect the solubility of corrosion products on and under the protective coatings.
Electrographic and Chemical Porosity Tests	Pores and active defects in nonmetallic coatings can be revealed by color indication or deposit formation. On nickel substrates, dimethylglyoxime, or steel, potassium ferricyanide (ferroxyl test) indicator can be applied to surface on filter paper while substrate is made the anode. Alternatively, a substrate immersed in acidic copper sulfate can be made the cathode to form copper nodules at conductive coatings defects.
Adhesion ASTM D 3359-02	Knife and fingernail test consists of cutting through the coating with knife or awl and dislodging coating with thumbnail or fingernail (pass/fail). The ASTM D 3359 test consists of “X” scribes or parallel cross-hatches followed by adhesive tape stripping of loosened coating.
T-Bend Adhesion ASTM D 4145	Combined flexibility and adhesion test consists of clamping end of coated flat metal panel in vise or similar tool, bending (convex) through 90°, reclamping to bend through 180° to give “0T” bend (where “T” is panel thickness and # (zero, 1, 2, ...) is the number of panel thicknesses). Rebending over the 180° bend gives a “1T” bend. Adhesive tape is pressed down along edge of bend and any loose coating stripped off.
	
Scab Test	Cyclic testing consisting of short salt exposure, short drying period, and long period of high humidity. Undercutting from scribe is measured.
Exterior Exposure ASTM D 1014	Method for conducting exterior exposure tests of paints on steel. Well-defined exposure setup, not necessarily equivalent to service tests.
Service Test/Data	Performance data of coatings systems under use conditions. Slowest evaluation method: provides tangible results.

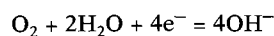
\*Note that dissolved CO<sub>2</sub> concentration at 0°C is three times that of concentration at 35°C and can affect corrosion.

which indicates that the acid reactant and the ferrous chloride (FeCl<sub>2</sub>) corrosion product exist largely in the ionic state in aqueous solution. The probability of this reaction occurring by the mechanism implied in the equation is very low because too many species must meet simultaneously. We may, however, conceive of this reaction occurring in two independent steps



In the two reactions, electron loss occurs at one site and electron gain occurs at another with the electrons linking the reactive sites through the conductive metal phase (Fe<sup>0</sup>).

The overall reaction takes place at a rate determined by the more difficult of these two steps. This simple concept, independent anodic and cathodic half-reactions, is the basis of the electrochemical mechanism of corrosion. The mechanism has profound effects on the corrosion protective properties of nonmetallic coatings materials. Some tests exploit the electrochemical mechanism to determine specific corrosion susceptibilities of coatings systems such as cathodic disbondment and pinhole detection. Coatings that are permeable to oxygen may be vulnerable to damage due to an alternative cathodic reaction





capable of causing high local pH and chemical degradation of the polymer or adhesive bonds. Thermodynamically this cathodic (reduction) reaction takes precedence over the hydrogen ion reduction reaction whenever oxygen is present at the cathodic reaction site.

### Corrosive Environmental Exposure

Corrosion occurs when all components of the process are present and capable of reaction (see preceding section). Basic test conditions include exposure of the coatings systems to an electrolyte containing reducible species (typically oxygen or hydrogen ion). More sophisticated testing would include closely replicating known corrosive conditions such as wet/dry cycles and multicomponent and multiphase chemical environments. Immersion, salt spray, and a partial pressure of sulfur dioxide corrosion tests correspond to water tank, marine, and combustion exhaust service environments, respectively. An important relationship exists between the corrosive environment used in the test procedures and the product's intended service use.

### Corrosion Effects

Distinction should be made between degradation due to corrosion and/or other processes. Corrosion can cause loss of coatings adhesion such as occurs with cathodic disbondment, blistering, or undercutting. Although adequate adhesion is necessary, greater adherence does not correspond to greater corrosion resistance. Exposing a coatings system to water can reduce the adhesion (wet adhesion), which is regained upon drying. Unless permanent damage occurs during the low adhesion period, no corrosion degradation results. The same may be true for other properties such as flexibility. Initial properties and property changes due to a corrosion environment may relate to corrosion protective properties. Clearly defining the relationship between measured properties and the intended use of the protective coatings is important.

### Noncorrosive Effects

There are many tests for coatings systems that provide useful information related to service requirements involving salts, fogs, immersion, scribes, radiation, heat, chemical, cold, and pressure transients. Whether such tests are applicable to the service intended for the coatings must be established and the test results must be interpreted in the context of corrosion protection performance. Ultraviolet (UV) resistance is not a useful property for the interior of water storage tanks. Long-term 100 % relative humidity and water immersion resistances are not necessarily appropriate for outdoor desert or climate-controlled indoor environments. Selecting tests without regard for the coatings' use may be detrimental to the development or qualification of a satisfactory coatings system.

## TESTS AND STANDARDS: SELECTION, APPLICATION, AND INTERPRETATION

### Available Tests and Standards

New and existing tests and standards are under continuous development and revision. ASTM is a leader of tests and

standards; other contributors, with various emphasis on specifications, are the federal government with Federal Test Method Standard 141C,<sup>2</sup> state government agencies, NACE International, Society of Automotive Engineers (SAE), Steel Structures Painting Council (SSPC), National Coil Coaters Association (NCCA), International Standards Organization (ISO), foreign systems (DIN), and commercial (e.g., automotive, architectural, electronics), proprietary, and military organizations. A comprehensive listing of these tests and standards is not the intent of this document.

Gaynes [1] and Munger [2] give descriptions and the framework for effective use of tests and standards. Gaynes [1] provides detailed descriptions including photographs, cross-listing ASTM to federal tests and a broader perspective encompassing the federal standard, miscellaneous tests, and some caveats of traditional testing. Munger [2] offers practical material directed towards large structures and provides a listing based on ASTM standards. Altmayer [3] compiled a table of 13 applicable corrosion tests for 30 metallic, inorganic, and organic coating/substrate combinations. The most commonly used tests are salt spray (ASTM B 117), acetic acid salt spray (ASTM G 85, Annex A1, formerly ASTM B 287), and the 100 % humidity (ASTM D 2247). A condensed listing with brief descriptions of tests selected from Altmayer [3], Mazia [4], ASM International [5], and others is given in Table 1. Additional tests are listed in Table 2, an edited and revised listing by Munger [2]. Hess [6] provides a very important auxiliary reference aiding in identifying the causes of paint film defects.

### Methods Selection

The large number of tests and methods makes selection difficult. Suppliers, users, and testers/researchers have different perspectives to help narrow the selection process. Obtaining corrosion resistance information enables a better focus. To aid in the selection process where no universal methodology exists, engage one or more from the following sections: (1) survey of practices; (2) specific practice by a successful coatings industry participant; (3) service life testing philosophy; and/or (4) a useful practical example involving cooperative efforts through better understanding (methodology).

#### Survey of Practices

A survey commissioned by the Federation of Societies for Coatings Technology (FSCT) was performed by Steel Structures Painting Council (SSPC) [7]. The full report [8] is available from FSCT and contains useful details including nonstandard tests and analyses. One portion of the report is particularly relevant to methods selections; a compilation of 102 coatings test users' responses is shown in Table 3, from which two conclusions are drawn: (1) most respondents used only one or two tests; and (2) the most prevalent test was salt spray. Salt spray testing is a crude approximation to highway environments involving deicing compounds [8] (see also fourth account below, Cooperative Practice Yielding Better Understanding) and is more useful for marine systems [8]. Coatings users may approach quality assurance with fewer tests than formulators [8]. Liu [9] presents a considerate case describing salt spray test usefulness or

<sup>2</sup> Standard 141C supersedes 141A and 141B.

**TABLE 2**—Coatings tests and methods pertinent to corrosion protection.<sup>a</sup>

NACE <sup>a</sup> or ASTM Standard	Title of Standard
<sup>a</sup> TM0174-91	Laboratory Methods for the Evaluation of Protective Coatings and Lining Materials in Immersion Service
B 117-02	Test Method of Salt Spray (Fog) Testing
B 368-85 (1990)	Method for Copper Accelerated Acetic Acid-Salt Spray (Fog) Testing (CASS Test)
B 457-67 (1993)	Test Method for Measurement of Impedence of Anodic Coatings on Aluminum
C 536-83 (1993)	Test Method for Continuity of Coatings in Glassed Steel Equipment by Electrical Testing
C 743-87 (1993)	Test Method for Continuity of Porcelain Enamel Coatings
D 522-92	Test Methods for Mandrel Bend Test of Attached Organic Coatings
D 523-89	Test Method for Specular Gloss
D 610-85 (1989)	Test Method for Evaluating Degree of Rusting on Painted Steel Surfaces
D 662-93	Test Method for Evaluating Degree of Erosion of Exterior Paints
D 714-87	Test Method for Evaluating Degree of Blistering of Paints
D 822-01	Practice for Conducting Tests on Paint and Related Coatings and Materials Using Filtered Open-Flame Carbon-Arc Light and Water Exposure Apparatus
D 823-95	Practices for Producing Films of Uniform Thickness of Paint, Varnish, Lacquer, and Related Products on Test Panels
D 870-02	Practice for Testing Water Resistance of Coatings Using Water Immersion
D 968-93	Test Methods for Abrasion Resistance of Organic Coatings by Falling Abrasive
D 1014-95	Test Method for Conducting Exterior Exposure Tests of Paints on Steel
D 1186-01	Test Method for Nondestructive Measurement of Dry Film Thickness of Nonmagnetic Coatings Applied to a Ferrous Base
D 1400-00	Test Method for Nondestructive Measurement of Dry Film Thickness of Nonconductive Coatings Applied to a Nonferrous Metal Base
D 1567-89 (1995)	Test Method for Testing Detergent Cleaners for Evaluation of Corrosive Effects on Certain Porcelain Enamels
D 1653-93	Test Method for Water Vapor Transmission of Organic Coating Films
D 1654-92	Test Method for Evaluation of Painted or Coated Specimens Subject to Corrosive Environments
D 1735-02	Practice for Testing Water Resistance of Organic Coatings Using Water Fog Apparatus
D 2197-98	Test Methods for Adhesion of Coatings by Scrape Adhesion
D 2247-02	Practice for Testing Water Resistance of Coatings in 100 % Relative Humidity
D 2248-01	Practice for Detergent Resistance of Organic Finishes
D 3258-80 (1987)	Test Method for Porosity of Paint Films
D 3273-94	Test Method for Resistance to Growth of Mold on the Surface of Interior Coatings in an Environmental Chamber
D 3276-96	Guide for Paint Inspectors (Metal Substrates)
D 3359-02	Test Methods for Measuring Adhesion by Tape Test
D 3361-01	Practice for Operating Light- and Water-Exposure Apparatus (Unfiltered Carbon-Arc Type) for Testing Paint, Varnish, Lacquer, and Related Products Using the Dew Cycle
D 3363-00	Test Method for Film Hardness by Pencil Test
D 4145-83	Test Method for Coating Flexibility of Prepainted Sheet
D 4585-99	Practice for Testing Water Resistance of Coatings Using Controlled Condensation
D 4587-01	Practice for Conducting Tests on Paint and Related Coatings and Materials Using a Fluorescent UV-Condensation Light- and Water-Exposure Apparatus
E 376-89	Practice for Measuring Coating Thickness by Magnetic-field or Eddy-Current (Electromagnetic) Test Methods
G 8-96	Test Method for Cathodic Disbonding of Pipeline Coatings
G 12-83	Test Method for Nondestructive Measurement of Film Thickness of Pipeline Coatings on Steel
G 42-96	Test Methods for Cathodic Disbonding of Pipeline Coatings Subjected to Elevated Temperatures
G 53-96	Practice for Operating Light- and Water-Exposure Apparatus (Fluorescent UV-Condensation Type) for Exposure of Nonmetallic Materials
G 60-01	Method for Conducting Cyclic Humidity Tests
G 80-88	Test Method for Specific Cathodic Disbonding of Pipeline Coatings
G 84-89	Practice for Measurement of Time-of-Wetness on Surfaces Exposed to Wetting Conditions as in Atmospheric Testing
G 85-02	Practice for Modified Salt Spray (Fog) Testing
G 87-02	Practice for Conducting Moist SO <sub>2</sub> Tests
G 90-94	Practice for Performing Accelerated Outdoor Weathering of Nonmetallic Materials Using Concentrated Natural Sunlight
G 92-86 (1992)	Practice for Characterization of Atmospheric Test Sites
J 2334 (SAE)	Cosmetic Corrosion Lab Test

<sup>a</sup>Revised from Munger [2], p. 310

uselessness based on years of experience. (See other chapters in this Manual on “Cabinet Tests” and “Automotive.”)

### A Specific Practice

The following tests constitute a generic test plan used by one industrial service company for coated metal in laboratory performance testing. A 4 in. by 12 in. (10.2 cm by 30.5 cm) coated panel is the preferred configuration. Before accelerated corrosion tests (ASTM B 117, G 85-A1, B 368, and G 85-A3), a scribe is introduced using ASTM D 3359,

Method A or D 1654, Section 5. Exposure times are 240–1000 h, depending on test and substrate. Additional corrosion tests (unscribed and ASTM D 714 evaluation) include hot humidity (ASTM D 2247, 100°F/100 % RH), condensing humidity (ASTM D 4585, 140°F), condensing humidity/UV (ASTM G 53, 150°F), water soak (ASTM D 870), and detergent soak (ASTM D 2248, 72 h). Scribed samples are prepared for ASTM D 1654 evaluation by scrape/rinse/dry, rinse/blow-off or 3M's #610 tape pull-off. Other noncorrosion tests (mainly adhesion) are also performed including T-Bend, Wedge Bend, Conical Mandrel, Impact (Direct/Reverse), MEK rub

**TABLE 3**—Survey results of 102 responses: Frequently Used Tests.

Test	% Respondents <sup>a</sup>
Salt Spray	52
Immersion	24
Outdoor	22
Ultraviolet/Condensation	20
Accelerated Weathering	14
Humidity/Condensation	10
Cathodic Disbondment	7
Adhesion	7
Atlas Cell Test (NACE TM0174)	4
Other Physical Tests	4
Other Chemical Tests	3
Flexibility	2

<sup>a</sup> Multiple tests used (total greater than 100%).

(cure test), Olsen Cup, Gravelometer, Pencil Hardness, Cross-Hatch, Dry Film Thickness, and Loss of Gloss. This battery of tests provides generous information about the coatings system, without establishing a direct link to service data. The test battery is necessarily extensive because the intent is to determine possible causes for service problems. A clear relationship between service and test data is necessary for problem resolution.

### Service Life Testing Methodology

In the example in the preceding paragraph, no rationale is given for the selection or application of the tests. Experience provides an important gauge for developing a useful set of tests. Dickie [10] suggested that a methodology be developed to provide rational guidance for service life testing, and proposed a general framework integrating laboratory experiments, field exposure history, and theoretical and empirical models. The central role of physical and chemical models of degradation processes in service life prediction was examined [10] and represents an important philosophical contribution for coatings testing. The methodology was first presented in a somewhat different form at an informal meeting of experts discussing coatings failure mechanisms [11]. (Correlation of test results with service life is discussed in several chapters in the section on Testing in Industries in this manual.)

### Cooperative Practice Yielding Better Understanding

AISI [12–14] has taken a leadership role to develop and evaluate methodology based on laboratory experiments, field exposure history, and theoretical and empirical models through an open forum of all interested parties (mainly North American automotive and steel industries), organized as the Corrosion Task Force of the AISI. The task force developed an improved laboratory-accelerated test for ranking the cosmetic corrosion resistance of coated automotive steel sheet products. This approach serves as a model for methodology development in areas of nonmetallic coatings corrosion testing.

### SUMMARY

- Many tests are available for evaluation of corrosion protective properties necessitating a test selection process.

- Understanding the protective mechanisms of coatings systems aids in developing methodologies for systems having long lives.
- The interpretation of the test results requires adequate correlation to service life data.
- Service results validation is difficult and often requires constrictively long times.
- Successful case histories and experiences provide the best means for useful evaluations until functional methodologies are devised.

### REFERENCES

- [1] Gaynes, N. I., *Testing of Organic Coatings*, Noyes Data Corporation, Park Ridge, NJ, 1977.
- [2] Munger, C. G and Vincent, D. V., *Corrosion Prevention by Protective Coatings*, Chapt. 12, 2nd ed., National Association of Corrosion Engineers, Houston, TX, 1999.
- [3] Altmayer, F., "Choosing an Accelerated Corrosion Test," *Metal Finishing*, 69th Guidebook and Directory Issue, Vol. 99, No. 1A, Elsevier, NY, January 2001, p. 579.
- [4] Athey, R. D., "Testing," *Metal Finishing Organic Finishing Guidebook and Directory*, Vol. 101, No. 10A, Elsevier, NY, October, 2003, p. 438.
- [5] Sandler, M. H., "Nonmetallic Coating Processes: Painting," *Metals Handbook*, Vol. 5: *Surface Cleaning, Finishing and Coating*, 9th ed., ASM International, Metals Park, OH, 1990, pp. 489–498, 527–531; and Mansfeld, F., "Electrochemical Methods of Corrosion Testing," *Metals Handbook*, Vol. 13A, ASM International, Metals Park, OH, 2003, p. 446.
- [6] *Hess's Paint Film Defects: Their Causes and Cure*, H. R. Hamburg and W. M. Morgans, Eds., Chapman and Hall, London, 1979.
- [7] Appleman, B. R., "Survey of Accelerated Test Methods for Anticorrosive Coating Performance," *Journal of Coatings Technology*, Vol. 62, No. 787, August 1990, pp. 57–67.
- [8] Appleman, B. R., "Survey of Accelerated Test Methods for Anti-Corrosive Coating Performance," Monograph prepared for Corrosion Committee of Federation of Societies for Coatings Technology, June 1990, available from FSCT, Blue Bell, PA.
- [9] Liu, T., "Is the Salt Fog Test an Effective Method to Evaluate Corrosion Resistant Coatings?" *Corrosion Control by Organic Coatings*, H. Leidheiser, Jr., Ed., National Association of Corrosion Engineers, Houston, TX, 1981, pp. 247–254.
- [10] Dickie, R. A., "Toward a Unified Strategy of Service Life Prediction," *Journal of Coatings Technology*, Vol. 64, No. 809, June 1992, pp. 61–64.
- [11] Funke, W., Leidheiser, H. Jr., Dickie, R. A., et al., "Unsolved Problems of Corrosion Protection by Organic Coatings: A Discussion," *Journal of Coatings Technology*, Vol. 58, No. 741, October 1986, pp. 79–86.
- [12] Townsend, H. E., Granata, R. D., McCune, D. C., Schumacker, W. A., and Neville, R. J., *Progress by the Automotive and Steel Industries Towards an Improved Laboratory Cosmetic Corrosion Test*, ACAP Conference Proceedings, P-250, SAE, Warrendale, PA, 1991.
- [13] Townsend, H. E., "Development of an Improved Laboratory Corrosion Test by the Automotive and Steel Industries," *Advanced Coatings Technology, Proceedings of the 4th Annual ESD Conference*, The Engineering Society, Ann Arbor, MI, 1994.
- [14] SAE J2334, Cosmetic Corrosion Lab Test, SAE, Warrendale, PA, 1997.

# Metal-Matrix Composites

*L. H. Hihara*<sup>1</sup>

METAL MATRIX COMPOSITES (MMCs) are metals that are reinforced with fibers or particles that usually are stiff, strong, and lightweight. The fibers and particles can be metal (e.g., tungsten), nonmetal (e.g., carbon or boron), or ceramic (e.g., silicon carbide (SiC) or (alumina)  $\text{Al}_2\text{O}_3$ ). The purpose for reinforcing metals with fibers or particles is to create composites that have properties more useful than that of the individual constituents. For example, fibers and particles are used in MMCs to increase stiffness [1], strength [1], and thermal conductivity [2], and to reduce weight [1], thermal expansion [3], friction [4], and wear [5].

Selection of the matrix metal and reinforcement constituent is usually based on how well the combination interacts to achieve desired properties. Interaction of the MMC with the environment is normally a secondary consideration; therefore, it is not uncommon for MMCs to have low resistance to corrosion. It is also not uncommon for MMCs to have corrosion behavior significantly different from what might be expected, based on the normal corrosion behavior of the MMC constituents. The corrosion resistance of the MMC is usually inferior to that of its monolithic matrix alloy, due to one or more of the following reasons:

1. Galvanic coupling of reinforcement constituent and matrix;
2. Formation of an interphase between the reinforcement constituent and matrix;
3. Microstructural contaminants and processing residuals in the MMC; and
4. Microstructural changes caused by the presence of the reinforcement constituents.

The corrosion behavior of aluminum, magnesium, lead, depleted uranium, stainless steel, titanium, copper, and zinc MMCs will be reviewed. Reinforcement constituents used in the aforementioned MMCs include boron, graphite, SiC,  $\text{Al}_2\text{O}_3$ , mica, quartz, tungsten, yttria, and zircon. The reinforcement constituents usually range from 10 to 60 vol. %. This review focuses on the corrosion properties of bulk MMCs and does not cover corrosion protection of MMCs, surface modification of MMCs, or MMCs used as coatings. Other reviews on corrosion of various types of MMC are available [6–12]. Methods and tests that can be used in a corrosion testing program to assess corrosion damage, determine corrosion mechanisms, and study specific types of corrosion will be discussed.

<sup>1</sup>Associate Professor, Department of Mechanical Engineering, University of Hawaii at Manoa, Honolulu, HI 96822.

## CORROSION SUSCEPTIBILITY OF MMCS

The effect of different types of reinforcement constituents on MMC corrosion behavior is discussed below. Due to the limited amount of information on MMC corrosion behavior, it is not feasible to have separate sections for effects of alloying elements, effects of microstructure, sensitivity to acidity/alkalinity, etc. MMCs are relatively new and specialized materials; therefore, only a limited number of corrosion studies have been conducted. Most studies relate the effects of the reinforcement constituents to overall MMC corrosion behavior.

### Aluminum MMCs

Corrosion research has focused primarily on aluminum MMCs, which is the only type of MMC that has become widely available [3]. Aluminum has relatively good corrosion resistance and is lightweight. Its density is  $2.7 \text{ g/cm}^3$ . Corrosion studies have been conducted on aluminum MMCs reinforced with boron, graphite, SiC,  $\text{Al}_2\text{O}_3$ , and mica. Corrosion of diffusion bonds, stress corrosion, and corrosion fatigue will also be discussed.

#### *Effect of Boron*

The primary use of boron/aluminum (B/Al) MMCs has been tubular struts in the mid-fuselage structure of the space shuttle. The use of B/Al MMCs instead of aluminum alloys (as planned in the original design) resulted in a 44 % savings in weight [13].

Boron filaments (BFs) consist of polycrystalline boron with a core of tungsten and tungsten borides, which form during processing [14]. B/Al MMCs are usually fabricated by diffusion bonding BFs between aluminum foils [15]. Aluminum borides (i.e.,  $\text{AlB}_{12}$  and  $\text{AlB}_2$ ) have been found at BF-matrix interfaces [16].

Crystalline boron has good chemical resistance and is not attacked by strong acids and bases, even though it is thermodynamically unstable in water [17]. Accordingly, BFs are relatively inert in aqueous solutions. No observable degradation of the BFs was observed after exposure to boiling, saturated, nickel chloride solutions for 16 s [18], or to 3 % NaCl solutions containing 0.1 % hydrogen peroxide ( $\text{H}_2\text{O}_2$ ) [19].

Pure boron (99.999 %) [20], as-manufactured (referred to as "virgin") BF with tungsten core shielded [20,21], virgin BF with tungsten core exposed [21], and BF extracted from aluminum matrices (not specified if tungsten core exposed)

FIG. 1—Micrograph of Gr/6061-T6 Al MMC. Graphite fiber volume fraction is approximately 50 %.

[22] are noble to aluminum in NaCl solutions. Therefore, galvanic corrosion of aluminum coupled to pure boron or BF is thermodynamically possible. Pure boron, however, is an insulator and cannot support electrical currents under normal conditions. Cathodic and anodic currents were unmeasurable on pure boron (99.999 %) electrodes in aerated NaCl solutions [20]. The conductivity of BFs is many orders of magnitude greater than that of pure boron, due to tungsten and tungsten borides in the core [14]. Galvanic currents, however, were also unmeasurable between virgin BF and 2024 aluminum or 6061 aluminum in 3.5 % NaCl solutions [22]. It was not specified whether solutions were aerated or deaerated and whether the tungsten core of the BFs was exposed. Galvanic currents were measurable between the aluminum alloys and BFs that were extracted from the matrix [22]. The extracted BFs were enveloped by a 4- $\mu\text{m}$ -thick layer of aluminum boride, which could not be positively identified as  $\text{AlB}_2$  or  $\text{AlB}_{12}$ . Galvanic currents measured between the aluminum alloys and aluminum boride (boride species not specified) were similar to those between the alloys and the extracted BFs. When the layer of aluminum boride was removed from the extracted BFs, the galvanic current ceased, indicating that the aluminum boride interphase is necessary for galvanic corrosion. In addition, B/Al MMCs were noble to the matrix alloy and active to the extracted BF and aluminum boride, which coincides with the mixed-potential theory. The corrosion rate of B/Al MMCs also increased when the BF content was increased from 18 to 46 vol. %, suggesting that corrosion rates increase as aluminum-boride cathodic sites increase. It was also noted that BF-matrix interface regions were preferentially corroded, but it was not determined if matrix near the interphase or the interphase itself was attacked. Others [19,20] have found that diffusion bonds in B/Al MMCs have been major sources

of corrosion. This is discussed in the subsection below entitled, *Effect of Diffusion Bonds and Microstructural Contaminants*.

#### *Effect of Graphite*

Continuous fiber Gr/Al MMCs (Fig. 1) are known to have high specific tensile strength and stiffness in the direction of the fiber axis. Limitations of shear, compression, and transverse strengths of the MMCs, however, have restricted their use [3]. Particulate Gr/Al MMCs have also been developed for potential use in tribological applications due to good resistance to wear and seizure [23,24].

In the presence of water, carbon has a small domain of thermodynamic stability in potential-pH space [25]. At active potentials, it is thermodynamically possible to form methane ( $\text{CH}_4$ ) by the reaction



but this has not been confirmed [25]. No  $\text{CH}_4$  was detected or visual fiber degradation observed when pitch-based graphite fibers were cathodically polarized [26]. At noble potentials, various carbon compounds may form during carbon oxidation [25], but carbon dioxide ( $\text{CO}_2$ ) and carbon monoxide ( $\text{CO}$ ) are believed to be the dominant reaction products [27]. During anodic polarization, pitch-based graphite fibers are oxidized to  $\text{CO}_2$  and  $\text{CO}$  with crevice formation [26]. Graphite compounds also form by the intercalation of ions between graphite planes during polarization [27]. In the open-circuit condition or when coupled to aluminum, however, graphite fibers do not usually exhibit visual degradation.

Graphite, which is an electrical conductor, can serve as an efficient cathode during galvanic corrosion in Gr/Al MMCs. Czyrklis [28] and others [29–31] have found that the

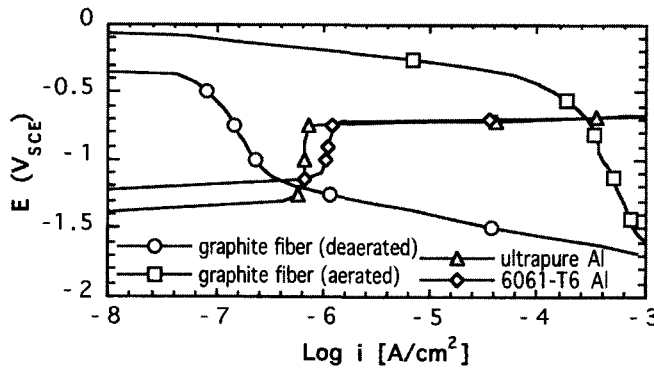


FIG. 2—Anodic polarization diagrams of ultrapure aluminum and 6061-T6 aluminum in deaerated 3.15 wt % NaCl plotted with the cathodic polarization diagrams of pitch-based graphite fibers (cross section exposed) in deaerated and aerated 3.15 wt % NaCl at 30°C. Scan rate = 0.1 mV/s.

open-circuit potential of a Gr/Al MMC is noble to the matrix alloy in deaerated NaCl solutions [28]. The open-circuit potential of a particulate Gr/Al MMC, however, was reported to be more active than the matrix material for a case in which the presence of graphite particles caused a large increase in the anodic currents [32]. Dull et al. [33] conducted polarization experiments on various Gr/Al MMCs in NaCl solutions, and found that dissolved oxygen greatly increases the corrosion rate, indicating that the main driving force for galvanic corrosion is oxygen rather than proton reduction in aerated solutions. Using the zero-resistance ammeter (ZRA) technique [34], Dash [35] showed that the galvanic-corrosion current density ( $i_{\text{GALV}}$ ) of a galvanic couple with a 5-to-1 area ratio of pure aluminum to pitch-based graphite fiber increased from less than  $1 \times 10^{-8}$  A/cm<sup>2</sup> in deaerated 3.5 wt % NaCl to  $1.5 \times 10^{-6}$  A/cm<sup>2</sup> in aerated 3.5 wt % NaCl. Hihara and Latanision [36] also found that  $i_{\text{GALV}}$  of galvanic couples consisting of equal areas of 6061-T6 aluminum and pitch-based graphite fiber was about 60 times greater in aerated 3.15 wt % NaCl solutions compared to deaerated solutions where  $i_{\text{GALV}}$  was equal to about  $3 \times 10^{-6}$  A/cm<sup>2</sup>. The galvanic effect has also been reported in particulate Gr/Al MMCs [37,38].

Figure 2 shows the anodic polarization diagrams of ultrapure aluminum (99.999 %) and 6061-T6 aluminum in deaerated 3.15 wt % NaCl with the cathodic polarization diagrams of pitch-based graphite fibers in deaerated and aerated 3.15 wt % NaCl. As shown in the figure, proton reduction on graphite will polarize aluminum to noble potentials that are less than the pitting potential  $E_{\text{PIT}}$ , explaining the negligible galvanic-corrosion rates in deaerated solutions. Oxygen reduction on graphite, however, polarizes aluminum into the pitting regime, which causes high galvanic-corrosion rates in aerated, chloride-containing solutions. Figure 3 shows  $i_{\text{GALV}}$  of 6061-T6 aluminum and ultrapure aluminum as a function of the area fraction of pitch-based graphite fiber (cross section exposed) in aerated 3.15 wt % NaCl [36]. Both ultrapure aluminum and 6061-T6 aluminum are represented by the same curve, since they have similar galvanic-corrosion behavior. Relatively new, nonequilibrium aluminum alloys containing approximately 20 at. % molybdenum or 26 at. % tungsten, with marked higher pitting

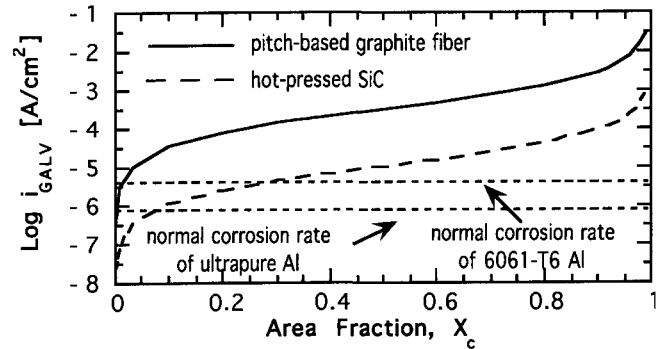
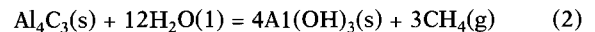


FIG. 3—Graphs showing  $i_{\text{GALV}}$  of ultrapure aluminum and 6061-T6 aluminum as a function of area fraction  $X_c$  of graphite fiber and SiC in aerated 3.15 wt % NaCl at 30°C.

potential (i.e., in excess of 1 V compared to pure aluminum) in chloride solutions, have been studied as potential new alloys for Gr/Al MMCs [39,40]. The results have been promising, as graphite fibers in aerated chloride solutions were incapable of polarizing the alloys to their pitting potentials, resulting in galvanic corrosion rates between the fibers and alloys up to three orders of magnitude lower than that with pure aluminum [39,40].

Another cause of degradation in Gr/Al MMCs is the presence of  $\text{Al}_4\text{C}_3$ . An aluminum carbide interphase forms by the reaction of aluminum and carbon [41]. In Gr/Al MMCs, the formation of  $\text{Al}_4\text{C}_3$  becomes substantial during processing at temperatures much higher than the liquidus temperature [42]. Portnoi et al. [43] showed that  $\text{Al}_4\text{C}_3$  in Gr/Al MMCs readily decomposes in water, producing  $\text{CH}_4$  and aluminum hydroxide  $\text{Al}(\text{OH})_3$ :



The hydrolysis rate of hot-pressed  $\text{Al}_4\text{C}_3$  (78 % theoretical density) was measured to be approximately 1 %/hr [44].

Aylor and Moran [45], who conducted polarization experiments on Gr/Al MMCs in seawater, also hypothesized that diffusion of carbon into aluminum could lower the integrity of the passive film, rendering it more susceptible to breakdown. Wielage [46] reported that the pitting potentials of various squeeze-cast Gr/Al MMCs were approximately 20 mV more active than that of the pure aluminum matrix material in a chloride solution. Aluminum carbide was found at the Gr fiber-matrix interfaces. Shimizu et al. [31], however, found that pitting potentials of a squeeze-cast, short fiber Gr/6061 Al MMC had pitting potentials similar to that of monolithic 6061 Al in a chloride solution.

#### Effect of Silicon Carbide

The SiC/aluminum (SiC/Al) MMCs are reinforced with SiC particles (P) (Fig. 4), whiskers (W), fibers, or monofilament (MF). In 1988, an aluminum tube in the catamaran *Stars and Stripes* '88 was replaced by a lighter SiC<sub>p</sub>/Al MMC tube having a 30.5-cm outer diameter [3]. Lightweight mirrors for telescopes have also been fabricated from SiC<sub>p</sub>/Al MMC foam [47].

The electrical resistivity of SiC depends on its purity. It ranges from about  $10^{13}$  to  $10^{-5}$   $\Omega$  cm [48]. Thus, in the un-pure state, the resistivity of SiC can be rather low. Some

FIG. 4—Micrograph of SiC/6061-T6 Al MMC. SiC volume fraction is 13 %.

SiC<sub>MF</sub> also have carbon cores and carbon-rich surfaces [49], with resistivities on the order of  $10^{-2} \Omega \text{ cm}$  [44]. Consequently, in aqueous solutions, SiC can serve as an inert electrode for proton and oxygen reduction. Depending on the type of SiC, galvanic corrosion with aluminum is possible.

In deaerated, chloride-containing solutions, SiC/Al MMCs and their matrix alloys passivate in the open-circuit condition [45,50]. Proton reduction alone cannot polarize the composites or the matrix alloys to  $E_{\text{PIT}}$ , since oxygen reduction is required for this. Accordingly, in aerated, chloride-containing solutions, the open-circuit potentials of SiC/Al MMCs and their matrix alloys are nearly equal to pitting potentials [50].

Galvanic corrosion between aluminum and SiC is possible in aerated chloride-containing environments. The degree of galvanic corrosion is strongly dependent on the type of SiC reinforcement. Figure 5 shows the anodic polarization diagrams of ultrapure aluminum and 6061-T6 aluminum in deaerated 3.15 wt % NaCl with the cathodic polarization diagrams of hot-pressed SiC, SiC<sub>MF</sub> (configurations with either carbon cores or carbon-rich surface exposed), pitch-based graphite fiber, and 6061-T6 aluminum in aerated 3.15 wt % NaCl. The figure shows that  $i_{\text{GALV}}$  of 6061-T6 aluminum coupled to hot-pressed SiC (of equal surface area) is about twice the normal corrosion current density ( $i_{\text{CORR}}$ ) of 6061-T6 aluminum. When 6061-T6 aluminum is coupled to SiC<sub>MF</sub> (of equal surface area),  $i_{\text{GALV}}$  is about 25 times greater than  $i_{\text{CORR}}$  of 6061-T6 aluminum. The influence of the carbon core and carbon-rich surface of the SiC<sub>MF</sub> is clearly seen in Fig. 5 where the polarization diagram of the SiC<sub>MF</sub> has a stronger resemblance to that of pitch-based graphite than that of hot-pressed SiC [44]. Galvanic current between Nicalon SiC fibers and an aluminum alloy was also measured in an aerated NaCl solution [29]. The galvanic current was 72  $\mu\text{A}$

(specimen areas not given) and 15 % of that between carbon fiber and the aluminum alloy.

For particulate SiC/Al MMCs, the galvanic corrosion behavior is likely to be more accurately represented by comparison to the hot-pressed SiC data, as opposed to the SiC<sub>MF</sub> and Nicalon SiC fiber data. From the polarization data in Fig. 5, galvanic-corrosion rates were calculated for ultrapure aluminum and 6061-T6 aluminum coupled to hot-pressed SiC exposed to aerated 3.15 wt % NaCl [36]. Figure 3 graphically shows  $i_{\text{GALV}}$  as a function of hot-pressed SiC area fraction. Galvanic corrosion between hot-pressed SiC and 6061-T6 Al would not exceed the normal corrosion rate of 6061-T6 Al in aerated 3.15 wt % NaCl until the SiC volume fraction exceeds approximately 0.3. Hence, based on

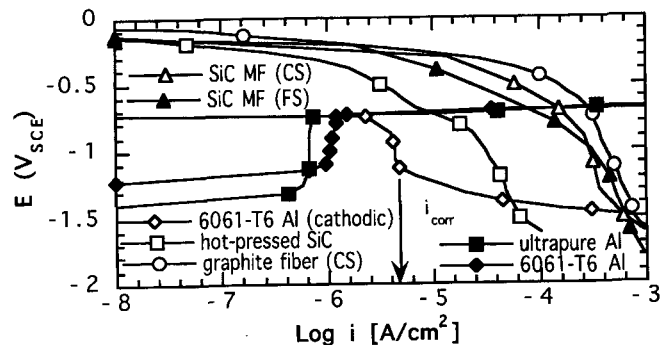


FIG. 5—Anodic polarization diagrams of ultrapure aluminum and 6061-T6 aluminum in deaerated 3.15 wt % NaCl plotted with the cathodic polarization diagrams of pitch-based graphite fiber, SiC<sub>MF</sub>, hot-pressed SiC, and 6061-T6 aluminum in aerated 3.15 wt % NaCl at 30°C. CS = cross section exposed. FS = fiber surface exposed. Scan rate = 0.1 mV/s.

Fig. 3, galvanic corrosion of particulate SiC/Al MMCs would increase with SiC content and become relatively noticeable only at higher SiC volume fractions; for example, in the electronic grade MMCs with 35–55 vol. % SiC.

Experimental results have generally indicated that the corrosion rate of particulate and whisker SiC/Al MMCs increase with SiC content in aerated, chloride-containing environments. Lore and Wolf [51] found that the degree of corrosion in SiC<sub>w</sub>/6061 Al MMCs exposed to chloride-containing solutions is proportional to the SiC content. Metzger and Fishman [6] reported the results of DeJarnette and Crowe who exposed 20 vol. % SiC<sub>p</sub>/2024 Al MMCs and monolithic 2024-T4 Al to aerated 3.5 wt % NaCl. The composite corroded about 40 % faster than the matrix alloy. Sun et al. [52] and Modi et al. [53] have also reported that corrosion rates of SiC<sub>p</sub>/Al MMCs were higher than that of the matrix alloys. Griffiths and Turnbull [54], however, found no evidence of galvanic corrosion in SiC/6061 aluminum MMCs with 20–30 wt % (17–27 vol. %, respectively) SiC particles. Rather, they showed that diffusion-limited oxygen reduction on SiC/Al MMCs in an NaCl solution was significantly greater than that of the monolithic alloy, which could not be attributed to the SiC content, but could be attributed to the increase in intermetallic particles in the MMC. Hence, it is possible that the increase in corrosion rates of the MMCs in comparison to the monolithic alloys could be the result of oxygen reduction on intermetallics. Observations contrary to that of Griffiths and Turnbull, however, have been made. Sun et al. [52] reported that the degree of corrosion increased with SiC particle content, but the intermetallic content was relatively constant.

Silicon carbide particles in SiC/Al MMCs have little effect on passive currents. In a chloride-free, sodium tetraborate-boric acid solution of pH 8.4, the passive current of a SiC<sub>w</sub>/6061 Al MMC was only slightly greater than that of monolithic 6061 aluminum [55]. In deaerated 0.1 N NaCl, the passive current densities (at potentials less than  $E_{PT}$ ) of 20 % SiC<sub>w</sub>/2024 Al and 20 % SiC<sub>w</sub>/6061 Al MMCs were actually slightly less than that of their monolithic matrix alloys. The passive current densities were on the order of  $10^{-5}$  A/cm<sup>2</sup> [50].

Silicon carbide also has little effect on  $E_{PT}$  [29,31,45, 50,54,56–59] indicating that the presence of SiC particles does not degrade the pitting resistance of passive films on aluminum. The pitting potential of a 20 vol. % SiC<sub>w</sub>/2024 Al MMC, however, was depressed by about 0.1 V [50]. Contrary to the relatively invariable behavior of  $E_{PT}$ , pit morphology is indirectly affected by the presence of SiC particles. Trzaskoma [60] found that pits on SiC<sub>w</sub>/Al MMCs were notably more numerous and much smaller in size, compared to pits on wrought and powder-compacted monolithic alloys during anodic polarization in 0.1 N NaCl. The pits nucleated at intermetallic particles (not SiC), which are smaller and more numerous in the MMCs than in the monolithic matrix alloys [60]. Apparently, SiC whiskers [60] and particles [54] enhance the precipitation of the intermetallic phases. The presence of SiC, therefore, may increase the number of intermetallic pit-nucleation sites but does not weaken the resistance of the passive film, as gaged by pitting potentials. Others have also observed pit nucleation at dendrite cores [61], near eutectic silicon [58,62] and intermetallic particles [62] in various SiC/Al MMCs.

The corrosion behavior of particulate SiC/Al MMCs is also sensitive to processing. The SiC particles have an indirect effect on corrosion behavior by altering the condition of the matrix metal. Processing conditions and the presence of SiC particles can affect void content [63], dislocation density [64], and the precipitation of active phases [65] in aluminum matrices. Paciej and Agarwala [63] found that certain solution heat treatments and high extrusion ratios improved corrosion resistance of a 20 % SiC<sub>p</sub>/7091 Al MMC. Bhat et al. [66] reported that extrusion improved the corrosion resistance of cast MMCs by reducing the amount of pores and agglomerates of SiC particles; and Ahmad and Abdul [67] found that the T4 temper improved corrosion resistance over O and F tempers due to a finer, more homogenous distribution of secondary phases. It has been suggested that corrosion near the SiC-Al interface could be caused by high dislocation density due to a mismatch of the coefficient of thermal expansion between SiC and aluminum [44,68,69], segregation of alloying elements to the SiC-Al interface [70], or the formation of Al<sub>4</sub>C<sub>3</sub>, which hydrolyzes in water. Silicon carbide reacts with molten aluminum to form Al<sub>4</sub>C<sub>3</sub> if the silicon activity is low [71]. Aluminum carbide has been identified as a source of corrosion for MMCs reinforced with particles [72] and SiC Nicalon fibers [29].

### *Effect of Alumina*

Particles and both short and continuous Al<sub>2</sub>O<sub>3</sub> fibers have been used to reinforce aluminum alloys. A short type of Al<sub>2</sub>O<sub>3</sub> fiber has been used to reinforce diesel-engine pistons [73].

The resistivity of Al<sub>2</sub>O<sub>3</sub> (99.7 % pure) is greater than about  $10^{14}$  Ω·cm [74], and therefore, galvanic corrosion between Al<sub>2</sub>O<sub>3</sub> fibers and aluminum is unlikely. In alkali and acidic solutions, Al<sub>2</sub>O<sub>3</sub> is thermodynamically unstable [75]; however, the short type of Al<sub>2</sub>O<sub>3</sub> fibers are resistant to hot concentrated alkalis and most hot acids [76]. It can be assumed for practical purposes that Al<sub>2</sub>O<sub>3</sub> fibers are inert in aqueous solutions to which Al<sub>2</sub>O<sub>3</sub>/Al MMCs are likely to be exposed.

The Al<sub>2</sub>O<sub>3</sub> reinforcements usually do not have significant effects on pitting potentials in chloride solutions [29,31, 56–58,77], although passive current densities below the pitting potential have been reported to increase with Al<sub>2</sub>O<sub>3</sub> content [77]. Microbial corrosion was also more significant on particulate MMCs in comparison to the monolithic alloy, indicating that the Al<sub>2</sub>O<sub>3</sub>/Al matrix interface may have aided biofilm formation [78].

Formation of interphases incorporating aluminum, oxygen, and alloying elements has been observed in some Al<sub>2</sub>O<sub>3</sub>/Al MMCs. Preferential corrosion near fibers and particles is sometimes noticed.

Continuous Al<sub>2</sub>O<sub>3</sub> fibers in an aluminum (2 % Li) MMC (containing 50 vol % of fibers) [79] were enveloped by a 2 to 3 μm thick Li<sub>2</sub>O·5Al<sub>2</sub>O<sub>3</sub> interphase, which formed during processing of the composite [6]. The corrosion resistance of the Al<sub>2</sub>O<sub>3</sub>/Al (2 % Li) MMC was compared to that of 6061-T6 aluminum and 2219-T87 aluminum in eight accelerated-corrosion tests that are often used for wrought aluminum alloys. Most of the test environments contained chlorides. In most cases, weight-loss data showed that the corrosion rate of Al<sub>2</sub>O<sub>3</sub>/Al (2 % Li) MMCs was slightly higher than that of 6061-T6 aluminum, but significantly lower than that of 2219-T87 aluminum. No severe interfacial corrosion was observed.



Continuous fibers in an aluminum (2 % magnesium) MMC [80] were enveloped by a thin layer of  $\text{MgAl}_2\text{O}_4$  through which bonding between fiber and matrix was made. Near the fibers, iron was detected and magnesium concentrations reached levels of about 10 %, suggesting that  $\text{Mg}_2\text{Al}_3$  clusters were present. Pits were found near the fibers after the composites were exposed to NaCl solutions containing  $\text{H}_2\text{O}_2$ . Yang and Metzger [80] attributed the pits to corrosion of  $\text{Mg}_2\text{Al}_3$ , which is rapidly attacked at low potentials. No attack of the  $\text{MgAl}_2\text{O}_4$  interphase was observed.

Preferential corrosion in the proximity of an unspecified type of  $\text{Al}_2\text{O}_3$  fiber in a 6061-T6 aluminum MMC was observed by Agarwala [81]. The MMC was exposed to 3.5 wt % NaCl (deaeration or aeration was not specified) for a 500-h period. No correlation was made between the microstructure and the region of corrosion.

Selective attack in the vicinity of  $\text{Al}_2\text{O}_3$  particles has been observed during anodic polarization [82] and in the open-circuit condition [58] in chloride solutions.

### *Effect of Mica*

Mica/aluminum (mica/Al) MMCs have been developed for potential use in applications where good antifriction, seizure resistance, and high-damping capacity are required [83].

Muscovite ( $\text{KAl}_3\text{Si}_3\text{O}_{10}(\text{OH})_2$ ) mica particles that are less than about 70  $\mu\text{m}$  in size are used in mica MMCs [84]. Galvanic corrosion between aluminum and muscovite should not be a problem, since muscovite is an insulator with resistivities that range from about  $10^{13}$  to  $10^{17} \Omega\cdot\text{cm}$  [85]. Muscovite is insoluble in cold water [86]; however, it has been reported that muscovite particles have a tendency to absorb moisture and then swell [87].

Mica particles were cast in various aluminum alloys [87, 88]. In 3.5 wt % NaCl solutions, the presence of mica particles depressed pitting potentials by approximately 20–30 mV, in comparison to the monolithic matrix alloys, suggesting that the presence of mica particles may slightly weaken the passive aluminum film. Corrosion behavior was also affected by the precipitation of secondary phases. In some cases, precipitates were preferentially attacked. Pits around and away from mica particles, interfacial corrosion of the mica-matrix interface, and exfoliation of mica particles were also observed.

Values of  $i_{\text{CORR}}$  (extrapolated from polarization diagrams) for nondeaerated 3.5 wt % NaCl ranged from about 3 to 10  $\mu\text{A}/\text{cm}^2$ , which was slightly less than that of the monolithic matrix alloys. Weight-loss data that were measured over a 32-day period showed that the MMCs corroded at higher rates than that of the alloys, contradicting trends observed in  $i_{\text{CORR}}$  data. The mica MMCs corroded at rates ranging from approximately 3.0 to 5.5  $\text{mg}\cdot\text{dm}^{-2}\cdot\text{day}^{-1}$ , which was approximately 1.5–2.0 times that of the monolithic alloys. The discrepancy in the trends of the weight-loss and  $i_{\text{CORR}}$  data could have resulted from several possibilities. Some of the weight loss could be due to nonelectrochemical reactions, such as the dissolution of dissolvable phases and the exfoliation of mica particles. The values of  $i_{\text{CORR}}$  were extrapolated from polarization curves that were generated after relatively short exposure times; whereas, the weight loss was assessed over a 32-day period.

### *Effect of Diffusion Bonds and Microstructural Contaminants*

B/Al and Gr/Al MMCs have been fabricated using techniques where aluminum foils, filaments, and precursor wires have been consolidated by diffusion bonding. The diffusion bonds, if of low integrity or if contaminated, may cause severe corrosion damage.

Sedriks et al. [20] and Bakulin et al. [19] found that  $E_{\text{CORR}}$  of B/Al MMCs was active to that of their monolithic matrix alloys in aerated NaCl solutions. That behavior does not appear to comply with the mixed-potential theory. Bakulin et al. [19], however, found that hot-pressed stacks of aluminum foil processed in the same way as the MMC (but without the BFs) have  $E_{\text{CORR}}$  values that are active to the MMCs. The only difference between the monolithic aluminum and the hot-pressed stacks of aluminum foil was crevices in the diffusion bonds between adjacent foils. The crevices, which are sources of additional anodic sites, can polarize the stacks to active potentials. Thus, the B/Al MMCs are actually noble to the matrix material processed in the same way, and the  $E_{\text{CORR}}$  values actually coincide with the mixed-potential theory. Sedriks et al. [20] found that increasing the volume fraction of BF caused anodic current densities (w.r.t. matrix area) to increase. This implies that BF-matrix interfaces, which increase with BF content, were also sources of anodic sites. Evans and Braddick [89] also reported that BF-matrix interface regions were severely attacked in an oxygenated NaCl solution. These reports indicate that the BF-matrix and foil-foil interfaces are major causes of corrosion.

Gr/Al MMCs that were fabricated by the Ti-B vapor deposit method [90] go through a processing sequence where a tow of graphite fibers is infiltrated with molten aluminum and solidified as a precursor composite wire. Bunches of wires are then diffusion bonded to consolidate larger components, such as plates and bars. Some of these composites have been susceptible to exfoliation (Fig. 6), which is the disbonding of precursor wires and aluminum foils caused by localized corrosion along wire-wire and wire-foil diffusion bonds. This form of corrosion is severe because composite plates can be rendered useless, even though corrosion in the bulk of the foils and precursor wires may not be severe. There have been some reports [91,92] of preferential corrosion of diffusion-bonded regions in marine environments. In severe cases of exfoliation, precursor wires are expelled from the sides of MMC plates [93].

The cause of exfoliation has been attributed [94] to residual microstructural chloride [95] that is trapped in the diffusion-bonded regions. The residual chloride originates from the Ti-B vapor deposit method, which uses titanium tetrachloride ( $\text{TiCl}_4$ ) and boron trichloride ( $\text{BCl}_3$ ) gases. The chloride is deposited on the skin of the precursor wires as the wires are extracted from the aluminum melt. Experiments have shown that in sodium sulfate solutions, where aluminum should be passive, the chloride-contaminated diffusion bonds corrode vigorously [94] (see subsection **Determination of Dissolution Behavior Using Polarization Techniques**.)

### *Effect of Reinforcement Constituents on Stress Corrosion in Al MMCs*

Stress corrosion studies have been conducted on continuous-fiber reinforced and particle-reinforced Al MMCs.

**FIG. 6—Exfoliation of Gr/6061-T6 Al MMC. MMC exposed to indoor environment.**

Studies have been conducted on unidirectional, continuous-fiber Gr/6061 Al [96], BF/2024 Al [20], BORSIC/2024 Al, BORSIC/6061 Al [97], and Nextel ( $\text{Al}_2\text{O}_3$ ,  $\text{SiO}_2$ ,  $\text{B}_2\text{O}_3$ )/6061 Al [98] MMCs. Stresses were applied either parallel or perpendicular to the fiber axis of unnotched specimens. The Gr/6061 Al MMCs were stressed parallel to the fiber axis in natural seawater. At high stresses, failure was stress-dependent and occurred in less than 100 h. At lower stresses, failure was primarily caused by extensive corrosion, and therefore, was relatively stress-independent. BF/2024 Al MMCs stressed parallel to the fiber axis at 80 % fracture strength in an NaCl solution did not fail in 1000 h, but failed after 500 h when  $\text{H}_2\text{O}_2$  was added to the NaCl solution. Extensive intergranular matrix corrosion and broken filaments at random sites were observed. The monolithic matrix alloy failed within 10 h under similar conditions. For BF/2024 Al MMCs stressed perpendicular to the fiber axis at 90 % yield strength in the NaCl and NaCl with  $\text{H}_2\text{O}_2$  solutions, failure occurred by intergranular matrix corrosion and separation at diffusion-bonded, fiber-matrix interfaces. Failure times decreased with increasing BF content. BORSIC/Al MMCs were stressed to 689 MPa along the fiber axis by three-point bending and exposed to synthetic sea-salt spray at 95°C and nearly 100 % relative humidity. The 6061 Al MMCs showed general corrosion attack without preference to tensile regions; whereas, the 2024 Al MMCs showed about a 2-to-1 depth-of-attack ratio comparing the tensile to the compressive surfaces, which may have been related to specimen orientation. Unlike the 6061 Al MMCs, the corrosion resistance of the 2024 Al MMC was sensitive to heat treatment. In the Nextel fiber MMC, the prevailing mode of failure was

attributed to extensive corrosion along the fiber-matrix interface and not stress-corrosion cracking in a pH 2 NaCl solution [98].

The stress corrosion behavior of particulate  $\text{Al}_2\text{O}_3$ /2014 [99],  $\text{SiC}_w$ /6061 [99],  $\text{SiC}_p$ /6061 [99], and  $\text{SiC}_p$ /2024 [100,101] MMCs were investigated in NaCl solutions. The  $\text{Al}_2\text{O}_3$ /2014 MMC was susceptible to stress corrosion cracking while subjected to three-point beam bending and alternate exposure and continuous immersions in an NaCl solution [99]. Under the same conditions, however, the 6061 Al MMCs reinforced with  $\text{SiC}_p$  and  $\text{SiC}_w$  were not susceptible to stress corrosion cracking [99]. Similarly,  $\text{SiC}_p$ /2024 MMCs were not prone to stress-corrosion cracking under constant strain at 75 % of ultimate tensile strength while exposed to an aerated NaCl solution [100]. Slow strain rate tension testing of  $\text{SiC}_p$ /2024 MMCs in an NaCl solution in the open-circuit condition indicated that the MMC lost up to 10 % of failure strength compared to exposure in air [101].

#### *Effect of Reinforcement Constituents on Corrosion Fatigue in Al MMCs*

Corrosion-fatigue studies have been conducted on Al MMCs reinforced with graphite fibers [96],  $\text{SiC}_w$  [102–105], and  $\text{SiC}_p$  [103,106]. Processing conditions and type of reinforcement affect corrosion-fatigue behavior. Unnotched Gr/6061 Al MMCs were exposed to natural seawater and stressed parallel to the fiber axis. The MMCs were processed with either silica ( $\text{SiO}_2$ )-coated or Ti-B-coated graphite fibers. For a given stress amplitude, the Ti-B type MMC had the longest corrosion-fatigue life, followed by the  $\text{SiO}_2$  type, and the monolithic matrix alloy. At low stress amplitudes

corresponding to longer exposure times, the  $\text{SiO}_2$  type MMC suffered premature failure due to extensive corrosion. In SiC/Al MMCs, fatigue crack rates of compact tension specimens are usually higher in NaCl solutions as compared to air [102] or argon [106]. Loading frequency affects corrosion-fatigue crack rates [106], but no consistent trends were observed. Fatigue [102] and corrosion-fatigue [106] crack rates are influenced by loading and extrusion or rolling direction. The nucleation of a crack was also observed at the bottom of a corrosion pit [105]. The shape of the reinforcement constituent may also have significant effects. Jones [104] developed a model based on crack-tip strain rate that is applicable to stress corrosion and corrosion fatigue. The model is relatively insensitive to slight variations in reinforcement volume fraction. The model predicts that crack rates are reduced by increasing the reinforcement constituent 1-to-d ratio, implying that MMCs reinforced with whiskers are more resistant to stress corrosion and corrosion fatigue than those reinforced with particles. This is in agreement with results of Hasson et al. [103] who found that  $\text{SiC}_w/6061$  Al MMCs have longer corrosion-fatigue lives than  $\text{SiC}_p/6061$  Al MMCs in salt-laden moist air.

### Magnesium MMCs

Very light composites can be fabricated from magnesium, which is one of the lightest structural metals. Its density is only  $1.7 \text{ g/cm}^3$ . Magnesium, however, is the most active structural metal in the electromotive series [107], which means that it has a very high tendency to corrode. Since magnesium is a very active metal, it is particularly susceptible to galvanic corrosion when in contact with noble reinforcement constituents. Corrosion studies have been conducted on magnesium MMCs reinforced with BF, graphite fibers,  $\text{SiC}_{MF}$ , and  $\text{Al}_2\text{O}_3$  fibers. Stress-corrosion behavior of an  $\text{Al}_2\text{O}_3/\text{Mg}$  MMC is included in the  $\text{Al}_2\text{O}_3$  section.

#### Effect of Boron

The general properties of BFs given in the subsection *Effect of Boron* (for **Aluminum MMCs**) also apply here. Pure boron is an insulator and a very poor cathode. Galvanic currents were unmeasurable between pure boron and magnesium in 0.005 N NaCl solutions [21,108] (it was not specified if solutions were deaerated or aerated). Galvanic currents, however, were measurable between virgin tungsten-core BF (cores either shielded or exposed) coupled to magnesium [108] and an MA2-1 magnesium alloy [21]. Galvanic currents were higher when tungsten cores were exposed [21,108]. This is not unexpected since pure tungsten was shown to be an effective cathode [21]. Since galvanic currents were unmeasurable between magnesium and pure boron, but measurable between magnesium and virgin BF (with tungsten cores shielded), it was suspected that the outer layer of BFs consisted of tungsten boride and not of pure boron [108]. It was also found that BF extracted from the matrix supported cathodic-current densities that were about five times that of virgin BFs [21]. The corrosion rates of actual BF/MA2-1 MMCs in 0.005 N and 0.5 N NaCl solutions were  $12.49 \text{ g/m}^2\text{day}$  and  $81.72 \text{ g/m}^2\text{day}$ , respectively, which were about six times the values of the monolithic matrix alloy in respective environments.

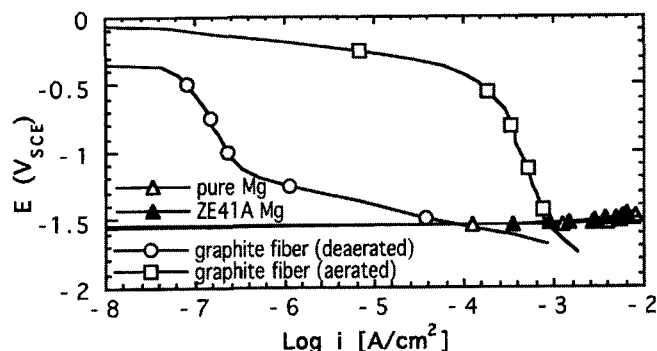


FIG. 7—Anodic polarization diagrams of pure magnesium and ZE41A magnesium in deaerated 3.15 wt % NaCl plotted with the cathodic polarization diagrams of pitch-based graphite fiber (cross section exposed) in deaerated and aerated 3.15 wt % NaCl at 30°C. Scan rate = 0.1 mV/s.

#### Effect of Graphite

The general properties of graphite given in the subsection *Effect of Graphite* (for **Aluminum MMCs**) also apply here. Figure 7 shows the cathodic polarization diagrams of pitch-based graphite (cross section exposed) in deaerated and aerated 3.15 wt % NaCl with the anodic polarization diagrams of pure magnesium and ZE41A magnesium in deaerated 3.15 wt % NaCl. Figure 7 reveals that galvanic-corrosion rates increase in aerated solutions. It should be noted that both anodic and cathodic curves of pure magnesium and ZE41A magnesium are practically insensitive to solution aeration, indicating that normal corrosion rates are virtually unaffected by dissolved oxygen. Figure 7 shows that galvanic corrosion of magnesium is not anodically controlled, and therefore galvanic-corrosion rates should increase with increasing area fraction of cathodic reinforcement material. Trzaskoma [109] showed that galvanic-corrosion current densities increased from about  $0.3 \times 10^{-3}$  to  $0.6 \times 10^{-3} \text{ A/cm}^2$  (based on magnesium area) as the graphite-to-magnesium area ratio was increased from 0.25 to 0.44. The galvanic couples consisted of AZ31B magnesium alloy and pitch-based graphite fiber with fiber ends and circumferential fiber surface exposed to an aerated, borated-boric acid solution of 8.4 pH containing 1000 ppm NaCl. Actual MMCs immersed in air-exposed 0.001 N NaCl suffered severe degradation within five days.

Czyrkliś [28] showed electrochemical evidence of galvanic corrosion in actual graphite/magnesium (Gr/Mg) MMCs. He measured open-circuit potentials and calculated corrosion current densities (by Tafel extrapolation) of a 40 % Gr/Mg MMC and its matrix alloy that were exposed to a deaerated 50 ppm-chloride solution. The open-circuit potential of the composite ( $-1.127 \text{ V}_{SCE}$ ) was about 0.3 V noble to that of the matrix alloy, and  $i_{CORR}$  of the composite ( $178 \text{ } \mu\text{A/cm}^2$ ) was about 40 times greater than that of the matrix alloy at 25°C. Czyrkliś also reported severe degradation of Gr/AZ91C Mg MMCs that were exposed to 50 ppm-chloride solutions and 95 % relative humidity atmospheres. Composite degradation was attributed to galvanic corrosion and to selective attack of  $\text{Mg}_{17}\text{Al}_{12}$  precipitates in the magnesium matrix.

Interphase formation of  $\text{Al}_4\text{C}_3$  was observed in a Gr/Mg (1 % aluminum) MMC produced by squeeze casting. The  $\text{Al}_4\text{C}_3$

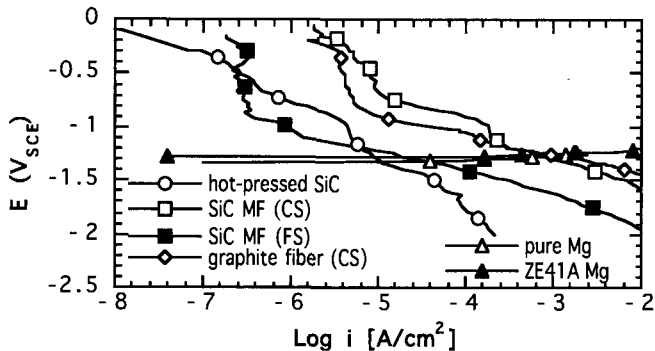


FIG. 8—Anodic polarization diagrams of pure magnesium and ZE41A magnesium plotted with cathodic polarization diagrams of hot-pressed SiC, SiC<sub>MF</sub>, and pitch-based graphite fibers in deaerated 0.5 M NaNO<sub>3</sub> at 30°C. Scan rate = 0.1 mV/s. CS = cross section exposed. FS = fiber surface exposed.

formation resulted from heat treatments at 500°C [110]. Degradation of these MMCs could be accelerated by both galvanic corrosion and Al<sub>4</sub>C<sub>3</sub> hydrolysis.

#### Effect of Silicon Carbide

The general properties of SiC given in the subsection **Aluminum MMCs** also apply here. Galvanic corrosion between magnesium and SiC depends to a large degree on the type of SiC reinforcement and on the presence of dissolved oxygen in solution. Figures 8 and 9 show anodic polarization diagrams of pure magnesium and ZE41A magnesium with cathodic polarization diagrams of hot-pressed SiC, SiC<sub>MF</sub> (with either carbon core or carbon-rich surface exposed) in deaerated and oxygenated 0.5 M sodium nitrate (NaNO<sub>3</sub>) solutions, respectively. Galvanic-corrosion rates (as determined by the mixed-potential theory) are greater in oxygenated solutions due to oxygen reduction occurring on the reinforcement materials (compare Figs. 8 and 9). Galvanic-corrosion rates are lowest between magnesium and hot-pressed SiC and highest between magnesium and SiC<sub>MF</sub> (with core exposed) [111]. The carbon-core and the carbon-rich surface appear to have a dominant effect on cathodic behavior of the SiC<sub>MF</sub>. The curves of SiC<sub>MF</sub> have a stronger resemblance to pitch-based graphite fiber (cross section exposed) than to hot-pressed SiC (Figs. 8 and 9). Similar

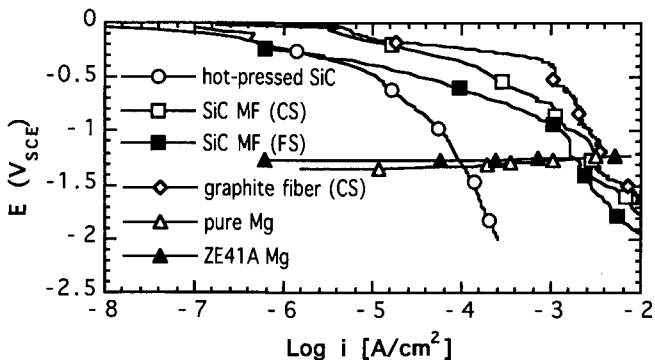


FIG. 9—Similar to Fig. 8, except the 0.5 M NaNO<sub>3</sub> solution is oxygenated.

results were obtained for sodium sulfate (Na<sub>2</sub>SO<sub>4</sub>) and NaCl solutions [112]. Nunez-Lopez et. al [113] conducted studies on particulate ZC71 magnesium alloy reinforced with 12 vol. % SiC particles ranging in size up to approximately 20 μm. Specimens exposed to salt spray tests did not show signs of galvanic coupling between the matrix and SiC particles. Preferential attack between SiC particles and the matrix was not observed. Instead, macroscopic anodic and cathodic regions developed. Corrosion spread over the MMC surface much more rapidly than on the monolithic alloy, but the local corrosion rates were approximately only three times greater on the MMC. The authors [113] speculated that the higher corrosion rates on the MMCs could have been caused by iron contamination of the magnesium matrix during processing in a steel crucible. Studies on a model MMC consisting of high-purity magnesium and well-separated SiC particles exposed to 3.5 wt % NaCl also did not show evidence of galvanic corrosion between the particles and matrix [114].

#### Effect of Alumina

The general properties given for Al<sub>2</sub>O<sub>3</sub> in the previous subsection of the same title (for aluminum MMCs) also apply here. Galvanic corrosion should not be expected in Al<sub>2</sub>O<sub>3</sub>/magnesium (Al<sub>2</sub>O<sub>3</sub>/Mg) MMCs, since Al<sub>2</sub>O<sub>3</sub> is an insulator. However, Levy and Czyrkis [115] found that continuous-fiber Al<sub>2</sub>O<sub>3</sub>/AZ91C MMCs were much more susceptible to corrosion in chloride-containing solutions compared to the matrix alloy. They did not specify if the solutions were deaerated. In a 50 ppm Cl<sup>-</sup> solution at 25°C, the corrosion rate of the composite was 0.78 mm/y compared to only 0.10 mm/y for the alloy. When the temperature was increased to 66°C, the corrosion rate of the composite dramatically increased to about 150 mm/y, while that of the alloy increased to only 0.13 mm/y. Corrosion rates were highest in 3.5 wt % NaCl at 25°C, where the composite corroded at an astronomical rate of about 350 mm/y compared to 3.6 mm/y for the alloy. In chloride-free environments, the composite showed equivalent or greater resistance to corrosion than the alloy. In distilled water at 25°C and 95 % relative-humidity environments at 25°C and 66°C, the corrosion rate of the composite and matrix alloy was less than 0.25 mm/y. The tremendously higher corrosion rates of the composites in the chloride-containing environments appear to be caused by the presence of the Al<sub>2</sub>O<sub>3</sub> fibers. It is unlikely that galvanic corrosion between the matrix and Al<sub>2</sub>O<sub>3</sub> fibers can take place, since Al<sub>2</sub>O<sub>3</sub> is an insulator. However, galvanic corrosion could be possible between the matrix and an interphase or precipitates, which potentially could form due to the presence of the Al<sub>2</sub>O<sub>3</sub> fibers. Czyrkis [116] reported that  $E_{CORR}$  of 35 % continuous-fiber Al<sub>2</sub>O<sub>3</sub>/AZ91C MMCs was more noble than that of the matrix alloy in 50 ppm Cl<sup>-</sup> solutions, indicating that galvanic corrosion is a possibility. It was not specified if the solutions were deaerated.

Evans [117] studied the stress-corrosion behavior of continuous-fiber Al<sub>2</sub>O<sub>3</sub>/ZE41A Mg MMC in an NaCl-potassium chromate (K<sub>2</sub>CrO<sub>4</sub>) solution. Unnotched and notched specimens stressed parallel to the fiber axis and exposed for approximately 100–1000 h in the NaCl-K<sub>2</sub>CrO<sub>4</sub> solution retained approximately 90 % of the strength in air. The matrix alloy and the MMC with the stress aligned perpendicular to the fiber axis retained only approximately 40–60 % of the strength in air.

## Lead MMCs

Lead is a relatively heavy metal with a density of  $11.4 \text{ g/cm}^3$ . Lead MMCs, therefore, are normally developed for applications where a combination of its structural, physical, and chemical properties are important. The corrosion behavior of pure lead MMCs in simulated, lead-acid battery environments has been studied to assess the feasibility of using these composites as positive electrode grids in place of conventional lead-based alloy grid materials. Lead can be alloyed with elements such as arsenic, antimony, or calcium to increase strength and stiffness. These elements, however, reduce corrosion resistance. Monolithic pure lead has very good corrosion resistance in lead-acid battery environments (which consists of sulfuric acid solutions), but is heavy and lacks sufficient mechanical strength. Pure lead, therefore, has been reinforced with strong, lightweight fibers in hopes of achieving the goals of increasing strength, reducing weight, and retaining the corrosion resistance of pure lead [118–120]. More recently, a study on the corrosion behavior of particulate lead-antimony alloy MMCs exposed in sodium chloride solutions has been conducted [121].

### Effect of Fibers

To simulate corrosion in lead-acid battery environments, Dacres et al. [118] and others [119,120] anodically polarized test materials at 1.226 V (versus mercury/mercurous sulfate reference electrode) in sulfuric acid solutions (of 1.285 specific gravity) at 50, 60, and/or 70°C. At 1.226 V, lead and water are oxidized to lead dioxide ( $\text{PbO}_2$ ) and molecular oxygen ( $\text{O}_2$ ), respectively [122,123]. About one third of the total anodic current is consumed in the oxidation of lead under these conditions [120].

$\text{Al}_2\text{O}_3$ , carbon, SiC, and glass-quartz fibers of various volume percents have been used in lead MMCs. Fabrication methods as well as fiber type may have significant effects on corrosion resistance. Several types of continuous-fiber  $\text{Al}_2\text{O}_3$ /lead ( $\text{Al}_2\text{O}_3/\text{Pb}$ ) MMCs [118,120] were examined. MMCs containing 5 % [120] and 7.5 % [118]  $\text{Al}_2\text{O}_3$  fibers showed good corrosion resistance. The 5 %  $\text{Al}_2\text{O}_3$  fiber MMC had gravimetric and Faradaic corrosion rates of 0.033 mm/y and 0.10 mm/y, respectively.  $\text{Al}_2\text{O}_3/\text{Pb}$  MMCs having 6 % [118], 10 % [120], 15 % [120], and 25 % [118]  $\text{Al}_2\text{O}_3$  fibers did not have acceptable corrosion resistance. Poor bonding between  $\text{Al}_2\text{O}_3$  fibers and the matrix allowed the electrolyte to diffuse into fiber-matrix interfaces, leading to accelerated corrosion [118] and swelling of the composite due to corrosion-product buildup [120].

Composites reinforced with carbon or graphite fiber were not resistant to corrosion [118,120]. Viala et al. [119] reported that the graphite fibers were oxidized. SiC fiber/Pb MMCs also did not have good corrosion resistance [119,120]. Viala et al. [119] reported that composites were destroyed by swelling due to formation of  $\text{PbO}_2$  in the bulk of the composites. The SiC fibers (which do not have carbon cores) were stable. The corrosion resistance of glass-quartz/Pb MMCs having 9.5 % fiber was not satisfactory, and gravimetric and Faradaic corrosion rates were 0.24 and 0.62 mm/yr, respectively [120]. Lead alloys containing calcium and tin had gravimetric and Faradaic corrosion rates of 0.49 and 1.35 mm/yr, respectively, also showing unsatisfactory corrosion

resistance [118,120]. The studies [118–120] have indicated that the penetration of electrolyte into the bulk of the composites, possibly through poorly bonded fiber-matrix interfaces or by oxidation of fibers, is a major factor governing degradation properties.

### Effect of Particles

A commercially available lead (80 %)-antimony (20 %) alloy was reinforced with 1, 3, and 5 wt % zircon ( $\text{ZrSiO}_4$ ) particles [121] and exposed to a 1 N NaCl solution. The particles should not induce galvanic corrosion. Weight loss measurements, made over a 72 h period, showed that weight loss of the lead MMCs increased with increasing zircon content. Heat treatment of the  $\text{ZrSiO}_4/\text{Pb-Sn}$  MMC at 200°C also improved resistance to weight loss.

## Depleted Uranium MMCs

Tungsten fiber/depleted uranium (W/DU) MMCs are the antithesis of the lightweight MMCs. W/DU MMCs were developed to create high-density materials. Uranium has a density of  $18.9 \text{ g/cm}^3$ .

DU corrodes galvanically when coupled to tungsten fibers in air-exposed 3.5 wt % NaCl solutions at room temperature [124]. The open-circuit potential of tungsten fiber ( $-0.25 \text{ V}_{\text{SCE}}$ ) is noble to that of the DU alloy ( $-0.80 \text{ V}_{\text{SCE}}$ ). The open-circuit potentials of the W/DU MMC and galvanic couples consisting of tungsten fiber and DU alloy of equal areas are  $-0.78 \text{ V}_{\text{SCE}}$  and  $-0.77 \text{ V}_{\text{SCE}}$ , respectively. These potentials fall between those of tungsten fibers and the DU alloy, which is consistent with the mixed-potential theory. The galvanic-corrosion current density measured between equal areas of tungsten fibers and the DU alloy was equal to about  $4 \times 10^{-5} \text{ A/cm}^2$ . In a 30-day exposure test in the NaCl solution, the W/DU MMC lost  $43.56 \text{ mg/cm}^2$ , which was about 1.3 times that of the DU alloy.

## Stainless Steel MMCs

Sintered, particulate composites consisting of ferritic 434L stainless steel and  $\text{Al}_2\text{O}_3$  particles have been developed for potential application in chemical processing plants, turbine blades, and heat exchanger tubes [125–127]. Austenitic 316L stainless steels reinforced with  $\text{Al}_2\text{O}_3$  and  $\text{Y}_2\text{O}_3$  have also been investigated for enhanced strength and wear resistance [128].

### Effect of Alumina

The corrosion behavior of sintered  $\text{Al}_2\text{O}_3/434\text{L}$  MMCs and sintered 434L alloy without  $\text{Al}_2\text{O}_3$  particles was examined [125–127]. The volume fraction of  $\text{Al}_2\text{O}_3$  particles in these materials ranged from 0 to 8 %. The effect of small amounts of titanium and niobium alloying elements on corrosion resistance was also investigated. Galvanic corrosion between 434L stainless steel and  $\text{Al}_2\text{O}_3$  should not occur since the latter is an insulator. Experiments were conducted in 1 N sulfuric acid ( $\text{H}_2\text{SO}_4$ ) [125–127] and 5 wt % NaCl [125] solutions at room temperature. It was not mentioned if solutions were deaerated. In 1 N  $\text{H}_2\text{SO}_4$  [125–127], there was no strong correlation between  $\text{Al}_2\text{O}_3$  content and corrosion behavior. The  $E_{\text{CORR}}$  and  $i_{\text{CORR}}$  values varied between materials,

**FIG. 10—Micrograph of SiC<sub>MF</sub>/Ti-15-3-3-3 MMC. Monofilament volume fraction is approximately 40 %.**

but clear trends relating  $E_{CORR}$  and  $i_{CORR}$  to  $Al_2O_3$  content or alloy composition were not conspicuous. One of the few generalities that could be made was that passive-current densities were within an order of magnitude of  $1 \text{ mA/cm}^2$  for almost all materials. Alloying with titanium and niobium tended to increase passive current densities. In the 5 wt % NaCl solutions,  $i_{CORR}$  of the MMCs was less than  $10 \text{ } \mu\text{A/cm}^2$  [125]. Upon polarization, all materials displayed active corrosion behavior in the NaCl solutions.

Particulate 316L stainless steel MMCs [128], fabricated using powder metallurgy, were reinforced with 3, 4, and 5 wt %  $Al_2O_3$  and additions of 2 wt % chromium diboride ( $B_2Cr$ ) or 1 wt % boron nitride (BN) for sintering aids. The density of the MMCs ranged from 86 to 96 % of the theoretical value. Unreinforced 316L specimens were also fabricated using powder metallurgy without sintering aids, resulting in 85 % of theoretical density. The test samples were immersed in 10 % sulfuric acid ( $H_2SO_4$ ) at room temperature for 24 h, 1 % hydrochloric acid (HCl) at room temperature for 24 h, and boiling 10 % nitric acid ( $HNO_3$ ) for 8 h. The pure, unreinforced 316L specimens passivated in the 10 %  $H_2SO_4$  solution; whereas, the corrosion rate of the MMC generally increased with increasing  $Al_2O_3$  content to a maximum value of approximately 4 mm/yr. Specimens with the BN sintering aids corroded at higher rates as compared to those with the  $B_2Cr$  sintering aids. The authors correlated this behavior to the local depletion of chromium in the matrix due to matrix reactions with BN, as compared to reactions with chromium-rich  $B_2Cr$ . The MMC performed better than the unreinforced 316L specimen in the 1 wt % HCl solution, but worse than the unreinforced specimen in the boiling nitric acid solution. There was no strong correlation between  $Al_2O_3$  content in the MMCs and the corrosion rates in 1 wt % HCl and boiling 10 wt %  $HNO_3$  solutions.

### *Effect of Yttria*

Yttria ( $Y_2O_3$ ) is an insulator and galvanic effects are not expected. The 316L stainless steel specimens discussed above [128] were also reinforced with 3, 4, and 5 wt %  $Y_2O_3$  and additions of 2 wt % chromium diboride ( $B_2Cr$ ) or 1 wt % boron nitride (BN) for sintering aids. In all solutions (i.e., sulfuric, hydrochloric, and nitric acid solutions), the  $Y_2O_3$  reinforced MMCs exhibited reduced corrosion resistance as compare to the  $Al_2O_3$  reinforced MMCs. The  $Y_2O_3$  MMCs were sintered to 88–96 % of theoretical density, and the  $Al_2O_3$  MMCs were sintered to 86–92 % of theoretical density. The  $Y_2O_3$  particles also showed better bonding to the matrix, probably forming a complex  $YCrO_3$  oxide, as compared to the  $Al_2O_3$  particles. It is possible that the formation of the reaction layer around the  $Y_2O_3$  particles may have depleted chromium from the matrix, resulting in reduced corrosion resistance, as compared to the  $Al_2O_3$ -reinforced MMCs.

### **Titanium MMCs**

Titanium MMCs have been developed for aerospace applications, as well as potential surgical implant materials. Silicon carbide MF/titanium ( $SiC_{MF}/Ti$ ) MMCs (Fig. 10) have utility in high-temperature applications requiring strong, lightweight materials. Titanium has a density of  $4.5 \text{ g/cm}^3$ . Structural  $SiC_{MF}/Ti$  MMCs have been used in prototype drive shafts, turbine-engine discs, compressor discs, and hollow fan blades; they are also candidate materials for the skin of the National Aerospace Plane [129]. Porous, particulate Ti MMCs have potential use as surgical implant materials, owing to the compatibility of titanium and bone growth [130]. Porous titanium is a good surgical implant material, because

bone growth is enhanced by the relatively low elastic modulus of titanium, and bone ingrowth is allowed by the porous structure. Porous titanium, however, has poor tribological properties and, therefore, MMCs that incorporate graphite to reduce friction, and incorporate titanium carbide to improve wear resistance are of interest [130].

#### *Effect of Graphite*

Porous titanium/graphite MMCs were processed and heat-treated to fabricate a porous titanium/graphite/titanium carbide (TiC) MMC [130]. Polarization tests were conducted in 0.9 wt % NaCl and lactated Ringer's solution for in vitro use. The  $E_{CORR}$  values of the Ti/graphite/TiC MMCs were more noble than that of pure Ti, as expected due to the presence of graphite and TiC. The anodic polarization current densities of the MMCs were significantly higher than that of pure monolithic titanium, which passivated. The authors attributed the higher corrosion rates of the Ti/graphite/TiC MMC to its porosity, which may have prevented complete passivation of the titanium matrix. Another possibility for the higher current densities could be the oxidation of graphite particles, and not dissolution of the titanium matrix (see subsection below).

#### *Effect of Silicon Carbide*

Corrosion studies on titanium alloy Ti-15-3-3-3 (15 wt % vanadium, 3 wt % chromium, 3 wt % tin, 3 wt % aluminum, balance titanium) [131] and titanium aluminide  $\alpha_2$ -Ti<sub>3</sub>Al (14 wt % aluminum, 21 wt % niobium, balance titanium) [132] reinforced with SiC<sub>MF</sub> have been conducted. The corrosion behavior of Ti-15-3-3-3/SiC<sub>MF</sub> MMC was investigated in 3.15 wt % NaCl. There was excellent agreement in the polarization diagrams of the actual MMC and that of a model utilizing the polarization diagrams of the individual constituents and the mixed-potential theory (see subsection **Determination of Dissolution Behavior Using Polarization Techniques**), indicating that the fabrication processing did not affect the dissolution behavior of the MMC constituents. The matrix passivated and the carbon cores and carbon-rich outer surface of the SiC<sub>MF</sub> oxidized. During anodic polarization, graphite oxidizes to CO<sub>2</sub> [94]. Zero-resistance ammeter studies showed that galvanic currents between the Ti-15-3-3-3 matrix and SiC<sub>MF</sub> were negligible. Based on the polarization diagrams, the galvanic current density cannot exceed that of the passive current density of Ti-15-3-3-3. The corrosion behavior of the  $\alpha_2$ -Ti<sub>3</sub>Al/SiC<sub>MF</sub> [132] was somewhat similar to that of the Ti-15-3-3-3/SiC<sub>MF</sub> MMC [131], with the exception that the  $\alpha_2$ -Ti<sub>3</sub>Al matrix is less resistant to pitting. During anodic polarization, the  $\alpha_2$ -Ti<sub>3</sub>Al/SiC<sub>MF</sub> pitted at approximately 1 V<sub>SCE</sub> in 0.5 N NaCl, which was approximately 0.5 V less than that of the monolithic matrix alloy. Some matrix pitting and crevice corrosion around the SiC<sub>MF</sub> were also observed after anodic polarization. The galvanic current density of the  $\alpha_2$ -Ti<sub>3</sub>Al/SiC<sub>MF</sub> MMC was negligible and limited to the passive current density of the  $\alpha_2$ -Ti<sub>3</sub>Al matrix [132].

#### **Copper MMCs**

Copper MMCs have been investigated for use in marine, electronic, and thermal applications. Copper is relatively heavy, with a density of 8.96 g/cm<sup>3</sup>. Reinforcements are

typically chosen to impart strength and stiffness, reduce weight, enhance thermal and electrical properties, improve machinability, and enhance wear resistance. Initial studies [7] were conducted on a wide variety of experimental copper and copper alloy MMCs for marine applications. The MMCs generally showed corrosion behavior that was similar to that of the monolithic alloys, although corrosion rates were higher for some of the MMCs. More recent corrosion studies have also added additional insight to corrosion mechanisms of copper MMCs.

#### *Effect of Graphite*

Copper MMCs have been reinforced with graphite particles and fibers. The particulate MMCs have been developed for sliding electrical contact materials [133], and improved machinability for lead-free copper alloys [134]. Fiber reinforced MMCs have been developed for applications requiring reduced-weight and high thermal conductivity [135]. Highly graphitized fibers have very high thermal conductivity, exceeding that of silver [3].

Sun et al. [136] examined the corrosion behavior of pure copper MMCs with 1.2, 5, 15, 25, and 40 vol % graphite particles and fiber-reinforced pure copper MMCs with 50 vol % graphite fibers in deaerated and aerated 3.5 wt % NaCl solutions. The corrosion potential of the particulate reinforced MMCs became more noble with increasing graphite content in both the deaerated and aerated solutions, as would be expected by increasing the content of the noble graphite particles. Polarization resistance generally decreased, with a few exceptions, with increasing graphite content in both deaerated and aerated solutions. This indicated that corrosion rates generally increased with graphite content, assuming that cathodic and anodic Tafel slopes remained relatively constant for the different MMC specimens (i.e., 1.2–40 vol % graphite). The corrosion rate is a function of both the polarization resistance and Tafel slopes. The 6 % porosity of the MMCs may have also been a factor regarding corrosion behavior. The corrosion potential of the fiber-reinforced MMC (50 vol % graphite fiber) was approximately as noble as the particulate MMC with 40 vol % graphite in the aerated solution, but was significantly more active than the particulate composite in the deaerated solution. This finding could be expected if the hydrogen evolution kinetics on the graphite fiber were significantly different from that of the graphite particles.

Rohatgi et al. [134] studied C90300 copper alloy reinforced with approximately 1–10 vol % graphite particles and 1 wt % Ti, added to enhance wettability of the graphite. The corrosion potentials of the MMCs increased with increasing graphite content in an aqueous solution containing ferric chloride, copper sulfate, and hydrochloric acid. Gravimetric measurements were made on specimens immersed for one year in an aqueous solution containing sodium bicarbonate, magnesium chloride, calcium chloride, sodium sulfate, and sodium chloride. The results showed insignificant weight gain (<0.25 %), indicating that the MMCs were resistant to corrosion in the test solution.

#### *Effect of Silicon Carbide*

Lee et al. [137] examined the corrosion behavior of pure copper MMCs reinforced with 0, 5, 10, and 20 vol % SiC particles

in a 5 wt % NaCl solution. The porosity of the materials ranged from 2.2 to 3.5 %, and generally increased with increasing SiC content. Corrosion potentials became more active, and corrosion current densities increased with increasing SiC content. The corrosion morphology indicated that there was significant corrosion at SiC-copper interfaces. Voids caused by porosity and SiC-copper interfaces both increased with increasing SiC content. Hence, the decrease in  $E_{CORR}$  with increasing SiC content is likely to have been caused by an increase in anodic currents from voids and SiC-copper interfaces. The SiC particles could also serve as cathodes, but due to their relatively high electrical resistivity, they are not as effective, for example, as graphite. Hence, any increases in cathodic currents with the increase in SiC content may not have been sufficient to shift  $E_{CORR}$  to positive values and overcome the effect of the higher anodic currents.

#### *Effect of Alumina*

A copper MMC reinforced with 2.7 vol %  $Al_2O_3$  was studied by Sun and Wheat [138] in deaerated and aerated 3.5 wt % NaCl. The corrosion potentials of the MMC were slightly more active (i.e., 0.01–0.02 V) than monolithic pure copper. The corrosion rates of the MMCs were comparable to monolithic copper. A galvanic effect with  $Al_2O_3$  is not expected due to its insulative nature.

#### **Zinc MMCs**

Zinc MMCs have been developed [139] for potential use as bearing materials. Zinc has a density of 7.14 g/cm<sup>3</sup>. An MMC with a ZA-27 zinc alloy matrix was cast with 1, 3, and 5 wt % graphite particles ranging in sizes from 100 to 150  $\mu$ m. Zinc alloys are known to have excellent wear and bearing characteristics [140]. Gravimetric corrosion tests were conducted at 23°C in:

1. SAE 40 grade lubricating oil that had been in service for six months in an internal combustion engine, and
2. 1 N hydrochloric acid (HCl).

The MMCs did not corrode in the previously-used lubricating oil. Interestingly, in the 1 N HCl, corrosion rates decreased with higher content of graphite, which is a noble conductor that can induce galvanic corrosion. Several hypotheses were made [139], such as the presence of the graphite network hindering the reaction between HCl and the matrix. Another possibility is that zinc ions in solution, acting as a cathodic inhibitor [141], may have eventually precipitated as zinc hydroxide on the cathodic graphite particles if the local pH resided in the correct range. This would also explain the decreasing corrosion rates with time that was observed. Similar behavior was noticed in graphite-aluminum couples in solutions containing zinc chloride [142].

### **METHODS FOR EVALUATING CORROSION DAMAGE**

Tests to evaluate corrosion damage of conventional monolithic alloys are not always applicable to MMCs. Under some circumstances, the reinforcement constituents that are left

in relief after matrix corrosion may interfere with measurements. There have been relatively few studies on MMC corrosion in comparison to monolithic metals. Tests that have been more commonly used for MMCs are gravimetric, and also those that assess loss of mechanical properties. The researcher should be able to use other tests that have been developed for monolithic alloys; however, data must be analyzed carefully to ensure that test results are valid since special problems are sometimes associated with MMCs. Further details regarding corrosion analysis of MMCs are provided below.

#### **Depth of Attack**

Depth of attack can be used to assess corrosion damage in MMCs. It may be more difficult, however, to assess the penetration depth in MMCs compared to that in monolithic metals because reinforcement constituents that are left in relief can prevent a depth gage from contacting the matrix surface, and thus, prevent the true depth of penetration from being measured. In particulate MMCs, the interference may be attenuated since reinforcement particles are free to detach from the matrix as they are undercut by corrosion. When reinforcements interfere with mechanical measurements, depth of penetration can be assessed metallographically. Samples may be mounted and polished, and penetration measurements can be made with a microscope and a calibrated eyepiece. Details for determining penetration depth are available in ASTM G 46, Recommended Practice for Examination and Evaluation of Pitting Corrosion.

#### **Gravimetric**

Gravimetric evaluation is often used to assess corrosion damage. Special problems, however, can be encountered when using gravimetric evaluation for MMCs. Results obtained from MMCs can be misleading, since corrosion is sometimes accompanied by weight gain. MMC samples can experience weight gain when corrosion products and moisture are trapped in composite microstructures, resulting in swelling of the MMC. Swelling of MMCs appears to be more troublesome with fiber-reinforced composites, as opposed to particulate composites. For details on gravimetric measurements, reference should be made to ASTM G 1, Recommended Practice for Preparing, Cleaning, and Evaluating Corrosion Test Specimens. This standard addresses metal alloys, and references should be followed for the matrix alloy in the MMC.

#### **Loss in Mechanical Properties**

Corrosion damage of MMCs is sometimes assessed by measuring a loss in strength. Changes in strength are measured before and after exposure to corrosion environments. These tests can be very useful for assessing corrosion damage in MMCs when corrosion appears to be mild on the surface, but penetrates deep into the bulk along diffusion bonds or reinforcement-matrix interfaces. Test specimens may take on various shapes and sizes, depending on the form of the stock material (e.g., wire, sheet, rod, etc.). Reference should be made to ASTM G 1 (7.3.2) and G 46 (7.5).



## TESTS FOR SPECIFIC CORROSION TYPES

Various tests can be performed on MMCs to obtain specific information on corrosion behavior. Tests used for monolithic metals can be applied to MMCs with some success. However, since MMCs may have properties significantly different from those of monolithic metals, conventional tests developed for monolithic metals may not always produce sought-after results when used to test MMCs.

### Determination of Dissolution Behavior Using Polarization Techniques

Dissolution behavior of MMCs can be determined by anodic polarization measurements. To ensure that the polarization setup is working properly, it should be checked against ASTM G 5, Reference Test Method for Making Potentiostatic and Potentiodynamic Anodic Polarization Measurements. The dissolution behavior of MMCs in specific environments can be determined by generating anodic polarization diagrams of the MMC. To determine the extent of matrix dissolution versus that of reinforcement dissolution, polarization diagrams of monolithic matrix metal and reinforcement constituents should be generated separately. The individual diagrams of the MMC constituents are then used to generate a polarization diagram of the MMC (here called a mixed-electrode diagram) using the mixed-potential theory. If good correlation exists between the polarization diagram of the actual MMC and the mixed-electrode diagram, the fraction of dissolution current originating from the matrix and from the reinforcement constituents can be determined. The results can be verified by examining the corrosion morphology of the MMC. For example, the anodic polarization diagrams of an actual  $\text{SiC}_{\text{MF}}$  (40 vol %)/Ti-15-3-3-3 MMC and that generated using the MMC constituents and the mixed-potential theory corresponding to a 3.15 wt % NaCl solution were in very good agreement (Fig. 11). Corrosion morphology studies confirmed that the high anodic currents measured on the MMC corresponded to oxidation of the carbon cores and carbon-rich surface of the  $\text{SiC}_{\text{MF}}$  [131].

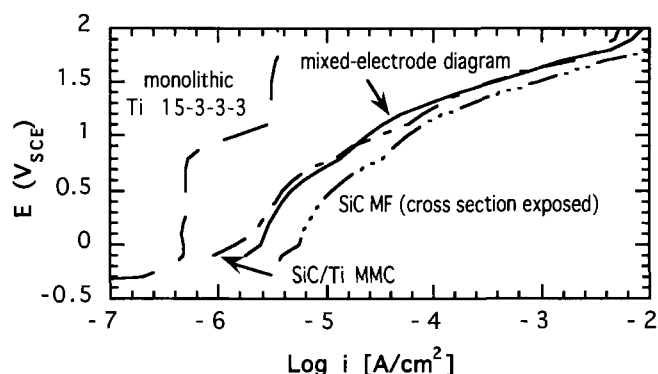


FIG. 11—Anodic polarization diagrams of SiC monofilament (cross section exposed), monolithic Ti-15-3-3-3, and  $\text{SiC}_{\text{MF}}$  (40 vol. %)/Ti-15-3-3-3 MMC exposed to deaerated 3.15 wt % NaCl at 30°C. Scan rate = 0.1 mV/s. A diagram for a composite consisting of 40 vol. % SiC monofilament was generated on the basis of the mixed-potential theory.

If there is poor correlation between the polarization diagram of the actual MMC and the mixed-electrode diagram, the discrepancy in dissolution behavior might be caused by formation of interphases or contaminants introduced in the MMC microstructure during processing. For example [94], Fig. 12 shows an anodic, mixed-electrode diagram generated from polarization diagrams of graphite fiber and 6061-T6 aluminum exposed to 0.5 M  $\text{Na}_2\text{SO}_4$ . The mixed-electrode diagram shows that 6061-T6 aluminum passivates during the anodic scan. The anodic polarization diagram of an actual Gr(50 vol %)/6061-T6 Al MMC, however, exposed to the same solution shows that pitting is induced at approximately  $-0.6 V_{\text{SCE}}$  (Fig. 12). The unexpected pitting was found to be caused by residual microstructural chloride [94] that was unintentionally introduced into the microstructure during processing [95]. Buonanno [143] later verified that the anodic polarization diagram of chloride-free Gr/Al MMCs traces the mixed-electrode diagram.

### Galvanic Corrosion between Matrix and Reinforcement Constituents under Immersed Conditions

Galvanic corrosion between the matrix and reinforcement constituents can be determined by several methods. The mixed-potential theory can be used with polarization data of the matrix metal and reinforcement constituents to estimate galvanic-corrosion currents and potentials. The intersection of the anodic polarization curve of the matrix metal with the cathodic polarization curve of a noble reinforcement constituent gives the galvanic-corrosion current and potential (refer to appendix of ASTM G 82, Guide for Development and Use of a Galvanic Series for Predicting Galvanic Corrosion Performance). When using this method, it should be noted that changes in electrochemical behavior of MMC constituents caused by MMC processing cannot be taken into consideration if virgin MMC constituents are used to obtain polarization data. The behavior predicted using virgin MMC constituents could be quite different compared to that of the actual MMC. Timonova et al. [21] showed that BF<sub>3</sub>

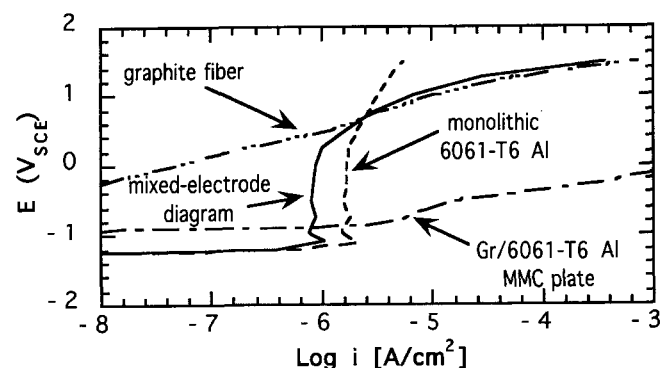


FIG. 12—Anodic polarization diagrams of pitch-based graphite fiber (cross section exposed), monolithic 6061-T6 aluminum, and Gr(50 vol. %)/6061-T6 Al MMC plate exposed to deaerated 0.5 M  $\text{Na}_2\text{SO}_4$  at 30°C. Scan rate = 0.1 mV/s. A diagram for a composite consisting of 50 vol. % graphite and 6061-T6 aluminum was generated on the basis of the mixed-potential theory.

extracted from a magnesium matrix supported cathodic-current densities that were about five times that of virgin BFs (see subsection *Effect of Boron* in **Magnesium MMCs**).

The galvanic-corrosion rate can also be determined from the open-circuit corrosion current of actual MMCs. To obtain the galvanic-corrosion current density, the local-corrosion current density [144] should be subtracted from the open-circuit current (of the MMC) that has been normalized with respect to matrix area. One difficulty would be to obtain an accurate estimation of the local-corrosion current density.

The zero-resistance ammeter technique (ASTM G 71, Practice for Conducting and Evaluating Galvanic Corrosion Tests in Electrolytes) can be used to measure galvanic-corrosion currents between monolithic pieces of the matrix metal and reinforcement constituents. One advantage of this technique is that galvanic-corrosion currents can be measured over long periods of time. If virgin MMC constituents are used, changes due to processing cannot be accounted for. Pohlman [22] showed that galvanic-corrosion currents between aluminum alloys and BFs extracted from an aluminum MMC were significantly greater than currents between aluminum alloys and virgin BFs. Aluminum borides that formed on the BFs during MMC processing were responsible for increasing galvanic-corrosion currents (see subsection *Effect of Boron* in **Aluminum MMCs**).

The three methods discussed above can be used to estimate galvanic-corrosion behavior. Advantages and disadvantages are associated with each method. Some comparisons between these methods have been made for Gr/Al [36] and SiC/Mg MMCs [111].

### Uniform Corrosion

Uniform corrosion of MMC matrices can be expected in environments that attack the matrix metal uniformly. In continuous-fiber MMCs, however, fibers will be left in relief as the matrix corrodes, whereas, in particulate MMCs, reinforcement particles fall free as they are undercut. Uniform corrosion rates of MMCs may be greater than that of the monolithic matrix alloys, due to galvanic action between the matrix and reinforcement constituents.

MMCs should be exposed to environments of interest and then inspected. If corrosion is uniform, corrosion rates can be assessed using recommendations in ASTM G 1. Electrochemical measurements can also be used to determine uniform corrosion rates. Refer to ASTM G 102, Calculation of Corrosion Rates and Related Information from Electrochemical Measurements. Note that when determining matrix corrosion rates, the corrosion current should be normalized with respect to the matrix area if reinforcements are inert.

### Pitting Corrosion

MMCs are susceptible to pitting in environments that induce pitting in the matrix metal. These environments usually contain halides and are oxidizing. In MMCs that have noble reinforcement constituents, galvanic corrosion between reinforcement constituent and matrix can accelerate pitting compared to the monolithic matrix alloy. The presence of the reinforcement constituents may also influence pitting by altering MMC microstructures. In SiC<sub>w</sub>/Al MMCs,

for example, pits were more numerous and much smaller in size compared to pits on monolithic alloys [60]. Apparently, the SiC whiskers enhance the precipitation of the intermetallic particles upon which pits nucleate [60] (see subsection *Effect of Silicon Carbide* in **Aluminum MMCs**).

MMC specimens should be exposed to environments of interest. The degree of pitting can be assessed using ASTM G 46. Pitting potentials may be obtained by generating anodic polarization diagrams of the MMCs. Refer to ASTM G 5 to ensure that the electrochemical setup is working properly. Electrochemical impedance spectroscopy has also been used to detect the onset of pitting in some MMCs [145].

### Stress Corrosion

Studies on stress-corrosion behavior of MMCs have been limited. Results for some aluminum and magnesium MMCs are summarized in the subsections on *Effect of Reinforcement Constituents on Stress Corrosion in Al MMCs*, and *Effect of Alumina* in Magnesium MMCs respectively. The type of tests that can be used will depend to some degree on the form in which the MMC is produced and whether or not the MMC can be precracked. Some types of MMCs are produced only in the form of relatively thin panels (e.g., less than about 0.25 cm), whereas other types are available in bars or tubes. It is sometimes impossible to properly precrack unidirectional, continuous-fiber MMCs because cracks do not always grow perpendicular to the direction of applied stress [146].

A variety of stress-corrosion testing methods, using unnotched, notched, and precracked specimens, have been well documented [147]. The following ASTM standards are also helpful in developing a stress-corrosion testing program: ASTM E 399, Test Method for Plane-Strain Fracture Toughness of Metallic Materials; G 30, Practice for Making and Using U-Bend Stress-Corrosion Test Specimens; G 38, Practice for Making and Using C-Ring Stress-Corrosion Test Specimens; G 39, Practice for Preparation and Use of Bent-Beam Stress-Corrosion Test Specimens; and G 49, Recommended Practice for Preparation and Use of Direct Tension Stress-Corrosion Test Specimens.

### Corrosion Fatigue

Relatively few studies on corrosion fatigue of MMCs have been conducted. Results for Gr/Al and SiC/Al MMCs are summarized in the subsection *Effect of Reinforcement Constituents on Corrosion Fatigue in Al MMCs*. An appropriate testing program will depend on the form of the MMC and the ability to precrack specimens, which is a problem in some MMCs. The practices for fatigue testing in ASTM Metals Test Methods and Analytical Procedures, Volume 03.01, should be helpful in selecting a testing scheme. Annex A.1 in ASTM E 647, Test Method for Measurement of Fatigue Crack Growth Rates, is particularly useful when doing corrosion-fatigue tests in aqueous environments.

## COMPARISON OF CORROSION BEHAVIOR BETWEEN MMCs

To some degree, the corrosion resistance of MMCs can be ranked based on the intrinsic corrosion resistance of the

matrix alloy. Within an MMC group, corrosion resistance can be further ranked based on the type of reinforcement constituent. For example, MMCs reinforced with graphite would have less resistance to corrosion than those reinforced with  $\text{Al}_2\text{O}_3$ , due to the degree of galvanic corrosion between reinforcement and matrix. It should be emphasized, however, that ranking by generalities may be misleading, since MMC corrosion properties can be highly sensitive to the effects of processing conditions. The formation of interphases, presence of microstructural contaminants, and microstructural changes in the matrix metal caused by reinforcement constituents may significantly deteriorate corrosion resistance. Two identical types of MMCs, but fabricated by different methods, may have very different corrosion resistances.

In the most general terms, titanium MMCs have the best resistance to corrosion due to the general and localized corrosion resistance of titanium. Aluminum MMCs reinforced with semi-conductors or insulators (i.e., SiC,  $\text{Al}_2\text{O}_3$ , and mica) were ranked next due to lack of significant galvanic action between reinforcement and matrix. Aluminum MMCs reinforced with conductors (i.e., graphite, carbon-coated  $\text{SiC}_{\text{MF}}$ ) are more susceptible to corrosion due to galvanic coupling with the reinforcements. Magnesium MMCs were ranked the least resistant due to the highly reactive magnesium matrix. Lead, and depleted uranium, stainless steel, copper, and zinc MMCs were not ranked since these MMCs and/or testing conditions were very specialized or limited. The above assessment is general and exceptions are likely.

## REFERENCES

- [1] Weeton, J. W., Peters, D. M., and Thomas, K. L., *Engineers' Guide to Composite Materials*, American Society for Metals, Metals Park, OH, 1987, p. 2-2.
- [2] Park, G. B. and Foster, D. A., in *International Technical Conference Proceedings, SUR/FIN'90*, Boston, MA, July 1990, American Electroplaters and Surface Finishers Society, pp. 1349-1369.
- [3] Harrigan, W. C., Jr., in *Metal Matrix Composites: Processing and Interfaces*, R. K. Everett and R. J. Arsenault, Eds., Academic Press, 1991, pp. 1-16.
- [4] Liu, Y., Rohatgi, P. K., Ray, S., and Barr, T. L., in *Conference Proceedings ICCM/8*, S. W. Tsai and G. S. Springer, Eds., 20H, Society for the Advancement of Material and Process Engineering (SAMPE), 1991.
- [5] Lim, T., Lee, C. S., Kim, Y. H., and Han, K. S., in *Conference Proceedings ICCM/8*, S. W. Tsai and G. S. Springer, Eds., 20E, Society for the Advancement of Material and Process Engineering (SAMPE), 1991.
- [6] Metzger, M. and Fishman, S. G., *Industrial and Engineering Chemistry. Product Research and Development*, Vol. 22, 1983, pp. 296-302.
- [7] Aylor, D.M., "Corrosion of Metal Matrix Composites," *Metals Handbook*, 9th ed., Vol. 13, *Corrosion*, ASM International, Metals Park, OH, 1987, pp. 859-863.
- [8] Turnbull, A., "Review of Corrosion Studies on Aluminium Metal Matrix Composites," *British Corrosion Journal*, Vol. 27, No. 1, 1992, p. 27.
- [9] Trzaskoma, P. P., "Corrosion," in *Metal Matrix Composites: Mechanisms and Properties*, R. K. Everett and R. J. Arsenault, Eds., 1991, Academic Press, pp. 383-404.
- [10] Hihara, L. H. and Latanision, R. M., "Corrosion of Metal Matrix Composites," *International Materials Review*, Vol. 39, No. 6, 1994, pp. 245-264.
- [11] Lucas, K. A. and Clarke, H., *Corrosion of Aluminium-Based Metal Matrix Composites*, Research Studies Press, England, John Wiley & Sons, New York, 1993.
- [12] Jones, R. H., "Metal Matrix Composites," in *Environmental Effects on Engineered Materials*, R. H. Jones, Ed., Marcel Dekker, 2001, pp. 375-390.
- [13] Buck, M. E. and Suplinskas, R. J., in *Engineered Materials Handbook on Composites*, Vol. 1, ASM International, Metals Park, OH, 1987, pp. 851-857.
- [14] Tsirlin, A. M., in *Strong Fibres (Handbook of Composites*, Vol. 1), W. Watt and B. V. Perov, Eds., Elsevier Science Publishers B. V., 1985, pp. 155-199.
- [15] Schwartz, M. M., *Composite Materials Handbook*, McGraw-Hill, New York, 1984.
- [16] Kim, W. H., Koczak, M. J., and Lawley, A., in *Proceedings of the 1978 International Conference on Composite Materials, ICCM/2*, Toronto, Canada, April 1978, The Metallurgical Society of AIME, pp. 487-505.
- [17] de Zoubov, N., Deltombe, E., and Pourbaix, M., in *Atlas of Electrochemical Equilibria in Aqueous Solutions*, M. Pourbaix, Ed., National Association of Corrosion Engineers, Houston, TX, 1974, pp. 158-167.
- [18] Porter, M. C. and Wolff, E. G., in *Advances in Structural Composites*, Vol. 12, *12th National Symposium and Exhibit*, Anaheim, CA, October 1967, Society for the Advancement of Material and Process Engineering, AC-14.
- [19] Bakulin, A. V., Ivanov, V. V., and Kuchkin, V. V., *Zashchita Metallov*, Vol. 14, No. 1, 1978, pp. 102-104.
- [20] Sedriks, A. J., Green, J. A., and Novak, D. L., *Metallurgical Transactions*, Vol. 2, 1971, pp. 871-875.
- [21] Timonova, M. A., Spiryakina, G. I., Stroganova, V. F., and Zolotareva, L. A., *Metallovedenie i Termicheskaya Obrabotka Metallov*, Vol. 11, 1980, pp. 33-35.
- [22] Pohlman, S. L., *Corrosion*, Vol. 34, 1978, pp. 156-159.
- [23] Gurbunov, V. G., Parshin, V. D., and Pamin, V. V., *Russ. Cast. Prod.*, 1974, p. 348.
- [24] Rao, N. A. P., Biswas, S., Rothagi, P. K., Santhanam, A., and Narayanaswamy, K., *Tribo. Int.*, Vol. 13, 1980, p. 171.
- [25] Van Muylder, J. and Pourbaix, M., in *Atlas of Electrochemical Equilibria in Aqueous Solutions*, M. Pourbaix, Ed., National Association of Corrosion Engineers, Houston, TX, 1974, pp. 449-457.
- [26] Hihara, L. H., "Corrosion of Aluminum-Matrix Composites," Ph. D. thesis, Massachusetts Institute of Technology, Cambridge, MA, 1989.
- [27] Kinoshita, K., *Carbon, Electrochemical and Physicochemical Properties*, John Wiley and Sons, New York, 1988.
- [28] Czyrkis, W. F., Paper 196, in *Conference Proceedings of 'Corrosion 85'*, Boston, MA, March 1985, National Association of Corrosion Engineers.
- [29] Coleman, S. L., Scott, V. D., and McEnaney, B., "Corrosion Behaviour of Aluminium-Based Metal Matrix Composites," *Journal of Materials Science*, Vol. 29, 1994, pp. 2826-2834.
- [30] Dutta, I., Elkin, L. R., and King, J. D., "Corrosion Behavior of a P130x Graphite Fiber Reinforced 6063 Aluminum Composite Laminate in Aqueous Environments," *Journal of the Electrochemical Society*, Vol. 138, No. 11, 1991, pp. 3199-3209.
- [31] Shimizu, Y., Nishimura, T., and Matsushima, I., "Corrosion Resistance of Al-Based Metal Matrix Composites," *Materials Science and Engineering A*, Vol. 198, 1995, pp. 113-118.
- [32] Modi, O. P., Saxena, M., Prasad, B. K., Jha, A. K., Das, S., and Yegneswaran, A. H., "Role of Alloy Matrix and Dispersoid on Corrosion Behavior of Cast Aluminum Alloy Composites," *Corrosion*, Vol. 54, No. 2, 1998, pp. 129-134.
- [33] Dull, D. L., Harrigan, W. C., Jr., and Amateau, M. F., "Final Report, The Effect of Matrix and Fiber Composition on Mechanical Strength and Corrosion Behavior of Graphite-Aluminum

- Composites," Aerospace Report No. ATR-76(7564)-1, The Aerospace Corporation, El Segundo, CA, 1977.
- [34] Brown, R. H. and Mears, R. B., *Transactions of the Electrochemical Society*, Vol. 74, 1938, p. 510.
- [35] Dash, L. C., "The Mechanism of Corrosion and Corrosion Control of Aluminum/Graphite Metal Matrix Composites," Ph.D. Thesis, Ohio State University, Columbus, OH, 1988.
- [36] Hihara, L. H. and Latanision, R. M., *Corrosion*, Vol. 48, No. 7, 1992, pp. 546–552.
- [37] Saxena, M., Jha, A. K., and Upadhyaya, G. S., "Corrosion Behaviour of Sintered 6061 Aluminium Alloy-Graphite Particle Composites," *Journal of Materials Science*, Vol. 28, 1993, pp. 4053–4058.
- [38] Saxena, M., Prasad, B. K., and Dan, T. K., "Corrosion Characteristics of Aluminium Alloy Graphite Particulate Composite in Various Environments," *Journal of Materials Science*, Vol. 27, 1992, pp. 4805–4812.
- [39] Schrecengost, T. R., Shaw, B. A., Wendt, R. G., and Moshier, W. C., "Nonequilibrium Alloying of Graphite-Reinforced Aluminum Metal Matrix Composites," *Corrosion*, Vol. 49, No. 10, 1993, pp. 842–849.
- [40] Wendt, R. G., Moshier, W. C., Shaw, B. A., Miller, P., and Olson, D. L., "Corrosion-Resistant Aluminum Matrix for Graphite-Aluminum Composites," *Corrosion*, Vol. 50, No. 11, 1994, pp. 819–826.
- [41] Becher, H. J., in *Handbook of Preparative Inorganic Chemistry*, Vol. 1, 2nd ed., G. Brauer, Ed., Academic Press, 1963, p. 832.
- [42] Kendall, E. G., in *Metal Matrix Composites*, Vol. 4, K. G. Kreider, Ed., Academic Press, 1974, pp. 319–397.
- [43] Portnoi, K. I., Timofeeva, N. I., Zambolotskii, A. A., et al., *Poroshkovaya Metallurgiya*, No. 2(218), 1981, pp. 45–49.
- [44] Hihara, L. H., "Corrosion of Aluminum-Matrix Composites," *Corrosion Reviews*, Vol. 15, Nos. 3–4, 1997, pp. 361–386.
- [45] Aylor, D. M. and Moran, P. J., *Journal of the Electrochemical Society*, Vol. 132, 1985, pp. 1277–1281.
- [46] Wielage, B. and Dörner, A., "Corrosion Studies on Aluminium Reinforced with Uncoated and Coated Carbon Fibres," *Composites Science and Technology*, Vol. 59, 1999, pp. 1239–1245.
- [47] Advanced Composite Materials Corporation Brochure, "Stablcel," Greer, SC, no year.
- [48] Ichinose, N., *Introduction to Fine Ceramics*, John Wiley and Sons, 1987, pp. 50–52.
- [49] Textron Specialty Materials, "Continuous Silicon Carbide Metal Matrix Composites," Company Report, no year.
- [50] Trzaskoma, P. P., McCafferty, E., and Crowe, C. R., *Journal of the Electrochemical Society*, Vol. 130, 1983, pp. 1804–1809.
- [51] Lore, K. D. and Wolf, J. S., in *Extended Abstracts*, Vol. 81-2, Denver, CO, October 1981, The Electrochemical Society, Abstract No. 154.
- [52] Sun, H., Koo, E. Y., and Wheat, H. G., "Corrosion Behavior of SiC/6061 Al Metal Matrix Composites," *Corrosion*, Vol. 47, No. 10, 1991, pp. 741–753.
- [53] Modi, O. P., Saxena, M., Prasad, B. K., Yegneswaran, A. H., and Vaidya, M. L., "Corrosion Behaviour of Squeeze-Cast Aluminium Alloy—Silicon Carbide Composites," *Journal of Materials Science*, Vol. 27, 1992, pp. 3897–3902.
- [54] Griffiths, A. J. and Turnbull, A., "An Investigation of the Electrochemical Polarisation Behaviour of 6061 Aluminium Metal Matrix Composites," *Corrosion Science*, Vol. 36, No. 1, 1994, pp. 23–35.
- [55] Golledge, S. L., Kruger, J., and Dacres, C. M., in *Extended Abstracts*, Vol. 85-2, Las Vegas, NV, October 1985, The Electrochemical Society, Abstract No. 146.
- [56] Roper, G. W. and Attwood, P. A., "Corrosion Behaviour of Aluminium Matrix Composites," *Journal of Materials Science*, Vol. 30, 1995, pp. 898–903.
- [57] Monticelli, C., Zucchi, F., Bonollo, F., Brunoro, G., Frignani, A., and Trabanelli, G., "Application of Electrochemical Noise Analysis to Study the Corrosion Behavior of Aluminum Composites," *Journal of the Electrochemical Society*, Vol. 142, No. 2, 1995, pp. 405–410.
- [58] Nunes, P. C. R. and Ramanathan, L. V., "Corrosion Behavior of Alumina-Aluminum and Silicon Carbide-Aluminum Metal-Matrix Composites," *Corrosion*, Vol. 51, No. 8, 1995, pp. 610–617.
- [59] Kiourtsidis, G. E., Skolianos, S. M., and Pavlidou, E. G., "A Study on Pitting Behaviour of AA2024/SiC<sub>p</sub> Composites Using the Double Cycle Polarization Technique," *Corrosion Science*, Vol. 41, 1999, pp. 1185–1203.
- [60] Trzaskoma, P. P., *Corrosion*, Vol. 46, 1990, pp. 402–409.
- [61] Kiourtsidis, G. and Skolianos, S. M., "Corrosion Behavior of Squeeze-Cast Silicon Carbide-2024 Composites in Aerated 3.5 wt.% Sodium Chloride," *Materials Science and Engineering A*, Vol. 248, 1998, pp. 165–172.
- [62] Buarzaiga, M. M. and Thorpe, S. J., "Corrosion Behavior of As-Cast, Silicon Carbide Particulate-Aluminum Alloy Metal-Matrix Composites," *Corrosion*, Vol. 50, No. 3, 1994, pp. 176–185.
- [63] Paciej, R. C. and Agarwala, V. S., *Corrosion*, Vol. 44, 1988, pp. 680–684.
- [64] Nutt, S. R. and Duva, J. M., *Scripta Metallurgica*, Vol. 20, 1986, pp. 1055–1058.
- [65] England, J. and Hall, I. W., *Scripta Metallurgica*, Vol. 20, 1986, pp. 697–700.
- [66] Bhat, M. S. N., Surappa, M. K., and Sudhaker Nayak, H. V., "Corrosion Behaviour of Silicon Carbide Particle Reinforced 6061/Al Alloy Composites," *Journal of Materials Science*, Vol. 26, No. 18, 1991, pp. 4991–4996.
- [67] Ahmad, Z. and Abdul Aleem, B. J., "Effect of Temper on Seawater Corrosion of an Aluminum-Silicon Carbide Composite Alloy," *Corrosion*, Vol. 52, No. 11, 1996, pp. 857–864.
- [68] Ahmad, Z., Paulette, P. T., and Aleem, B. J. A., "Mechanism of Localized Corrosion of Aluminum-Silicon Carbide Composites in a Chloride Containing Environment," *Journal of Materials Science*, Vol. 35, 2000, pp. 2573–2579.
- [69] Yao, H. -Y. and Zhu, R. -Z., "Interfacial Preferential Dissolution on Silicon Carbide Particulate/Aluminum Composites," *Corrosion*, Vol. 54, No. 7, 1998, pp. 499–503.
- [70] Garrard, W. N. C., "The Corrosion Behaviour of Aluminium-Silicon Carbide Composites in Aerated 3.5% Sodium Chloride," *Corrosion Science*, Vol. 36, No. 5, 1994, pp. 837–851.
- [71] Iseki, T., Kameda, T., and Maruyama, T., *Journal of Materials Science*, Vol. 19, 1984, pp. 1692–1698.
- [72] Park, J. K. and Lucas, J. P., "Moisture Effect on SiC<sub>p</sub>/6061 Al MMC: Dissolution of Interfacial Al<sub>4</sub>C<sub>3</sub>," *Scripta Materialia*, Vol. 37, No. 4, 1997, pp. 511–516.
- [73] Donomoto, T., Funatani, K., Miura, N., and Miyake, N., Paper 830252, Society of Automotive Engineers, March 1983.
- [74] Bolz, R. E. and Tuve, G. L., *CRC Handbook of Tables for Applied Engineering Science*, 2nd ed., CRC Press, 1973, p. 262.
- [75] Deltombe, E., Vanleughenaghe, C., and Pourbaix, M., in *Atlas of Electrochemical Equilibria in Aqueous Solutions*, M. Pourbaix, Ed., National Association of Corrosion Engineers, Houston, TX, 1974, pp. 168–176.
- [76] Greenwood, N. N. and Earnshaw, A., *Chemistry of the Elements*, Pergamon Press, 1984.
- [77] Fang, C.-K., Huang, C. C., and Chuang, T. H., "Synergistic Effects of Wear and Corrosion for Al<sub>2</sub>O<sub>3</sub> Particulate-Reinforced 6061 Aluminum Matrix Composites," *Metallurgical and Materials Transactions A*, Vol. 30A, March 1999, pp. 643–651.
- [78] Vaidya, R. U., Butt, D. P., Hersman, L. E., and Zurek, A. K., "Effect of Microbiologically Influenced Corrosion on the Tensile Stress-Strain Response of Aluminum and Alumina-Particle Reinforced Aluminum Composite," *Corrosion*, Vol. 53, No. 2, 1997, pp. 136–141.
- [79] Champion, A. R., Krueger, W. H., Hartmann, H. S., and Dhingra, A. K., in *Proceedings of the 1978 International Conference on*

- Composite Materials*, ICCM/2, Toronto, Canada, April 1978, The Metallurgical Society of AIME, pp. 883–904.
- [80] Yang, J.-Y. and Metzger, M., in *Extended Abstracts*, Vol. 81-2, Denver, CO, October 1981, The Electrochemical Society, Abstract No. 155.
- [81] Agarwala, V. S., in *Extended Abstracts*, Vol. 82-1, Montreal, Canada, May 1982, The Electrochemical Society, Abstract No. 15.
- [82] Bertolini, L., Brunella, M. F., and Candiani, S., "Corrosion Behavior of a Particulate Metal-Matrix Composite," *Corrosion*, Vol. 55, No. 4, 1999, pp. 422–431.
- [83] Rohatgi, P. K., Asthana, R., and Das, S., *International Metals Review*, Vol. 31, 1986, p. 115.
- [84] Nath, D., Bhat, R. T., and Rohatgi, P. K., *Journal of Materials Science*, Vol. 15, 1980, pp. 1241–1251.
- [85] Clauser, H. R., *The Encyclopedia of Engineering Materials and Processes*, Reinhold Publishing Corporation, 1963, p. 429.
- [86] Weast, R. C., *CRC Handbook of Chemistry and Physics*, 67th ed., B-116, CRC Press, 1986.
- [87] Nath, D. and Nambodhiri, T. K., *Composites*, Vol. 19, 1988, pp. 237–243.
- [88] Nath, D. and Nambodhiri, T. K., *Corrosion Science*, Vol. 29, 1989, pp. 1215–1229.
- [89] Evans, J. M. and Braddick, D. M., *Corrosion Science*, Vol. 11, 1971, pp. 611–614.
- [90] Harrigan, W. C., Jr. and Flowers, R. H., in *Failure Modes in Composites IV*, J. A. Cornie and F. W. Crossman, Eds., The Metallurgical Society of AIME, Warrendale, PA, 1979, pp. 319–335.
- [91] Vassilaros, M. G., Davis, D. A., Steckel, G. L., and Gudas, J. P., in *Mechanical Behavior of Metal-Matrix Composites*, J. E. Hack and M. F. Amateau, Eds., The Metallurgical Society of AIME, Warrendale, PA, 1983, pp. 335–352.
- [92] Pfeifer, W. H., in *Hybrid and Select Metal Matrix Composites: A State-of-the-Art Review*, W. J. Renton, Ed., American Institute of Aeronautics and Astronautics, New York, 1977, pp. 159–255.
- [93] Aylor, D. M. and Kain, R. M., in *Recent Advances in Composites in the United States and Japan*, ASTM STP 864, J. R. Vinson and M. Taya, Eds., ASTM International, West Conshohocken, PA, 1985, pp. 632–647.
- [94] Hihara, L. H. and Latanision, R. M., *Corrosion*, Vol. 47, 1991, pp. 335–341.
- [95] Hihara, L. H. and Latanision, R. M., *Materials Science and Engineering*, Vol. A126, 1990, pp. 231–234.
- [96] Davis, D. A., Vassilaros, M. G., and Gudas, J. P., *Materials Performance*, March 1982, pp. 38–42.
- [97] Dardi, L. E. and Kreider, K. G., in *Composite Materials: Testing and Design*, ASTM STP 546, ASTM International, West Conshohocken, PA, 1974, pp. 269–283.
- [98] Berkeley, D. W., Sallam, H. E. M., and Nayeb-Hashemi, H., "The Effect of pH on the Mechanism of Corrosion and Stress Corrosion and Degradation of Mechanical Properties of AA6061 and Nextel 440 Fiber-Reinforced AA6061 Composite," *Corrosion Science*, Vol. 40, No. 2/3, 1998, pp. 141–153.
- [99] Monticelli, C., Zucchi, F., Brunoro, G., and TrabANELLI, G., "Stress Corrosion Cracking Behaviour of Some Aluminium-Based Metal Matrix Composites," *Corrosion Science*, Vol. 39, Nos. 10–11, 1997, pp. 1949–1963.
- [100] Kiourtsidis, G. E. and Skolianos, S. M., "Stress Corrosion Behavior of Aluminum Alloy 2024/Silicon Carbide Particles ( $\text{SiC}_p$ ) Metal Matrix Composites," *Corrosion*, Vol. 56, No. 6, 2000, pp. 646–653.
- [101] Yao, H.-Y., "Effect of Particulate Reinforcing on Stress Corrosion Cracking Performance of a  $\text{SiC}_p$ /2024 Aluminum Matrix Composite," *Journal of Composite Materials*, Vol. 33, No. 11, 1999, pp. 962–970.
- [102] Yau, S. S. and Mayer, G., *Materials Science and Engineering*, Vol. 82, 1986, pp. 45–47.
- [103] Hasson, D. F., Crowe, C. R., Ahearn, J. S., and Cooke, D. C., in *Failure Mechanisms in High Performance Materials*, J. G. Early, T. R. Shives, and J. H. Smith, Eds., Cambridge University Press, 1984, pp. 147–156.
- [104] Jones, R. H., in *Environmental Effects on Advanced Materials*, R. H. Jones and R. E. Ricker, Eds., The Minerals, Metals, and Materials Society, Warrendale, PA, 1991, pp. 283–295.
- [105] Minoshima, K., Nagashima, I., and Komai, K., "Corrosion Fatigue Fracture Behaviour of a  $\text{SiC}$  Whisker-Aluminium Matrix Composite Under Combined Tension-Torsion Loading," *Fatigue and Fracture of Engineering Materials and Structures*, Vol. 21, 1998, pp. 1435–1446.
- [106] Buck, R. F. and Thompson, A. W., in *Environmental Effects on Advanced Materials*, R. H. Jones and R. E. Ricker, Eds., The Minerals, Metals, and Materials Society, Warrendale, PA, 1991, pp. 297–313.
- [107] Uhlig, H. H. and Revie, R. W., *Corrosion and Corrosion Control*, 3rd ed., John Wiley and Sons, New York, 1985.
- [108] Stroganova, V. F. and Timonova, M. A., *Metallovedenie i Termicheskaya Obrabotka Metallov*, October 1978, pp. 44–46.
- [109] Trzaskoma, P. P., *Corrosion*, Vol. 42, 1986, pp. 609–613.
- [110] Hall, I. W., *Scripta Metallurgica*, Vol. 21, 1987, pp. 1717–1721.
- [111] Hihara, L. H. and Kondepudi, P. K., *Corrosion Science*, Vol. 34, 1993, pp. 1761–1772.
- [112] Hihara, L. H. and Kondepudi, P. K., *Corrosion Science*, Vol. 36, 1994, pp. 1585–1595.
- [113] Nunez-Lopez, C. A., Skeldon, P., Thompson, G. E., Lyon, P., Karimzadeh, H., and Wilks, T. E., "The Corrosion Behaviour of Mg Alloy ZC71/ $\text{SiC}_p$  Metal Matrix Composite," *Corrosion Science*, Vol. 37, No. 5, 1995, pp. 689–708.
- [114] Nunez-Lopez, C. A., Habazaki, H., Skeldon, P., Thompson, G. E., Karimzadeh, H., Lyon, P., and Wilks, T. E., "An Investigation of Microgalvanic Corrosion Using a Model Magnesium-Silicon Carbide Metal Matrix Composite," *Corrosion Science*, Vol. 38, No. 10, 1996, pp. 1721–1729.
- [115] Levy, M. and Czyrkli, W. F., in *Extended Abstracts*, Vol. 81-2, Denver, CO, October 1981, The Electrochemical Society, Abstract No. 156.
- [116] Czyrkli, W. F., "Corrosion Evaluation of Metal Matrix Composite FP/Mg AZ91C," 1983 Tri-Service Corrosion Conference, Annapolis, MD, September 1983, U.S. Naval Academy.
- [117] Evans, J. T., *Acta Metallurgica*, Vol. 34, 1986, pp. 2075–2083.
- [118] Dacres, C. M., Reamer, S. M., Sutula, R. A., and Angres, I. A., *Journal of the Electrochemical Society*, Vol. 128, 1981, pp. 2060–2064.
- [119] Viala, J. C., El Morabit, M., and Bouix, J., *Materials Chemistry and Physics*, Vol. 13, 1985, pp. 393–408.
- [120] Dacres, C. M., Sutula, R. A., and Larrick, B. F., *Journal of the Electrochemical Society*, Vol. 130, 1983, pp. 981–985.
- [121] Seah, K. H. W., Sharma, S. C., Venkatesh, J., and Girish, B. M., "Corrosion Behaviour of Lead Alloy/Zircon Particulate Composites," *Corrosion Science*, Vol. 39, No. 8, 1997, pp. 1443–1449.
- [122] Burbank, J., *Journal of the Electrochemical Society*, Vol. 106, 1959, p. 369.
- [123] Burbank, J., Simon, A. C., and Willihnganz, E., in *Advances in Electrochemistry and Electrochemical Engineering*, Vol. VIII, P. Delahay, Ed., Wiley Interscience, 1971, p. 157.
- [124] Trzaskoma, P. P., *Journal of the Electrochemical Society*, Vol. 129, 1982, pp. 1398–1402.
- [125] Mukherjee, S. K., Kumar, A., and Upadhyaya, G. S., *Powder Metallurgy International*, Vol. 17, 1985, pp. 172–175.
- [126] Mukherjee, S. K., Kumar, A., and Upadhyaya, G. S., *British Corrosion Journal*, Vol. 20, 1985, pp. 41–44.
- [127] Mukherjee, S. K. and Upadhyaya, G. S., *Materials Chemistry and Physics*, Vol. 12, 1985, pp. 419–435.
- [128] Velasco, F., Antón, N., Torralba, J. M., and Ruiz-Prieto, J. M., "Mechanical and Corrosion Behaviour of Powder Metallurgy

- Stainless Steel Based Metal Matrix Composites," *Materials Science and Technology*, Vol. 13, No. 10, 1997, pp. 847–851.
- [129] Hughes, D., *Aviation Week Space Technology*, 28 November 1988, p. 91.
- [130] Blackwood, D. J., Chua, A. W. C., Seah, K. W. H., Thampuran, R., and Teoh, S. H., "Corrosion Behaviour of Porous Titanium-Graphite Composites Designed for Surgical Implants," *Corrosion Science*, Vol. 42, 2000, pp. 481–503.
- [131] Hihara, L. H. and Tamirisa, C., "Corrosion of SiC Monofilament/Ti-15-3-3-3 Metal-Matrix Composites in 3.15 wt.% NaCl," *Materials Science and Engineering A*, Vol. 198, 1995, pp. 119–125.
- [132] Saffarian, H. M. and Warren, G. W., "Aqueous Corrosion Study of  $\alpha_2$ -Ti<sub>3</sub>Al/SiC Composites," *Corrosion*, Vol. 54, No. 11, 1998, pp. 877–886.
- [133] Marcus, H. L., Weldon, W. F. and Persad, C., Technical Report Contract Number N62269-85-C0222, Austin, TX: University of Texas at Austin, February 1987.
- [134] Rohatgi, P. K., Nath, D., Kim, J. K., and Agrawal, A. N., "Corrosion and Dealloying of Cast Lead-Free Copper Alloy—Graphite Composites," *Corrosion Science*, Vol. 42, 2000, pp. 1553–1571.
- [135] Taylor, R. and Qunsheng, Y., "Thermal Transport in Carbon Fibre-Copper and Carbon Fibre/Aluminium Composites," in *Conference Proceedings ICCM/8*, S. W. Tsai and G. S. Springer, Eds., 18 D, Society for the Advancement of Material and Process Engineering (SAMPE), 1991.
- [136] Sun, H., Orth, J. E., and Wheat, H. G., "Corrosion Behavior of Copper-Based Metal-Matrix Composites," *Journal of Metals*, September 1993, pp. 36–41.
- [137] Lee, Y.-F., Lee, S.-L., and Lin, J.-C., "Wear and Corrosion Behaviors of SiC<sub>p</sub> Reinforced Copper Matrix Composite Formed by Hot Pressing," *Scandinavian Journal of Metallurgy*, Vol. 28, 1999, pp. 9–16.
- [138] Sun, H. and Wheat, H. G., "Corrosion Study of Al<sub>2</sub>O<sub>3</sub> Dispersion Strengthened Cu Metal Matrix Composites in NaCl Solutions," *Journal of Materials Science*, Vol. 28, 1993, pp. 5435–5442.
- [139] Seah, K. H. W., Sharma, S. C., and Girish, B. M., "Corrosion Characteristics of ZA-27-Graphite Particulate Composites," *Corrosion Science*, Vol. 39, No. 1, 1997, pp. 1–7.
- [140] Smith, W., *Structure and Properties of Engineering Alloys*, 2nd ed., McGraw-Hill, New York, 1993.
- [141] Boffardi, B. P., "Control of Environmental Variables in Water-Recirculating Systems," *Metals Handbook*, 9th ed., Vol. 13, *Corrosion*, ASM International, 1987, p. 487.
- [142] Hihara, L. H. and Latanision, R. M., "Suppressing Galvanic Corrosion in Graphite/Aluminum Metal-Matrix Composites," *Corrosion Science*, Vol. 34, No. 4, 1993, pp. 655–665.
- [143] Buonanno, M. A., "The Effect of Processing Conditions and Chemistry on the Electrochemistry of Graphite and Aluminum Metal Matrix Composites," Ph.D. Thesis, Massachusetts Institute of Technology, Cambridge, MA, 1992.
- [144] Wesley, W. A. and Brown, R. H., in *The Corrosion Handbook*, H. H. Uhlig, Ed., John Wiley and Sons, New York, 1948, pp. 481–496.
- [145] Mansfeld, F., Lin, S., Kim, S., and Shih, H., *Journal of the Electrochemical Society*, Vol. 137, No. 1, 1990, pp. 78–82.
- [146] Chawla, K. K., in *Metal Matrix Composites: Mechanisms and Properties*, R. K. Everett and R. J. Arsenault, Eds., Academic Press, 1991, pp. 235–253.
- [147] Sedriks, A. J., *Stress Corrosion Cracking Test Methods*, National Association of Corrosion Engineers, Houston, TX, 1990.

# Electrodeposits

*T. P. Moffat*<sup>1</sup>

ELECTRODEPOSITION OF METALLIC coatings has been extensively used as a means of corrosion control. In general, coatings are designed according to one of three different schemes. Electrodeposited coatings may be devised to act as corrosion-resistant barrier layers that separate the substrate from the aggressive environment. Alternatively, the well-known galvanic effects that arise from electrically coupling dissimilar metals may be used to provide active porous coatings, which cathodically or anodically protect the substrate. Electroplating a base metal with a barrier layer of gold is an example of the first strategy. Electrogalvanizing, or depositing zinc on steel, is an example of a sacrificial coating, while thin, porous, noble metal coatings such as palladium or platinum, which catalyze the proton-hydrogen reaction, may be used to anodically protect stainless steels.

In discussing the corrosion resistance of electrodeposited coatings, we are interested not only in the intrinsic chemical properties of the deposit, but must also give close attention to possible galvanic interactions between the coating and the substrate. This results from simultaneous exposure of the electrodeposited coating and the substrate due to either processing-related porosity or selective removal of the coating by mechanical or chemical means. Consequently, to be successfully implemented, the electrodeposited coating and substrate should be viewed as a composite system.

## INTRINSIC CORROSION RESISTANCE OF ELECTRODEPOSITED MATERIALS

In the simple case of free-standing electrodeposits, or deposits that completely cover the substrate, the corrosion behavior may be characterized by the standard procedures described in Sections III and IV of this manual. As with materials produced by other means, the corrosion performance of the deposit may be expected to be a sensitive function of the composition and microstructure, which are determined by the processing conditions. Interestingly, electrochemical deposition may be used to generate a variety of novel metastable materials. The deposition of certain metallic glasses or supersaturated single-phase materials offers the promise of remarkable corrosion resistance. For example, electrodeposited  $\text{Ni}_{51}\text{Cr}_{23}\text{P}_{26}$  metallic glass has been shown to exhibit corrosion characteristics superior to Hastelloy C-276 (Fig. 1) [1]. The nature of the passive film formed on Ni-Cr-P metallic

glasses has been investigated by X-ray photoelectron spectroscopy [2]. Oxidized phosphorus is found in the passive film as  $\text{CrPO}_4$  while phosphorus is enriched at the metal/film interface [2]. Thus, phosphorus chemistry in combination with the underlying homogeneous single-phase solid is responsible for the observed corrosion resistance. It is important to note that these single-phase materials cannot be made by traditional thermomechanical processing. In a similar fashion, much work has been performed concerning the corrosion resistance of  $\text{Ni}_{1-x}\text{P}_x$  alloys, which may be synthesized by electrolytic or electroless deposition [3]. Nonaqueous and molten salt electrolytes have also been used to produce a variety of interesting materials, ranging from photomagnetic cobalt-gadolinium films [4] to corrosion-resistant single phase aluminum-transition metal alloys [5]. Potentiodynamic polarization measurements of electrodeposited aluminum-manganese alloys in chloride media enable the pitting resistance of the materials to be assessed (Fig. 2) [6]. The unanticipated beneficial effect of manganese additions is revealed by the increase in the pitting potential for supersaturated solid solution  $\text{Al}^{97}\text{Mn}_3$  and glassy  $\text{Al}^{74}\text{Mn}^{26}$ . These results demonstrate that standard electrochemical techniques may be fruitfully employed to characterize the intrinsic behavior of electrodeposited materials. However, as noted earlier, electrodeposited coatings are often porous, or alternatively, the coating may be selectively removed by abrasion or scratching events. Galvanic corrosion processes, which may then occur at the discontinuities, must be carefully considered.

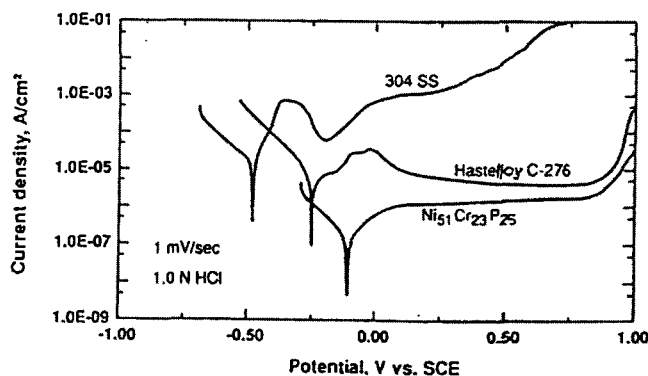


FIG. 1—The potentiodynamic *i*-*E* characteristics of electrodeposited  $\text{Ni}_{51}\text{Cr}_{23}\text{P}_{26}$  metallic glass compared to some conventional materials in 1 M HCl [1].

<sup>1</sup>N.I.S.T., Gaithersburg, MD 20899.

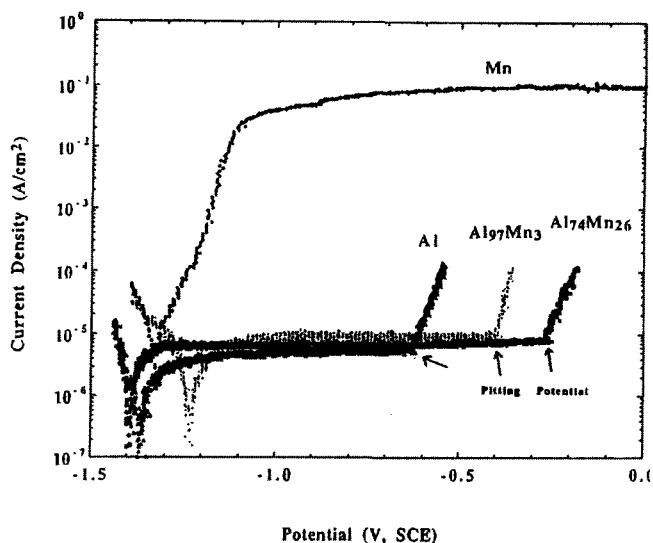


FIG. 2—The potentiodynamic  $i$ - $E$  characteristics of electrodeposited  $\text{Al}_{97}\text{Mn}_3$  and  $\text{Al}_{74}\text{Mn}_{26}$  compared to aluminum and manganese in 0.1 M NaCl, pH = 10, 0.2 mV/s. The enhanced pitting resistance of the Al-Mn alloys is revealed by the more positive pitting or breakdown potential [6].

## MECHANISMS OF CORROSION OF ELECTRODEPOSITED COATINGS

The electrochemical state of a corroding metal may be characterized by a mixed potential or free corrosion potential, and a corrosion rate or current density [7–9]. Both of these parameters are the result of the interaction of at least two partial processes, metal dissolution and the reduction of some oxidant, typically oxygen or protons. When there are two electrically conductive materials, which in general have different corrosion potentials and are electrically connected, the possibility for galvanic corrosion exists. This may be described using mixed potential or Evan's diagrams (Fig. 3) [7]. The figure shows the corrosion rate of Metals M and N before and after coupling. Before coupling, Metal M has a relatively positive corrosion potential and a low corrosion rate,  $i_{\text{corr}}(\text{M})$ , while Metal N corrodes at a higher rate,  $i_{\text{corr}}(\text{N})$ , at a more negative corrosion potential. When equal areas of these two metals are coupled (in a cell designed to ensure a homogeneous potential distribution), a mixed potential for the systems is established,  $E_{\text{couple}}$ , where the total oxidation rate equals the total reduction rate, i.e., conservation of charge. Thus, coupling results in a decrease of the corrosion rate of the metal, M, with the more positive corrosion potential, while the corrosion rate of the metal, N, with the more negative corrosion potential, is accelerated. The well-known galvanic series for metals and alloys immersed in a variety of media corresponds to a listing of the measured corrosion potentials and is often used to predict the effects of coupling two different materials. However, a more accurate assessment of galvanic effects may be obtained by measuring the current flow between coupled electrodes by using a zero-resistance ammeter (ZRA). If the individual potential-current characteristics of the coupled materials are known, then

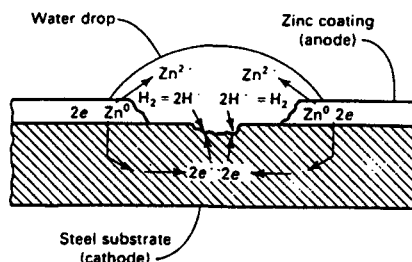
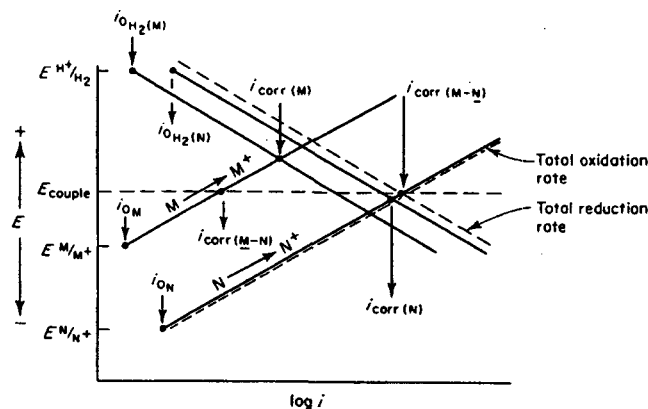


FIG. 3—A schematic Evan's diagram of cathodic protection of metal M (iron) that might be expected to occur due to the coupling with a more active metal N (zinc) [7].

sound predictions of galvanic corrosion effects may be generated and tested by using a ZRA. Further details on this particular method may be found in Section III of this manual.

From the preceding discussion, it is clear that an electrodeposited coating such as zinc may be used to protect substrates with a more positive corrosion potential such as iron. Thus, cathodic protection is implemented by the sacrificial coatings. Nonetheless, it is important to note that the zinc overlayer itself offers a degree of protection as a barrier coating, in addition to its action as a sacrificial anode. For example, in moist air zinc generally forms a thin, protective film of corrosion products, while bare steel rusts rapidly without protection. However, when zinc-coated steel is scratched exposing the iron substrate to an aqueous chloride solution, sacrificial dissolution of zinc protects the iron (Fig. 3). In contrast to the benefits of coating iron with zinc, electroplating a porous layer of corrosion-resistant metal, such as platinum, on a base metal substrate like zinc or iron leads to an acceleration of substrate dissolution, as shown in Fig. 4. This effect is accentuated due to the effects of geometry; namely, a large cathode to anode area ratio drives the anodic reaction at a higher rate. When two dissimilar materials are electrically connected in a cell with a homogeneous potential distribution, the corrosion rate of the anode is proportional to the area of the cathode. Table 1 demonstrates this effect from the coupling of two materials, chromium and "bright"



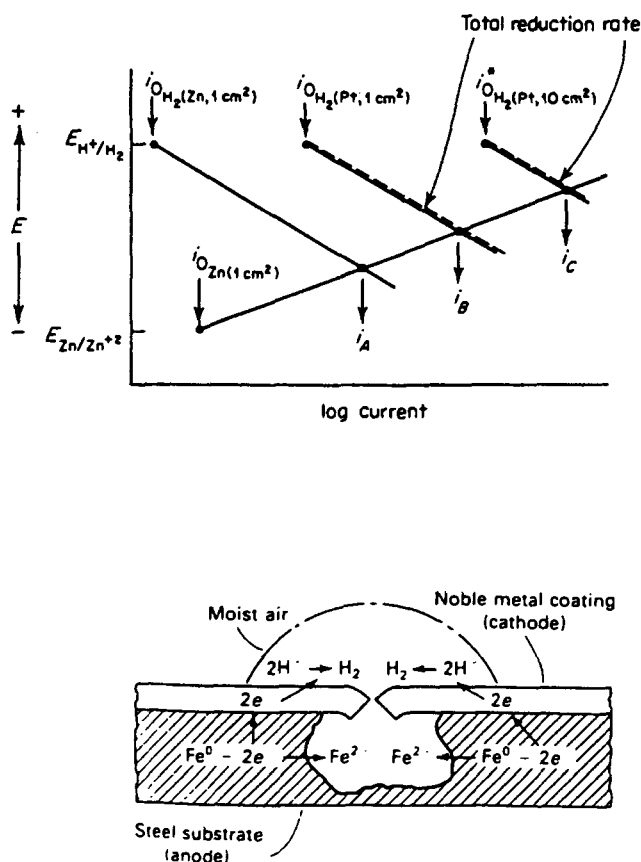


FIG. 4—A schematic Evan's diagram of accelerated substrate corrosion due to coupling of the base metal with a porous noble metal coating. The dramatic effect of the geometry, cathode/anode area ratio, is demonstrated [7].

TABLE 1—The influence of area ratio on the corrosion rate of bright nickel in contact with chromium in model rain water (pH 2.5).

Area Ratio Cr/Ni (Cr area = 6.3 cm <sup>2</sup> )	Anodic Current Density for Nickel Dissolution (mA/cm <sup>2</sup> )
1	0.0015
10	0.015
100	0.15
1000	1.3
10 000	6.8
20 000	17

nickel, which are relevant to the finishing of automobile bumpers [9].

It is important to note that the geometry associated with porous electroplated coatings can result in significant deviation from the uniform potential distribution associated with the simple mixed potential model described above [9]. In reality, the distributed nature of the pores may yield a highly nonuniform potential distribution. Furthermore, the occluded geometry of the pores, like that associated with pitting corrosion, may result in local solution chemistry markedly different from that of the bulk electrolyte. Likewise, the conductivity of the electrolytic medium is also

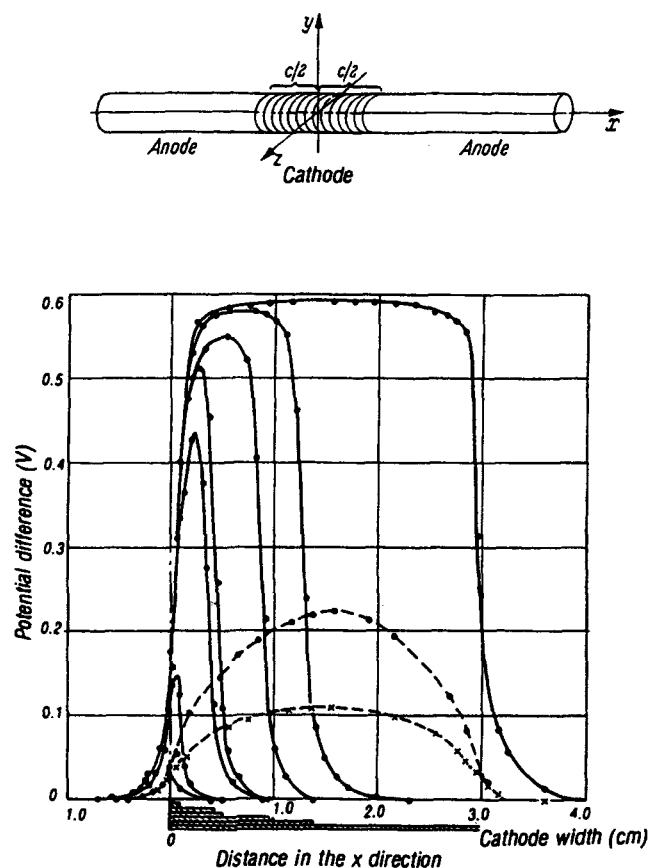


FIG. 5—Profiles of electrode potential, referred to the rest potential of zinc, at the surface of a rod shaped zinc/platinum/zinc short-circuited cell in acidic chloride media. The dashed lines represent platinum electrodes of varying length [9].

known to affect the potential distribution of an active galvanic cell. These effects are synonymous with the issue of controlling the throwing power in an externally driven electrolysis cell. Not surprisingly, the anodic current density is accentuated at regions adjacent to the cathode. The actual distribution is a sensitive function of the flaw, or pore size and distribution. This is demonstrated by using a scanning reference electrode to measure the potential distribution for a rod shaped zinc/variable length platinum/zinc short-circuited galvanic cell (Fig. 5). If the electrochemical parameters of the individual electrodes are known, it is possible to predict the corrosion rate from the measured potential distribution. However, as the dimensions of the flaw decrease, the potential field becomes more difficult to measure.

A major impediment to the extensive application of highly corrosion-resistant barrier coatings is the rapid pitting or perforation of the substrate that occurs at flaws in the coating (Fig. 4). The severity of the localized corrosion occurring at such pores may be reduced by appropriately designed multilayer electrodeposits. A coating system often used in automotive finishing provides an excellent example of this design philosophy (Fig. 6) [10]. The top layer of chromium has numerous microcracks that result in galvanic coupling with the "bright" nickel layer, which is sacrificial to the "semibright" nickel layer. The reactivity difference between

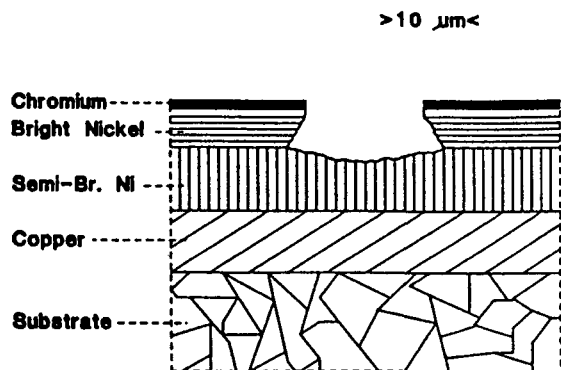


FIG. 6—Corrosion scheme for duplex nickel composite showing lateral penetration in the bright nickel layer, which helps prevent perforation of the substrate [10].

the respective nickel layers leads to enhanced lateral corrosion in the active bright nickel layer and retarded penetration of the semibright nickel layer. The potential difference between the nickel layers arises from the incorporation of sulfur in the bright nickel layer. The magnitude of the potential difference between the nickel layers is a sensitive function of the sulfur concentration. If the potential difference is too low,  $\approx$  less than 100 mV, enhanced lateral penetration may not occur. Consequently, controlling the activity of the organosulfur additives in the electrolytic bath is very important for maintaining good corrosion resistance. Likewise, the microcrack density in the chromium layer is an important parameter. Typically, finer dispersions of microcracks result in superior corrosion performance [11].

An interesting variation of the effect of galvanic coupling occurs with metals that exhibit active-passive transitions. When noble metals such as platinum, which are good catalysts for hydrogen reduction, are coupled to a metal with an active-passive transition below the reversible proton-hydrogen potential, spontaneous passivation may ensue (Fig. 7). Thus, a porous coating of noble metal on titanium, chromium, or stainless steels will result in anodic protection of the substrate.

In a similar fashion, care must be taken with sacrificial coatings to be sure that they will not be passivated in the application environment. For example, the position of zinc and iron in the galvanic series may be reversed in domestic water at temperatures above 71°C. The reversal is the result of the temperature dependence of the stability of the passivating corrosion product formed on zinc [12].

### Coating Porosity

From the preceding discussion, it is clear that coating porosity plays a central role in the corrosion behavior of electrodeposited coatings. This is particularly true for noble metal coatings that are designed to isolate the substrate from the aggressive environment. While a variety of means may be used to measure and control porosity, in electroplating practice coating thickness is the most frequently used parameter. For thin films, porosity is a sensitive function of the deposition parameters and substrate preparation, while

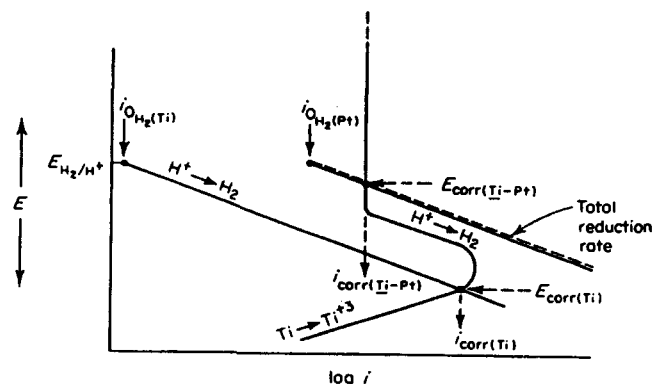


FIG. 7—Spontaneous passivation of an active-passive metal, such as titanium, by galvanically coupling to a noble metal such as platinum. The noble metal has a high rate constant for the proton-hydrogen reaction; thus, the corrosion potential of the system is near to the reversible potential for this reaction [7].

at greater thicknesses, it is controlled by the coating thickness [13–15]. A list of recommended thickness values for effective coverage of zinc, cadmium, and bright nickel/chromium coatings is available [16,17]. Likewise, a variety of destructive and nondestructive methods (see ASTM B 659, Guide for Measuring Thickness of Metallic and Inorganic Coatings, in Ref 18) are established for assessing coating thickness.

Several chemical staining methods exist for delineating the active pores in a coating [15,18]. Typically, the test involves using an indicator to reveal corrosion products that result from dissolution of the substrate at coating flaws or alternatively react with the substrate to highlight the flaws. Paper electrography, the ferroxyl, and the nitric acid vapor test are representative of the general methodology [15,18]. The electrographic technique involves making the substrate the anode in a two-electrode cell with filter paper soaked in a suitable electrolyte sandwiched between the electrodes. In the case of a corrosion-resistant coating on steel, flaws are identified by treating the filter paper with an indicator such as potassium ferrocyanide, which causes the precipitation of the iron dissolution products in the filter paper matrix, thus yielding an imprint of the defect population of the coating. Further details on this and other staining techniques may be found in the literature (ASTM B 765<sup>2</sup>) [18]. However, it must be remembered that porosity tests do not necessarily assess the pertinent corrosion performance, since this will depend on the actual service conditions.

### CORROSION TESTING OF ELECTRODEPOSITED COATING

Corrosion tests typically vary from simple exposure to the operational environment to laboratory-based accelerated exposure tests or more sophisticated electrochemical tests described in Sections III and VII of this manual. The corrosion

<sup>2</sup>Guide to the Selection of Porosity Test for Electrodeposits and Related Metallic Coatings.

testing of electrodeposits in microelectronic devices has been treated elsewhere [19], and a related chapter may be found in Section VII of this manual.

### Exposure Test

Salt spray-fog testing, ASTM B 117, Test Method of Salt Spray (Fog) Testing [18,20], has often been used to characterize the corrosion behavior of electrodeposited coatings. A copper-accelerated acetic acid salt spray (CASS) test (ASTM B 368<sup>3</sup>) [18] has been developed specifically for examining decorative copper/nickel/chromium composite coatings [18,20]. A similar test (Corrodokote) involving the application of a salt slurry followed by exposure to a humid environment has also been described (ASTM B 380<sup>4</sup>) [18,20]. The electrochemical basis of the CASS and Corrodokote test has been investigated [21]. A rating procedure exists for assessing the damage caused by these tests (ASTM B 537<sup>5</sup>), and a related test method is used specifically for quantifying the corrosion sites on copper-nickel-chromium multilayer deposits (ASTM B 651<sup>6</sup>) [18].

### Electrochemical Tests

A variety of standard electrochemical methods may be used to probe the corrosion behavior of electroplated coatings with a particular focus on assessing the effects of galvanic coupling between the coating and the substrate (ASTM G 5<sup>7</sup>, G 59<sup>8</sup>, G 61<sup>9</sup>, G 82<sup>10</sup>, G 102<sup>11</sup>, and G 106<sup>12</sup>) [22]. In accordance with the mixed potential treatment of galvanic corrosion, the corrosion potential and polarization resistance are expected to be a sensitive function of the anode/cathode area, i.e., porosity [13,14,20,23].

### Corrosion Potential Measurements

Measurement of the rest potential of a corrosion-resistant barrier coating on an active substrate provides a rapid and essential nondestructive means of assessing coating integrity. Mixed potential theory predicts that the corrosion potential

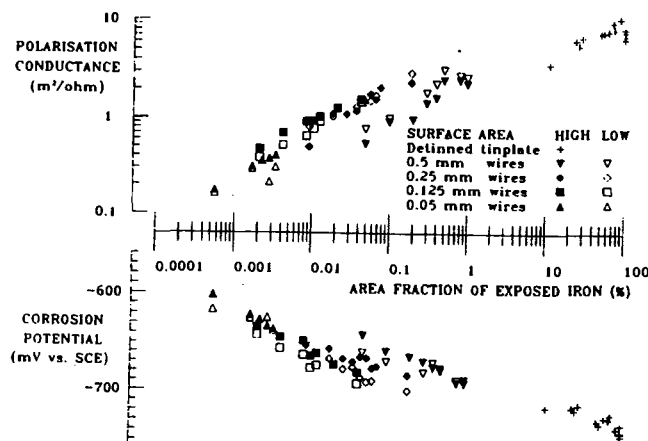


FIG. 8—Comparison between corrosion potential and polarization resistance measurements of the porosity of simulated tinplates [17].

will be a logarithmic function of the exposed substrate area,  $A^N$ . With an appropriate choice of electrolytes, the effect of the pores can be exaggerated by differential polarization, with a resultant increase in sensitivity and precision. A quantitative relationship [23] requires independent knowledge of the corrosion potential  $E_{\text{corr}}$ , corrosion rate  $i_{\text{corr}}$ , and the anodic  $b_a$  and cathodic  $b_c$  transfer coefficients of the Anodic A and Cathodic C electrode ( $A = N$  and  $C = M$ ) in

$$E_{\text{corr}} = C' - \frac{b_a^A b_c^C}{b_a^A + b_c^C} \log \frac{A^A}{A^C}$$

and

$$C' = \frac{E_{\text{corr}}^C b_a^A + E_{\text{corr}}^A b_c^C + b_a^A b_c^C \log i_{\text{corr}}^C / i_{\text{corr}}^A}{b_a^A + b_c^C}$$

(Fig. 3). This relationship has been demonstrated for a variety of systems ranging from gold coatings on copper [13,14] to tin overlayers on steel [23] (Fig. 8). However, there remains some uncertainty regarding the role of current distribution for systems with very high cathode/anode area ratios, i.e., high anodic current densities [20]. In practice, the dependence of the corrosion potential on the area of exposed substrate material may also be estimated by independent measurements of the exposed area, thus allowing a calibration curve to be obtained.

Corrosion potential measurements may also be used as an active probe of the effectiveness of a coating in service. An interesting example is the intergranular stress corrosion cracking (IGSCC) of 304 stainless steel piping in boiling water reactors, which represents a serious threat to operational longevity. The corrosion potential is the single most important environmental parameter in these systems. IGSCC of 304 SS only occurs at potentials above some critical value  $E_{\text{IGSCC}}$  (typically about  $-0.23$  SHE in high-temperature water) [24]. Consequently, a great deal of effort has been expended to displace the corrosion potentials below this value. Mixed potential theory predicts that the potential of a system may be dominated by coupling a metal with a particularly fast redox reaction. Noble metals are well-known catalysts for the hydrogen-proton reaction, which has a reversible potential below that of  $E_{\text{IGSCC}}$ . Thus, a porous noble metal coating on stainless steel will act to maintain the

<sup>3</sup>Method for Copper-Accelerated Acetic Acid-Salt Spray (Fog) Testing (CASS Test).

<sup>4</sup>Method of Corrosion Testing of Decorative Electrodeposited Coatings by the Corrodokote Procedure.

<sup>5</sup>Practice for Rating of Electroplated Panels Subjected to Atmospheric Exposure.

<sup>6</sup>Method for Measurement of Corrosion Sites in Nickel Plus Chromium or Copper Plus Nickel Plus Chromium Electroplated Surfaces with the Double-Beam Interference Microscope.

<sup>7</sup>Standard Reference Test Method for Making Potentiostatic and Potentiodynamic Anodic Polarization Measurements.

<sup>8</sup>Practice for Conducting Potentiodynamic Polarization Resistance Measurements.

<sup>9</sup>Test Method for Conducting Cyclic Potentiodynamic Polarization Measurements for Localized Corrosion Susceptibility of Iron, Nickel, or Cobalt-Based Alloys.

<sup>10</sup>Guide for Development and Use of a Galvanic Series for Predicting Corrosion Performance.

<sup>11</sup>Practice for Calculation of Corrosion Rates and Related Information from Electrochemical Measurements.

<sup>12</sup>Practice for Verification of Algorithm and Equipment for Electrochemical Impedance Measurements.

corrosion potential near the hydrogen-proton reversible potential (Fig. 7). The effective control of the corrosion potential of 316 SS, via an electrodeposited coating of palladium, has been demonstrated [25].

### Polarization Resistance Measurements

Mixed potential theory also allows predictions of the dependence of the polarization resistance on the exposed area of a galvanically active substrate. With due consideration for the influence of the total specimen area, as well as the surface roughness, an expression for the polarization resistance may be derived:

$$\frac{1}{A} \left( \frac{\Delta I}{\Delta E} \right) = K' + \frac{b_A}{b_A + b_c} \log \frac{A^A}{A} + \frac{b_c}{b_A + b_c} \log \frac{A^c}{A}$$

where

$$K' = \frac{E_{\text{corr}}^c - E_{\text{corr}}^A + b_c \log i_{\text{corr}}^c + b_A \log i_{\text{corr}}^A}{b_A + b_c} - \log \frac{b_A b_c}{2.3(b_A b_c)}$$

A recent publication [23] presents a summary of the systems that have been investigated to date. However, the influence of potential distribution is not considered in this model [9,20]. As with corrosion potential measurements, an independent calibration method demonstrates that with the appropriate electrolyte the polarization resistance is proportional to the exposed substrate area. For tin-coated steel tested in thiocyanate solution, favorable agreement is found between polarization resistance and corrosion potential measurements (Fig. 8).

### Chronopotentiometry

Chronopotentiometry, where the electrode potential is monitored as a function of time during galvanostatic polarization, is a particularly useful technique for characterizing the thickness and phase structure of electrodeposited multilayers. The corrosion performance of copper/semibright nickel/bright nickel/microcracked chromium composite coatings is a strong function of thickness of the various layers, as well the potential difference between the semibright and the sulfur containing bright nickel layer [10,11]. The potential difference must be sufficient to cause the bright nickel to corrode preferentially and sacrificially with respect to the semibright nickel. Chronopotentiometry may be used to assess effectively the thickness as well as the potential difference between the nickel layers. If a chromium layer is present, it is typically first removed with concentrated hydrochloric acid. The sample is then placed in the electrolyte under a constant galvanostatic imposed anodic current. A sharp transition in the potential occurs after the bright nickel layer has dissolved to expose the semibright nickel layer, which proceeds to dissolve until the copper substrate is exposed (Fig. 9). Assuming 100 % current efficiency, a coulometric analysis, according to Faraday's law, may be used to transform the time axis to an appropriate thickness scale. This test has been formalized as an ASTM standard known as the STEP Test (ASTM B 764<sup>13</sup>) [18].

<sup>13</sup>Test Method for Simultaneous Thickness and Electrochemical Potential Determination of Individual Layers in Multilayer Nickel Deposit.

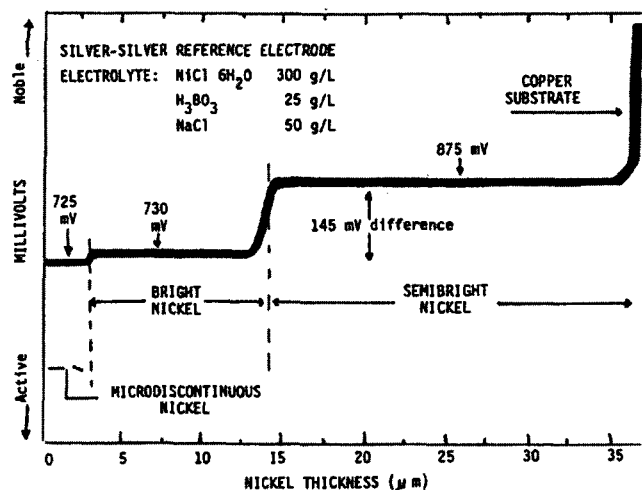


FIG. 9—Results of galvanostatic stripping of a duplex nickel deposit from a copper substrate (taken from ASTM B 764 [16]).

Chronopotentiometry has also been used to analyze the effects of different processing methods on the phase structure of coatings. The potential response of a variety of galvanostatically dissolved zinc-coated steel samples is highly sensitive to the presence of intermetallic layers that form at elevated temperatures [12].

### The EC Test

The EC Test (ASTM B 627<sup>14</sup>) [18,20,26] uses a combination of chronoamperometry and constant current coulometry to perform accelerated corrosion testing of copper/nickel/microcracked chromium multilayer electrodeposits on steel or zinc-based die castings. The test was designed to simulate the actual corrosion service expected for automotive trim in a metropolitan area such as Detroit [26]. The current-potential behavior for the individual constituents (Fig. 10) demonstrates that at potentials more positive than +0.1 V SCE, the dissolution rate is consistent with the anticipated ordering based on the Galvanic series. In the EC Test, the specimen is held potentiostatically at 0.3 V SCE, which preferentially initiates attack on the bright nickel layer. As the attack progresses, the measured current increases as the area of exposed nickel increases. When the current reaches a specific value, typically 3.3 mA/cm<sup>2</sup> (projected geometrical area), the regulation of the experiment is converted to galvanostatic control, thereby simulating corrosion control by the cathodic partial process (i.e., oxygen and proton reduction on microcracked chromium). The time of galvanostatic regulation corresponds to length of service. Penetration of the coating is ascertained by using chemical indicators, either in the electrolyte or after removal from the electrolyte, to reveal dissolution products emanating from the steel or zinc substrate. The test was found to be over 400 times faster than the CASS exposure test, and the mode of corrosion is found to be more representative of that observed in service [26].

<sup>14</sup>Test Method for Electrolytic Corrosion Testing.

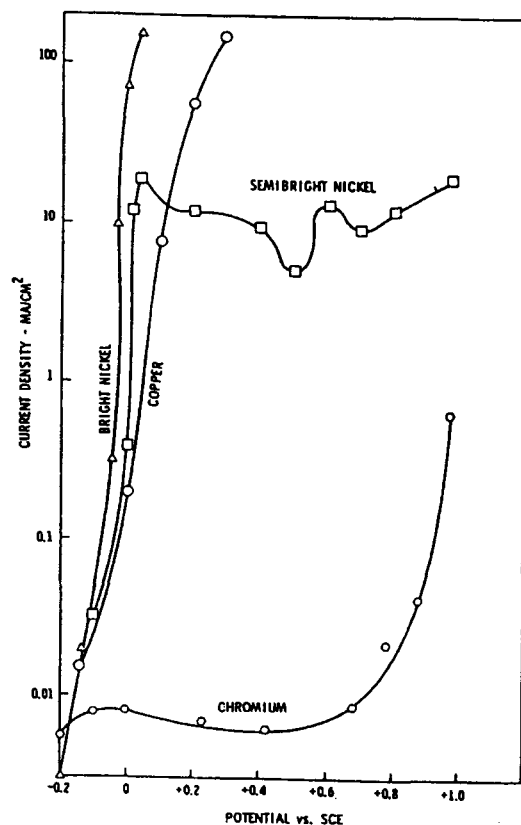


FIG. 10—Potentiostatic *i*-*E* curves for the constituents of the composite coating shown in Fig. 6 [20].

### In-Situ Imaging and Nondestructive Evaluation of Electrodeposited Coatings

During the last decade, significant developments have occurred that enable the in situ mapping of the potential distribution on a corroding surface. Both the scanning reference electrode (SRET) and, more recently, the scanning vibrating electrode technique (SVET) have been described [27]. In both techniques, a fine capillary tip electrode, which is rastered across the surface, is used to sense potential gradients. These methods may be used to image the sites of localized corrosion and related heterogeneities on surfaces and to determine their polarization characteristics. The SVET is currently able to resolve features down to 40  $\mu\text{m}$ , and a discussion of the limitations of the technique is available [27]. Defects in aluminized steel have been imaged in borate solution as shown in Fig. 11. The figure shows the result of repeated scanning of a single line in the X direction, which crosses over active sites, while the substrate potential was decreased from 1.1 to  $-0.9$  V. The polarization behavior of three specific sites may be compared. The two adjacent high current density sites at 1.1 V show a decrease in current density with decreasing potential. At negative potentials, the cathodic currents remained low at the two adjacent sites, while the cathodic currents observed from the third site increased. These results demonstrate that this technique allows the identification and examination of the character of different surface defects.

FIG. 11—A scanning vibrating electrode (SVET) image used to characterize the nature of defects in an aluminum-coated steel substrate as function of potential in a buffered borate solution [29].

Several other scanning probe techniques are under development, which may be used to examine the character of electrodeposited coatings. The scanning electrochemical microscope (SECM) is used to create a map of the chemical reactivity of a surface [28]. The technique involves using a redox couple to mediate the interaction between a rastered microelectrode probe and the substrate. This technique may be particularly useful for examining the character of thin noble metal coatings. For example, patches of gold on a glassy carbon electrode have been successfully imaged [28]. The resolution of this technique appears to be limited by the diameter of the probing microelectrode.

Other techniques such as magnetic force microscopy or SQUID magnetometry [29] may also find application in assessing the quality of electrodeposited materials. However, limitations on the sensitivity and spatial resolution of these methods need to be assessed.

## CONCLUSIONS

Electrodeposition enables the production of many novel corrosion-resistant alloys that may not be produced by conventional thermomechanical means. A variety of standard electrochemical methods may be used to examine the corrosion resistance of the electrodeposited material itself. However, the corrosion behavior of an electrodeposited coating must be viewed as a composite system due to possible galvanic interactions between the coating and substrate. An assortment of techniques is available for examining the corrosion behavior of these systems. Invariably, these methods all focus on the effects of coating porosity. It is important for the investigator to have a clear understanding of the goal of the test program (e.g., ranking of materials, quality control, study of mechanisms, etc.). Only through careful evaluation of all of the information can the most appropriate test for a particular situation be selected.

## ACKNOWLEDGMENTS

The author gratefully acknowledges the support of the Office of Naval Research, the N.I.S.T. Metal Matrix Competence Program, and David Lashmore.

## REFERENCES

- [1] Guilinger, T. R., Voytko, J. E., White, R. E., and Yin, K.-M., "Characterization of Amorphous Ni-Cr-P Electrodeposits," *Plating and Surface Finishing*, March 1993, p. 46.
- [2] Helfand, M. and Clayton, C. R., "Variable Angle XPS Studies of Passive Ni-P-Cr Metallic Glasses," *Corrosion, Electrochemistry and Catalysis of Metastable and Intermetallic*, C. R. Clayton and K. Hashimoto, Eds., The Electrochemical Society, Pennington, NJ, 1993.
- [3] Ratzker, M., Lashmore, D. S., and Pratt, K. W., "Electrodeposition and Corrosion Performance of Nickel-Phosphorus Amorphous Alloys," *Plating and Surface Finishing*, Vol. 76, 1986, p. 74.
- [4] Usuzaka, N., Yamaguchi, H., and Watanabe, T., "Preparation and Magnetic Properties of Co-Gd Amorphous Alloy Films by Electroplating Method," *Materials Science and Engineering*, Vol. 99, 1988, p. 105.
- [5] Searson, P. C. and Moffat, T. P., "Electrochemical Synthesis and Surface Modification," *Critical Reviews in Surface Chemistry*, Vol. 3, No. 314, CRC Press, 1994, pp. 171–238.
- [6] Moffat, T. P., Stafford, G. R., and Hall, D. E., "Pitting of Electrodeposited Al-Mn Alloys," *Journal of the Electrochemical Society*, Vol. 140, 1993, pp. 2779–2786.
- [7] Revie, R. W., *Uhlig's Corrosion Handbook*, 2nd ed., Wiley, New York, 2000, and Fontana, M. G. and Greene, N. D., *Corrosion Engineering*, McGraw-Hill, New York, 1978.
- [8] Gabe, D. R., *Principles of Metal Surface Treatment and Protection*, Pergamon Press, New York, 1978.
- [9] Kaesche, H., *Metallic Corrosion*, NACE, Houston, TX, 1985.
- [10] Lindsay, J. H. and Snyder, D. D., "Electrodeposition Technology in the Automotive Industry," *Electrodeposition Technology, Theory and Practice*, L. T. Romankiw and D. R. Turner, Eds., The Electrochemical Society, Pennington, NJ, 1987, p. 43.
- [11] DiBari, G. A., "Decorative Electrodeposited Nickel-Chromium Coatings," *Metal Finishing*, Vol. 75, June 1977, pp. 17–20; and Vol. 75, July 1977, pp. 17–24.
- [12] Payer, J. H., "Electrochemical Methods for Coatings Study and Evaluation," *Electrochemical Techniques for Corrosion*, R. Baboian, Ed., NACE, Houston, TX, 1977, p. 61.
- [13] Morrissey, R. J., "Electrolytic Determination of Porosity in Gold Electrodeposits," *Journal of the Electrochemical Society*, Vol. 117, 1970, p. 742; and Vol. 119, 1972, p. 446.
- [14] Morrissey, R. J., "Porosity and Galvanic Corrosion in Precious Metal Electrodeposits," *Electrochemical Techniques for Corrosion Engineering*, R. Baboian, Ed., NACE, Houston, TX, 1986, p. 167.
- [15] Clarke, M., "Porosity and Porosity Tests," *Properties of Electrodeposits: Their Measurement and Significance*, R. Sard, H. Leidheiser, and F. Ogburn, Eds., The Electrochemical Society, Pennington, NJ, 1975, p. 122.
- [16] Mazia, J. and Lashmore, D. S., "Electroplated Coatings," *Metals Handbook*, 9th ed., Vol. 13, ASM International, Metals Park, OH, 1987, p. 419.
- [17] Jones, A. R., "Corrosion of Electroplated Hard Chromium," *Metals Handbook*, 9th ed., Vol. 13, ASM International, Metals Park, OH, 1987, p. 873.
- [18] *Annual Book of ASTM Standards*, Vol. 02.05, *Metallic and Inorganic Coatings; Metal Powders, Sintered P/M Structural Parts*, ASTM International, West Conshohocken, PA, 2002.
- [19] Frankenthal, R. P., "Corrosion in Electronic Applications," *Properties of Electrodeposits: Their Measurement and Significance*, R. Sard, H. Leidheiser, and F. Ogburn, Eds., The Electrochemical Society, Pennington, NJ, 1975, p. 142.
- [20] Saur, R. L., "Corrosion Testing—Protective and Decorative Coatings," *Properties of Electrodeposits: Their Measurement and Significance*, R. Sard, H. Leidheiser, and F. Ogburn, Eds., The Electrochemical Society, Pennington, NJ, 1975, p. 170.
- [21] Petrocelli, J. V., Hospadaruk, V., and DiBari, G. A., "The Electrochemistry of Copper, Nickel and Chromium in the Corrodokote and CASS Test Electrolytes," *Plating*, Vol. 49, No. 1, 1962, pp. 50–59.
- [22] *Annual Book of ASTM Standards*, Vol. 03.02, *ASTM International*, West Conshohocken, PA, 2002.
- [23] Notter, I. and Gabe, D. R., "Polarization Resistance Methods for Measurement of the Porosity of Thin Metal Coatings," *Corrosion Science*, Vol. 34, 1993, p. 851.
- [24] Macdonald, D. D., "Viability of Hydrogen Eater Chemistry for Protecting In-Vessel Components of Boiling Water Reactors," *Corrosion*, Vol. 194, 1992, p. 48.
- [25] Niedrach, L. W., "Effect of Palladium Coatings on the Corrosion Potential of Stainless Steel in High Temperatures Water Containing Dissolved Hydrogen and Oxygen," *Corrosion*, Vol. 162, 1991, p. 47.
- [26] Saur, R. L. and Basco, R. P., "An Accelerated Electrolyte Corrosion Test and a Corrosion Analysis Procedure for the Nickel-Chromium Plating System," *Plating*, Vol. 53, 1966, p. 35; and Vol. 53, 1966, p. 320; and Vol. 53, 1966, p. 981.
- [27] Issacs, H. S. and Ishikawa, Y., "Application of the Vibrating Probe to Localized Current Measurements," *Electrochemical Techniques for Corrosion Engineering*, R. Baboian, Ed., NACE, Houston, TX, 1986, p. 17; Issacs, H. S., *Corrosion*, Vol. 46, 1990, p. 677.
- [28] Wipf, D. O. and Bard, A. J., "Scanning Electrochemical Microscopy, X. High Resolution Imaging on an Electrode Surface," *Journal of the Electrochemical Society*, Vol. 138, 1991, p. L4.
- [29] Hibbs, A. D., "Measurement of Electrochemical Corrosion Current Using a Multichannel Superconducting Quantum Interference Device Magnetometer," *Journal of the Electrochemical Society*, Vol. 139, 1992, p. 2447.

# Powder Metallurgy (P/M) Materials

*Erhard Klar<sup>1</sup> and Prasan K. Samal<sup>2</sup>*

A POWDER METALLURGY part is conventionally made by compacting a lubricated metal powder in a die to the desired shape followed by sintering in a protective atmosphere. Simple and complex parts with densities typically ranging between 80 and 90 % of theoretical and having the finished dimensions are produced at high production rates. The P/M process uses raw materials and energy efficiently and, hence, is cost effective.

The P/M materials developed during the first four decades of the 20th century included cemented carbides, composite electrical contacts, self-lubricating bronze bearings, and composite friction materials. The service lives of these materials were in general not limited by their corrosion resistances. With the sharp increase of iron-based sintered steel parts in the 1940s, however, corrosion resistance became of increasing importance. This culminated in the development of sintered stainless steels in the 1950s.

The bulk of sintered P/M carbon-, copper-, nickel-, and low-alloy steel parts are used without any further treatment for additional corrosion protection. The reason for this is that about 70 % of all P/M parts manufactured in North America are used in the automotive industry [1], and that a large majority of these parts are internal components of the automotive transmission, the engine, and the steering gears, where corrosion is not a problem. Farm, lawn and garden equipment, hardware, appliances, and business machines also contain many carbon- and low-alloy steel parts that sometimes require additional treatments for corrosion protection. A very simple treatment for corrosion protection consists of dipping the P/M parts in an oil. Alternately, P/M parts may be painted or coated mechanically (mechanical plating) [2]. Steam treatment [3,4] is an economical process applied to small iron and steel parts to improve their hardness, compressive strength, and corrosion resistance. It involves controlled oxidation with superheated steam. The parts become coated with a tightly adhering dark blue or black oxide ( $\text{FeO}$  and  $\text{Fe}_3\text{O}_4$ ), which is acceptable as final finish. Some sintered parts are impregnated with a resin, followed by plating with copper, nickel, cadmium, zinc, or chromium. More recently, a special coating process, called Dacronizing [5], was developed for the corrosion protection of ferrous P/M sensor rings used in anti-lock brake systems. It consists of a combination of steam treating, coating with

zinc flake and chromic acid, followed by impregnation and overcoating with a silicate slurry.

Sintered stainless steel parts are used generally in more severe corrosive environments. Due to their large surface areas and the presence of pores, these require special processing precautions to ensure good corrosion resistance. During the past ten years, the complex fundamental requirements for good corrosion resistance of sintered stainless steels have been described [6] and the industry is presently acquiring the know-how for mastering the practical aspects of these requirements. With appropriate process control and some modification of composition, it is now possible to manufacture sintered stainless steel parts passing the widely specified 100 h salt spray test (ASTM B 117, Test Method of Salt Spray/Fog Testing), and to even approach the corrosion resistances of wrought stainless steels [7,8].

Table 1 is a partial listing of the compositions of the common porous sintered P/M materials. Selected compositions of P/M materials possessing near theoretical full density (>99 %), sometimes called "full dense" or high-performance P/M materials, are shown in Table 2 [2,9]. Full dense P/M parts are made by liquid phase sintering, powder injection molding, extrusion, or hot isostatic pressing. Important full dense P/M materials include P/M superalloys, P/M tool steels, several P/M aluminum alloys, and many P/M specialty alloys. Owing to their refined microstructure and greater homogeneity, full dense P/M materials offer superior mechanical properties with equal or superior corrosion resistance, compared to their wrought or cast counterparts.

## CORROSION TESTING AND EVALUATION

Corrosion testing procedures and standards established for wrought alloys are generally applicable to full dense P/M materials. They are discussed in other chapters in this section. Among the porous P/M materials, sintered stainless steels are by far the most important materials whose corrosion testing is of commercial interest [6]. Only a very limited number of reports are published on the corrosion behavior of any other types of porous P/M materials. Therefore, the following discussion will be focused principally on sintered stainless steels. Details relating to the P/M process are covered only to the extent that they are relevant to corrosion resistance. For additional information, the reader is referred to other publications [2,10,11].

<sup>1</sup>Consultant, and <sup>2</sup>Manager, P/M Technology, North American Hoganas, Research Triangle Park, NC 27709.

TABLE 1—Compositions of selected sintered P/M materials.<sup>a</sup>

	Fe	C	Cu	Ni	Zn	Pb	Sn	Mo	Cr	Mn	Si	S	P	N
Carbon Steel F-0008	97.1–99.4	0.6–0.9												
Copper Steel FC-0208	93.2–97.9	0.6–0.9	1.5–3.9											
Nickel Steel FC-0205	91.9–98.7	0.3–0.6	0–2.5	1.0–3.0										
Low-alloy Steel FL-4605	94.5–97.5	0.4–0.7		1.7–2.0				0.4–0.8						
Stainless Steels SS-303L	rem.	0–0.03		8–13					17–19	0–2	0–1	0.15–0.30	0–0.20	
SS-316L	rem.	0–0.03		10–14				2–3	16–18	0–2	0–1	0–0.03	0–0.045	
SS-410	rem.	0–0.25							11.5–13	0–1	0–1	0–0.03	0–0.04	0.2–0.6
316LSC <sup>b</sup>	rem.	0.03 max	2	13–14			1	2–2.5	16.5–17.5	0.3 max	0.7–0.9	0.03 max	0.03 max	
Brass CZ-1000			88–91		rem.									
CZP-3002			68.5–71.5		rem.	1–2								
Bronze CT-1000			87.5–90.5				9.5							
Nickel Silver CNZ-1818	rem.		62.5–65.5	16.5–19.5										

<sup>a</sup>MPIF Standard 35, Material Standards for P/M Structural Parts, 2003 Edition, Metal Powder Industries Federation, Princeton, NJ.<sup>b</sup>Proprietary grade of SCM Metal Products, Inc.

TABLE 2—Nominal compositions of selected full dense P/M materials.

Superalloys <sup>a</sup>	Composition, %															
	C	Cr	Mn	W	Ta	Ti	Nb	Co	Al	Hf	Zr	B	Ni	Fe	V	V <sub>2</sub> O <sub>5</sub>
IN-100	0.07	12.5	3.2	...	...	4.3	...	18.5	5.0	...	0.04	0.02	rem	...	0.75	...
Rene 95	0.07	13.0	3.5	3.5	...	2.5	3.5	8.0	3.5	...	0.05	0.01	rem	...	...	...
MERL 76	0.02	12.4	3.2	...	...	4.3	1.4	18.5	5.0	0.4	0.06	0.02	rem	...	...	...
Low-carbon Astroloy	0.04	15.0	5.0	...	...	3.5	...	17.0	4.0	...	0.4	0.025	rem	...	...	...
MA 956	...	20.0	...	...	...	0.5	...	...	4.5	...	...	...	...	rem	...	0.5
MA 6000	0.05	15.0	2.0	4.0	2.0	2.5	...	...	4.5	...	0.15	0.01	rem	...	...	1.1
High-speed Steels <sup>a</sup>																
M2	0.85	4.2	5.0	6.3										rem	1.9	
T15	1.60	4.4		12.5				5.0						rem	4.8	
Aluminum Alloys <sup>b</sup>		Zn		Mg			Cu		Co			O				Al
X7090		7.3–8.7		2.0–3.0			0.6–1.3		1.0–1.9			0.2–0.6				rem
X7091		6.8–7.1		2.0–3.0			1.1–1.8		0.2–0.6			0.2–0.5				rem

<sup>a</sup>Ref 2.<sup>b</sup>Ref 6.

At present, there exists only one standard on corrosion testing and evaluation of sintered P/M parts, although many of the methods employed for wrought metals are used for sintered P/M parts with minor modification. In addition, a few nonstandardized tests are available.

## Atmospheric Testing

Many P/M parts are used in the equipment and machinery exposed to the atmosphere. However, systematic investigations into their corrosion resistances under atmospheric conditions, as they are known for many wrought metals, are not available for P/M parts. In most investigations, surface appearance and/or weight changes after certain length of exposure are reported [12], and occasionally changes in mechanical properties are reported. Recommendations in ASTM G 50, Practice for Conducting Atmospheric Corrosion Tests on Metals, are useful for this type of testing. One should keep in mind, however, that weight changes in sintered materials may be more difficult to interpret because of the presence of pores. The loss in weight due to the actual loss of material on the surface of the part may be undesirably compensated by the weight gain that occurs due to buildup of products of corrosion and moisture in the interior of the pores.

## Immersion Tests

Corrosion testing of P/M parts by immersion is useful for comparing the performance of various alloys, for optimization of P/M processing, and, with the mutual agreement

between the parties involved, as a criterion for acceptable quality.

## Immersion Tests with Mass Loss

ASTM G 31, Practice for Laboratory Immersion Corrosion Testing of Metals, may be followed for P/M parts where a loss in mass results due to reaction with the test solution. In comparison to wrought materials, the preparation of specimens or sintered parts for corrosion testing is usually minimal. In most cases the actual parts or specimens are tested in their as-sintered, or “secondary” treated, conditions. In fact, it would be counterproductive in most cases to clean the surfaces by mechanical means since this may result in material removal, and the new surfaces may differ in their compositions and structures from the original surface. The composition and structure of only the as-produced original surface has the most relevance to the corrosion resistance and the service life of the part. Cleaning by simply degreasing the P/M parts with an organic solvent is usually sufficient.

Corrosion rates of sintered steels have been reported for immersion testing in nitric [13], sulfuric [14–16], and acetic [17] acids. Compared to their wrought counterparts, the P/M parts exhibited much greater weight losses. In a more recent study, the authors reported a hydrogen sintered Nb-stabilized 444L stainless steel that was fully resistant in 2 % H<sub>2</sub>SO<sub>4</sub> [18].

## Immersion Tests without Mass Loss

Immersion testing without a resultant mass loss includes testing in neutral salt solutions. Developed by the authors,



a salt solution immersion test has now been standardized (ASTM B 895-99) and is widely used for sintered stainless steels. The procedure is simple, inexpensive, and flexible so that P/M parts producers also can use it in-house for optimizing their sintering process for stainless steels.

Each test is based on five or more pressed and sintered replicate specimens, which are exposed to a 5 % NaCl solution in individual jars at room temperature. The standardized test prescribes that the jars must be closed with lids, while the earlier version of the test was based on open jars or beakers. The specimens are examined visually at predetermined time intervals, for onset of staining or rusting, and thereafter for an estimation of the percentage of surface area covered by stain or rust, in accordance with the following four rating classes:

- A—sample free from any corrosion.
- B—up to 1 % of surface covered by stain or rust.
- C—1 to 25 % of surface covered by stain or rust.
- D—>25 % of surface covered by stain or rust.

A chart containing photographs of a series of specimens for each of the four rating classes is referred to, for maintaining accuracy of rating (Fig. 1). The time intervals between inspections are short at the beginning of the test, and are increased gradually as the test progresses. Table 3 shows a typical record of test data. Figure 2 shows a typical plot for the set of data listed in Table 3. From this plot, the mean lives (in hours) for the specified degrees of surface corrosion (on set, 1 % and 25 %) are obtained as the intersection points of the respective rating curves with the horizontal line at 50 %. If the specimens are not fabricated properly or handled carefully (such as affected by contaminations, wide variations in oxygen, nitrogen, or carbon contents, density variations, etc.), the scatter of the test data will increase.

With immersion testing in 5 % NaCl, corrosion resistances up to a C-rating (<25 % rust) usually have little effect on the mechanical properties of a P/M stainless steel part. At these levels of rusting, weight loss measurements are unreliable,

as some of the rust, as well as salt, may penetrate the pores and cause weight gains instead of weight losses. For applications that can tolerate larger amounts of corrosion, the determination of the amount of surface rust is often insufficient for part qualification. In cases of pitting, determination of number and depth of pits in porous materials is complex and their effects on mechanical properties are less severe in porous P/M parts than in wrought steel. In such cases it is often useful to remove surface rust (for instance, by sandblasting) and to provide photographic evidence of pitting in combination with relevant mechanical properties in accordance with Section 7.5 of ASTM G 46, Practice for Examination and Evaluation of Pitting Corrosion. Most of the other aspects of ASTM G 46 cannot be used readily for sintered materials because the size and shape of corrosion pits can be quite similar to those of the pores in sintered materials. Electrochemical testing (see subsection on *Electrochemical Tests*) appears to be the best technique for identifying pitting corrosion in sintered stainless steels.

### Salt Spray Tests

Salt spray testing in accordance with ASTM B 117 is being increasingly used in the P/M industry in recent years for qualifying new stainless steel parts or P/M substitutes for wrought parts. It may also be used for alloy development and process optimization. The neutral salt spray test is more aggressive than the neutral salt immersion test. The visual rating system described in the subsection on *Immersion Tests without Mass Loss* may also be used for salt spray testing. An extensive discussion of the corrosion resistances of sintered austenitic stainless steels processed under varying conditions is given in Refs 19 and 20. Testing and evaluation included electrochemical and neutral salt spray methods in accordance with ISO 3768 [21] and a visual rating scale from 10 to 0 in accordance with ISO 4540 [22]. In Ref 23 the neutral salt spray test is used on sintered 410L sensor rings for antilock brake systems.

### Electrochemical Tests

Electrochemical anodic polarization tests (ASTM G 5<sup>2</sup> and G 61<sup>3</sup>) are useful corrosion test methods for alloy and process development work on P/M materials. Reference 23 describes the application of potentiostatic anodic polarization to steam-treated P/M carbon steel in neutral salt and acidic environments. References 13 and 19 describe the application of potentiodynamic polarization to sintered austenitic stainless steels. These test methods are very effective in revealing metallurgical weaknesses of sintered stainless steels. Sintered stainless steels, due to their large surface areas, exhibit large corrosion currents, compared to the wrought stainless steels, and frequently the current rises with increasing potential. Furthermore, sintered stainless steels do not always exhibit a pronounced transition from

**FIG. 1—Photographic chart of sintered stainless steel transverse rupture specimens tested in 5 % aq. NaCl by immersion. Definition of ratings: A—sample free from any corrosion; B—up to 1 % of surface covered by stain or rust; C—1–25 % of surface covered by rust; D—>25 % of surface covered by rust.**

<sup>2</sup>Standard Reference Test Method for Making Potentiostatic and Potentiodynamic Anodic Polarization Measurements.

<sup>3</sup>Test Method for Conducting Cyclic Potentiodynamic Polarization Measurements for Localized Corrosion Susceptibility of Iron-, Nickel-, or Cobalt-Based Alloys.

TABLE 3—Example of corrosion rating chart for a set of six replicate specimens of sintered 316L stainless steel.<sup>a</sup>

Specimen No.	Hours Immersed in 5% aq. NaCl																		
	0.5	1	2	4	8	24	31	50	74	104	168	240	336	496	696	984	1368	1804	2282
1	A	A	A	A	A	A	A	A	A	B	B	B	C	C	C	C	D	D	D
2	A	A	A	A	A	A	A	A	A	A	B	B	B	B	C	C	C	D	D
3	A	A	A	A	A	A	A	B	B	B	B	C	C	C	D	D	D	D	D
4	A	A	A	A	A	A	A	A	A	B	B	B	B	C	C	C	C	C	D
5	A	A	A	A	A	A	A	A	A	B	B	B	B	C	C	C	C	C	C
6	A	A	A	A	A	A	A	A	A	B	B	B	B	C	C	C	C	C	D

<sup>a</sup>See Fig. 1 for definition of ratings.

the active to the passive state. As a result, the differences between initial passivation current,  $I_{\text{peak}}$ , and passive current,  $I_{\text{pass}}$ , may be smaller, and, at times,  $I_{\text{pass}}$  may be higher than  $I_{\text{peak}}$ . Also, sintered materials often show smaller differences between critical passivation current,  $I_{\text{peak}}$ , and passive current,  $I_{\text{pass}}$ . Metallurgical weaknesses show up as higher values of  $I_{\text{peak}}$  and  $I_{\text{pass}}$ , and lower values of the critical potential,  $E_{\text{pit}}$ . A larger critical passivation current means that the material is more difficult to passivate or remain passive. A higher passive current signifies a higher corrosion rate in the passive region. A lower critical potential signifies reduced pitting resistance.

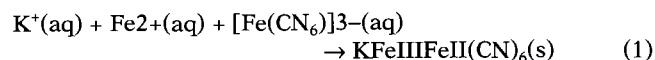
Figure 3 shows potentiodynamic curves for three P/M 316L stainless steel specimens sintered under three different conditions. These curves do not exhibit a pronounced transition from active to passive state, but do exhibit increase in corrosion current with increasing potential. Defining  $I_{\text{pass}}$  as the corrosion current in the passive region just before pitting initiates, it may be noted that the lowest  $I_{\text{pass}}$  is obtained with the specimen sintered at the highest sintering temperature (1350°C), in a 100 %  $\text{H}_2$  atmosphere and cooled rapidly.  $I_{\text{pass}}$  is higher for the specimens sintered in the nitrogen bearing atmosphere and for the lower sintering temperature in this atmosphere; both of these conditions increase the nitrogen content in the sintered stainless steels and cause precipitation of  $\text{Cr}_2\text{N}$  with attendant depletion of chromium in the grain boundaries and loss of corrosion resistance.

Table 4 summarizes electrochemical test data for 316L sintered in hydrogen and under vacuum [24]. In these examples, inferior corrosion resistance, documented also by neutral salt spray data, can be attributed to greater degrees of reoxidation of the surface of a specimen during cooling

in a higher dewpoint environment. Mathiesen and Maahn [19] have pointed out that in order to obtain qualitative correlation with neutral salt spray testing of sintered stainless steels of various densities, stepwise polarization must be employed. The slower polarization rate in stepwise polarization apparently enables the time-consuming buildup of localized attack in the pores, analogous to the mechanism of crevice corrosion.

### Ferroxyl Test

The ferroxyl test is mentioned in ASTM A 380, Practice for Cleaning and Descaling Stainless Steel Parts, Equipment, and Systems. It has recently been adapted as a rapid and simple corrosion test for sintered austenitic stainless steels [25] and for the detection of contamination of stainless steel powder with iron or low-alloy steel powders [26]. This test uses hexacyanoferrate (II/III) solutions with different chloride contents. Immersion of a sintered stainless steel part into such a solution develops, usually within minutes, a blue precipitate known as Turnbull's blue in accordance with



This test can reveal metallurgical weaknesses due to improper sintering conditions or due to contamination with iron. Agreement with salt spray testing and electrochemical

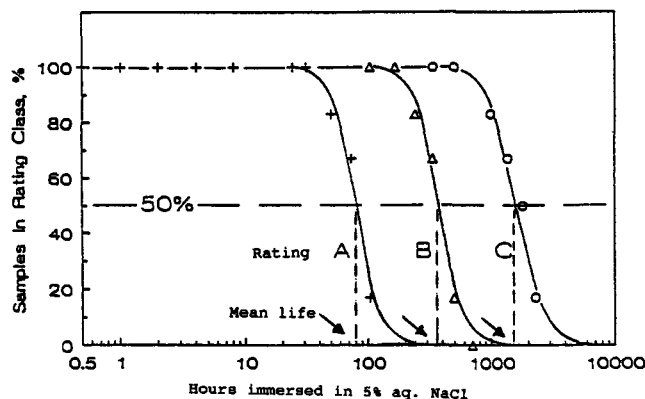
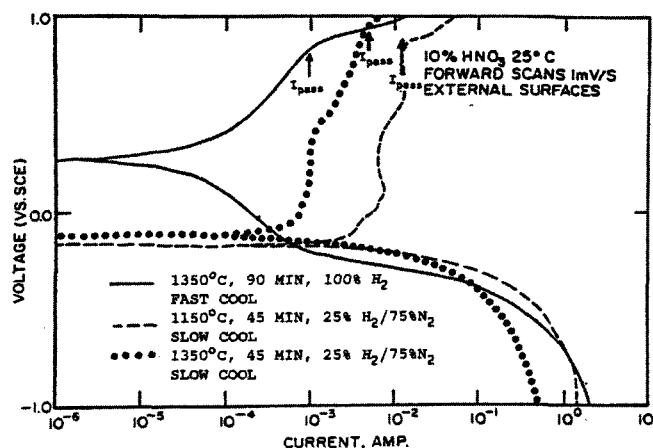


FIG. 2—Plot of percentage of replicate specimens with a given rating versus immersion time.

FIG. 3—Forward scan potentiodynamic corrosion curves for external surfaces of three sintered type 316L stainless steel samples in 10 %  $\text{HNO}_3$  at 25°C [13].  $I_{\text{pass}}$  increases with sintering in a nitrogen containing atmosphere, decreasing sintering temperature, and decreasing cooling rate.

**TABLE 4—Properties of sintered 316L, raw 316L powder, and wrought steel [15,24].**

TABLE 1. Properties of sintered SiO <sub>2</sub> , raw SiO <sub>2</sub> powder, and wrought steel [1, 2, 3].															
Sintering	°C min	H <sub>2</sub> (-30°C)				H <sub>2</sub> (-70°C)				Vacuum				Pwd	Wgt
		1120		1250		1120		1250		1120		1250			
		30	120	30	120	30	120	30	120	30	120	30	120		
Density	g/cm <sup>3</sup>	6.62	6.68	6.71	6.84	6.62	6.68	6.71	6.84	6.67	6.73	6.76	6.86		8.00
N	ppm	400	320	220	60	470	190	110	70	410	220	90	20	700	
O	ppm	2400	2400	2200	1500	2300	2000	1900	1700	2200	2200	2100	1800	1900	
C	ppm	230	220	190	130	240	250	170	110	60	60	20	10	180	300
I <sub>peak</sub>	μA/cm <sup>2</sup>	150	90	87	83	10	10	7	9	4	7	8	9		0
I <sub>pass</sub>	μA/cm <sup>2</sup>	29	21	28	19	14	10	12	11	9	13	12	7		0.5
E <sub>pit</sub>	mV SCE	250	243	243	333	345	370	330	395	368	410	363	405		665 <sup>a</sup>
E <sub>stp</sub>	mV SCE	269	213	188	163	238	275	188	163	263	238	175	150		538 <sup>b</sup>
NSS 1	h	36	60	48	24	1392	1278	1260	1512	1056	1008	420	240		1512
NSS 2	h	13	24	13	2	1512	1140	1260	60	1512	1008	324	24		

Pwd—Raw 316L powder. Wgt—Wrought 316L.

NSS—time to corrosion in Neutral Salt Spray test: 1—no pretreatment, 2—specimens filled with test solution.

<sup>a</sup>Measured with a crevice-free electrode.<sup>b</sup>Measured with a creviced electrode.**TABLE 5—Recommended test solution strengths and development times for Turnbull's blue [26].**

Material (300 Series SS)	Contaminant Powder	Solution Strength %		Development Time, min
		K <sub>3</sub> Fe(CN) <sub>6</sub>	NaCl	
Powder, not-lubed	Fe or 410L	0.1	0.1	<3
Powder, lubed <sup>a</sup>	Fe or 410L	0.25	0.25	120–180
Green Parts <sup>b</sup>	Fe or 410L	0.05	0.05	5–20
Green Parts <sup>b</sup>	Fe	0.1	0.1	<3

<sup>a</sup>Rinsed in acetone.<sup>b</sup>Density: 6.6 g/cm<sup>3</sup>, lubed.

measurements is moderate. However, this test is superior to the earlier established Copper Sulfate Test (ASTM A 380-88) for detecting less noble metal particles such as iron or low-alloy steel in austenitic stainless steel powders. Such particles, unless very fine, do not become alloyed or dissolved in the stainless steel during sintering and, therefore, give rise to galvanic corrosion. In the copper sulfate test the powder sample is covered with a saturated aqueous solution of copper sulfate, whereby the less noble contaminant particles become coated with metallic copper, and are thus readily identifiable under a low magnification stereo microscope. However, the copper sulfate test does not work with lubricated powders or green parts, whereas the ferroxyl test is not affected by presence of lubricant on powder surfaces. Also, unlike the copper sulfate test, in the ferroxyl test the blue precipitates formed in the interior of a green part or the powder mass grow rapidly in size, thus making it easy to examine. The high sensitivity of the ferroxyl test is commensurate with the fact that even traces of iron or low-alloy steel contamination can ruin the corrosion resistance of sintered stainless steel parts. Recommended test solutions and development times for the blue precipitate are shown in Table 5.

## PROCESSING AND QUALITY CONTROL OF SINTERED STAINLESS STEELS

This section briefly describes the critical process parameters that affect the corrosion resistance of sintered stainless steels in a chloride environment. The authors have observed that the most frequent processing problems in the stainless

steel parts producing industry are related to improper delubrication, excessive dewpoints in sintering furnaces, slow cooling rates after sintering, and contamination with iron or low-alloy steel powders. Improper delubrication can lead to high residual carbon or oxygen contents, or both, which in turn can cause intergranular and pitting corrosion. Excessive dewpoints of the sintering atmosphere most often result in the oxidation of the surface layers of the sintered parts during cooling. The amount of absorbed oxygen is usually too small to be identified by conventional oxygen analysis or to be noticed as discoloration of the surface. This condition produces low pitting resistance. Slow cooling rates may cause precipitation of carbides at the grain boundaries, in the same manner as sensitization occurs in wrought stainless steels. Slow-cooling in a nitrogen bearing atmosphere can lead to absorption of nitrogen on the surface of the part, forming chromium nitrides which will also impair corrosion resistance. Contamination with less noble metal powders produces galvanic corrosion.

A practical approach to process improvement for achieving good corrosion resistance in sintered stainless steels includes the following steps:

1. Testing of powders and pressed parts to assure freedom from contamination (Ferroxyl test).
2. Corrosion testing of sintered parts in accordance with the section on Corrosion Testing and Evaluation.
3. Comparison of corrosion resistance with published corrosion data.
4. Analysis of cause of inferior corrosion resistance, including analysis of samples for nitrogen, oxygen, and carbon contents, and examination of microstructure for presence of nitrides, oxides, and carbides.
5. Process modification to eliminate cause of inferior corrosion resistance as identified under (4).

Table 6 summarizes chloride corrosion resistances for various sintered and wrought stainless steels. These data were generated for a broad range of sintering conditions employed in the P/M industry. In all cases, processing was controlled to eliminate contamination of the specimens with less noble powders, to avoid or minimize precipitation of chromium carbides and chromium nitrides as well as loss of chromium during vacuum sintering [6,19,20]. Table 6 can be used by stainless steel parts producers to gage their

TABLE 6—Corrosion resistances of sintered and wrought stainless steels.

	Corrosion Test <sup>a</sup>	Corrosion Resistance Rating <sup>b</sup>		Sintered Density g/cm <sup>3</sup>	Sintering Atmosphere <sup>c</sup>	Comments			
		A hours	B hours			Sintering Temperature °C(°F)	Sintering Time, min	Type of Furnace <sup>d</sup>	Reference <sup>e</sup>
Sintered Stainless Steels									
303L	I		5	6.7–6.8	DA	1150(2100)	60	L	
303LSC <sup>d</sup>	I		500	6.7–6.8	DA	1150(2100)	60	L	
304L	I		100	6.7–6.8	DA	1150(2100)	60	L	
316L	I		500	6.7–6.8	DA	1150(2100)	60	L	
	I	400		6.7–6.9	V	1205(2200)	60	L	
	NSS	600		6.7	H <sub>2</sub>	1150(2100)	30	I	[16]
	NSS	1110		6.3	H <sub>2</sub>	1150(2100)	30	I	[16]
	NSS	1056		6.6–6.7	V	1120(2050)	30	L	[16]
316LSC <sup>d</sup>	I		1500	6.7–6.8	DA	1150(2100)	60	L	
	I	1000	1700	6.7–6.9	V	1205(2200)	60	L	
317	I	2400	4400	6.7–6.9	V	1205(2200)	60	L	
	NSS	>1500		6.7	H <sub>2</sub>	1150(2100)	30	I	
SS100 <sup>e</sup>	I	3400	5200	6.7–6.9	V	1205(2200)	60	L	
410L	I		200	7.0–7.1	V	1260(2300)	60	L	
434L	I		2200	7.0–7.1	V	1260(2300)	60	L	
Wrought Stainless Steels									
303	NSS	420							[16]
304	NSS	>1500							[16]
316	NSS	>1500							[16]
316L	I	5000							
	NSS	1512							[15]
410	I	200							
431	NSS	72							[16]
434	I	2200							

<sup>a</sup>I = by immersion in 5% NaCl; NSS = Neutral salt spray test [ASTM B 117; ISO 4540-1980(E)].

<sup>b</sup>A: time in h until appearance of first stain or rust spot; B: time in h until 1% of surface of specimen is covered with stain or rust.

<sup>c</sup>H<sub>2</sub> = hydrogen; DA = diss. ammonia; V = vacuum.

<sup>d</sup>Proprietary grades of SCM Metal Products.

<sup>e</sup>20 Cr17Ni5Mo.

<sup>f</sup>L = Laboratory; I = industrial.

<sup>g</sup>Data without reference numbers are author's data.

progress regarding process optimization for maximizing corrosion resistance. The data also show that it is possible to obtain satisfactory corrosion resistances in all three sintering atmospheres used by the P/M industry.

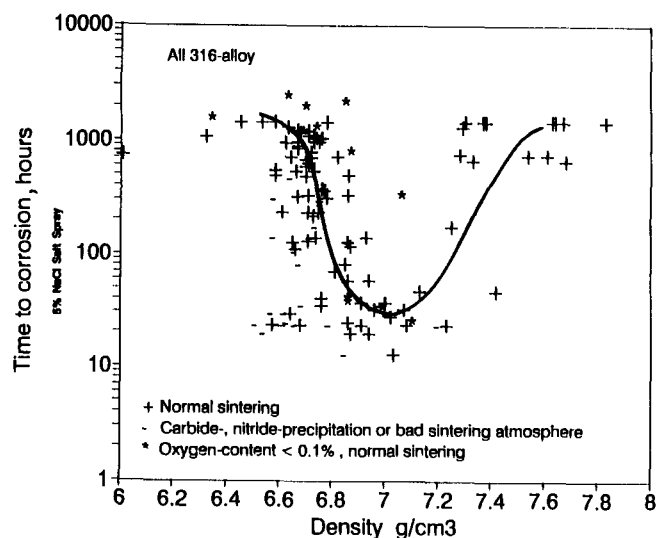


FIG. 4—Effect of sintered density upon corrosion resistance of pressed, sintered, repressed and annealed 317L [27].

Chemical analysis and metallographic examination can identify the causes of inferior corrosion resistance in many cases [6,19,20]. Quantitative data for intergranular corrosion in accordance with ASTM A 262, Practices for Detecting Susceptibility to Intergranular Attack in Austenitic Stainless Steels, are not available for sintered porous stainless steels.

For the lower alloyed austenitic stainless steels, say 18-8 and lower, after control of the metallurgical factors, there remains the detrimental effect of porosity giving rise to crevice corrosion. Crevice corrosion may be determined in accordance with ASTM G 48, Test Method for Pitting and Crevice Corrosion Resistance of Stainless Steels and Related Alloys by the Use of Ferric Chloride Solution. As shown in Fig. 4, for 317L type alloys, in the density range from about 6.6 to 7.4 g/cm<sup>3</sup>, the chloride corrosion resistance decreases with decreasing porosity reaching a minimum at around 7.2 g/cm<sup>3</sup>, and thereafter it increases as full density is approached. In these tests, the high densities were obtained by the use of a liquid phase sintering additive. To the left of the minimum, corrosion resistance decreases with decreasing pore size. To the right of the minimum, corrosion resistance improves as pores become increasingly closed-off or inaccessible to the surface. This type of crevice corrosion can be reduced or overcome by impregnation of the pores with a resin, metallurgical modification of the pore surfaces, or the use of higher alloyed stainless steels, particularly those containing higher concentrations of molybdenum.

## REFERENCES

- [1] White, D. G., "State of the North American P/M Industry," *Advances in Powder Metallurgy Particulate Materials*, Vol. 1, 1993, pp. 1-12.
- [2] *Metals Handbook, Ninth Edition, Vol. 7*, Powder Metallurgy, E. Klar Coordinator, ASM, Metals Park, OH, 1984.
- [3] Orzeske, D. J., "Steam Treatment Improves P/M Part Quality," *Industrial Heat Treating*, Vol. 63, May 1986, pp. 34-37.
- [4] Feinberg, D., *Surface Finishing of Powder Metallurgy Parts*, Metal Powder Industries Federation, Princeton, NJ, 1968.
- [5] Hanada, M., Amano, N., Takeda, Y., et al., "Development of a Powder Metallurgy Sensor Ring for Use in an Anti-lock Brake System," *International Congress and Exposition*, SAE Technical Paper Series 890407, Detroit, MI, 1989.
- [6] Maahn, E., Jensen, S. K., Larsen, R. M., and Mathiesen, T., "Factors Affecting the Corrosion Resistance of Sintered Stainless Steel," *Advances in Powder Metallurgy and Particulate Materials*, 1994, MPIF, Princeton, NJ, Vol. 7, pp. 253-271.
- [7] Reen, O. W., "Evaluating Stainless Steel Powder Metal Parts, II - Corrosion Resistance," *Precision Metals*, Vol. 35, No. 8, pp. 53-54.
- [8] Klar, E., "Corrosion of Powder Metallurgy Materials," *Metals Handbook, Ninth Edition, Vol. 13, Corrosion*, ASM, Materials Park, OH, 1987, pp. 823-845.
- [9] Pickens, J. R., "Review: Aluminum Powder Metallurgy Technology for High-Strength Applications," *Journal of Materials Science*, Vol. 16, 1981, pp. 1437-1457.
- [10] Fritz, V. L., *Powder Metallurgy Principles and Applications*, MPIF, Princeton, NJ, 1980.
- [11] *ASM Handbook, Vol. 7, Powder Metal Technologies and Applications*, ASM International, Materials Park, Ohio, 1998.
- [12] Schatt, W., *Pulvermetallurgie Sinter-und Verbundwerkstoffe*, Dr. Alfred Huttig Verlag, Pub., Heidelberg, 1986, p. 272.
- [13] Lei, G., German, R. M., and Nayar, H. S., "Corrosion Control in Sintered Austenitic Stainless Steels," *Progress in Powder Metallurgy*, Vol. 39, H. S. Nayar, S. M. Kaufman, and K. E. Meiners, Eds., Metal Powder Industries Federation, 1984, pp. 391-410.
- [14] Tikkanen, M. H., "Corrosion Resistance of Sintered P/M Stainless Steels and Possibilities for Increasing It," *Scandinavian Journal of Metallurgy*, Vol. 11, 1982, pp. 211-215.
- [15] Takeda, T. and Tamura, K., "Compacting and Sintering of Chrome-Nickel Austenitic Stainless Steel Powders," *H. B. Transl 8311 from Powder and Powder Metallurgy (Japan)*, Vol. 17, No. 2, 1970, pp. 70-76.
- [16] Kempster, A., Smith, J. R., and Hanson, C. C., "Chromium Diffusion Coatings on Sintered Stainless Steel," Metal Powder Report, MPR Publishing Services Ltd., England, June 1986, pp. 455-460.
- [17] Treharne, T. J., "Corrosion Inhibition in Sintered Stainless Steel," U. S. Patent 4,536,228, granted 20 August 1985.
- [18] Samal, P. K., Klar, E., and Nasser, S. A., "On the Corrosion Resistance of Sintered Ferritic Stainless Steels," *Advances in Powder Metallurgy and Particulate Materials*, MPIF, Vol. 2, 1997, pp. 16-99 to 16-112.
- [19] Mathiesen, T. and Maahn, E., "Corrosion Behavior of Sintered Stainless Steels in Chloride Containing Environments," *12th Scandinavian Corrosion Congress*, Helsinki, 1992, pp. 1-9.
- [20] Mathiesen, T., "Corrosion Behavior of Sintered Stainless Steel," Doctoral thesis (in Danish), Dept. of Metallurgy, Technical University of Denmark, 1993.
- [21] Dansk Standardiseringsrad, DS/ISO 3768, 1.udg., April 1980.
- [22] ISO 4540:1980, Metallic Coatings—Coatings Cathodic to the Substrate—Rating of Electroplated Test Specimens Subjected to Corrosion Tests, International Organization of Standardization, Geneva, Switzerland.
- [23] Santer, B. J. and Cash, B. E., "Effect of Surface Treatment on the Corrosion Properties of Ferrous Powder Metallurgy Parts," *Powder Metallurgy*, Vol. 17, No. 34, 1974, pp. 319-330.
- [24] Maahn, E. and Mathiesen, T., "Corrosion Properties of Sintered Stainless Steel," UK Corrosion 91, Manchester, *Proceedings*, 1991.
- [25] Mathiesen, T. and Maahn, E., "Corrosion Testing of Stainless Steels," *Metal Powder Report*, Vol. 49, No. 4, 1994, pp. 42-46.
- [26] Klar, E. and Samal, P. K., "On Some Practical Aspects Related to the Corrosion Resistance of Sintered Stainless Steels," *Proceedings of PM '94, Powder Metallurgy World Congress*, Paris, 6-9 June 1994, pp. 2109-2112.
- [27] Klar, E. and Samal, P. K., "Effect of Density and Sintering Variables on the Corrosion Resistance of Austenitic Stainless Steels," *Advances in Powder Metallurgy and Particulate Materials*, MPIF, Vol. 3, 1996, pp. 11-3 to 11-17.

# **Section VII: Testing in Industries**

*S. W. Dean, Jr., Editor*

# Automotive

*Robert Baboian<sup>1</sup>*

## INTRODUCTION

THE AUTOMOTIVE INDUSTRY has become one of the key sectors of the economy throughout the world. In industrialized countries it is estimated that between 10 and 16 % of the working population is employed in activities related to the automotive sector.

Passenger car production starts with the input of sheet metal, generally in coil form. The metal is cut and formed into 300–500 pieces, which are welded to form the body. It then passes through a paint line to the final assembly line where the assembled components (seats, carpets glass, engines, transmissions, suspensions, electrics, wheels, tires, brakes, etc.) are fitted to produce the finished vehicle.

Over the past 25 years, strategies to improve quality and reliability while reducing manufacturing costs and improve profit margins, have brought about considerable change in the industry. New designs, improved processing and new and/or improved materials and components have been developed to meet these challenges. The resulting improvements in corrosion resistance have led to extended warranties, which are currently 6–10 years for perforation and 1–5 years for cosmetic corrosion. Corrosion testing, such as laboratory accelerated tests, and the use of corrosion test track vehicles, has played a major role in the development of corrosion resistant vehicles. Today, the cost of conducting a corrosion test track study is estimated to be \$200,000 per vehicle. Therefore, the automotive industry has started to rely on other corrosion tests to determine performance characteristics of vehicles and components in service environments. This chapter addresses all of the testing technology used in the development of corrosion resistant vehicles.

## AUTOMOTIVE MATERIALS

The automobile has evolved into a complex multimaterial system that is exposed to a highly aggressive and wide range of environments. Its design includes auto-body and structural materials; hardware such as trim, bumpers, and brackets; engine; drive train and exhaust systems; electrical systems and systems incorporating liquid passages and reservoirs such as heat exchangers; hydraulic brake lines, fuel lines and tanks; and oil and transmission fluid reservoirs. Thus, the variety of materials used is extremely large. Table 1a

lists some of the metallic materials used in various automotive systems. Metallic and nonmetallic coatings used in the automotive industry are listed in Table 1b. Choice of these materials is determined by the specific application and nature of the environment.

The most significant changes that have occurred over the past three decades has been the transition from bare steel to pre-coated sheet steels such as galvanized steel. Other important changes include the increased use of aluminum alloys and of plastics and plastic composites. Also, use of lightweight magnesium has increased in recent years

## PROCESSING

Significant improvements in processing have been made over the past two decades. The most important are the steps in finishing the vehicle. Included here are the cleaning/phosphate processes, the electrocoat primer application, body sealing and wax augmentation coatings, and application of the topcoat. Other processing improvements include techniques to remove residual chemicals from components, improved electrodeposition processes and control of thickness, surface characteristics, chemistry, and metallurgy of metallic materials.

## DESIGN

Design improvements have played a major role in the development of corrosion resistant vehicles. Areas of entrapment, where salt, poultice and other materials could build up and provide a corrosive environment, have been eliminated to enhance corrosion resistance in vehicles. For example, wheel wells are now designed to have a sloping configuration so that corrosives can be washed or will drain out. Drain holes have been incorporated in areas so that corrosive liquid cannot accumulate. Sealers are used to eliminate crevices and joints where corrosives can build up. And, attempts have been made to reduce galvanic corrosion by avoiding dissimilar metal contact.

## AUTOMOTIVE ENVIRONMENT

The automotive environment can be categorized as (1) external exposure, (2) internal combustion exposure,

<sup>1</sup>RB Corrosion Service, Greenville, RI 02828.

**TABLE 1**—(a) Metallic materials used in the automotive industry.

Body Panels	Steel, coated steel (zinc, zinc-iron, zinc-nickel, aluminum), aluminum
Chassis	Steel, HSLA steel, coated steel (zinc, zinc-aluminum, aluminum), aluminum
Trim and Hardware	Chrome plated steel, stainless steel, aluminum, chrome plated zinc, stainless steel clad aluminum (bimetal), magnesium
Exhaust System	Steel, coated steel (zinc, zinc-aluminum, aluminum), stainless steel, Monel
Engine and Components	Iron, steel, aluminum, magnesium
Transmission	Steel, stainless steels, copper and alloys, nickel and alloys, aluminum
Fasteners	Steel, coated steel (wide range of metallic and nonmetallic coatings) aluminum
Cooling System	Copper and alloys, aluminum, steel, stainless steel, solder (lead-tin, tin, zinc) braze alloy (aluminum, copper)
Fuel System	Steel, coated steel (zinc, zinc-aluminum, zinc-nickel, aluminum, lead-tin, tin)
Brake System	Steel, coated steel (zinc, zinc-aluminum, lead-tin, tin) stainless steel cupro-nickel alloy
Electrical and Electronics	Aluminum, copper and alloys, coated steel (cadmium, chromium, nickel, copper, tin, lead) solder, beryllium, gold, silver stainless steels, magnesium

## (b) Coatings used in the automotive industry.

Precoated Steels	
Hot Dip	Zinc, zinc-iron, aluminum, aluminum (55%)-zinc, zinc-aluminum (5%), terne (lead-tin), nickel terne (nickel/lead-tin)
Electroplated	Zinc, zinc-iron, zinc-nickel, tin plate, tin free (chrome)
Organic/Precoat	Zinc-rich organic primer
Post-Applied (Protective and Decorative)	
Metallic	Cadmium, zinc, lead, copper, copper/nickel/chromium, nickel/chromium, chromium (microdiscontinuous), chrome flash, hard chromium, nickel-iron
Chemical Conversion Coatings	
Inorganic	Zinc phosphate, manganese phosphate, iron phosphate, black oxide, anodic oxide (aluminum), oxide/chromate, magnesium oxide
Organic Primers and Topcoats	
Organic Base	Epoxies, epoxy esters, polyesters, alkyds, vinyls, acrylics, oils, urethanes, cellulose
Pigments	Molybdates, lead, zinc, coloring
Other Organics	
Sealers	Asphaltic, rubber, vinyl, hot melts

and (3) internal functional liquids. Of these, the environment most investigated is external exposure.

### External Exposure

The severity of external automotive corrosion varies considerably throughout the world, due to differences in the chemistry of the environment [1–3]. The severest corrosion environments are in the snowbelt areas where deicing salts are used and along coastal areas where warm, humid, salt atmospheres exist. During the 20th century, the chemistry of the environment changed drastically. As a result of those changes, the corrosivity of the automobile environment increased.

To design automobiles for corrosion resistance, it is necessary to understand the nature of the environment and how materials react in that environment. Rain and snow are important to providing moisture to the environment. Atmospheric moisture and the conditions that produce fog and dew are also important. However, extensive studies and historic data have shown that moisture alone does not cause serious corrosion problems on automobiles.

Aggressive corrosive constituents include chlorides and pollutants. Marine environments are corrosive because of dissolved chlorides. A typical seawater composition has a sodium chloride content of about 3.5 %. However, this content will vary depending on location, such as that near tidal rivers or oceans. Splash and spray, which causes atmospheric redistribution of seawater, is extremely important in

marine environments. Larger seawater droplets fall out rapidly closer to the source. Smaller droplets distribute over a wide area while evaporating to an equilibrium size and deposit according to local weather conditions.

The data in Fig. 1 compiled by the Salt Institute (Washington, D.C.) on annual use of road salts in the United States show that use of sodium chloride and calcium chloride for ice and snow removal began to increase during the late 1950s. At that time, only one million tons per year of salt were used in the United States. By 1965, four million tons were used, and in 1979 usage peaked at twelve million tons. During the 1970s and 1980s, annual usage leveled at about ten million tons. During the 1990s, usage peaked at almost 20 million tons per year but varied in the range of 10–20 million tons. (See Fig. 1.) Approximately 5 % of the total usage is calcium chloride.

The rapid increase in the use of road salts during the 1960s was attributed to salt replacing abrasives. Further increase during the 1970s was attributed to changes in highway maintenance policy. Public awareness of the damaging effects of road salts during the 1980s may have prevented further increases. This pattern of road salt use has occurred throughout a large part of the industrialized world. Recent variations in usage have been attributed to variations in snowfall.

Atmospheric pollutants, such as sulfur dioxide, nitrogen oxides, hydrogen sulfide, ammonia ( $\text{SO}_2$ ,  $\text{NO}_x$ ,  $\text{H}_2\text{S}$ ,  $\text{NH}_3$ , respectively), and particulate matter, are known to have an effect on corrosion of metals [4]. The presence of  $\text{SO}_2$  in the



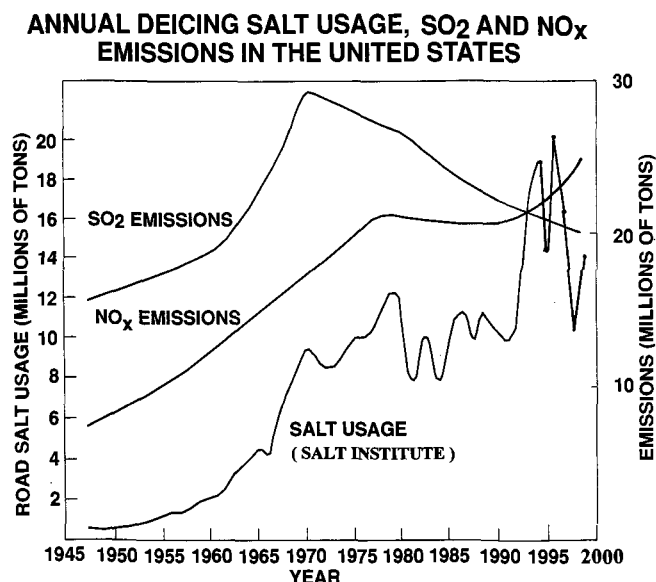
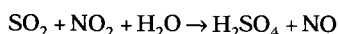


FIG. 1—Annual emissions and road salt usage in the United States.

atmosphere and its effect on corrosion has been studied very extensively. The complex reaction involves the SO<sub>2</sub> molecule striking a steel surface and converting to sulfuric acid as a result of oxidation and hydrolysis. This introduces reactive ions, increased conductivity, and a lower pH. The presence of hygroscopic sulfate corrosion products also lowers the critical humidity for corrosion reaction.

Study of the behavior of NO<sub>x</sub> has led to the conclusion that nitric acid forms on a steel surface. The conversion of SO<sub>2</sub> to sulfuric acid is enhanced in the presence of NO<sub>2</sub>, according to the reaction [5].



Increased corrosion rates have been measured for steel in the presence of both SO<sub>2</sub> and NO<sub>x</sub>. This synergistic effect may be important in the automobile environment because automobile emissions contain NO<sub>x</sub>.

Data in Fig. 1 compiled by the National Acid Precipitation Assessment Program (Washington, D.C.) on SO<sub>2</sub> and NO<sub>x</sub> emissions show that annual emissions have risen steadily in the United States peaking at 30 million tons for SO<sub>2</sub> in 1970 and 20 million tons of NO<sub>x</sub> in 1978 [6]. Although emissions have decreased during the 1980s and 1990s for SO<sub>2</sub>, the levels for NO<sub>x</sub> emissions increased. The current levels for both still remain quite high.

Atmospheric oxides of sulfur and nitrogen are emitted from both natural and anthropogenic sources. Examples of natural sources include volcanic activity and decomposition of organic materials (such as emissions from salt marshes). Anthropogenic sources are concentrated in the heavily industrialized zones. These emissions may be transported over great distances, because they are usually discharged from tall smokestacks. Thus, the long distance movement of air pollutants can affect areas remote from industry. Studies have shown that oxidation and hydrolysis reactions of SO<sub>2</sub> and NO<sub>x</sub> occur in the atmosphere yielding H<sub>2</sub>SO<sub>4</sub> and HNO<sub>3</sub>. (The residence time of SO<sub>2</sub> in the atmosphere is

estimated to be two to four days.) The resulting acid deposition in the form of acid rain, acid snow, acid fog, acid dew, and dry acid deposits is distributed over large areas.

The synergistic effect of road salts and acid deposition on corrosion has been investigated [1–4]. The combined effect of the chloride (a film disruptor on metals) and acids (which provide reducible hydrogen ions) can be much worse than the added separate effects. Thus, geographical areas that are subjected to both road salts and acid deposition are likely to be the most corrosive to automobiles.

Another important factor is the highly corrosive environment produced by the accumulation of dirt, vegetation, and other debris in metallic entrapment areas [7]. These areas remain wet almost continuously due to the presence of this poultice and produce a stationary electrolyte environment. The result is a concentrating effect of salts and acids similar to the phenomena observed in crevices. When steels are exposed to this poultice environment, the corrosion process becomes autocatalytic leading to rapid deterioration.

### Internal Combustion Exposure

Internal combustion produces water vapor and exhaust gases, which can condense in internal areas such as the exhaust system of automobiles [8,9]. This condensate chemistry includes sulfate, sulfite, nitrate, ammonium, carbonate, bicarbonate, and chloride ions. The acidity of the condensate is high due to the presence of nitric, hydrochloric, sulfuric, and sulfurous acids. Nitric acid is formed from atmospheric nitrogen, which is converted to oxides in the engine and then to the acid. Sulfuric and sulfurous acids are formed because fuels and lubricatory oils contain sulfur, which converts to sulfur dioxide and then reacts with water vapor to form these acids. In addition, catalytic converters are designed to convert SO<sub>2</sub> to SO<sub>3</sub> yielding acids. Chloride additives to fuels yield hydrochloric acid.

The temperature of the system is of great importance. If the system does not become hot enough (above the dew point), the condensate remains and concentrates. Thus, vehicles, which are driven for short distances are more susceptible to corrosion by exhaust gas condensates, sometimes referred to as cold-condensate corrosion [8]. Deterioration is also accelerated by stress (both cyclic and static) and by design configurations (such as at joints and welds).

Direct exhaust-gas impingement (erosion corrosion) can occur due to the high-velocity exhaust gas stream on the internal surfaces of the exhaust system. This effect is important at sharp bends and surfaces normal to the gas flow. The combination of particulate matter with hot corrosive gas produces this type of attack.

High-temperature oxidation of exhaust system components is governed mainly by the temperature encountered, as well as exhaust gas composition. Temperatures measured near the exhaust-manifold typically range up to 800°C and the skin temperature of metal components in this area can reach 600°C.

### Internal Functional Liquids

Internal functional liquids include engine coolants, engine oil, transmission fluid, hydraulic brake line fluid, fuels, etc.

The requirement of engine coolants is to transfer heat from the engine to the radiator where it is dissipated. Properties must include high specific heat, good thermal conductivity, low freezing point, high boiling point, chemical stability, and noncorrosivity. Since ethylene glycol provides a fairly good overall balance of these properties, it is used almost universally for automobile engine coolant in aqueous solution [10]. Typically, an ethylene glycol concentrate will also include a small amount of other glycols, chemical inhibitors, buffer or neutralizer, foam suppresser, dye, and a small quantity of water to dissolve the additives (ASTM D 3585, Specification for ASTM Reference Coolant, is a typical example of a formulated coolant). The concentrate is generally mixed with water for automotive service. The nature of the water used to dilute the ethylene glycol concentrate, and the type and length of service of the coolant will determine its corrosivity. Chloride-containing water, for example, can override the effect of inhibitors in the coolant and therefore will cause corrosion damage. Inhibitor depletion, and glycol breakdown to form acids, are also mechanisms whereby the coolant can become corrosive [11]. Metals and alloys exposed to engine coolants are copper, solder, brass, steel, cast iron, stainless steels, and aluminum.

Basic functions of engine oil are to provide lubricity, heat removal, and containment of contaminants [12]. The composition is about 75–90 % base stock (such as mineral oil) and 10–25 % additives such as viscosity index (VI) improvers, antioxidants, corrosion inhibitors, detergents, dispersants, and others such as antifoam agents. The aging of engine oil, as determined by the type of driving, can result in an aggressive liquid. Examples include oxidized oil due to exposure to heat and oxygen, loss of buffer when it is used up in neutralizing acids, and contamination by coolant, gasoline, and engine exhaust gases. Prolonged use of aged engine oil can lead to general corrosion, fretting, and erosion corrosion.

Automatic transmission fluid (ATF) performs many functions including lubrication, power transfer, hydraulic control, and cooling [13]. This fluid is extremely complex consisting of a base mineral oil (consisting of paraffinic, naphthenic, and aromatic hydrocarbons) and an additive package. Newer ATF compositions consist of synthetic base materials. The additives prevent fluid oxidation, corrosion, loss of lubricity, and foaming. Even though antioxidants, inhibitors, and stabilizers are added to the ATF, the base oil

can react with oxygen to form organic acids. The acidity is quantitatively measured as the total acid number (TAN). In addition, some additives such as organothiophosphates are reactive to some metals.

Hydraulic brake line fluids are usually polyglycols or silicones. Commercial brake fluids are hygroscopic and absorb moisture when exposed to humid atmosphere. Water contamination can also occur from atmospheric condensation. The result of this water contamination is a liquid with various degrees of corrosivity towards brake cylinders, the master cylinder, hydraulic brake line tubing, and other brake system components [14].

## CORROSION MECHANISMS

Corrosion mechanisms on automobiles are dependent on factors such as physical and chemical properties of the environment, materials, and the specific application. Table 2 is a summary of corrosion mechanisms according to specific application.

The most visible part of the automobile is the exterior body panel structure. Corrosion degradation is generally classified into structural (inside-out) and cosmetic (outside-in) corrosion. Structural corrosion in the auto-body leads to perforation, generally from the inside out (Fig. 2). This corrosion occurs at crevices and other entrapment areas where poulitice can build up and at failed coatings. Cosmetic corrosion is usually associated with painted auto-body panels (Fig. 3). Therefore, the quality and nature of the paint/metal system is very important. Paint coating failure can occur from a wide range of mechanisms including differential cells, cathodic disbondment, filiform corrosion, galvanic (bimetallic) effects, and fretting, and can occur at crevice geometries [1,2,15–27].

The chassis and undervehicle is most susceptible to mechanical damage because of its proximity to external road conditions [24] (Fig. 4). Usual corrosion mechanisms apply such as those due to the effect of stone impingement and crevice and uniform corrosion. Coatings failure can enhance deterioration as can poulitice built up in entrapment areas.

Trim and hardware are used for a number of reasons including styling, hiding welds, and protection from mechanical damage [28]. Trim materials such as stainless steel and anodized aluminum are susceptible to pitting, crevice corrosion,

TABLE 2—Corrosion mechanisms in automobile applications.

Body Panels—Structural	<b>Uniform</b> , pitting, <b>crevice</b> , fretting, <b>coating failure</b> , <b>poulitice</b>
Body Panels—Cosmetic	<b>Crevice</b> , <b>galvanic</b> , fretting, <b>coating failure</b>
Chassis	Uniform, pitting, <b>crevice</b> , fretting, stress cracking, coating failure, <b>poulitice</b>
Trim and Hardware	Uniform, <b>pitting</b> , <b>crevice</b> , <b>galvanic</b> , dealloying, intergranular, <b>coating failure</b>
Exhaust System	<b>Uniform</b> , pitting, crevice, dealloying, erosion, fretting, <b>intergranular</b> , stress cracking, <b>coating failure</b> , <b>high temperature oxidation</b>
Engine and Components	Uniform, pitting, crevice, galvanic, dealloying, <b>fretting</b> , intergranular, stress cracking, high temperature oxidation
Transmission	Uniform, crevice, galvanic, <b>fretting</b>
Fasteners	Uniform, <b>pitting</b> , <b>crevice</b> , <b>galvanic</b> , <b>fretting</b> , stress cracking, <b>coating failure</b>
Cooling System	Uniform, <b>pitting</b> , <b>crevice</b> , galvanic, dealloying, <b>erosion</b> , <b>cavitation</b> , intergranular
Fuel System	<b>Pitting</b> , crevice, coating failure
Brake System	<b>Pitting</b> , crevice, galvanic, <b>fretting</b> , <b>coating failure</b>
Electrical and Electronics	Uniform, <b>pitting</b> , <b>crevice</b> , <b>galvanic</b> , dealloying, <b>fretting</b> , stress cracking, <b>coating failure</b> , <b>corrosion product creep</b>

\*Primary mechanisms are in boldface.



FIG. 2—Structural corrosion (inside-out perforation) on automobile body.

and discoloration. Stainless steel trim materials can cause galvanic corrosion of painted auto-body steel. On the other hand, some trim materials such as aluminum and zinc die cast are anodic to auto-body steel and corrode sacrificially.

The exhaust system and engine are exposed to a dual (external and exhaust gas) environment. Therefore, the materials must be chosen to perform in more complex service conditions. High temperatures are important along with the chemistry of the exhaust gas condensate. Corrosion mechanisms include those normal in the external environment with the additional temperature factor [8,9].

Electrical and electronic systems are extremely susceptible to corrosion by the aggressive automobile environment [29–31]. Pitting, crevice and galvanic corrosion, and corrosion product creep are all important mechanisms, and in many cases these mechanisms are accelerated by leakage currents, which impose a potential bias on the materials. Fretting and coatings failure are also failure mechanisms.

## CONTROLLING AUTOMOTIVE CORROSION

### Exterior Exposure

The severe corrosivity of the automobile environment due to road salts and acid deposition has made it necessary for the industry to improve corrosion protection through (1) proper design, (2) choice of corrosion-resistant materials, (3) use of coatings and sealants, and (4) proper consumer maintenance [32–36].

Proper design has been recognized as an important aspect of automobile corrosion resistance. Thus, elimination of entrapment areas where moisture and poultice can be trapped, minimization of crevice configurations, elimination of unnecessary holes in body panels, provision of drainage holes, access for complete pretreatment and primer coverage, and elimination of dissimilar metal crevices are common practices in the design of automobiles.

Advancements in materials have been one of the most important factors in the development of corrosion-resistant automobiles. For automobile body and chassis parts, use of precoated sheet steel in critical areas, as demonstrated in Fig. 5, is one of the most effective methods of combating corrosion. Early on, hot dip galvanized steel and Zincrometal coated steel were used to prevent perforation corrosion from the inside out in auto-body applications. Today a wide range of materials is used including hot dip and electrodeposited zinc, zinc-iron, zinc-nickel, and zinc-nickel/organic composite coated steel. Other materials include aluminum and aluminum-zinc coated steels for exhaust systems and some structural components,terne (tin-lead) coated steel for fuel tanks, and tin coated steel [23–25].

Materials systems are used quite widely on automobiles for corrosion protection. For example, clad metals are commonly used in applications such as exterior trim and bumpers (stainless steel clad aluminum), windshield wiper socket (copper/steel/bronze), transition materials to join aluminum to steel (aluminum clad steel), and hydraulic brake line tubing (steel/SS/steel) [37]. A wide range of metallic coatings are produced by spraying, chemical vapor deposition, physical vapor deposition, electrodeposition, and electroless deposition [23–25].

FIG. 3—Cosmetic corrosion (outside-in) with red rust at painted auto-body steel.



FIG. 4—Severe undervehicle corrosion.

**FIG. 5—Critical areas and use of galvanized steel on automobile designed for corrosion resistance (courtesy of L. L. Peipho, General Motors Corporation, Milford Proving Grounds).**

New alloys have been introduced for specific automobile applications including type 434 stainless steel for exterior trim, type 409 and 430 stainless steels for exhaust systems, and 6XXX and 7XXX aluminum alloys for auto body and structural parts. Use of aluminum for body panels such as hoods and deck lids has prompted the development of new processing techniques for this material.

A wide range of inorganic and organic coatings and sealants is used to provide supplemental corrosion protection to automobiles [23–25]. Included are conversion coatings formed by interaction of the metal surface with constituents in solution to form an inert inorganic film. Some of these are phosphate, chromate, and various anodized and oxide coatings. Organic coatings are also used extensively and function as a barrier between the metal surface and the environment. These include primers, waxes, seam sealers, barriers to mechanical damage, and petroleum-based rust preventives.

The automobile paint system involves several different coatings [24,25]. Typically, a conversion coating such as phosphate is applied to a clean metal surface to improve corrosion protection and ensure good adhesion. Then, an epoxy primer is applied by dipping, spraying, or by electrodeposition. The most important advances in epoxy primer deposition have been in electrophoretic systems variously called electrocoating, E-Coat, or ELPO [2]. In this process, the metal substrate is immersed in an aqueous bath and coated with a charged organic primer under the influence of an electric field. The advantages here include uniform coverage, edge protection, penetration into enclosed areas, and full automation. In recent years, the industry has shifted from anodic to cathodic electrocoating [38]. The next step is usually a primer surfacer or guide coat for sealing and enhanced appearance. Finally, the topcoat is applied, usually in two or more steps including a base coat and a clear coat. These are generally enamels and urethanes. The performance of these complex painted auto-body materials in the aggressive automobile environment is understandably dependent on a number of factors.

Sealers play an important role in automobile corrosion protection by preventing water and contaminants from entering crevices and joints. They are usually rubber, vinyl, asphaltic, or hot melt or wax compounds [24,25]. The choice depends on the specific application such as at door hem flanges, brackets, fasteners, and body joints. Structural adhesives are also used to bond assemblies such as doors, decklids, and hoods, thereby sealing crevices and eliminating welds.

Consumer maintenance has become an important part of automobile corrosion protection. Automobile manufacturers have provided recommendations for maintenance in order to prevent deterioration from corrosion. The first defense is regular washing to remove road salts and other corrosive agents, and poultice. The procedure should ensure that mud and dirt is removed from entrapment areas underneath the vehicle. Drain holes should be cleaned out. The second defense includes repair of paint damage to avoid propagation of corrosion in these areas. Precautions should be taken to exclude corrosive agents from the interior such as driving in or splashing seawater or road deicing salt puddles on the vehicle.

### Internal Combustion

The service life of exhaust systems has been greatly extended through the use of more corrosion-resistant materials [8]. These include stainless steels (types 409 and 430), aluminum coated steels, and aluminum-zinc coated steels [39]. The use of catalytic converters presents some special problems because of the catalyzed oxidation reactions that take place in the exhaust gas stream. The converter itself must be highly corrosion-resistant because of its location near the exhaust manifold and the reaction to form acids such as sulfuric acid. Stainless steel is therefore widely used for the catalytic converter canister. More corrosion-resistant materials are also being used downstream from the converter.

### Liquid Passages and Reservoirs

Internal functional liquids generally have inhibitors in the formulation to minimize degradation due to corrosion. These inhibitors provide the necessary protection as long as they are present in the required concentration.

However, inhibitor depletion and acidity buildup due to decomposition of base organics can occur depending on the nature of vehicle use and maintenance practice. For example, engine coolant formulations contain a complex inhibitor package providing protection to component metals such as copper, steel, aluminum, solder, etc. [40,41]. When inhibitor depletion occurs, failure of an aluminum water pump due to corrosion can result but this component is easily replaced. When a transmission component fails due to corrosion, replacement is more costly and therefore more corrosion-resistant materials are generally used. For example, copper and brass may corrode in used automatic transmission fluid while steels and stainless steels are generally resistant in that environment. A proper maintenance schedule of replacement of these fluids is very important in maintaining corrosion protection within liquid passages and reservoirs.

## Electrical and Electronic Systems

Use of electrical and electronic components on automobiles has increased dramatically so that corrosion protection is important. The primary method is to minimize exposure to the environment by locating wiring and other components within the passenger compartment, by shielding or providing good drainage, and by sealing and coating [29,30]. Proper design, manufacturing, and quality are a precursor. However, failure can occur in electrical and electronic systems if proper precautions are not taken. For example, residual fluxes can cause corrosion problems because they can contain chlorides and may be hygroscopic. Examples of critical systems are connectors, switches, terminals, large housings and electrical connections, sensors, integrated circuits, and other electronic control devices. Various organic and inorganic coatings are used to exclude air, moisture, and chemical contaminants and to increase lubricity and reduce thermal degradation. These include paint, primer, varnish, resin, silicone compounds, oil, and greases. A wide range of sealed connectors has been developed for use on automobiles because even the best selection of base materials and plating cannot provide the necessary termination protection in the severe automotive environment. The problems associated with leakage currents (bias) have been addressed by ensuring that proper barrier coatings, sealing, and design are used.

## TEST METHODS

Corrosion testing has played a major role in the development of corrosion-resistant automobiles. The tests are generally classified as laboratory tests or field tests. The difference involves the nature of the environment. Laboratory tests simulate the environment, while field tests are conducted in the natural environment. Some tests combine a simulated environment and the natural environment. Although laboratory test results are obtained in shorter times, field test results are more reliable because they are conducted in the actual environment. The design and interpretation of laboratory tests are important in order to obtain useful information [1,42].

Test parameters are categorized according to chemical and physical effects. Chemical parameters involve the composition of the environment, i.e., concentration of constituents, pH, dissolved gases, etc. The complexity of the

automobile environment has been described above. The physical conditions include temperature, static or flowing solution or vapor, liquid or atmospheric volume, and mechanical factors such as stress and impingement. Finally, the duration of the test and exposure periods must be chosen carefully so that under- or over-exposure will not lead to incorrect design. Table 3 lists methods and guidelines that are used in the automobile industry for design and interpretation of corrosion tests.

## Laboratory Tests—External Exposure

Categories of laboratory (accelerated) tests are: electrochemical, immersion, cabinet, cyclic, and proving grounds. These accelerated tests require (1) selection of environmental and physical conditions representative of service exposure, (2) accelerated corrosion rates without a change in the mechanism, (3) reproducibility of results, and (4) acceleration factors which relate to service performance.

Electrochemical tests are rapid techniques to determine mechanisms, determine the effect of various parameters on corrosion rate, and screen out a large number of materials [43]. They usually involve measurement of corrosion potentials, corrosion currents, polarization curves, and electrochemical impedance. They are used to evaluate metals and alloys and the behavior of metallic, inorganic, and organic coatings. The simplest test involves the measurement of the corrosion potential and its use in conjunction with other measurements. A zero resistance ammeter (ZRA) is commonly used to measure corrosion currents between dissimilar metals and alloys. Controlled potential tests and anodic and cathodic polarization curves using potentiostats are the most commonly used electrochemical tests. These are powerful tools for investigating the effect of various parameters on corrosion behavior. These incorporate the use of cyclic polarization and polarization resistance for localized corrosion and corrosion rate measurements. Table 4 lists electrochemical tests that can be used for corrosion tests in the automobile industry.

Immersion tests are listed in Table 5 and consist of specimens immersed in a fluid of interest. Variations of the test can be used to enhance certain types of exposure such as partial immersion to create oxygen concentration cells, and alternate (cyclic) immersion to produce wetting and drying effects. The latter test, along with the ferric chloride spot test is used to determine the behavior of exterior stainless steel trim materials.

**TABLE 3**—Methods and guidelines for the design and interpretation of corrosion tests.

Practice for Preparation of Cold-Rolled Steel Panels for Testing Paint, Varnish, Conversion Coatings, and Related Coating Products	ASTM D 609
Test Method for Evaluation of Painted or Coated Specimens Subjected to Corrosive Environments	ASTM D 1654
Practice for Preparing, Cleaning, and Evaluating Corrosion Test Specimens	ASTM G 1 and ISO 8407
Test Method for Evaluating Degree of Rusting on Painted Steel Surfaces	ASTM D 610
Practice for Rating of Electroplated Panels Subjected to Atmospheric Exposure	ASTM B 537
Practice for Recording Data from Atmospheric Corrosion Tests of Metallic-Coated Steel Specimens	ASTM G 33
Practice for Examination for and Evaluation Pitting Corrosion	ASTM G 46
Practice for Conventions Applicable to Electrochemical Measurements in Corrosion Testing	ASTM G 3
Terminology Relating to Corrosion and Corrosion Testing	ASTM G 15 and ISO 8044
Guide for Applying Statistics to Analysis of Corrosion Data	ASTM G 16
Practice For Calculation of Corrosion Rates and Related Information from Electrochemical Measurements	ASTM G 102
Calculating of Economic Appraisals of Corrosion Control Measures	NACE RPO272

**TABLE 4—Electrochemical tests.**

Standard Reference Test Method for Making Potentiostatic and Potentiodynamic Anodic Polarization Measurements	ASTM G 5
Practice for Conducting Potentiodynamic Polarization Resistance Measurements	ASTM G 59
Test Method for Conducting Cyclic Potentiodynamic Polarization Measurements for Localized Corrosion Susceptibility of Iron, Nickel or Cobalt-Based Alloys	ASTM G 61
Practice for Measurement of Corrosion Potentials of Aluminum Alloys	ASTM G 69
Guide for Development and Use of Galvanic Series for Predicting Galvanic Corrosion Performance	ASTM G 82
Method for Conducting Cyclic Galvanostaircase Polarization	ASTM G 100
Practice of Calculation of Corrosion Rates and Related Information from Electrochemical Measurements	ASTM G 102
Practice for Electrochemical Impedance Measurements	ASTM G 106
Method for Electrochemical Reactivation (EPR)	ASTM G 108
Method for Electrochemical Critical Pitting Temperature	ASTM G 150

**TABLE 5—Immersion tests.**

Practice for Testing Water Resistance of Coatings Using Water Immersion	ASTM D 870
Practice for Laboratory Immersion Corrosion Testing of Metals	ASTM G 31
Practice for Evaluating Stress Corrosion Cracking Resistance of Metals in 3.5% Sodium Chloride Solution	ASTM G 44
Test Method for Pitting and Crevice Corrosion Resistance of Stainless Steels and Related Alloys by the Use of Ferric Chloride Solution	ASTM G 48
Testing of Metals for the Process Industry	NACE TM-01-69
Metallic Coatings—Accelerated Corrosion Tests	ISO 1462 and ISO 4540

Cabinet tests are the most commonly used laboratory tests in the automobile industry. These have been developed to simulate the effects of atmospheric corrosion [44]. Normally, a test chamber is used and the desired environment is introduced under controlled conditions. A list of these tests is given in Table 6. The simplest of these is the humidity test whereby the temperature and relative humidity within a chamber are controlled. A condensing humidity chamber, which operates at 100 % relative humidity and 38°C, provides

an environment whereby condensation occurs continuously on the specimens. The moist SO<sub>2</sub> test (Kesternich test, ASTM G 87) is a modification of the humidity test but is much more aggressive due to the presence of sulfur dioxide which converts to sulfuric acid. Another modification commonly referred to as the mixed flowing gas test (ASTM B 827) uses extremely low quantities of pollutants such as H<sub>2</sub>S, SO<sub>2</sub>, NO<sub>x</sub>, Cl<sub>2</sub>, and HCl with humidity to duplicate environments within the passenger compartment. This test is especially useful for electrical and electronic systems [45].

The most widely used cabinet test is the neutral salt spray (Fog) test (ASTM B 117), which consists of a fog of 5 % sodium chloride within the chamber at 35°C [46]. Controversy exists over the validity of B 117 as a performance test because corrosion mechanisms are not always the same as those observed in automobile service. Also, not all materials can be successfully evaluated in the test. However, the value of the salt spray test as a quality assurance test is well documented [46]. Several modifications to the salt spray test have been developed including acetic acid salt spray (ASTM G 85, Annex 1), copper accelerated acetic acid salt spray (ASTM B 368), acidified synthetic seawater fog (ASTM G 43, Method of Acidified Synthetic Seawater (Fog) Testing), and modified salt spray (ASTM G 85). ASTM G 85 also includes cyclic tests.

Cyclic corrosion tests have been developed to more accurately duplicate corrosion behavior observed in service [47–50]. They simulate the automobile environment by introducing a combination of conditions that exist in service. Testing consists of exposing specimens to at least two different environmental conditions and cycling from one environment to the other. There are a number of cyclic tests that have been developed specifically for determining the behavior of painted auto-body materials. In some cases, these tests are conducted in cabinets or in and out of cabinets. In other cases, the tests are not conducted within a cabinet. The various environmental conditions that have been used include salt spray, salt mist, aqueous immersion, temperature variation, humidity variations, ultraviolet (UV) light exposure, poultice, gravel or shot blasting, and drying. Cyclic tests are listed in Table 7.

A typical test developed by one of the automobile manufacturers and used widely, GM9540P, includes two accelerated

**TABLE 6—Cabinet tests.**

Test Method of Salt Spray (Fog) Testing	ASTM B 117, ISO9227, DIN 50016, and JIS-Z2371
Method of Acetic Acid-Salt Spray (Fog) Testing	ISO 3769
Method for Copper-Accelerated Acetic Acid-Salt Spray (Fog) Testing (CASS Test)	ASTM B368, ISO 3770, and JIS H8681
Method of Corrosion Testing of Decorative Electrodeposited Coatings by the CORRODKOTE Procedure	ASTM B 380
Practice for Conducting Mixed Flowing Gas (MFG) Environmental Tests	ASTM B 827
Practice for Testing Water Resistance of Coatings Using Water Fog Apparatus	ASTM D 1735
Test Method for Rust Protection by Metal Preservatives in the Humidity Cabinet	ASTM D 1748
Practice for Testing Water Resistance of Coatings in 100% Relative Humidity	ASTM D 2247
Guide for Testing Filiform Corrosion Resistance of Organic Coatings on Metal	ASTM D 2803
Practice for Testing Water Resistance of Coatings Using Controlled Condensation	ASTM D 4585
Method for Conducting Cyclic Humidity Tests	ASTM G 60
Practice for Modified Salt Spray (Fog) Testing	ASTM G 85
Practice for Conducting Moist SO Tests	ASTM G 87 and DIN 50018
Corrosion Tests in Artificial Atmosphere	ISO 7384
Accelerated Exposure Using Fluorescent UV Exterior Materials and Condensation Apparatus	SAE J2020
Tests in Artificial Atmospheres at Very Low Concentrations of Polluting Gases	ISO 10062

TABLE 7—Cyclic tests.

Chip Resistance of Surface Coatings	SAE J400
Laboratory Cyclic Corrosion Test	SAE J1563
Method for Conducting Cyclic Humidity Tests	ASTM G 60 and SAE J1047
Method for Conducting Moist SO Tests	ASTM G 87 and DIN 50018
Cyclic Corrosion Test (CCT)	JIS Z2371
Accelerated Outdoor Test by Intermittent Spraying of a Salt Solution (SCAB Test)	SS11 72 11, Swedish Standard
Performance of Substrates and/or Coatings Through Environmental Cycling	GM9505P
Corrosion Tests in Artificial Atmospheres	ISO 7384
Painted Sheet Metal Corrosion Test—Simulated Arizona Proving Ground	Ford TM—BI 123-01
Accelerated Corrosion Test for Cars and Trucks	Chrysler LP 461H-117
Volvo Scab Test	Volvo Std 1027, 1372
Cosmetic Corrosion Lab Test	SAE J2334
Accelerated Corrosion Test	GM 9540P
Practice for Modified Salt Spray (Fog) Testing	ASTM G 85
Corrosion Test Method for Automotive Materials	JASO M 609
Cosmetic Corrosion Test Method for Automotive Parts	JASO M 610

laboratory methods to evaluate assemblies and components. The test procedures provide a combination of cyclic conditions (salt solution ( $\text{NaCl}$ ,  $\text{CaCl}_2$  and  $\text{NaHCO}_3$ ), various temperatures, humidity and ambient environment) to accelerate metallic corrosion. The procedures are effective in evaluating a variety of mechanisms including galvanic, crevice, etc. [49].

One of the improved laboratory cyclic test procedures for cosmetic corrosion was developed during the 1990s by a joint Task Group of AISI and SAE. The extensive work of this Task Group resulted in the standard test SAE J 2334. The procedure is based on field correlated laboratory tests. The test has been shown to give an excellent correlation with five-year on vehicle tests in the aggressive environments such as Montreal, and also shows promise for perforation corrosion [51]. The test cycle consists of three stages; (1) humid stage-50°C, and 100 % RH, 6 hours duration; (2) salt application stage ( $\text{NaCl}$ ,  $\text{CaCl}_2$ , and  $\text{NaHCO}_3$  by immersion or misting)-15 minutes duration at ambient conditions; (3) dry stage-60°C and 50 % RH, 17 hours and 45 minutes in duration. Typically, J 2334 is conducted for 60–80 cycles when evaluating coated products.

Proving grounds tests (Table 8) include the operation of an automobile in a controlled environment to evaluate the performance of a fully assembled vehicle [52]. The test schedule varies from one facility to another but generally includes a driving schedule over various roads including highway travel, salt highway, gravel road, mud trough, and salt trough (Fig. 6). Also included are exposure to rain, snow, drying, elevated temperature, and controlled humidity. The period of time required to complete one set of exposure is termed a cycle, and usually a number of cycles is related to years of automotive service. One method to provide correlation to service performance is by use of coupons with known service behavior mounted on the test vehicle.

TABLE 8—Vehicle corrosion tests.

Proving Ground Vehicle Corrosion Test	SAE J1950
Method for Conducting Corrosion Coupon Tests	SAE J1293 and ASTM G 4
Atmospheric Exposure	ASTM G 33, G 50, G 92, SAE J1976, JIS Z2381, ISO 4542, ISO 8565, and ISO 9226
Automobile Corrosion Field Surveys	SAE P228

These are evaluated periodically to determine acceleration factors during the proving grounds test. Because these tests simulate service exposure but still represent accelerated conditions, considerable expertise is required for evaluation and interpretation of results. Some novel developments in proving ground testing include the use of specimens (including panels, parts, and components) mounted on trailers, which are pulled throughout the test schedule. A large amount of information can be obtained through this test procedure.

### Field Tests—External Exposure

When products or materials are exposed to the natural environment, they are considered field or service tests. Included in this category are atmospheric exposure, mobil test racks, fleet tests, and field surveys (Table 8).

Atmospheric exposure consists of placing specimens such as coupons, parts, components, on racks at stationary test sites [53]. The example in Fig. 7 shows bumpers under test at the marine splash and spray facility of the LaQue Center for Corrosion Technology at Wrightsville Beach, North Carolina. The nature of the site varies depending on geographic area and specific location within an area. Factors such as environmental chemistry (chlorides, pollutants,

FIG. 6—Proving ground test vehicle driven on salted highway strip.



FIG. 7—Marine splash and spray exposure test on vehicle bumpers.

etc.), time of wetness, temperature, humidity, hours of sunlight, and seasonal changes have an important effect on the corrosion rate and mechanism and, therefore, many atmospheric test sites for automobile materials are chosen based on these conditions. A warm, humid, marine site will be more aggressive than a rural site. The combination of marine chemistry with acid deposition is most aggressive. Frequently, test sites are located close to roads where deicing salts are used to obtain the desired automotive environment. Alternatively, the Volvo test consists of outdoor atmospheric exposure with periodic spraying with 5 % sodium chloride (Table 7). The more useful information from atmospheric corrosion tests is obtained when climatic and chemical information is available for the site.

Mobil test racks or plates are mounted on vehicles or trailers, which are subjected to normal driving conditions. They are mounted on various locations on vehicles such as the undervehicle as described in SAE J1293. However, these racks or plates are also mounted on bumpers, grilles, and truck trailers (Fig. 8). Panels, coupons, parts, and components are attached to these racks and are therefore exposed to driving conditions in the natural environment. Direct

FIG. 8—Corrosion test plate mounted on the front bumper of an automobile.

comparisons can therefore be made on the corrosion behavior of these materials.

Fleet tests are extremely valuable in providing direct information on corrosion behavior in specific locations. Groups of cars that are typically used for these tests are taxicabs, rental cars, municipally owned cars, and sales fleet cars. Because the operating parameters can be recorded through fleet record keeping, this type of test is probably the most reliable of all for automobile corrosion performance.

Field surveys are valuable because of the large number of vehicles that can be visually inspected over a short period of time [54]. In general, a location and time of year is chosen and a team of evaluators survey parking lots, streets, dealerships, etc., with survey sheets. Therefore, corrosion performance is based on inspection and evaluation of actual standard production vehicles exposed to natural environments and normal operating conditions. One drawback to field surveys is that actual driving conditions for each vehicle cannot be determined unless each owner is interrogated. However, the vehicle identification number (VIN) and odometer reading does provide important information.

Testing—Internal Combustion

The complex exhaust system environment including internal condensate corrosion, high-temperature oxidation, and exhaust-gas impingement makes it very difficult to obtain meaningful accelerated corrosion test results. Laboratory tests are generally based on exposure to synthetic exhaust gas condensate. A common test is the Walker Standard Accelerated Corrosion Test, which uses alternate immersion in hot synthetic muffler condensate [55]. Variations of this test are used depending on the particular components being considered [1,8,16]. The hottest area in the exhaust system exists from the catalytic converter back to the engine. Beyond the catalytic converter the temperature drops off but that area becomes susceptible to exhaust-gas condensation. Various test temperatures, immersion times, and condensate chemistries are used depending on the specific component and manufacturers' requirements (Table 9).

Controlled engine laboratory tests are valuable for evaluating internal exhaust system deterioration. These tests are conducted with actual engines to produce the exhaust gas, which is directed through the appropriate materials to be tested. This can be a coupon exposed to the exhaust stream or an actual exhaust system depending on the test design. The dew point temperature can be controlled such that condensation occurs within a temperature range. This control provides an acceleration factor for the test.

Fleet tests and surveys provide the most accurate information on exhaust system durability [39]. However, since this type of testing is not accelerated, long time periods are required to obtain meaningful results.

TABLE 9—Exhaust system tests.

Assessing Materials for Exhaust Systems—Condensate Corrosion	CUNA 07901 (Italian)
Walker Accelerated Corrosion Test	SAE P78
Determination of Sulfur Compounds in Automotive Exhaust	SAE J1280



**TABLE 10**—Tests on engine coolants.

Test Method for Corrosion Test for Engine Coolants in Glassware	ASTM D 1384
Method for Simulated Service Corrosion Testing of Engine Coolants	ASTM D 2570
Method of Testing Engine Coolants by Engine Dynamometer	ASTM D 2758
Test Methods for Cavitation-Erosion Corrosion of Aluminum Pumps	ASTM D 2809 and D 2966
Practice for Testing Engine Coolants in Car and Light Truck Service	ASTM D 2847
Test Method for Corrosion of Cast Aluminum Alloys in Engine Coolants Under Heat-Rejecting Conditions	ASTM D 4340
Engine Coolant Information Report	SAE J814
Engine Coolant Concentrate	SAE J1034 and SAE 1941
Principles of Engine Cooling Systems and Maintenance	SAE HS-40
Specification for ASTM Reference Coolant	ASTM D 3585

**TABLE 11**—Tests on automatic transmission fluid.

Copper Corrosion Test in Petroleum Products	ASTM D 130 and British Std. 1036
Test Method for Rust-Preventing Characteristics of Inhibited Mineral Oil in the Presence of Water	ASTM D 665
Chrysler Bench Oxidation Test (CBOT)	Chrysler Std. MS-4228D
Mercomatic Oxidation Test	Ford Std M2C138-CJ
Ford Thermal Stability Test	
Turbo Hydra-Matic Oxidation Test (THOT)	General Motors Stds, Dextron II Spec. M95-MAT-001
Turbo Hydra-Matic Cycling Test (THCT)	
Ford Aluminum Beaker Oxidation Test (ABOT)	Ford Std 801363

### Testing—Liquid Passages and Reservoirs

Laboratory tests to determine the behavior of materials and corrosivity of automotive fluids such as engine coolants, engine oils, automatic transmission fluids, and fuels involve exposure to the actual fluid as close to operating conditions as possible. In most cases, aging of the fluids due to their functional use produces a more corrosive liquid; therefore it is important that the test be conducted on used liquids or that aging of the fluid occur in-situ. Simple immersion tests can be used if chemical and physical environmental effects are introduced. This is not always possible and therefore simulated service tests have been developed. These laboratory bench tests simulate more

**TABLE 12**—Tests on automotive fluids.

<b>Brake Fluid</b>	
Motor Vehicle Brake Fluid	SAE J1703
Low Water Tolerant Brake Fluids	SAE J1705
Test Method for Detection of Copper Corrosion from Petroleum Products by the Copper Strip Tarnish Test	ASTM D 130
Corrosiveness and Oxidation Stability of Hydraulic Oils	ASTM D 4636
Testing Hydraulic Brake Line Tubing	SAE J1047
<b>Motor Oil, Grease, Lubricants</b>	
Engine Oil Tests	SAE J304
Detection of Copper Corrosion from Petroleum Products	ASTM D 130, D 849, and D 1743
Corrosion Preventive Properties of Lubricating Greases	ASTM D 1743
Corrosion Characteristics of Solid Film Lubricants	ASTM D 2649
<b>Fuels</b>	
Test Method for Rust-Preventing Characteristics of Inhibited Mineral Oil in the Presence of Water	ASTM D 665
Fuels and Lubricants Manual	SAE HS-23
Detection of Copper Corrosion from Petroleum Products	ASTM D 130

closely actual service conditions by using a model of a particular automobile function. Field service tests are the most reliable but also most time consuming and costly.

Corrosion testing of engine coolants is the most advanced in this group. These are divided into three categories including (1) laboratory tests, (2) engine tests, and (3) field service tests [10]. Tests under these categories are listed in Table 10. Laboratory tests have been the primary means for evaluating the corrosive effects of engine coolants and the effectiveness of the coolant inhibitor formulation. The most important of these is the Laboratory Glassware Test (ASTM D 1384). However, a wide range of other tests is used including electrochemical techniques. A simulated service test for engine coolants (ASTM D 2570) is also used quite widely and includes the use of a pump, radiator, thermostat housing, and a large pot to house test coupons. An extension of this test includes an actual operating engine, which is referred to as a no-load engine test (ASTM D 2758). Field service tests evaluate materials and inhibitor systems under actual vehicle operating conditions and are the most reliable. The test is described in ASTM D 2847.

The behavior of automatic transmission fluid (ATF) and its effect on materials has been a recent subject of investigation. Several tests are used to determine the behavior and include "bench" tests, laboratory motor-driven transmission tests, and field service tests [13,56]. These are listed in Table 11.

Laboratory tests for ATF include the copper corrosion test (ASTM D 130), rust test (ASTM D 665), the humidity cabinet test (ASTM D 1748), and a variety of glassware oxidation tests. Various bench tests are used by manufacturers to determine automatic transmission fluid oxidation stability. Important results obtained in these tests are the behavior of materials and corrosivity of the used fluids. Bench tests include the Chrysler CBOT (Chrysler Bench Oxidation Test), Ford's Mecromatic Test and its Thermal Stability Test, and General Motor's Turbo-Hydro-matic Cycling Test (THCT). The CBOT and Ford Thermal Stability test are glassware tests while the THOT, THCT, and Mercomatic involve transmissions mounted on test beds. These tests are designed

**TABLE 13**—Tests on electrical and electronics systems.

<b>See Tables 3-8</b>	
Electrical Equipment Design	SAE J1211
Acceptance Criteria for Integrated Circuits	SAE J1879
Corrosion Preventive Compound for Connectors	MIL-C-81309 and MIL-C-16173
Conformal Coating Performance	MIL-I-46955
Environmental Testing of Electronic and Associated Equipment	MIL-T-5422

TABLE 14—Standards used for corrosion tests.

	Metals and Alloys	Coatings
Body and Chassis	ASTM G 5, G 59, G 61, G 69, G 82, G 31, B 117, B 368, G 85, G 87, G 33, G 59, G 92, G 34 SAE J400, J1563, J1976, J2334	ASTM D 870, D 1735, D 1748, D 2247, D 4585, D 2933, D 2803, G 33, G 50, G 92, ISO 1462, 4540, 10062 SAE H2929M H1859M H1293, J1976, J2334
Trim and Hardware	ASTM G 5, G 59, G 61, G 69, G 82, G 48, B 117, B 368, G 85, G 87, G 33, G 50, G 92, B 380 SAE J1563, J1950, J1293, J1976, J1885	ASTM D 2803, D 1654, B 456, B 457, B 538, G 33, G 50, G 92 SAE J207, J1950, J1976

to deliberately oxidize the ATF under controlled conditions and the effects on materials and extent of oxidation are measured. In the latter tests, transmissions are run under cycling conditions to simulate those in actual driving. The behavior of copper wire, strip, or components is frequently used as a standard for corrosion resistance in the tests. Visual examination of copper content in the ATF are methods used for evaluation.

The most reliable information on ATF testing is obtained from lengthy and costly vehicle fleet tests. Taxicab service is generally chosen because shifting occurs more often with this type of service. In general, taxicabs are operated in large cities [approximately 6000 miles (966 km) per month] and ATF samples are taken every 10 000 miles (16 093 km). These are evaluated for physical and chemical characteristics (such as for copper). At the end of the test, the transmission is disassembled and evaluated for deterioration due to corrosion.

A laboratory immersion test for corrosion in hydraulic brake line fluid is described in Motor Vehicle Brake Fluid SAE J1703. This test includes the use of standard metal coupons for mass change and visual examination after immersion at 100°C in the brake fluid. Other tests are used to evaluate specific components in the braking system such as that described in SAE J1047 for hydraulic brake line tubing. Internal corrosion is not considered as important as external corrosion of the braking system and therefore only simple tests are used outside of on vehicle service tests.

Corrosion tests for hydraulic brake line fluid, as well as for motor oil, grease, and lubricants, are listed in Table 12. In addition, the effects of various fuels on materials have been of importance due to the effect of small amounts of water, which can become trapped in areas such as the fuel tank [57]. Various additives to fuels can prevent corrosion effects and include inhibitor packages and small amounts of alcohol and aromatics. Recently, corrosion testing of ethanol fuels has been of interest because small amounts of water as well as other contaminants (chlorides) cause severe corrosion to occur [58]. Tests for fuels include electrochemical polarization and immersion tests (Table 12).

### Testing—Electrical and Electronic Systems

Corrosion testing of electrical and electronic systems has generally followed the guidelines used for testing in external environments. A large degree of evaluation is performed in cabinet tests although the most accurate of these is the mixed flowing gas test. These are listed in Table 6. In addition, electrochemical tests (Table 4), immersion tests (Table 5), and various cyclic tests (Table 7) are used for laboratory purposes. Specific tests for these systems are listed in Table 13. Proving grounds and field tests are the most reliable but these are lengthy and costly procedures.

## TEST STANDARDS

Automobiles consist of a wide range of materials fabricated into various components and exposed to complex environments including external driving conditions and functional internal fluids and exhaust gas. Therefore, a wide range of corrosion tests is required in order to determine the corrosion behavior of materials in service. Corrosion standards are developed to ensure that results are reproducible and consistent. Several reviews have been published on this subject [59,60].

The wide range of standards used in the automobile industry is demonstrated in Table 14 by the long list for corrosion testing of body, chassis, trim, and hardware materials. These ASTM and SAE standards are prepared by volunteers representing various sectors of the industry including users, suppliers, and general interest participants. Tables 9 through 13 list standards used for other automotive systems including the exhaust system, cooling system, transmission system, brake system, electrical, and electronic systems.

Automotive companies develop their own standards if proprietary technology is involved or when suitable standards (ASTM, SAE, NACE, etc.) do not exist. These company standards become more valuable when they become the basis of a standards writing organization standard. Therefore, cooperative efforts to prepare automotive materials related standards at organizations such as ASTM, NACE, and SAE are extremely strong and active.

## REFERENCES

- [1] *Automotive Corrosion and Protection*, R. Baboian, Ed., NACE, Houston, 1992.
- [2] *Automotive Corrosion by Deicing Salts*, R. Baboian, Ed., NACE, Houston, 1981.
- [3] Baboian, R., "Chemistry of the Automotive Environment in Designing for Corrosion Prevention," SAE P-78, Warrendale, PA, 1978.
- [4] *Materials Degradation Caused by Acid Rain*, R. Baboian, Ed., ACS, Washington, DC, 1986.
- [5] Kucera, V., "Influence of Acid Deposition on Atmospheric Corrosion of Metals—A Review," *Materials Degradation Caused by Acid Rain*, R. Baboian, Ed., ACS, Washington, DC, 1986.
- [6] *Causes and Effects of Acid Deposition*, Vol. 1, Emissions and Controls, National Acid Precipitation Assessment Program, Washington, DC, 1987.
- [7] Baboian, R. and Turcotte, R. C., "Development of Poulitce Corrosion Tests for Automobiles," *Materials Performance*, Vol. 24, No. 12, 1985.
- [8] Patterson, W. R., "Materials Design and Corrosion Effects on Exhaust—System Life," *Designing for Automotive Corrosion Prevention*, SAE P-78, Warrendale, PA, 1978.

- [9] Chance, R. L. and Ceselli, R. G., "Corrosiveness of Exhaust Gas Condensate," SAE Paper 830585, Warrendale, PA, 1983.
- [10] Rowe, L. C., "Automotive Engine Coolants: A Review of Their Requirements and Methods of Evaluation," *Engine Coolant Testing: State of the Art*, ASTM STP 705, W. H. Ailor, Ed., ASTM International, West Conshohocken, PA, 1980.
- [11] Beynon, E., Cooper, N. R., and Hannigan, H. J., "Cooling System Corrosion in Relation to Design and Materials," *Designing for Automotive Corrosion Prevention*, SAE P-78, Warrendale, PA, 1978, p. 56.
- [12] SAE J1703: Engine Oil Tests, Society of Automotive Engineers, Warrendale, PA.
- [13] Deen, H. E. and Ryer, J., "Automatic Transmission Fluids—Properties and Performance," SAE Paper 841214, Warrendale, PA, 1984.
- [14] SAE J1703: Motor Vehicle Brake Fluid, Society of Automotive Engineers, Warrendale, PA.
- [15] "Designing for Automotive Corrosion Prevention," SAE Proceedings, P-78, Warrendale, PA, 1978.
- [16] *Proceedings of the Automotive Corrosion and Prevention Conference*, SAE P-136, 1983, P-188, 1986, P-228, 1989, P-250, 1991 and P-268, 1993, Warrendale, PA.
- [17] *Corrosion*, SAE SP-485, Warrendale, PA, 1981.
- [18] *Corrosion Protection, Resistance and Testing*, SAE SP-612, Warrendale, PA, 1985.
- [19] *Corrosion: Coatings and Steels*, SAE SP-649, Warrendale, PA, 1986.
- [20] *Corrosion Prevention*, SAE SP-1265, Warrendale, PA, 1997.
- [21] Granata, R. D., "Mechanism of Coatings Disbondment," *Automotive Corrosion and Protection*, R. Baboian, Ed., NACE, Houston, TX, 1992.
- [22] *Corrosion Prediction and Prevention in Motor Vehicles*, H. McArthur, Ed., John Wiley & Sons, NY, 1988.
- [23] "Cracking Down on Corrosion," AISI Report, AU-731, Southfield, MI, 1991.
- [24] "Prevention of Corrosion of Motor Vehicle Body and Chassis Components," SAE Technical Report HS J447, Warrendale, PA, 1981.
- [25] "Body Corrosion—A Comprehensive Introduction," SAE Technical Report J1617, Warrendale, PA, 1993.
- [26] "Corrosion in the Automotive Industry," *Metals Handbook*, 9th ed., Vol. 13, ASM, Materials Park, OH, 1987, p. 1011.
- [27] *Proceedings of the Wear and Corrosion Control Coatings for Automotive Applications Symposium*, Society of Manufacturing Engineers, Dearborn, MI, 1996.
- [28] Baboian, R., "Causes and Effects of Corrosion Relating to Exterior Trim on Automobiles," *Proceedings of the Corrosion Prevention Conference*, SAE P-136, Warrendale, PA, 1983.
- [29] Jones, M. M. and Welker, E. E., "Electrical Component Corrosion Prevention," *Designing for Automotive Corrosion Prevention*, SAE P-78, Warrendale, PA, 1978.
- [30] Cook, J. P. and Servais, G. E., "Corrosion Failures in Semiconductor Devices and Electronic Systems," *Proceedings of the Automotive Corrosion and Prevention Conference*, SAE P-136, Warrendale, PA, 1983.
- [31] Payer, J. H., "Effect of Environmental Stress of Reliability of Automotive Electronics," *Automotive Corrosion and Protection*, R. Baboian, Ed., NACE, Houston, TX, 1992.
- [32] Rowe, L. C., "Corrosion Principles Applied to Body Engineering Design," *Body Engineering Journal*, October 1977, p. 67.
- [33] Piepho, L. L., Singer, L., and Ostermiller, M. R., "Advancements in Automotive Corrosion Resistance," *Automotive Corrosion and Protection*, R. Baboian, Ed., NACE, Houston, TX, 1992.
- [34] Thompson, L., "Advances in Corrosion Protection Over the Past 10 Years," *Proceedings of the Wear and Corrosion Control Coatings for Automotive Applications Symposium*, SME, Dearborn, MI, 1996.
- [35] Dietz, R., "European Automotive Industry Design and Materials Philosophy," in *Proceedings of the Automotive Corrosion and Prevention Conference*, SAE P-250, Warrendale, PA, 1991.
- [36] "Status and Prospect of Japanese Automotive Anticorrosion Technology," *Proceedings of the Automotive Corrosion and Prevention Conference*, SAE P-250, Warrendale, PA, 1991.
- [37] Baboian, R., "Clad Metal Systems for Automobiles," *Automotive Corrosion and Protection*, R. Baboian, Ed., NACE, Houston, TX, 1992.
- [38] Vincent, J. J., "Automotive Cathodic Electrodeposition," *Automotive Corrosion and Protection*, R. Baboian, Ed., NACE, Houston, TX, 1992.
- [39] Gaugh, R. R., "Corrosion of Materials for Automotive Exhaust System," *Proceedings of the Automotive Corrosion and Prevention Conference*, SAE P-250, Warrendale, PA, 1991.
- [40] *Engine Coolant Testing: State of the Art*, ASTM STP 705, W. H. Ailor, Ed., ASTM International, West Conshohocken, PA, 1980.
- [41] *Engine Coolant Testing: Second Symposium*, ASTM STP 887, R. E. Beal, Ed., ASTM International, West Conshohocken, PA, 1984.
- [42] Rowe, L. C., "Fundamentals of Corrosion Testing," *Automotive Corrosion by Deicing Salts*, R. Baboian, Ed., NACE, Houston, TX, 1981.
- [43] *Electrochemical Technique for Corrosion Engineering*, R. Baboian, Ed., NACE, Houston, TX, 1986.
- [44] *Corrosion Testing and Evaluation, Silver Anniversary Volume*, ASTM STP 1000, R. Baboian and S. W. Dean, Eds., ASTM International, West Conshohocken, PA, 1990.
- [45] Abbott, W. H., "Field vs. Laboratory Experience in the Evaluation of Electronic Components and Materials," *Materials Performance*, Vol. 24, No. 8, 1985, p. 46.
- [46] Doppke, T. S. and Bryant, A. W., "The Salt Spray Test—Past, Present, and Future," *Proceedings of the Automotive Corrosion and Prevention Conference*, SAE P-136, Warrendale, PA, 1983.
- [47] *Cyclic Cabinet Corrosion Testing*, STP 1238, G. S. Haynes, Ed., ASTM, West Conshohocken, PA, 1995.
- [48] Brennan, P. and Grossman, S., "Introduction to Cyclic Corrosion Testing," *Proceedings of the Wear and Corrosion Control Coatings for Automotive Applications Symposium*, SME, Dearborn, MI, 1996.
- [49] Davidson, D. and Schumacher, W. A., "An Evaluation and Analysis of Commonly Used Accelerated Cosmetic Corrosion Tests Using Direct Comparisons with Actual Field Exposure," in *Proceedings of the 5th Automotive Corrosion and Prevention Conference*, P-250, SAE, Warrendale, PA, 1991.
- [50] Townsend, H. E., Granata, R. D., McCune, D. C., et al., "Progress by the Automotive and Steel Industries Toward an Improved Laboratory Cosmetic Corrosion Test," *Proceedings of the Automotive Corrosion and Prevention Conference*, SAE P-250, Warrendale, PA, 1991.
- [51] Townsend, H. E., "The Development of an Improved Laboratory Test by the Automotive and Steel Industries, in Advanced Coatings Technology," *Proceedings of the 4th Annual ESD Advanced Coatings Conference*, The Engineering Society, Ann Arbor, MI, 1994, and Townsend, H. E., "Laboratory Perforation Corrosion Tests of Autobody Steel Sheet, Corrosion Prevention, SP-1265, SAE, Warrendale, PA, 1997.
- [52] Schumacher, W. A., "Proving Ground Vehicle Corrosion Testing," *Proceedings of the Automotive Corrosion and Prevention Conference*, SAE P-136, Warrendale, PA, 1983.
- [53] Dean, S. W., "Atmospheric Corrosion—Testing and Evaluation," *Automotive Corrosion and Protection*, R. Baboian, Ed., NACE, Houston, TX, 1992.
- [54] Bryant, A. W. and Oldenburg, W. C., "1985 Body Corrosion Field Survey," *Proceedings of the Automotive Corrosion and Prevention Conference*, SAE P-188, Warrendale, PA, 1986.

- [55] *Standard Walker Accelerated Corrosion Test*, Engineering Materials Specification 5523, Walker Mfg. Co., Grass Lake, MI.
- [56] Friihauf, E. J., "Automatic Transmission Fluid Oxidation—A Comparison of Short Term with Long Term Testing," SAE Paper 790017, Warrendale, PA, 1979.
- [57] Bologna, D. J. and Page, H. T., "Corrosion Considerations in Design of Automotive Fuel Systems," *Designing for Automotive Corrosion Prevention*, SAE P-78, Warrendale, PA, 1978.
- [58] Walker, M. S. and Chance, R. L., "Corrosion of Metals and the Effectiveness of Inhibitors on Ethanol Fuels," *Proceedings of the Automotive Corrosion and Prevention Conference*, SAE P-136, Warrendale, PA, 1983.
- [59] Haynes, G. S., "Corrosion Standards Used in the Automotive Industry," *Automotive Corrosion and Protection*, R. Baboian, Ed., NACE, Houston, TX, 1992.
- [60] Durbin, C. O., "Corrosion Standards and Controls in the Automotive Industry," *Manual of Industrial Corrosion Standards and Control*, ASTM STP 534, F. H. Cocks, Ed., ASTM International, West Conshohocken, PA, 1973.

# Commercial Aircraft

A. A. Adjorlolo<sup>1</sup> and J. A. Marceau<sup>2</sup>

CORROSION OF AIRCRAFT STRUCTURE has plagued the airline industry since the use of metals in aircraft manufacture. It is costly both in unscheduled downtime and man-hours required for repair. The International Air Transport Association (IATA) reported in 1983 that corrosion cost the airlines between \$8 and \$20 per flight hour [1]. These numbers do not reflect the unscheduled downtime, both at the main bases and route stations, nor the additional corrosion inspections of aging airplanes recently mandated by the regulatory agencies. In fact, unlike fatigue damage, corrosion is extremely difficult to predict, i.e., when and where it will start, how fast it will progress, or how much damage it will cause. Because of this unpredictability, corrosion inspections are an integral part of an airline's maintenance program, and make up a significant part of its cost.

Corrosion problems on commercial aircraft are the result of combinations of factors whose causes can be found in the basic design, manufacturing, and operations of the aircraft. Some of these factors are summarized in Table 1 (manufacturer), and Table 2 (operator and service environment). These present unique problems to the manufacturer who must make the best design, materials, and process choices that are compatible with structural requirements and the economics of building and operating an airplane. In order to achieve these ends, corrosion testing must help establish requirements for structural materials and compatible finish systems, as well as a host of manufacturing aids, interior materials, and operational maintenance fluids that will

**TABLE 1**—Contributing causes of corrosion—manufacturer related.

Causes	Factors
Basic Design	<ul style="list-style-type: none"> <li>• Drainage</li> <li>• Crevices</li> <li>• Dissimilar metals</li> <li>• Finish system</li> <li>• Materials selection</li> <li>• Process selection</li> <li>• Access to structure</li> <li>• Pockets, cavities</li> </ul>
Manufacturing Processing	<ul style="list-style-type: none"> <li>• Metal finishing process control</li> <li>• Bonding process control</li> <li>• Training</li> <li>• Assembly</li> <li>• Handling</li> <li>• Storage</li> </ul>

<sup>1</sup>Senior specialist engineer and <sup>2</sup>retired senior principal engineer, respectively, The Boeing Company, Seattle, WA 98124.

**TABLE 2**—Contributing causes of corrosion—service related.

Causes	Factors
Finish Deterioration	<ul style="list-style-type: none"> <li>• Chipping</li> <li>• Scratches</li> <li>• Breaks around fasteners</li> <li>• Abrasion</li> <li>• Deposits</li> <li>• Age</li> </ul>
Environmental Conditions within Airplane	<ul style="list-style-type: none"> <li>• Skydrol (hydraulic fluid)</li> <li>• Condensation</li> <li>• Animals (cargo)</li> <li>• Fish (cargo)</li> <li>• Microbial growth</li> </ul>
Accidental Contamination	<ul style="list-style-type: none"> <li>• Lavatory spills</li> <li>• Galley spills</li> <li>• Cargo spills</li> <li>• Chemical spills</li> <li>• Mercury</li> <li>• Fire smoke and extinguisher residues</li> </ul>
Operational Environment	<ul style="list-style-type: none"> <li>• Seacoast</li> <li>• Tropical environment</li> <li>• Humidity</li> <li>• Industrial environment</li> <li>• Ground-air ground cycle</li> </ul>
Maintenance Problem Areas	<ul style="list-style-type: none"> <li>• Neglect</li> <li>• Improper repairs</li> <li>• Inadequate corrosion control program or lack of implementation</li> <li>• Inadequate training</li> <li>• Ignorance of corrosion</li> <li>• Plugged drain systems</li> </ul>

ensure the structural integrity of the aircraft during its useful life. In addition, anticipation and consideration of factors whose presence may at times be accidental in the operation of the airplane is necessary to the selection of the appropriate standardized corrosion tests. Sometimes test modifications, which account for these factors, are necessary. With over 44 years of service history on commercial jet aircraft, corrosion problems are being addressed systematically. Many improvements that are being incorporated into today's new aircraft would not have been possible without laboratory and outdoor corrosion tests.

## SERVICE ENVIRONMENTS

Environmental conditions inside and outside an airplane vary considerably from one operator to another. Factors

that determine environments include airplane interior configuration, an airline's geographic location, route structure, and world climatic conditions. The commercial jet airplane is designed to be a self-contained pressurized vessel, in order to create a comfortable living environment for flight durations of less than 1/2 h to longer than 12 h. Inside the fuselage, the air is conditioned for the comfort of passengers. Galleys (food stations) are provided for food and drink, and lavatories are provided for the needs of passengers.

Creating this comfortable environment also creates localized environments that are quite unique and very aggressive to structural components if these are not properly protected. For instance, fluids from food and drink spillage in galleys can migrate under floor panels. Trapped between the floor panels and the underlying structure, these fluids fester and cause corrosion of the structural component parts. The same is true for lavatory fluids, which can leak and become trapped between the flooring and floor structure. Further, excess fluids from galleys and lavatories will flow into the bilge, potentially creating further problems. In addition, entryways, e.g., passenger, service, and cargo, are exposed to the weather and occasional spills, which also add to the corrosive environment of the floor structure and bilge.

The rest of the fuselage interior is constantly exposed to condensing humidity caused by colder temperatures that result from the ground-air-ground flight cycle. This condensate is fairly benign compared to the fluids encountered under galleys and lavatories. However, this only means that corrosion will take longer to manifest itself.

The exterior surfaces of airplanes are always exposed to the elements, and are, hence, affected by world and local climatic conditions, e.g., rain, humidity, airborne industrial pollutants, hot and/or cold temperatures, dust, runway dirt, and spray from the oceans and seas. Corrosive contaminants trapped in exterior cavities and cove areas, e.g., wheel wells, wing front and rear spar cove areas, and fairing areas, are not washed off by rain in contrast to aerodynamic surfaces, thereby compounding potential corrosion problems.

## TECHNIQUES USED FOR CONTROLLING CORROSION

The primary defense for corrosion control of the airplane structure is the finish system. As a result, corrosion testing of metals and compatible finish systems is a significant factor in their selection. The tests for evaluating these materials and finishes depend on the function and the anticipated environmental exposure of the component parts. These same finishes are also used during repairs. It must be demonstrated that they can be applied locally over surface preparations accomplished in the field under less than optimum conditions. Techniques available to the airlines for controlling corrosion involve (1) maintaining drain holes open for proper drainage of condensed moisture, (2) restoring of the finish, and (3) applying corrosion inhibiting compound to protect further the paint in problem areas, and dislodge trapped moisture from joints and crevices.

Many of the corrosion tests described in the section titled **Use of Test Methods to Evaluate Corrosion** are routinely used in the aircraft industry to evaluate materials and finish systems. The tests specifically determine their performance during long-term service, usually relative to a current material finish or process. However, because laboratory tests represent relatively short-term exposures compared to the life of an airplane and cannot always simulate in-service airplane conditions, the rationale used to establish test duration and conditions must be relevant.

## In-Service Monitoring

Despite the obvious economic advantage of allowing airlines the ability to disassemble a structure for repairs only when corrosion is known to exist in certain areas, in situ monitoring of corrosion is not practiced in the industry. The resulting monitoring system's complexity, added weight, and future certification issues are certainly negative factors. The authors are aware of only one instance of experimentation with sensors in U.S. commercial aviation to detect the presence of moisture in certain areas prone to corrosion, such as floor support structure. A system using an optical fiber-based sensor and data acquisition system is being field-tested. This system has been described in a recent Aging Airplane conference [3].

Currently, in-service monitoring of corrosion on commercial airplanes is accomplished by inspection during routine maintenance checks. Although most airlines have corrosion control programs implemented in their maintenance programs, the regulatory agencies have recently required mandatory corrosion inspections based on calendar time rather than airplanes cumulative flight hours, as well as defining the specific areas to be inspected and at what frequency. For instance, a known problem area, such as the fuselage bilge, is inspected much more frequently than the crown (ceiling) area. These directed inspections, such as FAA-mandated Corrosion Prevention and Control Program (CPCP), assign levels of 1, 2, and 3 to corrosion findings. These levels relate to the amount of material blend-out required to remove the corrosion occurring between repeat inspections (level 1 or 2), and whether airworthiness concerns exist (level 3) with particular corrosion findings.

## Inspection

Inspection for corrosion is primarily by visual method, requiring very good access to the structure and the ability to recognize various forms of corrosion, their early signs in different metallic structures, or conditions leading to corrosion, such as finish damage and blocked drains. Other difficult to access areas may require borescope inspection. In some cases of hidden structure, such as lap joints, non-destructive inspection (NDI) techniques such as eddy current, or X-ray (radiography) may be used. Ultrasonic inspection has the advantage of detecting small cracks that may appear in corroded locations. Because some of these techniques may require significant amounts of material loss for detection, may be complex, and require high technician skills, visual observation of a partially opened lap joint is necessary to determine the full extent of the corrosion.

## SPECIFIC PROBLEM AREAS

Most corrosion problems on commercial aircraft are associated with aluminum alloys. This is consistent with the large use of corrosion-susceptible, high-strength or high-toughness alloys (approximately 78 %) in making the structure. Furthermore, all of the high-strength alloys used are susceptible to corrosion and must be protected appropriately. Corrosion protection of these alloys relies entirely on the protection systems used, i.e., anodizing, conversion coatings, primers, sealants etc. Most failures in the protection system occur at joints, faying surfaces, or crevices where water and aggressive electrolytes can become trapped for long periods of time. Crevices can be created by many conditions, e.g., joints, poorly adhering paint, insulation blankets against structure in wet areas, etc. When they exist in the highly corrosive areas described in the previous section, **Service Environments**, corrosion problems are greatly compounded. Other potentially corrosive conditions would include dissimilar metal couples, e.g., an aluminum-nickel-bronze bushing in an aluminum alloy housing, or an aluminum hinge fitting attached to a carbon fiber reinforced plastic control surface (e.g., elevator, aileron, etc.). Some of these conditions are unavoidable; therefore, it is extremely important that the proper finish protection schemes be incorporated.

## USE OF TEST METHODS TO EVALUATE CORROSION

The foregoing discussions on airplane corrosion problems, service environments, techniques for corrosion control, and problem areas underscore the need for comprehensive corrosion testing, including both sound rationale and methods. Table 3 summarizes the corrosion tests used in the commercial airplane industry. Shown are the names of the tests, how they are used, the type of information sought, and the type of comparative control used. These tests primarily address alloys, coatings, manufacturing aids or process evaluation, and also service conditions. The tests, particularly those from ASTM, lend themselves to multiple applications (for instance, there are many uses of the salt spray test—ASTM B 117, Test Method of Salt Spray (Fog) Testing). Alternately, there are multiple tests available to evaluate a particular corrosion issue (for instance, pitting can be evaluated using many different tests). The following is a more detailed discussion on why some of these tests are used in the selection of materials and processes.

### Materials Selection

The desirability of light structures for increasing payloads in commercial aircraft design dictates the use of materials with high strength-to-weight ratios. High-strength aluminum alloys, 7XXX series and 2XXX series, and their tempers, are evaluated for their integrity in environments likely to cause exfoliation and stress corrosion cracking (SCC). Steels must demonstrate that they are no more susceptible to hydrogen embrittlement and SCC than conventional high-strength, low-alloy (HSLA) steels. These represent

most commonly used alloys, and also the ones most susceptible to hydrogen embrittlement.

### Aluminum Alloy/Heat-Treat Evaluation

Exfoliation corrosion is the leaf-like degradation of high-strength aluminum alloys, due to corrosion product forming along the elongated grain paths of sheets, forgings, or extrusions. Susceptibility to exfoliation corrosion is predicted by testing in accordance with ASTM G 34, Test Method for Exfoliation Corrosion Susceptibility in 2XXX and 7XXX Series Aluminum Alloys [Exco Test], and ASTM G 85, Practice for Modified Salt Spray [Fog] Testing, Annex A2. However, exfoliation corrosion experienced in service by 7150-T6511 extruded alloys demonstrated, despite extensive prior testing, an important limitation of these accelerated tests. Exfoliation corrosion of this material, it was found, can initiate after a long incubation period detectable only after long natural outdoors exposure. This and all the other environmental factors responsible for exfoliation are difficult to assemble into one laboratory test, and ideally one would like to test in an outdoors environment for at least several years.

Several test methods are currently used for the testing of SCC in aluminum alloys: ASTM G 47, Test Method for Determining Susceptibility to Stress-Corrosion Cracking of High-Strength Aluminum Alloy Products, in conjunction with ASTM G 44, Practice for Evaluating Stress-Corrosion Cracking Resistance of Metals in 3.5 % Sodium Chloride Solution. The double cantilever beam test [2], and the breaking load test using ASTM G 139, Standard Test Method for Determining Stress-Corrosion Cracking Resistance of Heat-Treatable Aluminum Alloy Products Using Breaking Load Method, have also been used to that effect. The contrasting performance of stress corrosion resistant 7075-T73 aluminum alloy, the current standard, against that of 7079-T6, replaced by more SCC-resistant alloys in the late 1960s, is a reflection of the implementation of these two test methods.

### Testing of High-Strength Steels

Since most high-strength steels have requirements for chromium, low-embrittlement cadmium, or cadmium-titanium plating, their selection is dictated by their ability to be processed in a way that avoids the hydrogen-embrittling effects of these processes. Requirements for avoiding hydrogen embrittlement in AISI 4340 steel establish a baseline that must be met by any new alloy. A notch tensile test is generally performed using AISI 4340 as control material and evaluated according to ASTM F 519, Method for Mechanical Hydrogen Embrittlement Testing of Plating Processes and Aircraft Maintenance Chemicals.

### Paint Evaluation

Paints are used on a wide variety of materials and parts as a means of protecting the underlying metal and are generally the first line of defense. The paint itself must adhere to the substrate under dry, humid, or wet conditions, a requirement that underscores the critical nature of a base

TABLE 3—Corrosion tests conducted in the commercial airplanes industry.

General Test Name	Where Used (Alternate Test Name)	Information Sought	Control
EXCO (ASTM G 34)	Alloy evaluation	Resistance to exfoliation corrosion after 48 h immersion in test solution	Conventional alloy and/or thermomechanical treatment
Modified ASTM Acetic Acid Salt Intermittent Spray-MASTMAASIS (ASTM G 85)	Alloy evaluation	Resistance to exfoliation corrosion after 28 days exposure	Conventional alloy and/or thermomechanical treatment
3.5% NaCl Alternate Immersion (ASTM G 44)	Alloy evaluation	SCC resistance per ASTM G 47	Conventional alloy
Double Cantilever Beam	Alloy evaluation	Resistance to pitting of unstressed specimens	
Electrochemical Tests	Alloy evaluation	SCC growth rate, threshold $K_{ISCC}$	Conventional alloy
		Passivation characteristics (ASTM G 5)	Conventional alloy
		Corrosion rates	
		Pitting/protection potentials (ASTM G 61)	
		Corrosion potential (ASTM G 69)	
		Polarization resistance	
		Galvanic corrosion	
Notched Tension Test (ASTM F 519)	Paint/Coating evaluation	Impedance spectrum (ASTM G 106)	Conventional paint/coating
	Alloy evaluation	Resistance to hydrogen embrittlement	Conventional alloy
	Maintenance fluid evaluation	Potential to cause hydrogen embrittlement on AISI 4340 steel per ASTM F 519 Section 7.2	Conventional fluid
	Plating process evaluation	Resistance to hydrogen embrittlement of plated AISI 4340 per ASTM F 519 Section 7.3	Specification requirement per ASTM F 519, Sec. 7.3
Intergranular Attack/End Grain Pitting (IGA/EGP)	Manufacturing aid evaluation (deoxidizer/cleaner)	Potential to cause end grain pitting or intergranular attack in excess of recommended limits	Aluminum alloys 7178-T6514, 7075-T6511
Filiform Corrosion Test (ASTM D 2803)	Metal surface preparation processes and paint evaluation	Resistance to filiform corrosion $\frac{1}{8}$ in. (3.2 mm) beyond line scribed on a painted panel specimen preexposed to HCl vapor and held at 104 F at 80 % RH for 1000 h	Conventional organic coatings
Salt (Fog) Spray (ASTM B 117)	Alloy evaluation	General corrosion, pitting resistance after 30 days, 90 days, or 1 year exposure	Conventional alloy
or Modified Salt Spray (Fog) Test (ASTM G 85)	Chemical conversion coating/process evaluation	Resistance to pitting after 168 h exposure period (ASTM B 117 only per specification)	Conventional chemical coating/qualified process
or Outdoor Environmental Exposures	Anodizing/process evaluation	Resistance to pitting after 336 h exposure period (ASTM B 117 only per specification)	Conventional chemical coating/qualified process
	Paint/alloy evaluation (scribed line test)	Resistance of scribed line to corrosion after predetermined exposure period; loss of adhesion; blistering	Paint over conventional alloys or conventional paint over alloy
	Paint/alloy evaluation (fastener insulation test)	Resistance to corrosion around fastener heads; rating per ASTM D 1654	Paint over conventional alloys or conventional paint over alloy
	Paint/alloy evaluation (Al/CRES or CFRP coupling)	Resistance to corrosion aided by galvanic coupling; rating per ASTM D 1654	Paint over conventional alloys or conventional paint over alloy
	All adhesive bonding process evaluation (metal/metal) (Lap Shear Corrosion Test)	Reduction in lap shear strength after exposure for predetermined period	Qualified adhesive/primer over recommended surface preparation
	All adhesive bonding process evaluation (metal/metal) (Wedge Corrosion Test)	Crack growth rate after exposure to salt spray for 30, 60, and 90 days, or longer	Same as above
	All adhesive bonding process evaluation (metal/metal) (Double Cantilever Test)	Crack growth after exposure to neutral salt spray for 1 year or longer; Resistance to galvanic corr	Same as above
Titanium Compatibility Test	Manufacturing aids evaluation (lubricants/coolant)	Potential of fluid considered to cause pitting, cracking, or rough etching on titanium	Currently qualified material



TABLE 3—Corrosion tests conducted in the commercial airplanes industry. (continued)

General Test Name	Where Used (Alternate Test Name)	Information Sought	Control
Evaporation Corrosion Test	Manufacturing aids evaluation (lubricants/coolant)	Potential for pitting caused by fluid left to evaporate on machined alloy after 7 days	Currently qualified fluid
	Interior materials (silicone rubber-coated fabric, floor covering, carpet and underlay, thermal/acoustical insulation, flame-resistant polymer-coated fabric, Nomex felt, etc.)	Assessment of the corrosivity of water leachable species from tested materials left to evaporate on 2024-T3 aluminum after 7 days	Deionized or distilled water
	R & D (evaluation of corrosion inhibitors; maintenance fluids, and various extracts)	General corrosivity and pitting caused by water soluble extract from material of interest left to evaporate on 2024-T3 aluminum after 7 days.	Deionized, 3.5% NaCl, or distilled water
	Manufacturing aids evaluation (lubricants and coolants)	Resistance to general corrosion or staining caused by fluid entrapment on 7075-T6, 2024-T3 bare or clad Al alloys	Deionized, distilled water, or conventional fluid
	Maintenance fluids evaluation	Resistance to general corrosion or staining caused by fluid entrapment on 7075-T6, 2024-T3 bare or clad Al alloys	Deionized, distilled water, or conventional fluid
Immersion Test (ASTM F 483)	Manufacturing aids (lubricants and coolants) evaluation	Resistance to weight loss of AISI 4130 and 2024-T3, 7075-T6 Al alloys in fluid of interest	None—Allowable weight loss table
	Maintenance fluids evaluation	Resistance of selected aerospace aluminum, steel, titanium, and magnesium alloys, cadmium plate, to weight loss in fluid of interest; Resistance to galvanic corr.	None—Allowable weight loss table
Galvanic Entrapment	Manufacturing aids (cuttings fluids and greases) evaluation	Resistance to crevice corrosion caused by test fluid entrapment between drilled and fastened Al/Cad plated steel/Ti stackup	Deionized water, conventional fluid
Stress Corrosion Test	Manufacturing aids evaluation (lubricants and coolants)	Resistance to corrosion crack growth, pitting on precracked, 50 ksi (in.) <sup>a</sup> prestressed specimens immersed for 24 h in test fluid, and in ambient environment for 76 h minimum	Conventional fluid
Drip Test	Titanium/coating evaluation	Resistance to hydraulic fluid of coating and substrate at various temperatures (usually 450°F)	Bare 6Al-4V titanium specimen

surface preparation. The ability of the paint to protect against corrosion is evaluated using ASTM G 85 and ASTM B 117 for a test duration of 1000–3000 h on scribed surfaces, with fasteners installed, or on specimens galvanically coupled to a more noble metal. These tests are all designed to simulate accidental scratch marks, corrosion prone areas, or conditions that accelerate corrosion.

### Surface Finishes Evaluation

ASTM B 117 is the standard test used for evaluating the corrosion resistance of unpainted aluminum alloy surfaces when treated by anodizing, conversion coating, and for plating processes. Aluminum surfaces, which are anodized and then sealed for corrosion protection, must resist the salt spray environment for at least 336 h without pitting. Conversion

coated surfaces must resist at least 168 h. Cadmium plate on ferrous or copper alloys must also resist this environment for 96 h without showing base metal or cadmium corrosion. Although it is generally agreed in industry that the salt spray test is used too broadly, individual pass/fail criteria developed for each process have helped monitor process problems. Alternate testing methods (e.g., electrochemical tests) are under development, and have found limited use to aid in the evaluation of alloys and finishes.

### GENERAL REMARKS

The multiplicity of external environments, the unpredictability of various spillage inside an airplane, the influence of environmental and loading cycles on material and finishes,

and the long design life of an airplane account for the main difficulties encountered in performing the right laboratory corrosion test in commercial airplanes manufacturing. As a large amount of data from the commercial airplane fleet has become available, service history has emerged as the most important criterion in validating design choices, modifying the corrosion tests themselves, and developing better test acceptance criteria.

The history of airplane corrosion testing includes many successful tests that are now performed routinely, e.g., ASTM G 85 Annex A2 and ASTM G 44. Some other successful tests, such as the wedge test (ASTM D 3762, Test Method for Adhesive-Bonded Surface Durability of Aluminum), discovered as a result of bond line corrosion problems on airplanes, are not described here because they are not strictly corrosion tests. Many of the tests described here are ASTM standards. With others, standardization is being pursued, e.g., electrochemical impedance, or ANCIT (Aluminum-Nitrate Chloride Immersion Test), to replace EXCO [4]. Corrosion may never be totally eliminated from an airplane; however, further refinements in corrosion testing, made

possible by a better understanding of the fundamental interaction between environmental factors and dynamic loads, will take the airplane industry close to that goal.

## REFERENCES

- [1] International Air Transport Association (IATA), "Guidance Material on Design and Maintenance Against Corrosion of Aircraft Structures," DOC GEN/2637A, Issue 2, November 1983.
- [2] "Stress Corrosion Cracking of High Strength Aluminum Alloys," *Advances in Corrosion Science and Technology*, Vol. 2, M. G. Fontana and R. W. Staehle, Eds., Plenum Press, New York, 1972, pp. 115–335.
- [3] Elster, J. L., Trego, Angela, et al., "Corrosion Monitoring in Aging Aircraft Using Optical Fiber-Based Chemical Sensors," DOD / NASA / AFRL Aging Aircraft 2000 Conference, May 15–18, St. Louis, KS.
- [4] Lee, S. and Lifka, B. W., "Modification of the EXCO Test Method for Exfoliation Corrosion Susceptibility in 7XXX, 2XXX and Aluminum-Lithium Alloys," *New Methods for Corrosion Testing of Aluminum Alloys*, ASTM STP 1134, ASTM International, West Conshohocken, PA, 1992, pp. 1–19.

# Military Aircraft and Associated Equipment\*

*Earl C. Groshart<sup>1</sup>*

THIS CHAPTER DISCUSSES the reasons for running various corrosion tests on military equipment including airplanes and missiles, and the equipment needed to support them.

Military airplanes, missiles, space equipment, and the supporting equipment must be designed to operate for long periods of time in the most extremes of environment, from the Arctic Circle to the equator, from water to space. This defines ground temperatures from very cold [ $-60^{\circ}\text{F}$  ( $-51^{\circ}\text{C}$ )] to very hot [ $140^{\circ}\text{F}$  ( $60^{\circ}\text{C}$ )] and humidities from very low to saturated. The ambient air can have high levels of salt, industrial pollution, sand, and dust.

The life cycle management of military hardware requires that the various conditions of exposure of the hardware be determined. The many environments to which the hardware may be exposed must be determined, and a test program then must be designed to determine the acceptability of the hardware to those environments. The environments in question may range from transportation, storage, mission theater, and include spending time on aircraft carriers, air bases, or in hangers.

## SHIPPING/TRANSPORTATION OF EQUIPMENT

During this phase of the life of the aircraft, missiles, and equipment, it may be assumed that these items will be transported by truck, rail, airplane, or ship. These methods of transport will expose the hardware to high and low temperatures, high and low humidity, rain/hail, sand/dust, salt fog, temporary immersion, and reduced pressure. Corrosion tests to simulate shipping/transportation can be designed but usually are deferred to the more severe operational environmental tests.

## STORAGE/LOGISTIC SUPPLY

During this phase it can be assumed that equipment, parts, aircraft, and missiles are stored in either of two extremes: in environmentally controlled warehouses or sitting in the open on a dock or runway. Military space, office, computer, etc., equipment usually will be stored under conditions of

controlled humidity and temperature, but most other military equipment will likely see conditions of high and even condensing humidity, low and high temperature, conditions allowing fungus growth, and even those allowing chemical attack, (i.e., ground equipment moved to a warfare front). Because of mechanical damage, equipment in shipping crates and with packaging cannot be assumed to remain packaged during logistic supply and transport life phase. It therefore requires testing to withstand these environments. Testing is described later.

## THE MISSION

During its mission, military hardware is likely to be exposed to many extreme environments: high and low weather temperatures [ $-60^{\circ}\text{F}$  to  $140^{\circ}\text{F}$  ( $-51.1$  to  $60^{\circ}\text{C}$ )], fully wet conditions of rain and condensing humidity, including morning dew, blowing and settling sand and dust; salt fog, and chemical and biological attack.

## ENVIRONMENTAL TESTING

Testing to withstand the environments listed previously for the various life phases of military hardware involves not only testing of construction materials to help the designer find the best material for the job, but testing the unit after construction to see how well it can function after being placed into the various test environments. Only the equipment tests are crucial here since materials testing is covered fully in other areas.

### Humidity Testing

It is not enough to place an assembled hardware item into a chamber of high humidity. This will cause condensation of water onto the outside with some penetration into the inside through openings. The test is to cause moisture to penetrate into the hardware by raising and lowering the temperature while holding to relative humidity at 95 %. A common cycle is to start at room temperature (RT), the relative humidity (RH) at 95 %, raise the temperature to  $160^{\circ}\text{F}$  ( $71.1^{\circ}\text{C}$ ) within the next four hours, and add enough water to keep the humidity at 95 %. Hold the temperature under these conditions for 12 hours and then lower it back to RT while maintaining the 95 % RH in the next eight hours.

\* This chapter has been revised by Section VII Editor, S. W. Dean and Editor, R. Baboian.

<sup>1</sup> The Boeing Company, Seattle, WA 98124-2499.

Condensation will occur, but by removing water it can be held to a minimum. The test would consist of ten cycles, and at the end of the test the equipment is to be operated. A dry-out of some time may be allowed, and the severity of equipment damage is judged by any loss of operating efficiency. Other cycles can be used; for instance, to simulate the constant high humidity found in tropics, Mil-Std-810 has an "Aggravated Temperature-Humidity Cycle," where the temperature varies between 85 and 140°F (29.4 and 60°C), and the RH varies between 85 % for eight hours and 95 % for 16 hours; ten cycles usually are run and dry-out times are not allowed for equipment functioning tests.

### Temperature Shock

The purpose of the test is to determine if material in the assembled condition can withstand sudden changes of the temperature in the surrounding atmosphere without experiencing physical damage or detriment in performance.

As a result of exposure to extremes in temperature, operating equipment may bind, stick or have a slackening in tightness of moving parts, glass may shatter, and electrical part functions may change.

The test is conducted by starting at room temperature, raising it to a high temperature, say 160°F (71.1°C), and then lowering it to the low temperature, say -65°F (-53.9°C). Time should be allowed between the temperature changes, but the materials temperature should not reach equilibrium. The idea of this test is to see if the equipment can withstand air transport and be dropped in a cold environment to function without loss of efficiency and without broken or warped parts.

Variations of the test would hold the high temperature or the low temperature to see its effect on the equipment. The humidity can be varied during the entire test procedure. Effectiveness of the test is to operate without loss of efficiency at any temperature.

### Fungus

Equipment used in hot, humid environments is subject to fungus attack whether the material is fungus-resistant or not. This happens because organic contamination [fingerprints, oils, cleaning agents (soaps)] left on the hardware will support fungus growth. The tests are run to evaluate effects on performance of hardware that may or may not become contaminated with a fungus growth.

The test is conducted by inoculating the hardware with a selected group of fungus spores that have been cultured in an agar solution. After the culture has been sprayed onto the hardware sample, it is maintained in a warm, humid environment for 21 to 30 days. Evaluation of the test is to check on the viability of the spores. They should not live on the prepared agar for more than 18 to 20 days; if they do live they are probably living off contamination or nonfungus-resistant materials such as sleeving, wiring insulation, etc. Any loss of equipment efficiency also will be interpreted as test failure. Fungus tests are described in both Mil-Std-810 and in a number of ASTM tests such as ASTM D 3273 (Test Method for Resistance to Growth of Mold on the Surface of Interior Coatings in an Environmental Chamber). While

they are generally similar, the Mil-Std-810 test is conducted for military hardware.

### Salt Fog

Equipment salt fog tests are run to determine if conducting salts will cause malfunctioning of equipment. Salt fog tests may cause some corrosion of equipment which may cause the malfunction; however, if the equipment is known to require salt fog resistance it is more common to require that the materials of construction with their attendant finish system pass the tests for longer test times. The tests of equipment not intended for salt-containing environments are rarely run for longer than 48 h. Materials tests for equipment intended to resist salt environments are run in a neutral, 5 % salt fog exposure commonly at 500, 1000, and 5000 h. Tests are conducted according to ASTM B 117 [Test Method of Salt Spray (Fog) Testing] using a 5 % sodium chloride solution at a neutral pH. To simulate shipboard or seacoast operations, ASTM B 368 [Method for Copper-Accelerated Acetic Acid-Salt Spray (Fog) Testing (CASS Test)], which uses a copper ion and acetic acid as additives to the salt fog is used. In addition, ASTM G 85 [Standard Practice for Modified Salt Spray (Fog) Testing] is used. Annex 1 through 4 of this standard are used widely for this purpose.

After the equipment is exposed to the salt fog test it is required to operate without malfunctions. Drying out time may or may not be allowed.

### Low Pressure

Transportation of military equipment in unpressurized aircraft exposes hardware to a low-pressure environment that it was not designed to withstand. Low-pressure tests are therefore conducted on assembled equipment to check for pressure leaks, fluid leaks, evaporation of lubricants, failure of hermetic seals, etc. These types of failures may or may not lead to corrosion problems, but they certainly will lead to erratic operation or malfunction, or both. Missiles and space equipment are required to operate in low-pressure environments; however, low-pressure tests have caused sparks and corona that did not (or would not) show up at a lower altitude or higher-pressure environment. The tests are conducted by lowering the pressure in the chamber, allowing the equipment to outgas and come to equilibrium before it is operated. The conditions usually are optimized at ambient temperatures and the low pressures held for at least an hour. The equipment then may be operated either at low pressure or returned to ambient pressure and then operated.

### Solar Radiation—Sunshine

Military equipment may be subjected to long periods of time in areas of no protection from solar radiation. The heating effects of solar radiation differ from those of high air temperature alone in that the amount of heat absorbed or reflected depends on the roughness and color of the surface on which the radiation is incident. In addition to the differential expansion between dissimilar materials, changes in the intensity of solar radiation may cause components

to expand or contract at different rates, which can lead to severe stresses and loss of structural integrity. Long-term aging, especially of polymeric materials, also will be a problem. Mil-Std-810 Method 505.3 testing is used. For solar radiation effects (only) a minimum of 7–24 h cycles is suggested, for long-term aging, a minimum of 10–24 h cycles (Procedure 2, Method 505.3) for equipment occasionally exposed, and as much as 56 cycles for equipment continuously exposed is suggested.

### Rain

Rain tests are conducted to see if the hardware can function after it has been exposed to rain or complete wetting. Tests may be tailored as to the amount of rain and the duration of the exposure. The criteria for the test may be to check for leakage and, if leakage is allowed, determine if the operation will be affected. Mil-Std-810 Method 506.2 Procedure I is a convenient “blowing rain” test. This test is performed by allowing the rain to impinge on the test article for 30 min. The equipment can be operated during the last 15 min of the cycle. The equipment is rotated and the rain cycle repeated until all possible angles have been exposed. Less severe tests such as allowing a steady drip on equipment for a period of time (one week for example) also may be conducted according to Mil-Std-810.

### Sand and Dust

An airborne sand and dust environment, associated most often with the hot-dry regions of Earth, exist seasonally in other regions. Naturally occurring sand and dust storms are an important factor in the deployment of material, but with the increased mechanization of military operations, these cause less of a problem than do sand and dust associated with man’s activities. Consequently, this type of testing is important even when equipment may not be employed in hot-dry regions.

Some of the problems caused by sand and dust include abrasion and erosion of surfaces and finishes (generally paint finishes), penetration of seals, degradation of switch relays, contaminations of lubricated bearings and bushings, etc.

This test method is divided into two procedures. The small-particle procedure (dust, fine sand) is performed to ascertain the ability of equipment to resist the effects of dust particles that may penetrate into cracks, crevices, bearings, and joints. The test is run for 6 h at room temperature followed by 6 h at the high storage or high operating temperature. The second procedure, the blowing sand test, is performed to determine whether material can be stored and operated under blowing sand (149 to 850  $\mu\text{m}$  particle size) conditions without experiencing degradation of its performance, effectiveness, reliability, and maintainability due to the abrasion (erosion) or clogging effect of large, sharp-edged particles. The test duration is 90 min per face.

## STANDARDS AND SPECIFICATIONS

Up until recently, military specifications and standards (commonly known as Mil-Specs) dictated many aspects of system procurement to program offices and contractors.

Between 1994 and 2000, Acquisition Reform radically changed the way that military equipment was procured. During that period, the Department of Defense (DOD) reviewed over 29 000 detailed military specifications and standards in order to eliminate those that were no longer needed or replace them with nongovernment standards or performance specifications. While Mil-Spec reform did not eliminate the need for DOD military specifications and standards, it did dramatically shift the balance towards more commercial and performance-based specifications and standards [1].

One of the challenges of the reformed system is to identify and obtain copies of specifications and standards dealing with corrosion control [2]. The Acquisition Streamlining and Standardization Information System (ASSIST) database addresses this challenge. ASSIST provides a search capability for military, federal, and adopted nongovernment specifications and standards at the web site <http://assist.daps.dla.mil/online/start/>. One can use the ASSIST Quicksearch at the web site, <http://assist.daps.dla.mil/quicksearch/>, to view documents online. Information about other standards, specifications, and automated tools offered by the Defense Standardization Program Office can be obtained from the web site [www.dsp.dla.mil](http://www.dsp.dla.mil).

## CONCLUSION

Military equipment is exposed to every extreme of environment and is expected to function whenever called upon after long periods of exposure and nonfunctioning. It is because of these conditions that the specifications to which the equipment is built requires testing of the materials of construction for such materials properties as general corrosion resistance, susceptibility to stress corrosion cracking (SCC), and hydrogen embrittlement, as well as the severe testing of the equipment as delimited here. These tests are flexible as has been indicated, but should reflect the conditions under which the equipment must operate. The tests in detail as applied to military equipment are contained in Ref 3. ASTM tests are described in ASTM B 117, B 368, G 60, G 85, and D 4587 (Practice for Conducting Tests on Paint and Related Coatings and Materials Using a Fluorescent UV-Condensation Light- and Water-Exposure Apparatus). SAE tests are described in Ref 4. A search for standards and specifications by the military in dealing with corrosion control can be conducted at the web site in Ref 5.

## REFERENCES

- [1] “Beating Corrosion,” Special Issue, *AMPTIAC Quarterly*, Vol. 7, No. 4, 2003.
- [2] Grethlein, C. E., “Standardization is Needed to Fully Implement Corrosion Policy,” *AMPTIAC Quarterly*, Vol. 7, p. 30, 2003.
- [3] Mil-Std-810. Environmental Test Methods and Engineering Guidelines.
- [4] SAE-AIR 1167. Environmental Criteria and Test for Aerospace Ground Equipment in Support of Space Systems.
- [5] <http://assist.daps.dla.mil/quicksearch/>

# Pipeline

*Paul S. Rothman<sup>1</sup> and Walter T. Young<sup>2</sup>*

CORROSION TESTING OF pipelines is done for several reasons. One is to evaluate the pipeline condition to determine whether or not it is safe to operate. If repairs are needed, testing is performed to determine if repair is feasible or if replacement is needed. Testing is performed to track the pipe condition so that repair or replacement can be budgeted. Another reason for testing pipes is to evaluate the effectiveness of corrosion control measures, such as inhibitors for internal pipe surfaces or cathodic protection for internal or external surfaces. This chapter provides information on test techniques that can be applied to metallic pipes above ground or buried in an aqueous environment. Prior to discussing test techniques, the chapter will discuss briefly the materials and corrosion issues affecting pipelines. This chapter is by no means a detailed text on corrosion of pipelines, and the reader is encouraged to consult the references for further detail.

## PIPELINE MATERIALS

### Steel

Carbon and low-alloy steels are probably the most commonly used materials for pipes handling water, petroleum products, and some chemicals. Reference 1 provides a summary of the different specifications used for pipelines. Steel tends to corrode by both pitting and uniform surface deterioration [2]. Steel must usually be protected from corrosion both on the inside from the material being carried and on the outside from corrosion by the atmosphere, soil, or water that surrounds the pipe. External corrosion protection is provided by material selection, selective backfill, barrier coatings, stray current control, and cathodic protection. Internal corrosion protection can be provided by inhibitors, coatings, design process control, and materials selection.

### Stainless Steel

Stainless steel pipe is used primarily where corrosion products from carbon steel would cause unacceptable contamination of the product. Examples include jet fuel piping, food handling and other piping requiring FDA approval,

and chemical piping. There are many different variations of stainless steel alloys [3]. In general, stainless steels tend to corrode in a localized manner, resulting in pitting, crevice corrosion, stress corrosion cracking (SCC), and intergranular corrosion [4,5]. Corrosion will occur in any environment where access of the steel surface to oxygen is limited or uneven. Accelerated corrosion can occur in clay soils, soils containing chlorides, bacteria, marshy soils, and where stray currents are present. Stainless steel, under many conditions, requires protection from corrosion in the form of coatings and cathodic protection.

### Cast Iron and Ductile Iron

Cast (gray) iron and ductile iron are different in both chemical composition and metallurgy by virtue of the shape that the graphite takes in their microstructure [6]. Cast and ductile iron are used as wastewater piping and potable water piping. Alloyed cast iron is used to transport chemicals. Cast and ductile iron (other than the alloyed variety) corrode by pitting and uniform corrosion in water and in soils [2,3,7]. Gray cast iron, because of the interconnecting network of flake graphite, tends to retain its shape, but not its strength, even when severely corroded. This makes evaluation of the condition of gray cast iron difficult and requires that the "graphitized" layer be removed to perform a meaningful evaluation. The graphite in ductile iron is in the shape of nodules and does not have an interconnecting network. Ductile iron corrodes more like steel; however, graphite and corrosion products can also be difficult to evaluate without removing the corrosion products. Cast and ductile iron should be protected from corrosion when in a severely corrosive environment by using coatings, linings, and cathodic protection. Cast and ductile iron water piping are commonly lined with cement mortar [8]. Cast and ductile iron pipe also require protection against stray current corrosion.

### Galvanized Steel

Galvanized steel is carbon steel with either a hot dipped coating of zinc or a deposited layer of zinc (mechanically or electrolytically applied). The advantage of the zinc coating is that it provides increased corrosion resistance and some local cathodic protection to the steel if the layer is damaged. Galvanized steel is primarily used to transport water. The coating on hot dipped galvanized steel is primarily

<sup>1</sup>Principal Corrosion Engineer, The Port Authority of NY and NJ, New York, NY.

<sup>2</sup>Principal Engineer, Corpro Companies, West Chester, PA 19380.

a combination of several iron-zinc alloy layers [9]. This affects its ability to protect the steel by cathodic protection [10]. Galvanized steel will experience accelerated corrosion when buried in soils containing cinders, chlorides, and in alkaline ( $\text{pH} > 9$ ) or acidic ( $\text{pH} < 5$ ) soils. Therefore, galvanized steel is not recommended for buried applications without additional corrosion protection.

### Aluminum and Aluminum Alloys

Aluminum pipe is used where contamination of the contents with corrosion products is unacceptable, such as in jet fuel piping or alcohol. Aluminum pipe corrodes by pitting, intergranular corrosion, and uniform corrosion in soils and water [2]. In addition, aluminum is anodic (will corrode) when connected to most common engineering metals (bimetallic corrosion). Aluminum is also amphoteric; that is, it will corrode in either acidic or alkaline environments, i.e., below  $\text{pH} 4$  or above about  $\text{pH} 8.5$  [2,11]. Aluminum is corroded by copper or mercury in contaminated soils [12,13]. Aluminum is also corroded in tidal marsh, muck, and soils containing chlorides or cinders. Aluminum should be protected from corrosion by the use of coatings, linings, careful use of cathodic protection (because of possible deterioration in the alkaline environment created by cathodic protection), and by dielectric isolation from less active metals [14].

### Copper and Copper Alloys

Copper pipe is used primarily to transport water. Copper corrodes externally by pitting, crevice, uniform corrosion, and sometimes SCC. Copper can be corroded in soils containing cinders, chlorides, nitrogen compounds, inorganic and organic acids, cyanides, sulfides, and in salt tidal marsh soils [2,15]. Copper can also corrode internally due to the presence of high  $\text{CO}_2$  concentrations, high velocity at fittings and other flow restrictions, and by galvanic action resulting from bimetallic corrosion and corrosive flux in soldered joints.

## CORROSION ENVIRONMENTS

Factors affecting the corrosion of pipe include: soil resistivity, moisture content of the soil,  $\text{pH}$ , permeability of soil to moisture and air, soluble ion content of the soil, oxygen content, and the presence of corrosion-activating bacteria.

### Soil Resistivity

Resistivity is a measure of the soil's ability to conduct electrical current and is used as a guide in determining the corrosivity of the soil. Generally, soils with lower resistivity are more corrosive. Neither resistivity nor  $\text{pH}$  (described below) by themselves can be used to describe completely the corrosivity of the environment around the pipe. This is because other factors, such as aeration, drainage, and moisture levels have a significant impact on the corrosivity of soil. Very general resistivity guidelines are as follows:

<1000 $\Omega\text{-cm}$	Severely corrosive
1100–3000 $\Omega\text{-cm}$	Moderately corrosive
3100–10 000 $\Omega\text{-cm}$	Mildly corrosive
>10 000 $\Omega\text{-cm}$	Progressively less corrosive

It must be noted that the above guidelines are very qualitative and do not provide specific information as to corrosion rate, nor do they make distinctions about the performance of different materials, or the effect of bimetallic or other galvanic corrosion cells. For more information, the reader is referred to Refs 2, 16, and 17.

Lower resistivity soils can conduct more current and, therefore, tend to be more corrosive. The resistivity of a given soil can vary with the amount of moisture in the soil. Variations in resistivity can affect corrosion, because differential soil conditions create galvanic corrosion cells (e.g., oxygen concentration differential cells). Soil resistivity measurements are conducted according to ASTM G 57<sup>3</sup>, either in situ using the four-pin method or in the laboratory with a soil box. Of the two methods, field testing is preferable since it represents the actual conditions affecting the structure. Soil tested with a soil box should be measured with both the sample as-received and with the sample saturated with distilled water. Several soil measurements should always be taken, particularly when using the soil box, because soil characteristics are statistically distributed and resistivity will follow a normal probability function [18]. This fact can often be used to advantage, since it is only necessary to obtain representative data, which can be analyzed using normal and extreme value statistics [18,19].

### Moisture Content

Moisture is almost always found in soil. There is no critical moisture content for corrosion to occur, but greater quantities of water will increase the corrosivity of soil by increasing the amount of dissolved ions in the soil. Increasing water content will cause the resistivity to decrease, thus increasing the soil's conductivity and its ability to conduct corrosion current. Moisture content is measured by comparing the weight of the soil as-received with the weight after oven drying. A method to conduct this test is provided in ASTM D 2216<sup>4</sup>.

### Soil pH

Soil  $\text{pH}$  is a measure of the acidity or alkalinity of the soil, according to the following criteria [2]:

<4.5	extremely acid
4.5–5.0	very strongly acid
5.1–5.5	strongly acid
5.6–6.0	medium acid
6.1–6.5	slightly acid
6.6–7.3	neutral
7.4–7.8	mildly alkaline
7.9–8.4	moderately alkaline
8.5–9.0	strongly alkaline
>9.1	very strongly alkaline

It is generally considered that the corrosion of ferrous pipe in soil, where oxygen reduction is the cathodic reaction, is unaffected by  $\text{pH}$  unless the  $\text{pH}$  is below 4 or above 10. In

<sup>3</sup>Method for Field Measurement of Soil Resistivity Using the Wenner Four Electrode Method.

<sup>4</sup>Test Method for Laboratory Determination of Water (Moisture) Content of Soil and Rock.

soil with a pH below 4, the corrosion rate of iron increases above that found in neutral soils. The corrosion rate of iron in soil with pH above 10 decreases below that in more neutral soil. Variations in pH, even in the 4–10 range, cause corrosion by creating galvanic corrosion cells (called a pH differential corrosion cell). Corrosion rates of amphoteric metals, such as aluminum, are accelerated in soils with either strongly acidic or alkaline pH values. Soil pH is measured according to ASTM G 51.<sup>5</sup> The soil should be tested within 24 h of sampling. The soil pH is measured directly with pH and reference electrodes without adding any water.

### Permeability of Soil to Moisture and Air

Corrosion reactions depend on the presence of both moisture and oxygen. In general, soils that prevent the movement of either water or oxygen to the pipe surface will not be as corrosive as those that permit the ready movement of these items. Soil in the pipe ditch is generally more permeable than natural undisturbed soil.

### Soluble Ion Content

Significant ions include chlorides and sulfates. The higher the content of these ions, the more corrosive the soil. The amount of corrosion that occurs will depend on the quantity of moisture in the soil. Very dry soils are less corrosive than wet soils, even though both might contain high concentrations of dissolved salts. The soluble chloride and sulfate ion content of the soil can be measured by taking a water extract of the soil, measuring the chloride concentration of the extract, then calculating the chloride ion concentration in the original soil volume. The true concentration in parts per million (ppm) is given by

$$\frac{\text{Measured concentration of extract (mg/L)} \times \text{Mixed volume (L)} \times 10^6}{\text{Initial weight of solid sample (g)} \times 1000}$$

ASTM D 512<sup>6</sup> provides a method for measuring the chloride ion concentration of water. The sulfate ion content is measured in much the same way as the chloride ion test. ASTM D 516<sup>7</sup> provides a method of measuring the sulfate ion concentration in water. Titration methods and water testing kits can also be used. Soil chlorides can be found naturally in soils, or can be introduced by deicing salts and in a seacoast environment.

### Oxygen Content

Oxygen is essential for corrosion to occur in the pH range commonly found in soils. Soils such as clays restrict oxygen movement; therefore, these soils are prone to anaerobic conditions. Often, however, soils such as clays tend to promote galvanic corrosion cells that are caused by differences in oxygen concentration (differential concentration cell corrosion). Bacterial corrosion often occurs in clay soils because anaerobic conditions and organic matter promote bacterial growth. A common type of bacteria that causes

corrosion in soils is *desulfovibrio desulfuricans* anaerobic sulfate reducing bacteria.

The oxidation-reduction behavior of a soil is not frequently measured, because it is difficult to obtain reliable data in the field. Extraction of soil samples for laboratory analysis is likely to introduce oxygen into the sample that will adversely affect the accuracy of the data. Accurate data can be obtained with the soil in situ, but special probes are required. The use of redox potentials in evaluating the corrosivity of soils is discussed in Refs 20 and 21.

### Corrosion-Activating Bacteria

The presence of some forms of aerobic or anaerobic bacteria promotes corrosion, called microbiologically induced corrosion (MIC). The most common type of bacteria causing corrosion in soil is anaerobic sulfate reducing bacteria (SRB). Bacteria can cause the corrosion of ferrous and non-ferrous pipe. Identification and measurement of MIC can be accomplished by either laboratory analysis or by using several commercially available test kits.

For additional discussion on the relevance of soil characteristics, the reader is referred to ASTM STP 1013 and STP 1000 [22,23].

## CORROSION CONTROL

### Resistant Alloys

An acceptable life for underground pipelines can sometimes be realized through the use of corrosion-resistant piping. Copper, aluminum, and stainless steel piping are sometimes used for this purpose. All three alloys can have greater corrosion resistance than carbon steel or cast iron. However, they are not immune to corrosion and are often more susceptible to localized corrosion such as pitting, crevice corrosion, and SCC than carbon steel or cast iron. Further, corrosion protection in the form of coatings and cathodic protection are frequently used.

### Coatings and Linings

The purpose of a coating is to provide a barrier between the environment and the metal surface in order to prevent the corrosion cell from occurring. If the coating were a perfect barrier, then this would be satisfactory; however, experience has shown that coatings are rarely perfect barriers. Coatings contain defects that allow moisture to get through to the metal. Coatings are not always sufficiently bonded to the metal, due to contaminants on the metal surface or inadequate surface preparation or application. This allows osmotic transfer of moisture with subsequent blistering of the coating. Coatings can be damaged from soil stresses and mishandling and poor workmanship sometimes occurs, resulting in missed spots on the pipeline. If the pipe is not critical and if leaks are not a hazard or an economic problem, then coating alone might be justified; but normally, coating should be supplemented with cathodic protection.

Coatings are applied to carbon steel piping in atmospheric exposure, as this type of material is subject to general corrosion. Pitting attack can also occur on steel piping where

<sup>5</sup>Test Method for pH of Soil for Use in Corrosion Testing.

<sup>6</sup>Test Methods for Chloride Ion in Water.

<sup>7</sup>Test Methods for Sulfate Ion in Water.



conditions result in nonuniform collection of water and other aggressive contaminants. Coating of the piping in these areas is critical for the elimination of this form of accelerated corrosion attack. Coatings should also be applied to carbon steel, stainless steel, and ductile iron piping installed underground. The corrosion of all three of these ferrous materials can be of the pitting type, due to the inhomogeneity of the environment. Stainless steel, normally protected from corrosion by the formation of a passive oxide film, can corrode in a concentrated manner when buried in soil due to the inability to form a uniform oxide film. Therefore, the same corrosion resistance as that provided in above grade and internal exposure is not guaranteed when this material is buried. The same applies for aluminum piping. The application of coatings is generally part of a unified corrosion control program consisting of coatings and cathodic protection, so it is extremely important to select coatings systems that are compatible with the application of cathodic protection.

### Cathodic Protection

Cathodic protection is a very effective method of controlling corrosion on the exterior surfaces of metallic piping systems, including carbon steel, stainless steel, and ductile iron. It is most cost-effective when a quality coating system has been applied to the exterior surfaces of the pipe. Cathodic protection is of two types, galvanic anode and impressed current. The galvanic anode type uses metal ingots of a material more electrochemically active than the metal to be protected, to overcome the galvanic corrosion cells that exist on the pipe surface. This type of system usually requires that the pipe to be protected be electrically isolated from other metallic structures, such as copper water lines and grounding systems. In this manner, minimal current is required to achieve corrosion protection, and this current can be applied economically with a galvanic anode type system. If electrical isolation and effective coating do not exist, an impressed current type system is employed to produce the larger quantity of current required to achieve protection. The impressed current system uses inert anodes that serve as earth contact electrodes to supply the protective current to the protected structure. The current is generated by an external source of direct current, typically known as a "rectifier." The rectifier is an adjustable output current source that can deliver variable amounts of current based on the specific needs of the structure to be protected. The difference in operation between the two systems involves the consumption of the respective anodes. The galvanic anodes are consumed at a rate dependent on the current output and the consumption rate of the particular alloy. The consumption rate of typical impressed current anodes is much lower per ampere of current delivered. For example, a magnesium anode is consumed at a rate of 17 lb (7.7 kg) per ampere per year. A typical high silicon cast iron impressed current anode is consumed at a rate of 1 lb (0.45 kg) per ampere per year. Precious metal (platinized niobium and titanium) and mixed metal oxide coated titanium anodes have even lower consumption rates (on the order of milligrams per ampere per year of current discharge.) For more information, consult Refs 24 or 25.

### Stray Current Control

Stray currents are electrical currents on a pipeline caused by external sources. Examples of stray currents include: d-c or a-c powered transit systems, electric welding operations, currents from mining operations, and interference from cathodic protection systems on other structures. Stray current can cause corrosion where it discharges from the surface of the pipeline. For example, one ampere of d-c stray current causes the loss of 20 lb (9.1 kg) of iron per year. A-C stray current has about 1% of the effect of d-c strays on iron pipe, but a-c strays have a detrimental effect on aluminum [25]. Note that a-c stray current is not necessarily the same as induced a-c sometimes found on pipelines near a-c power transmission lines.

Corrosion by stray current is the result of the flow of current in other than intended paths. For example, in a d-c powered transit system, current that is intended to flow back to its source (the traction power substation) follows another path, exiting the rails, flowing into the ground, and is accumulated on a metallic structure such as a pipeline. The current flows along the pipeline, which acts as a low resistance conductor, until another low resistance path back to its source becomes available. The current discharges from the metallic structure into the soil and to its intended destination, the traction power substation negative bus. The problem involves the loss of metal at the point of discharge; for example, 20 lb (9.1 kg) of iron per year for every ampere of current discharging to earth.

The control of corrosion caused by stray current involves either reduction of the amount of current at the source or safe removal of the current from the corroding structure. The removal of the current from the structure involves the creation of a metallic path for the current to flow, rather than the electrolytic (soil) path. In order to create this metallic path, first the exact point of current discharge must be located through tests, and the quantity of current involved must be determined. The metallic path is provided after determining the quantity of current that must be "drained," and the characteristics that the drainage circuit must have. The resistance of the wire, its ampacity, and the exact point to which the current must be drained are examples of the characteristics that must be determined.

Standard tests for evaluating stray currents are rare. ASTM G 165, Practice for Determining Rail-to-Earth Resistance, provides a test method for measuring the resistance-to-earth of the running rails, which are used as the conductors for returning the train operating current to the substation in electric mass transit systems. For more information, consult Refs 25, 26, and 48.

### Above-Ground Installation

In some cases, external corrosion of buried structures can be eliminated by installing these structures above grade, rather than burying them. This has become common practice in plants, where space is available to relocate the underground facilities to above ground. This practice results in elimination of the invisible corrosion of the formerly buried structures, and replacement with a condition in which the structure can be seen and maintained. However, there

still remain corrosion control requirements. The structure must still be protected from atmospheric corrosion through the application and continual maintenance of corrosion coatings. A continuing program of visual inspection and maintenance of the coatings must be carried out to prevent the deterioration of the coating and the structure itself.

## Inhibitors

Chemicals can be added to the product in pipelines to control corrosion. These chemicals are called inhibitors. They control corrosion by forming barriers to isolate the metal surface from the environment or by controlling the anodic or cathodic corrosion reactions. Inhibitors are used to control corrosion by water (either condensed from the gas carrier or water being carried by the pipe) and salts (brine in petroleum pipelines, gathering pipelines, and oil wells). Inhibitors include oxygen scavengers, filming inhibitors, biocides, and passivating agents. For more information, see Ref 15.

## PROBLEM AREAS

### Welds and Mechanical Joints

Welds and mechanical joints can be areas where accelerated corrosion occurs for several reasons. Field coatings applied to joints are sometimes not of the same quality as shop-applied coatings on the remainder of the pipeline. This can lead to the environment penetrating to the metal and the formation of corrosion cells. Mechanical joints and rough welds can lead to crevice corrosion. Weld metallurgy also plays a role in corrosion. Welds containing high levels of sulfide inclusions can lead to localized corrosion of the weld metal.

### Mechanical Damage

Mechanical damage to the pipe can result in localized corrosion where the surface is scratched or dented, due to the formation of differential stress electrochemical corrosion cells. Corrosion can also occur if local damage occurs to the protective oxide film on the metal surface, resulting in an electrochemical corrosion cell between the clean metal and corroded metal. In the case of active-passive alloys, such as stainless steel, local damage to the protective oxide layer can result in an electrochemical corrosion cell.

### Bimetallic Couples

Corrosion caused by the connection of two or more different metals also occurs underground. This electrochemical corrosion cell is commonly referred to as bimetallic or galvanic corrosion. Typical examples include: brass or bronze valves connected to steel or cast iron pipes and stainless steel fasteners connected to steel or cast iron. These couplings of dissimilar metals will locally affect the corrosion rate. Aluminum can be severely corroded if directly connected to most other engineering alloys, such as steel, iron, copper, or stainless steel—dielectric isolation must be used.

## Stress Differences

Stress differences can result in localized electrochemical corrosion cells. An example is bolts used on joint fittings. The head and threaded areas of the bolt corrode at a faster rate than the body that is at a lower stress level.

## Environmental Cracking

### Hydrogen Damage

Atomic hydrogen generated at the surface by cathodic protection will diffuse into the metal. This atomic hydrogen can cause blistering of the metal, the formation of hydrides (in the case of titanium) that embrittle the titanium, and the embrittlement of steel (particularly high strength steel), martensitic stainless steel, high strength aluminum alloys (particularly 7000 series), and prestressed concrete. The embrittlement of the metal can cause cracks to form, which can grow and cause the structure to fail.

The prevention of hydrogen embrittlement depends on keeping the potential below the hydrogen evolution potential, which depends on the pH. In general, hydrogen is generated in neutral environments at  $-1044$  mV CSE. The lower the pH, the lower the hydrogen evolution potential. For aluminum, the polarized potential must be kept below  $-1200$  mV (CSE) to avoid alkali corrosion. For titanium, the maximum potential is  $-700$  mV (silver-silver chloride) to prevent hydriding. Overprotection levels are discussed in some cathodic protection criteria documents and might differ from these somewhat. For prestressed concrete, polarized potentials more negative than  $-1000$  mV CSE should be avoided.

### Stress Corrosion Cracking

Stress corrosion cracking is the cracking of a metal under an applied tensile stress in the presence of a corrosive environment. Many metals, including high strength steel, aluminum (2000 and 7000 series alloys), stainless steels, and brass alloys are susceptible to stress corrosion cracking. Cathodic protection generally reduces or eliminates stress corrosion cracking, because it stops the corrosion process. However, stress corrosion cracking of high strength pipeline steels caused by cathodic protection has occurred. This type of cracking occurs in a narrow potential range ( $-525$  to  $-725$  mV CSE) at a pH between 8 and 10.5, and is more likely at higher temperatures. The cracking occurs because of the formation of carbonates and bicarbonates at the steel surface. See Refs 27–30.

## CORROSION TEST METHODS

### Visual

Field evaluations consist of documenting both visual observations and measurements of corrosion on pipe sections. Evaluation of the environment also provides valuable information in the analysis of pipe corrosion. Visual methods are difficult to use on underground pipes because the pipe must be excavated to be examined; however, this is often the best way to evaluate the condition of a pipe. Carefully

obtained corrosion measurements can be analyzed using normal probability and extreme value statistics. There are no standards for performing this type of test. It is suggested that the locations for visual measurements be carefully selected from leak records, tapping excavation reports, close-interval survey test results (to be discussed), or soil corrosivity measurements (resistivity, pH, soil chemistry).

It is often difficult to evaluate the condition of a pipe by simple examination in the ditch because of the presence of corrosion products and deposits. Uncoated pipe should be thoroughly cleaned to remove all corrosion product and foreign matter (as in the evaluation of any corrosion, samples of the corrosion product should be retained for further analysis if the cause of the corrosion is unknown). This can be particularly true of gray cast iron, because the graphite matrix retains its shape and must be removed to reveal the remaining iron surface. Cleaning is often best accomplished using abrasive blasting. Care must be taken when using grit blasting not to erode away the pipe material itself, and grit blasting should not be used on thin pipes such as copper. For example, cast iron is harder than graphite and will not erode quickly, but if the blast nozzle is held in one place too long, the iron will erode. The graphite will be black in color and the cast iron a gray color.

Irregular surfaces and hard brownish deposits on the pipe are indicators that corrosion has occurred. Black or whitish deposits are indicators of possible anaerobic sulfate-reducing bacteria. Other visual methods rely on preparation of the pipe surface to remove graphite.

Visual inspection of the pipe in the ditch before pipe preparation includes the following steps:

- Clean the pipe surface to remove soil and debris.
- Document any obvious areas of corrosion or corrosion product accumulation.
- Evaluate black or whitish deposits for sulfate-reducing bacteria (SRB). A quick qualitative determination can be made using a 10 % hydrochloric acid solution in water. Place a drop of the solution on the deposit. An aroma of hydrogen sulfide (rotten eggs) indicates that SRB are present. Significant corrosion of the pipe might have occurred and further investigation is warranted. Wear safety glasses and gloves when handling the acid, and observe all necessary safety precautions. Commercial test kits are available that can provide a quantitative determination of the type and quantity of bacteria present.
- Obtain a general idea of the condition of gray cast iron pipe, especially when severely graphitized, by sounding the pipe with a hammer. A dull thud suggests extensive graphitization.
- Document all observations on data sheets and with photographs.

Further pipe evaluation is performed either by removing a sample from the pipe or cleaning a section of pipe for in situ measurements. Cleaning and measuring a section of pipe in the ditch provides the most accurate information, and the data are usable for statistical analysis. Extending the data from a single pipe section to the entire pipe run is not recommended beyond 1000 ft (305 m) or where the environment is known to vary significantly from that in the excavation.

## Pipe Coupon

Cut a coupon from the pipe using a pipe tapping tool, or cut a full circumferential coupon. Retain the coupon for further testing in the laboratory. Mark the sample to show the orientation of the sample on the pipe (top, side, bottom) and direction of flow. The full sample length should be at least 1 ft (30.5 cm). If possible, remove a 3-ft (0.9-m) length. The longer length will provide better information for statistical analysis. Put the sample in a plastic bag, seal the bag, and send it to the laboratory for further testing.

## Clean Pipe Section (In-Place Measurement)

Repair and safety equipment must be on-hand for any leak that might occur during the excavation or as a result of the cleaning procedure.

- Excavate a 10-ft (3-m) section of pipe, exposing the entire circumference of the pipe so that the entire pipe can be reached for examination.
- Document the condition of the pipe in writing and photographically before cleaning. Save samples of corrosion product before the pipe is cleaned for analysis.
- Sandblast the surface to remove all corrosion products. CAUTION: This can be hazardous! If the pipe shows extensive corrosion, extreme care must be exercised to avoid penetrating the pipe wall. Stop the cleaning operation if a wall penetration appears likely. The pipe surface after sandblasting should be a silver gray.
- Mark the cleaned surface into segments, each 1-ft (30.5-cm) long.
- Measure the depth of corrosion in each section, ensuring that the deepest corrosion is measured.
- Apply two coats of coal tar mastic coating to the pipe surface. Attach a sacrificial anode to the pipe section that was cleaned. This is necessary because the cleaned surface and old corroded surface form a galvanic corrosion cell. The clean pipe will corrode faster than the uncleaned pipe.

Coated pipe is somewhat more difficult to evaluate, because corrosion only occurs at coating holidays and sometimes under disbonded coating. Coating defects must be carefully examined and the condition of the pipe documented.

## Ultrasonic Inspection

Ultrasonic measurements can be used to supplement mechanical pit depth measurements and can be used in areas where the internal condition of the pipe must be determined. Ultrasonic measurements can be analyzed, using the same statistical approach as mechanical measurements. Additional information for ultrasonic inspection is found in ASTM E 212<sup>8</sup> and Ref 31.

There are several important considerations relative to ultrasonic measurements. One is the doubling effect of some digital gages when the thickness limitation of the transducer is reached. Another is the effect of coatings on the readings. Most pulse-echo instruments will provide inaccurate

<sup>8</sup>Practice for Ultrasonic Examination of Metal Pipe and Tubing.

information when the tester tries to read through an organic coating on the pipe. Coatings must be removed unless the equipment used compensates for the presence of the coating. The surface roughness of the pipe, both internal and external, plays an important role in the accuracy of the data. The surface must be relatively smooth. Roughness can make it either difficult or impossible to obtain accurate thickness data. It is sometimes necessary to grind the surface just enough to allow the transducer a flat surface. One very important consideration is the nature of the internal corrosion. Internal pitting that consists of narrow or widely scattered pits might be difficult to find with ultrasonics, because the probability of the transducer being immediately above a pit can be low. In that case, a scanning approach should be used to cover the widest area possible. A visual inspection of the pipe is a good idea if at all possible to determine the type of corrosion present.

### Instrumented Pigs

Instrumented or "smart pigs" using ultrasonic, eddy current, or mechanical measuring instrumentation can be effectively used to measure corrosion from the inside of the pipe. Instrumented pigs contain sensing devices that scan the pipe wall searching for defects. Ultrasonic devices work by measuring the time that it takes a high-frequency sound wave to travel across the pipe thickness and back to the transducer. The instrument is calibrated to measure this time as thickness of the pipe wall. Magnetic or eddy current devices work by sensing deviations in a magnetic flux field caused by corrosion pits or other defects that distort the flux field. For more information, consult Refs 32–34.

Magnetic flux inspection using pigs has been applied to small diameter cast iron and ductile iron water pipe as a means of measuring the internal and external corrosion of that pipe. Pipe up to 8 in. (200 mm) has been inspected using this technique [35].

### Statistical Evaluation

Corrosion, particularly pitting corrosion, tends to be distributed in a nonuniform manner. The depth of pits on a surface can be described by a normal probability curve. This can be used to advantage when evaluating a pipeline, because it is only necessary to measure a few representative areas and use statistics to determine the condition of the entire pipe. There are no standard test methods, but ASTM G 16<sup>9</sup> does describe statistical approaches to laboratory data, and applicable references can be found in Refs 36 and 37.

The corrosion data collected in the above-mentioned test provide information about the samples tested, but not necessarily about the pipe as a whole. That is why it is important not only to select sampling locations that represent the condition of the pipe run as a whole, but also include the worst case conditions. Whatever areas are selected, it is possible that more severe corrosion exists. Statistical analysis is a method that uses known data to predict the range of corrosion.

In order for a statistical analysis to provide useful results, the data must be taken in a systematic fashion. The corrosion measurements for both the field and laboratory evaluation, as described above, provide corrosion data at known and consistent intervals along the pipe sample. This provides usable data for the statistical analysis.

The statistical analysis procedure most useful in evaluating corrosion on pipes is the extreme value statistical method. The referenced publications provide details on extreme value statistics and their application to pipeline corrosion. The extreme value statistical approach analyzes the maximum pit depth (or minimum wall thickness) per unit length to estimate the range of corrosion data for the pipe. The results, of course, assume that the pipe run is in the same condition as the sample tested. The more samples tested, the greater the accuracy of the result.

Normal probability and extreme value statistics have already been discussed as means of evaluating corrosion and soil resistivity. Statistical methods have been applied to determine when steel tanks will fail [38]. Individual soil characteristics, such as resistivity, pH, and soluble ion content, are unsatisfactory methods of predicting the corrosion behavior of a structure in a particular soil. The statistical method is based on a regression analysis of all of the soil characteristics that affect corrosion as compared to actual corrosion of structures found in those soils. This method yields a mean time to corrosion failure (MTCF) as opposed to an actual corrosion rate. Its validity for structures other than steel tanks has not been demonstrated.

### Electrochemical Methods

#### *Polarization Techniques*

Polarization refers to the change in corrosion potential of a metal as an external current is applied. Plots of potential versus applied current are called polarization curves; these can be used to measure the corrosion rate of pipelines. ASTM G 59<sup>10</sup> and G 102<sup>11</sup>, normally used in the laboratory, are not directly usable on pipelines. Polarization curves to measure Tafel slopes (E-log I plots) have been used for years to measure corrosion currents and cathodic protection current requirements. Standard laboratory techniques must be modified to fit field conditions, since we are dealing with large working electrodes<sup>12</sup> rather than small electrodes as in a laboratory setting. Also, several factors are often present that are not found in the laboratory, such as the working electrode being coated and the possible presence of galvanic and stray currents. These factors make interpreting polarization data to determine corrosion rate difficult. Since all coatings contain defects (called holidays), the total area of pipe exposed and size and distribution of the holidays are often unpredictable and will affect the corrosion rate; i.e., one cannot use the total area of the pipe in the corrosion current density calculation. Concentration

<sup>10</sup>Practice for Conducting Potentiodynamic Polarization Resistance Measurements.

<sup>11</sup>Practice for Calculating the Corrosion Rates and Related Information from Electrochemical Measurements.

<sup>12</sup>The pipe is called the "working electrode" in electrochemical terminology.

<sup>9</sup>Guide for Applying Statistics to Analysis of Corrosion Data.

polarization effects on a large structure often affect the observation of the Tafel slope, thus making the measurements unreliable.

One method of getting around these problems is to use a small working electrode coupon connected to the pipe. The size of the electrode is based on a reasonable estimate of the holiday sizes on the pipe. The polarization curve is obtained by observing the potential on the known electrode. Such data must be evaluated carefully, since it represents only one point. On a long pipeline, several test locations should be evaluated. For more details on electrochemical polarization, the reader is advised to consult Refs 39 to 41 and 42.

### Potential Measurements

Corrosion testing often involves determining the relative level of electrical activity of various structures such as pipelines, storage tanks, and the like in the environment in which they are installed. These environments may be soil, water, or concrete, to name a few. In each case, the environment in which the structure is installed is the electrolyte that can and will support corrosion activity. Structure-to-electrolyte potential measurements may be used at various stages in the corrosion evaluation to determine the existence of corrosion activity. This is accomplished by measuring the "native" or "natural" potential of the structure. This involves using the circuit shown in Fig. 1. The measurements taken will indicate the electrical characteristics exhibited by the structure in its natural state. For example, for a pipeline installed in soil, the potential with respect to the soil by means of a standard reference electrode, taken at regular intervals along the pipeline will indicate the corrosion patterns affecting the pipeline, as described in the next section.

Once the potential pattern has been measured for a structure, potential measurements can also be used to evaluate the effects of the application of cathodic protection current. While a measured quantity of current is applied to a structure,

potential measurements are taken at locations where native potential measurements had been taken. The shift in potential as well as polarization effects due to the application of the current can be measured. These data can be used to determine the quantity of current required to achieve cathodic protection of the structure.

Potential measurements are also used to gage the effectiveness of a cathodic protection system, after it has been installed and is operating, in mitigating the corrosion activity detected by the native potential profile. The pipe-to-soil potential measurement has been established by corrosion engineers as a standard for determining the degree of cathodic protection on underground metallic structures. Various criteria have been promulgated; the three currently in use for steel structures are: (a) the achievement of a pipe-to-soil potential of  $-850$  mV referenced to a copper-copper sulfate electrode with cathodic protection current applied, (b) the achievement of a polarized potential of  $-850$  mV, and (c) the achievement of a  $100$  mV shift in potential due to cathodic polarization.<sup>13</sup> These measurements can be taken at distinct points along a structure, or continuously, as in the case of a close interval potential survey (see next section).

### Close Interval Survey

As discussed above, corrosion activity can be detected through the measurement of native structure-to-electrolyte potentials at regular intervals along a pipeline or similar structure. Techniques have been developed using sophisticated computerized data loggers to record the large numbers of potential readings that can be encountered during the course of such a survey. These data loggers in conjunction with personal computers can provide a continuous profile of the potential along miles of pipeline traversing all types of terrain. Some instrumentation can be linked to global positioning systems (GPS) synchronization software.

Figure 2 shows a typical pipe-to-soil potential profile on a pipe experiencing galvanic corrosion activity. This profile consists of a series of measurements with one reference electrode moved directly over the pipe, and a second reference electrode moved at a lateral distance remote from the pipe. In general, anodic areas exist at locations where the "over-the-pipe" potentials are more negative than "off-the-pipe" potentials. The anodic areas are at locations where the over-the-pipe potentials are of higher negative values than those measured in the cathodic areas. In the case of stray current interference, current is picked up on the pipeline, increasing the potential in the negative (cathodic) direction. At the point of stray current discharge, the potential is depressed (less negative). Therefore, the anodic areas in the case of interference currents are at locations where the potentials (both "over" and "off" the pipe) are of lower negative values than those at the cathodic areas. Figure 3 illustrates the typical profile for a stray current interference condition. Other types of corrosion conditions can be detected through the use of close interval potential surveys. These include the effects of coating damage, shorts to bare or grounded structures, and very aggressive soil environments [43].

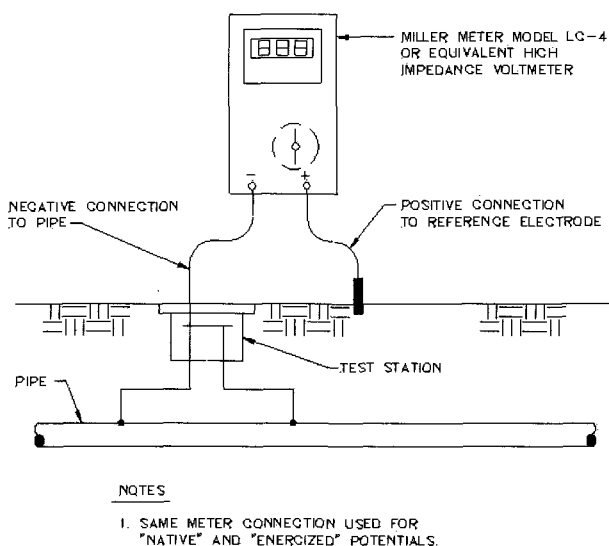


FIG. 1—Pipe-to-soil potential measurement (general).

<sup>13</sup>Practice for Preparing, Cleaning, and Evaluating Corrosion Test Specimens.

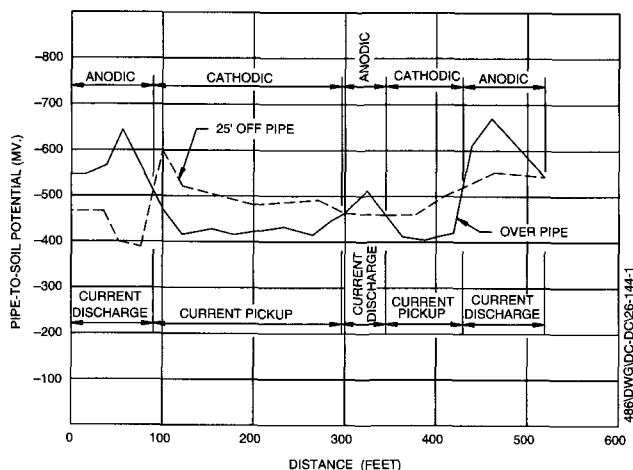


FIG. 2—Potential profile showing galvanic corrosion activity [41]. (Reprinted from Corrosion. © Copyright by NACE International. All Rights Reserved by NACE; reprinted with permission.)

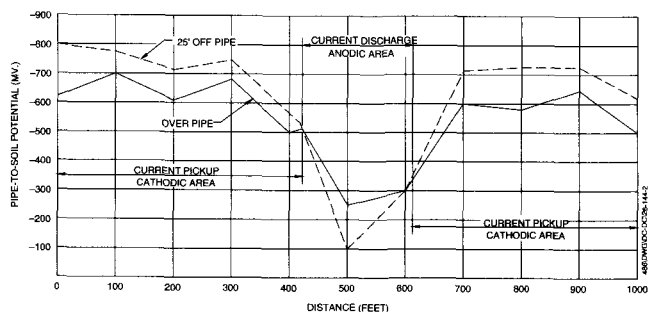


FIG. 3—Potential profile on pipe subject to exposure from cathodic protection interference [37]. (Reprinted from Corrosion. © Copyright by NACE International. All Rights Reserved by NACE; reprinted with permission.)

## Coupons

Coupons are relatively small pieces of metal, the same composition as the structure being evaluated, that are buried in the soil next to the structure. They are intended to measure the corrosivity of the soil where the structure is buried or is intended to be placed. If the structure already exists, the coupon should be connected to the structure in order to expose it to galvanic and stray currents, as well as the soil. Coupons can be evaluated after a period of time using mass loss (ASTM G 112) or polarization as previously discussed. Coupons should be large enough for pitting to develop. All coupons should be evaluated visually after exposure.

Commercially available coupon systems are available for measurement of cathodic protection data, and some are available for measurement of both polarization and corrosion rate data. Care must be exercised when using these methods to ensure that the coupons are installed in an area representative of the pipe and that the coupon size is representative of the coating holidays on the pipe. NACE International has published a state-of-the art report on the

application and interpretation of data from external coupons [44]. For additional information, see Refs 45 and 46.

NACE International has a series of test methods that are applicable to in situ testing. These are:

1. Standard Recommended Practice RP0189, On-Line Monitoring of Cooling Waters,
2. Standard Recommended Practice RP0775, Preparation, Installation, Analysis, and Interpretation of Corrosion Coupons in Oilfield Operations,
3. Standard Test Method TM0172, Determining Corrosive Properties of Cargoes in Petroleum Product Pipelines,
4. Standard Test Method TM0299, Corrosion Control and Monitoring in Seawater Injection Systems.

## Remote Monitoring

Recent advances in digital measurement systems and microprocessor-based monitoring and control systems have made the monitoring of cathodic protection systems for pipelines and complex piping networks more economical and accurate. Cathodic protection systems can be monitored on a continuous basis, and operational malfunctions such as power loss to impressed current rectifiers, lightning damage, and other component failure can be detected and alarms can be sent to owners and operators of these systems. The technology also includes the capability to perform detailed test protocols to evaluate the effectiveness of cathodic protection systems at critical locations, without the need for personnel to visit the locations. The testing can include anything from simple routine testing, such as pipe-to-soil potential at a test point, to simultaneous interruption of multiple rectifier units and the measurement of depolarization decay at selected test points. The outputs of the rectifier units and individual anodes can be both monitored and remotely adjusted. Additional information is contained in Ref 47.

## REFERENCES

- [1] ASM Metals Handbook, Vol. 1, Properties and Selection: Irons, Steels, and High Performance Alloys, 10th ed., ASM International, Materials Park, OH, 1990, pp. 327–336.
- [2] Romanoff, M., *Underground Corrosion*, National Bureau of Standards, Circular 579, NTIS PB-168 350, April 1957.
- [3] ASM Metals Handbook, Vol. 1, Properties and Selection: Irons, Steels, and High Performance Alloys, 10th ed., ASM International, Materials Park, OH, 1990, pp. 841–907.
- [4] Gerhold, W. F., Escalante, E., and Sanderson, B. T., "The Corrosion Behavior of Selected Stainless Steels in Soil Environments," NBSIR 81-2228(NBS), American Iron and Steel Institute, Washington, DC, February 1981.
- [5] Romanoff, M., *Underground Corrosion*, National Bureau of Standards, Circular 579, NTIS PB-168 350, April 1957, pp. 49–53.
- [6] ASM Metals Handbook, Vol. 1, Properties and Selection: Irons, Steels, and High Performance Alloys, 10th ed., ASM International, Materials Park, OH, 1990, pp. 12–55.
- [7] Gerhold, W. F., "Corrosion Behavior of Ductile Cast Iron Pipe in Soil Environment," *Journal AWWA*, December 1976, pp. 674–678.
- [8] AWWA Standard C104, Cement-Mortar Lining for Ductile Iron Pipe and Fittings for Water, AWWA, Denver, CO.

- [9] ASM Metals Handbook, Vol. 1, Properties and Selection: Irons, Steels, and High Performance Alloys, 10th ed., ASM International, Materials Park, OH, 1990, pp. 216–217.
- [10] Internal Corrosion of Water Distribution Systems, 2nd ed., AWWA Research Foundation, Denver, CO, 1996, pp. 127–212.
- [11] Young, W. T., "Evaluation of Highway Culvert Coating Performance," Final Report No. FHWA/RD-80/059, FHWA, Washington, DC, NTIS PB81 11546T, June 1980.
- [12] Godard, H. P., et al., *The Corrosion of Light Metals*, John Wiley & Sons, New York, 1967, p. 115.
- [13] Uhlig, H. H. and Revie, R. W., *Corrosion and Corrosion Control*, 3rd ed., John Wiley and Sons, New York, 1985, pp. 345–347.
- [14] NACE Standard RP0169, Control of External Corrosion on Underground or Submerged Metallic Piping Systems, NACE International, Houston, TX.
- [15] ASM Metals Handbook, Vol. 13, Corrosion, 9th ed., ASM International, Metals Park, OH, 1987, p. 621.
- [16] Chaker, V., "Corrosion Testing in Soils—Past, Present, and Future, Corrosion Testing and Evaluation," *Corrosion Testing and Evaluation: Silver Anniversary Volume*, ASTM STP 1000, R. Baboian and S. W. Dean, Eds., ASTM International, West Conshohocken, PA, 1990, pp. 95–111.
- [17] *Underground Corrosion*, ASTM STP 741, E. Escalante, Ed., ASTM International, West Conshohocken, PA, 1981.
- [18] Scott, G. N., "The Distribution of Soil Conductivities and Some Consequences," *Corrosion*, August 1958, pp. 396t–400t.
- [19] Fitzgerald, J. H., "Evaluating Soil Corrosivity—Then and Now," *Materials Performance*, Vol. 32, No. 10, October 1993, pp. 17–19.
- [20] Romanoff, M., *Underground Corrosion*, National Bureau of Standards, Circular 579, NTIS PB-168 350, April 1957, p. 154.
- [21] Booth, G. H., "Microbiological Corrosion," *British Corrosion Journal*, No. 2, 1967, pp. 104, 109, 116.
- [22] Palmer, J. D., "Field Soil Corrosivity Testing—Engineering Considerations," *Corrosion Testing and Evaluation: Silver Anniversary Volume*, ASTM STP 1000, R. Baboian and S. W. Dean, Eds., ASTM International, West Conshohocken, PA, 1990, pp. 125–138.
- [23] *Effects of Soil Characteristics on Corrosion*, ASTM STP 1013, V. Chaker and J. D. Palmer, Eds., ASTM International, West Conshohocken, PA, 1989.
- [24] Peabody, A. W., *Control of Pipeline Corrosion*, 2nd ed., NACE, Houston, TX, 2001.
- [25] *Corrosion*, L. L. Shreir, Ed., 3rd ed., Newnes-Butterworths, Boston, 1994.
- [26] Young, W. T. and McIntyre, W. B., "Stray Current Corrosion of Water Distribution Piping," Paper 390, *Corrosion/90*, Las Vegas, NV, NACE, Houston, TX.
- [27] Parkins, R. N., "Stress Corrosion Cracking of Pipelines," *Corrosion/96*, Paper 249, NACE International, Houston, TX.
- [28] Jaske, C. E., Beavers, J. A., and Harls, B. A., "Effect of Stress Corrosion Cracking on Integrity and Remaining Life of Natural Gas Pipelines," *Corrosion/96*, Paper 255, NACE International, Houston, TX.
- [29] Culbertson, D. L., "Use of Intelligent Pigs to Detect Stress Corrosion Cracking in Gas Pipelines," *Corrosion/96*, Paper 35, NACE International, Houston, TX.
- [30] Molan, R., Eliassen, S., Holt, T., and Rathje, S., "Possibility of Stress Corrosion Cracking in Submarine Pipelines," *Materials Performance*, August 1982, p. 50.
- [31] ASM Metals Handbook, Vol. 17, Nondestructive Evaluation and Quality Control, 9th ed., ASM International, Metals Park, OH, 1989, pp. 231–277.
- [32] Holm, W. K., "Magnetic Inspection Pigging Aids Pipeline Inspection," *Gas Industries*, March 1985, pp. 6–11.
- [33] Schmidt, J. T., "Magnetic Flux Leakage Inspection of Pipelines—An Operator's Viewpoint," *Materials Protection*, Vol. 33, No. 7, July 1994, pp. 53–57.
- [34] *Corrosion Detection Using Intelligent Pigs*, Corrosion Information Compilation Series, Pipeline Corrosion, NACE International, Houston, TX, 1999.
- [35] Staples, L. B., "A New Tool for Condition Evaluation of Cast and Ductile Iron Pipe," *Corrosion/96*, Paper 45, NACE International, Houston, TX, 1996.
- [36] Gumbel, E. J., *Statistics of Extremes*, Columbia University Press, New York, 1958.
- [37] Hawn, D. E., "Extreme Value Prediction of Maximum Pits on Pipelines," *Materials Protection*, March 1977, p. 29.
- [38] Bushman, J. B. and Mehalick, T. E., "Statistical Analysis of Soil Characteristics to Predict Mean Time to Corrosion Failure of Underground Metallic Structures," *Effects of Soil Characteristics on Corrosion*, ASTM STP 1013, V. Chaker and J. D. Palmer, Eds., ASTM International, West Conshohocken, PA, 1989.
- [39] Rowe, L. C., "Measurements and Evaluation of Pitting Corrosion," *Galvanic and Pitting Corrosion—Field and Laboratory Studies*, ASTM STP 576, ASTM International, West Conshohocken, PA, 1976, p. 203.
- [40] Scully, J. R., "Electrochemical Methods for Laboratory Corrosion Testing," *Corrosion Testing and Evaluation: Silver Anniversary Volume*, ASTM STP 1000, R. Baboian and S. W. Dean, Eds., ASTM International, West Conshohocken, PA, 1990.
- [41] Uhlig, H. H. and Revie, R. W., *Corrosion and Corrosion Control*, 3rd ed., John Wiley and Sons, New York, 1985, pp. 53–59.
- [42] Escalante, E., "Measuring the Corrosion of Metals in Soil," *Corrosion Testing and Evaluation: Silver Anniversary Volume*, ASTM STP 1000, R. Baboian and S. W. Dean, Eds., ASTM International, West Conshohocken, PA, 1990, pp. 112–124.
- [43] Husock, B., "Use of Pipe-to-Soil Potential in Analyzing Underground Corrosion Problems," *Corrosion*, Vol. 17, No. 8, August 1961, pp. 391–395.
- [44] "State of the Art Report on the Application and Interpretation of Data from External Coupons Used in the Evaluation of Cathodically Protected Metallic Structures," NACE International, Houston, TX, 2001.
- [45] *Cathodic Protection Monitoring for Underground Pipelines*, NACE Corrosion Information Compilation Series, Pipeline Corrosion, NACE International, Houston, TX, 1999.
- [46] Stears, C. D., Moghissi, O. C., and Bone, L., "Use of Coupons to Monitor Cathodic Protection of an Underground Pipeline," *Materials Performance*, February 1998, pp. 73–81.
- [47] Van Blaricum, V. L. and Norris, W. R., "Remote Monitoring Equipment for Cathodic Protection Systems," U. S. Army Construction Engineering Research Laboratories, Champaign, IL, FEAP User Guide 97/75, April 1997.
- [48] *Stray Current Corrosion: The Past, Present, and Future of Rail Transit Systems*, M. Szeliga Ed., NACE International, Houston, TX, 1994 (a compilation of papers on transit stray current).

# Highways, Tunnels, and Bridges

James B. Bushman<sup>1</sup> and Victor Chaker<sup>2</sup>

TRANSPORTATION IN THE UNITED STATES is essential to the physical and economic well-being of the country. In general, the transportation infrastructure in the United States has stood up well, leading to a false sense of security and to our taking it for granted. We are currently faced with the need to maintain, repair, and reconstruct the existing systems to extend their life expectancies, or to develop new technologies to replace them with more efficient and effective systems. To understand these challenges, an overview of the current material and testing procedures has been prepared.

## MATERIALS OF CONSTRUCTION

### Highways [1]

Highway design and construction use numerous materials, both metallic and nonmetallic. Most of the materials are controlled by standards adopted by the American Association of State Highway and Transportation Officials (AASHTO).

Metallic materials include but are not limited to the following:

- Steel forgings, carbon and alloy, for general use.
- Steel castings, carbon, for general application.
- Gray and ductile iron castings.
- High-strength steel bolts for structural steel joints.
- Carbon steel bars, cold-finished, standard quality.
- Structural steel.
- Steel sheet piling.
- Standard strength steel wire ropes and sockets for conventional catenary cable suspension bridges.
- Carbon steel reinforcing bars.
- Epoxy coated carbon steel reinforcing bars
- Stainless steel reinforcing bars.
- Stainless steel clad carbon steel reinforcing bars.
- Medium and ultra-high strength bar, rod, and cable in prestressed and post-tensioned concrete components.
- Ultra-high strength steel cables for cable stay suspension bridges.

Nonmetallic materials include but are not limited to the following:

- Fiberglass reinforced plastic (FRP) reinforcing bars.
- Timber, pressure-treated, and wood products.
- Portland cement concrete.

- Fly ash, silica fume, and ground granulated blast furnace slag.
- Corrosion inhibitors
- Bituminous material for paving
- Granulated rubber from used tires.

### Tunnels [2]

Steel, cast iron, or precast lining rings are installed in tunnels to support the ground. Tunnels in loose, noncohesive, or soft ground are generally driven by means of a steel shield, most often circular in shape, either in free air or under compressed air. The shield permits the excavation of soil and erection of primary lining under safe conditions and must be used in subaqueous tunnels. Some of the notable shield-driven tunnels include the Hudson River tunnels, which became part of the Hudson-Manhattan Railroad. The Holland Tunnel under the Hudson River began in 1922, followed by the three Lincoln Tunnels and the Midtown Tunnel under the East River.

All shield tunnels must have a primary lining to support the ground and take the thrust of the shove jacks. Traditionally, segmental cast iron liners have been used; other methods are ribs and lagging, fabricated steel liners, pressed steel liner plates, and precast concrete segmental liners.

#### Ribs and Wood Lagging

In tunnels that require a secondary lining for interior finish or smooth surface, steel ribs and wood lagging have been used in firm and relatively dry ground.

#### Precast Concrete Lining

Precast concrete liners have not yet found great use in the United States, except for the O'Rourke block used in a number of tunnels in Detroit. They are not watertight and require a secondary lining. Precast concrete segments were designed for a test section of the Baltimore subway tunnels, but were not competitive with steel liners.

In subway construction, concrete segmental liners generally do not receive a secondary lining, since slight seepage is tolerated.

#### Secondary Lining

A secondary lining is required if the primary lining consists of ribs and lagging or O'Rourke blocks, or if the tunnel interior needs a finish (as in highway tunnels). Rail tunnels with segmental metal or precast concrete usually do not receive a secondary lining.

<sup>1</sup>Principal Corrosion Engineer, Bushman & Associates, Inc., Corrosion Consultants, P.O. Box 425, Medina, OH 44256.

<sup>2</sup>Former Author, retired from Port Authority of NY/NJ.



Secondary linings are usually applied after primary linings have been in place for a period during which they have adjusted to the soil pressure and deformation, so that they have to absorb only long time secondary settlements.

In subaqueous tunnels, the thickness of the secondary lining may be governed by the requirement that its weight together with that of the rest of the structure be sufficient to counterbalance the buoyancy forces.

### *Poured Concrete Lining*

Generally used in highway tunnels, which receive a tile finish or other light reflecting surface, poured concrete lining will be of a minimum practical thickness for pouring and enclosure of conduits, fixtures for lighting, and other recessed equipment. The concrete is poured behind steel forms, starting at the invert. In tunnels with no watertight primary lining, the concrete secondary lining is placed as close to the face as possible.

Sprayed linings of cement mortar may be used to protect the interior of the steel primary linings. Acoustical lining may be sprayed directly to the primary lining or on a sprayed mortar lining for the reduction of train noise in rapid transit tunnels, particularly adjacent to the stations.

## **Bridges [1]**

### *Foundation*

Selection of foundation type must be based on an assessment of the magnitude and direction of loading, depth of suitable bearing materials, seismic activity, evidence of previous flooding, potential for liquid action, undermining or scour, swelling potential, frost depth, and ease and cost of construction.

Piling may be considered when footings cannot be founded on rock or on granular or stiff cohesive soils within a reasonable depth. Piles may be structural steel sections, steel pipe, precast concrete, cast-in-place concrete, prestressed concrete, timber, or a combination of materials. A steel foundation design must consider the possibility of corrosion, particularly in fill soil, low pH soil, and marine environment. Methods of protecting steel and steel reinforced concrete piling in corrosive environments include coating, wrapping, and cathodic protection.

A steel reinforced concrete pile foundation must consider the effect of sulfates, ground water or seawater, chlorides in soils, chemical waste, acidic ground water, and organic acids.

A timber pile foundation must consider the effect of decay from wetting and drying cycles and marine borers.

### *Retaining Walls*

Rigid gravity and semigravity walls can be constructed of reinforced concrete, while gravity walls can also be constructed of stone masonry or unreinforced concrete, or both.

Vertical wall elements may consist of discrete vertical elements and support retained soil with facing elements. Discrete vertical elements may include piles, caissons, drilled shafts, or augured cast piles. Structural facing may include wood, precast or cast-in-place concrete panels, wire or fiber-reinforced shotcrete, or metal elements such as sheet piles.

Mechanically stabilized earth systems may employ metallic strips or polymeric tensile reinforcements in the soil mass, and a discrete precast concrete facing.

Prefabricated modular wall systems generally employ interlocking soil filled reinforced concrete or steel modules or bins, which resist earth pressures by acting as gravity-retaining walls.

### *Super Structures and Fasteners*

Structural steels of all grades are selected with a modulus of elasticity of 200 000 kPa (29 000 000 psi) and a coefficient of linear expansion of 0.0000118 per °C (0.0000065 per °F).

Steel for pins, rollers, and expansion rockers may be carbon cold-finished standard quality, and steel forgings, carbon and alloy, for general industrial use.

Fasteners may be carbon steel bolts, power driven rivets, or high-strength bolts.

Weld metal should conform to the current requirements of the ANSI/AASHTO/AWS D1.5 Bridge Welding Code.

Cast steel should conform to AASHTO specifications for Steel Castings for Highway Bridges; Mild to Medium Strength Carbon Steel Castings for General Application; and corrosion-resistant Iron Chromium, Iron Chromium Nickel-based Alloy Castings for general application.

## **CORROSIVE ENVIRONMENTS**

Most of the materials used in transportation construction are exposed to one or more environments including atmospheric, soil, and water. The following section will outline the corrosive nature of each environment.

### **Atmospheric [3,15]**

Atmospheric corrosion is considered that which occurs from exposure of metals to atmospheric conditions, including precipitation and dew. Atmospheric corrosion damage includes general attack, cracking, and localized corrosion.

Although atmospheric corrosion has been recognized as a major cause of metal degradation for many years, it has been an ongoing challenge to make accurate predictions of the rate of atmospheric corrosion and the effectiveness of preventive measures.

Initial work done in this field showed that outdoor environments vary greatly in their corrosivity, that urban and industrial areas have substantially higher corrosion rates for most engineering materials than rural areas, and furthermore, that marine environments and locations within a mile or two of the ocean surf also suffer significantly higher corrosion rates than other inland areas.

It has been determined that sulfur dioxide and carbon dioxide from combustion of fossil fuels is the primary corrodent that differentiates industrial areas, and that chlorides from sea salt accelerated the corrosion in marine environments. In general, the acceleration of corrosion that occurs in marine atmospheres is different from that which occurred in industrial atmospheres in that it tends to cause localized corrosion in many alloys.

Recent atmospheric cleanup has caused the average sulfur dioxide concentration at the industrial ASTM Newark/Kearny

atmospheric exposure site to be lower than the rural ASTM State College site. Consequently, evaluation of the airborne contaminants from similar sites will enable engineers to select knowledgeably the appropriate material(s) and corrosion protection systems.

### Soils [4]

The characteristics of the soil are determined by the physical and mineralogical composition of the parent material, the contamination of the material over time by airborne salts and chemicals applied to the soil surfaces, and the natural processes of plant and animal life on and in the soil.

Chemical analyses of soils for corrosion purposes are usually limited to determination of the elements that are soluble in water. The base-forming elements are usually sodium, potassium, calcium, and magnesium. The acid-forming elements are carbonate, bicarbonate, chloride, nitrate, and sulfate. The nature and amount of soluble salts, together with the moisture content of the soil, generally determine the conductivity and corrosivity of the soil. The development of acidity in soils is a result of the natural processes of weathering and decay under humid conditions.

Bacteria may affect the chemical properties of soils. Certain types of bacteria are capable of fixing atmospheric nitrogen and converting nitrogenous material in the soil to a form useful for plant life. Other bacteria convert sulfur and sulfides to sulfates, and still others accomplish the reverse reaction.

The physical properties of soils important in corrosion are mainly those that determine the permeability of the soil to oxygen or air and to water. The particle size distribution of the soil is an important factor with respect to aeration and moisture content. In coarse texture soils such as sands and gravel, where there is free circulation of air, corrosion approaches the atmospheric type. Clay and silty soils are characterized in general by fine texture, high water-holding capacity, and by poor aeration and poor drainage. Variations in these characteristics within the same soil environment lead to higher corrosion rates compared to that experienced by atmospherically exposed materials.

#### *Factors Affecting Corrosion in Soils*

Since corrosion is an electrochemical process, it requires a potential difference between two points electrically connected and immersed in an electrolyte. Electrons flow from the anodic area through the metallic path to the cathodic area to complete the circuit. The anodic area is the most negative in potential and is the area that corrodes through the loss of metal ions to the electrolyte.

The factors affecting corrosion in soils are aeration, electrolyte, stray d-c currents, and miscellaneous:

1. Aeration affects the access of oxygen and moisture to the metal, consequently affecting corrosion. Oxygen causes corrosion by combining with the metal ions to form oxides, hydroxides, or salts of metal. If these corrosion products are soluble or removed from the anodic areas, corrosion proceeds, but if the products accumulate they may act as a protective layer to reduce corrosion or initiate localized corrosion because the corrosion products are more noble than the base metal.

FIG. 1

2. Electrolytes affect the flow of electrons. Moisture in soils helps the flow of electrons, thus promoting the corrosion process. The ions in the electrolyte determine the electrical conductivity as well as the acidity or alkalinity of the electrolyte, and the chemical reaction between the primary products of corrosion and the electrolyte.
3. The principal factor in the corrosion of metals in soils is the variation in potential that exists at different points or areas on the surface of the metal. Potential differences involve both the metal and the electrolyte. It may be affected by local variations in either one. The amount of current that flows through the cell as a result of the potential difference is dependent upon the electrical characteristics of the electrolyte and the polarization of the metal surfaces. The potential difference and the resulting corrosive current are not necessarily constant with time. The relative size of the anode and cathode areas is a factor in determining the rate of corrosion damage. For example, in a given environment, a small anode to large cathode area will always result in the highest penetration rate at the anode area.
4. Some of the miscellaneous factors affecting corrosion in soils are the effect of different soils in contact with the same metallic structure, different compaction and aeration in the case of backfill in a trench, and foreign material or stones in contact with the metal surface; bacterial action is another factor and is associated with aeration and the formation and presence of soluble salts. Porous backfills, such as sand and pea gravel, while giving good mechanical support to the structure, accelerate corrosion of metals buried in them by acting as "French Drains" providing ingress for aggressive surface pollutants such as fertilizers and de-icing salts.

### Waters [5,15]

At ordinary temperatures in neutral or near neutral water, dissolved oxygen is necessary for appreciable corrosion of iron. In air-saturated water, the initial corrosion rate may be high. This rate may diminish over a period of time as the iron oxide film is formed and acts as a barrier to oxygen diffusion. Since the diffusion rate at steady state is proportional to oxygen concentration, it follows that the corrosion rate of iron is also proportional to oxygen concentration.

In the absence of dissolved oxygen, the corrosion rate at room temperature is negligible both for pure iron and for steel.

Although in deaerated water iron does not corrode appreciably, the corrosion rate in some natural deaerated environments is found to be abnormally high. These high rates have been traced to the presence of sulfate-reducing bacteria. The bacteria thrive only under anaerobic conditions in the pH range of about 5.5–8.5. Certain varieties multiply in fresh waters and in soils containing sulfates, others in brackish water and seawater, and others exist in deep soils at temperatures as high as 60–80°C (140–175°F).

Sulfate-reducing bacteria reduce inorganic sulfates to sulfides in presence of hydrogen or organic matter, and are aided in this process by the presence of an iron surface. The aid which iron provides is to supply hydrogen which is normally adsorbed on the metal surface, and which the bacteria make use of in the reduction of  $\text{SO}_4$ . The bacteria therefore act essentially as depolarizers.

When corrosion is accompanied by hydrogen evolution (for example, iron corroding in hydrochloric acid), the corrosion rate doubles for every 10°C (18°F) rise in temperature.

When corrosion is controlled by diffusion of oxygen, the corrosion rate at a given oxygen concentration approximately doubles every 15–30°C (28–55°F) rise in temperature.

Since corrosion of ferrous metals in most environments involves both processes to some degree, in the absence of any other data, temperature is generally assumed to double the rate of corrosion every 10–15°C (18–28°F) below 80°C.

The effect of pH of an aerated pure (or soft) water on corrosion of iron at room temperature is high at the lower or acidic pH up to about pH of 4. It is stable between pH 4 and 10, then drops gradually to pH 14.

Within the range of about pH 4–10, the corrosion rate is independent of pH and depends only on how rapidly oxygen diffuses to the metal surface. The major diffusion barrier of hydrous ferrous oxide is continuously renewed by the corrosion process. Regardless of the pH of water within this range, the surface of iron is always in contact with an alkaline solution of saturated hydrous ferrous oxide, the pH of which is about 9.5. Within the acid region (pH 4), the surface pH falls, and iron is more or less in direct contact with the aqueous environment. The increased rate of reaction is then the sum of both an appreciable rate of hydrogen evolution and oxygen depolarization. Above pH 10, increase in alkalinity of the environment raises the pH of the iron surface. The corrosion rate correspondingly decreases because iron becomes increasingly passive in the presence of alkalis and dissolved oxygen. So long as oxygen diffusion through the oxide layer is controlling, which is the case within pH 4–10, any small variation in composition of a steel and its heat treatment, or whether it is cold-worked or annealed, has no bearing on corrosion properties provided the diffusion-barrier layer remains essentially unchanged. Oxygen concentration, temperature, and velocity of the water alone determine the reaction rate. These facts are important because almost all natural waters fall within the pH range 4–10. This means that whether a high- or low-carbon steel, or similarly a low-alloy steel, wrought iron, cast iron, or cold-rolled mild steel is exposed to fresh or seawater, all the observed corrosion rates in a given environment are essentially the same.

## CORROSION CONTROL TECHNIQUES

Seven primary corrosion prevention methods are available to reduce the corrosion of metals: material selection, electrical isolation, electrical bonding, environmental modification, inhibitors, coatings, and cathodic protection. Corrosion prevention methods are often used in conjunction with one another. Coatings are used to reduce current requirements in cathodic protection. Zinc is used as a cathodic protection system in coatings. The effects of two or more corrosion prevention systems can be synergistic or antisynnergistic. Two effects are synergistic if the combination of the two is more effective than the sum effect of the two.

### Material Selection

Alloying a metal with a noble metal can reduce its tendency to corrode. Alloys with active metals can reduce corrosion through passivity. A metal is considered passive when the potential for corrosion is large and the corrosion rate is small. Passivity is associated with a thin protective layer formed on the metal surface. An example is the use of an appropriate alloy of stainless steel in seawater.

### Electrical Isolation

Electrically separating one metal, which otherwise would be in direct contact with another dissimilar metal, can prevent the adverse effects of bi-metallic corrosion. A typical example is the use of di-electric unions where copper water pipe is connected to the steel tank of a hot water heater.

### Electrical Continuity

Where stray currents from a man-made source of direct current are a potential problem, metallic bonding the structure of concern to the source of the dc is often used to mitigate the corrosion that would otherwise occur. This is a common method of control where pipelines are subject to the adverse effects from stray currents generated by light rail transit systems, d-c welding machines, and impressed current cathodic protection systems installed on other nearby structures.

### Environmental Modification

Modification of the corrosion environment is a common control method. The corrosion environment can be made less damaging by the removal of active materials (oxygen or chemical composition of the electrolyte). The corrosion environment can be made less damaging by removing materials that reduce the extent or rate of formation of protective layers. A common example is the use of electro-chemical chloride removal systems on steel reinforced concrete structures.

### Inhibitors

A corrosion inhibitor is meant to be the addition of a chemical or chemicals to the fluid phase for its effect on the solid surface of the metal. In view of the fact that the corrosion inhibitor must be effective on the metal side of the

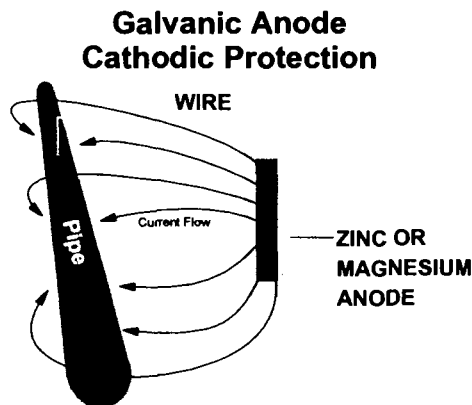


FIG. 2

metal/fluid interface, it is clear that a major aspect of corrosion inhibition is concerned with transport of the inhibitor to the interface. Also, the inhibiting particle must reach the solid surface to be effective, whether it is the material originally introduced or a derivative of the added substance. An example of this is the use of calcium nitrite as an admixed material in concrete, which will be exposed to high chloride environments.

### Coatings

Most coatings function by providing a resistive barrier between the metal to be protected and the environment. Common examples include coal tar epoxies, fusion bonded epoxies, and polyurethanes on buried steel pipelines and tanks. Some coatings provide protection by sacrificing themselves to protect the substrate metal. Galvanizing (zinc-coated) steel is an example. This is a form of cathodic protection. Some coating systems provide corrosion resistance by admixing a corrosion inhibitor to the coating prior to application.

### Cathodic Protection

Cathodic protection is an electrochemical polarization process that is widely and effectively used to limit corrosion. Simply stated, it is an electrical system whose energy operates in opposition to the natural electrochemical decomposition process of corrosion. All cathodic protection systems require the artificial development of an alternative corrosion cell with (-) electrons flowing from the artificially installed anode to the structure in the metallic path. It also requires the flow of (+) ions (atoms or molecules carrying electrical charge) from the anode to the structure by the electrolyte path and/or (-) ions in the opposite direction. For a constant current, the level of protection depends on the polarization slope of the cathodic reaction on the structure. Current can be supplied by a galvanic or impressed current system. In a galvanic system, the electrons flow because of the difference in half-cell potential between the metal of the structure and the cathodic protection anode metal, given that the anode metal is more reactive than the metal of concern. In an impressed current system, an

FIG. 3

a-c to d-c converter/power supply forces these electrons and ions to flow in the appropriate direction.

## SPECIFIC PROBLEM AREAS

### Highways

One example of the type of highway corrosion is the deterioration of culvert pipes. One of the materials used extensively is hot dip galvanized corrugated steel pipe. Accelerated corrosion on these culverts occurs on the invert of the pipe when an extremely aggressive water within the pipe is combined with a high flow rate providing an abrasive scouring action called "erosion-corrosion." For such conditions, remediation usually consists of paving the invert area.

### Tunnels

Many tunnel liners are made of cast iron rings. To date there is no known nondestructive method to test for graphitization on the outside surface of a tunnel. Ultrasonic methods were not effective because of the large graphitic grains. In one case, the length of graphitic grains were measured 1.1 mm (40 mils), and the wave length of sound used was 0.5 mm (18 mils) at the lowest frequency of 1 MHz. High scattering makes bistatic ultrasonic inspection methods unreliable, since the scattering within the specimen produces a background which when combined with increased attenuation of the ultrasound can obscure the backwall echo and make detection difficult. In another case, a large variation in sound velocity occurred between samples or between regions of the same sample. Since large variations in sound velocity correspond to large uncertainties in ultrasonic estimates of wall thickness, the observed grain size distribution raised questions about the suitability of ultrasonic methods for assessment of intact wall thickness. It is of interest to mention that the ultrasonically determined thickness consistently overestimated the thickness of the remaining wall thickness, which could lead to a false sense of security about the integrity of the liner section.

## Bridges

### *Deterioration of Concrete Bridges Due to Corrosion*

The primary cause for deterioration of concrete bridge components is the chloride-induced corrosion of the reinforcing steel. Wedging action resulting from the production of voluminous corrosion reaction products causes cracking and delamination at the steel rebar/concrete interface, ultimately leading to spalling of the concrete.

Normally, reinforcing steel is in a passive state due to the formation of a tenacious passive oxide coating called gamma ferric oxide on the steel surface created by the highly alkaline environment ( $\text{pH} > 12.5$ ) of concrete. However, the presence of chloride ions at the concrete/steel interface in excess of the reaction threshold level 0.5 kg to 1.0 kg of chloride ions/meter<sup>3</sup> concrete (1.0–2.0 lb of chloride ions/yard<sup>3</sup>) depassivates the steel, and corrosion will initiate. On bridges, the source of the chloride ion is usually deicing chemicals applied in the snow-belt areas in winter or salt spray with seawater in coastal areas.

### *Lead Paint [6]*

Highway agencies have been using lead-containing bridge paints for several decades. They have proven to be effective systems for protecting against corrosion and also are forgiving of surface preparation and application quality. Consequently, an estimated 70 % of existing highway bridges in the United States are painted with lead-containing systems. Unfortunately, lead compounds, including those used in bridge paint, are toxic to humans and other life forms. They are cumulative poisons that affect the central nervous system and can lead to debilitating illnesses and eventually death.

The major concern has been the potential entry of lead into the environment, and for this reason it has been regulated by the Environmental Protection Agency (EPA). The EPA has established national ambient air quality standards for lead at 1.5  $\mu\text{g}/\text{m}^3$  averaged over a 90-day period. Sand-blasting of paint containing lead frequently will produce airborne concentrations of lead greater than the maximum permissible by the EPA. However, normally these operations do not last as long as 90 days, resulting in a reduced average emission level. Another potential detrimental effect is the formation of silt deposits under the bridges, which can affect spawning grounds of fish. The pollution of soil by lead residues is a problem that tends to be localized, and good housekeeping can minimize this problem.

There is a variety of techniques that may be suitable for containing debris from the paint removal process. These include tarps and drapes, screens, rigid structure containments, dust collectors, vacuum blasting, power tools with vacuum attachment, and wheel blasting devices. The need for and efficiency of these techniques are highly dependent on the environmental conditions, structure configuration, and ability to take part or all of the structure out of service during the restoration process.

Waste disposal is a national problem extending beyond the scope of bridge paints. Procedures developed by other industries may be applicable to lead debris containment. The key to any approach is the economics of the processes. These numbers are often difficult to determine precisely because of the uncertain costs of hazardous waste disposal, and the larger uncertainties of whether a waste is hazardous to begin with.

It is important that the highway community continues to work with environmental agencies and regulators, because these groups usually have the final say in what is acceptable.

## TEST METHODS TO EVALUATE CORROSION

### Material Selection [7]

A large variety of materials, ranging from steel to concrete, is used by the engineer to construct bridges, roadways, tunnels, etc. The corrosion engineer is primarily interested in the chemical properties (corrosion resistance) of materials, but he or she must have knowledge of mechanical, physical, and other properties to assure desired performance. The properties of engineering materials depend upon their physical structure and basic chemical composition.

Selection of material must be done in conjunction with selection of the manufacturing method. It must be assumed that the material will be selected from among those candidate materials that meet all design and engineering requirements with emphasis on corrosion resistance or control, or both. Selecting a material for economy in manufacture involves consideration of several factors:

1. Raw material factors include chemical composition, form of mill product, size of mill product, material condition or temper, surface finish, and quality characteristics.
2. Processing factors include formability, machinability, weldability, response to heat treatment, and coatability.
3. General factors include quantity of material required, availability of grade and product form, plant standardization of grades and sizes, energy consumption, and availability of required processing equipment.

Because these factors are interdependent and strongly influenced by variables in the manufacture of the material and of the component made from it, none should be considered singly. Once all pertinent factors have been assembled, the different options should be evaluated for their effects on total cost. Standard specifications, such as those developed through ASTM, AASHTO, ASME, or NACE, may establish unified requirements for all of the selection factors described.

Corrosion tests are in two broad categories: (1) tests performed in the laboratory under controlled conditions, and (2) tests performed in the field under actual service conditions.

Tests performed in the laboratory give an early indication of what will happen in the field. These tests can be of a comparative nature where results are compared with known environments with known corrosion rates. These relative results can be very definitive. Field tests, on the other hand, take us one step closer to the end use. Some field tests will last from a few hours to a few days, while some ongoing testing/monitoring procedures may use months or even years.

### In-Service Monitoring

Monitoring the performance of materials while in actual service is very important, especially when it can be used to predict the life expectancy or remaining life.

### Atmospheric Environment [8]

One of the sensors used to measure the corrosivity of the atmosphere is the time-of-wetness. This is a moisture sensor that monitors the presence of surface moisture in conjunction with atmospheric corrosion testing. Both types Zn/Au and Cu/Au cells are equally effective. The time-of-wetness of a surface will vary not only from one locality to another and from one month or year to another, but also with type, size, and orientation of a specimen exposed to a given atmosphere.

### Soil and Natural Water Environments

Monitoring corrosion in soil and water extensively often uses reference electrodes. A reference electrode [9] is a pure metal in contact with a solution of known concentration of its own ion, and at a specific temperature develops a potential that is characteristic and reproducible; when coupled with another half-cell, an overall potential develops which is the sum of both half-cells.

Electrochemical sensors and techniques recently have been developed to test the corrosivity of the environment as well

as the corrosion rate of materials in several environments (Fig. 4). They have proven very useful and effective in predicting and controlling the corrosivity of the environment. One means gaining ever increasing use is the burial of small steel coupons of the same metal type as the structure in the same environment. The coupons are electrically connected to the structure and thus behave the same as the pipe itself. Metallic corrosion is usually an electrochemical process [10]. Electrochemical processes require anodes and cathodes in electrical contact and an ionic conduction path through an electrolyte. The electrochemical process includes electron flow between the anodic and cathodic areas, which quantify the rates of the oxidation and reduction reactions that occur at the surfaces. Monitoring this electron flow to or from the coupon provides the capability of assessing the kinetics of the corrosion process, including the continuing metal loss. These same coupons can be subjected to other electrochemical test methods for correlation with the current flow measurements. Finally, the coupons can be selectively retrieved for physical examination throughout the structure life.

Most forms of metallic corrosion, including uniform, localized, galvanic, dealloying, stress corrosion, and hydrogen-induced failure, can be tested by electrochemical techniques. Passivation, cathodic and anodic protection, and performance of barrier and sacrificial coatings on metals can be tested by electrochemical techniques [11]. Some of the more common techniques include Linear, ELogI and Tafel Polarization, Pitting Scans, and Variable Frequency Electrochemical Impedance Spectroscopy.

### Failure Analysis [12]

Failures of materials in service usually are traceable to misapplication resulting from: wrong choice of the material, improper treatment or fabrication of the material, an inadequately controlled environment, or improper design.

The technical literature is very reliable in helping the decision makers to select the appropriate material for the specific application and environment and can narrow the choice of materials to a manageable number of alternatives from which a final choice can be made quickly. Material suppliers are excellent sources of guidance in selection of proper alloys. Major suppliers of materials often maintain a staff of consultants to advise customers on the proper use of their material.

The sources of electrochemical driving force for corrosion reactions merit a special attention. The major causes for developing corrosion currents are given in Table 1.

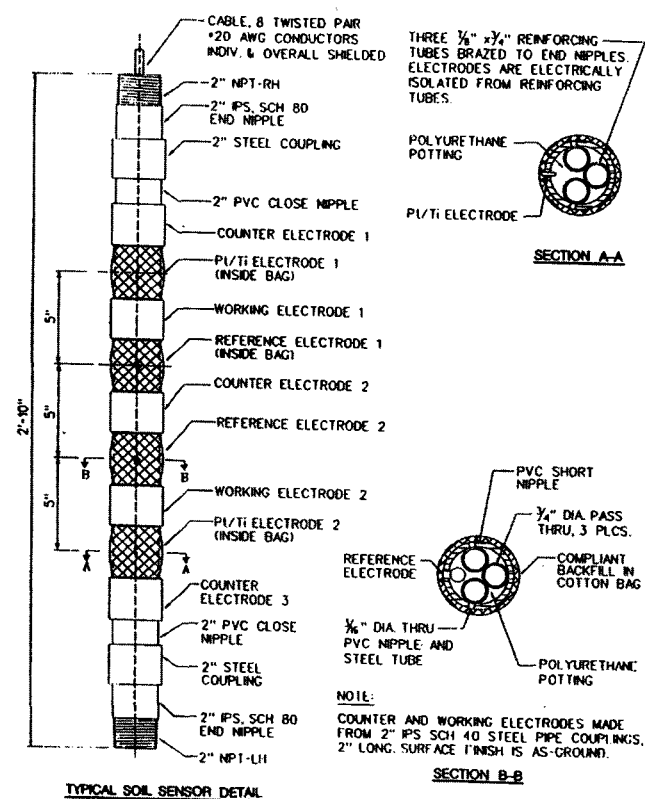


**FIG. 4—Soil sensor for electrochemical measurements, made of two reference electrodes, two working electrodes, and three counter-electrodes, all connected to their own shielded twisted pair cable. At the terminal box, they can be accessed in various combinations depending on the tests required. It also has two platinized titanium electrodes equally spaced with the reference electrodes to allow for the measurement of the average soil resistivity by the Wenner four-electrode method. The two working electrodes can be designed to represent the different conditions of the structure being monitored.**

**TABLE 1—Causes of corrosion currents.**

• Impurities in the metal.	• Differential pre-exposure to air or oxygen.
• Orientation of grains.	• Differential concentration or composition of solution.
• Grain boundaries.	• Differential aeration.
• Different grain size.	• Differential heating.
• Different thermal treatment.	• Differential illumination.
• Surface roughness.	• Differential agitation.
• Local scratches or abrasions.	• Contact with dissimilar metals.
• Difference in shape.	• Externally applied potentials.
• Difference strain.	• Complex cells.

**TABLE 2**—Classification of corrosion attack.

By Visual Appearance:	By Case of Attack:
<ul style="list-style-type: none"> <li>• Uniform, general attack.</li> <li>• Pitting (sometimes caused by a crevice).</li> <li>• Intergranular corrosion.</li> <li>• Selective leaching (may be uniform).</li> </ul>	<ul style="list-style-type: none"> <li>• Galvanic or bimetallic corrosion.</li> <li>• Crevice corrosion or concentration cell corrosion.</li> <li>• Erosion-corrosion.</li> <li>• Stress corrosion (sometimes intergranular).</li> </ul>

SOURCE: Fontana, M. G. and Greene, N. D., *Corrosion Engineering*, McGraw Hill, New York, 1967.

Much can be deduced from examination of materials that have failed in service. It is often possible by visual examination to decide what corrosion mechanisms have been responsible for the material degradation and what corrective measures are required to solve the problem. Fontana and Greene list eight common forms of corrosion based on the physical appearance of a corroded part, given in Table 2.

The corrosion engineer often finds himself confronted with a corroded sample taken from a failed structure. Usually some stopgap action must be taken immediately so that the structure can be placed in service as soon as possible. Then a decision must be made for further action to avoid recurrence of the failure. Often this involves planning and conducting a test program under simulated conditions to determine the factors responsible for the failure [18].

## TEST METHODS

### ASTM [13]

The following standards have been developed by ASTM Committee G 01 on Corrosion of Metals and is annually updated and printed in Volume 03.02, Section 3. They can be used to test materials selected for a transportation application:

- G 33 Practice for Recording Data from Atmospheric Corrosion Tests of Metallic-Coated Steel Specimens.
- G 46 Practice for Examination and Evaluation of Pitting Corrosion.
- G 50 Practice for Conducting Atmospheric Corrosion Tests on Metals.
- G 51 Test Method for pH of Soil for Use in Corrosion Testing.
- G 52 Practice for Exposing and Evaluating Metals and Alloys in Surface Seawater.
- G 57 Method for Field Measurement of Soil Resistivity Using the Wenner-Four Electrode Method.
- G 60 Method for Conducting Cyclic Humidity Tests.
- G 78 Guide for Crevice Corrosion Testing of Iron-Base and Nickel-Base Stainless Alloys in Seawater and Other Chloride-Containing Aqueous Environments.
- G 79 Practice for Evaluation of Metals Exposed to Carbonization Environments.
- G 84 Practice for Measurement of Time-of-Wetness on Surfaces Exposed to Wetting Conditions as in Atmospheric Corrosion Testing.
- G 87 Practice for Conducting Moist SO<sub>2</sub> Tests.
- G 91 Practice for Monitoring Atmospheric SO<sub>2</sub> Using the Sulfation Plate Technique.
- G 101 Guide for Estimating the Atmospheric Corrosion Resistance of Low-Alloy Steels.

- G 104 Test Method for Assessing Galvanic Corrosion Caused by the Atmosphere.
- G 109 Test Method for Determining the Effects of Chemical Admixtures on the Corrosion of Embedded Steel Reinforcement in Concrete Exposed to Chloride Environments.

### NACE Standards [14]

The following standards have been developed by NACE:

- RP0169 Control of External Corrosion on Underground or Submerged Metallic Systems.
- RP0172 Surface Preparation of Steel and Other Hard Materials by Water Blasting Prior to Coating or Recoating.
- RP0281 Method for Conducting Coating (Paint) Panel Evaluation Testing in Atmospheric Exposures.
- RP0187 Design Considerations for Corrosion Control of Reinforcing Steel in Concrete Structures.
- RP0287 Field Measurement of Surface Profile of Abrasive Blast Cleaned Steel Surfaces Using Replica Tape.
- RP0290 Cathodic Protection of Reinforcing Steel in Atmospherically Exposed Concrete Structures.
- RP0390 Maintenance and Rehabilitation Considerations for Corrosion Control of Existing Steel Reinforced Concrete Structures.

### Others

The main organization that develops standards for transportation is the American Association of State Highway and Transportation Officials (AASHTO) [1].

For standard specifications for transportation materials and methods of sampling and testing: Part 1 of the standard is for specifications and Part 2 of the standard is for conducting the tests.

## DISCUSSION

### Unresolved Issues

Many of the existing infrastructures contain elements in need of research to reveal long-term potential problems. This section enumerates two of these issues as an example to stimulate the engineer's thinking.

**Case No. 1:** Many of our infrastructures are built on soils containing aggressive chemical ions and moisture, supported on steel piles. There are no available data on the corrosion rate of such piles exposed to these types of soils, nor the long-term durability of such combinations, nor is there any standard test procedure for evaluating this over the structural life. It should be noted that one set of soldier piles supporting a 60-story office building in a marine environment was recently inspected by basement sidewall excavation. The 27 in. web by 14 in. flange by 75 ft deep piles had suffered more than 15 % web loss in less than three years service.

**Case No. 2:** Many tunnels were built with cast iron rings flanged and bolted together. One surface of the cast iron is exposed to soils and water of various corrosivity. It is

necessary to have a nondestructive method to evaluate that surface, especially to determine the degree of graphitization. Ultrasonic equipment was used unsuccessfully, in some cases, where the graphite fibers were large enough to obstruct the sound signal.

**Case No. 3:** Most bridge decks and substructures constructed or rehabilitated within the last 20 years have been constructed with fusion-bonded epoxy coated reinforcing bars. There are some test data that support the effectiveness of this methodology in solving the chloride induced corrosion activity over the first 20 years of use. These researchers hypothesize that the reduction in corrosion is due both to the coating serving as a barrier between the steel surface and chloride contaminated concrete, and also due to the coating electrically isolating the upper mat rebar from the lower mat rebar eliminating what is commonly called "macro-cell corrosion" [16,17].

On the other hand, other researchers have proposed that while the coating is indeed stopping the corrosion where the coating is intact, that the process will activate after 20–30 years of service when the chlorides permeate the new concrete where coating holidays exist. If this is the case, and presuming accelerated attack occurs, perforation of the bar will occur at a substantially increased rate. The corrosion product may not be of sufficient volume to spall the concrete providing visual warning of the problem, but could result in substantial structural strength degradation over time.

## Outlook for the Future

The advancements in many of the technical fields, especially the computer field, are impacting positively on corrosion testing, detection, design, monitoring, and life prediction. For example, one solution for Case No. 1 could be the design of a sensor and a computerized program to monitor the corrosion rate at different sites and at different depths. The information can be fed to another computer program to project future performance. The model can be updated with the results of the new data collected until the program is perfected. A sketch of such a sensor developed for use in soils is shown in Fig. 1.

Case No. 2 may be resolved by either a technique using magnetic flux leakage, or a technique using time-resolved infrared radiometry.

The principle of the first technique can be understood if a plate is thought of as the "keeper" of an electromagnet of field strength approximately 1000 gauss (tesla). Depending on the permeability of the keeper material and the thickness of the plate, most of the magnetic flux from the magnet will be confined within the plate itself. There is, however, a component of the field exterior to the plate. As the plate thickness changes, so does the exterior leakage field. Correspondingly, if the plate contained a nonmagnetic inclusion or had a part of its backwall replaced with nonmagnetic material, then the leakage flux would increase in the region of anomalous properties. As an extension of the method, if the field of the electromagnet varies sinusoidally, then the degree of flux penetration depends on the frequency of the field variation. In both cases, moving the electromagnet over the plate and measuring the leakage flux permits regions

that have graphite or other magnetic intrusions to be found. It may be possible to determine the degree of graphitization of an entire tunnel plate by varying the field modulation frequency at a fixed position in a single integrated measurement.

The principle of the second technique can be briefly explained as the measurement of surface temperature change of a solid object via infrared radiometry while the object is heated with an external source. The changes in temperature are typically less than 20°C. Since the surface temperature depends on the balance between the rate of heat input from the source and the rate of heat loss into the object, it will change as the rate of heat loss changes. In the case of a plate backed with another material of different thermal properties, the surface temperature changes with time during the heating pulse and then changes again at a time corresponding to the thermal diffusion time through the plate. The sign of the latter change depends on the relative thermal characteristics of the plate and the backing material. By measuring the time at which this second change occurs, the plate thickness can be determined.

Case No. 3 requires additional systematic testing, exhumation, and critical examination of existing structures involving dozens of bridge structures from different regions throughout the U.S. The structures, constructed with fusion bonded epoxy coated bar, must have been in service in high chloride environments for between 20 and 30 years. Part of the structure selection process has to include determination that chlorides have permeated to the rebar mat level at sufficient concentration levels to activate substantial corrosion if the structure were constructed from bare rebar.

If we are expected to resolve some or most of these problems, research funds will have to be budgeted and research programs will have to be developed and encouraged.

## REFERENCES

- [1] Standard Specifications for Transportation Materials and Methods of Sampling and Testing, American Association of State Highway and Transportation Officials (AASHTO), Washington, DC, 2001.
- [2] Bickel, J. O. and Kuesel, T. R., *Tunnel Engineering Handbook*, Krieger Publishing Company, Malabar, FL, 1992.
- [3] Dean, S. W., "Corrosion Testing of Metals under Natural Atmospheric Conditions," *Corrosion Testing and Evaluation, Silver Anniversary Volume, ASTM STP 1000*, R. Baboian and S. W. Dean, Eds., ASTM International, West Conshohocken, PA, 1990.
- [4] Chaker, V., "Corrosion Testing in Soils—Past, Present, and Future," *Corrosion Testing and Evaluation, Silver Anniversary Volume, ASTM STP 1000*, R. Baboian and S. W. Dean, Eds., ASTM International, West Conshohocken, PA, 1990.
- [5] Uhlig, H. and Revie, W. R., *Corrosion and Corrosion Control*, John Wiley and Sons, New York, 1985.
- [6] Appleman, B. R., "Lead Paint Regulations Challenge Bridge Workers," Steel Structures Painting Council, Pittsburgh, PA, (SSPC 89-02).
- [7] *Metals Handbook, Selection for Economy in Manufacture*, American Society for Metals, Metals Park, OH.
- [8] Sereda, P. J., et al., "Measurement of the Time-of-Wetness by Moisture Sensors and Their Calibration," *Atmospheric Corrosion of Metals, ASTM STP 767*, S. W. Dean and E. C. Rhea, Eds., ASTM International, West Conshohocken, PA, 1982.



- [9] Brasumas, A. de S., "Glossary of Corrosion Related Terms," *NACE Basic Corrosion Course*, NACE, Houston, TX 77218-8340.
- [10] Scully, J. R., "Electrochemical Methods for Laboratory Corrosion Testing," *Corrosion Testing and Evaluation, Silver Anniversary Volume, ASTM STP 1000*, R. Baboian and S. W. Dean, Eds., ASTM International, West Conshohocken, PA, 1990.
- [11] *Corrosion Testing and Evaluation, Silver Anniversary Volume, ASTM STP 1000*, R. Baboian and S. W. Dean, Eds., ASTM International, West Conshohocken, PA, 1990, pp. 376–378.
- [12] Verink, E. D., "Analysis and Correction of Corrosion Failures," *NACE Basic Corrosion Course*, NACE, Houston, TX 77218.
- [13] *1994 Annual Book of ASTM Standards*, Vol. 03.02, Wear and Erosion; Metal Corrosion, Section 3, Metals Test Methods and Analytical Procedures, ASTM International, West Conshohocken, PA, 1994.
- [14] *NACE 2001 Book of Standards*, NACE, Houston, TX 77084-4906.
- [15] "Marine Corrosion in Tropical Environments", S. W. Dean, G. H. Delgadillo, and J. B. Bushman, Eds., *ASTM STP 1399*.
- [16] Effectiveness of Epoxy-Coated Rebar: Final Report to Pennsylvania Department of Transportation, Project No: 94-05.
- [17] Performance of Epoxy-Coated Rebars in Bridge Deck; FHWA-RD-96-092.
- [18] G161-00 Standard Guide for Corrosion-Related Failure Analysis.

# Marine—Piers and Docks

James F. Jenkins<sup>1</sup>

## COMMONLY USED CONSTRUCTION MATERIALS AND SELECTION CRITERIA

THE MOST COMMONLY USED materials for construction of piers and docks are reinforced or prestressed concrete, steel, and timber. Composite materials are used primarily for mechanical applications such as pipe hangers and railings, but the use of composite materials in structural applications such as piling and gratings continues to increase. Other metals, primarily stainless steels and aluminum alloys, are often used for mechanical applications and fasteners. The primary criteria for selection of materials for marine piers and docks are past experience, cost, and availability. However, corrosion testing is used to evaluate candidates for many specific applications. This testing is commonly in the form of the evaluation of either full-scale or subscale components, but direct testing of base materials is also performed in many cases.

### Reinforced and Prestressed Concrete

The interactions between reinforced concrete, prestressed concrete and the marine environment are very complex. From the corrosion standpoint, the primary consideration is protection of the embedded steel from attack by the aggressive marine environment. This protection may rely solely on the ability of the ordinary concrete cover to protect the embedded steel or may be augmented by the addition of corrosion inhibitors to the concrete, by coating of the steel, by cathodic protection, or a combination of one or more of these methods.

While ordinary carbon or alloy steel is used most commonly for reinforcement or prestressing of concrete, stainless steels have been used in construction of piers with special service requirements [1] or in critical areas on other structures [2]. Other materials such as reinforced plastics and nickel-copper alloy 400 have been used also to a limited extent or have been proposed for use as reinforcement for concrete in piers and docks. Stainless steel clad carbon steel is a relatively new development and its use for reinforcement of marine structures currently is being evaluated. Epoxy-coated carbon steel reinforcement also has been used successfully in many marine applications, but some failures have occurred.

### Carbon, Alloy, and Stainless Steel

Carbon and low-alloy steels are the predominant alloys used for construction of waterfront structures. In most applications the steels are protected by protective coatings in the atmospheric, splash, and intertidal zones (including metallic and elastomeric sheathing) and are protected by either cathodic protection alone or by a combination of coatings and cathodic protection in the immersion zone. Use of stainless steels is limited predominantly to mechanical applications rather than structural applications. The use of stainless steel fasteners is common.

### Timber

Timber is used widely in the construction of waterfront facilities. Its durability is limited by biological attack, primarily due to marine boring organisms in the immersion zone and termite and fungus attack in the atmospheric zone. Due to recent success in reducing levels of pollutants in many harbor facilities, marine borer activity has increased greatly in many harbors. In many cases, the life of timber in these locations has decreased to the point that alternative materials are more cost-effective for repair or new construction. In addition, many of the traditional treatments for timber to reduce biological attack are now regulated for environmental reasons, thus either making them unavailable or more costly to use. Thus, although timber continues to be used, it is being supplanted by other materials particularly in the submerged and intertidal zones of many marine structures.

### Other Metals

The use of metals other than steel usually is limited to mechanical rather than structural applications. Aluminum alloys are, however, sometimes used in structural applications, primarily in the atmospheric zone. Copper-nickel and nickel-copper alloys are used also for sheathing of structures in the intertidal and splash/spray zones.

### Composite Materials

Composite materials such as reinforced plastics are used widely in mechanical applications in waterfront structures. They also have been used in the repair of timber structures as structural bracing. Composite pilings have good resistance to environmental deterioration, but their mechanical

<sup>1</sup>P.E., 329 Drake Street, Cambria, CA 93428

properties such as strength and creep resistance have limited their acceptance for marine structures.

### Selection Criteria

The most commonly used criteria for selection of materials for use in waterfront structures are least first-cost and prior experience. This is unfortunate as least first-cost construction usually does not result in least life-cycle costs when maintenance, repair, and facility life are considered. Prior experience also may not be reliable, particularly if the experience is from a different geographical location or from a structure with a different set of service conditions. In addition, differences in materials, changes in the local environment, and differences in corrosion protection and maintenance may limit the applicability of past experience to new construction.

Selection criteria may be based on a required level of corrosion resistance to meet safety and reliability requirements. More likely, selection will be based on economic considerations. Least first-cost usually is not appropriate and some type of evaluation of life-cycle cost is preferred. There are many methods for making such life-cycle cost analyses. The discounted cash flow method is ideally suited to life-cycle cost analyses that consider both first costs and costs for maintenance and repair over the system lifetime [3].

### Cost of Material

The procurement costs of the materials for initial construction are often the easiest cost data to obtain, and too often are used inappropriately as the sole criteria for materials selection. Materials costs based on a price per pound or other quantity usually are very misleading when used in lieu of total system costs to evaluate alternatives. Usually, in order to ensure that actual life-cycle costs are minimized, other cost factors such as maintenance and repair must be considered.

### Cost of Final Structure

All costs of the structure must be considered, such as the cost of materials, transportation of the materials to the construction site, construction, supervision, and inspection. From this information, first costs for the entire structure may be determined and compared for each of the alternative materials being considered. For example, when comparing the relative cost of a structure reinforced with an epoxy-coated steel versus stainless steel, the labor costs associated with the handling and inspection of the epoxy coated steel, along with the labor and materials costs for retouching of the inevitable coating defects and damage prior to pouring the concrete must be considered. In the case of stainless steel, these labor costs are avoided.

### Cost of Maintenance and Repair

Over the projected life of the structure, the total cost of maintaining the structure, including the costs of inspection, maintenance, and repair, easily can exceed the initial cost. Economic analyses such as the discounted cash flow method allow the designer to minimize the annual cost of ownership of a system by balancing the various costs involved. In many cases, reduction in maintenance through

the use of more expensive, but more corrosion-resistant materials in initial construction can reduce life-cycle cost. Economic analysis allows the designer to balance these cost factors properly.

### Strength

Strength alone is a poor criterion for selection of materials for waterfront structures. High-strength materials usually are not only more expensive than lower strength materials, but are often more susceptible to brittle fracture or corrosion. In many designs for marine structures, stiffness rather than strength is the primary structural consideration and low-strength materials used in thicker sections can have an advantage in section stiffness that can compensate for their lower strength.

### Deterioration Resistance

Resistance to deterioration is an important factor, but the cost of corrosion-resistant materials must be balanced against the benefit of their use in terms of extended life or reduced costs of maintenance and repair.

### Constructability

Construction of marine structures requires specialized knowledge and equipment. This knowledge and equipment exists for traditional materials and configurations. Traditional materials and construction techniques have evolved based on successful experience. With changing materials availabilities and costs, as well as changing environmental considerations, costs of maintenance, and other economic factors, these traditional materials and construction techniques may not be the most cost-effective alternatives. Innovative designs and materials that require variations from traditional construction practices may involve considerable extra expense in the development of new construction techniques and equipment. While the extra costs associated with the use of innovative materials or construction techniques may be justified, the costs must be established and evaluated in terms of overall life-cycle costs.

## CORROSIVE ENVIRONMENTS ENCOUNTERED

Waterfront structures are exposed to a variety of marine environments. The resistance of materials to each of these environments may vary considerably, as well as applicability of various forms of corrosion control in mitigating the anticipated corrosion. The waterfront environment can be divided into five exposure zones: sediment, immersion, intertidal, splash/spray, and atmospheric. In most cases, a single type of material will be used for the sediment, immersion, and intertidal zones. In some cases another material may be used for the splash and spray and atmospheric zones of the structure. An example of this would be the use of a reinforced concrete deck over steel pilings. Due to differences in corrosion activity between these zones, the corrosion performance of many materials is substantially different when exposed to two or more of these zones. Figure 1, taken from Ref 4, shows the result of a classical experiment where the corrosion of a continuous strip of

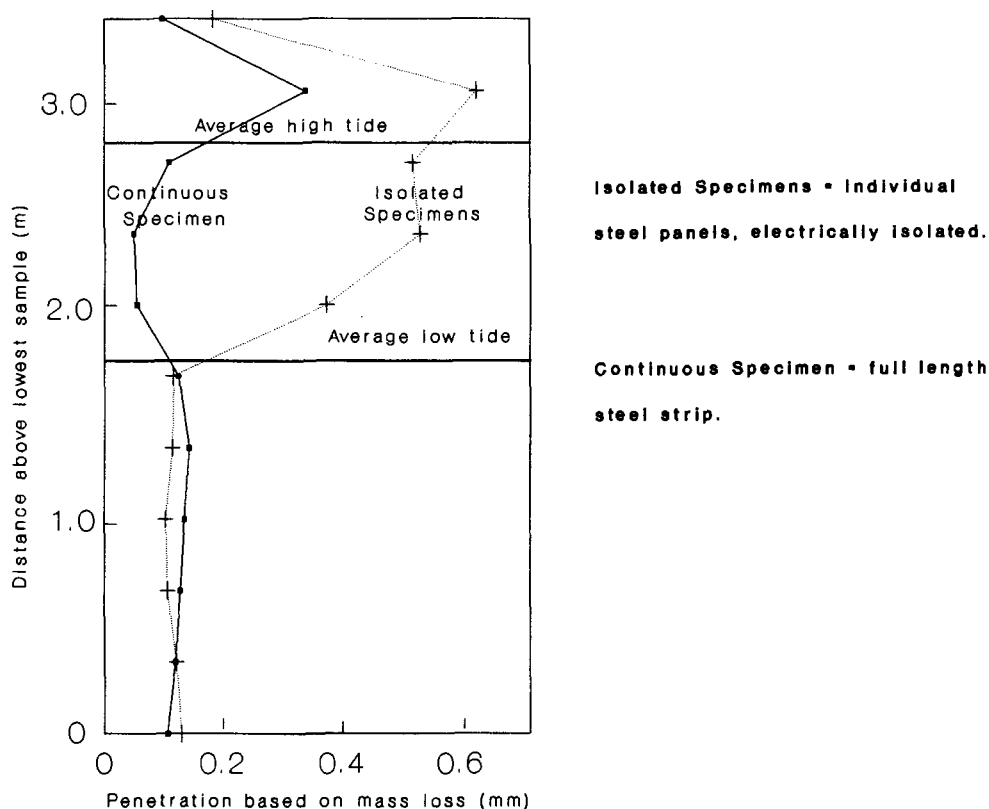


FIG. 1—Variation of corrosion with depth-isolated versus continuous specimens [4].

carbon steel exposed to three marine environment zones is compared to the corrosion of electrically isolated carbon steel panels exposed in the same zones. In this case, corrosion in the intertidal zone on the continuous strip was reduced compared to that of the isolated specimens due to an oxygen concentration cell where the continuously immersed steel was anodic to the steel in the intertidal zone. This effect also is commonly encountered in steel reinforced concrete pilings where the most severe corrosion frequently is encountered just below the intertidal zone where a difference between the highly oxygenated intertidal zone and the lower oxygen immersed zone results in a differential oxygen cell. If the damage is repaired by partial jacketing, the jacket simply drives this differential aeration cell lower on the piling and accelerated corrosion occurs at the bottom of the partial jacket. In other cases, corrosion can be greatly accelerated at the boundary between these zones such as at the mud line.

### Sediment Zone

The sediment zone consists of those portions of the structure that are exposed continuously or intermittently to the bottom sediments. The depth of this zone may vary due to natural sediment movement or to dredging. The sediments usually are characterized by a low oxygen content. In some cases, the conditions are anaerobic and hydrogen sulfide may be present. Cathodic protection can be effective in controlling corrosion of many metals in the sediment zone.

Coatings frequently are used to control the corrosion of steel in the sediment zone by application of the coating prior to emplacement of the structure. *In-situ* coating maintenance usually is not practical.

### Immersion Zone

In this zone the material is exposed continuously to seawater, or in estuarine locations, to brackish or fresh water. Behavior of materials in this zone differs depending upon the geographical location of the structure but is controlled predominantly by the salinity, oxygen content, temperature, and intensity of fouling. Cathodic protection can be effective in controlling corrosion of many metals in the immersion zone. Coating prior to emplacement frequently is used in the immersion zone, but *in-situ* maintenance coating usually is not cost effective due to the high cost of underwater surface preparation and the difficulty of effective coating application.

### Intertidal Zone

Corrosion in the intertidal zone is affected by intermittent immersion conditions. This zone is characterized by the composition of the immersion environment, the composition of the atmospheric environment, and the nature of the tidal variation. When exposed to the air, large amounts of oxygen are available. This affects the corrosion of many metals. For steel exposed to both the immersion and

intertidal zone, corrosion in the intertidal zone may be reduced due to “galvanic coupling” between the steel exposed to both the immersion and intertidal zone. For reinforcing steel in concrete, the intertidal zone is usually the zone of maximum attack. Cathodic protection is effective in mitigating corrosion in this zone and also can mitigate the accelerated attack caused by interzone interactions. Protective coatings, including metallic sheathing, frequently are used to control corrosion in the intertidal zone. Coatings can be maintained either by the use of rapidly curing coatings applied at low tide, coatings that can cure underwater, or preferably by the use of cofferdams that can provide a dry environment for surface preparation, coating application, and curing.

### **Splash and Spray Zone**

The splash and spray zone is often the most aggressive zone on marine structures. In this zone the high availability of oxygen is not offset by galvanic interaction between zones. In many cases, the highest rate of attack is at the boundary between the intertidal and the splash and spray zone. Conventional cathodic protection of steel in this zone generally is not effective, but the steel in reinforced concrete may be protected effectively in this zone using cathodic protection as the concrete is electrically conductive due to entrained water. Coatings frequently are used for corrosion control in the splash and spray zone.

### **Marine Atmosphere Zone**

Above the splash and spray zone, the marine atmospheric environment is characterized by the climatic conditions such as temperature and relative humidity, but is still usually contaminated by salt. Protection of steel in the marine atmosphere zone is primarily through protective coatings. Cathodic protection can be used to protect reinforcing steel in atmospherically exposed concrete.

### **Other Substances Encountered**

The real environment of marine piers and docks contains many potentially corrosive substances. These materials must be considered in the testing and selection of materials. They are of primary importance in the atmospheric zone but also can be of importance in other exposure zones. For example, bird droppings are an inevitable feature of marine pier and dock environments. They can be extremely aggressive toward many materials, particularly the aluminum alloys. Materials handled during loading and unloading operations also can be corrosive and potential contact of these materials with the construction materials must be considered during materials testing and selection.

## **TECHNIQUES USED FOR CORROSION CONTROL**

For permanent installations, few commonly used construction materials have sufficient inherent resistance to corrosion to perform adequately without the use of some

form of corrosion control. In order for the selection of the most cost-effective combination of materials and corrosion control techniques, the efficacy of the corrosion control technique for specific materials must be determined. This normally requires testing. This testing may be performed by accelerated laboratory tests in order to find the most promising alternatives. The most promising alternatives may be compared in field tests.

### **Protective Coatings**

Protective coatings are widely used for controlling corrosion of marine structures. For proper selection of coatings, many factors must be considered including the zone of exposure, degree of shelter, the substrate to be protected, and the potential for recoating. Testing for determination of coating performance must consider all of these pertinent factors in order to provide a valid basis for selection of coatings. While there are no specific standards for coating piers and docks, standards for other marine structures such as NACE RP-0176 (Corrosion Control of Fixed Offshore Platforms Associated with Petroleum Production) contain information that is applicable to marine piers and docks.

### **Cathodic Protection**

Cathodic protection is used widely for the protection of submerged steel in waterfront structures. It also can provide considerable benefit in the intertidal zone and can even reduce the usually high corrosion rate experienced at the boundary between the intertidal zone and the splash and spray zone. Cathodic protection also is used to prevent corrosion of the soil side of steel in marine structures such as sheet steel bulkheads. Cathodic protection also is effective in the control of the corrosion of reinforcing steel in concrete in all exposure zones in waterfront structures. Particularly for impressed current systems, it is important to select materials for the cathodic protection system components such as rectifiers and junction boxes with consideration of the environment to which they will be exposed. When considering cathodic protection, periodic inspection and maintenance is required for proper system operation. The costs for inspection and maintenance must be considered in the overall cost of cathodic protection. While there are no specific standards for cathodic protection of piers and docks, information in NACE RP0176 (Corrosion Control of Fixed Offshore Platforms Associated with Petroleum Production) and NACE RP-0187 (Design Considerations for Corrosion Control of Reinforcing Steel in Concrete) contain information that is applicable to marine piers and docks.

### **Design**

Proper consideration of materials performance in the design process can be the difference between a successful structure and an unsuccessful one. Often simple changes, such as the inversion of structural shapes to provide drainage as shown in Fig. 2, can result in significant improvement in corrosion performance with little or no effect on

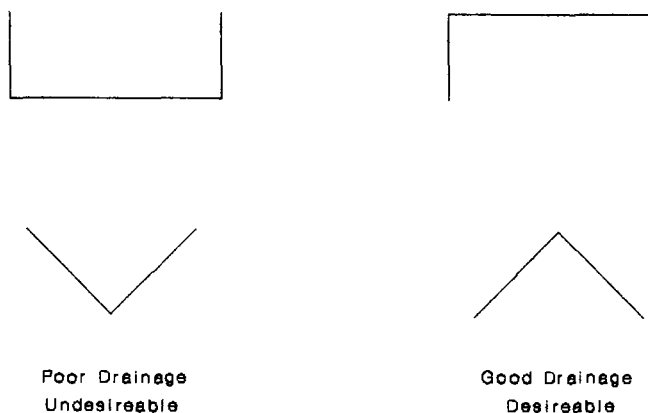


FIG. 2—Effect of orientation on drainage.

cost. When selecting materials, the design features that affect the actual environment that will be encountered must be considered. Elimination of crevices and pockets and avoidance of sharp corners and edges where coatings are to be used are other common design features that can improve resistance to deterioration in many structures.

## SPECIFIC PROBLEM AREAS

Rational design and materials selection must be based on an economic analysis of alternatives. In order to determine the actual costs of the alternatives, projected system life and the need for inspection, maintenance, and repair costs must be known. While there is a great deal of information available on the performance of a wide variety of materials in marine environments, these data are difficult to apply to the projection of system life. Most of the quantitative information on corrosion performance is for isolated specimens and does not address the interzone interactions and effect of design features that occur on real structures. Most of the limited amount of published information derived from the evaluation of actual structures is not quantitative and thus is difficult to use in the design of new structures.

## USE OF TEST METHODS TO EVALUATE CORROSION

There are standard test methods that can be used in the corrosion testing of materials in marine environments, but for corrosion testing of components and systems, the applicability of standard methods is predominantly limited to the evaluation of the corrosion that occurs rather than the overall performance of the tests.

### Materials Testing

Techniques and standards for testing of materials for marine structures are described in Chapter 12 of this manual. These techniques and standards generally are suitable for testing in sediment, submerged, and intertidal environments.

Atmospheric testing techniques and standards described in Chapter 11 are applicable to the splash/spray and atmospheric zones. As indicated previously, these tests give useful information for the design of marine structures but in many cases, additional information on the performance of components and component interactions is needed. Full-scale or subscale testing usually is required for the adequate assessment of techniques and materials for maintenance and repair of marine structures. This testing is required not only to determine the performance of the systems but also to derive cost information applicable to the specific application.

## Performance Assessment

Through the inspection of existing marine structures, significant information on the performance of materials and protective systems can be obtained. Routine inspections for condition assessment or maintenance control are seldom adequate for determining material performance. Quantitative performance data are required for assessment of material performance. Many standard methods are available for the assessment of the various forms of materials deterioration and are given in the section on Field Tests in Seawater (Chapter 12) and in other sections of this manual. Nondestructive testing techniques also can be used for quantitative assessment of deterioration of marine structures. ASTM Standards D 610, D 1654, G 40, G 46 and G 56 contain information that can be used to evaluate corrosion on marine structures. ASTM G 15 gives the terminology applicable to the evaluation on many forms of corrosion that commonly occur on marine structures.

For the assessment of the performance of cathodic protection in mitigating corrosion on marine structures, it is important that adequate records are maintained regarding the performance of the cathodic protection system. In many cases, when the performance of cathodic protection systems is being assessed, it is apparent that the cathodic protection system is capable of providing effective corrosion control but has not been operated and maintained properly. This must not be interpreted as an inadequacy of the technology, but only as the inability of the operators to properly apply the technology.

The performance of many systems for maintenance and repair associated with corrosion of marine structures is difficult to assess, as the performance of these systems is highly dependent upon the skill of the maintenance and repair personnel. In evaluation of such systems, it is advisable to evaluate the effect of personnel skill levels on the efficacy of the techniques and material by using the same maintenance and repair technique applied by several individuals or crews. The primary evaluation should be of the ability of the systems to mitigate corrosion, so the corrosion assessment techniques and standards outlined previously can be used.

## TEST METHOD DEVELOPMENT

*In-situ* exposures using actual structures, full-scale structural elements, or subscale structural elements exposed to the appropriate zones at the specific site for the actual

structure are preferred. Similar tests performed at a different test site usually will provide adequate results if the locations have similar environmental conditions.

Environmental simulation is less desirable as many of the actual environmental conditions as well as the interaction between materials exposed to more than one exposure zone are difficult to simulate in the laboratory.

Accelerated testing has little application to the generation of the performance data necessary for the evaluation of systems for marine structures. It is difficult, if not impossible, to quantitatively predict structure life from such tests. Accelerated testing, however, can be useful in screening candidate materials and systems so that the best alternatives can be evaluated in *in-situ* tests.

Standard laboratory type electrochemical tests can be used to establish the mechanisms of corrosion of materials in marine structures but have little application in providing the performance data required for design, maintenance, or repair. Electrochemical techniques such as ASTM G 71 (Guide for Conducting and Evaluating Galvanic Corrosion Tests in Electrolytes) can be used to determine field performance of materials in practical field structures. In addition, many electrochemical techniques can be adapted to field conditions for the assessment of the performance of components and systems in actual or subscale structures. Examples of such techniques are electrochemical techniques for determining the activity of reinforcing steel in concrete in atmospheric exposures (ASTM C 876).

## TEST METHODS/STANDARDS

Other than applicable standards for the evaluation of corrosion of materials and materials testing in surface seawater given in Chapter 12 of this manual, there are few if any industry-wide standards for evaluating the performance of materials or systems for marine structures.

## OUTLOOK

Due to rapid changes in the cost and availability of conventional construction materials used for marine structures, and the development (or increasing acceptance of) newer materials such as stainless steel for concrete reinforcement and composite materials, the economic balance reflected by conventional practice often is no longer valid. The challenge is to realistically evaluate alternative systems in terms of performance and cost so that new construction and the maintenance and repair of existing structures can be accomplished in a manner that adequate service is obtained at the lowest life-cycle cost.

### Need for Testing Standardization

While the lack of standardization of methods for testing of materials and systems has not been a severe impediment in the past, there is an increased need to rely upon evaluation of actual in-service structures to better establish system life for marine structures. It would be highly beneficial if the marine structure industry would develop a cooperative effort to evaluate existing structures using standardized procedures and techniques so that the information could be published in a form that could be used effectively for future design, maintenance, and repair.

## REFERENCES

- [1] Jenkins, J. F., "Validation of Nitronic 33 in Reinforced and Prestressed Concrete," *Naval Civil Engineering Laboratory Technical Note N 1764*, April 1987.
- [2] *Materials for Marine Systems and Structures*, D. F. Hasson and C. R. Crowe, Eds., Academic Press, Inc., 1988, p. 361.
- [3] *ASM Handbook*, Volume 13, "Corrosion," 1987, p.369.
- [4] LaQue, F. L., *Marine Corrosion Causes and Prevention*, John Wiley & Sons, New York, 1975, pp. 50–52.

# Electric Power

*P. Mayer<sup>1</sup> and A. D. Pellgrini<sup>2</sup>*

CORROSION OF ELECTRIC POWER transmission lines has been a primary cause of in-service equipment degradation. An integral part of the effort to mitigate corrosion processes is the use of standard and nonstandard testing methods for their prevention, correct recognition, and damage extent determination. Corrosion testing also serves multiple functions in equipment design, manufacture, and service life extension.

In the following, a detailed description of all applicable test procedures and devices that have been employed in the corrosion control of power lines will not be attempted. Instead, attention will be directed principally to those corrosion testing methods that are used most frequently in the current practice.

Power transmission is a mature technology that evolved into an optimized system with a very high reliability, based on utilization of traditional low-cost materials and maintenance procedures with a predictable performance. As a result, line equipment can reliably reach the designed operating and asset life with periodic maintenance. Most of the equipment, which has been properly maintained, is in such a good condition at the end of its design life that it is often more economic to refurbish rather than dismantle and build new lines. Consequently, the most frequently employed corrosion tests are those used for quality control during manufacture, performance maintenance scheduling, and condition assessment and service life extension.

## MATERIALS OF CONSTRUCTION AND ENVIRONMENT

The power transmission system in North America consists of equipment that has been built up since the turn of the century. Although the design of individual components has changed, the materials of construction remained virtually the same: steel and cast iron (bare, painted, or galvanized), aluminum alloys and copper alloys, porcelain, glass, and wood. Coatings and inhibitors are used to enhance the corrosion resistance of these materials.

For atmospheric service, zinc dust paints (linseed oil or alkyd) continue to outperform other classes of paints, as

they can be applied directly over some rust with minimal cleaning. For underground service, single component asphaltic and two-compound epoxy mastics are applied most frequently, since a higher degree of surface cleaning, such as abrasive blasting, is feasible. These are, in general, a group of coatings formulated to inhibit corrosion, rather than just provide physical barrier and aesthetic characteristics. In addition, cathodic protection is used to permanently protect the buried steel components. The continued integrity and soundness of the power system components depend mainly on the control of corrosion.

The severity of metal loss and aging process is governed by aggressivity of the environment. Traditionally, the atmospheric environment is classified as industrial, marine, urban, or rural. Recently, efforts have been made to classify the atmospheric corrosivity based on atmospheric data (estimated) or standard panel testing (measured). The atmospheric corrosivity categories range from benign to severely corrosive. This classification is practical for design, scheduling of maintenance, and refurbishment planning.

Corrosion of buried power line components is governed by diffusion of dissolved oxygen in the water entrapped in the soil, resulting in average corrosion rate of zinc and bare steel to be about the same. Copper and lead, which form barrier corrosion films, show lower corrosion rates in the same soils. In marshy and swampy areas, anaerobic sulfate-reducing bacteria (SRB) enhance significantly the corrosion rate of steel. The soils are classified into five classes, which have been found to correlate with the soil resistivity as measured by the Wenner four-pin method. The soil corrosivity range from very low (Resistivity > 10 000  $\Omega\text{cm}$ ), low (Resistivity > 5000 to 10 000  $\Omega\text{cm}$ ), moderate (Resistivity > 2000 to 5000  $\Omega\text{cm}$ ), high (Resistivity > 1000 to 2000  $\Omega\text{cm}$ ), to very high (Resistivity < 1000  $\Omega\text{cm}$ ).

## CORROSION PROBLEMS

Numerous studies have shown that corrosion is the main cause of power line deterioration, and that it affects all components [1].

There are ten broad classes of significant corrosion damages that lead to loss of component function or integrity, or both, if not remedied:

- General corrosion
- Pitting corrosion

<sup>1</sup>Principal Engineer, Kinectrics, 800 Kipling Avenue, Toronto, Ontario, M8Z 5S4, Canada.

<sup>2</sup>President, EP and CC Consulting, 42 Aragon Avenue, Toronto, Ontario, M1T 1X7, Canada.



- Crevice corrosion
- Exfoliation corrosion
- Stress corrosion
- Corrosion fatigue
- Hydrogen embrittlement
- Galvanic corrosion (dissimilar metal, differential, aeration)
- Stray-current corrosion
- Coating damage and deterioration
- Microbial induced corrosion
- Rotting of wood.

## TECHNIQUES FOR CORROSION CONTROL

The main emphasis in power line corrosion control is to select materials resistant to a specific environmental attack and to galvanize ferrous materials (carbon steel and cast iron). This approach is used in the design of new lines and is supplemented by selective use of coatings and cathodic (galvanic) protection. The in-service methods are limited to application of coatings, cathodic protection, and inhibitors.

## NEW POWER LINES

Corrosion testing of new line equipment is often introduced in the product qualification stage and as a part of the quality control during manufacturing. To a lesser degree, corrosion tests are performed to select or screen materials of construction.

For example, connectors used in power equipment and overhead lines are qualification-tested to determine the component resistance to stress corrosion cracking (SCC). Aluminum alloy connectors are subjected to an immersion test [2], in which the connector is attached to the largest conductor for which it is designed and torqued to the reusable stress value, and then immersed in a 7 % NaCl solution for a period of 300 h. For a component to pass, there shall be no visible signs of SCC. This testing is done after the materials were screened using ASTM tests (ASTM G 44<sup>3</sup>, G 47<sup>4</sup>, and G 64<sup>5</sup>) to establish the immunity to SCC. Similarly, copper base alloy connectors [2] are subjected to and shall pass the requirements of the “season cracking” test (ASTM B 154<sup>6</sup>). Attempts have been made in the past to substitute this test with the Mattsson’s solution test (ASTM G 37<sup>7</sup>), due to toxicity and stringent requirements for the disposal of mercurous nitrate.

Other line components, such as conductors, tower steel, and bolts, are not tested routinely for resistance to corrosion, although there is a need for corrosion durability improvements of these components.

<sup>3</sup>Practice for Evaluating Stress-Corrosion Cracking Resistance of Metals in 3.5% Sodium Chloride Solution.

<sup>4</sup>Test Method for Determining Susceptibility to Stress-Corrosion Cracking of High-Strength Aluminum Products.

<sup>5</sup>Classification of Resistance to Stress-Corrosion Cracking of Heat-Treatable Aluminum Alloys.

<sup>6</sup>Method for Mercurous Nitrate Test for Copper and Copper Alloys.

<sup>7</sup>Practice for Use of Mattsson’s Solution of pH 7.2 to Evaluate the Stress-Corrosion Cracking Susceptibility of Copper-Zinc Alloys.

Accelerated weathering tests are being used to develop new long lasting polymeric insulators to replace high-density ceramic and glass.

Tests to determine the aggressivity of environment are used in design of new lines to determine the need for additional corrosion protection of the lines to resist particularly polluted atmosphere, aggressive soil, or water. Coatings and cathodic protection are frequently added to safeguard the lines and to match the service life of other components.

## IN-SERVICE LINES

In recent years, the emphasis of power line operators is on predictive/preventive maintenance to ensure reliable and safe operation. Breakdown maintenance is becoming a thing of the past. Crucial elements of this approach are consistent application of the most up-to-date technological know-how and systematic surveillance of the power lines.

Corrosion tests are an integral part of a wide variety of methods (techniques and tools) employed to establish the condition of overhead lines for maintenance and refurbishment. Although the information needs for maintenance are different from those for refurbishment, the investigation and surveillance methodologies are practically identical. To establish an overall condition of the line for a refurbishment program, a detailed “snapshot in time” is needed. In comparison, a limited periodic survey continuing across the whole system over a long duration is needed to determine maintenance requirements.

The most common method of power line inspection is visual assessment, performed from the ground by foot-patrol or from the air during routine aerial (helicopter) surveillance. This is a very efficient method, but must be used in conjunction with instrumental, chemical, biological, electrical, and electrochemical methods, followed by laboratory failure analysis to obtain a true picture of the line condition.

## FOUNDATIONS

Degradation of foundations enclosed in concrete or grillage-type can be best assessed by excavation. This is the most rigorous method, since it allows the determination of the extent and type of corrosion attack, including possible involvement of microbial induced corrosion. To minimize excavation at every footing, tests to indicate the presence of stray current or a galvanic corrosion, or both, can be used. The stray current and galvanic corrosion can be identified by a potential survey of the footings with a Cu/CuSO<sub>4</sub> half cell reference electrode. The magnitude of the stray current can be measured by using special clip-on d-c ammeters.

New galvanized steel footings, when buried, will exhibit a potential between -0.85 and -1.1 V with reference to Cu/CuSO<sub>4</sub>. After the galvanizing is lost, the newly exposed bare steel surface will have potential between -0.5 and -0.7 V. Corroded steel with a heavy scale will have a potential between -0.3 and -0.5 V. In addition to a potential survey, an electrochemical polarization technique can be used to determine the rate of galvanic corrosion [3]. The device operates by passing a small current between the tower footing

and a probe inserted into the ground nearby. These currents disturb the electrochemical processes at any active corrosion site, and the resulting changes in potential are measured with reference to Cu/CuSO<sub>4</sub> half cell in contact with the ground close to the footing. The level of current required indicates severity of the corrosion process in progress. This instrument provides results that are a useful guide to the relative condition of the footings, but not absolute measure of the metal wastage [3]. For concrete footings, the magnitude of the potential readings is greatly affected by the high resistance of the concrete. Experience and knowledge is required to interpret these readings.

## TOWERS AND TOWER STEEL

Determining correctly the type and extent of power line tower component damage is essential for proper assessment of the structure condition and recommendation for plan of action to ensure safe and reliable operation. Component damage is defined as degradation leading to the loss of the load bearing capacity, which would, if not remedied, lead to tower failure.

The type and extent of the component damage caused by corrosion are determined during field inspection from [4]:

- Detailed visual inspection,
- Measuring loss of cross section and physical shape deformation,
- Measuring protective (galvanizing and/or painted) coating loss, and
- Measuring contamination of surfaces.

During visual inspection, the type of corrosion damage is established at locations where the protective coating was lost. The extent of corrosion damage must be accurately determined to: assess structure's fitness for service condition; estimate the remaining service life; and recommend maintenance, refurbishment, or replacement of the line. The techniques, methods, and instruments used to gage corrosion attack for field or laboratory use, or both, are readily available. These inspection and testing methods are standardized to ensure reproducible results.

The breakdown of protective coating occurs usually by a combination of erosion and physical damage. The extent of erosion (loss of thickness) of an intact coating can be measured by a variety of methods. These include destructive scribing, magnetic pull-off, magnetic flux, eddy current, ultrasonics, etc., gages.

The extent of protective paint loss can be determined using standard methods for evaluating the degree of rusting on steel surfaces (see ASTM D 610<sup>8</sup> and Ref 5) and paint coating degradation (ASTM D 660<sup>9</sup>, D 662<sup>10</sup>, D 714<sup>11</sup>, and D 772<sup>12</sup>).

<sup>8</sup>Test Method for Evaluating Degree of Rusting on Painted Steel Surfaces.

<sup>9</sup>Test Method for Evaluating Degree of Checking of Exterior Paints.

<sup>10</sup>Test Method for Evaluating Degree of Erosion of Exterior Paints.

<sup>11</sup>Test Method for Evaluating Degree of Blistering of Paints.

<sup>12</sup>Test Method for Evaluating Degree of Flaking (Scaling) of Exterior Paints.

Changes in color are an indication of the galvanized coating condition. As galvanizing weathers, it loses its brightness and turns dull gray and becomes progressively darker gray as it gradually erodes. Appearance of yellow and reddish-brown color indicates that the pure zinc coating was lost and the corrosion reddened the zinc-iron amalgam layer. This is the optimal time to paint the structure [6]. When the coating is lost, the surface of the bare steel becomes covered with dark-brown corrosion scale. The galvanizing is considered failed when 5 % of the surface is covered by a dark-brown color. As the percentage of this corroded area increases, higher levels of cleaning are required to remove the corrosion scales, before the paint coating can be applied. If the corrosion is allowed to progress to more than 50 % of the surface area, other corrosion problems, such as hydrogen embrittlement, cracking, pitting, reduced cross section, etc., evolve. Paint coating may no longer be feasible and structure replacement becomes the only option.

The contamination of tower surfaces with aggressive chemicals can lead to enhanced corrosion and deterioration of protective coatings. Although the methods of detection and determination of surface contamination are not standardized, several test methods [7] are accepted by the industry. Surface contamination analysis kits are available [8] to measure pH, chlorides (detection limit 40 ppm) and soluble ferrous ions (detection limit approximately 3 ppm). In most cases, these detection limits are sufficient to establish aggressivity of the operating environment and surface cleanliness before painting.

## WOOD STRUCTURES

Wood pole condition has traditionally been assessed by the sound of an impact on the pole or from the condition of a cored sample of the wood. Recent developments include nondestructive test procedures that offer more refined assessment of wood pole conditions. A device based on the measurement of the passage of ultrasound through the wood was developed [9]. The condition of the pole can be assessed, provided there is an adequate database to calibrate the signal delay time against the measured strength of the particular wood species. The device can only indicate the condition at and above the ground line.

## HARDWARE

Corrosion is a contributing factor to wear damage to hardware caused by aeolian vibration. This damage is very difficult to detect from the ground [10]. Initially, X-ray equipment was taken to the field to enable internal cracks or strand breaks to be detected within clamps or conductors. This was a cumbersome, slow, and costly procedure, and had to be done with the line de-energized. More recently, a line technique using a gamma ray source on hot sticks has been developed that permits detection of the internal damage in a practical manner.

In highly corrosive environments, such as marine, effect of atmospheric corrosion on hardware materials can be

established by using 'CLIMAT' devices [11]. These devices consist of aluminum wires wound tightly around threaded plastic rods. The mass loss of the wire during a 90-day period is measured to indicate the level of corrosion activity and allows mapping of the area in terms of air aggressivity index (Atmospheric Corrosivity Index). These data are valuable to schedule maintenance and evaluate new materials.

## INSULATORS

In marine and highly polluted environments, the steel components of insulators corrode at an accelerated rate. Galvanizing protection is lost early, and the remaining steel forms voluminous oxide scales. The growth of these scales induces large stresses in the ceramic parts leading to cracking, spalling, and failures [12]. The ceramic insulator cracking can be detected by electrical resistance testing.

## OVERHEAD GROUND WIRES

Galvanized steel overhead ground wires age during service, and corrosion is a major contributing factor to this process. A simple technique, based on standard torsional ductility test (ASTM E 558<sup>13</sup>), is being used to determine the remaining life. Based on experience, wire that would break in less than six turns is at the end of the service life and immediate replacement is required. Levels of corrosion and torsional strengths provide planning tools for replacement of the overhead ground wires before in-service failures occur.

## CONDUCTORS

The service life of power lines is limited by the deterioration of the most vulnerable component: the conductor. The deterioration processes include a combination of creep, fatigue, and corrosion. Both traditionally used materials in conductor construction (aluminum alloy and galvanized steel) are prone to corrosion. It was shown [13] that the aluminum alloys suffer from accelerated corrosion in coastal areas, while inland in industrial areas the corrosion attack of the galvanized steel core is most prevalent.

The helicopter borne infrared sensors were employed [14] to inspect power lines for aluminum corrosion. This method is suitable for detection of severe corrosion with many strands distorted and bulging. Early corrosion damage cannot be effectively detected.

The condition of the steel core is a key indicator of the remaining useful life of the conductor. The first step in this assessment is the use of a galvanized steel corrosion detector on in-service lines. Two similar devices have been developed and tested: one based on eddy current technique [15] and the second one using electromagnetic induction [16,17] principle to detect the conductor damage. Following this assessment, samples are removed from the lines and remaining service life is determined using the torsional ductility test (ASTM E 558).

To prioritize maintenance and refurbishment and to select the most suitable materials of construction, the aggressivity of the environment must be established. Passive corrosion tests are the most economical way of mapping large areas accurately. The CLIMAT test [11] and a test [13] comprising of zinc cans and aluminum wire twisted around steel bolts are used most frequently.

## CLOSING REMARKS

Most of the corrosion problems in power transmission can be reliably detected and assessed using conventional and well-established corrosion testing instruments, practices, and methods. The data, from field or laboratory, are essential information for the implementation of ameliorative measures. The corrosion control technology available today can, in a cost-effective way, protect reliability, performance, and safety of transmission lines.

## REFERENCES

- [1] Havard, D. G., "State-of-the-Art Study on Refurbishment of Overhead Lines," Canadian Electrical Association, Report No. ST-342, Montreal, Quebec, 1992.
- [2] Ontario Hydro Standard Specification: "Connectors: Electric Power," M-244-89, Ontario Hydro, Toronto, Ontario, issued April 1989.
- [3] Vorauer, A., "Grillage Corrosion Surveys Using the Tower Leg Integrity Monitor-1989 Results," Ontario Hydro Research Division Report No. 90-102-K, Toronto, Ontario, 1990.
- [4] Mayer, P., Robbins, S., and Pellegrini, A. D., "Automated Diagnostic System for Power Transmission Structures," Paper No. 9498, presented at Corrosion'94, Baltimore, NACE International, Houston, TX, 1994.
- [5] SSPC-Vis-2, Guide to Visual Standard No. 2, "Guide to Standard Method of Evaluating Degree of Rusting on Painted Steel Surfaces," 1982.
- [6] Long, D. J., "The Painting of Galvanized Transmission Towers and Substation Structures," *The Journal of Protective Coatings and Linings*, November 1987.
- [7] Trimber, K. A., "Detection and Removal of Chemical Contaminants in Pulp and Paper Mills," *The Journal of Protective Coatings and Linings*, November 1988.
- [8] KTA SCAT KIT, available from KTA Tator, Inc., Pittsburgh, PA, 15275.
- [9] Goodman, J. R. and Bodig, J., "Survival Prediction of Wood Pole Utility Structures," *Proceedings of Probabilistic Methods Applied to Electric Power Systems*, Pergamon Press, 1986, pp. 441-450.
- [10] Dixon, L. B., "Transmission Line Diagnostic Techniques," *International Conference on Revitalizing Trans. and Distr. Systems*, IEE, London, 1987.
- [11] Doyle, D. P. and Wright, T. E., "A Rapid Method of Predicting Adequate Service Lines for Overhead Conductors in Marine Atmospheres," IEEE Paper 71CP 172-PWR, 1971.
- [12] Maddock, B. J., Almutt, J. G., Ferguson, J. M., et al., "Some Investigations of the Aging of Overhead Lines," CIGRE Paper 22-09, Paris, France, 1986.
- [13] Manning, M. I., Crouch, A. G., Ferguson, J. M., and Lloyd, B., *International Conference on Revitalizing Trans. and Distr. Systems*, IEE, London, 1987.
- [14] Fisher, S. A., Funnel, I. R., and Larsen, S. T., "The Detection of Overhead Line Conductor Damage by Helicopter Borne Thermal

<sup>13</sup>Method for Torsion Testing of Wire.

- Images," Sixth International Symposium on High Voltage Engineering, New Orleans, 1989.
- [15] Sutton, J. and Lewis, K. G., "The Detection of Internal Corrosion in Steel-Reinforced Aluminum Overhead Power Line Conductors," *Proceedings, UK Corrosion '86*, Vol. 1, 1986, Birmingham, UK, pp. 345-359.
- [16] Komoda, M. T., Kawashima, T., Minemura, M., et al., "Electromagnetic Induction Method for Detecting and Locating Flaws on Overhead Transmission Lines," *IEEE Transactions, Power Delivery*, Vol. 5, No. 3, July 1990, pp. 1484-1490.
- [17] Japan IERE Council, Annual Report, Electrical Utilities' R&D—1989-90, Japan IERE Council Document, RA-90, 1991.

# Nuclear Power

*George J. Licina<sup>1</sup>*

MINIMIZING CORROSION IS a primary objective of nuclear power plant design. Such plants use corrosion-resistant alloys and high purity and well controlled water chemistries in critical systems to achieve that objective. Despite such measures, nuclear plants have experienced localized corrosion and environmentally assisted cracking in several plant components. These corrosion events have had significant ramifications on plant operability due to the extremely stringent requirements on component reliability and containment of radio-nuclides. Standards devoted to assessing susceptibility to localized corrosion and stress-corrosion cracking (SCC) have been used to qualify materials and remedial countermeasures. In many cases, the evolution of nuclear plant designs has required development of new standards.

## BACKGROUND

Nuclear power plants convert heat energy from the fission of uranium ( $^{235}\text{U}$ ) into high-quality steam. The steam is used to run large steam turbines and generate electricity. Large amounts of electric power can be produced inexpensively with very long refueling intervals (nominally 18 months or more) and small operating staffs. These typically large plants (600–1200 MWe) are an excellent source for providing “base load” electricity; however, their large size and the long time from design to commercial operation represent a huge investment of time and resources.

The total quantity of fuel material used and the volume of wastes generated by a nuclear plant per kW is very small; however, the radioactive nature of much of the waste requires that they be contained and closely monitored well beyond the life of the plant. The potential dangers of radioactivity to operating personnel, the general public, and other living creatures dictate designs with multiple barriers to the release of fission and activation products. The reliability of each barrier must meet exacting standards to assure that releases to the environment, including leaks to the air or water supply, do not occur.

Corrosion problems in nuclear plants have almost always been associated with localized corrosion phenomena or environmentally assisted cracking. For example, steam generator tubes in pressurized water reactors (PWRs) have experienced wastage and thinning, SCC, intergranular attack,

pitting corrosion, and “denting.” In boiling water reactors (BWRs), recirculation system piping has been degraded by intergranular stress corrosion cracking (IGSCC), especially at weldments. Irradiation assisted stress corrosion cracking (IASCC) has degraded reactor internal structural components. The zirconium alloys used for fuel cladding have been subject to hydriding, SCC, underdeposit corrosion (for example, under crud), and nodular corrosion. The occurrence of rapid general corrosion, pitting, underdeposit corrosion, and microbiologically influenced corrosion (MIC) have prompted increased attention to nuclear service water systems.

## MATERIALS OF CONSTRUCTION AND SPECIFIC CONCERNS

### General

Reliability is far and away the major concern with components in nuclear power plants. Component reliability must be assured for plant safety and to protect the investment in the plant. The very stringent regulations related to release of radioactivity to the environment drive much of the materials selection, environmental controls, and inspection requirements of nuclear plants. Unlike fossil-fueled plants, where repairs of leaking or flawed components are a routine fact of life, the availability of diverse and redundant systems for containment of radioactivity requires a far greater reliability of systems and components in nuclear systems.

### Materials of Construction

#### Primary Systems

Both BWRs and PWRs use zirconium alloys for fuel cladding. The “neutron economy” afforded by low cross section materials, such as zirconium, is critical for efficient operation of the reactor’s core. Zirconium alloys also exhibit good resistance to corrosion in water/steam environments as well as to the high-temperature fission products (the fission of the uranium produces iodine, cesium, cadmium, etc.). The fuel cladding thus represents the first containment barrier to radioactive products. Fuel cladding is also subject to high heat fluxes. The effects of heat flux and neutron and gamma irradiation can be synergistic with the aggressiveness of the high-temperature water environment, producing corrosion

<sup>1</sup>Associate, Structural Integrity Associates, San Jose, CA 95118.

effects that are more severe than those encountered out-of-reactor or in nonheat transfer applications.

Reactor internals include both fixed and movable components. Examples of such components are control rods (movable), in-core instrumentation (fixed and movable), the core shroud, core plate, jet pumps, top guide, and steam separators and steam dryers (all fixed). Austenitic stainless steels are used for the majority of these components for their corrosion resistance. In other specific applications such as in the control rod drives and jet pumps, precipitation-hardened nickel-base alloys (for example, Alloy X-750, UNS N07750) are used where greater corrosion resistance and strength are required.

### Reactor Coolant Systems

Heat transport system piping in most PWRs (Fig. 1) is fabricated from carbon and low-alloy steels, for strength and economy, and clad with roll bonded or weld deposited corrosion-resistant cladding (either stainless steel or high-nickel alloys).<sup>2</sup> Nickel-base alloys are used extensively as weld fillers for cladding and for joints between alloy steels and stainless steels for their superior corrosion resistance.

The primary coolant in PWRs is circulated through the core, where it absorbs heat, through the reactor coolant piping, and to the steam generators where it transfers its heat to a second, high-purity water loop. The water in the secondary loop is heated to steam. That steam is expanded in the turbine where the thermal energy is converted to mechanical energy in order to generate electricity.

The piping arrangement in a BWR is different from that of a PWR. In the BWR, only a single coolant loop is used (Fig. 2). The same water that is heated in the core to produce steam is expanded in the turbine. The water is further cooled in the condenser and is returned to the core as feedwater. Water is rapidly recirculated through the core at about seven to ten times the mass flow rate of steam, most often using jet pumps. Flow from the recirculation pumps "drives" the jet pumps, which have no moving parts. About a third of the flow from the vessel is returned to the recirculation loop. Water in the recirculation loop (Fig. 3) is pumped through a header, through riser pipes, and discharged to the jet pumps, providing the jet pumps' driving flow. In the jet pumps, water in the downcomer region is accelerated through the jet pump, then discharged into the lower core plenum.

Flow proceeds from the lower plenum, through the core. The steam and water are separated; the steam is then dried and passed to the turbine. Other flow (see above) returns to the recirculation system. Feedwater is introduced to the annulus between the core shroud and reactor vessel (Fig. 4). The recirculation system piping is a primary pressure boundary for the high-pressure, high-temperature reactor coolant. Type 304 stainless steel was selected for recirculation system piping and numerous other auxiliary systems (such as the reactor water cleanup system, residual heat removal system, core spray, and other emergency core cooling systems) for its corrosion resistance and adequate mechanical properties. Failures of weld heat affected zones

<sup>2</sup>Stainless steels, typically Type 304, are used in many PWR plants.

FIG. 1—Diagram of a typical PWR piping arrangement [1].

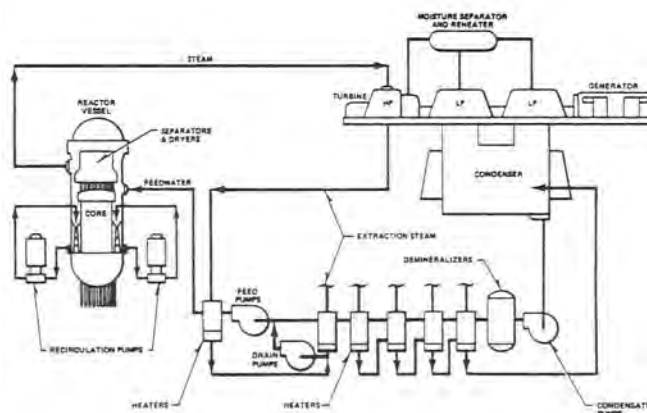


FIG. 2—Diagram of a typical BWR piping arrangement. (Courtesy of GE Nuclear, San Jose, CA.)

(HAZs) by IGSCC in the oxidizing environment resulting from water radiolysis in the core have shown the selection of these stainless steels, at least grades with carbon contents of 0.04 % and above, to have been a poor choice. Remedies, implemented in the most recent designs and in some retrofits, involved the use of special grades with very low carbon contents to avoid sensitization (and higher nitrogen to compensate for decreased mechanical strength), special welding procedures to minimize sensitization, and other remedial procedures to reduce residual stresses at welds. Decreasing the oxidizing power of the high-temperature water environment has also been implemented. This is accomplished by injecting hydrogen into the feedwater to recombine with the oxygen produced by radiolysis.

The BWR also uses some carbon steel and low-alloy steel for steam and other piping (to avoid IGSCC, when corrosion resistance is adequate) and a limited amount of nickel-base alloys (e.g., for reactor vessel/piping safe ends).

### Pressure Vessels and Heat Transfer Components

The key pressure vessels in the PWR system were discussed in the prior section, Reactor Coolant Systems. PWR vessels, including the reactor vessel, steam generator shells,

BWR reactor pressure vessels operate at much lower internal pressures than those of a PWR, of the order of the saturation pressure of steam at reactor operating temperatures (1000 psi/6.89 MPa at 288°C). As a result, BWR reactor vessels (Fig. 6) can be much larger than those of PWRs, which permits much of the equipment (such as jet pumps, steam driers, and steam separators) to be contained within the vessel. These pressure vessels are fabricated from low-alloy steels (SA-533, Grade B; SA-508, Class 2; UNS K12539, K12766) for strength and economy and weld clad with stainless steel for corrosion resistance.

The steam generators in PWRs provide the boundary between the primary (i.e., radioactive) and secondary (non-radioactive) systems. Service experience has proven the steam generator to be a key, if not the key piece of equipment for PWRs. Corrosion problems in the steam generators have been the principal cause of PWR downtime.

Nickel-base alloys (Alloys 600, 690, and 800; UNS N06600, N06690, and N08800) are most commonly selected for steam generator tubes for their good heat transfer properties and excellent resistance to all forms of corrosion. The thin-walled steam generator tubes have no corrosion allowance; hence, essentially any degradation constitutes a failure of the tube.

Like the steam generator shell, tubesheets are fabricated from low-alloy steels for their strength and economy. In some designs, the tubesheets are clad with stainless steel or nickel-base alloys for corrosion resistance.

On the secondary side of the steam generator (i.e., where the steam is actually generated), carbon steel tube support plates have been used (Fig. 7). This selection was based upon economics since the support plates have minimal structural function and represent a small area exposed to the coolant; the amount of iron released to the system from corrosion of the spacers can easily be accommodated by the cleanup system. Selection of carbon steel support plates (for example, SA-515, Grade 6; UNS K02401) proved to be a poor choice. Corrosion of the support plates, especially those with drilled holes, resulted in a thick, adherent magnetite corrosion product. The magnetite buildup caused a significant change in support plate dimensions (a decrease in the size of the holes), producing stresses that were sufficient to deform ("dent") steam generator tubes. Ferritic or martensitic stainless steel tube support plates are used in newer designs.

#### *Power Conversion and Auxiliary Systems*

The power conversion system and the balance of plant components for nuclear plants are similar to those for fossil plants with a few significant differences. First, fossil plants are generally much smaller than nuclear plants; hence, many of the key components in the power conversion system are smaller. Second, fossil plants generally operate at significantly higher temperatures (i.e., steam may be superheated from a few degrees to hundreds of degrees). The requirements on the power conversion system are, therefore, much different. The great emphasis on reliability of nuclear units often affects design and materials selection of power conversion or balance of plant components. Finally, the "diverse and redundant" design philosophy inherent in the design of nuclear plants requires greater numbers of heat exchangers, pumps, and valves, and far more piping in the

**FIG. 3—BWR recirculation loop. (Courtesy of GE Nuclear, San Jose, CA.)**

and pressurizer (Fig. 5), operate at pressures of the order of 2000 psi (13.8 MPa) and temperatures of up to 625°F (330°C). These vessels are fabricated from low-alloy steels (for example ASME SA-302, Grade B; SA-533, Grade B; SA-508, Classes 1, 2, and 3; UNS K12022, K12359, K12042, and K12766) and clad (usually weld clad) with stainless steels or nickel-base alloys. The alloy steel provides adequate strength at a reasonable cost for the thick-walled vessels. The stainless steel cladding provides corrosion resistance.

**FIG. 4—Jet pump. (Courtesy of GE Nuclear, San Jose, CA.)**



**FIG. 5—(a) Westinghouse Model F Recirculating Steam Generator (from Ref 1); (b) ABB Combustion Engineering System 80® Recirculation Steam Generator (reproduced with permission from Combustion Engineering, Inc., Windsor, CT); (c) Babcock & Wilcox Once-Through Steam Generator.**

**FIG. 6—BWR reactor pressure vessel. (Courtesy of GE Nuclear, San Jose, CA.)**

balance of plant than in a fossil-fired unit of comparable power output. Many of these systems operate very infrequently. The most common operational conditions for many of these systems is a monthly or quarterly demonstration of their operability to assure their functionality in the event of an accident.

Nuclear units use all of the commonly used condenser materials including brass (particularly Admiralty and aluminum brass), copper-nickel (90-10 and 70-30), stainless

steels, and titanium tubes, and Muntz metal and stainless steel tubesheets. Many retubed condensers have used specialty alloys such as titanium or the so-called super ferritic (high chromium; very low carbon; molybdenum contents to 4 %) or super austenitic (basically 20 % Cr-25 %Ni and up to 6 %Mo) or duplex stainless steels to eliminate pitting, SCC, and MIC. Tube replacements, with titanium or super stainless steels, have been performed most often in saline cooling waters; however, the critical nature of some heat

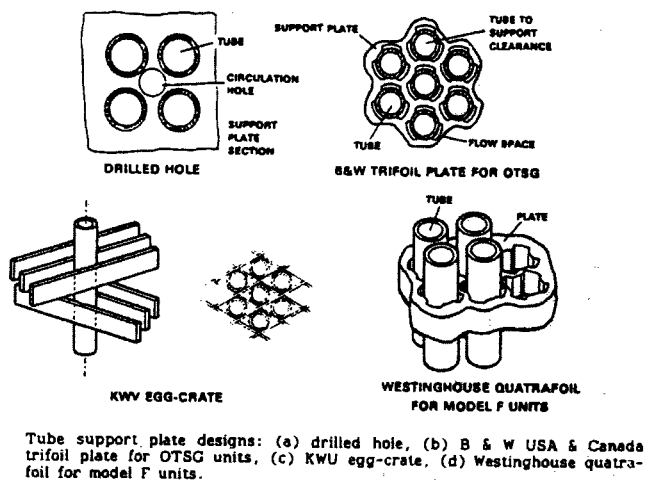


FIG. 7—PWR steam generator tube support plate designs [11].

exchangers and the insidious nature of underdeposit corrosion and MIC have prompted the use of such alloys in freshwater-cooled systems.

Carbon and low-alloy steels are most commonly used in the condensate system for economy and their adequate resistance to corrosion. Austenitic stainless steels have also been used in some systems and in key components. Copper alloys have also been used in some locations, although much less frequently.

Copper alloys (Admiralty, copper-nickel) and austenitic stainless steels are the most commonly used materials for feedwater heater tubing based upon their resistance to general and localized corrosion, erosion-corrosion, and SCC, and adequate heat transfer performance [1,2]. Carbon and low-alloy steels are most often used for the shells of such heaters for economy and availability.

Much of the materials selection for service water systems and closed cooling water systems is dictated by the water source (e.g., carbon steel for fresh waters; coated or lined steel, copper alloys, or stainless steels for saline waters). Coatings, linings, copper alloys, stainless steels, super austenitics, super ferritics, and titanium have been used for replacements.

### Failure Modes

Fine cracks or localized regions of attack, resulting from SCC, corrosion fatigue, or localized corrosion, are the most common corrosion failure modes in nuclear facilities. Small leaks can be a major concern in nuclear power plants where the release of radioactive products to the environment or leakage of extremely expensive materials such as heavy water from CANDU plants must be avoided. The CANDU plants are a type of heavy water moderated process using natural uranium; the name is an acronym for Canadian Deuterium Uranium. The other major concern with small cracks or fine pits is their potential to act as initiation sites for cracks that could lead to large leaks or unstable cracking and loss of coolant events. Almost without exception, the toughness of the alloys used for piping and vessels is sufficiently high that nuclear piping and vessels are structurally

stable, even with such flaws present. This assurance of "leak-before-break" is a critical criterion of nuclear plant reliability.

Radiation buildup, the result of general metal loss to the heat transport system and the deposition of activated corrosion products on metal surfaces, can represent a serious corrosion concern unique to nuclear plants, as radiation levels can limit worker exposure and hinder maintenance. The dissolution of metal and subsequent loss of the metal to the system also has other potential ramifications as maintenance activities such as refueling operations depend upon a high degree of water clarity. Nuclear plants are designed with minimal corrosion allowance on heat transfer surfaces, unlike the large fireside corrosion allowance designed into fossil-fueled plants. The relatively low operating temperatures, high purity water, and the extensive use of corrosion-resistant alloys permit the waterside corrosion allowances to be minimized. This is driven by requirements for water clarity and radiation buildup. Since much of the in-vessel maintenance must be performed using water for shielding, the clarity of the water is extremely important.

### TYPICAL ENVIRONMENTS, METALLURGICAL CONDITIONS, AND CORROSION PROBLEMS

The PWR primary system operates at  $-320^{\circ}\text{C}$  and 13.8 MPa, with a room temperature pH of approximately 10 (6.8 to 7.4 at temperature), and a hydrogen overpressure to suppress radiolysis. Boric acid is added for reactivity control (i.e., higher concentrations early in a fuel cycle; progressively lower as the enriched uranium is depleted). LiOH is added for pH control. The PWR primary system environment is relatively benign, even at the temperatures and pressures at which the system operates. Some components, particularly steam generators and control rod drive mechanism penetrations, have experienced primary water stress corrosion cracking (PWSCC), a phenomenon first discovered by Coriou in the 1960s [3]. Cracking is intergranular and does not appear to be associated with any particular metallurgical anomaly. The major concerns with PWSCC are radioactive contamination of the non-radioactive water/steam environment (e.g., from steam generator leaks) or the potential for a loss of coolant event from cracking in control rod drive mechanism attachments to the reactor vessel head.

PWR steam generators are exposed to the high-pH, hydrogen-rich primary water environment on the tube side (inner side) and high-purity, deoxygenated water on the secondary side. The method for corrosion control in the secondary circuit has evolved from a coordinated phosphate treatment to the all volatile treatment (AVT) that is used presently. Different AVT treatments have included hydrazine and ammonia, hydrazine and morpholine, and the use of alternate amines. Crevices on the secondary side, where impurities can concentrate, and other locations where deposits develop thermal gradients that enhance the concentration of impurities, have produced aggressive local environments (e.g., oxygen concentration cells, both acidic and caustic pH excursions) that have led to pitting, IGA, and SCC [1,2,4]. Figure 8 summarizes steam generator failure history.

**FIG. 8—Steam generator failure history [12].**

The single-cycle BWR historically has used very high purity water (conductivity  $<1\mu\text{S}/\text{cm}$ ) at essentially a neutral pH. More recent experience has shown that control to levels far less than  $1\mu\text{S}/\text{cm}$  ( $\sim 0.10\mu\text{S}/\text{cm}$ ) can be achieved in large operating plants. The radiolytic decomposition of water in the BWR core, however, produces oxidizing species (oxygen and hydrogen peroxide) that make the environment far more aggressive, particularly to the heat affected zones of stainless steel welds. All these factors produce a mildly oxidizing environment that, in concert with the sensitized microstructure and tensile stress, produce IGSCC of austenitic stainless steel.

In both PWRs and BWRs, the carbon steel feedwater train can be susceptible to flow-assisted corrosion and erosion-corrosion effects, especially at extremely low oxygen concentrations. Thinning of this piping, generally at areas of high turbulence, is dependent upon temperature, pH, and oxygen content. Oxygen additions are made to some feedwater lines to assure the formation of a protective magnetite film.

The main heat removal system (for example, the main condenser and associated equipment) and service water systems (which provide cooling for auxiliary equipment such as pumps, room coolers, chillers, etc., fire protection, and reactor heat removal systems used under accident and other shutdown conditions) for both BWRs and PWRs are exposed to environments that are controlled by the site's water source; that is, the cooling water may be seawater, brackish water, or a fresh water (lake, river, or pond). Fresh waters may range from the acidic to the highly alkaline. The pH and concentration of dissolved minerals (particularly calcium and magnesium salts) or metals (manganese or iron) can have a strong influence on the corrosivity of the water. Corrosion under deposits and MIC can result in a variety of such environments. Oxygen and flow rate are key factors in determining the aggressiveness of the environment. Very high flow rates produce flow-assisted corrosion and, eventually, erosion-corrosion, especially on copper alloys and carbon steels. Low flow rates encourage deposition and underdeposit corrosion and MIC.

The importance of corrosion in these balance of plant (BOP) systems increased tremendously for nuclear plant owners in the 1980s. Leakage and functional failures in safety-related and nonsafety-related cooling systems as a result of general corrosion, localized corrosion (especially

underdeposit corrosion), and MIC became critical issues. Several plants in the United States have completely replaced service water system piping, others have initiated planning for such a replacement, and the remainder have been faced with the need for local repairs, often on buried piping that is essentially inaccessible. Utilities are in the process of learning the importance of monitoring for corrosion and deposition and the necessity for early detection and actions to mitigate corrosion. The phenomenon of MIC is even more complex since the presence of living organisms makes it extremely dynamic. Many of the standard approaches to monitoring and control are not applicable. Similarly, the toxicity of many of the standard water treatments for biological control have significant environmental and administrative ramifications on storage and discharge. Most of the methods for testing MIC susceptibility in the laboratory or in service are still under development.

## TESTING FOR CORROSION

### Purpose of Testing and Types of Tests

Corrosion tests are performed for selection or qualification of materials (including materials to be used for repairs or replacements), for monitoring (to assess corrosion or to track process controls such as water treatments), or to supplement and assist with failure analyses.

Streicher [5] has identified five categories of corrosion test methods:

1. Plant service (i.e., how components behave in actual service)
2. Tests in process streams or cooling waters
3. Laboratory tests in plant solutions
4. Laboratory tests with reagent chemicals in place of plant solutions
5. Mechanism tests

Test types 1 or 2 are most useful for monitoring of performance in existing facilities. These test types are most useful for evaluating the performance of existing or candidate replacement materials or for monitoring mitigation treatments. Type 2 tests may include immersion or electrochemical tests. Corrosion (or SCC) may be accelerated by loading the specimen, forming a crevice (using a washer or other means), or by increasing temperature. Test types 3 and 4 have been used and continue to be used to qualify materials for various service environments including those where general corrosion, localized corrosion, or SCC are concerns. The corrosive conditions may be enhanced by using more concentrated solutions, higher temperature, greater aeration or acidity, creviced conditions, applied electrochemical potentials, or stress. Mechanism tests (Type 5) often incorporate environments or loading conditions that have little correspondence to plant conditions; however, they have been formulated to provide a useful indication of a particular characteristic that may be correlated with long-term service exposure. For example, the pitting resistance of stainless steels and nickel-base alloys may be compared by using a ferric chloride solution to determine the critical temperature

above which pitting or crevice corrosion occurs (ASTM G 48, Test Methods for Pitting and Crevice Corrosion Resistance of Stainless Steels and Related Alloys by Use of Ferric Chloride Solution), by determining the key electrochemical potentials for pit initiation and pit growth (hysteresis loop) in chloride solutions (ASTM G 61, Test Method for Conducting Cyclic Potentiodynamic Polarization Measurements for Localized Corrosion Susceptibility of Iron, Nickel, or Cobalt-Based Alloys), or using the electrochemical technique for determining the critical pitting temperature (ASTM G 150, Test Method for Electrochemical Critical Pitting Temperature of Stainless Steels) [6,7]. These values are not directly applicable to plant service but provide a useful basis for comparing different alloys.

Similarly, ASTM A 262, Practices for Detecting Susceptibility to Intergranular Attack in Austenitic Stainless Steels, is a mechanism test used to screen alloys for their resistance to intergranular attack (IGA) associated with the precipitation of chromium carbides. This standard has been used to rank alloys and treatments for their relative degree of sensitization and to infer their resistance to IGSCC. ASTM A 262 provides a method for evaluating the sensitization of stainless steels. Both IGA and IGSCC have been shown to be strongly dependent upon sensitization.

## Test Methods

The majority of the corrosion testing done for the initial qualification of materials in the environments encountered in nuclear power plants was based upon that predominant in fossil-fueled power plants and in nuclear-powered submarines where water is the heat transfer fluid. The extensive use of corrosion-resistant alloys, the lower temperatures used in nuclear plants, and the carefully controlled or high-purity environments of nuclear plants suggested that corrosion problems should be at a minimum. Early work, to qualify materials for the first generation of reactors, indicated that localized corrosion and SCC would not be expected in BWR or PWR environments. Those tests showed that control of chlorides and other aggressive anions would avoid corrosion problems. Those tests did not include some of the subtle environmental effects produced in the nuclear plants such as radiolytic decomposition of water in the BWR core to produce hydrogen peroxide and oxygen or the aggressive underdeposit environment in PWR steam generators. Many of the tests used to evaluate SCC resistance of material/environment pairs used deformation-controlled loading conditions (U-bends or C-rings) and test times of the order of thousands of hours. Such methods include:

- ASTM G 30, Practice for Making and Using U-Bend Stress Corrosion Test Specimens
- ASTM G 38, Practices for Making and Using C-Ring Stress Corrosion Test Specimens
- ASTM G 39, Practice for Preparation and Use of Bent-Beam Stress Corrosion Test Specimens
- ASTM G 49, Practice for Preparation and Use of Direct Tension Stress Corrosion Test Specimens
- ASTM G 58, Practice for Preparation of Stress Corrosion Test Specimens for Weldments

The constant deflection methods were, in many cases, inadequate to predict the corrosion effects that would be encountered in long-term service in the various reactor and coolant systems. For example, in constant deflection tests, load relaxation at temperature results in a much lower stress level in the specimen and a less aggressive test.

The slow strain rate test (SSRT) was developed to overcome the deficiencies of deformation-controlled SCC tests. Experience with turbine rotor steels had revealed that U-bends, C-rings, and the like might not crack in environments that would produce cracking in long-term service. Even constant load tests (actively loaded specimens exposed to aggressive environments) would underpredict SCC susceptibility when tests were run for times of the order of (only) thousands of hours. In the SSRT, a tension specimen is actively loaded at a slow, nearly constant, strain rate in the environment of interest. That environment may be the actual plant environment or may be accelerated by using a higher concentration of the species responsible for the attack (e.g., oxygen, chloride, hydroxide) or an applied potential. The slow and continuous strain rate produces deformation at the crack tip that maximizes the interaction of the corrosion and the crack tip strain. That method initiates cracks and causes film rupture events at the tips of existing cracks. Under the proper conditions, the bare metal surfaces (continue to) interact with the environment, resulting in crack advance. Considerable development work has been devoted to establishing optimum strain rates for the test. The SSRT has been used extensively for investigating the cause of IGSCC in BWRs and continues to be used for selection and qualification of replacement materials and remediation processes. The test produces results that look like those from a tensile stress-strain curve (Fig. 9). Like a tension test, the test always produces a failure. Typical test times are of the order of days to a month when extension rates from  $10^{-7}$  to  $10^{-6}$  in./in./s ( $10^{-7}$  to  $10^{-6}$  s $^{-1}$ ) are used. The interpretation of the test results may be compared to the results for the same material exposed to an environment where little or no environmental degradation occurs based upon one or more of the "tensile test" parameters (maximum stress, elongation

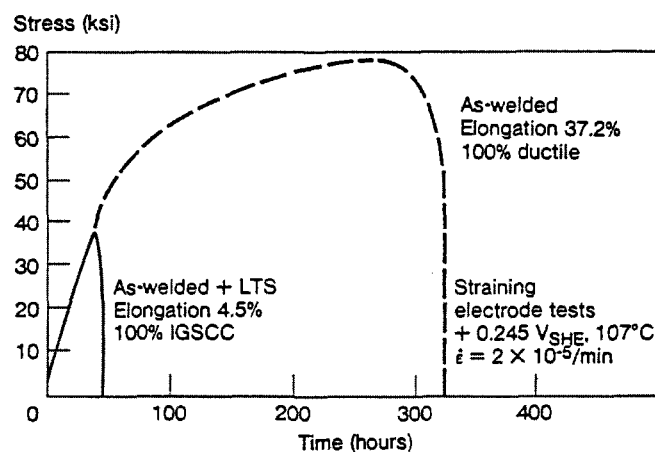


FIG. 9—Slow strain rate test, typical curve. (Copyright © 1980. Electric Power Research Institute. EPRI WS-79-174, Volume 1. Reprinted with permission.)

to failure, reduction of area, etc.). There is now a standardized version of this test, ASTM G 129, Practice for Slow Strain Rate Testing to Evaluate the Susceptibility of Metallic Materials to Environmentally Assisted Cracking. While the test is very useful for identifying materials that are susceptible to SCC, assessing the degree of susceptibility to be expected in service is more difficult. Efforts toward standardization of such interpretations continue.

ASTM A 262 is probably the most commonly used mechanism (Type 5) test for corrosion testing in support of nuclear reactor materials. It provides a qualitative measure of the degree of sensitization (DOS). The electrochemical potentiokinetic reactivation (EPR) test [8] provides a rapid method for generating a more quantitative measure of DOS. This test (see ASTM G 108, Test Method for Electrochemical Potentiokinetic Reactivation (EPR) Test Method for Detecting Sensitization of AISI Type 304 and 304L Stainless Steels) involves polarizing a polished sample (including pipe work in the field) at a controlled rate, then reversing the direction of polarization and returning to the open circuit potential. The area under the curve, normalized for the grain boundary area exposed (Fig. 10a), provides a quantitative measure of the degree of sensitization. The "double loop" method is similar, but is less critical regarding specimen preparation and provides the quantitative measure as a relative peak height. See Fig. 10b, and Chapter 7—*Electrochemical Tests*. Standards for the testing and interpretation of results have been under review within ASTM for a number of years.

Other methods that have been, and continue to be used are:

- ASTM G 4, Method for Conducting Corrosion Coupon Tests in Plant Equipment
- ASTM G 61, Test Method for Conducting Cyclic Potentiodynamic Polarization Measurements for Localized Corrosion Susceptibility of Iron-, Nickel-, or Cobalt-Based Alloys

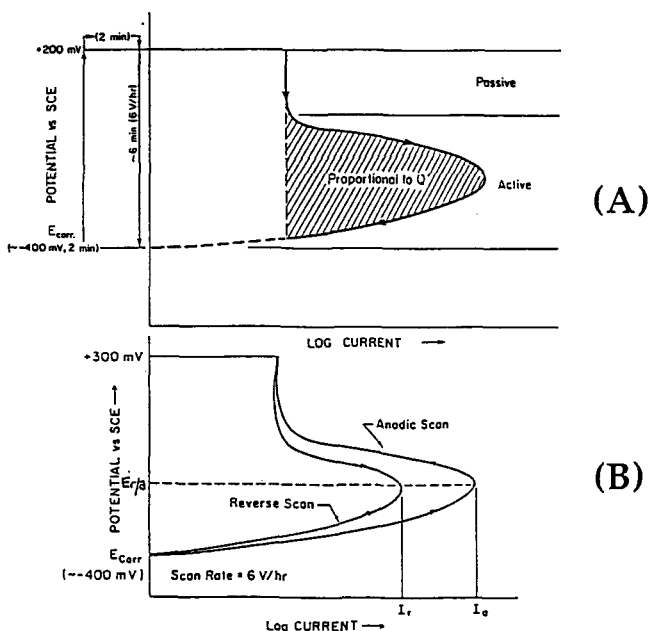


FIG. 10—EPR, typical curve (from G DLEPR-XX, G01.08.03 working draft version).

- ASTM G 5, Standard Reference Test Method for Making Potentiostatic and Potentiodynamic Anodic Polarization Measurements
- ASTM G 2, Test Method for Corrosion Testing of Zirconium, Hafnium, and Their Alloys at 680°F or in Steam at 750°F
- ASTM G 96, Practice for On-Line Monitoring of Corrosion in Plant Equipment (Electrical and Electrochemical Methods)
- ASTM G 111, Guide for Corrosion Tests in High Temperature or High Pressure Environment, or both
- ASTM G 102, Practice for Calculation of Corrosion Rates and Related Information from Electrochemical Methods
- ASTM G 46, Practice for Examination and Evaluation of Pitting Corrosion
- ASTM G 106, Practice for Verification of Algorithm and Equipment for Electrochemical Impedance Measurements.

### Future Outlook

Several unresolved issues remain in the area of corrosion testing for nuclear power plants. These include:

- IGA and IGSCC in PWR steam generator tubing (secondary side). The effect of different, "customized" microstructures such as those for cold-worked nickel-base alloys or (intentionally) heavily twinned materials (to eliminate intergranular crack propagation) on IGA and IGSCC need to be resolved.
- IASCC in BWR environments has been observed in highly irradiated components. Threshold levels of irradiation and methods to assess susceptibility and mitigate IASCC have been defined [9] but require standardization.
- Standard test methods are also required to qualify alternative approaches to environmental controls such as hydrogen water chemistry (HWC). HWC has been shown to be effective for protection of recirculation system piping against IGSCC (at the expense of higher radiation levels); however, the higher levels of hydrogen injection required to protect components in the reactor vessel may not be tolerable from a radiation dose ( $^{16}\text{N}$  carryover in steam) perspective.
- Primary water stress corrosion cracking (PWSCC) has been observed in PWR steam generator tubing, control rod drive mechanism penetrations, and bolting materials. Methods to evaluate susceptibility of components, mechanisms, and methods for qualifying alternate materials for resistance to this specific form of IGSCC are required.
- The nuclear industry has learned the value of on-line monitoring to provide an early warning of corrosion problems. Standard methods for automated and on-line methods (including measurements made at reactor system temperatures and pressures) need to be developed.
- The importance of corrosion effects in balance of plant (BOP) components in nuclear plants increased dramatically in the 1980s. BOP problems such as MIC, pitting, and underdeposit corrosion had a dramatic effect on plant performance. Methods for monitoring and for selecting materials for resistance to pitting and crevice corrosion exist. Additional standard methods for MIC testing are under development [10].

## REFERENCES

- [1] *The ASME Handbook on Water Technology for Thermal Power Systems*, P. Cohen, Ed., The American Society of Mechanical Engineers, New York, 1989.
- [2] "Corrosion in the Nuclear Power Industry," *Metals Handbook, Ninth Edition, Volume 13, Corrosion*, ASM International, Metals Park, OH, 1987.
- [3] Coriou, H., Grall, L., LeGall, M., and Vettier, S., Third Colloque de Metallurgie, Corrosion, (Seche et. Aquise), Centre d'Etudes Nucleaires de Saclay, 1959, North Holland Publishing Co., Amsterdam, 1960, pp. 161–169.
- [4] Welty, C. S., Jr. and Blomgren, J. C., "Steam Generator Issues," *Proceedings of the Fourth International Symposium on Environmental Degradation of Materials in Nuclear Power Systems—Water Reactors*, D. Cubicciotti, Ed., NACE, Houston, TX, 1990.
- [5] Streicher, M. A., "Classification and Application of Corrosion Tests," presented at ASTM Symposium on Application of Accelerated Corrosion Tests to Service Life Prediction of Materials, Miami, FL, 16–17 November 1992.
- [6] Garner, A., "Materials Selection for Bleached Pulp Washers," *Pulp and Paper Canada*, Vol. 82, 1981, T414.
- [7] Kolts, J. and Sridhar, N., "Temperature Effects in Localized Corrosion," *Corrosion of Nickel-Base Alloys*, ASM, Metals Park, OH, 1985.
- [8] Clarke, W. L., "The EPR Technique for the Detection of Sensitization in Stainless Steels," NUREG/CR-1095, 1981.
- [9] Andresen, P. L., Ford, F. P., Murphy, S. M., and Perks, J. M., "State of Knowledge of Radiation Effects on Environmental Cracking in Light Water Reactor Core Materials," *Proceedings of 4th International Symposium on Environmental Degradation of Materials in Nuclear Power Systems—Water Reactors*, D. Cubicciotti, Ed., NACE, Houston, TX, 1990.
- [10] *Microbiologically Influenced Corrosion Testing*, ASTM STP 1232, J. R. Kearns and B. J. Little, Eds., ASTM International, West Conshohocken, PA, 1994.
- [11] Theus, G. J. and David, D. L., "Corrosion in Steam Generating Systems," *Corrosion in Power Generating Equipment*, M. O. Speidel and A. Atreus, Eds., Plenum Press.
- [12] Jones, R. L., "Corrosion Experience in U.S. Light Water Reactors—A NACE 50th Anniversary Perspective," CORROSION/92, Paper 168, NACE, Houston, TX, 1993.

# Steam Generation

Otakar Jonas<sup>1</sup>

THIS CHAPTER COVERS corrosion and corrosion testing for the water side and steam side of utility and industrial steam generation, fossil fuel, and nuclear units. It does not cover primary cycles of nuclear units, fire side in fossil fuel fired steam generators, gas turbines, and cooling water systems.

## INTRODUCTION

The cost of corrosion and scale of steam cycle components in all types of cycles (fossil and nuclear utility, industrial) is still very high [1–3]. Recent studies determined that the total cost of corrosion in the United States is \$276 billion/year, including the \$6.9 billion/year cost to electric utilities [1]. The main cost is for the replacement power or lost production; it is about ten times higher than the cost of repairs. Scale and deposits often reduce the steam generating capacity and thermodynamic efficiency. There are also safety issues, such as stress corrosion of turbine blade attachments, deaerator cracking, and flow accelerated corrosion of piping. The high cost of corrosion led to intensive research into corrosion behavior of the materials used, characterization of the chemistry of corrosive environments, and introduction of corrosion into component design.

### Critical Areas

The following are current critical areas where corrosion dramatically impacts safety and reliability of the steam generating equipment:

- break before leak or before other warnings
- corrosion cracking of carbon steel welds in hot water
- stress corrosion cracking (SCC) in nuclear pressurized water reactor (PWR) and boiling water reactor (BWR) cycles
- corrosion fatigue of turbine blades, boiler tubes, and PWR cycle components
- other corrosion failures of boiler tubes
- corrosion cracking of deaerator welds
- flow accelerated corrosion (FAC) of feedwater and wet steam piping
- corrosion of condenser and feedwater heater tubing

## Corrosion Mechanisms and Root Causes of Problems

All the known corrosion mechanisms active in aqueous environments have been found to be active on the water side and steam side of the steam generation cycles. The most frequently found mechanisms include high-cycle and low-cycle corrosion fatigue, SCC, pitting, general and crevice corrosion (often under deposits), FAC, fretting, oxidation, and exfoliation. The most costly mechanisms are corrosion fatigue and SCC. During the last two decades, FAC received a lot of attention because of several catastrophic failures of carbon steel piping and the effect of the corrosion products generated by FAC on other cycle components, such as boilers and PWR steam generators. The root causes of most of the corrosion problems include design, water chemistry and operation, and material selection. The design root causes include high local steady and vibratory stresses, high flow velocity and turbulence (leading to FAC) and heat transfer conditions which can lead to concentration of corrosive impurities.

Because of the intensive research and application of the research to problem correction, over 90 % of these corrosion problems are understood, the mechanisms and root causes can be identified, and there are engineering solutions to these problems. Major contributions have been made by Electric Power Research Institute, main vendors of equipment, and by technical societies such as ASME [4], the American Society for Materials International (ASM) [5], ASTM, American Nuclear Society (ANS), and the National Association of Corrosion Engineers (NACE).

## Equipment Description

The steam-generating cycles of interest in this chapter include industrial and utility drum boiler cycles, utility once-through boiler cycles (super critical and subcritical), fluidized bed boiler cycles, combined cycles with gas and steam turbines, cogeneration cycles, pressurized water reactor and boiling water reactor cycles, and geothermal steam generation. An example of a utility drum boiler cycle is given in Fig. 1. The figure also indicates major impurity transport mechanisms around the cycle that can dramatically influence impurity concentration on the cycle component surfaces and corrosion. A link in the communication between different engineering disciplines on corrosion and water and steam chemistry is provided by the Mollier Diagram

<sup>1</sup>P.E., Ph.D. consultant, Jonas Inc., Wilmington, DE 19803.



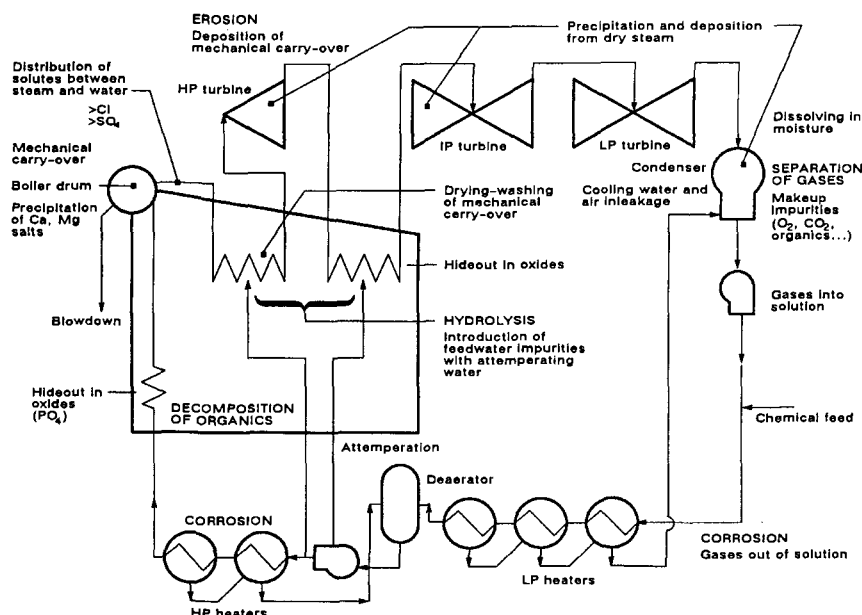


FIG. 1—A typical electric utility drum boiler cycle with sources of chemical impurities and their concentration mechanisms and transport [10,13].

(enthalpy-entropy), which can characterize the steam and water properties as well as impurity behavior and corrosion Fig. 2. Additional information on cycle designs, water chemistry, and corrosion can be found in Refs 4 to 24.

### Objectives of Corrosion Testing

The objectives of corrosion testing and associated monitoring of chemical, stress, and thermodynamic conditions in steam generating cycles are:

- to provide corrosion characteristics of materials for cycle and component design and selection of water treatment
- to provide data for troubleshooting and root cause analysis
- to help in life assessment and failure analysis
- to prevent leaks, breaks before leaks, and other catastrophic failures.

### MATERIALS OF CONSTRUCTION AND SELECTION CRITERIA

The highest proportion of the materials used in steam generation cycles are carbon and low-alloy steels. Austenitic and martensitic stainless steels are used for selected high-duty components such as for turbines blades, pumps, and valves, and there is a small quantity of superalloys used for special applications. Copper alloys, stainless steels, and titanium are used for condenser tubing, and copper alloys and carbon and stainless steels are used for feedwater heater tubing. A higher proportion of stainless steels and superalloys is used in nuclear cycles. Table 1 gives a list of typical materials used in steam generating cycles.

The most important criterion for the selection of materials is the reliability of steam cycle components during a typical 30-year design life. This is important because of the

high cost of replacement power or lost production in industrial steam generation.

Strength to weight considerations are important in rotating components such as in steam turbines. The cost of material is often a wrong consideration, leading to the selection of the cheapest material and poor component reliability. Typical components where the selection of the least expensive material leads to poor reliability include condensers and feedwater heaters.

Prevention and minimization of corrosion is achieved by a combination of design (steady and vibratory stresses, heat flux, and flow), feedwater and boiler water treatment (control of pH and corrosion potential, and control of impurity concentration), and operation (control of impurity ingress and stress and temperature conditions) (Fig. 3). These corrosion control measures are discussed in Refs 4–6 and 9–19.

### CORROSIVE ENVIRONMENTS

Normal steam cycle environments are not corrosive. They passivate the cycle component surfaces and promote formation of protective oxides such as magnetite, hematite, and spinel. Pure, low-oxygen hot water and steam are good passivating agents, and where impurities are present, alkalizing agents such as ammonia, sodium phosphate, and other water treatment chemicals are added [4,5,11–14].

The large variety of corrosive environments is unique for the steam generation industry. This is because the pressure around the steam cycle changes from vacuum to hundreds of atmospheres (thousands of psi) and the temperature from ambient to over 600°C (1100°F). This changes the aqueous environment from low-temperature water to high-temperature pressurized water, to wet, saturated, and superheated steam. Concentrations of impurities in these

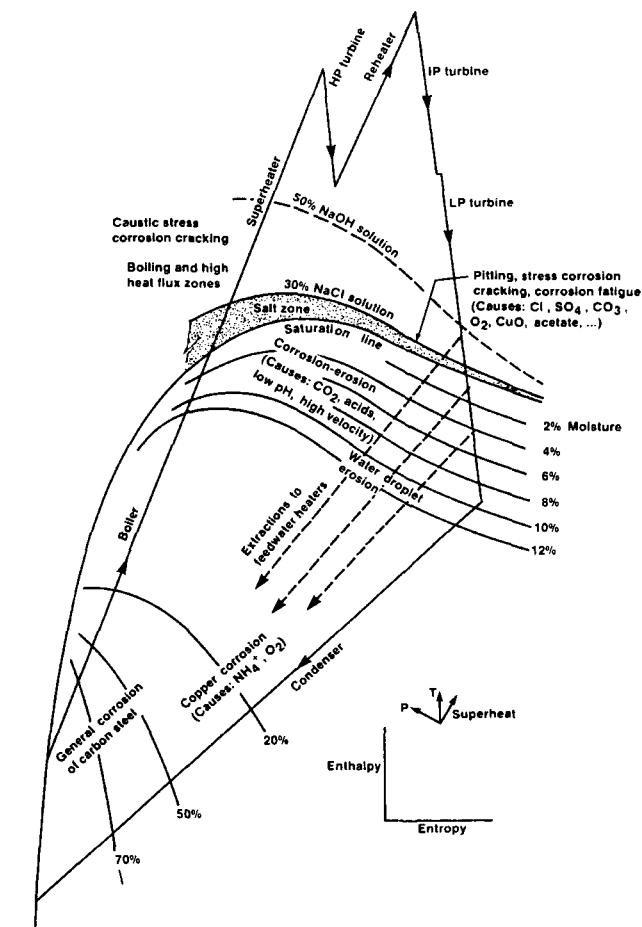


FIG. 2—A Mollier (enthalpy-entropy) diagram combining information on cycle water and steam properties, chemistry, and corrosion [6,10].

aqueous solutions and at component surfaces vary from low ppb to almost 100 %. Over 150 different chemical species have been identified in water, steam, and in deposits on boiler, turbine, and other surfaces [6,11–17]. Typical environments are listed in Table 2 and the sources of chemical impurities and their transport and concentration mechanisms are for a utility drum boiler cycle indicated in Fig. 1.

The cycle components also have to be protected against corrosion during inactive periods such as boiler layup, during which the environments are different from those experienced during operation. The layup protection is typically provided by nitrogen blanketing, or by wet layup with elevated pH and oxygen scavengers in aqueous solutions. Without layup protection, oxygen and CO<sub>2</sub> from air can interact with wet, possibly salt-covered surfaces and cause pitting and other forms of corrosion.

Preservatives, machining and cleaning fluids, dry lubricants (MoS<sub>2</sub> and graphite), and Loctite can also corrosively interact with steam cycle materials.

TABLE 1—Typical materials used in steam-generating units.

Type of Materials (examples)	Applications
Carbon Steels SA106, 212B, 515, 1020, A36, A-302 (0.5 Mo)	Piping, tubing, boiler drums, turbine casing, pressure vessels, turbine rotors, pumps
Low-Alloy Steels NiCrMoV, CrMoV, 0.5Cr-0.5Mo, 0.5Cr-0.5Mo, 1.25Cr, 0.5Mo, 2.25Cr-1Mo, 9Cr-1Mo	Turbine rotors, high-temperature piping and tubing, cast and forged pressure vessels
Austenitic Stainless Steels Types 304, 316, 321, 347, 308, 309 weld metal	High-temperature piping and tubing, nuclear piping, condenser tubing, stationary blades, pumps
Ferritic and Martensitic Stainless Steels AISI403, 422, 630 AL6X-N, Sea-cure	Turbines blades, condenser tubing
Superalloys Inconel 600, 630, Incolloy 800, Pyromet 860, Reactalloy 26, Incolloy 901	PWR steam gen. and other tubes, high-temperature bolts
Stellite (6B)	Erosion shields, valve seats, support keys
Copper Alloys Aluminum bronze, copper-nickel, Admiralty brass, Monel, bronze, muntz metal	Condenser and heater tubing, tube sheets, pump impellers, coolers
Titanium pure, Ti6-4, and other alloys	Condenser tubing, low-pressure turbine blades

A link between the environment and corrosion is provided by the relationship between the “at temperature” pH and corrosion potential (Fig. 4). These relationships are calculated or measured for specific materials, environments, and temperatures. It should be realized that the at temperature pH can be very different from that in a room temperature sample (Fig. 5). This is an important factor for proper simulation of service environments.

The most severe corrosive environments are encountered in the areas where corrosive impurities concentrate. These impurities can concentrate on heat transfer surfaces such as in boiler and steam generator tubes where the surface temperature is above the saturation temperature of the boiling water, and on the surfaces in superheated and saturated steam where the impurities concentrate by precipitation from a steam solution and deposition [4,5,11,14]. Figure 6 shows the gradient of concentration of sodium hydroxide at the surface of a boiler tube.

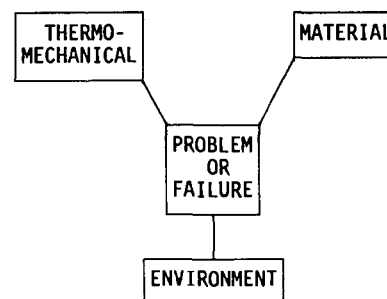


FIG. 3—Three components of corrosion control in steam generating cycles.

TABLE 2—Typical steam cycle environments.

	pH	Conductivity, $\mu\text{S}/\text{cm}$
Noncorrosive		
Pure and treated deaerated feedwater and boiler water	7.0 to 10.5	0.1 to 10
Drum boiler water, phosphate, AVT and NaOH water treatments	9.2 to 12	5 to 5000
Steam: dry, saturated, and wet	7.0 to 9.8	0.1 to 10
Corrosive—Concentrated Solutions		Concentration, %
NaOH on boiler and turbine surfaces	>13	1 to 90
Salts and acids on boiler and turbine surfaces	3 to 8	0.1 to 30
Corrosive—Oxygen and $\text{CO}_2$		Concentration of $\text{O}_2$ , ppb
Condensate and feedwater-aerated	<9	20 to 5000
System fill water		~7000
Corrosive—High Flow Velocity and Turbulence		
Feedwater, condensate, wet steam	5 to 9	$\text{O}_2 < 4$ ppb, reducing environment

In industrial steam cycles, oxygen and  $\text{CO}_2$  from air in return condensate and the chemicals from various industrial processes are the main corrosives. Where organic chemicals leak or are added into the steam cycle, their decomposition products often include organic acids and  $\text{CO}_2$ . Thermal decomposition of organics can occur at temperatures as low as  $150^\circ\text{C}$ .

## CORROSION CONTROL

Corrosion control in steam-generating systems is by a combination of design, material selection, water treatment, and

operation. Marginal design is responsible for most of the corrosion failures in utility equipment. Because most of the corrosion is localized, corrosion cracking and other forms of corrosion in the areas of high heat flux and impurity concentration is often controlled by control of surface stress. Control of flow velocity and heat transfer conditions is also essential. Cycle materials must be compatible with the water treatment chemicals selected for feedwater and boiler water treatments. The combination of copper alloys and ferrous materials in the steam cycle is not recommended because the pH region for the best protection is different for each of these two groups of materials. In general, the cycle materials do not have to be

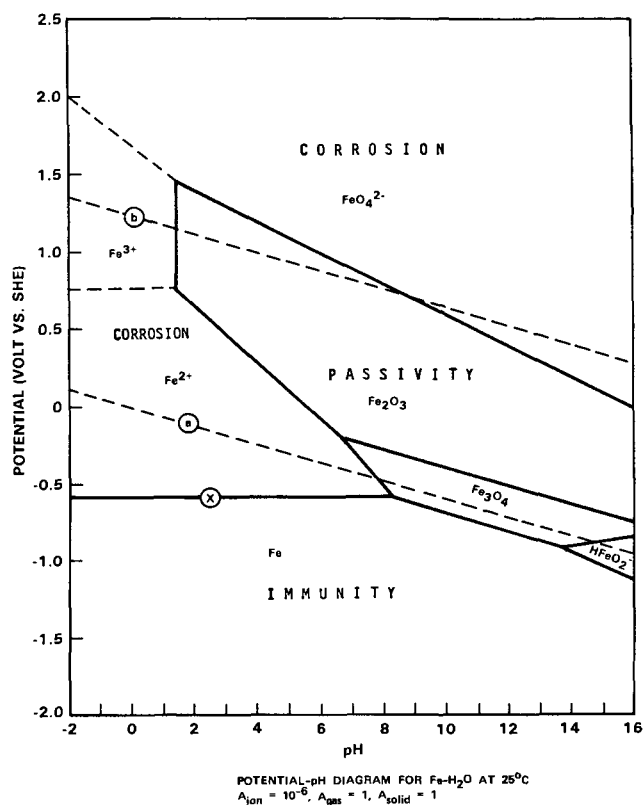


FIG. 4—Potential-pH diagram for iron in water, providing a link between the chemistry of aqueous environment, material, and corrosion [34].

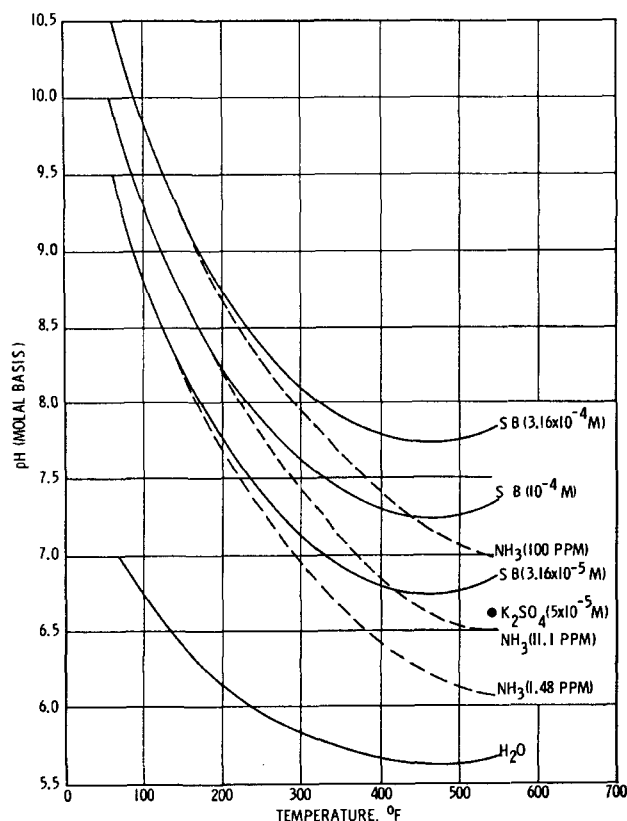


FIG. 5—Dependence of pH of aqueous solutions on temperature, SB = Strong base.

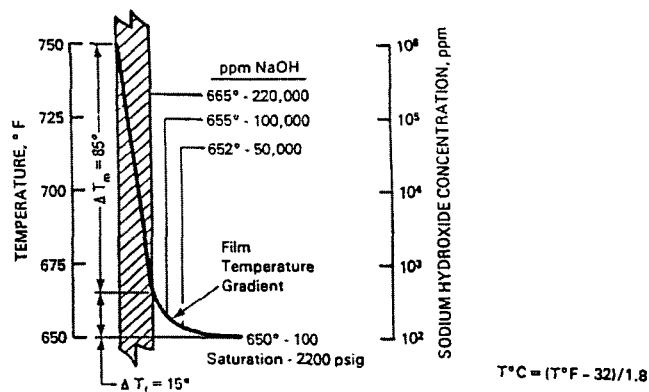


FIG. 6—Concentration gradient of sodium hydroxide at the surface of a boiler tube; a result of heat transfer which elevates the ID surface temperature above the saturation temperature of pure water.

extremely corrosion-resistant because the maintenance of a protective oxide layer achieved by control of pH and oxygen concentration is sufficient for a long, reliable operation.

With a few exceptions, coatings and linings are not used on the water and steam sides. In an EPRI project, about 50 turbine blade coatings have been evaluated, but none of these are being routinely applied. To reduce steam side oxidation in reheaters and superheaters, chromizing and chromating have been developed but these treatments are also not routinely applied. There is little use of composite materials with the exception of condenser tube sheets, which could be made of explosively clad stainless steel or titanium on carbon steel, and of the surfaces in the primary cycles of nuclear units where carbon or low alloy steels are protected by weld-deposited stainless steels. In pulp mill black liquor recovery boilers, stainless steel clad boiler tubes are often used.

Various types of water treatments, aimed at maintaining low concentrations of impurities and alkaline pH [6,11,12,14] are usually successful in long-time protection against corrosion. The water treatments include removal of dissolved and suspended impurities from makeup and feedwater (external treatment) and feeding alkaline additives, oxygen scavengers, and other chemicals (internal treatment). Water chemistry control also includes deaeration, boiler blowdown, sampling, monitoring, prevention of impurity ingress, and periodic mechanical and chemical cleaning.

## SPECIFIC PROBLEM AREAS

Specific problems associated with the steam generation industry include strong interactions of corrosive environment, heat transfer, and operating and residual stresses. These interactions, in a very large system, can result in unforeseen corrosion and corrosion cracking and component failures. Caustic gouging, hydrogen damage, corrosion fatigue, and pitting of boiler tubes [15], deaerator cracking [21] and pitting, corrosion fatigue and stress corrosion in turbines [17] are the most frequent problems specific to steam generation.

Other major problems include many types of corrosion in PWR steam generators, stress corrosion of austenitic stainless steels in superheaters and feedwater heaters [22], FAC of carbon steel piping [19], corrosion of condenser tubing [23], and steam oxidation of superheaters and reheaters leading to exfoliation and solid particle erosion [24]. Most of these problems are summarized in Ref 5. **The challenge** in corrosion control during operation is that large surface areas (several acres) must be controlled for many years, based on a few water and steam samples analyzed for 10 to 20 chemical parameters (such as pH, conductivity, oxygen, sodium, and chloride).

One of the most dangerous consequences of slow, long-time corrosion is the situation where a *break before leak* occurs. This occasionally happens in pressure vessels and piping. In all instances, the break before leak occurs because the structure, weakened by undetected corrosion, is overloaded by pressure or stress transients beyond its point of resisting to fracture.

A recently recognized generic problem is *corrosion cracking of carbon steel welds* such as in deaerators [21], blow-down flash tanks, steam accumulators, and piping. Also recently recognized is a large number of flow-assisted corrosion failures due to high velocity, low pH, low oxygen, and low chromium contents in carbon steel [19]. The safety related problems are summarized in [25].

The corrosion failure mechanisms specific to the steam generation industry include corrosion fatigue (low-cycle and high-cycle) and SCC. Often, this cracking is preceded by pitting.

The specific component **design problem** is that water chemistry and corrosion are not included in design codes and design practices and often not even understood by mechanical designers. For many steam cycle components, the number of new corrosion design variables, such as  $K_{ISCC}$  (threshold stress intensity for SCC),  $\sigma_{SCC}$  (threshold stress for SCC),  $\Delta K_{th}$  (threshold stress intensity amplitude for corrosion fatigue crack propagation), and stress corrosion, corrosion fatigue, and pit growth rates need to be included in design. Designers should also realize that the traditional approach of selecting higher strength materials for higher stresses can lead to susceptibility to SCC and corrosion fatigue.

## CORROSION TEST METHODS

Almost all known test methods applicable to aqueous solutions [26–30] (see Sections III, IV, and V) have been extensively used for material and design evaluation and in failure analysis of steam cycle materials. Many of these methods have been adapted for field testing. Corrosion variables that need to be known in design and failure analysis are, together with the applicable corrosion test methods, listed in Table 3, Table 3 also lists the corrosion test methods that have been applied for in-service monitoring.

The standard methods used include ASTM [27], ANS, NACE, and numerous other methods [26,28,29]. Many important methods are not yet standardized such as the stress corrosion cracking test method [30], and autoclave testing methods [31,32] Table 3 gives a list of the more common test methods and the tested corrosion parameters.

TABLE 3—Corrosion test methods and tested properties.

Test Method	To Determine
<b>GENERAL CORROSION AND MISCELLANEOUS TESTS</b>	
Coupons, U-bends	Corrosion and pitting rate
Polarization	Corrosion rate, pitting and transition potentials
Crevice	Crevice corrosion
Galvanically Coupled Dissimilar Metal Coupons	Couple potential, crevice corrosion, pitting
Flow Accelerated Corrosion	Effects of pH, O <sub>2</sub> , temp., velocity, and corrosion rate
Radioactive Tracer and Isotope Implantation	Corrosion and erosion rate
<b>STRESS CORROSION</b>	
U-bend, C-rings, Tension, and Bent-beam Specimens	$\sigma_{SCC}$ initiation time
Fracture Mechanics Specimens	$K_{ISCC}$ da/dt, incubation time
Constant Strain Rate	Compare materials and environments
Polarization—Anodic	Transition potential
<b>CORROSION FATIGUE (HIGH AND LOW CYCLE)</b>	
Fatigue—Standard and Ultrasonic Tests	Fatigue limit, cycles to crack initiation
Fracture Mechanics Specimens	$\Delta K_{th}$ da/dN
Fretting	Crack initiation
<b>FIELD TESTS</b>	
All methods listed above and many NDT methods are used for corrosion rate, crack growth rate, and other parameter determination in field tests. Test specimens are in autoclaves or directly inside steam cycle components.	
Corrosion-generated Hydrogen in Steam	Boiler tube, feedwater system, and PWR steam generator support plate corrosion
<i>In situ</i> pH and Corrosion and ORP potentials	Susceptibility to general and localized corrosion
Chemical Analysis of Fe, Cu, Ni, Zn in Feedwater, Condensate, and Boiler Water	Corrosion of tubing and piping (general and flow accelerated corrosion)

## Corrosion Test Approach

A simulation of the actual service environment and stress and temperature conditions is essential for proper representation in corrosion testing for steam cycle applications. The service environments can be estimated theoretically through thermodynamic calculations of the chemistry of solutions at component surfaces [33] and through calculation of the potential-pH diagrams [34]. The advantage of field testing or testing in autoclaves taking water and steam from actual operating cycles is that the environment is very representative of the actual conditions, including the changes during load transients, startups, and shutdowns.

In environmental simulations in laboratory testing, the corrosion potential and pH are the most important variables. The difference between oxidizing and reducing conditions is important for all types of corrosion (in particular for stress corrosion, corrosion fatigue, and flow accelerated corrosion).

## Accelerated Tests

Because of the need to develop reliable data representative of a long-time operation, extrapolation of test results and accelerated tests are often necessary. Corrosion cracking tests are accelerated by the use of higher stress intensity and fatigue stresses and by higher cycling frequencies for corrosion fatigue (ultrasonic fatigue testing). Tests can also be accelerated by using higher test temperature and then extrapolating to lower temperatures. Test environments that can accelerate stress corrosion and corrosion fatigue include dry hydrogen

sulfide and polythionates. It is always controversial how representative are the results of the accelerated testing. Corrosion rates, crack propagation rates, and crack growth incubation times are very difficult to determine with the use of accelerated testing.

## In-Service Monitoring

Because of the complex and changing corrosion environment in many steam cycle components, in-service monitoring is necessary to prevent failures. Corrosion situations can be evaluated through periodic nondestructive testing, water and steam chemistry assessments [11], and field testing of corrosion coupons for general corrosion, pitting, stress corrosion, and corrosion fatigue.

Equipment exists to also monitor the temperature pH, corrosion and redox potentials, and the corrosion hydrogen that is always produced during corrosion by aqueous solutions [35]. Periodic analysis of condensate, feedwater, and boiler water samples for iron and copper gives a good indication of general corrosion and flow accelerated corrosion.

The new technical field of Diagnostic Engineering aimed at an "incipient failure detection" and "predictive and preventive maintenance" is becoming a part of in-service monitoring [36].

## Special Methods

Special nonstandard corrosion specimens have been designed for field and laboratory testing and fracture mechanic

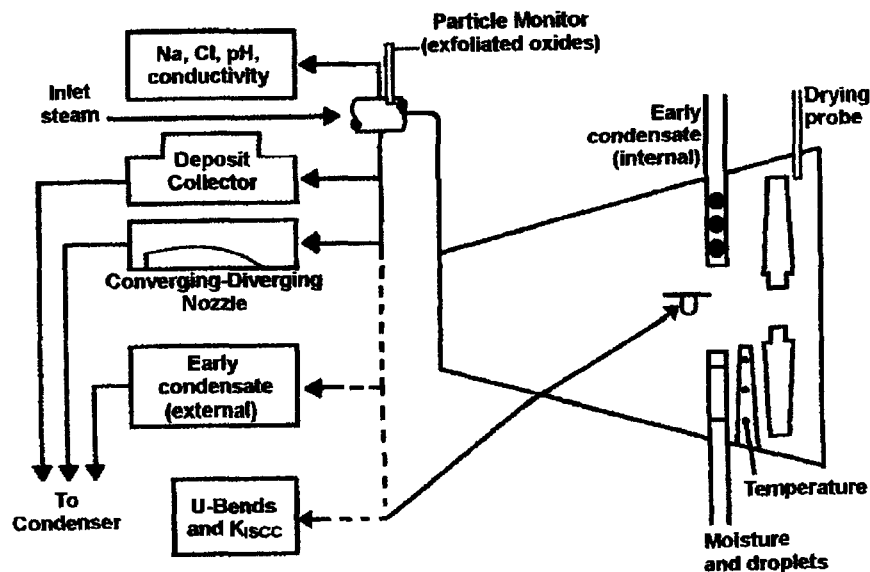


FIG. 7—LP turbine troubleshooting instrumentation that can identify chemical and corrosive conditions.

specimens are often used for stress corrosion and corrosion fatigue crack growth rate testing. For simulation of heat transfer and flow conditions, test methods are often custom-designed. For example, corrosion of PWR steam generator crevices [39] and new types of boilers and steam generators is evaluated by, often long-time, model testing.

### Detection of Corrosion

In corrosion testing, corrosion is detected visually, with optical and electron microscopy, or by electrochemical measurements. In general corrosion and FAC, thickness can be measured ultrasonically or by eddy current probes in tubing. In corrosion cracking tests, crack propagation is measured visually, ultrasonically, by magnetic particle inspection, or by the electric potential method. General corrosion in aqueous solutions can also be measured by monitoring the concentration of corrosion-generated hydrogen.

### Instrumentation

Several diagnostic tools are available for monitoring corrosion, water droplet and solid particle erosion, and for determining deposition rates and deposit composition and morphology in turbines (Fig. 7). The deposits collected with a Steam Turbine Deposit Collector, Converging-Diverging Nozzle for LP turbines, or Converging Nozzle for HP turbines can be analyzed using optical and SEM microscopy, energy dispersive X-ray spectroscopy, X-ray diffraction, and wet chemistry methods [18,37,38]. The results of the deposit analysis can be used to predict deposition and corrosion inside the turbine, and to assess boiler carry-over and the effects of steam and water chemistry upsets.

Several instruments have been developed that can be used to determine the corrosivity of the wet steam environment. One such instrument is the Drying Probe for Wet Steam Stages, which simulates the evaporation of moisture and the

concentration of low volatility impurities on hot surfaces. A Boiler Carry-over Monitor has recently been developed that can be used for the monitoring of high boiler carry-over and the % moisture in process and heating steam and the steam used for oil recovery. Early Condensate Samplers are used to collect samples of steam moisture in turbines. The condensate is collected and withdrawn for analysis while saturated steam is vented into the turbine space.

A Particle Flow Monitor for Exfoliated Oxides is used to determine number and size distributions of oxide particles or water droplets in steam.

### Discussion

It is anticipated that in the near future, important corrosion variables will be included in component design by the component manufacturers and in design codes, including ASME Pressure Vessel Code. For this step, more standard test methods which would be reproducible by different test laboratories are needed.

It is also expected that corrosion considerations will be more emphasized in the steam cycle design and material selection so that all materials of construction of the steam system will be compatible with the water treatment used. In design component integrity monitoring and failure analysis, the combination of the effects of corrosive environment, stress, flow velocity, and thermal conditions must be considered.

### REFERENCES

- [1] Payer, J. H., et al., *Economic Effects of Metallic Corrosion in the U.S.*, Appendix B, Part II, A Rep. to the NBS by Battelle Columbus Labs., NBS Spec. Publ. 511-2, U.S. Dept. of Commerce, NBS, 1978.

- [2] Jonas, O., "Cost of 'Corrosion and Scale' in Electric Utilities," Paper presented at the EPRI Symposium on Fossil Utility Water Chemistry, Atlanta, 11–13 June 1985.
- [3] Jonas, O., "Reducing Corrosion Costs in U.S. Industrial Steam Generation," *Materials Performance*, February 1993.
- [4] *The ASME Handbook on Water Technology for Thermal Power Systems*, P. Cohen, Ed., The American Society of Mechanical Engineers, New York, 1989.
- [5] *Metals Handbook, Ninth Edition, Vol. 13, Corrosion*, ASM International, Metals Park, OH, 1987, pp. 927–1010.
- [6] Jonas, O., "Steam," *Kirk-Othmer Encyclopedia of Chemical Technology*, Vol. 21, 3rd ed., John Wiley and Sons, New York, 1983.
- [7] *Steam/Its Generation and Use*, 39th ed., Babcock & Wilcox Company, New York, 1978.
- [8] *Combustion, Fossil Power Systems*, G. Singer, Ed., 3rd ed., Combustion Engineering, Inc., Windsor, CT, 1991.
- [9] *Corrosion in Power Generating Equipment*, M. O. Speidel and A. Atrens, Eds., Plenum Press, New York, 1984.
- [10] *Low Temperature Corrosion Problems in Fossil Power Plants—State of Knowledge*. EPRI, Palo Alto, CA, December 2003, 1004924.
- [11] "Interim Consensus Guidelines on Fossil Plant Cycle Chemistry," Electric Power Research Institute, Palo Alto, CA, CS-4629, June 1986.
- [12] *PWR Secondary Water Chemistry Guidelines, Revision 5*, Electric Power Research Institute, Palo Alto, CA, TR-102134-R5, June 2000.
- [13] *BWR Water Chemistry Guidelines—Revision 2*, Electric Power Research Institute, Palo Alto, CA, TR-103515-R2, February 2000.
- [14] Jonas, O. and Pebler, A., "Characterization of Operational Environment for Steam Turbine-Blading Alloys," Electric Power Research Institute, Palo Alto, CA, *Topical Report CS-2931*, August 1984.
- [15] B. Dooley and W. McNaughton, *Boiler Tube Failures: Theory and Practice, Vol. 2: Water-Touched Tubes*, EPRI, Palo Alto, CA, 1996.
- [16] *Turbine Steam Path Damage: Theory and Practice*, EPRI, Palo Alto, CA, June 1998, AP-108943.
- [17] Jonas, O., "Steam Turbine Corrosion," *Materials Performance*, Vol. 24, No. 2, February 1985, pp. 9–18.
- [18] Jonas, O. and Dooley, B., "Steam Chemistry and its Effects on Turbine Deposits and Corrosion," *57th International Water Conference*, Pittsburgh, October 1996.
- [19] Jonas, O., "Control Erosion/Corrosion of Steels in Wet Steam," *Power*, March 1985, p. 102.
- [20] *Flow-Accelerated Corrosion in Power Plants*, EPRI, Palo Alto, CA, 1998, TR-106611-R1.
- [21] Jonas, O., "Deaerators, An Overview of Design, Operation, Experience, and R & D," *Proceedings of the American Power Conference*, Vol. 49, Illinois Institute of Technology, Chicago, 1987, p. 979.
- [22] "Corrosion-Related Failures in Feedwater Heaters," Electric Power Research Institute, Palo Alto, CA, *Final Report CS-3184*, July 1983.
- [23] "Corrosion Related Failures in Power Plant Condensers," Electric Power Research Institute, Palo Alto, CA, *Final Report NP 79–730*, August 1980.
- [24] "Solid Particle Erosion of Utility Steam Turbines: 1985 Workshop," Electric Power Research Institute, Palo Alto, CA, *Proceedings CS-4683*, August 1986.
- [25] Jonas, O., "Safety Issues in Fossil Utility and Industrial Steam Systems," *Materials Performance*, May 2001.
- [26] "Corrosion Testing and Evaluation," in *Metals Handbook, Ninth Edition, Vol. 13, Corrosion*, ASM International, Metals Park, OH, 1987, pp. 191–316.
- [27] *2004 Annual Book of ASTM Standards, Vol. 03.02, Erosion and Water, Metal Corrosion*, ASTM International, West Conshohocken, PA.
- [28] "Techniques for Corrosion Measurement," *Proceedings of the Corrosion/92 T-3L Symposium*, NACE, Houston, TX, 1992.
- [29] *Symposium on Stress Corrosion Testing, ASTM STP 425*, ASTM International, West Conshohocken, PA, 1967, pp. 317–341.
- [30] ASTM Standard E 1681-03: Test Method for Determining a Threshold Stress Intensity Factor for Environment-Assisted Cracking of Metallic Material, ASTM International, West Conshohocken, PA, January 1993.
- [31] Dynamic Corrosion Testing of Metals in High Temperature Water, NACE Standard TM0274, National Association of Corrosion Engineers (NACE), Houston, TX, June 1992.
- [32] Autoclave Corrosion Testing of Metals in High Temperature Water, NACE Standard TM0171, National Association of Corrosion Engineers (NACE), Houston, TX, 1992.
- [33] Lindsay, W. T., "Chemistry of Steam Cycle Solutions: Principles," in *The ASME Handbook on Water Technology for Thermal Power Systems*, P. Cohen, Ed., ASME, New York, 1989, pp. 341–544.
- [34] "Computer-Calculated Potential pH Diagrams to 300°C," Electric Power Research Institute, Palo Alto, CA, *Final Report NP-3137*, June 1983.
- [35] Jonas, O., et al., "Evaluation and Application of a New Dissolved Hydrogen Analyzer," Paper IWC-85-27 46th International Water Conference, Pittsburgh, PA, November 1985.
- [36] Jonas, O., "Diagnostic Monitoring—An Overview," *Power*, January 1992, pp. 61–64.
- [37] Jonas, O., "Monitoring of Steam Plants," *Materials Performance*, April 2003.
- [38] Jonas, O. and Mancini, J., "Steam Turbine Problems and Their Field Monitoring," *Materials Performance*, March 2001.
- [39] "Tube-to-Tube Joint Test," Electric Power Research Institute, Palo Alto, CA, *Final Report NP-3013*, March 1983.

# Flue Gas Desulfurization

Harvey S. Rosenberg<sup>1</sup>

Eldon R. Dille<sup>2</sup>

## DESCRIPTION OF MATERIALS OF CONSTRUCTION USED AND SELECTION CRITERIA

A VARIETY OF CONSTRUCTION materials has been used in flue gas desulfurization (FGD) systems on utility boilers. They can all be classified into three major categories: metals, organics, and nonmetallic inorganics.

### Metals

Metals ranging from carbon steel to stainless steels and nickel-based alloys have been used in most components of FGD systems. Unlined carbon steel is used where the flue gas is above the acid dewpoint and/or where alkaline conditions are maintained, such as most of the components of spray dryer FGD systems, inlet ducts upstream of the wet/dry interface of all FGD systems, lime/limestone storage silos, and fresh lime/limestone storage tanks and piping. Under acidic conditions, the carbon steel must be protected by a lining or by other corrosion-control techniques. Alternatively, corrosion-resistant alloys are used under these conditions. Stainless steels (e.g., Type 316L, 317L, 317LMN, 904L, 254 SMO<sup>®</sup>, 25-6MO<sup>®</sup>, and AL6XN<sup>®</sup>) and nickel-based alloys (e.g., G-3, G-30, 625, C-276, C-22<sup>®</sup>, 622, 686, and 59) have been used in FGD system components such as prescrubbers, absorbers, spray nozzles, reheaters, and dampers. In critical locations with more aggressive environments, such as reheaters, outlet dampers, outlet ducts, and gas mixing zones, nickel-based alloys (e.g., alloys 625, G-3, C-276, C-22<sup>®</sup>, 622, 686, and 59) and titanium (grades 2 and 7) have been used.

Because of the relatively high cost of nickel-based and titanium alloys, a significant cost savings can be realized by using thin claddings of these alloys over carbon steel plates, rather than solid alloy plates, for absorbers, dampers, ductwork, and stack liners. Clad plate can be manufactured by hot rolling, explosive bonding, or welding the cladding and base plate together [1,2]. However, these methods are generally applicable only to new FGD systems, because existing systems already have the substrate (e.g., carbon steel) in place. A recently adopted method that is applicable to both new and retrofit construction is called "wallpapering" (NACE RP-0292, Installation of Thin Metallic Wallpaper Lining

in Air Pollution Control Equipment and Other Process Equipment) [3,4]. This method, which has been used in the chemical industry for many years, involves plug welding thin sheets, usually 1.6 mm (1/16 in.) thick, of an alloy such as C-276, C-22<sup>®</sup>, 622, 686, or 59 to the carbon steel substrate. A new practice (NACE International, NACE RP-0199, Installation of Stainless Chromium-Nickel Steel and Nickel-Alloy Roll-Bonded and Explosion-Bonded Clad Plate in Air Pollution Control Equipment) for clad lining is now available [5]. This practice offers guidance for an excellent means of providing protection using thin corrosion-resistant materials.

The most frequently reported failures for alloys in FGD components are pitting and crevice corrosion. General corrosion, erosion-corrosion, or stress corrosion cracking (SCC) also can occur. Many environmental factors are responsible for the failures, but high levels of chloride combined with low pH play a major role [6]. Fluoride also can be a factor, but its role is complex. For example, acid fluorides are especially corrosive to certain alloys such as titanium [7]. However, fluoride forms complex ions with species such as aluminum, magnesium, and silicon, which are typically present in fly ash. However, field corrosion failure analysis studies have shown that the fluoride ion is interacting with the chloride ion in limestone based FGD systems to cause severe crevice and pitting corrosion [8,9]. Elevated temperatures, such as those encountered in prescrubbers and reheaters, are thought to influence SCC susceptibility, while erosive particulates play a role in influencing erosion-corrosion in prescrubbers [10].

### Organics

Organics linings have been used extensively in various FGD components, including prescrubbers, absorbers, tanks, outlet ducts, and stacks. These linings include polyesters, vinyl esters, epoxies, novolac epoxy, novolac phenolic epoxy, fluoroelastomers, and rubber. Organic linings are attractive because they can provide the lowest initial cost for many of these components. The linings are generally applied in liquid form by brushing, rolling, spraying, or troweling. To provide an effective barrier, the organic linings used in FGD systems are often applied in several layers. This decreases the probability of through-thickness pinholes and achieves a greater permeation thickness than typical coatings. Moreover, the polyester, vinyl ester, epoxy, novolac epoxy, and novolac phenolic epoxy linings often contain a mica flake or glass flake filler that further

<sup>1</sup> Research leader, Guild Associates, Hilliard, OH 43026.

<sup>2</sup> Consultant, Specialists in Solutions, Inc., 9401 Wildwood Drive, Highland, IN 46322.



decreases the permeability and provides reinforcement. Mica flake-filled linings are generally not as abrasion-resistant as glass flake-filled linings. In components where high abrasion resistance is required, linings reinforced with glass cloth or inert matting along with abrasion-resistant pigments silicon dioxide, aluminum oxide, tungsten carbide have been used. Although rubber is an organic lining, it is often placed in a separate category because it is applied in sheet rather than liquid form. Three types of sheet rubber have been used for lining absorbers: natural (gum), neoprene, and chlorobutyl. Of these, the rubber industry generally considers chlorobutyl to be the preferred material for this application. Chlorobutyl rubber has low moisture permeability.

Failure of organic linings can occur by blistering, disbonding, and wear from abrasive slurries [11]. Blistering of organic linings immersed in liquids is greatly increased when a thermal gradient is present [12]. Excursions to hot flue gas temperatures can damage or destroy organic linings. Fluoroelastomer linings can withstand excursions up to 260°C (500°F) and are resistant to chemical attack and abrasion. However, they are relatively permeable to moisture and with the use of scrubbed flue gas in the outlet duct, less than desirable coating life has been obtained. In addition, fluoroelastomer coatings are generally more expensive than other types of organic linings. Rubber sheet linings offer excellent resistance to abrasion, but rubber is a flammable material, so care must be taken to prevent ignition of these sheet linings by external sources. It is good practice to label the external surfaces of rubber sheet-lined absorbers indicating the presence of a rubber lining. Close attention to product specification and application is required to prevent short life and inconsistent performance of rubber linings [13].

Fluoroelastomer, fluoropolymer, and fluorinated elastoplastic materials, as well as rubber, are used in expansion joints, typically with fabric reinforcement. The cost of the fluoroelastomer materials may be an order of magnitude higher than that of rubber materials, but longer life expectancy, higher temperature tolerance, and better overall operating performance can easily offset the higher installed cost. Mixing reprocessed fluoroelastomer scrap with virgin fluoroelastomer can reduce the cost of the material, but physical properties critical to the performance of expansion joints are impaired. The causes of failure of fluoroelastomer expansion joints include thermal degradation induced by temperature excursions or thermal cycling, acid attack, and mechanical damage.

Fiberglass-reinforced plastic (FRP, known as glass-reinforced plastic (GRP) in Europe) is used to fabricate mist eliminators, piping and spray headers, and stack liners. Various polymeric resins are used including polyester, vinyl ester, and novolac vinyl ester. The typical operating temperature range of the FRP structures is 82°C (180°F) to 177°C (350°F). FRP also is a flammable material that must be protected against ignition from external sources. The types of FRP failures include mechanical damage, laminate degradation, physical damage, and fire. The causes of failure are inadequate engineering, poor fabrication quality, abrasion, temperature excursions, and, depending on the resin, chemical attack, e.g., acid hydrolysis of polyester.

## Nonmetallic Inorganics

Nonmetallic inorganic materials are used in prescrubbers, spray nozzles, slurry pumps, outlet ducts, and stacks. The materials include prefired bricks and shapes, ceramic tiles, borosilicate foamed-glass blocks, hydraulically-bonded concretes and mortars, and chemically-bonded concretes and mortars, all of which are used as lining materials where temperature resistance, chemical resistance, or abrasion resistance are required. Acid-resistant bricks are commonly used as construction materials for stack liners. A potential failure cause of these bricks is mechanical stress from dimensional changes during service. Also, several free-standing brick flues have been found to lean toward the outer concrete shell. This problem appears to be associated with mixing bypassed gas and scrubbed gas in the stack, thus creating temperature and moisture gradients that cause one side of the flue to expand more than the other side. A free-standing brick flue that is constantly wet with scrubbed FGD gas does not lean [14].

Borosilicate foamed-glass blocks bonded with urethane-modified asphaltic mastic have been used to line outlet ducts and stacks. The combination of these two materials results in a lining that is resistant to permeation by aggressive condensate and can handle continuous temperatures to 205°C (400°F) and excursions to 370°C (700°F). The urethane-modified asphaltic mastic has a temperature limit of 82°C (180°F). However, as the mastic between the bricks is reduced to char by high temperatures, the char provides insulation for the remaining mastic. Moreover, the thermal insulating properties of the glass block and the flexibility of the membrane material contribute to the good performance of the lining. However, the foamed borosilicate glass can be mechanically damaged easily, and failures can occur due to abrasion, puncturing, and cracking. Also, scale that forms on the lining cannot be easily removed. These problems can be minimized by applying a topcoat of chemically bonded mortar over the borosilicate foamed-glass blocks.

Hydraulic-setting, cement-bonded concretes (hydraulic concretes) are used as linings for prescrubbers, outlet ducts, and stacks. These concretes contain aluminate to withstand temperatures of 260°C (500°F) without strength degradation. However, in sulfuric acid solutions (pH < 4), the cement is attacked due to dissolution of the calcium aluminate. This dissolution of the bond results in loosening of the aggregate and erosive wear of the lining [15].

Chemically bonded mortars are commonly used to bond acid-resistant brick stack liners. Chemically bonded concrete mixes can also be used as linings. These materials generally contain siliceous aggregates, a sodium silicate, potassium silicate, or colloidal silica bond phase, and a silicofluoride, phosphate, or organic bond gelling agent. They may also contain potassium fluoride. Since chemically bonded concretes can withstand hot, acidic environments, they offer an abrasion-resistant alternative to organic linings. However, they have a higher permeability than most organic linings and are subject to cracking, so that any condensed acid will reach the substrates to which they are applied. In many cases, an organic membrane is used under a chemically bonded concrete lining to provide additional protection to the carbon steel substrate. While this measure increases the

time for acidic condensate to reach the substrate, it can complicate repair procedures. When the membrane fails due to permeation by acidic species, the concrete must be removed to repair or replace the membrane [16].

### Cost Considerations

The prime objective in selecting construction materials for FGD systems is to choose the most cost-effective or optimum material for each component, i.e., the one meeting the design requirements at the least cost over the life of the facility. A large ratio in the purchase costs of alternative materials may be reduced if installed costs are considered. The reduction can result if the labor costs involved in the installation are significant compared to the difference in the cost of the materials. In addition to installed cost, it is necessary to consider repair and/or replacement cost over the 20- to 30-year design life of the plant when specifying the most economical materials available for the intended service conditions. Certain materials such as organic linings cannot be expected to last the plant lifetime without periodic maintenance touchup, repair, or replacement.

## DESCRIPTION OF CORROSION ENVIRONMENTS ENCOUNTERED

The environment in an FGD system depends upon three factors: temperature, chemistry, and abrasiveness. ASTM has identified three levels of severity, from 1 (mild) to 3 (severe), for classifying these three environmental factors (see Table 1) [17]. Figure 1 is a schematic diagram of environmental severity levels in the major components of a wet FGD system. In all of the three digit codes shown, the first digit represents temperature, the second digit represents chemistry, and the third digit represents abrasiveness. (A code of zero for a given environmental factor denotes that the factor does not exist or is not applicable for a specific operating condition.) For example, the mildest condition encountered can be coded 1-1-1 and represents a temperature below 60°C (140°F), a pH greater than 3 with low concentrations of chloride and fluoride (as defined in Table 1), and low-velocity fluid flow with no direct impingement by particulates. An example of this mild condition is a mist eliminator (see Fig. 1). By contrast, the most severe condition can be coded 3-3-3 and represents a temperature above 93°C (200°F), an acid concentration greater than 15 % with high concentrations of chloride and fluoride, and very high-velocity fluid flow with impingement by entrained particulates.

An example of this severe condition is the inlet of a venturi prescrubber.

Several species in solution have been found to affect the corrosion of alloys in FGD systems. However, most of these species are considered trace elements in scrubbing liquors. Notable exceptions are chlorine and fluorine, both of which are present in coal. Depending on the source, the makeup water can also contribute chlorides and fluorides to the FGD system. When the water balance is tightly closed, dissolved ionic species such as chlorides become highly concentrated. Chloride ions cause both general and localized corrosion in alloys. The corrosion rate for a given alloy is a function of chloride concentration, pH, temperature, and in many instances, the concentrations of trace elements present at levels below 2000 ppm, e.g., aluminum, copper, and iron [18,19]. Uncomplexed fluoride ions can cause localized attack in the heat-affected zone (HAZ) of welded austenitic stainless steels, and can be catastrophic to titanium. In addition to having its own effect on corrosion rates, aluminum, dissolved from fly ash, can react with fluorides to form the complex ions  $AlF_2^{+1}$  and  $AlF^{+2}$ . If there is sufficient aluminum, free fluoride will not be available.

## TECHNIQUES USED FOR CONTROLLING CORROSION AND MATERIALS DEGRADATION

The most important technique for avoiding materials problems is to ensure that the selected material is designed to give satisfactory service in a given environment. The applicability of an alloy in the temperature range of a wet FGD environment is mainly a function of pH and chloride concentration. Because the condensate in an outlet duct or flue can have a pH of 2.5 or lower, a more corrosion-resistant alloy should be used for these components than for an absorber, where the pH of the scrubbing liquor is typically above 5.0. (However, under upset conditions, the pH may drop to 2.0 or lower). The chloride concentration in the scrubbing liquor depends primarily upon the type of coal burned in the boiler. In addition, chlorides are provided by the water balance and the type of makeup water. If there is carryover of scrubbing liquor from the mist eliminator, the chloride concentration in the outlet duct can increase because of evaporation of water during periods of bypass of the absorber. Stainless steel Types 316L, 317LMN, 904L, 254SMO, 25-6MO<sup>®</sup>, and AL6XN<sup>®</sup> have been successfully used in absorber vessels when the chloride concentration is within the applicable range for these alloys. In some FGD reaction tank vessels,

TABLE 1—ASTM classification system for environmental factors in FGD systems.<sup>a</sup>

Level of Severity	Temperature	Chemistry	Abrasiveness
1	Ambient to 60°C (140°F)	pH >3 with <100 ppm F <sup>-</sup> and <1000 ppm Cl <sup>-</sup>	Low velocity fluid flow with no direct impingement of particulates (e.g., duct wall)
2	60° to 93°C (140° to 200°F)	pH 0.1 to 6 with 100 to 1000 ppm F <sup>-</sup> and 1000 to 10 000 ppm Cl <sup>-</sup> , or saturated flue gas	High velocity fluid flow, spray impingement, or strong agitation (e.g., absorber spray zone)
3	Above 93°C (200°F)	Greater than 15 % acid with >1000 ppm F <sup>-</sup> and >10 000 ppm Cl <sup>-</sup> , or intermittent wet/dry zones	Very high velocity fluid flow with impingement of entrained particulates (e.g., venturi throat)

<sup>a</sup>Adapted from Ref 13.

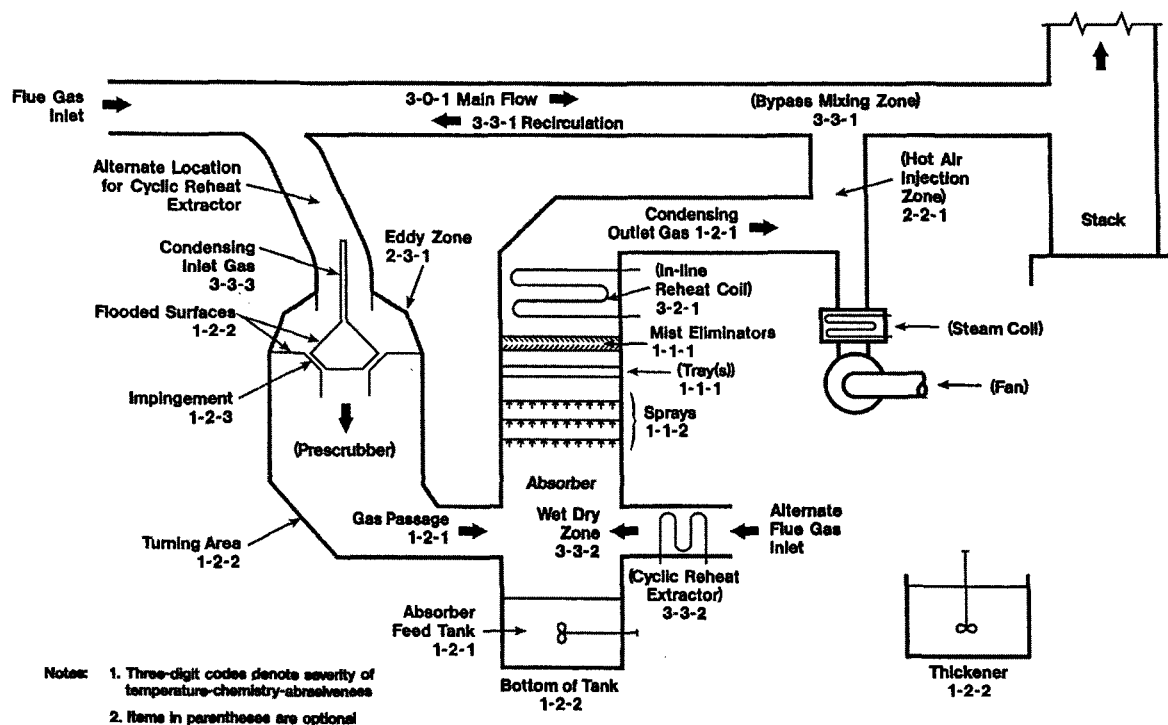


FIG. 1—Schematic diagram of environmental severity levels in wet FGD systems (adapted from Ref 13).

for example, a potential adjustment protection system has been successfully used to control thio-sulfate pitting, chloride/fluoride pitting, crevice corrosion, and general corrosion of all submerged stainless steels Types 317L, 317LMN, and 904L. This combination of stainless steels with the potential adjustment protection system allows the use of an alternative cost effective technique for corrosion control in FGD reaction tanks made of otherwise susceptible materials [20]. In outlet ducts exposed to both scrubbed flue gas and untreated flue gas, the use of a highly corrosion-resistant alloy, such as alloys C-276, C-22®, 622®, 686®, or 59® is generally required to prevent corrosion [21].

In certain cases, it may be possible to modify the environment, i.e., temperature, chemistry, or abrasiveness, to extend the useful life of a material. Temperature modifications in an FGD system can be accomplished only by a limited number of practical methods. These practical methods include: (1) water sprays to protect against thermal excursions, and (2) insulation to reduce thermal gradients. The scrubbed flue gas can be reheated by a variety of methods to prevent, for example, formation of acidic condensate on the floor of the outlet duct or to downstream fans in wet FGD systems. However, most reheat methods increase the capital and operating costs of an FGD system, increase the energy consumption of the system, and create materials problems of their own. Bypass reheat can avoid an increase in energy consumption, but it creates an extremely aggressive environment in the mixing zone of the bypassed gas and the scrubbed gas. Therefore, bypass to the outlet duct or stack for reheat or emergencies should be avoided, if possible.

The process chemistry can be modified by using additives or by minimizing the chloride and fluoride concentrations

in the scrubbing liquor. The use of additives that inhibit oxidation of sulfite to sulfate reduces gypsum deposition, which, in turn, can reduce crevice corrosion that tends to occur under deposits. The use of additives that buffer the pH of the scrubbing liquor may help prevent pH excursions that can cause failure of alloys.

Several methods are available for minimizing the chloride and fluoride concentrations in the scrubbing liquor. These include using a separate quench loop, operating the FGD system with an open water balance, or using sludge stabilization with fly ash and lime so that a considerable amount of water can be purged with the scrubber effluent. A minor reduction of chloride and fluoride concentrations also can be achieved by using river water or well water, rather than cooling tower blowdown, for makeup. Since the chloride and fluoride ions are primarily products of coal combustion, these non-coal related methods for reducing chloride and fluoride only result in minor reductions.

The abrasive effects of fly ash on downstream FGD components also can be minimized by using a separate quench loop, but in conjunction with a venturi prescrubber. Alternatively, a high-efficiency particulate collection device can be used upstream of a wet FGD system.

Aside from the use of linings, other corrosion protection techniques include cathodic protection and corrosion inhibitors. Impressed Current Cathodic Protection (ICCP) technology is attractive because it avoids the use of expensive alloys. The Electric Power Research Institute (EPRI) has developed a system that allows cathodic protection to be applied to duct walls having thin films of condensate, rather than immersed in a liquid [22]. EPRI also has evaluated the performance of several inhibitors on the corrosion behavior

of alloys in a pilot-scale scrubber. The data suggest that the use of corrosion inhibitors in FGD systems is possible, but the results from this particular study were not very encouraging [23].

Another electrochemical technique, potential adjustment protection (PAP), was patented by the Pulp and Paper Research Institute [24]. PAP is an electrochemical corrosion protection technique that is used to protect stainless steel in oxidizing chloride environments. The technique uses a DC current source to move the electrochemical potential of the protected surface in the negative direction. This technique is not cathodic protection (CP) in the traditional sense. Although both CP and PAP move the potential in the electronegative direction, CP requires the set potential to be in the immunity region as depicted by the Pourbaix Diagrams. PAP, on the other hand, takes advantage of the passive film available in stainless steel/oxidizing environment and the set potential is in the passive zone. Some of the economic advantages of PAP versus CP are smaller current source requirements and lower anode consumption. This technique has now been used on 14 FGD stainless steel reaction tanks [25].

Another technique for avoiding corrosion is the use of FRP (GRP in Europe) for FGD components such as absorbers and tanks. FRP vessels as large as 30 m (100 ft) in diameter can be fabricated on site by using a spinning process to produce multiple layers of material [26]. After an initial 3 m (10 ft) high cylindrical section is spun, it is hoisted to the top of the mandrel and another 3 m (10 ft) section is wound, overlapping the first. The overall height of the structure is limited by the mechanical properties of the composite unless external support is provided. A potential problem is abrasion from spray impingement and from highly agitated slurries. The interior surface of a FRP FGD vessel can be lined with an abrasion-resistant lining thus providing additional vessel life.

## SPECIFIC PROBLEM AREAS

### Welding

The quality of the welding is critical in FGD components constructed of stainless steels or nickel-based alloys. Achieving quality control of alloy welding requires stringent specifications, qualified fabricators and installation contractors, and thorough inspection and nondestructive testing of the welds [27]. A great deal of care must be taken to avoid iron contamination during fabrication (e.g., welding by using stainless steel tools and ceramic abrasives). In order to preclude rust blooms, any embedded iron must be removed by an acid pickling treatment. Heat input should be minimized by the use of small diameter welding electrodes and stringer passes to avoid carbide precipitation and hot cracking. Crevice type defects should be avoided or removed by grinding. Assuming that the proper alloy and welding electrodes have been selected for the service environment, the quality of the welds is the next most critical item. Leaking welds can cause discharges of process fluids, which, in turn, can deteriorate external equipment. Corrosion of welds can cause a loss of structural integrity of the welded component, e.g., ductwork, absorbers, and internal supports.

Thin metallic linings require good welding procedures and inspections in order to achieve leak tight welds. Improper welding results in flaws and pinholes in the seal welds between the overlapped alloy sheets. Because of these flaws, liquid can get behind the sheets and cause corrosion of the substrate. Also, during plug welding of the alloy sheets to the substrate, the proper welding material and care must be used to insure that the iron dilution does not adversely affect the corrosion resistance of the weld. One approach is to cover the plug weld with a seal-welded patch of the alloy lining.

### Fire Protection

In cases where combustible linings are used, fire protection should be provided by an automatic water spray system [28]. The system should be designed so that the spray patterns are not obstructed and the lining is completely covered by the spray. The spray nozzles should include corrosion-resistant blowoff caps to prevent plugging. The scrubbing liquor spray nozzles are not suited for fire protection in prescrubbers or absorbers. There have been a few costly fires in FGD systems where the ignition source has been linked to cutting and welding operations during maintenance procedures. Absorbers can contain a large quantity of combustible materials, including plastic mist eliminators and packing, as well as flammable linings. For example, the plastic materials may be as much as 1.2 m (4 ft) in height and 15 m (50 ft) in diameter. The fire hazard is most prevalent when the unit is down for periodic maintenance. Typically, the access hatches are open, allowing a high volume of air movement; the fire loading may be increased due to the presence of combustible scaffolding; and ignition sources may be present because of cutting and welding activities.

The National Fire Protection Association (NFPA), in Report No. NFPA 850, has recognized the fire hazard associated with FGD systems during outage and construction activities [29]. The NFPA committee responsible for this document is considering a revision to enhance guidance. The proposed revision will include identification of hazards for combustible-lined equipment, and will suggest closing the outlet damper during cutting and welding operations to reduce airflow through the equipment [28].

## USE OF TEST METHODS TO EVALUATE CORROSION AND DEGRADATION

Continuous, on-line corrosion monitoring can be used to operate FGD systems at optimal efficiency while avoiding high corrosion rates. Conventional corrosion monitors are designed for use in bulk liquids and do not function satisfactorily in the thin condensate films that form on the surfaces of FGD ducts. Recent EPRI research has made use of an advanced electrochemical method of corrosion surveillance developed by the Corrosion and Protection Centre Industrial Services (CAPCIS) in England [30]. This method allows on-line monitoring of corrosion activity in either thin condensate films or bulk liquids. EPRI introduced the CAPCIS system to the U.S. electric utility industry in 1985, sponsoring several field demonstrations.

An electrochemical monitoring system that tracks the rate and depth of permeation of aggressive chemicals in the walls of FRP or other nonmetallic vessels also is available [31]. The system uses a set of conductivity probes mounted at various depths in the wall of an FRP component. The probes can be attached during fabrication, before final installation, or as a retrofit for equipment already installed.

Methods to evaluate materials performance are used both for materials selection and for failure analysis. Materials selection can be based on field surveys, exposure tests in commercial units, or laboratory test results [21]. Field surveys represent long-term results from actual test environments, but the environmental conditions usually are not well-defined or constant. Exposure tests in commercial units may or may not be realistic, depending upon the test method approach. This point is discussed in the next section. Laboratory tests with simulated flue gas run the risk of missing the effects of trace constituents, which typically are not present in simulated environments. Laboratory tests with selected trace elements may not be indicative of the effect of these elements on materials performance in the field.

Failure analysis involves documentation of environmental conditions, inspection of the failed component, collection of samples of the failed material, any deposits on the material, and any liquids that condensed on or contacted the material, and appropriate laboratory analyses of the collected samples. The laboratory results and the background information are analyzed in an attempt to deduce the failure mechanism and/or the failure cause [32].

### Test Method Approach

Coal has been described as garbage of a previous eon. Thus, because coal contains very many of the elements in the periodic table, it is difficult to simulate the environment in an FGD system. The scrubbed flue gas from coal-fired power plants typically contains nitrogen, carbon dioxide ( $\text{CO}_2$ ), oxygen, water vapor ( $\text{H}_2\text{O}$ ), sulfur dioxide ( $\text{SO}_2$ ), sulfur trioxide ( $\text{SO}_3$ ), nitric oxide ( $\text{NO}$ ), nitrogen dioxide ( $\text{NO}_2$ ), hydrogen chloride ( $\text{HCl}$ ), hydrogen fluoride ( $\text{HF}$ ), trace organics, fly ash, and solids carried over from the absorber slurry. The concentration of species such as  $\text{HCl}$  and  $\text{HF}$  are very low in the scrubbed gas, but can be significant if some flue gas is bypassed for reheat. In one of the early FGD bypass reheated outlet ducts, the scale on the walls of the duct was 10 % potassium fluoride ( $\text{KF}$ ) [8].

If gas cylinders are used to prepare simulated flue gas for exposure testing, many cylinders may be required to run long exposure periods. If a combustion source is used to supply flue gas, it is difficult to match the composition of flue gas from a large pulverized coal-fired boiler. Maintaining the proper ratio of  $\text{NO}$  to  $\text{NO}_2$  is a special problem because  $\text{NO}$  oxidation to  $\text{NO}_2$  is a function of the temperature, the initial  $\text{NO}$  concentration, the oxygen concentration, and the gas residence time in the exposure chamber. The usual procedure is to use simulated flue gas with the same  $\text{SO}_2$  concentration as actual flue gas, but with different concentrations of other species. This procedure can produce erroneous results.

Many species are typically present at various concentrations in FGD outlet duct condensate [15]. Those typically present at concentrations greater than 100 mg/L include aluminum,

calcium, iron, potassium, magnesium, sodium, chlorine, fluorine, sulfate ( $\text{SO}_4^{2-}$ ), borate ( $\text{B}_4\text{O}_7^{2-}$ ), and phosphate ( $\text{PO}_4^{3-}$ ). Species present in the range of 10–100 mg/L include manganese, selenium, silicon, tin, titanium, vanadium, zinc, and nitrate ( $\text{NO}_3^-$ ). Several species, including barium, beryllium, cadmium, lead, and antimony, are present at concentrations less than 10 mg/L. The pH ranges from less than 1.0 to about 2.5, depending on FGD system operating parameters. In preparing solutions for exposure testing, solubility problems need to be considered. If precipitation occurs in a solution the composition changes. Also, if some species typically present in FGD condensate are omitted from the test solution, the results can be erroneous. As previously mentioned, trace elements can affect corrosion rates.

Many of the exposure tests in commercial units have involved the use of spools or racks of different materials placed in various locations inside an FGD system [33]. Although this type of testing can provide comparative data for materials, it may not provide accurate corrosion or degradation rates. By using more corrosion racks, at many locations inside an FGD system, there is a good probability that one or more of the corrosion racks will experience the desired corrosion rates. The environment in the bulk gas stream, in which the specimens are usually placed, is not the same as at a duct wall, where condensation can occur. In some field tests, the specimens were directly mounted on the duct wall so that they experienced the same conditions as the wall [34]. Test coupons were mounted using bolts of the same alloy as the duct wall. To avoid galvanic corrosion of alloy coupons, the coupons were insulated from the bolts and the substrate with fluoropolymer film and washers.

### Methods Used

Laboratory exposure tests are usually conducted in chambers similar to that described in ASTM B 117, Test Method of Salt Spray (Fog) Testing. Because the environment is more corrosive than the salt fog described in ASTM B 117, the variations described in ASTM G 85, Practice for Modified Salt Spray (Fog) Testing, are often used. Some investigators have used a modified procedure in which the test coupons are mounted over holes on the outside wall of the exposure chamber so that they can be subjected to a thermal gradient [35]. Outside mounting of the coupons also affords the opportunity to conduct in situ electrochemical impedance measurements.

Electrochemical impedance spectroscopy (EIS) is an AC technique for determining the components of an analog electric circuit that represents an electrochemical process [36]. Electrochemical impedance is the ratio of the change in potential to the change in current ( $\Delta E/\Delta I$ ) and is determined from the applied potential and the response current as a function of frequency ( $\omega$ ) in an electrochemical cell, when potential and current are linearly related. The impedance,  $Z$ , is a complex number incorporating both the magnitude of  $\Delta E/\Delta I$  and the phase shift between  $E$  and  $I$ . EIS can give extremely valuable mechanistic information for analyzing the corrosion behavior of alloys [37] and for analyzing the performance of coatings [38].

Two ASTM test methods are particularly useful for characterizing organic resin linings and bricks, respectively. These

methods include ASTM D 1653, Test Methods for Water Vapor Transmission of Organic Coating Films; and ASTM C 20, Test Methods for Apparent Porosity, Water Absorption, Apparent Specific Gravity, and Bulk Density of Burned Refractory Brick and Shapes by Boiling Water.

Two additional test methods regarding bricks are worthy of mention. One is a laboratory test in which the moisture expansion that occurred in service is recovered as a shrinkage during heating of a brick sample in a dilatometer [14]. The dilatometer measures thermal expansion as a function of temperature. Shrinkage causes a hysteresis in the thermal expansion curve so that the heating and cooling curves do not coincide. The shrinkage is determined from the difference in the curves at room temperature.

The other method is a field test to document the amount of lean in a free-standing brick flue. A laser beam is used to project a target onto the interior surface of a flue in four compass directions spaced 90° apart. In each direction, the target is tracked at predetermined incremental elevations for the entire height of the stack. The precise position of the target is determined by a triangulation method using two Kern electronic theodolites (precision optical tooling instruments) and a computerized data acquisition system. The data from each compass direction provide a profile of the interior surface of the flue. Opposing wall profiles are used to calculate centerline profiles, which give the amount of lean as a function of height [14].

Standard laboratory techniques are used to characterize samples for a failure analysis. These techniques include metallography, scanning electron microscopy (SEM), electron probe microanalysis (EPMA), X-ray diffraction (XRD), Fourier transform-infrared analysis (FTIR), and analytical chemistry.

## COMMENTS

New materials and innovative applications of existing materials are continually being developed for use in FGD system components. Some of the interesting recent developments include multifunctional epoxy linings with improved environmental resistance, thermal spraying alloy coatings on carbon steel substrates, centrifugal slurry pumps constructed of erosion-resistant cast alloys, solid ceramic ball valves to control slurry flow rates, round and rectangular ductwork constructed of sandwich panels (face sheets welded to a truss core), and structures made of high-strength fabric and sturdy support systems for constructing absorbers, outlet ducts, and stacks or stack liners. Some of these materials or applications may require the development of new testing methods and standards. A test method for continuous monitoring of organic resin lining performance in FGD systems would be very useful if it could be developed.

## REFERENCES

- [1] Morse, S. L. and Stevens, C. E., "Alloy C-276 Clad Steel Plate for Handling Scrubbed Flue Gases," *Proceedings of the 1990 Air Pollution Seminar*, Paper No. 9, NACE, Houston, TX, 1990.
- [2] Cerny, M. X. and Dormer, C. G., "Resista-Clad Plate in Flue Gas Desulfurization Units," *Proceedings of the 1987 Air Pollution Seminar*, Paper No. 21, NACE, Houston, TX, 1987.
- [3] Richard, R. L., "Economics of a C-276 Outlet Duct Wallpaper Retrofit at Public Service Indiana Gibson #5," *Proceedings of the 1987 Air Pollution Seminar*, Paper No. 4, NACE, Houston, TX, 1987.
- [4] NACE International RP-0292: Installation of Thin Metallic Wallpaper Lining in Air Pollution Control and Other Process Equipment, NACE International, Houston, TX.
- [5] NACE International RP-0199: Installation of Stainless Chromium-Nickel Steel and Nickel-Alloy Roll-Bonded and Explosion-Bonded Clad Plate in Air Pollution Control Equipment, NACE International, Houston, TX.
- [6] Koch, G. H. and Beavers, J. A., "Laboratory and Field Evaluation of Materials for Flue Gas Sulfurization Systems," *Proceedings of the Seventh Symposium on Flue Gas Desulfurization*, Paper No. 2D, U.S. Environmental Protection Agency, Research Triangle Park, NC, 1982.
- [7] Koch, G. H., Beavers, J. A., and Christman, T. K., "Materials Testing in Synthetic FGD Environments," Report CS-2740, Electric Power Research Institute, Palo Alto, CA, 1984.
- [8] Dille, E. R. and Lempke, T., "FGD Corrosion at the R. D. Morrow, Sr. Generating Plant," Solving Corrosion Problems in Air Pollution Equipment Seminar, PCA-IGCI-NACE, Denver, CO, 1981.
- [9] Dille, E. R., "Tame the Latest FGD-System Corrosion Pest: Fluorides," *Power Magazine*, August 1983.
- [10] Beavers, J. A. and Koch, G. H., "Review of Corrosion Related Failures in Flue Gas Desulfurization Systems," *Corrosion*/82, Paper No. 202, NACE, Houston, TX, 1982.
- [11] Leidheiser, H. Jr., White, M. L., Granata, R. D., and Vedage, H. L., "Mechanisms of Failure of Coatings Used in Flue Gas Desulfurization Systems," Report CS-4546, Electric Power Research Institute, Palo Alto, CA, 1986.
- [12] Montle, J. F., "Unexplained Coating Phenomena with Some Partially Baked Answers," *Corrosion*/71, Paper No. 53, NACE, Houston, TX, 1971.
- [13] Ellis, P. F. and Cassidy, P., "Specification Guidelines for Flue Gas Desulfurization Rubber," Report CS-5528, Electric Power Research Institute, Palo Alto, CA, 1987.
- [14] Rosenberg, H. S., Kistler, C. W. Jr., Brust, F. W., Dille, E. R., et al., "Leaning Brick Stack Liners," Report GS-6520, Electric Power Research Institute, Palo Alto, CA, 1989.
- [15] Rosenberg, H. S., Koch, G. H., Meadows, M. L., and Stewart, D. A., "Materials for Outlet Ducts in Wet FGD Systems," *Materials Performance*, Vol. 25, No. 2, February 1986, pp. 41-55.
- [16] Rosenberg, H. S., Koch, G. H., Kistler, C. W. Jr., et al., "Performance of Linings in FGD Systems," *Proceedings: First Combined Flue Gas Desulfurization and Dry SO<sub>2</sub> Control Symposium*, Paper No. 9C-4, Electric Power Research Institute, Palo Alto, CA, 1988.
- [17] Accortt, J. I., et al., *Manual of Protective Linings for Flue Gas Desulfurization Systems*, ASTM STP 837, ASTM International, West Conshohocken, PA, 1984.
- [18] Koch, G. H., Thompson, N. G., and Means, J. L., "Effects of Trace Elements in Flue Gas Desulfurization Environments on the Corrosion of Alloys—A Literature Review," Report CS-4347, Electric Power Research Institute, Palo Alto, CA, 1986.
- [19] Mansfeld, F., "The Effects of SO<sub>2</sub> Scrubber Chemistry on Corrosion," Report CS-4847, Electric Power Research Institute, Palo Alto, CA; Pal Dille, E. R. and Shim, W., "History of Electrochemical Protection of Flue Gas Desulfurization Reaction Tanks," Paper No. 0580, *Corrosion*/2000, NACE International, Houston, TX, 2000.
- [20] Dille, E. R., "Using Electrochemical Protection to Prolong Service Life of Scrubbers and Associated Equipment," *AIR-POL, update/98, Corrosion*/98, NACE International, San Diego, CA, March 1998.
- [21] Rosenberg, H. S., Hindin, B., and Radcliffe, P. T., "Guidelines for FGD Materials Selection and Corrosion Protection," *Proceedings of the 1992 Air Pollution Seminar*, NACE, Houston, TX, 1992.

- [22] Koch, G. H., Pednekar, S. P., Patterson, E. H., and Syrett, B. C., "Corrosion Control by Impressed Current Cathodic Protection in the Outlet Duct of a Pilot Wet Scrubber," *Proceedings of the 1990 SO<sub>2</sub> Control Symposium*, Paper No. 4B-5, Electric Power Research Institute, Palo Alto, CA, 1990.
- [23] Phull, B. S., Lee, T. S., Martin, N. H., and Syrett, B. C., "Corrosion Inhibitors for Flue Gas Desulfurization Systems," *Materials Performance*, Vol. 27, No. 2, February 1988, pp. 12–20.
- [24] US Patent 4,285,232: Monitor Assembly for Electrochemical Corrosion Protection of Stainless Steel Bleach Plant Washers, Garner, Andrew, Pulp and Paper Research Institute of Canada, August 25, 1981.
- [25] Dille, E. R. and Shim, W., "Electrochemical Protection of Flue Gas Desulfurization Reaction Tanks," Paper No. 0580, *Corrosion/2000*, NACE International, Houston, TX 2000.
- [26] Selley, J. and Kamody, J., "Build a Durable FGD System with FRP," *Chemical Engineering Progress*, Vol. 87, No. 9, September 1991, pp. 86–92.
- [27] Cantrell, G., Pickett, C. B., Froelich, D. A., and Pattison, D. C., "Quality Control of Alloy Welding in Flue Gas Desulfurization Installations," *Proceedings of the 1990 Air Pollution Seminar*, Paper No. 12, NACE, Houston, TX, 1990.
- [28] Adcock, R. C., Biggins, J. B., Fringeli, R. E., et al., "Clean Air Act Amendments: Overview of Gas and Electric Utility Fire Protection," Draft Report, M&M Protection Consultants, Chicago, 1991.
- [29] "Recommended Practice for Fire Protection for Fossil-Fueled Steam and Combustion Turbine Electric Generating Plants," Report No. NFPA 850, National Fire Protection Association, Quincy, MA, 1990.
- [30] Gearey, D. and Cox, W. M., "Multitechnique Corrosion Monitoring in Flue Gas Desulfurization Systems: Phase I," Report CS-5605, Electric Power Research Institute, Palo Alto, CA, 1988.
- [31] "Conductivity Probe Guards Against FRP Degradation," *Chemical Engineering*, Vol. 98, No. 7, July 1991, p. 163.
- [32] Rosenberg, H. S., "Performance Analysis of Materials in Wet FGD System Components," Report, Electric Power Research Institute, Palo Alto, CA, 1994.
- [33] Hoxie, E. C. and Tuffnell, G. W., "A Summary of INCO Corrosion Tests in Power Plant Flue Gas Scrubbing Systems," *Resolving Corrosion Problems in Air Pollution Control Equipment*, NACE, Houston, TX, 1976, pp. 65–71.
- [34] Koch, G. H., Kistler, C., and Mirick, W., "Evaluation of Flue Gas Desulfurization Materials in the Mixing Zone: R. D. Morrow Sr. Generating Station," Report CS-5476, Electric Power Research Institute, Palo Alto, CA, 1987.
- [35] Rosenberg, H. S. and Spangler, J. M., "Effect of Environmental Parameters on the Performance of Coatings in FGD Ductwork," Report TR-102162, Electric Power Research Institute, Palo Alto, CA, 1993.
- [36] Gabrielli, C., "Identification of Electrochemical Processes by Frequency Response Analysis," Issue 2, Technical Report/83, Solartron Instrumentation Group, Burlington, MA, 1984.
- [37] Kendig, M. W. and Mansfeld, F., "Corrosion Rates from Impedance Measurements: An Improved Approach for Rapid Automatic Analysis," *Corrosion*, Vol. 39, No. 11, November 1983, pp. 466–467.
- [38] Kendig, M. and Scully, J., "Basic Aspects of the Application of Electrochemical Impedance for the Life Prediction of Organic Coatings on Metals," *Corrosion/89*, Paper No. 32, NACE, Houston, TX, 1989.

# Electronics

Robert Baboian<sup>1</sup>

FAILURE IN ELECTRONICS DUE TO corrosion has become a significant factor because of the extremely complex systems (microchips, integrated circuits, computers, etc.) that have been developed and the increasing demand on their reliability. Electronics are now a part of all industries, ranging from transportation industries to medical and consumer products. Technological advances have resulted in the development of sophisticated components with closer spacing so that extremely low levels of corrosive contaminants can cause failure. Testing for this type of behavior is difficult and costly. Further advances in electronics can only be made where corrosion issues are addressed and reliability is maintained. Many publications have appeared in the technical literature on the subject of corrosion in electronics with more and more emphasis on testing [1–10].

## MATERIALS

Electronic materials include a broad range of metals and alloys depending on the specific system, equipment, and components. The system as a whole can include structural materials such as steels, copper, nickel and their alloys, aluminum, and titanium. The system can also include structural materials used for cabinets as well as those used for electronic components. The broadest range of materials used in electronics is in components including integrated circuits, printed circuit boards, contacts, connectors, switches and relays, grounding contacts, and thermal contacts. Table 1 lists various electrical components and includes important materials of construction. Materials used for integrated circuit conductors are aluminum based alloys, often alloyed with silicon and copper, and more recently copper. Conductors and connectors in PC boards are typically made of copper and are soldered with lead-tin alloys or complex additives to these metals. Contacts are fabricated from a range of materials but mainly copper plated with tin, nickel, or gold for added corrosion resistance.

Coupled with the materials used in electronics, the design of electronic devices plays an important role in corrosion behavior. For example, silicon based integrated circuit elements are spaced less than 0.2 microns. Minimum linewidth in state-of-the-art PC boards is less than 100 microns. On hybrid integrated circuits, line spacings may

be less than 5 microns (10). The tolerance for corrosion becomes extremely small with these designs and materials.

## ENVIRONMENTS

Electronics are exposed to a wide range of outdoor and indoor environments generally considered as atmospheric exposure. The corrosion behavior is determined by the actual environment, which can be as benign as a simple low humidity, purified atmosphere, indoor location, to the aggressive environment existing at a pulp and paper mill or on an automobile, which is subjected to road salt splash and spray. The electronics design as well as the nature of the environment are important because failures in printed circuit boards, integrated circuits, and other components have been known to occur even in extremely low levels of moisture and contaminants. Electronics components are mostly indoor or sheltered from direct exposure to liquid splash, spray, rain, snow, etc., and therefore the environment is considered atmospheric exposure.

Materials used in electronics are susceptible to corrosion in a wide range of environments. For example, sulfidation of silver in H<sub>2</sub>S occurs in dry as well as humid air. However, moisture in the form of humidity is generally required for atmospheric corrosion to occur. When the humidity is increased, a moisture film can form on the metallic surface and can yield an increased rate of corrosion. The duration of time at which this occurs is referred to as time of wetness (TOW). However, the humidity at which wetness occurs is dependent on a number of factors including the nature of the material, surface roughness and composition, temperature, and surface contamination including atmospheric pollutants. Since the nature and significance of the moisture film is dependent on very complex and synergistic interactions among a large number of variables, this subject has received a great amount of attention and has resulted in conflicting points of view. This behavior is significant because corrosion tests must be designed properly and include the effects of complex and synergistic reactions. Otherwise, the test environments will not represent those to which electronics are exposed.

In some cases, a critical humidity exists above which significant corrosion occurs. This behavior has been described for steel in SO<sub>2</sub> [11]. However, many of the materials used in electronics do not exhibit this behavior. Copper in SO<sub>2</sub>, for example, corrodes at a steadily increasing rate with

<sup>1</sup>RB Corrosion Service, 84 Ruff Stone Rd., Greenville, RI 02828.



**TABLE 1**—Electrical components.

Component	Design	Materials
Printed Circuit Board	Metallic conductor separated by insulating materials	Copper, copper alloys, copper clad materials, epoxy, resins, ceramics, woven glass fiber, electroplate, solder, tin, lead, conformal coatings
Contacts	Electrical contact maintained by mechanical force	Base Metal—copper alloys, steels (clad) Contact Surface—gold, palladium, silver-palladium, silver, tin, tin-lead, copper
Connectors	Electrical connections between systems or boards	Spring Material—beryllium copper, stainless steels Contact Surface—gold, palladium, silver, silver-palladium, tin, tin-lead
Switches and Relays	Cyclic electrical connection	Copper alloys, steels, stainless steels, electroplate and contact surface materials
Grounding contacts	For shielding	Copper, steels, aluminum, nickel, tin, tin-lead and contact surface materials
Thermal contacts	Heat sinks	Copper, aluminum
Integrated circuits	Small dimension complex systems	Gold, silver, aluminum, Kovar, solder, glass, ceramic, silicon, silicon dioxide, silicon nitride, tungsten

**TABLE 2**—Environmental pollutants causing corrosion.

Pollutant	Sources	Susceptible Metals
Sulfur Dioxide (SO <sub>2</sub> )	Fossil fuel combustion, petrochemical industries, pulp and paper industry, metal producing industry	Most metals
Nitrogen Dioxide (NO <sub>2</sub> )	Auto & truck emissions, fossil fuel combustion, various industries	Copper, brass, synergistic with SO <sub>2</sub>
Hydrogen Sulfide (H <sub>2</sub> S)	Pulp & paper industries, chemical industry, sewage plants, garbage dumps, oil refineries, animal shelters, volcanic activity, swamp areas, marine tidal areas	All copper and silver based metals
Chlorine (Cl <sub>2</sub> ) but most important is chlorine containing gases.	Bleaching plants in industries, metal production, PVC plants, cleaning agents	Most metals synergistic with other pollutants
Ammonia and Its Salts (NH <sub>3</sub> and NH <sub>4</sub> <sup>+</sup> )	Fertilizer, animal and human activity, detergents	All copper based alloys, nickel, silver
Chloride (Cl <sup>-</sup> )	Sea salt mist, road salt areas	Most metals
Soot (Carbon)	Combustion, auto and truck emissions, steel production	Synergistic with other pollutants; provides cathodic sites for most metals
Ozone	Formed in polluted areas, highest concentrations in smog	Strong oxidant to produce acids which attack most metals
Mineral Acids (H <sub>2</sub> SO <sub>4</sub> , HCl, HF, HNO <sub>3</sub> )	Pickling industry, chemical industry, metals production, semiconductor industry	Most metals, glass, ceramics
Organic acids	Wood, packing material, animals, preservatives	Long-term effects on some metals

increasing humidity, while in the absence of pollutants, its corrosion rate is very low, even at 100 % relative humidity. The presence of certain atmospheric pollutants therefore enhances corrosion by reaction on the surface in the presence of moisture to form corrosive species or corrosion products, or both. Their properties are different for each metal and therefore the corrosion behavior will vary. Some pollutants that can cause corrosion in electronics are listed in Table 2, along with their sources and effects on electronic materials. This table does not include the wide range of submicron atmospheric particles including various compounds of sulfate, chloride, nitrate, sodium, ammonium, potassium, magnesium, and calcium [12]. These particles deposit on surfaces and react with moisture to form corrosive electrolytes. Sulfate and ammonium ions are the most common ones found in particulates in outdoor and indoor environments.

Another source of contamination is chemicals from outgassing of organic materials. These vapors from sealants, resins, plastics, coatings, and packing materials can be emitted in closed areas and therefore can reach appreciable concentrations [1]. Examples are: acetic acid from silicone sealants; sulfurous vapors from polysulfide sealants; phenols from phenolic resins; ammonia from molded resins; organic acids from adhesives; amines from epoxy; sulfurous

vapors from paper, cardboard, and insulation; and formic and acetic acids from wood. Rubbers, plastics, and adhesives are also known to have residual acids that can leach out to cause corrosion problems. For example, residual acrylic acid in acrylate adhesives has caused pitting in stainless steel. Many types of rubber outgas sulfur or hydrogen sulfide, or both, which will react with copper and silver alloys. Such rubber can be found in furniture, carpet backing, rubber bands, etc.

Another group of contaminants causing failure in electronics is residual chemicals. These are generally introduced during manufacturing and include fluxes, cleaning compounds, plating solutions, and metal processing fluids. Also included here are chemicals from fingerprints and saliva. Many of these include chlorides, and when these contaminants, such as residual chloride flux, are not removed, corrosive electrolytes are formed.

## CLASSIFICATION OF ENVIRONMENTS

Classification of TOW has been included in ISO 9223, Corrosion of Metals-Classification of the Environment, and has been documented by the Nordic Research Project, as shown in Table 3, which includes six TOW classes where

**TABLE 3**—Classification of time of wetness (TOW).

Category	Time of Wetness		Example of Occurrence
	Hours/Year	% of Year	
$\tau_1$	<10	<0.1	Indoor air with climatic control
$\tau_2$	10–250	0.1–3	Indoor air in normal rooms for living or working conditions
$\tau_3$	250–1000	3–10	Indoor air storage rooms
$\tau_4$	1000–2500	10–30	Indoor air in some production rooms. Outdoor air in cold zone, dry zone, parts of temperate zone
$\tau_5$	2500–5500	30–60	Outdoor air in parts of temperate zone, parts of warm zone. Indoor air in animal houses.
$\tau_6$	>5500	>60	Outdoor air in tropical zone. Indoor air in greenhouse.

Source: Ref 1.

**TABLE 4**—Classification of corrosivity of copper reactivity.

Severity Level	Copper Reactivity (A first month exposure)	Explanation of Severity Level
G1 Mild	<300	Corrosion is not a factor in determining reliability.
G2 Moderate	<1000	The effects of corrosion are measurable and may be a factor in determining equipment reliability.
G3 Harsh	<2000	There is high probability that corrosive attack will occur. Environmental control or specially designed and packaged equipment is recommended.
GX Severe	>2000	Only specially designed and packaged equipment would be expected to survive. Specification of equipment in this class is a matter of negotiation between user and supplier.

Source: ANSI/ISA Standard SP71.

**TABLE 5**—Classification of corrosivity by pollutant level.

Class	Temperature °C	Relative Humidity, %	Pollutant Level, ppb		
			Cl <sub>2</sub>	NO <sub>2</sub>	H <sub>2</sub> S
I	—	—	Negligible	Negligible	Negligible
II	30	70	10 ± 3	200 ± 50	10 ± 5
III	30	75	20 ± 5	200 ± 50	100 ± 20
IV	50	75	50	200	200

Source: Ref 13.

$\tau_1$  to  $\tau_3$  are for indoor conditions and  $\tau_4$  to  $\tau_6$  mainly apply to outdoor environments [1].

Classification of corrosivity has been treated by Abbott in his pioneering work at Battelle [13]. Subsequently, other researchers have made contributions to the development of classification systems and these have been incorporated in standards developed throughout the world [14–16]. Since corrosivity depends on a wide range of factors, including material, physical and chemical properties of the environment, a classification system should be based on these factors. However, the complex interaction of these factors requires that some simplification be made. In general, two systems of classification are used. One is based on corrosion

of copper measured in the environment. The other is based on the levels of relative humidity and pollutants.

Classification according to copper corrosion is used because it is used widely in electronics. Also, copper provides a good representation of how many metals behave in environments. Several reports describe the use of copper where coupons are exposed for at least one month (three to twelve months for low levels of corrosivity) and the amount of corrosion product is determined by weight gain or cathodic reduction, or both [17–20]. Table 4 gives a classification of corrosivity according to copper reactivity as described in ANSI/ISA-SP71.

Classification according to levels of relative humidity and pollutants has gained wide acceptance, especially in combination with copper coupons. One classification of corrosivity is listed in Table 5 with 70–75 % relative humidity, 30–50°C temperature, and the indicated levels of H<sub>2</sub>S, NO<sub>2</sub>, and Cl<sub>2</sub> [21]. These classes of corrosivity are confirmed with copper coupons with no corrosion effect on reliability in a Class I environment, and with corrosion effects above that level. Other pollutants from the list in Table 2 can also be used to classify corrosivity; however, these three are the most commonly used. Since chlorine converts to hydrogen chloride in these tests, some researchers use the end product hydrogen chloride since it is a more exact procedure.

In some cases, the systems of classification are not adequate and can be related to specific factors. For example, behavior of silver contacts in sulfide environments can only be correlated with silver test material. In general, where local conditions vary significantly, correlation may be poor.

## CORROSION MECHANISMS

Corrosion mechanisms in electronic components have been the subject of intense study. Since electronics are largely found indoors and/or within packages or cabinets, the mechanisms leading to corrosion problems are not easily defined. Problems are compounded by the fact that these systems are fabricated by a number of complex processes and consist of a variety of dissimilar materials. Miniaturization and the requirement for high component density has resulted in smaller components, closer spacing, and thinner metallic paths. Thus, the effect of bias potentials and small defects is magnified.

Bias potentials provide corrosion mechanisms due to both anodic reaction and cathodic reaction. These reactions include the formation of acidic or alkaline electrolytes, and ion migration. Pore corrosion and corrosion product creep, galvanic corrosion, and fretting corrosion in connectors are other important mechanisms with electronics. Many of these mechanisms occur due to processing related corrosive residues.

Uniform and localized corrosion mechanisms are all-important in electronic systems and are described elsewhere in this manual. However, some extremely important mechanisms of degradation are unique to this field of interest [22–26]. Pore corrosion is one of these and is frequently associated with noble metal coatings such as gold on copper/nickel [23,24]. Defects in the noble metal coatings give rise to galvanically accelerated pitting of the underlying

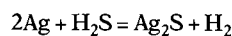
base metal. When that process occurs, the corrosion products (for example from copper) can migrate over the surface of the metal coating (such as gold).

Several mechanisms of migration are known to cause problems in electronics and involve metal migration and ion migration [1–4,9,22,23].

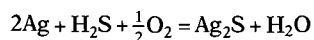
Metal migration occurring electrolytically involves: (1) electrodisolution, (2) ion transport, and (3) electrodeposition [25]. The metallic material is oxidized producing ions that are transported through an electrolyte by electrical migration, diffusion, or convection, and then cathodic reduction of the metal ions at dendritic nucleation sites [25]. Failure results due to the resulting conductive path formed across the dielectric between biased electrodes. This behavior has been reported for silver, gold, copper, and tin on devices such as integrated circuits and circuit boards.

Ion migration involves movement of metal ions over a surface away from the source metal [26,27]. The phenomenon is commonly referred to as corrosion product creep. The mechanism is not well understood, but it is known to occur in humid or dry environments depending on the materials. Tarnish films that form on copper in environments containing  $\text{H}_2\text{S}$  and high humidity can creep over adjoining gold surfaces causing increased contact resistance of the gold [26]. Silver iodide, formed when silver is exposed to dry iodine vapor, will creep over tantalum [27]. The latter mechanism involves silver ion migration in silver iodide and electronic conduction in the silver iodide. The driving force in the copper/gold system is thought to involve the local galvanic cell between the dissimilar metals. However, a mechanism involving conductive copper oxide is possible.

One of the most widely investigated effects is the atmospheric sulfidation of silver used in electronics. The mechanisms of silver corrosion in polluted dry and humid atmospheres have been studied [28]. For example, the reaction of silver and  $\text{H}_2\text{S}$  in air can occur directly



or by reaction with oxygen



The latter reaction mechanism is favored by most researchers. The presence of  $\text{NO}_2$  with  $\text{H}_2\text{S}$  greatly enhances silver sulfidation and when high relative humidity is added, the rate of sulfidation is extremely rapid and is limited by gas-phase diffusion even at high flow rates. Therefore, the solid-state transport of silver atoms from the bulk is faster than the interfacial reaction and does not affect the rate.

The silver sulfidation studies serve a very important point to demonstrate the complexity of mechanisms due to synergistic environmental effects. These synergistic effects are not well understood and are difficult to produce during testing unless specific conditions are met. One can easily understand how improper tests can yield results that do not duplicate actual service behavior.

Another phenomenon in electronics degradation is whisker growth, defined as filamentary growth on metallic materials [22–29]. Whiskers can be metallic or inorganic compounds. Although this behavior is still under investigation, it is reported to be a form of induced recrystallization

related to metallurgical imperfections and occurs under the influence of stress. Whiskers grow on tin, zinc, cadmium, and silver and can grow long enough to short out circuitry. Fretting is important in electronics because it can cause loss in electrical continuity in contacts, connectors, and other systems [30]. It occurs under relative motion at a contacting interface in a reactive environment. The relative motion may be produced by vibration, differential thermal expansion, or cyclic contact.

The mechanism of degradation due to the deposition of airborne particles has recently received attention [31]. When the system is exposed to moderately elevated relative humidity (typically 60 %), the critical humidity of the deposited particle is exceeded and the surface absorbs sufficient moisture to form an electrolyte solution. Various corrosion mechanisms including uniform and localized types can therefore occur, leading to failures.

## CORROSION OF COMPONENTS

Structural materials that are directly exposed, such as in cabinets, housings, and heat sinks, are fabricated from materials such as steels, stainless steels, brass, zinc, aluminum, and other metals and alloys with appropriate properties. The types of corrosion encountered in these structures depend on the environment and material as would be expected. Both uniform and localized corrosion can be important when cosmetic corrosion is of concern. In structural applications, crevice corrosion, corrosion fatigue, stress corrosion cracking (SCC), galvanic corrosion, and intergranular corrosion causing reduction in mechanical properties are important.

Printed circuit boards are generally fabricated with copper conductors separated by insulating materials and also incorporate several other metals. These systems are susceptible to corrosion when residual chemicals such as fluxes exist, and outgassing of insulating or adhesive materials such as epoxy or resin occurs. Galvanic corrosion and metal migration due to bias potentials is common under these conditions. Corrosion product creep and metal migration can cause shorting and failure.

Contacts are fabricated with a wide range of materials including gold, silver, and tin. Gold is either clad or electroplated on a substrate metal, usually a conductive material such as copper. When electroplated, a nickel underlayer is used to act as a diffusion barrier. Pore corrosion in the gold electroplate and/or corrosion product creep (usually from copper) can lead to failure. To prevent sticking and erosion, cadmium oxide is incorporated into silver in high current contact applications. With tin, the main cause of failure is fretting. An increase in resistance between contact surfaces is most destructive and is generally a direct result of corrosion reactions.

Connectors are a critical part of an electronic system. Corrosion mechanisms at connector interfaces include pore corrosion, corrosion product creep, fretting, and SCC and general attack. Pore corrosion in connectors is associated with surfaces plated with gold or other precious metals. Corrosion product creep in connectors usually involves copper corrosion products originating from exposed base

metal areas such as at edges with migration distances approaching 8 mm in several months. Fretting is mainly associated with tin in aggressive environments and where relative motion exists in the connector contact surfaces. Precious metals are also affected by fretting under more severe conditions. In some environments, SCC of connector base metals can occur. Copper alloy is susceptible to SCC in ammonia containing atmospheres. Some precious metal surfaces are susceptible to general corrosion in specific environments, which can affect contact resistance. One example is sulfur reacting with silver surfaces.

Switches and relays are also required to maintain conductive contact surfaces as well as thousands or millions of cycles of operation. The same corrosion mechanisms, such as fretting, exist with these devices as observed with connectors and contacts. However, the mechanical requirements can lead to additional wear and erosion corrosion problems.

The requirement to maintain electrical continuity in grounding and electromagnetic interference (EMI) shielding requires that corrosion in the contact areas be avoided. Galvanic corrosion, where dissimilar metals must be bonded, can lead to an increase in electrical resistance and loss in grounding. The same effect can occur with thermal contacts with the additional effect of higher temperatures.

Integrated circuits (IC) are highly intolerant to corrosion due to their small dimensions [5]. One example of a packaged IC consists of a silicon chip mounted on a metal support or frame, small gold wires to attach an aluminum pad on the circuit to external pins, and a plastic, epoxy, or silicone encapsulating material to protect the chip and wire connections. The frame is made from copper, Kovar, alloy 42, or nickel and is selectively plated with gold or silver. This encapsulated package with soldered or plated leads is extremely complex and therefore is susceptible to many corrosion mechanisms. The behavior of the package in a humid environment is highly dependent on the quality of the encapsulation. Moisture permeation, residual deposits such as chlorides, and atmospheric contaminants in contact with the silicon device will contribute to corrosion. Even minimal amounts of these contaminants and the resulting corrosion reactions can cause circuit failure. Examples include corrosion at the gold wire/aluminum pad galvanic

couple and electromigration of silver and, in rare cases, gold causing shorting. The external surface of the IC package is also susceptible to corrosion reactions because of direct exposure to the environment under bias conditions. The IC package leads are generally soldered or plated. Corrosion product creep can short the leads, SCC of the lead (such as alloy 42) can occur, and in some cases tin whiskers can grow with tin plated parts resulting in shorting.

## CORROSION TESTS AND STANDARDS

Accelerated corrosion testing of electronic components differs substantially from traditional accelerated corrosion testing. Most mature accelerated tests have been developed to evaluate the performance of structural materials in rather corrosive environments. Therefore, structural electronic systems such as cabinets, housings, and accessories are tested conventionally. However, electronic components usually function in environments that are comparatively mild where corrosion mechanisms and rates can be unique. The amount of corrosion that can cause failure is quite small when compared to that for other applications. Therefore, results of traditional tests must be evaluated carefully in order to determine if the resulting corrosion mechanisms are those encountered in real life. Also, new and improved tests have been developed specifically for electronic systems. It is of great importance to note that systems that are energized as in service may behave differently because of bias voltages and other effects. Therefore this factor must be taken into account when conducting corrosion tests. Where appropriate, electronic systems and devices should be active/energized during corrosion testing. A list of tests along with their use and standard designation is shown in Table 6. In addition to those listed in Table 6, a number of important standards are used in determining both the susceptibility and the decrease in corrosion protection of various metallic coatings used in electronics applications. Two of these are; ASTM B 765, Guide for the Selection of Porosity Tests for Electrodeposited and Related Metallic Coatings, and, ASTM B 809, Test Method for Porosity in Metallic Coatings by Humid Sulfur Vapor. Other ASTM standards for plated coatings include B 488 (Gold), B 545

TABLE 6—Environmental tests and standards for electronics corrosion.

Test	Standard	Use
Humidity (noncondensing)	IEC 68-2-3	Use and storage at high humidity
Humidity (condensing)	ASTM D 1735, D 2247, DIN 50017	Use and storage at high humidity where condensation occurs
Humidity (cyclic)	IEC 68-2-30, MIL-T-5422	Use and storage at high humidity where condensation occurs
Thermal (cold)	IEC 68-2-1	Use and storage at low temperature, adhesion of plating and coatings, physical distortion
Thermal (hot)	IEC 68-2-2	Use and storage at high temperature, long-term aging of organics and oxidation of metals
Salt Spray (Fog)	ASTM B 117, IEC 68-2-11, ISO 9227	Not recommended but used for coatings and systems
AASS	ASTM G 85, ISO 3769	Not recommended but used for coatings and systems
CASS	ASTM B 368, ISO 3770	Not recommended but used for coatings and systems
Cyclic Salt Spray	ASTM D 2933, SAE J1563	Electronic housings, cabinets, units
Sulfur Dioxide (SO <sub>2</sub> )	ASTM G 87, IEC 68-2-42, DIN 40 046	Noble metal coatings (porosity test)
Hydrogen Sulfide (H <sub>2</sub> S)	IEC 68-2-43, DIN 40 046	Noble metal coatings (porosity test)
Nitric Acid	ASTM B 735, ISO 4524/2	Porosity in gold coatings
Sulfurous Acid/SO <sub>2</sub>	ASTM B 799	Porosity in gold and palladium coatings
Paper Electrography	ASTM B 741	Porosity in gold coatings

(Tin), B 679 (Palladium), B 689 (Nickel), B 700 (Silver) and B 867 (Palladium-Nickel).

## ELECTROCHEMICAL TESTS

Electrochemical tests are powerful tools for determining the corrosion behavior of materials. One of the most important applications of these techniques in electronics is the determination of porosity in precious metal coatings [32]. For example, corrosion potential measurements and controlled potential tests are used to determine porosity in gold electrodeposits on copper/nickel. It is possible to calibrate the techniques so that exposed base metal due to porosity can be estimated. The potential techniques offer advantages of simplicity and high sensitivity at very low levels of porosity. Electrochemical tests are also valuable in evaluating and selecting detergents that are not harmful to electrical components in response to the industry's need to move away from chlorofluorocarbon-based cleaning agents towards aqueous based systems. These electrochemical techniques have been reviewed elsewhere in this manual.

## ENVIRONMENTAL TESTS

Environmental tests for electronics can be divided into two groups based on the information they provide.

The first group includes those tests that do not provide any corrodent other than humidity and oxygen. Such tests are constant humidity exposure, temperature cycling, and temperature/humidity cycling. For these tests, the level of cleanliness of the sample (residual chemicals) is a major variable. The types of questions answered in these tests are: Can a soldering flux be changed without causing corrosion problems? Is there a corrosive agent in organics such as an epoxy that will outgas and lead to corrosion of adjacent electronic components? Is the cleaning operation adequate to remove contaminants? Will corrosion occur during storage, shipping, and handling? Will electrical properties of insulating materials change due to moisture permeation? Will the device remain hermetic?

In running the first group of tests, care must be taken to ensure that the test chambers do not introduce any contaminant other than humidity and oxygen. Very low levels of hydrogen chloride or hydrogen sulfide will introduce corrosion variables that will affect most electronic metals. In general, the noncondensing humidity test is conducted in a chamber at high relative humidity and temperature for a selected period of time. The most common of these for IC packages is the 85°C-85 % relative humidity-bias (THB) test. Higher temperatures have been used in these tests in order to accelerate the effects. However, for general use, the most common condition is 98 % relative humidity at 30–60°C. Condensing humidity tests are commonly conducted in cabinets at 100 % relative humidity and 38°C. Table 6 lists commonly used standards for humidity testing.

Thermal tests, both cold and hot, are conducted to provide information on electronics use or storage at temperature. The performance of materials at low temperature (–40°C) or at elevated temperature is critical in many

applications. Thus, the mechanical properties of plastics, platings, and coatings, the stress relaxation and aging properties of materials, and the heat dissipating properties, can be determined.

Use of cyclic humidity, cyclic temperature, and cyclic bias are common to introduce conditions of condensation, distortions and electrolysis, and determine coating adhesion properties. The combination of physical distortion due to cyclic temperature, humidity producing condensation, and potential bias producing migration is important in determining the resistance and effect of moisture ingress in electronics.

The second group of tests answer questions such as: Are materials selected sensitive to corrosive air pollutants? Do the coatings provide an adequate barrier to corrodents? Are cabinet materials sufficiently corrosion-resistant to protect sensitive components? This group of tests introduces the corrodent and include salt spray (fog) and corrosive gas chamber tests [33]. Cabinet tests using salt fog (Table 6) are the most widely used corrosion tests for electronic systems. Although the salt spray test is not generally recommended for use as a performance test in electronics because corrosion mechanisms are not representative of those observed in service, the aggressive salt mist test is used widely for quality assurance of various systems and components. Other tests include the acetic acid salt spray and the CASS tests, which are also used for quality assurance of coatings. It should be mentioned that cyclic salt spray tests have been developed to incorporate the exposure to ambient atmosphere, hot and cold, and humidity as well as salt spray [33]. These cyclic salt spray tests are more reliable for performance testing, but still must be used with caution.

Several cabinet tests with a single gas environment are used for noble metal coatings in electronics. The most well-known is the Kesternich test and several variations on this test, which uses SO<sub>2</sub> at very high levels (0.1–1 %) at room temperature and 75–100 % relative humidity. A similar group of tests with H<sub>2</sub>S have been used, also with relatively high levels of this pollutant. In general, these single gas tests have been used for porosity in gold and other noble metal coatings, especially on nickel and copper underlayers.

It has been recognized that single gas tests with very high levels of SO<sub>2</sub> or H<sub>2</sub>S do not represent conditions to which electronics systems are exposed. Recent trends in accelerated testing of electronics have centered around environments consisting of flowing gas and low level multi-component gas mixtures, which simulate synergistic environments found in service [13,34–36]. Pollutant formulations usually contain very diluted mixtures of hydrogen sulfide, chlorine, nitrogen dioxide, and sulfur dioxide with continuous flow at 25–30°C and 70–85 % relative humidity. Various combinations and levels (in the ppb range) of these pollutants at specific temperature and relative humidities provide a range of aggressivity as shown in Table 5 [21]. The four classes of environments in Table 5 closely approximate the chemistries found in various service environments and the mechanisms observed in the corrosion of electronic materials. Examples include pore corrosion in noble metal coatings (especially gold), corrosion product creep, and electromigration under bias conditions. The multiplication factor relating the aggressivity of the mixed flowing gas test to

TABLE 7—Mixed flowing gas test conditions for electronics corrosion.

Source	Temp, °C	Relative Humidity, %	Pollutant				Air Flow Velocity, M/sec
			Cl <sub>2</sub>	NO <sub>2</sub>	H <sub>2</sub> S	SO <sub>2</sub>	
Nordic Research Project <sup>a</sup>	25	85	10	650	—	450	
Nordic Research Project <sup>a</sup>	25	75	—	1800	—	250	
Battelle (Class II) <sup>b</sup>	30	70	10	200	10	—	0.3
Battelle (Class III) <sup>b</sup>	30	70	20	200	100	—	0.3
IBM <sup>c</sup>	30	70	3	610	40	350	0.5
Texas Instruments <sup>d</sup>	30	70	10	200	100	—	0.3

<sup>a</sup>Zakipour, C. and Leygraf, C., *Journal of the Electrochemical Society*, Vol. 133, 1986, p. 21.  
<sup>b</sup>Abbat, W. H., *Proceedings, Holm Conference on Electrical Contacts*, Chicago, 1987, p. 47.  
<sup>c</sup>Gore, R., Witsks, R., and Chao, J., *Proceedings, Holm Conference on Electrical Contacts*, Chicago, 1989, p. 123.  
<sup>d</sup>Haynes, G. and Babolan, R., *Materials Performance*, Vol. 29, No. 9, 1990, p. 68.

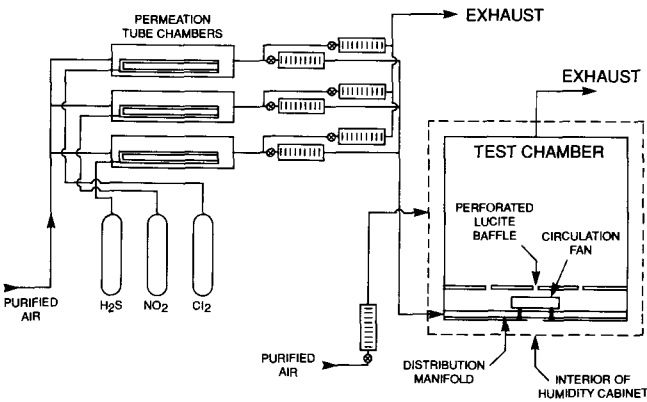


FIG. 1—Schematic of a three-pollutant gas, flowing mixed gas system.

TABLE 8—Standards for mixed flowing gas tests and associated measurements.

Standard	Title
ASTM B 808	Test Method for Monitoring of Atmospheric Corrosion Chambers by Quartz Crystal Microbalances
ASTM B 810	Test Method for Calibration of Atmospheric Corrosion Test Chambers by Change in Mass of Copper Coupons
ASTM B 825	Test Method for Coulometric Reduction of Surface Films on Metallic Test Samples
ASTM B 826	Test Method for Monitoring Atmospheric Corrosion Tests by Electrical Resistance Probes
ASTM B 827, ISO 10062	Practice for Conducting Mixed Flowing Gas (MPG) Environmental Tests

field service is determined through the use of copper or silver coupons, or both. The amount of coupon corrosion for a specific time as determined by cathodic reduction or weight gain, or both, is compared to results of coupon exposure in the appropriate field service environment. Table 7 lists some mixed flowing gas test conditions used in laboratories and Fig. 1 shows a diagram of a typical apparatus. Table 8 is a list of standards describing methods for conducting mixed flowing gas tests.

In both groups of tests described here, standard metal coupons should be included in each test to ensure that the test chamber is giving reproducible results. Copper coupons are a good standard because copper is commonly used in electronic devices, it is sensitive to most corrosives, and its oxide thickness is easily measured by coulometric reduction.

Control sample components with well-documented behavior can be used as a comparison. This information is valuable to determine if the chamber is reproducing corrosion effects previously observed.

There are literally thousands of tests used by industrial organizations for specific applications in electronics. Some are very specific, such as the nitric acid test for porosity in gold, (ISO 4524/2), for effects of vibration (IEC 68-2-6), for temperature (IEC 68-2-14), for solder (IEC 68-2-20), and for solderability (IEC 68-2-54). It is very common for laboratories to modify existing standardized tests to suit their specific needs. The technical literature will frequently describe these test conditions.

CHARACTERIZATION OF CORROSION PRODUCTS

The importance of surface and chemical analysis techniques in electronics corrosion testing cannot be overstated. These powerful tools contribute to solving problems and elucidating corrosion mechanisms in simple and complex systems. Chemical analysis techniques include infrared (IR), ultraviolet (UV), and RAMAN spectroscopy; X-ray diffraction; atomic adsorption; emission and mass spectroscopy; gas and liquid chromatography; and optical and transmission electron microscopy. Surface analytical techniques include electron spectroscopy for chemical analysis (ESCA), Auger, secondary ion mass spectroscopy (SIMS), and ion scattering spectroscopy (ISS). These important techniques used in conjunction with corrosion tests are described in another section of this manual.

SUMMARY

Environmental corrosion is having an increasing impact on the reliability of electronics. This chapter has reviewed the nature of the environment to which electronics are exposed and describes the classification of environments as reported in the literature.

Electronics corrosion is a unique subject because it occurs largely indoors or inside packages or cabinets. Therefore, classical corrosion tests do not generally apply. In addition, many failure mechanisms are unique to these systems and therefore are not treatable by classic corrosion kinetic fundamentals. This chapter therefore describes the various corrosion mechanisms important in electronics and lists the various test methods that are used in the industry.

## REFERENCES

- [1] Henricksen, J., Hienonen, R., Imrell, T., et al., "Corrosion of Electronics," Bulletin No. 102, Swedish Corrosion Institute, Stockholm, Sweden, 1991.
- [2] Guttenplan, J., "Corrosion in the Electronics Industry," *Corrosion*, ASM Handbook Vol. 13, ASM, Metals Park, OH, 1987, p. 1107.
- [3] White, E., Slenski, G., and Dobbs, B., "Case Histories and Failures of Electronics and Communications Equipment," *Corrosion*, ASM Handbook, Vol. 13, ASM, Metals Park, OH, 1987, p. 1113.
- [4] "Design Guidelines for Prevention and Control of Avionic Corrosion," NAVMAT P 4855-2 Department of the Navy, June 1983.
- [5] *Electronic Packaging and Corrosion in Microelectronics*, M. Nicholson, Ed., ASM, Metals Park, OH, 1987.
- [6] *Corrosion of Electronic Materials and Devices*, J. Sinclair, Ed., PV91-2, The Electrochemical Society, Pennington, NJ, 1991.
- [7] Peterson, P., *Corrosion of Electronic and Magnetic Materials*, ASTM STP 1148, ASTM International, West Conshohocken, PA, 1992.
- [8] *Reliability of Metals in Electronics*, PV91-3, H. S. Rathore, Ed., The Electrochemical Society, Pennington, NJ, 1995.
- [9] Frankenthal, R. P., "Electronic Materials, Components and Devices," *Uhlig's Corrosion Handbook*, 2nd ed., W. Revie, Ed., John Wiley and Sons, NY, 2000; Frankenthal, R. P. and Becker, W. H., *Journal of the Electrochemical Society*, Vol. 126, 1979, p. 1718.
- [10] Frankel, G. S., "Corrosion of Microelectronics and Magnetic Storage Devices," *Corrosion Mechanisms in Theory and Practice*, P. Marcus and J. Oudar, Eds., Marcel Dekker, Inc., NY, 1995.
- [11] Vernon, W., *Transactions of the Faraday Society*, Vol. 27, 1931, p. 255.
- [12] Sinclair, J. D., Psota-Kelty, L. A., Weshler, C. J., and Shields, H. C., "Indoor/Outdoor Concentrations and Indoor Surface Concentrations and Indoor Surface Accumulations of Ionic Substances," *Atmospheric Environments*, Vol. 24A, 1990, p. 627.
- [13] Abbott, W. H., "The Development and Performance Characteristics of Mixed Flowing Gas Test Environments," IEEE, Proceedings of the 33rd Holm Conference, Chicago, 1987.
- [14] ISO 9223, Corrosion of Metals; Classification of the Environment, International Standards Organization, Geneva.
- [15] IEC-721-3 Classification of Environmental Conditions, International Electrotechnic Commission, Geneva.
- [16] ANSI/ISA-SP71, Environmental Conditions for Process Measurements and Control Systems-Airborne Contaminants Instrument Society of America, Research Triangle Park, NC.
- [17] Abbott, W., "Comparison of Electronic Component Degradation in Field and Laboratory Environments," *Materials Performance*, Vol. 30, No. 6, 1991, p. 55.
- [18] Sharp, S., "Protection of Control Equipment from Atmospheric Corrosion," *Materials Performance*, Vol. 29, No. 12, 1990, p. 43.
- [19] Haynes, G. and Baboian, R., "Creep in Mixed Gas Tests," *Materials Performance*, Vol. 29, No. 9, 1990, p. 68.
- [20] Krumbein, S., Newell, B., and Pascucci, V., "Monitoring Environmental Tests by Coulometric Reduction of Metallic Control Samples," *Journal of Testing and Evaluation*, November 1989, p. 357.
- [21] Abbott, W., "Corrosion Still Plagues Electronic Packaging," *Electronic Packaging and Production*, August 1989, p. 28.
- [22] Guttenplan, J. and Violette, D., "Corrosion Related Problems Affecting Electronic Circuitry," *Materials Performance*, Vol. 29, No. 4, 1990, p. 76.
- [23] Rice, D., "Corrosion in the Electronics Industry," Paper 323, Corrosion/85, NACE, March 1985.
- [24] Baker, R. G., "Corrosion and Plating Problems in Electronics Equipment for the Communications Industry," Paper 83, Corrosion/73, NACE, 1973.
- [25] Steppan, J., Roth, J., Hall, L., et al., "Review of Corrosion Failure Mechanisms During Accelerated Tests, Electrolytic Metal Migration," *Journal of the Electrochemical Society*, Vol. 134, No. 1, 1987, p. 175.
- [26] Tierney, V., "The Nature and Rate of Creepage of Copper Sulfide Tarnish Films over Gold," *Journal of the Electrochemical Society*, Vol. 128, 1981, p. 1321.
- [27] Ilschner-Gensch, C. and Wagner, C., "Local Cell Action during the Scaling of Metals, I," *Journal of the Electrochemical Society*, Vol. 105, 1958, p. 198.
- [28] Volpe, L. and Peterson, P. J., IBM Technical Report TR 02.1449, IBM, San Jose, CA, March 1988.
- [29] *Guide to the Selection and Use of Electroplated and Related Finishes*, ASTM STP 785, F. A. Lowenheim, Ed., ASTM International, West Conshohocken, PA, 1982, p. 48.
- [30] Antler, M., "Survey of Contact Fretting in Electrical Connectors," *IEEE Transactions*, Vol. CHMT-8, No. 1, 1985.
- [31] Comizzoli, R., Frankenthal, R., Lobnig, R., et al., "Corrosion in Electronic Materials and Devices by Submicron Atmospheric Particles," ECS-Interface, Fall 1993, p. 26.
- [32] Morrissey, R., "Porosity and Galvanic Corrosion in Precious Metal Electrodeposits," *Electrochemical Techniques in Corrosion Engineering*, R. Baboian, Ed., NACE, Houston, TX, 1986, p. 167.
- [33] Haynes, G. S., "Review of Laboratory Corrosion Tests and Standards," *Corrosion Testing and Evaluation: Silver Anniversary Volume*, ASTM STP 1000, R. Baboian and S. W. Dean, Eds., ASTM International, West Conshohocken, PA, 1990.
- [34] Cosack, V., "Survey of Corrosion Tests with Pollutant Gases and Their Relevance for Contact Materials," *Proceedings of the 13th International Conference on Electric Contacts*, Lausanne, 1986, p. 316.
- [35] Rice, D. W., Cappell, R. J., Phipps, P. B., and Peterson, P. J., in *Atmospheric Corrosion*, W. H. Ailor, Ed., John Wiley & Sons, NY, 1982, p. 651.
- [36] Lorenzen, J. A., *Proceedings*, 17th Annual Tech Meeting of the Institute of Environmental Science, Los Angeles, 1971, p. 110.

# Telecommunications

*George Schick<sup>1</sup>*

## CORROSIVE ENVIRONMENTS

THE TELECOMMUNICATION CABLE plant is exposed to three basically different environments: aerial, underground, and buried.

Aerial plant is exposed to rain, condensate moisture, manmade pollutants (e.g., acid rain and emissions from chemical plants), and natural corrosives (e.g., airborne salt particles at sea coastal areas).

An underground plant is located in ducts and manholes. These locations may be full or partially full of water and silt. The water may contain soluble salts characteristic of the local environment, de-icing salts, industrial effluents, and microbiological species (such as sulfate-reducing bacteria). The silt may contribute to formation of differential aeration-type corrosion cells. Stray DC currents usually cause the highest rate of corrosion in the underground plant. These currents originate at such places as DC electrified rail transportation systems, mining operations, welding operations, and cathodic protection rectifiers of buried plant (e.g., gas pipelines). In some cities where steam is sent through pipes for heating various buildings, steam leaking from these pipes can ruin nearby communication cables, partially by the high temperatures and partially by water from condensation inside the cable.

A buried plant is directly exposed to local soil, water, contaminants, and stray currents.

## MATERIALS

### Cables and Closures

In the past the copper conductor pairs in telecommunication cables were insulated with paper pulp, and the outer sheath, which serves as an electric shield and provides corrosion-resistant physical protection, was made of a lead alloy containing 1.0 mass% antimony. The connections (splices) between the individual conductors were enclosed either in lead sleeves or in closures consisting of two galvanized half shells of gray cast iron, held together with stainless steel bolts and nuts. Although there is still a considerable amount of lead-sheath cable, lead sleeves, and galvanized cast iron closures, the modern telecommunication cable plant relies heavily on plastics as the material of construction.

The cables in the modern telecommunication plant, which is to a large extent today's plant, contain polyethylene-insulated

copper conductors (PIC). The shielding is accomplished in most cables with corrugated aluminum. The primary function of the shield is to reduce noise due to electric and magnetic fields from transmission and distribution power lines or other interfering sources. The shielding also protects from electrical transients such as power surges and lightning [1]. In some cables the aluminum shield is surrounded with corrugated steel for increased mechanical protection from rodents or stones. Other cables use copper-clad stainless steel for mechanical and corrosion protection. The outer jacket is made of polyethylene, an inexpensive, lightweight material that provides corrosion protection and mechanical protection to the underlying metallic shield(s). It also prevents water from entering the cable core. The connections (splices) are enclosed mainly in plastic closures, although galvanized cast-iron splice closures have been used in the past with polyethylene-jacketed cables.

The modern telecommunication plant increasingly relies on the use of optical fiber cables. The individual fibers inside the cable are coated with an epoxy acrylate polymer. Some of the cables are constructed of totally dielectric materials; others may have a steel strength member in the center in the center of the core. The outer jacket in each case is made of polyethylene. The connections of individual fibers are placed into sealed polymer closures.

The various cable constructions may have some additional components to keep corrosive elements, primarily water, out of the cable core. High-pair-count toll cables with paper-pulp wire insulation are usually pressurized with dry air to keep moisture out of the cable core. PICs may have insulation defects; to avoid corrosion of the positively energized conductors and noise-causing leakage currents at such defect sites, the cores of some cables are filled with cable filling compounds (e.g., wax in mineral oil or rubber in mineral oil) to keep water out. Many of the multipair cable sheath designs use a bituminous compound on the outer surface of the corrugated steel shield to protect against corrosion that could occur if the outer polyethylene jacket is damaged. Filled cables are usually connected with splice closures where the splices are protected with encapsulating compounds. In optical fiber cables the corrugated-steel shield is coated with a thin layer of polymer film to protect against corrosion if the outer polyethylene jacket is damaged.

Submarine optical fiber cables are generally protected by armor to resist mechanical damage and prevent floating of the cable. This armor may consist of helically wound galvanized

<sup>1</sup>Consultant, 9 Sutton Place, Apt. 1, Westwood, NJ 07675.



steel or stainless steel wires, with or without polyethylene jacketing. In some cables, the armor is made of corrugated steel covered with a polyethylene outer jacket. Galvanized steel, and to a lesser extent stainless steel, corrodes in water, and the corrosion process generates hydrogen. Another cause of hydrogen formation is hydrogenase, an enzyme that catalyzes the formation of hydrogen in hydrogen producing bacteria (*clostridium acetobutylicum*) in anaerobic bottom sediments. If fermentable carbohydrates are present (e.g., sugar) these bacteria cause hydrogen production. This hydrogen can enter the fibers and cause signal losses. These signal losses can be quite high in the 1300 nm transmission window. The signal loss increases with water depth because the partial pressure of hydrogen increases with the overall pressure [1].

Hermetically sealed lead, copper, or aluminum can keep hydrogen out of optical fiber cables in excess of the design life of the cable [1].

### Aerial Cable Hardware

The aerial cable plant is located on telephone poles. The support hardware, made of galvanized steel, is attached to the poles and holds in place the galvanized-steel strands that span the space between the poles. The cables themselves are lashed to the strands with galvanized-steel or stainless steel lashing wires. The various splice closures are also attached to the strand with galvanized-steel hardware. Some cables have built-in strands ("Figure 8" cables). Both the cable and the strand are jacketed with polyethylene, and the two jackets are attached to each other with a continuous web of polyethylene. This cable provides corrosion protection to the strand and saves the cost of lashing.

The telephone poles are mechanically secured with galvanized-steel guys, guy rods, and guy anchors. Although the guy anchors are located below grade, their corrosion can affect the aerial plant. Guy anchors may pick up stray currents at one location and transmit these currents to a discharge location where they cause stray-current corrosion. For this reason, in stray-current areas the aboveground guys are isolated with nonmetallic insulating bolts. The corrosion of guy rods and anchors also depends on the corrosiveness of the soil.

Protectors of telecommunication equipment, often mounted on the sides of homes or in basements, which provide electrical protection to the telecommunication equipment user against lightning and power faults, are exposed to environments similar to those of the aerial plant. Some of these protectors, which include a stressed copper alloy cap and cage, are placed in a phenolic housing. Ammonia or ammonium compounds can cause stress-corrosion cracking (SCC) of some of the stressed copper-base alloys, resulting in failure of the protector.

### Manholes

Manholes are located 500–800 ft (152.4–243.8 m) apart in the underground plant. They are mostly reinforced concrete chambers with built-in support hardware. Manholes are the structures where the cables are pulled into the duct system, the cable ends are spliced together, and in some of them,

signal reinforcing and signal equalizing circuits are placed, enclosed in watertight and airtight closures. In the past these closures were made of galvanized steel and galvanized cast iron. The newer types are made of polymers. Even the polymer closures contain some exposed metals, e.g., brass air pressure valves and grounding elements. Because of exposure to lightning and power fault, manholes also contain copper or tin-coated copper bonding ribbons to create equipotential conditions for electric safety.

Electronic Equipment Enclosures (EEEs) (Controlled Environment Vaults (CEVs), Walk-In Cabinets, Cabinets and Huts) are remote telecommunication centers that fulfill some of the functions of central offices (COs) but are located closer to the subscriber loop. EEEs can be constructed of reinforced concrete, steel, or fiberglass. All these locations have their own power and are required to be grounded. Regardless of the material of construction, the grounding electrodes may be stray-current pick up or discharge points; thus, they can corrode or cause corrosion elsewhere. If the material of construction is steel, corrosion problems of this material also have to be taken into account.

## CORROSION CONTROL TECHNIQUES

There are two fundamentally different methods of controlling corrosion in the telecommunication cable plant.

In the design and manufacturing stages, corrosion control is based on the selection of corrosion resistant materials and SCC-resistant alloys, heat treatment (reduced SCC and hydrogen stress cracking susceptibility), jacketing (polymer), coating (paint, bituminous compound, noble or sacrificial metal), and filling compounds (cables, splice closures).

After the plant is in place, local corrosion problems have to be taken into account. These corrosion problems do not exist everywhere, and built-in corrosion control would be prohibitively expensive. The primary corrosion control at this stage is protection against the effects of stray DC currents. Preventing or minimizing the pickup of stray current, draining the stray currents back to their source through low resistance bonds, and applying cathodic protection, can accomplish this. Other corrosion problems of the in-place telecommunication cable plant are discussed below.

An example of galvanic effects is the steel reinforcing bar in concrete in contact with the galvanized steel support hardware. In flooded manholes, the potential of reinforcing bar in concrete is around  $-0.2$  V versus a  $\text{Cu}/\text{CuSO}_4$  reference electrode. The potential of galvanized-steel support hardware against the same reference electrode is around  $-1.0$  V. This galvanic cell can lead to rapid corrosion of the galvanized-steel support hardware. This corrosion can be controlled by intentional insulation between the reinforcing bars and the support hardware.

An example of differential aeration type corrosion is lead-sheathed cable in partially silt-filled ducts. The area of the lead covered with silt is in contact with an environment that has a relatively low concentration of dissolved oxygen, while the area in water is in contact with an environment that has a relatively high concentration of dissolved oxygen. The

potential differences between these areas can be 300–400 mV. The low concentration areas are the corroding anodes, and these differential aeration cells, can lead to localized perforation of the lead cable sheath. This kind of corrosion problem can be resolved with distributed sacrificial duct anodes or replacement with polyethylene-jacketed cable.

Microbiologically induced corrosion can occur in manholes filled or partially filled with stagnant water. Under these anaerobic conditions in the presence of sulfates and some organic materials, sulfate-reducing bacteria (SRB) can proliferate and cause support-hardware failure within a few years. In manholes with high SRB content, the galvanic relationship between copper and steel can change, and copper may become the corroding anode. This condition can lead to bonding-ribbon failures and electrical protection problems. This type of corrosion problem can be resolved with environmental control (e.g., an oxidizing agent sprayed on the SRB-covered areas) or with cathodic protection.

## SPECIFIC PROBLEM AREAS

For electrical safety reasons, the telecommunication cable plant has to be grounded and bonded. This means that some bare metallic components of the plant have to be directly exposed to corrosive environments. Some of these alloys are not particularly corrosion resistant, and at some locations they require corrosion-control measures. An example of such a condition is where the galvanized-steel support hardware is part of the ground in a flooded manhole.

Bonding and grounding can also lead to inadvertent formation of galvanic corrosion cells. Grounding to copper water service pipe, and grounding a telephone cable shield to the multigrounded power cable neutral, can complete the circuit of a galvanic cell where the lead cable sheath is the corroding anode (Fig. 1). Although this problem can be resolved with an insulating joint in the shield of a vertical pole-mounted cable, the cause of the problem is difficult to track down. The reason is that different craft persons may make the grounding to the water pipe and bonding to the power cable neutral at different times.

In the modern optical fiber cable plant, hydrogen permeation into the fiber can cause considerable signal losses. Corrosion of the armor wires on submarine optical fiber

cables is a major cause of hydrogen formation, and without the presence of an effective barrier, hydrogen will enter the fibers. This problem can be resolved only by cable design changes.

## USE OF TEST METHODS TO EVALUATE CORROSION

### Tests for Materials Selection and Performance

Corrosion evaluation of the telecommunication cable plant components is started at the time of earliest availability. At this point, the corrosion test methods are geared toward establishment of corrosion resistance of the exposed bare metallic components in the environment for which they are intended. The test methods are also directed toward evaluation of galvanic compatibility of components made from more than one alloy, and the effectiveness of noble or sacrificial metallic coatings. Test methods are also used to establish susceptibility to SCC and hydrogen stress cracking. Other tests are used to establish whether or not low contact resistance can be maintained between exposed contacting elements (e.g., ground connectors and grounding clamps).

Some of the telecommunication cable plant components are made with metals embedded in polymers, and the metals are exposed to the corrosive environment only at very small areas (e.g., edges or small defect sites on the polymer). Test methods are used to evaluate the penetrability of the metal-to-polymer interface and the ensuing progressive corrosion of the metal.

These corrosion evaluation test methods of new or replacement components often lead to material or design changes to upgrade their performance. An extensive soil burial test program, using 52 different telephone cable shielding systems at six different test locations, was conducted by the USA's Rural Electrification Administration (REA) and the National Bureau of Standards between 1968 and 1974 [3]. The results of this study strongly affected the design of telephone cable shields.

In another program the corrosion resistance of aluminum, copper and copper clad stainless steel has been studied in four different soils for three years [4].

### In-Service Monitoring

The original corrosion test methods used to select the materials for manufacturing the telecommunication plant components cannot prevent all possible corrosion failures. Some corrosion problems may occur due to local conditions (e.g., stray DC currents or heavy industrial pollution). Corrosion of the cable plant is monitored by periodic field-testing and, for areas of prior corrosion failures, by centralized testing. The periodic field tests consist of potential surveys against reference electrodes along the cable routes to establish corrosion areas, potential changes perpendicular to the cables to establish the location of current pickup and discharge points, and current measurements (magnitude and direction) to further find the source of corrosion current. When the source of a corrosive stray current is suspected to be the rectifier of a "foreign plant's" cathodic

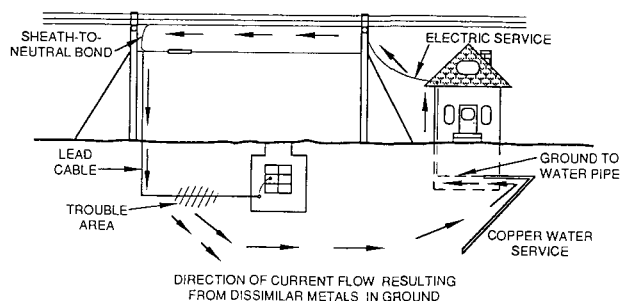


FIG. 1—Galvanic cell in the telecommunications cable plant.

protection system (interference) or an HVDC ground electrode, a joint field test is conducted together with the representatives of the "interfering" and the "affected" plants. During these tests, the interference current is periodically turned on and off so that the effect on the other plants can be measured. Other "dynamic" stray-current effects (e.g., stray currents from a DC electrified rail transportation system) on the cable plant can be measured with recording voltmeters. A testing technique that can pinpoint the area of maximum corrosion exposure on the cable, and can determine if a particular stray-current source is the cause of the observed effect is the simultaneous measurements of cable-to-earth potential ( $V_g$ ) and cable-to-interfering plant potential ( $E_1$ ). The measured data are plotted in correlation curves (Fig. 2) [5].

In order to facilitate joint testing, the owners of the affected plants send representatives to periodic meetings to organize and prepare the joint tests. Such voluntarily formed groups are called Corrosion Coordinating Committees.

When corrosion surveys have established the location and source of corrosion problems on a telecommunication cable plant, the next step is to establish mitigation measures. These measures can include placement of insulating joints to limit current pickup by the cable shield in cable entrance facilities (CEFs), some building entrances, vertical riser cables on telephone poles, and, under special conditions, in manholes. Most of these measures consist of placing low-resistance drainage bonds to return stray DC currents to their source without causing corrosion. If the stray current

source is a DC electrified rail transportation system (dynamic stray-current source), a reverse-current switch may have to be installed, in series with the bond, to stop current flow in the wrong direction (from the source to the cable).

Application of either the impressed-current or galvanic-anode type of cathodic protection can counteract the corrosion currents.

Centralized testing monitors the major corrosion areas and their mitigation measures. The potential of a permanent reference electrode, the operation of a cathodic protection rectifier, and the current on a bond wire can be brought to a test desk in a central office via dedicated wire pairs in cables, and they can be monitored at that location.

### Analysis of Simulated Field Failures

Sometimes, despite extensive corrosion testing, some components of the telecommunication cable plant may fail in the field. Often these failures are caused by unforeseen field conditions or by the presence of unexpected corrosives. To establish the source and mechanism of corrosion failure, these components are exposed to simulated field conditions, and the results are compared to the field failures. Some examples of simulated field failures are described below.

Type 410 (UNS S41000) stainless steel bolts, holding together galvanized cast-iron splice closures, failed in flooded manholes after being in service for three to four months. The field failures were simulated using samples assembled with the highest permissible torque, and with and without the use of molybdenum disulfide antiseize compound. To accelerate the failure time, some samples were charged with hydrogen using a power supply and a platinum anode. The results showed failures identical to those that occurred in the field. The cause of the failures was hydrogen, generated by the galvanic cell formed between zinc and stainless steel. The failures were accelerated by the fact that the martensitic (410 type) stainless steel is susceptible to hydrogen stress cracking, and the sulfide of the molybdenum disulfide on the stainless steel surface acted as a catalytic poison for the  $2H \rightarrow H_2$  reaction. The solution to the problem was to change to austenitic stainless steel, eliminate the molybdenum disulfide, and limit the torque.

Galvanized steel manhole support hardware and copper and tin-coated copper bonding ribbons failed in manholes after relatively short exposure times (1–4 years). Examination of these manholes indicated the following: (1) all these manholes smelled of hydrogen sulfide, (2) the hardware and bonding ribbons were coated with black slimy corrosion products, either directly visible or under a rust covering, and (3) when the black slime was wiped away, the metal underneath appeared clean, shiny, and pitted. Microbiological analysis of the water and the black compound indicated the presence of SRB (desulfovibrio desulfuricans). Laboratory tests of small size samples (1 in. by 1 in. (25.4 mm by 25.4 mm) galvanized steel, 3 in. by 0.5 in. (75.2 mm by 12.7 mm) copper and tin-coated copper bonding ribbons) were exposed individually and coupled in 30-L test vessels under anaerobic conditions. This ensured a large corrosive liquid volume to exposed surface area ratio. Potential measurements versus time indicated rapid corrosion of zinc.

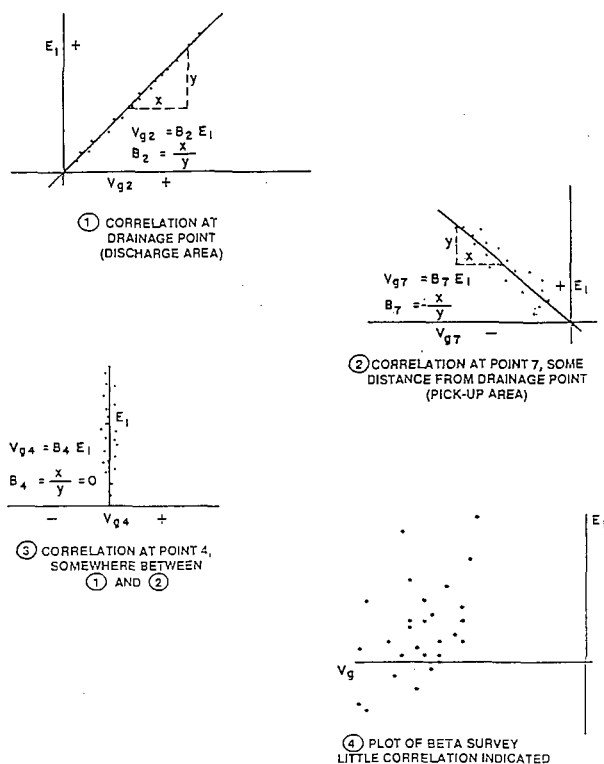


FIG. 2—Cable-to-earth vs. cable-to-rail correlation curves (Beta survey).

Mass loss measurements established high rates of corrosion for steel and copper. Potentiodynamic polarization measurements showed that in SRB environment, copper becomes anodic to steel.

In separate laboratory and field experiments, it has been established that spraying 5.25 wt% of sodium hypochlorite (NaOCl) solution on the black corrosion products can provide relief from this type of corrosion problem for one or more years.

## TEST METHOD APPROACH

The test method approach depends on several factors; thus, the test developer has to ask several questions to determine the best approach.

- What constitutes corrosion failure (e.g., loss of strength, perforation, increased contact resistance)?
- How well is the corrosive environment characterized?
- Is there a predominant component of the environment that causes corrosion (e.g., marine, industrial)?
- Can the test be accelerated without rendering it meaningless?
- Is the electrochemistry of the reaction well understood?
- What is the most important failure mode that requires detection (mass loss, loss of tensile strength, local penetration, formation of high resistance film between contacting elements resulting in high contact resistance, cracking)?
- How much time is allocated for testing?

## Environmental Simulation

This approach is useful if the environment is well characterized and a few weeks or months have been allocated for the test; examples include: exposure to salt spray to simulate sea coastal areas, exposure to 3.5 wt% NaCl solution for submarine environment, Kesternich chamber test (humid SO<sub>2</sub> and CO<sub>2</sub> mixture) for industrial environment [6], and mixed flowing gas tests for a range of environments.

## Acceleration

Accelerated corrosion tests are appealing because the allocated time is often very short. Generally, increased temperature, increased concentration of some of the corrosive species, increased or decreased pH, and applied DC current can all increase the rate of corrosion. However, these acceleration factors can be misused for the sake of saving time, and the test may become meaningless.

Some examples where acceleration can be beneficial are as follows:

- Moderately increased temperature to accelerate a reaction that is naturally occurring in the plant.
- Increased concentration of corrosive species in a SCC test (e.g., Mattsson's solution [7]).
- Acidified salt solution exposure to test for the effect of corrosive liquid penetration to a metal-to-polymer interface.
- In all cases it is important to insure that the mechanisms of corrosion are not changed by the acceleration technique.

## Electrochemical Test Methods

Electrochemical test methods evaluate various corrosion characteristics of metals and alloys in a relative short time. Among these characteristics that can be evaluated electrochemically are:

- Corrosion rates, if the corrosion reaction is well defined.
- Galvanic relationships of metals and alloys in various environments.
- Passive range of potentials of active-passive alloys.
- Susceptibility to pitting.

## Detection of Corrosion

Laboratory tests are used to detect corrosion of metals used in various cable plant components. These tests are conducted to establish whether or not a material is suitable for a given component. Corrosion of individual test components can be tested under both laboratory and field conditions. The in-place plant can only be tested under field conditions.

The materials testing may include corrosion studies based on: mass loss, pitting depth, loss of tensile strength, time for SCC or hydrogen stress cracking, and color changes at coating defect sites.

The components can be tested for: SCC to evaluate the effects of applied and residual manufacturing tensile stresses; leakage resistance after salt spray or temperature-humidity cycling tests; and contact resistance after a salt spray test, temperature-humidity cycling, or a hydrogen sulfide exposure test.

The in-service cable plant is tested to establish the presence or absence of stray direct currents, the galvanic corrosion effect of "foreign" plants, the corrosivity of local environmental conditions, and the corrosive effect of "long cells" formed by the changes in the environment. The corrosion of the in-place plant is detected through potential surveys, current tests, soil resistivity tests, redox potential tests, and pH tests.

## Methods Used

The test methods used to evaluate the corrosion of materials and plant components are described in Bellcore Technical Advisories (TAs), Technical References (TRs), and Generic Requirements (GRs). Many of the tests in these documents include and reference ASTM, UL, ANSI/NEMA, and MIL standards. Some of the test methods are specific to the telecommunication industry and can be found only in TAs\*, TRs\*, and GR\*s. Manufacturing and purchase of telecommunication plant components are based on these documents, thus, available to the manufacturers and to companies that sell them. The methods used for in-plant testing are described in Bell System Practices (BSPs)\*\* and licensed Bellcore documents.<sup>2</sup>

<sup>2</sup>Since the writing of this chapter Bell Communications Research became Lucent Technologies and Bell Telephone Laboratories became Lucent Technologies. The \* and \*\* marked documents are available from Lucent Technologies, Morristown, NJ\* and Lucent Technologies, Murray Hill, NJ\*\*.

### Test Methods for Corrosion Evaluation of Materials and Components

ASTM B 117, Test Method of Salt Spray (Fog) Testing, is widely used for testing the effectiveness of telecommunication equipment closures to protect the equipment inside from airborne ionic compounds. The test is also used to evaluate the corrosion resistance of the closure itself under extreme corrosive conditions. The testing time is usually 30 days, and the effectiveness to protect electrical equipment inside the closure is measured by resistances between tip and ring, tip and ground, and ring and ground during and after the test. This test is described in detail in TR-TSY-009 [2]. The salt fog test is also used (four days exposure) to evaluate cable shield bonding clamps. The test and the requirements are described in TA-TSY-001001 [8].

Temperature cycling with humidity is used to test equipment closures to see if condensate (moisture) forms on the inside wall. The condensate moisture may cause electronic noise on the telephone lines, and in combination with DC, electrolytic corrosion. Two different temperature-humidity cycles are used for testing telecommunication equipment. One is described in Fig. 3 and the other in Fig. 4. Temperature-humidity cycling with power is described in military standards MIL 883C [10] and MIL 202F [11].

The rain test is used to evaluate the water tightness of various closures and cabinets. For this test the top and all sides of closures are exposed to continuous water spray for 1 h at an operating pressure of 0.352 kg/cm<sup>2</sup>. The test is described in detail and the pass/fail criteria are given in UL 497 [12].

The dust exposure test is used to evaluate the tightness of closures against wind-blown dust. For this, closures are exposed to a blast of compressed air mixed with dry, Type 1 general-purpose Portland cement using a suction type blast gun. The cement is applied at a rate of 2.27 kg/min. Dust particles, besides causing mechanical damage to equipment, can also act as nucleation sites for condensate moisture. Water-soluble components of dust may form corrosive electrolytes on equipment under DC power. The test is described in detail in ANSI/NEMA 250 [13].

ASTM G 37, Practice for Use of Mattsson's Solution of pH 7.2 to Evaluate the Stress-Corrosion Cracking Susceptibility of Copper-Zinc Alloys [7], is used to evaluate manufacturing and applied stresses in components made of copper-zinc alloys.

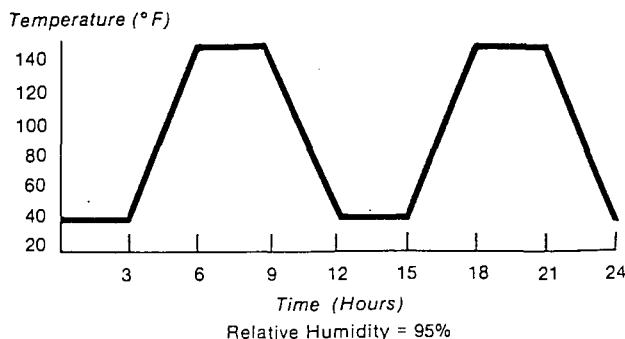


FIG. 3—Temperature-humidity cycling for repeater housings in carrier systems.

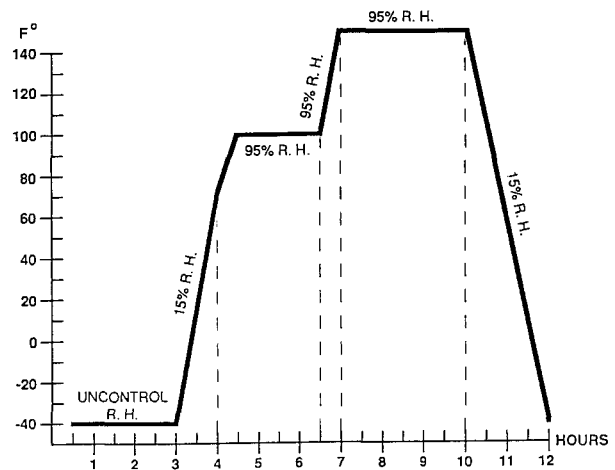


FIG. 4—Temperature-humidity cycling for cable shield bonding clamps.

The hydrogen sulfide test is used to evaluate bonding and grounding hardware of outdoor telecommunication equipment. This test consists of continuous exposure of bonding and grounding hardware, in contact with conductors, in a test chamber containing 10–15 ppm hydrogen sulfide and 75 % relative humidity at  $25 \pm 2^\circ\text{C}$  for 4, 10, or 21 days. The test is conducted according to IEC 68-2-43 [13]; the contact resistance after the test is measured according to EIA 364-B [15].

Two tests [2] are used to determine the porosity of gold contacts used in outdoor equipment: (1) a nitric acid vapor test (exposure of gold-plated specimens in a desiccator containing 300 mL nitric acid for 1 h at  $24 \pm 3^\circ\text{C}$  and a maximum relative humidity of 60 %); and (2) an alkaline polysulfide test (the specimen is immersed for 60 s in a solution made of sodium sulfide, water, and excess flower of sulfur, filtered and diluted to a specific gravity of 1.142, and made alkaline with sodium hydroxide).

A corrosion test for steam resistant optical fiber cable was developed: 30.2 cm long samples are cut from the cable and 7.6 cm of the outer polyethylene jacket is removed from the middle of the sample. The ends of these cable samples are closed with rubber stoppers. The cable samples are exposed to wet, salty sand in an autoclave for 60 days at  $130^\circ\text{C}$ . The test and the requirements for evaluation of the test results are described in TA-NWT-0011322 [16].

The salt-water corrosion test is used to evaluate submarine splice closures. For this test a splice closure and its outer housing are immersed in aerated 3.5 % sodium chloride solution for 180 days. The test is described in TA-TSY-041 [17]. The same closures are also exposed to a similar test using artificial fresh water (ASTM D 2570, Method for Simulated Service Corrosion Testing of Engine Coolants).

### In-Plant Testing

Table 1 describes the documents used for various in-plant testing.

TABLE 1

Document #	Subject	Ref. #
BSP 877-100-100	Cooperative testing through Corrosion Coordinating Committees	18
BSP 877-101-100	Basic objectives of corrosion testing in cable plants	19
BSP 877-102-100	Fundamentals of lead cable sheath corrosion and its control	20
BSP 877-104-101	Potential and current distribution in stray-current areas	21
LP-RPES-COR	Buried fuel tank corrosion testing and protection	22
BSP-877-110-100	Flowchart-based corrosion testing and mitigation process	23
BSP-877-200-100	Routine corrosion surveys potential and current measurements	24
BSP-877-201-100	Corrosion testing of underground plant by duct surveys	25
BSP-877-205-100	Corrosion testing in non-stray-current areas and data analysis	26
BSP-877-206-100	Centralized testing of corrosion control equipment	27
BSP-877-207-100	Copper sulfate half-cell	28
BSP-877-208-100	Corrosion testing equipment	29
LP-RPES-COR	Corrosion testing of the underground and buried plant	30
LP-RPES-COR001	Corrosion testing of plastic repeater housing with metal parts	31

## SUMMARY

The telecommunication plant is made of a number of metal and non-metal components, exposed to various corrosive environments. Man-made effects, such as DC stray currents, can further accelerate corrosion of the plant.

The metals of construction and some plant components are tested before manufacturing for corrosion resistance in the environments to which they will be exposed. Laboratory tests and field exposures are used for this purpose. The plants are also tested after exposure to the environment to establish the local corrosion effects, especially those caused by DC stray currents.

The metals and plant components are tested by methods described in national standards. Some of the plant components and the in-place plant are tested according to methods and requirements developed by the telecommunication industry.

## REFERENCES

- [1] NACE International Publication 10C198, "Technical Committee Report: Corrosion of Cable Shielding for Telecommunications Cable," NACE International, Houston, TX, May 1998.
- [2] Outdoor Telephone Network Interfaces, Bellcore TR-TSY-009, Bellcore, Livingston, NJ, 1987.
- [3] Gerhold, W. F. and McCann, J. P., "Corrosion Evaluation of Underground Telephone Cable Shield Materials," Paper 31, CORROSION/76, NACE, Houston, TX, 1976.
- [4] Haynes, G. S. and Baboian, R., "A Comparative Study of the Corrosion Resistance of Cable Shielding Materials," *Materials Performance*, Vol. 18, No. 2, 1979, pp. 45-56.
- [5] AT&T, "Corrosion Practices-Design of Drainage Wires," BSP 877-300-100, AT&T Co., Winston-Salem, NC, 1947.
- [6] ASTM G 87, Standard Practice for Conducting Moist SO<sub>2</sub> Tests, ASTM Annual Book of Standards, Vol. 0.3.02, ASTM International, West Conshohocken, PA, 2002.
- [7] ASTM G 37, Standard Practice for Use of Mattsson's Solution of pH 7.2 to Evaluate the Stress Corrosion Cracking Susceptibility of Copper-Zinc Alloys, ASTM Annual Book of Standards, Vol. 0.3.02, ASTM International, West Conshohocken, PA, 1995, pp. 129-131.
- [8] "Generic Requirements for Cable Shield Bonding Clamps," Bellcore TA-TSY-001001, Bellcore, Livingston, NJ, 1989.
- [9] "Repeater Housings for T1, T1C, T1D and T1G Carrier Systems," Bellcore TR-TSY-006, Bellcore, Livingston, NJ, 1984.
- [10] Military Standard MIL 883C, Test Method 1.4, Moisture Resistance, 1981.
- [11] Military Standard MIL 202F, Test Method 106E, Moisture Resistance, 1981.
- [12] Protectors for Paired Communications Circuits, Rain Test, UL 497, 1992.
- [13] Enclosures for Electrical Equipment [1000 Volts Maximum], ANSI/NEMA 250, 1998.
- [14] IEC Standard 68-2-43, Basic Environmental Testing Procedures, Part 2: Hydrogen Sulphide Test for Contacts and Connections, International Electrotechnical Commission, Geneva, Switzerland, 1976.
- [15] EIA 364-B, Low Level Contact Resistance Test Procedure for Electrical Connectors, Electronic Industries Alliance, 1990.
- [16] "Generic Requirement for Steam Resistant Optical Cable," Bellcore TA-NWT-001322, Bellcore, Livingston, NJ, 1992.
- [17] Submarine Splice Closures for Fiber Optic Cable, Bellcore TA-TSY-041, Livingston, NJ, 1988.
- [18] AT&T, "Cooperative Arrangements for Controlling Corrosion of Underground Structures," BSP 877-100-100, AT&T Co., Winston-Salem, NC, 1960.
- [19] AT&T, "General Principles Involved in Control of Cable Sheath Corrosion," BSP 877-101-100, AT&T Co., Winston-Salem, NC, 1946.
- [20] AT&T, Corrosion of Underground Lead Sheath Cable, Fundamental Considerations, BSP 877-102-100, AT&T Co., Winston-Salem, NC, 1965.
- [21] AT&T, "Voltage and Current Distributions in Stray Current Areas," BSP 877-104-101, AT&T Co., Winston-Salem, NC, 1946.
- [22] "Engineering Design Considerations for Corrosion Control of Underground Fuel Tanks," Bellcore LP-RPES-COR, Bellcore, Livingston, NJ, 1987.
- [23] AT&T, "Engineering and Implementation Methods System [EIMS] for Corrosion Testing and Mitigation of the Underground and Buried Plant," BSP 877-110-100, AT&T Co., Winston-Salem, NC, 1978.
- [24] AT&T, "Routine Surveys," BSP 877-200-100, AT&T Co., Winston-Salem, NC, 1966.
- [25] AT&T, "Duct Surveys," BSP 877-201-100, AT&T Co., Winston-Salem, NC, 1941.
- [26] AT&T, "Test Methods and General Procedures, Non-Stray Current Areas," BSP 877-205-100, AT&T Co., Winston-Salem, NC, 1966.
- [27] AT&T, "Centralized Testing," BSP 877-206-100, AT&T Co., Winston-Salem, NC, 1966.
- [28] AT&T, "Copper Sulphate Half-Cell," BSP 877-207-100, AT&T Co., Winston-Salem, NC, 1961.
- [29] AT&T, "Instruments and Associated Equipment for Corrosion Measurements," BSP 877-208-100, AT&T Co., Winston-Salem, NC, 1979.
- [30] "Impressed Current Cathodic Protection for Corrosion Control of Underground and Buried Cable Plant," Bellcore, LP-RPES-COR, Bellcore, Livingston, NJ, 1987.
- [31] Corrosion Testing and Mitigation for Hardware in Plastic Repeater Housings, Bellcore LP-RPES-COR001, Bellcore, Livingston, NJ, 1987.

# Metals Processing

*Terry A. DeBold<sup>1</sup>*

THE SELECTION OF APPROPRIATE tests for materials evaluation requires consideration of pertinent forms of corrosion and details of the environment and methods of fabrication. Mechanical properties, cost, and material availability are also important. This chapter describes the rationale of test selection and supplies background on corrosion testing.

## MATERIAL SELECTION

A wide variety of metals is produced for industries such as automotive, aerospace, marine, energy, chemical processing, etc. Materials include aluminum, titanium, stainless steel, nickel- and cobalt-base alloys, tool steels, and materials for electronic, magnetic, and expansion applications. Regardless of the metal, the same selection process can be used.

### Corrosion Resistance

First, candidate materials must be selected to resist corrosion in the service environment without "overalloying" to increase the cost. All forms of corrosion and effects of fabrication, as discussed below, must be considered.

### Mechanical Properties

Strength is usually the first mechanical property considered, but factors such as hardness, fatigue, impact, and stress-rupture properties are also important for many applications.

### Fabrication

The material chosen must be able to be welded, machined, cold-headed, etc., as necessary without undue cost or difficulty.

### Total Cost

This value analysis of the material includes initial alloy price, installed cost, and the expected life of the finished product. Improved machinability, headability, weldability, or simplified heat treatment may justify higher material cost. A more costly product that provides longer service may be less expensive than lost time for outages to replace a less expensive material.

<sup>1</sup>Specialist, Stainless Alloy R&D, Carpenter Technology Corporation, P.O. Box 14662, Reading, PA 19612-4662.

## Product Availability

The availability, including minimum purchase requirements, is also an important consideration in selecting the most practical and economical material.

## FORMS OF CORROSION

All forms of corrosion must be considered at the beginning of any test program, before discounting attack modes that are not likely to occur. Corrosion types can be divided into general (or uniform) attack and localized corrosion, in which extensive attack can occur in a very small area. Localized corrosion can be more difficult to observe.

Several forms of corrosion are shown following Fig. 1a (no corrosion), as follows: (1b) uniform attack or general corrosion, (dissolution over the entire surface); (1c) galvanic corrosion, (attack of less resistant material in a couple); (1d) erosion corrosion (increased attack due to relative motion of surface and corrosive solution); (1e) fretting (materials under load are subjected to vibration, and slip at the point of contact); (1f) crevice corrosion, (pitting at a gasket or deposit); (1g) pitting; (1h) exfoliation (subsurface attack with a laminated appearance); (1i) selective leaching, (removal of one element from a solid alloy by corrosion); (1j) intergranular (selective attack of grain boundaries); (1k) stress-corrosion cracking (SCC), (cracking in a specific medium in the presence of a tensile stress); (1l) corrosion fatigue (susceptibility to fatigue increased by a corrodent). Also, hydrogen embrittlement is a form of SCC in which hydrogen is produced by local corrosion, e.g., in a crack or pit, and results in crack propagation.

Many materials experience several of the above forms of corrosion. Some forms of attack are more prevalent in certain materials, e.g., exfoliation is well known in aluminum alloys and selective leaching can occur in copper-zinc alloys. A more complete description of corrosion types is found elsewhere in this book and is discussed in the literature [1-3].

## FACTORS THAT INFLUENCE CORROSION RESISTANCE

In addition to the alloy composition, several factors affect corrosion resistance and must be considered in testing programs.

FIG. 1—Several forms of corrosion that occur in metals and metallic alloys [29].

### Effects of the Service Environment and Operation

Tables and isocorrosion charts are available to document experience with general, or uniform, corrosion in relatively pure chemicals at various temperatures and concentrations. An example is shown in Fig. 2. The selection of a material, or the proper test to evaluate a material, often includes more than consideration of uniform attack in pure chemicals. The presence of impurities can accelerate or retard general corrosion, e.g., chlorides (and some other halides) can cause pitting or SCC. Crevices due to the design or adherent deposits can be sites of attack, particularly in the presence of chlorides. Higher velocity of the corrodent can (a) reduce attack if deposits and the resulting crevice attack

are prevented, or (b) increase attack if erosion-corrosion occurs. Both localized and general corrosion can be accelerated by variations in pH; aeration can have different effects depending upon the material/environment system. Also, corrosion may be increased by heat transfer. Examples include: (a) a heat exchanger where steam produces high metal temperatures to heat a corrosive solution, and (b) a cold metal wall where corrosive condensate forms from hot gases.

### Effects of Material Processing and Fabrication

The material condition, fabrication, and finish can also affect its service. Corrosion resistance, particularly SCC, can depend upon whether a material is annealed, hardened, or cold-worked, etc. Welding or stress relieving can affect intergranular or SCC resistance. Smoother surfaces, free of scale and other foreign particles, generally exhibit better resistance. Passivation can be useful for stainless steels to remove free iron contamination, which can cause rusting of resistant materials.

Service life can also be affected by galvanic contact with a dissimilar metal. The less resistant material tends to be dissolved and may experience general corrosion, pitting/crevice corrosion, or SCC. Hydrogen may be liberated at the more resistant metal, making hydrogen embrittlement an issue if the material is susceptible. Stray currents, e.g., from a DC power source, may have the same effect as dissimilar metal contact.

The literature includes additional information regarding the factors affecting corrosion [1-3]. Also, several corrosion data summaries are available to assist in material selection [4-9]. Many of these include consideration of several modes of corrosion and the effects of impurities. All of the above issues must be considered when evaluating a material for service. Testing of an unstressed-annealed material when the material in service will be bent, welded, or stress-relieved may result in a service failure regardless of satisfactory test results.

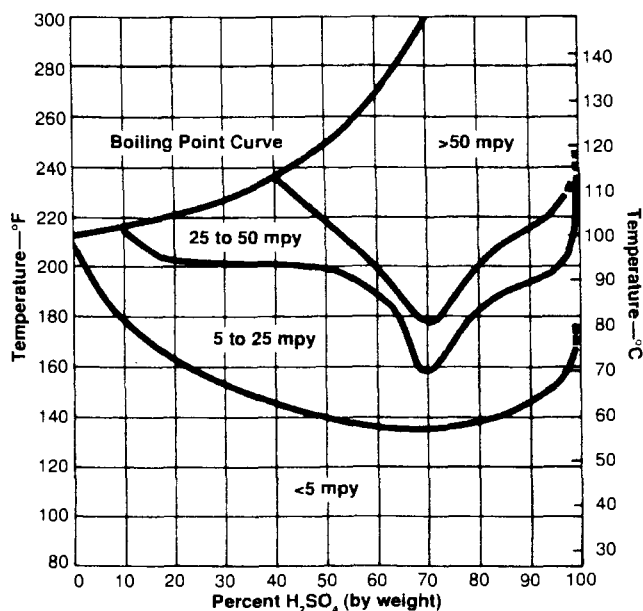


FIG. 2—Example isocorrosion chart for UNS N08020 in reagent grade sulfuric acid.



## RATIONALE OF TEST SELECTION

The corrosion testing performed in the metals processing industries is generally based on customer need. Corrosion tests may be chosen in order to select the correct material or allow the producer to develop a new alloy. Yet probably the largest volume of testing is conducted on established products for quality control purposes. The following section discusses the reasons for the various types of testing and provides concepts that can be used to design testing programs.

### Quality Control Tests

Quality control tests are frequently standardized and often are designed to detect susceptibility to a specific form of attack rather than simulate service. Standardization provides the opportunity for interlaboratory testing to develop precision (repeatability and reproducibility) and bias (deviation from accepted reference values) information before the test is used. ASTM provides a volume, *Standards on Precision and Bias for Various Applications*, for use in this work [10].

Knowledge of precision and bias is important if acceptance criteria are to be established. Confidence in the values obtained is necessary when a test is used to separate acceptable and unacceptable material. Generally, the establishment of acceptance criteria requires extensive testing of the product forms of interest.

Also, quality control tests are frequently brief and relatively inexpensive. Typically, they must be completed before shipment; delays, or excessive testing costs are not desired by either producer or user.

Discussion of the test objectives by user and producer is essential. Communication facilitates agreement regarding frequency of sampling, specimen location, orientation, and surface finish. Testing must be sufficient to guarantee quality without excessive cost or delay. Tests are often performed on each heat and heat treat lot to verify that the material composition and annealing practice were satisfactory. The specimen location may be chosen to provide a typical sample (generally midradius of a bar) or to evaluate

the area most likely to see service (e.g., the surface). In some cases, specimen location is chosen to restrict the amount of material wasted in cutting. Specimens are generally oriented longitudinally unless the transverse properties or resistance of the cross section is essential to service. In most cases, the equivalent of a 120 grit paper finish is provided, although smoother surfaces are sometimes required.

Perhaps the best-known quality control tests are those contained in the ASTM A 262, *Practices for Detecting Susceptibility to Intergranular Attack in Austenitic Stainless Steels*. These are summarized in Table 1 and discussed further in the testing section below.

### Simulated-Service Tests

Simulated-service tests facilitate specimen observation and control of the test environment versus in-plant tests. Tests for material selection or development generally simulate the service environment, including impurities and possibly factors such as heat transfer and aeration. Communication with the end user is essential to select the optimum tests and accomplish goals with minimum expense. Generally, these tests are not standardized. Fabrication information, such as welding or cold forming, is needed to assure that the material is evaluated in the condition that will see service. ASTM G 58, *Practice for Preparation of Stress-Corrosion Test Specimens for Weldments*, describes procedures for making and using welded stress-corrosion specimens. Also, details of the design and operation of the unit are needed to determine whether the effect of crevices must be evaluated.

Some means of acceleration is necessary to predict years of service using only weeks or months of testing. Several means have been used to accelerate these tests, including (a) use of higher temperatures, lower pH, or increased concentrations of deleterious impurities, (b) use of slow strain rate or electrochemical techniques, (c) use of increased stresses or precracked specimens, and (d) use of metallographic examination or measurement of very small weight losses to detect attack initiation. Examples are provided in the Test Descriptions section below.

TABLE 1—ASTM intergranular corrosion tests.

ASTM Standard	Test Media	Test Duration	Applicable Alloys
A 262-A	Oxalic acid etch	Etch test	Screening for selected alloys in other A 262 practices
A 262-B	$\text{Fe}_2(\text{SO}_4)_3\text{-H}_2\text{SO}_4$	120 h	UNS S30400, S30403, S31600, S31603, S31700, S31703, S32100, S34700, J92500, J92600, J92800, J92900, J92999, J93000
A 262-C	$\text{HNO}_3$ (Huey Test)	240 h <sup>a</sup>	Same as A 262-B <sup>b</sup>
A 262-E	$\text{Cu-CuSO}_4\text{-16 \%H}_2\text{SO}_4$	24 h <sup>c</sup>	UNS S20100, S20200, S30100, S30400, S30403, S30409, S31600, S31603, S31609, S31700, S31703, S32100, S34700
A 262-F	$\text{Cu-CuSO}_4\text{-50 \%H}_2\text{SO}_4$	120 h	UNS J92800, J92900
G 28-A	$\text{Fe}_2(\text{SO}_4)_3\text{-H}_2\text{SO}_4$ (similar to A 262-B)	24/120 h	UNS N10276, N06455, N06007, N06200, N06686, N06985, N08020, N06600, N06625, N08800, N08825, N06022, N06030, N06059, N08367
G 28-B	$\text{H}_2\text{SO}_4 + \text{HCl} + \text{FeCl}_3 + \text{CuCl}_2$	24 h	UNS N10276, N06022, N06059, N06200, N06686
A 763-W	Oxalic acid etch (similar to A 262-A)	Etch test	UNS S44400, S44626, S44660, S43035, XM27
A 763-X	$\text{Fe}_2(\text{SO}_4)_3\text{-H}_2\text{SO}_4$ (similar to A 262-B)	24/120 h	UNS S43000, S44600, S44700, S44800, XM27
A 763-Y	$\text{Cu-CuSO}_4\text{-50 \%H}_2\text{SO}_4$ (similar to A 262-F)	96/120 h	UNS S44600, S44626, S44660, S44735, S44700, S44800, XM27
A 763-Z	$\text{Cu-CuSO}_4\text{-16 \%H}_2\text{SO}_4$ (same as A 262-E)	24 h	UNS S43000, S43400, S43600, S44400, S43035

<sup>a</sup> Shorter duration permitted in some cases.

<sup>b</sup> The nitric acid test has also been applied less frequently to other austenitic, ferritic, and martensitic grades.

<sup>c</sup> Typically 24 h.

### In-Plant and Field Testing

Materials producers frequently supply specimens to users for exposure to plant environments. Comparison of several materials has been facilitated by exposing racks containing plate or sheet coupons along with stressed specimens, as shown in Fig. 3. A concern of both metals producers and users is that the specimens tested be in the condition that will see service. This has resulted in the use of welded U-bend specimens to incorporate the cold-forming and welding effects that may occur in fabrication. The crevice at the restraining bolt provides an evaluation of crevice corrosion resistance. Because crevice geometry and tightness are important variables, a reproducible crevice design is essential.

After testing for as long as possible, the specimens are evaluated by mass loss, visual, and binocular examination and in some cases by metallographic techniques. Generally, these tests can be accelerated only by severe bending or possibly by the application of a tight crevice, and the initiation of corrosion must be detected by careful weighing and examination.

Other plant test specimen designs and evaluation techniques are available. Some fit in restricted spaces and/or monitor electrochemical parameters. Examples of such fixtures, electrode polarization probes, appear in Fig. 4. These allow monitoring of the corrosion process and can detect changes in plant operation that cause excessive attack.

Information regarding field testing is contained in ASTM G 4, Guide for Conducting Corrosion Coupon Tests in Field Applications, while practices for handling samples are found in ASTM G 1, Practice for Preparing, Cleaning, and Evaluating Corrosion Test Specimens. Related information dealing with field testing in the atmosphere and seawater is found in ASTM G 50, Practice for Conducting Atmospheric Corrosion Tests on Metals and ASTM G 52, Practice for Exposing and Evaluating Metals and Alloys in Surface Seawater. Procedures for field failure analysis are found in ASTM G 161, Standard Guide for Corrosion-Related Failure Analysis.

### TEST DESCRIPTIONS

This section provides comments on the utility of several tests, according to the principles discussed above. A more complete description of corrosion testing appears elsewhere in this manual.

**FIG. 3—Twelve-in. (30.5 cm) long rack with stressed and unstressed specimens for exposure in plant environments (photograph courtesy of Metal Samples Co., Inc., Munford, AL).**



**FIG. 4—Two (top) and three (bottom) electrode polarization probes for exposure in plant environments (photograph courtesy of Metal Samples Co., Inc., Munford, AL).**

### Intergranular Corrosion Tests

The theory and application of intergranular corrosion tests have been discussed in the literature [11]. The tests included in ASTM A 262, as summarized in Table 1, are frequently used for quality control of austenitic stainless steels. These methods detect susceptibility to intergranular corrosion and the test solutions may be quite different than the service environments. These tests are frequently used to evaluate the effectiveness of the heat treatment used prior to shipment of a material. The alloys that may be evaluated by each practice (e.g., Types 304 or 316) are specified as well as the procedure for using the several tests. Comments regarding a few of the tests are useful.

ASTM A 262 Practice A is a rapid procedure in which specimens are electrolytically etched and examined metallographically for attack at the grain boundaries. It has been widely used as a quality control screening test to approve acceptable material. Specimens that fail the oxalic acid test are then evaluated by one of the other tests in ASTM A 262 and are accepted or rejected based on these results. Although the oxalic acid etch test is done quickly, it can be tedious, because examination of all fields is required.

The accelerated Strauss test, ASTM A 262 Practice E (copper-copper sulfate-16 % sulfuric acid test), is also a popular quality control test because it is brief (typically 24 h) and includes an acceptance criterion. After exposure, specimens are bent to expose intergranular attack. Material with attack fails, while unattacked material passes. Experience is important in specimen evaluation to separate "cracks" due to attacked grain boundaries from mechanical cracks that may have occurred in bending. Different laboratories have obtained varying results upon examination of the same set of specimens [12].

Three tests from ASTM A 262 provide corrosion rates: Practices B, C, and F. Practice B requires a 120 h exposure and is generally more popular than Practice C, which requires 240 h of boiling time. Also, Practice C detects susceptibility to attack, which may not affect service in environments other than highly-oxidizing media (such as nitric acid).

Use of these tests requires work and communication between user and producer to establish the maximum acceptable corrosion rate. In one example of this process for austenitic stainless steels, hundreds of specimens representing several product forms were evaluated in ASTM A 262 tests to compare actual corrosion rates with the specified maximum rate [13].

Related standards for determination of intergranular corrosion are ASTM A 763, Practices for Detecting Susceptibility of Intergranular Attack in Ferritic Stainless Steels, and ASTM G 28, Test Methods of Detecting Susceptibility to Intergranular Corrosion in Wrought, Nickel-Rich, Chromium-Bearing Alloys. As seen in Table 1, many of these methods are similar to the ASTM A 262 practices.

### Stress-Corrosion Cracking Tests

SCC behavior often is not as reproducible as intergranular corrosion penetration rates. Initiation and propagation of stress-corrosion cracks can depend upon many factors, including variation in pH and chloride content in crevices, amount of dissolved oxygen, and stress distribution in the material. Because of this, and the longer duration associated with testing, SCC tests have seen limited use as quality control techniques.

Several environments and specimen designs are available for SCC evaluation [14]. ASTM G 36, Practice for Evaluating Stress-Corrosion Cracking Resistance of Metals and Alloys in a Boiling Magnesium Chloride Solution, provides a more severe environment than generally found in service. Resistance in this test depends largely on the nickel content and most austenitic and duplex stainless steels are readily cracked.

Sodium chloride solutions appear to provide environments more representative of service than ASTM G 36. Boiling 25 % sodium chloride, acidified to pH 1.5 with phosphoric acid, provides a less severe environment, which has been used to evaluate stainless steels (see ASTM G 123, Test Method for Evaluating Stress-Corrosion Cracking of Stainless Alloys with Different Nickel Content in a Boiling Acidified Sodium Chloride Solution). Acceleration of cracking in this environment has been accomplished by severely stressing the material using U-bend specimens. See ASTM G 30, Practice for Making and Using U-Bend Stress-Corrosion Test Specimens. Other statically-stressed samples described in ASTM standards include: C-rings (G 38), bend-beams (G 39), and direct tension (G 49).

Several means are available to accelerate SCC tests. Dynamic testing can be an effective method to obtain results rapidly in environments that simulate service. Slow strain rate tension (SSRT) tests are performed by pulling a specimen to failure at strain rates of  $10^{-7}$  to  $10^{-4}$  s<sup>-1</sup> in a corrosive environment [15,16]. See ASTM G 129, Practice for Slow Strain Rate Testing to Evaluate the Susceptibility of Metallic Materials to Environmentally Assisted Cracking. Elongation (or time to fail) and reduction in area are compared to data for specimens pulled in an inert environment. Indications of corrosion susceptibility include the presence of attack on the fracture surface, secondary cracks along the gage section, and reduction in ductility figures (Fig. 5). SSRT methods have been used as acceptance tests for critical materials used in oil field applications and an example of the type of data obtained is shown in Table 2.

Dynamic testing has also been used in the nuclear power industry as a quality control test to identify material that is susceptible to SCC in reactor-water environments. The rising-load test has been performed by loading precracked, Charpy-type specimens in three-point bending using a constant

**FIG. 5—Tested slow strain rate tension specimens showing (a) poor ductility and secondary cracks indicating susceptibility to SCC, and (b) increased ductility versus Fig. 5a and absence of secondary cracking indicating improved resistance.**

extension rate. In this procedure, specimens have been tested in both air and deionized water. The stress intensity at maximum load and the time for the load to drop to one half its maximum value are recorded. Curves for exposures in a test environment and in air are shown in Fig. 6 for a susceptible heat of UNS N07750 and for a more resistant material, UNS N07716. More resistant materials are characterized by (a) higher ratios of the maximum stress intensity in the test environment versus that in an inert air environment, and (b) longer time for the load to decrease to half its maximum value (0.5 P<sub>max</sub>). Although the UNS N07716 was highly resistant, the fluctuation in load during the early part of the curve and the slightly lower maximum stress intensity (c.f. the air test) suggest slight susceptibility to attack. The rising load test is another example of a method that uses dynamic loading and is able to obtain results quickly in an environment that generally simulates long-term exposure.

Design criteria for corrosive environments can be obtained using fracture mechanics specimens. The critical stress intensity for SCC can be determined and is designated K<sub>ISCC</sub>. Frequently, however, the stress intensity after a predetermined test duration is used as a K<sub>f</sub> or final stress intensity rather than monitoring the crack growth to confirm

**TABLE 2**—Example slow strain rate test data for UNS N07716 0.250 in. (0.635 cm) diameter gage with a strain rate of  $4 \times 10^{-6}$ /s.

Environment	% R.A.	Time to Failure, h	R.A. (brine)	TF (brine) <sup>a</sup>	Secondary Cracking	Fracture Surface
			R.A. (inert)	TF (inert)		
Inert	54.8	25.8	...	...	...	...
	55.9	25.9	...	...	...	...
Sour brine	53.9	25.7	0.97	0.99	No	Slight attack
	53.1	26.6	0.96	1.03	No	Slight attack

Inert environment was helium at 177°C (350°F); sour brine was deaerated 100 000 ppm Cl<sup>-</sup>, 150 psi (1.03 MPa) H<sub>2</sub>S, 150 psi CO<sub>2</sub> (added at room temperature) and 10 g/L elemental sulfur; tests at 177°C (350°F).

<sup>a</sup>TF—time to failure.

that crack arrest has occurred. It is obviously important to differentiate between these two types of results.

The double-cantilever beam (DCB) specimen has been used in oil field and other applications [17] and is described in NACE Standard Test Method, Laboratory Testing of Metals for Resistance to Sulfide Stress Cracking in H<sub>2</sub>S Environments (TM0177) (Fig. 7). Thickness of DCB samples used in the oil field has often been restricted by the size of the product form under evaluation. In many applications, thicker samples are preferred as described in ASTM G168, Standard Practice for Making and Using Pre-Cracked Double-Beam Specimen.

Frequently, the DCB specimen is precracked to provide a sharp notch and accelerate hydrogen embrittlement or stress-corrosion processes. Machining and measuring the specimen and deflection as well as precracking parameters

and determination of the crack length require considerable care and expertise. Some material/environment systems allow evaluation in relatively short exposures, e.g., 14 days, based on experience with crack propagation rates (see TM0177). Most materials require a longer evaluation (e.g., one month or more) and the delay is usually objectionable for a quality control test.

The effect of test duration is demonstrated by a method used by the Navy to compare materials for aircraft parts. A single-edge notched (and precracked) cantilever beam specimen is deadweight loaded and exposed to 3 1/2 % NaCl. The time-to-fail at various stress intensities is plotted in Fig. 8. The stress intensity after 1000 h exposure has been used as a measure of resistance, although lower values have been obtained if the specimens are allowed to continue for 10 000 h.

### Pitting and Crevice Corrosion

Pitting and crevice corrosion tests frequently are less reproducible than intergranular corrosion tests. Pit initiation can be influenced by factors such as surface finish, localized differences in the test solution, and nonmetallic inclusions in the microstructure. Crevice corrosion can be dependent upon these variables as well as geometry and tightness of the crevice [18,19]. Propagation of attack in pits and in crevices occurs by a similar mechanism, but depends upon the local pH and chloride content in the attacked area. Additional data regarding pitting corrosion can be found in Ref 20.

Frequent use has been made of ASTM G 48, Test Methods for Pitting and Crevice Corrosion Resistance of Stainless Steels and Related Alloys by the Use of Ferric Chloride Solution. Specimens are immersed in ferric chloride or acidified ferric chloride and are evaluated by visual examination and mass loss. A related document, Guide for Crevice Corrosion Testing of Iron-Base and Nickel-Base Stainless Alloys in Seawater and Other Chloride-Containing Aqueous Environments is found in ASTM G 78.

Ferric chloride has also been used in Test Method C of ASTM A 923, Test Methods for Detecting Detrimental Intermetallic Phase in Wrought Duplex Austenitic/Ferritic

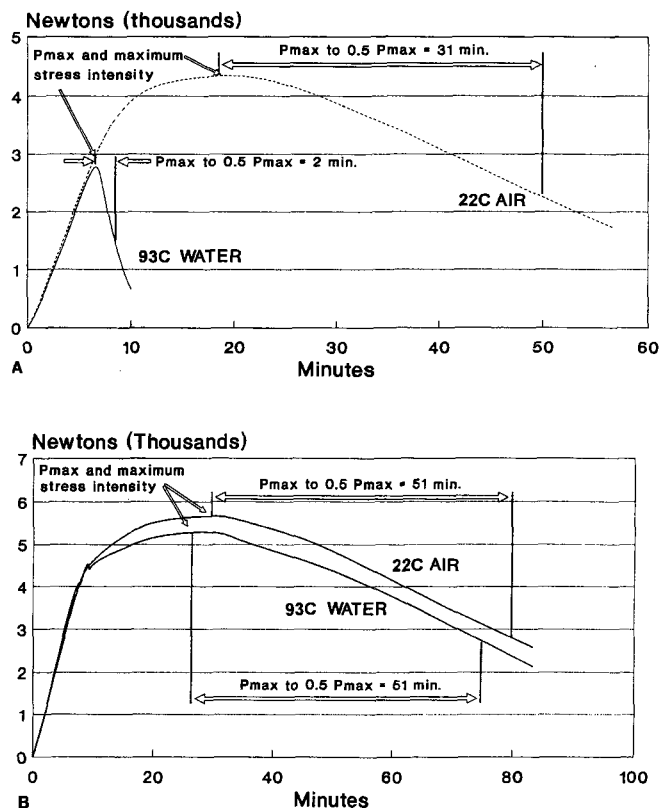


**FIG. 6**—Example of rising load curves in 93°C water and inert air environments for (a) a highly susceptible heat of UNS N07750, and (b) improved resistance demonstrated by UNS N07716.

**FIG. 7**—Double-cantilever beam specimen with side groove.

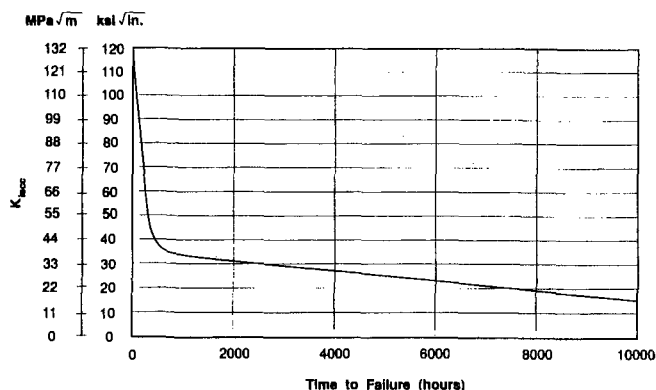


FIG. 8—SCC results for single-edge notched and precracked cantilever beam specimens of UNS K92580 (52 HRC) in 3.5 % NaCl at room temperature.

Stainless Steels. In this method, ferric chloride has been used to detect the precipitation of harmful intermetallic phases rather than indicate the performance of the steel in other corrosive environments.

Pit or crevice depth and pit density may be determined according to ASTM G 46, Standard Guide for Examination and Evaluation of Pitting Corrosion, but this can be labor-intensive. Results for highly resistant and very susceptible materials can be reproducible, but data for replicates with marginal resistance can be quite variable. Because of this variation these tests are generally difficult to use for quality control purposes.

Determination of the critical pitting or critical crevice temperature is often used as an alternative to comparing the severity of attack on several samples [21–23]. Procedures for this testing are described in Methods C and D of ASTM G 48. Specimens are immersed for a given period (e.g., 72 h) at a temperature that is not expected to cause attack. Fresh specimens are then exposed at 5°C increments for the same duration until the temperature at which attack occurs (critical temperature) is determined. For many materials, the critical temperatures of replicate specimens fall within a  $\pm 5^\circ\text{C}$  variation. Retesting of the same specimen can affect the critical temperature [24]. Testing may be initiated just below the critical temperature, if it can be estimated. If not, this technique can require many specimens and a few weeks to find the critical temperature.

Critical pitting temperature can be rapidly obtained using electrochemical equipment to maintain a preset potential, increase temperature and detect the onset of corrosion by monitoring corrosion current [24]. In ASTM G 150, Test Method for Electrochemical Critical Pitting Temperature Testing of Stainless Steels, a pre-set potential provides consistent conditions and a potential-independent critical pitting temperature. Sensitive detection of attack using the current allows an accelerated evaluation.

Resistance to pitting or crevice corrosion has been estimated by using the composition to calculate a PRE-number, where larger numbers indicate better resistance. A typical equation has been:

$$\text{PRE} = \% \text{Cr} + 3.3(\% \text{Mo}) + 16(\% \text{N}) \quad (1)$$

Actually, the coefficients can vary for comparisons of alloys with widely different molybdenum or nitrogen contents. For example, critical crevice temperatures were determined using ASTM G 48, Method D for several high-nitrogen alloys [25]. These included materials considered for use in medical devices such as BioDur® 108 Alloy (21 %Cr-22 %Mn-1 %Mo-1 %N-Fe) and UNS S20910, a 22 %Cr-13 %Ni-5 %Mn-2 %Mo-0.3 %N-Nb-V-Fe alloy. Both alloys demonstrated good resistance in these tests, but the 1 % nitrogen alloy was superior. While nitrogen was beneficial, regression indicated that its effect was not as strong as indicated in the above equation. Using regression, the equation obtained to compare alloys with nitrogen contents varying over the range of approximately 0.3 % to >1 % was:

$$\text{PRE} = \% \text{Cr} + 3.2(\% \text{Mo}) + 8(\% \text{N}) \quad (2)$$

While the data presented here may not be sufficient to specify nitrogen coefficients, they do demonstrate that care must be taken whenever using such equations to be certain the expression describes the alloys of interest.

### Rusting and Pitting in Corrosive Atmospheres

Automobiles and military equipment frequently are exposed to marine environments and road salt. Beach test sites are available, but simulations in the laboratory are convenient. The ASTM B 117, Method of Salt Spray (Fog) Testing, has been widely used for this purpose to evaluate rusting, pitting, and SCC. Martensitic stainless steels and maraging steels have been exposed to salt spray (and other NaCl environments) to evaluate resistance to SCC prior to use in military equipment and fasteners. Ferritic and austenitic stainless steels have been tested to evaluate resistance to rusting prior to use in automotive applications.

Rusting, pitting, and SCC tests frequently provide results with poor reproducibility. The percent surface rusted after a salt spray test can also be quite variable. The amount of rust covering a specimen after the salt spray test varies if the rust initiates at the top of the coupon and runs down over the test surface or initiates at the bottom and covers only a small portion of the specimen (Fig. 9). Rusting is also dependent upon the surface finish; smoother finishes are usually more resistant. Because of these factors, it is difficult to use the salt spray test for quality control.

Alternative atmospheric cabinet simulation tests are available, including ASTM G 87, Practice for Conducting Moist  $\text{SO}_2$  Tests and ASTM G 85, Practice for Modified Salt Spray Testing. Service in environments where humidity or moisture varies may be simulated by cyclic humidity or alternate immersion tests. See ASTM G 60, Test Method for Conducting Cyclic Humidity Tests and ASTM G 44, Practice for Exposure of Metals and Alloys by Alternate Immersion in Neutral 3.5 % Sodium Chloride Solution.

### Tests to Evaluate Passivation

Alloys with increased chromium content, such as stainless steels, employ a thin, invisible, passive film to provide corrosion

BioDur® Alloy is a trademark of CRS Holdings, Inc. a subsidiary of Carpenter Technology Corporation.

**FIG. 9—Variation in percent rust on 3/4 in. (1.9 cm) diameter conical test surface after ASTM B 117 salt spray exposure due to rust initiation at (a) bottom and (b) top.**

resistance. This film forms rapidly on clean surfaces with exposure to the air. These materials are frequently passivated in acid to optimize corrosion resistance, but for most applications it is likely that the film formed by these treatments is no better than that formed in air. The major purpose of passivation is to remove free iron, i.e., shop dirt containing very small bits of carbon or tool steel. Free iron particles become lodged on the surface of a resistant material and produce rust. Passivation in nitric acid (sometimes with sodium dichromate) or citric acid is performed to remove these free iron particles. Passivation also removes some or all of the sulfides of free-machining stainless steel [26]. Procedures for passivation are found in ASTM A 967, Standard Specification for Chemical Passivation Treatments for Stainless Steel Parts.

It is frequently desirable to test passivated parts to determine if the passivation has effectively removed free iron from machining operations. Both ASTM A 967 and ASTM A 380, Practice for Cleaning and Descaling Stainless Steel Parts, Equipment, and Systems, provide several methods to accomplish this. These include water immersion and high humidity tests which can be completed in as little as one day.

The salt spray test is frequently requested to verify the effectiveness of passivation treatments. This is a more severe environment than necessary to rust iron and frequently it has caused red staining of properly-passivated lower-alloy stainless steels. The salt spray test can, therefore, produce

spurious failures when used to evaluate the passivation of Types 410 and 430 as well as free-machining grades Type 416 and 303. The salt spray test may be useful to evaluate the passivation of more resistant specimens, such as Type 316 and polished Type 304.

ASTM A 380 and A 967 also include the copper sulfate test as a rapid method to provide a gross indication of free iron presence. This test is performed using a copper sulfate-sulfuric acid solution that plates copper when iron is dissolved from the surface. If the test parameters are not carefully controlled, this test can cause undesirable copper plating on properly-passivated material. To avoid spurious failures, the solution and specimen should be at room temperature and specimens should be handled with plastic or stainless tongs and exposed separately, rather than lying together in a basket. According to ASTM A 380, this test is not to be used for martensitic and lower-chromium ferritic stainless steels of the 400 series, because it will show a positive reaction on these materials.

### Electrochemical Tests and Effects

Electrochemical tests provide a means to understand the corrosion process, simulate service conditions, or accelerate evaluation of a material [27]. ASTM G 3, Practice for Conventions Applicable to Electrochemical Measurements in Corrosion Testing; ASTM G 5, Standard Reference Test Method for Making Potentiostatic and Potentiodynamic Polarization Measurements and ASTM G 61, Standard Test Method for Conducting Cyclic Potentiodynamic Polarization Measurements for Localized Corrosion Susceptibility of Iron-, Nickel-, or Cobalt-Based Alloys provide background in some of these techniques.

An example of a potentiodynamic curve for Type 430 stainless is found in Fig. 10. Early in the scan at more active potentials, high current indicates a significant amount of corrosion is occurring. At slightly higher potentials, a passive

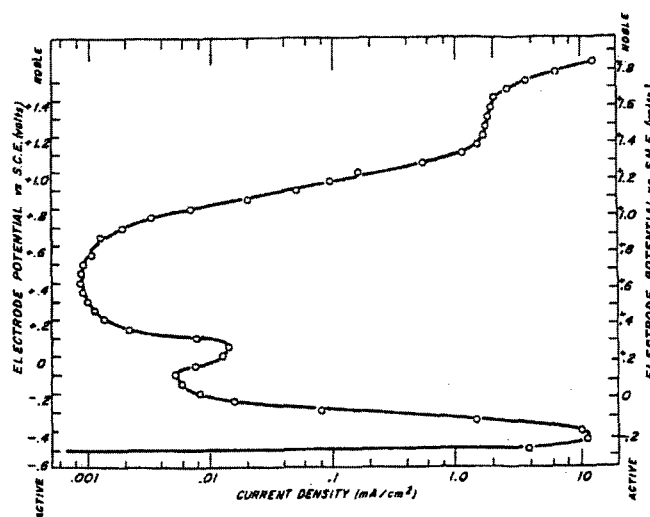


**FIG. 10—Typical anodic polarization plot for Type 430 stainless steel in 1.0 N sulfuric acid (from ASTM G 3, Practice for Conventions Applicable to Electrochemical Measurements in Corrosion Testing).**

film forms on stainless steels and corrosion (current) is minimum. Still higher potentials cause pitting and increased current results. After exceeding the pitting potential, the scan may be reversed to determine the reduction in potential required for the material to repassivate (not shown). This is indicated by low current, similar to that on the initial scan. Materials with improved resistance repassivate more readily at higher potentials during the return scan.

Electrochemical scanning techniques indicate the ability of a material to resist a given environment or repassivate after corrosion initiates. These tests can compare materials without waiting for pit initiation or for sufficient time to obtain measurable general corrosion rates. Although these tests can be done quickly, relating the results to long-term behavior in mill environments can require extensive expertise.

Other electrochemical techniques have been used for rapid detection of intergranular precipitation. Single- and double-loop electrochemical potentiokinetic reactivation scans are used to detect intergranular precipitation in Types 304 and 304L stainless steels [28]. The single-loop test is described in ASTM G 108, Test Method for Electrochemical Reactivation (EPR) for Detecting Sensitization of AISI Type 304 and 304L Stainless Steel. In single- and double-loop tests, the specimen potential is scanned through the active region, where corrosion at chromium-depleted grain boundaries causes current flow (Fig. 11). Larger current peaks indicate increased susceptibility to intergranular attack. The double-loop test includes an initial scan in the anodic direction to remove any surface condition that could affect resistance during the return scan. Experience has shown that material susceptible to intergranular attack in an EPR test can also be susceptible to intergranular SCC in other environments. Several of these tests can be conducted in one day, making these methods attractive for quality control; however, appropriate electrochemical equipment is required.

Electrochemical techniques have also been used to provide a rapid test in ASTM F 746, Test Method for Pitting or Crevice Corrosion of Metallic Surgical Implant Materials. A specimen is anodically polarized to stimulate pitting and then returned to a less positive preset potential to determine if repassivation will occur. This is repeated at successively higher preset potentials until the final, or critical potential is determined. More resistant materials display higher critical potentials. This relatively brief test does not wait for pits to initiate and reduces variability by maintaining the potential of the specimen.

Galvanic techniques have been used to assess the compatibility of dissimilar metals in an electrolyte. These methods are described in ASTM G 71, Guide for Conducting and Evaluating Galvanic Corrosion Tests in Electrolytes. A galvanic series is one way of predicting the attack of a less-resistant metal due to its contact with a more resistant metal in an electrolyte. See ASTM G 82, Guide for Development and Use of a Galvanic Series for Predicting Galvanic Corrosion Performance.

Electrochemical data have been used to calculate corrosion rates. It is useful to compare these corrosion rates with those from immersion tests to confirm that similar rates are obtained. Information regarding polarization resistance and determination of corrosion rates from electrochemical data

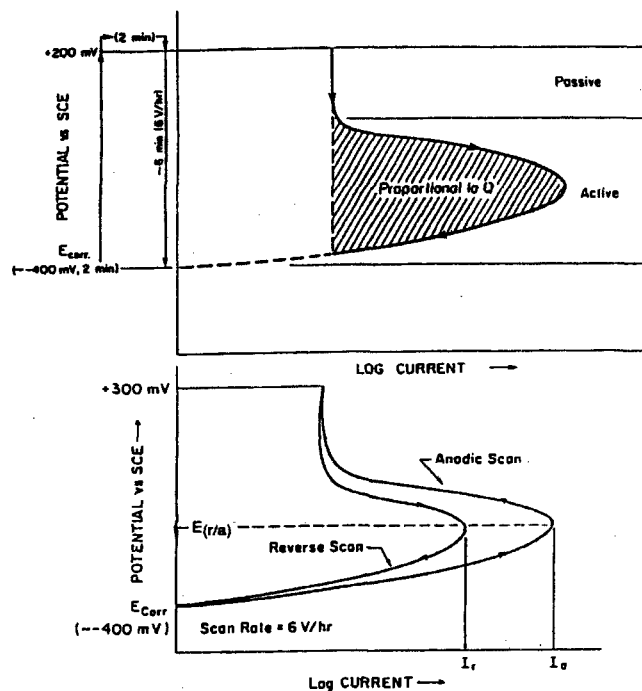


FIG. 11—Schematic polarization curves for the (a) single-loop and (b) double-loop EPR test methods on Type 304 stainless steel. (Courtesy of the ASTM G01.08 task group on “EPR Testing”.) SCE—saturated calomel electrode;  $I_r$ —maximum current in return scan;  $I_a$ —maximum current in initial, forward scan.

are found in ASTM G 59, Test Method for Conducting Potentiodynamic Polarization Resistance Measurements and ASTM G 102, Practice for Calculation of Corrosion Rates and Related Information from Electrochemical Measurements.

## SAMPLING AND STATISTICAL ANALYSIS

Unfortunately, prolonged test time and increased cost often prevent the development of statistical data in corrosion studies. Frequently, only duplicate specimens are evaluated, although three to five specimens are frequently used in the ASTM B 117 salt spray environment. Triplicate specimens are often suggested for pitting, crevice, and SCC tests. One useful reference is the ASTM G 16, Guide for Applying Statistics to Analysis of Corrosion Data.

## TEST PROCEDURES, RECORDS, AND EQUIPMENT CALIBRATION

In addition to the procedures provided by standards organizations, it is advisable for metals producers to maintain internal procedures manuals. Pertinent information may include details regarding specimen heat treatment or preparation, location and type of equipment and materials to be used, specific user test requirements, report scope and format, along with disposition of records following testing.

ASTM G 107, Guide for Formats for Collection and Compilation of Corrosion Data for Metals for Computerized Database Input, provides an extensive list of parameters that may be recorded to fully describe the test and its results. (Related information is found in ASTM G 135, Standard Guide for Computerized Exchange of Corrosion Data for Metals.) It is generally recommended that gages and all measuring devices be calibrated according to a set schedule and procedure.

## FUTURE TESTING NEEDS AND DIRECTIONS

Continued emphasis may be expected on interlaboratory testing and establishment of precision and bias for standard test methods. Equally necessary for quality control is extensive evaluation of the product forms of interest to establish acceptance criteria that discriminate between satisfactory and unsatisfactory material. While rapid and inexpensive tests will be used for most quality control tests, an increase in more sophisticated techniques such as electrochemical testing and slow strain rate techniques is expected. Additional work is necessary to improve reproducibility of rusting, pitting/crevice, and SCC tests. In some cases, control of the specimen potential may improve test reproducibility.

## REFERENCES

- [1] Fontana, M. G. and Greene, N. D., *Corrosion Engineering*, McGraw-Hill, NY, 1978.
- [2] Uhlig, H. H., *Corrosion and Corrosion Control*, Wiley, NY, 1971.
- [3] Metals Handbook, *Corrosion*, 9th ed., Vol. 13, ASM International, Materials Park, OH, 1987.
- [4] Graver, D. L., *Corrosion Data Survey—Metals Section*, 6th ed., National Association of Corrosion Engineers, Houston, 1985.
- [5] LaQue, F. L. and Copson, H. R., *Corrosion Resistance of Metals and Alloys*, Reinhold, NY, 1963.
- [6] Rabald, E. R., *Corrosion Guide*, Elsevier, NY, 1968.
- [7] Berg, F. F., *Corrosion Diagrams*, Vdi-Verlag, Dusseldorf, 1969.
- [8] Friend, W. Z., *Corrosion of Nickel and Nickel-Base Alloys*, Wiley, NY, 1980.
- [9] Sedriks, A. J., *Corrosion of Stainless Steels*, Wiley, NY, 1979.
- [10] ASTM Standards on Precision and Bias for Various Applications, 3rd ed., ASTM International, West Conshohocken, PA, 1988.
- [11] Streicher, M. A., "Theory and Application of Evaluation Tests for Detecting Susceptibility to Intergranular Attack in Stainless Steels and Related Alloys—Problems and Opportunities," *Intergranular Corrosion of Stainless Alloys*, ASTM STP 656, R. F. Steigerwald, Ed., ASTM International, West Conshohocken, PA, 1978.
- [12] Walker, W. L., Variations in the Evaluation of ASTM A 262, Practice E, Results, NEDO-24171, 79NED3, General Electric Co., San Jose, January 1979.
- [13] Brown, M. H., "Behavior of Austenitic Stainless Steels in Evaluation Tests for the Detection of Susceptibility to Intergranular Corrosion," *Corrosion*, Vol. 30, No. 1, January 1974, pp. 1–12.
- [14] *Stress Corrosion Testing*, ASTM STP 425, ASTM International, West Conshohocken, PA, 1976.
- [15] Parkins, R. N., "Development of Strain-Rate Testing and Its Implications," *Stress Corrosion Cracking—The Slow Strain-Rate Technique*, ASTM STP 665, G. M. Ugiansky and J. H. Payer, Eds., ASTM International, West Conshohocken, PA, 1979, pp. 5–25.
- [16] McIntyre, D. R., "Ranking Materials for Extreme Sour Gas Service Using the Slow Strain Rate Method," *Hydrogen Embrittlement: Prevention and Control*, ASTM STP 962, L. Raymond, Ed., ASTM International, West Conshohocken, PA, 1988, pp. 178–189.
- [17] Heady, R. B., "Evaluation of Sulfide Corrosion Cracking Resistance in Low Alloy Steels," *Corrosion*, Vol. 33, No. 3, March 1977, pp. 98–107.
- [18] Oldfield, J. W. and Sutton, W. H., "Crevice Corrosion of Stainless Steels—I. A Mathematical Model," *British Corrosion Journal*, Vol. 13, No. 1, 1978, pp. 13–22.
- [19] Oldfield, J. W. and Sutton, W. H., "Crevice Corrosion of Stainless Steels—II. Experimental Studies," *British Corrosion Journal*, Vol. 13, No. 3, 1978, pp. 104–111.
- [20] *Galvanic and Pitting Corrosion—Field and Laboratory Studies*, ASTM STP 576, ASTM International, West Conshohocken, PA, 1976.
- [21] Brigham, R. J. and Tozer, E. W., "Temperature as a Pitting Criterion," *Corrosion*, Vol. 29, No. 1, January 1973, pp. 33–36.
- [22] Brigham, R. J., "Temperature as a Crevice Corrosion Criterion," *Corrosion*, Vol. 30, No. 11, November 1974, pp. 396–398.
- [23] Hibner, E. L., "Modification of Critical Crevice Temperature Test Procedures for Nickel Alloys in a Ferric Chloride Environment," *Materials Performance*, March 1987, pp. 37–40.
- [24] Davis, G. O. and Streicher, M. A., "Initiation of Chloride Crevice Corrosion on Stainless Alloys," NACE Corrosion/85 paper 205.
- [25] Gebeau, R. C. and Brown, R. S., "Corrosion Resistance and Strength of Biodur<sup>82</sup> 108 Alloy, A Nickel-Free Austenitic Stainless Steel," *Structural Biomaterials for the 21st Century*, M. Niinomi, et. al. Ed., The Minerals, Metals and Materials Society, 2001, pp. 157–164.
- [26] DeBold, T. A., "Passivating Stainless Steel Parts," *Machine and Tool Blue Book*, Vol. 81, No. 11, November 1986, pp. 74–77.
- [27] *Electrochemical Corrosion Testing*, ASTM STP 727, ASTM International, West Conshohocken, PA, 1981.
- [28] Kearns, J. R., draft of new "Standard Test Methods for Single and Double Electrochemical Potentiokinetic Reactivation (EPR) for Detecting Sensitization of AISI Type 304 and 304L Stainless Steels," ASTM Subcommittee G01.08, September 1992.
- [29] Henthorne, M., "Fundamentals of Corrosion," *Chemical Engineering*, 17 May 1971, pp. 127–132.



# Chemical Processing

*Bert Moniz<sup>1</sup> and Shi Hua Zhang<sup>2</sup>*

## To Find What You Need

THE OBJECT OF THIS chapter is to help plant and project engineers understand how corrosion data are generated and used, in order to optimize chemical plant performance and prevent process safety incidents.

To understand *who needs corrosion data*, see:

### Purpose of Corrosion Testing

To understand how to conduct corrosion tests, see:

### Field, Laboratory, and Pilot Plant Testing

#### Coupon Testing

#### Probe Testing

#### Specialized Testing

To understand what value to place on corrosion data, see:

### Confidence in Corrosion Data

### Creation of a Computerized Corrosion Test Database

## INTRODUCTION

Corrosion testing and corrosion monitoring with coupons and corrosion-monitoring probes are used to select materials of construction, determine failure mechanisms, and study corrosion in process environments. Corrosion coupons provide data on the average corrosion response, and corrosion monitoring probes provide data on instantaneous corrosion response. Corrosion testing procedures are required during process research and development, pilot plant operation, plant start-up, and plant operation. ASTM standards [1] provide a wealth of information on corrosion testing, but are not absolute guides.

Even with effective corrosion test programs, many unexpected failures occur in chemical processes. There are several reasons. The corrosion behavior of a material is a combination of the property of the metal (composition and condition) and of the environment. Corrosion can take many forms, from general to localized. An acceptable rate of general corrosion may not translate into successful performance if there is also localized corrosion, such as pitting or stress corrosion cracking. There is no universal corrosion test for all situations, and sometimes a combination of corrosion test techniques may be required to raise one's level of confidence.

<sup>1</sup>Principal Consultant and <sup>2</sup>Senior Research Engineer, Dupont Company, Wilmington, Delaware.

## PURPOSE OF CORROSION TESTING

Corrosion testing is used to select materials of construction, and to monitor the performance of selected materials of construction in service. Availability of the materials should be considered when developing corrosion test programs. Corrosion acceptance testing is performed to ensure that specific corrosion-resistant alloys are manufactured without impairing their corrosion resistance.

## To Select Materials of Construction

The first purpose of corrosion testing is to select materials of construction. The materials of construction to be considered for the test should be the kinds of materials from which process equipment and components are usually fabricated.

### Pressure Containment Equipment

Tanks, heat exchangers, pressure vessels, columns, etc. are usually built of a wide range of materials made to ASME or equivalent codes. If non-code approved alloys are considered, the likelihood of their being approved for fabrication must be weighed.

### Piping and Fittings

Manufacturers of pipe and fittings provide a wide range of wrought materials to ASTM or other standards. Some cast products are also made, e.g., for fittings. Corrosion testing programs may choose from a relatively wide range of alloys.

### Valves and Pumps

Valve and pump bodies are cast in a relatively small range of off-the-shelf materials, and it is difficult to obtain materials outside the range. Cast materials are less homogeneous than wrought materials, and may not exhibit the same corrosion resistance, especially when repair welded and not re-solution annealed. Cast equivalents are not readily available to match every standard wrought composition. For example, manufacturers of valves supply CF3-M (equivalent to wrought alloy 316L) off the shelf, but CF-3 (equivalent to 304L) is more difficult to obtain.

### Engineered Items

Filters, dryers, blenders, etc., are made from standardized off-the-shelf wrought alloys. Equipment manufacturers are familiar with their fabrication techniques. Corrosion testing

should focus on off-the-shelf materials, favored for cost and delivery.

### *Instrumentation*

Pressure transducers, flowmeters, level controls, etc., are also made from a relatively small range of off-the-shelf wrought alloys. Delicate wetted parts of instruments, e.g., rupture discs, may need to be more corrosion resistant than more robust parts.

### *Gaskets and Seals*

Polymers and elastomers are usually specified by proprietary name. Use of ASTM specifications and standard descriptions is not common. When evaluating materials for gaskets and seals, obtain a sample of the actual product to make a test specimen. Do not use a generic material, since the details of composition and manufacture can have a significant impact on performance.

### *Effect of Welding and Forming*

Heat and/or mechanical deformation may lead to loss of corrosion resistance. Welding may cause severe problems for certain materials: for example, sensitization of the base metal in the heat-affected-zone, or molybdenum segregation of weld metal. Welded specimens are often tested to study potential problems. Specimens may be deformed to study the effect of residual stresses from forming or welding. U-bend specimens are often exposed. If space is restricted, a Brinell hardness indentation can be used on a flat specimen to create a region of high residual stress.

### *Corrosion Acceptance Testing*

Certain nickel alloys and stainless steels may develop poor corrosion resistance to some environments if improperly manufactured. The need for corrosion acceptance testing is created because the alloy producer exerts insufficient control of either the final rolling temperature, annealing temperature, or the relationship between thermal treatment and mechanical treatment via forging, rolling, swaging, etc., to create product forms. Corrosion acceptance testing is supplementary standardized corrosion evaluation testing to determine if purchased materials are in the correct condition and exhibit corrosion resistance comparable to baseline standards. Satisfactory performance in a corrosion acceptance test is not necessarily evidence of satisfactory performance for any real world service environment.

Corrosion acceptance testing is covered by ASTM standards A763 (for ferritic stainless steels) [2], A262 (for austenitic stainless steels and nickel alloys) [3], and A923 (for duplex stainless steels) [4]. It is time consuming and increases project costs, because all product forms require testing, such as plate, tube, fittings, etc. With wrought stainless steels, specifying and receiving low carbon grades largely eliminates acceptance testing; it may still be necessary for some aggressive process environments. Duplex stainless steels require corrosion evaluation testing in all instances because of their inherent tendency to form intermetallic compounds that reduce their corrosion resistance. Nickel alloys that precipitate molybdenum-rich phases during thermal and mechanical treating operations may require

corrosion acceptance testing, to verify that their corrosion resistance was not impaired.

A producer who has supplied a specific nickel alloy for many years will have developed the thermal and mechanical processing know-how for the alloy. Experienced producers rely on statistical process control, coupled with sample testing to qualify their alloys. New producers may meet the ASTM compositional specifications for the alloys, but do not necessarily understand the thermal and mechanical processing needed for creating the best metallurgical condition in the alloy. For new producers, corrosion acceptance testing of various product forms made from each heat of the alloy is usually necessary.

## **To Anticipate Process Chemistry Effects**

The second reason for corrosion testing is to understand how the process environment affects materials performance, and also how corrosion impacts the process. This may require ingenuity in devising tests or studies.

### *Metal Ion Contamination*

For some chemical processes, low levels of metal ion contaminants may alter the product and/or chemical reactions. One source of contamination could be the corrosion reaction. Even if a material of construction has an acceptable corrosion rate to meet mechanical integrity requirements, low levels of metal ions introduced into the system by corrosion may not be acceptable.

### *Presence of Water in Process*

Water can influence corrosion significantly. It can react, pass through unreacted, or accumulate in one part of a system. For example, water might accumulate in a distillation column and form a very corrosive second phase. The top of the column might be too cold to allow the water to leave from the top, and the bottom of the column might be too hot to allow the water to leave from the bottom. The column must be fabricated of material resistant to the second phase, instead of lesser materials that would be adequate for other phases.

The applicability of some materials of construction is critically dependent on the presence of water in the process. For example, stainless steels in chlorinated hydrocarbons may be severely attacked if the amount of water increases above a few hundred parts per million (ppm). Titanium, on the other hand, depends on a minimum amount of water to maintain passivity. Corrosion monitoring with probes may be used to signal the start of accelerated corrosion if the required level of water is violated.

### *Nonstandard Operations*

Nonstandard operations hint at the need for supplementary corrosion testing. For example, chemical cleaning operations are sometimes more damaging towards the materials of construction than the process itself. Hydrochloric acid is often used for chemical cleaning because of its low cost and rapid dissolution of metal oxides. Hydrochloric acid affects specific materials of construction, such as stainless steels, by means other than general corrosion.

Hydrochloric acid can result in pitting and stress corrosion cracking. Carbon steels can tolerate a relatively high corrosion rate during hydrochloric acid cleaning, provided an inhibitor is added, because cleaning operations are short and other damage mechanisms are not a factor.

### *Effect of pH*

pH is sometimes a useful indicator of a chemical's corrosiveness: the lower the pH, the greater the amount of free acid present and the more corrosive the solution. A solution of pH 4 contains very little free acid, but nonetheless is quite aggressive towards carbon steel. As a rule of thumb, the minimum pH for using carbon steel is 5. Some metals such as zinc, aluminum, and lead are susceptible to corrosion in highly alkaline solutions. Except for these metals, pH alone is not usually an important indicator of corrosiveness. The pH of organic solvents, in particular, can be difficult to relate to corrosiveness.

### *Utilities*

The quality of cooling water and steam must be considered when selecting materials of construction. The chosen materials may be resistant on the process side, but fail on the utility side. For example, 316 stainless steel may be applicable for vertical heat exchanger tubing that handles a weak organic acid on the process side, but it may fail from chloride stress cracking on the waterside. A duplex stainless steel may be a better choice.

### *Fitness-for-Service Evaluations*

The ability to predict future corrosion is an important aspect of an equipment inspection program. Commonly used guidance documents are API Inspection Codes API 510 (for pressure vessels) [5], API 570 (for piping) [6], and API 653 (for storage tanks) [7]. Knowledge of the amount and type of corrosion expected will affect the scope and type of inspection planned. A complete evaluation of an equipment inspection includes determining the remaining life of equipment and setting an appropriate inspection interval. API 579 "Fitness-For-Service" [8] is a resource document referenced from the API inspection codes for determining the remaining life of equipment subject to corrosion damage. A fitness-for-service assessment requires an estimation of the future corrosion allowance (FCA) for the intended future operating period. This information typically comes from a combination of past inspection data and corrosion rate data for the component material in a substantially similar environment.

## **Institutional Requirements for Corrosion Data**

Corrosion data is used at various stages in the lifecycle of a chemical plant project, principally to assist in development of process flowsheets and select materials and fabrication methods. The required level of depth varies at each stage of the project.

### *Concept Stage*

At the concept stage, process developers review alternative preliminary flow sheets and provide sketchy parameters. The materials engineer looks for showstoppers that indicate the need for an alternative process, such as excessive temperatures

or corrosive environments. The need for exotic materials in one scheme may direct developers to an alternate process.

### *Business Planning Stage*

At the business planning stage, process evaluators assess the profitability of the process and look to the materials engineer for common materials versus exotic materials with significant cost impact.

### *Process Definition Stage*

At the process definition stage, process and project engineers develop an approximate cost for the proposed project, within 25 %. The materials engineer sharpens the pencil on materials selection for the process flow sheet, and arbitrates key decisions that may affect project cost. Materials changes that are made to reduce cost must be carefully considered.

### *Production Design Basis Stage*

At the production design basis stage, all design information is coordinated by process and project engineers into a package for design contractors to bid against. At this stage, materials selection recommendations must be changed into specification information. For example, it is not sufficient to say, "Use 316 for tubing." The applicable ASTM specification and subdetails must be provided.

### *Production Design*

At the production design stage, the project has been approved. Process and project engineers develop the design and specification, and prepare fabrication drawings. Locations for corrosion testing or monitoring are specified at this time. An outside design contractor is often responsible for the details, and must be familiar with the client's requirements and internal standards. Availability of materials also affects the production design stage.

### *Construction and Startup*

Construction forces are contractors, often working in parts of the world unfamiliar to the client. Construction forces must be familiar with client's standards and idiosyncrasies, and good communication is essential. Potential surprises in materials availability, or practices such as quality of test water must be dealt with expeditiously, or costs/delays will increase. Well-developed, complete, and available corrosion data, including performance of back up materials, is invaluable at the construction and startup stage.

### *Plant Operation and Management of Change*

After the plant is started up, operators, technical and maintenance, assume responsibility for day-to-day running of the plant. A startup corrosion test program is often instituted. It provides valuable information when changes are considered. Materials modifications fall under management of change rules imposed by process safety management regulation, such as OSHA 1910.119 [9] in the United States. Management of change is either subtle or discrete. For example, replacement in kind requires no justification, but change of design does.

Examples of replacement in kind, which require no additional corrosion data, are:

- Replacing a flanged section of pipe with a new section of identical material and size, along with new flange gaskets, in accordance with site pipe specifications;
- Replacing internal components of a pump using genuine OEM components, exact duplicate, or rebuilt original components.

Examples of change of design, which require supporting corrosion data, are:

- Increasing temperature, pressure, or flow in a piping system;
- Changing material of construction (such as piping, gaskets, valve packing, fasteners, substituting metals with different hardness, heat treatment, or metallurgy);
- Changing valve trim or materials on a control valve.

## FIELD, LABORATORY, AND PILOT PLANT TESTING

Whenever it is decided that the existing corrosion data sources are inadequate, a decision must be made on how to develop the corrosion data. A corrosion test is designed to provide useful information to meet the end purpose. Corrosion tests may be run in the field, laboratory, or pilot plant. Use of standardized test procedures described in ASTM [10–12] may guarantee success, providing the vagaries and subtleties of the corrosive environment are understood and accommodated in the test.

A chemical process may involve a complex variety of inorganic and organic chemicals. When the process composition is known and invariable, testing to select appropriate materials of construction, or searching the literature, is relatively easy. However, the role of contaminants, and the process parameters of temperature, pressure, velocity, and species concentration must be considered for their effects on corrosion and how they affect the design of a corrosion test. Additionally, changes in process parameters, such as when reactants are blended in, or exothermic reactions, must be considered. Ask the process engineer what contaminants may be present, such as the chloride ion, or species containing sulfur.

When applicable, one must test materials at the actual temperature to which they will be exposed in the process. This is not necessarily the process temperature, and it may require special techniques such as hot-wall testing or cold-finger testing.

A corrosion test requires the following steps:

- Define the type of test needed, including any special safety considerations,
- Run the test by exposing the samples,
- Monitor the solution composition, if necessary,
- Examine the samples after testing for types of attack and quantify the amount of attack.

### Test Location

Simulation of location is the single most important element of a corrosion test. The process flow diagram should be reviewed to identify those locations with the most corrosive

conditions, based on material balance compositions and predicted contaminants. In a field test, the location must be selected to obtain the required type of exposure. For example, condensing conditions where phase separation has occurred may be more corrosive than fully immersed conditions. In a laboratory or specialized test, the conditions at the selected location(s) must be simulated.

Figure 1 is a schematic flow sheet indicating various types of corrosive conditions that may occur at various locations in typical chemical processes. The type of corrosion expected at a process location must be modeled if it is likely to be an issue in successful operation of the plant.

The principal types of test locations are as follows:

*Continuous immersion* is where exposure is to stagnant or flowing liquid. It is usually the easiest location in which to expose samples or to simulate. Continuous immersion is the most important location for developing basic data in stagnant or free-flowing portions of the process. Agitation can influence corrosion test data significantly because it helps maintain a high level of oxygen in solution. Oxygen accelerates corrosion of some metals and retards corrosion of metals that form a passive film. If oxygen is not permitted in the process, a nitrogen pad is usually employed. Slurries and process media that contain solids—these include catalysts, reactants, and products—require special consideration in corrosion testing. Moving slurries can cause erosion-corrosion; stagnant slurries aggravate crevice corrosion.

*Splash zone* is where the exposure is to splashing or spraying liquid. Splash zone is sometimes more corrosive than continuous immersion. For example, chlorides may concentrate through alternate wetting and drying, leading to pitting or stress corrosion cracking in the splash zone. This is more likely to occur when the splash zone is a hot surface.

*Solution line* is the boundary that is formed on a material surface when two phases have a stable interface that remains in one location for an extended time. The exposure alternates between continuous and partial immersion. The solution line level may change due to agitation, or when a vessel or tank is filled by different amounts. Solution line effects cause oxidant levels at the metal surface to fluctuate,

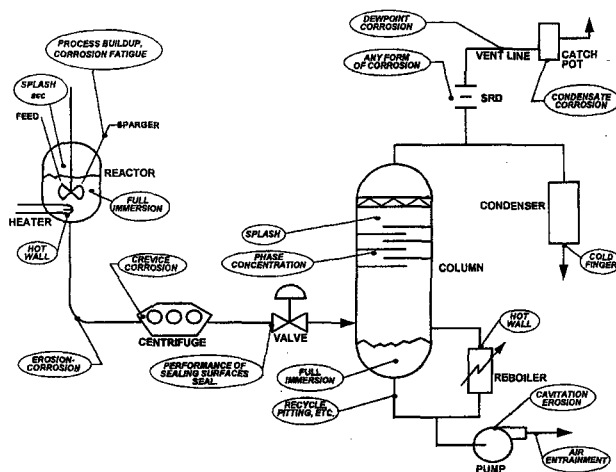


FIG. 1—Various types of corrosion occur in a chemical process.

and can be extremely corrosive to materials like carbon steels. Froth can also create solution line conditions. Solution line exposure is particularly important when evaluating materials for scrubbers, demisters, and columns. Strip-like coupons that completely extend through the susceptible zone may be positioned at the solution line to capture the effect.

*Condensate zone* is where the exposure is to droplets of condensing gases. As with splash zone, the condensate zone may be more corrosive than continuous immersion. Condensate can be extremely corrosive, depending on the distribution of components in a process. The problem may occur in distillation columns or condensers, where aggressive species partition or concentrate. For condensate exposure, one must design the coupon location carefully to ensure the coupon is actually exposed to the condensate.

*Gaseous zone* is where exposure is to vapor in the space above a liquid or to gas phase alone. Under most conditions, the gaseous zone is not usually corrosive until the vapor condenses and forms a corrosive condensate.

## Field Testing

Field corrosion testing consists of coupon testing and probe testing. Coupon exposure times typically range from one to three months. Probes are exposed for as long as a specific condition is under investigation, sometimes for the life of the process.

### *Managing System for Coupon Testing*

Field coupon testing employs small flat and/or U-bend [10,13] samples to average the effects of real world solution contaminants and process transients. Full immersion conditions are easy to reproduce. Splash, waterline, condensing, velocity, and hot wall conditions are more difficult to reproduce. Management of field coupon testing requires effective handoffs between different job functions on the plant site.

In most chemical manufacturing companies, a project, process, maintenance, or reliability engineer makes the initial request. A materials engineer determines coupon selection and exposure time. A planner may requisition the coupons, which are usually mounted on test racks. Maintenance installs the coupons and production alerts when they may be removed. Maintenance removes and decontaminates the coupons, and sends them to a qualified laboratory for analysis. After cleaning, weighing, and examining, the materials engineer calculates corrosion rates and creates a report [10,14], which is communicated to the requestor.

### *Considerations for Electrical and Electrochemical Probe Selection*

Probes consist of electrical resistance (ER) and linear polarization resistance (LPR). They are described in more detail in the section on Probe Testing. The first consideration for probe selection is the conductivity of the process environment. ER probes are the only option for nonconductive processes and for gaseous environments. The desired response time is critical in selecting ER probes. LPR probes provide instantaneous corrosion rate data in conductive environments, but may not be applicable where exposure is

intermittent, such as in spray or splash or solution line zones. ASTM G96 describes probe testing [15].

Probes may be fixed or retractable, and access for removal or replacement of elements is an important consideration. Intrinsic electrical safety requirements must be followed. Probe materials of construction, including sealing compounds used for insulation, must be compatible with the concentrations, temperature, and pressure of species in the chemical process.

In critical locations, consider using more than one probe (redundancy) if it is the primary method of monitoring corrosion.

Roles and responsibilities in procuring, installing, maintaining, and monitoring data from corrosion probes must be defined.

## Laboratory Testing

Laboratory corrosion testing is performed under simulated process conditions, either to help materials selection, or, by isolating specific process variables, to determine corrosion mechanisms. Laboratory testing consists of coupon testing and specialized testing.

Most laboratory testing is performed in glassware at atmospheric pressure, though some testing is carried out in autoclaves. The size of the glassware usually limits coupon exposure locations to liquid and vapor locations, unless a specialized testing, such as the three-position flask, is used. Velocity effects are limited to mild stirring with an agitator or magnetic stirrer.

The simplest type of laboratory test consists of exposing coupons to the liquid phase only. Simple immersion tests are performed using some form of glassware, such as a flask or a resin kettle, and a condenser for refluxing. A typical setup is a 1000-mL flask containing 500 mL of liquid. Laboratory coupon testing is described in ASTM G31 [16].

Factors affecting laboratory testing include the following:

### *Volume of Solution*

The solution volume should be 125 mL/square inch of exposed coupon area at a minimum [16].

### *Exposure Time*

It is usually 100–250 h (about 4–10 days). When relatively high rates of general corrosion are expected, a popular guideline is minimum exposure time (in hours) = 2000/expected corrosion rate in mils per year (mpy). Therefore, if a corrosion rate of 20 mpy is anticipated, one should expose the coupon for about four days (100 h). Certain types of corrosion, such as crevice corrosion, pitting, and stress corrosion cracking, occur only after relatively long incubation periods. If coupon exposure times are too short, they will not be detected during corrosion testing. Examining coupons under a microscope after the test helps reveal whether incipient pitting or crevice corrosion occurred. Incipient corrosion might be an indication of borderline performance. When pitting or crevice corrosion are factors, coupons should be exposed for a minimum of 250 h, and perhaps 1–3 months. Alternatively, electrochemical techniques such as cyclic potentiodynamic polarization might be used to reveal a tendency for crevice corrosion or pitting.

### *Cross Contamination Effects*

During running of the test, check the coupons regularly for signs of excessive corrosion or degradation. If these conditions are found, the test should be concluded, unless it is the purpose of the test. The test solution should also be checked for signs of color changes, which may indicate contamination by corrosion products, or solution degradation. Unless these effects are under investigation, terminate the test. The performance of certain metals is altered when cross contamination from corrosion of other coupons takes place. For example, titanium's corrosion resistance to a reducing acid improves when corrosion of stainless steels puts nickel and chromium ions into solution. Zirconium, on the other hand, may perform worse than expected under these conditions.

### *Stability of Solution*

If the process reaction time is short relative to the required exposure time, two techniques can be used to increase the exposure of coupons to reactants. One technique is to run the reaction repeatedly with fresh reactants until sufficient exposure time is obtained. Another is to use an electrochemical technique such as potentiodynamic polarization.

### *Representative Solution*

When simulating conditions such as concentration or condensation, it is useful to know the exact composition of the condensate. Thermodynamic modeling may be used to calculate the composition of the condensate. Contaminants, such as oxygen or chlorides, also need to be accounted for if they are present in the plant solution.

### *Simulating Location*

Basic laboratory corrosion tests are performed by exposing coupons (to the liquid phase only) at atmospheric pressure. Some testing is performed in autoclaves.

### **Pilot Plant Testing**

Pilot plant corrosion testing offers a few advantages over laboratory testing. For example, more coupons may be exposed at a specific location because the equipment is larger. It may seem that pilot plant testing offers longer exposure times compared with laboratory testing. However, available exposure periods between key process changes may amount to a few batches, so that the accumulated exposure time is relatively short. Effective pilot plant corrosion testing has other challenges.

### *Ease of Access*

Locating coupons where they can be easily installed and removed is a prime consideration, because coupons must be removed whenever there are significant changes to the process parameters. The test locations must not interfere with instrumentation or other items.

### *Frequent Process Parameter/Feedstock Changes*

The explicit purpose of most pilot plant testing is to optimize process parameters, so it is difficult to capture a stable set of conditions under which coupons or probes are exposed. Furthermore, the equipment is not usually designed for optimum location of coupons or probes.

### *Coordination Between Personnel to Optimize Data Quality*

Since most pilot plant test programs have low priority for collecting materials data, the greatest challenge for the materials engineer is in establishing communication and motivation. For examples, component failures are discarded before a qualified person examines them, or coupons are not removed between major campaign changes.

## **COUPON TESTING**

Coupon testing is the most widely used method of gathering corrosion data, on account of its versatility and ease of interpretation. Coupon testing is described in ASTM G4 [11].

### *Coupon Design*

Most corrosion coupons are 1/8-in.-thick flat, rectangular shaped specimens, identified by stamping. This is the least expensive design to manufacture. The U-bend coupon is the most common mechanically stressed coupon, and is used to determine susceptibility to stress cracking [13].

Flat and U-bend coupons may be supplied with an autogenous or butt weld [13]. With a butt weld, the weld profile is retained and not machined off, to duplicate the condition of process equipment, except on U-bend coupons. Autogenous welding (application of a locally melted region on base metal that contains no filler metal) does not always simulate real-world conditions. If welding of the coupon with filler metal is not possible, for example with thin stock, a sensitizing heat treatment may be preferred.

### *Sensitizing*

This is a heat treatment applied to specific stainless steels and nickel alloys to simulate the formation of microscopic compounds that reduce corrosion resistance. Sensitizing may occur in welding, hot forming, or certain types of heat treatments. Although welding is the most common cause of sensitization in process equipment, welded coupons may not sensitize because they contain insufficient weld passes compared with actual process equipment. Thus, the cumulative time spent in the sensitizing temperature range is insufficient for sensitizing to occur. A sensitizing heat treatment is relatively severe compared with the heat input from welding. It is an extreme test to indicate the potential for corrosion susceptibility from welding, or a stress relief heat treatment.

### *Surface Finish*

Coupons are normally 120 grit finished, which is reasonably close to the mill finish found on process equipment. A double disc ground surface is closer to mill finish, and improves reproducibility of results, because it creates a cleaner surface than 120 grit.

### *Electrical Insulation*

Coupons must be electrically isolated from one another with washers and insulating spacers made of TFE. Washers may be flat faced or serrated (with radial grooves). Serrated washers are used when susceptibility to crevice corrosion is to be studied [17], as in the case of a chloride-containing

process. Ceramic washers are used above 200°C, where PTFE is subject to creep.

### Test Rack Design

For field and pilot-plant testing, coupons are mounted on test racks designed to prevent them from detaching during exposure and to protect them from mechanical abuse. Do not weld racks directly to pressure containing parts without a qualified procedure and qualified welder, in accordance with pressure vessel code requirements.

The pipeline insertion rack is the most common design, and is installed at flanges in piping, nozzles, and manways. It can accommodate a useful number of coupons and is easily inserted and removed. It is relatively expensive to fabricate because a significant amount of stock must be discarded. The number of coupons is limited by the internal diameter of the piping, the space in the equipment, the length of the rack, and potential flow restrictions. A flat bar rack is a cheaper design. It is bolted to a tab welded to a blind flange attached to a manway. Pressure vessel code welding requirements may apply. The flat bar rack eliminates the need for additional gaskets, but is harder to install and remove.

Rack material must resist the process environment. Fasteners are susceptible to failure from crevice corrosion underneath the insulating TFE sleeve. Fasteners should have provisions to guard against mechanical loosening (for example, double nutting). They may require upgrading to a more resistant material in severely corrosive environments.

See Fig. 2 for photograph of corrosion test rack.

### Procurement of Coupons and Racks

The items shown in Fig. 3 should be considered when procuring coupons and racks.

### Interpreting Coupon Data

Metal coupon data are relatively easy to use for materials selection purposes from calculation of corrosion rate and observations on the appearance of the coupon. For nonmetallic materials, the problem is to define what constitutes failure. For example, when is color change, flaking, swelling, or tackiness acceptable, and when do they indicate potential failure?

### Interpreting Metal Coupon Corrosion Data

To calculate corrosion rate, one must know coupon dimensions, weight before test, material density, exposure time, and weight after cleaning. For a field test, periods when the process is down are subtracted from the total exposure time to obtain the actual exposure time. ASTM G31 provides a method of calculating corrosion rate [16]. To interpret corrosion rates on metals, use the following guidelines.

- Use 0.2 mpy as the maximum acceptable rate for reactive metals that can embrittle by taking up hydrogen from the corrosion reaction (for example, titanium, zirconium, and tantalum). Hydrogen uptake may occur from self-corrosion or when these metals are the cathodic member of a galvanic couple.

FIG. 2—Corrosion test racks must be designed for easy insertion and removal from equipment and piping.

Item	✓
Coupon materials	
Coupon design	
Coupon weld filler metal	
Coupon heat treatment	
Coupon surface finish	
Coupon spacer type (e.g. serrated washer)	
Rack type and dimensions	
Rack material	
Fastener material	
Identification of coupons	

FIG. 3—Checklist for corrosion coupon and test rack procurement.

- Use 1 mpy as the acceptable rate for product purity. The acceptable corrosion rate is usually determined by purity requirements. Thus, for greater accuracy, back-calculate the maximum allowable corrosion rate from the maximum amount of metallic ion contamination allowed in the product. Estimate the available area of metal in the process equipment and piping that contributes to corrosion and factor it into the corrosion rate.
- Use 5 mpy as the maximum acceptable rate for clad or relatively expensive metals, such as stainless steel.
- Use 10 mpy as the maximum acceptable rate for carbon steel with a thin film lining. Linings less than 10 mils thick (for example, baked phenolics) contain holidays, which are tiny holes through to the base metal created during curing of the lining. If the corrosion rate of the base metal is excessive, the lining will tend to pop from the surface. A carbon steel coupon should be exposed concurrently when a thin film lining is being evaluated such as in ASTM C868 [18].
- Use 5–25 mpy as the maximum acceptable rate when a corrosion allowance can be incorporated into a relatively inexpensive material of construction, such as carbon steel. Process equipment is generally designed for a service life of 10–20 years, and the design includes a corrosion allowance.

In addition to calculating the corrosion rate, the type and severity of local corrosion on the coupon should be noted by examining the coupon under a binocular microscope. The maximum depth of localized corrosion should be recorded.

Figure 4 shows the effects of localized corrosion in process equipment.

#### *Interpreting Polymer and Elastomer Coupon Data*

Polymer and elastomer coupons are evaluated differently from metallic materials [19]. The testing and evaluation of

polymers and elastomers are more difficult. They are less standardized than metals, and deductions between "generic" types are difficult to make because of the effects of various fillers, additives, and processing variables that must be taken into account.

A rule of thumb for evaluating polymer and elastomer coupons is to measure a key dimension (e.g., thickness), weight, and hardness before testing. After testing, the same measurements are taken immediately, and repeated after the sample has been stored under vacuum for at least 24 h.

Localized Corrosion Type	Potential Effect on Process Equipment
Corrosion fatigue	Catastrophic failure
Crevice corrosion	Loss of surface conformance, e.g. at a gasket surface, or local wall thinning, leading to leakage
Erosion-corrosion	Local thinning, e.g. at an elbow, leading to leakage
Galvanic corrosion	Possible embrittlement of cathodic member of couple, in the case of tantalum, titanium, zirconium. Thinning of anodic member of couple in other cases.
Microstructure-related	Various effects, leading to loss of net structural thickness
Pitting	Pinhole leaks
Stress corrosion cracking	Network of fine cracks, leading to leakage or catastrophic failure

FIG. 4—Effects of localized corrosion are less predictable than general corrosion.

Appearance	Description
Abrasion/Erosion	Wearing away of the surface by the scouring action of the process environment
Blistering	A cavity or sac that deforms the surface of the material, which may have burst and become flattened
Chalking	The formation of a powdery residue on the surface, resulting from degradation
Collapse	The densification of cellular material caused by the breakdown of the structure
Color Change	Alteration of color or surface texture, such as sheen
Cracking	Fractures or separations that extend through the surface layers, which may or may not extend through the thickness of the material
Crazing	Fine cracks at or under the surface
Creep	Dimensional change with time under load
Delamination	Separation of layers of material in the laminate
Dissolution	Solvation of the material
Flaking	Detachment of pieces of material from the substrate or bulk, often preceded by cracking, crazing, or blistering.
Orange Peel	Pitted or uneven texture, visible to the naked eye, resembling an orange peel
Popcorning	The formation of reaction products in the spaces of a sintered material, which causes the material to collapse
Shrinking	Decrease in dimensions
Sintering/Densification	Bonding of adjacent surfaces of particles in the material
Spalling	Cracking or rupture resulting in the detachment of portions of the surface or bulk of the material
Swelling	Increase in dimensions over original, usually by solvent uptake
Tackiness	Sticky or gummy character of the material surface
Warping	Change in the original contour or shape of the material, without swelling

FIG. 5—Polymer and elastomer coupons appearance must be documented.



The idea behind vacuum containment is to permit solvents to evaporate from the coupons. Often, the sample returns to its original condition after vacuum treatment, or after being allowed to stand for a few days in the atmosphere.

Documentation of physical appearance is also required. Figure 5 defines typical physical observations for polymer and elastomer coupons.

Polymer and elastomer coupon data must be used in the context of the application. If the application is structural, such as for an FRP tank, mechanical property data are also required. If the application is fully contained, such as an O-ring, dimensional and hardness change, coupled with visual observations, may provide sufficient information to make a decision. In all cases, it is useful to discuss the results with a qualified person, such as the supplier of the material.

### *Interpreting Lining Coupon Data*

Linings are often evaluated in the type of cell described in ASTM C 868 [18]. In the test cell, two lined panels are exposed simultaneously to test liquid, to study the effect of chemical attack and permeation on the lining system. The tests are often conducted for six months, and visual observations may be conducted during the period. At the end of the test, the lined panels are given a thorough examination, and may also be destructively evaluated for loss of adhesion, substrate corrosion, and hardness change.

### *Glass-lined Steel Coupons*

Glass-lined steel is used in applications requiring cleanliness and high corrosion resistance. Dumbbell-shaped glass-lined coupons may be obtained from the manufacturers of glass-lined equipment to evaluate performance. As with metal coupons, the corrosion rate of glass-lined steel coupons is calculated from surface area, weight loss, glass density, and exposure time.

In equipment designed for severe chemical exposure, glass linings are 40–90 mils thick (nominally 60 mils). The minimum thickness before reglassing is required is 30 mils. The remaining thickness adjacent to the substrate is known as ground coat and has poor corrosion resistance. A vessel with general corrosion should be reglassed when the lining thickness reaches 30 mils. Once the ground coat is exposed, corrosion will proceed at an unacceptable rate. Also, other failure modes such as thermal shock, electrostatic discharge, etc., control glass life. A rule of thumb for the maximum acceptable uniform corrosion rate on a glass-lined steel coupon is 8 mpy.

## **PROBE TESTING**

Probes are used to measure corrosion rate on-line. There are two basic types of probes, electrical resistance (ER) and linear polarization resistance (LPR). Probe testing is described in ASTM G 96 [15]. Probe data may be read on a hand-held meter or downloaded periodically to a computer and/or hand-held meter. These systems require no permanent fields cables.

However, more value is obtained when the output from corrosion probes is connected to transmitters that convert

probe data to a 4–20 mA signal output to the distributed control system (DCS). Thus, it is possible to integrate probe signals to process parameters. Integration with DCS requires cabling, which is more expensive.

In all cases, the need for intrinsic safety barriers must be evaluated. Instrumentation must conform with the electrical classification of the operating area.

### *Electrical Resistance*

The sensing element of an ER probe may be a wire, tube, or cylinder made of the test material. The principle of ER corrosion monitoring is based on measurement of electrical resistance of the sensing element. This is a function of its thickness, which depends on how much corrosion it has experienced. The higher the sensitivity of the probe, the shorter its life. A cylindrical element probe with 25 mils life will take 20 h to detect a corrosion rate of 100 mpy. A tube element probe with 2 mils life will detect a corrosion rate of 100 mpy in 2 h. Thus, the thicker the probe element the less the sensitivity, but the longer the life, and vice versa. However, thicker element probes, such as cylindrical element, are less fragile than thinner element probes, such as wire element. The maximum life of standard ER probes is 25 mils. See Fig. 6 for photo of an ER probe.

ER probes have certain limitations. Resistance is a function of temperature, so that large or rapid temperature swings generate noisy signals. Conductive deposits, such as metal plating out on the probe surface, will decrease resistance, and read a negative corrosion rate. ER probes are not effective in detecting localized corrosion, because the resistance change is not proportional to the local penetration of the corrosion attack.

### *Linear Polarization Resistance*

With LPR, a small electrical potential of approximately 20 mV is applied between two electrodes. The anode is made of the test material. The current response as a result of the applied potential is measured within minutes and converted to corrosion rate. LPR probes are rated to 200–250°C and pressures to 5000 psi. See Fig. 7 for photo of an LPR probe.

**FIG. 6—ER probes may be made of wire, tube, or cylinder.**

FIG. 7—LPR probes are limited to conductive environments.

Corrosion Type	Test	Test Type
Coating degradation	AC impedance	Electrochemical
Condensing surface	Demo flask	Coupon
Condensing surface	Cold finger	Coupon
Erosion corrosion	Rotating electrode	Electrochemical
Erosion corrosion	Velocity test loop	Coupon
Galvanic corrosion	Zero resistance ammetry	Electrochemical
Galvanic corrosion	Potentiodynamic polarization	Electrochemical
General – conducting liquids	Linear polarization resistance	Electrochemical
General – conducting liquids	Tafel extrapolation	Electrochemical
General – nonconducting liquids	AC impedance	Electrochemical
General and localized	Electrochemical noise	Electrochemical
Heated surface	Hot wall	Coupon
Pitting/crevice corrosion	Cyclic potentiodynamic polarization	Electrochemical
Stress corrosion cracking	Slow strain rate	Coupon
Stress corrosion cracking	Siphon	Coupon

FIG. 8—Specialized corrosion tests are usually conducted in the laboratory.

The success of LPR probes is dependent on the conductivity of the process, and the expected corrosion rate. LPR probes are limited to process environments with conductivities greater than 100 microSiemens/cm. The conductivity of tap water may vary between 100 and 1000 microSiemens/cm. Performance is sensitive to fouling, bridging, or short-circuiting.

Attributes of LPR probes are rapid data collection and ability to sense process excursions. These attributes allow them to be used as a process control and for on-line monitoring of corrosion rate.

## SPECIALIZED TESTING

Specialized testing techniques are used to confirm data or simulate corrosion phenomena that are beyond the capabilities of simple laboratory corrosion tests. They are generally performed in the laboratory, and in general require extensive data interpretation. See Fig. 8.

### Coating Degradation—AC Impedance [20,21]

AC impedance measurement offers an advanced electrochemical method of studying degradation processes for organic or nonconductive coatings. Generally, the degradation of coatings in aggressive environments consists of two sub-processes: water or moisture permeation into the coatings, and under-film corrosion when the water approaches the metal substrate. The AC impedance method is mainly used to monitor water permeation and under-film corrosion occurring in coatings during a period of immersion in an electrolyte.

AC impedance relies on the ability to monitor the behavior of a coating that absorbs water by modeling it as a capacitor. By measuring capacitance increase as a function of immersion time, the diffusion coefficient of water and the amount of saturated water within the coating film can be calculated. In addition, any severe under-film corrosion can be monitored by a drastic decrease in the coating resistance and charge transfer resistance.

With improved electronics technology, the measurement of electrochemical impedance over a wide range of frequencies has become fairly straightforward. During the impedance measurement, very small AC signals, which do not significantly disturb the electrode system, are applied. This makes the measurement in situ and nondestructive. Furthermore, the information on the uncompensated solution resistance, electrode polarization resistance, double layer capacitance, as well as resistance of the coating film or passive film on the metal surface, can be obtained in the same measurement.

#### *Condensing Surfaces—Three Position Flask [22]*

A three-position flask (Demo flask) may be used to simulate three exposure locations simultaneously: fully immersed, vapor, and condensate. For the condensate part of the exposure, coupons can be exposed to drips of condensate directly under a condenser, or they can be immersed in a heel of condensate before it is returned to the working container or sent elsewhere. When cross contamination effects are likely, the coupons should be exposed to the drips, not to the heel, and the coupons should be exposed in sequence that minimizes cross contamination effects. See Fig. 9 for sketch of a three-position flask.

#### *Condensing Surfaces—Cold Finger [22]*

The equipment described above is fabricated from glass and operates at essentially atmospheric pressure. For study of processes operated under pressure, the condensing exposure

is achieved by locating a cold finger in the lid of an autoclave. The cooling fluid circulated from a constant temperature bath through the cold finger controls the condensing temperature. As in the atmospheric test apparatus, a helpful addition to the pressure reactor is the ability to collect liquid and condensed vapor samples under operating conditions for analysis. The chemistries are often very different between the liquid and condensed vapor phase samples, and knowing them helps one to correlate the measured corrosion rates to solution chemistry.

#### *Erosion Corrosion—Rotating Electrode [23]*

In this test, a metal sample is rotated in the solution. A rotating cylinder is used to simplify fluid dynamics equations so that corrosion rate can be correlated with shear stress or mass transfer, which in turn can be related to velocity effects in piping and equipment. The same electrochemical techniques used on static samples are applicable to the rotating cylinder electrode. By coupling the samples to electrochemical measuring equipment, one can measure qualitatively the effects of stepped velocity changes in one experiment.

#### *Erosion Corrosion—Velocity Test Loop [23]*

To evaluate the effect of slurries or moving liquids on corrosion, a special test loop may build through which the solid-containing medium or high velocity medium is circulated by means of a pump. Tubular specimens are relatively easy to obtain. They may be exposed in the velocity test loop, and have a nice response to erosion corrosion calculations.

#### *Galvanic Corrosion—Zero Resistance Ammetry [24]*

A zero-resistance ammeter is connected between two metals, and the galvanic current is directly measured as a function of time. At the same time, a reference electrode can also be used to monitor the galvanic couple potential, which can be used to determine the galvanic corrosion if a third metal is to be connected with this couple. Most commercial potentiostats can be used as a zero-resistance ammeter by changing the electrode connections.

#### *Galvanic Corrosion— Potentiodynamic Polarization [24]*

A cathodic polarization curve of the metal with a noble corrosion potential and an anodic polarization curve of the metal with a negative corrosion potential are plotted. The two polarization curves are overlapped. The intersection of two polarization curves is the amount of galvanic current that will be produced when these two metals are in contact with each other. One important point to mention is that, due to the different surface areas of two metals, they receive the same galvanic current (instead of the same current density) during galvanic corrosion. To determine the galvanic current when the two polarization curves are overlapped, they should be modified to use current, not current density, as the x-axis.

#### *General Corrosion in Conducting Liquids— Linear Polarization Resistance [25]*

In linear polarization, the voltage of a test electrode is perturbed 20–30 mV above or below the corrosion potential.

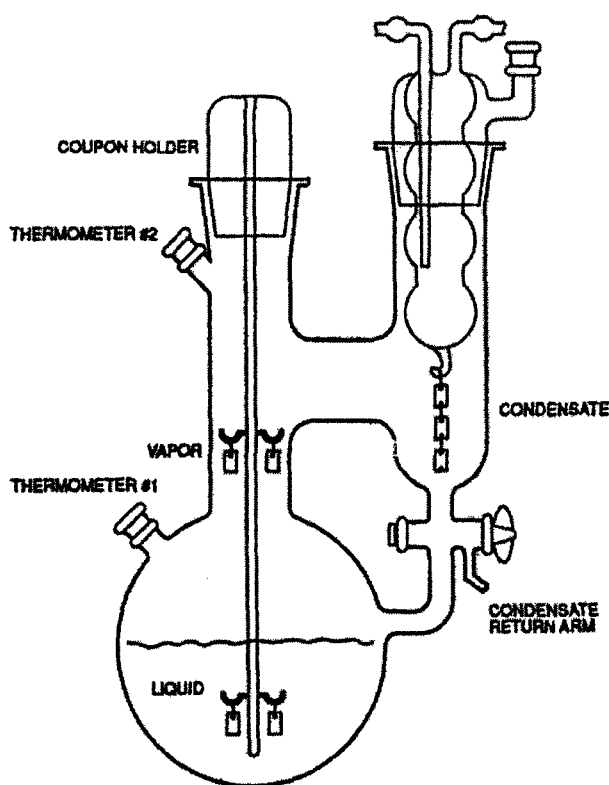


FIG. 9—Three-position flask allows corrosion in three phases to be simulated.

This is called applying a polarization overpotential. When it is small, the polarization overpotential has a linear relationship with polarization current, similar to Ohm's Law. Hence, the relationship (potential divided by current) is called polarization resistance. The corrosion rate is inversely proportional to the polarization resistance.

Linear polarization resistance can be applied to corrosion systems with electrochemical activation control, such as carbon steels and some stainless steels in low concentrations of sulfuric acid. For corrosion systems with a mass transport control or passivating systems, such as carbon steels in water with a pH between 5 and 10, the linear polarization equation is not valid. Additionally, the normal fluctuation of corrosion potential during the measurements can significantly affect the accuracy of the measurements. Under most circumstances, a larger polarization than 10 mV may be used to increase the signal/noise ratio. However, it may put the system out of the linear region, introducing some additional errors in the measurements.

#### General Corrosion in Conducting Liquids— Tafel Extrapolation [25]

A polarization curve is plotted for the metal in the corrosive environment. When the polarization curve is obtained, the anodic and cathodic polarization curves in the Tafel region (region of strong polarization) are extrapolated to the open-circuit, or corrosion potential. The corrosion rate is determined by the intersection between the Tafel straight lines and the horizontal line of corrosion potential. See Fig. 10.

The major error with Tafel extrapolation is the effect of concentration polarization introduced when the applied current is large. The theoretical basis of this method is only valid for the corrosion systems with an electrochemical control. If the applied current is significant, some corrosion systems may come under mass transport control, or at least under mixed electrochemical and mass transport control. This will make it very difficult to define the Tafel region from the polarization curve, introducing errors in the extrapolation process. Tafel extrapolation is not applicable in highly resistive environments: for example, glacial acetic acid.

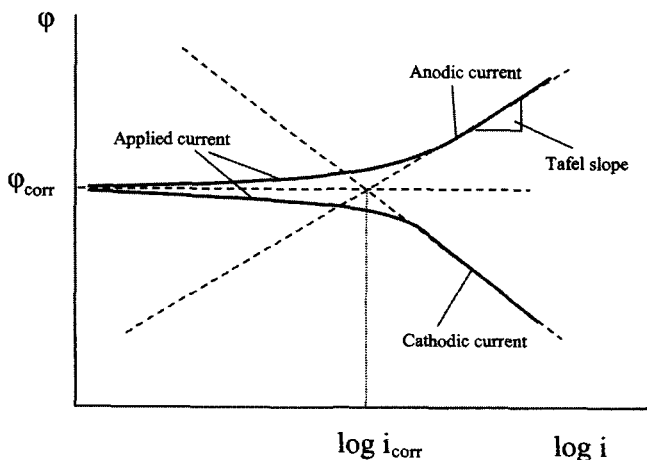


FIG. 10—Polarization plot for Tafel extrapolation.

#### General Corrosion in Nonconducting Liquids— AC Impedance [26]

Electrochemical polarization, which relies on dc, is limited to highly conducting liquids >100 microSiemens/cm. The ac impedance technique is more suitable for measurements in poorly conducting media, and does not suffer from the same limitation as dc electrochemical techniques. For more details, see Coating Degradation—AC Impedance.

#### General and Localized Corrosion— Electrochemical Noise [27–29]

Electrochemical noise measurement is a relatively new tool compared to other electrochemical methods. It is a sensitive electrochemical method especially for monitoring the localized corrosion, such as pitting and crevice corrosion, although it is also used for monitoring general corrosion as well. Since it was introduced over 20 years ago, the research in seeking the theoretical explanation has lagged far behind its practical applications. The general phenomenal observation is that when corrosion, especially localized corrosion, is initiated on the surface of metals, a spectrum of electrochemical noise is concurrently created, and the characterization of this spectrum of electrochemical noise is an indication of the severity of general corrosion and the form of corrosion.

There are two kinds of electrochemical noise, the electrode potential noise and cell current noise. The potential noise can be measured in two ways. One is by measuring the potential difference between two identical metal electrodes. The advantage of this method is the elimination of the effect of other factors on the electrochemical noise measurement, such as the temperature and fluctuation of environmental conditions. This is because the electrode potential of two identical electrodes should change at the same time when environmental conditions fluctuate. In addition, two identical electrodes configuration is easily made as an electrochemical sensor. The other way for monitoring potential noise is by using a reference electrode, by which the potential difference between the reference electrode and the metal of interest is measured. The current noise is measured by using a zero resistance ammeter, which is connected between two identical electrodes. If it is required, the potential noise of the two identical electrodes can also be monitored at the same time by using an extra reference electrode.

Several parameters can be derived and calculated from the electrochemical noise data obtained, which may be used to determine the severity of general corrosion and the types of corrosion. However, the theoretical explanation of some of the parameters is still under debate. The only generally accepted parameter is the electrochemical noise resistance,  $R_n$ , which is defined as the ratio of the standard deviations of potential noise and current noise ( $R_n = \sigma_v/\sigma_i$ ). This parameter is thought to be equivalent to the polarization resistance  $R_p$ , which can be used to estimate general corrosion rate.

The other parameters include the pitting index, which is defined as the standard deviation of current noise divided by the mean current ( $PI = \sigma_i/I_{mean}$ ), and the power spectral density of a noise, which can be calculated using the MEM (maximum entropy method) and the FFT (fast Fourier

transform). They have been proposed for the identification of localized corrosion. Due to their theoretical limitations, these parameters should be used with precautions.

#### Heated Surface—Hot Wall [22]

For assessing the effects of a heat transfer surface on corrosion, the hot wall tester may be used. One style includes a flat end soldering gun held against the sample on one side, which is sealed at the edges and exposed to a solution on the other side. The solution temperature can be controlled up to boiling, and the heat applied to the sample can be varied by the electrical input to the soldering gun. The combination produces a heat transfer effect across the sample thickness.

#### Pitting and Crevice Corrosion— Cyclic Potentiodynamic Polarization

The basic electrochemical method for evaluating the susceptibility of metals to pitting and crevice corrosion is covered by ASTM G 61 [30]. An anodic polarization curve is measured by a cyclic potentiodynamic polarization method using a specific scanning rate, from which breakdown potential and protection potential can be determined. See Fig. 11.

The evaluation criteria are as follows: the more noble the breakdown potential, obtained at a fixed scan rate, the less susceptible the alloy to the initiation of pitting; and the more noble the protection potential, the less likely is crevice corrosion. When the breakdown potential and protection potential are almost the same value, the possibility for pitting corrosion to occur is almost nonexistent.

Since the values of both breakdown potential and protection potential are significantly affected by the scanning rate, supplementary electrochemical methods are used to overcome this limitation (for example, if by using a supplementary potentiostatic method, the potential of metal may be maintained at a constant value while the corresponding polarization current is recorded as a function of time). If

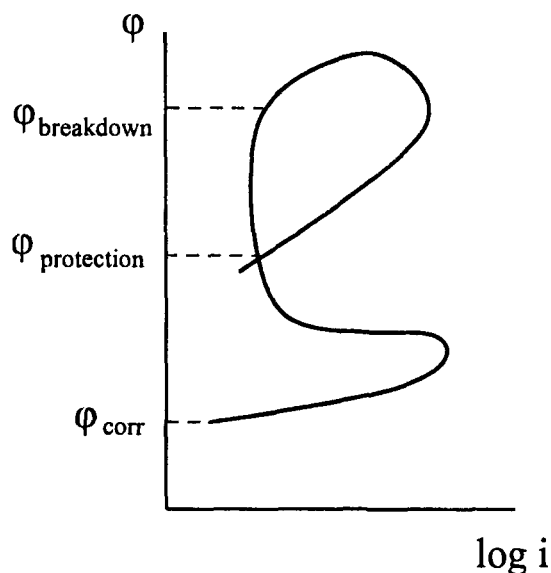


FIG. 11—Anodic polarization curve for passive corrosion systems.

the recorded current increases with time, the maintained potential should be above the breakdown potential. If the recorded current substantially decreases with time, the maintained potential should be below the protection potential. When using the potentiostatic method in conjunction with cyclic potentiodynamic polarization, the region of each potential is roughly estimated.

#### Stress Corrosion Cracking—Slow Strain Rate

The need to wait three months or longer for results in the U-bend test is often impractical, especially when a material decision for plant equipment may have to be made, sometimes within days. The slow strain rate test offers a rapid way to assess stress corrosion cracking susceptibility. The slow strain rate test is described in ASTM G 129 [31].

The key to the test procedure is that by straining the sample at a selected slow strain rate, the passive film is disrupted. This disruption in the passive film affords an opportunity for a stress corrosion crack to initiate quickly in a susceptible alloy. Results may be obtained in one to five days, depending on the strain rate. By contrast, the U-bend test takes much longer to run, because disruption or breakdown of the passive film with possible crack initiation is generally a very slow process. In the slow strain rate test, the sample is pulled to failure at a preselected strain rate in a tensile machine surrounded by the environment. If stress corrosion cracking is not a problem, the sample will fail by ductile tensile overload with the fracture surface showing the classical dimpled fractured surface under a scanning electron microscope. If stress corrosion cracking occurs, there are many secondary cracks associated with the primary fracture, and there will be a significant reduction in ductility (percent elongation and

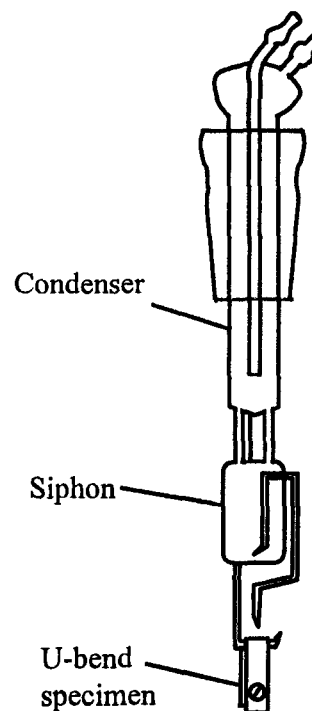


Fig. 12—Siphon test allows concentration of aggressive species to be simulated.

percent reduction in area) compared to a similar sample tested in an inert environment.

In some systems (for example, 304 stainless steel in hot water with low levels of chloride), the slow strain rate method gives false negative results. It is because the mechanism of failure requires pitting to be initiated before cracking can occur. Most slow strain rate tests are not run long enough for the slow pitting initiation step to occur. Alternatively, an electrochemical assist can be provided to initiate pitting before the straining occurs.

In general, the slow strain rate test is a conservative test and a useful method for determining whether an alloy is resistant to stress corrosion cracking in a plant solution.

#### *Stress Corrosion Cracking—Siphon Test*

The siphon apparatus can be used with a three-position flask (see Fig. 11) to assess the tendency for chloride stress corrosion cracking to occur on a stressed U-bend exposed to the condensing liquid [22]. The setup provides an alternating wet/dry condition. The condensed liquid fills the cup that empties when full by a siphon action with the liquid flowing across the sample surface. During the filling stage, the liquid film on the U-bend has a chance to flash off, concentrating the chlorides as would occur in a plant situation. See Fig. 12 for sketch showing siphon test arrangement.

## CONFIDENCE IN CORROSION TEST DATA

Corrosion data come from many sources. It is not produced to a common format and displays considerable variation in quality. Understand the source and quality of corrosion data before using it. The reliability of corrosion data sources may be categorized broadly.

#### *Plant Equipment Performance Data from Identical Process*

Plant equipment performance data in an identical process usually provide a high level of confidence. The data may correlate corrosion test exposure information (coupon or probes) with wall thickness monitoring of process equipment and inspection data on type of corrosion.

#### *Field Corrosion Coupon Data from Identical Process*

This also provides high confidence. Field corrosion coupon data provide corrosion rates and localized corrosion information, but may not provide insight into process upsets.

#### *Plant Equipment Performance or Field Coupon Data from a Similar Process*

Even slight differences in temperature, feedstock, impurities, or cooling water source make the data less reliable. However, corrosion data from a similar process provide information to improve the accuracy of a test program.

#### *Pilot Plant Corrosion Data*

Pilot plant corrosion data are often compromised by frequent process parameter and feedstock manipulations during test campaigns. Under these conditions, it is difficult to relate materials performance to process performance,

unless specific test campaigns are dedicated to corrosion data collection. Documentation is often inadequate.

#### *Laboratory Corrosion Data*

Laboratory corrosion tests are designed to simulate the process. Short test times and inability to capture every nuance of the process are limitations. However, laboratory corrosion testing provides important evidence of conditions that might depassivate active-passive alloys, such as increase in temperature or a threshold concentration of an aggressive species.

#### *Thermodynamic and Kinetic Modeling*

Thermodynamic modeling can be extremely useful in understanding the process chemistry and its influence on corrosion and corrosion data, particularly with respect to the speciation of the liquid phase and the potential for solids formation. Software codes for aqueous and nonaqueous systems are available from many sources, but care must be exercised in their use. Special attention should be paid to the source of the thermodynamic data and/or the source of experimental data used to develop the thermodynamic parameters.

Kinetic modeling of corrosion phenomena has made great advances in the past decade, and some software products are capable of predictions for simple systems. The available tools are extremely useful for extrapolation and relative performance if the corrosion mechanism is understood and model parameters have been derived from trusted data. Materials of construction should not be chosen based on predictions from unvalidated kinetic modeling tools. Rather, use the modeling tools to narrow the selection process and minimize the number of corrosion test experiments required.

#### *Corrosion Literature*

The corrosion literature contains gems, but is nonuniform. It requires a specialist to interpret conclusions, because the authors do not have the same goals as the nonspecialist reader, or even objectives similar to other specialists when performing their studies. Keywords included with the literature do little to help the nonspecialist.

#### *Commercial Data Publications*

The weakness of commercial data lies in nonuniform presentation format between different publications. Data are merged from many sources, and smoothed down to the lowest common denominator. Often, the simpler the presentation format, the lower the value of the information. Data from different publications may be in disagreement.

#### *Manufacturers' Data*

Data from materials suppliers is useful and offers insight into the performance of specific materials. What is omitted from materials suppliers' data is sometimes more revealing than what is included. Much of the information is developed under laboratory conditions in pure solutions. Manufacturers are reluctant to supply corrosion data that can be used for direct comparison of their alloys with competing products. ASTM G 157 [32] categorizes 15 test environments that cover a spectrum of processes in the chemical process

industry. It is recommended that new or existing alloys be exposed to these environments. However, manufacturers are reluctant to develop data that allow direct comparison with competing alloys.

### *Process Literature*

Most process literature provides very little information on materials performance.

## **CREATION OF A COMPUTERIZED CORROSION TEST DATABASE**

It is difficult to compare information between sources. On account of the vagaries of chemical process environments, it is important to develop a database that captures essential information on one's proprietary processes. ASTM standard G 107 [33] may be used as a guide. The amount of information it requires may be daunting. A business should decide what minimum essential elements of corrosion data should be captured in its proprietary corrosion test database.

Before deciding what fields require documentation, ask the question, "Will the information collected assist with the design of the plant, or when management of change justification is required during the life of the plant?" A computerized corrosion test database brings together three main types of information, which are materials, corrosion, and performance.

### *Materials Data*

Describe materials from which the test specimens are made with sufficient accuracy to understand the effect of formation, fabrication, heat treatment, or surface finish on performance. With metals, it is relatively easy to use standard descriptions to indicate composition, such as UNS

designation. Most specimens are exposed in the annealed condition. If another heat treatment is used, such as sensitization, it should be included in the documentation.

Polymers and elastomers are not described with the same degree of precision as metals. When describing them in the database, the ASTM generic name or manufacturer's trade-name is not sufficient. Other unique identification features (such as part number, if the specimen is taken from a component) are required for polymer and elastomer samples.

### *Corrosion Data*

Minimum essential data on the corrosive environment are shown in Fig. 13.

### *Performance Data*

Type of information to be recorded depends on the materials from which the test specimens are made. For metals, calculated corrosion rate and type/depth of localized corrosion must be documented. For polymers and elastomers, measured property changes, such as thickness or hardness, are documented, in addition to appearance change. The information for polymers and elastomers is usually recorded immediately after the coupons are removed and after a designated interval, to provide time for them to stabilize. In all cases, performance data may be linked to a photographic record of the coupons.

## **Acknowledgments**

The authors acknowledge contributions from DuPont peers Mike Dorsey, Sherryl Fox, Steve Grise, John Ludman, Tony Pezone, and Brian Saldanha. Sheldon Dean (formerly Air Products and Chemicals Corporation), Srinu Kesavan (FMC Corporation), and Roger Turcotte (FMC Corporation) are acknowledged for enhancing the draft.

Feature	Why Document
Test type	Lab, field, pilot plant are pointers to value of data
Test time	Required to calculate corrosion rate
Exposure	Type of exposure affects decision making
Coupon or probe location	Pinpoints where coupons are in equipment
Site Name	For internal benchmark
Product	Provides alert to vagaries of process
Responsible party	Provides a key contact who knows more
Process step	Provides link to other data sources
Active Corrosives	Important corrosives influence rate of attack
Weight percent or ppm	Quantities of species present influence corrosivity
Temperature - average	Temperature influences corrosivity
Temperature - maximum	Peak temperature attained may influence corrosivity
Pressure	Helps capture all important process parameter elements
Agitation	Relative motion of process environment influences corrosivity
Sparging	Degree of gas entrainment/blanketing influences corrosivity
pH	For some metals, pH influences corrosivity

FIG. 13—Minimum essential documentation of the corrosive environment is required to create an effective computerized test database.

## REFERENCES

- [1] *Annual Book of ASTM Standards*, Vol. 03.02, ASTM International, West Conshohocken, PA.
- [2] ASTM Standard A 763, Standard Practices for Detecting Susceptibility to Intergranular Attack in Ferritic Stainless Steels, *Annual Book of ASTM Standards*, Vol. 03.02, ASTM International, West Conshohocken, PA.
- [3] ASTM Standard A 262, Standard Practices for Detecting Susceptibility to Intergranular Attack in Austenitic Stainless Steels, *Annual Book of ASTM Standards*, Vol. 03.02, ASTM International, West Conshohocken, PA.
- [4] ASTM Standard A 923, Standard Test Methods for Detecting Detrimental Intermetallic Phase in Wrought Duplex Austenitic/Ferritic Stainless Steels, *Annual Book of ASTM Standards*, Vol. 03.02, ASTM International, West Conshohocken, PA.
- [5] API 510: Pressure Vessel Inspection Code. Maintenance, Inspection, Rating, Repairs and Alterations, American Petroleum Institute.
- [6] API 570: Piping Inspection Code: Inspection, Repair, Alteration and Rerating of In Service Piping Systems, American Petroleum Institute.
- [7] API 653: Tank Inspection, Repair, Alteration, and Reconstruction, American Petroleum Institute.
- [8] API 579: Fitness-for-Service, American Petroleum Institute.
- [9] OSHA 29 CFR 1910.119, Safety Management of Highly Hazardous Chemicals, Occupational Safety and Health Administration.
- [10] ASTM Standard G 1, Practice for Preparing, Cleaning, and Evaluating Corrosion Test Specimens, *Annual Book of ASTM Standards*, Vol. 03.02, ASTM International, West Conshohocken, PA.
- [11] ASTM Standard G 4, Guide for Conducting Corrosion Tests in the Field, *Annual Book of ASTM Standards*, Vol. 03.02, ASTM International, West Conshohocken, PA.
- [12] ASTM Standard G 5, Reference Test Method for Making Potentiostatic and Potentiodynamic Anodic Polarization Measurements, *Annual Book of ASTM Standards*, Vol. 03.02, ASTM International, West Conshohocken, PA.
- [13] ASTM Standard G 30, Practice for Making and Using U-bend Stress-corrosion Test Specimens, *Annual Book of ASTM Standards*, Vol. 03.02, ASTM International, West Conshohocken, PA.
- [14] ASTM Standard G 5, Reference Test Method for Making Potentiostatic and Potentiodynamic Anodic Polarization Measurements, *Annual Book of ASTM Standards*, Vol. 03.02, ASTM International, West Conshohocken, PA.
- [15] ASTM Standard G 96, Guide for On-line Monitoring of Corrosion in Plant Equipment (Electrical and Electrochemical Methods), *Annual Book of ASTM Standards*, Vol. 03.02, ASTM International, West Conshohocken, PA.
- [16] ASTM Standard G 31, Standard Practice for Laboratory Immersion Corrosion Testing of Metals, *Annual Book of ASTM Standards*, Vol. 03.02, p. 101, ASTM International, West Conshohocken, PA.
- [17] ASTM Standard G 78, Guide for Crevice Corrosion Testing of Iron-base and Nickel-base Stainless Alloys in Seawater and other Chloride-containing Aqueous Environments, *Annual Book of ASTM Standards*, Vol. 03.02, ASTM International, West Conshohocken, PA.
- [18] ASTM Standard C 868, Test Method for Chemical Resistance of Protective Lining, *Annual Book of ASTM Standards*, Vol. 04.05, ASTM International, West Conshohocken, PA.
- [19] NACE TM0196-96, Chemical Resistance of Polymeric Materials by Periodic Evaluation, National Association of Corrosion Engineers.
- [20] Macdonald, J. R., *Impedance Spectroscopy*, John Wiley & Sons, 1987.
- [21] *Electrochemical Impedance-Analysis and Interpretation*, ASTM STP 1188, J. R. Scully, D. C. Silverman, and M. W. Kendig, Eds., ASTM International, West Conshohocken, PA, 1993.
- [22] Demo, J. J., "Chemical Processing," Chapter 73, *Manual on Corrosion Tests and Standards*, ASTM International, West Conshohocken, PA, 1996, p. 666.
- [23] Lichtman, J. Z., Kallas, D. H., and Rufolo, A., "Evaluating Erosion Damage," in *Handbook of Corrosion Testing and Evaluation*, W. H. Ailor, Ed., John Wiley & Sons, 1971, pp. 453-472.
- [24] Hack, H. P. and Taylor, D., "Evaluation of Galvanic Corrosion," *ASM Handbook*, Vol. 13, p. 234.
- [25] Scully, J. R. and Taylor, D. W., *Electrochemical Methods of Corrosion Testing*, *ASM Handbook*, Vol. 13, p. 212.
- [26] Chechirlian, S., Keddam, M., and Takenouti, H., "Specific Aspects of Impedance Measurements in Low Conductivity Media," *Electrochemical Impedance—Analysis and Interpretation*, ASTM STP 1188, J. R. Scully, D. C. Silverman, and M. W. Kendig, Eds., ASTM International, West Conshohocken, PA, 1993, p. 23.
- [27] Bertocci, U. and Huet, F., *Corrosion*, Vol. 51, No. 2, 1995, p. 131.
- [28] Bertocci, U., Gabrielli, C., Huet, F., and Keddam, M., *Journal of Electrochemical Society*, Vol. 144, No. 1, January 1997, p. 31.
- [29] Mansfeld, F. and Xiao, H., *Journal of Electrochemical Society*, Vol. 140, No. 8, August 1993, p. 2205.
- [30] ASTM Standard G 61: Test Method for Conducting Cyclic Potentiodynamic Polarization Measurements for Localized Corrosion Susceptibility for Iron-, Nickel-, or Cobalt-based Alloys, *Annual Book of ASTM Standards*, Vol. 03.02, ASTM International, West Conshohocken, PA.
- [31] ASTM Standard G 129: Practice for Slow Strain Rate Testing to Evaluate the Susceptibility of Metallic Materials to Environmentally Assisted Cracking, *Annual Book of ASTM Standards*, Vol. 03.02, ASTM International, West Conshohocken, PA.
- [32] ASTM Standard G 157, Guide for Evaluating the Corrosion Properties of Wrought Iron- and Nickel-Based Corrosion Resistant Alloys for the Chemical Process Industry, *Annual Book of ASTM Standards*, Vol. 03.02, ASTM International, West Conshohocken, PA.
- [33] ASTM Standard G 107, Guide for Formats for Collection and Compilation of Corrosion Data for Metals for Computerized Database Input, *Annual Book of ASTM Standards*, Vol. 03.02, ASTM International, West Conshohocken, PA.



# Pulp and Paper

Angela Wensley<sup>1</sup>

THE SPECTRUM OF CORROSION environments in the pulp and paper industry is perhaps greater than that encountered elsewhere in the chemical process industries [1]. Aqueous environments range from acidic to neutral to basic, and from reducing to oxidizing. High-temperature environments include molten salts and boiler flue gases. Many of these environments are unique to the pulp and paper industry. Figure 1 is a schematic diagram of an integrated pulp and paper mill. Process equipment includes pressure vessels, boilers, kilns, storage tanks, towers, and large machines with rolls that rotate at high speed. This paper reviews the corrosion testing methods used for each of the major pulp and paper process environments.

Pulp and paper process environments are negatively affected by trends to higher production rates and increasingly stringent environmental laws. Higher production can place greater mechanical demands on equipment, as well as increase corrosivity of certain processes (e.g., simply by increasing the temperature). Requirements to discharge less, or even zero, effluent cause the increased recycle of corrosive elements that build up in concentration in process streams [2–4]. Environmental demands are requiring the development of new pulp and paper process technologies [5].

For many years, the pulp and paper industry depended heavily on carbon steels and 300-series austenitic stainless steels as materials of construction. There was heavy reliance on equipment suppliers for materials selection and repair advice. When failures occurred, incremental improvements in materials selection were made; for example, moving from Type 304 to Type 316 to Type 317 stainless steel. Beginning in the mid-1970s, several pulp and paper companies set up their own materials and corrosion laboratories with the aim of solving corrosion problems through proper materials selection, and to assist with materials selection for new process technologies. There has been a trend toward the application of duplex stainless steel for corrosion protection. The use of stainless steels in the pulp and paper industry is the subject of a recent publication jointly sponsored by TAPPI and the Nickel Development Institute [6].

Corrosion researchers working in or for the pulp and paper industry have developed or adapted their own corrosion test methods and standards relevant to the pulp and paper environments, in addition to using published standards. Corrosion test methods used within the pulp and paper industry

include a variety of corrosion coupon exposures and electrochemical procedures, including polarization testing, linear polarization, and corrosion potential monitoring in:

- simulated process environments,
- actual process environments,
- samples of process solutions,
- ASTM, NACE, and TAPPI standard environments.

Davies [7] summarized several of the ASTM standard recommended practices used for corrosion testing in the pulp and paper industry in the 1980s. These included:

- ASTM Standard Recommended Practice G1, Preparing, cleaning, and evaluating corrosion test specimens;
- ASTM Standard Recommended Practice G4, Conducting plant corrosion tests;
- ASTM Standard Recommended Practice G50, Conducting atmospheric corrosion tests of metals;
- ASTM Standard Recommended Practice G48, Pitting and crevice corrosion resistance of stainless steels and related alloys by the use of ferric chloride solution;
- ASTM Standard Recommended Practice G35, Determining the susceptibility of stainless steels and related nickel-chromium-iron alloys to stress corrosion cracking in polythionic acids.

There has been a greater reliance on developing test methods applicable to actual or simulated process solutions, rather than testing in “standard” solutions (e.g., ferric chloride), which are not relevant to pulp and paper processes.

## THE PAPER MACHINE

In a paper machine, a pulp suspension (approximately 2 % pulp in “white water”) is formed into a sheet, dewatered, pressed, and dried into paper. Paper machines operate at higher speeds than pulp machines. Wensley and Moskal have published a review of corrosion in paper machines [8].

## Environments

White waters can vary tremendously in composition among different paper machines, and may contain ions such as thiosulfate, chloride, and sulfate, plus additives to control pH, microbiological activity, drainage/retention, or other product qualities. Thiosulfate is a pitting agent that can be present from hydrosulfite brightening. Chloride is

<sup>1</sup>Pulp and Paper Corrosion Specialist, Angela Wensley Engineering Inc., White Rock, BC, Canada V4B 1K1.

**FIG. 1—A schematic example of an integrated pulp and paper mill.**

present from wood floated in from the ocean, the recycling of other process effluents, and carry-over from the bleach plant. Recycling of process streams in order to minimize effluent has increased both the temperature of the white water and the concentrations of corrosive species. Increased production demands have resulted in higher machine speeds and greater loading of components such as suction roll shells.

Austenitic and duplex stainless steels are the major metallic materials of construction for white water service, particularly for the headbox, piping, and also for suction roll shells. Bronze, once widely used for forming wires and suction roll shells, is used less because of its inherently poor corrosion resistance in modern white water environments. Poor welding quality can undermine the corrosion resistance of stainless steels, especially if the thiosulfate and chloride levels are high. Corrosion under surface deposits including scales, pulp mats, or microbiological growths

can require higher alloy compositions for corrosion resistance. Ultrahigh-strength low-alloy steels and various types of cast iron are used in the less corrosive areas of the paper machine.

Nonmetallic, composite, and ceramic materials are also used in paper machine construction, particularly on the wet forming end where low friction and dimensional stability are critical. Tile linings are used in tanks and wire pits, and corrosion-resistant coatings are used to protect the carbon steel structural beams in paper machines.

Alloy development for suction roll shells has barely kept pace with the ever-increasing performance demands and white water corrosivity in paper machines. Bronze, martensitic stainless steels, early-generation duplex stainless steels, precipitation hardening stainless steels, and later-generation duplex stainless steels have all been used for the manufacture of suction roll shells. Today, the preferred materials for suction roll shells in severe service are duplex

stainless steels with low residual stress and high chromium content to resist pitting. These shells are produced either by centrifugal casting or the by rolling and welding of plate where the final welded assembly is annealed. The history of corrosion studies of suction roll shells has been summarized by Bowers [9].

## Corrosion Testing

Corrosion testing for paper machines has included a variety of electrochemical, pitting, microbiologically influenced corrosion (MIC), corrosion fatigue, and structural coatings tests.

### *Electrochemical Corrosion Testing*

Cyclic anodic polarization procedures based upon ASTM G5 (Reference Test Method for Making Potentiostatic and Potentiodynamic Anodic Polarization Measurements) have been used to evaluate the localized corrosion resistance of stainless steel alloys in paper machine white waters. The difference between the open circuit or naturally occurring corrosion potential and the pitting breakdown potential of various materials has been reported by many investigators [10–13]. Bowers [14] called the difference between the breakdown potential and the potential of the cathodic/anodic current reversal the “margin of safety.” He also noted the effect of the sulfate to chloride concentration ratio on localized corrosion of Types 304 and 316L stainless steels. These results permitted alternative materials of construction to be ranked and their limits of resistance to be defined.

Variations of the test have been developed by others. In a polarization testing program to compare the localized corrosion resistance of Type 316L stainless steel from different sources, Wensley [13] found that machinable 316L was inferior to conventional 316L at comparable molybdenum contents. She noted that crevice corrosion at the electrode holder can interfere with the measurement of the pitting potential, but that the formation of corrosion crevices can be prevented by using an insulating varnish. A reproducible crevice site was made by means of a Viton O-ring. Bennett and Federowicz [10] used paper rings to simulate crevices under pulp deposits in a study of the effect of chloride on stainless steels.

Castillo and Caudill [15] used both linear polarization resistance and electrochemical noise to study the effect of process changes on the corrosion of Types 316 and 316L stainless steels. Wensley et al. [16] used linear polarization resistance to study the corrosion of bronze in various white water systems in a newsprint mill.

### *Pitting Corrosion Testing*

Theories that corrosion fatigue cracks initiate at corrosion pits have prompted interest in the pitting resistance of suction roll alloys. Reid and Wensley [17] used potentiodynamic pitting scans to evaluate duplex suction roll materials, as did Castillo et al. [18,19]. The pitting resistance of duplex stainless steels was studied extensively by Sriram and Tromans [20]. They conducted potentiodynamic pitting tests in conjunction with electron microscopy, concluding that pitting of the ferrite and austenite phases was dependent on the partitioning of alloy elements and nitrogen enrichment. Yoshitake [21] evaluated a new alloy via pitting tests in 6 % FeCl<sub>3</sub>.

Increased temperature and chloride concentration resulting from closing up the white water system of a mill could result in localized corrosion if the temperature exceeds the critical pitting temperature for the alloy of construction. Conventional electrochemical techniques often result in crevice corrosion, which may be nonreproducible and mask the initiation of pitting. The “Avesta cell” in which the crevice is continuously flushed with distilled water permits an electrochemical determination of the critical pitting temperature. The critical pitting temperature of 316L stainless steel was defined as the temperature at which the breakdown potential dropped about 200 mV as the corrosion reaction changed from transpassive corrosion to pitting [11,12]. Data obtained using the Avesta cell showed that the corrosion resistance of Type 316L stainless steel varied from heat to heat.

Newman et al. [22–24] have aided the understanding of thiosulfate effects on the corrosion of Type 304 stainless steel in paper machine white water. One of their tests was the “scratch method” [24] that was used to investigate pitting at various ratios of thiosulfate to sulfate, with chloride and bisulfite additions in simulated white water further defining the limits of corrosion resistance for stainless steels.

Varjonen et al. [25] studied the pitting corrosion resistance of Type 316 stainless steel in white waters containing thiosulfate using an Avesta Cell, where the pitting breakdown could be studied without interference from crevice corrosion. Salonen et al. [26] and Laitinen et al. [27] used the contact electric resistance (CER) method to study the effect of thiosulfate on the films formed on Type 304 stainless steel. In the CER method, the resistance of the films formed on metal surfaces can be studied as a function of potential. Stable passive films have a high electrical resistance, whereas unstable (or absent) films have a low electrical resistance.

### *Microbiologically Influenced Corrosion Testing*

White water environments are typically 40–60°C and contain dissolved organic nutrients that promote the formation of slimes and biofilms, sulfate ions also provide food for sulfate reducing bacteria. MIC is a particular concern in alkaline papermaking environments. Many mills have converted from acid papermaking (with the addition of alum) to alkaline papermaking in order to produce longer lasting papers. Corrosion considerations in alkaline papermaking have been summarized by Bowers [28]. MIC of austenitic and duplex stainless steels in paper machine environments has been investigated [29]. These investigations included polarization tests of surfaces under biofilms. Carpen et al. [30] simulated the MIC that occurs at splash zone areas of paper machines. NACE has published a book on MIC that is an aid in identifying problems [31].

### *Corrosion Inhibitor Testing*

Magar [32] evaluated inhibitors in white water by means of the linear polarization resistance technique in a search for effective inhibitors to prevent corrosion of bronze suction rolls. A galvanodynamic testing method was used by DeBerry and Ellis [33] in order to study inhibition of corrosion of a duplex stainless steel alloy.

### Corrosion Fatigue Testing

Significant research and testing has been devoted to corrosion fatigue resistance of paper machine suction roll shells [34]. Unfortunately, the results from the various tests used by the various manufacturers have been difficult to compare. Furthermore, their tests do not predict actual performance in the paper machines and cannot be related directly to roll loads or geometries. Experience gained over a long period of time has remained the best guide to selection of suction roll alloys. The tests used are summarized below.

The rotating beam bending test using the RR Moore machine in accordance with TAPPI Technical Information Paper 0402-09 [35] has been the most popular procedure. The fatigue life (number of cycles to failure) is plotted as a function of applied cyclic stress. The mean stress is zero in these tests so the effects of residual stresses are not tested. Unfortunately, most suction shells contain significant residual stresses from casting or weld repairing, and high residual stresses are believed to be responsible for the short service life of some suction shell alloys. Suction shell roll life cannot be predicted from the test results, and the stress fields produced in the test coupons cannot be directly related to those in operating rolls.

Jaske and Castillo [36] used RR Moore rotating beam fatigue machines to study several roll materials with simulated white water solutions dripped onto the test specimen surface. Castillo et al. [19] used rotating bending tests to evaluate the corrosion fatigue resistance of duplex stainless steel suction roll alloys. Yoshitake et al. [21] also used this method.

Glogowski and Castillo [37] used the reverse plate bending test to evaluate cast bronze alloys in paper mill white waters. Rectangular bars with holes drilled to simulate those in suction rolls were tested in accordance with TAPPI Technical Information Paper 0402-08 with simulated white water containing thiosulfate wicked into the holes [38]. This test is better than the rotating beam test as a simulation of the fatigue that occurs at suction roll holes, since it incorporates a drilled hole geometry.

Castillo and Michel [18] used uniaxial fatigue testing to demonstrate the performance of a duplex steel. The axial fatigue tests were done with a Krouse axial mechanical test machine. The mean load was varied to apply a stress to the specimen to simulate the effect of residual tensile stresses in a suction roll, for a number of different stress ratios. The specimens were sprayed with simulated white water during testing. The crack length was measured during their testing via a thin foil crack measuring gage. Log-log plots of the crack growth rate versus the stress intensity range were presented.

Fracture mechanics principles and test methods have been used to determine the corrosion fatigue behavior in well-characterized mechanical conditions. Kelley et al. [39] conducted fatigue tests in a hydraulic fatigue machine using notched compact tension fracture mechanics specimens (ASTM E647, Test Method for Measurement of Fatigue Crack Growth Rates) in a simulated acidic white water. Both crack initiation and propagation were studied. In the crack initiation tests, three holes were drilled in the path of the crack in order to simulate holes in a suction roll.

Yeske [40–42] investigated crack propagation in the corrosion fatigue of suction roll alloys using compact tension

specimens. A correlation with service performance and tensile stresses in the rolls was observed.

Paper machine components other than suction rolls can experience corrosion fatigue cracking. Dorsch et al. [43] used a full size felt roll journal as a laboratory fatigue test specimen in simulated white waters containing thiosulfate ions.

### Structural Coatings Testing

Corrosion resistance of paints for structural steel in paper machine environments has been studied by Bennett and Magar [44,45]. A short-term laboratory testing method was developed to evaluate maintenance coatings. The test method used coupons with one half initially coated and the other half left bare to corrode in the environment, and then later the bare half was coated to simulate a repair coating in the field. Salt fog and Atlas cell immersion tests were also conducted on the paint panels. Rendahl et al. [46] used in-plant exposures of paint test panels.

## THE BLEACH PLANT

Strong oxidizing agents are used in the bleach plant to remove the pulp fiber color produced by chemical pulping, i.e., from dark brown to white. There is widespread consumer demand for white paper. The bleaching operation is accomplished in several stages with various bleaching agents. The stages are identified by the oxidant used, e.g., chlorine (C-stage), chlorine dioxide (D-stage), hypochlorite (H-stage), oxygen (O-stage), peroxide (P-stage), and ozone (Z-stage). Caustic extraction (E-stage) is used between bleaching stages to remove lignin.

Chlorine ( $\text{Cl}_2$ ) and chlorine dioxide ( $\text{ClO}_2$ ) bleaching are carried out in towers (usually carbon steel) lined with non-metallic materials. The bleached pulp is typically washed in a rotary drum washer or diffusion washer after exposure to the bleaching chemicals. For many years, Type 317 stainless steel was the "standard" material of construction for the bleach plant washers. Increased recycle and conversion to  $\text{ClO}_2$  bleaching has resulted in increased corrosivity of bleach plant process streams, requiring stainless steels that contain higher concentrations of molybdenum, nickel-based alloys, or titanium. Bardsley has reviewed the metallurgies required in the new bleaching processes [47].

### Environments

Chlorine-based bleaching created the most corrosive environments in the bleach plant prior to the use of  $\text{ClO}_2$ , with the  $\text{Cl}_2$  providing both high oxidizing potentials and being a source of chloride ions that served as localized (pitting and crevice) corrosion agents. Chlorine bleach washers typically operated under acidic conditions that further promoted localized corrosion of stainless steels in the presence of chloride ions. Chlorine bleaching has been replaced by  $\text{ClO}_2$  because of potential release of organochlorines to the environment. Acidic  $\text{ClO}_2$  bleaching environments are similar to chlorine bleaching environments in their corrosivity to stainless steels. Near-neutral pH  $\text{ClO}_2$  environments have been observed to severely corrode nickel-base alloys. Increased

recycle has led to higher temperatures (60–80°C) that promote localized corrosion.

Alternative bleaching agents using oxygen, ozone, and peroxide have been developed. The environments produced in these stages do not appear to be as corrosive to stainless steels, but peroxide can be highly aggressive to titanium.

## Corrosion Testing

Bleach plant corrosion testing has included corrosion coupon testing, electrochemical testing, electrochemical protection testing, and nonmetallic materials evaluation. Coupon exposure tests have been used to rank candidate materials for these applications. Nonmetallic materials including thermoplastics, thermosets, brick, and tile are widely used in the bleach plant.

### Corrosion Coupon Testing

Members of the TAPPI Corrosion and Materials Engineering Committee conducted cooperative research programs based on field coupon studies in operating bleach plants to evaluate candidate materials for bleach washers [48,49]. Unwelded alloys were tested in Phase 1 and welded alloys were tested in Phase 2 [50,51]. Phase 1 testing [48] used circular test coupons on spool racks, with PTFE spacer washers to allow crevice corrosion to take place under the washers. The multi-crevice Anderson washer was included on the test spools. This washer is described in ASTM STP 576 [52]. In the Phase 2 research program, over 1000 coupons were exposed in a number of bleach washers [53]. Fabricated pipe spools were used in some testing [54,55]. Garner [53] described additional visual and metallographic examination of welded stainless steel bleach plant coupons. Statistical review of the results was performed by Beetham [56].

The pitting resistance of stainless alloys has been ranked using the ferric chloride ( $\text{FeCl}_3$ ) test. This method appears to be appropriate, since it is likely that  $\text{FeCl}_3$  itself may be formed in bleach plant corrosion deposits when ferrous salts are oxidized by  $\text{ClO}_2$ . The  $\text{FeCl}_3$  test establishes a critical temperature above which pitting will occur [57–64]. Pitting resistance is determined in 6 %  $\text{FeCl}_3$ , in accordance with ASTM G 48 (Test Method for Pitting and Crevice Corrosion Resistance of Stainless Steels and Related Alloys by the Use of Ferric Chloride Solution) or in 10 %  $\text{FeCl}_3$  [61,62]. This test provides a conservative limit for the maximum temperature at which a material can be used, and the results are consistent with field experience. Critical crevice corrosion temperatures are measured [59] by means of ASTM G 78 (Guide for Crevice Corrosion Testing of Iron-Base and Nickel-Base Stainless Alloys in Seawater and Other Chloride-Containing Aqueous Environments with Anderson Washers). Wallen [63] evaluated alloys for highly oxidizing bleach plant environments in  $\text{FeCl}_3$  and in other simulated environments. Audouard [64] has used  $\text{FeCl}_3$  testing to evaluate alloys for highly oxidizing bleach plant environments.

Wensley et al. [65–68] conducted tests for several years with duplex stainless steels, highly alloyed austenitic stainless steels, and nickel-base alloys in a  $\text{ClO}_2$  washer using creviced coupons. These tests revealed that in near-neutral D-stage environments all the stainless steels suffered crevice

corrosion and that nickel-base alloys experienced general corrosion due to transpassive dissolution. The crevice washers actually protected the nickel-base alloys from thinning beneath the crevices. All stainless steel alloys experienced crevice corrosion. Test-to-test exposure time variations were normalized by dividing maximum crevice depths for each alloy by the maximum crevice depth observed for a Type 317L standard test corrosion coupon that was exposed in each test.

Many corrosion coupon tests were done in  $\text{Cl}_2$  and mixed  $\text{Cl}_2/\text{ClO}_2$  bleach plant environments in the 1990s to investigate the phenomenon of transpassivation of both nickel-base and iron-base alloys [69–76]. In-plant corrosion coupon testing of stainless alloys has been done in ozone bleaching environments [77]. Both in-plant and laboratory corrosion coupon testing has been done in  $\text{H}_2\text{O}_2$  bleaching environments [78–82].

### Electrochemical Testing

Bleach plant environments are amenable to conventional polarization testing, although the presence of the oxidant prevents measurement of the complete polarization curve. For this reason, polarization testing is normally carried out in simulated solutions without the addition of the oxidant.

To avoid problems with crevice corrosion at the electrode holder, an Avesta cell was used in investigations of the effect of post-weld cleaning on corrosion resistance of austenitic and duplex stainless steels in a simulated  $\text{ClO}_2$  liquor [11,83,84].

Potentiodynamic anodic polarization techniques were used by Bennett [85] in laboratory testing to study Type 316L stainless steel in  $\text{ClO}_2$  bleaching environments. Other researchers used electrochemical testing via an anodic scan with reversal to locate the pitting potential and the repassivation potential [59].

Electrochemical polarization testing has been done to evaluate the corrosion behavior of iron-base and nickel-base alloys in  $\text{ClO}_2$  environments [62,75,86–93], in oxygen bleaching environments [94], in ozone bleaching environments [95–97], in peracetic acid bleaching environments [97], and of titanium and zirconium in  $\text{H}_2\text{O}_2$  bleaching environments [98–100].

### Electrochemical Protection Testing

Electrochemical protection of bleach washers has permitted the continued use of lower alloyed stainless steels, while washing conditions have become more corrosive. Electrochemical protection was applied successfully in an early chlorine dioxide washer [101]. Electrochemical protection at slightly cathodic potentials was commercially applied for C- and D-stage washers [51,102–106]. The effectiveness of electrochemical protection has been assessed by means of coupons [104].

### Nonmetallic Materials Evaluation

The widespread application of fiberglass-reinforced plastic (FRP) composites has prompted comparative testing for resistance to bleaching solutions [107]. Coupons were prepared in accordance with ASTM C 581 (Practice for Determining Chemical Resistance of Thermosetting Resins Used in Glass Fiber-Reinforced Structures Intended for Liquid

Service). Bishop and Cowley [108] have described methods for determining the depth of surface corrosion and the moisture content of resins. They have done considerable in-plant coupon testing in  $\text{ClO}_2$  bleaching environments [109–111].

Bergman [112] described innovative methods for evaluating the performance of fiber-reinforced ester plastics. The techniques include water absorption measurements, mechanical and acoustic emission tests, and light transmission. Using these methods, he has determined failure mechanisms and has compared the performance of alternative materials. Later work has used infrared spectral analysis for both the identification of materials and for estimating the maximum temperature to which the laminate has been exposed; other tests include differential scanning calorimetry and dye staining [113]. These methods revealed the role of water-related damage on FRP performance. Petersson and Bergman [114] have studied the resistance of polymeric materials exposed in the field to various bleaching environments.

## CHEMICAL PULPING

In kraft chemical pulping, wood chips are digested (cooked) using “white liquor” in batch or continuous digesters to produce the pulp. “Black liquor” (spent white liquor containing dissolved lignin) is a by-product of the cooking process. Black liquor is extracted from the digester where it is recovered in flash tanks. Black liquor is also obtained by washing the pulp. The washing is done in brownstock washers. Some black liquor is returned to the digester. Most of the black liquor is subsequently concentrated in evaporators to produce “strong” or “heavy” black liquors that are sent to the recovery boiler to be burned as a fuel. Smelt (a mixture of molten salts that collects in the bottom of the recovery boiler) is dissolved in water to create “green liquor.” The green liquor is recausticized using lime that converts it to the white liquor used for chemical pulping.

Several reviews of corrosion and protection of batch and continuous digesters are available [115,116], as well as for the corrosion of flash tanks [117]. Carbon steel is used extensively for kraft process equipment, including liquor tankage and digesters. Many carbon steel continuous digesters have experienced stress corrosion cracking (SCC) at welds in the impregnation zone at the top of the digester [118,119] where post-weld heat treatment was not mandated by the construction code. The phenomenon of rapid thinning of carbon steel continuous digesters has been increasingly reported through the 1990s [120]. The rapid thinning appears to be related to changes in operation that produce higher temperatures and lower concentrations of NaOH between the wash, extraction, and cooking screens in the digester.

Stainless steel and nickel-base alloys are also used in kraft pulping systems. Some stainless steels can experience SCC, general corrosion thinning, or intergranular attack in alkaline liquors. Piping, tubes (liquor heater and evaporator), tankage, and some process vessels other than digesters have been constructed using Type 304L austenitic stainless steel. Continuous digesters have austenitic stainless steel screens, downcomer piping, and nozzles. Stainless steel composite

plate (typically carbon steel plate roll-bonded using Types 304L, 316, or 321) has been used to construct numerous vessels including many digesters. The current trend is to construct both batch and continuous digesters and ancillary vessels such as flash tanks, level tanks, and steaming vessels from solid duplex stainless steel, particularly Type 2205. Duplex stainless steel and nickel-base alloys have been used for tubes in liquor heaters and for the construction of bottom scrapers in continuous digesters. These applications require strict quality control to ensure optimum performance of the protective coating(s).

Stainless steel or nickel-base alloy weld overlays have been used to extend the life of both continuous and batch digesters. Other corrosion protective measures for digesters include anodic protection and thermal spray coating [116].

## Environments

White liquors, the most concentrated alkaline pulping liquors, are solutions containing the following inorganic compounds: sodium hydroxide ( $\text{NaOH}$ ), sodium sulfide ( $\text{Na}_2\text{S}$ ), sodium thiosulfate ( $\text{Na}_2\text{S}_2\text{O}_3$ ), sodium sulfate ( $\text{Na}_2\text{SO}_4$ ), sodium carbonate ( $\text{Na}_2\text{CO}_3$ ), and sodium chloride ( $\text{NaCl}$ ). A typical white liquor contains 100 g/L  $\text{NaOH}$ , 35 g/L  $\text{Na}_2\text{S}$ , 5 g/L  $\text{Na}_2\text{S}_2\text{O}_3$ , 5 g/L  $\text{Na}_2\text{SO}_4$ , 20 g/L  $\text{Na}_2\text{CO}_3$ , and 1 g/L  $\text{NaCl}$ . White liquor is regarded as being the most corrosive of the alkaline pulping liquors, although higher corrosion rates can be obtained with black liquors at higher temperatures. The strength of white liquors is typically described in terms of the parameter “sulfidity” with higher sulfidity liquors generally having higher concentrations of  $\text{Na}_2\text{S}$ . Green liquor has a comparable inorganic composition, except that it has a lower concentration of  $\text{NaOH}$  than does white liquor. White liquor prior to addition to the digester is typically at 90–100°C. White liquor is usually mixed with black liquor and the chips prior to being added to either batch or continuous digesters. Black liquors have an appreciable organic content. Extractives from some wood species are known to make black liquors much more corrosive. Evaporated black liquors have a higher solids content than do weak black liquors and tend to have relatively high concentrations of both  $\text{NaOH}$  and  $\text{Na}_2\text{S}_2\text{O}_3$ .

The  $\text{NaOH}$  is consumed during either batch or continuous cooking. In a batch digester, the  $\text{NaOH}$  concentration decreases over the duration (approximately 2 h) of a batch cook, and the  $\text{NaOH}$  may eventually be completely depleted. Despite the depletion of  $\text{NaOH}$  in batch cooking, there have been rare occurrences of SCC in batch digesters.

Most of the white liquor is added at the top of a continuous digester, and the  $\text{NaOH}$  concentration is decreased at lower elevations, although there is the possibility of adding white liquor at lower elevations. In some cooking processes, white liquor is added directly at the top and/or to recirculated liquor that is removed from the digester, heated, and then re-introduced into the digester. The caustic concentration in the impregnation zone is high enough to support SCC of carbon steel welds that contain high residual welding stresses. In the wash zone near the bottom, the liquor may be nearly depleted in  $\text{NaOH}$ .

## Corrosion Testing

There has been much corrosion coupon testing in kraft and soda liquors. Electrochemical polarization, linear polarization resistance testing, and contact electrical resistance testing have also been used.

### *Corrosion Coupon Testing*

Wensley and Charlton [121,122] performed coupon studies to determine the effect of liquor composition on general, galvanic, and SCC in white liquors and to determine the effect of steel composition on corrosion rates. Strom [123] tested corrosion coupons of stainless steels in green and black liquors. Wensley and Champagne [124] also did laboratory corrosion coupon testing in white, green, weak black, strong black, and digester extraction (flash tank) liquors to investigate the effect of sulfidity on corrosion of carbon and stainless steels.

Clarke and Stead performed corrosion coupon testing in flash tank liquors [125]. Al-Hassan et al. have done coupon studies in condensed black liquor vapours [126]. Evaporator liquors have been studied recently [127–130]. The evaporator testing included SCC test specimens in the form of U-bends prepared in accordance with ASTM G 30 (Standard Practice for Making and Using U-Bend Stress Corrosion Test Specimens).

Thompson et al. [131] investigated the effects of sand on corrosion and erosion in simulated kraft white liquor using a reciprocating wear tester. Nadezhdin and Cardin [132] studied erosion-corrosion of stainless steels in simulated batch digester cooking liquor using coupons subjected to daily abrasive cleaning. These studies are relevant since sand trapped in the bark of logs moved on the earth can be introduced with the chips in mills where de-barking is not efficient.

Corrosion coupon studies in digesters and in the laboratory using digester liquors have been reported by a number of researchers [133–142]. Some have investigated the effect of organic species—including the addition of catechols—on corrosion in digester liquors using laboratory autoclaves [133,139–141]. Singh et al. [139,140] made liquors using pilot plant digester cooks with various hardwood and softwood species starting with the same white liquor source. They investigated the corrosion of both carbon steel and stainless steel at 170°C. Troselius [141] prepared synthetic liquors to which various inorganic and organic compounds were added to investigate the effects on the corrosion of stainless steel at 170°C. Ramo [142] investigated the influence of sulfur anions on the corrosion of stainless steels in simulated inorganic digester liquors in autoclaves.

### *Electrochemical Polarization Testing in White Liquors*

The earliest study of constituents in white liquor was reported by Ruus and Stockman [143]. Mueller [144,145] was one of the first workers to describe the active/passive corrosion of steel in white liquor. The important effect of polysulfide was explained by Roald [146,147] based on polarization testing and consideration of modern mixed electrode theory. Wensley and Charlton [148] performed potentiodynamic polarization tests to study the effects of various liquor constituents including polysulfide, thiosulfate, and sulfate on the corrosion of carbon steel at 90°C that is relevant to clarifiers

and storage tanks. The effect of passive film composition on stable passivity was studied by Crowe and Yeske [149] who investigated the corrosion of carbon steel in simulated kraft liquor via polarization testing, mass loss, and corrosion potential measurements to determine the effects of liquor components.

Uusitalo [150] analyzed iron sulfides via X-ray analysis to determine their influence on corrosion behavior. Tromans [151] conducted anodic polarization tests and used electron microscopy and including electron diffraction to reveal that sulfide incorporated into the  $\text{Fe}_3\text{O}_4$  film impaired passivation. Honda et al. [152] performed extensive analysis of surface corrosion films in simulated liquor. Clarke and Singbeil [153] completed potentiodynamic polarization scans in white liquor, green liquor, and weak wash liquor at 90°C to investigate the effect of polysulfides on corrosion of carbon and stainless steels.

### *Linear Polarization Resistance Testing*

LPR testing is typically done in accordance with ASTM Standard G 96. Yeske [154] measured the corrosion rates of carbon steels in alkaline sulfide environments using the LPR technique and described the use of the silver/silver sulfide reference electrode. These techniques were developed further by Crowe and Yeske [155] and used with real mill liquors for on-line monitoring of corrosion rates. The corrosion rates were found to be related to liquor composition with a strong flow effect. Crowe [156] also used LPR testing for on-line corrosion monitoring in white liquor clarifiers. Leinonen et al. [157] used the LPR method to monitor corrosion in a batch digester.

### *Contact Electric Resistance Testing*

The contact electric resistance technique has been applied by Ramo et al. [142] to study the corrosion and passivation of stainless steels and of chromium plated stainless steels in alkaline pulping liquors.

### *Hot Plate Boiling Corrosion Testing*

Audouard et al. and Dupouiron [158–160] simulated the performance of stainless steels in batch digesters during filling after a cook. Their studies were conducted under heat transfer conditions where white liquor was sprayed onto metal surfaces heated above the boiling point. They measured corrosion potentials, redox potentials, and polarization resistance and performed polarization tests in white and black liquors and mixtures of both at temperatures up to 170°C.

### *Electrochemical Corrosion Monitoring in Digesters*

Electrochemical corrosion monitoring in batch [157,161] and continuous digesters [162] has been accomplished using reference electrode probes that permit the measurement of the corrosion potential. The corrosion potential of the digester wall has been measured with respect to molybdenum, stainless steel, and silver/silver sulfide reference electrodes. Pawel et al. [163] have used electrochemical noise to monitor corrosion in a continuous digester.

### *Electrochemical Polarization Testing in Autoclaves*

Crowe and Tromans [164,165] performed polarization tests for carbon steel at 150°C in alkaline sulfide solutions

using an autoclave and an external silver/silver sulfide reference electrode. They developed potential-pH diagrams indicating thermodynamically stable compounds at given potentials and pH that were used to interpret the observed corrosion behavior.

Wensley [166–171] conducted extensive potentiostatic polarization studies in continuous digester liquors (mainly extraction liquors) and in batch digester liquors to obtain “corrosion polarization curves” showing the corrosion rate versus potential behavior for numerous materials of construction. “Corrosion polarization curves” show the actual relationship between potential and the anodic process of corrosion without the interference of competing anodic and cathodic reactions that otherwise makes it difficult to distinguish corrosion processes in potentiodynamic polarization curves. The potentiostatic tests were done at individual potentials in the range from –250 to +100 mV versus a molybdenum reference electrode, the range of possible corrosion potentials that materials may be experienced in digester environments. Materials investigated included carbon steels (of both low and high silicon contents), austenitic stainless steels, duplex stainless steels, various weld metal overlays, and thermal spray coatings. Specimens were held for a period of five days at each selected potential, then removed, cleaned, and mass loss corrosion rates were determined. This test method is also well suited to investigating the effects of temperature and NaOH concentration in the liquor and the effects of silicon and chromium contents in carbon steels and stainless steel, respectively [170].

#### *Anodic Protection*

Mueller [172] and then Banks et al. [173] described the anodic protection of batch digesters. These systems maintain the surface potential in the passive range, at more positive potentials to the active/passive transition where corrosion may be substantial and cracking may occur. Banks successfully used a molybdenum oxide reference electrode. Bennett [174] described anodic protection of a continuous soda digester, but molybdenum reference electrodes failed in those tests. Anodic protection has been used in some continuous digesters to mitigate corrosion and SCC [118,175–177]. Yeske et al. described the anodic protection of a white liquor clarifier [178], and Munro described the protection of white and green liquor tankage [179].

Thin layer activation coupons have been used to continuously monitor corrosion rates in continuous digesters, and to verify the effectiveness of anodic protection systems [180]. The surface of a thin layer activation coupon is irradiated to a shallow depth and monitoring is performed with a Geiger counter from outside the digester wall. Subtracting for effects of half-life decay, the corrosion rate can be estimated from the decreased activity of the coupon.

#### *Stress Corrosion Cracking Tests*

The catastrophic failure of a continuous digester by SCC revealed the need to better understand SCC of steels in alkaline sulfide solutions [118]. SCC was subsequently found in many other digesters [181]. SCC rates were measured by examination of double cantilever beam fracture mechanics specimens with various stress intensity factors, which were exposed in the failed digester after repairs were made [118].

Singbeil and Tromans [182–184] investigated the SCC of carbon steel in alkaline sulfide solutions in the laboratory by means of slow strain rate tests (SSRT) and fracture mechanics tests with precracked loaded double cantilever beams. Cracking occurred at active/passive transition potentials. Subsequent research [185–187] showed that there were two active/passive transitions and that cracking was associated with formation of a sulfide containing film. The fast scan/slow scan potentiodynamic techniques did not predict the potential range for SCC. Crack propagation rates, as a function of stress intensity, were investigated via fracture mechanics tests.

Yeske and Guzi [188] published results of SSRT done by using liquor samples continuously drawn through the test cell from a digester impregnation zone. They monitored corrosion potentials over a period of several months and discovered that the corrosion potential entered the cracking zone during digester upsets. Similar monitoring has been conducted by others [189–191]. Crowe [192] described slow strain rate testing, which revealed that the cracking zone varied at different mills and the susceptibility to SCC increased with increasing liquor concentration.

Ring weld tests have been used to evaluate the use of various weld materials to minimize residual stress induced cracking [193]. These were prepared and tested in accordance with ASTM G 58 (Practice for Preparation of Stress Corrosion Test Specimen for Weldments) and ASTM G 31 (Practice for Laboratory Immersion Corrosion Testing of Metals). The ring weld technique was modified for use in evaluating resistance to SCC along with stress relief, shot peening, sealed thermal spray coatings, and weld overlays of Alloy 82 and of Type 309L stainless steel [194].

High-temperature and pressure tests (weight loss, electrochemical measurements, and U-bends) were conducted by Honda et al. [152] with austenitic, ferritic, and duplex stainless steel alloys in alkaline sulfide solutions at 150°C. Dupoirion [160] reported on SCC tests conducted in white liquors using the constant load test.

Kivisäkk [195] used SSRT to study the SCC of carbon and stainless steels in white liquor. Specimens were prepared to ISO Standard 7539-4, Corrosion of Metals and Alloys—Stress Corrosion Testing—Part 4: Preparation and Use of Loaded Tension Specimens. The SSRT was done in accordance with ISO Standard 7539-7, Corrosion of Metals and Alloys—Stress Corrosion Testing—Part 7: Slow Strain Rate Testing.

#### *Sensitization*

Susceptibility of austenitic stainless steels to intergranular attack has been evaluated using ASTM A 262 (Practices for Detecting Susceptibility to Intergranular Attack in Austenitic Stainless Steels) and by ASTM G 108 (Test Method for Electrochemical Reactivation (EPR) for Detecting Sensitization of AISI Type 304 and 304L Stainless Steels). The former method involves electrolytic etching in oxalic acid, while the latter is an electrochemical reactivation test that measures the charge associated with corrosion of the chromium-depleted regions surrounding precipitated carbide particles. Wensley [135] performed sensitization tests using these standard procedures and also measured the rate of intergranular attack of stainless steel specimens in digester liquors. Continuous digester extraction liquors were found



to be an environment that produced severe intergranular attack of stainless steels that had been heat treated in the sensitization temperature range, even when the steels were of low carbon content.

Susceptibility of duplex stainless steels to formation of undesirable intermetallic phases is typically done using ASTM A 923 (Test Methods for Detecting Detrimental Intermetallic Phase in Wrought Duplex Austenitic/Ferritic Stainless Steels). The application of ASTM A 923 to testing of weldments is recommended in TAPPI TIP 0402-29 [196].

#### *Liquor Heater Corrosion*

Austenitic and duplex stainless steels, and nickel-base alloy tubes (both welded and seamless) have been used for digester liquor heater tubes. Stress corrosion and general thinning have been reported. Wensley [197] described methods for acceptance testing of tubing that included microstructural examination and testing of ring samples in boiling magnesium chloride using a procedure similar to ASTM G 36 (Practice for Performing Stress-Corrosion Cracking Tests in a Boiling Magnesium Chloride Solution).

#### *Brownstock and Black Liquor System Corrosion*

Corrosion in brownstock and post-oxygen washers has been investigated by Bennett and Magar [198] using electrochemical procedures. Their results showed that corrosion is affected by pH, chloride concentration, temperature, and aeration. These tests were complemented with instantaneous corrosion rate measurements by linear polarization resistance methods and by weight loss tests.

Corrosion in white liquor has been studied extensively, but there is little information available on black liquor, aside from some work by Mueller [172], Wensley [124], and Singh [139,140]. Mass loss tests in synthetic liquors containing inorganic and organic constituents of black liquors have been done at the University of Virginia [199].

Pepper and Voruganti [200] used ASTM C 581 (Practice for Determining Chemical Resistance of Thermosetting Resins Used in Glass-Fiber-Reinforced Structures Intended for Liquid Service) to investigate several FRP composites for use in brownstock washing environments.

#### *Sulfite Pulping Corrosion*

Sulfite pulping is a process that uses mildly acidic sulfite solutions instead of the very alkaline solutions used in kraft pulping. Murarka et al. [201] published results of corrosion tests in acidic condensates in vapor phase sulfite pulping using a batch type laboratory reactor in which acid was condensed and collected. He devised a means to prevent corrosion due to the acid condensation.

## MECHANICAL PULPING

Mechanically processed pulps are produced by wet grinding wood chips at high temperatures or with chemical additions to enhance the breakup of the wood. Originally, mechanical pulping processes involved the grinding of whole logs against rotating grindstones. Today, most mechanical pulping takes place inside pressurized refiners where wood chips are passed between counter-rotating discs faced with

wear-resistant refiner plates. Refiner plates are made from white cast iron (or hardened steels) or from stainless alloys. Steaming vessels used for mechanical pulping processes may have to be constructed from nickel-base alloys to avoid SCC beneath the deposits and general corrosion due to acidic condensate formation.

## Environments

Mechanical pulping aqueous environments are similar to paper machine white waters. In chemi-thermo mechanical pulping, however, the addition of sulfur ions can increase corrosivity. Pressurized presteaming of wood chips from seaborne logs can result in environments conducive to chloride SCC and also to the evolution of wood acids that can cause corrosion in the vapor phase. Wear is a more significant problem than corrosion in mechanical pulping environments.

## Corrosion Testing

Corrosion in mechanical pulping processes was investigated by Crowe [202] via weight loss tests and potentiodynamic polarization tests. Vapor phase condensate corrosion was more severe than liquid phase corrosion.

#### *Refiner Plate Corrosion and Wear Testing*

The corrosion and wear of refiner plates was studied by Rideout et al. [203] via potentiostatic and potentiodynamic anodic polarization measurements conducted similar to ASTM G 5. An experimental test cell that sealed against the surface of a refiner plate was developed, since coupons were difficult to cut from the hard plates. Thompson and Garner studied wear of refiner plate alloys [204,205] with a device that simulated abrasion under corrosive conditions. The alloy specimens were placed in the wall of a circular test chamber with an impeller at the center of the chamber. Wasikowski [206] evaluated wear with a pin-on-disc type machine, as well as cavitation erosion testing using a vibrating horn device according to ASTM G 32, Test Method for Cavitation Erosion Using Vibratory Apparatus. Thompson [207] used the vibrating horn method to test refiner materials. Reid and Lawn [208] have described inspection techniques for refiner discs. Thompson [209] developed a "clashing wear tester" for studying the wear of refiner plates in the laboratory.

## THE RECOVERY BOILER

Spent pulping chemicals are reduced and recovered in a molten salt (smelt) by combustion in the recovery boiler. The primary fuel is black liquor containing the lignin and myriad other combustible organic compounds, together with the inorganic chemicals from the pulping liquor. The black liquor is concentrated to  $\geq 65\%$  solids by evaporation before being burned in the recovery boiler. Steam generated by the recovery boiler is used for other process applications, including chemical and mechanical pulping, bleach plant mixers, and paper machine dryers. The reduced molten inorganic salts, called smelt, are drained from the bottom of the

boiler into water in the dissolving tank, producing green liquor. TAPPI [210] has summarized recovery boiler operation including corrosion problems. Bruno [211] has also published a review of recovery boiler corrosion.

The boiler has a water-circulating tube wall (waterwall) construction. A layer of smelt freezes on the fireside of the wall due to cooling from the water in the tubes, and this frozen smelt provides a barrier between the tube and the reducing and/or oxidizing gases. Gas composition has been implicated as a major determinant of the corrosion rate on the fireside surfaces. The lower waterwall is the most critical component. Unlike conventional boilers, a waterwall tube leak cannot be tolerated in a recovery boiler, since a smelt-water reaction has the potential for a catastrophic explosion.

As production demands have led to increasingly higher operating temperatures and pressures, protection of carbon steel waterwall tubes has involved studding, application of weld overlay or thermal spray, or the use of composite (stainless-clad carbon steel) or chromized (diffusion-coated carbon steel) tubes to provide resistance to sulfidation and oxidation on the fireside.

The upper furnace is also subject to corrosion in the superheater, the generating section, the economizer, and the precipitator.

## Environments

There are many different high temperature environments in a recovery boiler [210]. On the fireside of the boiler there is the molten smelt and the char bed in the bottom of the boiler. There is an oxidizing environment in the lower furnace where air is injected at up to four elevations for the combustion of the heavy black liquor that is sprayed into the boiler. Waterwall tubes are normally subjected to sulfidation. The use of composite tubes in the lower waterwalls has been successful in resisting sulfidation. The lower waterwall tubes may also have liquor running down them. At primary and secondary air ports, there are local environments that promote preferential corrosion and cracking of composite tubes.

At higher elevations, there is fume and carry-over with the flue gases that cause deposits to form on the superheater, generating bank, and economizer tubes. Deposits may be molten depending on the concentrations of chloride and potassium. Superheater temperatures are usually between 300°C at the steam inlet and 500°C at the outlet. Although there are a variety of materials used in superheaters, ranging from chromium-molybdenum steels to stainless steels and nickel-base alloys, changing materials offers little improvement when superheater deposits are molten.

## Corrosion Testing

Corrosion testing for recovery boilers has involved both laboratory tests in simulated smelt-gas environments and the use of probes inserted directly into recovery boilers.

### *Waterwall Tube Laboratory Testing*

Early research on recovery boiler corrosion conducted in Sweden and Finland was summarized by Moberg [212]. This work involved a field study and some laboratory

investigations in the gas phase and in smelt in a hot gas atmosphere. The effects of alloying elements, temperature, gas composition, and surface treatments were studied. The gas phase testing was completed by thermogravimetric procedures. Tests in synthetic smelt involved periodic dipping of the specimen in the molten phase, followed by exposure to the gas. Field tests were conducted via installation of tube specimens from various materials used in the lower furnace.

Other laboratory smelt tests [213,214] have included placing metal samples into ceramic boats, covering them with salts, and then exposing them in hot gas.

Recovery boiler corrosion fireside testing has been the subject of an extensive research project by the American Forest and Paper Association. Singbeil and Garner [215] published an extensive review of test methods from these studies. The American Forest Products and Paper Association support has produced a standard laboratory test at the Pulp and Paper Research Institute of Canada for the investigation of lower furnace corrosion [216–218] based on sulfidation processes that allow a clearer definition of complex variables.

The Institute of Paper Science and Technology has investigated the corrosion of waterwall materials through laboratory tests in furnaces having a controlled atmosphere, isothermal testing, “single spike” testing, and “double spike” testing [219–222]. The “spikes” were temperature excursions—for example, from a 320°C baseline temperature to 30 min at a maximum temperature of 480°C.

### *Air Port Composite Tube Corrosion*

Local wastage of the stainless steel cladding from composite tubes at ports in the waterwall (particularly primary and secondary air ports) has been attributed to hydroxide condensation [223,224]. The localized corrosion of stainless steel cladding from composite tubes at air ports of recovery boilers has been shown by deposit analysis to be a cyclical mechanism. Laboratory tests in molten salt supported the theory that this corrosion is caused by molten NaOH [225].

Other laboratory tests have confirmed that Type 304L stainless steel is rapidly corroded by molten hydroxide mixtures and that Alloys 600, 625, and 825 have resisted such corrosion [226]. Colwell [227] conducted mass loss experiments in molten NaOH at 320°F and demonstrated that Type 304L stainless steel corrodes more rapidly than carbon steel.

Tran et al. studied the kinetics of carbonation of molten alkali hydroxides [228], the air flow pattern [229], and the corrosion of Type 304L stainless steel by molten hydroxides at air port openings [230]. The presence of oxygen was found to make the corrosion inevitable in the presence of molten hydroxides. Electrochemical testing showed that a galvanic cell is set up between carbon steel and stainless steel with the latter protecting the former.

Falat [231] evaluated alternative primary air port materials in situ and also measured air port temperatures using thermocouples. He came to the conclusion that the corrosion of the stainless steel composite tube cladding could be better explained if the corrodent was molten smelt. Oxidation of molten smelt could produce the thermal spikes that he observed.

Estes et al. [232] used electrodes to study the basicity of molten salt mixtures and performed weight loss tests that

demonstrated that the chromium oxide film that forms on chromium metal can experience very rapid mass loss in molten hydroxides.

### *Composite Tube Corrosion and Cracking*

Many reports of corrosion and cracking in the floor composite tubes in recovery boilers were published in the 1990s [233]. Some cracking was branched like SCC and some cracking was straight, resembling fatigue. This led to several investigations of floor tube corrosion and cracking. Mäkipää [234–236] studied the corrosion of boiler tube materials in experimental melts containing polysulfides. His tests suggested that high nickel composite tube alloys had superior resistance to corrosion. Backman et al. [237] sampled smelts from recovery boiler floors and found that sulfur, chlorine, and potassium were enriched in the bottom layer near the floor. They prepared mixtures of salts and measured their conductivity. Molten deposits could exist at temperatures as low as 320°C when the mixture contained polysulfide.

Swindeman et al. [238] performed isothermal fatigue tests at 600°C on simulated Type 304L stainless steel cladding, using techniques conforming to ASTM E 606. They concluded that the cracking observed in the floor tubes was not due to thermal fatigue alone. Prescott and Singbeil [238] performed SCC testing using U-bends made in accordance with ASTM G 30 and found that SCC can occur in hydrated solutions of sodium sulfide that resemble those that exist during water washing. Tran et al. [240,241] did further investigations into the drying behavior of waterwash solutions by measuring electrical conductivity in a cell that could be heated at a controlled rate. They found that smelt solutions could not be dried out easily at temperatures below 180°C. Hanninen [242] investigated thermal fatigue using a fatigue testing device based on high frequency induction heating that cycled in the range between 300°C and 700°C. He also investigated SCC using U-bends. Hanninen's work suggested SCC was the mechanism of floor tube cracking.

Keiser et al. have reported on the cracking of floor composite tubes [243–247]. They examined samples of cracked floor tubes that had been removed from recovery boilers, measured residual stresses in tubes, and monitored temperature fluctuations using thermocouples. Svensson et al. [248] developed a probe for monitoring resistivity, temperature, and linear polarization resistance in recovery boiler floors.

### *Primary Air Port Composite Tube Corrosion and Cracking*

Closer inspection of recovery boilers that detected cracking of floor composite tubes also led to the discovery of cracking in primary air port composite tubes [249,250]. Some of the primary air port cracking had a branched appearance characteristic of SCC, and some of the cracking was straight, resembling fatigue. Keiser et al. [251] characterized the environments at primary air port openings and found that the cracking occurred in those openings where the temperature was above approximately 350°C and where the temperature fluctuated rapidly.

### *Superheater, Generating Bank, and Economizer Corrosion*

Field tests have been conducted using air-cooled probes fitted with samples of materials [213,252]. Tran et al. [253] used air-cooled probes to collect deposits from the fireside in the superheater and generating section, and then performed lab studies of sodium bisulfate ( $\text{NaHSO}_4$ ) corrosion. Backman et al. [254] used air-cooled probes to obtain samples of superheater deposits for electron microscopy and chemical analysis. Other probes with detachable steel ring samples were used to measure corrosion rates.

Laboratory studies of superheater, generating bank, and economizer corrosion have involved investigations of acidic sulfate deposits. Tran et al. [255–258] performed corrosion tests in a quartz tube furnace having a controlled atmosphere. Klower and White [259] used a chamber furnace to study the corrosion of stainless steels and nickel-base superheater tube alloys in synthetic molten salts. These specimens were repeatedly dip-coated with liquid salt to simulate the periodic formations of molten deposits on superheater tubes. Mäkipää et al. [260,261] studied the scaling of longitudinal tube samples in oxidizing and neutral gas laboratory environments and with air-cooled probes in recovery boilers. The scales were studied using high-temperature contact electric resistance and thermogravimetric analysis. Backman et al. [262] also studied the corrosion of superheater materials in different salt mixtures using a furnace with controlled atmosphere.

### *Near Mud Drum Corrosion*

Generating bank tubes have experienced corrosion adjacent to the mud drum in some recovery boilers. Thompson et al. [263] reported field and laboratory results. First, an in situ conductivity probe was used to determine when corrosive salts formed in the boiler at the mud drum/tube area. Then, erosion testing in the laboratory indicated that removal rates were insufficient to account for the tube wastage. Guzi [264] described an automated ultrasonic inspection procedure for use during boiler outages to detect near mud drum corrosion of generating tubes.

### *Electrostatic Precipitator Corrosion*

Corrosion of the electrostatic precipitator that is used to remove the dust from flue gases that exit the boiler, has been a problem as design and operating techniques have evolved. An intensive research program by Thompson and Yeske [265] has overturned the widely accepted belief that acid condensation was causing the corrosion. In fact, water condensation was found to be the major cause. Flush mounted electrical resistance monitoring probes were used to measure instantaneous corrosion rates. A cooled conductivity probe was used for dewpoint measurement, and weld pad thermocouples were used for temperature measurement.

### *Fluidized Bed Boiler Corrosion*

Corrosion of superheater tubes in fluidized bed boilers is caused by low melting point deposits. Salmenoja et al. [266–268] and Orjala et al. [269] used air-cooled probes to investigate the corrosion of various materials and to sample the deposits.

## DISCUSSION

Corrosion testing in the pulp and paper industry is based both on standards developed for other industries and on methodologies developed by individual researchers in the pulp and paper industry. Relatively few corrosion test standards have been developed for the pulp and paper industry. Corrosion testing has been most often performed either to investigate the performance of alternative materials in existing processes or to assess the effects of process modifications on existing materials of construction. As new processes create new problems, new test procedures will continue to be devised.

Corrosion test methods that are developed must be practical and provide useful results that are understandable to mill personnel. These methods should be embodied in standards to permit comparison of results by different investigators—allowing, for example, the evaluation of the performance of various suppliers' products.

There is a need to focus on chemical analysis of process environments, deposits, and metals in conjunction with the corrosion studies to better describe root cause mechanisms. Corrosion testing prior to equipment purchases will aid in the selection of appropriate materials and educate process engineers about the effects that their decisions have on long-term equipment performance.

The capability for on-line corrosion monitoring of equipment would certainly aid in correlating process changes or upsets with episodes of corrosion of equipment. This would ensure maximum equipment life when process modifications are anticipated that could have negative effects on corrosion resistance.

## REFERENCES

- [1] ASM Handbook, Vol. 13, 9th ed., ASM, Metals Park, OH, 1987.
- [2] Clarke, S. and Singbeil, D., *Proceedings of the 7th International Symposium on Corrosion in the Pulp and Paper Industry*, TAPPI, Atlanta, GA, 1992, pp. 11–22.
- [3] Ulmgren, P., *Proceedings of the 8th International Symposium on Corrosion in the Pulp and Paper Industry*, Swedish Corrosion Institute, Stockholm, 1995, pp. 223–232.
- [4] Clarke, P. H., Singbeil, D. L., and Thompson, C. R., *Proceedings of the 9th International Symposium on Corrosion in the Pulp and Paper Industry*, CPPA, Montreal, QC, 1998, pp. 131–138.
- [5] Yeske, R. and Garner, A., *Proceedings of the 7th International Symposium on Corrosion in the Pulp and Paper Industry*, TAPPI, Atlanta, GA, 1992, pp. 1–9.
- [6] *Stainless Steels and Specialty Alloys for Pulp and Paper Mills*, Tuthill, A. H., Ed., The Nickel Development Institute, Reference Book Series No. 11025, Toronto, Ontario.
- [7] Davies, R. D., *Appita*, Vol. 39, No. 6, 1986, pp. 472–476.
- [8] Wensley, D. A. and Moskal, M. D., *Paper Machine and Suction Roll Corrosion*, Chapter XXIII of *Pulp and Paper Manufacture*, Vol. 7, *Paper Machine Operation*, TAPPI Press, Atlanta, 1991, pp. 594–614.
- [9] Bowers, D. F., Paper 144, *Corrosion/86*, NACE, Houston, TX, 1986.
- [10] Bennett, D. C. and Federowicz, C. J., *Materials Performance*, Vol. 21, No. 4, 1982, pp. 39–43.
- [11] Davidson, R. M., Alfonsso, E., and Runnsjo, G., Paper 542, *Corrosion/90*, NACE, Houston, TX, 1990.
- [12] Qvarfort, R., *Corrosion Science*, Vol. 28, 1958, p. 135.
- [13] Wensley, D. A., *Materials Performance*, Vol. 28, No. 11, 1989, pp. 68–71.
- [14] Bowers, D. F., *TAPPI Journal*, Vol. 61, No. 3, 1978, pp. 57–61.
- [15] Castillo, A. P. and Caudill, D. L., Paper 374, *Corrosion/97*, NACE, Houston, TX, 1997.
- [16] Wensley, A., Dykstra, H., and Augustyn, A., *Proceedings of the 1997 TAPPI Engineering Conference*, TAPPI, Atlanta, GA, 1997, pp. 489–496.
- [17] Reid, D. C. and Wensley, D. A., *TAPPI Journal*, Vol. 72, No. 3, 1989, pp. 57–61.
- [18] Castillo, A. P. and Michel, G. M., *Proceedings of the 1991 TAPPI Engineering Conference*, TAPPI, Atlanta, GA, 1991, pp. 757–765.
- [19] Castillo, A. P., Michel, G. M., and Rogers, J. C., *TAPPI Journal*, Vol. 72, No. 6, 1989, pp. 193–197.
- [20] Sriram, R. and Tromans, D., "Pulp and Paper Research Institute of Canada Post-Graduate Research Laboratory Report PGRL 423," February 1989.
- [21] Yoshitake, A., Sakashita, M., Amako, S., et al., *Proceedings of the TAPPI Engineering Conference*, TAPPI, Atlanta, GA, 1991, pp. 767–773.
- [22] Newman, R. C., Sieradzki, K., and Isaacs, H. S., *Metallurgical Transactions A*, Vol. 13A, 1982, pp. 2015–2026.
- [23] Garner, A. and Newman, R. C., Paper 186, *Corrosion/91*, NACE, Houston, TX, 1991.
- [24] Newman, R. C., Wong, W. P., Ezuber, H., and Garner, A., Paper 202, *Corrosion/87*, NACE, Houston, TX, 1987.
- [25] Varjonen, O., Carpen, L., and Ehrnsten, U., *Proceedings of the 8th International Symposium on Corrosion in the Pulp and Paper Industry*, Swedish Corrosion Institute, Stockholm, 1995, pp. 254–262.
- [26] Salonen, T., Saario, T., and Likonen, J., Paper 426, *Corrosion/94*, NACE, Houston, TX, 1992.
- [27] Laitinen, T., Likonen, J., and Heinonen, M., *Proceedings of the 8th International Symposium on Corrosion in the Pulp and Paper Industry*, Swedish Corrosion Institute, Stockholm, 1995, pp. 271–283.
- [28] Bowers, D. F., *TAPPI Journal*, Vol. 69, No. 1, 1986, pp. 62–66.
- [29] Varjonen, O. A., Hakkarainen, T. J., and Marmo, S. A., Paper 190, *Corrosion/91*, NACE, Houston, TX, 1991.
- [30] Carpen, L., et al., Paper 01245, *Corrosion 2001*, NACE, Houston, TX, 2001.
- [31] *A Practical Manual on Microbiologically Influenced Corrosion*, G. Kobrin, Ed., NACE, Houston, TX, 1993.
- [32] Magar, I. J., *TAPPI Journal*, Vol. 75, No. 3, 1992, pp. 167–171.
- [33] DeBerry, D. W. and Ellis, P. F., Paper 346, *Corrosion/88*, NACE, Houston, TX, 1988.
- [34] Danielsson, E., Johansson, R., and Liljas, M., *Proceedings of the 6th International Symposium on Corrosion in the Pulp and Paper Industry*, NACE, Houston, TX, 1989.
- [35] TAPPI TIP 0402-09, Rotating Bar Bending Fatigue Testing in a Corrosive Environment, TAPPI, Atlanta, GA, 1984.
- [36] Jaske, C. E. and Castillo, A. P., *Materials Performance*, Vol. 26, No. 4, 1987, pp. 37–43.
- [37] Glogowski, P. E. and Castillo, A. P., *TAPPI Journal*, Vol. 71, No. 6, 1988, pp. 95–100.
- [38] TAPPI TIP 0402-08, Plate Bending Fatigue Testing in a Corrosive Environment, TAPPI, Atlanta, GA, 1984.
- [39] Kelley, C., Vestola, J., Sailas, V., and Pelloux, R., *TAPPI Journal*, Vol. 58, No. 11, 1975, pp. 80–85.
- [40] Yeske, R. A., *TAPPI Journal*, Vol. 71, No. 3, 1988, pp. 47–54.
- [41] Yeske, R. A., *Materials Performance*, Vol. 26, No. 10, 1987, pp. 30–38.
- [42] Yeske, R. A., Revall, M. A., and Thompson, C. M., *Proceedings of the 1993 TAPPI Engineering Conference*, TAPPI, Atlanta, GA, 1993, pp. 721–729.
- [43] Dorsch, T. J., Reid, C., and Hong, I., *Proceedings of the 1997 TAPPI Engineering Conference*, TAPPI, Atlanta, GA, 1997, pp. 803–817.

- [44] Magar, I. J., *Proceedings of the 7th International Symposium on Corrosion in the Pulp and Paper Industry*, TAPPI, Atlanta, GA, 1992, pp. 173–179.
- [45] Bennett, D. C. and Magar, I. J., *Proceedings of the 6th International Symposium on Corrosion in the Pulp and Paper Industry*, NACE, Houston, TX, 1989.
- [46] Rendahl, B., Igetoft, L., and Forsgren, A., *Proceedings of the 8th International Symposium on Corrosion in the Pulp and Paper Industry*, Swedish Corrosion Institute, Stockholm, 1995, pp. 5–13.
- [47] Bardsley, D. E., *Proceedings of the 8th International Symposium on Corrosion in the Pulp and Paper Industry*, Swedish Corrosion Institute, Stockholm, 1995, pp. 75–82.
- [48] *Corrosion Resistance of Alloys to Bleach Plant Environment*, A. H. Tuthill and J. D. Rushton, Eds., TAPPI, Atlanta, GA, 1980.
- [49] Rushton, J. D., *TAPPI Journal*, Vol. 65, No. 5, 1982, pp. 115–121.
- [50] Tuthill, A. H., *Materials Performance*, Vol. 24, No. 9, 1985, pp. 43–49.
- [51] Hill, J. B. and Tuthill, A. H., *Proceedings of the 4th International Symposium on Corrosion in the Pulp and Paper Industry*, NACE, Houston, TX, 1983, pp. 142–148.
- [52] Anderson, D. B., "Statistical Aspects of Crevice Corrosion in Sea Water," in *Galvanic and Pitting Corrosion—Field and Laboratory Studies*, ASTM STP 576, R. Baboian, et al., Eds., ASTM International, West Conshohocken, PA, 1976, pp. 231–242.
- [53] Garner, A., *Proceedings of the 1985 TAPPI Engineering Conference*, TAPPI, Atlanta, GA, 1985.
- [54] Tuthill, A. H. and Garner, A., *TAPPI Journal*, Vol. 73, No. 6, 1990, pp. 147–151.
- [55] Tuthill, A. and Garner, A., Paper 319, *Corrosion/92*, NACE, Houston, TX, 1992.
- [56] Beetham, M. P., *Proceedings of the 1986 TAPPI Engineering Conference*, TAPPI, Atlanta, GA, 1986, pp. 665–681.
- [57] Crowe, D. C. and Tuthill, A. H., *Proceedings of the 1990 TAPPI Engineering Conference*, TAPPI, Atlanta, GA, 1990, pp. 9–16.
- [58] Garner, A., *Pulp Paper Canada*, Vol. 86, No. 12, 1985, pp. 200–207.
- [59] Audouard, J. P., Desestret, A., and Catelin, D., *Proceedings of the 1985 TAPPI Engineering Conference*, TAPPI, Atlanta, GA, 1985, pp. 55–62.
- [60] Sharp, W. B. A. and Laliberte, L., Paper 16, *Corrosion/78*, NACE, Houston, TX, 1978.
- [61] Garner, A., *Pulp Paper Canada*, Vol. 82, No. 12, 1981, T414-T425.
- [62] Garner, A., *Corrosion*, Vol. 37, 1981, pp. 178–184.
- [63] Wallen, B., Liljas, M., and Stenvall, P., Paper 322, *Corrosion/92*, NACE, Houston, TX, 1992.
- [64] Audouard, J. P. and Charles, J., *Proceedings of the 1994 TAPPI Engineering Conference*, TAPPI, Atlanta, GA, 1994, pp. 153–159.
- [65] Wensley, D. A., Reid, D. C., and Dykstra, H., Paper 537, *Corrosion/90*, NACE, Houston, TX, 1990.
- [66] Wensley, D. A. and Reid, D. C., Paper 193, *Corrosion/91*, NACE, Houston, TX, 1991.
- [67] Wensley, D. A., Reid, D. C., Brown, D. J., and Christie, D. W., *Proceedings of the 1991 TAPPI Engineering Conference*, TAPPI, Atlanta, GA, 1991, pp. 499–509.
- [68] Wensley, D. A. and Reid, D. C., Paper 433, *Corrosion/93*, NACE, Houston, TX, 1993.
- [69] Nadezhdin, A., et al., Paper 320, *Corrosion/92*, NACE, Houston, TX, 1992.
- [70] Tuthill, A. H. and Bardsley, D. E., Paper 323, *Corrosion/92*, NACE, Houston, TX, 1992.
- [71] Agarwal, D. C. and White, F., Paper 324, *Corrosion/92*, NACE, Houston, TX, 1992.
- [72] Nadezhdin, A. and Timbers, G., Paper 432, *Corrosion/93*, NACE, Houston, TX, 1992.
- [73] Nordstrom, J. and Bergquist, A., *Proceedings of the 1994 TAPPI Engineering Conference*, TAPPI, Atlanta, GA, 1994, pp. 21–29.
- [74] Bardsley, D. E., *Proceedings of the 8th International Symposium on Corrosion in the Pulp and Paper Industry*, Swedish Corrosion Institute, Stockholm, 1995, pp. 75–82.
- [75] Troslius, L. and Andreasson, P., *Proceedings of the 9th International Symposium on Corrosion in the Pulp and Paper Industry*, Ottawa, 1998, pp. 103–109.
- [76] Back, G. and Singh, P. M., *Proceedings of the 10th International Symposium on Corrosion in the Pulp and Paper Industry*, Technical Research Center of Finland, Helsinki, 2001, pp. 301–322.
- [77] Pohjanne, P. and Siltala, M., *Proceedings of the 1999 TAPPI Engineering Conference*, TAPPI, Atlanta, GA, 1999, pp. 1303–1314.
- [78] Korvela, T., Paper 422, *Corrosion/94*, NACE, Houston, TX, 1994.
- [79] Wyllie, W. E., Brown, B. E., and Duquette, D. J., Paper 421, *Corrosion/94*, NACE, Houston, TX, 1994.
- [80] Varjonen, O. A. and Hakkarainen, T., Paper 421, *Corrosion/94*, NACE, Houston, TX, 1994.
- [81] Schutz, R. W., Xiao, M., and Korvela, T., Paper 427, *Corrosion/94*, NACE, Houston, TX, 1994.
- [82] Andreasson, P., *Proceedings of the 8th International Symposium on Corrosion in the Pulp and Paper Industry*, Swedish Corrosion Institute, Stockholm, 1995, pp. 119–126.
- [83] Christie, D. W., *Proceedings of the NACE Canadian Western Regional Conference*, 24–27 February 1992, Edmonton, Alberta.
- [84] Christie, D. W., *Proceedings of the 7th International Symposium on Corrosion in the Pulp and Paper Industry*, TAPPI, Atlanta, GA, 1992, pp. 87–95.
- [85] Bennett, D. C., *Corrosion*, Vol. 40, No. 1, 1984, pp. 1–5.
- [86] Arlt, N., et al., Paper 434, *Corrosion/93*, NACE, Houston, TX, 1993.
- [87] Arlt, N., Paper 577, *Corrosion/95*, NACE, Houston, TX, 1995.
- [88] Wallen, B., et al., *Proceedings of the 8th International Symposium on Corrosion in the Pulp and Paper Industry*, Swedish Corrosion Institute, Stockholm, 1995, pp. 65–74.
- [89] Hakkarainen, T., *Proceedings of the 9th International Symposium on Corrosion in the Pulp and Paper Industry*, Ottawa, 1998, pp. 97–101.
- [90] Pulkkinen, E., et al., *Proceedings of the 1999 TAPPI Engineering Conference*, TAPPI, Atlanta, GA, 1999, pp. 1293–1301.
- [91] Hakkarainen, T. J., *Proceedings of the 1999 TAPPI Engineering Conference*, TAPPI, Atlanta, GA, 1999, pp. 1351–1363.
- [92] Hakkarainen, T. J., Paper 00588, *Corrosion 2000*, NACE, Houston, TX, 2000.
- [93] Betova, I., et al., *Proceedings of the 10th International Symposium on Corrosion in the Pulp and Paper Industry*, Technical Research Center of Finland, Helsinki, 2001, pp. 323–335.
- [94] Clarke, S. and Risk, M., *Proceedings of the 1995 TAPPI Engineering Conference*, TAPPI, Atlanta, GA, 1995, pp. 559–563.
- [95] Klarin, A. and Pehkonen, A., *Proceedings of the 8th International Symposium on Corrosion in the Pulp and Paper Industry*, Swedish Corrosion Institute, Stockholm, 1995, pp. 96–103.
- [96] Pohjanne, P., Paper 376, *Corrosion/97*, NACE, Houston, TX, 1997.
- [97] Salo, T., et al., *Proceedings of the 9th International Symposium on Corrosion in the Pulp and Paper Industry*, Ottawa, 1998, pp. 125–130.
- [98] Reichert, D. L., Paper 467, *Corrosion/96*, NACE, Houston, TX, 1996.
- [99] Been, J. and Tromans, D., *Proceedings of the 9th International Symposium on Corrosion in the Pulp and Paper Industry*, Ottawa, 1998, pp. 111–117.
- [100] Clarke, S. J. and Clarke, P. H., *Proceedings of the 9th International Symposium on Corrosion in the Pulp and Paper Industry*, Ottawa, 1998, pp. 119–123.
- [101] Robinson, J. M., Stiles, C. O., and Hutchison, M., *TAPPI Journal*, Vol. 50, No. 5, 1967, pp. 91A–93A.
- [102] *Pulp Paper Canada*, Vol. 82, No. 1, 1981, pp. 16–19.
- [103] Laliberte, L. H. and Garner, A., *TAPPI Journal*, Vol. 64, No. 1, 1981, pp. 47–51.
- [104] Garner, A., *Materials Performance*, Vol. 21, No. 5, 1982, pp. 43–46.
- [105] Laliberte, L. H., *Proceedings of the 4th International Symposium on Corrosion in the Pulp and Paper Industry*, NACE, Houston, TX, 1983, pp. 157–159.

- [106] Linder, B., *Proceedings of the 4th International Symposium on Corrosion in the Pulp and Paper Industry*, NACE, Houston, TX, 1983, pp. 166–173.
- [107] Cowley, T. W. and Robertson, M. A., *Materials Performance*, Vol. 30, No. 7, 1991, pp. 46–49.
- [108] Bishop, T. N. and Cowley, T. W., *Proceedings of the 1992 TAPPI Engineering Conference*, TAPPI, Atlanta, GA, 1992, pp. 197–203.
- [109] Bishop, T. and Cowley, T. W., Paper 423, *Corrosion/94*, NACE, Houston, TX, 1994.
- [110] Thompson, M. and Cowley, T. W., *Proceedings of the 1995 TAPPI Engineering Conference*, TAPPI, Atlanta, GA, 1995, pp. 595–606.
- [111] Bishop, T. and Cowley, T. W., *Proceedings of the 9th International Symposium on Corrosion in the Pulp and Paper Industry*, Ottawa, 1998, pp. 83–95.
- [112] Bergman, G., *Proceedings of the 6th International Symposium on Corrosion in the Pulp and Paper Industry*, NACE, Houston, TX, 1989, pp. 386–400.
- [113] Bergman, G., *Proceedings of the 7th International Symposium on Corrosion in the Pulp and Paper Industry*, NACE, Houston, TX, 1992, pp. 131–135.
- [114] Petersson, K. and Bergman, G., *Proceedings of the 8th International Symposium on Corrosion in the Pulp and Paper Industry*, Swedish Corrosion Institute, Stockholm, 1995, pp. 104–118.
- [115] Wensley, A., Paper 00589, *Corrosion 2000*, NACE, Houston, TX, 2000.
- [116] Wensley, A., Paper 01423, *Corrosion 2001*, NACE, Houston, TX, 2001.
- [117] Wensley, A., *Proceedings of the 10th International Symposium on Corrosion in the Pulp and Paper Industry*, Technical Research Center of Finland, Helsinki, 2001, pp. 379–398.
- [118] Wensley, D. A., *Proceedings of the 6th International Symposium on Corrosion in the Pulp and Paper Industry*, NACE, Houston, TX, 1989, pp. 7–19.
- [119] Wensley, D. A., *TAPPI Journal*, Vol. 72, No. 8, 1989, pp. 211–215.
- [120] Wensley, D. A., *Proceedings of the 1993 TAPPI Engineering Conference*, TAPPI, Atlanta, GA, 1993, pp. 71–74.
- [121] Wensley, D. A. and Charlton, R. S., *Proceedings of the 3rd International Symposium on Corrosion in the Pulp and Paper Industry*, NACE, Houston, TX, 1980, pp. 20–29.
- [122] Wensley, D. A., *Proceedings of the 5th International Symposium on Corrosion in the Pulp and Paper Industry*, CPPA, Montreal, 1986, pp. 15–22.
- [123] Strom, S., *Proceedings of the 7th International Symposium on Corrosion in the Pulp and Paper Industry*, TAPPI, Atlanta, GA, 1992, pp. 105–109.
- [124] Wensley, A. and Champagne, P., Paper 281, *Corrosion/99*, NACE, Houston, TX, 1999.
- [125] Clarke, S. J. and Stead, N. J., Paper 282, *Corrosion/99*, NACE, Houston, TX, 1999.
- [126] Al-Hassan, S., et al., Paper 00594, *Corrosion 2000*, NACE, Houston, TX, 2000.
- [127] Klarin, A. and Kottila, M., *Proceedings of the 1996 TAPPI Engineering Conference*, TAPPI, Atlanta, GA, 1996, pp. 299–306.
- [128] Klarin, A., *Proceedings of the 10th International Symposium on Corrosion in the Pulp and Paper Industry*, Technical Research Center of Finland, Helsinki, 2001, pp. 469–483.
- [129] Kottila, M. and Rauscher, J. W., *Proceedings of the 10th International Symposium on Corrosion in the Pulp and Paper Industry*, Technical Research Center of Finland, Helsinki, 2001, pp. 485–495.
- [130] Andreasson, P., *Proceedings of the 10th International Symposium on Corrosion in the Pulp and Paper Industry*, Technical Research Center of Finland, Helsinki, 2001, pp. 497–508.
- [131] Thompson, C. B., Thomson, J. M., and Ko, P. L., *Proceedings of the 1993 TAPPI Engineering Conference*, TAPPI, Atlanta, GA, 1993, pp. 711–720.
- [132] Nadezhdin, A. and Cardin, B., *Proceedings of the 10th International Symposium on Corrosion in the Pulp and Paper Industry*, Technical Research Center of Finland, Helsinki, 2001, pp. 399–407.
- [133] Kannan, S. and Kelly, R., Paper 578, *Corrosion/95*, NACE, Houston, TX, 1995.
- [134] Troselius, L., *Proceedings of the 8th International Symposium on Corrosion in the Pulp and Paper Industry*, Swedish Corrosion Institute, Stockholm, 1995, pp. 46–57.
- [135] Wensley, A., Paper 465, *Corrosion/96*, NACE, Houston, TX, 1996.
- [136] Nadezhdin, A., Therrien, P., and McDonald, R., *Proceedings of the 1996 TAPPI Engineering Conference*, TAPPI, Atlanta, GA, 1996, pp. 275–290.
- [137] Nadezhdin, A. and McDonald, R., *Proceedings of the 9th International Symposium on Corrosion in the Pulp and Paper Industry*, Ottawa, 1998, pp. 39–53.
- [138] Clarke, S. J., Paper 01418, *Corrosion 2001*, NACE, Houston, TX, 2001.
- [139] Anaya, A. and Singh, P. M., Paper 01422, *Corrosion 2001*, NACE, Houston, TX, 2001.
- [140] Singh, P. M., et al., *Proceedings of the 10th International Symposium on Corrosion in the Pulp and Paper Industry*, Technical Research Center of Finland, Helsinki, 2001, pp. 409–425.
- [141] Troselius, L., *Proceedings of the 10th International Symposium on Corrosion in the Pulp and Paper Industry*, Technical Research Center of Finland, Helsinki, 2001, pp. 455–467.
- [142] Ramo, J., et al., *Proceedings of the 10th International Symposium on Corrosion in the Pulp and Paper Industry*, Technical Research Center of Finland, Helsinki, 2001, pp. 441–453.
- [143] Ruus, L. and Stockman, L., *Svensk Papperstid.*, Vol. 56, No. 22, 1953, pp. 857–865.
- [144] Mueller, W. A., *Canadian Journal of Technology*, Vol. 34, 1956, pp. 162–181.
- [145] Mueller, W. A., *TAPPI Journal*, Vol. 40, No. 3, 1957, pp. 129–140.
- [146] Roald, B., *Norsk Skogind.*, Vol. 10, No. 8, 1957, pp. 285–289.
- [147] Landmark, P. and Roald, B., *Norsk Skogind.*, Vol. 15, No. 8, 1961, pp. 342–347.
- [148] Wensley, D. A. and Charlton, R. S., *Corrosion*, Vol. 36, 1980, pp. 385–389.
- [149] Crowe, D. C. and Yeske, R. A., Paper 435, *Corrosion/88*, NACE, Houston, TX, 1988.
- [150] Uusitalo, E., *Suomen Kemistehti*, Vol. 31B, 1958, pp. 367–371.
- [151] Tromans, D., *Journal of the Electrochemical Society*, Vol. 127, 1980, pp. 1253–1256.
- [152] Honda, M., Tamada, K. K., and Kobayashi, Y., Paper 191, *Corrosion/91*, NACE, Houston, TX, 1991.
- [153] Clarke, S. and Singbeil, D., Paper 375, *Corrosion/97*, NACE, Houston, TX, 1997.
- [154] Yeske, R. A., Paper 245, *Corrosion/84*, NACE, Houston, TX, 1984.
- [155] Crowe, D. C. and Yeske, R. A., *Materials Performance*, Vol. 25, No. 6, 1986, pp. 18–26.
- [156] Crowe, D. C., *Proceedings of the 1995 TAPPI Engineering Conference*, TAPPI, Atlanta, GA, 1995, pp. 203–208.
- [157] Leinonen, H. and Lassila, P., *Proceedings of the 10th International Symposium on Corrosion in the Pulp and Paper Industry*, Technical Research Center of Finland, Helsinki, 2001, pp. 427–439.
- [158] Audouard, J. P., Desestret, A., Vallier, J., et al., *Proceedings of the 3rd International Symposium on Corrosion in the Pulp and Paper Industry*, NACE, Houston, TX, 1980, pp. 30–39.
- [159] Audouard, J. P., *Proceedings of the 4th International Symposium on Corrosion in the Pulp and Paper Industry*, Swedish Corrosion Institute, Stockholm, 1993, pp. 43–47.
- [160] Dupoirion, F., et al., Paper 420, *Corrosion/94*, NACE, Houston, TX, 1994.
- [161] Leinonen, H., Paper 00590, *Corrosion 2000*, NACE, Houston, TX, 2000.

- [162] Kiessling, L., *Proceedings of the 8th International Symposium on Corrosion in the Pulp and Paper Industry*, Swedish Corrosion Institute, Stockholm, 1995, pp. 12–19.
- [163] Pawel, S. J., et al., *Proceedings of the 10th International Symposium on Corrosion in the Pulp and Paper Industry*, Technical Research Center of Finland, Helsinki, 2001, pp. 227–242.
- [164] Crowe, D. C. and Tromans, D., *Corrosion*, Vol. 44, 1988, pp. 142–148.
- [165] Crowe, D. C. and Tromans, D., *Proceedings of the 5th International Symposium on Corrosion in the Pulp and Paper Industry*, CPPA, Montreal, 1986, pp. 159–167.
- [166] Wensley, A., *Proceedings of the 8th International Symposium on Corrosion in the Pulp and Paper Industry*, Swedish Corrosion Institute, Stockholm, 1995, pp. 26–37.
- [167] Wensley, A., *Proceedings of the 1996 TAPPI Engineering Conference*, TAPPI, Atlanta, GA, 1996, pp. 291–298.
- [168] Wensley, A., Moskal, M., and Wilton, W., Paper 378, *Corrosion/97*, NACE, Houston, TX, 1997.
- [169] Wensley, A. and Dykstra, H., *Proceedings of the 1997 TAPPI Engineering Conference*, TAPPI, Atlanta, GA, 1997, pp. 1527–1536.
- [170] Wensley, A., *Proceedings of the 9th International Symposium on Corrosion in the Pulp and Paper Industry*, Ottawa, 1998, pp. 27–37.
- [171] Wensley, A., *Electronic Proceedings of the 2001 TAPPI Engineering Conference*, TAPPI, Atlanta, GA, 2001.
- [172] Mueller, W. A., *TAPPI Journal*, Vol. 42, No. 3, 1959, pp. 179–184.
- [173] Banks, W. P., Hutchison, M., and Hurd, R. M., *TAPPI Journal*, Vol. 50, No. 2, 1967, pp. 49–55.
- [174] Bennett, D. C., *Proceedings of the 3rd International Symposium on Corrosion in the Pulp and Paper Industry*, NACE, Houston, TX, 1980, pp. 323–329.
- [175] Singbeil, D., *Proceedings of the 6th International Symposium on Corrosion in the Pulp and Paper Industry*, NACE, Houston, TX, 1989, pp. 109–116.
- [176] Pullianen, M. and Savisalo, H., *Proceedings of the 6th International Symposium on Corrosion in the Pulp and Paper Industry*, NACE, Houston, TX, 1989.
- [177] Kiessling, L., *Proceedings of the 1989 TAPPI Engineering Conference*, TAPPI, Atlanta, GA, 1989, pp. 659–666.
- [178] Yeske, R. A., Hill, E., and Mindt, S., *Proceedings of the 5th International Symposium on Corrosion in the Pulp and Paper Industry*, CPPA, Montreal, 1986, pp. 219–225.
- [179] Munro, J. L., *Proceedings of the 7th International Symposium on Corrosion in the Pulp and Paper Industry*, TAPPI, Atlanta, GA, 1992, pp. 117–130.
- [180] Boulton, L. H., Wallace, G., Barry, B. J., et al., *Proceedings of the 6th International Symposium on Corrosion in the Pulp and Paper Industry*, NACE, Houston, TX, 1989, pp. 67–83.
- [181] Chakrapani, D. G., *Proceedings of the 6th International Symposium on Corrosion in the Pulp and Paper Industry*, NACE, Houston, TX, 1989, pp. 20–34.
- [182] Singbeil, D. and Tromans, D., *Proceedings of the 3rd International Symposium on Corrosion in the Pulp and Paper Industry*, NACE, Houston, TX, 1980, pp. 40–46.
- [183] Singbeil, D. and Tromans, D., *Journal of the Electrochemical Society*, Vol. 128, 1981, pp. 2065–2070.
- [184] Singbeil, D. and Tromans, D., *Journal of the Electrochemical Society*, Vol. 129, 1982, pp. 2669–2673.
- [185] Singbeil, D. and Garner, A., *First Semi-Annual Progress Report of the Research Program to Investigate Cracking of Continuous Digesters*, PPRIC, Pointe Claire, QC, July 1983.
- [186] Singbeil, D. and Garner, A., *Corrosion*, Vol. 41, No. 11, 1985, pp. 634–639.
- [187] Singbeil, D. and Garner, A., *Materials Performance*, Vol. 24, No. 10, 1983, pp. 9–15.
- [188] Yeske, R. A. and Guzi, C. E., *TAPPI Journal*, Vol. 69, No. 5, 1986, pp. 104–108.
- [189] Reid, D. C., Section Head, MacMillan Bloedel Research, Private communication with author, 1984.
- [190] Ostlund, S., Erhenfeldt, B., Sandberg, B., and Linder, M., *Proceedings of the 6th International Symposium on Corrosion in the Pulp and Paper Industry*, NACE, Houston, TX, 1989, pp. 48–59.
- [191] Thorpe, P. H., *Proceedings of the 6th International Symposium on Corrosion in the Pulp and Paper Industry*, NACE, Houston, TX, 1989, pp. 84–94.
- [192] Crowe, D. C., *Proceedings of the 6th International Symposium on Corrosion in the Pulp and Paper Industry*, NACE, Houston, TX, 1989, pp. 35–47.
- [193] Boulton, L. H. and Miller, N. A., *Appita*, Vol. 36, No. 2, 1982, pp. 126–129.
- [194] Singbeil, D. and Garner, A., *Materials Performance*, Vol. 27, No. 2, 1988, pp. 38–46.
- [195] Kivisäkk, U., *Proceedings of the 8th International Symposium on Corrosion in the Pulp and Paper Industry*, Swedish Corrosion Institute, Stockholm, 1995, pp. 38–45.
- [196] TAPPI TIP 0402-29, Qualification of Welding Procedures for Duplex Stainless Steels, TAPPI, Atlanta, GA, 2001.
- [197] Wensley, D. A., *Proceedings of the 1990 TAPPI Engineering Conference*, TAPPI, Atlanta, GA, 1990, pp. 219–230.
- [198] Bennett, D. C. and Magar, I. J., *Proceedings of the 7th International Symposium on Corrosion in the Pulp and Paper Industry*, TAPPI, Atlanta, GA, 1992, pp. 111–116.
- [199] Kannan, S., Bastek, D., and Kelly, R. G., Paper 289, *Corrosion/92*, NACE, Houston, TX, 1992.
- [200] Pepper, T. and Voruganti, V., *Proceedings of the 9th International Symposium on Corrosion in the Pulp and Paper Industry*, Ottawa, 1998, pp. 79–95.
- [201] Murarka, S. K. and Dwars, W. T. A., *Pulp Paper Canada*, Vol. 87, No. 6, 1986, pp. 127–131.
- [202] Crowe, D. C., Report 1, Project 3606, Institute of Paper Chemistry, Appleton, WI, August 1988.
- [203] Rideout, D. J., Hopkins, R. M., and Molgaard, J., *Pulp Paper Canada*, Vol. 83, No. 5, 1982, pp. 54–58.
- [204] Thompson, C. B. and Garner, A., *Proceedings of the 1985 TAPPI Engineering Conference*, TAPPI, Atlanta, GA, 1985, pp. 223–231.
- [205] Thompson, C. B. and Garner, A., *TAPPI Journal*, Vol. 71, No. 6, 1988, pp. 95–100.
- [206] Wasikowski, P. L., *Proceedings of the 1987 CPPA Annual Meeting*, 1987, pp. A189–A196.
- [207] Thompson, C. B., *Proceedings of the 1989 CPPA Annual Meeting*, 1989, pp. A125–A135.
- [208] Reid, C. and Lawn, S., *Pulp Paper Canada*, Vol. 93, No. 4, 1992, pp. 18–23.
- [209] Thompson, C. and Brown, K., *Proceedings of the 9th International Symposium on Corrosion in the Pulp and Paper Industry*, Ottawa, 1998, pp. 145–152.
- [210] Adams, T. N., Ed., “Kraft Recovery Boilers,” TAPPI, Atlanta, GA, 1997.
- [211] Bruno, F., *Proceedings of the 10th International Symposium on Corrosion in the Pulp and Paper Industry*, Technical Research Center of Finland, Helsinki, 2001, pp. 27–44.
- [212] Moberg, O., *Proceedings of the 1st International Symposium on Corrosion in the Pulp and Paper Industry*, NACE, Houston, TX, 1974, pp. 125–136.
- [213] Plumley, A. L., Lewis, E. C., and Tallent, R. G., *TAPPI Journal*, Vol. 49, No. 1, 1966, pp. 72A–81A.
- [214] Tallent, R. G. and Plumley, A. L., *TAPPI Journal*, Vol. 52, No. 10, 1969, pp. 1955–2959.
- [215] Singbeil, D. and Garner, A., *Proceedings of the 1988 TAPPI Engineering Conference*, TAPPI, Atlanta, GA, 1988, pp. 163–180.
- [216] Singbeil, D. and Thompson, R., *Proceedings of the 7th International Symposium on Corrosion in the Pulp and Paper Industry*, TAPPI, Atlanta, GA, 1992, pp. 325–330.



- [217] Singbeil, D. L. and Frederick, L., *Proceedings of the 1994 TAPPI Engineering Conference*, TAPPI, Atlanta, GA, 1994, pp. 463–513.
- [218] Singbeil, D. L., et al., *Proceedings of the 1996 TAPPI Engineering Conference*, TAPPI, Atlanta, GA, 1996, pp. 649–680.
- [219] Colwell, J. A. and Fonder, G. J., *Proceedings of the 8th International Symposium on Corrosion in the Pulp and Paper Industry*, Swedish Corrosion Institute, Stockholm, 1995, pp. 150–157.
- [220] Al-Hassan, S. J., Fonder, G. J., and Singh, P. M., *Proceedings of the 9th International Symposium on Corrosion in the Pulp and Paper Industry*, Ottawa, 1998, pp. 255–259.
- [221] Al-Hassan, S. J., Fonder, G. J., and Singh, P. M., Paper 280, *Corrosion/99*, NACE, Houston, TX, 1999.
- [222] Singh, P. M., Al-Hassan, S. J., Stalder, S., and Fonder, G., *Proceedings of the 1999 TAPPI Engineering Conference*, TAPPI, Atlanta, GA, 1999, pp. 1047–1060.
- [223] Wensley, D. A., *Proceedings of the 1986 Kraft Recovery Operations Seminar*, TAPPI, Atlanta, GA, 1986, pp. 231–245.
- [224] Wensley, D. A., *Materials Performance*, Vol. 26, No. 11, 1987, pp. 53–55.
- [225] Lunn, M. A., Sharp, W. B. A., Andrews, J. D., et al., *Proceedings of the 6th International Symposium on Corrosion in the Pulp and Paper Industry*, NACE, Houston, TX, 1989, pp. 151–162.
- [226] Paul, L. D., Barna, J. L., Danielson, M. J., and Harper, S. L., *Proceedings of the 1992 TAPPI Engineering Conference*, TAPPI, Atlanta, GA, 1992, pp. 321–330.
- [227] Colwell, J. A., *Proceedings of the 7th International Symposium on Corrosion in the Pulp and Paper Industry*, TAPPI, Atlanta, GA, 1992, pp. 231–241.
- [228] Tran, H., Mao, X., and Barham, D., *Proceedings of the 1992 TAPPI Engineering Conference*, TAPPI, Atlanta, GA, 1992, pp. 363–369.
- [229] Kuhn, D. C. S., Mao, T., and Tran, H. N., *Proceedings of the 1993 TAPPI Engineering Conference*, TAPPI, Atlanta, GA, 1993, pp. 215–222.
- [230] Tran, H. N., Katiforis, N. A., Utigard, T. A., and Barham, D., *Proceedings of the 1994 TAPPI Engineering Conference*, TAPPI, Atlanta, GA, 1994, pp. 427–433.
- [231] Falat, L., *Proceedings of the 8th International Symposium on Corrosion in the Pulp and Paper Industry*, Swedish Corrosion Institute, Stockholm, 1995, pp. 165–178.
- [232] Estes, M., et al., *Proceedings of the 9th International Symposium on Corrosion in the Pulp and Paper Industry*, Ottawa, 1998, pp. 231–235.
- [233] Eilersson, T. and Leijonberg, A., *Proceedings of the 7th International Symposium on Corrosion in the Pulp and Paper Industry*, TAPPI, Atlanta, GA, 1992, pp. 259–265.
- [234] Mäkipää, M., Backman, R., and Hamalainen, M., *Proceedings of the 1996 TAPPI Engineering Conference*, TAPPI, Atlanta, GA, 1996, pp. 681–692.
- [235] Mäkipää, M. and Backman, R., *Proceedings of the 9th International Symposium on Corrosion in the Pulp and Paper Industry*, Ottawa, 1998, pp. 199–207.
- [236] Mäkipää, M., Oksa, M., and Pohjanne, P., *Proceedings of the 10th International Symposium on Corrosion in the Pulp and Paper Industry*, Technical Research Center of Finland, Helsinki, 2001, pp. 73–87.
- [237] Backman, R., et al., *Proceedings of the 10th International Symposium on Corrosion in the Pulp and Paper Industry*, Technical Research Center of Finland, Helsinki, 2001, pp. 57–72.
- [238] Swindeman, R. W., Keiser, J. R., Maziasz, P. J., and Singbeil, D. L., *Proceedings of the 9th International Symposium on Corrosion in the Pulp and Paper Industry*, Ottawa, 1998, pp. 209–220.
- [239] Prescott, R. and Singbeil, D. L., *Proceedings of the 9th International Symposium on Corrosion in the Pulp and Paper Industry*, Ottawa, 1998, pp. 185–188.
- [240] Tran, H., Habibi, B., and Jia, C., *Proceedings of the 1999 TAPPI Engineering Conference*, TAPPI, Atlanta, GA, 1999, pp. 1061–1069.
- [241] Tran, H., Habibi, B., and Piroozmand, F., *Proceedings of the 10th International Symposium on Corrosion in the Pulp and Paper Industry*, Technical Research Center of Finland, Helsinki, 2001, pp. 45–55.
- [242] Hanninen, H., Pihjanne, P., Saarinen, P., and Kiesi, T., *Proceedings of the 10th International Symposium on Corrosion in the Pulp and Paper Industry*, Technical Research Center of Finland, Helsinki, 2001, pp. 103–116.
- [243] Keiser, J. R., et al., *Proceedings of the 9th International Symposium on Corrosion in the Pulp and Paper Industry*, Ottawa, 1998, pp. 213–220.
- [244] Keiser, J. R., Paper 283, *Corrosion/99*, NACE, Houston, TX, 1999.
- [245] Keiser, J. R., et al., *Proceedings of the 1999 TAPPI Engineering Conference*, TAPPI, Atlanta, GA, 1999, pp. 1099–1107.
- [246] Keiser, J. R., et al., *Proceedings of the 1999 TAPPI Engineering Conference*, TAPPI, Atlanta, GA, 1999, pp. 1109–1120.
- [247] Keiser, J. R., et al., *Electronic Proceedings of the 2000 TAPPI Engineering Conference*, TAPPI, Atlanta, GA, 2000.
- [248] Svensson, C., et al., *Proceedings of the 10th International Symposium on Corrosion in the Pulp and Paper Industry*, Technical Research Center of Finland, Helsinki, 2001, pp. 243–255.
- [249] Dykstra, H., Risebrough, N., and Wensley, A., *Proceedings of the 1999 TAPPI Engineering Conference*, TAPPI, Atlanta, GA, 1999, pp. 1071–1090.
- [250] Wensley, A. and Woit, B., *Electronic Proceedings of the 2001 TAPPI Engineering Conference*, TAPPI, Atlanta, GA, 2001.
- [251] Keiser, J. R., et al., *Proceedings of the 10th International Symposium on Corrosion in the Pulp and Paper Industry*, Technical Research Center of Finland, Helsinki, 2001, pp. 89–102.
- [252] Morris, K. W., Plumley, A. L., and Rocznak, W. R., *Proceedings of the 3rd International Symposium on Corrosion in the Pulp and Paper Industry*, NACE, Houston, TX, 1980, pp. 47–57.
- [253] Tran, H. N., Barham, D., Reeve, D. W., et al., *Proceedings of the 5th International Symposium on Corrosion in the Pulp and Paper Industry*, CPPA, Montreal, 1986, pp. 201–207.
- [254] Backman, R., Hupa, M., and Uppstu, E., *Proceedings of the 5th International Symposium on Corrosion in the Pulp and Paper Industry*, CPPA, Montreal, 1986, pp. 243–249.
- [255] Poon, W., Barham, D., and Tran, H., *Proceedings of the 1992 TAPPI Engineering Conference*, TAPPI, Atlanta, GA, 1992, pp. 349–361.
- [256] Tran, H. N., Poon, W., and Barham, D., *Proceedings of the 1993 TAPPI Engineering Conference*, TAPPI, Atlanta, GA, 1993, pp. 207–213.
- [257] Tran, H., Mapara, N., and Barham, D., *Proceedings of the 1995 TAPPI Engineering Conference*, TAPPI, Atlanta, GA, 1995, pp. 421–431.
- [258] Tran, H., Khan, K., and Barham, D., *Proceedings of the 9th International Symposium on Corrosion in the Pulp and Paper Industry*, Ottawa, 1998, pp. 261–266.
- [259] Klower, J. and White, F. E., *Proceedings of the 8th International Symposium on Corrosion in the Pulp and Paper Industry*, Swedish Corrosion Institute, Stockholm, 1995, pp. 179–188.
- [260] Mäkipää, M., Oksa, M., and Koivisto, L., Paper 01424, *Corrosion 2001*, NACE, Houston, TX, 2001.
- [261] Mäkipää, M., et al., *Proceedings of the 10th International Symposium on Corrosion in the Pulp and Paper Industry*, Technical Research Center of Finland, Helsinki, 2001, pp. 157–180.
- [262] Backman, R., et al., *Proceedings of the 10th International Symposium on Corrosion in the Pulp and Paper Industry*, Technical Research Center of Finland, Helsinki, 2001, pp. 137–155.
- [263] Thompson, R., Singbeil, D., Guzi, C., and Streit, D., *Proceedings of the 7th International Symposium on Corrosion in the Pulp and Paper Industry*, TAPPI, Atlanta, GA, 1992, pp. 309–318.
- [264] Guzi, C. E., *Proceedings of the 8th International Symposium on Corrosion in the Pulp and Paper Industry*, Swedish Corrosion Institute, Stockholm, 1995, pp. 127–137.
- [265] Thompson, C. M., Yeske, R. A., Hendrickson, K. A., and McTee, R. J., Paper 61, *Corrosion/89*, NACE, Houston, TX, 1989.



- [266] Salmenoja, K., Makela, K., and Backman, R., *Proceedings of the 8th International Symposium on Corrosion in the Pulp and Paper Industry*, Swedish Corrosion Institute, Stockholm, 1995, pp. 189–206.
- [267] Salmenoja, K. and Makela, K., *Proceedings of the 1996 TAPPI Engineering Conference*, TAPPI, Atlanta, GA, 1996, pp. 707–713.
- [268] Salmenoja, K. and Makela, K., *Proceedings of the 9th International Symposium on Corrosion in the Pulp and Paper Industry*, Ottawa, 1998, pp. 221–230.
- [269] Orjala, M., et al., *Proceedings of the 10th International Symposium on Corrosion in the Pulp and Paper Industry*, Technical Research Center of Finland, Helsinki, 2001, pp. 117–136.

# Petroleum Production and Refining

*R. N. Tuttle*<sup>1</sup>

THE PETROLEUM INDUSTRY is usually divided into oil and gas production, refining, and oil and gas products. These encompass a wide variety of corrosive environments that must be considered during the process of materials selection and corrosion control management. The corrosive environments include acid gases, such as carbon dioxide (CO<sub>2</sub>) and hydrogen sulfide (H<sub>2</sub>S), and salt water. Refinery operations involve complex chemical systems and many corrosive environments. Management of these systems involves a wide range of activities by the producing, refining, and service companies.

## OIL AND GAS PRODUCTION

Oil and gas production involves the production of oil and gas, along with associated salt water and corrosive acid gases, such as CO<sub>2</sub> and H<sub>2</sub>S. Mineral acids are also often used during producing operations to improve well performance. The producing operations involve wells, piping used for gathering the oil and gas and associated fluids, and facilities for separating and treating the fluids. The wells vary widely in size, depth, and corrosive environments encountered. Temperature may range from roughly 77 to 482°F (25–250°C) and pressures from atmospheric to 25 000 psi (175 MPa). The wells contain a range of carbon steel tubular goods ranging in size from 2- to 24-in. (50- to 600-mm) diameter. Stainless steels and other corrosion resistant alloys (CRAs) are often used for corrosive environments, particularly for deep wells. Liners and FRP pipes are also used for the lower temperature and shallower wells when corrosive environments are encountered.

The produced fluids are separated into three streams: natural gas, liquid hydrocarbon (crude oil or hydrocarbon condensate), and produced water and solids. The liquid hydrocarbon stream is treated to remove the produced water before being shipped to a refinery. The produced water can vary in composition from condensed water to brine. The brine may contain a range of soluble salts at concentrations as high as 25 %. The produced water stream may be treated prior to disposal or re-injection. The gas stream may be further treated in a gas plant to separate the various hydrocarbon fractions and to remove the H<sub>2</sub>S and CO<sub>2</sub>. If the wells produce significant concentrations of H<sub>2</sub>S, it is removed

and converted to sulfur. If the wells produce very high concentrations of CO<sub>2</sub>, it is removed, and when possible re-injected to improve hydrocarbon recovery.

Selection of a material or method to control corrosion often depends on whether the produced fluids are sweet or sour. "Sour" is defined as the presence of sulfur compounds above some arbitrary concentration, and "sweet" is defined as "not sour." A crude oil is typically considered sour if it contains more than approximately 2 % total sulfur; although, the definition of "Sour" crude oil is often determined by the material and process needs of the refining operation.

For gas systems, the definition of sour is considered to be a gas in which the H<sub>2</sub>S partial pressure is greater than 0.05 psi (0.34 kPa). This is based on the NACE Standard MR0175 Sulfide Stress Cracking Resistant Metallic Materials for Oil-field Equipment. Sour multiphase systems (gas, crude oil, water) are treated separately in MR0175. An ISO (International Standards Organization) standard is currently being developed based upon MR0175 and documents prepared by the European Federation of Corrosion (EFC). This document is in FDIS stage as ISO 15156/MR0175.

## Corrosion During Well Drilling

Seamless steel pipe manufactured to API Specification 5D for Drill Pipe is used during the drilling operations. Available grades are E-75, X-95, G-105, and S-135 with specified minimum yield strengths (SMYS) of 75, 95, 105, and 135 ksi (517, 655, 724, 931 MPa), respectively. Drill pipe lengths are connected by tool joints, which involve a threaded pin and a box coupling. The couplings are friction welded to the pipe.

Corrosion fatigue and sulfide stress cracking (SSC) are potential problems during drilling operations. Service stresses and corrosion are the primary factors in drill pipe corrosion fatigue. Inadvertent air entry into the drilling mud system is the prime component of drill pipe corrosion. Internal coatings are often used to reduce general corrosion and to minimize corrosion fatigue. Oxygen scavengers and corrosion inhibitors are often used to minimize drill pipe corrosion.

Drill pipe failures because of SSC may occur when sour gas enters the drill hole during drilling operations. Control of the drilling environment, as outlined in NACE Standard MR0175, reduces the potential for entry of H<sub>2</sub>S into the well. The environmental control methods include use of water-based mud with a pH >10 and addition of sulfide

<sup>1</sup>Tuttle and Associates, Houston, TX.

scavengers. Alternatively, oil-based mud may be used to minimize water wetted steel surfaces.

NACE Publication 1D177 [1] describes corrosion monitoring techniques for drilling operations. Some components of drilling equipment may be fabricated from corrosion resistant alloy (CRA). CRA selection may involve laboratory testing, such as that described below for producing wells.

## Corrosion During Production

Most wells are completed with carbon or low-alloy steel casing, tubing, and liners. These are purchased to API Specification for Casing and Tubing (Spec 5CT). The specified minimum yield strength (SMYS) ranges from 40 to 125 ksi (280 to 860 MPa). Maximum hardness values are specified for those grades commonly used in sour service. Use of CRA in most wells is limited to special wellhead or downhole equipment. However, it is becoming more common to use CRA for tubing and wellheads for wells with corrosive environments.

The composition of produced gas varies widely in both the amount of heavier than methane hydrocarbons and the amount of  $H_2S$  and  $CO_2$  present. A gas condensate well may produce only gas at the bottom of the well, but may produce both gas and hydrocarbon liquids at the surface. The liquids at the surface are a result of condensation because of temperature and pressure changes.

Oil wells generally produce gas in addition to crude oil. Oil wells often require artificial lift as pressures decline. Artificial lift wells use rod pumps, submersible pumps, or gas lift. Injection wells are used in enhanced recovery operations or for disposal of produced water. In enhanced recovery, the injected fluids include steam, water, carbon dioxide, or polymer solutions.

Carbon dioxide in combination with a condensed or produced water phase is the primary cause of corrosion in producing wells. Chlorides present in produced water may increase corrosion. Localized severe corrosion in sweet wells may occur as a result of either high velocity or metallurgical factors. The latter effect, called ringworm corrosion, can be minimized by full-length heat treatment of well tubing.

Presence of hydrogen sulfide has an inhibiting effect on carbon dioxide corrosion, but introduces the possibility of harmful effects such as SSC of high strength carbon steels. Temperature, a major factor in the corrosiveness of produced fluids, can range from about 77°F (25°C) in shallow wells to above 482°F (250°C) in deep wells. Oxygen is generally not a corrosion factor in production wells, since the produced fluids are normally anaerobic (this may not be true for wells that are artificially lifted). The crude oil or hydrocarbon liquids often provide protection from corrosion by forming a water-repelling film on the metal surface, particularly in those wells with a high oil/water ratio.

In enhanced recovery, materials selection and corrosion control measures may significantly differ from those used during the primary production phase. Thus, additional corrosion testing may be required during the selection of corrosion control measures. For example, in some water and steam floods, the produced fluids may change during the well or facility life from sweet to sour because of increased

$H_2S$ . This change may result in potential SSC and other cracking mechanisms. Sulfate-reducing bacteria (SRB) activity in the water phase is the primary cause of the  $H_2S$  increase. As a result, chemical treatment with a biocide may be required.

## Inhibition of Producing Wells

Corrosion inhibitors are often used to control downhole corrosion and related equipment. Inhibitors are organic amine compounds combined with fatty acids. These wet the steel surfaces and form organic films. They are applied either continuously or intermittently. Continuous treatment is commonly done by direct injection into the casing-tubing annulus or by injection into the bottom of the well via small diameter tubing. Inhibitor concentrations in the produced fluids are typically in the range of 5–50 ppm. Intermittent treatments may involve simple batch injections or squeezing an inhibitor concentrate into the producing formation (squeeze method). In many cases, the inhibitor program is managed and conducted by a service company through a joint agreement with the oil company. This service includes inhibition and monitoring. Selection of a specific inhibitor and its treatment schedule is based on field experience supplemented by in-house laboratory testing. Inhibition is generally easier to achieve in sour systems than in sweet systems, because of the lower corrosion rates and the greater attraction of the inhibitors to sulfide surfaces. Inhibition is less attractive for deep wells, because of low inhibitor effectiveness at the high temperatures, and the complications of inhibitor injection.

*Inhibitor Testing*—There are no standardized laboratory tests for evaluating oilfield inhibitors. A number of tests have been described in the literature, but none has been adopted by NACE. The ideal test would determine the inhibitor effectiveness for the specific well fluids, would evaluate any secondary effects (e.g., emulsion problems), and would measure persistence of the inhibitor film.

NACE Publication 1D182 [2] describes a wheel test method that has been used for a number of years to evaluate film persistent inhibitors for oilfield applications. The publication outlines the general features of the method, leaving many details to be standardized by the user. The test involves exposing a steel specimen to a mixture of inhibitor, crude oil, and synthetic brine in a glass bottle that has been purged first with nitrogen to remove oxygen, then with either carbon dioxide or hydrogen sulfide to simulate sweet or sour conditions. The bottle is placed on a wheel and rotated in a controlled temperature cabinet for a specified time. Following this filming treatment, the specimen is transferred to a bottle containing uninhibited oil and brine, and the test repeated. Corrosion rates are measured after one or more exposures to uninhibited fluids. The method can also be used to evaluate inhibitors for continuous treatment by determining the percent protection for a given inhibitor concentration, or by determining the inhibitor concentration necessary to achieve a 90 % reduction in corrosion rate.

NACE Standard Recommendations for Selecting Inhibitors for Use as Sucker Rod Thread Lubricants (MR0174) suggests test methods for evaluating corrosion inhibitors in thread lubricants used to prevent both galling and corrosion of sucker rod threads and box cavities.

Testing inhibitors for application in deep wells is difficult because of the need to evaluate the inhibitor stability and effectiveness at high temperatures and pressures. For example, tests have been made with sour brine at 392°F (200°C) and 19 000 psi (130 MPa) pressure. In addition, flow loops are often used to simulate operating conditions.

#### *Inhibition During Acidizing Treatments*

Acidizing treatments are used to stimulate production by the acidic dissolution of undesirable materials on the walls of the producing formation or by pumping acid into the formation to improve permeability. Hydrochloric acid (HCl) is used for limestone formations. Hydrofluoric acid (HF) is added to the HCl for silicate formations. Inhibitors are added to the acid to protect steel tubing during the short period of exposure to acid during injection, and the following period when partially spent acid is returned to the surface. Suppliers use a variety of nonstandardized tests for acid inhibitor evaluation.

A unique field test for detecting the presence of inhibitor in acid is described in NACE Standard Practice for Handling and Proper Usage of Inhibited Oilfield Acids (RP0273), and in API Recommendations for Proper Usage and Handling of Inhibited Oilfield Acids (Bull. D15). These are designed for detecting the presence of an inhibitor, and not for comparing different inhibitors. The test consists of exposing steel wool to the test acid in a 1-mL-narrow-neck ampoule, placing the ampoule neck-down in a beaker of water that had been heated to boiling temperature, and measuring the time required for the ampoule to float to the surface due to the buoyancy provided by hydrogen generated by corrosion of the steel wool.

#### *Coating and Linings*

Protection of well tubing by organic coatings or linings may be economically attractive. The following standards have been developed to ensure that the coatings selected are adequate for a specific system, or that application of the coating is done in an acceptable manner. These standards are periodically modified and the latest version should be used.

NACE Standard Practice for the Application of Internal Plastic Coatings for Oilfield Tubular Goods and Accessories (RP0191) addresses initial inspection of equipment to be coated, surface preparation, coating application, coupling/connection makeup, and quality control.

NACE Standard Practice for Care, Handling, and Installation of Internal Plastic Coatings for Oilfield Tubular Goods and Accessories (RP0291). This standard addresses the practical aspects in the use of coated tubing.

NACE Test Method for Evaluation of Internal Plastic Coatings for Corrosion Control of Tubular Goods in an Aqueous Flowing Environment (TM0183) compares performance of coatings under identical conditions.

NACE Test Method for Evaluation of Internal Plastic Coatings for Corrosion Control of Tubular Goods by Autoclave Testing (TM0185) complements NACE Standard TM0183.

NACE Test Method for Holiday Detection of Internal Tubular Coatings of Less than 10 Mils (0.25 mm) Dry Film Thickness (TM0384) defines apparatus and procedure for holiday detection in nonconductive coating film.

NACE Test Method for Holiday Detection of Internal Tubular Coatings of 10 to 30 Mils (0.25 to 0.76 mm) Dry Film Thickness (TM0186) complements NACE Standard TM0384.

#### **Materials for Sulfide Stress Cracking (SSC) Resistance**

Sulfide stress cracking (SSC), a form of hydrogen embrittlement, is a serious problem in the oil industry because of the potentially catastrophic nature of a failure of high strength carbon steel casing, tubing, or surface equipment. Inhibition is not a reliable means to prevent SSC because treatment interruptions could lead to failure. Control of SSC is accomplished by careful specification and quality control of equipment for sour wells. Materials that are acceptable for service in sour environments are defined in NACE Standard MR0175. This standard is updated annually.

Of the large number of SSC test methods that have been used to evaluate materials for this service, five have survived: uniaxial load tensile test, Shell bent beam test, C-ring test, double-cantilever-beam test, and slow strain rate test. The first four of these are incorporated in NACE Test Method for Laboratory Testing of Materials for Resistance to Sulfide Stress Cracking in H<sub>2</sub>S Environments (TM0177). Following are comments on these methods [3].

##### *A. SSC of Carbon and Steels—General Test Features*

Tension and beam specimens are cut parallel to the axis of the tubing, since most SSC failures of the tubing have been transverse to the tubing axis. C-ring specimens are used to evaluate effects that have resulted in cases of longitudinal cracking. The test environment was selected to provide hydrogen absorption by the specimen equivalent to that expected in the most severe well environment. This is accomplished by using a solution saturated with H<sub>2</sub>S at atmospheric pressure (15 psia [0.0003 MPa]) at pH 3. This low pH being is obtained by adding 0.5 % acetic acid. Five percent sodium chloride (NaCl) is added to simulate typical produced water. This test solution is commonly called "NACE solution" or "TM0177 solution A."

Other test solutions (e.g., Solution B) are also available to represent mild environments. Test temperature is normally 77°F (25°C), since tests have shown this temperature to be in the most severe range for hydrogen embrittlement effects. Test durations of 21–30 days are consistent with the observed rapid failure of susceptible materials. In testing CRA, the test specimen is commonly coupled to carbon steel to provide a severe hydrogen absorption condition.

##### *B. Acceptability Criteria*

NACE has not adopted acceptability criteria for any of these methods, leaving this decision to the user. In early laboratory tests, all tubular steels tested in a severe test environment failed by cracking if strained to a sufficient degree [4]. However, field experience had shown that primarily only high-strength steels, above approximately 80 ksi (550 MPa) yield strength, were subject to failure. From this fact it was concluded that normal field conditions were such that severe straining did not occur, and that

susceptibility of steels to cracking was related to the strain required for failure. Thus, it became a matter of correlating field experience with laboratory test results to define acceptability criteria.

#### *C. TM0177 Method A (NACE Standard Tensile Test)*

This method uses a smooth tension bar specimen as described in ASTM A 370, Test Methods and Definitions for Mechanical Testing of Steel Products, and ASTM G 49, Practice for Preparation and Use of Direct Tension Stress-Corrosion Test Specimens. The test results in an apparent threshold stress for failure in 30 days, expressed as percent of yield strength. API Spec 5CT requires that the threshold stress for failure in this test be determined for Grades C-90 and T-95 using NACE TM0177, with an acceptance criterion of at least 80 % of the SMYS. An advantage of this test is that it uses a specimen with a well-defined stress state. One drawback is that the presence of nonmetallic inclusions may lead to hydrogen-induced cracking (HIC) related failures in lower strength steels at lower threshold stress values than normally expected for such steels [5].

#### *D. TM0177 Method B (NACE Standard Bent-Beam Test)*

This three-point constant deflection bent-beam test is based on the Shell Sc test that was used extensively in the development of SSC-resistant steels [6]. The Sc test makes use of a small beam with stress raisers in the form of two small holes drilled in the center of the beam. The beam is loaded with a screw at the center point and is supported at each end. Multiple tests are made with measured variations in the beam deflection.

A statistical determination is made of the beam deflection required for a 50 % probability of failure in 21 days. The deflection value is converted to a pseudomaximum stress value in ksi (1000 psi), which is divided by 10 to give the Sc value. The Sc value becomes a number for rank ordering the SSC resistance of the steel being tested. Typically, susceptible steels such as API Grade P-110 (ISO 11960) steel would have Sc values in the 2–5 range. By contrast, resistant steel like API Grade J-55 would have Sc values from 15 to 20.

The critical acceptance criteria ranging from 10 to 12 Sc, depending upon yield strength, was developed by correlating lab data with field experience [4]. An artificial number was used for the test result rather than a stress or strain value for the test result, in an attempt to discourage anyone from assuming that a critical stress or strain value obtained in such an arbitrary test could be used as a design parameter. The 50 % probability of failure concept has an advantage as compared to the threshold stress approach because it is less influenced by an erratic test result.

Other advantages of the Sc test are: (1) Sc values for different materials could include values on both sides of the acceptability criterion, thus providing a tool for research on improved steels since one would have a measure of the nearness to the desired goal; (2) the test evaluates the effect of plastic strain, a critical factor in SSC failures; and (3) the small area of maximum strain allows evaluating SSC susceptibility of localized areas and minimizes inclusion-related hydrogen effects. A major limitation of the Sc test is

that the constant deformation feature de-emphasizes crack growth factors.

#### *E. TM0177 Method C (NACE Standard C-Ring Test)*

This test uses an un-notched C-ring type specimen machined from tubing or bar stock as described in ASTM G 38, Practices for Making and Using C-Ring Stress-Corrosion Test Specimens. A conventional bolt assembly is used to apply the load. Test duration is 30 days. Specimens are exposed at varying levels of outer fiber stress, and an apparent threshold stress for failure is determined. The advantage of this test is that it evaluates the effect of circumferential stress and, thus, serves as an adjunct to the TM0177 tension test when testing tubular goods. Comparison of results from the two tests can be used to detect an anisotropic effect.

#### *F. TM0177 Method D (NACE Standard Double-Cantilever-Beam Test)*

The double-cantilever-beam (DCB) test uses fracture mechanics techniques to evaluate the SSC resistance of tubular steels [7]. It employs a 9.5 by 25 by 100 mm (0.375 by 1.0 by 4.0 in.) specimen with side grooves and loaded with a double taper wedge. In some cases, the specimen is precracked. Typical test duration is 14 days.

The DCB test has the major advantage of providing a critical stress intensity number, which has general engineering acceptance. In contrast to the Sc test, the DCB test emphasizes crack growth and arrest factors rather than crack initiation factors. The fact that the DCB test provides a rank-ordering number rather than a failure/no failure result makes it useful in the development of improved steels and alloys. One disadvantage is the specimen size, which limits its application, although subsize specimens, 4.8-mm (0.188-in.) thick, and curved specimens are acceptable.

#### *G. Slow Strain Rate Test*

The slow strain rate (SSR) test has seen only limited use in testing the SSC resistance of low-alloy steels. One reason may be the difficulty of establishing a criterion for failure in borderline cases. However, SSR tests have been useful in evaluating the effect of environmental variables on SSC of steels, the criterion being changes in either elongation or reduction in area. Also, SSR tests have proved to be valuable in evaluating the stress corrosion cracking (SCC) susceptibility of CRAs.

### **Corrosion Resistance Alloy (CRA) Selection**

Use of CRA is competitive with inhibition in deep, high-pressure wells, particularly in those locations where inhibitor supply may be a space and logistic problem. CRA includes stainless steels (austenitic, ferritic, martensitic, and duplex), nickel-based alloys, cobalt-based alloys, and titanium alloys. Economics is a major factor in alloy selection. The 13 Cr tubing has often been used in gas wells for low H<sub>2</sub>S wells. Tubing materials selection for a deep well could involve price increments between alloys of \$1 to 3 million. High-strength CRA is used to minimize costs. SMYS values of 150 ksi (1000 MPa) are common. The CRA is often cold-worked to achieve the required yield strength.

Corrosion concerns with CRA involve general corrosion, crevice corrosion, hydrogen embrittlement, and stress corrosion cracking (SCC). General corrosion and crevice corrosion data are usually obtained as an adjunct to stress corrosion testing. Evaluation of cracking resistance requires testing for resistance to both hydrogen embrittlement and anodic SCC. Separate tests are required. Hydrogen embrittlement evaluations are obtained in NACE TM0177 tests as described above, with coupling to carbon steel or with an applied potential to ensure a severe cathodic condition. The complexity of testing for SCC resistance is such that no standardized tests have been adopted. The generalized approaches that have been used are discussed in the following paragraphs.

It has been found that many CRAs of interest for downhole tubulars are subject to SCC in the  $H_2S/CO_2$ /chloride system under some conditions of temperature, pH, and chloride content. Presence of small amounts of oxidant in the form of elemental sulfur, resulting either from sulfur present in the produced fluids, or by reaction of  $H_2S$  with oxygen from air contamination, increases markedly the probability of SCC of many alloys. NACE MR0175 provides guidelines for selection of CRA.

#### A. Testing CRAs for SCC Resistance

The mechanistic differences between SSC and SCC (anodic type) have a significant influence on the test methods used. Stated simply, the critical variable in SSC of carbon and low-alloy steels is the stress (strain) required to initiate and sustain cracking in an arbitrarily selected severe environment. In SCC, the critical variables are the electrochemical polarization characteristics of the metal/environment system that control the anodic processes involved in crack initiation and growth. Therefore, alloy SCC susceptibility comparisons are done by determining the critical environmental factors (e.g., temperature,  $H_2S$  partial pressure, chloride concentration) required to cause failure of a severely stressed specimen.

Because of the wide spectrum of potentially severe environments for SCC of CRA, rank ordering of alloy susceptibility has become one of comparing SCC resistance under fixed stress conditions as a function of environmental variables such as temperature, hydrogen sulfide partial pressure, pH, chloride concentration, and the presence or absence of free sulfur. Selection of a CRA for a specific use requires finding SCC-resistant materials whose environmental limits, as defined by this matrix of environmental data, are beyond the expected environmental limits of the specific use.

The favored test methods correspond to TM0177 Method A (smooth tensile test), TM0177 Method C (C-Ring test), and the SSR test. Many test environments have been used. These include TM0177 Solution A and a 25 % sodium chloride (NaCl) solution containing 1 g/L elemental sulfur. Tests are commonly made at temperatures of 194–446°F (90–230°C) in the presence of  $H_2S$  and  $CO_2$  at pressures as high as 5000 psi (35 MPa). Temperature, chlorides, and  $H_2S$  partial pressure are common test variables.

SSR testing is often favored for screening because of the short time required. The test details follow those of conventional methods for SSR testing. Dimensions of the test section

of the uniaxial tension specimen are commonly 3.8-mm (0.150-in.) diameter by 25-mm (1.0-in.) long, with an overall diameter of about 6 mm (0.25 in.). A typical extension rate for such a specimen is  $1 \times 10^{-4}$  mm/s ( $4 \times 10^{-6}$  in./s). Failure is determined primarily by metallographic examination of the fracture. Common practice is to plot failure/no failure data on a  $H_2S$  partial pressure versus temperature graph for tests with common pH, chloride, and free sulfur content. Problems with this method include reproducibility related to surface finish, and failure to detect the effect of some metallurgical changes [8–10].

### Artificial Lift Wells Material Selection

Wells that fail to produce through natural means are usually artificially produced by other means, such as gas lifted by a separate source of gas or by mechanical means such as sucker rod pumps.

#### A. Sucker Rods

One means of producing the wells is through the use of downhole pumps where the energy to operate the pump is provided by the use mechanical rods (sucker rods) that are lifted and lowered by surface operated equipment. Sucker rods are subject to failure by fatigue and corrosion fatigue. Although corrosion fatigue failures can be controlled in part by design and operating factors, and by corrosion inhibition, the corrosion fatigue properties of individual sucker rod materials can be a factor in failure frequency. Laboratory testing has not been a satisfactory means of predicting corrosion fatigue of sucker rods because of the difficulty of reproducing well conditions. This has led to use of a technique for field testing to give reliable data for rod selection.

#### B. Sucker Rod Pumps

NACE Standard for Metallic Materials for Sucker Rod Pumps for Hydrogen Sulfide Environments (MR0176) supplements API Specification for Subsurface Sucker Rod Pumps and Fittings (Spec 11AX). NACE Standard MR0176 provides recommended materials for nine environments with varying degrees of abrasion and hydrogen sulfide corrosion.

### Testing Nonmetallic Materials

The following standards have been developed for testing nonmetallic seal materials used in oilfield equipment:

NACE Standard Worksheet for the Selection of Oilfield Nonmetallic Seal Systems (RP0491) provides information on test conditions, test media, test procedures, equipment, and reports for  $CO_2$  environment testing under pressures greater than atmospheric.

NACE Test Method for Evaluating Elastomeric Materials in Sour Gas Environments (TM0187) measures the ability of elastomeric materials to withstand static exposure to elevated pressure and vapor phase sour gas environments. It is designed for testing O-rings or sheet specimens of elastomeric vulcanites.

NACE Test Method for Evaluating Elastomeric Materials in Carbon Dioxide Decompression Environments (TM0192)

measures the effect of rapid depressurization on elastomeric materials subjected to elevated pressures in dry carbon dioxide environments. It is designed for testing O-rings or other specimens of elastomeric vulcanites.

### Monitoring Downhole Corrosion

Downhole specimens are rarely used for monitoring because of the costs and complications involved. Indirect monitoring of downhole corrosion conditions has been done with specimens or electrical resistance probes installed at the wellhead. These have been used for monitoring inhibition treatments, always with the reservation that such exposure does not accurately simulate downhole conditions.

In some wells, it is possible to obtain an indication of downhole corrosion by analysis of produced fluids for iron. This method is described in NACE Standard Practice for Monitoring Corrosion in Oil and Gas Production with Iron Counts (RP0192). It has been used effectively for monitoring inhibition in wells where corrosion follows a general, nonlocalized pattern, and where the corrosion products are water-soluble (e.g., in sweet wells).

In the case of pumped wells where tubing, rods, and pump are pulled periodically for maintenance, visual inspection is used to evaluate progress of corrosion. These records together with records of corrosion-related failures of downhole equipment serve as a means of monitoring effectiveness of mitigation procedures.

For flowing wells, periodic inspection of tubing by inspection tools, usually mechanical caliper type, are used for monitoring both general corrosion and pitting corrosion. In the latter case, statistical treatment of the pit depth data by extreme value techniques has been used to provide derived data that can provide a time-dependent graph of progress of corrosion (i.e., effectiveness of mitigation procedures). Video cameras are also used to evaluate well conditions.

Monitoring casing for both internal and external corrosion can be done with combinations of mechanical and electromagnetic methods to measure internal and external corrosion damage. For cathodically protected casing, NACE Standard Practice for Application of Cathodic Protection for Well Casings (RP0186) includes a description of a downhole potential survey tool that determines if the protective current from the cathodic protection anodes is reaching the desired depth.

### Water Injection Wells and Facilities

Produced water is usually re-injected into special wells for disposal or to maintain reservoir pressure. Two aspects of water injection corrosion control differ from those involved in producing wells. The first is the need to reduce suspended solids to very low values to avoid plugging the formation at the bottom of the injection well. These solids include steel corrosion products, as well as scales. Sulfide corrosion products are of major concern because of their low solubility. Metal sulfide products can occur because of reactions between metal and the  $H_2S$  from the sour gas or the  $H_2S$  generated by sulfate reducing bacteria.

Secondly, oxygen can result in undesirable corrosion products, and can result in severe pitting in either sweet or

sour systems, which creates the need for close control of oxygen contamination. A common control limit on oxygen contamination of injection water is 20 ppb. Thus, water treatment of injected water may include corrosion inhibition, scale inhibition, bactericides, and oxygen scavengers [11].

#### A. Solids Control

NACE Test Methods for Determining Water Quality for Subsurface Injection Using Membrane Filters (TM0173) describes methods for evaluating water quality of injection water. NACE Test Methods for Laboratory Screening Tests to Determine the Ability of Scale Inhibitors to Prevent the Precipitation of Calcium Sulfate and Calcium Carbonate from Solution (for Oil and Gas Production Systems) (TM0374) is used to rank order scale inhibitors at 158°F (70°C).

#### B. Materials Selection

Extensive use is made of nonmetallic materials and alloys to minimize corrosion effects. This includes plastic and nonmetallic piping and internal coatings (e.g., cement lining, organic coatings). For detailed information on alloys see NACE Standard for Selection of Metallic Materials to be used in All Phases of Water Handling for Injection into Oil-Bearing Formations (RP0475).

#### C. Corrosion Testing

Suppliers usually provide the laboratory evaluation (using conventional test methods) of corrosion inhibitors, scale inhibitors, bactericides, and oxygen scavengers. User companies generally provide evaluation by field monitoring with corrosion specimens. Crevices may be incorporated in specimens to evaluate the possibility of localized corrosion, such as that related to oxygen contamination.

### Surface Piping

Horizontal piping systems used to collect and transport well fluids introduce problems of phase separation resulting in stratified corrosive water and gas phases that complicate inhibition control and monitoring. In addition, there is the possibility of oxygen and bacterial (SRB) contamination that can accelerate corrosion. Control of internal corrosion of steel surface piping generally involves inhibition or plastic lining.

Control of external corrosion of steel piping is generally achieved with coatings plus cathodic protection. Testing related to external environments (soil, seawater) to which oilfield piping may be exposed is handled elsewhere (see Section V of this manual).

#### A. Corrosion Inhibition

Water removal may eliminate the need for inhibition of pipelines. Presence of 1 % or less water in crude oil is not considered sufficient to create a corrosion problem. Corrosion in gas pipelines can be avoided by dehydrating the gas to reduce the water dew point to values below the lowest temperature expected.

In water-containing systems, inhibitor selection is based on considerations and tests described above for downhole inhibition with one added constraint: the need to provide

inhibition for stratified flow conditions that may exist. This requires inhibition systems that can provide protection in the upper vapor phase of pipeline, as well as in the separated water phase at the bottom of the pipe. The latter condition often prevails at low spots in the line. Improved protection can be obtained by periodically pigging the line to distribute inhibitor over the entire internal surface and to remove liquid water.

### *B. Hydrogen Effects*

In sour service piping systems, control of SSC is accomplished by using acceptable materials as defined by NACE Standard MR0175. For example, all grades of steel pipe listed in API Spec 5L (ISO 3183-3) with specified minimum yield strengths of 65 ksi (Grade X-65) or less are listed as acceptable by MR0175. However, weldments in these low-strength pipes, including both seam welds made by the manufacturer and circumferential welds made in the field, are expected to conform to MR0175 requirements for SSC resistant welds, i.e., hardness of 22 HRC maximum. Microhardness surveys of cross sections of typical welds are normally used to evaluate weld susceptibility to SSC.

One additional control factor outside the scope of MR0175 is the need to select steels that are resistant to hydrogen blistering and related cracking phenomena, i.e., HIC and stress orientated hydrogen induced cracking (SOHIC). HIC is sometimes called stepwise cracking. In this discussion, HIC will be the term used to identify the effects of hydrogen-related cracking related to hydrogen blistering.

HIC differs from SSC in two major aspects: (1) HIC is observed with lower strength steels, and (2) HIC is associated with inclusions in the steel or with anomalous structures such as midwall banding. Crack initiation results from formation of molecular hydrogen at inclusions and discontinuities in the steels, and crack growth results from applied and residual stresses aided by the embrittling effect of hydrogen.

These effects have been encountered primarily in steel plate used for vessel construction or for fabrication of welded pipe. The major industry problem has been with welded pipe made from controlled rolled plate. Cases of pipe rupture have been attributed to HIC. Seamless pipe is less subject to these effects, but is not considered to be immune. HIC may be prevented by the manufacturer's control of the inclusion number, size, and shape, particularly sulfide inclusions [12].

### *C. Testing Steels for HIC Resistance*

Evaluation of steels is done via tests that measure the number and size of subsurface cracks following exposure to a standard hydrogen sulfide solution. NACE Test Method Evaluation of Pipeline and Pressure Vessel Steels for Resistance to Hydrogen-Induced Cracking (TM0284) defines a test procedure, but does not set criteria for acceptability. The specimen is cut from a steel pipe or plate in the as-manufactured condition, and exposed for 96 h to H<sub>2</sub>S-saturated synthetic seawater prepared according to ASTM D 1141, Specification for Substitute Ocean Water. The number, location, and dimensions of subsurface cracking are measured. From these data, two factors are calculated: crack length

ratio (CLR) and crack thickness ratio (CTR). Values approaching zero are the desired goals. In the absence of standard criteria, individual users specify CLR and CTR limits. It has been suggested that a lower pH test environment, such as that provided by the TM0177 Solution A, would be more representative of severe pipeline conditions [13].

### *D. Testing CRAs for Pipelines*

Pipeline usage of CRAs introduces an aspect of testing not covered in downhole applications. This is the need to evaluate the corrosion characteristics of weldments. At present, the principal alloys for pipelines are duplex stainless steels, high molybdenum austenitic stainless steels, and some nickel-base alloys. The latter alloys may be used as cladding inside steel piping. Hot-isostatic pressing (HIP) and weld overlaying are used for some equipment items. Corrosion factors introduced by welding include HAZ effects, sensitization, microstructure of weldments, and weld dilution. With appropriate modifications, the test methods described above for downhole applications can be used.

### *E. Monitoring Pipeline Corrosion*

Procedures for monitoring corrosion of pipelines and related surface facilities using retrievable specimens are described in NACE Standard Practice for Preparation and Installation of Corrosion Coupons and Interpretation of Test Data in Oilfield Operations (RP0775). One of the main concerns in the use of such specimens is the problem of location, since corrosion is generally associated with a separate water phase. In some cases, special dropout pots are used to trap a water phase to provide a severe location for specimens. Electric resistance probes can be used in place of specimens. In locations where there is a continuous water phase and fouling is not a problem, polarization type probes can be used [14,15].

Hydrogen probes have been used in sour systems to evaluate the effect of mitigation methods on hydrogen absorption resulting from sulfide-related corrosion. These measurements are of particular value in situations where blistering or HIC is of concern. A hydrogen probe consists of a closed-end steel tube that is inserted in the process stream and equipped with a device (pressure gage or analytical instrument) to measure the rate of hydrogen transmission through the tube wall, thus providing a measure of the effectiveness of inhibition or other means employed to reduce the amount of atomic hydrogen entering the steel. Similar measurements can be made with a hydrogen patch, which is a hydrogen collecting chamber attached to the outer wall of a vessel or pipe [16].

Pipeline corrosion can be monitored by pushing "smart pig" instruments through the line to measure local and general metal loss (by electromagnetic means). Related instruments have been developed that can make ultrasonic measurements of wall thickness. These methods are used to detect the presence of both external corrosion and internal corrosion. In some instances, video camera techniques can be used to evaluate the condition of internal pipe surfaces. Caliper type measurements can be made in those relatively short lines that permit use of a cable to pull the instrument



through the line. Smart pig techniques that do not necessitate shutting down the line are preferred.

### Field Tanks and Vessels

Field production tanks and treating vessels are protected from internal corrosion by coatings with or without added cathodic protection. NACE Standard Practice for Liquid-Applied Internal Protective Linings and Coatings for Oilfield Production Equipment (RP0181) provides guidelines for equipment design, lining selection, application, and inspection. For catalyzed coal tar epoxy linings, NACE Standard Method of Lining Lease Production Tanks with Coal Tar Epoxy (RP0372) applies. Lining selection is generally governed by experience, with new type linings being evaluated by field exposure of suitable test panels. NACE Standard Practice for Design, Installation, Operation, and Maintenance of Internal Cathodic Protection Systems in Oil Treating Vessels (RP0575) is a general cathodic protection guide that includes design criteria, system selection, and monitoring.

### Offshore Structures

The complexity of offshore production platforms and associated pipelines necessitates specialized seawater corrosion control methods. Coatings are used to protect steel components in the atmospheric zone with CRAs used for special items. The splash zone represents a special case, with either special coatings and/or CRAs being used. Control of corrosion of submerged steel equipment is by cathodic protection via either sacrificial anodes or impressed current. Standards covering some of these control measures are listed below:

NACE Standard Practice for Corrosion Control of Steel, Fixed-Offshore Platforms Associated with Petroleum Production (RP0176) gives guidelines for corrosion control by coatings and cathodic protection.

NACE Standard Practice for Metallurgical and Inspection Requirements for Cast Sacrificial Anodes for Offshore Applications (RP0387).

NACE Standard Practice for Metallurgical and Inspection Requirements for Offshore Pipeline Bracelet Anodes (RP0492).

NACE Standard Impressed Current Test Method for Laboratory Testing of Aluminum Anodes (TM0190).

## OIL REFINING

Oil refining involves many processes including distillation, thermal cracking, catalytic cracking, hydrocracking, hydrotreating, catalytic reforming, alkylation, isomerization, and polymerization. Secondary processes include hydrogen production from steam and methane, amine treating of gas streams to remove hydrogen sulfide, sulfur production by oxidation of separated hydrogen sulfide, and sour water stripping to remove hydrogen sulfide and ammonia. Hydroprocesses involve pressures in the range 400–2600 psi (3–18 MPa) and temperatures of the order of 840°F (450°C). A schematic refinery flow diagram is given in Fig. 1. Refining

processes, and related corrosion environments, are subject to change with time resulting from changes in refinery feedstock, changes in market demand for individual products, and process improvements.

Corrosive components in refinery feedstock are sulfur compounds (hydrogen sulfide and organic sulfides), nitrogen compounds, organic acids (principally naphthenic acids), and inorganic salts present in entrained produced water. During the refining process, sulfur compounds are converted to hydrogen sulfide, nitrogen compounds are converted to ammonia and hydrogen cyanide, and inorganic salts may be converted to hydrochloric acid. Treating chemicals include alkanolamines (for removal of hydrogen sulfide and carbon dioxide), sulfuric acid, hydrofluoric acid, and sodium hydroxide.

The two major corrosive environments that occur in oil refining are high-temperature nonaqueous corrosion and aqueous phase corrosion. High-temperature corrosion is either sulfidation, or naphthenic acid corrosion, external oxidation, high-temperature hydrogen attack, or carburization/decarburization reactions. Aqueous phase corrosion results from many complex environments involving combinations of hydrogen sulfide, carbon dioxide, ammonia, hydrogen cyanide, hydrochloric acid, plus treating chemicals (amines, acids, alkalies).

Detailed reviews of oil refining corrosion problems and control methods are given in a book by White and Ehmke [18]. Oil refining corrosion problems are generally solved by making appropriate materials selection based on accumulated industry experience as reflected in published papers plus API and NACE committee reports. Neutralization and inhibition are used in some cases. Monitoring is generally by inspection supplemented by analysis of process streams (e.g., acidity) and by special probes.

### Corrosion Control

#### A. High-Temperature Corrosion

Sulfidation of steel can occur at temperatures above 450°F (230°C), necessitating the use of alloys, generally chromium steels and stainless steels. Alloy selection is influenced by temperature and the sulfur content of the crude oil. In hydroprocesses, temperature and the hydrogen sulfide content of the process stream are the critical factors. In addition, high-temperature hydrogen attack may occur with carbon steels at temperatures above about 430°F (220°C), the latter being dependent on hydrogen partial pressure. Resistance to hydrogen attack is provided by chromium and molybdenum-containing steels selected using the experience summarized in the well-known “Nelson Curves” and in API Recommended Practice 941, Steels for Hydrogen Service at Elevated Temperatures and Pressures in Petroleum Refineries and Petrochemical Plants. This publication is updated periodically.

Some crude oils contain significant concentrations of organic acids, mainly naphthenic acids, which are corrosive to carbon steel at temperatures above about 400°F (200°C), and may require the use of molybdenum-containing austenitic stainless steels (i.e., AISI 316 and 317). Determination of when to use alloys is done by analysis of the crude oil for acid content using ASTM D 974, Test Method for Acid and



5. Hydrogen blistering of steel equipment can occur whenever hydrogen sulfide and water are present. Presence of cyanides may aggravate the effect. Control can be achieved either by selection of resistant steels or by injection of polysulfides. Monitoring of polysulfide treatment is by use of hydrogen probes. Selection of steels resistant to hydrogen blistering and the related stress-oriented hydrogen induced cracking (SOHIC) is accomplished by steel specifications aimed at minimizing sulfide inclusion content and morphology, and confirming the steel quality by tests with NACE Standard TM0284. The latter test method was developed originally for use with piping. It is being adapted to include steel plate as used in refinery vessels.
6. Corrosion of materials in sour water stripping operations involves complex mixtures of sulfides, cyanides, carbonates, and chlorides. Corrosion control is by alloy selection.

## OIL PRODUCTS

Transport of gasoline and other refined products in steel pipelines may result in corrosion products that can create a product contamination problem. Internal corrosion of the pipeline can also have an adverse effect on pipeline capacity. Corrosion results from condensation of a water film on the pipe wall plus dissolved air or SRB in the product. Corrosion control is commonly achieved by adding a corrosion inhibitor. Evaluation of inhibitor performance can be done using NACE Test Method for Antirust Properties of Cargoes in Petroleum Product Pipeline (TM0172). This test method is a modification of ASTM D 665, Test Method for Rust-Preventing Characteristics of Inhibited Mineral Oil in the Presence of Water.

Rust problems during usage of certain refined products, such as steam turbine oils, are controlled by addition of corrosion inhibitors. Evaluation of the performance of these inhibitors is done using ASTM D 665 or ASTM D 3603, Test Method for Rust-Preventing Characteristics of Steam Turbine Oil in the Presence of Water (Horizontal Disk Method).

Presence of small amounts of some sulfur compounds in certain refined products (gas and liquid) can have a corrosion effect on copper alloy components of users' equipment that adversely affects their function. For example, copper corrosion products could cause plugging of metering and pilot valves. Consequently, product specifications may call for the product to pass a copper corrosion test such as ASTM D 1838, Test Method for Copper Strip Corrosion by Liquefied Petroleum (LP) Gases, or ASTM D 130, Test Method for Detection of Copper Corrosion from Petroleum Products by the Copper Strip Tarnish Test, or ASTM D 4048, Test Method for Detection of Copper Corrosion from Lubricating Grease.

Specification restrictions on the total amount of sulfur compounds allowed in commercial natural gas to avoid copper corrosion problems are typically 0.25 grain sulfur per 100 standard cubic feet (SCF) (6 mg S per m<sup>3</sup>). This

restriction for commercial natural gas does not meet the requirements of NACE Standard MR0175, which limits the H<sub>2</sub>S to 0.05 psi partial pressure for resistance to SSC.

## Acknowledgments

The author wishes to thank D. J. Truax and Dick Horvath for their assistance in reviewing the technical content of this chapter.

## REFERENCES

- [1] "Monitoring Techniques for the Control of Drill Pipe, Casing, and Other Steel Components in Contact with Drilling Fluids," NACE Publication ID177, *Materials Performance*, Vol. 16, No. 2, February 1977, p. 9.
- [2] "Wheel Test Method Used for Evaluation of Film-Persistent Inhibitors for Oilfield Applications," NACE Publication ID182, *Materials Performance*, Vol. 21, No. 12, December 1982, p. 45.
- [3] Treseder, R. S., "A Comparison of Sulfide Stress Cracking Tests," *Corrosion Testing and Evaluation: Silver Anniversary Volume, ASTM STP 1000*, R. Baboian and S. W. Dean, Eds., ASTM International, 1990, p. 312.
- [4] Treseder, R. S. and Swanson, T. M., *Corrosion*, Vol. 24, No. 2, February 1968, p. 31.
- [5] Greer, J. B., *Materials Performance*, Vol. 16, No. 9, September 1977, p. 9.
- [6] Fraser, J. P., Eldredge, G. G., and Treseder, R. S., *Corrosion*, Vol. 14, No. 11, November 1958, p. 37.
- [7] Heady, R. B., *Corrosion*, Vol. 33, No. 3, March 1977, p. 98.
- [8] McIntyre, D. R., Kane, R. D., and Wilhelm, S. M., *CORROSION/86*, Paper 149, NACE, Houston, TX, 1986.
- [9] Ikeda, A., Tsuge, H., and Ueda, M., *CORROSION/89*, Paper 7, NACE, Houston, TX, 1989.
- [10] Ahluwalia, H., *CORROSION/93*, Paper 136, NACE, 1993.
- [11] Dunlop, A. K., in *Corrosion Inhibitors*, C. C. Nathan, Ed., NACE, 1973, p. 76.
- [12] "Plastic Liners for Oilfield Pipelines," NACE Publication 35101, NACE, Houston, TX.
- [13] van Gelder, K., Simon Thomas, M. J. J., and Kroese, C. J., *Corrosion*, Vol. 42, No. 1, January 1986, p. 36.
- [14] Hay, M. C., *Materials Performance*, Vol. 30, No. 12, December 1991, p. 43.
- [15] "Use of Galvanic Probe Corrosion Monitors in Oil and Gas Drilling and Production Operations," NACE Publication 1C187, NACE, Houston, TX, 1987.
- [16] Asperger, R. G. and Hewitt, P., *Materials Performance*, Vol. 25, No. 8, August 1986, p. 47.
- [17] "Monitoring Internal Corrosion in Oil and Gas Production Operations with Hydrogen Probes," NACE Publication 1C184, NACE, Houston, TX, 1984.
- [18] White, R. A. and Ehmke, E. F., *Materials Selection for Refineries and Associated Facilities*, NACE, Houston, TX, 1991.
- [19] Gutzeit, J., *Materials Performance*, Vol. 16, No. 10, October 1977, p. 24.
- [20] Piehl, R. L., *Materials Performance*, Vol. 27, No. 1, January 1988, p. 37.
- [21] The Role of Stainless Steel in Petroleum Refining, American Iron and Steel Institute, Washington, DC, April 1977.

# Food and Beverage

W. E. Clayton<sup>1</sup> and B. Tholke<sup>1</sup>

## MATERIALS OF CONSTRUCTION USED AND SELECTION CRITERIA

IN THE FOOD AND BEVERAGE INDUSTRY, the workhorse materials are the "300 series" austenitic stainless steels (i.e., S30400, S30403, S31600, and S31603). S30100 and 30200 are used, but less frequently. The 300 series alloys are used because they resist corrosion attack by most environments in the industry, are easily fabricated, do not cause contamination of the products, and are readily sanitized [1–3]. As with any industry, there are many other unique materials that are also used. In neutral or slightly acid environments where chlorides are significant, chloride-resistant stainless steel and/or other high alloy materials are used [4]. Duplex stainless steels are being used more and more frequently [5,6]. In some services like fats and edible oil, copper or copper-containing alloys should be avoided.

Complying materials with FDA/USDA regulations for contact with foods and beverages during manufacture, processing, and handling is a very significant issue. Users should be cautious about generic claims of materials being "FDA approved."

Another unique factor in the food and beverage industry is that the finish and polish of the equipment is often a consideration. There are concerns about microbial sterility on the inside of process equipment [2,7,8]. Of concern are both the type of surface finish on the material and the assurance that fabrication and welding practices prevent cracks or crevices. Surface finish is a valid consideration to cleanability. Eliminating crevices is a very important concern to maintaining cleanliness. Many plants want the outside of the equipment to be "gleaming stainless steel" to give the appearance of purity and high quality to both visitors of the plant and also to plant personnel. Although this is not directly related to process needs, it is a frequent consideration.

Much of the equipment is frequently sterilized and must resist modest cleaning with various kinds of antibacterial solutions [4]. The most common is hot water with a low concentration of hypochlorite. Most of the common stainless steels will handle this type of cleaning without significant problems as long as the cleaning cycle is not too long and there are no serious problems with residue buildup or leaving the cleaning solution in the equipment

afterwards. Steam cleaning is also frequently a part of the cleaning cycle. Quality of cleaning water should properly be maintained to prevent chloride build up and other contaminants. Connolly [3] describes cleaning solutions typically used in wine, brewery, and sugar industries.

There are some environments where the iron contamination of stainless steel during fabrication must be removed prior to operation. This is most often done with nitric acid or nitric-hydrofluoric acid rinsing. The 300 series stainless steels and other high alloys can be a benefit in avoiding loss of flavor, taste, color, or bouquet.

## TYPICAL CORROSIVE ENVIRONMENTS ENCOUNTERED

There is no single or small group of appropriate environments that adequately describes the "food and beverage industry." However, the industry handles aqueous-based solutions that frequently contain acidic chlorides [4]. When the chloride-containing aqueous solutions are modest in temperature, they are typically handled with the S30400/S31600 type stainless steels. However, at higher temperatures more chloride-resistant alloys are needed and must be used. The author's experience is that in most food and beverage services, pitting of S30400/S31600 stainless steel usually occurs only over 60°C and usually the temperature must be over 70°C for stress-corrosion cracking (SCC). However, the temperature to have pitting or SCC can vary widely due to pH, inhibitor effect of other ingredients, or the many other factors well known about chloride corrosion of stainless steel [9]. Pitting and stress corrosion can occur at temperatures much lower than 60 to 70°C [10].

Typical examples of chloride corrosion of stainless steel in the food and beverage industries have been described by Richardson and Godwin [4] and Page [11]. Many food environments are multiphase. Even if the overall chloride level is low, chlorides can be very high in an aqueous phase and highly corrosive.

Other parts of the industry may be based upon fats and edible oils, which typically are not corrosive to even carbon steels as long as the carbon steel equipment can stand the cleaning cycles. The author's experience is that carbon steels are widely used for fats and oils and typically resist corrosive attack well up to 90°C. When fatty acids are present in hot fats and edible oils, stainless steel must be used over 90°C. Also, copper or iron pickup can cause rancidity.

<sup>1</sup>The Procter & Gamble Company, Cincinnati, OH 45224.

S30400 and S31600 are widely used in the brewery and wine industry [12–15] although stress corrosion resistant alloys are needed at high chloride levels [16]. Typical corrosion environments and materials used in the brewery and wine industry are described by Dreyman [17] and Connolly [3].

The 300 stainless series alloys are widely used in dairy [3,18,19] and citrus juice [20] industries. S44400 has been reported [5,13] to be effective in brewery, meat processing, hot water tanks, and similar services where chlorides are present. The 300 series stainless steels are also commonly used for vegetable processing [21].

Some foods require heating to moderately high temperatures during processing in order to sterilize the product. The specific composition of the solution and temperature governs whether or not the environment is highly corrosive [3].

In some food services, wear and abrasion of moving parts and processing equipment can be significant. The wear and abrasion resistance becomes the dominant factor rather than corrosion. Materials often used to eliminate wear and abrasion include hard-faced cobalt or nickel-based alloys for cutting, scraping, conveying, mincing, and atomizing [22]. Electroless nickel plating is sometimes used on carbon steel parts [23]. S44400 has been used for conveyor parts where corrosion resistance similar to S30400 is needed [24]. The author's experience is that precipitation hardenable stainless steel alloys like S17400 are also surprisingly successful for mechanical process equipment when corrosion resistance similar to S30400 is needed but galling must be avoided.

As mentioned above, it is common to clean food processing equipment with sanitizing solutions. For example, in fats and oils processing equipment, there is a need to clean out the equipment with caustic in order to remove organics. Steam cleaning is a common requirement. Almost all equipment is sanitized at some frequency and this often involves chloride environments [4,7]. Clean-in-place systems are usually used.

## TECHNIQUES USED FOR CONTROLLING CORROSION AND MATERIALS DEGRADATION

In the food and beverage industry, the most common approach for controlling corrosion is to use resistant alloys. Because of concerns over contamination of the product, it is not as common to use other approaches for corrosion control. However, linings and coatings are used for shipping by truck, barge, or rail.

Another significant criterion in selecting materials is that they must comply with FDA/USDA regulations for contact with foods and beverages for the specific service [7,8]. Many people do not understand or recognize the process for obtaining such approval. There are two possible methods or directions of approval to consider: (1) external FDA/USDA approval where approval is obtained from the manufacturer/supplier of the material and generally cannot be established or determined by the user company. It is common practice to request that an officer of the company supplying the material of the construction sign a statement on their company letterhead that the material complies with FDA or USDA

regulations for food/beverage contact and include the basis for such approval. Caution should be used when using notes in product catalogues that refer to a material being FDA or USDA approved; and (2) internal FDA/USDA approval where the user needs to evaluate their own manufacturing, processing, or handling process to assure that corrosion products or chemicals leached from organic materials do not contaminate the product. With the extensive use of austenitic stainless steel, FDA/USDA concerns exist mostly with nonmetals.

## SPECIFIC PROBLEM AREAS

Chloride corrosion is the major corrosion problem. The other major specific problem area is assuring that materials used comply with FDA/USDA regulations for contact with foods and/or beverages during manufacture, processing, and handling [2,7].

Material selection and/or processing requirements to assure cleanliness and sterility are critical. For example, welding to assure that crevices are not present at a level that would allow microbial growth in service is a significant consideration. However, some overly zealous people often specify mirror finishes or flush ground welds as a requirement. Usually this extreme is not necessary. Modest surface finishes as well as welds on the inside of equipment that are ground smooth, but not flush, to a 150 silicon carbide grit (30 to 35 rms) finish with fabrication consistent with 3A Dairy Standard [25] are usually adequate in most services. Care should be taken that the grinding and polishing operation does not cause contaminants, usually steel, to be imbedded into the surface. Austenitic stainless steel has been shown to sanitize easily even when the surface has been abraded [2,26].

As mentioned earlier, external appearance of a shiny polished stainless steel is also a frequent consideration.

## THE USE OF TEST METHODS TO EVALUATE CORROSION

Standard corrosion test methods are used. Immersion [27,28], intergranular [29], and electrochemical [30] (for aqueous solution) are the most commonly used ones. Any of the specialized testing methods described by Sprowls [31] might be used for special testing conditions.

## NEW MATERIALS SELECTION

Standard laboratory immersion tests described in the previous section above are used. U-bend stress corrosion [9,32] tests and multiple crevice washer tests for crevice corrosion [33] are used to evaluate localized corrosion.

High-temperature chlorides can require unique chloride resistance testing [9]. In aqueous solutions, it is common to use electrochemical testing to evaluate pitting potential or crevice corrosion. In nonaqueous base solutions, this must usually be evaluated by in-service tests in pilot plants or in existing process equipment.

Wear related or abrasion related problems can only be determined by actually testing hardware in full scale service. Accelerated tests have not proven successful in reflecting most service and performance.

### In-Service Monitoring

In-service monitoring is seldom used in the food and beverage industry except in testing alternatives for known problem areas.

### Failure Analyses

Normal "after the fact" failure analysis is used [34]. There is no standard approach for simulating field failures and lab simulation is infrequently used.

### Test Method Approach

Materials are normally evaluated by using field sample racks in pilot plant or full scale equipment. Electrochemical tests are sometimes used in aqueous solutions to evaluate the likelihood or propensity for localized corrosion due to pitting or crevice corrosion.

### Methods Used

Industry standard field and/or laboratory immersion tests described above are common and adequate for most food and beverage service applications. Single sided tests for linings and coatings [35] are used.

## ADDITIONAL COMMENTS AND DISCUSSION

The problems in the food and beverage industry are typically unique to specific services within those industries. Many of the chloride-resistant stainless steels, duplex stainless steels [5], and high-alloy materials have been used in specific applications with good success [3].

One of the problem areas for food and beverage equipment that is often neglected has to do with the use of jacketed heating and cooling vessels. Sometimes there is a process need to alternately heat a batch process with steam in a jacket and then use cooling water in the same jacket. If chlorides are present in the cooling water, this often can lead to chloride stress-corrosion cracking in the jacketed system. Alternative processing methods or chloride-resistant materials must be used in these cases.

## GENERAL REMARKS

Most food and beverage services are handled with the 300 series stainless steels. The issues relating to complying with FDA/USDA regulations for contact with foods and beverages during manufacture, processing, and handling must be carefully evaluated, especially for nonmetallic materials. However, with few exceptions, most of the problems in the industry relate to FDA/USDA approval, microbes, or to

chloride corrosion. The vast bulk of the equipment used in the industry is S30400, S30403, S31600, and S31603 stainless steel and works very satisfactorily.

## REFERENCES

- [1] Puyear, R. B., "To Process Food, 200,000 Tonnes of Stainless," *Nickel*, Vol. 8, No. 2, December 1992, p. 9.
- [2] Holah, J. T. and Thorpe, R. H., "Cleanability in Relation to Bacterial Retention on Unused and Abraded Domestic Sink Materials," *Journal of Applied Bacteriology*, Vol. 69, 1990, pp. 599-608.
- [3] Connolly, B. J., "The Use of Stainless Steel and Nickel Alloys to Combat Corrosion in the Brewing, Dairy, Wine and Food Industries," *British Corrosion Journal*, Vol. 5, September 1970, pp. 209-216.
- [4] Richardson, J. A. and Godwin, A. W., "Localized Corrosion of Stainless Steel during Food Processing," *British Corrosion Journal*, Vol. 8, November 1973, pp. 258-263.
- [5] Redmond, J. D., "Solving Brewery Stress Corrosion Cracking Problems," *MBAA Technical Quarterly*, Vol. 21, No. 1, 1984.
- [6] Lyle, F. F., "Stress Corrosion Cracking Susceptibility of Weldments in Duplex Stainless Steels," *MTI Publication No. 33*, National Association of Corrosion Engineers, Houston TX, 1989, p. 1.
- [7] Pearce, M. O. and Pettibone, J. S., "Stainless Steel and Hygiene," Presentation, 2nd National Stainless Steel Fair, 15-17 July 1987, Sao Paulo, Brazil.
- [8] Pettibone, J. S., "Burgers, Fries, Coke and Stainless Steel," *Proceedings, Nickel Metallurgy, Vol. 2, Industrial Applications of Nickel, Canadian Institute of Mining and Metallurgy and Nickel Development Institute, 17-20 August 1986, NiDi Technical Series No. 10009*, pp. 1-6.
- [9] McIntyre, D. R. and Dillon, C. P., "Guidelines for Preventing Stress Corrosion Cracking in the Chemical Process Industries," *MTI Publication No. 15*, National Association of Corrosion Engineers, Houston, TX, 1989, pp. 111-145.
- [10] McIntyre, D. R., "Environmental Cracking," *Process Industries Corrosion—Theory and Practice*, B. J. Moniz and W. I. Pollock, Eds., National Association of Corrosion Engineers, Houston, TX, 1986, p. 26.
- [11] Page, G. C., "Corrosion Failures of Types 304 and 316 Stainless Steels in the Food Industry," *Materials Performance*, July 1989, pp. 58-63.
- [12] Tachis, G., "Linguistic Purity, World-Famous Wine and Maintenance-Free Tanks," *Nickel*, Vol. 2, No. 2, December 1986, pp. 8-9.
- [13] "Fermenter Tanks for Canada's Two Big Brewers in Ni Stainless," *Nickel*, Vol. 6, No. 2, December 1990, p. 6.
- [14] Chorley, D. M., "Depend Heavily on Nickel Stainless for Microbrewery Process Equipment," *Nickel*, Vol. 6, No. 3, March 1991, p. 12.
- [15] Ribeca, J., "Umbrian Makers of Olive Oil, Wine Prompt Tank Manufacturing Business," *Nickel*, Vol. 8, No. 3, March 1993, p. 12.
- [16] Rahoi, D. W., "The Stress-Cracking Limitations and Corrosion Resistance of Austenitic Stainless Steels and Nu ELI-T 18-2 in Brewery and Related Applications," Paper 106, CORROSION 84, NACE, 1984.
- [17] Dreyman, E. W., "Corrosion in the Brewery Industry," *Metals Handbook, Ninth Edition, Volume 13*, ASM International, Metals Park, OH, pp. 1221-1225.
- [18] "Producing Yogurt or Ice Cream? Nickel Stainless Means Hygiene," *Nickel*, Vol. 3, No. 2, December 1987, p. 8.
- [19] de Caprio, I. G., "How Stainless Steels Help to Combat Famine in the World," *Nickel*, Vol. 1, No. 1, September 1985, p. 6.

- [20] "Take a Reefer. Gut it and Add Stainless Tanks. Presto! A New Orange Juice Ship," *Nickel*, Vol. 3, No. 2, December 1987, p. 12.
- [21] Smith, C. A., "Stainless Steel in the Food Processing Industry," *Anti-Corrosion*, April 1984, pp. 7-8.
- [22] Kirchner, R. W., Crook, P., and Asphahani, A. I., "Wear/Corrosion-Resistant, High Performance Alloys for the Food Industries," Paper 102, CORROSION 84, NACE, 1984.
- [23] Duncan, R. N. and Arney, T. L., "Performance of Electroless Nickel Coatings in Food Products," Paper 101, CORROSION 84, NACE, 1984.
- [24] Dundas, H. J., Bond, A. P., and Watanaabe, H., "Corrosion Behavior of Type 304 and 444 Stainless Steel in Food and Beverage Environments," Paper 104, CORROSION 84, NACE, 1984.
- [25] 3-A, Accepted Practices for Permanently Installed Sanitary Product-Pipelines and Cleaning Systems, Number 605-02, International Association of Milk, Food and Environmental Sanitarians, United States Public Health Service, The Daily Industry Committee.
- [26] Holah, J. T., "Tests Show Stainless Offers Better Cleanability," *Nickel*, Vol. 8, No. 3, March 1993, p. 2.
- [27] Sprowls, D. O., "Immersion Tests," *Metals Handbook, Ninth Edition, Volume 13*, ASM International, Metals Park, OH, pp. 220-224.
- [28] Natalie, C. A., "Evaluation of Uniform Corrosion," *Metals Handbook, Ninth Edition, Volume 13*, ASM International, Metals Park, OH, pp. 229-230.
- [29] Corbett, R. A. and Saldanha, B. J., "Evaluation of Intergranular Corrosion," *Metals Handbook, Ninth Edition, Volume 13*, ASM International, Metals Park, OH, pp. 229-230.
- [30] Scully, J. R., "Electrochemical Methods of Corrosion Testing," *Metals Handbook, Ninth Edition, Volume 13*, ASM International, Metals Park, OH, pp. 216-219.
- [31] Sprowls, D. O., "Corrosion Testing and Evaluation," *Metals Handbook, Ninth Edition, Volume 13*, ASM International, Metals Park, OH, pp. 191-317.
- [32] Sprowls, D. O., "Evaluation of Stress Corrosion Cracking," *Metals Handbook, Ninth Edition, Volume 13*, ASM International, Metals Park, OH, pp. 252.
- [33] Kain, R. M., "Evaluation of Crevice Corrosion," *Metals Handbook, Ninth Edition, Volume 13*, ASM International, Metals Park, OH, pp. 305-308.
- [34] Wyatt, L. M., Bagley, D. S., and Moore, M. A., "An Atlas of Corrosion and Related Failures," *MTI Publication No. 18*, National Association of Corrosion Engineers, Houston, TX, 1989.
- [35] TM0174-74, "Laboratory Methods for the Evaluation of Protective Coatings Used as Lining Materials in Immersion Service-Item #53023," *NACE 1991 Book of Standards*, National Association of Corrosion Engineers, Houston, TX, 1991.

# Water Handling Systems

*Bennett P. Boffardi<sup>1</sup>*

CORROSION MONITORING IS an integral part of any water treatment program. It is used to determine treatment effectiveness and to establish the optimum level of chemical treatment that is most cost effective, not necessarily the cheapest per pound.

The purpose of corrosion monitoring is to assess or predict corrosion behavior of the system. Basically, there are two objectives to monitoring: (1) to obtain information on the condition of the operational equipment, and (2) to relate this information to the operating variables (i.e., pH, temperature, water quality, chemical treatment, etc.). Meeting these objectives will provide the following results:

1. Increased life of the plant.
2. Improved quality of the plant's product.
3. Prediction of maintenance needs at the plant.
4. Reduction in plant's operating costs.

Corrosion monitoring is standard practice in the water treatment industry. The plant engineer can use this information to predict equipment life. Monitoring helps the engineer identify significant factors responsible for corrosion problems and assures implementation of solutions.

Corrosion monitoring is a diagnostic tool. It provides information for the solution of corrosion problems. Knowledge of corrosion trends can be very valuable. Frequently, several variables might appear to be significant, and the ability to correlate corrosion rates with a single variable under specific conditions can be vital. As a logical extension of its diagnostic capabilities, corrosion monitoring is used to assess the effectiveness of a solution to a specific water treatment problem.

Corrosion monitoring can be used to provide operational information. If corrosion can be controlled by maintaining a single variable (e.g., temperature, pH, chemical treatment, etc.) within limits previously determined, then that variable can be used to predict changes in corrosion patterns as the limits are exceeded in both a positive and negative direction. An extension of this technique is to use a monitored variable to control chemical addition directly through automatic feed systems.

The particular corrosion monitoring techniques selected depend upon their applicability to the system and the information being sought. Some techniques provide information that is effectively instantaneous. Other techniques provide

a measure of corrosion rate. Others measure total corrosion or the remaining metal thickness, while others provide information on the overall system.

Most corrosion monitoring techniques are best suited to situations where corrosion is of a general nature, but some techniques provide at least some information on localized attack, such as pitting.

No one monitoring technique will provide all the necessary data to properly evaluate the efficacy of the treatment program. More than one technique may be necessary to monitor a particular system.

An overview of the various corrosion monitoring techniques used in cooling water systems is shown in Tables 1–3. The essential information is listed in Table 1, whereas Table 2 lists some of the characteristics of the monitoring techniques. Table 3 is a summary chart of the various monitoring techniques overall.

## CORROSION COUPONS

The most obvious method of assessing the corrosivity of a cooling water system to a specific material is to expose a specimen or coupon made of that material for a given time in the flowing water. Coupons are made from specific alloys, which have been cleaned and preweighed with a known surface area. Coupons vary widely in size and shape. Some commonly used coupons are 12.5 mm (1/2 in.) wide, 75 mm (3 in.) in length, and 1.6 mm (1/16 in.) thick, having an approximately 2155 mm<sup>2</sup> (3.4 in.<sup>2</sup>) surface area. At selected time intervals, the coupons are removed, cleaned, and reweighed to determine the metal loss.

The weight loss is converted to overall thickness loss or average corrosion rate expressed in millimeters per year, mm/y, as follows:

$$\text{mm/y} = 3.65(\Delta W)/[(A)(d)(D)]$$

where

- $\Delta W$  = weight change, mg,
- $A$  = coupon surface area, cm<sup>2</sup>,
- $d$  = metal density, g/cm<sup>3</sup>, and
- $D$  = exposure time, (days).

Conversion to English units, mils per year (mpy), requires the above equation to be multiplied by 39.4.

Corrosion coupons are highly susceptible to initial corrosion because the metal surface is in an "active" state due to surface preparation. Coupons should not be touched during

<sup>1</sup>Consultant, Boffardi and Associates, Inc., Pittsburgh, PA 15102.



TABLE 1—Corrosion monitoring.

Method	Measures	Applications
Coupon Testing	Average corrosion rate expressed as uniform corrosion in mm/y. Weight change over 30 to 90 days duration.	Most suitable for uniform corrosion under steady conditions. Can indicate localized attack, i.e., pitting, underdeposit, galvanic, etc. Coupons made from most engineering alloys.
LPR	Instantaneous corrosion rate is measured by electrochemical polarization of $\pm 10$ mV between two electrode probes. Pitting tendency can be measured.	Suitable for most engineering alloys. Probe must be placed in fluid of sufficient conductivity to provide accurate rate. Alloy multiplier required for materials other than carbon steel.
ER	Metal loss is determined from resistance change of a corroding metal element. Uniform corrosion rates are calculated from resistance reading. Does not measure localized corrosion.	Suitable for measurements in low conductivity environments, either liquid or vapor. Elements made from most engineering alloys. Element design a function of probe life and sensitivity.
Analytical	Concentrations of dissolved or suspended species in fluid systems including pH and conductivity. Does not measure corrosion.	Determines water quality level of chemical treatment, inhibitory and antagonistic species, dissolved and suspended corrosion by-products.
Heat transfer units	Visual observation of corrosion attack on heat transfer surface. Unit can determine corrosion rate from weight loss of heated surface.	Most suitable in simulating conditions in heat exchanger for corrosive attack. Heat transfer tubes can be made from most engineering alloys.
Test Heat Exchanger	Determines the effect of velocity, heat flux, chemical treatment on corrosion, scale, and fouling.	Most suitable in simulating conditions of critical plant heat exchanger. Heat transfer tubes can be made from most engineering alloys.

TABLE 2—Monitoring technique characteristics.

Method	Time Interval for Measurement	Type of Information	Response to Changing Condition	Plant Environment	Type of Corrosion	Ease of Interpretation
Coupon Testing	Long-term duration, 30 to 90 days	Average uniform corrosion rate	Poor	Any	Uniform and localized attack	Simple
LPR	Instantaneous	Corrosion rate, pitting index	Fast	Conductive	Uniform	Simple
ER	Short duration	Integrated corrosion rate	Moderate	Any	Uniform	Simple
Analytical	Fast	Species influencing corrosive attack	Fast	Any	Not applicable	Moderate
Heat Transfer Units	Long-term duration, 30 to 90 days	Corrosion rate, scale, and fouling	Moderate	Any	Uniform and localized attack besides deposition	Difficult

installation and monitoring processes. Use of plastic gloves when handling the coupons is highly recommended. Normally, 30 days is a typical test period for low corrosivity water (under 0.25 mm/y or 10 mpy). Low-corrosivity water usually contains chemical treatments to stifle corrosion attack. Exposure periods less than 30 days can yield misleading results. Frequently, long-term tests are required, up to 90 days' exposure. During this time frame, three sets of coupons are normally placed in a test rack and changed in sequence of 30-, 60-, and 90-day intervals. Normally, the longer the exposure period, the lower the measured average corrosion rate, and the more closely the coupons will approximate conditions in the system. Figure 1 graphically shows the decrease in corrosion rate with exposure time. Steady state is normally achieved in the 60- to 90-day time frame.

Screws and nuts made of nylon or plastic should be used to hold the coupons to the coupon holder. Mixed metallurgy should be avoided. Copper-base screws and nuts should not be used to hold carbon steel or stainless steel coupons. Galvanized screws and nuts should never be used.

Coupons having large amounts of deposits or tuberculation may indicate insufficient chemical treatment, unstable water characteristics, or highly corrosive conditions. Alternatively, deposits may have been transported from elsewhere

in the system. Heavy, uniform deposits will reduce corrosion rates, since they can act as a protective barrier.

General guidelines for acceptable uniform corrosion depend upon the coupon metallurgy. Low-carbon steel (mild steel) corrosion rates less than 0.13 mm/y (5 mpy) are considered good, rates between 0.13 to 0.25 mm/y (5 to 10 mpy) are fair, and rates greater than 0.25 mm/y (10 mpy) are poor. Copper-base alloys, such as admiralty and 90:10 copper nickel, should have rates under 0.013 mm/y (0.5 mpy). Above this value is considered excessive. General classification of corrosion rates is shown in Table 4.

Coupon installation should be placed in a coupon test rack shown in Fig. 2. Note that the broad face of the coupon is vertical to prevent deposits from settling during periods of low flow. It is important that the flow rate through the rack corresponds to heat exchanger flow rate.

Too high a flow rate will keep debris off of the coupons and may initiate erosion attack on copper-base alloys. Low flow rates may result in excessive corrosion and fouling. Normally, flow rates of 1–2 m/s (3 to 5 ft/s) are adequate. The coupon rack should be connected to the return riser to the tower or at the exit of the hottest part of the system using plastic piping or any other material that will not influence coupon corrosion rates. For example, do not use galvanized pipe, copper pipe, or brass valves to connect the

test loop to the riser. Note in Fig. 2 the use of an optional strainer. The strainer should be used in water systems known to have high-suspended solids or assorted foreign matter, or both.

Flow through the coupon rack can be controlled using an orifice control valve, but this valve is subject to plugging. A plugged orifice control valve will have reduced flow or no flow at all, resulting in high coupon corrosion rates. A rotameter valved at the end of the coupon rack will give more flexibility and accuracy in controlling water velocity. A strainer in the system will prevent plugging of the fluid control valve. Cooling water discharge from the rack should go to a sump (drain, tower basin, etc.) and not be plumbed back into the cooling system. The outflow of the rack must be open to the atmosphere.

In a high-rise building the cooling tower is normally placed on the roof and the corrosion rack is in the mechanical room, which are frequently in the basement. In this situation, the corrosion rack is plumbed between the downcomer and the riser. Materials of construction for the corrosion rack should be made of stainless steel to provide rigidity and have minimal influence on the coupons. Use of carbon steel or galvanized steel is not recommended as construction materials. Coupon placement in the rack follows the galvanic series, starting from the active end. That is, aluminum, carbon steel, stainless steel, and then copper-base alloys.

Coupon corrosion studies are simple to perform. This is the most direct method, aside from inspection of the actual

plant equipment, to determine the efficacy of a treatment. Coupon evaluation allows simple comparison between different alloys, which provides visual examination for localized attack, such as pitting, crevice attack, dealloying, or any other form of nonuniform attack. However, there are limitations to coupon evaluation. Coupons provide weight loss determination of corrosion rates. This consists of accumulated loss of material over the period of exposure. Therefore, coupons cannot determine the time or magnitude of corrosion upsets within the exposed time frame. Finally, 30–90 days are needed to allow sufficient weight change to be meaningful. This 30- to 90-day exposure can sometimes indicate differences between short-term and long-term corrosion rates.

## LINEAR POLARIZATION-RESISTANCE METER (LPR)

The linear polarization-resistance (LPR) technique is the only corrosion monitoring method that allows corrosion rates to be measured in real time. Although limited to electrolytically conducting liquids, the response time and data quality of this technique make it superior, where applicable, to all other forms of corrosion monitoring.

LPR is particularly useful as a method to rapidly identify corrosion upsets and, thus, evaluate remedial action, reducing and minimizing unscheduled downtime, thereby prolonging plant life.

Two LPR devices are presently in use, a three-electrode probe (working, counter, and reference electrodes) and a two-electrode probe. In the author's opinion, the three-electrode system is a better-designed corrosion monitor; however, it accounts for a small percentage of LPRs used to monitor corrosion rates in industrial water treatment systems. The two-electrode LPR device is used by most water treatment vendors and industrial plants. It will be the only LPR device discussed.

The basic operation of the LPR instrument uses two electrodes made of the material of interest, i.e., carbon steel, Admiralty, 90:10 copper nickel, etc. One of the electrodes acts as an anode, the other as a cathode. During the operation of the instrument, a very small voltage of 20 mV is applied across the electrodes. In this region, the polarization curves approach linearity, hence the term LPR. The applied potential divided by the measured current  $i_{\text{meas}}$  is a resistance term called Polarization Resistance, or  $R_p$ . The resistance to current flow between the two electrodes of the LPR probe is the sum of polarization resistance values at each electrode and the resistance of the solution between the electrodes ( $R_s$ ).

TABLE 3—Monitoring devices.

Systems	Coupon	LPR	ER	Analytical	Test Heat Exchanger
Once-through Cooling	X	X	X	X	
Closed System Cooling	X	X		X	
Open Recirculating Cooling	X	X		X	X

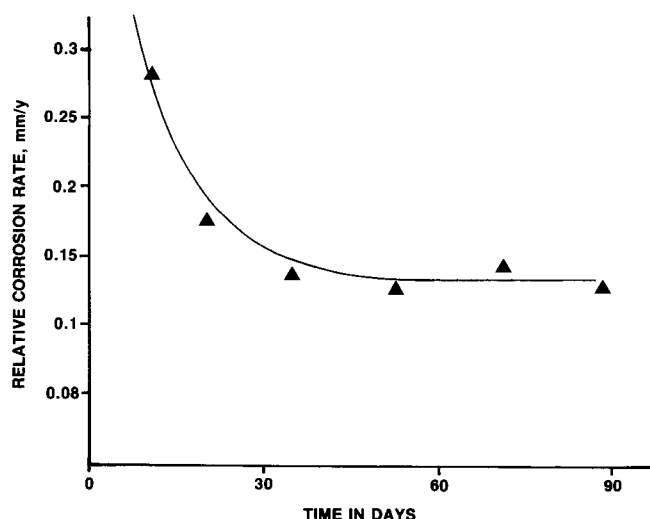


FIG. 1—Relative carbon steel corrosion rate versus elapsed time.

TABLE 4—Qualitative classification of corrosion rates.

Corrosion Rate (mm/y)		Description
Carbon Steel	Copper-Base Alloys	
<0.03	0 to 0.003	Negligible or excellent
0.03 to 0.08	0.003 to 0.006	Mild or very good
0.08 to 0.13	0.006 to 0.009	Good
0.13 to 0.20	0.009 to 0.0125	Moderate to fair
0.20 to 0.25	0.0125 to 0.03	Poor
>0.25	>0.03	Very poor to severe

$$\Delta E = i_{\text{meas}} (2R_p + R_s)$$

In addition to general or uniform corrosion, localized corrosion (pitting) may occur in a system. A Pitting Index or Imbalance measurement can be obtained from some LPR meters. The electrochemical current generated is a qualitative measurement or index. If the imbalance reading (pitting) is low compared to the corrosion reading, pitting is probably minimal. High imbalance reading compared to a general corrosion rate can indicate that pitting or crevice corrosion will be the main form of attack. When a general corrosion rate reading is about the same as the imbalance index, then some pitting is indicated but the pits will probably be broad and shallow.

The LPR probe should be installed perpendicular to the water flow in a representative water stream which is part of the piping system or at the end of the coupon test rack, as shown in Fig. 2. The probe must be installed such that water flows between the two electrodes in order to avoid fouling of the electrodes. An aligning pin at the male cable connector of the probe indicates the electrode position as shown in Fig. 2. The two electrodes should project into the flowing water, with the probe lead flush with the pipe wall as shown in Fig. 3.

Serious errors in corrosion rate measurements may occur in low-conductivity water due to solution resistivity effects. This situation tends to occur at moderate to high corrosion rates and is manifested by indicating lower corrosion rates than actual. The operating range for various LPR instruments can be obtained from the manufacturer.

The LPR probe alloy multiplier should be used when electrodes are made from materials other than carbon steel. The purpose of the multiplier is to convert the built-in constants that are specific for carbon steel to other alloys. Corrosion rate multipliers account for the specific alloy's anodic reactions, the valency of the anodic reactions, the alloy equivalent weight, and the alloy density. LPR electrodes should be changed periodically and at least annually.

Corrosion rates obtained with LPR instruments provide rate data directly and within a few minutes. This instrument is well suited to applications where upsets or other accelerated corrosive conditions can be detected quickly so that remedial action can be taken. The corrosion rates obtained with the meter assume uniform corrosion with a tendency to predict pitting attack. Deposits on the electrodes can bias the pitting index value. If the index value is high, the probe should be removed and the electrode visually examined for debris. Bridging the electrodes with conductive deposits will affect both the general corrosion value and the pitting index.

The LPR reading may not agree with the coupon corrosion rate. The LPR data are real time and measure the corrosion rate at the time of measurement. Coupon rates are an accumulated average mass loss, taking into account all corrosion that has occurred during its exposure period. Coupon mass losses are a direct measure of corrosion rate, whereas LPR data are generated from electrical currents, which are influenced by other factors. The main advantage of LPR devices is the rapid detection of sudden changes in system operating parameters or chemical levels.

Details on how to calculate corrosion rates from electrochemical measurements can be obtained from ASTM G 102, Practice for Calculation of Corrosion Rates and Related Information from Electrochemical Measurements.

## ELECTRICAL RESISTANCE METER (ER)

The electrical resistance (ER) technique is an online method of monitoring corrosion rates. It is universally applicable to all types of corrosive environments, i.e., conductive to poorly or nonconductive media (such as deionized or potable waters) and vapor phase systems (such as steam).

There are many manufacturers of ER instruments. ER meters measure the change in resistance of a metal element as it corrodes. The metal element or probe is usually in the

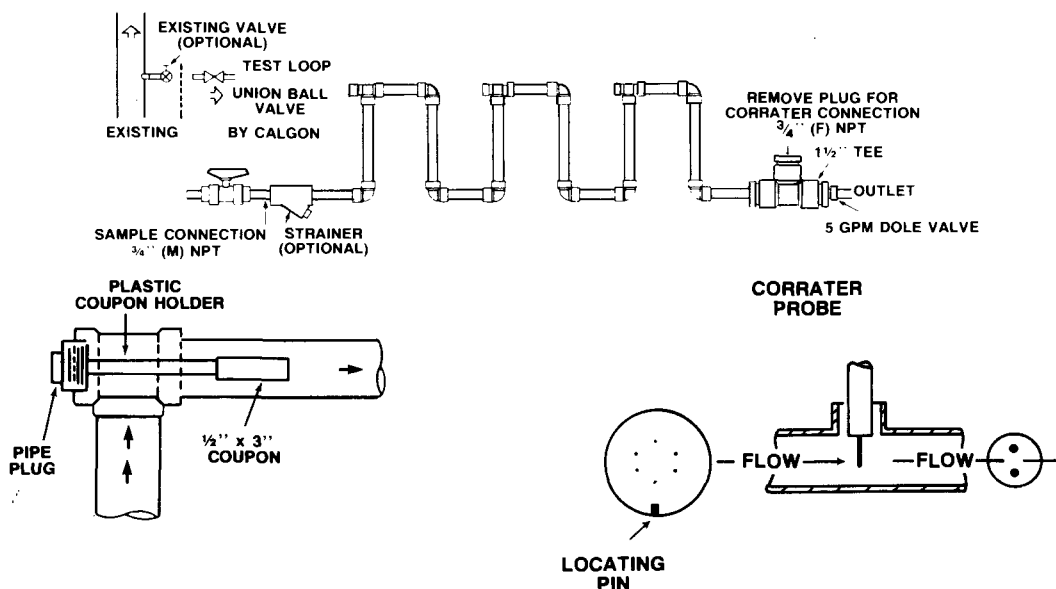


FIG. 2—Corrosion test rack installation.

form of a wire, strip, or tube. When it corrodes uniformly, the change in electrical resistance is proportional to corrosion

$$R = K/A$$

where  $R$  is the probe resistance,  $A$  is the cross-sectional area of the metal element, and  $K$  is a constant and a function of probe metallurgy, element length, and resistivity. As the probe element corrodes, its cross-sectional area is reduced, increasing its electrical resistance. Thus, the measurement of electrical resistance is inversely proportional to the remaining metal in the probe. Therefore, increases in the measured resistance signal increase the metal loss to corrosion. The probe is internally temperature compensated for changes in the probe constant, which is temperature dependent.

The advantage of the ER meters is their ability to measure corrosion in liquids, vapor phases, and in inaccessible locations. The liquid does not have to be conductive or have a minimum conductivity as with the LPR systems. However, corrosion rates are not instantaneously determined. The time frame required to determine corrosion rates is a function of probe element and metal loss. Also, the ER probes are suitable only for uniform corrosion. There is no pit index built into the instrument. Any pits developed on the element will cause rapid penetration and indicate excessively high corrosion rates.

Typical probe elements are shown in Fig. 4. Appropriate response time information for any given probe can be obtained from the manufacturer. The corrosion rate is calculated from the change in dial reading on the instrument.

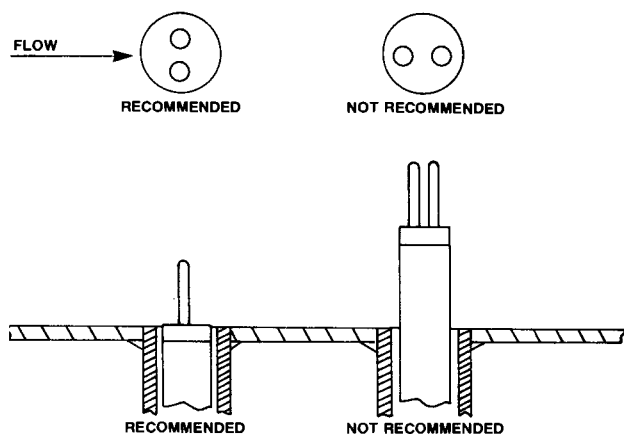


FIG. 3—Installation of LPR probe.

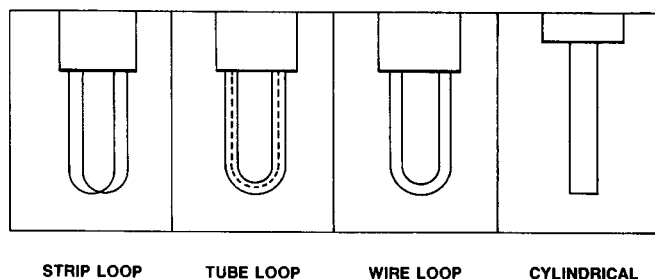


FIG. 4—Electrical resistance element design.

$$\text{Corrosion rate (mm/y)} = \frac{9.3 \times 10^{-3} \times \Delta D \times PF}{T}$$

where  $\Delta D$  is the change in the dial reading,  $PF$  is the probe factor (supplied with each probe), and  $T$  is the elapsed time in days. ER probes must be allowed to corrode for a period of time before accurate corrosion rate measurements can be made. The time duration depends upon the corrosion rate. The higher the rate, the shorter the time period and vice versa.

Probe placement in the fluid should be similar to LPR electrode placement; that is, the probe element should protrude into the fluid. Flow should pass the element. There is no specific orientation for the probe element.

Figure 5 shows a plot of dial setting or metal loss from the ER meter versus time, which can give an indication of corrosion rates. A large change in slope represents an increase in corrosion, whereas a zero slope indicates no significant increase in corrosion.

Generally, LPR is the preferred technology for on-line monitoring of corrosion in highly conductive waters such as those in industrial recirculating cooling water systems. The preference is based on two factors: 1) the relative instantaneous nature of the LPR, and 2) the distortional effect that even a single pit has on the ER measurement and reducing the usable life of the ER probe.

## CHEMICAL ANALYSIS

Water parameters relevant to the corrosion process can be provided through chemical analysis. This monitoring technique does not directly indicate corrosion rate but provides information on factors that can influence the corrosion process. It measures parameters that are known to be associated with acceptable or unacceptable corrosion processes within a system.

A thorough water analysis is not required of every water sample. However, there are core analyses that should be performed to determine the operating state of the system. It is good practice to periodically obtain complete analyses so that seasonal variations in water composition can be tracked.

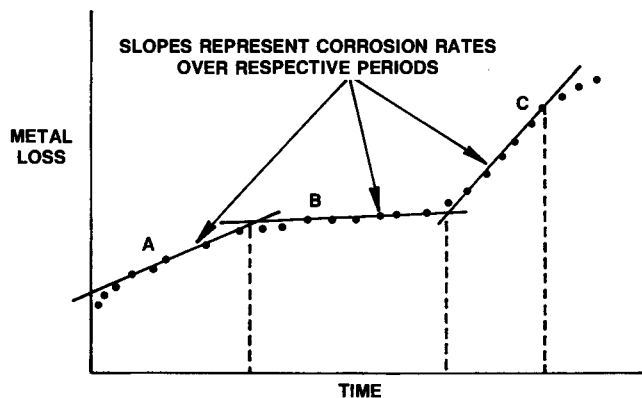


FIG. 5—Electrical resistance meter dial setting versus time. A is a medium corrosion rate, B is essentially no corrosion, and C is a high corrosion rate.

TABLE 5—Analytical parameters.

Species	Impact on Operating System
pH	Corrosion or scale-forming tendency.
P Reading	Monitor buffering capacity, differentiates $\text{OH}^-$ , $\text{CO}_3^{2-}$ , and $\text{HCO}_3^-$ .
M Reading	Provides data for calculating $\text{CaCO}_3$ potential. Includes all hydrogen titratable species, i.e., $\text{PO}_4^{3-}$ , $\text{SiO}_2$ , polymers. If pH/alkalinity relationship is outside of norm, then additional alkalinity value may be due to other titratable species.
Conductivity	Estimates total dissolved solids.
Suspended Solids	Monitors general water quality or turbidity.
Orthophosphate	Monitors inhibitor concentration and/or reversion.
Polyphosphate	Monitors inhibitor concentration.
Organic Phosphate	Monitors inhibitor concentration.
Total Organic Carbon	Monitors overall water quality.
Calcium, Total	Monitors potential hardness scale deposition.
Calcium, Dissolved	Monitors hardness scale deposition if value is different from calcium, total.
Magnesium, Total	Monitors potential deposition.
Magnesium, Dissolved	Monitors potential silicate or hydroxide deposition if value differs from magnesium, total.
Aluminum, Total	Monitors possible inhibitor adsorption, reducing corrosion protection if concentration $>0.1$ mg/L.
Aluminum, Dissolved	Monitors possible inhibitor adsorption, if concentration $>0.1$ mg/L. Loss of 3.5 mg/L of phosphate per 1 mg/L of aluminum.
Copper, Total	Monitors potential copper corrosion reducing steel corrosion protection if concentration $>0.1$ mg/L.
Copper, Dissolved	Monitors potential copper corrosion. Acceptable level $<0.05$ mg/L.
Zinc, Total	Monitors potential zinc scale deposition and level of treatment needed to inhibit/disperse solids.
Zinc, Dissolved	Monitors background levels and active synergist.

A “well check” analysis is also advisable. This consists of a thorough analysis when the plant is operating properly and corrosion rates are meeting the objectives. The well check can then be used as base line data when corrosion rates are outside the norm and analyses are being performed to determine the cause.

Parameters to be determined for a thorough analysis and their impact on corrosion/deposit are shown in Table 5.

## DISSOLVED OXYGEN MONITORING

Oxygen is the common cathodic reduction species found in water, which is responsible for continued corrosive attack on some engineering materials, such as low carbon steel. However, passive engineering alloys utilize the oxygen to form thin, tenacious, and adherent protective oxide films. Some common alloys with protective films are stainless steels, nickel alloys, copper-base alloys and aluminum alloys. The oxygen concentration at ambient temperatures and atmospheric pressure is approximately 6–8 mg/L. An increase in temperature decreases oxygen solubility, whereas an increase in pressure increases oxygen solubility.

In open cooling water environments, oxygen cannot be economically removed as an antagonistic species. Appropriate cathodic inhibitors control its impact on corrosion.

In boilers, it is a common practice to remove the oxygen from the water, since it is a major corrodent. Removal is through a combination of physical and chemical means. Deaerators physically remove the oxygen by purging the boiler feed water with steam, which heats and degases the water. Oxygen content can be reduced to 5–7  $\mu\text{g/L}$  by this method. Further reduction of oxygen is required and this is achieved through the use of chemical oxygen scavenger. The combination of deaeration and oxygen scavenger can reduce the oxygen content to zero.

Oxygen measurements can be made directly and continuously using online monitors or by wet chemical analysis.

## OXIDATION REDUCTION POTENTIAL (ORP)

Oxygen reduction potential (ORP), or redox potential, is the potential of a reversible oxidation-reduction electrode measured with respect to a reference electrode, corrected to the hydrogen electrode, in an electrolyte. It is an online, real-time measurement. In water treatment, ORP is used to control the addition of oxidizing biocides, such as chlorine, chlorine dioxide, bromine, hydrogen peroxide, ozone, etc. The presence of these chemicals will raise the ORP value. When an ORP probe is placed in the open recirculating cooling water environment in the absence of an oxidant, its value is taken as an initial set point. The addition of an oxidizing biocide increases the ORP value. The actual ORP reading depends upon concentration and activity of the oxidant or biocide, temperature of the system, contaminants and nutrients, pH and other parameters. Usually, at recommended concentrations of oxidizing biocides, the ORP value increases hundreds of millivolts depending upon the above parameters. Maintaining the recirculating water at the higher oxidizing potential assures adequate disinfection.

ORP measurements are similar to pH measurements. A typical ORP cell uses a platinum surface for measuring half of the potential and a silver-silver chloride in potassium chloride as a reference electrode. Maintenance of an ORP system is similar to that of a pH electrode; that is the ORP electrode should remain in the water circuit at all times.

Electrodes are replaced approximately every two years. The electrodes are cleaned in 5 % hydrochloric acid solution to remove any hard-water deposits that may form and interfere with the reference junction.

Quinhydrone is used to calibrate the ORP electrodes. By placing the quinhydrone in a known pH solution, a standard mV reading is achieved. An ORP value of 87 is obtained in a quinhydrone solution at pH 7, and 240 mV at pH 4. Other calibration protocol exists for higher ORP readings in the 600 mV range.

## HEAT TRANSFER SYSTEMS

Fouling and deposit monitors are used primarily to track the buildup of scale or deposits on heat transfer surfaces. The heat transfer tube can also be used as a tubular corrosion coupon to monitor corrosion under heat transfer conditions.

These units are designed to simulate heat exchangers under as near actual operating conditions as possible, taking into account ease of use and simplicity in design. Figure 6 shows a simplified schematic. An electric resistance heating element is used to impose a heat load on the tubular metal surface. The metal test specimen is inside a glass outer jacket in which water flows in the annular space. The glass tube makes it possible to visually examine the metal surface for deposit buildup or corrosion attack.

Heat flux ( $W/m^2$ ), which is the heat transfer rate ( $W$ ) divided by the exposed metal tube surface area ( $m^2$ ), is constant as long as no deposits accumulate on the specimen. However, deposits coming from hardness salts, corrosion by-products, silt, process contamination, biomass, etc., can form on the heated surface, raising the surface temperature. If the surface temperature becomes excessive, there is temperature cutoff switch to protect the device.

It is important to gather as much information about the system using fouling and deposit monitors as possible. Periodic visual inspection of the heat transfer tube is necessary to qualify the buildup of deposit. At the termination of the test, the tube deposit should be collected and chemically analyzed. Photographs of the deposits on the tube can be useful in describing the type of buildup. Also, photographs after the tube has been cleaned can be used to document the type of corrosion attack that has occurred, e.g., uniform, underdeposit, pitting, etc.

After the tube has been cleaned, the corrosion rate of the heat transfer tube should be determined. This rate should be compared with nonheat transfer coupons to determine the impact of heat flux.

## TEST HEAT EXCHANGER

The test heat exchanger is a monitoring tool that evaluates a heat transfer surface for corrosion and deposition. The test heat exchanger is only as good a monitoring or evaluating piece of equipment as its ability to duplicate or represent system conditions. The factors inherent in plant heat exchanger equipment that determine the corrosion and deposition of exchanger surfaces are:

- Product temperature, which determines metal skin temperature.
- Water flow velocity in the tube, which can influence fouling rate. Low velocities of 0–0.6 m/s (0–<2 ft/s) can result in more severe fouling. Average velocities of 1–2 m/s (3–5 ft/s) would correspond to normal rate of deposition. High velocities of 2–4 m/s (6–12 ft/s) will result in less fouling.
- Heat flux, a major influence on scale/deposition rate. Corrosion rates will also be influenced but to a lower degree. Heat flux of 0–6300  $W/m^2$  (0–2000  $BTU/ft^2-h$ ) are considered low. Heat flux of 6300–15 800  $W/m^2$  (2000–5000  $BTU/ft^2-h$ ) are average. Heat flux of 15 800–31 500  $W/m^2$  (5000–10 000  $BTU/ft^2-h$ ) are considered high.
- Cooling water temperature, which accepts heat from the plant exchanger.

FIG. 6—Corrosion deposit test unit.

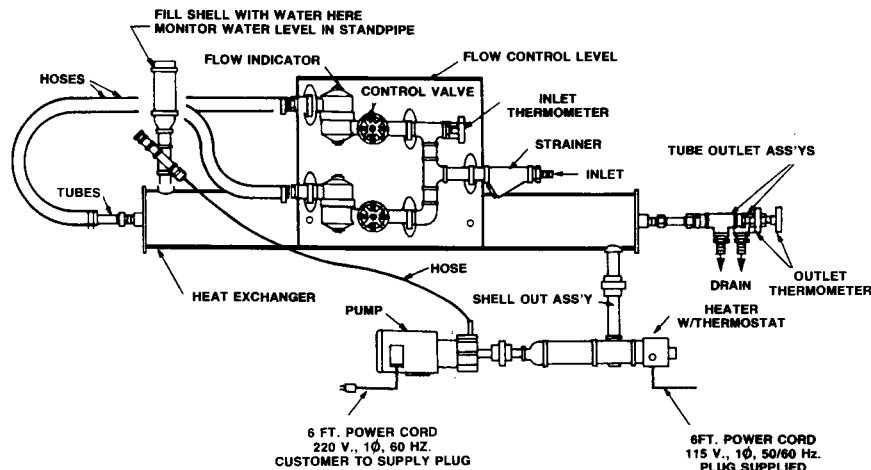


FIG. 7—Field evaluation test heat exchanger.

In order to obtain reliable results from a test heat exchanger, the above factors must be determined from the plant exchanger in the system that is to be duplicated. Once the plant parameters have been determined, they should be duplicated as nearly as possible in the test unit and held constant. Figure 7 is a schematic of a typical two-tube test heat exchanger. It is used to simulate tube side water conditions in a plant exchanger. Heated water or steam on the shell side is used to heat the tubes.

The flow of cooling water to the tubes must be controlled to maintain system velocity. An inlet water strainer is used to eliminate foreign objects, which can restrict flow. A valve ahead of a flow indicator controls flow.

The flow of hot liquid on the shell side is pumped through the exchanger and the temperature controlled by a thermostat. Thermometers on the inlet and outlet waters are used to determine temperature differential  $\Delta T^{\circ}\text{C}$ . Once the operating parameters have been selected and established, they should be checked and recorded on a per day or per shift basis.

The two-tube heat exchanger can be used to compare treatment, metallurgy, and the impact of heat flux on deposition by varying the flow in one of the tubes. At the end of the monitoring test period, which is at least 30 days, the heat transfer tubes should be evaluated for scale deposition, fouling, and corrosion. Analysis usually includes:

1. Cutting the tubes in half for visual inspection on both the heat transfer and nonheat transfer surfaces (tube extension outside the shell).
2. Scraping the deposits from the tube for analysis.
3. Brushing and chemically cleaning the tube to examine tube surface for general and localized corrosion.

These heat exchanger devices require considerable time and expertise to properly operate. They are not commonly used because of manpower commitment and ancillary expenses.

## CONCLUSION

A wide range of corrosion monitoring techniques is used in water treatment to systematically measure the corrosion or degradation of equipment and distribution piping. Corrosion monitoring is a viable tool to assess the performance of any chemical treatment program. There is no one technique that is universally applicable. The wide variety of corrosion monitoring tools can be used in any industry, and, although there are limitations on each technique, they provide a practical means to monitor corrosion behavior. More details on the various monitoring techniques can be found in the technical literature. Selected references include:

## REFERENCES

- [1] Ailor, W. H., *Handbook on Corrosion Testing and Evaluation*, John Wiley & Sons, Inc., NY, 1971.
- [2] ASTM D 2776, Test Methods for Corrosivity of Water in the Absence of Heat Transfer (Electrical Methods), *Annual Book of ASTM Standards*, ASTM International, West Conshohocken, PA.
- [3] ASTM G 96, Practice for On-line Monitoring of Corrosion in Plant Equipment (Electrical and Electrochemical Methods), *Annual Book of ASTM Standards*, ASTM International, West Conshohocken, PA.
- [4] ASTM G 102, Practice for Calculation of Corrosion Rates and Related Information from Electrochemical Measurements, *Annual Book of ASTM Standards*, ASTM International, West Conshohocken, PA.
- [5] NACE Standard TM0286, Cooling Water Test Units Incorporating Heat Transfer Services, NACE International, Houston, TX.
- [6] NACE Standard RP0189, Recommended Practice On-line Monitoring of Cooling Waters, NACE International, Houston, TX.

# Medical and Dental

*Anna C. Fraker<sup>1</sup>*

MEDICAL AND DENTAL MATERIALS are in the class of materials called biomaterials. Biomaterials are used in the body to replace body components or assist in retaining or restoring body functions. Biomaterials include synthetic materials, modified natural materials, biosynthetic materials, systems engineered materials, and morphological protein molecules that can send signals of direction to cells [1]. Synthetic biomaterials may be metallic, ceramic, polymeric, or a combination of these as needed to meet the needs of intended application.

Materials discussed in this chapter are metals. Some types of corrosion behavior discussed also apply to combinations of metals with ceramics or polymers. Information given in this chapter may serve as a guide for future assessment of metals and alloys considered for use as biomaterials.

Electrochemistry, a science of major importance to the medical and dental materials industry, was applied for the first time to medical materials in the 1930s [2,3]. Today, corrosion testing is conducted by the medical and dental materials industries and other research organizations to determine if materials planned for use in body environments are corrosion-resistant. Corrosion resistance assures that little or no ion release or degradation due to corrosion will occur during use in the body environment. In vitro corrosion test data can be used to screen and characterize the corrosion behavior of the materials, to determine chemical reactions, and to help predict suitability and stability in use. The application of corrosion testing to materials or devices is one of the first steps in developing or improving medical and dental materials and devices. Existing corrosion test methods using potentiostatic/galvanostatic techniques have been refined, ASTM recommended test methods have been developed, and alternating current (AC) impedance tests have been used to address specific problems of the medical and dental materials industry. New approaches to corrosion testing are required for porous coatings, surface layer coatings, and other modifications. Surface analysis techniques, such as Auger spectroscopy and electron spectroscopy for chemical analysis, are coupled with corrosion measurements to give a better understanding of the corrosion reactions and to characterize the interfacial surface of the implant. Scanning electrochemical microscopy (SECM), high-speed scratch testing and step-polarization impedance spectroscopy testing are techniques used to provide information

on surface variability, local electrochemical and mechanical phenomena and electrical properties of surface oxides [4]. A review of corrosion of biomaterials gives the environmental effects and test methods and susceptibility of implants to various types of corrosion [5].

The results of extensive corrosion testing, biocompatibility studies, and clinical evaluation have been used to select the corrosion-resistant metals and alloys that are in use as implants today. In addition, there are new materials being introduced as well as modifications of the currently used ones. Additional information on the biological and chemical reactions at the body/biomaterial interface would be useful in determining short- and long-term effects on the body and in preparing the biomaterial for its intended use.

This chapter provides general information on composition, mechanical properties, and corrosion behavior of some medical and dental metals used at present. References are provided for obtaining detailed information, and regulations and economics are discussed briefly. There is a wealth of information on medical and dental materials research that is not cited here and active investigations are continuing.

## GENERAL AND DESCRIPTIVE INFORMATION ON DEVICES AND MATERIALS

### Implants

The numbers of metallic surgical implants and dental implants in the U.S. are each in the range of 500 000 to 1 000 000 and are expected to increase. Projections of the U.S. Census Department are that the U.S. population over 65 years of age will increase 34 % from 1997–2015. This increase in the over 65 population is large when compared with the increase in population of all ages estimated to be 16 % for the same period. The total cost of a total hip joint may range from \$12 000–\$20 000, with 20 % of this cost being for materials (prosthesis). The total cost of a single dental implant may range from \$1000–\$1500, with the implant cost approximately 20 % of the total cost. Medical devices, equipment, and supplies comprise a \$100 B–\$200 B industry both in the U.S. and in the world [6]. U.S. firms are major suppliers in the worldwide market for medical devices, equipment, and supplies [6]. The World Health Organization (WHO) projects an increase in the over 65 population from 390 million in 1997 to 800 million in 2025.

<sup>1</sup>Retired, formerly Metallurgist, National Institute of Standards and Technology, Gaithersburg, MD 20899.



The success of the artificial hip joint replacement increased in the 1950s and 1960s. Charnley [7] and others introduced a joint that consisted of a metal femoral component articulating against an ultrahigh molecular weight polyethylene acetabular component with both components being inserted using polymethylmethacrylate cement. The success rates today, for periods of up to ten years, exceed 95 %. Current expectations for the life of total hip prostheses are 15–20 years if all aspects of the joint, installation, and patient's activities are optimized. The improved fixation of today using porous implants with and without cement as well as the introduction of new alloys and coatings and other biomaterials may further advance the service life of artificial hips. Biocompatibility increases in importance for porous implants since both surface area and time of implant duration increase. Some aspects of biocompatibility of metals, ceramics, and polymers have been discussed previously [8].

The success rate of dental implants increased dramatically during the 1980s [9]. Improved materials, selection of appropriate materials, and advanced technology have resulted in an improved implant/bone interface attachment that is responsible for the increased success. Success of dental implants is measured by the absence of mobility, no radiolucency between the bone and implant, and no other adverse symptoms or problems. The most successful dental implant today is the endosseous implant where the implant is anchored into the bone and osseointegrated. Success rates can be as high as 95 % over a five-year period [10,11]. Titanium and Ti-6Al-4V are the most widely used materials for the implants. The effects of surface treatment on the surface oxides of titanium have been shown [12,13]. Titanium was the material of choice for Branemark, who correlated the dental implant surface preparation and purity with the histology results of the interfacial bone [14].

The first requirement for an implant material is biocompatibility. The material must not cause any adverse reaction in the body. A second requirement is that the material must be corrosion resistant in the body environment. Corrosion resistance ensures that metal ions will not be released into the body, and the device will retain its integrity and not degrade due to corrosion. A third requirement is that the device must have sufficient mechanical strength and fatigue strength. A fourth requirement is appropriate design for the intended use. Crevices should be avoided to provide good corrosion resistance. A fifth requirement is the appropriate surface treatment. When the device is implanted into the bone, the surface of the device is the part that interfaces and could interact with body fluids and tissue. Surface treatment controls the nature of the surface and is important as a means of improving biocompatibility.

### Development of Surgical Implant Materials

Historical accounts of man's attempts to restore body functions are given in various references [15–23]. After the discovery of aseptic techniques in the 1860s by Joseph Lister [23] and the resulting decrease in infection, it became evident that the metals being used for repairs in the body were a limiting factor. Efforts were made to determine the most appropriate metals. Stainless steels began to be used

in 1926, and the cobalt-based alloys were first used in the mid-1930s [4]. Titanium was determined to be corrosion resistant in the body in the 1950s [24,25] and reported to be biocompatible [26] in 1973. Titanium and the alloy Ti-6Al-4V were not introduced as implants until the 1960s, and were not used much until the 1970s. The 1980s, 1990s, and 2000s saw increased use of titanium and its alloys for surgical and dental implants and for other dental uses.

Other modifications to surgical implants began to occur in the 1970s and continue until the present. Porous coatings were applied by arc plasma spraying [27] and by sintering of spheres [28] and wires [29]. The surface porosity was created for the purpose of providing better attachment of the implant to the tissue, making it possible to attach an implant without the use of polymethylmethacrylate cement. Further efforts to improve bony attachment to the implant involved applying a coating of hydroxyapatite,  $\text{Ca}_{10}(\text{PO}_4)_6(\text{OH})_2$ , to the porous metal implant [30]. Various aspects of hydroxyapatite coatings are the subjects of numerous papers and studies today.

Another technique that has been investigated for improving the attachment of bone to the device is bone growth stimulation by the application of electrical currents [31,32]. Some bone growth increase was observed in the initial stages, but not in later stages. Recent studies of electrical stimulation on bone growth give results ranging from detrimental and no improvement to improvement initially.

Metallurgical processing played an important role in the improvement of surgical implants in the 1970s and 1980s. This is evidenced by the improved fatigue strength of cobalt-chromium-molybdenum alloys due to annealing, thermomechanical processing, and forging [33–36]. The influence of heat treatment on corrosion-fatigue [37,38] and fatigue strength [39] of Ti-6Al-4V and titanium alloys, and duplex annealing of stainless steels [40] showed the benefits of metallurgical processing. A review article on modern processing of metal implants covers a number of processes that are being used as well as new possibilities for the future, and discusses properties that accompany various processing methods [41]. Surface ion implantation of nitrogen into Ti-6Al-4V has been done to improve the wear resistance [42]. Noble elements have been ion implanted into the surface to improve corrosion resistance [43]. Wear resistance is an important property for both medical and dental devices and materials [44,45].

### Metallic Dental Materials

Dental materials must serve to restore the function of the original biological tooth or part, and the restoration should be aesthetically acceptable if possible. Aesthetics present additional challenges in materials bonding and potential corrosion problems. Tarnish and corrosion of dental alloys [46] and descriptions of dental materials [47] have been discussed previously. Some of the reported earliest uses of synthetic materials in the body were for dental purposes [15,16,18,48,49].

A discussion of some dental uses of synthetic materials and associated repairs follows. Amalgams (based on mixing  $\text{Ag}_3\text{Sn} + \text{Hg}$ ) [50], and (sometimes) gold foil or gold powder are used for direct fillings. Acid assisted consolidation of

precipitated, nanosize silver powder is being studied as a potential process for direct fillings [51]. Cobalt-chromium, nickel-chromium, and titanium-based alloys are used for crowns and partial dentures (fixed and removable), although iron-based and other alloys have been used. Gold, palladium, nickel, and cobalt-based alloys are the predominant systems used for crowns and restorations involving fusing porcelain to metal. Metals used as dental implants and support structures include cobalt-chromium, nickel-chromium, stainless steel, titanium, and titanium alloys. Titanium and Ti-6Al-4V are the most widely used dental implant materials. Stainless steel, cobalt-chromium, nickel-titanium shape-memory alloy, and beta-titanium alloys are used for orthodontic wires. Gold solders, silver solders, and other special solders are used for joining metals.

### Other Uses

Metals are used in the cardiovascular area including heart valves, heart pacemaker leads, and heart pacemaker cases. These metals include titanium, titanium alloys, cobalt-chromium alloys, and cobalt-nickel alloys. Metals used for aneurism clips include cobalt-chromium-molybdenum alloys, cobalt-nickel-chromium-molybdenum alloys, and, previously, stainless steels were used. Metal seeds are used for fractionated hyperthermia treatment of prostate disease, and corrosion analysis showed the alloy, PdCo may be suitable for the seed implants [52].

### CAUTION—Magnetic Resonance Imaging

The use of magnetic resonance imaging (MRI) devices is not recommended for individuals with electrically, magnetically, or mechanically activated implants such as cardiac pacemakers, hearing aids, etc. The magnetic field will interfere with the operation of these devices and could destroy the device. MRI is not recommended for individuals who have aneurysm clips. MRI is not recommended for individuals who have metal clips or other implanted devices that are ferromagnetic, as these devices could be moved out of position. It may be best not to use MRI with individuals who have metallic implants. Sometimes, it is not known what type of metal is implanted and there is the possibility of heat generation by the metals. There is a Federal Register notice [53,54] regarding MRI devices, and some information is available regarding specific metals and devices that do not preclude the use of MRI.

## TYPES OF METALS USED

### Surgical Implant Alloys

Metals and alloys used for surgical implants in the U.S. include 316L stainless steel, cobalt-chromium-molybdenum, cobalt-chromium-tungsten-nickel, cobalt-nickel-chromium-molybdenum, titanium, Ti-6Al-4V, and tantalum. Variations of these alloys, including other alpha-beta titanium alloys, beta titanium alloys, Ti-Ni memory alloy, nitrogenated stainless steel and other cobalt alloys have ASTM-F4 specifications and are being used or considered for surgical implant use. Chemical compositions of selected metals and alloys are given in Table 1. Effects of various elements in alloys can be significant and are discussed in metallurgical texts and handbooks [49]. In some cases, small differences in composition result in alloy phase and microstructural changes that can alter corrosion and mechanical property behavior. There is an ASTM F-4 specification for each variation of the alloys and forms such as wrought, wire, coating powders.

Mechanical property data for selected alloys are given in the specifications of Table 2. One requirement for a load bearing implant is that it be strong enough to support the load. The high modulus of elasticity of these materials and the resulting stiffness can act to shield the bone from the stress necessary to produce new bone growth. Efforts of substituting other materials or composites with a lower modulus of elasticity have not been successful due to lack of strength and fatigue failure. Fatigue fracture is a risk if the materials are too weak, and the avoidance of fatigue is the reason for applying the previously mentioned special thermomechanical processing, forging, and annealing treatments to the alloys.

The compositions and mechanical property data in Tables 1 and 2 are taken from ASTM International Specifications [55]. There are other metals and alloys that have been approved under *market clearance* (510K) for use in the United States by the Food and Drug Administration and other alloys in use in other countries that are not listed here. Chemical and mechanical property data for alloys not in Tables 1 and 2 are available through ASTM specifications.

The composition of 316L stainless steel used for surgical implants is of the austenitic type which has a face centered cubic (fcc) crystal structure and the highest corrosion resistance for this kind of iron alloy. A compositional or processing change that produces a different crystal structure in this

TABLE 1—Compositions of selected metals and alloys.

Metal/Alloy	Co	Cr	Ni	Mo	Fe	Ti	C	Other
Stainless Steel, F138	—	17.0-19.0	13.0-15.0	2.0-3.0	Bal.	—	0.030	Max. 0.5Cu, 2.0Mn, 0.025P, 0.75Si, 0.20S, 0.10N
Co-Cr-Mo, Cast, F75	Bal.	27.0-30.0	1.0	5.0-7.0	0.75	—	0.35	1.0Si, 1.0Mn
Co-Cr-W-Ni, Wrought, F90	Bal.	19.0-21.0	9.0-11.0	—	3.0 Max.	—	0.05-0.15	14.0-16.0W, 1.0-2.0Mn, Max.- 0.4Si, 0.04P, 0.03S
Co-Ni-Cr-Mo, Wrought, F562	Bal.	19.0-21.0	33.0-37.0	9.0-10.5	1.0 Max.	1.0 Max.	0.025 Max.	Max.- 0.15Mn, 0.15Si, 0.015P, 0.010S
Titanium, F67	—	—	—	—	0.20 Max.	Bal.	0.10 Max.	Max.- 0.03N, 0.015H, 0.18O
Ti-6Al-4V, Wrought, F136	—	—	—	—	0.25 Max.	—	0.08 Max.	5.5-6.5Al, 3.5-4.5V, Max.- 0.05N, 0.12H, 0.13O
Tantalum, F560	—	—	0.010	0.020	0.010	0.010	0.010	0.015O, 0.010N, 0.0015H, 0.10Nb, 0.05W, 0.005Si

TABLE 2—Mechanical properties of metals and alloys.

Metal or Alloy	Yield Strength, MPa	Tensile Strength, MPa	Modulus of Elasticity, GPa	Elongation, %
316L stainless steel, annealed	207	517		40
316L stainless steel, cold-worked	689	862	200	12
Co-Cr-Mo, cast	450	655	248	8
Co-Cr-Mo, thermomechanically processed	827	1172		12
Co-Cr-W-Ni, wrought	379	896	242	
Co-Ni-Cr-Mo, annealed	241-448	793-1000	228	50
Co-Ni-Cr-Mo, cold-worked and aged	1586	1793		8
Titanium, Grade 1	170-310	240		24
Titanium, Grade 4	483-655	550	110	16
Ti-6Al-4V, ELI annealed	827	896	124	10
Tantalum, annealed	138	172		
Tantalum, cold-worked	345	480		

iron alloy is to be avoided. Chromium must be present within the range designated to give adequate corrosion resistance, but chromium is a ferrite former, and ferrite has a body centered cubic (bcc) crystal structure. Molybdenum, another ferrite former, is added in a mass fraction at 2–3 % to increase corrosion resistance (especially pitting resistance). Molybdenum content must not exceed a mass fraction at 3 % as amounts above this could result in ferrite formation and could lower corrosion resistance to oxidizing environments. Nickel is added as an austenitic stabilizer. Since carbon, also an austenite stabilizer, is more soluble in austenite than in ferrite, the nickel addition helps to keep the carbon in solution and prevent formation of martensite. Carbon serves to strengthen the stainless steel, but the carbon must remain in solution. Users and producers should be aware that improper heat-treating causes sensitization to corrosion via chromium carbide formation that depletes grain boundary areas of chromium necessary for corrosion resistance. Sensitization results in intergranular corrosion, and also cracking and pitting. Stainless steel must be in the cold-worked condition to have adequate mechanical properties for a load bearing implant. Nitrogen, another austenitic stabilizer, is added to stainless steel for strengthening, improving mechanical properties, and increasing corrosion resistance. Nitrogen, like carbon, must be in solid solution, or similar precipitated phases as with carbon, can occur. The influence on corrosion of stainless steel is synergistic with elemental additions, heat treatment and/or processing due to changes that occur in the microstructure such as precipitates, phase formation, and solid solution chemistry. Metallurgical aspects of stainless steel, the use stainless steels as implants, and stainless steels without nickel also have been discussed [56].

Titanium alloys undergo phase changes from hexagonal close packed (hcp), alpha phase, to bcc, beta phase, at a temperature near 882°C. The alpha/beta transus temperature and the relative amounts of the two phases are dependent on the composition. Aluminum, oxygen, tin, and zirconium are alpha stabilizers (hcp phase). Chromium, vanadium, molybdenum, niobium, iron, and manganese are beta phase (bcc) stabilizers. Corrosion-fatigue behavior of titanium alloys is directly related to microstructures that result from composition, heat treatment, and cooling procedures. Heat treatment and cooling rates are important aspects of the microstructural formation due to the phase

changes. The use of unalloyed titanium [57] and beta titanium alloys as implants has been described [58,59].

Cobalt-chromium-molybdenum alloys can be strengthened by carbide formation and alloying with refractory metals (such as molybdenum) that go into solution. Further strengthening can be accomplished with forged or hot isostatically pressed (HIP) materials that have microstructures showing twinning and smaller carbide phases [49]. Cooling rates must be controlled carefully to prevent agglomeration of carbides that could reduce the fatigue strength. Microstructures of cast Co-Cr-Mo alloys show large grains with visible carbide phases present where  $\text{Cr}_{23}\text{C}_6$  is the principal carbide formed but  $\text{Cr}_7\text{C}_3$  and the  $\text{M}_6\text{C}$  type, where M is cobalt and molybdenum, also form [35,36,60]. The use of cobalt alloys as implants has been described [61].

## Dental Alloys

Dental alloy properties, compositions, and uses are discussed in detail elsewhere [45,47,62,63,64]. Representative compositions of base metal alloys are given in Table 3. There are four types of gold alloys, and these are represented in Table 4. Other precious metal alloys that are widely used include gold with palladium ranging up to a mass fraction at 50 % plus silver or zinc. High palladium alloys may have up to a mass fraction at 80 % palladium, with platinum, silver, tin, copper, and gallium. High-noble, single-phase alloys have the highest corrosion resistance and would be recommended, but this does not rule out exceptions or considerations on a case-by-case basis [64].

The constituents of alloy powders used with mercury to form amalgams are mass fractions at 66.7–75.5 % silver, 25.3–27.0 % tin, 0–6.0 % copper, and 0–1.9 % zinc. Spherical particles of the Ag-Cu eutectic, mass fractions at 72 % Ag-28 % Cu, are added to conventional alloy powders in a ratio of 1 part Ag-Cu:2 parts conventional powder to produce an improved amalgam. If formation of the  $\text{Sn}_{7-8}\text{Hg}$  phase occurs, increased corrosion will result. Copper additions usually prevent the formation of the  $\text{Sn}_{7-8}\text{Hg}$  phase. Physical property measurements of dental amalgams showed that copper additions resulted in low static creep and high compressive strength and comparable tensile strength and dimensional change when compared with conventional alloys [65]. There are many variations of the composition ranges for the alloy powders.

TABLE 3—Compositions of representative dental alloys.

Use/Alloy	Co	Cr	Ni	Mo	Fe	Ti	C	Other
<b>Crown &amp; Bridge</b>								
Ni-Cr	—	12.5-20.0	66.0-81.0	1.5-7.0	0-0.8	—	0.0-0.2	1.8-3Al, 0-3.2Mn, 0-3.0Si, 0-2.1Be, 0-2.9B
Fe-Cr	0.8	29.0	6.0	2.5	46	—	0.35	
Cu-Al			5.0	—	3.0 Max.	—	—	72Cu, 20.0Al, 0.7Mn
<b>Partial Denture</b>								
Co-Cr	60.0-62.5	26.0-32.0	0-2.7	5.0-5.8	0-2.6	—	0.3-0.5	0.3W, 0.1Pt, 0.05Ga
<b>Wires</b>								
18-8 stainless steel	—	17.0-19.0	8-10	—	Bal.	—	0.08-0.2	2.0 Mn
TiNi (Nitinol)	1.4	—	48.6	—	—	50.0	—	—
Co-Cr-Ni	40	20	15	7.0	15.0	—	0.15	—
Beta titanium	—	—	—	11.5	—	Bal.	—	—
<b>Implants</b>								
Titanium, F67	—	—	—	—	—	Bal.	0.10 Max.	Max.-0.03N, 0.015H, 0.18O
Ti-6Al-4V, Wrought, F136	—	—	—	—	0.25 Max.	—	0.08 Max.	5.5-6.5Al, 3.5-4.5V, Max.-0.05N, 0.012H, 0.13O
Co-Cr-Mo	Bal.	27.0-30.0	0.3-1.0	5.0-7.0	0.75-1.0	—	0.35	1.0Si, 1.0Mn
Co-Cr-W-Ni	Bal.	19.0-21.0	9.0-11.0	—	3.0	—	0.05-0.15	14.0-16.0W, 1.0-2.0Mn, 0.4Si, 0.04P, 0.03S

TABLE 4—Typical compositions (wt%) of cast dental gold alloys [12].

No. and Type	Au	Ag	Cu	Pd	Pt	Zn
<b>Yellow golds</b>						
Type I Soft	79-92.5	3-12	2-4.5	0.5 max	0.5 max	0.5 max
Type II Medium	75-78	12-14.5	7-10	1-4	1	0.5
Type III Hard	62-78	8-26	8-11	2-4	3	1
Type IV Extra Hard (partial denture)	60-71.5	4.5-20	11-16	5 max	8.5 max	1-12
<b>White golds</b>						
Type III Hard	65-70	7-12	6-10	10-12	4	1-2
Type IV Extra Hard (partial denture)	60-65	10-15	9-12	6-10	4.8	1-2
Type IV Extra Hard (partial denture)	23-30	25-30	20-25	15-20	3-7	0.5-1.5

Solders are composed primarily of gold, silver, or copper with and without tin and zinc. Other metallic materials used for dental fillings in place of amalgams include cold welded silver powder [51] as mentioned earlier.

### Surface Modification

The corrosion resistance of some of the materials, especially stainless steel, can be improved by increasing the thickness of the film through further oxidization. ASTM F 86, Practice for Surface Preparation and Marking of Metallic Surgical Implants, is applicable to the iron alloys and cobalt- and nickel-based alloys. One of the final steps in ASTM F86 is a passivating treatment. Studies [66] showed that passivation treatments in either HNO<sub>3</sub> or oxygenated isotonic sodium chloride had a beneficial effect on the corrosion rate of 316 stainless steel and cobalt-chromium alloys, but had a negligible effect on the corrosion rate of titanium. The use of oxygenated isotonic NaCl was recommended for titanium and titanium alloys over HNO<sub>3</sub>. Other studies recommended the use of isotonic saline for the final washing of titanium and its alloys [14]. Steam and dry heat sterilization produce surface changes that reduce the corrosion rate for stainless steel, have a lesser effect for titanium, and have a negligible effect for Co-Cr alloys [66]. If the thicker oxide formed during passivation is not stable in the

body environment, this oxide provides an avenue for increased metal ion release. Measurements of the open circuit electrode potential over time for these metals exposed to Hanks' solution, a simulated body fluid, show that in vitro potential reaches the same value for these materials regardless of the initial oxide coating [67]. "Natural" oxide films on titanium range in thickness from 0.5-7 nm, depending on alloy composition, environmental exposure, and temperature [68].

Carbon coating of titanium and Ti-6Al-4V [69] and noble metal ion implantation followed by dealloying to enrich the percent of noble element in the surface [70] are examples of other methods used to improve corrosion resistance. Promising treatments such as these need further study, especially regarding corrosion-fatigue, susceptibility to pitting, and long-term behavior. Indications are that the carbon coating on the cobalt-chromium-molybdenum alloy causes a decrease in corrosion resistance due to chromium depletion in the matrix [71].

Hydroxyapatite is the main mineral constituent of bone, and it was expected to accelerate bone formation and to have the added benefit of shielding the bone from the metal. Initially, the accelerated bone growth occurs. Questions regarding hydroxyapatite coatings include the chemical composition of the coating after application, the nature of the metal/coating interface, the strength of the metal/coating

interface bond, and the needed thickness of the coating. The chemistry of hydroxyapatite has been discussed [72]. There are numerous literature references on hydroxyapatite and hydroxyapatite coatings.

## MINIMIZATION OF CORROSION

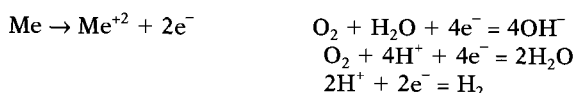
### Corrosion of Metals and Alloys

Base metals and alloys used in medical and dental devices are corrosion-resistant due to the presence of an oxide film on the surface that is protective [49]. These materials are not corrosion-resistant initially as is evident from their positions in the electromotive force series. The galvanic series, a listing of electrode potentials measured in seawater, indicates the changes in the noble and active tendencies of these materials in practical use for this given environment. Passivity is dependent on environmental factors such as solution pH, temperature, ions, oxygen, etc. Some ways of minimizing corrosion of these materials follow. Others are given in the discussion of the types of corrosion that can occur.

1. The surface preparation procedures described in ASTM F 86 passivate stainless steels and cobalt alloys. Titanium materials do not require this passivation. It is not clear what the ideal surface for the metal implants should be, and this will continue to be an aspect of studies relating to interfaces of these materials with the body. The condition of the surface may influence ion release.
2. Another way to minimize corrosion is to shield the metal from the body by a coating such as the hydroxyapatite coatings, but this procedure presents problems of cracking of the hydroxyapatite coating and integrity of bonding of the hydroxyapatite to the metal.
3. An important consideration for the minimization of corrosion of load bearing implants is to control the microstructure and surface conditions to give the highest corrosion-fatigue strength.

Corrosion of metal implants has been reviewed previously [5,18,49,73], and references are cited to numerous other studies relating to corrosion of implants. In vivo testing is covered in Chapter 42 of this manual. Corrosion occurs initially due to difference in potential of the anodic and cathodic sites and the tendency to establish the most stable system for a metal in an environment. The change in free energy associated with electrochemical reactions is  $\Delta G = -nFE$ , where  $\Delta G$  is the change in free energy,  $n$  is the number of electrons,  $F$  is the Faraday constant, and  $E$  is the cell potential. A negative  $\Delta G$  increases the tendency for corrosion to occur. During corrosion, one equivalent weight of metal ions is released for every 96 500 coulombs (1 Faraday) of electricity passed through the solution. Representative chemical reactions in an aqueous environment are:

- (1) anodic (loss of electrons) (2) cathodic (gain of electrons)



At physiological pH 7.4, the most probable reduction reaction is  $\text{O}_2 + \text{H}_2\text{O} + 4\text{e}^- = 4\text{OH}^-$ . At the corrosion potential,

the open circuit potential of a metal in a given environment, anodic and cathodic reactions occur at equal rates. Extensions of the anodic and cathodic curves result in Evan's diagrams that are used to show which reaction is controlling the corrosion process. One of the reactions, either anodic or cathodic, often dominates the process, and there will be a shift in the slope of the anodic or cathodic line to indicate this control. These reactions occur at cathodic and anodic sites on the metal or these sites can be on dissimilar metals that are electrically connected. The driving force for corrosion reactions to occur is the difference in potential between the anodic and cathodic sites.

ASTM G 3 (Practice for Conventions Applicable to Electrochemical Measurements in Corrosion Testing) [74] and Refs 49, 55, and 73 show the schematics for the apparatus for corrosion measurements and schematic drawings for cathodic and anodic polarization diagrams and polarization plots. ASTM G 5 (Standard Reference Test Method for Making Potentiostatic and Potentiodynamic Anodic Polarization Measurements) [74] and ASTM F 4 [55] test methods and practices describe the setup and procedures for making potentiostatic and potentiodynamic anodic polarization measurements. A cyclic polarization curve that contains both the cathodic and anodic portions provides data that can be used to describe corrosion behavior in terms of passivity, breakdown, corrosion rate, and susceptibility to pitting.

Pourbaix diagrams [75] are plots that describe the thermodynamically stable chemical species that exist for various pH and potential values for a given metal and set of electrolyte conditions. These diagrams indicate potential/pH ranges of immunity, corrosion, and passivity and are useful as guides to study effects of electrode potential and solution pH.

## TYPES OF CORROSION CONSIDERED

Many of the types of corrosion are localized in nature. These various types of corrosion will be described briefly here and additional information may be found in other references and chapters of this manual. The types of corrosion are pitting, crevice corrosion, fretting, corrosion-fatigue, stress-corrosion cracking (SCC), intergranular corrosion, and galvanic corrosion. In addition to the localized types of corrosion, the chemical dissolution or change of surface films that occurs after implantation is important. Interface reactions and initial reactions of the implant with the body are recognized as factors in implant success.

### Pitting

Pitting is an extreme and severe form of localized corrosion where the anode usually is smaller than the cathode, resulting in a high current density at the pit site and release of significant amounts of metal ions. Pitting causes visible and unknown damage as well as the release of metal ions. Pit initiation can result from a break in the protective film, inclusions or defects in the metal, defects in the film, etc. The first corrosion test method developed by the ASTM Joint F4/G1 Corrosion Section, ASTM F 746, was for screening materials for susceptibility to pitting or crevice corrosion, or both [55,74]. Pitting corrosion also can be assessed

by studying the pit propagation rate [76,77]. Pitting cannot be tolerated for surgical implant materials for a number of reasons, including the release of metal ions and the possibility of serving as a crack initiator in the relatively small piece. The cyclic polarization method of ASTM G 61 (Test Method for Conducting Cyclic Potentiodynamic Polarization Measurements for Localized Corrosion Susceptibility of Iron-, Nickel-, or Cobalt-based Alloys) [74] can be used for determining a tendency to pitting. This analysis is based on hysteresis in the return curve compared to the original curve, but interpretation of these cyclic polarization curves is required since other parameters can be responsible for the hysteresis. Pitting resistance of implant metals [78] and of Co-Cr-Mo [79–81] and Co-Ni-Mo alloys [81] has been studied.

### Crevice Corrosion

Crevice corrosion is a localized attack similar to pitting that occurs when an area of the metal is shielded from the environment. This can happen at threaded junctions, screw heads, etc. Metals and alloys not susceptible to pitting can undergo crevice corrosion. Crevice corrosion often can be avoided by design. In vitro tests [79] of Co-Cr-Mo indicated that crevice corrosion possibly could occur. In vivo tests in animals after two years showed no crevice corrosion of Co-Cr-Mo [80,81].

### Corrosion-Fatigue

Corrosion-fatigue occurs as a result of the complementary action of corrosion and mechanical damage. ASTM F 1801-97 is a Standard Practice for Corrosion Fatigue Testing of Metallic Implant Materials [55]. One of the most important requirements for load bearing implants, subjected to cyclic motion, is corrosion-fatigue resistance. Materials that undergo degradation in a corrosive environment do not have a corrosion-fatigue limit in the S/N (stress or applied shear strain amplitude versus number of cycles to failure) curves, below which there is no failure [49]. Fatigue tests of 316L stainless steel [82,83] and Co-Cr-Mo [84] in aqueous solution show a decrease in fatigue strength when compared to the fatigue strength measured in air. Comparison of results [37,85] showed only a slight decrease of fatigue strength for the Ti-6Al-4V alloy when tested in Hanks's solution instead of air. Another aspect of fatigue measurements, cycle frequency, may not significantly affect the fatigue strength when testing in air, but corrosion-fatigue measurements made in a corrosive medium are affected by cycle frequency. High frequencies in corrosion-fatigue testing will result in higher fatigue strengths compared to fatigue strengths from test runs at low frequencies that simulate in vivo loading in walking, such as 1 Hz. A frequency of 1 Hz has been used for many corrosion-fatigue tests. Microstructures and surface conditions influence corrosion-fatigue strength. Corrosion-fatigue measurements of implant metals and effects of heat treating Ti-6Al-4V have been discussed, and it was shown that the corrosion-fatigue life could be increased by heat treating at 900°C and rapid quenching [85]. The rate of quenching is difficult to control. The specification for Ti-6Al-4V, ASTM F 136 (Specification for Wrought Titanium 6Al-4V ELI Alloy for Surgical Implant

Applications) [55] is for the annealed form and contains specific microstructural requirements.

### Stress Corrosion Cracking

Stress corrosion cracking (SCC) is the result of a metal being subjected to a tensile stress in a corroding medium [86]. SCC appears to be complex and more than one mechanism may be involved. One mechanism involves film rupture and dissolution, where preferred anodic dissolution of the crack tip is enhanced due to plastic deformation that occurs at the area exposed by the break in the film. Another postulated mechanism involves the absorption of ions in the strained areas at the crack tip resulting in weakening the bonds within the metal and the film. Another possible explanation is that SCC is a series of brittle fractures. SCC is different from corrosion-fatigue in that the load is static. Fractures resulting from SCC exhibit more branching than those from the more direct paths of corrosion-fatigue fractures. Hydrogen embrittlement is related to SCC and corrosion fatigue, but the difference is that hydrogen embrittlement is caused by the absorption of hydrogen. This hydrogen absorption embrittles the metal and causes cracking. Studies of Co-Cr-Mo alloys in Ringer's solution showed these alloys to be subject to hydrogen embrittlement [87]. SCC generally is not considered to be a problem with surgical implant metals in use at present, and it is mentioned here for information.

### Fretting Corrosion

Fretting, a complementary process of wear and corrosion occurs when a small amplitude relative oscillatory motion between two surfaces that are in contact causes a disruption of the passive film. The passive film is removed by abrasion and other damage, leaving the underlying metal to repassivate by forming another oxide film. Debris produced can serve to accelerate abrasion, and debris can be released into the body. Implant metals require an oxide film for passivity, and will be subject to crevice corrosion. Fretting can occur in articulating devices or at screw plate junctions and in other similar arrangements. When possible, it is best to avoid circumstances or designs in which fretting could occur and to make efforts to prevent it. Wear is an aspect of fretting, and is an important consideration for articulating joints [44] and for dental uses [45].

### Intergranular Corrosion

Grain boundaries or areas adjacent to grain boundaries can become depleted or enriched in elements or compounds. Grain boundaries are regions of crystallographic disorder where contaminants and second phase precipitation are found. This can cause the grain boundary or adjacent area to become either anodic or cathodic to the rest of the grain, and the result is intergranular corrosion.

### Galvanic Corrosion

Galvanic corrosion occurs between dissimilar metals that are in contact and have a difference in potential. The less

noble metal is the anode and the other metal is the cathode. The surface area ratio of the anode to the cathode is important. Reactions at a small anode relative to the cathode will produce high current densities while low current densities result if the ratio is reversed and the anode is large. There are cases where combining dissimilar metals results in improved protection for the less noble alloy. Titanium combined with platinum in acid solutions is an example of this [62,79]. In the case of titanium/platinum, the corrosion potential of the titanium is moved from the active region to the passive region. Combining dissimilar metals for any application, and especially for implants, should not be done without applying corrosion principles and testing. Tests of selected surgical implant metals [88–91] indicate that it would be possible to use coupled or dissimilar metals. Recent analyses of numerous retrieved total hip prostheses made of two of these selected metals [91–93], Co-Cr-Mo head coupled with a Ti-6Al-4V stem for the femoral component, gave conflicting reports. One study [92] included 48 of these coupled metal hip prostheses and concluded that no corrosion had occurred in a period below 9.8 months but corrosion had occurred in all components that had been in place longer than 40 months. Another study, involving analysis of 18 Co-Cr-Mo/Ti-6Al-4V prostheses and eight alumina/Al<sub>2</sub>O<sub>3</sub>/Ti-6Al-4V prostheses that had been implanted for 36–60 months, showed no evidence of corrosion or pitting on either of the metal surfaces. Fretting had occurred in one instance with the Co-Cr-Mo/Ti-6Al-4V prosthesis and in two cases with the alumina/Ti-6Al-4V prosthesis [93]. A report of eight Co-Cr-Mo/Ti-6Al-4V prostheses that had been taken from a larger sample showed no significant alloy corrosion at the interfaces. This report cautioned against usage of the combined materials if any motion could occur at the contact zone [94]. Other laboratory studies indicated that coupling cobalt and titanium alloys did not result in short term corrosion unless fretting occurred [95]. A discussion of possible mechanisms for corrosion of the coupled alloys concluded that controlled laboratory electrochemical testing correlated with retrieval studies is needed [96]. While it is useful to combine the advantages of two different alloys in a single prosthesis, the coupling may cause corrosion problems even when not predicted from corrosion tests that do not consider fretting. The problems may arise from design or reduced tolerances arising from manufacturing or surgical placement that permits micromotion between parts. Micromotion may destroy the passive film and negate conditions that otherwise would have permitted the use of dissimilar metals.

In dentistry, the presence of amalgams and various alloys in the mouth poses potential corrosion problems if an electrical connection occurs. Growing numbers of dental implants increase the possibility for corrosion in the mouth, and consideration should be given to suprastructure metals that are used with implants.

## DESCRIPTION OF CORROSION ENVIRONMENTS

Environments used in vitro testing are saline in nature with various additions. A comparison of in vitro and in vivo

**TABLE 5**—Composition of Hanks' solution.

Solution A
160 g NaCl + 8 g KCl + 4 g MgSO <sub>4</sub> 7H <sub>2</sub> O in 800 mL H <sub>2</sub> O
Solution B
2.8 g CaCl <sub>2</sub> in 100 mL H <sub>2</sub> O
Solution C
A + B + 100 mL H <sub>2</sub> O + 2 mL CHCl <sub>3</sub> (chloroform)
Solution D
1.2 g Na <sub>2</sub> HPO <sub>4</sub> 7H <sub>2</sub> O + 2.0 g KH <sub>2</sub> PO <sub>4</sub> H <sub>2</sub> O + 20.0 g glucose + 2 mL CHCl <sub>3</sub> in 800 mL H <sub>2</sub> O—diluted to 1000 mL
Solution E
1.4% NaHCO <sub>3</sub> = 7 g NaHCO <sub>3</sub> in 500 mL H <sub>2</sub> O
Final Solution
50 mL C + 50 mL D + 24 mL E + 900 mL H <sub>2</sub> O + few drops of chloroform

**TABLE 6**—Composition of Ringer's and modified Krebs-Ringer solutions.

(a) 8.6 g NaCl + 0.30 g KCl + 0.33 g CaCl <sub>2</sub> + water to make 1000 mL
(b) To 900 mL of 0.154 mol/L NaCl, add 20 mL 0.154 mol/L KCl and 20 mL 0.11 mol/L CaCl <sub>2</sub>
(c) Krebs-Ringer—100 parts by volume of 0.154 mol/L NaCl + 4 parts 0.154 mol/L KCl + 3 parts 0.11 mol/L CaCl <sub>2</sub> + 1 part 0.154 mol/L MgSO <sub>4</sub> + 21 parts 0.16 phosphate buffer.

**TABLE 7**—Composition of Fusayama's solution.

0.400 g NaCl + 0.400 g KCl + 0.795 g CaCl <sub>2</sub> 2H <sub>2</sub> O + 0.690 NaH <sub>2</sub> PO <sub>4</sub> H <sub>2</sub> O + Na <sub>2</sub> S 9H <sub>2</sub> O + 1.00 Urea + H <sub>2</sub> O to make 1000 mL.
--

tests recommended isotonic sodium chloride as an appropriate test solution for implant metals [97]. The study showed that the corrosivity of in vivo exposure for stainless steel and the corrosivity of titanium were less in vivo than in isotonic saline. Two common testing solutions relating to simulated body fluids are Hanks' and Ringer's physiological solutions. The compositions of these solutions are given in Tables 5 and 6, respectively. Table 6 gives compositions for (a) Ringer's, (b) Ringer's, and (c) Krebs-Ringer solutions. One of the artificial solutions for simulating conditions in the mouth is Fusayama's solution [98], and the content of this is given in Table 7. Proteins, amino acids, serum, or other substances, as appropriate, may be added as needed to these solutions. Ideally, Hanks's and Ringer's solutions have a pH of 7.4, the normal body pH. Fusayama's solution has a pH of 5.5, similar to the pH found in the mouth. The body pH usually is 7.4, but in cases of a wound or infection, the pH can vary from 5.4 to 7.8 [26]. Environments in in vivo testing are discussed in Chapter 42 of this manual.

## SPECIFIC PROBLEM AREAS

Problem areas include planned or inadvertently occurring coupled metals, localized corrosion such as pitting or corrosion-fatigue, and wear and fretting corrosion. Modified surfaces represent new materials that need characterization for bonding, chemistry, durability, interfaces, and appropriate thickness. Surface characterization and control on increasingly finer scales will be required.

## USE OF TEST METHODS AND PROCEDURES TO EVALUATE CORROSION

Test methods used to evaluate corrosion of medical and dental materials are found in Refs 55 and 74. Useful information and guidance on specimen preparation and testing parameters are available in the literature. The schematic drawing in Fig. 1 from ASTM G 5 [74] shows a setup for exposing a test specimen to a selected environment for corrosion testing. The main components of the test cell are the working electrode (we—specimen), the auxiliary electrode (aux—counter-electrode), and the selected reference electrode (sce—saturated calomel electrode). The reference electrode may be bridged as shown or with an adapter in the same testing container, and the bridge tip should be near the surface of the working electrode. The electrodes in the test cell must be isolated except for the part that is in the testing solution. There should be no solution/air interface at the water line, and shielding, such as glass tubing, should be used. The auxiliary electrode should have a larger surface area than the working electrode, and should be opposite the working electrode area that is being tested. Geometry is important. A surrounding counter-electrode would be best for a round specimen. Surface preparation of specimens should be the same and, for some tests, should be that of the intended use. Selected testing solutions as given in Tables 5 through 7 can be used and kept at a temperature of 37°C, which is the body temperature. The elements of this setup can be used in combined mechanical property/corrosion testing such as corrosion-fatigue, fretting, or SCC.

Potentiostatic and potentiodynamic anodic polarization measurements often are applied to medical and dental materials, and test methods in ASTM G 5 and ASTM F 4 can be used as guides along with published literature. These methods involve applying a potential to the specimen and

measuring the current. Information obtained from these tests includes the corrosion potential, the passive region (in degree and size), and the breakdown potential. ASTM G 61 is a related test method and is for conducting cyclic potentiostatic polarization measurements. This test method provides information on susceptibility to localized corrosion. Setting the applied potential to include the cathodic portion of these curves provides data for determining corrosion rates using the Stern-Geary equation [99]. ASTM G 59 (Practice for Conducting Potentiodynamic Polarization Resistance Measurements) describes a method for conducting potentiodynamic, polarization resistance measurements to determine corrosion rates using the Stern-Geary equation [99]. ASTM F 746 (Test Method for Pitting or Crevice Corrosion of Metallic Surgical Implant Materials) is a recommended practice for determining susceptibility to pitting and crevice corrosion. A standard practice for verification of algorithm and equipment for electrochemical AC impedance measurements is given in ASTM G 106 (Standard Practice for Verification of Algorithm and Equipment for Electrochemical Impedance Measurements). The AC impedance method has been used for measurements of coated surfaces [100].

## REGULATIONS

Medical and dental materials and devices are regulated by the Food and Drug Administration (FDA). The Medical Device Amendments of 1976 amended the Food Drug and Cosmetic Act of 1938 to include medical devices and diagnostic products [101]. This gave the FDA the authority to establish regulations and standards. Devices were defined to be in three classes: I, II, III. Dental materials for many applications such as fillings, crowns and bridges, solders, and restraining wires are in Classes I and II. Many of the dental materials have the approval of the American Dental Association (ADA), but this is not a necessary requirement. Dental implants are controlled by the FDA and are in Class III. The three classes may be described as follows.

Class I, General Controls—a device that is under controls other than standards and premarket approval to assure safety and effectiveness.

Class II, Performance Standards—a device for which controls are not sufficient to assure safety and effectiveness, and performance standards are needed.

Class III, Premarket Approval—a device for which insufficient information exists to assure that general controls and performance standards would provide reasonable assurance of safety and effectiveness. This device is life sustaining, life supporting, or may be implanted in the body, and represents a potentially unreasonable risk of illness or injury. Devices in this category are required to have approved applications for premarket approval.

All of the medical devices and the dental implants discussed in this paper fall in Class III. Devices, including designs and materials that were used prior to 1976 were allowed to continue based on past successful experience. Since 1976, devices could be given market clearance, without clinical testing, if it could be shown that these devices were substantially equivalent to devices used prior to 1976 or to another device that had

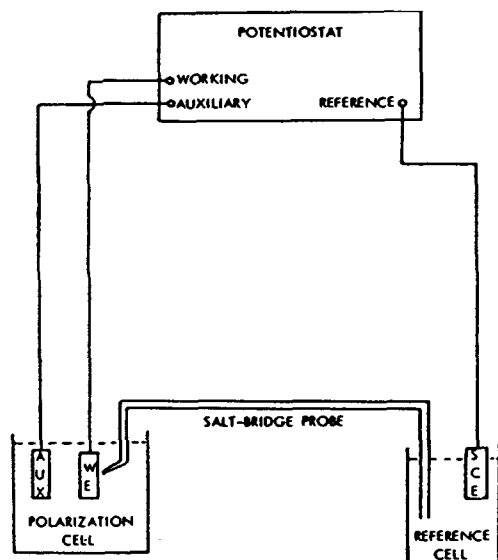


FIG. 1—Schematic potentiostatic anodic polarization experimental set-up.



obtained premarket approval. Premarket approval is different from market clearance in that premarket approval requires clinical testing according to a protocol from the FDA and market clearance does not. Congress passed the Safe Medical Device Act of 1990 [102], which went into effect in 1992. The 1990 Act did the following and more:

1. Established mandatory device reporting of failures, provided for post-market surveillance including the authority of the FDA to require additional studies on a device that is already on the market;
2. Gave revised rules for Class II performance standards, labeling guidelines, standards, and Class I general controls.

The 1997 FDA Modernization Reform Act [103] that took effect in February 1998 provides guidance for using FDA recognized consensus standards such as some standards of the ASTM and gives assistance for speeding up FDA approval of some medical devices. The premarket application for market clearance, 510K, may be *special* requiring only a 30 day review and modification, *abbreviated* if FDA approved consensus standards apply, or *traditional* requiring a full review. Some low risk devices are exempted from filing requirements. Experts outside the FDA are permitted to review some intermediate risk devices, and this allows the FDA more time to review devices that are considered high risk. A piece of legislation that helps protect producers of raw materials, The Biomaterials Access Assurance Act, became law in August 1998 [6]. This law exempts suppliers of raw materials from liability in lawsuits involving medical devices if the suppliers met the device manufacturer's requirements and were not negligent in any way.

The United States and the European Union (EU) have entered in Mutual Recognition Agreements (MRA), one of which is for medical devices [6]. The agreement provides for selected medium risk devices for export to the U.S. to be reviewed by the European assessment body based on FDA standards. Devices exported from the U.S. to the EU would be reviewed in the U.S. based on the EU's Medical Device Directive (MDD). While it is not practical to have MRAs throughout the world, the Global Harmonization Task Force (GHTF) composed of the U.S., EU, Canada, Australia, and New Zealand, with some Asian observers, is considering establishing uniform medical device regulations.

## OUTLOOK FOR THE FUTURE

Advances in technology and materials will continue to be studied and used, when possible, by the medical and dental industries to produce improved materials and devices. The Safe Medical Device Act of 1990 mandates reporting of failures, and this will provide data for making improvements. Future improvements also will result from other planned investigations involving retrieval and analysis of medical and dental devices. ASTM F 561, Practice for Analysis of Retrieved Metallic Orthopaedic Implants [55], gives guidelines regarding retrieval and analysis.

ASTM International established the F-4 Committee on Medical and Surgical Materials and Devices in 1964. The ASTM has established a Tissue Engineering Products

Division that will address standards for Tissue Engineering. Information on future developments in biomaterials can be obtained through the ASTM, references given here, and other sources. Corrosion testing will continue to be a part of the analysis of failures and the development of materials and methods.

## REFERENCES

- [1] Horowitz, E., "The Changing World of Biomaterials," Standards Alumni Assoc., Quarterly Meeting, National Institute of Standards and Technology, Jan. 18, 2001.
- [2] Masmonteil, F., *Presse' Medical*, Vol. 43, 1935, p. 1915.
- [3] Venable, C. S., Stuck, W. P., and Beach, A., *Annals of Surgery*, Vol. 105, 1935, p. 917.
- [4] Gilbert, J. L., "Novel Electrochemical Techniques for Analysis of Metallic Biomaterials Surfaces," *Medical Plastics and Biomaterials Magazine*, May 1998.
- [5] Bundy, K. J., "Corrosion and Other Electrochemical Aspects of Biomaterials," *Crit. Rev. Biomed. Eng.* 1994, Vol. 22, Nos. 3-4, pp. 139-251.
- [6] *U.S. Industry and Trade Outlook 1999*, published annually, U.S. Department of Commerce, International Trade Administration, The McGraw-Hill Companies, NY, 1999, pp. 45:4-7.
- [7] Charnley, J., *Journal of Bone and Joint Surgery*, Vol. 42B, 1960, p. 28.
- [8] Williams, D. F., "Biocompatibility of Clinical Implant Materials," *Metals and Ceramics*, Vol. 1, and *Polymers*, Vol. 2, CRC Press, Inc., Boca Raton, FL, 1981.
- [9] Shulman, L. B., *Consensus Development Conference Statement on Dental Implants*, National Institutes of Health, 15 June 1988, pp. 7, 43.
- [10] Horowitz, E. and Hahn, H., "Advanced Dental Implant Composite Coatings," *Transactions, First International Conference on Oral Implants for Dentistry*, February 10-12, 1990, Tokyo, Japan, p. 145.
- [11] Dental Materials, Kirk-Othner Encyclopedia of Chemical Technology, Vol. 7, J. A. Tesk, Ed., John Wiley, 1993, pp. 980, 1012-1014.
- [12] Fraker, A. C., Van Orden, A. C., Sung, P., and Hahn, H., "Corrosive Response of the Interface Tissue to Dental Implants," *Implant Prosthodontics: Surgical and Prosthetic Techniques for Dental Implants*, M. J. Fagan, Jr. et al., Eds., Yearbook Medical Publishers, Littleton, MA, 1991, pp. 293-304.
- [13] Wisby, A., Gregson, P. J., Peter, L. M., and Tuke, M., "Effect of Surface Treatment on the Dissolution of Titanium-based Implant Materials," *Biomaterials*, Vol. 2, No. 5, Jul., 1991, pp. 470-473.
- [14] Branemark, P. I., *Journal of Prosthetic Dentistry*, Vol. 50, 1983, pp. 339-410.
- [15] Bechtol, C. O., Ferguson, A. B. Jr., and Laing, P. G., *Metals and Engineering in Bone and Joint Surgery*, The Williams and Wilkins Company, Baltimore, 1959.
- [16] Venable, C. S. and Stuck, W. G., *The Internal Fixation of Fractures*, Charles C. Thomas, Springfield, IL, 1947.
- [17] Ludwigson, D. C., *Metals Engineering Quarterly*, Vol. 5, No. 3, 1965, pp. 1-6.
- [18] Hoar, T. P. and Mears, D. C., *Proceedings of The Royal Society (London)*, SCR.A294 (1439), 1966, pp. 486-510.
- [20] Williams, D. F. and Roaf, R., *Implants in Surgery*, W. B. Saunders, Philadelphia/London, 1973.
- [21] Icart, J. F., *Journal de Medecine, Chirurgie, Pharmacie*, Paris, Vol. 44, 1775, pp. 164, 169.
- [22] Hansmann, H., *Verein Deutsches Gesellschaft fur Chirurgie*, Vol. 15, 1886, p. 134.

- [23] Lister, J., *British Medical Journal*, Vol. 2, 1883, p. 855.
- [24] Jergesen, F. H., *Studies of Various Factors Influencing Internal Fixation as a Method of Treatment of Fractures of the Long Bones*, National Research Council, 1981.
- [25] Leventhal, G. C., *Journal of Bone and Joint Surgery*, Vol. 33, 1951, p. 473.
- [26] Laing, P., *Orthopedic Clinics of North America*, Vol. 4, No. 2, 1973, pp. 249–275.
- [27] Hahn, H. and Palich, W. J., *Journal of Biomedical Materials Research*, Vol. 4, 1970, p. 571.
- [28] Welsh, R. P., Pilliar, R. M., and MacNab, I., *Journal of Bone and Joint Surgery*, Vol. 53-A, No. 5, 1971, pp. 963–967.
- [29] Galante, J., Rostocker, W., Luek, R., and Ray, R. D., *Journal of Bone and Joint Surgery*, Vol. 53-A, No. 1, 1971, pp. 101–114.
- [30] Ducheyne, P., Hench, L. L., Kagan, A., et al., *Journal of Biomedical Materials Research*, Vol. 14, 1980, pp. 225–237.
- [31] Salman, N. N., "The Effect of Direct Electrical Current Stimulation on the Bone Growth into Porous Polymeric, Ceramic and Metallic Implants," Ph.D. thesis, Clemson University, 1980.
- [32] Brighton, C. T., *Symposium on Electrically Induced Osteogenesis, The Orthopedic Clinics of North America*, Vol. 15, No. 1, 1984.
- [33] Devine, T. M. and Wulff, J., *Journal of Biomedical Materials Research*, Vol. 9, No. 2, 1975, pp. 151–167.
- [34] VanderSande, J. B., Coke, J. R., and Wulff, J., *Metallurgical Transactions A*, Vol. 7A, 1976, pp. 389–397.
- [35] Kilner, T., Pilliar, R. M., Weatherly, G. C., and Allibert, C., *Journal of Biomedical Materials Research*, Vol. 16, No. 1, 1982, pp. 63–79.
- [36] Kilner, T., "The Relationship of Microstructure to the Mechanical Properties of a Cobalt-Chromium-Molybdenum Alloy Used for Prosthetic Devices," Ph.D. thesis, University of Toronto, 1984.
- [37] Imam, M. A., "Effect of Microstructure on Fatigue Properties in Ti-6Al-4V," Ph.D. thesis, The George Washington University, 1978.
- [38] Imam, M. A., Fraker, A. C., Harris, J. S., and Gilmore, C. M., "Influence of Heat Treatment on the Fatigue Lives of Ti-6Al-4V and Ti-4.5Al-5Mo-1.5Cr," *Titanium Alloys in Surgical Implants*, ASTM STP 796, H. A. Luckey and F. Kubli, Jr., Eds., ASTM International, West Conshohocken, PA, 1983, pp. 105–119.
- [39] Yue, S., Pilliar, R. M., and Weatherly, G. C., *Journal of Biomedical Materials Research*, Vol. 18, 1984, pp. 1043–1058.
- [40] Cigada, A., Rondelli, Vincantini, B., et al., *Journal of Biomedical Materials Research*, Vol. 23, 1989, pp. 1087–1095.
- [41] Pilliar, R. M., *Biomaterials*, Vol. 12, No. 2, 1991, pp. 95–101.
- [42] Buchanan, R. A., Rigney, E. D. Jr., and Williams, J. M., *Journal of Biomedical Materials Research*, Vol. 21, 1987, pp. 355–366.
- [43] Buchanan, R. A., Lee, I. S., and Williams, J. M., *Journal of Biomedical Materials Research*, Vol. 24, 1990, pp. 309–318.
- [44] Dowson, D., "Friction and Wear of Medical Implants and Prosthetic Devices," *ASM Handbook, Friction, Lubrication and Wear Technology*, Vol. 18, ASM, Materials Park, OH, 1992, pp. 656–664.
- [45] Powers, J. M. and Bayne, S. C., "Friction and Wear of Dental Materials," *ASM Handbook, Friction, Lubrication and Wear Technology*, Vol. 18, ASM, Metals Park, OH, 1992, pp. 665–681.
- [46] Mueller, H. J., "Tarnish and Corrosion of Dental Alloys," *ASM Handbook, Corrosion*, Vol. 13, ASM, Metals Park, OH, 1986, pp. 1337–1366.
- [47] Tesk, J. A., "Dental Materials," *Kirk-Othner Encyclopedia of Chemical Technology*, John Wiley, New York, 1993.
- [48] Reithe, P., *Tsch. Zahmaertzl. Z.*, Vol. 21, 1966, p. 301.
- [49] Fraker, A. C., "Corrosion of Metallic Implants and Prosthetic Devices," *Metals Handbook, Corrosion, Ninth Edition*, Vol. 13, ASM, Materials Park, OH, 1986, pp. 1324–1335.
- [50] Waterstrat, R. M. and Okabe, T., "Dental Amalgam," *Intermetallic Compounds—Principles and Practice*, J. H. Westbrook and R. L. Fleischman, Eds., Vol. 2, John Wiley and Sons, New York, 1995, pp. 575–590.
- [51] Johnson, C. E., Kelley, D. R., et al., "Acid Assisted Cold Welding and Intermetallic Formation and Dental Applications Thereof," U.S. Patent No. 5,711,866, Jan. 27, 1998.
- [52] Paulus, J. A., Parida, G. R., Tucker, R. D., and Park, J. B., "Corrosion Analysis of NiCu and PdCo Thermal Seed Alloys Used as Interstitial Hyperthermia Implants," *Biomaterials*, Dec., 1997, pp. 1609–1614.
- [53] Food and Drug Administration, "Magnetic Resonance Diagnostic Device-Panel Recommendation and Report on Petitions for MR Reclassification," *Federal Register*, Vol. 53, No. 46, 9 March 1988, pp. 7575–7579.
- [54] Shellock, F. G., Morsioli, S., and Kanal, E., "MR Procedures and Biomedical Implants, Materials and Devices: 1993 Update," *Radiology*, Vol. 189, No. 2, 1993, pp. 587–599.
- [55] *Annual Book of ASTM Standards*, Medical Devices, Emergency Medical Services, Vol. 13.01, ASTM International, West Conshohocken, PA, 1994 and 2000.
- [56] Disegi, J. and Eschbach, L., "Stainless Steel in Bone Surgery," *Injury*, Suppl. 4, Dec. 31, 2000, pp. 2–6.
- [57] Pohler, O. E., "Unalloyed Titanium for Implants in Bone Surgery," *Injury*, Suppl. 4, Dec. 31, 2000, 31, pp. 7–13.
- [58] Disegi, J. A., "Titanium Alloys for Fracture Fixation Implants," *Injury*, Suppl. 4, Dec. 31, 2000, pp. 14–17.
- [59] Long, M. and Rack, H. J., "Titanium Alloys in Total Joint Replacement—A Materials Science Perspective," *I Biomaterials*, Vol. 19, No. 18, Sept., 1998, pp. 1621–1639.
- [60] Gomez, M., Mancha, H., Sakinas, A., Rodriguez, J. L., Escobedo, J., Castro, M., and Mendez, M., "Relationship Between Microstructure and Ductility of Investment Cast ASTM F-75 Implant Alloy," *J. Biomed. Mater. Res.*, Vol. 34, No. 2, Feb. 1997, pp. 157–163.
- [61] Marti, A., "Cobalt-Base Alloys Used in Bone Surgery," *Injury*, Suppl. 4, Dec. 31, pp. 18–21.
- [62] Johansson, B. I., Lucas, L. C., and Lemons, J. E., *Journal of Biomedical Materials Research*, Vol. 23, No. A3, 1989, pp. 349–361.
- [63] Leinfelder, K. F., "An Evaluation of Casting Alloys Used for Restorative Procedures," *J. Am. Dent. Assoc.*, Vol. 128, No. 1, Jan. 1997, pp. 37–45.
- [64] Wataha, J. C., "Biocompatibility of Dental Casting Alloys: A Review," *Prosthet. Dent.*, Vol. 83, No. 2, Feb. 2000, pp. 223–234.
- [65] Malhotra, M. L. and Asgar, K., "Physical Properties of Dental Silver-Tin Amalgams with High and Low Copper Contents," *J. Am. Dent. Assoc.*, Vol. 96, No. 3, Mar. 1978, pp. 444–450.
- [66] Revie, R. W. and Greene, N. D., *Corrosion Science*, Vol. 9, 1969, pp. 755–770.
- [67] Fraker, A. C., Ruff, A. W., Sung, P., et al., "Surface Preparation and Corrosion Behavior of Titanium Alloys for Surgical Implants," *Titanium Alloys in Surgical Implants*, ASTM STP 796, H. A. Luckey and F. Kubli, Jr., Eds., ASTM International, West Conshohocken, PA, 1983, pp. 755–770.
- [68] Solar, R. J., "Corrosion Resistance of Titanium Surgical Implant Alloys: A Review," *Corrosion and Degradation of Implant Materials*, ASTM STP 684, B. C. Syrett and A. Acharya, Eds., ASTM International, West Conshohocken, PA, 1979, pp. 259–273.
- [69] Buchanan, R. A., Rigney, E. D., Jr., and Griffin, C. D., "Effectiveness of ULTI Carbon Coatings in Reducing the Metal Ion Release Rate from Ti and Ti-6Al-4V," *Transactions 11th Annual Meeting*, Society for Biomaterials, VIII, 1985, p. 88.
- [70] Buchanan, R. A., Lee, I.-S., and Williams, J. M., *Journal of Biomedical Materials Research*, Vol. 24, 1990, pp. 309–318.
- [71] Black, J., Oppenheimer, P., Morris, D. M., et al., *Journal of Biomedical Materials Research*, Vol. 21, 1987, pp. 1213–1230.
- [72] Tung, M. S. and Sung, P., "Calcium Phosphate Type Reference Material: Development, Preparation, and Characterization," *Characterization and Performance of Calcium Phosphate Coatings for Implants*, ASTM STP 1196, E. Horowitz and J. E. Parr, Eds., ASTM International, West Conshohocken, PA, 1994, pp. 99–110.

- [73] Kruger, J., "Fundamental Aspects of the Corrosion of Metallic Implants," *Corrosion and Degradation of Implant Materials*, ASTM STP 684, B. C. Syrett and A. Acharya, Eds., ASTM International, West Conshohocken, PA, 1979, pp. 107–127.
- [74] *Annual Book of ASTM Standards*, Wear and Erosion: Metal Corrosion, Vol. 3.02, ASTM International, West Conshohocken, PA, 1994.
- [75] Pourbaix, M., *Atlas of Electrochemical Equilibria in Aqueous Solutions*, Pergamon Press, 1966.
- [76] Syrett, B. C., *Corrosion*, Vol. 33, 1977, p. 221.
- [77] Syrett, B. C., "The Application of Electrochemical Techniques to the Study of Corrosion of Metallic Implant Materials," *Electrochemical Techniques for Corrosion*, R. Baboian, Ed., National Association of Corrosion Engineers, Houston, TX, 1977, pp. 93–100.
- [78] Syrett, B. C. and Wing, S. S., *Corrosion*, Vol. 34, No. 4, 1978, pp. 138–145.
- [79] Lucas, L. C., Buchanan, R. A., Lemons, J. E., and Griffin, C. D., *Journal of Biomedical Materials Research*, Vol. 16, No. 6, 1982, pp. 799–810.
- [80] Hodge, F. G. and Lee, T. S. III, *Corrosion*, Vol. 31, 1975, p. 111.
- [81] Syrett, B. C. and Davis, E. E., "Crevice Corrosion of Implant Alloys—A Comparison of In Vitro and In Vivo Studies," *Corrosion and Degradation of Implant Materials*, ASTM STP 684, B. C. Syrett and A. Acharya, Eds., ASTM International, West Conshohocken, PA, 1979, pp. 229–244.
- [82] Colangelo, V. J., *Journal of Basic Engineering*, Vol. 91, No. 4, Series D, 1969, pp. 581–586.
- [83] Cahoon, J. R. and Holte, R. N., *Journal of Biomedical Materials Research*, Vol. 15, 1981, pp. 137–145.
- [84] Bolton, J. D. Hayden, J., and Humphreys, M., *Engineering Medicine*, Vol. II, No. 2, 1982, pp. 89–113.
- [85] Imam, M. A., Fraker, A. C., and Gilmore, C. M., "Corrosion Fatigue of 316L Stainless Steel, Co-Cr-Mo Alloy and ELI Ti-6Al-4V," *Corrosion and Degradation of Implant Materials*, ASTM STP 684, B. C. Syrett and A. Acharya, Eds., ASTM International, West Conshohocken, PA, 1979, pp. 128–143.
- [86] Pugh, E. N., "Stress Corrosion Cracking," *Encyclopedia of Materials Science and Engineering*, Pergamon Press, 1982.
- [87] Edwards, B. J., Louthan, M. R., Jr., and Sisson, R. D., "Hydrogen Embrittlement of Zimaloy: A Cobalt-Chromium-Molybdenum Orthopedic Implant Alloy," *Corrosion and Degradation of Implant Materials (Second Symposium)*, ASTM STP 859, A. C. Fraker and C. D. Griffin, Eds., ASTM International, West Conshohocken, PA, 1985, pp. 11–29.
- [88] Fontana, M. G. and Greene, N. D., *Corrosion Engineering*, McGraw-Hill, New York, 1967.
- [89] Mears, D. C., *Journal of Biomedical Materials Research*, Vol. 9, No. 4, 1975, pp. 133–148.
- [90] Griffin, C. D., Buchanan, R. A., and Lemons, J. E., *Journal of Biomedical Materials Research*, Vol. 17, 1983, p. 489.
- [91] Lucas, L. C., Buchanan, R. A., and Lemons, J., *Journal of Biomedical Materials Research*, Vol. 15, 1981, pp. 731–747.
- [92] Collier, J. P., Mayor M. B., Jensen, R. E., and Surprenant, H. P., "Corrosion of Mixed Alloy Femoral Hip Components," *Implant Retrieval Symposium Transactions*, Vol. XV, Society for Biomaterials, 1992, p. 60.
- [93] Sauer, W., Kovacs, P., Beals, N., and Cuckler, J., "Corrosion at Head/Taper Interfaces: A 3.5 Year Follow-Up of Modular Head/Ti-6Al-4V Femoral Stem Prostheses," *Implant Retrieval Symposium Transactions*, Vol. XV, Society for Biomaterials, 1992, p. 56.
- [94] Justice, T. A., Lucas, L. C., and Lemons, J. E., "Investigations of 2-15 Year Retrieved Ti-6Al-4V/Co-Cr-Mo Total Hip Prostheses," *Implant Retrieval Symposium Transactions*, Vol. XV, Society for Biomaterials, 1992, p. 57.
- [95] Brown, S. A., Flemming, C. A., Kawalee, J. S., Placko, H. E., Vassaux, C., Merritt, K., Payer, J. H., and Kraay, M. J., "Fretting Corrosion Accelerates Crevice Corrosion of Modular Hip Tapers," *J. Appl. Biomater.*, Spring, Vol. 6, No. 1, 1995, pp. 19–22.
- [96] Bundy, K. J. and Collier, J. P., "Mechanistic Studies of Corrosion of Galvanically Coupled Alloys Used in Modular Total Hip Replacement Devices," *Implant Retrieval Symposium Transactions*, Vol. XV, Society for Biomaterials, 1992, p. 55.
- [97] Revie, R. W. and Greene, N. D., *Journal of Biomedical Materials Research*, Vol. 3, 1969, pp. 465–470.
- [98] Meyer, J. M. and Nally, J. N., "Influence of Artificial Salivas on the Corrosion of Dental Alloys," *11th Annual Cong. IADR – Continental European*, Div., Brussels, Sept., 1974, pp. 20–21.
- [99] Stern, M. and Geary, A. L., *Journal of the Electrochemical Society*, Vol. 104, 1957, pp. 56–63.
- [100] Bundy, K. J. and Luedemann, R. E., "Characterization of the Corrosion Behavior of Porous Biomaterials by AC Impedance Techniques," *Quantitative Characterization and Performance of Porous Implants for Hard Tissue Applications*, ASTM STP 953, J. E. Lemons, Ed., ASTM International, West Conshohocken, PA, 1987, pp. 137–150.
- [101] Medical Device Amendments, Public Law 94-295, United States Food and Drug Administration, Bureau of Medical Devices and Radiological Health, 1976.
- [102] Code of Federal Regulations, Vol. 21, pt. 872.3640, Office of Federal Register, National Archives and Records Administration, Washington, DC, April 1990.
- [103] FDA Modernization Act of 1997: Guidance for the Recognition and Use of Consensus Standards; Availability, Federal Register: Vol. 63, No. 37, February 25, 1998, pp. 9561–9569.

# Pharmaceutical

David F. Jensen<sup>1</sup>

## GENERAL NATURE OF THE PHARMACEUTICAL INDUSTRY

IN THE PHARMACEUTICAL INDUSTRY, a number of business factors exist that tend to discourage a consistent approach to technical issues such as corrosion testing. Some of the major issues are as follows:

1. In many processes the volumes are small and very expensive, creating an economic justification for testing of all processes that is difficult to support. This leads to equipment that is flexible and can handle varied process conditions and chemistries.
2. Being first on the market with a pharmaceutical product is of major business importance. Because speed is a major issue, many technical issues (i.e., corrosion) are frequently "over engineered" from the standpoint of good engineering practices. This allows flexible equipment to be capable of handling varied conditions and chemistries to support rapid product development. This then limits the need for corrosion testing of all processes.
3. Many reactions are multi-step syntheses, frequently requiring varied chemicals and reaction conditions. Many of the reaction components are proprietary and uncommon to traditional corrosion engineering data sources. Attempting to simulate these varied uncommon chemicals and chemical environments is difficult at best.
4. In many cases the chemistry of the process is still being modified well into development, and some even into production. Successful corrosion control depends on teamwork in which all parties of the project team are aware of process changes being considered and can develop a materials compatibility strategy accordingly.
5. The percentage of products that survive from discovery to production is very small. The time from product decision to production is very small. This also drives the need for flexible equipment, and limits the ability to corrosion testing for a specific process.

Decisions regarding materials of construction are most often made using the knowledge of operating and technical personnel, and the experiences from similar chemistries, rather than testing. Factors, such as the design life of the equipment, future use for the equipment after the process

for which it is being designed is obsolete, etc., are considerations. Most pharmaceutical processes are run as campaigns that may only represent 10 % equipment use. Therefore, most equipment is not dedicated to a given process but is used for several processes. The uncertainty of the ultimate uses of the equipment has led to a fail-safe tendency to overspecifying equipment, particularly regarding the materials of construction.

## TYPES OF EQUIPMENT

In general, equipment used in the pharmaceutical industry can be divided into three categories: processing equipment, ancillary systems, and utility systems. Processing equipment can be defined as equipment used to react, transfer, hold, or in any manner come in contact with the final product or any of the intermediates leading up to the final product. Some examples of processing equipment are stills, reactors, fermentors, receivers, filtration equipment, drying equipment, crystallizers, heat exchangers, sampling systems, blending equipment, and filling equipment.

Ancillary systems are defined as those necessary for production but in which product contact is not an issue. Some examples are solvent and waste storage vessels, scrubbers, neutralization systems, and venting systems.

Utility systems are unique and in part defined as traditional utility systems and in part as processing equipment. Part of the system is supplying noncontact utilities and part of the system is supplying products that contact the final product or intermediates. One example of these dual systems is the water systems. There are the traditional cooling waters for jackets and heat exchangers, but also there are varied "clean" water systems that supply water that are used in processing intermediates or final products, as well as, being used as part of the final product formulation.

## DESCRIPTION OF MATERIALS

Construction materials of choice for processing equipment product contact surfaces are glass-lined, nickel-chromium-molybdenum alloys such as Hastelloy® C-276 (UNS-N10276) or Hastelloy® C-22 (UNS-N06022), and 300 series stainless steels, with the most common being 304L (UNS-S30403) or 316L (UNS-S31603). In addition, some construction materials often used only for product transfer or condenser

<sup>1</sup>David F. Jensen, Engineering Consultant, Eli Lilly and Company, Tippecanoe Labs, TL27, 1650 Lilly Road, Lafayette, IN 47909.

operations are tantalum, Teflon® (PTFE), and graphite. Other materials considered for special applications are titanium, zirconium, and superaustenitic stainless steels containing 6 % molybdenum, such as Allegheny-Ludlum AL-6XN® (UNS-08637) or Avesta 254-SMO® (UNS-S31254).

The effects of corrosion on processing equipment can be a source of contamination. Pitting presents a potential for batch-to-batch or product-to-product contamination, and material removed in the corrosion process becomes a product contaminant.

Materials of construction for ancillary systems are commonly carbon steel, fiberglass-reinforced plastic (FRP), epoxy- or phenolic-lined, stainless steel, and concrete. Many times waste transfer lines will change from a product contact material (near the process equipment) to carbon steel, stainless steel, or polyethylene (near the ancillary equipment). Vent lines are particularly troublesome and require special attention. Smooth surfaces (noncorrugated) with proper sloping to avoid areas for condensation and debris accumulation are essential to minimize corrosion. Smooth and sloping surfaces are also needed to aid in cleaning between campaigns.

Surface finishes are considerations regarding cleanability, particularly in processes where sterility is a major issue. Generally, if the environment is conducive to corrosion, corrosion will occur regardless of the surface finish.

## ENVIRONMENT AND ENVIRONMENTAL FACTORS

Liquid phase is the most common medium in pharmaceuticals. The most common environments include aqueous solutions, and solvents such as acetone, methylene chloride, acetates, and alcohols. Environmental factors include temperature, pH, halogen levels, and oxidizing/reducing atmospheres. Process temperatures typically range from  $-70^{\circ}\text{C}$  to  $+150^{\circ}\text{C}$ . Low temperature is a concern mainly relating to the material's mechanical properties. For example, carbon steel develops brittle characteristics and many of the elastomers, that have high chemical resistance, lose their elastomeric properties below  $-20^{\circ}\text{C}$ . The pH values range from lows of less than 1 and highs of 14. Chloride levels greater than 100 ppm are normally viewed as a corrosion concern, especially at pH values less than neutral. At elevated temperatures and high stress levels even a few ppm of chlorides can promote corrosion. Strong oxidizing environments such as hydrogen peroxide, sodium hypochlorite, and ozone generally

are not major corrosion concerns. Since hydrochloric acid is used and handled in varied concentrations and ways, this is an ongoing challenge.

Most often the chemistry of the process is the driving force for corrosion concerns. Reducing environments are generally not a concern. Erosion from high flow areas such as agitation is not usually a problem or a concern. In the waste handling areas, constant variation in chemistries and conditions are the challenge, making testing more difficult.

## TESTING

The decision to test is usually driven by unusual chemistry such as a new catalyst, reaction components, or reaction conditions. Immersion/mass loss method is primarily used in conjunction with microscopic examination. Process fluids from production or pilot runs are primarily used to best simulate potential corrosion. The test methods are custom designed based, in part, on cost and the ability to obtain sufficient quantities of test fluids, and handle the process conditions. Process conditions are tested outside the process control limits (e.g., temperatures, pH) to better accentuate the corrosion potential. These extremes have to be tempered by the stability of the products in the stream. For wall thicknesses greater than 0.250 in. (6.35 mm), a uniform loss of less than 10 mil/year (0.26 mm/year) is considered structurally acceptable. Significantly lower levels of uniform loss are of concern for product or process contamination issues. Microscopic examination is used to determine potential localized corrosion concerns, such as pitting or stress cracking. Indications of pitting or stress corrosion in stamped areas of the coupon are of particular concern. U-bend tests are rarely used because of insufficient test fluid quantities and availability.

## UNRESOLVED ISSUES IN CORROSION TESTING

More affordable corrosion tests need to be developed with consideration given to the nature of the pharmaceutical industry. The ability to corrosion test in small test volumes (e.g., 50 mL or less), perform accelerated corrosion tests with temperature sensitive products, and perform testing in systems that cannot be run in glass would be a considerable step in promoting corrosion testing.

# **Section VIII: CORROSION-RELATED STANDARDS**

*H.P. Hack and R. Baboian, Editors*

# Corrosion-Related Standards

*H.P. Hack and R. Baboian, Section Editors*

## AMERICAN PETROLEUM INSTITUTE (API)

### Tubular Goods

- RP 5L2 Internal Coating of Line Pipe for Non-Corrosive Gas Transmission Service  
 RP 5L7 Unprimed Internal Fusion Bonded Epoxy Coating of Line Pipe

### Storage Tanks

- RP 12R1 Setting, Maintenance, Inspection, Operation and Repair of Tanks in Production Service  
 RP 575 Inspection of Atmospheric & Low-Pressure Storage Tanks  
 RP 651 Cathodic Protection of Aboveground Storage Tanks  
 RP 652 Lining of Aboveground Petroleum Storage Tank Bottoms  
 Std 653 Tank Inspection, Repair, Alteration and Reconstruction  
 RP 1604 Closure of Underground Petroleum Storage Tanks  
 RP 1615 Installation of Underground Petroleum Storage Systems  
 RP 1631 Interior Lining of Underground Storage Tanks  
 RP 1632 Cathodic Protection of Underground Petroleum Storage Tanks and Piping Systems  
 Std 2610 Design, Construction, Operation, Maintenance & Inspection of Terminal and Tank Facilities

## AMERICAN WATER WORKS ASSOCIATION (AWWA)

- C116/A21.16 ANSI Standard for Protective Fusion-Bonded Epoxy Coating for the Interior and Exterior Surfaces of Ductile-Iron and Gray-Iron Fittings for Water Supply Service  
 C203 Coal-Tar Protective Coatings and Linings for Steel Water Pipelines—Enamel and Tape—Hot Applied (Includes addendum C203a)  
 C205 Cement-Mortar Protective Lining and Coating for Steel Water Pipe—(100 mm) and Larger—Shop Applied  
 C209 Cold-Applied Tape Coatings for the Exterior of Special Sections, Connections, and Fittings for Steel Water Pipelines  
 C210 Liquid-Epoxy Coating Systems for the Interior and Exterior of Steel Water Pipelines  
 C213 Fusion-Bonded Epoxy Coating for the Interior and Exterior of Steel Water Pipelines  
 C214 Tape Coating Systems for the Exterior of Steel Water Pipelines  
 C218 Coating the Exterior of Aboveground Steel Water Pipelines and Fittings  
 C222 Polyurethane Coatings for the Interior and Exterior of Steel Water Pipelines and Fittings  
 D102 Coating Steel Water-Storage Tanks  
 D104 Automatically Controlled, Impressed-Current Cathodic Protection for Interior of Steel Water Tanks  
 D130 Flexible-Membrane-Lining and Floating-Cover Materials for Potable Water Storage

## ASME INTERNATIONAL

- B31G Manual: Determining Remaining Strength of Corroded Pipelines: Supplement to B31 Code-Pressure Piping

## ASTM INTERNATIONAL

### Corrosion of Metals

- A 262 Standard Practices for Detecting Susceptibility to Intergranular Attack in Austenitic Stainless Steels  
 A 763 Standard Practices for Detecting Susceptibility to Intergranular Attack in Ferritic Stainless Steels  
 G 1 Standard Practice for Preparing, Cleaning, and Evaluating Corrosion Test Specimens  
 G 2 Standard Test Method for Corrosion Testing of Products of Zirconium, Hafnium, and their Alloys in Water at 633°K or in Steam at 673°K [Metric]  
 G 4 Standard Guide for Conducting Corrosion Coupon Tests in Field Applications  
 G 15 Standard Terminology Relating to Corrosion and Corrosion Testing  
 G 16 Standard Guide for Applying Statistics to Analysis of Corrosion Data  
 G 28 Standard Test Methods of Detecting Susceptibility to Intergranular Corrosion in Wrought, Nickel-Rich, Chromium-Bearing Alloys

## 852 CORROSION TESTS AND STANDARDS MANUAL

- G 31 Standard Practice for Laboratory Immersion Corrosion Testing of Metals
- G 34 Standard Test Method for Exfoliation Corrosion Susceptibility in 2XXX and 7XXX Series Aluminum Alloys (EXCO Test)
- G 44 Standard Practice for Exposure of Metals and Alloys by Alternate Immersion in Neutral 3.5% Sodium Chloride Solution
- G 46 Standard Guide for Examination and Evaluation of Pitting Corrosion
- G 48 Standard Test Methods for Pitting and Crevice Corrosion Resistance of Stainless Steels and Related Alloys by Use of Ferric Chloride Solution
- G 52 Standard Practice for Exposing and Evaluating Metals and Alloys in Surface Seawater
- G 54 Standard Practice for Simple Static Oxidation Testing
- G 66 Standard Test Method for Visual Assessment of Exfoliation Corrosion Susceptibility of 5XXX Series Aluminum Alloys (ASSET Test)
- G 67 Standard Test Method for Determining the Susceptibility to Intergranular Corrosion of 5XXX Series Aluminum Alloys by Mass Loss After Exposure to Nitric Acid (NAMLT Test)
- G 78 Standard Guide for Crevice Corrosion Testing of Iron-Base and Nickel-Base Stainless Alloys in Seawater and Other Chloride-Containing Aqueous Environments
- G 79 Standard Practice for Evaluation of Metals Exposed to Carburization Environments
- G 107 Standard Guide for Formats for Collection and Compilation of Corrosion Data for Metals for Computerized Database Input
- G 109 Standard Test Method for Determining the Effects of Chemical Admixtures on the Corrosion of Embedded Steel Reinforcement in Concrete
- G 110 Standard Practice for Evaluating Intergranular Corrosion Resistance of Heat Treatable Aluminum Alloys by Immersion in Sodium Chloride + Hydrogen Peroxide Solution
- G 111 Standard Guide for Corrosion Tests in High Temperature or High Pressure Environment, or Both
- G 112 Standard Guide for Conducting Exfoliation Corrosion Tests in Aluminum Alloys
- G 117 Standard Guide for Calculating and Reporting Measures of Precision Using Data from Interlaboratory Wear or Erosion Tests
- G 135 Standard Guide for Computerized Exchange of Corrosion Data for Metals
- G 142 Standard Test Method for Determination of Susceptibility of Metals to Embrittlement in Hydrogen Containing Environments at High Pressure, High Temperature, or Both
- G 146 Standard Practice for Evaluation of Disbonding of Bimetallic Stainless Alloy/Steel Plate for Use in High-Pressure, High-Temperature Refinery Hydrogen Service
- G 157 Standard Guide for Evaluating the Corrosion Properties of Wrought Iron- and Nickel-Based Corrosion Resistant Alloys for the Chemical Process Industries
- G 161 Standard Guide for Corrosion-Related Failure Analysis
- G 170 Standard Guide for Evaluating and Qualifying Oilfield and Refining Corrosion Inhibitors in the Laboratory

### Corrosion of Non-Metals

- G 131 Standard Practice for Cleaning of Materials and Components by Ultrasonic Techniques
- G 166 Standard Guide for Statistical Analysis of Service Life Data

### Corrosion of Pipeline Coatings

- G 6 Standard Test Method for Abrasion Resistance of Pipeline Coatings
- G 8 Standard Test Methods for Cathodic Disbonding of Pipeline Coatings
- G 9 Standard Test Method for Water Penetration into Pipeline Coatings
- G 11 Standard Test Method for Effects of Outdoor Weathering on Pipeline Coatings
- G 12 Standard Test Method for Nondestructive Measurement of Film Thickness of Pipeline Coatings on Steel
- G 17 Standard Test Method for Penetration Resistance of Pipeline Coatings (Blunt Rod)
- G 19 Standard Test Method for Disbonding Characteristics of Pipeline Coatings by Direct Soil Burial
- G 20 Standard Test Method for Chemical Resistance of Pipeline Coatings
- G 42 Standard Test Method for Cathodic Disbonding of Pipeline Coatings Subjected to Elevated Temperatures
- G 62 Standard Test Methods for Holiday Detection in Pipeline Coatings
- G 80 Standard Test Method for Specific Cathodic Disbonding of Pipeline Coatings
- G 95 Standard Test Method for Cathodic Disbondment Test of Pipeline Coatings (Attached Cell Method)

### Atmospheric Corrosion

- B 117 Standard Practice for Operating Salt Spray (Fog) Apparatus
- B 368 Standard Test Method for Copper-Accelerated Acetic Acid-Salt Spray (Fog) Testing (CASS Test)



B 537	Standard Practice for Rating of Electroplated Panels Subjected to Atmospheric Exposure
B 810	Standard Test Method for Calibration of Atmospheric Corrosion Test Chambers by Change in Mass of Copper Coupons
B 827	Practice for Conducting Mixed Flowing Gas (MFG) Environmental Tests
D 2059	Standard Test Method for Resistance of Zippers to Salt Spray (Fog)
D 4585	Standard Practice for Testing Water Resistance of Coatings Using Controlled Condensation
G 7	Standard Practice for Atmospheric Environmental Exposure Testing of Nonmetallic Materials
G 33	Standard Practice for Recording Data from Atmospheric Corrosion Tests of Metallic-Coated Steel Specimens
G 50	Standard Practice for Conducting Atmospheric Corrosion Tests on Metals
G 60	Standard Test Method for Conducting Cyclic Humidity Tests
G 84	Standard Practice for Measurement of Time-of-Wetness on Surfaces Exposed to Wetting Conditions as in Atmospheric Corrosion Testing
G 85	Standard Practice for Modified Salt Spray (Fog) Testing
G 87	Standard Practice for Conducting Moist SO <sub>2</sub> Tests
G 90	Standard Practice for Performing Accelerated Outdoor Weathering of Nonmetallic Materials Using Concentrated Natural Sunlight
G 91	Standard Practice for Monitoring Atmospheric SO <sub>2</sub> Using the Sulfation Plate Technique
G 92	Standard Practice for Characterization of Atmospheric Test Sites
G 101	Standard Guide for Estimating the Atmospheric Corrosion Resistance of Low-Alloy Steels
G 113	Standard Terminology Relating to Natural and Artificial Weathering Tests of Nonmetallic Materials
G 116	Standard Practice for Conducting Wire-on-Bolt Test for Atmospheric Galvanic Corrosion
G 140	Standard Test Method for Determining Atmospheric Chloride Deposition Rate by Wet Candle Method
G 141	Standard Guide for Addressing Variability in Exposure Testing on Nonmetallic Materials
G 147	Standard Practice for Conditioning and Handling of Nonmetallic Materials for Natural and Artificial Weathering Tests
G 149	Standard Practice for Conducting the Washer Test for Atmospheric Galvanic Corrosion
G 156	Standard Practice for Selecting and Characterizing Weathering Reference Materials Used to Monitor Consistency of Conditions in an Exposure Test

### Environmentally Influenced Cracking

A 143	Standard Practice for Safeguarding Against Embrittlement of Hot-Dip Galvanized Structural Steel Products and Procedure for Detecting Embrittlement
B 577	Standard Test Methods for Detection of Cuprous Oxide (Hydrogen Embrittlement Susceptibility) in Copper
B 858	Standard Test Method for Determination of Susceptibility to Stress Corrosion Cracking in Copper Alloys Using an Ammonia Vapor Test
C 692	Standard Test Method for Evaluating the Influence of Thermal Insulations on External Stress Corrosion Cracking Tendency of Austenitic Stainless Steel
F 326	Standard Test Method for Electronic Measurement for Hydrogen Embrittlement from Cadmium-Electroplating Processes
F 519	Standard Test Method for Mechanical Hydrogen Embrittlement Evaluation of Plating Processes and Service Environments
F 945	Standard Test Method for Stress-Corrosion of Titanium Alloys by Aircraft Engine Cleaning Materials
G 30	Standard Practice for Making and Using U-Bend Stress-Corrosion Test Specimens
G 35	Standard Practice for Determining the Susceptibility of Stainless Steels and Related Nickel-Chromium-Iron Alloys to Stress-Corrosion Cracking in Polythionic Acids
G 36	Standard Practice for Evaluating Stress-Corrosion-Cracking Resistance of Metals and Alloys in a Boiling Magnesium Chloride Solution
G 37	Standard Practice for Use of Mattsson's Solution of pH 7.2 to Evaluate the Stress-Corrosion Cracking Susceptibility of Copper-Zinc Alloys
G 38	Standard Practice for Making and Using C-Ring Stress-Corrosion Test Specimens
G 39	Standard Practice for Preparation and Use of Bent-Beam Stress-Corrosion Test Specimens
G 41	Standard Practice for Determining Cracking Susceptibility of Metals Exposed Under Stress to a Hot Salt Environment
G 47	Standard Test Method for Determining Susceptibility to Stress-Corrosion Cracking of 2XXX and 7XXX Aluminum Alloy Products
G 49	Standard Practice for Preparation and Use of Direct Tension Stress-Corrosion Test Specimens
G 58	Standard Practice for Preparation of Stress-Corrosion Test Specimens for Weldments
G 64	Standard Classification of Resistance to Stress-Corrosion Cracking of Heat-Treatable Aluminum Alloys

## 854 CORROSION TESTS AND STANDARDS MANUAL

- G 103 Standard Test Method for Performing Stress-Corrosion Cracking Resistance of Low Copper 7XXX Series Al-Zn-Mg-Cu Alloys in Boiling 6% Sodium Chloride Solution
- G 123 Standard Test Method for Evaluating Stress-Corrosion Cracking of Stainless Alloys with Different Nickel Content in Boiling Acidified Sodium Chloride Solution
- G 129 Standard Practice for Slow Strain Rate Testing to Evaluate the Susceptibility of Metallic Materials to Environmentally Assisted Cracking
- G 139 Standard Test Method for Determining Stress-Corrosion Cracking Resistance of Heat-Treatable Aluminum Alloy Products Using Breaking Load Method
- G 148 Standard Practice for Evaluation of Hydrogen Uptake, Permeation, and Transport in Metals by an Electrochemical Technique
- G 168 Standard Practice for Making and Using Precracked Double Beam Stress Corrosion Specimens

### **Wear and Abrasion**

- D 2809 Standard Test Method for Cavitation Corrosion and Erosion-Corrosion Characteristics of Aluminum Pumps with Engine Coolants
- F 897 Standard Test Method for Measuring Fretting Corrosion of Osteosynthesis Plates and Screws
- G 32 Standard Test Method for Cavitation Erosion Using Vibratory Apparatus
- G 40 Standard Terminology Relating to Wear and Erosion
- G 65 Standard Test Method for Measuring Abrasion Using the Dry Sand/Rubber Wheel Apparatus
- G 73 Standard Practice for Liquid Impingement Erosion Testing
- G 75 Standard Test Method for Determination of Slurry Abrasivity (Miller Number) and Slurry Abrasion Response of Materials (SAR Number)
- G 76 Standard Test Method for Conducting Erosion Tests by Solid Particle Impingement Using Gas Jets
- G 77 Standard Test Method for Ranking Resistance of Materials to Sliding Wear Using Block-on-Ring Wear Test
- G 83 Standard Test Method for Wear Testing with a Crossed-Cylinder Apparatus
- G 98 Standard Test Method for Galling Resistance of Materials
- G 99 Standard Test Method for Wear Testing with a Pin-on-Disk Apparatus
- G 105 Standard Test Method for Conducting Wet Sand/Rubber Wheel Abrasion Tests
- G 118 Standard Guide for Recommended Data Format of Wear Test Data Suitable for Databases
- G 119 Standard Guide for Determining Synergism Between Wear and Corrosion
- G 134 Standard Test Method for Erosion of Solid Materials by a Cavitating Liquid Jet
- G 163 Standard Guide for Digital Data Acquisition in Wear and Friction Measurements

### **Soils**

- G 51 Standard Test Method for Measuring pH of Soil for Use in Corrosion Testing
- G 57 Standard Test Method for Field Measurement of Soil Resistivity Using the Wenner Four-Electrode Method
- G 97 Standard Test Method for Laboratory Evaluation of Magnesium Sacrificial Anode Test Specimens for Underground Applications
- G 158 Standard Guide for Three Methods of Assessing Buried Steel Tanks
- G 160 Standard Practice for Evaluating Microbial Susceptibility of Nonmetallic Materials by Laboratory Soil Burial
- G 162 Standard Practice for Conducting and Evaluating Laboratory Corrosion Tests in Soils
- G 165 Standard Practice for Determining Rail-to-Earth Resistance

### **Electrochemical Testing**

- B 457 Standard Test Method for Measurement of Impedance of Anodic Coatings on Aluminum
- G 3 Standard Practice for Conventions Applicable to Electrochemical Measurements in Corrosion Testing
- G 5 Test Method for Making Potentiostatic and Potentiodynamic Anodic Polarization Measurements
- G 59 Standard Practice for Conducting Potentiodynamic Polarization Resistance Measurements
- G 61 Standard Test Method for Conducting Cyclic Potentiodynamic Polarization Measurements for Localized Corrosion Susceptibility of Iron-, Nickel-, or Cobalt-Based Alloys
- G 69 Standard Test Method for Measurement of Corrosion Potentials of Aluminum Alloys
- G 71 Standard Guide for Conducting and Evaluating Galvanic Corrosion Tests in Electrolytes
- G 82 Standard Guide for Development and Use of a Galvanic Series for Predicting Galvanic Corrosion Performance
- G 96 Standard Guide for On-Line Monitoring of Corrosion in Plant Equipment (Electrical and Electrochemical Methods)

G 100	Standard Test Method for Conducting Cyclic Galvanostaircase Polarization
G 102	Standard Practice for Calculation of Corrosion Rates and Related Information from Electrochemical Measurements
G 106	Standard Practice for Verification of Algorithm and Equipment for Electrochemical Impedance Measurements
G 108	Standard Test Method for Electrochemical Reactivation (EPR) for Detecting Sensitization of AISI Type 304 and 304L Stainless Steels Exposed to Chloride Environments
G 150	Standard Test Method for Electrochemical Critical Pitting Temperature Testing of Stainless Steels

### Electrodeposited Coatings

B 380	Standard Test Method of Corrosion Testing of Decorative Electrodeposited Coatings by the Corrodokote Procedure
B 545	Standard Specification for Electrodeposited Coatings of Tin
B 605	Standard Specification for Electrodeposited Coatings of Tin-Nickel Alloy
B 650	Standard Specification for Electrodeposited Engineering Chromium Coatings on Ferrous Substrates
B 651	Standard Test Method for Measurement of Corrosion Sites in Nickel Plus Chromium or Copper Plus Nickel Plus Chromium Electroplated Surfaces with the Double-Beam Interference Microscope
B 680	Standard Test Method for Seal Quality of Anodic Coatings on Aluminum by Acid Dissolution
B 689	Standard Specification for Electroplated Engineering Nickel Coatings
B 733	Standard Specification for Autocatalytic (Electroless) Nickel-Phosphorus Coatings on Metal
B 734	Standard Specification for Electrodeposited Copper for Engineering Uses
B 735	Standard Test Method for Porosity in Gold Coatings on Metal Substrates by Nitric Acid Vapor
B 741	Standard Test Method for Porosity in Gold Coatings on Metal Substrates by Paper Electrography
B 765	Standard Guide for Selection of Porosity Tests for Electrodeposits and Related Metallic Coatings
B 809	Standard Test Method for Porosity in Metallic Coatings by Humid Sulfur Vapor ("Flowers-of-Sulfur")

### Applications

A 380	Standard Practice for Cleaning, Descaling, and Passivation of Stainless Steel Parts, Equipment, and Systems
B 76	Standard Test Method for Accelerated Life of Nickel-Chromium and Nickel-Chromium-Iron Alloys for Electrical Heating
B 78	Standard Test Method of Accelerated Life of Iron-Chromium-Aluminum Alloys for Electrical Heating
B 154	Standard Test Method for Mercurous Nitrate Test for Copper and Copper Alloys
C 739	Standard Specification for Cellulosic Fiber (Wood-Base) Loose-Fill Thermal Insulation
C 876	Standard Test Method for Half-Cell Potentials of Uncoated Reinforcing Steel in Concrete
D 130	Standard Test Method for Detection of Copper Corrosion from Petroleum Products by the Copper Strip Tarnish Test
D 610	Standard Test Method for Evaluating Degree of Rusting on Painted Steel Surfaces
D 665	Standard Test Method for Rust-Preventing Characteristics of Inhibited Mineral Oil in the Presence of Water
D 849	Standard Test Method for Copper Strip Corrosion by Industrial Aromatic Hydrocarbons
D 876	Standard Test Methods for Nonrigid Vinyl Chloride Polymer Tubing Used for Electrical Insulation
D 1141	Standard Practice for Substitute Ocean Water
D 1193	Standard Specification for Reagent Water
D 1280	Standard Test Method for Total Immersion Corrosion Test for Soak Tank Metal Cleaners
D 1384	Standard Test Method for Corrosion Test for Engine Coolants in Glassware
D 1414	Standard Test Methods for Rubber O-Rings
D 1611	Standard Test Method for Corrosion Produced by Leather in Contact with Metal
D 1654	Standard Test Method for Evaluation of Painted or Coated Specimens Subjected to Corrosive Environments
D 1743	Standard Test Method for Determining Corrosion Preventive Properties of Lubricating Greases
D 1838	Standard Test Method for Copper Strip Corrosion by Liquefied Petroleum (LP) Gases
D 2247	Standard Practice for Testing Water Resistance of Coatings in 100 % Relative Humidity
D 2251	Standard Test Method for Metal Corrosion by Halogenated Organic Solvents and Their Admixtures
D 2570	Standard Test Method for Simulated Service Corrosion Testing of Engine Coolants
D 2649	Standard Test Method for Corrosion Characteristics of Solid Film Lubricants
D 2671	Standard Test Methods for Heat-Shrinkable Tubing for Electrical Use
D 2758	Standard Test Method for Engine Coolants by Engine Dynamometer

## 856 CORROSION TESTS AND STANDARDS MANUAL

D 2803	Standard Guide for Testing Filiform Corrosion Resistance of Organic Coatings on Metal
D 2847	Standard Practice for Testing Engine Coolants in Car and Light Truck Service
D 3263	Standard Test Methods for Corrosivity of Solvent Systems for Removing Water-Formed Deposits
D 3310	Standard Test Method for Determining Corrosivity of Adhesive Materials
D 3316	Standard Test Method for Stability of Perchloroethylene with Copper
D 3482	Standard Test Method for Determining Electrolytic Corrosion of Copper by Adhesives
D 3603	Standard Test Method for Rust-Preventing Characteristics of Steam Turbine Oil in the Presence of Water (Horizontal Disk Method)
D 4048	Standard Test Method for Detection of Copper Corrosion from Lubricating Grease
D 4340	Standard Test Method for Corrosion of Cast Aluminum Alloys in Engine Coolants Under Heat-Rejecting Conditions
D 4627	Standard Test Method for Iron Chip Corrosion for Water-Dilutable Metalworking Fluids
E 712	Standard Practice for Laboratory Screening of Metallic Containment Materials for Use With Liquids in Solar Heating and Cooling Systems
E 745	Standard Practices for Simulated Service Testing for Corrosion of Metallic Containment Materials for Use With Heat-Transfer Fluids in Solar Heating and Cooling Systems
E 937	Standard Test Method for Corrosion of Steel by Sprayed Fire-Resistive Material (SFRM) Applied to Structural Members
F 359	Standard Practice for Static Immersion Testing of Unstressed Materials in Nitrogen Tetroxide (N <sub>2</sub> O <sub>4</sub> )
F 482	Standard Test Method for Corrosion of Aircraft Metals by Total Immersion in Maintenance Chemicals
F 483	Standard Test Method for Total Immersion Corrosion Test for Aircraft Maintenance Chemicals
F 746	Standard Test Method for Pitting or Crevice Corrosion of Metallic Surgical Implant Materials
F 1089	Standard Test Method for Corrosion of Surgical Instruments
F 1110	Standard Test Method for Sandwich Corrosion Test

## INTERNATIONAL ELECTROTECHNICAL COMMISSION (IEC)

60068-2-18	Environmental testing—Part 2 –18: Tests—Test R and guidance: Water
60068-2-43	Environmental testing—Part 2: Tests—Test Kd: Hydrogen sulphide test for contacts and connections
60068-2-60	Environmental testing—Part 2: Tests—Test Ke: Flowing mixed gas corrosion test
60068-2-66	Environmental testing—Part 2: Test methods—Test Cx: Damp heat, steady state (unsaturated pressurized vapour)
60068-2-67	Environmental testing—Part 2: Tests—Test Cy: Damp heat, steady state, accelerated test primarily intended for components
60068-2-74	Environmental testing—Part 2: Test Xc: Fluid contamination
TR 60355	An appraisal of the problems of accelerated testing for atmospheric corrosion
60426	Test methods for determining electrolytic corrosion with insulating materials
60512-11-7	Electrochemical components for electronic equipment—Basic testing procedures and measuring methods—Part 11: Climatic tests—Section 7: Test 11g: Flowing mixed gas corrosion test
60512-11-14	Electromechanical components for electronic equipment—Basic testing procedures and measuring methods—Part 11: Climatic tests—Section 14: Test 11p: Flowing single gas corrosion test
60695-5-1	Fire hazard testing—Part 5: Assessment of potential corrosion damage by fire effluent—Section 1: General guidance
TR1 60695-5-2	Fire hazard testing—Part 5: Assessment of potential corrosion damage by fire effluent—Section 2: Guidance on the selection and use of test methods

## INTERNATIONAL ORGANIZATION FOR STANDARDIZATION (ISO)

### Coatings

1462	Metallic coatings—Coatings other than those anodic to the basis metal—Accelerated corrosion tests—Method for the evaluation of the results
3160-2	Watch cases and accessories—Gold alloy coverings—Part 2: Determination of fineness, thickness, corrosion resistance and adhesion
4536	Metallic and non-organic coatings on metallic substrates—Saline droplets corrosion test (SD test)
4538	Metallic coatings—Thioacetamide corrosion test (TAA test)
4539	Electrodeposited chromium coatings—Electrolytic corrosion testing (EC test)
4540	Metallic coatings—Coatings cathodic to the substrate—Rating of electroplated test specimens subjected to corrosion tests
4541	Metallic and other non-organic coatings—Corrodokote corrosion test (CORR test)
4542	Metallic and other non-organic coatings—General rules for stationary outdoor exposure corrosion tests

4543	Metallic and other non-organic coatings—General rules for corrosion tests applicable for storage conditions
4623	Paints and varnishes—Filiform corrosion test on steel
4623-1	Paints and varnishes—Determination of resistance to filiform corrosion—Part 1: Steel substrates
6988	Metallic and other non-organic coatings—Sulfur dioxide test with general consideration of moisture
TR 8502-1	Preparation of steel substrates before application of paints and related products—Tests for the assessment of surface cleanliness—Part 1: Field test for soluble iron corrosion products
10289	Methods for corrosion testing of metallic and other inorganic coatings on metallic substrates—Rating of test specimens and manufactured articles subjected to corrosion tests
11997-1	Paints and varnishes—Determination of resistance to cyclic corrosion conditions—Part 1: Wet (salt fog)/dry/humidity
11997-2	Paints and varnishes—Determination of resistance to cyclic corrosion conditions—Part 2: Wet (salt fog)/dry/humidity/UV light
12944-1	Paints and varnishes—Corrosion protection of steel structures by protective paint systems—Part 1: General introduction
12944-2	Paints and varnishes—Corrosion protection of steel structures by protective paint systems—Part 2: Classification of environments
12944-3	Paints and varnishes—Corrosion protection of steel structures by protective paint systems—Part 3: Design considerations
12944-4	Paints and varnishes—Corrosion protection of steel structures by protective paint systems—Part 4: Types of surface and surface preparation
12944-5	Paints and varnishes—Corrosion protection of steel structures by protective paint systems—Part 5: Protective paint systems
12944-6	Paints and varnishes—Corrosion protection of steel structures by protective paint systems—Part 6: Laboratory performance test methods
12944-7	Paints and varnishes—Corrosion protection of steel structures by protective paint systems—Part 7: Execution and supervision of paint work
12944-8	Paints and varnishes—Corrosion protection of steel structures by protective paint systems—Part 8: Development of specifications for new work and maintenance

## **Metals and Alloys**

3651-1	Austenitic Stainless Steels—Determination of resistance to intergranular corrosion of stainless steels—Part 1: Austenitic and ferritic-austenitic (duplex) stainless steels—Corrosion test in nitric acid medium by measurement of loss in mass (Huey test)
3651-2	Determination of resistance to intergranular corrosion of stainless steels—Part 2: Ferritic, austenitic and ferritic-austenitic (duplex) stainless steels—Corrosion test in media containing sulfuric acid
6509	Corrosion of metals and alloys—Determination of dezincification resistance of brass
6957	Copper alloys—Ammonia test for stress corrosion resistance
7384	Corrosion tests in artificial atmosphere—General requirements
7441	Corrosion of metals and alloys—Determination of bimetallic corrosion in outdoor exposure corrosion tests
7539-1	Corrosion of metals and alloys—Stress corrosion testing—Part 1: General guidance on testing procedures
7539-2	Corrosion of metals and alloys—Stress corrosion testing—Part 2: Preparation and use of bent-beam specimens
7539-3	Corrosion of metals and alloys—Stress corrosion testing—Part 3: Preparation and use of U-bend specimens
7539-4	Corrosion of metals and alloys—Stress corrosion testing—Part 4: Preparation and use of uniaxially loaded tension specimens
7539-5	Corrosion of metals and alloys—Stress corrosion testing—Part 5: Preparation and use of C-ring specimens
7539-6	Corrosion of metals and alloys—Stress corrosion testing—Part 6: Preparation and use of pre-cracked specimens
7539-7	Corrosion of metals and alloys—Stress corrosion testing—Part 7: Slow strain rate testing
7539-8	Corrosion of metals and alloys—Stress corrosion testing—Part 8: Preparation and use of specimens to evaluate weldments
8044	Corrosion of metals and alloys—Basic terms and definitions
8407	Corrosion of metals and alloys—Removal of corrosion products from corrosion test specimens
8565	Metals and alloys—Atmospheric corrosion testing—General requirements for field tests
8993	Anodized aluminium and aluminium alloys—Rating system for the evaluation of pitting corrosion—Chart method

8994	Anodized aluminium and aluminium alloys—Rating system for the evaluation of pitting corrosion—Grid method
9223	Corrosion of metals and alloys—Corrosivity of atmospheres—Classification
9224	Corrosion of metals and alloys—Corrosivity of atmospheres—Guiding values for the corrosivity categories
9225	Corrosion of metals and alloys—Corrosivity of atmospheres—Measurement of pollution
9226	Corrosion of metals and alloys—Corrosivity of atmospheres—Determination of corrosion rate of standard specimens for the evaluation of corrosivity
9227	Corrosion tests in artificial atmospheres—Salt spray tests
9400	Nickel-based alloys—Determination of resistance to intergranular corrosion
9591	Corrosion of aluminium alloys—Determination of resistance to stress corrosion cracking
10062	Corrosion tests in artificial atmosphere at very low concentrations of polluting gas(es)
10270	Corrosion of metals and alloys—Aqueous corrosion testing of zirconium alloys for use in nuclear power reactors
11130	Corrosion of metals and alloys—Alternate immersion test in salt solution
11303	Corrosion of metals and alloys—Guidelines for selection of protection methods against atmospheric corrosion
11306	Corrosion of metals and alloys—Guidelines for exposing and evaluating metals and alloys in surface sea water
11463	Corrosion of metals and alloys—Evaluation of pitting corrosion
11474	Corrosion of metals and alloys—Corrosion tests in artificial atmosphere—Accelerated outdoor test by intermittent spraying of a salt solution (Scab test)
11782-1	Corrosion of metals and alloys—Corrosion fatigue testing—Part 1: Cycles to failure testing
11782-2	Corrosion of metals and alloys—Corrosion fatigue testing—Part 2: Crack propagation testing using precracked specimens
11845	Corrosion of metals and alloys—General principles for corrosion testing
11846	Corrosion of metals and alloys—Determination of resistance to intergranular corrosion of solution heat-treatable aluminium alloys
11881	Corrosion of metals and alloys—Exfoliation corrosion testing of aluminium alloys
11972	Corrosion-resistant cast steels for general applications
14713	Protection against corrosion of iron and steel in structures—Zinc and aluminium coatings—Guidelines
14993	Corrosion of metals and alloys—Accelerated testing involving cyclic exposure to salt mist, “dry” and “wet” conditions
15324	Corrosion of metals and alloys—Evaluation of stress corrosion cracking by the drop evaporation test
16701	Corrosion of metals and alloys—Corrosion in artificial atmosphere—Accelerated corrosion test involving exposure under controlled conditions of humidity cycling and intermittent spraying of salt solution

## Applications

2160	Petroleum products—Corrosiveness to copper—Copper strip test
4404	Petroleum and related products—Determination of the corrosion resistance of water-containing fire-resistant fluids for hydraulic systems
4952	Structural steels with improved atmospheric corrosion resistance
6251	Liquefied petroleum gases—Corrosiveness to copper—Copper strip test
6315	Road vehicles—Brake linings—Seizure to ferrous mating surface due to corrosion—Test procedure
9455-12	Soft soldering fluxes—Test methods—Part 12: Steel tube corrosion test
9455-15	Soft soldering fluxes—Test methods—Part 15: Copper corrosion test
TR 10129	Plain bearings—Testing of bearing metals—Resistance to corrosion by lubricants under static conditions
TR 10217	Solar energy—Water heating systems—Guide to material selection with regard to internal corrosion
TR 10271	Dentistry—Determination of tarnish and corrosion of metals and alloys
TS 12928	Lubricants, industrial oils and related products (class L)—Family R (Products for temporary protection against corrosion)—Guidelines for establishing specifications
13402	Surgical and dental hand instruments—Determination of resistance against autoclaving, corrosion and thermal exposure (available in English only)
13806	Vitreous and porcelain enamels—Corrosion tests in closed systems

## NACE INTERNATIONAL

### General

RP0197	Standard Format for Computerized Electrochemical Polarization Curve Data Files
RP0198	The Control of Corrosion Under Thermal Insulation and Fireproofing Materials—a Systems Approach

RP0199	Installation of Stainless Chromium—Nickel Alloy Roll-Bonded and Explosion-Bonded Clad Plate in Air Pollution Control Equipment
RP0294	Design, Fabrication, and Inspection of Tanks for the Storage of Concentrated Sulfuric Acid and Oleum at Ambient Temperatures
RP0300	Pilot Scale Evaluation of Corrosion and Scale Control Additives for Open Re-circulating Cooling Water Systems
RP0390	Maintenance and Rehabilitation Considerations for Corrosion Control of Existing Steel-Reinforced Concrete Structures
RP0487	Considerations in the Selection and Evaluation of Rust Preventives and Vapor Corrosion Inhibitors for Interim (Temporary) Corrosion Protection
RP0497	Field Corrosion Evaluation Using Metallic Test Specimens
RP0590	Recommended Practice for Prevention, Detection, and Correction of Deaerator Cracking
RP0690	Standard Format for Collection and Compilation of Data for Computerized Material Corrosion Resistance Database Input
TM0193	Laboratory Corrosion Testing of Metals in Static Chemical Cleaning Solutions at Temperatures Below 93°C(200°F)
TM0299	Corrosion Control and Monitoring in Seawater Injection Systems
TM0397	Screening Tests for Evaluating the Effectiveness of Gypsum Scale Removers
TM0398	Laboratory Corrosion Testing of Metals in Static Cleaning Solutions at Temperatures Above 100°C (212°F)
TM0399	Test Method for Phosphonate in Brine
TM0498	Standard Test Method for Measuring the Carburization of Alloys for Ethylene Cracking Furnace Tubes
TM0499	Immersion Corrosion Testing of Ceramic Materials

### **Cathodic Protection**

RP0169	Control of External Corrosion on Underground or Submerged Metallic Piping Systems
RP0572	Design, Installation, Operation, and Maintenance of Impressed Current Deep Groundbeds
RP0174	Corrosion Control of Electric Underground Residential Distribution Systems
RP0575	Design, Installation, Operation, and Maintenance of Internal Cathodic Protection Systems in Oil Treating Vessels
RP0675	Control of Corrosion on Offshore Steel Pipelines
RP0176	Corrosion Control of Steel, Fixed Offshore Platforms Associated with Petroleum Production
RP0177	Mitigation of Alternating Current and Lightning Effects on Metallic Structures and Corrosion Control Systems
RP0180	Cathodic Protection of Pulp and Paper Mill Effluent Clarifiers
RP0285	Control of External Corrosion on Metallic Buried, Partially Buried, or Submerged Liquid Storage Systems
RP0186	Application of Cathodic Protection for Well Casings
RP0286	The Electrical Isolation of Cathodically Protected Pipelines
RP0387	Metallurgical and Inspection Requirements for Cast Sacrificial Anodes for Offshore Applications
RP0388	Impressed Current Cathodic Protection of Internal Submerged Surfaces of Steel Water Storage Tanks
RP0100	Cathodic Protection of Pre-stressed Concrete Cylinder Pipelines
RP0193	External Cathodic Protection of On-Grade Metallic Storage Tank Bottoms
RP0194	Criteria and Test Methods for Cathodic Protection of Lead Sheath Cable
RP0196	Galvanic Anode Cathodic Protection of Internal Submerged Surfaces of Steel Water Storage Tanks
RP0492	Metallurgical and Inspection Requirements for Offshore Pipeline Bracelet Anodes
RP0572	Design, Installation, Operation and Maintenance of Impressed Current Deep Groundbeds
RP0575	Internal Cathodic Protection Systems in Oil-Treating Vessels
TM0294	Testing of Embeddable Anodes for Use in Cathodic Protection of Atmospherically Exposed Steel-Reinforced Concrete
TM0497	Measurement Techniques Related to Criteria for Cathodic Protection on Underground or Submerged Metallic Piping Systems

### **Oil Production**

MR0174	Recommendations for Selecting Inhibitors for Use as Sucker Rod Thread Lubricants
MR0175	Sulfide Stress Cracking Resistant Metallic Materials for Oil Field Equipment
MR0176	Metallic Materials for Sucker Rod Pumps for Hydrogen Sulfide Environments
RP0175	Control of Internal Corrosion in Steel Pipelines and Piping Systems
RP0181	Liquid Applied Internal Protective Linings and Coatings for Oil Field Production Equipment

RP0273	Handling and Proper Usage of Inhibited Oilfield Acids (API Bulletin D-15) (Joint API-NACE Project)
RP0278	Design and Operation of Stripping Columns for Removal of Oxygen from Water
RP0475	Selection of Metallic Materials to be Used in All Phases of Water Handling for Injection into Oil Bearing Formations
RP0775	Preparation and Installation of Corrosion Coupons and Interpretation of Test Data in Oil Production Practice
RP0191	The Application of Internal Plastic Coatings for Oilfield Tubular Goods and Accessories
RP0192	Monitoring Corrosion in Oil and Gas Production with Iron Counts
RP0291	Care, Handling, and Installation of Internal Plastic Coatings for Oilfield Tubular Goods and Accessories
RP0296	Guidelines for Detection, Repair and Mitigation of Cracking of Existing Petroleum Refinery Pressure Vessels in Wet H <sub>2</sub> S Environments
RP0472	Methods and Controls to Prevent In-Service Environmental Cracking of Carbon Steel Weldments in Corrosive Petroleum Refining Environments
RP0475	Selection of Metallic Materials to be Used in all Phases of Water Handling for Injection into Oil-Bearing Formations
RP0491	Worksheet for the Selection of Oilfield Non-metallic Seal Systems
TM0173	Methods for Determining Water Quality for Subsurface Injection Using Membrane Filters
TM0177	Testing of Metals for Resistance to Sulfide Stress Cracking at Ambient Temperatures
TM0187	Evaluating Elastomeric Materials in Sour Gas Environments
TM0275	Performance Testing of Sucker Rods by the Mixed String, Alternate Rod Method
TM0284	Evaluation of Pipeline Steels for Resistance to Stepwise Cracking
TM0374	Laboratory Screening Tests to Determine the Ability of Scale Inhibitors to Prevent Precipitation of CaSO <sub>4</sub> and CaCO <sub>3</sub> from Solution
TM0194	Field Monitoring of Bacterial Growth in Oilfield Systems
TM0197	Laboratory Screening Test to Determine the Ability of Scale Inhibitors to Prevent the Precipitation of Barium Sulfate and/or Strontium Sulfate from Solution (For Oil and Gas Production Systems)
TM0198	Slow Strain Rate Test Method for Screening Corrosion-Resistant Alloys (CRAs) for Stress Corrosion Cracking in Sour Oilfield Service
TM0296	Evaluating Elastomeric Materials in Sour Liquid Environments
TM0298	Evaluating the Compatibility of FRP Pipe and Tubulars with Oilfield Environments

### Process and Power Industries

RP0170	Protection of Austenitic Stainless Steel from Polythionic Acid Stress Corrosion Cracking During Shutdown of Refinery Equipment
RP0173	Collection and Identification of Corrosion Products
RP0182	Initial Conditioning of Cooling Water Equipment
RP0189	On-Line Monitoring of Cooling Waters
RP0472	Methods and Controls to Prevent In-Service Cracking of Carbon Steel (P-1) Welds in Corrosive Petroleum Refining Environments
RP0292	Installation of Thin Metallic Wallpaper Lining in Air Pollution Control and Other Process Equipment
TM0169	Laboratory Corrosion Testing of Metals for the Process Industries
TM0171	Autoclave Corrosion Testing of Metals for the Process Industries
TM0274	Dynamic Corrosion Testing of Metals in High Temperature Water
TM0286	Cooling Water Test Units Incorporating Heat Transfer Surfaces
TM0199	Standard Test Method for Measuring Deposit Mass Loading (Deposit Weight Density) Values for Boiler Tubes by the Glass-Bead-Blasting Technique

### Pipeline Coatings

MR0274	Material Requirements in Prefabricated Plastic Films for Pipeline Coatings
RP0185	Extruded Polyolefin Resin Coating Systems for Underground or Submerged Pipe
RP0274	High Voltage Electrical Inspection of Pipeline Coatings Prior to Installation
RP0275	Application of Organic Coating to the External Surface of Steel Pipe for Underground Service
RP0276	Extruded Asphalt Mastic Type Protective Coatings for Underground Pipelines
RP0375	Application and Handling of Wax-Type Protective Coatings and Wrapper Systems for Underground Pipelines
RP0190	External Protective Coatings for Joints, Fittings and Valves on Metallic Underground or Submerged Pipelines and Piping Systems
RP0200	Steel-Cased Pipeline Practices
RP0375	Wax Coating Systems for Underground Piping Systems



RP0490	Holiday Detection of Fusion-Bonded Epoxy External Pipeline Coatings of 250 to 760 microns (10 to 30 mils)
RP0492	Metallurgical and Inspection Requirements for Offshore Pipeline Bracelet Anodes

### Protective Coatings

TM0174	Laboratory Methods for the Evaluation of Protective Coatings Used as Lining Materials in Immersion Service
TM0183	Evaluation of Internal Plastic Coatings for Corrosion Control
TM0184	Accelerated Test Procedures for Screening Atmospheric Surface Coating Systems for Offshore Platforms and Equipment
TM0185	Evaluation of Internal Plastic Coatings for Corrosion Control of Tubular Goods by Autoclave Testing
TM0186	Holiday Detection of Internal Tubular Coatings of 10 to 30 mils (0.25 to 0.76 mm) Dry Film Thickness
TM0384	Holiday Detection of Internal Tubular Coatings of Less Than 10 mils (0.25 mm) Dry Film Thickness
TM0192	Evaluating Elastomeric Materials in Carbon Dioxide Decompression Environments
TM0196	Chemical Resistance of Polymeric Materials by Periodic Evaluation
TM0297	Effects of High-Temperature High-Pressure Carbon Dioxide Decompression on Elastomeric Materials
RP0178	Design, Fabrication and Surface Finish of Metal Tanks and Vessels to be Lined for Chemical Immersion Service
RP0184	Repair of Lining Systems
RP0188	Discontinuity (Holiday) Testing of Protective Coatings
RP0281	Method for Conducting Coating (Paint) Panel Evaluation Testing in Atmospheric Exposure
RP0287	Field Measurement of Surface Profile of Abrasive Blast Cleaned Steel Surfaces Using a Replica Tape
RP0288	Inspection of Linings on Steel and Concrete
RP0372	Method for Lining Lease Production Tanks with Coal Tar Epoxy
RP0376	Monolithic Organic Corrosion Resistant Floor Surfacing
RP0386	Applications of a Coating System to Interior Surfaces of Covered Railroad Hopper Cars in Plastic, Food and Chemical Service
RP0487	Considerations in the Selection and Evaluation of Interim Petroleum-Based Coatings
RP0190	External Protective Coatings for Joints, Fittings, and Valves on Metallic Underground or Submerged Pipeline and Piping Systems
RP0297	Maintenance Painting of Electrical Substation Apparatus Including Flow Coating of Transformer Radiators
RP0295	Application of a Coating System to Interior Surfaces of New and Used Rail Tank Cars
RP0298	Sheet Rubber Linings for Abrasion and Corrosion Service
RP0394	Application, Performance and Quality Control of Paint-Applied, Fusion-Bonded Epoxy External Pipe Coating
RP0395	Fusion-Bonded Epoxy Coating of Steel Reinforcing Bars
RP0398	Recommendations for Training and Qualifying Personnel as Railcar Coating and Lining Inspectors
RP0399	Plant Applied, External Coal Tar Enamel Pipe Coating System: Application, Performance and Quality Control
RP0495	Guidelines for Qualifying Personnel as Abrasive Blasters and Coatings and Linings Applicators in the Rail Industries
RP0591	Coatings and Concrete Surfaces in Non-Immersion and Atmospheric Service
RP0592	Application of a Coating System to Interior Surfaces of New and Used Rail Tank Cars in Concentrated (90 to 98%) Sulfuric Acid Service
RP0692	Application of a Coating System to Exterior Surfaces of Steel Rail Cars

### SAE INTERNATIONAL

J401	Selection and Use of Steels
J1434	Wrought Aluminum Applications Guidelines
J1562	Selection of Zinc and Zinc-Alloy (Hot-Dipped and Electrodeposited) Coated Steel Sheet
J1677	Tests and Procedures for SAE Low-Carbon Steel and Copper Nickel Tubing
J1755	Guidelines for Usage of Stainless Steel and Bimetal for Exterior Automotive Bright Trim
J2334	Cosmetic Corrosion Lab Test

### STEEL STRUCTURES PAINTING COUNCIL (SSPC)

#### Surface Preparation (SP)

SP COM	Surface Preparation Commentary for Steel and Concrete Substrates
SP 1	Solvent Cleaning
SP 2	Hand Tool Cleaning

SP 3	Power Tool Cleaning
SP 5/NACE 1	White Metal Blast Cleaning
SP 6/NACE 3	Commercial Blast Cleaning
SP 7/NACE 4	Brush-Off Blast Cleaning
SP 8	Pickling
SP 10/NACE 2	Near-White Blast Cleaning
SP 11	Power Tool Cleaning to Bare Metal
SP 12/NACE 5	Surface Preparation and Cleaning of Steel and Other Hard Materials by High- and Ultrahigh-Pressure Water Jetting Prior to Recoating
SP 13/NACE 6	Surface Preparation of Concrete
SP 14/NACE 8	Industrial Blast Cleaning

### Technology Reports (TR)

TR 1/NACE 6G194	Thermal Pre-Cleaning
TR 2/NACE 6G198	Wet Abrasive Blast Cleaning

### Abrasives (AB)

AB 1	Mineral and Slag Abrasives
AB 2	Cleanliness of Recycled Ferrous Metallic Abrasives
AB 3	Newly Manufactured or Re-Manufactured Steel Abrasives

### Painting Systems (PS) and Coating Systems (CS)

PS COM	Commentary on Painting Systems
PS Guide 1.00	Guide for Selecting Oil Base Painting Systems
PS 1.09	Three-Coat Oil Base Zinc Oxide Painting System (Without Lead or Chromate Pigment)
PS 1.10	Four-Coat Oil Base Zinc Oxide Painting System (Without Lead or Chromate Pigment)
PS 1.12	Three-Coat Oil Base Zinc Chromate Painting System
PS 1.13	One-Coat Oil Base Slow Drying Maintenance Painting System (Without Lead or Chromate Pigments)
PS Guide 2.00	Guide for Selecting Alkyd Painting Systems
PS Guide 3.00	Guide for Selecting Phenolic Painting Systems
PS Guide 4.00	Guide for Selecting Vinyl Painting Systems
PS 4.02	Four-Coat Vinyl Painting System (For Fresh Water, Chemical, and Corrosive Atmospheres)
PS 4.04	Four-Coat White or Colored Vinyl Painting System (For Fresh Water, Chemical, and Corrosive Atmospheres)
PS Guide 7.00	Guide for Selecting One-Coat Shop Painting Systems
PS Guide 8.00	Guide to Topcoating Zinc-Rich Primers
PS 9.01	Cold-Applied Asphalt Mastic Painting System with Extra-Thick Film
PS 10.01	Hot-Applied Coal Tar Enamel Painting System
PS 10.02	Cold-Applied Coal Tar Mastic Painting System
PS 11.01	Black (or Dark Red) Coal Tar Epoxy Polyamide Painting System
PS Guide 12.00	Guide to Selecting Zinc-Rich Coating Systems
PS 12.01	One-Coat Zinc-Rich Painting System
PS 13.01	Epoxy Polyamide Painting System
PS 14.01	Steel Joist Shop Painting System
PS Guide 15.00	Guide for Selecting Chlorinated Rubber Painting Systems
PS 15.01	Chlorinated Rubber Painting System for Salt Water Immersion
PS 15.02	Chlorinated Rubber Painting System for Fresh Water Immersion
PS 15.03	Chlorinated Rubber Painting System for Marine and Industrial Environments
PS 15.04	Chlorinated Rubber Painting System for Field Application Over a Shop-Applied Solvent Base Inorganic Zinc-Rich Primer
PS 16.01	Silicone Alkyd Painting System for New Steel
PS Guide 17.00	Guide for Selecting Urethane Painting Systems
PS 18.01	Three-Coat Latex Painting System
PS Guide 19.00	Guide for Selecting Painting Systems for Ship Bottoms
PS Guide 20.00	Guide for Selecting Painting Systems for Boottoppings
PS Guide 21.00	Guide for Selecting Painting Systems for Topsides
PS Guide 22.00	Guide for Selecting One-Coat Preconstruction or Prefabrication Painting Systems
CS 23.00(I)	Interim Specification for the Application of Thermal Spray Coatings (Metallizing) of Aluminum, Zinc, and Their Alloys and Composites for the Corrosion Protection of Steel
PS 24.00	Latex Painting System for Industrial and Marine Atmospheres, Performance-Based

PS 26.00	Aluminum Pigmented Epoxy Coating System Materials Specification, Performance-Based—Type I, for Use over Blast Cleaned Steel, Type II, for Use over Hand Cleaned Steel
PS 27.00	Alkyd Coating System Materials Specification, Performance-Based

### Paints and Coatings (PAINT)

Paint COM	Commentary on Paint Specifications
Paint 5	Zinc Dust, Zinc Oxide, and Phenolic Varnish Paint
Paint 8	Aluminum Vinyl Paint
Paint 9	White (or Colored) Vinyl Paint
Paint 11	Red Iron Oxide, Zinc Chromate, Raw Linseed Oil, and Alkyd Primer
Paint 12	Cold-Applied Asphalt Mastic (Extra Thick Film)
Paint 15	Steel Joist Shop Primer
Paint 16	Coal Tar Epoxy-Polyamide Black (or Dark Red) Paint
Paint 17	Chlorinated Rubber Inhibitive Primer
Paint 18	Chlorinated Rubber Intermediate Coat Paint
Paint 19	Chlorinated Rubber Topcoat Paint
Paint 20	Zinc-Rich Primers (Type I, Inorganic, and Type II, Organic)
Paint 21	White or Colored Silicone Alkyd Paint
Paint 22	Epoxy-Polyamide Paints (Primer, Intermediate, and Topcoat)
Paint 23	Latex Primer for Steel Surfaces
Paint 24	Latex Semigloss Exterior Topcoat
Paint 25	Zinc Oxide, Alkyd, Linseed Oil Primer for Use Over Hand Cleaned Steel, Type I and Type II
Paint 25.1BCS	Zinc Oxide, Alkyd, Linseed Oil Primer for Use Over Blast Cleaned Steel
Paint 26	Slow Drying Linseed Oil Black Maintenance Primer, (Without Lead and Chromate Pigment)
Paint 27	Basic Zinc Chromate-Vinyl Butyral Wash Primer
Paint 28	Water-Borne Epoxy Primer for Steel Surfaces
Paint 29	Zinc Dust Sacrificial Primer, Performance-Based
Paint 30	Weld-Through Inorganic Zinc Primer
Paint 31	Single-Package Waterborne Alkyd Primer for Steel Surfaces, Performance-Based
Paint 32	Coal Tar Emulsion Coating
Paint 33	Coal Tar Mastic, Cold Applied
Paint 34	Water-Borne Epoxy Topcoat for Steel Surfaces
Paint 35	Medium Oil Alkyd Primer (Air Dry/Low Bake), Type I and Type II
Paint 36	Two-Component Weatherable Aliphatic Polyurethane Topcoat, Performance-Based
Paint 101	Aluminum Alkyd Paint (Type I, Leafing and Type II, Non-Leafing)
Paint 102	Black Alkyd Paint
Paint 103	Black Phenolic Paint
Paint 104	White or Tinted Alkyd Paint
Paint 106	Black Vinyl Paint
Paint 108	High-Build Thixotropic Leafing Aluminum Paint

### Paint Application (PA)

PA COM	Commentary on Paint Application
PA 1	Shop, Field, and Maintenance Painting of Steel
PA 2	Measurement of Dry Coating Thickness with Magnetic Gages
PA Guide 3	A Guide to Safety in Paint Application
PA Guide 4	Guide to Maintenance Repainting with Oil Base or Alkyd Painting Systems
PA Guide 5	Guide to Maintenance Painting Programs

### Qualification Procedures (QP)

QP COM	Commentary on Qualification Procedures
QP 1	Standard Procedure for Evaluating Painting Contractors (Field Application to Complex Industrial Structures)
QP 2	Standard Procedure for the Qualification of Painting Contractors (Field Removal of Hazardous Coatings from Complex Structures)
QP 3	Standard Procedure for Evaluating Qualifications of Shop Painting Applicators
QP 4	Standard Procedure for Evaluating the Qualifications of Contractors Disturbing Hazardous Coatings During Demolition and Repair Work
QP 5	Standard Procedure for Evaluating Qualifications of Coating and Lining Inspection Companies

**Technology Guides (GUIDE)**

Guide 6	Guide for Containing Debris Generated During Paint Removal Operations
Guide 9	Guide for Atmospheric Testing of Coatings in the Field
Guide 10	Guide to Specifying Coatings Conforming to Volatile Organic Compound (VOC) Content Requirements
Guide 11	Guide for Coating Concrete
Guide 13	Guide for the Identification and Use of Industrial Coating Material in Computerized Product Databases
Guide 14	Guide for the Repair of Imperfections in Galvanized or Inorganic Zinc Coated Steel Using Organic Zinc-Rich Coating

**Test Panel Preparation Methods (ME)**

ME 1	Uncontaminated Rusted Steel
------	-----------------------------

# Author Index

## A

Adjorlolo, A. A., 687  
Alhassan, Safaa J., 525, 531  
Aylor, Denise M., 362

## B

Baboian, Robert, 558, 673, 754  
Bagnall, Chris, 465  
Baker, Brian A., 434  
Berke, Neal S., 405  
Boffardi, Bennett P., 826  
Brossia, C. S., 221, 448  
Bundy, K. J., 500  
Bushman, James B., 706

## C

Chaker, Victor, 706  
Clayton, W. E., 822  
Cohen, Arthur, 565  
Colwell, Richard L., 66  
Cooper, Kevin R., 266  
Corbett, Richard A., 139  
Cagnolino, Gustavo A., 221  
Cramer, Stephen D., 49  
Crook, P., 591

## D

Dean, Sheldon W., Jr., 159  
DeBold, Terry A., 769  
DeVan, Jack H., 465  
Dexter, Stephen C., 509  
Dille, Eldon R., 746  
Dunn, Darrell S., 221

## E

Efird, K. Daniel, 425  
Ellor, James A., 205  
Escalante, Edward, 181

## F

Fairer, Philippa, 175, 380  
Fraker, Anna C., 834

## G

Gangloff, Richard P., 302  
Glaeser, W. A., 273  
Goodwin, Frank E., 525, 531  
Granata, Richard D., 632  
Groshart, Earl C., 693

## H

Hack, Harvey P., 233  
Hausler, Rudolf H., 480  
Haynie, Fred H., 83  
Hibner, Edward L., 580  
Hihara, L. H., 637  
Hillis, James E., 537  
Hinshaw, E. B., 617  
Hopkins, Alfred G., 76

## I

Interrante, C. G., 322

## J

Jenkins, James F., 170, 716  
Jensen, David F., 846  
Jonas, Otakar, 738  
Jones, Barnie P., 49  
Jordan, D. L., 558

## K

Kane, Russel D., 147  
Kearns, Jeffrey R., 221  
Kelly, R. G., 211  
Klar, Erhard, 664  
Komp, M. E., 558  
Krisher, A. S., 413

## L

Lawson, Herbert H., 343  
Licina, George J., 727  
Lifka, Bernard W., 547  
Lisagor, W. Barry, 289

## M

Marceau, J. A., 687  
Martin, James W., 585  
Mayer, P., 722  
Meade, Cynthia L., 131  
Moffat, T. P., 656  
Moniz, Bert, 779  
Moser, K. D., 617

## P

Pawel, Steven J., 465  
Pellgrini, A. D., 722  
Perkins, Allan, 187  
Pettit, F. S., 457  
Puyear, Robert B., 418

## R

Raymond, L., 322  
Repp, John, 205  
Roberge, Pierre R., 89  
Rosenberg, Harvey S., 746  
Rothman, Paul S., 696

## S

Samal, Prasan K., 664  
Schick, G., 762  
Schrock, Steven L., 465  
Scully, John R., 107  
Schutz, Ronald W., 598  
Shifler, David A., 362, 448  
Silverman, David C., 59  
Simpson, T. C., 620  
Sinclair, J. D., 349  
Smith, Gaylord D., 194, 434  
Sprowls, Donald O., 266  
Sridhar, Narasi, 221  
Streicher, Michael A., 244

## T

Tholke, B., 822  
Tortorelli, Peter F., 465  
Townsend, H. E., 620  
Tuttle, R. N., 812

## V

Van Orden, Ann Chidester, 278  
Velva, Lucien, 387

## W

Wensley, Angela, 795

## Y

Yau, Te-Lin, 61  
Young, Walter T., 175, 380, 696

## Z

Zhang, Shi Hua, 779

# Subject Index

65% nitric acid test, 250–251

## A

Abbreviations, ASTM, 14–16

AC impedance, 788–790

Accelerated tests, 743, 766

Acetic acid salt spray (fog) tests, 132

Acidified synthetic sea water (fog) test, 134

Acidity

aluminum and aluminum alloys, 550

lead and lead alloys, 534

magnesium and magnesium alloys, 541

Acidizing treatments, 814

Acids

copper and copper alloys, 568

stainless steels, 587–588

Acronyms, 12–13

Additives, concrete, 406, 409

Aerations, soils, 390, 392

Aerospace, hydrogen damage, 329–331

Agitated tests, 148

Air, dew point, 38–42

Air port composite tube corrosion, 804–805

Aircraft, *see* Commercial aircraft

Alkalinity

aluminum and aluminum alloys, 550

copper and copper alloys, 569

lead and lead alloys, 534

magnesium and magnesium alloys, 541

stainless steels, 588

Allihn condensers, 252–253

Alloying effects, stainless steels, 585

Alloys

coefficients of thermal expansion, 36

common names, 5–6

density, 25, 33

equivalent weight values, 28–29

resistant, pipeline, 698

sensitization, 124–125

Alternating current methods,

microbiological effects, 514–515

Alumina, effect on

aluminum metal-matrix composites, 641–642

copper metal-matrix composites, 649

magnesium metal-matrix composites, 645

stainless steel metal-matrix composites, 646–647

Aluminum and aluminum alloys, 547–556

acidity/alkalinity, 550

addition, stainless steels, 585

alloying effect, 547

anodized, single frequency impedance test, 126

compatibility with chemicals, 551

crevice corrosion, 551

environmental factors, 550–551

exfoliation corrosion, 266–267, 552, 554

filiform corrosion, 553, 555–556

galvanic corrosion, 551, 555

heat treatment evaluation, commercial aircraft, 689

hydrogen role, 549

intergranular corrosion, 552, 554

ions, 550

liquid metals, 551

mechanical treatments, 548–549

metal-matrix composites, 637–644

alumina effect, 641–642

boron effect, 637–638

effect of diffusion bonds and microstructural contaminants, 642

graphite effect, 638–639

mica effect, 642

reinforcement constituent effect, 642–644

silicon carbide effect, 639–641

as metallic coatings, 622–623

metallurgical treatments, 547

mill and foundry products, 549

natural protective films, 547

pipeline, 697

pitting corrosion, 552, 554

precracked specimens, 555

protective coatings, 547, 549–550, 556

seawater corrosion, 376

smooth specimens, 554–555

staining corrosion, 553–554

stress corrosion cracking, 553–554

test methods, 551–553

test selection factors, 547

uniform corrosion, 553

Aluminum brass, 566

Aluminum bronzes, 567

Ammonia test, copper and copper alloys, 569–570

Anaerobic bacteria, 391

Anions, 390

Anode/cathode area ratio, galvanic corrosion, 235

Anodic protection, chemical pulping, 802

Anodic reaction, 391

Anodized aluminum corrosion test, 125

ANSI/NEMA 250, 767

API standards, 781, 851

Aqueous corrosion testing, 526, 593–595

Aqueous environments, steels, 559

Aqueous media, titanium, passivity, 599–601

Aqueous phase corrosion, oil refining, 820–821

Artificial intelligence, applications, 99–102

ASME B31G, 851

ASTM A 143, 853

ASTM A 239, 527–528

ASTM A 242, 558, 562–563

ASTM A 262, 64, 71, 125, 140, 143–144, 244, 247, 250, 252–253, 255, 261–262, 386, 505, 582, 586, 588, 669, 735–736, 771–773, 802, 851

ASTM A 370, 173, 815

ASTM A 380, 345–346, 585, 668, 776, 855

ASTM A 393, 251

ASTM A 514, 558

ASTM A 517, 558

ASTM A 572, 558

ASTM A 588, 558, 562–563

ASTM A 606, 558

ASTM A 708, 251

ASTM A 763, 143, 244, 248, 252–253, 255, 261–262, 587–588, 771, 773, 851

ASTM A 767, 410

ASTM A 775, 409

ASTM A 852, 558, 562

ASTM A 876, 563

ASTM A 884, 410

ASTM A 923, 586, 774, 803

ASTM A 967, 585, 776

ASTM B 29, 532

ASTM B 69, 526

ASTM B 76, 200–201, 445, 855

ASTM B 78, 201, 445, 855

ASTM B 80, 538

ASTM B 90, 538

ASTM B 93, 538

ASTM B 94, 538

ASTM B 107, 538

ASTM B 117, 127, 131–132, 135, 348, 372, 527–529, 535, 538–539, 542, 544–545, 554, 556, 561, 570–571, 577, 624, 626–627, 633–635, 660, 666, 669, 680, 684, 689–691, 694–695, 751, 758, 767, 775, 777, 852

ASTM B 154, 569, 855

ASTM B 162, 134

ASTM B 201, 526–528

ASTM B 240, 526

ASTM B 275, 537

ASTM B 287, 633–634

ASTM B 368, 132, 134, 571, 577, 633, 635, 660, 680, 684, 694, 758, 852

ASTM B 380, 132, 134, 528, 571, 660, 680, 684, 855

ASTM B 418, 525

ASTM B 456, 684

ASTM B 457, 126, 635, 684, 854

ASTM B 488, 758

ASTM B 499, 527–528

ASTM B 537, 138, 168, 660, 679, 853

ASTM B 538, 125, 633, 684

ASTM B 545, 758, 855

ASTM B 568, 527–528

ASTM B 577, 853

- ASTM B 605, 855  
 ASTM B 627, 125, 661  
 ASTM B 650, 855  
 ASTM B 651, 660, 855  
 ASTM B 659, 659  
 ASTM B 661, 529  
 ASTM B 669, 526  
 ASTM B 679, 759  
 ASTM B 680, 855  
 ASTM B 689, 759, 855  
 ASTM B 695, 621  
 ASTM B 696, 621  
 ASTM B 700, 759  
 ASTM B 733, 855  
 ASTM B 734, 855  
 ASTM B 735, 758, 855  
 ASTM B 741, 758, 855  
 ASTM B 765, 659, 758, 855  
 ASTM B 758, 799  
 ASTM B 808, 760  
 ASTM B 809, 758, 855  
 ASTM B 810, 356, 361, 760, 853  
 ASTM B 825, 760  
 ASTM B 826, 760  
 ASTM B 827, 132, 134–136, 356, 361, 680, 760, 853  
 ASTM B 843, 538, 539  
 ASTM B 845, 356, 361  
 ASTM B 858, 569, 853  
 ASTM B 867, 759  
 ASTM C 494, 409  
 ASTM C 536, 635  
 ASTM C 581, 799, 803  
 ASTM C 692, 140, 143, 853  
 ASTM C 739, 855  
 ASTM C 743, 635  
 ASTM C 868, 785, 787  
 ASTM C 876, 57, 408–409, 721, 855  
 ASTM D 130, 683, 821, 855  
 ASTM D 512, 698  
 ASTM D 516, 698  
 ASTM D 522, 635  
 ASTM D 523, 635  
 ASTM D 572, 157  
 ASTM D 609, 679  
 ASTM D 610, 138, 635, 679, 720, 724, 855  
 ASTM D 660, 724  
 ASTM D 662, 635, 724  
 ASTM D 664, 820  
 ASTM D 665, 683, 821, 855  
 ASTM D 714, 138, 635, 724  
 ASTM D 772, 724  
 ASTM D 822, 633, 635  
 ASTM D 823, 635  
 ASTM D 849, 683, 855  
 ASTM D 870, 132, 635, 680, 684  
 ASTM D 876, 855  
 ASTM D 968, 635  
 ASTM D 974, 819  
 ASTM D 1014, 635  
 ASTM D 1141, 374, 517, 633, 855  
 ASTM D 1186, 635  
 ASTM D 1193, 57, 615, 855  
 ASTM D 1280, 855  
 ASTM D 1384, 141, 143, 577, 683, 855  
 ASTM D 1400, 635  
 ASTM D 1414, 855  
 ASTM D 1567, 635  
 ASTM D 1611, 855  
 ASTM D 1653, 635  
 ASTM D 1654, 138, 164, 545, 625, 635, 679, 684, 690, 720, 855  
 ASTM D 1735, 132, 635, 680, 684, 758  
 ASTM D 1743, 683, 855  
 ASTM D 1748, 132, 684  
 ASTM D 2010, 160, 345  
 ASTM D 2059, 853  
 ASTM D 2197, 635  
 ASTM D 2216, 388  
 ASTM D 2247, 132, 135, 626, 634–635, 680, 684, 758, 855  
 ASTM D 2248, 635  
 ASTM D 2251, 855  
 ASTM D 2434, 389  
 ASTM D 2488, 387, 389  
 ASTM D 2570, 141, 143, 683, 767, 855  
 ASTM D 2578, 143  
 ASTM D 2649, 683, 855  
 ASTM D 2671, 855  
 ASTM D 2688, 177, 383, 415, 528–529, 535  
 ASTM D 2758, 141, 683, 855  
 ASTM D 2776, 528–529, 535  
 ASTM D 2803, 132, 135, 680, 684, 690, 856  
 ASTM D 2809, 683, 854  
 ASTM D 2847, 683, 856  
 ASTM D 2933, 684, 758  
 ASTM D 2937, 387  
 ASTM D 2966, 683  
 ASTM D 2980, 389  
 ASTM D 3258, 635  
 ASTM D 3263, 856  
 ASTM D 3273, 635, 694  
 ASTM D 3276, 635  
 ASTM D 3310, 856  
 ASTM D 3316, 856  
 ASTM D 3359, 633, 635  
 ASTM D 3361, 635  
 ASTM D 3363, 635  
 ASTM D 3482, 856  
 ASTM D 3585, 676, 683  
 ASTM D 3603, 821, 856  
 ASTM D 3632, 157  
 ASTM D 3794, 135  
 ASTM D 3963, 410  
 ASTM D 4048, 821, 856  
 ASTM D 4145, 633, 635  
 ASTM D 4170, 276  
 ASTM D 4340, 683, 856  
 ASTM D 4584, 853  
 ASTM D 4585, 635, 680, 684  
 ASTM D 4587, 635, 695  
 ASTM D 4627, 856  
 ASTM D 4636, 683  
 ASTM D 4739, 820  
 ASTM D 5894, 132, 134, 372, 374  
 ASTM D 6294, 135  
 ASTM D 6396, 157  
 ASTM D 6899, 137  
 ASTM E 3, 173, 179–180, 385–386  
 ASTM E 8, 242, 326, 331  
 ASTM E 10, 445  
 ASTM E 80, 386  
 ASTM E 112, 124  
 ASTM E 203, 455  
 ASTM E 212, 701  
 ASTM E 376, 527, 635  
 ASTM E 380, 17–18, 21–22, 57  
 ASTM E 399, 333, 606, 651  
 ASTM E 456, 53  
 ASTM E 466, 310  
 ASTM E 468, 311  
 ASTM E 527, 57  
 ASTM E 558, 725  
 ASTM E 606, 311, 375, 805  
 ASTM E 647, 313–315, 375, 798  
 ASTM E 673, 77  
 ASTM E 712, 157, 856  
 ASTM E 739, 375  
 ASTM E 745, 856  
 ASTM E 807, 179–180, 385–386  
 ASTM E 827, 78  
 ASTM E 937, 856  
 ASTM E 983, 79  
 ASTM E 984, 79  
 ASTM E 995, 79  
 ASTM E 1049, 375  
 ASTM E 1064, 455  
 ASTM E 1078, 79  
 ASTM E 1127, 79  
 ASTM E 1217, 80  
 ASTM E 1290, 333, 336–337  
 ASTM E 1325, 53  
 ASTM E 1488, 52  
 ASTM E 1505, 80  
 ASTM E 1523, 79  
 ASTM E 1524, 375  
 ASTM E 1681, 333–338, 374–375  
 ASTM E 1820, 333  
 ASTM F 4, 836, 839, 842  
 ASTM F 67, 504  
 ASTM F 75, 504  
 ASTM F 86, 504  
 ASTM F 90, 504  
 ASTM F 113, 562  
 ASTM F 136, 504, 840  
 ASTM F 138, 503  
 ASTM F 139, 504  
 ASTM F 326, 328, 853  
 ASTM F 359, 856  
 ASTM F 482, 856  
 ASTM F 483, 856  
 ASTM F 519, 328–331, 337, 689–690, 853  
 ASTM F 560, 504  
 ASTM F 562, 504  
 ASTM F 563, 504  
 ASTM F 620, 504  
 ASTM F 621, 504  
 ASTM F 688, 504  
 ASTM F 745, 504  
 ASTM F 746, 119, 178, 218, 227, 384, 503, 505, 777, 842, 856  
 ASTM F 748, 504  
 ASTM F 763, 504  
 ASTM F 799, 504  
 ASTM F 897, 385–386, 503, 505, 854  
 ASTM F 945, 853  
 ASTM F 961, 504  
 ASTM F 981, 504  
 ASTM F 1058, 504  
 ASTM F 1089, 505, 856  
 ASTM F 1091, 504  
 ASTM F 1108, 504  
 ASTM F 1110, 856  
 ASTM F 1113, 328  
 ASTM F 1295, 504  
 ASTM F 1314, 504  
 ASTM F 1341, 504  
 ASTM F 1350, 504  
 ASTM F 1377, 504  
 ASTM F 1472, 504  
 ASTM F 1537, 504  
 ASTM F 1580, 504  
 ASTM F 1586, 504  
 ASTM F 1624, 337–338  
 ASTM F 1713, 503  
 ASTM F 1801, 840  
 ASTM F 1813, 504  
 ASTM F 1875, 503  
 ASTM F 1940, 328, 331  
 ASTM F 2004, 504  
 ASTM F 2005, 504  
 ASTM F 2063, 504

- ASTM F 2066, 504  
 ASTM F 2068, 505  
 ASTM F 2082, 504  
 ASTM F 2129, 140, 143  
 ASTM G 07, 344  
 ASTM G 1, 23, 43, 57, 63, 138, 143, 145, 172–173, 177, 180, 183, 192, 198, 206–208, 211, 242, 345–346, 375, 383, 400, 406, 445, 455, 527–528, 535, 544, 552, 554, 560, 562–563, 602, 619, 625, 649, 651, 679, 772, 795, 851  
 ASTM G 2, 613–614, 736, 851  
 ASTM G 3, 27, 57, 59–60, 140, 143, 177, 383, 401, 555, 588, 606, 679, 776, 839, 854  
 ASTM G 4, 57, 143, 157, 177–178, 192, 211, 383, 560, 604, 613, 619, 681, 736, 772, 784, 795, 851  
 ASTM G 5, 57, 60, 109, 140, 143, 226, 229, 401, 455, 505, 555, 561, 588, 604, 606, 628, 649, 651, 660, 666, 680, 684, 690, 736, 776, 797, 803, 839, 842, 854  
 ASTM G 6, 852  
 ASTM G 7, 853  
 ASTM G 8, 635, 852  
 ASTM G 9, 852  
 ASTM G 11, 852  
 ASTM G 12, 635, 852  
 ASTM G 15, 57, 174, 205, 226, 266, 375, 381, 560–561, 580, 679, 720, 851  
 ASTM G 16, 52, 57, 171, 173–174, 178, 193, 212, 346, 374–375, 384, 406, 560–561, 679, 777, 851  
 ASTM G 17, 852  
 ASTM G 19, 852  
 ASTM G 20, 852  
 ASTM G 26, 633  
 ASTM G 28, 64, 143, 244, 254, 258–259, 261, 263, 582, 584, 593, 595, 606, 771, 773, 851  
 ASTM G 30, 164, 167, 171, 174, 193, 242, 293, 299, 375, 385–386, 505, 554, 562, 583, 589, 593, 604, 606, 735, 773, 805, 853  
 ASTM G 31, 57, 62, 64, 140, 143–144, 177, 185, 207, 375, 383, 454, 528–529, 535, 544, 560, 581–582, 588, 593, 595, 597, 602, 613, 619, 665, 680, 684, 783, 785, 802, 852  
 ASTM G 32, 172, 174, 179, 276, 373, 375, 385–386, 595–597, 803, 854  
 ASTM G 33, 166–167, 238, 346, 406, 528–529, 679, 681, 684, 713, 853  
 ASTM G 34, 140, 143, 173–174, 267–268, 270–271, 548, 552, 554, 684, 689, 690, 852  
 ASTM G 35, 140, 143, 295, 583, 589, 604, 606, 795, 820, 853  
 ASTM G 36, 140, 143, 295, 298, 505, 562, 580, 583, 589, 593, 597, 604, 606, 773, 803, 853  
 ASTM G 37, 295, 570, 767, 853  
 ASTM G 38, 57, 164, 167, 171, 174, 179, 193, 293–294, 375, 505, 554, 564, 583, 589, 606, 735, 815, 853  
 ASTM G 39, 164, 167, 171, 174, 179, 193, 294, 375, 385–386, 505, 554, 562, 583, 589, 735, 853  
 ASTM G 40, 57, 179, 385, 720, 854  
 ASTM G 41, 295, 562, 589, 607, 853  
 ASTM G 42, 635, 852  
 ASTM G 43, 133–134, 633, 680  
 ASTM G 44, 143, 295, 299, 375, 554–555, 562, 583, 589, 680, 689–690, 775, 852  
 ASTM G 46, 57, 63, 71–72, 138, 143, 145, 173–174, 178, 184, 193, 211, 223, 242, 346, 375, 384, 400, 406, 505, 527–528, 552, 554, 561, 581, 589, 605, 616, 619, 649, 651, 666, 679, 713, 720, 736, 775, 852  
 ASTM G 47, 179, 299, 375, 385–386, 554, 604, 689, 690, 853  
 ASTM G 48, 140, 143, 212, 222–225, 384, 583, 589, 593, 597, 606, 669, 680, 684, 774–775, 795, 799, 852  
 ASTM G 49, 143, 164, 167, 179, 294–295, 375, 385–386, 505, 554, 562, 564, 589, 606, 735, 815, 853  
 ASTM G 50, 57, 143, 164, 166–167, 238, 240, 344, 346, 528–529, 554, 560, 562, 588, 625, 665, 681, 713, 772, 795, 853  
 ASTM G 51, 400, 535, 698, 713, 854  
 ASTM G 52, 170–174, 374, 560, 572, 713, 772, 852  
 ASTM G 53, 633, 635  
 ASTM G 54, 201, 437, 445, 610, 852  
 ASTM G 56, 720  
 ASTM G 57, 57, 399–400, 528–529, 535, 697, 713, 854  
 ASTM G 58, 164, 167, 171, 174, 179, 295, 385–386, 554, 589, 735, 771, 802, 853  
 ASTM G 59, 57, 60, 109, 111, 177, 184, 208–210, 375, 383, 401, 408, 455, 505, 561, 584, 588, 628, 660, 680, 684, 702, 854  
 ASTM G 60, 143, 348, 561, 635, 680–681, 695, 713, 775, 853  
 ASTM G 61, 60, 118–119, 140, 143, 178, 193, 215, 226, 228–229, 375, 384–386, 401, 406, 455, 505, 528–529, 561, 584, 628, 660, 666, 680, 684, 690, 735, 736, 776, 791, 840, 842, 854  
 ASTM G 62, 852  
 ASTM G 64, 385–386, 853  
 ASTM G 65, 595–597, 854  
 ASTM G 66, 173–174, 268, 270, 552–554, 852  
 ASTM G 67, 244, 554, 852  
 ASTM G 69, 59, 213, 555, 680, 684, 690, 777, 854  
 ASTM G 71, 57, 61, 140, 143, 171, 174, 179, 226, 238, 239, 242, 375, 384–385, 401, 505, 535, 561, 651, 721, 777, 854  
 ASTM G 72, 157  
 ASTM G 73, 172, 174, 179, 276, 373, 375, 385–386, 854  
 ASTM G 75, 140, 143, 854  
 ASTM G 76, 275, 854  
 ASTM G 77, 854  
 ASTM G 78, 63, 140, 143, 171, 174, 178, 193, 226, 375, 384, 589, 604, 713, 774, 799, 852  
 ASTM G 79, 201–202, 445–446, 713, 852  
 ASTM G 80, 635, 852  
 ASTM G 82, 57, 59, 117, 171, 174, 178–179, 234, 239, 242, 375, 384–385, 535, 555, 650, 660, 680, 684, 777, 854  
 ASTM G 83, 854  
 ASTM G 84, 159, 167, 238, 344, 347, 359, 635, 713, 853  
 ASTM G 85, 132, 212–213, 268, 272, 372, 554, 556, 561, 571, 633–635, 681, 684, 689–691, 694, 751, 758, 775, 853  
 ASTM G 86, 157  
 ASTM G 87, 132, 135, 348, 527–529, 561, 626, 635, 680–681, 684, 713, 758, 853  
 ASTM G 90, 635, 853  
 ASTM G 91, 160, 167, 345, 527–528, 713, 853  
 ASTM G 92, 167, 238, 345, 347, 528–529, 560, 635, 681, 684, 853  
 ASTM G 94, 157  
 ASTM G 95, 852  
 ASTM G 96, 111, 177, 189–190, 193, 210, 383, 415, 736, 783, 787, 854  
 ASTM G 97, 239, 539, 854  
 ASTM G 98, 595, 597, 854  
 ASTM G 99, 854  
 ASTM G 100, 119, 217, 226, 375, 628, 680, 855  
 ASTM G 101, 167, 562–563, 713, 853  
 ASTM G 102, 28–30, 57, 60, 109, 177, 185, 190, 193, 679–680, 702, 736, 777, 829, 855  
 ASTM G 103, 295, 554, 854  
 ASTM G 104, 713  
 ASTM G 105, 854  
 ASTM G 106, 61–62, 112, 140, 143, 401, 408, 529, 628, 660, 680, 690, 736, 842, 855  
 ASTM G 107, 61, 65, 89, 778, 852  
 ASTM G 108, 61, 124–125, 140, 143, 180, 244, 257, 261, 385, 680, 736, 777, 802, 855  
 ASTM G 109, 407–409, 563, 713, 852  
 ASTM G 110, 244, 552, 554, 852  
 ASTM G 111, 157, 736, 852  
 ASTM G 112, 266, 268, 270, 554, 852  
 ASTM G 113, 853  
 ASTM G 116, 164, 167, 241–242, 345, 347, 561, 853  
 ASTM G 117, 212–213, 852  
 ASTM G 118, 854  
 ASTM G 119, 57, 854  
 ASTM G 123, 295, 298, 583, 589, 773, 854  
 ASTM G 124, 157  
 ASTM G 129, 157, 298, 337, 375, 555, 561, 589, 736, 773, 791, 854  
 ASTM G 131, 852  
 ASTM G 134, 854  
 ASTM G 135, 90, 778, 852  
 ASTM G 139, 299, 375, 689, 854  
 ASTM G 140, 160, 345, 853  
 ASTM G 141, 853  
 ASTM G 142, 157, 852  
 ASTM G 146, 157, 852  
 ASTM G 147, 853  
 ASTM G 148, 123–124, 401, 854  
 ASTM G 149, 164–165, 167, 241–242, 853  
 ASTM G 150, 120, 218, 589, 680, 735, 775, 855  
 ASTM G 156, 853  
 ASTM G 157, 223, 792, 852  
 ASTM G 158, 854  
 ASTM G 160, 854  
 ASTM G 161, 65, 792, 852  
 ASTM G 162, 185, 854  
 ASTM G 163, 854  
 ASTM G 165, 699, 854  
 ASTM G 166, 852  
 ASTM G 168, 297, 336, 589, 774, 854  
 ASTM G 170, 157, 852  
 ASTM G 472, 606  
 Atmospheric corrosion, metals processing, 775  
 Atmospheric exposure tests, 159–168  
 copper and copper alloys, 568  
 corrosion inhibitors, 493–494  
 exposure program, 163  
 galvanic corrosion, 240–242  
 indoor atmospheres, 162–163, 166  
 monitoring variables, 159–161



outdoor exposure, 165–166  
 powder metallurgy materials, 665  
 principles, 159–163  
 program development, 163  
 site monitoring/evaluation of  
   environment, 166–167  
 specimens, 163–165  
 types of exposures, 159  
**Atmospheric environment**  
   classification, 161–162, 343  
   highways, tunnels, and bridges, 707–708,  
   712  
   service test, 199  
   steels, 559  
**Atmospheric gaseous pollutants, design**  
   guidelines, 350  
**Atmospheric particulate matter, design**  
   guidelines, 350  
**Auger electron spectroscopy, 77–79**  
**Austenitic stainless steels, 586**  
**Autoclaves, 801–802**  
**Automobiles, 673–684**  
   automatic transmission fluid, 676  
   cabinet tests, 680  
   controlling corrosion, 677–679  
   corrosion mechanisms, 676–677  
   cyclic tests, 680–681  
   design improvements, 673  
   electrical and electronic systems, 679  
   electrochemical tests, 679–680  
   engine oils and coolants, 676  
   environment, 673–676  
   external exposure, 674–675  
   field tests, external exposure, 681–682  
   immersion tests, 679–680  
   internal combustion exposure, 675  
   internal functional liquids, 675–676  
   laboratory tests, external exposure,  
   679–681  
   liquid passage and reservoirs, 678  
   materials, 673  
   metallic materials, 674  
   processing, 673  
   test methods, 679–684  
   testing, 682–684  
**Automotive fasteners, 331**  
**Automotive radiators, accelerated**  
   corrosion testing, 576–577  
**AWWA standards, 851**  
**Axial heating rate, liquid metals, 470**

**B**

**Bacteria**  
   corrosive, 176  
   pipeline, 698  
**Bar steel, 562–563**  
**Barnacle electrode, 123, 328**  
**Basquin equation, 304**  
**Bent-beam test, oil and gas production,**  
   815  
**Beverage, *see* Food and beverage**  
**BI 103–01, 132, 135**  
**BI 104–01, 132**  
**BI 104–02, 132**  
**BI-123–01, 132**  
**Bias effects, indoor atmospheres, 355**  
**Bimetallic couples, pipeline, 700**  
**Biofilms, 367, 509–510**  
**Biofouling, copper and copper alloys, 568**  
**Biological activity test, soils, 401**  
**Biological factors, freshwater, 381**  
**Biological organisms, seawater, 366**  
**Black liquor system corrosion, 803**

**Bleach plant, 798–800**  
**Block designs, 55–56**  
**BNF jet test, copper and copper alloys,**  
   573  
**Bode phase angle and magnitude plots,**  
   113, 127  
**Boron, effect on metal-matrix**  
   composites, 637–638, 644  
**Bottom up approach, 92**  
**Box-and-Whisker plots, 91–93**  
**BQ 105–01, 132**  
**Brasses, 565–566**  
**Breakaway corrosion, high-temperature**  
   corrosion, 196  
**Bridges, *see* Highways, tunnels, and**  
   bridges  
**British Std 1036, 683**  
**Brownstock and black liquor system**  
   corrosion, 803  
**BSI Code of Practice 7361 Part 1, 525**  
**BSP standards, 768**  
**Burner, rigs simulation, 458–459**

**C**

**C-ring test, oil and gas production, 815**  
**Cabinet corrosion tests, 131–138**  
   acetic acid salt spray (fog) tests, 132  
   acidified synthetic sea water (fog) test,  
   134  
   automobiles, 680  
   CASS test, 134  
   corrodokote test, 134  
   corrosive gas tests, 135  
   cyclic acidified salt fog test, 133–134  
   cyclic corrosion tests, 136–138  
   cyclic salt fog/UV exposure, 134  
   dilute electrolyte cyclic fog/dry test, 134  
   evaluation of results, 137–138  
   filiform tests, 135  
   humidity tests, 134–135  
   mixed flowing gas, 136  
   salt spray (fog) test, 131–132  
   sal/SO<sub>2</sub> spray (fog) test, 134  
**Cables, telecommunications, 762–763**  
**Cadmium, as metallic coatings, 623**  
**Capillary water, 389**  
**Carbon steel, 376, 716**  
**Carbonates, in seawater, 366**  
**Carbonation, concrete, 406**  
**Carburization, 198, 201, 437–440**  
**Case-based reasoning, 101–102**  
**CASS test, 134, 571**  
**Cast iron, pipeline, 696**  
**Catastrophic corrosion, high-temperature**  
   corrosion, 196  
**Cathodic protection, 394**  
   concrete, 410  
   highways, tunnels, and bridges, 710  
   piers and docks, 719  
   pipeline, 699  
**Cathodic reaction, 392**  
**Cations, 390**  
**Cavitation, 274, 276**  
   copper and copper alloys, 573  
   freshwater, 386  
   seawater, 370  
**CCT, 132**  
**Ceramics, molten salts, 461–463**  
**Chemical cleaning procedures, 43–45**  
**Chemical etching, 69–70**  
**Chemical processing, 779–793**  
   anticipating process chemistry effects,  
   780–781  
   computerized test database, 793  
   confidence in data, 792–793  
   coupon testing, 784–787  
   electrical resistance probe, 787  
   field testing, 783  
   institutional requirements, 781  
   interpreting data, 785–787  
   laboratory testing, 783–784  
   linear polarization, 787–789  
   materials selection, 779–780  
   pilot plant testing, 784  
   probe testing, 787–788  
   specialized testing, 788–792  
   test location, 782–783  
**Chemical pulping, 800–803**  
**Chemical vapor deposition, 621**  
**Chloride, ingress into concrete, 406**  
**Chromium and chromium alloys, as**  
   metallic coatings, 623  
**Chromium carbide precipitates, 249**  
**Chromium-iron alloys, phase**  
   formation, 73  
**Chronopotentiometry, electrodeposited**  
   coatings, 661  
**Chrysler LP 461H-117, 681**  
**Chrysler Std MS-4338D, 683**  
**CLIMAT test, 347**  
**Close interval survey, pipeline, 703**  
**Closures, telecommunications, 762–763**  
**CO<sub>2</sub> corrosion, modeling, 100**  
**Coal ash corrosion, 442**  
**Coating degradation, 788–789**  
**Coatings**  
   AC impedance, 788–790  
   aluminum and aluminum alloys, 556  
   highways, tunnels, and bridges, 710  
   magnesium and magnesium alloys, 545  
   in oil and gas production, 814  
   piers and docks, 719  
   pipeline, 698  
   *see also* Electrodeposited coatings;  
   Metallic coatings on steel;  
   Nonmetallic coatings; Protective  
   coatings and films  
**Cobalt-base alloys, 591–597**  
   aqueous corrosion testing, 593–595  
   compositions, 591  
   galling test, 596  
   hot corrosion testing, 597  
   investment castings, 595  
   microstructures, 592–593  
   oxidation testing, 597  
   stress corrosion cracking, 593–594  
   wear testing, 595–597  
**Coefficients of thermal expansion, 36**  
**Coffin-Manson equation, 304**  
**Commercial aircraft, 687–692**  
   aluminum alloy/heat-treat evaluation, 689  
   controlling corrosion, 688  
   high-strength steel testing, 689  
   hydrogen damage, 329–331  
   in-service monitoring, 688  
   inspection, 688  
   materials selection, 689  
   paint evaluation, 689, 691  
   problem areas, 689  
   service environments, 687–688  
   surface finishes evaluation, 691  
**Composite materials, piers and docks,**  
   716–717  
**Composite tube corrosion and cracking,**  
   805  
**Computer modeling, galvanic corrosion,**  
   239–240, 242

- Concrete, 405–410
  - additives, 406, 409
  - carbonation, 406
  - cathodic protection, 410
  - chloride ingres, 406
  - complexities associated with corrosion evaluation, 405–406
  - environment, 405
  - field testing, 408–409
  - laboratory testing, 406–408
  - membranes, 410
  - outdoor exposures, 406
  - reinforced and prestressed, 716
  - reinforcing bar coatings, 409–410
  - resistivity, 405
  - sealers, 410
  - solution tests in concrete-like solutions, 406–407
  - standards, 409
  - testing in laboratory specimens, 407–408
- Condensate zone, 783
- Condensers, 250, 572–573
- Condensing surfaces, 789
- Conductivity, exfoliation corrosion, 269
- Conductors, electric power, 725
- Confidence limits for the mean, 84
- Constant phase elements, 114
- Contact electric resistance testing, chemical pulping, 801
- Continuous immersion, 782
- Conversion factors, 18–19
  - corrosion rate, 24
  - reference potentials, 27
- Cooling waters, polluted, copper and copper alloys, 568
- Copper-accelerated salt spray test, 134
- Copper and copper alloys, 565–578
  - acids, 568
  - alkalies and ammonia, 569
  - aluminum brass, 566
  - aluminum bronzes, 567
  - ammonia tests, 569–570
  - atmospheric exposure, 568
  - automotive radiators, 576–577
  - biofouling, 568
  - BNF jet test, 573
  - brasses, 565–566
  - cavitation tests, 573
  - classification, 565
  - copper-beryllium alloys, 567
  - copper-bismuth, 567
  - copper-bismuth-selenium, 567
  - copper nickels, 567
  - copper-silicon alloys, 567
  - electrical resistance tests, 573–574
  - erosion-corrosion tests, 574–575
  - galvanic corrosion tests, 575–576
  - high copper alloys, 565
  - hydrochloric acid spray test, 571–572
  - inhibited alloys, 567
  - liquid metal embrittlement, 569
  - mercurous nitrate test, 569
  - metal-matrix composites, 648–649
  - microbiologically influence corrosion testing, 577–578
  - modified salt spray (fog) testing, 571
  - nickel silvers, 567
  - organic compounds, 569
  - oxidation test, 575
  - oxidizing salts, 569
  - phosphor bronzes, 567
  - pipeline, 697
  - pitting corrosion, in condenser tubes, 572–573
  - polluted cooling waters, 568
  - potentiostatic tests, 576
  - protective film, 565
  - salt droplet test, 571
  - salt spray test, 570–571
  - salts, 569
  - seawater corrosion, 376, 568, 572
  - selection for environments, 567–569
  - smelting, refractories, 578
  - in soils, 394–395, 568, 576
  - stainless steels, 585
  - steam, 568
  - stress corrosion cracking, in Mattsson's solution, 570
  - testing in water, 568, 572
  - tin brasses, 566
- Copper-beryllium alloys, 567
- Copper-bismuth, 567
- Copper-bismuth-selenium, 567
- Copper-nickel alloys, 279, 567
- Copper-silicon alloys, 567
- Copper sulfate-sulfuric acid tests, 251–253
- Copper-zinc alloys, seawater corrosion, 376
- Corrodokote test, 134, 571
- Corrosion, forms, 91
- Corrosion acceptance testing, 780
- Corrosion agents, soils, 390
- Corrosion attack, classification, 713
- Corrosion currents, causes, 712
- Corrosion failure analysis, 50–51
- Corrosion fatigue, 302–318
  - aluminum metal-matrix composites, reinforcement constituents, 643–644
  - common elements of experiments, 310
  - component service life prediction, 318
  - crack detection, 311
  - crack length measurement, 314
  - cyclic strain-induced dissolution, 316
  - data analysis and evaluation, 311, 315–316
  - definition, 303
  - effect of applied polarization, 308
  - electrode potential, 308–309
  - environmental cell design, 311–313
  - factors controlling, 303–308
  - fracture mechanics methods, 312–316
  - frequency effects on crack propagation, 306–307
  - future research, 318
  - life prediction, 317–318
  - loading frequency, 305–308
  - magnesium and magnesium alloys, 540–541
  - measurement of crack solution pH and potential, 317
  - mechanical driving forces, 304–308
  - mechanical variables, 304
  - mechanisms, 303
  - medical and dental materials, 840
  - metal-matrix composites, 651
  - metallurgical variables, 309–310
  - nomenclature, 302–303
  - programmed stress intensity experimentation, 316
  - pulp and paper, 798
  - relationship with stress corrosion cracking, 310
  - small crack methods, 316–317
  - smooth specimen  $\Delta\epsilon(N)$ , 311–312
  - smooth specimen  $\Delta\sigma$ -life method, 310–311
  - stages, 303
  - sulfur ion content, 309
- Corrosion index, pipeline risk evaluation, 97–99
- Corrosion inhibitors, 480–497
  - atmospheric testing, 493–494
  - chemical stability, 481
  - compatibility, 481
  - corrosion product layers, 490
  - corrosion rate measurements, 487–488
  - cost effectiveness, 486
  - direct hydrogen measurements, 488
  - electrical resistance measurements, 489
  - electrochemical impedance spectroscopy, 492–493
  - electrochemical noise measurements, 493
  - environment conditioning, 496
  - flow and pressure effects, 494–495
  - galvanic measurements, 493
  - high pressure testing, 494
  - highways, tunnels, and bridges, 709–710
  - historical perspective, 480–481
  - importance of system analysis, 481
  - indirect hydrogen measurements, 488–489
  - interphase, 490–491
  - IR-problem, 490
  - iron counts, 488
  - linear polarization, 490
  - metallurgy selection, 495–496
  - performance characteristics, 486–487
  - pH and flow effects, 484–485
  - physical stability, 481
  - pipeline, 700
  - practical applications, 491–492
  - precorroded surface inhibition, 496–497
  - producing wells, 813–814
  - protection and inhibitor adsorption, 482–483
  - pulp and paper, 797
  - quality criteria, 481–482
  - steady state corrosion rate, 485
  - surface preparation, 495
  - test procedures, 483–484
  - thermal stability, 481
  - transport phenomena, 481
- Corrosion potential
  - distribution, galvanic corrosion, 237
  - measurements, electrodeposited coatings, 660
  - pitting, 213
- Corrosion prediction, polarization scans, 100
- Corrosion product
  - chemical cleaning procedures, 43–45
  - deposition, liquid metals, 472
  - electrolytic cleaning procedures, 46
  - iron counts, 488
  - layers, corrosion inhibitors, 490
- Corrosion rate, 346
  - calculation, 23
  - conversion factors, 24
  - conversion to mass loss and penetration rate, 109
  - measurements, corrosion inhibitors, 487–488
- Corrosion resistance, electrodeposited coatings, 656
- Corrosion resistance alloy, 815–816, 818
- Corrosion sample analysis, high-temperature gases, 444–445
- Corrosion tests, 49–58
  - block designs, 55–56
  - completely randomized designs, 54–55
  - crude oil systems, 431
  - curve fitting, 53–54
  - data reliability levels, 51–52

define goals and objectives, 49–51  
 design, 51–56  
 designing experiments, 54–56  
 determining number of observations, 53  
 develop test protocol, 56  
 engineering, 56–57  
 factorial designs, 55  
 hydrocarbon gas systems, 430  
 industrial chemicals, 422–423  
 modifications, 57  
 probability sampling, 53  
 produced water systems, 430–431  
 randomization, 53–55  
 seawater, 371–374  
 statistical basis, 52–53  
 statistical modeling, 53–54  
 statistical tests, 56  
 Corrosion yard instrumentation, 345  
 Corrosive gas tests, 135, 355–356, 360  
 Coupon testing  
   bleach plant, 799  
   chemical processing, 784–787  
   chemical pulping, 801  
   glass-lined steel, 787  
   indoor atmospheres, 359–360  
   industrial waters, 415  
   organic liquids, 454  
   pipe, 701, 704  
   pitting, 211–213  
   surface finish, 602–603, 784  
   water handling systems, 826–828  
 Covariance of independent variables, 87  
 Crack closure, 305  
 Crack propagation, corrosion fatigue, 312–316  
 Cracking, environmental, 122–125  
 Crevice corrosion, 221–229, 791  
   aluminum and aluminum alloys, 551  
   ASTM G 48, 222–225  
   ASTM G 78, 226  
   critical potentials, measurement, 228–229  
   depassivation pH, measurement, 229  
   electrochemical critical temperature, 227–228  
   electrochemical tests, 226–229  
   freshwater, 178, 384  
   industrial chemicals, 421  
   mechanisms, 221–222  
   medical and dental materials, 840  
   metals processing, 774–775  
   nickel and nickel alloys, 583  
   non-electrochemical tests, 222, 226  
   seawater, 171, 369  
   stainless steels, 589  
   steels, 561  
   titanium, 604–605  
 Critical potentials, measurement, 228–229  
 Critical temperature tests, 224–225  
 Cross contamination effects, 784  
 Crude oil, 427–429  
 CUNA 07901, 682  
 Current density, 59–61  
 Curve fitting, 53–54  
 Cyclic acidified salt fog test, 133–134  
 Cyclic corrosion tests, 136–138  
 Cyclic polarization, electrochemical tests, 215  
 Cyclic potentiodynamic polarization, 61, 118–119, 791  
 Cyclic salt fog/UV exposure, 134  
 Cyclic strain-induced dissolution, corrosion fatigue, 316  
 Cyclic tests, metallic coatings on steel, 627

## D

Data, 59–65, 89  
   compilation, 89  
   current, 59–61  
   electrochemical test, 59–62  
   impedance, 61  
   localized corrosion, 63  
   overcoming knowledge gaps, 91–92  
   potential, 59  
   quality, 90–91  
   standardized recording formats, 89–90  
   statistical analysis, 86–88  
   stress corrosion cracking, 64  
   velocity sensitive corrosion, 64–65  
 Dealloying, 278–286  
   ASTM and NACE standards, 285  
   dissolution and reprecipitation model, 281–282  
   electrochemical tests, 284  
   enhance diffusion models, 280  
   freshwater, 386  
   fundamentals, 278–279  
   immersion tests, 283–284  
   ISO standards, 285  
   metallographic analysis, 72–73  
   microstructural examination, 284  
   oxide formation model, 281  
   parting limit, 282–283  
   percolation model, 281  
   seawater, 370  
   service performance versus test results, 284–285  
   surface diffusion, 280–281  
   testing techniques, 283–284  
   use of standards in industry, 285  
   volume diffusion model, 279–280  
 Deep ocean testing, seawater corrosion testing, 172–173  
 Degree of protection, corrosion inhibitors, 483  
 Delayed failure, hydrogen damage, 326–327  
 Density, 25, 33–35  
 Dental materials, 835–838  
   *see also* Medical and dental materials  
 Depassivation pH, measurement, 229  
 Deposit etchants, 69–70  
 Depth of attack, metal-matrix composites, 649  
 Dew point, 38–42, 359  
 Differential flow cell technique, industrial waters, 417  
 Diffusion, metallic coatings, 621  
 Diffusion bonds, effect on aluminum metal-matrix composites, 642  
 Diffusion coefficient, 197  
 Diffusivity, 322–323  
 Digesters, 801  
 Dilute electrolyte cyclic fog/dry test, 134  
 DIN 40046, 758  
 DIN 50017, 132, 758  
 DIN 50018, 132, 135, 680–681  
 DIN 50021, 132  
 DIN 50908, 564  
 DIN 50916, 569, 680  
 Direct current polarization technique, microbiological effects, 513  
 Disk pressure tests, 331–332  
 Dissolution and reprecipitation model, dealloying, 281–282  
 Dissolution behavior, metal-matrix composites, 650  
 Dissolved oxygen monitoring, water handling systems, 831  
 Dissolved salts, soils, 390

Docks, *see* Piers and docks  
 Double-cantilever beam test, 336, 815  
 Dual cell techniques, microbiological effects, 516  
 Ductile iron, pipeline, 696  
 Ductility, hydrogen damage, 325–326  
 Duplex stainless steels, 587  
 Dust, military aircraft and equipment, 695  
 Dynamic testing, stress corrosion cracking, 298

## E

EC test, electrodeposited coatings, 661  
 Economizer, 805  
 EIA 364-B, 767  
 EIA RS-364–50, 353, 356, 361  
 Electrochemical potentiokinetic reactivation tests, simplified, 261  
 Electric heater wire tests, high-temperature corrosion, 200  
 Electric power, 722–725  
 Electrical and electronic systems, automobiles, 679  
 Electrical continuity, highways, tunnels, and bridges, 709  
 Electrical insulation, coupons, 784–785  
 Electrical isolation, highways, tunnels, and bridges, 709  
 Electrical resistance  
   copper and copper alloys, 573–574  
   industrial waters, 415  
   measurements, corrosion inhibitors, 489  
 Electrical resistance probes, 189–190  
   chemical processing, 787  
   microbiological effects, 516  
   seawater, 374  
   soils, 396  
 Electrical resistivity, soils, 399  
 Electrochemical behavior, tantalum, 617  
 Electrochemical tests, metallic coatings on steel, 627–629  
 Electrochemical behavior, niobium, 618  
 Electrochemical corrosion measurements, high-temperature/high-pressure corrosion testing, 152–153  
 Electrochemical critical temperature, 227–228  
 Electrochemical factors, stress corrosion cracking, 291–292  
 Electrochemical impedance, 101–102, 112–114  
 Electrochemical impedance spectroscopy  
   corrosion inhibitors, 492–493  
   freshwater, 383  
   metallic coatings on steel, 628  
   microbiological effects, 514–515  
   seawater, 373  
 Electrochemical kinetic data, obtaining corrosion rates, 108–109  
 Electrochemical laboratory tests, soils, 401–402  
 Electrochemical measurements  
   corrosion inhibitors, 489–493  
   soils, 184–186  
 Electrochemical mechanism, 632–634  
 Electrochemical methods, pipeline, 702–703  
 Electrochemical noise, 61–62, 121, 790–791  
   microbiological effects, 516  
   measurements, corrosion inhibitors, 493  
   organic coating, 127  
   resistance, 115–117  
 Electrochemical polarization

- chemical pulping, 801–802
  - freshwater, 384
  - soils, 184–185
  - Electrochemical potentiokinetic reactivation tests, 255–258
  - Electrochemical probes, 190–191, 783
  - Electrochemical reactivation technique, 61
  - Electrochemical test data, 59–62
  - Electrochemical tests, 107–127, 207–210, 213
    - alloy sensitization, 124–125
    - anodized aluminum corrosion test, 125
    - automobiles, 679–680
    - barnacle electrode technique, 123
    - bleach plant, 799
    - characterization of anodized surfaces and conversion coatings, 127
    - crevice corrosion, 226–229
    - critical temperature tests, 218
    - cyclic polarization, 215–217
    - cyclic potentiodynamic polarization methods, 118–119
    - dealloying, 284
    - electrochemical impedance methods, 112–114
    - electrochemical impedance spectroscopy, 126–127
    - electrochemical noise, 121, 127, 218–219
    - electrochemical noise resistance, 115–117
    - electrodeposited coatings, 660
    - electrolytic corrosion test, 125
    - electronics, 759
    - evaluation of protective coatings and films, 125–127
    - exfoliation corrosion, 269
    - frequency modulation methods, 114–115
    - galvanic corrosion, 117–118, 239, 242
    - galvanostatic measurements, 217
    - metals processing, 776–777
    - nickel and nickel alloys, 584
    - organic liquids, 455
    - paint adhesion on a scribed surface test, 125
    - passivity and localized corrosion, 118–122
    - permeation method, 123–124
    - polarization methods, 109–117
    - potential probe methods, 118
    - potential step-down or scan-down methods, 119–120
    - potentiodynamic methods, 122–123
    - potentiostatic measurements, 217–218
    - powder metallurgy materials, 666–667
    - pulp and paper, 797
    - scratch repassivation, 120, 122
    - seawater, 372–373
    - shot noise methods during pitting, 121–122
    - single frequency impedance test, 126
    - specimen mounting, 213–215
    - statistical distribution in critical potentials, 120–121
    - Tafel extrapolation, 110
    - telecommunications, 766
    - tribo-ellipsometric methods, 122
  - Electrode potential, corrosion fatigue, 308–309
  - Electrode reaction, thermodynamics and kinetics, 107–109
  - Electrodeposited coatings, 656–662
    - chronopotentiometry, 661
    - corrosion mechanisms, 657–659
    - corrosion potential measurements, 660–661
    - corrosion resistance, 656
  - corrosion testing, 659–662
    - EC test, 661
    - electrochemical tests, 660
    - in-situ imaging and nondestructive evaluation, 662
    - polarization resistance, 661
    - porosity, 659
    - salt spray-fog testing, 660
  - Electrolyte chemistry, freshwater, 381–382
  - Electrolyte flow, effects on freshwater
    - corrosion testing, 179
  - Electrolyte flow rate, 235–236
  - Electrolytic cleaning procedures, 46
  - Electrolytic corrosion test, 125
  - Electrolytic etching, 69
  - Electrolytic polishing, 69
  - Electromotive series, 395
  - Electronics, 754–760
    - classification of environments, 755–756
    - corrosion mechanisms, 756–757
    - corrosion of components, 757–758
    - corrosion products, 760
    - electrochemical tests, 759
    - environmental tests, 759–760
    - environments, 754–755
    - materials, 754
    - tests and standards, 758–759
  - Electrostatic precipitator, 805
  - Elements, physical properties, 32
  - Energy storage batteries, lead and lead alloys, 535–536
  - Engine coolants, 676
  - Engine oils, 676
  - Enhanced diffusion models, dealloying, 280
  - Ennoblement, seawater, 371
  - Environmental cracking, 370, 373–374, 700
  - Environmental deterioration analysis
    - logic diagram, 98
  - Environmental factors, stress corrosion cracking, 291
  - Environmental hydrogen embrittlement, 325
  - Environmental modification, highways, tunnels, and bridges, 709
  - Environmental simulation, telecommunications, 766
  - Environmentally assisted cracking, 122–125
  - Erosion corrosion, 275–276, 494, 789
    - copper and copper alloys, 574–575
    - factors controlling, 273–274
    - freshwater, 386
    - mechanisms, 273
    - seawater, 370
  - Error, 83
  - Etching, sample, 69–71
  - Evans diagram, 233–235
  - Exfoliation corrosion, 266–272
    - aluminum and aluminum alloys, 266–267, 552–554
    - classification, 270
    - electrochemical and conductivity tests, 269
    - evaluation of test results, 269–270
    - immersion tests, 268–269
    - relation to service conditions, 267
    - specimen inspection, 270–271
    - test controls, 272
    - test duration, 269
    - test procedures, 267–269, 271–272
    - test specimens, 269
  - Expert Systems, 99–100
  - External corrosion direct assessment, buried pipelines, 402–404
  - Extreme value statistics, 85, 94
- ## F
- Factorial designs, 55
  - Factorial experiments, 55, 85–86
  - Failure, 64
    - factors and subfactors controlling occurrence, 91
  - Failure analysis, 91, 712–713
  - Failure modes, nuclear power, 733
  - Faraday's equation, constants, 30
  - Faraday's law, 109, 242
  - Fault tree analysis, 95–96
  - Ferric sulfate-50% sulfuric acid test, 253
  - Ferritic stainless steel, 248, 586–587
  - Ferroxyl test, powder metallurgy materials, 667–668
  - Fibers, effect on lead metal-matrix composites, 646
  - Field tanks and vessels, 819
  - Filiform corrosion, 135, 553, 555–556
  - Fine particles, indoor atmospheres, 357–360
  - Fire protection, flue gas desulfurization, 750
  - Fitness-for-service evaluations, 781
  - Fixturing, 66–67
  - Flow induced localized corrosion, 494
  - Flow rate, effect on corrosion, 176
  - Flue gas desulfurization, 746–752
    - corrosion control, 749–750
    - corrosion environments, 749
    - fire protection, 750
    - materials of construction, 746–748
    - test methods, 750–752
    - welding, 750
  - Fluidized bed boiler, 805
  - Fog testing, copper and copper alloys, 571
  - Food and beverage, 822–824
  - Forced-convection loops, liquid metals, 476
  - Ford Std M2C138-CJ, 683
  - Ford TM-BI 123–01, 681
  - Foundations
    - electric power, 723–724
    - selection of type, 707
  - Foundry products, aluminum and aluminum alloys, 549
  - Four-point bend tests, 336–337
  - Fracture mechanics testing, hydrogen damage, 332–339
  - Free found water, 389
  - Frequency modulation methods, 114–115
  - Freshwater, 380–386
    - biological factors, 381
    - corrosion forms, 382
    - dealloying, 386
    - electrolyte chemistry, 381–382
    - factors affecting corrosion, 175–176
    - metallurgy, 381
    - process conditions, 381
    - resistance probes, 383
    - water chemistry, 380–381
    - weight loss testing, 382
  - Freshwater corrosion testing, 175–180
    - cavitation, 386
    - design, 177
    - electrochemical impedance spectroscopy, 383
    - electrochemical polarization, 384
    - electrolyte flow effects, 179
    - erosion corrosion, 386
    - exposure methods, 176–179
    - fretting corrosion, 386
    - galvanic corrosion, 178–179, 384, 386
    - intergranular corrosion, 180, 386
    - pitting and crevice corrosion, 178, 383–384

polarization, 382–383  
 stress-corrosion cracking, 179–180, 386  
 uniform corrosion, 177–178, 382–383  
 Fretting corrosion, 274–275  
   factors controlling, 275  
   medical and dental materials, 840  
 Fretting fatigue, 275–276  
 Fretting wear, tests, 276  
 Fugacity, 323–324  
 Fungus, military aircraft and equipment, 694  
 Fusayama's solution, 841

## G

Galvanic corrosion, 117–118, 191, 233–242, 789  
   aluminum and aluminum alloys, 551, 555  
   anode/cathode area ratio, 235  
   atmospheric tests, 240–242  
   between matrix and reinforcement constituents, 650–651  
   computer modeling, 239–240, 242  
   copper and copper alloys, 575–576  
   corrosion inhibitors, 493  
   current and potential distributions, 237  
   direct measurement, 117–118  
   electrochemical reactions, 233  
   electrochemical tests, 239, 242  
   electrolyte flow rate, 235–236  
   factors controlling, 237–238  
   freshwater, 178–179, 384, 386  
   lead and lead alloys, 535  
   measured currents, 236–237  
   medical and dental materials, 840–841  
   metal-matrix composites, 650–651  
   mixed potential theory, 235  
   seawater, 171, 369–370  
   soils, 185  
   standards, 242  
   steels, 561  
   testing techniques, 238–241  
 Galvanic couples, exposure, 238–239, 241–242  
 Galvanic protection, zinc, 525–526  
 Galvanic series, 234–235  
 Galvanized steel, pipeline, 696–697  
 Galvanostatic methods, 119, 217  
 Gas pipeline, risk assessment, 95–96  
 Gaseous zone, 783  
 Gases  
   lead and lead alloys, 534–535  
   physical properties, 31  
   *see also* High-temperature gases  
 Gaskets, 780  
 General corrosion, 171, 588, 601–604  
 General Motors Std Dextron II Spec., 683  
 General Motors Std M95-MAT-001, 683  
 Glass-lined steel coupons, 787  
 Glossary, 7–11  
 GM 4298P, 626  
 GM 4299P, 132  
 GM 4465P, 132, 626  
 GM 4476P, 132  
 GM 9102P, 138, 625  
 GM 9505P, 132, 681  
 GM 9511P, 132  
 GM 9540P, 132, 137, 375, 680–681  
 GM 9682P, 132  
 Grain refining, magnesium and magnesium alloys, 539  
 Graphite, effect on metal-matrix composites, 638–639, 644–645, 648  
 Gravimetric corrosion rates, 544–545, 581, 649

Gravitational water, 389  
 Greco-Latin square, 85–86  
 Grinding, sample, 67–68  
 Ground synthetic dust mixture, indoor atmospheres, 357–358

## H

Hafnium, 613–616  
   test solutions, 615  
 Hammett acidity function, 450  
 Hanks' solution, 841  
 Hardware  
   aerial cable, 763  
   electric power, 724–725  
 Health hazards, lead, 536  
 Heat tinting, 70  
 Heat transfer, industrial chemicals, 421  
 Heat transfer components, nuclear power, 728–729  
 Heat transfer systems, water handling systems, 832  
 Heat treatment, magnesium and magnesium alloys, 539  
 Heated surface, 791  
 High pressure environments, 154–156  
 High pressure testing, corrosion inhibitors, 494  
 High-temperature corrosion, 194–202  
   aluminum and aluminum alloys, 550–551  
   carburization corrosion tests, 201  
   chemical thermodynamic and physical principles, 196–197  
   electric heater wire tests, 200  
   kinetics, 194–196  
   magnesium and magnesium alloys, 542  
   metallographic analysis, 74  
   modes, 197  
   molten salt corrosion tests, 201  
   oil refining, 819–820  
   residual fuel oil corrosion tests, 200  
   service testing, 198–201  
   specimen preparation, 198–199  
   steels, 559  
   sulfur corrosion tests, 200–201  
   testing in environments, 197–198  
 High temperature environments, 155–156  
 High-temperature gases, 434–436  
   Brinkley method, 438  
   carburization and metal dusting, 437–440  
   coal ash corrosion, 442  
   corrosion sample analysis, 444–445  
   environments, 435–537  
   kinetics, 436  
   laboratory and field testing controls, 435  
   mass change analysis, 445  
   materials for test equipment, 442–443  
   metallographic analysis, 444–445  
   oxidation, 436  
   oxidation rate laws, 436–437  
   reference materials, 435  
   sample preparation, 434–435  
   service test standards, 445–446  
   structural changes, 445  
   sulfidation, 441–443  
   testing, 437, 439  
   thermodynamics, 436  
 High-temperature/high-pressure corrosion testing, 147–157  
   agitated tests, 148  
   ASTM standards, 157  
   dissolved gas effects, 151

electrochemical corrosion  
   measurements, 152–153  
 factors affecting environments, 149–150  
 in high-purity water, 157  
 hydrogen effects, 151  
 hydrogen permeation measurement, 153–154  
 mechanical property testing, 154  
 NACE standards, 156–157  
 oxygen effects, 150–151  
 pressurized corrosion tests, 147–149  
 refreshed and recirculating tests, 148–149  
 safety, 154–155  
 simulation of service environments, 155–156  
 special test conditions, 150–151  
 static tests, 148  
 test conditions, 147  
 test variations, 151–154  
 windowed test vessels, 152  
 High velocity flow testing, seawater, 373  
 Highways, tunnels, and bridges, 706–714  
   coatings, 710  
   corrosive environments, 707–709  
   electrical continuity, 709  
   environmental modification, 709  
   failure analysis, 712–713  
   future, 714  
   in-service monitoring, 711–712  
   inhibitors, 709–710  
   material selection, 709, 711  
   materials of construction, 706–707  
   problem areas, 710–711  
   unresolved issues, 713–714  
 Hot corrosion testing, cobalt-base alloys, 597  
 Hot dip coating, 620  
 Hot plate boiling corrosion testing, chemical pulping, 801  
 Hot wall, 791  
 Humidity tests, 134–135, 355, 359, 545  
 Hydrocarbon gas systems, corrosion testing, 430  
 Hydrochloric acid spray test, 571–572  
 Hydrogen  
   in aluminum and aluminum alloys, 549  
   diffusible concentration, 123–124  
   effects, oil and gas production, 818  
   measurement of concentration, 327  
   nickel and nickel alloys, 581  
   niobium, 618  
   role in titanium, 601  
   tantalum, 617  
   testing, titanium, 607–609  
 Hydrogen damage, 322–339  
   ASTM E 1681, 333–336  
   ASTM F 326, 328  
   ASTM F 519, 329–331  
   ASTM F 1113, 328  
   ASTM F 1459, 331–332  
   ASTM F 1624, 337–338  
   ASTM F 1940, 328, 331  
   ASTM G 129, 337  
   ASTM G 168, 336  
   cantilever bend tests, 335–336  
   delayed failure, 326–327  
   diffusivity, 322–323  
   ductility effects, 325–326  
   environmental hydrogen embrittlement, 325  
   fracture mechanics testing, 332–339  
   fugacity, 323–324

hydrogen concentration measurement, 327  
 internal hydrogen embrittlement, 325  
 interpretation of test results, 327  
 mechanical testing, 328–331  
 notch effect, 326  
 pipeline, 700  
 potential, 328  
 principles, 322–339  
 process control, 328–329  
 ripple loads, 333  
 solubility, 323  
 stress corrosion cracking, 325  
 temperature and strain rate, 328  
 test selection, 338–339  
 three-point and four-point bend tests, 336–337  
 trapping behavior, 324  
 Hydrogen embrittlement cracking tests, 151, 202, 371  
 Hydrogen induced cracking, 94–95, 818  
 Hydrogen measurements  
   corrosion inhibitors, 488–489  
   high-temperature/high-pressure corrosion testing, 153–154  
 Hydrogen probes, 191

## I

IEC 60068-2-18, 856  
 IEC 60068-2-43, 767, 856  
 IEC 60068-2-60, 856  
 IEC 60068-2-66, 856  
 IEC 60068-2-67, 856  
 IEC 60068-2-74, 856  
 IEC 60426, 856  
 IEC 60512-11-14, 856  
 IEC 60512-11-7, 856  
 IEC 60695-5-1, 856  
 IEC 68-2-1, 758  
 IEC 68-2-11, 758  
 IEC 68-2-2, 758  
 IEC 68-2-3, 758  
 IEC 68-2-30, 758  
 IEC 68-2-42, 758  
 IEC 68-2-43, 758  
 IEC TR 60355, 856  
 IEC TR 60695-5-2, 856  
 Ignition testing, titanium, 609  
 Immersion corrosion, zinc, 529  
 Immersion critical crevice-corrosion temperature, 224–225  
 Immersion critical pitting temperature, 224–225  
 Immersion testing, 139–146  
   automobiles, 679–680  
   cleaning specimens, 145  
   cyclic test procedure, 144  
   dealloying, 283–284  
   evaluation of results, 145  
   exfoliation corrosion, 268–269  
   molten salts, 460–461  
   physical parameters, 141  
   precautions and validity of results, 145–146  
   principles, 139–141  
   seawater, 372  
   simple tests, 144  
   simulation and acceptance testing, 144  
   specimen preparation, 144–145  
   test conditions, 139–141  
   test duration, 141  
   titanium, 604  
   types, 141–144  
 Immersion zone, piers and docks, 718

Impedance, 61  
 Impingement angle, 273–274  
 Implants, 834–837  
 In-plant testing, 187, 767–768, 772  
 In-service monitoring  
   commercial aircraft, 688  
   food and beverage, 824  
   highways, tunnels, and bridges, 711–712  
   steam generation, 743  
   telecommunications, 764–765  
 In-situ imaging, electrodeposited coatings, 662  
*In vivo* environments, 500–505  
 Indoor atmospheres, 349–361  
   coarse particle testing, 356–357, 360  
   corrosive gas testing, 355–356, 360  
   description of environment, 349–353  
   dewpoint monitoring, 359  
   field testing, 359–360  
   fine particle concentrations, 351  
   fine particle testing, 357–360  
   ground synthetic dust mixture, 357–358  
   metal coupon exposures, 359–360  
   standards, 360–361  
   testing for thermal, humidity, and bias effects, 355, 359  
   testing of electronic equipment, 354  
   unique aspects of testing, 353–354  
   variables, 354–355  
 Industrial applications, 187–193  
   corrosion test specimens, 189  
   crevice corrosion, 191  
   electrical resistance probes, 189–190  
   electrochemical probes, 190–191  
   galvanic corrosion, 191  
   hydrogen probes, 191  
   in-plant testing, 187  
   maintaining device installation, 188–189  
   measurement technologies, 187–188  
   online monitoring, 191–192  
   specimens, 189  
   standards, 192–193  
   stress corrosion cracking, 191  
   testing precautions, 192  
 Industrial chemicals, 418–423  
   batch and continuous processes, 418–423  
   chlorides and halides, 421  
   contaminating chemicals, 421–422  
   corrosion testing, 422–423  
   crevice corrosion, 421  
   heat transfer, 421  
   pH, 419–420  
   pressure and temperature effects, 419  
   test design, 422  
   unique aspects, 418–423  
   velocity, 421  
 Industrial waters, 413–417  
   coupon tests, 415  
   differential flow cell technique, 417  
   distribution in a process plant, 413  
   electrical and electrochemical methods, 415  
   laboratory testing, 414  
   miniature heat exchanger with combined corrosion and fouling evaluation, 416  
   plant testing, 414–416  
   synthetic crevice devices, 416  
   test exchangers, 415–416  
   thin layer activation, 416  
 Inspection, commercial aircraft, 688  
 Instrumented pigs, pipeline, 702  
 Insulators, electric power, 725

Intergranular attack, evaluating susceptibility, 259–261  
 Intergranular corrosion, 64, 244–264, 386  
   65% nitric acid test, 250–251  
   aluminum and aluminum alloys, 552, 554  
   annealing effect, 247  
   associated with precipitates, 245  
   copper sulfate-sulfuric acid tests, 251–253  
   electrochemical potentiokinetic reactivation tests, 255–258  
   ferric sulfate-50% sulfuric acid tests, 253  
   freshwater corrosion testing, 180  
   future developments, 261–264  
   grain-boundary imperfection effect, 245  
   grain-face corrosion rate, 245  
   medical and dental materials, 840  
   metals processing, 772–773  
   nickel and nickel alloys, 582  
   nickel-rich chromium-bearing alloys, 257–259  
   nitric-hydrofluoric acid tests, 255  
   origin of evaluation tests, 250  
   oxalic acid etch tests, 253–255  
   precipitates at grain boundaries, 249  
   principles, 244–247  
   seawater, 370  
   testing strategy, 259–261  
   weld decay zone, 262  
 Intergranular cracking, copper and copper alloys, 569  
 Internal combustion exposure, automobiles, 675  
 Internal functional liquids, automobiles, 675–676  
 Internal hydrogen embrittlement, 325  
 International System of Units, 17  
 Internet, 102  
 Interphase, in presence of corrosion inhibitors, 490–491  
 Intertidal zone, piers and docks, 718–719  
 Ion scattering spectroscopy, 81  
 IR-problem, corrosion inhibitors, 490  
 Iron, pipeline, 696  
 ISO 1462, 375, 680, 684, 856  
 ISO 2160, 858  
 ISO 3160-2, 856  
 ISO 3183-3, 818  
 ISO 3231, 132, 135  
 ISO 3651, 857  
 ISO 3768, 666  
 ISO 3769, 680, 758  
 ISO 3770, 680, 758  
 ISO 4404, 858  
 ISO 4524-2, 758  
 ISO 4536, 856  
 ISO 4538, 856  
 ISO 4539, 856  
 ISO 4540, 168, 375, 666, 684, 856  
 ISO 4541, 132, 856  
 ISO 4542, 168, 681, 856  
 ISO 4543, 857  
 ISO 4623, 375, 857  
 ISO 4952, 858  
 ISO 6251, 858  
 ISO 6351, 858  
 ISO 6270-1, 132  
 ISO 6957, 569, 857  
 ISO 6988, 857  
 ISO 7253, 132  
 ISO 7384, 375, 680–681, 857

ISO 7441, 164, 168, 240, 242, 857

ISO 7539, 375

ISO 7539-1, 174, 857

ISO 7539-2, 171, 174, 857

ISO 7539-3, 171, 174, 857

ISO 7539-4, 857

ISO 7539-5, 171

ISO 7539-5, 174, 857

ISO 7539-6, 555, 857

ISO 7539-7, 555, 562, 857

ISO 7539-8, 857

ISO 7549-6, 564

ISO 8044, 679, 857

ISO 8407, 173-174, 679, 857

ISO 8565, 168, 681, 857

ISO 8993, 174, 375, 857

ISO 8994, 168, 174, 375, 858

ISO 9223, 168, 348, 560, 755, 858

ISO 9223-6, 162

ISO 9224, 168, 348, 560, 858

ISO 9225, 168, 348, 858

ISO 9226, 168, 348, 681, 858

ISO 9227, 132, 680, 758, 858

ISO 9400, 858

ISO 9455, 858

ISO 9591, 375, 858

ISO 10062, 132, 680, 684, 760, 858

ISO 10270, 858

ISO 10289, 857

ISO 11130, 858

ISO 11303, 168, 858

ISO 11306, 375, 858

ISO 11463, 375, 858

ISO 11474, 858

ISO 11782, 375

ISO 11782, 375, 858

ISO 11845, 375, 858

ISO 11846, 858

ISO 11881, 858

ISO 11972, 858

ISO 11997, 857

ISO 13402, 858

ISO 13806, 858

ISO 14713, 858

ISO 14993, 858

ISO 15156, 812

ISO 15324, 858

ISO 16701, 858

ISO 65092, 857

ISO corrosion classification system,  
outdoor atmospheres, 347

ISO DIS 16701, 132

ISO TC 156, 161

ISO TR 8502-1, 857

ISO TR 10129, 858

ISO TR 10217, 858

ISO TR 10271, 858

ISO TR 12928, 858

## J

JASO M 609, 681

JASO M 610, 132, 681

JIS H8681, 680

JIS Z2371, 132, 680-682

JIS Z2381, 681

## K

Kettle test, 484

Kinetic modeling, 792

Kinetics, high-temperature gases, 36

Kohler principle of illumination, 70-71

Krebs-Ringer solution, 841

## L

Langelier saturation index, 380-381

Langmuir isotherm, 483

Latin square design, 55-56

Lawrence gage, 328

Lead and lead alloys, 531-536

acidity/alkalinity, 534

corrosion, 533-534

effects of alloying, 532

environment, 536

galvanic corrosion, 535

gases, 534-535

metal-matrix composites, 646

microstructural effects, 532

mill products, 532-533

natural protective films, 531-532

salt spray, 535

salts, 534-535

sensitivity to environmental factors,  
534-535

soil, 394-395, 534-535

solubility, 533

world consumption, 531

Lead-antimony, 532

Lead-calcium, 532

Lead-copper, 532

Lead paint, bridges, 711

Lead-silver, 532

Lead-tin, 532

Life prediction, 92-94, 317-318

Linear polarization

chemical processing, 787-789

chemical pulping, 801

corrosion inhibitors, 490

industrial waters, 415

Linear polarization-resistance meter,  
water handling systems, 828-829

Linear rate law, 436

Linear reaction kinetics, high-  
temperature corrosion, 194-195

Linear regression, 86-87

Linings, pipeline, 698

Liquid drop erosion, 274

Liquid impingement erosion, tests, 276

Liquid metal embrittlement, 73-74, 569

Liquid metals, 465-477

aluminum and aluminum alloys, 551

axial heating rate, 470

circulation type, 470

containment surface condition, 468

corrosion product deposition, 472

environment, 465

exposure temperature, 468-469

exposure time, 471

external environment effect, 472

forced-convection loops, 476

heat input/removal zones, 470

large engineering experiments, 476-477

loop temperature differential, 471

mechanical stress, 470-471

monometallic or multi-metal/alloy

containment system, 471-472

nickel and nickel alloys, 581

reactive impurity content, 469

refluxing capsules, 474

rotating cylinder technique, 475

seesaw capsules, 474-475

specimen examination, 473

stainless steels, 588

static isothermal capsules, 473-474

test procedures, 472-473

test specimen configuration, 471

thermal-convection loops, 475-476

thermophysical condition, 467-468

unique aspects, 465-467

use of capsules for pre-exposure, 475

variables, 467-472

velocity, 469

Liquids, physical properties, 31

Liquor heater corrosion, 803

Localized corrosion, 63, 119-120

Log-normal distribution, 85

Logarithmic reaction kinetics, high-  
temperature corrosion, 195-196

Loop temperature differential, liquid  
metals, 471

Low pressure, military aircraft and  
equipment, 694

LP-463PB-10-01, 132

LP-463PB-22-01, 132

LP-463PB-45-01, 132

LP-RPES-COR, 768

## M

Macrofouling films, seawater, 367

Magnesium and magnesium alloys,  
537-545

compositional effects, 537-539

contaminant tolerance limits, 538

corrosion characteristics, 537-541

corrosion testing, 544-545

elevated temperature, 542

environmental factors, 541-544

galvanic corrosion, 542-544

gravimetric corrosion rates, 544-545

humidity tests, 545

ions/salts, 541

metal fasteners, 543

metal-matrix composites, 644-645

metallurgical treatment effect, 539-540

mill products, 540

organic compounds, 542

painted corrosion performance, 545

protective films, 537

stress-corrosion cracking, 540-541

Magnesium-zinc alloys, 540

Magnetic resonance imaging, cautions with  
medical and dental materials, 836

Maintenance steering group system, 96-98

Manganese, stainless steels, 585

Manholes, telecommunications, 763

Marine atmosphere zone, piers and  
docks, 719

Martensitic stainless steels, 587

Mass change analysis, high-temperature  
gases, 445

Mass loss tests, 109, 206-208

Mass transport overpotential, 110

Mattsson's solution, 570

Mechanical coatings, steel, 621-622

Mechanical damage, pipeline, 700

Mechanical polishing, 68

Mechanical property testing, high-  
temperature/high-pressure  
corrosion testing, 154

Mechanical pulping, 803

Mechanical stress, liquid metals, 470-471

Mechanical treatments, aluminum and  
aluminum alloys, 548-549

Medical and dental materials, 834-843

corrosion environments, 841

corrosion evaluation, 842

corrosion-fatigue, 840

crevice corrosion, 840

dental alloys, 837-838

fretting corrosion, 840

- future, 843
  - galvanic corrosion, 840–841
  - implants, 834–835
  - intergranular corrosion, 840
  - metallic dental materials, 835–836
  - minimization of corrosion, 839
  - MRI cautions, 836
  - pitting, 839–840
  - problem areas, 841
  - regulations, 842–843
  - stress corrosion cracking, 840
  - surface modification, 838–839
  - surgical implant alloys, 836–837
  - Membranes, concrete, 410
  - Mercurous nitrate test, copper and copper alloys, 569
  - Mercury, aluminum and aluminum alloys effect, 551
  - Metal coupon exposures, indoor atmospheres, 359–360
  - Metal dusting, 74, 437–440
  - Metal ion contamination, 780
  - Metal-matrix composites, 637–652
    - aluminum, 637–644
      - alumina effect, 641–642
      - boron effect, 637–638
      - effect of diffusion bonds and microstructural contaminants, 642
      - graphite effect, 638–639
      - mica effect, 642
      - reinforcement constituent effect, 642–644
      - silicon carbide effect, 639–641
    - comparison of corrosion behavior, 651–652
    - copper, 648–649
    - corrosion fatigue, 651
    - depleted uranium, 646
    - depth of attack, 649
    - dissolution behavior, 650
    - galvanic corrosion, 640–641, 650–651
    - gravimetric evaluation, 649
    - lead, 646
    - loss in mechanical properties, 649
    - magnesium, 644–645
    - pitting corrosion, 651
    - stainless steel, 646–647
    - stress corrosion, 651
    - titanium, 647–648
    - uniform corrosion, 651
    - zinc, 649
  - Metallic coatings on steel, 620–630
    - aluminum and aluminum alloys, 622–623
    - cabinet tests, 626–627
    - cadmium, 623
    - chemical vapor deposition, 621
    - chromium, 623
    - corrosion resistance, 623–624
    - corrosion testing, 624–630
    - cyclic tests, 627
    - diffusion, 621
    - electrochemical impedance spectroscopy, 628
    - electrochemical tests, 627–629
    - electroplating, 620–621
    - functions, 620
    - hot dip coatings, 620
    - mechanical coating, 621–622
    - physical vapor deposition, 621
    - simulated service, 625
    - static atmospheric testing, 625–626
    - terne, 623
    - thermal spray, 621
  - tinplate, 623
  - zinc and zinc alloys, 622, 624
  - Metallographic analysis, 66–75
    - corrosion due to phase changes, 73
    - dealloying, 72–73
    - general corrosion, 73
    - high temperature corrosion, 74
    - high-temperature gases, 444–445
    - liquid metal embrittlement, 73–74
    - metal dusting, 74
    - oxidation, 74
    - pitting, 71–72
    - sample selection, 66–75
    - stress corrosion cracking, 71
    - sulfidation, 74
  - Metallurgical treatments, aluminum and aluminum alloys, 547–548
  - Metallurgy
    - impact on corrosion, 176
    - selection, corrosion inhibitors, 495–496
  - Metals
    - density, 33
    - equivalent weight values, 28–29
    - flue gas desulfurization, 746
  - Metals processing, 769–778
    - corrosive atmospheres, 775
    - crevice corrosion, 774–775
    - electrochemical tests, 776–777
    - factors influencing corrosion resistance, 769–770
    - forms of corrosion, 769
    - future testing needs, 778
    - in-plant and field testing, 772
    - intergranular corrosion tests, 772–773
    - materials selection, 769
    - passivation, 775–776
    - pitting, 774–775
    - procedure manuals, 777–778
    - quality control tests, 771
    - sampling and statistical analysis, 777
    - service environment and operation, 770
    - simulated-service tests, 771
    - stress-corrosion cracking, 773–774
    - test selection, 771
  - Metric practice guide, 20–21
  - Mica, effect on aluminum metal-matrix composites, 642
  - Microbiological activity, soils, 390–391
  - Microbiological effects, 509–519
    - alternating current methods, 514–515
    - direct current polarization technique, 513
    - dual cell techniques, 516
    - electrical resistance probes, 516
    - electrochemical noise, 516
    - field tests, 518–519
    - microelectrode techniques, 515
    - multiple crevice assembly, 517
    - open circuit corrosion potential, 512
    - performing test without influence of microbes, 517–518
    - pitting potentials, 514
    - polarization resistance, 513
    - potentiodynamic sweep techniques, 514
    - proper sampling techniques, 511–512
    - redox potential, 512–513
    - remote crevice assembly, 517
    - scanning vibrating probe techniques, 515
    - Tafel polarization, 513–514
    - unique aspects, 509–510
    - variables, 510–511
  - Microbiologically influenced corrosion testing, 577–578, 698, 797
  - Microelectrode techniques,
    - microbiological effects, 515
  - Microstructural contaminants, effect on aluminum metal-matrix composites, 642
  - Microstructure, 559, 586
  - MIL 202F, 767
  - MIL 883C, 767
  - MIL-A-81801, 526
  - MIL-C-16173, 683
  - MIL-C-81309, 683
  - MIL-I-46955, 683
  - MIL-STD-810, 132, 694–695
  - MIL-STD-810E, 349–361
  - MIL-STD-810E-14, 353, 356, 360–361
  - MIL-T-5422, 683, 758
  - Military aircraft and equipment, 693–695
  - Mill products, 540, 549, 587
  - Miniature heat exchange, with combined corrosion and fouling evaluation, 416
  - Mixed flowing gas, 136
  - Mixed-potential theory, 117, 235
  - Modeling
    - bottom up approach, 92
    - extreme value statistics, 94
    - mathematical, 92–94
    - top down approach, 95–99
  - Moisture content, pipeline, 697
  - Molten salts, 457–463
    - ceramics, 461–463
    - controlled laboratory testing, 459–460
    - high-temperature corrosion, 201
    - immersion test, 460–461
    - simulation burner rigs, 458–459
    - test condition selection, 457
    - thick deposits, 461
    - thin deposits, 458–461
  - Molybdenum
    - stainless steels, 586
    - carbide precipitates, 249
  - Monitoring devices, installation, 188–189
  - Monometallic containment system, liquid metals, 471–472
  - Mounting, 66–67
  - MTI standards, 143
  - Multi-metal/alloy containment system, liquid metals, 471–472
  - Multiple crevice assembly, 223–224, 517
  - Multiple regression analysis, 87
  - Multiplication factors, 22
- N
- NACE 3D170, 193
  - NACE MR0174, 813, 859
  - NACE MR0175, 193, 812, 814, 818, 821, 859, 812
  - NACE MR0176, 816, 859
  - NACE MR0274, 860
  - NACE RP0100, 859
  - NACE RP0169, 395, 713, 859
  - NACE RP0170, 820, 860
  - NACE RP0172, 168, 713
  - NACE RP0173, 375, 560, 860
  - NACE RP0174, 396, 859
  - NACE RP0175, 859
  - NACE RP0176, 168, 719, 819, 859
  - NACE RP0177, 396, 859
  - NACE RP0178, 861
  - NACE RP0180, 859
  - NACE RP0181, 819, 859
  - NACE RP0182, 860
  - NACE RP0184, 861
  - NACE RP0185, 860



NACE RP0186, 817  
 NACE RP0187, 563, 713, 719  
 NACE RP0188, 861  
 NACE RP0189, 193, 860  
 NACE RP0190, 819, 860–861  
 NACE RP0191, 814, 860  
 NACE RP0192, 817, 860  
 NACE RP0193, 859  
 NACE RP0194, 859  
 NACE RP0196, 859  
 NACE RP0197, 858  
 NACE RP0198, 858  
 NACE RP0199, 859  
 NACE RP0200, 860  
 NACE RP0272, 679  
 NACE RP0273, 814, 860  
 NACE RP0274, 396, 860  
 NACE RP0275, 860  
 NACE RP0276, 860  
 NACE RP0278, 860  
 NACE RP0281, 186, 713, 861  
 NACE RP0285, 396  
 NACE RP0286, 396, 859  
 NACE RP0287, 713, 861  
 NACE RP0288, 861  
 NACE RP0290, 713  
 NACE RP0291, 814, 860  
 NACE RP0292, 860  
 NACE RP0294, 859  
 NACE RP0295, 861  
 NACE RP0296, 860  
 NACE RP0297, 861  
 NACE RP0298, 861  
 NACE RP0300, 859  
 NACE RP0372, 819, 861  
 NACE RP0375, 396, 819, 860  
 NACE RP0376, 861  
 NACE RP0386, 861  
 NACE RP0387, 239, 819, 859  
 NACE RP0388, 859  
 NACE RP0390, 713  
 NACE RP0394, 861  
 NACE RP0395, 861  
 NACE RP0398, 861  
 NACE RP0399, 861  
 NACE RP0472, 820, 860  
 NACE RP0475, 817, 860  
 NACE RP0487, 396, 859, 861  
 NACE RP0490, 861  
 NACE RP0491, 816, 860  
 NACE RP0492, 819, 859, 861  
 NACE RP0495, 861  
 NACE RP0497, 859  
 NACE RP0502, 395, 403  
 NACE RP0572, 859  
 NACE RP0575, 859  
 NACE RP0590, 859  
 NACE RP0591, 168, 861  
 NACE RP0592, 861  
 NACE RP0675, 859  
 NACE RP0690, 859  
 NACE RP0692, 168, 861  
 NACE RP0775, 143–144, 193, 560, 818, 860  
 NACE TM0169, 178, 193, 560, 860  
 NACE TM0170–70, 168  
 NACE TM0171, 143, 157, 177–178, 561, 860  
 NACE TM0172, 821  
 NACE TM0173, 817, 860  
 NACE TM0174, 143, 635, 861  
 NACE TM0175–75, 168  
 NACE TM0177, 156, 563, 774, 814, 818, 860  
 NACE TM0183, 814, 861  
 NACE TM0184, 861  
 NACE TM0185, 143, 156, 814, 861

NACE TM0186, 814, 861  
 NACE TM0187, 816, 860  
 NACE TM0192, 861  
 NACE TM0193, 859  
 NACE TM0194, 860  
 NACE TM0196, 861  
 NACE TM0197, 860  
 NACE TM0198, 156, 860  
 NACE TM0199, 860  
 NACE TM0270, 561  
 NACE TM0274, 143, 157, 178, 383, 561, 860  
 NACE TM0275, 860  
 NACE TM0284, 143, 564, 821, 860  
 NACE TM0286, 143, 416, 860  
 NACE TM0294, 859  
 NACE TM0296, 860  
 NACE TM0297, 861  
 NACE TM0298, 860  
 NACE TM0299, 859  
 NACE TM0374, 143, 382, 817, 860  
 NACE TM0384, 814, 861  
 NACE TM0398, 859  
 NACE TM0399, 859  
 NACE TM0497, 859  
 NACE TM0498, 859  
 NACE TM0499, 859  
 Near mud drum, 805  
 Near surface techniques, 81  
 Nernst equation, 107–108  
 NES M0140, 132  
 NES M0158, 132  
 Neural networks, 100–101  
 Nickel and nickel alloys, 580–584  
   alloying effects, 580  
   aqueous solution variables, 581  
   crevice corrosion, 582  
   depth of attack measurements, 581  
   electrochemical testing, 584  
   environmental factors, 581  
   gravimetric, 581  
   hydrogen, 581  
   intergranular corrosion, 582  
   liquid metals, 581  
   metallurgical factors, 580  
   microstructural effects, 580–581  
   pitting corrosion, 581, 583  
   stainless steels, 585  
   stress corrosion cracking, 583  
   uniform corrosion, 581–582  
 Nickel-chromium-molybdenum alloys,  
   seawater corrosion, 376  
 Nickel-copper alloys, seawater corrosion,  
   376  
 Nickel-rich chromium-bearing alloys,  
   257–259  
 Nickel silvers, 567  
 Nickel-chromium-iron alloys, phase  
   formation, 73  
 Niobium, 585, 618–619  
 Nitric-hydrofluoric acid test, 255  
 Nitridation, high-temperature corrosion, 198  
 Nitrogen, stainless steels, 585  
 Nondestructive evaluation,  
   electrodeposited coatings, 662  
 Nonmetallic coatings, 632–636  
   cooperative practice yielding, 636  
   corrosion effects, 634  
   corrosive environmental exposure, 634  
   materials, 632  
   noncorrosive effects, 634  
   service life testing, 636  
   test method selection, 634–636  
 Nonmetallic inorganics, flue gas  
   desulfurization, 747–748

Nonmetallic materials, 100–101, 799–800,  
   816–817  
 Nonstandard operations, chemical  
   processing, 780–781  
 Normal distribution, 84  
 Notches, hydrogen damage, 326  
 Nova rupture risk, 96  
 Nuclear power, 727–736  
   corrosion problems, 733–734  
   corrosion testing, 734–736  
   failure modes, 733  
   future, 736  
   materials of construction, 727–728  
   power conversion and auxiliary  
     systems, 729, 732–733  
   pressure vessels and heat transfer  
     components, 728–729  
   reactor coolant systems, 728–733

## O

Offshore structures, 819  
 Oil and gas production, 812–819  
   artificial lift wells material selection, 816  
   coatings and linings, 814  
   corrosion, 812–814  
   corrosion resistance alloy, 815–816  
   field tanks and vessels, 819  
   HIC resistance, 818  
   hydrogen effects, 818  
   inhibition, 813–814  
   monitoring corrosion, 817–819  
   offshore structures, 819  
   oil products, 821  
   oil refining, 819–921  
   sulfide stress cracking, 814–815  
   surface piping, 817–819  
   testing nonmetallic materials, 816–817  
   water injection wells and facilities, 817  
 Oil products, 821  
 Oil refining, 819–921  
 Oilfield corrosion test environments,  
   156–157  
 Online monitoring, industrial  
   applications, 191–192  
 Open circuit corrosion potential,  
   microbiological effects, 512  
 Optical etching, 70  
 Organic coatings, 127, 394  
 Organic compounds, 542, 569, 746–747  
 Organic liquids, 448–456  
   cathodic process, 454  
   corrosion types, 448–449  
   coupon testing, 454  
   electrochemical testing, 455  
   environment, 448–449  
   environmental variables, 451–454  
   field testing, 455–456  
   surface film, 453  
   unique aspects, 449–451  
   variables, 449  
   water content, 450, 452  
 Outdoor atmospheres, 343–348  
   acidity/alkalinity, 541  
   corrosion yard instrumentation, 344–345  
   ISO corrosion classification system,  
     347–348  
   laboratory simulation tests, 348  
   site selection and preparation, 343–344  
   special testing procedures, 346–347  
   stainless steels, 588  
   terminology, 344  
   test specimens and identification,  
     345–346

Overhead ground wires, electric power, 725  
 Overvoltage values, 26  
 Oxalic acid etch tests, 253–255  
 Oxidation  
   high-temperature, 197, 436  
   metallographic analysis, 74  
 Oxidation rate laws, high-temperature gases, 436–437  
 Oxidation reduction potential, water handling systems, 831  
 Oxidation testing, 575, 597  
 Oxide formation model, dealloying, 281  
 Oxidizing salts, copper and copper alloys, 569  
 Oxygen  
   content, pipeline, 698  
   dissolved, in seawater, 365–366  
   in sodium, 469  
   in soils, 390, 392

## P

- Paint, evaluation in commercial aircraft, 689, 691  
 Paper machine, 795–798  
 Paper, *see* Pulp and paper  
 Parabolic rate law, 436  
 Parabolic reaction kinetics, high-temperature corrosion, 195  
 Parabolic rate law, 436–437  
 Particle induced X-ray emission, 81  
 Particles  
   effect on lead metal-matrix composites, 646  
   transport, indoor atmospheres, 352  
   *see also* Fine particles  
 Parting limit, 282–283  
 Passivation, metals processing, 775–776  
 Penetration rate, corrosion rate conversion to, 109  
 Percolation model, dealloying, 281  
 Performance assessment, piers and docks, 720  
 Permeation method, 123–124  
 Petroleum production and refining, 425–433, 812–821  
   corrosion testing, application to new production, 431–432  
   crude oil, 427–429, 431  
   environments, 425–427  
   gas and gas condensate phases, 426  
   hydrocarbon gas systems, corrosion testing, 430  
   laboratory corrosion testing, 429–431  
   liquid water phase, 426–427  
   physical phases, 425  
   preventing changes in solution chemistry, 431  
   produced water systems, corrosion testing, 430–431  
   sweet/sour, 425  
   temperature and pressure, 426  
   oil and gas production, 812–819  
 pH  
   in chemical processing, 781  
   corrosion inhibitors, 484  
   industrial chemicals, 419–420  
   seawater, 366  
   soils, 390, 400  
 Pharmaceutical materials, 846–847  
 Phase transport-controlled erosion, seawater, 370  
 Phosphor bronzes, 567  
 Physical properties, 31–32, 37  
 Physical vapor deposition, 621  
 Pickling, zirconium and hafnium, 614  
 Piers and docks, 716–721  
   composite materials, 716–717  
   corrosion control, 719–720  
   corrosive environments, 717–719  
   design, 719–720  
   immersion zone, 718  
   intertidal zone, 718–719  
   marine atmosphere zone, 719  
   materials selection, 717  
   need for standardization, 721  
   performance assessment, 720  
   problem areas, 720  
   protective coatings, 719  
   reinforced and prestressed concrete, 716  
   sediment zone, 718  
   splash and spray zone, 719  
   test methods, 720–721  
   wood, 716  
 Pilot plant testing, chemical processing, 784  
 Pipe coupon, 701  
 Pipeline, 696–704  
   above-ground installation, 699–700  
   bimetallic couples, 700  
   buried, external corrosion direct assessment, 402–404  
   close interval survey, 703  
   corrosion control, 698–700  
   corrosion environments, 697–698  
   corrosion resistance alloy, 818  
   coupons, 701, 704  
   electrochemical methods, 702–703  
   environmental cracking, 700  
   in-place measurement, 701  
   instrumented pigs, 702  
   materials, 696–697  
   mechanical damage, 700  
   monitoring corrosion, 818–819  
   oil and gas production, 817–819  
   remote monitoring, 704  
   statistical evaluation, 702  
   stress differences, 700  
   ultrasonic inspection, 701–702  
   visual evaluation, 700–701  
   welds, 700  
 Pipeline risk evaluation, corrosion index, 97–99  
 Pit propagation rate test, 218  
 Pitting, 63, 211–220, 791  
   alteration of test methods, 213  
   aluminum and aluminum alloys, 552, 554  
   causes, 93  
   copper and copper alloys, in condenser tubes, 572–573  
   corrosion potential, 213  
   coupon testing, 211–213  
   critical temperature tests, 218  
   cyclic polarization, 215–217  
   electrochemical noise, 218–219  
   electrochemical tests, 213–219  
   exposure environments, 212–213  
   freshwater, 178, 383  
   galvanostatic measurements, 217  
   medical and dental materials, 839–840  
   metal-matrix composites, 651  
   metallographic analysis, 71  
   metals processing, 774–775  
   nickel and nickel alloys, 581, 583  
   potentiostatic measurements, 217–218  
   predictive capabilities, 219  
   pulp and paper, 797  
   salt spray (fog) testing, 212–213  
   seawater, 369  
   Seawater corrosion testing, 171  
   shot noise methods, 121–122  
   soils, 392–393  
   specimen preparation, 211–212  
   stainless steels, 588–589  
   steels, 561  
   titanium, 605–606  
 Pitting potentials, microbiological effects, 514  
 Plate steel, 562–563  
 Polarization methods, 109–117  
   concentration effects, 110–111  
   freshwater, 382–383  
   metal-matrix composites, 650  
   pipeline, 702–703  
 Polarization resistance, 60, 111–112  
   electrodeposited coatings, 661  
   measurements, complications, 112  
   microbiological effects, 513  
   solution resistance, 110  
 Polarization scans, corrosion prediction, 100  
 Polishing, 68–69  
 Population, 83  
 Potential, 59, 120–121  
 Potential mapping, soils, 185  
 Potential measurements, pipeline, 703  
 Potential probe methods, 118  
 Potentiodynamic methods, 122–123  
 Potentiodynamic polarization, 789  
 Potentiodynamic sweep techniques, microbiological effects, 514  
 Potentiostatic tests, 119, 217–218, 576  
 Poured concrete lining, 707  
 Powder metallurgy materials, 664–669  
   atmospheric testing, 665  
   electrochemical tests, 666–667  
   ferrozyl test, 667–668  
   immersion tests, 665–666  
   salt spray tests, 666  
   sintered stainless steels, 668–669  
 Power conversion and auxiliary systems, 729, 732–733  
 Precast concrete lining, 706  
 Precipitation-hardening alloys, stainless steels, 587  
 Precorroded surfaces, inhibition, 496–497  
 Pressure vessels, nuclear power, 728–729  
 Pressurized corrosion tests, 147–149  
 Probability distribution, 83–84, 84–85  
 Probability functions, propagation, 94–99  
 Probability sampling, 53  
 Probe testing, chemical processing, 787–788  
 Process control, hydrogen damage, 328–329  
 Produced water gas systems, corrosion testing, 430–431  
 Programmed stress intensity experimentation, corrosion fatigue, 316  
 Protective coatings and films  
   aluminum and aluminum alloys, 547, 549–550, 556  
   copper and copper alloys, 565  
   electrochemical evaluation, 125–127  
   metallic, on steel, 628  
   stainless steels, 585  
 Pulp and paper, 795–806  
   bleach plant, 798–800  
   chemical pulping, 800–803  
   corrosion fatigue, 798  
   corrosion inhibitors, 797

electrochemical testing, 797  
 mechanical pulping, 803  
 microbiologically influenced corrosion, 797  
 pitting, 797  
 recovery boiler, 803–805  
 structural coatings testing, 798

## Q

Quality control tests, metals processing, 771

## R

Rain, military aircraft and equipment, 695  
 Randomization, 53–55  
 Reactor coolant systems, nuclear power, 728–733  
 Redox potential, microbiological effects, 512–513  
 Reference potentials, conversion factors, 27  
 Refiner plate corrosion and wear testing, 803  
 Refluxing capsules, liquid metals, 474  
 Refractories, copper smelting, 578  
 Reinforcement constituents, aluminum metal-matrix composites  
   effect on corrosion fatigue, 643–644  
   effect on stress corrosion, 642–643  
 Remote crevice assembly, microbiological effects, 517  
 Remote monitoring, pipeline, 704  
 Replication, 83  
 Residual fuel oil corrosion tests, high-temperature corrosion, 200  
 Resistance probes, freshwater, 383  
 Resistivity, 399–400, 405  
 Retaining walls, 707  
 Ringer's solution, 841  
 Ripple loads, hydrogen damage, 333  
 Risk assessment, gas pipeline, 95–97  
 Rotating cylinder technique, liquid metals, 475  
 Rutherford Backscatter Spectroscopy, 81

## S

SAE 1941, 683  
 SAE H1293, 684  
 SAE H1859M, 684  
 SAE H2929M, 684  
 SAE HS-23, 683  
 SAE HS-40, 683  
 SAE J207, 684  
 SAE J304, 683  
 SAE J400, 681, 684  
 SAE J401, 861  
 SAE J814, 683  
 SAE J1034, 683  
 SAE J1047, 681, 683, 684  
 SAE J1211, 683  
 SAE J1280, 682  
 SAE J1293, 681, 682, 684  
 SAE J1434, 861  
 SAE J1562, 861  
 SAE J1563, 627, 681, 684, 758  
 SAE J1677, 861  
 SAE J1703, 683, 684  
 SAE J1705, 683  
 SAE J1755, 861  
 SAE J1879, 683  
 SAE J1885, 684  
 SAE J1950, 625, 681, 683  
 SAE J1976, 681, 684

SAE J2020, 680  
 SAE J2334, 132, 136–137, 527, 627, 630, 635, 681, 684, 861  
 SAE P78, 682  
 SAE P228, 681  
 SAE USCAR-1, 132  
 Safety, high-temperature/high-pressure corrosion testing, 154  
 Salinity, seawater, 366  
 Salt droplet test, copper and copper alloys, 571  
 Salt spray (fog) testing, 131–132  
   copper and copper alloys, 570–571  
   electrodeposited coatings, 660  
   lead and lead alloys, 535  
   military aircraft and equipment, 694  
   modified, copper and copper alloys, 571  
   pitting, 212–213  
   powder metallurgy materials, 666  
   seawater, 372  
 Salt water, *see* Seawater  
 Salts  
   copper and copper alloys, 569  
   lead and lead alloys, 534–535  
   stainless steels, 588  
   *see also* Molten salts  
 Salt/SO<sub>2</sub> spray (fog) test, 134  
 Sample, 66  
   definition, 83  
   etching, 69–71  
   fixturing and mounting, 66–67  
   grinding, 67–68  
   metallographic interpretation, 71  
   polishing, 68–69  
   selection, 66  
 Sand, military aircraft and equipment, 695  
 Scanning auger microscopy, 78  
 Scanning electron microscopy, 72  
 Scanning force microscopy, 81  
 Scanning Kelvin probe, 81–82  
 Scanning tunneling microscopy, 81  
 Scanning vibrating probe techniques, microbiological effects, 515  
 Scratch repassivation, 120, 122  
 Sealers, concrete, 410  
 Seals, 780  
 Seawater, 362–376  
   biological organisms, 366–367  
   composition, 263  
   corrosion mechanisms, 369–371  
   dealloying, 370  
   deep ocean, 364  
   dissolved oxygen, 365–366  
   ennoblement, 371  
   environmental zones, 362–364  
   heavy metals, 368–369  
   hydrogen embrittlement, 371  
   mud, 364  
   pH and carbonates, 366  
   phase transport-controlled corrosion, 370  
   salinity effect, 366  
   splash/spray, 363  
   standards, 374–375  
   submerged/shallow ocean, 363–364  
   sulfides, 368  
   temperature effects, 364–365  
   tidal zone, 363  
   turbulence, 368  
   under-deposit attack, 369  
   uniqueness, 364  
 Seawater corrosion testing, 170–174, 371–374  
   cavitation, 370

copper and copper alloys testing, 568, 572  
 corrosion performance of materials, 375–376  
   crevice corrosion, 171, 369  
   deep ocean testing, 172–173  
   duration of exposure, 171  
   electrochemical impedance spectroscopy, 373  
   electrochemical testing, 372–373  
   electrical resistance probes, 374  
   environmental cracking, 370, 373–374  
   erosion corrosion, 370  
   field evaluation, 374  
   galvanic corrosion, 171, 369–370  
   general corrosion and pitting, 171  
   high velocity flow testing, 373  
   immersion testing, 372  
   in-service testing, 374  
   intergranular corrosion, 370  
   laboratory evaluation, 371–372  
   number of specimens, 171  
   pitting, 369  
   salt spray (fog) testing, 372  
   simulated service testing, 374  
   slow strain test, 373  
   specimen configuration, 170–171  
   specimen evaluation, 173  
   specimen exposure and retrieval, 172–173  
   specimen preparation, 171–172  
   static testing, 172  
   stress corrosion, 171  
   ultrasonic measurements, 374  
   velocity testing, 172, 367–368  
 Secondary ion mass spectroscopy, 80  
 Secondary neutral mass spectroscopies, 80–81  
 Sediment zone, piers and docks, 718  
 Seesaw capsules, liquid metals, 474–475  
 Sensitization, 784, 802–803  
 Service testing  
   high-temperature corrosion, 198–200  
   nonmetallic coatings, 636  
 Sheet steel, 562  
 Shot noise methods, pitting, 121–122  
 SHRP C 103, 410  
 $\sigma$  phase formation, metallographic analysis, 73  
 Silicon stainless steels, 586  
 Silicon carbide, effect on metal-matrix composites, 639–641, 645, 648  
 Simulated field failures, telecommunications, 765–766  
 Simulated-service tests, 625, 771  
 Single phase flow, 64–65  
 Sipon test, 792  
 Slow-strain-rate tension tests, 337–338  
 Slow strain rate test, 373, 606, 791–792, 815  
 Small crack methods, corrosion fatigue, 316–317  
 Smooth specimen  $\Delta\sigma$  life method, corrosion fatigue, 310–311  
 Sodium, oxygen in, 469  
 Soil resistivity, pipeline, 697  
 Soils, 181–186, 387–404  
   aeration and oxygen content, 390, 392  
   anaerobic bacteria, 391  
   biological activity tests, 401  
   burial site, 182  
   cleaning and examination of specimens, 183  
   considerations for physical measurements, 182

- copper and copper alloys, 568, 576
- corrosion, 391–395
- corrosion protection, 394
- definition and classification, 387–388
- direct and indirect measurements, 395–396
- dissolved salts and corrosion agents, 390
- disturbance of natural soils, 391
- electrical resistance probe, 396
- electrochemical laboratory tests, 401–402
- electrochemical measurements, 184–186
- external corrosion direct assessment, buried pipelines, 402–404
- factors affecting corrosion, 708
- field and laboratory tests, 396–397
- galvanic corrosion, 185, 392–394
- highways, tunnels, and bridges, 708, 712
- lead and lead alloys, 534, 535
- maintaining records, 181
- measurement for ions, 400–401
- microbiological activity, 390–391
- moisture, 388–389
- permeability to moisture and air, 698
- pH, 390, 400, 697–698
- pit depth, 184
- pitting corrosion, 392–393
- potential mapping, 185–186
- potential measurement in situ, 397–398
- redox potential, 397–398
- resistivity, 399–400
- specimen design, 181–182
- specimen emplacement, 182–183
- specimen retrieval, 183
- steels, lead, and copper, 394–395
- stray current corrosion, 392
- stress-corrosion cracking, 393
- stress induced failure, 184
- weight loss, 183–184
- zinc, 529
- Solar radiation, military aircraft and equipment, 694–695
- Solubility, 323
- Soluble ion content, pipeline, 698
- Solution line, 782–783
- Solution, stability, 784
- Solvents, physical properties, 452
- Specimen preparation, 144–145, 198–199, 211–212
- Splash zone, 719, 782
- Spray zone, piers and docks, 719
- Sputter rates, 79
- SS117211, 527–529, 681
- Staining corrosion, 553–554
- Stainless steels, 585–589
  - acids, 587–588
  - alkalis, 588
  - alloying effects, 585
  - aluminum addition, 585
  - austenitics, 586
  - composition, 247
  - concrete, 410
  - copper, 585
  - crevice corrosion, 589
  - duplex, 587
  - ferritics, 586–587
  - general corrosion, 588
  - grain boundary composition, 246
  - intergranular corrosion, 588
  - liquid metals, 588
  - manganese, 585
  - martensitic, 587
  - metal-matrix composites, 646–647
  - microstructure, 586
  - mill products, 587
  - molybdenum, 586
  - nickel, 585
  - niobium, 585
  - nitrogen, 585
  - outdoor atmospheres, 588
  - piers and docks, 716
  - pipeline, 696
  - pitting corrosion, 588–589
  - precipitation-hardening alloys, 587
  - protective film, 585
  - salts, 588
  - seawater corrosion, 376
  - silicon, 586
  - sintered, processing and quality control, 668–669
  - in soils, 395
  - stress corrosion cracking, 100–101, 589
  - titanium, 586
  - susceptibility to intergranular attack, 247–250
  - weld-decay zones, 249
- Static atmospheric testing, metallic coatings on steel, 625–626
- Static isothermal capsules, liquid metals, 473–474
- Static testing, 148, 172
- Statistical methods, 83–88
  - analysis of variance, 87–88
  - covariance of independent variables, 87
  - data analysis, 86–88
  - design experiments, 85–86
  - factorial experiments, 85–86
  - metals processing, 777
  - multiple regression analysis, 87–88
  - probability distribution, 84–85
  - stress corrosion cracking data, 299
  - terminology, 83
- Statistical modeling, 53–54, 94
- Steady state corrosion rate, corrosion inhibitors, 485
- Steam, copper and copper alloys, 568
- Steam generation, 738–744
  - accelerated tests, 743
  - corrosion control, 741–742
  - corrosion mechanisms, 738
  - corrosive environments, 739–741
  - critical areas, 738
  - detection of corrosion, 744
  - equipment description, 738–739
  - in-service monitoring, 743
  - materials of construction, 739–740
  - problem areas, 742
  - test methods, 742–744
  - testing objectives, 739
- Steels, 558–564
  - aqueous environments, 559
  - atmospheric environment, 559
  - bar, plate and structural shapes, 562–563
  - crevice corrosion, 561
  - electric power towers, 724
  - engineering properties, 620
  - environmental effects, 559
  - galvanic corrosion, 561
  - high-strength, commercial aircraft, 689
  - high-strength low-alloy, 558
  - high temperatures, 559
  - metallurgical effects, 558–559
  - microstructure, 559
  - pipeline, 696
  - pitting corrosion, 561
  - sheet and strip, 562
  - in soils, 394–395, 559
  - stress corrosion cracking, 561–562
  - test methods, 560–562
  - testing considerations, 559–560
  - tubular products, 563–564
  - uniform corrosion, 560–562
  - wire, 564
  - see also* Metallic coatings on steel
- Stockholm sign invariant convention, 59
- Strain rate, hydrogen damage effect, 328
- Stray current corrosion, 392–393, 699
- Stress corrosion cracking, 64, 191, 289–300, 791–792
  - alloying additions, 290–291
  - aluminum and aluminum alloys, 553–554
  - aluminum metal-matrix composites, reinforcement constituents, 642–643
  - chemical pulping, 802
  - cobalt-base alloys, 593–594
  - copper and copper alloys, in Mattsson's solution, 570
  - correlation of test results with service performance, 298
  - dealloying, 279
  - dynamic testing, 298
  - electrochemical factors, 291–292
  - environmental factors, 291
  - expert systems, 99
  - freshwater, 179–180, 386
  - hydrogen damage, 325
  - magnesium and magnesium alloys, 540–541
  - mechanical stress conditions, 292
  - medical and dental materials, 840
  - metal-matrix composites, 651
  - metallographic analysis, 71
  - metallurgical factors, 291
  - metals processing, 773–774
  - nickel and nickel alloys, 583
  - pipeline, 700
  - precracked specimens, 295–297
  - principles, 289–290
  - relationship with corrosion fatigue, 310
  - seawater corrosion testing, 171
  - stainless steels, 100–101, 589
  - standards, 299–300
  - statistical treatment of data, 299
  - steels, 561–562
  - test environments, 295
  - test specimens, 293–295
  - testing techniques, 292–298
  - titanium, 600, 606–607
- Stress induced failure, soils, 184
- Strip steel, 562
- Structural coatings testing, pulp and paper, 798
- Structural shapes, steels, 562–563
- Structure significant items, 97
- Sucker rods, 816
- Sulfidation, 74, 441–443
- Sulfide stress cracking, oil and gas production, 814–815
- Sulfides, seawater, 368
- Sulfite pulping corrosion, 803
- Sulfur-containing environments, 159–160, 197–198
- Sulfur corrosion tests, high-temperature corrosion, 200–201
- Sulfur ion content, corrosion fatigue, 309
- Sunshine, military aircraft and equipment, 694–695
- Superheater, 805
- Surface analysis, 76–82
  - auger electron spectroscopy, 77–79
  - comparison of techniques, 77
  - ion scattering spectroscopy, 81

limitations, 76  
 near surface techniques, 81  
 particle induced x-ray emission, 81  
 principles, 76–77  
 Rutherford backscatter spectroscopy, 81  
 scanning force microscopy, 81  
 scanning Kelvin probe, 81–82  
 scanning tunneling microscopy, 81  
 secondary electron microscopy-energy dispersive  
 X-ray spectroscopy, 81  
 secondary ion mass spectroscopy, 80  
 secondary neutral mass spectroscopies, 80–81  
 in situ methods, 81–82  
 surface analysis by laser ionization, 81  
 X-ray photoelectron spectroscopy, 79–80  
 Surface analysis by laser ionization, 81  
 Surface diffusion, dealloying, 280–281  
 Surface finish, coupons, 784  
 Surface modification, medical and dental materials, 838–839  
 Surface piping, oil and gas production, 817–819  
 Sustained load cracking, titanium, 608  
 Synthetic crevice devices, industrial waters, 416  
 Synthetic dust mixture, indoor atmospheres, 357–358

## T

TA-NWT-0011322, 767  
 TA-TSY-001001, 767  
 TA-TSY-041, 767  
 Tafel approximation, 108  
 Tafel expression, 109–110  
 Tafel extrapolation, 110, 372, 790  
 Tafel polarization, microbiological effects, 513–514  
 Tantalum, 617–619  
 TAPPI TIP 0402–08, 798  
 TAPPI TIP 0402–09, 798  
 TAPPI TIP 0402–29, 803  
 Telecommunications, 762–768  
 accelerated tests, 766  
 aerial cable hardware, 763  
 cables and closures, 762–763  
 corrosion control, 763–764  
 corrosion detection, 766  
 corrosion evaluation, 767  
 corrosive environments, 762  
 electrochemical tests, 766  
 environmental simulation, 766  
 in-plant testing, 767–768  
 in-service monitoring, 764–765  
 manholes, 763  
 problem areas, 764  
 simulated field failures, 765–766  
 test methods, 764–766  
 Temperature, hydrogen damage effect, 328  
 Temperature shock, military aircraft and equipment, 694  
 Tensile test, oil and gas production, 815  
 Terminology, 7–11, 83  
 Terne, as metallic coatings, 623  
 Test heat exchanger, 415–416, 832–833  
 Thermal-convection loops, liquid metals, 475–476

Thermal spray, 621  
 Thermodynamics, 436, 792  
 Thin layer activation, industrial waters, 416  
 Three-point bend tests, 336–337  
 Threshold stress intensity factor, hydrogen damage, 333–336  
 Tilting-furnace capsules, 474–475  
 Time domain, 61–62  
 Tin brasses, 566  
 Tin-free steel, 623  
 Tinplate, as metallic coatings, 623  
 Titanium, 598–611  
 commercial alloys, 598–599  
 corrosion resistance, mechanism, 598–599  
 coupon surface finish, 602–603  
 crevice corrosion, 604–605  
 density values, 604  
 failure prediction, 94  
 forms of corrosion, 601–602  
 general corrosion testing, 601–604  
 hydrogen role, 601  
 hydrogen testing, 607–609  
 ignition testing, 609  
 immersion testing, 604  
 metal-matrix composites, 647–648  
 metallurgical factors, aqueous media, 600–601  
 oxidation tests, 610–611  
 passivity in aqueous media, 599–601  
 pitting, 605–606  
 protective oxide film, 600  
 slow-strain-rate testing, 606  
 stainless steels, 586  
 stress corrosion cracking, 600, 606–607  
 surface corrosion products, 603  
 sustained load cracking, 608  
 Titanium alloys, seawater corrosion, 376  
 Top down approach, 95–99  
 Towers, electric power, 724  
 TR 1/NACE 6G194, 862  
 TR 2/NACE 6G198, 862  
 TR-TSY-009, 767  
 Tribo-ellipsometric methods, 122  
 Tunnels, *see* Highways, tunnels, and bridges

## U

Ultrasonic inspection, pipeline, 701–702  
 Ultrasonic measurements, seawater, 374  
 Uncontrolled experiments, 86  
 Uniform corrosion, 205–210  
 aluminum and aluminum alloys, 553  
 electrochemical tests, 207–210  
 mass loss tests, 206–208  
 metal-matrix composites, 651  
 nickel and nickel alloys, 581–582  
 steels, 560–562  
 theory, 205–206  
 Unit symbols, ASTM, 14–16  
 Units, relationships, 22  
 Uranium, depleted, metal-matrix composites, 646

## V

Variance, 84, 87–88  
 VDA 621–415, 132

Velocity sensitive corrosion, 64–65  
 Velocity testing, 172  
 Vibratory polishing, 68–69  
 Volume diffusion model, dealloying, 279–280  
 Volvo Std 1027, 681  
 Volvo Std 1372, 681

## W

Water  
 chemistry, effect on corrosion, 175–176  
 content, organic liquids, 450, 452  
 copper and copper alloys, 568  
 highways, tunnels, and bridges, 708–709, 712  
 physical properties, 37  
 potable, copper and copper alloys testing, 572  
 presence in chemical processing, 780  
*see also* Industrial waters  
 Water handling systems, 826–833  
 chemical analysis, 830–831  
 corrosion coupons, 826–828  
 dissolved oxygen monitoring, 831  
 electrical resistance meter, 829–830  
 heat transfer systems, 832  
 linear polarization-resistance meter, 828–829  
 oxidation reduction potential, 831  
 test heat exchanger, 832–833  
 Water injection wells and facilities, 817  
 Waterwall tube laboratory testing, 804  
 Wear testing, cobalt-base alloys, 595–597  
 Web, 102  
 Weibull distribution, 85  
 Weight loss corrosion rate measurements, corrosion inhibitors, 487–488  
 Weight loss testing, freshwater, 382  
 Welds, 262, 700, 750, 780  
 Well drilling, 812–813  
 Wenner four-electrode method, 399  
 Wet deposition, 160  
 White liquors, 801  
 Windowed test vessels, 152  
 Wire, steels, 564  
 Wood, 716, 724

## X

X-ray photoelectron spectroscopy, 79–80

## Y

Yttria, effect on stainless steel metal-matrix composites, 647

## Z

Zinc-aluminum coatings, 622  
 Zinc and zinc alloys, 525–529  
 immersion corrosion, 529  
 metal-matrix composites, 649  
 as metallic coatings, 622, 624  
 Zinc-nickel coatings, 622  
 Zirconium, 613–616

[www.astm.org](http://www.astm.org)

ISBN 0-8031-2098-2

ASTM Stock# MNL20-2ND